

1001

Early response to microgravity in the analysis of whole transcriptome and live imaging. Masahiro Chatani¹, Akiko Mantoku¹, Kazuhiro Takeyama¹, Hiroya Morimoto¹, Takehiko Ito¹, Naoki Tanigawa², Koji Kubota², Hiromi Suzuki³, Satoko Uchida³, Fumiaki Tanigaki⁴, Masaki Shirakawa⁴, Yoshio Takano⁵, Akira Kudo¹. ¹Tokyo Institute of Technology, Japan, ²Chiyoda Corporation, Japan, ³Japan Space Forum, Japan, ⁴Japan Aerospace Exploration Agency, Japan, ⁵Tokyo Medical & Dental University, Japan

Introduction: In early on-orbit, it is known that alterations of fluid shift and blood pressure occur rapidly in the astronaut's body. However, other affection including the molecular mechanism of response to microgravity is unclear. We previously reported that mineral density was decreased in the pharyngeal bone region caused by the activation of osteoclasts in medaka fish systematically reared during two months in spaceflight. In this presentation, we examined initial response to microgravity *in vivo*.

Methods: In 2012, medaka fish 6 weeks after hatch were launched to the international space station (ISS) and preserved by RNAlater at early on-orbit; two and half days after launch. Alteration of the gene expression level was examined by the whole transcriptome analysis using HiSeq. In 2014, we performed again the space experiment for real-time tracing of cell signals *in vivo* in ISS. The transgenic medaka larvae after hatch were embedded in a gel and observed by fluorescent microscopy in ISS via remote operation from Tsukuba space center. For this experiment, we established 4 reporter medaka lines; TRAP-GFP/Osterix-DsRed, TRAP-GFP/Osteocalcin-DsRed, Cox2-GFP/TRAP-DsRed, and RANKL-GFP/MMP9-DsRed.

Results and discussion: Whole transcriptome analysis via RNAs extracted from whole-body tissues showed up-regulation of several genes, which are related to stress response, including KLF family. Gene ontology analysis suggested promotion of DNA replication in the flight group. In addition, RNAs extracted from the pharyngeal bone and teeth region showed significant up-regulation of osteoblast- and osteoclast-related genes, indicating that bone cells were preferentially reactive to microgravity. Live imaging of the pharyngeal region in medaka larvae after hatch showed the significant increase of osterix-DsRed and osteocalcin-DsRed signals in the flight medaka group, suggesting that microgravity initially promoted the osteoblast differentiation in early on-orbit.

Disclosures: Masahiro Chatani, None.

1002

1,25-Dihydroxyvitamin D Alters Human Skeletal Muscle Mitochondrial Oxygen Consumption through Changes in Mitochondrial Number and Nuclear mRNA Expression. Zachary Ryan¹, Theodore Craig¹, Clifford Folmes², Xuwei Wang³, Ian Lanza⁴, Niccole Schaible⁵, Jeffrey Salisbury⁶, K. Sreekumaran Nair⁴, Andre Terzic², Gary Sieck⁵, Rajiv Kumar¹. ¹Division of Nephrology & Hypertension, Department of Medicine, USA, ²Division of Cardiovascular Diseases, Department of Medicine, USA, ³Division of Biomedical Statistics & Informatics, Department of Health Sciences Research, USA, ⁴Division of Endocrinology, Department of Medicine, USA, ⁵Department of Physiology, Biophysics & Biomedical Engineering, USA, ⁶Department of Biochemistry & Molecular Biology, USA

Vitamin D deficiency is associated with muscle weakness and a myopathy that respond to therapy with vitamin D3. Furthermore, the vitamin D3 analogs, 1,25(OH)2D3 and 1(OH)D3, have been shown to reduce falls in humans. The goal of this study was to assess the mechanisms by which 1,25(OH)2D3 alters skeletal muscle function.

Since skeletal muscle is critically dependent upon oxidative metabolism and ATP synthesis for muscle contraction, we examined whether 1,25(OH)2D3 directly alters mitochondrial function in human skeletal muscle cells. Extracellular flux analysis was utilized to assess the impact of 1,25(OH)2D3 on the rate of skeletal muscle mitochondrial oxygen consumption (OCR). 1,25(OH)2D3 treatment induced a dose-dependent increase in the OCR of human muscle cell primary cultures. Indices of mitochondrial function including basal, ATP-dependent and maximal OCR increased following treatment of cells with 1,25(OH)2D3 without associated changes in glycolytic rates. 1,25(OH)2D3-treatment also increased mitochondrial volume and fragmentation. Vitamin D3 and analogs including 25-hydroxyvitamin D3, 24R,25-dihydroxyvitamin D3 and 1-hydroxyvitamin D3, decreased or did not change mitochondrial OCR. To examine the mechanism by which mitochondrial oxygen consumption is altered by 1,25(OH)2D3, we first confirmed the expression of the vitamin D receptor (VDR) in human skeletal muscle biopsies from normal subjects and in primary cultures of skeletal muscle cells. Knock-down of the VDR in primary cultures of human skeletal muscle cells with a VDR-specific silencing RNA, blocked 1,25(OH)2D3-dependent increases in the OCR. Next generation, whole transcriptome sequencing of mRNAs from 1,25(OH)2D3-treated skeletal muscle cells revealed VDR-dependent changes in the expression of 1947 mRNAs including eighty three nuclear mRNAs encoding mitochondrial proteins. Transcripts that were regulated in skeletal muscle cells by 1,25(OH)2D3 were involved in Janus kinase and signal transducer and activator of transcription, growth factor signaling and cytokine signaling and cell adhesion.

1,25(OH)2D3 alters skeletal muscle mitochondrial activity, volume and the expression of nuclear messenger RNAs encoding mitochondrial and cellular proteins via vitamin D receptor-dependent mechanisms.

Disclosures: Rajiv Kumar, None.

1003

Glucocorticoids induce bone and muscle atrophy by distinct mechanisms upstream of atrogenin1 and MuRF1. Amy Y. Sato¹, Ernie Au¹, Danielle Richardson¹, Nicoletta Bivi², Meloney Cregor¹, Kevin McAndrews¹, Hannah M. Davis¹, Teresa Zimmers³, Lilian I. Plotkin¹, Teresita Bellido¹. ¹Indiana University School of Medicine, USA, ²Eli Lil, USA, ³Indiana University Department of Surgery, USA

Excess glucocorticoids (GC), either endogenous as with aging or when used as immunosuppressants, leads to loss of mass in bone and muscle. We investigated herein whether the same or different mechanisms mediate GC-induced osteopenia and sarcopenia. Mice receiving GC for 14 or 28 days (slow release pellets, 2.1 prednisolone mg/kg/day) exhibit 90% reduction in bone formation rate in tibial cancellous, endocortical, and periosteal surfaces; as well as 15% decrease in lean body mass and ~20% decrease in the mass of the tibialis anterior and the gastrocnemius muscles. Expression of the atrophy-associated genes atrogenin1 and MuRF1 was increased in tibia/vertebra and tibialis anterior muscle from GC-treated mice. Moreover, these genes were upregulated by addition of the GC dexamethasone to differentiated primary cultures of calvaria derived osteoblasts, Ob-6 osteoblastic cells, MLO-Y4 osteocytic cells and undifferentiated (myoblasts) and differentiated (myotubes) C2C12 muscle cells. GC also increased the expression of the Notch ligands Dll1 and Jag1, Notch1-4 receptors and Notch target genes Hey1 and Hes1 in tibialis anterior muscles *in vivo*. Moreover, GC decrease C2C12 myotube diameter by ~20%, and the Notch inhibitor GSIXX prevented this effect. In contrast, GC did not increase components of the Notch signaling pathway in bone *in vivo* or in Ob-6 or MLO-Y4 cells *in vitro*. Instead, GC activated the FAK-related kinase Pyk2 in bone cells *in vitro*. Further, whereas WT littermates lost 5% spinal BMD in response to GC, Pyk2 KO mice were resistant to bone loss and gained 5% spinal BMD. In contrast, GC induced similar decreases in lean body mass (8%) and tibialis anterior and gastrocnemius muscle mass (19-25%) in WT and Pyk2 KO mice. Thus, GC activate different signaling pathways (Pyk2 in bone and Notch signaling in muscle), which converge in up-regulation of the same genes atrogenin1 and MuRF1 leading to loss of tissue mass. These findings provide the basis for combination therapy with Pyk2 and Notch inhibitors to treat GC-induced osteopenia and sarcopenia.

Disclosures: Amy Y. Sato, None.

1004

Suppressing Sclerostin Activity Alleviates Radiotherapy-Induced Osteoporosis by Accelerating DNA Repair in Osteoblasts and Their Progenitors. Tiao Lin¹, Abhishek Chandra², Xiaoyuan Ma³, Wei-Ju Tseng³, Keith Cengel⁴, Xiaowei Liu³, Ling Qin³. ¹University of Pennsylvania, USA, ²Departments of Orthopaedic Surgery, Perelman School of Medicine, University of Pennsylvania, USA, ³Departments of Orthopaedic Surgery, Perelman School of Medicine, University of Pennsylvania, USA, ⁴Departments of Radiation Oncology, Perelman School of Medicine, University of Pennsylvania, USA

Radiotherapy eliminates tumor cells but has untoward effects on neighboring normal tissues including bone, causing acute and chronic problems such as osteoradionecrosis, osteoporosis, and fractures. We have previously established a clinically relevant focal radiation model in rodent and demonstrated that PTH injections prevented bone loss in irradiated bone by stimulating beta-catenin to promote cell survival after radiation. Since a black box warning of PTH makes it an unlikely option for cancer patients, we explored whether activating Wnt canonical pathway via Sclerostin antibody (Scl-Ab) could be a superior alternative as it has no evidence for cancer concerns. To demonstrate its *in vivo* efficacy, we focally irradiated right distal femoral metaphysis of 2-month-old male C57BL/6 mice at a clinically relevant dosage (8 Gy at day 1 and 3) and treated mice with either vehicle or Scl-Ab (100 mg/kg) weekly. Compared to contralateral femurs, irradiated ones exhibited significant decreases in bone volume fraction (21%) and stiffness (56%) after 4 weeks. Strikingly, Scl-Ab not only blocked such structural deterioration but also improved bone quality in the radiated area to the same levels of non-radiated area. Interestingly, trabecular bone in sclerostin (SOST) KO mice was resistant to radiation, confirming that suppressing SOST activity is effective in reversing radiation-induced bone damage. Histomorphometry analysis revealed that, while radiation greatly reduces osteoblast number and activity and almost eliminates their progenitors, Scl-Ab treatment significantly increases osteoblast number (2.5 fold), mineral surface (4.7 fold), and CFU-F number (1.4 fold). *In vitro*, Wnt3a, a canonical Wnt ligand, almost completely mitigated radiation-induced apoptosis in osteoblasts and their progenitors by activating beta-catenin. We identified Ku70, a critical DNA repair protein, as a critical mediator of Wnt3a/beta-catenin-induced DNA repair after radiation. Lineage tracing using Col2-Cre Rosa-Tomato mice, in which all bone marrow mesenchymal progenitors, adipocytes, osteoblasts, and osteocytes are Td+, demonstrated that Scl-Ab reverted radiation-induced marrow adiposity by switching the fate of progenitors

from adipogenesis to osteogenesis. Taken together, our studies provide proof-of-principle evidence for a novel use of Scl-Ab as a therapeutic treatment for radiation-induced osteoporosis and establish molecular and cellular mechanisms that support such treatment.

Disclosures: Tiao Lin, Novartis

1005

Loss of DNMT3b in Chondrocytes Leads to Impaired Angiogenesis and Delayed Fracture Repair. Cuicui Wang*¹, Jie Shen¹, Tzong Jen Sheu², Regis O'Keefe¹. ¹Washington University in St. Louis, USA, ²University of Rochester Medical Center, USA

While cell signaling mediated by local and systemic factors has been extensively investigated, there is less understanding of the role of epigenetic changes in the regulation of bone regeneration. The DNA methyltransferase enzymes (DNMTs) DNMT3a and DNMT3b have tissue specific expression patterns and create unique methylation signatures to regulate gene expression. Using a stabilized murine tibia fracture model we find that *Dnmt3b* is induced early in fracture healing, peaks at 10 days post fracture (dpf), and then declines to nearly undetectable levels by 28 dpf. DNMT3b expression was cell and stage specific. High levels were observed in mesenchymal progenitor cells and in proliferating and prehypertrophic chondrocytes within the fracture callus. To determine a functional role for *Dnmt3b* in fracture healing the gene was conditionally deleted in chondrocytes in fractures of *Agc1Cre^{ERT2};Dnmt3b^{fl/fl} (Dnmt3b^{Agc1ER})* mice by daily administration of tamoxifen (10 mg/kg body weight; dpf 1-7). Fracture callus in mice with gene deletion had delayed chondrogenesis, prolongation of endochondral bone formation with persistence of cartilage matrix, and a delay in the later events of angiogenesis, ossification and bone remodeling. Biomechanical studies demonstrated markedly reduced strength in *Dnmt3b^{Agc1ER}* fractures and confirmed the delay in repair. The angiogenic response was assessed by MicroCT and showed a marked reduction in both vessel number and volume at 10 and 14 dpf in *Dnmt3b^{Agc1ER}* mice. Immunohistochemistry showed decreased PECAM expression, consistent with the reduced angiogenesis. Finally, *in vitro* angiogenesis assays with HUVECs revealed that loss of DNMT3b in chondrocytes significantly reduced capillary tube formation and endothelial migration; however, HUVEC proliferation and apoptosis appeared largely unaffected. To identify specific angiogenic factors involved in the decreased callus vascularization, a protein array was performed using media isolated from cell cultures of control and DNMT3b LOF chondrocytes. Several angiogenic factors, including OPN, PAI1, SDF-1/CXCL12, and TIMP1 are reduced in chondrocytes following loss of DNMT3b. Altogether, our findings establish that epigenetic modulation mediated by DNMT3b is a key event that occurs during the endochondral bone repair process, with gene ablation leading to impaired angiogenesis and delayed fracture repair.

Disclosures: Cuicui Wang, None.

1006

High Bone Mass is associated with bone-forming features of osteoarthritis at non-weight bearing joint sites, independent of Body Mass Index. Aaron Murphy¹, Sarah Hardcastle¹, Martin Williams², George Davey Smith³, Jon H Tobias¹, Celia Gregson^{*4}. ¹Musculoskeletal Research Unit, School of Clinical Sciences, University of Bristol, United Kingdom, ²Department of Radiology, North Bristol NHS Trust, United Kingdom, ³MRC Integrative Epidemiology Unit at the University of Bristol, United Kingdom, ⁴University of Bristol, United Kingdom

Objectives

We have previously reported associations between High Bone Mass (HBM) and (a) radiographic knee osteoarthritis (OA), in part mediated by increased body mass index (BMI) in HBM cases and (b) enthesophytes and osteophytes, suggestive of a bone-forming phenotype in HBM. In this study we aimed to determine (i) whether HBM is also associated with OA at non weight-bearing skeletal sites, (ii) if OA at these sites also displays a bone-forming phenotype and (iii) whether increased BMI contributes to any association found.

Methods

HBM cases (identified by screening 335,115 DXA scans; defined by BMD Z-scores $\geq +3.2$) from the UK-based HBM study were compared with unaffected family controls. A single blinded assessor graded AP dominant hand radiographs from cases and controls for features of OA (osteophytes and joint space narrowing (JSN) (0-3), subchondral sclerosis (0-1)) at the index Distal Interphalangeal Joint (DIPJ) and 1st Carpometacarpal Joint (CMCJ)), using an atlas. Analyses used logistic regression, adjusting *a priori* for age and gender. The role of BMI as a mediating factor was explored by further adjusting for BMI in regression models in Stata v11. A second assessor graded 40 randomly selected radiographs: inter and intra-rater reliability Kappas all ≥ 0.6 .

Results

315 HBM cases (mean age 61.2 years, 75% female) and 184 controls (54.2 years, 84% female) were included. Osteophytes (grade ≥ 1) were more common in HBM (DIPJ: 67% vs. 45%, CMCJ: 70% vs. 50%), with adjusted OR [95% CI] 1.78 [1.11, 2.85], $p=0.017$ and 1.84 [1.19, 2.85], $p=0.006$ respectively; whilst no differences were seen in JSN. Subchondral sclerosis was more common amongst HBM cases than

controls, but was explained by age & gender adjustment. Further adjustment for BMI failed to attenuate the OR for osteophytes in HBM cases vs. controls; DIPJ 1.69 [1.05, 2.74], $p=0.031$ and 1st CMCJ 1.71 [1.09, 2.67], $p=0.019$.

Conclusion

Our findings support a positive association between HBM and OA in non-weight-bearing joints which is independent of BMI. This HBM-associated OA is characterised by osteophytes, consistent with a bone forming phenotype, rather than JSN reflecting cartilage loss. It is possible that the same systemic factors (e.g. genetic architecture) which govern HBM may also increase the risk of bone-forming OA.

Disclosures: Celia Gregson, None.

1007

Osteoarthritis and chronic back pain as predictors of postmenopausal falls. Nadia Afrin^{*1}, Heli Koivumaa-Honkanen², Toni Rikkonen¹, Heikki Kröger¹, Risto Honkanen¹. ¹University of Eastern Finland, Finland, ²Department of psychiatry, University of Eastern Finland, Finland

Introduction: Musculoskeletal diseases increase falling risk in the elderly. There is less information about this association in postmenopausal women.

Objective: The purpose of this study was to evaluate if and how musculoskeletal diseases predict falls in postmenopausal women.

Methods: Study design was prospective cohort by using Kuopio Osteoporosis Risk Factor and Prevention (OSTPRE) Study cohort. Information about musculoskeletal diseases and use of analgesics as exposure variables were obtained from the year 1999 enquiry and about falls in preceding 12 months as the outcome variable in 2004 enquiry. The study population consisted of 8955 women with complete information about falls and exposure variables. Women were fallers if they reported at least two falls per year (n=2069). Falls were classified into slip (n=727) and nonslip (n=1068) falls. There were 204 women with Rheumatoid arthritis, 1424 with Osteoarthritis, 1073 with Sciatica and 665 women with other back pain. Logistic regression was used as the statistical method.

Results: The women were 57-66 years old in 1999. History of osteoarthritis, sciatica and chronic back pain predicted slip falls as follows: (OR 1.3, 95% CI 1.1-1.5), (OR 1.2, 95% CI 1.0-1.5) and (OR 1.4, 95% CI 1.2-1.8) but rheumatoid arthritis did not do it (OR 0.8, 95% CI 0.5-1.3). The corresponding risks of nonslip falls were: 1.6 (95% CI 1.4-1.8), 1.6 (95% CI 1.4-1.8), 1.5 (95% CI 1.3-1.8) and 1.0 (95% CI 0.7-1.5) respectively. After adjusting for smoking, life satisfaction, self-rated health and number of chronic health disorders did not considerably change the strength of predictions.

Conclusion: Falling tendency is increased by history of main musculoskeletal diseases except rheumatoid arthritis in postmenopausal women.

Disclosures: Nadia Afrin, None.

This study received funding from: Academy of Finland

1008

Subchondral Bone in Human Osteoarthritic Knees Is Characterized By Trabecular Rod Loss and Trabecular Plate Stiffening. Yan Chen^{*1}, Bin Zhou², Ji Wang², Weimei Zhao³, FKL Leung⁴, Xu Cao⁵, William Lu⁶, X Edward Guo². ¹Department of Orthopaedics & Traumatology, Faculty of Medicine, the University of Hong Kong; Bone Bioengineering Laboratory, Department of Biomedical Engineering, Columbia University, USA, ²Bone Bioengineering Laboratory, Department of Biomedical Engineering, Columbia University, USA, ³Department of Orthopaedics & Traumatology, Faculty of Medicine, the University of Hong Kong, Hong Kong, ⁴Department of Orthopaedics & Traumatology, Faculty of Medicine, the University of Hong Kong; Shenzhen Key Laboratory for Innovative Technology in Orthopaedic Trauma, the University of Hong Kong Shenzhen Hospital, Hong Kong, ⁵Department of Orthopaedic Surgery, School of Medicine, Johns Hopkins University, USA, ⁶The University of Hong Kong, Hong Kong

Subchondral bone sclerosis leads to cartilage damage in osteoarthritis (OA). However, treatment with antiresorptive drugs attenuates OA cartilage erosions, suggesting that bone sclerosis may be accompanied by bone loss in OA. Thus, we aimed to evaluate trabecular plate and rod microstructural changes in subchondral bone based on the individual trabecula segmentation (ITS) technique and corresponding mechanical properties in human OA knees. Tibial plateaus were collected from knee OA patients (n=102) undergoing total knee arthroplasty, and from cadaver donors (n=25) without arthritis or bone diseases. The tibial plateaus were scanned using micro computed tomography (μ CT) at 17.3 μ m. Five cubic subchondral bone subregions were extracted from external, central, internal, anterior and posterior areas of both medial and lateral condyles, respectively, and subjected to ITS and μ CT based micro finite element (μ FE) analysis. The specimens were then processed for cartilage evaluation using the OARS system. On medial condyle and in internal and central subregions on lateral condyle where OA was severe, OA group has decreased rod volume fraction and number, while increased rod thickness and length, increased bone volume fraction (BV/TV), plate volume fraction (pBV/TV) and thickness than control group. However, trabecular plate number did not differ.

Moreover, OA group has dramatically increased plate to rod ratios but lower plate-plate, plate-rod and rod-rod junction density. In addition, axial bone volume fraction was drastically higher in OA group, indicating that the orientation of the trabecular bone network was more axially aligned than control group. These striking differences in trabecular bone microstructure resulted in much higher bone stiffness, as assessed by elastic moduli, in OA group. In external, anterior and posterior subregions on lateral condyle where OA was mild, the changes of most ITS parameters were similar to those on medial condyle, while BV/TV, pBV/TV and elastic moduli did not differ, suggesting that trabecular plate and rod changes in subchondral bone may proceed OA changes in cartilage. We found that subchondral bone within human OA knee is characterized by trabecular rod loss and trabecular plate stiffening. These changes lead to uneven distribution of trabecular bone density, and may increase focal shear stresses in cartilage. Trabecular rod loss probably precedes plate stiffening, and thus may play an important role in OA progression.

Disclosures: Yan Chen, None.

1009

A novel method for the assessment of joint space width and subchondral bone texture. Richard Ljuhar^{*1}, Astrid Fahrleitner-Pammer², Helena Canhao³, Hans Peter Dimai². ¹Braincon Technologies, Vienna, Austria; ²University of Technology, Vienna, Austria, At, ³Medical University Graz, Division of Endocrinology & Metabolism, Austria, ³Faculdade Medicina Universidade Lisboa, Portugal

OBJECTIVE: Assessment of osteoarthritis (OA) of the knee usually involves AP and lateral radiographs to evaluate medial and lateral joint spaces, but perspective errors and low reproducibility are limiting factors. In addition to joint space width, subchondral bone area may provide important information on the status of OA. However, no adequate standard has been developed so far to quantify subchondral changes. The method described here combines assessment of joint space width (JSW) and fractal analyses of the adjacent subchondral bone area to discriminate between patients with and without OA.

METHODS: The study included 274 standardized knee radiographs from 110 patients with OA, and 164 controls. Knee joint space analysis was performed at the medial and lateral compartment, applying a gradient based algorithm for automated detection of critical landmarks and joint space contour. Furthermore, subchondral bone texture was assessed by using fractal analysis at predefined regions of the proximal tibia. A matrix of 3x8 ROIs was used to gain sufficient textural information (FIG.). Self-similarity of the texture, reflecting 2D projection of the 3D trabecular structure, has been used to calculate the Bone Structure Value (BSV) which provides indirect information on bone quality.

RESULTS: Comparing mean BSVs of the control group and the OA group, a deviation of 7.04% in mean values was determined. The odds ratio showed that the control group had a 6.5 times higher probability to be measured with a BSV above 0.33 than the OA group. A combination of both, JSW & BSV showed a further increase in discriminative power between the control group and OA patients. The most powerful combination of JSW and BSV enabled a discrimination between control/OA in 97.83% of cases. Differences in BSV were found between left/right knee and male/female. Furthermore, a rising BMI was identified to be linked to lower BSV values.

CONCLUSIONS: The novel method described here is sufficient to discriminate between subjects with and without OA. Furthermore, fractal analysis alone may provide information on bone quality aspects. Future work should therefore also focus on the potential role of fractal analysis (in a possible combination with JSW assessments) to serve as a fracture risk assessment tool.



BSV_JSWSampleKneeOA

Disclosures: Richard Ljuhar, None.

1010

Effects of a Multi-modal Exercise Program on BMD, Muscle Function, Knee Cartilage Structure, Defects and Bone Marrow Lesions in Older Adults: An 18 month RCT. Robin Daly^{*1}, Jenny Gianoudis¹, Yuanyuan Wang², Christine Bailey³, Peter Ebeling⁴, Carvl Nowson¹, Kerrie Sanders⁵, Flavia Cicuttini², Keith Hill⁶. ¹Centre for Physical Activity & Nutrition Research, Deakin University, Australia, ²Department of Epidemiology & Preventive Medicine, Monash University Medical School, Alfred Hospital, Australia, ³NorthWest Academic Centre, The University of Melbourne, Western Health, Australia, ⁴School of Clinical Sciences, Monash University, Australia, ⁵Institute for Health & Ageing, Australian Catholic University, Australia, ⁶School of Physiotherapy & Exercise Science, Curtin University, Australia

Osteoporosis and osteoarthritis (OA) often coexist in older adults. While progressive resistance training (PRT) and weight-bearing impact exercise (Ex) are recommended to improve bone and muscle health and function, few studies have simultaneously examined the effects of such programs on knee and cartilage health in older adults. The aim of this study was to examine the effects of a multi-modal Ex program on bone, muscle and cartilage health in community-dwelling older adults at risk for falls and fracture. This was an 18-month RCT consisting of a 12-month structured and supervised intervention followed by a 6-month translational phase. 162 adults aged 60+ years were randomised to Ex (n=81) or a usual-care control group (n=81). Ex consisted of high velocity PRT, weight-bearing activities (60-180 impacts/session) and balance training 3 days per week for 18 months. Outcome variables included: DXA hip and spine BMD and total body lean mass (LM), and muscle strength, power and function (leg press, stair climb, 4-square test, TUG, sit-to-stand). MRI of the left knee was used to assess tibial cartilage volume, cartilage defects (CD) [tibiofemoral (TF) and patella] and TF bone marrow lesions (BMLs) in a subset of 120 participants. We assessed changes in CD and BMLs as both have been linked to increased cartilage loss and may be indicative of incipient OA. A total of 150 participants (93%) completed the study (97/120 had repeat MRI scans). Ex attendance averaged 55% (range 0-98%). After 18 months there were significant Ex-induced improvements in FN BMD (1.9%, P<0.001), muscle strength, power and function (net benefits 6-15%, P<0.05-<0.001) relative to Con, but no Ex effect on LM. The rate of loss in tibial cartilage volume was similar in both groups (Ex vs Con: medial, -2.5% vs -1.5%, P=0.27; lateral, -3.2% vs -2.5%, P=0.33), and an equal proportion of participants in the Ex and Con group demonstrated progression of CD (Ex vs Con; TF medial, 14% vs 15%; lateral 26% vs 28%; patella 12% vs 19%) and BMLs (Ex vs Con, TF medial 14% vs 17%; lateral 7% vs 5%). Furthermore, tibial cartilage loss was no different between the groups when stratified by the presence of CD or BMLs at baseline. In conclusion, this study indicates that a multi-modal, targeted bone loading exercise program is safe and effective for improving bone health and muscle function in older adults at increased risk of falls and fracture, with no adverse effects on knee cartilage structure.

Disclosures: Robin Daly, None.

1011

Activin Receptor Type IIA (ACVR2A) Functions Directly in Osteoblasts as a Negative Regulator of Bone Mass. Brian Goh^{*}, Vandana Singhal, Angelica Herrera, Thomas Clemens, Se-Jin Lee, Douglas DiGirolamo. Johns Hopkins University School of Medicine, USA

Bone and skeletal muscle mass are highly correlated in mammals, suggesting the existence of common anabolic signaling networks that serve to coordinate the development of these anatomically adjacent tissues. The activin signaling pathway is an attractive candidate to fulfill such a role. Our group and others have previously reported that mice treated with soluble activin receptors demonstrate both increased skeletal muscle mass and bone mass. In the present study, we have generated mice with conditional deletion of ACVR2A, ACVR2B, or both, specifically in osteoblasts, in order to determine the contribution of activin signaling in osteoblasts in regulating bone mass. Immunohistochemistry localized ACVR2A and ACVR2B to osteoblasts and osteocytes in trabecular and cortical bone. Primary mouse osteoblasts expressed major activin receptor signaling components, including ACVR2A, ACVR2B, and ACVR1B (ALK4), and demonstrated increased levels of phosphorylated Smad2/3 upon exposure to activin ligands. In vitro, osteoblasts lacking ACVR2B did not show significant changes in differentiation, however, osteoblasts deficient in ACVR2A exhibited enhanced differentiation by measures of alkaline phosphatase activity, mineral deposition, and increased transcriptional expression of *Osterix*, *Osteocalcin*, and *Dmp1*. To test the importance of activin receptor signaling in osteoblasts in vivo, we analyzed the skeletal phenotypes of mice selectively lacking these receptors in osteoblasts and osteocytes (Osteocalcin-Cre). Similar to the lack of effect noted in vitro, ACVR2B deficient mice demonstrated no significant change in any bone parameter. By contrast, both male and female mice lacking ACVR2A had significantly increased femoral trabecular bone volumes at six weeks of age. Further, compound mutant mice lacking both ACVR2A and ACVR2B demonstrated sustained increases in trabecular bone volume, similar to ACVR2A single mutants, in both male and female mice at six and twelve weeks of age. Taken together, these data indicate that activin signaling, predominantly through ACVR2A, functions directly in osteoblasts as a negative regulator of bone mass.

Disclosures: Brian Goh, None.

1012

Six-month of Spaceflight and 1 Year Follow-Up Revealed Differential Responses of Cortical and Trabecular Bone Dependent on Bone Localization and Starting Bone Status. Laurence Vico^{1*}, Myriam Normand², Bert Van Rietbergen³, Nicolas Vilayphiou⁴, Hervé Locrelle², Mohamed Zouch⁵, Maude Gerbaix², Galina Vassilieva⁶, Ivan Morukov⁶, Thierry Thomas².
¹University of St-Etienne, France, ²INSERM-U1059, Biologie du Tissu Osseux, University of Lyon, France, ³Eindhoven University of Technology, Netherlands, ⁴SCANCO Medical AG, Switzerland, ⁵Laboratory of Cardio-Circulatory, Respiratory, Metabolic, & Hormonal Adaptations to the Muscular Exercise, Faculty of Medicine Ibn-El-Jazzar, University of Sousse, Tunisia, ⁶INSTITUTE OF BIO-MEDICAL PROBLEMS, Russia

Introduction

Using pQCT, we previously found that the weight-bearing tibial site displayed trabecular and cortical bone losses after 6-month space exposure while the radius, being a non-weight bearing bone, did not exhibit any bone loss. During a 6-month follow-up survey after landing tibial bone loss persisted, suggesting that the time needed to recover is longer than the mission duration (Vico et al., Lancet 2000). In a new series of crewmembers, we aimed to better assess structural and mechanical changes and beyond 6-months after space sojourns up to one year to appreciate if and when bone is regained.

Methods

We measured bone density, microarchitecture and micro-finite element-derived bone strength at the distal radius and tibia using HR-pQCT in 13 spacemen [mean age 43.6 (35-54 years old)] who sojourned in the International Space Station (ISS) during 6 months. Measurements were done before flight, immediately after landing, and after 3, 6, and 12 months follow-up.

Results

Despite inter-individual variability among crewmembers, statistical analysis revealed the following alterations.

Radius: as found in previous missions, no significant bone loss was seen immediately after the flight. However, from 3 to 12 month post-flight Ct.Th and ultimate load, and at 12 month for trabecular BV/TV or density, declines were evidenced.

Tibia: we confirmed in these crewmembers a loss of bone during flight at both cortical and trabecular levels. One year after reentry, the recovery was effective for cortical thickness but not for trabecular BV/TV or density, and ultimate load.

In tibia, a negative correlation was found between Ct.Th preflight and the change in Ct.Th during flight ($R^2 = 0.41$, $p < 0.05$) showing that the thinner the initial cortex is the higher the inflight loss is.

Conclusion

Overall these results highlight the importance of analyzing different skeletal sites and compartments on long-term time journeys. A striking discovery of this study is the fact that the radius shows a progressive increase in fragility after reentry, suggesting that the return to ground following long-term space travel might be fraught with unsuspected skeletal recovery uncertainties.

1013

Osteolineage Notch ligand Jagged1 is critical for maintaining homeostatic trabecular bone mass. Rialnat Lawal^{1*}, Benjamin Frisch², Matthew Hilton³, Laura Calvi². ¹University of Rochester Medical Center, USA, ²University of Rochester, USA, ³Duke University School of Medicine, USA

Notch signaling regulates the progenitor subset of osteolineage cells and osteoblastic differentiation. While Notch receptors have been evaluated extensively, the specific contribution of individual Notch ligands is unknown. Parathyroid Hormone (PTH) regulates the expression of the Notch ligand Jagged1 in osteoblastic cells. Therefore, in the current study we examined if loss of osteolineage Jagged1 in vivo affects bone homeostasis. Selective deletion in osteolineage cells was achieved through excision of floxed Jagged1 alleles in the presence of Prx1 promoter-driven Cre recombinase expression, targeting mesenchymal stem cells (MSCs) and their progeny (P Jag1 mice). P Jag1 mice were viable and fertile and did not exhibit any skeletal abnormalities at 2 weeks or 1 month of age. At 2 months of age however, P Jag1 mice had increased trabecular bone mass without changes in cortical bone compared to wild-type (WT) littermates. Dynamic histomorphometric analysis revealed that osteoblastic activity was increased as demonstrated by significantly increased mineral apposition rate. Immunohistochemical analysis showed increased numbers of osteocalcin positive mature osteoblasts in P Jag1 mice. Also increased phenotypically defined Lin-/CD45-/CD31-/Sca1-/CD51+ osteoblastic cells were measured by flow cytometric analysis. Surprisingly, phenotypically defined Lin-/CD45-/CD31-/Sca1+/CD51+ MSCs were unchanged in P Jag1 mice as measured by flow cytometric analysis, while functional osteoprogenitor (OP) cell frequency, measured by Von Kossa+ colony formation, was decreased. Together these data suggest that osteolineage Jagged1 is critical for maintenance of the OP pool. Coupled with the increase in mature osteoblast numbers and activity, P Jag1 mice had increased osteoclastic activity, suggesting that trabecular increases are not due to osteoclastic defects. Since PTH increases osteoblastic Jagged1, we sought to understand if a role for osteolineage Jagged1 exists in PTH-mediated bone anabolism. PTH-dependent bone anabolism resulted in a significantly greater increase in BV/TV in P Jag1 hind limbs compared to WT. These findings demonstrate a critical role of osteolineage Jagged1 in bone homeostasis, where Jagged1 restricts the transition of OP to maturing osteoblasts. This novel role of Jagged1 not only identifies a regulatory loop maintaining appropriate populations of osteolineage cells, but also provides a novel approach to increase trabecular bone mass, particularly in combination with PTH, by specific modulation of Jagged1.

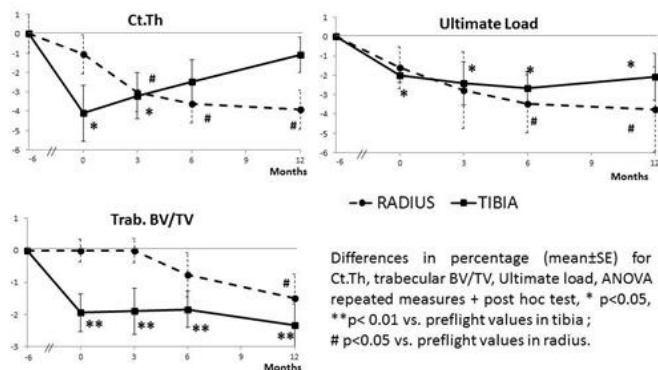
Disclosures: Rialnat Lawal, None.

1014

MMP14 Is a Novel Target of PTH Required for Osteocytic PTH Receptor-Driven Bone Remodeling and Mineral Apposition. Jesus Delgado-Calle^{*}, Gretel G. Pellegrini, Monica Feustel, Kevin McAndrews, Teresita Bellido. Indiana University School of Medicine, USA

PTH has profound effects on the skeleton by acting on osteocytes through mechanisms still unraveling. We report that matrix metalloproteinase (MMP) 14 expression is increased in bones from transgenic mice with constitutive activation of the PTH receptor in osteocytes (caPTHRIOT). Daily injections of PTH (100ng/g) for 1 month also increased MMP14 expression in WT mice, but not in mice with conditional deletion of the PTHR1 in osteocytes. These results demonstrate that MMP14 is a target gene of the osteocytic PTH receptor. MMP14 has been shown to be required for bone formation and maintenance of osteocytic processes during skeletal development; however, its potential role in PTH regulation of bone remodeling is unknown. To address this question we blocked MMP14 activity by injecting the neutralizing MMP14 antibody KD014 (30 mg/kg, sc 2x/wk) to 1 month old caPTHRIOT mice or WT littermate controls. After 2 months, caPTHRIOT mice injected with KD014 exhibited ~10% lower total, spinal and femoral BMD, lower BV/TV in the distal femur (-15%), trabecular thickness (-50%), cortical bone area (BA/TA) (-25%), and cortical thickness (-50%), compared to saline injected caPTHRIOT mice. These effects were preceded by reduction in serum bone formation markers Alp and P1NP and the bone resorption marker CTX after 1 month of treatment in caPTHRIOT mice. Furthermore, the high periosteal and endocortical mineral apposition rate (1.7 and 2.3-fold) and bone formation rate (2.8 and 2.4-fold) exhibited by the caPTHRIOT mice were reversed to WT levels by KD014 treatment. In contrast, WT mice were not affected by KD014. Unexpectedly, the effect of KD014 on bone mass and bone formation occurred even when Sost remained low and Wnt target genes (Axin2, Bmp1 and Smad6) and osteoblast markers (Runx2, col1A, and Osx) remained high in caPTHRIOT mice treated with KD014. In contrast, the elevated expression of Alp, Enpp1, Enpp3 and Ank, key genes involved in extracellular phosphate metabolism and hydroxyapatite deposition, was reversed to WT levels in KD014-treated caPTHRIOT mice. Moreover, KD014 decreased the hydroxyapatite content of caPTHRIOT bones in both trabecular and cortical compartments, as quantified by micro-CT. These results demonstrate that MMP14 is a novel target of PTH required for bone remodeling and mineral apposition driven by PTH receptor signaling in osteocytes, and suggest that regulation of extracellular phosphate metabolism is crucial for full bone anabolism by PTH.

Disclosures: Jesus Delgado-Calle, None.



Figure

Disclosures: Laurence Vico, None.

This study received funding from: CNES and ESA

1015

Mineral remodeling characterized by carbonate ion substitution is associated with MMP-13 in both HYP and wild-type mice during pregnancy and lactation. Courtney McEachon¹, Carolyn Macica², Steven Tommasini^{1*}. ¹Yale University, USA, ²Frank H. Netter, M.D., School of Medicine at Quinnipiac University, USA

The skeleton plays a major role in the homeostasis of calcium and phosphate and acts as a reservoir for these essential minerals. We previously used HYP mice, a murine model of X-linked hypophosphatemia (XLH), to study how impaired mineral metabolism affects skeletal adaptations to the increased mineral demands of pregnancy and lactation. The data revealed that both HYP and wild-type mice undergo a form “mineral remodeling” in which phosphate in the mineral matrix is replaced with carbonate. This unique form of remodeling provides phosphate for the developing fetus in the latter phases of development and for lactation without significant net maternal bone loss. However, the mechanism is unknown. We hypothesized that mineral mobilization was facilitated by osteocyte expression of matrix metalloproteinase-13 (MMP-13), which degrades the collagen matrix, freeing up mineral ions for phosphate homeostasis. Here, we analyzed the spatial distribution of the matrix composition of bone in wild-type and HYP mice. Regions of cortical bone were isolated around pores in synchrotron radiation-based FTIR maps and images of MMP-13 immunostaining. Using a custom Matlab algorithm, we measured carbonate ion substitution, collagen cross-linking, and MMP-13 as a function of distance relative to a pore's edge. Our results show the spatial co-localization of MMP-13 expression, carbonate substitution, and collagen cross-linking around intracortical porosities consisting of unmineralized osteoid and osteocyte lacunae (Fig. 1). The highest levels of MMP-13 and carbonate substitution corresponded to alterations in collagen cross-linking and occurred within 5 to 10µm of a pore. Quantitatively, carbonate substitution decayed exponentially as a function of distance, as did the ratio of reducible to non-reducible cross-links. Alterations in matrix composition occurred in both wild-type and HYP, but HYP had a 50% higher baseline of carbonate substitution throughout the skeleton in both the pregnant and lactating states. Together with the elevated expression of MMP-13 in HYP, the data point to a higher osteocyte-mediated contribution to mineral homeostasis due to lack of trabecular bone available for osteoclastic resorption. Also consistent with our hypothesis, these data suggest this mechanism of “mineral remodeling” protects the skeleton from excessive bone loss during periods of high mineral demand and may be essential to the rapid recovery of bone following cessation of lactation.

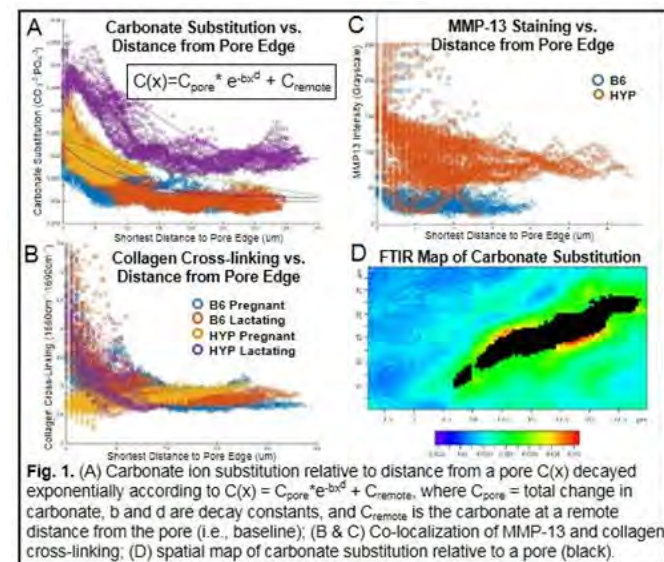


Fig. 1

Disclosures: Steven Tommasini, None.

1016

Inducible WNT16 Inactivation Demonstrates that WNT16 is a Major Regulator of Cortical Bone Thickness in Adult Mice. Sofia Moverare Skrtic^{*1}, Petra Henning¹, Jianyao Wu¹, Karin Gustafsson¹, Klara Sjögren¹, Marie Lagerquist¹, Fu-Ping Zhang², Matti Poutanen², Ulf Lerner¹, Claes Ohlsson¹. ¹Center for Bone & Arthritis Research at the Sahlgrenska Academy, Sweden, ²Department of Physiology, Institute of Biomedicine & Turku Center for Disease Modeling, University of Turku, Finland

Although substantial progress has been made in the therapeutic reduction of vertebral fracture risk in individuals with osteoporosis, non-vertebral fracture risk has been improved only marginally by currently available treatments, defining an unmet medical need. Our previous unbiased human genome-wide association studies revealed that the WNT16 locus is a major determinant of cortical bone thickness and nonvertebral fracture risk and our subsequent mechanistic studies using global and cell-specific deletion of *Wnt16* in mice demonstrated that osteoblast-derived WNT16 is a key regulator of cortical bone thickness and fracture susceptibility (1-3). However, these mechanistic studies were based on mouse models with lifelong global or tissue-specific inactivation of *Wnt16*, not being able to separate between developmental effects and effects on adult bone metabolism.

To investigate the role of WNT16 specifically for adult cortical bone homeostasis, *Wnt16* was conditionally ablated in adult male mice through tamoxifen-inducible Cre-mediated recombination using *CAG-CreER;Wnt16^{lox/lox}* mice. At 10 weeks of age, tamoxifen was administered i.p. for 4 consecutive days using two different doses, 0.25 and 1 mg/mouse/day, respectively. *CAG-CreER* mice did not have a cortical bone phenotype and, therefore, tamoxifen-treated *CAG-CreER;Wnt16^{lox/lox}* mice were compared with tamoxifen-treated *Wnt16^{lox/lox}* mice at 14 weeks of age.

Tamoxifen dose-dependently substantially decreased the *Wnt16* mRNA levels in the cortical bone of *CAG-CreER;Wnt16^{lox/lox}* mice compared to tamoxifen-treated *Wnt16^{lox/lox}* mice (0.25 mg/mouse/day, $-80.9 \pm 7.0\%$; 1 mg/mouse/day, $-96.3 \pm 1.1\%$, $p < 0.01$). In addition, tamoxifen dose-dependently decreased femur cortical bone thickness in the adult *CAG-CreER;Wnt16^{lox/lox}* mice (0.25 mg/mouse/day $-10.9 \pm 1.3\%$; 1 mg/mouse/day, $-14.1 \pm 2.7\%$, $p < 0.05$). Notably, when evaluated in all mice, cortical bone thickness was directly associated with *Wnt16* mRNA levels in cortical bone ($r = 0.52$, $p = 0.006$), supporting a crucial role of WNT16 in the regulation of cortical bone thickness.

These findings demonstrate that WNT16 regulates cortical bone thickness in adult mice. We propose that new treatment strategies targeting the adult regulation of WNT16 might be useful to reduce fracture risk at cortical bone sites.

References

¹Estrada et al *Nature Genetics* 2012;44:491-501; ²Zheng et al *PLoS Genetics* 2012; 8:e1002745; ³Moverare-Skrtic et al *Nature Medicine* 2014;20:1279-88

Disclosures: Sofia Moverare Skrtic, None.

1017

Osteoclast-Specific Deletion of Mef2C Causes High Bone Mass Independent of Sost. Nicole M. Collette¹, Deepa K. Murugesu¹, Crista S. Yee², Nicholas R. Hum¹, David Gravano², Jennifer O. Manilav², Alex G. Robling³, Gabriela G. Loots¹. ¹Lawrence Livermore National Laboratory, USA, ²University of California, Merced, USA, ³Indiana University, USA

Mef2C is a transcription factor that binds to *ECR5*, a *Sost* transcriptional regulatory region, and is required for *Sost* expression in osteocytes. *Mef2C* conditional deletion in osteoblasts and osteocytes causes high bone mass (HBM). We have shown that ablation of *Mef2C* in *Mef2C^{CKO}* mice using an osteoblast-specific (*Coll-Cre*) results in *Sost*-dependent HBM; conditional deletion of *Mef2C* with an osteocyte-specific (*Dmp1-Cre*) *Cre* deleter also resulted in HBM. The HBM phenotype in *Mef2C^{CKO}; Coll-Cre* mice was driven by increased bone formation, whereas the HBM phenotype in *Mef2C^{CKO}; Dmp1-Cre* mice was driven by both increased bone formation and decreased bone resorption. To determine whether the HBM phenotype observed in *Mef2C^{CKO}; Dmp1-Cre* mice was attributed solely to *Sost* down-regulation, we characterized bone parameters of *Sost^{KO}; Mef2C^{CKO}; Dmp1-Cre* mice. We found *Sost^{KO}; Mef2C^{CKO}; Dmp1-Cre* mice to have a bone volume: total volume (BV/TV) ratio of over 83% by mCT, or ~700% more bone than control mice, and 2X more bone than *Sost^{KO}* alone, suggesting that *Mef2C* has a significant *Sost*-independent effect on bone mass. Subsequently, we found robust *Mef2C* expression, but no *Sost* expression, in osteoclasts. We also found that *Rosa26-LacZ* reporter mice crossed with the *Dmp1-Cre* allele, but not the *Col1-Cre* allele, expressed in osteoclasts. We hypothesized that *Mef2C* plays a dual role in bone metabolism, as an anti-anabolic and pro-catabolic transcriptional mediator, such that conditional loss of *Mef2C* in osteoclasts impairs osteoclast function and reduces resorption, independent of *Sost*. To determine whether *Mef2C* has a role in osteoclasts, we examined the bone parameters of *Mef2C^{CKO}; Ctsk-Cre*. Immunofluorescent staining confirmed the expected loss of *Mef2C* in *Mef2C^{CKO}; Ctsk-Cre* osteoclasts, while osteoblast/osteocyte expression of both *Mef2C* and *Sost* were unaffected. We found *Mef2C^{CKO}; Ctsk-Cre* femurs to have HBM, approximately 25% BV/TV, compared to 9.4% for *Mef2C^{CKO}* controls. In addition, *Sost^{KO}; Mef2C^{CKO}; Ctsk-Cre* compound mice had 2X more bone mass than *Sost^{KO}*, supporting a new role for *Mef2C* in osteoclasts. To determine whether *Mef2C* is involved in osteoclast differentiation, we quantified osteoclast

precursor populations and found early osteoclast precursors to be 50% reduced in *Mef2C^{KO}*; *Ctsk-Cre* bone marrow compared to wildtype or *Sost^{KO}* controls, suggesting that *Mef2C* significantly influences osteoclast differentiation.

Disclosures: , None.

1018

Sclerostin Antibody (Scl-Ab) Increased Bone Mass and Strength in a Mouse Model of Osteogenesis Imperfecta Caused by Wnt1 Mutation. Kyu Sang Joeng¹, Ming-Ming Jiang¹, Terry Bertin¹, Hao Ding², Yuqing Chen¹, Xiaohong Bi², Catherine Ambrose², Brendan Lee¹, Yi-Chien Lee^{*1}. ¹Baylor College of Medicine, USA, ²University of Texas Health Science Center at Houston, USA

Background: Osteogenesis Imperfecta (OI) is a brittle bone disease characterized by low bone mass and multiple bone fractures. Recently, our laboratory and others have identified *WNT1* mutations in patients with OI. We have also established and described a mouse model of OI caused by *WNT1* mutations (*swaying* mouse model). Current treatment options for OI mostly focus on bisphosphonate therapy; however, because of its questionable efficacy in some OI patients and concerns about long-term administration, it is necessary to explore new treatment strategy. Sclerostin is a potent inhibitor of WNT signaling, and several studies have shown that the inhibition of sclerostin greatly enhances bone formation. Therefore, we hypothesized that Scl-Ab treatment could be beneficial for treating *WNT1* related OI and tested this hypothesis using our *swaying* mouse model.

Methods: In this study, we followed two treatment regimens: from week 3 to week 8 (the early treatment group) and from week 9 to week 14 (the late treatment group). *swaying* mice and wild-type littermates were subcutaneously administered vehicle or 25 mg/kg Scl-Ab twice a week for 6 weeks (n=4-10 per group). Bone mass was assessed by microCT, bone strength by three-point bending, and matrix composition by Raman spectroscopy.

Results: First, the Scl-Ab treated *swaying* mice in the early treatment group exhibited reduced fracture rate from 90% (vehicle treated *swaying* mice) to 12.5% fracture rate (Scl-Ab treated *swaying* mice). microCT analysis showed that Scl-Ab treated *swaying* mice exhibited significantly increased bone volume per tissue volume in both the femur and lumbar spine (p-value < 0.01) in both early and late treatment groups. Three point bending analysis at the femur confirmed that the Scl-Ab treated *swaying* mice show increased bone strength parameters including maximum load, stiffness, and post-yield energy. Finally, Raman analysis demonstrated that the Scl-Ab treated *swaying* mice have increased bone collagen content in bone matrix.

Conclusions: These results suggest that Scl-Ab treatment significantly rescued the low bone mass phenotype and increased bone strength in *swaying* mice. These results support future investigations of a potential clinical benefit of Scl-Ab in the management of OI patients with *WNT1* mutations.

Conflict of Interest: Amgen and UCB Pharma provided Scl-Ab for this study

Disclosures: Yi-Chien Lee, None.

1019

Romosozumab (Sclerostin Antibody) Improves Bone Mass and Bone Strength in Ovariectomized Cynomolgus Monkeys After 12 Months of Treatment. Michael S Ominsky^{*1}, Aurore Varela², Susan Y Smith², Jacquelin Jollette², Elisabeth Lesage², Sabina Buntich¹, Rogely W Boyce¹. ¹Amgen Inc., USA, ²Charles River Laboratories Preclinical Services, Canada

Romosozumab, a sclerostin antibody, is a bone-forming agent under clinical investigation for the treatment of osteoporosis. To examine its effects on bone quality over the duration of proposed clinical treatment in a remodeling species, bone mass and strength were assessed in ovariectomized (OVX) cynomolgus monkeys treated for 12 mos.

Cynomolgus monkeys (≥9 yrs) were OVX and 4 mos later were treated with weekly sc injections of either vehicle (Veh) or 3 or 30 mg/kg romosozumab for 12 mos, or 30 mg/kg romosozumab for 6 mos followed by Veh for 6 mos (n=6-16/group). Doses provided a 1x and 20x multiple of clinical exposure.

Bone mass increased dose dependently throughout the skeleton, with 12-mo DXA BMD increases from predose of 14-19% (3 mg/kg) and 24-26% (30 mg/kg) at the lumbar spine and proximal femur. By pQCT, cortical thickness (Ct.Th) increased by 23% from predose at the tibial diaphysis due to geometric changes on both periosteal and endocortical surfaces with 30 mg/kg; increased Ct.Th was also observed *ex vivo* at the femoral neck, femoral diaphysis, and L3 vertebra relative to OVX-Veh. Trabecular bone mass and thickness also increased robustly with both doses of romosozumab. Despite a transient 2% reduction in cortical vBMD at the radius at mo 6, 1 yr of romosozumab at either dose did not affect cortical porosity in the rib, tibia, or humerus, and ash-based tissue mineralization in the humerus or vertebra.

Significant improvements in bone strength were observed, with peak load significantly increased with 30 mg/kg at the femoral diaphysis (21%) and femoral neck (53%), and with 3 and 30 mg/kg in lumbar vertebral bodies (62-131%) and cancellous cores (91-156%), relative to OVX-Veh. Bone mass remained positively correlated with strength at these sites, with no changes in material properties calculated from bending tests at the femoral diaphysis and humeral cortical beams. These bone quality measures were also maintained in the group that transitioned to Veh at mo 6, despite a gradual loss of bone mass.

Romosozumab treatment of OVX cynomolgus monkeys for 12 mos resulted in marked improvements in bone mass, cortical geometry, and bone strength. Romosozumab maintained bone quality as reflected in mass-strength regressions, calculated material properties, and ash analysis. These results support the bone efficacy and safety profile of romosozumab and suggest that treatment-related BMD improvements should yield improved bone strength in osteoporosis patients.

Disclosures: Michael S Ominsky, Amgen
This study received funding from: Amgen Inc.

1020

Neutralizing Antibody and Orally Active Small Molecule Inhibitors of the Secreted WNT Inactivating Lipase NOTUM Stimulate Cortical Bone Formation in Ovariectomized Rodents. Robert Brommage^{*}, Andrea Thompson, Melanie Shadoan, Jeff Liu, Sabrina Jeter-Jones, Jie Cui, David Potter, Dawn Bright, Faika Mseeh, Jennifer Bardenhagen, Gwenn Hansen, Peter Vogel, James Tarver, David Powell, Qingyun Liu, Brian Zambrowicz. Lexicon Pharmaceuticals, USA

WNT signaling, involving WNTs, FZDs, LRP6, Sclerostin, DKK1 and SFRP4, plays a key role in bone formation and identification of additional genes in this pathway can provide novel therapeutic approaches to treat osteoporosis. NOTUM is a secreted enzyme that inactivates WNTs by removing a palmitoleic acid group essential for activity. Male and female Notum KO mice have normal soft tissue histology, bone length and trabecular bone parameters, but elevated cortical bone thickness (9 cohorts, total KO N=165) with increased strength. Enzymatic and cell-based assays of NOTUM activity were employed to screen both a chemical library and antibodies generated against mouse NOTUM. Neutralizing antibody 2.78.33 had IC50 potencies of 37 and 4 nM in enzymatic and cell-based assays, respectively. Small molecule (SM) LP-935001 had IC50 potencies of 0.4 and 12 nM in enzymatic and cell-based assays, respectively. Exposure of differentiating MC3Tc-E1 osteoblasts to NOTUM conditioned medium prevented mineralization, which was reversed by cotreatment with SM inhibitors. Eight weeks following surgery, sham-surgery and OVX mice were treated with Ab 2.78.33 (10 mg/kg weekly) for 4 weeks starting at 24 weeks of age. Treatment increased cortical thickness (P < 0.01) similarly in sham and OVX mice in midshaft femur (12%), vertebral body (9%) and femoral neck (6%). Triple fluorochrome labeling on days 7 (calcein), 14 (alzarin) and 21 (demeclocycline) showed 3-fold elevations in midshaft femur endocortical MS at 7 and 14 days but minimal activity at 21 days. BFR was elevated 4-fold between 7 and 14 days. Sixty-three weeks following surgery, OVX rats were treated with LP-935001 (daily oral gavage at 1 and 5 mg/kg) for 12 weeks starting at 80 weeks of age. High dose treatment increased (P < 0.02) cortical bone thickness in midshaft femur (6%), distal tibia (9%), pelvis (12%), vertebral body (7%) and femoral neck (6%). Bone strength was elevated (P < 0.01) in midshaft femur (13%), midshaft tibia (7%) and femoral neck (15%). Two courses of double fluorochrome labeling showed 3.6- and 3.2-fold elevations in distal tibia endocortical BFR during 1 to 3 weeks (alzarin) and 9 to 11 weeks (calcein) of treatment, respectively. These findings demonstrate NOTUM is a WNT inhibitory factor reducing bone formation. As a secreted enzyme inhibitable by neutralizing antibodies and orally active SMs, NOTUM is a potential drug target for stimulating endocortical bone formation and treating osteoporosis.

Disclosures: Robert Brommage, None.
This study received funding from: Lexicon Pharmaceuticals

1021

Parathyroid hormone administration regulates osteoprogenitor numbers and decreases their differentiation into the adipocytic lineage *in vivo*. Henry M. Kronenberg¹, Noriaki Ono², Deepak H. Balani^{*1}. ¹Massachusetts General Hospital & Harvard Medical School, USA, ²University of Michigan, School of Dentistry, USA

The contribution of mature osteoblasts to the bone anabolic response induced by parathyroid hormone (PTH) has been studied extensively. However, the role of osteoprogenitors in fuelling that anabolic response is poorly understood. Recently our group identified osteoprogenitors in young postnatal mice. Using a lineage-tracing strategy, we showed that Sox9 promoter/enhancer labels progenitors with multilineage potential and self-renewing capabilities *in vivo*. In this study we show that Sox9 promoter/enhancer actively labels the multi-potential skeletal progenitors in older mice. Further, we hypothesized that PTH may regulate the numbers of Sox9⁺ progenitors *in vivo* and preferentially direct them towards the osteoblastic lineage, thereby contributing to its anabolic action. To understand if PTH affects proliferation and/or differentiation of progenitors, we utilized a creER-mediated lineage-tracing strategy using 6-8 week old Sox9creER²;Rosa26-tdTomato. Osteocalcin (Ocn)-GFP triple transgenic mice. Mice received 2 mg tamoxifen first and 24h later were started on daily subcutaneous injections of PTH or vehicle for 3, 7 and 21 days. No Tomato⁺ signal was seen in the absence of tamoxifen confirming the non-leakiness of the cre recombinase. Both flow cytometry and histology showed that Tomato⁺ cells were significantly increased in mice that received PTH in a dose and time-dependent manner. PTH increased the proliferation of these cells as corroborated by an *in vivo* EdU assay. The increase in the numbers of Tomato⁺ cells was seen as soon as 3 days after PTH administration in the primary spongiosa, periosteal and the endocortical surfaces. On Day 3 Tomato⁺ cells were not yet Ocn-GFP⁺. On Day 7 and Day 21 we

observed several Tomato⁺ cells that also expressed Ocn-GFP present on bone surfaces and buried as osteocytes. Strikingly, following 21 days of daily PTH injections, mice that were subjected to PTH withdrawal for 4 weeks showed a significant increase in bone marrow adiposity. A fraction of adipocytes was Tomato⁺, which was not observed in corresponding controls. We present novel observations wherein we successfully label adult multi-potential skeletal progenitors and witness increase in proliferation and their differentiation into osteoblastic lineage subsequent to PTH administration. We also show that on PTH withdrawal there is a reduction in the number of Tomato⁺ osteoblasts and concomitant replacement of bone marrow by Tomato⁺ adipocytes.

Disclosures: Deepak H. Balani, None.

1022

Peripheral Nerves Provide Essential Cellular Components for Heterotopic Ossification. Elizabeth Salisbury*, Za Waunya Lazard, Eric Beal, Corinne Sonnet, Eleanor Davis, Elizabeth Olmsted-Davis, Alan Davis. Baylor College of Medicine, USA

We have previously developed an animal model of heterotopic ossification (HO), in which we deliver cells producing bone morphogenetic protein 2 (BMP2) to the skeletal muscle of mice. This leads to the recruitment of key cellular players, including transient brown adipocytes (tBAT), chondrocytes, and osteoblasts, that ultimately contribute to bone formation within the muscle. Using this model, we have shown the tBAT formed during HO derives from a cell within the perineurium (nerve sheath) of peripheral sensory nerves. In the studies presented here, we determined that the osteoblasts also have a neural origin and have further characterized the progenitor populations within the nerve. Within the first day following BMP2 induction, we observed a population of cells in the endoneurium (inner nerve layer) expressing the osteoblast markers *osterix* and *dlx5*. However, two days after delivery of BMP2, these cells disappear from the endoneurium and FACS analysis showed these cells to now be found within the blood. In order for these osteoprogenitor cells to exit the nerve and enter the general circulation, they must cross the blood-nerve-barrier (BNB), which protects the microenvironment of the nerve, into the endoneurial vessels. At this time, these osteoprogenitors began to express the tight junction molecule *claudin5*, which may assist these cells in traversing the BNB. In later days, these *osterix*/*claudin5*⁺ cells exit the bloodstream by extravasation to the area of bone formation. To further characterize both the endoneurial and perineurial progenitors within the nerve, we utilized lineage tracing mice. *Wnt1* is a marker of neural crest stem cells. Using an inducible-*Wnt1* Cre fluorescent reporter mouse, we observed what appear to be fluorescent osteoblasts within the site of bone formation, suggesting a unique neural pool of osteoprogenitors. In addition, we found the tBAT perineurial progenitors co-express the glutamate aspartate transporter (GLAST). Interestingly, GLAST expression has been reported within chondrocytes, as well as astrocytic neuroglia. We employed an inducible-GLAST reporter mouse to track this perineurial population, by correlating expression of tBAT (UCP1, ADRB3), chondrocytes (*sox9*), and astrocytes (GFAP). Collectively, these data suggest the peripheral nerves give rise to multiple, key cell types that not only coordinate the formation of, but are also progenitors for, cartilage and bone during HO.

Disclosures: Elizabeth Salisbury, None.

1023

α SMA⁺ macrophages skewed from hematopoietic stem cells by vitamin D3 initiate myelofibrosis and subsequent osteosclerosis. Kanako Wakahashi*¹, Kentaro Minagawa¹, Noboru Asada¹, Yuko Kawano¹, Mari Sato¹, Hiroki Kawano¹, Akiko Sada¹, Shigeaki Kato², Kotaro Shide³, Kazuya Shimoda³, Toshimitsu Matsui¹, Yoshio Katayama¹. ¹Hematology, Kobe University Graduate School of Medicine, Japan, ²Soma Central Hospital, Japan, ³Gastroenterology & Hematology, Miyazaki University, Japan

Myelofibrosis is frequently complicated with osteosclerosis (MF/OS). The pathogenesis is largely unknown and bone marrow (BM) transplantation is the only curable therapy in clinic. Here, we established a novel MF/OS model. We transplanted wild-type (WT) BM cells into lethally irradiated vitamin D receptor (VDR) ^{-/-} mice and found that hematopoietic stem cells (HSCs) selectively disappeared at 3 weeks after transplantation followed by the death of vast majority of mice due to BM failure in 3 months. Since VDR ^{-/-} mice show normal hematopoiesis, we transplanted VDR ^{-/-} BM into lethally irradiated VDR ^{-/-} recipients, which resulted in survival with no BM failure. These data suggested that the loss of VDR ^{+/+} HSCs was due to the exposure to high vitamin D3 (vitD) in VDR ^{-/-} microenvironment. BM cavity at 1-2 months after transplantation of WT BM into VDR ^{-/-} recipients was occupied by spindle shaped cells and silver fibers with prominently increased trabecular bones mainly in metaphysis. This was initiated by the hematopoietic cells since CD45+lineage-c-kit+ cells isolated from WT CAG-EGFP transgenic mice as donor source induced MF/OS in VDR ^{-/-} recipients. Monotonous fibroblastic cells in metaphysical BM were composed of two distinct populations with mutual distribution, 1) GFP+F4/80+ donor-derived macrophages and 2) GFP-*osterix*⁺ host-derived preosteoblasts. Both populations were positive for α SMA. Importantly, VDR mRNA level in HSCs was 30 times higher than lineage⁺ mature hematopoietic cells, and low vitD diet prevented our model from the development of MF/OS. Furthermore, macrophage depletion by clodronate liposome also inhibited the MF/OS. Thus, the true pathogenesis is likely

that α SMA⁺ macrophages as MF-initiating cells are perhaps directly differentiated from HSCs by the strong vitD signal in BM microenvironment, and drive the activity of preosteoblasts as a major producer of collagen fibers which is the origin of OS. In human MF patients, JAK2 V617F is a major disease-initiating mutation. And JAK2 V617F transgenic (JAK2 Tg) mice display MF/OS. We confirmed that marrow fibroblastic cells of JAK2 Tg mice were composed of α SMA+CD169+ macrophages and α SMA+*osterix*⁺ osteoblastic cells. A preliminary data showed that VDR ^{-/-} JAK2 Tg BM induced less severe fibrosis compared to VDR ^{+/+} JAK2 Tg BM when transplanted into WT recipients. We propose that the inhibition of vitD signaling or macrophage-targeted strategies could be novel therapeutic choices for this disease.

Disclosures: Kanako Wakahashi, None.

1024

Bone lining cells are a major source of osteoblasts during bone remodeling. Brya Matthews*¹, Igor Matic¹, Xi Wang¹, Danka Grecevic², Ivo Kalajzic¹. ¹University of Connecticut Health Center, USA, ²University of Zagreb, Croatia

Mesenchymal stem cells are thought to provide a continuous supply of mature osteoblasts during bone remodeling. However, under certain conditions, bone-lining cells (BLCs) can activate into matrix producing osteoblasts. The ability to identify BLCs and understand their role in bone physiology has been very limited. We propose a novel mechanism of bone remodeling that introduces BLCs as a major source of osteoblasts and preosteoblasts in adult bone. To selectively identify BLCs we labeled osteoblasts and a subset of osteocytes using 10kb-Dmp1CreER12/Ai9 (iDMP-Ai9) mice following tamoxifen treatment (Cre directed Tomato expression). Labeled cortical surface decreased from >90% one day after labeling to 40% by 21 days and then remained stable up to 180 days later. Matrix producing osteoblasts remained labeled long after they would be expected to undergo apoptosis or maturation to osteocytes, suggesting continuous activation of BLCs. To distinguish the fate of BLCs from osteoblasts we crossed the Col2.3 Δ TK suicide gene into iDMP-Ai9 mice. Following ganciclovir treatment, cuboidal osteoblasts were absent, while flat BLCs were labeled. After 21 days of recovery, new osteoblasts form, and new areas of active bone surface are covered by iDMP-Ai9 expressing osteoblasts indicating activation of BLCs. EdU staining demonstrated DNA synthesis and cell division of labeled cells. Similar studies using α SMACreER12, a marker of mesenchymal progenitors, showed contribution to marrow fibrosis, but minimal contribution of α SMA-labeled bone marrow cells to bone formation during recovery. A large proportion of BLCs express mesenchymal stem cell markers while osteoblasts do not (*Sca-1* – 41% vs <1% in Col2.3GFP+ cells, CD51 – 60-80% vs 10-20%, *LepR* – 22% vs 3%), and BLCs have the ability to form colonies and mineralized nodules in vitro, but not adipocytes. Transplanted BLCs can participate in healing of a calvarial defect and differentiate into osteoblasts and osteocytes. In contrast, endogenous BLCs did not make a major contribution to fracture callus formation, or healing of a tibial hole defect. Furthermore we evaluated whether glucocorticoid treatment affects activation of BLCs. Prednisolone treatment in mice following osteoblast ablation showed reduced activation of lining cells after 7 days and delayed the recovery of bone parameters. Our results define the bone lining cell as a major source of proliferating and mature osteoblasts during bone remodeling.

Disclosures: Brya Matthews, None.

1025

Osteocyte-specific Deletion of Cathepsin K Prevents Increased Bone Turnover, Bone Loss and Bone Fragility during Lactation in Mice. Sutada Lotinun*¹, Riku Kiviranta², Vincent Carpentier³, Lynn Neff³, Daniel Brooks⁴, Mary Boussein⁴, Roland Baron⁵. ¹Department of Oral Medicine, Infection & Immunity, Harvard School of Dental Medicine, USA & Department of Physiology & STAR on Craniofacial & Skeletal Disorders, Faculty of Dentistry, Chulalongkorn University, Thailand, ²Department of Medical Biochemistry & Genetics & Department of Medicine, University of Turku, Finland, ³Department of Oral Medicine, Infection & Immunity, Harvard School of Dental Medicine, USA, ⁴Center for Advanced Orthopedic Studies, Beth Israel Deaconess Medical Center, & Harvard Medical School, USA, ⁵Department of Oral Medicine, Infection & Immunity, Harvard School of Dental Medicine & Harvard Medical School, Endocrine Unit, Massachusetts General Hospital, USA

Lactation induces a substantial loss of bone mass in order to provide adequate amounts of calcium to pups through milk production, a process that involves not only osteoclasts and bone resorption but also osteocytes and perilacunar osteolysis (Qing H. et al, J Bone Miner Res, 27:1018-1029 2012). Interestingly, lactation results in enlarged osteocytic lacunae, presumably through perilacunar osteolysis, and induces the expression of cathepsin K (Ctsk) and TRAP in osteocytes. To determine whether the induction of Ctsk in osteocytes contributes to the increased resorption and perilacunar osteolysis induced by lactation, we crossed 10kb DMPI-Cre with Ctsk^{fl/fl} mice to specifically delete Ctsk in late osteoblasts and osteocytes. This resulted in a significant deletion of Ctsk in osteocytes. At steady state, targeted deletion of Ctsk in osteocytes had no effect on bone remodeling and homeostasis in female mice. As

expected, lactating control mice showed increased bone resorption (N.Oc/B.Pm, 1.13^{0.23} vs 1.89^{0.20} mm⁻¹) and decreased bone formation rate per tissue volume (88.32^{9.19} vs 66.04^{5.34} %/year), leading to decreased cancellous bone volume (5.97^{0.54} vs 4.02^{0.23} %) and significantly altered mechanical properties, decreasing max bending moment, failure moment, bending stiffness and estimated strength. Strikingly, this lactation-induced increased remodeling and bone loss was prevented in the absence of Ctsk in osteocytes (N.Oc/B.Pm, 1.89^{0.20} vs 0.48^{0.08} mm⁻¹; BFR/TV, 66.04^{5.34} vs 101.47^{5.51} %/year; BV/TV, 4.02^{0.23} vs 5.52^{0.40} %). Lactation also increased osteocyte lacunar area (23.28^{1.32} vs 31.23^{1.31} μm^2) and osteocyte density (4.99^{0.38} vs 6.54^{0.31} $\times 10^{-4}/\text{cm}^3$) in cortical bone and deletion of Ctsk in osteocytes prevented these changes. Furthermore, deletion of Ctsk in osteocytes also prevented the negative effects of lactation on the mechanical properties of bone. In summary, deleting Ctsk in osteocytes prevented the alterations in bone formation, bone resorption, perilacunar osteolysis, bone volume and biomechanical properties induced by lactation. Our data therefore demonstrate that Ctsk expression in osteocytes contributes to the increased remodeling, bone loss and deterioration of mechanical properties observed during lactation, providing genetic evidence that Ctsk contributes to the regulation of bone remodeling and homeostasis exerted by osteocytes.

Disclosures: Sutada Lotinun, None.
This study received funding from: Merck

1026

Rho-Pkn3 Pathway Regulates the Bone-resorbing Activity of Osteoclasts under Wnt5a-Ror2 Signaling. Shunsuke Uehara^{*1}, Hideyuki Mukai², Teruhito Yamashita³, Takashi Nakamura⁴, Shigeaki Kato⁵, Akira Kikuchi⁶, Michiru Nishita⁷, Yasuhiro Minami⁷, Nobuyuki Udagawa⁸, Naoyuki Takahashi³, Yasuhiro Kobayashi³. ¹Matsumoto Dental University, Jp, ²Biological Research Center, Kobe University, Japan, ³Institute for Oral Science, Matsumoto Dental University, Japan, ⁴Department of Biochemistry & Integrative Medical Biology, School of Medicine, Keio University, Japan, ⁵Soma Central Hospital, Japan, ⁶Department of Molecular Biology & Biochemistry, Graduate School of Medicine, Osaka University, Japan, ⁷Department of Physiology & Cell Biology, Graduate School of Medicine, Kobe University, Japan, ⁸Department of Biochemistry, Matsumoto Dental University, Japan

We previously reported that Wnt5a induces the RANK expression in osteoclast precursors through Ror2-JNK signaling, which in turn, facilitates osteoclast differentiation. Although Ror2 is highly expressed in osteoclasts, it is still unclear whether Wnt5a-Ror2 signaling is involved in the bone-resorbing activity of osteoclasts. Osteoclast-specific Ror2 conditional knock-out mice (*Ror2* cKO) were generated by crossing *Ror2^{fl/fl}* mice with cathepsin K-Cre (*Ctsk^{Cre/+}*) mice. MicroCT analysis of femurs revealed that bone volume in *Ror2* cKO was higher than that in control (*Ror2^{+/+}*; *Ctsk^{Cre/+}*) mice. In addition, serum CTX, a bone resorption marker, was lower in *Ror2* cKO. Osteoclast number in femurs and serum ALPase activity, a bone formation marker, remained the same in *Ror2* cKO. These results suggest that increased bone mass in *Ror2* cKO is due to the impaired bone-resorbing activity of osteoclasts. Osteoclasts formed from bone marrow cells of *Ror2* cKO showed the low bone-resorbing activity on dentine slices due to a defect in actin ring formation. Wnt5a activated both Rho and Rac in control osteoclasts, but not in *Ror2* cKO osteoclasts. Overexpression of constitutively active (CA)-RhoA, but not CA-Rac1, rescued the bone-resorbing activity of *Ror2* cKO osteoclasts. To clarify the mechanisms by which Rho regulates the bone-resorbing activity of osteoclasts, we examined the expression of Rho effectors using real-time RT-PCR. Among 13 Rho effectors, the expression of *Pkn3* (encoding protein kinase N3; Pkn3) was significantly increased during osteoclast differentiation. Phosphorylation levels of Pkns were lower in osteoclasts from *Ror2* cKO than those from control mice. This result suggests that Wnt5a-Ror2 signaling regulates the kinase activity of Pkns including Pkn3. MicroCT analysis showed that the bone volume of femurs from *Pkn3^{-/-}* mice was higher than that from wild-type mice (WT). Serum CTX was lower in *Pkn3^{-/-}* mice. Osteoclast number in femurs from *Pkn3^{-/-}* mice was comparable to that from WT. These results suggest that the bone-resorbing activity of osteoclasts in *Pkn3^{-/-}* mice is impaired. Osteoclasts from *Pkn3^{-/-}* mice showed the suppressed bone-resorbing activity *in vitro*. The enforced expression of full-length Pkn3 rescued the bone-resorbing activity of *Pkn3^{-/-}* osteoclasts, but that of Pkn3 lacking proline rich region did not. Taken together, Wnt5a-Ror2 signaling regulates the bone-resorbing activity of osteoclasts through Rho-Pkn3 pathway.

Disclosures: Shunsuke Uehara, None.

1027

Maternal Obesity Programs Senescence Signaling and Glucose Metabolism in Fetal Osteoblastic Cells. Jin-Ran Chen^{*1}, Oxana P. Lazarenko², Michael L. Blackburn², Thomas M. Badger², Kartik Shankar². ¹University of Arkansas for Medical Science, Arkansas Children's Nutrition Center, USA, ²University of Arkansas for Medical Sciences & Arkansas Children's Nutrition Center, USA

Nutritional status during intrauterine and early postnatal life impacts the risk of chronic diseases, presumably via epigenetic mechanisms. However, evidence on the impact of gestational events on regulation of bone development is sparse. Here, we designed studies both in rodents and humans to investigate the effects of maternal obesity on bone development. First, female Sprague-Dawley rats were fed either a low-fat AIN-93G control diet or a high fat diet (HFD) (45% fat calories) for 10 wks starting at 6 wks of age. After 10 wks of these diets, lean (from control diet) and obese (from HFD) female rats were time-impregnated (n=6 per group) by control diet male rats. At gestational day 18.5 (E18.5), all fetuses were taken and embryonic osteogenic calvarial cells (EOCCs) were isolated. We found epigenetic regulation of polycomb-regulated genes in embryonic rat from HFD obese dams. Increased enrichment of repressive histone mark H3K27me3 on the gene bodies of IGF1 and TCFAP2 in synergy with decreased H3K27me3 at the promoter of BMP4 was associated with increased cell senescence signaling in EOCCs. BMP4 and EGR1 dependent p53/p21-mediated increase of cell senescence signaling and decreased aerobic glycolysis were imprinted in HFD-EOCCs resulting in decreased osteoblast differentiation potential. Second, twenty four pregnant women [12 obese (pre-pregnancy BMI ≥ 30 Kg/m²) and 12 lean (pre-pregnancy BMI 19 - 25 Kg/m²)] were recruited during last three years. Upon delivery, placentas and umbilical cords (UCs) were collected and cells from the UC matrix were isolated as UC human mesenchymal stem cells (UC MSCs). The UC MSCs were counted and plated in growth media in a single well of a six-well plate. Cells were expanded until the third passage after which they were fluorescently labeled with antibodies against CD13, CD29, CD44, CD90, CD105, CD31, CD34, and CD45 and analyzed via FACS. The UC MSCs of obese mothers displayed less potential toward osteoblastogenesis and more toward adipogenesis. These human MSCs and placentas from obese mothers not only exhibited increased cell senescence signaling and decreased glucose metabolism but also insulin resistance. These findings indicate fetal pre-osteoblastic cell senescence signaling and glucose metabolism programming by maternal obesity in both rodents and humans. *Supported in part by ARS CRIS #6251-51000-005-03S (JRC).*

Disclosures: Jin-Ran Chen, None.

1028

Roles of Mineralization Heterogeneity and Porosity in the Fracture Resistance of Human Cortical Bone. Mathilde Granke^{*1}, Alexander J Makowski², Sasidhar Uppuganti¹, Jeffrey S Nyman². ¹Vanderbilt University Medical Center, USA, ²Vanderbilt University Medical Center, VA Tennessee Valley Healthcare System, USA

The association between rare atypical femoral fractures and long-term use of bisphosphonates has drawn attention to the loss of heterogeneity in tissue mineralization as a possible mechanism contributing to skeletal fragility. However, there are conflicting reports on whether increased or reduced heterogeneity exists between osteoporotic fracture and control cases, and there is little experimental evidence that heterogeneity is even a determinant of fracture resistance. Based on computational models suggesting that tissue heterogeneity at the microstructural level promotes fracture resistance, we hypothesized that the age-related decrease in fracture toughness in human cortical bone is partly explained by a decrease in heterogeneity of tissue mineralization.

A cortical bone sample was obtained from the lateral mid-diaphysis of 39 human femurs (19 male, 20 female, age = 65 \pm 20 yrs [24-101]) and machined into a single-edge notched beam specimen. Fracture toughness testing of the beam (crack propagating normal to osteon direction) provided the resistance to crack initiation (K_{init}) and overall crack toughness (J). Then, a cross-section adjacent to the fracture path (~2.5 mm x 4.5 mm) was imaged by backscattered SEM (1 μm pixel size). Images were segmented to obtain the distribution of porosity and calibrated using standard materials to convert grey levels into tissue mineralization (wt % Ca) (Fig. 1).

An age-related decrease in K_{init} was significantly associated with micro-structural differences, namely greater intracortical porosity characterized by the presence of larger pores but lower lacunar porosity (Table 1). Resistance to fracture was also negatively correlated with the degree of mineralization ($C_{a,mean}$, $C_{a,peak}$). Mineral heterogeneity ($C_{a,width}$) did not correlate with fracture resistance properties (Table 2). However, an inverse relationship existed between K_{init} and the occurrence of hypomineralization ($C_{a,low}$) in bones from females (r=-0.50, p=0.027). Including gender as a covariate, non-lacunar porosity and hypomineralization explained 46% of the variance in resistance to crack initiation.

These results suggest that the heterogeneity of mineralization existing across numerous osteons and interstitial sites within the cortex is not a major determinant of fracture resistance of human femur cortical bone. However, it does not preclude other types of heterogeneity (e.g. at the osteonal/interstitial interface) from affecting bone fragility.

1030

Cartilage β -Catenin Signaling Plays a Key Role in the Development of Ankylosing Spondylitis. Tianqian Hui*, Wanqing Xie, Shan Li, Chundo Oh, Hee-Jeong Im, Di Chen. Rush University Medical Center, USA

Ankylosing spondylitis (AS) is an autoimmune disease of spine and joint and cartilage is the major tissue affected by this disease. Up-regulation of Wnt/ β -catenin signaling has been reported in patients with AS. In this study, we determined if activation of β -catenin signaling in chondrocytes is the key event leading to destructions of the spine and disc tissues during the development of AS. We have generated chondrocyte-specific β -catenin conditional activation mice (β -cat(ex3)Col2ER), by breeding β -cat(ex3)lox/lox mice with Col2-CreERT2 transgenic mice. 1) We found that severe destruction of disc tissues in 3- and 6-month-old β -cat(ex3)Col2ER mice, including severe loss of cartilage tissues in endplate, disorganized annular fibrosus (AF) and nucleus pulposus (NP) tissues and large amounts of osteophyte formation in the entire spine. 2) We have recently generated immortalized rat AF and NP cell lines (immortalized AF and NP cells have been passed over 50 generations and they maintain proliferation and differentiation properties). We found that treatment with BIO, a GSK-3 β inhibitor (mimic β -catenin activation), stimulated Top-flash reporter activity (6-15 folds) in both AF and NP cells after 24 h treatment. BIO induced Mmp13 (8 and 11 folds) and Ccl2 (6 and 11 folds) expression in AF and NP cells. 3) To determine if Mmp13 is a key downstream target of β -catenin signaling, we generated (β -cat(ex3)/Mmp13)Col2ER double mutant mice and found that deletion of Mmp13 significantly reversed defects observed in disc tissue of β -cat(ex3)Col2ER mice. 4) In addition to the disc tissues, we also observed severe damage and loss of proteoglycan and defects in cartilage structure in the facet joint in 4- and 9-month-old β -cat(ex3)Col2ER mice, demonstrated by Alcian blue and Safranin O staining. 5) CCL2 has been demonstrated as a key mediator in osteoarthritis pain. In the present studies we found that Ccl2 was significantly up-regulated by the activation of β -catenin signaling in both AF and NP cells. We then determined changes in pain-related behavior in 4-9 month old β -cat(ex3)Col2ER mice. The β -cat(ex3)Col2ER mice had significantly increased pain sensitivity as evidenced by lower von Frey thresholds ($P < 0.001$), and this pain behavior sustained throughout the entire experimental period (9 months). Also rearing counts were reduced in 4-9 month old β -cat(ex3)Col2ER mice compared to Cre-negative controls ($P = 0.007$) so does ambulation counts ($P = 0.013$). Taking consideration of our previous observations from β -cat(ex3)Col2ER mice with osteoarthritis phenotype in knee joint and temporomandibular joint, the findings observed in disc and facet joint tissues of β -cat(ex3)Col2ER mice largely resemble key features found in patients with AS. Our findings suggest that activation of β -catenin signaling in cartilage tissue may be the key event leading to spine and joint destruction in patients with AS.

Disclosures: Tianqian Hui, None.

1031

Reduced osteoclast TGF β signaling in the aged skeleton impairs the coupling of bone resorption to bone formation through reduced osteoclast Wnt1 expression. Megan Weivoda*¹, Ming Ruan¹, Christine Hachfeld¹, Larry Pederson¹, Rachel Davey², Jeffrey Zajac², Jennifer Westendorf¹, Sundeep Khosla¹, Merry Jo Oursler¹. ¹Mayo Clinic, USA, ²University of Melbourne, Australia

Osteoclasts secrete factors that couple bone resorption and formation. These processes are uncoupled with age through unclear mechanisms, resulting in age-related bone loss. TGF β is abundant in the bone and is released and activated by osteoclasts. We have shown that conditioned media from TGF β -treated osteoclasts stimulates pre-osteoblast migration and differentiation. Because the concentration of TGF β in bone matrix decreases with age, we hypothesized that reduced osteoclast TGF β signaling contributes to age-related uncoupling of bone resorption and formation. Dominant negative TGF β receptor (Tgfr-2) was expressed in osteoclasts using Ctsk promoter Cre mice (Tgfr2^{Cre/KO}). MicroCT analysis of 5 month-old animals revealed osteopenia in Tgfr2^{Cre/KO} mice with significant reductions in femur and vertebral BV/TV. Histomorphometry of the femurs showed no change in osteoclast numbers; however, osteoblast numbers and bone formation rates were reduced 60% in Tgfr2^{Cre/KO} mice. Mineral apposition rates were unchanged, indicating that the reduced bone formation rate was not a result of impaired osteoblast function. Microarray was utilized to identify genes induced in TGF β -treated osteoclasts and data was validated by qPCR. Of interest, 2ng/mL TGF β induced Wnt1 expression >1000-fold. Wild type osteoclasts cultured on bone, a source of matrix-TGF β , also exhibited Wnt1 induction; this induction was impaired in Tgfr2^{Cre/KO} osteoclasts. IHC of Tgfr2^{Cre/KO} femurs revealed a 53% reduction in osteoclast Wnt1 in vivo. To determine whether osteoclast TGF β signaling was disrupted with aging, we performed IHC on young and old (4 and 26 month) femurs. Consistent with the age-related decrease in matrix TGF β , phospho-SMAD2/3, a marker of Tgfr signaling, was significantly reduced in old bone osteoclasts in vivo. Osteoclasts derived from young and old bone marrow showed similar inductions of Wnt1 expression by exogenous and young bone matrix-TGF β . However, culture of osteoclasts derived from young bone marrow on old bone matrix resulted in a 72% reduction in matrix-induced Wnt1, and IHC revealed that osteoclast Wnt1 expression was reduced 64% in old mice in vivo. These data demonstrate that impaired Tgfr signaling in osteoclasts causes osteopenia by reducing osteoblast numbers and establish a novel paradigm by which TGF β stimulated osteoclasts are a key source of factors such as Wnt1 that promote osteoblastic bone formation at sites of bone resorption.

Disclosures: Megan Weivoda, None.

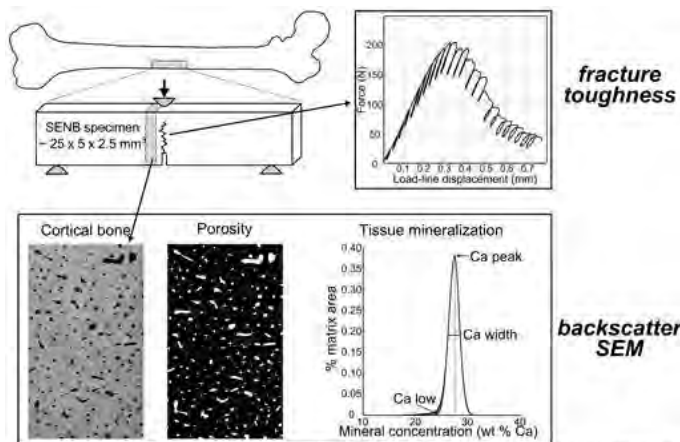


Figure 1: Schematic of the study design. Following fracture toughness testing, a polished cross-section adjacent to the crack propagation site was imaged with quantitative backscattered scanning electron microscopy. SEM images were segmented to separate the mineralized matrix from the pores which encompass the intracortical porosity (pore larger than 100 μ m² that include Haversian canals, Volkmann's canals, resorption cavities) and the lacunar porosity (occupied by osteocytes). The distribution of the calcium concentration within the matrix was characterized by the following parameters: Ca mean (average Ca concentration), Ca peak (most frequent Ca concentration), Ca width (full width half maximum of Ca concentration), and Ca low and Ca high (spread of the distribution on the low and high concentration sides, respectively, defined as the deviation of the mineral distribution from a Gaussian curve).

Table 1: Spearman rank correlation between fracture toughness properties and porosity (r (pval))

| Fracture toughness properties | Intracortical porosity (%) | Pore area median (μ m ²) | Pore area IQR (μ m ²) | Pore area 95 th percil (μ m ²) | Pore density (#/mm ²) | Lacunar porosity (%) |
|---|----------------------------|---|--|--|-----------------------------------|----------------------|
| K _{IC} (MPa.m ^{0.5}) | -0.41 (0.019) | -0.28 (0.088) | -0.32 (0.048) | -0.33 (0.039) | 0.29 (0.069) | 0.40 (0.012) |
| J (kJ/m ²) | -0.15 (0.375) | -0.14 (0.407) | -0.20 (0.226) | -0.19 (0.247) | 0.20 (0.231) | 0.27 (0.103) |

Table 2: Spearman rank correlation between fracture toughness properties and mineral distribution parameters (r (pval))

| Fracture toughness properties | Ca mean (wt% Ca) | Ca peak (wt% Ca) | Ca width (wt% Ca) | Ca low (wt% Ca) | Ca high (wt% Ca) |
|---|------------------|------------------|-------------------|-----------------|------------------|
| K _{IC} (MPa.m ^{0.5}) | -0.27 (0.092) | -0.30 (0.063) | -0.33 (0.434) | 0.11 (0.514) | 0.02 (0.927) |
| J (kJ/m ²) | -0.45 (0.005) | -0.47 (0.002) | 0.07 (0.679) | 0.08 (0.669) | -0.15 (0.372) |

Fig1

Disclosures: Mathilde Granke, None.

1029

Discovery of PCO371, an orally active small-molecule PTH1R agonist for the treatment of hypoparathyroidism. Hiroshi Noda*, Eri Joyashiki, Maiko Hoshino, Tomoyuki Watanabe, Yoshikazu Nishimura, Tohru Esaki, Kotaro Ogawa, Masaru Shimizu, Hidetomo Kitamura, Tatsuya Tamura, Haruhiko Sato, Yoshiki Kawabe. Research Division, Chugai Pharmaceutical Co., Ltd., Japan

Parathyroid hormone (PTH) plays a primary role in maintaining serum calcium (Ca). Hypoparathyroidism (hypoPT) is a rare disease characterized by hypocalcemia and lack of PTH. Conventional therapy of hypoPT, high doses of oral Ca and active vitamin D analogs, can increase the risk of hypercalciuria. Human PTH(1-84) has recently been approved as a treatment option for hypoPT. It would maintain serum Ca while reducing Ca and requirements of vitamin D analogs by replacing the missing hormone. However, due to its short half-life, multiple injections are necessary to maintain serum Ca at a steady level. Since hypoPT is a chronic disorder, there exists an unmet need for orally bioavailable small-molecule which can mimic PTH.

The pharmacological actions of PTH are mediated via the PTH1R, a class B GPCR. No orally active small molecule agonists of the PTH1R have yet been reported. To identify such small molecule agonist, we used a cell-based high throughput screening with LLC-PK1 cells transfected with the human PTH1R (hPTH1R) by using urokinase plasminogen activator activity as a readout. Hit-compounds found from our compound library were optimized to identify a chemical candidate, PCO371, 1-({3,5-dimethyl-4-[2-({4-oxo-2-[4-(trifluoromethoxy)phenyl]-1,3,8-triazaspiro[4.5]dec-1-en-8-yl]sulfonyl)ethyl]phenyl}-5,5-dimethylimidazolidine-2,4-dione). In COS-7 cells transfected with the hPTH1R, the compound stimulated cAMP production and PLC activation in a dose-dependent manner, but not in cells transfected with vector alone. PCO371 displaced ¹²⁵I-labeled hPTH(1-15) that was bound to the membranes in those cells. PCO371 also stimulated Ca release in fetal rat long bone cultures as well as hPTH(1-34) did. These results suggest that PCO371 acts as a full agonist on the PTH1R. Single oral administration of PCO371 showed calcemic and hypophosphatemic actions in thyroparathyroidectomized (TPTX) rats; the effects were more potent and long-lasting than those of hPTH(1-34). In 4-week repeated dosing studies in TPTX rats, once-daily oral PCO371 increased serum Ca to the normal range. Co-treatment with once-daily oral PCO371 and alfacalcidol normalized serum Ca, and also reduced urinary Ca excretion and the requirements of alfacalcidol. These results indicate that PCO371 is the first example of an orally active small-molecule PTH1R agonist that can mimic the biological functions of PTH. It would provide a new option for the treatment of patients with hypoPT.

Disclosures: Hiroshi Noda, Chugai Pharmaceutical Co., Ltd.

This study received funding from: Chugai Pharmaceutical Co., Ltd.

1032

A Hajdu Cheney Mutant Mouse Exhibits Profound Osteopenia. Ernesto Canalis*, Lauren Schilling, Kyeong Lee, Stefano Zanotti. UConn Health, USA

Notch receptors play a critical role in skeletal development and bone homeostasis. Hajdu Cheney Syndrome (HCS) is a devastating disease characterized by acro-osteolysis, severe osteoporosis with fractures and sudden death. HCS is associated with a gain-of-function of NOTCH2, where point mutations in exon 34 lead to a truncated and stable protein product lacking sequences necessary for its degradation. Despite the skeletal manifestations reported in HCS, mechanisms underlying the bone loss are not known. To understand the disease process, we created a mouse model harboring a Notch2 mutant allele reproducing the mutation found in subjects with HCS manifesting pronounced osteoporosis with fractures. The mutation, 6946C>T in humans and 6955C>T in mice, creates a STOP codon at glutamic acid 2319 in mice, upstream the PEST domain required for Notch degradation. Sequences necessary for Notch2 transcriptional activity are preserved. The 6955C>T mutation was introduced into the Notch2 locus by homologous recombination, verified by DNA sequencing, and mice characterized following removal of the selection cassette. Notch target genes were increased in bone and osteoblast cultures from Notch2Q2319X mice, demonstrating Notch signal activation in the skeleton. Homozygous Notch2Q2319X mutants exhibited newborn lethality, whereas heterozygous mice had pronounced cancellous and cortical bone osteopenia. Compared to littermate controls, microcomputed tomography of Notch2Q2319X mutants revealed a 50-55% decrease in cancellous bone volume and markedly decreased connectivity. Cortical thickness, total and cortical cross-sectional areas were decreased by 20-40%. Histomorphometry revealed a ~30% increase in osteoclast number and eroded surface, and a modest decrease in bone formation. Flow cytometry of bone marrow cells revealed a 20-25% increase in osteoclast precursors in Notch2Q2319X mice, and bone marrow mononuclear cells had an increased capacity to form multinucleated osteoclasts in response to M-CSF and RANK-L, explaining the enhanced bone resorption. Osteoblast cultures exhibited decreased alkaline phosphatase and osteocalcin expression and increased RANK-L mRNA. In conclusion, a genetically engineered HCS mutant mouse recreates the human disease and exhibits pronounced osteopenia due to an increase in the osteoclast precursor cell pool and osteoclastogenesis leading to increased bone resorption. For the first time, the skeletal pathogenesis of HCS is explained.

Disclosures: Ernesto Canalis, None.

1033

Decreased cancellous bone mass in a murine model of type 1 diabetes is caused by cell autonomous effects of FoxOs in committed osteoblast precursors and their descendants. Srividhya Iyer*¹, Li Han², Serra Semahat Ucer², Ha-Neui Kim², Aaron Warren², Julie Crawford², John Fowlkes³, Stavros Manolagas², Maria Almeida². ¹Central Arkansas VA Healthcare System, Univ of Arkansas for Medical Sciences, USA, ²Center for Osteoporosis & Metabolic Bone Diseases, Central Arkansas Veterans Healthcare System, University of Arkansas for Medical Sciences, USA, USA, ³Barnstable Brown Diabetes & Obesity Center, University of Kentucky College of Medicine, UK Healthcare, USA

Type1 diabetes (T1D) is associated with osteopenia and increased risk of fragility fracture, as well as poor fracture healing. These skeletal abnormalities are often associated with reduced serum markers of bone formation. As in humans, murine models of T1D generated via genetic or pharmacologic means exhibit decreased bone formation and low bone mass. However, the molecular mechanisms responsible for these effects remain unknown. Nonetheless, insulin increases the proliferation and differentiation of osteoblastic cells in vitro and mice lacking the insulin receptor in osteoblasts have reduced osteoblast numbers and decreased trabecular bone mass. Insulin signaling suppresses the activity of the FoxO transcription factors; and FoxOs inhibit osteoprogenitor proliferation and bone formation by sequestering β -catenin away from TCF-mediated transcription. Prompted by this evidence we investigated here whether FoxOs are responsible for the low bone mass in T1D. To do this, we used mice lacking FoxO1,3,4 in Osx1-Cre expressing cells (FoxO1,3,4^{Osx1-Cre}) and their control littermates (FoxO1,3,4^{fl/fl}). At 4 weeks of age males of both genotypes (n=10-14 per group) were injected with vehicle or 40 μ g/g body weight of streptozotocin (STZ) for five days to induce T1D. Ninety percent of the STZ-injected mice had elevated blood glucose levels (>250 mg/dl) and were considered diabetic. Forty days later mice were sacrificed and micro-CT analysis revealed that the diabetic FoxO1,3,4^{fl/fl} mice had reduced spinal cancellous bone volume, as compared to their non-diabetic controls. These changes were associated with lower trabecular thickness, but unchanged trabecular number. In contrast, cancellous bone volume or trabecular thickness was unaffected in diabetic FoxO1,3,4^{Osx1-Cre} mice. Similar results were obtained in the cancellous bone of the femur. In line with its effect on bone mass, diabetes caused a reduction in vertebral strength in FoxO1,3,4^{fl/fl} mice but not in FoxO1,3,4^{Osx1-Cre} mice. Nonetheless, in difference to cancellous bone, diabetes reduced femoral cortical thickness in both FoxO1,3,4^{fl/fl} and FoxO1,3,4^{Osx1-Cre} mice. Ongoing histologic analysis should elucidate the cellular mechanisms responsible for the differential effects of diabetes in cortical versus cancellous bone. Taken together, our results strongly suggest that FoxOs mediate the deleterious effects of T1D on cancellous bone.

Disclosures: Srividhya Iyer, None.

1034

Protein Phosphatase 5 (PP5) conveys negative effect of rosiglitazone on bone by inversely regulating PPAR γ and Runx2 activities. Lance A. Stechshulte*¹, Piotr J. Czernik², Edwin R. Sanchez³, Beata Lecka-Czernik¹. ¹Department Orthopaedic Surgery, Center for Diabetes & Endocrine Research, University of Toledo, College of Medicine & Life Sciences, USA, ²Micro Tomografix Ltd., USA, ³Department of Physiology & Pharmacology, Center for Diabetes & Endocrine Research, University of Toledo, College of Medicine & Life Sciences, USA

Energy metabolism and bone mass are interconnected. Conditions with compromised energy balance, such as diabetes, obesity, and aging, are associated with increased risk of fractures due to decreased bone mass and/or bone quality. This implicates an existence of a common mechanism regulating energy and bone metabolism. Two transcription factors, PPAR γ and Runx2, are key regulators of mesenchymal stem cells (MSCs) differentiation toward adipocytes (AD) or osteoblasts (OB), respectively. PPAR γ and Runx2 are subjected to posttranslational modifications, which determine their activities. Dephosphorylation of PPAR γ at S112 and S273 is required for activation of pro-AD and insulin sensitizing activities, whereas phosphorylation of Runx2 at S319 is required for pro-OB activity. Upon rosiglitazone (Rosi) treatment, which promotes MSCs commitment toward AD and away from the OB lineage, both PPAR γ and Runx2 undergo dephosphorylation which increases PPAR γ and suppresses Runx2 activity. We have recently identified the Protein Phosphatase 5 (PP5) as a specific enzyme inversely regulating PPAR γ and Runx2 activities associated with phosphorylation. In the presence of Rosi, PP5 binds to PPAR γ and Runx2 in the cell nuclei and dephosphorylates both. Knockdown of PP5 in marrow MSCs decreased PPAR γ and increased Runx2 activity and correlated with increased phosphorylation of both factors. Most importantly, PP5 deficiency rendered marrow MSCs unresponsive to pro-AD and anti-OB effects of Rosi suggesting that *in vivo* PP5 may convey negative effects of Rosi on bone. To test this hypothesis, WT and mice deficient in PP5 (PP5-KO) were treated with Rosi for 8 wks at the dose of 20 mg/kg/d. In response to this treatment, WT animals gained 80% of body weight and doubled fat content, whereas PP5-KO mice were resistant to these effects. Most importantly, while Rosi administration resulted in 50% decrease in bone mass of WT, there was only 13% decrease in bone mass of PP5-KO animals. An analysis of gene expression in the OBs freshly isolated from femora endosteal surface indicated that in WT Rosi decreased the expression of OB-specific transcription factors, Osterix and Dlx5, whereas it did not affect the expression of these factors in OBs isolated from PP5-KO mice. In conclusion, PP5 mediates negative effect of Rosi by upregulating PPAR γ and suppressing Runx2 activity. These results also suggest that PP5 is the immediate target for Rosi. This possibility is currently being tested.

Disclosures: Lance A. Stechshulte, None.

1035

Hydrogen Sulfide Is a Novel Regulator Of Bone Formation Implicated In The Bone Loss Induced by Estrogen Deficiency. Francesco Grassi*¹, Abdul Malik Tyagi², Jonathan Adams², Lindsey D. Walker², Jau-Yi Li², John W Calvert³, Laura Gambari⁴, Gina Lisenoli⁴, Jerid Robinson², Roberto Pacifici⁵. ¹Laboratorio RAMSES, Istituto Ortopedico Rizzoli, Italy, ²Division of Endocrinology, Metabolism, & Lipids, Emory University, USA, ³Cardiothoracic Research Laboratory, Department of Surgery, Emory University, USA, ⁴Lab di Immunoreumatologia e Rigenerazione Tissutale, Istituto Ortopedico Rizzoli, Italy, ⁵Division of Endocrinology, Metabolism, & Lipids, Immunology & Molecular Pathogenesis Program, Emory University, USA

Critical for the bone wasting effect of estrogen deficiency is a potent stimulation of bone resorption that is only partially mitigated by an increase in bone formation. The mechanism that prevents bone formation from increasing as much as bone resorption in estrogen deficient humans and animals is unknown. Hydrogen sulfide (H₂S) is a gasotransmitter produced by mammalian tissues known to regulate stromal cell (SC) function and bone formation. To investigate whether H₂S plays a role in ovariectomy (ovx) induced bone loss, serum H₂S levels were measured in 14 week old WT mice, 4 weeks after ovx or sham operation. Serum H₂S was reduced by 55% in ovx mice compared to sham controls. The whole bone marrow (BM) and BM SC mRNA levels of the two key H₂S-generating enzymes, cystathionine β -synthase (CBS) and cystathionine γ -lyase (CSE), were 70-90 % lower in samples from ovx than sham operated mice, demonstrating that estrogen deficiency impairs the SC production of H₂S. To attest to relevance, sham and ovx mice were treated in vivo with the H₂S-donor, GYY4137 (50mg/kg/day IP) or vehicle for 4 weeks starting at surgery or 4 weeks after surgery. GYY4137 normalized the serum levels of H₂S in ovx mice, increased histomorphometric and biochemical indices of bone formation, and completely prevented or reversed the loss of trabecular bone induced by ovx. GYY4137 also blocked or reversed by ~80% the loss of cortical bone. In ovx mice GYY4137 increased CFU-ALP formation, an index of SC commitment to the osteoblastic lineage, and SC differentiation into osteoblasts, as determined by measurements of ALP, RUNX2, Collagen 1, BSP, Osterix mRNA levels. GYY4137 also decreased SC apoptosis. Moreover, H₂S increased the BM mRNA levels of WNT16, WNT2b and WNT6, resulting in Wnt activation in SCs. Studies in human cells showed that β -estradiol induces the expression of CBS and CSE in human BM SCs (hSCs) and confirmed that

H₂S-releasing drugs induce osteogenic differentiation of hSCs. Finally, silencing of CBS and CSE by siRNA abrogated hSCs ability to form mineralized nodules *in vitro*. In summary, our findings show that regulation of H₂S levels is a novel mechanism by which estrogen stimulates osteoblastogenesis and bone formation in mice and humans. Blunted production of H₂S contributes to ovx induced bone loss by limiting the compensatory increase in bone formation elicited by ovx. Restoration of H₂S levels is a potential novel therapeutic approach for postmenopausal osteoporosis.

Disclosures: Francesco Grassi, None.

1036

FGFR3 Modulates Fracture Repair by Controlling the Balance of Intramembranous and Endochondral Bone Formation. Simon Kelley^{*1}, Chunying Yu², Heather Whetstone², Benjamin Alman³. ¹The Hospital for Sick Children, Toronto, Ontario, Canada, Canada, ²The Hospital for Sick Children, Canada, ³Duke University, USA

Fibroblast growth factor receptor 3 (*fgfr3*) mutations cause skeletal dysplasias with disparate phenotypes. Gain-of-function mutations are characterized by disproportionate short stature, whereas loss-of-function mutations are characterized by tall stature. *Fgfr3* is known to be a negative regulator of chondrocyte proliferation affecting long bone growth through endochondral ossification. However we observed that individuals with achondroplasia showed enhanced bone regeneration during distraction osteogenesis (intramembranous ossification) for surgical limb lengthening, thus we hypothesized that *fgfr3* affects mesenchymal proliferation and osteoblast differentiation, which act in concert with its known effects on chondrocyte function to manifest in the abnormal healing of bone fractures. To investigate the role of *fgfr3* in fracture healing we used an established murine semi-stabilized tibia fracture model in genetically modified *fgfr3* knockout mice and their wild type (WT) controls. Fractures were harvested and analyzed at critical time points (Post Fracture Day 3, 7, 14 and 21) using histomorphometry, micro-CT and gene expression analysis (qPCR) to assess fracture callus structure and composition. We showed that *fgfr3* modulates the size and structure of healing fracture callus with the *fgfr3* mutant calli showing peak callus size earlier than their WT controls (PFD7), yet showing reduced callus size at the later time points (PFD14, PFD21) suggesting an acceleration of fracture repair. Despite the overall rapidity of healing, the structural integrity of the healed mutant fractures was diminished. Enhanced endochondral bone formation in *fgfr3*^{+/-} mice accounted for the rapidity of bone healing however early peripheral subperiosteal bone formation from the intramembranous pathway was diminished in *fgfr3*^{+/-} mice suggesting that *fgfr3* has a role in switching between the two major systems of bone formation. Using bone marrow MSCs (BM-MSCs) from *fgfr3*^{+/-} and WT mice an in-vitro colony forming unit-fibroblast (CFU-F) assay, BrdU assay, limiting dilution and qPCR were performed demonstrating that *fgfr3* regulates the number, and proliferative ability of osteochondral progenitors. BM-MSC Colony forming unit-osteoblast (CFU-O), colony forming unit-chondrocyte (CFU-C) assays and qPCR revealed that under-expression of *fgfr3* decreases osteogenic differentiation but increases chondrogenic differentiation recapitulating those findings identified in the fracture model in-vivo. Thus we showed that *fgfr3* affects fracture healing by acting as a switch between intramembranous and endochondral ossification. Modulation of *fgfr3* signaling may offer the ability to direct progenitor cells towards specific bone regenerative pathways, which has enormous appeal for the enhancement of skeletal regeneration and repair.

Disclosures: Simon Kelley, None.

1037

Intermittent PTH Alleviates Abnormalities of Bone Tissue Heterogeneity Associated with Prolonged Bisphosphonate Treatment by Inducing Substantial New Bone Formation. Allison Altman^{*1}, Yong-Hoon Jeong², Wei-Ju Tseng¹, Chantal de Bakker¹, Ling Qin¹, Lin Han³, Do-Gyoon Kim², X. Sherry Liu¹. ¹University of Pennsylvania, USA, ²Ohio State University, USA, ³Drexel University, USA

Postmenopausal osteoporosis is often treated with bisphosphonates (BP, eg, alendronate, ALN), but over-suppression of bone turnover by long-term BP may reduce bone mineral heterogeneity, increasing the risk of atypical fractures. Our recent study demonstrated that intermittent PTH following long-term ALN in ovariectomized (OVX) rats efficiently improved bone mass and microarchitecture (FigA). The objective of this study was to test whether switching from ALN to PTH would alleviate abnormalities of tissue heterogeneity induced by ALN.

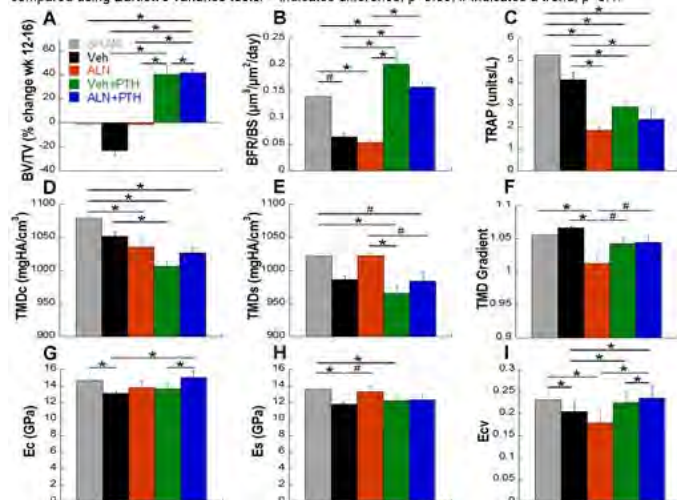
30 4-mo-old rats underwent OVX (n=24; 6x4 groups) or Sham (n=6) surgery. Treatment began at 6-mo-old (wk 0) for OVX rats: Veh (saline wk 0-16); ALN (28µg/kg 2x/wk wk 0-16); Veh+PTH (saline wk 0-12 & PTH 40µg/kg 5x/wk wk 12-16); ALN+PTH (ALN wk 0-12 & PTH wk 12-16). Bone formation (BFR/BS) was assessed by *in vivo* µCT-based dynamic analysis (wk 15&16 scanned@10.5µm) and resorption assessed by serum TRAP. The L2 vertebra were subjected to µCT (3.5µm) and nanoindentation to assess tissue mineral density (TMD) and modulus (E) at both the inner trabecular region (TMDc and Ec) and the edges (TMDs and Es).

In vivo dynamic analysis indicated a 16% lower BFR/BS in ALN vs. Veh, and a 212% and 147% higher BFR/BS in PTH and ALN+PTH vs. Veh, respectively (FigB). Serum TRAP in treatment groups were 42-55% lower than Veh (FigC). TMDs and Es tended to increase in ALN vs. Veh (4% p>0.1 & 13% p<0.1, respectively) with no difference in TMDc or Ec (FigDEGH). However, TMD gradient (TMDc/TMDs) and

the coefficient of variation of E (Ecv) were 5% and 13% lower in ALN vs. Veh, respectively (FigFI), indicating reduced heterogeneity in both tissue mineralization and material mechanical properties. PTH following ALN resulted in a trend of 4% lower TMDs than ALN alone. Moreover, bone tissue heterogeneity was restored as shown by a 3% higher mineralization gradient and 31% greater Ecv in ALN+PTH vs. ALN alone. Interestingly, TMDs was significantly correlated with Es (r=0.58, p<0.01) but TMDc and Ec was not correlated, suggesting that during the mineralization process (bone surface), TMD is a primary determinant of material properties, but once complete (bone center) TMD plays a lesser role.

In summary, prior treatment with ALN does not diminish the potential for PTH to increase new bone formation. By altering the tissue mineralization, PTH acts to alleviate abnormalities in heterogeneity of tissue mechanical properties induced by prolonged ALN treatment.

Figure. (A) Bone volume fraction (BV/TV) percent change during wks 12-16 at the tibia compared using repeated measures ANCOVA covaried by wk 12 BV/TV. (B) µCT-based bone formation rate (BFR/BS) from wk 15-16. (C) Serum TRAP analysis. At L2: (D) central TMD (TMDc), (E) surface TMD (TMDs), (F) surface-central TMD gradient. (G) central modulus (Ec), surface modulus (Es), and modulus coefficient of variation (Ecv) compared using Bartlett's variance tests. * indicates difference, p<0.05; # indicates a trend, p<0.1.



Figure

Disclosures: Allison Altman, None.

1038

Genome-wide analysis of DNA methylation identifies a novel locus associated with bone mineral density. John Morris^{*1}, Pei-Chien Tsai², Fei Gao³, Vincenzo Forgetta⁴, Yudong Xia³, Celia Greenwood⁵, Elin Grundberg², Tim Spector², Jun Wang³, Jordana Bell², Brent Richards⁵. ¹McGill University, Ca, ²King's College London, United Kingdom, ³BGI-Shenzhen, China, ⁴Lady Davis Institute for Medical Research, Canada, ⁵McGill University, Canada

Osteoporosis is a common, complex disease characterized by increased bone fragility, often resulting in fracture. Bone mineral density (BMD) is measured to diagnose osteoporosis and estimate fracture risk. Studying the genetic determinants of BMD has led to novel disease pathophysiology insights. We sought to study epigenetic associations with BMD, as DNA methylation levels are known to influence or be secondary to disease phenotypes. To assess epigenetic associations with BMD, we undertook a genome-wide association study of DNA methylation levels. Methylation levels were estimated using methylated DNA immunoprecipitation sequencing (MeDIP-seq) to identify differentially methylated regions (DMRs) associated with BMD measured at the forearm, femoral neck, and lumbar spine in the TwinsUK cohort, in 890, 1,518, and 1,397 twins, respectively. An intergenic DMR on chromosome 6q21 was found to be significantly associated with forearm BMD ($P = 5.3 \times 10^{-9}$). Through the usage of publicly available functional genomics data, we have linked the DMR to an enhancer putatively interacting with PRDM1, a gene regulating osteoclastogenesis. Using multiple public data repositories for 3D nuclear conformations (Rao *et al.* 2014, *Cell* 159: 1665), enhancer RNAs (FANTOM5), DNaseI hypersensitivity sites (ENCODE), and epigenetic marks (Epigenome Roadmap), we find evidence that the region encompassing the DMR likely contains a regulatory element of PRDM1, in that it is in close 3D proximity to the PRDM1 promoter and the DNA at these two regions is coincidentally open in relevant cell types such as monocytes, an osteoclast precursor cell. Moreover, recent work suggests rare genetic variants are nominally associated with forearm BMD at this locus. Further work is underway to validate these and any other genetic associations with BMD at this locus. This study represents the most comprehensive genome-wide analysis to date of the role of methylation in BMD. This work forms a basis for future studies that will refine the definitive role of epigenetic mediated effects at this osteoclast locus.

Disclosures: John Morris, None.

1039

Def6 restrains osteoclastogenesis and inflammatory bone resorption. Nikolaus Binder¹, F. Patrick Ross¹, Christine Miller¹, Lionel B. Ivashkiv¹, Georg Schett², Alessandra Pernis¹, Steven R. Goldring¹, Baohong Zhao^{*1}. ¹Hospital for Special Surgery, USA, ²University of Erlangen-Nuremberg, Germany

Abnormal generation and/or function of osteoclasts lead to pathological bone resorption in inflammatory disorders such as rheumatoid arthritis (RA). Def6, a novel type of guanine nucleotide exchange factor (GEF), plays an important role in the activation of lymphocytes by regulating IRF4 activity and/or exerting its function in conjunction with Swap70, the only other molecule with high homology to Def6. Recent studies show that IRF4 and Swap70 negatively regulate physiological osteoclast differentiation and function, respectively. In addition, Def6 deficiency leads to the development of RA like joint disease with bone erosion in a mouse model. These findings stimulated us to explore the role of Def6 in osteoclastogenesis and inflammatory osteolysis, as well as to investigate its underlying mechanisms of action. In this study, we found that osteoclast precursors from Def6 deficient mice (*Def6*^{-/-}) demonstrated enhanced sensitivity to RANKL in the early differentiation phase. Def6, unlike Swap70, did not affect actin ring formation or the function of osteoclasts. As TNF-alpha is a key pathogenic factor driving inflammatory bone resorption in RA, we next investigated the role of Def6 in TNF-mediated osteoclastogenesis. We found that lack of Def6 markedly enhanced TNF-alpha-induced osteoclastogenesis both *in vitro* and *in vivo* and resulted in increased bone resorption in a TNF-alpha-induced inflammatory osteolysis mouse model. In human system, Def6 levels were decreased in osteoclast precursors obtained from RA patients and were elevated after TNF blockade therapy. Furthermore, the osteoclastogenic capacity of the RA cells was significantly inversely correlated with Def6 expression levels, indicating that Def6 functions as an inhibitory factor in limiting enhanced osteoclast formation and bone destruction in RA. Mechanistically, we found that Def6 suppressed osteoclastogenesis and the expression of key osteoclastogenic factors NFATc1 and c-Fos by regulating an endogenous IFN-beta mediated autocrine feedback loop. Our data identify Def6 as a novel negative regulator of osteoclastogenesis in both physiological and inflammatory conditions and provide a novel mechanism for regulation of osteoclastogenesis driven by the Def6-IFN-beta axis. These results identify Def6 as an attractive therapeutic target to prevent bone destruction in inflammatory arthritis.

Disclosures: Baohong Zhao, None.

1040

Gna13 gain-of-function to protect mice from inflammatory bone loss in rheumatoid arthritis through inhibiting AKT activity in osteoclasts. Mengrui Wu^{*1}, Wei Chen², Yun Lu², Guochun Zhu², Liang Hao², Yi-Ping Li². ¹The University of Alabama at Birmingham, USA, ²UAB, USA

Current resorption inhibitors are effective but far from ideal due to negative side effects (e.g., jaw osteonecrosis and increased bone fragility). Thus, a need for better therapeutic agents is compelling, and endogenous inhibitors may serve as powerful new therapeutic targets in osteoclast-related bone diseases. We found that knockdown of Gna13 *in vitro* and osteoclast-specific conditional knockout (CKO) of Gna13 *in vivo* promoted osteoclast differentiation and function via PI3K/Akt signaling. The average nuclei number of osteoclasts and average size of actin rings were increased in the absence of Gna13 (by 200% and 300%, respectively), which can be reversed by PI3K inhibitor LY294002 and AKT inhibitor MK2206HCl at a dose-dependent manner. On the other hand, over-expression of the constitutively active form of Gna13 (Gna13CA) in monocytes/macrophages and RAW264.7 cells inhibits osteoclast formation by 85%, which can be partly rescued by overexpression of the constitutively active form of AKT (AKTCA). Furthermore, we tested whether an AAV (adeno-associated virus) overexpressing Gna13CA *in vivo* would protect mice from inflammatory bone destruction induced by lipopolysaccharide (LPS) or in the Rheumatoid arthritis mice model induced by TNF α . In the LPS-injection model, both WT and Gna13 CKO mice were subjected to subcutaneous injection over calvaria with LPS or PBS. LPS induced mice showed a 2-fold increase in the number of osteoclasts and 3-fold more bone resorption. While the absence of Gna13 further promotes osteoclastogenesis and bone loss, local administration of AAV-G13CA over calvaria had a marked inhibitory effect on excessive osteoclast formation and bone destruction by LPS, by 60% and 50% respectively. TNF α transgenic mice automatically developed arthritis rheumatology accompanying excessive osteoclast formation and bone destruction. Local administration of AAV-G13CA over metacarpal bones largely reduced the number of osteoclasts and bone loss in the TNF α transgenic mice, by 90% and 72% respectively. Interestingly, cartilage destruction was also inhibited by 75% and swelling was also relieved after AAV-G13CA treatment. In summary, we demonstrated that Gna13 negatively regulates osteoclast fusion and function by inhibiting PI3K/AKT signaling, and Gna13-gain-of-function could serve as a potential and powerful therapeutic treatment to inflammatory bone loss.

Disclosures: Mengrui Wu, None.

1041

The translational repressor Musashi-2 promotes osteoclastogenesis by regulating Numb/Notch signaling. Toshifumi Fujiwara^{*1}, Shiqiao Ye¹, Haibo Zhao². ¹Center for Osteoporosis & Metabolic Bone Diseases, Division of Endocrinology & Metabolism, Department of Internal Medicine, University of Arkansas for Medical Sciences & the Central Arkansas Veterans Healthcare System, USA, ²Central Arkansas VA Healthcare System, Univ of Arkansas for Medical Sciences, USA

Notch receptors are transmembrane proteins that play an essential role in cell fate decisions and the regulation of proliferation and differentiation during development and adult life in mammals. Upon ligand binding, Notch receptors are cleaved by a γ -secretase complex. As a result, the Notch intracellular domain (NICD) is released from the plasma membrane and translocates to the nucleus, where it induces the expression of Notch target genes, including *Hes1*. Mounting evidence indicates that Notch signaling modulates RANKL-induced osteoclast (OC) differentiation *in vitro* and *in vivo*. Numb, an endogenous repressor of intracellular Notch signaling, inhibits osteoclastogenesis through degradation of NICD. Musashi (Msi) 1 and 2 are members of a family of RNA-binding proteins that activate Notch signaling through the translational repression of Numb. Msi1 also modulates tumor cell cycle progression and proliferation by inhibiting the translation of the cyclin-dependent kinase inhibitor p21WAF-1. Aberrant activation of Msi2 promotes acute myeloid leukemia in humans. Here, we report that Msi2, but not Msi1, is predominantly expressed in bone marrow macrophages (BMMs). Both mRNA and protein expression of Msi2 were dramatically increased during OC differentiation. Knocking-down Msi2 expression in BMMs by lentivirus-mediated shRNAs markedly decreased the formation of TRAP+ multinucleated OCs, as evidenced by diminished mRNA and protein expression of OC marker genes, such as TRAP, Cathepsin K, and NFATc1. In addition, loss of Msi2 in BMMs, pre-OCs or mature OCs led to an increase in Numb levels and a significant decrease in both NICD2 and *Hes1*. On the other hand, depletion of Notch2 or *Hes1* expression by shRNAs attenuated OC formation without changing Msi2 expression, suggesting that Msi2 regulates Notch activation in OC lineage cells through Numb. Msi2 deficiency had no effects on BMM proliferation, cell cycle progression, as well as the levels of p21WAF-1, cyclin D1 and D2. Moreover, deletion of Msi2 in OC precursors attenuated RANKL-induced NF κ B activation and promoted OC apoptosis, as demonstrated by increased DNA fragmentation and increased levels of cleaved caspase 3 and poly (ADP-ribose) polymerase. These results indicate that RANKL induces Msi2, which in turn activates Notch signaling during OC differentiation. Hence, Msi2 is critical for RANKL-induced osteoclastogenesis, at least in part, by regulating Numb/Notch/ NF κ B signaling.

Disclosures: Toshifumi Fujiwara, None.

1042

Osteoclast-derived exosomal miR-214 inhibits osteoblastic bone formation. Defang Li^{*}, Jin Liu, Baosheng Guo, Chao Liang, Lei Dang, Aiping Lu, Ge Zhang. Institute for Advancing Translational Medicine in Bone & Joint Diseases, School of Chinese Medicine, Hong Kong Baptist University, Hong Kong SAR, China

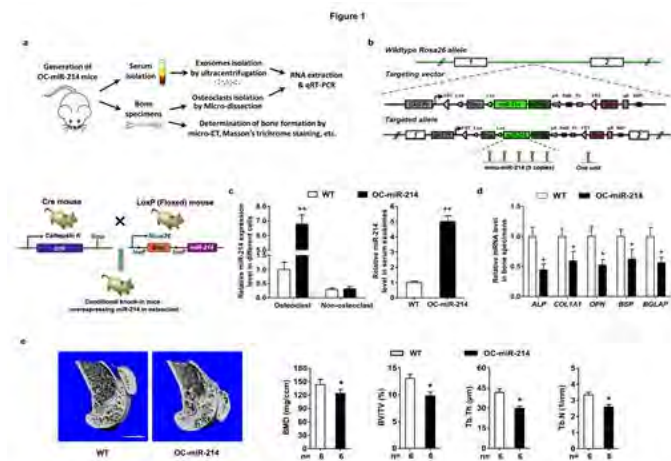
Introduction: Emerging evidences indicate that osteoclasts may direct osteoblasts to regulate bone formation, and that the dysregulation of microRNAs (miRNAs) plays a crucial pathophysiological role on skeletal disorders with a reduction in bone formation. Our previous work demonstrated that exosomal miR-214 transferred from osteoclast could inhibit osteoblast activity *in vitro*. Here we further showed that osteoclast-derived exosomal miR-214 could inhibit osteoblastic bone formation *in vivo*.

Experimental Design: (1) Study 1: To investigate whether osteoclastic miR-214 could inhibit bone formation in the conditional knock-in mice overexpressing miR-214 in osteoclast (OC-miR-214 mice). (2) Study 2: To examine whether exosomal miR-214 secreted from miR-214-overexpressed osteoclast (derived from OC-miR-214 mice) could inhibit bone formation *in vivo*.

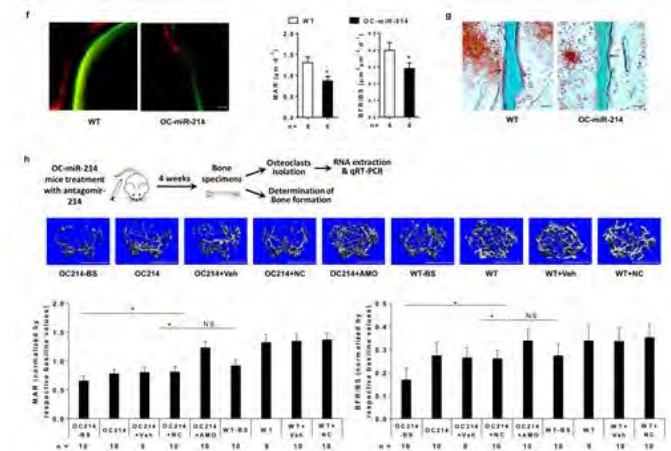
Results: In study 1, we successfully generated OC-miR-214 mice. The osteoclastic and serum exosomal miR-214 level was significantly higher in OC-miR-214 mice than those in WT mice (Fig 1a-c). In contrast, the intra-osseous mRNA levels of the bone formation marker genes *ALP*, *COL1A1*, *OPN*, *BSP* and *BGLAP* were all remarkably reduced in OC-miR-214 mice (Fig 1d). The micro-CT and bone histomorphometric analysis for the distal femora showed that poorly organized trabecular architecture, lower bone mass and lower bone formation in OC-miR-214 mice when compared to those in WT mice (Fig 1e-g). After treatment with antagomir-214, the above parameters were reversed and ameliorated at the distal femur in OC-miR-214+AMO mice (Fig 1h).

In study 2, the intra-osseous fluorescence signal was detected in mice administrated with PKH67-labelled exosomes derived from OC-miR-214 osteoclasts (Fig. 2a-b). Then, we isolated osteoblasts (*Alp*-positive cells) from bone marrow cells by fluorescence activated cell sorting. As expected, the intra-osteoblasts miR-214 level was elevated in mice administrated with PKH67-exosomes (Fig. 2c). Furthermore, the intra-osseous mRNA levels of *ALP*, *COL1A1*, *OPN*, *BSP* and *BGLAP* were remarkably decreased in mice treated with the exosomes (Fig 2d). Furthermore, the micro-CT and bone histomorphometric analysis for the distal femora showed that poorly organized trabecular architecture, lower bone mass and lower bone formation in mice after treatment with the exosomes when compared with the control group (Fig

2e-g).Conclusions: Osteoclast-derived exosomal miR-214 could inhibit osteoblastic bone formation.



Results-1



Results-2



Results-3



Results-4

Disclosures: Defang Li, None.

Figure 1 Decreased bone formation in osteoclast-specific miR-214 knock-in mice is rescued by osteoclast-specific miR-214 inhibition. (a) The conditional knock-in mice overexpressing miR-214 in osteoclast were generated. The miR-214 level, bone formation marker genes mRNA expression levels and bone formation-associated parameters were examined. (b) Schematic diagram for conditional miR-214 knock-in mouse (ROS26-miR-214 knock-in mice), targeting vector and targeted allele (left) and development strategy of OC-miR-214 mice (right). One unit includes the mma-miR-214 stem-loop, a 200 bp 5' flanking sequence, and a 200 bp 3' flanking sequence. (c) miR-214 levels in osteoclasts (Ctsk positive cells) versus non-osteoclasts (Ctsk negative cells) (left) and serum exosomes (right) from WT and OC-miR-214 mice. (d) The mRNA expression levels of marker genes (*Alp*, *Collagen-I*, *Opn*, *BSP* and *Bglap*) in bone specimens determined by Real-time PCR in WT and OC-miR-214 mice. (e) The representative micro-CT images of three-dimensional trabecular architecture (left) and the value of micro-CT parameters (BMD, BV/TV, Tb.Th and Tb.N) (right) at the proximal tibiae collected from WT and OC-miR-214 mice. (f) The value of dynamic bone histomorphometric parameters (MAR, BFR/BS) (left) and the representative images of new bone formation assessed by double calcein labeling (right) at the distal femur collected from WT and OC-miR-214 mice. Scale bars, 20 μ m. (g) Osteoid formation indicated by Masson's trichrome staining in the distal femur of WT and OC-miR-214 mice. Scale bars, 10 μ m. (h) The effect of osteoclast-targeted (D-Asp)-liposome-antagomir-214 in OC-miR-214 mice determined by micro-CT and dynamic bone histomorphometric analysis. Representative images showing three-dimensional trabecular architecture (top) and bone histomorphometric parameters (MAR, BFR/BS) showing the bone formation (bottom) in each group. Scale bars, 2 mm. **Note:** The data were presented as mean \pm s.d. * P <0.05. OC214: OC-miR-214 mice, OC214-BS: age-matched OC-miR-214 mice that were sacrificed before treatment as baseline, Veh OC-miR-214 mice treated with (D-Asp)-liposome (vehicle) alone, NC: OC-miR-214 mice treated with (D-Asp)-liposome-antagomir negative control, AMO: OC-miR-214 mice treated with (D-Asp)-liposome-antagomir-214.

Figure 2

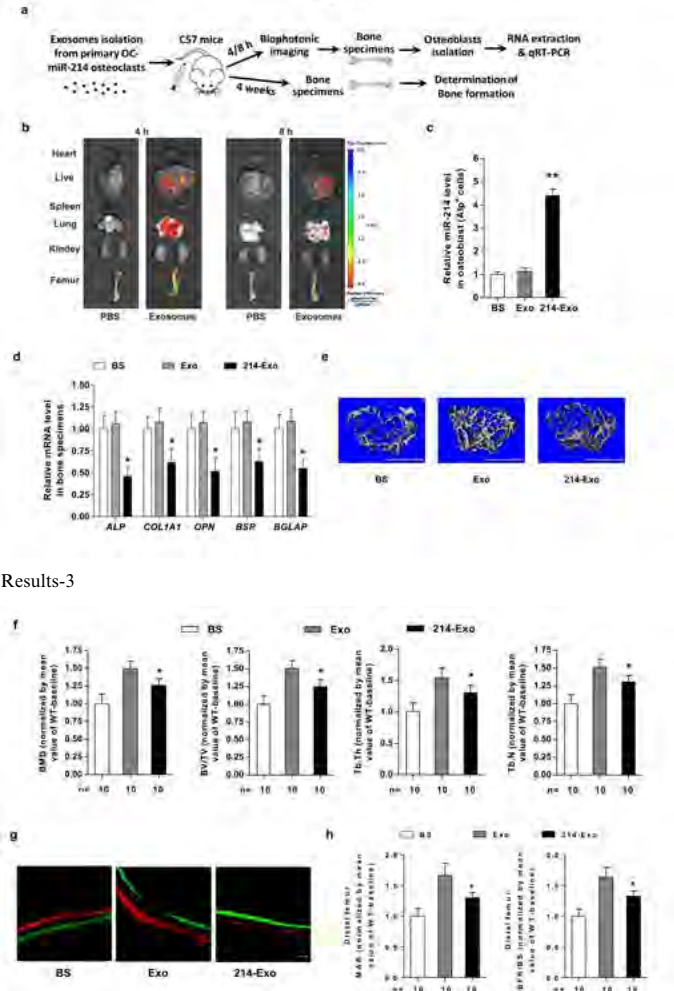


Figure 2 Exosomal miR-214 secreted from primary osteoclast inhibits bone formation *in vivo*. (a) C57 mice were injected with PKH67-labelled exosomes purified from OC-miR-214 osteoclasts. The distribution and the effect of PKH67-exosomes were analyzed. (b) The tissue distribution of fluorescence signal in mice by biophotonic imaging at 4 h and 8 h after administration with 100 μ g purified PKH67-exosomes. (c) The miR-214 levels in *Alp*⁺ osteoblasts isolated from C57 mice by fluorescence activated cell sorting at 8 h after administration with purified PKH67-exosomes. (d) The mRNA expression levels of *Alp*, *Collagen-I*, *Opn*, *BSP* and *Bglap* in bone tissues determined by real-time PCR in mice administered with purified exosomes, mouse GAPDH mRNA was used as the internal control. (e) Representative micro-CT images for three-dimensional trabecular architecture at distal femur in mice administered with purified exosomes. Scale bars, 1 mm. (f) Micro-CT parameters for bone mass (BMD, BV/TV) and trabecular architecture (Tb.Th and Tb.N) at distal femur in mice administered with purified exosomes. (g) Representative fluorescence microscopic images of double calcein labeling at distal femur in mice administered with purified exosomes. Scale bars: 20 μ m. (h) Bone histomorphometric parameters (MAR and BFR/BS) at distal femur in mice administered with purified exosomes. **Note:** All data were presented as the mean \pm s.d. * P <0.05 vs. PBS group. BS: 12-week-old female C57BL/6 mice as baseline, Exo: mice administered with purified exosomes derived from osteoclasts (control), 214-Exo: mice administered with purified exosomes derived from OC-miR-214 osteoclasts (derived from OC-miR-214 mice).

Results-4

Disclosures: Defang Li, None.

1043

Osteoclast lineage cells are a crucial source of Wnt proteins in load-induced bone modeling. Megan Weivoda^{*1}, Ming Ruan¹, Christine Hachfeld¹, Larry Pederson¹, Jean Vacher², Richard Lang³, Bart Williams⁴, Jennifer Westendorf¹, Sundeep Khosla¹, Merry Jo Oursler¹. ¹Mayo Clinic, USA, ²IRCM, Canada, ³Cincinnati Childrens, USA, ⁴Van Andel Institute, USA

Wnt signaling is essential for normal skeletal development. However, the source of skeletal Wnt proteins remains unclear. We previously demonstrated that mature osteoclasts secrete Wnt proteins. Therefore, we hypothesized that osteoclasts are a source of Wnt proteins in the developing skeleton. Real time PCR was utilized to measure Wnt expression during osteoclast differentiation and a genetic mouse model was employed to test the effect of impaired-osteoclast lineage Wnt secretion on skeletal development. Bone marrow macrophages expressed Wnts 2a, 2b, 3a, 4, 5a, 5b, 6, 7a, 7b, 9b, 10a, 10b, and 16. Wnts 1, 5b, 9a, and 11 transcripts increased with osteoclast differentiation whereas Wnts 2a, 2b, 3a, 4, 5a, 6, 7a, 7b, 9b, 10a, 10b, and 16 decreased. Mature osteoclasts expressed Wnt1, 2b, 3a, 4, 5a, 5b, 6, 7b, 9a, 10b, and 11. The membrane-associated chaperone, Wntless (Wls), is required for Wnt secretion. Transgenic CD11b-Cre mice were crossed with Wls flox mice to obtain animals with Wls selectively deleted in the osteoclast lineage. Homozygous deletion of Wls in the CD11b lineage was embryonic lethal; therefore, CD11b positive Wls F/+ mice (CD11b/Wls^{Het}) were assessed at 8 weeks of age. Analysis of bone marrow derived osteoclast conditioned-media confirmed that CD11b/Wls^{Het} osteoclasts secreted less Wnt protein. Ex vivo μ CT of CD11b/Wls^{Het} femurs showed significantly reduced bone volume, trabecular number, and trabecular thickness, with increased trabecular spacing and plate-like structure in cancellous bone. CD11b/Wls^{Het} femurs had reduced cortical thickness at the metaphysis and diaphysis with decreased periosteal perimeter. In contrast, μ CT analysis of CD11b/Wls^{Het} vertebrae showed no significant change in trabecular or cortical parameters, suggesting that osteoclast derived Wnt proteins play a role in mechanical load-induced long bone modeling. Histomorphometry of the CD11b/Wls^{Het} femurs showed significant increases in osteoclast number and modestly reduced osteoblast numbers on the periosteal and trabecular surfaces. Interestingly, CD11b/Wls^{Het} femurs showed a 70% reduction in bone formation rate on the periosteal surface. These data support that the osteoclast lineage is an important source of Wnt proteins in skeletal development, and may be involved in mechanical-load induced bone modeling.

Disclosures: Megan Weivoda, None.

1044

RANKL/OPG double deficient medaka unveils the decision system for the bone resorption site in a whole-body. Masahiro Chatani^{*1}, Yoshiro Takano², Takeshi Todo³, Akira Kudo¹. ¹Tokyo Institute of Technology, Japan, ²Tokyo Medical & Dental University, Japan, ³Osaka University, Japan

Introduction: Bone shape is determined with bone resorption of osteoclasts. Osteoclast differentiation is enhanced by RANKL or inhibited by OPG. However, it is unclear how RANKL and OPG co-operatively regulate bone resorption in a whole body. We previously established the live imaging system using medaka fish, which allowed observation of an osteoclast behavior in a whole-body (Chatani et al., 2011). To clarify the mechanism of how RANKL and OPG control the site of bone resorption in a whole-body, we examined bone modeling during medaka development.

Methods: RANKL-deficient and OPG-deficient medaka were established by using Tilling (Targeting induced local lesions in genomes) and TALEN (Transcription activator-like effector nucleases) methods, respectively. Osteoclasts were live-imaged by using the TRAP promoter-GFP or DsRed transgenic line. To examine the function of OPG and RANKL, we performed cross-breeding of OPG^{-/-} medaka and RANKL^{-/-} medaka.

Results and discussion: We found three significant phenotypes of bone resorption. Firstly, OPG^{-/-}:RANKL^{+/+} medaka induced numerous osteoclasts that absorbed bones of the vertebral body and fin ray, whereas no osteoclasts existed on the vertebral body and fin ray in WT, suggesting that OPG inhibited osteoclast differentiation on the bone surface in WT. Secondly, to examine the role of RANKL in homozygous mutation of the OPG gene, we examined OPG^{-/-}:RANKL^{+/+} medaka. Contrary to expectation, osteoclasts were specifically localized at neural and hemal arches, suggesting the threshold for RANKL-dependent osteoclastogenesis limit on the vertebral body in this mutant. In addition, osteoclasts gathered at only edges of fin rays to degrade bone tissues, indicating the existence of a site where osteoclasts preferentially differentiate with a help of RANKL. Lastly, OPG^{-/-}:RANKL^{-/-} medaka indicated that osteoclasts, which were differentiated in the RANKL-independent pathway, were localized at neural and hemal arches with a defect of bone modeling, and no osteoclasts were observed at the edge of fin ray, indicating the existence of a RANKL/OPG-independent manner that determines osteoclast location on the bone surface. Taken together, our results suggested that the promotion of pre-osteoclast differentiation is regulated by both of RANKL and OPG, and the location of pre-osteoclasts is determined in the RANKL/OPG-independent manner.

Disclosures: Masahiro Chatani, None.

1045

The MicroRNA miR-23a Cluster Regulates the Differentiation of Osteoblasts into Osteocytes. Huan-Chang Zeng^{*}, Yangjin Bae, Yuqing Chen, Terry Bertin, Brian Dawson, Elda Munivez, Jianning Tao, Brendan Lee. Baylor College of medicine, USA

Recent studies have shown that microRNAs play important regulatory roles in skeletal development. However, how microRNAs can control osteocyte differentiation is unknown. The miR-23a cluster is one of the most enriched group of microRNAs in bone and has been reported to be involved in osteogenesis *in vitro*. We generated transgenic mice overexpressing this cluster with the collagen type I (Col1a1-2.3kb) promoter and found significantly increased density of osteocytes. In addition, the transgenic mice exhibited low bone mass phenotype by micro-computed tomography (μ CT) along with decreased numbers of osteoblasts, decreased mineral apposition rate but no significant change of the numbers of osteoclasts by histomorphometric analysis. Real-time PCR analysis of calvarial RNAs revealed increased expression of osteocytic markers including *Dmp1* and *Fgf23* and decreased expression of the mature osteoblast marker *Ocn*. To study the loss of function of this microRNAs cluster, we generated transgenic mice expressing microRNA decoys with the same Col1a1-2.3kb promoter. Although these mice also exhibited low bone mass, histomorphometry showed significantly decreased osteocyte density, opposite that of the gain of function. RNA-Seq and Ingenuity Pathway Analysis of bones from transgenic mice suggested that TGF- β as the potential signaling pathway contributing to osteocytic phenotype. Moreover, *Prdm16*, a negative regulator of TGF- β pathway, was the candidate target of the miR-23a cluster. Consistent with this, we observed transgenic TGF- β reporter activity was increased in the bones of the miR-23a cluster gain of function mice and decreased in the transgenic decoy loss of function mice. When we treated the miR-23a cluster transgenic mice with the TGF- β neutralizing antibody, ID11, at 6 weeks of age for 6 weeks, the low bone mass and osteocyte phenotype was rescued. Finally, *in vitro* osteogenic differentiation of the bone marrow stroma cells from the miR-23a cluster transgenic mice showed increased *Sost* expression as expected, and this increased expression could be suppressed by overexpression of *Prdm16*. Taken together, we identified that the miR-23a cluster could regulate osteocyte differentiation by TGF- β signaling pathway through its target *Prdm16*.

Disclosures: Huan-Chang Zeng, None.

1046

Class IIa HDACs are required for PTH-mediated suppression of SOST in osteocytes. Marc Wein^{*1}, Elizabeth Williams², Nicolas Govea², Shigeki Nishimori², Kenichi Nagano³, Daniel Brooks², Roland Baron³, Mary Bouxsein², Paola Divieti-Pajevic², Henry Kronenberg². ¹Massachusetts General Hospital, USA, ²MGH Endocrine Unit, USA, ³Harvard School of Dental Medicine, USA

Purpose: Intermittent PTH stimulates new bone formation by osteoblasts, in part by suppressing expression of the Wnt pathway inhibitor sclerostin (encoded by the gene SOST) in osteocytes. The signaling pathway between PTH receptor signaling and SOST suppression involves inhibition of MEF2 action, but otherwise is unknown. In chondrocytes, PTHrP blocks MEF2 through actions on class IIa HDACs. Therefore, we hypothesized that class IIa HDACs might similarly block MEF2 activity on the SOST gene in osteocytes. The purpose of this study is to determine the role of class IIa HDACs in PTH-mediated suppression of SOST in osteocytes. **Methods:** The skeletal phenotype of 8 week old global HDAC5^{-/-}, HDAC4^{fl/fl};DMP1-Cre, and double HDAC4/5 knockout (HDAC4^{fl/fl};HDAC5^{-/-};DMP1-Cre, "DKO") mice was determined by histology, micro-CT, and histomorphometry. Bone RNA was collected 90 minutes after a single pharmacologic dose of PTH (300 μ g/kg), and levels of SOST and RANKL were determined by RT-qPCR and semi-quantitative immunohistochemistry. The murine osteocytic cell line Ocy454 was used to study mechanisms of PTH-mediated SOST suppression *in vitro*. HDAC4 and HDAC5 were depleted from Ocy454 cells by CRISPR/Cas9-mediated genome editing and shRNA, respectively. **Results:** DKO mice show cortical osteopenia, woven bone, and increased osteocyte density. None of these phenotypes are present in either class IIa HDAC single knockout strain. DKO mice show 2.5-fold elevated SOST levels at baseline in bone RNA, and fail to suppress SOST mRNA and sclerostin protein in response to acute PTH administration *in vivo*. Each single HDAC null strain shows normal PTH-mediated SOST suppression. PTH-stimulated RANKL upregulation is intact in DKO mice. In Ocy454 cells, PTH stimulates the dephosphorylation of HDAC4 at S246 and HDAC5 at S259/279, and promotes the nuclear translocation of these two proteins. Ocy454 cells lacking both HDAC4 and HDAC5 also fail to down-regulate SOST in response to PTH, while RANKL upregulation occurs normally. **Conclusions:** PTH stimulates the nuclear translocation of HDAC4 and HDAC5 in osteocytes. Both HDAC4 and HDAC5 are required for PTH-stimulated SOST suppression *in vivo* and *in vitro*. The dramatic cortical bone phenotypes present in HDAC4/5 DKO mice are unlikely to be due solely to increased SOST levels, indicating that other functionally important targets for these proteins must exist.

Disclosures: Marc Wein, None.

1047

SOST Downregulates Notch Signaling and Reverses the Effects of Notch in Osteocytes. Stefano Zanotti*, Lauren Schilling, Ernesto Canalis. UConn Health, USA

Notch receptors play a critical role in cell fate decisions. Activation of Notch1 in undifferentiated and mature osteoblasts impairs osteoblast differentiation/function, whereas Notch activation in osteocytes causes a distinct phenotype characterized by a pronounced increase in bone mass due to a suppression of cancellous bone resorption and enhanced cortical bone formation. The osteocyte-specific phenotype of the Notch1 activation is attributed to a downregulation of *Sost* and upregulation of *Tnfrsf11b* expression in the bone microenvironment. To explore the contributions of the *Sost* downregulation to the effects of Notch in osteocytes, Notch1 signaling was activated in the context, or not, of *SOST* overexpression. Notch1 activation in osteocytes was achieved by crossing dentin matrix protein (*Dmp1*)-Cre transgenics with *RosaNotch* mice to delete an intervening loxP flanked STOP cassette and allow expression of the Notch intracellular domain under the control of the *Rosa26* promoter. To determine whether the suppression of *Sost* expression by Notch1 contributed to the high bone mass phenotype of the osteocyte-specific Notch activation, *Dmp1-Cre⁺/+;RosaNotch* mice were crossed with hemizygous *Dmp1-SOST* transgenics. The pronounced increase in cancellous bone observed in femurs from *Dmp1-Cre⁺/+;RosaNotch* mice was no longer observed in the context of *SOST* overexpression, and *Dmp1-Cre⁺/+;RosaNotch;Dmp1-SOST* mice were not substantially different from wild type mice. The mechanisms responsible for the reversal of the phenotype by *SOST* involved the downregulation of Notch signaling since *Dmp1-Cre;RosaNotch;Dmp1-SOST* mice had 60 to 80% inhibition of Notch target gene (*Hey1*, *Hey2* and *HeyL*) expression when compared to *Dmp1-Cre;RosaNotch* mice, suggesting that sclerostin reverses the effects of Notch1 in osteocytes by downregulating Notch signaling. The effects of Notch1 in osteocytes were secondary to activation of the canonical pathway, which requires interactions with *Rbpj²*, and they were fully reversed in the context of *Rbpjk* inactivation. In conclusion, by downregulating Notch signaling sclerostin reverses the high bone mass osteocyte-specific Notch1 phenotype indicating that intact Wnt signaling is required for Notch activity in these cells.

Disclosures: *Stefano Zanotti*, None.

1048

Targeted Disruption of BMP Signaling Through Type IA Receptor (BMPRIA) in Osteocyte Suppresses SOST and RANKL, Leading to a Dramatic Increase in Bone Density and Mechanical Strength. Nobuhiro Kamiya*¹, Harry Kim². ¹Tenri University, Japan, ²Texas Scottish Rite Hospital for Children, USA

BMPs are known as ectopic bone inducers. The FDA approved BMP2 and BMP7 for clinical use. However, our recent studies demonstrated challenging evidence that BMP signaling in osteoblasts can negatively regulate endogenous bone mass because loss of BMP receptor IA (BMPRIA) in osteoblasts dramatically increased bone mass in mice. Although more than 90% of bone cells are osteocytes, roles of BMP signaling in osteocytes are largely unknown. The purpose of this study was to investigate BMP function in osteocytes and prove our concept. We generated conditional knockout mice (cKO) with osteocyte-specific deletion of BMPRIA under DMP1 promoter (*Dmp1Cre⁺;Bmpr1a^{flx/flx}*) and compared them with controls (*Dmp1Cre⁺;Bmpr1a^{flx/flx}*). The resulting cKO bones were dramatically sclerotic as assessed by X-ray. Micro CT revealed significantly increased bone parameters in cKO femur and spine (i.e. more than 100% increase in trabecular bone volume, thickness, number, and mineral density). H&E staining demonstrated increased trabecular bone and thickened cortical bone in cKO femur. Osteoclast number assessed by TRAP staining was reduced in cKO bones. These findings were consistent with results from bone histomorphometry (i.e. significantly increased bone volume and reduced osteoclast number in cKO bones). In addition, osteoid volume was increased and bone formation rate was reduced in cKO bones. Interestingly, serum protein levels of SOST and RANKL, as well as gene expression levels of *Sost* and *Rankl* in bones, were significantly reduced in cKO mice. Beta-catenin staining levels as well as Wnt target genes (*Tcf1*, *Tcf3*) were increased in cKO bones. Mechanical strength was better in cKO mice (i.e. max force, displacement, and work failure were increased in cKO femurs). For osteocyte-morphometry, lacuna numbers were significantly increased in cKO bones. Osteocyte shape was disorganized and osteocyte dendrite network was immature assessed by SEM. These results suggest that loss of BMP signaling specifically in osteocytes dramatically increases bone mass presumably through simultaneous inhibition of RANKL and SOST (i.e. osteoclast inhibition and Wnt activation together). It is reported that RANKL and SOST are more expressed by osteocytes than osteoblasts. Thus, BMP signaling through BMPRIA can play more important roles in osteocytes than osteoblasts by controlling RANKL and SOST. This study proves the concept that BMP signaling can negatively regulate endogenous bone mass *in vivo*.

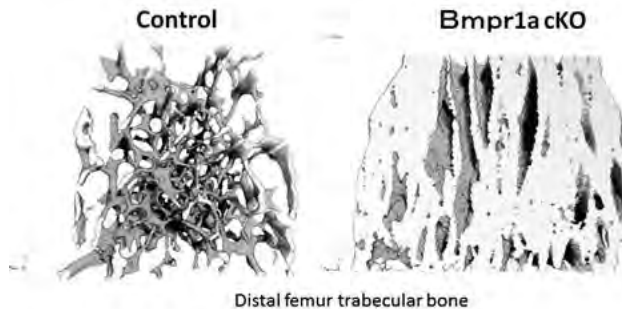


Figure 1

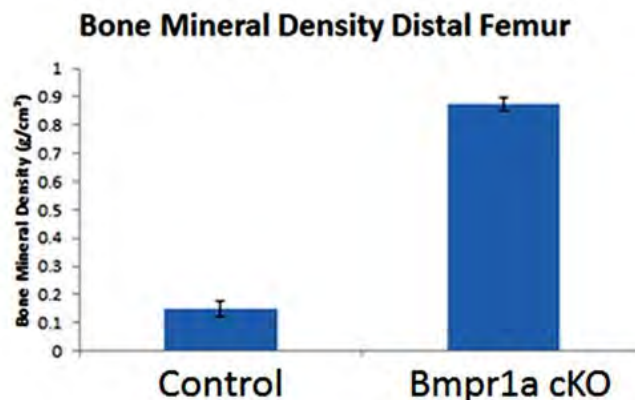


Figure 2

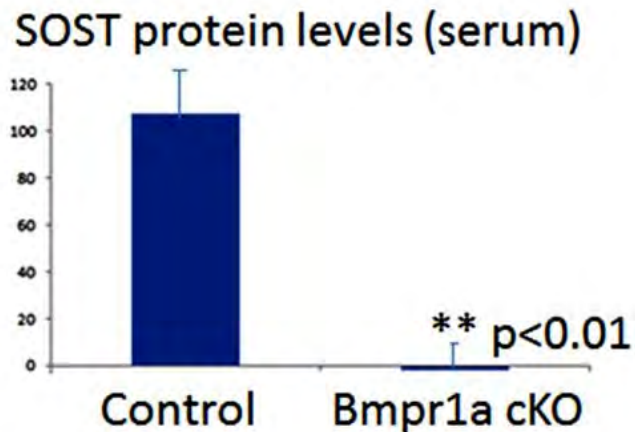


Figure 3

Disclosures: *Nobuhiro Kamiya*, None.

1049

CYR61 Regulates Bone Turnover Through Inhibiting Sclerostin Expression and Angiogenesis in Osteocytes. Gexin Zhao*¹, Chinmay Bhoot², Karen Lyons². ¹UCLA Department of Orthopaedic Surgery, USA, ²University of California, Los Angeles, USA

Cysteine-rich protein 61 (CYR61/CCN1), is found in mineralized tissues and plays an integral role in the differentiation of the osteogenic cells. CYR61 expressed in osteoblast(OBs) and osteocytes(OCy) in bone; however, the role of CYR61 in bone remains unclear. To address this, we generated 3 strains of mice with a conditional deletion of CYR61 in OBs using *OSXcre(pre-OB)*, *COL1cre(OB)* and *OCNcre(mature OB)*. By μ -CT analysis, 3month old male mice exhibited lower BMD and BV/TV within the trabecular bone of femurs, and a decrease in thickness of the cortical bone[Fig1]. This demonstrated that CYR61 is an important protein in OBs and OCy for acquisition of bone mass. Analysis of CYR61 localization demonstrated that mature OBs and OCy are the major source of expression. In accordance, there is no

significant difference in the phenotypes of mice lacking CYR61 in osteoprogenitors vs. mature OBs.

WNT signaling has been shown to be critical in OB differentiation and function [Ref1], and McClung et al. reported neutralization of a bone-specific WNT inhibitor, sclerostin(SOST), can protect patients from osteoporosis[Ref2]. We demonstrated that, at the in vivo level, the mRNA of SOST is increased in *CYR61^{flx/flx}/OCNcre* cortical bone. This increase was also confirmed through immunostain[Fig2]. Moreover, during the osteogenic induction of MSCs, isolated from *CYR61^{flx/flx}* mice and infected by Adenovirus-Cre, SOST mRNA levels were also significantly up regulated in mutants[Fig2]. This increase in SOST in bones lacking CYR61 may contribute to the lower bone mass in these mutants.

CYR61 has been shown previously to exhibit pro-angiogenic activity. To test whether CYR61 impacts vascularization in bone, we found that a lack of CYR61 leads to a decrease in vascular endothelial growth factor (VEGF) expression in the cortical bone of *CYR61^{flx/flx}/OCNcre* mice[Fig3]. This is also confirmed through angiogenesis assays on mouse metacarpals cultured ex vivo, which showed a significant decrease in vascularization. These findings also hold in vivo as the mutant mice show less vascularization by immunostain[Fig3]. Since the VEGF promoter is known to have binding sites for β -catenin/TCF[Ref3], the decreased VEGF may be due to SOST inhibiting WNT signalling and therefore inhibiting VEGF expression. These observations suggest that CYR61 is an important regulator of SOST and VEGF levels to mediate bone dynamics, and CYR61 may be a potential target for treatment for osteoporosis.

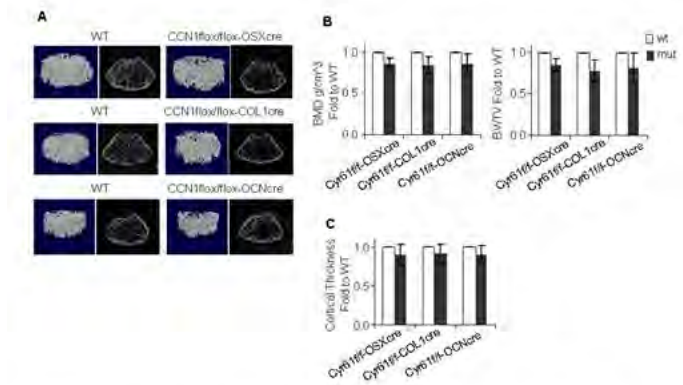


Fig1. Decreased bone mass in mice *CCN1^{flx/flx}/OSXcre*, *CCN1^{flx/flx}/COL1cre* and *CCN1^{flx/flx}/OCNcre* by μ -CT analysis. A. 3D and 2D μ -CT images of the trabecular bone of femur. B. BMD and BV/TV of the trabecular bone of femur. C. Cortical thickness of the femur. n=4

Fig1

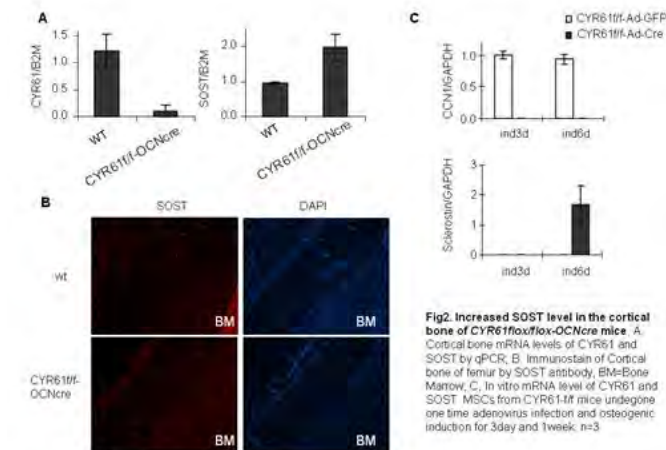


Fig2. Increased SOST level in the cortical bone of *CYR61^{flx/flx}/OCNcre* mice. A. Cortical bone mRNA levels of *CYR61* and *SOST* by qPCR. B. Immunostain of Cortical bone of femur by SOST antibody. BM= Bone Marrow. C. In vitro mRNA level of *CYR61* and *SOST* MSCs from *CYR61^{flx/flx}* mice undergone one time adenovirus infection and osteogenic induction for 3day and 1week. n=3

Fig2

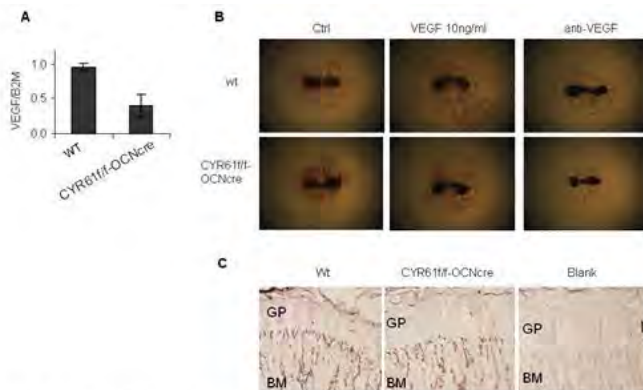


Fig3. Decreased VEGF level when knockout *CYR61* in OBs in vivo and ex vivo. A. Cortical bone mRNA levels of *CYR61* and *SOST* by qPCR. B. Mouse metacarpals cultured ex vivo for 14days with VEGF or anti-VEGF antibody, immunostained by CD31 antibody. C. Immunostain of Cortical bone of femur by CD31 antibody. BM= Bone Marrow, GP=Growth Plate.

Fig3

[Ref1] Lerner et al., *J Intern Med.* 2015 doi: 10.1111/joim.12368.

[Ref2] McClung et al., *N Engl J Med.* 2014; 370: 412-20.

[Ref3] Zhang et al., *Cancer Res.* 2001 Aug ;61(16):6050-4.

Ref

Disclosures: Gexin Zhao, None.

1050

Osteocyte-specific HIF-1 α Signaling Regulates Bone Mass and Protects Mice From Osteoporotic Bone Loss. Steve Stegen^{*1}, Ingrid Stockmans¹, Karen Moermans¹, Peter Carmeliet², Geert Carmeliet¹. ¹Laboratory of Clinical & Experimental Endocrinology, KU Leuven, Belgium, ²Angiogenesis & Neurovascular Link, Vesalius Research Center, VIB, & Angiogenesis & Neurovascular Link, Vesalius Research Center, KU Leuven, Belgium

Deeply embedded within the bone matrix, osteocytes depend on adequate oxygen and nutrient delivery to maintain the functioning of the osteocyte network. Cells respond to decreases in oxygen tension, by activating hypoxia-inducible factor (HIF), which is regulated by the prolyl hydroxylase (PHD) oxygen sensors. The role of PHDs in osteocytes remains however unknown.

We therefore generated mice lacking *Phd2* specifically in osteocytes (*PHD2^{ost}*) by crossing *Phd2^{lox/lox}* mice with mice expressing the Cre recombinase under the control of the DMP1 promoter, resulting in osteocytic HIF-1 α , but not HIF-2 α , stabilization. Trabecular and cortical bone mass was increased in 10-week old *PHD2^{ost}* mice compared to wild-type (WT) mice, evidenced by micro-CT analysis. This phenotype resulted from enhanced bone formation together with decreased resorption. Osteoblast number and activity was increased in mutant mice, evidenced by serum osteocalcin levels and static and dynamic histological analysis. Moreover, *PHD2^{ost}* mice displayed an increase in the number of viable osteocytes in cortical bone, which were however more randomly organized. Bone resorption in *PHD2^{ost}* mice was reduced as shown by a decrease in serum CTx levels and number of osteoclasts, quantified on TRAP-stained histological sections. Intriguingly, we found a decrease in bone *Sost* expression, but not *Dmp1* or *Phex*, which could in part explain the changes in bone mass accrual. Activation of the HIF pathway generally leads to enhanced angiogenesis, an effect linked with increased bone formation. The number and size of blood vessels was increased in the bones of *PHD2^{ost}* mice, likely resulting from the elevated bone *Vegf* transcript levels.

As osteocytes also control bone mass during pathology, we subjected *PHD2^{ost}* to unloading and ovariectomy, two models of osteoporosis. Both hindlimb suspension

and ovariectomy resulted in a decrease in trabecular and cortical bone mass in WT mice, while PHD2^{0/-} mice were protected from bone loss.

Together, the high bone mass in PHD2^{0/-} mice is caused by enhanced bone formation and reduced resorption, and was associated with an increase in the number of blood vessels. Furthermore, we show that activation of the HIF pathway in osteocytes protects mice during hindlimb unloading and ovariectomy.

Disclosures: Steve Stegen, None.

1051

Vitamin K2 treatment prevents postmenopausal bone loss and microarchitectural deterioration of trabecular bone. Sofie Hertz Roenn*, Torben Harsloef, Steen Boenloekke Pedersen, Bente Langdahl. Department of Endocrinology & Internal Medicine, Aarhus University Hospital, THG, Denmark

Background: Clinical studies suggest, that vitamin K2 prevents bone loss and protect against fractures. Vitamin K2 is suggested to affect bone through the bone matrix protein osteocalcin (OC). OC is produced by the osteoblast in an undercarboxylated form (ucOC) that is carboxylated with vitamin K2 as a cofactor. Carboxylated OC promotes mineralization of bone. The aim of the study was to investigate the effect of vitamin K2 on bone mass and quality. **Methods:** In this randomized placebo-controlled double blinded clinical trial, 142 postmenopausal women (60-80 years old) with osteopenia were treated with vitamin K2 (375 µg MK-7) or placebo. Both groups also received vitamin D3 (38 µg/day) and calcium (800 mg/day). Bone mineral density and -quality were assessed by DXA and HRpQCT at baseline and after 1 year. **Results:** BMD of the lumbar spine was unchanged within groups without difference between groups. Total hip BMD decreased significantly in the placebo-group (-0.64±0.44 %, p<0.01), whereas no change was seen in the K2-group. There was no significant difference between groups. HRpQCT of the tibia showed a reduction in trabecular number within the placebo-group (-3.5±2.2 %, p<0.01) but no change in trabecular number within the K2-group (-0.1±1.9 %, p=0.87). The difference between groups was significant (-3.4±2.9 %, p=0.02). Trabecular thickness increased within the placebo-group (+4.0±2.2 %, p<0.01), whereas no change occurred within the K2-group (+0.2±1.7 %, p=0.9). The difference between groups was significant (+3.8±2.8 %, p<0.01). There was no change in BMD. HRpQCT of the radius showed a decrease in total BMD within the placebo-group (-1.7±1.5 %, p=0.03) and within the K2-group (-1.2±0.9 %, p=0.01), without differences between the groups. In both tibia and radius, cortical area and thickness were reduced and trabecular area were increased in both groups (p<0.05 for all) without differences between groups. **Conclusion:** The results suggest that vitamin K2 may prevent the age-related decline in bone mineral density at the hip, however, there was no significant difference between the two groups. The HRpQCT results suggest that vitamin K2 may prevent microarchitectural deterioration by preventing the age-related loss of trabeculae. The concomitant increase in trabecular thickness can be explained by loss of the thinnest trabeculae and trabecularization of the endocortical bone. There is need for long-term investigations of the effect of vitamin K2 on bone.

Disclosures: Sofie Hertz Roenn, None.
This study received funding from: Orkla

1052

Bone's Material Composition and Microstructure are Compromised in Women Sustaining Atypical Femoral Fractures During Antiresorptive Therapy. Cherie Chiang*¹, Ego Seeman², Ali Ghasem Zadeh², Sandra Iuliano², Peter Ebeling³, Hanh Nguyen³, Roger Zebaze². ¹Austin Health, Australia, ²Austin Health, University of Melbourne, Australia, ³Monash Medical Centre, Monash University, Australia

Purpose: Anti-resorptive agents like the bisphosphonates reduce the rate of remodelling and fracture risk. However, they may also compromise bone's material strength by reducing the removal of microdamage, by facilitating secondary mineralization of unremodelled matrix and by allowing accumulation of pentosidine crosslinks. Atypical femoral fractures (AFF) are associated with bisphosphonate exposure, but the micro-architecture and bone material composition in affected patients are not well described. The aims of this study were to determine whether women with AFFs have high matrix mineral density and high cortical porosity, relative to age-matched women who sustained typical femoral fragility fractures while receiving anti-resorptive treatment.

Methods: We performed a prospective study comparing patients on anti-resorptive agents who sustained AFFs and controls sustaining low trauma 'typical' fractures while receiving anti-resorptive agents. Patients with AFFs were identified according to the ASBMR taskforce revised definition. Controls with typical fractures were identified from the Austin Health Fracture Capture database and matched by age, gender and duration of anti-resorptive therapy. Bone micro-architecture of the distal tibia and radius were quantified at baseline using high resolution peripheral micro-computed tomography (HRpQCT). The bone matrix mineralisation density and its distribution were quantified using StrAx1.0 (StraxCorp, Melbourne, Australia), an image processing software which use an algorithm to separate bone from background and then separate bone into its cortical, transitional zone and trabecular compartments without thresholding.

Results: Cases with AFF, 19 females with AFF (age: 73.9 ± 7.6 yrs, anti-resorptive treatment: 6.5 ± 2.8 yrs) compared with 23 referent 'controls' - women with typical fractures (age 72.5 ± 9.3 yrs, anti-resorptive treatment: 5.0 ± 3.2 yrs), had higher femoral neck T score (-1.7 vs -2.3, p = 0.018), higher radius cortical volumetric BMD (864.3 vs 808.8, p = 0.01), and lower cortical porosity (44.6 vs 49.2%, p = 0.01). The higher proportion of more fully mineralised bone matrix did not achieve significance (0.23 vs 0.09%, p = 0.06).

Conclusions: Women with AFF have reduced porosity and reduced mineralisation heterogeneity with elevated matrix mineral density relative to women receiving bisphosphonates following typical fragility fractures. These characteristics may assist in managing patients on long term bisphosphonates.

Disclosures: Cherie Chiang, None.

1053

Effects of Abaloparatide on Major Osteoporotic Fracture Incidence in Postmenopausal Women with Osteoporosis - Results of the Phase 3 ACTIVE Trial. Lorraine Fitzpatrick*¹, Greg Williams¹, Willard Dere², Alan Harris¹, Ming-Yi (Tristan) Hu¹, Kate Banks¹, Gary Hattersley¹. ¹Radius Health, USA, ²U of Utah Medical Center, USA

Abaloparatide (ABL) is an osteoanabolic analog of PTHrP being developed for the treatment of postmenopausal osteoporosis (PMO). Of particular concern in these women are major osteoporotic fractures, because these are associated with a higher level of morbidity or increased mortality risk. As has been previously reported from the ACTIVE Phase 3 trial, treatment with ABL significantly reduced the incidence of new vertebral, non-vertebral and clinical fractures while significantly increasing bone mineral density (BMD) in the lumbar spine, total hip and femoral neck. In the ACTIVE double-blind, placebo-controlled Phase 3 fracture prevention trial, postmenopausal osteoporotic women were randomized to receive 18-months of either daily ABL 80-mcg SC, matching placebo (PBO) SC, or open label teriparatide (TPTD) 20-mcg SC. Patients also received calcium and vitamin D supplements. Of the 2,463 patients who were randomized (ITT population), 1,901 (77.9%) completed the study. There were no apparent differences between the groups in baseline demographics or characteristics. 44.5% of patients had a prevalent vertebral fracture, 46.8% had a recent history of least 1 non-vertebral fracture. As part of the ACTIVE study the incidence of major osteoporotic fractures, defined as clinical fractures of the upper arm, the forearm (including wrist), the hip, the shoulder and/or the vertebral spine (spine and/or tailbone) was analyzed. ABL significantly reduced major osteoporotic fracture (n=824, fracture rate (FR) 1.2%) by 67% (HR 0.33, 95% CI 0.16, 0.68) compared to placebo-treated subjects (n=821, FR 3.8%) (p=0.0014) whereas TPTD (n=818, FR 2.7%) was not significantly different from PBO (HR 0.70, 95% CI 0.41, 1.21, p=0.2028). The difference between ABL and TPTD was significantly different (p=0.0437). In conclusion, 18-months of ABL significantly decreased the incidence major osteoporotic fractures in postmenopausal women with osteoporosis when compared to PBO and TPTD. The overall safety and efficacy results suggest that ABL may provide an effective treatment option in the management of PMO.

Disclosures: , Radius Health
This study received funding from: Radius Health, Inc.

1054

Effects of Denosumab on Bone Matrix Mineralization: Results From the Phase 3 FREEDOM Trial. David W Dempster*¹, Jacques P Brown², Susan Yue³, Delphine Farlay⁴, Sebastien Rizzo⁴, Jenny Song³, Andrea Wang³, Rachel B Wagman³, Georges Boivin⁴. ¹Columbia University & Helen Hayes Hospital, USA, ²Laval University & CHU de Quebec-(CHUL) Research Centre, Canada, ³Amgen Inc., USA, ⁴INSERM UMR 1033, Université de Lyon, France

Purpose: Low fracture incidence has been demonstrated in women with postmenopausal osteoporosis treated with denosumab (DMAB) for up to 9 years in the FREEDOM Extension (Papapoulos *WCO-IOF-ESCEO* 2015). Several assessments have evaluated effects of DMAB treatment at the tissue level (Reid *JBMR* 2010; Brown *JBMR* 2014) and showed low remodeling consistent with mechanism of action. While reduced bone matrix heterogeneity has been observed in huRANKL mice treated with DMAB for 6 months (Misof *ASBMR* 2011), assessment in clinical biopsies has not been performed. Here, we report the effects of DMAB on bone matrix mineralization in women who underwent transiliac crest bone biopsy in FREEDOM.

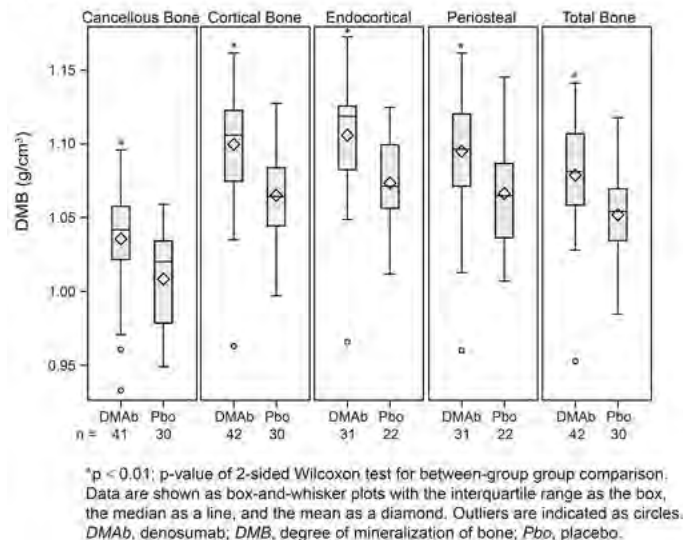
Methods: FREEDOM was a 3-year randomized, double-blind, placebo (Pbo)-controlled study in postmenopausal women who received Pbo or 60 mg DMAB subcutaneously every 6 months (Cummings *NEJM* 2009). A subset of women underwent transiliac crest bone biopsies at year 2 and/or 3 (Reid *JBMR* 2010). In the current study, bone matrix mineralization was assessed in a blinded fashion by digitized quantitative microradiography and analyzed using a Matlab program (Montagner *J X-Ray Sci Technol* 2015). The mean degree of mineralization of bone (DMB) and the heterogeneity index (HI) of the distribution of DMB were calculated for cancellous and cortical bone, endocortical and periosteal sub-compartments of cortical bone, and total bone (cancellous and cortical combined).

Results: In this analysis, 72 bone biopsy samples (42 DMAB, 30 Pbo) from a subset of the FREEDOM bone biopsy assessment (N = 115) were evaluated and analyzed.

Demographics for subjects in this matrix mineralization substudy were comparable to the FREEDOM study. Treatment with DMAB resulted in a significant increase in mean DMB compared with Pbo-treated subjects (Figure) and these findings were consistent across cancellous and cortical compartments ($p < 0.01$). A significantly lower HI was observed in total bone and in all compartments assessed in the DMAB-treated group ($p < 0.05$), consistent with reduced bone turnover in response to DMAB therapy.

Conclusions: Treatment of women with postmenopausal osteoporosis with DMAB resulted in increased bone matrix mineralization and a lower HI compared with Pbo. These data are consistent with expected results based on observations with other antiresorptives (Bala *Eur J Endocrinol* 2011) and with mechanism of action.

Figure



Figure

Disclosures: David W Dempster, Eli Lilly, Amgen; Eli Lilly, Merck, Amgen; Eli Lilly This study received funding from: Amgen Inc.

1055

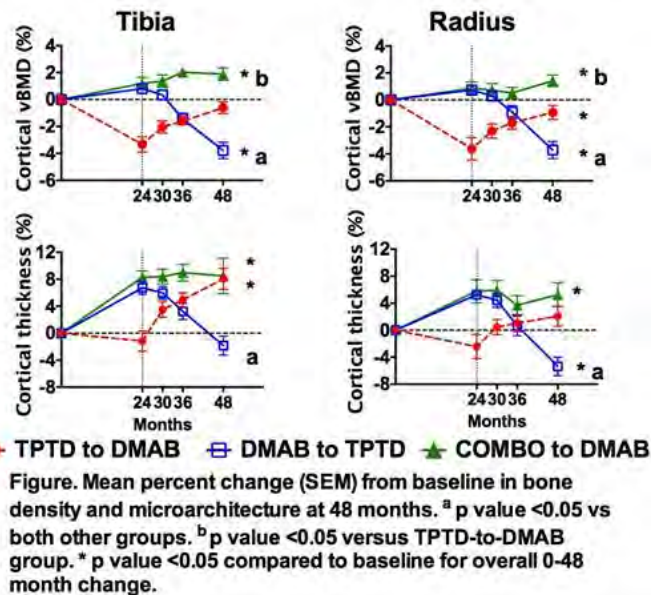
Effect of Denosumab (DMAB) and Teriparatide (TPTD) Transitions on Peripheral Bone Mineral Density (BMD) and Microarchitecture: The DATA-Switch HR-pQCT Study. Joy Tsai^{1*}, Alexander Uihlein², Sherri-Ann Burnett-Bowie¹, Robert Neer¹, Padrig Tuck¹, Paul Wallace¹, Mary Bouxsein³, Benjamin Leder¹. ¹Massachusetts General Hospital, USA, ²Northwestern University, USA, ³Beth Israel Deaconess Medical Center, USA

Background: In postmenopausal women, switching from TPTD to DMAB is associated with progressive BMD gains whereas the opposite transition results in progressive decreases in radial BMD and transient decreases at the hip and spine. The effects of these drug transitions on peripheral volumetric and compartmental BMD and microarchitecture are unknown.

Methods: Postmenopausal osteoporotic women completing the DATA study were eligible to enroll in DATA-Switch. Women who received DMAB 60mg every 6 months for 2-years were switched to TPTD (n=27) for years 3-4 and women who received either TPTD 20 µg daily (n=27) or TPTD+DMAB (n=23) switched to DMAB alone. Total, trabecular and cortical density (Tot.vBMD, Tb.vBMD, Ct.vBMD), cortical thickness (Ct.Th) and trabecular microarchitecture of the radius and tibia were measured by high-resolution pQCT.

Results: After a total of 4-years of therapy, the increase in volumetric cortical density at the radius and tibia was greatest in women who received combination therapy followed by DMAB ($P < 0.005$ for all comparisons) (Fig). Specifically, in women switched from TPTD to DMAB, 24-months of DMAB increased or maintained Tot.vBMD, Tb.vBMD, Ct.vBMD, and Ct.Th at both sites, resulting in net 4-year tibia changes of 3.3%, 3.0%, -0.6%, and 8.1%, respectively and net 4-year radius changes of 0.4%, 1.8%, -0.9%, and 2.0%, respectively (Table). In women switching from both drugs to DMAB alone, 24-months of DMAB maintained Tot.vBMD, Tb.vBMD, Ct.vBMD, and Ct.Th, resulting in net 4-year tibia increases of 5.4%, 2.8%, 1.9%, and 8.5%, respectively, and 4-year radius increases of 2.9%, 1.0%, 1.4%, and 5.3%. Conversely, women switching from DMAB to TPTD experienced decreases in Tot.vBMD, Ct.vBMD, and Ct.Th and no change in Tb.vBMD resulting in net 4-year tibia changes of -1.1%, -3.7%, -1.9%, and 1.6%, respectively, and 4-year radius changes of -3.7%, -3.7%, -5.4%, and -1.2%. Trabecular microarchitectural changes were small and did not differ between groups.

Conclusions: DMAB increases Ct.vBMD and Ct.Th in women treated with TPTD whereas the use of TPTD after DMAB results in decreases in these parameters. Whether TPTD-induced Ct.vBMD decreases represent as yet under-mineralized new bone is unclear. Combination therapy followed by DMAB results in the greatest cumulative improvements in peripheral cortical microarchitecture and further supports the therapeutic potential of combined DMAB/TPTD in patients with severe osteoporosis.



Figure

Disclosures: Joy Tsai, None.

This study received funding from: Eli Lilly Inc, Amgen Inc

1056

Effect of Odanacatib on Bone Density and Estimated Bone Strength in Postmenopausal Women: a CT-Based Sub-study of the Phase 3 Long-Term Odanacatib Fracture Trial (LOFT). Bente Langdahl^{1*}, Tobias DeVilliers², Tony M. Keaveny³, Klaus Engelke⁴, Harry Genant⁵, Shabana Ather⁶, Hilde Giezek⁶, Antonio Lombardi⁶, Albert Leung⁷, Anne de Papp⁶. ¹Aarhus University Hospital, Denmark, ²Mediclinic Panorama & Department of Obstetrics & Gynaecology, University of Stellenbosch, South Africa, ³University of California & O.N. Diagnostics, USA, ⁴Bioclinica-Synarc Germany, Germany, ⁵University of California, USA, ⁶Merck & Co., Inc., USA, ⁷Formerly Merck & Co., Inc., USA

Purpose: Odanacatib (ODN), a selective oral inhibitor of cathepsin K, is in development for the treatment of osteoporosis. In the Phase 3, Long-Term ODN Fracture Trial (LOFT; NCT00529373) of postmenopausal women with osteoporosis, ODN significantly reduced fracture risk and led to progressive increases in BMD at the lumbar spine and total hip (TH) compared with placebo (PBO). The incidence of adverse events (AEs) and serious AEs has been previously presented. Major cardiovascular events overall were generally balanced; however, there were numerically more adjudicated strokes with ODN than with PBO. Final blinded adjudication of major cardiovascular events is ongoing. In a substudy of LOFT, we evaluated the effect of ODN on volumetric BMD (vBMD) of trabecular and cortical bone by quantitative computerized tomography (QCT) and estimated whole-bone strength using finite element analysis (FEA).

Methods: Women ≥ 65 years without a baseline radiographic vertebral fracture (Vfx) and a TH or femoral neck (FN) BMD T-score between -2.5 and -4.0, or with a prior Vfx and a TH or FN T-score between -1.5 and -4.0, were randomized (1:1) to ODN 50 mg/week or PBO. All patients received vitamin D3 (5600 IU/week) and calcium as required to achieve ~ 1200 mg/day. In this sub-study, 164 women (78 ODN, 86 PBO) were enrolled at 10 centers in Denmark and South Africa. The key endpoints included % change from baseline in trabecular vBMD at the spine (primary) and cortical vBMD at the TH (secondary) at 24 months. Additional QCT endpoints included other trabecular, cortical and integral parameters at the spine and hip and estimated whole-bone strength using FEA. Analysis of spine and hip QCT scans was performed using Medical Image Analysis Framework. All endpoints were analysed by a Longitudinal Data Analysis model.

Results: Baseline characteristics in the sub-study population were similar to those in the overall LOFT population. Treatment with ODN significantly increased trabecular, cortical and integral vBMD, at the spine (L1) and TH compared with baseline and PBO (Table 1). ODN increased whole-bone estimated strength at the L1 vertebra and proximal femur, as assessed by FEA, while this remained stable or decreased in the PBO group (Table 2).

Conclusions: In postmenopausal women with osteoporosis, ODN compared with PBO increased trabecular, cortical and integral vBMD in the spine and TH and increased the estimate of whole-bone strength at the spine and hip as assessed by FEA.

Table 1. Differences between ODN 50 mg once weekly and placebo in QCT measurements of vBMD at the spine (total vertebral body) and total hip after 24 months of treatment (FAS population)^a

| Treatment | N | % change from baseline | | P value |
|-----------------------------------|----|-------------------------------|---------------------|---------|
| | | LS mean (95% CI) ^b | Difference (95% CI) | |
| Spine (L1) trabecular vBMD | | | | |
| ODN 50 mg weekly | 46 | 8.05 (4.48, 11.62) | 8.92 (3.90, 13.93) | <0.001 |
| Placebo | 48 | -0.87 (-4.37, 2.64) | | |
| Spine (L1) cortical vBMD | | | | |
| ODN 50 mg weekly | 46 | 8.28 (6.66, 9.89) | 6.89 (4.62, 9.16) | <0.001 |
| Placebo | 48 | 1.39 (-0.19, 2.97) | | |
| Spine (L1) integral vBMD | | | | |
| ODN 50 mg weekly | 46 | 8.59 (6.57, 10.61) | 8.52 (5.70, 11.35) | <0.001 |
| Placebo | 48 | 0.06 (-1.91, 2.04) | | |
| Total hip trabecular vBMD | | | | |
| ODN 50 mg weekly | 51 | 6.19 (1.24, 11.14) | 13.25 (6.36, 20.13) | <0.001 |
| Placebo | 55 | -7.06 (-11.82, -2.30) | | |
| Total hip cortical vBMD | | | | |
| ODN 50 mg weekly | 51 | 3.29 (2.33, 4.24) | 2.76 (1.43, 4.10) | <0.001 |
| Placebo | 55 | 0.52 (-0.39, 1.44) | | |
| Total hip integral vBMD | | | | |
| ODN 50 mg weekly | 51 | 4.31 (3.11, 5.52) | 5.34 (3.67, 7.02) | <0.001 |
| Placebo | 55 | -1.03 (-2.19, 0.13) | | |

^aFAS, Full-Analysis-Set population, consisting of all randomized participants who took ≥1 dose of blinded study treatment and had a baseline and at least one on-treatment measurement available.

^bLongitudinal data analysis model with terms for treatment, stratum and interaction between treatment and time as fixed effects (LS means weighted for stratum size).

1057

Analysis of Signaling Downstream of PTHrP in Chondrocytes through Genetic Manipulation. Shigeki Nishimori*, Marc N. Wein, Henry M. Kronenberg, Massachusetts General Hospital, USA

Purpose: Parathyroid hormone-related protein (PTHrP) suppresses chondrocyte hypertrophy. Using mouse genetics, Eric Olson's group showed that Histone Deacetylase (HDAC) 4 suppresses chondrocyte hypertrophy (Vega, Cell 2004) by blocking the action of Myocyte Enhancer Factor (Mef) 2, which drives chondrocyte hypertrophy (Arnold, Dev Cell 2007). By *in vitro* experiments, Andrew Lassar's group showed that PTHrP works upstream of this pathway (Kozhemyakina, MCB 2009). The purpose of this study is systematic genetic analyses of the PTHrP/HDAC4/Mef2 axis.

Methods: We studied mediators downstream of PTHrP in a model of PTHrP overexpression driven by the Collagen 2 promoter (Weir, PNAS 1996). This transgenic mouse has only round proliferating chondrocytes in long bones until one week after birth. PTHrP *in situ* hybridization confirmed that the deletions detailed below did not affect PTHrP overexpression.

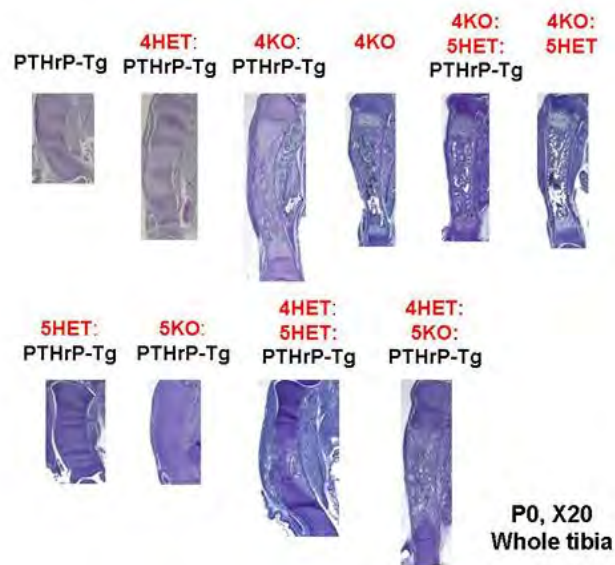
Results: In contrast to the PTHrP-Tg mouse, the HDAC4-HET: PTHrP-Tg mouse has small areas of flat and hypertrophic chondrocytes as well as 50% longer tibia at birth. Surprisingly, the PTHrP-Tg phenotype is almost reversed in the HDAC4-KO: PTHrP-Tg mouse, which has an entire growth plate, bone, and bone marrow at birth. However, several differences between HDAC4-KO: PTHrP-Tg and HDAC4-KO suggest that PTHrP action is mediated by additional mediators, presumably other Class II HDAC proteins (HDAC5, 7, 9).

The phenotype of the HDAC4-KO: HDAC5-HET: PTHrP-Tg mouse is exactly the same as that of the HDAC4-KO: HDAC5-HET mouse, indicating that HDAC5 is an additional mediator of PTHrP signaling. The phenotype of this mouse further suggests that HDAC7 and 9 may not serve as mediators of PTHrP action.

HDAC5-KO or HET have no effect on the PTHrP-Tg phenotype, indicating that HDAC4 alone is sufficient to mediate transgenic PTHrP signaling. However, HDAC5 has a clear role brought out in the context of HDAC4 heterozygosity: in that setting, removal of one or both alleles of HDAC5 blocks PTHrP action.

To investigate a downstream mediator of Mef2 action, we analyzed the HDAC4-HET: Runx2-HET: PTHrP-Tg mouse. This mouse has only round and flat chondrocytes at birth and not the hypertrophs seen in the HDAC4-HET: PTHrP-Tg mouse; this demonstrates the role of Runx2 in driving hypertrophy.

Conclusions: HDAC4 and HDAC5 are the essential downstream mediators of PTHrP signaling. Runx2 works downstream of Mef2 to induce chondrocyte hypertrophy.



Systematic deletions of HDAC4 and 5 in the PTHrP-Tg mouse

Disclosures: Shigeki Nishimori, None.

1058

Distinct modes of Sox9 action in transcriptional regulation of the developing mammalian chondrocyte. Shinsuke Ohba*¹, Xinjun He², Hironori Hojo², Andrew P. McMahon². ¹The University of Tokyo, Japan, ²W.M. Keck School of Medicine of the University of Southern California, USA

Sox9, an HMG-box-containing transcription factor, is required for chondrocyte specification and differentiation. To understand the modes of Sox9 action in transcriptional programs regulating these processes, we here compared Sox9 association at chondrocyte targets to a broad catalogue of regulatory indicators of chromatin organization and transcriptional activity in rib chondrocytes isolated from

Table 1

Table 2. QCT measurements of estimated strength by FEA of the vertebral body and total hip after 24 months of treatment with ODN 50 mg once weekly or placebo (FAS population)

| | N | Mean % change from baseline (95% CI) ^a |
|--|----|---|
| Compressive strength of vertebral body (L1) | | |
| ODN 50 mg weekly | 46 | 8.98 (5.99, 11.98) |
| Placebo | 47 | -0.77 (-4.16, 2.61) |
| Strength under fall loading conditions at total hip | | |
| ODN 50 mg weekly | 55 | 3.80 (2.29, 5.31) |
| Placebo | 56 | -3.10 (-4.43, -1.77) |

As there were no pre-specified hypotheses for FEA endpoints, analysis was restricted to descriptive statistics.

^aConfidence intervals assuming normality.

Table 2

Disclosures: Bente Langdahl, Amgen, Lilly, Merck; Lilly, Novo Nordisk, Orkla; Amgen, Lilly, Merck, UCB
 This study was sponsored by Merck & Co. Inc., Kenilworth, NJ, USA.

mouse neonates. Chromatin immunoprecipitation sequencing (ChIP-seq) for Sox9 identified 27,656 Sox9-associated regions on the chondrocyte genome. These regions resolved into two distinct classes: Class I regions closely associating with transcriptional start sites (TSSs) and Class II regions outside of the local TSS domains. Class I regions were not enriched with Sox motifs, but co-bound by p300 and RNA pol II. Class I ChIP-seq signal intensities were highly correlated with the expression level of the associated genes that were enriched with general regulators of basal cell activities. In contrast, Class II regions were associated with chondrocyte genes and showed active and tissue-specific enhancer signatures including H3K4me2, H3K27ac, RNA pol II, and p300. The level of expression of the associated genes correlated with the number of enhancer modules grouping into super-enhancer clusters (Cell 153:307, 2013). *De novo* motif analyses identified Sox dimer motifs as the over-represented motifs in Class II regions. Cartilage-specific enhancer activities of Class II regions were verified by *in vivo* reporter assays. The enhancer activities were increased when an individual element was multimerized or endogenous Sox dimer motifs were substituted with the optimum consensus motif predicted from the whole Class II data set; mutations into the endogenous motif cancelled the activities. In addition, electrophoresis mobility shift assay revealed that the Sox9-binding affinities of the endogenous motifs were lower than those of the optimum motif. These data suggest that multiple cooperative Sox9-bound distal enhancers each with a sub-optimal Sox9-binding affinity ensure appropriate expression of chondrocyte genes, whereas Sox9 also engages indirectly through a likely association with the basal transcriptional complex to regulate basal cell activities. Thus, this study reveals Sox9 regulatory landscape in relation to chromatin organization on the genome of the *in vivo* chondrocytes, and will contribute to the identification of gene regulatory networks in skeletal development.

Disclosures: Shinsuke Ohba, None.

1059

Epidermal Growth Factor Receptor (EGFR) Signaling Is Critical for Maintaining Articular Cartilage and Preventing Osteoarthritis Progression. Haoruo Jia^{*1}, Basak Doyran², Wei Tong¹, Xianrong Zhang³, Motomi Enomoto-Iwamoto⁴, Lin Han², Ling Qin¹. ¹Department of Orthopaedic Surgery, School of Medicine, University of Pennsylvania, USA, ²School of Biomedical Engineering, Science & Health Systems, Drexel University, USA, ³Department of Physiology, School of Basic Medical Sciences, Wuhan University, China, ⁴Department of Surgery, The Children's Hospital of Philadelphia, USA

Osteoarthritis (OA) is a degenerative joint disease characterized by destruction of articular cartilage and aberrant subchondral bone remodeling. We previously identified EGFR as an important signaling pathway for cartilage matrix degradation during endochondral ossification. To delineate its role in articular cartilage maintenance and OA progression, we generated cartilage-specific EGFR knockout mice (Col2-Cre *Egfr^{fllox/Wa5}*, CKO) and their WT (*Egfr^{fllox/+}*) and *Wa5* (*Egfr^{Wa5/+}*, an EGFR dominant negative allele) siblings. At the adult stage, CKO mice had a significantly thinner articular cartilage layer (60% of WT) with less chondrocyte number (41% of WT) and a higher percentage of hypertrophic chondrocytes (CKO 73% vs WT 47%), while *Wa5* cartilage had similar alterations but to a much lesser extent. Osteophytes in knee joints were observed in some CKO mice but never in WT or *Wa5*. Histological analyses revealed that chondrocytes in CKO had much lower EGFR signaling, less proliferation and more apoptosis, compared to those in controls. Primary chondrocyte culture confirmed that activating EGFR stimulates cell proliferation and survival and inhibits their terminal differentiation. Interestingly, atomic force microscopy-based nanoindentation on the medial condyle cartilage of CKO mice detected a significant decrease (78%) in effective indentation modulus (Eind), suggesting that EGFR is indispensable for maintaining the biomechanical function of cartilage. Male mice at 3 months of age underwent surgical destabilization of medial meniscus in the right knees to induce OA. Three months later, WT developed mild-to-moderate OA (Makin score: 6.0 ± 0.5), *Wa5* exhibited advanced OA (11.5 ± 0.5), and CKO had the most severe OA (14.0 ± 0.0) with a complete loss of entire cartilage layer restricted at the medial side. Moreover, we observed a local and drastic subchondral bone plate (SBP) thickening (4.5-fold) only under the cartilage damage area. This was correlated with locally reduced sclerostin amount by osteocytes within SBP and increased number of osteoblasts lining SBP surface. Since subchondral trabecular bone was not altered, we reason that SBP sclerosis is caused by increased mechanical loading after cartilage depletion. Hence, we provide the first direct evidence that chondrogenic EGFR signaling is critical for articular cartilage homeostasis and OA development and that local crosstalk between cartilage and SBP plays an important role in accelerating OA progression.

Disclosures: Haoruo Jia, None.

1060

Phlpp1 Deletion Increases Fgf18 Expression and Protects Against Post-Traumatic Osteoarthritis. Elizabeth Bradley^{*1}, Lomeli Carpio¹, Derek Amanatullah¹, Sanjeev Kakar¹, Lauren Ta¹, Alexandra Newton², Jennifer Westendorf¹. ¹Mayo Clinic, USA, ²University of California, USA

Osteoarthritis (OA) is a degenerative joint disease and leading cause of disability. Although Fgf18 is an emerging candidate, there are no FDA-approved disease

modifying OA drugs (DMOADs). We recently identified the protein phosphatase Phlpp1 as an effector of chondrocyte differentiation *in vitro*. Phlpp1 dephosphorylates and inactivates Akt2 other substrates to arrest matrix production and induce apoptosis. The purpose of this study was to determine if Phlpp1 contributes to OA disease progression and inhibits proper endochondral bone formation in humans and mice. PHLPP1 was highly expressed in human articular cartilage from OA patients, but was undetectable by IHC in articular cartilage samples from FNFx specimens (Fig 1A). To determine if Phlpp1 contributes to OA progression, we evaluated the effects of Phlpp1 deficiency on OA progression in mice using the DMM model. Phlpp1^{-/-} mice showed significant reductions in OARSI scores and subchondral bone thickening (Fig 1B), suggesting that loss of Phlpp1 is protective against OA progression. To elucidate the mechanism of this protective effect, we examined the effects of Phlpp1 deficiency during endochondral bone formation. Phlpp1 null mice exhibit reduced bone density likely due to increased osteoclast formation and growth plate abnormalities, including increased chondrocyte proliferation and matrix production. Furthermore, Phlpp1 deficiency promoted expression of Fgf18 (Fig 1C), a growth factor that facilitates chondrogenesis, chondrocyte proliferation and cartilage regeneration in surgically-induced models of osteoarthritis. Erk1/2 activity and chondrocyte proliferation were also elevated. Chemical inhibition of the Fgf18 receptor, FgfR3, abrogated the increased Erk1/2 phosphorylation observed in Phlpp1 null chondrocytes. Furthermore, blocking FgfR or MEK1/2 signaling suppressed proliferation induced by Phlpp1 deficiency. Phlpp inhibitors also augmented Erk1/2 phosphorylation, matrix content and Fgf18 production (Fig 1D&E). These results demonstrate that suppression of Phlpp1 expression and/or activity is protective against cartilage degeneration. Phlpp1 therefore contributes to cartilage development and OA progression and may be a therapeutic target for OA treatment.

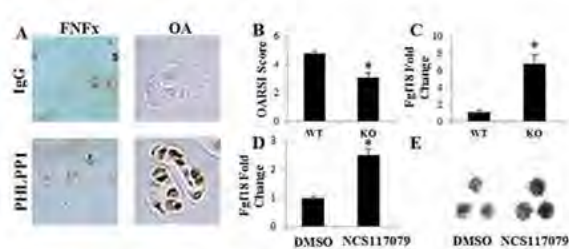


Figure 1. (A) PHLPP1 IHC in human articular cartilage from patients undergoing total joint arthroplasty for OA or FNFx. (B) OARSI scores from DMM surgeries performed on WT or Phlpp1^{-/-} mice. (C) Fgf18 expression was determined in Phlpp1^{-/-} cells by qPCR. (D-E) Fgf18 expression and Alcian blue staining of WT micromasses treated with the Phlpp1 inhibitor NCS117079. *p<0.05.

Figure 1

Disclosures: Elizabeth Bradley, None.

1061

The Role of Fibroblast Growth Factor 2 Isoforms in Osteoarthritis. Patience Meo Burt^{*1}, Marja Hurley², Thomas Doetschman³. ¹University of Connecticut Health Center, USA, ²UCONN Health, USA, ³University of Arizona, USA

Osteoarthritis (OA) is the leading cause of chronic disability in the U.S., characterized by the loss of articular cartilage and changes in underlying bone. There is no effective therapy for OA. Mice deficient in fibroblast growth factor 2 (FGF2) develop accelerated and more severe spontaneous OA. Thus, FGF2 plays a role in cartilage maintenance, but a comprehensive analysis is indicated since the *Fgf2* gene encodes multiple protein isoforms including high molecular weight isoforms (HMW) with nuclear localization sequences and low molecular weight isoform (LMW) that is exported from cells. We utilized mice in which all FGF2 isoforms are knocked-out (*Fgf2^{ALLKO}*), mice in which only the FGF2HMW isoforms are knocked-out (*Fgf2^{HMWKO}*) that have increased bone mineral density (BMD) compared to wild-type (WT) littermates, and mice in which the FGF2LMW isoform is knocked-out (*Fgf2^{LMWKO}*) that have decreased BMD compared to WT littermates. We hypothesized that *Fgf2^{LMWKO}* mice will develop OA whereas *Fgf2^{HMWKO}* mice will not develop OA compared with WT littermates. To assess for signs of OA, knee joints from 2, 6 and 9 month old *Fgf2^{ALLKO}*, *Fgf2^{HMWKO}* and *Fgf2^{LMWKO}*, and their WT littermate mice underwent digital x-ray imaging and microCT analysis. To determine articular cartilage integrity, Safranin-O staining was performed. Immunohistochemistry was used to examine expression of cartilage degrading metalloproteinases MMP-13 and ADAMTS-5. X-rays revealed no evidence of OA in 2 month-old mice of all genotypes. As shown in Figure 1, x-rays of 6 month-old mice confirmed OA in knees of *Fgf2^{ALLKO}*. Interestingly osteophyte formation, thinning of the subchondral bone at 6 months, and thickening of the bone was observed at 9 months in *Fgf2^{LMWKO}* knees, which was not present in *Fgf2^{HMWKO}* or WT mice. MicroCT analysis of *Fgf2^{LMWKO}* knees revealed changes in trabecular architecture indicative of OA compared to WT, while changes observed in *Fgf2^{HMWKO}* mice were minor compared to their WT controls (this was also observed at 2 years of age). Safranin-O staining (Figure 2) was decreased

and metalloproteinase labeling was increased in articular cartilage and synovium of *Fgf2^{LMWKO}* mice only. Overall, these results suggest that lack of the LMW isoform of FGF2 contributes to the progression of OA, and they offer insight into a factor that causes the disease, while being a potential therapeutic target for OA.



Figure 1

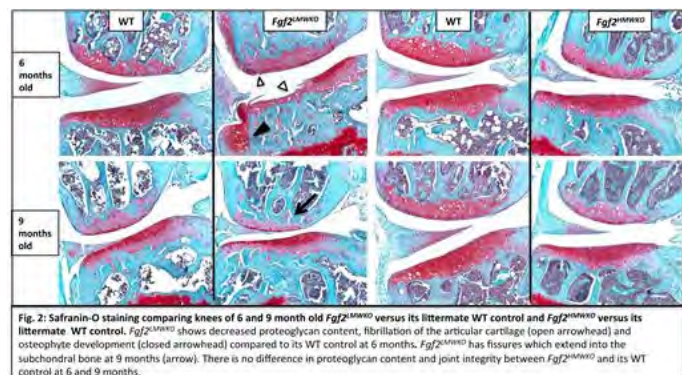


Figure 2

Disclosures: Patience Meo Burt, None.

1062

Sost Protects Mouse Joints from Post Traumatic Mediated Cartilage Degradation by Inhibiting MMP-Activity. Jiun Chiun Chang^{*1}, Blaine A. Christiansen², Nicole M. Collette³, Aimy Sebastian⁴, Deepa K. Muruges³, Sarah Hatsell⁵, Aris N. Economides⁵, Craig D. Blanchette³, Gabriela G. Loots⁵. ¹University of California, Merced, USA, ²UC Davis Medical Center, USA, ³Lawrence Livermore National Laboratories, USA, ⁴University of California Merced, USA, ⁵Regeneron Pharmaceuticals, USA

Sclerostin (*Sost*), a Wnt antagonist and a potent negative regulator of bone formation has recently been implicated in regulating chondrocyte function in osteoarthritis (OA). *Sost* levels were found to be elevated in regions of damaged cartilage in a sheep surgical model of OA raising the possibility that *Sost* may have a protective role in post-traumatic osteoarthritis (PTOA); however the mechanism is not yet known. To determine how *Sost* up-regulation may protect the joint from cartilage degradation, we examined the progression of OA using a noninvasive tibial compression model of PTOA in transgenic mice (*TG*) overexpressing *SOST* from a human bacterial artificial chromosome or lacking *Sost* (*KO*). OA development was examined histologically and by micro-computed tomography (μ CT) at 1 day, 6-, 12-, and 16- weeks post injury (PI). Histologically, *TG* injured joints displayed a less severe OA phenotype than injured *WT* or *KO* joints, while *KO* injured joints exhibited accelerated cartilage loss. Quantification of osteophyte formation by μ CT at 16 weeks PI found *TGs* to contain ~49% less and *KOs* ~28% more osteophyte volume than *WT* injured joints. To determine whether *Sost* interferes with the initial catabolic response in cartilage, we quantified the activity of matrix metalloproteinases (MMP) shortly after the injury. Fluorescent MMPsense substrate was administered intravenously PI and MMP activity was quantified 3 days PI. *TG* injured joints displayed ~2-fold less MMP activity than *WT* or *KO* injured joints; MMP activation was similar in *WT* and *KO* injured joints. Intra-articular administration of recombinant *Sost* PI also significantly reduced the activity of MMPs relative to PBS injected controls. Next, we quantified gene expression using RNA sequencing (RNASeq) at 1 day post injury and compared injured and uninjured *WT* and *KO* joints. In this analysis, 84 and 78 transcripts were found to be up-regulated >2-fold in *WT* and *KO* injured joints, respectively. In particular, we found MMPs 2/3/9/13 transcripts to be significantly up-regulated in both *KO* and *WT* injured joints, and the level of up-regulation was significantly higher in *KO* than in *WT* injured joints. Preliminary data suggest that MMP14, an enzyme involved in MMP activation is up-regulated in injured *WT* and *KO* joints, but reduced in *TG* injured joints, suggesting that *SOST* overexpression protects the injured joint from subsequent cartilage degradation by inhibiting the transcription of MMPs and MMP activating enzymes.

Disclosures: Jiun Chiun Chang, None.

1063

Increasing Pediatric Wrist Fracture Rates May Have Major Implications for Future Adult Fracture Burden. Daniel Jerrhag¹, Martin Englund², Ingmar Petersson³, Lennart Landin¹, Magnus Karlsson¹, Bjorn Rosengren^{*1}. ¹Skåne University Hospital Malmö, Lund University, Sweden, ²Clinical Epidemiology Unit, Orthopaedics, Clinical Sciences Lund, Lund University; Epidemiology & Register Centre South, Skåne University Hospital Lund, Sweden, Sweden, ³Orthopaedics, Clinical Sciences Lund, Lund University; Epidemiology & Register Centre South, Skåne University Hospital Lund, Sweden, Sweden

Background

Much effort has been put into monitoring fracture risk in the senior population in order to predict fracture burden in the future. As children with fracture have lower peak bone mass (a determinant of osteoporosis in old age) and higher adult fracture risk it may be possible already today to partly discern the vector of fragility fracture risk in the far future. This would be especially important as estimations have suggested that 50% of the children of today will live 100 years or more.

We set out to examine the current epidemiology of wrist fractures in children, the most common pediatric fracture, and relate results to older pediatric fracture data (from 1950s and onwards) for those at risk of fragility fractures today (current age up to 80 years).

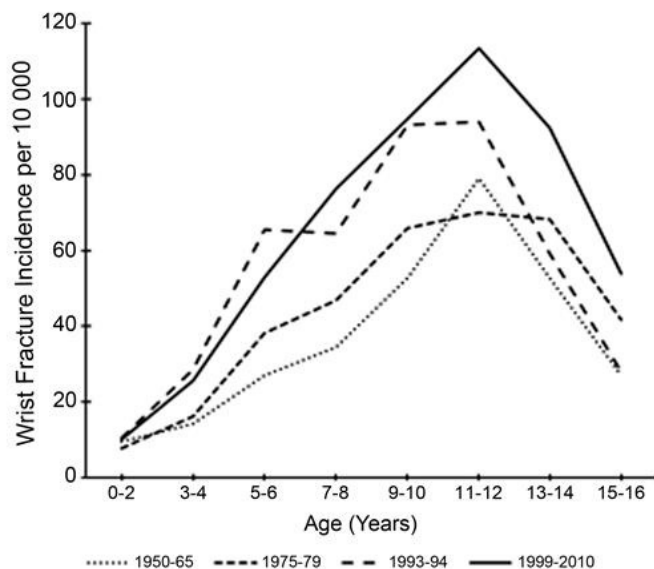
Methods

By use of official in- and out-patient register data in the Skåne region in Sweden we ascertained distal forearm fractures in children aged <17 years during the years 1999-2010 (2.8 million patient years) and estimated overall and age- and sex- specific rates and time trends and compared the results to earlier estimations in the same region from 1950 and onwards.

Results

During the examination period (1999-2010) the overall wrist fracture rate was 63 per 10 000 patient years (75 in boys and 51 in girls). This was an increase compared to earlier (+50% compared to 1950s) with the age specific difference most evident during puberty (Figure) and with a statistically significant different age-rate distribution (Poisson interaction between curves $p < 0.001$). It should be noted that there also within the period of examination (1999-2010) was a statistically significant increase in annual age-adjusted rates for both boys (+1.5 per 10 000 and annum (95%CI 0.7, 2.3)) and girls (+1.2 (0.8, 1.7)) which may further enhance risk increments.

Conclusion: These data suggest that the number of fragility fractures in the future may increase not only on the basis of the projected life-span increase but also due to an increased fracture risk. The origin of the 50% increase in pediatric wrist fracture rate between current children and those aged up to 80 years today (children in the 1950s) remains to be revealed but may be associated to a more sedentary lifestyle with digital amusements and lower physical activity but could also be related to changes in risk behavior



Pediatric wrist fracture rate per age-group and period

Disclosures: Bjorn Rosengren, None.

1064

Increased Physical Activity in Childhood Reduces Fracture Risk - an 8-Year Intervention Study in 3 534 Children. Marcus Coster*, Jesper Fritz, Jan-Ake Nilsson, Magnus Dencker, Bjorn Rosengren, Magnus Karlsson. Lunds Universitet, Sweden

Purpose: Physical activity (PA) in childhood is associated with high bone mass and superior neuromuscular function, but the long-term musculoskeletal and fracture risk effects are unclear. Method: We conducted a population based clustered randomized controlled PA intervention trial (RCT) in one school where the intervention included 40 minutes of moderate PA per school day for 8 years in 1 339 children (aged six to eight years at study start). 2 195 children in three other schools who continued with the national standard of 60 minutes of PA per week served as controls. We then registered incident fractures during the study period through our regional radiographic archive and estimated annual fracture incidences and risk ratios (RR). We also correlated year of intervention with RR to sustain fracture that year by Spearman's correlation coefficient. In a sub-cohort of 234 children we also measured spine bone mineral content (BMC) and bone mineral density (BMD) with DXA and muscle strength as peak torque (PT) in knee extension (ext) and flexion (flex) by a computerized dynamometer (BiodexÜ). We present data as means with 95% CI. Results: The RR of fracture in intervention children (compared to controls) decreased with each year of extra PA (r=-0.86, p=0.007) so that the RR in the intervention group after eight years was 0.48 (95% CI 0.25, 0.91). The gain in bone mass was greater in the intervention children (compared to the controls), with a mean difference in spine BMD gain of 0.03 g/cm² (95% CI 0.00, 0.06), in PText of 6.5 Nm (95% CI 0.4, 12.6), and in PTflex of 7.7 Nm (95% CI 3.5, 11.9). Conclusion: A population-based pediatric PA intervention program that begins before puberty and continues for eight years induces a highly clinically and statistically significant fracture risk reduction, probably due to PA-induced benefits in BMD and muscle function. We can explain 74% of the variance in the diminished fracture risk during the study period by the intervention.

Disclosures: *Marcus Coster, None.*

1065

Are Psychiatric Illnesses and the Medications Used to Treat Them FRAX-Independent Risk Factors? The Manitoba BMD Cohort. William Leslie*¹, James Bolton¹, Suzanne Morin², Sumit Majumdar³, Lisa M. Lix¹, Helena Johansson⁴, Anders Oden⁴, Eugene MClouskey⁴, John Kanis⁴, Jitender Sareen¹. ¹University of Manitoba, Canada, ²McGill University, Canada, ³University of Alberta, Canada, ⁴University of Sheffield Medical School, United Kingdom

Background: FRAX is used for fracture risk assessment in the general population, but its applicability to specific patient subgroups remains incompletely investigated. Psychiatric illnesses and medications used to treat them may adversely impact bone metabolism and increase fracture risk, but have not been systematically studied in relation to FRAX. Methods: From a clinical DXA registry for Manitoba, Canada, we identified women and men age =40 y with baseline DXA in 1996-2011. Population-based data were used to identify FRAX covariates (with alcohol / substance abuse as a proxy for high alcohol intake), mutually exclusive psychiatric diagnoses (most responsible over 3 y prior to DXA), mutually exclusive categories of psychiatric medications (exposure defined by medication possession ratios over 1 y prior to DXA as low if <0.5 and high if >0.5), incident non-trauma major osteoporotic fractures (MOF) and hip fractures (HF). Results: We studied 71,271 women and men (age 64 y [SD 11], 90% female). During 485,322 y (median 7 y), 5750 (8.1%) patients sustained an incident MOF, 1579 (2.2%) an incident HF and 8998 (12.6%) died. Psychiatric diagnoses were depression in 6824 (9.6%), anxiety 6425 (9.0%) and schizophrenia 203 (0.3%); psychiatric medications were used by 21,915 (30.7%) of which 12,263 (17.2%) had high exposure. High exposure to selective serotonin reuptake inhibitors (SSRI), antipsychotics and benzodiazepines were each associated with increased risk for both MOF and HF (adjusted for FRAX with BMD and osteoporosis treatment). Psychiatric diagnoses were not independently associated with fractures when adjusted for psychiatric medications. FRAX with BMD provided significant fracture discrimination in subgroups defined by psychiatric diagnoses or psychiatric medication use (c-statistic MOF 0.66 to 0.73, HF 0.72 to 0.84), similar to the general population (MOF 0.69, HF 0.82). However, FRAX underestimated 10-y fracture risk for subgroups with depression (observed vs. expected ratios MOF 1.29, HF 1.51), or high exposure to SSRI (ratios MOF 1.36, HF 1.57), non-lithium mood stabilizers (ratios MOF 1.63, HF 1.98), antipsychotics (ratios MOF 1.60, HF 2.71) or benzodiazepines (ratios MOF 1.13, HF 1.31). Conclusions: Psychiatric illnesses and medications used to treat them were associated with increased risk for fracture. FRAX underestimated fracture risk in those with depression and high exposure to SSRI, mood stabilizers, antipsychotics and benzodiazepines.

Fracture risk, stratification and calibration (10-y observed/expected) with psychiatric diagnoses and medications.

| | MOF with BMD HR (95% CI)* | HF with BMD HR (95% CI)* | MOF with BMD c-statistic** | HF with BMD c-statistic** | MOF with BMD 10y Obs/Exp*** | HF with BMD 10y Obs/Exp*** |
|-----------------------|------------------------------|-----------------------------|-------------------------------|------------------------------|--------------------------------|-------------------------------|
| Depression | 1.06 (0.96-1.17) | 1.06 (0.87-1.30) | 0.69 (0.67-0.71) | 0.83 (0.81-0.86) | 1.29 (1.18-1.39) | 1.51 (1.25-1.77) |
| Anxiety | 1.06 (0.96-1.16) | 0.94 (0.78-1.13) | 0.69 (0.67-0.71) | 0.84 (0.81-0.87) | 1.13 (1.03-1.23) | 1.18 (0.95-1.40) |
| Schizophrenia | 1.21 (0.75-1.97) | 1.12 (0.48-2.63) | 0.73 (0.60-0.85) | 0.72 (0.52-0.92) | 1.28 (0.68-1.88) | 1.97 (0.25-3.68) |
| SSRI | 1.43 (1.27-1.60) | 1.48 (1.18-1.85) | 0.69 (0.66-0.72) | 0.84 (0.81-0.87) | 1.36 (1.22-1.50) | 1.57 (1.22-1.92) |
| Tricyclics | 1.05 (0.93-1.19) | 1.21 (0.96-1.51) | 0.69 (0.66-0.72) | 0.79 (0.75-0.83) | 1.08 (0.95-1.22) | 1.43 (1.09-1.78) |
| Other antidepressants | 1.27 (1.06-1.52) | 1.06 (0.71-1.58) | 0.66 (0.61-0.70) | 0.79 (0.74-0.86) | 1.32 (1.06-1.58) | 1.46 (0.82-2.10) |
| Lithium | 0.80 (0.45-1.42) | Insufficient # | 0.75 (0.59-0.90) | Insufficient # | 1.03 (0.42-1.64) | Insufficient # |
| Mood stabilizers | 1.41 (1.12-1.77) | 1.24 (0.80-1.92) | 0.69 (0.63-0.76) | 0.81 (0.73-0.89) | 1.63 (1.24-2.01) | 1.98 (1.02-2.95) |
| Antipsychotics | 1.43 (1.15-1.77) | 2.14 (1.52-3.02) | 0.68 (0.63-0.74) | 0.80 (0.74-0.86) | 1.60 (1.28-1.91) | 2.71 (1.81-3.60) |
| Benzodiazepines | 1.15 (1.04-1.26) | 1.21 (1.05-1.47) | 0.70 (0.67-0.72) | 0.77 (0.74-0.80) | 1.13 (1.03-1.23) | 1.31 (1.09-1.53) |

Fracture risk, stratification and calibration with psychiatric diagnoses and medications.

Disclosures: *William Leslie, None.*

1066

Predicting Imminent Risk for Fracture in Patients With Osteoporosis Using Commercially Insured Claims Data. M Bonafede¹, N Shi¹, R Barron², X Li², DB Crittenden², D Chandler². ¹Truven Health Analytics, USA, ²Amgen Inc., USA

Purpose

Several risk factors contribute to long-term fracture risk. However, few studies have identified individuals at imminent risk for fracture, defined as risk within the next 12 or 24 months. We aimed to identify risk factors associated with imminent first and subsequent fracture.

Methods

This was a retrospective cohort study using commercially-insured and Medicare supplemental data for patients aged ≥50 years with osteoporosis, a new fragility fracture claim (index date; fracture cohort) or no fracture claim (control cohort) from January 1, 2006 to September 30, 2012, and continuously enrolled ≥24 months prior to index date. Patients with a fracture in the 24-month pre-index period were excluded. Risk factors for imminent first fracture were identified by logistic regression models that included >60 potential risk factors assessed in the 12 or 24 months prior to index date; controls were randomly assigned an index date within the study period. Cox proportional hazards regression models were used to identify risk factors for subsequent fracture for up to 12 months following the index fracture.

Results

Of the 1,324,571 patients with an osteoporosis diagnosis, 163,186 patients met all inclusion criteria, and 19.7% of these had a fracture. Using data from 12 months prior to fracture, predictors more strongly associated with imminent first fracture were mainly fall-related risk factors, including previous falls, wheelchair use, psychoactive medication use (narcotics, SSRIs, and muscle relaxants), every additional decade after age 50, and mobility impairment (Table). In patients with a first fracture, risk factors for subsequent fracture included prior vertebral fracture (HR [95%CI] 1.62 [1.46-1.80], driven by risk of subsequent vertebral fracture), poor health reflected by a higher Charlson comorbidity index (4+, HR [95%CI] 1.26 [1.02-1.56] or 3, HR [95%CI] 1.22 [1.02-1.48]), antidepressant use (HR [95%CI] 1.21 [1.07-1.37]), and every additional decade after age 50 (HR [95%CI] 1.17 [1.12-1.22]). Similar findings were observed with data from 24-months pre-index. Conclusions

Recent falls, psychoactive medications, mobility impairment, older age, and impaired health status predict imminent risk for fracture within 12 or 24 months. Most of these factors also indicate risk of subsequent fracture. Patients with these characteristics warrant prompt intervention for fracture prevention, including potential lifestyle modifications and osteoporosis therapy.

Table. Factors Associated With Imminent Risk of First Fracture Within 12 and 24 Months

| Predictor | 12 Months Prefracture Odds Ratio (95%CI) | 24 Months Prefracture Odds Ratio (95%CI) |
|--------------------------------------|--|--|
| Falls | 6.67 (6.03-7.37) | 4.43 (4.09-4.80) |
| Narcotic use | 2.11 (2.05-2.18) | 1.85 (1.79-1.92) |
| Every additional decade after age 50 | 2.00 (1.98-2.03) | 1.97 (1.94-2.00) |
| Wheelchair use | 1.79 (1.61-2.00) | 1.80 (1.64-1.97) |
| SSRI use | 1.47 (1.41-1.52) | 1.41 (1.36-1.46) |
| Charlson comorbidity index score* 4+ | 1.46 (1.35-1.59) | 1.49 (1.38-1.62) |
| Mobility impairment | 1.46 (1.41-1.51) | 1.39 (1.34-1.43) |
| CNS disease | 1.41 (1.30-1.52) | 1.34 (1.25-1.43) |
| Muscle relaxant use | 1.40 (1.34-1.47) | 1.29 (1.25-1.35) |
| Charlson comorbidity index score* 3 | 1.40 (1.31-1.50) | 1.42 (1.32-1.52) |

p < 0.0001 for all.
*Reference category: Charlson comorbidity index = 0.

Table

Disclosures: *M Bonafede, Truven Health Analytics, Amgen*
This study received funding from: Amgen Inc. & UCB Pharma

1067

Vertebral Fracture Risk in Diabetic Elderly Men: The MrOS Study. Nicola Napoli*¹, Ann Schwartz², Anne Schafer², Peggy Cawthon³, Neeta Parimi², Joseph M. Zmuda⁴, Eric S. Orwoll⁵, Andrew R. Hoffman⁶, Elsa S. Strotmeier⁴, Elizabeth Barrett-Connor⁷, Dennis M. Black². ¹University Campus Bio-Medico di Roma, Italy, ²University of California San Francisco, USA, ³California Pacific Medical Center Research Institute, USA, ⁴University of Pittsburg, USA, ⁵Oregon Health & Science University, USA, ⁶Stanford School of Medicine, USA, ⁷University of California San Diego, USA

Type 2 diabetes (T2DM) is associated with a 50-80% increased risk of hip fractures as well as 30-70% increased risk of fracture of the humerus and foot. However, to date, very limited information is available on the vertebral fracture (VFs) risk in diabetic men. Moreover, although BMD is strongly associated with vertebral fractures in the general population, previous results have shown no association between bone mineral density (BMD) and vertebral fractures in T2DM.

The aim of this study was to evaluate whether the prevalence and incidence of VFs in T2DM men is higher than in their non-DM counterparts and to examine whether the association between lumbar spine BMD and VF is similar in T2DM and non-DM men.

We used data from the Osteoporotic Fractures in Men (MrOS) Study that enrolled 5,994 men (≥65 years). Men without fasting glucose (n=306) or baseline spine x-ray (n=34) were excluded. Diabetes (ascertained by self-report, use of diabetes medication or elevated fasting glucose) was reported in 875 men of whom 80 used insulin. Spine BMD was measured with dual x-ray absorptiometry (DXA) and QCT. Morphometric VFs were identified on spine x-rays at baseline and at 2nd visit on average 4.6 years later, using standard methods. Prevalent VF was defined as semi quantitative score (SQ) ≥2; incident VF was defined as an increase of ≥1 SQ from baseline.

We used logistic regression analysis to a) examine the effect of diabetes status on prevalent and incident VFs and b) estimate the effect of BMD obtained by DXA or QCT as a risk factor for prevalent and incident VFs in T2DM and non-DM men. T2DM men had higher spine aBMD (by DXA), integral and trabecular vBMD (by QCT) (p<0.001 for all examined parameters). Prevalence of VF was not higher in T2DM (6.97%) vs. non-DM men (7.67%) in models adjusted for age, clinic site, race or after adjustment for BMI, aBMD or vBMD (Table 1). Similarly, risk of incident VFs was not higher in T2DM vs. Non-DM men in all analyzed models (Table 1). However, power to detect modest associations was limited. Spine aBMD was negatively associated with prevalent VFs in T2DM [OR=0.69 (0.52-0.91)] and non-DM men [OR 0.56 (0.49-0.63)](p for interaction 0.18). Results were similar for vBMD.

In conclusion, T2DM is not associated with increased risk of prevalent or incident VFs in elderly men. Lower BMD is associated with higher risk of prevalent VFs in DM as well as non-DM men.

| Model adjusted for | Prevalent vertebral fractures OR (95%CI) | Incident vertebral fractures OR (95%CI) |
|---------------------------------|--|---|
| Model 1: age, race, clinic site | 0.91 (0.74-1.18) | 1.05 (0.68-1.62) |
| Model 2: Model 1, BMI | 0.93 (0.70-1.25) | 1.10 (0.71-1.71) |
| Model 3: Model 2, spine aBMD | 1.05 (0.78-1.40) | 1.28 (0.81-2.00) |
| Model 4: Model 2, spine vBMD | 1.30 (0.89-1.88) | 1.40 (0.78-2.53) |

Diabetes and risk of morphometric vertebral fracture in older men

Disclosures: Nicola Napoli, None.

1068

The Burden of Osteoporosis Is Set to Increase Worldwide: Secular Trends in High Fracture Probability 2010-2040. Anders Odén¹, Eugene McCloskey¹, John Kanis¹, Nicholas Harvey*², Helena Johansson¹. ¹Centre for Metabolic Diseases, University of Sheffield, United Kingdom, ²MRC Lifecourse Epidemiology Unit, University of Southampton, United Kingdom

The burden of osteoporosis has been defined in terms of bone mineral density, fracture incidence and quality of life, but no studies have explored the prevalence of high fracture risk globally. The aim of this study was to quantify the number of individuals worldwide aged 50 years or more at high risk of osteoporotic fracture in 2010 and 2040. For both men and women, a threshold of high fracture probability was set at the age-specific ten-year probability of a major fracture (clinical vertebral, forearm, humeral or hip fracture), equivalent to that of a woman with a prior fragility fracture, an average BMI (24kg/m²) but no other clinical risk factors. All available country-specific FRAX models (covering 78% of the world population) were used to calculate the prevalence of high risk worldwide and by continent through application to the population demography for each country. The burden of disease over time was estimated from future population projections up to 2040 in each geographical region using the medium variant of UN projections. Globally, in 2010, 3.1% of men and 18.2% of women aged at least 50 years had a fracture probability above the fracture threshold, comprising 21 million men and 137 million women. The greatest number of

men and women at high risk were from Asia (55%), followed by Europe (17%). Worldwide, the number of high-risk individuals is expected to double over the next 40 years. Increases were noted for all regions but were particularly marked in Africa and Latin America. The most modest rise (by 30%) was seen for Europe. In conclusion, individuals with high probability of osteoporotic fractures comprise a very significant disease burden to society, particularly in Asia, and this burden is set to increase markedly in the future. These analyses identify the population who might be targeted for interventions to prevent future fracture and thus may usefully inform future health policy.

Disclosures: Nicholas Harvey, None.

1069

Intensive bisphosphonate therapy aimed at normalising bone turnover in Paget's disease increases the risk of fractures and requirement for orthopaedic procedures: The PRISM-EZ trial. Adrian Tan*¹, Jemma Hudson², William Fraser³, Peter Selby⁴, Graeme MacLennan², Stuart Ralston¹. ¹University of Edinburgh, United Kingdom, ²University of Aberdeen, United Kingdom, ³University of East Anglia, United Kingdom, ⁴University of Manchester, United Kingdom

The optimal management strategy for Paget's disease of bone (PDB) is unclear but it has been suggested that bisphosphonates should be given with the aim of maintaining biochemical markers within the normal range. Here we report upon the long term outcome of treatment in the PRISM-extension with Zoledronic acid study (PRISM-EZ) in which 502 PDB patients who had already participated in the PRISM study (Langston *et al* JBMR 2010) were treated for a further 3 years using the same treatment allocation. Patients in the symptomatic group (n=232) were treated with bisphosphonates only if they had bone pain, whereas those in the intensive group (n=270) were given bisphosphonates even in the absence of symptoms with the aim of maintaining alkaline phosphatase levels (ALP) within the normal range. Zoledronic acid was the treatment of choice in the intensive group. Baseline characteristics of the treatment groups were similar and both groups had already been treated in PRISM for an average of 4.3 years. At baseline mean levels of ALP were significantly lower in the intensive group (p=0.02) and the difference between groups increased as the study progressed. For example, at year 1, the mean ± SD normalized ALP was 0.71 ± 0.30 (intensive) vs. 1.01 ± 0.81 (symptomatic) (p<0.001). The values were similar at years 2 and 3. There was no difference between the groups in pain or quality of life assessed by the SF36 questionnaire and analgesic use was similar. Fractures were more common in the intensive group (26 vs. 13) as were orthopaedic procedures (15 vs. 8). A time to event analysis correcting for baseline characteristics showed that the risk of fractures and requirement for orthopaedic procedures as a combined endpoint was significantly increased in the intensive group (HR = 1.85, 95% CI (1.04-3.27)). About 25% of the fractures and 50% of the orthopaedic events occurred in Pagetic bone with a non-significant trend for more events in the intensive group. There was no significant difference in number or type of adverse events between groups overall, but osteonecrosis of the jaw developed in one patient in the intensive group. We conclude that intensive bisphosphonate therapy confers no clinical benefit in patients with PDB and may be harmful. Treatment should be directed at treating symptoms rather than normalizing ALP values

Disclosures: Adrian Tan, None.

This study received funding from: Arthritis Research UK

1070

Extended Conventional Therapy in Adult Patients with X-linked Hypophosphatemia: Effects on Enthesopathy and Dentition. Jessica Connor*¹, Elizabeth Olear¹, Lee Katz¹, Suher Baker², Ragbir Kaur², Christine Simpson¹, John Sterpka¹, Jane Zhang³, Robert Dubrow¹, Karl Insogna¹, Thomas Carpenter⁴. ¹Yale University, USA, ²Yale-New Haven Hospital, USA, ³Veterans Affairs Connecticut Health Care System, USA, ⁴Yale University School of Medicine, USA

In X-linked hypophosphatemia (XLH), renal phosphate loss leads to rickets, osteomalacia and bowed legs. Affected children are treated with phosphate and active vitamin D metabolites, which improve most skeletal outcomes. Dental abscesses occur frequently, and calcification of tendons and ligaments (enthesopathy) occur in adults. It is unclear whether medical treatment has any long-term effects on extent of enthesopathy or dental abscess formation. Our objective was to investigate the relationship of conventional XLH therapy to enthesopathy and dental disease in adult XLH patients.

We performed a cross-sectional study in 52 XLH patients >18 yrs of age. Treatment exposure since diagnosis was recorded in detail. The number of enthesopathy sites were identified by comprehensive radiographic survey, and self-reported abscess histories were recorded. PHEX mutation analysis was performed. Biochemical measures included serum phosphorus and FGF23, as well as diurnal PTH levels, calculated as area under the curve for 26 hrs (PTHauc). Exposure to treatment was modeled as both proportion of life with treatment and proportion of adult life with treatment by dividing total treatment yrs by age and total treatment yrs over age 17 by yrs of life over 17, respectively. Multiple linear regression was used to

explore associations between treatment exposure and extent of enthesopathy with age, sex, mutation severity, and PTHaC as covariates. Multiple logistic regression was used to assess the association between treatment and odds of having severe dental disease (> 5 abscesses) with age, sex, and mutation status as covariates.

Neither proportional treatment exposure during adulthood, nor throughout the total life span were associated with the extent of enthesopathy ($P>0.85$). Age, BMI, and sex were significant predictors of enthesopathy for both proportional models ($P<0.01$). PTHaC was associated with the extent of enthesopathy ($p=0.05$) for the adult treatment exposure model. Proportion of both adult life and of total life with treatment were significantly associated with severity of dental disease ($P<0.008$). Those with no treatment in adulthood were 25.1 times more likely to experience severe dental disease compared to those treated 100% of adulthood. Extending treatment into adulthood appears beneficial for the prevention of dental disease, however does not seem to either promote or prevent enthesopathy.

Disclosures: Jessica Connor, None.

1071

Asfotase alfa: Sustained Efficacy and Tolerability in Children with Hypophosphatasia Treated for 5 Years. Cheryl Rockman-Greenberg^{*1}, Katherine L Madson², Amy Reeves², Scott Moseley³, Tatjana Odrlić³, Michael P Whyte². ¹University of Manitoba, Canada, ²Shriners Hospital for Children, USA, ³Alexion Pharmaceuticals, USA

Background. Hypophosphatasia (HPP) is the rare inherited metabolic disease caused by loss-of-function mutation(s) within the gene that encodes the tissue-nonspecific isoenzyme of alkaline phosphatase (TNSALP). The resulting TNSALP deficiency can cause a spectrum of complications in children including premature loss of primary teeth, rickets, poor growth, muscle weakness, compromised physical function, and pain. In 2014, we reported that children 5-12 years old with HPP and treated with asfotase alfa, a recombinant bone-targeted human TNSALP, experienced rapid improvement in skeletal mineralization and physical function, sustained through 3 years (1, 2).

Aims/Objectives. Report the 5 year experience using asfotase alfa to treat these children.

Methods. The outcome assessments of this Phase II, open-label, ongoing extension study of asfotase alfa (6 mg/kg/wk; SC) in patients 5-12 years old include change in HPP-related skeletal manifestations assessed by a 7-point Radiographic Global Impression of Change (RGI-C) scale (-3=severe worsening; +3=near-complete/complete healing); functional ability/disability assessed by 6-Minute Walk Test (6MWT), the Bruininks-Oseretsky Test of Motor Proficiency, 2nd Edition (BOT-2) Strength and Agility composite score, and Child Health Assessment Questionnaire (CHAQ) Disability Index; and safety.

Results. 12/13 patients completed the original 6-month study, entered the extension phase, and received ≥ 5 years of treatment. The most common treatment-related adverse events (AEs) were mild-to-moderate injection site reactions in all patients (e.g., erythema, macule, and lipohypertrophy; 1 event of injection site atrophy assessed as severe). There were no deaths or AEs leading to withdrawal. Significant healing of HPP-related skeletal manifestations was sustained at 5 years (median [min, max] RGI-C: +2.2 [+1.7, +2.7]; $p=0.0005$). Normalization of physical function was sustained through 5 years across the 6MWT, BOT-2 Strength and Agility score, and CHAQ Disability Index (Table 1).

Conclusion. Asfotase alfa was tolerated well over 5 years of treatment. Normalization of HPP-related skeletal manifestations and functional ability is sustained through 5 years of asfotase alfa treatment in children with HPP.

Madson, 2014 PAS3808.202

Madson, *JBMR* (2014)29:Suppl 1

Table 1. Outcomes at 5 years of asfotase alfa treatment

| Outcome | Normal Reference range for healthy peers | Median (min, max) | | Change from Baseline p-value |
|--|--|------------------------------|-----------------|------------------------------|
| | | Baseline (n=13) ¹ | 5 years (n=12) | |
| 6MWT, % predicted of healthy normal | :80%-120% | 61% (29%, 82%) | 83% (70%, 104%) | 0.0002 |
| BOT-2 Strength and Agility, standard score | 40-60 | 28 (20, 37) | 46 (33, 64) | <0.0001 |
| CHAQ Disability Index ² | 0=no disability | 1 (0, 2.25) | 0 (0, 1) | 0.0002 |

¹6MWT, 6-Minute Walk Test. ²BOT-2, the Bruininks-Oseretsky Test of Motor Proficiency, 2nd Edition. ³One patient withdrew after 1 month for elective surgery. ⁴CHAQ, Child Health Assessment Questionnaire (range 0-3).

Table 1. Outcomes at 5 years of asfotase alfa treatment

Disclosures: Cheryl Rockman-Greenberg, Honoraria and travel support from Alexion Pharmaceuticals

This study received funding from: Alexion Pharmaceuticals

1072

Type I Collagen C-Propeptide Cleavage Site Mutations: Bone Fragility with High Bone Mass. Tim Cundy^{*1}, Chumei Li², Shehla Mohammed³, Emma Duncan⁴, Aideen McInerney-Leo⁴, Paul Roschger⁵, Klaus Klaushofer⁵, Peter Byers⁶. ¹Faculty of Medical & Health Sciences University of Auckland, New Zealand, ²McMaster University, Canada, ³Guys Hospital, United Kingdom, ⁴University of Queensland, Australia, ⁵Ludwig Boltzmann-Institut für Osteologie, Austria, ⁶University of Washington, USA

Osteogenesis imperfecta (OI) is characterized by low bone mass and skeletal fragility. Most cases of OI result from mutations in COL1A1 and COL1A2, which encode the pro α 1(I) and pro α 2(I) chains, respectively, of type I procollagen. In addition to the core triple helical domain characterized by the repeating Gly-Xaa-Yaa triple, these chains contain amino (N)-terminal and carboxyl (C)-terminal regions. Directed by sequences in the carboxyl-terminal domain, these chains combine in a 2:1 ratio into a trimeric structure that then propagates the triple helical collagen structure in a C- to N-terminal direction. Following secretion in the pericellular domain the N-terminal and C-terminal propeptides are cleaved by proteases: in the case of the C-propeptide by BMP1, at an Ala-Asp dipeptide in each chain [1218-1219 in pro α 1(I) and 1119-1120 in pro α 2(I)]. Mutations in BMP1 result in a severe form of OI with a relatively high bone mass and Lindahl et al have described two OI patients with heterozygous mutations at the C-propeptide cleavage site with normal or high bone mass.* We describe here the clinical and laboratory findings in a larger group of 18 subjects (age 3-77) with C-propeptide cleavage site mutations in COL1A1 (A1218T in 5 subjects from 2 families; D1219E in 4 subjects, 1 family) or COL1A2 (D1120N in 5 subjects, 1 family; D1120A in 4 subjects, 1 family). The age at first fracture ranged from infancy to age 17; half had fractured a femur by age 25. Stature was normal (mean height, 47th centile). The sclerae were white and dentinogenesis imperfecta absent or mild, but two patients had fibro-osseous dysplasia of the mandible; deafness was a feature in one family. Radiographs were remarkable for thickened cortices and spinal osteosclerosis. Spine bone density (DXA) was significantly elevated: mean z-score +2.2 (SD 2.3) – with a marked sex difference (male +0.9 (1.2); female +3.6 (2.5), $p=0.016$). Heterotopic calcification was a feature in some families, and quantitative backscattered electron imaging of a bone biopsy showed a shift in mineral density distribution towards exceptionally high bone matrix mineralization although, paradoxically, histology showed an excess of unmineralized osteoid. In this still relatively small sample, we confirm that OI patients (particularly females) with C-propeptide cleavage site mutations have increased bone mineral density. The basis for this remains unknown. Retention of propeptide sequences conceivably could result in more space for mineral within and between fibrils. However, in vitro studies showed that the C-terminal propeptides are still removed from type I procollagen by enzymatic cleavage. The absence of abnormal fibrils suggests that there is an alternative cleavage site. The clinical features appear to be similar in those with COL1A1 and COL1A2 mutations.* K Lindahl et al Hum Mutation 2011 32: 598-609

Disclosures: Tim Cundy, None.

1073

Change in Fracture Risk After Bariatric Surgery from a Pattern Associated with Obesity to a Pattern Typical of Osteoporosis: A Study Using Healthcare Administrative Databases. Catherine Rousseau^{*1}, Sonia Jean², Philippe Gamache³, Stefane Lebel⁴, Fabrice Mac-Way¹, Laëtitia Michou¹, Claudia Gagnon⁵. ¹Endocrinology & Nephrology Unit, CHU de Quebec Research Centre; Department of Medicine, Laval University, Canada, ²Institut national de santé publique du Québec; Department of Medicine, Laval University; University of Sherbrooke, Canada, ³Institut national de santé publique du Québec, Canada, ⁴Quebec Heart & Lung Institute, Canada, ⁵Endocrinology & Nephrology Unit, CHU de Quebec Research Centre; Department of Medicine, Laval University; Institute of Nutrition & Functional Foods, Canada

Purpose: To investigate whether fracture risk by site change after bariatric surgery.

Methods: This retrospective, population-based cohort study used healthcare administrative databases to compare fracture risk by site of patients who had undergone bariatric surgery between 2001 and 2012 in the province of Quebec, Canada, with the one of age- and sex-matched non-bariatric obese and non-obese controls. Fracture risk by site was also compared before vs. after surgery (or index date) for each group. Fractures were identified using a validated algorithm (sensitivity >80% for most fracture sites) and were grouped as: lower extremity (knee, foot, ankle, tibia and fibula), upper extremity (shoulder, humerus, elbow, forearm, wrist), spine and hip/femur/pelvis. Multivariate conditional Poisson regression models were adjusted for past fracture, comorbidities (cardiovascular disease, hypertension, diabetes, renal failure, chronic obstructive pulmonary disease, depression, osteoporosis, hypothyroidism), material and social deprivation and area of residence.

Results: 10 662 individuals who underwent bariatric surgery (72.6% women; mean age (SD), 42 (11) years), 31 986 obese and 31 986 non-obese matched controls were followed for a mean of 4.2 years (min-max: <1-12 years). Before surgery (or index date), the risk of lower extremity fractures was higher while the one of upper extremity fractures was lower in both the bariatric and obese control groups compared with the

non-obese group (Table 1). However, the risk of central fractures (spine, hip, femur, pelvis) was similar between groups. After surgery, the risk of sustaining a lower extremity fracture decreased by 33% in the bariatric group compared with pre-surgery (Table 2), being still higher than the one observed in the non-obese group although not statistically significant (Table 3). There was however a two-fold increase in upper extremity fractures and a three-fold increase in pelvic, hip or femur fractures following surgery (Table 2). There was no change in the risk of spine fractures post surgery (but the *n* was small). Fracture risk in the obese and non-obese control groups remained stable for all sites before and after the index date.

Conclusions: These results suggest that fracture risk change after bariatric surgery from a pattern associated with obesity to a pattern typical of osteoporosis. Fracture risk assessment and management should be part of postoperative clinical care.

| | Bariatric group (n=10 662) | | Control group of obese individuals (n=31 986) | | Control group of non-obese individuals (n=31 986) | |
|------------------------------|-------------------------------|--------------------------|--|--------------------------|--|----------------------|
| | n (%) | Adjusted RR ³ | n (%) | Adjusted RR ³ | n (%) | Adj. RR ³ |
| Fractures, n | 1 285 | | 2 892 | | 2 463 | |
| Fracture sites, n (%) | | | | | | |
| Lower extremity ¹ | 820 (63.8) | 1.60 (1.44-1.78) | 1 718 (59.4) | 1.37 (1.26-1.49) | 1 237 (50.2) | REF |
| Upper extremity ² | 365 (28.4) | 0.85 (0.74-0.98) | 969 (33.5) | 0.90 (0.83-0.99) | 1 027 (41.7) | REF |
| Spine | 39 (3.0) | 1.06 (0.68-1.66) | 81 (2.8) | 1.01 (0.73-1.41) | 82 (3.3) | REF |
| Hip, femur, pelvis | 61 (4.7) | 0.99 (0.69-1.25) | 124 (4.3) | 0.93 (0.69-1.25) | 117 (4.7) | REF |

Data are presented as n (%) or RR (95% CI).

¹ Includes fractures of the knee, foot, ankle, tibia and fibula.

² Includes fractures of the shoulder, humerus, elbow, forearm and wrist.

³ RR adjusted for material and social deprivation, area of residence and number of comorbidities using multivariate conditional Poisson regression model.

Table 1. Comparison of fracture risk by site before surgery (or index date) among groups

| | Bariatric group (n=10 662) | | Control group of obese individuals (n=31 986) | | Control group of non-obese individuals (n=31 986) | |
|------------------------------------|-----------------------------------|----------------------------------|--|----------------------------------|--|----------------------------------|
| | Before surgery (or index date) | After surgery (or index date) | Before surgery (or index date) | After surgery (or index date) | Before surgery (or index date) | After surgery (or index date) |
| Lower extremity¹ | | | | | | |
| Crude RR | REF | 0.66 (0.56-0.78) | REF | 0.85 (0.76-0.94) | REF | 0.92 (0.81-1.04) |
| Adjusted RR ² | REF | 0.67 (0.56-0.79) | REF | 0.86 (0.77-0.95) | REF | 0.92 (0.81-1.04) |
| Upper extremity³ | | | | | | |
| Crude RR | REF | 1.98 (1.66-2.36) | REF | 1.04 (0.92-1.16) | REF | 1.09 (0.96-1.23) |
| Adjusted RR ² | REF | 2.06 (1.75-2.47) | REF | 1.06 (0.93-1.21) | REF | 1.09 (0.96-1.23) |
| Spine | | | | | | |
| Crude RR | REF | 1.41 (0.87-2.35) | REF | 1.05 (0.69-1.61) | REF | 1.01 (0.66-1.56) |
| Adjusted RR ² | REF | 1.52 (0.88-2.61) | REF | 1.04 (0.67-1.59) | REF | 1.05 (0.68-1.61) |
| Hip, femur, pelvis | | | | | | |
| Crude RR | REF | 2.88 (1.92-4.71) | REF | 1.21 (0.86-1.71) | REF | 1.22 (0.87-1.72) |
| Adjusted RR ² | REF | 2.99 (1.98-4.54) | REF | 1.29 (0.91-1.83) | REF | 1.27 (0.89-1.80) |

Data are presented as RR (95% CI).

¹ Includes fractures of the knee, foot, ankle, tibia and fibula.

² Adjusted for comorbidities (cardiovascular disease, hypertension, diabetes, renal failure, chronic obstructive pulmonary disease, depression, osteoporosis, hypothyroidism), material and social deprivation and area of residence.

³ Includes fractures of the shoulder, humerus, elbow, forearm and wrist.

Table 2. Comparison of fracture risk by site before and after surgery (or index date) for each group

| | Bariatric group (n=10 662) | Control group of obese individuals (n=31 986) | Control group of non-obese individuals (n=31 986) |
|------------------------------------|-------------------------------|--|--|
| Lower extremity¹ | | | |
| Crude RR | 1.43 (1.18-1.73) | 1.30 (1.14-1.50) | REF |
| Adjusted RR ² | 1.18 (0.96-1.44) | 1.29 (1.11-1.49) | REF |
| Upper extremity³ | | | |
| Crude RR | 1.94 (1.62-2.31) | 0.91 (0.79-1.06) | REF |
| Adjusted RR ² | 1.57 (1.30-1.89) | 0.88 (0.76-1.03) | REF |
| Spine | | | |
| Crude RR | 2.04 (1.14-3.65) | 1.04 (0.63-1.71) | REF |
| Adjusted RR ² | 1.67 (0.85-3.27) | 0.98 (0.59-1.63) | REF |
| Hip, femur, pelvis | | | |
| Crude RR | 3.69 (2.47-5.50) | 1.06 (0.71-1.60) | REF |
| Adjusted RR ² | 2.45 (1.58-3.79) | 0.94 (0.62-1.45) | REF |

Data are presented as RR (95% CI).

¹ Includes fractures of the knee, foot, ankle, tibia and fibula.

² Adjusted for comorbidities (cardiovascular disease, hypertension, diabetes, renal failure, chronic obstructive pulmonary disease, depression, osteoporosis, hypothyroidism), material and social deprivation and area of residence.

³ Includes fractures of the shoulder, humerus, elbow, forearm and wrist.

Table 3. Fracture risk by site after surgery (or index date) for each group vs. the non-obese group

Disclosures: Catherine Rousseau, None.

1074

Natural History and Prognostic Factors of Fibrous Dysplasia of Bone in a Modern Cohort of 372 Patients The Francedys Study. [Johanna Benhamou¹](#), [Deborah Gensburger²](#), [Claude Maessien³](#), [Roland Chapurlat^{2*}](#). ¹Université de Lyon, France, ²INSERM UMR 1033, France, ³APHP, France

Fibrous dysplasia of bone (FD) is a rare genetic bone disease that can be responsible for fracture, bone pain and deformity. The prognosis may be difficult to establish because of the coexistence of patients with benign forms of the disease and some others who are severely affected. Their distinction has not been well established so far. We have analyzed the data from the French National Reference Center for FD. Patients can obtain a consultation on their own rapidly (< 2 months) or be referred. We have established a database from standardized electronic medical records. We have made descriptive statistics of the various forms of FD and examined the prognostic factors by multivariable logistic regression analysis, with a parsimonious stepwise method. The primary outcome was a clinically relevant composite index combining bone pain (analogic scale = 3/10) and incident fragility fracture. In our modern (recruitment after 1990) cohort of 372 patients, the median age at diagnosis was 23. The revealing symptom (median age = 18) was bone pain in 44% of patients, a fracture in 9% but the diagnosis was fortuitous in 25% of cases. Monostotic forms represented 58% of patients and polyostotic forms 42%. The femur was the most commonly affected bone (44% of patients), followed by the skull (38%). Twelve percent of patients had McCune-Albright syndrome (MAS). With a median duration of follow-up of 7 years among 211 patients, we observed an incidence of fragility fracture of 17% and 51% of patients had no bone pain at the end of follow-up (with or without bisphosphonate therapy). A delay in diagnosis was defined by an interval of more than 6 months between first symptoms and diagnosis, that was observed in 30% of patients. In univariate analysis, younger age at diagnosis, renal phosphate wasting, a polyostotic form and prevalent fracture were predictors of a poorer prognosis, but in the multivariate model, the polyostotic form was the only significant predictor (OR = 2.04 [1.29; 3.27]). The predictors of surgical treatment were a younger age at diagnosis and first symptoms, the polyostotic forms, renal phosphate wasting, MAS and prevalent fracture, but none could emerge significantly in a multivariable analysis. In conclusion, in a national reference center for FD, one patient on follow-up out of six had incident fragility fracture. A polyostotic form was the main risk factor of a poorer outcome.

Disclosures: Roland Chapurlat, None.

1075

H₂O₂ generated in the mitochondria of osteoclasts is required for the loss of cortical bone mass caused by estrogen or androgen deficiency, but not aging. Semahat Serra Ucer^{*1}, Srividhya Iyer², Li Han², Shoshana M Bartell³, Aaron D Warren³, Julie A Crawford², Christine Rutlen², Robert L Jilka², Maria Jose Almeida², Stavros C Manolagas². ¹University of Arkansas for Medical Sciences, USA, ²Center for Osteoporosis & Metabolic Bone Diseases, Central Arkansas Veterans Healthcare System, University of Arkansas for Medical Sciences, USA, ³Central Arkansas Veterans Healthcare System, University of Arkansas for Medical Sciences, USA

Loss of bone mass caused by acute sex steroid deficiency or aging in mice is associated with an increase in reactive oxygen species (ROS). Nonetheless, the former is a state of high bone turnover with increased resorption and formation, albeit unbalanced, while the latter is a state of low turnover and decreased formation. Recent genetic evidence has revealed that H₂O₂ accumulation is important for the differentiation of osteoclasts; and that the anti-resorptive effects of sex steroids in the cortical versus the cancellous compartment are mediated by different mechanisms. Here, we examined the contribution of osteoclast H₂O₂ to the loss of bone mass caused by ovariectomy (OVX), orchidectomy (ORX), or old age, using transgenic mice in which the gene for human catalase - a potent H₂O₂ inactivating enzyme - has been targeted to the mitochondria of LysM-Cre expressing cells (MitoCat;LysM-Cre). Six weeks following OVX of 12-week old LysM-Cre littermate control mice, ROS levels in the bone marrow were increased and cancellous and cortical bone mass were decreased, as compared to sham-operated mice. MitoCat;LysM-Cre mice, however, were protected from the OVX-induced increase in ROS and the cortical bone loss, but not the loss of cancellous bone. Similar to the OVXed MitoCat;LysM-Cre mice, MitoCat;LysM-Cre ORXed at 18 weeks of age and analyzed 6 weeks later were protected from the loss of cortical, but not cancellous, bone. MitoCat;LysM-Cre mice were also protected from the ORX-induced increase in osteoclast number at the endocortical, but not cancellous, bone surface. Furthermore, administration of the antioxidant N-acetylcysteine to C57BL/6J mice prevented the loss of cortical, but not cancellous, bone caused by OVX or ORX. Finally, we aged ovary-intact female MitoCat;LysM-Cre mice and littermate controls and examined their skeletal phenotype at 22 months. Both genotypes exhibited the expected age-related decline in cortical and cancellous bone mass. However, in spite of the higher bone mass seen at 6 months in the MitoCat;LysM-Cre mice, at 22 months both cancellous and cortical bone mass were indistinguishable from the controls. These results demonstrate that the pathogenetic mechanisms responsible for the loss of cortical bone in acute sex steroid deficiency are different than those responsible for the loss of cancellous bone, and also different from the mechanisms causing loss of cortical bone with old age.

Disclosures: Semahat Serra Ucer, None.

1076

A Spontaneous Mutation in Dock7 Results in Extreme Age-Related Loss of Trabecular Bone and Sympathetic Nervous System-Related Bone Loss. Phuong T Le^{*1}, Kathleen Bishop¹, Katherine J Motyl¹, Daniel J Brooks², Kenichi Nagano³, Roland Baron⁴, Mary L Bouxsein², Clifford J Rosen¹. ¹Maine Medical Center, USA, ²Beth Israel Deaconess Medical Center, Harvard Medical School, USA, ³Harvard School of Dental Medicine, USA, ⁴Harvard School of Medicine & of Dental Medicine, USA

Misty mice (*m/m*) have a loss of function mutation in Dock7, a guanine nucleotide exchange factor, resulting in low bone mass, uncoupled bone remodeling, reduced bone formation, decreased osteoblast migration and altered Wnt signaling. In addition, *m/m* exhibit a reduction of preformed brown adipose tissue activity leading to compensatory increases in sympathetic nervous system (SNS) activity and browning of peripheral white adipose depots. Propranolol administration only partially rescues the low bone mass phenotype. Importantly, with advanced age, the skeletal phenotype becomes even more pronounced. We hypothesized that synergy between cell autonomous and non-cell autonomous factors exaggerate the process of age-related bone loss. To test this hypothesis, we first analyzed the static and dynamic histomorphometric parameters of *m/m* and their littermate controls (+/+) at 52 weeks of age. In 52 wk old *m/m*, femoral BV/TV (p=0.003) and Tb.N. (p<0.0001) were significantly reduced by μ CT analysis. However, histomorphometry revealed only 4/10 *m/m* and 8/9 +/+ exhibited any trabecular bone in tibia sections (p=0.027 by chi square). In contrast to 16 wk old *m/m*, neither osteoclast numbers nor surface area was changed at 52 wks of age. Osteoblast numbers were undetectable in *m/m* and marrow adipocytes were elevated 3.5 fold over +/+ (p=0.014). Consistent with reduced bone formation, gene expression of *Alp*, *Col-1*, and *Runx-2* was significantly decreased (p=0.001, .0002, and 0.01 respectively) in *m/m* whole bone. In combination with reduced appositional growth observed by μ CT analysis, these data suggest a defect in periosteal expansion and an acceleration of age-related bone loss in the absence of Dock7. Next, to test the importance of the increased SNS activity as the driver of bone loss in *m/m*, we crossed *m/m* with β 2AR^{-/-}. In mice wildtype for the *Misty* mutation, β 2AR^{-/-} alone had 8.8 \pm 0.4% (p=0.01) increase in femoral aBMD over +/+ at 8 wks of age. Interestingly, female β 2AR^{-/-}, *m/m* exhibited a 6.2 \pm 0.2% (p=0.007) increase

in femoral aBMD over β 2AR^{+/-}, *m/m*, but the β 2AR^{-/-}, *m/m* failed to gain BMD compared to β 2AR^{+/-}, *m/m*. Thus, loss of a single allele in the β 2AR resulted in increased aBMD due to modulation of SNS signaling in the *m/m*. In summary, the low bone mass and age-related bone loss observed in *m/m* results from both changes in SNS activity and a cell autonomous role for Dock7 in bone.

Disclosures: Phuong T Le, None.

1077

Velcade Enhances Fracture Repair in Aged Mice by targeting Mesenchymal Stem Cells. Hengwei Zhang^{*1}, Xing Li², Michael Zuscik², Brendan Boyce², Lianping Xing². ¹University of Rochester, USA, ²University of Rochester, USA

The Ubiquitin Proteasome System(UPS) influences the differentiation of mesenchymal stem cells(MSCs) to osteoblasts(OBs) during skeletal development and remodeling by regulating the stability of the essential osteoblastogenic proteins, Runx2 and JunB. However, the role of the UPS during fracture healing has not been studied well. We hypothesize that UPS activity is elevated in aging, leading to reduced MSC-OB differentiation and delayed fracture repair, which can be reversed by Velcade, a clinically used proteasome inhibitor. To test this, we performed open tibial fractures in 3-month-old(young) and 20-month-old(aged) C57BL6 mice, treated with Velcade(0.6mg/kg/day, ip, x4) or saline(Ctl), and examined callus volume by microCT and did biomechanical testing. Compared to Ctl, Velcade significantly increased callus volume in both young (3.5 \pm 1.1 vs 1.1 \pm 0.4 mm3) and aged (3.2 \pm 0.8 vs 2.1 \pm 0.4 mm3) mice and also increased bone strength (maximum torque: young: 28 \pm 4 vs 21 \pm 3 N.mm & aged: 19 \pm 2.8 vs 13 \pm 1.4 N.mm). To study if Velcade increases MSC frequency as a cellular mechanism, we examined the percentage of CD45-CD105+Sca1+ MSCs in fracture callus by flow cytometry. Aged mice had significantly fewer MSCs than young mice (%CD45-CD105+Sca1+: 1 \pm 0.2% vs. 1.5 \pm 0.3%), and Velcade significantly increased MSC frequency in the aged population (%CD45-CD105+Sca1+: 3.3 \pm 0.6% vs. 1 \pm 0.2% in Ctl). To determine if Velcade affects protein ubiquitination and degradation, we measured ubiquitinated protein levels in the fracture callus. Compared to young mice, aged mice had higher levels of total ubiquitinated proteins. Velcade increased the levels of key stem cell and osteoblast proteins known to be degraded via the UPS, including Runx2, JunB and stem cell factor Sox2. To investigate if Velcade stimulates proliferation of MSCs in fracture callus, we fractured tibiae of Nestin-GFP mice. We observed >10-fold increase in Nestin+ cells in fracture callus 10 days post-fracture, and among these 70% are CD105+Sca1+, 41% are α SMA+, and 60% are LeptinR+, and all are osteocalcin-. Velcade increased the % of Nestin+ and Nestin+ /BrdU+ cells by 4-10- and 2-fold, respectively. Thus, increased activation of the UPS may contribute to impaired fracture healing in aging by promoting the degradation of proteins involved in MSC proliferation and OB differentiation. Inhibition of USP activity with drugs such as Velcade would be a potential new therapeutic approach for patients with impaired fracture healing.

Disclosures: Hengwei Zhang, None.

1078

SIRT6 Deficiency Culminates in Low-Turnover Osteopenia. Toshifumi Sugatani^{*1}, Olga Agapova², Hartmut Malluche³, Keith Hruska². ¹Washington University in St. Louis School of Medicine, USA, ²Washington University School of Medicine, USA, ³University of Kentucky, USA

Sirtuin 6 (SIRT6) is a chromatin-related Class III histone deacetylase enzyme. Recently, it has been reported that SIRT6^{-/-} mice reveals severe premature aging phenotypes including osteopenia. Yet, no detailed skeletal investigation was performed in the study and the underlying molecular mechanisms of SIRT6 in bone metabolism are unclear. Hence, we investigated the bone phenotypes of SIRT6^{-/-} mice in detail, and studied the role of SIRT6 in osteoblastogenesis in culture.

Micro-CT and bone histomorphometry revealed that SIRT6^{-/-} mice produces a low-turnover osteopenia caused by impaired bone formation and bone resorption, which is a similar mechanism to age-related bone loss.

Consistent with the in vivo findings, quantitative alizarin red stain assays revealed drastically reduced osteoblastic mineralization in SIRT6^{-/-} osteoblasts. Osteoclast formation assays revealed that the number of TRAP+ cells were remarkably reduced in SIRT6 deficiency. Taken together, these findings indicate that SIRT6 positively regulates osteoblastogenesis and osteoclastogenesis as a decisive intrinsic factor.

Next, we analyzed the expression of Runx2 and Osx during SIRT6^{-/-} osteoblastogenesis. Surprisingly, Runx2 and Osx levels were gradually up-regulated in time-depend fashion in SIRT6^{-/-} osteoblastogenesis. Given that Runx2 and Osx negatively control osteoblastogenesis at a late stage, excessively elevated Runx2 and Osx in SIRT6^{-/-} osteoblasts may lead to impaired osteoblastic development and bone mineralization.

We found that SIRT6 interacts with Runx2 and Osx, and SIRT6 is recruited and deacetylates histone H3 at Lysine 9 (H3K9) at their target gene promoters, such as Runx2, Osx, ALP, osteocalcin, and Dkk1. Therefore, SIRT6^{-/-} osteoblasts produced the excessive expression of Dkk1 caused by the hyperacetylation of H3K9 in the promoter of Dkk1, a potent negative regulator of osteoblastogenesis. Moreover,

osteoprotegerin, an inhibitor of osteoclastogenesis, was excessively expressed in SIRT6^{-/-} osteoblasts, although osteoprotegerin is not target for Runx2 and Osx. In fact, nuclear accumulation of β -catenin was diminished by conditioned media harvested from SIRT6^{-/-} osteoblasts culture media and NFATc1 levels were also attenuated by the conditioned media during osteoclastogenesis. Taken together, the resulting up-regulation of Dkk1 and osteoprotegerin levels may impair bone remodeling, leading to osteopenia with a low bone turnover in SIRT6^{-/-} mice.

This is first demonstration that the structural changes of chromatin by loss of SIRT6 leads to functional changes that are important determinants of gene expression-related with bone remodeling. In addition, since SIRT6^{-/-} mice reveal characteristic features of low-turnover osteopenia in humans, the cellular and molecular mechanisms of SIRT6 in bone turnover could be potential therapeutic targets for age-related bone loss.

Disclosures: Toshifumi Sugatani, None.

1079

Overexpression of Sirt1 in Mesenchymal Stem Cells Stimulates Skeletal Growth and Osteoblastic Bone Formation. Quanquan Yan^{*1}, Qian Zhang¹, Jianliang Jin¹, Dengshun Miao². ¹Nanjing Medical University, China, ²Nanjing Medical University, Peoples republic of china

Previous study has demonstrated that Sirt1 haploinsufficiency resulted in a significant reduction in bone mass characterized by decreased bone formation and increased marrow adipogenesis, however, it is unclear whether overexpression of Sirt1 in bone marrow mesenchymal stem cells (BM-MSCs) plays an anti-osteoporotic role. To investigate this, we generated a transgenic mouse model overexpressing Sirt1 in BM-MSCs (Prx1-Sirt1^{1E}) and analyzed their skeletal phenotype. The expression levels of Sirt1 were significantly higher in skeletal tissue and BM-MSCs of Prx1-Sirt1^{1E} mice than in those of wild-type mice. Compared to wild-type mice, body weight and size, skeletal size, cortical and trabecular bone volume, osteoblast number, ALP- and type I collagen-positive areas, total numbers of CFU-f, mRNA expression levels of Runx2, ALP, type I collagen and osteocalcin were all significantly increased in the Prx1-Sirt1^{1E} mice. Furthermore, ROS levels were reduced significantly, whereas mRNA levels of anti-oxidative enzymes including SOD1 and 2 and glutathione peroxidase 1 (GPX1) were up-regulated in bony tissues of the Prx1-Sirt1^{1E} mice. We previously have demonstrated that Bmi1 deficiency displayed osteoporotic phenotype with a significant down-regulation of Sirt1 protein expression, therefore we crossed Prx1-Sirt1^{1E} mice with Bmi1^{-/-} mice to generate Bmi1^{-/-} mice with Sirt1 overexpression in BM-MSCs for comparison with the Bmi1^{-/-} and wild-type littermates. Overexpression of Sirt1 in Bmi1^{-/-} mouse BM-MSCs resulted in a longer lifespan, significantly increased body weight and improvement in skeletal growth and osteoblastic bone formation in the Bmi1^{-/-} mice, although the defects were not completely rescued. Furthermore, mRNA levels of anti-oxidative enzymes including SOD1 and 2, and glutathione peroxidase 1 and protein levels of SOD2 and FOXO3a were down-regulated in bony tissues of the Bmi1^{-/-} mice, importantly, Sirt1 overexpression in the Bmi1^{-/-} mice rescued this down-regulation. Taken together, these results demonstrated that overexpression of Sirt1 in BM-MSCs enhanced osteoblastic bone formation and partially rescues the defects in skeletal growth and osteogenesis in the Bmi1^{-/-} mice by inhibiting oxidative stress, consequently, support that Sirt1 is a target for promoting bone formation as an anabolic approach for treatment of osteoporosis.

Disclosures: Quanquan Yan, None.

1080

Discovery of MicroRNAs in Synovium in Regulating Inflammation Leading to Bone Erosion in Rheumatoid Arthritis. Yukiko Maeda^{*1}, Nicholas Farina², Melissa Matzelle³, Paul Fanning³, Jane Lian⁴, Ellen Gravalles³. ¹University of Massachusetts Medical School, Us, ²Department of Biochemistry, University of Vermont, USA, ³University of Massachusetts Medical School, USA, ⁴University of Vermont, USA

Articular bone erosion in rheumatoid arthritis (RA) is a consequence of synovial inflammation that results in significant disability. Synovial cells secrete inflammatory cytokines and RANKL promoting osteoclastogenesis and inhibition of osteoblast function. MicroRNAs (miRNAs) are key regulators of skeletal remodeling and are associated with RA pathogenesis. We hypothesized that miRNAs derived from synovial tissues play a regulatory role in erosion in RA through effects on osteoblasts. Using the serum transfer model of RA, we performed expression profiling of qPCR based 756 miRNAs in pooled synovial samples from non-arthritic and arthritic mice and compared this data set to gene expression from array data. We identified 417 up-regulated genes that are predicted targets of 72 down-regulated miRNAs (1.5 fold or >); and, 536 down-regulated genes as predicted targets of 59 up-regulated miRNAs. Gene ontology analysis of the miRNA-targeted genes revealed significant enrichment of skeletal pathways involved in osteoblast function, including Wnt/ β -catenin signaling. Principal component analysis identified 22 miRNAs with the greatest statistical significance ($P < 0.01$) of expression changes between non-arthritic and arthritic mice. Among these, 11 miRNAs were predicted to target numerous Wnt and BMP signaling pathway components. We validated their expression in isolated synovial fibroblasts and in whole synovium by qPCR and showed that 4 miRNAs were down-regulated by TNF. Target genes of these miRNAs, GSK3 β , Sfrp2, Tbl1

and Osx, were up-regulated at the erosion sites in bone. Among these 11 miRNAs, miR-221 was significantly up-regulated during peak inflammation. Since miR-221 is known to be upregulated in RA patients, we examined the role of miR-221 in osteoblasts. Transfection of miR-221 into primary murine calvarial osteoblasts suppressed osteoblast differentiation and mineralization. A predicted target gene of miR-221, DKK2 that is essential for bone mineralization is suppressed by miR-221 at the protein level. Tcf-1, a downstream target of Wnt signaling is also down regulated by miR-221. These results suggest that miR-221, derived from inflamed synovial tissues, regulates skeletal pathways and osteoblast differentiation in RA. Overall, our data support the hypothesis that miRNAs derived from inflamed synovium contribute to bone erosion, not only by increasing osteoclast activity, but also by inhibiting bone formation in RA.

Disclosures: Yukiko Maeda, None.

1081

Selective Antagonism of Beta 2 Adrenergic Receptor Enhances Periosteal Anabolic Response to Mechanical Stimulation in Aged Mice. Sundar Srinivasan, DeWayne Threet, Philippe Huber, Brandon Ausk, Leah Worton, Ronald Kwon, Steve Bain, Ted Gross, Edith Gardiner^{*}. University of Washington, USA

Mechanical stimulation of young bone is anabolic but the aged bone response to loading is muted. Autonomic dysregulation is common in the aged. The sympathetic nervous system (SNS) directly suppresses bone formation under physiological load through osteoblastic beta 2 adrenergic receptor (β 2AR). Pharmacological tests of a potential SNS role in the osteoblastic response to mechanical stimulation using the non-selective β AR antagonist propranolol gave equivocal results, perhaps explained by evidence that β 1AR and β 2AR mediate opposing effects on bone mechanical response *in vivo*. We therefore hypothesized that selective antagonism of only β 2AR would enhance bone mechanotransduction in senescent mice. Aged female C57 mice (22 mo) underwent a 3d/wk, 3wk cantilever bending regimen of right tibia (1700 μ e normal strain, 50 cycles/bout). Mice (4-5/group) randomly received injection of saline or the β 2AR-selective antagonist Butaxamine (3 mg/kg) 0.5 h prior to loading. Mice received calcein labels (d10, d19) for dynamic histomorphometry of the periosteal surface of both loaded (right) and contralateral (left) tibia midshafts. Neither loading nor Butax alone altered osteoblast function but there was a vigorous anabolic response to loading in the Butax treated mice, with p.MAR (+154%), p.MS (+56%) and p.BFR (+282%) all elevated in right vs left tibiae of the Butax group. Further, loading plus Butax treatment significantly augmented p.MAR, p.MS and p.BFR compared to loading plus saline injection (+165%, +59% and +223%, respectively). To estimate synergistic benefit, we determined the ratio for combined effect of load plus Butax versus additive effects of these factors. p.MAR and p.BFR were both synergistically increased, as the interaction between loading and Butax treatment was significant ($p \leq 0.05$) with ratios (combined/additive) of 21.8 and 5.0 respectively. Thus although Butax alone is not sufficient to initiate periosteal osteoblast activity in the aged mouse tibia, when Butax treatment was combined with a mildly osteogenic mechanical loading waveform, osteoblast function was elevated to levels 50% greater than previously observed in young adult mice subjected to equivalent loading. These data suggest that modest exercise preceded by Butax treatment may produce a robust anabolic response in the senescent skeleton. This treatment combination thus holds significant promise as a potential clinical intervention in osteoporosis and other low bone mass disorders.

Disclosures: Edith Gardiner, None.

1082

PHOSPHO1, a Novel Skeletal Regulator of Energy Metabolism. Karla Oldknow^{*1}, Nik Morton², Manisha Yadav³, Carmen Huesa⁴, Mathieu Ferron⁵, Gerard Karsenty⁶, Zohreh Khavandgar⁷, Anvona Guntur⁸, Vicky MacRae⁹, Monzur Murshed⁷, Calvin Vary¹⁰, Clifford Rosen¹⁰, José Luis Millán³, Colin Farquharson¹¹. ¹The Roslin Institute, The University of Edinburgh., United Kingdom, ²The University of Edinburgh, United Kingdom, ³Sanford Burnham Medical Research Institute, USA, ⁴University of West Scotland, United Kingdom, ⁵Institut de recherches cliniques de Montréal (IRCM), Canada, ⁶Columbia University Medical Center, USA, ⁷McGill, Canada, ⁸Maine Medical Center Research Institute, USA, ⁹Roslin Institute University of Edinburgh, United Kingdom, ¹⁰Maine Medical Center Research, USA, ¹¹The Roslin Institute, The University of Edinburgh, United Kingdom

Cell-specific gene deletions in mouse and human genetic studies have identified bone as an endocrine organ capable of regulating whole-body glucose metabolism. We now show that the ablation of PHOSPHO1, a bone specific phosphatase, indispensable for bone mineralization, confers a remarkable degree of protection against obesity and diabetes in mice. *Phospho1*^{-/-} mice (35 day-old) have lower blood glucose (mmol glucose/L), (WT, 9.31 \pm 0.31; *Phospho1*^{-/-}, 7.76 \pm 0.39, $p < 0.01$) and improved glucose and insulin tolerance. Food intake (g/gBW/day): WT, 0.126 \pm 0.006; *Phospho1*^{-/-}, 0.117 \pm 0.006, $p = 0.29$) and energy expenditure are comparable between

35 day-old WT and *Phospho1^{-/-}* mice fed a control diet. At this age there is no difference in BW. *Phospho1^{-/-}* mice (120 day-old) resist obesity on a high fat diet (BW: WT, 38.0±1.54 g, *Phospho1^{-/-}*, 32.4±1.26 g, p<0.05; visceral fat weight: WT, 13.2±1.34g; *Phospho1^{-/-}*, 5.56±1.61g; p<0.01). Despite a 20-fold increase in *Esp* expression (negative regulator of osteocalcin (OCN)), in *Phospho1^{-/-}* osteoblasts (osb) the serum levels of undercarboxylated OCN were normal, suggesting an OCN-independent mechanism of PHOSPHO1-regulated energy metabolism. A key marker of insulin sensitivity in bone (AKT phosphorylation) was elevated (p<0.05) in *Phospho1^{-/-}* mice following a sub-maximal *in vivo* administration of insulin (1mU/g), with no changes noted in liver, muscle and fat. *Phospho1^{-/-}* osb showed an enhanced response to mitochondrial stress parameters *in vitro*, suggestive of improved respiration and increased basal mitochondrial activity. The latter was associated with elevated GLUT4 expression. Furthermore, *Phospho1^{-/-}* osb conditioned medium (OCM), but not WT OCM increased basal insulin sensitivity (AKT and GSK phosphorylation) in WT primary osb, decreased insulin-stimulated sensitivity of INS1e cells and increased insulin stimulated sensitivity in 3T3-L1 cells. *Ucp1* expression and acute cold studies suggested a white adipose tissue browning phenotype in *Phospho1^{-/-}* mice. Mass spectrometry analysis identified >100 differentially expressed proteins in *Phospho1^{-/-}* serum associated with the regulation of glycolysis and gluconeogenesis. Furthermore, these candidates displayed enrichment for microRNA Mir34a and the transcription factor hepatocyte nuclear factor 1, both reported to regulate hepatic glucose homeostasis. These data support the notion that further, yet undefined osb derived factors contribute to whole body energy metabolism.

Disclosures: Karla Oldknow, None.

1083

Critical Role of Galanin in the Hypothalamic Neuronal Regulation of Bone Density and Energy Expenditure by AP-1 Antagonists. Anna Idelevich^{*1}, Kazusa Sato², Glenn Rowe³, Francesca Gori⁴, Roland Baron². ¹Harvard University, USA, ²Harvard Medical School, Harvard School of Dental Medicine, USA, ³Beth Israel Deaconess Medical Center, USA, ⁴Harvard Medical School, Harvard School of Dental Medicine, MGH Endocrine Unit, USA

The hypothalamus regulates whole body metabolism and the skeleton. Virus-mediated stereotaxic gene delivery of Δ FosB, a splice isoform of FosB and an antagonist of AP1, in the ventral hypothalamus (VHT) of mice increases both energy expenditure and bone density. Several hypothalamic neurons are involved in the regulation of metabolism, including the arcuate nucleus (ARC) AgRP NPY, POMC, and CART neurons, as well as ventromedial nucleus (VMN) SF1 neurons, but their specificity for energy and/or bone regulation is unknown. The aim of this study was to identify the individual AP1-responsive neuronal circuits in the VHT that mediate the metabolic and/or skeletal effects, and determine the mechanisms by which they exert their actions. For this purpose, we generated Cre-inducible lentiviral vectors expressing AP1 antagonists (Δ FosB, Δ 2 Δ FosB and DNJunD) or the AP-1 agonist FosB. The expression of these factors was restricted to specific neuronal types by stereotaxic delivery into the VHT of mice expressing Cre-recombinase under the control of neuron-specific promoters, including AgRP-Cre, CART-Cre, NPY-Cre, POMC-Cre, and SF1-Cre. Despite the classically divergent functions of CART and AgRP neurons in energy balance, AP-1 inhibition in either neuron type resulted in increased energy expenditure, lower fat mass with smaller adipocytes and higher bone density. In contrast, AP-1 blockade in SF-1 neurons reduced bone density while increasing energy expenditure, demonstrating differential regulation of bone by distinct hypothalamic nuclei. To elucidate the molecular mechanisms underlying the bone and energy effects, we analyzed VHT gene expression and identified galanin as a potential downstream target of Δ FosB. Accordingly, global deletion of galanin, VHT delivery of the galanin receptor antagonist M35 or silencing of galanin by combining Δ FosB overexpression with galanin shRNA in the same Cre-inducible vector demonstrated that VHT neuronal AP1 machinery mediates both its metabolic and bone effects via the upregulation of galanin in AgRP and/or POMC neurons.

In conclusion 1) Selective inhibition of AP-1 in one of the ARC neuronal subtypes is sufficient to stimulate total body metabolism, decrease fat and increase bone density 2) ARC, but not VMN, mediates the AP-1 inhibition-dependent increase in bone mass, and 3) Downstream of AP1 galanin acts as a central factor common to and/or affecting several types of hypothalamic neurons to regulate bone and energy.

Disclosures: Anna Idelevich, None.

1084

Osteocyte-specific ablation of Ppar γ increases bone mass and improves energy metabolism. Nicolas Bonnet^{*1}, Mirko Trajkovski², Beatrice Desvergne³, Serge Ferrari⁴. ¹University Geneva Hospital (HUG), Switzerland, ²Laboratoire des maladies métaboliques, Medical faculty, University of Geneva, Switzerland, ³Center for integrative Genomics, Faculty of Biology & Medicine, University of Lausanne, Switzerland, ⁴Service des Maladies Osseuses, Medical faculty, University of Geneva, Switzerland

Ppar γ is a master transcriptional regulator of energy metabolism, and both Ppar γ haploinsufficient mice and osteoblast-targeted Ppar γ -deficient mice have increased bone mass and osteoblastogenesis. Here we investigated the role of Ppar γ in late osteoblast/osteocytes (ocy) on bone (re)modeling and energy metabolism. For this purpose Ppar γ -loxP were crossed with Dmpl-cre mice to generate Ocy-Ppar γ -/- (KO) and -Ppar γ /+ (WT) male mice. Tissue and cell specificity of Ppar γ deletion were confirmed by western blot and immunostaining. Metabolic rate and tissue temperature were evaluated by labmaster system and infrared camera. At 3 months of age, total body lean and fat mass, handgrip strength as well as glucose tolerances test (GTT) were comparable in KO and WT. However femoral BMD was significantly higher in KO (78.6±1.3 vs 73.4±2.1mg/cm² in WT, p<0.001). Trabecular and cortical microstructure respectively evaluated at the distal and midshaft femur was improved in KO: BV/TV +28.6%, TbTh +12.5%, CtTV +9.8%, CtBV +12.0% and CtTh +4.5% compared to WT (all p<0.05). Periosteal BFR was higher in KO (+66.5% vs Ppar γ /+, p<0.05), whereas no significant differences were observed at endocortical surfaces. In contrast CTx was decreased in KO (8.6±0.6 vs 12.9±0.5ng/ml in WT, p<0.001). From 3 to 9 months of age, BMD did not further increase in KO but remained higher compared to WT (89.9±2.1 vs 80.6±1.7mg/cm², p<0.001). Age-related changes in fat and lean mass were attenuated in KO (total fat +11.1% and lean -1.9% vs +30.8% and -6.1% respectively in WT, p<0.01). At 9 months of age, handgrip strength, VCO₂/VO₂ and heat production were higher in KO (+33.2%, +4.3% and +13.7% vs WT, p<0.001) without significant differences in food intake. Body temperature was also higher, particularly in the BAT-rich neck region, and in the limbs, i.e musculo-skeletal region (respectively +4.3% and +3.8% vs WT, p<0.001). As a result, GTT was improved in the KO mice (AUC-38.4% vs WT, p<0.01). In conclusion, Ocy-specific ablation of Ppar γ increased periosteal bone formation and lowered bone turnover, resulting in high bone mass from a younger age. Moreover, Ppar γ expression in osteocytes regulates respiratory exchange ratio and metabolic rate, causing age-related changes in body composition and glucose homeostasis. These observations suggest a role for Ocy-Ppar γ in diabetes bone disease. What component of osteocyte is responsible for the metabolism energy effect of Ppar γ remains to be determined.

Disclosures: Nicolas Bonnet, None.

1085

Fibrillin-1 Regulates Skeletal Stem Cells Fate Determination through Modulation of Local TGF β . Silvia Smaldone^{*1}, Francesco Ramirez². ¹Mount Sinai School of Medicine, USA, ²Ichan School of Medicine at Mount Sinai, USA

A full understanding of the microenvironmental factors controlling the activities of skeletal stem cells (a.k.a., mesenchymal stem cells [MSCs]) in the adult bone marrow holds great promise for developing new therapeutic strategies to mitigate age-related diseases of bone and cartilage degeneration. Bone loss is an understudied manifestation of Marfan syndrome (MFS), a multisystem disease associated with mutations in the extracellular matrix protein and TGF β modulator fibrillin-1. Previous characterization of osteopenia in mice with MFS has implied that fibrillin-1 restricts osteoblast maturation and TGF β driven, osteoblast-dependent, osteoclastogenesis. As MFS mice die from ruptured aneurysm at ~3 month of age, osteopenia progression was studied in mice with conditional inactivation of Fbn1 gene in the developing limbs (*Fbn1^{Prx1-/-}* mice). Longitudinal studies showed that progressive bone loss in *Fbn1^{Prx1-/-}* mice is accounted for by decline of bone formation, secondary to premature depletion of MSCs, combined with constitutively enhanced bone resorption. Significant paucity of marrow adipose tissue in the long bones of *Fbn1^{Prx1-/-}* mice, together with reduced adipogenic potential of cultured marrow cells, suggested an additional defect in MSC differentiation. The finding that an *Fbn1*-silenced osteoprogenitor cell line cultured in adipogenic induction media, yielded fewer than normal adipocytes and exhibited relatively lower PPAR γ levels corroborated this postulate. Consonant with fibrillin-1 modulation of TGF β bioavailability, cultures of marrow stromal cells from *Fbn1^{Prx1-/-}* limb bones showed greater activation of normal amounts of latent TGF β . In line with this finding, systemic TGF β neutralization improved bone mass and trabecular microarchitecture along with normalizing the number of MSCs, osteoprogenitor cells and marrow adipocytes. Lastly, reduced frequency of hematopoietic stem cells (HSC) in bone marrow of adult *Fbn1^{Prx1-/-}* mice, which *in vitro* co-culture experiments with WT GFP-CD45+ cells correlated to fibrillin-1 deficient stroma, suggested that fibrillin-1 constitute an essential structural component of the bone marrow niche. Collectively our findings advance the current understanding of MSC biology, which are necessary for improving regenerative therapies to ameliorate the conditions of patients affected by skeletal disorders.

Disclosures: Silvia Smaldone, None.

1086

MiR-144 Inhibits Tumor Growth and Metastasis in Osteosarcoma via Targeting ROCK1. Jing Li^{1*}, Xiaoling Zhang², Kerong Dai³, Qian Chen⁴.

¹Department of Orthopaedics, Alpert Medical School/Rhode Island Hospital, Brown University, USA, ²The Key Laboratory of Stem Cell Biology, Institute of Health Sciences, Shanghai Institutes for Biological Sciences, Chinese Academy of Sciences & Shanghai Jiao Tong University School of Medicine, China, ³Shanghai Key Laboratory of Orthopaedic Implant, Department of Orthopaedic Surgery, Shanghai Ninth People's Hospital, Shanghai Jiao Tong University School of Medicine, China, ⁴Brown University School of Medicine, USA

Abstract

Purpose

Osteosarcoma (OS) is the most prevalent bone tumor in children and young adults. Several miRNAs have been found expressed differentially in osteosarcoma, thus their function may be implicated in the onset and progression of osteosarcoma. Previous studies have shown that Rho-associated, coiled-coil containing protein kinase 1 (ROCK1), a pivotal downstream effector of RhoA/ROCK signaling pathway, is strongly upregulated in osteosarcoma clinical specimens and may be a therapeutic target of this disease. We wondered whether the deregulation of ROCK1 was associated with miRNA regulation.

Methods

The expression levels of miR-144 and ROCK1 in osteosarcoma cell lines and clinical samples were quantified by quantitative real-time PCR and Western blotting. The effect of miR-144 on migration and invasion was measured by wound healing assay and transwell migration assay. Cell cycle distribution was analyzed by flow cytometry. Human osteosarcoma cells were injected into the tibia of athymic mice to induce a tumor. One week after injection, mice were treated by way of multi-point intratumoral injection of miR-144 twice a week. Tumor growth was monitored over time using an in vivo imaging system. Tumors and lungs were harvested at sacrifice for real-time PCR and immunohistochemical staining.

Results

In this study, we found that miR-144 was downregulated in both osteosarcoma cell lines and clinical specimens. ROCK1 was identified as a direct target of miR-144. Overexpression of miR-144 decreased the protein levels of ROCK1 and then influenced the signal transduction of RhoA/ROCK signaling pathway. miR-144 suppressed the proliferation of OS cells by mediating the expression of cell-cycle regulatory molecules and by arresting cells in the G0/G1 phase of the cell cycle. Both migration and invasion of OS cells was inhibited by miR-144. Furthermore, miR-144 intratumoral administration in mice reduced the tumor size and pulmonary metastasis, and prolonged the survival time of tumor-bearing mice.

Conclusions

We reveal for the first time that overexpression of miR-144 represses osteosarcoma cell growth and tumorigenesis, and inhibits osteosarcoma cell migration and pulmonary metastasis. These findings suggest that miR-144, which is downregulated in osteosarcoma, may contribute to osteosarcoma pathogenesis by targeted inhibition of ROCK1 both in vitro and in vivo, and could be a new therapeutic approach for the treatment of disease.

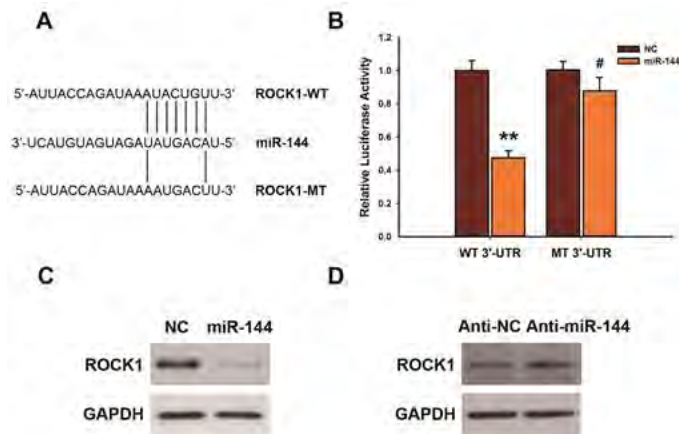


Figure 1

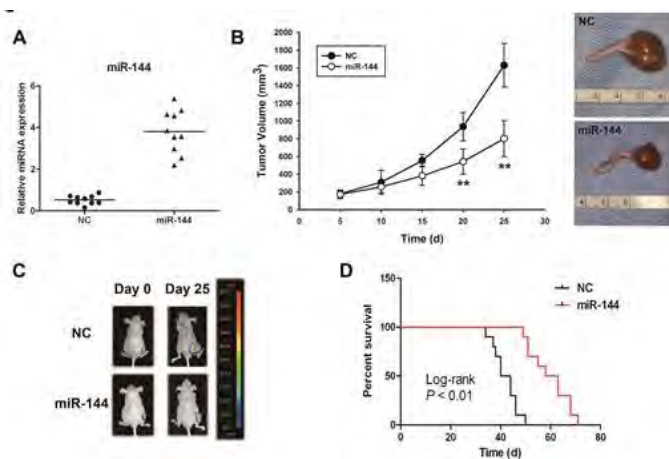


Figure 2

Disclosures: Jing Li, None.

1087

Vitamin D Status and Bone Mineralization: A Histomorphometric Analysis.

Neil Binkley^{1*}, Joan Lappe², KM Davies³, Robert Recker². ¹University of Wisconsin, Madison, USA, ²Creighton University Osteoporosis Research Center, USA, ³Creighton University Osteoporosis Research Program, USA

Background: How to define vitamin D insufficiency is controversial. Vitamin D deficiency impairs bone mineralization. As such, it is reasonable that histomorphometric evidence of mineralization impairment could be used to define vitamin D insufficiency. Indeed, a prior report from cadaveric specimens found osteoid minimization when serum 25(OH)D was ≥ 30 ng/mL. However, it is not known if blood 25(OH)D levels obtained at autopsy are directly comparable to ante-mortem values. Additionally, autopsy specimens (given their absence of tetracycline labeling) do not allow assessment of dynamic variables. Here we report the association of serum 25(OH)D with bone histomorphometric data in postmenopausal women early in menopause.

Methods: 50 women participated in a study evaluating the effect of menopause on histomorphometric variables (previously reported) had transiliac bone biopsies performed 12 months after their last menses. Oral tetracycline was administered prior to transiliac biopsy, which was performed and evaluated in standard manner. In addition to static histomorphometry, dynamic parameters were determined including bone formation rate/bone surface (BFR/BS) calculated as mineral apposition rate (MAR) corrected for obliquity times mineralizing surface/bone surface (MS/BS). MS/BS is the mineralizing surface divided by the total trabecular surface. Activation frequency (Ac.f), the annual probability of new remodeling site activation, was calculated as (BFR/BS)/wall thickness where wall thickness is the mean distance between cement lines (corrected for obliquity) and trabecular surface. Serum 25(OH)D was measured by RIA or competitive protein binding assay. Correlations between histomorphometric results and 25(OH)D were performed using Excel.

Results: Static histomorphometric parameters (osteoid thickness, osteoid volume/bone volume and osteoid surface) were unrelated to 25(OH)D (data not shown). In contrast, MS/BS (figure a) and Ac.f (figure b) were positively correlated ($p < 0.05$) with 25(OH)D concentration.

Conclusion: The increase in bone remodeling seen in early postmenopausal women is strongly dependent on serum 25(OH)D. The mechanism(s) underpinning these results, and the optimal value to facilitate bone mineralization, remain to be defined. Further study of the relationship of dynamic bone parameters with circulating vitamin D metabolites is needed.

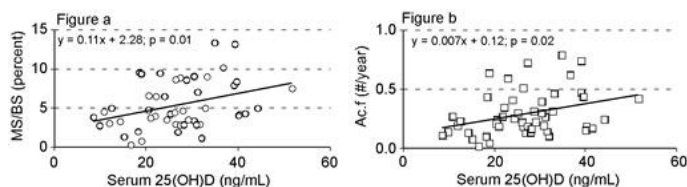


Figure a and b

Disclosures: Neil Binkley, None.

Interactions of Genetic Variants and Vitamin D Intake on Serum Vitamin D Level: A large-Scale Genome-Wide Association Meta-analyses in Caucasians from the SUNLIGHT Consortium. Yi-Hsiang Hsu^{*1}, Hugues Aschard², Alana Cavadin³, Alexis Frazier-Wood⁴, Brent Richards⁵, Carola Zillikens⁶, Caroline Hayward⁷, Chiao-Feng Lin⁸, Ching-Ti Liu⁹, David Karasik⁸, Denise Houston¹⁰, Diane Berry¹¹, Elina Hypponen¹¹, Evropi Theodoratou¹², Guillaume Pare¹³, Harry Campbell¹², Jill McDonald¹⁴, Jim Wilson¹², John Todd¹⁵, Karl Michaelsson¹⁶, Klaus Badenhoop¹⁷, Kurt Lohman¹⁸, L. Adrienne Cupples¹⁹, Leo-Pekka Lytikainen²⁰, Lina Zgaga¹², Marcus Kleber²¹, Maria Timofeeva²², Marjo-Riitta Jarvelin²³, Mika Kahonen²⁰, Olli Raitakari²⁴, Pamela Lutsey²⁵, Ronald Booi²⁶, Rui Li²⁷, Stefan Pilz²⁸, Steve Kritchinsky¹⁰, Terho Lehtimäki²⁰, Vera Mikkilä²⁹, Winfried Maerz³⁰, Thomas Wang³¹, Peter Kraft², Douglas Kiel³². ¹HSL Institute for Aging Research, Harvard Medical School, USA, ²Dept. Epidemiology, Harvard School of Public Health, USA, ³Queen Mary, University of London, United Kingdom, ⁴Department of Pediatrics, Baylor College of Medicine, USA, ⁵McGill University, Jewish General Hospital, Departments of Medicine, Human Genetics, Epidemiology & Biostatistics, Canada, ⁶Erasmus Medical Center, Department of Internal Medicine, Netherlands, ⁷MRC Human Genetics Unit MRC IGMM, University of Edinburgh Western General Hospital, United Kingdom, ⁸Hebrew SeniorLife Institute for Aging Research, USA, ⁹Dept. Biostatistics, Boston University, USA, ¹⁰Wake Forest University School of Medicine, USA, ¹¹Univ. College London Institute of Child Health, United Kingdom, ¹²Centre for Population Health Sciences, The University of Edinburgh, College of Medicine & Veterinary Medicine, United Kingdom, ¹³McMaster University Clinical Epidemiology & Biostatistics, Canada, ¹⁴Harvard School of Public Health, USA, ¹⁵University of Cambridge, JDRF/WT Diabetes & Inflammation Laboratory, United Kingdom, ¹⁶Department of Surgical Sciences, Uppsala University, Sweden, ¹⁷University of Frankfurt am Main, Germany, ¹⁸Division of Public Health Sciences, Department of Biostatistical Sciences, Wake Forest School of Medicine, USA, ¹⁹Dept. Biostatistics, Boston Univ., USA, ²⁰School of Medicine, University of Tampere, Finland, ²¹Medical Faculty of Mannheim, University of Heidelberg, Germany, ²²The MRC Institute of Genetics & Molecular Medicine at The University of Edinburgh, United Kingdom, ²³Faculty of Medicine, School of Public Health, Imperial College London, United Kingdom, ²⁴Department of Clinical Physiology, University of Turku, Finland, ²⁵Epidemiology & Community Health, University of Minnesota, USA, ²⁶Biomedical Imaging Group, Erasmus Medical Center, Netherlands, ²⁷Genetic epidemiology, McGill University, Canada, ²⁸Medical University of Graz, Austria, ²⁹Division of Nutrition, University of Helsinki, Finland, ³⁰Synlab Center of Laboratory Diagnostics Heidelberg GmbH, Germany, ³¹Division of Cardiovascular Medicine, Vanderbilt University Department of Medicine, USA, ³²Hebrew SeniorLife Institute for Aging Research & Harvard Medical School, USA

Vitamin D plays a complex role in calcium homeostasis, PTH regulation, and promotion of overall health. Maintenance of serum 25(OH)D₃ levels may be critical to skeletal health, cardiovascular health as well as lower mortality rate. A wide range of factors influence the intake, production, and metabolism of vitamin D and thereby contribute to serum 25(OH)D₃ levels. High heritability (70%) of 25(OH)D₃ levels suggests that genetic factors also play a role. The serum response to vitamin D intake is quite variable suggesting that both genetics and environment factors may involve an individual's handling of dietary vitamin D. To investigate the interaction between genetic variants and Vitamin D intake on serum 25(OH)D₃ concentration, we performed a genome-wide association (GWAS) meta-analysis in 34,915 Caucasian men and women using data obtained from 16 cohort studies. Single nucleotide variants (SNVs) were genotyped and un-genotyped SNVs were imputed based on HapMap II project with a total of 2.5M SNVs available for analyses. In each study, we performed a multiple linear regression analyses to estimate the genetic effect of each single SNV and their interaction with vitamin D intake on serum 25(OH)D₃ concentration. Covariates included age, sex, BMI, season of vitamin D measurement and ancestral genetic background. We considered two statistical tests for interactions, (1) a 1 degree of freedom test of the interaction term only (SNVs-Vitamin D intake); and (2) a 2 degrees of freedom joint test of SNVs main effect and the interaction term. An inverse-variance fixed effect meta-analysis was used to combine results from 16 studies. Several genome-wide significant associations ($p < 5 \times 10^{-8}$) with serum 25(OH)D₃ concentration were found for SNVs located in or near *AMDHD1*, *CYP24A1*, *DHCR7*, *GC* and *NADSYN1* genes. We identified several genome-wide significantly associated SNVs ($p < 5 \times 10^{-8}$) potentially interacting with vitamin D intake. These SNVs are located in or near *AMDHD1*, Chr9 *LOC101929563*, *CHD11AP2A2*, *CYP2R1*, *FAR2*, *KLF7*, *LPIN1* and *SEM6A* genes. In summary, our analysis identified potential SNVs-vitamin D intake interactions, suggesting the relationships between vitamin D intake and serum

25(OH)D₃ concentration may be mediated by genetic variation. To validate these findings, a replication study in independent samples is underway.

Disclosures: Yi-Hsiang Hsu, None.

1089

Effects of High Dose Vitamin D Supplementation on Bone metabolism in Pregnant Women with Hypovitaminosis D – a Randomized Controlled Trial. Gitte Bloch Rasmussen^{*1}, Leif Mosekilde², Tanja Sikjaer³, Peter Vestergaard⁴, Lene Heickendorff⁵, Niels Ulbjerg⁶, Bente Langdahl², Lars Rejnmark³. ¹Aarhus Universitetshospital, Denmark, ²Department of Endocrinology & Internal Medicine, Aarhus University Hospital., Denmark, ³Department of Endocrinology & Internal Medicine, Aarhus University Hospital, Denmark, ⁴Department of Endocrinology, Aalborg University Hospital, Denmark, ⁵Department of Clinical Biochemistry, Aarhus University Hospital, Denmark, ⁶Department of Obstetrics & Gynecology, Aarhus University Hospital., Denmark

Purpose: To study the effects of supplementation with high doses of vitamin D during pregnancy on maternal bone metabolism.

Methods: The study was designed as an investigator-initiated double-blind, randomized, placebo-controlled, parallel-group trial. Women, aged 20-40 years, with P-25OHD < 50 nmol/L all planning pregnancy (N=193), were randomized to a daily supplementation with 70 µg (2800 IU), 35 µg (1400 IU) vitamin D₃ (VitD₃), or placebo. Supplementation was initiated before conception and continued until 16 weeks post partum (PP). Main outcome measures were bone mineral density (BMD) and trabecular bone score (TBS) as assessed by DXA scans at time of inclusion and four months PP. Biochemical markers of bone turnover were measured every three months throughout the study.

Results: A total of 90 women gave birth. Vitamin D supplementation did not affect birth weight. In response to supplementation, P-25OHD levels increased dose-dependently reaching a peak level at the time of giving birth of 118 ± 29 in the 70 µg/day group, 98 ± 32 in the 35 µg/day group, and 60 ± 23 in the placebo group. Four months PP, most women 86% were breast feeding their infants with no differences between groups. Biochemical measurements and paired BMD were available from respectively 84 and 68 women who completed the trial. Within each of the three supplemented groups, BMD at most sites and TBS were significantly decreased 16 weeks after giving birth compared with the pre-pregnancy measurement ($p < 0.001$). Changes in BMD from pre-pregnancy to 16 weeks PP did not differ between groups at the lumbar spine ($p=0.51$), total hip ($p=0.35$), whole body ($p=0.31$), or for TBS ($p=0.52$). At the femoral neck BMD decreased 4.8% in the women treated with 70 µg VitD₃ daily compared to placebo ($p=0.03$). In contrast, the mid distal forearm BMD increased significantly 0.6% in the group treated with 70 µg VitD₃ group compared with the placebo group ($p=0.03$). Changes in plasma levels of bone turnover markers during pregnancy and breast feeding did not differ significantly between groups.

Conclusion: Pregnant women with vitamin D insufficiency experienced no major beneficial effects of high dose vitamin D supplementation. The pregnancy associated decrease in BMD was not prevented by vitamin D supplementation. Our finding of an aggravated BMD loss at the femoral neck in response to a daily supplement of 70 µg VitD₃ calls for caution on use of high dose vitamin D supplementation during pregnancy.

Disclosures: Gitte Bloch Rasmussen, None.

1090

A randomized, double-blind, placebo-controlled clinical trial on the treatment of vitamin D insufficiency in postmenopausal women. Karen Hansen^{*1}, R. Erin Johnson², Kaitlin Chambers³, Michael G. Johnson³, Christina C. Lemon³, Tien Nguyen Thuy Vo³, Sheeva Marvdashti³. ¹University of Wisconsin, Us, ²St. Lukes Hospital, USA, ³University of Wisconsin, USA

Experts debate optimal 25(OH)D levels for musculoskeletal health. We designed a clinical trial to directly address this controversy. We performed a randomized, double-blind, placebo-controlled clinical trial in postmenopausal women with 25(OH)D levels 14-27 ng/mL by HPLC. We excluded women >75 years old, with hypercalcemia, nephrolithiasis, cancer within five years (excluding skin cancer), malabsorption, glomerular filtration rate <45 mL/minute, adult fragility fracture of the hip, spine or wrist, spine or hip T-score <-2.49, use of bone-active medications within the past 6 months including bisphosphonates, estrogens, calcitonin, teriparatide, oral corticosteroids, anticonvulsants, or vitamin D intake >400 IU/day. The high-dose vitamin D arm received a loading dose (50,000 IU daily x 15 days) to quickly raise 25(OH)D >30 ng/mL, with sham loading of yellow placebo capsules in other arms to maintain blinding. After loading, subjects in the high-dose arm took vitamin D 50,000 IU every 15th day for one year, the low-dose arm took vitamin D 800 IU daily and yellow placebo capsules every 15th day, and the placebo arm ingested daily white placebo and every 15th day yellow placebo capsules. Outcomes were the between-arm one-year changes in total fractional calcium absorption, spine, hip and total body bone mineral density and trabecular bone score. We also measured Timed-Up-and-Go and 5-Sit-to-Stand tests and pain (visual analog scale) at 0, 30, 60, 120, 240 and 365 days. We performed Bonferonni correction of p-values for multiple statistical comparisons. After controlling for baseline absorption, total fractional calcium

absorption increased 1% (10 mg/day) in the high-dose arm, but decreased 2% in low-dose (p=0.005 vs. high-dose) and decreased 1.3% placebo (p=0.03 vs. high-dose) arms. We found no between-arm changes in spine, total hip, mean femoral neck or total body bone mineral density, trabecular bone score or Timed-Up-and-Go score. When controlling for pain, the high-dose arm had the greatest improvement in the 5-sit-to-stand test score vs placebo (p=0.02), but the absolute change (0.4 seconds) was not clinically significant. Hypercalciuria occurred 7 (4 subjects), 1 and 1 times in the high-dose, low-dose and placebo arms (p=0.19). High-dose vitamin D therapy increased calcium absorption but the effect was small and did not translate into changes in bone mineral density. Study results do not support recommendations to maintain serum 25(OH)D levels at or above 30 ng/mL. Instead, our study results support the Institute of Medicine's conclusion that vitamin D repletion is a serum 25(OH)D level of =20 ng/mL.

Disclosures: Karen Hansen, None.

1091

A Randomized Trial Investigating Impact of Vitamin D Replacement on Indices of Insulin Resistance in Elderly Overweight Subjects. Ghada El-Hajj Fuleihan*¹, Rafic Baddoura², Georges Halabi², Asma Arabi³, Robert Habib³, Maya Rahme³, Singh Ravinder⁴, Moustapha Kassem⁵, Ziyad Mahfoud³, Rose Daher³, Mohamad Kassir³. ¹American University of Beirut-Medical Center, Lebanon, ²Hotel Dieu de France, Lebanon, ³American University of Beirut, Lebanon, ⁴Mayo Clinic, USA, ⁵Odense University Hospital, Denmark

Introduction: Hypovitaminosis D, obesity and diabetes are prevalent in the Middle East, but the impact of vitamin D replacement on indices of insulin resistance, in subjects from this region is unclear.

Objective:

To investigate in a randomized clinical trial (RCT) the impact of high dose vitamin D compared to the Institute of Medicine (IOM) recommended daily allowance (RDA) on indices of insulin resistance in overweight elderly ambulatory individuals.

Methods:

This is a one year, double blind, multicenter RCT of 257 subjects, randomized by center and gender, to calcium citrate 1000 mg and the equivalent of 600IU or 3500 IU of vitamin D3 daily. Exclusion criteria were the presence of diabetes, defined by a fasting blood sugar exceeding 126 mg/dl, or a hemoglobin A1C exceeding 6.4%, the intake of oral hypoglycemic agents, of GFR<30 ml/min, or the presence of severe chronic illnesses. Routine biochemistries, hormonal levels, serum hydroxyvitamin D (25OHD, by LCMS) were measured at entry, 3, 6 and 12 months. The primary outcomes were indices of insulin resistance: McCauley, HOMA and QUICKI. The study had a power of 80%, to pick up a delta in HOMA between the 2 groups of 0.9 (SD 2.1), p=0.05. Numbers represent mean (SD).

Results:

222 subjects completed the study, age 71(4) years, BMI 30 (4) kg/m², 31% were normal, and 69% had impaired fasting glucose or abnormal HgA1C, 55% were female subjects, 45% were on anti-hypertensive, and 30% on lipid lowering drugs. Baseline clinical and biochemical characteristics were comparable between the two groups. 25OHD rose from 20(7) to 26 (6.9) ng/ml in the low-dose, and from 20.9(8.2) to 35.9 (9.8) ng/ml in the high-dose arm, p<0.0001 within and between arms at 1 year. There was a significant rise in FBS within each group, a rise that was not explained by any drift in laboratory performance over the study period, nor by the intake of statins. There were no detectable differences in FBS, nor in any of the indices of insulin resistance, between the two groups at one year (Table). In the multivariate analyses, BMI, but not vitamin D treatment or age, predicted insulin sensitivity indices at one year.

Conclusion:

High dose vitamin D did not improve insulin resistance in elderly overweight individuals. Regardless of the vitamin D dose, an unexpected rise in fasting glucose, that correlated with the rise in 25OHD, and exceeded the anticipated rise in FBS in an aging overweight population, was observed.

Table: Indices of glycemia and insulin resistance in high dose and low dose arms at entry and 1 year.

| | High Dose | | Low dose | |
|--------------------------|-------------|--------------|-------------|---------------|
| | Baseline | 12 months | Baseline | 12 months |
| BMI (kg/m ²) | 30.5±4.3 | 30.6±4.6 | 29.8±4.5 | 29.7±4.7 |
| FBS (mg/dl) | 94.1 ± 9.6 | 99.6 ± 12* | 93.4 ± 9.3 | 97.2 ± 13.3* |
| HbA1c | 5.8 ± 0.3 | 5.8 ± 0.4 | 5.8 ± 0.3 | 5.8 ± 0.4 |
| Triglyceride (mg/ml) | 133.9±69.6 | 139.7±75.8 | 133.8±70.5 | 132.4±62 |
| Insulin (pmol/L) | 76.5 ± 42 | 75.7 ± 36.9 | 70.6 ± 53 | 73.5 ± 52.7 |
| McAuley ³ | 6.84 ± 1.4 | 6.82 ± 1.5 | 7.12 ± 1.6 | 6.93 ± 1.4 |
| HOMA ² | 2.54 ± 1.5 | 2.66 ± 1.5 | 2.30 ± 1.8 | 2.50 ± 2 |
| QUICKI ¹ | 0.34 ± 0.02 | 0.33 ± 0.026 | 0.34 ± 0.02 | 0.34 ± 0.026* |

*p<0.05 within groups baseline and 12 months
 †p<NS independent t-test for all variables, at 12 months low dose vs. high dose
 ‡ (McAuley's Index, $\exp[2.62 - 6.28 \ln(\text{insulin in micromoles per millilitre})] - 0.31 \ln(\text{triglycerides in millimoles per litre})$)
 § (McAuley et al. Diabetes care 2001)
 †† HOMA2s: $[\text{glucose in milligrams per deciliter}] \times \text{insulin in micromoles per millilitre} / 405$ (Matthews et al. Diabetologia 1985)
 ‡‡ (QUICKI): $1 / [\log(\text{glucose in milligrams per deciliter}) + \log(\text{insulin in micromoles per millilitre})]$ (Katz et al. JCEM 2000)
 Conversion: Insulin: $\mu\text{U/mL} \times 1.378 = \text{pmol/L}$
 Triglycerides: $\text{mg/dL} \times 0.0113 = \text{mmol/L}$ (Dilbert A. Fisher et al. Endocrinology Test Selection and Interpretation 2nd edition)

(Table)

Disclosures: Ghada El-Hajj Fuleihan, None.

1092

The Effects of a Longer-Term, Low-Protein Diet on Calcium Absorption and Kinetic Measures of Bone Turnover in Young Women. Jessica Bihuniak*¹, Rebecca Sullivan², Tania Huedo-Medina¹, Irina Rosewater³, Donna Caseria⁴, Kimberly O'Brien⁵, Jane Kerstetter¹, Karl Insogna². ¹Allied Health Sciences, University of Connecticut, USA, ²Internal Medicine Endocrinology, Yale University, USA, ³Internal Medicine Endocrinology, Yale University, USA, ⁴Yale New Haven Hospital, USA, ⁵Cornell University, USA

Increasing dietary protein causes a rise in urine Ca (UCa) while with restricted protein intakes less Ca appears in the urine. Balance studies in the 1970's indicated no change in intestinal Ca absorption as dietary protein increased, which led to the conclusion that the increase in UCa was due to loss of skeletal Ca. However, we have found that in the short term, increasing dietary protein from 1.0 to 2.1 g/kg results in an increase in UCa that is not accompanied by increased bone resorption. Instead the increase in UCa can be nearly quantitatively explained by a concomitant increase in intestinal Ca absorption. Moreover, we recently reported that long-term whey protein supplementation in older adults with adequate protein intakes is not detrimental to bone.

Dietary protein studies have largely focused on the impact of increasing dietary protein on Ca economy. The long-term consequences of low protein intakes on Ca metabolism have been less well studied. The purpose of this study was to use stable Ca isotopes to accurately quantify the longer-term consequences of a protein-restricted diet on Ca absorption and bone turnover. We studied 11 premenopausal women consuming a low protein diet (0.7 g/kg) for 6.5-weeks and assessed Ca absorption and kinetics measures of bone turnover at day 5 (acute changes) and week 6 (new steady state). Mixed-effects longitudinal modeling was conducted with time (i.e. visit) as the fixed effects for each of the continuous dependent variables. Data are expressed as β -coefficient (95% CI). Restricting dietary protein for 6.5-weeks resulted in significant declines in intestinal calcium absorption (%) [-0.43 (-0.77,-0.09); P=0.02] as well as the percent of UCa from the diet [-0.13 (-0.22,-0.04); P=0.01]. This was accompanied by an increase in the fraction of UCa originating from bone [0.13 (0.04,0.22); P=0.01] and increases in serum PTH (pmol/L) [0.18 (0.02,0.33); P=0.03]. We also observed a trend towards more negative bone balance (mmol Ca) [-0.15 (-0.33,0.02); P=0.08].

These data indicate that a diet low in protein, defined as an intake level below the current RDA (0.8 g/kg), causes calcium malabsorption, a rise in PTH and a larger contribution of bone to UCa. In the aggregate, these findings are consistent with the conclusion that a protein-restricted diet induces unfavorable changes in Ca economy in young women.

Disclosures: Jessica Bihuniak, None.

1093

Reference Ranges and Characteristics of Spine Bone Mineral Apparent Density in U.S. Children – Results from the Bone Mineral Density in Childhood Study. Babette Zemel^{1*}, Karen Winer², Andrea Kelly³, Joan Lappe⁴, John Shepherd⁵, Sharon Oberfield⁶, Vicente Gilsanz⁷, Heidi Kalkwarf⁸. ¹Children’s Hospital of Philadelphia, USA, ²NICHHD, USA, ³The Children’s Hospital of Philadelphia, USA, ⁴Creighton University, USA, ⁵University of California San Francisco, USA, ⁶Columbia University, USA, ⁷Children’s Hospital Los Angeles, USA, ⁸Cincinnati Children’s Hospital & Medical Center, USA

The 2014 ISCD Pediatric Positions Statement recommended height Z-score adjusted (HtZ-adj) bone Z-scores or spine bone mineral apparent density (BMAD) for clinical assessment of bone health in children, especially for those with short stature. Low spine BMAD has been associated with increased fracture risk in children with health conditions that threaten bone health, but reference ranges for U.S. children are not available.

The main objective of this study was to develop spine BMAD reference ranges for African American (AfrAm) and Non-African American (non-AfrAm) youth, ages 5 to 20 years. In addition, we aimed to determine (a) whether this measure minimized the distorting effects of short or tall stature on spine bone density; and (b) whether it was a stable measure (tracked well) over time in comparison to the HtZ-Adj spine BMD-Z and unadjusted spine BMD-Z.

We used data from the Bone Mineral Density in Childhood Study, a mixed longitudinal cohort of healthy children, ages 5 to 20 years, from 5 U.S. centers followed over 6 years (~10,000 observations). Spine scans were acquired on Hologic densitometers (QDR4500/Delphi/Discovery models). Height Z-scores (HtZ) were calculated using the CDC2000 growth charts. Tanner stage was assessed by physical exam. LMS Chartmaker was used to create reference ranges separately for AfrAm and non-AfrAm males and females. For each group, Pearson correlations were used to (1) evaluate associations between spine Z-scores and HtZ; and (2) assess the stability of spine Z-scores during growth, by calculating the “tracking correlations” for children in Tanner stages 1 and 2 at baseline with their year 6 values.

Smoothed reference percentile values for BMAD are shown in Table 1. Correlations between HtZ and BMAD Z-scores ranged from 0.00 to 0.13; the range for HtZ-adj BMD-Z was -0.02 to -0.27, and both were lower than for unadjusted spine BMD Z (0.25 to 0.35) across sex and ancestry groups. The range of tracking correlations from baseline to year 6 for puberty stages 1 and 2 was similar for all Z-scores (range BMAD-Z: 0.61 to 0.79; HtZ-adj BMD-Z: 0.73 to 0.81; unadjusted Spine BMD-Z: 0.61 to 0.79). Both BMAD-Z and HtZ-adj BMD-Z correct for effects of short and tall stature on spine BMD Z-scores and track well over time. BMAD is more easily computed than HtZ-adjBMD. These findings support the use of spine BMAD for assessment of bone health in children.

| Spine Bone Mineral Apparent Density | | | | | | | | | | |
|-------------------------------------|------------------|-------|-------|-------|-------|----------------------|-------|-------|-------|-------|
| age | African American | | | | | Non-African American | | | | |
| | L | S | 2nd | 50th | 98th | L | S | 2nd | 50th | 98th |
| Females | | | | | | | | | | |
| 5 | 0.746 | 0.130 | 0.147 | 0.197 | 0.250 | -0.707 | 0.125 | 0.145 | 0.183 | 0.241 |
| 6 | 0.746 | 0.130 | 0.148 | 0.198 | 0.251 | -0.651 | 0.128 | 0.145 | 0.183 | 0.241 |
| 7 | 0.746 | 0.129 | 0.150 | 0.200 | 0.253 | -0.578 | 0.128 | 0.145 | 0.184 | 0.242 |
| 8 | 0.746 | 0.129 | 0.152 | 0.202 | 0.255 | -0.450 | 0.127 | 0.146 | 0.186 | 0.243 |
| 9 | 0.746 | 0.127 | 0.155 | 0.205 | 0.259 | -0.225 | 0.128 | 0.147 | 0.189 | 0.246 |
| 10 | 0.746 | 0.126 | 0.161 | 0.212 | 0.267 | 0.116 | 0.130 | 0.149 | 0.194 | 0.251 |
| 11 | 0.746 | 0.123 | 0.171 | 0.224 | 0.281 | 0.494 | 0.132 | 0.154 | 0.204 | 0.261 |
| 12 | 0.746 | 0.120 | 0.184 | 0.239 | 0.299 | 0.732 | 0.131 | 0.163 | 0.218 | 0.277 |
| 13 | 0.746 | 0.117 | 0.197 | 0.255 | 0.316 | 0.716 | 0.124 | 0.178 | 0.234 | 0.295 |
| 14 | 0.746 | 0.114 | 0.209 | 0.268 | 0.331 | 0.536 | 0.114 | 0.194 | 0.248 | 0.308 |
| 15 | 0.746 | 0.112 | 0.217 | 0.277 | 0.341 | 0.328 | 0.107 | 0.206 | 0.257 | 0.316 |
| 16 | 0.746 | 0.110 | 0.223 | 0.284 | 0.348 | 0.160 | 0.102 | 0.213 | 0.262 | 0.321 |
| 17 | 0.746 | 0.108 | 0.228 | 0.289 | 0.353 | 0.049 | 0.099 | 0.218 | 0.266 | 0.324 |
| 18 | 0.746 | 0.108 | 0.231 | 0.292 | 0.356 | -0.015 | 0.098 | 0.220 | 0.268 | 0.326 |
| 19 | 0.746 | 0.107 | 0.233 | 0.294 | 0.358 | -0.047 | 0.097 | 0.222 | 0.269 | 0.327 |
| 20 | 0.746 | 0.107 | 0.234 | 0.295 | 0.360 | -0.057 | 0.096 | 0.222 | 0.269 | 0.327 |
| Males | | | | | | | | | | |
| 5 | 1.692 | 0.137 | 0.125 | 0.180 | 0.226 | 0.535 | 0.128 | 0.134 | 0.177 | 0.224 |
| 6 | 1.633 | 0.136 | 0.128 | 0.183 | 0.229 | 0.535 | 0.128 | 0.135 | 0.178 | 0.226 |
| 7 | 1.574 | 0.135 | 0.131 | 0.186 | 0.233 | 0.535 | 0.128 | 0.135 | 0.178 | 0.227 |
| 8 | 1.513 | 0.133 | 0.134 | 0.189 | 0.236 | 0.535 | 0.128 | 0.137 | 0.180 | 0.228 |
| 9 | 1.449 | 0.132 | 0.137 | 0.192 | 0.240 | 0.535 | 0.127 | 0.138 | 0.181 | 0.230 |
| 10 | 1.372 | 0.131 | 0.141 | 0.195 | 0.244 | 0.535 | 0.127 | 0.140 | 0.184 | 0.233 |
| 11 | 1.270 | 0.129 | 0.146 | 0.199 | 0.249 | 0.535 | 0.126 | 0.143 | 0.187 | 0.237 |
| 12 | 1.131 | 0.127 | 0.153 | 0.206 | 0.257 | 0.535 | 0.125 | 0.147 | 0.192 | 0.243 |
| 13 | 0.952 | 0.123 | 0.162 | 0.215 | 0.269 | 0.535 | 0.123 | 0.153 | 0.200 | 0.252 |
| 14 | 0.745 | 0.120 | 0.174 | 0.227 | 0.283 | 0.535 | 0.121 | 0.163 | 0.211 | 0.265 |
| 15 | 0.530 | 0.116 | 0.187 | 0.240 | 0.298 | 0.535 | 0.119 | 0.175 | 0.225 | 0.282 |
| 16 | 0.330 | 0.112 | 0.199 | 0.251 | 0.311 | 0.535 | 0.117 | 0.185 | 0.237 | 0.295 |
| 17 | 0.164 | 0.109 | 0.208 | 0.259 | 0.321 | 0.535 | 0.115 | 0.192 | 0.246 | 0.305 |
| 18 | 0.041 | 0.107 | 0.214 | 0.265 | 0.328 | 0.535 | 0.114 | 0.197 | 0.251 | 0.312 |
| 19 | -0.037 | 0.105 | 0.217 | 0.268 | 0.331 | 0.535 | 0.113 | 0.200 | 0.255 | 0.315 |
| 20 | -0.081 | 0.105 | 0.219 | 0.270 | 0.333 | 0.535 | 0.112 | 0.202 | 0.256 | 0.317 |

Table 1

Disclosures: Babette Zemel, None.

1094

Skeletal Maturation and Genetically Determined Population Ancestry in Non-Obese, Pre-Pubertal Children. Alessandra Chesi^{1*}, Sani M. Roy², Jonathan A. Mitchell³, Heidi J. Kalkwarf⁴, Joan M. Lappe⁵, Vicente Gilsanz⁶, Sharon E. Oberfield⁷, John A. Shepherd⁸, Soroosh Mahboubi², Karen Winer⁹, Andrea Kelly², Struan F.A. Grant¹, Babette S. Zemel¹, Shana McCormack². ¹Children’s Hospital of Philadelphia, USA, ²Children’s Hospital of Philadelphia, USA, ³University of Pennsylvania, USA, ⁴Cincinnati Children’s Hospital Medical Center, USA, ⁵Creighton University School of Medicine, USA, ⁶University of Southern California Los Angeles, USA, ⁷Columbia University Medical Center, USA, ⁸University of California San Francisco, USA, ⁹NIH, USA

Previous studies have suggested that advanced skeletal maturation in African-American children compared to their non-African-American counterparts is largely accounted for by environmental factors, including nutritional status.

We evaluated the effects of population ancestry, as determined by genome-wide genotyping data, on skeletal maturation in a cohort of non-obese, pre-pubertal children.

The Bone Mineral Density in Childhood Study (BMDCS) included serial simultaneous bone age assessments, anthropometrics, Tanner staging, and body composition data by DXA, along with self-reported population ancestry. The first available bone age assessment for each child (as rated by two expert radiologists according to the standards of Greulich and Pyle) was included. Genetic markers were used to estimate degree of African and European admixture. Body mass index (BMI) z-scores were calculated using CDC 2000 standards. Pre-pubertal (Tanner I) children with BMI >3rd and <95th percentile were included.

The sample included 1,000 subjects, mean age 7.5 ± 1.7 years, 48% female, and 17% African-American, mean BMI z-score 0.19 ± 0.76. The difference between bone age and chronological age was higher in self-reported AA vs non-AA girls (by 4.9 months, p=0.00029) and also higher in AA vs non-AA boys (by 5.5 months, p=0.00016). When defined using genetic markers, proportion of African ancestry was positively associated with the difference between bone age and chronologic age (for girls, c=0.19, p=0.00040 and for boys, c=0.14, p=0.0056). In multivariate regression

analyses after accounting for lean mass, fat mass, height, and age, proportion of African admixture was independently associated with more advanced skeletal maturation in both girls ($b=0.35$, $p=0.017$) and boys ($b=0.37$, $p=0.011$). In addition, increased fat mass was independently associated with skeletal maturation after accounting for ancestry and the clinical covariates in both girls ($b=0.06$, $p=0.01$), and boys ($b=0.09$, $p=0.0013$). The effect of lean mass reached statistical significance in boys ($b=0.07$, $p=0.045$ in boys), and near-significance in girls ($b=0.06$, $p=0.06$).

In non-obese, pre-pubertal girls and boys, skeletal maturation is more advanced in proportion to degree of African ancestry, even after accounting for body composition and size. A better appreciation of ancestry-specific differences in skeletal maturation may inform our understanding of corresponding variations in bone and metabolic health.

Disclosures: Alessandra Chesi, None.

1095

Are we still accruing bone mineral content during the third decade of life?

Adam Baxter-Jones¹, Stefan Jackowski², Augusta Rosie Hatton³, Saija Kontulainen². ¹University of Saskatchewan, USA, ²University of Saskatchewan, Canada, ³McGill University, Canada

Introduction: The importance of maximizing bone mineral accrual during the initial two decades of life, the growing years, is clearly recognized. In a five year window around peak height velocity (PHV) approximately 40% of total body bone mineral content (TB BMC) is accrued. The timing of the attainment of peak bone mass (PBM) is suggested to occur anywhere between 15 and 30 years of age. This suggests that little is known about the accrual of TB BMC during the third decade of life, when growth has ceased. Using data from the Saskatchewan Pediatric Bone Mineral Accrual Study (PBMAS) we have previously suggested that TB PBM occurs 6 years post PHV; the end of the second decade of life, approximately 18 and 20 years of age for females and males respectively. The primary purpose of this study was to continue to measure bone accrual in this cohort during the third decade of life. The secondary purpose was to identify sex differences. **Methods:** One hundred and fifty four participants (79 males and 75 females) were drawn from the PBMAS (1991-2011). TB BMC was measured by DXA (cv 0.6%) continuously for 20 years after the attainment of PHV; age range 11 to 34 years of age. Median number of visits was 10 (range 1 to 14). Biological age (BA) was calculated in years from PHV (at PHV BA=0). Percentage increases in TB BMC between PHV and the thirteen BA categories from 8 to 20 years were calculated and compared between BA categories, alpha set to 0.05. **Results:** At a BA of 8 years there was an increase of 40.3% (SD 9.2%) in TB BMC from PHV. At 20 years post PHV the average increase from PHV was 39.4% (SD 6.9%). There were no significant differences in percentage increases between the thirteen BA categories from 8 to 20 years of age ($p>0.05$). No sex specific significant differences were found in accruals from PHV in any of the thirteen BA categories ($p>0.05$). **Conclusions:** These results substantiate our previous observations that PBM occurs at 6 years post PHV and that when aligned by biological rather than chronological age percentage accrual with age is the same in females and males. Unlike some previous studies we found no evidence of accrual in the third decade of life. Although TB BMC did fluctuate during the 15 years preceding the attainment of PBM, the changes appear to be within the error of the measurement.

Disclosures: Adam Baxter-Jones, None.

1096

Effects of maternal calcium supplementation on childhood bone growth differs between males and females. Kate Ward¹, Landing Jarjou², Ann Prentice¹.

¹MRC Human Nutrition Research, United Kingdom, ²MRC The Gambia Unit, Gambia

In a population accustomed to low calcium intakes (approximately 300mg/d) we have described sex differences in the longitudinal effects on bone growth and mineralization of calcium supplementation during childhood¹⁻³. In a separate study of maternal calcium supplementation during pregnancy (ISCRTN96502494)⁴ we have measured childhood bone at age 8-12 years. The aim was to investigate whether there were effects of maternal calcium supplementation on childhood height, weight, bone size and mineralisation, measured using DXA and pQCT, and if so, whether they differed by sex.

In rural Gambia (West Africa) 447 children (216 males; 231 female), mean (SD) age 9.3(0.1)y, 9.2(0.1)y, respectively were measured. Their mothers were randomized to receive 1500mg/d calcium carbonate (Ca), or placebo (P), from 20wk gestation to term; children were not supplemented. At birth, no effects of supplement on infant growth were found^{4,5}. At age 8-12 years, DXA (whole body, spine, hip) and pQCT (tibia) scans were performed. Differences in childhood bone outcomes (DXA: bone mineral content (BMC), bone area (BA); pQCT cortical content, bone cross-sectional area (XSA) and cortical area were tested for a supplement effect using linear regression including sex, length at 52 weeks, current age and a sex-supplement interaction as covariates.

Results are summarized in Table 1. Girls whose mothers were in the Ca group were significantly shorter, lighter and had lower BMC and smaller bones (BA, XSA) with less cortical area than those whose mothers were in the P group. In contrast, there was a trend for boys whose mothers were in the Ca group to be taller, heavier, with greater

BA and BMC than boys whose mothers who received P. There were significant sex-supplement interactions for most anthropometric and bone measures.

Maternal calcium supplementation has affected height, skeletal size and mineralisation at 8-12 y and the differences were divergent in boys and girls. These data highlight the importance of not assuming more is necessarily better for bone health in populations accustomed to lower calcium intakes than international recommendations and that the effects differ between males and females.

¹Prentice, Am J Clin Nutr 2012; 96; ²Ward, J Clin Endocrinol Metab 2014 ;99; ³Ward, Proceedings of International Children's Conference on Bone Health, 2015; ⁴Jarjou, Am J Clin Nutr 2006;83; ⁵Goldberg et al. Am J Clin Nutr 2013;98.

KW, LJ are joint first authors

Table 1: Anthropometry, DXA and pQCT results, supplement differences by sex

| | Boys | | Girls | | Sex-sup int |
|-----------|------|---------|-------|---------|-------------|
| | S-P | P-value | S-P | P-value | P-value |
| Height | +0.5 | 0.3 | -1.0 | 0.04 | 0.03 |
| Weight | +2.1 | 0.2 | -3.3 | 0.03 | 0.01 |
| WB-BMC | +2.6 | 0.2 | -3.3 | 0.08 | 0.03 |
| WB-BA | +1.4 | 0.3 | -2.9 | 0.03 | 0.01 |
| LS-BMC | +3.9 | 0.09 | -4.4 | 0.03 | 0.007 |
| LS-BA | +2.1 | 0.1 | -1.9 | 0.1 | 0.03 |
| Hip-BMC | +0.5 | 0.8 | -5.5 | 0.02 | 0.07 |
| Hip-BA | -0.0 | 0.9 | -3.1 | 0.04 | 0.1 |
| Tib-Area | +2.2 | 0.2 | -3.7 | 0.04 | 0.02 |
| Tib-cBMC | +1.7 | 0.4 | -3.6 | 0.06 | 0.04 |
| Tib-CortA | +1.9 | 0.3 | -4.1 | 0.02 | 0.01 |

Key: sex-sup int = results for sex by supplement interaction, WB-wholebody, LS-lumbar spine, tib = tibia 50% site; data are presented as percent differences supplement minus placebo.

Table 1

Disclosures: Kate Ward, None.

1097

Pediatric bone density is influenced by physical activity and genetic variation at known bone density loci. Jonathan Mitchell¹, Alessandra Chesi², Okan Elci², McCormack Shana², Sani Roy², Heidi Kalkwar³, Joan Lappe⁴,

Vicente Gilsanz⁵, Sharon Oberfield⁶, John Shepherd⁷, Andrea Kelly², Struan Grant², Babette Zemel². ¹University of Pennsylvania, USA, ²Children's Hospital of Philadelphia (CHOP), USA, ³Cincinnati Children's Hospital Medical Center, USA, ⁴Creighton University, USA, ⁵Children's Hospital Los Angeles, USA, ⁶Columbia University Medical Center, USA, ⁷University of California San Francisco, USA

Physical activity (PA) mechanically loads the skeleton to increase pediatric bone mineral density (BMD). In addition, genome wide association studies (GWAS) have identified 66 loci that influence BMD and some of these loci may impact skeletal mechanosensitivity. We aimed to determine if GWAS-implicated BMD loci influenced associations between PA and bone mineral content (BMC) and BMD in childhood.

We leveraged the six-year prospective longitudinal study design of the 'Bone Mineral and Density in Childhood Study', comprised of European ancestry children (N=689, 52.4% female). Our outcome variables were femoral neck (FN), total hip (TH) and spine areal-BMD (aBMD) Z-scores, and total body less head (TBLH) bone mineral content (BMC) Z-score, estimated by dual energy X-ray absorptiometry. Our primary exposures included self-report PA and single nucleotide polymorphisms (SNPs) at 66 GWAS-implicated BMD loci, plus interaction terms for PA and each SNP. Linear mixed models were used to analyze our data, by sex, adjusted for age, Tanner stage, BMI and dietary calcium. We applied the Benjamini and Hochberg (BH) method to correct for the multiple testing of 66 loci. Our findings are categorized as follows: 1) interaction P-values that survive BH correction and 2) interaction P-values <0.05 and a genotype specific PA association P-value <3.9x10⁻⁴.

In males, statistical interactions involving SNPs at the *WNT5B* (TBLH-BMC) and *CYLD* loci (FN aBMD) survived BH correction. For example, the effect of PA on TBLH-BMC-Z depended on rs4283041 genotype (BMD-lowering 'risk' C allele) at *WNT5B* ($P=1.1x10^{-4}$); each hour per day (h/d) of PA increased TBLH-BMC-Z for CC homozygotes ($\beta=0.04$, $P=3x10^{-2}$), but not for the TT homozygotes ($\beta=-0.03$, $P=0.078$). In females, rs7195617 (risk G allele) at *AXIN1* interacted with PA to influence TH aBMD-Z ($P=3.9x10^{-4}$); each h/d of PA increased TH aBMD-Z for GG homozygotes ($\beta=0.06$, $P=4x10^{-3}$), but not for AA homozygotes ($\beta=-0.01$, $P=0.310$). Secondary statistical interactions were observed for the following loci in males at ≥ 1 skeletal sites: *DNM3*, *MHC*, *SPTBN1*, *WNT5B*, *C16orf38/CLCN7*, *LEKRI*, *RANKL/AKAP11*, *C6orf97* and *HOXC6*. A secondary statistical interaction was observed for the *FUBP3* locus in females for TH aBMD.

PA may be particularly effective for promoting bone accretion in children with certain genetic backgrounds. These gene-PA interactions findings will aid in developing future strategies to promote optimal bone accretion during childhood.

Disclosures: Jonathan Mitchell, None.

1098

Deficits in Bone Strength in Girls with a Distal Radius Fracture Track 1 Year after Fracture. Mikko Maatta*¹, Heather Macdonald², Douglas Race², Lindsay Nettlefold², Kishore Mulpuri³, Heather McKay². ¹University of British Columbia, Canada, ²Centre for Hip Health & Mobility, Canada, ³British Columbia Children's Hospital, Canada

We recently reported⁽¹⁾ impaired bone strength in girls with low to moderate energy distal radius fractures (Fx) compared with girls with no history of forearm fractures (NF). In this study we aimed to determine whether bone strength deficits were still present in Fx girls after 12-months.

We assessed the non-dominant (NF) and non-fractured (Fx) distal radius (7% site) bone microstructure at baseline and 12 months using high-resolution pQCT (Scanco Medical) in 95 girls (12.1 ± 1.7 y; 41 Fx, 54 NF). Morphological outcomes included total area (Tt.Ar) and bone mineral density (Tt.BMD), trabecular bone volume ratio (BV/TV), trabecular thickness (Tb.Th) and number (Tb.N), cortical area (Ct.Ar), BMD (Ct.BMD), thickness (Ct.Th) and porosity (Ct.Po). We used finite element analysis to estimate bone strength (failure load, FLoad; ultimate stress, UStress⁽²⁾). We calculated load-to-strength ratio as a ratio of the estimated fall load applied to the outstretched arm after a fall from standing height⁽³⁾ and FLoad. We used one-way ANOVA to compare anthropometry (height (cm), weight (kg), forearm length (mm), body fat and lean mass (kg); DXA, Hologic QDR 4500W). We fit multivariable linear regression to compare 12-month change in bone outcomes as well as bone measures at 12-months between groups adjusting for maturity (Tanner stage), height, ethnicity and body fat at baseline.

During the 12-month follow-up Fx girls gained more body fat than NF girls (1.3 vs 0.7 kg, p<0.05). Fx girls had a smaller increase in FLoad (190 vs. 273 N, p=0.02) and Tt.BMD (6.4 vs. 13.7 mg HA/cm³, p=0.03) compared with NF group. At follow-up, Fx girls had lower bone strength (FLoad: -15%, UStress: -24% and load-to-strength ratio: 11%, p≤0.02) compared with NF girls. Fx girls also had lower Tt.BMD, BV/TV, Tb.Th, Ct.Ar and Ct.Th than NF girls (7-11%, p≤0.03).

We did not observe a catch-up period for bone outcomes in girls with a distal radius fracture. This implies that the bone deficits may track across growth and place girls with a low to moderate energy fractures at greater risk for a recurrent fracture. Greater increases in body fat in Fx girls may be an indication of physical inactivity, which might further increase the risk of future fracture.

References

1. Määttä et al. Osteoporos Int 26:1163-1174.
2. MacNeil & Boyd Bone 42:1203-1213.3. Chiu & Robinovitch J Biomech 31: 1169-1176.

Disclosures: Mikko Maatta, None.

1099

Leukemia Inhibitory Factor Receptor (LIFR) Signaling Regulates Breast Cancer Cell Dormancy and Bone Colonization. Rachel Johnson*¹, Alyssa Merkel², Julie Sterling², Joshua Johnson³, Joy Wu³, Amato Giaccia⁴. ¹Stanford University, USA, ²Department of Veterans Affairs, Tennessee Valley Healthcare System (VISN 9), Vanderbilt University Medical Center, USA, ³Department of Medicine, Stanford University, USA, ⁴Department of Radiation Oncology, Stanford University, USA

Breast cancer cells frequently metastasize to the bone marrow, where they may enter a dormant state and remain undetected for years. The tumor-bone interactions that enable cells to exit dormancy are not well understood. Recent findings indicate that the leukemia inhibitor factor (LIF) LIF receptor (LIFR), a member of the interleukin-6 family cytokines, suppresses breast cancer metastases to lung, but it is unknown whether LIFR signaling is involved in bone metastasis. Since LIF inhibits *in vitro* growth of MCF7 breast cancer cells, which home to the bone and lay dormant, we proposed that LIF provides a pro-dormancy signal to breast cancer cells in the bone, and that loss of the LIFR would enable these cells to colonize the bone. Characterization of breast cancer cells with low (MCF7, D2.0R, PyMT, SUM159) and high metastatic potential (MDA-MB-231, D2A1, 4T1BM2) revealed that the former rapidly phosphorylate STAT3-Y705 and induce SOCS3 mRNA levels in response to LIF (3-18 fold, p<0.01-p<0.0001), suggesting that LIF may act as a pro-dormancy factor to disseminated breast cancer cells. In contrast, breast cancer cells that readily metastasize to bone lack a functional LIFR and do not induce STAT3/SOCS3 signaling. Genetic knockdown of LIFR in MCF7 cells converts them to an invasive phenotype in 3D cultures and significantly (p<0.05-0.001) reduces genes associated with dormancy (TSP1 39%, TPM1 27%, P4HA1 26%, miR-190 70%, Selenbp1 29% lower) and a cancer stem cell phenotype (Notch1 48%, Casp3/Scal 29%, Tert 21%, Sox2 71% lower), suggesting that loss of LIFR drives cells toward a proliferative, aggressive phenotype. Intracardiac inoculation of MCF7shLIFR cells resulted in significantly enhanced osteolysis (2.7-fold, p<0.01) over controls. To determine whether extreme low-oxygen conditions of the bone marrow may drive

quiescent tumor cells to exit dormancy, MCF7 cells were cultured in anoxic conditions, resulting in dramatic down-regulation of the LIFR (63%, p<0.01) and SOCS3 (46%, p<0.05) mRNA levels. Furthermore, data mining of The Cancer Genome Atlas database revealed that as hypoxia gene activity increases in invasive breast cancer patients, their LIFR mRNA levels decrease (n=1104 patients, p<0.0001), providing a mechanism by which hypoxia may drive tumor recurrence in bone. These data indicate that LIFR signaling in breast cancer cells maintains dormancy and that anoxic conditions may drive the loss of LIFR, allowing tumor cells to colonize the bone marrow.

Disclosures: Rachel Johnson, None.

1100

The Wnt-miR-218-axis promotes breast cancer -induced osteolytic disease. Hanna Taipaleenmaki*¹, Mohammad Q Hassan², Yukiko Maeda³, Andre van Wijnen⁴, Eric Hesse⁵, Janet L Stein⁶, Gary S Stein⁶, Jane B Lian⁶. ¹University Medical Center Hamburg-Eppendorf, Germany, ²Department of Oral & Maxillofacial Surgery, School of Dentistry, University of Alabama at Birmingham, USA, ³Department of Cell Biology, University of Massachusetts Medical School, USA, ⁴Department of Biochemistry & Molecular Biology, Department of Orthopedic Surgery, Mayo Clinic, USA, ⁵Heisenberg-Group for Molecular Skeletal Biology, Department of Trauma, Hand & Reconstructive Surgery, University Medical Center Hamburg-Eppendorf, Germany, ⁶Department of Biochemistry & Vermont Cancer Center, University of Vermont College of Medicine, USA

Signaling pathways crucial in bone development, including Wnt and BMP, are also upregulated in breast cancer cells to cause aggressive tumor growth in the skeleton. Homing of breast cancer cells to bone is facilitated by their ability to express many osteoblast-related genes ('osteomimicry'). We thus asked if osteogenic miRNAs are aberrantly expressed in bone metastatic tumor cells to support the osteomimetic properties. miR-218 is highly expressed in osteoblasts and promotes osteogenic differentiation. Interestingly, we found that miR-218 expression is also significantly up-regulated in bone metastatic MDA-MB-231 breast cancer cells and is not detectable in normal MCF-10A mammary epithelial cells, suggesting a positive role of miR-218 in bone metastasis. Indeed, ectopic expression of miR-218 in MDA-MB-231-Luc cells promoted tumor growth in the bone microenvironment *in vivo* whereas inhibition of miR-218 resulted in impaired growth. Aggressive intratibial tumor growth was accompanied by increased osteoclast activity and bone resorption in the presence of miR-218, while antagonizing miR-218 protected from development of osteolytic lesions. Signaling pathway analyses revealed a positive correlation between aberrant miR-218 expression and high activation of endogenous, metastasis promoting Wnt signaling pathway, demonstrated by the Wnt-responsive TopFlash reporter assay and expression of the Wnt transcriptional mediators. Mechanistically, miR-218 directly targets several inhibitors of Wnt and BMP signaling including Sclerostin, DKK2, sFRP-2, and TOB1, which were validated by 3'UTR, western blot and gene expression analyses. Consequently, ectopic expression of miR-218 further increased Wnt activity in MDA-MB-231 cells while inhibition of miR-218 decreased Wnt signaling. Importantly, bone sialoprotein (BSP) and osteopontin (OPN), both reported to be elevated in serum of breast cancer patients, CXCR-4, a chemokine receptor directly linked to bone metastasis and PTHrP, the key cytokine promoting cancer-induced osteolysis were all upregulated in the presence of miR-218. Inhibition of Wnt signaling abolished the miR-218-induced elevation, indicating a Wnt-dependent activation of these metastatic genes. We conclude that miR-218 activates Wnt signaling to enhance metastatic properties of breast cancer cells and the cancer-induced osteolytic disease, and is therefore an attractive novel therapeutic intervention to prevent the disease progression.

Disclosures: Hanna Taipaleenmaki, None.

1101

Reciprocal Interactions between Sensory Neurons and Tumor Cells Promote Breast Cancer Progression in Bone, Secondary Visceral Metastasis and Bone Pain. Tatsuo Okui*¹, Masahiro Hiasa¹, Yuki Nagata¹, Fletcher White², G David Roodman¹, Toshiyuki Yoneda¹. ¹Department of Medicine, Hematology Oncology, Indiana University School of Medicine, USA, ²Department of Anesthesia, Paul & Carole Stark Neurosciences Research Institute, USA

Breast cancer (BCa) has a strong predilection for spreading to bone, contributing to increased morbidity and mortality. BCa in bone causes intractable bone pain and subsequently disseminates to visceral organs, resulting in secondary metastasis and increased mortality. Thus, inhibition of bone metastasis is an important goal for managing BCa patients. Interactions between BCa cells and the cellular and molecular elements of the bone microenvironment have been shown to be critical to the pathophysiology of bone metastasis. However, the contribution of the sensory neurons (SN) to bone metastasis is totally unknown. Using the 4T1 mouse BCa model, we tested the hypothesis that bone SN contributes to the progression of BCa bone metastasis, development of secondary metastasis and bone pain via reciprocal

interactions with BCa cells. We first examined the effects of SN on 4T1 BCa. F11 SN cell conditioned medium (CM) stimulated cell proliferation and migration and epithelial-mesenchymal transition of 4T1 cells. We detected high levels of hepatocyte growth factor (HGF) in F11 CM, which increased phosphorylation of the HGF receptor, c-Met, in 4T1 cells. All of these effects were blocked by crizotinib, a c-Met tyrosine kinase inhibitor, or c-Met knockdown in 4T1 cells. Importantly, blocking HGF effects by 4T1 c-Met knockdown or crizotinib in mice injected intratibially with 4T1 cells (4T1 mice) markedly reduced osteolytic lesion size and secondary lung metastasis from bone. These results suggest that SN-produced HGF contributes to bone colonization and secondary metastasis of 4T1 BCa. We next examined if 4T1 BCa has reciprocal effects on SN. We found that 4T1 cells produced high mobility group box 1 (HMGB1) and that 4T1 CM increased F11 neurite sprouting that was blocked by a HMGB1 neutralizing antibody. The 4T1 mice had elevated serum levels of HMGB1 and progressive bone pain with increased sprouting of calcitonin gene-related peptide-positive SN in bone. The HMGB1 antibody or FPS-ZM1, an antagonist of the HMGB1 receptor, RAGE, reduced bone pain. These results suggest that HMGB1 produced by 4T1 BCa increases SN sprouting to enhance bone pain. In conclusion we show that reciprocal direct interactions between BCa and bone-innervating SN appear critical to the progression of BCa bone metastasis, secondary visceral metastasis from bone and induction of bone pain. Disruption of these interactions may provide a novel therapeutic approach for treatment of BCa patients.

Disclosures: *Tatsuo Okui, None.*

1102

EpCAM Promotes Bone Metastases of Breast Cancer by Conferring Cancer Stem-like and Epithelial Properties. Toru Hiraga^{*1}, Susumu Ito², Hiroaki Nakamura¹. ¹Matsumoto Dental University, Japan, ²Shinshu University, Japan

Epithelial cell adhesion molecule (EpCAM), also known as CD326 and epithelial-specific antigen (ESA), has been implicated in multiple cellular functions, such as cell signaling, migration, proliferation, and differentiation as well as cell adhesion. Clinical studies showed that EpCAM is highly expressed in various cancers, including breast cancer, and its overexpression is associated with a poor prognosis. EpCAM is also widely recognized as a marker for circulating tumor cells (CTCs) in peripheral blood, disseminated tumor cells (DTCs) in bone marrow, and cancer stem cells (CSCs). Here, we examined the roles of EpCAM in the development of bone metastasis of breast cancer by using well-characterized animal models. EpCAM-negative and -high-expressing (EpCAM^{neg} and EpCAM^{pos}) cells were firstly isolated from mouse breast cancer cell lines by fluorescence-activated cell sorting. Morphological and real-time RT-PCR data showed that EpCAM^{neg} and EpCAM^{pos} cells exhibited mesenchymal and epithelial phenotypes, respectively. Flow cytometric analysis showed that, during serial subcultures of monolayers after cell sorting, the EpCAM^{pos} population gradually decreased while an EpCAM^{neg} population was generated from EpCAM^{pos} cells in a time-dependent manner. In contrast, EpCAM^{neg} cells did not produce an EpCAM^{pos} population, suggesting that EpCAM^{pos}, but not EpCAM^{neg}, cells possess self-renewal and differentiation potentials. Tumor sphere formation in suspension cultures and tumorigenicity in the orthotopic mammary fat pad of mice were significantly greater in EpCAM^{pos} cells than in EpCAM^{neg} cells. The development of bone metastases induced by an intracardiac injection was markedly increased in mice inoculated with EpCAM^{pos} cells. Furthermore, intracardiac inoculations of the unsorted parental cancer cells demonstrated that the EpCAM^{pos} population in cancer cells that colonized in bone was significantly higher than that in the parental cells. These results suggest that the expression of EpCAM in breast cancer cells is associated with CSC-like phenotypes and contributes to the promotion of bone metastases by enhancing tumorigenicity. Our results also support the possibility that the epithelial phenotypes of EpCAM-expressing cells confer advantageous properties for the development of bone metastases, at least after entering the circulation. Thus, EpCAM may be a potential target for therapeutic interventions to treat bone metastases of breast cancer.

Disclosures: *Toru Hiraga, None.*

1103

Lysyl oxidase endows colon cancer cells with the ability to thrive in the bone marrow and promotes bone metastasis formation. Caroline Reynaud^{*1}, Laura Ferreras², Marie Brevet³, Philippe Clezardin⁴. ¹INSERM Unité 1033UFR de Médecine Lyon-Est (domaine Laënnec), Fr, ²INSERM Unité 1033UFR de Médecine Lyon-Est, France, ³Hospices Civils de Lyon - Accueil, France, ⁴INSERM & University of Lyon, France

Lysyl oxidase (LOX) catalyzes the cross-linking of collagens and elastin in the extracellular matrix, thereby regulating the tensile strength of many tissues, such as in bone. In cancer, LOX plays a critical role in facilitating tumor growth and metastasis formation in soft tissues. Whether tumor-derived LOX also enables bone metastasis is unknown. In this study, we first showed by immunohistochemistry using patients' tumor specimens, that LOX was expressed in the desmoplastic tumor stroma of pairs of colorectal carcinomas and their matching bone metastases. Preclinical experiments showed that LOX overexpression in different colon carcinoma cell lines enhanced the

formation of osteolytic lesions in animals by promoting both skeletal tumor burden and osteoclast-mediated bone resorption. Additionally, LOX treatment of animals enhanced bone metastasis caused by parental colorectal carcinoma cells. Conversely, the pretreatment of animals with the LOX inhibitor β -aminopropionitrile or the silencing of LOX in colorectal carcinoma cells drastically reduced the formation of osteolytic lesions. Furthermore, we demonstrated that LOX was involved in the early migration of tumor cells into the bone marrow.

In vitro, LOX directly enhanced the attachment of colon cancer cells to type-I collagen, but not to fibronectin. Preliminary experiments also indicated that LOX-overexpressing colorectal carcinoma cells were more prone to adhere to components of the osteoblastic niche, such as osteoblasts or mesenchymal stem cells. Thus, LOX may promote engraftment of colon cancer cells in the osteoblastic niche. Tumor-derived LOX could also promote osteoclast differentiation by enhancing the secretion of osteolytic factors from colon cancer cells such as IL-6. Additionally, the activation of an IL-6 autocrine loop led to cancer cell survival.

In conclusion, our findings provide novel evidence that LOX endows colon cancer cells with the ability to thrive in the bone marrow microenvironment and stimulate osteoclast-mediated bone destruction.

Disclosures: *Caroline Reynaud, None.*

1104

Dickkopf-related protein 1 (Dkk1) exerts immune suppressive effects in cancer by regulating expansion and function of myeloid derived suppressor cells. Lucia D'Amico^{*1}, Aude Helene Capietto¹, Ali Zaman¹, David Bumpass², Roberta Faccio³. ¹Washington University School of Medicine, USA, ²Orthopaedic Surgery, Washington University School of Medicine, USA, ³Department of Orthopedics, Washington University School of Medicine, USA

Emerging evidence suggest the importance of tumor-stroma interactions during tumor progression. Changes in the stromal compartment can promote tumor growth by recruiting and activating a heterogeneous population of immature myeloid cells, often referred to as myeloid-derived suppressor cells (MDSC), that can suppress T cell responses and thus facilitate tumor proliferation. These findings raise a critical question: how is MDSC generation and/or activation driven by the stromal compartment at a primary or metastatic site? We recently found that downregulation of β -catenin in MDSC drives MDSC generation and their ability to inhibit T cell responses in mice and cancer patients. Our new data demonstrate that the Wnt/ β -catenin inhibitor Dkk1 suppresses β -catenin in MDSC during tumor progression. Mice bearing subcutaneous (sc) Lewis Lung Carcinomas (LLC) show increased Dkk1 levels in circulation, produced by tumor-associated fibroblasts and by osteoblasts and osteocytes in bone. To investigate whether Dkk1 promotes MDSC expansion during tumor progression, α -Dkk1 or IgG control Abs (20 mg/kg) were administered 3x/week to WT mice sc injected with LLC. Strikingly, we find that tumor growth is significantly decreased and β -catenin expression in MDSC is restored following α -Dkk1Ab treatment ($p=0.019$). Dkk1 neutralization significantly reduces the % of MDSC in bone marrow and at tumor site while T cell recruitment is increased. To directly test the effects of α -Dkk1Ab on MDSC functionality, we examined the immune suppressive effects of MDSC on T-cell proliferation after Dkk1 targeting. We find that MDSC isolated from tumor bearing mice treated with α -Dkk1Ab have reduced ability to suppress T cell proliferation ($p=0.02$). Next, to determine whether MDSC are the main target of Dkk1 pro-tumor effects, we turned to β -catenin^{fl/fl}/LysMCre c.KO mice to delete β -catenin in MDSC. We find that Dkk1 neutralization fails to reduce tumor growth and MDSC expansion in mice lacking β -catenin in MDSC. Similarly to MDSC from tumor-bearing mice, MDSC isolated from human donors incubated with serum from breast cancer patients in the presence of recombinant Dkk1 show reduced expression of β -catenin target genes. These findings demonstrate that Dkk1 directly targets MDSC in mice and humans and drives MDSC expansion and activation. Our work reveals a novel immunomodulatory role for Dkk1 in regulating tumor-induced immune suppression via targeting β -catenin in MDSC.

Disclosures: *Lucia D'Amico, None.*

1105

Deletion of the Transcriptional Coactivators YAP and TAZ in Mesenchymal Progenitors Promotes Osteoblastogenesis and Increases Bone Mass. Jinhu Xiong^{*1}, Marilina Piemontese¹, Yuko Fujiwara¹, Priscilla Baltz¹, Charles O'Brien². ¹University of Arkansas for Medical Sciences & Central Arkansas Veterans Healthcare System, USA, ²Central Arkansas VA Healthcare System, Univ of Arkansas for Medical Sciences, USA

YAP (Yes associated protein) and TAZ (transcriptional co-activator with PDZ-binding motif) are related transcriptional coactivators that control organ size in a redundant manner. In vitro studies have suggested that high matrix stiffness enhances osteoblast differentiation from mesenchymal progenitors by promoting YAP and TAZ nuclear translocation. However, other studies show that YAP and TAZ suppress osteoblast differentiation. Thus, in vitro studies have not provided consistent results regarding the role of YAP and TAZ in osteoblast differentiation. Here, we deleted

genes for YAP and TAZ from mesenchymal progenitors using the Prx1-Cre transgene, which leads to recombination in all mesenchyme-derived cells in the limbs. Complete loss of YAP and TAZ in mesenchymal progenitors caused embryonic lethality. However, mice with haploinsufficiency of YAP and complete lack of TAZ in mesenchymal progenitors, referred to here as Prx1-Cre;YAP^{fl/+};TAZ^{fl/0}, developed normally. We then analyzed the skeletal phenotype of these mice at 5 weeks of age. Deletion of YAP and TAZ was confirmed by low levels of their mRNAs in the tibia. Micro-CT analysis of the femur revealed high cancellous bone volume with increased trabecular number, trabecular thickness, and decreased trabecular separation in Prx1-Cre;YAP^{fl/+};TAZ^{fl/0} mice compared to control littermates. Femoral cortical thickness was also elevated in Prx1-Cre;YAP^{fl/+};TAZ^{fl/0} mice. Ex vivo culture of bone marrow mesenchymal progenitors from Prx1-Cre;YAP^{fl/+};TAZ^{fl/0} mice showed increased osteoblastogenesis with increased expression of osteoblast marker genes such as osterix, osteocalcin, and collagen 1a1. These results demonstrate that loss of YAP and TAZ in Prx1-Cre-expressing cells promotes osteoblastogenesis and increases both cancellous and cortical bone in young mice, suggesting that these transcriptional regulators inhibit osteoblast differentiation.

Disclosures: *Jinhu Xiong, None.*

1106

Assessing the Skeletal Phenotype of Compound Gja1^{+/-} Runx2^{+/-} Mice. Atum Buo*, Joseph Stains. University of Maryland, School of Medicine, USA

The coupling of osteoblasts and osteocytes by connexin43 (Cx43)-comprised gap junctions permits the sharing of second messengers that coordinate bone cell function and bone mass accrual. However, details are lacking as to the molecular events by which Cx43 converts shared second messengers into signals that converge onto essential osteogenic processes. Previously, we have shown that Cx43 expression modulates the transcriptional activity of Runx2 in MC3T3 cells in vitro. Here, we sought out to determine whether Cx43 is able to regulate the activities of Runx2 in vivo. To achieve this, we used a compound heterozygous breeding strategy to generate mice that are doubly heterozygous for the Cx43 gene (Gja1) and the Runx2 gene. We hypothesized that if Cx43 and Runx2 indeed functionally intersect to regulate osteogenesis in vivo, then the dual hemizyosity of both Cx43 and Runx2 should manifest a skeletal phenotype not visible in wild-type or singly hemizygous animals. To assess skeletal phenotype, we performed micro-CT analysis on femur and skull specimens of 8 week-old Gja1^{+/-} Runx2^{+/-} compound mice, as well as wild-type and single Gja1^{+/-} and Runx2^{+/-} mice for controls. Cortical bone analysis reveals that in both male and female mice, compound Gja1^{+/-} Runx2^{+/-} mice have a marked increase in tissue area, endosteal and periosteal bone perimeter, as well as a striking increase in porosity in comparison to all other genotypes. This indicates that compound hemizyosity of Gja1 and Runx2 resembles the endosteal widening phenotype seen in conditional osteoblast-specific Gja1-knockout mouse models. Furthermore, micro-CT analysis of skulls reveals an interparietal bone defect in compound hemizygous mice. Consistent with this finding, whole-body alizarin red and alcian blue staining of 2 day-old Gja1^{+/-} Runx2^{+/-} neonates displays elements of the skull that are even less mineralized than the characteristically hypomineralized skull of Runx2^{+/-} neonates. In summary, these findings provide preliminary evidence that Cx43 and Runx2 functionally intersect in vivo to regulate bone formation and contribute to the skeletal phenotype of Cx43 conditional knockout mice. Ongoing studies will assess the osteogenic potential of cells from these compound animals, expand the characterization of the cranial phenotype and attempt to rescue the osteoblast dysfunction observed in Cx43 deficient cells by overexpressing Runx2.

Disclosures: *Atum Buo, None.*

1107

DOK3 Affects Bone Homeostasis by Regulating Osteoblast and Osteoclast Differentiation and Function. Mary Beth Humphrey*¹, Junjie Xing¹, Courtney Long². ¹University of Oklahoma Health Sciences Center, USA, ²University of Hamberg-Eppendorf, Germany

Bone homeostasis is maintained by the balance of osteoblasts (OB) mediated bone formation and osteoclasts (OC) mediated bone resorption. RANKL promotes OC differentiation but requires costimulation of immunoreceptor tyrosine-based activation motif (ITAM)-adapters such as DAP12. Downstream of tyrosine kinases (DOK) are cytosolic adaptors which assemble multi-molecular signaling complexes that function to limit tyrosine kinase receptor mediated signaling. Recently, we found that DOK3 negatively regulates DAP12 signaling and inflammatory cytokine production in response to toll-like receptor (TLR) stimulation of macrophages. To test the hypothesis that DOK3 negatively regulates DAP12 signaling in osteoclasts, bone micro-architecture, histomorphometry, and histology of sex matched 16 week old wild type (WT) and DOK3-deficient (DOK3 KO) mice were evaluated. In vitro derived OC from DOK3 KO and WT bone marrow were analyzed for morphology and function. The MCSF and RANKL signaling pathways was investigated. OB differentiation was analyzed by alizarin red S staining and expression of OB markers. Our results show that DOK3 KO mice have significantly reduced trabecular bone mass at the tibia and femur whereas cortical bone is unchanged. Histomorphometry revealed significant decreases in OB surface, numbers, and perimeter but normal bone formation and mineral apposition rates. In vivo, OC numbers were similar between WT and DOK3 KO. In vitro derived OB from DOK3 KO mice had reduced calcified nodules and

mineralization compared to WT. Compared to WT OB, expression of alkaline phosphatase and collagen $\alpha 1$ was decreased in DOK3 KO OB. Mechanistically, decreased OB differentiation was related to failure to achieve sustained WNT3a and β -catenin expression. In vitro derived OC assays revealed that DOK3 pre-OC had increased proliferation in response to MCSF and were more sensitive to RANKL with increased OC differentiation and resorptive capacity.

Restoration of DOK3 expression in DOK3 KO pre-OC significantly reduced OC numbers and decreased resorption. Mechanistically, DOK3 regulates osteoclastogenesis by sequestering of Grb2, Sos1, Lab or Cbl and thus inhibiting Syk and Erk activation. Thus, DOK3 modulates bone remodeling by promoting OB differentiation and inhibiting osteoclastogenesis and bone resorption. Our studies have revealed DOK3 as novel mediator of osteoblastogenesis in vitro and in vivo.

Disclosures: *Mary Beth Humphrey, None.*

1108

Telomerase Expression Marks Transitional Growth-Associated Skeletal Progenitor/Stem Cells. Diana Carlone*, Rebecca Riba-Wolman, Luke Deary, Alessio Tovaglieri, Dana Ambruzs, Manasvi Shah, Benjamin Mead, David Breault. Boston Children's Hospital, USA

Skeletal progenitor/stem cells (SSCs) play a critical role in postnatal bone growth and maintenance. Recently, distinct SSC populations were shown to contribute to bone formation in a temporal-specific manner. Telomerase (Tert) activity prevents cellular senescence and is required for maintenance of stem cells in regenerative tissues. Here we investigate the role of mTert-expressing cells in postnatal bone development. Quantitative RNA analysis of long bones revealed that mTert is expressed predominantly at weaning (3-4 weeks), suggesting these cells are temporally regulated and mark a discrete developmental time point between rapid bone growth and bone maintenance, which we have termed "transitional growth". We next investigated the location of mTert-expressing cells using our mTert-GFP mouse model, which faithfully recapitulates endogenous telomerase activity. mTert-GFP+ cells were detected within the metaphyseal stroma, with ~75% of them residing adjacent to CD31+ vascular cells, consistent with the proposed location for SSCs. In addition, GFP+ cells were detected within the growth plate and articular cartilage as well as in the bone marrow adjacent to trabecular and cortical bone, regions also proposed to house progenitor/stem cells. mTert-expressing cells exhibited a 30-fold enrichment in CFU-F forming capacity, persisted long-term and contributed to multiple mesenchymal lineages. In vivo lineage-tracing studies showed that mTert+ cells contribute to the majority of bone-forming cells during endochondral bone growth with a subset persisting into adulthood. Additional studies revealed that mTert+ cells give rise to Osx+ osteoprogenitor cells, reinforcing the concept that a hierarchy of progenitor/stem cells exists within the bone. Taken together, these data show that mTert expression marks a distinct SSC population during the transition stage between rapid bone growth and bone maintenance. Additional studies are currently underway to identify the molecular mechanisms and signaling pathways responsible for the age-dependent expression of mTert.

Disclosures: *Diana Carlone, None.*

1109

DNA Damage Checkpoint Pathway Modulates The Regulation of Skeletal Growth and Osteoblastic Bone Formation by Parathyroid Hormone-Related Peptide. Ying Zhang*¹, Guangpei Chen¹, Zhen Gu¹, Andrew Karaplis², David Goltzman², Dengshun Miao³. ¹Nanjing Medical University, China, ²McGill University, Canada, ³Nanjing Medical University, Peoples republic of china

We previously demonstrated that parathyroid hormone-related peptide (PTHrP) 1-84 knockin (*Pthrp* KI) mice displayed early senescence, skeletal growth retardation and defective osteoblastic bone formation. To determine whether oxidative stress and DNA damage response pathways were involved in the regulation by PTHrP of skeletal growth and development *in vivo*, we examined alterations of oxidative stress and DNA damage response related molecules in *Pthrp* KI skeletal tissue. Our results demonstrated that ROS levels, protein expression levels of the DNA damage marker g-H2AX and the DNA damage response markers p-Chk2 and p53 were up-regulated significantly, whereas mRNA expression levels of anti-oxidative enzymes including SOD1 and 2, catalase, glutathione reductase (GSR) and glutathione peroxidase 4 (GPX4) were down-regulated in *Pthrp* KI skeletal tissues. We therefore further disrupted the DNA damage response pathway by Chk2 deletion in *Pthrp* KI (*Chk2^{-/-}Pthrp* KI) mice, and compared them with *Chk2^{-/-}*, *Pthrp* KI, and WT littermates. Deletion of Chk2 in *Pthrp* KI mice resulted in a longer lifespan, increased body weight and improvement in skeletal growth, although *Pthrp* KI mice were not normalized. At 2 weeks of age, skeletal growth parameters, including length of long bones, size of epiphyses and width of growth plates, BMD, cortical and trabecular bone volume, osteoblast numbers, and ALP and type I collagen positive bone areas, the mRNA expression levels of Runx2, ALP, and osteocalcin, and the numbers of total CFU-F and ALP positive CFU-F were increased in *Chk2* mice, and reduced in both *Pthrp* KI and *Chk2^{-/-}Pthrp* KI mice compared to WT mice; however these parameters were increased in *Chk2^{-/-}Pthrp* KI mice compared to *Pthrp* KI mice.

Furthermore, gene expression levels of SOD1 and 2, catalase, GSR and GPX4 in skeletal tissues were up-regulated significantly, whereas senescence-associated tumor suppressor genes including p16, p19, p53, p21 and p27 were down-regulated in *Chk2*^{-/-} mice compared to wild-type mice and in *Chk2*^{-/-}*Pthrp* KI mice compared to *Pthrp* KI mice. Our results demonstrate that deletion of *Chk2* in *Pthrp* KI mice can partially rescue defects in skeletal growth and osteoblastic bone formation by enhancing endochondral bone formation and osteogenesis. These studies therefore indicate that the DNA damage checkpoint pathway may function downstream in the action of PTHrP to regulate skeletal growth and development.

Disclosures: Ying Zhang, None.

1110

Transition of Chondrocytes into Osteoblasts in Endochondral Bones Requires Active Canonical Wnt Signaling. Xin Zhou^{*1}, Ailing Huang², Klaus von der Marck³, Benoit de Crombrughe², Venkata Battula², Michael Andreeff².
¹MD Anderson Cancer Center, USA, ²UT MD Anderson Cancer Center, USA, ³University of Erlangen-Nuremberg, Germany

Recent lineage tracing studies demonstrated that mature chondrocytes, both in cartilage primordia and in established growth plates, as well as chondrocytes in bone repair calluses, were a major source of osteoblasts during endochondral ossification.

To test whether chondrocyte-derived cells might be present in the bone marrow, FACS was performed using 3.5-month *Coll10a1-Cre; ROSA26-YFP* mice. We found that about 0.1% of the total nucleated bone marrow cells were YFP⁺. Likewise in *Coll10a1-Cre; Osx^{fllox/+}* mice, in which *EGFP* expression marks *Osx*-expressing cells after Cre-mediated *LoxP* recombination of the *Osx^{fllox}* allele, GFP⁺ cells were present in the bone marrow. Both the YFP⁺ and the GFP⁺ bone marrow cells, isolated either directly from bone marrow or from a bone marrow MSC culture, were positive for mesenchymal progenitor cell (MSC) markers (Sca1, CD140a, CD140b, CD105), negative for the hematopoietic cell marker CD45 and the erythroid cell marker Ter119. Moreover, the cultured YFP⁺ or GFP⁺ bone marrow cells displayed clonogenic, osteogenic, chondrogenic and adipogenic capacities *in vitro*. Interestingly, more than 30% of the cells, in a bone marrow MSC culture of 4-month-old *Coll10a1-Cre; Osx^{fllox/+}* mice, were GFP⁺. These results provide evidence that hypertrophic chondrocyte-derived mesenchymal progenitor cells were indeed present in the bone marrow and that a significant fraction of the total bone marrow mesenchymal progenitor cells were *Osx*-expressing cells derived from mature hypertrophic chondrocytes. This suggests the hypothesis that the hypertrophic chondrocytes to osteoblasts transition might proceed first through a dedifferentiation and then a redifferentiation step.

Inactivation of β -catenin in hypertrophic chondrocytes led to marked decrease in trabecular formation (Golovchenko *et al*, Bone 2013), suggesting that Wnt signaling may play an important role in regulating hypertrophic chondrocytes to osteoblasts transition. In 2-week-old *Coll10a1-Cre; Ctnnb1^{fllox/fllox}; ROSA-tomato* mice, only tomato⁺ bone marrow cells, but no tomato⁺ osteoblasts were observed on trabecular and endosteal surfaces, and no tomato⁺ osteocytes within the cortex, implying that Wnt signaling is needed for chondrocyte-derived progenitors to differentiate into mature osteoblasts.

Disclosures: Xin Zhou, None.

1111

Sarcopenia and age-related muscle impairment: histology and imaging in a close relationship. Umberto Tarantino^{*1}, Jacopo Baldi¹, Manuel Scimeca², Elena Bonanno², Elena Gasbarra³, Eleonora Piccirilli⁴. ¹University of Rome Tor Vergata, orthopaedics & traumatology, Italy, ²University of Rome Tor Vergata, Anatomic Pathology Department, Italy, ³University of Rome Tor Vergata, orthopaedics & traumatology, Italy, ⁴University of Rome Tor Vergata, Department of orthopaedics & traumatology, Italy

Background: Sarcopenia is a pathological condition of impaired muscle quality that may be predictive of an increased fragility fracture risk in the elderly. In the elderly the muscle patrimony becomes poorer in terms of power, strength and resistance. In this context, our experience aims to describe in a multimodal way macro- and micro-structural changes that muscle tissue undergoes during the physiological aging process using histological analysis and Nuclear Magnetic Resonance imaging. **Methods:** We performed vastus lateralis biopsies in 25 women with osteoporosis (OP group) and in 25 women underwent surgery for hip osteoarthritis (OA group). Patients were clinically characterized performing DeXA, T-score and after radiographic assessment by Kellgren-Lawrence scale. The study was approved by the local Ethical Committee. Immunohistochemistry was performed to evaluate muscle fibers type, fast and slow, satellite cells activity, myostatin and CD44, bone-muscle cross-talk molecules and BMP-2 and BMP-4 and mineralization markers. A Magnetic Resonance Diffusion tensor Imaging protocol was performed; we evaluated the T1, T2, Fractional Anisotropy and the Mean Diffusivity. **Results:** in this study we measured vastus lateralis musculature diffusion properties of OP subjects and compared them with OA patients. Our findings revealed in OP a preferential type II fiber atrophy. The analysis of DTI parameters reveals that the FA was significant lower in OP as compared to OA subjects. The correlation analysis showed a strong significant correlation between DTI parameters and the muscle fat of OP and OA subjects. In particular, a positive correlation was found between FA and fat fraction.

In addition, Our results clearly indicate a similar pattern of BMP-2 and BMP-4 expression in bone and muscle tissues. In particular, we demonstrated that muscle tissues of elderly patients frequently express BMPs close to degenerated areas or adipose tissue. However, the expression of these molecules was significantly higher in osteoarthritis group as compared with osteoporotic patients. **Conclusion:** Our experience demonstrates the usefulness of new diagnostic techniques for understanding pathophysiological mechanisms shared by sarcopenia and osteoporosis. Our DTI analysis showed that the MD and the three eigenvalues were significantly higher in OP as compared to OA subjects. Moreover, an opposite trend was obtained for the FA parameter. The finding that both the activity of satellite muscle stem cells and bone remodeling are related to the same factors, BMP-2 and BMP-4, could shed new light on molecular mechanism of more relevant bone-muscle related diseases of the elderly, such as sarcopenia, osteoarthritis and osteoporosis.

Disclosures: Umberto Tarantino, None.

1112

Evaluation of cutpoints for low lean mass and slow gait speed in predicting death in the National Health and Nutrition Examination Survey 1999-2004. Ching-Lung Cheung^{*1}, Karen Lam², Bernard Cheung². ¹The University of Hong Kong, Hong kong, ²University of Hong Kong, Hong kong

Background: Sarcopenia is commonly defined as loss of muscle mass with limited muscle function or strength. Different cutpoints of low lean mass and slow gait speed have been proposed by different professional working groups. We compared the performance of different cutpoints of low lean mass and slow gait speed in predicting death. **Methods:** We analyzed data of participants aged 65 or above from the continuous National Health and Nutrition Examination Survey conducted between 1999 and 2004 (N=2,841), and the subsequent follow-up data on mortality up to December 31, 2006. For low lean mass, cutpoints based on appendicular lean mass (ALM) alone, ALM adjusted for body mass index (ALMBMI) and ALM adjusted for height squared (ALMH2) were evaluated. For slow gait speed, the cutpoints based on 0.7m/s, 0.8m/s, 0.9m/s, and 1.0m/s were evaluated. A Cox-proportional hazard regression model with adjustment for multiple confounding factors was used for the association analyses. **Results:** For low lean mass, the cutpoints based on ALMBMI (<0.512 in women and <0.789 in men) showed the most significant association and highest hazard ratio (HR) with death (HR=1.72; 95% CI: 1.28-2.29; P<0.001). Similar associations were observed in sex-specific analyses. All cutpoints of low lean mass had similar AUC values, except the AUC of low ALMBMI was shown to be significantly higher than that of ALMH2 in men. For slow gait speed, all cutpoints tested showed significant association with death in the full model (P<0.001), while the cutpoint 0.9m/s showed the highest HR (HR=2.39; 95% CI: 1.79-3.20). Similar associations were observed in sex-specific analyses and all cutpoints of low gait speed had similar AUC values. In addition, participants with both low ALMBMI and low gait speed (<0.9m/s) had the highest HR (HR=3.67; 95% CI: 2.42-5.57; P<0.001) when compared to participants with low ALMBMI only, low gait speed only, or without low ALMBMI or low gait speed. **Conclusions:** Low lean mass defined by ALMBMI showed the strongest association with death; while slow gait speed (cutpoints ranging from 0.7m/s to 1.0m/s) showed significant association with death, with the strongest association being observed for the cutpoint of 0.9m/s. Further studies validating the cutpoints are warranted before using them in clinical settings.

Disclosures: Ching-Lung Cheung, None.

1113

Hyperparathyroidism is Associated with Osteosarcopenia in Older Individuals with a History of Falling. Pushpa Suriyaarachchi^{*1}, Fernando Gomez², Carmen L. Curcio², Ruth Huo³, Derek Boersma¹, Oddom Demontiero¹, Piumali Gunawardene⁴, Gustavo Duque⁴. ¹Musculoskeletal Ageing Research Program, Sydney Medical School Nepean, The University of Sydney, Australia, ²Research Group on Geriatrics & Gerontology, Faculty of Health Sciences, International Association of Gerontology & Geriatrics Collaborative Centre, University of Caldas, Colombia, ³Faculty of Medicine, University of New South Wales, Australia, ⁴Musculoskeletal Ageing Research Program, University of Sydney, Australia

BACKGROUND: In older persons, the combination of osteopenia/osteoporosis and sarcopenia (osteosarcopenia) has been proposed as a subset of frail individuals at higher risk of institutionalization, falls and fractures. Therefore, identification of the risk factors for osteosarcopenia is pivotal. Although vitamin D has been associated with a higher risk of osteosarcopenia, the role of parathyroid hormone (PTH) in this syndrome remains unknown. In this study, we evaluated the role of PTH in a population of older individuals with a history of falling.

METHODS: This is a cross sectional study of 760 subjects (mean age=79, 65% women) assessed between 2009-2014 at the Falls and Fracture Clinic, Nepean Hospital (Penrith, Australia). Assessment included medical history, physical examination, bone densitometry and body composition by DXA, posturography, grip strength, gait parameters (GaitRITE), and blood tests for nutrition and secondary causes of sarcopenia and osteoporosis. Patients were divided in 4 groups: 1) Osteopenic (BMD<-1.0 SD in femoral neck); 2) sarcopenic (following the European Consensus criteria); 3) osteosarcopenic and; 4) non-sarcopenic/non-osteopenic. Difference between the groups was assessed using with one-way ANOVA and X² analysis. Multivariable

linear regression evaluated the association between the groups and PTH levels adjusted for age, vitamin D, renal function and albumin.

RESULTS: Our analysis showed that 24% of the subjects had high PTH (>6.8 pmol/L). These subjects were older (81 ± 3, p<0.01), reported a higher number of falls/year (3 ± 1, p<0.01), and showed lower grip strength (18 ± 1Kg, p<0.06), limits of stability (108 ± 6, p<0.008), BMD (-0.7 ± 0.2, p<0.02), and gait velocity (55 ± 6cm/sec, p<0.01). Compared with the other groups, subjects with high PTH showed increased prevalent osteosarcopenia (6.88; CI: 0.9-52).

CONCLUSION: In summary, we have reported an independent association of high PTH levels with osteosarcopenia in a population at high risk of falls and fractures. As a potential mechanism, the chronic elevation of PTH could have a catabolic effect on both muscle and bone, which may be independent of serum levels of vitamin D. In conclusion, our results suggest an important role of PTH in osteosarcopenia that deserves further exploration.

Disclosures: Pushpa Suriyaarachchi, None.

1114

Greater Grip Strength is associated with Larger Cortical Thickness in Men and Larger Bone Size in Women: The Framingham Osteoporosis Study. Robert McLean¹, Xiaochun Zhang², Kerry Broe², Ching-An Meng², Elizabeth Samelson¹, L Adrienne Cupples³, Marian Hannan¹, Mary Bouxsein⁴, Douglas Kiel¹. ¹Hebrew SeniorLife Institute for Aging Research & Harvard Medical School, USA, ²Hebrew SeniorLife Institute for Aging Research, USA, ³Boston University School of Public Health, USA, ⁴Beth Israel Deaconess Medical Center & Harvard Medical School, USA

The sensitivity of bone to mechanical loading might underlie the observation that age-related loss of muscle strength is associated with bone loss. Greater grip strength has consistently been associated with higher areal bone density across several studies of older adults, though fewer have examined bone volumetric density and structure, and results have been mixed. Further, we are aware of only one previous study of grip strength and bone microarchitecture in older men, while none have examined women. Thus, our understanding of the relation between age-related changes in muscle and bone is incomplete. Our objective was to determine the association of grip strength with distal radius bone density, size and microarchitecture among 402 men and 541 women aged ≥50 years in the community-based Framingham Offspring cohort. At the non-dominant arm, grip strength (kg) was measured by hand-held dynamometer (maximum of 3 trials), and bone size, microarchitecture and density of the distal radius were assessed by HR-pQCT (Scanco Medical AG). For men and women separately, analysis of covariance was used to calculate least squares-adjusted mean (SE) bone measures for sex-specific quartiles of grip strength, and test for linear trends, adjusting for age, height and weight. Mean age in the study population was 70 years (range 51-92). Mean grip strength was 37 kg in men and 21 kg in women. From quartile 1 (low) to quartile 4 (high), total cross-sectional area increased in women (P for trend<0.0001), while a similar trend in men had a P for trend=0.06. Cortical thickness increased across quartiles in men (P trend=0.006), but not in women. In both sexes, grip strength was not associated with cortical porosity, trabecular thickness, trabecular number, nor with cortical bone area fraction (cortical area/total area). Density did not increase across grip strength quartiles, though in women there was suggestion of a decrease in total density with increasing grip strength quartile (P trend=0.046). We found that at the non-weight bearing distal radius, greater grip strength was associated with larger bone cross-sectional area, particularly in women, but with larger cortical thickness in men only. Our results suggest that while mechanical loading does not seem to influence bone density at the distal radius, it may contribute to bone size. Findings also indicate that the response of cortical bone to loading may differ between men and women.

Least squares-adjusted* mean (SE) distal radius bone density, size and microarchitecture for quartiles of grip strength among men and women in the Framingham Osteoporosis Study.

| Men | Q1 | Q2 | Q3 | Q4 | P trend |
|--|--------------------|---------------------|---------------------|---------------------|---------|
| | (4-31 kg) n=105 | (32-36 kg) n=107 | (37-42 kg) n=94 | (43-68 kg) n=96 | |
| Total area (mm ²) | 373 (6) | 378 (6) | 386 (6) | 389 (7) | 0.06 |
| Cortical bone area fraction (%) | 0.20 (0.01) | 0.20 (0.01) | 0.21 (0.01) | 0.21 (0.01) | 0.10 |
| Cortical thickness (mm) | 0.937 (0.020) | 0.925 (0.019) | 0.978 (0.020) | 1.012 (0.021) | 0.006 |
| Cortical porosity (%) | 4.23 (0.17) | 4.34 (0.16) | 4.45 (0.17) | 4.22 (0.18) | 0.89 |
| Trabecular thickness (mm) | 0.069 (0.001) | 0.071 (0.001) | 0.069 (0.001) | 0.070 (0.001) | 0.71 |
| Trabecular number (mm ⁻¹) | 2.2 (0.03) | 2.2 (0.02) | 2.3 (0.03) | 2.3 (0.03) | 0.23 |
| Total density (mg/cm ³) | 325 (6) | 326 (6) | 331 (6) | 342 (7) | 0.07 |
| Cortical density (mg/cm ³) | 949 (5) | 947 (5) | 950 (5) | 960 (6) | 0.21 |
| Trabecular density (mg/cm ³) | 184 (4) | 189 (4) | 187 (4) | 191 (4) | 0.29 |
| Women | Q1 | Q2 | Q3 | Q4 | P trend |
| | (5-17 kg) n=132 | (18-20 kg) n=137 | (21-24 kg) n=139 | (25-44 kg) n=133 | |
| Total area (mm ²) | 240 (4) | 247 (3) | 257 (3) | 268 (4) | <0.0001 |
| Cortical bone area fraction (%) | 0.21 (0.01) | 0.21 (0.01) | 0.20 (0.01) | 0.20 (0.01) | 0.02 |
| Cortical thickness (mm) | 0.820 (0.016) | 0.806 (0.015) | 0.783 (0.016) | 0.796 (0.016) | 0.21 |
| Cortical porosity (%) | 3.60 (0.15) | 3.84 (0.14) | 3.69 (0.14) | 3.69 (0.15) | 0.89 |
| Trabecular thickness (mm) | 0.066 (0.001) | 0.064 (0.001) | 0.063 (0.001) | 0.063 (0.001) | 0.12 |
| Trabecular number (mm ⁻¹) | 1.9 (0.04) | 1.9 (0.03) | 1.9 (0.03) | 1.9 (0.03) | 0.67 |
| Total density (mg/cm ³) | 307 (6) | 300 (5) | 292 (5) | 291 (6) | 0.046 |
| Cortical density (mg/cm ³) | 965 (5) | 959 (5) | 956 (5) | 957 (5) | 0.24 |
| Trabecular density (mg/cm ³) | 149 (4) | 148 (3) | 148 (3) | 145 (4) | 0.50 |

*Adjusted for age, height and weight

table

Disclosures: Robert McLean, Policy Analysis Inc
This study received funding from: Friends of Hebrew SeniorLife & research grant from the Investigator-Initiated Studies Program of Merck Sharp & Dohme

1115

Sarcopenia Predicts Fracture Risk in 65-year Old Healthy Community-dwellers. Andrea Trombetti*, Mélyny Hars, Emmanuel Biver, Thierry Chevalley, Serge Ferrari, René Rizzoli. Division of Bone Diseases, Geneva University Hospitals & Faculty of Medicine, Switzerland

Sarcopenia is associated with an increased risk of adverse outcomes, including falls. However, the contribution of low skeletal muscle mass to fracture risk remains unknown. Various thresholds for low lean mass have been proposed for sarcopenia definition, but their ability to predict hard outcomes like incident fractures is not established. In this study, we investigated the prevalence of low lean mass and its association with 3-year fracture incidence in a homogeneous cohort of healthy 65-year old community-dwellers. Nine hundred thirteen subjects (729 women; age 65.0 ± 1.4 years), enrolled in the Geneva Retirees Cohort (GERICO) study, were prospectively followed-up. Total (TLM) and appendicular (ALM) lean masses were assessed using DXA. The various thresholds proposed by Baumgartner et al, the European Working Group on Sarcopenia in Older People (EWGSOP 1 and 2), the International Working Group on Sarcopenia (IWG), or the Foundation for the National Institutes of Health Sarcopenia Project (FNIH) were applied. Low trauma clinical fracture incidence over a 3-year period was recorded. The associations between lean mass and incident low trauma fractures were assessed using univariate and multivariate logistic regression models. During an average follow-up of 3.4 ± 0.9 years, 40 (4.4%) participants sustained at least one incident low trauma fracture. The prevalence of low lean mass was 11.2%, 17.1% and 3.5% according to Baumgartner or EWGSOP 1, EWGSOP 2 or IWG, and FNIH thresholds, respectively. Baseline ALM and TLM were lower in subjects with incident fractures compared to those without fractures (17.2 ± 3.3 vs 18.6 ± 4.3 kg, p<0.02, for ALM; 41.2 ± 7.0 vs 43.7 ± 8.8 kg, p<0.04, for TLM). After adjusting for sex, age, length of follow-up and FRAX probability with BMD, low lean mass was associated with a 2.3 (CI95%: 1.0-5.1; p<0.05) (Baumgartner or EWGSOP 1 threshold) and 1.3 (CI95%: 0.6-2.7; ns) (EWGSOP 2 or IWG threshold)-fold increase in low trauma fracture risk. No patient with FNIH low lean mass criteria experienced any low trauma fracture. Our results show that low appendicular lean mass, as defined with Baumgartner or EWGSOP 1 threshold, is a predictor of incident fractures in a large cohort of healthy 65-year old community-dwellers, independently of FRAX score. The increased risk is clearly related to the threshold for low lean mass selected. Whether assessing in addition muscle function improves low trauma fracture risk prediction remains to be determined.

Disclosures: Andrea Trombetti, None.

1116

Poor peripheral nerve function increases the risk of injurious falls: the Health, Aging and Body Composition Study. Elsa S. Strotmeyer*, Mary E. Winger¹, Jane A. Cauley¹, Robert M. Boudreau¹, Teresa M. Waters², Julie M. Donohue¹, Steven M. Albert¹, Ann V. Schwartz³, Suzanne Satterfield², Sasa Zivkovic¹, Aaron I. Vinik⁴, Melissa Garcia⁵, Tamara B. Harris⁵, Anne B. Newman¹. ¹University of Pittsburgh, USA, ²University of Tennessee Health Science Center, USA, ³University of California, San Francisco, USA, ⁴Eastern Virginia Medical School, USA, ⁵National Institute on Aging, USA

Older adults have subclinical sensorimotor nerve declines, though the relationship to injurious falls is unknown. Clinical neuropathy has been associated with fractures; however age-related impairments and non-fracture injuries have not been investigated. Sensorimotor nerve function in the Health, Aging and Body Composition Study (Medicare-eligible at 1997/98 baseline, 52% women, 38% black, 22% diabetes) was related to incident injurious falls from linked Medicare claims. Monofilament detection (10-g/1.4-g), sensory vibration threshold (inability to detect: >131 μ), peroneal motor nerve conduction velocity (NCV, low: <40 m/s) and amplitude (CMAP, low: <1 mV) were assessed at 7/00-6/01 exam (N=2,399). Injurious falls from clinic exam to 12/31/08 were identified from Medicare claims for N=2,375 (99%) as fall code (E880-888) plus non-fracture injury (N=161), and/or fracture code (800-829) with (N=91) or without (N=367) a fall code. Traumatic, intentional or pathologic injuries were excluded (N=38). Censoring performed at initial injurious fall (N=619 in 3.8 ± 2.4 years), or at earliest date of: Medicare fee-for-service end (N=1), last follow-up (N=13), death (N=525), or 12/31/08 claims dataset end (N=1217) in 6.9 ± 2.1 years. Fracture injuries were more likely from inpatient hospital claims compared to non-fracture injuries (28% vs. 3%; p<0.05). Participants with injurious falls were more likely to be white (71% vs. 58%), women (65% vs. 47%), older (age 77 ± 3 vs. 76 ± 3 years), and had lower BMI (26.8 ± 4.9 vs. 27.6 ± 4.8 kg/m²), all p<0.001. Cox regression models for each sensorimotor measure were developed for total fall injuries and stratified by fracture injuries, adjusted for demographic, BMI, lifestyle factors, comorbidity, leg strength and medications (total count and with potential to affect falls). Sensitivity analyses removing injuries possibly unrelated to falls (e.g., vertebral fracture) were consistent. In adjusted models (Table 1), 1.4-g and 10-g insensitivity increased incident injurious fall risk. Vibration threshold and motor CMAP/NCV were not related when including fracture injuries. When fall injuries with or without fractures were stratified, associations were largely consistent though inability to detect vibration was also related to increased risk of non-fracture injuries. Sensory, though not motor, nerve impairment increased injurious fall risk, and simple monofilament tests may be a particularly important predictor in older adults.

1118

Genetic or Pharmacological Ablation of Fgf23 Ameliorates Progression of Chronic Kidney Disease in Mice. OLENA ANDRUKHOVA¹, Svetlana Slavic², Sathish Kumar Murali², Bill Richards³, Reinhold G. Erben². ¹INST. OF PHYSIOLOGY, PATHOPHYSIOLOGY & BIOPHYSICS, Austria, ²Department of Biomedical Sciences, University of Veterinary Medicine, Austria, ³Amgen Inc, USA

Clinical studies have shown that circulating fibroblast growth factor 23 (FGF23) is associated with disease progression, cardiovascular risk, and mortality in patients with chronic kidney disease (CKD). Here, we sought to elucidate further the role of Fgf23 and its co-receptor Klotho in the pathogenesis of CKD in mice by a dual approach, using genetic loss-of-function together with pharmacological inhibition models. CKD was induced by 5/6 nephrectomy in 3-month-old wild-type (WT) mice, vitamin D receptor (VDR) mutant mice, Fgf23-/-VDR?? (Fgf23/VDR), and Klotho-/-VDR?? (Klotho/VDR) compound mutant mice. All mice were kept lifelong on a rescue diet enriched with calcium, phosphorus, and lactose to prevent secondary hyperparathyroidism in VDR mutant mice. Sham-operated (SHAM) mice served as controls. In addition, SHAM and CKD WT, VDR, and Klotho/VDR mice were treated with low dose anti-FGF23 antibody (anti-FGF23Ab, 50 µg per mouse, two times per week) over 8 week post-surgery. This dose of anti-FGF23Ab reduced circulating Fgf23 in CKD mice to Sham control levels. Genetic ablation of Fgf23 in Fgf23/VDR compound mutant or treatment of WT and VDR CKD mice with anti-FGF23Ab partially or completely protected against the CKD-induced weight loss, increase in mortality, reduction in glomerular filtration rate, albuminuria, volume expansion, hypernatremia, hypercalcemia, hyperphosphatemia, hypertension, and left ventricular functional impairment observed in untreated and vehicle-treated WT and VDR mice, 8 weeks post-surgery. Moreover, anti-FGF23Ab treatment of Klotho/VDR CKD mice, which were characterized by the highest circulating Fgf23 concentrations among all CKD groups, reduced the increased mortality and accelerated disease progression observed in these mice to levels found in Fgf23/VDR mutants, demonstrating that Fgf23 also has Klotho independent effects at high circulating levels. Genetic ablation or pharmacological inhibition of Fgf23 prevented hypercalcemia and volume overload in CKD mice by down-regulating renal sodium-transporting molecules, and increasing urinary excretion of sodium and calcium. Collectively, our data suggest that elevated Fgf23 contributes to the pathogenesis of CKD in a vitamin D hormone- and partially Klotho-independent manner. Hence, our study may provide a mechanistic explanation for the association between circulating FGF23 and disease progression in CKD patients.

Disclosures: OLENA ANDRUKHOVA, None.

1119

Inhibition of Fibroblast Growth Factor Receptor Signaling Partially Rescues Hypophosphatemic Rickets in FGF2 High Molecular Weight Isoform Transgenic Mice. Liping Xiao^{*}, Erxia Du, Patience Meo Burt, Marja Marie Hurley. University of Connecticut Health Center, USA

Vitamin D and phosphates improves serum phosphate (Pi) and rickets in some X-linked hypophosphatemic rickets (XLH) patients but increases circulating FGF23, which further complicates therapy. Mice harboring high molecular weight FGF2 isoforms (HMWTg) in osteoblast lineage phenocopy human XLH and Hyp murine model of XLH and HMWFGF2 was upregulated in bones of Hyp mice. Since abnormal FGF receptor signaling is important in XLH, HMWTg mice were used to examine the effect of the FGFR inhibitor NVP-BGJ398 (BGJ398, Novartis) on hypophosphatemic rickets.

Five week old HMWTg or Vector control male mice were orally gavaged with BGJ398 50mg/kg or Vehicle, 3 times/week, for 8 weeks. Body weight, tail length, bone mineral density (BMD) and bone mineral content (BMC) were measured biweekly. At 8 weeks, serum was collected to measure calcium (Ca), Pi, FGF23 and PTH and 24h urine to measure Pi. Mice were labeled with calcein and xylene orange (XO) 7 and 2 days prior to sacrifice. Femur and tibia length was measured and Digital x-rays and micro-CT was performed on excised bones. BGJ398 normalized serum Pi, reduced urine Pi, decreased serum PTH but further increased FGF23 (Table 1).

BGJ398 normalized tail, tibia and femur length but further decreased vertebral BMD and BMC and femur BMD in HMWTg (Table 1). Micro-CT of vertebrae (Table 2) showed further decreased BV/TV, Trab.Number and increased Trab Spacing with BGJ398 treatment. Micro-CT of femurs (Table 3a) showed increased Trabecular Tissue density in BGJ398 treated HMWTg. BGJ398 rescued abnormal architecture (arrow head) and mineral defect in cortical bone (arrow) (Figure 1) and increased cortical thickness, reduced porosity, increased endosteal perimeter and cortical tissue density in HMWTg (Table 3b). Histologic examination of femurs (Figure 2) revealed that BGJ398 improved cancellous bone (black arrow head), cortical bone structure (black arrow), growth plate, and double labeling in cortical bone (white arrows) in HMWTg. BGJ398 increased osteoclast number and surface, double labeled surface, MAR and bone formation rate in femur trabeculae of HMWTg.

We conclude that BGJ398 partially rescued hypophosphatemic rickets and could be considered as a new treatment for XLH. However, BGJ398 treatment increased serum FGF23 that could further exacerbate the mineralization defect. Furthermore HMWFGF2 may have effects on bone matrix mineralization independent of FGFR.

Table 1. Final adjusted Cox regression models for sensorimotor nerve impairment predicting total fall injuries, non-fracture injuries, and fractures.

| | Total fall injuries (N=619/2375) | Non-fracture fall injuries (N=161/2375) | Fracture injuries (N=458/2375) |
|--|----------------------------------|---|--------------------------------|
| Hazard Ratio (95% Confidence Interval) | | | |
| Sensory nerve | | | |
| Monofilament insensitivity, 10-g | 1.5 (1.1, 2.0) [†] | 2.4 (1.5, 3.9) [†] | 1.2 (0.9, 1.8) |
| 1.4-g | 1.3 (1.1, 1.6) [†] | 1.3 (0.9, 1.9) | 1.3 (1.1, 1.6) [†] |
| Inability to detect vibration >131µ | 1.1 (0.8, 1.6) | 2.2 (1.3, 3.8) [†] | 0.9 (0.6, 1.5) |
| Motor nerve | | | |
| NCV <40 m/s | 1.1 (0.9, 1.4) | 1.2 (0.8, 2.0) | 1.1 (0.8, 1.5) |
| CMAP <1 mV | 1.2 (0.9, 1.6) | 1.5 (0.9, 2.5) | 1.1 (0.8, 1.6) |

[†]p-value<0.01. Age, sex, race, site, diabetes (yes/no), BMI and total number of medications were retained in all models, with additional covariates removed at p>0.1. Modified Mini-Mental State score was retained in all models for total fall injuries and non-fracture fall injuries, and Cystatin C>1.0 mg/L in 1.4-g/10-g insensitivity models for total fall injuries and non-fracture fall injuries and in vibration model for total fall injuries.

Table 1

Disclosures: Elsa S. Strotmeyer, None.

1117

Erythropoietin and FGF23 cross-talk during iron-deficiency anemia. Erica Clinkenbeard^{*}¹, Keith Stayrook², Hitesh Appaiiah³, Taryn Cass⁴, Emily Farrow⁵, Mircea Ivan⁶, Rebecca Chan⁷, Ernestina Schipani⁸, Thomas Clemens⁹, Kenneth White⁴. ¹Indiana University-Purdue University Indianapolis, USA, ²Department of Pharmacology & Toxicology, Indiana University School of Medicine, USA, ³Department of Medical & Molecular Genetics Indiana University School of Medicine, USA, ⁴Department of Medical & Molecular Genetics, Indiana University School of Medicine, USA, ⁵Department of Pediatrics, University of Missouri-Kansas City School of Medicine, USA, ⁶Department of Medicine/Hematology-Oncology, Indiana University School of Medicine, USA, ⁷Herman B Wells Center for Pediatric Research, Indiana University School of Medicine, USA, ⁸Departments of Orthopaedic Surgery & Medicine/Endocrinology, University of Michigan School of Medicine, USA, ⁹Department of Orthopaedic Surgery, Johns Hopkins School of Medicine, USA

The mechanisms controlling FGF23-mediated phosphate metabolism during normal and disease conditions remain unclear. We previously determined that anemia/hypoxia increased bone FGF23. This finding is important for late onset autosomal dominant hypophosphatemic rickets (ADHR) where FGF23 is elevated during iron deficiency, and in CKD, where conjoint manifestations of anemia/iron deficiency, high serum FGF23, and defects in phosphate metabolism occur. Herein, our goal was to identify the molecular mechanisms controlling FGF23 production during anemia. In this regard, we first tested the role of the transcription factor Hypoxia inducible factor-1 alpha (HIF1α). In vitro studies using iron chelators demonstrated significant HIF-reporter activity (10-fold; p<0.05), and HIF1α knock-down resulted in 95% reduction of FGF23 mRNA (p<0.02) in UMR-106 and U2OS osteoblastic cells. In vivo, mice lacking HIF-1α in osteoblasts [HIF1α^{fl/fl}/OCN-cre] or lacking both HIF-1α and HIF-2α in osteoprogenitors [HIF1/2^{fl/fl}/OSX-cre] were provided iron-restricted diets to induce anemia. In contrast to in vitro studies, upon induction of anemia conditional null mice retained similar abilities as Cre⁺ littermates to increase FGF23 mRNA (>40-fold) and total protein (16-fold). Serum erythropoietin (EPO) dramatically rose in the HIF-null mice (40-60 fold, p<0.01), therefore this hormone was next tested as an independent FGF23 regulator. In concert with positive indicators of EPO delivery, including splenomegaly and elevated bone transferrin receptor (5-fold; p<0.01), EPO injections dose-dependently increased FGF23 mRNA and total protein (>40-fold maximal; p<0.01), as well as doubled intact FGF23 (p=1x10⁻⁶) in WT and HIF1α^{fl/fl}/OCN-cre⁺ mice. Next, the juvenile cystic kidney ('Jck') PKD/CKD mouse model was tested over a 4-20 week time course and found to have iron deficiency and anemia at 12 weeks of age concomitant with elevated EPO and FGF23. EPO administration to 6-week old Jck caused an early rise in intact FGF23 to levels greater than in age-matched WT mice (686.3 vs 407.2 pg/mL; p<0.01). Together, our findings demonstrate that in addition to HIF-dependent pathways, EPO drives FGF23 production, and in conditions of renal insufficiency may increase secretion of active FGF23. Considering the overlapping toxicity of EPO/ESAs and FGF23, our findings have significant implications for optimizing emerging and current interventions for syndromes involving disturbed iron and phosphate metabolism.

Disclosures: Erica Clinkenbeard, None.

Table 1. Body weight, tail, tibia, femur length, BMD, BMC, serum and urine biochemistry

| | Vector Mice Vehicle | HMWTg Mice Vehicle | HMWTg Mice BGJ398 |
|------------------------------------|---------------------|--------------------|-------------------|
| Body Weight (g) | 25.77±0.57 | 23.47±0.70* | 23.39±0.84* |
| Tail Length (mm) | 81.27±0.20 | 78.10±0.73* | 89.90±0.93# |
| Total BMD (g/cm ³) | 0.052±0.001 | 0.051±0.001 | 0.050±0.001 |
| Total BMC (g) | 0.286±0.006 | 0.296±0.008 | 0.293±0.004 |
| Vertebrae BMD (g/cm ³) | 0.048±0.001 | 0.044±0.001* | 0.040±0.001*# |
| Vertebrae BMC (g) | 0.028±0.001 | 0.026±0.001 | 0.023±0.001* |
| Tibiae Length (mm) | 17.25±0.28 | 15.24±0.24* | 16.59±0.21# |
| Tibiae BMD (g/cm ³) | 0.048±0.000 | 0.051±0.001* | 0.048±0.001 |
| Tibiae BMC (g) | 0.016±0.000 | 0.017±0.001 | 0.017±0.001 |
| Femur Length (mm) | 14.96±0.10 | 14.34±0.17* | 16.06±0.16*# |
| Femur BMD (g/cm ³) | 0.054±0.001 | 0.051±0.001 | 0.049±0.002* |
| Femur BMC (g) | 0.021±0.001 | 0.019±0.001 | 0.020±0.001 |
| Serum Pi (mg/dL) | 8.37±0.30 | 7.31±0.20* | 9.26±0.60# |
| 24h Urine Pi (mg) | 0.17±0.20 | 1.48±0.25* | 1.01±0.21 |
| Serum Ca (mg/dL) | 9.29±0.18 | 9.24±0.13 | 9.02±0.31 |
| Serum PTH (pg/mL) | 225.68±16.57 | 278.14±16.74* | 54.59±8.43*# |
| Serum FGF23 (pg/mL) | 315.37±15.09 | 941.75±322.64* | 1536.71±117.77* |

*: Compared with Vector Vehicle p<0.05; #: Compared with HMW Vehicle p<0.05

Figure 1. X-ray and Micro-CT analysis of femurs

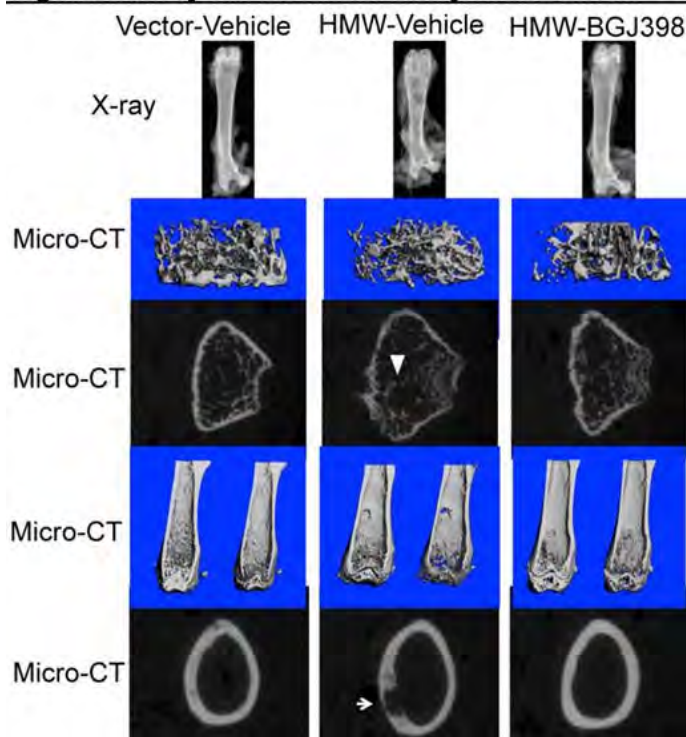


Figure1

Figure 2. Alizarin red & alcian blue staining and calcein & xylenol orange labeling of femurs

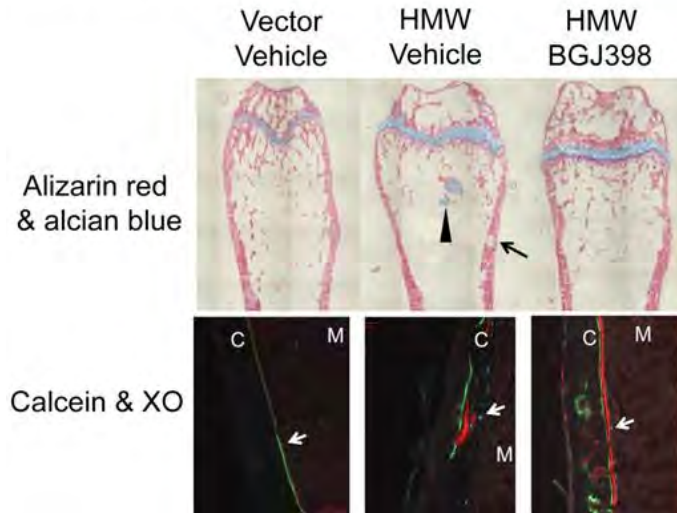


Figure2

Disclosures: Liping Xiao, None.

1120

Sorting Nexin 27 Links PTHR Trafficking to the Retromer for Postnatal Bone Growth. Audrey Chan^{*1}, Euphemie Landao¹, Thomas Clairfeuille², Pei Ying Ng¹, Genevieve Kinna², Li Shen Loo³, Tak Sum Cheng¹, Ming Hao Zheng¹, Rohan Teasdale², Wanjin Hong³, Brett Collins², Nathan Pavlos¹. ¹Cellular Orthopaedic Laboratory, School of Surgery, University of Western Australia, Australia, ²IMB, University of Queensland, Australia, ³Institute of Molecular & Cell Biology, A*STAR, Singapore

During postnatal life, longitudinal bone growth relies upon the ability of its cellular residents to receive and respond to local and systemic stimuli through a complement of transmembrane signalling receptors (cargo). The parathyroid hormone receptor type 1 (PTHr) is a class B GPCR critical for bone growth, remodelling, and mineral ion metabolism. In response to stimulation, PTHr is rapidly

Table1

Table 2. Micro-CT analysis of vertebrae

| | Vector Mice Vehicle | HMWTg Mice Vehicle | HMWTg Mice BGJ398 |
|--|---------------------|--------------------|-------------------|
| Vertebrae BV/TV (%) | 18.63±0.78 | 14.43±0.59* | 10.02±0.41*# |
| Vertebrae Trab. Thickness (µm) | 47.93±0.60 | 43.67±0.91* | 40.84±0.36*# |
| Vertebrae Trab. Number (1/mm) | 4.38±0.11 | 3.93±0.10* | 3.47±0.07*# |
| Vertebrae Trab. Spacing (µm) | 230.18±6.35 | 257.26±6.53* | 286.92±5.59*# |
| Vertebrae Connec. Density (1/mm ³) | 151.91±7.67 | 198.62±20.67* | 97.59±1.78*# |

*: Compared with Vector Vehicle p<0.05; #: Compared with HMW Vehicle p<0.05

Table2

Table 3. Micro-CT analysis of femurs

| 3a. Trabecular | Vector Mice Vehicle | HMWTg Mice Vehicle | HMWTg Mice BGJ398 |
|--|---------------------|--------------------|-------------------|
| BV/TV (%) | 13.17±0.73 | 12.04±1.28 | 11.74±1.04 |
| Trab. Thickness (mm) | 51.12±1.11 | 57.78±2.43* | 54.63±4.11 |
| Trab. Number (1/mm) | 4.51±0.08 | 3.93±0.34 | 3.91±0.12* |
| Trab. Spacing (µm) | 221.57±3.93 | 273.68±29.48 | 266.28±17.62* |
| Connec. Density (1/mm ³) | 97.96±5.29 | 91.59±8.76 | 104.00±6.59 |
| Tissue Density (mg/ccm HA) | 619.9±7.4 | 583.8±8.6* | 607.3±4.8# |
| 3b. Cortical | Vector Mice Vehicle | HMWTg Mice Vehicle | HMWTg Mice BGJ398 |
| Thickness (mm) | 0.18±0.00 | 0.16±0.00* | 0.17±0.00* |
| Porosity (%) | 0.009±0.000 | 0.023±0.004* | 0.010±0.001# |
| Endosteal Perimeter (mm) | 3.29±0.04 | 3.47±0.06* | 3.70±0.04*# |
| Periosteal Perimeter (mm) | 4.34±0.08 | 4.70±0.18 | 5.06±0.05* |
| Segmented Bone (mm ²) | 0.71±0.01 | 0.72±0.02 | 0.75±0.02 |
| Mask (mm ²) | 0.72±0.01 | 0.74±0.02 | 0.76±0.02 |
| Sub-Endosteal Area (mm ²) | 0.86±0.02 | 0.96±0.04* | 1.09±0.02*# |
| Sub-Periosteal Area (mm ²) | 1.58±0.03 | 1.70±0.05 | 1.85±0.04*# |
| Tissue Density (mg/ccm HA) | 1193.9±6.1 | 1098.44±10.9* | 1128.57±8.9*# |

*: Compared with Vector Vehicle p<0.05; #: Compared with HMW Vehicle p<0.05

Table3

internalised and recycled from early endosomes to the plasma membrane (PM) via the retromer sorting ensemble. Sorting Nexin 27 (SNX27), a PDZ-domain containing member of the Phox-homology (PX) family of SNXs, is an endosome-associated cargo adaptor that operates in unison with the retromer to ensure the fidelity of cargo selection during activity-dependent endosome-to-PM retrieval. Here we show that SNX27 functions as a crucial regulator of postnatal bone growth by linking PTHR trafficking to the retromer endosome-to-PM recycling pathway. Using micro-computed tomography (microCT) and histomorphometry we demonstrate that mice lacking SNX27 exhibit severe disturbances in postnatal bone growth. Analysis of long bones of 4-week-old SNX27-deficient mice revealed a drastic reduction in bone size and net volume, decreased trabecular number, and a conspicuous growth plate defect. Mechanistically, we demonstrate that these abnormalities are attributable, in part, to cell-autonomous disturbances in the signalling, trafficking and function of the PTHR. By co-immunoprecipitation and isothermal titration calorimetry (ITC) we show that PTHR is a direct SNX27 binding cargo whose affinity is enhanced by an order of magnitude in the presence of the retromer. At the atomic level, we demonstrate that PTHR associates electrostatically with the binding pocket of SNX27-PDZ domain via its canonical C-terminal PDZ-binding motif (PDZbm: E-T-V-M) and identify several upstream amino acids critical to the high affinity SNX27-PDZ: PTHR-PDZbm interaction. In response to agonist stimulation, we demonstrate that PTHR is internalised into early endosomes, an event that coincides with the rapid mobilisation of SNX27 and recruitment of the retromer complex. Finally, we show that depletion of the SNX27-retromer by shRNA knockdown misdirects PTHR trafficking to lysosomes, resulting in a net reduction of PTHR expression at the cell surface. Therefore, SNX27 serves as endosomal cargo adaptor that links PTHR trafficking to the retromer to preserve bone growth and homeostasis throughout postnatal life.

Disclosures: Audrey Chan, None.

1121

Thyroid Hormone Receptor β (TR β) Signaling is Critically Involved in Regulating Secondary Ossification via Promoting Transcription of the IHH Gene in the Epiphysis. Weirong Xing¹, Patrick Aghajanian², Heather Watt², Catrina Alarcon², Subburaman Mohan². ¹Musculoskeletal Disease Center, Jerry L. Pettis Memorial Veteran's Admin., USA, ²Jerry L. Pettis Memorial VA Medical Center, USA

We recently demonstrated that thyroid hormone (TH) is indispensable for the initiation and progression of the secondary ossification center (SOC) at the epiphysis. TH action is mediated through two nuclear TH receptors, TR α and TR β . The ligand binding TR α is ubiquitously expressed and is the most abundant form of TR expressed in bone. While the role of TR α is well established, less is known about the relevance of TR β -mediated signaling in bone development. A two day treatment of Tshr^{-/-} mice with TH increased the TR β mRNA level at day 7 by 3.4 fold (P<0.001) but had no effect on the TR α mRNA level at the proximal tibial epiphysis. Accordingly, treatment of serum-free cultures of tibia-derived cells from 3-day old mice treated with T3 increased TR β expression by 2.1 and 13-fold, respectively, at 24 and 72 h. To determine the role of TR β signaling, we evaluated the effects of GC1, a TR β -specific agonist, on bone formation in vivo in the epiphysis. TH deficient Tshr^{-/-} mice were treated daily for 10 days (day 5-14) with GC1 (0.2 or 2 μ g/day) or vehicle and the amount of bone formed at the proximal tibial epiphysis was quantitated by micro-CT at postnatal day 21. GC1 treatment at 0.2 or 2.0 μ g increased BV/TV by 225% and 263% of vehicle treatment (P<0.001), respectively. Two day treatment with GC1 (0.2 μ g/day) increased expression levels of IHH by 100-fold, osterix by 15-fold and osteocalcin by 59-fold (all P<0.001) compared to vehicle at day 7 in the proximal tibial epiphysis. While expression of type X collagen was increased by 238-fold (P<0.001), type II collagen expression was reduced by 25% (P<0.05). Since IHH is a key regulator of endochondral ossification and since the distal promoter regions of the IHH genes of different species each contain TH responsive elements (TREs), we next evaluated if TH acts directly on the IHH gene to promote transcription. We inserted a 1 kb portion (-5918 to -4919) of the mouse IHH promoter containing putative TREs in front of the TK minimal promoter of the pTAL-SEAP reporter gene and found that a 1 nM GC1 treatment increased alkaline phosphatase activity by 20-fold (P<0.01) compared to vehicle at 48 h in chondrocytes. In conclusion, our data demonstrate a novel role for TR β in secondary ossification at the epiphysis that involves transcriptional up-regulation of the IHH gene.

Disclosures: Weirong Xing, None.

1122

Osteocytic JAK/STAT signalling controls corticalization of long bones by estradiol and testosterone-dependent mechanisms. Daechul Cho¹, Narelle McGregor¹, Brett Tonkin², Holly Brennan², Rachelle Johnson², Roger Zebaze³, David Handelsman⁴, T John Martin², Natalie Sims^{*1}. ¹St. Vincent's Institute of Medical Research, Australia, ²St. Vincent's Institute of Medical Research, Australia, ³Austin Health, University of Melbourne, Australia, ⁴ANZAC Research Institute, The University of Sydney, Australia

Cortical morphology at the metaphysis of long bones is a key determinant of bone strength in old age. Cortical bone in this region forms by coalescence of trabeculae arising from the growth plate, but the control of this process is poorly understood.

SOCS3 (Suppressor of Cytokine Signalling 3) is a JAK/STAT inhibitor specific for glycoprotein 130 (gp130), leptin and G-CSF receptors. Male and female mice lacking SOCS3 in osteocytes (DMP1Cre.SOCS3^{fl/fl} (f/f)) had significantly higher trabecular bone volume (BV/TV, by micro CT) at 6 weeks of age (4.5-fold, p<0.01) compared to DMP1Cre.SOCS3^{w/w} controls (w/w). At 12 weeks of age, both male and female f/f mice had greater osteoid surface, volume, osteoblast surface and mineralizing surface (p<0.01), but bone mass phenotypes were sex-divergent: male f/f BV/TV was half of male w/w (p<0.05) while female f/f BV/TV was 7-fold higher (p<0.001) than female w/w. There were no alterations in bone length. The female f/f high bone mass was most dramatic in the metaphysis where trabecular bone was continuous with, and indistinguishable from, highly porous cortical bone, suggesting defective metaphyseal corticalization.

To determine whether estrogen was responsible for this phenotype, male and female f/f and w/w mice were orchietomized (ORX) or ovariectomized (OVX) at 6 weeks of age, and treated until 12 weeks of age with 17- β -estradiol (E₂) or non-aromatizable dihydrotestosterone (DHT) by slow-release silastic implant. In w/w mice these E₂ and DHT doses prevented OVX and ORX-associated bone loss, respectively. In female f/f mice, OVX reduced BV/TV and partially restored cortical integrity; E₂ prevented these changes. DHT normalized the female f/f phenotype such that trabecular and cortical bone were readily distinguished. When male f/f mice were treated with E₂, the phenotype fully recapitulated that of female f/f mice: cortical bone in the metaphysis was highly porous and indistinguishable from abundantly calcin-labelled trabecular bone.

These data suggest that trabecular coalescence, required for compartmentalization of cortical and trabecular bone, is controlled not by longitudinal growth, or the activity of cells at the growth plate, but rather by SOCS3 inhibitory actions in the osteocyte. In this model of high osteoblast activity, testosterone promoted trabecular coalescence while estradiol prevented it, pointing to sex steroid-dependency in the process of trabecular coalescence during formation of strong cortical bone.

Disclosures: Natalie Sims, None.

1123

Osteoblast-Activated Notch1 signaling in Hematopoietic Cells Induces Acute Myeloid leukemia. Marta Galán-Díez^{*1}, Aruna Kode¹, Sanil J Manavalan¹, Julie Teruva-Feldstein², Govind Bhagat³, Ellin Berman⁴, Stavroula Kousteni³. ¹Columbia University Medical Center, USA, ²Mount Sinai Health System, Icahn School of Medicine at Mount Sinai, USA, ³Columbia University, USA, ⁴MSKCC, USA

An activating mutation of b-catenin in osteoblasts induces acute myeloid leukemia (AML) in mice (*Ctmb1*^{CAosb} mice) through upregulation of *Jagged1* expression in the same cells. As a result, Notch signaling is activated in long term hematopoietic stem cell progenitors (LT-HSC cells). Activated β -catenin/Notch signaling was also identified in a subset of AML patients, indicating the relevance of these observations to human disease. To obtain genetic proof of this mechanism, we inactivated Notch signaling specifically in HSCs of *Ctmb1*^{CAosb} mice by inactivating either the Notch1 or the Notch2 receptor. Bone marrow cells isolated from mice lacking *Notch1* or *Notch2* in HSCs were transplanted into the liver of 2 day-old, lethally-irradiated *Ctmb1*^{CAosb} mice. Overall chimerism, 2 weeks after transplantation, reached 50%-70% in all examined tissues with 67%-80% chimerism within the LT-HSC population, the Leukemia Initiating Population in the *Ctmb1*^{CAosb} mice. Notch signaling was decreased as tested by the expression of Notch transcriptional targets. Recipients of *Notch2*-deficient hematopoietic cells had blasts and dysplastic neutrophils in their peripheral blood, their numbers ranged from 18-75% and 20-70%, respectively, within 20 days following transplantation. Transplanted mice maintained low body weight and died within 5 weeks following transplantation. In contrast, transplantation of *Ctmb1*^{CAosb} neonates with *Notch1*-deficient hematopoietic cells prevented AML development, progressively increased body weight and rescued lethality as transplanted *Ctmb1*^{CAosb} mice survived for the entire observation period of 31 weeks. To examine the leukemogenic potential of *Jagged1*/Notch signaling in human disease we co-cultured CD34+ cells isolated from healthy individuals with U2OS human osteosarcoma cells overexpressing *Jagged1*. Exposure of CD34+ cells to *Jagged1* favored myeloid lineage specification. At the same time, it induced myeloid block, an event indicating an increase in early myeloid progenitors that arrest in an undifferentiated state and usually leads to the development of myeloid blasts. Taken together, these results indicate that activation of Notch signaling in HSCs can mediate the leukemogenic signal of osteoblasts and that this event is facilitated by the Notch1 receptor. Moreover, the results suggest that, similar to mice, activation of *Jagged1*/

Notch signaling from osteoblasts to hematopoietic progenitors can induce myeloid bias and arrest in human cells.

Disclosures: Marta Galán-Diez, None.

1124

NOTCH Signaling in Skeletal Progenitors is a Critical Determinant in Fracture Repair and Nonunion. Cuicui Wang^{*1}, Jason Inzana², Anthony Miranda³, Zhaoyang Liu², Jie Shen⁴, Regis O'Keefe⁴, Hani Awad², Matthew Hilton³. ¹Washington University in St. Louis, USA, ²University of Rochester, USA, ³Duke University, USA, ⁴Washington University in St. Louis, USA

Fracture nonunions develop in 10-20% of fractures, resulting in prolonged disability. Current data suggests that bone union during fracture repair is achieved via proliferation and differentiation of skeletal progenitors within periosteal tissues surrounding bone, while bone marrow stromal/stem cells (BMSCs) and other skeletal progenitors may also contribute. The NOTCH signaling pathway is a critical maintenance factor for BMSCs during skeletal development, although the precise role for NOTCH and the requisite nature of BMSCs following fracture is unknown. To determine whether NOTCH and/or BMSCs are required for fracture repair, we performed non-stabilized and stabilized fractures on NOTCH mutant mice with targeted gene deletion in different cell lineages, including BMSCs, committed chondrocytes, and committed osteoblasts. We demonstrate that non-stabilized tibia fractures on Prx1Cre;RBPjkf/f mutants displayed characteristics most commonly observed in human hypertrophic nonunions, while Agc1CreERT2;RBPjkf/f and Col1Cre;RBPjkf/f fractures healed normally. Although the Prx1Cre;RBPjkf/f mutants did form a substantial external callus involving periosteal progenitors, they did not develop an appropriate internal callus which ultimately resulted in fracture nonunion. Furthermore, Prx1Cre;RBPjkf/f mutants exhibited a marked reduction in the BMSC pool, indicating that BMSCs are a vital component of fracture repair that likely acts to form the internal callus providing stability to the fracture and promoting healing. Similarly, rigidly fixed femur fractures on Prx1Cre;RBPjkf/f mutants also resulted in fracture nonunion that strongly resembles those seen in atrophic nonunion patients, suggesting that insufficient stabilization is not absolutely required for fracture nonunion in these mutants. Taken together, our findings provide the first genetic evidence whereby NOTCH signaling removal specifically within skeletal progenitors results in BMSC depletion and fracture nonunion, while NOTCH removal in committed chondrocytes and maturing osteoblasts leads to no impairment in fracture healing. Our use of multiple fracture modalities has proven the requisite role for BMSCs and NOTCH signaling within BMSCs during fracture repair, irrespective of fracture stability and vascularization. Finally, this work strongly supports the concept that different skeletal progenitor populations contribute to the fracture repair process in unique ways.

Disclosures: Cuicui Wang, None.

1125

Transplanted Hematopoietic Stem Cells form Functional Osteoblasts that Deposit Collagen and Repair Bone in a Mouse Model of Osteogenesis Imperfecta. Yongren Wu¹, Hai Yao¹, Makio Ogawa¹, Amanda LaRue², Meenal Mehrotra^{*3}. ¹Medical University of South Carolina, USA, ²Medical University of South Carolina, Ralph H Johnson VAMC, USA, ³Medical University of South Carolina & Research Services, Ralph H Johnson VAMC, USA

Osteogenesis imperfecta (OI), an autosomal dominant disorder caused by mutation in one of the two genes that encode type I collagen, is the most common hereditary bone disease. At present there is no cure for OI. One of many strategies that are being tested experimentally involves stem cells. Previously we have shown that transplantation of bone marrow (BM) cells highly enriched for hematopoietic stem cells (HSCs) can ameliorate bone defects seen in OI mice. We have also demonstrated that HSCs give rise to osteoblasts during normal bone turnover as well as non-stabilized fracture repair. Therefore, we hypothesized that HSC transplantation will lead to replacement of affected osteoblasts with normal cells leading to correction of collagen defects and preventing OI pathologies. Thus, transplantation of a clonal population derived from a single EGFP⁺ HSC into irradiated OI mice (*oim*; B6C3F₁ *ala-Coll1a2^{oim}*) was used to test our hypothesis. Dramatic improvements were observed on micro-CT analysis of tibia including increase in bone volume, trabecular number and trabecular thickness with a concomitant decrease in trabecular spacing in clonally engrafted *oim*. Analysis of control *oim* demonstrated continued deterioration in bone parameters. Mechanical testing of humerus exhibited an increase in parameters such as stiffness in clonally engrafted *oim* when compared to control *oim*, similar to that seen in normal mice. Dynamic histomorphometry showed a significant increase in mineral apposition rate in engrafted *oim* as compared to control *oim*. Paraffin sections of decalcified bones showed the presence of numerous GFP⁺ cells within bone which stained positive for osteocalcin, demonstrating that HSCs engraft in bone and differentiate to osteoblasts. Picosirius red staining of sections from clonally engrafted *oim* showed the presence of structurally improved collagen when compared to control *oim*. The collagens extracted from clonally engrafted *oim* contained a mixture of both $\alpha 1$ and $\alpha 2$ chains, similar to those from normal mice,

while those from control *oim* shown presence of only $\alpha 1$ chain. Immunofluorescent staining demonstrated that the GFP⁺ cells in bone (HSC-derived) were the ones which secreted Col1a2. These data indicate that HSC transplantation leads to clinical improvements in *oim* and that HSC-derived osteoblasts are functional. These findings are significant in that they can be applied to long-term studies to enhance and accelerate bone healing in OI.

Disclosures: Meenal Mehrotra, None.

1126

Identification of a Distinct Progenitor Cell within Long Bones that Gives Rise to Bone Marrow Adipocytes In Vivo. Ryan Berry^{*1}, Tracy Nelson¹, Rose Webb¹, Clifford Rosen², Matthew Rodeheffer¹, Mark Horowitz¹. ¹Yale University, USA, ²Maine Medical Center Research Institute, USA

Marrow adipose tissue (MAT) was identified in the bone marrow (BM) more than a century ago but has recently been associated with age, metabolic disease and low bone volume, highlighting the importance of studying this often neglected adipose tissue depot. However, little is known about the origin, development and function of MAT, as the identity of the BM adipocyte precursor (AP) cell is unknown. We have performed lineage tracing of BM adipocytes following induction of BM adipogenesis with either rosiglitazone-enriched diet or lethal irradiation and BM reconstitution to determine the ontogeny of BM adipocytes and identity of BM AP cells. Irradiation of double fluorescent mT/mG reporter mice (which harbor a constitutively expressed membrane targeted tdTomato cassette (mT) upstream of a Cre-responsive membrane targeted eGFP cassette (mG)) followed by reconstitution with C57BL/6 (B6) BM resulted in the presence of tdTomato traced BM adipocytes, indicating that BM APs do not reside within the transplanted BM but are irradiation-resistant cells within the host bone that likely line the endosteum. Following either irradiation/reconstitution or 8 wks of rosiglitazone diet, all BM adipocytes were eGFP⁺ and therefore traced in Adiponectin-Cre:mT/mG, Prx1-Cre:mT/mG, Twist2-Cre:mT/mG and Osx1-Cre:mT/mG mice. BM adipocytes were uniformly tdTomato⁺ and therefore untraced in Vav1-Cre:mT/mG and Myf5-Cre:mT/mG mice. In contrast, using a lipid-specific dye we are unable to visualize any adipocytes in non-induced BM. Between 50-70% of BM adipocytes were eGFP⁺ in Pdgfra-Cre:mT/mG mice depending on the type of induction. Importantly, only 20-25% of BM adipocytes were eGFP⁺ in OCN-Cre:mT/mG mice regardless of the type of induction. We have shown that all adipocytes in classical WAT depots are traced in Pdgfra-Cre:mT/mG mice. We have recently discovered that white adipocytes are uniformly untraced in Osx1-Cre:mT/mG mice. Therefore the uniform tracing of BM adipocytes by the endosteal cell/osteoblast promoters Osx1, Prx1 and Twist2 coupled with the absent or non-uniform tracing of BM adipocytes by Myf5 and Pdgfra indicate that BM adipocytes compose an adipose tissue depot that is distinct from brown or white adipose tissue. Our work supports the idea of a bi-potent "mesenchymal stem cell" lining the endosteum that generates both osteoblasts and BM adipocytes, but future work will decipher if distinct sub-populations of cells give rise to adipocytes and osteoblasts in vivo.

Disclosures: Ryan Berry, None.

1127

Deletion of PTH/PTHrP Receptor in Osteoprogenitors Deregulates Local Bone Marrow Vasculature in Mice. Cristina Panaroni^{*}, Joy Wu, Joshua Johnson, Ke Yuan, Vinicio de Jesus Perez. Stanford University School of Medicine, USA

Osteogenesis and angiogenesis in skeletal tissues are coupled via paracrine factors and cell-cell interactions. Osterix-expressing (Osx) cells, here referred as osteoprogenitors, co-invade cartilage with growing vessels during endochondral bone formation. Early in mouse life, Osx cells are detected in bone tissue and bone marrow (BM) stroma adjacent to or in contact with blood vessels. Parathyroid hormone (PTH) acting through the PTH/PTH-related peptide receptor (PPR) promotes bone growth but also alters the bone marrow microenvironment by relocating blood vessels to sites of new bone formation and expanding hematopoietic and mesenchymal stem cells. Disruption of PPR in mature osteoblasts and osteocytes not only reduces trabecular bone formation but also impairs endochondral angiogenesis. We have previously reported that ablation of PPR in osteoprogenitors (Osx-PPRKO mice) results in severe osteopenia. Here we show that deletion of PPR in osteoprogenitors disrupts bone marrow vasculature in proximity to trabecular bone. In vivo fluorescent labeling of the vascular networks in Osx-PPR KO mice revealed a reduction in BM blood vessels, especially along the endosteal bone surface. Immunostaining of frozen bone sections for the endothelial marker CD31 demonstrated a reduction of CD31⁺ endothelial cells specifically along the trabeculae. To examine whether osteoprogenitors directly regulate angiogenesis, we performed an *in vitro* matrigel tube formation assay seeding endothelial cells in the presence or absence of Osx sorted cells. We found that the presence of Osx cells increased by 22% the total tube length, by 27% the total tube number, by 33% the total branching points and by 50% the total loops formed by endothelial cells. However, expression of PPR in Osx cells was not required. We therefore performed PCR array analysis of 84 genes involved in endothelial cell biology in sorted osteoprogenitors from Osx-PPR KO and control mice, and found that genes involved in vasoconstriction, coagulation, chemotactic activity and inflammatory response were significantly upregulated, whereas the expression of VEGF-A gene, the major contributor to vessel sprouting and endothelial cell proliferation, was 50% reduced in Osx-PPR KO cells. In

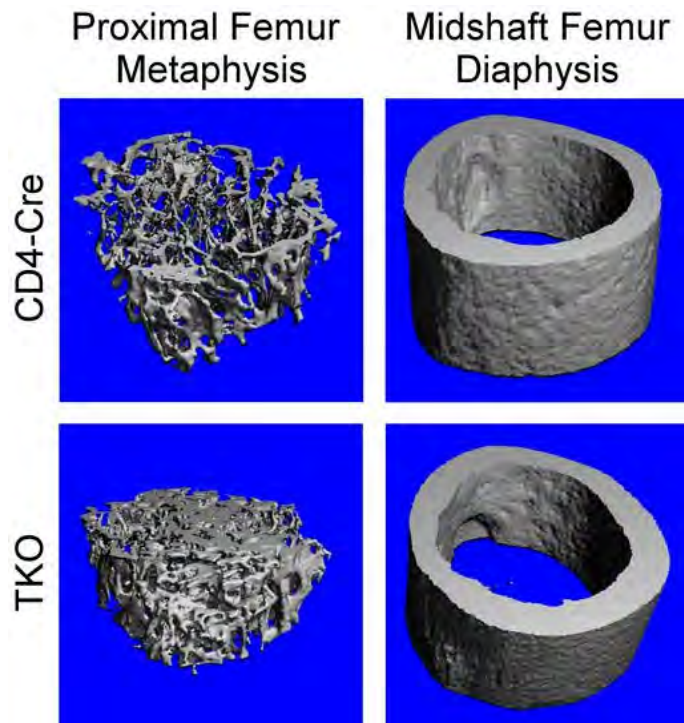
summary, these data indicate that Osterix-expressing cells actively support angiogenesis and PPR signaling in osteoprogenitors locally regulates the BM vasculature.

Disclosures: Cristina Panaroni, None.

1128

T-cell specific deletion of TIEG alters chemokine expression profiles and results in increased bone mass in mice. Malayannan Subramaniam^{*1}, AKM Khryul Wara², Fang Fang², Kevin Pitel¹, Mark Feinberg², John R. Hawse¹. ¹Mayo Clinic, USA, ²Harvard Medical School, USA

TGF β Inducible Early Gene-1 (TIEG) is known to play important roles in skeletal development and has been shown to be critical for optimal TGF β , BMP and estrogen signaling in bone. Recently, TIEG has been shown to play a central role in mediating CD4⁺ T-cell effector functions and in the development of T-regulatory cells through its control of TGF- β 1 signaling and FOXP3 expression. Based on these observations, as well as the known roles of the immune system in regulating bone metabolism and skeletal homeostasis, we sought to examine the effects of CD4⁺ T-cell specific deletion of TIEG on the mouse skeleton. Two-month old CD4-Cre control and T-cell specific TIEG knockout (TKO) mice were first analyzed using pQCT of the right tibia. Minimal differences were detected within the tibial metaphysis with the exception of a 10% increase in total density in TKO mice. However, substantial differences in multiple cortical parameters were detected at the tibial diaphysis as significant increases in total content (22%), total density (7%), cortical content (25%), cortical density (5%), cortical area (22%), cortical thickness (14%), periosteal circumference (9%) and endosteal circumference (5%) were observed in TKO mice relative to CD4-Cre controls. Micro-CT analysis of the femoral metaphysis revealed increased bone volume (61%), bone volume/tissue volume (50%), trabecular number (10%) and trabecular thickness (40%) with a concomitant decrease in trabecular spacing (7%) in TKO mice (see Figure). At the femoral diaphysis, increased bone volume (25%) and bone volume/tissue volume (7%) was also observed in TKO mice relative to controls (see Figure). At the cellular level, TKO CD4⁺ T-cells had increased expression of INF γ and decreased expression of RANKL and TRAF6. In response to CD3 activation, TKO CD4⁺ T-cells exhibited higher expression of INF γ , IL-2, IL-4, and IL-17 compared to controls. Since RANKL and TRAF6 are critical for osteoclastogenesis, and since INF γ and IL-4 are known to inhibit osteoclastogenesis, these data suggest that loss of TIEG expression in CD4⁺ T-cells may impair differentiation of osteoclast precursors *in vivo* leading to the observed increases in bone mass of TKO mice. These data for the first time identify TIEG as an important osteoimmunological molecule due to its ability to regulate skeletal homeostasis through the functions of CD4⁺ T-cells and provide a novel model system for further elucidating our understanding of osteoimmunology.



Figure

Disclosures: Malayannan Subramaniam, None.

1129

Conditional Disruption of *miR17~92* in Osteoclasts Results in Activation of Functional Activity of Osteoclasts and Substantial Loss of Trabecular Bone in Mice. Kin-Hing William Lau^{*1}, Virginia Stiffel¹, Matilda Sheng². ¹Jerry L. Pettis Memorial VA Medical Center, USA, ²Loma Linda University, USA

This study sought to investigate the potential regulatory role of *miR17~92* in osteoclast resorption by examining the skeletal effects of conditional disruption (cKO) of the *miR17~92* cluster in osteoclasts, which were generated by crossing *miR17~92* LoxP mice with *Ctsk*-Cre mice. The average knockdown of *miR17~92* in osteoclasts of cKO mutants was >70%. The body weight of cKO mutants and wild-type (WT) littermates was not different, but the femur length was reduced by 6%. pQCT analysis of femur reveals that cKO mutants had 28.8% decrease in Tb.BMC, 12.4% decrease in Tb.BMD, along with 6.8% increase in endosteal circumference. The low bone mass phenotype was confirmed by μ -CT analyses, which shows that cKO mutants had significantly ($p < 0.01$ for each) lower Tb.BV (\downarrow 50.2%), Tb.BV/TV (\downarrow 53.5%), Tb.Conn-Dens (\downarrow 41.6%), Tb.N (\downarrow 31.6%), Tb.Th (\downarrow 10%), Ct.BV (\downarrow 8.4%), and Ct.Th (\downarrow 5.3%), along with 37.4% increase in Tb.Sp. *In vitro*, the total number of marrow-derived osteoclasts (generated by treating osteoclast precursors with RANKL/c-MSF for 6 days) formed from cKO precursors was not greater than those derived from same number of WT precursors, while the average number of nuclei in *miR17~92* cKO osteoclasts was almost twice as many as that in WT osteoclasts. The average size of derived osteoclasts of cKO mutants was almost twice ($p < 0.05$) as large as that of WT osteoclasts. The average size of resorption pits created by cKO osteoclasts was also twice as large as those formed by WT osteoclasts ($p < 0.05$). In addition, the expression level of several genes known to be associated with osteoclast activation (*ATP6v0d2*, *Igfb3*, *Mmp9*, *OC-Stamp*, and *Oscar*), but not those genes associated with osteoclastogenesis (*Rank*, *Traf6*, *Acp5*, *Mitf*, and *Nfatc1*), was significantly ($p < 0.05$) increased in cKO osteoclasts, suggesting that disruption of *miR17~92* in osteoclasts enhances osteoclast activity and not osteoclastogenesis. The *Ctsk*-Cre-mediated disruption of *miR17~92* did not have discernible effect on the growth plate. There was also no significant difference in MAR or in BFR/B.Pm between cKO mice and WT littermates. The B.Pm of cKO mice was increased by 48.7%; a finding consistent with an increased bone turnover. There were also no significant differences in cellular ALP activity in osteoblasts or bone nodule forming ability of stromal cells of cKO mutants *in vitro*. In conclusion, *miR17~92* has an important regulatory function in osteoclast activity but not in osteoclastogenesis.

Disclosures: Kin-Hing William Lau, None.

1130

DNA Demethylation Ameliorates Inflammatory Bone Loss in Scurfy Mice by Modulating both Myeloid and Lymphoid lineages. Tim Chen^{*1}, Gaurav Swarnkar¹, Gabriel Mbalaviele², Yousef Abu-Amer³. ¹Department of Orthopaedic Surgery, Washington University School of Medicine, USA, ²Division of Bone & Mineral Diseases, Department of Internal Medicine, Washington University School of Medicine, USA, ³Department of Orthopaedic Surgery & Cell Biology & Physiology, Washington University in St. Louis School of Medicine, USA

Inflammatory responses contribute to the development of copious disorders including cancer and osteolysis. The interplay between inflammation and bone loss is well established. Epigenetic modulation is one of the most promising approaches for cancer therapy. Decitabine, a cancer treatment drug used for hematological malignancies, hypomethylates DNA by inhibiting DNA methyltransferases (DNMTs). Given the growing evidence of epigenetic regulation in inflammatory diseases and scarce information regarding its role in osteolysis, we tested the role of decitabine as a therapeutic agent to treat inflammatory bone diseases. We have recently reported that scurfy (*Sf*) mice, which lack Foxp3⁺ Treg cells exhibit severe osteopenia ensuing from myeloid lineage skewing, vast increase of granulocyte/macrophage progenitors (GMPs) and osteoclast (OC) precursors induced by pathogenic CD4⁺ T cell-mediated hypercytokinemia. Using *Sf* as a therapeutic model for inflammatory bone loss, we injected 16-day-old *Sf* and WT mice with decitabine or PBS. After 2 weeks, inflammatory indices were dramatically reduced in treated mice evident by weight gain, lack of dermatitis and skin ulcers. Mice were then sacrificed for *ex vivo* osteoclastogenesis, μ CT and FACS analysis for hematopoietic progenitors and lineage cells. Interestingly, not only *in vivo* decitabine treatment greatly inhibited the OC potential of unfractionated bone marrow cells, this inhibitory effect appeared to be more profound for *Sf* derived cells. FACS analysis revealed significant reduction of the frequency of GMPs and OC precursors in decitabine-treated *Sf* mice. More intriguingly, the frequencies of both CD4⁺ helper and CD8⁺ cytotoxic T cells were both greatly increased in the bone marrow and spleen of decitabine-treated *Sf*, implying that decitabine not only affected the myeloid but also the lymphoid lineage. Indeed, direct treatment with decitabine inhibited hyper-osteoclastogenesis of *Sf* bone marrow cell culture in a dose dependent manner (0.4-10 nM). Co-culture of CD4⁺T cells and bone marrow macrophages showed CD4⁺T cells derived from decitabine-treated *Sf* lost their osteoclastogenic activity compared to CD4⁺T cells from PBS treated *Sf* mice. μ CT analysis also revealed increased bone mass in decitabine treated *Sf* mice compared to PBS treated *Sf* controls. Taken together, our data unraveled the

potential for targeting epigenetic pathways as ways to treat inflammatory bone loss similar to hematological malignancies.

Disclosures: Tim Chen, None.

1131

Osteolytic Macrophages in Inflammatory Bone Resorption of Cherubism Mice Lacking c-Fos. Mizuho Kittaka*, Joshua Prather, Tomoyuki Mukai, Teruhito Yoshitaka, Yasuyoshi Ueki. University of Missouri-Kansas City School of Dentistry, USA

TRAP-positive (+) multinucleated osteoclasts are regarded as the exclusive bone-resorbing cells in pathological inflammatory bone resorption. This consensus is based on observations that bone destruction is absent in osteoclast-free animal models of inflammatory bone disease such as TNF- α transgenic mice deficient in c-Fos. Therefore, we hypothesized that ablation of osteoclasts would rescue the inflammatory bone destruction in *Sh3bp2^{KIKI}* mice, a knock-in (KI) mouse model of cherubism (*Sh3bp2^{KI}*). These mice exhibit TNF- α -dependent macrophage inflammation and increased RANKL-induced osteoclastogenesis resulting in inflammatory bone destruction. To test this hypothesis, we created *Sh3bp2^{KIKI}* mice on a c-Fos-deficient background. Surprisingly, although less severe than on a c-Fos^{+/+} background, the bone erosion was still present in *Sh3bp2^{KIKI}/c-fos^{-/-}* mice by micro-CT analysis. This bone erosion occurred even though no TRAP+ cells were detected in *Sh3bp2^{KIKI}/c-fos^{-/-}* mice. H&E staining showed inflammatory infiltrates surrounding joints and on the surface of long bones in *Sh3bp2^{KIKI}/c-fos^{-/-}* mice, presumably responsible for the bone erosion. Elevation of serum TNF- α levels and inflammatory infiltrates in liver, stomach, and lymph nodes were observed. Gene expression levels of *Mmp-9*, *-12*, and *-14* were increased in inflamed joints of *Sh3bp2^{KIKI}/c-fos^{-/-}* mice compared to *Sh3bp2^{+/+}/c-fos^{-/-}* mice, while *cathepsin K* expression was comparable. Tissue staining with antibodies against CD68 and MMP-9 showed that the cellular infiltrates at the eroded bone surfaces were positive for both. Levels of serum ICTP, a marker for bone resorption by MMPs, were elevated in *Sh3bp2^{KIKI}/c-fos^{-/-}* compared to *Sh3bp2^{+/+}/c-fos^{-/-}* mice, while serum CTX levels, another marker by cathepsin K, were not significantly increased. To test if bone erosion is observed in a different osteoclast-deficient model, *Sh3bp2^{KIKI}* mice on a *Rankl^{-/-}* background were created. The *Sh3bp2^{KIKI}/Rankl^{-/-}* mice showed bone erosion, but which was less severe than *Sh3bp2^{KIKI}/c-fos^{-/-}* mice. These results suggest that macrophages that express MMPs carry out the bone erosion in *Sh3bp2^{KIKI}/c-fos^{-/-}* mice with a mechanism that is independent of TRAP+ osteoclasts. Our data further suggest that gain-of-function of SH3BP2 and loss-of-function of c-Fos are required for the development of osteolytic macrophages that play a critical role in this unique mechanism of inflammatory bone resorption.

Disclosures: Mizuho Kittaka, None.

1132

A role for V-ATPase V0 domain subunit *el* in bone homeostasis. Tak Cheng*¹, Hua Ying¹, An Qin², Nathan Pavlos¹, Euphemia Landao¹, Qing Jiang³, Kerong Dai², Ming-Hao Zheng¹. ¹Centre for Orthopaedic Research, School of Surgery, The University of Western Australia, Australia, ²Shanghai Key Laboratory of Orthopaedic Implant, Department of Orthopaedics, Shanghai Jiao Tong University School of Medicine, China, ³Australian-China Joint Centre for Bone & Joint Disease, Nanjing University, China

Vacuolar-type H⁺-ATPases (V-ATPases) proton pumps function to acidify a diverse range of intracellular organelles required to sustain cellular homeostasis. In osteoclasts (OCs), V-ATPases are uniquely enriched on the surface of the ruffled border membrane where they serve to acidify the underlying extracellular milieu, a prerequisite for bone resorption. The mammalian V-ATPase complex is composed of at least 14 subunits (organized into two functionally and structurally distinct domains, the cytoplasmic V1 and the membrane-embedded V0), of which the hydrophobic V0 domain *e* subunit(s) (i.e. *el* and *e2* paralogs) remain poorly characterized. Here, using the Cre-LoxP system, we demonstrate that *el* is the major functional isoform expressed in OCs. Whereas mice with conditional knockout (cKO) of the *e2* isoform in either mature OCs (Cathepsin K (CtsK^{Cts}) or OC precursors (RANK^{Cts}) have normal bone mass, conditional deletion of the *el* counterpart results in severe OC-rich osteopetrosis (CtsK^{Cts}-*el* cKO mice; designated *el*^{DOC} herein) and/or embryonic lethality (RANK^{Cts}-*el* cKO), respectively. Histomorphometric assessment revealed that the marrow spaces of femurs from *el*^{DOC} mice were completely occluded by unresorbed bone. Consistently, deletion of *el* significantly impaired the bone resorptive function of OCs derived from *el*^{DOC} spleen cells, but did not alter overall OC differentiation. Mechanistically, this impairment is due to a disruption in extracellular and intracellular acidification as evidenced by live cell confocal microscopy and *in vitro* acidification assays. Interestingly, loss of *el* resulted in destabilization of the V-ATPase complex with reduced expression of V0 $\alpha 3$ subunit and uncoupling of V1 and V0 domain assembly. This disruption was further confirmed by Bioluminescence Resonance Energy Transfer (BRET) proximity assays which found that the integrity of the V0 domain was compromised due to reduced association between critical V0 subunits. Collectively, our data indicate that the V-ATPase V0 domain *el* subunit is an integral component of the OC acidification machinery.

Disclosures: Tak Cheng, None.

1133

Deletion of Plekhm1 in mice increases bone mass by attenuating osteoclast lysosome secretion and bone resorption. Toshifumi Fujiwara*¹, Shiqiao Ye¹, Takashi Nakamura², Stavros C Manolagas¹, Haibo Zhao³. ¹Center for Osteoporosis & Metabolic Bone Diseases, Division of Endocrinology & Metabolism, Department of Internal Medicine, University of Arkansas for Medical Sciences & the Central Arkansas Veterans Healthcare System, USA, ²Department of Biochemistry & Integrative Medical Biology, School of Medicine, Keio University, Japan, ³Central Arkansas VA Healthcare System, Univ of Arkansas for Medical Sciences, USA

Mutations of Plekhm1 (Plk1), a lysosome adaptor protein, cause osteopetrosis in humans and incisor-absent (ia) rats, due to impaired lysosome trafficking and ruffled border (RB) formation in osteoclasts (OCs). To elucidate the mechanism(s) by which Plk1 regulates lysosomal secretion we generated mice with global deletion of Plk1 in C57BL/6J mice, by crossing Plk1-floxed mice with Hypoxanthine guanine phosphoribosyl transferase (HPRT)-Cre (Plk1;HPRT); as well as mice with OC-specific Plk1 deletion using LysM-Cre (Plk1;LysM), or Cathepsin K (CTSK)-Cre (Plk1;CTSK). All three models had normal tooth eruption and bone development as well as normal osteoblast differentiation and bone formation. Plk1;LysM mice displayed a transient and mild increase in trabecular bone mass (BV/TV), but only in females. Both female and male Plk1;CTSK and Plk1;HPRT, on the other hand, had over a 30% increase in BV/TV at 2-month and 5-month of age as compared to their littermate controls, measured by micro-CT and histomorphometry. OC generation from Plk1 null bone marrow macrophages was indistinguishable from controls. Similarly, actin-ring formation and microtubule organization were normal in Plk1 null OCs. However, the resorptive capacity of Plk1 null OCs was markedly reduced. Specifically, a series of morphological, functional, and live cell imaging studies revealed that loss of Plk1 caused an accumulation of enlarged lysosomes around the nuclei and loss of OC RB. Yet, the biogenesis and lytic functions of lysosomes and the formation of autophagosomes in OCs were unaffected. Using immunoprecipitation (IP) and mass spectrometry we identified several novel Plk1 interacting proteins in OCs, including Def8, Fam98a, and Ndel1. These interactions were confirmed by co-IPs in 293T cells. Further, we determined that Def8 bound to the C-terminal part of Plk1 and this promoted Plk1's interaction with Rab7, a lysosome-associated small GTPase. Fam98a and Ndel1, both of which regulate vesicular trafficking on microtubules, interacted with N-terminal of Plk1. More importantly, knocking down the expression of these genes in OCs by shRNAs dramatically inhibited lysosome secretion and bone resorption. These results demonstrate that Plk1 is indispensable for bone homeostasis in mice as is the case in rats and humans. Furthermore, our work has uncovered a molecular apparatus linking lysosomes to microtubules through Plk1-Rab7 for lysosome transportation/secretion and bone resorption in osteoclasts.

Disclosures: Toshifumi Fujiwara, None.

1134

Actin cytoskeleton regulators Nck1 and Nck2 are required for supporting osteoblastic migration, bone formation and bone mass under the control of IGF-1 and for suppressing osteoclastic bone loss. Smriti Aryal A.C*¹, Yoichi Ezura¹, Yayoi Izu¹, Masaki Noda¹. Department of molecular pharmacology, Tokyo medical & dental university, Japan

Nck are actin cytoskeleton regulators. Mammals carry 2 Nck genes Nck1 & Nck2 (collectively termed Nck). To elucidate Nck actions in bone cells, mice carrying floxed Nck2 & Nck1-/- were crossed to transgenic mice expressing cre recombinase under the control of 2.3kb type I collagen (osteoblast specific) & Cathepsin K (osteoclast specific) promoters. Our data showed that osteoblast specific Nck-dKO (Ob-Nck-dKO) bone showed significant reduction in trabecular BV/TV & number resulting in osteoporosis. Bone histomorphometry showed significant reduction in mineral apposition rate, bone formation rate, mineralized surface per bone surface, osteoblast number & surface along with alteration in osteoblast shape in Ob-Nck-dKO bone compared to Ct. qRT-PCR showed significant reduction in osteoblast genes in Ob-Nck-dKO bone. *In vitro* migration, mineralized nodule formation & shape of Ob-Nck-dKO primary osteoblast were significantly altered. Furthermore, Nck1 overexpressing osteoblast showed increase in migration & motility. Bodian staining of Ob-Nck-dKO cortical bone showed significant reduction of the osteocyte processes. To examine *in vivo* effects of Nck on bone formation & osteoblast spreading, bone marrow ablation (BMA) & calvaria defect experiments were conducted. 3D μ CT after 1 week of BMA showed significant reduction of BV/TV in Ob-Nck-dKO bone compared to Ct. To examine osteoblast spreading, 2 calvaria defects were made on the parietal bone of wild type mice, defects were then implanted with Dil labelled Ct & Nck.dKO cell pellets, after 1 week BV/TV & spreading of defect with Nck.dKO cells were significantly reduced compared to Ct cells. To know the mechanism for Nck induced osteoblast migration, migration assay using Ct & Nck.dKO cells towards IGF-1 was done, which showed significant suppression of Nck.dKO osteoblast migration towards IGF-1. Co-immunoprecipitation showed binding of Nck to IRS-1 in osteoblast after IGF-1 stimulation, suggesting that IGF-1R couple IRS-1 to Nck and mediates the signaling required for osteoblast migration. Moreover, 3D μ CT of osteoclast specific Nck-dKO (Oc-Nck-dKO) bone showed significant reduction in trabecular BV/TV, number & separation compared to Ct. Oc-Nck-dKO bone showed significant increase in osteoclast genes & reduction in serum & urinary calcium levels

compared to Ct. Taken together, our data shows that Nck are required for supporting osteoblast migration, bone mass under IGF-1 stimulation & for suppressing osteoclast bone loss.

Disclosures: *Smriti Aryal A.C. None.*

1135

Heritability and Genetic Correlations for Bone Microarchitecture: The Framingham Study Families. David Karasik^{*1}, Yanhua Zhou², Mary L. Bouxsein³, Kerry E. Broe⁴, L. Adrienne Cupples², Serkalem Demissie², Douglas P. Kiel⁵. ¹Hebrew SeniorLife; Bar Ilan University, USA, ²Biostatistics, BU School of Public Health, USA, ³BIDMC, USA, ⁴Institute for Aging Research, HSL, USA, ⁵HSL, USA

Genetic factors contribute to the risk of long bone fractures; however, there is no data on whether the genetic variance captured by volumetric bone mineral density (vBMD) and bone microarchitecture measured with advanced imaging is above and beyond that for conventional areal bone mineral density (aBMD). This study aimed to estimate the heritability (h^2) of bone cortical and trabecular microstructure indices, measured by high-resolution peripheral quantitative computed tomography (HRpQCT) and the extent to which they share genetic regulation with femoral neck aBMD measured by DXA. Bone microarchitecture was measured by HR-pQCT (Scanco Medical, AG) at the distal tibia (n=1,059) and distal radius (n=1,022) in adults of European ancestry from the Offspring Cohort of the Framingham Heart Study. Femoral neck (FN) aBMD was measured by DXA (Lunar DPX-L). Heritability estimates (h^2) were calculated, adjusting for covariates (age, sex, and menopause (in women)) and bivariate genetic correlation analysis was performed, using a variance components model.

Estimates of h^2 adjusted for covariates ranged from 0.533 (cortical porosity) to 1.0 (total cross-sectional area, CSA) in the tibia, and from 0.207 (trabecular number) to 0.926 (cortical porosity) in the radius. Additional adjustment for FN BMD had no major effect on h^2 estimates (Table 1). In bivariate analysis, there was a high genetic correlation between multivariable-adjusted cortical vBMD at the tibia and radius (RhoG=0.960), while correlations between cortical vBMD and FN aBMD were much lower (RhoG=0.389 and 0.352, at the tibia and radius, respectively). Environmental correlations (RhoE) were negligible (Table 2).

Here we report data from extended families from population-based cohort, men and women. Our study suggests that, in adults of European ancestry, bone microarchitecture indices are heritable. Moreover, high RhoG between vBMD of the radius and tibia suggests that there is common genetics that governs vBMD regardless of the specific long bone; lower genetic correlation between cortical vBMD of the radius and tibia and aBMD of the hip might suggest that there are unique factors for peripheral cortical vBMD that are not captured by aBMD. These results point toward importance of further work to identify the specific variants underlying genetic susceptibility to long bones fracture, bone density and structure.

TABLE 1: Heritability of Bone Microarchitecture before and after adjustment for FN BMD

| Trait | Radius | | Tibia | |
|--------------------------------------|-------------|---------------------|-------------|---------------------|
| | Covariates* | Covariates + FN BMD | Covariates | Covariates + FN BMD |
| Total CSA (mm ²) | 0.885±0.115 | 0.870±0.116 | -1.0 | -1.0 |
| Cortical vBMD (mg/cm ³) | 0.784±0.133 | 0.788±0.144 | 0.680±0.132 | 0.689±0.138 |
| Cortical thickness (mm) | 0.600±0.128 | 0.550±0.135 | 0.947±0.107 | 0.960±0.112 |
| Cortical porosity (%) | 0.526±0.187 | 0.545±0.198 | 0.533±0.191 | 0.623±0.188 |
| Trabecular BMD (mg/cm ³) | 0.590±0.145 | 0.620±0.154 | 0.568±0.132 | 0.551±0.130 |
| Trabecular Number (1/mm) | 0.207±0.166 | 0.206±0.172 | 0.562±0.136 | 0.554±0.135 |
| Total Density (mg/cm ³) | 0.706±0.120 | 0.684±0.129 | 0.809±0.100 | 0.766±0.115 |

* Age, Sex, menopause

TABLE 2: Genetic and environmental correlations (adjusted for age, sex, menopause (in women), and height):

| | Cortical vBMD-radius | Cortical vBMD-tibia | FN BMD |
|----------------------|----------------------|---------------------|-------------|
| Cortical vBMD-radius | | 0.960±0.192 | 0.352±0.157 |
| Cortical vBMD-tibia | 0.061±0.285 | | 0.389±0.168 |
| FN BMD | -0.391±0.306 | -0.148±0.266 | |

Genetic correlations (ρ_g) above the diagonal; environmental correlations (ρ_e) below the diagonal.

Tables

Disclosures: *David Karasik. None.*

1136

Whole-genome sequencing and deep imputation identifies non-coding variants near *EN1* with large effects on bone mineral density. Vince Forgetta^{*}, Brent Richards. McGill University, Canada

Presented by Vincenzo Forgetta on behalf of the UK10K and GEFOS.seq Consortia.

The extent to which low-frequency (minor allele frequency [MAF] between 1-5%) and rare (MAF $\leq 1\%$) variants contribute to medically relevant complex traits in the general population is largely unknown. Bone mineral density (BMD), a highly heritable trait and a major predictor of osteoporotic fractures. While dozens of common genetic variants have been found to be associated with BMD, only one rare population-specific coding variant has been identified to date. To identify non-common variants in the general population associated with BMD, we performed a large-scale meta-analysis derived from whole-genome sequencing from the UK10K consortium (n=2,882), whole-exome sequencing (n= 3,549), deep imputation of genotyped samples using a combined UK10K/1000Genomes reference panel (n=26,534), and *de-novo* replication genotyping (n= 20,271) in 27 population-based

cohorts of European ancestry (n_{total} = 53,236). We identified a low-frequency novel non-coding variant near *EN1* with an effect size that is 4-fold larger than that of the mean of previously reported common variants for lumbar spine BMD (rs11692564[T], MAF = 1.7%, replication effect size = +0.20 standard deviations [SD], $P_{meta} = 1.7 \times 10^{-14}$). Upon combined discovery and replication meta-analysis, three additional novel non-coding variants encompassing *EN1*, two being of low-frequency, also achieved genome-wide significance ($P < 1.2 \times 10^{-8}$) for lumbar spine or femoral neck BMD. Meta-analysis of 29,103 cases and 311,229 controls found 3 of 4 variants to be strongly associated with decrease risk of fracture, including the lead variant rs11692564[T] (OR = 0.83 [95% CI: 0.76-0.91] $P = 4.7 \times 10^{-5}$). Using an *En1*^{Crefllox} mouse model, we observed that conditional loss of *En1* results in low bone mass, likely as a consequence of high bone turn-over. We also identified a novel low-frequency non-coding variant with an effect on forearm BMD which is 2.2-fold larger than that of any previously reported common variants near *CPED1* and *WNT16* (rs148771817[T], MAF = 1.1%, replication effect size = +0.39 SD, $P_{meta} = 1.1 \times 10^{-11}$). All identified low-frequency variants were not present in the HapMap reference panel, illustrating the utility of using larger whole genome sequencing-based reference panels for deep imputation of rare and low-frequency genetic variants. Lastly, a comprehensive analysis also revealed enrichment in genetic associations with BMD for functional variants, as measured by evolutionary constraint or their deleterious effect on protein coding genes. These findings provide evidence that low-frequency non-coding variants have large effects on BMD in the general population, thereby providing rationale for whole-genome sequencing-based approaches to study the genetic architecture of complex medically-relevant traits in the general population.

Disclosures: *Vince Forgetta. None.*

1137

Femoral Neck BMD is the Preferred Site in the Assessment of Hip Fracture in Elderly Men. (10 Year Follow Up of MrOs Sweden). Helena Johansson^{*1}, Anders Odén², Magnus Karlsson³, Mattias Lorentzon⁴, Björn Rosengren³, Östen Ljunggren⁵, Claes Ohlsson⁴, Nicholas Harvey⁶, Eugene McCloskey⁷, John Kanis⁷, Dan Mellström⁴. ¹Centre for Metabolic Bone Diseases, University of Sheffield Medical School, Sweden, ²Centre for Bone & Arthritis Research (CBAR), Sahlgrenska Academy, University of Gothenburg, Gothenburg, Sweden; Centre for Metabolic Bone Diseases, University of Sheffield, Sheffield, UK; Sweden, ³Clinical & Molecular Osteoporosis Research Unit, Department of Clinical Sciences, Lund University & Department of Orthopedics, Skane University Hospital, Malmö, Sweden, Sweden, ⁴Centre for Bone & Arthritis Research (CBAR), Sahlgrenska Academy, University of Gothenburg, Gothenburg, Sweden, Sweden, ⁵Department of Medical Sciences, University of Uppsala, Uppsala, Sweden, Sweden, ⁶MRC Lifecourse Epidemiology Unit, University of Southampton, Southampton, UK; NIHR Southampton Biomedical Research Centre, University of Southampton & University Hospital Southampton NHS Foundation Trust, Tremona Road, Southampton, UK, United Kingdom, ⁷Centre for Metabolic Bone Diseases, University of Sheffield, Sheffield, UK, United Kingdom

Low bone mineral density (BMD) is a well-established risk factor for hip fracture. The aim of the present study was to determine the relative performance characteristics of total hip (TH), femoral neck (FN) and trochanteric (Tr) BMD in the prediction of all hip fractures, cervical fractures and peritrochanteric hip fracture.

We studied the relationship between baseline BMD measured by DXA (Lunar Prodigy in two centers and Hologic QDR 4500-A-Delphi in one, instruments cross-calibrated) and incident hip fracture by site among 2984 elderly men drawn from the general population and recruited to the MrOS study in Sweden. Men were followed for up to 12.2 years (average 8.6 years). An extension of Poisson regression was used to investigate the relationship between BMD and the hazard function of fracture expressed as a gradient of risk (GR=HR/SD decrease).

During follow up 198 men sustained one or more hip fractures (6.6%). 109 incident hip fractures were cervical and 85 were peritrochanteric. The performance characteristics are presented in the Table. For all hip fracture outcomes, the highest GR was provided by FN BMD and was significantly better than Tr BMD. For cervical fractures FN BMD outperformed BMD at other sites, statistically significantly so in the case of Tr BMD. For peritrochanteric fracture the GRs were similar at all BMD sites. The associations were similar when adjusted for radiographic vertebral fracture and other fractures at baseline. The GRs were stable with age and time since baseline.

Although measurements of BMD at all regions of the hip predicted incident hip fracture, femoral neck BMD appeared to perform best across all hip fracture types and thus may constitute the preferred site of measurement in elderly men.

1139

Table. GR (95% CI) for hip fracture at different sites of BMD measurement (adjusted for age)

| BMD site | Outcome hip fracture | | |
|--------------|----------------------|-------------------|------------------|
| | All | Cervical | Trochanteric |
| Total hip | 2.40 (2.05-2.80) | 1.87 (1.51-2.31) | 3.06 (2.37-3.94) |
| Femoral neck | 2.68 (2.24-3.22) | 2.28 (1.81-2.88) | 3.06 (2.33-4.01) |
| Trochanter | 2.17 (1.87-2.52)* | 1.61 (1.31-1.98)* | 2.94 (2.28-3.78) |

* Significantly different from FN BMD

Table

Disclosures: Helena Johansson, None.

1138

FRAX underestimates hip fracture risk in older men with CKD. Thomas Nickolas*¹, Stephanie Shiau¹, Kyle Nishiyama¹, Natalia Cortez¹, Elizabeth Shane¹, Maria Rodriguez-Barradas², David Rimland², Cynthia Gibert², Roger Bedimo², Amy Justice³, Julie Womack³, Michael Yin¹. ¹Columbia University, USA, ²Veterans Affairs Medical Center, USA, ³Yale University, USA

Fracture incidence rates are 4- to 14-fold greater in patients with severe chronic kidney disease (CKD, eGFR <30 mL/minute and ESRD) than in the general population. However, fracture risk screening is discouraged in patients with severe CKD despite their predisposition to fractures. This is because measurement of bone mineral density (BMD) by dual energy X-ray absorptiometry is not recommended by the Kidney Disease Improving Global Outcomes guidelines. Thus, validation of methods that predict fracture independent of BMD in patients with severe CKD is needed. The World Health Organization's FRAX[®] tool predicts 10-year risk of major osteoporotic (MOP) and hip fracture without BMD, but no studies have validated its calibration in patients with severe CKD. We hypothesized that FRAX[®] would be well calibrated to predict 10-year risk of MOP and hip fractures in patients with eGFR <30 mL/minute. We used The Veterans Aging Cohort Study Virtual Cohort (VACSVC) to compare the calibration of FRAX[®] without BMD across ranges of kidney function. VACSVC is a prospective study of HIV-infected Veterans matched with uninfected Veterans by age, sex, race/ethnicity, and geographic region. We included 13,668 men age 50-70 years with complete data in 2000 to approximate all but two factors (history of secondary osteoporosis and parental hip fracture) for modified-FRAX calculation without BMD and 10-year observational data for incident fragility fracture. Accuracy of the modified-FRAX calculation was compared by observed/estimated (O/E) ratios of fracture. eGFR was estimated by CKD-EPI formula, CKD stage was defined by National Kidney Foundation criteria, and normal kidney function was ≥60mL/min. None of the patients were on dialysis and 1.1% (N=160), 1.0% (N=142) and 7.5% (N=1031) of patients had CKD stages 5, 4 and 3 respectively (Table). For MOP fractures, calibration of the modified-FRAX was similar across CKD stages. For hip fractures, modified-FRAX underestimated risk by 10-fold for subjects with severe CKD (Stages 4 and 5). When the analysis was restricted to the 9,307 uninfected subjects, modified-FRAX underestimated hip fracture risk by 9- and 15-fold for CKD stages 4 and 5, respectively. These findings question the utility of FRAX for prediction of fragility fracture, especially at the hip in older male CKD patients. These data require validation in other CKD cohorts and support the need for the development of an accurate CKD-specific fracture prediction tool.

| Table 1 | N | Observed | Expected | O/E | 95% CI |
|------------------------------------|-------|----------|----------|-------|-------------|
| Major osteoporotic fracture | | | | | |
| CKD Stage 5 | 160 | 5 | 3.44 | 1.46 | 0.61, 3.50 |
| CKD Stage 4 | 142 | 7 | 3.94 | 1.78 | 0.85, 3.73 |
| CKD Stage 3 | 1031 | 35 | 32.53 | 1.08 | 0.77, 1.50 |
| Normal Kidney Function | 12335 | 516 | 336.66 | 1.53 | 1.41, 1.67 |
| Hip fracture | | | | | |
| CKD Stage 5 | 160 | 4 | 0.39 | 10.23 | 3.84, 27.26 |
| CKD Stage 4 | 142 | 5 | 0.47 | 10.64 | 4.43, 25.56 |
| CKD Stage 3 | 1031 | 6 | 3.70 | 1.62 | 0.73, 3.61 |
| Normal Kidney Function | 12335 | 143 | 30.79 | 4.64 | 3.94, 5.47 |

Table

Disclosures: Thomas Nickolas, None.

Altered trabecular microarchitecture in youth with type 1 diabetes mellitus. DEBORAH MITCHELL*, Mary Bouxsein, Madhusmita Misra. MASSACHUSETTS GENERAL HOSPITAL, USA

Type 1 diabetes (T1D) confers a significantly elevated risk of fracture which is only partially explained by low areal bone mineral density (aBMD). As microarchitecture is an important additional determinant of bone strength, the goal of this study was to investigate the degree to which microarchitecture is affected in T1D. Since the onset of T1D is typically in early childhood, we hypothesized that microarchitectural deficits would be apparent in growing children. This was a cross-sectional study of 83 girls ages 10-16 years (16 T1D and 67 controls). Subjects with T1D were at least 1 year post-onset. Microarchitecture of the distal radius (7% site) and tibia (8% site) was assessed by high-resolution peripheral quantitative computed tomography (HR-pQCT), and micro-finite element analysis was used to estimate bone strength. Mean duration of disease in T1D was 4.6 ± 2.8 years, and mean HgbA1c since onset was 8.6 ± 1.2%. The groups were well-matched for age, bone age, race, and height. Weight was higher among T1D subjects, leading to a higher BMI Z-score (0.9 ± 0.6 vs. 0.2 ± 0.9, p<0.001). Groups did not differ for serum calcium, phosphate, 25-hydroxyvitamin D, and parathyroid hormone. Z-scores for aBMD at the spine and subtalar body did not differ between groups, and these comparisons remained non-significant after adjustment for BMI Z-score. As shown in Figure 1, at the radius, T1D had higher total cross-sectional area (p=0.02 after adjustment for bone age and BMI Z-score). This difference was driven by higher trabecular area (adjusted p=0.03) while cortical thickness was non-significantly lower in T1D. As shown in Figure 2, while cortical volumetric BMD (vBMD) did not differ between groups, trabecular vBMD was lower at the tibia in T1D (adjusted p=0.04). There were no differences in trabecular number, but trabecular thickness trended lower in T1D at the tibia (adjusted p=0.07). Between-group differences in trabecular parameters at the radius were similar though not statistically significant. Cortical porosity did not differ between groups. Estimated failure load did not differ at the radius but was lower at the tibia in T1D (adjusted p=0.04). Overall, though aBMD did not differ between groups, we detected unfavorable trabecular vBMD and microarchitecture in T1D, particularly at the distal tibia. These results suggest that impaired trabecular bone contributes to the fracture risk in T1D, and that this insult occurs early in the course of the disease.

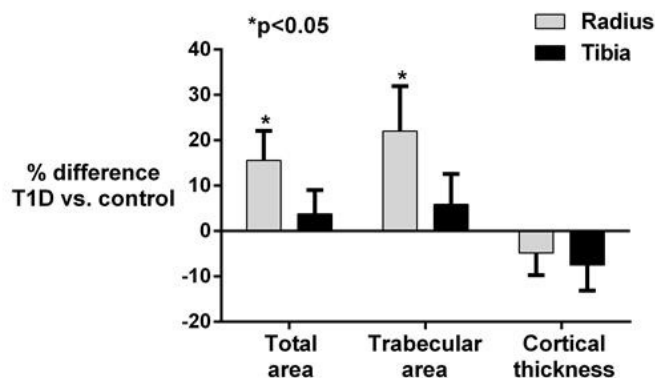


Figure 1

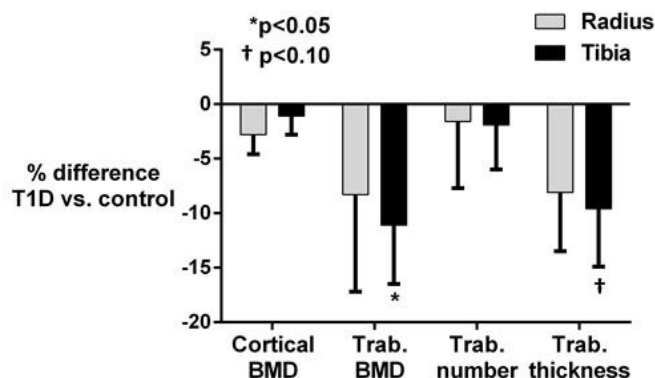


Figure 2

Disclosures: DEBORAH MITCHELL, None.

1140

Reference Point Microindentation Supplements Existing Clinical Factors for Improved Fracture Risk Assessment at the Femoral Neck. Thomas Jenkins¹, Louise Coutts¹, Stefania D'Angelo², Douglas Dunlop³, Richard Oreffo⁴, Cyrus Cooper², Nicholas Harvey⁵, Philipp Thurner⁶. ¹Bioengineering Science Research Group, Faculty of Engineering & the Environment, University of Southampton, Southampton, UK, United Kingdom, ²MRC Lifecourse Epidemiology Unit, University of Southampton, Southampton, United Kingdom, ³University Hospital Southampton NHS Trust, Southampton, United Kingdom, ⁴Centre for Human Development, Stem Cells & Regeneration, Institute for Developmental Sciences, Faculty of Medicine, University of Southampton, Southampton, United Kingdom, ⁵MRC Lifecourse Epidemiology Unit, University of Southampton, Southampton, UK, United Kingdom, ⁶Vienna University of Technology, Austria

Current approaches to fracture risk assessment, combining BMD and clinical risk factors, most frequently in FRAX[®], do not incorporate any direct measure of bone biomechanical properties. A new technique, Reference Point micro-indentation (RPI), which permits such a direct assessment of bone quality, appears to discriminate patients with fragility fracture from controls through *in vivo* measurements at the tibia¹, but it is unclear how this relates to testing at the site of most clinically devastating fracture, the femoral neck.

Femoral neck samples were collected at surgery following low trauma hip fracture (n= 46; 17 male, 83 (IQR 77-87) years), and compared with 16 cadaveric femoral neck samples, free from bone disease, obtained from a tissue bank (7 male; 65 (IQR 61-74) years). RPI measures (Biodent HfcTM, ActiveLife Scientific) were compared between fracture patients and controls using Mann-Whitney U-tests, and discriminative ability using ROC analysis. A subset of fracture patients returned for DXA assessment (Hologic Discovery), and BMD values for cadaveric samples were retrieved using a phantom-calibrated micro-computed tomography device (HMX, Nikon) in radiography mode.

The RPI measured Total Indentation Depth (TID) was higher in femoral neck samples from osteoporotic fracture patients (131.3 µm) than that of cadaveric controls (105.9 µm) p < 0.001. This difference persisted with adjustment for age, sex, BMI and height (p < 0.001). TID demonstrated good discrimination between fracture and controls using ROC analysis (AUC = 0.89). RPI appeared to measure a property distinct from existing clinical factors with low correlation between TID and each of FRAX probability (r = 0.31, p = 0.026, n = 53), and BMD (r = -0.32, p = 0.063, n = 35). The clinical thresholds for FRAX and BMD did not identify the majority of individuals in the fracture group (60% to 86%), and yet, in this subset the ROC values are still high for TID (AUC = 0.88 to 0.93) showing potential to supplement current techniques, together having a sensitivity up to 100% (for an 80% specificity). Alternatively, summation of normalised TID to normalised BMD or FRAX probability also resulted in an improved AUC (0.95 To 0.99).

In conclusion, the RPI technique at the femoral neck discriminated fracture cases from controls independent of BMD and traditional risk factors. The approach, in its clinical form, may therefore usefully add to risk assessment, and requires testing in prospective cohorts.

[1] Diez-Perez *et al*, JBMR, 25(8), 2010

We gratefully acknowledge funding from EPSRC (EP/J008192/1) and University of Southampton alumnus, Mike Russell.

Disclosures: Philipp Thurner, None.

1141

Bisphosphonates reduce fracture risk in postmenopausal women with diabetes: Results from FIT and HORIZON trials. Ann Schwartz^{*1}, Eric Vittinghoff¹, Douglas C. Bauer¹, Steven R. Cummings², Andrew Grey³, Michael R. McClung⁴, Nicola Napoli⁵, Ian R. Reid³, Anne L. Schafer¹, Robert B. Wallace⁶, Dennis M. Black¹. ¹University of California, San Francisco, USA, ²California Pacific Medical Center, USA, ³University of Auckland, New Zealand, ⁴Oregon Osteoporosis Center, USA, ⁵Universita Campus Bio-Medico di Roma, Italy, ⁶University of Iowa, USA

Type 2 diabetes is associated with increased fracture risk but also with higher bone density, reduced bone formation, and higher levels of advanced glycation end-products. There is concern that the anti-fracture efficacy of bisphosphonate therapy may be reduced in diabetic patients. To test this hypothesis, we performed a post hoc subgroup analysis of combined individual-level data from two randomized placebo-controlled trials, the Fracture Intervention Trial (FIT) of alendronate (ALN) and the Health Outcomes and Reduced Incidence with Zoledronic Acid (ZOL) Once Yearly-Pivotal Fracture Trial (HORIZON-PFT). Baseline diabetes (DM) was identified from self-report, DM medication use, or an elevated fasting glucose (≥ 126 mg/dl) or non-fasting glucose (> 200 mg/dl). Incident non-vertebral fractures were centrally adjudicated. Morphometric vertebral fractures were ascertained from spine x-rays at annual visits. For clinical fracture, Cox models were used to estimate treatment efficacy in DM and non-DM women, with stratification of the baseline hazard by trial and diabetes status. For morphometric vertebral fractures, logistic regression was used, with DM status and trial as covariates. In FIT 6,459 postmenopausal women

with femoral neck (FN) T-score ≤ -1.6 received daily ALN (5-10 mg) or placebo (PBO) for up to 4 years. DM status could not be determined for 38 participants who were excluded from these analyses. In HORIZON-PFT 7,736 postmenopausal women with osteoporosis based on FN T-score and/or baseline vertebral fracture received a once-yearly infusion of ZOL (5 mg) or PBO for up to 3 years. At baseline in FIT and HORIZON-PFT, respectively, mean age was 68 and 73 years and mean BMI was 25.1 and 25.3 kg/m². There were 87 of 869 DM and 1,411 of 13,288 non-DM women with ≥ 1 non-vertebral fracture. There were 44 of 769 DM and 786 of 12,312 non-DM women with ≥ 1 morphometric vertebral fracture. Compared with placebo, treatment reduced risk of non-vertebral and morphometric vertebral fractures in DM and non-DM women (figure). In DM, relative risk of non-vertebral fracture was 0.52 (95% CI 0.33-0.80) and of morphometric vertebral fracture was 0.34 (95% CI 0.18-0.67), comparing bisphosphonate treatment with placebo. This post hoc analysis of randomized trial data indicates that, among postmenopausal women with low bone density and/or prevalent vertebral fracture, bisphosphonates reduce fracture incidence in those with diabetes.

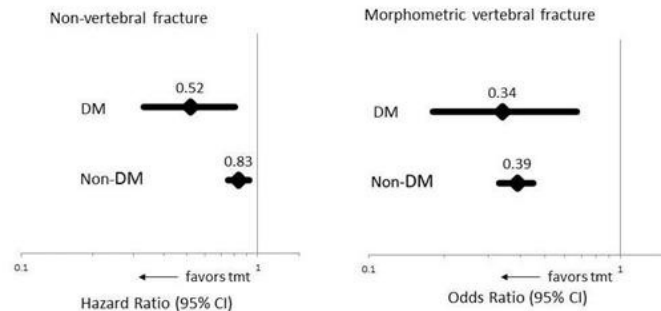


Figure. Relative risk of fracture, comparing bisphosphonates with placebo, in DM and non-DM women

Disclosures: Ann Schwartz, Chugai Pharmaceutical

1142

Eighteen Months of Treatment with Abaloparatide Followed by Six Months of Treatment with Alendronate in Postmenopausal Women with Osteoporosis – Results of the ACTIVEExtend Trial. Felicia Cosman^{*1}, Paul Miller², Gary Hattersley³, Edith Lau⁴, Peter Alexandersen⁵, Thomas Hala⁶, Sorica Mustatea⁷, Bettina Storgaard Nedergaard⁸, Annesofie Krogsaa⁹, Jan Slesinger¹⁰, Cristiano Zerbin¹¹, Ivo Valter¹², Zydrune Visockiene¹³, Beata Jendrych¹⁴, Carolina A Moirera Kulak¹⁵, Farid Marquez¹⁶, Alan Harris³, Greg Williams³, Ming-Yi (Tristan) Hu³, D. Black¹⁷, BJ Riis¹⁸, Luis Russo¹⁹, C. Christiansen²⁰. ¹Helen Hayes Hospital, ²Colorado Center for Bone Research, USA, ³Radius Health, USA, ⁴CCBR Hong Kong, China, ⁵CCBR Vejle, Denmark, ⁶CCBR Pardubice, Czech Republic, ⁷CCBR Bucharest, Romania, ⁸CCBR Aalborg, DK, Denmark, ⁹CCBR Ballerup, DK, Denmark, ¹⁰CCBR Brno, Czech Republic, ¹¹CEPIC Sao Paulo, Brazil, ¹²CCBR, Estonia, ¹³CCBR Vilnius, Lithuania, ¹⁴CCBR Warsaw, Poland, ¹⁵SEMPR Curitiba, Brazil, ¹⁶Palm Springs Research Center, USA, ¹⁷UC San Francisco, USA, ¹⁸Nordic Bioscience Herlev, Denmark, ¹⁹CCBR Rio de Janeiro Brazil, ²⁰Nordic Bioscience Herlev, Denmark, Denmark

Abaloparatide (ABL) is an osteoanabolic analog of PTHrP being developed for the treatment of postmenopausal osteoporosis (PMO). The ACTIVE trial was a double-blind, placebo-controlled (PBO) Phase 3 fracture prevention trial in which 2463 women with PMO were randomized to receive 18-months of daily subcutaneous administration of ABL 80 µg, PBO, or teriparatide (TPTD) 20 µg. All patients received calcium and vitamin D supplements. As has been previously reported, treatment with ABL significantly reduced the incidence of new vertebral, non-vertebral and clinical fractures while significantly increasing bone mineral density (BMD) in the lumbar spine (LS), total hip (TH) and femoral neck (FN) (Miller, ENDO 2015, Miller, ECTS 2015). In addition, more subjects treated with ABL experienced BMD increases in LS, TH and FN when compared to those treated with PBO or TPTD. In the ACTIVEExtend trial, subjects enrolled in the ACTIVE trial, who completed 18 months of treatment with either ABL or PBO, and who were deemed eligible were offered up to 24 additional months of treatment with alendronate (ALEN) at a dose of 70 mg per week. The objectives of the ACTIVEExtend trial are to assess the vertebral and non-vertebral fracture rate, BMD change, and safety associated with 6 months of treatment with ALEN following 18 months of treatment with ABL. Additional endpoints are to provide information on fracture rate, BMD change and safety after 24 months of ALEN treatment following treatment with ABL. 91% of eligible subjects from the ACTIVE trial (N=1139) were enrolled, and will undergo clinical fracture assessment, BMD, bone marker, and safety evaluations every 6 months for 24 months, as well as vertebral fracture assessments at months

6 and 24. All subjects will have completed their first six months of treatment; and the rates of vertebral and clinical fractures, changes in BMD, and safety results will be presented.

Disclosures: Felicia Cosman, Radius Health
This study received funding from: Radius Health, Inc.

1143

Romozosumab Improves Strength at the Lumbar Spine and Hip in Postmenopausal Women With Low Bone Mass Compared With Teriparatide.

TM Keaveny¹, DB Crittenden², MA Bolognese³, HK Genant⁴, K Engelke⁵, B Oliveri⁶, JP Brown⁷, BL Langdahl⁸, YC Yang², A Grauer², C Libanati⁹. ¹UC Berkeley, Berkeley & O.N. Diagnostics, USA, ²Amgen Inc., USA, ³The Bethesda Health Research Center, USA, ⁴UCSF & Synarc Inc., USA, ⁵Synarc Germany, Germany, ⁶Hospital de Clínicas, INIGEM, Argentina, ⁷Laval University & CHU de Québec (CHUL) Research Centre, Canada, ⁸Aarhus University Hospital, Denmark, ⁹UCB Pharma, Belgium

Purpose

Romozosumab is a bone-forming agent that inhibits sclerostin. In a phase 2 study (NCT00896532), 12 months of romozosumab increased DXA BMD in postmenopausal women with low bone mass (McClung *NEJM* 2014). A subset of these women underwent spine and hip quantitative computed tomography (QCT) imaging, confirming the BMD gains (romozosumab vs teriparatide integral volumetric BMD gains of 17.7% vs 12.9% at the spine and 4.1% vs 1.2% at the hip). To investigate the effects of romozosumab on bone strength, we performed a finite element analysis (FEA) on these QCT scans.

Methods

This international randomized study enrolled postmenopausal women with lumbar spine, total hip, or femoral neck T-scores ≤ -2.0 and ≥ -3.5 . In this analysis, subjects received blinded subcutaneous romozosumab 210 mg monthly, placebo, or open-label teriparatide (20 mcg daily). QCT scans were performed at the L1 & L2 lumbar vertebrae and proximal femur at baseline and month 12. Subject-specific vertebral strength for a simulated compression overload and femoral strength for a simulated sideways fall was estimated blinded-to-treatment using an FDA-approved non-linear 3D FEA (VirtuOst, O.N. Diagnostics). Whole-bone and compartment strength changes were estimated. The “cortical” compartment was defined as all bone within 2 mm and 3 mm of the periosteal surface for the spine and hip, respectively, plus any high-density bone (>1.0 g/cm³ of apparent density); the trabecular compartment was defined as all other bone.

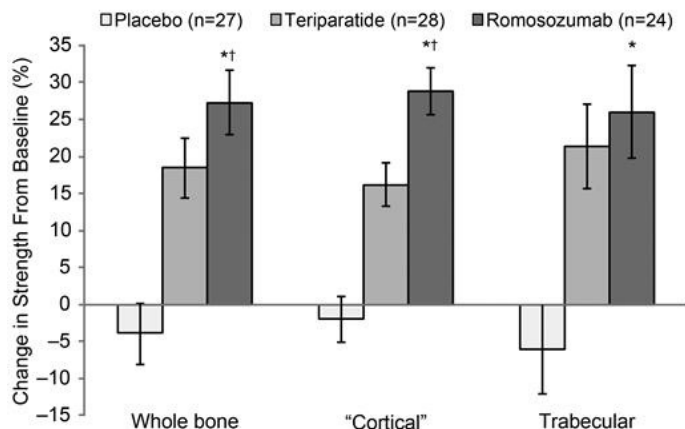
Results

At the spine, romozosumab increased strength from baseline by 27.3% at month 12, which was substantially higher than placebo (-3.9%) and teriparatide (18.5%; Figure A). This strengthening effect was due to contributions from both the “cortical” and trabecular compartments. At the hip, despite a small sample size for the romozosumab group, strength increased compared with baseline for romozosumab (3.6%), but did not change for placebo or teriparatide (Figure B). Again, both “cortical” and trabecular compartment changes contributed to the overall strengthening observed with romozosumab.

Conclusions

Romozosumab increased strength at the spine and hip over 12 months, with strength improving in the “cortical” and trabecular compartments at both sites. These strength improvements, documented using a validated method for assessing fracture risk and monitoring treatment, confirm and extend existing data and support romozosumab evaluation in the ongoing phase 3 clinical program.

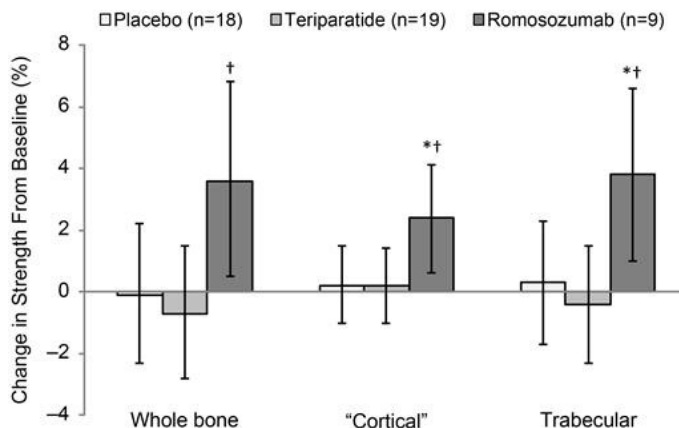
Figure A. Percentage Change (95% CI) in FEA-Estimated Strength at Month 12 for the Lumbar Spine



*P < 0.05 compared with placebo; †P < 0.05 compared with teriparatide. ANCOVA model compared the treatment arms from baseline to month 12 adjusting for baseline quantitative computed tomography FEA value and geographic region. FEA, finite element analysis.

Figure A

Figure B. Percentage Change (95% CI) in FEA-Estimated Strength at Month 12 for the Hip



*P < 0.05 compared with placebo; †P < 0.05 compared with teriparatide. ANCOVA model compared the treatment arms from baseline to month 12 adjusting for baseline quantitative computed tomography FEA value and geographic region. FEA, finite element analysis.

Figure B

Disclosures: TM Keaveny, Amgen, AgNovos Healthcare; O.N. Diagnostics
This study received funding from: Amgen Inc. & UCB Pharma

1144

Efficacy of Odanacatib in Postmenopausal Women With Osteoporosis: Subgroup Analyses of Data From the Phase 3 Long-Term Odanacatib Fracture Trial (LOFT).

Kenneth G. Saag¹, Peter Alexandersen², Claude-Laurent Benhamou³, Nigel Gilchrist⁴, Johan Halse⁵, E. Michael Lewiecki⁶, Kurt Lippuner⁷, Michael McClung⁸, Masataka Shiraki⁹, Carolyn A. DaSilva¹⁰, Nadia Verbruggen¹¹, Boyd B. Scott¹⁰, Antonio Lombardi¹⁰.

¹University of Alabama at Birmingham, USA, ²Center for Clinical & Basic Research, Denmark, ³Hôpital d'Orléans-la-Source, France, ⁴The Princess Margaret Hospital, New Zealand, ⁵Osteoporoseklinikk, Norway, ⁶New Mexico Clinical Research & Osteoporosis Center, USA, ⁷Bern University Hospital, Switzerland, ⁸Oregon Osteoporosis Center, USA, ⁹Research Institute & Practice for Involuntary Diseases, Japan, ¹⁰Merck & Co., Inc., USA, ¹¹MSD Europe Inc., Belgium

Background/Purpose: Odanacatib (ODN), a selective oral inhibitor of cathepsin K, is in development for the treatment of osteoporosis. In the Phase 3, Long-Term Odanacatib Fracture Trial (LOFT; NCT00529373) of postmenopausal women with osteoporosis, ODN significantly reduced fracture risk and led to progressive increases in BMD at the lumbar spine (LS) and total hip (TH) compared to placebo. The incidence of adverse events (AEs) and serious AEs has been previously presented. Major cardiovascular events overall were generally balanced but there were numerically more adjudicated strokes in the ODN group. Final blinded adjudication of all major cardiovascular events is ongoing. Pre-specified subgroup analyses evaluated the efficacy of ODN in different patient subgroups.

Methods: Women aged ≥ 65 years without a baseline radiographic vertebral fracture (VFX) and a TH or femoral neck (FN) BMD T-score between -2.5 and -4.0 or with a prior VFX and a TH or FN T-score between -1.5 and -4.0 were randomized (1:1) to ODN 50 mg/week or placebo. All patients received vitamin D₃ (5600 IU/week) and calcium as required to achieve ~ 1200 mg/day. Treatment effects on the primary endpoints (new and worsening morphometric vertebral, incident hip, and non-VFX) were investigated in subgroups of patients, including baseline age, race, intolerance to bisphosphonates, prior radiographic VFX, and baseline BMD.

Results: 16,713 women were randomized (16,071 included in analyses) at 387 centers in 40 countries. Baseline mean age was 72.8 years, 57% Caucasian, 46.5% with prior VFX. Mean BMD T-scores were: LS -2.7, TH -2.4, and FN -2.7. The risk reduction of ODN vs. placebo for primary fracture endpoints was generally consistent across all subgroups. For morphometric VFX, the relative risk reductions (RRR) for participants with or without a prior VFX were 51% and 60%, respectively; for age groups < 70 and ≥ 70 years, the RRRs were 57% and 53%, respectively (Table). RRR for morphometric VFX based on baseline LS BMD T-score tertiles (≥ -2.22 ; $-3.25 <$ to < -2.22 ; ≤ -3.25) were 54%, 47% and 58%, respectively. In bisphosphonate-intolerant patients, the RRR for morphometric VFX, hip and non-VFX were 52%, 48% and 17% respectively consistent with the overall study population.

Conclusion: In postmenopausal women with osteoporosis, the effect of ODN vs. placebo was generally consistent among various predefined subgroups in reducing the risk of new and worsening morphometric vertebral, hip and non-VFX.

Table. Interval-censored analysis of time to first morphometric vertebral fracture and time to first adjudicated osteoporotic fracture (hip and non-vertebral): subgroup analyses (Full-Analysis-Set population; base study)

| | ODN 50 mg OW versus Placebo OW | | | | | |
|---|-------------------------------------|-------------------|------------------|-------------------|----------------------------|-------------------|
| | Morphometric vertebral ^a | | Hip ^b | | Non-vertebral ^b | |
| | N | HR (95% CI) | N | HR (95% CI) | N | HR (95% CI) |
| Overall | 13,680 | 0.46 (0.40, 0.53) | 16,071 | 0.53 (0.39, 0.71) | 16,071 | 0.77 (0.68, 0.87) |
| No prior vertebral fracture | 7367 | 0.40 (0.31, 0.52) | 8601 | 0.48 (0.31, 0.74) | 8601 | 0.77 (0.63, 0.93) |
| Prior vertebral fracture | 6313 | 0.49 (0.41, 0.59) | 7470 | 0.58 (0.38, 0.87) | 7470 | 0.77 (0.65, 0.92) |
| Age, years | | | | | | |
| <70 | 4501 | 0.43 (0.32, 0.58) | 5067 | 0.53 (0.27, 1.05) | 5067 | 0.80 (0.63, 1.02) |
| ≥70 | 9179 | 0.47 (0.40, 0.56) | 11,004 | 0.53 (0.38, 0.74) | 11,004 | 0.76 (0.65, 0.88) |
| Race | | | | | | |
| Caucasian | 7561 | 0.42 (0.35, 0.52) | 9085 | 0.46 (0.31, 0.69) | 9085 | 0.77 (0.66, 0.90) |
| Asian | 2442 | 0.57 (0.41, 0.79) | 2832 | 0.56 (0.25, 1.26) | 2832 | 0.87 (0.60, 1.25) |
| Other | 3677 | 0.47 (0.34, 0.64) | 4154 | 0.67 (0.38, 1.18) | 4154 | 0.71 (0.54, 0.93) |
| Baseline BMD | | | | | | |
| Lumbar spine BMD T-score | | | | | | |
| ≥ Top tertile (-2.22) | 4168 | 0.42 (0.30, 0.58) | 4961 | 0.50 (0.29, 0.85) | 4961 | 0.85 (0.68, 1.06) |
| Bottom tertile (-3.25) to < top tertile (-2.22) | 4283 | 0.53 (0.39, 0.70) | 4948 | 0.35 (0.19, 0.66) | 4948 | 0.67 (0.53, 0.85) |
| < Bottom tertile (-3.25) | 4232 | 0.46 (0.36, 0.59) | 4923 | 0.65 (0.38, 1.08) | 4923 | 0.75 (0.60, 0.95) |
| Total hip BMD T-score | | | | | | |
| ≥ Top tertile (-2.08) | 4456 | 0.50 (0.38, 0.67) | 5171 | 0.48 (0.24, 0.95) | 5171 | 0.77 (0.62, 0.97) |
| Bottom tertile (-2.65) to < top tertile (-2.08) | 4429 | 0.38 (0.29, 0.50) | 5158 | 0.40 (0.21, 0.77) | 5158 | 0.81 (0.64, 1.02) |
| < Bottom tertile (-2.65) | 4208 | 0.46 (0.37, 0.59) | 5012 | 0.63 (0.42, 0.95) | 5012 | 0.74 (0.59, 0.92) |

^aAnalyses based on generalized linear model for binary data with cloglog link and terms for time interval, treatment, stratum, geographic region, subgroup and treatment by subgroup interaction.
^bAnalyses were based on Cox proportional hazards model with terms for treatment, stratum and geographic region.

Table

Disclosures: Kenneth G. Saag, Amgen, Merck; Amgen, Lilly, Merck
 This study was sponsored by Merck & Co. Inc., Kenilworth, NJ, USA.

1145

Hip BMD by DXA Can Reliably Estimate Reduction in Hip Risk in Osteoporosis Trials: A Meta-Regression. Dennis M. Black*¹, Eric Vittinghoff¹, Richard Eastell², Mary Bouxsein³, Charles McCulloch¹, Peggy M. Cawthon⁴, Steven R. Cummings⁵, Stephanie L. Harrison⁵, Anne de Papp⁶, Victor Dishy⁷, Andreas Grauer⁸, Ursula Klause⁹, Bruce H. Mitlak¹⁰, Bruce Schneider¹¹, Sanya Fanous-Whitaker¹², Jeff Zachwieja¹³, Chiyuan A. Zhang¹, Douglas C. Bauer¹. ¹University of California, San Francisco, USA, ²University of Sheffield, United Kingdom, ³Harvard University, USA, ⁴San Francisco Coordinating Center; California Pacific Medical Center, USA, ⁵San Francisco Coordinating Center, California Pacific Medical Center, USA, ⁶Merck & Co., Inc., USA, ⁷Daichi Sankyo, Inc., USA, ⁸Amgen Inc., USA, ⁹Roche Diagnostics Corporation, Indianapolis, USA, ¹⁰Eli Lilly & Co., USA, ¹¹Food & Drug Administration, USA, ¹²Foundation for the National Institutes of Health, USA, ¹³Dairy Research Institute, USA

Hip fractures (hip fx) are the most serious consequence of osteoporosis, and it is therefore critically important to develop new agents that can reduce hip fx risk. However, due to the relatively low rate of hip fx, randomized trials have become large and prohibitively expensive. To facilitate future drug development, it would be valuable to have a surrogate measure that could be used to design more efficient RCTs. The potential value of changes in DXA BMD to predict fracture reductions was studied in 2 meta-regressions (2002), one for spine and the other for non-vertebral fractures (NVFx). However, since 2002, new trials with >45,000 additional subjects and adding data for 5 new drugs (Zoledronate, Denosumab, Lasofoxifene, Basedoxifene and Tibolone) have been published. Moreover, no studies have addressed the relationship between BMD changes and hip fx reduction.

We performed a study-level meta-regression to examine the relationship between change in total hip BMD and fracture reductions including aany osteoporosis treatment trials published through March, 2015. We searched the literature for placebo-controlled trials of anti-resorptive or anabolic drugs in which hip fx and NVFx were adjudicated and change in BMD was measured in osteoporotic women. Trials with <5 hip fx were excluded. We modeled the relationship between estimates of the effect of treatment on change in BMD (active-placebo % difference at study end) and log of relative risk of hip fx and NVFx using linear models weighted by study size. We identified 14 trials including about 73,000 women for hip fx, and 30 trials with >75,000 women for NVFx (mean follow-up 3 yrs, range 1-4). For hip fx (figure), the results showed a strong relationship between active-placebo total hip BMD change and reduction in hip fracture risk. For example, for 2 drugs with 2% vs 6% hip BMD effect, the model predicted a 10% vs. 59% reduction for hip fx (r²=0.57, p<.0001). For NVFx, the relationship was weaker: comparable risk reductions were 6% vs 21% (r²=0.14, p=0.004).

We conclude that on a study level, the difference between active vs. placebo change in DXA hip BMD with treatment can strongly predict fracture reductions for that treatment, particularly for hip fx. Further evaluation is warranted to determine the extent to which changes in DXA hip BMD, perhaps augmented with bone turnover and other imaging data, may be useful as a surrogate for hip fx reductions in future trials.

Disclaimer: Dr. Schneider's contributions are an informal communication and represent his own best judgment. These comments do not bind or obligate FDA.

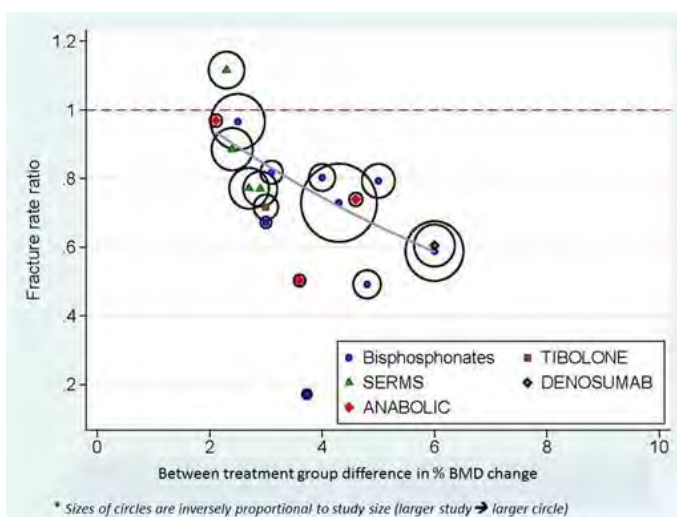


Figure: Relationship of % difference in total hip BMD (active v placebo) to Relative Risk for Hip Fx

Disclosures: Dennis M. Black, None.

1146

Relationship Between Total Hip BMD T-score and Incidence of Nonvertebral Fracture With up to 8 Years of Denosumab Treatment. S Ferrari*¹, C Libanati², CJF Lin², S Adami³, JP Brown⁴, F Cosman⁵, E Czerwiński⁶, LH de Gregório⁷, J Malouf⁸, J-Y Reginster⁹, NS Daizadeh², A Wang², RB Wagman², EM Lewiecki¹⁰. ¹Geneva University Hospital, Switzerland, ²Amgen Inc., USA, ³University of Verona, Italy, ⁴Laval University & CHU de Québec Research Centre, Canada, ⁵Helen Hayes Hospital, USA, ⁶Krakow Medical Center, Poland, ⁷CCBR, Brazil, ⁸Universitat Autònoma de Barcelona, Spain, ⁹University of Liège, Belgium, ¹⁰New Mexico Clinical Research & Osteoporosis Center, USA

Purpose: The relationship between BMD T-score and fracture risk has not been established in patients on therapy. We previously reported that denosumab (DMAB) treatment over 8 years enables a substantial proportion of women with osteoporosis to achieve non-osteoporotic BMD T-scores (Ferrari, ASBMR 2014). Further improvement in T-score would only be meaningful if it is associated with fracture reductions; thus, we investigated the relationship between total hip BMD T-score and the incidence of nonvertebral fracture through 8 years of DMAB therapy.

Methods: For these analyses, women received DMAB for 3 years during the FREEDOM trial (N=3902). A large subset of these women enrolled in the Extension and received DMAB for up to an additional 5 years, for a total of up to 8 years of continued treatment (N=2343). A repeated-measures model was first used to estimate each subject's BMD T-scores during the entire follow-up, specifically at each unique nonvertebral fracture time among all subjects at risk at the time of each fracture. Cox's proportional-hazards model was then fitted with time to nonvertebral fracture as the response and total hip BMD T-score time course as a time-dependent covariate.

Results: The incidence of nonvertebral fracture was lower with higher total hip BMD T-score throughout a wide and clinically relevant T-score interval (Figure). For example, total hip BMD T-scores of -2.5 and -1.5 were associated with 1-year nonvertebral fracture incidences of about 3.0% and 2.0%, respectively. The relationship flattened at a T-score somewhere between -2.0 and -1.0, similar to what is known to occur in untreated subjects. This inverse relationship between total hip BMD T-score and nonvertebral fracture incidence was maintained regardless of age or prior fracture (data not shown).

Conclusions: Higher total hip BMD T-scores during DMAB treatment were associated with a lower incidence of nonvertebral fractures, which is similar to the relationship previously established in treatment-naïve patients. Improvements of similar magnitude in BMD would result in different reductions in fracture risk depending on the baseline BMD value. Our findings highlight the importance of BMD measurement in patients on osteoporosis treatment as a predictor of fracture risk and support the concept that a specific T-score should be further evaluated as a practical goal for therapy.

1148

Wnt1 Regulates Bone Homeostasis by Regulating the Function of Osteoblasts. Kyu Sang Joeng*, Brendan Lee, Yi-Chien Lee, Ming-Ming Jiang, Terry Bertin, Yuqing Chen, Baylor College of Medicine, USA

Many studies have shown that canonical WNT/ β -catenin signaling regulates bone homeostasis; however, the key WNT ligand involved in this process was largely unknown. Recently, *WNT1* mutations have been reported to cause Osteogenesis Imperfecta (OI) and early-onset osteoporosis. Interestingly, our lineage tracing experiments suggested that *Wnt1* is expressed in a subset of osteocytes. Based on these studies, we hypothesized that *Wnt1* expressed in osteocytes regulates bone homeostasis. To test our hypothesis, we generated an osteocyte-specific *Wnt1* loss-of-function mouse model (*DMP1-Cre; Wnt1^{fl/fl}*). Interestingly, *DMP1-Cre; Wnt1^{fl/fl}* mice exhibit spontaneous tibial fractures (70% fracture rate) and severe low bone mass (4-fold decrease in trabecular BV/TV and 40% reduction in cortical bone diameter). Subsequent histomorphometric analyses showed that the osteopenic phenotype is due to decreased osteoblast activity, but not due to changes in osteoclasts. To confirm WNT1 function in bone, we next generated an osteocyte-specific *Wnt1* gain-of-function mouse model (*DMP1-Cre; Rosa26^{Wnt1/+}*). As expected, the *DMP1-Cre; Rosa26^{Wnt1/+}* mice exhibited a dramatic increase in trabecular bone mass (5-fold increase in BV/TV) and cortical bone diameter (50% increase) resulting solely from increased osteoblast activity. To confirm WNT1 function in osteoblasts, we overexpressed *Wnt1* in mouse stromal cell lines (ST2). The expression of *Wnt1* dramatically enhanced osteoblast differentiation and mineralization *in vitro*. Taken together, our data strongly support that *Wnt1* expressed in osteocytes functions in bone homeostasis by regulating osteoblast activity. To understand the genetic mechanism driving these effects, we generated *DMP1-Cre; Rosa26^{Wnt1/+}; β -catenin^{fl/fl}* mice to assess whether β -catenin mediates WNT1 function in bone formation. We hypothesized that, if WNT1 signaling is mediated by β -catenin, *DMP1-Cre; Rosa26^{Wnt1/+}; β -catenin^{fl/fl}* mice would recapitulate the phenotypes of *DMP1-Cre; β -catenin^{fl/fl}* mice. Interestingly, *DMP1-Cre; Rosa26^{Wnt1/+}; β -catenin^{fl/fl}* mice phenocopied the cancellous bone phenotype of *DMP1-Cre; β -catenin^{fl/fl}* mice, whereas the cortical bone diameter of *DMP1-Cre; Rosa26^{Wnt1/+}; β -catenin^{fl/fl}* mice was significantly increased compared to *DMP1-Cre; β -catenin^{fl/fl}* mice. These results suggest that β -catenin mainly mediates WNT1 function in cancellous bone formation, while both β -catenin dependent and independent mechanisms mediate WNT1 function in cortical bone formation.

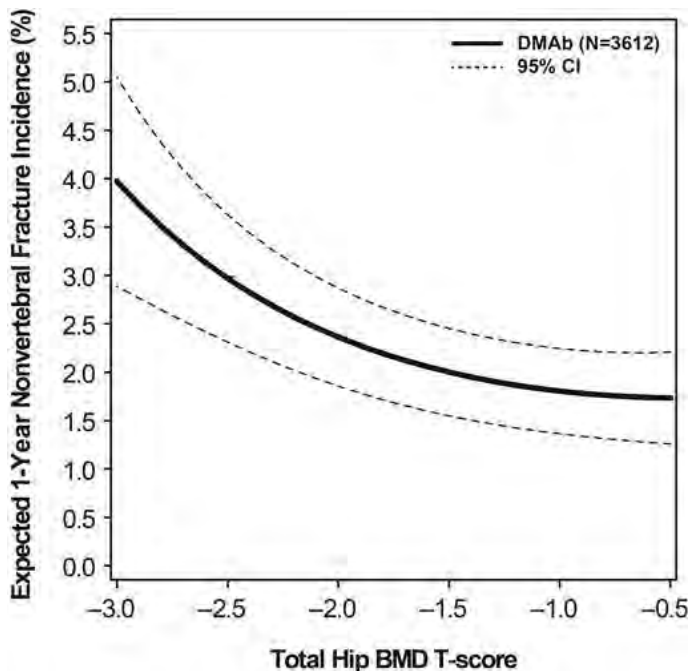
Disclosures: Kyu Sang Joeng, None.

1149

Critical and Interrelated role of Parathyroid Klotho and CaSR in Regulating PTH Synthesis and Parathyroid Gland Growth. Yi Fan*¹, Tadatashi Sato¹, Michael Densmore¹, Hannes Olauson², Tobias E. Larsson², Hakan Toka³, Beate Lanske¹. ¹Harvard School of Dental Medicine, USA, ²Karolinska Institute, Sweden, ³Nephrology & Hypertension, Eastern Virginia Medical School, USA

The parathyroid gland (PTG) maintains mineral ion homeostasis by detecting low serum-Ca²⁺ and secreting PTH. The Calcium-Sensing Receptor (CaSR) is a key component in this system. Klotho (KL) is also expressed in the PTG and is a co-factor for Fibroblast Growth Factor-23 (FGF23), which suppresses PTH in a regulatory feedback mechanism. To determine the specific role of KL in the PTGs and to test possible interactions between KL and CaSR in PTH regulation, we generated mice with PTG-specific deletion of KL (PTG-KL-KO), CaSR (PTG-CaSR-KO) and both (PTG-DKO) using Cre-LoxP recombination. We utilized ROSA26^{tdTomato} mice to visualize and collect PTGs. Mutant mice lacking CaSR either alone or in combination with KL were severely growth retarded, and developed osteomalacia and rickets-like abnormalities. In particular, PTG-DKO mice exhibited a significantly lower body weight with a more severe skeletal phenotype and shorter life expectancy than PTG-CaSR-KO mice. To explore a potential interaction between KL and CaSR in PTG-tissues to modulate mineral ion homeostasis, we compared serum biochemistries at P10. Ablation of KL alone in PTG had no effect, whereas both PTG-CaSR-KO and PTG-DKO mice displayed hypercalcemia, hypophosphatemia and significantly elevated PTH, iFGF23 and 1,25(OH)D levels. Most notably, PTG-DKO mice had markedly higher serum PTH, iFGF23 and 1,25(OH)D when compared to PTG-CaSR-KO mice, indicating a suppressive function of KL on the PTG in the absence of CaSR. CaSR ablation also resulted in significantly decreased KL expression on mRNA and protein levels. The moderately to severely elevated serum PTH in PTG-CaSR-KO and PTG-DKO mice might depend on KL gene-dosage effects. Moreover, mice deleted for CaSR displayed PTG hyperplasia. Dual ablation of KL and CaSR resulted in a further enlargement of PTG size with more severe and disrupted morphological structure when compared to CaSR deletion alone. Immunostaining to assess the PTH expression pattern showed that CaSR ablation leads to increased PTH protein expression. Interestingly, in the extremely hyperplastic PTG of PTG-DKO mice, some areas of altered structure failed to express PTH protein due to increased apoptosis. Real-time PCR analyses showed no differences in PTH mRNA expression level, suggesting that parathyroid cell population might be disrupted by KL and CaSR deletion. Our results indicate a critical and interrelated role of KL and CaSR in modulating PTH biosynthesis and PTG structure.

Disclosures: Yi Fan, None.



N=number of subjects randomized to DMAP in FREEDOM who had an observed total hip BMD T-score at FREEDOM baseline and ≥ 1 observed total hip BMD T-score during FREEDOM or the Extension.

Figure

Disclosures: S Ferrari, MSD, Amgen, Oscare; MSD, Amgen, GSK, UCB, Lilly, Agnovos
This study received funding from: Amgen Inc.

1147

Bmp2 Controls the Runx2/Osx Transition and Regulates Mineral Metabolism in Osteoblasts. Valerie Salazar*¹, Luciane Capelo², Satoshi Ote³, Vicki Rosen³. ¹Harvard School of Dental Medicine, Us, ²Universidade Federal de São Paulo, Brazil, ³Harvard School of Dental Medicine, USA

Bone morphogenetic proteins (BMPs) and canonical Wnts (cWnts) control many aspects of skeletal development, postnatal bone growth, and adult skeletal homeostasis. Current therapies based on BMP or cWnt signaling are developed and approved for use in humans, and yet the underlying mechanisms by which each pathway regulates osteoblast differentiation and function remain poorly understood. Among all BMPs expressed in bone, *Bmp2* is sufficient to induce ectopic bone formation, and is necessary in *Prx1*⁺ cells for bones to grow properly in width and acquire biomechanical stability. We monitored Wnt-induced osteoblast differentiation in a variety of murine osteoprogenitor cell types with reduced or ablated expression of endogenous *Bmp2*. As expected, *wild type* (*WT*) osteoprogenitors underwent differentiation and produced a mineralized matrix when cultured with rWnt3a. However, Wnt3a-induced osteoblast differentiation was not observed in limb bud cells stably expressing *Bmp2* RNAi, nor in primary bone marrow stromal cells where floxed alleles of *Bmp2* had been removed using either Adeno-Cre or endogenously expressed *Prx1-Cre*. Responsiveness to Wnt3a could be fully rescued, and even enhanced, by complementation with recombinant BMP2. To test the significance of these results *in vivo*, we induced cWnt signaling by removing a single copy of *Dkk1* in mice that were otherwise *WT* (*Dkk1^{+/-}*) or lacked *Bmp2* in *Prx1*⁺ cells of the limb (*Dkk1^{+/-}; Bmp2^{Prx1:Ala}*). By 2 weeks of age, *Bmp2^{Prx1:Ala}* mice had developed narrow appendicular bones with a ~75% decrease in moment of inertia, and this cortical phenotype was not improved by compound haploinsufficiency of *Dkk1*. Importantly, *Bmp2^{Prx1:Ala}* cells express essential molecules of cWnt signaling machinery, and are able to upregulate Tcf/Lef-target genes in a manner equivalent to *WT* cells following exposure to Wnt3a. Moreover, *Bmp2^{Prx1:Ala}* cells express a wide variety of other BMP ligands. Despite this, microarray analysis revealed that *Bmp2^{Prx1:Ala}* cells treated with Wnt3a fail to progress through the *Runx2/Osx* checkpoint, and do not upregulate many genes required for mineral metabolism including *Alpl* and *Phospho1*. By stark contrast, *Bmp2^{Osx1:Ala}* cells treated with Wnt3a differentiate and mineralize normally. In summary, these data point to pre-Osx1⁺ progenitors as a primary source and target of *Bmp2*, and uncover a previously unknown role for *Bmp2* in osteoblast mineral metabolism that is not compensated for by other BMPs or canonical Wnts.

Disclosures: Valerie Salazar, None.

Chondrogenesis is an essential physiological phase of endochondrogenesis but not separated from osteogenesis. Yinshi Ren^{*1}, Yan Jing¹, Xin Zhou², Junjun Jing¹, Jingya Wang¹, Jian Feng¹. ¹Baylor College of Dentistry, USA, ²The University of Texas MD Anderson Cancer Center, USA

For decades, it has been widely accepted that hypertrophic chondrocytes undergo apoptosis prior to endochondral bone formation and that chondrogenesis is a separate physiological process from osteogenesis. However, new studies suggest that chondrocytes can directly transform into bone cells using a cell lineage tracing process. In this study, we initially found only modest numbers of apoptotic cells but high levels of anti-apoptotic *Bcl-2* expression in hypertrophic chondrocytes, indicating that most hypertrophic chondrocytes do not undergo apoptosis. Interestingly, we also revealed dividing hypertrophic chondrocytes by BrdU staining, and high alkaline phosphatase activity (early bone marker) (Fig.1). An ex vivo culture of newborn cartilage on a chick chorioallantoic membrane showed that after 5 days, the cells on the periphery of the explants had begun to express *Col1* (bone marker) and produce bone-like matrices (Fig.2). The cartilage-specific cell lineage tracing approach in mice containing Rosa 26tdTomato (tracing marker), 2.3 *Col1*GFP (bone cell marker), and *Aggrecan* CreERT2 (one-time Tamoxifen-induced) or *Col10*-Cre (activated from E14.5 throughout adult stage) proved the direct transformation of chondrocytes into bone and endothelial cells in vivo (Fig.3). Importantly, deletion of *Bmpr1a* in chondrocytes (via crossing *Bmpr1a* flox and *Aggrecan* CreERT2 with one-time the Tamoxifen induction) led to a lack of cartilage and striped subchondral bone, but replaced it by intramembranous bone in the metaphysis (due to a compensated bone formation by the perichondrium), which greatly destroyed the normal shape and structure of long bone and led to a short status (Fig.4). This finding supports the novel concept that the chondrogenesis is an initial phase of endochondrogenesis, in which some of these chondrocytes undergo apoptosis, some divide, some become bone cells, and some give rise to endothelial cells for de novo vessel formation in subchondral bone formation. Taken together, this multi-pronged approach not only demonstrates that a majority of chondrocytes directly transform into bone and blood vessel cells, but also challenge the dogma that chondrogenesis is a separate process from osteogenesis during endochondral bone formation.

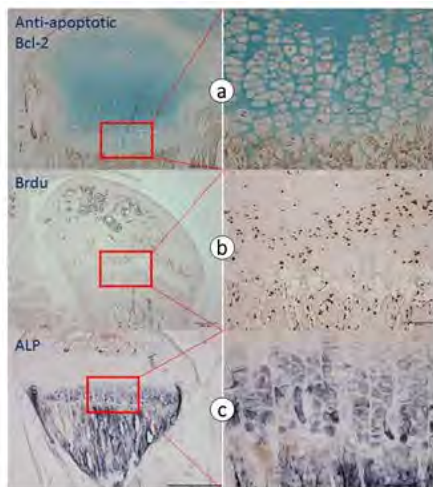


Figure 1. *Bcl-2*, *BrdU* and *ALP* expression in hypertrophic chondrocytes in wild type long bone. a), Anti-apoptotic marker *Bcl-2* is highly expressed in hypertrophic chondrocytes, indicating most of these cells may have another cell fate rather than apoptosis. b), Hypertrophic chondrocytes have the proliferating capability shown by *BrdU* labeling. c), High *ALP* activity in hypertrophic chondrocytes.

Figure 1

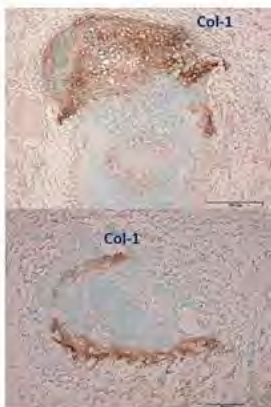


Figure 2. *Col-1* expression of ex-vivo cartilage culture on chick chorioallantoic membrane. Condyle cartilage is carefully dissected out from new born mice embryo and cultured on the chick chorioallantoic membrane. *Col-1* (bone marker) is strongly expressed on the periphery of the explants after 5 days of culture, indicating cartilage cells can directly transform into bone cells and lay down bone matrix ex-vivo.

Figure 2

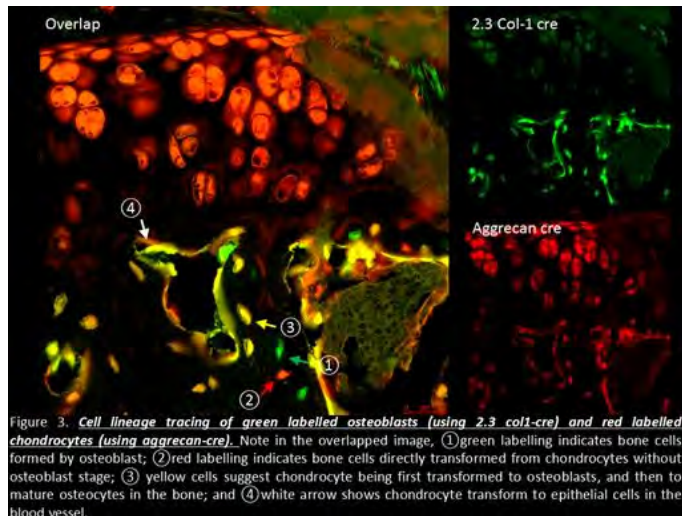


Figure 3

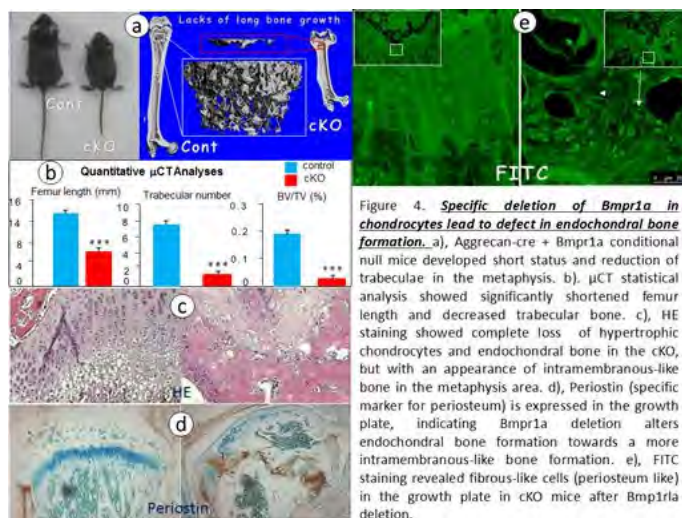


Figure 4

Disclosures: Yinshi Ren, None.

1151

An Sp7/Dlx transcriptional complex specifies mammalian osteoblasts. Hironori Hojo^{*1}, Shinsuke Ohba¹, Xinjun He¹, Lick Pui Lai¹, Andrew McMahon¹. ¹USC Broad-CIRM Center, USA, ²Dept. of Bioengineering, Univ. of Tokyo, Japan

Sp7/osterix encodes a key transcriptional regulator essential for mammalian osteoblast specification. To identify *Sp7*'s osteoblast regulatory program *in vivo*, we engineered a new mouse allele of *Sp7* by gene targeting. This allele produces a normally functioning fusion protein with a C-terminal addition of a Biotin-3xFLAG cassette to facilitate biochemical characterization of *Sp7* targets. We performed chromatin immunoprecipitation with FLAG antibody and DNA sequencing (ChIP-seq) using isolated neonatal calvarial osteoblasts. In addition, we obtained an osteoblast transcriptional profile by RNA-sequencing of neonatal calvarial osteoblasts. Bioinformatic analysis of these data sets identified *Sp7* engagement at putative regulatory regions for a large number of osteoblast-enriched genes. *In vitro* studies confirmed activities of the several predicted enhancers including those flanking *Coll1a1*, *Runx2* and *Notch2*. Transgenic mouse analysis of the *Notch2* enhancer verified osteoblast specific enhancer activity. Unexpectedly, *de novo* motif analysis on the *Sp7* ChIP-seq data identified an AT-rich sequence (AT-motif) as the primary *Sp7* interaction site; *Sp*-family members are known to bind to a GC-rich consensus motif. Functional analysis demonstrated that this AT-motif was required for *Sp7*-mediated enhancer activation but *Sp7* fails to bind this target sites, raising the possibility that partner proteins mediate *Sp7* with genomic targets. Bioinformatics, biochemical and *in vitro* expression analyses revealed that *Dlx*-family members were highly expressed in osteoblasts, bound to the AT-motif directly, and underwent protein-protein interactions with *Sp7*. Further *Sp7* and *Dlx5* ChIP-seq analysis showed that most of *Sp7* binding regions in genome were shared with *Dlx5*, an identical AT-motif that recovered from *Sp7* ChIP-seq on primary osteoblasts was the most enriched sequence

in the shared regions, and a positive correlation was observed in the strength of engagement exhibited by Sp7 and Dlx5. Gain- and loss-of-function studies showed that the transcriptional complex has synergistic effects on the transactivation of their targets and the Dlx members were required for Sp7 to associate with DNA and induce target gene expressions. Together these data support a novel model of Sp7 action. In this, Sp7 does not directly bind DNA targets. Instead, Dlx-family members bind to an AT-motif within osteoblast enhancers and recruit Sp7 to activate osteoblast-specific gene regulatory programs.

Disclosures: Hironori Hojo, None.

1152

AMPK favors the Smurf1-dependent ubiquitination of Runx2 in vivo. Junko Shimazu*, Jianwen Wei, Gerard Karsenty. College of Physicians & Surgeons, Columbia University, USA

The regulation of osteoblast differentiation by glucose taken up by the mesenchymal progenitor cells relies in large part on the ability of glucose to inhibit the activity of AMPK that would otherwise promote the ubiquitination of Runx2. An involvement of AMPK in protein ubiquitination has never been reported in any cell type before. Therefore it is important to decipher the molecular bases of this novel function of AMPK and to verify them in vivo. To address these questions we tested whether E3 ubiquitin ligases expressed in osteoblasts and known to be involved in Runx2 degradation could be phosphorylated and activated by AMPK. Using a bioinformatics analysis we identified Serine 148 in the E3 ubiquitin ligase Smurf1 that is involved in Runx2 degradation, as a putative AMPK phosphorylation site. Through the use of a specific phosphor-antibody directed against Smurf1 when phosphorylated at Serine 148 we could demonstrate that AMPK phosphorylates Smurf1 at Serine 148 in osteoblasts and that this post-translational modification is necessary for Smurf1 ability to ubiquitinate Runx2. To demonstrate the in vivo relevance of this cascade AMPK-Smurf1-Runx2, we generated mice in which Serine 148 in Smurf1 was mutated to alanine to prevent its phosphorylation. The resulting Smurf1ki/ki mice were born at the expected mendelian ratio. A Western blot analysis showed that Runx2 is markedly more abundant in the bones of Smurf1ki/+ mice and even more in those of Smurf1ki/ki mice thus establishing in vivo the importance of this phosphorylation event for the function of Smurf1. Alcian blue/alizarin red staining of skeletal preparations of showed a premature closure of cranial suture in the skull of Smurf1ki/ki newborn mice as well as significantly longer clavicles. To demonstrate that these phenotypic abnormalities were caused in part by an increase in Runx2 activity we generated and analyzed Smurf1Ki/+; Runx2+/- mice. Alcian blue/alizarin skeletal preparations showed that there was already a significant rescue of the cleidocranial dysplasia phenotype otherwise present in Runx2+/- mice in the Smurf1Ki/+; Runx2+/- mice analyzed. Runx2+/-; Smurf1Ki/ki mice are currently being generated. These results identify for the first time a role for AMPK signaling in the ubiquitination of Runx2 and identify a single Serine residue in the E3 ubiquitin ligase Smurf1 as carrying the brunt of its function.

Disclosures: Junko Shimazu, None.

FR0002

Increased Micro Crack Density in Patients with Low Turnover Renal Osteodystrophy. Logan Burgess*¹, Constance Wood¹, David Pienkowski¹, Hanna Mawad¹, Hartmut Malluche². ¹University of Kentucky, USA, ²University of Kentucky Medical Center, USA

Renal Osteodystrophy (ROD) is a common abnormality in patients with chronic kidney disease (CKD). Patients with ROD experience bone fractures more than 4 times the normal rate. Previous work in our laboratory showed that patients with ROD and high bone turnover have abnormal bone mineralization; this was not observed in patients with ROD and low bone turnover. Patients with low turnover; however, were reported to have more fractures than patients with high turnover. The present study was conducted to evaluate bone microdamage (an important parameter governing bone quality and load-bearing mechanical competence) in patients with low versus high bone turnover ROD.

Anterior iliac crest double tetracycline-labeled bone biopsies received sequentially in the Bone Diagnostic and Research Laboratory at the University of Kentucky were screened to identify 7 patients with high turnover ROD and 7 patients with low turnover ROD. Inclusion criteria were signed informed consent from female Caucasian patients aged 40-70 years with CKD stage 5D and ROD with low or high bone turnover diagnosed from undecalcified histologic bone sections. Men and patients of non-Caucasian races were excluded to focus on the patient group with the highest fracture risk.

Bone samples were stained with basic fuchsin under vacuum using an established protocol. Bone quality was assessed by measuring microcracks in 100 µm thin undecalcified sections using bone histomorphometry software at 40X magnification. Crack number, crack length, and accompanying area of mineralized bone were measured in a total of 50 optical fields for each sample. Data were analyzed by using analyses of covariance (SAS Institute).

Adjusted for bone area, the mean number of cracks was 2.2X greater in low turnover bone compared to high turnover bone (p=0.016). Mean crack length was not significantly different for high versus low turnover and was not correlated with bone area. This is the first study showing an increased number of microcracks in low turnover bone in patients with ROD adjusted for turnover-related changes in bone area. These findings are consistent with previous studies demonstrating an increase in microcrack number in low turnover canine bone treated with bisphosphonates. These results may offer a contributory mechanism for the increased fracture risk in this population and call for the early diagnosis and management of low bone turnover.

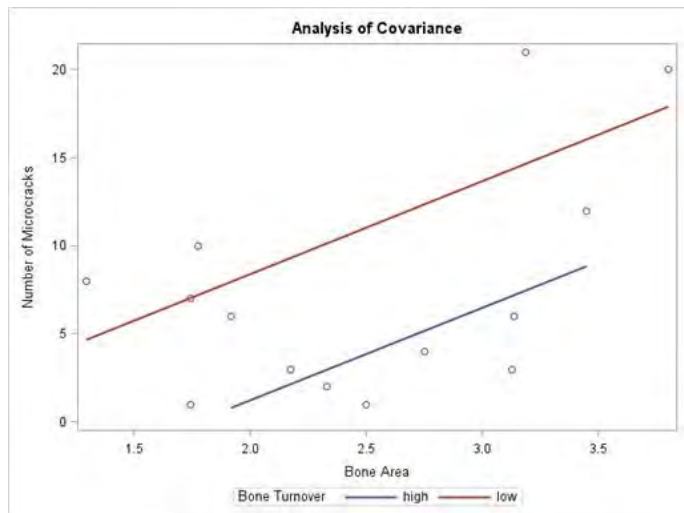


Figure 1

Disclosures: Logan Burgess, None.

FR0005

TBK1 Plays A Critical Role In Myeloma-Induced Osteoclast Formation. Quanhong Sun*, Peng Zhang, Juraj Adamik, Deborah Galson. University of Pittsburgh, USA

Increased osteoclast (OCL) formation is the hallmark of multiple myeloma (MM) bone disease, yet the underlying molecular mechanisms are incompletely understood. Our study showed that conditioned media (CM) from cultures of the human MM cell line MM1.S increased OCL formation by both the OCL precursor cell line 4B12 and mouse primary bone marrow monocyte (BMM) cultures when exposed to the MM-CM (1:100) for the M-CSF plus RANKL-driven differentiation stage. The MM-CM exposure increased expression of both IL-6 and RANK mRNA at day 2 (D2) over the RANKL-induced increases in cultures in control media. However, we found that BMM cultures treated with MM-CM only during the M-CSF-driven proliferation stage (D-3 to D0) demonstrated a more dramatic increase of both OCL formation and the nuclei number per OCL than those exposed to the MM-CM only during the differentiation stage (D0 to D3) or during both stages, although all three MM-CM

exposure paradigms were effective at increasing OCL numbers. We have previously reported that TBK1, an IKK family member with roles in innate immunity, is not required for normal OCL formation in vitro, but is required for the measles virus nucleocapsid protein (MVNP) enhancement of OCL formation and IL-6 production resulting in a pagetic OCL phenotype. We hypothesized that perhaps TBK1 plays a similar role in another model of inflammatory OCL formation such as MM-induced OCL formation. Therefore, we examined TBK1 in MM-CM treated BMM proliferation cultures. MM-CM exposure during the BMM proliferation phase resulted in a dose-dependent increase in expression of IL-6, RANK, and TBK1 mRNA at D0 compared to BMM cultures in control media. We reported that an increased ratio of TBK1 to optineurin (OPTN) enhanced OCL formation. Western blot analyses of TBK1 and OPTN revealed that MM-CM added after the proliferation phase, but in the absence of RANKL, increased total TBK1 protein and the TBK1/OPTN ratio within 12 h. Further, MM-CM increased the level of activated TBK1 (phosphoS172-TBK1) within 2 min. Of key interest, knockdown of TBK1 in BMM significantly attenuated the ability of MM-CM to affect OCL differentiation without altering OCL differentiation in control media. These data suggest MM cells require TBK1 to enhance OCL formation and that targeting TBK1 would decrease multiple myeloma bone disease, a major source of the mortality and morbidity in multiple myeloma patients.

Disclosures: Quanhong Sun, None.

FR0008

Unraveling the Vitamin D Paradox in African Americans. Mageda Mikhail*, John Aloia, Louis Ragolia, Shahidul Islam. Winthrop University Hospital, USA

Context: African Americans have a lower total serum 25-hydroxyvitamin D [25(OH)D] but superior bone health. This has been referred to as a "paradox". A recent publication found that free serum 25(OH)D is the same in black and white women. However, the study was criticized because an indirect method was used to measure free 25(OH)D.

Objective: We hypothesized that although total serum 25(OH)D is lower in African Americans, free serum 25(OH)D measured directly would not differ between races.

Design: White and black healthy postmenopausal women were matched for age and BMI. Serum total 25(OH)D, PTH, 1,25(OH)2D, vitamin D binding protein (VDBP) and bone density were measured. Direct measurement of serum free 25(OH)D was carried out using ELISA.

Setting: Ambulatory research unit in a teaching hospital.

Outcome: Cross-racial comparison of serum free 25(OH)D.

Results: A propensity match resulted in selection of a total of 164 women. Total 25(OH)D was lower in black women (19.5±4.7 vs. 26.9±6.4 ng/ml) but direct measurement of free 25(OH)D revealed almost identical values (5.25±1.2 vs. 5.25±1.3 ng/ml) between races. VDBP was significantly lower in blacks when using a monoclonal based ELISA (151±73 vs. 264.8±95 mcg/ml), but not a polyclonal based ELISA. Serum PTH, 1,25(OH)2D and bone density were higher in African Americans.

Conclusion: VDBP is lower in black women. Free serum 25(OH)D is the same across races despite the lower total serum 25(OH)D in black women.

Disclosures: Mageda Mikhail, None.

FR0014

Bone Remodeling in Patients With Hypoparathyroidism Treated for 3 Years With Recombinant Human Parathyroid Hormone, rhPTH(1-84), in the Open-Label RACE Study. Michael Mannstadt*¹, John P. Bilezikian², Bart L. Clarke³, Tamara J. Vokes⁴, Mark L. Warren⁵, Hjalmar Lagast⁶, Dolores M. Shoback⁷, Michael A. Levine⁸. ¹Massachusetts General Hospital Harvard Medical School, USA, ²College of Physicians & Surgeons, Columbia University, New York, NY, USA, ³Mayo Clinic Division of Endocrinology, Diabetes, Metabolism, & Nutrition, Rochester, MN, USA, ⁴University of Chicago Medicine, Chicago, IL, USA, ⁵Endocrinology & Metabolism, Physicians East, PA, Greenville, NC, USA, ⁶NPS Pharmaceuticals, Inc, Bedminster, NJ, USA, ⁷SF Department of Veterans Affairs Medical Center, University of California, San Francisco, San Francisco, CA, USA, ⁸Children's Hospital of Philadelphia, Philadelphia, PA, USA

Deficient endogenous parathyroid hormone (PTH) in hypoparathyroidism patients is associated with marked abnormalities of bone metabolism, which can lead to aberrations in bone microarchitecture and increased bone mineral density (BMD). In the pivotal phase III placebo-controlled trial and in a phase III, dose-blind, fixed-dose study, rhPTH(1-84) treatment improved mineral homeostasis and bone-remodeling characteristics in patients with hypoparathyroidism. We report on skeletal indices from patients who completed the Month 36 visit in the ongoing, long-term, open-label rhPTH(1-84) study.

Patients with hypoparathyroidism who completed either or both of the phase III studies initiated open-label treatment with subcutaneous rhPTH(1-84) at 25 or 50 µg/

day. Doses could be up-titrated to 50, 75, or 100 µg/day as needed to reduce conventional treatment with oral calcium and active vitamin D and to maintain serum calcium at 8.0–9.0 mg/dL. Because patients had completed the previous phase III studies, baseline was defined as the start of rhPTH(1-84) treatment. Bone turnover was evaluated by serum levels of bone turnover markers (BTMs), and BMD was assessed by dual-energy x-ray absorptiometry. Data are shown as mean ± SD.

This interim analysis included patients who were assessed at the Month 36 study visit as of September 30, 2014. Between baseline and Month 36, optimized albumin-corrected serum calcium levels were maintained (baseline, 8.4±0.7 mg/dL; Month 36, 8.2±0.7 mg/dL) and serum phosphorus decreased (baseline, 4.8±0.6 mg/dL; Month 36, 4.2±0.7 mg/dL). BTMs increased from low-normal levels between baseline and Month 36, indicating increased bone turnover. 3-year values were lower than peak values of BTMs achieved earlier in the time course (Table). There were very small changes in BMD at Month 36, with the lumbar spine trending upward and the other sites trending downward (Table). The most frequently reported adverse events were hypocalcemia (35%), muscle spasm (29%), nausea (27%), and paresthesia (25%). 3-year rhPTH(1-84) treatment in adults with hypoparathyroidism was associated with sustained improvements in mineral and bone homeostasis, as indicated by maintenance of serum calcium, decreases in serum phosphorus, increases in serum BTMs, and reductions in most BMD Z-scores. The results provide further support for the long-term efficacy and safety of rhPTH(1-84) treatment for hypoparathyroidism.

Table. Effects of rhPTH(1-84) on Bone Parameters

| | Baseline | | Maximum Value* | | Month 36 | |
|---|---------------------|----|------------------------|----|---------------------------|----|
| | Mean ± SD | n | Mean ± SD | n | Mean ± SD | n |
| Bone Turnover Markers | | | | | | |
| Bone-specific alkaline phosphatase (BSAP), µg/L | 9.6±3.3 | 48 | 20.7±12.2 [†] | 45 | 15.6±9.4 | 37 |
| Cross-linked C-telopeptide of type 1 collagen (CTX), ng/L | 213±172 | 48 | 699±469 [‡] | 47 | 480±457 | 36 |
| Aminoterminal propeptide of type 1 collagen (P1NP), µg/L | 34±20 | 49 | 201±161 [§] | 46 | 130±115 | 36 |
| | Actual Values | | | | Mean Change From Baseline | |
| Bone Mineral Density | Baseline, Mean ± SD | n | Month 36, Mean ± SD | n | Month 36, Mean ± SD | n |
| g/cm ² | | | | | | |
| Lumbar spine (L1–L4) | 1.27±0.19 | 45 | 1.29±0.19 | 38 | 0.01±0.10 | 36 |
| Hip (total) | 1.12±0.16 | 44 | 1.10±0.17 | 36 | -0.02±0.07 | 34 |
| Hip (femoral neck) | 0.99±0.19 | 44 | 0.98±0.19 | 36 | -0.02±0.08 | 34 |
| Distal one-third radius | 0.79±0.11 | 45 | 0.77±0.12 | 37 | -0.03±0.07 [¶] | 35 |
| Z-score | | | | | | |
| Lumbar spine (L1–L4) | 2.14±1.43 | 45 | 2.46±1.46 | 38 | 0.24±0.84 | 36 |
| Hip (total) | 1.52±1.10 | 44 | 1.56±1.17 | 36 | -0.05±0.51 | 34 |
| Hip (femoral neck) | 1.35±1.24 | 44 | 1.34±1.16 | 36 | -0.05±0.61 | 34 |
| Distal one-third radius | 0.94±0.82 | 45 | 0.49±1.03 | 37 | -0.44±0.76 [¶] | 35 |

*Over 36 months of rhPTH(1-84) treatment, assessed at baseline, Weeks 8, 16, 24, 40 and 52, and every 4 months thereafter.

[†]Peak value occurred at Month 16, [‡]Peak value occurred at Week 40, [§]Peak value occurred at Week 52.

[¶]p=0.016, ^{¶¶}p<0.002.

Table

Disclosures: Michael Mannstadt, NPS Pharmaceuticals, Inc
This study received funding from: NPS Pharmaceuticals, Inc

FR0018

PTH(1-84) Treatment is Safe and Effective in Hypoparathyroidism for Seven Years. Mishaela Rubin*, Natalie Cusano, Wen-Wei Fan, Yasmine Delgado, Farnoosh Mahdavi, Juviza Rodriguez, Aline Costa, Donald McMahon, John Bilezikian. Columbia University, USA

Hypoparathyroidism (HypoPT) is a rare disorder in which PTH is absent from the circulation. The biochemical profile includes hypocalcemia, hyperphosphatemia and hypercalciuria, while the densitometric hallmark is above average bone mineral density (BMD). We previously found that PTH(1-84) treatment for 6 years improves these abnormalities. Yet because HypoPT is a lifelong condition, there is a need to extend these findings. We now report 7-year data on the efficacy and safety of PTH(1-84) treatment in HypoPT.

Twenty one HypoPT subjects (46.5 ± 3 yrs; 17 female; duration HypoPT 19 ± 3 yrs) were studied. Etiologies were postsurgical (n=11), autoimmune (n=9) and DiGeorge (n=1). Baseline medications were calcium 3289 ± 288 mg/d; calcitriol 0.73 ± 0.1 µg/d; vitamin D 6669 ± 5112 IU/d and HCTZ 10.5 ± 4 mg/d. Serum calcium was 8.5 ± 0.2 mg/dL, undetectable PTH levels and serum phosphate of 4.4 ± 0.2 mg/dL; BMD measurements (g/cm²) were lumbar spine (LS) 1.230 ± 0.05; femoral neck (FN) 0.970 ± 0.04, total hip (TH) 1.079 ± 0.04 and distal 1/3 radius (DR) 0.731 ± 0.01.

PTH(1-84) was started at 100 µg every other day and changed after 3 yrs to doses ranging from to 25–100 µg/d. Calcium supplementation fell by 60% to 1307 ± 343 mg/d (p=0.0001) as did calcitriol by 56% to 0.32 ± 0.1 µg/d (p=0.006). Vitamin D intake and HCTZ dose did not change. Serum calcium remained stable (8.5 ± 0.2 to 8.7 ± 0.2 mg/d; p=NS) while 24-hr urinary calcium decreased by 32% from 262 ± 29 to 178 ± 26 mg (p=0.03). There was no change in serum phosphate, Mg or creatinine (0.99 ± 0.04 to

1.07 ± 0.1 mg/dL; p=NS), while total alkaline phosphatase increased (69.1 ± 4 to 79.1 ± 3.2 U/L; p=0.04). BMD increased by 4.6 ± 1.7% at LS (p=0.01), 3.0 ± 1.3% at TH (p=0.02), did not change at FN and fell 3.6 ± 1.4% at DR (p=0.02). One kidney stone and 3 minor fractures occurred. An elevation of serum calcium above the upper limit of normal occurred in only 5% of all measurements.

These data suggest that 7 years of PTH(1-84) treatment in HypoPT maintains normal calcium metabolism. Reductions in calcium and calcitriol requirements and urinary calcium excretion were maintained along with normal serum calcium levels. BMD changes were consistent with site-specific effects of PTH. These data, the longest-term clinical experience with continuous PTH treatment for any condition, suggest that PTH(1-84) is a safe and effective long-term option in HypoPT.

Disclosures: Mishaela Rubin, NPS Pharma

This study received funding from: NPS Pharma

FR0025

Does Cortical Bone Loss Precede Menopause? Ashild Bjornerem*¹, Ali Ghasem-Zadeh², Roger Zebaze², Xiaofang Wang², Minh Bui³, John L Hopper³, Ego Seeman². ¹UiT The Arctic University of Norway, Norway, ²Endocrine Centre, Austin Health, Australia, ³Centre for Epidemiology & Biostatistics, School of Population & Global Health, University of Melbourne, Australia

Remodelling is slow before menopause and there is little compelling evidence of a negative bone balance at the level of the basic multicellular unit. Bone loss is held to be predominantly trabecular in origin before menopause with appearance of cortical bone loss after menopause. We hypothesized that shortly before menopause cortical bone loss occurs by intracortical and endocortical remodeling, so porosity will increase, as 80% of the skeleton is cortical, most bone loss will be cortical, not trabecular.

Images of the distal tibia were obtained using high-resolution peripheral quantitative computed tomography (HR-pQCT; Scanco Medical) in 249 pre-, 32 peri- and 103 postmenopausal women aged 27–75 years at baseline of a twin study in 2008–2009, Melbourne, Australia. During an average of 3.1 years (SD 0.7) follow-up, 173 women remained pre-, 49 changed from pre- to peri-, and 30 from peri- to postmenopausal. Total, trabecular and cortical volumetric bone mineral density (vBMD), and cortical porosity of the total cortex, compact cortex, outer and inner transitional zones were quantified using the StrAx1.0 software, and annual changes were calculated.

In women who remained premenopausal and were below 40 years of age at baseline, cortical and trabecular vBMD decreased annually by 1.7 and 1.0 mg HA/cm³ respectively, and porosity of each cortical compartment increased by 0.1–0.2% (all p<0.05). In women 40–45 years of age, cortical vBMD decreased by 4.9 mg HA/cm³, and porosity increased by 0.2–0.5% (all p < 0.001). In women > 45 years of age, cortical vBMD decreased by 8.1 mg HA/cm³ and porosity increased by 0.4–0.8% (all p<0.001), no trabecular bone loss was detected in these two groups.

In premenopausal aged 40–54 years becoming perimenopausal, cortical vBMD decreased by 10.6 mg HA/cm³ and porosity increased by 0.4–0.8% (all p<0.001). In perimenopausal women aged 46–55 years becoming postmenopausal, cortical vBMD decreased by 15.9 mg HA/cm³ and porosity increased by 0.5–1.5% (all p<0.001). In both groups, no trabecular bone loss was detected. In postmenopausal women aged 49–75 years, cortical and trabecular vBMD decreased by 9.9 and 0.7 mg HA/cm³ respectively, porosity increased by 0.3–0.9% (all p<0.01).

Of the distal tibia total bone loss of 157 mg HA between 27 and 75 years of age; 4, 11, and 85% occurred before, across and after menopause, respectively, and 72% was cortical and 28% trabecular.

We infer that intracortical and endocortical remodeling produces modest cortical bone loss before menopause, most bone is lost after menopause and cortical exceeds trabecular bone loss.

Disclosures: Ashild Bjornerem, None.

FR0028

Effect of Teriparatide Treatment on Vertebral Strength in Postmenopausal Women with Osteoporosis Assessed Using a Patient-Specific Finite Element Model of the Disc-Vertebra-Disc Unit. Chuhee Lee¹, Margaret A Paggioli¹, Eugene V McCloskey¹, Nicola FA Peel², Jennifer S Walsh¹, Richard Eastell¹, Lang Yang*¹. ¹University of Sheffield, United Kingdom, ²Sheffield Teaching Hospitals NHS Foundation Trust, United Kingdom

Teriparatide (TPTD, PTH 1-34) treatment increases BMD, but the increase is not sufficient to explain the reduction in fracture risk entirely. The aim of this study was to apply a novel patient-specific finite element (FE) model of the disc-vertebra-disc (DVD) unit to quantify the effect of TPTD treatment on vertebral strength. In an open-label single-centre study, 20 postmenopausal women (age 64.4 ± 15.4 years) with osteoporosis (BMD T score < -2.5 at spine or hip) were treated with TPTD (FORSTEO, 20 micrograms daily) for 104 weeks. QCT scans of the lumbar spine were performed at baseline, 26, 52 and 104 weeks with a resolution of 0.62x0.62x0.62 mm³. The DVD FE models of the L2 vertebrae were generated using brick elements.

Transverse-isotropic, elastic-perfectly plastic material properties were assigned to the vertebra. Linear-elastic properties were used for the nucleus pulposus and annulus ground matrix, whereas 4 fibre layers were embedded in the annulus matrix to simulate collagen fibres. A pure compressive loading condition was simulated. Vertebral strength was defined using a 0.2% offset method in the load-displacement curve. Percentage changes from baseline were calculated at individual level. TPTD treatment increased not only the densitometric variables but also the FE-estimated vertebral strength (Table 1 and Figure 1). The mean (SE) percentage increases at the year-2 visit were 11% (2%) for DXA L1-L4 BMD, 22% (6%) for QCT L1-L3 vBMD and 30% (8%) for the FE estimated strength, respectively. In conclusion, vertebral strength derived from the in vivo DVD FE model shows a larger treatment effect relative to the baseline value than densitometric variables.

Table 1. Mean (SD) of the measurements at each visit

| | Baseline | Week 26 | Week 52 | Week 104 |
|--------------------------------------|-------------|--------------|--------------|--------------|
| DXA L1-L4 BMD (g/cm ²) | 0.73 (0.04) | 0.77 (0.05)* | 0.79 (0.04)* | 0.82 (0.05)* |
| QCT L1-L3 vBMD (mg/cm ³) | 86 (17) | 96 (20) | 104 (20)* | 103 (22)* |
| L2 DVD FE strength (N) | 1318 (251) | 1540 (327)* | 1668 (268)* | 1698 (332)* |

* indicates that the mean is significantly different from the baseline value at P<0.05

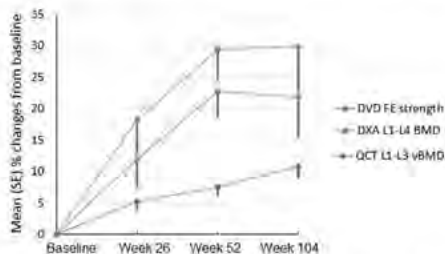


Figure 1. Mean (SE) percentage changes from baseline

Table 1 and Figure 1

Disclosures: Lang Yang, None.

FR0029

Effect of Transforming Growth Factor-Beta Inhibition on the Fracture Resistance of Bone in a Mouse Model of Type 2 Diabetes. Jeffry Nyman¹, Stephen O'Brien², Sasidhar Uppuganti³, Amy Creecy³, Mathilde Granke³, Paul Vozyian³, Kuber Sampath². ¹Vanderbilt University Medical Center, USA, ²Genzyme Research Center, USA, ³Vanderbilt University, USA

Individuals with type 2 diabetes (T2D) are twice as likely to suffer a fracture as non-diabetics of the same age. A lower BMD does not explain this increase in fracture risk, suggesting that diabetes deleteriously affects bone quality. The inhibition of TGF-β with a monoclonal antibody (GC1008 for humans, 1D11 for rodents) is a potential treatment for diabetic nephropathy. Since TGF-β signaling is inversely related to bone quality, we hypothesized that treating diabetic mice with 1D11 increases the fracture resistance of bone. The unknown effect of diabetes on bone material properties for the KK-Ay mouse model of T2D motivated two parallel experiments: i) non-diabetic a/a mice vs. diabetic KK-Ay/a mice and ii) 13C4 (control antibody) vs. 1D11 (anti-TGF-β antibody) in diabetic KK-Ay/a mice. One kidney was removed from all 41 female KK-Ay/a mice at 9 wks of age. They were then fed a high fat diet (24% kcal fat), while 12 age-matched female a/a mice ate a control diet (12% kcal fat). At 12 wks of age, diabetic mice were given 13C4 (n=14) or 1D11 (n=13) at 5 mg/kg (ip 3x/wk) for 12 weeks. After euthanasia, the femoral mid-shaft was imaged by μCT to obtain tissue mineral density (Ct.TMD), structural parameters, and porosity and ii) subjected to 3pt bending to estimate material properties. The femur metaphysis was also analyzed by μCT. All KK-Ay mice weighed more than the non-diabetic mice, and 1D11-treatment did not significantly lower circulating levels of glucose (Fig. 1). Diabetic mice had higher BV/TV and significantly greater Tb.Th than the non-diabetic mice. BV/TV, Tb.Th, and Tb.N were higher for 1D11- than for 13C4-treated diabetic mice. Moreover, 1D11-treatment rescued the diabetes-related decrease in Tb.TMD. Although structurally bigger (higher Imin), the femoral cortex was thinner for the diabetic mice with treatment having no effect. Ct.TMD was also lower for diabetic bone, but 1D11-treatment did not increase Ct.TMD as it did for trabecular bone. Cortical porosity was higher with diabetes, and 1D11-treatment lowered this porosity. There were no significant differences in structural or material strength of bone between the control and T2D mice. Instead, toughness was lower for the diabetic animals. Although 1D11-treatment did not prevent this loss in toughness, it did increase bone strength (Table 1). As in humans, diabetes in KK-Ay mice increases cortical porosity. TGF-β inhibition could ameliorate diabetes-related decrease in material strength.

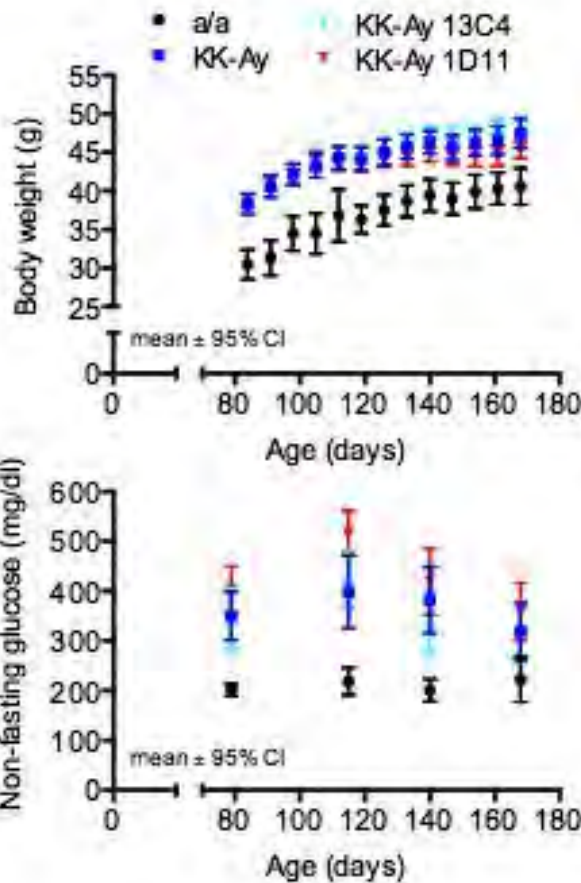


Figure 1. Differences in body weight and blood glucose between non-diabetic and diabetic KK-Ay mice.

| Parameter | Unit | Effect of Diabetes (no antibody) | | | Effect of Treatment (KK-A/a) | | | a/a vs. 1D11 |
|-------------------------|----------------------|----------------------------------|---------------|----------------------|------------------------------|---------------|----------------------|------------------|
| | | a/a | vs. KK-A/a | p-value [†] | 13C4 | vs. 1D11 | p-value [†] | |
| Femur Diaphysis | | | | | | | | |
| I _{min} | mm ⁴ | 0.227 (0.025) | 0.257 (0.035) | 0.0225 | 0.260 (0.025) | 264 (0.017) | 0.896 | 0.0055 |
| Ct.Th | mm | 0.203 (0.006) | 0.190 (0.014) | 0.0474 | 0.183 (0.011) | 0.187 (0.005) | >0.99 | 0.0005 |
| Ct.TMD | mgHA/cm ³ | 1378 (9) | 1356 (9) | <.0001 | 1353 (8) | 1350 (10) | 0.577 | <.0001 |
| Ct.Po | % | 4.75 (0.64) | 7.89 (1.85) | 0.0002 | 8.56 (2.60) | 6.60 (0.86) | 0.0156 | 0.0243 |
| Rigidity | N/mm ² | 1971 (343) | 2166 (203) | 0.575 | 2138 (201) | 2367 (259) | 0.0812 | 0.0035 |
| Peak Moment | N.mm | 72.9 (6.8) | 75.8 (7.0) | 0.460 | 76.1 (4.8) | 82.3 (6.1) | 0.0379 | 0.0031 |
| Strength | MPa | 245 (20) | 237 (11) | >0.99 | 237 (14) | 252 (11) | 0.0317 | 0.301 |
| Toughness | N/mm ² | 2.80 (0.54) | 2.20 (0.65) | 0.0521 | 2.35 (0.57) | 1.97 (0.61) | 0.191 | 0.0066 |
| Femur Metaphysis | | | | | | | | |
| BV/TV | mm ³ | 0.095 (0.024) | 0.129 (0.025) | 0.0576 | 0.113 (0.014) | 0.302 (0.066) | <.0001 | <.0001 |
| Tb.N | mm ⁻¹ | 2.95 (0.28) | 3.17 (0.23) | 0.325 | 3.12 (0.16) | 4.40 (0.49) | 0.0001 | <.0001 |
| Tb.Th | mm | 0.049 (0.003) | 0.055 (0.005) | 0.0136 | 0.051 (0.003) | 0.074 (0.007) | <.0001 | <.0001 |
| Tb.Sp | mm | 0.335 (0.031) | 0.313 (0.023) | 0.0432 | 0.312 (0.016) | 0.232 (0.022) | <.0001 | <.0001 |
| Tb.TMD | mgHA/cm ³ | 1111 (14) | 1097 (19) | 0.0427 | 1079 (17) | 1147 (17) | <.0001 | <.0001 |

[†]p-values were adjusted using Holm-Sidak's method or Dunn's method (non-parametric) for multiple pairwise comparisons.

Table 1. Selected properties of cortical and trabecular bone - mean (SD).

Disclosures: Jeffry Nyman, Genzyme
This study received funding from: Genzyme Corporation

FR0034

Lossing Trabecular Plate and Rod Number in Wrist Fractures. Bin Zhou¹, Will Smith², Ji Wang³, Yue Yu³, Kyle Nishiyama⁴, Emily Stein⁴, Elizabeth Shane⁴, X.Edward Guo³. ¹Columbia University, USA, ²Biomedical Engineering, Columbia University, USA, ³Biomedical Engineering Department, Columbia University, USA, ⁴Department of Medicine, Columbia University, USA

Trabecular plates and rods determine biomechanical properties of trabecular bone and individual trabecula segmentation (ITS) based plate-rod parameters have been shown to provide additional power to discriminate groups of patients with fragility fractures and vertebral fractures, independent of areal bone mineral density. We hypothesized that wrist fracture patients (WFX) also have abnormal trabecular plate and rod microstructure and compromised bone strength compared with healthy controls (C). We applied ITS and nonlinear micro finite element (μFE) analyses to high-resolution peripheral quantitative computed tomography (HR-pQCT) scans of

distal radius (DR) and tibia (DT) from wrist fracture patients and their matched controls.

Areal BMD (aBMD) of the spine, hip and forearm by DXA and HR-pQCT scans (*XtremeCT*, *Scanco Medical*) of the DR and DT were performed on postmenopausal women with (69±8 years, n=50) and without (69±6 years, n=50) wrist fracture history. ITS was applied to segment the trabecular bone network into individual trabecular plates and rods to measure plate- and rod-related microstructural parameters. Bone stiffness, yield strength and failed tissue fraction in cortical, trabecular plate and rod were calculated based on μ FE analyses.

Mean DXA T-scores were in the osteopenic range at all sites and were not different between WFX and C. At the DR, plate and rod bone volume fraction (pBV/TV, rBV/TV), plate and rod trabecular number (pTb.N, rTb.N), plate-plate and plate-rod junction density (P-P Junc.D, P-R Junc.D) and axial bone volume fraction (aBV/TV) were 25%, 10%, 8%, 4%, 22%, 19% and 20% lower in WFX than C (Fig, p<0.05). At the DT, pBV/TV, pTb.N, P-P Junc.D, P-R Junc.D and aBV/TV were 17%, 6%, 14%, 10% and 14% lower in WFX (p<0.05). Bone stiffness and yield strength were 13% and 16% lower at the DR, and 11% and 12% lower at the DT in WFX (Table). Trabecular plate compression failed fraction was 26% and 17% lower and rod compression failed fraction was 17% and 12% lower in WFX, at the DR and DT respectively.

In conclusion, despite similar aBMD by DXA, postmenopausal women with prior wrist fracture have lower plate and rod bone volume, fewer trabecular plates and rods, less connectivity between rods and plates at both the DR and DT, and lower bone stiffness and strength. Application of ITS, μ FE and failure analyses to HR-pQCT scans of the DR and DT can discriminate postmenopausal women with and without wrist fractures independent of aBMD.

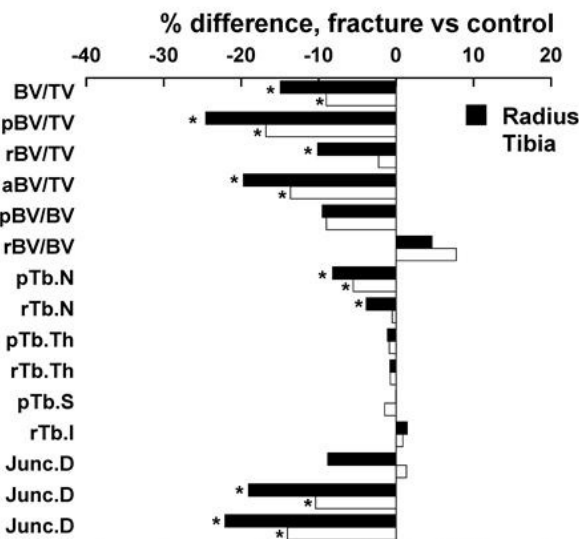


Figure. Comparison of percent difference in HR-pQCT based ITS measurements between radius fracture and control subjects. *indicates significant difference.

Figure

| | Radius | | Tibia | |
|---|-----------------|------------------|-------------------|--------------------|
| | fracture | control | fracture | control |
| Stiffness (N/mm) | 58617.34±3008.7 | 67599.14±5381.5* | 183042.44±40619.9 | 207775.94±42941.6* |
| Yield Force (N) | 3312.64±812.6 | 3942.14±1008.7* | 11207.44±2702.2 | 12759.04±989.1* |
| Yield energy (mJ) | 138.34±40.8 | 190.44±50.9* | 596.44±134.2 | 615.14±49.4* |
| Elastic energy (mJ) | 141.14±37.7 | 171.74±47.9* | 496.14±128.6 | 571.24±46.1* |
| Plastic energy (mJ) | 17.24±4.1 | 18.74±3.9* | 40.34±9.1 | 43.94±7.3* |
| Cortical compression failure fraction | 0.0674±0.025 | 0.0764±0.028 | 0.0894±0.041 | 0.1014±0.041 |
| Cortical tension failure fraction | 0.0594±0.015 | 0.0584±0.017 | 0.140±0.029 | 0.1134±0.028 |
| Trabecular compression failure fraction | 0.0544±0.02 | 0.0684±0.025* | 0.0834±0.021 | 0.1064±0.031* |
| Trabecular tension failure fraction | 0.0424±0.023 | 0.0574±0.03* | 0.0734±0.027 | 0.0934±0.032* |
| Plate compression failure fraction | 0.0584±0.025 | 0.0784±0.028* | 0.0914±0.024 | 0.1094±0.032* |
| Plate tension failure fraction | 0.0774±0.021 | 0.0944±0.021* | 0.0894±0.015 | 0.1014±0.015* |
| Rod compression failure fraction | 0.0534±0.019 | 0.0644±0.023* | 0.0784±0.02 | 0.1034±0.032* |
| Rod tension failure fraction | 0.0324±0.022 | 0.0464±0.03* | 0.0684±0.039 | 0.0974±0.063* |

Table. Mechanical properties percent differences between fracture and control. *indicates significant difference.

Table

Disclosures: Bin Zhou, None.

FR0035

Nanomechanical Properties of Human Bone with Varying Continuous Bisphosphonate Treatment Durations. David Pienkowski^{1*}, Constance L. Wood², Hartmut H. Malluche³. ¹University of Kentucky, USA, ²Department of Statistics, University of Kentucky, USA, ³Nephrology: Bone & Mineral Metabolism, USA

Oral bisphosphonates (BPs) have well-known short-term benefits on bone mass for patients with osteoporosis, but reports of atypical fractures with longer-term BP use generate concerns for adverse bone quality changes. Deformation resistance is a key aspect of bone quality and is determined by extrinsic structure and intrinsic material properties. The present study sought to quantify changes in the material properties of human bone from patients treated with BPs for varying durations. Iliac crest bone samples (n=82) from Caucasian females aged 40 – 80 years diagnosed with osteoporosis and continuously treated with oral BPs for varying (0.2 – 16 years) durations were studied. Bone samples (n=12) from comparable subjects with osteoporosis never exposed to BPs were also studied. Exclusion criteria were: osteogenesis imperfecta, genetic bone diseases, osteomalacia, hyperparathyroid bone disease, chronic kidney or Paget's disease, endocrine abnormalities, drug/alcohol abuse, and non-oral BP bone metabolism altering drugs. Young's modulus (a metric of intrinsic material deformation resistance) was measured in all samples using an established nanoindentation technique. Modulus was calculated at 30 sites (6 trabeculae X 5 sites/trabeculae (left & right edges (E), left & right middles (M), and center (C)) per sample. Repeated measures polynomial regression was used to model the relationships among patient age, modulus, and BP treatment duration at each of the 3 (E,M,C) trabecular locations. Adjusted for patient age, modulus differed by trabecular location (p<0.0001) and displayed a quadratic relationship (p-values of coefficients for linear and 2nd-order terms were 0.0039 and 0.0233) with BP treatment duration. These relationships showed: 1) increasing modulus with increasing BP treatment duration, 2) modulus peaks of 16.20, 16.80, and 17.30 GPa at E, M, and C at 8.52 years of BP treatment, 3) modulus declines with longer BP treatment duration. The observed peak and subsequent decline in modulus are novel and consistent only with our prior study showing a similar quadratic relationship between bone strength calculated from finite element analyses of trabecular structure and varying BP treatment duration. Unlike short-term modulus increases, modulus declines with longer-term BP treatment duration are unclear. Data from this and our prior study show that BP treatment duration is related to changes in both the extrinsic and intrinsic properties of human bone.

Disclosures: David Pienkowski, None.

FR0041

Multiscale characterization of material properties of cortical tissue from patients with atypical femoral fractures. Ashley Lloyd^{1*}, Bernd Gludovatz², Christoph Riedel³, Emma Luengo¹, Joseph Lane⁴, Robert Ritchie⁵, Björn Busse³, Eve Donnelly¹. ¹Cornell University, USA, ²Lawrence Berkeley National Laboratory, USA, ³University Medical Center Hamburg-Eppendorf, Germany, ⁴Hospital for Special Surgery, USA, ⁵University of California, Berkeley, USA

Bisphosphonates (BPs) reduce fracture risk in postmenopausal women by up to 50%. However, prolonged BP treatment has been associated with rare atypical femoral fractures (AFFs) characterized by transverse brittle morphology. Because BPs reduce remodeling, they could alter bone tissue material properties. However, mechanical properties of tissue from patients with AFFs have yet to be studied.

Thus, the objectives of this study were to compare the nanoscale mechanical and compositional properties, and the microscale fracture properties, of bone tissue from patients with AFFs to those of patients with typical fragility fractures and patients without fractures.

Biopsies of proximal femoral cortical bone adjacent to the fracture site were obtained from postmenopausal women during fracture repair surgery (fracture groups), or total hip arthroplasty (non-fracture group). Patients were allocated to four groups: atypical fractures, all with history of BP use (+BP Atypical: n=7, age 73 ± 12y, BP 9.3 ± 4y); typical fragility fractures with and without BP use (+BP Typical: n=6, age 88 ± 6y, BP 9.5 ± 6y; -BP Typical: n=6, age 85 ± 3y); and non-fracture without history of BP use (-BP Non-fx: n=5, age 69 ± 5.5y).

Mineral composition was assessed with quantitative backscattered electron imaging and Raman imaging. Nanomechanical properties were assessed with nanoindentation. Fracture properties were assessed with in-situ fracture toughness testing of cortical beams (~0.5x0.5x5mm). Cortical microstructure and crack paths were assessed with micro-computed tomography.

Raman mineral:matrix ratio was greater in atypical samples compared to controls (+BP Atypical vs. +BP Typical +18%, vs. -BP Non-fx +29%). Distributions of tissue mechanical and compositional properties showed trends toward atypical samples having narrower distributions than controls with significant differences versus non-fracture controls (Raman crystallinity -34% p<0.05, modulus -29% p<0.10, hardness -31% p<0.05) (Fig. 1). Preliminary analysis shows propagation of cracks through cortical bone in relation to osteons in atypical fracture samples and controls (Fig. 2). The elevated tissue mineralization in atypical samples suggests increased tissue age and increased brittleness relative to controls. The decrease in heterogeneity is consistent with a reduction in overall bone toughness due to a loss of intrinsic toughening behavior. Both are consistent with the transverse fracture morphology

observed radiographically.

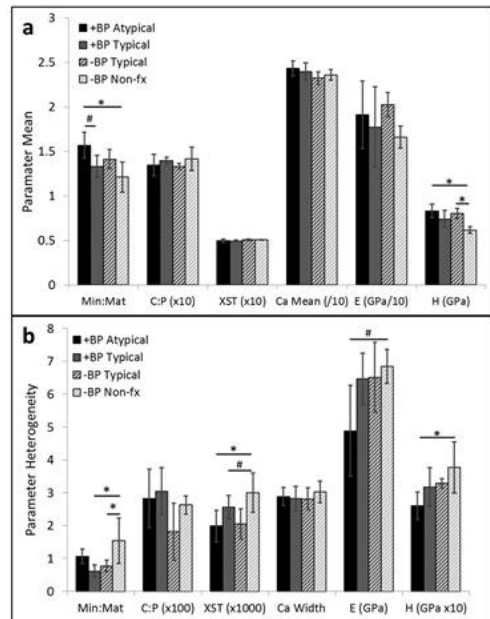


Fig. 1 Comparison of compositional parameters measured by Raman microscopy (Min:Mat: mineral to matrix ratio, C:P: carbonate to phosphate ratio, XST: crystallinity) and qBEI (Ca mean, Ca width), and nanomechanical properties measured by nanoindentation (E: reduced modulus, H: hardness). *p<0.05 #p<0.10 (a) Parameter means (b) Parameter distribution widths

Figure 1

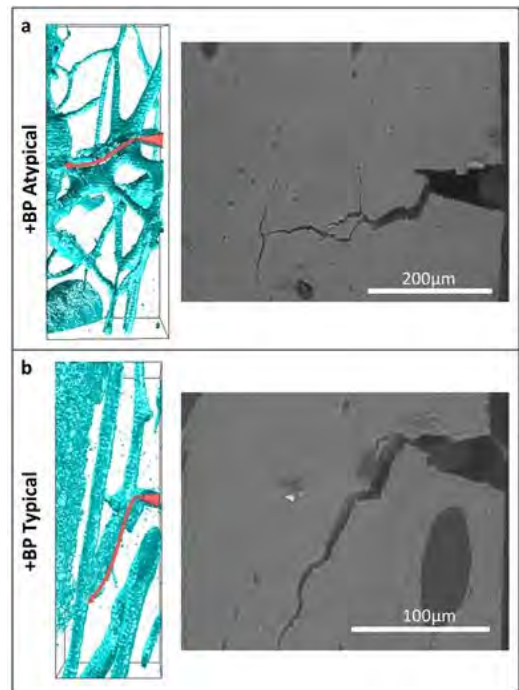


Fig. 2 Comparison of fracture behavior in (a) +BP Atypical vs. (b) +BP Typical samples showing (right) electron backscatter image of in situ fracture toughness tests of microbeams and (left) reconstruction of μCT image of haversian canals and crack path (notch and direction of crack path in red)

Figure 2

Disclosures: Ashley Lloyd, None.

FR0042

Osteocyte Lacunar Characteristics as a Function of Genotype and Age in Bone Tissue. Valerian Peterson¹, Brad Hugenroth¹, Brett Rosauer¹, Diane Cullen¹, Mohammed Akhter^{*2}. ¹Creighton University, USA, ²Creighton University Osteoporosis Research Center, USA

The purpose of this study is to examine and compare the osteocyte lacunar characteristics in mouse femurs representing different genotype and age. It is hypothesized that osteocyte lacunar properties in bone tissue are a function of genotype and age. To test this hypothesis we used two mouse genotypes (high bone

mass [HBM], and C57BL/6J wild type [WT]) and two age groups (6 and 22 months old). Femurs from HBM (n=12) and WT (n=12) mice representing two age groups (6 and 22 months) were embedded in quick setting plastic (EpoThin Resin) in order to help cut 300 to 400 μm thick sections. Each femoral section's anatomical was identified and scanned using high resolution MicroXCT-200 (Carl Zeiss/Xradia Inc.). All scans were done using 40X objective lens to obtain the best possible resolution of 0.6μm pixel size. Each femur was scanned at the anterior-medial site with a field of view (FOV) of 0.5mm x 0.5mm, and 1000 images/specimen were collected with a scan time of 3 to 4hrs. All images were analyzed using Avizo 8.1software (FEI) to segment the osteocyte lacunar voids in the bone tissue. The lacunar voids with different sizes are shown in cortical bone with part of the mineral removed digitally (Figure -1). The voids range (50 μm³ to 610 μm³) that best represents the osteocyte lacunar were analyzed for their average volume (μm³), surface area (μm²), and density (#/mm³) along with an average distance from adjacent lacunae (μm) and void sphericity. A two way ANOVA was used to determine the genotype- and age- related differences (P<0.05). Osteocyte lacunar properties showed both genotype- and age-related differences in some of the measured properties (Table-1). While lacunar volume showed no difference due to genotype and age, the surface area was greater in HBM at younger age when compared to WT. There is a significant age-related increase in the lacunar density for WT which was also greater than HBM at older age. The near neighbor distances decrease with age in WT and remained lower than HBM at older age. Sphericity, a measure of a lacunar void being a true sphere (Sphericity =1) or ellipsoid (Sphericity < 1), suggest that WT lacunar voids are more spherical than those in HBM in younger age only. We conclude that there is both genotype- and age-related influence on osteocyte lacunar characteristic in some of the measured variables, and that may play a major role in skeletal health and response to exercise (mechanical stimuli).



Figure-1. Osteocyte lacunae shown in the anterior-medial quadrant of mid shaft-femur.

Figure-1. showing osteocyte lacunar distribution

| Table-1 | Volume [μm ³] | Surface Area [μm ²] | Density [# /mm ³] | Distance [μm] | Sphericity |
|----------|---------------------------|---------------------------------|-------------------------------|---------------|----------------|
| 6 month | | | | | |
| WT | 173±36 | 205±27 | 4902±9826 | 249±31 | 0.724±0.0189 |
| HBM | 194±18 | 234±14* | 4322±9427 | 261±31 | 0.6918±0.0264* |
| 22 month | | | | | |
| WT | 181±18 | 214±13 | 62109±5244* | 236±14* | 0.7215±0.0158 |
| HBM | 173±27 | 209±25* | 4902±12478* | 272±13* | 0.7175±0.0406 |

* Age-related diff (P<0.05); * Genotype-related diff (P=0.05); * Age-related trend (P<0.1); Mean ± std

Table-1. Data for the osteocyte lacunar characteristics

Disclosures: Mohammed Akhter, None.

FR0043

Unloading conditions negatively affects bone homeostasis via endothelial-osteoblast-osteoclast interactions in vitro and in vivo. Vimal Veeriah*, Mattia Capulli, Angelo Zanniti, Nadia Rucci, Anna Teti, University of L'Aquila, Italy

Skeletal homeostasis is a major target of mechanical unloading. Endothelial cells (ECs) are sensitive to mechanical stimuli and to bone-seeking factors, therefore we hypothesized that ECs are implicated in the regulation of bone metabolism during unloading. ECs were subjected to MicroGravity, then Conditioned Media (MG-EC-CM) were collected and used to treat mouse primary osteoblasts. MG-EC-CM increased osteoblast proliferation (+1.5-fold;p=0.003) and decreased Alkaline Phosphatase (ALP) activity (-53%;p<0.001) and matrix nodule formation (-66%;p=0.010) compared to unit gravity EC-CM. MG-EC-CM increased osteoblast RANKL expression and osteoclastogenesis in osteoblast-bone marrow mononuclear cell co-cultures (+56%;p<0.001). It also induced the expression of the osteoblast differentiating factor, Lipocalin 2 (Lcn2) (+48-fold;p<0.001), whose silencing rescued ALP activity (+52%;p=0.024), decreased RANKL expression and reduced osteoclast formation (-38%;p=0.004), with no effect on osteoblast proliferation. MG-EC-CM enhanced osteoblast NO-Synthase 2 (NOS2) and CycloOxygenase 2 (COX2) expression, while inhibition of NOS2 or NO signaling reduced osteoblast proliferation and rescued ALP activity (+38%;p=0.004). Nuclear translocation of the Lcn2/NOS2 transcription factor, NF-kB, was observed in MG-EC-CM-treated osteoblasts and in MG-ECs, alongside a high expression of the NF-kB activator, IL-1β (+96-fold;p=0.002), with NF-kB inhibition reducing osteoblast proliferation and rescuing ALP. Lcn2 (+22-fold) and NOS2 (+12-fold) were also incremented in ex-vivo calvaria cultured with MG-EC-CM, and in tibias and calvarias (p=0.021) injected in-vivo with MG-EC-CM. Furthermore, the tibias of in-vivo models of mechanical unloading, including tail-suspended mice and mice treated with botulin A toxin to induce transient muscle paralysis, featuring decreased bone mass, showed higher expression of IL-1β (+5.8-fold;p=0.004), Lcn2 (+10-fold;p=0.002) and NOS2 (+23-fold;p=0.001), suggesting their involvement in the in-vivo EC-osteoblast crosstalk. We conclude that, MG-EC-CM induces Lcn2 and NOS2 in osteoblasts through IL-1β. Lcn2 impairs osteoblast differentiation and enhances RANKL expression and osteoclastogenesis, while NOS2 increases osteoblast proliferation. Targeting this EC-osteoblast-osteoclast regulatory loop could help improve the bone phenotype in unloading conditions.

Disclosures: Vimal Veeriah, None.

FR0044

Effects of 1 Month Spaceflight and 8 Days Recovery on Bone Structural and Quality Properties of Mice. Maude Gerbaix*¹, Vasily Gnyubkin¹, Delphine Farlay², Hélène Follet², Patrick Ammann³, Norbert Laroche¹, Boris Shenkman⁴, Guillemette Gauquelin-Koch⁵, Laurence Vico¹. ¹INSERM U1059, Biologie du Tissu Osseux, Université de Lyon, France, ²UMR-U1033-INSERM, Université de Lyon, France, ³Hôpitaux Universitaires de Genève (HUG), Switzerland, ⁴Institute for Biomedical Problems, Russian Academy of Sciences, Russia, ⁵Centre National d'Etudes Spatiales, France

Introduction

Site specific loss of bone mass is commonly observed after spaceflight both in human and rodent. However, bone quality response to flight and earth recovery remains poorly known. This study aims to characterize bone intrinsic properties alterations after spaceflight and to determine the bone events occurring during short term recovery.

Methods

Two groups of five C57/Bl6 male mice exposed to one month of spaceflight on the Russian Bion-M1 satellite were compared (Andreev-Andrievskiy A. et al., PloS One 2014). One group was euthanized 12 hours after landing (Flight), the other 8 days later (Flight+Rec). A ground synchronous control group (Ground Control) was placed in the same housing, climate and food conditions as two others during one month. Bone structure was evaluated by microCT, osteoclast activity by TRAP staining and intrinsic bone qualities by nanoindentation, microradiography and infra-red spectroscopy.

Results

At femur, spaceflight significantly decreased BV/TV, Ct.Th and increased TRAP+ osteoclasts at the periosteal surface. Nano indentation indicated a significant decrease in cortical plastic and elastic properties (modulus, hardness and working energy). One week of recovery tended to rescue these properties mainly at the third trochanter. Nevertheless, Ct.Th remained smaller in the Flight+Rec vs flight groups.

At vertebrae, spaceflight significantly decreased BV/TV which tended to be rescued by recovery. Degree of mineralization and mineral and collagen intrinsic quality (mineralization index, crystallinity, mineral and collagen maturity) remained unchanged.

Conclusions

One month of spaceflight severely altered the bone structure and intrinsic mechanical properties of femur without affecting mineralization and collagen of vertebrae. Interestingly, one week of recovery primarily tended to rescue the bone structure of vertebrae. Femur cortical plastic and elastic properties almost recovered whereas its cortex remained thinner. A better understanding of the adaptation of

trabecular and cortical compartments to microgravity and recovery as well as their intrinsic properties could help anticipate spationauts bone loss.

| | Ground Control | Flight | Flight+Rec |
|---------------------|----------------|------------|------------|
| Femur BV/TV (%) | 4.8±0.9 | 1.7±0.4* | 2.2±0.8 |
| Femur Ct.Th (mm) | 0.206±0.0 | 0.194±0.0* | 0.175±0.0* |
| Vertebrae BV/TV (%) | 12.1±1.0 | 7.8±0.7* | 11.3±1.5 |

Data are mean ± SE *p<0.05 Flight vs Ground Control #p<0.05 Flight+Rec vs Flight

Effects of Spaceflight and recovery on bone micro architecture parameters

Disclosures: Maude Gerbaix, None.

This study received funding from: CNES

FR0051

Greater Bone Accrual Occurs in African American Youth Before and After Puberty Compared to Euro-American Youth. Laura Armas*¹, Patrice Watson¹, Vicente Gilsanz², Thomas Hangartner³, Heidi J. Kalkwarf⁴, Kalkwarf⁴, Sharon Oberfield⁵, John Shepherd⁶, Karen K. Winer⁷, Babette Zemel⁸, Joan M. Lappe¹. ¹Creighton University, USA, ²Children's Hospital Los Angeles, USA, ³Wright State University, USA, ⁴Cincinnati Children's Hospital Medical Center, USA, ⁵Columbia University, USA, ⁶University of California at San Francisco, USA, ⁷Unice Kennedy Shriver National Institute of Child Health & Human Development, USA, ⁸Children's Hospital of Philadelphia, USA

African American (AfrAm) adults have higher bone mass than people of European ancestry (EuAm) of the same sex and age, and this difference is not present at birth. Greater peak bone mass is achieved through higher rates of bone accrual. Our purpose is to investigate when the greatest difference occurs in bone accrual between AfrAm and EuAm children. The BMDCS was a multicenter cohort study with 2014 subjects, ranging in age from 5 to 19 yrs who were evaluated annually for up to 7 visits. Bone mineral content (BMC) and areal bone mineral density (aBMD) of total body, lumbar spine and hip were acquired by DXA and Tanner staging (TS) was assessed by physical exam. Each pair of consecutive DXA's on a given subject was converted into a single observation of velocity: ((BMC at 2nd visit – BMC at 1st visit)/ time between visits (yrs)). Observations were categorized by ancestry group, sex, and TS. (See Table.) TS was further classified as pre-pubertal if TS was 1 at start and end of velocity interval, and as post-pubertal if TS was 5 at the start and end of the interval. In boys and in girls, mixed effects regression was used to investigate the effects of ancestry on BMC and aBMD velocity in pre-pubertal, peri-pubertal and post-pubertal groups, and on BMC/ BMD increase from start to end of peri-puberty, defined as TS 2 at beginning of interval to TS 4 at end of interval. Ancestry group differences during peri-puberty: BMC and BMD velocity were strongly associated with TS, and ancestry by TS interactions were observed. The model was used to compare total BMC/BMD accrual (gm) during peri-puberty, and no significant ancestry group differences were observed in either sex or at any bone site. Ancestry group differences in BMC/BMD velocity: 1) prepuberty, significantly higher accrual velocities in AfrAm. AfrAm boys had higher velocities for TBBMC/BMD, hip BMC/BMD, and spine BMD. AfrAm girls had higher velocities for TBBMC. 2) post-puberty, significantly higher accrual velocities in AfrAms. AfrAm boys had higher velocities for TBBMC/BMD and hip BMC. AfrAm girls had higher velocities for spine BMD. Findings from this large cohort are in agreement with previous findings that AfrAm have higher bone accrual than whites during pre-puberty and not during peri-puberty. In addition, we conclude that AfrAm vs EuAm BMC/BMD differences may be partially accounted for by differences in accrual velocity in post-puberty. 1. Hui SL, Perkins AJ, Harezlak J et al. 2010 Velocities Of Bone Mineral Accrual in Black and White American Children J Bone and Mineral Metabolism 25:1527-1535

Counts of observations (Obs) and subjects (SS) by sex, race and pubertal category

| | EuAm | EuAm | EuAm | EuAm | AfrAm | AfrAm | AfrAm | AfrAm |
|-------------|------|------|-------|-------|-------|-------|-------|-------|
| | Boys | Boys | Girls | Girls | Boys | Boys | Girls | Girls |
| | Obs | SS | Obs | SS | Obs | SS | Obs | SS |
| Prepuberty | 459 | 193 | 372 | 187 | 161 | 81 | 106 | 57 |
| Peripuberty | 738 | 240 | 839 | 281 | 347 | 113 | 344 | 119 |
| Postpuberty | 618 | 198 | 509 | 168 | 282 | 99 | 363 | 101 |

Table

Disclosures: Laura Armas, None.

FR0052

Maternal Gestational Vitamin D Supplementation and Offspring Bone Mass: A Multicentre Randomised, Double-Blind, Placebo-Controlled Trial (MAVIDOS). Cyrus Cooper¹, Nicholas C Harvey¹, Nicholas J Bishop², Stephen Kennedy³, Aris T Papageorgiou³, Robert Fraser⁴, Saurabh V Gandhi⁴, Stefania D'Angelo¹, Sarah R Crozier¹, Rebecca J Moon¹, Nigel K Arden⁵, Elaine M Dennison¹, Keith M Godfrey¹, Hazel M Inskip¹, Inez Schoenmakers⁶, Ann Prentice⁶, Zulf Mughal⁷, Richard Eastell⁸, David M Reid⁹, Kassim Javaid⁵, MAVIDOS Study Group¹. ¹MRC Lifecourse Epidemiology Unit, University of Southampton, United Kingdom, ²Academic Unit of Child Health, Sheffield Children's Hospital, University of Sheffield, United Kingdom, ³Nuffield Department of Obstetrics & Gynaecology, John Radcliffe Hospital, University of Oxford, United Kingdom, ⁴Sheffield Hospitals NHS Trust (University of Sheffield), United Kingdom, ⁵Oxford NIHR Musculoskeletal Biomedical Research Unit, Nuffield Department of Orthopaedics, Rheumatology & Musculoskeletal Sciences, The Botnar Research Centre, University of Oxford, United Kingdom, ⁶MRC Human Nutrition Research, Elsie Widdowson Laboratory, United Kingdom, ⁷Central Manchester University Hospitals, United Kingdom, ⁸Academic Unit of Bone Metabolism, University of Sheffield, United Kingdom, ⁹School of Medicine & Dentistry, Medical School, University of Aberdeen, United Kingdom

There is increasing evidence that maternal gestational vitamin D insufficiency might adversely influence offspring bone development. We evaluated the efficacy of 1000IU/day cholecalciferol during pregnancy for optimisation of neonatal bone mass in a UK multicentre randomised double-blind placebo-controlled trial (MAVIDOS, ISRCTN82927713).

Pregnant women with a serum 25-hydroxyvitamin D [25(OH)D] 25-100nmol/l at 12 weeks gestation were randomised to either 1000IU cholecalciferol/day or matched placebo until delivery. Plasma 25(OH)D concentration was measured in a central laboratory at 14 and 34 weeks gestation (Diasorin Liaison). Within two weeks after birth, whole body bone mineral content (BMC) of the offspring was assessed by dual-energy X-ray absorptiometry.

DXA information was available for 665 infants for the intention to treat analysis. Whole body BMC was non-significantly greater in infants born to mothers supplemented with vitamin D (61.6 ± 11.7 g vs 60.5 ± 11.1 g, $p=0.21$). However, in a pre-specified analysis, there was an interaction between treatment allocation and season of birth ($p=0.04$), such that infants born in winter months (December-February) to mothers randomised to cholecalciferol had greater BMC than infants of mothers randomised to placebo (63.0 ± 10.8 g vs 57.5 ± 10.9 g, $p=0.004$), a difference >0.5 SD. Similar patterns were observed for bone area and bone mineral density. At 34 weeks gestation, mean 25(OH)D was greater (68.2 ± 21.9 nmol/l vs 43.4 ± 22.4 nmol/l, $p<0.001$) and the proportion of women with vitamin D insufficiency [25(OH)D <50 nmol/l] reduced (16.6% vs 63.5%, $p<0.001$) in the women who had received the vitamin D supplement compared to placebo. In the placebo group, 25(OH)D declined from 14 to 34 weeks in women who delivered in winter or spring, but increased in those who delivered in summer or autumn (all $p<0.001$). These seasonal differences were entirely removed by vitamin D supplementation, with 25(OH)D rising from 14 to 34 weeks irrespective of season of birth ($p<0.001$). No safety issues were identified.

Maternal supplementation with 1000IU/day cholecalciferol during pregnancy increases bone mass in offspring born during winter months, and prevents the seasonal decline in 25(OH)D in these mothers. These findings have implications for public health policy relating to antenatal vitamin D supplementation. CC and NCH are joint first author.

Disclosures: Cyrus Cooper, None.

FR0053

The Effect of Insulin Resistance on the Cortical Bone-IGF-I Relationship in Children. Joseph Kindler¹, Norman Pollock², Emma Laing¹, Kathleen Hill Gallant³, Stuart Warden⁴, Connie Weaver³, Munro Peacock⁵, Carlos Isaacs², Richard Lewis¹. ¹The University of Georgia, USA, ²Georgia Regents University, USA, ³Purdue University, USA, ⁴Indiana University, USA, ⁵Indiana University School of Medicine, USA

During pubertal maturation, insulin-like growth factor I (IGF-I) plays a key role in bone mass accrual and cortical bone expansion. Although normal maturational growth is accompanied by fluctuations in insulin resistance, excessive insulin resistance during adolescence has been identified as a negative predictor of appendicular cortical bone size and strength. The aim of this study was to determine whether the relationships between IGF-I and cortical bone geometry differ among children with normal and higher insulin resistance. Participants included 61 healthy black and white boys and girls (mean \pm SD age 11.3 ± 1.2 years). Tibia and radius cortical bone and muscle cross-sectional area (MCSA) were assessed via peripheral quantitative computed tomography (Stratec XCT 2000) at the 66% site relative to the

distal growth plate. In sera, IGF-I (ng/ml) was measured by ELISA, insulin (uU/mL) by RIA, and glucose (mmol/L) by the enzymatic Autokit glucose method. The homeostasis model assessment of insulin resistance (HOMA-IR) was calculated ($\text{[insulin} \times \text{glucose]} / 22.5$). Based on the HOMA-IR cutoff of 4.0, normal ($n=30$) and higher ($n=31$) insulin resistance groups were determined. Multiple linear regression analyses were conducted adjusting for race and sex. Subsequent analyses were performed controlling for MCSA. In all children, IGF-I was a positive predictor of tibia cortical bone mineral content (Ct.BMC; $\beta=0.31$, $p<0.01$), area (Ct.Ar; $\beta=0.34$, $p<0.01$), and thickness (Ct.Th; $\beta=0.34$, $p<0.01$), and polar strength strain index (pSSI; $\beta=0.25$, $p<0.05$). The relationship with Ct.Th persisted after leg MCSA adjustment ($\beta=0.24$, $p<0.05$). However, these relationships were modified when children were divided by insulin resistance status. In the normal insulin resistance group: 1) IGF-I positively predicted tibia Ct.BMC ($\beta=0.47$, $p<0.01$; $\beta=0.32$, $p<0.05$), Ct.Ar ($\beta=0.44$, $p=0.01$; $\beta=0.28$, $p<0.05$) and Ct.Th ($\beta=0.61$, $p<0.01$; $\beta=0.59$, $p<0.01$) with and without MCSA-adjustment; 2) IGF-I positively predicted radius Ct.BMC ($\beta=0.53$, $p<0.01$), Ct.Ar ($\beta=0.49$, $p<0.01$), Ct.Th ($\beta=0.43$, $p<0.05$), and pSSI ($\beta=0.45$, $p<0.05$); and 3) after controlling for MCSA, IGF-I positively predicted radius volumetric density ($\beta=0.50$, $p<0.05$) and Ct.BMC ($\beta=0.32$, $p<0.05$). Conversely, IGF-I was not associated with any cortical bone outcomes among children with higher insulin resistance. To our knowledge, this is the first study to identify insulin resistance as an important factor involved in the cortical bone-IGF-I relationship.

Disclosures: Joseph Kindler, None.

FR0054

Decreased bone mass in perinatally HIV-infected school-aged South African children on antiretrovirals. Stephen Arpadi¹, Stephanie Shiau¹, Renate Strehlau², Francoise Pinillos², Faezah Patel², Louise Kuhn¹, Ashraf Coovadia², Sarah Ramteke¹, Jonathan Kaufman³, Michael Yin¹. ¹Columbia University Medical Center, USA, ²University of the Witwatersrand, South Africa, ³Mount Sinai School of Medicine, USA

Background: Decreased bone mineral content (BMC) and bone mineral density (BMD) by dual-energy X-ray absorptiometry (DXA) have been described in children with HIV-infection. However, no studies have been conducted in resource limited settings, where $>90\%$ of HIV-infected youth now live.

Methods: We present baseline results of the bone sub-study of CHANGES, a prospective, two-year observational cohort study of 220 HIV+ and 180 HIV- prepubertal South African children who initiated ART before age 2. Weight- (WAZ) and height- (HAZ) Z-scores were calculated using WHO standards and CD4 and HIV RNA levels were measured. BMC and BMD of the whole body (WB) and lumbar spine (LS, L1-4) by DXA were assessed using a Hologic Discovery W densitometer (Hologic Inc, Bedford, MA). Reference curves from the BMD in Childhood Study were used to generate Z-scores for WB and LS BMC (Kalkwarf 2007). All measures were compared between HIV+ and HIV- children by t-tests and chi-squared tests.

Results: 220 HIV+ children (49.1% male) and 180 HIV- children (55% male) were included. HIV+ children were younger than controls (mean age 6.4 vs. 7.1 years, $p<0.01$). All HIV+ children were on antiretroviral therapy (ART). Half were on a ritonavir-boosted lopinavir-based and half were on an efavirenz-based regimen, both in combination with two nucleoside reverse transcriptase inhibitors, including lamivudine and abacavir or stavudine, but not tenofovir. Mean duration on ART was 5.6 years. 93.2% had HIV RNA <400 cps/mL at the time of evaluation. Mean CD4% was 37.3. HIV+ children had lower mean WAZ (-0.82 vs -0.56 , $p<0.01$) and HAZ (-1.37 vs -1.16 , $p=0.03$) than HIV-children. WB BMC and BMD were lower in HIV+ compared to HIV- children, and the difference remained significant after adjustment for weight and height ($p<0.01$) (Table 1). Similarly, LS BMC and BMD were lower in HIV+ compared to HIV- children, but not after adjustment for weight and height. Similar patterns were observed with WB and LS BMC Z-score. When analysis was limited to 60 HIV+ and 53 HIV- children with normal growth (WAZ and HAZ between -1 and 1), WB BMC, WB BMD, LS BMC and LS BMD remained lower in the HIV-infected group.

Conclusions: Despite early initiation of ART and excellent virologic control, in this sample of South African school aged children, HIV+ children receiving ART have lower indices of bone quality by DXA compared to HIV- controls. Differences cannot entirely be accounted for by smaller body size alone.

Table 1

| Measurement | HIV+ | HIV- | P-value |
|-----------------------------|-----------------|-----------------|---------|
| WB BMC (g) | 416 \pm 98 | 496 \pm 123 | <0.001 |
| WB BMD (g/cm ²) | 0.51 \pm 0.06 | 0.56 \pm 0.07 | <0.001 |
| LS BMC (g) | 14.5 \pm 3.1 | 16.1 \pm 3.4 | <0.001 |
| LS BMD (g/cm ²) | 0.46 \pm 0.06 | 0.49 \pm 0.07 | <0.001 |
| WB BMC Z-score | -3.32 \pm 1.8 | -2.06 \pm 1.6 | <0.001 |
| LS BMC Z-score | -2.18 \pm 1.6 | -1.59 \pm 1.3 | <0.001 |

Table 1

Disclosures: Stephen Arpadi, None.

FR0055

Growth, Body Mass Index, Bone Health And Ambulatory Status Of Boys With Duchenne Muscular Dystrophy (DMD) Treated With Daily Versus Intermittent Oral Glucocorticoid Regimen. Nicola Crabtree¹, Raja Padidela², Nicholas Shaw¹, Wolfgang Hogler¹, Helen Roper³, Imelda Hughes², Judith Adams⁴, Anjali Daniel², Zulf Mughal². ¹Birmingham Children's Hospital, United Kingdom, ²Royal Manchester Children's Hospital, United Kingdom, ³Heart of England Hospital, United Kingdom, ⁴Manchester Royal Infirmary, United Kingdom

Oral glucocorticoids (GC; prednisolone dose of 0.75 mg/kg/day), help to preserve muscle strength and prolong independent walking in boys with DMD. This study compared longitudinal growth, body mass index (BMI), bone mineral density (BMD), vertebral fractures (VFs) and ambulatory status in boys with DMD on daily (DAILY) or intermittent (INTER; 10 days on & 10 days off), oral GC regimens.

Fifty DMD boys from two centres were included in the study; 25 boys each were on the DAILY or the INTER regimen. Size adjusted lumbar spine BMD (LS BMAD), total body less head BMD (TBLH), VF assessment and forearm pQCT data were analysed in all boys at three time points; baseline, 1 and 2 years.

At their first (baseline) assessment, there were no significant differences in mean (SD) age (8.3 (2.5) years) or any of the bone parameters, but DAILY boys were already shorter ($p=0.013$) with higher BMI ($p=0.014$). There were no documented VFs; however 1 DAILY and 3 INTER boys had suffered long bone fractures. All DAILY boys were still ambulant whereas 5 INTER boys had already stopped walking. Prior to the 2 year assessment, 6 of the DAILY boys had sustained symptomatic VFs and were subsequently commenced on IV bisphosphonate therapy; these boys were excluded from further follow-up bone parameter comparisons. At 2 years, 6 DAILY boys and 10 INTER boys had lost ambulation and the difference in height between DAILY and INTER boys had increased significantly ($p<0.001$). The DAILY boys also had significantly higher BMI SDS but lower BMAD and TBLH Z-Scores. Most notably, significantly more DAILY boys had VFs compared to INTER boys (13 DAILY versus 4 INTER; $p = 0.015$). Only 2 of the 16 boys with VFs also had low BMAD ($z<-2$); in contrast 14 had low TBLH BMD Z-scores and 11 had low trabecular BMD Z-scores.

Boys on a daily GC regimen appear to remain ambulant longer but at the cost of significantly greater VFs, greater adiposity and markedly diminished growth. In contrast, the boys on the intermittent GC regimen had fewer fractures but lost ambulation earlier. In both groups, LS BMAD was a poor predictor of VFs.

Disclosures: Nicola Crabtree, None.

FR0057

EphB/ephrin-B interactions regulate stromal cell fate determination and bone marrow support. Stan Gronthos¹, Thao Nguyen¹, Louise Purton², Koichi Matsuo³, Agnes Arthur⁴. ¹University of Adelaide, Australia, ²St. Vincent's Institute of Medical Research, Australia, ³School of Medicine Keio University, Japan, ⁴School of Medical Sciences, Australia

Bone marrow mesenchymal stromal/stem cells (BMSC) residing within a perivascular niche, are essential for regulating skeletal tissue homeostasis, including bone formation and repair. However, the molecular signals that maintain multipotential MSC populations within the stem cell niche and the mechanisms that drive their support of hematopoiesis are not well understood. The tyrosine kinase receptor, EphB4, mediates cross-talk between BMSC and hematopoietic populations during bone remodelling, fracture repair and arthritis, through its interactions with the ligand, ephrin-B2. The present study demonstrated that BMSC transgenic EphB4 mice (EphB4 Tg), over-expressing EphB4 under the control of collagen type-1 promoter, exhibited higher frequencies of osteogenic cells and hematopoietic stem/progenitor cells, correlating with a higher frequency of long-term culture-initiating cells (LTC-IC), compared to wildtype mice. EphB4 Tg stromal feeder layers displayed a greater capacity to support LTC-IC in vitro, where blocking EphB4/ephrin-B2 interactions decreased LTC-IC output. Similarly, shRNA mediated EphB4 knock-down in human bone marrow stromal cells reduced their ability to support high ephrin-B2 expressing CD34+ hematopoietic stem/progenitor cells in LTC-IC cultures. Notably, irradiated EphB4 Tg mouse recipients displayed enhanced bone marrow reconstitution capacity and enhanced homing efficiency of transplanted donor hematopoietic stem/progenitor cells relative to wildtype controls. Studies examining the expression of hematopoietic supportive factors produced by stromal cells indicated that CXCL12, Angiopoietin-1, IL-6, FLT-3 ligand and osteopontin expression were more highly expressed in EphB4 Tg stromal cells compared to wildtype controls. These findings indicate that EphB4 facilitates stromal mediated support of hematopoiesis, and constitute a novel component of the HSC niche.

Disclosures: Stan Gronthos, None.

FR0058

Inhibition of FGF-23 Signaling Ameliorates Anemia in a Mouse Model of Chronic Kidney Disease. Despina Sitara¹, Lindsay Coe^{2*}, Regina Goetz², Moosa Mohammadi², Stefano Rivella³. ¹New York University College of Dentistry, USA, ²New York University, USA, ³Weill Cornell Medical College, USA

We recently reported that Fibroblast Growth Factor-23 (FGF-23), the primary regulator of phosphate homeostasis and vitamin D metabolism, also regulates erythropoiesis. High FGF-23 levels are associated with several diseases including Chronic Kidney Disease (CKD) and correlate with declining renal function and disease progression. Anemia is a common complication in CKD caused by insufficient renal production of erythropoietin (EPO), the hormone responsible for red blood cell production (RBC) in the bone marrow (BM). The primary physiological stimulus of Epo induction is hypoxia through activation of the hypoxia inducible factors (HIFs). We recently reported that administration of FGF-23 in wild-type mice rapidly decreases erythropoiesis and the hematopoietic stem cell (HSC) pool size, whereas genetic inactivation of Fgf-23 results in increased red blood cell (RBC) production and HSC frequency in the circulation and BM of young adult mice and in fetal livers. Moreover, our data show that loss of Fgf-23 is associated with significantly high EPO levels and increased HIF mRNA expression, suggesting a novel role for FGF-23 as a negative regulator of erythropoiesis. Therefore, our hypothesis is that high FGF-23 levels may contribute to the development of anemia in CKD and, if so, blocking FGF-23 signaling may present a viable treatment option for CKD patients. To test this, we used a mouse model of CKD induced by 5/6 nephrectomy (Nx) and injected them with a competitive inhibitor of FGF-23 binding to its receptor. 5/6 Nx mice exhibit significantly lower EPO levels, however, treatment with the FGF-23 inhibitor results in significantly elevated Epo levels compared to vehicle-treated mice. This increase in Epo is due to an induction of HIF mRNA expression. Most importantly, we found that treatment of 5/6 Nx mice with the FGF-23 inhibitor restores erythroid cell production to normal levels. Taken together, our data show that blocking FGF-23 signaling improves erythropoiesis and ameliorates anemia in a mouse model of CKD, suggesting a novel therapeutic strategy for the treatment of anemia associated with CKD and other diseases.

Disclosures: Lindsay Coe, None.

FR0059

Megakaryocytes: Regulators of Bone Mass and Hematopoiesis. Marta Alvarez^{*}, LinLin Xu, Evan Himes, Brahmananda Chitteti, Ying-Hua Cheng, Andrew Engle, David Olivos, Paul Childress, Edward Srour, Melissa Kacena. Indiana University School of Medicine, USA

Emerging evidence demonstrates that megakaryocytes (MK) play a key role in regulating skeletal homeostasis and hematopoiesis. Recent reports show that MK reside in close proximity to hematopoietic stem cells (HSC). Genetic depletion of MK resulted in mitotic activation of HSC suggesting that MK maintain HSC quiescence. Other studies demonstrated that following irradiation, surviving MK migrate to endosteal surfaces whereby numbers of osteoblast (OB) lineage cells dramatically increase and promote engraftment of transplanted HSC. Our studies have shown that MK markedly increase proliferation of OB lineage cells while simultaneously inhibiting differentiation. We also showed that less mature OB lineage cells are better able to support hematopoiesis.

Here we investigated if MK directly impact hematopoiesis or whether they indirectly support HSC function through their interaction with OB lineage cells. Our data strongly suggest that LSK (Lin-Sca+CD117+, an enriched HSC population) co-cultured with MK and OB generate significantly higher numbers of colony forming cells (a gauge of HSC function) compared to LSK co-cultured with either MK or OB alone. The functionality of this in vitro data was confirmed in vivo with transplantation studies which showed increased engraftment in mice transplanted with LSK cells co-cultured with OB and MK compared to LSK cells co-cultured with OB alone (Figure 1). To test if loss of MK negatively impacts osteoblastogenesis and consequently hematopoiesis through impeding the hematopoiesis enhancing activity of OB, we generated conditional knockout (CKO) mice where cMpl, the receptor for the main MK growth factor, thrombopoietin (TPO), was deleted specifically in MK (cMpl^{fl/fl} x PF4Cre). Unexpectedly, these mice exhibited a 10-fold increase in platelet numbers, megakaryocytosis, a dramatic expansion of phenotypically defined hematopoietic precursors, and a remarkable 20-fold increase in the bone volume fraction (Figure 2).

Collectively, these data indicate that while MK modulate HSC function, this activity is in part mediated through interactions with OB and suggest an intricate and complex role for TPO and MK in HSC regulation. While work is needed to further elucidate mechanisms, understanding the coordinated interaction between MK, OB, HSC, and TPO/cMpl should inform the development of novel treatments to enhance HSC recovery following myelosuppressive injuries, as well as bone loss diseases, such as osteoporosis.

FR0060

Osteoblast Fibronectin Stimulates Myelopoiesis and Affects the Behavior of Myeloid-Derived Cells *In Vivo*. Stephanie Rosnagl^{*1}, Sabrina Kraft¹, Eva Altrock¹, Carla Sens¹, Katrin Rau¹, Verena Klemis¹, Inaam Nakchbandi². ¹University of Heidelberg & Max-Planck Institute of Biochemistry, Germany, ²Max-Planck Institute of Biochemistry & University of Heidelberg, Germany

Osteoblasts affect hematopoietic stem cell differentiation. They also produce fibronectin isoforms that affect their own differentiation (J Bone Miner Res 2010). The aim of this work was therefore to determine whether osteoblast fibronectin affects hematopoiesis.

Conditional deletion of fibronectin in differentiating osteoblasts (cKO) resulted in a 30% decrease in myeloid cells in the bone marrow due to defective differentiation of the progenitors without affecting peripheral blood counts. Osteoblasts produce several fibronectin isoforms. An isoform containing the extra domain A (EDA-FN) enhanced myelopoiesis *in vitro* while other isoforms did not. EDA-FN binds to $\alpha 4\beta 1$, $\alpha 9\beta 1$ and enhances binding to $\alpha 5\beta 1$ integrin. Further studies identified $\alpha 5\beta 1$ integrin as the mediator of CD11b differentiation in response to EDA-FN.

The myeloid cells of the bone marrow can differentiate to myeloid-derived suppressor cells (MDSCs). Fibrosis represents a wound healing process where MDSCs prevent an excessive immune response. Indeed, induction of liver fibrosis in mice resulted in enhanced fibrosis in cKO animals that have less MDSCs. Another function of MDSCs is the detrimental inhibition of the immune response against tumors. A decrease in MDSCs in cKO animals was therefore associated with enhanced defense against cancer and suppressed cancer growth in two different cancer models. Adoptive transfer experiments injecting *in vitro* differentiated CD11b+ cells in mice with cancer cells confirmed the causal relationship between EDA-mediated CD11b differentiation and effects on cancer growth. Thus, the presence of EDA during CD11b+ cell differentiation is responsible for the anti-inflammatory behavior of these cells.

We next wondered whether EDA affects the immune signature of myeloid cells. The mRNA expression of cytokines involved in MDSCs response was evaluated in various types of isolated CD11b+ cells. The pro-inflammatory factors IL-6, iNOS and IFN- γ were higher and the anti-inflammatory Arg-1 was lower in cells from healthy cKO bone marrow, cKO tumors, or *in vitro* differentiated CD11b+ cells not exposed to EDA. Thus, EDA supports the differentiation of CD11b+ cells with anti-inflammatory immune profile.

In summary, EDA-containing fibronectin originating from the osteoblasts acts via $\alpha 5\beta 1$ to enhance the differentiation of anti-inflammatory myeloid cells. While this is beneficial under normal wound healing conditions and fibrosis, it contributes to enhanced cancer growth.

Disclosures: Stephanie Rosnagl, None.

FR0063

NELL-1 induces Expansion of Sca-1+ Mesenchymal Stem Cell Population for Bone Formation. Aaron James^{*1}, Jia Shen², Greg Asatrian², Swati Shrestha², Ben Wu³, Xinli Zhang², Kang Ting², Chia Soo⁴. ¹University of California, Los Angeles, USA, ²Division of Growth & Development & Section of Orthodontics, School of Dentistry, USA, ³Department of Bioengineering, School of Engineering, USA, ⁴UCLA Division of Plastic Surgery & Department of Orthopaedic Surgery & the Orthopaedic Hospital Research Center, University of California, Los Angeles, USA

Introduction: Recombinant (r)NELL-1 has been studied as an alternative osteoinductive factor to BMP2 (Bone Morphogenetic Protein2) in pre-clinical orthopaedic models. Moreover, rNELL-1 has been recently described as a novel systemic agent that reverses osteoporotic bone loss. This study aims to identify a mechanism of action that unifies both the local and systemic bone-forming effects of rNELL-1. **Methods:** The local and systemic effects of rNELL-1 were examined across animal models, including (1) NELL-1 deficient mice, (2) intramedullary rNELL-1 injection in the rat, (3) systemic rNELL-1 injection in the mouse, and (4) non-human primate spinal fusion. Intramedullary rNELL-1 injection was performed utilizing a TCP carrier, while systemic injection was via repeated rNELL-1 intravenous injection. Interlumbar spinal fusion in primates was performed using a scaffold composed of demineralized bone matrix and rNELL-1 (up to 1.7mg/ml). In each model, stem cell populations were analyzed using a combination of FACS for stem cell markers (including Sca-1 and Stro-1), CFU assays, and immunostaining for Sca-1+ MSC. Bone formation was confirmed by a combination of radiologic (micro computed tomography), histologic, static and dynamic histomorphometric, and immunohistochemical analyses. **Results:** NELL-1 deficient mice demonstrated marked reductions in the numbers of Sca-1+CD45- bone marrow MSC (Fig. 1A), reduction in stem cell content, and a significant osteoporotic phenotype (Fig. 1B). rNELL-1 treatment had converse effects on stem cell content and bone formation. Either local intramedullary or systemic rNELL-1 injection showed increased numbers of Sca-1+CD45- bone marrow MSC (~75% increase in cell number, Fig. 1C), increased MSC content (CFU-F assays), accompanied by an increase in bone anabolic markers, and microCT based bone measurements (Fig. 1D). Finally, rNELL-1 implantation in a non-human primate spinal fusion model led to 100% fusion rates (Fig. 1E), significantly increased BV/TV and BMD, and histological evidence of bony bridging. Significantly, more Sca-1+ MSC were identified within the marrow cavity of newly formed trabecular

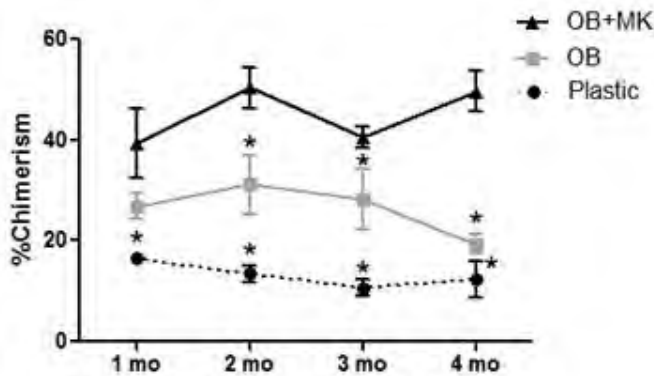


Figure 1 % engraftment from LSKs co-cultured with OB+MK, OB, or LSK alone.

Figure 1



Figure 2 Micro-Computed Tomography of Wild-type and cMpl CKO femurs from 3-month old mice.

Figure 2

Disclosures: Marta Alvarez, None.

bone with rNELL-1 treatment (Fig. 1F). Discussion: In summary, rNELL-1 induces bone formation across small and large animal models either via local implantation or intravenous delivery. NELL-1 induces an expansion of Sca-1+ cells and MSC content in bone marrow milieu, resulting in clinically significant bone anabolism and repair.

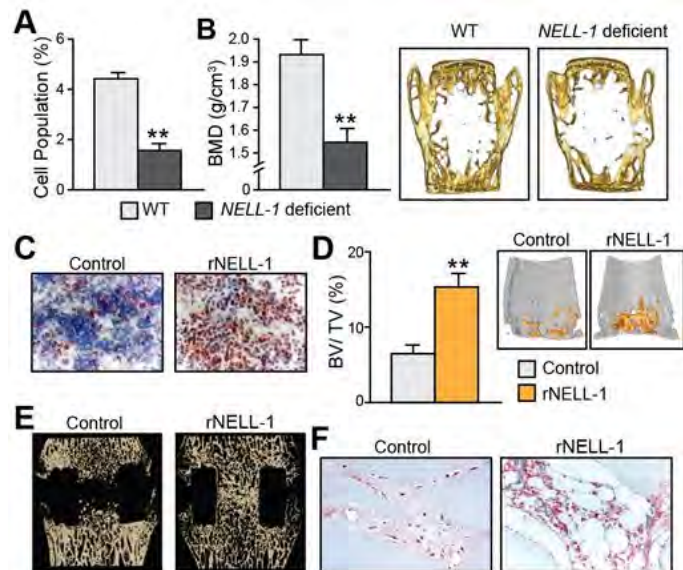


Figure 1

Disclosures: Aaron James, None.

FR0066

N-cadherin in Osteolineage Cells Modulates the Tumor Environment. Francesca Fontana¹, Jacqueline Kading², Jingyu Xiang³, Marcus Watkins⁴, Katherine Weilbaecher³, Roberto Civitelli⁴. ¹Bone & Mineral Diseases, USA, ²Division of Bone & Mineral Diseases, Washington University School of Medicine in St Louis, USA, ³Division of Molecular Oncology, Washington University School of Medicine, USA, ⁴Division of Bone & Mineral Diseases, Washington University School of Medicine, USA

Tumor establishment and growth entail interactions with the environment through cell-cell contact and secretory factors. N-cadherin (Ncad) in tumor cells has been shown to promote migration and metastases in animals; it was also proposed to facilitate engraftment and growth of disseminated tumor cells (DTC) in bone via adhesion to osteogenic cells. We and others have shown that Ncad is expressed in bone cells, and genetic ablation of the Ncad gene (*Cdh2*) in osteolineage cells leads to low bone mass and reduced osteoprogenitor number, while it accelerates osteogenic differentiation via increased Wnt and PTH signaling. To determine the role of Ncad in interactions between bone and tumor cells, we conditionally deleted *Cdh2* using a Cre recombinase driven by a doxycycline-repressible *Sp7* promoter *Cdh2^{fl/fl};Sp7-Cre* (cKO), and inoculated cKO and wild type mice with breast cancer cell (BCC) lines derived from a MMTV-PYMT tumor in a Black6 background. Moderately stunted growth was observed among cKO mice (20% lower body weight at 3 months vs. wild type, $p=0.004$), and this was prevented by perinatal doxycycline treatment – which suppresses *Sp7-Cre* expression – without effects on tumor growth. Crossing of *Sp7-Cre* mice with the *Ai9* reporter mice revealed effective targeting of 7.6% (range 5-9%) of total bone marrow cells (by FACS). Surprisingly, 2% (range 0.7-3%) of tumor-associated stromal cells were also targeted by *SP7-Cre*, implying a biologic effect of the tumor on the host microenvironment. Injection of a murine breast cancer cell line (MMTV) and a bone-metastatic derivative line (BO1) in the mammary fat pad and tibia of cKO resulted in similar tumor growth relative to control mice at both sites. However, subcutaneous inoculation of the BO1 line resulted in larger tumors in cKO than in wild type mice by caliper measurement (20% by day 10 and 30% by day 12; two-way ANOVA for genotype vs. time <0.001). Bone marrow DTC, detected through GFP expression (10^1 - 10^3 per million bone marrow cells), were observed in the presence of subcutaneous primary tumors as well as months after tumor resection, without significant differences between cKO and wild type mice. Our results suggest that Ncad is dispensable for the engraftment and growth of BCC to the bone; however, we find that Ncad plays an unexpected role as a negative regulator of stromal support of tumor growth via paracrine or endocrine mechanisms.

Disclosures: Francesca Fontana, None.

FR0067

Pivotal role of TAK-1 in tumor growth and bone destruction in myeloma: therapeutic impact of TAK-1 inhibition. Jumpei Teramachi^{1*}, Masahiro Hiasa¹, Asuka Oda¹, Hirofumi Tenshin¹, Ryota Amachi¹, Takeshi Harada¹, Shingen Nakamura¹, Hirokazu Miki², Isturo Endo¹, Tatsuji Haneji¹, Toshio Matsumoto¹, Masahiro Abe¹. ¹Tokushima University, Japan, ²Tokushima University Hospital, Japan

Multiple myeloma (MM) has a unique propensity to develop and expand almost exclusively in the bone marrow and generates destructive bone disease. We have reported that Pim-2 is overexpressed in MM cells and their surrounding cells, namely bone marrow stromal cells (BMSCs) and osteoclasts, in bone lesions, and that treatment with Pim inhibitors markedly suppressed MM tumor growth while preventing bone destruction in MM-bearing animal models, indicating Pim-2 as an important therapeutic target in MM. We recently found TGF- β -activated kinase-1 (TAK-1) as an upstream mediator responsible for Pim-2 up-regulation. In the present study, we therefore aimed to clarify the role of TAK-1 in tumor growth and bone destruction in MM. TAK-1 was constitutively over-expressed in MM cells while only marginally in normal peripheral blood mononuclear cells. The TAK-1 inhibitor LLZ1640-2 dose-dependently suppressed cell growth, and induced caspase-dependent apoptosis in MM cells. LLZ1640-2 almost completely abolished TNF- α -induced NF- κ B, p38MAPK and ERK activation and IL-6-induced STAT3 activation in MM cells. LLZ1640-2 as well as TAK-1 knock-down decreased VCAM-1 expression and IL-6 production in BMSCs, and MM cell adhesion to BMSCs to impair BMSC support of MM cell growth. Interestingly, phosphorylation of TAK-1 was induced in BMSCs and MC3T3-E1 preosteoblastic cells by addition of cytokines known as inhibitors of osteoblastogenesis in MM, including IL-3, IL-7, TNF- α , TGF- β and activinA, as well as MM cell conditioned media (MMCM), suggesting TAK-1 as a common mediator to suppress osteoblastogenesis in MM. Furthermore, LLZ1640-2 abolished up-regulation of Pim-2, an inhibitory mediator of osteoblastogenesis, in BMSCs and MC3T3-E1 cells by MMCM to restore mineralized nodule formation. Moreover, the TAK-1 inhibition up-regulated in MC3T3-E1 cells phosphorylation of Smad1/5 and p38MAPK by BMP-2 while suppressing Smad2/3 phosphorylation by TGF- β , suggesting potentiation of BMP-2-mediated anabolic signaling. TAK-1 was also up-regulated along with osteoclastogenesis. TAK-1 inhibition by LLZ1640-2 suppressed the induction of c-fos and NFATc1 as well as osteoclastogenesis in RAW264.7 preosteoclastic cells by MMCM or rRANK ligand. Finally, treatment with LLZ1640-2 potently suppressed MM growth in MM models with intratibial injection of murine 5TGM1 MM cells. Taken together, these results suggest that TAK1 plays a pivotal role in MM tumor growth and bone destruction, and that TAK1 may become an efficacious therapeutic target in MM.

Disclosures: Jumpei Teramachi, None.

FR0069

The anti-diabetic drug Metformin reduces tumour burden and osteolytic bone disease in Multiple Myeloma in vivo. Siobhan Webb^{*}, Rosie Butler, Amanda Bacon, Ann Snaith, Sarah Gooding, Jessica Whitburn, Claire Edwards. University of Oxford, United Kingdom

Multiple myeloma (MM) is a fatal haematologic malignancy characterised by accumulation of malignant plasma cells in the bone marrow (BM), and severe lytic bone disease. Metformin is widely prescribed in diabetes, and recently associated with improved outcomes in diabetic patients with MM, suggesting a potential anti-myeloma effect of metformin. Our aim was to investigate the effect of metformin within the myeloma-bone microenvironment *in vitro* and *in vivo*. C57Bl/KaLwRij mice were inoculated with 5TGM1MM cells and treated with metformin either from time of tumour inoculation (met-cont) or from time of established tumour (met-delay). MM-bearing mice treated with metformin exhibited a decrease in myeloma-specific serum paraprotein as compared to control (Control; 4.29mg/ml \pm 0.3mg/ml, met-cont; 1.51mg/ml \pm 0.6mg/ml, $p<0.001$, met-delay; 0.7mg/ml \pm 0.7mg/ml $p<0.001$). MicroCT analysis demonstrated a significant decrease in osteolytic lesion number in MM-bearing mice treated with metformin (Control; 26 \pm 3.6, met-cont; 11.4 \pm 0.7 $p<0.001$, met-delay; 9 \pm 1.5 $p<0.01$). Histomorphometry revealed an increase in BV/TV of metformin mice compared to untreated MM (MM; 2.6% \pm 0.41, met-cont; 4.0% \pm 0.43 $p<0.05$, met-delay; 4.4% \pm 0.46 $p<0.05$). Metformin also increased osteoblast number (MM; 1.86/mm \pm 0.5, met-delay; 4.7/mm \pm 0.7, $p<0.01$, met-delay; 6.5/mm \pm 1.4 $p<0.01$) and decreased osteoclast number (MM; 2.86/mm \pm 0.4, met-cont; 1.6/mm \pm 0.1 $p<0.05$, met-delay; 1.2/mm \pm 0.2, $p<0.05$), as well as increasing trabecular thickness and decreasing trabecular separation compared to untreated MM. Interestingly, metformin had no significant effect on non-tumour mice, suggesting that the effect of metformin to reduce MM bone disease may be indirect, in response to the decrease in tumour burden. Metformin induced a dose-dependent decrease in MM cell viability. Metformin treatment of MM cells decreased IGF-1 gene expression and induced apoptosis, detected by increased cleaved caspase-3 and PARP. Metformin had no effect on BM stromal cell (BMSC) viability. BMSC-conditioned media (CM) had a protective effect against the anti-MM effects of metformin at 24h that was lost by 72h. In contrast, BMSC CM protected against the anti-MM effects of the proteasome inhibitor bortezomib at all time points. Our studies demonstrate a strong anti-tumour effect of metformin in the MM-bone microenvironment, suggesting that metformin may be effective for the treatment of MM and associated bone disease.

Disclosures: Siobhan Webb, None.

FR0072

Long-term Safety of Denosumab Through Greater than 48 Doses in Giant Cell Tumor Patients. Susan Bukata¹, Madhuri Sudan², William Mendanha³, Neal Chawla³, Kamalesh Sankhala³, Sant Chawla³.¹UCLA, USA, ²Department of Epidemiology, UCLA School of Public Health, USA, ³Sarcoma Oncology Center, USA

Giant cell tumors of the bone (GCTB) are aggressive lytic tumors characterized by local invasion and limited non-surgical treatments. Stromal cells involved with GCTB express surface RANK ligand which is used to activate the osteolytic properties of the giant cells within the lesion. Denosumab is a RANK ligand inhibitor that has been shown to be effective in neutralizing this pathway, stopping the lytic destruction of the bone by the tumor. Because denosumab does not eliminate the stromal tumor cells, surgery is still required to clear the tumor.

In patients with unresectable tumors, long-term denosumab treatment has offered an opportunity to maintain tumor stability. We present a cohort of 42 such patients on 120 mg denosumab monthly (after 3 loading doses at 7 day intervals) who have received on average 48 doses of medication (Table 1). Safety, tumor stability, and patient comfort have been excellent. In addition, this cohort offers a unique opportunity to assess the long-term safety of multiple doses of denosumab, as they have now received more denosumab than osteoporosis patients would receive in a lifetime.

This patient population demonstrated a remarkably good safety profile on this medication. Myalgia (64%) and tooth pain (36%) were the most common complaints during treatment. Fourteen percent of patients complained of peripheral neuropathy, and other less common complications included eczema (10%), infection (10%), and cellulitis (10%). Osteonecrosis of the jaw (ONJ) also occurred in 10% of patients, and two patients developed atypical femur fractures. Only one case of ONJ was seen through the first 50 doses of medication (first case of ONJ occurred after 25 doses), with a notable increase in ONJ after 70 doses (Figure 1). Although tooth pain was seen frequently in patients with ONJ (75%), many patients without ONJ also complained of tooth pain (32%). Giant cell tumor suppression was maintained with rapid and sustained pain improvement with the therapy for all patients.

Conclusion: Long-term, high frequency dosing of denosumab in a population of giant cell tumor patients demonstrated a good safety profile and sustained tumor suppression. Complications did increase with prolonged dosing, but no complications occurred within the first 25 doses.

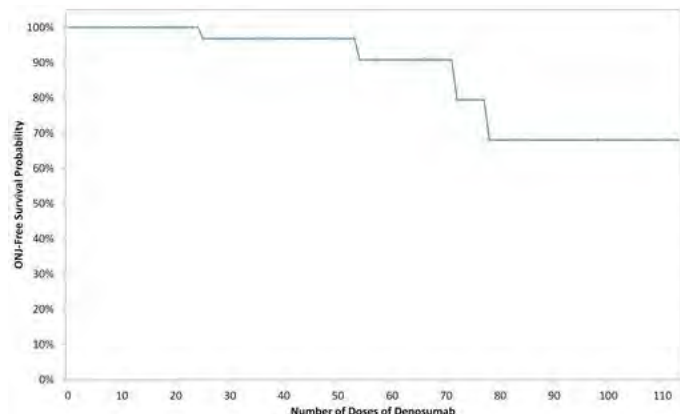


Figure 1. Probability of ONJ-free Survival by Total Number of Doses of Denosumab Administered

| | Total (n=42) |
|------------------------------------|--------------------|
| Mean (SD) age at start (years) | 33.7 (12.7) |
| Sex | |
| Men | 16 (38.1%) |
| Women | 26 (61.9%) |
| Total length of treatment (weeks)* | |
| Mean (SD) | 180.4 (110.1) |
| Median (Min, Max) | 160.8 (4.1, 440.6) |
| Total number of doses* | |
| Mean (SD) | 47.8 (27.5) |
| Median (Min, Max) | 43.0 (4, 113) |
| Osteonecrosis of jaw | 4 (9.5%) |
| Fracture | 2 (4.8%) |
| Infection | 4 (9.5%) |
| Rash/cellulitis | 4 (9.5%) |
| Tooth pain | 15 (35.7%) |
| Myalgia, joint pain, thigh pain | 27 (64.3%) |
| Eczema/psoriasis | 4 (9.5%) |
| Peripheral neuropathy | 6 (14.3%) |
| *Up to date of ONJ occurrence | |

Table 1. Patient Characteristics

*Disclosures: Susan Bukata, amgen; amgen
This study received funding from: Amgen*

FR0075

A novel p53 isoform-dependent accelerated aging that causes osteoarthritis in mice. Yasuhiko Kawakami^{*}, Robyn Leary, Keianna Vogel, Hiroko Kawakami, Anindya Bagchi. University of Minnesota, USA

Purpose: Although aging is a major risk factor of osteoarthritis (OA), how aging affects OA is poorly understood. The goal of this proposal is to determine the role of the senescence-specific novel p53 isoform, found in our study, in OA development in mice. **Background:** We previously generated a mutant allele in mice, in which the D4Mit190-51 region on chromosome 4 is duplicated on one chromosome (duplicated allele: dp) and is deleted in another chromosome (deficiency allele: df). The df/dp alleles are a balanced chromosome and the mice are indistinguishable from wild type (WT) mice. However, dp/+ mice that harbor three copies of D4Mit190-51 region exhibited perinatal death with signs of cell senescence, a hallmark of aging. By following up this study, we succeeded in rescuing the dp/+ mice by genetically reducing p53 dosage, given that this locus indirectly regulates p53 on chromosome 11. This suggests that increased p53 activity caused the dp/+ mouse phenotype. **Methods:** By using collected tissue we examined knee joint tissue integrity by histological examination. We also performed RT-PCR with various primer sets and isolated a novel splice isoform of p53 from senesced dp/+ mouse embryonic fibroblasts (MEFs), which we termed as s-p53 (senescence-specific p53). Series of biochemical analyses were used to determine function of s-p53. **Results:** We found early lethality of df/dp; p53+/- mice (3-6 months of age) without tumor formation, compared to WT and p53+/- mice. The df/dp; p53+/- mice died by tumor, similar to p53+/- mice. By histological examination of the knee joint, we found early onset of joint cartilage degeneration of df/dp; p53+/- mice, compared to WT, p53+/- and p53+/- mice. Doxycycline-dependent inducible expression of s-p53 induced p21 expression and cell senescence in wild type cells, but not in p53+/- cells. By co-immunoprecipitation assays, we found that wild type p53 and s-p53 form a complex. In transmission electron microscopy analysis of MEFs, we found nuclear envelope blebbing in dp/+ cells, a characteristic of progeria. The blebbing phenotype was partially and completely rescued in dp/+; p53+/- and dp/+; p53+/- cells, respectively. **Conclusion:** Our results support the model that s-p53 forms complex with full length p53 and enhances p53 activity, which leads to cellular senescence, and that this process causes chondrocyte senescence and accelerated joint cartilage degeneration in mice.

Disclosures: Yasuhiko Kawakami, None.

FR0076

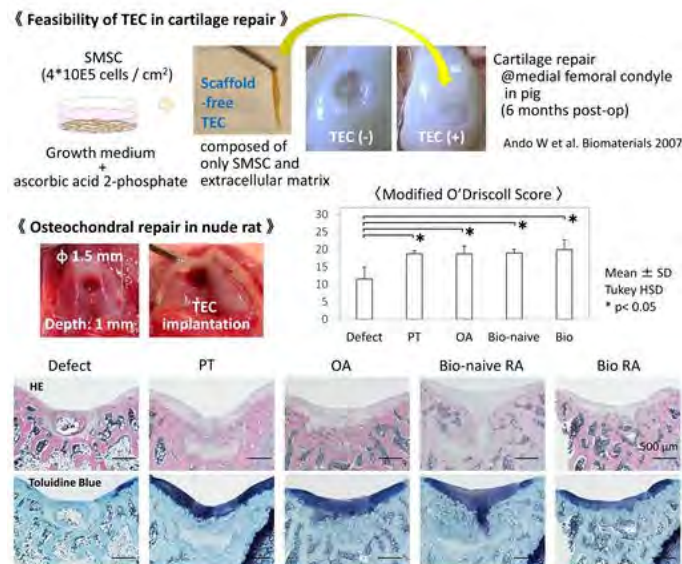
Cartilage repair ability of scaffold-free tissue engineered construct(TEC) derived from osteoarthritis(OA) and rheumatoid arthritis(RA) patients' synovial mesenchymal stem cells(SMSC). Kota Koizumi*, Kosuke Ebina, Makoto Hirao, Takaaki Noguchi, Yukihiro Yasui, Norihiko Sugita, Hideki Yoshikawa, Norimasa Nakamura. Department of Orthopaedics, Osaka University Hospital, Japan

Purpose: We have developed scaffold-free TEC composed of SMSC and its cartilage-repairing efficacy in focal chondral defect of pig has been demonstrated. In addition, clinical trial of autogenic TEC in cartilage repair of the patients with traumatic knee injury (defined as control group; Ctrl) is on going in Osaka University Hospital. But autogenic TEC implantation have limitations such as multiple surgeries and cell culture period. Establishment of allogenic TEC bank may be useful in overcoming these problems. In this study, we evaluated the features and feasibility of SMSC and TEC derived from the patients with OA or RA, which can be obtained abundantly from routine surgeries compared with Ctrl.

Methods: 25 patients were divided into 4 groups (group name; female/total number, mean age = Ctrl; 2/6, 38.6, OA; 4/6, 71.2, RA without biologics (Bio-naive RA); 5/6, 67, RA with biologics (Bio RA); 6/7, 72.4). We analyzed the following items. 1:Proliferative ability of SMSC by WST-1 assay 2:Weight and volume of TEC composed of same cell number (1.52*10E6 / 6well dish) 3:Cytokine gene expression of TEC by qRT-PCR 4:Chondrogenesis of TEC by qRT-PCR and GAG component 5:Osteochondral repair at femoral trochlea groove (diameter1.5 × depth1mm) using TEC in nude rat (F344/NJcl/rnu, male, 12 week-old; evaluated by modified O'Driscoll score 8weeks after implantation)

Results: In every item, SMSC or TEC from OA and RA showed equivalent quality and quantity compared with Ctrl (mean ± SD, Ctrl / OA / Bio-naive RA / Bio RA). 1:Proliferation rate (Day3/Day1) 2.0 ± 0.16 / 1.8 ± 0.4 / 1.7 ± 0.3 / 1.7 ± 0.2, 2: Weight - Volume (mg - mm3); 5.9 ± 1.1 - 5.7 ± 1.2 / 6.1 ± 0.9 - 5.6 ± 0.7 / 6.5 ± 0.8 - 6.3 ± 0.8 / 5.7 ± 1.4 - 5.4 ± 1.3, 3: No significant difference in gene expression of IL1 β , IL6 and IL10 among all groups, 4: GAG component (%); 2.9 ± 0.4 / 3.1 ± 0.3 / 2.9 ± 0.75 / 3.2 ± 0.6, No significant difference in gene expression of SOX9, COL2 and ACAN, 5: All groups showed significantly better repair than defect group. (18.8 ± 0.8 / 18.8 ± 2.2 / 19 ± 1.0 / 20.0 ± 2.8 / Defect 11.5 ± 3.3)

Conclusions: Regardless of its higher age and inflammatory character, TEC derived from the patients with OA or RA showed similar quality and quantity compared with that from post-trauma patients. TEC from OA and RA patients may be promising source of cartilage repair and allogenic TEC bank, although further investigation with larger scale may be required.



Feasibility of TEC in cartilage repair

Disclosures: Kota Koizumi, None.

FR0077

CK2.1, a novel BMP receptor mimetic peptide, induces cartilage formation *in vivo*. Hemanth Akkiraju*, Jonathan Avallone², Padma Srinivasan², Jeremy Bonor¹, Catherine Kirn Safran¹, Anja Nohe². ¹University of Delaware, USA, ²University of Delaware, Biological Sciences, USA

CK2.1 is a novel mimetic peptide based on the Bone Morphogenetic Protein (BMP) receptor type I sequence. Our research shows that this peptide CK2.1 induced chondrogenesis in C3H10T1/2 cells as well as in bovine chondrocytes. Here we demonstrate that systemic injection of the CK2.1 into the tail vein of 8 week old mice led to increased articular cartilage formation without chondrocyte hypertrophy. These

results are in sharp contrast to Bone Morphogenetic Protein 2 (BMP2) injections that led to increased trabecular bone and cartilage as well as chondrocyte hypertrophy. Fluorescence staining of articular cartilage shows that CK2.1 injected group had increased collagen type IX production but not collagen type X or MMP13. Furthermore second harmonic generation (SHG) imaging shows an increase in collagen fibrillar structure. CK2.1 acts by releasing Casein Kinase II (CK2) from the BMP receptor type I and activating the Smad signaling pathway. CK2.1 also induced COMP expression and upregulated *SOX9*, *CREB* and *NKX3.2* (genes associated with chondrogenesis). However, *ME2C*, *RUNX2* and *IHH* (genes associated with chondrocyte hypertrophy) were downregulated. These data show for the first time that CK2.1 induced chondrogenesis *in vitro* and enhance articular cartilage formation *in vivo* when injected systemically into mice. New therapeutics to treat Osteoarthritis or regenerate damaged cartilage are desperately needed and currently unavailable. Therefore CK2.1 maybe a new valuable treatment option for the restoration of cartilage defects in humans.

Disclosures: Hemanth Akkiraju, None.

FR0078

HIF1 α / β -catenin interaction prevents cartilage damage by inhibiting MMP13 expression in mice. Wafa Bouaziz*, Johanna Sigaux², Claire-Sophie Devignes¹, Thomas Funck-Brentano³, Hang-Korng Ea¹, Dominique Modrowski², Sylvain Provot², Martine Cohen-Solal¹, Eric Hay⁴. ¹INSERM U1132 University paris7, France, ²INSERM U1132, France, ³AP-HP, France, ⁴INSERMU1132 Université Paris 7, France

Purpose: Low oxygen tension (hypoxia) regulates chondrocyte differentiation and metabolism. HIF1 α is a crucial hypoxia factor for chondrocyte growth and survival. Few data focused on the role of hypoxia in the regulation of cartilage remodeling and maintenance in osteoarthritis (OA). Wnt/ β -catenin is a major chondrocyte regulator that might be down-regulated to preserve cartilage from damage. Here we investigated the role of HIF1 α and Wnt/ β -catenin to modulate MMP-13 and cartilage loss.

Methods: To determine the effect of HIF1 α in cartilage, we used mice with conditional deletion of HIF1 α in chondrocytes (Col2CreERT; fl/fl HIF1 α or ?HIF1 α chon) and WT (fl/fl HIF1 α) mice underwent destabilization of the medial meniscus (DMM) to induce OA. Hypoxia was monitored using Pimidazole probe in OA and undamaged cartilage. Cellular mechanisms were assessed using primary chondrocyte cultures of fl/fl HIF1 α mice. HIF1 α was modulated by siRNA strategy for the inhibition and by transduction of VHL resistant HIF1 α for stabilization.

Results: In WT mice, DMM decreased hypoxia levels in the articular cartilage along with a decrease HIF1 α expression. After DMM, ?HIF1 α chon mice showed increased cartilage breakdown and MMP-13 expression compared to WT mice. Chondrocytes cultured in hypoxic conditions (1%) showed that activation of Wnt/ β -catenin signaling was unable to induce the expression of the catabolic genes (Mmp-13, Mmp3), this effect being reversed by HIF1 α knock-down. Immunoprecipitation revealed decreased β -catenin/TCF4 complexes in hypoxia in favor of β -catenin/HIF1 α complexes. Moreover, chip assay and transactivation analysis demonstrated that HIF1 α inhibited the binding of β -catenin to Wnt responsive elements reducing the formation of β -catenin/TCF4 transcriptional activity, and thereby the expression of Mmp13. Finally, blockade of β -catenin/TCF4 direct interaction by PKF 118-310 alleviated the OA phenotype and Mmp13 downregulation.

Conclusions: We here demonstrated that HIF1 α is a negative regulator of MMP13 transcription and Wnt signaling through the direct interaction of HIF1 α / β -catenin. Our study sheds new light on the role of HIF1 α / β -catenin interaction in OA and brings new insights into the impact of hypoxia in regulating Wnt signaling in articular cartilage.

Disclosures: Wafa Bouaziz, None.

FR0080

ADAMTS-12 protects against inflammatory arthritis through interacting with and inactivating proinflammatory CTGF. Jianlu WEI*, Wenyu Fu, Qingyun Tian, Chuanju Liu. Hospital for Joint Diseases of NYU, USA

It has been reported that ADAMTS-12 is a susceptibility gene for rheumatoid arthritis (RA) development (Nah et al, Mol. Med. Rep., 2012). In addition, we previously reported that ADAMTS-12 could directly bind to and degrade cartilage oligomeric matrix protein (COMP), and its level was significantly increased in RA patients (Liu, Nature Reviews Rheumatology, 2009; Liu et al, J Biol. Chem., 2006; Guo et al, Arthritis & Rheumatology, 2010). However, ADAMTS-12 was also reported to be required for normal inflammation (Angela et al, J Biol. Chem., 2012). These previous reports promoted us to determine whether ADAMTS-12 plays an important role in the pathogenesis of inflammatory arthritis, and if so what is the molecular mechanism involved. To address this issue, we established collagen-induced arthritis (CIA) model in ADAMTS-12 deficient mice and their control littermates. ADAMTS-12 deficient mice developed more severe inflammatory arthritis and exhibited increased bone and joint destruction when compared with their control littermates. Accelerated disease onset, significant increase in the arthritis severity score and arthritis incidence, were observed in ADAMTS-12 deficient mice. Histological analysis of whole ankle joints demonstrated a significant increase in synovitis, pannus formation and destruction of bone and cartilage in ADAMTS-12 deficient mice.

Furthermore, ADAMTS-12 deficient CIA mice exhibited higher level of ROR γ expression and lower level of Foxp3 expression, indicating the ratio of Treg/Th17 was reduced in ADAMTS-12 deficient mice. In addition, the isolated CD4+T cells produced more pro-inflammatory but less anti-inflammatory cytokines. Mechanistic studies revealed that ADAMTS-12 associated with connective tissue growth factor (CTGF), a molecule which is known to play a pro-inflammatory and pro-osteoclastogenesis role in the pathogenesis of inflammatory arthritis (Kazuhsa et al, Arthritis & Rheumatology, 2013). Yeast-Two-Hybrid (Y2H) assay with various ADAMTS-12 deletion mutants demonstrated that C-terminal mucin and TSP motifs of ADAMTS-12 were required and sufficient for binding CTGF. ADAMTS-12 digested and inactivated CTGF in the in vitro systems. In addition, elevated CTGF was observed in ADAMTS-12 deficient mice, and intra-articular injection of CTGF blocking antibody attenuated the enhanced inflammation seen in ADAMTS-12 deficient CIA model. Comparison of inflammation and bone loss between ADAMTS-12 deficient and ADAMTS-12/CTGF double deficient CIA models is ongoing. Collectively, ADAMTS-12 turns to be a critical regulator of inflammatory arthritis, through, at least in part, interacting with and inactivating CTGF. These findings not only provide novel insights into the role of ADAMTS-12 in the pathogenesis of inflammatory arthritis in vivo, but may also lead to the development of novel therapeutic intervention strategies for rheumatoid arthritis.

Disclosures: Jianlu WEI, None.

This study received funding from: funding from NIH

FR0081

Retinoic Acid Receptor Gamma Agonists Promote Endochondral Ossification And Facilitate Cartilage-to-Bone Transition Together With beta-catenin-Lef/Tcf Signaling. Kenta Uchibe^{*1}, Agnese DiRocco², Matthew Johnson³, Sayantani Sinha², Colleen Larmour², Struan Grant³, Maurizio Pacifici², Motomi Enomoto-Iwamoto², Masahiro Iwamoto². ¹Okayama University Children's Hospital of Philadelphia, Jp, ²Translational Research Program in Pediatric Orthopaedics, The Children's Hospital of Philadelphia, USA, ³Divisions of Human Genetics & Endocrinology, The Children's Hospital of Philadelphia, USA

Chondrocytes in the growth plate undergo maturation and hypertrophy, regulate matrix remodeling, mineralization and blood vessel invasion, and promote endochondral bone formation. Previous studies have shown that the retinoic acid receptor gamma (RAR γ) functions as ligand-less form and maintains matrix homeostasis in prehypertrophic zone of growth plate. Expression level of RAR γ transcripts was high and rapidly decreased in hypertrophic zone (HZ) while RAR α and RAR β transcripts were detectable by RT-PCR but were less than 7% of RAR γ transcript. Surprisingly, immunostaining showed that RAR γ was present in HZ. Since the concentration of the endogenous active retinoid reaches to a physiological level at the chondro-osseous junction, RAR γ in HZ may bind to retinoids and regulate hypertrophic chondrocyte function. To address this question, we isolated mouse epiphyseal chondrocytes, treated them with a specific RAR γ agonist and performed RNAseq. Expression patterns of key growth plate genes were markedly altered by agonist treatment including: a reduction in cartilage matrix genes and their associated regulators Sox5, Sox6 and Sox9 as well as an induction of expression of genes encoding matrix proteases (ADAMTSs and MMPs), angiogenesis-inducing factors and mineralization-related factors. Interestingly, many genes up-regulated by the RAR γ agonist did not harbor typical RAR/RXR binding sites, suggesting that they were not direct targets but rather were indirectly impacted by cross-talk with other signaling pathways. Indeed, genes such as MMPs and VEGF are known to have binding sites for Lef/Tcf protein family members that act as gatekeepers for Wnt/ β -catenin signaling. To explore a possible relationship between RAR γ function and Wnt/ β -catenin signaling, we administered the RAR γ agonist NRX204647 from P10 to P16 to β -catenin conditional knockout mice (Col2CreER; floxed β -catenin CKO) and control (floxed β -catenin) littermates both receiving tamoxifen at P5 and P7. NRX204647 treatment accelerated replacement of growth plate to bone, leading to growth plate closure in control mice by 3 weeks of age, whereas 80% of treated CKO mutants did not show such a phenotype. The results indicate that stimulation of ligand bound RAR γ function promotes maturation in growth plate chondrocytes, thus facilitating cartilage to bone transition. The findings also suggest that RAR γ function is in part mediated by Wnt/ β -catenin signaling.

Disclosures: Kenta Uchibe, None.

FR0082

The role of macro-autophagy in cartilage homeostasis. Andrei Chagin^{*1}, Karuna Vuppalapati², Thibault Boudierlique², Phillip Newton². ¹Karolinska Institutet, Sweden, ²Karolinska Institute, Sweden

Macro-autophagy is a process of catabolic degradation of unnecessary intracellular material, which is encapsulated in a double-membrane vehicle called autophagosome and then delivered to lysosomes. The process of macro-autophagy is tightly controlled by mTOR (mechanical target of rapamycin) signaling pathway, which suppresses autophagy.

Here we explored the role of macro-autophagy in cartilage tissues by genetically inactivating indispensable autophagy genes Atg5 or Atg7 utilizing collagen2-driven Cre mouse strain and respected floxed strains.

Inactivation of autophagic process diminished chondrocyte survival in both epiphyseal growth plate and in articular cartilage. Accordingly, autophagy-deficient mice initially develop moderate growth retardation whereas osteoarthritis is developed with aging. Interestingly, surgery-induced osteoarthritis was autophagy-independent in this model. Diminished chondrocyte survival in the absence of autophagy led to cascade-dependent chondrocyte apoptosis associated with cytochrome C release by mitochondria. Finally, we also observed that pharmacological inhibitors of autophagy, in particular bafilomycin and chloroquine, unexpectedly activated mTOR signaling pathway in autophagy-independent manner and this activation is chondrocyte- but not osteoblast-specific. Summarizing, we demonstrated that macro-autophagy is an important mechanism supporting chondrocyte survival and facilitating cartilage homeostasis both at the growth plate level and at the articular surface.

Disclosures: Andrei Chagin, None.

FR0083

Scleraxis cells contribute to the development of trauma-induced and genetic HO. Shailesh Agarwal^{*1}, Shawn Loder¹, Cameron Brownley¹, John Li¹, Hsiao Hsin Sung¹, Laura Mangiavini¹, Ammar Qureshi², Kristoffer Sugg¹, Shuli Li¹, Christopher Mendias¹, Nobuhiro Kamiya³, Bin Zhao⁴, Vesa Kaartinen¹, Thomas Davis², Jonathan Forsberg², Ernestina Schipani⁵, Yuji Mishina¹, Benjamin Levi¹. ¹University of Michigan, USA, ²Naval Medical Research Center, USA, ³Tenri University, USA, ⁴Albert Einstein College of Medicine, USA

Introduction: Heterotopic ossification is the pathologic development of ectopic bone. Two groups of patients are at risk for HO – those with trauma and burn injuries, and those with mutations in the type I BMP receptor, *ACVRI*. Despite the varying presentation of patients with HO and the differing etiologies, we hypothesize that the progenitor cells that develop into HO lesions are of the same cell lineage in all different settings. In this study, we tested this hypothesis.

Methods: Three different models of trauma-induced HO were used to identify HO progenitor cells: 1) mouse burn and Achilles' tendon transection (burn/tenotomy), 2) intramuscular BMP scaffold with cardiotoxin, and 3) rat muscle blast injury. Burn/tenotomy was additionally performed in *Scx-Cre/R26^{RFP}* mice, in which RFP marks the scleraxis-lineage. Additional genetic mouse models included Cre-induced constitutively active *Acvr1* transgenic mice (*ca-Acvr1^{floxWT}*) were bred with *Nfatc1-Cre*, *Ub-Cre-ERT*, *Ckmm-Cre*, and *Coll-CreERT*. All animals were euthanized at the appropriate time points and tissue sectioning was performed for histologic analysis. Pentachrome was used to identify cartilage, mature HO, and surrounding tissue. Immunostaining for pSmad 1/5, Scleraxis, Tenomodulin, and Sox9 was performed.

Results: All three models of trauma-induced HO, and *Nfatc1-Cre/ca-Acvr1^{floxWT}* mutant mice consistently developed HO lesions. Three weeks after burn/tenotomy, ectopic cartilage had robust presence of cells expressing scleraxis, tenomodulin, and SOX9 (Fig 1A). In *Scx-Cre/R26^{RFP}* mice, a vast majority of cells in mature HO expressed RFP. Cells along the periphery actively expressed SOX9, scleraxis, and tenomodulin. In the rat blast and intramuscular BMP scaffold models, cells forming HO lesions co-expressed scleraxis, tenomodulin, and SOX9. *Nfatc1-Cre/ca-Acvr1^{floxWT}* mice developed HO lesions exclusively in proximity to ligaments and tendons, despite recombination in tissues such as skin and muscle. HO lesions in mutants co-stained for scleraxis, tenomodulin, and SOX9 as well (Fig 1B). HO was not observed in mice expressing *ca-Acvr1* with muscle- or osteoblast-specific Cre drivers (*Ckmm-Cre* and *Coll-CreERT* respectively).

Conclusions: Our findings show that independent of etiology, scleraxis(+) cells contribute substantially to HO lesions. Furthermore, despite *ca-Acvr1* expression within multiple tissue types, only expression within tendons and ligaments appears to result in HO.

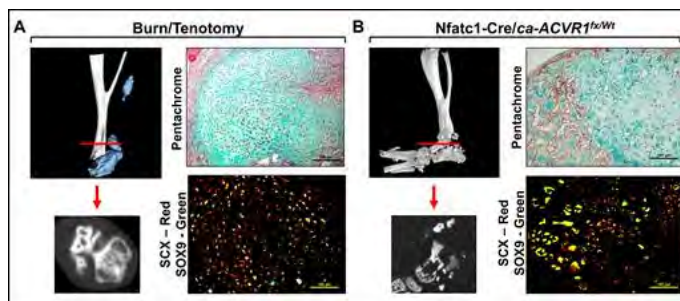


Fig 1

Disclosures: Shailesh Agarwal, None.

FR0084

CNBP controls Chondrocyte Hypertrophy and Hypertrophic Chondrocyte Cell Size by Spatially and Temporally Regulating the Expression of Sox9 and Runx2. Yun Lu*, Wei Chen, Guochun Zhu, Yi-Ping Li. Department of Pathology, University of Alabama at Birmingham, USA

How chondrocyte hypertrophy and hypertrophic chondrocyte cell size are regulated is a fundamental question in bone biology. However, which factor(s) regulates the events still remains largely unknown. Cellular Nucleic acid Binding Protein (CNBP) is highly conserved among vertebrates. Functionally, CNBP binds single-stranded nucleic acids and may act as a molecular chaperone, thus regulating both transcription and translation. Recently, we found that CNBP cartilage specific knockout through the CNBP^{Loxp}/Loxp Col2a1-Cre (CKO) approach resulted in very large hypertrophic chondrocytes, which were about three-fold larger than that in wild type (WT) mice. Meanwhile, the immature chondrocytes of CNBP CKO mice experienced early hypertrophy. As a result, the limbs of CNBP CKO mice are extremely short, indicating the importance of normal chondrocyte hypertrophy and cell size. We hypothesized that CNBP regulates chondrocyte hypertrophy and controls hypertrophic chondrocyte cell size by spatially and temporally regulating the expression Sox9 and Runx2. To test this hypothesis and characterize the mechanism, we studied the function of CNBP at the histological, cell, and molecular levels respectively. Newborn IHC stain of Col X in the resting and proliferation zones confirms that the immature chondrocytes of CNBP CKO mice are undergoing hypertrophy. The expression of Sox9, which has been noted to block immature chondrocyte maturation into hypertrophic cells, was dramatically reduced in CNBP CKO mice. On the other hand, Runx2, as a vital transcriptional factor to trigger chondrocyte hypertrophy, is ectopically and highly expressed in the chondrocyte resting and proliferation zones, but poorly expressed in the pre-/hypertrophic zone of the growth plate in CNBP CKO mice. Surprisingly, IGF-1, which is essential for the third phase of the chondrocyte hypertrophy process, is highly expressed in CNBP CKO mice. Taken together, our study reveals that CNBP is a novel key negative regulator of chondrocyte hypertrophy initiation and cell size and spatially and temporally regulates the expression of Sox9 and Runx2 in chondrocytes. The insight of this study not only improved our understanding of the mechanism underlying how CNBP regulates chondrocyte hypertrophy and hypertrophic chondrocyte cell size, but it will also facilitate the design of novel treatment approaches for aging, congenital, degenerative skeletal and metabolic bone disorders and diseases by targeting CNBP.

Disclosures: Yun Lu, None.

FR0085

Histone Deacetylase 3 Controls Extracellular Matrix Remodeling and Proinflammatory Signals in Chondrocytes. Lomeli Carpio*, Elizabeth Bradley¹, Amel Dudakovic¹, Andre van Wijnen¹, Meghan McGee-Lawrence², Jennifer Westendorf¹. ¹Mayo Clinic, USA, ²Georgia Regents University, USA

Histone deacetylase (Hdac) inhibitors are emerging epigenetic therapies for cancer, arthritis, and epilepsy; however, these drugs inhibit multiple Hdacs and have detrimental effects on the pre- and post-natal skeleton. Several Hdacs contribute to endochondral bone formation. In this study, we defined the cell autonomous role of Hdac3 in chondrocyte maturation by deleting it pre- and post-natally in type II collagen alpha 1 (Col2a1) expressing chondrocytes. Hdac3-CKOCol2 mice rarely survived embryogenesis. The few that survived birth were hypomorphic for Hdac3 expression, runted, and had severely reduced cancellous and cortical bone density. To overcome the prenatal lethality, postnatal Hdac3 deficiency was induced with a tamoxifen-inducible Col2a1 Cre model (Hdac3-CKOCol2ERT). At 4-weeks of age, these animals had residual hypertrophic cartilage and increased osteoclast activity in the primary spongiosa. By 8 weeks, these animals had compromised bone architecture, with significant decreases in trabecular bone, but greater cortical bone thickness, which is likely a compensation for disrupted growth plate maturation during development. Erk1/2 phosphorylation and matrix metalloproteinases (Mmp-3 and Mmp-13) were elevated in Hdac3-depleted immature mouse chondrocyte micromass cultures and the growth plates of the Hdac3-CKOCol2ERT mice. RNA sequencing was used to assess Hdac3-dependent global changes in gene expression. Functional annotation clustering for Hdac3-deficient IMCs showed increases in genes related to inflammatory and immune responses and reductions in genes related to the extracellular matrix, bone development and ossification. Among the differentially regulated proinflammatory cytokines, chemokines, and their respective receptors in Hdac3-depleted chondrocytes, interleukin-6 was significantly elevated. Downstream of this immune response mechanism, Stat3 phosphorylation was increased in Hdac3-deficient chondrocytes. These results show that chondrocyte-specific Hdac3 deletion alters gene expression in a number of cellular processes, including initiation of proinflammatory responses, which can increase Mmp expression. Altogether, these results indicate that Hdac3 controls the temporal and spatial regulation of gene expression and downstream signaling factors in chondrocyte maturation to ensure proper ossification during long bone development.

Disclosures: Lomeli Carpio, None.

FR0086

PRC2 controls chondrocyte proliferation, differentiation and hypoxic adaptation by suppressing aberrant activation of multiple signaling pathways. Fatemeh Mirzamohammadi*¹, Garyfallia Papaioannou², Erinn Rankin³, Huanfeng Xie⁴, Jennifer Inloes⁵, Stuart H. Orkin⁶, Ernestina Schipani⁷, Tatsuya Kobayashi⁸. ¹Massachusetts General Hospital & Harvard Medical School, USA, ²Massachusetts general hospital & harvard medical school, USA, ³Stanford cancer institute, USA, ⁴Dana-Farber Cancer Institute, USA, ⁵Endocrine Unit, Massachusetts General Hospital, USA, ⁶Boston Children's Hospital & Dana-Farber Cancer Institute, USA, ⁷University of Michigan, USA, ⁸Endocrine Unit, Massachusetts General Hospital & Harvard Medical School, USA

Histone modifications regulate gene expression through altering chromatin structure. Trimethylation on lysine residue 27 of histone 3 (H3K27me3), catalyzed by the polycomb repressive complex 2 (PRC2), controls cell fate determination and stem cell function by suppressing expression of genes that regulate cellular differentiation. However, the role of PRC2-mediated gene repression in somatic tissues remains largely unknown. To investigate the role of PRC2 in skeletal development, we genetically ablated PRC2 function in chondrocytes by deleting *Eed*, an essential component of PRC2. *Eed*-deficient mice exhibited a growth defect and kyphoscoliosis. *Eed*-deficiency led to decreased chondrocyte proliferation and accelerated differentiation, and caused ectopic cell death in the central area of the growth plate. Multiple signaling pathways, including the Wnt and TGF- β signaling pathways were upregulated in *Eed*-deficient chondrocytes. Suppression of the Wnt signaling using Wnt-C59, a Porcupine enzyme inhibitor, rescued accelerated chondrocyte differentiation and ameliorated kyphoscoliosis in mutants. We also found that *Eed*-deficient chondrocytes showed reduced expression of *Hif1a*, a critical transcription factor for hypoxia adaptation, which likely induced chondrocyte cell death in the hypoxic region of the growth plate. We found that the upregulation of TGF- β signaling in *Eed*-deficient chondrocytes was responsible for the *Hif1a* mRNA downregulation. In summary, our study demonstrates that PRC2 function is essential for normal skeletal development. PRC2-mediated gene regulation controls differentiation and proliferation, and hypoxic adaptation of chondrocytes by suppressing aberrant activation of multiple signaling pathways. Our study suggests a paradigm in which PRC2 continuously plays an essential role in lineage-committed, differentiated somatic cells.

Disclosures: Fatemeh Mirzamohammadi, None.

FR0088

Partial pharmacological repression of PPAR γ balances energy metabolism and increases bone mass. L.A. Stechschulte¹, P.J. Czernik², F. Tausi¹, C.A. Corzo³, A. Asteian³, M. Cameron³, T.M. Kamenecka³, P.R. Griffin³, B. Lecka-Czernik*¹. ¹Department of Orthopaedic Surgery, Center for Diabetes & Endocrine Research, University of Toledo, College of Medicine & Life Sciences, USA, ²Micro Tomografts Ltd., USA, ³Department of Molecular Therapeutics, The Scripps Research Institute, Scripps Florida, USA

The armamentarium to fight diabetes is constantly expanding into therapies targeting particular mechanisms controlling glucose levels; however treatments which increase cellular responsiveness to insulin are the most effective. Unfortunately, PPAR γ full agonists, TZDs, cause adverse effects including weight gain and bone fractures. Besides glucose metabolism, PPAR γ also regulates marrow mesenchymal stem cells (MSCs) commitment toward osteoblast and adipocyte lineage by either acting directly on MSCs or indirectly by changing milieu of marrow microenvironment. We have previously showed that PPAR γ anti-osteoblastic and insulin sensitizing activities can be separated by using ligands of different chemical structures. Recently, a new class of insulin sensitizers and selective modulators of PPAR γ activity has been developed in efforts to curb the adverse effect on weight gain, but their effect on bone remains unknown. Here, we demonstrate that SR10171 compound, a partial inverse agonist of PPAR γ , normalizes energy metabolism and increases bone mass by modulating directly osteocyte activities. Treatment of mice with SR10171 at the dose which normalizes glucose tolerance, results in increased trabecular and cortical bone mass due to increased bone formation and bone turnover. SR10171 decreases SOST and increases RANKL expression both *in vivo*, in osteocytes isolated from femora of treated mice, and *in vitro*, in treated MLO-A5 cells. At the same time, SR10171 is neutral for direct effect on osteoblast differentiation. Treatment of marrow MSCs does not have an effect on differentiation and expression osteoblast and adipocyte gene markers; however osteoblasts isolated from endosteal surface of femora of treated mice have increased activity of Wnt signaling and expression of osteoblast-specific gene markers. Beneficial effects on bone are independent of SR10171 metabolic activity. SR10171 increases energy metabolism and normalizes fat function in animals with diet induced obesity, but unlike rosiglitazone it is neutral in animals with balanced energy metabolism. Our data suggest that SR10171 modulates energy metabolism in an on-demand manner, while having sustained anabolic activity on bone regardless of animal metabolic status. These results demonstrate a possibility for developing a compound which may act as insulin sensitizer with simultaneous anabolic effect on bone.

Disclosures: B. Lecka-Czernik, None.

FR0089

PTHrP-derived Peptides Restore Bone Mass and Strength in Diabetic Mice: Additive Effect of Mechanical Loading. Marta Maycas^{*1}, Kevin A McAndrews², Amy Y Sato³, Gretel G Pellegrini³, Drew M Brown⁴, Matthew R Allen³, Lilian LI Plotkin², Pedro Esbrit⁵, Aranca Gortazar⁶, Teresita M Bellido⁷. ¹Anatomy & Cell Biology, Indiana University School of Medicine, USA, ²Department of Anatomy & Cell Biology, Indiana University School of Medicine; Roudebush Veterans Administration Medical Center, USA, ³Department of Anatomy & Cell Biology, Indiana University School of Medicine, USA, ⁴Department of Anatomy & Cell Biology, Indiana University School of Medicine, USA, ⁵Instituto de Investigación Sanitaria (IIS)-Fundación Jiménez Díaz, Universidad Autónoma de Madrid (UAM) & Red Temática de Investigación Cooperativa en Envejecimiento y Fragilidad (RETICEF), Spain, ⁶Universidad San Pablo-CEU School of Medicine Madrid Spain, Spain, ⁷Department of Anatomy & Cell Biology, Indiana University School of Medicine; Department of Medicine, Division of Endocrinology, Indiana University School of Medicine; Roudebush Veterans Administration Medical Center, USA

There is an unmet need to treat bone fragility in patients with diabetes mellitus. We examined herein the effectiveness of N- and C-terminal fragments of parathyroid hormone related peptide (PTHrP), in combination with mechanical loading, in counteracting skeletal deterioration in a mouse model of type 1 diabetes. Diabetes was induced in 4-month-old male C57BL/6 mice by 5 consecutive daily ip injections of streptozotocin (45 mg/kg). Four weeks after injections, glucose levels were significantly higher in streptozotocin-injected mice compared to non-diabetic control mice receiving saline (382±105 vs 179±27 mg/dL). At this time, diabetic mice were separated in 3 groups and received 3 consecutive daily sc injections of PTHrP(1-37) (50 µg/kg), PTHrP(107-111) (7 µg/kg), or vehicle, followed by loading of the right ulnae for 1 min at 120 cycles/day at 3 different magnitudes ranging from 1,995 to 2,500 g strain. All mice were sacrificed 12 days thereafter. Diabetic mice receiving vehicle exhibited a significant lower femoral BMD compared to non-diabetic controls (decreased by 14.9%). In contrast, diabetic mice treated with either PTHrP(1-37) or PTHrP(107-111) showed a gain of 3.4% and 3.5%, respectively, in femoral BMD, similar to non-diabetic controls. Moreover, the decrease in trabecular thickness in the distal femur and in cortical thickness at the mid-diaphysis exhibited by diabetic mice was reversed by both PTHrP peptides. Furthermore, diabetic mice exhibited significantly lower mechanical (ultimate force and stiffness) and material (ultimate stress and toughness) properties quantified by femoral 3-point-bending, which was restored to non-diabetic control levels by both PTHrP peptides. In addition, CTX, a bone resorption marker, was increased in diabetic mice and reversed to non-diabetic control levels by both PTHrP peptides. Higher magnitude loading was needed in diabetic mice to increase periosteal MAR and BFR/BS compared to non-diabetic controls. In addition, loading increased MAR and BFR/BS to higher levels in diabetic mice treated with either PTHrP peptide compared to diabetic mice receiving vehicle. In conclusion, these PTHrP peptides partially restored bone loss and strength, reversed increased resorption induced by diabetes, and worked additively with mechanical loading to enhance periosteal bone formation in the appendicular skeleton of diabetic mice. Thus, this short treatment with both PTHrP peptides reversed skeletal deterioration in diabetes.

Disclosures: *Marta Maycas, None.*

FR0090

Δ FosB in the ventral hypothalamus prevents the age-related dysregulation of metabolic homeostasis in mice. Kazusa Sato^{*1}, Anna Idelevich¹, Glenn Rowe², Francesca Gori¹, Roland Baron¹. ¹Harvard School of Dental Medicine, USA, ²Cardiovascular Institute, Beth Israel Deaconess Medical Center, Harvard Medical School, USA

Aging is associated with a high risk of developing osteoporosis and also impaired glucose tolerance. The hypothalamus plays a critical role in bone homeostasis as well as energy balance and glucose metabolism through endocrine and neuronal pathways that are only partially elucidated.

ΔFosB is a naturally truncated form of FosB that antagonizes AP-1 transcription. In mice, overexpression of ΔFosB under the control of the enolase 2 (ENO2) promoter, which drives expression in bone, adipose tissues, and the ventral hypothalamus (VHT), results in increased bone mass, decreased adipose mass due to increased energy expenditure, and favored glucose metabolism due to increased insulin sensitivity. Moreover, adeno-associated virus (AAV)-mediated expression of ΔFosB in the VHT phenocopies the bone, energy and glucose phenotypes of ENO2-ΔFosB mice, suggesting a dominant role of ΔFosB in the VHT.

The present study determined whether ΔFosB is implicated in the development of the age-related dysregulation of bone and glucose homeostasis, and evaluated the contribution of ΔFosB in the VHT to these regulation systems. To this end, we analyzed the bone and metabolic profiles of aged (40-50 weeks) ENO2-ΔFosB mice and C57BL/6 mice 35-40 weeks after stereotaxic injection of AAV encoding ΔFosB (AAV-ΔFosB) or GFP (AAV-GFP) as control exclusively in the VHT.

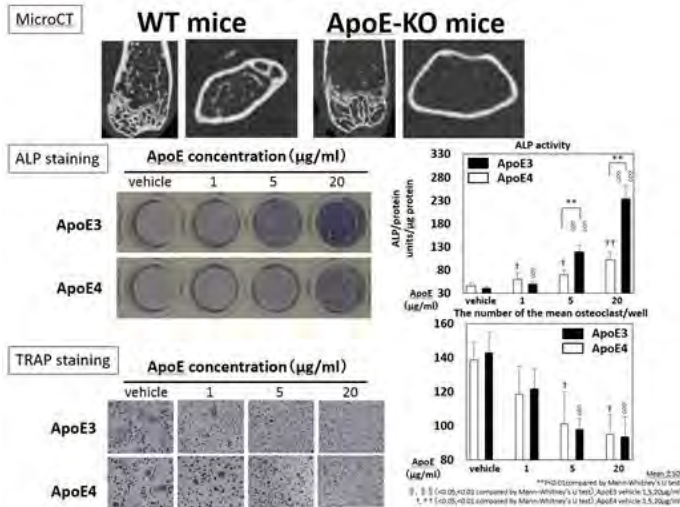
In comparison to control littermates, aged ENO2-ΔFosB mice had increased femoral BV/TV and Tb.Th by 28% and 39%, respectively, as well as increased energy expenditure and decreased abdominal adiposity. During glucose tolerance test, aged ENO2-ΔFosB mice maintained lower glucose levels (AUC 22.0±0.3 vs 16.1±1.5 *10³ mg/dl*min) with significantly lower insulin levels (AUC 1096±16 vs 54±5 ng/ml*min), due to markedly increased insulin sensitivity. This was in contrast to the glucose intolerance associated with severe hyperinsulinemia and exacerbated insulin resistance observed in aged control mice. Similarly, aged AAV-ΔFosB mice were protected from abdominal adiposity due to increased energy expenditure compared to aged AAV-GFP mice. Aged AAV-ΔFosB mice were more glucose tolerant (AUC 38.6±1.6 vs 30.1±1.3 *10³ mg/dl*min) with lower insulin response (AUC 456±64 vs 218±19 ng/ml*min) and increased insulin sensitivity as observed in aged ENO2-ΔFosB mice. Taken together, these results suggest that the VHT signaling downstream of ΔFosB has protective effects against age-related metabolic changes.

Disclosures: *Kazusa Sato, None.*

FR0091

Apolipoprotein E (ApoE) plays a crucial role in maintaining trabecular and cortical bone mass by promoting osteoblastic differentiation via ERK1/2 pathway and suppressing osteoclast differentiation by down-regulation of c-Fos and NFATc1. Takaaki Noguchi^{*1}, Kosuke Ebina², Makoto Hirao², Kota Koizumi², Hideki Yoshikawa². ¹Osaka University, Japan, ²Department of Orthopaedic Surgery, Graduate School of Medicine, Osaka University, Japan

It is well known that hyperlipidemia is tightly associated with osteoporosis, while its detailed mechanism remains unknown. ApoE plays a major role in the lipid metabolism and its deficiency leads to severe hyperlipidemia. The aim of this study is to clarify the effect of ApoE on bone metabolism. Females ApoE knockout mice (ApoE-KO) (n=8) and control C57BL/6 wild type mice (WT) (n=8) were fed with normal chow for 48-weeks and sacrificed. 3D trabecular structure of the femur was measured by microCT, and the number of osteoclasts was evaluated by TRAP staining in distal femur. ApoE-KO and WT mice calvaria were used to investigate osteoblastic differentiation, and murine bone marrow derived macrophages (BMDM) and human peripheral blood monocytes (PBMC) were used to investigate osteoclastogenesis under RANKL and M-CSF stimulation. The finding of microCT revealed that ApoE-KO mice showed severe osteoporosis compared to WT mice, which were evaluated by cancellous bone quantity (BV/TV: 3.3v.s.16.6%; P<0.001) and cortical bone quantity (Cv/Av: 31.8v.s.37.9%; P<0.01). ApoE-KO mice showed significantly larger number of osteoclasts per bone surface compared to WT mice (8.6v.s.4.5/mm; P<0.05). Recombinant human ApoE3 and ApoE4 protein (rh-ApoE3/E4) significantly promoted ALP activity (0→20µg/ml ApoE3: 40.5→233.7units/µg protein; P<0.01, 0→20µg/ml ApoE4: 46.0→102.2units/µg protein; P<0.01) and osteoblast-related mRNA (*ALP*, *osteocalcin*) expression in a dose dependent manner by using WT mice calvaria, and ApoE3 had significantly stronger effect compared with ApoE4. Western blot (WB) analysis showed that ApoE3 strongly down-regulated the phosphorylation of ERK1/2, which was up-regulated in ApoE-KO mice as compared with WT mice calvaria. On the other hand, rh-ApoE3/E4 significantly inhibited osteoclasts formation (0→20µg/ml ApoE3: 142.3→93.4/well; P<0.05, 0→20µg/ml ApoE4: 138.5→95.0/well; P<0.05) and osteoclast-related mRNA (*c-Fos*, *NFATc1*, *TRAP*, *Cathepsin K*) expression in a dose dependent manner by using BMDM. Furthermore, rh-ApoE3 significantly inhibited bone resorption activity by using PBMC (0→5µg/ml: 99692→2608µm²/well; P<0.05). WB analysis showed that ApoE3 suppressed c-Fos protein expression. Our findings revealed that ApoE plays a crucial role in bone metabolism by up-regulating osteoblastic differentiation and down-regulating osteoclastogenesis. Therapeutic strategy targeting ApoE may be a promising in treating both osteoporosis and lipid metabolism dysfunction.



ASBMR 2015 figure

Disclosures: Takaaki Noguchi, None.

FR0093

Impaired Bone Accrual during Obesity occurs by a Neuropeptide Y-dependent Mechanism in the Osteoblast. Natalie Wee¹, Nikki Lee², Ronaldo Enriquez¹, Herbert Herzog², Paul Baldock¹. ¹Skeletal Metabolism, Osteoporosis & Bone Biology Program, Garvan Institute of Medical Research, Australia, ²Eating Disorders, Neuroscience Program, Garvan Institute of Medical Research, Australia

Diet-induced obesity (DIO) is detrimental to cancellous bone mass, the effect on cortical bone is less clear, as is the mechanisms involved.

Neuropeptide Y (NPY) is a powerful modulator of energy and bone metabolism. Central overexpression of NPY reduces bone formation and results in bone loss. In diet-induced obesity (DIO), NPY is upregulated, suggesting a potential inhibition of bone formation in obese mice. In this study, we aimed to determine the contribution of NPY to bone loss during DIO and to evaluate whether blocking osteoblastic Y1 receptors would be protective.

6-week old WT and NPYKO mice were fed either a chow or a HFD (23% fat) for 10 weeks. Obesity and bone mass was monitored by DXA. Post-cull, femurs were evaluated using microCT and histomorphometry. We also examined an osteoblastic-specific NPY, Y1 receptor KO mouse (Y1f3.6cre) using a high fat feeding model for 8 weeks.

WT mice on HFD had increased body weight compared to chow (by ~14%), due to increased fat mass (Chow ~3.3g; HFD ~ 7.3g of fat). NPYKO were less susceptible to DIO with no difference in body weight; however, fat mass was significantly increased (WT~3.0g; HFD~5.1g). In WT, HFD reduced the accrual of whole body BMC (WBBMC) over the 10 weeks compared to chow, with WBBMC reduced by ~ 26%. In contrast, NPYKO mice had greater WBBMC, and importantly, bone accrual was unaffected by HFD. Femoral cortical bone mass in HFD WT was reduced by 20%, independent of the positive effects of weight bearing, and again attributed to changes in fat mass. In NPYKO, cortical bone mass was not different between HFD and chow. Thus, suggesting that DIO affects bone mass via NPY-mediated mechanisms.

Additionally, NPYKO partially attenuated DIO-induced cancellous bone loss: HFD WT had 40% less BV/TV whilst HFD NPYKO had a 20% reduction in BV/TV compared to chow.

Bone from Y1f3.6cre mice was also unaffected by HFD, thus this effect can be directly regulated by NPY responses in the osteoblast.

In summary, we establish the critical role of NPY on inhibition of bone accrual during obesity. We also show that inhibition of osteoblastic NPY signalling using Y1f3.6cre is protective of DIO bone loss, highlighting the role of peripheral NPY signalling in this process and a potential therapeutic avenue.

Disclosures: Natalie Wee, None.

FR0095

Increased G_s Signaling in Osteoblasts Increases Metabolic Activity and Reduces Whole Body Adiposity. Corey Cain*, Joel Valencia, Kate Jordan, Edward Hsiao. University of California, San Francisco, USA

Purpose: Osteoblasts are thought to affect both systemic adiposity and metabolism through secreted factors. G_s-GPCR signaling is a potent regulator of both osteoblast and adipocyte development, but it is unclear if G_s-GPCRs in osteoblasts can have systemic effects beyond the bone. ColII(2.3)⁺/Rsl⁺ mice, which express the engineered G_s-GPCR receptor Rsl in ColII(2.3) expressing osteoblastic cells, have a 5-15 fold

increase in trabecular bone formation, a 2.8 fold reduction in total body fat, and a 11 fold reduction in tibial bone fat. The goal of this study is to use the ColII(2.3)⁺/Rsl⁺ mice to understand how changes in osteoblastic G_s-GPCR signaling regulate osteoblast metabolic activity and whole body adiposity.

Results: ColII(2.3)⁺/Rsl⁺ mice showed increased respiration (VO₂ and VCO₂) but a reduced respiratory exchange ratio (RQ) despite no changes in food intake and ambulatory movement. The mice had significant reductions in serum adipokines leptin and adiponectin, with increased serum GLA-osteocalcin and the metabolically active GLU-osteocalcin. Fasting blood glucose and insulin levels showed no alterations in ColII(2.3)⁺/Rsl⁺ mice. Glucose and insulin tolerance tests revealed that ColII(2.3)⁺/Rsl⁺ mice had increased insulin sensitivity that was independent of food intake in paired feeding experiments. 3T3-L1 pre-adipocytes differentiated with either control or ColII(2.3)⁺/Rsl⁺ serum showed comparable adipocyte differentiation. qPCR analysis of adipogenic genes in ColII(2.3)⁺/Rsl⁺ bones indicated a block in the development of mature adipocytes in the bone marrow, possibly resulting from increased Wnt signaling in ColII(2.3)⁺/Rsl⁺ bones. Seahorse glycolytic and mitochondrial stress tests, which measures cellular glycolytic and oxidative metabolism, of ColII(2.3)⁺/Rsl⁺ digested bone cells revealed increased glucose utilization but no significant alterations to the rate of oxygen consumption.

Conclusions: Our findings suggest that increased G_s-GPCR signaling in osteoblasts increases osteoblast metabolic activity and can reduce peripheral adiposity. Furthermore, osteoblast G_s-GPCR activity reduced mature adipocyte development in ColII(2.3)⁺/Rsl⁺ bones through Wnt signaling, however, the reduction in peripheral adipose tissues was most likely from increased GLU-osteocalcin by osteoblasts. These results suggest that targeting G_s-GPCR in osteoblasts can have potential non-skeletal advantages for treating obese patients with osteoporosis or bone fractures.

Disclosures: Corey Cain, None.

FR0096

Mitochondrial Sirtuin-3 Regulates Skeletal Homeostasis. Linh Ho¹, Yong Pan², Emilie Besnard³, Theresa M. Roth⁴, Yuva Nishida³, Chia-Lin Tsou³, ChePing Ng³, Eric M. Verdin³, Robert A. Nissenson⁴. ¹UCSF, USA, ²Edison Pharmaceuticals, 350 North Bernardo Avenue, Mountain View, CA 94043, USA, USA, ³Gladstone Institutes, University of California San Francisco, San Francisco, CA 94158, USA, USA, ⁴Endocrine Research Unit, VA Medical Center & Departments of Medicine & Physiology, University of California San Francisco, San Francisco, CA, USA, USA

Among seven sirtuins in mammals, mitochondrial Sirt3 has been identified as an essential metabolic regulatory enzyme that plays an important role in metabolism, reducing oxidative stress and promoting efficient energy production with aging by the reversible deacetylation of mitochondrial proteins. However, the role of Sirt3 in skeletal homeostasis has yet to be studied. Using Sirt3 overexpression and Sirt3 knockout (Sirt3KO) mice in a C57BL/6 background, we now report that Sirt3 is a negative regulator of bone mass. Sirt3 transgenic (Sirt3Tg) male mice exhibited a significant reduction in cortical thickness at the tibio-fibular junction (TFJ) (0.201 ± 0.003 vs. 0.220 ± 0.004 mm in Sirt3Tg and WT mice, respectively, P=0.012). Osteoblastogenesis was unaffected by Sirt3 overexpression, but there was almost 2 fold decrease in osteoclastogenesis (P<0.05) by Sirt3KO bone marrow cells grown in the presence of macrophage colony-stimulating factor 1 (CSF1) and receptor activator of nuclear factor kappa-B ligand (RANKL). Accordingly, there was 2.5 fold increase in the number of tartrate resistant acid phosphatase (TRAP) positive cells/bone surface in Sirt3Tg mice compared with WT (P< 0.03). Upon histological analysis, Sirt3Tg mice exhibited an increased number of adipocytes in the tibia when compared to WT mice (92 ± 6.0 vs. 11 ± 0.1 in Sirt3Tg and WT mice, respectively, P<0.05). BMSCs from Sirt3Tg mice displayed an enhanced ability to differentiate into Oil Red O positive adipocytes compared to BMSCs from WT mice (adipocyte area per square millimeter of the Sirt3Tg is 1.274 ± 0.150 compared to the WT 0.642 ± 0.036, P=0.04). In contrast, BMSCs from Sirt3KO mice displayed reduced adipogenesis compared to BMSCs from WT mice (1.001 ± 0.073 adipocyte area per square millimeter of the Sirt3KO compared to 1.673 ± 0.077 of the WT, P<0.001). Interestingly, adipocytes differentiated from Sirt3KO bone marrow cells displayed reduced expression of macrophage colony-stimulating factor 1 (P<0.01), suggesting a role for Sirt3 in adipogenesis linked to induced osteoclastogenesis. In summary, Sirt3 promotes favorable metabolic effects in bone marrow cells and bone loss *in vivo*. The positive energetic effects of Sirt3 in bone marrow cells are associated with increased adipogenesis and increased osteoclastogenesis. These findings demonstrate that Sirt3 is an important regulator of skeletal homeostasis *in vivo*, and identify Sirt3 as a novel therapeutic target for the treatment of osteoporosis.

Disclosures: Linh Ho, None.

FR0099

Metabolic Regulation of Osteoclast Differentiation by Hif1 α in Human Osteoclastogenesis. Koichi Murata*, Min Joon Lee, Seveon Bae, Sehwan Mun, Kyung-Hyun Park-Min, Lionel Ivashkiv. Hospital for Special Surgery, USA

Osteoclast differentiation is considered to be an energy-demanding process. However, molecular mechanisms regulating metabolic adaptation during osteoclastogenesis, to meet the increased demand for adenosine triphosphate, is not fully understood, especially in human. Hypoxia-inducible factor 1 (HIF1) is the major oxygen homeostasis regulator by low oxygen tensions. HIF1 stimulates glycolytic energy production by transactivating genes involved in extracellular glucose import (e.g. GLUT1) and enzymes responsible for glycolytic breakdown of intracellular glucose (e.g. PFK1). It also downregulates oxidative phosphorylation within the mitochondria by transactivating genes such as PDK1 and MX11. Although most knowledge regarding HIF-1 has been derived from studies following hypoxic stress, HIF1 stabilization has also been found in non-hypoxic settings. Here we show that Hif1 α is stabilized by RANKL stimulation and orchestrates metabolic adaptation during osteoclastogenesis even in normoxia.

We treated human osteoclast precursors (OCPs) with RANKL in a time-dependent manner and analyzed the expression of metabolic genes. Not only mTOR, which regulates growth and metabolism by integrating information on nutrient, energy, and oxygen levels, but also adenosine monophosphate (AMP)-activated protein kinase (AMPK), a sensor of increased AMP and adenosine diphosphate was induced and activated by RANKL stimulation, suggesting that RANKL promotes OCPs into energy-demanding and consuming status (Figure 1). RNA sequencing revealed 1761 genes were induced by more than 1.5 fold at 48 h after RANKL stimulation compared to 24 h time point of RANKL stimulation. We also found that 53 RANKL-induced genes were HIF1 α target. Immunoblotting showed the expression of HIF1 α protein could not be observed within 24 h of RANKL stimulation; however, it was detected at 48 h after RANKL stimulation in normoxia (Figure 2). Concomitantly, expressions of HIF1 α target genes, including GLUT1, GLUT3, VEGFA, PHD3 and LDHA, were induced at 48 h after RANKL treatment. Furthermore, siRNA-mediated knockdown of HIF1 α suppressed osteoclastogenesis, and osteoclast-related gene expression, including TRAP, CathepsinK, ITGB3, and DC-STAMP, supporting the important role of Hif1 α in osteoclastogenesis, even in normoxia (Figure 3).

In conclusion, Hif1 α is stabilized by RANKL stimulation and orchestrates metabolic adaptation during osteoclastogenesis even in normoxia.

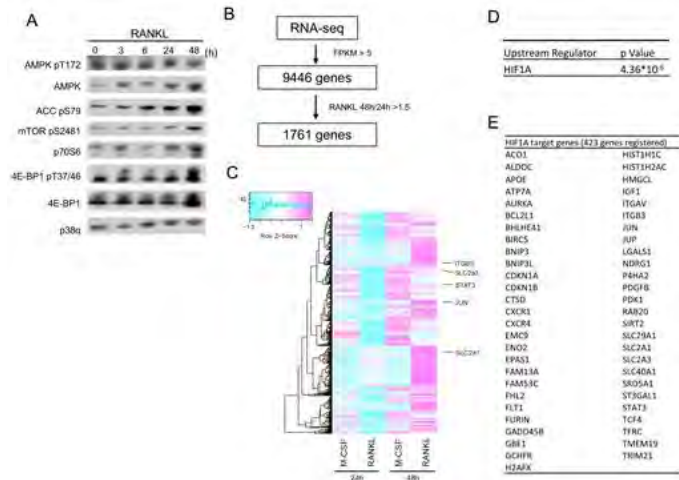


Figure1

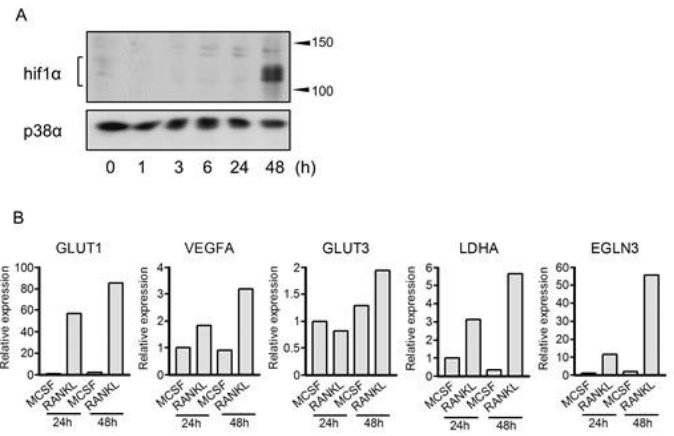


Figure2

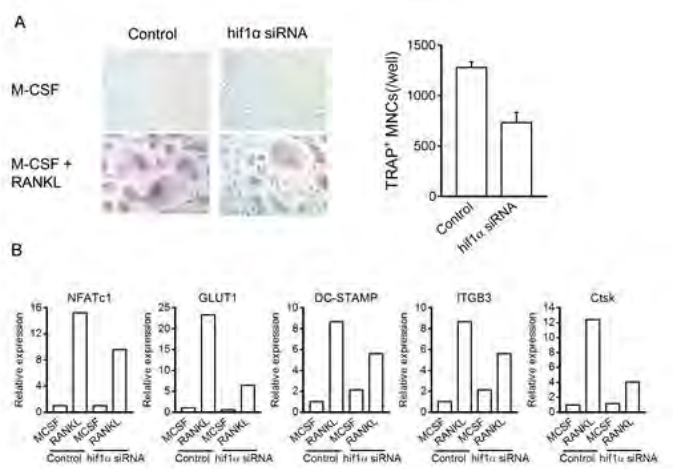


Figure3

Disclosures: Koichi Murata, None.

FR0101

Both phosphate replacement and high fat diet cooperatively improve survival and bone quality in Ebf1-deficient mice. Jackie Fretz*¹, Tracy Nelson², Ben-Hua Sun², Rose Webb², Nancy Troiano², Steven Tommasini². ¹Yale University School of Medicine, USA, ²Yale School of Medicine, USA

The transcription factor Early B Cell Factor 1 (Ebf1) is not only important for maturation of B lymphocytes, but has also been revealed to be integral for maturation of several cell lineages from mesenchymal progenitors. Whole body knockout mice have many problems including low bone mineral density and are severely runted. Our investigations have revealed that Ebf1-deficient mice have impaired renal maturation and function. The mice waste phosphate and calcium in urine, are hypophosphatemic, hypoalbuminuric, and exhibit alterations in proximal tubule and glomerular maturation in the peripheral cortex. Last year we reported that administration of a high phosphate diet (1.5%), high fat diet (45%), or combination diet in animals during the 6-12th weeks of life increased bone density and quality and improved survival of the KO mice. This year we report that administering specialized diets between the 3rd and 12th week of life improved survival from 10% in chow fed animals to 42.8% with high phosphate alone, 50% with high fat alone, and 75% with a combination high fat and phosphate diet. The extended time course provided an even greater improvement in linear growth with all modified diets (compared to chow fed mice) restoring the growth rate to that of WT and heterozygous littermates. Kidney health, as assessed through urine analysis, serology, histology, and circulating FGF23 were all improved with phosphate alone, and further enhanced by the addition of high fat. Biomechanical assessment of bone quality (by micro-CT, histology, and 4 point bending) revealed that phosphate alone provided significant improvement in bone quality, but that these parameters were also further enhanced by addition of high fat into the diet. These results demonstrate that dietary modification to counteract the renal insufficiency present in Ebf1-deficient mice: 1) significantly improves the overall health of the animals, 2) restores linear growth, 3) improves bone quality, and 4) slows

progression of renal failure. Furthermore, the results suggest that circulating lipids and possibly maintenance of adipose mass influences the severity of renal disease and associated renal osteodystrophy resulting from Ebf1-deficiency. These results provide novel insights into the mechanisms underlying the renal insufficiency present in Ebf1-deficient mice and provide intriguing evidence for an interaction of phosphate and circulating lipids to bone and kidney health.

Disclosures: Jackie Fretz, None.

FR0102

Genetic keratin inactivation corrects the altered osteoblast function, bone formation and osteopenia in F508delta-Cftr mice, a murine model of cystic fibrosis. Carole Le Henaff^{*1}, Mélanie Faria², Aurélie Hatton², Danielle Tondelier², Caroline Marty¹, Mylène Zarka¹, Kurt Zatloukal³, Valérie Geoffroy¹, Aleksander Edelman², Isabelle Sermet², Pierre J. Marie¹. ¹INSERM UMR-1132 & University Paris Diderot, Sorbonne Paris Cité, France, ²INSERM U-1151, Faculté de Médecine Paris Descartes, France, ³Institute of Pathology, Medical University of Graz, Austria

Mice with the prevalent F508del mutation in the cystic fibrosis conductance regulator (Cftr) gene display reduced bone formation and osteopenia, but the underlying molecular mechanisms are unknown, which precludes the development of an efficient therapeutic strategy. In this study, we hypothesized that the microfilament keratin 8 (K8) which is known to interact with F508del-CFTR in epithelial cells, may play a role in osteoblast dysfunctions and bone loss induced by the F508del-Cftr mutation in mice. We found that osteoblasts isolated from wild type (WT) or F508del-Cftr mice express CFTR and the microfilament keratin 8 (K8) at the mRNA and protein levels. Analysis of bones of K8 null WT mice (K8^{-/-}) showed that inactivation of K8 led to long bone loss due to decreased bone mineral apposition rate (MAR) and bone formation rate (BFR) assessed by histomorphometric analysis. In marked contrast, K8 inactivation in F508del-Cftr mice fully rescued the decreased bone mass and altered microarchitecture induced by the mutation, as shown by bone histomorphometry and microCT analyses. The beneficial effect of K8 inactivation on bone mass in F508del-Cftr mice resulted from enhanced osteoblast activity as documented by the expression of phenotypic osteoblast genes (Runx2, Alp, Coll1a1, Oc) in bone and increased MAR and BFR, with no change in bone resorption parameters. Mechanistically, K8 inactivation in F508del-Cftr mice led to correct the overactive NF- κ B signaling and the decreased Wnt-beta-catenin signaling induced by the mutation in osteoblasts, as evidenced by Opg, Axin and Wisp1 expression in K8^{-/-}F508del-Cftr osteoblasts and by increased beta-catenin immunohistochemistry in vertebral bone of K8^{-/-}F508delta-Cftr mice. Knowing that the abnormal K8-F508del-CFTR interaction is a functional defect of F508del-CFTR in epithelial cells, we tested the effect of 407, a compound that binds to the F508del-NBD1 domain and acts as a protein-protein interaction inhibitor. We found that treatment with 407 corrected the abnormal NF- κ B transcription and Wnt-beta-catenin target gene expression and restored normal phenotypic gene expression in F508del-Cftr osteoblasts in vitro. In vivo, the injection of 407 for 4 days restored beta-catenin immunohistochemistry in vertebral bone and rescued long bone formation in F508del-Cftr mice, as indicated by correction of both MAR and BFR. Collectively, the data indicate that K8 plays a central role in the osteoblast dysfunctions induced by the prevalent F508del-Cftr mutation in mice, and suggests that K8 in relation with F508del-CFTR is a new target for therapeutics to correct the altered osteoblast bone formation and osteopenia in cystic fibrosis.

Disclosures: Carole Le Henaff, None.

FR0103

Matrix deposition and mineralization in heterozygous and homozygous mouse embryos with Gly610 to Cys substitution in the triple helical region of the α 2(I) collagen chain. Lynn Mirigian¹, Elena Makareeva¹, Shakib Omari¹, Anna Roberts-Pilgrim¹, Edward Mertz¹, Sergey Leikin^{*2}. ¹NICHHD, NIH, USA, ²National Institutes of Health, USA

Glycine substitutions in the triple helical region of type I collagen are the most common mutations resulting in severe forms of osteogenesis imperfecta (OI). The G610C mouse with a Gly610 to Cys substitution in the α 2(I) chain is the only model that produces moderately severe OI in heterozygous (het) and lethal OI in homozygous (hom) animals, as expected for dominant negative mutations. Here, we investigated extracellular matrix formation and mineralization in wild type (wt), het and hom G610C embryos and neonates on C57BL/6J background as well as in osteoblast and embryonic fibroblast cultures from these animals. At gestational day E18-19, we observed close to the expected 1:2:1 ratio of wt:het:hom embryos, all of which had similar size and appeared to be viable. Yet, all hom pups recovered within hours of birth were dead while most heterozygous and wild type pups survived to weaning. Skeletal staining and X-ray radiography of newborn hom animals revealed underdevelopment and undermineralization of calvaria, gross deformities of many other bones, and multiple fractures. Newborn het animals exhibited significant variability, ranging from severe bone malformations like in hom mice to almost normal bone appearance like in wt mice. In culture, heterozygous embryonic fibroblasts deposited 2-3 times less collagen/cell than their wt counterparts but approximately the same amount of collagen/cell as their hom counterparts.

Consistently, the skin of E18.5 het and hom embryos had similar reduced weight fraction of collagen and increased weight fraction of glycosaminoglycans compared to wt embryos. While het cells secreted equal number of molecules with and without the mutant α 2(I) chain, the matrix deposited by them in culture and skin of E18.5 embryos contained only 30% of mutant molecules. Deficient deposition of the latter into the matrix was at least in part caused by their reduced thermal stability and premature denaturation after secretion, before their incorporation and stabilization in collagen fibers. The amount of matrix deposited by cultured het osteoblasts was restored to almost wt level by treatment of the cells with rapamycin, suggesting that deficient matrix deposition was caused primarily by malfunction of the cells rather than secreted mutant molecules. Analysis of matrix mineralization *in vivo* and in culture also pointed to abnormal osteoblast differentiation and function as the primary cause of bone pathology.

Disclosures: Sergey Leikin, None.

FR0105

MS-275 administration rescues cleidocranial dysplasia (CCD) phenotypes of Runx2+/- mice. Han-sol Bae^{*}, Won-joon Yoon, Young-dan Cho, Rabia Islam, Hye-rim Shin, Bong-soo Kim, Kyung-mi Woo, Jeong-hwa Baek, Hyun-mo Ryoo. Seoul National University, South Korea

Cleidocranial dysplasia (CCD) is an autosomal-dominant skeletal disorder caused by haploinsufficiency of Runx2, a key regulator of bone growth and differentiation. We previously reported that RUNX2 protein stability and its transcriptional activity require a serial post-translational modification process including phosphorylation, isomerization and acetylation. In the absence of the final acetylations, Runx2 undergoes perishing ubiquitination process. Aim of this study was to evaluate whether post-translational stabilization of Runx2 by an HDAC inhibitor (HDACi) could overcome phenotypes of genetic haploinsufficiency of Runx2. Runx2^{+/+} and Runx2^{+/-} mice were mated and MS-275, a Class I HDAC-specific inhibitor, was administered in pregnant mice at critical time points of bone development, then littermates treated with or without MS-275 were analyzed just after birth (P1). Systemic administration of MS-275 remarkably improved most of the skeletal deformities associated with Runx2^{+/-}; cranial bone development and clavicle maturation, spinal bone maturations, and mandible growth. In molecular level, MS-275 administration in Runx2^{+/-} mice stimulated Runx2 acetylation, thereby recovering hypomorphic expression of active Runx2 through enhanced stabilization of the protein so that Runx2 protein level was comparable that of wild-type mice. In addition, Runx2 transacting activity in Runx2^{+/-} calvarial osteoblasts was substantially recovered by the MS-275 treatment. On the other hand MS-275 neither caused pregnant mice to die, show toxic behaviors nor did it affect littermate numbers. Moreover, other class of HDACi, such as SAHA and valproic acid, didn't show any effects on Runx2^{+/-} bone defects. Conclusively, MS-275 could be applied for intervention of CCD phenotypes as a drug and its mechanism of action strongly suggested HDACi could open a new therapeutic regimen for diseases requiring bone regeneration.

Disclosures: Han-sol Bae, None.

FR0106

Osteocyte-specific Overexpression of Human WNT16 Increases both Cortical and Trabecular Bone Density and Improves Bone Strength in Mice. Imranul Alam^{*1}, Austin Reilly¹, Charishma Kasipathi¹, Mohammed Alkhouli¹, Rita Gerard-O'Riley¹, Dena Acton¹, Amie Gray¹, Kyung-Eun Lim², Alexander Robling², Michael Econs¹. ¹Indiana University School of Medicine, USA, ²Anatomy & Cell Biology, USA

Several genome-wide association studies identified common variants in WNT16 gene that were associated with bone mineral density (BMD) and risk of fracture across multiple populations. In addition, studies involving both global and conditional knockout of Wnt16 in mice revealed that Wnt16 is a critical regulator for cortical BMD and strength. Recently, we demonstrated that osteoblast-specific overexpression of human WNT16 increased both cortical and trabecular bone mass and structure in mice. To further identify the cell-specific role of Wnt16 in bone homeostasis, we created transgenic (TG) mice over-expressing human WNT16 in osteocytes on B6 background using Dmp1 promoter. We compared bone density, micro-architecture and strength phenotypes between TG and wild-type (WT) mice at 6 and 12 weeks of age in both male and female. Compared to WT mice, Dmp1-WNT16 TG mice exhibited significantly higher ($p < 0.005$) whole body aBMD (9-16%) and BMC (11-21%) in both male and female (Figure 1). Spinal aBMD and BMC were also significantly greater (13-20%; $p < 0.005$ and 14-26%; $p < 0.05$, respectively) in the TG mice in both sexes. ρ CT analysis of trabecular bone at distal femur at 12 weeks of age revealed 2-fold (male) and 5-fold (female) higher ($p < 0.0005$) BV/TV, 29% (male) and 50% (female) higher Tb.N, 21% (male) and 50% (female) higher Tb.Th with 23% (male) and 35% (female) lower Tb.Sp in the TG mice compared to WT littermates (Figure 1). The cortical bone at midshaft femur showed 10-11% higher ($p < 0.001$) B.Ar/T.Ar and 4-6% higher ($p < 0.05$) cortical thickness in the TG mice. Femur biomechanics test at 12 weeks of age identified 12% higher ultimate force (UF), 7% higher stiffness (S) and 10% higher energy to UF in male TG mice compared to male WT littermates whereas female TG mice displayed significantly higher ($p < 0.05$) values for UF (17%), S (11%), energy to UF (35%) and energy to failure (16%)

compared to female WT mice (Figure 1). Our data indicate that overexpression of WNT16 in osteocytes increased both cortical and trabecular bone mass and improved bone strength, particularly in female. WNT16 has high potential for therapeutic interventions to treat osteoporosis or other low bone mass and high bone-fragility conditions.

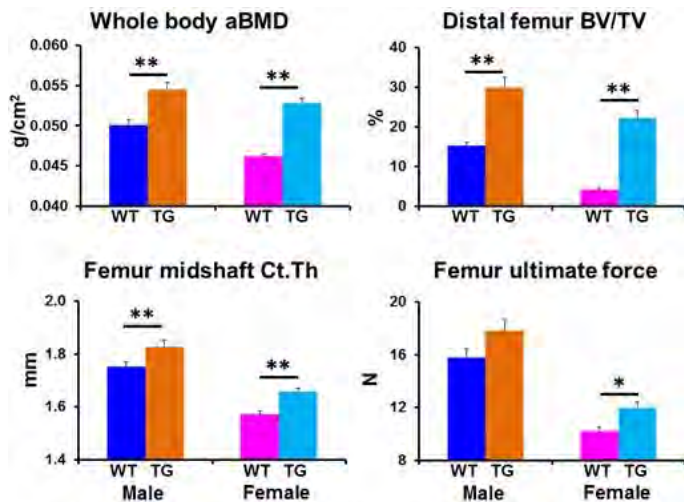


Figure 1. Bone mass and strength improved significantly in *Dmp1-WNT16* transgenic mice in both male and female. WT: wild-type; TG: Transgenic * $p < 0.05$; ** $p < 0.005$

Figure 1

Disclosures: Inranul Alam, None.

FR0107

PHOSPHO1 is Essential for Normal Bone Fracture Healing. Mina Morcos¹, Hadil Al-Jallad², Jose Luis Millan³, Reggie C Hamdy⁴, Monzur Murshed⁵. ¹McGill University, Canada, ²Division of Paediatric Orthopaedic Surgery, Shriners Hospital for Children, Montreal, Canada, ³Sanford-Burnham Medical Research Institute La Jolla, CA, USA, USA, ⁴Division of Paediatric Orthopaedic Surgery, Shriners Hospital for Children, Montreal. Department of Medicine, McGill University, Montreal, QC, Canada, Canada, ⁵Department of Molecular Genetics, Shriners Hospital for Children, Montreal. Department of Medicine, McGill University, Montreal, QC, Canada. Faculty of Dentistry, McGill University, Montreal, QC, Canada, Canada

Introduction: Bone fracture healing is regulated by a series of complex physicochemical and biochemical processes. One of these processes is bone mineralization, which is vital for normal bone development, its biomechanical competence and fracture healing. Phosphatase, orphan 1 (PHOSPHO1), a bone-specific phosphatase, has been shown to be involved in the mineralization of the extracellular matrix in bone. It can hydrolyze phosphoethanolamine and phosphocholine to generate inorganic phosphate, which is crucial for bone mineralization. *Phospho1*^{-/-} mice show hypomineralized bone and spontaneous fractures. All these data led to the hypothesis that PHOSPHO1 is essential for bone mineralization and its structural integrity. However, no study to our knowledge has shown the effects of PHOSPHO1 on bone fracture healing. In this study, we examined how PHOSPHO1-deficiency might affect the healing and quality of the fractured bones in *Phospho1*^{-/-} mice. **Materials and methods:** We performed rodded immobilised fracture surgery on the right tibia of control wild type (WT) and *Phospho1*^{-/-} mice (n=16 for each group) at 8 weeks of age. Bone was left to heal for 4 weeks and then the mice were euthanized and their tibias were analysed using Faxitron X-ray analyses, microCT, histology and histomorphometry. **Results:** Our microCT and X-ray analyses revealed that the appearance of the callus and several static parameters of bone remodeling at the fracture sites were markedly different in WT and *Phospho1*^{-/-} mice. We observed a significant increase of BS/BV, BS/TV and trabecular number and decrease in trabecular thickness and separation in *Phospho1*^{-/-} callus in comparison to the WT callus. These observations were further confirmed by histomorphometry. The increased bone mass at the fracture sites of *Phospho1*^{-/-} mice appears to be caused by increased bone formation as there is a significant increase of osteoblast number, while osteoclast numbers remained unchanged. There was a marked increase of osteoid volume over bone volume (OV/BV) in the *Phospho1*^{-/-} callus. Interestingly, the amount of osteoid was markedly higher at the fracture sites than that of normal trabecular bones. The mechanical properties of these fractured bones are currently being analyzed by 3-point bending tests. **Conclusion:** Our work suggests that PHOSPHO1 plays an integral role during bone fracture repair. PHOSPHO1 can be an interesting target to improve the fracture healing process.

Disclosures: Mina Morcos, None.

FR0110

Integrating genome-wide association and co-expression network data for novel BMD gene discovery. Gina Calabrese¹, Larry Mesner², Joseph Stains³, Steven Tommasini⁴, Mark Horowitz⁴, Clifford Rosen⁵, Charles Farber^{*2}. ¹University of Virginia, USA, ²University of Virginia, USA, ³University of Maryland, USA, ⁴Yale, USA, ⁵Maine Medical Research Institute, USA

Over the last seven years, genome-wide association studies (GWAS) have identified >70 associations for fracture, bone mineral density (BMD) and other fracture-related quantitative traits. While these data represent a treasure-trove of information on novel genes regulating bone strength, it has proven difficult to identify causal genes at associations using genetic data alone. Here, we hypothesized that analyzing GWAS data in the context of a co-expression network could identify putative regulators of BMD and causal GWAS genes. Our approach is based on the idea that groups of causal genes will influence BMD through the same process (e.g. osteoblast-mediated bone formation) and genes involved in the same process are often co-expressed. Therefore, we determined the module membership in a mouse bone co-expression network of 127 genes located in 64 BMD GWAS associations. We found that 25 of the 127 genes were members of two network modules (6 and 9; enrichment $P \leq 0.002$). We previously demonstrated that genes in modules 6 and 9 play key roles in the activity and function of osteoblasts. Of the 25 genes, 18 are well-known regulators of osteoblast activity and BMD, such as *Lrp5*, *Sp7* and *Tnfrsf11b*, demonstrating our ability to recover known BMD genes. To determine if the seven novel candidates were involved in the regulation of BMD, we queried BMD data collected on newly created mouse knockouts by the International Mouse Phenotyping Consortium. Knockout mice for two (*Tcf7l2* and *Spnb2*) of the seven had been characterized. Mice heterozygous for a null allele of *Tcf7l2* (*Tcf7l2*^{+/-}) had increased ($P=0.018$) BMD. In addition, BMD was decreased in female *Spnb2*^{+/-} mice and increased in male *Spnb2*^{+/-} mice (interaction $P=0.0002$). For an additional novel gene, *MARK3*, the network data predicted that it was involved in the regulation of osteoblast differentiation by altering the expression of module 9 genes. We showed that *Mark3* knockdown decreased osteoblast commitment, but increased osteoblast differentiation and mineralization. Additionally, *Mark3* knockout mice had increased femoral BMD, trabecular bone volume fraction (BV/TV) and cortical thickness and specifically altered the expression of module 9 genes. Together, our results identify *Tcf7l2*, *Spnb2* and *Mark3* as novel regulators of BMD and potential causal genes at their respective associations. Our results also highlight the power of using co-expression network data to inform human GWAS.

Disclosures: Charles Farber, None.

FR0111

A Murine Model with Conditional FGF23 Deletion. Erica Clinkenbeard^{*1}, Taryn Cass², Julia Hum², Matt Allen³, Teresita Bellido³, Kenneth White². ¹Indiana University-Purdue University Indianapolis, USA, ²Department of Medical & Molecular Genetics Indiana University School of Medicine, USA, ³Department of Anatomy & Cell Biology Indiana University School of Medicine, USA

Phosphate homeostasis is maintained through FGF23 endocrine actions between bone and kidney. Characterized animal models involving FGF23 are highly informative, defining novel aspects of mineral metabolism. However, these models are limited by shortened life span, inability of fine FGF23 control, and infertility of the global knockout. To improve understanding of FGF23-mediated phosphate handling, a novel conditional-null mouse targeting deletion of FGF23 exon 2 was generated. Initial crosses of the floxed-FGF23 (*FGF23*^{fl/fl}) mice to ubiquitous *Ella*-cre mice were performed. Mice genotyped as fully recombined (*FGF23*^{Δ/Δ}) had undetectable serum intact FGF23 corresponding with elevated serum phosphate ($p < 0.05$) and increased kidney *Cyp27b1* ($p < 0.05$), thus recapitulating the global *FGF23*^{-/-} phenotype. To test functionality of this model, *FGF23*^{fl/fl} and *FGF23*^{Δ/Δ} first underwent targeted recombination with the early osteoblast 2.3kb *Col1a1* (2.3Col)-cre. After challenge with a high phosphate and low calcium diet, Cre⁺ mice had 2-2.4 fold increases in serum intact FGF23 ($p < 0.01$). At baseline, *FGF23*^{fl/fl} and *FGF23*^{Δ/Δ}/Cre⁺ mice exhibited ~50% lower intact FGF23 (133-144 pg/ml vs 75-66 pg/ml; $p < 0.05-0.02$). With dietary challenge, Cre⁺ mice had significantly elevated serum phosphates versus Cre⁻ mice ($p < 0.05-0.02$), whereas intact FGF23 remained restricted to below baseline, control-diet levels (63-88% reduction). *FGF23*^{Δ/Δ}/DMP1-Cre⁺ also had lower basal intact FGF23; however, Cre⁺ mice were less resistant to phosphate challenge (42-46% reduced; $p < 0.05-0.01$) consistent with recombination in more mature FGF23-producing cells. Next, the *FGF23*^{Δ/Δ}/Col2.3-cre was bred onto the Hyp background. As opposed to global *FGF23*^{-/-}/Hyp mice, which assume the biochemical and skeletal FGF23-null phenotype, *FGF23*^{Δ/Δ}/Col2.3-cre⁺/Hyp mice had 5% of the intact FGF23 versus Hyp mice and body and tail lengths comparable to WT. Additionally, μ CT analysis showed *FGF23*^{Δ/Δ}/Col2.3-cre⁺/Hyp had largely normal femur shape and increased metaphyseal trabecular BV/TV at 85+1.09% vs 3+0.9% in Hyp and 13.2+0.01% in WT. In summary, we developed a novel mouse model that undergoes conditional recombination of FGF23, and with bone-specific targeting this animal had reduced hormone levels that were resistant to phosphate challenge. Thus, the ability to suppress FGF23 non-lethally in vivo represents a useful genetic tool to address new questions isolating FGF23 bioactivity in normal and disease states.

Disclosures: Erica Clinkenbeard, None.

FR0112

Limb-specific Klotho Expression Is Required for FGF23 Production During Renal Failure. Jovana Kaludjerovic¹, Hirotaka Komaba¹, Tadatoshi Sato¹, Takenobu Ishii¹, Hannes Olausson², Tobias Larsson², Reinhold Erben³, Beate Lanske¹. ¹Harvard School of Dental Medicine, USA, ²Karolinska Institutet, Sweden, ³University of Veterinary Medicine, Austria

FGF23 has been proposed to be the initial adaptive response to development and progression of acute and chronic kidney disease. Since membrane Klotho (mKL) is expressed in osteoblasts and osteocytes – the major sites of FGF23 synthesis – we hypothesized that mKL may be required by FGF23 locally to induce an autocrine positive feedback loop. We conditionally deleted mKL from long bones in mice using Prx1-Cre and challenged these mice with renal failure by feeding them an adenine diet for 8 weeks. At 16 weeks of age, all mice fed adenine diet had reduced body weight, kidney atrophy, high urea concentrations (80-120 mg/dL) and hyperphosphataemia, confirming induction of renal failure. No differences in these parameters were seen between adenine fed *KL^{fl/fl}* and *Prx1-Cre;KL^{fl/fl}* mice. However, limbs of adenine fed *Prx1-Cre;KL^{fl/fl}* mice did not respond with an increase in *Fgf23* mRNA expression that was observed in adenine fed *KL^{fl/fl}* mice. As such, adenine fed *Prx1-Cre;KL^{fl/fl}* had significantly lower serum iFGF23 levels than adenine fed *KL^{fl/fl}* mice, higher expression of renal 1 α -hydroxylase, hypercalcaemia and severe kyphosis. To validate the results, findings were confirmed in 5/6 NTX *Prx1-Cre;KL^{fl/fl}* mice. Preliminary histomorphometric analyses of femurs (n=4-7/group) showed that *Prx1-Cre;KL^{fl/fl}* had increased number of trabecular osteocytes and osteocyte lacunae volume in response to uremia; but have significantly less mineralized volume, trabecular thickness and connectivity than uremic *KL^{fl/fl}* mice. Osteoblasts cultured from calvaria of newborn *KL^{fl/fl}* mice and stained with alizarin red showed that loss of mKL results in reduced bone mineralization. Therefore, our data is the first to show that limb-specific mKL plays an important role in regulating mineral ion homeostasis and more importantly FGF23 production. This novel data suggests that mKL expression in bone cells might provide a sensing mechanism for the need of FGF23.

Disclosures: Jovana Kaludjerovic, None.

FR0113

Sustained expression of a soluble form of α Klotho prevents aortic calcification and disease phenotypes during chronic hyperphosphatemia. Julia Hum¹, Linda O'Bryan², Arun Tatiparthi³, Robert Johnson⁴, Jonathan Wilson⁴, Erica Clinkenbeard⁵, Tarvn Cass⁵, Rosamund Smith², Kenneth White⁵. ¹Indiana University School of Medicine, USA, ²Biotechnology Discovery Research, Eli Lilly & Company, USA, ³Lead Optimization Pharmacology & Toxicology, Covance Laboratories Inc., USA, ⁴Investigational Pathology, Eli Lilly & Company, USA, ⁵Department of Medical & Molecular Genetics, Indiana University School of Medicine, USA

α Klotho (α KL), the co-receptor for FGF23, is expressed as a membrane-bound protein (mKL) that forms heteromeric complexes with FGF receptors (FGFRs) to initiate intracellular signaling. A circulating form of α KL (cKL) also arises from endoproteolytic cleavage of mKL, however its role in phosphate handling remains unclear. The goal of the present study was to isolate cKL activity in the absence of native α KL, as renal α KL expression during CKD falls with disease progression. In WT mice, and in α KL-null mice where basal serum intact FGF23 levels are already high, 4-week delivery of adeno-associated virus (AAV2/8) carrying cKL (AAV-cKL) at 1011gc/20g mouse resulted in significantly elevated FGF23, compared to respective genotype controls (p<0.05). Consistent with these observations, AAV-cKL induced a >200-fold elevation of bone FGF23 mRNA in WT mice, and a 25-fold increase in already-elevated FGF23 mRNA in α KL-null mice. The α KL-null serum phosphate levels showed >20% reduction with cKL delivery (p<0.01 vs controls). This effect was independent of PTH, which remained suppressed in α KL-null compared to WT animals. Importantly, AAV-cKL prevented aortic calcification in α KL-null mice as tested by μ CT (74% less aorta mineral content, 72% reduced mineral volume; p<0.01), also confirmed by histology. In vitro, UMR-106 cells treated with cKL+FGF23 increased p-ERK1/2 activity, as well as FGF23 mRNA (12-fold; p<0.001), whereas cKL or FGF23 alone had minimal effects. EGFR1 mRNA, a marker for FGFR signaling activity, also responded with a 40-fold maximum increase (p<0.0001), and pretreatment with MEK (10 μ M; U0126) and FGFR inhibitors (80 μ M; PD173074) ablated p-ERK1/2 and EGFR1 responses. Additionally, a novel UMR-106 line with deletion of FGFR1 via CRISPR could not elevate FGF23 mRNA in response to cKL+FGF23. EGFR1 was similarly blunted in this line following treatment with cKL+FGF23 (78%), FGF2 (92%), and FGF8 (86%; all p<0.01). In summary, we demonstrated in a model of hyperphosphatemia and vascular calcification that sustained cKL expression reduced serum phosphate levels and prevented aortic calcification, in the absence of effects on PTH. cKL also stimulated FGF23 in an FGFR1-dependent manner in bone cells. Collectively, these findings support that stable cKL delivery may improve severe manifestations arising from alterations in phosphate homeostasis.

Disclosures: Julia Hum, None.

This study received funding from: Eli Lilly and Company

FR0115

AMG 416 Prevented Cortical Porosity and Preserved Bone Strength in 5/6 Nephrectomized Rats with Established Secondary Hyperparathyroidism. Longchuan Yu¹, Frank Asuncion¹, Shawn Alexander¹, Kelly Hensley¹, Chun-Ya Han², Denise Dwyer³, Qing-Tian Niu¹, Marina Stolina¹, Charley Dean Jr¹, Michael Ominsky¹, William Richards¹, Xiaodong Li¹. ¹Amgen Inc., USA, ²Amgen, Inc., USA, ³Amgen, Inc, USA

Continuous elevation of parathyroid hormone (PTH) is catabolic to cortical bone, causing deterioration in cortical bone structure (eg, cortical porosity), and is a major factor for increased fracture risk in chronic kidney disease. AMG 416, a peptide agonist of calcium-sensing receptor, reduces PTH levels in patients on hemodialysis with secondary hyperparathyroidism (SHPT) in clinical studies. We hypothesized that AMG 416 would prevent the cortical bone deterioration by reducing PTH in a rat model of established SHPT. Twelve-week-old male 5/6 nephrectomized (5/6 Nx) rats were fed a special diet containing high phosphate (0.9%) and low calcium (0.6%) to further induce SHPT. Sham-operated rats were used as non-SHPT controls. Following 8 weeks on the special diet, rats were chosen with a baseline PTH level > 750 pg/mL (SHPT rats) and were subcutaneously injected daily with vehicle or AMG 416 for 6 weeks. Prior to treatment, SHPT rats had significant increases in serum creatinine (2-fold), blood urea nitrogen (BUN, 3-fold), PTH (5-fold), FGF-23 (13-fold) and osteocalcin (12-fold, a marker of bone turnover) compared with the non-SHPT controls. Serum creatinine and BUN continued to increase in both vehicle- and AMG 416-treated SHPT rats during the treatment period. PTH, FGF-23 and osteocalcin continued to increase in vehicle-treated SHPT rats, but were significantly reduced in AMG 416-treated SHPT rats (-96%, -64% and -38%, respectively at day 42). At the end of treatment, vehicle-treated SHPT rats had significantly increased cortical porosity (8.3% in SHPT vs 0.07% in non-SHPT) and lower energy to failure (-30%), a bone strength endpoint, compared with non-SHPT controls. In contrast, cortical porosity was significantly lower (-72%) and energy to failure was significantly greater (+54%) in the AMG 416-treated SHPT rats than in vehicle-treated SHPT rats. These results demonstrated that AMG 416 prevented cortical porosity and preserved bone strength by reducing PTH in 5/6 Nx rat model of established SHPT.

Disclosures: Xiaodong Li, Amgen Inc.

This study received funding from: Amgen Inc.

FR0117

Continuous PTH Treatment Induces Bone Loss through G α S Signaling in T cells. Jau-Yi Li¹, Jerid W. Robinson², Abdul Malik Tyagi², Jonathan Adams², Neal M. Weitzmann², Roberto Pacifici². ¹Emory University School of Medicine, USA, ²Emory University, USA

Hyperparathyroidism in humans and continuous PTH treatment (cPTH) in mice stimulate bone resorption and cause bone loss by regulating RANKL production by osteocytes and osteoblasts. T cells markedly potentiate the bone catabolic effect of cPTH by secreting the osteoclastogenic cytokine TNF, a factor that potentiates the osteoclastogenic activity of RANKL. TNF produced by T cells is required for cPTH to expand Th17 cells and induce the production of the osteoclastogenic factor IL-17. IL-17 is an upstream cytokine that induces RANKL production by osteocytes and osteoblasts. PTH binding to its receptor PPR activates G protein α (G α S). Activation of G α S has been shown to induce the differentiation of Naive CD4+ cells into Th17 cells. Therefore, cPTH could further upregulate Th17 differentiation by activating G α S in naive CD4+ T cells. To investigate this hypothesis, we generated G α S^{ACD4,8} mice by crossing C57BL6 G α S fl/fl mice with C57BL6 CD4-Cre mice. The targeted genetic deletion of G α S with CD4-Cre occurs at the CD4+CD8+ double positive stage of T cell development. Consequently both CD4+ and CD8+ T cells from G α S^{ACD4,8} mice lack G α S expression. We found that in vivo cPTH treatment (80 μ g/kg/day subcutaneously for 2 weeks) increased the frequency of BM Th17 ~3 fold in control G α S fl/fl mice, but not in G α S^{ACD4,8} mice. μ CT measurements revealed that cPTH induced significant losses of femoral trabecular and cortical bone in G α S fl/fl mice but not in G α S^{ACD4,8} mice. Furthermore, cPTH increases serum CTX (a marker of bone resorption) in G α S fl/fl but not in G α S^{ACD4,8} mice. Conversely, cPTH increases serum PINP (a marker of bone formation) in all strains. Signaling events downstream of G α S include cAMP generation and activation of L-type calcium channels. The latter contributes to Th17 cell differentiation. To determine if Ca²⁺ influx is required for Th17 cell expansion induced by cPTH, we fed mice with water with or without the L-type calcium channel blocker diltiazem and infused them with vehicle and cPTH. Diltiazem blocked the increase in the number of BM Th17 cells, and the loss of cortical and trabecular bone induced by cPTH. Moreover, diltiazem blocked the increase in serum CTX levels but not the increase in serum PINP induced by cPTH. In summary, these findings demonstrate that cPTH causes bone loss by expanding Th17 cells via C α S/cAMP/Ca²⁺ signaling. Calcium channel blockers may thus represent novel therapeutic strategies for hyperparathyroidism.

Disclosures: Jau-Yi Li, None.

FR0118

CRISPR-mediated RUNX2 Deletion Delineates Mechanisms of Gene Expression throughout Osteoblast Differentiation and Mineralization. Mark Meyer*, Nancy Benkusky, J. Wesley Pike. University of Wisconsin-Madison, USA

RUNX2 (CBFA1) is a vital transcription factor for osteoblast maturation and function. RUNX2 forms complexes with transcription factors at enhancers located near essential osteoblast genes and contributes to their expression. Using a CRISPR/Cas9 deletion approach, we generated a unique cell culture knockout model of RUNX2 in UAMS-32P cells, a clonal osteoblastic line that stably expresses hPTH1R. Unlike its parental counterpart, these RUNX2 KO cells cannot differentiate or mineralize and exhibit retarded growth, all functions restored via lentivirus mediated re-expression of RUNX2. Many osteoblastic genes have distal enhancers that are RUNX2 dependent, as loss of RUNX2 greatly affects the binding of other factors to the same, or neighboring, enhancers as assayed by direct ChIP analysis. Accordingly, we see large reductions in the expression of genes that include *Enpp1/3*, *Bmp4*, and *Mmp13*; *Hdac4*, however, was only modestly reduced. Loss of RUNX2 prevents Osterix (*Sp7*), *Alpl*, *Igf1bp5*, and *Col2a1* expression, consistent with the cell's lack of differentiation. Finally, RUNX2 deletion had no effect on the expression of *Mgp*, *Cbs*, or several additional *Hdac* genes despite significant RUNX2 binding at major enhancers for these genes. The CRISPR approach was also used to prepare additional daughter cell lines containing mutations specifically within the *Mmp13* gene locus that permitted evaluation of the effects of 1,25(OH)₂D₃ on *Mmp13* expression. This enabled us to demonstrate a dual interplay between RUNX2 and the VDR at *Mmp13* and at sites across the UAMS-32P genome as well. These mutant lines have also allowed us to explore the impact of PTH and forskolin on the expression of *Mmp13* and other bone genes. PTH regulation of *Mmp13* is believed to be mediated through a region proximal to the promoter that is RUNX2 dependent and involves both HDAC4 and PKA signaling. However, deletion of this region in UAMS-32P cells had little effect on *Mmp13* expression induced by either PTH or the VDR. On the other hand, the activity of PTH at *Mmp13* was fully abrogated by deletion of a RUNX2-enriched enhancer located 30 kb up-stream of the *Mmp13* gene as well as through global deletion of RUNX2. Our CRISPR mouse model of *Mmp13* expression, now established, will allow us to confirm principles of *Mmp13* gene regulation *in vivo*, extend our understanding of *Mmp13* expression by RUNX2, and explore atherosclerotic disease models in which aberrant *Mmp13* expression may be involved.

Disclosures: Mark Meyer, None.

FR0120

LRP6 Is Required For PTH-Induced SOST Suppression. CHANGJUN LI*¹, Liang Xie², Xu Cao², Mei Wan². ¹Johns Hopkins University School of Medicine, USA, ²Department of Orthopaedic Surgery, Johns Hopkins University School of Medicine, Baltimore, MD 21205, USA, USA

Parathyroid hormone (PTH) suppresses the expression of a bone formation inhibitor sclerostin (SOST) in osteocytes by inducing nuclear accumulation of histone deacetylases (HDACs) to inhibit the myocyte enhancer factor 2 (MEF2)-dependent SOST bone enhancer. We previously demonstrated that lipoprotein receptor-related protein 6 (LRP6) mediates intracellular signaling activation elicited by PTH in osteoblastic lineage cells. Importantly, LRP6 is indispensable for PTH anabolic action on bone in mice. Here, we investigated whether LRP6 mediates the inhibitory effect of PTH on SOST using osteoblast-specific LRP6-knockout (LRP6 KO) mice, which were generated by crossing mice expressing the Cre recombinase driven by the human osteocalcin promoter (OC-Cre) with mice expressing loxP-flanked Lrp6 (*Lrp6^{fl/fl}*). Immunohistochemical analysis revealed that LRP6 expression was detected in most (approximately 75%) of the osteocytes in cortical bone of femora in wild type mice, but only in a small portion (about 23%) of osteocytes in femurs of the KO mice. Thus, LRP6 is deleted in most of the osteocytes in LRP6 KO mice. An increased level of SOST mRNA expression was detected in femur tissue from LRP6 KO mice relative to their wild type littermates. The number of osteocytes expressing sclerostin was also increased in bone tissue of LRP6 KO mice, indicating a negative regulatory role of LRP6 on SOST/sclerostin. We then examined the changes of SOST gene and sclerostin in osteocytes in femur tissue from WT mice and LRP6 KO mice after daily injection of either PTH(1-34) or vehicle for 4 weeks. Intermittent PTH treatment significantly suppressed SOST mRNA expression in femur tissue and the number of sclerostin+ osteocytes in WT mice relative to vehicle-treated mice, while this effect of PTH was much less significant in LRP6 KO mice. Thus, the suppressive effect of PTH on SOST/sclerostin in osteocytes was alleviated by LRP6 deficiency. It is known that HDACs interact with MEF2 transcription factor, and the MEF2-HDAC axis mediates the effect of PTH on SOST repression. In PTH-treated mice, MEF2C and 2D were down-regulated and the HDACs were also changed in osteocytes of femur tissue as detected by both immunohistochemical analysis and qRT-PCR. The changes of MEFs and HDACs were abrogated in LRP6 KO mice. Therefore, LRP6 mediates PTH effect on HDAC-MEF-SOST axis, providing an additional dimension to the current understanding of LRP6-mediated PTH bone action.

Disclosures: CHANGJUN LI, None.

FR0122

The large variant of the stimulatory G protein alpha-subunit XL α s mediates early postnatal regulation of renal phosphate handling by enhancing IP3/DAG signaling. Qing He*¹, Yan Zhu¹, Braden Corbin¹, Antonius Plagge², Murat Bastepe¹. ¹Massachusetts General Hospital, USA, ²University of Liverpool, United Kingdom

GNAS encodes the alpha-subunit of the stimulatory G protein (G α s), as well as its large variant XL α s. Through production of cAMP, G α s mediates the actions of multiple molecules, including parathyroid hormone (PTH), which promotes phosphate excretion and vitamin D activation in renal proximal tubules. PTH also activates G α _{q/11} signaling to regulate renal phosphate handling. XL α s can mimic the actions of G α s and mediate PTH-induced cAMP signaling when overexpressed. However, although alterations in XL α s level/activity are implicated in various diseases, its cellular roles have remained unclear. Here we determined that XL α s is expressed in renal proximal tubules early postnatally. At postnatal day 2 (P2) XL α s knockout mice (XLKO) exhibited hyperphosphatemia/hypocalcemia with elevated plasma PTH and 1,25 dihydroxyvitamin D. The level of sodium-phosphate co-transporter Npt2a was increased in renal brush border membranes, as well as the renal expression of vitamin D metabolizing enzymes Cyp27b1 and Cyp24a1. In addition, PTH-induced reduction of serum phosphate and downregulation of Npt2a were significantly blunted. Nevertheless, PTH-induced urinary cAMP excretion was modestly increased. Instead, XLKO pups showed repressed basal and PTH-stimulated G α _{q/11} signaling with diminished IP3 generation and reduced levels of certain PKC isoforms in proximal tubules. Hyperphosphatemia and elevated renal Cyp27b1 mRNA in XLKO pups, as well as reduced PKC levels in proximal tubules, were rescued by proximal tubule-specific overexpression of XL α s. Overexpression of XL α s in transgenic mice and in transfected HEK293 cells promoted G α _{q/11} signaling basally and in response to PTH. Thrombin, another agonist that stimulates G α _{q/11} signaling via its own endogenous receptor, also induced higher IP3 generation in HEK293 cells transfected with XL α s cDNA than in vector transfected cells. Moreover, XL α s expression recovered thrombin-induced IP3 generation in G α _{q/11}-/- HEK293 cells in which G α _q and G α ₁₁ were ablated through the use of CRISPR/Cas technology. Our findings indicate that XL α s mediates proximal tubular PTH actions during early postnatal development by mimicking, at least partly, the actions of G α _{q/11} to promote IP3/DAG signaling.

Disclosures: Qing He, None.

FR0124

Androgen receptor signaling in mesenchymal lineage cells suppresses soluble RANKL production, cancellous osteoclast number, and B lymphopoiesis. Semahat Serra Ucer*¹, Srividhya Iyer², Ha-neui Kim², Shoshana M Bartell², Aaron D Warren³, Li Han², Julie A Crawford², Charles A O'Brien², Maria Jose Almeida², Stavros C Manolagas². ¹University of Arkansas for Medical Sciences, USA, ²Center for Osteoporosis & Metabolic Bone Diseases, Central Arkansas Veterans Healthcare System, University of Arkansas for Medical Sciences, USA, ³Central Arkansas Veterans Healthcare System, University of Arkansas for Medical Sciences, USA

Androgens are critical for the acquisition and maintenance of bone mass in both the cortical and cancellous bone compartment, but the cellular and molecular mechanisms responsible for these effects remain poorly understood. It has been shown earlier that the anti-resorptive effects of androgens on cancellous bone result from androgen receptor (AR) signaling in cells of the mesenchymal lineage and a decrease in osteoclast numbers – but not from direct actions on osteoclasts. In addition, osteocyte-derived RANKL is critical for bone remodeling in the cancellous compartment in mice; the number of B lymphocytes increases in the bone marrow of rodents after loss of either estrogen or androgens; and B lymphocyte-derived RANKL contributes to the loss of cancellous bone caused by estrogen deficiency (OVX). In search of molecular mechanisms of the anti-resorptive effects of androgen on cancellous bone, male AR^{fl/y};Prx1-Cre mice and AR^{fl/y} littermates were euthanized at 16 weeks of age. In addition, C57BL/6 wild type mice were sham operated or orchidectomized at 20 weeks of age and euthanized 6 weeks later. In both experiments, bone marrow plasma was obtained at the time of harvest and soluble RANKL levels as well as the percentage of pre B (B220⁺/CD43⁺) and B (CD19⁺) lymphocytes were determined. Both AR deletion from cells of the mesenchymal lineage or orchidectomy (ORX) increased the levels of soluble RANKL by 85% and 248%, respectively. Similarly, AR deletion or ORX increased the percentage of pre B lymphocytes in the bone marrow by 32% and 161%, and the percentage of B lymphocytes by 27% and 133%, respectively. Nonetheless, RANKL mRNA levels on a per cell base was no different in B lymphocytes from either model. Collectively, our findings support the conclusion that androgen signaling via the AR expressed in cells of the mesenchymal lineage and their descendants, most likely osteocytes, restrains soluble RANKL production as well as the total number of B cells expressing RANKL rather than the expression level per B cell; and thereby restrains osteoclastogenesis. The greater increase in soluble RANKL and B lymphocyte percentage in the bone marrow of androgen deficient mice, as compared to mice with the targeted AR deletion in mesenchymal progenitors (AR^{fl/y};Prx1-Cre), raises the possibility that direct effects of androgens on other cell types, including B lymphocyte themselves, also contribute to their influence on RANKL and cancellous bone resorption.

Disclosures: Semahat Serra Ucer, None.

FR0125

Conditional knockout of progesterone receptor in the osteoprogenitor cells, but not in the mature osteoblasts, increases trabecular bone formation. Zhendong Zhong^{*1}, Weihua Sun², Haiyan Chen², Yu-an Lay², Nancy Lane², Wei Yao². ¹University of California, Davis, USA, ²Musculoskeletal Research Unit, Department of Medicine, University of California Davis Medical Center, Sacramento, CA 95817, USA., USA

Sexual dimorphism in bone is well known; men tend to have higher peak bone mass than women. Our laboratory and another group previously reported that global progesterone receptor knockout (PRKO) mice displayed a high-bone-mass phenotype (Rickard, 2008; Yao, 2010). **Methods.** To further elucidate the role of progesterone receptor (PR) in osteoprogenitor cells and osteoblasts, bone-specific PR conditional knockout mice were generated in our laboratory by crossing PR-flox mice to either Prx1-Cre or Bglap-cre mice. Bone mass acquisition, bone turnover and bone mechanical properties were evaluated at the age of 2 and 6 months in both sexes. **Results.** We first used genetic fate-mapping approaches (PR-cre;tdTomato; Col1(2.3kb)-GFP) to demonstrate that the PR could be expressed by the cells on bone surface (primarily trabeculae) after 1 month of age, and these PR+ cells rarely expressed mature osteoblast marker Col1a1. PR protein measured by western blot was only detected at the femoral epiphysis and metaphysis, but not at the diaphysis. In line with the PR expression pattern in bone, no significant skeletal change was identified in Bglap-Cre-driven (mature osteoblast-specific) PR conditional knockout mice. In contrast, we observed 50-100% higher trabecular bone volume in distal femurs, as well as significantly higher serum osteocalcin levels, in Prx1-Cre-driven heterozygous/homozygous male and homozygous female PR knockout mice at 2 and 6 months of age. Bone size and femur length were similar between Prx1-Cre-driven mutant and WT controls. No significant phenotypic change was observed in cortical bone of femurs from 6-month-old Prx1-Cre;PR-flox mice by microCT analyses and 3-point bending tests, probably due to the lack of PR expression in the diaphyses. Mechanistically, we found ~40% higher MSC-like population (CD105+CD29+Scal+CD45-) in bone marrow stromal cells from male homozygous Prx1-Cre;PR-flox knockout mice at 2 and 6 months of age; and the PR-deficient BMSCs exhibited higher osteogenic differentiation in vitro. Further investigations are ongoing to decipher the PR signaling cascades involved in bone formation and attainment of peak bone mass. **Conclusions.** Inactivation of the PR in Prx1+ osteoprogenitor cells resulted in higher trabecular bone mass and bone formation in both sexes. Our results reveal PR in osteoprogenitor cells to be a potential target for bone mass augmentation.

Disclosures: Zhendong Zhong, None.

FR0126

ER α Expression in T Lymphocytes is Dispensable for Estrogenic Effects in Bone. Karin Gustafsson^{*1}, Annica Andersson², Helen Farman², Vikte Lionikaite², Petra Henning², Jianyao Wu², Sara Windahl², Merja Nurkkala Karlsson², Angelina Bernardi², Ulrika Islander², Sofia Skrtic², Klara Sjögren², Claes Ohlsson², Marie Lagerquist². ¹University of Gothenburg, Sweden, ²Centre for Bone & Arthritis Research, Institute of Medicine, University of Gothenburg, Sweden

It is well established that estrogen withdrawal has deleterious effects in the skeleton and that estrogen signaling, via estrogen receptor alpha (ER α), counteracts this negative effect. ER α signaling in mesenchymal cells, including osteoprogenitor cells, is known to affect bone mass. However, T lymphocytes are implicated to be involved in bone loss caused by estrogen deficiency and we recently showed that ER α expression in hematopoietic cells affects the degree of bone response to estrogen treatment. The aim of this study was therefore to determine the role ER α expression in T lymphocytes both for ovariectomy (ovx)-induced bone loss and for the estrogen treatment response in bone.

Lck-ER $\alpha^{fl/fl}$ mice, lacking ER α expression in T cells, were generated by crossing Lck-Cre mice with ER $\alpha^{fl/fl}$ mice, carrying a floxed ER α exon 3, and compared to ER $\alpha^{fl/fl}$ littermates. The effectiveness of ER α gene deletion was demonstrated by an 84% (p<0.001) reduction in ER α mRNA levels in T lymphocytes (CD3-positive cells) in thymus. 12-week-old mice were sham-operated or ovx and treated with estradiol (E2; 167ng/mouse/day) or vehicle for 4 weeks. At termination the mice were subjected to a DEXA scan and the tibiae were dissected and analyzed using pQCT.

The total bone mineral density (BMD), measured by DEXA, did not differ between sham-operated Lck-ER $\alpha^{fl/fl}$ mice and ER $\alpha^{fl/fl}$ controls. OvX decreased total body BMD to a similar extent in both genotypes (Lck-ER $\alpha^{fl/fl}$; -4.2%, p<0.05, ER $\alpha^{fl/fl}$; -5.7%, p<0.05) and the estrogenic responses in total body BMD were equal (Lck-ER $\alpha^{fl/fl}$; +16%, p<0.001, ER $\alpha^{fl/fl}$; +18%, p<0.001). No significant difference in trabecular BMD, measured by pQCT, was detected between sham-operated mice Lck-ER $\alpha^{fl/fl}$ mice and ER $\alpha^{fl/fl}$ controls and the decrease was equal in both genotypes after ovx (Lck-ER $\alpha^{fl/fl}$; -35%, p<0.01, ER $\alpha^{fl/fl}$; -23%, p<0.001). Furthermore, the E2 response in trabecular BMD was similar in Lck-ER $\alpha^{fl/fl}$ mice (+281% p<0.001) and ER $\alpha^{fl/fl}$ controls (+338% p<0.001).

In conclusion, ER α expression in T lymphocytes is not required for ovx-induced bone loss or the estrogen treatment response in bone.

Disclosures: Karin Gustafsson, None.

FR0127

The role of osteocyte estrogen receptor beta (ER β) in regulating skeletal growth, aging, and the skeleton's anabolic response to physical stimuli. Maxime Gallant¹, Haisheng Yang¹, Whitney Bullock², Teresita Bellido³, Russell Main^{*1}. ¹Purdue University, USA, ²Indiana University Purdue University Indianapolis, USA, ³Indiana University School of Medicine, USA

Sex hormones are key contributors to skeletal health. However, the effects of estradiol on skeletal anabolic pathways are still not well defined. While osteocytes are critical regulators of bone formation, osteocyte estrogen receptor alpha (ER α) has limited effects in the growing skeleton and response to mechanical load. These results call for a better understanding of skeletal ER β , which has been proposed as an inhibitor of skeletal mechanotransduction. Our goal is to characterize the role of osteocyte ER β in regulating bone structure during growth, aging, and the response to mechanical stimuli. Mice lacking osteocyte ER β were generated by Cre-LoxP recombination driven by DMP1-8kb-Cre. Male and female mice with osteocyte deletion of ER β (KO) and littermate control mice (LC) were (i) sacrificed at 4 or 7wks old or (ii) began 2wks of unilateral tibial loading at 10 or 26wks old (12 and 28wks old at sacrifice). Serum estradiol and testosterone analyses were conducted in 4, 7, and 28wks old. MicroCT analyses of the tibiae and L5 vertebrae were conducted and genotypic differences tested by t-test. Load-genotype interactions were tested by linear mixed model with repeated measures.

We found no genotype-related differences in serum hormones. There were few phenotypic differences between KO and LC mice at 4, 7, or 12wks of age. Osteocyte-specific ER β deletion had sex-dependent effects on bone mass at 28wks. Tibial midshaft Ct.Ar (+17%) and proximal cancellous BV/TV (+83%) were increased in male KO relative to LC mice. By contrast, cancellous BV/TV was reduced in 28wk female KO relative to LC mice (-38%). Similar cancellous patterns were seen in L5. While loading had an anabolic effect in the cancellous and cortical tissues in 12wk old tibiae, no interactive effect of genotype was found. 28wk female mice showed a strong midshaft response to load, but no genotypic interaction. At a site 37% of the tibia's length from the proximal end, 28wk female KO mice showed a greater load-induced increase in Ct.Ar than LC mice (+46% vs. +35%). Similarly, Tb.Th in the proximal tibia increased more in the 28wk female KO mice than in LC mice (+28% vs. +8%). 28wk old male mice did not respond strongly to tibial loading.

Osteocyte ER β plays an important role in regulating bone turnover in adult mice and the anabolic response to physical stimuli, especially in adult female mice. The cellular mechanisms underlying these structural outcomes are presently being investigated.

Disclosures: Russell Main, None.

FR0128

Common polymorphism in Vitamin D 25-hydroxylase gene (CYP2R1) abrogates promoter activity and is associated with low serum 25OHD in a Caucasian pediatric cohort. Jeff Roizen^{*1}, Alex Casella², Jonathan Bradford², Meizan Lai², Hakon Hakonarson², Michael Levine². ¹The Childrens Hospital of Philadelphia, USA, ²The Children's Hospital of Philadelphia, USA

Optimal bone and mineral metabolism, as well as immune and cardiovascular function, depend on normal vitamin D metabolism. Ineffective sunlight exposure and inadequate dietary vitamin D each have well understood roles in the pathophysiology of vitamin D deficiency; however, the extent to which common variations or polymorphisms in genes encoding vitamin D metabolizing enzymes contribute to vitamin D homeostasis remains unknown. Several genome wide association studies (GWAS) have identified significant associations between serum [25(OH)D] and single nucleotide polymorphisms (SNPs) in or near the locus for CYP2R1, the gene encoding the principal vitamin D 25-hydroxylase enzyme. To examine whether SNPs in the CYP2R1 promoter alter transcriptional activity we introduced single base changes corresponding to the minor alleles of several SNPs into the 5 kb CYP2R1 promoter fragment that directs transcription of firefly luciferase in a hybrid reporter construct. Reporter constructs containing the wild type CYP2R1 promoter reporter or the minor allele of promoter SNPs (rs2060793, rs10741657, rs1562902, rs16930609 and rs7949459) plus a Renilla luciferase reporter were used to transfect LnCap cells, a human prostate carcinoma cell line that expresses CYP2R1 in a regulated fashion. The wild-type promoter showed significantly (p < 0.001 one way ANOVA) greater activity than a promoterless luciferase reporter (3.58 \pm 0.51 vs 1.00 \pm 0.00 (mean \pm SD)). Four of the five promoter polymorphisms (rs2060793, rs10741657, rs1562902 and rs16930609) showed similar luciferase activity compared to wild-type promoter (2.73 \pm 0.35 to 3.51 \pm 0.29 (mean \pm SD)). By contrast, the SNP rs7949459 showed an 85% reduction in luciferase activity compared to wild type promoter (0.58 \pm 0.07 vs 3.58 \pm 0.51, p < 0.001). This SNP is in high linkage disequilibrium with the commonly nearby SNPs identified in GWAS for 25(OH)D (for each of rs10500804, rs10741657, and rs10766192, D > 0.98). The 1000 Genomes database indicates that the minor allele of this SNP occurs in more than 10% of the population, however, it is not present on chips used for genotyping in GWAS. Therefore we used IMPUTE2 to determine the presence of this allele in a sample of 440 Caucasian children representing a population based cohort recruited by the Center for Applied Genomics at CHOP (info score of 0.933). Using logistic regression we tested for an association between allelic dosage and serum 25(OH)D levels expressed as quartiles. Presence of a

single rs7949459_T allele was associated as a continuous variable with 25(OH)D (beta= -0.35, SE=0.15, p=0.02). Our biochemical results provide evidence that this common genetic variation in *CYP27R1* has significant effects on transcription of *CYP27R1*, and our genetic studies provide a functional context for interpreting GWAS that show relationships between circulating 25(OH)D and *CYP27R1*.

Disclosures: Jeff Roizen, None.

FR0129

Conditional Knockout of Osteoblast Vitamin D Receptor and CYP27B1 Implicates Cell-Specific Receptor Signaling but Not Cell-Specific 1,25-dihydroxyvitamin D Production in the Maintenance of Trabecular and Cortical Bone Mass in Male and Female Mice. Tsui-Hua Chen, Amanda Herberger*, nathan liang, Alfred Li, daniel Bikle, wenhan chang, Dolores Shoback, UCSF, USA

Many tissues important in systemic calcium (Ca²⁺), phosphate, and bone homeostasis express both the vitamin D receptor (VDR) and CYP27B1 (1-alpha hydroxylase) and thus can locally produce and respond to 1,25-dihydroxyvitamin D [1,25-(OH)₂D] in an autocrine/paracrine manner. Such tissues include the parathyroid, kidney, and bone. Progress has been slow in understanding the role of locally produced 1,25-(OH)₂D on VDR actions in both local and distant endocrine actions of 1,25-(OH)₂D since global knockout (KO) mice show altered serum minerals and hormones as well as secondary bone and cartilage pathology. To test the role of the osteoblast (OB) VDR and of OB-produced 1,25-(OH)₂D, we generated OB-specific conditional KO's of VDR [^{OB}VDR(-/-)] and of CYP27B1 [^{OB}CYP27B1(-/-)] by crossing floxed VDR (gift of S. Kato) and floxed CYP27B1 (gift of R. St-Arnaud) with mice expressing Cre recombinase under control of the rat 2.3 kb Col1 promoter (gift of D. Rowe). We assessed mass and microstructure by computed tomography (CT) of trabecular (Tb) and cortical (Cort) bone at the distal femur and tibio-fibular junction, respectively, and mineral and hormonal parameters in male and female homozygous KO mice and control littermates at 12 weeks of age. Tb bone volume/tissue volume (BV/TV) was significantly greater in both female and male ^{OB}VDR(-/-) vs control mice – with increased connectivity and decreased structural model index (SMI) in females and increased Tb thickness in males (see Table; N=18-26 mice). Cort BV/TV and Cort thickness were significantly greater in both female and male ^{OB}VDR(-/-) vs control mice (see Table). In contrast, mice with deletion of CYP27B1 in OB's were not significantly different in their Tb and Cort bone parameters compared with their control littermates of the same sex (not shown; N=18-24 mice). Serum Ca²⁺, phosphate and alkaline phosphatase levels did not differ in ^{OB}VDR(-/-) vs control mice or in ^{OB}CYP27B1(-/-) vs control mice of either sex (data not shown, N=18-24 mice). Thus, the VDR expressed in OB's plays a key role in maintaining skeletal homeostasis in both male and female mice. Targeted inactivation of VDR produces mild osteopenia at both Tb and Cort bone sites. Local production of 1,25-(OH)₂D, however, is not required for maintenance of adult bone mass and structural properties in mice of either gender, supporting the dominance of endocrine vs paracrine/autocrine sources of 1,25-(OH)₂D in bone metabolism.

| | Control (N=18) | ^{OB} VDR (-/-) (N=18) | P value |
|---|-----------------|--------------------------------|--------------------|
| FEMALE | | | |
| Trabecular Parameter | | | |
| BV/TV (%) | 0.0663 ± 0.0033 | 0.0813 ± 0.0045 | 0.006 |
| Connectivity density (1/mm ³) | 91.4 ± 7.8 | 119.1 ± 12.1 | 0.0032 |
| SMI | 2.776 ± 0.047 | 2.586 ± 0.058 | 0.0077 |
| Number (1/mm ³) | 3.484 ± 0.081 | 3.656 ± 0.136 | ns |
| Thickness (mm) | 0.0427 ± 0.0018 | 0.0444 ± 0.0011 | ns |
| Spacing (mm) | 0.2931 ± 0.0072 | 0.2826 ± 0.0114 | ns |
| Cortical Parameter | | | |
| BV/TV (%) | 0.6515 ± 0.0047 | 0.6756 ± 0.0090 | 0.013 |
| Thickness (mm) | 0.2089 ± 0.0023 | 0.2232 ± 0.0050 | 0.007 |
| MALE | | | |
| Trabecular Parameter | | | |
| BV/TV (%) | 0.1423 ± 0.0052 | 0.1603 ± 0.0094 | 0.05 |
| Connectivity density (1/mm ³) | 278.6 ± 17.1 | 275.9 ± 16.8 | ns |
| SMI | 2.151 ± 0.058 | 2.011 ± 0.077 | ns |
| Number (1/mm ³) | 5.334 ± 0.124 | 5.134 ± 0.1451 | ns |
| Thickness (mm) | 0.0427 ± 0.007 | 0.0482 ± 0.0018 | 0.004 |
| Spacing (mm) | 0.1877 ± 0.0045 | 0.1966 ± 0.0059 | ns |
| Cortical Parameter | | | |
| BV/TV (%) | 0.6470 ± 0.0047 | 0.7114 ± 0.0054 | < 0.0001 |
| Thickness (mm) | 0.2283 ± 0.0033 | 0.2662 ± 0.0045 | < 0.0001 |

VDR-Table

Disclosures: Amanda Herberger, None.

FR0131

A transcriptomic analysis of cortical versus cancellous bone from mechanically-loaded murine tibiae reveals ERα-dependent differential changes in gene expression. Natalie Kelly*¹, John Schimenti¹, F Patrick Ross², Marjolein van der Meulen¹. ¹Cornell University, USA, ²Hospital for Special Surgery, USA

In postmenopausal osteoporosis decreased estrogen signaling, in part via the receptor ERα, contributes to reduced bone mass. Mechanical loading increases bone mass differentially in cortical (Ct) and cancellous (Cn) bone at the tissue level. We recently showed that mice lacking ERα in osteoblasts and osteocytes (pOC-ERαKO) had an increased adaptive response to mechanical loading in Cn bone [1], but little is known about the molecular mechanisms. Here we used RNA-seq to identify molecular changes during Ct and Cn adaptation to tibial loading in pOC-ERαKO and littermate control (LC) mice.

Tibiae from LC and pOC-ERαKO mice (10-wk female) underwent one session of mechanical loading with the contralateral tibia as control [3]. Three hours (LC, n=4; pOC-ERαKO, n=2) and 24 hours (LC, n=4) after loading a Cn core was removed from the Ct shell of the metaphysis, and RNA was isolated (LC: Ct and Cn; pOC-ERαKO: Cn only) [2]. mRNA was processed for RNA-seq (100bp, single-end). Sequences were aligned (TopHat), and differential expression determined by a paired design (DE >1.5-fold, EdgeR). Enriched pathways were determined (DAVID).

Ct and Cn bone respond differently at 3 and 24h in LC: More genes were DE in Ct than Cn bone at 3h (43 vs 18), with only 11 genes common to both sites (fig 1A). In both sites, a majority of genes were upregulated. Wnt signaling was enriched in Ct and Cn bone, while hedgehog signaling was enriched only in Ct. At 24 hours, more genes were DE in Ct than Cn (57 vs 32), with 12 shared genes (fig 1B). More genes were upregulated in Ct (60%) and downregulated in Cn (66%). Enriched pathways included melanogenesis in Ct and tight junction in Cn. Loaded Ct bone shared 4 genes between time points (*Wnt1*, *Wnt10b*, *Prgs2*, *Mt2*), while loaded Cn bone shared 1 gene (*Timp1*).

pOC-ERαKO response increased in Cn bone over LC at 3h: More genes were DE in Cn bone of pOC-ERαKO mice than LC (71 vs 18). The fold-change of the 12 shared genes was 1.3-4.2X higher in pOC-ERαKO than LC mice (figure 2).

The increased gene expression in Cn bone of pOC-ERαKO agrees with our previous tissue-level data showing enhanced response to loading [1]. RNA-seq analysis of *in vivo* mechanical loading response in Ct and Cn bone separately provides transcriptome level data to identify new research targets and identify estrogen's role in mechanotransduction.

[1] Melville et al. 2015 [2] Kelly et al. 2014 [3] Lynch et al. 2010

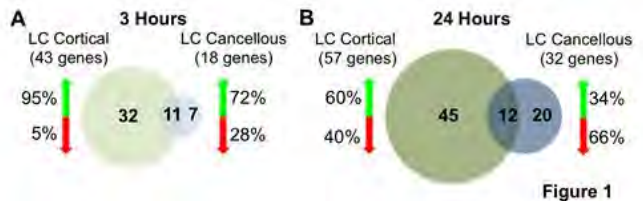


Figure 1

Fig 1

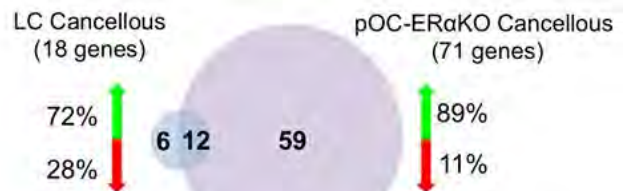


Figure 2

Fig 2

Disclosures: Natalie Kelly, None.

FR0132

Inhibition of BMP 2/4 Signaling Reduces Enhanced Cancellous Bone Response to Mechanical Loading in Female ERα-Deficient Mice. Katherine Melville¹, Gina Surita¹, Natalie Kelly¹, R Scott Pearsall², John Schimenti¹, F Patrick Ross³, Marjolein Van Der Meulen*¹. ¹Cornell University, USA, ²Accelaron Pharma, USA, ³Hospital for Special Surgery, USA

Estrogen and BMPs regulate bone homeostasis and adaptation to mechanical loading. Cortical and cancellous bone mass decreased in female mice lacking ERα in mature osteoblast [1]. In contrast, blocking signaling through BMPRIA increased bone mass in a time- and dose-dependent manner in mice [2]. These pathways interact *in vitro* and are implicated in adaptation to loading, but have not been studied *in vivo*. Our goal was to examine whether blocking BMP signaling affected (a) skeletal

phenotype and (b) the response to mechanical loading *in vivo* and whether ER α modulated the response.

We bred female osteoblast-specific ER α KO (pOC-ER α KO) and littermate control (LC) mice [1]. At 10 weeks of age, *in vivo* mechanical loading was applied to the left tibia daily for 2 weeks (7N peak load [1], n=20 mice/gp). We administered either placebo or a soluble BMPRI1 Fc ligand trap (RAP-661, 5 mg/kg ip, 2x/wk) to each genotype during the loading period (n=10/gp). Cortical and cancellous morphology of tibiae, femora and vertebrae were analyzed by microCT. Sections were stained for TRAP (osteoclasts, N.Oc/BS) and pro-collagen I (osteoblast activity, N.Ob/BS). Femora and L5 vertebrae were failed in 3-point bending or compression, respectively. Data were analyzed by ANOVA; p<0.05 was significant.

In both genotypes, inhibiting BMP 2/4 signaling increased bone mass in the cortical and cancellous vertebra but not in the femur. In the vertebra, blocking BMPRI1A increased cortical bone mass more in LC than in ER α KO mice, but strength was increased similarly.

At the tibial metaphysis, inhibiting BMP signaling attenuated the loading response in cortical and cancellous bone in both genotypes. However, the increased response to loading in pOC-ER α KO was eliminated when BMPRI1A was blocked. Tb.Th increased 18% in LC and 29% in pOC-ER α KO placebo mice, but only 3% in LC and 9% in pOC-ER α KO without BMP signaling. In the cancellous metaphysis, blocking BMP signaling suppressed bone formation with loading but did not alter resorption. In the diaphysis adaptation to loading was not altered by blocking BMP signaling.

Blocking BMPRI1A signaling increased bone mass site- and genotype-specifically. Inhibition of BMP signaling dramatically increased bone mass in the vertebra and cancellous tibial metaphysis along with increased strength in the vertebra, but did not affect the diaphysis. BMP 2/4 signaling appears to be needed for the cancellous response to loading.

[1] Melville+ 2015; [2] Baud'huin+ 2012

Disclosures: Marjolein Van Der Meulen, None.
This study received funding from: Acceleron

FR0133

Low Magnitude Mechanical Loading Regulates Repair Events in Cortical Bone Defect Healing. Robert Carrera¹, Vittoria Flamini², Benson George³, Daniel Hunter³, Bo Liu³, Gurpreet Singh³, Jill Helms³, Philipp Leucht⁴, Alesha Castillo⁵. ¹Department of Bioengineering, Stanford University, USA, ²Department of Mechanical & Aerospace Engineering, New York University, USA, ³Department of Surgery, Stanford University School of Medicine, USA, ⁴Departments of Orthopaedic Surgery & Cell Biology, New York University School of Medicine, USA, ⁵Departments of Mechanical & Aerospace Engineering & Orthopaedic Surgery, New York University, USA

Introduction: The purpose of this work was to (1) develop an *in vivo* murine model to study the influence of mechanical loading on bone regeneration, and (2) to use this model to determine the effects of loading on cellular events during repair. Early postoperative weight-bearing is an important aspect of orthopaedic rehabilitation, though its effects on cellular and molecular events in bone regeneration are not completely understood¹. We describe a novel *in vivo* system consisting of a mechanically loaded, stable cortical defect injury in the mouse tibia, and present data showing the influence of early loading on proliferation and cellular differentiation. **Methods:** Bilateral mono-cortical tibial defects were created in B6 adult mice (n=40); this defect typically heals via intramembranous ossification². Tibiae were subjected to 4 consecutive days of *in vivo* axial compressive loading (4 N, 2 Hz, 60 cycles)(Fig. 1A) beginning on post-surgical day (psd) 2. Non-loaded tibiae served as controls. *In vivo* μ CT images of defects were acquired on days 2, 5, 8, 10, and 14. The ROI included the regenerate and surrounding cortices. Percent change in bone volume (% Δ BV) at each time point, relative to psd 2, was calculated for each tibia. Mice were euthanized on days 5, 10, and 14. Longitudinal sections were assessed for proliferation and differentiation. A linear elastic FE model at psd 2 was developed and strains were computed for a 4 N point load. **Results:** Highest compressive strains (700-1100 μ ε) were observed at the posteromedial edge of the defect, with strains reaching ~300 μ ε in tension at the anterior edge (Fig 1). % Δ BV was significantly lower in loaded versus control tibiae at psd 8 and 10 relative the first day of loading (psd 2) (Fig 2) by a T-test (α =0.05). Loaded defects displayed increased proliferation (Fig 3) and greater amounts of cartilage (Fig 4) at the periosteum and within the regenerate at psd 10 and 14. **Conclusion:** Low magnitude loading in the inflammatory phase (psd 2) delays mineralization and remodeling by prolonging the proliferative phase and initiating a robust endochondral response. The primary advantage of this model is that it combines a well-described and tightly regulated sequence of repair events with a highly controlled mechanical stimulus, a system amenable for studying effects of physical signals on distinct components of the regenerative cascade. Refs: 1. Betts and Müller, *Front Endocrinol* 2014. 2. Leucht et al., *Bone* 2007.

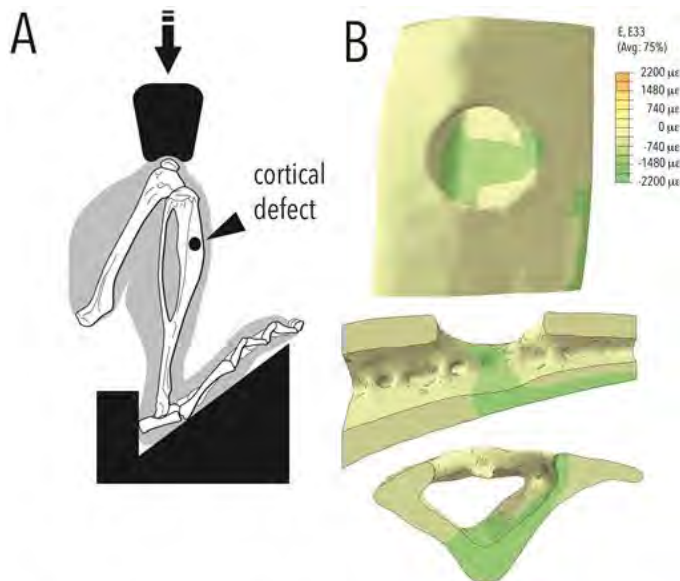


Figure 1. (A) Axial compressive loading of the tibial defect. (B) Estimated longitudinal strain around the defect using FE analysis.

Figure 1

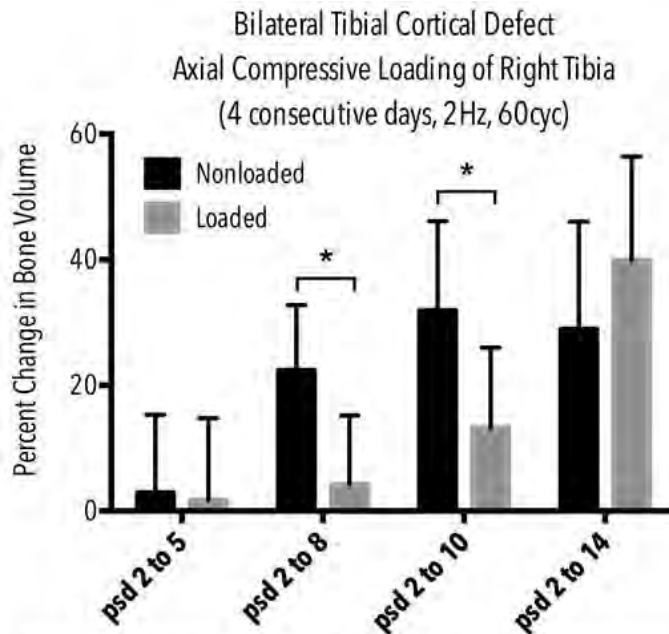


Figure 2. Percent change in bone volume in loaded and nonloaded control defects as measured by *in vivo* longitudinal microCT scanning. *p<0.05

Figure 2

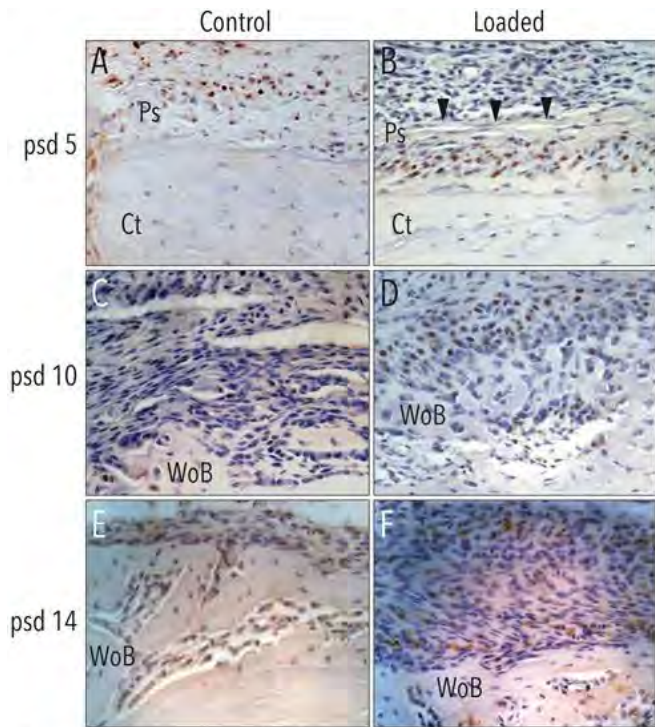


Figure 3. Assessment of proliferation by PCNA staining (shown in brown). (A) Proliferating cells are observed at the periosteal surface above the newly formed bone adjacent to the defect in control defects. (B) Loaded defects displayed an elevated periosteum (black arrows) containing many proliferating cells. (C-F) Increased numbers of proliferating cells is maintained at psd 10 and 14. Ps=periosteum. Ct=cortical bone. WoB=woven bone.

Figure 3

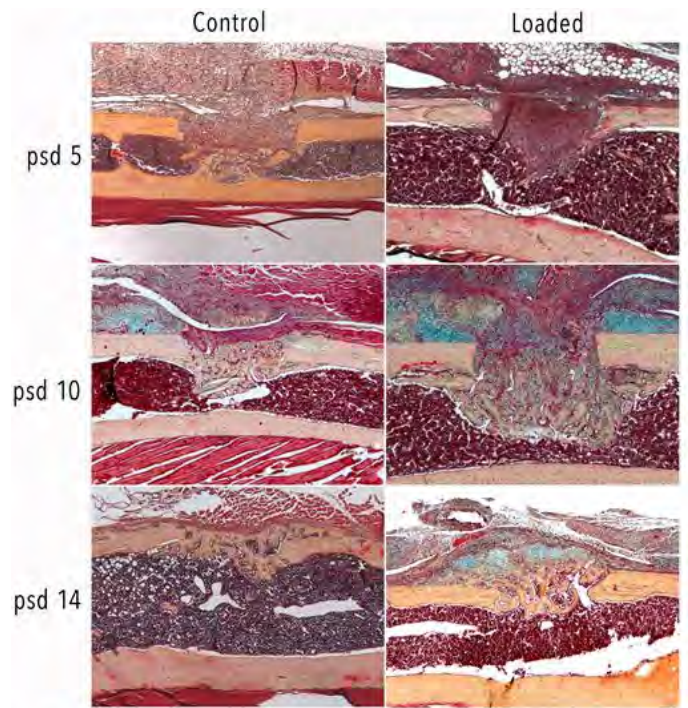


Figure 4. Histological appearance of loaded and nonloaded control defects at psd 5, 10, and 14. Exuberant amounts of cartilage and fibrocartilage are observed above the defect on psd 10 and 14 in loaded defects. In addition, the regenerate is larger in loaded defects on psd 10 compared to controls.

Figure 4

Disclosures: Alesha Castillo, None.

FR0134

Mechanical unloading sensitive miR-138 targets MACF1 to regulate bone formation. [Airong Qian](#)*¹, [Zhihao Chen](#)², [Yasir Arfat](#)², [Lifang Hu](#)², [Peng Shang](#)³, [Ge Zhang](#)⁴. ¹Northwestern Polytechnical University, Peoples republic of china, ²Key Laboratory for Space Bioscience & Biotechnology, Institute of Special Environmental Biophysics, School of Life Sciences, Northwestern Polytechnical University, Xi'an 710072, China, China, ³Key Laboratory for Space Bioscience & Biotechnology, Institute of Special Environmental Biophysics, School of Life Sciences, Northwestern Polytechnical University, China, ⁴nstitute for Advancing Translational Medicine in Bone & Joint Diseases, School of Chinese Medicine, Hong Kong Baptist University, Hong Kong, China, China

MicroRNAs (miRNAs) are an abundant class of evolutionarily conserved, short (about 22 nt long), single-stranded RNA molecules that have emerged as important post-transcriptional regulators of gene expression. Computational predictions indicate that more than 50% of all human protein-coding genes are potentially regulated by miRNAs. miRNAs play critical roles in diverse biological and cellular processes including metabolism, differentiation and apoptosis. Reportedly, miRNAs have been identified as indispensable regulators of osteoblasts differentiation and bone formation.

This study aimed to identify specific miRNAs and their regulatory roles in the process of MACF1-induced osteogenic differentiation. We investigated specific miRNAs and their regulatory roles in hind limb unloading (HLU) mice. Eight week old male BALB/c mice underwent HLU and their femur and tibia were harvested to extract total bone RNAs after four weeks of suspension. We have identified thirteen up regulated and one down-regulated miRNAs to be differentially expressed and their expression was verified by quantitative real time PCR. Especially, elevated levels of miR-138 correlated with a lower degree of bone formation in whole bone samples of HLU mice were presented (Fig 1).

Target prediction analysis tools were used to predict MACF1 as a direct target of miR-138. To investigate the effects of role of miR-138 in regulating the bone formation, specific inhibitors antagomir-138 and antagomir-NC is designed. Then Transfect antagomir to preosteoblast MC3T3-E1 by lipofectamine 2000, researching miRNA function on bone formation in vitro. MACF1 is specially higher with using

antagomir-138 than antagomir-NC and control by qPCR analysis. Staining of calcium deposition by Alizarin red in MC3T3-E1 cells after treatment with antagomir-138 shows that miR-138 downregulate bone formation (Fig 2). Further, *in vitro* analysis confirmed the osteoblasts activity and matrix mineralization were enhanced by antagomir-138. Predominantly, we found an inhibitory role of miR-138 in regulating the bone formation in HLU mice and *in vivo* pretreatment with antagomir-138, partly recovered the bone loss caused by HLU. Taken together, these results suggest that *in vivo* inhibition of miRNA by anti-miR could represent a potential therapeutic strategy for ameliorating bone loss.

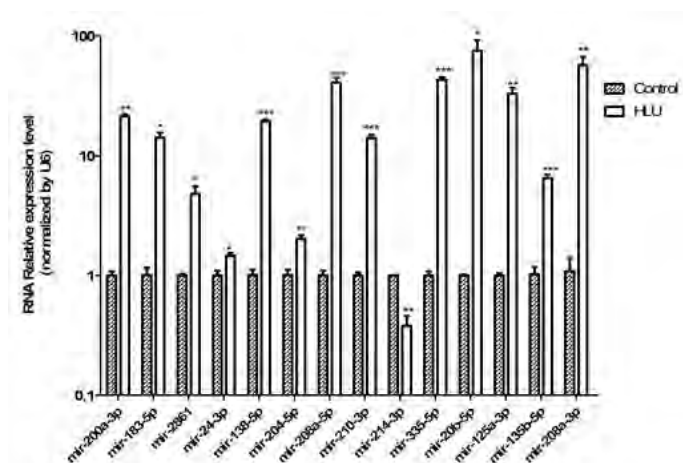


Fig 1 Screen the noncoding RNAs targeting MACF1 by qPCR from HLU mice.

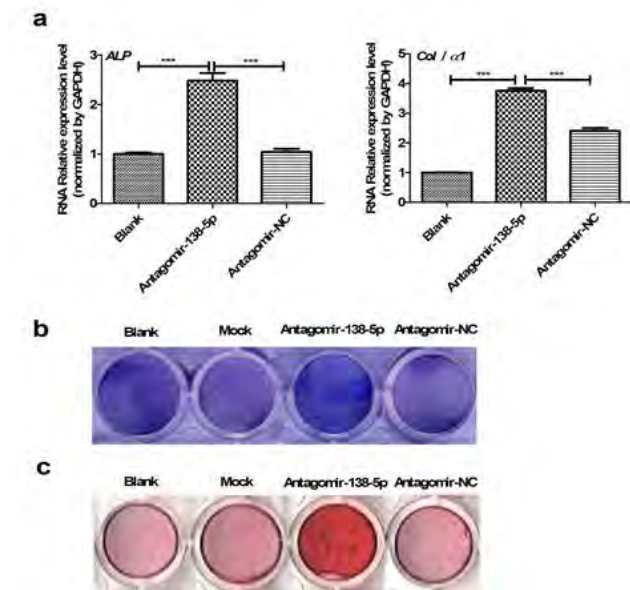


Fig 2. Antagomir138 promotes ALP, Collagen I expression and osteoblast mineralization

Disclosures: Airong Qian, None.

FR0135

Pre-exercise through Moderate Treadmill Running Enhances Healing of Wounded Tendons in Aging Rats. Jianying Zhang*, Ting Yuan, James H-C Wang. University of Pittsburgh School of Medicine, USA

Aging leads to degenerative changes in tendons, while appropriate exercise enhances their mechanical strength. In young mice (2.5 months) tendons, we previously showed that moderate treadmill running (MTR) induces anabolic changes such as increasing tendon stem/progenitor cell (TSC) numbers and collagen production. It is known that adult stem cells play a vital role in tissue homeostasis, remodeling and repair. Therefore, in this study we aimed to test the hypothesis that MTR enhances tendon healing potential in aging rats through TSC-based mechanisms.

In this study, we used 24 rats (20 months), which were divided into MTR and control groups. Rats in the MTR group ran 5 days/week at the speed of 13 meter/min for 15 min/day in the first week and for 30 min/day for the next 4 weeks. Control rats freely roamed in cages. After MTR, a 2mm window defect was created in the patellar tendons of all rats and TSCs were isolated from the excised tendons for *in vitro* culture. Then, the effect of MTR on aging rat tendons was tested both *in vitro* and *in vivo*.

Our results showed that *in vitro* culture of TSCs from rats in the MTR group formed larger colonies with higher TSC numbers when compared to the controls (Fig. 1). Besides, flow cytometry revealed that MTR significantly increased the expression of stem cell markers, SSEA-1 and Stro-1 (Fig. 2), and qRT-PCR showed the up-regulation of Nanog and OCT-4 by MTR (Fig. 3). Gross morphology of patellar tendons revealed high vascularization and unhealed wounds in the controls after 4 weeks (Fig. 4A) while defects in the MTR group appeared 50% healed (Fig. 4B). After 8 weeks, the wound was still visible in the controls (Fig. 4C) while the tendon was completely healed in the MTR group (Fig. 4D). Moreover, H&E staining showed better collagen fiber organization in the MTR group while in the controls the collagen fibers were disorganized and had large holes (Fig. 5).

These findings indicate that pre-exercise in the form of MTR can enhance healing of injured aging tendons by inducing anabolic effects such as increasing TSC proliferation and stemness, which may improve tendon function and quality of tendon repair after an injury. This study reveals the TSC-based mechanisms behind the beneficial effects of pre-exercise on tendons and may help devise clinical rehabilitation protocols to treat tendon injuries in aging patients.

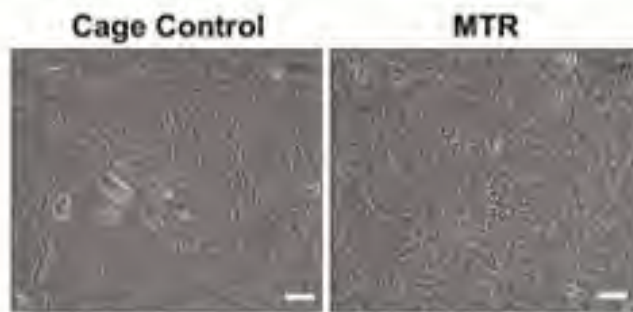


Fig. 1 Morphology of TSCs from aging rats in the cage control and MTR groups. Bar - 100µm.

Fig 1

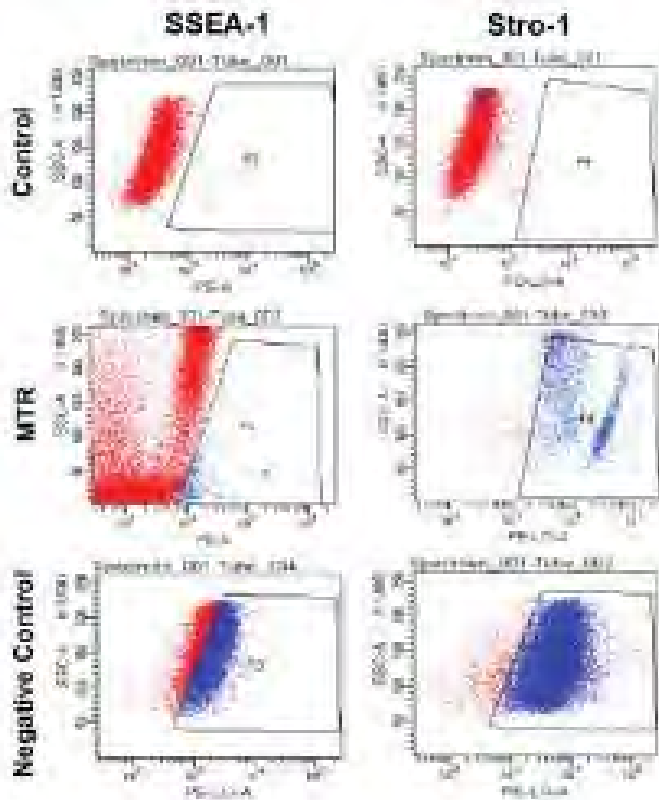


Fig. 2 Flow cytometry analysis of stem cell markers, SSEA-1 and Stro-1, in TSCs of aging rats from the cage control and MTR groups.

Fig 2

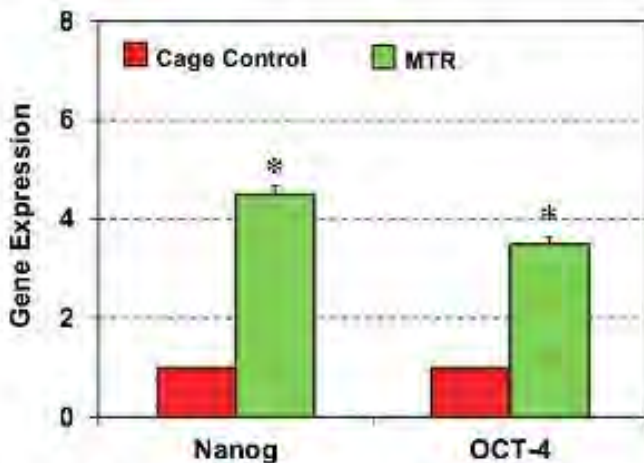


Fig. 3 qRT-PCR analysis of stem cell marker genes, Nanog and OCT-4, in TSCs from aging rats in the cage control and MTR groups.

Fig 3

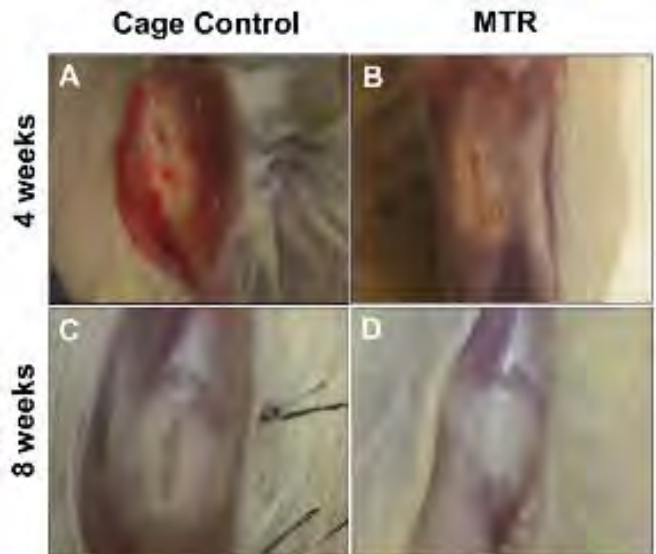


Fig. 4 Gross appearance of patellar tendon window defect in rats from the cage control and MTR groups.

Fig 4

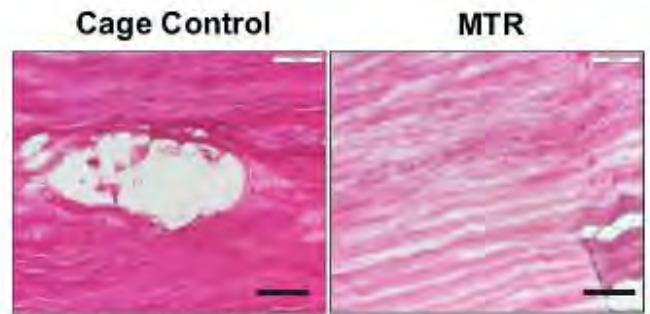


Fig. 5 H&E staining of patellar tendon sections of rats in the cage control and MTR groups. 20x magnification. Bar - 100µm.

Fig 5

Disclosures: Jianying Zhang, None.

FR0136

Preosteoclasts Mediate Bone Modeling by Secretion of PDGF-BB and Induction of CD31^{hi}Emcn^{hi} Vessels. Hui Xie¹, Zhuying Xia², Weicheng Xu³, Genevieve Brown⁴, Mei Wan³, X. Edward Guo⁴, Xu Cao³. ¹Johns Hopkins Medical Institution, USA, ²Xiangya Hospital, Central South University, China, ³Department of Orthopaedic Surgery, Johns Hopkins University School of Medicine, USA, ⁴Department of Biomedical Engineering, Columbia University, USA

Bone is modeled in adaptation of mechanical loading changes. The molecular and cellular mechanism is still under investigation. We have found that preosteoclasts secrete platelet-derived growth factor-BB (PDGF-BB) to induce cortical bone formation and CD31^{hi}Emcn^{hi} vessels, a specific vessel subtype that couples angiogenesis and osteogenesis essential for new bone formation during bone modeling and growth. Here we report that mechanical loading and unloading regulate bone modeling by modulating the formation of preosteoclasts and consequently the PDGF-BB secretion and CD31^{hi}Emcn^{hi} vessel formation. In brief, the number of preosteoclasts and CD31^{hi}Emcn^{hi} endothelial cells in periosteum, periosteal bone formation and cortical bone mass were dramatically increased after four weeks of mechanical loading in wild-type mice, whereas CD31^{hi}Emcn^{hi} vessels, periosteal bone formation and cortical bone mass were not changed in osteoclast lineage-specific PDGF-BB conditional knockout mice. Interestingly, the number of preosteoclasts

was also increased in osteoclast lineage-specific PDGF-BB conditional knockout mice, indicating that PDGF-BB secreted by preosteoclasts regulates bone modeling. Conversely, following three weeks of hind-limb unloading, wild-type mice experienced substantial decline in preosteoclast number in both periosteum and trabecular bone. Bone marrow PDGF-BB level, CD31^{hi}Emcn^{hi} endothelial cell number, trabecular and periosteal bone formation, trabecular and cortical bone mass were decreased accordingly. The alterations in hind-limb unloading mice were partly rescued by a cathepsin K inhibitor, which has been shown to stimulate formation of preosteoblasts and subsequent formation of CD31^{hi}Emcn^{hi} vessels by secretion of PDGF-BB. Taken together, mechanical loading-modulated formation of preosteoclasts mediates bone modeling by secretion of PDGF-BB and induction of CD31^{hi}Emcn^{hi} vessels.

Disclosures: Hui Xie, None.

This study received funding from: Merck

FR0137

Simulated Space Radiation: Murine Skeletal Responses during Recovery and with Mechanical Stimulation. Yasaman Shirazi-Fard*¹, Ann-Sofie Schreurs¹, Tiffany Truong¹, Candice Tahimic¹, Joshua Alwood¹, Alesha Castillo², Ruth Globus¹. ¹NASA Ames Research Center, USA, ²New York University, USA

Simulated space radiation at doses similar to those of solar particle events or a round-trip sojourn to Mars (1-2Gy) may cause skeletal tissue degradation and deplete stem/progenitor cell pools throughout the body. We hypothesized that simulated space radiation (SSR) causes late, time-dependent deficits in bone structure and bone cell function reflected by changes in gene expression in response to anabolic stimuli. We used a unique sequential dual ion exposure (proton and iron) for SSR to investigate time-dependence of responses in gene expression, cell function, and microarchitecture with respect to radiation and an anabolic stimulus of axial loading.

Male 16-wk C57BL/6J mice (n=120 total, n=10/grp) were exposed to 0Gy (Sham), ⁵⁶Fe (2Gy, positive control dose), or sequential ions for SSR (1Gy ¹H/⁵⁶Fe/¹H) by total body irradiation (IR), and the tissues were harvested 2 or 6 mo. later. ⁵⁶Fe caused a significant reduction in BV/TV compared to Sham (-38%) and SSR (-29%); however BV/TV for SSR group was not different than Sham 2-mo post-IR. Both ⁵⁶Fe and SSR caused significant reduction in Tb.N compared to Sham (-38% and -12%, respectively). Tb.N for ⁵⁶Fe was also significantly lower than SSR (-30%). To assess the response to anabolic stimuli, we subjected subsets of Sham and SSR groups to rest-inserted axial loading 1-month post-IR (-9N, 60 cycles/day, 3 days/wk, 4 wks). There were main effects of both mechanical loading and radiation to reduce BV/TV, and a main effect of mechanical loading to reduce TbTh, and a main effect of radiation to reduce TbN. Axial loading increased BV/TV by 19% and 17%, Tb.Th by 20% and 15% in Sham and SSR groups, respectively, and Tb.N remained unchanged. *Ex vivo* culture of marrow cells to assess growth and differentiation of osteoblast lineage cells 6 months post-IR showed that both ⁵⁶Fe and SSR exposures significantly impaired colony formation compared to Sham (both by ~84%), as well as nodule mineralization (-75% and -51% respectively). Additional analyses of cancellous bone microarchitecture (6 mo) and gene expression (2&6 mo) post-IR are in progress.

Results indicate that SSR caused persistent impairment of osteoblast colony formation and nodule mineralization 6-mo post-IR. Sequential ¹H/⁵⁶Fe/¹H exposure (1Gy) was not as detrimental on bone microarchitecture compared to a maximal dose (2Gy ⁵⁶Fe) for damaging HZE particles. Contrary to hypothesis, SSR did not suppress the ability of the bone to respond to mechanical stimuli.

Disclosures: Yasaman Shirazi-Fard, None.

FR0138

Sirtuin 1's Role as a Negative Regulator of the Anabolic Response to Mechanotransduction in Mature Osteoblasts. Elizabeth Rendina-Ruedy*¹, Nicole Fleming², Rashmi Pandey¹, Guillaume Vignaux², Heather Durai², Daniel Perrien³. ¹Vanderbilt University Medical Center, VA Tennessee Valley Healthcare System, USA, ²Vanderbilt University Medical Center, USA, ³VA Tennessee Valley Healthcare System, Vanderbilt University Medical Center, USA

Disuse experienced by astronauts/cosmonauts and bedridden patients leads to rapid and dramatic bone loss or osteoporosis, predisposing these populations to an increased risk of fracture. Moreover, bone mineral density upon return to normal loading is slow, possibly incomplete, and the mechanisms controlling this anabolic response are poorly understood. Sirtuin 1 (Sirt1) is a NAD⁺-dependent deacetylase originally described for its role in prolonging life. Female mice that are globally hemizygous for Sirt1 or with osteoblast-conditional deletion of Sirt1 using Col1a1-Cre or Osr-Cre have a low bone mass phenotype and treatment with the Sirt1 activators, resveratrol or SRT2104, reduces bone loss during hindlimb suspension (HS) in mice. However, the role of Sirt1 in disuse osteoporosis and/or recovery of bone remains unclear. This study tested the hypothesis that Sirt1 reduces disuse-induced bone loss and promotes recovery of bone upon return to normal ambulation. Fourteen (14) wk-old, male *Sirt1*^{fl/fl} and *2.3kbCol1a1-Cre;Sirt1*^{fl/fl} mice (*Sirt1*^{Ob-/}) underwent HS or normal ambulation (Con) for 3 wks. At the end of this period, a cohort of the HS mice were released from tail suspension and allowed to recover/reambulate (HSRA) for an additional 3 wks. Trabecular and cortical bone volume and structure in the femur were assessed by *ex vivo* μ CT. The *Sirt1*^{fl/fl}-Con and *Sirt1*^{Ob-/}-Con mice had a

similar bone phenotype; and following disuse, they experienced similar, significant decreases in trabecular bone volume (-37%) as well as deterioration of trabecular architecture within the respective genotype. Interestingly, however, the *Sirt1*^{Ob-/}-HSRA mice had a higher trabecular bone volume (~24%) compared to the *Sirt1*^{fl/fl}-HSRA mice, demonstrating a hypersensitive anabolic response during reambulation. These data suggest that the endogenous activity of Sirt1 does not play a role in disuse-induced bone loss, but Sirt1 may function as a negative regulator of the anabolic responses of osteoblasts and osteocytes during recovery from disuse. Continued investigation is underway to explore the mechanism by which Sirt1 exerts this effect which could lead to the development of novel therapeutic targets capable of enhancing the recovery from disuse osteoporosis.

Disclosures: Elizabeth Rendina-Ruedy, None.

FR0139

β -catenin deletion in osteocytes does not prevent load-induced bone formation. Kyung Shin Kang*, Alexander Robling, Indiana University, USA

Osteocytes are the major mechanosensory cell type in bone. Wnt/Lrp5 signaling in osteocytes is essential for modulating mechanotransduction. The putative downstream cascade for this receptor/ligand complex involves activation of β -catenin (β -cat); thus β -cat might be essential for the response to loading, much like the upstream mediator Lrp5 is required. Alternatively, other downstream mechanisms might transduce mechanical information originating from Lrp5 that do not require β -cat. We sought to understand whether osteocytic β -cat regulates mechanotransduction in bone by deleting both copies of β -cat from ^{10kb}Dmp1-expressing cells. Because β -cat^{fl/fl} mice that harbor the ^{10kb}Dmp1-Cre transgene do not survive beyond 8-12 wks, and mechanotransduction studies are most informative when conducted after the growth phase is completed (16 wks of age), we chose an inducible Cre model (^{10kb}Dmp1-CreERT2) which allows for postnatal activation of Cre to recombine the floxed β -cat alleles (β -cat^{fl/fl}). We injected tamoxifen (TAM; 20 mg/kg IP) or corn oil (OIL; vehicle) into 16-wk old transgenic (TG) and non-transgenic (NTG) mice 6 and 3 days prior to the first loading bout, and again 3 and 9 days after loading began. All mice underwent ulnar loading (2 Hz, 2.85 N; 180 cyc.) of the right arm 3 dy/wk for 1 wk. Fluorochrome labels were injected 5 and 12 dy after loading began for use in histomorphometry. BMD was measured pre-induction and at sacrifice to monitor skeletal changes due to β -cat loss. TAM-treated TG mice exhibited significantly reduced whole body (9-12% decrease; p<0.05) and spinal (32-24% decrease; p<0.05) BMD, compared to control mice (TAM-treated NTG mice, and OIL-treated TG and NTG mice). In the nonloaded control ulna, β -cat mutation resulted in a 65-73% (p<0.05) reduction in MS/BS, compared to the control groups, but MAR was unaffected by β -cat deletion. TAM-treated TG mice exhibited a significant response to mechanical loading. Load-induced bone formation (226 μ m³/ μ m²/yr) in TAM-treated TG mice was significantly less (p<0.05) in absolute terms that that exhibited by the control groups (380-490 μ m³/ μ m²/yr), but when normalized to the nonloaded control ulna (i.e., rBFR/BS), TAM-treated TG mice were equally responsive to loading as control mice. Our data indicate that the osteogenic response to loading can occur in the absence of osteocytic β -cat, suggesting that other downstream mediators of Lrp5 might participate in transducing load induced Wnt signaling.

Disclosures: Kyung Shin Kang, None.

FR0140

β -catenin gainofunction mutation in osteocytes confers protective effects from disuse-induced bone loss. Whitney Bullock*, Alexander Robling, Indiana University, USA

Wnt signaling is a key modulator of bone metabolism, including response to the mechanical environment. Although portions of the extracellular and transmembrane components of Wnt signaling, such as Sost and Lrp5, have been explored in the bone mechanotransductive response, the intracellular downstream signaling molecules, such as β -catenin, have received only cursory investigation. In the canonical Wnt pathway, activation of downstream mediator β -catenin by Wnt co-receptors Lrp5/6 leads to stabilization of β -catenin and changes in gene expression. Activating mutations in Lrp5 or genetic deletion of Sost in mice leads to an osteoprotective phenotype when mechanical stimulation is removed by disuse models (tail suspension or Botox-induced muscle paralysis). To date, it is unclear what downstream molecular mechanisms are altered in this mechanotransductive response, or if increased levels of β -catenin would generate the same osteoprotective phenotype. We hypothesized that the constitutive activation of β -catenin would have an osteoprotective effect and would diminish disuse-induced bone loss. β -catenin gain-of-function mutant mice (floxed exon 3) were crossed with the tamoxifen-inducible ^{10kb}Dmp1-CreERT2 transgenic mice to selectively activate β -catenin postnatally in osteocytes. Mice were given tamoxifen (20 mg/kg) or corn oil (vehicle) at 12 weeks of age to induce recombination/deletion of the floxed 3rd exon, and consequent stabilization of β -catenin. These mice were then subjected to disuse by hind limb suspension or by unilateral Botox-induced muscle paralysis (Botox; 20 U/kg) of the right lower limb for four weeks. As expected, control mice (oil-treated TG mice) subjected to disuse by tail-suspension and muscle paralysis lost a significant amount of femoral BMD (13.1 \pm 4.1% and 22.3 \pm 6.2% reduction, respectively [p<0.05]), whereas ground or saline control mice maintained femoral BMD (5.8 \pm 4.0 and 1.1 \pm 9.1% increase [NS], respectively), over the 4 week experiment. However, mice with transgene-induced activation of β -catenin did not lose bone mass in the hind limbs (3.8 \pm 6.9% decrease in

tail suspended and $13.0 \pm 11.0\%$ decrease in Botox treated [NS]). In summary, constitutive activation of β -catenin in osteocytes of adult mice had osteoprotective effects during disuse in both muscle paralysis and tail suspension models, suggesting that β -catenin might be a therapeutic target for bone wasting conditions caused by mechanical disuse.

Disclosures: Whitney Bullock, None.

FR0141

Actin Cytoskeletal Structure Influences MSC Lineage through Balanced Activity of LARG GEF and ARHGAP18. William Thompson¹, Sherwin Yen², Zhihui Xie², Gunes Uzer², Buer Sen², Maya Styner², Keith Burridge², Janet Rubin². ¹Indiana University, USA, ²University of North Carolina Department of Medicine, USA

The quantity and quality of bone depends on mesenchymal stem cell (MSC) differentiation, where adipogenic commitment depletes the available pool for osteogenesis. Cell architecture influences lineage decisions, as the cytoskeleton aligns critical elements that regulate responses to the physical environment. Disruption of the actin cytoskeleton, and RhoA activity, tip MSC fate in favor of adipogenesis. Mechanical strain suppresses MSC adipogenesis by cytoskeletal enhancement through activation of RhoA via Fyn/mTORC2/AKT signaling. Two distinct protein families direct RhoA activity, GEFs (RhoA activators) and GAPs (RhoA deactivators). In fibroblasts, ARHGAP18, a little studied GAP, suppresses RhoA leading to decreased stress fiber formation and motility, while the GEF LARG regulates RhoA activation in response to force. We hypothesized that ARHGAP18 and LARG influence MSC commitment by regulating cytoskeletal structure through control of RhoA. Knockdown of LARG resulted in accelerated adipogenesis and repression of basal RhoA activity. Importantly, mechanical activation of RhoA was almost entirely inhibited following LARG depletion and the anti-adipogenic effects of strain were prevented. This implicates LARG as the GEF responder to substrate strain in MSCs, controlling both RhoA activity and mechanical biasing against adipogenic lineage. In contrast, shRNA knockdown of ARHGAP18 increased basal RhoA activity and actin stress fibers; yet, no synergistic enhancement of RhoA was observed following mechanical strain. As the actin cytoskeleton modulates MSC fate, we reasoned that ARHGAP18 should affect MSC differentiation. In ARHGAP18 null MSCs adipogenesis was suppressed, as assessed by Oil-Red-O staining and Western blot of fat markers. Moreover, ARHGAP18 knockdown enhanced osteogenic commitment, confirmed by alkaline phosphatase staining and PCR of *Osx* and *Ocn*. This suggests that ARHGAP18 is a critical tonic inhibitor of MSC cytoskeletal assembly, returning RhoA to an "off state". In contrast, LARG is recruited during dynamic mechanical strain, and as such its absence has less effect on the resting RhoA state. In summary, control of RhoA cycling between on and off states is determined by ARHGAP18 when quiescent, with LARG playing a dominant role in the actin remodeling resulting from active mechanical input. Thus, both of these GTP exchangers converge on RhoA to regulate the MSC response to static and dynamic physical factors, influencing lineage allocation.

Disclosures: William Thompson, None.

FR0142

Disruption of nucleo-cytoskeletal connectivity increases intranuclear actin and enhances MSC differentiation. Gunes Uzer¹, Buer Sen¹, Zhihui Xie¹, William Thompson², Guniz Bas¹, Maya Styner¹, Janet Rubin¹. ¹University of North Carolina, USA, ²Indiana University, USA

The cell cytoskeleton (CSK) not only modulates cell signaling and differentiation, but also - through LINC (Linker of Nucleoskeleton and Cytoskeleton) connections - distributes force into the nucleus thus altering gene expression by mechanisms currently unknown. We recently showed that disconnecting the nucleus from the CSK by disrupting the LINC complex limits the ability of mesenchymal stem cells (MSCs) to respond their mechanical environment. As similar disruptions in LINC underlie clinically significant premature aging and muscle wasting disorders, and these are associated with increased fat infiltration in bone, we hypothesized that nucleocytoskeletal connectivity as facilitated by LINC would affect MSC fate selection. Using murine MSC, we first showed that dislocation of the actin binding element of LINC complex -Nesprin with siRNA targeting the Nesprin anchoring proteins SUN1 and 2 (siSUN) - increased adipogenic differentiation as represented by increased fatty acid binding protein (150% of to control siRNA, $p < 0.001$) and Adiponectin (250%, $p < 0.001$). Decreased β catenin is associated with adipogenesis; indeed, siSUN treatment decreased nuclear β catenin (68%, $p < 0.001$). Surprisingly, when siSUN treated cells were cultured under osteogenic conditions; we found increased osteocalcin mRNA (500%, $p < 0.001$) and protein (390%) compared to control siRNA. This suggested that mechanically isolating the nucleus from the CSK by disrupting LINC connectivity might generally enhance ongoing gene expression. Increased nuclear actin is known to enhance gene expression; in fact, we recently showed that cofilin-mediated influx of nuclear G-actin strongly promotes osteogenesis in MSCs. Thus, we next considered if disconnecting F-actin from the nuclear envelope by disrupting LINC might result in increased free monomeric G-actin which could be translocated into the nucleus. We found that siSUN treatment was associated with actin accumulation in the cell nucleus (220% compared to control siRNA, $p < 0.001$). We are currently investigating whether the increased bicameral differentiation of LINC deficient cells

requires the cofilin-dependent nuclear transport of actin. Further, we are interested in how actin might alter the nucleoskeleton, potentially leading to activation of heterochromatin associated genes, such as osteogenic *Runx2*. These findings suggest novel mechanisms by which cytoskeletal cues regulate MSC lineage decisions.

Disclosures: Gunes Uzer, None.

FR0143

Distinct subcellular activation patterns of Src and FAK by interstitial fluid flow and cytokines. Qiaoqiao Wan¹, Hiroki Yokota², Sungsoo Na³. ¹Department of Biomedical Engineering, Purdue University, USA, ²Department of Biomedical Engineering, Indiana University Purdue University Indianapolis, USA, ³Indiana University-Purdue University Indianapolis, USA

In the chondrocytes of patients with osteoarthritis (OA), the elevated level of inflammatory cytokines such as interleukin 1 β (IL1 β) and tumor necrosis factor α (TNF α) have been reported. These cytokines contribute to degrading cartilage matrix. Therefore, blocking the action of these cytokines is a potential strategy to prevent cartilage degradation. Accumulating evidence suggests that mechanical loading contributes to the regulation of cartilage homeostasis. However, the underlying mechanisms are not clear as to how varying magnitudes of mechanical loading trigger differential intracellular signaling pathways at sub-cellular levels.

Tyrosine kinases such as Src and FAK are known to play a crucial role in OA progression. To investigate activation patterns of Src and FAK at sub-cellular microdomains, we used lipid raft-targeting (Lyn-FAK and Lyn-Src) and non-lipid raft-targeting (KRas-FAK and KRas-Src) biosensors based on fluorescence resonance energy transfer (FRET). The C28/I2 human chondrocytes were grown in a three-dimensional (3D) cell culture system using collagen-coupled agarose gels to mimic the physiologically relevant cell environment. The activities of Lyn-Src, KRas-Src and Lyn-FAK were up and down regulated by high (>10 μ /min) and moderate (5 μ /min) interstitial fluid flow, respectively (Fig. 1A-C), but KRas-FAK did not respond to the flow (Fig. 1D). We also found that Src regulation by fluid flow was blocked by inhibition of FAK (Fig. 1E, F), while inhibition of Src did not affect FAK activities (Fig. 1G, H), suggesting that FAK is necessary for flow-induced Src activity. In contrast, Src was necessary for inflammatory cytokine-induced FAK activation (Fig. 2). Furthermore, we developed a 3D ex vivo system that uses bovine and murine cartilage explants. This system in conjunction with 3D FRET imaging allowed us to visualize sub-cellular signaling activities of Src and FAK that closely mimic in vivo conditions. We found that intermediate loading can inhibit inflammatory cytokine-induced activities of Lyn-Src, KRas-Src and Lyn-FAK, but not KRas-FAK (Fig. 3).

In summary, our findings of the distinct sub-cellular activation patterns of FAK and Src suggest the different mechanisms of mechanical loading- and cytokine-induced signaling. By selectively regulating Src and FAK activities, moderate fluid flow appear to interact with Src/FAK signaling and contribute to cartilage health.

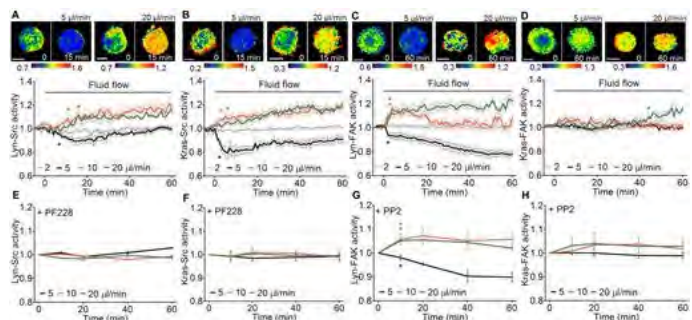


Figure 1

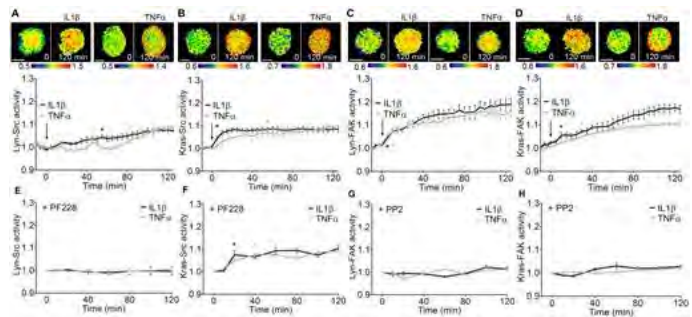


Figure 2

FR0145

Ectopic Tendon Mineralization After Injury Is Progressive, Deteriorates Tendon Biomechanical Properties And Involves BMP Signaling. Kairui Zhang¹, Shuji Asai², Michael Hast³, Louis Soslowsky³, Motomi Enomoto-Iwamoto^{*1}. ¹Children's Hospital of Philadelphia, USA, ²Nagoya University, Japan, ³University of Pennsylvania, USA

Heterotopic ossification (HO) is ectopic bone formation occurring outside of the normal skeleton, and may limit range of motion and cause pain. HO can be caused by traumatic events (acquired HO) or genetic disorders (hereditary HO). The former is generally self-limited while the latter is progressive and life threatening. Ectopic tendon mineralization can be found as a sequel to tendon injuries. Clinical retrospective studies have reported that mineralization is found in 14–62% of cases following percutaneous or open repair of the Achilles tendon. In this study, we utilized a mouse tendon injury HO model to determine whether ectopic tendon mineralization affects biomechanical property and whether BMP signaling is also involved in this condition as previously suggested in other HO. A complete transverse incision was made at the midpoint of the right Achilles tendon in 8-week-old female CD-1 or C57/BL6 mice and the gap was left open. Ectopic cartilaginous mass formation was found in the injured tendon by 4 weeks after surgery and ectopic mineralization was detected by radiographical and histological inspections at 8–10 weeks postsurgery. Ectopic mineralization grew over time and volume of the mineralized materials of 6 months postsurgery samples was about 2.5 fold bigger than that of 10 weeks samples, indicating that injury-induced ectopic tendon mineralization is progressive. In vitro mechanical testing showed that mid-substance modulus in the 6-months samples was significantly lower than that in the 10-weeks samples. The 6-months samples showed a higher circular variance of collagen alignment than the 10-weeks samples, indicating that collagen fibers in injured tendons became more disorganized over time. To determine the signaling pathway involved in ectopic tendon mineralization, we analyzed gene expression in injured tendon one week after surgery. We found huge increases in expression levels of various TGF β /BMP signaling related genes. Immunohistochemical analysis revealed that both phospho-Smad1/5/8 and phospho-Smad2/3 were highly up-regulated in ectopic chondrogenic lesion. Treatment with the BMP receptor kinase inhibitor (LDN193189: 3 mg/kg daily IP injection for 2 weeks) significantly inhibited injury-induced tendon mineralization. These findings indicate that injury-induced ectopic tendon mineralization is progressive and detrimental to tendon biomechanical properties, and involves BMP signaling.

Disclosures: Motomi Enomoto-Iwamoto, None.

FR0146

Low Intensity Pulsed Ultrasound Can Promote Stem Cell Proliferation during Fracture Healing but Varied by the Acoustic Wave Patterns. Yi-Xian Qin¹, Hua Yue^{*2}, Guoxian Feng², Li Huang², Jingyu Wang², Devi Zhang², Jingbo Liu², Kartik Grover². ¹State University of New York at Stony Brook, USA, ²Stony Brook University, USA

Recent studies have shown that low intensity pulsed ultrasound (LIPUS) has effects on acceleration of fresh fracture healing. Ultrasound exposure has mechanotransductive properties that allow inducing mechanical stimulation in bone cells and activate osteogenesis leading to bone formation. The objective of this study was to evaluate the effect of plain and focus ultrasound in fracture healing under hindlimb suspension (HLS) in a rat model, and MSC activations.

76 Sprague-Dawley rats (Female, 12 weeks old, 350–400g) were randomly divided into 4 groups (n=18 per group): 1) Fracture+HLS+Focused Ultrasound (FUS), 2) Fracture+HLS+Plain Ultrasound (PUS), 3) Fracture+HLS, and 4) Fracture+FUS. All the animals underwent surgeries on mid-shaft of right femur, and an accurate 2mm defect was made. LIPUS of 3 MHz, pulse width of 200ms, and intensity of 100mW/cm² for 20 min/day and 5 days/week. Immediately sacrificed the animals, the bone marrow was flushed out from the fracture area by dulbecco's modified eagle medium (DMEM) and then centrifuged and washed by sterilized phosphate buffer solution (PBS). The surface marker expression of MSCs, including CD29, CD90.1, CD11b, CD45 and CD49e, was analyzed by flow cytometry assay. The mid-shaft and the callus part of the right femur were scanned at 18 microns resolution using microCT (μ CT40, Scano Medical). Turnover Markers were analyzed by Serum/Plasma ALP, PINP, TRACP level by an Elisa Kit or EIA kit (Biovision or IDS). Three-point bending was performed to determine the stiffness and strength of right femur for all 4 groups. All results were statistical analyzed with One-way ANOVA on Tukey's protocol, with significance set at $p < 0.05$.

MSCs numbers and percentage in the bone marrow after 2 weeks ultrasound therapy were varied from 131, 503, 115, and 169 (Group 1-4), indicating PUS has most effective on MSC numbers (Fig. 1a), while the MSC numbers changed at week 4, 224, 153, 114, and 161 (Group 1-4) (Fig. 1b). There is no significant difference of mechanical stiffness between PUS and FUS in femurs, but both significantly higher than fracture plus LIPUS and fracture alone groups (Fig. 2).

This study suggested that both PUS and FUS has positive effects on accelerating MSCs recruitment in bone fracture area during the fracture healing process under disuse condition. However, PUS played an important role in the early phase of bone regeneration, whereas FUS had an effect on MSCs recruitment after 4 weeks of stimulation.

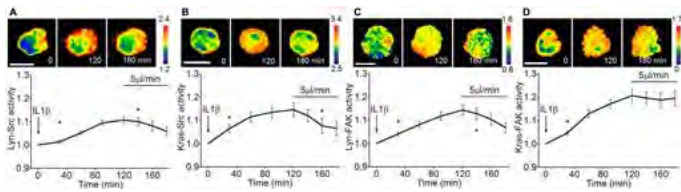


Figure 3

Disclosures: Qiaoqiao Wan, None.

FR0144

Diminished Mechanoresponsiveness with Skeletal Maturation occurs via a Sclerostin-Independent Pathway. Laia Albiol^{*1}, Annette I. Birkhold², David Pflanz², Tobias Thiele², Ina Kramer³, Michaela Kneissel², Georg N. Duda², Sara Checa², Bettina M. Willie². ¹Julius Wolff Institut, Charit \ddot{e} – Universit \ddot{a} tsmedizin Berlin, Germany, ²Julius Wolff Institute, Charit \ddot{e} Universit \ddot{a} tsmedizin, Germany, ³Novartis Pharma, Switzerland

An apparent loss in mechanoresponsiveness with maturation and aging may contribute to bone loss observed already in adulthood. We reported female C57Bl/6 adult mice had a reduced cortical bone formation response to loading (1200 μ c tibial midshaft) compared to young mice. Loading reduces SOST/sclerostin expression, however sclerostin independent pathways have been shown to be involved in the cortical bone formation response to loading in young mice. Thus, we hypothesized that reduced mechanoresponsiveness with skeletal maturation occurs through sclerostin independent pathways. Female 10 and 26 week old SOST knockout (KO) and littermate wild-type (WT) C57Bl/6 mice underwent 2 weeks of cyclic compressive loading of the left tibia (right tibia=control, n=7/genotype/age, 216 cycles/d, f=4 Hz, emax=900 μ c). In vivo microCT of the midshaft was performed at days 0 and 15. Images were registered and voxels were labeled as newly formed, quiescent or resorbed bone. 3D dynamic in vivo morphometry was used to quantify mineralized and eroded normalized volume (MV/BV, EV/BV), normalized surface area (MS/BS, ES/BS) and thickness/depth (MTh, ED) (Fig.1a). ANOVA assessed within-subject, between-subject and interaction effects for absolute values and interlimb differences (?interlimb=loaded - control limb). Age affected (re)modeling: MV/BV and MTh were lower ($p < 0.001$ and $p = 0.046$) and all resorption parameters were higher in adult compared to young mice ($p < 0.001$). Genotype affected MTh, ES/BS, ED ($p < 0.018$). Loading increased MV/BV and MS/BS ($p < 0.001$) and decreased ES/BS ($p = 0.003$). The formation (MV/BV) response to loading was reduced with skeletal maturation in WT (young: 142%, adult 38%) and SOST KO mice (young: 206%, adult 81%; %?= (loaded - control)/control \times 100); all formation parameters had a greater response to loading in 10 than 26 week old SOST KO and WT mice (loading and age interaction, < 0.010). Similar results were observed for interlimb differences; 10 week old had a greater formation response to loading compared to 26 week old mice (< 0.010). SOST KO had a greater ?MS/BS ($p < 0.016$) in response to loading than WT mice. Our study indicates sclerostin independent pathway(s) contribute to the reduced bone formation response at maturation in mice. Our data suggest the anabolic and catabolic benefits of loading in combination with sclerostin inhibition are age-specific. Studies are required to confirm this in humans and identify signaling pathways contributing to reduced mechanoresponsiveness with skeletal aging.

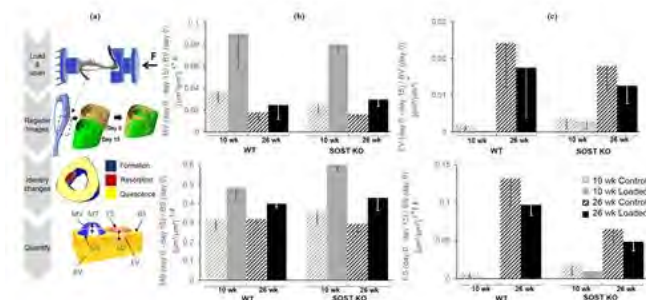


Fig 1: (a) Methods. (b) Formation parameters. (c) Resorption parameters; Mean \pm SD, \dagger loading effect, *

Disclosures: Laia Albiol, None.

This study received funding from: Novartis Pharma

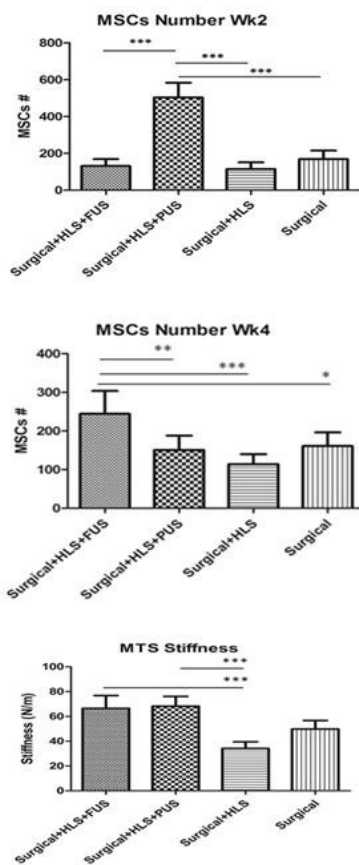


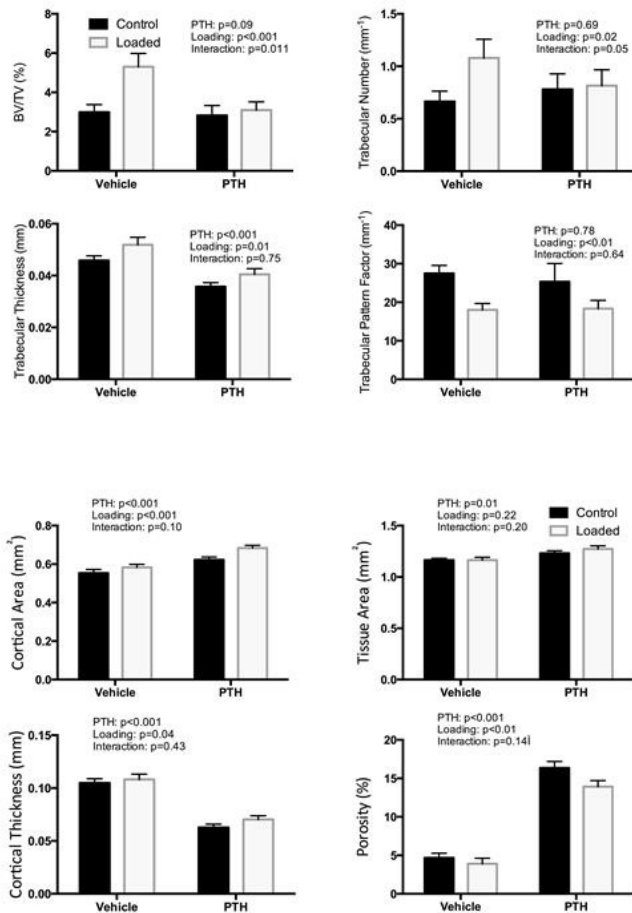
Fig.1a. MSCs numbers in bone marrow after 2 weeks experiment: A: MSCs numbers in Group 2 VS Group 1, $P<0.001$; B: MSCs numbers in Group 2 VS Group 3, $P<0.001$; C: MSCs numbers in Group 2 VS Group 4, $P<0.001$; Results are expressed as the mean \pm SD, * $P<0.05$, ** $P<0.01$, *** $P<0.001$

Fig.1b. MSCs numbers in bone marrow after 4 weeks experiment: A: MSCs numbers in Group 2 VS Group 1, $P=0.007$; B: MSCs numbers in Group 2 VS Group 3, $P<0.001$; C: MSCs numbers in Group 2 VS Group 4, $P=0.017$. Results are expressed as the mean \pm SD, $n = 9$. * $P<0.05$, ** $P<0.01$, *** $P<0.001$.

Fig. 2. Stiffness of right femur after 4 weeks study: A: Stiffness in Group 1 VS Group 3, $P<0.001$; B: Stiffness in Group 2 VS Group 3, $P<0.001$. Results are expressed as the mean \pm SD, * $P<0.05$, ** $P<0.01$, *** $P<0.001$.

In conclusion, in aged, as in young mice, mechanical loading alone is osteogenic in both cortical and trabecular bone compartments. iPTH is also osteogenic in cortical bone but, unlike its effects in young mice, it acts independently of the mechanostat. In trabecular bone iPTH does not have the dramatic osteogenic effect seen in young mice (1) and appears to reduce rather than enhance the positive effects of the mechanostat. The mechanism of this age-related dislocation of the effects of iPTH and mechanical loading needs to be determined.

Sugiyama et al., Bone 2008. DOI 10.1016/j.bone.2008.12.026



Figure

Disclosures: Joanna Price, None.

This study received funding from: Wellcome Trust Integrated Training Fellowship

FR0149

Risedronate and Mechanical Loading Have Additive Effects Increasing Bone Mass in Cortical, but Not Cancellous, Bone in Aged Mice. Peter Delisser*¹, Henry Todd¹, Lee B Meakin¹, Gabriel L Galea¹, Lance E Lanyon¹, Sara H Windahl², Joanna S Price³. ¹School of Veterinary Sciences, University of Bristol, United Kingdom, ²Centre for Bone & Arthritis Research, Institute of Medicine, Sahlgrenska Academy, Gothenburg, Sweden & School of Veterinary Sciences, University of Bristol, United Kingdom, ³School of Veterinary Sciences, University of Bristol, United Kingdom

In young adult mice the osteogenic response to artificial mechanical loading is unaffected by bisphosphonates suggesting that it primarily involves adaptive osteogenic modelling without accompanying resorption [1]. The aim of the present study was to use bisphosphonates to determine whether the mechanically adaptive response is similar in aged mice.

Female 19-month-old C57BL/6J mice were administered vehicle (saline) or the bisphosphonate Risedronate (15µg/kg) by daily subcutaneous injections from day zero. From day four, the right tibiae were subjected to loading every second day for two weeks, with the left limb as an internal non-loaded control. Mice were killed on day 21. Cortical and trabecular bone was analysed by µCT.

Loading resulted in greater trabecular thickness (Tb.Th) and increased cortical bone mass in the proximal tibia (37% site) by increasing cortical area (Ct.Ar), cortical thickness (Ct.Th), total tissue area (Tt.Ar) and polar moment of inertia (PMI) despite an increase in medullary area (Ma.Ar). As expected, loading had no significant effect on cortical bone in the distal tibia (75% site). Risedronate reduced trabecular structure model index (SMI), increased Ct.Th in both cortical sites and increased PMI in the

Fig. 1a, 1b, 2

Disclosures: Hua Yue, None.

FR0147

Withdrawn

FR0148

Parathyroid hormone’s enhancement of bones’ osteogenic response to loading in young mice is lost in the cortical bone of old mice, and reversed in their trabeculae. Lee Meakin, Henry Todd, Peter Delisser, Alaa Moustafa, Gabriel Galea, Sara Windahl, Lance Lanyon, Joanna Price*. University of Bristol, United Kingdom

Decreased effectiveness of bones’ adaptive response to mechanical loading contributes to age-related bone loss. Thus therapies that enhance the effectiveness of “the mechanostat” could stimulate structurally appropriate increases or maintenance of bone mass and so reduce the incidence of fragility fractures. In cortical bone of young mice, intermittent administration of parathyroid hormone (iPTH) and loading interact synergistically to increase bone mass (1). This interaction could be particularly valuable in the elderly. Here we assessed the effects of loading and iPTH in cortical and trabecular bone of old mice.

19-month-old female C57BL/6 mice (n=32) were administered 0, 25, 50 or 100µg/kg iPTH by daily subcutaneous injection for 4 weeks. Their tibiae were examined at 37% of the bone’s length from the proximal end. Histological and mCT analysis revealed potent iPTH dose-related effects on cortical (re)modelling; periosteally-enclosed area, cortical area and porosity were increased and cortical thickness decreased. iPTH had no effect of loading-related strain measurements at the same site. 30 similar mice were given the medium, submaximal, 50 µg/kg iPTH dose or vehicle daily for 6 weeks with concurrent minimally osteogenic non-invasive axial mechanical loading (40 cycles, 10s rest period, peak strain 1750µε on the medial aspect of the tibia, three times weekly) of the right tibia for the final 2 weeks of iPTH treatment. In trabecular bone of the proximal tibia iPTH alone had no effect, however, it abrogated the load-related increase in BV/TV by reducing the increase in trabecular number, with no effect on the increase in trabecular thickness. In cortical bone at the 37% site loading reduced the iPTH-associated increase in porosity. The osteogenic effects of iPTH and loading on periosteally-enclosed area and cortical area were additive but not synergistic.

37% site. The combination of risedronate and loading did not alter the loading-related increase in Tb.Th but additively increased Ct.Ar, Ct.Th and PMI in the proximal tibia. Risedronate pre-treatment prevented the loading-related increase in Ma.Ar observed at the 37% cortical site. Loading did not alter the increase in Ct.Th due to risedronate treatment in the distal tibia.

In conclusion, the lack of any observed effect of risedronate on trabecular bone mass in these old mice differs from that reported in young mice [1], demonstrating that observations in the young cannot necessarily be extrapolated to the old. To the extent that the situation in old mice can be extrapolated to old humans, it appears that in cortical bone, risedronate treatment potentially confers the clinical benefit of increased bone mass. This benefit is increased when risedronate treatment is combined with loading since there is an additive positive increase in a number of cortical bone parameters, due to increased periosteal expansion unaccompanied by endosteal resorption.

1. Sugiyama et al (2011) Bone 49 133-139

Disclosures: Peter Delisser, None.

FR0151

A Natural Antibody Against Oxidized Phospholipids Causes Bone Anabolism. Elena Ambrogini^{1*}, Shuling Wang², Xuchu Que², Fumihiko Yamaguchi², Annick Deloose¹, Kanan Vyas¹, Michela Palmieri¹, Stuart B Berryhill¹, Robert S Weinstein¹, Sotirios Tsimikas², Stavros C Manolagas¹, Joseph L Witztum², Robert L Jilka¹. ¹Center for Osteoporosis & Metabolic Bone Diseases, University of Arkansas for Medical Sciences & the Central Arkansas Veterans Healthcare System, USA, ²Department of Medicine, University of California, San Diego, USA

Oxidation of LDL is thought to be a fundamental mechanism of atherogenesis. Oxidized phospholipids (OxPL) in oxidized LDL (OxLDL) serve as ligands mediating the uptake of OxLDL by macrophage scavenger receptors and promoting inflammatory gene expression in endothelial cells and macrophages. E06 is an IgM natural antibody that recognizes the phosphocholine moiety of OxPL in OxLDL and on apoptotic cells. E06 prevents both the uptake of OxLDL by macrophage scavenger receptors and the pro-inflammatory activity of OxPL. We generated LDL receptor-KO (LDLR-KO) mice expressing a single chain variant of E06 (E06-scFv) as a transgene under the control of the ApoE promoter (LDLR-KO;E06-Tg mice). The E06-scFv is expressed in liver and macrophages, and leads to atheroprotection in LDLR-KO mice fed a high fat diet (HFD). Mouse models of atherosclerosis caused by HFD also exhibit decreased bone mass. We therefore studied LDLR-KO mice and LDLR-KO;E06-Tg mice to determine if OxPL play a role in bone homeostasis. At two months of age, male LDLR-KO;E06-Tg mice were placed on HFD containing 0.5% cholesterol and 21% milk fat; LDLR-KO mice were fed either HFD or normal chow. At 6.5 months, LDLR-KO mice on HFD had lower femoral bone mass as compared to LDLR-KO mice fed chow, as determined by DXA BMD. LDLR-KO;E06-Tg mice, however, were protected from the adverse effect of HFD on femoral BMD observed in the LDLR-KO mice. At 7.5 months, mice were euthanized and vertebrae and femurs were analyzed by micro-CT. LDLR-KO mice on HFD had decreased cortical diaphyseal thickness resulting from a decrease in periosteal perimeter. Strikingly, LDLR-KO;E06-Tg mice did not exhibit a decrease in cortical thickness. This, however, resulted from a decrease in the endosteal perimeter due to increased bone formation (determined by tetracycline labeling) – not a reversal of the suppressive effect of the HFD on periosteal apposition. Cancellous bone mass in the femur and vertebra was indistinguishable in LDLR-KO mice fed HFD vs chow. More surprisingly, LDLR-KO;E06-Tg mice exhibited a profound increase in femoral cancellous bone mass as compared to the other two groups. E06-scFv does not possess antibody effector functions other than the ability to neutralize OxPL. Therefore, our data suggest that OxPL - generated from a variety of sources, including inflammatory and apoptotic cells - restrain bone formation. Hence, neutralization of OxPL with an antibody could be a novel strategy for bone anabolism.

Disclosures: Elena Ambrogini, None.

FR0152

Activation of Protein Kinase A in Mature Osteoblasts Promotes a Remarkable Bone Anabolic Response. Liana Tascou¹, Thomas Gardner¹, Hussein Anan², Charlie Yongpravat¹, Christopher Cardozo³, William Bauman³, Francis Lee¹, Daniel Oh¹, Hesham Tawfeek^{3*}. ¹Columbia University, USA, ²SacredHeart Hospital/Temple University, USA, ³James J Peters VA Medical Center, USA

Protein kinase A (PKA), a major serine/threonine kinase, is directly activated by cAMP after G-protein alpha S (Gs) or Gs-coupled receptor stimulation. This study determined whether PKA activation in the osteoblast cells is sufficient to mediate a bone anabolic response. Thus, a constitutively active form of the PKA (CA-PKA) catalytic subunit was conditionally expressed in the osteoblast lineage cells of mice (CA-PKA-OB mouse) by crossing 2 mouse lines, a 2.3-kb alpha1(I)-collagen promoter-Cre mouse (Coll-Cre mouse) with a floxed-CA-PKA mouse (FF-CA-PKA mouse). Primary osteoblast cells from the CA-PKA-OB mice exhibited higher basal PKA activity than that of the osteoblast cells from control mice. Micro CT analysis revealed that constitutive PKA activation in osteoblast cells of female mice

led to a more than 10-fold increase in femur (p=0.0001) but only 20% increase in L5 vertebral (p=0.009) bone volume/total volume (BV/TV) compared to control littermates. Femur cortical thickness and volume were also higher in the CA-PKA-OB mice. Interestingly, the three-dimensional structure model index (TRI-SMI) was significantly reduced both in femur (-8 ± 6 vs 3 ± 0.4, p=0.0008) and L5 (-0.6 ± 0.3 vs 0.4 ± 0.1, p=0.0001) of the CA-PKA-OB mice, reflecting an increase in the number of plates vs rods. In agreement with improved bone micro-architecture, femurs from the CA-PKA-OB mice had a 55% greater load to failure (p<0.001) and were 45% stiffer (p<0.001) compared to those of control mice. Furthermore, the CA-PKA-OB mice had enhanced bone turnover with a predominance of bone formation (serum PINP, 35 ± 5 vs 13 ± 4, p=0.001) over that of resorption (serum CTX, 23 ± 4 vs 16 ± 2, p=0.007). In summary, these findings demonstrate that constitutively activated PKA in mature osteoblasts is sufficient to increase bone mass and improve bone architecture and mechanical properties. PKA in osteoblasts is, therefore, an important target for designing new bone anabolic drugs for treating osteoporosis and diseases that are associated with bone loss.

Disclosures: Hesham Tawfeek, None.

FR0156

Gpr39 deficient mice have increased bone mass during aging as a result of accelerated osteoblast differentiation. Noam Levaot^{1*}, Milena Pesic², Gail Guterman-Ram², Avelet Orenbuch². ¹Ben-Gurion University of the Negev, Israel, ²Department of Physiology & Cell Biology, Ben-Gurion University of the Negev, Israel

G coupled protein receptors (GPCRs) are a diverse group of receptors that play a pivotal role in regulation of both resorption and formation of bone. Recently, a novel GPCR, GPR39 was shown to be expressed in osteoblast cell lines, but the role of GPR39 in the regulation of bone homeostasis was not explored. In order to elucidate the role for GPR39 in bone metabolism we investigated the bone phenotype of GPR39 deficient mice (GPR39^{-/-}).

These mice had normal body length, weight and bone mass at the age of 12 weeks when the skeleton reach maturation. However, micro CT analysis of trabecular bone in the femurs of aging six month old mice revealed a significant increase of 32% in the trabecular bone fraction, compared to wild type littermates. Increased trabecular bone in these mice was a result of higher trabecular numbers and thickness. In order to test whether increased bone mass was a result of attenuated resorption by osteoclasts we analyzed the serum levels of CTX-1 peptide. No significant difference in the levels of CTX-1 was observed. In addition, histomorphometric analysis showed normal numbers and distribution of TRAP stained osteoclasts in GPR39^{-/-} bone sections. On the other hand, serum levels of PINP-1, a marker for bone formation, showed significant increase in GPR39^{-/-} mice indicating bone formation is higher in these aging mice. In vitro, isolated bone marrow mesenchymal stem cells (BMSCs) from GPR39^{-/-} mice formed mineralization nodules as early as 7 days, a time point were no mineralization nodules were observed in cultures of wild type BMSCs. This enhanced mineralization was unlikely a result of increased osteoprogenitor numbers as colony-forming-unit fibroblasts and expression of the early osteoprogenitor markers Runx2 and Osterix showed no difference between GPR39^{-/-} and wild type BMSCs. However, mRNA expression analysis showed ordered but early and much higher expression of osteoblast and osteocytes regulating genes, suggesting that the osteoblast differentiation program is accelerated in the absence of GPR39. Thus our data suggest an inhibitory role for GPR39 in regulation of osteoblast differentiation. This assumption was further supported by our observation that GPR39 mRNA levels drop significantly during osteoblast differentiation of BMSCs in vitro.

Our data reveal a novel role for the receptor GPR39 in regulation of bone homeostasis and suggest that its absence leads to accelerated osteoblast differentiation and bone formation.

Disclosures: Noam Levaot, None.

FR0157

Intermittent Parathyroid Hormone Enhances Osseointegration of a Physiologically Loaded Tibial Implant in Ovariectomized Mice. Xu Yang^{1*}, Aleksey Dvorzhinskiv¹, Vinicius Ladeira Craveiro¹, Caroline Briat¹, Benjamin Ricciardi¹, F. Patrick Ross¹, Marjolein van der Meulen², Mathias Bostrom¹. ¹Hospital for Special Surgery, USA, ²Cornell University, USA

Introduction: Cementless total knee replacements primarily rely on cancellous bone for their initial stability and long term fixation. With a novel physiologically-loaded mouse tibial implant model, we have previously demonstrated that intermittent parathyroid hormone (iPTH) enhances osseointegration and strength of the bone-implant interface in intact mice. In the current study, we used this model to determine the effects of ovariectomy (OVX) and post-implantation iPTH on peri-implant cancellous bone mass and fixation strength.

Methods: Study Design: The titanium implant manufactured by 3-D printer has a smooth surface of the proximal side of the plateau to articulate with the native femur and a roughened surface of the stem to facilitate bone on-growth and initial stability. The implant was pressed fit into the medullary canal of the mouse tibia (Fig 1). The mice tolerated the implant well and started weight bearing immediately after surgery.

Female C57BL/6 mice received OVX or sham surgery (n=20/group) at age of 12 weeks and an implant in right tibia at 16 weeks. From day 1 post-implantation, the mice were given PTH (S.Q., 40 µg/kg/day) or vehicle (n=10/treatment/group), 5 days/week, until euthanasia 4 weeks post-implantation. **Microcomputed Tomography (microCT):** Both tibiae of each mouse were scanned by microCT. Bone volume fraction (BV/TV) was measured in the left tibial metaphysis and two regions in the right tibia (Fig 2). **Mechanical Testing:** The implant was pulled out of the tibia under displacement control to failure. Maximum load was calculated from the load-displacement curve. **Statistical Analyses:** The differences with surgery and treatment were assessed with two-way ANOVA. The alpha was 0.05.

Results: OVX decreased BV/TV of cancellous bone in left tibiae 8 weeks post surgery. iPTH did not affect BV/TV in OVX or sham mice (Fig 3A). OVX decreased cancellous mass in both the peri-implant and distal to implant regions of the right tibiae 4 weeks post-implantation. PTH enhanced cancellous mass in both of these two regions of both OVX and sham mice (Fig 3B and C). OVX lowered the maximum load of pull out testing. PTH enhanced the maximum load of both OVX and sham mice (Fig 4).

Discussion: OVX decreased peri-implant cancellous bone mass and fixation strength post-implantation. iPTH rescued bone mass and fixation strength. These results will lead to translational studies and may eventually benefit patients receiving cementless joint replacements.



Figure 1. Dimension and use of a novel titanium tibial implant. The implant was manufactured using three-dimensional metal printing. Top left: Implants shown in top, front, and side views. Implants were placed on a dime for size comparison. Bottom left: Secondary electron microscopy image of the implant showing the roughened surface. Right: Lateral radiograph of the knee with tibial implant in situ.

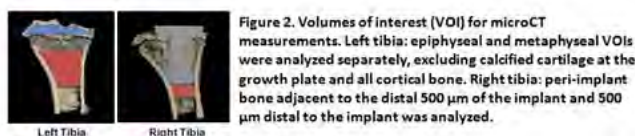


Figure 2. Volumes of interest (VOI) for microCT measurements. Left tibia: epiphyseal and metaphyseal VOIs were analyzed separately, excluding calcified cartilage at the growth plate and all cortical bone. Right tibia: peri-implant bone adjacent to the distal 500 µm of the implant and 500 µm distal to the implant was analyzed.

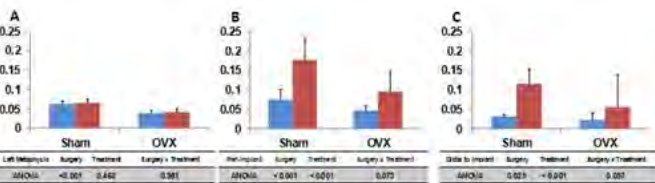


Figure 3. Bone volume fraction measured by microCT in: A. left metaphysis, B. right peri-implant region, and C. right distal to implant region. p values of ANOVA are shown in the table below each graph.

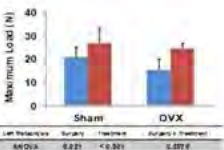


Figure 4. Maximum load of pull-out testing. p values of ANOVA are shown in the table below each graph.

Figure 1, 2, 3 and 4

Disclosures: Xu Yang, None.

This study received funding from: Smith & Nephew, Inc.

FR0159

Overexpression of Bmi1 in Mesenchymal Stem Cells Mediates Intracrine Actions of PTHrP in Regulating Skeletal Growth and Development. Guangpei Chen^{*}, Ying Zhang¹, Wanxin Qiao¹, Andrew Karaplis², Xiang-Jiao Yang², David Goltzman², Dengshun Miao³. ¹Nanjing Medical University, China, ²McGill University, Canada, ³Nanjing Medical University, Peoples republic of china

We previously demonstrated that Bmi1 deficiency resulted in an osteoporotic phenotype by inhibiting bone marrow mesenchymal stem cell (BM-MSC) proliferation and differentiation into osteoblasts. To investigate whether overexpression of Bmi1 in BM-MSCs can stimulate osteogenesis, we generated a transgenic mouse model overexpressing Bmi1 in BM-MSCs (Prx1-Bmi1^{Tg}). The expression levels of Bmi1 were significantly higher in skeletal tissue and BM-MSCs of Prx1-Bmi1^{Tg} mice than in those of wild-type mice, and body weight and size, skeletal size, cortical and trabecular bone volume, osteoblast number, ALP-positive and type I collagen-positive areas, total numbers of CFU-f and ALP⁺ CFU-f were all significantly increased in the Prx1-Bmi1^{Tg} mice. We then crossed Prx1-Bmi1^{Tg} with Bmi1^{-/-} mice and found that Bmi1 overexpression in BM-MSCs in the Bmi1^{-/-} background not only largely rescued

the osteoporotic phenotype of Bmi1^{-/-} mice, but also significantly prolonged their lifespan. In PTHrP (1-84) knockin (Pthrp KI) mice, Bmi1 expression is reduced and premature osteoporosis occurs. We demonstrated that Bmi1 and PTHrP were colocalized to cellular nuclei and interacted physically; therefore we crossed Prx1-Bmi1^{Tg} mice with Pthrp KI mice. BM-MSC overexpression of Bmi1 in the Pthrp KI background resulted in a longer lifespan, increased body weight, and improvement in skeletal growth and osteoblastic bone formation in the Pthrp KI mice, although the defects were not completely rescued. Levels of anti-oxidative enzymes including SOD1 and 2, catalase, glutathione reductase and glutathione peroxidase 1 were up-regulated in bony tissues of the Prx1-Bmi1^{Tg} mice, but down-regulated in the Pthrp KI mice, and importantly, Bmi1 overexpression in the Pthrp KI mice rescued this down-regulation. In contrast, the tumor suppressor genes p16, p19, p53 and p21 were down-regulated in bony tissues of the Prx1-Bmi1^{Tg} mice, but up-regulated in the Pthrp KI mice and Bmi1 overexpression in the Pthrp KI mice rescued their up-regulation. Taken together, these results demonstrate that overexpression of Bmi1 in BM-MSCs partially rescues the defects in skeletal growth and osteogenesis in the Pthrp KI mice by inhibiting oxidative stress and inactivating p16 and p19 signaling pathways. These studies therefore indicate that the PTHrP-Bmi1 signaling axis plays an essential role in regulating skeletal growth and development.

Disclosures: Guangpei Chen, None.

FR0160

Pyk2-Deletion Enhances Bone Mass through Estrogen Signaling in Osteoblasts and Osteoclasts. Sumana Posritong^{*}¹, Pierre P. Eleniste², Evan R. Himes², Melissa A. Kacena², Angela Bruzzaniti¹. ¹Indiana University School of Dentistry, USA, ²Indiana University School of Medicine, USA

An imbalance between osteoclast (OC) and osteoblast (OB) activity can lead to low bone mass and osteoporosis. The activity of the proline-rich tyrosine kinase 2 (Pyk2) is important for bone remodeling. Pyk2-deficient mice (Pyk2-KO) exhibit high bone mass which is due to both increased OB activity and decreased OC function. We found that Pyk2-KO mice are protected from ovariectomized (OVX) induced bone loss and that estrogen (E2)-supplemented Pyk2-KO OVX mice exhibit a greater increase in bone mass than wild-types (WT). To determine if Pyk2-deficiency promotes the anti-resorptive or bone-promoting actions of E2, we performed several *in vitro* studies. Calvarial OBs were cultured in osteogenic media with or without E2 for up to 28 days. E2-stimulation led to an increase in Pyk2 protein levels in WT OBs. On the other hand, ER α (but not ER β) was lower in Pyk2-KO than WT OBs. Further, QPCR studies revealed significantly higher c-fos mRNA levels in Pyk2-KO OBs, consistent with increased OB proliferation, which remained high after E2 treatment. Alkaline phosphatase (ALP) activity was also significantly higher in Pyk2-KO OBs (13.8 ± 1.7 nM/ml) than WT OBs (6.8 ± 0.7). Importantly, E2-treatment further increased ALP activity in Pyk2-KO OBs (28.1 ± 1.8) but had no effect on WT OBs. Similarly, calcium deposition (mineralization) was higher for Pyk2-KO OBs (7.4 ± 1.1 µg/ml Ca²⁺) than WT OBs (2.5 ± 0.1) and E2 further increased calcium deposition by Pyk2-KO OBs (12 ± 0.3) but not WT OBs. Next, we examined the effects of E2 on RANKL and OPG which control OC differentiation. In the absence of E2, Pyk2-KO OBs showed a higher RANKL/OPG ratio (1.5-fold) than WT OBs, which was reduced to 0.9-fold in E2-treated Pyk2-KO OBs. Finally, E2 decreased the survival of mature Pyk2-KO OCs (-38%) to a greater extent than WT OCs (-24%). Together, these results suggest that Pyk2 plays an important role in the E2/ER α -signaling pathways to regulate both bone formation as well as OC number *in vitro* and *in vivo*.

Disclosures: Sumana Posritong, None.

FR0161

Skeletal Anabolism By Concurrently Targeting the PTH1R and CaSR. Christian Santa Maria^{*}¹, Alfred Li², Zhiqiang Cheng², Fuqing Song², Dolores Shoback³, Chia-Ling Tu², Wenhan Chang². ¹UCSF, USA, ²San Francisco Veterans Affairs Medical Center, USA, ³University of California, San Francisco, USA

Intermittent parathyroid hormone, PTH(1-34) is the only approved osteoanabolic therapy for osteoporosis. However, its use is limited to a short-term with a relatively low dose due to adverse hypercalcemic effects and oncogenic potential in bone. A better understanding of the mechanisms underlying the actions of PTH(1-34) is required to enhance this therapy. Our recent studies have shown that increases in local [Ca²⁺] activate the extracellular Ca²⁺-sensing receptor (CaSR) in osteoblasts (OBs) to promote bone accrual and maturation. To determine whether the calcium-mobilizing effects of PTH(1-34) activate OB CaSRs to produce osteoanabolic responses, we tested whether co-injecting a calcimimetic, an allosteric CaSR agonist that can stimulate OB CaSRs directly, enhances the anabolic effects of PTH(1-34) and whether ablating CaSRs in early OB lineage blocks the effects in OBCaSR-KO mice. We found that treatment with PTH(1-34) or calcimimetic alone produced hypercalcemia or hypocalcemia, respectively, 3 hrs after injections in wild-type (Wt) C57/B6 mice. Co-injections with calcimimetics normalized the hypercalcemic effects of PTH(1-34) (p<0.01). Skeletal analyses by μ CT showed that PTH(1-34) alone increased trabecular bone mass and thickness by \approx 8% (p<0.05) in distal femurs compared to vehicle-injected controls. When a calcimimetic was co-injected with PTH(1-34), there were robust increases in trabecular bone mass (\approx 21% or 2.5 fold

over PTH(1-34) treatment alone, $p < 0.05$) and in thickness ($\approx 17\%$, $p < 0.05$). Co-injections of calcimimetic with PTH(1-34) also significantly increased cortical bone size, volume, and thickness at tibiofibular junction by 8-10% ($p < 0.01$), and bone strength as indicated by a 10% increase in failure load ($p < 0.01$) in 3-point bending tests, all which were absent with PTH(1-34) treatment alone. In OBCaSR-KO mice, the osteoanabolic effects of combined PTH(1-34)/calcimimetic treatment were completely abrogated, supporting our hypothesis that OB CaSRs play an essential role in mediating skeletal responses to the treatment. Our findings suggest novel synergistic actions of PTH(1-34) and of Ca^{2+} itself in producing skeletal anabolism and may inform preclinical regimens to restore osteoporotic skeleton and augment healing of injured bones.

Disclosures: Christian Santa Maria, None.

FR0162

The Effects of Systemic Hedgehog Pathway Modulation on Fracture Healing. Jennifer McKenzie*, Evan Buettmann, Matthew Silva, Michael Gardner. Washington University in St. Louis, USA

The role of the Hedgehog (Hh) pathway in regulating skeletal development has been extensively studied; however its role in skeletal repair is less well understood. In this study we sought to determine the effects of pharmacological Hh pathway activation on fracture repair in a healing-challenged model. It has been shown that older rodents demonstrate less robust fracture healing, characterized by delayed periosteal bridging and a downregulation of hedgehog related gene expression. Expression of *Ihh*, *Gli1* and *Ptch1* during fracture healing of aged mice (18mo) is diminished when compared to younger mice (10 wk). Specifically, *Ihh* expression in older mice was reduced to less than 50% of expression in young mice at both 3 and 7 days post fracture. Therefore, we hypothesized that Hh pathway activation will overcome the age-related decline in Hh signaling and improve radiographic and histologic aspects of fracture healing. Using the *Gli1-Cre-ERT2;Ai14* mice we were able to localize Hh signaling in the fracture callus at 5 and 7 days post fracture. Strong Hh activity was seen in the woven bone and the periphery of the cartilaginous area of the callus. Daily dosing of Hh agonist (Hh-Ag1.5) or vehicle for 28 days was well-tolerated by the mice and demonstrated sustained activation of the Hh pathway (*Gli1*, *Ptch1* upregulation by qPCR by >200 and 300% , respectively). In addition, 28 days of treatment with Hh agonist increased trabecular bone formation compared to vehicle treated group (60% increase in BV/TV). This demonstrated the potent bone anabolic effect of enhanced Hh signaling. Assessment of microCT at 2 weeks post fracture in aged (18mo) mice demonstrated improved callus BMD in the Hh agonist treatment group (Figure 1). In summary, the Hh pathway is important in regulating fracture healing and pharmacological modulation may lead to enhanced healing.

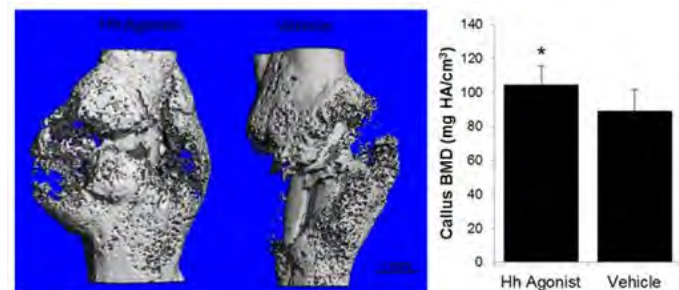


Figure 1. Daily systemic treatment with Hh agonist improved fracture healing.

Disclosures: Jennifer McKenzie, None.

FR0164

Crosstalk between Sensory Neuropeptides Regulating Heterotopic Ossification in Tendon. Ceren Tuzmen*, Phil Campbell, Lee Weiss. Carnegie Mellon University, USA

Heterotopic ossification (HO) of soft tissues is a costly medical problem with no effective cure. It is usually predisposed by neurogenic and musculoskeletal trauma, where systemic release of certain factors leads to overexpression of bone morphogenetic proteins (BMPs). BMP-2, one of the most studied of the BMPs, has been shown to be involved in most common cases of HO by promoting osteogenic differentiation of primitive stem cells into osteocytes at an anatomical site ectopic to bone. Despite advances in understanding the pathophysiology of HO, the associated cellular and molecular mechanisms are not well understood. The peripheral nervous system acting via specific neuromediators plays an active role in regulation of cellular and extracellular changes observed in ossified tendons. Sensory neuropeptides, including substance P (SP) and calcitonin gene-related peptide (CGRP), are upregulated in patients with injured or degenerative tendons, as well as in animal disease models and they are known to be involved in BMP-2 induced osteogenic differentiation *in vitro*. In this study, we assessed the effect of SP and/or CGRP on BMP-2 induced osteogenic differentiation *in vitro* and on tendon HO *in vivo*. Unique

to this study is to deliver SP and/or CGRP using biopatterning technology which enables spatial control of the tendon microenvironment.

Our *in vitro* and *in vivo* data suggest a possible connection between SP and CGRP pathways and the BMP-2 pathway. *In vitro*, neither of the treatments had significant effect on BMP-2 induced alkaline phosphatase activity (Fig1). However, SP alone significantly enhanced while CGRP had no effect on BMP-2 induced mineralization (Fig2). *In vivo*, SP promoted HO but CGRP had no effect on tendon HO (Fig3). Remarkably, when SP and CGRP are delivered together, both *in vitro* and *in vivo*, CGRP was able to counteract the effect of SP on BMP-2-induced mineralization and bone formation in tendon (Fig2,3). In conclusion, we were able to spatially promote and further reverse HO in Achilles tendons using biopatterning as delivery system. To our knowledge there is no other study reported that involves administration of SP and/or CGRP in tendon to elucidate the effect of these neuropeptides in tendon HO as well as the interaction between SP and CGRP related to tendon HO.

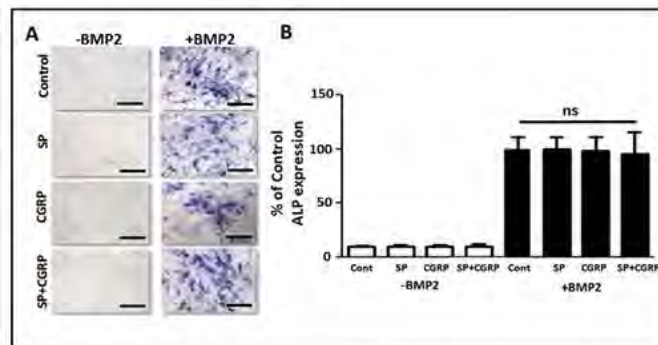


Figure 1 Pluripotent C2C12s cultured with neuropeptides \pm BMP-2. A. Cells cultured in normal growth medium (Control); growth medium with SP, CGRP, SP and CGRP; with or without BMP-2. Blue stands for the Alkaline Phosphatase (ALP) stain. All treatments have a final concentration of 100ng/ml. Scale bar: 200 μ m. B. Quantification of ALP staining for each experimental group are normalized to control. n=9.

Figure 1

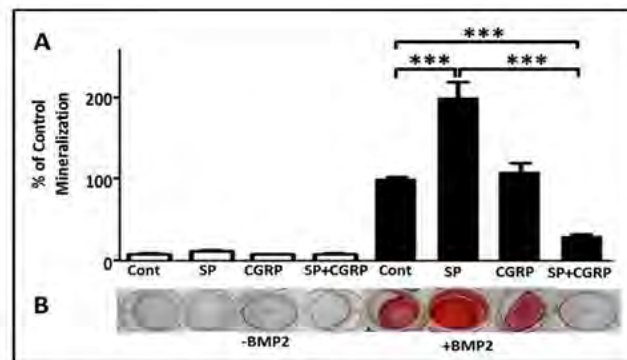


Figure 2 Pre-osteoblastic MC3T3s cultured in osteogenic media with neuropeptides \pm BMP-2. A. Quantification of Alizarin Red Stain (ARS) for each experimental group are normalized to control. n=6-9. *** indicates $p \leq 0.001$. B. Whole plate images of pre-osteoblasts stimulated with SP, CGRP, SP and CGRP, with or without BMP-2. Red stands for ARS. All treatments have a final concentration of 100ng/ml. Controls did not receive any treatment.

Figure 2

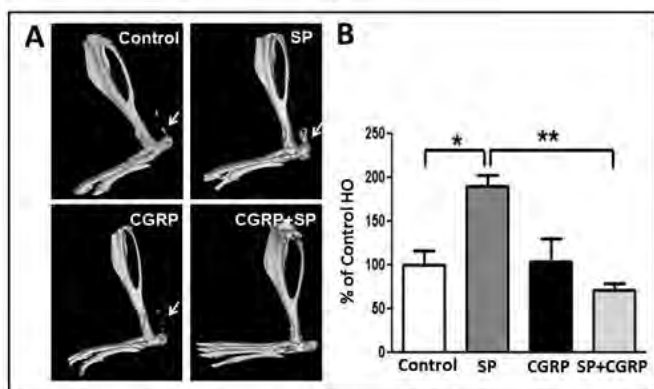


Figure 3. Biopatterned constructs implanted to Achilles tendon of mice. **A.** μ CT scans of the operated legs 6 weeks post-surgery, control legs received constructs with no treatment. **B.** Quantification of HO around calcaneus and mid-tendon, all measurements are normalized to control. $n=4-6$, * indicates $p<0.05$, ** indicates $p<0.01$.

Figure 3

Disclosures: Ceren Tuzmen, None.

This study received funding from: NIH

FR0166

LRP4 in osteoblasts suppresses bone formation and promotes osteoclastogenesis and bone resorption. Wen-Cheng Xiong*, Lei Xiong, Georgia Regents University, USA

LRP4 (low-density lipoprotein receptor related protein 4) is a member of the LDL receptor family, whose mutations have been identified in patients with high bone-mass such as sclerosteosis and Van Buchem diseases. However, it remains unknown how LRP4 regulates bone-mass homeostasis in vivo. Here we provide evidence that LRP4 null mutation or specific mutation in osteoblast-lineage cells increased cortical and trabecular bone-mass, which was associated with elevated bone formation and impaired bone resorption. This phenotype was not observed in osteoclast-selective LRP4 knock-out mice. Mechanistic studies indicate that loss of LRP4 function in osteoblast-lineage cells increased serum levels of sclerostin, a key factor for bone mass homeostasis that interacts with LRP4, but abolished the inhibition of Wnt/ β -catenin signaling and osteoblastic differentiation by sclerostin. Concomitantly, sclerostin-induction of RANKL (receptor activator of nuclear kappa B ligand) was impaired, leading to a lower ratio of RANKL over OPG (osteoprotegerin) (a key factor for osteoclastogenesis). Taken together, these results support the view for LRP4 as a receptor of sclerostin to inhibit Wnt/ β -catenin signaling and bone formation, and identify LRP4 as a critical player in bone-mass homeostasis.

Disclosures: Wen-Cheng Xiong, None.

FR0167

Milk fat globule-epidermal growth factor 8 (MFG-E8) is a novel anti-inflammatory factor in rheumatoid arthritis in mice and men. Martina Rauner*¹, Elise Albus², Kathrin Sinnigen², Maria Winzer², Sylvia Thiele², Anke Hannemann³, Sylvia Grossklauss⁴, Triantafyllos Chavakis⁴, Mark Udey⁵, Lorenz Hofbauer². ¹Medical Faculty of the TU Dresden, Germany, ²Department of Medicine III, Technische Universität Dresden, Germany, ³University of Greifswald, Germany, ⁴Department of Clinical Pathobiochemistry & Institute for Clinical Chemistry & Laboratory Medicine, Technische Universität Dresden, Germany, ⁵Dermatology Branch, Center for Cancer Research, National Cancer Institute, USA

Milk fat globule-epidermal growth factor 8 (MFG-E8) mediates the clearance of apoptotic cells and is implicated in the pathogenesis of autoimmune and inflammatory diseases. As MFG-E8 has recently also been shown to influence bone metabolism, we investigated its role in the pathogenesis of rheumatoid arthritis (RA) and the subsequent bone destruction. The regulation of MFG-E8 by inflammation was assessed in osteogenic cells *in vitro*, in arthritic mice and in patients with RA. K/BxN arthritis was applied to MFG-E8 knock-out mice to assess its role in the pathogenesis of arthritis. Stimulation of osteoblasts with LPS and TNF- α down-regulated the expression of MFG-E8 by 30-35% in a receptor-dependent manner. MFG-E8-deficient osteoblasts responded to LPS with a stronger production of the pro-inflammatory cytokines TNF and IL-6. *In vivo*, MFG-E8 mRNA levels were 52% lower in paw extracts of collagen-induced arthritic mice and 24-42% lower in the serum of arthritic mice using two different arthritis models. Similarly, patients with RA ($n=93$) had lower serum concentrations of MFG-E8 (-21%) as compared to healthy controls ($n=186$). In a subgroup of patients who had a moderate to high

disease activity at the time of measurement ($n=21$), serum concentrations of MFG-E8 rose when remission or low disease activity had been achieved after successful treatment (+49%). Finally, MFG-E8-deficient mice subjected to K/BxN arthritis exhibited a stronger disease burden, an increased number of neutrophils and CD3-positive T cells in the joints, and a more extensive local and systemic bone loss, which was associated with an increased number and activity of osteoclasts. Thus, MFG-E8 is a relevant factor in the pathogenesis of RA and subsequent bone destruction. Whether MFG-E8 qualifies as a novel biomarker or therapeutic target for the treatment of RA needs to be addressed in further studies.

Disclosures: Martina Rauner, None.

FR0168

Tanshinol reverses the impaired bone formation of Glucocorticoid-induced osteoporosis in rats: a role for KLF15. Liao Cui¹, Yajun Yang*², Yanjie Su², Yahui Chen², Yuyu Liu², Tie Wu². ¹Guangdong Medical College, Peoples republic of china, ²Department of Pharmacology, Guangdong Key Laboratory for R & D of Natural Drugs, Guangdong Medical College, China

Objective: Decreased bone formation is responsible for the pathogenesis of glucocorticoid-induced osteoporosis (GIO), while the mechanism remains to be elucidated. Krueppel-like factor 15 (KLF15), a direct GR target gene, exerts an extensive role in pathophysiologic progression of diverse diseases. This study aims to investigate the action of Tanshinol (termed D(+)- α -3,4-dihydroxyphenyl lactic acid), a botanical antioxidant, on bone metabolism involving in KLF15-dependent regulation of Wnt/FoxO pathway in GIO rats. Methods: KLF15 mRNA level of bony tissue were detected in 4-month-old female Sprague-Dawley rats administered prednisone acetate (GC, 5mg/kg), GC plus Tanshinol (Tan, 16mg/kg) and GC plus Resveratrol (Res, 5mg/kg, positive control) for 14 weeks. Micro-CT, histomorphometry, biomechanical assay, serum biomarkers of bone turnover, and gene or protein expression analysis in bone tissue were investigated. Cell viability, cell apoptosis, capacity of bone formation, oxidative stress level, Wnt signaling and FoxO3a pathway were measured in C2C12 cells and MC3T3-E1 cells exposed to dexamethasone (Dex, 1 μ M) in the presence or absence of KLF siRNA or overexpression of KLF15. Results: Tanshinol exerted a preventive effect on impairment of bone formation and bone architecture, and the following decreased bone mass (%BV/TV) and bone quality in association with inhibition of the increased KLF15 mRNA level in GIO rats. Furthermore, Tanshinol maintained bone homeostasis involving in up-regulation of Wnt signaling and counteracted osteoblastic apoptosis elicited by oxidative stress via down-regulation of FoxO3a pathway in GIO rats. Further evidence *in vitro* confirmed that Tanshinol counteracted the GR-dependent activation of KLF15 cascade pathway, contributing to activation of Wnt signaling and the subsequent bone formation, and to inhibition FoxO3a pathway and the following caspase 3-dependent apoptosis in the two cell lines treated with Dex in a synergistic manner with KLF15 siRNA. In addition, transcription activity of Tcf-luc was stimulated by KLF15 siRNA and suppressed by overexpression of KLF15 in the two cell lines treated with Dex, especially in the presence of Tanshinol, which were adverse to the alterations of FoxO3a-Luc. Conclusion: Tanshinol attenuates reduction of Wnt-mediated bone formation and FoxO3a-triggered osteoblastic apoptosis in GIO via inhibition of KLF15-dependent pathway. The study may provide a novel target to treat GIO.

Disclosures: Yajun Yang, None.

FR0169

Annexin A5 inhibits bony outgrowth at tendon/ligament insertion sites. Akemi Shimada*¹, Yoshinori Arai², Satoshi Wada³, Hisashi Ideno⁴, Taichi Kamiyunt³, Kazuhisa Nakashima⁴, Koichiro Komatsu⁴, Teruhito Yamashita⁵, Yoichi Ezura⁶, Norio Amizuka⁷, Ernst Pöschl⁸, Bent Brachvogel⁹, Yoshiki Nakamura³, Akira Nifuji⁴. ¹Tsurumi University School of Dental Medicine, Japan, ²Nihon University, School of Dentistry, Japan, ³Department of Orthodontics, Tsurumi University School of Dental Medicine, Japan, ⁴Department of Pharmacology, Tsurumi University School of Dental Medicine, Japan, ⁵Division of Hard Tissue Research, Institute for Oral Science, Matsumoto Dental University, Japan, ⁶Department of Molecular Pharmacology, Medical Research Institute, Tokyo Medical & Dental University, Japan, ⁷Department of Developmental Biology of Hard Tissue, Division of Oral Health Science, Graduate School of Dental Medicine, Hokkaido University, Japan, ⁸School of Biological Sciences, University of East Anglia, Norwich Research Park, Norwich, United Kingdom, ⁹Experimental Neonatology, Department of Pediatrics & Adolescent Medicine, Center for Biochemistry, Medical Faculty, University of Cologne, Germany

Formation and remodeling of insertion sites of tendon/ligament to bone (enthesis) has remained unclear. Annexin a5 (Anxa5), which belongs to the annexin family of calcium-dependent phospholipid binding proteins, is known to have many functions as mechanical sensor in osteoblast, signal molecule in cell apoptosis, and regulator of

cell membrane repair. Previous studies suggested that Anxa5-deficient mouse in which lacZ was inserted into Anxa5 gene (*Anxa5^{lacZ}*) displayed no obvious changes in skeletal development by 3 months of age. In the present study, we analyzed skeletal phenotypes in detail in adult *Anxa5^{lacZ}* mice. We observed that Anxa5 was strongly expressed at articular cartilage, periosteum, and tendon/ligament insertion sites to bone by lacZ staining. At 4 weeks of age, there were no obvious difference in bone morphology between wild and *Anxa5^{lacZ}* mice. After 7 weeks of age, however, increase of bony outgrowth at enthesis in *Anxa5^{lacZ}* mice was observed, while there were no obvious differences in morphology of long bones. These phenotypes were commonly observed in long bones as well as mandibular bones. To examine the contribution of muscle movements on the bony outgrowth at enthesis, we performed tenotomy in mice in which movement of anterior tibial muscle was impaired by surgical releasing muscle from enthesis at 12 weeks of age. In the tenotomy mice, bony outgrowth of tibial bone in *Anxa5^{lacZ}* mice were decreased to comparable levels to that of wild mice after 8 weeks of operation. These results suggest that Anxa5 inhibits the bony outgrowth at enthesis which depends on mechanical stimuli brought by muscle movements.

Disclosures: Akemi Shimada, None.

FR0170

Fusion Induced Hypertrophy of Skeletal Muscle Is Modulated By Pin1 through the Smad3 Pathway. Rabia Islam*, Won-joon Yoon, Young-dan Cho, Woo-Jin Kim, Han-sol Bae, Hye-rim Shin, Bong-soo Kim, Kyung Mi Woo, Jeong-Hwa Baek, Hyun-Mo Ryoo. Seoul National University, School of Dentistry, Department of Molecular Genetics, South Korea

The regulation of skeletal muscle fusion is necessary for normal embryo development as well as for the repair of damaged muscle in adult life. We had previously observed that the enzyme Peptidyl-prolyl cis-trans isomerase NIMA-interacting 1 (Pin1) is involved in osteoclast fusion. The objective of this study was to find out if Pin1 is also involved in the fusion induced hypertrophy of myoblasts. *Pin1^{-/-}* mice have neurodegenerative features so we selected the *Pin1^{+/-}* mice as a genetic model to analyze the effect of Pin1 in muscle fusion. Different hind limb muscles from *Pin1^{+/+}* and *Pin1^{+/-}* mice were collected and processed for histological analysis. In vitro studies were carried out with the common model for muscle, C2C12 myoblast cell line. We compared the *Pin1^{+/+}* and *Pin1^{+/-}* muscle cross sections and found that *Pin1^{+/-}* muscles had increased bulk as indicated by the weight and distribution of the muscle fiber CSA (cross sectional area). *Pin1^{+/-}* mice had complete recovery of muscle weight and myofiber size in an earlier time point than *Pin1^{+/+}* mice after muscle injury was inflicted by injecting cardio toxin from *Naja mossambica*. The number of nascent myofibers formed after muscle injury was also higher in *Pin1^{+/-}* mice. We found that overexpression of Pin1 suppressed myoblast fusion in vitro also. Low dose of Pin1 inhibitor, DTM (0.01 μ M) treatment actually caused more enhanced fusion than higher dosage (1 μ M). With very high concentration of DTM (10 μ M) treatment fusion was reduced even in the absence of cytotoxicity. The R-Smads 1, 2 and 3 are well known targets of Pin1. In muscle we found only p-Smad3, a key signaling mediator for the major regulators of skeletal muscle hypertrophy Tgf- β and myostatin pathway, was decreased with minimal inhibition of Pin1. With low dose of Pin1 inhibitor treatment total Smad3 expression level was decreased in vitro and in *Pin1^{+/-}* muscle in vivo. We observed that Pin1 is crucial for maintaining the stability of Smad3 and preventing Smad3 ubiquitination. Our results show that the dosage of Pin1 protein is very critical for regulation of the Smad3 signaling pathway to maintain the muscle bulk. This knowledge of the basic molecular mechanism behind myoblast fusion can contribute to the development of therapeutics for muscle repair in debilitating diseases.

Disclosures: Rabia Islam, None.

FR0172

Identification of Muscle-derived Mesenchymal Stem Cells in Traumatic Heterotopic Ossification. Zijun Zhang*, Reed Michell², Lew Schon². ¹Union Memorial Hospital, USA, ²MedStar Union Memorial Hospital, USA

Heterotopic ossification (HO) is a pathological condition that muscles calcify. Local muscle damage and fracture/osteotomy are often associated with the development of HO. The source of cells in the muscle that contribute to the HO develop is unclear. In muscles, there are two types of progenitor cells that are potent in differentiation: satellite cells and mesenchymal stem cells (M-MSCs). Both of them have been demonstrated are capable of osteogenic differentiation. This study was designed to differentiate the source of cells that participate in the development of HO.

HO surgical model: Surgery that included osteotomy of great trochanter and muscle injury (O+M) was performed on the right hip of mice to simulate the tissue condition for HO formation. Muscle injury was done by clamping the gluteus maximus and gluteus medius for 5 min. For controls, either osteotomy of great trochanter (O) or muscle injury (M) was performed on mice. Mice in groups O+M, O and M, were euthanized at days 1, 3, 5 and 10. Gluteus maximus and gluteus medius were collected for muscle digestion. The isolated cells were cultured in an osteogenic medium for 3 weeks and osteogenesis was examined with gene expression of type I collagen, osteocalcin and Runx2.

For cells harvested on 1 day post surgery, gene expression of type I collagen, osteocalcin and Runx2 was not significantly different among groups M, O and M+O. In group O, muscle cells that harvested on days 3, 5 and 10 moderately increased the

expression of type I collagen over the time, comparing with the corresponding time-points in group M. Other osteogenic genes such as Runx2 and osteocalcin, however, were not up-regulated in the cells of both groups O and M. Notably, the expression of type I collagen, Runx2 and osteocalcin by the cells of group M+O harvested on days 3, 5 and 10 was significantly increased, compared with the corresponding ones in groups M and O. Furthermore, the expression of type I collagen, Runx2 and osteocalcin by the cells of group M+O was gradually increased from day 1 to day 10.

Flow cytometry was performed on cells isolated from groups M, O, and M+O (day 10) for the expression of CD73, CD90, CD105, CD56 and PDGFR-alpha (CD140). In general, M-MSCs isolated from groups M, O and M+O (day 10) had similar expressions profiles of common MSC surface markers, except the expression of CD90 was lower in the groups O and M+O than in group M. CD56, representing myogenic progenitors, was highly expressed in M-MSCs isolated from group M (day 10), as compared with groups O and M+O (day 10) ($p < 0.05$). CD140, also known as platelet-derived growth factor receptor α (PDGFR-alpha), is a specific marker of M-MSCs. Among the three experimental groups, CD140 was expressed the highest in group M+O (day10), followed by group O and group M ($p < 0.05$).

The data indicate that M-MSCs, rather than muscle satellite cells, participate in HO formation in the muscles.

Disclosures: Zijun Zhang, None.

FR0174

Increased Glycolytic Fast-twitch Skeletal Muscle Growth in Mice has Beneficial Effects on Both Loaded and Non-loaded Skeletal Sites. Joshua Farr*, Glenda Evans¹, Thomas White¹, Daniel Fraser¹, Kenneth Walsh², Sundeep Khosla¹, Nathan LeBrasseur¹. ¹Mayo Clinic, USA, ²Boston University, USA

In addition to mechanically loading bone, skeletal muscle may stimulate bone formation via secreted factors, or "myokines". To advance this concept, we examined the skeletal phenotype of a unique skeletal muscle-specific conditional transgenic mouse expressing a constitutively active form of Akt1. Activation of the Akt1 transgene by administration of doxycycline (DOX) results in hypertrophy of glycolytic fast-twitch muscle fibers (Cell Metab 7:159-72, 2008).

Akt1 transgenic mice (4 week-old female) were administered either DOX (n = 14) or vehicle (n = 11) for 6 weeks. All mice underwent *in vivo* pQCT scanning of the tibia at baseline and end of study. μ CT scans were performed on excised femurs and lumbar spines following sacrifice. Quadriceps and gastrocnemius weights were recorded and lean and fat mass were quantified by EchoMRI. At the study midpoint, physical activity was monitored over a 48-hour period using a Comprehensive Laboratory Animal Monitoring System.

At baseline, the two groups of mice were of similar weight with no differences any bone or soft tissue parameters. Physical activity levels did not differ between the groups. DOX-mediated transgene activation caused a doubling in both quadriceps and gastrocnemius weights ($p < 0.001$). These increases in muscle mass contributed to a modestly greater gain in total body lean mass in DOX- compared to vehicle-treated mice (+39% vs +23%, $p = 0.09$) and an attenuated accrual of fat mass (+14% vs +44%, $p < 0.05$). At the end of the study, pQCT analysis of the tibia revealed that DOX-treated mice had significantly thicker cortices than vehicle-treated mice (+7.2%, $p < 0.05$), resulting mainly from periosteal expansion (+3.2%, $p < 0.05$). μ CT analysis of the femur confirmed that DOX-treated mice had thicker cortices than vehicle-treated mice (+5.6%, $p < 0.05$). Finally, DOX-treated mice had significantly (all $p < 0.05$) better trabecular microarchitecture at the lumbar spine compared to vehicle-treated mice (i.e., increased trabecular number [+12.0%] and thickness [+6%]; decreased trabecular separation [-10.9%] and SMI [-15.3%]).

Collectively, these results suggest that glycolytic fast-twitch skeletal muscle growth has beneficial effects on the skeleton at both loaded (femur and tibia) and non-loaded (spine) sites. Future studies utilizing this model may provide new insights into the "crosstalk" between skeletal muscle and bone, and ultimately lead to the identification of novel musculoskeletal therapeutic targets.

Disclosures: Joshua Farr, None.

FR0177

Free Fatty Acid Induced Insulin Resistance in Human Synovocytes: A Potential Link Between Obesity and Osteoarthritis. Eric Schott*, Daisuke Hamada², Robert Maynard¹, Michael Zuscik¹, Robert Mooney³. ¹Center for Musculoskeletal Research, University of Rochester Medical Center, USA, ²Department of Orthopedics, Tokushima University Hospital, Japan, ³Department of Pathology, University of Rochester Medical Center, USA

Obesity-induced type 2 diabetes (T2D) is an established major risk factor for the development of osteoarthritis (OA). To address the molecular basis of this comorbid interaction, we previously demonstrated high-fat (HF) diet-induced T2D in mice leads to increased pro-inflammatory cytokine expression, including TNF and IL-6, in the synovium of the knee. Consistent with this, we also showed that TNF expression is increased in the synovium from obese/T2D OA patients compared to non-obese control subjects. Importantly, synovium from obese/T2D patients is insulin resistant, evidenced by decreased insulin-induced phosphorylation

of Akt compared to the non-obese synovium. Moreover, we have established that synovial insulin resistance may promote OA since TNF-induced catabolic enzyme and pro-inflammatory cytokine expression in human fibroblast-like synoviocytes (FLSs) is significantly blunted by insulin. It is known that in the obese state, increased free fatty acid (FFA) levels lead to upregulation of pro-inflammatory cytokines and insulin resistance. Therefore, we hypothesize that the accelerated progression of OA in obesity is, in part, due to elevated saturated FFA levels leading to increased cytokine expression and impaired insulin signaling in the synovium. To address this hypothesis *in vitro*, FLSs from non-diabetic patients were treated with palmitic acid (PA), the most abundant saturated FFA in the circulation. PA induced an inflammatory response with expression of IL-6 and MMP13 increasing in a dose dependent manner. Importantly, PA also induced insulin resistance in FLSs in less than 60 min, as demonstrated by a 75% blunting of phosphorylation of Akt in response to insulin. Toll-like receptor 4 (TLR4), the receptor for lipopolysaccharide (LPS), has been implicated as a mediator of PA-induced insulin resistance in various cells. When FLSs were treated with LPS, insulin signaling was impaired as reflected by decreased insulin-dependent pAkt levels, though the effect was less than that of PA, suggesting more than one pathway mediates the effect of PA on FLSs. Taken together, these data demonstrate that PA increases the expression of pro-inflammatory cytokines and induces insulin resistance. This may be an important mechanism mediating the increased OA risk in obesity.

Disclosures: Eric Schott, None.

FR0179

Therapeutic effects of a novel FGFR1 inhibitor on osteoarthritis. Yangli Xie^{*1}, Wei Xu², Siru Zhou², Zuqiang Wang², Junlan Huang², Xianding Sun², Wanling Jiang², Xiaolan Du², Lin Chen². ¹Third Military Medical University, Peoples republic of china, ²Center of Bone Metabolism & Repair, Department of Rehabilitation Medicine, State Key Laboratory of Trauma, Burns & Combined Injury, Trauma Center, Institute of Surgery Research, Daping Hospital, Third Military Medical University, China

Objective. Fibroblast growth factors (FGFs) and their receptors (FGFRs) play important roles in articular cartilage homeostasis. Our previous study revealed that genetic inhibition of Fibroblast growth factor receptor 1 in knee cartilage attenuates the degeneration of articular cartilage in adult mice, suggesting that FGFR1 may be a potential therapeutic target for treating osteoarthritis. This study aims to investigate whether a novel FGFR1 inhibitor, GL-141 (screened through molecular docking approach by collaborators) has therapeutic effects on osteoarthritis.

Methods. Human articular chondrocytes were incubated with FGFR1 inhibitor followed by IL-1 β for 24 hours, then the expression levels of adams-5, mmp-13 and aggrecan were detected by real-time PCR, the protein level of MMP-13 were detected by western blot. Surgical destabilization of the medial meniscus (DMM) was performed to induce experimental murine OA. Intra-articular injections of 10 μ l of GL-141 were administered twice weekly for 4 and 8 weeks. Articular cartilage damage was analyzed by histology using the OARSI histologic scoring system at 4 and 8 weeks after surgery. MMP-13, type II collagen, type X collagen expressions were analyzed by immunohistochemistry.

Results. The mRNA levels of adams-5 and mmp-13 were increased and the mRNA level of aggrecan was decreased in human articular chondrocytes after IL-1 β treatment, as compared to those in vehicle-treated human articular chondrocytes. Treatment with GL-141 resulted in a remarkable reduction in the IL-1 β stimulated mRNA levels of adams-5 and mmp-13 and a marked increasing of aggrecan mRNA level in human articular chondrocytes. MMP-13 protein level was increased after IL-1 β treatment in articular chondrocytes. In the presence of FGFR1 inhibitor, the degree of increase in the protein level of MMP-13 was attenuated in IL-1 β treated chondrocytes. Intra-articular injection of GL-141 attenuated the DMM-induced cartilage destruction and matrix loss in mice knee joints. Inhibitor-treated mice showed higher Type II collagen expression and lower MMP-13 and type X collagen expression in articular cartilage than that in mice that underwent vehicle treatment.

Conclusion. GL-141 treatment reduced the catabolic events induced by IL-1 β in human articular chondrocytes. Intra-articular injection of GL-141 attenuates the degeneration of articular cartilage in mice.

Disclosures: Yangli Xie, None.

FR0181

Communication of Cyclic AMP by Connexin43 Gap Junctions Influences Osteoblast Signaling and Gene Expression. Aditi Gupta^{*}, Hidayah Anderson, Margaret Ren, Joseph Stains. University of Maryland School of Medicine, USA

While connexin43 (Cx43) containing gap junctions play an important role in bone modeling and remodeling, very little is known about the biologically relevant second messengers communicated by Cx43 in bone. In this study, we have used MC3T3-E1 mouse osteoblast and UMR106 rat osteosarcoma cells to test the hypothesis that cyclic AMP (cAMP) is a second messenger communicated by bone cells that impacts osteoblast function. Overexpression of Cx43 in these cells enhanced the responsiveness of a cAMP-response element driven transcriptional reporter (CRE-luc) and enhanced phospho-CREB levels following treatment with prostaglandin E2 (PGE2), forskolin

or expression of a constitutively active Gs-alpha. In addition, activation of cAMP-dependent signaling led to an increase in ERK1/2 activation, an effect that was also enhanced by Cx43 expression. The protein kinase A (PKA) inhibitor H89 blocked the increase in phospho-CREB levels and CRE-luc transcriptional activity, as well as the activation of ERK1/2. Notably, the enhancement of signaling caused by Cx43 expression in PGE2 treated cells was not accompanied by a further increase in cAMP levels as determined by an ELISA assay, suggesting that the cAMP was shared between cells rather than Cx43 enhancing cAMP production. In support of this point, using a novel assay in which one set of cells express a constitutively active Gs-alpha (donor cells) were co-cultured with a second set of cells expressing a cAMP-response element driven transcriptional reporter (acceptor cells), we showed that when both the donor cells and acceptor cells express Cx43, then we could detect robust activation of the CRE-luc reporter in the acceptor cells, indicating communication of the cAMP-dependent signal. This stimulation was not seen when the donor and acceptor cells were co-cultured in a transwell chamber where cell-to-cell contacts were not formed between the donor and acceptor cell populations, nor when the cells did not both express Cx43. Finally, we showed that Cx43 increased the cAMP-dependent expression of RANKL in UMR-106 cells in culture and enhanced the repression of Sost, implying a potential mechanism for the modulation of tissue remodeling. In total, these data demonstrate that Cx3 can communicate cAMP to impact signal transduction cascades and the expression of key bone effector molecules.

Disclosures: Aditi Gupta, None.

FR0182

Intravital imaging of coupling between osteoblasts and osteoclasts by using multiphoton microscopy. Masayuki Furuya^{*1}, Junichi Kikuta², Hiroki Mizuno², Shigeto Seno³, Hiroki Maeda⁴, Kazuya Kikuchi⁴, Hideo Matsuda³, Hideki Yoshikawa¹, Masaru Ishii². ¹Department of Orthopaedics, Graduate School of Medicine, Osaka University, Japan, ²Department of Immunology & Cell Biology, Graduate School of Medicine & Frontier Biosciences, Osaka University, Japan, ³Department of Bioinformatic Engineering Graduate school of Information Science & Technology, Osaka University, Japan, ⁴Department of Material & Life Sciences, Graduate School of Engineering, Osaka University, Japan

Background/Purpose: Bone is constantly remodeled by bone-resorbing osteoclasts (OCs) and bone-forming osteoblasts (OBs). Although it has long been believed that bone homeostasis is tightly regulated through communication between OBs and OCs ('coupling'), the fundamental process and the dynamics have remained elusive. Previously we originally established an intravital bone imaging system with multiphoton microscopy and reported the dynamics of OCs and osteoclast precursor monocytes *in vivo*. This study aimed to reveal the mechanism of coupling and investigate the effects of parathyroid hormone (PTH) on coupling in living bone tissues by using an intravital bone imaging system.

Methods: For visualizing coupling between OBs and OCs, we generated the double fluorescently-labeled mice (Col2.3-ECFP/TRAP-tdTomato mice) by crossing Col2.3-ECFP mice where ECFP was expressed in Col1a1⁺ OBs with TRAP-tdTomato mice where tdTomato was expressed in TRAP⁺ OCs. We observed calvaria bone tissues of Col2.3-ECFP/TRAP-tdTomato mice by using an advanced intravital bone imaging system with multiphoton microscopy that we have previously reported. We investigated the function of OCs by means of a pH-sensing fluorescent chemical probe which we previously developed to detect the acidification by bone-resorbing OCs *in vivo*. In addition for examining the effects of PTH, teriparatide (40 μ g/kg/day) was administered by subcutaneous injections 5 days a week. 0, 1, 3, or 6 weeks after the initiation of the treatment, images were acquired.

Results: We succeeded in visualizing the interaction of OBs with OCs in live bone tissues. In normal condition we could observe some clusters of OBs and OCs respectively. In boundary areas between OBs and OCs, there were a few interaction areas, where OCs had some synapse like projections to OBs. We also found that treatment of PTH increased bone volume by the anabolic effect of PTH, the number of OBs and OCs, and the number of interaction areas *in vivo*. Furthermore we could demonstrate that OCs interacting with OBs have lower ability of bone resorption than non-interacting OCs in live bone tissues. **Conclusion:** By visualizing *in vivo* behaviors of OBs and OCs simultaneously, we found a few areas with interaction of OBs with OCs in normal condition. In addition, we revealed that PTH could not only increase the number of OBs and OCs, but also the number of interaction areas and inhibit bone resorption in live bone tissues.

Disclosures: Masayuki Furuya, None.

FR0183

Matrix Vesicles Mediate the Cell-to-Cell Transmission of MicroRNA-125b as an Inhibitor of Osteoclastic Bone Resorption. Yuichiro Takei^{*1}, Yuko Nakao², Tomoko Minamizaki¹, Yasumasa Irie², Faisal Ahmed², Hiroataka Yoshioka¹, Shumpei Niida³, Kotaro Tanimoto¹, Yuji Yoshiko¹. ¹Hiroshima University Institute of Biomedical & Health Sciences, Japan, ²Hiroshima University Graduate School of Biomedical & Health Sciences, Japan, ³Biobank, National Center of Geriatrics & Gerontology, Japan

Matrix vesicles (MVs) play a key role during the initial stages of bone mineralization. MVs bud off from the osteoblast plasma membrane and located at the osteoid matrix. Mineralization regulatory molecules are accumulated in MVs, and initial hydroxyapatite crystals form within these microstructures. Additionally, MV-derived TGF- β and IGF-I are released from the matrix during bone resorption and contribute to bone formation. In our global analysis of microRNAs (miRs) in osteoblasts, we identified that miR-125b and let-7c are selectively transported into MVs. Because these miRs may be targeted to genes involved in bone formation and resorption, we investigated whether MV mediates osteoblastogenesis and/or osteoclastogenesis by a miR-dependent mechanism. We examined the effects of MVs on mouse osteoblastic MC3T3-E1 cells and mouse macrophage RAW-D cells. MVs were isolated by collagenase and ultracentrifugation from human and rodent osteoblasts. MVs had no obvious effects on proliferation and osteogenic differentiation in MC3T3-E1 cells. The vesicles, however, suppressed RANKL-dependent osteoclast (OC) formation from RAW-D cells. In accordance with this, cells with MVs expressed reduced levels of OC marker genes including *Acp5*, *Ctsk* and *Destamp*. These effects were mimicked in primary mouse macrophages. We confirmed that MVs are incorporated relatively quickly and accumulated in RAW-D cells but not MC3T3-E1 cells. Treatment of MVs increased levels of miR-125b but not let-7c in RAW-D cells. Besides being a suppression of RANKL-dependent OC formation, transfection of miR-125b decreased the expression of its predicted target gene, *Prdm1*, and OC marker genes in RAW-D cells. To determine whether miR-125b affects bone resorption in vivo, we used a mouse lipopolysaccharide (LPS)-induced calvarial osteolysis model. miR-125b partially inhibited LPS-dependent osteoclastic osteolysis, when administered subcutaneously over the calvaria. These findings suggest MV-mediated miRs transfer from osteoblasts to osteoclasts, which provides new insights into the importance of MVs for cell-to-cell interactions in bone.

Disclosures: Yuichiro Takei, None.

FR0184

New Insight into Collagen Assembly Dynamics in Osteoblasts by Live Cell Imaging. Michael Grillo^{*1}, LeAnn Tiede-Lewis², Lora McCormick¹, Charlotte Phillips³, Hong Zhao¹, Sarah Dallas¹. ¹University of Missouri - Kansas City, USA, ²University of Missouri-Kansas City, USA, ³University of Missouri - Columbia, USA

Type I collagen, the major bone matrix protein, consists of heterotrimers of two $\alpha 1(I)$ chains and one $\alpha 2(I)$ chain, encoded by the COL1A1 and COL1A2 genes. Although the collagen biosynthetic pathway is well understood, the dynamic process by which collagen is assembled into extracellular fibers is less clear. We previously generated transgenic mice expressing GFP-tagged $\alpha 2(I)$ collagen driven by the 3.6kb-COL1A1 promoter. To gain new insight into collagen assembly dynamics we have developed immortalized osteoblast-like cell lines. One cell line expresses GFP-tagged collagen. Another co-expresses GFP-collagen and RFP-actin (p^{cmv}LifeAct-TagRFP). The third co-expresses GFP-collagen and a membrane-targeted TdTomato. Widefield and confocal live-cell imaging was performed on these cell lines with or without transfection of an endoplasmic reticulum imaging probe (CellLightER-RFP) or golgi probe (CellLight Golgi-RFP). Dual imaging of GFP-collagen and ER-RFP showed that prior to addition of ascorbate GFP-collagen was localized in the ER. After ascorbate addition, collagen condensed into intracellular vesicle-like structures that continued to co-localize with ER-RFP. A small proportion of GFP-collagen co-localized with the golgi-RFP probe. These findings were confirmed by immunostaining for ER and golgi markers on fixed col-GFP osteoblasts and immunostaining for wild-type collagen and ER in primary osteoblasts. The collagen-containing vesicles showed extensive intracellular movement to localized regions in the cell, followed by formation of extracellular fibers. Collagen assembly was highly dynamic, with motile cells exerting considerable forces on the fibers, resulting in stretching and distortion. Time-resolved confocal imaging suggested that thicker collagen fibers formed by cell-mediated stretching of smaller "mesh-like" fibers to condense them into rope-like structures. Dual imaging of GFP-collagen/ActinRFP cells seeded at low density on wild-type cells allowed visualization of collagen deposition by individual cells and showed assembly in a circular/perinuclear arrangement that appeared to be due to cell rotation/centrifugal collagen placement. Collagen was deposited only in areas where the cell body or processes had been, suggesting active cell placement. Our data show that collagen assembly is highly dynamic and involves internal movement of collagen-containing vesicles to localized regions of the cell and physical molding of fibers via cell-generated forces.

Disclosures: Michael Grillo, None.

FR0185

Structure-Function Analysis of Connexins as Active Regulators of Signal Transduction in Osteoblasts. Megan Moorer^{*}, Carla Hebert, Joseph Stains. UMB, USA

Gap junctions allow signaling between osteoblasts and osteocytes, coordinating bone remodeling. While gap junctions are generally thought of as passive conduits for small molecules to be shared between cells, we hypothesize that connexins actively contribute to downstream signaling by assembling a specific subset of effectors to the gap junction. We propose that, in addition to having unique permeability (e.g., Cx43 forms a pore permeable to <1kD molecules, and Cx45 forms a pore permeable to <0.3kD molecules), each connexin can assemble a unique "interactome" that can affect downstream signaling and bone cell function. In support of this hypothesis, several studies show that the unconserved, C-terminal domain (or tail) of connexins can associate with a variety of signaling complexes. Here, we examine the influence of this C-terminal tail on osteoblast signaling and function. We look at the function of two connexins, Cx43 and Cx45, which generally have opposing function in osteoblast biology. In addition, we have generated chimeric connexins, which fuse the Cx43 pore with the Cx45 C-terminal tail (Cx43pore-Cx45tail) and vice versa (Cx45pore-Cx43tail), to test the function of the C-terminus on osteoblastic signaling and function. Luciferase reporter assays performed in UMR106 or MC3T3 cells showed that expression of an intact Cx43 increased the transcriptional activity of a beta-catenin reporter (TOPflash), a Runx2 reporter (pOSE2-Luc), a cAMP-response element reporter (CRE-luc), a MAPK sensitive serum response element luciferase reporter (SREluc) and an NFkB sensitive reporter. In contrast, expression of an intact Cx45, or a Cx43pore-Cx45tail or Cx45pore-Cx43tail chimera either inhibited or had minimal impact on the transcriptional activity from these reporters. These results were confirmed by immunoblots from transfected cells. In addition, an intact Cx43 stimulated the expression of Sp7/Osterix, bglap/osteocalcin, coll1a1, lox, axin2 and excl12. In contrast, Cx45 attenuated the expression of most of these genes, while the chimeras were generally intermediate between the two. In total, these data suggest that both the pore and tail of Cx43 and Cx45 are required for their ability to affect osteoblast signaling and gene expression, implying that gap junctions need to not only pass signals back and forth, but also must be able to recruit the appropriate effector molecules in order to affect cell function.

Disclosures: Megan Moorer, None.

FR0186

A Novel Role of miR-150 in Bone Homeostasis. Fouad Moussa^{*1}, Gregory Sondag¹, Thomas Mbimba¹, Kimberly Novak², Scott McDermott³, Favez Safadi². ¹Kent State University, USA, ²NEOMED, USA, ³SUMMA Health System, USA

MicroRNA is a small non-coding RNA that consists of about 22 nucleotides, which targets mRNA and triggers its degradation or repress translation. MiR-150 is highly expressed in immature B cell stage, and targets c-Myb, a transcription factor that is important for lymphocytes development. However, the role of miR-150 on bone has not been documented. Our laboratory shows that miR-150 is expressed in mouse long bone and calvaria, and its expression is increased with age, thus, suggesting that miR-150 might play a role in bone homeostasis. Here, we show a novel role of miR-150 in osteoblast differentiation and function, where miR-150 gene expression is maximum at early stage (cell proliferation) and decreases at later stage (matrix mineralization) of osteoblastogenesis in vitro. To further determine the role of miR-150 in osteoblast function in vivo, we obtained the miR-150 knockout mice (miR-150 KO) and characterized their skeletal phenotype. MiR-150 KO mice have decreased bone mass associated with less bone volume to tissue volume ratio; decreased trabecular number associated in increased trabecular separation. This phenotype was evident as early as 4-weeks of age. Furthermore, we observed a significant reduction of ex vivo bone marrow-derived mesenchymal stem cells (MSCs) proliferation. Interestingly, there was an increase in osteoblast differentiation and function compared to wild type (WT) MSCs. We further examined osteoclast-mediated bone resorption in vivo and found that CTX1 levels was significantly reduced in miR-150 KO compared to WT mice. To determine the mechanism by which miR-150 plays in regulating bone cell differentiation and function, osteoactivin/gpmb, a bone anabolic factor is regulated by miR-150 through its 3'-UTR. OA expression was increased in miR-150 KO compared to WT bone cells. These results explained, at least in part, the mechanism of miR-150 in regulating bone cell differentiation and function. Taken together, these data suggest that miR-150 is a novel target for bone-related genes that might play a role in bone homeostasis and regulating MSCs proliferation, osteoblast and osteoclast differentiation and function. In addition, miR-150 can also be utilized as a therapeutic potential to treat osteoporosis, or used as a diagnostic tool for bone-related diseases.

Disclosures: Fouad Moussa, None.

FR0187

Alternative NF- κ B as a Regulator of Osteogenesis. Jennifer Davis^{*1}, Deborah Novack². ¹Washington University in St. Louis, USA, ²Washington University School of Medicine, USA

The alternative (alt) NF- κ B pathway has been shown to regulate both osteoblasts (OB) and osteoclasts (OC), complicating interpretation of bone phenotypes in global KO animals. In order to support the hypothesis that alt NF- κ B is a cell-intrinsic regulator of osteogenesis, we used transgenic mouse models to modulate alt NF- κ B in the OB lineage. NIK and IKK α are both critical upstream kinases for alt NF- κ B activation. We generated Osx-Cre:IKK α ^{fl/fl} (cKO) mice to ablate alt NF- κ B signaling in the OB lineage. NIKDT3 (NT3) is a constitutively active, lox-Stop-lox allele of NIK placed in the ROSA26 locus. Osx-Cre:NT3^{+/+} (cACT) mice were generated to activate alt NF- κ B signaling in the OB lineage. Recombination of alleles was induced by doxycycline withdrawal at weaning, and controls (CON) were Cre negative littermates.

As expected based on global KO studies, levels of collagen Ia and osteocalcin were higher in OB cultures from cKO animals, while OB from cACT animals had severely blunted levels. However, *in vivo* microCT analysis revealed no significant difference in trabecular or cortical bone parameters between cKO mice and CON at ages up to 6 months. 16 week old cACT mice showed an increase in cortical parameters (Ct.Th and Ct.BV, but no change in TV), not apparent at 6 and 12 weeks, a finding opposite to the expected decrease in bone mass. We next used *in vivo* axial tibial compression (2000 μ e; 4 Hz, 1200 cycles/day, 5 days/week, 2 weeks) to examine responses to mechanical anabolic stimulus between cKO, cACT, and CON animals at 16 weeks of age. Dynamic histomorphometry at the tibial mid-shaft in cKO mice showed no increase in Ps.BFR/BS, Ps.MAR, or Ps.MS/BS compared to CON. Surprisingly, cACT animals displayed an enhanced response to loading with increased Ps.BFR/BS and Ps.MS/BS.

In summary, the *in vitro* OB phenotype of cKO and cACT animals is consistent with reports in the alt NF- κ B global KO mice. However, we observe no difference in cKO bone phenotype either basally or after anabolic stimulus suggesting that loss of alt NF- κ B is not critical for OB differentiation and/or function *in vivo*. The finding that cACT animals have increased cortical bone mass and bone formation after *in vivo* loading suggests that pathological alt NF- κ B activation may impact osteogenesis. Taken together, our results indicate that the role of this pathway *in vivo* is complex and potentially context and/or age-dependent.

Disclosures: Jennifer Davis, None.

FR0188

Collagen production of osteoblasts revealed by ultra-high voltage electron microscopy. Rumiko Hosaki-Takamiya¹, Mana Hashimoto¹, Tomoyo Tanaka¹, Takashi Yamashiro², Hiroshi Kamioka^{*3}. ¹Department of Orthodontics, Okayama University Graduate School of Medicine, Dentistry, & Pharmaceutical Sciences, Japan, ²Department of Orthodontics & Dentofacial Orthopedics, Graduate School of Dentistry, Osaka University, Japan, ³Okayama University Graduate School of Medicine, Dentistry, & Pharmaceutical Sciences, Jp

In the bone, collagen fibrils form a lamellar structure called "twisted plywood-like model." For this unique structure, the bone can withstand various mechanical stresses. But the formation of this structure has not been elucidated due to the difficulty in observing collagen fibrils production of the osteoblasts via currently available methods. This is because the formation occurs in the very limited space between the osteoblast layer and bone matrix. In this study, we used ultra-high voltage electron microscopy (UHVEM) to observe collagen fibrils production three-dimensionally. UHVEM has 3 MV acceleration voltage and enables us to use thicker sections. We observed collagen fibrils that were beneath the cell membrane of osteoblasts elongated to outside of the cell. We also observed that osteoblasts produced collagen fibrils with polarity. By using AVIZO software, we observed collagen fibrils produced from osteoblasts along the contour of the osteoblasts towards the bone matrix area. Immediately after releasing from the cell, the fibrils run randomly and sparsely. But as they recede from the osteoblast, the fibrils began to run parallel to the definite direction and became thick and we observed a periodical stripe at that area. Furthermore, we also observed membrane structures wrapped around filamentous structures inside the osteoblasts. The filamentous structures had densities similar to the collagen fibrils and a columnar form and diameter. Our results suggested that collagen fibrils run parallel and thick, which may be related to the lateral movement of the osteoblasts. UHVEM is a powerful tool for observing collagen fibrils production.

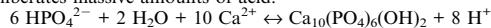
Disclosures: Hiroshi Kamioka, None.

FR0189

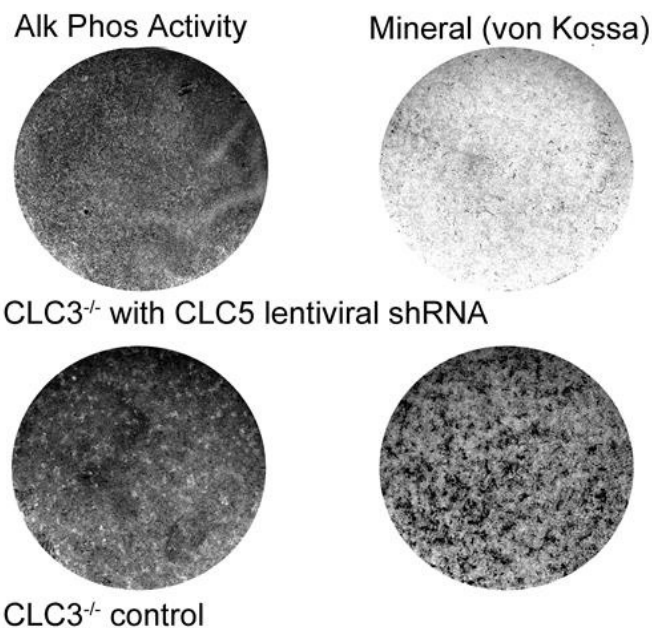
Double knockout of CLC3 and CLC5 in murine osteoblasts eliminates all mineralization. Quitterie C. Larrouture^{*1}, Deborah J. Nelson², Paul H. Schlesinger³, Peter A. Friedman⁴, Irina Tourkova⁵, Li Liu⁶, Harry Blair⁷.

¹Department of Pathology University of Pittsburgh, USA, ²Dept of Neurobiology, Pharmacology & Physiology, University of Chicago, USA, ³Department of Cell Biology, Washington University, USA, ⁴Department of Pharmacology & Chemical Biology, University of Pittsburgh, USA, ⁵Department of Pathology, University of Pittsburgh, & Pittsburgh Veteran's Affairs Medical Center, USA, ⁶Department of Pathology, University of Pittsburgh, USA, ⁷University of Pittsburgh, USA

Bone formation is mediated by a tight epithelium-like layer of secretory osteoblasts. The new bone matrix is separated from the extracellular fluid by tight junctions. The osteoblasts, and deeper layers of osteocytes of a bone forming osteon, are connected by gap junctions that couple the unit functionally. The osteon makes osteoid, mainly type I collagen, and then mineralizes it. Mineral formation, in a sealed space, liberates massive amounts of acid:



By removing the acid, mineralization can be driven to completeness efficiently over a wide range of interstitial fluid variations. This effectively mirrors osteoclast acidification of the resorption compartment to solubilize mineral. In both cases we envision multiple coordinated transporters moving protons across the osteoblast or osteoclast cell body at neutral pH. Previously, we showed that sodium hydrogen exchangers 1 and 6 (NHE1 and 6) move massive amounts of acid out of active osteoblasts at the *basolateral surface*. The pdz organizing protein, sodium hydrogen exchange regulatory factor 1 (NHERF1), also at the basolateral surface, is essential for efficient of bone formation and for phosphate transport via the neutral phosphate transporter-2 (Npt2). The unresolved central activity, crucial to active mineral deposition, was hypothesized to be *high capacity transporter(s) moving protons from the extracellular matrix space into the osteoblast cytoplasm*. We studied proton transport in membrane vesicles of mineralizing osteoblasts, which was consistent with Cl⁻ dependent H⁺ uptake. Matching these results with the identity of pumps, channels and exchangers significantly expressed in mineralizing osteoblasts we identified the chloride-proton exchangers as probable candidates. CLC3 and 5 expression is increased by large amounts (20-100 fold) in mineralizing osteoblasts. These transporters occur at the apical secretory surface as well as in the canalicular system. The CLC3 KO has mildly disordered mineralization with increased CLC5 expression compensating. We isolated mesenchymal stem cells from CLC3 ko mice, and used lentiviral CLC5 shRNA expression to create double KO MSCs. Phenotypes were validated by Western blots and PCR. In the double KO, no extracellular mineral is produced (Figure). Thus, osteoblast apical Cl⁻/H⁺ exchange imports acid from mineral formation. This acid is removed by basolateral Na⁺/H⁺ exchange to maintain osteoblast cytosolic pH.



Normal alk phos but no mineral in CLC3/5 double KO osteoblasts

Disclosures: Quitterie C. Larrouture, None.

FR0190

Multi-Modal High-Content Imaging Reveals Relationships Between Cell Signaling and Mineralization in Zebrafish. Claire Watson*, Edith Gardiner, Werner Kaminsky, Ronald Kwon. University of Washington, USA

The generation of new bone requires activation of specific signaling cascades in a temporally and spatially distinct manner. However, until recently, a direct comparison between the dynamics of these signaling events and the formation of mineralizing bone has been precluded by the lack of strategies to simultaneously visualize these relationships *in vivo*. The optical clarity of the zebrafish caudal fin allows for high content imaging of cell signaling in real time by taking advantage of fluorescent reporter strains. Previously, we demonstrated the potential to measure crystalline mineral accrual during fin regeneration using quantitative birefringence imaging (Rotopol microscopy [1]). Building on these findings, in this study, we developed a high-content, multi-modal imaging system for tandem imaging of fluorescent reporters and bone mineralization within the same tissue. The system consisted of a motorized rotating polarizer integrated into a fully motorized Zeiss Axio Imager.M2 high-content fluorescence microscope, with custom software enabling interfacing between systems. We applied this imaging strategy to directly examine the relationships between canonical Wnt signaling and *sp7* (*osterix*) expression (using the Tg(7xTCF-Xla.Siam:GFP)ia4 and Tg(sp7:EGFP) reporter fish, respectively) with changes in cell metabolism (indicated by NADH autofluorescence) and mineralization (via Rotopol acquired birefringence) during bone formation and maturation in the regenerating zebrafish fin (Fig 1A). The first segment of bone distal to the amputation plane was analyzed for each of these parameters during the first 8 days post amputation (dpa) to examine early bone maturation (Fig 1B). We find that acute activation of NADH is followed by Wnt signaling and subsequent expression of *sp7* at this site. Interestingly, increases in mineralization coincide with second and third peaks in NADH autofluorescence. Furthermore, we find that mineralization is not complete even at 26 dpa in some fish. Using Rotopol imaging in concert with high resolution fluorescent imaging for the first time, we demonstrate that this system can be used to examine relationships between core bone formation events and maturation into fully mineralized bone.

Disclosures: Claire Watson, None.

FR0191

Regulation of matrix mineralization and bone vascularization by pigment epithelium-derived factor (PEDF). Heeseog Kang*, Joan C. Marini. NIH/NICHD, USA

Pigment epithelium-derived factor (PEDF), encoded by SERPINF1, is a potent anti-angiogenic and neurotropic factor. Null mutations in SERPINF1 cause recessive type VI osteogenesis imperfecta (OI), a progressive deforming OI characterized by broad bands of unmineralized osteoid and a fish-scale pattern of bone under polarized light. Serpinfl (-/-) mice were reported to have delayed *in vitro* mineralization and increased mineral-to-matrix ratio, giving rise to decreased trabecular bone mass and brittle bone. However, it remains to be elucidated how PEDF contributes to bone matrix mineralization. Furthermore, we recently reported a novel connection of PEDF and the transmembrane protein BRIL, expressed during osteoblast mineralization. A loss-of-function BRIL mutation (IFITM5 (c.119C>T; p.S40L)) causes atypical type VI OI with decreased SERPINF1 expression, while the type V OI gain-of-function IFITM5 mutation (c.-14C>T) increased SERPINF1 expression and PEDF secretion. Here, we investigated the differentiation of murine serpinfl (-/-) calvarial osteoblasts. We show that serpinfl expression increases during early osteoblast differentiation and then decreases in terminally differentiated osteoblasts. Osteoblasts from serpinfl (-/-) mice exhibited delayed nodule formation and mineralization, compared with WT osteoblasts. We examined expression of osteogenesis marker genes during differentiation of calvarial osteoblasts by real-time PCR. Serpinfl (-/-) osteoblasts exhibited lower expression of ifitm5, demonstrating a mutual feedback loop regulating transcription of these proteins. Several osteoblast differentiation markers (colla1, osteocalcin, and phex) were significantly lower than in WT cells during matrix mineralization. The delayed mineralization was accompanied by the reduced expression of mineralization markers, such as alkaline phosphatase and phospho1, while expression of the mineralization inhibitor, osteopontin, was increased. Moreover, the absence of PEDF significantly decreased expression of sost (sclerostin), an antagonist of the canonical wnt signaling. The reduced sost expression was consistent with the elevated expression of vegfa and ptgs2 (COX-2), the wnt target genes. The resultant increase in VEGF-to-PEDF ratio may underlie the increased bone vascularization previously in serpinfl (-/-) mouse bones. Taken together, these results suggest that PEDF plays a role in coordinating bone matrix mineralization and bone vascularization.

Disclosures: Heeseog Kang, None.

FR0193

Loss of galectin-3 leads to retention of bone mass in aging female mice. Kevin Maupin*¹, Kevin Weaver², Carol Flegler³, Stanley Flegler³, Tao Yang², John Wang³, Bart Williams². ¹Van Andel Institute Graduate School, USA, ²Van Andel Research Institute, USA, ³Michigan State University, USA

Osteoporosis is a growing health concern in the United States due to an aging population. Thus, there is a need to identify novel targets to control bone homeostasis. Galectin-3 (Gal3) is a chaperone protein which functions in numerous cell processes both intracellularly via protein-protein interactions and extracellularly by binding specific glycans on glycoproteins. Gal3-deficient mice have normal reproduction and lifespan, but are protected against fibrosis. Because Gal3 is highly expressed by bone cells and regulates the deposition of collagen in fibrosis models, we hypothesized that Gal3-deficient mice would have altered bone matrix deposition.

When we compared the femurs of aging (12, 24, 36, and 48wks) Gal3-deficient mice to their wildtype littermates by microcomputed tomography (μ CT), we found that Gal3-deficient mice had a sex-dependent bone phenotype. While males showed no difference in measured bone parameters, Gal3-deficient females had increased trabecular bone volume fraction (BV/TV) and were protected against age related loss of trabecular bone mineral density (BMD). At 36wks, there was an increase in the polar moment of inertia (MMI) of female Gal3-deficient femurs, which suggested an improvement in cortical bone strength. Mechanical testing by 4-point bending revealed that the Gal3-deficient bones had no changes in absolute strength or stiffness. However, there was a decrease in the maximum strain and Young's modulus of elasticity, which meant that there was a decrease in the quality of the bone matrix. We used scanning electron microscopy to observe the collagen of the cortical bone and found that despite normal cortical BMD, there was abnormal mineralization of the collagen fibrils. We also wanted to know whether the bone phenotype is dependent upon abnormal osteoblast function, so we made an osteoblast conditional knockout mouse line by crossing mice with floxed Gal3 alleles (*Lgals3-flox*) to mice expressing cre-recombinase driven by the human osteocalcin promoter (*OCN-cre*). Consistent with the globally Gal3-deficient mice, the *OCN-cre;Lgals3-flox* mice also showed a sex-dependent increase in trabecular bone mass and mineralization. The results of this study identify a novel sex-dependent regulation of the extracellular matrix by Gal3 in bone. While further experimentation is necessary, our data provides support for the development of Gal3 targeted therapies to prevent bone loss during aging.

Disclosures: Kevin Maupin, None.

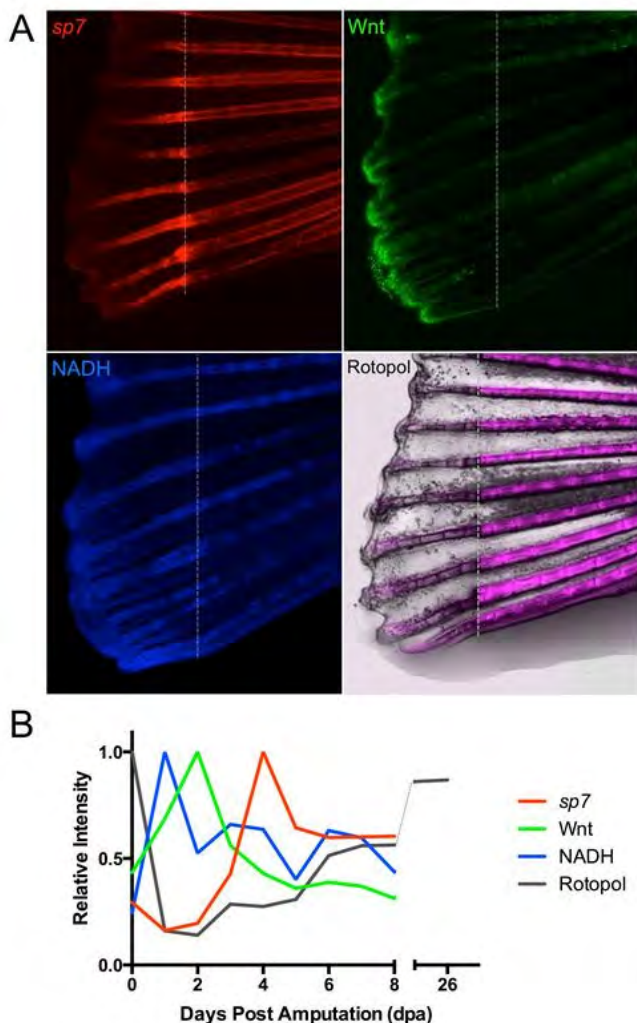


Figure 1

FR0194

microRNA Regulation of Circadian Rhythm in the Osteoblastic Lineage. Spenser Smith*, Neha S. Dole, Tiziana Franceschetti, Anne M. Delany, UConn Health, USA

Disruption of circadian rhythm is associated with many diseases, including cancer, metabolic syndrome and bone loss. In bone, genes critical for normal homeostasis display circadian rhythm. Rhythm is maintained by clock genes, including *Bmal1* and *Per1-3*, which interact in a series of transcriptional and post-transcriptional feedback loops. In non-skeletal tissues, microRNAs (miRNAs) were shown to be important for controlling circadian rhythm; however, miRNAs maintaining rhythm in bone have not been determined. Here, we identify miR-433 as a regulator of rhythmic gene expression in the osteoblast lineage.

Hif1 α and *Igf1* are critical osteoblast genes displaying circadian rhythm. Using Luciferase reporter-3'UTR assays, we demonstrated that these genes are novel miR-433 targets. *In vivo*, we saw that miR-433 displays robust rhythmicity in mouse calvaria. Its expression pattern was anti-phasic in relation to *Bmal1*, peaking after light removal. However, in primary mouse mesenchymal cells synchronized with a short pulse of dexamethasone, miR-433 did not display rhythmicity. This suggests that a systemic factor establishes miR-433 rhythm *in vivo*.

miR-433 was recently shown to target the glucocorticoid receptor (Riester et al.), and rhythmic secretion of glucocorticoids is critical for synchronizing local clocks in peripheral tissues by activating transcription of *Per* genes. Moreover, as circulating glucocorticoid levels fluctuate diurnally, so does the sensitivity of tissues to glucocorticoids. We hypothesized that miR-433 helps maintain circadian rhythm in osteoblasts by regulating glucocorticoid signaling. To determine if miR-433 regulates circadian rhythm *in vitro*, its activity was inhibited using a doxycycline-inducible competitor (miR-433 tough decoy) in stably transduced C3H10T1/2 cells. Although miR-433 inhibition did not affect *Bmal1* rhythm, it dramatically altered *Per2* amplitude, period length, and phase. miR-433 inhibition also dampened rhythmicity of *Runx2* mRNA. Inhibiting miR-433 activity amplified the dexamethasone-stimulated expression of glucocorticoid responsive genes *Dusp1* and *Per2*, demonstrating increased glucocorticoid sensitivity. Overall, we found that miR-433 displays a circadian rhythm in calvaria, targets mRNAs with rhythmic expression and regulates sensitivity to glucocorticoid signaling. We speculate that miR-433 can modify responsiveness of peripheral tissues to variations in circulating glucocorticoids and alter bone metabolism.

Disclosures: Spenser Smith, None.

FR0195

Osteoblast-specific deletion of Sclerostin rescues ovariectomy-induced bone loss, in adult female mice, but does not significantly improve bone parameters in adult males. Cristal S. Yee¹, Nicole M. Collette¹, Deepa K. Muruges¹, Aris N. Economides², Alexander G. Robling³, Gabriela G. Loots⁴. ¹Lawrence Livermore National Laboratories, USA, ²Regeneron Pharmaceuticals, USA, ³Indiana University, USA, ⁴Lawrence Livermore National Laboratory, USA

Estrogen deficiency causes rapid bone loss followed by skeletal fragility and ovariectomy (OVX) in rodents can effectively recapitulate these osteoporotic phenotypes. Sclerostin (Sost) is a negative regulator of bone formation and blocking its function *via* antibodies has shown great therapeutic promise by increasing both bone mass in humans and animal models. Sclerostin deletion in *Sost* knockout mice (*Sost*^{KO}) causes high bone mass (HBM) similar to Sclerosteosis patients. Both 3- and 6- month old *Sost*^{KO} mice have >150% and >300% more bone volume/total volume (BV/TV), respectively, than aged matched controls, and it has been postulated that the main source of skeletal Sost is the osteocyte. To examine temporal and cell-type specific contributions of Sost to bone metabolism, we investigated the skeletal phenotypes of mice with conditional *Sost* (*Sost*^{KO}) deletions initiated (1) in the limb mesenchyme (*Prx1-Cre*); (2) in embryonic osteoblasts (*Coll-Cre*); or (3) in adult osteoblasts (*Coll-ER-Cre*). *Prx1-Cre* deletes alleles in the early limb bud mesenchyme, between E9.5-E10.5. These cells represent the osteochondral progenitors (chondrocytes, adipocytes, osteoblasts, osteocytes) of the appendicular skeleton, and *Prx1-Cre* leaves the axial skeleton unperturbed. At 16 weeks of age, microCT (mCT) analysis of *Sost*^{KO}; *Prx1-Cre* distal femurs showed 200% more BV/TV than controls. The lumbar vertebrae, region of the skeleton where *Sost* alleles should remain intact, also showed a significant increase (60%) in BV/TV compared to controls. *Sost*^{KO}; *Coll-Cre* femurs displayed 75% more BV/TV than controls, while *Sost* deletion initiated by tamoxifen (TMX) injection at 22- weeks of age in *Sost*^{KO}; *Coll-ER-Cre* male mice caused no significant changes in the bone mass in 28- weeks old femurs compared to PBS or TMX treated *Sost*^{KO}; *Coll-ER-Cre* controls. However, *Sost* deletion initiated at 22- weeks of age significantly improved the bone parameters of *Sost*^{KO}; *Coll-ER-Cre* females that were ovariectomized at 16 weeks of age, and indicated a complete rescue from the effects of ovariectomy on bone mass. We found osteoblast deletion of *Sost* after OVX in females to significantly increase BV/TV by 130%, suggesting that the high bone turnover in OVX may rapidly propagate *Sost* deletion from osteoblasts to osteocytes, rescuing the LBM phenotype.

Disclosures: Cristal S. Yee, None.

FR0196

Serum Amyloid A3: A Novel Means by Which Preosteoclasts Inhibit the Anabolic Effects of PTH. Shilpa Choudhary*, Sui-Pok Yee, Renata Rydzik, Estus Thomas, Douglas Adams, Joseph Lorenzo, Carol Pilbeam, University of Connecticut Health Center, USA

Absence of cyclooxygenase 2 (*Cox2*), the major enzyme regulating prostaglandin production, enhances the bone formation response to PTH infusion in mice without affecting resorption. We identified Serum amyloid a3 (*Saa3*) as a *Cox2*-dependent inhibitor of PTH-stimulated cAMP production and osteoblast (OB) differentiation *in vitro* and showed that *Saa3* is secreted by preosteoclasts (POCs). We generated *Saa3* knockout (KO) mice using the CRISPR/Cas9 approach in a CD1 background and confirmed by PCR and sequencing. The goal of this study was to determine if *Saa3* knockout enhanced osteogenic responses to PTH *in vitro* and anabolic responses to PTH *in vivo*. In primary OB cultures, conditioned media from WT but not *Saa3* KO POCs inhibited PTH-stimulated cAMP production and cAMP-regulated *Ramp3* expression. In bone marrow stromal cell cultures, PTH stimulated markers of OB differentiation only in *Saa3* KO cultures. Male WT and KO mice (n=3/group; 3 month old) were infused with vehicle or hPTH 1-34 (40 μ g/kg/d) via ALZET pump for 12 days. Bone mineral density (BMD) was measured at the beginning and end of infusion. PTH decreased BMD in WT mice but increased BMD in KO mice. μ CT analysis of vehicle-infused WT and KO distal femur showed no differences. PTH infusion increased trabecular BV/TV, Conn.Dens and Tb.N and decreased Tb.Sp in KO femurs relative to WT. There were no differences in cortical parameters with PTH infusion. PTH increased serum PINP, a marker of bone formation, only in KO mice but increased serum CTX, a marker of resorption, equally in WT and KO mice. Gene expression was performed on whole tibiae. *Saa3* was undetectable in vehicle-infused tibiae and markedly induced by PTH in WT tibiae. Other members of the serum amyloid family, *Saa1* and 2, were unchanged by PTH infusion. PTH increased expression of the cAMP-regulated gene, *Ramp3*, only in KO tibiae but increased expression of *Rankl* and *Cox2* similarly in both WT and KO tibiae. PTH increased the bone formation-related genes—*Runx2*, *Osteocalcin*, *Igf1* and the Wnt family gene, *Wnt10b*—only in KO tibiae. PTH infusion decreased expression of the Wnt antagonists, *Sost* and *Dkk1*, only in KO tibiae. These results demonstrate that the effects of *Saa3* knockout on responses to PTH appear to mimic the effects previously seen with *Cox2* knockout. Thus, it seems likely that *Cox2*-dependent production of *Saa3* is a novel mechanism by which osteoclast lineage cells regulate the anabolic responses of osteoblast lineage cells to PTH.

Disclosures: Shilpa Choudhary, None.

FR0197

Constitutive Activation of NF- κ B, Mimicking Inflammation, Inhibits Osteoblast Function by Inducing Glycolysis and mTORC2. Gaurav Swarnkar¹, Tim (Hung-Po) Chen¹, Gabriel Mbalaviele¹, Yousef Abu-Amer². ¹Washington University School of Medicine, USA, ²Washington University in St. Louis School of Medicine, USA

Inflammatory signals elicit bone catabolic responses through increased bone resorption by osteoclasts (OC) coupled with decreased bone formation by osteoblasts (OB), resulting in net bone loss. Whereas the mechanisms underlying inflammatory OC activity have been well-studied, those governing OB function remain elusive. The transcription factor NF- κ B which is considered as the centerpiece mediator of inflammation and essential for normal bone development, has also been shown to regulate cellular metabolism. Hence, this study was designed to investigate if IKK2/NF- κ B activation, an index of inflammation, cellular metabolism and function of OB. To this end, we conditionally deleted or constitutively activated IKK2 (IKK2ca) during OB differentiation using Sp7cre (early stage), Coll1cre and DMP1cre (late stage) mice. micro-CT analysis indicates that deletion of IKK2 using Sp7cre results in increased basal level of bone volume. In contrast, mice expressing IKK2ca under Sp7cre show a decrease in bone volume compared with WT, suggesting that IKK2 activation in OB mediates inflammation-induced catabolic effect. However, deletion using DMP1cre did not change bone parameters, yet activation with DMP1cre resulted in a moderate decrease in bone mass and connectivity density compared with WT controls. Analysis of Coll1cre-induced regulation of NF- κ B is ongoing. These results suggest that NF- κ B is more important in early stage of OB differentiation. Mechanistically, we found that expression of IKK2ca but not IKK2-Kinase dead in calvarial OB changed cellular metabolism towards increased aerobic glycolysis and decreased OB function. We found increased expression of glycolytic enzymes, including Hexokinase 2 and Lactate dehydrogenase in OB expressing IKK2ca compared to control cells. These cells also showed increased glucose uptake and consumption with increase in lactate production. IKK2ca expression also resulted in increased expression of sclerostin, DKK1, and RANKL along with decreased expression of OB genes (ALP, OCN). Further, consistent with reports that suggest that IKK2 regulates mTORC1/2 signaling, we found that IKK2ca expression in OB upregulates mTORC2 signaling evident by increase in expression of mTOR/Rictor. Further details of the mechanism underlying IKK2 mediated regulation of mTOR and OB metabolism are under investigation. Our study highlights the mechanism by which inflammation alters OB metabolism leading to impaired osteoblastogenesis

Disclosures: Gaurav Swarnkar, None.

FR0198

Effects of Osteoblast-Specific Gαs Over-Expression on Skeletal Development using a Transgenic Mouse Model. Lucia Zhang*¹, Kim Sugamori¹, Colin Claridge¹, Ariana Dela Cruz¹, Marc Grynpas², Jane Mitchell³. ¹University of Toronto, Canada, ²Lunenfeld-Tanenbaum Research Institute of Mount Sinai Hospital, Canada, ³Department of Pharmacology & Toxicology, University of Toronto, Canada

Gαs is a heterotrimeric G protein that transduces signals from activated G protein-coupled receptors on the cell surface to stimulate intracellular signaling cascades. In bone cells, Gαs is known to play a central role in mediating processes that regulate skeletal development, maintenance, and repair. Clinically, alterations in Gαs activity are associated with many bone disorders. Constitutive activity of Gαs results in McCune-Albright syndrome and fibrous dysplasia, while a 50% reduction in Gαs activity results in pseudohypoparathyroidism and Albright hereditary osteodystrophy. Our lab has previously found there is a 2.4 fold variation in Gαs protein levels in lymphocytes from children suggesting there is significant variability in Gαs levels in human cells. To examine the effects of increased osteoblastic Gαs expression on bone *in vivo*, we have created a transgenic mouse model of Gαs over-expression in osteoblasts (Gs-Tg mice) driven by the 3.6 kb Col1A1 promoter.

At both the RNA and protein levels, expression of total Gαs was significantly increased specifically in bone and teeth of Gs-Tg mice compared to wild-type (WT) mice. MicroCT assessment of bone microarchitecture showed cortical bone from 9-week old Gs-Tg mice had a modest reduction in volumetric bone mineral density (vBMD) compared to age-matched WT mice. Conversely, trabecular bone displayed significantly increased vBMD in Gs-Tg mice, accompanied by increased trabecular number and bone volume. Furthermore, static and dynamic histomorphometry analyses were conducted to examine differences at the cellular level. Static histomorphometry revealed gross abnormalities in the growth plates of 9-week old Gs-Tg mice compared to WT mice, with loss of the normal organization of growth plate chondrocytes. In concordance, dynamic histomorphometry displayed calcin green labelling that could not be quantified as it was both disorganized and diffuse. Follow-up analyses in female Gs-Tg mice revealed there is some disruption of the growth plate present at 3-weeks of age, progressed at 9 weeks, and was not resolved after skeletal maturity at 26-weeks of age. In summary, our findings suggest that osteoblastic Gαs over-expression leads to aberrant skeletal development in which cortical bone and trabecular bone are differentially affected.

Disclosures: Lucia Zhang, None.

FR0199

Promotion of osteoblast differentiation and nodule formation through Ucm a as a direct transcriptional target of Runx2 and Osterix. Yeon-Ju Lee*¹, Seung-Yoon Park², So-Jeong Lee¹, Eun-Hye Lee¹, Soon-Young Kim¹, Je-Yong Choi³, Yeo Hyang Kim⁴, Jung-Eun Kim⁵. ¹Dept. of Molecular Medicine, CMRI, BK21 Plus KNU, Kyungpook National University School of Medicine, South Korea, ²Dept. of Biochemistry, School of Medicine, Dongguk University, South Korea, ³Dept. of Biochemistry & Cell Biology, CMRI, BK21 Plus KNU, Kyungpook National University School of Medicine, South Korea, ⁴Dept. of Pediatrics, Kyungpook National University Hospital, South Korea, ⁵Kyungpook National University School of Medicine, South Korea

Runx2 and Osterix (Osx) are the master transcription factors in bone formation. Nonetheless, genes acting downstream of both Runx2 and Osx have yet to be fully characterized. Here, we investigate the downstream targets of both Runx2 and Osx in osteoblasts. In DNA microarray analysis using Runx2/Osx double heterozygous embryos, the expression of unique cartilage matrix-associated protein (Ucm a) was significantly decreased. In contrast, Ucm a expression was increased in osteoblasts overexpressing both Runx2 and Osx. Ucm a expression was initiated mid-way through osteoblast differentiation and continued throughout the differentiation process. Transcriptional activity of the Ucm a promoter was increased upon transfection of the cells with both Runx2 and Osx. Runx2- and Osx-mediated activation of the Ucm a promoter was directly regulated by Runx2- and/or Sp1-binding sites within its promoter. During osteoblast differentiation, the formation of mineralized nodules in Ucm a-overexpressing stable clones occurred earlier and was more enhanced than that in the mock-transfected control. In contrast, osteoblast differentiation and nodule formation were significantly reduced in Ucm a-knockdown cells. Mineralized nodule formation was strongly augmented in osteoblasts or partially rescued in Ucm a-knockdown cells cultured in a medium containing Ucm a proteins. Collectively, our data demonstrate that Ucm a is a novel downstream gene regulated by both Runx2 and Osx and it stimulates osteoblast differentiation and nodule formation.

Disclosures: Yeon-Ju Lee, None.

FR0200

Runx2 Gene Deletion in Odontoblast Fails to Disrupt Dentin Synthesis. Mitra Adhami*¹, John C. Clarke¹, Haiyan Chen¹, Harunur Rashid¹, Kayla King¹, Mohammad Hassan¹, Yang Yang², Amjad Javed³. ¹School of Dentistry, University of Alabama at Birmingham, USA, ²Department of Pathology, University of Alabama at Birmingham, USA, ³University of Alabama at Birmingham, USA

Runx2 transcription-factor is essential for lineage commitment of undifferentiated oral mesenchyme toward odontoblast. Global deletion of Runx2 results in arrested tooth development prior to the bell stage. Runx2 deficient dental-mesenchyme fails to commit to the odontoblast lineage and lack morphological features characteristic of differentiated odontoblast. However, due to early lethality of global null mice, the specific role of Runx2 for development of functional odontoblast remains unknown. Here we determine Runx2 requirement during odontogenesis. Runx2 gene was deleted in committed odontoblast using 2.3kbCol1a1-Cre transgene which is turned on in dental-mesenchyme during embryonic development. We confirmed specific deletion of Runx2 in committed odontoblast by two independent reporter lines. To our surprise, Runx2^{CKO} mice were born alive and were similar to wild-type littermates in size and body-weight. Newborn heads sectioned sagittally showed normal tooth morphogenesis in homozygous mutants. Incisors and multi-cusped 1st and 2nd molar were noted in wild-type and Runx2^{CKO} littermates. Consistent with normal tooth-morphogenesis, both odontoblasts and ameloblasts were polarized and well differentiated in Runx2^{CKO} mutants at birth. Expression levels of dentin matrix genes were similar in tooth organs of WT and Runx2^{CKO} littermates. Thus Runx2 activity in committed odontoblast is not essential for embryonic tooth development. We also evaluated molars after eruption. The size, length and width of crowns and roots of molars in Runx2^{CKO} mice were comparable to wild-type mice. Furthermore, a well-defined predentin, dentin and cementum layer was present in both wild-type and Runx2^{CKO} mice. Equal number, spacing and thickness of odontoblast tubules were noted in both littermates. Finally, the periodontal ligament was integrated into surrounding alveolar-bone in both wild-type and Runx2^{CKO} mice. In sharp contrast, Runx2 mutants exhibited significantly low bone mass by 1 month of age. Decreased bone formation was associated with decreased gene expression of osteoblast markers and impaired collagen assembly in the extracellular matrix. We further show that osteoblast function, and not number, is disrupted in Runx2^{CKO} mice. Taken together our data demonstrate that despite critical requirement during lineage commitment of dental mesenchyme, Runx2 is not essential in odontoblasts for tooth development.

Disclosures: Mitra Adhami, None.

FR0202

Dividing Growth Plate Chondrocytes Transdifferentiate into Osteoblasts and Provide a Major Source of De Novo Osteoblasts throughout Postnatal Growth in Mice. Patrick Aghajanian*¹, Shaohong Cheng¹, Catrina Alarcon¹, Subburaman Mohan². ¹Jerry L Pettis VA Medical Center, USA, ²Jerry L. Pettis Memorial VA Medical Center, USA

It has long been believed that during endochondral ossification osteoblast progenitors are delivered via the vasculature to form bone matrix that replaces the cartilage. In contrast to this model, we recently demonstrated that epiphyseal chondrocytes transdifferentiate into bone forming osteoblasts during the early postnatal growth period in mice. To determine if transdifferentiation of chondrocytes represents a major source of De Novo osteoblasts at different bone forming sites, we genetically labeled proliferating chondrocytes with tamoxifen-induced Col2-CreERT2 using Tomato (Tom) expression and followed the fate of labeled cells over a period of 16 weeks. Col2-Cre-ERT2; ROSA-tdTomato mice were administered a single dose (100 ug) of tamoxifen at postnatal day 3 and were euthanized at weeks 1, 2, 3, 6, 12 and 16. Immunohistochemistry of frozen bone sections were performed using chondrocyte and osteoblast markers. Our data show that many proliferating chondrocytes originating in the growth plate (physis) have the potential to transdifferentiate into osteoblasts which populate both the primary and secondary spongiosa during postnatal growth. Similarly, proliferating chondrocytes in the epiphysis predominantly contribute to bone forming osteoblasts at the secondary ossification center (SOC). Co-expression studies using osteoblast markers indicate colocalization of Tom with matrix proteins, bone sialoprotein II (BSP) and alkaline phosphatase (ALP), as well as osterix (OSX), all of which are indicators of osteoblast differentiation, in both the SOC and in trabecular bone. These events occur as early as 7 days after tamoxifen injection and continue to occur until at least 16 weeks of age. As early as 3 weeks of age, Tom labeled cells can be seen composing populations of trabecular bone and trabecular lining cells as far as 2.2 mm deep from the growth plate and 3.5 mm from the growth plate in 16 week mice. Quantitative studies indicate that 50% or more of OSX and BSP-positive osteoblasts in the primary and secondary spongiosa regions as well as epiphysis contained Tom. Taken together, our data show that dividing chondrocytes can transdifferentiate into bone matrix producing osteoblasts throughout postnatal growth and represent a major source of osteoblasts at different skeletal sites. Therefore, mechanisms that promote the chondrocyte-osteoblast transdifferentiation process should provide novel therapeutic opportunities towards development of anabolic skeletal therapies for osteoporosis.

Disclosures: Patrick Aghajanian, None.

FR0203

Histone H2B Monoubiquitination is Required for Bone Development. Zeynab Najafova^{*1}, Peng Liu², Dominik Saul³, Hiroaki Saito⁴, Wanhua Xie⁵, Simon Baumgart⁵, Ahmed Mansouri⁶, Eric Hesse⁴, Stephan Sehmisch³, Jan Tuckermann², Steven A. Johnsen⁵. ¹University Medical Center Goettingen, Germany, ²Institute for General Zoology & Endocrinology, University of Ulm, Germany, ³Department of Trauma Surgery & Orthopedics, University Medical Center Goettingen, Germany, ⁴Department of Trauma-, Hand- & Reconstructive Surgery, University Medical Center Hamburg, Germany, ⁵Clinic for General, Visceral & Pediatric Surgery, University Medical Center Goettingen, Germany, ⁶Max Planck Institute for Biophysical Chemistry, Molecular Cell Differentiation Group, Germany

The complexity of lineage-specific transcriptional regulation is controlled by an intricate network of tissue-specific transcription factors and epigenetic regulatory mechanisms. Perturbation of these epigenetic mechanisms frequently leads to developmental defects and/or cancer. Thus, therapeutic strategies which specifically target these mechanisms offer an ideal approach for a number of clinical conditions such as aging-related bone loss. Histone H2B monoubiquitination (H2Bub1) is carried out by the obligate heterodimeric Rnf20/40 E3-ligase complex and is associated with transcriptional elongation on active genes. Surprisingly, despite its global correlation with active gene transcription, we previously demonstrated a specific role for H2Bub1 and its upstream regulatory pathway in controlling osteoblast (OB)-specific gene transcription during OB differentiation of mesenchymal stem cells (Karpiuk et al., 2012, Mol Cell). To address the significance of H2Bub1 for bone development *in vivo*, we generated a bone-specific Rnf40 conditional knockout (KO) mouse model. *Ex vivo* differentiation studies confirmed a role for Rnf40 and H2Bub1 in OB differentiation as revealed by decreased alkaline phosphatase activity/expression, mineralization and expression of Runx2 and Sp7 in KO OBs. Surprisingly, γ CT analysis revealed increased bone mass in homozygous OB-specific KO mice while bone histomorphometry demonstrated a decreased bone formation rate. Consistently, biomechanical loading studies showed reduced bending parameters (Stiffness, Yield load, Fmax (Strength) and Failure Load). Thus, these findings suggest that while H2Bub1 is required for OB differentiation, its absence results in increased bone mass associated with reduced bone strength and formation, a finding frequently associated with decreased osteoclast activity. Consistently, Rnf40-deficient OBs showed significantly reduced Rankl expression. Altogether, these data suggest that H2Bub1 is a defining epigenetic regulator of osteoblast-osteoclast coupling *in vivo* and provide a basis for future studies to investigate the potential of its regulatory pathway for the treatment of conditions such as aging-related osteoporosis.

Disclosures: Zeynab Najafova, None.

FR0204

miR-322 and Its Target Protein Tob2 Modulate Osterix mRNA Stability. Beatriz G3mez Molina^{*}, Edgardo Rodr3guez-Carballo, Francesc Ventura. University of Barcelona, Spain

The aim of our study was to perform a miRNA expression profile in BMP-treated cells and to analyze the biological impact of their modulation in osteoblast differentiation. We performed a screening of BMP-regulated miRNAs in C2C12 cells and focused on miR-322, a down-regulated miRNA. miR-322 was also repressed in MC3T3-E1 and BM-MSCs after BMP treatment. We also carried out miR-322 gain- and loss-of-function experiments in C2C12 and MC3T3-E1 in order to determine whether miR-322 affects osteoblast differentiation. Overexpression of miR-322 significantly increased *Osx*, *Runx2* and *Msx2* mRNA at basal levels and after BMP-2 stimulation. Concordantly, miR-322 increased OSX protein levels, revealing that miR-322 enhances the BMP-2 response. Furthermore, we confirmed the regulation of *Osx* mRNA by miR-322 in differentiated BM-MSCs using a lentiviral approach.

Putative targets of miR-322 were analyzed *in-silico* and *Tob2* was identified as a potential target. The characterization of the specific *Tob2* 3'-UTR sequence bound by miR-322 was possible due to the generation of *Renilla* luciferase reporter plasmids carrying wild-type or mutant *Tob2* 3'-UTR. Only wild-type construct was significantly inhibited after cotransfection with miR-322 in C2C12 and MC3T3-E1 cells, allowing us to demonstrate that miR-322 acts as an inhibitor of *Tob2*.

Previous studies identified *Tob* not only as a general regulator of mRNA decay but also as a specific regulator through its binding to CPEB2-4 (cytoplasmic polyadenylation element-binding protein) and further recruitment of the Cnot7 deadenylase to the target mRNAs. mRNA decay assays in C2C12 and MC3T3-E1 cells evidenced that ectopic expression of *Tob2* reduced the half-life of *Osx* transcripts. Moreover, accumulation of miR-322 led to significant stabilization of *Osx* mRNA.

To further prove direct binding of *Tob2* and CPEB2-4 to *Osx* prior to specific decay, we developed RNA pulldown assays using oligonucleotides corresponding to *Osx* 3'-UTR sequences found to form secondary stem-loop structures compatible to those shown to bind CPEB2-4. Either expressed alone or in combination, ectopic CPEB4 and *Tob2* were able to bind specifically to *Osx* RNA.

In conclusion, our results demonstrate a new molecular mechanism controlling osteogenesis through the miR-322/*Tob2* regulation of specific target mRNAs. This

regulatory circuit provides a clear example of a complex miRNA-transcription factor network for fine-tuning the osteoblast differentiation program.

Disclosures: Beatriz G3mez Molina, None.

FR0205

Osteoblast-derived FGF9 Regulates Skeletal Homeostasis. Liping Wang^{*1}, Marcia Abbot², Theresa Roth³, Linh Ho³, Lalita Wattanachanya³, Rebecca Hayden³, Robert Nissenon⁴. ¹VA Medical Center, San Francisco, USA, ²Endocrine Unit, San Francisco VA Medical Center, Canada, ³Endocrine Unit, San Francisco VA Medical Center, USA, ⁴Endocrine Unit, San Francisco VA Medical Center; Department of Medicine & Physiology, University of California, USA

FGF9 has complex and important roles in skeletal development and repair. We have previously observed that FGF9 expression in osteoblasts (OBs) is regulated by G protein signaling and therefore the present study was done to determine whether OB-derived FGF9 was important in skeletal homeostasis. To directly test this idea, we deleted functional expression of FGF9 in OBs using a 2.3kb collagen type I promoter-driven Cre transgenic mouse line. Both FGF9 knockout (KO) and wild type (WT) mice were maintained in an FBV/N background. μ CT revealed that 3 month old male FGF9 KO mice displayed a 26% ($p < 0.001$) decrease in cancellous BV/TV, an 11% ($p < 0.001$) decrease in trabecular thickness in the distal femur and a 5.9% ($p = 0.05$) decrease in cortical thickness (Ct.Th) at the tibiofibular junction, compared to age and sex matched WT mice. Strikingly, FGF9 deficiency in OBs did not affect bone mass in female mice (KO vs. WT: cancellous %BV/TV, 13.8 ± 0.6 vs. 12.9 ± 0.5 ; Ct.Th, 236 ± 5.6 vs. $232 \pm 4.1 \mu\text{m}$). Histomorphometry of the distal femur confirmed that significant changes were seen in male KO mice only. There was a 39% ($p < 0.01$) decrease in cancellous BV/TV and a 52.7% ($p < 0.05$) decrease in bone formation rate at the distal femur in male KO mice. Continuous treatment of mouse BMSCs with FGF9 (5 ng/ml) from day 0 to day 20 inhibited mouse BMSC mineralization while acute treatment (5 ng/ml) on BMSC cultures at day 3 for 24h increased the progenitor cell proliferation, as determined by BrdU incorporation. Strikingly, BMSCs from male mice were more responsive to FGF9 than were BMSCs from female mice. There was a 209% ($p < 0.01$) increase in BrdU labeled male cells and a 76% ($p < 0.05$) increase in BrdU labeled female cells, when compared to sex matched, vehicle treated control cells. In a previous study, heterozygous loss of Akt1 was shown to be deleterious to OB precursor development, leading to lower bone mass in male (but not female) mice (Mukherjee A et al., PLoS One. 2014, 9: e93040). In the present study, we found that inhibition of Akt activity by adding an Akt inhibitor, MK-2206 ($1 \mu\text{M}$) completely prevented the stimulatory effect of FGF9 (5 ng/ml) on OB precursor proliferation *in vitro*. Our results demonstrate that mature OBs are a biologically important source of FGF9, positively regulating skeletal homeostasis in male mice. Osteoblast-derived FGF9 may serve a paracrine role to maintain the osteogenic progenitor cell population through activation of Akt signaling.

Disclosures: Liping Wang, None.

FR0206

Ablation of a mitochondrial stress sensor, cyclophilinD, increases osteogenicity of MSCs and reduces bone degeneration. Roman Eliseev^{*}, Jerry Madukwe. University of Rochester, USA

The goal of this project was to elucidate the effect of genetic ablation of a mitochondrial stress sensor, cyclophilin D (CypD), in CypD knock-out (KO) mice on bone marrow mesenchymal stromal (a.k.a. stem) cells (MSC) and on bone degeneration. MSCs are precursors of osteoblasts, adipocytes and chondrocytes. Our data and the literature indicate that MSC osteogenic function is highly dependent on the ability of these cells to activate mitochondria and maintain high levels of oxidative metabolism. Under the conditions of oxidative stress observed in aging and upon loss of hormone stimulation, mitochondria become less functional leading to cell demise and whole tissue dysfunction. Opening of the mitochondrial permeability transition (MPT), a large non-selective pore gated by CypD, is the major mechanism of such a mitochondrial dysfunction. Our previous data indicated improved bone quality and biomechanical properties and preservation of oxidative metabolism in 13-month old CypD KO mice when compared to the age-matched wild type mice. We are now presenting our new data indicating that genetic ablation of CypD prevented aging-associated decline in MSC CFU's and increased their osteogenic potential while reducing MSC adipogenic potential. On a tissue level, in 13-month old CypD KO mice we observed reduced bone loss, absence of bone marrow fat, no change in osteoblast numbers but improved osteoblast function measured with bone formation rate, and higher osteocyte numbers when compared to the age-matched wild type mice. Overall, our data indicate that protecting and enhancing mitochondrial metabolism by targeting CypD/MPT and de-sensitizing mitochondria for stress, improves MSC osteogenic function and prevents adipogenic shift leading to reduced bone degeneration in aging.

Disclosures: Roman Eliseev, None.

FR0207

Identification of a Subpopulation of Periosteal and Endosteal Prx1-Expressing Cells in Postnatal Long Bones and Their Contribution to Fracture Repair. Alessandra Esposito^{*1}, Ye Ping², Tieshi Li³, Joe Temple³, Anna Spagnoli³. ¹Rush University Medical School, USA, ²UNC of Chapel Hill, USA, ³Rush University Medical Center, USA

The regenerative ability of bones after fracture implies the existence of adult progenitors. However, the nature of these progenitors is still elusive. Although it is evident that the periosteum is critical to fracture repair, the cell population(s) that govern its regenerative ability are largely unknown. Furthermore, there is evidence that the endosteum contributes to the intramembranous callus by providing progenitor(s) derived from the bone marrow interfacing the bone. To identify potential adult skeletal progenitors, we used Prx1CreERGFPRosaLacZ mice in which Tamoxifen (TAM) induces Prx1Cre-driven recombination resulting in bGal expression. For early postnatal study, TAM was given at P3 and tibias obtained at P6, P9, P12, P19, P15, P18 and P21. We found that at P6 and P9, most of the Prx1-bGal cells localized in the endosteum. By P12, in addition to endosteum, Prx1-bGal cells were detected in the periosteum. By P15 and P21, Prx1-bGal cells were found in the periosteum, endosteum, within the cortical bones, growth plates and secondary ossification centers as osteoblasts, lining cells, and chondrocytes. In older mice (16-18 weeks) 4OHTAM was given for 5 days and mice sacrificed either 6 or 28 days later. At both chasing times, we found Prx1-bGal cells within the periosteum (mostly) and the endosteum. In the longer term chasing study, we also found Prx1-bGal cells within the cortical bones and growth plates. We next evaluated Prx1-bGal+ pattern in fracture repair using two timelines for TAM administration. Study 1 was aimed at labeling cells that express Prx1 during repair (4OHTAM 3 days before and 2 days after fracture), Study 2 at tracing cells that express Prx1 before fracture and their progenies (4OHTAM for 5 days starting 33 days before fracture). Mice were euthanized 7 days post-fracture. In both studies, we found a large number of Prx1-bGal cells within the periosteum and endosteum facing the fracture line. Differently from Study 1, Study 2 showed Prx1-bGal cells within the callus as bone and cartilaginous cells. At the periosteal and endosteal sites in unfractured as well as fractured mice, Prx1-bGal cells, were perivascular, surrounding PECAM+ and vWF+ endothelial cells, and co-expressed the pericyte markers aSMA and NG2. Our studies indicate that we have identified a population of periosteal and endosteal Prx1+ pericytes that seem to contribute to fracture repair. Studies are in progress to further characterize the nature of Prx1+ cells.

Disclosures: Alessandra Esposito, None.

FR0208

Large-scale Bone Regeneration by Cells Intermediate between Chondrocytes and Osteocytes. Gage Crump^{*}, Sandeep Paul, Simone Schindler, Sofia Bougioukli, Jay Lieberman, Francesca Mariani, University of Southern California, USA

The repair of extensive bone injuries remains a clinical challenge. While bone repair often involves a cartilage intermediate, the role of chondrocytes in this process has remained unclear. We have found that the adult lower jawbone of zebrafish can undergo extensive regeneration following resection, and that it does so through an unusual skeletal cell type with properties intermediate between chondrocytes and osteoblasts. During jawbone regeneration, these cells initially produce cartilage matrix while expressing genes associated with both chondrocyte and osteoblast development. Shortly thereafter, regenerating chondrocytes directly produce mineralized matrix and become embedded in mature bone. By analyzing adult viable *ihha* mutants, we find that *Ihh* signaling causes periosteal progenitors to shift from making osteoblasts during bone homeostasis to making chondrocyte-like cells during bone regeneration. Together, our studies highlight that jawbone regeneration utilizes a progenitor program distinct from endochondral development. Moreover, we observe a remarkably similar process during mouse rib bone regeneration, and we are testing if rib periosteal cells are able to heal critical sized bone defects in other parts of the mouse. We therefore propose periosteal-derived hybrid cartilage/bone cells as a novel therapeutic for critical sized bone defects in patients.

Disclosures: Gage Crump, None.

FR0209

Mesenchymal Progenitors Promote Vasculogenesis to Initiate the Formation of Secondary Ossification Center in the Epiphyseal Cartilage. Wei Tong^{*1}, Motomi Enomoto-Iwamoto², Haoruo Jia³, Ling Qin³. ¹Perelman school of medicine, USA, ²Department of Surgery, The Children's Hospital of Philadelphia, USA, ³Department of Orthopaedic Surgery, University of Pennsylvania, USA

Endochondral ossification in long bones proceeds via the development of a diaphyseal primary ossification center (POC) in embryo and an epiphyseal secondary ossification center (SOC) after birth. While POC formation has been extensively studied, the initiation and expansion of SOC are largely uncharacterized. Tomato (Td)+ cells of Col2-Cre Rosa-Td mice were recently identified as mesenchymal

progenitors that constantly replenish osteoblasts and osteocytes in POC. At P4, while most epiphyseal chondrocytes were Td+, those located at cartilage surface had much higher Td signal than those inside cartilage and were termed Td^{high} cells. Since later all osteoblasts, osteocytes, and osterix+ osteoprogenitors within SOC were Td^{high}, those Td^{high} cells at cartilage surface are likely mesenchymal progenitors responsible for subchondral bone formation. At P5, using a whole mount staining with 3D image reconstruction (100 um thickness), we observed that Td^{high} cells started to penetrate into cartilage at discrete surface sites, followed by endothelial progenitor cells. At P6, cartilage canals were initiated at these sites. The canal wall, which consists of Td^{high} cells, endothelial progenitors, and chondrocytes, was again preceded by VEGF+ Td^{high} cells leading the front edge. Inside the canal, there was a cone-shaped and dense cell cluster, including Td^{high} cells, vessels, and CD45+ cells, with the base at the cartilage surface. Those Td^{high} cells were proliferative and they migrated either as perivascular cells or as single cells. Interestingly, there was a space about 30 um long between the canal wall and the cell cluster where only erythrocytes were detected. The canal wall was distinctly labeled by an antibody against the aggrecan-degraded product (VIPEN). The unique initiation and structure of cartilage canal strongly suggest that mesenchymal progenitors play a leading role in promoting vasculogenesis, a de novo vessel formation process, and together with chondrocytes creating a path for canal protrusion. In vitro, mesenchymal progenitors greatly stimulate migration and vessel assembly of endothelial progenitors. After P8, the expansion of SOC was led by blood vessel growth followed by Td^{high} progenitors, the same mechanism by which the growth plate is remodeled into bone. In summary, using a powerful 3D imaging approach, we discovered a novel crosstalk between mesenchymal progenitors and endothelial progenitors that initiates SOC formation.

Disclosures: Wei Tong, None.

FR0210

Notch Signaling Mediates Skeletal Sex Differences. Stefano Zanotti^{*}, Ernesto Canalis, UConn Health, USA

Women attain a lower peak bone mass and are more prone to cancellous bone loss than men. Similarly, maturing female mice have less cancellous bone volume than male littermates. The skeletal disadvantage suffered by female rodents is explained by a decrease in osteoblastogenesis due to a suppressed capacity of progenitor cells to become osteoblasts. However, the mechanisms responsible for sex differences in skeletal microarchitecture and osteoblastic cell maturation are not known. Since Notch activation in immature osteoblasts suppresses their differentiation and decreases bone mass, we asked whether sensitization of female mice to the effects of Notch in osteoblast precursors mediates sex-dependent skeletal effects. To answer this question, we generated dual Notch1/Notch2 conditional null C57BL/6 mice in Osterix-expressing cells and compared them to Notch1/Notch2 conditional littermate controls of the same sex. Postnatal Notch1 and Notch2 inactivation in osteoblast precursors precluded the influence of sex on cancellous bone volume and microarchitecture, indicating that Notch receptors are responsible for sex differences in skeletal microarchitecture. To establish whether Notch mediates the impact of sex on osteoblastogenesis, bone marrow stromal cells from conditional Notch1/Notch2 mice were infected with an adenoviral vector where the cytomegalovirus (CMV) promoter governs Cre expression (Ad-CMV-Cre), or a control vector (Ad-CMV-GFP). Notch downregulation enhanced osteoblastogenesis in cells from female, but not from male, mice. Moreover, suppression of Notch activity in cells from wild-type mice confirmed these findings, indicating that Notch signaling mediates sex differences in osteoblastogenesis. To determine whether canonical Notch signaling, which requires the DNA-binding protein Rbpjk, is responsible for the sex differences, we assessed the capacity for osteoblastogenesis of bone marrow stromal cells from conditional Rbpjk mice. Rbpjk downregulation following infection with Ad-CMV-Cre did not change the influence of sex on osteoblast differentiation. These results suggest that Rbpjk-independent, or non-canonical, Notch signaling mediates sex differences in osteoblastogenesis. In conclusion, Notch1 and Notch2 determine skeletal sexual dimorphism, and the effect on osteoblastogenesis is mediated by non-canonical mechanisms.

Disclosures: Stefano Zanotti, None.

FR0211

A Novel Interferon Regulatory Factor-8 (IRF8) Mutation is Associated with Osteoclast-Mediated Idiopathic Tooth Root Resorption. Vivek Thumbigere Math^{*1}, Brian Foster², Anthony Neely³, Hiroaki Yoshii⁴, Keiko Ozato⁴, Martha Somerman². ¹National Institutes of Health, USA, ²National Institute of Arthritis & Musculoskeletal & Skin Diseases (NIAMS), USA, ³University of Detroit-Mercy School of Dentistry, USA, ⁴National Institute of Child Health & Human Development, USA

Multiple idiopathic root resorption is a form of periodontal disease often noted in middle age with unknown etiology. Previous case reports of familial pattern suggest a genetic susceptibility to the disease. Following IRB approval from the University of Detroit Mercy School of Dentistry and the National Institutes of Health (NIH), dental/medical histories, x-rays, saliva samples, and extracted teeth were collected from a kindred (3 affected and 3 unaffected members) exhibiting idiopathic root resorption. On examination, the proband and the affected son and daughter exhibited severe root resorption of multiple teeth, but no other significant medical history.

Micro-CT of exfoliated teeth revealed a unique pattern of severe cervical root resorption distinct from tooth decay. Whole exome sequencing performed using saliva identified SNPs in twenty-three candidate genes that co-segregated with the resorption phenotype, including a novel autosomal dominant missense mutation in IRF8. Primarily expressed in immune cells, IRF8 is a key regulator of inflammation and bone metabolism, and its repression mediates osteoclastogenesis by enhancing nuclear factor of activated T cells c1 (NFATc1) activity. The identified amino acid change (G388S) in IRF8 was localized to a highly conserved C-terminal motif, leading to altered serine phosphorylation motifs and phosphoserine binding domains, and is predicted to cause a large shift in 3D protein folding. These data suggest that the G388S mutation would impair IRF8 heterodimerization with other transcription factors including NFATc1, thereby producing overactive osteoclasts that target the periodontia. Consistent with these predictions, we noted *Irif8^{-/-}* mice, when compared to WT mice, exhibited increased osteoclast activity in the periodontia, widened periodontal ligament (PDL) space and alveolar bone loss. Following induction of periodontal inflammation, these findings were exacerbated including irregularities in tooth root surfaces. In conclusion, this study identifies a novel mutation associated with multiple idiopathic root resorption and results indicate that IRF8 is a key factor in maintaining periodontal tissue homeostasis.

Disclosures: Vivek Thumbigere Math, None.

FR0212

Osteoclastic miR-214 targets PTEN to increase bone resorption. Jin Liu*¹, Defang Li², Baosheng Guo², Lei Dang², Aiping Lu², Ge Zhang^{2,1}, Hong kong, ²Institute for Advancing Translational Medicine in Bone & Joint Diseases, Hong Kong Baptist University, Hong kong

Introduction: Emerging evidences indicate the unique role of microRNAs in regulating bone resorption. Our preliminary study showed that elevated osteoclastic miR-214 associated with increased bone resorption in both postmenopausal osteoporosis and osteolytic bone metastasis, suggesting a potential role of osteoclastic miR-214 in regulating bone resorption. It was documented that miR-214 could target PTEN in cancer cells (Yang et al. 2008). Moreover, PTEN was shown to participate in regulating osteoclast function (DeMambro et al. 2012). Thus, we postulated that osteoclastic miR-214 could target PTEN to regulate bone resorption.

Objectives: To investigate whether osteoclastic miR-214 could target PTEN to regulate bone resorption.

Methods: We performed qPCR, TRAP staining, western blotting and luciferase reporter assays to determine the role of osteoclastic miR-214 during osteoclast differentiation *in vitro*. We applied qPCR, ELISA, western blotting, microCT and bone histomorphometric analysis to examine the role of osteoclastic miR-214 in regulating bone resorption in our established osteoclast-specific miR-214 knock-in (OC-miR-214) mice.

Results: In the *in vitro* study, we found that the miR-214 level gradually increased during osteoclast differentiation (Fig. 1). The mRNAs level of *TRAP* and *CTSK* and the area of TRAP+ cells could be suppressed by antagomiR-214 and promoted by agomiR-214 during osteoclast differentiation (Fig. 2). Moreover, a series of *in vitro* experiments showed that miR-214 could functionally target the 3'UTR of *PTEN* mRNA to promote osteoclast activity (Fig. 3). In the *in vivo* study, we found that the intrasosseous mRNA level of osteoclast marker genes and serum bone resorption biomarker were all higher in OC-miR-214 mice when compared to WT mice (Fig. 4 a, b). The intrasosseous PTEN protein level was lower in OC-miR-214 mice when compared to WT mice (Fig. 4c). Micro-CT imaging revealed poorly organized trabecular architecture at distal femur in OC-miR-214 mice when compared to WT mice (Fig. 4d). Bone histomorphometry analysis showed higher level of bone resorption-related parameters in OC-miR-214 mice when compared to WT mice (Fig. 4e). In addition, the above bone phenotype in OC-miR-214 mice could be markedly attenuated after treatment with antagomir-214 encapsulated by our established osteoclast-targeting delivery system (Liu et al. 2015) (Fig. 4f, g).

Conclusions: Osteoclastic miR-214 could target PTEN to increase bone resorption.

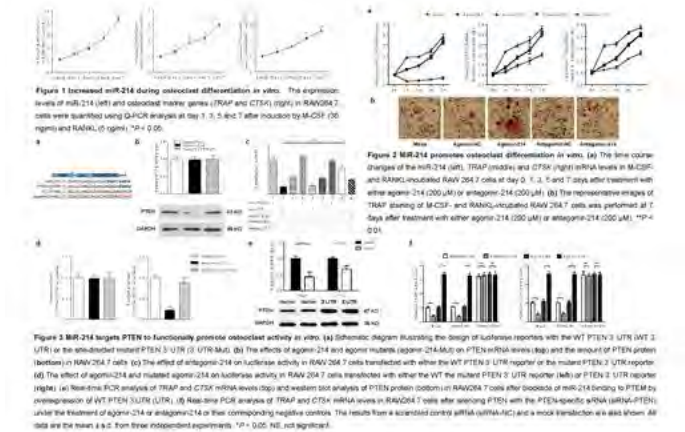


Figure 1, 2 & 3

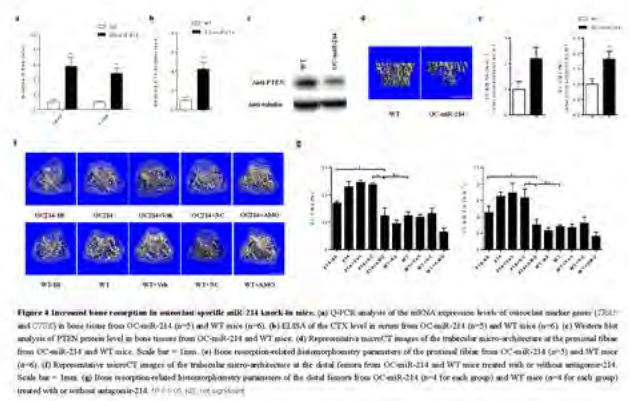


Figure 4 Increased bone resorption in osteoclast-specific miR-214 knock-in mice. (a) qPCR analysis of the mRNA expression levels of osteoclast marker genes (TRAP and CTSK) in bone tissue from OC-miR-214 (n=5) and WT mice (n=6). (b) ELISA of the CTX level in serum from OC-miR-214 (n=5) and WT mice (n=6). (c) Western blot analysis of PTEN protein level in bone tissue from OC-miR-214 and WT mice. (d) Representative micro-CT images of the trabecular micro-architecture of the proximal tibia from OC-miR-214 and WT mice. Scale bar = 1mm. (e) Bone resorption-related histomorphometry parameters of the proximal tibia from OC-miR-214 (n=5) and WT mice (n=6). (f) Representative micro-CT images of the trabecular micro-architecture at the distal femur from OC-miR-214 and WT mice treated with or without antagomir-214. Scale bar = 1mm. (g) Bone resorption-related histomorphometry parameters of the distal femur from OC-miR-214 (n=4 for each group) and WT mice (n=4 for each group) treated with or without antagomir-214. *P < 0.05, **P < 0.01, ***P < 0.001.

Figure 4

Disclosures: Jin Liu, None.

FR0213

Ostm1 expression in mature osteoclasts is both necessary and sufficient to prevent osteopetrosis. Jean Vacher*¹, Monica Pata², Marie Solange Mutabaruka^{2,1} Institut De Recherches Cliniques De Montréal, Canada, ²IRCM, Canada

Autosomal recessive malignant osteopetrosis is an inherited bone disorder resulting from defective hematopoietic derived osteoclasts. We have characterized the *Ostm1* gene (*Ostm1*) responsible for the spontaneous recessive murine osteopetrotic *gl* mutation and functional rescue of hematopoietic defects in myeloid and lymphoid lineages including osteoclast, B and T cells, was attained in *gllgl*-PU.1-*Ostm1* BAC transgenic mice. Characterization of *gllgl* hematopoiesis showed that *gllgl* multipotent cells can differentiate into all lineages and that the osteoclast lineage is significantly stimulated. In contrast the mature *gllgl* osteoclasts are poorly functional and display cytoskeletal defects. To definitively establish the osteoclast autonomous role of *Osm1*, first we targeted *Ostm1* expression specifically to mature osteoclasts under the control of the CathepsinK (*Ctsk*) promoter in transgenic mice. Several transgenic lines with differential expression levels of the *Ctsk-Ostm1* transgene were established and *gllgl* *Ctsk-Ostm1* transgenic mice were generated. Phenotypic rescue of osteopetrosis in these progenies was demonstrated as dosage dependent and correlated with transgene expression levels. However, these *gllgl* transgenic mice did not thrive normally and died prematurely with a lifespan of 8-9 weeks due to neuronal degeneration. Second, we generated a conditional *Ostm1* floxed allele that reproduces the first *OSTM1* mutation we described resulting from *OSTM1* exon 5 skipping. The potential of the floxed allele to reproduce a complete *Ostm1* loss of function was validated with the ubiquitously expressed *Meox-Cre* deleter mice. *Ostm1^{lox/lox}* *Meox-Cre⁺* progenies compared to control littermates exhibited smaller size, severe osteopetrosis with major increase of bone mass and die ~3 weeks. This result demonstrates that the *Ostm1^{lox}* allele we generated can recapitulate, under systemic ablation, an osteopetrotic phenotype similar to the spontaneous *Ostm1* null mutation in *gllgl* mice. Specific mature osteoclast conditional ablation was induced using the CathepsinK-Cre deleter mouse. Ablation of *Ostm1* in *Ostm1^{lox/lox}* *Ctsk-Cre⁺* was concomitant with osteoclast maturation and reached ~100% efficiency in fully mature OCLs produced *ex vivo*. *In vivo*, loss of *Ostm1* in mature osteoclasts resulted in severe osteopetrosis with massive increased bone mass, inefficient bone resorption and early death ~3 weeks of age. All these features closely recapitulate the skeletal phenotypes that we characterized in the spontaneous osteopetrotic *Ostm1*-null *gllgl* mouse mutant. Together our studies demonstrate that the *Ostm1* expression in mature osteoclasts is necessary and sufficient to prevent osteopetrosis.

Disclosures: Jean Vacher, None.

FR0217

Conditional abrogation of *Atm* in osteoclasts leads to reduced bone mass in mice. Toru Hirozane*, Takahide Tohmonda, Masaki Yoda, Yoshiaki Toyama, Morio Matsumoto, Hideo Morioka, Keisuke Horiuchi, Masaya Nakamura. Keio University School of Medicine, Japan

Introduction Ataxia-telangiectasia mutated (ATM) plays a major role in response to DNA damage. We previously found that ATM is activated during osteoclastogenesis (Fig1); however, the potential function of ATM in bone metabolism is not well-understood.

To address this issue, we generated mutant mice in which ATM is specifically disrupted in osteoclasts (*Atm-Ctsk* mice).

Methods

Atm floxed mice were crossed with Cathepsin K-Cre recombinase transgenic mice to specifically inactivate ATM in osteoclasts. Bone morphometric analysis and μ CT analysis were done using the femur collected from 3-week-old and 9-week-old male *Atm-Ctsk* and their littermate control mice. In vitro osteoclast formation assay was performed using bone marrow cells harvested from 9-week-old male *Atm-Ctsk* and control mice. The number of multinucleated osteoclasts was enumerated and the pit formation assay was performed. The expression levels of osteoclast-related transcripts and proteins were evaluated by quantitative PCR and western blotting, respectively.

Results and Discussion

Bone morphometric analysis and μ CT analysis showed reduced cancellous bone mass in *Atm-Ctsk* mice compared to control mice (Fig2). However, there was no increase in the osteoclast number or resorption activity in *Atm-Ctsk* mice compared to control mice. Of note, we found that the expression of the osteoclast-derived coupling factors, including *Wnt10b* and *Bmp6*, was reduced in ATM-deficient osteoclasts compared to control cells, and that RANKL-induced NF κ B signaling was suppressed in ATM-deficient osteoclasts. These observations indicate that the decreased bone volume in *Atm-Ctsk* mice was in part derived from the defect in producing coupling factors that are involved in stimulating osteoblastic bone formation in osteoclasts lacking ATM.

Conclusion

Atm-Ctsk mice exhibited reduced bone mass possibly due to the defects in producing coupling factors that are involved in stimulating bone formation following bone resorption by osteoclasts.

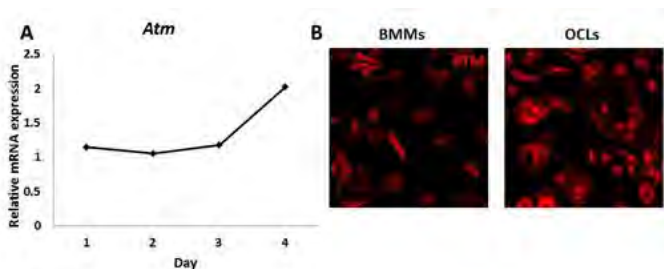


Figure 1.

ATM is activated during osteoclast differentiation.

(A) Time-course changes of *Atm* transcript expression in bone marrow macrophages (BMMs) treated with soluble RANKL. (B) Immunostaining of ATM in BMMs and osteoclasts (OCLs). Note the nuclear localization of ATM in OCLs but not in BMMs.

figure 1

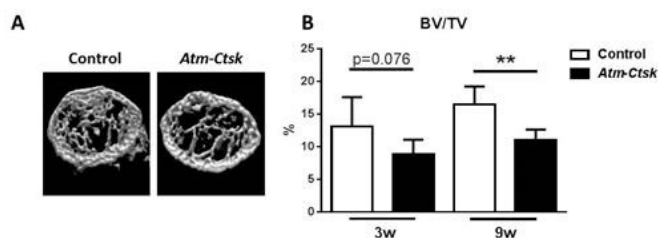


Figure 2.

Reduced cancellous bone mass in *Atm-Ctsk* mice.

(A) μ CT images of the distal femur of Control and *Atm-Ctsk* mice. (B) Bone volume fraction (BV/TV %) of the proximal tibia of 3 and 9-week-old mice. Statistical significance was evaluated by Student's t test. ** $p < 0.01$

figure 2

Disclosures: Toru Hirozane, None.

FR0218

Correlating RANK Ligand/RANK Binding Kinetics with Osteoclast Formation and Function. Julia Warren^{*1}, Steve Teitelbaum², Wei Zou², Nidhi Rohatgi², Corinne Decker², Christopher Nelson², Daved Fremont². ¹Washington University in St. Louis School of Medicine, ²Washington University in Saint Louis, USA

The interaction between Receptor Activator of NF- κ B Ligand (RANKL) and its receptor RANK is essential for the differentiation and bone resorbing capacity of the osteoclast. Osteoprotegerin (OPG), a soluble homodimer, acts as a decoy receptor for RANKL and thus inhibits osteoclastogenesis. An imbalance in the RANKL/RANK/OPG axis, with decreased OPG and/or increased RANKL, is associated with diseases that favor bone loss, including osteoporosis. Recently, we established a yeast surface display system and screened libraries of randomly mutated RANKL proteins to identify mutations that abolish binding to OPG while preserving recognition of RANK. These efforts yielded several RANKL variants possessing substantially higher affinity for RANK compared to their wild-type (WT) counterpart. Using recombinant RANKL mutant proteins, we find those with increased affinity for RANK produce more robust signaling in osteoclast lineage cells and have greater osteoclastogenic potential. Our results are the first to document gain of function RANKL mutations. They indicate that the physiological RANKL/RANK interaction is not optimized for maximal signaling and function, perhaps reflecting the need to maintain receptor specificity within the tumor necrosis factor superfamily (TNFSF). Instead, we find, a biphasic relationship exists between RANKL/RANK affinity and osteoclastogenic capacity. In our panel of RANKL variants, this relationship is driven entirely by manipulation of the kinetic off-rate. Our structure-based and yeast surface display-derived insights into manipulating this critical signaling axis may aid in the design of novel anti-resorptive therapies as well as provide a paradigm for design of other receptor-specific TNF superfamily ligand variants.

Disclosures: Julia Warren, None.

FR0221

Sirtuin1 (Sirt1) activation suppresses osteoclastogenesis by deacetylating FoxOs. Ha-Neui Kim^{*1}, Li Han², Srividhya Iyer¹, Serra Ucer², Aaron Warren², Haibo Zhao², Rafael de Cabo³, Charles O'Brien², Stavros Manolagas², Maria Almeida². ¹Univ. Arkansas for Medical Sciences, Central Arkansas VA Healthcare System, USA, ²University of Arkansas for Medical Sciences & the Central Arkansas Veterans Healthcare System, USA, ³National Institute on Aging, USA

Activation of Sirt1 – an NAD⁺ dependent deacetylase – by natural or synthetic compounds like resveratrol, SRT2104, and SRT3025 attenuates the loss of bone mass caused by ovariectomy, aging, or unloading in mice. Conversely, Sirt1 deletion in osteoclast progenitors increases osteoclast number and bone resorption. Sirt1 deacetylates FoxO1, 3, and 4 and thereby modulates their activity; and FoxO1, 3, and 4 restrain osteoclastogenesis and bone resorption. Here, we tested the hypothesis that the anti-resorptive effects of Sirt1 activators require FoxO deacetylation. We report that FoxO1 acetylation was increased by knocking-down Sirt1 or adding RANKL to bone marrow macrophages (BMM) from C57BL/6J mice; this effect of RANKL was prevented by SRT3025. Further, transduction of a wild-type (WT) FoxO1 construct into BMM from mice lacking FoxO1,3,4 reversed the increased cyclinD1, macrophage proliferation, and osteoclastogenesis. In contrast, transduction of a FoxO1 mutant in which all six acetylation sites could not be de-acetylated (KQ-FoxO1), had no effect. In line with this result, SRT2104 or SRT3025 decreased cyclinD1 levels, proliferation, and osteoclast number in BMM from FoxO replete control mice. All the effects of the Sirt1 activators were absent in cells from littermate mice lacking FoxOs. Additionally, SRT3025 increased the expression of the FoxO-target genes catalase and heme oxygenase-1 in control BMMs, but this effect was greatly attenuated in cells lacking FoxOs. Furthermore, transfection of WT-FoxO1 into Raw264.7 macrophages increased the activity of a FoxO-luciferase reporter while KQ-FoxO1 had no effect, strengthening the evidence that deacetylation promotes FoxO-mediated transcription. Finally, SRT3025 decreased the protein levels of components of mitochondrial complex II (Sdhb), III (Uqcrc2), IV (Cox1) and V (Atp5a1), as well as ATP production in BMM from control mice, but not in BMM from mice lacking FoxOs, suggesting that the anti-osteoclastogenic effects of Sirt1 activation result from impaired mitochondria activity. These results, along with earlier findings that the osteoblastogenic effects of Sirt1 are also mediated by FoxOs, demonstrate that the dual anti-osteoporotic efficacy of Sirt1 stimulators (i.e. decreasing bone resorption and promoting bone formation) is indeed mediated via FoxO deacetylation.

Disclosures: Ha-Neui Kim, None.

FR0223

Alternative NF- κ B Regulates RANKL-induced Osteoclast Differentiation and Mitochondrial Biogenesis via Independent Mechanisms. Rong Zeng*, Roberta Faccio, Deborah Novack, Washington University in St. Louis, USA

Mitochondrial biogenesis, the generation of new mitochondrial DNA and proteins, has been linked to OC differentiation and function. In this study we used mutations in key alternative NF- κ B pathway proteins, RelB and NIK, to dissect the complex relationship between mitochondrial biogenesis and osteoclastogenesis. In precursors lacking either NIK or RelB, RANKL is unable to increase mitochondrial DNA or expression of proteins in the oxidative phosphorylation chain, associated with lower oxygen consumption rates. Transgenic OC precursors expressing constitutively active NIK showed normal RANKL-induced mitochondrial biogenesis compared to controls, but had larger mitochondrial dimensions and increased oxygen consumption rates, suggesting increased mitochondrial function in the mutant cells. To deduce the mechanism for mitochondrial biogenesis defects in NIK- and RelB-deficient precursors, we examined expression of several genes known to control this process. PGC-1 β , but not PGC-1 α , PPRC1 or ERR α , were significantly decreased in RelB-/- and NIK-/- cells. Because PGC-1 β has been reported to positively regulate both mitochondrial biogenesis and differentiation in OCs, we retrovirally overexpressed PGC-1 β in RelB-/- cells. Surprisingly, exogenous PGC-1 β did not affect differentiation, nor restore RANKL-induced mitochondrial biogenesis. Thus, while downstream of RelB, PGC-1 β is not the key mediator of RANKL-induced mitochondrial biogenesis in OCs. To determine whether the blockade in osteoclastogenesis in RelB-deficient cells precludes mitochondrial biogenesis, we rescued RelB-/- differentiation with overexpression of NFATc1. Mitochondrial parameters were unaffected by retrovirus-driven NFATc1 in either WT or RelB-/- cultures, and bone resorption in the latter was not restored. Our data demonstrate that alternative NF- κ B regulates mitochondrial biogenesis in response to RANKL stimulation in OC precursors, but this process is independent of NFATc1. Furthermore, the inability of PGC-1 β to drive mitochondrial biogenesis in the absence of RelB indicates that there is cell type-specificity in the regulation of mitochondria.

Disclosures: Rong Zeng, None.

FR0225

Function of novel splicing variant of receptor activator of NF- κ B. Riko Kitazawa*¹, Ryuma Haraguchi², Yosuke Mizuno³, Yasuhiro Kobayashi⁴, Sohei Kitazawa². ¹Department of Diagnostic Pathology, Ehime University, Japan, ²Department of Molecular Pathology, Ehime University Graduate School of Medicine, Japan, ³Department of Diagnostic Pathology, Ehime University Hospital, Japan, ⁴Institute of Oral Science, Matsumoto Dental University, Japan

Receptor activator of NF- κ B (RANK) is a member of the tumor necrosis factor receptor (TNFR) family expressed in osteoclast precursors, and RANK-RANK ligand (RANKL) signaling is a key system for differentiation, activation and survival of osteoclasts. We have identified a novel alternative splicing variant of mouse and human RANK gene (vRANK) that contains an intervening exon between exons 1 and 2 of full-length RANK (fRANK) mRNA. Since this novel exon contains a stop codon, vRANK encodes short truncated amino acids that have a portion of the signal peptide of fRANK and additional amino acids that show no homology to previously reported domains. By transient transfection of RAW264.7 cells with vRANK-GFP and -Flag expressing constructs, vRANK was found localized mostly in the cytoplasm and partly in the cell membrane, but was not secreted into the culture supernatant. In the HL60 human myelomonocytic leukemic cell line, vRANK expression was induced by PMA or TGF- β in the presence of Vitamin D3 in an ERK-dependent manner. The presence of Sam68 binding sites located around intervening exon-intron junctions also signifies the importance of the ERK pathway in vRANK expression. When overexpressed *in vitro*, vRANK in mouse pre-osteoclastic RAW264.7 cells decreased the formation of TRACP-positive multinucleated giant cells and negated the anti-apoptotic effect of sRANKL. When systemically overexpressed *in vivo*, the CAGCre+/vRANK mouse showed high fatality before weaning; a 13-week survivor displayed severe cardiac dilatation with cardiomyopathy and bronchopneumonia. When selectively overexpressed among the RANK-positive monocyte-macrophage lineage *in vivo*, the RANKCre+/vRANK mouse displayed reduced bone mass with almost normal osteoclastic activity. Taken together, these results suggest that vRANK is a novel bioactive peptide that not only reduces the number of RANKL-induced mature osteoclasts, but also exhibits profound systemic cytopathic effects. We are now creating CTSKCre+/vRANK mice to analyze the effects of vRANK on mature osteoclasts.

Disclosures: Riko Kitazawa, None.

FR0226

Loss of PARP1 Poly-ADP-ribosylating Function is Necessary for Osteoclast Differentiation. Chao Qu*¹, Chun Wang¹, Gaurav Swarnkar¹, Jacqueline Kading¹, Michael Hottiger², Yousef Abu-Amer¹, Roberto Civitelli¹, Gabriel Mbalaviele³. ¹Washington University School of Medicine, USA, ²University of Zurich, Switzerland, ³Washington University in St. Louis School of Medicine, USA

Poly(ADP-ribose) polymerase 1 (PARP1) catalyzes the formation of poly-ADP-ribose (PAR) polymers by transferring several ADP-ribose units from nicotinamide adenine dinucleotide (NAD⁺) onto acceptor proteins, a post-translational modification termed PARylation. Emerging evidence implicates PARP1 in cell differentiation, but its role in bone metabolism remains unknown. We find that M-CSF induces massive PARylation of proteins, including PARP1, in mouse bone marrow macrophages (BMM), an effect that is PARP1-dependent as silencing or selective inhibition of this enzyme decreases protein PARylation by >95%. Our other *in vitro* findings indicating that retroviral-mediated PARP1 overexpression inversely correlates with the survival of BMM suggest that attachment of PAR units to PARP1 in response to M-CSF may be a survival signal that restrains the action of this enzyme in the osteoclast (OC) lineage. Consistent with this view, and the overall prediction that PARP1 negatively regulates OC formation, we find that PARP1 protein abundance is completely suppressed in BMM cultures after 3-day exposure to RANKL, via increased protein degradation without interference with mRNA expression. Mechanistically, we established a sequence of biological events during RANKL-driven osteoclastogenesis whereby PARP1 is highly PARylated in BMM, cleaved in OC lineage-committed BMM by caspase-1, a component of the intracellular NLRP3 inflammasome complex, and finally degraded in late OC precursors, thus enabling OC maturation. Notably, genetic or pharmacological blockade of the inflammasome, not only preserve PARP1 protein abundance, but also inhibits OC formation induced by M-CSF and RANKL, strengthening the notion that PARP1 negatively affects OC differentiation. Consistent with these results, knock-in mice (2-week-old and 8-week-old) globally expressing an uncleavable PARP1 mutant (gain-of-function) consistently exhibit 30-40% higher bone mass compared to wild-type littermates, owing to decreased OC differentiation and bone resorption, while bone formation is unaffected. Conversely, in states of pronounced PARP1 degradation and reduced PARylation responses such as those associated with inflammasome hyperactivation, OC development is accelerated. These results indicate that protein PARylation is one of the mechanisms through which PARP1 inhibits OC differentiation, and reveal an important role of this post-translational modification in modulating bone resorption and homeostasis.

Disclosures: Chao Qu, None.

FR0228

Lineage Tracing of Cathepsin-K in Bone and Other Tissues. Farzin Takyar*¹, Ryan Berry², Lynda Bonewald³, John J Wysolmerski⁴, Mark C Horowitz². ¹Yale University, School of Medicine, USA, ²Department of Orthopaedics & Rehabilitation, Yale School of Medicine, USA, ³School of Dentistry, University of Missouri-Kansas City, USA, ⁴Section of Endocrinology & Metabolism, Yale School of Medicine, USA

The cathepsin K inhibitor, Odanacatib, has been shown to increase periosteal bone formation through unknown mechanisms. Using *CatKCre;R26R* mice we recently showed that some periosteal cells express CatK. To determine the origin of these cells, we performed lineage tracing using fluorescent *mTmG* reporter mice bred to *CatKCre* mice. The *mTmG* model is useful for lineage tracing because expression of Cre-recombinase in progenitor cells results in the permanent expression of eGFP in both progenitor and daughter cells. 10 day-old *CatK-Cre;mTmG* mice show eGFP (CatK expression) within osteoclasts at the primary spongiosum and along the endosteal surface of the cortex. We also observed scattered CatK expression within the periosteum. In 6-wk-old mice, an almost continuous layer of periosteal cells at the bone surface express CatK with scattered eGFP+ osteoclasts along the endosteum and trabeculae. Chondrocytes and bone marrow (BM) cells are CatK-negative at either age. There is also a prominent eGFP+ population of cells with a stellate appearance in the skin and smaller numbers of cells in skeletal muscle, the medulla of the kidney and in some fat depots. In order to identify if eGFP+ periosteal cells arise from hematopoietic stem cells in the BM, *mTmG* mice were lethally irradiated and reconstituted with BM from *CatK-Cre;mTmG* mice. eGFP+ osteoclasts were readily detected in the BM of reconstituted mice but no GFP+ cells were present along the periosteum, showing that CatK+ BM-derived cells do not home to the periosteal surface. Isolation of periosteal cells followed by flow cytometry characterized GFP+ cells as predominantly negative (75.7%) for the common leukocyte marker, CD45. A minor population of GFP+ cells (14.3%) was positive for CD11b (which is a monocyte/macrophage marker), while just over half of the GFP+ cells (53.3%) were Ly6C+, a monocyte marker. These findings indicate that periosteal catK+ cells are not likely to be derived from the bone marrow macrophage/osteoclast lineage. Finally, ovariectomy of 10-week-old *CatK-Cre;mTmG* mice did not change the numbers or distribution of GFP+ cells on the periosteum suggesting that these cells are not affected by estrogen withdrawal. Furthermore, neither unloading nor loading altered CatK expression in periosteal cells. In summary, our data suggest that the periosteum contains a resident population of CatK+ cells that may be a target of Odanacatib's periosteal effects.

Disclosures: Farzin Takyar, None.

This study received funding from: Supported in part by a research grant from Investigator-Initiated Studies Program of Merck Sharp & Dohme Corp. The opinions expressed in this paper are those of the authors and do not necessarily represent those of Merck Sharp & Dohme Corp.

FR0230

STAT5 is a key transcription factor for IL-3-mediated inhibition of RANKL-induced osteoclastogenesis. Semun Seong^{*1}, Jongwon Lee², Jung Ha Kim², Kabsun Kim², Inyoung Kim², Lothar Hennighausen³, Nacksung Kim². ¹Chonnam National University Medical School, South Korea, ²Department of Pharmacology, Medical Research Center for Gene Regulation, Chonnam National University Medical School, South Korea, ³Laboratory of Genetics & Physiology, National Institute of Diabetes & Digestive & Kidney Diseases, National Institutes of Health, USA

Among diverse cytokines involved in osteoclast differentiation, IL-3 has been known to inhibit RANKL-induced osteoclastogenesis. However, the mechanism underlying IL-3-mediated inhibition of osteoclast differentiation has not fully understood. In the present study, we demonstrated that STAT5 activated by IL-3 inhibited RANKL-induced osteoclastogenesis through induction of Id genes. Over-expression of STAT5 inhibited RANKL-induced osteoclastogenesis. However, RANKL regulated neither STAT5 expression nor activation during osteoclast differentiation. STAT5 deficiency prevented IL-3-mediated inhibition of osteoclastogenesis, suggesting that STAT5 plays an important role in IL-3-mediated inhibition of osteoclast differentiation. In addition, IL-3-induced STAT5 activation upregulated expression of Id1 and Id2 genes, negative regulators of osteoclastogenesis. Over-expression of ID1 or ID2 in STAT5-deficient cells reversed osteoclast development recovered from IL-3-mediated inhibition. Moreover, micro-computed tomography and histomorphometric analysis revealed that STAT5 conditional knockout mice had reduced bone mass with increased number of osteoclasts. Furthermore, STAT5 conditional knockout mice showed that IL-3 less effectively inhibited RANKL-induced osteoclast differentiation than wild-type mice in RANKL injection model. Taken together, our data suggest that STAT5 activation is a key transcription factor for IL-3-mediated inhibition of RANKL-induced osteoclastogenesis through Id gene expression.

Disclosures: Semun Seong, None.

FR0231

Analysis of an in Vitro Reconstitution System of Bone Cell Network by Two-Photon Microscopy. Atsuhiko Hikita^{*1}, Tadahiro Iimura², Yusuke Oshima², Shin Yamamoto², Takeshi Imamura². ¹Graduate School of Medicine, The University of Tokyo, Japan, ²Ehime University, Japan

[Purpose] To establish a system to reconstitute cellular network of osteoblasts, osteoclasts and osteocyte with matrices synthesized by osteoblast lineage cells, and to capture cellular events in bone metabolism. [Methods] Calvarial osteoblasts were harvested from newborn C57BL/6J mice and cultured under osteoblast differentiation condition for 4 weeks. Bone marrow macrophages from Ctsk-Cre x flox-tdTomato mice were co-cultured with differentiated osteoblasts for 3 weeks under co-culture condition, followed by a culture again in osteoblast differentiation condition. During the culture period, cells were observed using a multiphoton confocal microscopy system (A1R+MP, Nikon). Collagen fibers of matrices were also detected by second harmonic generation without labeling. Acquired images were processed and analyzed by NIS-Elements (Nikon) and IMARIS (Bitplane AG). [Results] Inside the nodule formed in osteoblast differentiation culture, cells with many processes were observed. By immunofluorescence staining, expression of DMP-1 and sclerostin was detected, which suggested these cells were osteocytes. During the osteoblast differentiation culture, increase of matrices and appearance of osteocytes were observed. Osteoblasts on the nodule changed their shape from cuboidal to flat, which was quantitatively demonstrated by image analysis. When bone marrow macrophages were co-cultured in this system, most of osteoclasts were formed on the nodule, suggesting the presence of supporting cells for osteoclasts in the nodule. Increase of osteoclasts and progression of matrix destruction were observed during the co-culture condition. Flat osteoblasts were found in the resorption pits formed by osteoclasts. When culture medium was changed again to osteoblast differentiation condition, flat osteoblasts became cuboidal, and newly synthesized matrices filled the resorption pits almost completely, which suggest the coupling of matrix resorption and formation occurred in this system. [Conclusion] A novel reconstitution system of bone cell network was established. By analyzing this system using two-photon microscopy, cellular events in bone modeling and remodeling such as coupling of matrix resorption and formation were observed.

Disclosures: Atsuhiko Hikita, None.

FR0232

Characterization of a New Cre Model Targeting Osteocytes. Delphine Maurel^{*1}, Mark L Johnson², Stephen E Harris³, Marie A Harris³, Lynda F Bonewald². ¹Department of Oral & Craniofacial Sciences, USA, ²Oral & Craniofacial Sciences, USA, ³UT Health Science Center at San Antonio, USA

Transgenic mice are widely used to delete or overexpress genes in a cell specific manner to advance bone biology. While numerous Cre models exist to target gene recombination in osteoblasts and osteoclasts, there are few that target osteocytes. Our goal was to create a spatial and temporal conditional Cre model using tamoxifen to induce Cre expression in osteocytes using the Sost Bac construct containing the 5' and 3' regions of the Sost gene (Sost ERT2 cre).

Using RP24-178J4 BAC (157Kb) with the Sost gene, recombineering was used to replace the ATG region with the CreERT2 cassette, and the frt-neo-frt cassette was then removed with l-arabinose inducible flip recombinase. Four founder lines were created by pronuclear injection of the SostBAC-CreERT2 construct. The founder lines were crossed with the td tomato reporter mice (AI9, Jackson Laboratory). CreERT2 + and CreERT2 - male and female mice were injected at 2 or 5 mo of age with tamoxifen diluted in corn oil (53 to 555mg/kg, divided in 5-6 injections in consecutive days) or vehicle (corn oil). Tail vertebrae were taken at baseline before tamoxifen injection and the mice were sacrificed 1 month later. Bones and organs (28 total) were fixed and cryosectioned (10um) in order to image and quantitate the red signal using fluorescent microscopy and to identify any off target effects.

Out of the four founder lines, only one showed specific and strong signal in osteocytes (See figure below). No signal was observed in any surface bone cell, nor in bone marrow or in muscle. While no expression was observed in the 2 day old pup, by 2 months of age some osteocytes were positive, and the osteocyte expression became more 'leaky' with age. The percentage of positive osteocytes was increased following tamoxifen injection, especially in males (40-90% positive cells versus 20-37% in females). No expression was observed in any other organ, however with tamoxifen injection, a few positive cells were observed in kidney, eye, lung, heart and brain. Many of the positive cells were associated with blood vessels, but very few blood vessels contained these positive cells. All the other organs analyzed were negative (28 organs in total).

To conclude, this model is a useful tool to delete targeted genes in osteocytes as well as to image potential changes in the osteocyte network under various conditions.



Tail vertebrae imaged with brightfield, DAPI and TRITC

Disclosures: Delphine Maurel, None.

FR0233

Gene Expression and Local in vivo Environment (LivE) Imaging of Osteocyte Subpopulations in trabecular mouse bone. Andreas Truesse^{*1}, Felicitas Flohr², Gisela Kuhn², Ralph Müller². ¹ETH Zurich, Institute for Biomechanics, Switzerland, ²ETH Zurich, Institute for Biomechanics, Switzerland

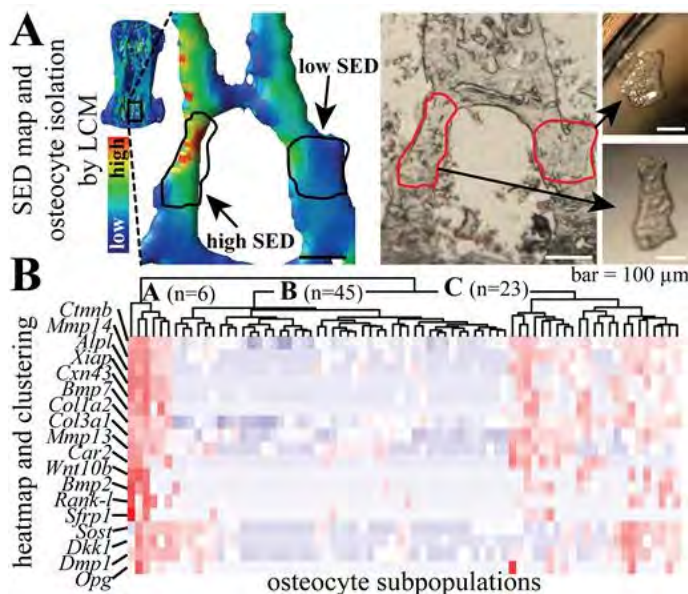
Bone constantly remodels itself to adapt to changes in its physiological environment. Osteocytes (Ot) are thought to coordinate this remodeling process with cellular signals that result in increased or decreased bone formation or resorption activity on nearby marrow-bone interfaces. To investigate these signaling events, we have developed a local in vivo environment (LivE) imaging technique based on in vivo micro-computed tomography (microCT) imaging and micro finite element (microFE) analysis in combination with laser capture microdissection (LCM) and high throughput gene expression assays. LivE imaging allows us to quantify the mechanical and remodeling microenvironment of hundreds of individual Ots over several weeks. Here, we used LivE imaging in trabecular mouse bone to show that the Ot's microenvironment is locally linked to its gene expression pattern.

To do so, the 6th caudal vertebrae of adult female C57BL/6 mice (n=9) were imaged 2 weeks prior and again 24h prior to sacrifice by in vivo microCT. 3D dynamic morphometric parameters were assessed and local strain energy density (SED) was simulated by microFE analysis. Cryosections were cut and registered into 3D microCT data. In these cryosections, Ots were identified, mapped into the microCT coordinate system and grouped according to their local SED values (high or low) and according to the past remodeling activity on the nearby marrow-bone interface

(forming, quiescent or resorbing). By LCM, Ots ($n = 689$) were then isolated in subpopulations ($n = 74$, figure A) containing nine Ots on average and their gene expression was analyzed using a microfluidic platform. Ot subpopulations were clustered according to their expression patterns (consisting of 18 individual gene expression levels) using unsupervised hierarchical clustering.

Three cluster (A, B, C) were distinguished (figure B), Ots from cluster A had a 3.3x increased chance to be found in the resorbing group and Ots from cluster C had a 1.8x higher chance to be found in the high SED group. Furthermore, Live imaging showed that Ots of the resorbing group blocked bone formation activities by Sfrp1, a WNT antagonist and increased perilacunar matrix resorption by MMPs (Mmp13, Mmp14). Ots in areas of high SED increased WNT signaling related gene expression (β -catenin and connexin43) to enhance bone formation. Additionally, genes involved in perilacunar matrix remodeling (Alpl, Colla2, Dmp1, Mmp14) were upregulated, indicating active remodeling of Ot's perilacunar matrix. Finally, the expression levels of bone morphogenic growth factors (Bmp2, Bmp8) were increased in these Ots, thus indicating an anabolic effect within the high SED group.

In conclusion, Live imaging helps to understand how Ots contribute to the dynamic remodeling of trabecular bone on the molecular level.



A) Osteocyte isolation from high & low SED. B) Gene expression heatmap & hierarchical clustering.

Disclosures: Andreas Truessel, None.

FR0236

Reduction in microRNA21 promotes apoptosis and increases RANKL in osteoblastic cells and with aging. Hannah Davis^{*1}, Emily Atkinson¹, Julia Harris¹, Rafael Pacheco-Costa², Arancha Gortazar³, Mircea Ivan¹, Angela Bruzzaniti⁴, Teresita Bellido¹, Lillian Plotkin¹. ¹Indiana University School of Medicine, USA, ²Federal University of Sao Paulo School of Medicine, Brazil, ³San Pablo-CEU University School of Medicine, Spain, ⁴Indiana University School of Dentistry, USA

Mice lacking connexin (Cx) 43 in osteocytes exhibit apoptotic osteocytes preferentially located near endocortical bone surfaces containing osteoclasts. However, the mechanism by which osteocytes lacking Cx43 undergo apoptosis and the potential consequences for osteoclast development are unknown. Silencing Cx43 in MLO-Y4 osteocytic cells increased cell death about 3-fold, which was abolished by the caspase3 inhibitor DEVD demonstrating death by apoptosis. Apoptosis of Cx43-deficient osteocytes was accompanied by reduced levels of the microRNA (miR) 21, which promotes survival in various cell types but of unknown function in osteoblastic cells. Similar to silencing Cx43, reduction of miR21 expression by transfecting a specific oligonucleotide inhibitor induced apoptosis of control osteocytes. Conversely, transfection of an oligonucleotide miR21-mimic reversed the increased apoptosis of Cx43-deficient osteocytes. These results demonstrate that reduction of miR21 is sufficient to increase osteocyte apoptosis and that apoptosis of Cx43-deficient osteocytes is due to reduced miR21 expression. Earlier evidence showed that Cx43-deficient osteocytes express increased RANKL and decreased OPG levels in vivo and in vitro. We now found that soluble (s) RANKL was increased 4-fold in conditioned media (CM) from Cx43-deficient osteocytes compared to control osteocytes. In addition, 12-fold more osteoclasts were induced by CM from Cx43-deficient osteocytes compared to control osteocytes, under suboptimal concentrations of sRANKL (40ng/ml) and MCSF (10ng/ml). Moreover, 5-fold more osteoclasts developed from non-adherent bone marrow precursors co-cultured with Cx43-deficient osteocytes compared to control osteocytes. Further, inhibition of apoptosis with DEVD prevented the increase in RANKL, but not the decrease in OPG

expression in Cx43-deficient osteocytes. Similar to Cx43-deficient mice, old mice exhibit increased osteocyte apoptosis and elevated endocortical bone resorption. Consistent with these similarities, bones from 24-month-old C57BL/6 mice exhibit reduced expression of both Cx43 and miR21 compared to 4-month-old mice. We conclude that miR21 lies downstream of Cx43 in the control of osteocyte apoptosis; and that the increased osteoclastogenic potential of Cx43-deficient osteocytes is a consequence of osteocyte apoptosis. Our findings reveal a novel Cx43/miR21/RANKL pathway in osteocytes that could be targeted to treat bone fragility with aging.

Disclosures: Hannah Davis, None.

FR0237

Bone microarchitecture anomalies and vascular expression of osteocytes markers in low serum parathormone CKD rats with vascular calcification.

Sarah-Kim Bisson¹, Roth-Visal Roth², Sylvain Picard², Richard Larivière², Mohsen Agharazi², Fabrice Mac-Way^{*3}. ¹CHU de Québec Research Center, l'Hôtel-Dieu de Québec Hospital, Laval University, Quebec, CANADA, Canada, ²CHU de Québec Research Center, l'Hôtel-Dieu de Québec Hospital, Division of Nephrology, Department of Medicine, Laval University, Quebec, CANADA, Canada, ³CHU de Québec Research Center, l'Hôtel-Dieu de Québec Hospital, Division of Nephrology, Faculty & Department of Medicine, Laval University, Quebec, CANADA, Canada

INTRODUCTION: The mechanisms underlying bone and vessels anomalies are poorly understood in chronic kidney disease (CKD). Vascular calcification is a tightly regulated process involving the transdifferentiation of vascular smooth muscle cells into "osteoblasts-like" cells. The aim of this study is to determine the anomalies of bone microarchitecture in CKD rats with vascular calcification and to evaluate whether if calcified vessels express osteocytes markers.

METHODS: CKD, low serum parathormone (PTH) level and vascular calcification in Wistar rats were induced by 5/6 nephrectomy and high calcium, phosphate and vitamin D (Ca/P/VitD) supplementation. These rats were compared to CKD and normal rats fed with a normal diet. Tibia bones and thoracic aortas were harvested 4-6 weeks after CKD induction. The markers of vascular remodeling and osteoblastic differentiation (RunX2, BMP-2, α -SMA and osteocalcin) were analyzed by qPCR and immunofluorescence on thoracic aortas. The expression of osteocytes markers (sclerostin, DMP-1, DKK-1) was performed on the thoracic aortas by immunofluorescence and western-blot. Serum levels of sclerostin were also determined. Cortical and trabecular bone microarchitecture assessment were performed by Micro-Ct and histomorphometry analysis.

RESULTS: CKD rats given a Ca/P/Vit D supplementation developed vascular calcification and induced low serum PTH level as compared to control and CKD rats fed a normal diet. In the thoracic aortas, markers of osteoblastic differentiation (RunX2, BMP-2, osteocalcin) were increased only in CKD rats with vascular calcification while α -SMA was significantly reduced. Sclerostin, DMP-1 and DKK-1 were all highly expressed in areas of calcification from thoracic aortas (Figure 1). Furthermore, serum levels of sclerostin were increased only in rats with vascular calcification. Cortical bone mineral content and thickness were significantly decreased in CKD rats with vascular calcification as compared to control while trabecular thickness, osteoid volume and surface were dramatically increased (Table 1).

CONCLUSIONS: In this CKD model of vascular calcification and low serum PTH levels, there is increased expression of osteocytes markers in calcified vessels. Furthermore, cortical and trabecular bone compartments are differently affected. These results emphasize the central role of bone metabolism and osteocytes in the development of vascular calcification in CKD.

Figure 1. Expression of sclerostin, DKK1 and DMP1 in thoracic aortas from CKD rats with vascular calcification

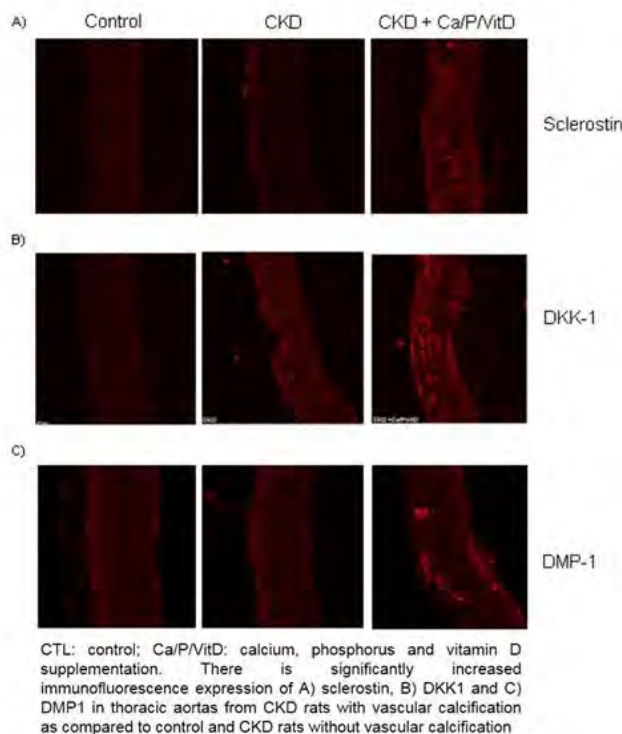


Figure 1

Table 1. Trabecular and cortical bone parameters in CKD rats with vascular calcification

| | Control | CKD | CKD + Ca/P/VitD |
|----------------------------------|---------------|---------------------------|----------------------------|
| Trabecular bone | | | |
| Bone volume/Tissue volume (%) | 12.38 ± 2.71 | 8.87 ± 0.73 | 10.84 ± 2.14 |
| Trabecular thickness (µm) | 53.66 ± 2.34 | 47.88 ± 1.70 | 77.77 ± 6.35 ^{ab} |
| Trabecular number | 2.27 ± 0.45 | 1.85 ± 0.11 | 1.35 ± 0.19 |
| Osteoid volume/Bone volume (%) | 2.59 ± 2.19 | 0.90 ± 0.02 | 17.76 ± 2.88 ^{ab} |
| Osteoid thickness (µm) | 19.34 ± 9.91 | 6.90 ± 0.18 | 21.11 ± 1.04 |
| Osteoid surface/Bone surface (%) | 0.31 ± 0.12 | 1.21 ± 0.24 | 2.88 ± 1.02 ^a |
| Cortical bone | | | |
| Thickness (mm) | 0.740 ± 0.017 | 0.714 ± 0.013 | 0.679 ± 0.023 ^a |
| Inner perimeter (mm) | 4.77 ± 0.13 | 4.46 ± 0.16 | 4.48 ± 0.11 |
| Outer perimeter (mm) | 14.03 ± 0.34 | 12.25 ± 0.29 ^a | 13.92 ± 0.37 ^b |
| Bone mineral content (mg) | 39.22 ± 0.98 | 34.10 ± 0.64 ^a | 35.60 ± 0.88 ^a |

Values are expressed as Mean ± SEM

CKD: chronic kidney disease, Ca/P/VitD: calcium, phosphate and vitamin D supplementation.

^ap < 0.05 compared to control

^bp < 0.05 compared to CKD

Table 1

Disclosures: Fabrice Mac-Way, None.

FR0238

EphrinB2 acts differently in osteoblasts and osteocytes to control bone strength and matrix composition. [Christina Vrahnas](#)¹, [Ingrid Poulton](#)², [Huynh Nguyen](#)³, [Mark Forwood](#)³, [Keith Bamberg](#)⁴, [Mark Tobin](#)⁴, [T John Martin](#)², [Natalie A Sims](#)². ¹St. Vincent's Institute, Australia, ²St. Vincent's Institute of Medical Research, Australia, ³Griffith University, Australia, ⁴Australian Synchrotron, Australia

Deletion of ephrinB2, a receptor tyrosine kinase stimulated by parathyroid hormone, in osteoblasts and osteocytes (*OsxCre.EfnB2^{fl/fl}*) delayed bone mineralization, resulting in osteoid-rich compliant bones that broke at a lower force in 3-point

bending tests. Deletion of ephrinB2 in osteocytes (*Dmp1Cre.EfnB2^{fl/fl}*) also resulted in bones that broke at a lower force, however they were more brittle with a 30% reduction in toughness, energy absorbed at failure and a 40% reduction in ultimate strength. Their phenotype was not associated with a change in cortical tissue mineral density or bone formation rate. To determine the cause of altered strength in these two mouse models, we have used synchrotron-based Fourier-Transform Infrared Microscopy (sFTIRM) to assess cortical bone composition.

Tibial sections from 12 week old female *Dmp1Cre.EfnB2^{fl/fl}*, *OsxCre.EfnB2^{fl/fl}* mice and littermate *Cre+* controls (*w/w*) (n = 13/ group) were analyzed 1.5mm below the growth plate starting at the periosteal edge of the lateral cortex, in three 15µm² regions, concluding in the more mature bone.

While cortical composition was unchanged in *OsxCre.EfnB2^{fl/fl}* bones, sFTIRM revealed that the *Dmp1Cre.EfnB2^{fl/fl}* bones had a 12% higher mineral:matrix (p<0.05) and 37% higher carbonate:mineral (p<0.05) ratio than *w/w* controls, even in newly formed bone at the periosteal edge. This suggests that the brittleness relates to altered primary mineralization, and not prolonged secondary mineralization. *Dmp1Cre.EfnB2^{fl/fl}* bones also had altered collagen orientation (13% lower amide I:amide II, p<0.001) that may underlie their high mineral content. Regression analysis with 3-point bending data showed that while the energy absorbed to failure correlated with amide content of *w/w* bones (r² = 0.40, p<0.05), this relationship failed in *Dmp1Cre.EfnB2^{fl/fl}* mice. Instead, ultimate strength of *Dmp1Cre.EfnB2^{fl/fl}* bones was determined by the carbonate:mineral ratio (r² = 0.50, p<0.05); an abnormal relationship that was not upheld in *w/w* controls.

While ephrinB2 deletion in the entire osteoblast lineage delayed bone mineralization but retained normal cortical composition, its absence in osteocytes promoted carbonate deposition within the bone matrix, leading to increased brittleness. These data highlight two stage-specific roles of ephrinB2 during osteoblast/osteocyte differentiation: in osteoblasts ephrinB2 promotes osteoid maturation while in osteocytes ephrinB2 limits the carbonate content of the matrix.

Disclosures: Christina Vrahnas, None.

FR0239

FGF9 Potently Induces Dmp1 Expression and Early Osteocyte Markers in a Cell Model of Osteocyte Differentiation. [Lora McCormick](#)^{*}, [Kun Wang](#), [LeAnn Tiede-Lewis](#), [Hong Zhao](#), [Yixia Xie](#), [Lynda Bonewald](#), [Dallas Sarah](#). University of Missouri-Kansas City, USA

In humans and in rodent models aging is associated with a dramatic loss in osteocyte connectivity and dendricity, which has features in common with age-related neurodegeneration. We therefore hypothesized that the molecular mechanisms controlling osteocyte dendrite formation, maintenance and dendrite degeneration may overlap with mechanisms regulating neurogenesis/neurite formation and neurodegeneration. To investigate this a recently generated cell line, OmGFP66, was used, which expresses a membrane-targeted GFP driven by the *Dmp1* promoter. When differentiated over a 21 day timecourse this cell line expresses early then late osteocyte markers. It also forms "mini-bone" structures with a highly organized bone-like appearance and dendritic GFP-positive osteocytes embedded in clearly defined lacunae. Using a neurotrophin/receptor targeted qPCR array, OmGFP66 cells were shown to robustly express 33 genes related to neurogenesis/neurite formation, 17 of which were enriched in "mini-bone" structures compared to the undifferentiated cell monolayer. FGF9, which plays key roles in glial cell development/repair, neuronal cell differentiation/survival, sex determination and chondrogenesis, was enriched 18 fold in "mini-bone" structures compared to the cell monolayer in day 15 cultures. qPCR showed that FGF9 expression in OmGFP66 cells and IDG-SW3 cells, another model of osteocyte differentiation, increased over a 28 day timecourse by 33 and 94 fold, respectively, with FGF9 highly enriched in OmGFP66 "mini-bones" compared to the cell monolayer at every time point. Treatment with recombinant FGF9 potently induced *Dmp1*-GFP expression in early undifferentiated or late differentiated OmGFP66 cells and also in IDG-SW3 cells. qPCR analysis confirmed a 12 fold upregulation of *Dmp1* expression with FGF9 treatment and a 2 fold upregulation of PHEX in early differentiating OmGFP66 cells. Alkaline phosphatase was down-regulated. Live cell imaging showed a rapid induction of *Dmp1*-GFP after only 3 hrs of FGF9 treatment in OmGFP66 cells, that the FGF9-induced cells were highly polymorphic and that in differentiated cultures the induced cells were localized around the "mini-bones". Live cell imaging also suggested that FGF9 stimulated extension and retraction of dendrites in embedded osteocytes. These data identify the glial cell differentiation factor FGF9 as a potent inducer of *Dmp1* expression that may play a role in initiating the transition from osteoblast to osteocyte.

Disclosures: Lora McCormick, None.

FR0246

To measure or not to measure? Vitamin D and parathyroid hormone in patients with clinical risk factors for osteoporosis. [Oliver Bock](#)^{*}¹, [Silke Nicklisch](#)¹, [Christiane Weinberg](#)², [Ute Dostmann](#)¹. ¹Promedio - Integrated Medicine, Germany, ²German Osteoporosis Screening Center, Germany

Background: Vitamin D deficiency is associated with higher incidence of falls and fractures and plays a role in the pathophysiology of many chronic diseases. Despite the large amount of studies published on vitamin D, the threshold for a sufficient serum 25(OH)D concentration remains subject to a considerable debate. There has also been no clear consensus on the assessment and treatment of vitamin D deficiency.

Objective: To examine the prevalence of vitamin D deficiency or insufficiency and its impact on calcium/phosphate homeostasis as well as on bone turnover in a major German cohort of individuals with defined clinical risk factors (CRF) for osteoporosis and fractures (acc. to German DVO Guideline 2009, and QFracture Score 2013).

Results: In 2014 we examined a total of 7,253 patients (mean age = 62.6 yrs (SD 13.9); women 64.4%, men 35.6%) with CRF for osteoporosis and fractures. The prevalence of 25(OH)D serum levels <75 nmol/l was 87.7%. 25(OH)D serum levels below 50 nmol/l (deficiency) and 25 nmol/l (severe deficiency) have been detected in 55.0% and 15.7% of patients, respectively. Elevated PTH levels (>65 ng/l) have been found in 20.9% of 5,119 samples tested - with an inverse correlation to 25(OH)D serum levels (p<0.05) and positive relationship to increased bone turnover markers (B-AP, OC, DPD). The prevalence of secondary hyperparathyroidism (sHPT) was highest in patients with severe Vitamin D deficiency (35.3%) but common also in patients with 25(OH)D serum levels between 50 and 75 nmol/l (13.5%). In 29 further cases elevated PTH levels were attributed to primary hyperparathyroidism (pHPT). Five patients had mild hypercalcemia of (formerly unknown) malignancy, uncovered by PTH serum levels <2.5 ng/l. **Conclusion:** In our opinion the high prevalence of vitamin D deficiency or insufficiency with or without secondary hyperparathyroidism in a major cohort of patients at risk for osteoporosis demonstrates the importance of measurements of 25(OH)D and PTH serum levels for differential diagnostic and therapeutic purposes. The results put into question the approach adopted in various national guidelines which do not recommend 25(OH)D routine measurements. Furthermore, additional consideration of PTH serum levels may contribute to a more adequate estimate of individual vitamin D supplementation needs.

Disclosures: Oliver Bock, Promedio - Integrated Medicine

FR0248

Improved Risk Assessment Using Lumbar Spine Trabecular Bone Score (TBS) to Adjust Fracture Probability: The Manitoba BMD Cohort. William Leslie^{*1}, Helena Johansson², Anders Oden², Eugene MCloskey², Didier Hans³, John Kanis². ¹University of Manitoba, Canada, ²University of Sheffield Medical School, United Kingdom, ³Lausanne University Hospital, Switzerland

Background: Lumbar spine trabecular bone score (TBS), a DXA-derived image texture measurement, is a risk factor for osteoporotic fracture independent of FRAX clinical risk factors and femoral neck BMD. Our aim was to determine whether applying a TBS adjustment to fracture probability was beneficial in terms of risk reclassification and treatment qualification.

Methods: Using a registry containing all clinical DXA results for Manitoba, Canada, we identified 34,316 women age 40-100 years (mean 64 years) with baseline spine and hip DXA (Prodigy, GE Healthcare), FRAX input variables, blinded lumbar spine TBS measurement (TBS iN Sight[®] version 2.1, Med-Imaps), and minimum 5 years of observation (to March 31, 2013). Population-based health services data were used to identify non-trauma major osteoporotic fractures (MOF) and hip fractures (HF). MOF and HF probability were estimated using FRAX with femoral neck BMD (Canadian tool) without and with the TBS adjustment. Risk re-categorization was assessed using net reclassification improvement (NRI) for individual FRAX-based intervention criteria (fixed MOF 20%, fixed HF 3%, age-specific MOF) and three national clinical practice guidelines (CPGs) (Osteoporosis Canada, US National Osteoporosis Foundation [NOF], UK National Osteoporosis Guideline Group [NOGG]).

Results: Overall proportions of women reclassified with the TBS adjustment to FRAX were small (less than 5%). However, for women close to an intervention cut-off (MOF 20%+5% [absolute], HF 3%+1% [absolute], age-specific+20% [relative]) reclassification rates were much higher (17.5%, 17.9%, 25.3%, respectively); reclassification rates were <1% otherwise. During mean 8.8 years of follow up, 3503 (10.2%) women experienced an incident MOF and 945 (2.8%) women experienced an incident HF. There was a small but significant improvement in overall NRI for all individual FRAX-based intervention criteria (range 0.7-1.8%) and all three national CPGs (range 0.5-1.1%). NRI was greater in women younger than age 65 years compared with women age 65 years and older.

Conclusion: A small but significant improvement in MOF and HF risk assessment was seen by using lumbar spine TBS to adjust FRAX probability. The improvement in risk classification was not specific to a particular CPG, and was observed for CPGs from three different countries. Almost all of the benefit in terms of risk re-categorization was seen in individuals close to the intervention threshold.

Proportion reclassified and NRI for individual FRAX intervention criteria and three national CPGs.

| | MOF 20% | Hip 3%* | Age-specific | Canada | NOF | NOGG |
|--------------------------|---------|---------|--------------|--------|--------|--------|
| Reclassification | | | | | | |
| All subjects | 2.6% | 2.8% | 4.5% | 2.3% | 1.2% | 2.8% |
| Close to cutoff** | 17.5% | 17.9% | 25.3% | 15.4% | 4.4% | 14.6% |
| NRI fractures | 1.4% | 3.0% | 1.7% | 1.1% | 1.0% | 2.1% |
| p-value | <0.001 | <0.001 | <0.001 | 0.002 | <0.001 | <0.001 |
| NRI non-fractures | -0.4% | -1.1% | -1.0% | -0.3% | -0.5% | -0.9% |
| p-value | <0.001 | <0.001 | <0.001 | 0.001 | <0.001 | <0.001 |
| NRI total | 1.1% | 1.8% | 0.7% | 0.8% | 0.5% | 1.1% |
| p-value | 0.006 | <0.001 | 0.141 | 0.020 | 0.049 | 0.002 |

* For hip fracture prediction. ** MOF 20%+5%[absolute], HF 3%+1%[absolute], age-specific+20%[relative]. NOF = US National Osteoporosis Foundation. NOGG = UK National Osteoporosis Guidelines Group.

Proportion reclassified and NRI for individual FRAX intervention criteria and three national CPGs.

Disclosures: William Leslie, None.

FR0252

Contribution of Lumbar Spine BMD to Fracture risk in individuals with T-score discordance. Dunia Alarkawi^{*}, Dana Bliuc, Tuan Nguyen, John Eisman, Jacqueline Center. Garvan Institute of Medical Research, Australia

Context Bone mineral density (BMD) is an important predictor of fracture risk. Risk estimates are usually based on femoral neck (FN) BMD. However it is unclear how to address T-score discordance, where lumbar spine (LS) T-score is lower than FN T-score.

Objectives To examine the impact of LS BMD on fracture risk, specifically in individuals with lower LS T-score than FN T-score.

Design Prospective cohort from the Dubbo Osteoporosis Epidemiology Study of community-dwelling women and men aged 60+ years that had had both LS and FN BMD measured at their first visit, followed from April 1989 to December 2014.

Results Of 2270 women and 1373 men, 988 women and 264 men had lower LS T-score than FN T-score. Of those, 364 women and 60 men had a LS T-score lower than FN T-score by ≥1 SD (discordant group). In women with lower LS than FN T-score, each 1 SD lower LS T-score was associated with a 30% increase in fracture risk (HR 1.30, 95% CI 1.19-1.41, P<0.0001). However, there was no further increase in fracture risk for men with lower LS T-score than FN. Discordant women had a greater fracture risk than the rest of the women for all levels of FN T-score. This increased fracture risk was more apparent for lower levels of FN T-score and in older age groups. For example, with FN T-score -2, discordant women aged 60-69 had a 3% higher five-year absolute fracture risk than non-discordant women. In the 70-79 yr age group this risk was 11% higher and in the >80 group, it was 31% higher. Furthermore, an osteoporotic LS T-score increased ten year absolute fracture risk for women with either normal or osteopenic T-score by ~15%.

Conclusion This study demonstrates the significant contribution of lower LS BMD to fracture risk in individuals, over and above FN BMD. Women with lower LS T-score by ≥1 SD than FN T-scores had consistently higher absolute fracture risks regardless of their FN T-scores. However the risk increased exponentially with lower FN BMD and increasing age. The findings clearly indicate that a LS BMD lower than FN BMD should be incorporated into fracture risk calculation algorithms at least for women.

Disclosures: Dunia Alarkawi, None.

FR0254

Net Reclassification Improvement with FRAX Versus a Simpler Risk Assessment System: More is More. William Leslie^{*1}, Suzanne Morin², Sumit Majumdar³, Lisa Lix¹, Helena Johansson⁴, Anders Oden⁴, Eugene MCloskey⁴, John Kanis⁴. ¹University of Manitoba, Canada, ²McGill University, Canada, ³University of Alberta, Canada, ⁴University of Sheffield Medical School, United Kingdom

Background: There is much debate regarding the value of complex fracture risk assessment tools over simpler more intuitive tools. Indeed, Canadian clinical practice guidelines (CPG) go so far as to endorse both complex (WHO FRAX) and simple (Canadian Association of Radiologists and Osteoporosis Canada [CAROC]) tools. CAROC uses age, sex, femoral neck BMD and two clinical risk factors (prior fracture and prolonged glucocorticoid use) to assign semi-quantitative 10-year risk (low <10%, moderate 10-20%, high >20%). We compared net incremental benefit of using the complete FRAX tool vs CAROC tool. **Methods:** Using a registry with all clinical DXA results for Manitoba, Canada, we identified women and men age = 50 years undergoing baseline DXA in years 1996-2011. Population-based data were used to identify FRAX/CAROC covariates and incident major osteoporotic fractures (MOF). Net reclassification improvement (NRI) was used to quantify the differences between FRAX vs CAROC. **Results:** The study population included 54,493 women and men (mean age 67 years [SD 10], 90% female) among whom 4,508 (8.3%) sustained an incident MOF during mean follow up 6 years. FRAX and CAROC both provided good risk stratification and calibration (observed 10-year MOF with FRAX = low 6.6%, moderate 15.4%, high 30.4%; CAROC = low 6.7%, moderate 15.4%, high 28.7%), with identical risk categorization in 82.3% (FRAX higher 6.7%, CAROC higher 11.0%). NRI for FRAX vs CAROC was no different in those who experienced an incident MOF (-0.7%, P=0.23) but it was significantly greater for those who did not (+4.6%, P<0.001) as well as for the entire cohort (+3.9%, P<0.001). Subgroup analyses in 10,880 patients with prior fracture showed lower risk concordance (64.9%) and overall NRI was again significantly better with FRAX vs CAROC (+14.9%, P<0.001). Similar improvements in NRI with FRAX (all P<0.001) were seen in the following subsets of prior fracture patients: age < 65 (+17.1%), age = 65 (+8.4%), women (+10.9%), men (+22.1%). The NNF ("Number Needed to FRAX") to improve fracture prediction was 26 overall and 7 in those with a prior fracture. **Summary:** Both FRAX and CAROC provide good risk stratification and are well calibrated to the Canadian population, but FRAX provides a more accurate quantitative assessment of risk, particularly in those with prior fracture, compared with simpler semiquantitative systems.

Disclosures: William Leslie, None.

FR0261

Statistical Shape and Appearance Models and Statistical Parameter Mapping for Hip Fracture Discrimination: Not Better Than BMD or Less Robust. Oleg Museyko¹, Valérie Bousson², Jean-Denis Laredo², Judith Adams³, Andreas Friedberger⁴, Klaus Engelke⁵. ¹Inst of Med Physics, Univ of Erlangen, Germany, ²Service de Radiologie OstéoArticulaire, Hôpital Lariboisière, France, ³Clinical Radiology, The Royal Infirmary, Univ. of Manchester, United Kingdom, ⁴Inst of Med Physics, Univ. of Erlangen, Germany, ⁵University of Erlangen, Germany

Purpose: To investigate whether statistical parameters describing the 3D shape (SSM) of the proximal femur and its local BMD distribution (SAM: statistical appearance model) can discriminate subjects with and without acute osteoporotic hip fractures.

Methods: QCT datasets of the femur from 98 pm women (46 with acute hip fx) were used. SSM and SAM models were built by non-rigid registration of randomly selected segmented femurs to one femur. Models included unfractured subjects (ctrl) and fractured subjects (fx). SSM/SAM consisted of principal components (PC) of the registration displacement vectors (BMD values) for the whole sample set. SSM/SAM parameters that discriminated sig. between the two groups after adjust. for age, height, and weight were included into binary logistic regression to obtain odds ratios (OR) and AUC of the ROC curve. A stratified validation was performed by means of random partitioning of the whole sample into k partitions with k=1, 2, and 5. Then 1. The discrimination of SSM/SAM and int. BMD were compared. 2. A combined SSM-SAM model was compared with the combination of trochanteric trabBMD (TrTrabBMD) + neck cort. thickness (NeckCortTh). 3. In addition, statistical parameter mapping models (SPM) were built to find voxels on the normalized femur shape which were significantly different between ctrl and fx, forming a new analysis VOI.

Results: For both SSM and SAM, only one significant PC was found. The discriminative performance of SSM and SAM for k=1 is shown in the table. Performance of the combined shape-appearance model was sig. worse (AUC 0.71 [0.61,0.81]) than TrTrabBMD+NeckCortTh (AUC 0.79 [0.70,0.88]). SPM on shapes did not find any voxels with sig. difference between ctrl and fx; for BMD, 3% of voxels were sig. different forming a VOI which discriminated fracture with AUC 0.82 [0.74,0.91], but reduced to 0 and 1% voxels when analyzing to halves of the sample (k=2, see Fig).

Conclusions: The performance of SSM/SAM was not superior to BMD. Intersubject variations of shape not related to fracture were much larger than those related to fracture, indicating that sig. parameters in femur shape models may be quite "noisy". The observed discrimination may be just by chance. SPM on BMD discriminated best but was instable to subset-based validation due to the small number of significant voxels found, which may indicate that much more accurate registration is needed. BMD was a more stable discriminator for hip fractures.

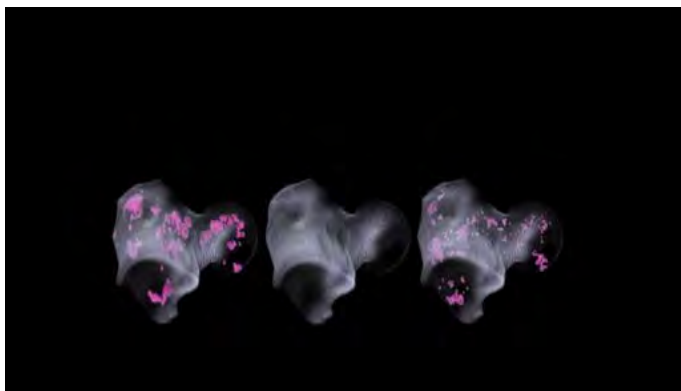


Table and Figure

Disclosures: Klaus Engelke, None.

FR0266

Multiple GWAS-Implicated Adult Height Loci Operate in the Context of Pediatric Bone Mineral Density and Content Determination. Alessandra Chesni^{*1}, Jonathan Mitchell², Kevin Basile³, Shana McCormack³, Sani Roy³, Heidi Kalkwarf⁴, Joan Lappe⁵, Vicente Gilsanz⁶, Sharon Oberfield⁷, John Shepherd⁸, Andrea Kelly³, Babette Zemel³, Struan Grant⁹. ¹Children's Hospital of Philadelphia, USA, ²University of Pennsylvania, USA, ³Children's Hospital of Philadelphia, USA, ⁴Cincinnati Children's Hospital Medical Center, USA, ⁵Creighton University School of Medicine, USA, ⁶University of Southern California, USA, ⁷Columbia University Medical Center, USA, ⁸University of California, USA, ⁹Children's Hospital of Philadelphia / University of Pennsylvania, USA

Height is a complex trait influenced by environmental and genetic factors operating in a number of biological pathways, including those related to hormone activity and bone accretion. The most recent meta-analysis of genome-wide association studies of adult height identified 697 variants corresponding to 423 distinct genomic loci, which collectively account for up to one-fifth of this trait's heritability. However, the physiological route by which these genetic variants influence an individual's overall height is not known.

Stature reflects skeletal size, which is achieved by bone mineral accretion during childhood growth. Thus, we investigated the effects of genetic variants known to associate with adult height on pediatric bone mineral content and density. We leveraged a prospective observational study of 691 participants of European ancestry enrolled in the Bone Mineral Density in Childhood Study (52% female), then sought further support from an additional cohort of 472 Caucasian subjects (51% female). Bone mineral content (BMC) and areal bone mineral density (aBMD) of the radius, hip, spine and total body (to estimate head and whole body BMC/aBMD) were assessed by dual energy X-ray absorptiometry (DXA) and expressed as age and sex-specific Z-scores. We further tested bone Z-scores adjusted for height-for-age Z-score to account for known effects of size on DXA outcomes. DNA was extracted from blood/saliva and genotyped using high-throughput technology. Genotyping of subjects was performed at the Children's Hospital of Philadelphia using the Illumina InfiniumTM II OMNI Express plus Exome BeadChip technology.

Three of the loci previously linked to adult height yielded Bonferroni-corrected significance for association with pediatric bone accretion at specific skeletal sites. These loci were rs3750972 at *TPCN2* for head aBMD in males ($P=5.48 \times 10^{-2}$; $\beta=-0.241$), rs6952113 at *C7orf58* (also known as *CPED1*) for both BMC and aBMD at the distal radius in females ($P=1.63 \times 10^{-5}$; $\beta=-0.250$ and $P=6.30 \times 10^{-8}$; $\beta=-0.317$, respectively), and rs2781373 at *MAX* with aBMD at the distal radius in females ($P=3.22 \times 10^{-5}$; $\beta=0.243$). These loci did not show any degree of significant association with height Z-score, nor did height adjustment of BMC/aBMD outcomes dramatically alter the significance of association of these loci to their respective skeletal phenotypes. Additionally, 19 other adult height loci demonstrated at least a nominally significant, directionally consistent association in both the discovery and replication cohorts for a variety of other skeletal phenotypes.

These results indicate that at least some of the genetic variants associated with adult height may be exerting their influence via alterations in pediatric bone accretion. Additionally, our data have implicated *TPCN2* and *MAX* as novel pediatric bone density loci.

Disclosures: Alessandra Chesni, None.

FR0305

Single Nucleotide Polymorphisms Are Associated with Circulating Bone Biomarkers in Young Adults undergoing Initial Military Training. Erin Gaffney-Stomberg^{*1}, Anna Shcherbina², Darrell Ricke³, Martha Petrovick², Laura Lutz⁴, Thomas Cropper⁵, Sonya Cable⁶, James McClung⁴. ¹USARIEM, USA, ²Massachusetts Institute for Technology Lincoln Laboratory, USA, ³Massachusetts Institute for Technology Lincoln Laboratory, Lexington, MA 02420, USA, ⁴US Army Research Institute of Environmental Medicine, USA, ⁵Lackland Air Force Base, USA, ⁶Initial Military Training Center of Excellence, USA

Initial military training (IMT) is associated with increased risk of stress fracture. Previous studies demonstrated that supplemental calcium (Ca) and vitamin D (vit D) provided daily throughout IMT reduced stress fracture incidence, suppressed PTH, and improved some measures of bone health compared to placebo. The purpose of this study was to determine whether previously identified single nucleotide polymorphisms (SNPs) in Ca and vit D related genes are associated with circulating biomarkers of bone metabolism in young adults entering IMT, and whether responses to Ca and vitamin D supplementation during IMT are modulated by genotype. Baseline associations between SNPs including the following genes: vit D receptor (VDR; n=6), vit D binding protein (VDBP; n=2), and 1-alpha-hydroxylase (CYP27B1), and circulating biomarkers were measured in fasting blood samples from volunteers (n=778) starting IMT. Volunteers were block randomized by race and sex to receive a Ca and vit D fortified food product (2000 mg Ca and 1000 IU vit D per day) or placebo throughout Army or Air Force IMT (7-9 wk). Habitual food intake during IMT was estimated using a food frequency questionnaire. Total Ca and vit D intakes were calculated as the sum of supplemental intake based on compliance

and dietary intake. Relationships between SNPs, Ca and vit D intake tertile, and change in biomarkers were evaluated in those who completed the trial (n=391). At baseline, circulating 25(OH)D was positively associated with the presence of the minor allele of a VDR gene SNP (rs1544410, B=1.39, p=0.02) and in a VDBP gene SNP (rs7041, B=3.65, p=2.82x10⁻¹⁴). In addition, presence of the minor allele of a second VDR SNP (rs2228570) was associated with lower circulating P1NP (B=-4.81, p=0.02), while presence of the minor allele in the CYP27B1 gene (rs10877012) was associated with higher CTX (B=2.99, p=0.03). In black/African American volunteers, those homozygous for the T allele of a VDR SNP (rs11568820) had greater increases in BAP with higher Ca and vit D intake (B=15.8, p<0.01) compared to volunteers carrying the C allele. These data suggest that VDR, VDBP and CYP27B1 SNPs are associated with 25(OH)D status and bone turnover and that a VDR SNP conferred a greater anabolic response to Ca and vit D intake in Black/African American volunteers.

Research supported by: USAMRMC.

Disclosures: Erin Gaffney-Stomberg, None.

FR0309

Prevention of osteoporotic fractures by black tea consumption. Richard Prince¹, Gael Myers², Jonathan Hodgson³. ¹Sir Charles Gairdner Hospital, Australia, ²Curtin University, School of Public Health, Australia, ³University of Western Australia, School of Medicine & Pharmacology, Australia

Previous studies, including our own, have demonstrated a beneficial effect of tea, a major source of dietary flavonoids, on bone structure. The association of black tea and flavonoid intake with the risk of fractures leading to hospitalization or death was examined in a prospective cohort study of women mean age over 80 years.

At baseline 1,188 women had their dietary intake assessed by a food frequency and beverage questionnaire. Complete ascertainment of 10 year, incident, verified osteoporotic fracture hospitalisation or death was determined through the Western Australian Hospital Morbidity Data system. Multivariate-adjusted Cox regression was used to examine the hazard ratios (HR) for incident fracture. Flavonoid intake was calculated using United States Department of Agriculture flavonoid databases.

Any osteoporotic fractures occurred in 288 (24.2%) women. Compared to women consuming £1 cup/week, for each 1 cup/day increase in tea intake there was a 9% decrease in the risk of any serious osteoporotic fracture (fully-adjusted HR 0.91; 95% CI:0.84, 0.99; P=0.027), the relationship was not significant after adjustment for BMD. Major osteoporotic fracture occurred in 212 (17.8%) women and hip fracture in 129 (10.9%) women Tea accounted for 75% of the total flavonoid intake. Compared to the lowest tertile of flavonoid intake, women in the highest tertile of flavonoid intake had a lower risk of serious osteoporotic fracture (HR: 0.65; 95% CI: 0.47, 0.88, actual risk 21.0% and 28%); major osteoporotic fracture (HR: 0.66; 95% CI: 0.45, 0.95; actual risk 15% versus 20%) and hip fracture (HR: 0.58; 95% CI: 0.36, 0.95, actual risk 8% versus 12%).

Women who drink black tea, a major dietary flavonoid, have a substantial lower fracture risk. The health benefits of tea may extend to the skeletal system.

Disclosures: Richard Prince, None.

FR0310

The Effect of Vitamin K1 and Vitamin D on Muscle Composition and Muscle Function: the ECKO RCT. Andy Kin On Wong¹, Marvam Hamidi², Lianne Tile², George Tomlinson³, Hanxian Hu², Judy Scher², Yuna Lee⁴, Lilian Thompson³, Reinhold Veith⁵, Robert Josse⁴, Sophie Jamal³, Gillian Hawker⁶, Angela M. Cheung². ¹University Health Network, Ca, ²UHN, Canada, ³University of Toronto, Canada, ⁴St. Michael's Hospital, Canada, ⁵Mount Sinai Hospital, Canada, ⁶Women's College Hospital, Canada

Objectives: 1) to determine the effect of vitamin K1 on changes in muscle function; 2) to evaluate how vitamin K modulates the relationship between muscle function and composition. Study design: A randomized double-blind placebo-controlled trial of vitamin K1 with prospective follow-up for 48 months. Outcomes: Muscle function was measured at 0, 24 and 48 months. Myotendinous density (MyD) was assessed at the distal tibia using HR-pQCT at the last study visit. Percentage undercarboxylated osteocalcin (%UCOC), serum vitamin K and triglyceride levels were measured at baseline, 12, 24, 36 and 48 months. Yale Physical Activity Energy Expenditure Summary Index (EESI) was determined at these same visits. Analyses: Effect of treatment on changes in muscle function variables was assessed using a general linear model (GLM). Factor analysis identified latent muscle constructs, which were also subjected to GLM. All GLMs adjusted for serum vitamin K/triglyceride ratio, EESI, serum vitamin D at 24 months, as well as age and body mass index (BMI). Latent growth curve models measured the effect of %UCOC at 24 months on trajectories of muscle function. The effect of treatment on how MyD relates to function was evaluated as an interaction term in linear regression analyses. Results: Among 428 (Vitamin K, N=211, Placebo, N=217) postmenopausal women, serum vitamin K was higher (p<0.001) in the vitamin K-treated group (23.4 ± 21.4 ng/mL) at 24 months compared to placebo (2.1 ± 2.3 ng/mL) (upheld after adjusting for age, BMI and triglycerides). Factor analyses yielded a locomotor function construct, and a balance construct. There was a non-significant trend towards maintained static balance in the vitamin K-treated group over 48 months compared to placebo (Fig 1). A smaller

%UCOC at 24 months was associated with a significantly faster rate of improved balance (construct) but not locomotor function (construct), which was preserved after adjusting for EESI and serum vitamin D (Table I). Higher serum vitamin D at 24 months was associated with increased locomotor function (construct) but not balance (B=0.001, SE(B)=0.0003, Beta=3.17, p<0.001, effect = 0.08%). MyD correlated with muscle function constructs more strongly in those treated with vitamin K than with placebo (Table II). Conclusions: Those with superior vitamin K status have mildly improved balance. Taking vitamin K may improve the ability to use muscle that is already present.

Table I. Effect of % undercarboxylated osteocalcin (%UCOC) at 24 months on the rate of change in the locomotor function (LMF) construct and the balance construct. Regression coefficients are expressed as unit rate per 1% increase in UCOC. Models are adjusted for age, BMI and the baseline value for the latent construct at minimum (Model A), plus concurrent changes in energy expenditure (Model B) and plus serum vitamin D at 24 months (Model C) cumulatively.

| N | | Model | B | SE(B) | Beta | P-Value | Effect (% of mean) |
|-----|---------|-------|---------|--------|-------|---------|--------------------|
| 427 | LMF | A | 0.0010 | 0.0004 | 2.35 | 0.009 | 0.08 |
| 426 | LMF | B | 0.0025 | 0.0018 | 1.42 | 0.078 | 0.19 |
| 378 | LMF | C | -0.0003 | 0.0006 | -0.47 | 0.317 | -0.02 |
| 427 | Balance | A | -0.0036 | 0.0018 | -2.05 | 0.020 | -0.68 |
| 426 | Balance | B | -0.0008 | 0.0004 | -2.26 | 0.011 | -0.16 |
| 378 | Balance | C | -0.0040 | 0.0020 | -2.03 | 0.021 | -0.74 |

Table I

Table II. Effect of vitamin K on the association between MyD and muscle function constructs. * covariates = timing of HR-pQCT scan, serum Vitamin K1/triglyceride ratio, serum vitamin D and serum calcium.

| Muscle Function Construct | Model R ² p-value | Interaction p-value | Placebo B (95% CI) Partial R ² | Vitamin K B (95% CI) Partial R ² |
|--|------------------------------|---------------------|---|--|
| Base model – adjusted for age and BMI (N=122) | | | | |
| Locomotor | 0.126 0.007 | 0.029 | N=60 0.003(-0.016,0.023) R ² =0.002 | N=62 0.036(0.005,0.068) R ² =0.072 |
| Balance | 0.133 0.005 | 0.026 | 0.034(-0.036,0.103) R ² =0.002 | 0.092(0.011,0.174) R ² =0.058 |
| Further adjusted for covariates* (N=90) | | | | |
| Locomotor | 0.413 <0.001 | 0.014 | N=47 0.002(-0.018,0.022) R ² = 0.001 | N=43 0.048(0.017,0.079) R ² = 0.144 |
| Balance | 0.402 <0.001 | <0.001 | -0.007(-0.022,0.009) R ² =0.015 | 0.107(0.016,0.198) R ² =0.091 |

Table II

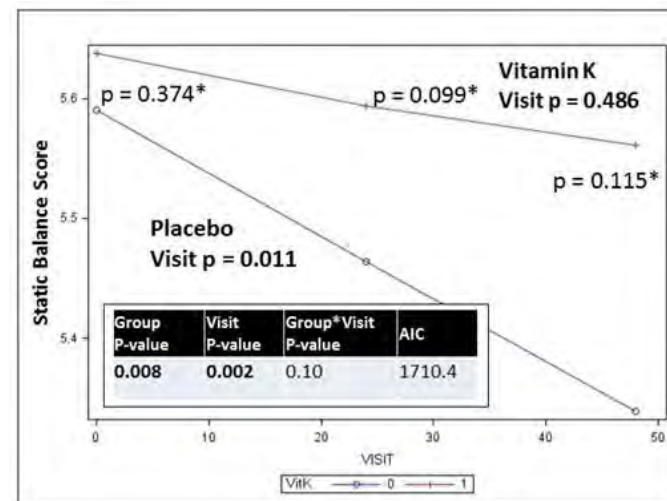


Figure 1

Disclosures: Andy Kin On Wong, None.

FR0311

Does Vitamin D Metabolism Differ by Race? Evaluation of Vitamin D Metabolites in American Indians and Caucasian Americans Prior to and Following Vitamin D₃ Supplementation. Neil Binkley¹, Ellen Fidler², Gretta Borchardt², Diane Krueger². ¹University of Wisconsin, Madison, USA, ²University of Wisconsin, USA

Objective: Serum 25(OH)D levels differ between races. It is often assumed that this is due to pigmentation with dark skinned individuals at higher risk for low 25(OH)D levels. However, whether racial differences exist in other circulating vitamin D metabolite levels, e.g., cholecalciferol (D₃) and/or 24, 25(OH)₂D (24,25D), or whether race affects the change in these metabolites following supplementation has received little study. Recently, liquid chromatography tandem mass spectrometry (LC-MS/MS) methodology has made measurement of D₃ and 24,25D more available. This report describes serum levels of these metabolites in American Indian (AI) and Caucasian American (CA) postmenopausal women and to evaluate change in these metabolites following oral vitamin D₃ supplementation.

Materials and Methods: Serum D₃, 25(OH)D and 24,25D were measured by LC-MS/MS in a study of 99 postmenopausal AI mean (SD) age 61.2 (7.3) years and a second study of 88 postmenopausal CA women mean (SD) age 64.2 (8.7) years. Inclusion/exclusion criteria for both studies were similar. The AI volunteers were randomly assigned to receive either 400 IU or 2500 IU of vitamin D₃ daily for six months; the CA women received 2300 IU of daily vitamin D₃ for four months. Vitamin D metabolites were measured at baseline and study conclusion.

Results: At baseline, mean serum 25(OH)D did not differ between AI (27.6 ng/mL) and CA (26.2 ng/mL) women. Baseline 24,25D was lower ($p < 0.0001$) in AI than CA (2.0 and 2.9 ng/mL respectively). Serum 24,25D was positively correlated ($p < 0.001$) with 25(OH)D in both AI and CA women. Following supplementation with 2300 or 2500 IU daily, a greater ($p < 0.001$) increase in 25(OH)D was observed in AI than CA women (18.1 vs. 11.9 ng/mL). After this supplementation, 24,25D increased similarly in AI and CA women. Serum D₃ was detectable (≥ 5 ng/mL) in only 9% of AI and 4% of CA women at baseline.

Conclusion: When compared to Caucasian postmenopausal women, serum 24,25D is lower, and the response to daily vitamin D₃ supplementation greater, in a cohort of postmenopausal AI women. This differing response suggests that reported racial differences in vitamin D status may reflect not only skin pigmentation, but also differences in vitamin D metabolism. It is possible that vitamin D intake and status recommendations should be race specific. Further study of potential racial differences in vitamin D metabolism is needed.

Disclosures: Neil Binkley, None.

FR0312

The Association between Maternal and Fetal 25OHD and Infant Size and Adiposity at Birth, 6 Months and 2 Years of Age. Mary Horan¹, Jean Donnelly¹, Malachi McKenna², Brenda Crosbie², Mark Kilbane², Fionnuala McAuliffe¹. ¹National Maternity Hospital, Ireland, ²St. Vincent's University Hospital, Ireland

Background: While the effects of vitamin D in pregnancy and offspring bone health are well established, there remains a dearth of knowledge on the effect of maternal vitamin D status on offspring size and adiposity. The aim of this study was to examine the association of early and late pregnancy and fetal 25-hydroxyvitamin D (25OHD) on offspring size and on adiposity at birth, at 6 months and at 2 years of age in a cohort from the ROLO (Randomised cOntrol trial of LOw glycaemic index diet versus no dietary intervention to prevent recurrence of fetal macrosomia study).-
Methods: 272 mother and infant pairs from the ROLO study were included in this analysis at 20 weeks gestation, 290 at 34 weeks gestation, 292 at birth, 160 at 6 months postpartum and 287 at 2 years postpartum. 25OHD was measured in mothers in early (13 weeks) and late (28 weeks) gestation, and in fetal umbilical cord blood samples at delivery. **Results:** According to Institute of Medicine 2011 Report, 30% in early pregnancy and 38% in late pregnancy were at risk of vitamin D deficiency (25OHD < 30 nmol/L). Birthweight was negatively associated with early pregnancy 25OHD ($p < 0.001$) and with fetal 25OHD ($p < 0.001$). Birth length was not associated with early, late or fetal 25OHD. Neonatal sum of all skinfolds and sum of subscapular and triceps skinfolds, which are measures of overall adiposity, were negatively associated with fetal 25OHD (respectively, $p = 0.001$, and $p = < 0.001$). At 2 years of age there was a negative association between weight-for-age z-score and early pregnancy 25OHD ($p < 0.041$). **Conclusion:** Maternal and fetal 25OHD were negatively associated with offspring size and adiposity at birth, at 6 months, and 2 years of age in a cohort at risk of macrosomia in whom risk of vitamin D deficiency was high. Improvement of vitamin D status in pregnancy remains a public health concern.

Disclosures: Malachi McKenna, None.

FR0314

A neuronal action of Sirtuin 1 Suppresses Bone Mass in young and aging mice. Na Luo¹, Ioanna Mosialou¹, Aruna Kode¹, Mattia Capulli², Stavroula Kousteni¹. ¹Columbia University Medical Center, USA, ²University of L'Aquila, Italy

The histone deacetylase Sirtuin 1 (Sirt1) has emerged as a regulator of several brain-dependent functions that are compromised with aging. We explored a potential role of Sirt1 in the neuronal control of bone mass through regulation of the activity of the sympathetic nervous system (SNS). We show that a modest increase in *Sirt1* expression in transgenic (*TgSirt1*) mice, compromised bone mass by suppressing bone formation and promoting bone resorption. The opposite effects of Sirt1 on the two compartments of bone remodeling correlated with an increase in SNS activity as indicated by increased expression of *Ucp1* in brown fat and elevated levels of urinary epinephrine and norepinephrine in *TgSirt1* mice. Decreased bone mass was observed at 1.5 month-old *TgSirt1* mice and persisted at 3, 6 and 12 months of age. The decrease in osteoblast numbers was more pronounced at 12 months of age indicating a progressive effect of Sirt1 functions with aging. High sympathetic tone in *TgSirt1* mice accounted for the decrease in bone mass as pharmacological inhibition of SNS signaling by daily administration of the beta adrenergic receptor inhibitor propranolol to *TgSirt1* mice for 4 weeks fully restored osteoblast and osteoclast numbers and rescued the low bone mass phenotype of these animals. To examine whether Sirt1 regulates bone mass through a central action, we generated mice lacking *Sirt1* in the brain by crossing mice carrying an allele of *Sirt1* in which exon 4 is floxed with *Synapsin-Cre* mice (*Sirt1^{brain}-/-* mice). Inactivation of *Sirt1* in the brain decreased SNS activity and increased bone mass by increasing bone formation and suppressing bone resorption in 3 month-old *Sirt1^{brain}-/-* mice. More directly related to Sirt1 biology, whereas the loss of bone mass in 3-month old *Sirt1^{+/+}* mice occurs only in female mice and only in the femur, we found that brain inactivation of *Sirt1* increased bone mass in both genders at this age. Likewise, whereas 7-month old female or male *Sirt1^{+/+}* mice do not have a bone phenotype, brain inactivation of *Sirt1* increased bone mass at 8 months of age. Collectively, these observations suggest that, in addition to its cell autonomous effects in osteoblasts and osteoclasts, Sirt1 controls bone mass by upregulation of SNS signaling. The neuronal effects of Sirt1 in the regulation of bone mass persist and become more pronounced during aging.

Disclosures: Na Luo, None.

FR0319

Glucocorticoids attenuate bone formation independently of FoxOs. Srividhya Iyer¹, Elena Ambrogini², Li Han², Shoshana Bartell², Ha-Neui Kim³, Aaron Warren², Julie Crawford², Stuart Berryhill², Stavros Manolagas², Maria Almeida². ¹Central Arkansas VA Healthcare System, Univ of Arkansas for Medical Sciences, USA, ²Center for Osteoporosis & Metabolic Bone Diseases, Central Arkansas Veterans Healthcare System, University of Arkansas for Medical Sciences, USA, USA, ³Center for Osteoporosis & Metabolic Bone Diseases, University of Arkansas for Medical Sciences, USA, USA

Administration of glucocorticoids causes rapid bone loss and increases the risk of fractures. Endogenous or exogenous glucocorticoid excess severely decrease the number of osteoblast and bone formation due to reduced production of new osteoblast precursors as well as premature apoptosis of mature osteoblasts. However, the molecular mechanisms responsible for these deleterious effects remain unclear. In vitro studies have suggested that glucocorticoids activate members of the FoxO family of transcription factors and thereby attenuate Wnt signaling in cultured osteoblast progenitors. Based on this and in vivo evidence that FoxOs suppress bone formation by sequestering β -catenin and preventing Wnt/TCF transcription in osteoprogenitors, we examined here whether FoxOs mediate the deleterious effects of glucocorticoids on bone formation. To this end, 5-month-old male mice lacking FoxO1, 3 and 4 in *Osx1-Cre* targeted cells (designated FoxO1,3,4^{*ΔOx1-Cre*}) and their littermate controls (FoxO1,3,4^{*fl/fl*}) were administered placebo or prednisolone (2.1 mg/kg/day) for 28 days, using slow-release pellets. Consistent with earlier evidence, prednisolone did not alter the cancellous bone volume at the spine or the distal femur in the control mice. Prednisolone administration, however, severely decreased mineralizing surfaces and bone formation rate (38% and 40%, respectively) as determined by dynamic histomorphometry in vertebral bone sections. As seen also before, the FoxO1,3,4^{*ΔOx1-Cre*} mice had increased cancellous bone at the spine and at the femoral metaphysis compared to the FoxO1,3,4^{*fl/fl*} littermates. Nevertheless, the decrease in mineralizing surface and bone formation caused by glucocorticoids in FoxO1,3,4^{*ΔOx1-Cre*} mice was indistinguishable from the controls. In agreement with the adverse effects on bone formation, prednisolone decreased the mRNA and protein levels of osteocalcin in both genotypes, measured in tibia shafts and serum, respectively. Taken together, these results demonstrate that the deleterious effects of glucocorticoids on bone formation do not result from the activation of FoxOs in cells of the osteoblast lineage.

Disclosures: Srividhya Iyer, None.

FR0320

Sost/sclerostin deficiency protects the murine skeleton from glucocorticoid-induced bone loss by inhibiting bone resorption. Amy Y. Sato*, Meloney Cregor, Jasmine Tzeggai, Kevin McAndrews, Jesus Delgado-Calle, Alexander G. Robling, Lilian I. Plotkin, Teresita Bellido. Indiana University School of Medicine, USA

The bone weakening effects of glucocorticoids (GC) oppose those promoted by activation of the Wnt/beta-catenin signaling pathway. Based on this evidence, we investigated here whether mice lacking the gene encoding the Wnt antagonist Sost (KO) are protected from the bone loss induced by GC excess. Female 4-month-old KO and wild type (WT) littermate controls (10 mice/group) were implanted with slow-release pellets containing placebo or prednisolone at two doses 1.4 or 2.1 mg/kg/day, for 4 weeks. Consistent with the previously demonstrated bone anabolism with Sost/sclerostin deficiency, KO mice displayed higher bone mineral density (BMD) compared to WT controls (+42, +55, and +64% for total, femoral, and spinal BMD); increased MS/BS (+32%), MAR (+44%), and BFR (+101%), increased circulating bone formation markers ALP (+43%) and P1NP (+72%), but no changes in bone resorption markers CTX or TRAP5b. GC induced the expected dose-dependent decrease in BMD in WT mice (total: -2.1 and -2.7% and spinal: -4.4 and -5%, $p < 0.05$). Both GC doses also reduced significantly trabecular thickness, cortical bone area (BA/TA) and cortical thickness in WT mice, quantified by micro-CT in L6 vertebra. In contrast, GC failed to decrease BMD at any site, or BA/TA, or reduce trabecular or cortical thickness in KO mice, demonstrating bone preservation. Unexpectedly, however, both doses of GC decreased MAR and BFR similarly in WT and KO mice (MAR: -38 vs -31% and BFR: -33 vs -34%, for WT and KO, respectively). Further, GC lowered circulating bone formation markers to a similar extent for both doses in WT and KO mice (ALP, 2wks: -36% vs -33% and P1NP, 2 and 4wks: -61% vs -67%, for WT and KO mice respectively). In contrast, GC raised circulating bone resorption markers (CTX: +32% and TRAP5b: +77%) and increased osteoclast number and surface (+40% and +80% for low and high dose, respectively) in WT mice, but not in KO mice at any dose or time point. Moreover, both GC doses increased Sost (1.6- and 2.2-fold) and decreased OCN (0.44- and 0.36-fold) and OPG (0.70- and 0.67-fold) expression in WT mice. In contrast, in the KO mice, GC decreased OCN expression (0.44- and 0.20-fold), but did not affect OPG expression. These findings demonstrate that the absence of Sost/sclerostin protects from GC-induced bone loss not by reversing the inhibition of bone formation, but instead by preventing downregulation of OPG and the consequent increase in bone resorption induced by GC.

Disclosures: Amy Y. Sato, None.

FR0321

NR2C2 gene regulated osteoblasts bone formation activity through mir34a TGF β signaling pathway. Eric Beier*¹, Hsin-chu Ho², Shen-chin Hsu³, John Holz⁴, Tzong-Jen Sheu⁵, I-Hui Su⁶, Edward Puzas⁵. ¹Rutgers, USA, ²Wan-Chuan Clinics, Fangliao General Hospital, Taiwan, ³Chung Shan Medical University Hospital Dept of Pharmacy, Taiwan, ⁴D'Youville College Department of Math & Natural Sciences, USA, ⁵University of Rochester, USA, ⁶Fangliao General Hospital, Taiwan

Nuclear receptor subfamily 2, group C, member 2 (NR2C2) belongs to a nuclear receptor superfamily without an identified ligand. The expression of NR2C2 is found in virtually all tissue types including cerebellum, skeletal tissue, pancreas, reproductive system. NR2C2^{-/-} mice have severe osteopenia. Its role within the skeletal system and signaling mechanisms are currently unknown.

To study how NR2C2 regulates skeletal integrity, we first characterized NR2C2-deficient mice compared with wild type mice. The mutant mice showed significantly lower bone density (50% compared to wild type mice) at 4 wks, and remained lower beyond 6 months. Flexure testing of femurs revealed a 30-50% decrease in stiffness and resistance to load in mutant mice. Trabecular bone properties in the femur (BV/TV, trabecular number, connection density) showed the same magnitude of decrease when comparing the deficient mice to wild type mice. Excessive bone resorption was ruled out as the major contributor to the osteopenia as osteoclast markers TRAcP5b, NTX, and CTX levels remained unchanged. However, serum osteocalcin (OC) levels were significantly lower in the mutant, and furthermore the remaining OC was primarily in the inactive gamma-carboxyglutamic form (Gla-OC). Therefore we hypothesize that the observed bone loss is predominantly a function of insufficient osteoblast bone formation activity. In support of this, dynamic histomorphometry by calcein-alizarine double labeling showed that the mineral apposition rate and bone formation rate were 65% and 50% lower respectively in deficient mice compared to wild type. Next, we isolated primary osteoblasts from the calvaria of NR2C2-KO and wild type mice. miRNA screening and RNA-Seq techniques demonstrated a reduction of transforming growth factor-beta (TGF-beta) signaling activity in deficient osteoblasts. Concordantly, we generated several TGF-beta luciferase reporter transgenic osteoblasts comprised of pBabe-NR2C2, pBabe-NR2C2 RNAi, and pBabe GFP, which similarly confirmed a link between NR2C2-deficiency and an impingement of TGF-beta signaling. On the other hand, over-expression of NR2C2 showed a consistent three-fold induction of TGF-beta luciferase activity compared to the control group (pBabe-GFP). In addition, the expression of miR-34a was increased and the corresponding miR-34a target TGF-beta-induced factor (TGIF) was decreased in mutant mice. This novel characterization of NR2C2 regulation of the

TGF-beta signaling pathway offers new mechanistic insights on NR2C2 regulation of osteoblast activity, in which NR2C2 insufficiency can produce a bone loss phenotype.

Conclusion: NR2C2 regulates TGF-beta signaling through the microRNA miR-34a, which subsequently reduces its downstream target TGIF. TGIF has been linked to lipid metabolism, a long-suspected ligand candidate for NR2C2. This data uncovers a new signaling axis that may help to understand how the NR2C2 orphan receptor regulates skeletal integrity.

Disclosures: Eric Beier, None.

FR0323

Skeletal Health in Healthy Postmenopausal Women Treated with Exemestane for the Primary Prevention of Breast Cancer: 3-year data from the nested bone strength substudy of the MAP.3 trial (MAP3BSS). Miranda Boggild*¹, Lianne Tile¹, George Tomlinson¹, Natasha Gakhal², Sandhya Pruthi³, John Robbins⁴, Shail Rawal¹, Sharmila Majumdar⁵, Sundeep Khosla³, James Ingle³, Harriet Richardson⁶, Paul Goss⁷, Angela Cheung¹. ¹University of Toronto, Canada, ²Women's College Hospital, Canada, ³Mayo Clinic, USA, ⁴UC Davis Health System, USA, ⁵UCSF University of California, San Francisco, USA, ⁶Queen's University, Canada, ⁷Harvard University, USA

Purpose: Exemestane is an oral steroidal aromatase inhibitor that lowers circulating estrogen levels and prevents breast cancer in postmenopausal women. Previously published data from a nested non-inferiority bone strength substudy of the MAP.3 trial (MAP3BSS) showed that exemestane had negative effects on bone at 2 years. In this analysis, we assessed the effect of exemestane on bone after 3 years of treatment.

Methods: Postmenopausal women in the MAP.3 trial (a placebo-controlled randomized trial of exemestane 25 mg/day for the primary prevention of breast cancer) who did not have osteoporosis (T-score > -2.0 at all sites), were not on bone medications, and have never had fragility fracture were recruited from 5 centres (2 US and 3 Canadian). Primary outcome was change from baseline to 3 years in total volumetric bone mineral density (BMD) at the distal radius as measured by HRpQCT. For all outcomes, we compared the percent change over time between groups with the Kruskal-Wallis test.

Results: Three hundred and sixty-two women (171 in the exemestane group, 191 in the placebo) participated in the MAP3BSS. Seventy-nine participants crossed over from the placebo to the exemestane group after unblinding at 2 years. This analysis included women who have taken up to 3 years of exemestane as compared to placebo. At baseline, median age was 61.2 years and median areal BMD T-scores at the lumbar spine and total hip by DXA were -0.41 and 0.12, respectively. From baseline to 3 years, the mean percent change in total volumetric BMD at the distal radius was -8.53% (95% CI -9.35 to -7.72) in the exemestane group, -7.59% (95% CI -8.71 to -6.47) in the women who crossed over from placebo to exemestane, and -2.33% (95% CI -3.93 to -2.04) in the placebo group ($p < 0.0001$). The decline in secondary bone outcomes continued to the third year of treatment and was significantly different compared to the placebo group (Table 1 and Figure 1).

Conclusions: Three years of exemestane for the prevention of breast cancer continued to have progressive negative effects on bone despite calcium and vitamin D supplementation. Further studies with long-term follow-up, including fracture risk, are needed to weigh the risks and benefits of using exemestane for the primary prevention of breast cancer.

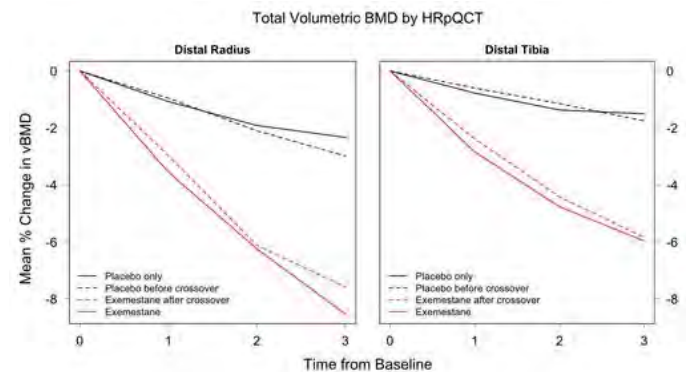


Figure 1

| Table 1. Mean percent change in secondary bone outcomes from baseline to 3 years | | | |
|--|---------------------------|------------------------|---------|
| Mean percent change (95% CI) | Exemestane | Placebo | P value |
| HRpQCT parameters | | | |
| Volumetric BMD at the distal tibia | -5.97 (-6.68 to -5.26) | -1.51 (-2.14 to -0.87) | <0.0001 |
| Cortical thickness at the distal tibia | -10.17 (-11.48 to -8.85) | -1.48 (-2.65 to -0.31) | <0.0001 |
| Cortical thickness at the distal radius | -11.80 (-13.16 to -10.45) | -2.30 (-3.74 to -0.86) | <0.0001 |
| Dual-energy X-ray absorptiometry (DXA) parameters | | | |
| Lumbar spine areal BMD | -2.96 (-3.70 to -2.22) | -0.41 (-1.97 to 1.15) | <0.0001 |
| Total hip areal BMD | -2.61 (-3.22 to -2.00) | -1.30 (-2.01 to -0.59) | 0.0003 |
| Femoral neck areal BMD | -3.34 (-4.10 to -2.59) | -2.04 (-3.01 to -1.08) | 0.0003 |

Table 1

Disclosures: *Miranda Boggild, None.*

FR0324

Bone Health in Glucocorticoid-Treated Men and Women. Edward Leib¹, Renaud Winzenrieth². ¹University of Vermont, USA, ²Med-Imaps, France

Edward S. Leib¹, Renaud Winzenrieth², (1) Dept. of Medicine, University of Vermont College of Medicine, Burlington, VT, USA (2) R&D Department; Med-Imaps, Berdeaux, France.

Introduction: Glucocorticoid (GC) treatment has been widely shown to have a negative impact on bone. The aim of this study is to investigate GC-induced effects on areal Bone Mineral Density (aBMD) and bone microarchitectural texture measured by Trabecular Bone Score (TBS).

Methods: 416 subjects aged 40 years and over who received GCs (=5 mg/day, for =3 months) were included in the study and matched with 1104 control subjects for sex, age and BMI. aBMD was measured at L1-L4 PA spine and at the femur (neck and total) by DXA, and TBS was evaluated at the spine. Clinical data, osteoporotic fractures (OPF) and dietary habits were documented in the medical report.

Results: Among the study population, 13.1% of the control subjects and 16.3% of the GC subjects sustained a prevalent osteoporotic fracture. GC-treated patients were characterized by a significant decrease of TBS (1.267 vs. 1.298, $p<0.001$) compared with control-matched subjects while no differences in BMD were observed at spine (1.060 vs. 1.056, $p=0.88$), femoral neck (0.858 vs. 0.848, $p=0.21$) or at total femur (0.903 vs. 0.899, $p=0.59$). These decreases were even more pronounced when fracture status was taken into account (1.222 vs. 1.298, $p<0.001$). The Odds Ratio (OR) for TBS was 1.44 [1.095–1.89] for OPF, whereas no significant ORs were found for BMD at spine ($p=0.36$), femoral neck ($p=0.61$) and total femur ($p=0.23$). The presence of a fracture was correlated with the same level of TBS as was GC treatment in subjects without fracture (?TBS=0.002, $p=0.66$). Those with fracture in the GC group had a greater decrease of TBS when compared to those without fracture (?TBS=-0.054, $p<0.01$) or to those with fracture in the control group (?TBS=-0.076, $p<0.001$). An influence on TBS by sex was also noted with a decrease in TBS of greater magnitude in GC men than in GC women (?TBS=-0.052 vs. ?TBS=-0.027) without differences in terms of age ($p=0.48$) and BMI ($p=0.08$).

Conclusion: GC-treated individuals have a significant deterioration of bone microarchitecture as assessed by TBS which is more marked in those with OP fracture and in men. TBS seems to be more sensitive than aBMD for GC-related fracture detection and should be a good surrogate indicator of bone health in such secondary osteoporosis.

Disclosures: *Renaud Winzenrieth, None.*

FR0325

Does a specific bone pattern exist in patient suffering from Cushing's disease?. Amandine Boisson¹, Renaud Winzenrieth², Antoine Tabarin³, Thierry Schaeverbeke¹, Nadia Mehzen-Cetre¹. ¹Rheumatology department, CHU Pellegrin, France, ²R&D department, Med-Imaps, France, ³Endocrinology Department, France

Rational: Rare studies conducted in patients with Cushing's disease (CD), a model of endogenous hypercortisolism, have pinpointed dissociation between the increased risk of fracture and apparently normal areal Bone Mineral Density (aBMD). The aim of this study was to evaluate the bone impact of CD assessed by TBS and aBMD, at various status.

Patients and methods: 50 subjects with CD status confirmed by biochemical evaluations (ACTH, UFC), presence of a pituitary adenoma or dynamic hormonal

levels were recruited. CD status defined as active disease (AD), eucorticism treated patients (EU) or corticotrope insufficiency with hydrocortisone supplementation (CIH). aBMD at spine and at the hip has been evaluated using a iDXA densitometer (GE-Lunar, Madison, USA) as well as TBS at spine using TBS iN Sight® v2.1 (Med-Imaps, France).

Results: Compared with the normal values for age, CD subjects have lower TBS value (TBS=1.26±0.13, Z-score TBS = -0.8 SD; $p<0.01$) whereas no differences have been obtained for aBMD at spine (Z-score=0.3 SD, $p=0.49$) or at total femur (Z-score=0.0 SD, $p=0.95$). Significant differences were obtained over CD subjects depending on the CD status without difference in terms of age (all $p>0.25$). Those with AD have a significant TBS alteration when compared with reference values (Mean Z-score TBS=-1.3 SD, $p<0.001$) despite a normal aBMD at spine (Z-score = 0.4 SD) or at total femur (Z-score = 0.2 SD). Subjects with EU have both normal aBMD and TBS values for age (Mean Z-scores of 0.5 and 0.0 SD respectively). In addition, CD subjects with CIH have both decrease of aBMD and TBS (Mean Z-scores of -0.6 and -0.7 SD respectively) without significances. AD subjects have significant lower TBS values than those with EU (Δ TBS=-0.104, $p<0.05$) or with CIH (Δ TBS=-0.048, $p<0.05$) without differences in terms of aBMD at any sites (all $p>0.05$). Men with AD had lower TBS values than women with AD (TBS = 1.105 vs. 1.244; $p<0.01$). In addition, CIH had lower TBS values than EU subjects (Δ TBS=-0.056, $p<0.05$). **Conclusion:** A specific bone pattern exists in CD subjects consisting in a marked alteration of the trabecular texture assessed by TBS despite a normal aBMD. This alteration seems to be gender related with a higher impairment in men. One striking findings of this study is that a specific bone pattern exists for each CD status and activity, and that CIH subjects, usually considered in remission, have also a bone pattern alteration.

Disclosures: *Amandine Boisson, None.*

FR0326

Endogenous Cortisol Levels Are Positively Correlated to Adrenal Androgens But Negatively to Total Testosterone and Estradiol Whereas Exogenous Glucocorticoids Suppress Both Adrenal and Gonadal Steroid Hormones in Elderly Men. Anna Nilsson¹, Claes Ohlsson², Mattias Lorentzon², Liesbeth Vandenput², Magnus Karlsson³, Ulf Lerner², Östen Ljunggren⁴, Dan Mellström². ¹Sahlgrenska University Hospital, Sweden, ²Center for Bone & Arthritis Research, Department of Internal Medicine & Clinical Nutrition, at the Institute of Medicine, Sahlgrenska Academy, Gothenburg University, Sweden, ³Clinical & Molecular Osteoporosis Research Unit Department of Clinical Sciences & Orthopaedic Surgery Lund University, Skåne University Hospital, Sweden, ⁴Department of Medical Sciences, University of Uppsala, Uppsala, Sweden, Sweden

Treatment with glucocorticoids is a strong risk factor for fragility fractures, due to several effects including suppression of gonadal hormones. We have studied the role of glucocorticoid treatment for bone density and fracture risk in the Swedish MrOS study (n=3014), and assessed the co-variation of endogenous cortisol levels to bone metabolism, bone density, and adrenal and gonadal steroid hormones in MrOS Sweden. Briefly, a population-based sample of 3014 men between 70 and 80 years of age was studied. Fractures were obtained from the radiology departments. Bone mineral density (BMD) was measured by dual energy x-ray absorptiometry, and hormone analyses were done by mass spectrometry.

The risk of fracture in men treated with glucocorticoids (n=59) tended to be higher 5 years after assessment (hazard ratio (HR) 1.82, $p=0.06$) but not after 10 years (HR 1.36, $p=0.23$). These men also had lower BMD at the total hip (0.87 ± 0.14 vs 0.93 ± 0.14 g/cm²) and clearly reduced serum levels of dehydroepiandrosterone (DHEA) (0.5 vs 1.8 ng/mL), DHEA-sulfate (0.2 vs 0.7 µg/mL), androstenedione (0.4 vs 0.8 ng/mL), total testosterone (12 vs 15 nmol/L) and estradiol (59 vs 77 pmol/L; $p<0.001$ for all comparisons in unpaired t-tests).

Fasting morning serum cortisol levels in men in MrOS Gothenburg excluding diabetics and glucocorticoid users (n=812), were strongly and positively correlated to DHEA ($r=0.31$) and androstenedione ($r=0.34$), but negatively to total testosterone ($r=-0.11$) and estradiol ($r=-0.10$) both in age-adjusted analyses and in models adjusted for age, body mass index (BMI), smoking, and renal function ($p<0.01-0.001$). There was a negative correlation between age-adjusted serum cortisol levels and BMD at the hip ($r=-0.08$, $p=0.02$) but not after adjustment for BMI, smoking, and renal function ($r=-0.04$, $p=0.29$). High serum cortisol was also associated with higher plasma glucose ($r=0.18$), serum insulin ($r=0.11$), systolic blood pressure ($r=0.11$), and C-reactive protein ($r=0.15$; $p<0.01-0.001$).

In conclusion, adrenal androgens were positively correlated to endogenous serum cortisol and suppressed by the use of exogenous glucocorticoids, as expected. Total testosterone and estradiol were low in subjects with high endogenous cortisol as well as in those using glucocorticoids. Low levels of DHEA have been suggested to increase fracture risk, and the role of DHEA in the development of glucocorticoid-induced osteoporosis needs to be further explored.

Disclosures: *Anna Nilsson, None.*

FR0327

Effects of Denosmab on vertebral fractures in patients with Glucocorticoid-Induced Osteoporosis. Ikuko Tanaka¹, Mari Ushikubo², Takashi Kato³, Keisuke Izumi², Kumiko Akiya², Hisaji Oshima². ¹NAGOYA Rheumatology Clinic, Japan, ²Tokyo Medical Center, Department of connective Tissue Disease, Japan, ³National Center for Geriatrics & Gerontology, Japan

Background) Bisphosphonates have been widely used for prevention and treatment of glucocorticoid-induced osteoporosis. In recent years, denosmab, a monoclonal antibody against RANKL, has been proven for effective treatment of primary osteoporosis. However, effects of denosmab for glucocorticoid-induced osteoporosis (GIO) was not clearly resolved.

Purpose) This study was conducted to clarify effects of denosmab on vertebral fractures in GIO.

Subjects and Methods) Patients with connective tissue diseases at Tokyo Medical Center was subjected for one-year longitudinal cohort study. The number of subjects was 200 (female; 175, age; 65+/-14 (mean +/- SD), prednisolone dosage at base line; 7.7+/-11 mg/day, prednisolone dosage during 1yr; 6.0+/-11mg/day, duration of prednisolone treatment; 11.7+/-11.3yr, prevalent vertebral fracture (Genant, H. 1996); 46.0%). Lumbar bone mineral densities (IBMD) were measured as %YAM with Lunar 3030 (GE). Incident vertebral fractures were analyzed with XP at thoracic and lumbar spines. Patients were treated with bisphosphonates (74%) or denosmab (26%).

Results) The value of IBMD (%YAM) at the base line was 82.1+/-14.7%. The rate of incident fractures during the follow-up period was 13.0%. 2) Clinical data at the base line were not statistically different between two treatment groups (sex, age, prevalent fracture, prednisolone dosage, and IBMD). However, increases in IBMD after 1 yr were larger in patients with denosmab than in those with bisphosphonates (3.22+/-0.45% vs 2.97+/-0.25%, respectively; p<0.02). A logistic regression analysis showed that statistically significant contributors for incident fractures were IBMD (5% decrease, OR; 1.30; 95%CI; 1.10-1.54, p<0.01), prednisolone dosages (5mg/day increase, 2.09, 1.30-3.34, p<0.01), prevalent fractures (3.87, 1.40-10.7, p<0.01), and denosmab treatment (vs bisphosphonates, 0.12, 0.02-0.56, p<0.01).

Conclusions) It is suggested that denosmab may be more effective than bisphosphonates for prevention of osteoporotic fractures in patients treated with glucocorticoids.

Disclosures: Ikuko Tanaka, None.

FR0331

Effects of Romosozumab in Japanese Women With Postmenopausal Osteoporosis: Phase 2 Trial Results. H Ishibashi¹*, DB Crittenden², A Miyauchi³, C Libanati⁴, J Maddox², L Chen², A Grauer². ¹Ina Hospital, Japan, ²Amgen Inc., USA, ³Miyauchi Medical Center, Japan, ⁴UCB Pharma, Belgium

Purpose: Romosozumab is a sclerostin inhibitor that rapidly increases BMD through a dual-effect on bone, causing increased bone formation and decreased bone resorption, as shown in a global phase 2 study in postmenopausal (PM) women with low bone mass (McClung *NEJM* 2014). Here we report the key results of a phase 2 dose-ranging study to assess the efficacy and safety of romosozumab in a Japanese population (NCT01992159).

Methods: This randomized, double-blind, placebo (Pbo)-controlled study enrolled PM Japanese women aged 55-85 years with a lumbar spine (LS), total hip (TH), or femoral neck (FN) DXA T-score ≤ -2.5 . Women were randomized to receive Pbo or 1 of 3 doses of subcutaneous romosozumab (70 mg, 140 mg, or 210 mg) monthly (QM) for 12 months. The primary endpoint was percentage change from baseline in LS BMD at month 12. Secondary endpoints included percentage change from baseline in LS BMD at month 6, TH and FN BMD at months 6 and 12, and percentage change from baseline in serum bone turnover markers.

Results: Women enrolled in the study (N=252) had a mean (SD) age of 68 (6.4) years and mean LS, TH, and FN T-scores of -2.7, -1.9, and -2.3, respectively. All romosozumab doses significantly increased BMD compared with Pbo at each of the 3 skeletal sites at month 12 (p<0.01). The largest improvements were observed with romosozumab 210 mg QM, which resulted in BMD gains from baseline of 16.9% and 4.7% at the LS and TH, respectively (Fig), and 3.8% at the FN, at month 12. All doses of romosozumab increased P1NP and reduced CTX vs Pbo by week 1 (p<0.0001). In the 210 mg QM group, P1NP levels peaked at month 1 (median increase 101.1%) and fell below Pbo levels by month 12; CTX levels were lowest at week 1 (median decline 45.6%) and were still below Pbo at month 12. Subject incidences of adverse events (AEs) and serious AEs were generally comparable between treatment groups. Numerical differences were observed between the total romosozumab vs Pbo groups for subject incidence of mild to moderate osteoarthritis AEs (6.9% vs 0%) and mild injection site reactions (3.7% vs 1.6%).

Conclusions: In this study of Japanese women with PM osteoporosis, romosozumab treatment resulted in rapid, large, and significant gains in BMD compared with Pbo and baseline, and the 210 mg QM dose showed the greatest efficacy. Romosozumab was generally well tolerated in this population. Global phase 3 studies evaluating the 210 mg QM dose for the treatment of osteoporosis are underway.

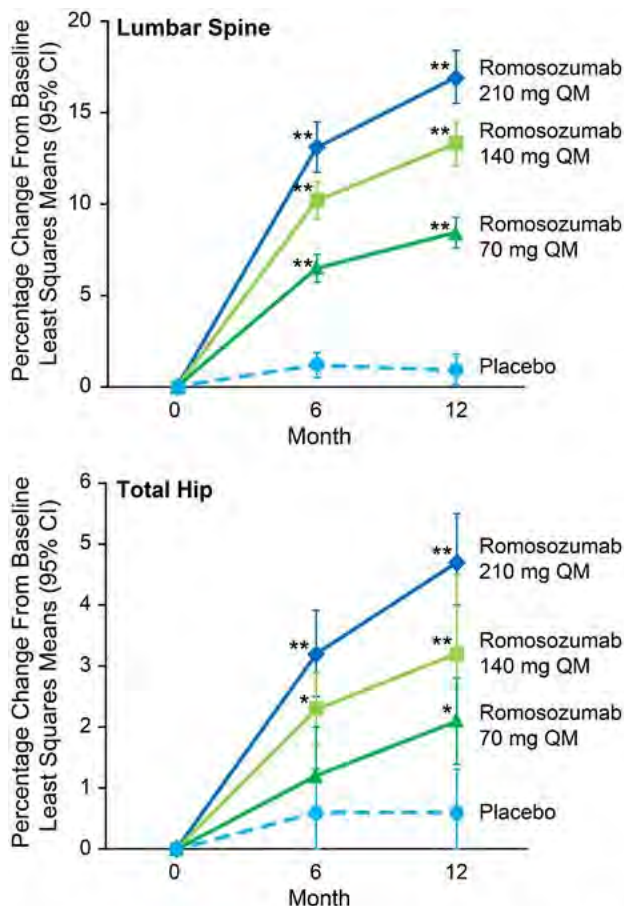


Fig. Percentage change in bone mineral density from baseline in women receiving placebo or romosozumab (70 mg, 140 mg, or 210 mg) every month for 12 months. Estimated least square means for the changes by linear models are presented. QM, every month. *p<0.01 vs placebo; **p<0.0001 vs placebo.

Figure

Disclosures: H Ishibashi, None.

This study received funding from: Amgen Inc. and UCB Pharma

FR0333

Response Rates for Hip, Femoral Neck and Lumbar Spine BMD are Higher for Patients Treated with Abaloparatide when Compared to Placebo or Teriparatide – Results of the ACTIVE Trial. Gary Hattersley¹*, Alan Harris¹, Greg Williams¹, D. Black², Ming-Yi (Tristan) Hu¹. ¹Radius Health, USA, ²UC San Francisco, USA

Abaloparatide (ABL) is an osteoanabolic analog of PTHrP being developed for the treatment of postmenopausal osteoporosis (PMO). It has recently been reported from the ACTIVE trial that ABL reduces the incidence and risk of new vertebral, non-vertebral and clinical fractures relative to placebo (PBO) and teriparatide (TPTD) (Miller et al, ENDO 2015). ACTIVE was a randomized, double-blind, placebo-controlled Phase 3 fracture prevention trial in which PMO women received 18-months of daily SC PBO, ABL 80 µg, or TPTD 20 µg. 2,463 patients were randomized (ITT population) and 1,901 (77.9%) completed treatment. All patients were also treated with calcium and vitamin D supplementation as per local practice. To determine if women treated with 18-months of ABL were more likely to have increases in BMD than those treated with either PBO or TPTD, a pre-specified responder analysis was performed comparing the percentage of subjects experiencing BMD gains of >3% at three anatomic sites (total hip (TH), femoral neck (FN), lumbar spine (LS)) at 6, 12, and 18 months. For the purposes of this analysis, a responder was defined as a patient with a gain at all three sites (TH, FN and LS). A Chi-square test or Fisher's Exact test was used to determine the difference in the number of responders between the two treatment groups (e.g., ABL vs. TPTD), as appropriate. At Month 6, 54% of patients treated with ABL exhibited a statistically significant % change BMD of >3% compared to 3.4% for PBO (p<0.0001) and 39.7% for TPTD (p<0.0001), the comparison between PBO and TPTD was also significant at this 6 months (p<0.0001). At Month 12, 33.1% of ABL treated patients had BMD increases of >3% compared to PBO (1.5%) or TPTD (19.7%), and at Month 18, 44.4% of ABL

treated patients had BMD increases of >3% compared to PBO (1.8%) or TPTD (31.9%). All of the differences were statistically significant, $p < 0.0001$. In conclusion, in women with PMO, more subjects treated with ABL experienced greater clinically relevant BMD increases at all 3 anatomical sites compared to those treated with TPTD or PBO.

Disclosures: Gary Hattersley, Radius Health
This study received funding from: Radius Health, Inc.

FR0352

Inhibition of Osteoclastogenesis and Inflammatory Bone Resorption by Targeting BET Proteins and Epigenetic Regulation. Kyung-Hyun Park-Min^{*1}, Elisha Lim¹, Min Joon Lee¹, Sung ho Park¹, Eugenia Giannopoulos¹, Anna Yarillina¹, Marjolein van der Meulen², Baohong Zhao¹, Nicholas Smithers³, Rab Prinjha⁴, Lionel Ivashkiv⁵. ¹Hospital for Special Surgery, USA, ²Cornell University, USA, ³GSK, United Kingdom, ⁴Epinova DPU, United Kingdom, ⁵Hospital for Special Surgery, USA

Epigenetics is becoming increasingly appreciated as a new area of research that may provide insights into the pathogenesis of inflammatory autoimmune diseases such as rheumatoid arthritis. Epigenetics refers to the control of gene expression by chromatin regulators that bind to DNA and by modifications of chromatin components such as histones and DNA (hydroxyl)methylation. Recent drugs targeting epigenetic processes have shown great promise for the treatment of cancers and inflammatory conditions. Receptor activator of nuclear kappa B ligand (RANKL) is a key inducer of osteoclastogenesis and emerging evidence suggests that RANKL-induced changes in chromatin state are important for osteoclastogenesis. However, these epigenetic mechanisms in osteoclasts are not well understood and have not been therapeutically targeted. Thus, we have investigated the epigenetic regulation of osteoclast differentiation and we find that the small molecule inhibitor, I-BET151, that targets bromo and extra-terminal (BET) proteins that 'read' chromatin states by binding to acetylated histones strongly suppresses osteoclastogenesis. I-BET151 treatment suppresses *in vivo* pathologic bone loss in TNF-induced inflammatory osteolysis, inflammatory arthritis and postovariectomy models. Transcriptome analysis identifies a MYC-NFAT axis important for osteoclastogenesis. I-BET151 inhibits expression of the master osteoclast regulator, NFATC1 by suppressing expression and recruitment of its newly identified upstream regulator MYC. Importantly, MYC is elevated in rheumatoid arthritis macrophages and its induction by RANKL is important for osteoclastogenesis and TNF-induced bone resorption. These findings implicate the importance of MYC and BET proteins in osteoclast differentiation and demonstrate that targeting an epigenetic molecule in osteoclasts can be effective in suppressing the pathological bone resorption. Taken together, our study opens up a new line of investigation in the understanding and therapeutic targeting of inflammatory and oestrogen deficiency-mediated pathological bone resorption.

Disclosures: Kyung-Hyun Park-Min, None.

FR0355

TBS and HbA1c but not BMD are Predictors of Incident Fractures in Type 1 Diabetes. Thomas Neumann^{*1}, Martin Keil², Gabriele Lehmann², Sabine Lodes², Bettina Kästner², Thomas Lehmann³, Michael Kiehnopf⁴, Didier Hans⁵, Olivier Lamy⁵, Ulrich-Alfons Müller², Gunter Wolf², Alexander Sämann². ¹Jena University Hospital, Germany, ²Jena University Hospital, Department of Internal Medicine III, Germany, ³Jena University Hospital, Institute of Medical Statistics, Computer Sciences & Documentation, Germany, ⁴Jena University Hospital, Institute of Clinical Chemistry & Laboratory Diagnostics, Germany, ⁵Lausanne University Hospital, Bone Disease Unit, Switzerland

Background

Fracture risk in type 1 diabetes (T1D) is reported to be greater compared with non-diabetic controls. Bone mineral density (BMD) underestimates the observed fracture rate in individuals with T1D. This study aimed to investigate potential risk predictors for incident fractures in middle-aged men and women with long-standing T1D.

Patients and Methods

105 individuals (52 males, 53 females, age 43.6 ± 8.7 years, diabetes duration 21.8 ± 10.4 years) were followed for 6.9 ± 0.3 years. Associations of traditional risk factors for fractures (e.g. age, gender, family history of osteoporosis and nicotine), BMD at lumbar spine (LS), femoral neck (FN) and total hip (TH), trabecular bone score (TBS) and HbA1c with incident fractures were analysed. Receiver operating characteristic (ROC) analysis of TBS and HbA1c were performed to identify potential threshold effects on incident fractures.

Results

BMD decreased at LS, FN and TH in females but only at FN in males. Only female gender was associated with greater decrease in BMD at lumbar spine and total hip in univariate regression analysis. At least one new fracture occurred in 18 individuals (17.1%), peripheral fractures in 17 and vertebral fractures in 3 individuals, with the first fracture event in all but 6 individuals. No differences appeared between

individuals with fracture and without for age (44.5 ± 8.2 vs. 43.4 ± 8.9 years, $p=0.510$) and BMD (LS: 1.099 ± 0.151 vs. 1.124 ± 0.108 g/cm², $p=0.405$; FN: 0.939 ± 0.129 vs. 0.941 ± 0.128 g/cm², $p=0.983$; TH: 1.011 ± 0.132 vs. 1.020 ± 0.143 g/cm², $p=0.976$). The 10-year risk for major osteoporotic fractures and hip fractures evaluated by FRAX[®] did not identify individuals with subsequent fractures. Individuals with fractures had higher HbA1c values (65.1 ± 12.6 vs. 57.9 ± 11.2 , $p=0.043$) and lower mean TBS scores (1.281 ± 0.125 vs. 1.369 ± 0.121 , $p=0.013$) at baseline. This association was confirmed by logistic regression analysis. The ROC curves showed that mean TBS score and HbA1c level can discriminate patients with incident fractures from those without fractures (AUC 0.72 [95% CI = 0.58 – 0.86; $P=0.003$] for combined mean TBS scores and HbA1c levels).

Conclusion

The occurrence of fractures in middle-aged men and women with T1D is high and not predictable with traditional parameters including BMD. Only HbA1c and mean TBS score are independently associated with incident fractures. Further studies in larger cohorts are needed to test a risk prediction model in T1D.

Disclosures: Thomas Neumann, None.

This study received funding from: Merck Pharma GmbH, Germany

FR0359

Bisphosphonate Therapy, and the Bone Protection Treatment Care Gap, in Men on Androgen Deprivation Therapy for Non-Metastatic Prostate Cancer. Lisa-Ann Fraser^{*}. Western University, Canada

Androgen deprivation therapy (ADT) is a mainstay of prostate cancer (PC) treatment, but is known to increase the risk of fracture. Although data from clinical trials support a bone density benefit to bisphosphonates (BP) used in men on ADT, no trials have shown a fracture benefit. We used population level data from Ontario, Canada to study whether treatment with a BP prevents fractures in men on ADT for non-metastatic PC. We conducted a nested-case control study among men ≥ 66 years diagnosed with PC and started on ADT between April 1, 2000 and March 31, 2010. ADT usage was defined as ≥ 6 months of continuous use of pharmacological ADT or bilateral orchiectomy. Men with a history of metastasis, or prior BP use were excluded. Cases were identified based on a new non-vertebral major osteoporotic fracture (MOF) occurring within 3 years of ADT initiation. Event-free controls were matched to cases (at a ratio of 5:1) on age, history of previous MOF, year of ADT initiation, and long-term care (LTC) vs community residence. Conditional logistic regression was used to estimate the odds ratio of MOF associated with BP use, controlling for possible confounding factors including comorbidities, medications, and health care utilization. A cohort of 18,726 men was identified. Only 10.4% were treated with a BP within 3 years of ADT initiation. Mean time between ADT initiation and the start of a BP was 402.3 days (SD: 334.5), median 350 days (IQR: 76-676). A total of 1,298 men experienced a MOF and were matched to 6,490 controls. In these 7,788 men, mean age was 78.5 (± 6) years, 8.8% had a prior osteoporotic fracture, and 1.1% resided in LTC. Bisphosphonates were used in 101 (7.8%) of cases and in 363 (5.6%) of controls. Bisphosphonates were not significantly associated with lower MOF incidence (adjusted OR=1.29, 95%CI 0.99-1.69). In this large study over 10 years we did not observe any reduction in MOFs with BP use in men with non-metastatic PC on ADT therapy. We suspect this negative result is due to the striking care gap in bone protection in these men. Current guidelines recommend bone assessment, and appropriate treatment, at the time of ADT initiation. However, in our cohort, only 10% of men were started on a BP within 3 years of ADT initiation. A bone treatment care gap exists in these men, which needs to be addressed before it is possible to study the real-world outcomes of BP intervention in this population.

Disclosures: Lisa-Ann Fraser, None.

FR0361

Fracture Risk Following Bariatric Surgery: A Study Using Healthcare Administrative Databases. Catherine Rousseau^{*1}, Sonia Jean², Philippe Gamache³, Stefane Lebel⁴, Fabrice Mac-Way⁵, Laëtitia Michou⁵, Claudia Gagnon⁶. ¹Department of Medicine, Laval University; Endocrinology & Nephrology Unit, CHU de Quebec Research Centre, Canada, ²Institut national de santé publique du Québec; Department of Medicine, Laval University; University of Sherbrooke, Canada, ³Institut national de santé publique du Québec, Canada, ⁴Quebec Heart & Lung Institute, Canada, ⁵Endocrinology & Nephrology Unit, CHU de Quebec Research Centre; Department of Medicine, Laval University, Canada, ⁶Endocrinology & Nephrology Unit, CHU de Quebec Research Centre; Department of Medicine, Laval University; Institute of Nutrition & Functional Foods, Canada

Purpose: To investigate whether bariatric surgery increases fracture risk.

Methods: This retrospective, population-based cohort study used healthcare administrative databases. Fracture incidence for patients who had undergone bariatric surgery between 2001 and 2012 in the province of Quebec, Canada, was compared with the one of age- and sex-matched non-bariatric obese and non-obese controls. Moreover, for each group, fracture incidence before vs. after surgery (or index date)

was compared. Fractures were identified using a validated algorithm (sensitivity >80% for most fracture sites). Multivariate conditional Poisson regression models were adjusted for past fracture history, comorbidities (cardiovascular disease, hypertension, diabetes, renal failure, chronic obstructive pulmonary disease, depression, osteoporosis, hypothyroidism), material and social deprivation and area of residence.

Results: 10 662 individuals who underwent bariatric surgery (72.6% women; mean age (SD), 42 (11) years) were matched with 31 986 obese and 31 986 non-obese individuals who did not undergo surgery. At index date, patients in the bariatric group were less likely to come from metropolitan areas, were more materially and socially disadvantaged, had more comorbidities and a higher prevalence of fractures. Mean follow-up was 4.2 years (min-max: <1-12 years). 415 bariatric patients (3.9%) suffered at least one fracture after surgery compared with 826 obese (2.6%) and 750 non-obese (2.3%) controls (p<0.0001). For the bariatric group, first fracture occurred after a mean of 3.6 years (Q1-Q3: 1.6-5.1 years) (Figure 1). Adjusted fracture risk was significantly higher in the bariatric group compared with the non-obese (R.R. [95% CI]=1.45 [1.27-1.66]) and the obese (R.R. [95% CI]=1.36 [1.19-1.55]) control groups. While fracture risk did not change significantly before and after the index date in the obese and non-obese controls, it was significantly higher pre- vs. post-surgery in the bariatric group (R.R. [95% CI]=1.19 [1.06-1.34]) (Table 1).

Conclusions: After a mean follow-up of 4.2 years, patients who undergo bariatric surgery are more likely to sustain a fracture than non-obese or obese controls. Moreover, fracture risk is higher by about 20% after surgery in the bariatric group. These results suggest that bariatric patients are a high-risk group for fractures and that fracture risk assessment and management should be part of postoperative clinical care.

| Group | Period | Crude RR (95% CI) ¹ | Adjusted RR (95% CI) ² |
|---|--------------------------------|--------------------------------|-----------------------------------|
| Bariatric group (n=10 662) | Before surgery (or index date) | REF | REF |
| | After surgery (or index date) | 1.16 (1.04-1.31) | 1.19 (1.06-1.34) |
| Control group of obese individuals (n=31 986) | Before surgery (or index date) | REF | REF |
| | After surgery (or index date) | 0.93 (0.86-1.01) | 0.95 (0.87-1.03) |
| Control group of non-obese individuals (n=31 986) | Before surgery (or index date) | REF | REF |
| | After surgery (or index date) | 1.01 (0.92-1.09) | 1.01 (0.93-1.10) |

RR = relative risk.

¹ Unadjusted RR using conditional Poisson regression model.

² RR adjusted for material and social deprivation, area of residence, history of fractures and number of comorbidities in the past 5 years using multivariate conditional Poisson regression model.

Table 1. Comparison of fracture risk before vs. after surgery (or index date) for each group

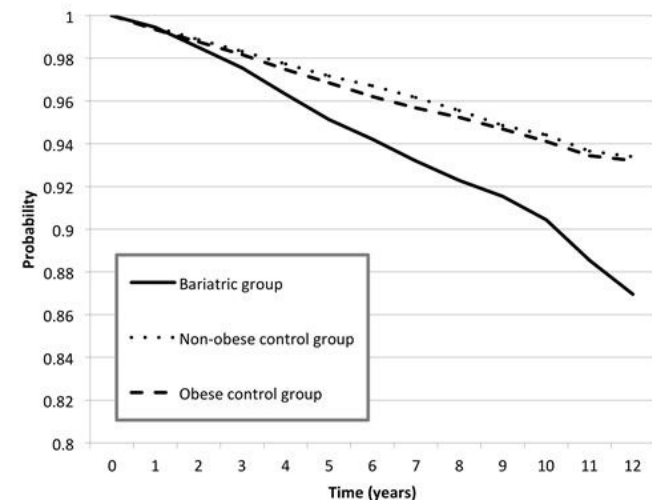


Figure 1: Survival without fracture by group

Disclosures: Catherine Rousseau, None.

FR0366

Sclerostin levels and changes in bone metabolism after bariatric surgery.

Christian Muschitz*¹, Roland Kocijan², Christina Marterer², Arastoo Rahbar Nia², Gabriela Katharina Muschitz³, Heinrich Resch², Peter Pietschmann⁴. ¹St. Vincent's Hospital, Austria, ²St. Vincent Hospital Vienna - Medical Department II, Austria, ³Division of Plastic & Reconstructive Surgery, Department of Surgery, Medical University of Vienna, Austria, ⁴Department of Pathophysiology & Allergy Research, Center for Pathophysiology, Infectiology & Immunology, Medical University of Vienna, Austria

Purpose: The role of sclerostin as a key regulator of bone formation remains unknown after Roux-en-Y gastric bypass (RYGB) or laparoscopic sleeve gastrectomy (SG). The objective was the evaluation of sclerostin and Dickkopf-1 (DKK-1) serum levels after surgery and correlations with bone turnover markers (PINP, CTX), parathyroid hormone (iPTH) and areal bone mineral density (BMD) changes at total body, lumbar spine and total hip. Methods: This was a prospective observational single-center two-arm study in premenopausal women with severe adipositas over 24 months. Prior to surgery and after 1, 3, 6, 9, 12, 18, and 24 months sclerostin, DKK-1, CTX, PINP and BMD were measured. Results: 52 premenopausal women (40.8 years, BMI 43.4) after RYGB and 38 premenopausal women (41.7 years, BMI 45.7) after SG were included. Sclerostin, CTX and to lesser extend PINP immediately increased after surgery and remained elevated during the entire study period (p<0.001). DKK-1 declined during months 3 - 9 (p<0.005) and then remained unchanged, serum phosphate continuously increased (p<0.001), iPTH remained in the upper normal limit. Sclerostin increases were significantly positively correlated with CTX and PINP increases and significantly negatively correlated with BMD loss. BMD independently declined regardless of RYGB and SG. Elevations of sclerostin, CTX, PINP, and phosphate but not DKK-1 and iPTH, were significant discriminating factors for BMD loss (AUC 0.920). Conclusions: Rapid and sustained increases of sclerostin, CTX and to lesser extend PINP causes an increase in bone metabolism and results in BMD loss at all skeletal sites.

Disclosures: Christian Muschitz, None.

FR0367

Strategies for the reduction of loss of bone and body lean mass after bariatric surgery.

Christian Muschitz*¹, Roland Kocijan², Judith Haschka², Christina Marterer², Arastoo Rahbar Nia², Gabriela Katharina Muschitz³, Heinrich Resch², Peter Pietschmann⁴. ¹St. Vincent's Hospital, Austria, ²St. Vincent Hospital - Medical Department II - Academic Teaching Hospital of Medical University of Vienna, Austria, ³Division of Plastic & Reconstructive Surgery, Department of Surgery, Medical University of Vienna, Austria, ⁴Department of Pathophysiology & Allergy Research, Center for Pathophysiology, Infectiology & Immunology, Austria

Purpose: Bariatric surgery causes ongoing weight loss, an increased bone turnover and loss of areal bone mineral density (aBMD) at different skeletal sites. The hypothesis of this study was to test if a specific postoperative intervention exerts different effects on bone metabolism, aBMD, body lean mass, and Trabecular Bone Score (TBS) compared to no intervention. In this prospective observational single-center two-arm study patients eligible for either laparoscopic Roux-en-Y gastric bypass (RYGB) or sleeve gastrectomy (SG) were randomly assigned into the two groups: The intervention group received preoperative vitamin D loading (28.000 IU/week for 8 weeks) and postoperative supplementation of vitamin D (16.000 IU/week), calcium citrate (500 mg/d), weight adjusted protein diet (range 50 - 110 g/day including protein supplementation), and physical exercise (Nordic walking 3x45 min/week). The non-interventional group received regular consultation for food intake behavior. The objectives were the evaluation of changes between the two groups of sclerostin (Scl) and Dickkopf-1 (DKK-1) serum levels, bone turnover markers (PINP, CTX), intact parathyroid hormone (iPTH), 25-OH vitamin D, areal bone mineral density (BMD) changes at total body, lumbar spine and total hip as well as body lean body mass, and changes of TBS. Measurements were performed prior to surgery and after 1, 3, 6, 9, 12, 18, and 24 months. Results: In each group 110 female and male patients with a median age of 41 years [IQR 34; 45] and a BMI of 44 kg/m² [IQR 41; 47] participated. Baseline characteristics of both groups did not differ with regard to type of surgery, serum values, and aBMD or body lean mass values. All investigated median values significantly changed within the groups regardless of RYGB or SG. At study endpoint in the intervention group median levels were lower for iPTH (51.8 vs 77.6 pg/mL), Scl (40.2 vs 53.0 pmol/L), CTX (0.524 vs 0.640 ng/mL; p<0.0001 for all) and PINP (41.5 vs 51.3 µg/L, p=0.004). Median levels were higher for 25-OH vitamin (32.5 vs 22.0 ng/mL), body lean mass (46.5 vs 42.6 kg), aBMD total body (1.178 vs 1.091 g/cm²), aBMD lumbar spine (1.272 vs 1.130 g/cm²), aBMD total hip (1.179 vs 1.064 g/cm², p<0.0001 for all), DKK-1 (25.9 vs 22.3 pmol/L, p=0.038), and TBS (1.226 vs 1.172, p=0.0067). Conclusions: Specific interventions for patients with RYGB and SG reduce high bone turnover, the loss of aBMD and body lean mass, as well as changes in TBS.

Disclosures: Christian Muschitz, None.

FR0369

Osteocyte production of PTHrP is necessary for normal osteocyte differentiation and bone remodeling. Niloufar Ansari¹, Patricia Ho¹, Jonathan Gooi², T John Martin¹, Natalie A Sims¹. ¹St. Vincent's Institute of Medical Research, Australia, ²Melbourne Medical School, University of Melbourne, Australia

Parathyroid hormone-related protein (PTHrP) is an autocrine/paracrine regulator in many tissues, including bone. Although *Pthrp* gene ablation is neonatal lethal in mice, heterozygotes were normal at birth but osteopenic by 12 weeks of age. That phenotype was recapitulated in mice with PTHrP knocked out in the osteoblast lineage. Since PTHrP is also expressed in osteocytes, we sought to determine the role of osteocytic PTHrP in bone.

We crossed mice carrying the DMP1.Cre transgene (10-kb promoter) with PTHrP-loxP mice to target PTHrP deletion to osteocytes (DMP1.Cre.PTHrP^{fl/fl}). DMP1.Cre⁺ PTHrP^{w/w} littermates were used as controls. Mice were born at the expected Mendelian ratios and grew normally. In 6 week-old DMP1.Cre.PTHrP^{fl/fl} mice and Cre⁺ PTHrP^{w/w} littermate controls, no significant differences were detected in periosteal or endocortical perimeter, cortical thickness, or in trabecular bone volume (BV/TV), trabecular number or separation (n=6-8/group). At 12 weeks of age however, BV/TV was 27% lower in male and 50% lower in female DMP1.Cre.PTHrP^{fl/fl} mice than in littermate controls (n=6-7/group, p<.05). Trabecular number was reduced to a similar extent in both males and females (both p=0.03), but trabecular thickness remained unchanged. The findings indicate a key role for osteocyte-derived PTHrP in bone remodeling in the adult skeleton, and in maintaining trabecular bone mass.

As a surrogate osteocyte system we used the OCY454 cell line; when these cells were differentiated for 14 days on plastic surfaces or on Alvetex scaffolds for 3D growth their mRNA levels for *Sost*, *Dmp1* and *Mepe* increased more than 50-100-fold. PTHrP treatment at this time point reduced *Sost* and *Mepe* mRNA levels by 70% and 80% respectively (p<0.01). Using shRNA, *Pthrp* mRNA levels were knocked down by 80% (compared to luciferase) but *Pthr1* mRNA levels were unaffected. PTHrP knockdown altered OCY454 cell differentiation such that *Sost* mRNA levels were >2-fold greater than luciferase control at day 7 of differentiation, and at day 14 *Mepe* and *Dmp1* were 3-4-fold higher. In addition, osteoblast markers *Alpl* and *Bglap* were reduced by PTHrP knockdown. This suggests that PTHrP deficiency pushes OCY454 cells towards an osteocytic phenotype. The results suggest osteocyte-derived PTHrP acting in an autocrine/paracrine manner is required for the normal differentiation of late-stage osteoblasts and osteocytes and maintenance of trabecular bone mass during adult bone remodeling.

Disclosures: Niloufar Ansari, None.

FR0370

A Complex Set of Distal Enhancers Linked to the Mouse *Tnfrsf11* Gene Direct Tissue-Specific and Hormone-regulated Expression of RANKL. Melda Onal^{*}, Hillary StJohn, Allison Danielson, Jon Markert, Wesley Pike. University of Wisconsin, USA

RANKL expression from the *Tnfrsf11* gene is regulated by numerous local and systemic factors whose activities are mediated via 10 enhancers (D1-D7, T1-T3) located 16kb to 155kb upstream of the *Tnfrsf11* transcriptional start site. Studies in osteoblastic cells have revealed inducible VDR and pCREB binding at D2 and Stat 3/5 binding at D6, suggesting that like D5, D2 mediates the induction of RANKL by PTH and 1,25(OH)₂D₃ whereas D6 mediates upregulation by IL-6 type cytokines. Similar studies in lymphocytes have revealed that T1 modulates RANKL expression in activated T cells. The importance of RANKL regulation by D5 *in vivo* has been previously described. Our recent studies indicated that the entire *Tnfrsf11* regulatory locus is required for tissue-specific expression of RANKL that is fully capable of rescuing the RANKL-null mouse phenotype. We therefore prepared 3 additional mouse strains containing genomic deletions of D2, D6 or T1 and examined the resulting phenotypes. Deletion of D2 or D6 did not alter lymphocyte expression of RANKL, whereas loss of D5 or T1 resulted in 15% and 80% decreases, respectively. Deletion of D5 or T1, but not D2 or D6, blunted the activation-induced increase in RANKL expression in T cells *ex vivo*. Loss of D5 and T1 enhancers also resulted in significantly lower RANKL expression in spleen and thymus. We also measured RANKL expression in the bones and in *ex vivo* stromal cultures of these enhancer null (KO) mice. Lack of D2 and D6, but not T1, blunted PTH- and LPS-induced increases in RANKL expression, respectively, both *ex vivo* and *in vivo*. Similar to D5KO mice, D2KO mice, but not D6KO or T1KO mice, exhibited an up to 50% reduction in RANKL expression in spine, tibia and femur shafts compared to wildtype controls. Decreased skeletal RANKL expression in D2KO mice led to decreased bone resorption and a progressive increase in cancellous bone mass, while lack of D6 or T1 had no effect on bone mass up to 12 months of age. These results suggest that D5, a multifunctional RANKL enhancer, operates in concert with both lineage- and factor-specific enhancers (D2, D6 and T1) to mediate RANKL expression in lymphoid and skeletal tissues. The organization of the *Tnfrsf11* gene highlights the increased regulatory complexity that has emerged experimentally from unbiased ChIP-seq analyses which describes most genes that encode factors involved in the regulation of key biological processes such as osteoclastogenesis.

Disclosures: Melda Onal, None.

FR0371

Deletion of a Distal Enhancer of the *RANKL* Gene Delays the Progression of Atherosclerotic Plaque Calcification in Hypercholesterolemic Mice. Soheil Shamsuzzaman^{*}, Melda Onal, Hillary St. John, J. Wesley Pike. University of Wisconsin-Madison, USA

Receptor activator of NF-κB ligand (RANKL) is a TNF-like factor which mediates osteoclast formation. Recent studies demonstrated the presence of RANKL in atherosclerotic lesions; however, its role in atherosclerotic plaque formation remains controversial. We and others have previously shown that an enhancer located 75kb upstream of the mouse *RANKL* gene's transcriptional start site designated as D5 is important for 1,25(OH)₂D₃ and PTH-induced expression of RANKL. Most importantly, deletion of the D5 enhancer results in reduced basal expression of RANKL in bone and lymphoid organs. Herein, we explore RANKL's role in atherosclerotic plaque formation *in vivo* in D5 enhancer-null mice. The D5^{-/-} mice were crossed with ApoE^{-/-} mice to obtain the ApoE^{-/-};D5^{-/-} mice; wild-type (WT) (ApoE^{+/+};D5^{+/+}) and D5^{-/-} (ApoE^{+/+};D5^{-/-}) littermates were used as controls. The animals were fed a high fat Western diet (HFD) to promote atherosclerosis. We analyzed the gene expression and atherosclerotic plaque formation after 12 and 18 weeks of HFD feeding. Bone density was higher in D5^{-/-} and ApoE^{-/-};D5^{-/-} mice due to reduced bone remodeling. RANKL was significantly elevated in aortic arches and thoracic aortas of ApoE^{-/-};D5^{+/+} and ApoE^{-/-};D5^{-/-} mice compared to controls; however, ApoE^{-/-};D5^{-/-} mice had lower RANKL compared to ApoE^{-/-};D5^{+/+} mice. Similarly, higher RANKL was identified in splenic T lymphocytes isolated from the ApoE^{-/-};D5^{+/+} mice and its level was reduced in ApoE^{-/-};D5^{-/-} mice. Osteogenic regulators *Runx2*, *Osx* (*Sp7*), *Opn* (*Spp1*), *Alpl* and *Mmp13* were elevated in aortic arches and thoracic aortas in the ApoE^{-/-};D5^{+/+} and ApoE^{-/-};D5^{-/-} animals as well; however, the smooth muscle cell markers Sm-α-actin (*Acta2*), Sm22α (*Tagln*) and Sm-MHC (*Myl11*) were reduced in ApoE^{-/-};D5^{+/+} and ApoE^{-/-};D5^{-/-} aortas. Atherosclerotic fatty streaks were identified in ApoE^{-/-};D5^{+/+} as well as ApoE^{-/-};D5^{-/-} mice after 12 weeks of HFD feeding. When analyzed by μCT, plaque calcifications were identified in 6 out of 8 ApoE^{-/-};D5^{+/+} mice whereas only 1 out of 8 ApoE^{-/-};D5^{-/-} mice developed plaque calcification when fed the HFD for 12 weeks. However, after 18 weeks of HFD challenge 100% of both ApoE^{-/-};D5^{+/+} and ApoE^{-/-};D5^{-/-} animals developed fatty streaks as well as plaque calcification. Our data suggest that RANKL D5 enhancer deletion delays the progression of atherosclerotic plaque calcification in mice. This work provides important insights into RANKL's regulatory role in atherosclerosis.

Disclosures: Soheil Shamsuzzaman, None.

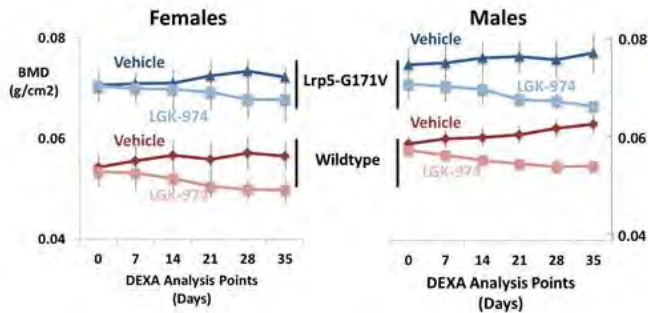
FR0373

Decreasing Bone Mass in Mice Containing the High-Bone-Mass Mutation LRP5-G171V through the inhibition of Porcupine by LGK974. Cassandra R. Zylstra-Diegel, Mitchell McDonald^{*}, Bart Williams. Van Andel Research Institute, USA

Wnt/B-catenin signaling is important in bone proliferation, differentiation, and remodeling. Missense mutations in LRP5, the co-receptor for the Wnt/B-catenin pathway, cause high bone mass (HBM) in humans. Studies looking at the mechanism of LRP5-HBM mutations have shown these patients have no change in serum levels of Wnt signaling antagonists such as DKK1, SOST, and sFRP4; and treating animals carrying these mutations with these antagonists has relatively minor effects on modulating bone density (and no effects on mice carrying transgenes specifically directing expression of the LRP5-G171V allele). Considering that the LRP5-HBM mutation may still require a Wnt ligand for signaling we speculated that treating LRP5-G171V knock-in mice with an inhibitor of Wnt secretion would decrease their bone mass.

We treated Lrp5-G171V^{K1/+} and wildtype littermates with LGK974, a small molecule Porcupine inhibitor that blocks Wnt secretion. The animals were treated daily for 35 days and DEXA was performed every 7 days to assess changes in bone mineral density (BMD). We found LGK974 significantly reduced BMD in both Lrp5-G171V^{K1/+} and wildtype animals. We are currently assessing cortical and trabecular morphology by μCT and assessing histological phenotypes by histomorphometry.

This study will help us better understand the mechanism of the LRP5-HBM G171V mutation and also confirms this mutation is Wnt ligand dependent. Treating LRP5-HBM mutation patients with LGK974 may offer a therapeutic treatment to alleviate the symptoms of high bone mass.



LGK974 decreases BMD in LRP5-G171V animals as determined by DEXA.

Disclosures: Mitchell McDonald, None.

FR0375

Role of FKBP12 in Signal Transduction by Mutant ALK2 Responsible for Fibrodysplasia Ossificans Progressiva. Aiko Machiya^{*1}, Mai Fujimoto¹, Sho Tsukamoto², Mai Kuratani², Satoshi Ohte², Naoto Suda³, Takenobu Katagiri². ¹Division of Pathophysiology, Research Center for Genomic Medicine, Saitama Medical University, Division of Orthodontics, Department of Human Development & Fostering, Meikai University School of Dentistry, Japan, ²Division of Pathophysiology, Research Center for Genomic Medicine, Saitama Medical University, Japan, ³Division of Orthodontics, Department of Human Development & Fostering, Meikai University School of Dentistry, Japan

Fibrodysplasia ossificans progressiva (FOP) is a rare hereditary disorder characterized by postnatal progressive heterotopic ossification in skeletal muscle. Twelve independent mutations in ALK2, a type I BMP receptor, have been identified from patients with FOP. The mutant forms of ALK2 were active in vitro without adding exogenous BMPs, indicating that they were gain-of-function mutations. It has been suggested that a decrease in binding affinity of ALK2 to FKBP12, which is a repressor of type I receptor kinases, is involved in the activation of the mutant ALK2. Recently, F198 and L199 residues in ALK2 have been shown to act as the binding site to FKBP12. In the present study, we examined the role of FKBP12 in the activation of ALK2 by analyzing biochemical characteristics of ALK2 carrying the mutations, including at the FKBP12-binding site (P197_F198del-insL mutant). Over-expression of those mutant ALK2, but not WT, induced ALP activity in the cooperation with Smad1 in C2C12 cells. The co-expression of FKBP12 markedly reduced the ALP activity and phosphorylated levels of Smad1/5. However, in the cultures of P197_F198del-insL mutant, neither ALP activity nor phosphorylated Smad1/5 levels were changed in the presence of FKBP12. FKBP12 did not change the binding ability of ALK2 to Smad1. Co-IP experiments revealed that the mutant ALK2, except the P197_F198del-insL mutant, showed weaker binding ability to FKBP12 than that of WT. In contrast, however, the P197_F198del-insL mutant did not bind to FKBP12, confirming that this mutant ALK2 has been changed structure in the FKBP12-binding site. These findings suggest that FKBP12 can repress the ALK2 activity in vitro through a direct interaction with ALK2 via the binding site. However, heterotopic ossification in the patient carrying the P197_F198del-insL mutation started at 11-year-old similar to other patients carrying typical mutation in ALK2, suggesting that heterotopic ossification in FOP is induced additional molecular mechanisms. Recently, we found that the mutant ALK2, including the P197_F198del-insL mutant, were hypersensitive to BMP type II receptors and were activated by them. FKBP12 failed to repress the ALP activity induced by the co-expression of BMP type II receptors and mutant ALK2, not only P197_F198del-insL but also other mutants. Taken together, our findings indicate that mutant ALK2 were activated by BMP type II receptors even in the presence of FKBP12. Phosphorylation of mutant ALK2 by the type II receptors may cancel the inhibitory activity of FKBP12 in FOP.

Disclosures: Aiko Machiya, None.

FR0380

The Clinical and Genetic Spectrum of Low Alkaline Phosphatase in Adults. Leyre Riancho-Zarrabeitia^{*1}, María T. García-Unzueta², Jair A. Tenorio³, Juan A. Gómez-Gerique², Pablo Lapunzina³, Jose Riancho⁴. ¹Service of Rheumatology, Hospital UM Valdecilla, Spain, ²Service of Clinical Analysis, Hospital UM Valdecilla, Spain, ³Inst. Medical Molecular Genetics, Hospital La Paz., Spain, ⁴University of Cantabria, Spain

Purpose.-Different from infantile forms, adult forms of hypophosphatasia have less severe manifestations and may go unrecognized. Low serum levels of alkaline phosphatase (ALP), the enzyme encoded by the ALPL gene, are a hallmark of hypophosphatasia. However, the clinical significance and the underlying genetics of low ALP in unselected populations are unclear. **Methods.**-In order to clarify this issue,

we performed a clinical and biochemical study of subjects with reduced serum ALP activity and sequenced the exons of the ALPL gene. **Results.**-Forty two adults with unexplained persistently low serum ALP were studied. There was a 3:1 female:male ratio. Age range was 20-77 yr. Although many subjects experienced minor complaints, such as mild musculoskeletal pain (60%), none had major health problems. ALPL mutations were found in 21 out of 42 subjects (50%). Twenty patients carried heterozygous mutations; whereas 1 had a homozygous mutation. Eight mutations were novel and had not been previously described. Eighteen of the 21 patients with mutations (86%) had a missense mutation; in 1 case the mutation caused a splice change and there were 2 frameshift mutations. Most mutations were located in exons 5 and 6 (12 aminoacid were mutated in 17 patients) and were predicted to have a damaging effect on the protein activity, both according to the structure-based Polyphen webtool and the evolutionary criteria proposed by Silvent. The presence of a mutated allele was associated with premature tooth loss (48% versus 12%; $p=0.04$), slightly lower levels of serum AP (30'6 vs 25'6 u/l; $p=0.002$) and higher levels of enzyme substrates, such as serum pyridoxal phosphate ($p<0.0001$) and urine phosphoethanolamine ($p<0.0001$), as well as mildly increased serum phosphate ($p=0.03$). Ten patients had pyridoxal phosphate levels above the normal range, a test frequently used when hypophosphatasia is suspected. All carried a gene mutation; predicted to be deleterious in 9 cases and of doubtful significance in one. **Conclusion.**-One half of adults with persistently low levels of total alkaline phosphatase had a mutated allele of the ALPL gene. Although clinical manifestations are usually mild, in about 50% of them enzyme activity is low enough to cause substrate accumulation and may predispose to disorders of the teeth and other calcified tissues.

Disclosures: Leyre Riancho-Zarrabeitia, None.

This study received funding from: Alexion

FR0382

Comparative effectiveness of FGF23 blocking antibodies versus daily or intermittent 1,25 dihydroxyvitamin D as therapies for X-linked hypophosphatemia in mice. Eva Liu^{*1}, Adalbert Raimann², Daniel Brooks³, Mary Bouxsein⁴, Marie Demay⁴. ¹Brigham & Women's Hospital & Massachusetts General Hospital, USA, ²Medical University Vienna, Massachusetts General Hospital, Austria, ³Massachusetts General Hospital, USA, ⁴Massachusetts General Hospital, Harvard Medical School, USA

X-linked hypophosphatemia (XLH) is characterized by elevated serum FGF23, leading to hypophosphatemic rickets. Current therapies, 1,25 dihydroxyvitamin D (1,25D) and phosphate supplementation, do not normalize skeletal growth or mineralization. Recent studies have shown that FGF23 blocking antibodies increase serum phosphate in adults with XLH. Therefore, Hyp mice (murine model for XLH) were treated from day 2 to 75 with a blocking FGF23 antibody (FGF23Ab, Amgen), daily 1,25D or intermittent high dose 1,25D. Litter-matched wild type (WT) and Hyp mice were treated with vehicle. Relative to Hyp controls, all treatments significantly increased serum phosphate and suppressed serum PTH, while maintaining normocalcemia. Daily 1,25D and FGF23Ab significantly suppressed urinary phosphate excretion. All treatments increased FGF23 mRNA in long bones. The FGF23Ab significantly increased serum 1,25D at day 35 relative to Hyp controls, but not at day 75.

Daily 1,25D normalized body weight, whereas FGF23Ab significantly increased but did not normalize body weight; intermittent 1,25D had no effect. All treatments significantly increased lumbar vertebral height and tail length, compared to Hyp controls. Hypophosphatemia leads to decreased p-Erk1/2 in the growth plate, decreased hypertrophic chondrocyte apoptosis and expansion of the hypertrophic chondrocyte layer. All treatments attenuated the rachitic phenotype of the Hyp growth plate, assessed by collagen type X *in situ* hybridization and increased p-Erk1/2 and hypertrophic chondrocyte apoptosis relative to Hyp controls.

MicroCT analyses (Table 1) showed that relative to WT mice, Hyp controls had shorter femurs and reduced cortical thickness (Ct.Th), cortical area (Ct.Ar), polar moment of inertia (pMOI), and trabecular bone volume (Tb.BV/TV). FGF23Ab increased femur length relative to Hyp controls, but not to the same extent as daily or intermittent 1,25D. Compared with Hyp controls, mice treated with daily 1,25D and FGF23Ab had significantly higher Ct.Th and Ct.Ar. Although FGF23Ab improved pMOI, unlike daily 1,25D it did not normalize this parameter. Intermittent 1,25D did not improve these parameters. No treatment improved Tb.BV/TV.

While all treatments improved growth plate maturation, these studies demonstrate the importance of 1,25D for long bone and vertebral growth and bone micro-architecture in XLH. The inability of FGF23Ab to sustain increased serum 1,25D levels suggests combined therapy may be beneficial.

Table 1: Bone microarchitecture of Hyp mice treated with daily 1,25D, FGF23 Ab, or intermittent 1,25D

| Femur microCT | Wild Type | Hyp Control | Daily 1,25D | FGF23 Ab | Intermittent 1,25D |
|--------------------------|------------|-------------------------|---------------------------|----------------------------|----------------------------|
| Femur Length (mm) | 14.8±0.4 | 10.6±0.6 ^a | 12.6±0.4 ^{a,b} | 11.3±0.5 ^{a,b} | 12.6±0.4 ^{a,b} |
| Midshaft Cortical | | | | | |
| Ct.Th (mm) | 0.148±0.01 | 0.051±0.01 ^a | 0.074±0.01 ^{a,b} | 0.067±0.008 ^{a,b} | 0.053±0.005 ^{a,b} |
| Ct.Ar (mm ²) | 0.74±0.09 | 0.38±0.06 ^a | 0.63±0.13 ^{a,b} | 0.51±0.08 ^{a,b} | 0.44±0.05 ^{a,b} |
| Tl.Ar(mm ²) | 2.08±0.26 | 2.16±0.19 | 2.58±0.21 ^{a,b} | 2.21±0.16 ^a | 2.16±0.09 ^a |
| Ct.Ar/Tl.Ar (%) | 35.83±2.46 | 17.71±2.24 ^a | 24.17±3.95 ^{a,b} | 23.13±2.40 ^{a,b} | 20.61±1.61 ^{a,b} |
| Cortical Porosity (%) | 5.52±0.81 | 34.35±5.16 ^a | 26.72±5.40 ^{a,b} | 22.80±7.04 ^{a,b} | 35.54±8.57 ^{a,b} |
| pMOI (mm ³) | 0.43±0.10 | 0.24±0.05 ^a | 0.46±0.11 ^a | 0.32±0.07 ^{a,b} | 0.27±0.04 ^{a,b} |
| Distal Trabecular | | | | | |
| BV/TV (%) | 17.08±4.31 | 9.66±1.53 ^a | 10.09±3.37 ^a | 10.28±2.66 ^a | 9.79±1.94 ^a |

Values are represented as average±SD

^a p value < 0.05 vs Wild Type
^b p value < 0.05 vs Hyp Control
^a p value < 0.05 vs Daily 1,25D
^b p value < 0.05 vs FGF23Ab

Table 1

Disclosures: *Eva Liu, None.*

FR0387

Bone impairment in primary hyperoxaluria (PH): an ultrastructural analysis.

Delphine Farlay^{*1}, Justine Bacchetta², Pierre Cochat³, Georges Boivin⁴.

¹INSERM, UMR1033; Université De Lyon, France, ²Service de Néphrologie, Rhumatologie et Dermatologie Pédiatrique, centre de Référence des Maladies Rénales Rares, Hôpital Femme Mère enfant, Bron; INSERM UMR1033, Université de Lyon, France, ³service de Néphrologie, Rhumatologie et Dermatologie Pédiatriques, Centre de Référence des Maladies Rénales Rares, Hôpital Femme Mère enfant, Bron; Université de Lyon, France, ⁴INSERM UMR 1033, Université de Lyon, France

Deposition of calcium oxalate crystals in the kidney and bone is a hallmark of systemic oxalosis. Patients with PH1 (less frequently PH2) present severe impaired renal function, and thus systemic oxalosis. Since the bone compartment stores massive amounts of oxalate, patients present with recurrent low-trauma fractures, bone deformations, severe bone pains and specific oxalate osteopathy on plain X-ray. The threshold of glomerular filtration rate at which this occurs is debatable and might be as high as 30 to 45 mL/min per 1.73m². The objective of the study is to present a single-centre experience of bone biopsies and bone ultrastructural analysis in cases with oxalosis. Data were obtained in 10 samples from 8 patients with oxalosis (16-68 years) who underwent iliac crest bone biopsy and bone quality analysis using modern methods (Microradiography, microindentation, Fourier Transform InfraRed Microspectroscopy, transmission electron microscopy) in addition to histomorphometry. Disseminated calcium oxalate deposits (whewellite) were found in the bone marrow space (with a granulomatous reaction) but not in the bone matrix. Calcium oxalate deposits were totally surrounded by macrophages and multinucleated giant cells, and a phagocytosis activity was sometimes observed. Very few calcium oxalate crystals were directly in close contact with the mineral substance of bone. Pathological deposits are composed of more or less numerous elongated, birefringent crystals identified as calciumoxalate monohydrate. Bone tissue close to oxalosis deposits was composed of apatite, the usual mineral component of bone tissue. Bone mineralization was not modified by the presence of calcium oxalate even in close vicinity. Mineral maturity and crystallinity index were also unchanged, indicating that age of bone mineral and crystal size/perfection were not significantly modified. However, a decrease in the CO3/PO4 ratio was found in the PH group compared to controls. Bone quality analysis also revealed a harder bone than normal, perhaps in relationship with decreased carbonate content in the mineral. This study reports in patients with oxalosis, the specific location of calcium oxalate deposits (whewellite) in the bone marrow space (with a granulomatous reaction) and not in the bone matrix. Bone hardness is increased, that could explain a more "brittle" bone. The formation and growth of calcium oxalate crystals in bone is independent of apatite. Despite these novel observations, the exact mechanisms leading to nucleation and growth of oxalate deposits are still unclear and deserve further studies.

Disclosures: *Delphine Farlay, None.*

FR0388

GORAB missense mutations disrupt RAB6 and ARF5 binding and Golgi targeting. Uwe Kornak^{*1}, Johannes Egerer², Denise Emmerich², Wing Lee Chan², Björn Fischer-Zirnsak², David Meierhofer³, Francis A. Bari⁴.
¹Charité-Universitätsmedizin Berlin, Germany, ²Institut fuer Medizinische Genetik und Humangenetik, Charité-Universitätsmedizin Berlin, Germany, ³Max Planck Institute for Molecular Genetics, Germany, ⁴Department of Biochemistry, University of Oxford, United Kingdom

Geroderma osteodysplastica is a hereditary segmental progeroid disorder leading to infantile osteoporosis and fractures caused by loss-of-function mutations in *GORAB*. The GORAB protein is prominently expressed in osteoblasts, where it localizes to the Golgi apparatus and interacts with the small GTPase RAB6. In this study we used different approaches to shed more light on the recruitment of GORAB to this compartment. We show that GORAB best co-localizes with trans-Golgi markers and is rapidly displaced upon Brefeldin A exposition indicating a loose association to Golgi membranes. A yeast two-hybrid screening revealed a specific interaction with the small GTPase ARF5 in its active, GTP-bound form. ARF5 and RAB6 bind to GORAB via the same internal Golgi-targeting RAB6 and ARF5 binding (IGRAB) domain. Two GORAB missense mutations identified in geroderma osteodysplastica patients fall within this IGRAB domain. GORAB carrying the mutation p.Ala220Pro had a cytoplasmic distribution and failed to interact with both, RAB6 and ARF5. In contrast, the p.Ser175Phe mutation displaced GORAB from the Golgi compartment to vesicular structures and selectively impaired ARF5 binding. Our findings indicate that the IGRAB domain is crucial for the Golgi localization of GORAB and that loss of this localization impairs its physiological function in osteoblasts and other matrix producing cells.

Disclosures: *Uwe Kornak, None.*

FR0389

Neonatal High Bone Mass With First Mutation Of the NF-κB Complex:

Heterozygous De Novo Missense (p.Asp512Ser) *RELA* (Rela/p65). Anja L

Frederiksen¹, Martin Larsen¹, Klaus Brusgaard¹, Deborah V Novack², Peter Juel Thiis Knudsen³, Henrik Daa Schroeder¹, Christina Eckhardt¹, William H McAlister², Steven Mumm², Morten Frost¹, Michael Whyte^{*4}.

¹Odense University Hospital, Denmark, ²Washington University School of Medicine, USA, ³University of Southern Denmark, Denmark, ⁴Shriners Hospital for Children, USA

Heritable disorders that feature high bone mass (HBM) are rare. The etiology is typically a mutation(s) within a gene that importantly regulates the differentiation and function of osteoblasts (OBs) positively, or osteoclasts (OCs) negatively. However, the molecular basis is unknown for approximately one-fifth of such entities. NF-κB signaling is a key regulator of bone remodeling and acts by enhancing OC survival while impairing OB maturation and function. The NF-κB transcription complex comprises five subunits. Deletion of the p50 and p52 subunits together causes osteopetrosis (OPT) in mice. However, mutations within the genes that encode the NF-κB complex, including the Rela/p65 subunit, have not been reported in humans. We describe a neonate who died suddenly and unexpectedly and was found at post-mortem to have HBM documented radiographically and by skeletal histopathology. Serum was not available for study. Radiographic changes resembled malignant OPT (see figure), but histopathological investigation showed morphologically normal OCs and evidence of intact bone resorption excluding OPT. Furthermore, mutation analysis was negative for eight genes associated with OPT. Instead, accelerated bone formation appeared to account for the HBM. Subsequently, trio-based whole exome sequencing revealed a heterozygous, de novo, missense mutation (p.Asp512Ser) in exon 11 of *RELA* encoding Rela/p65 that was then validated by bi-directional Sanger sequencing. Five unrelated patients with unexplained HBM did not show a *RELA* defect. Ours is the first report of a mutation within the NF-κB complex in humans. The missense change is associated with neonatal osteosclerosis apparently from *in utero* increased OB function rather than decreased OC action. This finding clarifies the importance for human skeletal homeostasis of the Rela/p65 subunit within the NF-κB pathway, and represents a new genetic cause of HBM.

FR0392

Appendicular lean mass index is associated with estimated bone strength at the distal radius and distal tibia in middle-aged and older adults. Jenna Gibbs¹, Lora Giangregorio¹, Andy Wong², Robert Josse³, Angela Cheung⁴.
¹University of Waterloo, Canada, ²University Health Network Osteoporosis Program, Canada, ³St. Michael's Hospital-University of Toronto, Canada, ⁴University Health Network-University of Toronto, Canada

Appendicular lean mass index (appendicular lean mass (kg) corrected by height squared (m²), ALMI) is widely used as the defining parameter of low muscle mass indicative of sarcopenia and is positively correlated with areal bone mineral density measured by dual energy X-ray absorptiometry (DXA). However, the association between ALMI and estimated bone strength measured by high-resolution peripheral quantitative computed tomography (HRpQCT) requires further investigation. Purpose: To determine whether there is an association between ALMI and estimated bone strength outcomes at the distal radius and distal tibia in middle-aged and older adults. Methods: Secondary data analysis of 197 adults (70 men and 127 women; age range 40-91 years) from the Canadian Multicentre Osteoporosis Study Toronto cohort was conducted. Sociodemographic, medical history, and medication characteristics were obtained by an in-person interviewer-administered questionnaire. Height and weight were measured. Total body DXA scans were performed to determine appendicular lean mass. HRpQCT scans were performed to assess bone microarchitecture at the distal radius and distal tibia. Finite element analysis was used to estimate failure load and ultimate stress from HRpQCT scans. Bivariate and multivariable linear regression analyses were used to examine the association between ALMI and bone strength outcomes. Results: Participants were a mean \pm SD age of 69.5 \pm 10.3 yr and had a mean \pm SD body mass index of 27.95 \pm 4.95 kg/m² and ALMI of 7.31 \pm 1.31 kg/m². ALMI was positively associated with failure load ($b=337.83$, SE=28.25, $p<0.001$ and $b=764.58$, SE=58.06, $p<0.001$) and ultimate stress ($b=2.17$, SE=0.47, $p<0.001$ and $b=2.00$, SE=0.42, $p<0.001$) at the distal radius and distal tibia, respectively. After adjusting for age, sex, prior fracture, calcium supplementation, estrogen replacement, osteoporosis medication use, and glucocorticoid use, ALMI explained 63.2% (F=41.6, $p<0.001$) and 57.7% (F=32.9, $p<0.001$) of the variance in failure load and 16.0% (F=5.5, $p<0.001$) and 15.8% (F=5.4, $p<0.001$) of the variance in ultimate stress at the distal radius and distal tibia, respectively. Conclusions: Our findings demonstrate that ALMI is a moderately strong positive correlate of failure load and may contribute to the preservation of bone strength. Future prospective studies are necessary to confirm the associations among ALMI, estimated bone strength, and incident fragility fractures.

Disclosures: Jenna Gibbs, None.

This study received funding from: CIHR Senior Investigator Award (A. Cheung); CIHR New Investigator Award, Canadian Foundation of Innovation, Ontario Ministry of Research and Innovation- Early Researcher Award (L. Giangregorio)

FR0397

Aging and caloric restriction significantly alter the microRNA cargo of exosomes and microvesicles in the bone marrow microenvironment. Colleen Davis¹, Amy Dukes¹, Sadanand Fulzele¹, Xingming Shi¹, William Hill¹, Carlos Isaacs¹, Yutao Liu¹, Mark Hamrick². ¹Georgia Regents University, USA, ²Georgia Health Sciences University, USA

Exosomes are small (40-100 nm) and microvesicles are larger (>100 nm) membrane-derived extracellular vesicles (EVs) that are released into the extracellular space by a variety of cell types. EVs derived from human bone marrow stromal cells (BMSCs) have been found to be enriched in microRNAs (miRNAs), and microvesicle- and exosome-derived transport of miRNAs is thought to represent a novel cellular and molecular pathway for epigenetic reprogramming of target cells. We tested the hypothesis that aging may contribute to bone loss by altering the microRNA profile of bone-derived EVs, and that caloric restriction might have a protective effect on the skeleton by suppressing these age-induced changes. We isolated EVs from bone marrow of young mice (3-4 mos) and aged mice (22-28 mo) fed ad-libitum and on caloric restriction using ExoQuick precipitation and centrifugation. Relative size and concentration of these extracellular vesicles was analyzed using nanoparticle tracking analysis (ZetaView), and the microRNA profile of the EVs assessed using microarray. These data indicate that the concentration and size distribution of EVs is similar between the young and aged mice; however, the miRNA profile differs significantly between the two age groups. Specifically, the microRNAs miR-141, miR-19b, and miR-183 are increased significantly in the aged mice, as assessed using either microarray or realtime PCR. Importantly, these miRNAs have been demonstrated previously to play key roles in suppressing osteogenesis and inducing cellular senescence. Caloric restriction (CR) is known to extend lifespan in vertebrates, and while CR inhibits bone mineral accrual during growth it can actually attenuate bone loss with aging. Our PCR data showed that CR can reverse the increased expression of miR-141, -19b, and -183 more than two-fold compared to aged mice fed libitum. Confocal imaging of BMSCs treated with labeled EVs demonstrate that BMSCs show uptake of EVs, indicating that exosomes and microvesicles are likely to play an important role in cell-cell communication within the bone marrow microenvironment. Moreover, changes in the microRNA cargo of these EVs with age may contribute to decreased bone formation and bone loss.

Disclosures: Mark Hamrick, None.

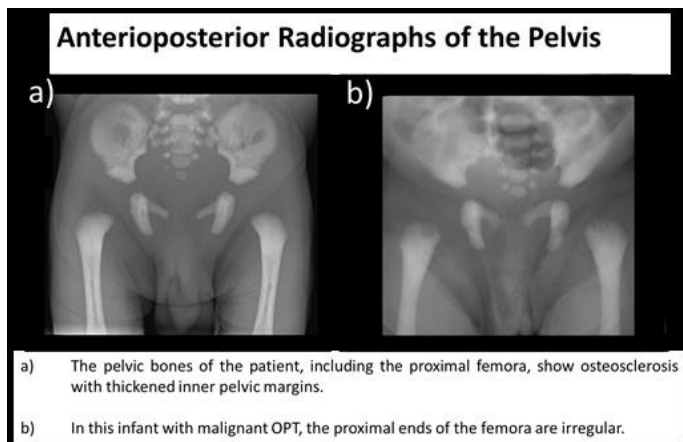


Figure 1

Disclosures: Michael Whyte, None.

FR0390

Advancing Muscle Measurement for Sarcopenia Assessment. Bjoern Buehring¹, Ellen Fidler², Yosuke Yamada³, Jessie Libber², Diane Krueger², Shubha Shankaran⁴, Gregg Czerwiec⁴, Chancy Fessler⁴, William Evans⁴, Scott Turner⁴, Marc Hellerstein⁴, Dale Schoeller⁵, Neil Binkley². ¹University of Wisconsin, Madison, USA, ²Osteoporosis Clinical Research Program, University of Wisconsin - Madison, Madison, USA, ³National Institute of Health & Nutrition, Japan, ⁴KineMed, Inc., USA, ⁵Department of Nutritional Sciences, University of Wisconsin-Madison, USA

Sarcopenia (SP), the age related decline in muscle mass and function, is common and associated with falls and fractures. Muscle function predicts adverse outcomes better than does muscle mass, possibly due to limitations of current clinically available mass assessment methods. Specifically, DXA measured lean mass is largely water, both intra- and extracellular. Extracellular water does not decline with advancing age thereby blunting the ability to detect age-related muscle loss. It is likely that newer mass methodologies, e.g., bioelectric impedance spectroscopy (BIS) and creatine (*methyl-d*₃) dilution (D₃-C) provide more accurate mass assessment. Here, we hypothesized that BIS and D₃-C measured muscle mass will better correlate with muscle function than does DXA measured lean mass.

In this ongoing study, muscle function and mass assessments were performed in 20 community dwelling individuals age 70+. Grip strength, gait speed, timed up and go (TUG), and chair rise time were assessed in standard manner. Jumping mechanography (JM) was used to measure weight-corrected jump power. DXA body composition was obtained using a GE Lunar iDXA, BIS with an Impedimed SFB7 device and D₃-C was administered orally. Descriptive statistics and linear correlations between total lean/muscle mass and functional tests were performed.

This preliminary analysis included 17 women and 3 men, mean age 81.8 \pm 6.3. Total body lean mass [mean (SD)] by DXA was 38.9 (7.0) kg, BIS total body intracellular water (ICW) was 16.6 (3.2) kg and D₃-C total muscle mass 20.6 (5.5) kg. Correlations between DXA lean mass, BIS and D₃-creatine measured muscle mass were good (R²-values ~0.82). Grip strength was highly correlated with D₃-C measured mass (R² = 0.60) and also with BIS and DXA (R² = 0.49 and 0.39 respectively). The other functional tests were not significantly related to mass. A marker of muscle composition/quality, the BIS leg ICW/total leg water ratio correlated with gait speed, jump power and TUG (R² = 0.29 – 0.68).

In conclusion, these preliminary data suggest that advances in measurement of muscle mass and quality, i.e., D₃-C and BIS, will likely improve the correlation with functional status in older adults. Including BIS and D₃-C in larger studies of adverse health outcomes e.g., falls and fractures, are needed for validation. These methods have potential to improve clinical assessment of muscle mass/quality and thus become an integral part of sarcopenia diagnosis and treatment.

Disclosures: Bjoern Buehring, Kinemed Inc

This study received funding from: GE Lunar and Kinemed, Inc.

FR0399

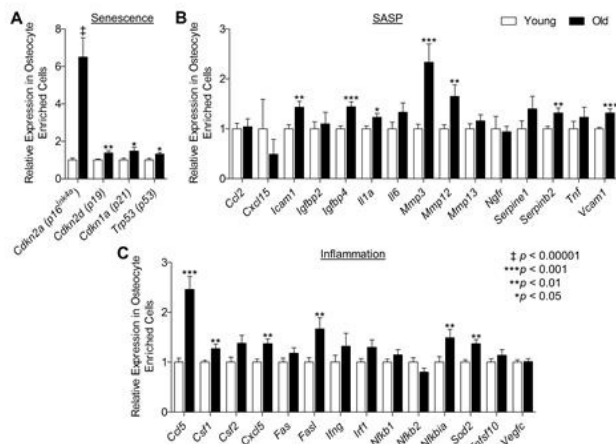
Identification of Senescent Cells in the Bone Microenvironment: A Key Role for Osteocytes in Skeletal Aging. Joshua Farr*, David Monroe, Matthew Drake, Daniel Fraser, Tamara Tchkonja, Nathan LeBrasseur, James Kirkland, Sundeep Khosla, Mayo Clinic, USA

Cellular senescence is a fundamental mechanism by which cells cease dividing and undergo distinct phenotypic alterations, characterized by upregulation of *p16^{Ink4a}* (a robust biomarker and principle mediator of senescence) and secretome changes. Senescent cells accumulate in multiple tissues with aging where they secrete pro-inflammatory factors and matrix remodeling proteins. Accordingly, they have been hypothesized to promote degenerative pathologies, including osteoporosis. Thus, senescent cells and their senescence-associated secretory phenotype (SASP) are increasingly recognized as promising therapeutic targets. However, it is unclear which cell type(s) in the bone microenvironment is most prone to senescence with aging.

Thus, from young (6-month) and old (24-month) mice, we measured expression of senescence, SASP and pro-inflammatory markers *in vivo* via qPCR in highly enriched preparations of B cells, T cells, myeloid cells, osteoprogenitors, osteoblasts and osteocytes, all rapidly isolated using novel approaches without *in vitro* culture.

In both young and old mice, *p16^{Ink4a}* was not expressed in B cells, T cells, osteoblasts or osteoprogenitors. With aging, however, *p16^{Ink4a}* expression increased markedly (+6.5-fold, $p < 0.00001$; Fig. A) in the osteocyte-enriched fraction, as did other senescence mediators (*p19*, *p21*, *p53*, all $p < 0.05$; Fig. A). These increases correlated with higher abundance of an *in vivo* senescence biomarker (senescence-associated β -galactosidase). Corresponding with this age-associated accumulation of senescent osteocytes, were significant increases in the expression of multiple SASP (Fig. B) and pro-inflammatory (Fig. C) markers in the old vs young osteocyte fractions. Finally, several of these same SASP and pro-inflammatory markers were dramatically upregulated (>30-fold) in myeloid cells with aging.

When interpreted in the context of accumulating evidence demonstrating osteocyte control of myeloid lineage cells (e.g., osteocyte RANKL production leading to osteoclast development from myeloid progenitors), our data point to the provocative hypothesis whereby with aging, a subset of osteocytes become senescent and produce a SASP signal that is communicated to neighboring myeloid lineage cells. These myeloid lineage cells may in turn amplify this signal, resulting in excessive production and secretion of pro-inflammatory cytokines and chemokines, thereby creating a toxic local microenvironment that may contribute to age-related bone loss.



Figure

Disclosures: Joshua Farr, None.

FR0403

Requirement of nitric oxide in bone development and homeostasis informed by genetic deficiency of argininosuccinate lyase. Zixue Jin*, Jordan Kho, Monica Grover, Brian Dawson, Ming-Ming Jiang, Yuqing Chen, Terry Bertin, Brendan Lee, Baylor College of Medicine, USA

Although nitric oxide (NO) donors have been shown to have the potential to increase bone density, the effect is dependent on many factors and recent studies suggest NO may exhibit biphasic function on bone formation. The precise mechanism of NO regulation of bone development and homeostasis is unclear due to complexity of animal models. NO is enzymatically produced by three nitric oxide synthases (NOS1,2, however, analyses have been limited by the potential redundancy of the three NOS isoforms. Argininosuccinate lyase (ASL) is the only mammalian enzyme capable of generating arginine, the sole precursor for NOS-dependent NO synthesis. Moreover, we recently showed that it is also required for channeling extracellular L-arginine to NOS for NO production. Hence, deletion of ASL leads to a cell autonomous deficiency of NOS-dependent NO production due to combined loss of

endogenous arginine production and extracellular arginine channeling. As such, it serves as a powerful model for NOS-dependent NO production in biological processes. To study NO function in bone development and remodeling, we generated novel mouse models with conditional deficiency of ASL in osteoblastic lineage cells. Interestingly, we found that early deletion of ASL in osteoblasts using *ostx1-Cre* mice (*Asl^{flox/flox} osx-Asl cKO*) led to high bone mass. In contrast deletion of ASL in more mature osteoblasts using mouse type I collagen *Cre* mice (*Asl^{flox/flox} colla1-Asl cKO*) led to low bone mass. Mechanistically, we found that *Osx-Asl cKO* mice had dramatically decreased expression of RANKL, thereby reducing bone resorption. In contrast, *colla1-Asl cKO* mice showed suppressed bone formation with down-regulation of bone formation markers such as *Runx2*, *Osterix* and *Colla1*. Furthermore, *ex vivo* osteoblast differentiation was also decreased in *colla1-Asl cKO* mice compared with WT mice. In the context of postmenopausal osteoporosis, we found *colla1-Asl cKO* were resistant to ovariectomy (OVX) induced bone loss. This suggests that NO down-regulation may be a mechanism for estrogen deficiency induced bone loss. In conclusion, we established new mouse models to study NO function in bone by conditional deletion of ASL in osteoblastic cells. Our findings reveal that osteoblast autonomous NO depletion has biphasic and stage-dependent effects on bone formation and bone resorption, respectively.

Disclosures: Zixue Jin, None.

FR0404

A transcription factor *Zfhx4* functions as a transcriptional platform for Osterix during endochondral ossification. Eriko Nakamura*, Kenji Hata², Michiko Yoshida², Tomohiko Murakami², Yoshifumi Takahata², Makoto Abe³, Satoshi Wakisaka³, Toshiyuki Yoneda⁴, Riko Nishimura⁵. ¹Osaka University, Japan, ²Osaka University Graduate School of Dentistry, Dep Mol Cell Biochemistry, Japan, ³Osaka University Graduate School of Dentistry, Dep Oral Anat Dev Biol, Japan, ⁴Indiana University School of Medicine, USA, ⁵Osaka University Graduate School of Dentistry, Japan

Several transcription factors, including *Sox9*, *Runx2*, and *Osterix* play critical role in endochondral ossification. Considering the complex but harmonious regulation in endochondral ossification, it is possible that unknown transcription factors are involved in this biological event. To address this, we performed microarray analyses using mouse limb bud cells and isolated a novel transcription factor *Zfhx4* containing 4 homeobox and 22 zinc finger domains. *Zfhx4* is putatively proposed to be responsible for the 8q21.11 Microdeletion Syndrome, characterized by micrognathia, camptodactyly, and syndactyly. We first generated the *Zfhx4* knockout (KO) mice and examined the phenotype. *Zfhx4* KO mice died of respiratory failure within a day after birth. *Zfhx4* KO mice exhibited trivertebra thoracic cavity, malformation of skull and proximal skeletal elements and cleft palate. Histological analyses and *in situ* hybridization analyses indicated that endochondral ossification was arrested at hypertrophic stage in the *Zfhx4* KO mice. Although differentiation of chondrocytes into resting, proliferating and hypertrophic chondrocytes seemed normal, calcification and degradation of cartilage matrices was markedly suppressed in the *Zfhx4* KO mice. In addition, *MMP13* expression was dramatically down-regulated in the femur of *Zfhx4* KO mice at E15.5. Because these findings are similar to phenotype observed in the cartilage-specific conditional *Osterix* KO mice, we next examined interaction between *Zfhx4* and *Osterix*. Fluorescent imaging analyses showed co-localization of *Zfhx4* with *Osterix*, but not with *Runx2*. Co-immunoprecipitation experiments also indicated the physical association of *Zfhx4* with *Osterix*. Moreover, overexpression of *Zfhx4* up-regulated the *MMP13* gene promoter, which is one of the direct targets of *Osterix*. These results suggest that *Zfhx4* is a critical transcriptional factor that interacts with *Osterix* and regulates the late stage of endochondral ossification. Thus, *Zfhx4* seems to function as a transcriptional platform for *Osterix*.

Disclosures: Eriko Nakamura, None.

FR0405

AP-1 factor interacts with *Sox9* during mammalian chondrocyte hypertrophy. Xinjun He¹, Shinsuke Ohba², Hironori Hojo¹, Andrew McMahon¹. ¹University of Southern California, USA, ²University of Tokyo, Japan

Sox9 is essential for chondrocyte specification and differentiation. Despite extensive genetic and biochemical studies, the interplay and interactions of *Sox9* in the progression of chondrocyte development is not well understood. Our previous study on chromatin immunoprecipitation and sequencing (ChIP-seq) of *Sox9* in neonatal mouse rib chondrocyte revealed a *Sox9* regulated network of chondrocyte enhancers (see presentation by Ohba et al.). Interestingly, in addition to the expected *de novo* recovery of a *Sox9* binding sequence through motif analysis, analysis of the ChIP-seq data also demonstrated a highly significant enrichment of an AP-1 factor-binding motif in the *Sox9* ChIP-seq dataset. The AP-1 factor comprises Fos and Jun-related family members. Expression studies revealed localized expression of *Jun* and *Fos2* (a Fos-relative) overlapping *Sox9* cells in the proximal prehypertrophic/early hypertrophic subset of the *Coll10a1*+ hypertrophic chondrocytes, suggesting that AP-1 factor and *Sox9* may co-regulate chondrocyte gene activity in this segment of the growth plate. Though the action of *Sox9* in hypertrophy is controversial, *Sox9* levels are highest in prehypertrophic chondrocytes and *Sox9* removal specifically within this population blocked hypertrophic chondrocyte development. Clearly, *Sox9* is essential for continued progression of chondrocytes to maturing hypertrophic chondrocytes.

To directly determine AP-1 complex engagement in the hypertrophic process, we performed ChIP-seq for Jun (c-Jun). Intersection of Sox9 with Jun binding data showed that Jun is co-bound at most Sox9 interacting cis-regulatory modules. Further, the strength of interaction as determined by recovery of sequence reads was highly correlated and co-bound regions were strongly associated with skeletal development-related genes. These data suggest AP-1 factors act in conjunction with Sox9 to regulate chondrocyte hypertrophy. Consistent with this view, knockdown or inhibition of AP-1 factors in chondrocytes attenuated Sox9 controlled endochondral hypertrophy, supporting the argument that AP-1 complexes modulate Sox9 function during this process. Functional analysis identified Sox9 and AP-1 binding motifs in a *Coll10a1* distal enhancer responsible for Sox9 and AP-1 regulation of *Coll10a1* expression in hypertrophic chondrocytes. These data, together with biochemical studies of Sox9 and AP-1 factor interactions with their targets and each other, lead to complex model of target output to be presented at the meeting.

Disclosures: Xinjun He, None.

FR0406

Bardet-Biedl Syndrome 3 Is Involved in the Development of Cranial Base. Makiri Kawasaki^{*1}, Tadayoshi Hayata², Yayo Izu¹, Yoichi Ezura¹, Masaki Noda¹. ¹Department of Molecular Pharmacology, Medical Research Institute, Tokyo Medical & Dental University, Japan, ²Department of Biological Signaling & Regulation, Faculty of Medicine, Project Office of Ph.D program in Life Science Innovation, Japan

Craniofacial dysmorphology presented in various genetic disorders could be a key for diagnosing the disease, and may also become a key for understanding its etiology. The patients of a typical ciliopathy, Bardet-Biedl syndrome (BBS) manifest characterized craniofacial abnormalities such as high-arched palate, mid-facial hypoplasia and hypo-odontia. However, the mechanisms involved in such phenotype have not been investigated enough. Here, we aimed to reveal morphological phenotype of the BBS mouse model by focusing on developmental craniofacial abnormalities. BBS3 is one of the causative genes for human BBS. Thus, we analyzed skeletal phenotype of the BBS3 knockout (KO) mice at E18.5. 3D micro-CT analysis revealed hypoplasia of basi-sphenoid in the midline, a loss of pre-sphenoid, and dysplasia of distal maxillae with 100% penetrance in Bbs3-KO embryos. Skeletal preparation revealed cleaved intrasphenoidal / sphenoid-occipital synchondrosis. Furthermore, intrasphenoidal synchondrosis was shortened longitudinally. Tooth germs of incisors were lost in Bbs3-KO embryos with nearly 100% penetrance. Histological analysis demonstrated that while the binate prechordal cartilages were formed almost normally, they were not fused in the midline and space between the cartilages was filled with fibroblastic cells in the cranial base of Bbs3-KO embryos. Mandibles, calvarias and occipital bones were morphologically normal. Our results demonstrate that Bbs3-KO embryos present severe defects in cranial base midline constructs. Impaired fusion of prechordal cartilages antecedent to the mineralization may be the cause. In addition, since skeletal elements constructing the craniofacial region are mostly derived from cranial neural crest cells (CNCCs), and their migration, proliferation and differentiation are tightly regulated by sonic hedgehog (Shh) signaling that takes place in primary cilia, our results may suggest that impaired Shh signaling due to dysfunction of the cilium in CNCCs may be the cause of midface dysplasia.

Disclosures: Makiri Kawasaki, None.

FR0407

Bone-anabolic effects of histone methyltransferase EZH2 inhibition. Amel Dudakovic^{*1}, Emily Camilleri¹, Fuhua Xu¹, Scott Riester¹, Meghan McGee-Lawrence², Elizabeth Bradley¹, Christopher Paradise¹, Roman Thaler¹, Eric Lewallen¹, John Hawse¹, Malavannan Subramaniam¹, David Deyle¹, Noelle Larson¹, David Lewallen¹, Gary Stein³, Martin Montecino⁴, Jennifer Westendorp¹, Andre van Wijnen¹. ¹Mayo Clinic, USA, ²Georgia Regents University, USA, ³University of Vermont Medical School, USA, ⁴Universidad Andres Bello, Chile

Perturbations in skeletal development and bone degeneration can result in reduced bone mass and quality leading to greater fracture risk. Bone loss is mitigated by bone protective therapies, but there is a clinical need for new bone-anabolic agents. Here, we investigated if epigenetic enzymes regulating osteoblast differentiation can be leveraged for bone stimulatory applications. Expression screening for epigenetic regulators during osteoblast differentiation identified the histone methyltransferase Enhancer-of-Zeste homolog 2 (EZH2) as a potential target. Using loss-of-function models and pharmacologic inhibitors, we show that EZH2 not only controls early stages of mesenchymal cell commitment as reported but also maturation of pre-committed osteoblasts. Next-generation sequencing of mRNA (mRNASeq) and real-time quantitative PCR profiling establish that EZH2 inactivation promotes expression of bone-related gene regulators and extracellular matrix proteins. Mechanistically, enhanced gene expression is linked to decreased Histone 3 lysine 27 tri-methylation (H3K27me3) near transcriptional start sites in genome-wide chromatin immunoprecipitation analyses (ChIPSeq). Conditional genetic loss of Ezh2 in uncommitted mesenchymal cells (Prrx1-Cre) results in multiple skeletal patterning and bone defects, including shortened forelimbs, craniosynostosis and clinodactyly. Histological

analysis and mRNASeq profiling suggests that these effects are attributable to growth plate abnormalities and premature cranial suture closure due to precocious maturation of osteoblasts. Deletion of functional Ezh2 in the osteoblast lineage (Ox-Cre) generates normal appearing mice with a low bone mass phenotype at weaning (3 weeks), while the bone parameters become less prominent in early adulthood (8 weeks). Daily administration (five weeks) of an EZH2 inhibitor increases cortical bone density of female adult wild type mice. Strikingly, daily injection (six weeks) prevents cortical bone loss in an estrogen-deficient mammalian model (ovariectomy) for osteoporosis. Thus, although EZH2 is required for early skeletal patterning and development, inhibition of this enzyme has bone-anabolic and osteoprotective potential in adults.

Disclosures: Amel Dudakovic, None.

FR0408

Deletion of the Prolyl Hydroxylase Domain-containing Protein 2 (PHD2) Gene in Chondrocytes Promotes Endochondral Bone formation by Elevating HIF-1 α Signaling. Shaohong Cheng^{*1}, Weirong Xing², Sheila Pourteymoor², Catrina Alarcon², Subburaman Mohan². ¹VA Loma Linda Health Care Systems, USA, ²Jerry L Pettis VA Medical Center, USA

Endochondral bone formation (EBF) initiates from differentiation and ossification of chondrocytes at the avascular growth plates of long bones. The hypoxic growth plate cartilage requires hypoxia-inducible transcription factors (HIFs)- mediated pathways to maintain chondrocyte survival and differentiation. HIF protein is closely regulated by prolyl hydroxylase domain-containing protein 2 (Phd2) mediated proteasomal degradation. To determine the role of Phd2 in chondrocytes in regulating EBF, we conditionally disrupted the Phd2 gene in chondrocytes by crossing Phd2 floxed and Col2a1-Cre mice, and found massive increases in the trabecular bone mass of the long bones (145%) and lumbar vertebra (53%) of 12 week old Phd2 conditional knockout (cKO) mice. Trichrome staining of bone sections revealed increased bone in the primary and secondary spongiosa of cKO mice. Dynamic histomorphometry revealed that while the mineral apposition rate was unchanged, the bone formation rate was increased by 77% (p<0.01) due to a 62% increase (p<0.05) in osteoblast (OB) number in the trabeculae of cKO mice, measured as Osterix-positive cells. Bone resorption was decreased by 16% (p<0.05) in the cKO mice measured by Oc.S/B.S. (osteoclast surface per bone surface). To determine the mechanism for increased EBF, we measured expression levels of genes involved in the EBF process in the growth plates by quantitative RT-PCR. Expression levels of chondrocyte (Sox9, Col2 and aggrecan) as well as OB markers (ALP and BSP) were increased significantly in the cKO growth plate. Since the HIF pathway are the major target of Phds, we next examined HIF-1 α and HIF-2 α expression by immunohistochemistry, and detected a marked increase of HIF-1 α protein in the hypertrophic chondrocytes, while the HIF-2 α protein level was not changed in the cKO growth plate. Accordingly, expression levels of HIF-1 α targets, VEGF, Epo, and glycolytic enzymes (Glut1, Ldha1, Pdk1, Pkg1) were significantly upregulated in the growth plates of cKO mice compared to WT mice. This expression profile was recapitulated in vitro upon adenoviral Cre-mediated knockdown of Phd2 expression in chondrocytes-derived from Phd2 floxed mice. Based on our findings, we conclude that Phd2 deficiency leads to upregulation of HIF-1 α signaling and elevation of VEGF, Epo expression and glycolysis to promote chondrocyte survival and differentiation into osteoblasts and, thereby, EBF.

Disclosures: Shaohong Cheng, None.

FR0410

ER Stress Signaling Transducer IRE1 α Links ER Stress to Canonical Wnt Signaling in Regulating Postnatal Bone Development and Homeostasis. Shankar Revu^{*1}, Kai Liu¹, Konstantinos Verdelis¹, Alejandro Jose Almarza¹, Donna Stolz², Hong-Jiao Ouyang³. ¹School of Dental Medicine, University of Pittsburgh, USA, ²School of Medicine, University of Pittsburgh, USA, ³University of Pittsburgh, USA

The inositol-requiring enzyme 1 α (IRE1 α)/ X-box binding protein 1s (XBP1s) pathway is an evolutionarily conserved endoplasmic reticulum (ER) stress signal transduction pathway required for the development of secretory cells and organs, such as pancreatic β cells and salivary glands. However, it remains unknown whether IRE1 α is required for bone development and homeostasis. Recently, our laboratory found that the activation of IRE1 α /XBP1s signaling is a physiological event intrinsic to osteoblast differentiation and bone development. This prompted us to generate mice lacking osteoblast-specific IRE1 α (CKO), and their wild type littermates (WT), by breeding *Irel1^{Flox/Flox}* mice with *Osterix-Cre* mice. It was observed that IRE1 α -deficient osteoblasts exhibited exacerbated ER stress and consequently experienced activation of the PRKR-like endoplasmic reticulum kinase (PERK)/eukaryotic translation-initiation factor 2 α subunit (EIF2 α) signal transduction pathway, both in vivo and in vitro, compared with WT counterparts, as shown by immunohistochemical (IHC) staining and Western blot analysis for phosphorylated PERK (p-PERK) and EIF2 α (p-EIF2 α). Furthermore, IRE1 α CKO mice displayed osteoporosis/osteopenia with increased bone marrow fat, recapitulating the bone phenotypes resulting from loss-of-function of canonical Wnt signaling in mice. Consistent with this notion, IRE1 α -deficient osteoblasts had a reduced steady-state protein level of β -Catenin, a transcription factor central for canonical Wnt signaling, both in vivo and in

vitro, compared with WT counterparts, as shown by IHC staining and Western blot analysis, respectively. It was observed that IRE1 α deficiency did not affect the gene expression of β -Catenin in osteoblasts, both in vivo and in vitro, as shown by quantitative real-time PCR (qRT-PCR) analysis. Instead, IRE1 α deficiency resulted in compromised protein synthesis of β -Catenin in osteoblasts via its induction of p-EIF2 α , an inhibitor for global protein synthesis, as shown by ³⁵S pulse labeling assays. Taken together, our studies identified the ER stress signaling transducer IRE1 α as a novel regulator for postnatal bone development and homeostasis. In addition, we discovered that the p-EIF2 α -mediated regulation of β -Catenin protein synthesis is a novel molecular mechanism, by which ER stress affects canonical Wnt signaling in regulating postnatal bone development and homeostasis.

Disclosures: Shankar Revu, None.

FR0411

Matrix vesicle-mediated initiation of skeletal mineralization depends on PHOSPHO1 and PIT-1 function. Manisha Yadav*¹, Massimo Bottini², Pia Kuss², Esther Cory³, Robert Sah³, Laurent Beck⁴, Colin Farquharson⁵, Jose Luis Millan². ¹Sanford-Burnham Medical Research Institute, USA, ²Sanford Children's Health Research Center, Sanford-Burnham Medical Research Institute, USA, ³Department of Bioengineering, University of California San Diego, USA, ⁴Centre for Osteoarticular & Dental Tissue Engineering (LIOAD), Nantes, Cedex, France, France, ⁵The Roslin Institute, The University of Edinburgh, Easter Bush, Roslin, Midlothian, EH25 9RG, United Kingdom

We have previously shown that ablation of either the Phospho1 or Alpl gene, encoding PHOSPHO1 and tissue-nonspecific alkaline phosphatase (TNAP) respectively, lead to hyperostoidosis but that their chondrocyte- and osteoblast-derived matrix vesicles (MVs) are able to initiate mineralization. In contrast, the double ablation of Phospho1 and Alpl completely abolishes initiation and progression of skeletal mineralization. We argued that MVs initiate mineralization by a dual mechanism: PHOSPHO1-mediated intravesicular generation of Pi and phosphate transporter-mediated influx of Pi generated perivesicularly. To test this hypothesis, we generated mice with col2a1-driven cre-mediated ablation of Pit1 alone or in combination with a Phospho1 gene deletion. Pit1col2/col2 mice did not show any major phenotypic abnormalities, while severe skeletal deformities were observed in the [Phospho1^{-/-}; Pit1col2/col2] double knockout mice that were more pronounced than those observed in the Phospho1^{-/-} mice. Histological analysis of 15-day-old [Phospho1^{-/-}; Pit1col2/col2] bones showed growth plate abnormalities with a shorter hypertrophic chondrocyte zone and extensive hyperostoidosis. The [Phospho1^{-/-}; Pit1col2/col2] skeleton displayed significantly decreases in BV/TV%, trabecular number and bone mineral density with increased trabecular separation for both tibia and femur compared to Phospho1^{-/-} mice. Three-point bending analysis also showed that [Phospho1^{-/-}; Pit1col2/col2] bones exhibit decreased stiffness, decreased strength, and increased post-yield deflection. By atomic force microscopy we found that approximately 70% of [Phospho1^{-/-}; Pit1col2/col2] MVs were empty in comparison to about 20-30 % empty MVs for the WT, Phospho1^{-/-} and Pit1col2/col2 MVs. We also found a significant decrease in the number of MVs produced by both Phospho1^{-/-} and [Phospho1^{-/-}; Pit1col2/col2] chondrocytes. These data prove the involvement of Pit-1 function in the initiation of skeletal mineralization and it provides compelling evidence that PHOSPHO1 mediates MV biogenesis.

Disclosures: Manisha Yadav, None.

FR0412

Newly Identified FGFR2 Isoform Modulates FGF10-FGFR Signaling During Osteochondrogenesis. Kazuko Kagawa*¹, Hirotaka Yoshioka², Saki Okita³, Koh-ichi Kuremoto¹, Yuichiro Takei², Tomoko Minamizaki², Kotaro Tanimoto³, Kazuhiro Tsuga¹, Yuji Yoshiko². ¹Department of Advanced Prosthodontics, Hiroshima University Institute of Biomedical & Health Sciences, Japan, ²Department of Calcified Tissue Biology, Hiroshima University Institute of Biomedical & Health Sciences, Japan, ³Department of Orthodontics & Craniofacial Developmental Biology, Hiroshima University Institute of Biomedical & Health Sciences, Japan

Fibroblast growth factor (FGF) family consists of 22 members and plays diverse roles in angiogenesis, wound healing, embryonic development, and endocrine signaling. FGF activities are mediated by receptor tyrosine kinases and implicated in skeletal growth and its related disorders. Gain-of-function mutations in a common extracellular domain of FGF receptor (FGFR) 2 isoforms (type b and c) cause craniosynostosis and chondrodysplasia syndromes. FGF10, a major ligand for FGFR2b, is secreted from mesenchymal cells and regulates epithelial-mesenchymal interactions. Meanwhile, FGF10 regulates early chondrogenesis, and abrogation of FGF10 in an Apert syndrome mouse model rescues skeletal defects. Thus, FGF10-FGFR signaling during osteochondral development remains unclear. We generated transgenic mice expressing mouse FGF10 under the control of doxycycline. Fetuses were exposed to doxycycline from embryonic day 12.5, and FGF10 transgenic (TG) pups were compared with control littermates. Similar to FGF10- and FGFR2b-deficient mice, TG mice died shortly after birth. TG pups were smaller in size, while

limb and vertebral deformities were worthy of little attention. These mice showed craniomaxillofacial dysmorphology including rostrocaudal hypoplasia, developmental retardation in mandibular condylar cartilage, cleft palate and so on. Expression profiling of *Fgfr* genes in multiple tissues and cells suggested the presence of the additional alternative RNA splicing isoform of *Fgfr2* (*Fgfr2bc*). Among tissues and cells tested, this isoform was expressed in particular tissues/cells including mandibular condylar cartilage and ATDC5 cells. The predicted translation product of *Fgfr2bc* appears to include both exon 8- and 9-encoded residues (type b and c, respectively) and lack membrane-spanning and tyrosine kinase domains, suggesting a soluble form of FGFR2b (sFGFR2). sFGFR2 was identified in the conditioned media in ATDC5 cells and overexpressing sFGFR2 increased cell proliferation, suggesting that sFGFR2 may act as a decoy receptor for FGFs. Thus, a large amount of FGF10 may trap sFGFR2 and allow for enhancing other FGF-FGFR signaling pathways, with resultant skeletal anomalies in TG mice.

Disclosures: Kazuko Kagawa, None.

FR0413

Sex-related Differences in the Axial Skeletal Development of Newborns and Infants. Skorn Ponrartana¹, Patricia Aggabao¹, Naga Dharmavaram², Carissa Fisher¹, Tishya Wren¹, Vicente Gilsanz*³. ¹Children's Hospital Los Angeles, Keck School of Medicine, University of Southern California, USA, ²Children's Hospital Los Angeles, Keck School of Medicine, University of Southern California, USA, ³Children's Hospital Los Angeles, USA

Compared with boys of the same body mass, healthy prepubertal girls have less musculature and smaller vertebrae – phenotypic differences that account, at least in part, for the variance in vertebral fracture risk among sexes. The purpose of this study was to examine for pre- and early post-natal sex differences in the morphogenesis of the axial skeleton. Using magnetic resonance imaging techniques that allow for fast and reliable determinations of newborn and infant development without the need for sedation, we longitudinally characterized musculoskeletal development in 25 boys and 25 girls at birth, three months, and six months of age.

We found a striking sexual dimorphism in vertebral size at birth; on average, the lumbar vertebral cross-sectional area (CSA) was 9.6% smaller in newborn girls than boys (p=0.0004) – a difference that persisted even after accounting for gestational age, weight, body length, or paraspinal musculature. In contrast, the sexes were monomorphic with regard to paraspinal musculature at birth (p=0.95). As expected, the cross-sectional dimensions of the vertebrae increased during infancy in both sexes. The gains were, however, greater in boys than in girls, which further enhanced the sexual dimorphism in vertebral size. Whereas mean values for vertebral CSA increased from birth to 6 months of age by 54% (SD=10%) in boys, those in girls only increased by 35% (SD=13%); p < 0.0001. Among both sexes, the rate of growth was threefold higher during early infancy than from three to six months of age (32 ± 12% vs 10 ± 9%; p < 0.0001) and closely related to muscle development, consistent with knowledge that neonates experience a "mini-puberty" during the first three months of life. Regression analysis indicated that vertebral growth during early infancy was strongly related to differences in gains in paraspinal musculature (0.22 ± 0.63; p=0.001).

In conclusion, sex has a differential effect on the intrauterine programming of the axial skeleton, while differences in muscle development are key determinants of the sexual dimorphism in skeletal growth during infancy. The strong relations found between bone accrual and increases in muscle mass even in early postnatal life, stress the need for preventive strategies to start in childhood and be geared toward those infants with the smallest vertebrae and highest risk for developing vertebral fractures later in life.

Disclosures: Vicente Gilsanz, None.

FR0414

Suppression of Autophagy by Postnatal FIP200 Deletion Compromises Cortical Bone Development with Minimal Effect on Trabecular Bone Development. Li Wang*¹, Fei Liu². ¹University of Michigan, USA, ²University of Michigan School of Dentistry, USA

Autophagy is a conserved lysosomal-catabolic process, by which superfluous or damaged cellular material is delivered, degraded and then recycled to maintain cellular homeostasis and normal physiology. In previous study, we found that suppression of autophagy by ablation of focal adhesion kinase family interacting protein of 200 kD (FIP200), an essential component of mammalian autophagy, led to severe osteopenia in mice. In that study, FIP200 was deleted in osteoblast from embryonic stage with Osterix-Cre. Autophagy deficient mice had significant early postnatal skeleton growth retardation, which prevented us from concluding to what extent the osteopenic phenotype observed at later stages can be ascribed to the role of FIP200/autophagy at adult stage. To address this, we suppressed osteoblast autophagy in mice from 2 month old to 6 month old (4-month suppression group, male) and from 4 month old to 6 month old (2-month suppression group, female) by inducibly deleting FIP200 using doxycycline-controlled Tet-off Osx-Cre expression system (removed doxycycline food at 2 months of age and 4 months of age respectively). Bone morphology was evaluated in femur and vertebrae by microCT analysis. In contrast to the result from our previous mouse model, postnatal osteoblast autophagy suppression did not result

in notable trabecular BV/TV change in both femur (4 months and 2 months suppression groups) and vertebrae (2 months suppression group). However, we found that the tissue mineral density of trabecular bone had a small (3-5%) but statistically significant decrease ($p < 0.05$ for 4 months suppressing group femurs and 2 months suppression group vertebrae, $p = 0.08$ for 2 months suppression group femurs) in autophagy deficient mice, indicating the compromised bone quality. In both 4 months and 2 months suppression group, the femoral cortical area was significantly decreased (-6.3% and -6.8% respectively). To further determine the effect of autophagy deficiency on cortical bone, we measured the calvarial thickness and found that the calvaria thickness dramatically decreased (-29%, $p < 0.01$) in 4 months but not in 2 months suppression group. In summary, our preliminary data suggest that FIP200/autophagy has overlapping but different roles in bone development during later postnatal stage compared to early postnatal stage. FIP200/autophagy may play more important roles in regulating cortical bone development and remodeling compared to trabecular bone at later postnatal stage.

Disclosures: Li Wang, None.

FR0415

The role of Wnt signal modulator, sFRP4, in bone formation and metabolism.

Ryuma Haraguchi^{*1}, Riko Kitazawa², Yuuki Imai², Sohei Kitazawa².

¹Ehime University Graduate School of Medicine, Japan, ²Ehime university, Japan

Background: Activation of the Wnt signaling pathway leads to the buildup of bone strength and bone mass. Its excessive hyperactivity, however, leads to musculoskeletal tumors and the progression of articular disorders. Secreted Frizzled-related protein 4 (sFRP4) is a member of the secreted Wnt antagonist gene family that adequately fine-tunes its signal activity by direct binding to Wnt-ligands. We have previously reported that bone loss under the oxidative stress of diabetes and aging is related to the suppression of canonical Wnt pathways through the reactivation of sFRP4 gene expression by a unique epigenetic mechanism. To explore the functions of sFRP4 as a balancer molecule for Wnt signal activity in bone development, we engineered an sFRP4 knock-in mouse strain in which the sFRP4 gene locus was replaced by the LacZ reporter gene. In addition to genetic gene inactivation, the generation of the sFRP4-LacZ knock-in mouse provides the additional advantage of the highly sensitive and easy *in situ* detection of LacZ gene expression, for *in vivo* analysis of the gene expression of sFRP4. In this study, we investigated the details of sFRP4 expression patterns during long bone formation and the characteristic features of the bone phenotype in sFRP4-LacZ knock-in mice.

Finding: X-gal staining in sFRP4-LacZ knock-in mice revealed spatial-temporal Sfrp4 expression patterns in the developing limb. Until stage E16.5, LacZ expression was undetectable in limb bud tissues; it then became evident only in a restricted area of the diaphysis at E17.5. At the postnatal and puberty stages, strong LacZ expression was observed on the trabecular bone surface and the periosteum in the long bone shaft. Immunohistochemistry on the X-gal stained tissue sections showed that most of LacZ positive cells were Osterix-positive osteoprogenitor cells and Cathepsin K-positive osteoclasts. μ CT analysis of long bones revealed an increased trabecular BV/TV and bone mineral density, and reduced cortical bone thickness in sFRP4-LacZ $-/-$ mice compared with that in control mice. Histological analysis of sFRP4-LacZ $-/-$ mice trabecular bones confirmed the increased number of osteoprogenitor cells and the reduced number of normal osteoclasts. **Conclusion:** sFRP4 is expressed in dual osteogenic lineages, osteoblastic cells and osteoclasts, in the neonatal and postnatal skeleton. Inactivation of the sFRP4 gene in these cell lineages shows dramatic increase in trabecular bone volume with alteration in skeletal metabolism. These findings raise the possibility that sFRP4 is one of the key molecules that regulate the balance between cortical and trabecular bone volume by efficiently influencing both bone formation and bone absorption directly during long bone development and maintenance.

Disclosures: Ryuma Haraguchi, None.

FR0416

TrkA Signaling by Sensory Nerves is Required for Skeletal Development and Repair.

Ryan Tomlinson^{*1}, Zhi Li¹, Qian Zhang¹, Labchan Rajbhandari¹, Arun Venkatesan¹, David Ginty², Thomas Clemens¹. ¹Johns Hopkins University, USA, ²Harvard University, USA

The development and repair of the skeleton requires inductive signals from multiple cell types, which act in a sequential and hierarchical fashion to program lineage allocation of osteochondral progenitors. Critical to the early stages of this program is the invasion of blood vessels and sensory nerves, which appear simultaneously at sites of incipient bone formation. In contrast to the well-established role of angiogenesis in bone development and repair, relatively little is known about the function of sensory nerves in bone. Since nearly all sensory nerves in bone express TrkA, we first characterized the role of TrkA signaling during endochondral bone development. Using established reporter mice, we show that TrkA expressing sensory neurons of the dorsal root ganglion (DRG) project axons that reach perichondrial bone surfaces adjacent to primary ossification centers by E14, coincident with the appearance of NGF expressing perichondrial cells. To selectively disrupt TrkA signaling, we used mice harboring TrkA-F592A knockin alleles that render the endogenous TrkA kinase sensitive to inhibition by the membrane-permeable molecule 1NMPP1 (Chen X et al. 2005). The efficacy of this approach was confirmed *in vitro* by

demonstrating impaired axonal growth of TrkA-F592A DRG neurons exposed to 1NMPP1 and *in vivo* by reduced TrkA phosphorylation in DRGs from TrkA-F592A mice treated with 1NMPP1. To determine the requirement of TrkA signaling during endochondral bone formation, we analyzed femurs from newborn offspring of heterozygous TrkA-F592A mothers that received 1NMPP1 in their drinking water throughout pregnancy. The inhibition of TrkA signaling during embryogenesis significantly diminished bone volume, reduced innervation density, and decreased vascularity at birth. We also assessed the requirement of TrkA signaling during bone repair by subjecting adult TrkA-F592A mice to an ulnar stress fracture, a regenerative process that incorporates mechanosensation, angiogenesis, and osteogenesis. In this model, inhibition of TrkA signaling severely diminished woven bone formation during healing. Taken together, these studies demonstrate that TrkA signaling is required for normal endochondral bone development and stress fracture repair. We hypothesize that TrkA sensory nerves deliver key signaling molecules that initiate osteoblast lineage commitment and progression while also providing a template for vascular invasion of newly formed bone.

Disclosures: Ryan Tomlinson, None.

SA0001

FGF23 metabolism, a new paradigm for chronic kidney disease. Isabelle Picc*¹, Christopher Washbourne², Holly Nicholls², Jonathan Tang², William D. Fraser². ¹BioAnalytical Facility, University of East Anglia, United Kingdom, ²University of East Anglia- bioanalytical facility, United Kingdom

Introduction: Fibroblast growth factor-23 (FGF23) is a major regulator of phosphate metabolism often elevated in genetic hypophosphataemic disorders (XLH, ADHR) and in chronic kidney disease (CKD). Recent studies have identified relationships between FGF23 and various markers of iron status including ferritin. New assays measuring the intact form of FGF23 have been released.

Objective: To determine the relationship between ferritin and C-terminal and intact FGF23 concentrations in blood.

Method: FGF23 concentrations were measured using the second generation, two-site enzyme-linked immunosorbent assay for either C-terminal or intact FGF23 (immotopics Inc, CA, USA). Ferritin was measured on a COBAS 6000 (Roche Diagnostics, UK). Assay accuracy and precision were monitored using kit controls supplied by the manufacturers.

Results: We observed a weak correlation between measurements of C-terminal and intact FGF23 (Pearson's rho = 0.85 p<0.0001) suggesting that the turnover of FGF23 is not 100% and cleaved fractions can accumulate. We observed no statistically significant correlation of ferritin concentrations with either FGF23 C-terminal or intact. However high concentrations of ferritin were observed in samples showing low concentrations of C-terminal FGF23 (<140RU/mL) and intact FGF23 (<122pg/mL).

Conclusion: Although not statistically significant, we observed a negative relationship between concentrations of ferritin and FGF23 (Pearson's rho =-0.3 and rho = -0.2 for C-terminal and intact FGF23, respectively). A high concentration of C-terminal FGF23 is found in patients with CKD, especially in patients with end-stage renal disease usually regarded as a compensatory response to hyperphosphatemia. We observed a number of patients (16%) with retention of both C-terminal and intact FGF23 associated with low levels of ferritin suggesting that metabolism and/or excretion of FGF23 in CKD patients might be an iron-dependent enzyme mediated mechanism.

Disclosures: Isabelle Picc, None.

SA0002

See Friday Plenary Number FR0002.

SA0003

Sclerostin and FGF-23 Protein Expression in Bone of Patients With Various Stages of Decline in Kidney Function. Florence Lima*, Marie-Claude Monier-Faugere, Hanna W. Mawad, Harmut H. Malluche. University of Kentucky, USA

Renal osteodystrophy occurs in the early stages of chronic kidney disease (CKD) and progresses during loss of kidney function. Sclerostin and FGF-23, both produced by osteocytes, are increased in blood of patients with reduced kidney function. The aim of this study was to analyze the impact of decline in kidney function on sclerostin and FGF-23 protein expression in bone and to study their relationship with bone histomorphometry.

Thirty-six patients underwent anterior iliac crest biopsies after double-tetracycline labeling. Eleven patients were CKD-2, 16 were CKD-3 and 9 were CKD-4 to 5. Fourteen aged-matched patients without CKD were included as controls. Immunostaining was performed on undecalcified bone sections to quantify sclerostin and FGF-23 expression. Bone sections were also evaluated by histomorphometry for bone turnover, mineralization and volume.

Sclerostin expression in bone correlated positively with CKD stages (rho=0.50, P<0.001) with an increase from 3.8- to 5.1-fold starting at CKD-2 compared to those with non-CKD. This increase was progressive and significantly greater in cortical than cancellous bone (Figure 1A).

FGF-23 expression in bone correlated positively with CKD stages (rho=0.55, P<0.001) with an increase from 5.3- to 7.1-fold in patients starting at CKD-2 compared to those with non-CKD. No difference in FGF-23 expression was seen between trabecular and cortical bone (Figure 1B).

Sclerostin expression in bone correlated negatively with parameters of trabecular thickness, osteoid surface (rho=-0.50 and -0.51, respectively; P<0.05), osteoblast and osteoclast numbers and erosion depth (rho=-0.61, -0.60 and -0.60, respectively; P<0.01). FGF-23 bone expression correlated positively with cortical porosity (rho=0.75, P<0.001).

These data show a progressive increase in sclerostin and FGF-23 bone expression associated with decrease in kidney function. This is associated with changes in bone structure (decrease in trabecular thickness, increase in cortical porosity) and bone turnover (osteoblast and osteoclast numbers and erosion depth). These findings suggest that targeting the suppression of sclerostin and/or FGF-23 expression early in the course of loss of kidney function may be of interest to protect bone against renal osteodystrophy.

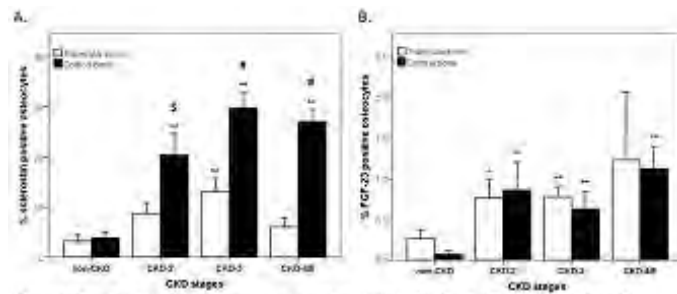


Figure 1-Quantification of positive osteocytes per total osteocyte number for (A) sclerostin and (B) FGF-23. Values are represented by mean and standard errors. * P<0.05 or ** P<0.01 for CKD stages 2 to 5 versus non-CKD. † P<0.05 or ‡ P<0.001 for trabecular versus cortical bone.

Figure 1

Disclosures: Florence Lima, None.

SA0004

Altered RNA Stability And A Gfi1-Induced Epigenetic Switch Regulate Runx2 Repression In Multiple Myeloma-Exposed Pre-Osteoblasts. Juraj Adamik*¹, Wei Zhao², Peng Zhang¹, Quanhong Sun¹, G. David Rodman³, Deborah L. Galson¹. ¹University of Pittsburgh, USA, ²Indiana University, USA, ³Indiana University & Veterans Administration Medical Center, USA

Multiple myeloma (MM) causes osteolytic bone lesions that rarely heal even after therapeutic remission. We reported that the MM-induced pro-inflammatory bone marrow microenvironment causes upregulation of the transcriptional repressor Gfi1 in bone marrow stromal cells (BMSC) via TNF α . Gfi1 represses the key osteoblast (OB) differentiation factor Runx2, resulting in impaired BMSC differentiation into OB. Proliferating pre-OB treated with TNF α or cocultured with 5TGM1 MM cells exhibited a rapid (1.5-3h) decrease in Runx2 mRNA and later (48h) the Runx2 gene became refractory to OB differentiation stimuli even after removal of the TNF α or MM cells. We showed that Gfi1 knockdown in pre-OB did not block the MM-induced rapid decrease of Runx2 mRNA, but it prevented the sustained repression of Runx2 following induction of OB differentiation for 2-4d. We found that the initial Runx2 decline is due to decreased mRNA stability. The Runx2 promoter in MC4 pre-OB cocultured with 5TGM1 MM cells (48h) had reduced activating acetylation (H3K9ac) levels and enhanced heterochromatic methylation (H3K27me3), consistent with decreased expression that stayed refractory to OB differentiation. BMSC from MM patients (3) compared to normals (2) also had decreased levels of H3K9Ac at the Runx2 gene promoter. Further, MM coculture induced binding of Gfi1 to the Runx2 promoter in pre-OB with increased occupancy at 36 and 48h, concomitantly with increased histone deacetylase HDAC1 (erases H3K9ac) and the PRC2 complex methyltransferase subunit EZH2 (adds H3K27me3). Ectopic Gfi1 also bound Runx2 and recruited these histone modifiers. The HDAC1 inhibitor MC1293 prevented Runx2 mRNA suppression in MM treated pre-OB. Interestingly, TNF α inhibited expression of H3K27me3 demethylases JmjC-domain-containing proteins UTX and JMJD3, and increased global H3K27me3 levels in pre-OB, further arguing for the role of PRC2 complex in Runx2 suppression. We found that Gfi1 knockdown pre-OB lacked MM-dependent HDAC1 recruitment, resulting in prevention of Runx2 deacetylation and rescue of differentiation-induced Runx2 mRNA expression. These data show that Gfi1 is required for the MM-induced epigenetic repression of Runx2. We report that MM cells utilize dual modes of suppressive effects on OB differentiation by reducing Runx2 mRNA stability in proliferating pre-OB and employing Gfi1 to recruit HDAC1 and EZH2 to establish long-term epigenetic suppression of Runx2 transcription.

Disclosures: Juraj Adamik, None.

SA0005

See Friday Plenary Number FR0005.

SA0006

The Relationship between Vitamin D Status and Clinical Outcomes of Patients with Hepatic Cirrhosis. Edward Marchese*¹, Francine Almeda², Isabel Camara², Thomas Layden², Stephanie Kliethermes², William Adams², Pauline Camacho². ¹Loyola University Stritch School of Medicine, USA, ²Loyola University Medical Center, USA

Purpose: Vitamin D insufficiency is prevalent amongst patients with hepatic cirrhosis due to a multitude of factors, including decreased dietary intake, limited sunlight exposure, and impaired hepatocyte function. In a previous report, we found an inverse correlation between vitamin D levels and frequencies of lung transplant rejection and infection. (Lowery et al 2012). Given the recognized immunoregulatory effect of vitamin D, we aimed to determine its impact on clinical outcomes in hepatic

cirrhosis patients. We utilized the frequency of hepatic decompensation, Child-Pugh (CP), and model for end-stage-liver disease (MELD) scores to quantify endpoints, as previously described by Bankuti et al. (2012). Additionally, bone density status of patients was assessed using dual energy x-ray absorptiometry (DXA) data.

Methods: A retrospective electronic medical chart review was conducted on consecutive patients seen at Loyola University Medical Center between 2009-2014, who had 25(OH) vitamin D levels measured after diagnosis of hepatic cirrhosis. Vitamin D sufficiency was defined as a 25(OH)D level of ≥ 30 ng/ml. Within a one-year timeframe, we tracked liver biochemistries, abdominal ascites, hepatic encephalopathy, and calculated CP and MELD scores for each patient. Chi-square and two-sample t-tests were used to compare demographic, laboratory, clinical, and DXA results between the groups.

Results: The cohort included 60 subjects (51.7% female) with a mean age of 58.2 ± 10.5 years. The mean 25(OH)D for sufficient patients ($n=24$) was 38.1 ng/ml versus 18.8 ng/ml ($p=.003$) in the insufficient group ($n=36$). Nine (38%) sufficient patients suffered from hepatic decompensation as compared to 27 (75%) in the insufficient cohort ($p=0.004$). The mean CP scores in the sufficient versus insufficient groups were 6.11 ± 1.05 and 7.65 ± 1.78 ($p<.001$). MELD scores were 8.47 ± 7.51 vs. 12.65 ± 5.13 for these groups, respectively ($p<.001$). There were no significant differences in femoral neck T-scores; however, there was a trend toward lower lumbar T-scores in the insufficient group as compared to the sufficient group (-1.14 ± 0.44 vs. 0.25 ± 0.46 , $p=0.06$).

Conclusions: Vitamin D status showed a strong inverse correlation between CP and MELD scores; however, its role in liver pathogenesis is not clearly defined. Additionally, the trend towards lower lumbar T-scores may indicate preferential decreases in bone mineral density of trabecular bone as compared to cortical bone.

Table 1 - Hepatic Decompensation

| | Insufficient (n=36) | Sufficient (n=24) | p-value |
|-----------------|---------------------|-------------------|---------|
| 25(OH)D (ng/mL) | 18.8 (6.4) | 38.1 (11.1) | |
| Decompensation | 27 (75%) | 9 (38%) | 0.004** |

Table 1

Table 2 - Hepatic Function

| | Insufficient (SD) | Sufficient (SD) | p-value |
|-----------------|-------------------|------------------|----------|
| Albumin | 2.94 (0.11) | 3.45 (0.11) | 0.001** |
| Total Bilirubin | 2.40 (0.46) | 1.18 (0.20) | 0.02** |
| INR Ratio | 1.31 (0.04) | 1.15 (0.03) | 0.003** |
| Platelet Count | 88.08 (7.53) | 139.90 (11.44) | <0.001** |
| CP | 7.65 (1.78) n=26 | 6.11 (1.05) n=17 | <0.001** |
| MELD | 12.65 (5.13) n=26 | 8.47 (7.51) n=17 | <0.001** |

Table 2

Table 3 - Bone Mineral Density

| | Insufficient | Sufficient | p-value |
|----------------------|--------------|--------------|---------|
| Lumbar Spine T-Score | -1.14 (0.44) | 0.25 (0.46) | 0.06 |
| Femoral Neck T-Score | -1.23 (0.19) | -1.20 (0.23) | 0.94 |

Table 3

Disclosures: Edward Marchese, None.

SA0007

Tumour-Induced Osteomalacia due to a Gluteal Phosphaturic Mesenchymal Tumour: A Case Report. Rachel Johnston¹, Brendan C. Dickson², Peter C. Ferguson², Ina Radziunas³, Sandra A. Kim⁴. ¹University of Toronto, Canada, ²Mount Sinai Hospital, University of Toronto, Canada, ³Women's College Hospital, Canada, ⁴Women's College Hospital, University of Toronto, Canada

Case:

A 47-year-old male sustained multiple rib fractures and a non-displaced fracture of the left hip, requiring a total hip replacement, after slipping on ice. Post-operatively, his hip pain worsened and he developed diffuse bony pain and proximal muscle weakness. Multiple occult pelvic fractures and a right hip stress fracture were identified on repeat imaging.

The patient was previously healthy, with no personal or family history of bone disease or cancer. There was no history of prior fragility fractures or glucocorticoid use. Physical examination was remarkable only for proximal myopathy.

Baseline bone density revealed a Z-score of -2.5 at the lumbar spine. His bone scan was consistent with osteomalacia. Biochemical work-up revealed hypophosphatemia, hyperphosphaturia, elevated alkaline phosphatase and undetectable calcitriol.

The diagnosis of tumour-induced osteomalacia (TIO) was confirmed based on elevated fibroblast growth factor-23 (FGF-23) level of >800 pg/mL (reference range 8-54 pg/mL). He was commenced on phosphate and calcitriol supplementation. An octreotide scan revealed a focal ovoid area of increased octreotide avidity deep to the left gluteal minimus muscle. CT-guided biopsy confirmed a phosphaturic mesenchymal tumour, mixed connective tissue variant (PMT). He underwent an uncomplicated surgical resection of the tumour, and had complete clinical and biochemical recovery at 3-month follow-up.

Discussion:

Phosphate plays a critical role in bone mineralization and cellular metabolism. Its homeostasis is regulated by FGF-23, parathyroid hormone and calcitriol through renal tubular reabsorption, bone mineralization, and intestinal absorption. Eighty to 95% of filtered phosphate is reabsorbed at the proximal convoluted tubule via the type IIa sodium-phosphate NaPi co-transporter. FGF-23 increases renal phosphate excretion by down-regulating the NaPi co-transporter and calcitriol conversion. Persistent hypophosphatemia may manifest as proximal myopathy and debilitating fragility fractures due to osteomalacia.

Conclusion:

TIO is a rare paraneoplastic process; inappropriately elevated levels of FGF-23 secreted from an occult PMT lead to renal phosphate wasting, hypophosphatemia, decreased calcitriol levels and subsequent fractures. PMT are notoriously difficult to localize. With tumour excision, prognosis is excellent, with complete symptomatic and biochemical resolution.

Disclosures: Rachel Johnston, None.

SA0008

See Friday Plenary Number FR0008.

SA0009

Genetic Variants Associated with Bisphosphonate-Associated Osteonecrosis of the Jaw: A Whole-Exome Sequencing Analysis. Yan Gong^{*1}, Joseph Katz², Alberto Riva¹, Noa Davis³, Issam Hamadeh¹, Bernadett Bella⁴, Janos Kosa⁴, Mihaly Vaszilko⁵, GIAN ANDREA PELLICIONI⁶, Peter Lakatos⁴, Jan Moreb¹, Taimour Langae¹. ¹University of Florida, USA, ²Department of Oral Medicine, College of Dentistry, USA, ³Micromedic Technologies Ltd, Israel, ⁴Semmelweis University Medical School, Hungary, ⁵Semmelweis University Dental School, Hungary, ⁶University of Bologna, Italy

Purpose: Osteonecrosis of the jaw (ONJ) is a rare and serious adverse drug event that was reported initially with bisphosphonates use and more recently with other drug classes such as RANKL inhibitors and anti-angiogenic agents. The purpose of this study is to identify functional genetic variants associated with ONJ in patients treated with intravenous (IV) bisphosphonates using a whole-exome sequencing approach.

Methods: Whole-exome sequencing analysis was performed on 46 multiple myeloma patients treated with IV bisphosphonates (zoledronate or pamidronate), including 23 individuals with ONJ and 23 age, gender and race-matched controls who did not develop ONJ after at least 24 months of IV bisphosphonate treatment. Standard bioinformatics analysis was applied and the reads were aligned to the human genome (version GRCh37/hg19) using bowtie (version 2.2.3). Variant calling was performed using GATK pipeline (version 3.2-2). The association of the variants with ONJ was performed in PLINK with Fisher's exact test and logistic regression controlling for age, gender and race. Variants with $p < 1.2 \times 10^{-7}$ were considered statistically significant and those with $p < 10^{-4}$ were considered suggestive.

Results: The patients had mean age of 63 years, 54% male and 96% were self-identified as Whites. An average of 3,667,001 SNPs per sample (min=3,441,884, max=4,048,829) were identified. After quality control steps, 427,367 variants were analyzed. In the Fisher's exact analysis, 5 SNPs had $p < 10^{-4}$. Four SNPs were associated with lower odds of ONJ including an intronic SNP rs795489 on *PRDX4* gene encoding peroxiredoxin 4 with odds ratio (OR) of 0.14 ($p = 2.16 \times 10^{-5}$), rs6504184 in the promoter region of gene *CCDC47* with OR of 0.13 ($p = 3.2 \times 10^{-5}$) and rs11074355 in *TMC7* gene with OR of 0.15 ($p = 4.4 \times 10^{-5}$). One SNP was associated with higher odds of ONJ: intronic SNP rs11938792 on chromosome 4 had OR of 22.93 ($p = 6.98 \times 10^{-5}$). The *TMC7* and *CCDC47* SNPs remained significant in the multiple logistic regression analysis.

Conclusions: We identified 5 novel variants that might be associated with ONJ in multiple myeloma patients treated with IV bisphosphonates. Functional analysis is warranted to understand the underlying mechanisms of these associations. If validated, these genetic variants could be used to guide personalized therapy for bisphosphonates for multiple myeloma patients.

Disclosures: Yan Gong, None.

This study received funding from: Micromedic

SA0010

KLF10 is a Critical Mediator of Wnt Signaling in Calcific Aortic Valve Disease. Nalini M. Rajamannan¹, John Hawse², Malayannan Subramaniam². ¹Mayo Clinic, Rochester MN, USA, ²Mayo Clinic, USA

We have previously demonstrated that β -catenin plays important roles in valve calcification with a specific osteogenic phenotype defined by increased bone mineral content and overall valve thickening. Recent studies indicate that KLF10, a transcription factor known to play critical roles in osteoblast differentiation and bone mineralization, may also be involved in mediating the Wnt signaling pathway in the skeleton. Therefore, we sought to determine if KLF10 participates in regulating Wnt signaling, as well as differentiation and mineralization in valve interstitial cells (VICs). As a first step, we analyzed the expression patterns of Wnt pathway genes in VICs prior to and following differentiation. Following exposure of VICs to osteogenic differentiation media, increased expression of Runx2, Sox9, and osteocalcin were observed compared to non-differentiated cells. Differentiated cells also stained positive with Von Kossa while undifferentiated cells stained negative confirming the induction of an osteogenic phenotype. As expected, transfection of VICs with Lef1, β -catenin or both resulted in activation of the canonical Wnt signaling top-flash reporter construct. Interestingly, expression of KLF10 also significantly up-regulated the top-flash reporter construct alone and further enhanced the activity of both Lef1 and β -catenin. These data suggested that KLF10, Lef1 and β -catenin interact with each other to form a transcriptionally active protein complex leading to enhanced Wnt signaling in VICs. This possibility was confirmed by the observation that KLF10 and β -catenin co-localize with one another in the nucleus of VICs following stimulation with Lf1 or treatment with TGF- β , a cytokine known to induce KLF10 expression and enhance osteogenic phenotypes. In an experimental model of hypercholesterolemia using LRP5 null mice, the expression levels of LRP6, KLF10 and Runx2 were significantly increased following cholesterol treatment of mice as compared to controls suggesting that hyperlipidemia may also enhance Wnt signaling via LRP6 and downstream KLF10. Taken together, these data implicate important roles for KLF10 in mediating Wnt signaling and LEF1 transcriptional activity in VICs, and imply a potential role for the canonical Wnt signaling pathway in the observed osteogenic bone phenotype in aortic valves.

Disclosures: Nalini M. Rajamannan, None.

SA0011

The association between vitamin D receptor gene polymorphisms (TaqI and FokI) and micro/macrovacular complications in postmenopausal women with type 2 diabetes. Juliana Maia de Almeida¹, Andreia Soares Silva², Rodrigo Feliciano do Carmo², Taciana Belmonte², Luiz Griz¹, Patricia Muniz Moura², Francisco Bandeira¹, Mirna De Sa³. ¹Division of Endocrinology & Diabetes, Agamenon Magalhães Hospital, University of Pernambuco Medical School, Recife, Brazil, ²Institute of Biological Sciences, University of Pernambuco Medical School, Recife, Brazil, ³University of Pernambuco Medical School, Brazil

Some studies have shown that vitamin D deficiency is associated with increased risk of developing type 2 diabetes (T2DM) and atherosclerotic cardiovascular disease but few studies have examined the association of vitamin D receptor (VDR) polymorphisms with these two common conditions as well as with the chronic complications of T2DM. Aims: To examine the associations between VDR polymorphisms (FokI and TaqI), T2DM and its chronic complications in postmenopausal women. Methods: This cross-sectional study analyzed 100 postmenopausal women with T2DM (mean age 65.7 \pm 7.18 years) and 100 postmenopausal women without diabetes in the control group (mean age 65.1 \pm 9.18 years; $p=0.1608$). We evaluated clinical and metabolic parameters and analyzed TaqI and FokI polymorphisms. Results: There were no significant differences in genotype and allele frequencies between patients and controls in either of the polymorphisms studied. In the group of patients with diabetes, there were no significant differences in either polymorphism in relation to stroke, retinopathy, nephropathy or neuropathy. However, in patients with T2DM and coronary artery disease (CAD) Ff genotype ($p=0.0361$) and the combination of Ff+ff genotypes were observed less frequently ($p=0.0462$) [Table 1]. Conclusions: Our data demonstrated a protective effect of FokI polymorphism for CAD in postmenopausal women with T2DM in the recessive model.

Key words: 1) Type 2 diabetes; 2) VDR; 3) Polymorphism; 4) Vitamin D

TABLE 1: Distribution of VDR (FokI) polymorphism genotypes and allele frequencies in T2DM patients according to the presence of coronary artery disease (CAD)

| VDR | CORONARY ARTERY | | P value ⁽¹⁾ | OR | CI 95% |
|------------------|-----------------|------------|------------------------|------|-----------|
| | YES n=18 | NO n=82 | | | |
| Genotype | | | | | |
| GG (FF) | 12 (67%) | 34 (42%) | - | | |
| AG (Ff) | 4 (22%) | 38 (46%) | 0.0361* | 0.29 | 0.09-1.01 |
| AA (ff) | 2 (11%) | 10 (12%) | 0.3072 | 0.57 | 0.11-2.96 |
| AG-AA (Ff-ff) | 6 (33%) | 48 (58%) | 0.0462* | 0.35 | 0.12-1.02 |
| Alleles n(%) | | | | | |
| G (F) | 28 (78%) | 106 (65%) | - | | |
| A (f) | 8 (22%) | 58 (35%) | 0.0907 | 0.52 | 0.22-1.22 |

* Statistically significant difference ($P < 0.05$)
(1) Chi-square test

TABLE 1

Disclosures: Mirna De Sa, None.

SA0012

The MicroRNA Signatures in the Patients with Lumbar Disc Herniation. Lili Chen¹, Xiaoya Zhou², Songlin Peng^{3,4}, Shishu Huang⁴, Sibylle Grad⁵, Mauro Ajimi⁵. ¹Shenzhen Institute of Advanced Technology, Chinese Academy of Sciences, Peoples republic of china, ²Center for Human Tissues & Organs Degeneration, Shenzhen Institute of Advanced Technology, Chinese Academy of Sciences, China, ³Shenzhen People's Hospital, Jinan University School of Medicine, China, ⁴State Key Laboratory of Oral Diseases, Sichuan University, China, ⁵AO Research Institute Davos Clavadelstrasse, Switzerland

Introduction: Lumbar disc herniation (LDH) is one of the major causes for back and sciatic pain that costs large medical expense. Accumulating evidence has indicated that microRNAs (miRNAs), a small non-coding RNA molecule, are associated with disc degeneration, the profile of miRNAs in the LDH patients with indication for laminectomy remains unclear.

Material methods: MicroRNA profiling was performed on plasma samples of 4 groups: LDH-young group (n=8, average age is 31), LDH-old group (n=8, average age is 56), healthy control-young group (n=4, average age is 20), healthy control-old group (n=6, average age is 58). The miRNAs expression were further validated by qRT-PCR.

Results: The miRNAs with p -values < 0.05 and fold change values ≥ 2 or ≤ 0.5 compared to healthy control were regarded as dysregulated miRNAs. 61 miRNAs were upregulated and 302 were downregulated in LDH-young group compared to healthy control-young group. In addition, there are 46 upregulated miRNAs and 115 downregulated in LDH-old group compared to healthy control-old group. In particular, 12 upregulated and 71 downregulated miRNAs expressed significant differences both in the LDH-young group vs healthy control-young group and the LDH-old group vs healthy control-old group. Among them, miR-224 was upregulated 4.04-, 16.99-fold in LDH-young and LDH-old groups compared to healthy control-young and healthy control-old groups, respectively ($p < 0.01$ for both). Besides, relative to old groups, miR-130b and miR-147b were downregulated significantly in young groups, both of which were reported to be associated with disc degeneration.

Conclusion: The selected miRNAs might play a vital role in the molecular pathogenesis of LDH and further research for the understanding of the functionality and pathological mechanism of the miRNAs in LDH is important and would shed new light on LDH.

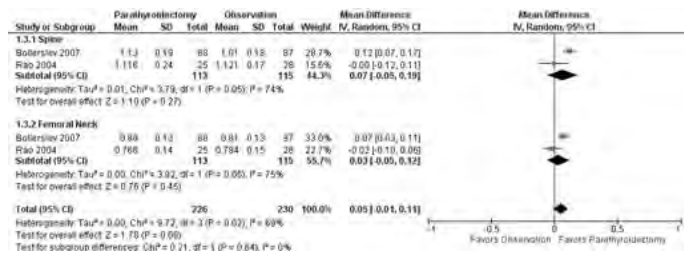
Key words: LDH, microRNAs, disc degeneration

Disclosures: Songlin Peng, None.

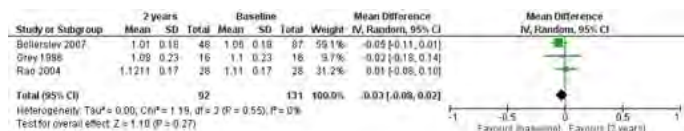
SA0013

Bone Mineral Density Changes and Fracture Risk in Patients with Asymptomatic Primary Hyperparathyroidism. Systematic Review and Meta-analysis. Spyridoula Maraka¹, Naykky Singh Ospina¹, Ana Espinosa De Ycaza², Rene Rodriguez Gutierrez³, Sina Jasmin⁴, Michael Gionfriddo⁵, Ana Castaneda-Guarderas⁵, Alaa Al Nofal⁶, Victor Montori¹, Robert Wermers². ¹Mayo Clinic, Division of Endocrinology, Knowledge & Evaluation Research Unit, USA, ²Mayo Clinic, Division of Endocrinology, USA, ³Mayo Clinic, Knowledge & Evaluation Research Unit, USA, ⁴Endocrinology, Mayo Clinic, ⁵Mayo Clinic, Knowledge & Evaluation Research Unit, USA, ⁶Mayo Clinic, Division of Pediatric Endocrinology, USA

Many patients with asymptomatic primary hyperparathyroidism (PHPT) have mild uncomplicated disease without indications for surgical intervention. A better understanding of the potential benefits of surgical intervention would help clinicians counsel these patients. The purpose of this study is to summarize the available evidence regarding changes in bone mineral density (BMD) and fracture risk in PHPT when comparing parathyroidectomy with active surveillance. We performed a computerized bibliographic search of published articles and citation review by an experienced medical reference librarian. We included randomized (RCT) and observational studies that evaluated the changes in BMD and fracture risk in patients with asymptomatic PHPT and no strong indications for surgery undergoing parathyroidectomy or active surveillance as treatment options. Trained reviewers independently screened for eligible studies, assessed risk of bias and extracted data in duplicate. Statistical analysis was performed following a random effect model. The search yielded 3141 articles for abstract screening of which 4 studies were included; 2 RCTs with 113 patients undergoing surgery and 115 surveillance and 2 single arm cohort studies of 124 patients followed with active surveillance. The BMD change (g/cm²) was 0.07 (95% CI: -0.05, 0.19) at the lumbar spine and 0.03 (95% CI: -0.05, 0.12) at the femoral neck when comparing these 2 treatment modalities at 2 years of follow up. When evaluating the patients followed by active surveillance the overall lumbar spine BMD change from baseline was -0.03 (95% CI: -0.08, 0.02) at 2 years of follow up. There were no reported fractures in any patients included in the RCT (53 patients) or in the 136 patients followed with active surveillance (follow up 12-123 months). Overall, studies had moderate to high risk of bias mainly driven by unclear allocation and attrition for RCTs and/or inappropriate patient selection and follow up for observational studies. The available evidence regarding the effects of surgical intervention versus active surveillance on bone health in patients with asymptomatic PHPT without strong clinical indications for parathyroidectomy is scarce. Available data suggest a minimal BMD gain at the spine and femoral neck in favor of parathyroidectomy and minimal BMD loss in patients with active surveillance. The confidence in these estimates is weakened by moderate to high risk of bias and imprecision.



Bone Effect



Bone Observation

Table1. Summary of Included Studies of patients with mild PHPT and without strong indications for surgical intervention

| Author | Year | Type of study | Inclusion Criteria | Patients with Surgery | Patients with Observation | Mean follow up time |
|------------|------|--|--|--|---------------------------|------------------------------|
| Bollerslev | 2007 | RCT | Untreated, asymptomatic PHPT; serum calcium 2.6-2.85 mmol/L Age 50-80 years No medications interfering with calcium metabolism | 88 | 87 | Final follow up at 24 months |
| Rao | 2004 | RCT | Age 50-75 years, mean albumin adjusted serum calcium between 10.1-11.5 mg/dL; intact PTH > 20 ng/L, normal renal function, serum creatinine less than 1.5 mg/dL, forearm bone mineral density within 2 SD adjusted for age, sex, race, absence of symptoms and complications from hypercalcemia or excess PTH, living 150 miles from the institution | 25 | 28 | At least 24 months |
| Rao | 2003 | Single arm | Patients discovered fortuitously with biochemical screening and without symptoms of hypercalcemia, nephrolithiasis, serum calcium > 12 mg/dL, serum creatinine > 1.5 mg/dL or forearm bone density > 2.5 SD below the mean for age, race and sex | NA | 108 | 12-120 months |
| Grey | 1996 | RCT (only arm with active surveillance used) | Postmenopausal women with mild PHPT and hypercalcemia detected incidentally. No concurrent systemic illness, untreated thyroid disease, hepatic or renal dysfunction, genital bleeding, estrogen therapy in the last 6 months, history of bisphosphonate use or fluoride therapy, steroids, anticonvulsant or thiazide | Hormone replacement therapy (not used) | 16 | 24 months |

PHPT; primary hyperparathyroidism

Included studies

Disclosures: Spyridoula Maraka, None.

SA0014

See Friday Plenary Number FR0014.

SA0015

Familial hypocalciuric hypercalcemia and primary hyperparathyroidism: different clinical manifestations in one family with a previously undescribed calcium-sensing receptor gene mutation. Melissa Sum¹, Robert Udelsman², Tobias Carling², Shonni Silverberg¹. ¹Columbia University Medical Center, Division of Endocrinology, USA, ²Yale University School of Medicine, Section of Endocrine Surgery, USA

Familial hypocalciuric hypercalcemia (FHH) is characterized by hypercalcemia without suppressed parathyroid hormone (PTH) levels and hypocalciuria. It has a benign course with an autosomal dominant inheritance pattern of a mutation in the calcium-sensing receptor (CaSR) gene. In primary hyperparathyroidism (PHPT), hypercalcemia is due to inappropriate PTH secretion and may be associated with skeletal and renal target organ effects. Families with mixed clinical pictures of FHH and PHPT have been described. We report the clinical characteristics of three family members with a previously undescribed mutation of the CaSR who present with three phenotypes. The mother, a 63-yr-old Caucasian woman, was referred for low bone density and a 30-year history of hypercalcemia. Evaluation (Table) revealed mild PHPT with hypercalcemia, hypercalciuria and a normal PO4. BMD was typical for PHPT: preserved at the lumbar spine, close to osteoporotic at the femoral neck, with severe osteoporosis at the 1/3 radius. She was diagnosed with PHPT and underwent subtotal parathyroidectomy. Intraoperative PTH predicted cure [baseline 89 to 14 pg/ml 15 min post-PTX]. Calcium fell to 8.5 mg/dl. Hypercalcemia was incidentally noted in her 35 yo son (Table), with low PO4, 25OHD and hypocalciuria. BMD was normal. FHH or familial hyperparathyroidism was suspected. Genetic testing identified a point mutation in the 7th exon of the CaSR gene leading to change (P798L) in the transmembrane domain and no MEN1 mutation. He was diagnosed with FHH. Screening of his 31 yo sister (Table) revealed hypercalcemia, urinary calcium at the upper normal range and normal BMD, consistent with asymptomatic PHPT. Genetic testing of the mother and daughter identified identical point mutations. In summary, three family members with identical CaSR mutations exhibited disparate clinical phenotypes: the mother had features of PHPT with both hypercalciuria and forearm osteoporosis; the son had FHH; the daughter had PHPT with increased urinary calcium excretion but no bone loss, and BMD was not lower at the cortical site. This

kindred, with autosomal dominant hypercalcemia caused by a previously undescribed point mutation of the transmembrane domain of the CaSR, includes members displaying clinical phenotypes of FHH and PHPT with and without skeletal sequelae. This kindred underscores the possibility of diverse phenotypic expression of unique mutations and highlights the expanding clinical spectrum of CaSR mutations.

| | MOTHER | DAUGHTER | SON |
|-----------------------------|----------------|----------------|----------------|
| Serum Calcium mg/dl | 11.3 | 11.1 | 11.2 |
| Serum PO ₄ mg/dl | 3.5 | 2.8 | 2.4 |
| PTH pg/ml | 63 | 64 | 40 |
| 24 h Urine Calcium mg | 251 | 250 | 44 |
| 25OHD ng/dl | 52 | 34 | 14.9 |
| | | | |
| Lumbar Spine | T-Score = -1.5 | Z-Score = -0.5 | Z-Score = -0.7 |
| Femoral Neck | T-Score = -2.4 | Z-Score = -0.1 | Z-Score = 0.4 |
| 1/3 Radius | T-Score = -3.6 | Z-Score = -0.3 | Z-Score = -0.7 |

Table

Disclosures: *Melissa Sum, None.*

SA0016

INTRAOPERATIVE PARATHYROID HORMONE MEASUREMENT AND OUTCOME FOLLOWING PARATHYROIDECTOMY IN PRIMARY HYPERPARATHYROIDISM. Patamaporn Lekprasert*, Catherine Anastasopoulou, Goral Panchal. Einstein Medical Center of Philadelphia, USA

BACKGROUND:

Primary hyperparathyroidism (PHPT) is the most common cause of hypercalcemia in an ambulatory setting. Surgery is the mainstay of the treatment. Focused parathyroidectomy and minimally invasive parathyroidectomy (MIP) are preferred operations in non-complicated patients given an advancement of pre-operative localizing, and rapid intraoperative parathyroid measurements (IOPTH).

STUDY DESIGN:

This is a retrospective study aimed to compare recurrent rate, persistent hypercalcemia rate, complications (infection, bleeding, and hypocalcemia), operative time, and length of hospital stay between MIP with IOPTH and conventional parathyroidectomy. We included all PHPT patients who underwent parathyroidectomy at our tertiary care hospital during January 2006 to January 2014. For MIP with IOPTH, intact parathyroid hormone (iPTH) was measured preoperatively, baseline before the excision of the gland, and at 5-, 10- and 20-minute intervals after the excision. MIP was considered complete after appropriate glands were excised and iPTH fell to less than 50% of baseline levels. Tertiary hyperparathyroidism patients were excluded.

RESULTS:

We included 220 patients who underwent surgery during the 8-year period; 131 patients underwent MIP with IOPTH, and 89 patients had conventional surgery. Patients were 29% men and 71% women. There was no difference in demographics, pre-operative serum calcium, and iPTH level between the 2 groups. Operation demonstrated 90% of patients had single adenoma, 7% had four-gland hyperplasia, and 3% had double adenomas. Recurrent rate was 6.7% in conventional group, and 6.1% in MIP group (p=0.266). Persistent hypercalcemia rate was 0% in conventional group, and 6.1% in MIP group (p=0.021). In the group of patients with persistent hypercalcemia, the IOPTH did not drop by 50% at 20 minutes after resection. The operative time and length of hospital stay were shorter in MIP group (81.03 vs 110.49 minutes, p = 0.032, and 1.94 vs 3.1 days, p = 0.034 respectively). There was no difference in post-operative complications between two groups. Ten out of 21 patients with persistent and recurrent HPTH underwent a second operation.

CONCLUSIONS:

MIP with IOPTH monitoring is safe, effective and helps to shorten the operative time and length of hospital stay compared to conventional parathyroidectomy.

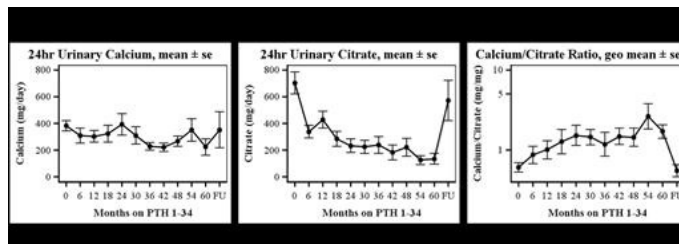
Disclosures: *Patamaporn Lekprasert, None.*

SA0017

Parathyroid Hormone (PTH) 1-34 Therapy Decreases Urinary Citrate in Hypoparathyroidism. Rachel Gafni*¹, Craig Langman², Lori Guthrie³, Beth Brillante¹, Robert James⁴, Nancy Yovetich⁴, Alison Boyce¹, Michael Collins¹. ¹National Institutes of Health, USA, ²Northwestern University & the Ann & Robert H Lurie Children's Hospital of Chicago, USA, ³NIDCR, National Institutes of Health, USA, ⁴Rho, Inc, USA

Many studies have shown that PTH therapy can effectively manage the hypocalcemia in patients with hypoparathyroidism (HPTH), with varying effects on

hypercalcemia. However, little is known about PTH's ability to decrease the renal comorbidities of HPTH: nephrocalcinosis (NC), nephrolithiasis (NL), and chronic kidney disease. Urinary citrate promotes the solubility of urinary calcium; hypocitraturia is a risk factor for NC/NL. The prevalence of hypocitraturia in PTH-treated HPTH patients is unknown. Urinary calcium (Ca), citrate (cit), and Ca/cit ratios were measured in 30 patients with HPTH receiving PTH 1-34 replacement therapy for up to 5 years in an ongoing study. Renal ultrasounds and CT scans were performed annually. Before PTH, mean \pm SD Ca excretion was elevated at 383 ± 203 mg/d (nl <250) and cit excretion was 703 ± 394 mg/day (nl 250-1190), with a geometric mean Ca/cit ratio of 0.61 mg/mg, 95% CL 0.46, 0.8 (target <0.7) (N=23). After 6 mos of PTH, urine Ca had not significantly changed (308 ± 242 mg/d, p=NS) while urine cit had decreased significantly (338 ± 203 mg/d, p<0.01), resulting in an increased Ca/cit (0.87 mg/mg, CL 0.52, 1.48; p=NS) (N=19) that became statistically significant with time (p=0.0078, repeated measures ANOVA, Fig). In 12 subjects, K-citrate (30-60 meq/d) was added with varying response. Overall, however, urinary cit levels remained low and Ca/cit remained elevated while on PTH. After stopping PTH, compared to the last measures on PTH, cit had risen to 572 ± 473 mg/d (p=0.0072), reducing the Ca/cit to 0.55 mg/mg, CL 0.37, 0.82 (p<0.0001) (N=10) without change in Ca (353 ± 427 mg/d). Urine pH, serum bicarbonate, and eGFR were unchanged throughout. On imaging, 12 subjects did not have NC/NL, 8 had NC/NL prior to PTH, and 8 developed NC/NL after starting PTH (with resolution in 2). Impaired urinary acidification leading to proximal renal tubular acidosis is a known effect of excess PTH, both experimentally and in primary hyperparathyroidism. Metabolic acidosis reduces tubular secretion of citrate, which may lead to hypocitraturia and increased NC/NL. Our data demonstrate that, while PTH therapy might be promising for hypocalcemia management in HPTH, hypocitraturia appears to be an untoward effect that may result in an increased risk of renal morbidity. Thus, with increasing use of PTH therapy in patients with HPTH, close monitoring and treatment for hypocitraturia may be indicated to prevent acceleration of NC/NL and compromised renal function.



Urinary calcium, citrate and calcium/citrate ratio before, during, and after PTH 1-34

Disclosures: *Rachel Gafni, Shire*

SA0018

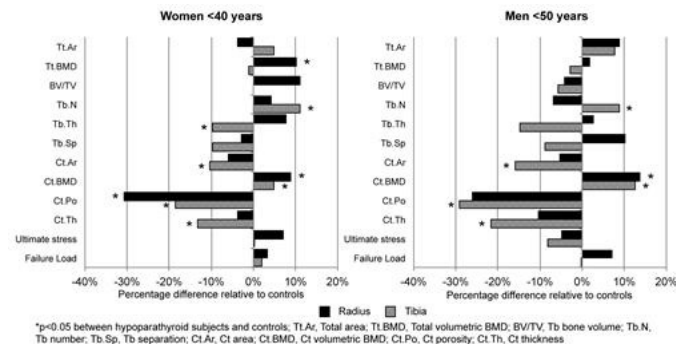
See Friday Plenary Number FR0018.

SA0019

Skeletal Microstructure and Estimated Bone Strength in Hypoparathyroidism. Natalie Cusano*¹, Kyle Nishiyama¹, Chengchen Zhang¹, Mishaela Rubin¹, Donald McMahon¹, X. Edward Guo², John Bilezikian¹. ¹Columbia University College of Physicians & Surgeons, USA, ²Columbia University Bone Bioengineering Laboratory, Department of Biomedical Engineering, USA

Hypoparathyroidism (HypoPT) is characterized by low bone turnover, above average areal bone mineral density (BMD), and abnormal structural indices by bone biopsy. Little is known about microstructure or bone strength in this PTH-deficiency disease. We studied 61 HypoPT subjects by high resolution peripheral quantitative computed tomography (HRpQCT, Scanco Medical) of the distal radius and tibia and estimated bone strength by finite element analysis (FEA). Demographics: 49 women/12 men; age 46 ± 12 (SD) years; etiology: 35 postsurgical, 25 idiopathic, 1 DiGeorge; duration 11 ± 11 years; serum calcium 8.6 ± 0.8 mg/dL; PTH 1.3 ± 3 pg/mL. We compared HypoPT subjects to published normative data from the 20-29 year-old female and male cohorts of the Canadian Multicentre Osteoporosis Study. We present here results for the premenopausal women <40 (n=18) and men <50 years (n=7). In both the women and men, areal BMD was above average at the lumbar spine (T-score +1.37, +1.88) and total hip (+1.26, +1.27); the 1/3 radius site was also above average for women (+0.55). HRpQCT results are summarized in the figure. At both the radius and tibia, cortical (Ct) volumetric BMD was increased in the HypoPT women and men compared to controls. Ct porosity was reduced at both the radius and tibia in women and at the tibia in men. At the tibia alone, Ct thickness was lower in women and men. Tb thickness was lower in women and Tb number was lower in women and men. Ultimate stress and failure load at both sites were similar for the HypoPT subjects vs. controls. We used a linear regression model that included age, sex and disease duration to further evaluate their relationships to bone strength in all subjects. At both radius and tibia, each 1-year increment in age decreased ultimate stress (-0.27, -0.21 MPa) and failure load (-15, -32 N) while each increment in disease duration improved these same indices (ultimate stress: +0.29, +0.34 MPa, failure load: +14, +37 N). Using non-invasive high resolution imaging, these data show abnormal micro-architecture in HypoPT subjects, giving additional evidence for the critical role of

PTH in establishing and maintaining bone quality. Despite above average areal BMD, estimated bone strength was not different from controls, consistent with registry data showing similar fracture incidence in HypoPT subjects vs. controls. Increasing disease duration appears to negate the adverse effects of increasing age on estimated bone strength in HypoPT.



HRpQCT results at the distal radius and tibia in HypoPT subjects

Disclosures: Natalie Cusano, None.

This study received funding from: NPS Pharma

SA0020

Age-related changes in 3D bone microstructure are more pronounced in the sub-endplate region than in the central region of human vertebral bodies.

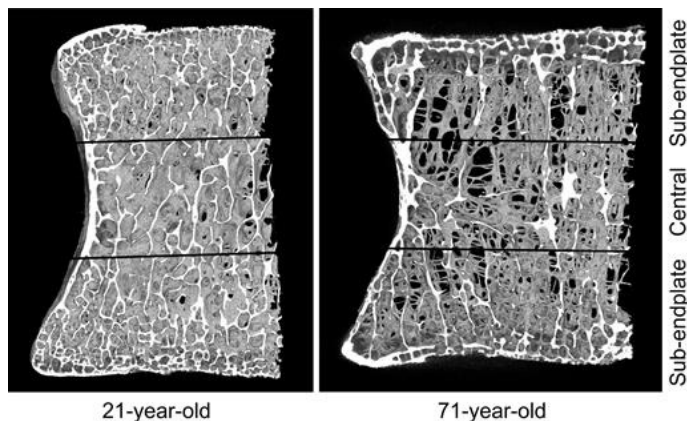
Jesper Thomsen¹, Ebbe Ebbesen², Annemarie Br uel³. ¹Aarhus University, Denmark, ²Department of Biomedicine, University of Aarhus, Denmark, ³Department of Biomedicine, Aarhus University, Denmark

Purpose: The 3D bone microstructure of the vertebral body of young individuals appears to be divided into three equally high horizontal regions: two adjacent to the endplates and one in the centre of the vertebral body. With increasing age this regional subdivision of the 3D microstructure of the vertebral bodies appears to vanish. Therefore, the aim of the study was to investigate the differences in the age-related changes in 3D microstructure of the sub-endplate region and the central region in human vertebral bodies.

Materials and Methods: The material comprised 80 9-mm-thick frontal slices of L2 from 41 women and 39 men aged 18 to 96 years with an even age-distribution. The bone samples were μ CT scanned at an isotropic voxel size of 18.5 μ m. By use of custom made software the vertebral bone specimens were divided into two regions: one spanning the central third and another spanning the two remaining thirds adjacent to the endplates. Standard 3D microstructural parameters were determined in each of the two regions.

Results: In both regions, BV/TV, Tb.N, and vBMD decreased significantly with age, structure model index (SMI), Tb.Sp, and bone material density increased significantly with age, while Tb.Th was independent of age. In the central region connectivity density (CD) and the degree of anisotropy (DA) were independent of age, while in the sub-endplate region these two parameters decreased and increased significantly with age, respectively. The slope of the fit lines was significantly larger for CD, Tb.N, and DA in the sub-endplate region than in the central region. Furthermore, the age-related changes in the 3D microstructural parameters CD, Tb.N, and DA were significantly different in the two regions.

Conclusion: The bone in the sub-endplate region is denser, more well-connected, and less mineralised, than the bone in the central region, and the trabeculae in the sub-endplate region is more closely spaced, more rod-like, and of similar thickness as in the central region. Finally, 3D bone microstructural parameters change significantly differently with age in the two regions. Therefore, caution should be exercised when examining the age-related changes of the 3D bone microstructure of human vertebral bone.



21-year-old

71-year-old

Vertebral body from a young and an old individual

Disclosures: Jesper Thomsen, None.

SA0021

Application of novel broadband ultrasound transducer in quantifying trabecular bone properties. Jian Jiao^{*1}, Xiaofei Li¹, Liangjun Lin¹, Yi-Xian Qin¹, Raffi Sahul², Ed Nesvjski². ¹Stony Brook University, USA, ²TRS Technologies Inc., USA

Ultrasound, as an oscillating mechanical wave, can be used to scan bones and its behavior in bone can reflect the structural and mechanical properties of that bone, such as density and Young's modulus. The technology of quantitative ultrasound (QUS) has been developed to measure bone properties and predicting fractures. Broadband ultrasound attenuation (BUA) has demonstrated high correlation to density in trabecular bones and it has been used as a good indicator for the femoral fracture risk. Ultrasound attenuation in bone is frequency dependant and it becomes strongly correlated in the frequency ranges from 0.3 to 0.7 MHz. In our study, a pair of conventional panametric confocal transducers which are manufactured by OLYMPUS, Inc. and a pair of novel broadband ultrasound transducers which are developed by Technologies, Inc. are respectively used to scan the same bone samples. The broadband transducers are fabricated from spiral-wrapping multiple piezoelectric PMN-PT single crystal of various center frequencies onto a flexible sheet and have a resonant frequency from 0.5MHz to 8MHz. To evaluate their application in bone scanning, three groups of trabecular bovine bone cubes were prepared, each group has five different degrees of decalcified samples. The confocal transducers scanning results indicate that with bone density loss by 23.94%, ultrasound velocity decreased from 1951.04 ± 77.49 m/s to 1591.24 ± 30.31 m/s, attenuation decreased from 18.75 ± 0.60 dB to 11.12 ± 0.95 dB, nBUA decreased from 22.77 ± 2.33 dB/MHz/cm to 10.14 ± 0.93 dB/MHz/cm. Comparing to the broadband transducers scanning results, the ultrasound velocity decreased from 1871.33 ± 148.14 m/s to 1532.90 ± 25.23 m/s, attenuation decreased from 21.07 ± 1.25 dB to 14.12 ± 2.35 dB, nBUA decreased from 33.27 ± 3.45 dB/MHz/cm to 22.49 ± 6.30 dB/MHz/cm. Due to multiple piezoelectric crystal structure, the broadband transducer has more harmonic waves and noise, but the broadband transducer is still good enough to use to quantify bone quality. Moreover, the wider frequency band can reveal more information than conventional single frequency transducer.

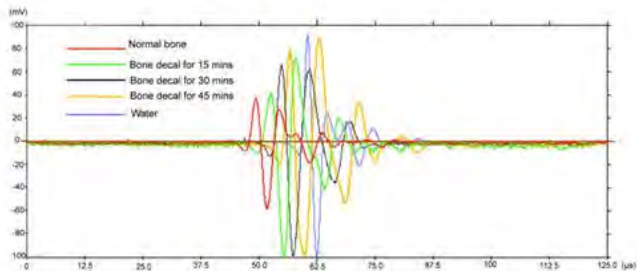


Figure 1. Single frequency OLYMPUS panametric transducer bone samples scanning waveforms

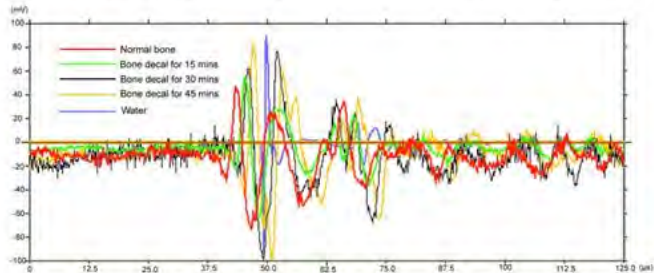


Figure 2. Broadband TRS transducer bone samples scanning waveforms

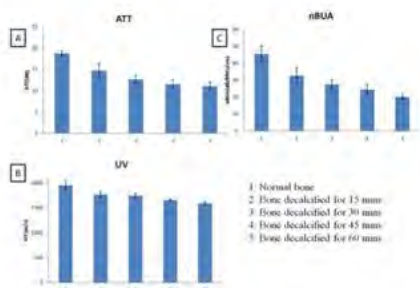


Figure 3. Single frequency OLYMPUS panametric transducer bone scanning result. (A) Ultrasound attenuation; (B) Ultrasound velocity; (C) Normalized broadband ultrasound attenuation

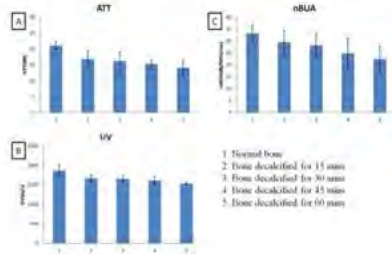


Figure 4. Broadband TRS transducer bone scanning result. (A) Ultrasound attenuation; (B) Ultrasound velocity; (C) Normalized broadband ultrasound attenuation

Bone scanning comparison between broadband TRS transducer and OLYMPUS panametric transducer

Disclosures: Jian Jiao, None.

SA0022

Bending Stiffness Predicts Bending Strength More Accurately than Cortical Diameter or Porosity in Cadaveric Human Ulnas. Gabrielle C. Hausfeld¹, Emily R. Ellerbrock², Jennifer M. Neumeyer², Tyler C. Beck², Maureen A. Dean², John R. Cotton³, Lyn Bowman^{*2}, Anne Loucks². ¹Honors Tutorial College, Ohio University, USA, ²Department of Biological Sciences, Ohio University, USA, ³Department of Mechanical Engineering, Ohio University, USA

Purpose: Cortical Porosity (CP) is measured to help identify individuals at high risk of fracture, but the *in vivo* method suffers from low image resolution and limitations in image processing and analysis. Increased bone fragility in post-menopausal women has been attributed to inadequate periosteal bone formation in compensation for endosteal bone resorption. Bone strength and stiffness are strongly

associated, and Mechanical Response Tissue Analysis (MRTA) measures ulna bending stiffness (k_B) noninvasively. The purpose of this study was to compare the accuracies with which ulna bending strength (F_{peak}) is predicted by CP, diameter, and k_B .

Methods: Fresh-frozen cadaveric human arms of 35 donors ($17 \leq \text{age} \leq 99$ yrs; $13 \leq \text{BMI} < 40$ kg/m²) were imaged with 250-820µm pixels by computed tomography (CT). In one day (1) an arm was thawed, (2) ulna k_B was measured by MRTA, (3) the arm was defleshed, and (4) ulna k_B and F_{peak} were measured by gold standard Quasistatic Mechanical Testing (QMT). Fractured ulnas were imaged with 10-15µm pixels by gold standard micro-computed tomography (µCT) in three 2mm cross-sections (33% and 55% of length from the distal end and adjacent to the fracture). The endosteum was located in 3D computer models made from 200 consecutive µCT slices at each site and CP was measured in CT and µCT images with *ImageJ*. Confounding of k_B by differences in ulna length (L) was corrected by computing ulna flexural rigidity ($EI = k_B L^3/48$). F_{peak} was related to CP, ID, EI and clinical predictors by simple and forward stepwise multiple regression.

Results: Standard errors of the estimate (SEE) for predictions of F_{peak} ($191 \leq F_{peak} \leq 1287$ N) appear in Table 1. ID at 55%L ($13 \leq ID \leq 23$ mm) predicted F_{peak} more accurately ($p=0.02$) than CP ($4 \leq CP \leq 64\%$) at any site. Predictions by ID in CT and µCT images were similar ($p=0.35$). As second predictors, body mass ($32 \leq BM \leq 129$ kg), height ($1.47 \leq Ht \leq 1.88$ m) and CP improved ($p \leq 0.02$) ID predictions similarly ($p \geq 0.24$). Predictions by EI_QMT ($10 \leq EI \leq 69$ Nm²) and EI_MRTA ($10 \leq EI \leq 74$ Nm²) were similar ($p=0.12$) and more accurate ($p \leq 0.02$) than CP, ID or both together. Only age explained any variance ($p \leq 0.03$) not explained by EI. No model with >2 predictors was significant.

Conclusions: Until MRTA is clinically available, the bending strength of ulnar cortical bone can be estimated more accurately by ID from CT images and other clinical data than by CP.

| Model | Predictor 1 | Predictor 2 | R ² | SEE (N) |
|-------|-------------|-------------|----------------|---------|
| 1 | EI_QMT | Age | 0.96 | 69 |
| 2 | EI_QMT | | 0.95 | 74 |
| 3 | EI_MRTA | Age | 0.93 | 86 |
| 4 | EI_MRTA | | 0.92 | 91 |
| 5 | ID_uCT_55% | BM | 0.86 | 120 |
| 6 | ID_uCT_55% | CP_FX | 0.85 | 127 |
| 7 | ID_uCT_55% | Ht | 0.84 | 128 |
| 8 | ID_CT_55% | BM | 0.84 | 130 |
| 9 | ID_CT_55% | Ht | 0.83 | 134 |
| 10 | ID_CT_55% | CP_55% | 0.80 | 147 |
| 11 | ID_uCT_55% | | 0.77 | 152 |
| 12 | ID_CT_55% | | 0.74 | 163 |
| 13 | ID_CT_33% | | 0.67 | 182 |
| 14 | ID_uCT_33% | | 0.64 | 193 |
| 15 | ID_uCT_FX | | 0.50 | 226 |
| 16 | CP_FX | | 0.46 | 235 |
| 17 | CP_33% | | 0.29 | 257 |
| 18 | CP_55% | | 0.33 | 262 |

Table 1

Disclosures: Lyn Bowman, None.

SA0023

Contra-Lateral Bone Loss in Post-Menopausal Women After a Distal Radius Fracture: A Two-Year Follow-Up HR-pQCT Study. Joost De Jong*¹, Frans Hever², Paul Willems³, Jacobus Arts³, Martijn Poeze⁴, Piet Geusens⁵, Bert van Rietbergen⁶, Joop van den Bergh⁷. ¹Maastricht University Medical Center, The Netherlands, ² Department of Surgery & NUTRIM, Maastricht University Medical Center, Maastricht, The Netherlands, Netherlands, ³Department of Orthopaedics & CAPRHI, Maastricht University Medical Center, Maastricht, The Netherlands, Netherlands, ⁴Department of Surgery, Maastricht University Medical Center, Maastricht, The Netherlands, Netherlands, ⁵Department of Rheumatology & CAPRHI, Maastricht University Medical Center, Maastricht, The Netherlands, Netherlands, ⁶Faculty of Biomedical Engineering, Eindhoven University of Technology, Eindhoven, The Netherlands, Netherlands, ⁷Department of Internal Medicine, Viecuri Medical Center Venlo & Maastricht University Medical Center, The Netherlands, Netherlands

After fracture of the lower limbs, e.g. a hip fracture, bone loss not only occurs at the fractured side but also at the contra-lateral side due to a period of immobilization. Whether bone loss also occurs at the contra-lateral side of the upper, non-weight bearing limbs, such as the distal radius, is unknown.

The contra-lateral distal radius of 14 post-menopausal women (aged 63.7±7.9 years) with a stable distal radius fracture was scanned by high resolution peripheral quantitative computed tomography (HR-pQCT) at baseline (1-2 weeks post-fracture), 12 weeks and 2 years post-fracture. Standard bone density and micro-structural parameters were assessed, and compression stiffness was calculated using finite element analysis (FEA). Furthermore, markers of bone formation (procollagen type-I N-terminal propeptide; PINP) and resorption (carboxy-terminal telopeptide of type I collagen; ICTP), and inflammation (C-reactive protein; CRP) were measured in venous blood samples. A mixed-effect model with random intercept and visit as fixed effect was used to compare the bone parameters between the three visits. Linear regression was used to assess the correlation between early changes (from baseline to 12 weeks post-fracture) in CRP, PINP and ICTP, and the changes in bone parameters from 12 weeks to 2 years post-fracture.

Ten patients (71%) used bisphosphonates (BP). During 2 years post-fracture, no significant changes occurred in total or trabecular bone density, nor in the trabecular micro-structure and neither in cortical perimeter or thickness at the contra-lateral side. For cortical density (Dcort) and compression stiffness (Scomp) an initial 12 week period without change was followed by a significant decrease of 4.0% (p<0.001) and 4.8% (p=0.005), respectively, at 2 years post-fracture. This change in Scomp correlated positively to the early change in PINP (ρ=0.676, p=0.011). The change in Dcort did not correlate to any of the early changes in PINP, ICTP or CRP. BP use did not affect the results.

Similar to weight-bearing limbs, contra-lateral bone loss was observed 2 years after a fracture at the forearm. Changes in Dcort and Scomp appear to be higher than reported during normal aging, in BP users and non-users. We conclude that a stable fracture at the distal radius is associated with bone and strength loss at the contra-lateral distal radius. Interestingly, a lesser decrease of PINP in the first 12 weeks correlated to less loss of bone strength after 2 years.

Disclosures: Joost De Jong, None.

SA0024

Determination of Elastic Modulus of Mouse Bones Using Data from BioDent Reference Point Indentation (RPI). Ganesh Thiagarajan*¹, Sruvan Kola², Mark Begonia², Mark Dallas², Vladimir Dusevich², Nuria Lara², Mark Johnson². ¹University of Missouri - Kansas City, USA, ²University of Missouri Kansas City, USA

Young's Modulus is a standard measurement of bone stiffness, and 3-point bending is a destructive test used to obtain this value. Reference Point Indentation (RPI) offers a nondestructive alternative to assess bone mechanical properties. However, little is known regarding RPI measurements and their association with widely accepted bone mechanical properties. This study aims to determine the Young's (indentation) Modulus of mouse bones using RPI measurements with the eventual goal of conducting longitudinal in vivo studies in mice. We developed a numerical analysis procedure using the Oliver-Pharr (O/P) method to estimate the indentation elastic modulus using the 1st cycle indentation depth hf and 1st cycle unloading slope at the peak load. Two methods were used to determine the area function: (1) Oliver-Pharr (O/P) and (2) Geometric. Indentations using BioDent were performed on PMMA and on mouse bones.

Femurs from 4-5 mo. and 1.5 yr. TOPGAL old mice were tested under 3-point bending to obtain the elastic modulus for comparisons with the indentation elastic modulus from RPI. Ulnae from mice were also indented and imaged via SEM to assess the damage at each site. The indentation modulus of PMMA calculated by the O/P (3.49-3.68 GPa) and Geometric (3.33-3.49 GPa) methods was similar to values in

literature (~3.5-4 GPa). When comparing the indentation elastic moduli from RPI vs. 3-point bending in 4-5 mo. old femurs, we found that the moduli from both the Geometric and O/P methods were similar to the 3-point bending modulus. In males, the indentation modulus from the Geometric (5.61±1.25 GPa) and O/P (5.53±1.27 GPa) methods was higher than the 3-point bending modulus (5.28±0.34 GPa). In females, the indentation modulus from the Geometric (7.45±0.86 GPa) and O/P (7.46±0.92 GPa) methods was also higher than the 3-point bending modulus (7.33±1.13 GPa). Further elastic modulus comparisons for each age group for mutant and control mice will be presented in detail along with SEM micrographs on mouse ulnae. Based on initial tests conducted on PMMA and mouse bones, RPI indentation modulus values compare well with the Young's modulus values obtained from 3-point bending. The findings of this study indicate that this method could be applied to mice in longitudinal in vivo studies to analyze the effects of anabolic agents on bone material properties.

Disclosures: Ganesh Thiagarajan, None.

SA0025

See Friday Plenary Number FR0025.

SA0026

Early changes in estimated bone stiffness and serum bone markers predict clinical outcome 2 years after stable distal radius fractures: An HR-pQCT exploratory study. Frans Hever*¹, Joost de Jong², Paul Willems³, Chris Arts³, Martijn Poeze¹, Piet Geusens⁴, Bert van Rietbergen⁵, Joop van den Bergh⁶. ¹Department of General Surgery & NUTRIM, Maastricht University Medical Center, Netherlands, ²Department of Rheumatology & NUTRIM, Maastricht University Medical Center, Netherlands, ³Department of Orthopaedic Surgery & CAPRHI, Maastricht University Medical Center, Netherlands, ⁴Department of Rheumatology & CAPRHI, Maastricht University Medical Center, Netherlands, ⁵Faculty of Biomedical Engineering, Eindhoven University of Technology, Netherlands, ⁶Department of Internal Medicine, Viecuri Medical Center Venlo & NUTRIM, Maastricht University Medical Center, Netherlands

Stable distal radius fractures are usually treated by cast immobilization. Functional outcome in this group is highly variable and cannot be predicted by fracture classification. Therefore, we aim to develop methods based on changes in bone micro-architectural parameters during the early stages of fracture healing to predict long-term functional outcome, which will aid in clinical decision making and can also serve as an early outcome measurement in clinical trials.

The development of high-resolution peripheral quantitative computed tomography (HR-pQCT) enables the in vivo assessment of bone microarchitecture and strength estimation with micro-finite elements analysis (μFEA). We hypothesized that HR-pQCT measurements at the fracture location reflect the healing response and are predictive of long-term functional outcome.

In this exploratory study we evaluated 15 patients up to 2 years after a stable distal radius fracture treated by cast immobilization. HR-pQCT scans were performed at 1-2 (baseline), 3-4, 6-8 and 12 weeks and 2 years postfracture. During study visits, pain and disabilities were assessed using the patient rated wrist evaluation (PRWE) questionnaire. Bone stiffness was estimated from the HR-pQCT scans at each time point using μFEA. In addition, markers of bone formation (procollagen type-I N-terminal propeptide; PINP), bone resorption (carboxy-terminal telopeptide of type I collagen; ICTP) and inflammation (CRP) were measured in venous blood samples. Area under the curve (AUC) in the first 3 months was used as a summary statistic to reflect the longitudinal changes between 1-2 and 12 weeks postfracture. Linear regression models were used to predict 2 year functional outcome by PRWE from early AUCs.

The changes from baseline to 12 weeks postfracture in torsional (ρ=-0.54; p=0.037) and bending stiffness (ρ=0.84; p<0.001), and PINP (ρ=0.62; P=0.014) were correlated with PRWE outcome after 2 years (table 1 and 2). Using regression analysis, these parameters predicted up to 50% of the variation in long-term functional outcome after stable distal radius fractures.

Although limitations of this study are the low number of patients and lack of validation of μFEA in metaphyseal fractures, our results indicate that early changes in torsional and bending stiffness as measured with HR-pQCT, and serum markers of bone formation are useful for the prediction of long term clinical outcome (pain and disability) after distal radius fractures.

| AUC | Spearman's Rho | P | R | R ² | Regression coefficient | P | Intercept |
|--------|----------------|--------|-------|----------------|------------------------|-------|-----------|
| S.comp | -0.263 | 0.343 | 0.193 | 0.037 | NS | 0.491 | NS |
| S.tors | -0.541 | 0.037 | 0.61 | 0.372 | -1.85x10 ⁻⁵ | 0.016 | 106.039 |
| S.bend | -0.843 | <0.001 | 0.732 | 0.536 | -1.22x10 ⁻⁵ | 0.002 | 101.094 |

AUC=area under the curve; S.comp=compression stiffness; S.tors=torsional stiffness; S.bend=bending stiffness; NS=not statistically significant

Table 1: AUC of bone stiffness correlated to PRWE score at 2 years follow up.

| AUC | Spearman's | | | | Regression | | Intercept |
|------|------------|-------|-------|----------------|-------------|-------|-----------|
| | Rho | P | R | R ² | coefficient | P | |
| PINP | 0,620 | 0,014 | 0,702 | 0,493 | 0,100 | 0,004 | -34,091 |
| ICTP | 0,184 | 0,512 | 0,072 | 0,005 | NS | 0,799 | NS |
| CRP | 0,014 | 0,959 | 0,126 | 0,016 | NS | 0,655 | NS |

AUC=area under the curve; PINP= procollagen type-I N-terminal propeptide; ICTP= carboxy-terminal telopeptide of type I collagen; CRP= C-reactive protein; NS=not statistically significant

Table 2: AUC of serum markers correlated to PRWE score at 2 years follow up.

Disclosures: Frans Heyer, None.

SA0027

Effect of Intermittent Radiation Exposure in vivo On Tibia Micro-Architecture in OVX Sprague-Dawley Rats Over 3 Months. Amanda Longo*, Sandra Sacco, Wendy Ward. Brock University, Canada

Recent advances in in vivo micro-computed tomography (μ CT) allow researchers to measure changes in tibia micro-architecture at multiple times throughout the lifespan and/or in response to an intervention. This is highly advantageous as it substantively reduces the number of animals required for long-term testing of an outcome. However, continued radiation exposure may have a negative impact on the skeletal region under investigation. The purpose of this study was to elucidate an effect of intermittent radiation exposure over a three-month period to micro-architecture of the tibia in the ovariectomized (OVX) rat and to determine if estrogen modulates this response. The right proximal tibia of three-month OVX or sham-operated Sprague-Dawley rats (n=12/group) was scanned one-week following OVX or sham-surgery and at 1, 2 and 3 months post-surgery. The contralateral proximal tibia was scanned at study endpoint only, 3 months post-surgery, to allow direct comparison with the right proximal tibia. All scans were performed using high-resolution parameters (18 μ m resolution, 60kV, 200 μ A, 1mm Al filter, 0.5° rotation step, SkyScan 1176) at a radiation dose of approximately 600mGy (TN-502RD-H, Best Medical Canada). A repeated measures ANOVA was performed to assess an effect of age and estrogen status. A two-way ANOVA was used to quantify an effect of the frequency of radiation exposure and estrogen status between left and right legs at study endpoint. As expected, there was an interaction of age and estrogen status for trabecular morphometry of the right proximal tibia: percent bone volume (p=0.002), trabecular number (p<0.001), trabecular separation (p<0.001), and structural model index (p<0.001). These findings support the role of estrogen in the maintenance of bone architecture with aging. Trabecular thickness increased with age in both OVX and sham-operated rats (p=0.007). There were no differences in bone micro-architecture between the left and right proximal tibia when exposed to a single or repeated scans, respectively. Moreover, having observed no interaction between estrogen status and frequency of radiation exposure, suggests that endogenous estrogen production does not alter the susceptibility of trabecular bone of the proximal tibia to the effects of either single or repeated scans. These findings provide support for the use of repeated in vivo scans by high-resolution μ CT in the well-characterized OVX rat model.

Disclosures: Amanda Longo, None.

SA0028

See Friday Plenary Number FR0028.

SA0029

See Friday Plenary Number FR0029.

SA0030

Effect of Varying Levels of Compositional Heterogeneity on Fracture Resistance in Cortical Bone. Ani Ural*. Villanova University, USA

The recent reports of atypical femoral fracture and its possible association with prolonged bisphosphonate use highlighted the importance of a thorough understanding of mechanical modifications in bone due to bisphosphonate treatment. The reduced compositional heterogeneity of bone is one of the modifications in bone due to extensive suppression of bone turnover. The goal of the current study is to evaluate the influence of varying levels of compositional heterogeneity on fracture resistance in human cortical bone using finite element modeling.

A transverse microscopy image of cortical bone from the mid-diaphysis of a 70-year-old male donor tibia was converted to a 3D finite element model which was inserted in a compact tension test specimen to evaluate the fracture resistance of the bone (Fig. 1). Crack formation and propagation was modeled by cohesive extended finite element method in the osteons and interstitial bone and by cohesive interface elements at the cement lines. Five models were generated including a model with homogeneous material properties (HM) and four heterogeneous models with 5 (HT1), 10 (HT2), 15 (HT3), and 20 (HT4) different material property groups in the microstructural region. Heterogeneous material properties were randomly assigned to each element in the microstructural region using a MATLAB script based on values reported in the literature. The average material properties were used for the

homogeneous model. The fracture response was assessed through crack growth path and the volume of cracked elements.

There was only 1% difference in the crack volume between HM and HT1 (Fig. 2a). On the other hand, the crack volume in HT2 and HT3 was reduced to 62% and 75% of HM, respectively. The crack volume increased for HT4 which had 92% of crack volume of HM. The crack growth paths exhibited mostly smooth crack growth for HM and HT1. HT2 and HT3 demonstrated extended uncracked sections of bone with low damage whereas this behavior was limited for HT4 (Fig. 2b-2f).

In summary, the results showed that although increasing heterogeneity enhanced the fracture resistance of bone, there is a threshold after which its beneficial effects were not as significant. These results provide new information on the relationship between varying levels of tissue heterogeneity and fracture resistance and may improve the understanding of the influence of material level changes due to prolonged bisphosphonate use on the fracture resistance of bone.

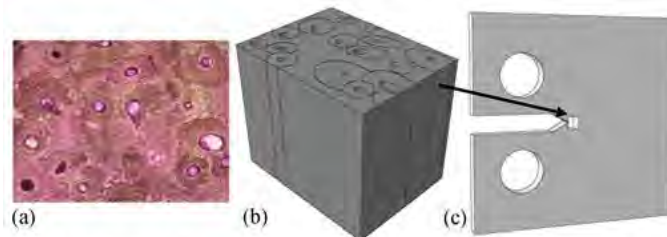


Figure 1: (a) Microscopy image of human cortical bone from a 70-year-old donor (b) 3D finite element model of the microscopy image in (a). (c) Finite element model of the compact tension specimen with a hole where the detailed microstructural bone volume is inserted.

Figure 1

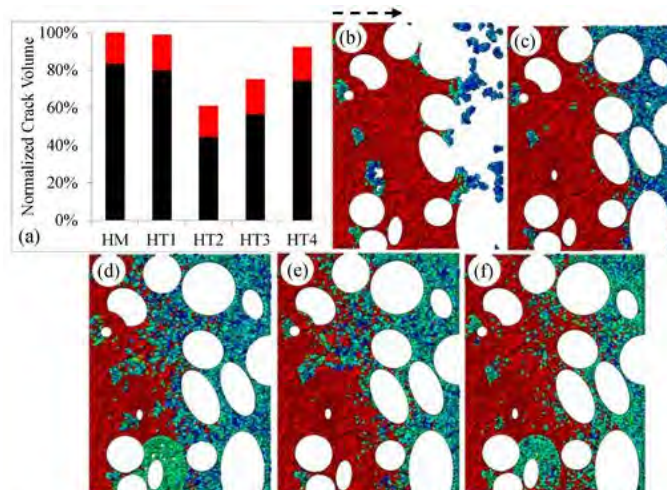


Figure 2: (a) Total crack volume in osteons and interstitial bone in heterogeneous and homogeneous models. Note that red and black denote the crack volume in osteons and interstitial bone, respectively. Planar view of crack growth in (b) HM (c) HT1 (d) HT2 (e) HT3 (f) HT4 models. Note that the colors show the accumulated damage where red is a full crack and dark blue means no damage. Dashed arrow shows the direction of crack growth.

Figure 2

Disclosures: Ani Ural, None.

SA0031

FES-Rowing Training Improves Bone Strength of the Paralyzed Legs in a Dose-Dependent Fashion. Leslie Morse*¹, Can Tan¹, Ricardo Battaglini², Rajiv Gupta¹, J.A. Taylor¹. ¹Harvard Medical School, USA, ²The Forsyth Institute, USA

Objective: To determine if the combination therapy of FES-rowing plus zoledronic acid (ZA) improves bone strength in participants with lower extremity paralysis.

Methods: This was a longitudinal comparative clinical trial, where 29 non-ambulatory volunteers with SCI were randomized into treatment (ZA, n = 13) or no treatment (n = 16), and all were enrolled in a 12-month FES-rowing exercise program.

Lower extremity computed tomography (CT) scans were obtained at baseline (all volunteers) and after 6 (n = 18) or 12 months (n = 27) of exercise (n=17 at all three time points). Axial stiffness of the proximal fibula (non-weight-bearing bone, reflecting the effect of ZA treatment alone), and proximal tibia and distal femur (reflective of weight-bearing and ZA treatment) were quantified via finite element analysis using reconstructed 3D models of volumetric CT scans. Effects of ZA treatment, exercise, and time were assessed via a linear mixed-effect model, repeated on each side (dominant vs non-dominant) nested within each subject with a random intercept, taking into account correlations between each bone within each side and subject.

Results: Volunteers were 37 + 2 (SE) years old with a BMI 26.0 + 1.0. All but five had adult-onset spinal cord injury (average age at injury 26 + 11) at C4 – T12 level, ASIA A – C. At the time of enrollment, volunteers were 2 months – 38 years post-injury (average 11 + 2 years). On average, volunteers exercised 1.6 + 0.1 times a week and the intensity of exercise varied substantially among volunteers. There was a time-dependent decline in fibula stiffness, which was prevented by ZA treatment (treatment x time effect $p < 0.01$). In contrast to the fibula, there was no decline in tibia stiffness for either rowing-only or rowing plus ZA treatment ($p > 0.2$ for time, treatment, or interaction effects), suggesting that both ZA treatment and exercise were effective at preventing bone loss. Furthermore, a subgroup analysis showed that gains in axial stiffness varied in a dose-dependent fashion based on the total amount of exercise performed in the rowing-only arm (1.3 + 4.3% at the tibia and 7.9 + 4.4% at the femur in the lowest rowing tertile versus 5.3 + 9.4% at the tibia and 15.7 + 16.8% at the femur, respectively).

Conclusions: Our results from the fibula confirm that ZA treatment prevents SCI-related osteoporotic bone loss. We also show that FES-row exercise alone improves bone strength in a dose-dependent fashion at mechanically stimulated sites, suggesting that FES-row training is an important therapeutic exercise that may reduce fracture risk after SCI.

Disclosures: *Leslie Morse, None.*

This study received funding from: No

SA0032

In vivo precision of three HR-pQCT-derived finite element models of the distal radius and tibia in postmenopausal women. Chantal Kawalilak*, Saija Kontulainen, Morteza Amini, Joel Lanovaz, James D Johnston. University of Saskatchewan, Canada

Objective. The objective of our study was to define and compare in vivo precision errors for 3 high-resolution peripheral quantitative computed tomography (HR-pQCT) based finite element (FE) models of distal radii and tibiae in postmenopausal women. Models include: a single-tissue model (STM), a cortical-trabecular double-tissue model (DTM) and one model scaled according to imaged density. Methods. Using HR-pQCT, we scanned the distal radius and tibia of 34 postmenopausal women (74.7 years), at two time points. Primary outcomes for each model included: bone stiffness (N/mm), apparent modulus (MPa), average von Mises stress (MPa), and failure load (kN). Precision errors (root-mean-square coefficient of variation, CV%; and 95% limits of agreement, LOA) were calculated. Multivariate ANOVA was used to compare mean CV% for all outcomes among the 3 FE models. Significance was accepted at $P < 0.05$. Results. At the distal radius, CV% precision for STM and DTM were $< 5.5\%$ (range: 2.8-5.4%) and $< 9.0\%$ for the scaled model (range: 2.6-8.7%). Compared to STM and DTM, the scaled FE model had significantly higher precision error for apparent modulus (mean CV% difference: 3.3-3.4%, $P < 0.020$) and von Mises stress (3.3%, $P = 0.001$). At the distal tibia, precision was $< 5.0\%$ for STM and DTM (range: 0.9-4.8%) and $< 2.5\%$ for the scaled model (range: 1.2-2.1%). The scaled FE model had statistically lower precision error for stiffness compared to the STM (-1.6%; $P = 0.034$). Conclusion. Overall, the scaled FE model appeared more precise for modeling the distal tibia whereas STM and DTM appeared more precise for modeling the distal radius. Qualitative analyses suggest that precision error differences between the FE models are due to different periosteal boundary definitions.

Disclosures: *Chantal Kawalilak, None.*

SA0033

Intravertebral Heterogeneity of Lumbar Vertebral Trabecular Bone Density Assessed from in vivo QCT is Weakly Associated with Lumbar Spine TBS Measured by DXA. Fjola Johannesdottir*¹, Arunima Awale², Paul Fein³, Brett Allaire⁴, Robert R. McLean⁵, Kerry E. Broe², Elizabeth J. Samelson⁵, Douglas P. Kiel⁵, Elise Morgan³, Mary L. Bouxsein⁶.

¹University of Cambridge, United Kingdom, ²Institute for Aging Research, Hebrew SeniorLife, USA, ³Boston University, USA, ⁴Beth Israel Deaconess Medical Center, USA, ⁵Hebrew SeniorLife Institute for Aging Research & Harvard Medical School, USA, ⁶Beth Israel Deaconess Medical Center, Harvard Medical School, USA

In vitro studies show that accounting for the spatial variation, or heterogeneity, of bone density within the vertebral body improves the prediction of vertebral strength compared to bone mass alone [1-3]. Trabecular Bone Score (TBS) is an index that

reflects very local variations in pixel gray-scale values from 2D lumbar spine DXA images. Low TBS values are associated with increased fracture risk, in some cases independently of aBMD [4]. Yet, the skeletal traits that influence TBS are not well understood. In particular, the relationships among TBS and measures of spatial variation in bone density are not known. Thus, we aimed to determine the association between DXA-derived TBS and the intravertebral heterogeneity in trabecular bone density measured by 3D QCT of lumbar vertebrae. Methods: We studied 230 individuals (124 women and 106 men, 44-81 years old) from the Framingham Heart Study cohort who had both 3D QCT and DXA scans of the spine within 6 months of each other. L3 vertebrae were analyzed for aBMD by DXA (Lunar Prodigy) and L3 TBS was computed from the DXA image using TBS iNsight software (V.2.1). QCT scans were analyzed to quantify average trabecular bone density (Tb.BMD) and the intravertebral heterogeneity in density in L3. For heterogeneity measures, we first subdivided the trabecular centrum into 5mm contiguous cubic regions and then measured the vBMD for each cube. Two global measures of heterogeneity were calculated from the cube vBMD values for a given vertebra: 1) the interquartile range (IQR); and 2) the quartile coefficient of variation (QCV) in cube vBMD values [3]. Correlation analyses were used to determine associations between variables. Results: TBS and QCT-derived average trabecular vBMD were moderately, positively correlated ($r = 0.29$, Table 1), whereas TBS and L3 aBMD were unrelated. TBS was weakly associated with the indices of intravertebral heterogeneity in trabecular bone density: IQR ($r = 0.13$, $p = 0.04$) and QCV ($r = -0.18$, $p = 0.005$). In conclusion, TBS by DXA was only weakly associated with global measures of the spatial variation in trabecular bone density assessed by QCT and was moderately correlated with average trabecular vBMD. These findings imply that DXA-based TBS does not reflect global heterogeneity of trabecular bone density throughout the vertebral centrum. Thus, the TBS index may reflect more localized density variations within the trabecular centrum and/or may be influenced by the cortical shell or posterior processes.

References: 1) Fields et al, JBMR 2009; 2) Wegrzyn et al, JBMR 2010; 3) Hussein et al, Osteopor Int 2013; 4) Silva et al, JBMR 2014

Table 1: Correlation coefficients

| | TBS _{L3} * | aBMD _{L3} * | Tb.BMD _{L3} ** | Tb.IQR _{L3} BMD** | Tb.QCV _{L3} BMD** |
|--------------------------|---------------------|----------------------|-------------------------|----------------------------|----------------------------|
| TBS _{L3} | 1 | ns | 0.29 ^b | 0.13 ^a | -0.18 ^a |
| aBMD _{L3} | | 1 | 0.60 ^b | 0.44 ^b | -0.24 ^b |
| Tb.BMD _{L3} | | | 1 | 0.44 ^b | -0.63 ^b |
| Tb.IQR _{L3} BMD | | | | 1 | 0.37 ^b |
| Tb.QCV _{L3} BMD | | | | | 1 |

*Pearson correlation, **Spearman correlation, ns: not significant, ^a $p < 0.05$, ^b $p < 0.001$

Tb.BMD: trabecular vBMD, IQR: interquartile range, QCV: quartile coefficient of variation

Table 1: Correlation coefficients

Disclosures: *Fjola Johannesdottir, None.*

SA0034

See Friday Plenary Number FR0034.

SA0035

See Friday Plenary Number FR0035.

SA0036

Withdrawn

SA0037

Rate of Change of Cortical Mass with Age over the Femoral Surface.

Graham Treece*¹, Andrew Gee¹, Carol Tonkin², Kenneth Poole¹.

¹University of Cambridge, United Kingdom, ²Nova Scotia, Canada, Canada

Purpose: Cortical bone mapping (CBM, Treece MedIA 2015) allows structural properties of the proximal femur, including cortical thickness and density, to be measured from QCT data and displayed as a colour map on the femoral surface. Here we apply CBM to a large cohort of women spanning a wide age range, to investigate in detail how the cortex changes with age at different parts of the femur.

Methods: Mindways Software Inc (Austin, TX, USA) recruited 630 Caucasian women aged 19-97 years (mean 47 ± 17 SD) from 1998 to 2002 at 11 centres in the USA. The cohort comprised women having BMD assessments as part of their clinical evaluation and volunteers who desired an assessment. QCT data, using the Mindways liquid K₂HPO₄ phantom, was obtained from below the lesser trochanter to above the femoral head. The data was collected for the purposes of FDA (510k) approval (K030330) and was subject to Investigational Review Board oversight. Of the 630, 11 were excluded due to incomplete scans and metalwork. For the remaining 619, CBM was used to measure cortical mass surface density (CMSD mg/cm², the product of cortical BMD and cortical thickness) across each proximal femur. All measurements were mapped onto a canonical surface and a model was fitted to the mapped data, explaining CMSD in terms of (1 + age + age²) and other confounding variables. Quadratic modelling allows for different rates of change at different ages and the possibility of detecting peaks.

Results: Figure 1 shows the mean CMSD, its rate of change at ages 30 and 80, and (where detectable) the age at which CMSD peaks. Of particular interest are the regions (a) and (b), where CMSD increases until late middle age before starting to plateau (a) or decline (b), and the region (c) where there is steady, significant loss of CMSD across the entire age range. In terms of hip fragility, region (c) is associated with cervical fracture and (b) with trochanteric fracture: our findings are consistent with cervical fractures being more strongly associated with age than are trochanteric fractures [Lofman OI 2002]. Cortical thickening with age in region (a) has been noted previously [Mayhew Lancet 2005]. Conclusion: CBM has produced a more detailed map of ageing across the proximal femur than has previously been available. This "healthy ageing" baseline might find application in finite element models, fracture studies and intervention planning (pharmaceutical and exercise).

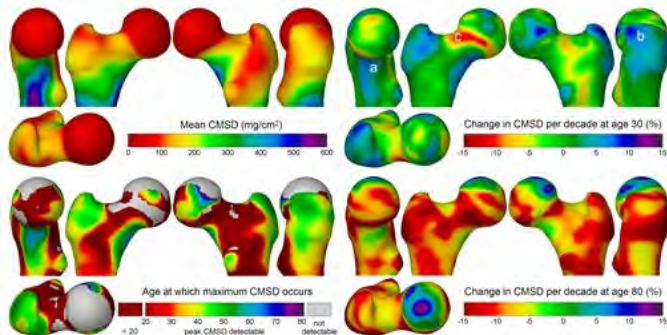


Figure 1. The distribution of cortical mass surface density (CMSD) in the proximal femur. Left top shows the average for women of age 20 to 90. Right column shows the rate of change per decade for young (age 30) and old (age 80) women. Bottom left is the age at which CMSD starts to decline.

Figure 1

Disclosures: *Graham Treece, None.*

SA0038

Sensitivity of Imaging Biomarkers for Detecting Postmenopausal Bone Loss. Wenli Sun^{*1}, Chamith Rajapakse¹, Mahdieh Bashoor-Zadeh¹, Jeremy Magland¹, Mona Al Mukaddam², Rhiannon Miller², Elizabeth A. Kobe², MICHELLE SLINGER², Peter J. Snyder¹, Felix W. Wehrli¹.
¹University of Pennsylvania, USA, ²UPenn, USA

Background: Declined estrogen levels following menopause lead to rapid loss of bone mass, increasing the risk of osteoporosis. The rate of postmenopausal bone loss is a key determinant of bone fracture risk later in life. Early detection of greater than normal bone loss in this population could guide pharmacological interventions, which are known to be effective in reducing fractures. Besides DXA BMD, various imaging modalities and biomarkers are currently available for in-vivo assessment of bone quality, including densitometric, structural, and strength measures. The purpose of this study was to determine which image-based bone outcomes are most affected following menopause.

Methods: This prospective study involved 90 postmenopausal women, aged 55-79 years (mean age = 65.1 ± 5.7 years). Microstructural MRI of the distal tibia and radius was performed on a 3T scanner using 4-channel surface coil at 0.137 mm x 0.137 mm x 0.410 mm voxel size. Structural parameters (bone volume fraction, surface curve ratio, erosion index, trabecular number, separation and thickness) were computed on the basis of these images using digital topological analysis and volumetric topological analysis. Trabecular and whole-section axial stiffness were measured from elastic modulus by finite element analysis. Cortical and trabecular BMD were assessed at the diaphysis and metaphysis, respectively, both in the tibia and radius by means of pQCT. Total hip and lumbar spine areal BMD were determined with DXA. 90 subjects were categorized into three age groups: 50-59 (n = 22), 60-69 (n = 46), and 70-79 (n = 22).

Results: Out of all the parameters measured, only whole-section stiffness and cortical BMD significantly declined with age ($p < 0.05$) in this cohort representing a narrow age range (Figure 1), suggesting that the decline is most likely due to the thinning of cortex rather than trabeculae. Loss of cortex with age in the distal tibia and radius is visually evident from the MR images (Figure 2). All tibial parameters were positively correlated with the corresponding ones at the radius ($R = 0.25 - 0.65$, $p < 0.05$), indicating the systemic nature of bone loss.

Conclusions: Measures involving only trabecular bone or 2D measures were not significantly different among the three groups in this cohort (age 55-79 years). Cortical bone parameters or those being a function of both cortical and trabecular bone (e.g., MRI stiffness and pQCT cortical BMD) were significantly decremented with age.

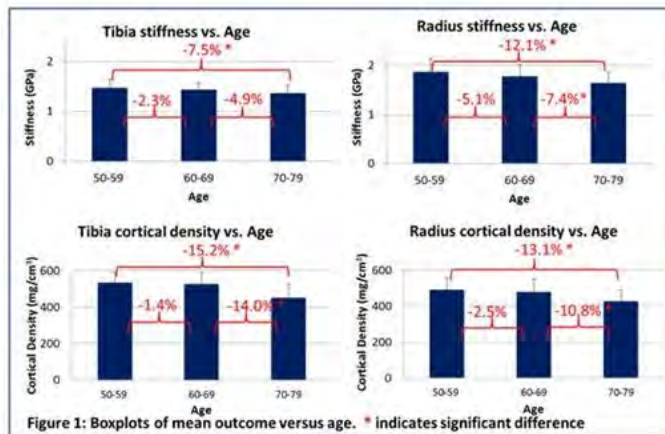


Figure 1

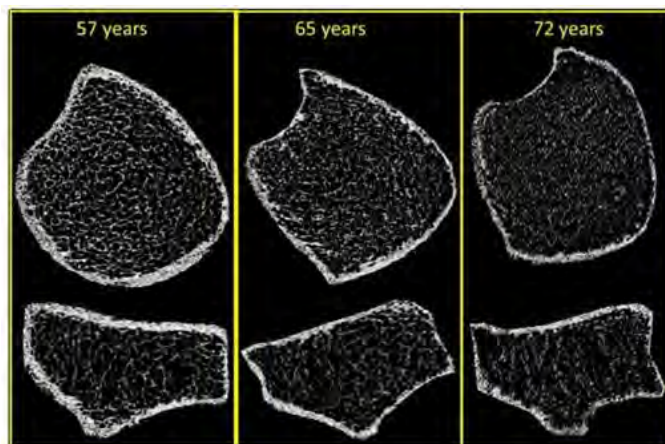


Figure 2: MRI BVF maps of distal tibia and radius of three representative postmenopausal women from three age groups. Note age-related thinning of cortex.

Figure 2

Disclosures: *Wenli Sun, None.*

SA0039

Variation in Cortical Bone Tissue Composition and Mechanical Properties show Significant Genetic Effects. Daniel Nicoletta^{*1}, Ellen Quillen², Arthur Nicholls¹, Don Moravits¹, Jennifer Harris², Shayna Levine², Travis Eliason¹, Matt Allen³, Jeff Nyman⁴, Todd Bredbenner¹, Lorena Havill².
¹Southwest Research Institute, USA, ²Texas Biomedical Research Institute, USA, ³Indiana University, USA, ⁴Vanderbilt University, USA

At the tissue level, cortical bone mechanical integrity is a complex, multivariate function of bone tissue composition and microstructural organization. Co-adaptation of these traits results in trait combinations that provide redundant strategies to provide nominally equivalent functionality. Combinations of traits that are sufficient for everyday loading may be suboptimal for atypical, traumatic loads. The aim of this study was to determine the degree to which normal population level variation in both individual and composite cortical bone mechanical and compositional traits is due to genetic variation. Cortical bone tensile test specimens were obtained from the femur mid diaphysis from 102 baboons (46 males, 56 females). (All animals died naturally or were sacrificed for reasons unrelated to this study). Specimens were monotonically loaded to failure under displacement control at a strain rate of 0.01%/sec. Elastic modulus (E, GPa), yield stress (0.2% offset method) (MPa), ultimate stress (MPa), strain at failure (%), toughness (MPa), and post-yield energy (MPa) were investigated. We also measured cortical porosity, apparent density, ash and water content, collagen crosslinks (pyridinoline (PY), deoxypyridinoline (DPD), pentosidine (PE)), and total collagen content for the same specimens. We identified independent, composite traits (combinations of the tissue composition and biomechanical traits) that describe variability within the group using principal components analysis (PCA). Using a variance decomposition approach, we quantified the contribution of additive genetic effects (heritability [h^2]) to variation in the individual as well as composite cortical bone traits. PCA resulted in a set of 11 composite traits that explains 100% of the variation in individual composition traits and 7 composite traits that explain 100% of the variation in the individual mechanical property traits. After accounting for age and sex effects, significant genetic effects were determined for ash content ($h^2=0.63$, $p=0.003$), DPD xlinks ($h^2=0.52$, $p=0.02$), PE xlinks ($h^2=0.39$, $p=0.03$), post yield energy ($h^2=0.53$, $p=0.007$), toughness ($h^2=0.48$, $p=0.01$), peak strain ($h^2=0.47$,

p=0.012), and three composite traits from the PCA: PC1 ($h^2=0.52$, $p=0.009$), PC3 ($h^2=0.38$, $p=0.04$), and PC5 ($h^2=0.40$, $p=0.04$). These results indicate that normal population level variation in individual bone composition, mechanical property, and complex composite traits are significantly influenced by genes.

Disclosures: Daniel Nicoletta, None.

SA0040

ESR1 and ESR2 Exert Opposing Influence on Bone's Susceptibility to Unloading. Jevantt Srinivas Sankaran^{*1}, Manasvi Varshney¹, Leah-Rae Donahue², Stefan Judex¹. ¹Stony Brook University, USA, ²The Jackson Laboratory, USA

Genetics is a strong determinant of bone's response to mechanical stimuli or absence thereof. Disparity in the amount of bone loss in astronauts/cosmonauts highlights the genetic control of bone loss. To identify genes that regulate this adaptation we performed a mouse linkage study to isolate genomic regions (Quantitative Trait Loci or QTL) that modulate this trait. These QTLs were processed to select bone related genes, yielding estrogen receptor 1 (ESR1) as a genetic target. ESR1 and ESR2 regulate estrogen signaling, critical for the maintenance of bone. Here, we determined whether ESR1 and ESR2 modulate bone loss induced by unloading. 9wk old, female ESR1 KO mice (ESR1^{-/-}, n=38), ESR2 KO (ESR2^{-/-}, n=20) were assigned to baseline control, age matched control, and hindlimb unloaded (HLU) groups. C57BL/6J (B6J, n=34) mice, the background strain of the KOs, were used as wild type (WT) controls. Following 2wk of hindlimb unloading, femurs were harvested and scanned via μ CT. In normal controls, ESR1^{-/-} mice had greater trabecular quantity than their WT counterparts without differences in the thickness of trabeculae. The differences between WT and ESR1^{-/-} mice ranged from 38% greater trabecular number (Tb.N) to 105% greater bone volume (BV) (all $P<0.05$). Between ESR2^{-/-} and WT mice, the differences ranged between 4% lower trabecular thickness (Tb.Th) to 17% greater BV (all $P<0.05$). BV/TV was unaffected by knocking out ESR2. In ESR1^{-/-} mice, unloading did not cause loss of trabecular bone while in WT-B6J mice, HLU significantly degenerated all trabecular indices. When the HLU responses were directly compared between the two strains, the degree of trabecular thinning was lower in HLU ESR1^{-/-} mice when compared to WT-B6J mice (Tb.Th: 7% vs. 19%, Gene*HLU, $P<0.05$). In contrast, ESR2^{-/-} mice exhibited a greater susceptibility to loss of weightbearing. When compared to WT mice, the trabecular compartment of ESR2^{-/-} mice exhibited greater losses in BV (56% ESR2^{-/-} vs. 32% WT), BV/TV (55% vs. 31%), Tb.N (14% vs. 5%) and Tb.Th (27% vs. 19%) (Gene*HLU, all $P\leq 0.05$). Both ESR1^{-/-} and ESR2^{-/-} mice had enhanced cortical architectural indices at baseline but their response to hindlimb unloading was similar to WT-B6J mice. Validation of ESR1 and ESR2 as contrasting modulators of trabecular adaptation during unloading may aid in development of specific drug targets to treat disuse bone loss.

Disclosures: Jevantt Srinivas Sankaran, None.

SA0041

See Friday Plenary Number FR0041.

SA0042

See Friday Plenary Number FR0042.

SA0043

See Friday Plenary Number FR0043.

SA0044

See Friday Plenary Number FR0044.

SA0045

Does premenarcheal gymnastics training benefit bone structural strength at the proximal femur after long-term retirement?. Marta Erlandson^{*1}, Stefan Jackowski², Adam Baxter-Jones¹. ¹University of Saskatchewan, Canada, ²University of Saskatchewan & Pivotal Therapeutics Inc, Canada

We have previously found that when adjusted for body size, a group of premenarcheal gymnasts had significantly greater indices of both axial strength and bending strength at the narrow neck (NN) and femoral shaft regions of the proximal femur (PF), as well as a greater bone strength index at the femoral shaft (S). It is thought that the mechanical loading experienced during growth increased their adolescent bone mass and positively influenced their adolescent bone geometry and architecture. If these bone adaptations were to be maintained when the gymnastics stimulus was withdrawn it could result in a decreased risk of developing osteoporosis and related fractures later in life. Therefore, the purpose of this investigation was to determine if the former gymnasts maintained the bone strength advantages after a long term retirement from gymnastics. A dual x-ray absorptiometry (DXA) scan of

the non-dominant hip was obtained in 23 retired female gymnasts and 22 controls, age range 22 to 30 years. Cross-sectional area (CSA), section modulus (Z), cortical thickness (CT) and buckling ratio (BR) at the NN, intertrochanter (IT), and S were estimated using hip structural analysis (HSA). Multivariate analysis of covariance (covariates: age, height, weight, age at menarche, and physical activity) was used to compare properties between retired gymnasts and controls. Adjusted means showed that gymnasts had 13% greater NN CSA (0.42 ± 0.15 cm², $p<0.05$), 13% greater NN Z (0.21 ± 0.10 cm³, $p<0.05$), 21% greater NN CT (0.05 ± 0.008 cm², $p<0.05$), 33% lower NN buckling ratio (-2.4 ± 0.63 , $p<0.05$), 11% greater IT CSA (0.61 ± 0.29 cm², $p<0.05$), 13% lower IT buckling ratio (-1.1 ± 0.39 , $p<0.05$), and 9% greater S CSA (0.42 ± 0.18 cm², $p<0.05$) compared to controls. These results suggest that former gymnasts maintain significantly better geometric and bone architectural properties at the hip 10 years after retirement from gymnastics training.

Disclosures: Marta Erlandson, None.

SA0046

Effect of Exercise Modality during Weight Loss on Bone Mineral Density in Overweight and Obese, Older Adults. Kristen Beavers^{*1}, Daniel Beavers², Sarah Martin¹, Anthony Marsh¹, Mary Lyles², Leon Lenchik², Barbara Nicklas². ¹Wake Forest University, USA, ²Wake Forest School of Medicine, USA

Purpose: Identification of weight loss therapies that minimize bone loss in older adults is critical. The purpose of this study was to determine whether resistance training (RT) attenuates loss of hip and spine BMD compared to aerobic training (AT) during caloric restriction (CR) in overweight and obese, older adults. Methods: We combined data from 2 5-month, randomized controlled trials of CR with either RT or AT in overweight and obese (BMI=27-45 kg/m²), older (65-79 years) adults, free from clinically diagnosed osteoporosis at baseline. The first study randomized participants to a structured RT program (3 days/week; 8 upper/lower body exercises, 3 sets, 10 repetitions at 70% 1 repetition maximum) with and without CR. The second study randomized participants to a structured AT program (4 days/week; 30 minutes at 65-70% heart rate reserve) with and without CR. We compared the effect of RT+CR versus AT+CR, only. All participants received a daily calcium (1200 mg) and vitamin D (1600 IU) supplement. BMD at the total hip, femoral neck, and lumbar spine (L1-L4) regions was assessed via DXA at baseline and 5-months. Results: Sixty-three and 60 participants completed the RT+CR and AT+CR interventions, respectively. Average age was 69.4 ± 3.5 years. 67% of the study sample was female, and 81% was Caucasian. Baseline BMI was lower in RT+CR (30.4 ± 2.2 kg/m²) than AT+CR (34.7 ± 3.7 kg/m²). Overall exercise compliance was excellent (>80% sessions attended for both RT and AT) and average weight loss was 5.7% (95% CI: 4.6-6.7%) and 8.2% (95% CI: 7.2-9.3%) in the RT+CR and AT+CR groups, respectively. After adjustment for age, gender, baseline BMI, baseline regional BMD, and weight change, differential treatment effects were observed for the total hip and femoral neck regions (both $p<0.05$), but not lumbar spine. Specifically, total hip (0.001 [95% CI: -0.003, 0.006] g/cm²) and femoral neck (0.008 [95% CI: -0.000, 0.016] g/cm²) BMD was unchanged in RT+CR participants, and modestly decreased in AT+CR participants (total hip: -0.008 [95% CI: -0.012, -0.003] g/cm²; femoral neck: -0.007 [95% CI: -0.014, 0.001] g/cm²). Conclusion: Exercise modality differentially effects change in BMD in older adults undergoing CR. Data suggest that AT+CR results in greater loss of hip and femoral neck BMD than RT+CR. Findings warrant replication from a long-term, randomized controlled trial.

Table 1. Baseline descriptive characteristics according to treatment group.

| Baseline Characteristics | RT+CR | AT+CR |
|---|--------------|--------------|
| | n=63 | n=60 |
| Age (years) | 70.0 ± 3.8 | 68.7 ± 3.1 |
| Female, n (%) | 37 (58.7) | 45 (75.0) |
| White, n (%) | 55 (87.3) | 45 (75.0) |
| Weight (kg) | 85.4 ± 11.7 | 92.4 ± 12.2 |
| BMI (kg/m ²) | 30.4 ± 2.2 | 34.7 ± 3.7 |
| Bone Medication Use*, n (%) | 4 (6.3) | 3 (5.0) |
| Year of Menopause** (years) | 46.0 ± 6.5 | 46.4 ± 8.4 |
| Total Hip aBMD (g/cm ³) | 0.96 ± 0.15 | 0.98 ± 0.13 |
| Total Hip T-score | -0.18 ± 1.04 | 0.15 ± 0.95 |
| Femoral Neck aBMD (g/cm ³) | 0.77 ± 0.13 | 0.78 ± 0.11 |
| Femoral Neck T-score | -0.93 ± 1.08 | -0.73 ± 0.95 |
| Lumbar Spine*** aBMD (g/cm ³) | 1.10 ± 0.22 | 1.10 ± 0.18 |
| Lumbar Spine T-score | 0.31 ± 1.91 | 0.42 ± 1.62 |

Data are presented as means ± SD or n (%).

*Prescription bone medication usage includes anabolic (i.e. Fosamax, Boniva, Actonel, Reclast, Evista, Prolia, Forteo) and catabolic (i.e. Dilantin, Lexapro, Prozac, Zolof, Cortisone, Prednisone) medications.

**Year of menopause acquired on a subset of participants (RT+CR=36 and AT+CR=45).

***Lumbar spine defined as L1-L4.

Table 1

Table 2. Unadjusted and adjusted 5-month treatment effects on regional BMD.

| Regional Change in BMD | RT+CR | AT+CR | p-value |
|------------------------------------|-----------------------|-------------------------|---------|
| | Mean (95% CI) | Mean (95% CI) | |
| Total Hip (g/cm ³) | | | |
| Unadjusted | 0.001 (-0.003, 0.005) | -0.008 (-0.012, -0.004) | <0.01 |
| Adjusted | 0.001 (-0.003, 0.006) | -0.008 (-0.012, -0.003) | 0.02 |
| Femoral Neck (g/cm ³) | | | |
| Unadjusted | 0.006 (-0.001, 0.013) | -0.005 (-0.011, 0.002) | 0.04 |
| Adjusted | 0.008 (-0.000, 0.016) | -0.007 (-0.014, 0.001) | 0.03 |
| Lumbar Spine* (g/cm ³) | | | |
| Unadjusted | 0.004 (-0.004, 0.011) | 0.011 (0.003, 0.018) | 0.20 |
| Adjusted | 0.008 (-0.000, 0.017) | 0.006 (-0.002, 0.015) | 0.78 |

Unadjusted estimates are based on a one-way ANOVA at 5-months. Model-adjusted estimates control for age, gender, baseline BMI, baseline regional BMD, and weight change.

*Lumbar spine defined as L1-L4.

Table 2

Disclosures: *Kristen Beavers, None.*

SA0047

Higher Levels of Habitual Physical Activity Results in Region-specific Gains in Cortical Mass Distribution in Pre-pubertal Boys, but not Girls. [Rachel L Duckham](#)¹, [Timo Rantalainen](#)¹, [Gaele Ducher](#)¹, [Briony Hill](#)², [Richard M Telford](#)³, [Rohan D Telford](#)⁴, [Robin M Daly](#)². ¹Centre for Physical Activity & Nutrition Research, Deakin University, Australia, ²Centre for Physical Activity & Nutrition Research, Deakin University, Australia, ³Centre for Research & Action in Public Health, University of Canberra, Australia, ⁴Medical School, College of Medicine, Biology & Environment, Australian National University, Canberra, Australia

Cortical bone is a non-uniform tissue, with its apparent mass and density varying around the bone cross-section. Targeted weight-bearing exercise during the pre-

pubertal years can improve bone mass, structure and cortical distribution at loaded sites, but less is known about the influence of habitual physical activity (PA). This study examined the effects of habitual PA on cortical bone density, geometry and its mass distribution in pre-pubertal children. A total of 245 girls and 241 boys aged 7-9 years had a pQCT scan to measure tibial mid-shaft (66%) total and cortical area, volumetric bone density, polar strength strain index (SSI_{polar}) and the mass/density distribution through the bone cortex (radial distribution divided into endo-, mid- and peri-cortical regions) and around the centre of mass (polar distribution). PA quartiles were generated based on daily step counts (pedometer, 7-days) for boys and girls separately. Boys were 1.4 cm taller (p<0.05) and had 16.6% less tibial fat CSA than girls (p<0.01). On average, 25% of boys and 15% of girls were classified as inactive based on the recommended cut-points of 12,000 and 10,000 steps per day, respectively. There were no gender differences in total and cortical bone area or density, but cortical mass in the lateral region was 6.7% (p<0.001) greater in boys versus girls. In contrast, peri-cortical density (outer third of cortical bone) was greater (0.7%, P<0.05) in girls. There were no differences in any of the bone parameters across the PA quartiles for either sex, with the exception that boys in the highest versus lowest quartile had 8.5% (p<0.05) greater cortical mass at the lateral region. When PA was categorized into high and low levels based on the recommended cut-points, boys in the high PA group had 4-6% greater cortical bone mass compared to the less active group across nearly all sectors of the tibia cortex. In girls, contrasting levels of PA had no effect on polar cortical bone mass distribution. In conclusion, higher levels of habitual PA resulted in small regional specific gains in mid-tibial cortical bone mass distribution, with no significant effect on whole cortical bone parameters, in pre-pubertal boys but not girls. While these findings suggest that higher levels of habitual PA may produce small structural changes in cortical bone in healthy pre-pubertal boys, the clinical relevance of these changes remains to be determined given there was no apparent effect on whole bone strength

Disclosures: *Rachel L Duckham, None.*

SA0048

Serum Sclerostin Decreases Following 12 Months of Resistance- or Jump-training in Men with Low Bone Mass. [Pam Hinton](#)^{*}, [Peggy Nigh](#), [John Thyfault](#). University of Missouri, USA

Purpose: We previously reported that 12 months of resistance training (RT, 2x/wk, N= 19) or jump training (JUMP, 3x/wk, N= 19) increased whole body and lumbar spine BMD and increased serum bone formation markers relative to resorption in physically active (≥4 hr/wk) men (mean age: 44 ± 2 y; median: 44 y) with osteopenia of the total hip or lumbar spine. The purpose of this secondary analysis was to examine the effects of the RT or JUMP intervention on potential mediators of the exercise effects on bone, specifically IGF-I, PTH and sclerostin. **Methods:** Fasting blood samples were collected after a 24-h period of no exercise at baseline and after 12 months of RT or JUMP. IGF-I, PTH and sclerostin were measured in serum by ELISA. The effects of RT or JUMP on IGF-I, PTH and sclerostin were evaluated using 2x2 repeated measures ANOVA (time, group). This study was conducted in accordance with the Declaration of Helsinki and was approved by the University of Missouri IRB. **Results:** There was a significant time main effect for serum sclerostin (p=0.012), such that sclerostin decreased ~7% from 39.2 ± 11.6 ng/mL at baseline to 36.8 ± 13.3 ng/mL after 12 months of RT or JUMP. IGF-I increased ~26% from 203 ± 71 ng/mL to 239 ± 109 ng/mL after 12 months of RT or JUMP (time main effect, p=0.036). PTH remained unchanged from baseline to 12 months. **Conclusion:** The beneficial effects of RT or JUMP on BMD and bone turnover in moderately active, osteopenic men are associated with decreased sclerostin and increased IGF-I.

SA0049

Spinal Bone Texture Assessed by Trabecular Bone Score (TBS) in Adolescent Girls with Anorexia Nervosa. Catherine Gordon^{*1}, Abigail Donaldson², Henry Feldman³, Jennifer O'Donnell⁴, Geetha Gopalakrishnan⁵. ¹Hasbro Children's Hospital & Brown University, USA, ²Division of Adolescent Medicine, Hasbro Children's Hospital & Alpert Medical School of Brown University, USA, ³Clinical Research Center, Boston Children's Hospital, USA, ⁴Division of Adolescent Medicine, Hasbro Children's Hospital, USA, ⁵Division of Endocrinology, Women & Infant's Hospital, USA

Purpose: Trabecular bone score (TBS) is a novel bone assessment tool that offers information beyond that afforded by standard dual-energy X-ray absorptiometry (DXA) bone mineral density (BMD) measurements. Adolescents with anorexia nervosa (AN) are known to exhibit deficits in both bone density and skeletal strength. Lumbar spine TBS was derived from spinal DXA measures to determine whether this assessment provided evidence of degraded bone microarchitecture in this patient group. This study also aimed to examine the relation of TBS to measures of axial and peripheral BMD and bone strength, anthropometrics, body composition, disease duration, and fracture among a sample of adolescent girls with AN. **Methods:** Fifty-seven females with AN, age 11-18 years, were enrolled from an urban eating disorders program. DXA BMD spinal measures were retrospectively analyzed for TBS. Findings were compared to clinical variables (height, weight, BMI, 25-hydroxyvitamin D); spine and whole body DXA measures of areal BMD and body composition; tibial peripheral quantitative computed tomography (pQCT) volumetric BMD measures and strength-strain index (SSI); and self-reported data (illness duration, amenorrhea, exercise, fracture, family history of osteoporosis, and antidepressant use). **Results:** TBS scores were abnormal in 44% of participants: 6 (11%) showed degraded and 19 (33%), partially degraded, microarchitecture. Spinal TBS correlated significantly ($p < 0.05$) with age, height, weight, BMI, absolute BMD and BMD Z-score at all skeletal sites. TBS was also correlated significantly ($p < 0.001$) with total volumetric BMD at the 3% tibial site, and SSI at both the 38% and 66% sites by pQCT; and lean body mass by DXA. Clinical variables that were not correlated with TBS included duration of amenorrhea or AN, fracture, body fat percentage, exercise, antidepressant use, family history of osteoporosis, vitamin D status, race or ethnicity. **Conclusions:** To our knowledge, this is the first study to test use of TBS as part of a skeletal evaluation in a pediatric population. TBS was abnormal in over 40% of adolescents with AN, and was strongly correlated with measures of areal and volumetric BMD, skeletal strength, body composition, and anthropometric measures. TBS is a novel, additional bone assessment method that indicates compromised bone health in adolescents with AN.

Disclosures: Catherine Gordon, None.

SA0050

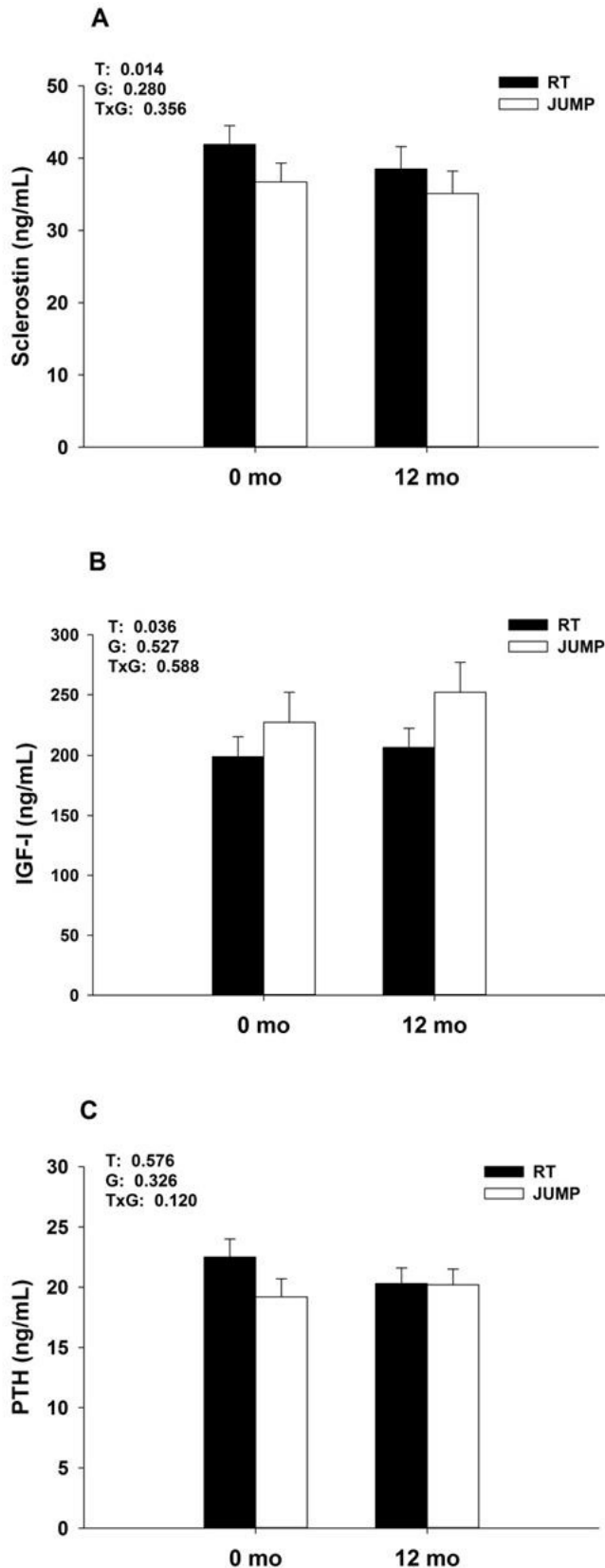
Weight Percentile is an Effective Predictor of Osteoporosis in Patients with Cerebral Palsy. A Cross Sectional Study Analyzed by Simulation and Data-mining Approaches. Abdulhafez Selim¹, Abeer Hegazy^{*2}. ¹Center for Chronic Disorders of Aging, PCOM, USA, ²Dammam Medical Complex Rehab Center, Saudi Arabia

Cerebral palsy (CP) is the most common physical disability in children and affects 3.6/1,000 children. Babies with CP may not gain weight at the same rate as other babies their age. In addition to poor linear growth, children with moderate to severe CP often sustain painful pathological fractures due to poor mineralization of bone. The risk of osteoporotic fracture is further complicated by the difficulty associated with BMD assessment due to limitations induced by difficult positioning and other artifacts in these children. Clinicians, therefore, need methods that can easily predict low BMD scores early on in order to prevent osteoporosis-related complications. We therefore conducted a cross-sectional study in order to satisfy this clinical need by identifying an effective prediction method.

The study included thirty CP patients of both genders, between 5 and 8 years of age. Case record forms were used to record full medical history including weight; height; BMI; mid-arm circumference; head circumference; triceps skin fold thickness; prenatal, perinatal and postnatal history; nutritional history; type of rehabilitation program and physiotherapy; and medications used. Weight, height, and BMI percentiles were classified into three categories: above 50th percentile (rank 3), at 50th percentile (rank 2), and below 50th percentile (rank 1). Ranked data were used for further analyses. Subjects underwent dual energy x-ray absorptiometry (DXA) scan and results were compared to reference values in children relative to age, gender and body size. The collected data was analyzed using correlation, step-wise regression, Bayesian simulation analysis, and data-mining approaches.

A significant correlation was observed between the weight percentile rank and BMD scores (0.8, P -value = 0.001). Stepwise regression analysis demonstrated that weight rank can effectively predict the BMD score (BMD score = $-3.7 + 0.8 * (\text{weight rank})$, $R^2 = 0.6$ and P -value < 0.00). The positive predictive value of this equation was found to be 100%. Simulation outcomes further demonstrated that subjects with weight below 50th percentile are at high risk of having low BMD scores (-2.9 ± 0.17). Additionally, data-mining analysis suggested that those patients with weight rank less than 50th percentile are likely to have a BMD score of -3 . Collectively, these data suggest that managing physicians can use patient's weight rank in order to effectively predict the BMD status. To our knowledge this is the first study that proposes a simplified yet effective approach for BMD prediction in CP patients.

Disclosures: Abeer Hegazy, None.



Sclerostin, IGF-I, PTH after RT or JUMP

Disclosures: Pam Hinton, None.

SA0051

See Friday Plenary Number FR0051.

SA0052

See Friday Plenary Number FR0052.

SA0053

See Friday Plenary Number FR0053.

SA0054

See Friday Plenary Number FR0054.

SA0055

See Friday Plenary Number FR0055.

SA0056

Maintenance on a Low Calcium Diet Results in an Osteocyte-Mediated Reduction of Long-Term Hematopoietic Stem Cell Engraftment. Benjamin Frisch^{*1}, Alexandra Goodman¹, Olga Bromberg¹, Xiaolin Tu², Teresita Bellido², Laura Calvi¹. ¹University of Rochester School of Medicine & Dentistry, USA, ²Indiana University Department of Anatomy & Cell Biology, USA

The bone marrow microenvironment, including osteolineage cells, is known to play a critical role in the regulation of hematopoietic stem cells (HSCs). Intermittent pharmacologic treatment with parathyroid hormone, PTH (1-34), is anabolic to bone, and increases HSCs in mice through microenvironmental signals, as HSCs do not express the PTH receptor (PTH1R). However, continuous PTH treatment is catabolic to bone, while its effects on HSCs are not known. We used a model of secondary hyperparathyroidism in which we maintained mice on a low calcium (LCa) diet in order to investigate the role of continuous PTH exposure on HSCs. In juvenile mice placed on the low calcium diet immediately upon weaning, PTH levels were significantly elevated as early as 7 days. Fourteen days on the LCa diet caused a significant reduction in long-term engraftment potential as measured by secondary competitive transplants over 22 weeks (Normal vs LCa diet donors, 2-way ANOVA $p \leq 0.001$, $N \geq 20$ mice/group), while there was no decrease in HSCs when adult mice were placed on the LCa diet. These data suggest that sustained PTH signaling decreases microenvironmental support for HSCs in juvenile mice. Osteocytes are the most abundant osteolineage cells in the bone and activation of PTH signaling specifically in osteocytes is anabolic. Osteocytes are also known to regulate multiple cellular components of the HSC niche. Therefore, we studied the role of osteocytic PTH signaling in our model using cre recombinase driven by the 8kb-DMP1 promoter to conditionally delete PTH1R in osteocytes (OCyPTHRko mice). In juvenile mice the lack of PTH signaling in osteocytes rescued the long-term engraftment defects, suggesting that PTH signaling in osteocytes mediates the loss of long-term HSC support caused by the LCa diet. In further support of a deleterious effect mediated by the PTH1R in osteocytes in the setting of continuous PTH, adult OCyPTHRko mice placed on LCa diet had superior long term HSC function. Our findings demonstrate that continuous exposure to elevated levels of PTH in a model of secondary hyperparathyroidism leads to osteocyte-mediated loss of long-term engraftment potential of HSCs in juvenile mice. These data also suggest that additional effects of continuous PTH, likely mediated by other HSC niche cellular populations, are instead supportive of LT-HSC function and that the relative contributions of niche populations to HSC regulation are modulated by age.

*Disclosures: Benjamin Frisch, None.***SA0057**

See Friday Plenary Number FR0057.

SA0058

See Friday Plenary Number FR0058.

SA0059

See Friday Plenary Number FR0059.

SA0060

See Friday Plenary Number FR0060.

SA0061

Radiation Injury Links Mineral Homeostasis to Hematopoietic Stem Cell Niche Activation. Corey Hoffman^{*}, Mark LaMere, Alexandra Goodman, Brandon Zaffuto, Benjamin Frisch, Laura Calvi, University of Rochester, USA

Hematopoietic Stem Cells (HSCs) reside at the apex of hematopoiesis, and are regulated by their bone marrow microenvironment or niche, including osteolineage cells. While hematopoietic injury is a major cause of morbidity and mortality following radiation, the role of the HSC niche in hematopoietic and HSC recovery after radiation is poorly understood. Recently an increase in endosteal osteoblasts was reported after radiation in mice, however the mechanism for this increase is not well-understood. We sought to investigate niche engagement at acute time points (24 and 48 hours) after sub-lethal (6.5Gy) total body irradiation (TBI). Using this in vivo model, we confirmed HSC loss and quantified osteoblastic (OBCs), mesenchymal (MSCs) and osteoprogenitor (OPs) populations after TBI. Phenotypic OBCs (CD45⁻, Lineage⁻, CD31⁺, CD51⁺, Sca1⁺) were expanded 1.73 Fold (31.78 ± 3.07 vs 55.13 ± 3.40 % of % non-hematopoietic cells $P=0.0005$, $N=6$ mice/group) and 1.83 Fold (29.63 ± 2.73 vs 54.12 ± 3.40 % non-hematopoietic cells $P=0.0002$, $N=6$ mice/group) 24 and 48 hours after 6.5Gy TBI. TBI caused a decrease in functional OPs from bone associated cells (36.11 ± 3.066 vs 3.444 ± 0.729 Colonies/ 10^4 Cells, $P=0.0005$, $N=3$ mice/group) and bone marrow (19.17 ± 2.798 vs 5.667 ± 1.5 Colonies/ 10^6 Cells, $P=0.01$, $N=3$ mice/group) as measured by CFU-AlkPhos 48 hours post TBI. Functional MSCs, measured by CFU-F, were also severely decreased 48 hours after TBI (44.11 ± 2.336 vs 26.00 ± 1.633 Colonies/ 10^4 Cells, $P<0.0001$, $N=3$ mice/group). We next determined if mineral homeostasis is affected by TBI. Hyperphosphatemia was seen at 18 and 24 hours after TBI, while mice had no concurrent measurable changes in ionized Ca⁺⁺. Concurrently there was a 10 fold increase in circulating Parathyroid Hormone (PTH) (0Gy vs 24 vs 48 hours: 31.91 ± 11.53 vs 305.5 ± 68.55 vs 331.5 ± 119.1 pg/mL, $P<0.005$, $N=7-17$ mice/group). Notably, PTH is known to improve hematopoietic recovery after radiation. Since PTH also known to activate OBCs to increase their ability to support HSCs, our data suggest that TBI increases circulating PTH in response to elevated PO₄³⁻, preventing hypocalcemia but also engaging the niche through OBC expansion, thus increasing HSC support. While further studies are needed to determine if the PTH increase is required for HSC recovery after TBI injury, our data demonstrate acute changes in mineral metabolism that may impact the hematopoietic response to TBI.

*Disclosures: Corey Hoffman, None.***SA0062**

Phosphate Restriction Leads to Low Bone Mass and Impaired Marrow Vasculature. Frank Ko^{*1}, Beth Bragdon², Amira Hussein², Louis Gerstenfeld², Marie Demay¹. ¹Massachusetts General Hospital, USA, ²Boston University School of Medicine, USA

Phosphate restriction in growing mice leads to rachitic expansion of the growth plate due to impaired hypertrophic chondrocyte apoptosis. Histological analyses of the long bones of phosphate restricted mice were performed to identify effects of phosphate restriction on osteogenesis. Dietary phosphate restriction was shown to be associated with a reduction in both trabecular and cortical bone. Recent investigations demonstrate that marrow angiogenesis and osteogenesis are coupled, with increased bone formation being associated with an increase in mature vessels expressing high levels of endothelial CD31 and endomucin. Thus, we investigated the relationship between bone and marrow vasculature in growing mice subjected to dietary phosphate restriction.

Mice were phosphate-restricted d28-50. Immunohistochemical staining for osteocalcin and Runx2 in the metaphysis revealed a significant decrease in the number of osteocalcin (Chow, 7.1 ± 1.7 /mm; Phosphate-restricted 0.4 ± 0.2 /mm) and Runx2 (Chow, 11.6 ± 5.8 /mm; Phosphate-restricted, 0.80 ± 0.6 /mm) expressing osteoblasts per mm metaphyseal trabecular bone surface in the phosphate-restricted mice relative to chow fed controls. This decrease in osteoblasts and osteoprogenitors was associated with decreased pSmad1/5/9 immunoreactivity in osteolineage cells. A significant decrease in TRAP positive osteoclasts was also observed in the metaphysis of phosphate-restricted mice (Chow 1.5 ± 0.7 /mm; Phosphate-restricted, 0.3 ± 0.5 /mm).

Metaphyseal blood vessel density, evaluated by microCT of Microfil perfused tibiae, demonstrated a significant reduction in vascular volume per total volume in the phosphate-restricted mice (Chow, 0.12 ± 0.05 mm³/mm³; Phosphate-restricted, 0.09 ± 0.02 mm³/mm³). Neither vessel diameter nor vessel separation was affected by phosphate restriction. In addition to decreasing the overall vasculature, phosphate deficiency markedly decreased mature vasculature evidenced by a dramatic reduction of vessels with endothelial expression of CD31 and endomucin.

In conclusion, phosphate restriction in mice resulted in decreased bone associated with a reduction in osteoprogenitors, osteoblasts and mature marrow vasculature. Decreased expression of pSmad1/5/9 suggests that phosphate restriction impairs osteogenesis and angiogenesis by attenuation of the BMP signaling pathway.

Disclosures: Frank Ko, None.

SA0063

See Friday Plenary Number FR0063.

SA0064

Aromatase Inhibitor-Induced Bone Loss Causes Muscle Weakness and Increased Progression of ER-Negative Breast Cancer in Bone in a Murine Model. Laura Wright^{*}, David Waning¹, Ahmed Harhash¹, Khalid Mohammad¹, Andrew Marks², Theresa Guise¹. ¹Indiana University, USA, ²Columbia University, USA

Adjuvant endocrine therapy using an aromatase inhibitor (AI) is a standard treatment for postmenopausal women with ER-positive breast cancer. Unfortunately, up to 50% of women treated with an AI develop muscle weakness, bone loss and joint pain that result in treatment discontinuation. Previous studies in our laboratory have demonstrated bone loss and muscle weakness in ovariectomized (OVX) mice. We therefore hypothesized that the combination of AI-OVX would cause more profound estrogen deprivation and bone loss than OVX alone, and that this high bone turnover state could alter the bone microenvironment in ways that accelerate the progression of breast cancer growth in bone and exacerbate muscle weakness systemically. Four-week female athymic nude mice underwent OVX or sham surgery and were treated daily with vehicle or AI (10µg/day; n=20/group). Three weeks after surgery and onset of treatment, serum levels of 17β-estradiol in OVX-AI mice were reduced by 56% (p<0.01; Calbiotech ELISA) and trabecular bone volume fraction at the proximal tibia was reduced by 67% (p<0.001; SCANCO viva40CT) relative to vehicle-sham. After confirming estrogen deficiency and bone loss, the same animals were inoculated with ER-negative MDA-MB-231 human breast cancer cells into the left cardiac ventricle and followed for cancer progression in bone. Since MDA-MB-231 cells are ER-negative, effects of estrogen deprivation on the tumor should be indirect and attributed to the microenvironment. Five weeks after inoculation, osteolytic lesion area increased by 110% (p<0.01, X-Ray) and tumor burden in bone assessed by histology was increased by 87% (p<0.01) in OVX-AI mice relative to sham-vehicle. Furthermore, ex vivo maximal contractile force of the extensor digitorum longus muscle was significantly reduced in OVX-AI mice (-12%, p<0.001) relative to sham-vehicle. Our murine studies confirm that AI treatment induces bone loss and skeletal muscle weakness, recapitulating effects in cancer patients. As hypothesized, the severe bone loss resulting from AI-induced estrogen depletion may prime the bone microenvironment for the development of breast cancer metastases to bone and potentiate muscle weakness. This model serves as an excellent tool to study the mechanisms of underlying musculoskeletal defects in cancer patients and to assess potential therapeutics. Ongoing studies will evaluate whether protection of bone with bisphosphonates can prevent AI-induced musculoskeletal complications in our model of breast cancer bone metastases.

Disclosures: Laura Wright, None.**SA0065**

Ectopic Production of FGF23 in Tumor-Induced Osteomalacia is Mediated by HIF-1α. Qian Zhang^{*}, Michele Doucet², Ryan Tomlinson², Xiaobin Han³, Darryl Quarles³, Michael Collins⁴, Thomas Clemens². ¹Johns Hopkins University, USA, ²Department of orthopaedic surgery, Johns Hopkins University, USA, ³University of Tennessee Health Science Center, USA, ⁴NATIONAL INSTITUTES OF HEALTH, USA

Tumor-induced osteomalacia (TIO) is a rare phosphate-wasting syndrome in which patients harboring non-malignant hemangioma/pericytomas overproduce fibroblast growth factor-23 (FGF23). In this study, we investigated the mechanisms responsible for increased FGF23 production in primary tumors recovered from patients with proven TIO. Our approach was informed by recent studies showing that deficiency in iron, a known regulator of HIF-1α, predisposes patients with Autosomal Dominant Hypophosphatemia to phosphate wasting. Freshly isolated tumor tissue was finely minced and cultured for 24 hours in DMEM medium containing 5% of fetal bovine serum. FGF23 levels measured by ELISA were increased within 1 hour and remained elevated throughout the culture period. Western blot analysis showed that expression of HIF-1α in the tumor tissue was also markedly elevated. Treatment of organ cultures with digoxin, which inhibits HIF-1α translation, profoundly suppressed HIF-1α protein levels with parallel reductions in FGF23 levels, suggesting that HIF-1α directly activates FGF23 expression. In accordance with this idea, overexpression of HIF-1α in SaOS2 osteoblasts increased FGF23 promoter activity while chromatin immunoprecipitation (ChIP) assays demonstrate HIF-1α occupancy at HRE elements within the FGF23 promoter. Finally, immunohistochemical analysis in fixed tumor tissue reveals that spindle-shaped tumor cells, immediately adjacent to blood vessels, coexpressed FGF23 and HIF-1α, and some of which were also positive for bone markers including osteocalcin. Based on these observations, we conclude that aberrant upregulation of HIF-1α secondary to a yet to be identified mutation, elevates FGF23 by transcriptionally activating its promoter. Based on previous reports of pediatric hemangiomas that spontaneously regress to adipose tissue through a HIF-1α dependent endothelial mesenchymal transition (EMT), we speculate that a similar phenomenon occurs in TIO whereby HIF-1α drives EMT to convert endothelial cells to bone-like cells that produce FGF23.

Disclosures: Qian Zhang, None.**SA0066**

See Friday Plenary Number FR0066.

SA0067

See Friday Plenary Number FR0067.

SA0068

Sympathetic Activation Alters the Bone Vasculature: Implication for Osteotropic Breast Cancer Metastasis. Patrick Mulcrone^{*}, J. Preston Campbell¹, Ana Lia Anbinder², Florent Elefteriou¹. ¹Vanderbilt University, USA, ²Universidade Estadual Paulista Campus de Sao Jose dos Campos, Brazil

Most cancer-related deaths are due to metastasis of the primary tumor. Breast cancer commonly metastasizes to the skeleton, an organ innervated by the sympathetic nervous system (SNS). Emotional stresses chronically activate the SNS, and such conditions have been associated with the progression of breast cancer, reduced survival, and increased recurrence. Preclinical evidence suggests that SNS activation promotes the establishment of breast cancer cells in bone, by increasing bone-derived RANKL expression and the migration of these cells toward RANKL-expressing osteoblasts. However, the receptor for RANKL is detected in only 30% of breast cancers; hence other mechanisms may contribute to the establishment of metastatic breast cancer cells in bone following SNS activation. We observed that isoproterenol (ISO), a beta1/2 adrenergic receptor (βAR) agonist used in mice to mimic sympathetic activation, induced the expression of *Vegfa* in bone in vivo and in osteoblast cultures in vitro. Because VEGF is pro-angiogenic and tumor cells depend on blood vessels to form distant metastases, we hypothesized that SNS activation may increase bone marrow vascular density, via effect on osteoblasts and *Vegf* expression, thus promoting the chance of metastatic breast cancer extravasation into the skeleton. To address this question, we measured the formation of CD31⁺ vessels in adult femurs in vivo by histomorphometric analyses and ex vivo, following osteoblastic βAR stimulation. Daily ISO treatment for 6 wks increased vessel area and number in WT mouse femurs, and this effect was blunted in mice lacking the β2AR (n>6/group, P=.0003). The conditioned media (CM) from MC3T3 osteoblasts treated with ISO for 24 hrs augmented blood vessel formation in an *ex vivo* metatarsal assay as compared to the CM of PBS-treated osteoblasts (n>3, P<.0001). VEGF treatment promoted HUVEC endothelial cell tube formation, whereas direct ISO treatment did not (n=3, P=.0076). Ongoing assays aim at determining the effect of VEGF blockade on bone vessel formation and on GFP-tagged MDA-231 breast cancer cell bone metastasis upon ISO treatment. These results suggest that the effect of stress/SNS activation on metastatic breast cancer cell establishment in the skeleton is mediated via the β2AR in osteoblasts, and an increase in bone VEGF and RANKL expression that promotes bone vascular density and homing in the bone marrow environment, respectively, contributing to higher chance of cancer cells engraftment.

Disclosures: Patrick Mulcrone, None.**SA0069**

See Friday Plenary Number FR0069.

SA0070

Up-regulation of the pH sensor TRPV1 in myeloma cells and their adaption to an acidic microenvironment. Ryota Amachi^{*}, Masahiro Hiasa², Jumpei Teramachi³, Asuka Oda⁴, Hirofumi Tenshin², Keiichiro Watanabe³, Shing Nakamura⁴, Hirokazu Miki⁴, Kumiko Kagawa⁴, Shiro Fujii⁴, Endo Itsuro⁴, Eiji Tanaka⁵, Toshio Matsumoto⁶, Masahiro Abe⁴. ¹University of Tokushima, Japan, ²Department of Biomaterials & Bioengineering, Institute of Biomedical Sciences, Tokushima University Graduate School, Japan, ³Department of Histology & Oral Histology, Institute of Biomedical Sciences, Tokushima University Graduate School, Japan, ⁴Department of hematology, endocrinology & metabolism, Institute of Biomedical Sciences, Tokushima University Graduate School, Japan, ⁵Department of Orthodontics & Dentofacial Orthopedics, Institute of Biomedical Sciences, Tokushima University Graduate School, Japan, ⁶Fujii Memorial Institute of Medical Sciences, Tokushima University, Japan

Myeloma (MM) cells preferentially grow and expand in acidic bone lesions in MM. We have demonstrated that MM cells in acidic bone lesions up-regulate their acid sensing to enhance the PI3K-Akt survival signaling to adapt to harsh acidic microenvironment in MM bone lesions. Transient receptor potential cation channel subfamily V member 1 (TRPV1), an acid-sensitive ion channel, is among major pH sensors expressed in cancer cells, including MM cells. In the present study, we therefore explored the regulatory mechanism of TRPV1 expression and its role in MM cell growth and survival in acidic conditions. The expression of *TRPV1* mRNA was up-regulated in all MM cell lines tested at pH6.8 compared to at pH7.4, which was abolished by addition of the PI3K inhibitor LY294002. Activation of the PI3K-Akt

pathway by rh IGF1 or cocultured with acid-producing OCs was able to enhance *TRPV1* mRNA expression in MM cells even at pH7.4, suggesting a critical role of the PI3K-Akt pathway in *TRPV1* expression in MM cells. Although MM cell viability was marginally affected at pH6.8, MM cells underwent cell death preferentially at pH6.8 than at pH7.4 by LY294002, and to a lesser extent by the *TRPV1* antagonist SB366791. Treatment with the *TRPV1* agonist resiniferatoxin induced the phosphorylation of Akt in MM cells even at pH7.4, indicating *TRPV1*-mediated activation of the PI3K-Akt survival signaling. To further clarify the mechanisms for acid-induced up-regulation of *TRPV1* in MM cells, we looked at nuclear localization of Sp1, a transcription factor responsible for *TRPV1* gene expression. Nuclear localization of Sp1 was enhanced in MM cells cultured at pH6.8 compared to those at pH7.4 in a manner inhibitable by LY294002; the up-regulation of *TRPV1* mRNA expression in acidic conditions was suppressed by the PI3K inhibition as well as treatment with terameprocol, a competitive inhibitor of Sp1 binding to promoter regions. Sp1 is also known as a transcription factor of *HDAC* genes. Together with our previous observation of the role of Sp1 in acid-induced gene repression by HDAC, these results collectively suggest that an acidic condition activates the PI3K-Akt pathway in MM cells, which induces Sp-1 nuclear localization and thereby *TRPV1* expression to form a progressive vicious cycle between acid sensing and survival signaling while altering gene expression in MM cells in acidic bone lesions in MM.

Disclosures: Ryota Amachi, None.

SA0071

ELISA measurement of circulating periostin in animal models of bone loss or bone formation, and identification of circulating and tissue-specific associated forms of periostin. Evelyne Gineys¹, Nicolas Bonnet², Cindy Bertholon¹, Aurélien Pagnon-Minot³, Olivier Borel¹, Daniel Hartmann³, Roland Chapurlat⁴, Serge Ferrari², Patrick Garnero¹, Philippe Clezardin¹, Jean-Charles Rousseau^{*1}. ¹INSERM UMR 1033, Lyon, France, ²University Geneva Hospital (HUG), Faculty of Medicine (UNIGE), Department of Internal Medicine Specialties, Service of Bone Diseases, Geneva, Switzerland, ³Novotec, France, ⁴INSERM UMR 1033 & Hospices Civils de Lyon, Lyon, France

Purpose: Matricellular protein periostin (PN) mediates the bone anabolic effect of parathyroid hormone (PTH) and is associated with metastasis from solid tumors. The aim of this study was to develop an enzyme-linked immunosorbent assay (ELISA) to measure PN levels in the serum of animals treated with intermittent PTH or inoculated with 4T1 breast cancer cells. Circulating- and tissue-associated forms of PN recognized by the antibodies used for the ELISA were also characterized.

Methods: We developed a sandwich ELISA using polyclonal antibodies raised against the recombinant mouse PN (Ab1) or the last C-Ter 22 amino acids (Ab2). In the "PTH model", mice (12 weeks old) were treated with intermittent PTH (40mg/kg/day) or vehicle for 5 weeks. In the "metastasis model", mice (5 weeks old) were inoculated iv with 4T1 cells and sacrificed at day 14 after tumor cell inoculation. Mice developed bone and lung metastases. Osteolytic lesions were monitored at day 13 by radiography. Lung metastases were assessed by histology and immunohistochemistry. At sacrifice, serum and tissues were collected and stored at -80°C. Using 2-D gel electrophoresis and western blotting, PN forms in the serum and bone and soft tissues of wild type mice were characterized and PN spot specificity was controlled using a model of Postn deficient mice. The ability of recombinant human cathepsin K to cleave the recombinant mouse PN (R&D) was also tested.

Results: In the "PTH model", serum PN levels were significantly increased compared to untreated animals, (+44%, mean ± SD: 2178 ± 198 vs 3139 ± 213 ng/ml, p=0.02). In contrast, in the "metastasis model", a significant decrease of serum PN levels was observed, compared to age-matched control mice (-26%, mean ± SD: 560 ± 100 vs 756 ± 64 ng/ml, p<0.002). In serum and tissues, the two antibodies recognized several PN spots differing according to their isoelectric points and molecular weights (MW). We found a "bone signature" corresponding to a 50 kDa PN fragment not recognized by Ab2. Additionally, PN was a substrate for cathepsin K, leading to the generation of fragments with a range of MWs similar to that found in the bone signature.

Conclusion: ELISA measurement of serum PN levels reflects variations of the bone metabolism that are associated with an anabolic treatment or cancer-induced bone disease. Additionally, we found that PN was cleaved by cathepsin K, enabling the identification of a "bone signature" in the animals.

Disclosures: Jean-Charles Rousseau, None.

SA0072

See Friday Plenary Number FR0072.

SA0073

Loss of the Vitamin D Receptor Promotes the Metastatic Potential of Human Breast Cancer Cells to Bone. Konstantin Horas^{*1}, Yu Zheng², Shu-Oi Chow², Colette Fong-Yee², Colin Dunstan², Hong Zhou², Markus Seibel². ¹ANZAC Research Institute, The University of Sydney, Australia, ²ANZAC Research Institute, Australia

Breast cancer is amongst the most prevalent malignancies globally with up to 40% of patients developing skeletal metastases. We have demonstrated that vitamin D deficiency, partly through an increase in bone turnover, accelerates the growth of human breast cancer cells in rodent models of bone metastasis. The purpose of the current study was to define the role of the vitamin D receptor (VDR) in systemic breast cancer spread to bone.

VDR expression was knocked down in the human breast cancer cell line, MDA-MB-231 (MDAVDR^{-/-}). Compared to non-target (NT) controls transfected with an empty vector, knockdown efficiency in MDAVDR^{-/-} cells was ~80%. MDAVDR^{-/-} and NT-cells were further transfected with a luciferase gene and injected into the left ventricle of female nude mice (n=11 for each, MDAVDR^{-/-} and NT). Systemic cancer cell spread and tumour growth were monitored by sequential *in vivo* bioluminescent imaging (BLI), high resolution X-ray and μ -CT imaging for a period of 30 days. Affected bones were analysed by histomorphometry and immunohistochemistry at endpoint (day 30).

Compared to NT controls, MDAVDR^{-/-} cells were characterised by a significant increase in cell migration and cell invasion *in vitro* (Fig.1A, B). Mice injected intracardially with MDAVDR^{-/-} cells developed more metastases at day 5 (p<0.01) and 10 (p=0.03), with light emission measurements generating significantly higher values at all time points in MDAVDR^{-/-} mice compared to animals injected with NT-cells (Fig.1C). After 20 days, multifocal metastases were detectable in all animals and tumours were visible on X-ray. Of note, mice injected with MDAVDR^{-/-} cells had significantly larger bone lesions compared to control mice (P<0.01).

We conclude that silencing the VDR in human breast cancer cells boosts their systemic metastatic potential, resulting in significantly greater tumour burden. Our results clearly indicate that the VDR itself has a critical function in controlling cancer cell behaviour and osteotropism.

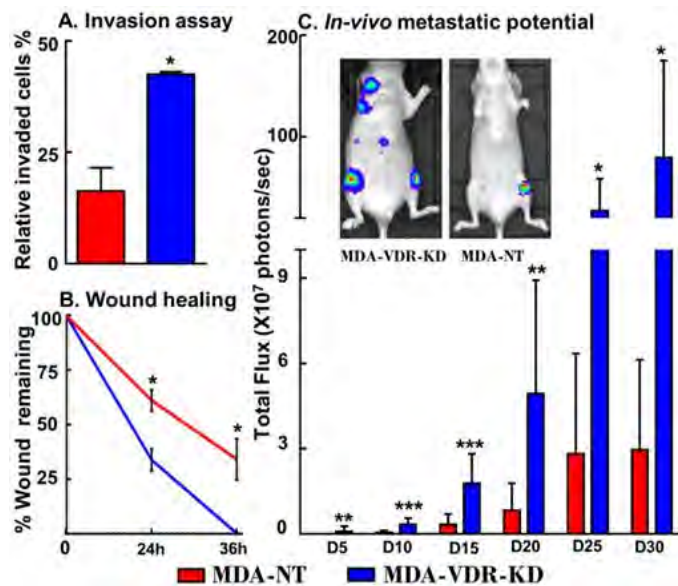


Figure 1

Disclosures: Konstantin Horas, None.

SA0074

Osteoclast TGF- β signaling-mediated basic-FGF promotes breast cancer bone metastasis. Xiangqi Meng¹, Alexandra Vander Ark¹, Priscilla Lee¹, Galen Hostetter¹, Neil A. Bhowmick², Lynn M. Matrisian³, Bart O. Williams¹, Cindy K. Miranti¹, xiaohong li¹. ¹Van Andel Institute, USA, ²Cedars Sinai Medical Center, USA, ³Pancreatic Cancer Action Network, USA

Breast cancer (BCa) bone metastases cause osteolytic bone lesions, which result from the interactions of metastatic BCa cells with osteoclasts and osteoblasts. Transforming growth factor beta (TGF- β) is a cytokine that functions as both tumor suppressor and oncogene, which plays important roles in advanced BCa bone metastasis. To understand the cell-specific role of TGF- β signaling in osteoclasts in BCa bone metastases, MDA-MB-231 BCa cells were intra-tibially or intra-cardially injected into *LysM^{Cre}/Tgfb2^{flloxE2/flloxE2}* knockout (*LysM^{Cre}/Tgfb2* KO) or *Tgfb2^{flloxE2/flloxE2}* mice. Metastatic bone lesion development was monitored by X-ray and compared by analysis of both lesion number and area. We found that *LysM^{Cre}/Tgfb2* knockout significantly decreased MDA-MB-231 induced bone lesion development in both the cardiac and tibial injection models. *LysM^{Cre}/Tgfb2* knockout inhibited the tumor cell proliferation, angiogenesis, and osteoclastogenesis in the metastatic bone microenvironment. Cytokine array analysis and ELISA results showed that basic fibroblast growth factor (bFGF) was down regulated in MDA-MB-231-injected tibiae from the *LysM^{Cre}/Tgfb2* KO group. Intravenous injection of the recombinant bFGF to *LysM^{Cre}/Tgfb2* KO mice rescued the inhibited metastatic bone lesion development. The mechanism by which bFGF rescued the bone lesion development was by promotion of tumor cell proliferation through the downstream MAPK-ERK-cFos pathway after binding to the FGF receptor 1 (FGFR1). Consistent with animal studies, we found that in human BCa bone metastatic tissues, TGF- β type II receptor (T β RII) and p-Smad2 were expressed in osteoclasts and tumor cells, and were correlated with the expression of FGFR1. Our studies suggest that osteoclast TGF- β signaling-mediated bFGF in the bone promotes BCa bone metastasis.

Disclosures: Xiangqi Meng, None.

SA0075

See Friday Plenary Number FR0075.

SA0076

See Friday Plenary Number FR0076.

SA0077

See Friday Plenary Number FR0077.

SA0078

See Friday Plenary Number FR0078.

SA0079

Organic Phosphate Regulates Chondrocyte Expression of Extracellular Matrix Genes and Osteocyte Associated Mediators (FGF23, Phex, MEPE) of Mineralization. Margaret Cooke^{*}, Louis Gerstenfeld. Boston University, USA

Introduction: A phosphate gradient in the cartilage growth plate increases from the proliferative to the hypertrophic region. Inorganic phosphate has been shown to regulate chondrocyte maturation and induce matrix mineralization and cell apoptosis. This study sought to determine the role of organic phosphate in chondroprogenitor development and mineralization. **Methods:** ATDC5 chondroprogenitor cells were cultured to confluence in growth media (50/50 DMEM/F12 with 10% FBS). At confluence, they were switched to a differentiating media (a-MEM, 5% FBS, 25ug/ml ascorbate-2-phosphate, 1X insulin-transferrin-selenium and with or without 54ug/ml β -glycerol phosphate (BGP). Cells were harvested at day 7, 14, 21, days and assayed for growth (MTT), differentiation (Alkaline phosphatase and gene expression [qRT-PCR]) and mineralization (Alizarin Red). **Results:** Across the 21 day time course of differentiation (SOX9) and overall growth was unaffected by BGP. While Collagen 2a1, Aggrecan, and Collagen 10a1 expression showed respective ~ 250, 5 and 200 fold increase with chondrocyte differentiation in the presence of BGP. The absence of BGP in the media led to a further ~2, 8 and 3 fold further increase in the expression of these genes respectively (Figure 1). Differentiation in the presence of BGP led to a 2.91 fold increase alkaline phosphatase activity and a 7.11 fold increase in mineralization with a 67% decrease in alkaline phosphatase activity and 31% decrease in mineralization seen in cultures in the absence of BGP (Figure 2). Strikingly, several genes associated with osteocytes were expressed by these cells including DMP1, FGF23, Phex and MEPE. Over the time course of differentiation BGP induced the expression of DMP1 ~12x and FGF23 ~400x while MEPE and Phex decreased over time by 50%. In the absence

of BGP both FGF23 and MEPE increased an additional ~3x and DMP1 and Phex decreased 25% to 50% respectively. **Conclusions:** This study demonstrates that organic phosphate directly controls chondrogenic differentiated functions. Moreover current studies suggest that chondrogenic cells express the same central molecular mediators that control mineralization and phosphate metabolism including FGF23, Phex as osteogenic cells. The regulation of these genes in the absence of BGP is comparable to that seen in a hypophosphatemia state in bone tissues. These studies suggest that organic phosphate as well as inorganic phosphate directly regulates in chondrocyte differentiation and function.

Figure 1

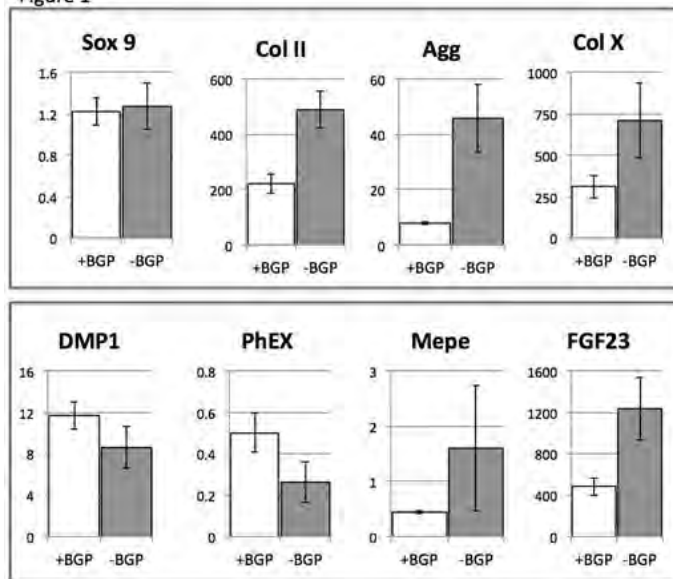


Figure 1

Figure 2

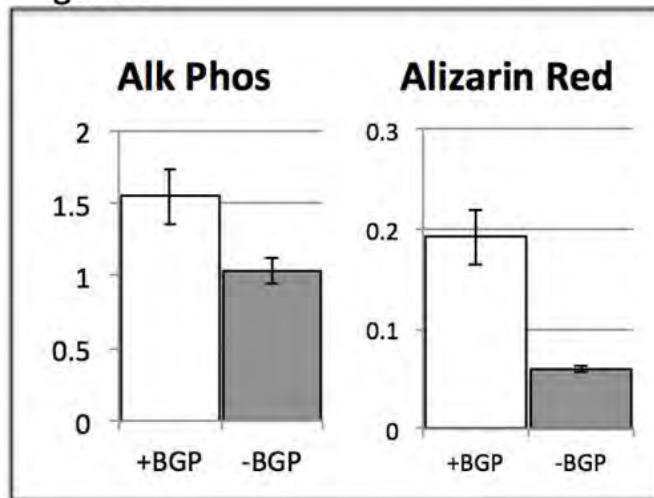


Figure 2

Disclosures: Margaret Cooke, None.

SA0080

See Friday Plenary Number FR0080.

SA0081

See Friday Plenary Number FR0081.

SA0082

See Friday Plenary Number FR0082.

SA0083

See Friday Plenary Number FR0083.

SA0084

See Friday Plenary Number FR0084.

SA0085

See Friday Plenary Number FR0085.

SA0086

See Friday Plenary Number FR0086.

SA0087

Estrogen deficiency exacerbates type 1 diabetes induced bone loss. Sandra Raetz*, Nara Parameswaran, Laura McCabe. Michigan State University, USA

Estrogen deficiency following menopause is associated with rapid bone loss, osteoporosis and increased fracture risk. Type 1 Diabetes (T1D), characterized by little or no insulin secretion and hyperglycemia, is also associated with bone loss and increased fracture risk. With better treatment options, T1D patients are living longer and therefore the number of patients having both T1D and estrogen deficiency is increasing. Little is known about the impact of type 1 diabetes and estrogen deficiency on bone health and density. To investigate this, 11 week old mice were ovariectomized (ovx) and T1D (blood glucose greater than 300 mg/dl) was induced by multiple low dose streptozotocin injection. As expected, ovx mice gained body and fat pad mass whereas T1D and T1D-ovx mice lost body and fat pad mass. MicroCT analysis of both distal femur and lumbar vertebrae trabecular bone indicated significant bone volume fraction (BVf) losses in all groups. However, while ovx and T1D mice lost roughly 50% BVf, the combination of T1D and ovx led to a BVf loss of 82% in the distal femur. A similar response was seen in the vertebrae. 2-way ANOVA analyses indicated a significant interaction between T1D and ovx resulting in greater bone loss. mRNA analysis of bone remodeling markers revealed no change in osteocalcin expression in ovx mice, but a significant decrease in both T1D and T1D-ovx mice. In addition, TRAP5b expression was only increased in the T1D-ovx mice. Taken together, our results show that T1D combined with estrogen deficiency can have a profound effect on bone health. Understanding the additive effects of estrogen deficiency and T1D on bone health is essential for fracture prevention in this patient population.

Disclosures: *Sandra Raetz, None.***SA0088**

See Friday Plenary Number FR0088.

SA0089

See Friday Plenary Number FR0089.

SA0090

See Friday Plenary Number FR0090.

SA0091

See Friday Plenary Number FR0091.

SA0092

IGFBP2/FOXC2 interactions: effects on body composition and bone mass. Victoria Demambro*¹, David Clemmons², Beata Lecka-Czernik³, Clifford Rosen¹. ¹Maine Medical Center Research Institute, USA, ²University of North Carolina Chapel Hill, USA, ³University of Toledo, USA

We have previously reported that *Igfbp2* *-/-* ovariectomized (OVX) females have 'browning' of the inguinal fat depot coinciding with reduced weight gain and intra-abdominal fat mass, as well as increased bone loss, insulin sensitivity and energy expenditure relative to OVX *+/+* mice. In addition, inguinal fat depots from OVX *-/-* mice were found to have a 10-fold increase in *Foxc2* expression compared to OVX *+/+* depots. *Foxc2* transgenic mice, on the other hand, are lean, insulin-sensitive, and have high bone mass due to increased bone formation associated with high bone turnover. These mice also exhibit a 10-fold increase in *Igfbp2* expression, suggesting a possible regulatory mechanism between IGFBP2 and FOXC2. The IGFBP2 molecule contains two Heparin Binding Domains (HBD), the first of which is thought to be

anabolic for bone. To test the effect of HBD1 on bone loss in an OVX model we treated ovariectomized 8-week-old *+/+* mice with HBD or control peptide for 4 weeks. Surprisingly, HBD-treated OVX mice did not gain as much weight as control-treated OVX mice (HBD1: 23.25 ± 0.8318 vs. CON: 25.87 ± 0.1848, *p*=0.003), which was primarily due to a reduction in fat mass (HBD1: 4.233 ± 0.3887 vs. CON: 6.300 ± 0.4716, *p*=0.007) accrual. MicroCT of the distal trabecular bone of the femur revealed that HBD treatment was able to partially rescue OVX-induced bone loss with an increase in BV/TV compared to controls (HBD1: 0.0196 ± 0.0023 vs. CON: 0.0134 ± 0.0011 *p*=0.036), however HBD-treated mice were still well below sham mice (SHAM: 0.0343 ± 0.0031). This increase in BV/TV was accompanied by modest increases in trabecular number and thickness with subsequent decreases in spacing. No changes in cortical bone were noted with treatment. Analysis of gene expression in the inguinal fat depot revealed a 2-fold increase in *Foxc2* transcripts in OVX HBD-treated mice relative to controls. Interestingly, in the absence of IGFBP2, up-regulation of *Foxc2* was noted, suggesting a possible inhibitory role of IGFBP2 on FOXC2. However, the increase in *Foxc2* expression with HBD treatment suggests a possible feedback loop between the two molecules. Further experiments will be required to determine the exact interaction between the two. Previous findings in humans have shown correlations between low levels of IGFBP2 and browning of white adipose tissue, with our findings suggesting that this browning could be directly mediated through FOXC2-dependent mechanisms.

Disclosures: *Victoria Demambro, None.***SA0093**

See Friday Plenary Number FR0093.

SA0094

Inability to Generate Bone Marrow Adipocytes Does Not Protect the Skeleton from Disuse-Induced Cancellous Bone Loss in Adult Male Mice. Jessica Keune*, Adam Branscum, Urszula Iwaniec, Russell Turner. Oregon State University, USA

Skeletal adaptation to disuse and spaceflight typically includes rapid site-specific bone loss due to unbalanced bone turnover. Bone marrow adiposity is also increased during disuse and spaceflight. Since osteoblasts and adipocytes are derived from the same precursors, it has been hypothesized that increased bone marrow adipogenesis during disuse occurs at the expense of osteoblast differentiation. We have recently demonstrated that bone marrow adipocytes are absent in *c-kit*-deficient *Kit^{w^{fl/y}}* mice. The goal of this study was to determine if a lack of marrow adipocytes confers resistance to disuse-induced bone loss. Male *Kit^{w^{fl/y}}* mice and their wild-type (WT) littermates were obtained at 4 weeks of age and housed singly at 32°C for the duration of study. At 16 weeks of age, animals within each genotype were randomly assigned to one of two groups, control or hindlimb-unloaded (HLU) with 10 mice/group, and unloaded for two-weeks. Control mice were single-housed in the same caging units as HLU mice and pair-fed to their respective genotype HLU counterparts. Cancellous bone in distal femur metaphysis was evaluated using micro-computed tomography and analyzed using two-way ANOVA. Effects of genotype, treatment and their interaction on cancellous bone volume and architecture in the distal femur metaphysis are shown in the table below. *Kit^{w^{fl/y}}* mice exhibited a high cancellous bone phenotype associated with higher connectivity density, trabecular number and thickness, and lower trabecular spacing. HLU resulted in lower cancellous bone volume fraction, connectivity density, trabecular number and trabecular thickness, and higher trabecular spacing. However, the magnitude of bone loss was greater in the marrow adipocyte-deficient *Kit^{w^{fl/y}}* mice. In summary, the absence of bone marrow adiposity was not protective against disuse-induced cancellous bone loss in mice. Indeed, the greater bone loss in marrow adipocyte-deficient *Kit^{w^{fl/y}}* mice suggest that marrow adiposity may have a protective role in limiting disuse-induced osteopenia.

| | Wild-type | | <i>Kit^{w^{fl/y}}</i> | | ANOVA (P<) | | |
|---|-------------|-------------|---------------------------------------|--------------|------------|-----------|-------------|
| | Control | HLU | Control | HLU | Genotype | Treatment | Interaction |
| Bone Volume/Tissue Volume (%) | 12.8 ± 0.4 | 9.5 ± 0.4 | 22.2 ± 0.9 | 15.2 ± 1.1 | <0.001 | <0.001 | 0.024 |
| Connectivity Density (1/mm ³) | 144.4 ± 7.2 | 101.8 ± 8.1 | 231.7 ± 9.1 | 139.3 ± 10.5 | <0.001 | <0.001 | 0.008 |
| Trabecular Number (1/mm) | 5.5 ± 0.1 | 5.0 ± 0.1 | 6.1 ± 0.1 | 5.4 ± 0.1 | <0.001 | <0.001 | NS |
| Trabecular Thickness (µm) | 42 ± 0 | 39 ± 1 | 50 ± 1 | 45 ± 1 | <0.001 | <0.001 | NS |
| Trabecular Spacing (µm) | 182 ± 3 | 201 ± 4 | 159 ± 3 | 186 ± 6 | <0.001 | <0.001 | NS |

Data are mean ± SE
NS, Not Significant

Femur Metaphysis

Disclosures: *Jessica Keune, None.***SA0095**

See Friday Plenary Number FR0095.

SA0096

See Friday Plenary Number FR0096.

SA0097

Sirt1 Stimulates Browning of Marrow Fat: From Mice To (Wo)men. Hanna Artsi*¹, Irina Gurt¹, Madi El-Haj¹, Ralph Müller², Gisela Kuhn², Gal Ben Shalom¹, Rotem Paz³, Einav Cohen-Kfir¹, Rivka Dresner-Pollak¹.
¹Hadassah-Hebrew University Medical Center, Israel, ²ETH Zurich, Institute for Biomechanics, Swaziland, ³TAU, Dept. of Zoology, Faculty of Life Science., Israel

Adipose tissue consists of 3 depots: visceral, subcutaneous and marrow. These depots are comprised of predominantly lipid storing white adipocytes (WAT), mitochondria-rich brown adipocytes (BAT), and presumably beige adipocytes bearing characteristics of both. The role of marrow adipose tissue (MAT) in metabolism and skeletal health remains elusive. Conditions associated with increased bone fragility including aging, osteoporosis, glucocorticoid excess, estrogen deficiency, anorexia nervosa and type 1 diabetes mellitus are associated with increased MAT. Moreover, the lineage origin of marrow adipocytes arising from marrow mesenchymal stem cell (BM-MSC) is unclear. Induction of BAT is a much desired goal for combating obesity and appears to be beneficial to bone health. The role of Sirtuin1, a key player in aging, metabolism and bone biology in MAT physiology is unknown and is the focus of this study. Studies were performed in 5-7-month-old Sirt1 haplo-insufficient 129/Sv (Sirt1^{+/-}) and WT female mice (Endocrinology;2011;152:4514-24), C3H10T1/2 over-expressing Sirt1, and human femoral BM-MSCs obtained from women who sustained an osteoporotic hip fracture. Whole body fat content and tibia MAT volume were assessed by DXA and osmium staining followed by ζ CT, respectively. WAT and BAT characteristic genes and proteins were determined by real time RT-PCR and western blotting in abdominal WAT, sub-scapular BAT, whole tibia extracts including MAT, primary murine tibial and human BM-BMCs cultures treated with the Sirt1 activator SRT3025. No difference in food intake, body weight, blood glucose, plasma FFA, whole body and tibial fat content were observed in Sirt1^{+/-} compared to WT mice. A marked 50% reduction in mRNA expression of the BAT characteristic genes: $\text{O}3\text{AR}$, Foxc2 , PRDM16 and $\text{PGC1}\alpha$ was found in BAT and whole tibiae derived from Sirt1^{+/-} compared to WT mice. A Sirt1 cell autonomous effect was confirmed by similar results in Sirt1^{+/-} vs WT-derived BM-MSCs cultures. Consistently, a reciprocal 2-fold increase in gene expression of BAT marker genes and in PRDM16 and $\text{PGC1}\alpha$ protein was observed in Sirt1 over-expressing C3H10T1/2 cells and in human BM-BMCs treated with SRT3025. These results indicate that Sirt1 is a regulator of the bone marrow adipocyte fate and stimulates browning of MAT in both murine and human cells. Whether Sirt1 activation in MAT enhances bone strength and favorably affects whole organism energy metabolism remains to be investigated.

Disclosures: Hanna Artsi, None.

SA0098

Thyroid Hormone Induces Browning of Bone Marrow Adipose Tissue via Activation of TR β Signaling. Richard Lindsey*, Sheila Pourteymoor, Catrina Alarcon, Subburaman Mohan. VA Loma Linda Healthcare System, USA

Mutant mouse models deficient in thyroid hormone (TH) action have recently shown that there is an important prepubertal period in which TH is critical for the regulation of skeletal growth and development. Furthermore, TH negatively regulates total body fat during the prepubertal growth period, an observation consistent with the well-established effects of TH to accelerate resting energy expenditure. Since bone marrow mesenchymal stromal (BMMS) cells differentiate into both adipocytes and osteoblasts, and since a relationship between bone marrow adipogenesis and osteogenesis has been predicted, we examined the effect of TH deficiency during the postnatal growth period on bone marrow adiposity in mice. We found that bone marrow adiposity, measured by DEXA, was increased by >20% ($P < 0.01$) in TH deficient (Tshr^{hyt/hyt}) mice at 3 weeks of age at multiple skeletal sites, and 10 day treatment with T3/T4 at a time when serum levels of T3/T4 normally increase (day 5-14) rescued this phenotype. Furthermore, treatment of TH deficient mice with a TH receptor (TR) β -specific agonist, GC-1, rescued the adipogenesis phenotype equally well, thus suggesting TH effects on adipose tissue are primarily mediated via TR β signaling. To further examine the mechanism for TH regulation of bone marrow adiposity, we tested the effects of TH on mRNA expression levels of markers of adipocyte differentiation using primary cultures of mouse BMMS cells and the ST2 mouse stromal cell line *in vitro*. We found that 1- or 6-day treatment with 10 ng/mL T3 significantly increased expression levels of several markers of brown/beige fat, including UCP-1, PGC-1 α , P2RX5, PAT2, PRDM16, and Zfp516. In BMMS cells, real-time RT-PCR measurements revealed a 3.5-fold increase in UCP-1, a 2.5-fold increase in PGC-1 α , 1.4-fold increase in P2RX5, and a 1.9-fold increase in PAT2 (all $P < 0.05$). In ST2 cells, T3 treatment caused a 2.6-fold increase in PGC-1 α , a 1.8-fold increase in P2RX5, a 14.4-fold increase in PAT2, and a 1.5-fold increase in Zfp516 (all $P < 0.05$). Moreover, 6-day treatment of ST2 cells with GC-1 produced a 1.6-fold increase in PRDM16. Based on our data, we conclude that 1) TH regulation of bone marrow adiposity is mediated primarily via activation of TR β signaling, and 2) the TH effect on energy metabolism may in part be due to increased production of brown/beige adipose tissue in bone marrow.

Disclosures: Richard Lindsey, None.

SA0099

See Friday Plenary Number FR0099.

SA0100

“Skeletal Alterations in Hyp (C57BL/6J-PhexHyp/J) Mouse Model of X-linked Hypophosphatemia (XLH) in humans”. Ed Berryman*¹, David Zakur², Cedo Bagi². ¹Pfizer Global Research & Development, USA, ²Pfizer Research & Development, Groton CT, USA

PURPOSE: Hypophosphatemia can impact various tissues and cause osteomalacia, rickets, rhabdomyolysis, cardiomyopathy, metabolic acidosis, and disruption of red blood cell function. Increased urinary excretion of phosphate due to impaired reabsorption is the key mechanism underlying X-linked hypophosphatemic rickets (XLH), a rare disease associated with skeletal abnormalities and growth retardation. This study was conducted to investigate the progression of skeletal alterations in the Hyp (C57BL/6J-PhexHyp/J) mouse that is frequently used as a model of XLH disease in humans. **METHODS:** Male and female wild type (WT) and Hyp mice were obtained at the age of 2, 4, and 6 months to evaluate differences in skeletal development over time. A Dynamic Weight Bearing (DWB) system was utilized to measure functional capacity of the musculoskeletal system, and evaluation via 3-point bending was used to assess femoral strength. X-ray and Micro-CT (mCT) were used to evaluate bone size, geometry and bone structure. Fluorescent labels were used to assess bone remodeling and paraffin histology was used for cellular analysis of bone and cartilage. **RESULTS:** Hyp mouse featured numerous changes in bone morphology and structure at all skeletal sites assessed including hock joint, femur, lumbar vertebrae, and mandible. Hyp mice exhibited shorter but wider bones, lower BMD, impaired structure and reduced strength relative to WT controls. **CONCLUSIONS:** Results from this study clearly showed genotype-related skeletal differences between the C57BL/6J mice and the C57BL/6J-PhexHyp/J mice. Similar to patients with XLH, the negative impact of lower hypomineralization and structural alteration were partially compensated in Hyp mice by an increase in bone diameter, however the bone strength was diminished.

Disclosures: Ed Berryman, Pfizer Inc.

This study received funding from: Pfizer Inc.

SA0101

See Friday Plenary Number FR0101.

SA0102

See Friday Plenary Number FR0102.

SA0103

See Friday Plenary Number FR0103.

SA0104

Monitoring of Collagen Replacement in a Transplant Model for Treatment of Osteogenesis Imperfecta Using GFP-Collagen Donor Mice. Molly Hulbert*¹, Hong Zhao¹, Richard Campos¹, Yixia Xie¹, Michael Grillo¹, Donna Pacicca², Charlotte Phillips³, Sarah Dallas¹. ¹University of Missouri - Kansas City, USA, ²Children's Mercy Hospital, Kansas City, USA, ³University of Missouri, USA

Osteogenesis Imperfecta (OI) is an inherited disorder of bone fragility which is mainly caused by mutations in COL1A1 and COL1A2 genes that encode type I collagen. The spectrum of disease ranges from perinatal lethal/severe forms with intrauterine fractures to milder forms with fewer fractures. There is no cure and treatment is limited to management of symptoms. Bisphosphonate treatment is the current standard of care but there is a need to develop new treatments due to concerns over the potential of long term bisphosphonates to impair bone remodeling.

Marrow and mesenchymal stem cell (MSC) transplantation is a potential treatment that could be of benefit in severe OI cases. As a novel model to optimize transplantation approaches for OI, we have generated transgenic mice expressing a GFP-tagged collagen construct driven by the 3.6kb-COL1A1 promoter. GFP-collagen expression is seen in bone, teeth, tendon, skin and other connective tissues. Collagen-GFP transgenic mice were used as donors for transplantation of marrow and MSC into the *oimloim* mouse model of OI. Male and female *oimloim* mice (6-12 wks) were injected with busulfan to ablate their marrow and were reconstituted with donor marrow from GFP-collagen mice. To provide osteoprogenitors, the mice also received intramedullary or intratibial MSC injections from GFP-collagen donors. One month after transplantation, OI mice with $\geq 80\%$ donor marrow reconstitution were evaluated to determine collagen replacement. 12 of 13 injected femurs and 5 of 5 injected tibias showed robust incorporation of GFP-collagen into bone, confirming both engraftment of osteoprogenitors and their contribution of donor collagen to host bone matrix. The donor-derived GFP-collagen was frequently seen as a thick, well defined seam on the endocortical bone surface. Quantitation of GFP+ve (donor-

derived) bone area compared to host bone area showed a mean replacement of $8.7\% \pm 2.1$ by 1 month. Deposition of GFP-collagen in adjacent bones that were not injected with MSC was only seen in 1 of 6 bones examined, suggesting the osteoprogenitors came from the injected MSC rather than donor marrow. This further suggests that the osteoprogenitors do not circulate. Together, these data show that the GFP-collagen mouse is a powerful model for evaluating replacement of OI-collagen with donor collagen and will be useful for developing strategies to enhance collagen replacement, such as treatment with bone anabolic or anti-resorptive agents.

Disclosures: Molly Hulbert, None.

SA0105

See Friday Plenary Number FR0105.

SA0106

See Friday Plenary Number FR0106.

SA0107

See Friday Plenary Number FR0107.

SA0108

The Skeletal Phenotype of *Serpinf1*- Null Mice. Hadil Al-Jallad*¹, Pierre Moffatt¹, Hazem Eimar², Faleh Tamimi², Marc McKee², Frank Rauch¹.
¹Shriners Hospital for Children, Canada, ²McGill University, Canada

Osteogenesis imperfecta (OI) type VI is caused by recessive loss-of-function mutations in *SERPINF1*, the gene coding for pigment epithelium derived factor (PEDF). Patients with OI type VI have undetectable circulating levels of PEDF, but the mechanism whereby lack of PEDF leads to bone disease is not clear. In the present study we assessed a *Serpinf1*-null mouse model. Primary osteoblast cultures from neonatal *Serpinf1*- mice did not produce PEDF and had decreased expression of osteoblast differentiation markers, alkaline phosphatase, Sp7, *Ank*, *Phospho 1* and *Enpp1*, whereas adiponectin expression was increased. Von Kossa staining showed fewer mineralization nodules in *Serpinf1*- cultures as compared to osteoblasts from wild type littermates. These data suggest that *Serpinf1* is important for osteoblast differentiation and that PEDF is required for mineralization. The skeletal phenotype of *Serpinf1*- mice was investigated at 20 weeks of age (*Serpinf1*^{+/+}, N=10; *Serpinf1*^{-/-}, N= 8). Serum PEDF was absent in *Serpinf1*- mice, but serum levels of C-terminal telopeptide of collagen type I and procollagen type I N-propeptide were similar to wild type mice. Micro-computed tomography (μ CT) of femurs, in addition to quantitative bone histomorphometry of femurs and vertebrae, showed no significant differences between *Serpinf1*- mice and their wild type littermates. Even though human OI type VI bone is characterized by a mineralization defect with increased unmineralized osteoid, *Serpinf1*- mice had an osteoid thickness, osteoid volume, mineral apposition rate, and bone formation rate similar to wild type mice. However, μ CT analyses of craniofacial bones showed a significant decrease in cranial length, maxillary length, palatine length, inter-molar distance and inter-zygomatic distance. Our results demonstrate that *Serpinf1*- mice have apparently normal axial and appendicular bone mineralization and bone mass, but have abnormalities in the craniofacial skeleton.

Disclosures: Hadil Al-Jallad, None.

SA0109

Targeted sequencing for monogenic causes of High Bone Mass: Predictions in LRP5 protein structure explain variation in the clinical severity of LRP5 High Bone Mass. Celia Gregson*¹, Lawrie Wheeler², Sarah Hardcastle³, Kathryn A Addison², Marieke Brugmans², Kate Ward⁴, Margaret Paggiosi⁵, Louise Appleton⁶, Jane Turton⁷, Michael Stone⁷, Joegi Thomas⁸, Rohan Agarwal⁹, Kenneth Poole⁹, Eugene McCloskey⁵, Eleanor Williams¹⁰, Alex Bullock¹⁰, George Davey Smith¹¹, Matthew A Brown², Jon H Tobias³, Emma L Duncan². ¹University of Bristol, United Kingdom, ²Human Genetics Group, University of Queensland Diamantina Institute, Australia, ³Musculoskeletal Research Unit, School of Clinical Sciences, University of Bristol, United Kingdom, ⁴MRC Human Nutrition Research Unit, Elsie Widdowson Laboratory, United Kingdom, ⁵Mellanby Centre for Bone Research, Academic Unit of Bone Metabolism, University of Sheffield, United Kingdom, ⁶NIHR Oxford Musculoskeletal Biomedical Research Unit, Nuffield Orthopaedic Centre, United Kingdom, ⁷Bone Research Unit, University Hospital Llandough, United Kingdom, ⁸James Paget University Hospital Foundation NHS Trust, United Kingdom, ⁹Department of Medicine, University of Cambridge, United Kingdom, ¹⁰Structural Genomics Consortium, University of Oxford, United Kingdom, ¹¹MRC Integrative Epidemiology Unit at the University of Bristol, United Kingdom

Rare monogenic high bone mass (HBM) disorders (e.g. due to *LRP5* or *SOST* mutations) augment understanding of bone regulatory pathways and can inform development of novel anabolic therapies for osteoporosis. We aimed to identify the genetic cause of presumed monogenic HBM and determine associated clinical characteristics in a large HBM population.

258 unrelated HBM cases identified from review of 335,115 DXA scans from 13 UK centers were assessed clinically and underwent targeted sequencing of known anabolic HBM loci: *LRP5* (exons 2, 3 & 4), *LRP4* (exons 25 & 26), *SOST* (exons 1 & 2) and the van Buchem's disease 52kb intronic deletion 3' of *SOST*. Family members were assessed for HBM segregation with identified variants. 3-D protein models were constructed for identified variants.

Two novel missense *LRP5* HBM mutations (c.C518T; p.T173M, c.C796T; p.R266C) were identified, plus 3 previously reported missense *LRP5* mutations (c.A593G; p.N198S, c.G724A; p.A242T, c.A266G; p.Q89R), associated with HBM in 11 adults from 7 families. Those with *LRP5* HBM (~population prevalence 5/100,000) displayed a variable phenotype of skeletal dysplasia with increased trabecular BMD and cortical thickness on HRpQCT, and fat mass accumulation in a gynoid distribution on DXA, compared with both non-*LRP5* HBM and controls. One woman carried a novel heterozygous nonsense *SOST* mutation (c.C530A; g.C3335A) predicted to prematurely truncate sclerostin; apart from mandible enlargement (ME) and BMD Z-scores L1 +3.5, Hip +1.7 she was asymptomatic.

Protein modelling suggests the severity of the LRP5-HBM phenotype corresponds to the degree of protein disruption and the consequent effect on SOST-LRP5 binding. We predict N198S directly disrupts SOST binding and the larger threonine side chain in A242T leads to steric clashes destabilising the SOST binding site, both correspond to severe HBM phenotypes (Z-scores +3.1 to +12.2, inability to float, ME, no fractures, 2 of 8 have nerve compression). Less disruptive structural alterations predicted from R266C, Q89R, T173M associate with less severe phenotypes (Z-scores +2.4 to +6.2, able to float, of 3 only 1 has ME, 1 high trauma fracture, 1 nerve compression).

Heterogeneity in LRP5-SOST interactions may have implications for the therapeutic effects of Wnt antagonists. Variants in known HBM loci account for a very small proportion of people with HBM, suggesting that either monogenic HBM mutations yet to be identified or polygenic inheritance is responsible.

Disclosures: Celia Gregson, None.

SA0110

See Friday Plenary Number FR0110.

SA0111

See Friday Plenary Number FR0111.

SA0112

See Friday Plenary Number FR0112.

SA0113

See Friday Plenary Number FR0113.

SA0114

Tiptoe Walking (*ttw*) Mice, Rodent Spinal Ligamentous Ossification Models, Exhibiting High Serum FGF23 Level. Ryuichi Watanabe*, Takeshi Miyamoto, Morio Matsumoto, Masaya Nakamura. Department of Orthopaedic Surgery, Keio University School of Medicine, Japan

Background:

Mouse models of ectopic ossification, tiptoe walking (*ttw*) mice, exhibit ectopic ossification of the posterior longitudinal ligament of the spine (OPLL) with extensive mineralization in Achilles tendon. The *ttw* mice demonstrate the accelerated bone formation in the cortical vertebrae, while showing the osteopenic changes in the cancellous vertebrae. Although aggravated ectopic mineralization has been reported in the *ttw* mice fed with high phosphate diet, the precise mechanism underlying ectopic ossification due to the disturbance in phosphate metabolism remains unknown. Thus, the objective of this study is to clarify the role of phosphate metabolism of the ectopic ossification in the *ttw* mice.

Methods and Results:

Serum levels of phosphate and FGF23 in *ttw* mice and control littermates fed with either normal or high phosphate diet that is 1.5 times higher phosphate concentration than normal diet were analyzed. Furthermore, ectopic ossification of spinal ligament was examined with micro CT scan. The level of serum phosphate in *ttw* mice placed on high phosphate diet was significantly lower than WT mice placed on high phosphate diet. Micro CT findings indicated that the ectopic calcification of spinal ligament in the *ttw* mice was strikingly worsened by high phosphate diet. Moreover, the *ttw* mice fed with high phosphate diet exhibited the accelerated osteopenic changes in the cancellous vertebrae. We found that the serum FGF23 level in the *ttw* mice placed on high phosphate diet was significantly higher than either the *ttw* mice placed on normal diet or WT mice placed on high phosphate diet. Therefore, we investigated whether the aggravation of spinal ligamentous calcification was due to the elevated serum FGF23 level with phosphate overload. Exhibiting high serum FGF23 level, *Phex* mice fed with high phosphate diet were analyzed ectopic ossification using CT scan. Micro CT analysis showed that ectopic calcification in the spinal ligament was not detected in *Phex* mice fed with high phosphate diet.

Summary:

We found that high phosphate diet exacerbated the spinal ligamentous ossification and osteopenic phenotypes in *ttw* mice. The serum FGF23 level was significantly elevated in *ttw* mice via high phosphate diet, however, the elevated serum FGF23 level with phosphate overload did not induce the development of ectopic spinal ligamentous ossification in *Phex* mice.

Disclosures: *Ryuichi Watanabe, None.*

SA0115

See Friday Plenary Number FR0115.

SA0116

Continuous Parathyroid Hormone Injection in Mouse Has Differential Effects on Osteoclast Activation in Primary and Secondary Spongiosa. Nobuhito Nango*¹, Shogo Kubota¹, Wataru Yashiro², Atsushi Momose², Shizuko Ichinose³, Koichi Matsuo⁴. ¹Ratoc System Engineering Co., Ltd., Japan, ²Institute of Multidisciplinary Research for Advanced Materials, Tohoku Univ., Japan, ³Research Center for Industry Alliances, Tokyo Medical & Dental University, Japan, ⁴Laboratory of Cell & Tissue Biology, Keio University School of Medicine, Japan

Parathyroid hormone (PTH) is used clinically to accelerate bone formation, but how it functions remains unclear. In this study, we determined the effect of continuous PTH injection especially on mouse primary trabecular bone. Seven-week-old mice implanted with osmotic pumps were continuously dosed with PTH. Tibiae were isolated after 144 h and proximal tibial growth plates were scanned using a Talbot phase method with synchrotron radiation (Fig. 1). We then compared sections of non-injected versus injected groups using backscattered scanning electron microscopy (SEM, Fig. 2). After continuous PTH injection, the longitudinal length of the calcified matrix of hypertrophic chondrocytes increased approximately 2-fold compared with that of the non-injected group (Fig. 2). In controls, vascular channels were invaded, transverse septa were resorbed, and bone formation occurred normally along remaining longitudinal septa (Fig. 1A). By contrast, in the injection group, we observed a hypertrophic chondrocyte zone expanded over a few hundred micrometers, mineralized cartilaginous matrix in the absence of resorption of transverse septa (Fig. 1B), deposition of bone matrix with low mineralization on the inner wall of chondrocytic lacunae (Fig. 1B), which retained their original ellipsoid form (Fig. 1B), and emergence of primary bone with two highly mineralized layers (Fig. 2B). Furthermore, injected animals exhibited calcified matrix with extremely greater bone volume and trabecular star volume in primary spongiosa but lower values of these parameters in secondary spongiosa relative to non-injected controls. These results indicate that continuous parathyroid hormone injection inhibits

osteoclast activation in the primary spongiosa and stimulates it in the secondary spongiosa. The Talbot phase method can measure slight differences in bone mineralization (Fig. 1). In the figure, bone with low mineralization is formed on septa (Fig. 1B). Thus, bone with low mineralization formed inside the lacuna without absorption of septa in the injected group (Fig. 1B), indicating that bone-forming osteoblasts appear before blood vessel penetration and osteoclast formation. The presence of double-layered primary bone with high mineralization suggests that blood vessel penetration stops in the middle of the two layers. We conclude that resorption of calcified cartilage by osteoclasts decreases in continuously PTH-injected mice.

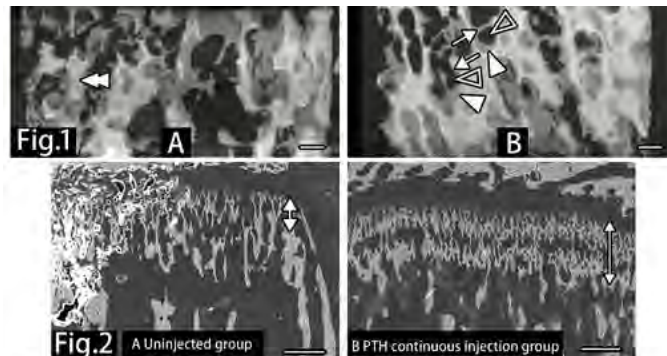


Fig.1 Talbot differential phase image generated by synchrotron radiation. (scale bar: 20 μ m) Gray image shows degree of mineralization. In the continuously PTH injected group, hypertrophic chondrocyte lacunae (\blacktriangleleft) remain, and bone with low mineralization (\blacktriangleleft) forms in lacunae. The mineralized septa (\blackleftarrow) also remains. In the uninjected group, the septa and mineralized matrix of hypertrophic chondrocytes are absorbed, and the new bone forms on the remaining matrix wall (\blackleftarrow).

Fig.2 Backscattered SEM image (scale bar: 200 μ m) In B the PTH injection group, primary bone layers (\blackleftrightarrow) extended approximately 300 μ m with double-layered, and the vascular path from the bone marrow to calcified cartilage lacunae was apparently blocked by the septa. In A the uninjected group, the thickness of the primary bone layer was approximately 100 μ m (\blackleftrightarrow). The lacuna septa were partly absorbed, and a path to the bone marrow was formed.

Fig.

Disclosures: *Nobuhito Nango, None.*

SA0117

See Friday Plenary Number FR0117.

SA0118

See Friday Plenary Number FR0118.

SA0119

Evaluation of Different Schedules of Teriparatide Injection on Sinus Bone Graft in Rabbit. Jisun Huh*¹, Ui-Won Jung², Kyeong-Mee Park¹, Jin-Sun Jeong¹, Kee-Deog Kim¹, Wonse Park³. ¹Department of Advanced General Dentistry, College of Dentistry, Yonsei University, South Korea, ²Department of periodontology, Research Institute for Periodontal Regeneration, College of Dentistry, Yonsei University, South Korea, ³Dental College, Yonsei University, USA

Purpose

This study evaluated two different teriparatide injection schedules-intermittent (5 times/week) and episodic (2 times/week) on sinus bone graft in rabbit.

Material and Method

25 New Zealand white rabbits were used. Bio-Oss was grafted on maxillary sinus. Rabbits were divided into 3 groups; 1) Saline (N=10), 2) PTH (N=10), 3) PTHalt (alternative injection group, N=5). Saline and PTH groups were injected intermittently 5 times a week for 2 weeks and PTHalt group was injected episodically 2 times a week for 4 weeks. Halves of Saline and PTH groups were sacrificed 2 weeks post op and the last halves of these 2 groups and PTHalt group were 4 weeks post op. Radiographic and histomorphometric analysis were performed.

Result

At 2 weeks new bone area (NB, %) of Saline and PTH groups were 5.72% and 7.19%. At 4 weeks NB of Saline, PTH and PTHalt groups were 15.18%, 14.50% and 10.00%. In the small region near the Schneiderian membrane, NB of PTH group was 14.24% and higher than Saline (8.56%) and PTHalt (6.61%) groups at 4 weeks. In total augmented area and all specific small regions near window, center and membrane, PTHalt group represented smaller NB than Saline and PTH groups.

Conclusion

The intermittent teriparatide injection improves new bone formation specifically near the Schneiderian membrane at 4 weeks healing period in sinus bone graft of rabbit. The episodic injection of teriparatide is not effective as intermittent injection.

Disclosures: *Jisun Huh, None.*

SA0120

See Friday Plenary Number FR0120.

SA0121

Sorting Nexin 27 Promotes Rapid Activity-dependent Recycling of the Parathyroid Hormone Receptor. Jennifer McGarvey^{*1}, Tatyana Mamonova¹, Shanna Bowman², W. Bruce Sneddon¹, Manojkumar Puthenveedu², Peter Friedman¹. ¹University of Pittsburgh, USA, ²Carnegie Mellon University, USA

The parathyroid hormone receptor (PTHr) is a GPCR that regulates mineral ion homeostasis and bone remodeling. Its C-terminal tail contains a Type I PDZ ligand that binds PDZ-domain containing proteins. Upon agonist stimulation, the PTHR is internalized into early endosomes and subsequently traffics to the retromer complex. Sorting nexin 27 (SNX27) is a cargo selector for the retromer complex that promotes recycling of surface receptors. We analyzed the role of SNX27 on PTHR trafficking in early endosomes. Co-immunoprecipitation, fluorescence polarization, and molecular modeling experiments show that SNX27 is a novel PTHR binding partner in the endomembrane system and establish the molecular determinants of the interaction. Endogenous SNX27 both colocalizes and co-immunoprecipitates with PTHR after treatment with PTH (1-34). Mutation of the C-terminal PDZ ligand of PTHR or deletion of the PDZ domain of SNX27 abolishes this interaction in co-immunoprecipitation assays. Molecular modeling suggests that the C-terminal motif of PTHR recognizes SNX27 PDZ domain through canonical PDZ-ligand interactions, supporting the biochemical data. Primary interactions occur through the GYGF core-binding motif of PDZ domain and the carboxy-terminal methionine at ligand position 0. We examined the binding affinity between PDZ domain of SNX27 and the PTHR ligand using fluorescent polarization binding assay. The measured dissociation constant $K_D = 1.7 \mu\text{M}$ is consistent with the molecular dynamics modeling prediction of PDZ-ligand binding of PTHR. We generated a PTHR construct tagged with the pH sensitive GFP variant super-ecliptic pHluorin (SEP) at the N-terminus to investigate recycling of the PTHR. TIRF-based, live cell imaging was used to measure the rate of receptor recycling by visualizing exocytic events at the cell surface. RNAi depletion of either SNX27 or Vps35, a component of the retromer complex, resulted in a 50% decrease in the rate of recycling of SEP-PTHr following agonist stimulation, and a similar effect was observed when actin was inhibited with Latrunculin A. Consistent with the role of SNX27 in retromer trafficking, RNAi depletion of SNX27 abolished PTHR interacting with retromer. We conclude that a portion of internalized PTH receptors are returned to the cell surface through a rapid recycling pathway that involves SNX27 and the retromer complex.

*Disclosures: Jennifer McGarvey, None.***SA0122**

See Friday Plenary Number FR0122.

SA0123

β 2-adrenergic Receptor Control of PTH Receptor Signaling. Jean-Pierre Vilaradaga¹, Frederic Jean-Alphonse^{*2}. ¹University of Pittsburgh, School of Medicine, USA, ²University of Pittsburgh, USA

Osteoblasts express several cell surface G protein-coupled receptors (GPCRs) that respond to multiple extracellular signals and regulate bone growth and turnover. A rational therapeutic approach targeting bone and mineral diseases thus requires a comprehensive understanding of osteoblast activity resulting from the integration of multiple GPCR signaling pathways. This is of particular relevance to parathyroid hormone (PTH) osteoanabolism mediated by the PTH receptor (PTHr) because β 2-adrenergic receptor (β 2AR)-deficient mice show no osteoanabolic activity after intermittent injection of PTH(1-34). Thus, β 2AR signaling is required for the osteoanabolic activity of PTHR. These findings raise the hypothesis that PTH anabolism is regulated by β 2AR signaling in osteoblasts, and that this regulation has therapeutic relevance for the treatment osteoporosis. Here we tested this hypothesis by determining the molecular and cellular mechanisms by which the β 2AR regulates PTHR signaling in cells, and develop in a systems biology approach a quantitative modeling of β 2AR-mediated the regulation of PTHR signaling in osteoblasts.

*Disclosures: Frederic Jean-Alphonse, None.***SA0124**

See Friday Plenary Number FR0124.

SA0125

See Friday Plenary Number FR0125.

SA0126

See Friday Plenary Number FR0126.

SA0127

See Friday Plenary Number FR0127.

SA0128

See Friday Plenary Number FR0128.

SA0129

See Friday Plenary Number FR0129.

SA0130

Pregnancy and Post-Lactation Recovery Rescue Low Bone Mass and Hypocalcemia in *Cyp27b1* Null Mice That Cannot Make Calcitriol. Brittany Gillies^{*1}, Brett A. Tonkin², Yue Ma¹, Beth J. Kirby¹, René St-Arnaud³, Natalie A. Sims², Christopher Kovacs¹. ¹Memorial University of Newfoundland, Canada, ²St. Vincent's Hospital & University of Melbourne, Australia, ³Shriner's Hospital & McGill University, Canada

Vdr null mice lack calcitriol's receptor and have hypocalcemia, hypophosphatemia, and rickets, but during pregnancy, *Vdr* nulls upregulate intestinal calcium absorption, mineralize osteoid, and increase BMC by 58%. They also lose a normal amount of BMC during lactation and restore it fully within 14 days after weaning. These data suggest that factors other than calcitriol upregulate intestinal calcium absorption and bone formation post-weaning. An alternative explanation is that the high calcitriol levels observed in *Vdr* null mice may act through non-genomic receptors to have these effects. If true, then loss of calcitriol itself should lead to effects that loss of VDR does not.

We tested this hypothesis by examining the calcitriol-deficient *Cyp27b1* null mouse line. Adult *Cyp27b1* null mice have hypocalcemia, hypophosphatemia, and rickets on a normal diet, but reportedly normal mineral metabolism when maintained on a "rescue" diet (high calcium, phosphorus and lactose). We studied sister *Cyp27b1* null and WT pairs raised on the rescue diet from weaning and mated at 10 weeks. Bones (DXA and μCT), blood, and urine were obtained at pre-pregnancy baseline, end pregnancy, end lactation, and days 7, 14, 21, and 28 of post-weaning recovery.

Litter sizes were equal between *Cyp27b1* null and WT. Compared to WT, and despite the rescue diet, at baseline *Cyp27b1* nulls were hypocalcemic (1.69 ± 0.14 vs. 1.98 ± 0.03 mM) with markedly increased PTH ($2,815 \pm 1,292$ vs. 8.4 ± 3.9 ng/l) and 30% lower BMC (0.42 ± 0.03 vs. 0.56 ± 0.02 g); μCT confirmed a rickets-like phenotype. During pregnancy serum calcium increased, PTH reduced, and BMD increased 45%, so that all values became equivalent to WT. During lactation, serum calcium of *Cyp27b1* nulls dropped to 1.11 ± 0.13 mM, PTH increased to $5,500 \pm 680$ ng/ml, and BMC declined to baseline. During post-weaning, serum calcium of *Cyp27b1* null normalized (1.89 ± 0.08 mM), PTH remained high, and BMC increased 40% to 0.54 ± 0.04 g.

In summary, pregnancy rescued hypocalcemia, secondary hyperparathyroidism, and low bone mass of *Cyp27b1* nulls. This implies increased intestinal calcium absorption and mineralization of rachitic bone via calcitriol-independent mechanisms. During lactation normal loss of BMC occurred. The increased BMC during post-weaning recovery suggests calcitriol-independent stimulation of new bone formation.

In conclusion, calcitriol-independent mechanisms regulate mineral and bone metabolism during pregnancy, lactation, and post-weaning.

*Disclosures: Brittany Gillies, None.***SA0131**

See Friday Plenary Number FR0131.

SA0132

See Friday Plenary Number FR0132.

SA0133

See Friday Plenary Number FR0133.

SA0134

See Friday Plenary Number FR0134.

SA0135

See Friday Plenary Number FR0135.

SA0136

See Friday Plenary Number FR0136.

SA0137

See Friday Plenary Number FR0137.

SA0138

See Friday Plenary Number FR0138.

SA0139

See Friday Plenary Number FR0139.

SA0140

See Friday Plenary Number FR0140.

SA0141

See Friday Plenary Number FR0141.

SA0142

See Friday Plenary Number FR0142.

SA0143

See Friday Plenary Number FR0143.

SA0144

See Friday Plenary Number FR0144.

SA0145

See Friday Plenary Number FR0145.

SA0146

See Friday Plenary Number FR0146.

SA0147

Withdrawn

SA0148

See Friday Plenary Number FR0148.

SA0149

See Friday Plenary Number FR0149.

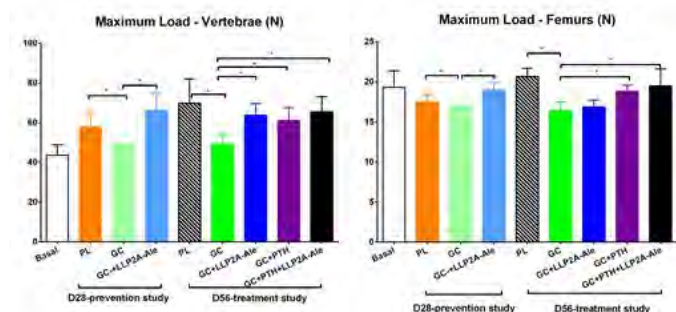
SA0150

A bone-seeking anabolic agent, LLP2A-Ale, prevented and restored glucocorticoid-induced bone loss. Nancy Lane¹, Yu-An Lay¹, Haley Berka¹, Lorna Ringwood¹, Alexander Kot¹, Haiyan Chen¹, Wei Yao².

¹University of California at Davis Medical Center, USA, ²University of California, Davis Medical Center, USA

Introduction. Glucocorticoid induced osteoporosis (GIOP) is the most common cause of secondary osteoporosis. Glucocorticoid (GC) treatment has prolonged effects on osteoblast maturation and activity. Currently, rhPTH (1-34) is on the only approved anabolic treatment that can restore bone mass and bone strength in GIOP. A bone-seeking compound, LLP2A-Ale that selectively targets the integrin $\alpha 4\beta 1$ on

the mesenchymal stem cell surface, can increase endogenous (MSC) recruitment to the bone surface, stimulate bone formation and increase bone mass. The purpose of this study was to determine if treatment with the LLP2A-Ale, or PTH or the combination treatment (LLP2A-Ale + PTH) could prevent GIOP or treat GIOP in a mouse model of GC excess. **Methods.** Four month old male mice of Swiss-Webster background were randomized to a prevention study with Placebo (PL), GC (2.8 mg/kg/d), GC + LLP2A-Ale (200 μ g/kg, IV at day 1) or a treatment study with PL, GC (2.8mg/kg/d) from day 1-60, LLP2A-Ale (300 μ g/kg at day 28), PTH (10 μ g/kg/d, 5x/wk) or GC +LLP2A-Ale + PTH from days 28 to 60. Mice were sacrificed at day 28 (prevention arm) or at day 60 (treatment arm). The study endpoints included a biochemical marker of bone turnover (PINP), surface-based bone turnover, bone mass and bone strength. **Results.** For the prevention study, GC alone reduced serum PINP levels by 45%, and trabecular bone mass and strength, while GC +LLP2A-Ale increased levels of PINP to 180% over PL (p<0.05), and prevented loss of bone mass and strength (Figure 1). For the treatment study, compared to GC alone, GC+LLP2A-Ale, PTH or LLP2A-Ale+PTH all significantly increased PINP, trabecular surface based bone formation, bone mass, and strength (p<0.05). Also, compared to GC alone, GC +LLP2A-Ale, PTH or and LLP2A-Ale + PTH all significantly increased both trabecular bone mass and strength at day 60 (p<0.05), and trabecular (treatment study) and cortical (prevention study) bone strength were not different from PL treated mice at day 60. (Figure). **Conclusion.** GC treatment significantly reduced both trabecular and cortical bone mass and strength. Treatment with GC+ LLP2A-Ale prevented these changes and GC+LLP2A-Ale, PTH or LLP2A-Ale+PTH completely restored both the bone mass and strength that was lost from the GC treatment. Additional studies with LLP2A-Ale are warranted to further evaluate the potential of this agent that can direct MSCs to bone surface for the treatment of GC induced osteoporosis and possibly osteonecrosis. **Methods.** Four month old male mice of Swiss-Webster background were randomized to a prevention study with Placebo (PL), GC (2.8 mg/kg/d), GC + LLP2A-Ale (300 μ g/kg, IV at day 1) or a treatment study with PL, GC (2.8mg/kg/d) from day 1-60, LLP2A-Ale (300 μ g/kg at day 28), PTH (10 μ g/kg/d, 5x/week, day 28-60) or GC +LLP2A-Ale + PTH from day 28 to 60. Mice were sacrificed at day 28 (prevention arm) or at day 60 (treatment arm). The study endpoints included a biochemical marker (PINP) and surface-based bone turnover, bone strength and assessments of angiogenesis including serum VEGF- and vascular density of the left femur (n=3/group) measured with microCT. **Results.** For the prevention study, GC alone reduced serum PINP levels by 45%, and trabecular bone mass and strength, while GC +LLP2A-Ale increased levels of PINP to 180% over PL (p<0.05), and prevented loss of bone mass and strength (Figure 1). For the treatment study, compared to GC alone, GC+LLP2A-Ale, PTH or LLP2A-Ale+PTH all significantly increased PINP, trabecular surface based bone formation, bone mass, and strength (p<0.05). Also, compared to GC alone, GC +LLP2A-Ale, PTH or and LLP2A-Ale + PTH all significantly increased both trabecular and cortical bone mass and strength at day 60 (p<0.05), and both trabecular and cortical bone strength were not different from PL treated mice at day 60. (Figure). Preliminary data on angiogenic effect of endogenous MSCs found that GC reduced serum levels of VEGF-A by 58% and blood vessel density by 88% compared to PL, and this decrease was reduced to 50% when the mice were treated with GC + LLP2A-Ale. **Conclusion.** GC treatment significantly reduced both trabecular and cortical bone mass and strength. Treatment with GC+ LLP2A-Ale prevented these changes and GC+LLP2A-Ale, PTH or LLP2A-Ale+PTH completely restored both the bone mass and strength that was lost from the GC treatment. Also, LLP2A-Ale treatment appeared to prevent GC induced reduction in serum VEGF-A levels and blood vessel density. Additional studies with LLP2A-Ale are warranted to further evaluate the potential of this agent that can direct MSCs to bone surface for the treatment of GC induced osteoporosis and possibly osteonecrosis.



GC-2A-Strength

Disclosures: Wei Yao, None.

SA0151

See Friday Plenary Number FR0151.

SA0152

See Friday Plenary Number FR0152.

SA0153

Cbl-PI3 Kinase Interaction Controls Osterix Expression And Regulates Periosteal Proliferation Upon Injury. Vanessa Scanlon, Bhavita Walia, Jungeun Yu, Peter Mave, Hicham Drissi, Archana Sanjay*. UConn Health Center, USA

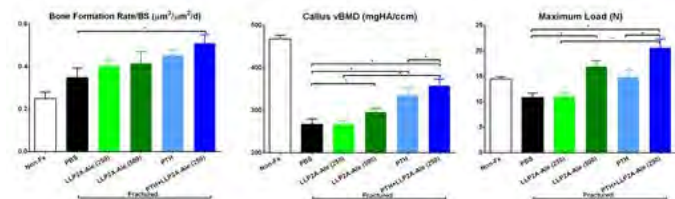
Tight regulation of Phosphatidylinositol kinase (PI3K) enzymatic activity is required for cell proliferation, differentiation and apoptosis. One major function of the adaptor and E3 ligase protein, Cbl, is to regulate PI3K activity by binding to the p85 regulatory subunit. We have reported that in mice where Cbl-p85 interaction is abrogated (YF mice) are osteopetrotic and have increased cortical thickness. Periosteum, a connective tissue covering the outer surface of long bones, is required for cortical bone modeling. To determine if the YF mutation alters the osteogenic potential of periosteal progenitors, we isolated periosteum from WT and YF long bones and cultured these cells in conditions that promote osteogenesis. We found that the osteogenic differentiation of YF periosteal cells was enhanced as evidenced by increased ALP activity and calcium content. RT-PCR analysis showed that although in YF cultures, expression levels of Runx2 were not altered, there was a significant upregulation in Osterix (Osx) expression. Immunofluorescence staining using anti-Osterix antibodies showed that under basal conditions compared to WT cells, YF cultures had increased numbers of cells with Osterix expression in the nucleus (WT 5.44%; YF 14% $p < 0.05$). While chemical inhibition of PI3K reduced the presence of Osx in WT cells, significantly higher numbers of cells with nuclear localization of Osx persisted in YF cultures (WT 1.74%; YF 10.4%, $p < 0.05$). To visualize Osx expression, we also bred both WT and YF mice with Osterix RFP reporter mice to generate WT-Osx-RFP and YF-Osx-RFP mice. To gain further insight into the process of initiation of periosteal bone formation and the role of Cbl-PI3K interaction in this process, we used a well-defined model of closed femoral fracture healing. Histological analysis of frozen sections showed that 3-days post fracture, compared to WT-Osx-RFP fractured femurs, YF-Osx-RFP showed a 2-fold increase in the periosteum thickness (WT 90.11um, YF188.8um, $p < 0.043$) and was largely comprised of Osterix-RFP+ cells. Additionally, in vivo EdU labeling showed that while there were very few EdU+ cells in intact WT or YF femurs, upon femoral fracture, proliferation of periosteal cells is enhanced in YF periosteum (WT 4.1%, YF 21.9%, $p < 0.052$). Cumulatively, these studies suggest that the Cbl-PI3K interaction controls cellular localization of Osterix regulating osteogenesis under basal and dynamic conditions of cortical bone modeling.

Disclosures: Archana Sanjay, None.

SA0154

Effect of LLP2A-Ale on fracture healing in growing mice. Wei Yao*¹, Yu-An Lav², Haiyan Chen², Alexander Kot², Nancy Lane². ¹University of California, Davis Medical Center, USA, ²University of California at Davis Medical Center, USA

Introduction. Bone fractures can result in surgery, increased physician visits, lost work time, and ongoing pain/disability. No FDA-approved medical treatment that augments fracture healing exists. A bone-seeking compound, LLP2A-Alendronate (LLP2A-Ale) that selectively binds integrin $\alpha 4\beta 1$ on endogenous mesenchymal stem cell (MSC) surfaces and increases MSC recruitment to bone surfaces, may stimulate callus formation and increase periosteal bone apposition. Our purpose is to find whether LLP2A-Ale alone, PTH alone or LLP2A-Ale+PTH accelerates healing in a murine fracture model. **Methods.** A closed fracture (fx) of the right mid-femur of two-month-old C57BL/6 male mice was created. A medullary pin was then placed to stabilize the fx and the wound was closed. The fx mice were divided into five groups (N=16/grp) and treated immediately with vehicle (VEH), LLP2A-Ale [250cg/kg (low dose-LD) or 500 μ g/kg (high dose-HD), IV at days 1 and 22], PTH (1-34) (20 μ g/kg/d, 5X/wk), or combined (LLP2A-Ale [LD]+PTH, COMBO). Unfractured, untreated mice (Non-Fx) (N=16) of equal age were included. Necropsy (N=8/grp) was conducted at Days 21 and 42 post-fx. Fx healing was assessed by measuring surface-based bone formation (BFR/BS) in the callus, callus volume/total volume (CV/TV), callus volumetric bone mineral density (vBMD), and right central femur maximum load (CFML). **Results.** At Day 21, PTH and COMBO groups had higher CV/TV than VEH ($P < 0.05$). At Day 42, callus BFR/BS was 40% higher in COMBO than VEH ($P < 0.05$). At Day 42, vBMD was 20%, 40%, and 50% greater in LLP2A-Ale (HD), PTH, and COMBO than VEH, respectively, and COMBO was better than either LLP2A-Ale (HD) or PTH (all $P < 0.05$). At Day 42, CFML was higher in LLP2A-Ale (HD), PTH, and COMBO than VEH, and COMBO was higher than PTH (all $P < 0.05$) (Figures 1-3). **Conclusion.** At Day 42 after fracture, LLP2A-Ale (HD) mice had higher callus vBMD and bone strength than VEH mice. COMBO mice had even higher callus vBMD and strength than any monotherapy. These results indicate a need for additional pre-clinical studies that use LLP2A-Ale alone or with PTH, to accelerate fracture healing.



d42-2A-Fx-callus

Disclosures: Wei Yao, None.

SA0155

Effects of Endoxifen, a Selective Estrogen Receptor Modulator, on Bone in Ovary-intact and Ovariectomized Rats. Anne Gingery*¹, Malavannan Subramaniam², Kevin Pitel², James N Ingle², Matthew P Goetz², Russell T Turner³, Urszula T Iwaniec³, Thomas C Spelsberg², John Hawse². ¹Mayo Clinic School of Medicine, USA, ²Mayo Clinic, USA, ³Oregon State University, USA

Endoxifen (END) has been identified as the predominant active metabolite of tamoxifen and is currently being developed as a novel hormonal therapy for the treatment of estrogen receptor positive breast cancer. We have previously shown that treatment with END increases cortical and cancellous bone in an ovariectomized (OVX) mouse model. We have extended these studies to a pre-clinical rat model to examine the effects of END in both intact and OVX animals. Four month old Sprague-Dawley rats (n=40) underwent either sham or OVX surgeries and were randomized to placebo or END (10mg/kg/day, for 35 days) treatment via oral gavage. Micro-CT analysis of the proximal tibial metaphysis revealed significantly greater bone volume per tissue volume (BV/TV), connectivity density, and trabecular number (Tb.N.) in END-treated OVX animals compared to vehicle-treated OVX, while trabecular spacing (Tb.Sp.) was significantly lower. Interestingly, BV/TV and Tb.Th. were also significantly greater in ovary-intact animals treated with END compared to vehicle. Cortical measurements (cross sectional volume, cortical volume and cortical thickness) at the tibial diaphysis were lower in END-treated animals compared to controls. Analysis of the vertebrae (LV5) revealed significant increases in BV/TV, Tb.N., Tb.Th., and reductions in Tb.Sp. in END-treated animals compared to vehicle controls, irrespective of gonadal status. END treatment resulted in no differences in serum levels of the bone resorption marker CTX1 in ovary-intact animals. However, CTX1 levels were significantly decreased in OVX END treated animals. The bone formation marker PINP was significantly reduced in both intact and OVX END-treated rats. Interestingly, END treatment also reduced serum sclerostin levels in both the intact and OVX setting. In summary, END enhanced many bone parameters in both ovary-intact and OVX rats. Importantly END improved many skeletal parameters in the ovary-intact pre-clinical rat model, making it an attractive therapeutic for pre-menopausal breast cancer patients where both estrogen deprivation and tamoxifen treatment result in bone loss.

Disclosures: Anne Gingery, None.

SA0156

See Friday Plenary Number FR0156.

SA0157

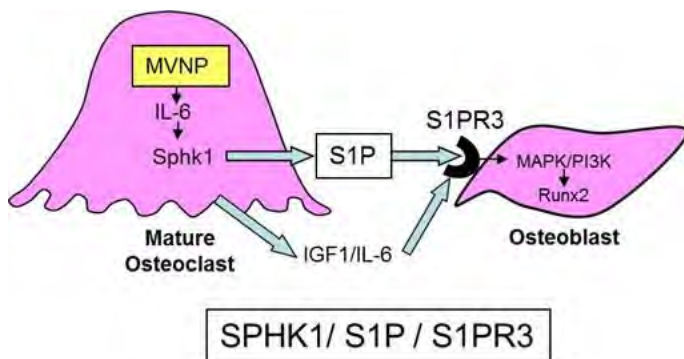
See Friday Plenary Number FR0157.

SA0158

Measles Virus Nucleocapsid Protein Expression in Osteoclasts Increases SPHK1/S1P/S1PR3 to Enhance Osteoblast Differentiation in Paget's Disease. Yuki Nagata*¹, Khalid Mohammad², Theresa Guise², Laëtitia Michou³, Jacques P. Brown³, Jolene J. Windle⁴, Noriyoshi Kurihara⁵, G. David Roodman⁶. ¹Indiana University-Purdue University Indianapolis, USA, ²Indiana University, Medicine/Endocrinology, USA, ³Department of Medicine, Laval University, CHU de Quebec Research Center, Canada, ⁴Human & Molecular Genetics, Virginia Commonwealth University, USA, ⁵Indiana University, Medicine/Hematology-Oncology, USA, ⁶Indiana University, Medicine/Hematology-Oncology, Roudebush VA Medical Center, USA

We reported that osteoclasts (OCLs) from 70% of Paget's disease (PD) patients express measles virus nucleocapsid protein (MVNP) and high levels of IL-6. Similarly, transgenic mice with MVNP targeted to OCLs (MVNP mice) express high levels of IL-6 and develop pagetic bone lesions that display highly localized increased bone resorption and formation. We recently found that OCLs expressing MVNP (MVNP-

OCLs) from PD patients and MVNP mice express increased IGF1 and ephrinB2 that was induced by IL-6. Further, IL-6 increased EphB4 on osteoblasts (OBs) and IGF1 further enhanced OB differentiation in MVNP mice. However, other factors also appear to be involved. Recently, sphingosine-1-phosphate (S1P) was identified as a coupling factor in bone remodeling. OCLs produce S1P which enhances bone formation through specific interactions with S1P-receptors on OBs. Therefore, we determined if S1P and its receptors also act as coupling factors in PD. We tested MVNP-OCLs from PD patients and healthy donors. MVNP-OCLs from PD patients and MVNP transduced human OCL highly expressed sphingosine kinase-1 (SPHK1), which phosphorylates sphingosine to form S1P, compared to normal or EV transduced human OCLs. We then examined if IL-6 contributed to the enhanced SPHK1 signaling in MVNP-OCLs. Treatment of OCL precursors from MVNP, MVNP/IL-6^{-/-}, IL-6^{-/-} and WT mice with RANKL for 5 minutes significantly increased p-SPHK1 in MVNP-OCL precursors compared to WT and MVNP/IL-6^{-/-} mice. IL-6^{-/-} OCL precursors had very low p-SPHK1 levels. Basal SPHK1 levels were increased in MVNP-OCL precursors. Western blot analysis of OBs from bone explants of WT and MVNP mice showed that S1P-receptor 3 (S1PR3) expression was higher in OBs from MVNP mice and was further increased by IL-6 and IGF1 (10ng/ml), which are secreted by MVNP-OCLs. Immunohistochemistry of bones from MVNP and WT mice confirmed increased SPHK1 in OCLs and S1PR3 expression in OB of MVNP mice compared to WT mice. To determine if S1P stimulates OB differentiation, OB derived from MVNP or WT mice were treated with S1P (50 ng/ml) for 3 days, and Runx2 assayed by Western blot. Runx2 levels were higher in OBs from MVNP mice compared to WT. Further, S1P increased the activation of Akt and Erk signaling in OBs from MVNP mice to a greater extent compared to WT OBs. These results suggest that IL-6 and IGF1 produced by MVNP expressing OCLs can enhance SPHK1/S1P/S1PR3 interactions to increase bone formation in PD.



Model of SPHK1/S1P/S1PR3 coupling in PD

Disclosures: Yuki Nagata, None.

SA0158

See Friday Plenary Number FR0158.

SA0159

See Friday Plenary Number FR0159.

SA0160

See Friday Plenary Number FR0160.

SA0161

See Friday Plenary Number FR0161.

SA0162

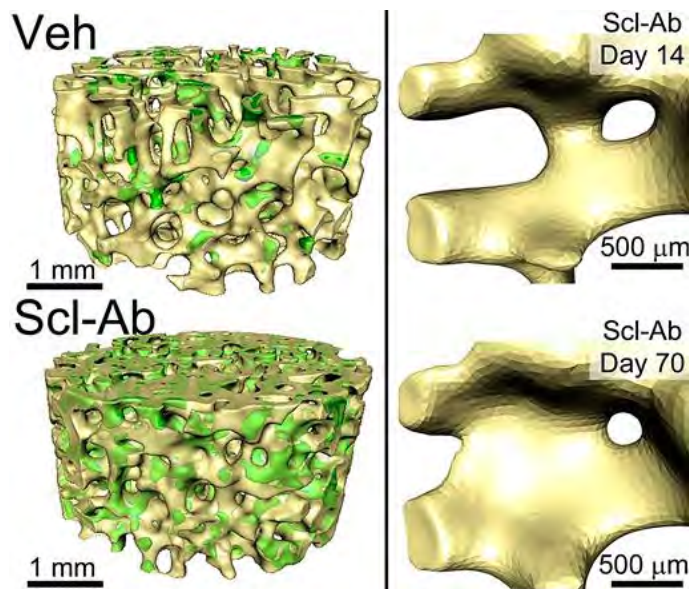
See Friday Plenary Number FR0162.

SA0163

Treatment with Sclerostin Antibody Converts Trabecular Rods into Trabecular Plates in Male Cynomolgus Monkeys. Jonathan Matheny*, Ashley Torres, Christopher Hernandez, Sibley School of Mechanical & Aerospace Engineering, Cornell University, USA

Trabecular microstructure with a more plate-like morphology has been associated with reduced risk of fragility fracture. Sclerostin antibody (Scl-Ab) treatment increases modeling-based bone formation and bone volume fraction while reducing bone resorption; however, the degree to which individual trabeculae are converted from rod-like to plate-like in response to treatment has not been examined. Here we used three-dimensional images of bone and bone formation markers to measure changes in rod-like and plate-like trabecular morphology associated with Scl-Ab

treatment. Specimens from a previously reported, IACUC approved study of adolescent (4-5-year-old) male cynomolgus monkeys were examined [1]. Animals had been treated bi-weekly with either Scl-Ab (romosozumab, 30 mg/kg, sc, n=6) or vehicle (Veh, n=6) for 10 weeks. Animals had received bone formation labels on days 14 and 24 (25 mg/kg tetracycline) and on days 56 and 66 (8 mg/kg calcein). Animals were euthanized at day 70. Cylindrical specimens of cancellous bone were obtained from the 5th lumbar vertebrae. Three-dimensional images of bone and formation markers were obtained using serial milling (0.7 X 0.7 X 5.0 um voxel size) and the volume of bone formed during the experiment was determined in three-dimensions (Shown in green, See Figure). Trabecular morphology was analyzed using Individual Trabecula Segmentation (ITS). Changes in trabecular microstructure (rod-like vs plate-like) over the 8 week period between the first and last bone formation label were determined by examining images of the specimens with and without the volume spanned by the formation labels. Over the 8 week period, 10% of rod-like trabeculae were converted to plate-like trabeculae in Scl-Ab treated animals compared to 4% in the Veh group (p=0.01). Plate bone volume fraction (pBV/TV) was higher in the Scl-Ab group relative to Veh (mean 43% v. 30%, p<0.05). Newly formed volume fraction (FV/TV) was also higher in Scl-Ab treated groups (9.0 v. 5.4%, p=0.02). Our results demonstrate that increased bone formation associated with Scl-Ab treatment not only increases bone volume fraction, but also provides additional improvements to trabecular bone microstructure by converting rod-like trabeculae to plate-like trabeculae. [1]. Ominsky, MS et al., JBMR 2011.



Sclerostin antibody treatment converts trabecular rods into trabecular plates

Disclosures: Jonathan Matheny, None.

This study received funding from: AMGEN

SA0164

See Friday Plenary Number FR0164.

SA0165

Fluoxetine Affects Bone Remodeling Via Peripheral, Serotonin-Independent, And Central, Serotonin-Dependent, Mechanisms. Maria J Ortuno Romero*¹, Riccardo Paone², J John Mann³, Patricia Ducy⁴. ¹Columbia University Medical Center, USA, ²Department of Biotechnological & Applied Clinical Sciences, University of L'Aquila, Italy, ³Division of Molecular Imaging & Neuropathology, Department of Psychiatry, College of Physicians & Surgeons, Columbia University, USA, ⁴Department of Pathology & Cell Biology, College of Physicians & Surgeons, Columbia University, USA

Clinical studies have reported a correlation between long-term use of Selective Serotonin Reuptake Inhibitors (SSRIs), are a class of drugs widely prescribed for anxiety disorders and decreased bone mass and/or the risk of fracture raising concerns about the broadening of SSRIs use in the general population. Using a combination of genetic, pharmacologic and in vitro approaches we have identified two distinct modes of action of SSRIs on bone remodeling explaining this observation.

First, SSRIs inhibit osteoclast differentiation and function through a direct, serotonin-independent, effect on osteoclasts. Indeed, treatment of primary osteoclasts with fluoxetine, one of the most frequently prescribed SSRIs, or with other SSRIs impairs several key aspects of osteoclast maturation. This inhibition is independent of fluoxetine's canonical mode of action on serotonin reuptake since it affects to same extent wild-type, *Tph1*-, *Tph2*- and *5Htt*-deficient osteoclasts. Instead, fluoxetine inhibits osteoclast biology by impairing Creb phosphorylation by the Ca²⁺-

calmodulin pathway, thereby limiting its activation of *Nfatc1* expression. This inhibitory effect on bone resorption could be observed in vivo in wild-type mice treated with fluoxetine for a short time (3 weeks). Gene expression analyses demonstrated a RANKL/OPG-independent inhibition of NFATc1 activity as the basis of this effect.

When the fluoxetine treatment was extended, however, a second mode of action overcame this direct inhibition of bone resorption. Mice treated for 6 weeks with fluoxetine showed a normalized bone resorption due to the combination of the direct inhibitory effect of fluoxetine on osteoclasts and of a RANKL/OPG-dependent increase in bone resorption. These mice also showed a decrease in bone formation, leading to bone loss. This second mode of action is dependent on brain serotonin signaling, as it could not be observed in *Tph2*^{-/-} mice, and is mediated by an increase of sympathetic output. Given this observation, we hypothesized that blocking sympathetic signaling could reverse the bone loss caused by a long-term fluoxetine treatment and co-treated wild-type mice with fluoxetine and a dose of the β -blocker that does not induce a bone phenotype by itself. This combined treatment indeed prevented fluoxetine-induced bone loss by normalizing bone formation and decreasing bone resorption, suggesting that long-term users of SSRIs could benefit from co-treatment with a low dose of β -blockers.

Disclosures: Maria J Ortuno Romero, None.

SA0166

See Friday Plenary Number FR0166.

SA0167

See Friday Plenary Number FR0167.

SA0168

See Friday Plenary Number FR0168.

SA0169

See Friday Plenary Number FR0169.

SA0170

See Friday Plenary Number FR0170.

SA0171

Histone 3 lysine 9 methyltransferase G9a is essential for the growth and differentiation of tenocytes. Satoshi Wada*¹, Hisashi Ideno², Akemi Shimada², Taichi Kamiunten¹, Yoshiki Nakamura¹, Kazuhisa Nakashima², Hiroshi Kimura³, Makoto Tachibana⁴, Akira Nifuji². ¹Department of Orthodontics, Tsurumi University School of Dental Medicine, Japan, ²Department of Pharmacology, Tsurumi University School of Dental Medicine, Japan, ³Graduate School of Bioscience & Biotechnology, Tokyo Institute of Technology, Japan, ⁴The Institute of Enzyme Research, The University of Tokushima, Japan

The growth and differentiation of tenocytes were regulated by genetic and epigenetic mechanisms. Posttranslational modifications of histone tails affect cell differentiation and gene expression by regulating chromatin. So far, however, the effects of epigenetic modifications on gene expression and differentiation in tenocytes remain unclear. In this study, we focus on expression and function of H3K9 methyltransferases (H3K9MTases), the enzymes mediating histone 3 lysine 9 (H3K9) methylation. Specifically, we investigated the functional roles of an H3K9MTase, G9a, in the growth and differentiation of tenocytes. First, we isolated tail tenocytes from neonatal mice by using collagen gel methods (Shimada et al. 2014) and examined the expression of H3K9MTases during tenocyte differentiation. Next, we investigated the localization of H3K9MTases in embryonic tendon tissues in mice by *in situ* hybridization (ISH). Finally, using tenocytes isolated from G9a-flox/flox mice, we deleted G9a by infecting the cells with Cre-expressing adenoviruses and investigated the effects of G9a deletion on the growth and differentiation of tenocytes. The mRNA expression levels of six H3K9MTases increased with the duration of tenocytes culture. Among them, G9a mRNA expression was relatively high in six H3K9MTases. By ISH, we observed that G9a mRNA was expressed in tenocytes, which were overlapped with or were adjacent to cells expressing tenomodulin. Using tenocytes isolated from G9a-flox/flox mice, we deleted G9a by Cre-expressing adenoviruses. We confirmed that G9a mRNA and protein expression levels decreased in the Cre-expressing adenovirus-infected tenocytes. Proliferation of G9a-null tenocytes decreased compared with that of control tenocytes. The mRNA expression levels of tendon-related genes were downregulated in G9a-null tenocytes. Similarly, tenomodulin protein expression was suppressed in G9a-null tenocytes compared with control cells. These results suggest that G9a expression is essential for the proliferation and differentiation of tenocytes, and that G9a play important roles in tendon development.

Disclosures: Satoshi Wada, None.

SA0172

See Friday Plenary Number FR0172.

SA0173

Therapeutic Potential of Myostatin (GDF8) in Protecting Immobilization-Induced Muscle Atrophy at an Adult Stage. Toshimi Tando*, Takeshi Miyamoto, Morio Matsumoto, Masaya Nakamura. Department of Orthopedic Surgery, Keio University School of Medicine, Japan

Femoral neck fracture is a big concern in the osteoporosis patients. Most cases of fractures are caused by falls, and at least some of the falls are due to sarcopenia, characterized by muscle weakness accompanied by muscle atrophy in elderly people. Myostatin (also named GDF8), a member of TGF β superfamily, was an inhibitor of muscle hypertrophy, and that was considered a therapeutic target to prevent muscle atrophy, however, the inhibitory effects of Myostatin in preventing muscle atrophy at an adult stage remain unclear. Therefore, the purpose of this study is to clarify the effects of Myostatin-inhibition in protecting muscle atrophy at an adult stage.

We utilized adult stage specific Myostatin conditional knockout (cKO, Mx Cre; *Myostatin*^{flox/flox}) or control (Ctl, *Myostatin*^{flox/flox}) mice, and performed two independent mouse immobilization induced muscle atrophy models, denervation of sciatic nerve or fixation of hind limb, in these mice. Gastrocnemius muscles were harvested from atrophic side (immobilized side) and non-atrophic side (sham operated side), and muscle weight and the expression of Atrogin-1 and MuRF1, both of which are ubiquitin ligases required for muscle atrophy, were analyzed.

Gastrocnemius muscle weight was equivalent between Ctl and cKO before the immobilization. Reduction of gastrocnemius muscle weight in immobilized compared with non-immobilized side was equally seen in Ctl and cKO mice. Elevation of both Atrogin-1 and MuRF1 expression in atrophic compared with non-atrophic muscles was also similarly seen in both Ctl and cKO mice. These results suggest that inhibition of Myostatin is not effective to prevent immobilization induced muscle atrophy.

Today, Myostatin is considered as a therapeutic target to prevent or treat sarcopenia. However, our results suggest that Myostatin is not a preferable target to protect the immobilization induced muscle atrophy at an adult stage.

Disclosures: Toshimi Tando, None.

SA0174

See Friday Plenary Number FR0174.

SA0175

Window of Opportunity: Circulating Osteoblast Precursors Were Decreased after Infiximab Therapy in Patients with Ankylosing Spondylitis. Seong-Ryul Kwon*¹, WON PARK¹, MIN-JUNG SON¹, MIE-JIN LIM², KYOUNG-HEE JUNG², SHIN-GOO PARK³. ¹INHA University Hospital, South Korea, ²Rheumatism Center, INHA University Hospital, South Korea, ³Department of Occupation & Environmental Medicine, INHA University Hospital, South Korea

Background

It was known TNF alpha blocker therapy had little or no effect on new bone formation or structural remodeling in patients with ankylosing spondylitis (AS).

Objective

We studied the differentiation and activity of osteoblast by novel cell culture technique of osteoblast in peripheral blood and other methods in candidates for infiximab therapy with AS and controls.

Methods

Male sixteen individuals with AS were enrolled. They met modified New York criteria and were candidates for infiximab therapy. Sex and age matched nineteen controls were also recruited. Peripheral blood mononuclear cells were collected and cultured in growth medium. Once cell multi-layering has been observed, cells were transferred to differentiation medium and cultured for 3 weeks. They were then fixed and stained with alizarin S stain to detect any calcified nodules. The optical density (OD) of alizarin S was measured for quantitative analysis.

We evaluated 1) the numbers of circulating osteoblast precursors in peripheral blood, 2) the OD of alizarin S red staining of circulating osteoblast precursors, 3) total procollagen type 1 N-terminal propeptide (PINP) as osteoprogenitor marker, osteocalcin as mature osteoblast marker in patients with AS and in healthy controls at baseline and 14 weeks after infiximab therapy in AS patients.

Results

The serum level of PINP (osteoprogenitor marker) was significantly higher in patients with AS than in the controls (p = 0.08), but that of osteocalcin (mature osteoblast marker) was not. The number of osteoblast precursor cells and optical density of alizarin S were decreased after infiximab therapy (p = 0.028 for optical density of alizarin S). The serum level of PINP was decreased after infiximab therapy (p = 0.002), but that of osteocalcin was increased (p = 0.007).

Conclusions

These results support the hypothesis, 'window of opportunity' that acute inflammation resolved completely but mature lesion could not alter the new bone formation.

Disclosures: *Seong-Ryul Kwon, Celltrion company, Korea, Republic of*

SA0176

Evaluation of Vitamin D Levels in Women with Carpal Tunnel Syndrome. Hyun Sik Gong*¹, Seung Hoo Lee². ¹Seoul National University Bundang Hospital, South Korea, ²Seoul National University, South Korea

Background: Carpal tunnel syndrome (CTS) is the most common compressive neuropathy in the upper extremity and commonly occurs in postmenopausal women. Recent studies suggest an association between vitamin D and peripheral nerve disorders. Vitamin D has been shown to improve myelination and recovery after nerve injuries, and low levels of vitamin D were associated with neuropathy in patients with diabetes or Sjögren's syndrome. Thus, we aimed to evaluate levels of vitamin D and their association with clinical features of CTS in women undergoing carpal tunnel release.

Methods: We measured vitamin D levels in 154 women (mean age, 57 ± 10 years) undergoing surgery for CTS and 388 control women (mean age, 56 ± 8 years) without neurologic symptoms. Patients with CTS were evaluated for electrophysiologic severity of the disease and perceived disability using the Disabilities of the Arm, Shoulder, and Hand (DASH) questionnaire. Vitamin D levels were compared between women with CTS and control women, and correlation analyses were performed between vitamin D levels and clinical features of CTS such as age, symptom duration, electrophysiologic severity, and perceived disability in CTS patients.

Results: Vitamin D levels were comparable between women with CTS and control women (mean ± standard deviation (SD), 20.6 ± 11.5 ng/ml and 20.8 ± 9.8 ng/ml, respectively; p = 0.801). However, CTS women less than 50 years of age (n = 40) had significantly lower levels of vitamin D (mean ± SD, 16.7 ± 8.1 ng/ml) than age-matched controls (n=107, mean ± SD, 20.7 ± 9.6 ng/ml, p = 0.021), while there were no such differences in other age groups. Lower vitamin D levels were associated with lower age of onset (r = 0.159, p = 0.048). Other clinical features did not correlate with vitamin D status.

Conclusions: In this study, CTS women less than 50 years of age had significantly lower levels of vitamin D than age-matched controls, and lower vitamin D levels were associated with lower age of onset. This study suggests a potential link between vitamin D status and the occurrence of CTS in women younger than 50 years of age. Further studies are necessary to explore the potential role of vitamin D in the pathogenesis of CTS.

Disclosures: *Hyun Sik Gong, None.*

SA0177

See Friday Plenary Number FR0177.

SA0178

Quantifying the Progression of Preclinical Osteoarthritis as an Organ Disease Using Co-Registered Analysis in Five Tissues (CRAFTs). Joseph Temple*¹, Tieshi Li², Alessandra Eposito², Anna Spagnoli². ¹University of North Carolina at Chapel Hill, USA, ²Department of Pediatrics, Rush University Medical Center, USA

It has become accepted that osteoarthritis (OA) is a complex organ disease involving inter-tissue regulation in the cartilage, subchondral bone, osteophyte border, synovium, and meniscus. As the established preclinical OA scoring technique (i.e. OARSI) centers on assigning cartilage grades to sampled histological slices, it provides semi-quantitative data about only one joint tissue and has histological limitations.

Here, we present Co-Registered Analysis in Five Tissues (CRAFTs), an imaging analysis platform designed to progressively quantify OA progression as an organ disease. To optimize precision, we developed a co-registration technique that uses validated anatomically invariant bone landmarks to uniformly align all scans. Briefly, murine post-traumatic OA was induced via surgical destabilization of the medial meniscus (DMM). Knees were harvested 2, 4, 8, 12, 16, and 20 weeks (W) post-operatively and scanned natively (no contrast) using Micro-Computed Tomography to evaluate OA-related bone changes (osteophytes, subchondral sclerosis, meniscal calcification). Knees were stained (1.0% phosphotungstic acid/70% EtOH, EPTA) and rescanned for cartilage damage and synovitis. DMM results were evaluated vs. controls (t test) and over time (ANOVA). Significance was set at p < 0.05 and there were n ≥ 10 samples per group.

On native DMM scans, we measured significant increases in the amount of mineralized tissue vs. controls in the subchondral bone (BV: 0.626 ± 0.018 vs. 0.558 ± 0.019), meniscus (TV: 0.118 ± 0.005 vs. 0.085 ± 0.004 mm³), and osteophyte border (TV: 0.037 ± 0.006 vs. 0.000 ± 0.000 mm³) at 2W. These changes progressively increased over time. On EPTA DMM scans, we quantified decreased matrix integrity vs. controls at 2W (Attenuation: 875.6 ± 14.0 vs. 938.2 ± 26.8 TU). Full thickness fissuring and significant volumetric cartilage loss were present at 8W (TV: 0.074 ± 0.004 vs. 0.087 ± 0.006 mm³). These results correlated with the OARSI scores, which were not significant at 2W (0.6 ± 0.4 vs. 0.3 ± 0.3, p = 0.109), but were significant at 8W (3.2 ± 1.1 vs. 0.4 ± 0.2). Significant synovitis was present at 12W (Thickness: 0.035 ± 0.008 vs. 0.020 ± 0.005 mm).

Our results suggest that CRAFTs is a high-precision technique capable of quantifying subtle OA changes and progression in multiple joint tissues. Excitingly, the simultaneous early pathology that we identified in multiple joint tissues further reinforces the concept of OA as a complex organ disease.

Disclosures: *Joseph Temple, None.*

SA0179

See Friday Plenary Number FR0179.

SA0180

Favorable Effects of anti TNF Therapy on Bone Turnover in Peripheral Blood Despite Inadequate Response of Inflammatory Markers in Seropositive RA Patients. Mie Jin Lim*¹, Won Park², Seong Ryul Kwon², Kyung Hee Jung². ¹Inha University Hospital, South Korea, ²Inha University Hospital, South Korea

Objectives

We investigated the circulating osteoclasts and osteoblast activity in peripheral blood before and 6 months after anti TNF- α therapy in seropositive RA patients.

Materials and Methods

Thirteen seropositive RA patients were enrolled. They had been refractory to disease modifying antirheumatic drugs (DMARDs) and were preparing for anti TNF- α Therapy including infliximab, adalimumab and etanercept. Peripheral blood mononuclear cells (PBMCs) were collected before and 6 months after anti TNF- α Therapy. PBMCs (1 x 10⁶ cells/well) were placed in a 96-well tissue culture plate and cultured for 14 days. Histochemical staining for tartrate resistant acid phosphatase (TRAP) was carried out using an acid phosphatase kit (Sigma 386-A, St. Louis, MO). TRAP positive giant cells with more than 3 nuclei were regarded as osteoclasts. To assess resorption potential of osteoclasts, PBMCs were also cultured on bone slices for 3 weeks under the same condition as described above. Osteoclasts were then removed and the pits were visualized with 0.1% toluidine blue. The areas of pits were quantified using a computerized image analysis program. PBMCs were also cultured, fixed and stained with alizarin S stain to detect any calcified nodules. The optic density measurement of total alizarin S solute was performed for quantitative analysis.

Results

After 6 months of anti TNF- α therapy, number of ex vivo cultured osteoclasts was reduced and the area of resorption pit decreased as shown in Table 1. The optic density of calcified nodules increased significantly. On the other hand, systemic inflammatory markers including erythrocyte sedimentation rate (ESR) and c-reactive protein (CRP) failed to show significant response after anti TNF therapy. Anti-TNF therapy reduced swollen and tender joint counts, resulting in improvement of RA disease activity.

Conclusion

The number of peripheral osteoclasts and osteoblast activity decreased after 6 months of anti TNF- α treatment despite inadequate response of inflammatory mediators. The clinical signs of patients also improved after anti TNF therapy.

| | Before TNF- α Therapy | 6 months after TNF- α therapy | p |
|---|------------------------------|--------------------------------------|--------|
| Number of osteoclasts (per well) | 586.8 ± 284.8 | 321.5 ± 131.7 | 0.013 |
| Area of resorption pit (mm ²) | 0.18 ± 0.113 | 0.08 ± 0.076 | 0.007 |
| Optic density from osteoblastic nodules (μ mol/well) | 125.2 ± 157.62 | 1215.5 ± 676.65 | 0.013 |
| Swollen Joint counts | 18 ± 6.9 | 8 ± 4.9 | 0.002 |
| Tender Joint Counts | 18 ± 6.4 | 8 ± 4.9 | 0.001 |
| ESR (mm/hr) | 28 ± 17.7 | 22 ± 28.3 | 0.2 |
| CRP (mg/L) | 13.8 ± 13.32 | 6.9 ± 17.08 | 0.2 |
| DAS28-ESR | 6.64 ± 0.9 | 4.48 ± 1.48 | <0.001 |
| DAS28-CRP | 6.33 ± 0.7 | 4.12 ± 1.08 | <0.001 |

Table 1

Disclosures: *Mie Jin Lim, None.*

SA0181

See Friday Plenary Number FR0181.

SA0182

See Friday Plenary Number FR0182.

SA0183

See Friday Plenary Number FR0183.

SA0184

See Friday Plenary Number FR0184.

SA0185

See Friday Plenary Number FR0185.

SA0186

See Friday Plenary Number FR0186.

SA0187

See Friday Plenary Number FR0187.

SA0188

See Friday Plenary Number FR0188.

SA0189

See Friday Plenary Number FR0189.

SA0190

See Friday Plenary Number FR0190.

SA0191

See Friday Plenary Number FR0191.

SA0192

TGF- β 1 Induces TRAF3 Autophagic Degradation leading to GSK-3 β -induced β -catenin Inactivation and Inhibition of Osteoblast Differentiation. Jinbo Li*¹, Zhenqiang Yao², Lianping Xing², Brendan F. Boyce². ¹University of Rochester Medical Center, USA, ²U of Rochester Medical Center, USA

TNF receptor-associated factor 3 (TRAF3) is an adaptor protein that transduces signaling of cytokines, including TNF and RANKL. Conditional deletion of TRAF3 (TRAF3 cKO) in myeloid cells resulted in osteoporosis due to increased osteoclast (OC) activity, and TRAF3 cKO in mesenchymal progenitor cells (MPCs) also led to early onset osteoporosis in the cKO mice. Importantly, we have found that TRAF3 protein levels are significantly lower in the bones of 18- than 3-m-old mice. These findings suggest that increased bone resorption and decreased formation in age-related osteoporosis could be linked to the reduced TRAF3 levels in bone with aging, but the mechanisms involved are unclear. We treated mouse and human MPCs with factors that regulate osteoblast (OB) differentiation and found that TGF- β 1 clearly reduced TRAF3 protein levels. Consistent with this, TGF- β 1 significantly inhibited ALP and Runx2 gene expression, OB differentiation (ALP⁺ OB area 5.4 ± 2.4 vs. 42 ± 15 mm²/well in veh) and nodule formation (mineral area 0.2 ± 0.1 vs. 41 ± 16 mm²/well in veh) from WT MPCs. Similar changes were observed in MPCs from TRAF3 cKO mice. Ubiquitination (Ub) followed by either proteasomal or autophagic degradation is a common mechanism to degrade proteins. We found that TGF- β 1 significantly increased TRAF3 Ub, and TGF- β R2 directly associated with TRAF3 in WT MPCs. Of note, TGF- β 1 significantly increased co-localization of TRAF3 with the lysosome protein LAMP2; the autophagy inhibitor, chloroquine, partially blocked this effect. We used TRAF3 cKO and WT mouse MPCs to identify potential signaling pathways regulated by TRAF3. We found that active β -catenin levels were significantly lower in the cKO than in WT MPCs, with no difference in total β -catenin protein levels; in contrast, levels of active GSK-3 β , which degrades β -catenin, were increased in the cKO MPCs. Importantly, the GSK-3 β inhibitors, lithium chloride and SB-216763, significantly increased active β -catenin protein levels and partially reversed the inhibition of OB differentiation in TGF- β 1-treated WT MPCs and of TRAF3 cKO MPCs. In summary, 1) TRAF3 protein levels are reduced in bone with aging; 2) TGF- β 1/TGF- β R2 signaling induces TRAF3 autophagic degradation; 3) GSK-3 β is activated in TRAF3 cKO MPCs and degrades β -catenin to inhibit OB differentiation. We conclude that prevention of TRAF3 degradation could be a novel strategy to reduce bone resorption and increase bone formation to treat age-related osteoporosis.

Disclosures: Jinbo Li, None.

SA0193

See Friday Plenary Number FR0193.

SA0194

See Friday Plenary Number FR0194.

SA0195

See Friday Plenary Number FR0195.

SA0196

See Friday Plenary Number FR0196.

SA0197

See Friday Plenary Number FR0197.

SA0198

See Friday Plenary Number FR0198.

SA0199

See Friday Plenary Number FR0199.

SA0200

See Friday Plenary Number FR0200.

SA0201

Oxidativestress-induced apoptotic insults to rat osteoblasts is attenuated by nitric oxide pretreatment via GATA-5-involved regulation of *Bcl-X_L* gene expression and protein translocation. Ruei-Ming Chen*¹, Gong-Jhe Wu², Yi-Ling Lin¹. ¹Taipei Medical University, Taiwan, ²Taipei Medical University Hospital, Taiwan

Nitric oxide (NO) has biphasic effects on regulating osteoblast survival and death. This study was aimed to evaluate the effects of NO pretreatment on hydrogen peroxide (HP)-induced osteoblast insults and the possible mechanisms. Exposure of osteoblasts prepared from rat calvarias to HP significantly increased intracellular reactive oxygen species levels, decreased alkaline phosphatase activity and cell survival, and ultimately induced cell apoptosis. However, NO pretreatment lowered HP-induced oxidative stress and apoptotic insults. In parallel, HP increased Bax levels and its translocation from the cytoplasm to mitochondria. NO pretreatment caused significant attenuations in HP-induced modulations in Bax synthesis and translocation. In contrast, pretreatment with NO enhanced levels and translocation of anti-apoptotic Bcl-XL protein in osteoblasts. RNA analyses further revealed that HP inhibited Bcl-XL mRNA expression without affecting Bax mRNA levels. In comparison, NO induced Bcl-XL mRNA production and alleviated HP-caused inhibition of this mRNA expression. As to the mechanism, HP suppressed RNA and protein levels of transcription factor GATA-5 in osteoblasts. Pretreatment with NO induced GATA-5 mRNA and protein expressions and simultaneously attenuated HP-induced inhibition of this gene's expression. Consequently, GATA-5 knockdown using RNA interference inhibited Bcl-XL mRNA expression and concurrently lowered NO's protection against HP-induced apoptotic insults. Therefore, this study showed that NO can protect osteoblasts from HP-induced apoptotic insults. The protective mechanisms are mediated by GATA-5-mediated transcriptional induction of Bcl-XL gene, and translocational modulation of Bcl-XL and Bax proteins.

Disclosures: Ruei-Ming Chen, None.

SA0202

See Friday Plenary Number FR0202.

SA0203

See Friday Plenary Number FR0203.

SA0204

See Friday Plenary Number FR0204.

SA0205

See Friday Plenary Number FR0205.

SA0206

See Friday Plenary Number FR0206.

SA0207

See Friday Plenary Number FR0207.

SA0208

See Friday Plenary Number FR0208.

SA0209

See Friday Plenary Number FR0209.

SA0210

See Friday Plenary Number FR0210.

SA0211

See Friday Plenary Number FR0211.

SA0212

See Friday Plenary Number FR0212.

SA0213

See Friday Plenary Number FR0213.

SA0214

Regulation of Osteoclasts by Scavenger Receptor-A. Larry Suva¹, Nisreen Akel², Jessica Webber³, Sean Parham⁴, Diarra Williams⁴, Frances Swain⁴, Dana Gaddy⁴, Steven Post³. ¹University of Arkansas for Medical Sciences, USA, ²UAMS Orthopaedic Surgery, USA, ³UAMS Department of Pathology, USA, ⁴UAMS Department of Orthopaedic Surgery, USA

The class A scavenger receptor (SR-A) is a multifunctional receptor predominantly expressed by macrophages critical for mediating ligand uptake, cell attachment and signaling. SR-A binds a broad array of macromolecular ligands including modified proteins and lipoproteins, nucleic acids, as well as a variety of microbial proteins. Since osteoclasts are derived from the monocyte/macrophage lineage, SR-A has the potential to significantly impact osteoclast development and function. In this study the impact of SR-A deletion on bone, muscle and fat was investigated. SR-A null mice (males and females) deficient in SR-AI, AII, and AIII on a C57Bl6 background were examined at 3, 4, 5 and 6 months of age and compared with WT age-matched controls. Body composition analyses demonstrated greater total lean and fat body mass in SR-A^{-/-} animals, with no significant difference in percent fat and lean body mass by DEXA, and no differences in food intake. In addition, the evaluation of long bones and spine by microCT confirmed a previously identified high trabecular bone mass phenotype, significantly increased BV/TV and Tb.N. with decreased Tb.Sp. in SR-A^{-/-} mice, with the phenotype apparent at even the earliest (3 month) time point. The cortical bone was also affected, with cortical thickness and periosteal perimeter both significantly increased. Histologically, the bone phenotype is explained by significantly decreased osteoclasts in SR-A^{-/-} compared to wild type mice, with no measurable differences in osteoblast or adipocyte progenitors. Interestingly, there appears to be an increase in the number of nuclei/osteoclast in SR-A^{-/-} mice. *Ex vivo* bone marrow cultures from wild-type and SR-A^{-/-} mice revealed a dramatic decrease in osteoclastogenesis in SR-A^{-/-} bone marrow and isolated bone marrow macrophages, along with mild suppression of osteoblastogenesis. The increased osteoclast nuclei per cell was reproduced *in vitro*, implicating SR-A as a novel regulator of cell fusion. These data suggest that the deletion of SR-A *in vivo* induces changes in osteoclast development that involve osteoclast differentiation, fusion and function. Collectively, SR-A is necessary for normal osteoclast development and we hypothesize a novel role for SR-A in the scavenging and removal of bone resorption debris by osteoclasts.

Disclosures: Nisreen Akel, None.

SA0215

The deletion of *Hdac4* in osteoblasts influences both catabolic and anabolic effects in bone. Teruyo Nakatani¹, Tiffany Chen², Eric Olson³, Nicola Partridge². ¹New York University College of Dentistry, USA, USA, ²New York University College of Dentistry, USA, ³University of Texas Southwestern Medical Center, USA

Histone deacetylase (Hdac4) is known to control chondrocyte hypertrophy and bone formation. Since the global knockout *Hdac4* mice do not survive to weaning, we cannot obtain samples for mature bone analysis nor treat the animals with PTH. To analyze the function of Hdac4 in bone, we generated osteoblast-specific knockout of *Hdac4* (*Hdac4*^{ob/-}). We crossed transgenic mice bearing col2.3 1a(1)-Cre recombinase with mice bearing loxP-*Hdac4*. To determine the effect of PTH on bone resorption in these mice, we conducted experiments infusing hPTH (1-34) with Alzet microosmotic pumps (8 mg/100g BW/day) or saline vehicle implanted subcutaneously on the back at a normal pumping rate of 0.25 ml/h for 14 days in 8 week old female *Hdac4*^{ob/-} and wild type (*Hdac4*^{fl/fl}) mice. The *Hdac4*^{ob/-} mice survive to adulthood but show a clear but mild bone phenotype. At 12 weeks of age, they have a shortened and irregular-shaped stiff tail due to shorter tail joints, with almost no growth plates. Similarly, the thickness of the tibial growth plate zone was shortened. MMP-13 and SOST mRNAs were increased in the distal femurs of *Hdac4*^{ob/-} mice. Immunohistochemistry showed that Mef2c and Runx2 were increased in cells of trabecular bone in *Hdac4*^{ob/-} mice, suggesting that Hdac4 inhibits their gene expression. It is likely that the increase in these transcription factors causes the increase in MMP-13 and SOST. Serum CTX, a marker of bone resorption was increased in *Hdac4*^{ob/-} mice with or without PTH treatment. Tibial cortical BV/TV, Cs/Th, and relative cortical area (RCA) were decreased in *Hdac4*^{ob/-} mice but PTH caused no further decrease in *Hdac4*^{ob/-} mice. Tibial trabecular thickness tended to decrease in *Hdac4*^{ob/-} mice and further decreased with PTH treatment. These results indicate that Hdac4 might inhibit bone resorption and also have an anabolic effect via inhibiting MMP-13 and SOST gene expression. Hdac4 influences cortical bone mass and thickness and knockout of *Hdac4* seems to prevent the catabolic effect of PTH in cortical bone.

Disclosures: Teruyo Nakatani, None.

SA0216

The effects of GPR43 allosteric agonist on bone. Myeongmo Kang¹, Namhee Kim¹, HeeJin Nam¹, Seong Hwan Kim², Dongdong Zhang¹, Bo Mi Park³, YuMie Rhee¹, Sung-Kil Lim³, ChuHyun Bae³. ¹Yonsei Univ., Sinchon-dong, Seodaemun-gu, Seoul, Korea, South Korea, ²Korea Research Institute of Chemical Technology, South Korea, ³Brain Korea 21 PLUS Project for Medical Science, Yonsei University, Seoul, Republic of Korea, South Korea

Absence of gut microbiota leads to increased bone mass associated with reduced number of osteoclasts (OCLs) per bone surface, decreased frequency of CD4⁺T cells and OCL precursor cells in bone marrow. Sodium butyrate, short chain amino acid increased alkaline phosphatase (ALP) activity of cloned osteoblastic cell line MC3T3-E1 by the stimulation of *de novo* enzyme synthesis and it decreased tartrate resistant acid phosphatase (TRAP)-positive multinucleated cells (MNC) formation from bone marrow cells. Short chain amino acids metabolized from fiber in gut stimulate both GPR41 and GPR43. CMTB is the first synthetic allosteric agonist for GPR43. To test the effects of CMTB on bone, we established stable cell line for expressing GPR43 and NFATc luciferase reporter. CMTB efficiently activated the reporter activity dose dependently. GPR43 was expressed bone marrow cells, preosteoclast extensively, meanwhile expression was low in mature osteoclast and primary cultured osteoblast cells. It suppressed the expression of Runx2, Osterix and RANKL induced by osteogenic media. It also inhibits significantly the osteoclastogenesis induced by RANKL and M-CSF. Furthermore it suppressed Alp expression in MC3T3E1 cells at the high dose, however it stimulated BMP4 induced ALP expression in C2C12 cells. Taken together, activation of GPR43 suppresses osteoclastogenesis and differentiation of osteoblast at the stage of preosteoblasts after enhancing the commitment of precursor cells into osteoblast lineage cells. The *in vivo* effects of GPR43 allosteric agonist will be presented in the meeting

Disclosures: ChuHyun Bae, None.

SA0217

See Friday Plenary Number FR0217.

SA0218

See Friday Plenary Number FR0218.

SA0219

Estrogen regulates the activity of avian medullary bone osteoclasts through Eph/ephrin signaling. Shinji Hiyama*¹, Ki-ichi Nakamori², Mineo Watanabe¹, Takashi Uchida¹. ¹Hiroshima University Institute of Biomedical & Health Sciences, Japan, ²Hiroshima University, Japan

Estrogen induces mammalian osteoclast apoptosis, which may be related to postmenopausal osteoporosis, while this hormone does not promote apoptosis of avian medullary bone (MB) osteoclasts. MB is a unique tissue of female birds, which acts as a calcium reservoir of egg-shell formation and remodeled in the bone marrow cavity under the powerful control of circulating estrogen. In this process, increased circulating estrogen does not facilitate apoptosis of osteoclasts, and osteoclasts are present as a resting state on the surface of MB. Until now, we reported using the avian medullary bone osteoclastogenesis model that estrogen had not effect on apoptosis of MB osteoclasts, while their activity and morphology were affected. Clarifying the difference between avian and mammalian osteoclast responses to estrogen may be helpful to identify additional roles of estrogen in bone. Recently, there are reported that Ephrin (Eph) receptors and its ligands, ephrin, are related to osteoclast activity. Therefore, we focused on the effects of estrogen on the expression of Eph receptors and its ligands in MB osteoclasts. Male Japanese quails were given a single injection of 17beta-estradiol (E2). After a couple of days, bone marrow cells were collected and cultured in the presence of RANKL/M-CSF for a week. Continued treatment of E2 did not effect to the expression of Eph receptors and its ligands. On the other hand, EphA2, EphA4 and EphrinB1 expression levels were decreased by transient exposure of E2 at late stage of culture. In this culture stage, intracellular pH of these cells had no effect, while the immunoresponse of MMP-9 of these cells was decreased by E2 treatment. These results suggest that Ephrin receptors and its ligands may regulate to avian osteoclast activity and these signaling may be regulated by estrogen. Further studies will determine the relationship between estrogen and Eph/ephrin signaling.

Disclosures: Shinji Hiyama, None.

SA0220

Lnk Deficiency leads to TPO-Mediated Osteoclastogenesis and Increased Bone Mass Phenotype. David Olivos*¹, Ying-Hua Cheng², Marta Alvarez², Adam Hooker², Wendy Ciovacco³, Brahmananda Chitteti⁴, Pierre Eleniste⁵, Mark Horowitz⁶, Edward Srour⁴, Angela Bruzzaniti⁵, Robyn Fuchs⁷, Melissa Kacena⁸. ¹Department of Orthopaedic Surgery, Indiana University School of Medicine; Department of Microbiology & Immunology, Indiana University School of Medicine, USA, ²Department of Orthopaedic Surgery, Indiana University School of Medicine, USA, ³Department of Orthopaedic Surgery, Indiana University School of Medicine; Department of Orthopedics & Rehabilitation, Yale University School of Medicine, USA, ⁴Department of Medicine, Indiana University School of Medicine, USA, ⁵Department of Oral Biology, Indiana University School of Medicine, USA, ⁶Department of Orthopaedics & Rehabilitation, Yale University School of Medicine, USA, ⁷Department of Physical Therapy, Indiana University School of Health & Rehabilitation Sciences, USA, ⁸Department of Orthopaedic Surgery, Indiana University School of Medicine; Department of Orthopaedics & Rehabilitation, Yale University School of Medicine, USA

The Lnk adapter protein negatively regulates the signaling of thrombopoietin (TPO), the main megakaryocyte (MK) growth factor. As expected Lnk-deficient (-/-) mice have increased TPO signaling and therefore increased MK number. Interestingly, several mouse models exist in which increased MK number leads to a high bone mass phenotype. Here we demonstrate that Lnk-/- mice also exhibit a high bone mass phenotype. While MK-mediated osteoblast proliferation contributes to the high bone mass phenotype, we also show that Lnk is expressed by cells of the osteoclast (OC) lineage. Moreover, when Lnk-/- OC progenitors are cultured in the presence of TPO, significantly more TRAP+ OCs are observed than in wild-type (WT) control cultures. However, in vitro, Lnk-/- OC bone resorbing activity is impaired. MicroCT and static histomorphometric analyses at 20 weeks found the distal femur of Lnk-/- mice to have significantly higher bone volume per total volume (BV/TV), increased trabecular number (Tb.N), and decreased trabecular separation (Tb.Sp) compared to WT mice. Of note, despite a significant increase in the number of OC per tissue area (N.Oc/T.Ar), and decreased bone formation rate per total volume (BFR/TV) in Lnk-/- mice compared to WT mice, Lnk-/- mice demonstrated a 2.5-fold greater BV/TV suggesting impaired osteoclast function in vivo, consistent with the in vitro results. Additionally, Lnk-/- mouse femurs exhibited increases in mid-shaft cross-sectional area and periosteal BFR compared to that observed in WT femurs. In agreement with this, Lnk-/- femurs had an increased polar moment or inertia. Lnk-/- cortical bone area and thickness was markedly reduced and biomechanical testing showed femurs to be less stiff, have reduced strength, and a decreased modulus compared to WT femurs. Taken together, these data suggest that Lnk both directly regulates bone mass through its actions on OC (impaired resorptive activity) while also indirectly regulating bone mass through its actions on MK which in turn regulate osteoblasts. Thus, targeting Lnk may serve as a novel therapeutic approach for treating bone loss diseases such as osteoporosis.

Disclosures: David Olivos, None.

SA0221

See Friday Plenary Number FR0221.

SA0222

A Transmembrane Osteoclastic Protein-Tyrosine Phosphatase (PTP-oc), a Positive Regulator of Osteoclast Activity, Is Regulated Post-transcriptionally in part by miR17 in Osteoclastic Cells. Matilda Sheng*¹, Virginia Stiffel², Mehran Amoui², Kin-Hing William Lau². ¹Jerry L. Pettis Memorial VA Medical Center & Loma Linda University, USA, ²Jerry L. Pettis Memorial VA Medical Center, USA

PTP-oc has been shown to be a positive regulator of functional activity of osteoclasts. This study sought to determine the mechanism by which PTP-oc is regulated. Accordingly, we found that PTP-oc is regulated post-transcriptionally as several resorption effectors increased PTP-oc mRNA levels without altering its promoter activity. To test if PTP-oc expression is regulated by miRNAs, we searched for potential miRNA target sites on PTP-oc mRNA and found three potential miRNA target sites; one of which is for *miR17*. We focused on *miR17*, because *miR17* has been shown to negatively regulate a structurally-related PTP (*PTPRO*). During the RANKL-induced osteoclast differentiation, there was a corresponding time-dependent reduction in *miR17* and a significant inverse relationship between the levels of *miR17* and *PTP-oc* mRNA. *miR17* in osteoclasts was suppressed by those resorption effectors that also upregulated PTP-oc. The pre-*miR17*-92-transfected osteoclasts showed ~2-fold increase in *miR17* and ~50% decrease in *PTP-oc* mRNA. The average size of osteoclasts derived from pre-*miR17*-92 transfected cells was 43 ± 8% smaller. To ascertain that the observed effects of *miR17* overexpression were not due to off-target effects, we transduced osteoclast precursors of *miR17*-92^{fllox/fllox} mice with a Cre-expressing adenoviral vector (Ad5-CMV-Cre) to delete *miR17*-92. The cellular *miR17* level in Ad5-Cre-transduced osteoclasts was <50% of that of Ad5-GFP-treated control cells. The average size of *miR17*-92 cKO osteoclasts was 35-40% larger than control osteoclasts. The average number of nuclei in *miR17*-92 cKO osteoclasts was also 75% more. The *miR17*-92 cKO cells showed an increase in *PTP-oc* mRNA level by 86 ± 32%, and the relative size of resorption pits formed by *miR17*-92 deficient osteoclasts was significantly larger (~2-fold). To confirm that these observed effects were caused by deficient *miR17*, we transfected osteoclast precursors with LNA-modified antisense inhibitor of mouse *miR17*-5p. Inhibition of *miR17* also yielded ~twice as large osteoclasts with more nuclei per cells as control-LNA oligo-treated cells. Importantly, transgenic mice with conditional disruption of *miR17*-92 in osteoclasts have very similar bone and osteoclast phenotypes to those of transgenic mice with conditional overexpression of PTP-oc in osteoclasts. In conclusion, PTP-oc is a target gene for *miR17* and that *miR17* regulates osteoclast activity in part through suppression of PTP-oc expression.

Disclosures: Matilda Sheng, None.

SA0223

See Friday Plenary Number FR0223.

SA0224

C/EBP α mediates osteoclast differentiation through SOX4 downregulation and promotes osteoclast activity by inducing cell survival. Joel Jules*¹, Wei Chen, Yi-Ping Li. University of Alabama at Birmingham, USA

The transcription factor CCAAT/enhancer binding protein α (C/EBP α) is essential for osteoclastogenesis by committing bone marrow macrophages (BMMs) into the osteoclast (OC) lineage. However, whether C/EBP α is also crucial for OC differentiation and function is unknown. It was reported that while treatment of BMMs with permissive levels of receptor activator of NF- κ B ligand (RANKL) was unable to stimulate OC differentiation, it was sufficient to prime BMMs into the OC lineage for tumor necrosis factor- α (TNF) and interleukin 1 (IL-1)-induced OC differentiation. Here, we utilized this strategy to investigate the role of C/EBP α in OC differentiation and thereby bypass its requirement for lineage commitment. C/EBP α overexpression in BMMs could induce OC differentiation and strongly up-regulate OC markers with RANKL-evoked OC lineage commitment. Accordingly, C/EBP α overexpression in different stages of osteoclastogenesis revealed that while C/EBP α played a stronger role in the early stages of osteoclastogenesis, it was also critical for the later stages and could also promote OC activity. Consistently, C/EBP α silencing in different stages of osteoclastogenesis drastically inhibited OC formation and significantly abrogated the expression of OC markers as well as OC activity. Notably, C/EBP α promoted OC activity by regulating cell survival. Importantly, ectopic expression of rat C/EBP α could rescue osteoclastogenesis in the C/EBP α depleted BMMs. TNF and IL-1 are known to stimulate bone loss in many inflammatory bone diseases, so we then investigated the role of C/EBP α in TNF- and IL-1-induced OC differentiation. C/EBP α overexpression in BMMs significantly enhanced RANKL-

mediated TNF- α /IL-1-induced OC differentiation and markedly induced bone loss in a mouse model of periodontitis. Given the established role of C/EBP α in regulating gene expression, we hypothesized that C/EBP α mediates OC differentiation by not inducing OC markers but also by repressing novel OC inhibitors. We found that C/EBP α negatively regulates the expression of SRY (sex determining region Y)-box 4 (SOX4) during osteoclastogenesis. Remarkably, SOX4 overexpression in BMMs drastically inhibited RANKL-induced osteoclastogenesis. Also, SOX4 overexpression inhibited OC differentiation by TNF or IL-1. Taken together, these results indicate that C/EBP α is critical for all stages of osteoclastogenesis. Significantly, our data support that C/EBP α may evolve as an important therapeutic target for bone loss.

Disclosures: Joel Jules, None.

SA0225

See Friday Plenary Number FR0225.

SA0226

See Friday Plenary Number FR0226.

SA0227

MKP-1 Regulates LPS-Induced Osteoclastogenesis by Regulating TRAIL Function. Michael Valerio*, Keith Kirkwood. Medical University of South Carolina, USA

Osteoclasts (OC) are specialized bone resorptive cells required for a physiologic bone turnover. Under pathologic conditions, the inflammatory microenvironment produced both pathogens and cytokines drives inflammatory OC and subsequent bone loss. MAP kinase phosphatase-1 (MKP-1, gene Dusp1), regulates p38 and JNK MAPK and was shown to regulate inflammatory OC by reducing inflammatory cytokines and chemokines. MKP-1 was also shown to attenuate apoptosis in cells stimulated with endotoxin LPS. TNF-related apoptosis-inducing ligand (TRAIL), a member of the TNF ligand superfamily, has been shown to be involved in regulating cell death by apoptosis, but more interestingly was shown to induce OC formation. Based on these observations, we aim to investigate the role of MKP-1 regulating TRAIL in LPS-stimulated OC. OC progenitors (dOCP) derived from WT and Dusp1 $^{-/-}$ mouse bone marrow (BM) were immunophenotyped as CD3-CD45R-GR1-CD11b/CD115+ and sorted via magnetic bead separation. Cells were primed with MCSF (25ng/ml) and RANKL (50ng/ml) for 48 hours, washed out and stimulated with LPS (100ng/ml) for up to 10 days. In some experiments, cells were also treated in the presence of inhibitors p38 (SB203580), JNK (SP600125), Erk (U0126) and NF κ B (BAY) alone or in combination. Additionally, some cells were treated with rTRAIL (250-500ng/ml) or TRAIL-R2 blocking Antibody (2ug/ml) prior to stimulation with LPS (100ng/ml). Treated cells were TRAP stained to measure osteoclast formation. RNA was extracted using Trizol and mRNA expression for Traf6 (Traf6), NFATc1 (Nfatc1), DR5 (TNFRsf10b) and Trail (Tnfsf10). Trail-R2 protein expression was measured using flow cytometry. In the current study, we reveal that OC stimulated with LPS have prolonged survival in the absence of MKP-1, along with significantly more expression of intracellular traf6 and cytokines TNF and NOS2 ($P < 0.05$). dOCP stimulated with LPS had 50-fold increase in Trail mRNA expression ($P < 0.05$) and significantly more protein expression compared to WT counterparts. Trail receptor 2 (DR5) is increased up to 3-fold in LPS stimulated cells lacking MKP-1 ($P < 0.01$). Blocking Trail R2 blunted LPS-induced OC formation in WT and Dusp1 $^{-/-}$ cells. rTRAIL (up to 500ng/ml) induced significantly more OC in Dusp1 $^{-/-}$ cells. In all, these results reveal that TRAIL expression is activated in the absence of MKP-1 but does not induce cell death, rather promotes OC survival.

Disclosures: Michael Valerio, None.

SA0228

See Friday Plenary Number FR0228.

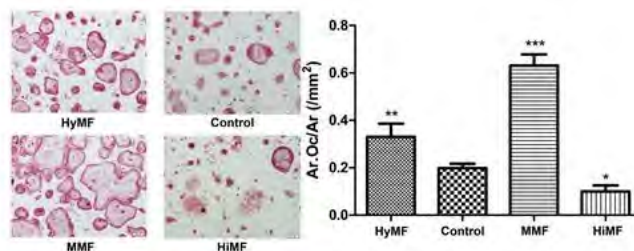
SA0229

Nitric Oxide Pathway is Involved in the Intensity-Dependent Biphasic Effects of Static Magnetic Fields on Osteoclastogenesis. Ting Huyan*¹, Jian Zhang², Dandan Dong², Jingbao Li², Huiyun Xu², Zhouqi Yang², Peng Shang². ¹Key Laboratory for Space Bioscience & Biotechnology, School of Life Sciences, Peoples republic of china, ²Key Laboratory for Space Bioscience & Biotechnology, Institute of Special Environmental Biophysics, School of Life Sciences, Northwestern Polytechnical University, China

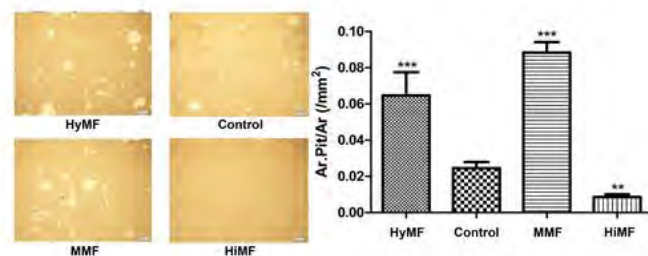
Numerous studies have demonstrated that certain magnetic fields have positive influence on human skeleton system. Static Magnetic Fields (SMF) is considered as a potential physical therapy to improve bone healing and keep bones healthy nowadays. In our previous study, it is showed that SMF which is increased progressively from hypo-magnetic field (HyMF, $< 5 \mu\text{T}$), weak magnetic field (WMF, $5 \mu\text{T} \sim 1 \text{mT}$), moderate SMF (MMF, $1 \text{mT} \sim 1 \text{T}$) to high SMF (HiMF, $> 1 \text{T}$), have intensity-

dependent biphasic effect on the osteoclasts differentiation. However, the mechanisms of SMF environment on osteoclastogenesis are inadequately understood till now and need to be further investigated. Nitric oxide is a short lived free radical involved in the regulation of bone turnover and bone cell function. The present study aims to investigate the co-relationship between nitric oxide pathway and SMF during osteoclast differentiation.

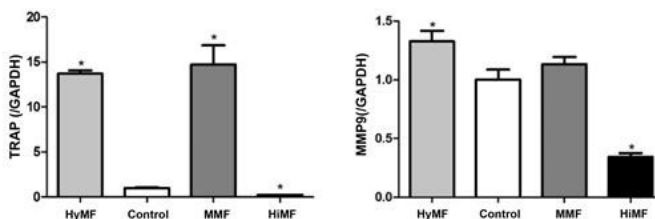
Our results showed that firstly HyMF and MMF had a positive effect on the osteoclasts formation and expression of marker gene Tartrate Resistant Acid Phosphatase (TRAP) and Matrix Metalloproteinase-9 in osteoclasts, but HiMF inhibited the formation and bone resorption activity of osteoclasts; secondly, the stronger SMF boosted the more nitric oxide production and endothelial nitric oxide synthase (NOS) activity. We hypothesized that nitric oxide pathway may play a vital role with SMF in the regulation of osteoclastogenesis. Further results demonstrated that sodium nitroprusside (SNP), a nitric oxide donor, had an inhibited effect on the elevated osteoclasts formation in HyMF and MMF, but N^G-Nitro-L-arginine methyl ester (L-NAME), a nitric oxide synthase inhibitor, rescued the inhibited osteoclast formation in HiMF. These findings indicate that nitric oxide pathway is involved in the intensity-dependent biphasic effect of SMF on osteoclastogenesis. Moreover, with regard to physical therapy in some bone disorders and maintenance of bone health, HiMF is preferable to HyMF and MMF which may cause negative effect to bone remodeling. In conclusion, these results will provide new horizons to our understanding of the SMF molecular mechanisms in osteoclastogenesis and HiMF may be a useful ancillary therapeutic modality in treating or preventing human osteoporosis.



Osteoclasts formation under SMF environments



Osteoclasts resorption activity under SMF environments



marker gene expression of osteoclast under SMF

old male ICR wild-type mice and Rankl^{-/-} mice were injected with human PTH (1-34; 80cg/kg) directly from the external jugular vein. After calcein injection, mice were sacrificed and the femora and tibiae were processed for paraffin- or epoxy resin-embedding or grind sections. These specimens were subjected to toluidine blue staining, von Kossa staining, observation under transmission electron microscopy (TEM) and fluorescence microscopy, and nanoindentation by atomic force microscopy (AFM). Furthermore, we fed Ca deficient diet to lactating mice, and fixed them after 12, 24, 36, 48 and 72 hours. Grind sections were used for nanoindentation by AFM and examined under confocal laser microscopy for detecting calcein labeling. Epoxy resin sections were used for von Kossa staining and TEM observation. Results and Discussion: Serum Ca concentration was increased at 1 hour after PTH administration with ligation of renal artery and vein in wild-type and Rankl^{-/-} mice. At six hours after PTH administration, enlarged osteocytic lacunae were observed mainly in the cortical bone, and von Kossa staining demonstrated broadly demineralized bone matrix surrounding the osteocytes. Under TEM, fragmented collagen fibrils and pieces of mineralized matrices were observed in the enlarged osteocytic lacunae with irregular shape of walls. In addition, calcein labeling was seen on the walls of some osteocytic lacunae. In lactating mice, the serum concentration of Ca was decreased at around 36-48 hours after feeding with Ca deficient diet. The osteocytic lacunae after 48 hours fed with Ca deficient diet, consistently, were enlarged, and sometimes labeled with calcein. It seems likely, therefore, that osteocytes erode the surrounding bone matrix, i.e., osteocytic osteolysis, and deposit minerals on their lacunae.

Disclosures: Hiromi Hongo, None.

SA0235

The treatment of human monocytes with the anti-microbial peptide LL-37 produces a novel bone forming cells with large inclusion bodies of LL-37. Zhifang Zhang*, Keith Le, Deirdre La Placa, John E. Shively. City of hope, USA

We previously showed that the antimicrobial peptide LL-37 induces human monocyte differentiation to a novel bone forming cell, termed monoosteophil, which exhibits the acceleration of bone repair in murine model. We here demonstrate that LL-37 is internalized by monocytes in the inclusion bodies. Over 1 hour to 16 hours, internalized LL-37 vesicles become larger vesicles in the cytosol. At the 4 hour time point, LL-37 positive vesicles are co-localized with Golgi but not ER, Mitochondria and lysosomes. At 16 hours, LL-37 positive vesicles even are co-localized with mitochondria and lysosomes. At day 6, LL-37 positive vesicles large as 10 micron long × 2 micron wide inclusion bodies and are not localized with mitochondria, ER, lysosome and Golgi. Interestingly, the concentration of LL-37 in the supernatant remains in the range of 3.8µM to 4.5µM from day 1 to day 6 with initial concentration of 5µM. Day 6 monoosteophil supernatant retains the ability to differentiate freshly isolated monocytes to monoosteophils according to morphology and unique monoosteophil surface markers integrin α3 and α6. Therefore, LL-37 remains intact during differentiation and form unique LL-37 inclusion bodies in the cytosol of monoosteophils.

Disclosures: Zhifang Zhang, None.

SA0236

See Friday Plenary Number FR0236.

SA0237

See Friday Plenary Number FR0237.

SA0238

See Friday Plenary Number FR0238.

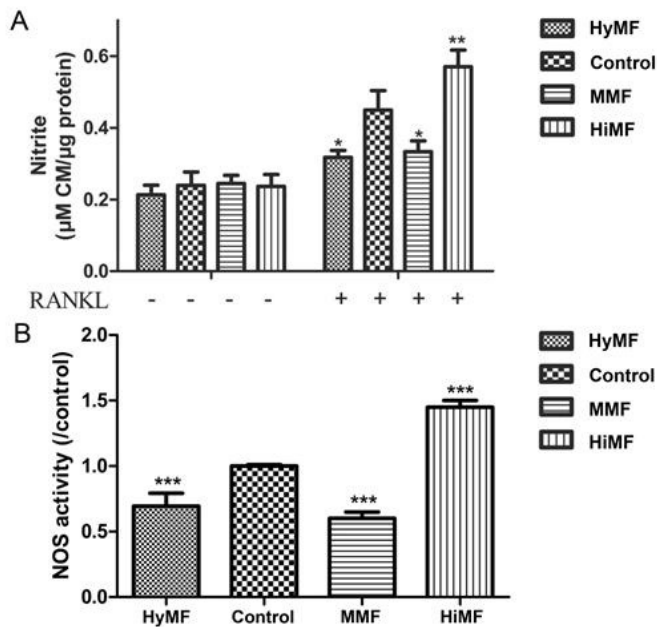
SA0239

See Friday Plenary Number FR0239.

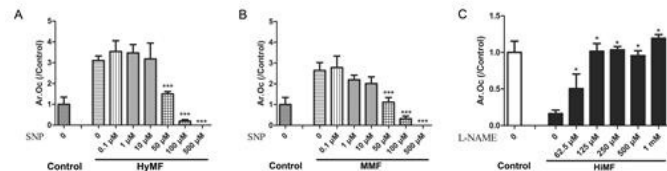
SA0240

Sclerostin enhances adipocyte differentiation in 3T3-L1 preadipocytes. Mayumi Ukita*¹, Taihiko Yamaguchi¹, Masato Tamura². ¹Crown & Bridge Prosthodontics, Graduate School of Dental Medicine, Hokkaido University, Japan, ²Biochemistry & Molecular Biology, Graduate School of Dental Medicine, Hokkaido University, Japan

Sclerostin, a secreted protein of the Sost gene product, is produced by osteocytes and is inhibited osteoblast differentiation and bone formation. Recently, a functional association between bone and fat tissue has been suggested, and a correlation between circulating sclerostin levels and the lipid metabolism in humans has been reported. However, the effects of sclerostin on adipogenesis remain unexplored. In the present study, we examined the role of sclerostin in regulating adipocyte differentiation using



nitric oxide production and NOS activity of osteoclasts under SMF



effect of nitric oxide donor and inhibitor in osteoclast formation under SMF

Disclosures: Ting Huyen, None.

SA0230

See Friday Plenary Number FR0230.

SA0231

See Friday Plenary Number FR0231.

SA0232

See Friday Plenary Number FR0232.

SA0233

See Friday Plenary Number FR0233.

SA0234

Histological examination on osteocytes and their lacunae after PTH administration or during lactation of mice fed with calcium deficient diet. Hiromi Hongo*¹, Muneteru Sasaki², Masami Saito³, Nobuyuki Udagawa⁴, Norio Amizuka⁵. ¹Hokkaido University, Japan, ²Division of Oral Implantology, Nagasaki University, Japan, ³Bruker AXS K. K., Japan, ⁴Department of Biochemistry, Matsumoto Dental University, Japan, ⁵Departments of Developmental Biology of Hard Tissue, Graduate School of Dental Medicine, Hokkaido University, Japan

Introduction: The idea of "osteocytic osteolysis" by injection of parathyroid hormone (PTH) or low calcium (Ca) diet has been proposed by Bélanger in 1960's. In addition, recent studies have suggested that the lactating mice might also show enlarged osteocytic lacunae. In order to clarify the occurrence of osteocytic osteolysis, we have examined osteocytes and their lacunae in mice after PTH administration and those in lactating mice fed with Ca deficient diet. **Materials and Methods:** Eleven-week

3T3-L1 preadipocytes. Oil red O stained-accumulated cytoplasmic lipid droplets and absorbance of oil red O staining were increased during adipogenic cultures in response to 5 ng/mL of sclerostin and further increased with increasing doses of sclerostin compared to sclerostin untreated cells. The mRNA expression level of adiponectin, lipoprotein lipase and fatty acid-binding protein 4 was also increased dose-dependently by sclerostin. Although sclerostin up-regulates CCAAT/enhancer binding protein (C/EBP) beta expression, cell proliferation and caspase3/7 activity did not alter by sclerostin in 3T3-L1 cells. TAZ is a transcriptional coactivator originally identified in a proteomic screen for 14-3-3 binding protein and is well-known for their regulation by Hippo signaling pathway. Recently, it is reported that TAZ is a downstream of the canonical Wnt signaling pathway independent Hippo pathway. Sclerostin reduced the TAZ responsive transcriptional activity using 8xGT10C-Lux, a synthetic luciferase reporter and TAZ-responsive ctgf gene expression which activated by Wnt3a. Although following transfection of 3T3-L1 cells with siRNA for the TAZ, the lipid deposits and adipogenic gene expression was increased, sclerostin could not alter adipocyte differentiation induced by siRNA for TAZ. These results show that sclerostin up-regulates adipocyte differentiation in 3T3-L1 cells, suggesting a possible role for the osteocyte derived sclerostin as a regulator of fat metabolism and of reciprocal regulation between bone and adipose tissue.

Disclosures: *Mayumi Ukita, None.*

SA0241

Biochemical markers of bone turnover and distal radial fracture in men: MR F study. Michael Prediger¹, Birgit Hanusch², Roger Francis³, Stephen Tuck², Harish Datta^{*4}. ¹Blood Sciences, The newcastle upon tyne hospitals nhs foundation trust, United Kingdom, ²Musculoskeletal Research Group, Institute of Cellular Medicine, Newcastle University, United Kingdom, ³Institute for Ageing & Health, Newcastle University, United Kingdom, ⁴Newcastle University, United Kingdom

It has been suggested that distal forearm fractures represent an early and sensitive marker of skeletal fragility in Caucasian men. We tested the hypothesis whether men with higher bone turnover, reflected by elevated levels of bone turnover markers (BTMs), would have an increased risk of distal radial fracture. We measured both the established as well as newer biochemical markers of bone turnover (BTMs). This investigation is an age- and gender-matched case-controlled study and subjects were recruited from one geographical location in the UK over a period of 24 months. Patients with distal forearm fracture were recruited within six months of the fracture; age-matched control subjects without fracture were recruited at any time throughout the investigation. All subjects were Caucasian males over 50 years. Fasting serum and plasma were collected from controls subjects (n=60) and men with distal radial fracture (n=60) after minimum of six months following fracture and stored at -80°C. The following serum BTMs were measured: type I collagen N-propeptide (PINP); β -terminal cross-linked telopeptide of type I collagen (CTX); sclerostin, fibroblast growth factor (FGF23); dickkopf-related protein 1 (DKK1). The fracture group had significantly lower BMD at the hip (mean (SD) femoral T-score of -0.953 (0.943) vs. -0.401 (0.975); $p < 0.001$) and at the lumbar spine BMD (-0.933 (1.392) vs 0.091 (1.750); $p < 0.01$). But there were no significant differences in age, weight, height or BMI. The concentration of the established BTMs PINP (38.94 (15.11) vs 33.5 (11.97), $p < 0.0005$) and CTX (0.45 (0.18) vs. 0.37 (0.18), $p < 0.05$) was significantly higher in the fracture group compared with the controls. In contrast, the serum concentration of sclerostin was lower in the fracture group (0.75(0.31) vs 0.89(0.51), $p < 0.05$). However, DKK1 and FGF23 showed no significant differences between the two cohorts. The correlation of BTMs with BMD revealed strong positive correlation between sclerostin and the lumbar spine (Pearson's $r = 0.400$, $p = 0.0001$) and total hip (Pearson $r = 0.266$, $p = 0.003$) Z-scores. Whereas PINP showed significant negative correlation with BMD with hip Z-score (Pearson's $r = -0.323$, $p = 0.0003$). The suppression of sclerostin concentration in fracture group is likely to reflect lower osteogenic activity and possible activation of bone formation following fracture. In conclusion, our findings show that men with distal radial fracture have increased bone turnover.

Disclosures: *Harish Datta, None.*

SA0242

Bone and serum manganese content in osteoporotic and normal subjects with hip replacement. Werner Maurer-Ertl¹, Joerg Friesenbichler¹, Ulrike Pirker-Frühaut¹, Michael Maier¹, Doris Wagner¹, Thomas Pieber¹, Andreas Leithner¹, Astrid Fahrleitner-Pammer^{*1}, Karin Amrein². ¹Medical University of Graz, Austria, ²Medical University of Graz, Division for Endocrinology & Metabolism, Austria

Introduction

Manganese (Mn) is an essential trace element required as cofactor in many enzymes, particularly in metabolism and in the antioxidant system. Recently, a pivotal role of manganese nutrition content has been suggested for the biomechanical properties of deer antlers (increased work to peak force). The purpose of this study was therefore to test if the manganese content in bone is different in subjects with and without osteoporosis.

Methods

In a cross-sectional, observational study, we sampled bone biopsies from the femoral neck and the corresponding iliac crest in patients with elective hip replacement for coxarthrosis or avascular necrosis of the femoral head. Dry ashed bone samples were used to assess manganese content. Blood samples and DXA measurements at the lumbar spine, the hip and the radius (Lunar, GE) were performed in all patients. Osteoporosis was defined by a T-Score ≤ 2.5 SD in DXA.

Results

38 patients aged 67 ± 13 years were included (17 men, 21 women, BMI 28.6 ± 8.6). There was no significant difference between osteoporotic and normal subjects neither for manganese bone content at the femoral neck (0.07 vs. 0.06 $\mu\text{g/g}$, $p = 0.78$), iliac crest (0.10 vs. 0.19 $\mu\text{g/g}$, $p = 0.24$) nor Mn serum levels (9.36 vs. 8.91 $\mu\text{g/l}$, $p = 0.61$). Mn serum levels did also not correlate with bone content (Pearson's correlation for femoral neck 0.200, $p = 0.24$; iliac crest 0.082, $p = 0.71$). Interestingly, the Mn content of the weight-bearing site (femoral neck) was almost threefold and significantly lower than at the non-weight-bearing site iliac crest (0.06 vs. 0.15 $\mu\text{g/g}$, $p < 0.01$)

Discussion

In this first human study on bone mineral Mn content of bone biopsies from weight-bearing and non weight-bearing sites, we found no significant difference between osteoporotic and normal subjects. Although we have not assessed biomechanical properties of bone, our small pilot study does not support a pivotal role in human bone biology as previously suggested in deer.

Disclosures: *Astrid Fahrleitner-Pammer, None.*

SA0243

Determinants of Serum FGF23 and Sclerostin in Elderly Hospitalized Individuals. Luigi Gennari^{*1}, Claudio Vitali², Stefano Rotatori³, Daniela Merlotti⁴, Gualberto Gussoni⁵, Daniele Diacinti⁶, Luigi Sinigaglia⁷, Antonella Valerio⁵, Aurora Patti⁸, Maria Stella Campagna⁸, Maria Beatrice Franci⁸, Barbara Lucani⁸, Stefano Gonnelli⁸, Ranuccio Nuti⁸. ¹University of Siena, Italy, ²Internal Medicine, Hospital of Piombino, Livorno, Italy, ³Department of Medicine Surgery & Neurosciences University of Siena, Italy, ⁴Division of Genetics & Cell Biology, San Raffaele Scientific Institute; Department of Medicine, Surgery & Neurosciences University of Siena, Italy, ⁵FADOI Foundation, Research Department, Italy, ⁶Section of Osteoporosis & Musculoskeletal Diseases, Department of Radiological, Oncological & Anatomical-Pathological Sciences, University "La Sapienza", Italy, ⁷Rheumatology, "G. Pini" Institute, Italy, ⁸Department of Medicine Surgery & Neurosciences University of Siena, Italy

Sclerostin (SCL) and FGF23 are osteocyte-secreted factors with a major role in bone turnover and mineral homeostasis. Despite their skeletal effects, variations in their circulating levels were also described in patients with diabetes, chronic renal failure (CRF) and/or cardiovascular disease. In order to better characterize the determinants of circulating SCL and FGF23 and their relationships with bone turnover or fractures we assessed their levels in peripheral blood samples from the POINT (Prevalence of Osteoporosis in Internal medicine) study cohort (n=1199 patients, mean age 75 ± 8 yrs), a cross-sectional multicenter sample that was specifically designed to assess the prevalence of morphometric vertebral fractures in patients hospitalized in Internal Medicine Units (*Bone 2015;74:114-20*). For each patient, the index of coexistent disease (ICED, which assesses the severity and the index of physical impairment for each disease category according to 5 levels of severity) was calculated. Serum SCL levels were positively correlated with CTX ($p < 0.05$), creatinine ($p < 0.0001$) and inversely with physical activity score ($p < 0.05$), while FGF23 levels were positively correlated with PTH ($p < 0.05$) and creatinine ($p < 0.05$). In the overall sample, serum SCL did not significantly differ between patients with or without prevalent fractures or morphometric vertebral fractures. A significant association was observed between FGF23 levels and prevalent nonvertebral fractures ($p < 0.005$) but not morphometric vertebral fractures. Either SCL or FGF23 levels progressively increased with the increase of comorbid conditions, particularly in subjects with the highest ICED levels of severity for cardiovascular disorders (mainly coronary heart disease), cerebrovascular diseases, diabetes and CRF. After exclusion of subjects with all those comorbid conditions, the association between FGF23 levels and fractures became nonsignificant, while serum SCL levels were significantly lower in patients with morphometric vertebral fractures than in patients without fractures (36.0 ± 14 vs. 41.5 ± 18 pmol/L, $p < 0.05$). The opposite association was observed when patients with cardiovascular disorders, diabetes and/or CRF were considered, with statistically significant higher levels of SCL in patients with morphometric fractures (58.3 ± 20 vs. 43.1 ± 19 pmol/L, $p < 0.01$). The mechanisms underlying the increase in either FGF23 or SCL levels in the presence of these extraskelatal disorders remain to be investigated.

Disclosures: *Luigi Gennari, None.*

SA0244

Examining phospholipids interference in LC-ESI-MS/MS measurements of 25-hydroxyvitamin D in long term storage samples. Jonathan Tang*¹, Holly Nicholls², Milka Budnik-Zawilska², John Dutton², Isabelle Picc², Chris Washbourne², William Fraser². ¹University of East Anglia, Norwich, UK, United Kingdom, ²University of East Anglia, United Kingdom

Background: Endogenous phospholipids in biological fluids present a major problem in liquid chromatography tandem mass spectrometry (LC-MS/MS) analysis. Due to their strong retention characteristics in reversed phase chromatography phospholipids are often very difficult to separate from analytes of interest. This co-elution leads to areas of suppression or enhancement in the chromatogram which in turn can cause analytical errors. The use of matrix matched reference standard materials with isotopically labelled internal standard are likely to improve accuracy of 25 hydroxyvitamin D (25(OH)D) measurements. However, we observed greater level of phospholipids present in human serum samples after long periods of -20°C storage, and found significant variability on 25(OH)D measurements when assayed retrospectively by isotopic dilution protein precipitation method.

Objective: We developed an approach to monitor and assess the level of phospholipids in samples and investigate the effects of long term storage on 25(OH)D measurements. We have developed an effectiveness phospholipid elimination technique using Supported Liquid Extraction (SLE) and evaluated improvement to assay recovery.

Method: Serum samples from a human vitamin D clinical study stored in -20°C for up to 10 years were selected from various time points and analysed retrospectively for 25(OH)D using protein precipitation and lipid removing extraction techniques. Phospholipids were monitored using *m/z* 184 Da productions.

Results: A near tenfold increase in phospholipids was observed in serum samples undergone long term storage samples and found to be directly proportional to the length of storage. Retrospective measurements of total 25(OH)D using non phospholipid removing method showed a maximum of 40.5% variability when compared to original measurement.

Conclusion: Our study showed phospholipids present in samples increases over time and have profound effect 25(OH)D measurements. We have developed sample clean up protocols using SLE that substantially reduce the presence of phospholipids and significantly improve analyte recovery in older samples. From our findings we concluded that phospholipid interference is a major concern that could result in misinterpretation of vitamin D measurements. Removal of phospholipid is essential in clinical studies involved the use of 25(OH)D measurement particularly in retrospective studies where samples from long term storage are used.

Disclosures: Jonathan Tang, None.

SA0245

Performance of a Novel Automated TRACP 5b Immunoassay in Renal Disease Patients. Jussi Hallee*¹, Jani Salmivaara², Henna Ek², Tiina Lehto³, Tommi Vaskivuo³. ¹Pharmatest Services Ltd, Finland, ²Valirx Finland Ltd, Finland, ³NordLab Oulu, Finland

Tartrate-resistant acid phosphatase isoform 5b (TRACP 5b) is released into the blood circulation from osteoclasts and is considered as a marker of osteoclast number. Human serum contains a closely related isoform TRACP 5a derived from inflammatory macrophages that has a different pH optimum and smaller active site space for substrates than TRACP 5b. A previously developed manual immunoassay for TRACP 5b (BoneTRAP®) uses a monoclonal antibody that binds both TRACP 5a and 5b, but no other interfering acid phosphatases in serum. The assay utilizes the difference in pH-optimum of TRACP 5a and 5b to minimize cross-reactivity to TRACP 5a. While the cross-reactivity of the assay to TRACP 5a is usually less than 10%, it can be a problem in cases with highly elevated TRACP 5a values. A recently developed automated TRACP 5b immunoassay uses the same monoclonal antibody than the manual assay, and a large substrate that does not fit into the active site of TRACP 5a, completely preventing cross-reactivity. Previous studies have shown that renal function has no effect on manually determined TRACP 5b values. In this study we have compared the manual and automated TRACP 5b assays for their performance in patients with impaired renal function. Serum samples were collected from 65 patients, including 38 patients with glomerular filtration rate (GFR) below 15 ml/min/1.73 m². C-terminal cross-linked telopeptides of type I collagen (CTX-I), intact procollagen I N-terminal propeptide (PINP), bone-specific alkaline phosphatase (BAP) and intact parathyroid hormone (PTH) were measured with automated assays. As expected, renal function had no effect on the manually determined TRACP 5b values, or the PINP and BAP values, while CTX-I and PTH values were substantially (3-5 -fold) elevated in patients with GFR under 15 ml/min/1.73 m². The correlation coefficient between the manual and automated TRACP 5b assays was 0.92, and renal function did not affect TRACP 5b values determined with the automated assay. We conclude that TRACP 5b measured with the automated assay can be used as a marker of bone resorption in patients with impaired renal function without the need to worry that renal function would affect the results. These results suggest that the method could be used to demonstrate elevated bone resorption due to renal osteodystrophy in end-stage renal disease patients.

Disclosures: Jussi Hallee, IDS Ltd
This study received funding from: IDS Ltd

SA0246

See Friday Plenary Number FR0246.

SA0247

Bisphosphonate Associated Femur Fractures Treated with Teriparatide. Michelle Lalinde*¹, Deborah Aggers¹, Tina Savage¹, Ed McCarthy², Paul Miller¹. ¹Colorado Center for Bone Research, USA, ²John Hopkins University, USA

We performed an uncontrolled longitudinal study examining the response of 24 months of teriparatide (20 mcg SQ daily) on bone remodeling in subjects with bisphosphonate-associated atypical sub-trochanteric femoral fractures. The primary endpoint of our study was to compare the mineralizing surface to bone surface (MS/BS) in the cancellous compartment of the iliac crest. This was assessed by bone biopsy using tetracycline labelling, pre- and post-12 months of teriparatide. The secondary endpoints of the study were to measure changes in bone turnover markers, fracture healing, and subjects' report of pain.

A total of 14 post-menopausal subjects (mean age 68.3 years) with a documented atraumatic diaphyseal femoral fracture within 12 months of screening were recruited. The mean duration of bisphosphonate exposure was 105 months (range: 36 -174 months). Bone turnover marker procollagen type 1 N-terminal propeptide (PINP) was obtained every six months during treatment. In addition, dual-energy x-ray absorptiometry (DXA) was performed at baseline, 12 and 24 months. CT scan was performed at baseline, month 12 and month 24, to assess for fracture healing.

Results revealed that there was heterogeneity in bone turnover at baseline when assessed by quantitative histomorphometry. The MS/BS (Figure 1), an indicator of osteoblast activity, increased in 12 out of the 14 subjects. The two subjects that did not have an increase in MS/BS also had a decrease in PINP at months 12 and 24. No subject sustained a new or worsening vertebral fracture while on treatment. However, two subjects sustained atypical femoral fractures on the contralateral femur side after 8 days and 254 days of teriparatide. One of these subjects also had no tetracycline labels. Eleven of the subjects had intramedullary rods in the femur prior to entry in the study. After 24-months of treatment, two of the three non-surgical subjects showed fracture site healing, assessed by CT scan. Using a visual analog pain scale (Figure 2), 13 of the subjects had improved pain scales at the fracture site from baseline to 24 months.

In this small sample size, the majority of subjects seemed to respond to teriparatide. However there appears to be a small portion of subjects who may be non-responders, as evidenced by inconsistency of fracture healing, bone markers and quantitative histomorphometry.

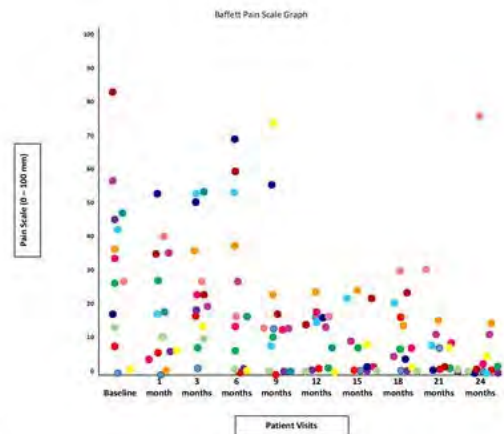


Figure 2

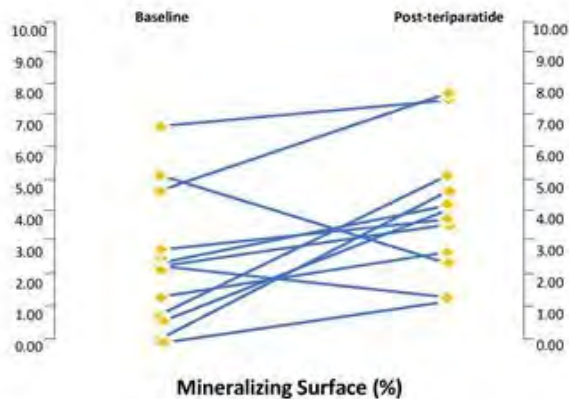


Figure 1

Figure 1

Disclosures: Michelle Lalinde, None. This study received funding from: Eli Lilly

SA0248

See Friday Plenary Number FR0248.

SA0249

Standardized Training For HR-pQCT Scan Positioning Reduces Inter-Operator Precision Errors: The MrOS Multicenter Study Experience.

SERENA BONARETTI*¹, NICOLAS VILAYPHIOU², ANDREW YU³, MARGARET HOLETS⁴, KYLE NISHIYAMA⁵, DANMEI LIU⁶, STEPHANIE BOUTROY⁷, ALI GHASEM-ZADEH⁸, STEVEN K. BOYD⁹, ROLAND CHAPURLAT⁷, HEATHER MCKAY⁶, ELIZABETH SHANE⁵, MARY L. BOUXSEIN¹⁰, THOMAS F. LANG³, SUNDEEP KHOSLA⁴, PEGGY M. CAWTHON¹¹, DENNIS M. BLACK¹², SHARMILA MAJUMDAR³, ERIC S. ORWOLL¹³, ANDREW J. BURGHARDT³. ¹University of California, San Francisco, USA, ²Scanco Medical AG, Brüttisellen, Switzerland, ³Department of Radiology & Biomedical Imaging, University of California, San Francisco, CA, USA, ⁴Division of Endocrinology, Metabolism & Nutrition, Department of Internal Medicine, College of Medicine, Mayo Clinic, Rochester, MN, USA, ⁵Division of Endocrinology, Department of Medicine, Columbia University Medical Center, New York, NY, USA, ⁶University of British Columbia, Vancouver, BC, Canada, ⁷INSERM UMR 1033, Université de Lyon, France, ⁸Department of Medicine, Austin Health, University of Melbourne, Melbourne, Australia, ⁹Department of Radiology, Cumming School of Medicine, University of Calgary, Calgary, Alberta, Canada, ¹⁰Center for Advanced Orthopaedic Studies, Beth Israel Deaconess Medical Center, Boston, MA, USA, ¹¹San Francisco Coordinating Center, California Pacific Medical Center Research Institute, San Francisco, CA, USA, ¹²Department of Epidemiology & Biostatistics, University of California, San Francisco, CA, USA, ¹³Division of Endocrinology, Bone & Mineral Unit, Oregon Health & Science University, Portland, OR, USA

The role of high-resolution peripheral quantitative tomography (HR-pQCT) in musculoskeletal research is rapidly expanding through its inclusion into multicenter clinical trials and observational cohort studies, such as the Osteoporotic Fractures in Men Study (MrOS, an observational study being conducted at 6 clinical sites). Previously¹, we found that positioning variability is an important source of imprecision. In this study, we aimed to reduce inter-operator positioning precision errors through standardized training.

The training procedure included theoretical and practical demonstrations led by a vendor representative and MrOS investigator, followed by simulated scan positioning exercises using software developed at UCSF. The software reproduced the graphical user interface of the XtremeCT (Scanco Medical AG) and provided the user with a series of scout images of the radius and tibia to perform simulated scan positioning. In this study, we enrolled 6 new operators with various background and no previous HR-pQCT experience, who required certification to perform HR-pQCT exams for MrOS. After successful completion of the software training and evaluation, operators performed a blinded positioning exercise to test intra- and inter-operator reproducibility. In these exercises, we measured positioning precision and the corresponding precision error in cortical and trabecular bone measurements. Results from the MrOS

trainees were compared to previously acquired data from experienced operators with a heterogeneous training history¹.

Intra-operator precision errors of the trainees were not significantly different compared to the experienced operators (e.g. Ct.Th: 3.2% vs. 3.5%), indicating that new operators achieved equivalent reliability to experienced operators (Table 1). Inter-operator precision errors of trainees in this study were half than errors of the experienced operators (e.g. Ct.Th: 4.9% vs. 8.4%, p<0.001) and approached the level of intra-operator precision. Thus the training regimen led to the new operators achieving a superior level of multicenter reproducibility.

In conclusion, we found that inter-operator variability in scan positioning can be significantly reduced with standardized training procedures in a controlled environment. With the purpose of making our training platform available to the community, we are developing a version of the training and evaluation tool that will be openly disseminated as a web application.

¹Bonaretti S. et al. ASBMR 2014

Table 1. Precision errors of reference line positioning and corresponding errors in bone and mechanical parameter measurements for radius and tibia for intra- and inter-operator reproducibility. "Experienced" refers to the operators involved in our previous study¹, who participated in the experiments without common training. "New" refers to MrOS operators enrolled in the present study, who participated in the experiments after common training. Details of the precision experiment were described in our previous study¹.

| RADIUS | Positioning Precision SD _{RMS} [mm] | BMD CV _{RMS} [%] | Ct.Th CV _{RMS} [%] | Tb.N CV _{RMS} [%] | L _{failure} CV _{RMS} [%] |
|------------------------|---|------------------------------|--------------------------------|-------------------------------|---|
| Intra-operator* | | | | | |
| Experienced | 0.24 ± 0.05 ^a | 1.39 ± 0.32 ^{a,c} | 3.17 ± 0.65 ^{a,c} | 0.47 ± 0.14 ^a | 0.42 ± 0.12 ^{a,c} |
| New | 0.28 ± 0.08 ^c | 1.50 ± 0.25 ^{a,c} | 3.46 ± 1.24 ^{a,c} | 0.69 ± 0.56 | 0.41 ± 0.11 ^a |
| Inter-operator | | | | | |
| Experienced | 0.68 ^{a,b,c} | 3.69 ^{a,b,c} | 8.40 ^{a,b,c} | 2.12 ^{a,b} | 1.17 ^{a,b,c} |
| New | 0.34 ^{b,c} | 2.09 ^{b,c} | 4.90 ^{a,b,c} | 1.32 ^b | 0.72 ^{a,b,c} |

(a)

| TIBIA | Positioning Precision SD _{RMS} [mm] | BMD CV _{RMS} [%] | Ct.Th CV _{RMS} [%] | Tb.N CV _{RMS} [%] | L _{failure} CV _{RMS} [%] |
|------------------------|---|------------------------------|--------------------------------|-------------------------------|---|
| Intra-operator* | | | | | |
| Experienced | 0.13 ± 0.07 ^a | 0.26 ± 0.15 ^{a,c} | 0.94 ± 0.50 ^{a,c} | 0.31 ± 0.18 ^a | 0.07 ± 0.03 ^{a,c} |
| New | 0.11 ± 0.03 ^{a,c} | 0.31 ± 0.06 ^a | 0.52 ± 0.29 ^{a,c} | 0.31 ± 0.05 | 0.06 ± 0.01 ^{a,c} |
| Inter-operator | | | | | |
| Experienced | 0.30 ^{a,b,c} | 0.61 ^{a,b,c} | 1.97 ^{a,b,c} | 0.85 ^{a,b} | 0.20 ^{a,b,c} |
| New | 0.16 ^{a,b,c} | 0.30 ^{b,c} | 1.02 ^{a,b,c} | 0.41 ^b | 0.08 ^{a,b,c} |

(b)

* Intra-operator vs. inter-operator comparison; p<0.001.
^a Experienced vs. new operator comparison; p<0.001.
^c Radius vs. tibia; p<0.001.
^a For intra-operator precision and corresponding bone parameters, values refer to mean ± standard deviation.
 SD_{RMS} [mm] = Root mean square of standard deviations.
 CV_{RMS} [%] = Root mean square of percentage coefficient of variations.
 BMD = bone mineral density; Ct.Th = cortical thickness; Tb.N = trabecular number;
 L_{failure} = failure load.

Table 1

Disclosures: SERENA BONARETTI, None.

SA0250

Vertebral strength index calculated by finite element method using bone material properties of non-diabetes subjects does not reflect the bone fragility of the patients with type 2 diabetes mellitus. Masahiro Yamamoto*, Nobuaki Kiyohara, Noriko Nakata, Toshitsugu Sugimoto, Shimane University Faculty of Medicine, Japan

Purpose: Patients with type 2 diabetes mellitus (T2DM) have an increased risk of vertebral fractures compared to non-T2DM controls independent of bone mineral density (BMD) (JBMR 2009), suggesting that poor bone quality causes increased bone fragility. It has been reported that the predictive power of vertebral fractures (VFs) in postmenopausal women by quantitative computed tomography-based nonlinear finite element method (QCT/FEM) was superior to that by BMD. However, availability of QCT/FEM for assessment of the bone fragility of the patients with T2DM remains unknown. The aim of this study is to investigate whether vertebral strength evaluated by QCT/FEM in the patients with T2DM is useful for assessment of bone fragility.

Methods: Vertebral strength index (VSI) of second lumbar spine calculated by QCT/FEM in the same method as the previous report (slice thickness: 2 mm, a pixel width: 0.35 mm, element: 2-mm tetrahedron and 2-mm triangular plates, Young's modulus and yield stress of each element: values calculated from the equations

obtained from non-diabetic patients reported by Keyak et al., and Poisson's ratio: 0.4). We compared parameters of bone metabolic markers including lumbar spine BMD and VSI between Japanese T2DM patients with and without vertebral fractures [54 postmenopausal women and 92 men over 50 years old].

Results: One or more vertebral fractures assessed by X-ray were observed in 20 women and 39 men whose mean ages were 65.6 and 63.4, respectively. VSI of men group was significantly higher than that of women (6.0 ± 2.1 vs. 4.3 ± 2.4 kN, respectively). Multiple regression analysis including independent variables of age, urinary NTX and spine BMD selected by simple regression analysis showed that VSI were significantly and inversely correlated with spine BMD and positively related with age in both genders. In contrast to the previous report, there was no significant difference in VSI between the subjects with and without VFs, even if multiple regression analysis was performed after adjusting for age, BMI, HbA1c, duration of T2DM and spine BMD.

Conclusion: The estimation of the bone strength of T2DM patients by established QCT/FEM using material properties obtained from non-diabetic subjects may be unable to reflect real bone fragility. This observation suggested that the poor bone quality of T2DM patients, in part, may be caused by inferior bone material strength compared with non-diabetic subjects.

Disclosures: Masahiro Yamamoto, None.

SA0251

A Method to Assess Bone Mineral in the Mandible Using the Norland DXA System. Jingmei Wang*¹, MinMin An², Fan Yang², Shao Yang Guan², Lei Liu², Wei Zhang², Tom Victor Sanchez³. ¹Bone Health Division, Norland at Swissray, China, ²Wuhu Second People's Hospital in Anhui Province, Wannan Medical College, China, ³Bone Health Division, Norland at Swissray, USA

The mandible is known to have high bone turnover, increased vascularity and greater susceptibility to osteoclast and osteoblast and has long been pursued by DXA as a site from which to monitor early change in response to treatment or disease. We evaluate a method developed to directly assess bone mineral in both the Body and Ramus of the mandible.

A Norland XR-800 was used to develop a procedure to evaluate bone mineral content in the Body and Ramus of the mandible. Patients were positioned on the scanner laying on their side with the head supported by a positioning platform so that the upper and lower mandibles were well superimposed on each other. A scan region width of 12cm centered over the mandible was set to start at the level of the eyebrow and end below the level of the chin. Scans were done with a resolution of 1.0x1.0mm and typically completed in a couple of minutes. The study of the mandible examined six dentate subjects—each undergoing four examinations with totally repeated positioning—to assess repeatability of the study. The studies were evaluated to assess the distribution of bone mineral content in the entire Body and Ramus of the evaluated mandibles and to assess repeatability of selected regions within the Body and Ramus of the mandibles.

Examining mandibular mineral distribution over 5x5mm regions demonstrated greater ranges of contents in the Body of the mandible—from lows of 0.141 gm to highs of 0.7gm—than seen in the Ramus—from lows of 0.141gm to highs of 0.42gm. The results point to considerable differences in how material is distributed and may indicate that both regions should be independently monitored to locate changes over time. Repeatability studies of an operator defined 10mmx10mm region showed average repeatability of 2.14% in the Body of the mandible—allowing an assessment of significant change with changes of 6.14%.

The study demonstrates that the Norland XR-800 when using specific positioners is able to document the distribution of bone mineral content in the Body and Ramus regions of the mandibles and can reflect relatively small changes in bone mineral in the Body of the mandible. Given that the mandible is reportedly able to undergo swift changes in bone, the documented repeatability of the study should allow swifter identification of changes in bone mineral content in subjects with changing bone density.

Disclosures: Jingmei Wang, None.

SA0252

See Friday Plenary Number FR0252.

SA0253

Correlation of albumin/globulin ratio (A/G ratio) with forearm bone mineral density in women above 50 years of age. Kayoko Furukawa*, Kunitaka Menuki, Yukichi Zenke, Yoshiaki Yamanaka, Hideyuki Hirasawa, Takafumi Tajima, Akinori Sakai. Department of Orthopaedic Surgery, University of Occupational & Environmental Health, Japan

[Objective] We aimed to determine whether blood test values correlates with bone mineral density by body part.[Subjects and Methods] We included data on 78

forearms of 78 women age 50 or older treated for distal radius fracture at our hospital from October 2007 to October 2012. All underwent DXA (dual-energy x-ray absorptiometry) scan of the 2nd-4th lumbar vertebrae, femoral neck, and forearm bone (divided into 3 parts: ultra distal [UD], mid distal [MD], and shaft [1/3]). The following blood test values were determined: ALB, A/G ratio, AST, ALT, LDH, ALP, GTP, Ca, P, BUN, Crea, eGFR, WBC, Hb, Hct, and PT-INR.[Statistical analysis] Using Pearson product-moment correlation coefficients, we analyzed the DXA scan results (lumbar vertebrae, femur, and 3 forearm parts) for correlations with age, height, weight, BMI, and blood test values.[Results] ALB, the A/G ratio, LDH, Hb, and PT-INR correlated positively with bone mineral densities of the forearm (UD, MD, and 1/3) and femur (neck), but not with those of the lumbar vertebrae. TP, AST, ALT, ?GTP, P, BUN, Crea, eGFR, WBC, Hb, and Hct did not correlate with any bone mineral density values. [Discussion] The A/G ratio had a stronger correlation with the bone mineral density of the proximal 1/3 (0.39), which has a high percentage of cortical bone, than with those of MD (0.38) and UD (0.26). The A/G ratio also correlated with femoral neck bone mineral density (0.23), but not with those of the lumbar vertebrae. Our results thus suggest a correlation between cortical bone amount and albumin metabolism.[Conclusions] Our statistical analyses identified correlations between blood test values and bone mineral density by body part in middle-aged and elderly females with distal radius fracture. Serum albumin and the A/G ratio correlated positively with forearm and femoral neck bone mineral densities, but not with lumbar vertebral bone mineral densities.

Disclosures: Kayoko Furukawa, None.

SA0254

See Friday Plenary Number FR0254.

SA0255

Clinical Applicability of TBS in Individuals with Small Bone Sizes and Low Bone Mineral Density by DXA: A Case Report. Bruno Camargos¹, Nathalia Gomes², Pedro Alvarenga*³, Caroline Silva³, Milena Leite³, Barbara Silva⁴, Angelica Tiburcio⁵. ¹Mater Dei Hospital, Brazil, ²Santa Casa de Belo Horizonte, Brazil, ³UNI-BH, Brazil, ⁴Uni-BH, Santa Casa de Belo Horizonte & Felicio Rocho Hospital, Brazil, Brazil, ⁵Santa Casa Hospital, Brazil

Measurement of areal bone mineral density (aBMD) by dual X-ray absorptiometry (DXA) is considered the gold standard for diagnosis of osteoporosis and fracture risk assessment. Nevertheless, DXA has a number of limitations. aBMD is influenced by bone size such that true BMD is underestimated in those with smaller bones and overestimated in those with larger bones. Accordingly, we have recently reported a case of a 50-yr-old man, with very short stature, with low BMD by DXA, but normal volumetric BMD (vBMD) by quantitative computed tomography (QCT). Trabecular bone score (TBS), a textural index of trabecular microarchitecture evaluated by pixel gray-level variations in the lumbar spine (LS) DXA image, appears to be independent of bone size. To this end, we aimed to assess TBS in this very short man, considering that TBS may also offer advantages over DXA in patients whose lower aBMD does not reflect bone strength.

Case report: A 50-yr-old man with SHORT syndrome (an acronym for Short stature, Hyperextensibility of joints and/or inguinal Hernia, Ocular depression, Rieger anomaly, and Teething delay) was referred to our Bone Unit for evaluation of osteoporosis. Further history revealed type 2 diabetes, hypertension, and glaucoma. His medications included insulin, enalapril, amlodipine, aspirin, simvastatin, and calcium supplements. Physical examination was remarkable for his short stature, 129 cm in height, distinctive facial features (facial gestalt), and low visual acuity. His BMI was normal at 21.9 Kg/m². Extensive evaluation ruled out secondary causes of osteoporosis. Lateral spine radiographs did not show vertebral fractures, and his medical history was negative for fragility fractures. BMD by DXA showed T-scores of -3.5 at the LS, -3.9 at the femoral neck, -2.9 at the total hip, and -3.1 at the 1/3 radius. QCT (QCT Pro 5.1, Mindways, Austin, TX) showed normal vBMD at the LS (L1-L2: 148 mg/cm³) and low, but not indicative of osteoporosis, vBMD at the femur (total hip: 112 mg/cm³; femoral neck: 117 mg/cm³). Site-matched LS TBS was then performed using TBS iNsite software (version 2.1; Medimaps, Switzerland). Remarkably, LS TBS was normal at 1.392.

We report a case of a man, with extremely short stature, with low BMD by DXA, but normal vBMD by QCT and normal TBS. These findings suggest that TBS may be helpful in selecting individuals whose lower aBMD seems to reflect their smaller bone geometry rather than reduced bone strength and fracture risk.

Disclosures: Pedro Alvarenga, None.

SA0256

Distal radius cortical microstructure and calculated strength predict incident fractures independently of FRAX in postmenopausal women. Emmanuel Biver*¹, Claire Durosier¹, Andrea Trombetti¹, Thierry Chevalley¹, Bert van Rietbergen², René Rizzoli¹, Serge Ferrari¹. ¹Division of Bone Diseases, Geneva University Hospitals & Faculty of Medicine, Switzerland, ²Department of Biomedical Engineering, Eindhoven University of Technology, Netherlands

The contribution of bone microstructure determination to fracture risk prediction, in addition to prior fractures, clinical risk factors and areal bone mineral density (aBMD), all integrated in FRAX tool, remains unknown. We investigated the independent contribution of bone microstructure alterations to fracture risk assessment in postmenopausal women. Seven hundred thirty seven women (age 65.0 ± 1.4 years), enrolled in the Geneva Retirees Cohort (GERICO) study, were prospectively followed for fracture occurrence over 3.4 ± 0.9 years. At baseline, cortical (Ct) and trabecular (Tb) bone density (vBMD) and microstructure at distal radius and tibia were assessed by HR-pQCT (Xtreme CT, Scanco Medical, Bassersdorf, Switzerland), in addition to aBMD by dual X-ray absorptiometry. Prior fragility fractures (FF) were defined as clinical fractures occurring after 45 yrs of age. Sixty one incident clinical fractures (excluding fingers, toes and skull) occurred in 58 women. Wrist (n = 15), ankle (n = 10), humerus (n=7), vertebrae (n=5) and rib (n = 5) were the most common sites. At baseline, the prevalence of FF and osteoporosis (OP) was higher in women with incident fracture than without incident fracture (FF 53% vs 27%, p<0.001, OP 33% vs 19%, p=0.012), whereas their FRAX probability of major fractures was 15.5% vs 11.8% (p<0.001). Radius and tibia Ct and Tb vBMD and most microstructure parameters were associated with incident fractures: hazard ratios [HR] for one standard deviation decrease of each parameter from 1.30 to 1.59, p<0.05 to 0.001. After adjustment for age and distal radius total aBMD, radius density and microstructure remained significantly associated with fracture risk: adjusted HR (95%CI) of 1.59 (1.09-2.27) for total vBMD, 1.69 (1.14-2.56) for Ct area, 1.39 (1.01-1.89) for Tb number (p<0.05 for all), and 1.96 (1.28-2.94, p=0.002) for stiffness. After adjustment for prior FF and OP status, radius Ct area [1.37 (1-1.89), p=0.047] and stiffness [1.37 (1-1.85), p=0.049] remained significantly associated with fracture risk. After adjustment for FRAX, radius Ct area [1.39 (1.04-1.85), p=0.028], Ct thickness [1.33 (1-1.79), p=0.047] or stiffness [1.37 (1.04-1.82), p=0.027] remained significantly associated with fracture risk. In conclusion, cortical variables predict incident fractures independently of prior FF and OP status, or FRAX, indicating the major role of cortical bone microstructure analysis in identifying women at increased risk of fracture.

Disclosures: Emmanuel Biver, None.

SA0257

High Rates of Prevalent Fracture in Bone Phenotypes Identified by Cluster Analysis of High Resolution Peripheral Quantitative Computed Tomography Parameters. Mark Edwards*¹, Danielle Robinson², Camille Parsons², Kate Ward³, Cyrus Cooper², Elaine Dennison². ¹MRC Lifecourse Epidemiology Unit, University of Southampton, United Kingdom, ²MRC Lifecourse Epidemiology Unit, University of Southampton, United Kingdom, ³MRC Human Nutrition Research, United Kingdom

High resolution peripheral quantitative computed tomography (HRpQCT) has been used to differentiate fracture from non-fracture cases. Studies have demonstrated specific components of bone structure to be deficient in fracture cases. However, these components are significantly correlated and so it may be more appropriate to explore different overall bone phenotypes and their relationships to fracture. The aim of this study was to identify clusters of bone microarchitecture in older men and women and relate them to fracture prevalence and areal BMD (aBMD). We studied 177 men and 159 women, aged 72.1-80.9 years, with HRpQCT (XtremeCT) images (voxel 82µm) of the distal radius. Standard image analyses were performed for assessment of macrostructure, regional densitometry, cortical porosity and trabecular microarchitecture. K-means partitioning cluster analysis was used to identify clusters in men and women separately. Prevalent fracture rates and femoral neck aBMD were determined for each cluster and the clusters were numbered in order of fracture prevalence. Forty four (24.9%) men and 48 (30.2%) women had fractures. Women with fractures were on average 1.7 years older and 3.1 years further from menopause than women who had not fractured (p<0.05). Although analyses were carried out separately in each sex, two morphologically-similar, high risk clusters were identified in each sex. "Cluster 1" contained 26 women (50.0% fractured) and 30 men (50.0% fractured) and denoted a phenotype with mean cortical thickness and cortical volumetric BMD around 1SD below and, in men, mean total and trabecular area more than 1SD above, the sex-specific cohort mean. "Cluster 2" contained 20 women (50.0% fractured) and 14 men (35.7% fractured) and showed a phenotype with mean trabecular density and trabecular number both more than 1 SD below the sex-specific cohort mean. Logistic regression showed fracture rates in these clusters to be significantly higher than the lowest fracture risk cluster (5) (p<0.05). Mean femoral neck aBMD was significantly lower than cluster 5 in women in cluster 1 and 2 (p<0.001 for both), and in men, in cluster 2 (p<0.001) but not 1 (p=0.220). We have identified a cluster (1) that describes a bone phenotype which differs from the conventional view of osteoporosis but with a

high proportion of fractures. In men, this phenotype was not associated with lower aBMD measured by DXA and therefore could be missed by current clinical assessments of osteoporosis.

Disclosures: Mark Edwards, None.

SA0258

Influence of vertebral fractures severity and pelvic parameters on global spinal balance in osteoporotic patients. Jacques Fechtenbaum¹, Adrien Etchet¹, Sami Kolta¹, Antoine Feydy², Christian Roux³, Karine Briot*³. ¹Cochin Hospital, rheumatology Department, France, ²Cochin Hospital, radiology Department, France, ³Paris Descartes University, Cochin hospital, Rheumatology Hospital, France

Purpose: Thoracic kyphosis and other postural parameters related to the postural adjustment strategy affect the biomechanical environment of the spine. These parameters can be influenced by vertebral fractures in elderly osteoporotic patients. This study aims to compare the spine curvatures, the pelvic parameters and the global spinal balance of patients aged above 50 years with and without osteoporotic vertebral fractures. Methods: Two hundred patients (95% women) aged 66.5 ± 13.6 years underwent a standardised lateral and antero-posterior full skeleton radiographs in the standing position, by EOS® (a low dose biplanar imaging system) in an upright weight-bearing position. VFs were evaluated according to Genant's classification and the spinal deformity index (SDI). Spinal (thoracic and lumbar Cobb's indices, thoracic tilt (T9 tilt) and lumbar tilt (L1 tilt)) and pelvic (pelvic tilt, sacral slope, and pelvic incidence) parameters were measured. Sagittal global spinal balance was measured using 2 parameters: the C7 plumb line (mm), and the spinosacral angle (SSA in degrees). We compared these parameters in patients with and without vertebral fracture, according to the location and the severity of VFs (SDI). We assessed the discriminative value of the global spinal parameters in patients with at least one vertebral fracture using Area Under the Curve (AUC). We also assessed the variables associated with abnormal SSA. Results: Sixty-nine patients had at least 1 VF, with a mean number of VF of 2.3 ± 1.7 and a mean SDI of 4.2 ± 4.5. In patients with only lumbar VFs (n=11), only lumbar parameters (lower lumbar Cobb's angle and sacral slope and higher lumbar tilt) were modified. In contrast, in patients having only thoracic VFs (N=34), both thoracic, lumbar and pelvic parameters were different than those in patients without VFs. The greater the SDI, the greater were the thoracic Cobb's angle and pelvic tilt and the lesser the lumbar Cobb's angle. Thoracic and lumbar tilts and sacral slope were not affected by SDI increase. The global spine balance assessed by C7 plumbline and SSA was significantly altered in patients with at least one VF, and there was a dose effect of the number and severity of VFs on global spinal balance, significant for all parameters for a SDI value >2. Discriminative value for identification of patients with at least one VF, as assessed by AUCs was 0.652 and 0.706 for C7 plumbline and SSA respectively. SSA has a higher discriminative value than C7 plumb line. For a SSA of 121.8°, sensitivity and specificity were 0.67 and 0.28. Using multivariate analysis, the variables significantly associated with abnormal SSA were: age (OR=0.933 [0.897 - 0.971], p=0.0006), SDI>0 (OR= 0.202 [0.099 - 0.410], p<0.0001) and pelvic incidence (OR= 1.075 [1.040 - 1.112], p<0.0001) with an AUC of the model of 0.8175. Conclusion: Global spinal balance is significantly altered in patients with at least one vertebral fracture with a dose-effect of the number and severities of VFs. Pelvic parameters are relevant in the assessment of global spinal balance.

Disclosures: Karine Briot, None.

SA0259

Nano-CT Analysis of Osteocyte Anomalies in Klotho-deficient Mice. Tomoko Minamizaki*¹, Kaoru Sakurai², Hirohisa Yoshioka³, Yuichiro Takei³, Katsuyuki Kozai⁴, Yuji Yoshiko³. ¹Hiroshima University Institute of Biomedical & Health Sciences, Japan, ²Department of Pediatric Dentistry, Hiroshima University Graduate School of Biomedical Sciences, Japan, ³Department of Calcified Tissue Biology, Hiroshima University Institute of Biomedical & Health Sciences, Japan, ⁴Department of Pediatric Dentistry, Hiroshima University Institute of Biomedical & Health Sciences, Japan

Osteocyte is the most abundant cell type in bone and plays a fundamental role in bone turnover. Morphological changes in osteocytes and osteocyte lacunae are closely related to bone loss and fragility associated with skeletal disorders. Mice homozygous for *Klotho* gene deletion (*kl/kl*) exhibit some aspects resembling human aging, including osteoporosis, and abnormal findings on osteocytes were described in *kl/kl* mice. Computed tomography (CT) is a non-destructive approach to provide three-dimensional x-ray images of the internal structure of an object. µCT for a small scale with increased resolution is often driven by the bone research field, allowing considerable success for bone morphometry in mouse models. However, conventional µCT is limited to cover the entire hierarchical assembly in some case, such as osteocyte parameters. Nano-CT achieves an isotropic voxel size of as low as 100 nanometers and is suitable for investigating the microstructure of bone. We then used nano-CT to determine multiple osteocyte parameters and mineralized bone in *kl/kl* mice versus wild type (WT) mice. Femurs were collected from 6-week-old male mice, fixed in 4% PFA and stored in 70% ethanol. The mid-portion of the diaphysis in the range of 2.4

mm thickness was scanned using SkyScan 1176 or SkyScan 2211 (Bruker), and imaging parameters were optimized to maximize spatial resolution. Reconstruction of raw data was performed using InstaRecon[®], and anisotropy in mineralized components and osteocyte parameters were determined by CT-Analyzer. Regardless of whether *Klotho* is deficient, the 3D orientation of mineralized components was mostly aligned transversely. Osteocyte lacunae were widely but not evenly distributed in *kl/kl* and WT bone. Total number of osteocyte lacunae in total bone volume was higher in WT mice, whereas the number of lacunae per mm³ was higher in *kl/kl* mice. Osteocyte lacunae less than 100 μm³ were distributed in *kl/kl* bone (12.5% of total lacunae) but not in WT bone. Osteocyte lacunar surface density in *kl/kl* mice was higher than that in WT mice. Thus, our data indicate morphological anomalies of osteocyte in *kl/kl* mice can be detected by nano-CT at the 3D microarchitecture level.

Disclosures: Tomoko Minamizaki, None.

SA0260

Racial and Ethnic Differences in Bone Structure in Young Adult Women and Men. Kristy Nicks^{*1}, Joshua N. Farr², Elizabeth J. Atkinson², Louise K. McCready², Sundeep Khosla². ¹Mayo Clinic, Us, ²Mayo Clinic, USA

Osteoporotic fractures are a major world-wide problem, and it is now well-established that significant geographic variability exists in fracture rates among racial and ethnic groups. A better understanding of factors that contribute to this variability might substantially influence our ability to provide new avenues for prevention and treatment. Primary determinants of fracture risk include bone mineral density (BMD) and bone structure. While several studies have examined racial and ethnic disparities in areal BMD (aBMD) by DXA, bone structural parameters have received insufficient attention. Thus, the purpose of this cross-sectional study was to utilize DXA and HRpQCT to examine aBMD as well as bone macro- and microstructure among healthy young African American (n = 45), Hispanic (n = 44), and Caucasian (n = 145) women and men, age 20-44 years, from Olmsted County, MN, USA. African American women had significantly higher DXA-derived total body aBMD than both Caucasian (by +3.2%) and Hispanic (by +4.8%) women, whereas total body aBMD did not differ between Caucasian and Hispanic women. Further, while no differences were observed in total body aBMD between African American and Caucasian men, Hispanic men had significantly lower total body aBMD than both African American (by -7.5%) and Caucasian (by -4.0%) men. HRpQCT analysis at the distal radius revealed that trabecular bone parameters were similar among the three groups of women, although African American women had significantly thicker trabeculae (by +6.4%) than Caucasian women. There were also no differences in radial cortical volumetric BMD among the three groups of women. By contrast, Hispanic women had significantly thinner radial cortices than both African American (by -12.3%) and Caucasian (by -11.7%) women. Interestingly, sex differences in HRpQCT-derived bone structural parameters were also observed among ethnic/racial groups. In particular, African American men had significantly thicker cortices at both the distal radius and tibia as compared to Caucasian (radius by +10.1%; tibia by 15.1%) and Hispanic (radius by +22.6%; tibia by +17.8%) men. In summary, these data suggest that trabecular and cortical bone structure may vary significantly by both sex and race/ethnicity, which likely contributes to differential fracture rates among these groups both in the United States and globally. Future studies in larger samples of racial/ethnically diverse populations are needed to extend these observations.

Disclosures: Kristy Nicks, None.

SA0261

See Friday Plenary Number FR0261.

SA0262

VITamin D and Omega-3 Trial (VITAL) bone health study: Clinical factors associated with Trabecular Bone Score in women and men. Anna Ross^{*1}, Amy Yue¹, Nancy Cook², JoAnn Manson², Julie Buring², Trisha Copeland³, Cindy Yu¹, Meryl LeBoff⁴. ¹Brigham & Women's Hospital, Endocrinology, Diabetes & Hypertension Division, USA, ²Brigham & Women's Hospital, Division of Preventive Medicine, Professor of Medicine, Harvard Medical School, USA, ³Brigham & Women's Hospital, Division of Preventive Medicine, USA, ⁴Brigham & Women's Hospital Professor of Medicine, Harvard Medical School, USA

The Trabecular Bone Score (TBS) is derived from textural analyses of spinal dual-energy X-ray absorptiometry (DXA) and is associated with bone microarchitecture and fracture risk. The aim of this study was to test whether baseline TBS differs by sex, race/ethnicity, body mass index (BMI) and other clinical variables.

Methods: The VITamin D and Omega-3 Trial (VITAL) is a double-blind, placebo-controlled trial assessing the role of vitamin D₃ (2000 IU/d) and/or omega-3 fatty acids (FA; 1 g/d) supplements in reducing risks of cancer and cardiovascular disease among 25,874 U.S. participants (men age ≥50 and women age ≥55). VITAL: Effects on Bone Structure and Architecture, an ancillary study among a VITAL subcohort, is determining effects of the interventions on bone with bone health phenotyping and clinical assessments at baseline and 2 yrs post-randomization (LeBoff et al. *Contemp Clin Trials* 2015). Baseline spinal BMD using DXA (Discovery

W, Hologic Inc, Bedford, MA) and TBS using TBS iNsite software (version 2.1; Medimaps Group, Geneva, Switzerland) were determined at L1-L4. Differences between unadjusted means were analyzed using analysis of variance or tests for trend.

Results (Table 1): TBS was measured in 609 participants (324 men and 285 women aged 63.7±6.0 yrs; BMI≤37 kg/m²). Mean TBS was greater in men than women (1.34±0.10 vs 1.31±0.08, p<0.001). Younger age was associated with higher TBS (p=0.02). TBS was lower at higher BMIs and in participants who used medications linked to fractures (p=0.003). TBS was lower in participants with a history of fragility fracture (trend p=0.07). History of diabetes was associated with lower TBS (1.30±0.13 vs 1.33±0.09, p=0.04). Alcohol consumption was positively associated with higher TBS (p=0.006). Greater physical activity ≥15.0 MET-hrs/wk was associated with higher TBS (p<0.001). Knee osteoarthritis was associated with lower TBS (p=0.02). There were no significant differences in TBS when analyzed according to race/ethnicity, multivitamin use, rheumatoid arthritis history, smoking status, or caffeine intake.

Summary: Higher TBS was associated with clinical variables including younger age, male sex, BMI<30 kg/m², higher MET-hrs/wk, moderate alcohol intake, and absence of diabetes, knee osteoarthritis, or medications linked to fracture. Ongoing follow-up studies at 2 yrs post-randomization will elucidate the effects of moderately high doses of vitamin D and/or omega-3 FA on TBS and other bone health measures.

| Table 1 | Variable | Total (%) | TBS mean (std) | P value |
|---------|---------------------------------------|-------------|----------------|---------|
| | Age | N=609 | | 0.02 |
| | 50-54 | 42 (6.9%) | 1.37 (0.09) | |
| | 55-64 | 327 (53.7%) | 1.33 (0.09) | |
| | 65-74 | 213 (35.0%) | 1.32 (0.09) | |
| | 75+ | 27 (4.4%) | 1.33 (0.09) | |
| | BMI categories | N=609 | | <.001 |
| | <18.5 | 4 (0.7%) | 1.31 (0.07) | |
| | 18.5-24.9 | 172 (28.2%) | 1.36 (0.07) | |
| | 25-29.9 | 274 (45.0%) | 1.34 (0.08) | |
| | 30-34.9 | 136 (22.3%) | 1.28 (0.10) | |
| | 35-37.0 | 23 (3.8%) | 1.23 (0.13) | |
| | Medications associated with fractures | N=597 | | 0.003 |
| | No | 539 (90.3%) | 1.33 (0.09) | |
| | Yes | 58 (9.7%) | 1.29 (0.09) | |
| | History fragility fracture | N=592 | | 0.07 |
| | No | 546 (90.3%) | 1.32 (0.11) | |
| | Yes | 46 (7.8%) | 1.30 (0.09) | |
| | Alcohol used | N=574 | | 0.006 |
| | 1=Never | 104 (18.1%) | 1.31 (0.10) | |
| | 2=Rarely<weekly | 40 (7.0%) | 1.31 (0.07) | |
| | 3=1-6/week | 240 (41.8%) | 1.33 (0.09) | |
| | 4=Daily | 190 (33.1%) | 1.34 (0.10) | |
| | Total met-hrs categories | N=609 | | <.001 |
| | <7.5 | 125 (20.5%) | 1.31 (0.09) | |
| | 7.5-14.9 | 79 (13.0%) | 1.31 (0.09) | |
| | >=15.0 | 405 (66.5%) | 1.34 (0.09) | |
| | Knee osteoarthritis | N=588 | | 0.02 |
| | Yes | 90 (15.3%) | 1.31 (0.10) | |
| | No | 498 (84.7%) | 1.33 (0.09) | |

Table 1

Disclosures: Anna Ross, None.

SA0263

A Preliminary Genome-Wide Association Study with Bone Mineral Density in Mexican Mestizo Postmenopausal Women. Marisela Villalobos-Comaran¹, Rogelio Jimenez-Ortega², Alma Parra-Torres², Anahi Gonzalez-Mercado³, Manuel Castillejos Lopez⁴, Zacarias Jimenez-Salas⁵, Manuel Quiterio⁶, Sandra Romero-Hidalgo¹, Bertha Ibarra⁷, Jorge Salmeron⁸, Rafael Velazquez-Cruz^{*2}. ¹Consorcio de Genómica Computacional, Instituto Nacional de Medicina Genómica, Mexico, ²Consorcio Genómica del Metabolismo Oseo, Instituto Nacional de Medicina Genómica, Mexico, ³Doctorado en Genética Humana, CUCS, Universidad de Guadalajara, Mexico, ⁴Unidad de Vigilancia Epidemiológica Hospitalaria, Instituto Nacional de Enfermedades Respiratorias, Mexico, ⁵Facultad de Salud Pública y Nutrición, Universidad Autónoma de Nuevo Leon, Mexico, ⁶Centro de Investigación en Salud Poblacional, Instituto Nacional de Salud Pública, Mexico, ⁷Instituto de Genética Humana "Enrique Corona Rivera". CUCS, Universidad de Guadalajara, Mexico, ⁸Centro de Investigación en Salud Poblacional, Instituto Nacional de Salud Pública, Mexico

Mexican population is composed mostly of Native American, European and a minimal contribution of African population. Osteoporosis, a disease characterized by low bone mineral density (BMD), is a common health problem in Mexican population. To date, Genome-wide SNP association (GWA) studies have provided an important opportunity to discover genes with sequence variants contributing to bone density variations. However, with a few exceptions, GWA studies have been focused on populations of European descent, and these results cannot, be directly extended to other populations, as the Mexican-Mestizo population. The aim of this

Disclosures: Susana Balcells, None.

SA0265

Genome-wide association study of bone mineral density, content and area measured at the axial and appendicular skeleton identifies four novel loci and suggests a possible reason why genetic loci are associated with bone mineral density at some sites but not others. John Kemp^{*1}, Carolina Medina-Gomez², Alessandra Chesi³, Carol Wang⁴, Joel Eriksson⁵, Nicole M. Warrington⁶, Vincent W.V. Jaddoe⁷, Babette S. Zemel⁸, Kun Zhu⁹, Liesbeth Vandenput⁵, Beate St. Pourcain¹⁰, Nicholas J. Timpson¹¹, André G. Uitterlinden², John Walsh⁹, Stephen Lye¹², Mattias Lorentzon⁵, George Davey-Smith¹¹, Claes Ohlsson⁵, Craig Pennell⁴, Struan F.A. Grant¹³, Jonathan H. Tobias¹⁴, Fernando Rivadeneira², David M. Evans¹⁵. ¹MRC Centre for Causal Analyses in Translational Epidemiology, Australia, ²Department of Internal Medicine, The Generation R Study Group, Department of Epidemiology, Erasmus University Medical Center, Rotterdam, The Netherlands & Netherlands Genomics Initiative (NGI)-sponsored Netherlands Consortium for Healthy Aging (NCHA), Netherlands, ³Division of Human Genetics, The Children's Hospital of Philadelphia, Philadelphia, PA, USA, ⁴School of Women's & Infants' Health, The University of Western Australia, Perth, Australia, ⁵Centre for Bone & Arthritis Research, Department of Internal Medicine & Clinical Nutrition, Sahlgrenska Academy, University of Gothenburg, Gothenburg, Sweden, ⁶University of Queensland Diamantina Institute, Translational Research Institute, Brisbane, Queensland, Australia, ⁷The Generation R Study Group, Department of Epidemiology & Department of Paediatrics, Erasmus University Medical Center, Rotterdam, Netherlands, ⁸Department of Pediatrics, Perelman School of Medicine, University of Pennsylvania, Philadelphia, PA, USA & Division of Gastroenterology, Hepatology & Nutrition, The Children's Hospital of Philadelphia, Philadelphia, PA, USA, ⁹Department of Endocrinology & Diabetes, Sir Charles Gairdner Hospital & School of Medicine & Pharmacology, The University of Western Australia, Perth, Australia, ¹⁰MRC Integrative Epidemiology Unit, School of Oral & Dental Sciences & School of Experimental Psychology, University of Bristol, Bristol, United Kingdom, ¹¹MRC Integrative Epidemiology Unit, University of Bristol, Bristol, United Kingdom, ¹²Samuel Lunenfeld Research Institute, Mount Sinai Hospital, Toronto, Canada, ¹³Division of Human Genetics & Endocrinology, The Children's Hospital of Philadelphia, Philadelphia, PA, USA & Department of Pediatrics, Perelman School of Medicine, University of Pennsylvania, Philadelphia, PA, USA, ¹⁴School of Clinical Sciences, University of Bristol, Bristol, United Kingdom, ¹⁵University of Queensland Diamantina Institute, Translational Research Institute, Brisbane, Queensland, Australia & MRC Integrative Epidemiology Unit, University of Bristol, Bristol, United Kingdom

Aim: Bone mineral density (BMD) can be expressed as the ratio of bone mineral content (BMC) to bone area (BA) reflecting differences in bone mass relative to size. Previously we identified several loci associated with BMD at some skeletal sites, but not at others. Our aim was to perform a follow-up study to elucidate why some BMD loci exhibit site specificity by studying how genetic effects on BMD variation are the result of processes influencing BMC and BA.

Methods: Genome-wide association (GWA) analyses were performed on 12,713 children and adolescents from 5 cohorts, using imputed genetic data in relation to site-specific DXA measures of BMD, BMC and BA [at the skull (SK), upper-limbs (UL) and lower-limbs (LL)]. Multiple linear regression models based on expected allelic dosages included sex, age, height, weight and ancestry informative principal components. Meta-analyses were conducted using an inverse variance fixed-effects method.

Results: Variants in four novel loci were associated at genome-wide significance: two with SK-BMD (*CSNK1G3*, $P=2 \times 10^{-8}$ and *KCNJ16*, $P=2 \times 10^{-8}$), one with LL-BMC (*PCDH20*, $P=5 \times 10^{-8}$) and one with LL-BA (*GDF5*, $P=7 \times 10^{-11}$). Across most loci, patterns of association with BMD were largely similar to those of BMC, suggesting that the majority of loci either influenced BMC independently of BA or that their influence on BMC is substantially larger than on BA. Variants in three loci exerted larger effects on BA when compared to BMC, resulting in complete attenuation of the association with BMD at the skull (*RPS6KA5*), upper limb (*GDF5*) and lower limb (*CPED1* and *GDF5*). Site-specific genetic associations previously observed for *CPED1* (i.e. variants associated with BMD of the skull and upper limbs, but not lower limbs), were replicated and appeared to be a consequence of variants affecting BA to a greater extent than BMC at particular skeletal sites (i.e. lower limbs), but not others (i.e. skull and upper limbs).

Conclusions: Most BMD-associated loci influence BMC to a larger degree than BA; however other loci exert equivalent or larger effects on BA relative to BMC and as such are unlikely to be detected by GWA studies of BMD. In some cases site-specific genetic effects on BMD appear to be modulated by larger effects on BA relative to BMC. Loci

study was perform an initial trial of genome-wide association study to identify genetic loci that influence bone mineral density in Mexican-Mestizo postmenopausal women. A total of 425 unrelated postmenopausal women of the state of Morelos were included in the stage 1, and 435 postmenopausal women of the state of Guadalajara, were included in stage 2. Risk factors were recorded and BMD was measured in total hip, femoral neck and lumbar spine using dual-energy X-ray absorptiometry. The stage 1 genotyping of 300,739 bi-allelic SNPs was performed using the Illumina HumanCytoSNP-12 v2.1 BeadChip. After QC steps, 225,635 SNPs and 411 Mexican mestizo women were retained for statistical analysis of stage 1. In this stage none SNPs pass the genome-wide significance level, but fifteen provided P values =5 x10-05 for Femoral Neck BMD and Lumbar Spine BMD. For stage 2, we focus on two SNPs located in the (6q25) region, because this region has been previously reported associated in European and Asiatic populations. Linear regression analyses adjusted by age, body mass index and ancestry, showed that these two SNPs were associated with Femoral Neck BMD under recessive model: rs17081341 located in the CCDC170 and the rs6904364 in the RMND1 genes, (P=0.020 and P=0.023, respectively). It is noteworthy, that the frequency of the SNP rs17081341 was lower in European and African population (MAF=0.03), that in Mexican population (MAF=0.17). In conclusion, our data replicate previous associations in the 6q25 region in European populations and suggest CCDC170 and RMND1 as a potential candidate genes for BMD variation in Mexican Mestizo postmenopausal women, however, the sample size is small for the type of study, therefore further studies in other Mexican populations and with a large sample size are needed.

Disclosures: Rafael Velazquez-Cruz, None.

SA0264

Exploring the *FLJ42280* Genomic Region to Identify Genetic Variants Associated with Osteoporosis. Neus Roca-Ayats¹, Marina Gerousi¹, Nuria Martinez-Gil¹, Esteban Czwan², Roser Urreiziti¹, Natalia Garcia-Giralte³, Guillem Pascual¹, Leonardo Mellibovsky³, Xavier Nogues³, Adolfo Diez-Perez³, Daniel Grinberg¹, Susana Balcells^{*1}. ¹Dept. Genetics, Fac. Biology, University of Barcelona, CIBERER, IBUB, Spain, ²Roche Diagnostics Deutschland GmbH, Germany, ³URFOA, IMIM, RETICEF, Parc de Salut Mar, Spain

Genome-wide association studies (GWAS) have identified a number of variants associated with bone mineral density (BMD) and osteoporotic fracture. Signals emerging from GWAS are frequently located in non-coding poorly studied regions. In addition, most of these GWAS SNPs are likely to be in linkage disequilibrium with ungenotyped causal variants. Recent studies have pointed out *FLJ42280* as a susceptibility gene for osteoporosis. In the meta-analysis of Estrada *et al.* (2012), an intronic SNP (rs4727338) was significantly associated with BMD and osteoporotic fracture. Likewise, other studies demonstrated correlation of other intronic SNPs (rs7781370, rs10429035 and rs4729260). Yet, *FLJ42280* is a poorly studied gene with unknown link with bone biology.

We aimed to explore the genetic variability of the *FLJ42280* locus associated with BMD by two approaches. On the one hand, we performed an eQTL analysis to determine whether the GWAS SNPs correlated with gene expression levels. We used 210 unrelated HapMap individuals' genotypes and expression levels from the whole-genome Illumina lymphoblastoid cell line gene expression data. None of these SNPs showed influence on expression levels of cis-genes. On the other hand, targeted resequencing of the *FLJ42280* region was carried out in two groups of 50 women from the BARCOS cohort (Spanish postmenopausal) presenting either extreme low bone mass (LBM) or high bone mass (HBM). In each woman, a 28 kb region was amplified in 7 overlapping fragments by LR-PCR. All amplicons were pooled into two groups, one of HBM and another of LBM, prior to massive parallel sequencing at 3600x coverage per pool with Roche's 454 Junior technology. After quality filtering, alignment and variant calling, the number and frequency of variants were statistically compared between the two groups and their overlap with functional elements from ENCODE was analyzed. Preliminary results are shown in Table 1. The number of low frequency variants (LFVs) was balanced between the two groups. As for frequency differences of all variants between the two groups these were all below the statistical power of the experimental design although we found 2 common variants and 7 LFV showing trend. We did find an undescribed downstream VNTR, but no significant difference in allele frequency distribution was found between the two groups. To further explore the most promising variants, they are currently being genotyped in the complete BARCOS cohort.

Table 1. Number and location of single nucleotide variants found in this study

| | Raw | Filtered | Coding | Regulatory regions* | Putative osteoblast enhancer | Active osteoblast enhancer |
|------------------------|-------|----------|--------|---------------------|------------------------------|----------------------------|
| Common Variants | 96 | 52 | 0 | 12 | 3 | 1 |
| LFV | 24243 | 59 | 1 | 16 | 1 | 0 |
| Total | 24339 | 111 | 1 | 28 | 4 | 1 |

* Either present in flanking regions 5'UTR, 3'UTR or introns; LFV: low frequency variants (MAF>5%)

Table 1

associated with height-adjusted BA (e.g. *GDF5*) may reflect examples of novel genetic influences on bone expansion occurring during periosteal bone growth.

Disclosures: John Kemp, None.

SA0266

See Friday Plenary Number FR0266.

SA0267

Decline in Vertebral Strength and Bone Mineral Density in Men and Women over the Year Post Hip Fracture. Denise Orwig^{*1}, David Kopperdahl², Tony Keaveny³, Rasheeda Johnson⁴, Jay Magaziner⁴, Marc Hochberg⁴. ¹University of Maryland, Baltimore, USA, ²O.N. Diagnostics, USA, ³University of California Berkeley, USA, ⁴University of Maryland School of Medicine, USA

Previous studies have shown the rate of decline in bone mineral density (BMD) at the femoral neck is greater than expected in older women over the year post hip fracture. Little is known, however, about changes in vertebral bone strength or BMD in men compared to women post hip fracture. The objective was to compare changes in vertebral BMD and bone strength, estimated using finite element analysis (FEA) of quantitative computed tomography (QCT) scans of the spine (T12-L1), over the year post hip fracture in men and women. QCT scans were performed at 2 and 12 months post hip fracture as part of an ancillary study of the Baltimore Hip Studies 7th cohort (BHS-7) (n=339), a prospective observational study designed to examine consequences of hip fracture in equal numbers of men and women. BHS-7 participants were =65 years, community-dwelling, and had surgical repair of a non-pathological hip fracture. This analysis includes 37 BHS-7 participants (21 men; 16 women) with 2- and 12-month QCT scans. Vertebral BMD and compressive strength were calculated using VirtuOst^U (O.N. Diagnostics, Berkeley, CA). BMD of trabecular centrum and the peripheral 2 mm of bone and their individual contributions to bone strength were also determined. Unpaired t-tests were used to compare women versus men with respect to baseline demographics and measurements of BMD and strength, and 10-month changes in BMD and strength; 95% confidence intervals of mean longitudinal changes were used to identify changes significantly different from zero. At 2 months post fracture, mean age, body mass index, and vertebral strength or any BMD measurement did not differ significantly by sex. Over the 10-month follow-up, vertebral strength and density of the whole vertebral body decreased significantly in women but not in men (Figure 1); however, the trajectory of decline did not differ significantly by sex. In men and women, for both BMD and strength, losses were predominantly due to loss of the trabecular bone rather than the peripheral (cortical) bone. In men, the heterogeneity in response was greater than in women: some men did not lose strength while others lost as much as the women, whereas all women lost strength. Data suggest that appreciable loss of vertebral strength can occur in women shortly after hip fracture, primarily due to the loss of trabecular bone; responses for women and men appear to differ, but additional study is required to further elucidate these sex effects.

Figure 1. Longitudinal change in vertebral strength and BMD by sex

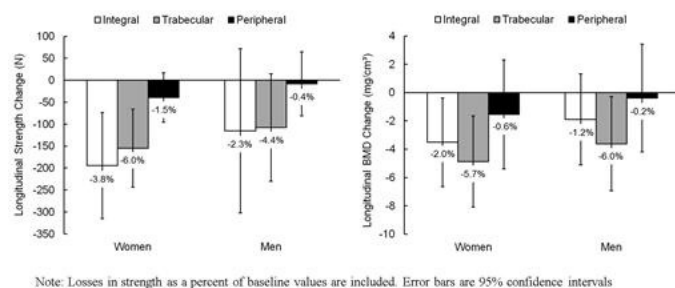


Figure 1. Longitudinal change in vertebral strength and BMD by sex

Disclosures: Denise Orwig, None.

SA0268

Delineating the relationship between leptin, fat mass, and bone mineral density: A mediation analysis. Lan T Ho Pham^{*1}, Thai Q Lai², Tuan V Nguyen³. ¹Ton Duc Thang University, Vietnam, ²Department of Rheumatology, People's Hospital 115, Vietnam, Vietnam, ³Garvan Institute of Medical Research; School of Public Health & Community Medicine, UNSW Australia; University of Technology Sydney, Australia, Australia

Background and Aim — Leptin is a hormone synthesized and secreted by adipocytes which act centrally to control fat mass. The effect of leptin on bone mineral

density (BMD) has been reported, but the role of fat mass in this relationship is not clear. The present study sought to test the hypothesis that the relationship between leptin and BMD is mediated by fat mass by using a model of mediation analysis.

Methods — The study involved 357 men and 870 women aged between 18 and 89 years (average 45). The individuals were randomly sampled from 4 districts within Ho Chi Minh City (Vietnam). BMD at the femoral neck, lumbar spine, and whole body was measured by DXA (Hologic QDR4500). Lean mass and fat mass (FM) were derived from the whole body DXA scan. Serum leptin was measured by enzyme-linked immunosorbent assay (ELISA) on the Elecsys System (Roche Diagnostics). We tested the hypothesis of mediation by fitting a series of regression models to the data, in which (i) BMD was expressed as a function of leptin alone, and then leptin and fat mass in combination, and (ii) fat mass as a function of leptin. From the estimated parameters of these models we computed the direct and indirect effects of leptin on the variation in BMD.

Results — In women, after adjusting for age, greater serum leptin levels were associated with greater BMD at the femoral neck (P=0.006), lumbar spine (P=0.0001) and whole body (P=0.06). Serum leptin levels were also highly correlated with whole body fat mass (r=0.57; P<0.0001). In the mediation analysis, the effect of leptin on BMD was primarily mediated through fat mass (P<0.001). The direct effect of leptin on BMD was not statistically significant (P=0.89), and this was observed for all BMD sites. The proportion of lumbar spine BMD variance that was attributable to direct effect of leptin, and indirect effect of fat mass was 0.4% and 6.5%, respectively.

In men, leptin was significantly associated with lumbar spine BMD, but not with femoral neck or whole body BMD. In the mediation analysis, the effect of leptin on lumbar spine BMD was mainly mediated by fat mass (P=0.02). The proportion of lumbar spine BMD that was attributable to direct effect of leptin, and indirect effect of fat mass was 0.2% and 5.1%, respectively. **Conclusions** — These results suggest that greater serum levels of leptin are associated with greater BMD, but the association is primarily mediated by fat mass. The direct effect of leptin on BMD is not negligible.

Disclosures: Lan T Ho Pham, None.

SA0269

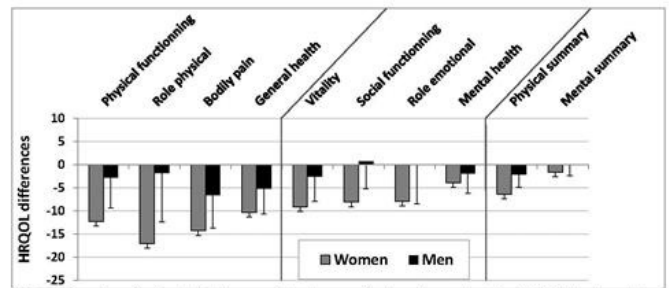
Rural First Nations Women Over Age 60 Years Have Lower Distal Forearm Bone Density for Age in Association with Low Vitamin D Status. Hope Weiler^{*1}, Kurtis Sarafin², William Leslie³. ¹McGill University, Canada, ²Health Canada, Canada, ³College of Medicine, University of Manitoba, Canada

Native First Nations (FN) Canadian women are at much higher fracture risk than the general population. Previously we demonstrated that FN women have lower bone mass in association with low vitamin D status despite similar dietary intakes to white (W) women in a representative urban population from Manitoba, Canada. Very few assessments have been conducted in FN women living in rural regions. The objective of this study was to capture measures of bone mass and vitamin D status in FN and W women residing in rural Manitoba. Women (n=262) 25 y of age and over were recruited from two rural Manitoba communities (one southern, one northern), between September 2005 and August 2011. Distal forearm and calcaneal bone mineral density (BMD) and Z-scores were assessed on the non-dominant side using a peripheral x-ray imager (PIXI, GE Lunar). Vitamin D status was assessed using total 25-hydroxyvitamin D (25OHD) as quantified using a chemiluminescent immunoassay (Liaison, Diasorin Inc.). Proportions surveyed during the UVB exposure period between April 1st and September 30th were balanced across the study (FN 51% and W 52%). Differences among ethnic and age groups were tested using mixed model ANOVA accounting for effects of season of sampling. Body mass index was not different between ethnic groups (FN 31.4 ± 7.1 vs W 29.8 ± 6.7, kg/m²). Vitamin D status was lower in FN women without main or interaction effects across age groups (FN 44.0 ± 19.8 vs W 66.3 ± 24.4 of 25OHD nmol/L, p<0.0001). No differences among ethnic groups were observed for BMD or Z-score of the calcaneus (data not shown), although women ≥ 60 y of age had lower BMD compared to the two younger groups (p<0.001). Forearm BMD was different across ethnic and age groups (p<0.003), and ethnicity-by-age interactions were observed for forearm BMD and Z-score (Table). FN women ≥ 60 y of age had lower BMD compared to all other age and ethnic groups and lower Z-score compared to white women of any age. These data suggest that BMD of the forearm is not different in First Nations and white women at younger ages, but factors associated with aging including lower vitamin D status may elevate risk of fracture in older First Nations women.

| Distal Forearm | Age Group (y) | n | First Nations Women | n | White Women |
|--------------------------|---------------|----|---------------------|----|---------------|
| BMD (g/cm ²) | 25 to 39.9 | 20 | 0.483 ± 0.063 | 39 | 0.494 ± 0.076 |
| BMD Z-score | | | -0.10 ± 1.05 | | +0.07 ± 1.27 |
| BMD (g/cm ²) | 40 to 59.9 | 41 | 0.439 ± 0.070 | 97 | 0.466 ± 0.065 |
| BMD Z-score | | | -0.57 ± 1.36 | | -0.18 ± 1.08 |
| BMD (g/cm ²) | ≥ 60 y | 13 | 0.328 ± 0.057* | 52 | 0.417 ± 0.071 |
| BMD Z-score | | | -1.38 ± 0.87** | | +0.34 ± 1.17 |

* p<0.001 vs all other groups; ** p<0.05 vs all White women values.

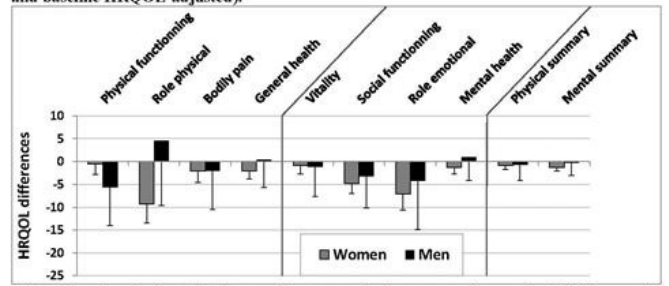
Figure 1: Age-adjusted HRQOL differences at baseline in those with osteoporosis compared to those without.



* Negative values indicate that those with osteoporosis have lower baseline HRQOL values than those without. Clinically relevant differences are differences ≥5 points in the 8 domains or >2-3 points in the summary scores.

Figure 1: Age-adjusted HRQOL differences at baseline

Figure 2: Differences in 10-year changes in HRQOL in those with osteoporosis at baseline compared to those who were still not diagnosed with osteoporosis at year 10 follow-up (age and baseline HRQOL-adjusted).



* Negative values indicate that those with osteoporosis have greater decrease in HRQOL over 10 years than those without. Clinically relevant differences are differences ≥5 points in the 8 domains or >2-3 points in the summary scores.

Figure 2: Differences in 10-year changes in HRQOL

Disclosures: *Claudie Berger, None.*

SA0271

Osteoporosis Prevention: Where are the barriers to improvement in patients and doctors?. Blandine Merle¹, Julie Haesebaert², Christian Dupraz³, Marie Aussedat³, Loïc Barraud³, Amélie Bedouet³, Cyril Motteau³, Virginie Simon³, Anne-Marie Schott⁴, Marie Flori³. ¹INSERM, France, ²pôle IMER, Hospices Civils de Lyon, France, ³Université Claude Bernard Lyon, France, ⁴Hospices Civils de Lyon, France

Despite numerous programs aiming at improving osteoporosis care, the prevention, diagnostic and treatment remain suboptimal. It is important to understand barriers to preventive care initiation to improve management of osteoporosis (OP). We implemented a qualitative study to explore the knowledge and representations regarding OP and its prevention of women, men and general practitioners in Region Rhône-Alpes, France. Four types of focus groups were conducted until data saturation, with women aged 50 to 85 years and men aged 60 to 85 years, with or without a history of fragility fracture or an osteoporosis diagnostic (referred to as "aware" or "unaware"). We involved 57 men, 23 aware and 34 unaware, in 7 focus-groups; and 45 women, 23 aware and 22 unaware in 9 focus groups. In parallel, semi-directed face-to face interviews were conducted with 16 general practitioners. A thematic analysis of transcripts was made with Nvivo 10 software. Results showed that osteoporosis is not considered as an illness but rather associated to old age by women and men who usually do not feel concerned, even if they had suffered a fragility fracture. No differences could be observed between aware and unaware patients. If OP was associated with bone fragility and fractures by women, for most of the men it was a women pathology which they deny. Fragility fracture was usually not linked to OP but to the fall. Men and women agreed with a healthy lifestyle although the benefits of dairy products, sun exposure and sport practicing were discussed. Pharmacological treatments were only mentioned by women, and always with suspicion due to their side effects. Women and men thought that their general practitioner is the right person to inform them about OP although it is rarely done, but women were more likely to be active in their health. For general practitioners, OP was associated with fragility fractures, women, menopause and old age but rarely with men. Bone mineral density measurement was regarded as the referent diagnostic test, but with questions as to when to prescribe, and difficulties to interpret the results. Biphosphonates were the reference treatment. Above all, they were waiting for clear and pragmatic guidelines to better manage this disease, and a better education of patients about OP. In conclusion, understanding barriers to osteoporosis care in patients and general practitioners will help to set up effective strategies to improve prevention and treatment.

Table

Disclosures: *Hope Weiler, None.*

SA0270

Longitudinal assessment of health-related quality of life in osteoporosis – data from the Canadian Multicentre Osteoporosis Study (CaMos). Claudie Berger¹, Wilma M. Hopman², Lisa Langsetmo³, Lawrence Joseph⁴, Suzanne N Morin⁴, Tanveer Towheed², Tassos Anastassiades², Jonathan D. Adachi⁵, David A. Hanley⁶, Jerilynn C. Prior⁷, Goltzman David⁴. ¹CaMos, McGill, Canada, ²Queen’s University, Canada, ³MUHC-RI, McGill University, Canada, ⁴McGill University, Canada, ⁵McMaster University, Canada, ⁶University of Calgary, Canada, ⁷University of British Columbia, Canada

There is evidence that osteoporosis is associated with lower health-related quality of life (HRQOL), even in the absence of fractures. However, little is known about the impact of osteoporosis on changes in HRQOL over time in women and men. Our objectives were to determine the associations between self-reported diagnosis of osteoporosis (with/without fracture) and HRQOL (SF-36 at baseline and 10-year longitudinal change) in a population-based cohort of women and men. Study population: CaMos participants age 50+. We stratified the cohort based on sex, reported diagnosis of osteoporosis, and presence of fragility fracture at baseline. Age-adjusted linear regressions were used to compare groups in terms of HRQOL. In longitudinal analysis (with further adjustment for baseline scores), we considered three diagnoses groups: never diagnosed, diagnosed at baseline, diagnosed during the 10-year follow-up. At baseline, there were 736 women and 42 men with osteoporosis and 4695 women and 2126 men without. Of those with osteoporosis, 266 (36.1%) women and 11 (26.2%) men had a prevalent fragility fracture. For women, baseline age-adjusted HRQOL differences between those with and without osteoporosis were substantial (Figure 1), with the osteoporosis group scoring lower on all 8 domains and both component summaries; in addition, most were clinically relevant. Men showed a similar pattern, although only 2 domains exceeded the threshold for clinical relevance. In women with osteoporosis, those who reported prevalent fractures had age-adjusted differences lower than those without a fracture, with 3 physically oriented scores attaining clinical relevance. For men, results suggest a lower HRQOL in those who reported prevalent fractures, but the sample size was too small to draw conclusions. For the changes over 10 years (Figure 2), those with osteoporosis were more likely to have greater declines in scores than those who were never diagnosed with osteoporosis; some differences in women were clinically relevant. A similar pattern was seen for those who developed osteoporosis over the follow-up, although the differences were smaller. Osteoporosis diagnosis appears to be associated with poorer HRQOL in women, which is compounded by the presence of fractures. In addition, having the disease, or developing it, is also associated with greater 10-year declines in HRQOL when compared to those who do not have it. Results appear similar for men, although the sample sizes were small.

Disclosures: *Blandine Merle, None.*

SA0272

A Prospective Study of Diuretic Use and Risk of Vertebral Fractures in Women. Julie M Paik^{*1}, Harold N Rosen², Catherine M Gordon³, Gary C Curhan¹. ¹Brigham & Women's Hospital, Harvard Medical School, USA, ²Beth Israel Deaconess Medical Center, USA, ³Hasbro Children's Hospital, Alpert Medical School of Brown University, USA

Purpose: Vertebral fractures are the most common type of osteoporotic fracture and are associated with significant disability and morbidity. Loop diuretics increase urinary calcium excretion, thereby affecting calcium balance. Although thiazide diuretics decrease urinary calcium excretion and preserve bone mineral density, they may also induce hyponatremia and several recent studies suggest hyponatremia to be associated with an increased fracture risk. The few studies to date examining the relation between loop diuretics, thiazides, and vertebral fracture risk have shown inconsistent results, which could be related to the assessment of vertebral fractures by self-report or administrative codes.

Methods: We conducted a prospective study of the relation between loop diuretic use, thiazide use, and vertebral fracture risk in a cohort of 56,974 women, 51-78 years of age in 1998, with no history of vertebral fracture, who were participating in the Nurses' Health Study. Use of furosemide or thiazides was assessed by questionnaire every four years. Dietary intake and vitamin supplement use were assessed from semi-quantitative food frequency questionnaires in the same years. All cases of self-reported vertebral fracture were confirmed by medical record review.

Results: In 1998, there were 5,362 women (9.4%) receiving thiazides and 1,070 women (1.9%) taking furosemide. Between 1998 and 2014, 343 incident vertebral fracture cases were documented. After adjustment for other potential risk factors, including intakes of calcium, vitamin D, protein, caffeine and alcohol, body mass index, physical activity, smoking status, and history of hypertension, diabetes, and osteoporosis, the relative risk of vertebral fracture for those women taking furosemide was 1.66 (95% confidence interval 1.14 to 2.43) compared with women who were not taking furosemide. After multivariate adjustment, the relative risk of vertebral fracture for women taking thiazides was 1.40 (95% confidence interval 1.07 to 1.83) compared with women who were not taking thiazides.

Conclusion: Diuretic use, both loop diuretics and thiazides, is associated with an increased risk of vertebral fractures in women. While the increased risk associated with loop diuretics could be related to increased calciuria, thiazides could potentially increase vertebral fracture risk by a mechanism other than urinary calcium handling such as thiazide-induced hyponatremia.

Disclosures: *Julie M Paik, None.*

SA0273

Can FRAX Predict Falls in Older Women?. Shreyasee Amin^{*}, Elizabeth Atkinson, Sara Achenbach, Jeremy Crenshaw, Kenton Kaufman, Sundeeep Khosla, L. Joseph Melton. Mayo Clinic, USA

Falls in the elderly can lead to fragility fractures. Fall prevention targeted at those with high fall risk could help reduce fractures. Although the fracture risk assessment tool, FRAX, does not directly incorporate fall risk, it does include some risk factors for falling. We examined whether FRAX scores could predict fall risk in older ambulatory women.

We studied 125 community-dwelling women, age ≥ 65 yrs, in whom 124 had femoral neck bone mineral density (FN BMD, g/cm²) and US-FRAX scores (% 10-yr risk for major osteoporotic fractures [FRAX-OP] and hip fractures [FRAX-Hip]) reliably determined. Falls were longitudinally tracked every two weeks for 1 yr by self-reported questionnaire. We divided subjects into 4 groups, using FRAX score cutoffs for osteoporosis [OP] treatment ($\geq 20\%$ for FRAX-OP and $\geq 3\%$ for FRAX-Hip) as the initial basis for groupings. We then examined whether FRAX scores (by groups and as a continuous variable) predicted falls using an Andersen-Gill model, adjusted for age and prior fall history.

The median (range) age, FN BMD and FRAX scores of women were 77 (65-92 yrs), 0.81 (0.54-1.20 g/cm²), 14.2 (3.3-56.9%, FRAX-OP) and 3.5 (0.1-45.8%, FRAX-Hip), respectively. There were 28 women (23%) with FRAX-OP $\geq 20\%$ and 67 (53%) with FRAX-Hip $\geq 3\%$. There were 47 women (38%) who reported a fall in the yr prior to their study visit. Compliance with all fall tracking questionnaires was 97.5%. Over follow-up, 73 women fell, 38 of whom had more than one fall, for a total of 157 falls over 125 person-yrs of follow-up [p-y] (1.3 falls/p-y). There was a trend for higher fall risk with greater FRAX score [see Table]. But the association appeared non-linear when using FRAX as a continuous variable in analyses, with decreasing fall risk in women having the very highest ($>25\%$, FRAX-OP and $>10\%$, FRAX-Hip) scores [data not shown]. Women with high FRAX scores were more likely to have a parent with hip fracture, increasing the FRAX score, but which may not necessarily have influenced fall risk. They also reported being less active, which may have reduced their likelihood for falling over follow-up.

We found a higher risk of future falls in older women with greater FRAX scores, including at scores below the recommendations for OP treatment. That said, the non-linear association we observed at the highest FRAX scores suggests that information beyond FRAX would still be necessary to distinguish those at high vs. low risk for falls.

| FRAX-OP Score [%]† (N-per-Group)‡ | Falls/† P-Yr | Hazard-Ratio- (95%-CI)‡ | FRAX-Hip Score [%]† (N-per-Group)‡ | Falls/† P-Yr | Hazard-Ratio- (95%-CI)‡ |
|--------------------------------------|-----------------|----------------------------|---------------------------------------|-----------------|----------------------------|
| <10 (N=26)‡ | 0.8‡ | reference‡ | <1.5 (N=31)‡ | 0.8‡ | reference‡ |
| 10-14.9 (N=41)‡ | 1.2‡ | 1.9 (0.8, 4.3)‡ | 1.5-2.9 (N=26)‡ | 0.9‡ | 1.3 (0.7, 2.6)‡ |
| 15-19.9 (N=29)‡ | 1.5‡ | 2.3 (1.1, 4.9)‡ | 3.0-5.9 (N=37)‡ | 2.0‡ | 2.5 (1.3, 4.9)‡ |
| ≥ 20 (N=28)‡ | 1.5‡ | 2.6 (1.1, 6.3)‡ | ≥ 6 (N=30)‡ | 1.2‡ | 1.8 (0.9, 3.9)‡ |

Table

Disclosures: *Shreyasee Amin, None.*

SA0274

Decreased serum albumin level and renal function are the risk for mortality after newly diagnosed vertebral fracture (Vfx) in Japanese subjects. Akiko Kuwabara^{*1}, Kiyoshi Tanaka², Tetsuo Nakano³. ¹Department of Health & Nutrition, Osaka Shoin Women's University, Japan, ²Kyoto Women's University, Japan, ³Department of Orthopaedic Surgery, Tamana Central Hospital, Japan

Purpose: It is well established that the prevalence of Vfx is higher, whereas that of hip fracture is lower in Japan than that in Europe or America. Recently, some reports described the higher mortality in subjects with Vfx in Japan. Few papers have been available, however, on the factors contributing the mortality after Vfx. In addition, mortality after recently occurred Vfx has not been reported in Japan. Thus we have studied the survival rate after freshly diagnosed Vfx. Methods. 774 subjects aged 78.8 \pm 8.6 years old with back or lumbar pain, and diagnosed as fresh Vfx by magnetic resonance imaging (MRI) were studied for their age, gender, number of prevalent Vfx, survival or the date of death, circulating levels of hemoglobin (Hb), albumin (Alb), C reactive protein, and estimated glomerular filtration rate (eGFR). The subjects who died within 30 days from baseline were excluded from the analyses. Cox's proportional hazard analysis was performed to assess the significant predictors for mortality. The cut-off levels of the variables for mortality were analyzed using the receiver operator characteristic (ROC) curve. Results. The median observation duration was 3.8 years. The survival rates of our Vfx patients were 91.3%, 84.6%, and 78.8% at one, 2, and 3 years after the diagnosis of fresh Vfx, respectively. Non-survivors had significantly higher age ($p<0.001$), higher serum CRP level ($p<0.001$), and lower Alb ($p<0.001$), Hb ($p=0.002$), eGFR ($p<0.001$) than survivors. Cox's proportional hazard analysis has shown that serum Alb level (hazard ratio (HR) =0.355) and eGFR (HR=0.993) were significant predictors for mortality. Based on the ROC curves, the cut-off levels were 3.6 g/dl and 60 mL/min/1.73m², respectively. Kaplan-Meier curves revealed that survival rates were significantly decreased in patients with both serum Alb level and eGFR below these cut-off levels. Conclusions. The present study has revealed that subjects with freshly diagnosed Vfx have high risk of mortality, to which hypoalbuminemia and impaired renal function have significantly contributed.

Disclosures: *Akiko Kuwabara, None.*

SA0275

Glucose Metabolism Status Is Not Associated With a Recent History of Falls, Recurrent Falls or Fractures – The Maastricht Study. Ellis de Waard¹, Annemarie Koster², Tom Melai³, Tineke van Geel⁴, Ronald Henry⁵, Miranda Schram⁵, Pieter Dagnelie⁶, Carla van der Kallen⁵, Simone Sep⁵, Coen Stehouwer⁵, Nicolaas Schaper⁷, Hans Savelberg³, Piet Geusens⁸, Joop van den Berg⁹. ¹NUTRIM School for Nutrition & Translational Research in Metabolism, Maastricht University, Department of Internal Medicine, Subdivision of Rheumatology, Maastricht, Netherlands, ²Maastricht University, Department of Social Medicine, Maastricht, Netherlands & CAPHRI School for Public Health & Primary Care, Maastricht University, Maastricht, Netherlands, ³NUTRIM School for Nutrition & Translational Research in Metabolism, Maastricht University, Department of Human Movement Science, Maastricht, Netherlands, ⁴NUTRIM School for Nutrition & Translational Research in Metabolism/CAPHRI School for Public Health & Primary Care, Maastricht University, Department of Family Medicine, Maastricht, Netherlands, ⁵Maastricht University Medical Centre, Department of Internal Medicine, Maastricht, Netherlands & CARIM School for Cardiovascular diseases, Maastricht University, Maastricht, Netherlands, ⁶CAPHRI School for Cardiovascular diseases/CAPHRI School for Public Health & Primary Care, Maastricht University, Maastricht, Netherlands & Maastricht University, Department of Epidemiology, Maastricht, Netherlands, ⁷Maastricht University Medical Centre, Department of Internal Medicine, Maastricht, Netherlands & CARIM School for Cardiovascular diseases/CAPHRI School for Public Health & Primary Care, Maastricht University, Maastricht, Netherlands, ⁸CAPHRI School for Public Health & Primary Care, Maastricht University Medical Centre, Department of Internal Medicine, Subdivision of Rheumatology, Maastricht, Netherlands, ⁹VieCuri Medical Centre, Department of Internal Medicine, Subdivision of Endocrinology, Venlo, Netherlands & NUTRIM, Maastricht University Medical Centre, Department of Internal Medicine, Subdivision of Rheumatology, Maastricht, Netherlands

Purpose: To compare the prevalence of past falls, recurrent falls and fractures in participants with normal glucose metabolism (NGM), impaired glucose metabolism (IGM) and type 2 diabetes (T2DM). Additionally, to examine the role of glucose metabolism regulation, insulin use and T2DM duration on falls, recurrent falls and fractures.

Methods: Baseline data of all participants over the age of 50 (N=2953) from The Maastricht Study, a population based cohort study with oversampling of patients with T2DM, was used. Glucose metabolism status was based on an oral glucose tolerance test and medication use. Data about past falls or fractures was obtained by questionnaires. Falls in the past year (yes vs. no), recurrent falls (>1 fall in the past year, yes vs. no) and fractures over the age of 50 (yes vs. no) were used for analysis.

Results: In total, 1577 participants had NGM, 468 had IGM and 908 had T2DM (mean duration 8.7 ± 7.1 years, mean HbA1c 52.1 ± 11.4 mmol/mol, 21.9% insulin user). A fall in the past year was reported by 881 (33.1%), recurrent falls by 204 (6.9%) and a fracture over the age of 50 by 176 (6.0%) participants. Adjusted for age, sex, BMI and physical activity, the odds ratios in IGM and T2DM compared to NGM were not different for falls (IGM: OR 0.94, 95% CI 0.74-1.17, T2DM: OR 1.12, 95% CI 0.86-1.47), recurrent falls (IGM: OR 1.10, 95% CI 0.71-1.69; T2DM: OR 1.29, 95% CI 0.79-2.10) or fractures (IGM: OR 1.09, 95% CI 0.70-1.71; T2DM: OR 1.39, 95% CI 0.84-2.30). Within the T2DM group, falls or fractures did not significantly differ between participants with poorly regulated (HbA1c >64 mmol/mol, N=107) and well-regulated (HbA1c ≤64 mmol/mol) diabetes (falls: 31.8% vs. 33.5%, p=0.75, fractures: 10.6% vs. 6.1%, p=0.16) and between insulin (N=199) and non-insulin users (falls: 36.5% vs. 32.5%, p=0.34, fractures: 9.9% vs. 5.8%, p=0.10). The prevalence of recurrent falls was significantly higher in the poorly regulated participants (13.0% vs. 6.7%, p=0.05) and in insulin users (13.1% vs. 6.0%, p<0.01). T2DM duration (>5 vs. ≤5 year) was not associated with the prevalence of falls (32.1% vs. 36.1%, p=0.28), recurrent falls (7.8% vs. 6.6%, p=0.59) or fractures (6.7% vs. 6.3%, p=0.88).

Conclusion: Glucose metabolism status is not associated with a recent history of falls, recurrent falls or fractures. Within the T2DM group, the prevalence of recurrent falls was higher in poorly controlled participants and in insulin users.

Disclosures: Ellis de Waard, None.

SA0276

High subcutaneous fat measured by DXA is associated with higher fracture risk in older men - the STRAMBO study. Pawel Szulc¹, François Duboueu², Roland Chapurlat². ¹INSERM UMR 1033, University of Lyon, Hôpital E. Herriot, Pavillon F, France, ²INSERM UMR 1033, University of Lyon, Hôpital Edouard Herriot, France

Obesity is associated with higher bone fragility. However, it is not clear whether visceral and subcutaneous fat have similar impact on fracture risk. In older men, high subcutaneous, but not visceral, fat mass was associated with low grip strength and poor physical performance (Szulc, ISCD Congress, 2015). Therefore, our aim was to assess the association between fat mass and fracture risk in older men. In a cohort of 802 men aged 60-88, a HOLOGIC Discovery A device was used to assess total hip bone mineral density (BMD) and body composition (including gynoid fat and visceral and subcutaneous compartments of android fat). Incident vertebral and non-vertebral fractures were recorded prospectively. Cox proportional hazards model was adjusted for age, hip BMD, prior fractures, self-reported ischemic heart disease and serum 25-hydroxycholecalciferol. During the follow-up (median 7 yrs), 82 men sustained low trauma fragility fractures. Higher body weight and fat mass were associated with higher fracture risk (per SD increase: HR= 1.33, 95%CI: 1.06-1.66, p<0.05 and HR= 1.46, 95%CI: 1.16-1.84, p<0.005). Gynoid fat and android fat were associated with higher fracture risk (per SD increase: HR= 1.55, 95%CI: 1.23-1.94, p<0.001 and HR= 1.38, 95%CI: 1.08-1.77, p=0.01). In the stepwise model, only gynoid fat was retained. The highest quintile of gynoid fat was associated with higher fracture risk (HR= 2.04 vs. four lower quintiles combined, 95%CI: 1.20-3.48, p<0.01). By contrast, the highest quintile of android fat was not associated with fracture risk (HR= 1.66 vs. lower quintiles combined, 95%CI: 0.93-2.94, p=0.10). Higher abdominal subcutaneous fat was associated with higher fracture risk (HR= 1.47 per SD, 95%CI: 1.15-1.87, p<0.005), whereas visceral fat and fracture tended to be associated (HR= 1.28 per SD, 95%CI: 0.98-1.64, p=0.06). When both were introduced in the stepwise model, only subcutaneous fat was retained. The highest quintile of abdominal subcutaneous fat was associated with higher fracture risk (HR= 1.94 vs. lower quintiles combined, 95%CI: 1.12-3.33, p<0.05). The highest quintile of visceral fat was not associated with the fracture risk (HR= 1.47 vs. lower quintiles combined, 95%CI: 0.82-2.62, p=0.20). In conclusion, in older men, higher subcutaneous fat is associated with higher incident fracture risk after adjustment for potential confounders.

Disclosures: Pawel Szulc, None.

SA0277

How Do Hip Fracture Rates in Long-term Care Compare with the Community?. Courtney Kennedy¹, Alexandra Papaioannou¹, George Ioannidis¹, Ruth Croxford², Cathy Cameron³, Sara Mursleen¹, Jonathan Adachi¹, Susan Jaglal³. ¹McMaster University, Canada, ²Institute for Clinical Evaluative Sciences, Canada, ³University of Toronto, Canada

Background: Individuals living in long-term care (LTC) homes are typically frailer and are at higher risk of falls than their community counterparts. In this study we compared patterns of hip fracture rates in LTC versus community-dwelling men and women. **Methods:** A retrospective cohort was defined using population-level health administrative data for all individuals aged 65 years and older living in Ontario, Canada between 2002-12. The LTC cohort was defined based on records indicating an LTC admission or a physician visit or prescription filled while residing in LTC. In Ontario, approximately 620 LTC facilities (nursing homes) are funded by the provincial health ministry and provide residential care for older adults who need access to 24-hour nursing, supervision, or higher levels of personal care assistance. Fractures were identified (ICD-10-CA diagnosis codes) from emergency department, inpatient records, and physician claims. Crude incident hip fracture rates were calculated for men and women separately, for age strata 65-74, 75-84, and 85+ years. **Results:** The LTC cohort was substantially older [n= 733,619; women=85.0 (SD 7.4); men=81.5 (SD 7.7)] than the community cohort [n= 17,419,498; women=74.8 (SD 7.0); men=73.5 (SD 6.4)]. There was a markedly higher hip fracture rate in institutionalized women in the two younger age strata (figure) compared with women residing in the community. However, by age 85+ hip fracture rates for women were similar regardless of institutionalization status. Men in LTC had higher hip fracture rates than community-dwelling men across all age strata (figure) and a similar distribution of rates as women residing in LTC. The substantial rise in fracture rates occurred by age 75 in LTC but not until age 85 in the community. During the study period, LTC residents contributed to 17% of all hip fractures in Ontario, despite being only 4% of the overall senior population age 65 years and older. **Discussion:** There was a considerable burden of hip fractures for both men and women residing in LTC. Women age 85 years and older had similar hip fracture rates irrespective of living arrangement (community versus LTC) indicating that these two groups may have a similar risk profile and degree of frailty.

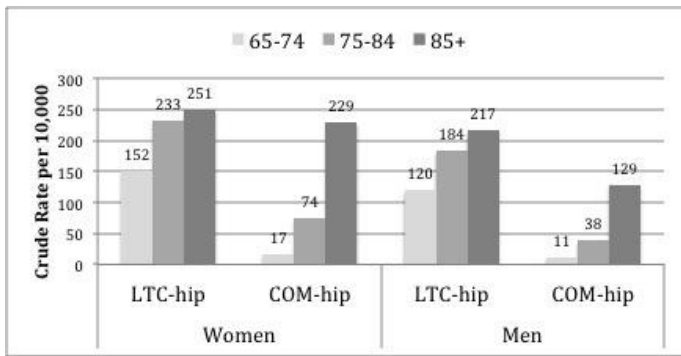


Figure
Disclosures: Courtney Kennedy, None.

SA0278

Humeral fractures in south-eastern Australia: epidemiology and risk factors. Kara Holloway¹, Gosia Bucki-Smith², Amelia Morse², Sharon Brennan-Olsen², Mark Kotowicz², David Moloney², Elizabeth Timney², Amelia Dobbins², Julie Pasco². ¹Barwon Health, Australia, ²School of Medicine, Deakin University, Australia

In this study, we report the epidemiology and risk factors for humeral fractures (proximal humerus and shaft) among men and women residing in south-eastern Australia.

Incident fractures during 2006 and 2007 were identified using X-ray reports (Geelong Osteoporosis Study Fracture Grid). Risk factors were identified using data from case-control studies conducted as part of the Geelong Osteoporosis Study.

During 2006 and 2007, there were 283 and 385 humeral fractures in males and females respectively. Of these, 105 males and 218 females had proximal humerus fracture. Median age of fracture was lower in males than females for proximal humerus (33.0 95%CI 17.3-63.1 years vs 71.2 95%CI 58.4-82.0 years), but not for humeral shaft (8.9 95%CI 5.6-16.4 years vs 8.5 95%CI 5.9-59.6 years). Most fractures were the result of a fall (>75%) onto an outstretched hand/arm or shoulder. For both sexes, proximal humerus fractures occurred mainly in older age groups (70-79 and 80+ years), whereas humeral shaft fractures followed a U-shaped pattern. Total incidence (age-standardised to the Australian population) of humerus fractures in males and females (per 100,000 person-years) were 109.9 (95%CI 109.4, 110.3) and 135.3 (95%CI 133.7, 136.9), respectively. In men, increased femoral neck BMD and younger age were protective of proximal humerus fracture, whereas prior fracture and high milk consumption were risk factors. For the humeral shaft, only prior fracture was identified as a risk factor. In premenopausal women, height and falls were both risk factors for proximal humerus fractures. For postmenopausal women, protective factors for proximal humerus fractures included a higher non-milk dairy consumption. Education and prior fractures were both risk factors. We were unable to determine risk factors for humeral shaft fractures in women due to small numbers of cases.

Males sustained proximal humerus fractures at a younger age than females. Most fractures were the result of a fall. Humeral shaft fractures in both sexes were sustained mainly in childhood, while proximal humerus fractures were sustained in older adulthood. Risk factors for adult humeral fractures in both sexes were identified and may be used as an indicator of individuals at high risk of humerus fractures.

Disclosures: Kara Holloway, None.

SA0279

Impact of osteonecrosis of the jaw on osteoporosis treatment in Japan: results of a questionnaire-based survey by the Adequate Treatment of Osteoporosis (A-TOP) research group. Akira Taguchi¹, Masataka Shiraki², Mayumi Tsukiyama³, Teruhiko Miyazaki³, Satoshi Soen⁴, Hiroaki Ohta⁵, Toshitaka Nakamura⁶, Hajime Orimo⁷. ¹Matsumoto Dental University, Japan, ²Research Institute & Practice for Involutional Diseases, Japan, ³Public Health Research Foundation, Japan, ⁴Department of Orthopaedic Surgery & Rheumatology, Nara Hospital, Kinki University School of Medicine, Japan, ⁵Department of Clinical Medical Research Center, International University of Health & Welfare, Women's Medical Center of Sanno Medical Center, Japan, ⁶National Center for Global Health & Medicine, Japan, ⁷Japan Osteoporosis Foundation, Japan

Purpose: The status of divergence between medical professionals and dentists may largely impact on patients who need antiresorptive therapy. It is necessary to first clarify how osteonecrosis of the jaw (ONJ) problems, especially drug holidays and cooperation between medical professionals and the dentists, impact on osteoporosis treatment in the real world of current Japan. Little is known about how drug holidays

affect osteoporosis treatment and how medical professionals and dentists cooperate to deal with ONJ in osteoporosis treatment. This study aimed to clarify the impact of ONJ on osteoporosis treatment in Japan. Methods: A structured questionnaire including 14 key clinical queries was sent to 488 medical professionals as part of the Japanese Osteoporosis Intervention Trial (JOINT)-04, and 206 responses were received. Results: A total of 173 respondents had received discontinuation requests from dentists. Of these, 28 respondents reported 30 adverse events including 10 fractures and one ONJ case. The respondents who refused discontinuation requests observed no cases of ONJ. Approximately 16% of respondents had experience of patients discontinuing osteoporosis treatment after tooth extraction under a drug holiday. Dentists requested discontinuations for many medications not associated with the incidence of ONJ. Approximately 76% of respondents had never requested oral health care from dentists before osteoporosis treatment and 72% reported no cooperation between dentists and medical professionals in their region. Conclusions: Our results suggest that drug holidays do not prevent ONJ but may increase adverse events and disturb osteoporosis treatment. Currently both medical professionals and dentists in Japan still continue to push their own treatment position. A forum to share information about ONJ among medical professionals, dentists and patients is needed.

Disclosures: Akira Taguchi, Ono; Asahi Kasei
This study received funding from: Grants-in-Aid from the Japan Society for the Promotion of Science (Nos. 24592849, 26463148 and 90119222)

SA0280

Low blood pressure cut points for fall injuries in community-dwelling elderly: the Health, Aging and Body Composition Study. Naoko Sagawa¹, Zachary A. Marcum², Robert M. Boudreau¹, Joseph T. Hanlon¹, Steven M. Albert¹, Suzanne Satterfield³, Ann V. Schwartz⁴, Aaron I. Vinik⁵, Jane A. Cauley¹, Tamara B. Harris⁶, Anne B. Newman¹, Elsa S. Strotmeyer¹. ¹University of Pittsburgh, USA, ²University of Washington, USA, ³University of Tennessee Health Science Center, USA, ⁴University of California, San Francisco, USA, ⁵Eastern Virginia Medical School, USA, ⁶National Institute on Aging, USA

Falls often result in injury and are an important cause of morbidity and mortality. Hypertension and low blood pressure (BP) are known risk factors of falls in the elderly. However, cut points for low BP vary among studies. We investigated if BP at various cut points is associated with fall injury in the Health, Aging and Body Composition Study using incident injurious falls from linked Medicare data. Injurious falls from clinic exam (7/00-6/01) to 12/31/08 were defined as any unique event from Medicare claims for N=2375 (99%) with a fall code (E880-888) plus non-fracture injury (N=161) or a fracture code (800-829) with/without (N=367) a fall code (N=458). Traumatic, intentional or pathologic injuries were excluded (N=38). We included 2,324 with BP data (52% women, 38% black). Initial injurious falls (N=609) occurred in 3.8 ± 2.4 years, with others censored at end of Medicare coverage (N=1) or last follow-up (N=12)/death (N=514)/Medicare dataset end date (N=1188) over 6.9 ± 2.1 years. Participants with injurious falls were more likely to be white (72% vs. 59%), women (65% vs. 47%), older (age 77 ± 3 vs. 76 ± 3 years), had lower BMI (26.7 ± 4.8 vs. 27.6 ± 2.8 kg/m²), and lower diastolic BP (DBP; 70.4 ± 11.1 vs. 71.9 ± 10.9 mmHg), all p < 0.01. They were more likely to have more prescription medications (3.6 ± 2.7 vs. 3.2 ± 2.5, p < 0.01) and cerebrovascular disease history (9% vs. 6%, p = 0.02); though no difference in systolic BP (SBP; 135.0 ± 20.6 vs. 135.2 ± 19.8 mmHg), pulse pressure (64.5 ± 18.3 vs. 63.3 ± 17.0 mmHg), antihypertensive medication use (56.8% vs. 59.9%), orthostatic hypotension (defined as decrease in SBP 20 mmHg or DBP 10 mmHg; 5.6% vs. 6.9%), or diabetes (21.0% vs. 21.5%) was found. Cut points for low DBP were based on literature (80, 90 mmHg) and J-curve phenomenon (60, 70 mmHg). Cox regression models for each cut point were built for fall injuries adjusted for demographics, BMI, lifestyle factors, comorbidity and medication use at baseline. Fall injury risk was higher in those with DBP ≤ 70 mmHg (HR=1.19; 95%CI: 1.01-1.40), and was attenuated by adjustment for the total number of medications (Table 1). SBP was not associated with fall injury risk. These results were consistent after stratifying for non-fracture and fracture injuries. DBP ≤ 70 mmHg identifies older adults at higher risk of fall injury. This relationship was accounted for in part by polypharmacy; however, it is unclear what aspect accounts for the risk and this will be the focus for future work.

Table 1: Cut points for diastolic blood pressure and incident fall injury.

| Cut points (Prevalence) | Model 1 | Model 2 | Model 3 | Model 4 |
|-------------------------|--|-------------------|------------------|------------------|
| | Hazard Ratio (95% Confidence Interval) | | | |
| ≤60mmHg (22%) | 1.27 (1.05-1.54)* | 1.24 (1.02-1.51)* | 1.19 (0.98-1.44) | 1.21 (0.99-1.49) |
| ≤70mmHg (57%) | 1.19 (1.01-1.40)* | 1.19 (1.01-1.40)* | 1.14 (0.97-1.34) | 1.14 (0.96-1.35) |
| ≤80mmHg (84%) | 1.00 (0.80-1.24) | 0.99 (0.80-1.24) | 0.95 (0.76-1.19) | 0.92 (0.73-1.17) |
| ≤90mmHg (97%) | 0.89 (0.56-1.43) | 0.87 (0.54-1.39) | 0.83 (0.52-1.33) | 0.80 (0.49-1.33) |

*p<0.05. Variables in Model 1 were kept in all models, additional covariates were removed at P>0.1. Model 1: adjusted for age, sex, race, site, BMI. Model 2: Model 1 + medication use (antidepressives, opioids, benzodiazepines, antipsychotics, antiepileptics, antihypertensives). Model 3: Model 1 + medication use (antidepressives, opioids, antiepileptics), total number of medications (includes antihypertensives since these were P>0.1). Model 4: Model 1 + antiepileptics, total number of medications, Modified Mini-Mental State score, 1.4-g/10-g monofilament insensitivity, Cystatin C>3.0 mg/L.

Table 1
Disclosures: Naoko Sagawa, None.

SA0281

Personality, Falls and Fractures: The Women's Health Initiative Observational Study (WHI-OS). Jane Cauley*¹, Stephen Smagula², Kathleen Hovey³, Jean Wactawski-Wende^{2,3}, Carolyn Crandall⁴, Meryl LeBoff⁵, Christopher Andrews⁶, Wenjun Li⁷, Mathilda Coday⁸, Marvan Sattari⁹, Hilary Tindle¹⁰. ¹University of Pittsburgh Graduate School of Public Health, USA, ²University of Pittsburgh, USA, ³State University of NY at Buffalo, USA, ⁴University of California, USA, ⁵Brigham & Women's Hospital, USA, ⁶University of Michigan, USA, ⁷University of Massachusetts Medical School, USA, ⁸The University of Tennessee Health Science Center, USA, ⁹University of Florida, USA, ¹⁰Vanderbilt University, USA

Traits of optimism and cynical hostility are features of personality that could influence the risk of falls and fractures in several ways. Personality may influence risk taking behavior or health behaviors i.e., physical activity. Alternatively, optimism has been associated with lower levels of inflammatory markers which have been linked to a lower risk of fractures. To test the hypothesis that personality influences fall and fracture risk, we studied 87,342 women enrolled in WHI-OS. The Life Orientation Test - Revised measures optimism with scores summed across 6-items. A sample question was "If something can go wrong for me, it will". Cynical hostility was assessed by the cynicism subscale of the Cook-Medley questionnaire. A sample question, "It is safer to trust nobody" is responded to by a true/false answer. Higher scores indicate greater optimism and hostility. Optimism and hostility were correlated at $r = -0.31$, p_2 times in the past year was modeled using repeated measures logistic regression. Average follow-up for fractures was 11.4 years; falls, 7.6 years. Women with the highest optimism scores were about 15% less likely to report 2 or more falls compared to women with the lowest optimism scores, Table. Similarly, highest hostility scores were associated with a 17% higher risk of falls. These associations were independent of many risk factors for falls. Higher optimism scores were also associated with about a 10% lower risk of hip, vertebral, lower arm and all fractures but this association was attenuated in multivariate models (MV). Women with the greatest hostility had a modest increased risk of any fracture, MV adjusted hazard ratio=1.06 (95% confidence intervals, 1.02-1.09) compared to women with lowest hostility but there was no association with other specific fracture types. Personality traits may influence the risk of falls above and beyond traditional risk factors. Associations with fractures were largely explained by other risk factors supporting conceptual models of how personality traits may prospectively influence biological outcomes. Whether interventions aimed at attitudes could reduce fall risks remains to be determined.

Repeated logistic regression of falls by optimism and hostility (n=87,342)

| | Age adjusted OR (95% CI) | Fully-adjusted ¹ OR (95% CI) |
|-------------------------|-----------------------------|--|
| Optimism | | |
| Continuous ² | 0.84 (0.83-0.85) | 0.93 (0.91-0.94) |
| Quartile 1: 6.0-21.0 | 1 (ref) | 1 (ref) |
| Quartile 2: 22.0-23.0 | 0.79 (0.76-0.82) | 0.88 (0.84-0.91) |
| Quartile 3: 24.0-25.0 | 0.71 (0.68-0.73) | 0.83 (0.80-0.87) |
| Quartile 4: 26.0-30.0 | 0.67 (0.64-0.70) | 0.85 (0.82-0.89) |
| Hostility | | |
| Continuous ¹ | 1.12 (1.11-1.14) | 1.06 (1.05-1.08) |
| Quartile 1: 0.0-1.0 | 1 (ref) | 1 (ref) |
| Quartile 2: 2.0-3.0 | 1.10 (1.06-1.15) | 1.05 (1.01-1.09) |
| Quartile 3: 4.0-5.0 | 1.18 (1.13-1.23) | 1.09 (1.05-1.14) |
| Quartile 4: 6.0-13.0 | 1.35 (1.29-1.40) | 1.17 (1.12-1.22) |

¹ Adjusted for age, weight, height, treated diabetes, ethnicity/race, clinic site, smoking status, general health status, current hormone therapy use, total calcium, total D intake, antidepressants, physical activity, and hypnotics.
² Odds ratio (OR) expressed as 1 SD; 95% confidence intervals.

Table
 Disclosures: Jane Cauley, None.

SA0282

Predictors of Imminent Fracture Risk in Women Aged 65 Years with Osteoporosis. Derek Weycker*¹, Rich Barron², Alex Kartashov³, John Edelsberg⁴, Barry Crittenden², Andreas Grauer². ¹Policy Analysis Inc. (PAI), USA, ²Amgen Inc., USA, ³Policy Analysis Inc., USA, ⁴Policy Analysis, USA

Background: Fractures are the major source of morbidity among women with osteoporosis. However, evidence on factors leading to imminent risk for hip or other

non-vertebral fracture within the next 12 months among women aged ≥ 65 years with osteoporosis is limited.

Methods: A retrospective cohort design and data from the Study of Osteoporotic Fractures (SOF)—which includes 20 years of prospectively collected data on osteoporosis care and outcomes—were employed. The study population comprised all women aged ≥ 65 years with osteoporosis (T-score ≤ -2.5 at total hip) in the Caucasian cohort. Hip and other non-vertebral fractures were ascertained over a 1-year follow-up period. Potential predictors of fracture were evaluated using multivariate regression models and included anthropometric measures, BMD, cognitive function, comorbidities, drug use, fracture/fall history, lifestyle variables, medical symptoms, physical function/performance, quality of life, and vision status.

Results: The study population included 2,499 women with osteoporosis who contributed 6,811 observations. During the 1-year follow-up, 2.2% had a hip fracture and 6.6% had any non-vertebral fracture (including hip). Independent predictors of hip and/or non-vertebral fracture included impaired cognitive function, total hip T-score, falls history, fracture history, and lower physical performance (Table).

Conclusions: Imminent fracture risk within 12 months among osteoporotic women is higher among those with a history of fracture, history of falls, lower BMD, physical dysfunction, and/or cognitive dysfunction. Careful consideration should be given to identifying this population so that those at imminent risk may be targeted for the appropriate therapy.

Table. Independent predictors of 1-year hip and non-vertebral fracture in osteoporotic women aged ≥ 65 years from multivariate regression models

| Risk Factors | Hazard Ratios* (95% CI) | |
|---|-------------------------|--------------------------|
| | Hip Fracture | Non-Vertebral Fracture** |
| Age (vs. referent: 65-74) | | |
| ≥ 75 to 79 | - | 0.9 (0.6-1.3) |
| ≥ 80 to 84 | - | 1.0 (0.7-1.4) |
| ≥ 85 | - | 1.4 (0.9-1.9) |
| Total Hip T-Score (vs. referent: > -3.0 to -2.5) | | |
| ≤ -3.5 | 2.3 (1.5-3.7) | 1.9 (1.5-2.5) |
| > -3.5 to -3.0 | 1.6 (1.0-2.6) | 1.6 (1.2-2.0) |
| No. of Falls in Last 12 Months (vs. referent: 0) | | |
| 1 | - | 1.2 (0.9-1.5) |
| ≥ 2 | - | 1.7 (1.3-2.2) |
| History of Fracture (vs. referent: no history)*** | | |
| Non-Vertebral Fracture | 1.6 (1.0-2.6) | - |
| Any Fracture | - | 1.4 (1.1-1.7) |
| Walking Speed (m/s) (vs. referent: > 1.0) | | |
| ≤ 0.70 | 1.0 (1.5-5.9) | 1.5 (1.1-2.1) |
| 0.70 to 1.0 | 2.6 (1.4-5.0) | 1.4 (1.1-1.9) |
| Short MMSE ≤ 23 (vs. referent: > 23) | 1.7 (1.2-2.4) | - |
| Use of Arms for Chair Stands or Poo/Very Poor Tandem Stair (vs. referent: no use of arms) | 1.7 (1.1-2.6) | - |
| Parkinson's or Stroke (vs. referent: without conditions) | - | 1.3 (1.0-1.8) |
| Smoker, Pack Years (continuous measure) | - | 1.0 (1.0-1.0) |
| Bisphosphonate Use (vs. referent: non-users) | 0.3 (0.1-0.9) | - |
| C statistic (95% CI) | 0.71 (0.67-0.76) | 0.62 (0.59-0.65) |

MMSE: Mini-Mental State Examination
 *Only hazard ratios for variables retained in the final model (i.e., those with p-values < 0.10) are reported; grouped dichotomous variables were retained if any of the grouped variables had a p-value < 0.10
 **Includes fracture of any non-vertebral site, defined—by SOF in a composite measure—as an incident, non-traumatic fracture of ankle, clavicle, elbow, face, foot, finger, hand, heel, hip, humerus, knee, lower leg, pelvis, rib, toe, upper leg, or wrist
 ***After age 50 years

Table
 Disclosures: Derek Weycker, Amgen Inc.
 This study received funding from: Amgen Inc.

SA0283

Recurrent major osteoporotic fracture in older men: the Osteoporotic Fractures in Men Study. Carrie Nielson*¹, Elizabeth Hooker¹, Jodi Lapidus¹, Lynn Marshall¹, Peggy Cawthon², Margaret Lee Gourlay³, Doug Bauer⁴, Jane Cauley⁵, Kristine Ensrud⁶, Nancy Lane⁷, Eric Orwoll¹. ¹Oregon Health & Science University, USA, ²California Pacific Medical Center, USA, ³University of North Carolina, USA, ⁴University of California, San Francisco, USA, ⁵University of Pittsburgh, USA, ⁶University of Minnesota, USA, ⁷University of California, Davis, USA

Background: Major osteoporotic fracture (MOF) is a risk factor for recurrent fracture and mortality. We examined characteristics of men with an incident MOF and the risk factors for a subsequent MOF, considering the competing risk of mortality.

Methods: The incidence rate of MOF, which included a hip, wrist, shoulder, or clinically detected spine fracture, was calculated in men age 65 or older in the Osteoporotic Fractures in Men (MrOS) study with at least 30 days of follow-up (N=5987). In the 585 men with an initial MOF (ages 65-98), potential risk factors from the study visit preceding the first MOF were evaluated for their associations with a subsequent MOF using Cox proportional hazards regression accounting for the competing risk of mortality. All models were minimally adjusted for age, clinic site, and race; and a multivariable model included all variables with $p < 0.2$ in minimally adjusted models.

Results: The incidence of first MOF in the full cohort was 9/1000 man-years and ranged from 5/1000 in men ages 65-69 to 28/1000 in those age 85 or older. In men with a first MOF, the incidence of second MOF was at least doubled in every age group (ranging from 31/1000 in 70-74 year old men to 71/1000 in 85+ men) and was highest after an initial clinical vertebral fracture (68/1000 man-years).

In men with an initial MOF, common conditions at the most recent clinic visit were frailty (27%), self-reported mobility limitations (29%), inability to complete a 6-

m narrow walk test (26%), osteopenia (56%) and osteoporosis (10%). 9% of men used an osteoporosis medication. Low BMD was a strong independent risk factor for subsequent MOF (HR: 1.5 per SD decrease in total hip BMD, 95% CI: 1.2-1.9). Contrary to expectation, *inability* to complete a 6-m narrow-walk test was independently associated with lower risk of recurrent fracture (HR: 0.5, 95% CI: 0.3-0.96).

Conclusions: The incidence of recurrent MOF rose dramatically after a first MOF in older men, and low BMD was a potentially modifiable risk factor. Further investigation of lifestyle and functional characteristics of men with an initial MOF may elucidate mechanisms by which inability to complete a narrow walk affects subsequent fracture. This research may have implications for improving rehabilitation and long-term fracture prevention following a first MOF. Identifying safe ways for older men to be active should be a priority to aid in recovery from the initial fracture and reduce the risk of a second fracture.

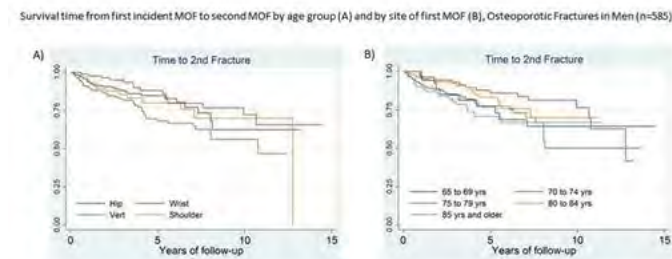


Figure: Survival time from first incident MOF

Disclosures: *Carrie Nielson, None.*

SA0284

Serum phosphate levels are associated with fracture risk: the Rotterdam Study. Natalia Campos¹, Nadia Koek², Bram C van der Eerden³, Fernando Rivadeneira⁴, Albert Hofman⁵, Johannes van Leeuwen³, André G Uitterlinden³, M Carola Zillikens³. ¹Erasmus MC, The Netherlands, ²Department of Internal Medicine, Erasmus Medical Center, Netherlands, ³Department of Internal Medicine Erasmus Medical Center, Netherlands, ⁴Department of Internal Medicine, Netherlands, ⁵Department of Epidemiology, Erasmus Medical Center, Netherlands

Abnormal serum phosphate levels (P) have been associated with specific bone mineral density (BMD) phenotypes, such as rickets/osteomalacia and tumoral calcinosis. Nevertheless, the nature of an association of phosphate levels with BMD and fracture risk in the general population is unknown. We tested these relations in elderly Dutch participants from the Rotterdam Study (RS). Fasting serum phosphate was measured with same technique across cohorts; BMD at the femoral neck (FN-BMD) and lumbar spine (LS-BMD) was assessed by dual X-ray absorptiometry (DXA). The association between P and BMD was tested through linear models using three cohorts (RS-I, RS-II and RS-III). We applied competing risk regression models to assess the relation between P and prospective all-type fracture risk in two RS cohorts (RS-I and RS-II). Basic adjustments included age, BMI and smoking. Betas (β (95% CI)) and hazard ratios (HR(95% CI)) were meta-analyzed applying fixed-effect model. Results are expressed per 1 mg/dL increase in P. In BMD analyses, the initial unadjusted significant association of P with BMD at both skeletal sites in women was abolished after adjustment for body mass index (LS-BMD: 0.003(-0.09 to 0.09); FN-BMD: 0.01(-0.06 to 0.07)). In men, P was inversely related only to LS-BMD (-0.13(-0.23 to -0.02)) and this association was not substantially modified after further adjustments for calcium and 25-hydroxyvitamin D levels (-0.11(-0.22 to -0.001)). We found a positive association between P and all-type fracture risk in both sexes (men: 1.54(1.20-1.97); women: 1.23(1.01-1.49); sex-combined: 1.35(1.15-1.58)). Results were similar after further adjustments for levels of calcium, 25-hydroxyvitamin D, kidney function (defined as creatinine-based estimated glomerular filtration rate) and BMD (men: 1.57(1.11-2.22); women: 1.30(1.04-1.64)), or after restricting analyses with subjects with normal kidney function (men 1.81(1.28-2.55); women: 1.25(1.01-1.55)). To conclude, P was negatively related to LS-BMD in men but not women, and no association with FN-BMD was found in either sex. P was positively related to all-type fracture risk in both sexes. Our findings suggest that increased P even within normal range might be deleterious for bone health in the normal population

Disclosures: *Natalia Campos, None.*

SA0285

Bone turnover status in older Hispanic women with type 2 diabetes: preliminary data from the Cameron County Hispanic Cohort in Texas. Nahid Rianon^{*1}, Scott Smith², Matthew Hnatow³, Susan Fisher-Hoch⁴, Joseph McCormick⁵, Catherine Ambrose⁶. ¹UTHealth The University of Texas Medical School at Houston, USA, ²NASA, USA, ³University of Texas Medical School at Houston, USA, ⁴University of Texas School of Public Health, Brownsville Regional Campus, USA, ⁵University of Texas School of Public Health Brownsville Regional Campus, USA, ⁶University of Texas Medical School at Houston, USA

Fracture risk is elevated in individuals with type 2 diabetes (T2D) although, paradoxically, bone mineral density (BMD) is similar or higher than those without diabetes. Bone turnover, which is normally higher in older osteoporosis patients, has been reported to be lower in T2D patients. Limited human studies have reported associations between higher glycated hemoglobin levels (HbA1c) and lower serum osteocalcin (a marker of bone turnover) in older T2D patients. As most of these studies were conducted among Caucasian and Asian populations, there is a gap in knowledge about bone turnover status in Hispanic populations where there is a higher than average prevalence of diabetes. Prevalence of T2D is about 30% in the Cameron County Hispanic Cohort (CCHC) in TX, mostly with high HbA1c. This homogeneous cohort provides a unique opportunity to evaluate bone turnover, monitor risk, and design prevention and treatment of fragility fracture in high risk Hispanic T2D individuals.

BMD was measured using DXA and serum samples analyzed for bone biochemical markers. We present the preliminary cross-sectional results from 23 Hispanic T2D women (≥ 65 years) from the CCHC at baseline and compared them with an age-matched cohort without diabetes from our outpatient osteoporosis clinic in Houston, TX.

Compared to the non-diabetic controls, the T2D individuals had similar femoral neck BMD ($p=0.62$) and T-scores ($p=0.59$). Serum osteocalcin, PTH, magnesium, and vitamin D levels were significantly ($p<0.05$) lower in T2D group. Serum calcium and phosphorous levels were higher in the T2D individuals (not statistically significant). These results are similar to those previously reported for Caucasian and Asian T2D cohorts, which report lower bone turnover in T2D individuals.

Anti-resorptive drugs are frequently prescribed as a first line agent for treating osteoporosis in older individuals with osteoporosis based on BMD or fragility fracture, assuming they have high bone turnover. Our results of lower bone turnover in older Hispanic T2D individuals, therefore, raises concern of even more suppressed bone turnover in this group if treated with anti-resorptive therapy, more so in those with high HbA1c. Further longitudinal research is recommended to answer such concerns. We will continue to monitor this T2D cohort to determine the trend of bone turnover, relationships between HbA1c and bone turnover markers, and risk of fracture in diabetic patients of Hispanic heritage.

Disclosures: *Nahid Rianon, None.*

SA0286

Circulating Sclerostin Level in the Elderly with and without Hip Fracture: A Prospective Case-Control Study. Ji WAN Kim^{*1}, Jai Hyung Park², Seong-eun Byun³, Jae Suk Chang⁴. ¹Haeundae Paik Hospital, Inje University, South Korea, ²Orthopaedic Surgery, Kangbuk Samsung Hospital, Sungkyunkwan University, South Korea, ³Orthopaedic Surgery, CHA Bundang Medical Center, CHA university, South Korea, ⁴Orthopaedic Surgery, Asan Medical Center, University of Ulsan, South Korea

Purpose Sclerostin is a protein secreted by osteocytes, and inhibits bone formation. The aim of this study was to compare the laboratory hallmark of osteoporosis and the serum sclerostin level between hip fracture patients and non-fracture group. Methods We conducted a prospective case-control study of 103 participants who admitted to our hospital for the surgery of hip fracture or osteoarthritis from April 2011 to Mar 2014. Serum specimens were collected, and clinical data including age, gender, height, weight, and bone mineral density (BMD), were obtained. After collecting data, case and control patients with available data were precisely matched according to sex and age. The 32 patients were enrolled into each group. We compared the sclerostin levels, laboratory parameters of bone and mineral metabolism and BMD. Results In the fracture group, the sclerostin level was 0.61ng/mL and 0.17ng/mL in the fracture group and control group, and this difference was statistically significant ($p=0.004$). The mean osteocalcin level was significantly lower (15.4ng/mL) in the fracture group than in the control group (21.8ng/mL, $p=0.048$). PTH level was higher in the fracture group (40.1 vs 28.6pg/mL, $p=0.010$), but both result were normal range (10-65pg/mL). There was no significant difference in the serum level of C-telopeptide and alkaline phosphatase, 25 (OH) D, phosphorus and calcium. Bone mineral density (BMD) was lower in the fracture group ($p<0.001$), but body mass index were not different in two groups. Conclusion The serum sclerostin level was higher and the serum osteocalcin level was lower in the fracture group. We concluded that lower ability of bone formation can be in charge of hip fracture besides low BMD.

Disclosures: *Ji WAN Kim, None.*

SA0287

Comparison of Vertebral Density, Structure, Strength, and Fracture Rate between Hong Kong Chinese and US Caucasian Older Men. Jian Shen¹, Lynn Marshall², Carrie Nielson³, David Lee⁴, Tony Keaveny⁴, Jodi Lapidus⁵, Dennis Black⁶, Jane Cauley⁷, Anthony Kwok⁸, Timothy Kwok⁸, John Schousboe⁹, Eric Orwoll³. ¹Oregon Health & Science University, USA, ²Department of Orthopedics & Rehabilitation, Oregon Health & Science University, USA, ³Department of Medicine, Bone & Mineral Unit, Oregon Health & Science University, USA, ⁴O.N. Diagnostics, USA, ⁵Division of Biostatistics, the Department of Public Health & Preventive Medicine, Oregon Health & Science University, USA, ⁶Department of Epidemiology & Biostatistics, University of California San Francisco, USA, ⁷Department of Epidemiology, Graduate School of Public Health, University of Pittsburgh, USA, ⁸Jockey Club Centre for Osteoporosis Care & Control, & Department of Medicine & Therapeutics, Chinese University, Hong Kong, ⁹University of Minnesota, USA

Osteoporotic fracture is a major public health problem in US and has become an increasingly important concern in Asia. However, differences between these two populations in vertebral structure, volumetric density (vBMD) and vertebral fracture rates are not well understood. Quantitative computed tomography (QCT) scans of the lumbar spine (L1-L2) were acquired in 318 Hong Kong (HK) Chinese and 177 US Caucasian men ≥ 65 yr (mean age: 75y for HK; 74y for US) who were randomly selected from the Osteoporotic Fractures in Men Study (MrOS) cohorts in HK and US. QCT image processing was performed centrally and calibrated to minimize the between-clinical site variation. Finite element analysis (FEA) was used to estimate vertebral strength under compressive loading. We used body weight and height to estimate a compressive force for forward bending at the waist, and a load-to-strength ratio was calculated. Areal BMD (aBMD) was assessed with DXA. Multivariable general linear models with linear contrast were used to compare least square means of the vertebral measures between the HK and US men adjusted for age, weight, height and US enrollment sites. Incident vertebral fractures were assessed (HK: 1544; US: 3978) using semiquantitative (SQ) scoring of lateral thoracic and lumbar radiographs. Fractures were defined as a change in SQ grade ≥ 1 from baseline to follow-up (mean: 3.99 y for HK; 4.56 y for US). We calculated the annualized binomial proportion and 95% confidence interval (CI) for a new or worsening of fracture. Compared to US Caucasian men, HK men were smaller in stature and had 13% lower areal lumbar spine aBMD, 11% smaller vertebral cross-sectional area and 13% lower total compressive strength (Table). After adjustment, these parameters did not differ between groups, although vertebral body height remained higher for the US. The two populations had similar vBMD (from QCT). The load-to-strength ratio was better (21% lower) in HK Chinese than in US Caucasians. Consistent with the trends for the load-to-strength ratio, the annualized vertebral fracture incidence was lower in HK Chinese at 0.68% (0.48%-0.88%) than in US Caucasian men at 1% (0.85%-1.13%). HK Chinese and US Caucasian men had similar vBMD, but differences in vertebral structure and strength that were mainly explained by body size. HK Chinese men had more favorable load-to-strength ratio and this biomechanical advantage appears to provide an explanation for their lower risk of vertebral fractures.

Table. Vertebral density, structure and strength by two populations^{*}

| | Hong Kong Chinese (n=318) | | US Caucasian (n=177) | | % Diff | P-value ¹ | P-value ² | P-value ³ |
|--|------------------------------|-------------------|-------------------------|---------------|---------|----------------------|----------------------|----------------------|
| | Mean \pm SD | Mean \pm SD | Mean \pm SD | Mean \pm SD | | | | |
| Bone density | | | | | | | | |
| DXA aBMD(g/cm ²) | 0.93 \pm 0.19 | 1.07 \pm 0.17 | -13 | <0.0001 | <0.0001 | 0.53 | | |
| Total vertebral vBMD (mg/cm ³) | 186 \pm 38 | 186 \pm 35 | 0 | 0.89 | 0.85 | 0.16 | | |
| Trabecular vBMD (mg/cm ³) | 101 \pm 34 | 101 \pm 27 | 0 | 0.9 | 0.75 | 0.24 | | |
| Bone Geometry | | | | | | | | |
| Min transverse cross-sectional area (mm ²) | 1223 \pm 144 | 1371 \pm 162 | -11 | <0.0001 | <0.0001 | 0.98 | | |
| Vertebral heights anterior (mm) | 26.1 \pm 1.6 | 28.2 \pm 1.9 | -7.4 | <0.0001 | <0.0001 | <0.0001 | | |
| Strength | | | | | | | | |
| Overall strength under compressive loading (N) | 6435 \pm 1939 | 7424 \pm 2071.2 | -13 | <0.0001 | <0.0001 | 0.57 | | |
| Trabecular strength (N) | 3340 \pm 1196 | 3944 \pm 1343 | -15 | <0.0001 | <0.0001 | 0.6 | | |
| Load-to-strength ratio | 0.254 \pm 0.073 | 0.32 \pm 0.092 | -21 | <0.0001 | <0.0001 | N/A | | |

¹ Unadjusted; ² adjusted for age and site; ³ adjusted for age, site, height and weight^{*} The difference between site-adjusted US and HK groups was compared via test of contrast of regression coefficient.

Vertebral density, structure and strength by two populations

Disclosures: Jian Shen, None.

SA0288

Insulin Resistance and Composite Indices of Femoral Neck Strength in Asians: the Fourth Korea National Health and Nutrition Examination Survey (KNHANES IV). Seong Hee Ahn^{*}, Hyeonmok Kim, Beom-Jun Kim, Seung Hun Lee, Woo Je Lee, Jung-Min Koh, Asan Medical Center, University of Ulsan College of Medicine, South Korea

Purpose: The fracture risk in type 2 diabetes mellitus with insulin resistance increases, despite relatively conserved bone mineral density (BMD). In this present

study, we investigated the relationship between insulin resistance and composite indices of femoral neck strength in Koreans.

Methods: This was a population-based, cross-sectional study from Korea National Health and Nutrition Examination Survey, including 1,243 men and 1,433 women. Insulin resistance was evaluated using the homeostasis model assessment-estimated insulin resistance (HOMA-IR) index. Femoral neck width and axis length were measured from hip dual-energy X-ray absorptiometry scans and combined with BMD, weight, and height to calculate composite indices of femoral neck strength relative to load: compression (CSI), bending (BSI) and impact strength indices (ISI).

Results: HOMA-IR showed an inverse relationship with CSI, BSI and ISI in both genders before and after adjusting for confounders ($P < 0.001-0.029$). CSI was more strongly associated with HOMA-IR than BSI and/or ISI in both genders ($P < 0.001-0.013$). When men were stratified according to HOMA-IR quartiles, all strength indices decreased as the quartile increased after adjusting for all potential confounders (P for trend $< 0.001-0.001$), and CSI and ISI did in women (P for trend = 0.012 and 0.002, respectively). Serum fasting insulin levels, but not glucose levels, were negatively associated with all strength indices regardless of confounders ($P < 0.001-0.044$).

Conclusion: Insulin resistance is associated with low femoral neck strength, particularly against the compressive load. These findings suggest a better approach to evaluate bone health in insulin-resistant individuals.

Disclosures: Seong Hee Ahn, None.

SA0289

Mortality risk following incident low-trauma osteoporotic fracture and subsequent fracture: 15-year prospective data from the Canadian Multicentre Osteoporosis Study (CaMOS). Thach Tran^{*}, Dana Bliuc¹, Dunia Alarkawi¹, Tuan Nguyen¹, John Eisman¹, Lisa Langsetmo², Jerilynn C Prior³, Robert G Josse⁴, Stephanie M Kaiser⁵, Christopher S Kovacs⁶, Claudie Berger², David Goltzman², David A Hanley⁷, Jonathan Adachi⁸, Teneke van Geel⁹, Piet Geusens⁹, Joop van den Bergh⁹, Jacqueline Center¹. ¹Garvan Institute of Medical Research, Australia, ²McGill University, Canada, ³University of British Columbia, Canada, ⁴University of Toronto, Canada, ⁵Dalhousie University, Canada, ⁶Memorial University, Canada, ⁷University of Calgary, Canada, ⁸McMaster University, Canada, ⁹Maastricht University, Netherlands

Data on long-term consequences of osteoporotic fracture other than spine and hip are scanty. This study examined the risk of premature mortality associated with different types of low-trauma fracture and subsequent fracture.

Participants in the Canadian Multicentre Osteoporosis Study, an on-going population-based cohort study of Canadians, were followed for 15 years with scheduled interviews and annual postal questionnaires. Incident fractures were identified from annual self-reports and deaths ascertained through contact with a member family or obituary review. 7687 participants (5525 women and 2162 men) aged ≥ 50 years had one or more subsequent visits. Age- and sex-specific standardized mortality ratios (SMRs) for specific fracture types were compared with the representative general Canadian population.

There were 1494 low-trauma fractures followed by 307 deaths in women, and 337 fractures followed by 97 deaths in men. Osteoporotic fractures doubled the risk of subsequent fracture (relative risk: 2.05, 95% confidence interval (CI): 1.84-2.28 in women and 2.55, 1.95-3.30 in men). Risk of death 5 years post-fracture was increased for participants sustaining low-trauma fracture (age-adjusted SMR: 2.38, 95% CI: 2.04-2.75 in women, and 2.63, 2.01-3.37 in men). The risk was increased after virtually every fracture type (see table). The SMR for most fracture types, except for hand, finger, foot and toe, were of similar effect size between women and men; but the risk of several types was not statistically significant presumably due to smaller numbers. Mortality risk was increased for a further 5 years after a subsequent fracture (SMR: 1.83, 95% CI: 1.37-2.39 in women and 2.23, 1.25-3.68 in men). SMRs were higher if fracture occurred before 75 years of age. The most parsimonious model predicting premature mortality included age, current smoking, comorbidities and fracture type. Higher education level was associated with lower risk for women, but not men. Excessive mortality for the first 5 years post fracture was found for virtually all incident low-trauma fractures. The risk was increased for an additional 5 years after subsequent fracture. This study highlights the need for early intervention to decrease subsequent fracture risk and potentially mortality.

Table: Age-adjusted standardized mortality ratios (SMR) for specific type of fracture

| Fracture types | Women | Men |
|------------------------------------|--------------------|--------------------|
| Clinical vertebral | 3.26 (2.15-4.74)* | 3.40 (1.47-6.71)* |
| Hip | 2.12 (1.52-2.88)* | 3.08 (1.80-4.94)* |
| Rib | 3.80 (2.48-5.57)* | 2.20 (1.26-3.57)* |
| Humerus | 1.88 (1.05-3.09)* | 4.09 (1.11-10.45)* |
| Forearm | 2.82 (1.98-3.91)* | 2.35 (0.64-6.02) |
| Pelvis | 1.97 (0.85-3.91) | 1.80 (0.22-6.51) |
| Upper Leg | 4.00 (1.09-10.24)* | 7.40 (0.90-26.76) |
| Lower Leg (knee, ankle, lower leg) | 2.06 (1.07-3.60)* | 1.33 (0.16-6.53) |
| Distal (hand, finger, foot, toe) | 1.29 (0.62-2.37) | 2.50 (0.91-5.44) |

Data presented as age-adjusted standardized mortality ratios (SMR) and 95% confidence interval.

*: statistical significance.

Age-adjusted standardized mortality ratios (SMR) for specific type of fracture

Disclosures: Thach Tran, None.

SA0290

Osteoporosis Treatment is Associated with Better Post-fracture Survival: A 15-Year Prospective Study from Canadian Multicentre Osteoporosis Study.

Dana Bliuc*¹, Thach Tran¹, Dunia Alarkawi¹, Tuan Nguyen¹, John Eisman¹, Claudie Berger², Lisa Langsetmo², David Hanley³, David Goltzman², Jerilynn Prior⁴, Robert Josse⁵, Stephanie Kaiser⁶, Christopher Kovacs⁷, Rick Adachi⁸, Tineke van Geel⁹, Piet Geusens¹⁰, Joop Van Den Bergh¹⁰, Jacqueline Center¹. ¹Garvan Institute of Medical Research, Australia, ²McGill University Health Center, Canada, ³University of Calgary, Canada, ⁴University of British Columbia, Canada, ⁵Toronto CaMOS Center, Canada, ⁶Halifax CaMOS Center, Canada, ⁷St John's CaMOS Center, Canada, ⁸Hamilton CaMOS Center, Canada, ⁹Maastricht University, Netherlands, ¹⁰Maastricht University Medical Center, Netherlands

Osteoporotic fractures are associated with increased risk of mortality. There is evidence that bisphosphonates not only reduce the risk of future fracture but may also reduce post-fracture mortality. This study aimed to examine the effect of osteoporosis medication on mortality risk following low trauma fracture in women and men aged 50+ years, participating in the ongoing population-based Canadian Multicentre Osteoporosis Study (CaMOS).

During 15 years of follow-up (1996-2011), 1165 incident low trauma fractures (971 and 194 in women and men, respectively) were reported. Bone mineral density, information on co-morbidities, medication, and lifestyle were obtained. Treatment groups were classified as: bisphosphonates (BP), and no treatment (NoRx). Osteoporotic fractures were classified into 4 groups: hip, clinical vertebral, proximal and distal skeleton. There were 932 participants treated with BP (841 women and 91 men), and 233 who did not receive any treatment for osteoporosis. Individuals on BP had a higher proportion of fracture risk factors, such as lower BMD, BMI and weight compared to NoRx. The proportion of vertebral fractures was also higher in BP group. There were 299 deaths (168 and 35 in women and men, respectively) over 7,126 person-years follow-up (6,077 and 1,048 in women and men, respectively). Independent predictors of mortality risk in the fracture cohort were older age, male gender, having at least one co-morbid disease, low BMD, lower weight and being inactive. Hip, clinical vertebral and proximal fractures were also independently associated with mortality risk. Notably, despite having a less favourable risk profile, BP treatment was associated with better survival compared to NoRx after adjusting for age, BMD and clinical factors in women [adjusted HR 0.35 (95% CI, 0.23-0.54)] with a similar, albeit non-significant, effect in men [adjusted HR 0.50 (95% CI, 0.39-1.46)]. The reduction in mortality rates was not due to a decrease in the risk of subsequent fracture [subsequent fracture adjusted HR 0.40 (95% CI, 0.26-0.62) and 0.73 (95% CI, 0.42-1.29) for women and men, respectively]. This study has a caveat. The proportion of people who did not receive any treatment (NoRx) is relatively small (20%). Although further analyses is required to assess whether treatment selection criteria may play a role in this outcome, these data suggest that bisphosphonates reduce the risk of post-fracture mortality, particularly in women.

Disclosures: Dana Bliuc, None.

SA0291

A Multi-Sector Public-Private Partnership Working Together to Improve America's Bone Health. Debbie Zeldow¹, David Lee*². ¹National Bone Health Alliance, USA, ²NBHA, USA

The National Bone Health Alliance (NBHA, www.nbha.org) is a public-private partnership launched in late 2010 that brings together the expertise and resources of its members to collectively promote bone health and prevent disease; improve diagnosis and treatment of bone disease; and enhance bone research, surveillance and evaluation. NBHA currently includes 53 participating organizations (29 non-profit

member organizations, 18 member companies and liaisons representing CDC, CMS, FDA, NASA and NIH).

The concept for NBHA stems from the 2004 Bone Health and Osteoporosis: A Report of the Surgeon General and the June 2008 Summit for a National Action Plan for Bone Health. NBHA's "20/20 vision" is to reduce the incidence of bone breaks 20% by the year 2020.

NBHA provides a platform for its collective voice to weigh in on subjects important to bone health, particularly vitamin D, calcium, bone mineral density reimbursement and utilization and the risks and benefits of the use of bone health therapies; communication among organizations interested in bone health; shared priorities to become reality through pooled funding; and working together towards the goals and recommendations of the National Action Plan.

Fracture Prevention CENTRAL: An online resource center which provides tools to support the implementation of a FLS program including resources, case studies, best practices, business plans and over a dozen webinars - www.FracturePreventionCENTRAL.org .

FLS Pilot: This demonstration study will assess 3 hospitals' adoption and implementation of a FLS across their communities and measure improvement in performance around selected quality measures.

Bone Turnover Marker Standardization Project: NBHA is leading the effort to standardize U.S. bone marker sample collection procedures and standardize bone turnover marker assays used in clinical laboratories through a variety of related efforts, including a bisphosphonate drug holiday study, inter-laboratory and inter-method comparison studies, patient sample collection procedure standardization and development of a standardized reference database project.

2Million2Many: This national awareness campaign is educating health care professionals and the public about the 2 million bone breaks in the U.S. each year that are not accidents but signs of osteoporosis. Campaign materials for both the consumer and provider are available - www.2Million2Many.org microsite.

Disclosures: David Lee, None.

SA0292

Awareness and Reasons for Lack of Post-Fracture Osteoporosis Therapy: A

Survey of Post-Menopausal Women. Denise Boudreau¹, Onchee Yu², Akhila Balasubramanian³, Jane Grafton², Jackie Saint-Johnson², Hiedi Wirtz³, Andreas Grauer³, Barry Crittenden³, Delia Scholes*⁴. ¹Group Health Research Institute, Wake island, ²Group Health Research Institute, USA, ³Amgen Inc., USA, ⁴Group Health Cooperative/Group Health Research Institute, USA

Purpose: Osteoporotic fractures cause patient morbidity and increase risk for future fracture. Effective drug therapies for osteoporosis (OP) are available, yet only a minority of women receives osteoporosis pharmacotherapy (OP-Rx) post-fracture. Reasons for lack of post-fracture OP-Rx are not well understood. We undertook the first large scale survey of women with recent osteoporotic fractures to characterize their beliefs about OP and their physician interactions, and to understand the factors associated with lack of post-fracture OP-Rx. Methods: A survey was mailed to 985 women, aged >55 years with an osteoporotic fracture in 2013-2014, who were enrollees of Group Health Cooperative, a large Northwest health plan. Receipt of OP-Rx in the 6 months post-fracture was determined from automated pharmacy data. The associations between factors of interest and non-receipt of post-fracture OP-Rx were assessed using age-adjusted modified Poisson regression with a robust sandwich estimator. Results: 634 women returned the survey (73% response rate, excluding 119 ineligible); mean age was 75 (SD 11.1) and 77% were white. Primary fracture sites were distal forearm (31%), hip (27%), spine (14%), and humerus (18%). 84% of women did not receive OP-Rx within 6 months post fracture. Even among the 11% of women who were on OP-Rx prior to fracture, 40% did not continue therapy following the fracture. Only 20% of all respondents believed that OP-Rx reduces risk of fracture. Women who were not concerned about OP or future fractures, did not think OP caused their fracture, did not think OP-Rx was effective in reducing fractures, or did not believe a fracture put them at risk for future fracture were at increased risk for non-receipt of OP-Rx (Table). Similarly, women who did not discuss OP management or fracture prevention with their physicians, and whose primary source of information on OP was the media or family and friends rather than their medical providers were also at higher risk for not receiving OP-Rx. Conclusions: The majority of women who suffered an OP fracture did not receive OP-Rx in the 6 months post-fracture. This study suggests that patient education about OP, the risk for future fracture after an initial fracture, and the potential benefits of therapy – through physician input or potentially other reliable sources – may help reverse the substantial under-treatment of women post-fracture.

Table. Association between patient perspectives and interactions with medical providers on non-receipt of osteoporosis pharmacotherapy (OP-Rx) within 6 months of osteoporotic fracture

| | | Relative Risk ¹ | 95% CI |
|--|-------------------------------------|----------------------------|-----------|
| Patient self-reported perspectives and beliefs on osteoporosis and fracture | | | |
| Concerned about their future risk of fractures | Not at all vs. very/somewhat | 1.13 | 1.05-1.21 |
| Concerned about osteoporosis | Not at all vs. very/somewhat | 1.21 | 1.14-1.28 |
| Believe a fracture puts them at risk for future fractures | No vs. yes | 1.17 | 1.09-1.25 |
| Believe osteoporosis caused their fracture | No vs. yes | 1.31 | 1.15-1.48 |
| Believe OP-Rx reduces risk of fracture | No vs. yes | 1.22 | 1.09-1.36 |
| Believe harms of OP-Rx outweigh benefits | Yes vs. no | 1.06 | 0.98-1.14 |
| Interactions with medical providers on osteoporosis and fractures | | | |
| Primary source of information on osteoporosis | Media vs. medical provider | 1.13 | 1.05-1.21 |
| | Family/friends vs. medical provider | 1.20 | 1.11-1.30 |
| PCP aware of fracture | No vs. yes | 1.08 | 1.00-1.17 |
| Told had osteoporosis by provider | No vs. yes | 1.25 | 1.16-1.36 |
| Provider recommendation to prevent fractures and/or manage osteoporosis | OP-Rx | (ref) | |
| | Other (e.g. supplements, diet) | 1.89 | 1.61-2.21 |
| | No recommendation | 1.85 | 1.57-2.19 |
| Contact with PCP post fracture | No vs. yes | 1.03 | 0.92-1.15 |
| Discussed preventing fractures | No vs. yes | 1.13 | 1.04-1.24 |
| Discussed managing osteoporosis | No vs. yes | 1.38 | 1.23-1.54 |
| Osteoporosis was among top 3 topics discussed at PCP visits | No vs. yes | 1.34 | 1.21-1.49 |
| Time spent with PCP | Not enough vs. enough | 0.92 | 0.78-1.08 |

Abbreviations: OP-Rx—osteoporosis pharmacotherapy; PCP—primary care provider
¹All risk estimates, except for age, are adjusted for age.

Table 1

Disclosures: Delia Scholes, Amgen
 This study received funding from: Amgen Inc.

SA0293

In-Hospital Assessment and Management of Falls in the Elderly. Anna O'Connor^{*1}, Monidipa Dasgupta², Lisa-Ann Fraser². ¹Schulich School of Medicine & Dentistry, University of Western Ontario, Canada, ²University of Western Ontario, Canada

Objectives: A thorough falls assessment can successfully reduce future fall events and injuries, making it an important part of fall care in the elderly presenting to hospital with a fall. However, the frequency with which patients receive such an assessment is not known. We sought to characterize the assessment and management of elderly patients presenting to hospital with a fall. **Methods:** Records from a tertiary care center between 2003-2014 were searched. A random sample of 180 charts (96 ED and 84 inpatient), describing visits for a "fall" in individuals = 65 year, were selected. Paper and electronic charts were reviewed using a detailed pre-specified data abstraction form. **Results:** Of the 180 patients studied, mean age was 80.2 years (SD=8.46), and 66.1% were women. Many (38.9%) lived at home with family, 20.6% lived alone, and 21.1% lived in nursing homes (NH) or assisted living. Fall related injuries were common with 59.5% sustaining a new fracture. Other serious consequences of falls included: need for a new assistive walking device (21%), new wheelchair dependence (6.3%), other permanent disability (1.7%), new admission to a nursing home (2.8%), and death (3.9%). In terms of falls assessment, only 1.1% of patient charts had documentation of the presumed etiology of their fall on the discharge summary. Similarly, orthostatic blood pressure was documented in 1.7% of patients, 2.2% had a visual assessment, 11.1% underwent formal assessment of cognition, and 17.8% had a medication review. Of the patients who were discharged, 19.2% had no follow-up arranged. Despite the fact that the majority of patients had new fractures, including 83 (46.1% of the cohort) lower limb fractures, only 30 (17.1%) were discharged on Vitamin D, 25 (14.3%) on calcium, and 17 (9.7%) on a bisphosphonate. **Conclusions:** Despite the serious health consequences in elderly patients who presented to the hospital with a fall, very few received a proper falls assessment or an adequate treatment plan. These results suggest a significant care gap and highlight an area of opportunity for future quality improvement.

Disclosures: Anna O'Connor, None.

SA0294

Miami Veterans Health Administration Fracture Prevention Program. Violet Lagari^{*1}, Andreina Rojas², Silvina Levis², Zeina Hannoush², Marilu Jurado², Daisy Acevedo², Ngina Muigai². ¹University of Miami, USA, ²University of Miami School of Medicine & Miami VA Health System, USA

Introduction
 Osteoporosis is a public health problem affecting more than 200 million people worldwide. Although the general awareness about osteoporosis and its consequences has been steadily increasing, rates of osteoporosis medication use after a fracture have declined significantly from 40.2% in 2002, to 20.5% in 2011. In 2012, an expert task force encouraged the implementation of a "fracture Liaison Service" to prevent secondary fractures which, when implemented, has shown to significantly improve

treatment for osteoporosis after an initial fracture. VA Office of Inspector General 2010 report stated that only 42% of veterans with osteoporotic fractures had received recommended management.

Methods

We identified veterans 50 years of age and older with an ICD-9 of fracture in calendar year 2012 who had one or more visits to a primary care provider (PCP) at Miami VA in 2012. We excluded patients with non-osteoporotic fractures, remote fractures, those who had a DXA scan, or were already on or declined treatment. Electronic medical records were reviewed to confirm eligibility criteria and generate a list stratified by PCP. A secure email message was sent to the PCPs listing the patients who had sustained an osteoporotic fracture and offering 3 different follow up options: start medical therapy, request an endocrinology e-consult or referral to endocrinology. We will reevaluate what measures were taken to improve care 6 months after the email was sent.

Conclusion

We expect that the implementation of an outpatient secondary fracture prevention program at the Miami VA will result in increased rates of treatment of veterans with osteoporotic fractures.

Disclosures: Violet Lagari, None.

SA0295

Osteoporosis-Related Knowledge, Self-Efficacy and Health Beliefs Among Chinese Breast Cancer Survivors. Evelyn Hsieh^{*1}, Qin Wang², Liana Fraenkel¹, Elizabeth Bradley³, Weibo Xia⁴, Karl Inosogna¹, Jennifer Smith⁵, Youlin Qiao², Pin Zhang². ¹Yale School of Medicine, USA, ²Cancer Institute & Hospital, Chinese Academy of Medical Sciences, China, ³Yale School of Public Health, USA, ⁴Peking Union Medical College Hospital, China, ⁵UNC Gillings School of Public Health, USA

Women with breast cancer (BC) are at increased risk for fracture. Understanding behavioral factors that influence adoption of fracture prevention measures in this population is critical. Utilizing concepts from the Health Beliefs Model, we sought to evaluate osteoporosis-related knowledge, self-efficacy, and health beliefs among a cohort of breast cancer survivors in China.

From April to August 2014, BC survivors at the Cancer Institute and Hospital of the Chinese Academy of Medical Sciences were invited to participate in this cross-sectional study. Eligibility criteria: 50-70 years of age, no history of prior osteoporosis or metabolic bone disease. Measures: A mandarin-language questionnaire including sociodemographic and fracture risk assessment, the International Physical Activity Questionnaire, a calcium and vitamin D intake scale, the Osteoporosis Knowledge Test (OKT), Osteoporosis Self-Efficacy Scale (OSES), and Osteoporosis Health Beliefs Scale (OHBS).

Two hundred women were enrolled with a mean age of 57.5 ± 4.9 yrs, and BMI of 24.9 ± 3.7 kg/m². Fifty-three percent reported high levels of physical activity, and on average women reported consuming calcium/vitamin D-rich foods more than once weekly. Mean OKT score was 11.9 ± 3.8 (scale: 0 to 26). OSES scores (scales: 0 to 100) reflected greater confidence for adopting dietary intake behaviors (89.3 ± 12.8) compared with exercise-related behaviors (66.8 ± 15.2). OHBS scores (scales: 6 to 30) showed high levels of health motivation (26.7 ± 2.9), high perceived benefit to exercise and dietary calcium intake (25.9 ± 3.6 and 23.6 ± 3.3, respectively), and relatively low perceived barriers to these activities (14.0 ± 3.9 and 14.0 ± 3.5, respectively). Logistic regression adjusted for age and BMI showed that high dietary calcium/vitamin D intake was associated with fewer perceived barriers to dietary calcium intake (OR 0.84, 95%CI 0.77-0.93, p=0.001), and high physical activity level was associated with fewer perceived barriers to exercise (OR 0.92, 95%CI 0.84-0.99, p=0.04) and higher self-efficacy (1.02, 95%CI 1.01-1.05, p=0.02).

Despite high risk for fracture, women in our study demonstrated only moderate levels of knowledge regarding osteoporosis. Perceived barriers to dietary calcium intake and physical activity, as well as self-efficacy regarding physical activity may influence uptake of these behaviors. Understanding these associations can aid development of targeted fracture prevention measures.

Disclosures: Evelyn Hsieh, None.

SA0296

Real-World Clinical and Economic Outcomes In Daily Teriparatide Patients in Japan. Russel Burge¹, Masayo Sato^{*2}, Tomoko Sugihara³. ¹Eli Lilly & Company, USA, ²Eli Lilly Japan K.K., Japan, ³Inventiv Health Clinical, USA

Purpose: To estimate clinical and economic outcomes for daily teriparatide (d-TPD) patients in Japan in real-world clinical practice.

Data and Methods: A large database (Medical Data Vision Co., Ltd.) with medical and pharmacy claims from 121 hospitals in Japan was used for this study. From April 2008-July 2013, 1244 patients with an index prescription of d-TPD and with 6+ months' pre- and post-index observation were identified. Administered via daily 20mcg subcutaneous injection, d-TPD is indicated for individuals at high risk of fracture. From this sample, 445 patients had 18+ months of follow up, and were the

study's focus. Descriptive analyses were conducted on clinical vertebral and nonvertebral fractures, health care resource use, and costs. D-TPD adherence was measured by medication possession ratio (MPR) (High MPR ≥ 0.8; 0.5 < Medium < 0.8, low MPR < 0.5). Adjusted analyses of Lower (low+medium) MPR vs High MPR for fracture incidence and hospital admissions were performed using Logistic and Poisson regression models with Log-link, controlling for cross-group differences in demographics and clinical characteristics. Adjusted cost analyses used Propensity Bin Bootstrapping, controlling for baseline characteristics.

Results: Baseline patient characteristics were: mean age 74.7 years (SD=8.9); 90% female; 87% aged 65+; 20% had 1+ fracture. Post-index, 249 and 196 patients had High and Lower MPR, respectively. Mean incident fractures/1000 patient years for Lower and High MPR patients were 77.4 and 57.7, respectively. Adjusted risk of fracture was greater in Lower MPR patients in Logistic (OR=1.67, 95% CI=0.791, 3.541) and Poisson models (Incidence ratio, IR=1.505, CI=0.764, 2.966), though not statistically significant. Mean hospital admissions, length of stays, and surgeries are summarized in Table 1. Adjusted risk of hospital admission was significantly greater in Lower vs. High MPR patients (Logistic model: OR=1.85, CI=1.169, 2.921; Poisson model: IR=1.47, CI=1.137, 1.904). During d-TPD use High MPR patients had numerically lower inpatient and total unadjusted costs vs. Lower MPR patients. Adjusted inpatient costs were significantly less in High MPR patients, but outpatient and pharmacy costs were greater.

Conclusions: Better adherence to daily teriparatide revealed numerically lower fracture risk, and significant reductions in hospital admissions and costs. The small sample size limited the robustness of these results, however.

Table 1: Health Care Resource Use and Costs For Daily Teriparatide Patients Per Patient Per Month, Post-Index (N=445)

| Health Care Resource Use, Unadjusted~ | Hospital Admissions | Hospital Length of Stay | Outpatient Visits | Surgeries |
|---------------------------------------|---------------------|-------------------------|-------------------|-------------------|
| 18-month MPR | Mean (SD) | Mean days (SD) | Mean (SD) | Mean (SD) |
| Lower (<=80%) (N=196) | 0.182 (0.61) | 3.321 (7.345) | 1.84 (1.551) | 0.085 (0.203) |
| High (>80%) (N=249) | 0.028 (0.07) | 0.565 (1.646) | 1.535 (0.867) | 0.054 (0.068) |
| | Inpatient Hospital | Outpatient | Pharmacy | Total |
| Costs, Unadjusted~ | Mean (SD) | Mean (SD) | Mean (SD) | Mean (SD) |
| Lower (<=80%) (N=196) | 95,790 (197,813) | 20,214 (21,272) | 60,940 (28,919) | 176,943 (201,910) |
| High (>80%) (N=249) | 21,503 (70,897) | 20,318 (24,043) | 64,780 (27,452) | 106,601 (91,133) |
| | Inpatient Hospital | Outpatient | Pharmacy | Total |
| Costs, Adjusted^ | Mean | Mean | Mean | Mean |
| Lower (<=80%) (N=196) | 35,961* | 14,404* | 27,981* | 78,345* |
| High (>80%) (N=249) | 22,064 | 20,274 | 64,119 | 106,457 |

Notes: Resource use means are per patient. All costs are in 2013 Japanese Yen. Abbreviations: SD = standard deviation. ~Unadjusted health care resource use and unadjusted costs were measured during d-TPD exposure time period. ^The adjusted costs were from Propensity Bin Bootstrapping, controlling for 6-month baseline patient demographics and clinical characteristics. All adjusted costs were measured over an 18-month post index period. *P<0.05 relative to high (MPR).

Table

Disclosures: Masayo Sato, Eli Lill and Company
This study received funding from: Eli Lilly and Company

SA0297

Reasons for Patient Non-Adherence to Recommended Osteoporosis Pharmacotherapy. Sylvie Hall*¹, Stephanie Edmonds², Yiyue Lou³, Peter Cram⁴, Douglas Roblin⁵, Kenneth Saag⁶, Fredrick Wolinsky⁷. ¹University of Iowa Hospitals & Clinics, USA, ²University of Iowa Carver College of Medicine, USA, ³University of Iowa College of Public Health, USA, ⁴University of Toronto, Canada, ⁵Kaiser Permanente, USA, ⁶University of Alabama at Birmingham, USA, ⁷University of Iowa College of Public Health, USA

Purpose: Half of all patients recommended for osteoporosis (OP) pharmacotherapy do not take their medications. The purpose of this study was to examine patients' reasons for not adhering to recommended OP pharmacotherapy and differences in patient characteristics among those who did and did not adhere in order to target interventions designed to increase pharmacotherapy adherence rates and improve bone health. Methods: We used participants from the Patient Activation after DXA Result Notification (PAADRN) study, a randomized controlled trial of 7,749 participants 50 years old or older presenting for DXA scans at three medical centers in the United States (site A, B, C). Participants were first interviewed at the time of their index DXA, and then 12 weeks later. For this study, we focused on the 790 participants who reported that their healthcare provider had recommended an OP medication at 12-weeks post-DXA. We compared those who reported starting the recommended medication (adherers) and those who did not (non-adherers) on a variety of factors including demographics, health habits, DXA impression, FRAX risk, and osteoporosis knowledge using Pearson Chi-squared tests for categorical variables, and two sample t-test for continuous variables. Results: Mean age was 66.8 (SD = 8.9), 87.2% were women, and 84.2% were white (Table 1). One-fourth (24.8%) reported that they did not start the recommended medication while 75.2% participants said that they did. Non-adherers had better scores on a measure of OP knowledge (p<0.05). Adherence did not differ by patient demographics. The most common

reasons for non-adherence were fear of side effects (28.3%), a dislike of taking medicine (13.7%), and the belief that the medicine would not help their condition (8.7%). Conclusions: Patients who are recommended for OP pharmacotherapy report that they decline treatment because of the fear of side effects or the belief that the medication will not help their condition; they also have better OP knowledge. These findings suggest that improved patient counseling regarding the side effects of OP treatment and the risk-benefit ratio for these medications could increase adherence rates. Providers should address these issues in discussions with their patients.

Table 1: Characteristics of PAADRN Participants Who Were Recommended to Take Medications after Baseline DXA

| Variable | Reported Not Taking the Medication (N=196; 24.8%) | Reported Taking the Medication (N= 594; 75.2%) | P-value |
|---|---|--|----------------|
| Age | | | |
| < 65, number (%) | 89 (45.4) | 229 (38.6) | 0.090 |
| ≥65, number (%) | 107 (54.6) | 365 (61.4) | |
| Gender | | | |
| Men, number (%) | 19 (9.7) | 82 (13.8) | 0.135 |
| Women, number (%) | 177 (90.3) | 512 (86.2) | |
| Race/Ethnicity | | | |
| White, number (%) | 162 (82.7) | 503 (84.7) | 0.445 |
| Black, number (%) | 29 (14.8) | 80 (13.5) | |
| Other, number (%) | 5 (2.6) | 11 (1.9) | |
| Health Insurance | | | |
| Private insurance, number (%) | 157 (80.1) | 464 (78.1) | 0.557 |
| Public health coverage, number (%) | 114 (58.2) | 371 (62.5) | 0.285 |
| Study DXA Results | | | |
| Normal, number (%) | 7 (3.6) | 27 (4.5) | 0.758 |
| Low BMD, number (%) | 74 (37.8) | 204 (34.3) | |
| Osteoporosis, number (%) | 115 (58.7) | 363 (61.1) | |
| FRAX Risk | | | |
| High, number (%) | 63 (32.1) | 205 (34.5) | 0.759 |
| Moderate, number (%) | 80 (40.8) | 226 (38) | |
| Low, number (%) | 53 (27) | 163 (27.4) | |
| Comorbidities (1 or more), number (%) | 41 (20.9) | 160 (26.9) | 0.094 |
| Mean (SD) of Correct Responses in the Osteoporosis and You Knowledge Scale | 81.04(14.8) | 77.86(17.8) | 0.0138* |
| Correctly Identified DXA Impression, number (%) | 139 (70.9) | 394 (66.3) | 0.235 |
| Current smoker, number (%) | 16 (8.2) | 76 (12.8) | 0.080 |
| Past smoker, number (%) | 70 (35.7) | 202 (34.1) | 0.674 |
| Current alcohol user, number (%) | 88 (44.9) | 263 (44.4) | 0.894 |
| Exercise | | | |
| None, number (%) | 54 (27.8) | 180 (31.4) | 0.250 |
| 1-2 times per week, number (%) | 33 (17) | 108 (18.8) | |
| 3-4 times per week, number (%) | 45 (23.2) | 118 (20.6) | |
| 5 or more times per week, number (%) | 62 (32) | 168 (29.3) | |
| Calcium Supplements, number (%) | 149 (76.4) | 476 (80.3) | 0.249 |

Reasons for Patient Non-Adherence to Recommended Osteoporosis Pharmacotherapy Table 1

Disclosures: Sylvie Hall, None.

SA0298

Relationship between Gastrointestinal Events and Compliance with Osteoporosis Therapy: An administrative claims analysis of US Managed Care Population. Ankita Modi*¹, Shiva Sajjan². ¹Merck & Co., Inc., USA, ²Merck & Company, USA

Background: A large proportion of women with osteoporosis (OP) do not comply with their prescribed OP therapies, which may lead to an increase in fracture risk. Occurrence of gastrointestinal (GI) events during the course of OP therapy may be one of the reasons for non-compliance.

Purpose: To estimate the rate of gastrointestinal (GI) events and their association with osteoporosis treatment compliance.

Method: A retrospective cohort study using a large US administrative claims database from 2007 through 2013 was conducted. Claims for osteoporotic women ≥65 years old continuously enrolled in a health plan for at least 2 years, a baseline year before and a follow-up year after the date of the first prescription of oral bisphosphonate (index date) were included. Women were excluded if they had a claim for any OP medication in the baseline year, or a diagnosis of Paget's disease or malignant neoplasm. Oral bisphosphonates were identified based on national drug codes and included alendronate, ibandronate, and risedronate. The medication possession ratio (MPR) was calculated as the total days supply of all OP medications received in the follow-up period divided by 365 days. Compliance was defined as MPR of ≥ 0.80. GI events were assessed using ICD-9 diagnosis or CPT procedure codes. Logistic regression analysis was used to examine the association of post-treatment GI events and compliance adjusting for baseline covariates such as age, OP fracture, GI events, use of gastro-protective agents, NSAIDs, glucocorticosteroids, estrogen and Charlson comorbidity Index.

Results: A sample of 45,031 women taking at least one oral bisphosphonate with mean (SD) age of 72 (7.4) years was identified. A total of 17,481 (38.8%) patients experienced at least one GI event during the follow-up period. Overall, only 14,071 (31.2%) patients were compliant with their oral OP therapy, compliance was even lower among those having GI event with only 27% (n=4,750) with an MPR \geq 0.80. Patients who experienced GI events after initiation of oral bisphosphonates were 24% less likely to comply with OP therapy as compared to patients who did not experience post-treatment GI events (odds ratio [95% CI], 0.76 [0.728–0.796]; $P < .001$).

Conclusions: The rate of GI events was high among elderly osteoporotic women initiating oral bisphosphonates. GI events were associated with low treatment compliance which may result in increased fracture risk among this population.

Disclosures: *Ankita Modi, Merck and Company*

This study received funding from: Merck and Company

SA0299

Safety concerns and treatment monitoring among senior Chinese orthopedists in the management of osteoporotic fracture: a nationwide survey in China.
Pan Wei, Li Senyuan*, Man Yi, Liu Xun. Novartis, China

Objectives: To understand the safety concerns and treatment monitoring among senior Chinese orthopedists from tertiary hospitals in the management of osteoporotic fracture.

Material and Methods: A questionnaire with multiple-choice items according to Chinese and several international osteoporosis guidelines and advice from orthopedic specialists was designed. The questionnaire was drafted in the manner of standard flow and was pre-tested, and its reliability and validity met statistical criteria. Face to face surveys were conducted and instructed by investigators among 509 orthopedists who are deputy directors and above in Mainland China. Tablet computers were used to save the questionnaire.

Results: In all, 484 effective questionnaires (95%) were confirmed, of them, 98% agreed risk of fracture recurrence would be increased if a patient has a history of fragility fracture. The most common choice for first-line treatment of osteoporosis is bisphosphonates (80%). Nearly a quarter (23%) held the opinion that using bisphosphonates has an effect on fracture healing and 29% did not. More than half (57%) knew that acute-phase response may occur after either oral or intravenous bisphosphonates administration, and more than two-thirds (73%) knew that acute-phase response rate of intravenous bisphosphonates would drop if oral bisphosphonates were administered before. Regarding long-term management of osteoporosis, most (63%) would suggest visiting department of orthopedics, while department of endocrinology and osteoporosis received same vote (17%). For bone mineral density re-evaluation: 85% would recommend it; 52% would recommend it every 12 months and 39% would recommend it every 6 months. Three-fifths of the respondents chose bone turnover markers could be monitored in their hospitals, 27% were negative about the feasibility, and 13% chose uncertain. For prescription of bisphosphonates, 68% would consider it appropriate if aminotransferase is more than 2 times the normal range.

Conclusion: This survey showed that anti-osteoporosis treatment received quite awareness among senior Chinese orthopedists, while treatment monitoring was less cared. Safety use of bisphosphonates was a major concern but it was not well understood.

Disclosures: *Li Senyuan, Novartis*

This study received funding from: Novartis

SA0300

Semi-Automated Radiology Report Screening to Facilitate a Fracture Liaison Service. Agnes Zak*¹, Ronilda Lacson², Sara Lee¹, Ramin Khorasani², Daniel Solomon³. ¹Brigham & Women's Hospital, USA, ²Center for Evidence-Based Imaging, USA, ³Harvard Medical School, USA

Purpose: Osteoporosis represents the major risk factor for fractures in patients over 60 years old, and associated costs are estimated to exceed \$25 billion in 2015. However, there is a large gap in identifying these patients for secondary treatment after an initial fracture. To facilitate identification of osteoporotic fractures at a large medical center, we developed a semi-automated tool that uses Natural Language Processing (NLP) to scan a hospital-wide database of radiology reports for possible osteoporotic fractures.

Methods: The NLP system uses pre-determined query terms, derived from confirmed osteoporotic fracture cases, to scan reports linked to CPT procedure and ICD-9 diagnosis codes associated with humeral, vertebral, and hip fractures. This tool was run on a weekly basis reviewing all relevant radiologic imaging reports (e.g. spine and hip imaging reports) generated in the prior week. A brief chart review (<5 minutes per fracture) was performed to confirm that fractures were likely due to osteoporosis.

Results: The system identified 2148 potential fractures over an 8-month period. After chart review, 1400 (65%) fractures were excluded, 919 for no confirmation of fracture and 419 for reasons believed to be unrelated to osteoporosis such as cancer or major trauma. The remaining 748 (35%) potential osteoporotic fractures were categorized into the 8 groups shown in the Figure. The majority of these potential fractures (56%) had actually occurred >8 weeks from radiology report date. A small

portion of the fractures (4%) were present in a population <50 years old at diagnosis. Additionally, 11% of fractures had occurred <8 weeks from report date in patients >50 years old. This group had three sub-categories including multiple anatomic fracture sites, patient mental status/native language/residency, and death indicator.

Conclusions: The use of a semi-automated NLP tool can rapidly screen for patients who may require follow-up osteoporosis care. This screening process will facilitate referral to a fracture liaison service for appropriate treatment, bridging the communicative gap between acute and primary care settings. Further modification of NLP qualifiers can enhance the accuracy of identified fractures and eliminate the need for manual, confirmatory chart review or target a specific category of fracture based on investigator interest.

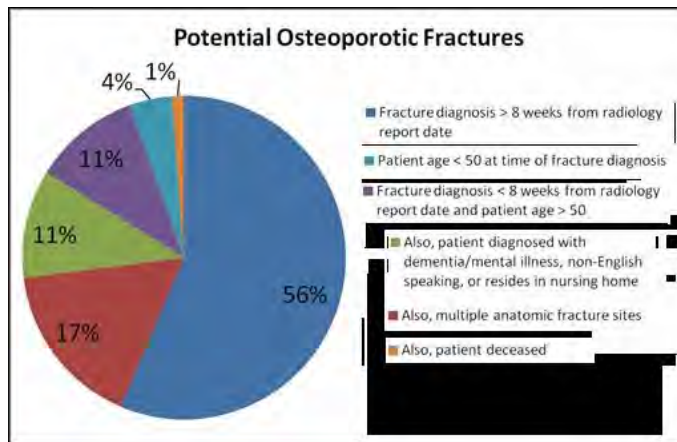


Figure 1

Disclosures: *Agnes Zak, None.*

SA0301

Serum calcium levels required for the increase in bone mineral density by the combination therapy of bisphosphonate and active vitamin D3 analog for the treatment of osteoporosis. Mayuko Kinoshita*¹, Muneaki Ishijima², Haruka Kaneko², Lui Liz³, Ryo Sadatsuki², Shinnosuke Hada², Anihar Yusp², Hidetoshi Nojiri⁴, Yuko Sakamoto⁵, Kazuo Kaneko². ¹Juntendo University, Japan, ²Department of Orthopaedics & Motor Organ, Juntendo University Graduate School of Medicine, Japan, ³Sportology Center, Juntendo University Graduate School of Medicine, Japan, ⁴Department of Orthopaedics, Juntendo Tokyo Koto Geriatric Medical Center, Tokyo, Japan, ⁵Department of Orthopaedics, Juntendo Nerima Hospital, Japan

Since vitamin D insufficiency is one of the risk factors for the decrease in BMD, the combination therapy of Bisphosphonates (BPs) and active vitamin D3 analog (aVD) in osteoporosis treatment has become widespread in Japan. We reported that there were the "non-responders" in this combination therapy and the risk factor for the non-responder was the 8.5-9.0 mg/ml of serum level of calcium (sCa) [reference range (8.5-10.5 mg/ml)] at baseline. The aim of this retrospective study was to find out the sCa levels to obtain the increase in BMD adequately. Since 2008 to 2013, 275 osteoporotic patients were started to use BPs. As the 166 were excluded, the remaining 99 female patients were included in this study. While BPs used in this study were alendronate, risedronate or minodronate. aVD used in this study were either alfacalcidol or eldcalcidol. In addition to age and body mass index (BMI), serum levels of 25(OH)D, Ca (sCa), Pi (sPi), intact PTH, bone turn markers including TRACP5b and BAP, lumbar spine (L2-L4) BMD (LS-BMD) and femoral neck BMD (H-BMD) were assessed for every 6 months for 2 years. Both LS-BMD ($p < 0.001$, 5.4%) and H-BMD ($p = 0.007$, 1.8%) of the patients were significantly increased by this combination therapy for 2 years. sCa level was also significantly increased within the reference range ($p < 0.001$), while intact-PTH, sBAP and TRACP5b were significantly decreased by this combination therapy for 2 years ($p < 0.001$). sCa level was peaked out about 9.5 mg/ml in 18 months. Multiple regression analysis revealed that the factor affects both the %LS-BMD ($r^2 = 0.452$, $p = 0.030$) and %H-BMD ($r^2 = 0.464$, $p = 0.030$) were the sCa level at first visit. Patients were divided into two groups in terms of sCa level for %LS-BMD and %H-BMD. The %LS-BMD after 6 month-treatment of the lower group (0.4%) was significantly different in comparison to that of the higher group (1.5%) ($p = 0.030$) and borderline sCa level was 9.0 mg/ml. Similarly for %H-BMD, the lower group (0.0%) was significantly different in comparison to that of the higher group (1.2%) ($p = 0.027$) and borderline sCa level was 9.3 mg/ml. When sCa level was 9.3 mg/ml or more, odds ratio for the increasing both %LS-BMD and %H-BMD by the combination therapy for next 6 months was 4.9 (95%CI: 1.87 to 12.71). In conclusion, the increase in BMD by the treatment of the combination therapy of BPs and aVD was associated with the sCa level before starting the treatment, even though it is within the reference range.

Disclosures: *Mayuko Kinoshita, None.*

SA0302

Hospitalizations for Osteoporosis-Related Fractures: Economic Costs and Clinical Outcomes. Derek Weycker¹, Xiaoyan Li², Rich Barron², Rebecca Bornheimer¹, Alex Kartashov¹, David Chandler^{*2}. ¹Policy Analysis Inc. (PAI), USA, ²Amgen Inc., USA

Background: Osteoporotic fractures frequently require inpatient care, and are associated with elevated risks of morbidity, mortality, and re-hospitalization. A comprehensive evaluation of healthcare costs, resource utilization, and outcomes associated with osteoporosis-related fractures treated in US hospitals was undertaken.

Methods: A retrospective design and data from the Premier Perspective Database (2010-2013) were employed. The Premier Database includes validated discharge records for all inpatient admissions from >400 geographically diverse US hospitals. The study population comprised patients aged ≥50 years who were hospitalized with a primary diagnosis of a closed or pathologic fracture commonly associated with osteoporosis; the first qualifying hospitalization was designated the “index admission”. Patients with evidence of major trauma or malignancy (or other [non-osteoporotic] conditions that may lead to pathologic fracture) during their index admission were excluded. Study measures included healthcare costs, length of stay (LOS), intensive care unit (ICU) use, and mortality during the index admission, as well as 60-day fracture-related re-hospitalization.

Results: A total of 268,477 patients were admitted to hospital (n=548 hospitals) with a primary diagnosis of an osteoporosis-related fracture; mean (SD) age was 78 (11) years, 75% were female, 69% had ≥2 comorbidities, and 82% of patients had a diagnosis code for accidental fall. For all fractures, mean (95% CI) hospital cost was \$12,839 (12,784-12,893), LOS was 5.1 (5.1-5.1) days, ICU use was 7.4% (7.3-7.5), and mortality was 1.5% (1.5-1.6); 60-day fracture-related re-hospitalization was 2.3% (2.2-2.4). Study measures for selected fracture types are presented in the Table.

Conclusions: Hospital costs associated with the treatment of osteoporosis-related fractures are high—especially among patients with fractures of the hip and femur, and those with multiple fractures—and are comparable to or exceed those for other serious conditions such as stroke, heart failure, and chronic obstructive pulmonary disease (COPD). Among patients with vertebral fractures—the second most common reason for admission—mortality and ICU use were notably high, and costs and LOS were higher than among those with non-vertebral fractures (excluding hip). Interventions that are effective in reducing fracture risk have the potential to yield substantial cost savings.

| | Type of Fracture | | | | |
|------------------------------------|----------------------|-----------------------|-----------------------|---------------------------|-------------------------------|
| | Hip (n=133,826) | Femur (n=12,813) | Spine (n=38,483) | Non-Vertebral* (n=96,370) | Multiple Fractures (n=28,370) |
| Cost—Total, \$ | | | | | |
| Mean | \$14,784 | \$16,423 | \$11,681 | \$10,668 | \$14,581 |
| Median | \$12,632 | \$13,920 | \$7,799 | \$6,289 | \$11,944 |
| 95% CI | (\$8,657 - \$14,812) | (\$16,175 - \$16,674) | (\$11,579 - \$11,822) | (\$10,599 - \$10,737) | (\$14,391 - \$14,771) |
| LOS, days | | | | | |
| Mean | 5.6 | 5.8 | 5.4 | 4.2 | 5.7 |
| Median | 5 | 5 | 4 | 3 | 5 |
| 95% CI | (5.0 - 5.4) | (5.2 - 5.9) | (5.3 - 5.4) | (4.2 - 4.3) | (5.0 - 5.8) |
| Mortality | | | | | |
| % | 2.1 | 3.8 | 1.5 | 0.8 | 3.8 |
| 95% CI | (2.0 - 2.2) | (1.3 - 2.0) | (1.3 - 1.6) | (0.7 - 0.8) | (1.8 - 2.0) |
| ICU Use | | | | | |
| % | 8.7 | 8.6 | 9.5 | 4.3 | 8.7 |
| 95% CI | (8.6 - 8.8) | (9.1 - 10.2) | (9.2 - 9.8) | (4.4 - 5.1) | (8.1 - 10.1) |
| 60-Day Fracture Re-Hospitalization | | | | | |
| % | 1.5 | 1.7 | 5.7 | 2.0 | 2.2 |
| 95% CI | (1.5 - 1.6) | (1.5 - 1.9) | (5.4 - 5.9) | (2.0 - 2.1) | (2.0 - 2.4) |

Table

Disclosures: David Chandler, Amgen Inc. This study received funding from: Amgen Inc.

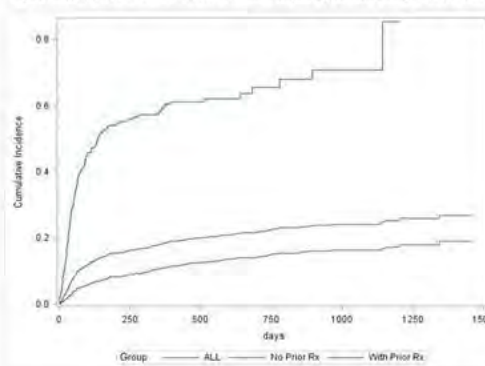
SA0303

More Evidence of a Broken Post-Fracture Care Process: A Call for a Fracture Liaison Service. Daniel Solomon^{*1}, Chih-Chin Liu², Mitch Harris². ¹Harvard Medical School, USA, ²Brigham & Women’s Hospital, USA

Background/Purpose: It has been widely noted that post-fracture osteoporosis treatment rates are dismal in typical practice settings. However, a careful examination of the process of post-fracture care at a large US medical center is lacking in the literature. In preparation for developing a Fracture Liaison Service (FLS), we examined a linked dataset that includes rich information from an electronic medical record (EMR) plus claims data from Medicare. Methods: We identified patients hospitalized with an acute fracture in 2008-2011 who were older than 65 years of age. Medicare data were linked with these patients using an exact matching system through insurance identification numbers. We examined the rates and timing of osteoporosis treatments after the index acute fracture. Cox proportional hazard regression models allowed us to identify pre-fracture variables associated with lack of treatment. As well, the post-fracture process of care was analyzed to determine possible reasons for lack of treatment (lack of diagnosis or visits for osteoporosis, lack of local primary care provider). Finally, we examined the rates of subsequent fractures among patients who did and did not receive post-fracture osteoporosis treatment. Results: We identified 1,586 patients with an acute hospitalized fracture who were Medicare eligible. The distribution of fracture type was as follows: 28.9% hip, 11.1% humerus, 11.9% pelvis, 36.2% spine, and 11.9% Wrist. The mean age of patients was 80.1±7.9 years, 72.1% were female, and 15.8% had evidence of a prior fracture in their

Medicare data. During follow-up, 19.2% had a medication for osteoporosis started or re-started. For patients with prior treatment for osteoporosis, this percentage was 56.1% and for those without prior treatment 12.1%. The types of medications included: calcitonin (5.9%), hormone replacement therapy (22.0%), IV bisphosphonates (18.8%), oral bisphosphonates (49.0%), raloxifene (2.6%), and teriparatide (1.6%). The median time until the start of such medications was 407 (interquartile range 111 - 868) days (see Figure). 29 (1.8%) patients died during follow-up. Conclusions: At one large US medical center, post-fracture osteoporosis treatment rates were sub-optimal. Further data will be presented describing the process of care post-fracture and subsequent fracture rates. These data will help us design a more targeted Fracture Liaison Service that serves patients at high risk of sub-optimal care.

Figure: Osteoporosis Treatment After Fractures, Adjusting for Competing Risk of Death



Figure

Disclosures: Daniel Solomon, None.

SA0304

Differential effect of dietary calcium intake on bone mineral density according to body size in older adults. Kyoung Min Kim^{*1}, Dong Hwa Lee¹, Soo Lim¹, Sung Hee Choi¹, Jae Hoon Moon¹, Jung Hee Kim², Sang Wan Kim³, Hak Chul Jang¹, Chan Soo Shin². ¹Seoul National University Bundang Hospital, South Korea, ²Seoul National University Hospital, South Korea, ³Boramae Hospital & Seoul National University College of Medicine, South Korea

Limited information suggests that calcium requirement for bone accretion is associated with skeletal size in growing phase. The objective of this study was to investigate whether the interactions between dietary calcium intake and bone mineral density (BMD) could be different according to the height in older adults.

This was a cross-sectional study of data from the Korea National Health and Nutrition Examination Survey from 2008 to 2010. A total of 7562 older adults aged 50 years and older (3425 men and 3938 women) were included and further stratified into three groups by ± 1SD of height in each gender: short, middle and tall groups. Dietary calcium intake was classified into three groups, less than 400 mg/d, 400-799 mg/d, and 800 mg/d or greater. All the study participants underwent dual-energy X-ray absorptiometry to estimate BMD at lumbar spine (LS), femur neck (FN) and total hip (TH)

Age and body mass index (BMI) showed significant differences between the dietary calcium intake groups in each height-group both in men and women, indicating lowest dietary calcium intake group provided significantly older age and lower BMI. In men, BMDs were positively associated with dietary calcium intake for LS, FN and TH in tall and medium groups adjusting for age, BMI and 25-hydroxy vitamin D (25OHD) levels, and the associations were stronger in tall group than those of middle group (p for trends <0.05, respectively). However, no significant differences were observed in short group for all skeletal sites in men. In women, LS BMD showed no significant differences according to dietary calcium intake in all height groups after adjusting same covariates. However, FN BMD were positively associated with dietary calcium intake in all height groups (p for trends <0.05, respectively). TH BMD showed significant differences according to dietary calcium intake in tall and short groups (P=0.033 in tall and P=0.042 in short group), whereas no significant difference in medium height group (P=0.089). The results of the present study demonstrate that the positive association between BMD and dietary calcium intake was more evident in tall and medium groups than those of short height group. These findings could suggest that the calcium requirement for bone health in older adults might be associated with skeletal size.

Disclosures: Kyoung Min Kim, None.

SA0305

See Friday Plenary Number FR0305.

SA0306

The Low Calcium Intake in Postmenopausal Women in the Czech Republic. Vaclav Vyskocil*¹, Frantisek Senk Senk², Pavel Novosad³, Olga Ruzickova⁴, Barbora Skyvarova². ¹Center for Metabolic Bone Diseases, Czech republic, ²Osteocenter Regional Hospital, Czech republic, ³Osteology Academy, Czech republic, ⁴Institut of Reseach Revmatology, Czech republic

The optimal dosage of calcium and vitamin D is very often discussed not only in regards to its effect on the reduction of the risk of fractures but recently also in connection with cardiovascular risk versus its benefit.

Authors of the mentioned centers used detailed questionnaires to determinate the average calcium intake from food and supplementation by patients measured in osteocenters and by that they followed the European study by O. Bruyer from 2007 which didn't contain Czech and Slovakian data.

Patients were divided into two groups, non-treated – with osteopenia using only supplementation and treated – using biophosphonates and supplementation. As a part of the acquired and evaluated data was also BMD in spine, neck and whole hip joint and also risk factors monitored with FRAX and vitamin D level, resp. 25(OH)D expressed in nmol/L.

According to the questionnaire survey it was discovered that only 57 percent of patients use supplementation regularly and from food they gain only about 200-300 mg of calcium per day. From the results of the survey, which has many limitations, comes out that the consumption of milk and dairy products is very low and the recommended values can't be reached without calcium supplementation. Most of the patients (from 60 to 70 percent) present a fluid intake 1-2 liters per day, only 4-5 percent present the intake under 1 liter per day. The vitamin D supplementation paradoxically seems to be better than the calcium saturation. Authors suppose that the acquired values of vitamin D are higher than reality. Very interesting is the high percentage of risk factors – the previous osteoporotic fracture is presented in 26 percent (in treated group 49 percent), menopause before 45th year of age occurred in 20 percent (in treated group only in 15 percent). The supplementation is regularly used only by 57 percent of patients in non-treated group and 76 percent in treated group. From the point of eating habits and fluid intake there weren't discovered any differences between the urban and country population and also the education didn't have any effect on these results.

The calcium intake from food was in both observed groups insufficient and up to 85 percent of patients in the non-treated group is without supplementation containing calcium.

The survey proved that the total calcium intake from food/supplementation by Czech women is, similarly to European women, low – in the non-treated group it was under 500 mg per day.

Disclosures: Vaclav Vyskocil, None.

This study received funding from: Pfizer static analysis

SA0307

Association of the Dietary Inflammatory Index, Bone Mineral Density and Risk of Fracture in Postmenopausal Women. Tonya Orchard*¹, Vedat Yildiz¹, Susan Steck², James Hebert², Rebecca Jackson¹. ¹Ohio State University, USA, ²University of South Carolina, USA

Objective: Evaluate the association of an anti-inflammatory diet pattern, as measured by the Dietary Inflammatory Index (DII), with changes in bone mineral density (BMD) and risk of fracture in postmenopausal women.

Methods: The inflammatory potential of the diet was estimated using DII scores calculated from the baseline food frequency questionnaire for participants of the Women's Health Initiative (WHI) Observational Study and Clinical Trials who reported no history of hip fracture at baseline (n=161,595). BMD was measured in a sub-group (n=10,290) at baseline and years 3, 6 and 9 using dual-energy X-ray absorptiometry. Fractures were reported annually; hip fractures were confirmed by medical record review. Percent changes in hip and spine BMD over 9 years of follow-up were analyzed by pair-wise comparisons by Quartile (Q1 = reference, most anti-inflammatory diet) of baseline DII scores. Cox proportional hazard models were used to compute hazard ratios for fractures adjusted for important covariates.

Results: Women with the most anti-inflammatory diet (Q1) were older, had a lower BMI, were more likely to be White, and reported higher calcium intake, more physical activity and more falls than women in Q4. Women in Q1 had a greater increase in spine BMD compared to women in Q4 at year 6 (0.85%; p=0.003), but no significant differences at years 3 or 9. Those in Q1 had lower mean hip BMD at baseline, but lost significantly less BMD at the hip (0.54%; p=0.012) over 9 years of follow-up versus Q4. Women with the most pro-inflammatory diet had a significantly higher risk of hip fracture in Cox models adjusted for age and race (Q4 HR: 1.12; 95% CI 1.02, 1.23; p for linear trend 0.01), but risk disappeared after multivariate adjustment (Q4 HR: 1.02; 95% CI 0.91 -1.15; p for linear trend 0.82). Conversely, in fully adjusted models, lower arm fracture and total fracture risk decreased by 8% (p for trend 0.02) and 5% (p for trend 0.01) respectively in women in Q4. In analyses

excluding women who reported taking hormones or bone-active medications or those in the active treatment arm of the WHI Hormone Therapy trial, the risk of hip fracture increased by 17% in women consuming the most pro-inflammatory diet although this was not statistically significant (Q4 HR: 1.17, 95% CI: 0.93-1.46; p for trend 0.35). In contrast, women in Q4 had a 14% lower risk of lower arm fractures (Q4 HR: 0.86; 95% CI 0.75, 0.99; p for trend 0.02), and a non-statistically significant lower total fracture risk (Q4 HR: 0.94; 95% CI 0.87, 1.01; p for trend 0.06).

Conclusion: An anti-inflammatory dietary pattern was associated with less loss of BMD in postmenopausal women, but this did not translate into reduced fracture risk.

Disclosures: Tonya Orchard, None.

SA0308

Comparative Study of Net Calcium Absorption of Two Different Pharmaceutical Formulations of Calcium Carbonate in Postmenopausal Women. Silvina Mastaglia*¹, Dana Watson², Julia Somoza³, Roxana Gainotti⁴, Graciela Brito², Beatriz Oliveri⁵. ¹Laboratorio De Enfermedades Metabólicas Óseas, CONICET-UBA, Argentina, ²Laboratorio de Enfermedades Metabólicas Óseas (INIGEM), CONICET-UBA, Argentina, ³Laboratorio de Enfermedades Metabólicas Óseas (INIGEM) CONICET-UBA, Argentina, ⁴Mautalen, Salud e Investigación., Argentina, ⁵Laboratorio de Enfermedades Metabólicas Óseas (INIGEM), CONICET-UBA, Argentina

Calcium supplementation, administered alone or associated to a specific medication for osteoporosis, would reduce bone mass loss and fracture risk in postmenopause. However, the adherence rate to calcium supplements is low, mainly due to low tolerance. New formulations with the same effect but better tolerance are required. **Objective:** To compare calcium (Ca) net absorption rate, between two different pharmaceutical formulations of calcium carbonate (PFCa) in postmenopausal women. **Materials and Methods:** Population: 11 postmenopausal women aged 58.9 ± 3yrs with a body mass index (BMI) 25.1 ± 2kg/m². **Inclusion criteria:** age: 55-65yrs, Menopause: ≥5yrs. Absence of osteoporosis (defined by T-score ≤-2.5 of Lumbar spine or Total femur or a history of osteoporotic fractures). **Exclusion criteria:** any medical condition and/or medication affecting mineral metabolism or intestinal Ca absorption. **Design:** comparative, randomized, prospective, open-label exploratory crossover study of calcium mousse versus calcium pills. **Intervention:** Participants were randomized in 2 groups to receive in two periods, 2 different PFCa (500mg): pill vs. mousse, with previous vitamin D₃ supplementation and adaptation periods for each. The parathormone (PTH) inhibition test and the area-under-the-curve (AUC) of calcium were studied. Blood samples were taken at baseline (after 12hrs fasting) and 1, 2 and 3 hrs after intake of the assigned PFCa. Urine samples (2hs) were obtained at -baseline, and after 2 and 4 hrs of PFCa intake. **Biochemical Determinations:** Serum: Calcium (Atomic absorption), phosphorus (Colorimetric); albumin (colorimetric), 25-hydroxyvitamin D (RIA), and iPTH (ECLIA). In urine: calculia/creatinuria. **Statistical Analysis:** Performed with SPSS 19.0 software for Windows (Inc. Chicago, IL, USA). The trapezoid rule was applied to assess AUC in time [R Development Core Team (2008).http://www.R-project.org]. An ANOVA model with 2 error terms was used to assess the sequence effect, period and formulation. **Results:** The highest inhibition PTH rates were observed after 2 hrs of PFCa (pill 38.2% vs. mousse 36.7%; p=ns). In Table 1, the analysis of the AUC_{0-3hrs} of both PFCa is shown. **Conclusion:** In this population sample, the absorption rate with mousse administration was similar to that one with pills. This data would be useful in clinical practice as it would allow a higher adherence to calcium supplementation with a greater therapeutic efficacy.

Table 1: Comparison of AUC_{0-3hrs} between two formulations of calcium carbonate

| Calcium carbonate | AUC _{0-3hrs} (log) | 95% CI | 90% CI (log) | Double unilateral Schnirmann test |
|-------------------|-----------------------------|-------------|--------------|-----------------------------------|
| Pills | 3.35 | (3.32;3.37) | | |
| Mousse | 3.36 | (3.33;3.38) | 97.6;101.4% | p<0.0001 |

Abbreviations: AUC: area under the concentration x time curve; CI: confidence interval

Table

Disclosures: Silvina Mastaglia, None.

This study received funding from: Lab. Pablo Cassaras (Pharmaceutical Laboratory)

SA0309

See Friday Plenary Number FR0309.

SA0310

See Friday Plenary Number FR0310.

SA0311

See Friday Plenary Number FR0311.

SA0312

See Friday Plenary Number FR0312.

SA0313

Systemic trabecular bone loss following femoral fracture in mice. Armaun Emami¹, Chrisoula Skouritakis², Clare Yellowley², David Fyhrie¹, Blaine Christiansen^{*3}. ¹UC Davis Medical Center, USA, ²UC Davis, USA, ³University of California - Davis Medical Center, USA

One of the most reliable predictors of future fracture risk is a previous history of fracture at any skeletal site, even after controlling for bone mineral density. The mechanisms of this association are not known, but it is possible that a bone fracture initiates a systemic bone resorption response that *actively compromises the skeleton*. However, the systemic loss of bone following a fracture has not been quantified, and the specific mechanisms of this bone loss have not been identified. The current study investigated trabecular bone loss at the L5 vertebral body and contralateral femur following a femur fracture in mice. We hypothesized that fracture would initiate a systemic loss of bone, which would be measurable at distant skeletal sites, and would be detectable for at least 6 weeks following fracture. Female C57BL/6 mice, 12 weeks old at injury, were subjected to transverse femur fracture (n = 36), sham surgery (n = 36; surgical placement of pin in medullary cavity), or no surgical procedure (control; n = 37). Mice were sacrificed 2, 4, or 6 weeks after fracture (n ~ 10 mice/group/time point), and L5 vertebrae and contralateral femurs were analyzed with microCT. Six mice from each group were retained for Open Field testing to quantify voluntary movement over a 24 hour period at 4 days, 2, 4, and 6 weeks post-fracture. Trabecular bone structure was significantly decreased in the L5 vertebral bodies and contralateral femurs of both fractured and sham mice by 2 weeks post-injury (Fig. 1). However, by 6 weeks there were no differences between experimental groups. Open Field testing showed that mice subjected to fracture or sham surgery exhibited less voluntary movement at 4 days post-injury compared to control mice. No differences were present at later time points. Consistent with our hypothesis, we found that femur fracture resulted in bone loss at distant skeletal sites 2 weeks post-injury, suggesting a possible systemic response to fracture. However, contrary to our hypothesis, we observed a recovery of bone by 4 or 6 weeks after fracture. Differences in voluntary movement at early time points after fracture partially explain the observed changes in bone. However, we believe that the magnitude of bone changes is not fully explained by decreased mechanical loading. Ongoing studies will quantify systemic inflammation, bone turnover, and other biological processes following fracture, and will investigate systemic bone loss and recovery in older mice.

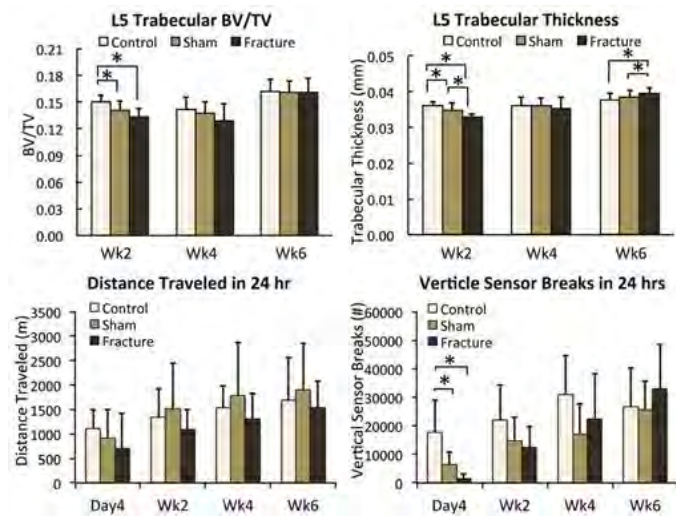


Figure 1: Results from microCT analysis of L5 trabecular bone and Open Field testing.

Disclosures: Blaine Christiansen, None.

SA0314

See Friday Plenary Number FR0314.

SA0315

Icariin Exerts Anabolic Effects on Osteoblasts via Rapid Estrogen Receptor α Signaling Pathways. Man-Sau Wong^{*1}, Ming-Xian Ho², Ling-Ping Zhou². ¹Hong Kong Polytechnic University, Hong kong, ²The Hong Kong Polytechnic University, Hong kong

Icariin, a prenylated flavonoid glucoside isolated from Herba Epimedii, has been shown to improve bone properties in both experimental and clinical studies. Our previous study demonstrated that the estrogenic anabolic actions of icariin in osteoblast-like cells involve estrogen response element (ERE)-independent and ligand-independent activation of estrogen receptor (ER). The present study aims to delineate the mechanism by which icariin activates ER in osteoblastic cells. The anabolic effects of icariin on pre-osteoblastic MC3T3-E1 and rat osteoblastic UMR106 cells were evaluated by its effects on cell proliferation, alkaline phosphatase (ALP) activities as well as bone specific gene expression (Runx2, collagen α 1, osterix) using real time RT-PCR. UMR 106 cells are co-treated with specific blockers (ER antagonist ICI182,780, MAPK inhibitor U0126 and PI3K inhibitor LY294002) to determine if specific signaling pathways are involved in mediating the actions of icariin. Its effects on the expression of signaling proteins and their phosphorylation were studied by using immunoblotting. The results showed that icariin (10-12 to 10-6 M) dose-dependently increased proliferation and alkaline phosphatase (ALP) activities in both MC3T3-E1 and UMR106 cells. In addition, runx2, collagen α 1 and osterix mRNA expression increased in response to icariin (10-6 M) in MC3T3-E1 cells. The anabolic effects of icariin on UMR 106 cells were completely abolished by co-treatment of UMR 106 cells with ICI182,780 (10-6 M), U0126 (10-5 M) and LY294002 (10-5 M), suggesting the involvement of ER, MAPK and PI3K in its actions. Icariin at 10-7 M rapidly stimulated ERK and Akt phosphorylation in UMR 106 cells in a time-dependent manner. In addition, icariin induced ER α phosphorylation at Ser118 and Ser 167 sites and such induction were attenuated by pre-treatment of UMR 106 cells with U0126 and LY294002. The results suggest that both MAPK and PI3K/Akt signaling pathways are involved in mediating the effects of icariin on ER α activation in osteoblastic cells. Taken together, this study provides evidence that the anabolic actions of icariin in osteoblasts are mediated by ligand-independent activation of ER α via rapid MAPK and PI3K/Akt pathway.

Disclosures: Man-Sau Wong, None.

SA0316

Withdrawn.

SA0317

RANKL Inhibition Reverses the Effects of Ovariectomy and IL-10 Deficiency on Bone Composition in a Mouse Animal Model. Eleftherios Paschalis^{*1}, Klaus Klaushofer², Sonja Gamsjaeger², Norbert Hassler², Hamad Alzoman³, Dimitris Tatakis⁴. ¹Ludwig Boltzmann Institute for Osteology, Austria, ²Ludwig Boltzmann Institute of Osteology at the Hanusch Hospital of WGKK & AUA Trauma Center Meidling, 1st Medical Dept., Austria, ³Division of Periodontics College of Dentistry, King Saud University, Saudi arabia, ⁴Division of Periodontology, College of Dentistry, The Ohio State University, USA

Ovariectomy and inflammatory bowel disease are risk factors for osteoporosis. Lack of interleukin-10 (IL-10) results in severe intestinal inflammation, accelerated alveolar bone loss, reduced bone mass, increased mechanical fragility, and suppressed bone formation. Osteoprotegerin (OPG) has been shown to reduce bone resorption under osteoporotic conditions caused by menopause or other conditions. In the present study, femurs from wildtype (WT), ovariectomized (OVX), IL-10 knockout (KO), ovariectomized and IL-10 deficient (OVX-KO) mice, as well as WT, OVX, KO, and OVX-KO mice treated with OPG (WT-OPG, OVX-OPG, KO-OPG, and OVX-KO-OPG, respectively) were analyzed by Raman microspectroscopy (spatial resolution ~ 1 μ m), in the area of trabecular bone. The monitored parameters were: mineral to matrix ratio (MM); glycosaminoglycan (GAG), lipids, and pyridinoline (PYD) content; mineral maturity/crystallinity (MMC). The results were expressed as a function of tissue age. Four tissue ages were examined: 3 based on the presence of fluorescent double labels (between the second label and the mineralizing front (TA1), between the two labels (TA2), and right behind the first label (TA3). Additionally, the geometrical center of the trabeculae (TA4; representative of old tissue) were analyzed. IL-10 deficiency resulted in significantly lower MM at all 4 tissue ages, with the lowest values evident in the OVX-KO animals. While lipids content was similar between WT and KO mice, OVX-KO had significantly lower values compared to KO at TA1. KO animals had significantly higher GAG content compared to WT at TA4, potentially signifying altered canaliculi network. Similarly, OVX-KO animals had a higher GAG content compared to KO animals at TA3 and TA4. OVX, KO, and OVX-KO animals had a significantly higher PYD content compared to WT at TA1, TA2, and TA3, while OVX-KO animal values were also higher compared to KO. MMC was significantly higher in OVX-KO vs OVX, and OVX-KO-OPG vs OVX-OPG animals

at TA4. No significant differences in any of the monitored parameters were evident when WT and WT-OPG animals were compared (negative control), suggesting that OPG does not induce any adverse changes to bone composition. The values for all parameters in OVX-OPG, KO-OPG, and OVX-KO-OPG animals were restored to WT ones. The results of the present study suggest that OPG treatment reverses the individual, as well as the combined effects of ovariectomy and IL-10 deficiency on bone composition.

Disclosures: Eleftherios Paschalis, None.

SA0318

Sexual Dimorphism in the Metabolic Response to Glucocorticoids – The Role of the Osteoblast. Sylvia Gasparini¹, Holger Henneicke², Sarah Kim², Lee Thai², Hong Zhou², Markus Seibel³. ¹ANZAC Research Institute, Australia, ²Bone Research Program, ANZAC Research Institute, The University of Sydney, Sydney, NSW, Australia, ³Department of Endocrinology & Metabolism, Concord Hospital, The University of Sydney, Sydney, NSW, Australia

We have recently demonstrated in male mice that the adverse metabolic outcomes of glucocorticoid (GC) therapy are mediated via the osteoblast-derived peptide osteocalcin (1). Since a sexual dimorphism in the response to exogenous GCs has been reported in rodents (2), the current study aims to determine if a similar mechanism applies in female mice.

We used a transgenic (tg) mouse model in which GC signaling has been selectively disrupted in osteoblasts and osteocytes via targeted overexpression of the glucocorticoid-inactivating enzyme, 11β-hydroxysteroid dehydrogenase type 2. Eight-week-old male (M) and female (F) wild-type (wt) and tg mice received either placebo (plc) or corticosterone (CS) at a dose of 50µg/ml or 75µg/ml dissolved in the drinking water for 4 weeks. Body weight and water intake were measured weekly. Body composition by DXA, insulin tolerance and osteocalcin (OCN) serum concentrations were assessed at baseline and endpoint.

Male and female mice consumed the same amount of water irrespective of treatment (~4ml/mouse/day). Wt male mice developed profound insulin resistance (IR) with both low and high dose CS while in female mice 50ug/ml CS had no effect on insulin sensitivity and 75ug/ml CS induced partial IR only (Fig 1a,c). In tg males exposed to CS, IR was attenuated while, remarkably, female tg mice were completely protected from GC-induced IR (Fig. 1a,c). Similarly, in male wt mice, GC treatment induced pronounced obesity (Fig. 1b,d), which was again attenuated in tg mice (Fat mass: M-50µg-wt +57% vs. M-50µg-tg +24%; p<0.05 & M-75µg-wt +70% vs. M-75µg-tg +35%; p<0.05). In female wt mice, only the higher dose of 75µg/ml CS invoked obesity (Fat mass: F-50µg-wt +3% vs. F-50µg-tg -0.7%; p=ns & F-75µg-wt +50% vs. F-75µg-tg +17%; p=0.1). In line with the observed metabolic differences, OCN serum concentrations were higher in CS-treated wt and tg females than in their respective male counterparts.

The metabolically protective effect of disrupted GC-signaling in osteoblasts was evident in both genders, demonstrating that the osteoblast plays a critical role in GC-induced dysmetabolism. Interestingly, however, female mice displayed a high degree of resilience to the adverse metabolic outcomes associated with GCs. This may in part be due to maintenance of higher circulating OCN levels.

1. Brennan-Speranza et al. J Clin Invest. 2012
2. Quinn M et al. Ann N Y Acad Sci. 2014

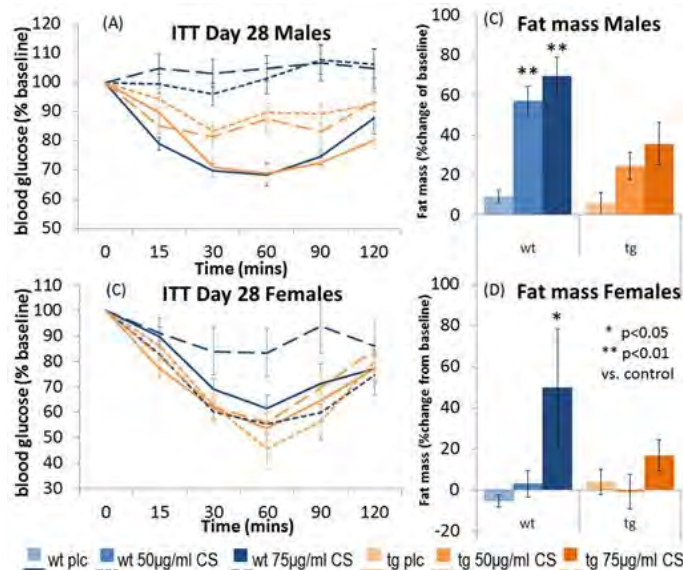


Figure 1. Disclosures: Sylvia Gasparini, None.

SA0319

See Friday Plenary Number FR0319.

SA0320

See Friday Plenary Number FR0320.

SA0321

See Friday Plenary Number FR0321.

SA0322

Effect of angiotensin-converting enzyme inhibitor on the fracture resistance of bone in mouse model of type 1 diabetes. Amy Creecy^{*1}, Sasidhar Uppuganti¹, Clay Bunn², Gael Cockrell³, Elizabeth Wahl³, Mallikarjuna Rettiganti³, John Fowlkes², Jeffrey Nyman⁴, Kathryn Thrailkill². ¹Vanderbilt University, USA, ²University of Kentucky, USA, ³University of Arkansas for Medical Sciences, USA, ⁴Vanderbilt University Medical Center, USA

Low areal bone mineral density (BMD) does not fully explain the 10-fold increase in fracture risk among individuals with type 1 diabetes (T1D). This suggests that insulin treatment alone partially corrects the deleterious effects of T1D on the ability of bone to resist fracture. T1D patients can also be treated with captopril, an angiotensin-converting enzyme (ACE) inhibitor, to prevent the progression of diabetic nephropathy. As a drug that causes vasodilation and improves kidney function, captopril (CAP) may exert positive effects on bone. Since CAP is not bone anabolic, we hypothesized that in diabetic mice it could partially prevent a decrease in material strength and toughness of bone (fracture resistance independent of structure). Over 5 days, streptozotocin (STZ, 40 mg/kg/day) or 100 mM citrate buffer alone was injected ip once daily into 11-wk old, male, DBA/2J mice. After confirming the development of hyperglycemia (>250 mg/ml), STZ-diabetic and control mice at 14 weeks of age were given free access to drinking water containing either CAP (~50 mg/kg/day) with 5 mg/ml ascorbic acid or just the ascorbic acid for 10 weeks. Upon sacrifice, the left femur was harvested for µCT analysis (12 µm voxel size), and three-point bend testing to determine treatment effects on cortical structure (diaphysis), trabecular architecture (metaphysis), and mechanical properties (diaphysis). CAP-treatment did not affect circulating levels of glucose or the body weight loss that follows STZ-induced diabetes, but it did lower the albumin-to-creatinine ratio (Table 1). With severe hyperglycemia, there was a decrease in bone toughness. CAP-treatment did not improve toughness, irrespective of diabetes. It also did not rescue the T1D-related decrease in the structural or material strength of bone. Interestingly, within the non-diabetic mice, the moment of inertia was actually lower for CAP- than for vehicle-treated mice. As for the metaphysis, CAP-treated, T1D mice had lower trabecular number and higher trabecular spacing than vehicle-treated, T1D mice with no effect of ACE inhibition on BV/TV in diabetic or control mice. Clinical studies investigating a positive association between ACE inhibitors and BMD in non-diabetics have been equivocal. Certainly, in poorly controlled diabetes, the likelihood of such inhibition helping to maintain fracture resistance is low.

| Parameter | Unit | Vehicle | | Captopril | | Veh. vs. Captopril | |
|------------------------------|----------------------|----------------|---------------|----------------|---------------|--------------------|---------|
| | | Control (n=10) | T1D (n=16) | Control (n=10) | T1D (n=16) | T1D p | Conf. p |
| Non-bone measurements | | | | | | | |
| Body weight | Mg | 28.8 (2.3) | 18.7 (1.6) | <.0001 | 26.8 (2.5) | 18.5 (2.7) | <.0001 |
| Blood glucose | mg/dL | 125.9 (34.8) | 594.9 (114.4) | <.0001 | 137.8 (18.6) | 560.56 (144.7) | <.0001 |
| ACR ^a | µg/mg | 56.7 (21.2) | 195.1 (148.6) | 0.0005 | 85.0 (38.2) | 89.1 (42.6) | 0.99 |
| Femur Diaphysis | | | | | | | |
| I _{min} | mm ⁴ | 0.072 (0.005) | 0.048 (0.005) | <.0001 | 0.064 (0.005) | 0.047 (0.005) | <.0001 |
| Cl.Ar | mm ² | 0.77 (0.03) | 0.54 (0.04) | <.0001 | 0.74 (0.03) | 0.53 (0.04) | <.0001 |
| Cl.Ti | mm | 0.21 (0.01) | 0.16 (0.01) | <.0001 | 0.2 (0.01) | 0.15 (0.01) | <.0001 |
| Cl.TMD | mgHA/cm ³ | 1405 (10) | 1395 (14) | 0.18 | 1396 (9) | 1389 (14) | 0.36 |
| Cl.Po | % | 1.83 (0.12) | 2.64 (0.26) | <.0001 | 1.9 (0.11) | 2.68 (0.2) | <.0001 |
| Peak Moment | N.mm | 40.9 (2.8) | 21.7 (5.2) | <.0001 | 39.8 (3.4) | 23.1 (5.2) | <.0001 |
| Rigidity | N/mm ² | 1361 (164) | 694 (191) | <.0001 | 1161 (149) | 754 (202) | <.0001 |
| Modulus | GPa | 18.8 (1.6) | 14.7 (3.9) | 0.002 | 18.6 (1.5) | 15.9 (3.4) | 0.18 |
| Strength | MPa | 299 (25) | 222 (49) | <.0001 | 308 (16) | 237 (47) | 0.0003 |
| Toughness | N/mm ² | 1.89 (0.31) | 1.07 (0.40) | <.0001 | 2.00 (0.44) | 1.10 (0.31) | <.0001 |
| Femur Metaphysis | | | | | | | |
| BV/TV | mm ³ | 0.067 (0.012) | 0.043 (0.007) | <.0001 | 0.063 (0.006) | 0.039 (0.009) | <.0001 |
| Tb.N | mm ⁻¹ | 3.82 (0.31) | 3.30 (0.19) | <.0001 | 3.77 (0.16) | 3.10 (0.26) | <.0001 |
| Tb.Th | mm | 0.038 (0.002) | 0.027 (0.001) | <.0001 | 0.036 (0.002) | 0.027 (0.002) | <.0001 |
| Tb.Sp | mm | 0.27 (0.02) | 0.31 (0.02) | 0.0003 | 0.27 (0.01) | 0.33 (0.03) | <.0001 |
| Tb.TMD | mgHA/cm ³ | 1014 (15) | 965 (17) | <.0001 | 1001 (6) | 963 (27) | <.0001 |

^aAdjusted p-values using a step-down Bonferroni used to keep the overall family-wise error rate under 0.05; ^balbumin-creatinine-ratio (ACR) by ELISA and by enzymatic assay, respectively.

Table 1. Selected properties as mean (SD) determined at sacrifice or from ex vivo analysis

Disclosures: Amy Creecy, None.

SA0323

See Friday Plenary Number FR0323.

SA0324

See Friday Plenary Number FR0324.

SA0325

See Friday Plenary Number FR0325.

SA0326

See Friday Plenary Number FR0326.

SA0327

See Friday Plenary Number FR0327.

SA0328

Longitudinal Cohort Study of Once Weekly Teriparatide in Glucocorticoid-Induced Osteoporosis in Japanese Patients. Ikuko Tanaka^{*1}, Mari Ushikubo², Takashi Kato³, Keisuke Izumi², Kumiko Akiya², Hisaji Oshima². ¹NAGOYA Rheumatology Clinic, Japan, ²Tokyo Medical Center, Department of connective Tissue Disease, Japan, ³National Center for Geriatrics & Gerontology, Japan

Background) Weekly teriparatide (wTPT) developed in Japan has been shown to be effective in reducing risk of new vertebral fracture and increasing bone mineral density in primary osteoporosis. In the present study we investigated effects of wTPT on vertebral fractures in glucocorticoid induced osteoporosis.

Subjects and Methods) Patients with connective tissue diseases at Tokyo Medical Center was recruited for one-year longitudinal cohort study. The number of subjects was 168 (female; 145, age; 64±/15 (mean +/- SD), prednisolone dosage at base line; 8.4±/9.9 mg/day, prednisolone dosage during 1yr; 6.7±/5.5mg/day, duration of prednisolone treatment; 10.4±/10.8yr, prevalent vertebral fracture (Genant, H. 1996); 41.4%). Lumbar bone mineral densities (IBMD) were measured as %YAM with Lunar 3030 (GE). Incident vertebral fractures were analyzed with XP of the thoracic and lumbar spines. Patients were treated with bisphosphonates (87%) or wTPT (13%).

Results) The value of IBMD (%YAM) at the base line was 82.8±/16.3%. The rate of incident fractures during the follow-up period was 15.5%. 2) Sex, age, prevalent fracture, and IBMD were not different between two treatment groups. However, prednisolone dosages at the base line were statistically increased in patients with wTPT than bisphosphonates (19.3±/4.2 vs 6.5±/0.5, p<0.01). Increases in IBMD after 1 yr were not different in these two groups. Incident vertebral fractures were seen in 16.2% in patients with bisphosphonates and 10.0% in those with wTPT.

3) A logistic regression analysis revealed that statistically significant factors for incident fractures were IBMD (1% decrease, OR; 1.74; 95%CI; 1.18-2.59, p<0.01), prednisolone dosages (1mg/day increase, 1.09, 1.03-1.15, p<0.01), prevalent fractures (3.37, 1.23-9.20, p<0.01), and wTPT treatment (vs bisphosphonates, 0.12, 0.11-0.81, p<0.01). Conclusions) Our results suggested that wTPT might be effective for prevention of osteoporotic fractures in patients treated with glucocorticoids.

Disclosures: *Ikuko Tanaka, None.*

SA0329

Role of Trabecular Bone Structure Analysis in Glucocorticoid-Induced Osteoporosis. Ikuko Tanaka^{*1}, Mari Ushikubo², Takashi Kato³, Keisuke Izumi², Kumiko Akiya², Hisaji Oshima². ¹NAGOYA Rheumatology Clinic, Japan, ²Tokyo Medical Center, Department of connective Tissue Disease, Japan, ³National Center for Geriatrics & Gerontology, Japan

Background) Although glucocorticoid induced osteoporosis (GIO) is known as a sever secondary osteoporosis, sufficient markers for prediction of incident fracture have not been elucidated. Recently, Trabecular Bone Structure (TBS) has been developed for a novel predictor of osteoporosis. The purpose of this study was to clarify a role of TBS in GIO.

Subjects and Methods) Patients with connective tissue diseases at Tokyo Medical Center was subjected for one year longitudinal cohort study. The number of subjects was 232 (female; 204, age; 65±/15 (mean +/- SD), prednisolone (PSL) dosage at base line; 9.1±/12.8 mg/day, PSL dosage during 1y; 6.7±/5.9mg/day, prevalent vertebral fracture (Genant, H. 1996); 46.7%). Lumbar bone mineral densities (IBMD) were measured as %YAM with Lunar 3030 (GE). TBS values were calculated with TBS (medimaps). Incident vertebral fractures were analyzed with XP at thoracic and lumbar spines. Medications during this study were bisphosphonates (65%), denosmab (26%), weekly teriparatide (9%).

Results) 1) The value of IBMD (%Young Adult Mean; %YAM) at the base line was 81.5±/15.6%, and that of TBS was 1.268±/0.107. The rate of incident fractures during the follow-up period was 14.1%. 2) TBS was significantly correlated with IBMD (r=0.695, p<0.001) and the age (r=-0.603, p<0.001). 3) A logistic regression analysis revealed that incident fractures could be predicted (87.1%) with IBMD (per

5% decrease; OR; 1.32, 95%CI; 1.08-1.81; p<0.01), daily prednisolone dosages (per 5mg/day increase; 1.47; 1.20-1.81; p<0.01), and the prevalent fractures (3.63; 1.33-9.89; p<0.02). When TBS data were added to this analysis, TBS (1.78; 1.10-2.86; p<0.02) was extracted instead of IBMD.

Conclusions) TBS analysis of the lumbar spine DXA data might be useful for prediction of prevalent fractures in GIO.

Disclosures: *Ikuko Tanaka, None.*

SA0330

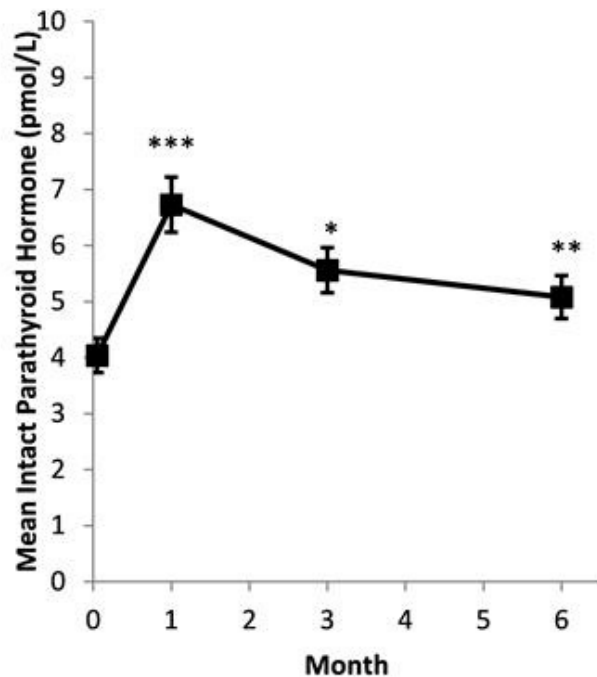
Anabolism versus Antiresorption (AVA Study): A Comparison of the Mechanism of Action (MOA) of Teriparatide (TPTD) and Denosumab (DMAB) in Postmenopausal Women with Osteoporosis Using Quadruple Fluorochrome Labeled Bone Histomorphometry. David Dempster^{*1}, Hua Zhou¹, Robert Recker², Jacques Brown³, Christopher Recknor⁴, E. Michael Lewiecki⁵, Paul Miller⁶, Sudhaker Rao⁷, David Kendler⁸, John Krege⁹, Jahangir Alam⁹, Kathleen Taylor¹⁰, Boris Janos¹¹, Valerie Ruff¹⁰. ¹Regional Bone Center, Helen Hayes Hospital, USA, ²School of Medicine, Creighton University, USA, ³Groupe de Recherche en Maladies Osseuses, Laval University, Canada, ⁴United Osteoporosis Centers, USA, ⁵New Mexico Clinical Research & Osteoporosis Center, USA, ⁶Colorado Center for Bone Research, USA, ⁷Bone & Mineral Research Laboratory, Henry Ford Health System, USA, ⁸Prohealth Clinical Research, Canada, ⁹Eli Lilly & Company, USA, ¹⁰Lilly USA, LLC, USA, ¹¹Eli Lilly Canada Inc., Canada

Purpose: The reported increase in endogenous intact parathyroid hormone (iPTH) levels 1-3 months after a dose of DMAB, an antiresorptive bone agent, has led to the speculation that elevation in iPTH could result in early stimulation of bone formation. The AVA study was conducted to evaluate the effects of DMAB vs TPTD, a well-established anabolic agent. A quadruple fluorochrome labeling method was used to compare changes from baseline (BL) in bone histomorphometric indices with changes in iPTH over the same period. Methods: This study compared TPTD (20 µg/day) with DMAB (60 mg once) for 6 months in postmenopausal women with osteoporosis. Fasting bone turnover markers (BTMs) and iPTH were collected at BL, 1, 3, and 6 months. Patients underwent fluorochrome labeling at BL and during treatment before a trans-iliac bone biopsy at 3 months. The primary objective was change from BL in mineralizing surface/bone surface (MS/BS) in the cancellous envelope. Dynamic and static histomorphometric indices were assessed in cancellous, endocortical, intracortical, and periosteal envelopes. Results: In the DMAB group, iPTH increased from BL and peaked at month 1, remaining above BL at months 3 and 6 (Figure). Even so, histomorphometric indices of bone formation in the cancellous envelope were higher in the TPTD than the DMAB group at month 3 (Table). Except for mineral apposition rate (MAR), these indices increased with TPTD and decreased with DMAB treatment from BL to month 3. Similar findings were observed in other envelopes. TPTD increased BTMs from BL: procollagen type I N-terminal propeptide (PINP) starting at month 1 and carboxyterminal cross-linking telopeptide of type I collagen (CTX) starting at month 3. In the DMAB group, PINP and CTX decreased from BL at all time points. Conclusion: This study is the first to use a quadruple fluorochrome labeling method to compare longitudinal changes from BL to month 3 between an antiresorptive and anabolic drug at the tissue level. Histomorphometric data confirm and BTM data support the opposing MOA of the 2 drugs on bone remodeling. The increase in iPTH after DMAB administration was associated with marked decreases in indices of bone formation in all envelopes, inconsistent with DMAB causing early indirect anabolic action. In contrast, TPTD increased histomorphometric indices and BTMs of bone formation in all envelopes, consistent with an anabolic MOA in trabecular and cortical bone.

| | Cancellous Envelope Median (interquartile range) | | | | | |
|--|---|----------------------------|----------------------------|----------------------------|---------------------------|---------|
| | TPTD (N=31) | | DMAB (N=35) | | TPTD vs. DMAB p-Values | |
| | Baseline | Month 3 | Baseline | Month 3 | Baseline | Month 3 |
| MS/BS (%) | 5.22 (2.63, 7.39) | 18.73 (11.13, 26.64) | 4.78 (2.68, 6.19) | 0.96 (0.44, 1.93) | 0.523 | <0.001 |
| BFR/BS (mm ³ /mm ² /year) ^a | 0.0096 (0.0051, 0.0148) | 0.0366 (0.0226, 0.0543) | 0.0091 (0.0048, 0.0115) | 0.0014 (0.0005, 0.0033) | 0.414 | <0.001 |
| MAR (µm/day) ^a | 0.55 (0.48, 0.58) | 0.57 (0.49, 0.59) | 0.52 (0.45, 0.54) | 0.41 (0.30, 0.48) | 0.043 | <0.001 |
| Ac.f (cycle/year) ^{a,b} | NA | 1.41 (0.88, 2.02) | NA | 0.06 (0.02, 0.14) | NA | <0.001 |

Abbreviations: Ac.f = activation frequency; BFR/BS = bone formation rate/bone surface; DMAB = denosumab; MAR = mineral apposition rate; MS/BS = mineralizing surface/bone surface; N = number of samples; NA = not applicable; TPTD = teriparatide
 Note: p-values are from non-parametric tests (Wilcoxon Sign and Rank Sum tests)
^a Samples with single label only imputed to 0.3 µm/day; samples with no label = missing (MAR) or assigned a value of zero (BFR/BS, Ac.f)
^b Ac.f cannot be calculated at baseline

Table. Dynamic Indices of Bone Formation



*** $p < 0.001$; ** $p < 0.01$; * $p < 0.05$; SE=standard error
 Baseline: N=35, Month 1: N=35, Month 3: N=28, Month 6: N=34.
 p-values from t-test

Figure. Mean (SE) Change from Baseline in Intact Parathyroid Hormone in Patients Treated with DMAb

Disclosures: David Dempster, Merck; Amgen; Eli Lilly and Company
 This study received funding from: Eli Lilly and Company

SA0331

See Friday Plenary Number FR0331.

SA0332

Incidence of Clinical Fracture in Osteoporosis Patients with Daily Teriparatide in the Japan Fracture Observational Study (JFOS): Interim Report. Saeko Fujiwara¹, Ryoichi Takayanagi², Masayo Sato³, Mika Tsujimoto³, Takanori Yamamoto³, Hiroyuki Enomoto³, Satoshi Soen⁴. ¹Health Management & Promotion Center, Hiroshima Atomic Bomb Casualty Council, Japan, ²Department of Medicine & Bioregulatory Science, Graduate School of Medical Sciences, Kyushu University, Japan, ³Medicines Development Unit Japan, Eli Lilly Japan K.K., Japan, ⁴Department of Orthopaedic Surgery & Rheumatology, Nara Hospital, Kinki University Faculty of Medicine, Japan

Background: Due to the rapid growth of the elderly population, the number of patients with osteoporosis and fragility fractures has been increasing in Japan. Although teriparatide 20 $\mu\text{g/day}$ (TPTD) has been broadly approved for osteoporosis treatment, the evidence of TPTD use in a daily clinical setting is limited in Japan. Therefore, we conducted the Japan Fracture Observational Study (JFOS) to investigate the incidence of clinical fracture and safety profile in osteoporosis patients who initiated TPTD. We report an interim analysis of results of 12-month observation. **Methods:** JFOS is a 24-month, multicenter, prospective, observational study in Japan. TPTD-naive patients with osteoporosis at high risk of fracture were included. The incidence of clinical fracture, the percent changes from baseline in bone mineral density (BMD) and serum levels of procollagen type 1 aminoterminal propeptide (PINP), and treatment emergent adverse events (AEs) were observed at up to 12 months after initiating TPTD. **Results:** A total of 1810 patients (90.1%: women) were analyzed at baseline. Mean age (SD) was 76.9 (7.9) years. Two-thirds of patients had prevalent vertebral fractures and 34.3% of patients had 2 or more fractures. One-third of patients received bisphosphonates prior to TPTD. The cumulative incidences of clinical vertebral and non-vertebral fractures were 1.1% and 1.8% at 6 months, and 1.4% and 2.3% at 12 months, respectively. The mean of BMD for the lumbar spine (L2-L4) and total hip were 0.70 g/cm^2 and 0.55 g/cm^2 at baseline, and increased by 8.9% (95% confidence interval [CI]: 7.8 to 9.9) and 0.8% (95% CI: -0.8 to 2.4) at 12

months, respectively. The median PINP serum level was 43.9 $\mu\text{g/L}$ at baseline. The median percent change was increased by 159.0% at 3 months and 187.7% at 6 months. Drug related treatment emergent AEs and serious AEs were reported from 110 (6.1%) and 39 (2.2%) patients, respectively. **Conclusion:** JFOS is the first large observational study to investigate the effectiveness of TPTD as a primary objective in osteoporosis patients in Japan. The cumulative incidence of clinical fracture was not substantially increased over time after initiating TPTD. An increase in PINP was observed in 3 months. Lumbar spine BMD was increased at 12 months. These findings are consistent with the results of previous studies and can contribute to evidence-based osteoporosis management in Japan.

Disclosures: Saeko Fujiwara, None.

This study received funding from: Eli Lilly Japan K.K.

SA0333

See Friday Plenary Number FR0333.

SA0334

Time course of disassociation of bone formation signals with bone mass and bone strength in sclerostin antibody treated ovariectomized rats. Yanfei Ma*, Qianqiang Zeng, Matthew Hamang, Mary D Adrian, Jonathan Lucchesi, Sarah E Raines, Stuart A Kuhstoss, Victor Obungu, Henry U Bryant, Venkatesh Krishnan, Eli Lilly & Company, USA

Sclerostin is a glycoprotein produced by osteocytes that negatively regulates osteoblastic bone formation. Neutralizing sclerostin with a monoclonal antibody stimulates bone formation and increases bone mass in animals and humans. To understand the anti-sclerostin antibody mechanism of action, we studied the time course response of serum bone formation signals correlating with rate and extent of accrual of bone mass and bone strength in a sclerostin antibody treated skeleton. Rats were ovariectomized (OVX) at 6 months of age and permitted to lose bone for 2 months to establish osteopenia. Rats were then treated with a chimeric sclerostin-antibody (Scl-ab) at 20 mg/kg sc once weekly and sacrificed at baseline, weeks 2, 3, 4, 6, 7, and 8 post treatment. In Scl-ab treated rats, the bone formation biomarkers N-terminal procollagen type I (PINP) and osteocalcin (OCN) rapidly increased at week 1, peaked around week 3, and returned to OVX control level at week 6. Lumbar vertebral (LV) osteoblast surface increased 88% at week 2, bone formation rate/bone surface (BFR/BS) was increased by 157% at week 4 and they returned to OVX control level at week 4 and 6, respectively. Similar to lumbar vertebrae, endocortical and periosteal BFR/BS increased rapidly and peaked around week 4 to 585% and 313%, of the vehicle control, respectively. BFR/BS remained higher than OVX control on both periosteal and endocortical surfaces through week 8. Micro-CT analysis showed Scl-ab treatment completely restored OVX induced bone mineral density (BMD) loss in LV, femoral neck (FN) and mid femur between weeks 4 to 6 and BMD continued to increase at all 3 sites through week 8. Biomechanical tests showed a similar linear improvement in bone strength through 8 weeks of Scl-ab treatment in mid-femur and FN, but bone strength begins to plateau between weeks 6 and 8 for LV. These data indicate sclerostin-antibody treatment results in rapid and robust increase in bone formation, however notably, bone anabolic response in cortical bone takes longer to reach its plateau than it does in trabecular bone. Bone mineral density and bone strength continue to improve even after the majority of objective bone formation serum signals have returned to the control level in osteopenic rats. Collectively, these results suggest that treatment with anti-Sclerostin antibodies represents a rapid build-up of bone mass followed by a more sustained and continued favorable impact on bone quality.

Disclosures: Yanfei Ma, Eli Lilly and Company

This study received funding from: Eli Lilly employee

SA0335

Transdermal Delivery of Abaloparatide: Optimization of the Pharmacokinetic Profile in Cynomolgus Monkeys. Hila Bahar*, Daniel Dohmeier², Joan Moseman², Ying Zhing², Alan Harris¹, Ken Brown², Gary Hattersley¹. ¹Radius Health, USA, ²3M Drug Delivery Systems, USA

Abaloparatide (ABL) is a novel analog of hPTHrP (1-34) being developed for the treatment of postmenopausal osteoporosis. In the ACTIVE Phase 3 clinical trial, 18 months of daily subcutaneous (SC) injection of ABL reduced the incidence of new vertebral, non-vertebral and clinical fractures while significantly increasing bone mineral density (BMD) in the lumbar spine, total hip and femoral neck. Transdermal (TD) delivery provides a promising alternative to SC injection and has the potential to improve patient convenience and compliance. We are currently evaluating a novel microneedle based transdermal technology (sMTS) developed by 3M Drug Delivery Systems to deliver ABL. In a completed phase 2 clinical study ABL-TD demonstrated dose dependent and significant BMD gains at the spine and hip. However, these BMD increases were lower than those achieved with ABL-SC. The difference in the pharmacokinetic (PK) profile between ABL-TD and SC may account for the reduced efficacy seen with ABL-TD. To select an optimized TD patch we compared the PK profiles of modified patch configurations and formulations in cynomolgus monkeys. Blood samples were collected at baseline and following TD or SC dosing, after 5, 10, 20, 30, 60 and 90 minutes, and ABL analyzed by LC-MS/MS. Consistent with clinical

PK, application of the parent formulation of ABL-TD resulted in rapid ABL delivery, with a C_{max} comparable to ABL-SC, but an earlier T_{max}, shorter half-life (T_{1/2}), and lower AUC. In contrast, application of an optimized ABL-TD patch resulted in an enhanced PK profile, with longer T_{1/2}, an AUC which increased by approximately 2-fold compared to the original patch, while retaining rapid delivery and C_{max} similar to SC. Overall the PK profile was comparable to SC injection. This optimized TD patch was well tolerated as evaluated using a modified Draize scoring system. Together, these results suggest that ABL-TD patch formulation can be optimized to achieve a PK profile comparable to SC injection and may have the potential to enhance the efficacy of ABL-TD.

Disclosures: Hila Bahar, Radius Health

This study received funding from: Radius Health, Inc.

SA0336

A Revisit to Safety Evaluation of Calcium/Phosphate Metabolism in A 12-Month, Randomized, Controlled Study on Alendronate/Vitamin D₃ versus Calcitriol in Chinese Osteoporotic Women. Zhen Lin Zhang¹, Er Yuan Liao², Wei Bo Xia³, Hua Lin⁴, Qun Cheng⁵, Li Wang⁶, Yong Qiang Hao⁷, De Cai Chen⁸, Hai Tang⁹, Yong De Peng¹⁰, Li You¹⁰, Liang He¹¹, Zhao Heng Hu¹², Chun Li Song¹³, Fang Wei¹⁴, Jue Wang¹⁴, Lei Zhang¹⁴, Arthur C Santora¹⁵. ¹Shanghai Sixth People's Hospital, Shanghai Jiaotong University, China, ²The Second Xiangya Hospital, Central South University, China, ³Peking Union Medical College Hospital, China, ⁴Nanjing Drum Tower Hospital, China, ⁵Huadong Hospital Affiliated to Fudan University, China, ⁶Tianjin Hospital, China, ⁷Shanghai Ninth People's Hospital, China, ⁸West China Hospital, West China School of Medicine, Sichuan University, China, ⁹Beijing Friendship Hospital, Capital Medical University, China, ¹⁰Shanghai First People's Hospital, China, ¹¹Beijing Jishuitan Hospital, China, ¹²Peking University People's Hospital, China, ¹³Peking University Third Hospital, China, ¹⁴Global Medical Affairs, Merck Sharp & Dohme China, China, ¹⁵Merck Research Laboratories, Rahway, NJ, USA, USA

Purpose: In a 12-month randomized study in Chinese osteoporotic women, weekly alendronate 70mg/vitamin D₃ 5600 IU (ALN/D5600) was superior on BMD increase over calcitriol 0.25µg daily, a Chinese guideline recommended therapy recognized to have a low risk of both hypercalcemia and hypercalciuria. However, very few randomized controlled studies evaluated these safety endpoints in Chinese patients. Our purpose was to summarize key safety endpoints related to calcium (Ca) and phosphate (P) in this controlled study.

Methods: All treated patients (n=215) in the original study were included in this safety reanalysis. Patients received concomitant Ca supplements 500mg daily. Specific measures including mean serum Ca, P and 24-h urine Ca were analyzed at baseline and several time points in 1 year. Changes exceeding predefined limits—hypercalcemia (serum Ca>2.60mmol/L), hyperphosphatemia (serum P>1.46 mmol/L with an increase>20% of baseline) and hypercalciuria (24-h urine Ca>7.5mmol/L with an increase>25% of baseline)—were assessed. Mixed model repeated measures were applied to compare within and between-group differences; Chi-Square test was used to compare proportions.

Results: In ALN/D5600 treated group, a decrease in mean serum Ca occurred at Month 6 (-0.04mmol/L, p<0.05 vs. baseline) but resolved at Month 12 (p=NS vs. baseline). Patients had lower Ca levels by ALN/D5600 treatment compared with calcitriol throughout the study (p-values <0.05). Mean serum P levels generally suggested a similar trend. ALN/D5600 treatment exhibited a small increase in mean 24-h urine Ca whereas a significant increase (1.1 mmol/L, 0.9mmol/L, at Month 6, 12, p<0.05) was shown in the calcitriol group. ALN/D5600 resulted in lower 24-h urine Ca levels compared with calcitriol at Month 6 (4.9 vs 6.1 mmol/L) and 12 (5.2 vs. 5.9 mmol/L) (p-values <0.05). One event of hypercalcemia (0.9%) and hyperphosphatemia (0.9%) occurred in the calcitriol group; 3 episodes of hyperphosphatemia (2.8%) were seen in the ALN/D5600 group. The incidence of hypercalciuria was higher in the calcitriol group at Month 6 with marginal insignificance (9.4 vs.18.5%, p=0.05) but was similar between groups at Month 12 (12.3 vs. 13.0%).

Conclusions: Hypercalciuria was uncommon with no sustained increases observed in either treatment. Calcitriol 0.25µg daily was favourable for Ca/P safety with a greater incidence of hypercalciuria at Month 6. Further studies are required to establish safety for calcitriol higher doses.

Disclosures: Arthur C Santora, Merck; Merck

This study received funding from: MSD China Holding Co., Ltd., China

SA0337

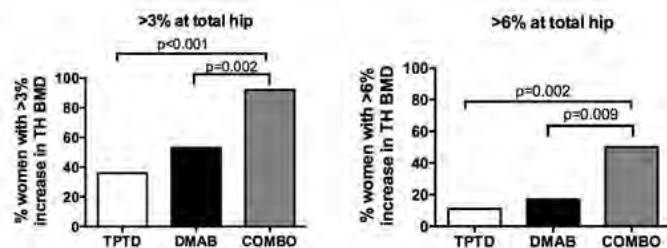
Bone Mineral Density Response Rates with Teriparatide, Denosumab, or Both: a Responder Analysis of the DATA Study. Paul Wallace¹, Alexander Uihlein², Sherri-Ann Burnett-Bowie¹, Robert Neer¹, Benjamin Leder¹, Joy Tsai¹. ¹Massachusetts General Hospital, USA, ²Northwestern University, USA

Background: Both antiresorptive and anabolic osteoporosis medications increase bone mineral density (BMD) but the patient response varies between them depending on the anatomic site. In this analysis, we wished to determine the differential rates of BMD response at the hip and spine among postmenopausal osteoporotic women treated with either teriparatide (TPTD), denosumab (DMAB) or both medications (COMBO).

Methods: 94 postmenopausal women (ages 51-91) at high fracture risk and without recent bisphosphonate exposure were randomized to receive TPTD (20 mcg SC daily), DMAB (60 mg SC every 6 months), or both medications for 24 months. BMD of the total hip (TH), femoral neck (FN), and lumbar spine (LS) were assessed by DXA at each visit. The 82 subjects who completed all 2 years were included in this analysis. Responders were defined as having 2-year BMD increases of >3% as this value meets or exceeds the least significant change for DXA measurements. An "excellent response" was defined a BMD increase of >6%. Between-group differences in response rates were analyzed using 2-sided Chi-square tests.

Results: Over 24 months, TH BMD increased by >3% in 36%, 53%, and 92% of women in the TPTD, DMAB, and COMBO groups, respectively (COMBO vs. TPTD p<0.001; COMBO vs. DMAB p=0.002). TH BMD increased by >6% in 11%, 17%, and 50% of women (COMBO vs. TPTD p=0.002; COMBO vs. DMAB p=0.009). FN BMD increased by >3% in 46%, 57%, and 83% of women in the TPTD, DMAB, and COMBO groups, respectively (COMBO vs. TPTD p=0.006; COMBO vs. DMAB p=0.036), and increased by >6% in 21%, 27%, and 50% of women (COMBO vs. TPTD p=0.031; COMBO vs. DMAB p=0.078). In the LS, BMD increased by >3% in 85%, 93%, and 100% of women in the TPTD, DMAB, and COMBO groups, respectively (p=NS for all comparisons), and increased by >6% in 63%, 78%, and 100% of women (COMBO vs. TPTD p=0.001, COMBO vs. DMAB p=0.016). There were no significant differences in the response rates between TPTD and DMAB groups.

Summary and Conclusions: The BMD response in subjects treated with combined DMAB/TPTD was higher than the rates in the monotherapy groups with 19/24 subjects in the COMBO group achieving >3% BMD gains at all 3 sites. Moreover, 50% of subjects in the COMBO group achieved hip BMD increases >6%, and 100% experienced LS BMD increases >6%. These results support the potential use of combined DMAB/TPTD in postmenopausal osteoporotic women, especially those at a very high risk of fracture.



Figure

Disclosures: Joy Tsai, None.

This study received funding from: Amgen Inc, Eli Lilly Inc

SA0338

Withdrawn.

SA0339

Design of the Foundation for NIH Bone Quality Project: Pooled individual-level measurements of BMD, bone strength, and bone turnover as surrogates for fracture risk reduction. Douglas C. Bauer^{*1}, Jean L. Hietpas¹, Mary Bouxsein², Richard Eastell³, Charles McCulloch¹, Anne DePapp⁴, Andreas Grauer⁵, Ursula Klause⁶, Bruce H. Mitlak⁷, Bruce Schneider⁸, Sanya Fanous-Whitaker⁹, Steven R. Cummings¹⁰, Dennis M. Black¹. ¹University of California, San Francisco, USA, ²Harvard Medical School, USA, ³University of Sheffield, United Kingdom, ⁴Merck & Co., Inc., Kenilworth, NJ, USA, USA, ⁵Amgen Inc., USA, ⁶Roche Diagnostics Corporation, Indianapolis, USA, ⁷Eli Lilly & Co., USA, ⁸Food & Drug Administration, USA, ⁹Foundation for the National Institutes of Health, USA, ¹⁰San Francisco Coordinating Center, California Pacific Medical Center, USA

Development of new treatments for osteoporosis has become prohibitively expensive due to the need for increasingly large fracture endpoint studies, particularly for hip fracture. Valid surrogate outcomes that accurately predict anti-fracture treatment efficacy could greatly decrease drug development time and costs. Imaging as well as bone turnover markers, alone or in combination, might be useful as surrogate endpoints, but individual trials are too small to be conclusive. Instead, pooling individual participant data from multiple trials increases sample size, ensures a consistent approach and allows predefined subgroup analyses. This strategy would allow optimal estimation of the relationship between potential surrogates and fracture outcomes.

The FNIH Bone Quality Project is collecting and pooling data from nearly 100,000 randomized participants enrolled in osteoporosis treatment trials. This Project is led by investigators from UCSF in collaboration with academic, regulatory, and industry co-investigators. The study aims include critical evaluation of 1) Imaging-derived bone strength measurements (QCT/finite element analysis (FEA) and DXA) and 2) Bone turnover markers (BTMs) for use in drug development and patient management.

To achieve these aims, we plan to systematically collect individual data from randomized trials with fracture endpoints. Imaging-based biomarkers include DXA and hip strength estimated by FEA from baseline and follow-up QCT images analyzed centrally (ON Diagnostics, Berkeley, CA) without knowledge of treatment group. Serum biomarkers will include commercially available BTMs, such as PINP and CTX. Once assembled, we will perform a series of individual-level meta-analyses to assess change in each biomarker as a predictor of anti-fracture efficacy for hip, non-spine and vertebral fracture. Pooled measurements of short-term changes in BTMs over 3-12 months will also be analyzed to identify their value to predict long-term treatment benefit.

This project represents a novel collaboration between academic investigators, the FNIH, the FDA and multiple pharmaceutical and diagnostic companies. Successful analysis of the pooled data may help establish the utility of imaging and biochemical biomarkers for both drug development and clinical care.

Disclaimer: Dr. Schneider's contributions are an informal communication and represent his own best judgment. These comments do not bind or obligate FDA.

Disclosures: Douglas C. Bauer, None.

SA0340

Determinants of Change in Bone Mineral Density during Bisphosphonate Holiday. Li Hao Richie Xu^{*1}, Beverley Adams-Huet¹, John Poindexter¹, Naim Maalouf². ¹UT Southwestern Medical Center, USA, ²University of Texas Southwestern Medical Center, Dallas, USA

Background: Due to concerns about potential side-effects related to prolonged bisphosphonate (BP) use, a drug holiday has been suggested for some BP-treated patients with osteoporosis (OP). However, there is limited information on the evolution of bone mineral density (BMD) during a BP holiday.

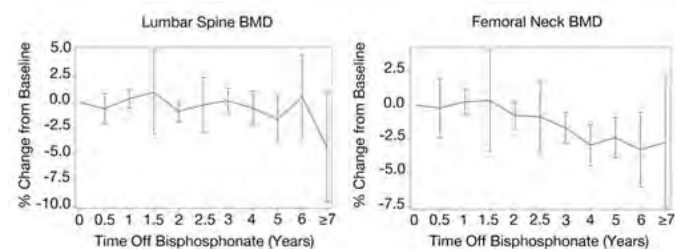
Objectives: To describe the change in BMD during a BP-holiday and assess its determinants.

Methods: A retrospective review was conducted on OP patients at a single specialty clinic who were treated with oral BP for > 2 yrs and then discontinued their BP for a drug holiday. Included were patients with at least one BMD measurement while on BP and one measurement > 1 yr after BP discontinuation. All BMD measurements were on a single DXA instrument. Excluded were patients with CKD, disuse osteoporosis, 1ry hyperparathyroidism, or concomitant glucocorticoid use. Demographic, clinical, densitometric and laboratory characteristics at the time of BP cessation were assessed as predictors of BP change in univariable and multivariable models.

Results: This analysis included 175 OP patients (13% men, 87.4% Caucasian, 7.4% Asian, 5.1% other race). At time of BP cessation, mean age was 66.5 yrs, BMI 24.5 Kg/m², T-score at L-spine (LS):-1.4 and femoral neck (FN):-1.8. Median duration on BP was 4.8 yrs. During BP holiday, patients were followed for a median of 3.1 yrs, with a median 2 follow-up DXA scans. On average, there was a significant decline in BMD at FN (-0.46%/yr; 95% CI -0.75 to -0.16; p=0.003) but not at LS (-0.28%/yr; 95% CI -0.62 to +0.05; p=0.10). FN BMD tended to drop after 1.5 yrs of BP holiday, while LS BMD was stable for 5 yrs after BP cessation (Figure). The fraction of patients whose T-score declined from >-2.5 at start of holiday to <-2.5 by the 5th yr of holiday was 8% for the LS and 11% for the FN. In univariable models, significant predictors associated with change in BMD at the FN were duration off BP therapy, BMI, Asian race, and urine DPD/Cr at time of BP discontinuation. Duration off

therapy, Asian race and BMI remained significantly associated with FN BMD decline in the multivariable model.

Conclusions: In 175 patients followed with serial DXA scans during BP holiday, FN BMD was more likely to decline over time than LS BMD. In addition to duration off BP and higher bone turnover, significant predictors of decline in BMD included lower BMI and Asian race. These data may help identify individuals who require closer BMD monitoring during BP holiday.



Change in BMD During Bisphosphonate Holiday

Disclosures: Li Hao Richie Xu, None.

SA0341

Effect of Denosumab on BMD Outcomes in Persistent Patients in a Prospective Observational Study. DL Kendler^{*1}, SL Silverman², E Siris³, JP Brown⁴, DT Gold⁵, EM Lewiecki⁶, C Simonelli⁷, G Quinn⁸, S Yue⁹, B Stolshek⁹, C Recknor¹⁰. ¹University of British Columbia, Canada, ²Cedars-Sinai Medical Center, UCLA School of Medicine, & OMC Clinical Research Center, USA, ³Columbia University Medical Center, USA, ⁴Laval University & CHU de Québec (CHUL) Research Centre, Canada, ⁵Duke University Medical Center, USA, ⁶New Mexico Clinical Research & Osteoporosis Center & University of New Mexico School of Medicine, USA, ⁷Health East Osteoporosis Care, USA, ⁸Sarnia Statistics Ltd, United Kingdom, ⁹Amgen Inc., USA, ¹⁰United Osteoporosis Centers, USA

Purpose

Although clinical trial data help characterize therapeutic efficacy in a very select population, understanding real-world effectiveness is of interest as patient populations may be more heterogeneous. In addition, persistence with therapy in the community may be suboptimal compared with clinical trials; studies report that up to 82% of patients prescribed osteoporosis therapy discontinue medication within a year (Cramer, 2007). The clinical efficacy of denosumab (DMAb) has been well characterized in the Fracture REduction Evaluation of Denosumab in Osteoporosis every 6 Months (FREEDOM) trial and other studies. To understand clinical outcomes in the community experience, we conducted a posthoc analysis to evaluate BMD response in postmenopausal women treated for osteoporosis in a 24-month prospective observational study.

Methods

In this 24-month, multicenter, single-arm study in the United States and Canada, 935 women were enrolled within 4 weeks of starting DMAb treatment, regardless of prior treatment. No assessments, clinical procedures, or changes in routine patient management were required. Persistence with DMAb was assessed at 12 and 24 months, defined as receiving ≥2 injections and ≥4 injections, respectively, and no 2 consecutive injections more than 6 months + 8 weeks apart. DXA assessment was not required to participate in the study and was collected as available. This analysis was conducted in patients who were persistent at 12 or 24 months and had both baseline and follow-up DXA scans at the same anatomical site (lumbar spine or femoral neck) during 12 or 24 months, respectively. DXA scans were analyzed at local study sites without central reading.

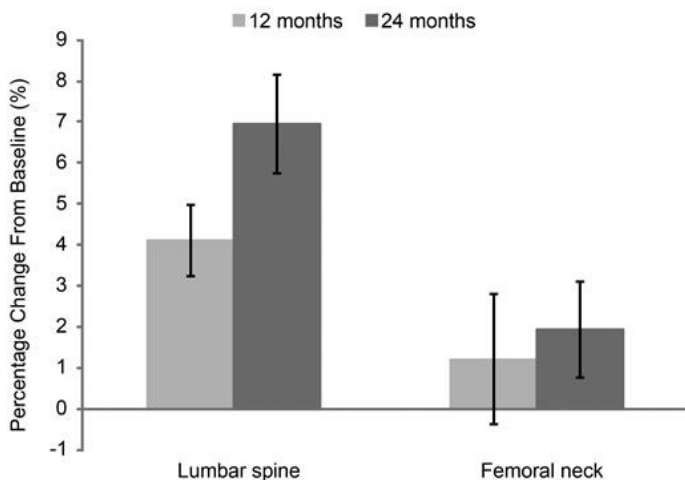
Results

Of the 374 patients with a baseline DXA and at least 1 follow-up DXA, 190 were persistent and had 12-month DXA BMD, and 154 were persistent and had 24-month DXA BMD. As expected, BMD increased over time (Figure). Mean BMD at the lumbar spine increased from baseline by 4.1% at 12 months and 7.0% at 24 months. At the femoral neck, BMD increased by 1.2% at 12 months and 1.9% at 24 months. At the 12- and 24-month time points, the percentage of patients with increased BMD was 81% and 88% at the lumbar spine and 57% and 67% at the femoral neck, respectively.

Conclusions

DMAb improved BMD in most persistent patients in a real-world setting. Moreover, the changes observed in routine clinical practice were similar to the efficacy achieved in DMAb clinical trials.

Figure. Improvement in DXA BMD in Patients Persistent With Denosumab



Values are means (95%CI).

Figure

Disclosures: DL Kendler, Pfizer, Merck, Lilly, Amgen; Lilly, Amgen, GSK; Amgen, Lilly, AstraZeneca, Astellas
This study received funding from: Amgen Inc.

SA0342

Effect of Glucocorticoid, Bisphosphonate Therapy and Disease Activity on Metacarpal Shaft Morphology: A Longitudinal pQCT Study. Inna galli-Lysak¹, Harald M Bonel², Peter M Villiger¹, Daniel Aeberli³. ¹Dept. of Rheumatology, Immunology & Allergy University of Bern, Inselspital, Switzerland, ²Institute for Diagnostic, Interventional & Paediatric Radiology, University of Bern, Inselspital, Switzerland, ³Dept. of Rheumatology, Immunology & Allergy University Hospital, Switzerland

Introduction: We established a protocol for measuring volumetric bone mineral density (vBMD) of the metacarpal shaft using peripheral quantitative computed tomography (pQCT). In a recently published cross-sectional study patients with rheumatoid arthritis (RA) had a 19% increase in cross-sectional area (CSA) at the midshaft with a reduction in cortical thickness by 10% compared to healthy controls. There was an inverse association between bone erosiveness (activity of RA) and cortical thickness. The aim of this study was to quantify the effect of glucocorticoid and bisphosphonate (BP) therapy on metacarpal shaft morphology.

Method: Consecutive postmenopausal RA patients fulfilling the American College of Rheumatology Criteria and consecutive postmenopausal healthy controls were recruited. pQCT-measurements at 50% of total metacarpal shaft of the third metacarpal bone were at baseline and follow-up. Use of BP, glucocorticoids, biologics and disease modifying anti-rheumatic drugs (DMARDs) was monitored from baseline to follow-up using patient records. Anti-CCP antibodies (ACPA) positivity, bone erosiveness (Rating Score), and disease activity (DAS28) were assessed at baseline and follow-up. Follow-up measurements were considered as valid when circumference and bone shape corresponded to baseline measurement. The following parameters were measured or calculated: total metacarpal, cortical and medullary CSA, and cortical density. To compare relative changes with muscle force, we measured muscle CSA at 60% of total radial length, and handgrip strength by sphygmomanometer. Individuals with neoplasia, anti-oestrogen or anti-testosterone therapy, HRT, osteoanabolic therapy or additional concomitant diseases or medication were excluded. For statistical analysis we used one way ANOVA or two sided Man Whitney Test.

Results: 40 consecutive postmenopausal patients with RA and 40 consecutive postmenopausal healthy controls (matched for age, height, and weight) were included. Mean follow-up was 54 months (RA patients: mean 51 months, range 24-82; controls: mean 57 months, range 23-78; p=0.122). 18 RA patients were on BP, 22 were BP-naïve. Compared to healthy controls or BP-naïve RA patients, RA patients on BP were older, had lower handgrip strength and lower forearm muscle density (p<0.01). At baseline RA patients on BP had lower cortical CSA, lower cortical thickness and bigger medullary CSA (p≤0.002). Compared to baseline BP-naïve RA patients and healthy controls showed relative increase of medullary CSA of 11% and 8%, and a reduction of cortical thickness, cortical CSA and cortical density of 6%, 4% and 1.5% (p<0.015). In RA patients on BP a relative reduction of cortical thickness was found (4%, p<0.01). Overall, glucocorticoid use ≥5mg/d had a significant negative effect on change of cortical density, cortical CSA and cortical thickness over time and a positive effect on medullary CSA. DAS28 ≥ 3.2 was positive correlated with change of cortical density. There was a trend of increased cortical CSA and cortical thickness when correlated with handgrip. ACPA positivity correlated neither with change of bone density nor geometry in a linear regression model.

Conclusion: Healthy controls, BP-naïve RA patients and RA patients on BP have an endosteal and periosteal drift at the shaft of the third metacarpal bone over time. Glucocorticoid use, disease activity and handgrip are influencing factors of metacarpal shaft morphology.

Disclosures: Daniel Aeberli, None.

SA0343

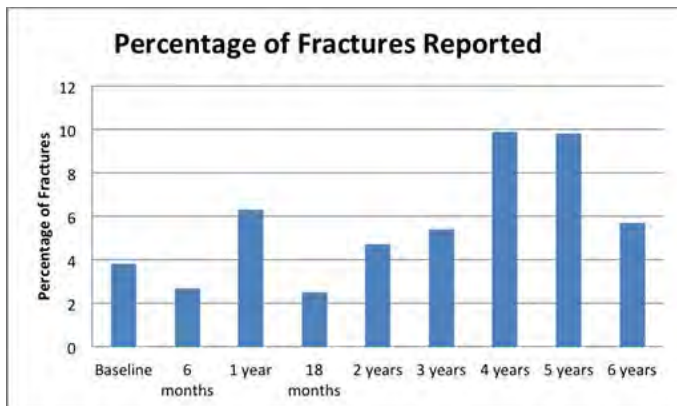
Fractures during Bisphosphonate Drug Holidays. Brittany Bindon^{*1}, Cara Clure², Neelam Balasubramanian³, William Adams³, Stephanie Kliethermes³, Jasmin Sandhu³, Pauline Camacho⁴. ¹Loyola University, USA, ²Loyola University Chicago Stritch School of Medicine, USA, ³Loyola University Medical Center, USA, ⁴Loyola University Osteoporosis & Metabolic Bone Disease Center, USA

Introduction: Atypical femoral fractures and osteonecrosis of the jaw have been associated with prolonged bisphosphonate (BP) therapy for osteoporosis. Currently, there is minimal data on safe duration of BP drug holidays. AACE guidelines (2010) recommend a holiday after 4-5 years of BP treatment for patients with moderate fracture risk and after 10 years for patients at high risk. The FDA advocates for clinicians to evaluate the need for BP therapy after 3-5 years and if a patient is at high risk, a holiday may not be "advisable". Our aim was to determine the clinical and laboratory parameters associated with increased fracture risk in patients on BP drug holiday.

Methods: A retrospective chart review was conducted of 401 patients with low bone mass and osteoporosis who began a BP drug holiday between 2004 and 2013 at Loyola University Osteoporosis and Metabolic Bone Disease Center. Collected parameters included demographics, prior therapy, bone mineral density (BMD), bone turnover markers (BTMs), PTH, calcium, Vitamin D, and clinical reports of fractures.

Results: BPs used prior included alendronate (62%), risedronate (34%), ibandronate (13%), and zoledronic acid (7%) and specific therapy did not affect fracture rates. The mean duration of treatment was 6 years ± 3.23. 62 (15.8%) patients developed a fracture during follow up. The yearly frequency of fractures ranged from 3.7-9.9%, peaking at 9.9% and 9.8% during years 4 and 5, respectively. The mean age of the fracture group was lower than the non-fracture group, almost approaching significance (69.24 years ± 12.26 vs 66.42 ± 10.18, p=0.053). Compared to the non-fracture group, the fracture group had significantly lower femoral neck BMD (0.75 gms/cm² ± 0.12 vs 0.79 ± 0.10, p = 0.02), and lumbar spine T scores (-2.13 ± 0.99 vs -1.78 ± 0.79, p = 0.01). Individuals in the fracture group had a larger increase in 25-OHD than those in the non-fractured group (9.23 ng/mL ± 21.39 vs 16.58 ± 20.61, p = 0.046). There were no significant differences when comparing changes in BMD and BTMs. Overall, there was a significant increase in bone alkaline phosphatase from the first to the last visit (p < 0.001), and more prominent with risedronate than alendronate (2.39 mcg/L ± 0.82 vs 1.27 ± 0.45).

Conclusion: Patients who begin BP drug holidays at high risk of fracture based on age and BMD warrant close follow-up. Fracture risk analysis needs to be regularly assessed during the drug holiday and treatment resumed accordingly.



Percentage of Fractures Reported

Disclosures: Brittany Bindon, None.

SA0344

Increased femoral cortical thickness in patients with atypical femur fractures; the Quebec Registry for Atypical Femur Fractures. Suzanne Morin^{*1}, Thomas Moser², Benoit Godbout³, Etienne Belzile⁴, Michelle Wall⁵, Laetitia Michou⁶, Louis-Georges Sainte-Marie², Jacques A de Guise⁷, Jacques P Brown⁶. ¹McGill University, Canada, ²Université de Montréal, Canada, ³Centre de Recherche du CHUM, Canada, ⁴Université Laval, Canada, ⁵McGill University Health Center Research Institute, Canada, ⁶Centre de recherche du CHU de Québec, Canada, ⁷Centre de recherche CHUM, Canada

Purpose: The 2014 American Society for Bone and Mineral Research (ASBMR) task force includes the presence of generalized increase in cortical thickness of the femoral diaphyses as a minor criterion in its case definition of atypical femur fracture (AFF). However, data on are lacking.

Methods: We determined femoral cortical thickness in 16 Caucasian women with AFF (cases) who agreed to participate in the Quebec Atypical Femur fracture registry and compared it to 16 ethnicity-, age-, height- and cumulative bisphosphonate exposure- matched women without fractures (controls). Using the EOS™ low irradiation 2D-3D X-Ray scanner, bilateral lower extremities examinations were obtained. We measured and compared differences in the cortical thickness ratio (CTR=medial + lateral cortices thickness in mm/femur diameter in mm, Niimi R et al. *JBMR* 2015; 30: 225-231) at 4 cm and 12.5 cm below the lesser trochanter, and the lateral cortical thickness every mm along the diaphysis from the lesser trochanter to the distal condyles in one non-operated femur between cases and controls.

Results: We identified 16 Caucasian women (mean age 69.1[8.7] years, height 157.4 [5.0] cm, 11 diaphyseal fractures (D) and 5 subtrochanteric fractures (ST), and a mean cumulative bisphosphonate use duration 12.4 [4.7] years) with AFF, and recruited 16 ethnicity-, sex-, age- and height-matched controls (mean age 68.8 [7.7] years, height 156.3 [7.0] cm, and mean cumulative bisphosphonate use duration 10.4 [3.3] years). CTR at 4 cm and 12.5 cm below the lesser trochanter were statistically different between cases and controls: 0.55 [0.05] and 0.60 [0.04] versus 0.49 [0.05], 0.54 [0.07] respectively, p < 0.001. (Table1). Measurements of CTR along the entire femur diaphysis revealed thicker cortices in cases with ST and D AFF versus their controls (p < 0.04) (Figure1). In those with ST fractures the location of highest thickness in the lateral cortex was at 2.5 cm below the lesser trochanter (9 mm) whereas in those with a D fracture, this was located at 11.5 cm below the less trochanter (8.2 mm) and in controls at 10 cm (7.1 mm).

Conclusion: We have documented increased cortical thickness ratio and lateral cortical thickness in patients with AFF compared to their matched controls with similar exposure to bisphosphonates. This supports inclusion of this criterion in the ASBMR task force definition of AFF.

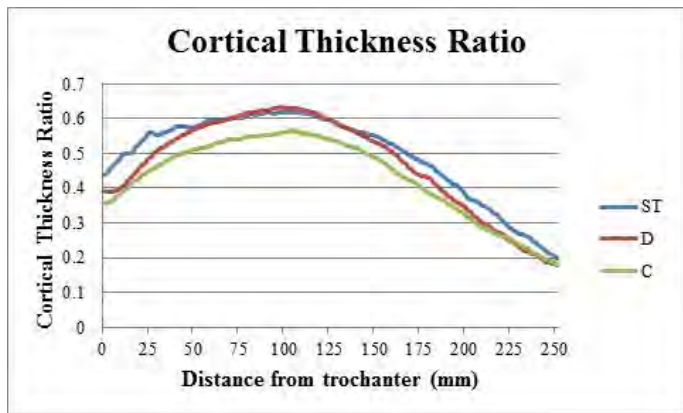


Figure Cortical Thickness Ratio distal to the lesser trochanter in participants with subtrochanteric

Table 1. Clinical characteristics of participants with atypical femur fractures (cases) and without atypical femur fractures (controls)

| Characteristics | AFF (N=16) | Controls (N=16) | p value | |
|-----------------------------|-------------|-----------------|------------|-------|
| Age, years | 69.1 (8.7) | 68.8 (7.7) | 0.65 | |
| Height, cm | 157.4 (5.0) | 156.3 (7.0) | 0.36 | |
| Bisphosphonate use, years | 12.4 (4.7) | 10.4 (3.3) | 0.10 | |
| Weight, kg | 66.2 (7.6) | 59.6 (11.8) | 0.13 | |
| Bone Mineral Density | | | | |
| Lumbar spine T-score | 14 | -1.4 (1.1) | -2.7 (0.6) | <0.01 |
| Femoral Neck T-score | 14 | -1.7 (0.7) | -2.5 (0.7) | 0.01 |

Table 1. Clinical characteristics of participants with atypical femur fractures (cases) and without

Disclosures: *Suzanne Morin, Amgen; Merck; Amgen; Eli Lilly*

SA0345

Molecular investigations of bone quality from osteoporotic women treated with Alendronate or Strontium Ranelate after 12 months. Guillaume Falgavrac^{*1}, Bernard Cortet², Cecile Olejnik³, Guillaume Penel³. ¹PMOI EA4490, France, ²Service de Rhumatologie, Hôpital Roger Salengro, CHRU de Lille, France, ³PMOI (Physiopathologie des Maladies Osseuses et Inflammatoires), EA4490, Faculté de Chirurgie Dentaire, University of Lille, Health & Law, France

Osteoporosis impairs the bone quality. Alendronate (ALN) and Strontium Ranelate (SrRan) are effective treatments in the field of osteoporosis. Their clinical benefits are recognized but their mechanisms at molecular level need to be elucidated. The aim of this work was to compare the effects of ALN and SrRan on bone quality at molecular level for a 12 month-period.

Paired iliac crest biopsies were harvested on postmenopausal osteoporotic women (50-84 years) at baseline (M0, n=10) and after 12 months (M12, n=10) for each treatment (ALN/SrRan). New and old bone was located by Back Scattered Electron images. Sr fixed in bone was located by elemental images. Raman microspectroscopy was done on new and old bone. The physico-chemical parameters (PCP) were assessed from Raman spectra (Olejnik et al 2014, Osteoporosis Int.): mineralization ratio, type-B carbonatation, crystallinity, collagen quality (hydroxyproline/proline and crosslinks ratio) and relative non-collagenous content (PG/AmideIII). The results were interpreted as function of the tissue age, the treatment and the nature of bone.

As the tissue age increases, the PCP showed that the mineralization, the type-B carbonatation and the crystallinity increases in cortical (ct) and trabecular (tb) bone, independently of the treatment as reported by Gamsjaeger et al (2014, JBMR).

Regarding the treatment, the mineralization increased (+9.3%, p=0.0026) in tb and PG/Amide III increased (+8.5%, p=0.0030) in ct and tb between ALN-M0 and ALN-M12 in new bone. The type-B carbonatation (-9.6%, p<0.0001) and the crystallinity (-1.8%, p=0.017) decreased in ct and tb new bone between SrRan-M0 and SrRan-M12. The PG/AmideIII (-8.3%, p=0.0047) decreased in tb new bone between SrRan-M0 and SrRan-M12. No difference was observed between M0 and M12 in old bone for both drugs.

The fact that ALN suppresses the bone remodeling and enhances the secondary mineralization process, explains the increase of the mineralization. A different mechanism may occur at the molecular level following SrRan intake, which could explain the release of carbonate and the decrease of crystallinity. Both drugs may have an opposite effect on the mineralization mechanism of collagen matrix according to PG/AmideIII. In conclusion these findings indicate that the effects of ALN and SrRan at molecular level are different. These data provide new insight in the mechanism of action of both ALN and SrRan.

Disclosures: *Guillaume Falgavrac, None. This study received funding from: SERVIER*

SA0346

Response to Denosumab in Patients attending a Specialist Bone Clinic. Triona McNicholas^{*1}, Breffni Drumm², Patrick O'Donoghue², Georgina Steen², Kevin McCarroll², JB Walsh², James Mahon², Rosaleen Lannon². ¹St James's Hospital, Dublin, Ireland, ²Bone Health Unit, St James's Hospital, Ireland

Background:

Denosumab has been available for the treatment of severe osteoporosis since October 2010. It is an anti-resorptive agent which has been shown to reduce fracture risk and increase bone mineral density (BMD). It is indicated in post-menopausal women with osteoporosis at high risk of fracture and has been shown to reduce the incidence of vertebral, non-vertebral and hip fractures.

Method:

Using an electronic database we reviewed records of subjects who were prescribed denosumab at our bone health clinic. 191 patients who had been commenced on denosumab between October 2010 and January 2013. Of these, 125 patients had a repeat DXA between the date they commenced denosumab and March 2015. We recorded the change in T-score in the AP spine and the total hip in these patients.

Results:

Looking at the 125 follow up DXAs available; mean age was 76 ± 10.54 years and mean time to follow-up DXA was 1.92 ± 1.08 years. 116 subjects had spinal results and 115 had hip results. Reasons for non-availability of spine or hip scores include vertebrae not suitable for analysis due to fracture or degenerative disease or bilateral hip replacements respectively.

Mean T-scores at baseline in spine and total hip were -2.82 and -2.42 respectively. Spinal T-scores improved in 91 subjects with an average relative improvement in T-score of 0.63SD (+/-0.42). In 18 subjects T-score deteriorated an average of 0.42SD (+/-0.41). T-score in the AP spine remained unchanged in 7 subjects. Hip T-scores improved in 70 subjects with an average relative improvement in T score of 0.34 (+/-0.23). In 24 subjects T-score deteriorated an average of 0.49SD (+/-0.87). T Score in the Hip remained unchanged in 21 subjects. Overall T-scores improved by 15% at the spine and 9% at the total hip.

Conclusion:

These results show that in 125 patients on denosumab with follow up DXA attending a tertiary clinical setting there is an improvement in T score in the AP spine in 78.45% of patients and in the hip in 60.87% of patients. Reasons for lack of response will require further analysis of factors such as duration of treatment,

previous treatment as well as bone turnover markers and vitamin D and fracture history.

Disclosures: *Triona McNicholas, None.*

SA0347

Short-term functional recovery between immediate- and delayed bisphosphonate treatment in patients with femoral neck fractures: a randomized controlled trial. Aasis Unnanuntana, Panai Laohaprasitiporn*, Atthakorn Jarusriwanna, Wachirapan Narktang. Siriraj Hospital, Thailand

Objective: The objective of this study was to compare the short-term functional recovery between immediate- and delayed bisphosphonate treatment in femoral neck fractured patients who were treated with hemiarthroplasty. Methods: We conducted a randomized controlled trial study at a university hospital in Bangkok, Thailand during June 2013 – June 2015. Eighty-six patients who underwent hemiarthroplasty after femoral neck fractures were included and allocated into two groups: immediate- and delayed treatment groups. Both groups received risedronate 35 mg/week either at 2 weeks (immediate group) or 3 months (delayed group) post-operation and additional calcium and vitamin D supplementation. Functional recovery were assessed by using the de Morton Mobility Index, Barthel index, EuroQoL-5D, visual analog scale, timed get-up and go test, and 2-minute walk test (2MWT) at 2 weeks as baseline data and either at 6 weeks or 3 months after surgery. Results: Most patients were female with an average age of 77 years. The patients' demographic and baseline clinical information were similar in both groups (Table 1). At 3 months follow-up, the functional outcome of both groups improved significantly. There were no statistically significant differences in any of the functional outcomes between the two groups at both 6-week and 3-month follow-up (Table 2). Although the average distance walked within 2 minutes in the immediate treatment group was higher than that of delayed treatment group (44.8 and 40.6 meters for immediate and delayed treatment groups, respectively), the difference was not statistically significant (p-value = 0.085). Discussion and conclusion: Hip fracture in the elderly carries high morbidity and mortality and can lead to another fragility fracture. Bisphosphonate is proved to be an effective drug used to prevent osteoporotic fracture. Because there is a concern regarding bisphosphonate effect on fracture healing, most orthopaedic surgeons delayed the initiation of bisphosphonate therapy for few months after fracture fixation. Since delayed bisphosphonate treatment did not adversely affect functional recovery after hemiarthroplasty, this treatment can be postponed in femoral neck fractured patients. During the first few months after surgery, the focus of treatment should be on normalization of calcium and vitamin D levels. Once corrected, the pharmacological treatment of osteoporosis can then be initiated.

Table 1 Patients' demographics and clinical characteristics

| Clinical variables | Early BIS (N=43) | Late BIS (N=43) | p-value |
|---|------------------|-----------------|---------|
| Age (years) | 78 ± 8.43 | 76 ± 8.16 | 0.366 |
| Sex (Female, %) | 23 (76.7) | 25 (78.1) | 0.891 |
| Side (Right side, %) | 10 (33.3) | 19 (59.4) | 0.040* |
| Body mass index (kg/m ²) | 21.92 ± 3.26 | 23.39 ± 4.29 | 0.136 |
| Charlson comorbidity index (%) | | | |
| - 0-1 | 28 (93.3) | 29 (90.6) | |
| - 2-3 | 2 (6.7) | 3 (9.4) | 0.696 |
| - more than 3 | 0 (0) | 0 (0) | |
| Cementless femoral component (%) | 26 (86.7) | 28 (87.5) | 0.922 |
| Preoperative ambulatory status (%) | | | |
| - with assisting device | 7 (23.3) | 11 (34.4) | 0.338 |
| - without assisting device | 23 (76.7) | 21 (65.5) | |
| Estimated glomerular filtration rate (mL/min/1.73m ²) | 74.99 ± 19.04 | 70.09 ± 19.01 | 0.328 |
| Serum calcium level (mg/dL) | 9.02 ± 0.51 | 9.12 ± 0.51 | 0.343 |
| Serum 25(OH)D level (ng/mL) | 24.22 ± 9.84 | 24.65 ± 9.73 | 0.757 |
| Baseline bone mineral density (T-score) | | | |
| - Lumbar spine | -1.43 ± 1.80 | -1.72 ± 1.21 | 0.466 |
| - Femoral neck | -2.44 ± 1.00 | -2.07 ± 1.21 | 0.300 |
| - Total hip | -2.27 ± 1.10 | -2.06 ± 0.88 | 0.406 |

Continuous data was presented as mean ± SD

BIS = bisphosphonate; SD = standard deviation; 25(OH)D = 25-hydroxyvitamin D

Table 1

Table 2 Changes of the outcome measures at postoperative 6-week and 3-month follow-up

| Outcome measures | Early BIS (N=43) | Late BIS (N=43) | p-value |
|--|------------------|-----------------|---------|
| de Morton Mobility index | | | |
| - baseline | 39.70 ± 8.95 | 38.50 ± 10.98 | 0.910 |
| - 3-month follow-up | 63.45 ± 18.14 | 64.16 ± 19.04 | 0.883 |
| Barthel index score | | | |
| - baseline | 56.83 ± 17.98 | 59.69 ± 17.08 | 0.524 |
| - 3-month follow-up | 86.72 ± 14.53 | 86.61 ± 16.70 | 0.785 |
| EQ-5D | | | |
| - baseline | 60.83 ± 18.53 | 62.31 ± 16.80 | 0.691 |
| - 3-month follow-up | 76.48 ± 15.08 | 77.58 ± 14.66 | 0.776 |
| Visual analog scale | | | |
| - baseline | 2.43 ± 1.76 | 3.06 ± 2.64 | 0.412 |
| - 6-week follow-up | 1.23 ± 1.33 | 1.27 ± 1.57 | 0.814 |
| - 3-month follow-up | 0.76 ± 0.99 | 1.32 ± 1.45 | 0.124 |
| Two-minute walking test (meters) | | | |
| - baseline | 16.22 ± 9.80 | 16.45 ± 8.35 | 0.751 |
| - 6-week follow-up | 30.93 ± 17.19 | 31.51 ± 17.89 | 0.952 |
| - 3-month follow-up | 44.84 ± 21.67 | 40.60 ± 26.55 | 0.085 |
| Timed get-up-and-go test (seconds) | | | |
| - baseline | 72.00 ± 45.59 | 66.13 ± 51.09 | 0.762 |
| - 6-week follow-up | 39.16 ± 29.53 | 36.26 ± 18.12 | 0.909 |
| - 3-month follow-up | 27.10 ± 18.16 | 31.35 ± 19.64 | 0.350 |
| Use of walking assisting device at 3-month follow-up (%) | | | |
| - none | 10 (34.5) | 10 (32.3) | |
| - cane | 4 (13.8) | 5 (16.1) | 0.962 |
| - walker | 15 (51.7) | 16 (51.6) | |

BIS = bisphosphonate

Table 2

Disclosures: *Panai Laohaprasitiporn, None.*

SA0348

Skeletal-site Heterogeneity in the Association Between Bisphosphonate Use and Incident Non-vertebral Fracture. Lisa Langsetmo*¹, Claudie Berger², David Goltzman³, Suzanne Morin³, David Hanley⁴, Stephanie Kaiser⁵, Jerilynn Prior⁶, Brian Lentle⁶, Millan Patel⁶, Nancy Kreiger⁷, Sophie Jamal⁷, Robert Josse⁷, Jacques Brown⁸, Jonathan Adachi⁹, Alexandra Papaioannou⁹, Kenneth Davison¹⁰, Wojciech Olszynski¹¹, Christopher Kovacs¹², William Leslie¹³, Tassos Anastassiades¹⁴, Tanveer Towheed¹⁴.

¹Canadian Multicenter Osteoporosis Study, Canada, ²Canadian Multicenter Osteoporosis Study, Canada, ³McGill University, Canada, ⁴University of Calgary, Canada, ⁵Dalhousie University, Canada, ⁶University of British Columbia, Canada, ⁷University of Toronto, Canada, ⁸University of Laval, Canada, ⁹McMaster University, Canada, ¹⁰University of Victoria, Canada, ¹¹University of Saskatchewan, Canada, ¹²Memorial University, Canada, ¹³University of Manitoba, Canada, ¹⁴Queen's University, Canada

We have previously reported that the use of antiresorptives among women was associated with a decrease in all non-vertebral fractures during the period 1996-2003; this overall skeletal benefit is consistent with clinical trial results. The implications of the decline in hormone therapy and increase in bisphosphonate use since the original study are unclear. In addition, the effect of treatment may be skeletal site-specific and vary over time.

We assessed the association between bisphosphonate use (current vs none) among postmenopausal women and men age 50 years and older and incident non-vertebral fracture within the CaMos cohort from Years 5-15 (2000-12). We also considered exposure duration (≤ 5y, 6-10y, >10y) and fracture site (hip, forearm, rib, upper arm, leg, other non-vertebral fracture) in secondary analysis (women only). We used a nested case-control study design with time-varying exposure and selected 4 controls (if available) per case matched on age, prior fracture history, low BMD (binary), osteoporosis diagnosis, and time period (women only). Additional covariates included education, smoking, alcohol, BMD (continuous), and for women included hormone therapy and propensity score (probability of bisphosphonate use based on demographics/medical history). There were 641 non-vertebral fracture cases in women with 2447 matched controls, and 129 cases in men with 431 matched controls.

Current bisphosphonate use was not associated with overall fracture risk in men (OR=1.11, 95% CI: 0.61, 2.02) or in women (OR: 1.03, 95% CI: 0.82, 1.30). There was no variation by duration of use in women (55% of users had 6+ years). There was apparent heterogeneity by fracture site among women, with current use associated with a reduction in hip fracture risk (OR:0.47, 95% CI: 0.26, 0.83) and an increase in forearm fracture risk (OR=1.66, 95% CI 1.03, 2.69); associations for other fracture sites fell between these extremes. The observed associations between bisphosphonate use and site-specific fracture risk also did not differ by duration of use. Comparison of the estimates to those obtained without matching indicated substantial confounding by indication.

The present study showed possible skeletal site-specific variation in women, but failed to demonstrate an association between bisphosphonate use and all non-vertebral fracture in women or men; the hypothesized duration effects were not present. Possible residual confounding by indication precludes strong conclusions.

Disclosures: Lisa Langsetmo, None.

This study received funding from: Amgen, Merck, Eli Lilly, Novartis

SA0349

Surgical treatment following Atypical Femur Fractures and functional outcomes: the Quebec Atypical Femur Fracture Registry. Prism Schneider^{*1}, Edward Harvey², Michelle Wall², Etienne Belzile³, Jacques P. Brown⁴, Suzanne Morin¹. ¹McGill University, Canada, ²McGill University Health Center Research Institute, Canada, ³Université Laval, Canada, ⁴Centre de recherche CHU de Quebec, Canada

Purpose

Atypical femur fractures are rare events leading to uncertainty as to best surgical therapeutic options. We aim to describe surgical treatment following AFF and functional outcomes 6 months after fracture diagnosis.

Methods

We reviewed all X-rays from patients who agreed to participate in the Province of Quebec (Canada) Atypical Femur Fracture Registry to characterize type, location, and surgical treatment of each AFF. Functional outcomes before and 6 months following fracture were determined by an interviewer-administered questionnaire using the Level of Lower Extremity Function Scale (LEFS).

Results

To date, 51 participants have been recruited in the Registry (total of 76 AFF) with a mean age of 69 (\pm 9) years, 90% women (Table). All were exposed to bisphosphonates with an average cumulative duration of use of 10.5 [4.7] years. Incomplete subtrochanteric AFF (sAFF) were more often treated non-operatively (n = 9) compared with operatively (n = 3), similarly incomplete diaphyseal AFF (dAFF) were more often treated non-operatively (n = 18) compared to operatively (n = 12). In patients who underwent surgery, sAFF were most often treated with a long cephalomedullary nail (CMN) (n = 9 complete; n = 2 incomplete) compared to a short CMN (n = 3). Complete dAFF were treated with a long CMN (n = 10) compared to intramedullary nail (IMN) (n=9; greater trochanteric start n = 6; piriformis entry n = 3). Similarly, incomplete dAFF were treated either with CMN (n = 3) vs. IMN (n = 4; greater trochanteric start= 3). Patients with unilateral complete AFF showed greater improvement in LEFS from pre-fracture diagnosis (25.3 ± 19.9) to 6-month after (32.7 ± 7.5) with surgical fixation, when compared to patients with unilateral incomplete AFF from pre-diagnosis (43.8 ± 13.9) to 6-month follow-up (43.0 ± 17.9) without surgical fixation. Patients with bilateral AFF who underwent surgical fixation of only one side (n = 7), mean baseline LEFS was 64.9 ± 15.6 , compared to 6-month follow-up LEFS of 54.0 ± 9.8 , demonstrating a lack of return to baseline function ($p = 0.09$).

Conclusion

Treatment of AFF varied from non-operative treatment to surgical fixation for both complete and incomplete fractures using CMN or IMN implants. Clinical guidelines are needed for optimal timing of surgical fixation for incomplete AFF or for optimal implant use in complete fractures. Functional outcomes vary in patients and may be related in part to surgical treatment.

| Characteristics | AFF |
|---------------------------------|----------------|
| Age, years | 69 (9) |
| Women | 46 (90) |
| Height, cm | 158.3 (7.5) |
| Weight, kg | 67.1 (19.6) |
| BMI, kg/m ² | 26.8 (3.5) |
| Caucasian | 47 (92) |
| Asian | 4 (8) |
| Comorbid condition count | 3.6 (1.6) |
| Previous Fragility Fracture | 11 (60) |
| Prior Bisphosphonate Use | |
| Bisphosphonate | 51 (100) |
| Alendronate | 42 (82) |
| Risedronate | 12 (24) |
| Zoledronic Acid | 7 (14) |
| Etidronate | 3 (6) |
| Cumulative years of use, years | 10.5 (4.7) |
| Daily Supplemental Intake | |
| Vitamin D, UI/day | 1049.6 (376.3) |
| Calcium, mg/cidor | 828.0 (295.6) |
| Bone Mineral Density | N |
| Femoral neck T-score | -1.8 (0.7) |
| Lumbar spine T-score | -1.7 (1.4) |
| Mechanism of Injury | |
| No fall | 40 (78) |
| Fall from standing height | 11 (22) |
| Pre-fracture Pain | |
| Present | 37 (73) |
| Duration, median (IQR)*, months | 6 (1-12) |

Table. Characteristics of Quebec Atypical Femur Fracture Registry participants

Disclosures: Prism Schneider, None.

SA0350

The Bone-Protective Effects of a Novel Selective Estrogen Receptor Modulator (SERM) pERD in Ovariectomized Rats. Jukka Morko^{*1}, Carsten Möller², ZhiQi Peng¹, Jukka Vääräniemi¹, Katja M Fagerlund¹, Tiina A Suutari¹, Jenni Bernoulli¹, Jukka P Rissanen¹, Andrea Wagenfeld², Arndt Schmitz², Jussi M Halleen¹. ¹Pharmatest Services Ltd, Finland, ²Bayer Pharma AG, Germany

Selective estrogen receptor modulators (SERMs) are a diverse class of compounds that bind to estrogen receptors (ERs) and agonize or antagonize estrogen action in different tissue types. Due to a broad spectrum of physiological and pathological processes contributed by ERs, SERMs provide a potential therapeutic benefit for a variety of diseases. In this study, we characterized the effects of a novel SERM pERD on bone in a rat ovariectomy (OVX) model of postmenopausal osteoporosis, and we compared the effects of pERD treatment with the effects of 17 β -estradiol (E2) and raloxifene (RAL). E2 was used as a complete agonist and RAL as a reference SERM exhibiting agonist activity on bone and being used in clinical practice. Female Sprague-Dawley rats were ovariectomized or SHAM-operated at 3 months of age. Treatment of rats was started on one day after the operations and continued once a day for 8 weeks. OVX rats were treated with pERD at 1, 3 or 10 mg/kg/d *p.o.*, E2 at 4 μ g/kg/d *s.c.*, RAL at 1 mg/kg/d *p.o.* or with vehicle, and SHAM-operated rats were treated with vehicle. Treatment effects on bone were studied by peripheral quantitative computed tomography (pQCT), bone histomorphometry and by measuring serum levels of bone turnover biomarkers. In metaphyseal trabecular bone, treatment with pERD at 1, 3 and 10 mg/kg/d prevented an OVX-induced reduction in bone mineral density (BMD), bone mineral content (BMC), bone volume fraction (BV/TV) and trabecular number (Tb.N). The effects of pERD were associated with a prevention of OVX-induced increase both in osteoclastogenesis (N.Oc/B.Pm and Oc.S/BS) and bone turnover and formation (MS/BS, MAR, BFR/BS and BFR/BV). In diaphyseal cortical bone, treatment with pERD at 1 and 3 mg/kg/d prevented an OVX-induced increase in cortical BMC, cortical bone area and periosteal perimeter. In circulation, treatment with pERD at 1, 3 or 10 mg/kg/d prevented an OVX-induced increase in serum levels of cross-linked telopeptides of type I collagen (CTX-I), N-terminal mid-fragment of osteocalcin (OC), and procollagen type I N-terminal propeptide (PINP). These effects of pERD treatment were similar with the effects of E2 and RAL indicating a bone-protective agonist activity for pERD in metaphyseal trabecular bone at 1-10 mg/kg/d and in diaphyseal cortical bone at 1-3 mg/kg/d. The maximal efficacy of pERD was lower than the efficacy of E2 presenting pERD as a novel partial agonist in bone in young adult OVX rats.

Disclosures: Jukka Morko, Pharmatest Services Ltd, Employee

SA0351

Why Do Bisphosphonates Compromise Bone Formation?. Pia Jensen^{*1}, Thomas Levin Andersen², Pascale Chavassieux³, Jean-Paul Roux³, Jean-Marie Dealisse². ¹Vejele Hospital, Denmark, ²Department of Clinical Cell Biology, Vejele Hospital, Denmark, ³INSERM Unité 1003, Université de Lyon, France

Bisphosphonates (BP) are widely used to reduce osteoclastic bone resorption in osteoporotic patients. However, BPs also reduce bone formation, an effect commonly considered as a consequence of decreased resorption. Still, direct effects of BPs on the osteoblast lineage were reported in preclinical models. Furthermore, refined analyses of remodeling sites in adult human bone recently revealed pools of osteoprogenitors in areas likely to be exposed to BPs, raising the question of an effect of BPs on osteoblast recruitment. These areas included reversal surfaces and so-called bone remodeling compartment canopies, which are not taken into account in classical bone histomorphometry. The aim of the present study was to investigate whether BPs affect these putative osteoblast recruitment sites, by re-analyzing bone sections of the initial clinical study that addressed the effect of alendronate on patients with postmenopausal osteoporosis (PMO).

Goldner trichrome-stained sections of transiliac bone biopsies of PMO patients treated with alendronate (10 mg/d, n=25) or placebo (n=64) for 24-36 months, were assessed for classical histomorphometric parameters, i.e. extent of cancellous bone surface showing erosion, osteoid, osteoclasts, and osteoblasts. Reversal surfaces, defined as eroded surfaces without osteoclasts, were also assessed. Reversal surfaces were subdivided into active and arrested, depending on whether they were leading to bone formation or not, as based on our earlier studies. All surfaces were evaluated for the presence or absence of a canopy. The activation frequency of bone formation was also determined.

BP treatment significantly decreased bone resorption and formation parameters. Of note, BPs induced an increase in the extent of arrested reversal surfaces ($p < 0.01$) and a decrease in the prevalence of canopy ($p < 0.01$), indicating an impaired delivery of osteoprogenitors at the resorption sites. This view was strengthened by the negative relation between the proportion of reversal surface that was arrested and the prevalence of canopy ($p < 0.001$), the extent of osteoid ($p < 0.0001$), the extent of osteoblast surface ($p < 0.0001$), and the activation frequency of bone formation ($p < 0.05$).

We conclude that a previously unrecognized reason why BPs compromise bone formation in PMO is that BPs induce an arrest of remodeling cycles due to deficient osteoblast recruitment. These data deserve attention when treating osteoporotic patients with BPs.

Disclosures: Pia Jensen, None.

SA0352

See Friday Plenary Number FR0352.

SA0353

Risk of hip fracture increases with diabetes mellitus (DM): Results from the Kailun cohort in China. Shivani Sahni^{1*}, Katherine Tucker², Chunpeng Ji³, Junjuan Li³, Shouling Wu³, Xiang Gao⁴. ¹Hebrew SeniorLife, Institute for Aging Research & Harvard Medical School, USA, ²University of Massachusetts, Lowell, MA, USA, ³Kailun Hospital, China, ⁴The Pennsylvania State University, USA

Osteoporosis affects almost 70 million older Chinese and causes ~687,000 hip fractures in China each year. By the year 2050, more than 50% of all osteoporotic hip fractures will occur in Asia. Limited data from Western countries suggests that type 2 diabetes (T2D) may increase fracture risk in older adults though data on pre-diabetes is less clear. Considering the overall high prevalence of diabetes (11.6%) and pre-diabetes (50.1%) in Chinese adults, it is vital that we examine the association of diabetes and osteoporosis in Chinese populations that will aid in targeting specific risk factors of fracture in older adults with diabetes or pre-diabetes.

We examined the association of impaired fasting glucose (IFG) and T2D with the risk of hip fracture over 5 years in men and women from the Kailun cohort in China.

Men and women (n=101,510) with baseline information on IFG and T2D were followed for hip fracture from 2008-2013. After excluding those with CHD/stroke, baseline report of hip fractures and missing data, we included 95,526 participants in the analyses. Hip fracture was defined as the first fracture of the proximal femur and was confirmed by review of medical records. Participants with no medical history of diabetes treatment and fasting plasma glucose concentration <5.6 mg/dL were categorized as not having diabetes. Participants with fasting plasma glucose concentration between 5.6 and 6.9 mmol/L were categorized as having IFG. Participants who had fasting glucose concentration ≥7 mmol/L or reported active diabetes treatment during the survey were categorized as having T2D. Cox-proportional hazards regression estimated Hazard Ratios (HR) adjusting for age, smoking, height, weight, menopausal status (in women), physical activity, alcohol intake and C-reactive protein. Individuals without diabetes were considered as the reference group.

The mean age was 52 y (range: 18-98), 20% were women, 23% had IFG, and 11% had T2D. During 5.4 years of follow-up (521,782 person years), there were 183 incident hip fractures. Those with T2D had 60% greater risk of hip fracture compared to those without T2D (Table). Those with IFG appeared to have 30% greater risk of hip fracture compared to those without T2D, but this did not reach statistical significance. Further adjustment strengthened the results among those with T2D.

These findings suggest that older Chinese adults with T2D have greater risk of hip fracture than those without T2D. Future work should examine if these associations persist after adjustment for insulin use and baseline bone mineral density.

Table. Association of impaired fasting glucose and type 2 diabetes with risk of hip fracture in older men and women from the Kailun cohort in China.

| | Hazard Ratios and 95% Confidence Intervals [HR (95%CI)] by Diabetes Status | | |
|---------|--|--------------------------|-------------------|
| | Diabetes Status | | |
| | Without diabetes | Impaired fasting glucose | Diabetes |
| Cases/N | 99/62,678 | 41/21,829 | 43/11,019 |
| Model 1 | Ref | 1.30 (0.90-1.88) | 1.60 (1.08-2.36) |
| Model 2 | Ref | 1.29 (0.89, 1.88) | 1.85 (1.24, 2.77) |

Model 1 adjusted for age, smoking, height, weight and menopausal status (in women). Model 2 adjusted for model 1 and physical activity, alcohol and C-reactive protein.

Table

Disclosures: Shivani Sahni, PAI, Inc.; General Mills Bell Institute of Health and Nutrition

SA0354

Serum Sclerostin Levels in Liver Transplantation Patients at Risk of New-Onset Diabetes Mellitus: Response to Oral Glucose Tolerance Test. Guillermo Martinez Diaz-Guerra^{1*}, Gonzalo Allo², Mercedes Aramendi², Sonsoles Guadalix², Soledad Librizzi², David Lora², Carlos Jiménez², Federico Hawkins². ¹University Hospital 12 Octubre, Spain, ²University Hospital 12 de Octubre, Spain

INTRODUCTION: Several studies have found that sclerostin (SCL) is increased in patients with diabetes mellitus (DM) and could have a role in the increased risk of fractures in these patients. SCL has not been investigated in new onset diabetes after transplantation (NODAT) and, particularly, the acute effect of increasing plasma glucose on SCL remains unknown. The aim of our study is to evaluate serum SCL levels in a cohort of patients with liver transplantation (LT) at risk of developing

NODAT and its response after an oral glucose overload. PATIENTS AND METHODS: 85 LT patients (50 M, 35 F) without previous DM were studied. A 75 g oral glucose tolerance test was performed (OGTT) and ADA diagnostic criteria were followed. Serum SCL (Enzyme immunoassay, TECO medical) was measured in fasting, 60 and 120-minute samples during OGTT. MANOVA test were used to evaluate the evolution of SCL levels (from baseline to 120-minute). RESULTS: Mean age was 58.6 ± 12.5 years. Minimum study time since LT was 6 months and mean time since LT was 9.7 ± 5.7 years. 48 patients (64%) showed normal glucose tolerance (NGT), 31 (36.4%) impaired glucose tolerance (IGT) and 6 NODAT (7.05%). SCL levels were significantly higher in NODAT patients at baseline compared to NGT (p<0.001) and IGT (p<0.01). Age and fasting plasma glucose were independently associated with SCL (multiple linear regression, standardized β coefficient 0.29, p=0.006; 0.24, p<0.05 respectively). After OGTT, SCL showed a significant decrease which was more pronounced in the NODAT group (% of change -0.32 ± 0.64, p=0.01), although remained higher during the test compared to the other groups. CONCLUSIONS: Our results show that serum SCL levels are positively correlated with plasma glucose and age, and higher in patients with NODAT than in patients with IGT or NGT. After an OGTT, SCL decreases particularly in patients with NODAT. More studies are necessary to evaluate the role of high SCL levels in NODAT and bone loss.

Disclosures: Guillermo Martinez Diaz-Guerra, None.

SA0355

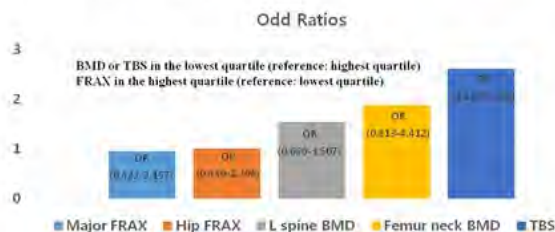
See Friday Plenary Number FR0355.

SA0356

The better performance of TBS in the prediction of vertebral fractures in postmenopausal diabetic women compared to BMD or FRAX score. Yong Jun Choi^{*}, Insun Song, Yoon-Sok Chung. Ajou University School of Medicine, South Korea

Introduction Type 2 diabetes has been associated with fracture risk, but paradoxically greater bone mineral density. The trabecular bone score (TBS) derived from the dual x-ray absorptiometry (DXA) image is proposed as an index of bone microarchitecture that associated with bone quality. The aim of this study is to compare the performance of TBS, bone mineral density (BMD), Fracture Risk Assessment Tool (FRAX) score in the prediction of vertebral fractures in diabetic patients. Subjects and Methods This cross-sectional study enrolled total 187 Korean postmenopausal diabetic women. Lateral plain radiographs of the thoracolumbar spine, and BMD of lumbar spine and femur neck were obtained using DXA. TBS was obtained by TBS iNsite Software program with DXA images. The FRAX probability was computed using the algorithm available online at <http://www.shef.ac.uk/FRAX> (South Korea version). Vertebral fractures (VFs) were detected by Genant semi-quantitative method and graded according to their severity (grade 0-3). Results Among the subjects, 77 women (41.2%) had vertebral fractures and 110 women (58.8%) did not. The mean of TBS was significantly lower in subjects with VFs (1.27±0.12) than without VF (1.31±0.11), (p=.006). However, there was no significant difference in lumbar spine and femur neck BMD between the subjects with VFs and without VFs (p>.05). TBS were also significantly decreased according to the number or severity of VFs. However, lumbar spine BMD did not showed significant decrease according to the number or severity of VFs. Odds ratios (ORs) for VFs for TBS in the lowest quartile (vs. highest quartile reference) was the higher (OR 2.617, 95% CI 1.120-6.116) compared to ORs for BMD in the lowest quartile (vs. highest quartile reference) and ORs for FRAX score in the highest quartile (vs. lowest quartile reference). Conclusion TBS showed the better performance in the prediction of VFs in postmenopausal diabetic women. These results suggest that TBS could be more useful tools to predict radiographic VFs in postmenopausal diabetic women than BMD or FRAX.

Odd Ratios (95% CI) for vertebral fracture(s) with BMD or TBS or FRAX



Figure

Disclosures: Yong Jun Choi, None.

SA0357

BMD and TBS status in adult patients suffering from Polio. D Grados Canovas¹, Silvana Di Gregorio², Luis Del Rio*², E Bonel², Manuel Garcia², Renaud Winzenrieth³. ¹Departament of Rheumatology, Hospital San Rafael, Spain, ²Cetir Grup Mèdic, Spain, ³R&D department, Med-Imaps, France

Objective: Assess TBS to categorize skeletal status in adult subjects with history limbs Poliomyelitis sequelae.

Method: We scan total body, lumbar spine (LS) and both hips in 59 patients with history of poliomyelitis infection and limb. Differences between affected extremities and opposites were assessed in terms of BMD and TBS (TBS® Insight v2.1; Medimaps). Subjects were stratified using BMD T-score (minimum T-score of the scanned sites). TBS results were categorized as normal (TBS-N, >1.350); partially deteriorated (TBS-PD, [1.250 -1.350]), and significantly deteriorated (TBS-SD, ≤1.250).

Results: The left limb was the extremity most affected in this group (32 vs 21). 6 patients had both extremities affected. 15% of patients had normal BMD at femur, 49% had normal LS BMD while only 36% had TBS-N. After stratifications, osteopenic patients (47% at the femur and 42% at LS) or TBS-PD (39%) were detected similarly. In osteoporotic patients, lowest BMD T-score was found at the femur (37%, mainly at the affected limb) while only 8% were osteoporotic at LS. TBS-SD was found in 25% of these patients. Spondyloarthritis and scoliosis signs were found in 25 patients. Among them, 16.7% were osteoporotic at affected femoral side although a normal BMD at L1-L4 and at the opposite femur. All of them had a deteriorated TBS (TBS-PD and TBS-SD). TBS value is associated negatively with the fat mass ($r=-0.36$, $p<0.005$) and with the legs lean mass ($r=-0.44$, $p<0.001$) while Spine BMD was neither associated with lean nor fat mass. A positive borderline association between lean mass and BMD at Femur was observed ($r=0.26$, $p=0.049$). No correlations were obtained between TBS and BMD at all sites. Polio subjects had a significant lower TBS value (TBS Z-score=-0.6 SD; $p<0.001$) when compared with normal values for age and thus independently of the gender. It seems that TBS alteration is more pronounced in mean than in women as reported by a lower TBS z-score (-0.83 vs -0.44 SD).

Conclusion: TBS seems to be more sensitive than BMD to identify patients suffering from Polio. Postural instability could increase irregular mechanical charges to lumbar spine and unaffected femur that may decrease the BMD sensitivity to classify patients. Interestingly, TBS was negatively associated with the fat and lean mass while BMD at femur was associated positively with lean mass. This differentiating associations have to be investigated in further study.

Disclosures: Luis Del Rio, None.

SA0358

Risk Factors For The Development Of Osteoporosis After Spinal Cord Injury. A 12-Month Follow-up Study. Laia Gifre*¹, Joan Vidal², Josep Lluís Carrasco³, Africa Muxi⁴, Enric Portell², Ana Monegal⁵, Núria Guanabens⁵, Pilar Peris⁵. ¹Hospital Clinic Barcelona, Spain, ²Guttmann Neurorehabilitation Institute. Universitat Autònoma de Barcelona, Spain, ³Public Health Department, University of Barcelona, Spain, ⁴Nuclear Medicine Department. Hospital Clínic of Barcelona, Spain, ⁵Rheumatology Department, Hospital Clinic of Barcelona, Spain

Introduction: Spinal cord injury (SCI) has been associated with a marked bone loss after injury and a consequent increased risk of osteoporosis and fractures. The aim of this study was to analyze the factors associated with osteoporosis development short-term after SCI. Methods: We included patients with complete recent SCI (<6 months) evaluating bone turnover markers (PINP, bone ALP and sCTX), 25-OH-vitamin D (25OHD) levels and lumbar and femoral BMD (Lunar, Prodigy) at baseline, and 6 and 12 months after SCI. The risk factors for osteoporosis analyzed included: age, gender, BMI, toxic habits, bone turnover markers, 25OHD levels, lumbar and femoral BMD, level, severity and type of SCI and days-since-injury. Osteoporosis was defined according to WHO criteria. Covariates at baseline were used as markers of osteoporosis at 12 months, with their diagnostic and prediction ability being assessed by computing their sensitivity, specificity and predictive values. The area under ROC curves (AUC) was analyzed, and relative risk ratios (RR) to evaluate the increase of risk of osteoporosis development at 12 months were calculated. Results: Thirty-five patients aged 35-16 years were included, and 52% developed osteoporosis during the 12-month follow-up. These latter patients had lower BMD values at femur and lumbar spine and higher bone turnover markers at baseline. Total femur BMD showed an excellent diagnostic ability (AUC=0.92; 95%CI, 0.81-1), and lumbar BMD (AUC=0.78; 95%CI, 0.6-0.97), bone ALP (AUC=0.77; 95%CI 0.57-0.96) and PINP (AUC=0.75; 95%CI, 0.54-0.95) had good diagnostic ability. On multivariate analysis the principal factors related to osteoporosis development were: baseline total femur BMD (<1gr/cm2 (RR, 3.86; 95%CI, 2.74-4.22, $p<0.0001$) and lumbar BMD <1.2gr/cm2 (RR, 2.32; 95%CI, 1.53-2.59, $p=0.0002$), with a high probability for osteoporosis development when both parameters were below these cut-off values (0.97 probability of osteoporosis). Increased risk for osteoporosis was also associated with increased baseline values of bone ALP (>14 ng/mL) (RR, 2.40; 95%CI, 1.10-5.23, $p=0.041$) and PINP (>140 ng/mL) (RR, 3.08; 95%CI, 1.10-8.57, $p=0.017$). Conclusions: Evaluation of BMD at the lumbar spine and femur short-term after SCI is a simple, effective method for predicting the development of osteoporosis during the first year after SCI.

Our results also indicate the need to evaluate and treat these patients shortly after injury.

Disclosures: Laia Gifre, None.

This study received funding from: Work funded by a grant from Fundació La Marató de TV3.

SA0359

See Friday Plenary Number FR0359.

SA0360

Compromised Trabecular Microstructure in Young Adults with Cystic Fibrosis. Melissa Putman¹, Logan Greenblatt*², Padrig Tuck², Ahmet Uluer³, Leonard Sicilian⁴, Allen Lapey⁵, Catherine M. Gordon⁶, Mary Bouxsein⁷, Joel Finkelstein². ¹Massachusetts General Hospital/Children's Hospital Boston, USA, ²Massachusetts General Hospital, Endocrine Unit, USA, ³Boston Children's Hospital, Division of Respiratory Diseases, USA, ⁴Massachusetts General Hospital, Pulmonary Division, USA, ⁵Massachusetts General Hospital, Pediatric Pulmonary Division, USA, ⁶Hasbro Children's Hospital, Divisions of Adolescent Medicine & Endocrinology, USA, ⁷Massachusetts General Hospital, USA

Purpose: The risk of fracture is increased in patients with cystic fibrosis (CF). Although areal bone mineral density (aBMD) by DXA and bone microarchitecture by high-resolution peripheral quantitative computed tomography (HR-pQCT) are often compromised, these factors do not seem to account for all of the increase in fracture risk in these patients. Individual trabecular segmentation (ITS)-based morphological analysis of HR-pQCT images segments trabecular bone into individual plates and rods of different alignment and connectivity, which are important determinants of trabecular bone strength. We sought to determine whether alterations in ITS are present in patients with CF and may help explain some of their increased fracture risk.

Methods: 30 patients with CF (18 women, 12 men), ages 18-40 years (mean 25 ± 5) underwent DXA of the hip and HR-pQCT scans of the radius and tibia with further assessment of trabecular microstructure by ITS. They were compared with 60 healthy controls matched for age (+2 yrs), gender, and race using generalized linear models. Multivariable linear regression was performed adjusting for BMI and BMI plus total hip aBMD.

Results: As expected, BMI was lower in patients with CF than in controls (20.8 vs 25.2 kg/m², $p<0.01$). Plate volume fraction, thickness, and density as well as plate-plate and plate-rod connectivity were reduced and axial alignment of trabeculae was lower in CF subjects at both the radius and the tibia ($p<0.05$ for all). At the radius, adjustment for BMI eliminated most of these differences. At the tibia, however, reductions in plate volume fraction and number, axially aligned trabeculae, and plate-plate connectivity remained significant after adjustment for BMI alone and for BMI and aBMD ($p<0.05$ for all).

Conclusions: Young adults with CF have compromised plate-like and axially aligned trabecular morphology with less connectivity between trabeculae. Although the lower BMI in patients with CF may account these differences at the radius, neither differences in BMI nor in aBMD fully account for trabecular microstructural deficits at the tibia. These findings indicate that ITS provides unique information about bone integrity and thus it may help explain a portion of fracture risk in CF patients not accounted for by BMD and/or bone microarchitecture.

Table 1: ITS Results (mean ± SE)

| ITS Parameter | Radius | | Tibia | |
|--|------------------------------|--------------------|--------------------------------|--------------------|
| | CF Subjects | Healthy Volunteers | CF Subjects | Healthy Volunteers |
| Plate bone volume fraction (pBV/TV) | 0.104 ± 0.008 ^a | 0.127 ± 0.006 | 0.136 ± 0.008 ^{a,b,c} | 0.173 ± 0.006 |
| Rod bone volume fraction (rBV/TV) | 0.170 ± 0.004 | 0.174 ± 0.003 | 0.131 ± 0.006 ^b | 0.150 ± 0.004 |
| Axial bone volume fraction (aBV/TV) | 0.111 ± 0.006 ^a | 0.128 ± 0.004 | 0.133 ± 0.006 ^{a,b,c} | 0.154 ± 0.004 |
| Trab plate number density (pTbN, 1/mm) | 1.45 ± 0.02 ^a | 1.54 ± 0.02 | 1.50 ± 0.023 ^{a,b,c} | 1.62 ± 0.016 |
| Trab rod number density (rTbN, 1/mm) | 1.91 ± 0.02 | 1.90 ± 0.02 | 1.71 ± 0.03 | 1.78 ± 0.02 |
| Mean trab plate thickness (pTbTh, mm) | 0.203 ± 0.002 ^a | 0.210 ± 0.001 | 0.217 ± 0.003 ^{a,b,c} | 0.229 ± 0.002 |
| Mean trab rod thickness (rTbTh, mm) | 0.211 ± 0.001 ^{a,b} | 0.214 ± 0.002 | 0.217 ± 0.001 | 0.216 ± 0.001 |
| Mean trab rod length (rTbL, mm) | 0.651 ± 0.002 | 0.644 ± 0.003 | 0.655 ± 0.004 | 0.649 ± 0.003 |
| Plate-Rod junction density (P-R JuncD, 1/mm ³) | 4.21 ± 0.17 ^a | 4.64 ± 0.12 | 3.66 ± 0.18 ^{a,b} | 4.69 ± 0.13 |
| Plate-Plate junction density (P-P JuncD, 1/mm ³) | 2.10 ± 0.11 ^a | 2.42 ± 0.08 | 2.17 ± 0.08 ^{a,b,c} | 2.74 ± 0.06 |

^a $p<0.05$ on unadjusted analysis comparing CF subjects with age, gender, and race-matched healthy volunteers; ^b $p<0.05$ after adjustment for BMI; ^c $p<0.05$ after adjustment for BMI and total hip aBMD

Table 1

Disclosures: Logan Greenblatt, None.

This study received funding from: Vertex Investigator Initiated Studies Grant

SA0361

See Friday Plenary Number FR0361.

SA0362

Inflammatory focal bone destruction in femoral heads with end-stage hemophilic arthropathy: A study on clinic samples with micro-CT and histologic analyses. Shanxing Zhang^{*1}, Hongting Jin², Peijian Tong³.
¹Zhejiang Chinese Medical University, Peoples republic of china, ²Institute of Orthopaedics & Traumatology of Zhejiang Province, China, ³Department of Orthopaedics Surgery, the First Affiliated Hospital of Zhejiang Chinese Medical University, China

Abstract Introduction In addition to systematic bone loss, focal bone destruction has a high prevalence in hemophilic arthropathy (HA) affected joints, but the mechanism remains unclear. Purpose We performed this study on clinic samples to explore the focal bone destruction in femoral heads suffered with end-stage HA. Methods 21 femoral heads from HA patients and 19 femoral heads from rheumatoid arthritis (RA) patients were collected when they underwent total hip replacement. Micro-CT scanning and histologic analysis, including tartrate-resistant acid phosphatase (TRAP) staining of subchondral bone were performed to evaluate the bone destruction and osteoclasts activity by counting osteoclasts in each random field (magnification 5 ×). RANKL, OPG as well as pro-inflammatory cytokines, such as TNF-α and IL-1β in subchondral bone were detected by immunohistochemistry (IHC) method. The IHC photos were quantitative analyzed with software by detecting the integral optical density (IOD) of the tissue around the subchondral bone. Results Severe focal bone lesions were observed in all of the HA and RA femoral heads by micro-CT imaging and histologic analysis. The mean percentage of lesion volume to total volume of the femoral heads from HA patients was significantly higher than those from RA patients (8.2 ± 3.0% versus 6.0 ± 2.6%, P=0.019). There was no significant difference in osteoclasts numbers in subchondral bone between HA and RA groups. By IHC analysis, high expression of RANKL, TNF-α, IL-1β and low expression of OPG were observed in subchondral bone in femoral heads derived from HA and RA patients, and there were no significant differences in the expression of RANKL, OPG, TNF-α and IL-1β in femoral heads derived from HA and RA patients. Conclusion Our findings demonstrated the focal bone destruction coupled with inflammatory osteoclastogenesis at subchondral bone in femoral heads from patients with end-stage HA, and that was similar to the changes in the femoral heads of RA patients, so maybe proper therapeutic interventions are required. Keywords: Hemophilia; Hemophilic arthropathy; Bone destruction; osteoclastogenesis; Inflammation; Femoral head

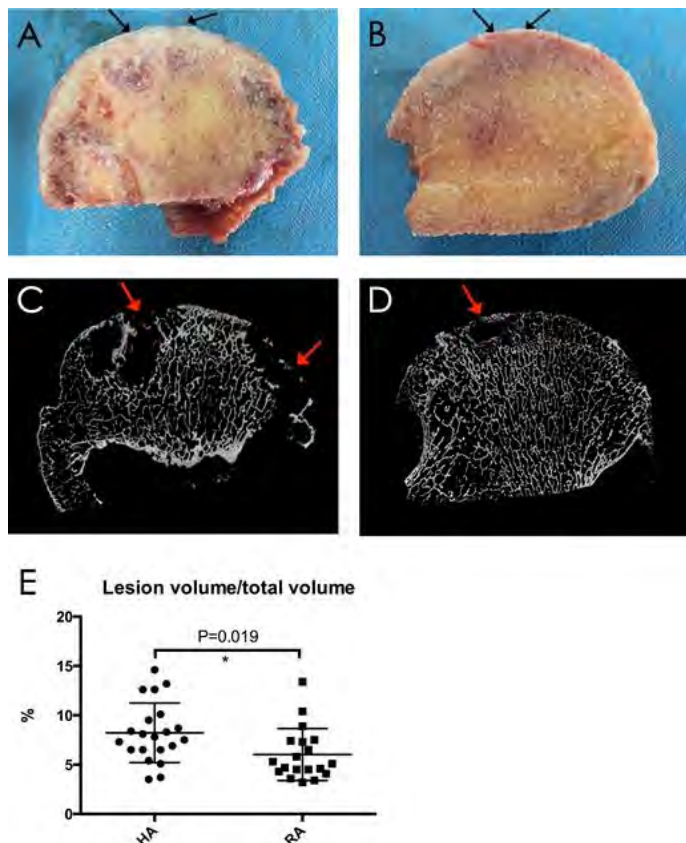


Fig 1

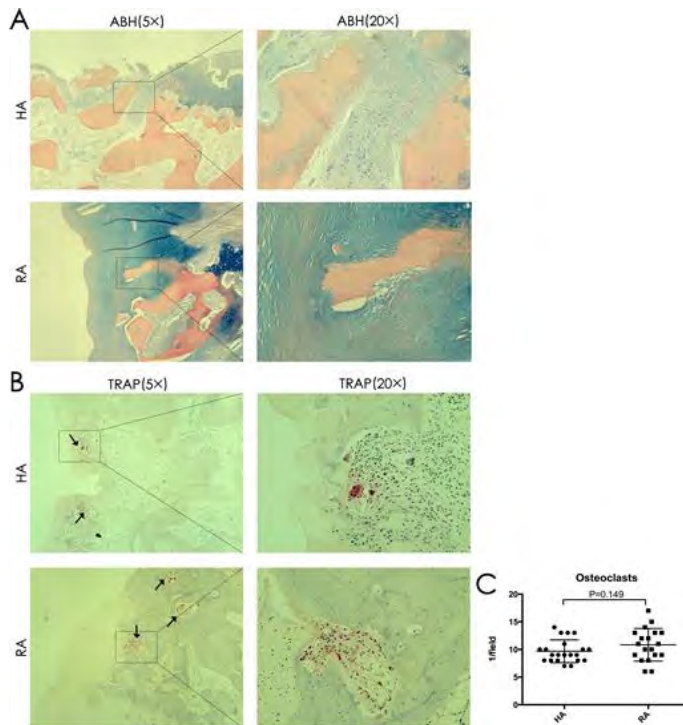


Fig 2

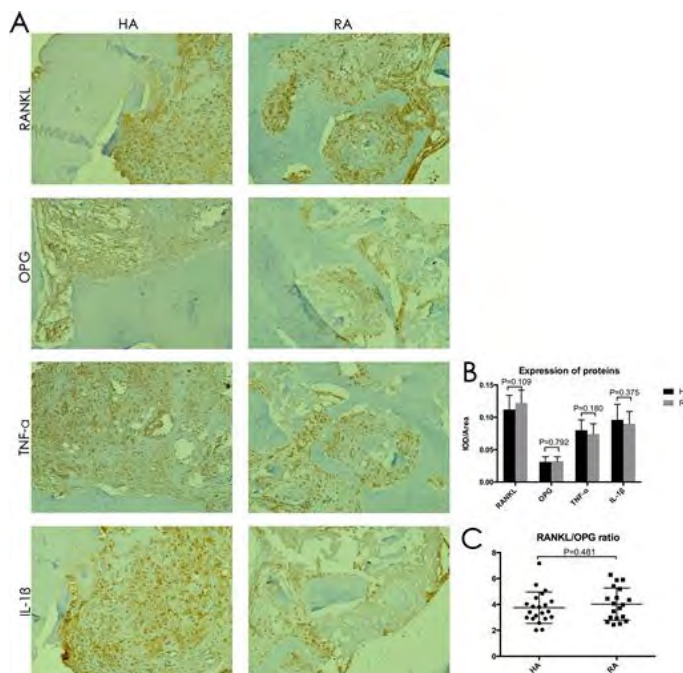


Fig 3

Disclosures: Shanxing Zhang, None.
 This study received funding from: the program for Zhejiang Leading Team of S&T Innovation and the program for Key Laboratory of Zhejiang Province

SA0363

Microarchitectural and Biomechanical Effects of PTH Excess due to Primary or Renal Secondary Hyperparathyroidism. Emily Stein^{*}, Thomas Nickolas¹, Kyle Nishiyama¹, Donald McMahon¹, Nientara Anderson¹, Anna Kepley¹, X. Edward Guo², Shonni Silverberg¹, Elizabeth Shane¹.
¹Columbia University College of Physicians & Surgeons, USA, ²Columbia University, USA

Whether the skeletal effects of parathyroid hormone (PTH) excess differ according to etiology of hyperparathyroidism (HPT) is not known. We compared postmenopausal women (PM) with primary (PHPT) and secondary (SHPT) hyperparathyroid-

ism to determine whether primary and secondary elevations in PTH have similar effects on bone mass, microarchitecture and strength. We hypothesized that women with PHPT and SHPT from chronic kidney disease would have similar skeletal abnormalities, with greatest deficits in cortical (Ct) bone.

PM women with PHPT (n=50), SHPT (n=28), and controls (C; n=55; normal PTH and renal function) had calciotropic hormones, bone turnover markers, and areal BMD (aBMD) of lumbar spine (LS), total hip (TH), femoral neck (FN), and 1/3 radius (1/3R) by DXA. Trabecular (Tb) and Ct volumetric BMD (vBMD) and microarchitecture were measured by high resolution peripheral computed tomography (HRpQCT) of the distal radius and tibia. Whole bone stiffness was estimated by finite element analysis.

Subjects were 69 ± 8 yrs, had BMI 27 ± 6 kg/m², 76% were Caucasian. Women with SHPT had higher BMI, were older and more likely to be Latina (52% vs 8% PHPT and 15% C; p<0.01). Intact and whole PTH levels were highest in SHPT (Table 1). All groups were 25OHD sufficient. DXA and HRpQCT were compared after adjusting for age, race and BMI. aBMD was similar at the LS and 1/3R, but tended to be lower in SHPT at the TH (p=0.08) and FN (p=0.09). In contrast with the DXA findings, women with PHPT had the most abnormalities by HRpQCT (Table 2). At the radius, Ct deficits were most pronounced, with lower Ct area, thickness and density compared to controls. Total density was lower and Tb density tended to be lower in PHPT, although Tb microarchitecture did not differ. Whole bone stiffness was lower in both HPT groups compared to controls. There were no significant findings at the tibia.

In summary, women with PHPT and SHPT had similar bone stiffness that was decreased compared to controls. Despite higher PTH levels in SHPT, skeletal abnormalities were greatest in PHPT, with cortical deficits predominating. That biomechanical impairment was similar in both HPT groups despite better vBMD in SHPT suggests the importance of factors other than elevated PTH in determining fragility in patients with SHPT and CKD.

Table 1. Demographics and Biochemistries (mean \pm SE)

| | PHPT | SHPT | C | p |
|------------------------------|-----------------|------------------------------|---------------|--------|
| Age (yrs) | 68 \pm 1 | 74 \pm 2 ^A | 68 \pm 1 | <0.01 |
| BMI (kg/m ²) | 27 \pm 1 | 31 \pm 1 ^A | 25 \pm 1 | <0.01 |
| iPTH (pg/ml) | 88 \pm 7* | 151 \pm 10 ^A * | 40 \pm 6 | <0.001 |
| wPTH (pg/ml) | 46 \pm 3* | 62 \pm 4 ^A * | 21 \pm 3 | <0.001 |
| Calcium (mg/dl) | 10.6 \pm 0.1* | 9.4 \pm 0.1 | 9.4 \pm 0.1 | <0.001 |
| Creatinine (mg/dl) | 0.8 \pm 0.0 | 1.9 \pm 0.1 ^A * | 0.8 \pm 0.0 | <0.001 |
| 25OHD (ng/ml) | 37 \pm 3 | 31 \pm 7 | 34 \pm 4 | 0.71 |
| 1,25OHD ₃ (pg/ml) | 81 \pm 5* | 47 \pm 7 ^A | 48 \pm 5 | <0.001 |

*p<0.01 for PHPT or SHPT vs. C, ^Ap<0.01 for SHPT vs. PHPT

Table 1. PHPT vs SHPT Demographics and Biochemistries

Table 2. Comparison of HRpQCT in PHPT, SHPT and C (mean \pm SE)

| RADIUS | PHPT | SHPT | C | p |
|-------------------------------|------------------|-----------------|-----------------|-------|
| Ct.Ar (mm ²) | 39 \pm 1* | 42 \pm 2 | 46 \pm 1 | <0.01 |
| Ct.Th (mm) | 0.61 \pm 0.02* | 0.67 \pm 0.04 | 0.72 \pm 0.02 | <0.01 |
| Ct.D (mgHA/cm ³) | 796 \pm 10* | 828 \pm 15 | 848 \pm 10 | <0.01 |
| Tot.D (mgHA/cm ³) | 252 \pm 10* | 277 \pm 14 | 297 \pm 9 | <0.01 |
| Tb.D (mgHA/cm ³) | 112 \pm 6 | 123 \pm 9 | 131 \pm 6 | 0.07 |
| Tb.N (1/mm) | 1.7 \pm 0.0 | 1.8 \pm 0.1 | 1.8 \pm 0.1 | 0.23 |
| Stiffness (kN/mm) | 26.8 \pm 1.1* | 28.7 \pm 1.6* | 31.7 \pm 1.1 | <0.01 |

*p<0.01 vs. C, p values adjusted for age, race and BMI

Abbreviations: Ct.Ar cortical area, Ct.Th cortical thickness, Ct.D cortical density, Tot.D total density, Tb.D trabecular density, Tb.N trabecular number.

Table 2. PHPT vs SHPT HRpQCT

Disclosures: Emily Stein, None.

SA0364

Prevalence of low bone mineral density, osteopenia, osteoporosis and its associated risk factors in female ballet dancers. Tânia Amorim^{*1}, Lygeri Dimitriou², George Metsios³, Matthew Wyon³, Alan Nevill³, Andreas Flouris⁴, José Maia⁵, José Carlos Machado⁵, Franklim Marques⁵, Nuno Adubeiro⁶, Luísa Nogueira⁶, Kerry Matthews³, Yiannis Koutedakis⁷.

¹University of Wolverhampton, UK; ²University of Porto, Portugal, United Kingdom, ³University of Middlesex, United Kingdom, ⁴University of Wolverhampton, United Kingdom, ⁵University of Thessaly, Greece, ⁶University of Porto, Portugal, ⁷Polytechnic Institute of Porto, Portugal, ⁷University of Thessaly; University of Wolverhampton, Greece

PurposeConcerns have been voiced over the possible deleterious effects of professional dance training environment on dancers' bone health. The aim of the present study was to determine low bone mineral density (BMD) prevalence,

osteopenia and osteoporosis and its associated risk factors in female ballet dancers. MethodsDancers were recruited from professional ballet companies and vocational ballet dance schools in Portugal and England. Aged and sex-matched controls (non-dancers) were also drafted from both countries. All participants provided written informed consent and were subsequently scanned at the lumbar spine (LS) and non-dominant arm using Dual-Energy X-Ray Absorptiometry. Osteopenia and osteoporosis were diagnosed in professionals and matched controls based on the American College of Sports Medicine criteria for athletes, and low BMD was diagnosed in vocational dancers (and respective controls) according to the International Society of Clinical Densitometry criteria for children. Participants were also asked to complete a menstrual history questionnaire. ResultsOne hundred and twenty-nine professional dancers (28.2[±]9.5yrs), 99 matched controls (28.9[±]10.9yrs), 109 vocational dancers (13.4[±]2.4yrs) and 56 student controls (13.7[±]2.2yrs) volunteered. Compared with their controls, professional dancers revealed a significantly higher prevalence of osteopenia and osteoporosis at the arm (36.7% vs. 16.2%, p<0.001 and 24.2% vs. 1%, p<0.001, respectively). Although not significant, a higher prevalence of osteopenia at the LS (12.4% vs. 9.1%, p>0.05) was also found. A significantly higher prevalence of low BMD at the arm (9.2% vs. 0%, p<0.01) and LS (16.4% vs. 5.5%, p<0.01) was found in the vocational dancers compared to controls. Logistic regression analysis revealed that vocational dancers are more likely to develop low BMD at the LS (OR=0.2; 95% CI: 0.08-0.73) and arm (OR= 0.1; 95% CI: 0.02-0.98) than controls. In both vocational and professional dancers, neither body weight (Kg) nor menstrual disturbances (oligo-amenorrhea) were predictors of low BMD/osteoporosis (p>0.05). ConclusionElements of low BMD and osteoporosis are present in female vocational and professional dancers at both impact (LS) and non-impact sites (arm). It seems that known associated factors for low BMD and osteoporosis do not explain the aforementioned results.

Disclosures: Tânia Amorim, None.

SA0365

Prevalence of Morphometric Vertebral Fracture in Brazilian Women with Human Immunodeficiency Virus (HIV) Infection. Érico Carvalho¹, Francisco Bandeira^{*2}, Zoraya Barros¹, Demócrito Filho³, Heloisa Melo⁴, Maria de Fátima Albuquerque⁵, Ulisses Montarroyos⁶, Ricardo Ximenes⁷. ¹Serviço de Infectologia, Universidade de Pernambuco, Recife, Pernambuco, Brasil., Brazil, ²University of Pernambuco, Brazil, ³Departamento de Medicina Clínica, Universidade de Pernambuco, Recife, Pernambuco, Brasil., Brazil, ⁴Departamento de Medicina Clínica, Universidade de Pernambuco, Recife, Pernambuco, Brasil., Brazil, ⁵Serviço de Endocrinologia, Hospital Agamenon Magalhães, Recife, Pernambuco, Brasil, Brazil, ⁶Departamento de Medicina Tropical, Universidade Federal de Pernambuco, Recife, Pernambuco, Brasil., Brazil, ⁷Departamento de Medicina Clínica, Universidade de Pernambuco, Recife, Pernambuco, Brasil., Brazil, ⁷Departamento de Medicina Tropical, Universidade Federal de Pernambuco, Recife, Pernambuco, Brasil, Brazil

Introduction: Some studies have suggested that adults with HIV infection have a high prevalence of low bone mass (LBM), as well as increased risk for clinical fractures but few data are available regarding morphometric vertebral fractures (MVf) and its associated factors particularly in women. The aim of this study was to determine the prevalence of MVf by the semi-quantitative (SQ) and by the algorithm-based qualitative (ABQ) methods in Brazilian women living with HIV. Subjects, Methods and Results: We studied 386 women (63.1 % premenopausal) aged 44 ± 9.3 years, with a mean time of 7 years with HIV infection, of whom 90% were using highly active anti-retroviral therapy (HAART) for more than 6 years. Spine X-rays were reviewed by two observers. The inter-observer agreement (IOA) for each method was calculated by Kappa. The association with bone mineral density (BMD) as well as clinical and laboratory factors were evaluated. The prevalence of MVf was 10.1% for the SQ method and 8.8% for the ABQ method (IOA SQ: $\kappa = 0.338$, 95% CI 0.243 to 0.432; p<0.001; ABQ: $\kappa = 0.211$, 95% CI 0.113 to 0.31; p<0.001) and there was a sharp increase after the age of 50 (Figure 1). In univariate analysis MVf was associated with LBM but this did not remain significant after adjustment for age, and no association was found with factors related to HIV or HAART. Conclusions: We found a high prevalence MVf in women with HIV infection using both SQ and ABQ methods and age was the most important associated factor. Keywords: Vertebral fractures, low bone mass, osteoporosis, HIV.

Figure 1- Prevalence of morphometric vertebral fracture by age in women living with HIV

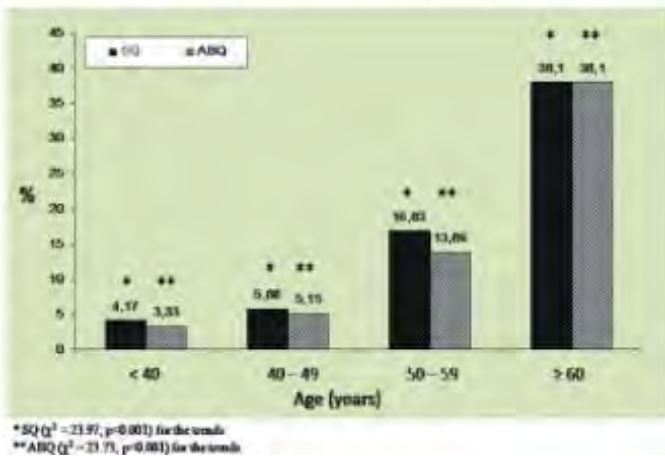


Figure 1

Disclosures: Francisco Bandeira, None.

SA0366

See Friday Plenary Number FR0366.

SA0367

See Friday Plenary Number FR0367.

SA0368

B Cells Contribute to Bone Erosion in Rheumatoid Arthritis by Directly Inhibiting Osteoblast Differentiation. Wen Sun*, Nida Meednu, Hengwei Zhang, Xing Li, Teresa Owen, Alex Rosenberg, Brendan Boyce, Jennifer Anolik, Lianping Xing. University of Rochester Medical Center, USA

Rheumatoid arthritis (RA) is an autoimmune inflammatory disorder characterized by increased osteoclast-mediated joint bone erosion accompanied by decreased osteoblast (OB)-mediated bone formation. B cell depletion therapy (BCDT) effectively attenuates joint tissue damage in many RA patients. B cells promote osteoclast formation by secreting RANKL and activating other immune cells such as T cells. However, the effects of B cells on OB function in RA have not been studied. Here we investigated the effects of B cells on OB differentiation and bone erosion using TNF transgenic (TNF-Tg) mice, a mouse model of RA. Immunofluorescent staining of knee joint sections from TNF-Tg mice showed B220+ B cell aggregates at sites of joint erosion and in the subchondral bone area, and some of these localized adjacent to osteocalcin+ OBs. We co-cultured bone marrow (BM)-derived CD19+ B cells from TNF-Tg or WT littermate control (Ctl) mice with WT bone-derived mesenchymal progenitor cells (MPCs) in OB-inducing medium and found that TNF-Tg B cell cultures had significantly decreased alkaline phosphatase+ (ALP+) areas and Runx2 expression (Runx2/actin: 0.3 ± 0.03 vs. 1.1 ± 0.14 in Ctl). RNA sequencing pathway analyses of CD19+ B cells from WT BM, TNF-Tg BM and synovium revealed that 225 pathways were dysregulated in TNF-Tg BM B cells vs. WT BM B cells and 377 pathways were dysregulated in TNF-Tg synovial B cells vs. TNF-Tg BM B cells. Among these, the expression of inflammatory cytokines (TNF, Oncostatin M and IL6) and chemokines (CCL3), known to inhibit MPC-OB differentiation were markedly elevated. qPCR confirmed increased TNF expression by TNF-Tg B cells (TNF/actin: 4.6 ± 1.2 in TNF-Tg synovium vs. 0.7 ± 0.4 in TNF-Tg BM and 0.3 ± 0.1 in WT BM). TNF neutralizing antibody blocked OB inhibition induced by TNF-Tg B cells (ALP+ area: 17.3 ± 2.9 vs. 9.3 ± 1.5 mm² in IgG). TNF-Tg mice given BCDT (murine anti-CD20) had decreased joint erosion (patellar bone volume: 0.7 ± 0.05 vs. 0.6 ± 0.01 mm³ in IgG, $p < 0.05$) and increased numbers of osteocalcin+ OBs (OB#/mm bone surface: 26 ± 4.6 vs. 16.4 ± 3.1 in IgG, $p < 0.05$). BM cells from BCDT-treated TNF-Tg mice had increased OB differentiation (CFU-ALP#: 53.2 ± 8.9 vs. 20.5 ± 5.2 in IgG). We conclude that B cells inhibit OB differentiation in RA by secreting TNF and perhaps other OB inhibitors and thus contribute to bone loss in affected patients. BCDT therefore should preserve bone mass in RA patients by inhibiting bone resorption and stimulating bone formation.

Disclosures: Wen Sun, None.

SA0369

See Friday Plenary Number FR0369.

SA0370

See Friday Plenary Number FR0370.

SA0371

See Friday Plenary Number FR0371.

SA0372

Essential Role of RANKL Expressed in Chondrocytes in Endochondral Ossification. Patrick Aghajanian*, Shaohong Cheng, Weirong Xing, Heather Watt, Catrina Alarcon, Sheila Pourteymoor, Subburaman Mohan. Jerry L. Pettis Memorial VA Medical Center, USA

The long bones of the skeleton are formed by endochondral ossification, a process in which bones are first formed as cartilage templates, which are replaced subsequently by bone. RANKL and OPG are known to be expressed in hypertrophic chondrocytes and have been predicted to be involved in regulating expression of proteases involved in the dissolution of cartilage. Since thyroid hormone (TH) is essential for normal skeletal growth and development, we evaluated if the RANKL/OPG axis is involved in TH regulation of endochondral ossification. A two day treatment of TH deficient Tshr-/- mice with T3/T4 increased the RANKL mRNA level by 390% ($P < 0.001$) and decreased OPG expression by 40% ($P < 0.01$) compared to vehicle treatment at day 7. Accordingly, treatment of serum-free cultures of metatarsal-derived cells from 3-day old mice treated with T3 increased RANKL expression by 2.5-fold but decreased OPG expression by 50% ($P < 0.01$). Furthermore, T3 treatment increased RANKL expression and decreased OPG expression in both primary chondrocytes and the established ATDC5 chondrocyte cell line. To evaluate the role of a TH-induced increase in RANKL action in chondrocytes in regulating endochondral ossification, we conditionally disrupted RANKL expression in chondrocytes of Col2-Cre-ERT2 mice carrying RANKL floxed alleles by administration of a single dose of tamoxifen (Tam, 100 μ g) at day 5 when TH levels start to increase. Trabecular (Tb.) BMD was reduced by 21% ($P < 0.05$, $n = 7$) in the tibial epiphysis of Tam treated Cre+ve RANKL floxed mice compared to the Cre-ve RANKL floxed control mice that was caused by reduced Tb. number and increased Tb. separation. We next determined the mechanism for the TH effect on RANKL expression. Since T3 increased osterix (SP7) expression in chondrocytes and since the RANKL promoter contains a perfect SP7 response element but not a TRE, we evaluated if the TH effect on RANKL expression in chondrocytes was mediated via osterix. We found that knockdown of osterix expression by lentiviral shRNA decreased osterix expression by 70% and RANKL expression by 60%. Furthermore, the T3-induced increase in RANKL expression failed to occur in the osterix knockdown ATDC5 cells. By contrast, overexpression of osterix increased RANKL expression by 3-fold ($P < 0.01$). Based on these data, we conclude that RANKL expressed in chondrocytes is critically involved in mediating the TH effects on endochondral bone formation and that the TH effect on RANKL expression is mediated via osterix.

Disclosures: Patrick Aghajanian, None.

SA0373

See Friday Plenary Number FR0373.

SA0374

Mutations preventing regulated exon skipping of a receptor tyrosine kinase cause a developmental disorder of osteogenesis. Peter Kannu*¹, Ben Alman², Stephen Robertson³, Carol Wise⁴, Haemish Crawford⁵, Lori Karol⁶, Mary Gray³, Rebekah Jobling², Linda Vi², Heather Whetstone², Raymond Poon², Angela Weng², Gino Sommers², Christian Marshall², Lucie Dupuis², Andrew Howard². ¹Hospital for Sick Children Toronto, Canada, ²Hospital for Sick Children, Canada, ³University of Otago, New Zealand, ⁴Texas Scottish Rite Hospital for Child, USA, ⁵Starship Children's Hospital, New Zealand, ⁶Texas Scottish Rite Hospital for Children, USA

Osteofibrous dysplasia (OFD) is a proliferative fibro-osseous condition affecting bone with an onset in early childhood. Typically, affected individuals develop tibial bowing and spontaneous non-healing fractures. Radiolucent lesions centered on the periosteal surface of the shafts of the tibia and fibula are visualized radiographically. We identified mutations in a gene encoding a receptor tyrosine kinase, in three families segregating an autosomal dominant form of OFD and in a fourth sporadic case. All mutations abolished the splice inclusion of an exon in transcripts resulting in receptors lacking a juxtamembrane cytoplasmic domain. Our mouse data indicate that

exclusion of this domain is a physiologically regulated event in the periosteum which is spatially partitioned during development. Forced induction of this exon skipping event in vitro retarded osteoblastic differentiation in vitro and inhibited matrix mineralisation. To further characterize the mutation effect, comprehensive immunohistological analysis on human samples was undertaken. Histology demonstrated alkaline phosphatase positive fibroblast-like cells in the stromal tissue, which may be due to an increased number of osteoblast progenitor cells. To confirm the mutation effect on osteoblast differentiation, proliferation and function, cells derived from affected patient bone samples obtained at surgery were cultured and differentiated in osteogenic media. Abnormal fibro-osseous bone cells from the tibial fracture site were compared to the cells obtained from unaffected proximal tibial bone. When cultured in osteogenic differentiation media, fracture site-derived osteoblasts displayed considerably higher levels of mineralization compared to the cells from the unaffected tibial bone. Moreover, the fracture site osteoblasts proliferated more rapidly compared to the control cells. To examine the effect of the receptor tyrosine kinase mutation on osteoclast differentiation and function in vitro, osteoclasts were differentiated from patient peripheral blood mononuclear cells and an age and gender matched control. Mutant osteoclasts showed decreased bone resorption. Together these data indicate that the production of this mutant receptor isoform is a developmentally regulated event during mammalian embryonic development and mutations which render this alternative splice event constitutional subvert core functions of this receptor that regulate osteogenic functions within the periosteum.

Disclosures: Peter Kannu, Hospital for Sick Children
This study received funding from: Rare Disease Foundation

SA0375

See Friday Plenary Number FR0375.

SA0376

A Longitudinal, Prospective, Long-Term Registry of Patients with Hypophosphatasia. Lothar Seefried¹, Wolfgang Högler², Craig Langman³, Agnès Linglart⁴, Etienne Mornet⁵, Keiichi Ozono⁶, Cheryl Rockman-Greenberg⁷, Camille Bedrosian⁸, Kenji P Fujita⁸, Alex Cole⁸, Priya Kishnani⁹.
¹University of Würzburg, Germany, ²Birmingham Children's Hospital, United Kingdom, ³Northwestern University & Lurie Children's Hospital, USA, ⁴Paris-Sud University, APHP & INSERM U1169, France, ⁵Centre Hospitalier de Versailles, France, ⁶Osaka University, Graduate School of Medicine, Japan, ⁷University of Manitoba, Canada, ⁸Alexion Pharmaceuticals, USA, ⁹Duke University Medical Center, USA

Hypophosphatasia (HPP) is a rare, inherited metabolic disease characterized by bone mineralization defects and osteomalacia, as well as systemic manifestations including seizures, respiratory insufficiency, muscle weakness, nephrocalcinosis, and pain. The biochemical hallmark of HPP is low serum alkaline phosphatase activity, resulting from loss-of-function mutations in the gene encoding tissue non-specific alkaline phosphatase. HPP presents a broad spectrum of disease severity classically defined by age at onset of symptoms (perinatal/infantile, juvenile, adult, odontohypophosphatasia [isolated dental symptoms only], and "benign" prenatal), with recognized overlap between, and range of severity within, these forms. The rarity of HPP combined with its variable expressivity presents considerable challenges in the diagnosis and understanding of the disease. Here we describe the design of an HPP Registry, which will enable better characterization and understanding of the epidemiology and clinical course of HPP through collection of demographic and longitudinal clinical data.

This multinational, observational, prospective, long-term registry will enroll ≥ 500 patients. Patients of any age with HPP will be included, except for those participating in Alexion-sponsored clinical trials. Sites will conduct the study in accordance with local regulations. Available patient data will be collected retrospectively via chart review at baseline and thereafter at intervals ≤ 6 months in the course of routine clinical care. Performance of new clinical procedures is not required. Data collected will include patient demographics; method of diagnosis; HPP disease history including dates of onset and diagnosis; family history; clinical manifestations; and genotype. Data from medical and laboratory assessments specific to HPP will be recorded. Standardized questionnaire instruments will be used to quantify patient-reported burden of disease, functional status/disability, and quality of life.

The HPP Registry will provide a detailed longitudinal profile of patients with HPP including demographics, diagnosis patterns, genotype-phenotype correlations, country-specific findings, and impact of HPP on activities of daily living and quality of life.

Disclosures: Lothar Seefried, Honoraria from Alexion Pharmaceuticals
This study received funding from: Alexion Pharmaceuticals

SA0377

A novel frameshift mutation c.1362_1399del38 (p.Gly456Alafs330) in exon 12 of the ALPL gene in two siblings and their previously undiagnosed mother with hypophosphatasia: a case report. Cedric Ng^{*}, Pisit Pitukcheewanont. Children's Hospital, Los Angeles, USA

Background: Hypophosphatasia (HPP) is a rare disorder characterized by low serum alkaline phosphatase (alk phos) and elevated pyridoxal-5'-phosphate (PLP) levels causing defective mineralization of the bone. There are at least 285 reported mutations in the ALPL (alkaline phosphatase, liver/bone/kidney) gene. **Clinical Case:** A: is the 4 year old Japanese-Caucasian male with premature loss of his primary teeth, a low serum alk phos of 99 U/L, an elevated PLP level >100 ug/L, no history of skeletal demineralization, fractures, or bone pain. A diagnosis of HPP was made. B: is the fetal sibling of A aborted at 23 weeks gestation and had clinical signs of HPP, with severe skeletal abnormalities on fetal ultrasound. Both siblings have compound heterozygous mutations of the ALPL gene and share a missense mutation in exon 5 (c.407G>A amino acid change with p.R136H or R119H genotype) from their father previously reported in the literature as pathogenic in a 3 year old compound heterozygote with bone affected HPP. They also share a previously unreported heterozygous frameshift mutation in exon 12 of the ALPL gene (c.1362_1399 del38) from their mother resulting in a premature stop codon, p.Gly456Alafs330. The father has no clinical or biochemical evidence of HPP, a normal serum alk phos of 41 U/L and a normal serum PLP level (46.6 ug/L). He is heterozygous for the missense mutation in exon 5 of the ALPL gene and given that he is unaffected, this suggests that the mutation he shares with his children is non-pathogenic. The mother has both clinical and biochemical evidence of HPP, a low serum alk phos level of 29 U/L, an elevated serum PLP level (>100 ug/L), and is heterozygous for a frameshift mutation in exon 12 of the ALPL gene. Because the two siblings and their mother all have characteristics of HPP, this suggests that the frameshift mutation they share is pathogenic. **Conclusion:** We report a novel frameshift mutation in exon 12 of the ALPL gene (c.1362_1399 del38 - p.Gly456Alafs330) in two siblings and their previously undiagnosed mother with HPP. This result suggests an autosomal dominant inheritance pattern. Genetic testing and counseling should be considered for additional siblings in the future.

Disclosures: Cedric Ng, None.

SA0378

Hypophosphatasia: Natural History Study Of 101 Children From Inpatient Investigations Over 25 Years At A Single Research Center. Michael P Whyte¹, Deborah Wenkert¹, William H McAlister², Karen E Mack¹, Fan Zhang¹. ¹Center for Metabolic Bone Disease & Molecular Research Shriners Hospitals for Children - St Louis, USA, ²Department of Pediatric Radiology, Mallinckrodt Institute of Radiology at St. Louis Children's Hospital, Washington University School of Medicine, USA

Hypophosphatasia (HPP) is the inborn-error-of-metabolism that features deficient activity of the "tissue-nonspecific" isoenzyme of alkaline phosphatase (TNSALP). Clinical hallmarks are tooth loss and rickets or osteomalacia caused by extracellular accumulation of inorganic pyrophosphate, an inhibitor of mineralization. Dominant versus recessive transmission of nearly 300 typically missense mutations in the TNSALP gene underlies the disorder's remarkably broad-ranging expressivity. In 2015, cross-sectional data from our inpatient investigations, spanning 25 years, of 173 affected children validated and expanded the nosology for HPP in pediatric patients (Bone 75:229-39).

Here, we investigated longitudinally the natural history of HPP in children by assessing several key parameters in this cohort: z-scores for height, weight, grip-strength, and spine and hip DXA BMD. Weight and BMD z-scores were further analyzed after adjusting for stature using the equations we published in 2012 to calculate "height-age" for the preteenage patients (JCD 15:267-74).

At least one study readmission (407 total) had occurred for 101 patients (Table). They had been classified by increasing HPP severity, determined by age at presentation. There were 28 odonto HPP, 28 mild childhood HPP, 37 severe childhood HPP, and 8 survivors of infantile HPP with mean follow-up (first-last admissions) of 5.9, 6.1, 7.0, and 8.2 years, respectively. Eighteen patients had been studied "across" puberty. Cohort and group mean height z-scores, that reflected the HPP nosology, did not change with patient aging (including across puberty) ($ps > 0.1$). Mean weight z-scores for chronologic-age and after height-adjustment increased for the pre-teenage patients in all four groups, in keeping with pediatric trends for healthy children. After stature adjustment, mean weight z-scores were in the normal range for all patient groups. Mean grip-strength z-scores were not changed by aging. Spine and hip BMD z-scores calculated routinely for chronologic age did not change with patient aging, whereas the height-corrected BMD z-scores for the pre-teenage patients showed improvements in the spine, but not hip.

We found that mean z-scores for height, grip-strength, and hip BMD remained stable, whereas mean weight and spine BMD z-scores increased, in children with HPP. Our observations should aid prognostication and help assess treatment for children with HPP.

| Table | Ages (Years) During, And Years Between, First Versus Last Admission | | | | | | |
|------------------|---|---------------|------------------|---------------|------------------|-----------|------------------|
| | # Pts | First | | Last | | Interval | |
| | | Mean Age (SD) | Range (min, max) | Mean Age (SD) | Range (min, max) | Mean (SD) | Range (min, max) |
| Odonto | 28 | 4.9 (3.5) | 1.7-15.8 | 10.8 (4.3) | 3.7-20.9 | 5.9 (3.3) | 1.0-12.9 |
| Mild Childhood | 28 | 4.3 (2.4) | 1.3-10.0 | 10.4 (4.3) | 3.9-20.0 | 6.1 (3.7) | 1.0-16.7 |
| Severe Childhood | 37 | 4.9 (3.6) | 0.8-14.0 | 11.9 (5.8) | 1.5-20.9 | 7.0 (4.4) | 0.7-19.4 |
| Infantile | 8 | 2.2 (1.9) | 0.5-6.3 | 10.5 (5.7) | 2.2-17.2 | 8.2 (5.3) | 1.0-15.8 |
| Total | 101 | 4.5 (3.2) | 0.5-15.2 | 11.1 (5.0) | 1.5-20.9 | 6.5 (4.0) | 0.7-19.4 |

Ages (Years) During, And Years Between, First Versus Last Admission

Disclosures: Michael P Whyte, None.

This study received funding from: Alexion Pharmaceuticals Inc. Cheshire, CT

SA0379

Pseudohypophosphatasia: Mutation Identification And 46-Year Follow-Up Of The Original Patient. Katherine L. Madson^{*1}, Sabrina S Gill², Steven Mumm³, Michael P. Whyte¹. ¹Center for Metabolic Bone Disease & Molecular Research, Shriners Hospitals for Children - St Louis, USA, ²Division of Endocrinology, University of British Columbia, Canada, ³Division of Bone & Mineral Diseases, Washington University School of Medicine, USA

We present a 46-year follow-up of the patient with pseudohypophosphatasia (pseudoHPP) reported by Scriver and Cameron in 1969 (NEJM 281: 604-06). She presented at 3 mos-of-age with hypotonia, broadened cranial sutures, metaphyseal changes, and elevated urinary phosphoethanolamine (PEA), all consistent with HPP. However, her serum alkaline phosphatase (ALP) activity was not low, but normal; hence, "pseudoHPP". Hypercalcemia persisted for the first 4 months-of-life, but then remitted. Rickets was reported to have nearly resolved by four years-of-age. Subsequently, most serum phosphorus levels were slightly elevated consistent with HPP. PEA was still elevated at age 18 and 19 years. As a young adult, iliac crest biopsy showed osteomalacia and normal osteoblast ALP staining. In 1986, Cole et al documented that her urinary inorganic pyrophosphate and plasma pyridoxal 5'-phosphate levels, both ALP substrates, were elevated (NEJM 314: 992-3). Serum creatinine and estimated GFR have been normal despite medically-controlled hypertension and unilateral renal calcification since age 27 yrs. Meneire's disease developed in 2005. Her low-trauma long bone fractures heal slowly, or become non-unions. The right humerus and all lower extremity long bones are rodged. Spinal stenosis, with seemingly paradoxical calcification of dura throughout the lumbar spine, has developed. Pelvic "non-union" fractures cause pain, and one extends through the left sacral ala causing L5 weakness and foot drop. She reports that teriparatide therapy from 2009-2011 was ineffective for healing fractures. This disabled former clinical dietician has been wheelchair bound since 2013. At age 51 years, her height is 141 cm (Z=-3.4) and weight 42 kg (Z=-2.4).

Serum ALP activity remains normal for age, varying from 67-102 U/L at ages 19-50 years using different laboratory assays.

In 2008, we found she carried a common American *TNSALP* mutation (c.1250A>G). Further analysis showed an additional and unique mutation (c.1355 A>G), not reported in two databases. She also has an intron polymorphism, a SNP, and a homologous alanine substitution.

Apparently, this novel combination of *TNSALP* changes in relatively close proximity within the homodimer creates an enzyme with normal in-vitro catalytic activity, under the artificial conditions of the laboratory assay, yet poor enzymatic activity in-vivo toward natural substrates resulting in a distinct and life-long form of HPP.

Disclosures: Katherine L. Madson, None.

SA0380

See Friday Plenary Number FR0380.

SA0381

Accumulation of osteopontin in the absence of PHEX decreases *NaPT2A* expression. Nilana Barros^{*1}, Gabrielly Chiarantin², Raquel Neves², Adriana K Carmona², Marc McKee³. ¹Federal University of Sao Paulo, Brazil, ²UNIFESP, Brazil, ³McGill University, Canada

X-linked hypophosphatemia (XLH/HYP) is the most prevalent form of inherited rickets in humans, characterized by hypophosphatemia related to defective renal phosphate reabsorption associated with growth retardation, osteomalacia and dental abscesses. XLH occurs as consequence of inactivating mutations in the *PHEX* gene (phosphate-regulating gene with homologies to endopeptidases on the X chromosome). In vivo mouse studies have shown that the absence of *PHEX* leads to the release of a circulating factor(s) that decreases mineralization and inhibits sodium/phosphate co-transporter *NaPT2A*, which mediates reabsorption of phosphate in the kidneys. Recently we demonstrated that the mineral-binding bone extracellular matrix protein osteopontin (OPN) is a physiologically relevant substrate for *PHEX*, whose inactivation by *PHEX* normally promotes bone mineralization. In the present study,

we have extended these observations to show that OPN and a derived OPN fragment (ASARM peptide; acidic serine- and aspartate-rich motif) modulate *NaPT2A* expression.

Using a constructed *PHEX*-deficient human osteoblast cell line (MG-63 osteoblasts treated with shRNAi-*PHEX*) we show that, in the absence of *PHEX*, OPN accumulates and decreases *NaPT2A* mRNA and protein expression when conditioned media or extract were applied to human kidney (HK-2) proximal tubule epithelial cell cultures. In addition, we postulated that the absence of *PHEX* could influence FGF-23 expression via the indirect effect of OPN accumulation. We demonstrate that although FGF-23 is not inactivated by *PHEX*, OPN and FGF-23 are both increased in the shRNAi-*PHEX* osteoblasts, as similarly observed in the murine model of XLH, the Hyp mouse. In conclusion, these results provide new insight into circulating humoral factors that might influence phosphate handling in the kidney whose alterations contribute to the osteomalacic XLH phenotype, and they suggest that OPN and its fragments may be involved in this process and influence FGF-23 expression. Supported by FAPESP and CNPq.

Disclosures: Nilana Barros, None.

SA0382

See Friday Plenary Number FR0382.

SA0383

Osteogenesis Imperfecta in Sweden - Genetic Epidemiology, Prevalence and Genotype-phenotype Correlations. Katarina Lindahl^{*1}, Eva Åström², Carl-Johan Rubin³, Giedre Grigelioniene⁴, Barbro Malmgren⁵, Östen Ljunggren⁶, Andreas Kindmark⁶. ¹Dept. of Medical Sciences, Uppsala University, Sweden, ²Department of Women's & Children's Health Karolinska Institutet & Neuropediatric Unit Astrid Lindgren's Children's Hospital at Karolinska University Hospital Stockholm Sweden, Sweden, ³Department of Medical Biochemistry & Microbiology, Uppsala University, Sweden, ⁴Department of Molecular Medicine & Surgery, Karolinska Institutet, Stockholm, Sweden, Sweden, ⁵Department of Clinical Science, Intervention & Technology, Division of Paediatrics, Karolinska University Hospital, Huddinge, Sweden & Department of Dental Medicine, Division of Pediatric Dentistry, Karolinska Institutet, Huddinge, Sweden, Sweden, ⁶Department of Medical Sciences, Uppsala University, Sweden

Background: Osteogenesis imperfecta (OI) is a rare connective tissue disorder leading to bone fragility, spanning from mild to intrauterine lethality in severity. Collagen I mutations are causative in 90%, and recently several non-collagen genes have been reported to account for the remaining 10%. There are no population-based studies determining the genetic epidemiology of OI, and no extensive genotype-phenotype studies on >100 families outside of North America.

Subjects and methods: Here, detailed clinical phenotypes were recorded, and the *COL1A1* and *COL1A2* genes were Sanger-sequenced in 164 Swedish OI-families (223 individuals). Collagen I negative families were also analyzed by MLPA-technique. Averages for bone mineral density (BMD Z-score), height (Z-score) and yearly fracture rate were calculated and related to OI- and mutation type. Furthermore, gender and age correlations were studied. Population and diagnosis data were retrieved from official Swedish national databases.

Results: Individuals were classified according to Sillence: type I n=151 (101 families), type II n=1, type III n=29 (26 families), and type IV n=42 (37 families). A typical OI-causing collagen I mutation was found in 132 families (75 qualitative and 57 quantitative). Noteworthy mutations included: five mutations located in the *COL1A1* C-propeptide, four mutations located in lethal clusters of *COL1A2* described by Marini et. al., two mutations causing OI-EDS, and one *COL1A1* C-terminal cleavage site mutation causing a high bone mass phenotype.

C-terminal helical mutations in both the $\alpha 1$ - and $\alpha 2$ -chains were associated with dentinogenesis imperfecta (DI) (p<0.0001 vs. 0.0049), while only N-terminal $\alpha 1$ -chain mutations were associated with blue sclera (p=0.0110). DI was strongly associated with classical dominant OI, as none of the 32 collagen I mutation negative families had this phenotype clinically (p<0.0001). When comparing individuals with OI types III and IV, blue sclera was associated with collagen I mutations (p=0.0094). Comparing the most frequent amino-acid substitution glycine to serine, $\alpha 2$ -alterations were associated with a milder phenotype (p=0.0031); these individuals were taller, had a higher BMD, fewer fractures, and a lower frequency of intramedullary rodding. Patients with OI type I caused by qualitative vs. quantitative mutations were shorter (p<0.0001), but did not differ considering fracture rate or BMD. Males with OI type I had a lower BMD (p=0.0482), but were taller (p=0.0265), and had a lower frequency of DI (p=0.0258).

The children in this cohort were estimated to represent >95% of the entire Swedish pediatric OI-population. The prevalence of OI type I, III and IV was 5.16, 0.89 and 1.35/100 000 respectively (7.40/100 000 overall), which extrapolated corresponds to approximately 9.50/100 000 affected pregnancies. This corresponds to what has been estimated, but not unequivocally proven in any population. Collagen I sequencing was performed in the family of 97% of known pediatric cases, with causative mutations found in 87%. OI type I was caused by qualitative mutations in 32% out of which 91% were glycine substitutions.

Conclusion: Here, the genetic epidemiology in >95% of an entire OI-population is described for the first time, and data presented may be helpful in genotype-phenotype predictions. The prevalence of OI types I, III and IV in Swedish children was 7.40/100 000.

Disclosures: Katarina Lindahl, None.

SA0384

Raloxifene reduces skeletal fractures in homozygous OIM male mice. Alycia Berman^{*1}, Drew Brown², Zachary Bart³, Erin McNerny³, Jason Organ², Chris Newman², Matthew Allen², Joseph Wallace³. ¹Indiana University - Purdue University Indianapolis, USA, ²Indiana University School of Medicine, USA, ³Indiana University Purdue University Indianapolis, USA

Osteogenesis imperfecta (OI) is a genetic disease of Type I collagen that results in brittle bone behavior that is characterized by reduced toughness. Based on previous work in our laboratory showing that raloxifene can significantly improve bone toughness through non-cellular mechanisms, we hypothesized that raloxifene would improve the mechanical properties of OI bone. In experiment 1, eight-week old WT and homozygous OIM male mice were treated for eight weeks with subcutaneous saline vehicle (VEH) or raloxifene (RAL) injections. Endpoint measures included DXA, microcomputed tomography (uCT), and fracture toughness. In vivo skeletal fractures, assessed by projection CT images of the right and left femora (fig. 1), were significantly reduced ($p = 0.014$) in OI-RAL (17%) compared to OI-VEH (46%). There were no fractures in either WT treatment group. RAL significantly increased both DXA-based BMD ($p < 0.01$) and CT-based trabecular BV/TV in WT (+10% and +11%) and OI (+13% and +43%). Fracture toughness, assessed at crack initiation, maximum load, and crack instability, was lower in OI mice compared to WT (43%, 49%, and 46%, respectively), and tended to be higher in both genotypes in response to RAL treatment. In experiment 2, tibiae from a different cohort of wild type (WT) and homozygous OIM mice were soaked in raloxifene (RAL, 2uM) for 14 days at which time mechanical properties were assessed by 4 point bending and compared to non-soaked bones. RAL significantly increased post-yield displacement (75% in WT, 472% in OI; $p < 0.004$ for both) and post-yield work (79% in WT, 451% in OI; $p < 0.002$ for both), with no effect on ultimate load or stiffness, in both WT and OIM animals. The results of these studies show that raloxifene reduces the incidence of fracture in this mouse model of OI. Furthermore, they show that raloxifene's effects are likely the result of both cellular (increased bone mass) and non-cellular (presumably changes in hydration) mechanisms, raising the possibility of new approaches to treating bone fragility associated with OI.

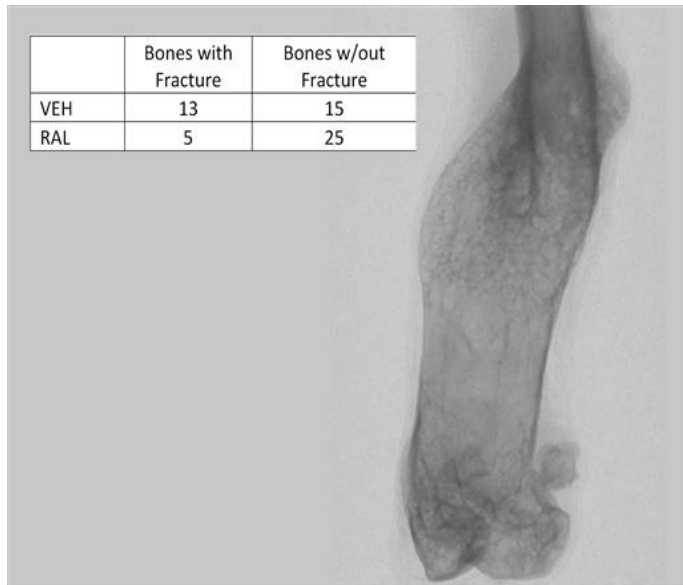


Fig. 1: In vivo skeletal fracture assessment

Disclosures: Alycia Berman, None.

SA0385

The Effectiveness of Bisphosphonate Treatment in Osteogenesis Imperfecta on Bone Biomarkers and Fracture Rates. Jay Shapiro^{*1}, Evelise Brizola², Adutu Kantipuly³. ¹Kennedy Krieger Institute, Johns Hopkins, USA, ²Kennedy Krieger Institute, USA, ³Johns Hopkins School of Public Health, USA

Problem Statement: Bisphosphonate (BP) therapy for Osteogenesis Imperfecta (OI) is accepted as the "standard" for both children and adults. However, questions exist regarding the long term effectiveness of BP in decreasing fractures. **Method and Results:** We have assessed the effect of BP treatment on bone biomarkers and fracture

rates in children and adults with OI. This includes 19 children, ages birth to 18 years, treated with IV pamidronate. They are divided into two groups: treatment responders with < 2 fractures/year during treatment (n=5) and non-responders with > 2 fractures/year during treatment (n=14). Only type I patients were found in the responder group. The non-responder group included Types I, III, IV. No significant difference was found between groups for mean values of vitamin D, serum total alkaline phosphatase, C-telopeptides, or osteocalcin. However, there was a difference between the responder and non-responders in mean duration of treatment ($p = .02$): responder 42.6 ± 8.1 months, vs. non-responder 72.7 ± 10.97 months. 34 adult patients who received a minimum of 3 years of BP treatment experienced 41 fractures 10 years prior to treatment and 57 fractures in the 10 years following treatment ($p > 0.05$). Treatment responses for metabolic and bone related biomarkers did not show a significant difference over a 5 year period of observation between 34 adults treated with BP and 12 non-treated controls. **Discussion:** Two meta-analyses (Dwan, 2014, Hald, 2014) conclude that BPs effect on decreasing fracture incidence is "unclear" or "inconclusive". Meta-analysis by Shi (2015) concluded that BP decrease fracture rate in children but not in adults as previously reported. Bishop et al. reported risdrionate to decrease fracture rate in children after one year of treatment but that incidence rose to non-treatment rates during a 2-3 year extended treatment period. Rauch et al. (2006) observed marked histologic effects of BP treatment on bone tissue in the first 2-4 years of pamidronate treatment but no significant effect afterwards. **Conclusion:** Conflicting data exists on the effectiveness of oral and IV BP in OI. Certain children and adults do not decrease fracture incidence in response to BP. Response of bone biomarkers does not differentiate responders from non-responders in children or adults. Current evidence questions whether prolonged treatment with IV BP is associated with a sustained decrease in fracture rate.

Disclosures: Jay Shapiro, None.

SA0386

An overview of the etiology, clinical manifestations, management strategies and complications of hypoparathyroidism. Tayyab Khan^{*1}, Hamid Syed², Aliya Khan². ¹Department of Medicine, Western University, Canada, ²McMaster University, Canada

Hypoparathyroidism is an uncommon endocrine disease characterized by absent or inappropriately low levels of Parathyroid hormone (PTH), with low serum calcium and elevated phosphate levels, and presents unique therapeutic challenges. While evidence gathered over the last decade has led to an increased understanding of this condition, data regarding disease manifestations in the Canadian population are lacking.

We established a Canadian registry of patients with hypoparathyroidism and reviewed baseline data with respect to etiology, presenting symptoms, current treatment and complications of this condition. The study was approved by the Research Ethics Board at McMaster University and all patients provided informed consent.

Most patients (47/65; 72.3%) had postsurgical hypoparathyroidism, followed by idiopathic/autoimmune disease (12/65; 18.5%), pseudohypoparathyroidism (4/65; 6.1%) and congenital hypoparathyroidism (2/65; 3.1%). The mean age of onset was 46 years (Range: 10 years – 75 years). Paresthesias in the upper and lower extremities were the most common presenting symptom and experienced by approximately 50% of patients. Approximately 16% of patients reported tetany and 14% had seizures. 42% of patients required hospitalization at the time of presentation. Current treatment options were reviewed and almost all patients were receiving calcium supplements (90.1%) with calcitriol being used by 92.3%; 22 patients (33.8%) were on hydrochlorothiazide and 4 patients (6.1%) were receiving parathyroid hormone. Complications were reviewed and 10 patients had brain imaging completed with 8 having evidence of basal ganglia calcification. 11 of 28 (39.3%) patients who received an abdominal ultrasound showed evidence of nephrolithiasis or nephrocalcinosis. Renal impairment was present in 68.4% who had chronic kidney disease Stage II or higher, over an average disease duration of 10 years. Based on bone densitometry by dual energy xray absorptiometry in the men and women over the age of 50 years evaluating BMD at either the lumbar spine, femoral neck, total hip or one third radial site 25% of the patients had low bone density while another 25% had osteoporosis. Amongst these patients 8% had experienced fragility fractures. Our findings provide interesting insights into the etiology, symptomatology, treatment strategies and complications of hypoparathyroidism in a Canadian population. Skeletal health does require further evaluation and assessment of bone strength would be of value in this patient population.

Disclosures: Tayyab Khan, None.

SA0387

See Friday Plenary Number FR0387.

SA0388

See Friday Plenary Number FR0388.

SA0389

See Friday Plenary Number FR0389.

SA0390

See Friday Plenary Number FR0390.

SA0391

Appendicular Lean Mass and Anxiety Disorders: A Potential Regulatory Role for Skeletal Muscle on Brain Function. Julie Pasco^{*1}, Mark Kotowicz², Sharon Brennan-Olsen¹, Kara Holloway¹, Felice Jacka¹, Michael Berk¹, Shae Quirk¹, Amanda Stuart¹, Lana Williams¹. ¹Deakin University, Australia, ²Deakin University & Barwon Health, Australia

Purpose: Skeletal muscle contraction produces neurotrophic factors that have a critical role in the pathophysiology of common mental disorders. Furthermore, skeletal muscle activity modulates immune function and redox status that impact neurological pathways. We aimed to examine the relationship between appendicular lean mass (ALM, lean mass of arms and legs combined) and the likelihood for incident anxiety disorders.

Methods: This nested case-control study utilises data from the 10-year and 15-year follow-up phases of the Geelong Osteoporosis Study (GOS). Cases were women with incident anxiety disorders, identified using the Structured Clinical Interview for DSM-IV-TR (SCID-I/NP). Controls were women who had no history of anxiety and remained anxiety-free during the five-year period of follow-up. The exposure of interest was ALM (expressed in SD units), measured by dual energy x-ray absorptiometry at the 10-year follow-up, together with socioeconomic status and health behaviours. Clinical and psychiatric data were available for 745 participants. Those with prostheses (n=26) or pre-existing anxiety at 10-year follow-up (n=100) were excluded; thus, 619 women (age 21-84 years) were included in the analysis.

Results: There were 71 cases. Cases were younger than controls (median age (IQR): 40 (27-55) vs 50 (37-64) years, $p<0.001$) and were more likely to be sedentary (24% vs 13%, $p=0.02$), otherwise no other differences were detected between the groups. Mean ALM (SD) for cases was 7.05 compared with 7.17 for controls and this difference was not significant. However, after adjusting for age, greater ALM was protective against anxiety (OR 0.75, 95%CI 0.57-0.99, $p=0.04$). This relationship was attenuated by accounting for physical inactivity (adjusted OR 0.77, 95%CI 0.58-1.01, $p=0.06$) but remained unaffected by further adjustment for height, smoking, alcohol use and socioeconomic status. No effect modifiers were identified.

Conclusions: These data suggest that lower ALM may increase the risk of subsequent anxiety disorders in women and that the relationship is explained, at least in part, by a sedentary lifestyle. This finding warrants further investigation into muscle wasting as a risk factor for the common mental disorders.

*Disclosures: Julie Pasco, None.***SA0392**

See Friday Plenary Number FR0392.

SA0393

Body compositions differently affect bone mineral density in men and women throughout the lifespan : the Korean National Health and Nutrition Examination Survey (KNHANES) 2008-2011. Yoo Mee Kim^{*}, Se Hwa Kim, Jung Sun Yoo, Eun Yeong Choe, Young Jun Won. Department of Internal Medicine, Catholic Kwandong University College of Medicine, International St. Mary's Hospital, South Korea

Body mass index (BMI) is an important bone modulating factor in postmenopausal women. BMI is the best way of determining obesity, however, it has limits discriminating lean mass and fat mass. As aging proceeds, BMI changes little but muscle mass decreases and fat mass increases. Thus, BMI alone is not enough to evaluate body composition. Moreover, it is uncertain which component of body compositions mostly affects bone mineral density (BMD) in men and women throughout the lifespan. We therefore evaluated the relationship between body composition and BMD from age 10 to 97 years (y) old. This population-based, cross-sectional study is from the Korea National Health and Nutrition Examination Surveys (KNHANES) 2008-2011. The subjects who performed both body composition analysis and BMD by dual energy X-ray absorptiometry were enrolled. The total number of subjects were 20,704. The mean age was 45.3 ± 19.0 y (M, n=9,077, 10-93 y) and 46.7 ± 18.5 y (F, n=11,627, 10-97 y). The subjects were divided into 2 age groups by 50 y. Anthropometric data, lean mass (LM), appendicular skeletal muscle mass (ASM), fat mass (FM), fat percentage (FP), lumbar spine (LS) BMD, and total hip (TH) BMD were compared between 2 age groups by gender. Blood pressure, smoking, alcohol, and exercise history were compared as well. All body compositions were evaluated for correlations with LS or TH BMD. LM or ASM, and FM or FP were included in multivariate analysis for LS or TH BMD controlling for age and height in

each age group by gender. BMI and waist were higher in older men and women than younger subjects. Lower LM, ASM, and FM but similar FP were observed in older men. In older women, LM and ASM were lower, while FM and FP were higher than younger women. Anthropometric data or body composition parameters significantly correlated with both LS and TH BMD in all age groups of both gender. After adjusting for age and height, LM and ASM strongly affected LS and TH BMD in both age groups of men and women. FM and FP significantly affected LS and TH BMD in both young and old women and also in old men, but it negatively affected LS and TH BMD only in young men group. In conclusion, considering different contribution of age, height, and gender to BMD, LM and ASM are important positive independent predictors of LS and TH BMD in both men and women across the lifespan. However, FM and FP negatively affect BMD in young men but they positively affect BMD of old men and also women throughout the lifespan.

*Disclosures: Yoo Mee Kim, None.***SA0394**

Characteristics of Regional Bone Mineral Density and Soft Tissue Composition in Japanese Elderly Women with Sarcopenia. Shinjiro Takata^{*}. Tokushima National Hospital, National Hospital Organization, Japan

The term sarcopenia was proposed by Irwin Rosenberg to describe an age-related decrease of muscle mass (Am J Clin Nutr 1989; 59:1231-3). The European Working Group on Sarcopenia in Older People (EWGSOP) recommends using the presence of both low muscle mass and low muscle function (strength or performance) to make a diagnosis of sarcopenia (Age and Ageing 2010; 39:412-423). The purpose of this study was to clarify the characteristics of regional bone mineral density (BMD) and soft tissue composition in Japanese elderly women with sarcopenia.

One hundred and thirty-three Japanese elderly women aged 65 years or more were divided into two groups, sarcopenia group (n=54) and control group (n=79). No significant differences were found between these two groups with regard to age, body height, body weight, and body mass index. The mean BMD of the second to fourth lumbar vertebrae (L2-4BMD), total body BMD, and soft tissue composition were measured by DXA using Hologic Discovery W (Waltham, MA, USA). Regional BMD (g/cm^2) was measured in the head, arms, legs, ribs, thoracic vertebrae, lumbar vertebrae, and pelvis. Lean mass (g) and fat mass (g) of the head, arms, legs, and trunk were measured. Skeletal mass index (SMI) is the appendicular skeletal mass in kilograms measured by dual energy X-ray absorptiometry divided by the square of the height in meters (kg/m^2). SMI of the sarcopenia group was less than 5.4 (kg/m^2).

The BMDs of the arms, legs, and femoral neck as well as the L2-4BMD of the sarcopenia group were significantly lower than those of the control group ($p<0.05$). The lean masses of the arms, trunk, and legs of the sarcopenia group were significantly lower than those of the control group ($p<0.05$), whereas the fat masses of the arms and legs of the sarcopenia group were significantly greater than those of the control group ($p<0.05$).

The major findings of this study were that the BMDs and skeletal muscle masses of the arms and legs were significantly lower than those of the control group, whereas the fat masses of the arms and legs of the sarcopenia group were significantly greater than those of the control group. These results show that sarcopenia in Japanese women aged 65 years or more is associated with osteopenia or osteoporosis in addition to low muscle function.

*Disclosures: Shinjiro Takata, None.***SA0395**

Physical exercise may prevent sarcopenia in elderly women. Samu Sjölöblom^{*}, Juha Suuronen, Toni Rikkinen, Risto Honkanen, Heikki Kröger, Joonas Sirola. University of Eastern Finland, Finland

Purpose: The aim of the study was to examine the relationship between physical exercise and sarcopenia and the components of sarcopenia in Finnish postmenopausal women. This is a cross-sectional study.

Material and Methods Study sample: a population-based cohort of 591 Finnish postmenopausal women (mean age 67.9; range 65-72) from the Osteoporosis Fracture Prevention (OSTPRE-FPS) study. Outcome measures: Relative skeletal muscle index (RSMI) and fat percent were measured by dual X-ray absorptiometry (DXA). Moreover, grip strength, quadriceps strength and 10 m walking test were measured. The study sample was divided into sarcopenic and non-sarcopenic groups according to quartiles of relative skeletal muscle mass index (RSMI) (appendicular muscle mass ($\text{kg}/\text{height}(\text{m})^2$), hand grip strength (kPa) and walking speed. The amount of physical exercise was asked by exercise diary. The number of women who walked was 489, skied 191, cycled 268, did gym 178 and swam 267. The analyses were adjusted for: strenuousness of exercise, age, height, weight, the level of serum vitamin D and hormone therapy (HT), consumption of alcohol and smoking.

Results: The logistic regression analysis revealed that the amount of cycling was negatively associated with sarcopenia in non-adjusted model ($p=0.007$, OR=0.807, Confidence interval 0.692-0.942) and in adjusted model ($p=0.035$, OR=0.817, CI=0.677-0.986). Moreover, the amount of swimming had a negative association with

sarcopenia in non-adjusted model ($p=0.018$ OR=0.841, CI 0.729-0.971) but not in adjusted model ($p=0.071$). In linear regression cycling was positively associated with RSMI in non-adjusted model ($p=0.002$) and in adjusted model ($p=0.001$). Moreover, walking had a positive association with grip strength in non-adjusted model ($p=0.006$) and in adjusted model ($p=0.008$). Cycling was positively associated with quadriceps strength in non-adjusted model ($p=0.023$) but not in adjusted model. The amount of walking and skiing was positively associated with walking speed in non-adjusted model ($p=0.036$ and 0.049 , respectively) but not in adjusted model. Finally, cycling and skiing was negatively associated with fat percent ($p=0.028$ and $p=0.001$, respectively) and in adjusted model the p -values were 0.033 and 0.277.

Conclusion Physical exercise may prevent sarcopenia and decrease fat mass. Cycling might be the most suitable form of exercise in elderly women to prevent sarcopenia.

Disclosures: Samu Sjöblom, None.

SA0396

Vitamin D Status and Muscle Strength among Ethnic Minorities Residing in Northeast Scotland. Nor Aini Jamil¹, Stuart Gray², William Fraser³, Helen Macdonald^{*2}. ¹University of Aberdeen & Universiti Kebangsaan Malaysia, United Kingdom, ²University of Aberdeen, United Kingdom, ³University of East Anglia, United Kingdom

Vitamin D may play a role in muscle strength, yet little is known about how this is affected by emigrating from low to high latitudes. The aims of this longitudinal study were (1) to examine vitamin D status and muscle strength changes among ethnic minorities from sunnier climates after arriving in Northeast Scotland (Aberdeen, 57°N) and (2) to investigate the relationship between vitamin D status on muscle strength. A total of 66 healthy adults (73% Asians (96% Southeast Asians), 15% Africans and 12% Middle Easterners) aged 19-41 years took part with 58% seen within 3 months of arriving in Scotland. Participants attended visits every 3 months for fifteen months. At each visit, fasted blood samples were collected for analysis of serum total 25-hydroxyvitamin D (25(OH)D) by dual tandem-mass spectrometry. Maximal voluntary contraction (MVC) was measured using a Takei digital grip dynamometer (both arms) and a Biodex dynamometer (right knee extension). Skin type (I-VI) was determined using a CM-2600d spectrophotometer (inner arm). Dietary vitamin D intake and sunlight exposure were assessed by questionnaires. Mean(SD) baseline 25(OH)D was lower in Middle Easterners (16.9(6.8)) nmol/L, $p=0.010$ compared to Asians (31.1(13.1)) nmol/L and Africans (32.4(10.9)) nmol/L. Mixed model analysis showed that ethnicity, longer duration in Scotland, increasing age and lighter skin colour were associated with lower 25(OH)D concentrations. Recent holiday, greater body surface exposure area and total dietary vitamin D intake (including supplements) were significant positive predictors of 25(OH)D. There was no association between vitamin D status and grip strength ($p=0.23$), although grip strength increased over time possibly due to improved technique. For knee strength, there was a trend for a positive association between 25(OH)D and knee isometric strength. The model predicted that for each 1 nmol/L increase in 25(OH)D, peak torque increased by 1 Nm ($p=0.06$). Whilst vitamin D status was associated with lower limb muscle strength among ethnic minorities residing in northeast Scotland, the study design does not prove causality.

Disclosures: Helen Macdonald, None.

SA0397

See Friday Plenary Number FR0397.

SA0398

Fracture Repair and Effects of Aging on Macrophages at the Fracture Callus. Mary Nakamura^{*1}, Erene Niemi², Yang Frank³, Ted Mclau³, Ralph Marcucio³. ¹University of California, San Francisco/San Francisco VA Medical Center, USA, ²UCSF/SFVAMC, USA, ³Orthopaedic Trauma Institute, SFGH, UCSF, USA

Delayed healing and non-union during fracture healing is common in the elderly. We propose that age-related changes in myeloid cells promote dysfunctional bone regeneration during fracture repair. We isolated fracture callus cells from aged or young animals for flow cytometric and gene expression analysis. Aged (24 months) or young (10-12 weeks) mice undergo closed non-stable tibial fracture. At indicated time points a defined area around the fracture callus is removed, skin/muscle eliminated and bone marrow discarded. The remainder of the fracture callus is minced and digested with collagenase. Isolated cells are washed, and stained for flow cytometry. Samples from aged and young animals are analyzed simultaneously, 5 animals/group/time point. Days 1, 3, 5, 7 and 10 were examined using multicolor analysis to examine F4/80 positive cells (macrophages) using lineage markers to gate out T cells, B cells, NK cells, and granulocytes. Tissue macrophages are identified as Lin^{neg}, CD11b⁺, F4/80^{hi}, Ly-6C^{lo/hi} and stained for additional markers. Live hematopoietic cell gates use CD45 and sytox blue (or dead red) staining.

Day 1 cellular analysis demonstrates similar distribution of immune cells in the aged and young fracture callus including T cells, B cells, NK cells, macrophages and granulocytes. Initial macrophages in aged and young fracture callus were phenotypically similar. F480/CD11b⁺ cells are predominantly Ly6C⁺ and MHC Class II negative. Macrophage number increases about 4-8 fold at Day 3 in the aged and young fracture callus. By Day 3, numerical and phenotypic differences between the aged and young macrophages in the fracture callus emerge. In the young fracture callus, 2 fold more F480⁺ cells particularly Ly6C⁺/MHC Class II⁻ cells are found in the young compared with aged callus, with other cells in both the aged or young, Ly6C⁺ MHC Class II⁺. At Day 7, total macrophage number decreases in both the aged and young fracture callus. At Day 10, macrophage number again rises with a marked change in Ly6C⁺ and MHC Class II⁺ cells number, with a greater increase in the young compared with the aged fracture callus. RNAseq analysis of Isolated fracture callus macrophages comparing cells from aged and young fracture calluses is in progress. Our data suggests that decreased recruitment and/or proliferation of inflammatory macrophages in addition to changes in macrophage phenotype with aging likely contribute to abnormalities in fracture healing seen with aging.

Disclosures: Mary Nakamura, None.

SA0399

See Friday Plenary Number FR0399.

SA0400

Restraining mitochondrial H₂O₂ generation in cells of the mesenchymal lineage abrogates the adverse effects of aging on the murine skeleton. Maria Almeida^{*1}, Serra Semahat Ucer¹, Srividhya Iyer², Ha-Neui Kim¹, Li Han¹, Christine Rutlen¹, Shoshana Bartell¹, Aaron Warren¹, Julie Crawford¹, Robert Jilka¹, Stavros Manolagas¹. ¹Center for Osteoporosis & Metabolic Bone Diseases, Central Arkansas Veterans Healthcare System, University of Arkansas for Medical Sciences, USA, USA, ²Central Arkansas VA Healthcare System, Univ of Arkansas for Medical Sciences, USA

Generation of reactive oxygen species (ROS) is an inevitable consequence of aerobic metabolism and it occurs mainly in the mitochondria from the escape of electrons passing through the electron transport chain. Of the ROS species, H₂O₂ has the highest oxidative activity and intracellular concentration. An increase in ROS has been associated with the decreased bone formation caused by old age as well as the increased resorption caused by sex steroid deficiency in mice. Increased ROS in osteoblasts and osteocytes decreases bone formation. On the other hand, H₂O₂ generation is a critical requirement for osteoclastogenesis and bone resorption. We have generated mice in which a transgene for human catalase - a potent H₂O₂ inactivating enzyme - has been targeted to the mitochondria (MitoCat) of cells of the mesenchymal lineage using Prx1-Cre (MitoCat;Prx1-Cre). Bone marrow derived osteoblasts from MitoCat;Prx1-Cre mice had 2-fold higher catalase activity as compared to wild-type, Prx1-Cre, or MitoCat-flox stop (FS) control mice. Catalase activity in kidney, liver, spleen, or cultured macrophages was, however, indistinguishable from littermate controls. Femoral cancellous and cortical bone volume in young adult males or females (3 and 6 month of age, respectively) was indistinguishable from littermate controls as determined by micro-CT. MitoCat-FS control mice aged to 22 months exhibited the expected age-related decline in cortical thickness and cortical bone volume as compared to 6 month-old mice of the same genotype. In contrast, the cortical thickness of 22 month old MitoCat;Prx1-Cre mice was indistinguishable from young adults. Elsewhere in this meeting, we report that mice in which MitoCat has been targeted to cells of the osteoclast lineage (MitoCat;LysM-Cre) are protected from the increase in osteoclast number at the endocortical surface as well as the loss of cortical bone mass caused by loss of sex steroids in females or males. The MitoCat;LysM-Cre mice, however, are not protected from the adverse effects of old age. This genetic evidence indicates that increased H₂O₂ generation with old age in cells of the mesenchymal lineage is a seminal culprit of the loss of cortical bone. In contrast, increased H₂O₂ generation in cells of the osteoclast lineage is the culprit of the loss of cortical bone caused by acute sex steroid deficiency, but not old age. Hence, the mechanisms of cortical bone loss in the two conditions are distinct.

Disclosures: Maria Almeida, None.

SA0401

Synergistic Effects of Metformin and Sitagliptin on Mesenchymal Stem Cells Maintenance and Differentiation During Aging. Sudharsan Periyasamy-Thandavan^{*1}, Sadanand Fulzele², Alexandra Aguilar-Pérez³, Maribeth Johnson⁴, Mark Hamrick³, Carlos Isales⁵, William Hill³. ¹Georgia Regents University & Charlie Norwood VAMC, USA, ²Department of Orthopaedic Surgery, Georgia Regents University, USA, ³Department of Cellular Biology & Anatomy, Georgia Regents University, USA, ⁴Department of Biostatistics, Georgia Regents University, USA, ⁵Department of Neuroscience & Regenerative Medicine, Georgia Regents University, USA

An imbalance between bone resorption and bone formation leads to osteoporosis, one of the most ubiquitous diseases affecting over 45 million elderly Americans. Several studies suggest that the age-related osteoporosis is mostly initiated by decline in the regenerative capacity of its resident stem cells. Mesenchymal Stem Cells (MSCs) are multipotent stem cells that can differentiate into osteoblasts. MSCs secrete SDF-1, which is required for CXCR4 regulated activation of BMP2 receptors driving osteogenic differentiation. SDF-1 is also critical in MSC survival within the bone marrow (BM) microenvironment by increasing autophagy. However, BM SDF-1 levels are altered with age, and are linked to an age-associated reduction of autophagy and bone loss. AMP-activated protein kinase (AMPK) has emerged as a key sensing mechanism in the regulation of cellular energy homeostasis by mediating autophagy, and plays a major role in bone physiology by regulating the differentiation of osteoblasts. The combination of metformin and sitagliptin, two FDA-approved antihyperglycaemic drugs, has been shown to possess enhanced therapeutic efficacy in patients over either alone. In the present study, we explored the potential connection between defective AMPK and the SDF-1 mediated autophagic signaling pathways on BM MSC maintenance, survival and osteogenic differentiation during aging. We used Sca1+ Lin- MSCs isolated from 6 and 24 month old male C57BL/6J mice (n=6; passage 3). qPCR analysis showed a significant reduction in critical osteogenic and autophagic genes with age. We examined the effect of metformin treatment, with, or without, sitagliptin, in 24 month MSCs on SDF-1 and autophagy induction at different time points. Metformin in combination with sitagliptin synergistically induced SDF-1 expression via the AMPK-autophagic signaling pathway in a time dependent manner. It also regulated the ability of MSCs to migrate. Likewise, the metformin-sitagliptin combination treatment significantly increased the osteogenic matrix deposition and its mineralization. Collectively, these data suggested that the pAMPK signaling pathway regulates SDF-1 expression, MSC survival and osteogenic potential thereby enhancing the regenerative and osteogenic capacity of aged MSCs. Our novel findings are significant in that they open new therapeutic avenues to potentially reduce osteoporotic bone loss through regulation of the SDF-1 and AMPK pathways.

Disclosures: Sudharsan Periyasamy-Thandavan, None.

SA0402

Measurement of Fluoride in Rat and Monkey Urine. Florence Poitout-Belissent, Luc Huard, Rana Samadfam, Melanie Felix, Jeffrey McCartney, Smith Susan Y.^{*}. Charles River Laboratories, Canada

Exposure to compounds with fluoride results in fluoride incorporation in bones and tooth enamel, and excretion in urine. Assessment of fluoride concentration is important after administration of fluoride compounds as an excess of sodium fluoride may lead to proximal renal tubular injury. An excessive concentration of fluoride in urine has been correlated with dental fluorosis in humans. Urine fluoride evaluation is challenging because it is present only in trace amounts, and its transformation into ionic form is necessary for measurement. Common methods of analysis are high performance liquid chromatography and ion specific electrode after acid extraction.

We validated a method for the determination of fluoride concentration using a buffer extraction of the fluoride and an ion specific electrode perfectION[®], in urine of rats and cynomolgus monkeys.

Method: Urine was collected overnight at room temperature from animals deprived of food and water. 1 mL of urine was diluted 1:1 with a 5% sodium EDTA in buffer deionized water/Total Ionic Strength Adjustment Buffer, placed in a water bath at 95°C for 15 minutes, cooled at room temperature, and measured with the ion selective electrode.

Results: measurement range was 0.01 to 10.0 mg/L.

Precision intra-assay coefficient of variation (CV) was 0.1 to 0.3% in rats, 0.4 to 0.6% in monkeys. Inter-assay CV was 3.6 to 5.9% in rats, 1.5% in monkeys.

Accuracy was determined using a commercial Sodium Fluoride (NaF) control solution: CV was 0.3 to 4.9% rats, 3.6 to 4.0% monkeys.

Linearity of dilution range was 0.0164 to 5.92 mg/L in rats, 0.0163-5.33 mg/L in monkeys.

Extraction efficiency was evaluated by calculation of the recovery in five individual samples spiked at two different concentrations of NaF. Recovery ranged between 89.5 and 121% in monkeys, 97.6 and 115% in rats.

Samples were stable up to 3 months at -20°C for both species.

Reference range was 1.25-6.39 mg/L rats, 0.598-5.41 mg/L monkeys for an overnight collection.

In conclusion: The fluoride buffer extraction and ion specific electrode measurement method is simple, rapid, and suitable for the determination of trace amounts of fluoride in urine in rats and monkeys.

Disclosures: Smith Susan Y., None.

SA0403

See Friday Plenary Number FR0403.

SA0404

See Friday Plenary Number FR0404.

SA0405

See Friday Plenary Number FR0405.

SA0406

See Friday Plenary Number FR0406.

SA0407

See Friday Plenary Number FR0407.

SA0408

See Friday Plenary Number FR0408.

SA0409

Diet Derived Phenolic Acid Regulates Bone Accretion and Senescence Signaling. Jin-Ran Chen^{*1}, Oxana P. Lazarenko², Michael L. Blackburn², Thomas M. Badger². ¹University of Arkansas for Medical Science, Arkansas Children's Nutrition Center, USA, ²University of Arkansas for Medical Sciences & Arkansas Children's Nutrition Center, USA

A blueberry (BB) supplemented diet has been previously shown to significantly stimulate bone formation in rapidly growing male and female rodents. Phenolic acids (PAs) are metabolites derived from polyphenols found in fruits and vegetables as a result of the actions of gut bacteria, and the levels of these PAs were found significantly higher in the serum of rats fed a BB-containing diet. We have characterized the effect on stimulating osteoblastogenesis of one such BB-associated serum PA, 3-(3-hydroxyphenyl) propionic acid (PPA). To more fully understand the mechanistic actions of PPA on bone formation, we administered four different doses of PPA (0.1, 0.5, 1 and 5 mg/kg/d) to one-month-old female C57Bl mice for thirty days. We found that stimulation of osteoblast differentiation and proliferation occurred in PPA treated osteoblastic cells. Using peripheral quantitative CT scan (pQCT) analysis, we demonstrated differences in bone phenotypes between control and PPA-treated animals, i.e., trabecular bone mineral densities were significantly higher in 0.5 to 5 mg/kg/d PPA-treated animals compared to their controls. Furthermore, static and dynamic histomorphometric analyses showed that osteoblast number and mineralizing surface per bone surface (Ms/Bs) were significantly increased in 1 and 5 mg/kg/d PPA-treated animals compared to un-treated controls. Bone formation rate was significantly increased in 0.5, 1 and 5 mg/kg/d PPA-treated animals compared to un-treated controls. After aspiration of bone marrow, femur bone protein and RNA were isolated for Western blot and real-time PCR analysis of signaling transduction. We found that PPA was able to suppress bone senescence signaling as evaluated by measuring senescence associated beta-galactosidase activity, p53 and p21 expression in bone. Suppression of PPAR γ expression in bone by PPA was associated with increased bone mass dose-dependently. In conclusion, PPA is capable of altering the mesenchymal stem cell differentiation program and merits investigation as a potential dietary therapeutic alternative to drugs for degenerative bone disorders. *Supported in part by ARS CRIS #6251-51000-005-03S (JRC).*

Disclosures: Jin-Ran Chen, None.

SA0410

See Friday Plenary Number FR0410.

SA0411

See Friday Plenary Number FR0411.

SA0412

See Friday Plenary Number FR0412.

SA0413

See Friday Plenary Number FR0413.

SA0414

See Friday Plenary Number FR0414.

SA0415

See Friday Plenary Number FR0415.

SA0416

See Friday Plenary Number FR0416.

SU0001

Bone Deficits in Chronic Kidney Disease and the Effect of Renal Transplantation on Mechanical Competence. Chamith Rajapakse*¹, Wenli Sun², Michelle Slinger¹, Elizabeth Kobe¹, Rhiannon Miller¹, Felix Wehrli¹, Mary Leonard³. ¹University of Pennsylvania School of Medicine, USA, ²University of Pennsylvania, USA, ³Stanford School of Medicine, USA

Abnormal vitamin D and mineral metabolism are a universal complication of advanced chronic kidney disease (CKD). Secondary hyperparathyroidism results in abnormal trabecular microarchitecture and cortical thinning. Renal transplantation (RTxp) corrects many of the risk factors for bone deficits; however, glucocorticoid therapy and persistently elevated PTH levels may further compromise strength. The objective of this study was to use MRI-based finite-element analysis to assess bone mechanical competence at the time of RTxp, compared with controls, and to examine changes after RTxp.

Sixty RTxp recipients (52% male, 32% preemptive), ages 20-60 years, were enrolled at transplantation and compared with 104 healthy controls (49% male), ages 19-60 years. MRI of the distal tibia was performed on a 1.5 Tesla scanner (Siemens Tim Trio, Erlangen, Germany) using a 2-channel surface coil at 0.137 mm x 0.137 mm x 0.410 mm voxel size. Trabecular bone parameters and stiffness of the whole section were computed on the basis of these images using digital topological and finite element analysis, respectively.

Within controls, bone volume fraction (BV/TV) was inversely associated with age ($p=0.001$) and greater in males ($p<0.001$). At baseline, RTxp recipients had lower BV/TV, Tb.N, higher Tb.Sp, and lower stiffness, adjusted for age and sex ($p < 0.05$) (Figure 1). In CKD patients, from baseline to 6 months following renal transplantation, stiffness significantly decreased by 3% ($p=0.01$). During 6-12 and 12-24 months, stiffness increased by 4% and 1%, respectively, however these changes were not statistically significant.

Further analysis is needed to determine if trabecular and cortical bone compartments are differentially affected by CKD and renal transplantation.

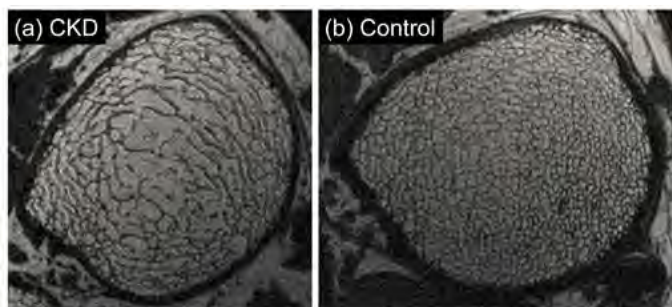


Figure 1: (a) Baseline MR image of the distal tibia metaphysis obtained from a 26-year old Caucasian female CKD patient and (b) a healthy control subject with the same age, race, and sex. Compared to the control, the CKD patient shows decreased Tb.N, increased Tb.Sp, and thinned cortex, which contribute to decreased stiffness, consistent with the overall baseline results from the study.

Figure 1

Disclosures: Chamith Rajapakse, None.

SU0002

Specific microRNA signatures in CKD patients focusing on the risks of calcifications and ROD. Barbara Obermayer-Pietsch*¹, Matthias Ulbing¹, Alexander Kirsch², Schweighofer Natascha³, Bettina Leber⁴, Sandra Lemesch⁵, Alexander Rosenkranz⁶, Helmut Müller⁴, Kathrin Eller⁶, Vanessa Stadlbauer⁵. ¹Medical University Graz, Austria, ²Medical University Graz, Dept. Internal Medicine, Division of Nephrology, Austria, ³Medical University Graz, Dept. Internal Medicine, Div. Endocrinology & Metabolism, Austria, ⁴Medical University Graz, Dept. Surgery, Div. of Transplant Surgery, Austria, ⁵Medical University Graz, Dept. Internal Medicine, Div. Gastroenterology, Austria, ⁶Medical University Graz, Dept. Internal Medicine, Div. Nephrology, Austria

Introduction:

Calcification of vessels - mainly in the tunica media - with additional demineralisation of bone is typical for patients suffering from chronic kidney disease (CKD). In this project, we analyse samples from CKD patients with a focus on microRNAs (miRNAs) as new biomarkers for vascular calcification. Our aim is to find a pattern of miRNAs indicating vascular calcification and/or mineralisation changes in the course of the disease and after kidney transplantation.

Methods:

Serum and plasma samples of 73 patients in CKD stages 3 – 5; 67 post RT (renal transplantation) patients as well as 36 healthy controls are analysed in the study. Additional 25 patients in CKD stage 5 were prospectively followed before, and already some of them during and after RT. Known biomarkers for calcification have been measured using ELISA techniques. A miRNA profile of CKD patients

compared to healthy controls has been established using a nCounter® miRNA Expression Assay. Deregulated miRNAs were further analysed in qPCR experiments.

Results:

PTH, FGF23 and osteocalcin were significantly increased in late stage CKD patients. When analysing more than 800 miRNAs, significant differences were found in 37 of them when comparing CKD patients of stage 5 and healthy controls. These miRNAs were related to vascular smooth muscle cell (VSMC) biology and bone metabolism. 12 miRNAs of them were followed for further analysis. In subsequent experiments especially 4 miRNAs emerged showing a different expression level comparing the patient and control groups.

Discussion:

miRNAs have been shown to have a biological association to vascular calcification, bone metabolism or differentiation of VSMCs to osteoblast-like cells. They are deregulated to a considerable extent in CKD patients. These pathways may be important during the development of calcified and vascular tissue in the course of kidney disease. miRNA signatures could become early diagnostic markers indicating the risk of vascular calcification or bone demineralisation in this high risk group.

Disclosures: Barbara Obermayer-Pietsch, None.

This study received funding from: Austrian Research Promotion Agency, Austrian Jubilee Fund

SU0003

The Effect of Kidney Disease on Bone Metabolism in Mice may be Modulated by the Initial Bone Characteristics. Ryan Clark*¹, Chelsea Heveran², William Schroeder¹, Moshe Levi¹, Virginia Ferguson², Karen King¹. ¹University of Colorado School of Medicine, USA, ²University of Colorado Boulder, USA

Patients with kidney disease have altered bone metabolism including high or low resorption and/or formation. The combination and degree of alterations cannot easily be predicted based on the type or severity of kidney dysfunction. To test our hypothesis that genetic variation contributes to variation in metabolic bone disorders we induced kidney dysfunction in two different mouse strains.

We created moderate chronic kidney disease (CKD) in 10 week old male C57Bl/6 and FVB mice by first removing one kidney and then 2/3 of the other one week later (5/6 nephrectomy). Additional mice received sham surgeries. Mice were euthanized 11 weeks later (N = 12/group). From each mouse, mRNA was extracted from one femur for qRT-PCR, protein from one tibia for Western blot analysis, while the remaining femur was imaged with micro computed tomography (μ CT) and then subjected to 3-point bending.

The Wnt pathway was upregulated with CKD in the C57Bl/6 strain. Gene expression increased significantly ($P<0.05$) for low-density lipoprotein receptor-related protein 5 (LRP5), secreted frizzled-related protein-4 (sFRP4, a Wnt inhibitor), and receptor for advanced glycation end products (RAGE, a downstream target). Conversely, sFRP4 protein appeared to increase in (Fig. 1, N=2/group). The Wnt pathway was unchanged or down-regulated with CKD in the FVB strain. Dickkopf-related protein 1 (DKK1, a Wnt inhibitor) and RAGE mRNA significantly decreased and sFRP4 protein appeared to decrease (Fig. 1).

Femur mechanical and structural properties were diminished with CKD but more severely for the FVB. Three-point bending strength at maximum load decreased (-10.6%; $P=0.03$) and fracture load at the femoral neck decreased (-10.0%; $P=0.01$) for the FVB but not for the C57Bl/6. Femur cortical diaphysis thickness decreased (-10.0%; $P=0.01$) for the FVB but not for the C57Bl/6 despite an equivalent loss of bone mineral density (both strains: -1.9%; $P<0.05$). Our data indicate that these two genetically different strains exhibit opposite reactions in response to decreased kidney function. Therefore, we propose the hypothesis that the initial bone traits may modulate the effect of CKD on subsequent bone metabolism. Our data are consistent with an osteocyte response to CKD in which FVB osteocytes more efficiently suppress the Wnt pathway resulting in more severely affected bone. Our study is limited in that the data do not show whether bone loss is due to increased resorption and/or decrease formation.

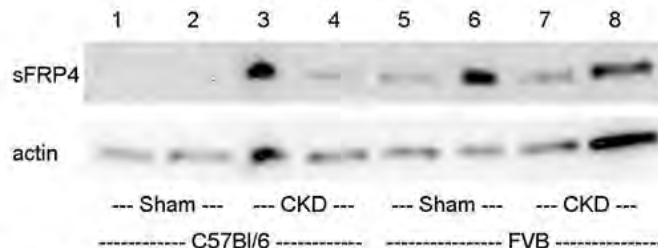


Fig. 1: Western blot analysis of protein - 10 μ g each lane - from C57Bl/6 (lanes 1-4) and FVB (lanes 5-8) mice. Mice were either sham operated (lanes 1, 2, 5, and 6) or operated to create moderate CKD (5/6 nephrectomy; lanes 3, 4, 7, and 8). Note: We believe that a calcium impurity caused lane 3 to run poorly.

Fig. 1

Disclosures: Ryan Clark, None.

SU0004

The Impact of Arteriovenous Fistula on Bone Density and Structure assessed by HR-pQCT. Stephanie Boutroy*¹, Justine Bacchetta², Solenne Pelletier³, Cyrille Confavreux⁴, Denis Fouque⁵, Roland Chapurlat⁴. ¹INSERM UMR1033 & Université de Lyon, France, ²INSERM UMR1033, Service de Néphrologie et Rhumatologie Pédiatrique, Hôpital Femme Mère Enfant, Université de Lyon, France, ³INSERM UMR1033, Département de Néphrologie, Hôpital Edouard Herriot, Université de Lyon, France, ⁴INSERM UMR1033, Département de Rhumatologie, Hôpital Edouard Herriot, Université de Lyon, France, ⁵Département de Néphrologie, Hôpital Edouard Herriot, Université de Lyon, France

Objectives

Maintenance hemodialysis is usually performed through an arteriovenous fistula (AVF). However, the impact of AVF on the underlying bone is largely unknown with only one study having reported decreased forearm aBMD assessed by DXA on the AVF side in 30 hemodialysis patients. Our aim was to evaluate the impact of AVF on volumetric BMD and bone microstructure assessed by High Resolution peripheral QCT (HR-pQCT).

Patients and methods

Fifty four patients (51 ± 16yrs, 20 women, 34 men) undergoing hemodialysis with a functioning AVF were included in this study. They underwent HR-pQCT (XtremeCT, Scanco Medical, Switzerland) of both radius.

Results

Total and cortical volumetric densities were significantly decreased by 3% and 2% (p<0.05) on the AVF radius side compared to the non-AVF radius. Cortical area and thickness were also decreased by 6% (p<0.05) while no difference was observed for the trabecular bone.

When comparing patients with radiolarial (distal) AVF (n=32) to those with humero-cephalic (proximal) AVF (n=22), the magnitude of the difference between the AVF and non AVF radius were similar in the two fistula localizations groups although patients with a humero-cephalic AVF were significantly older (57 ± 15 vs. 46 ± 16 yrs) with an increased dialysis duration (42 ± 32 vs. 25 ± 33 months).

Conclusions

This study shows a cortical impairment by HR-pQCT on the AVF radius side in patients undergoing maintenance hemodialysis with a functioning AVF, but the presence of an AVF seems to have no consequence on trabecular BMD and microstructure.

Disclosures: *Stephanie Boutroy, None.*

SU0005

Vertebral Fractures in Patients with End-Stage Renal Disease Undergoing Dialysis. Jerzy Przedlacki*¹, Paweł Żebrowski², Ewa Wojtaszek², Mariusz Mieczkowski², Agnieszka Grzejszczak³, Paweł Kulicki⁴, Małgorzata Koscielska⁴, Maria Kaszyńska², Joanna Matuszkiewicz-Rowińska². ¹Medical University of Warsaw, Poland, ²Chair & Department of Nephrology, Dialysis & Internal Diseases, Medical University of Warsaw, Poland, ³Chair & Department of Nephrology, Dialysis, & Internal Diseases, Medical University of Warsaw, Poland, ⁴Chair & Department of Nephrology, Dialysis & Internal Medicine, Medical University of Warsaw, Poland

Patients with end-stage renal failure treated with dialysis are in a high risk of bone fracture. In our everyday practice the clinically overt vertebral fractures (VFr) are recognized only, with the spine X-ray. There are no reports on the real frequency of VFr in this group of patients. The aim of the study was to assess the frequency of the low-energy VFr in dialysis patients. One hundred eight patients from our one dialysis center (62 males and 46 females; 74 hemodialysis and 34 peritoneal dialysis patients) aged 59.7 ± 13.7 years were examined. The observation was carried out during 2010-2013. Densitometric Vertebral Fracture Assessment (VFA) was done with the use of Discovery A, Hologic machine in 74 patients in 2010, and in 34 next years. Control tests were repeated every one or second year in all patients. Genant method of VFr assessment was used. In the case of the new VFr, X-ray was done to confirm it. The whole examined spine (T4-L4) was visible in 28 patients (25.9%). All but 2 lumbar vertebrae in 1 patient were visible. Altogether, 15 VFr (5 thoracic and 10 lumbar) were recognized in 9 patients (8.3%; 8 HD and 1 CAPD patients; 6 males and 3 females). In 1 male patient only VFr was diagnosed before the study with X-ray. There were wedge deformity in 4 thoracic vertebrae (2 of grade 1 and 2 of grade 2) and in 2 lumbar vertebrae (grade 1) and biconcave deformity in 1 thoracic vertebra (grade 1) and in 8 lumbar vertebrae (4 of grade 1 and 4 of grade 2). There was no statistically significant difference between fractured and not-fractured patients depending on the method of dialysis, gender and age. There were only 3 fractured patients with DXA spine and 2 with DXA hip osteoporotic result (in accordance to WHO criterion, T-score ≤ -2.5). Vertebral fractures seems to be frequent in dialysis patients but it is not possible to relate these results to general Polish population (data not available) and other dialysis patients. Most of them were not clinically overt and none of them was of grade 3. Densitometric VFA was useful in diagnosis of VFr. It is reasonable to perform VFA assessment in dialysis patients as the routine procedure because the new VFr gives information on the increased further fracture risk.

Disclosures: *Jerzy Przedlacki, None.*

SU0006

Radiation And Hypoxia Cooperatively Suppress Orofacial Mesenchymal Stem Cell Survival. Pinky Salat¹, Weihua Li¹, Sunday Akintoye*². ¹University of Pennsylvania, USA, ²University of Pennsylvania School of Dental Medicine, USA

BACKGROUND: Combination of radiotherapy and surgery is the standard of care for management of head and neck cancers. However, radiotherapy often leads to the complication of osteoradionecrosis (ORN) that further undermines the quality of life of cancer survivors. ORN pathogenesis is associated with development of a hypoxic-hypovascular-hypocellular tissue condition as tissue oxygen tension plays a vital role in critical cellular processes such as proliferation, growth factor expression and differentiation. Bone mesenchymal stem cells (MSCs) modulate bone healing and homeostasis and also display site-dependent disparity in responsiveness to irradiation. This study tested the hypothesis that radiation cooperates with hypoxia to suppress survival of orofacial (jaw) MSCs (OFMSCs) with consequent depletion of osteoprogenitor cell populations essential for post-irradiation healing and recovery. **METHODS:** Early passage human OFMSCs were subjected to two external stress modalities: 5 Gy irradiation followed by severe hypoxia (0.1% oxygen tension) for 6 hours in a modular hypoxic chamber (Billups-Rothenburg MIC-101). Appropriate control groups +/- radiation and/or +/- hypoxia were included in the experimental plan. Cell survival was assessed using WST-1 proliferation assay and western blotting was used to assess survival markers pAKT/TotalAKT and pERK1/2/TotalERK1/2, apoptotic markers p21 and MDM2 and hypoxic marker HIF-1α. **RESULTS:** Exposure to radiation, hypoxia or combination of both suppressed OFMSC survival and upregulated HIF-1α level but phosphorylation of AKT and ERK1/2 were unchanged. While p21 level was unaffected by hypoxia alone, radiation combined with or without hypoxia promoted p21 expression levels. MDM2 was upregulated only by radiation. **CONCLUSIONS:** Hypoxia apparently cooperates with radiation to suppress OFMSCs survival, a factor that may relate to ORN pathogenesis.

Disclosures: *Sunday Akintoye, None.*

SU0007

Association between Vitamin D deficiency and low HDL levels in Type 2 diabetics with Acute Coronary Syndrome. Fernando Gondin¹, Maria do Socorro Azevedo¹, Luiz Henrique Griz², Arianna Chacon¹, Breno Coimbra¹, Nathália Brito¹, Mirna de Sá*¹, Francisco Bandeira¹. ¹Division of Endocrinology & Diabetes, Agamenon Magalhães Hospital, University of Pernambuco Medical School, Recife, Brazil, ²Aluisio Borba Griz & Argentina Maciel Griz, Brazil

Epidemiological studies have suggested an association between vitamin D deficiency and the risk of cardiovascular disease but few data are available in patients with acute coronary syndrome, particularly in women with type 2 diabetes (T2DM).

This was a cross-sectional study comprising 321 diabetic women, stratified into two groups according to the presence or not of acute coronary syndrome (ACS) with the following characteristics: age (66.81 ± 11.38 yr x 63.62 ± 7.92 yr), duration of diabetes (mean ± SD: 9.03 ± 8.16 x 10.21 ± 8.08 yr), Body mass index (BMI): 27.16 ± 4.69 x 29.43 ± 5.87 kg/m², Waist circumference (WC): 93.05 ± 13.23 x 98.03 ± 11.57 cm, total serum cholesterol (93.05 ± 13.23 x 197.24 ± 49.07 mg/dl), LDLC (98.99 ± 32.11 x 113.43 ± 42.75 mg/dl), HDLC (40.84 ± 9.68 x 50.44 ± 13.82 mg/dl), triglycerides (196.78 ± 91.44 x 164.83 ± 82.31 mg/dl), 25OHD (7.56 ± 19.92 x 25.60 ± 8.51 ng/ml, p < 0.001) and PTH levels (42.25 x 49.20 ± 45.98 ± 28.28 pg/ml). No significant differences were found between the groups with respect to age (p = 0.106), diagnosis of hypertension (p = 0.554), duration of diabetes (p = 0.405) and PTH levels (p = 0.543). There was a statistically significant difference between BMI (p = 0.024) and WC (p = 0.016), with lower values among patients with ACS. Despite having lower BMI and WC values, ACS patients had lower serum 25OHD levels (p < 0.001) and serum HDLC cholesterol (p < 0.001). The other component of serum lipid profile also showed significant differences with the ACS group with lower total cholesterol (p < 0.001) and LDLC (p = 0.048). Only serum triglycerides were higher in the ACS group (p = 0.029).

Our data demonstrates an independent association between vitamin D deficiency and reduced HDLC in women with type 2 diabetes with ACS

Disclosures: *Mirna de Sá, None.*

SU0008

Determination of Severe Suppression of Bone Turnover in Women with Atypical Femoral Fracture after Long-term Bisphosphonate Treatment. Shijing Qiu*¹, George Divine, Saroj Palnitkar, Mahalakshi Honasoge, Sudhaker D Rao, Henry Ford Hospital, USA

Inhibition of bone turnover is an effective therapeutic for osteoporosis. However, severe suppression of bone turnover (SSBT) by antiresorptive drugs, especially bisphosphonates (BP), is likely to cause accumulation of aged bone with increased fragility. Until now, there is still no clear definition or diagnostic criteria for SSBT. Most authors defined SSBT as absence of tetracycline labeling in cancellous bone.

Since bone remodeling occurs not only on cancellous but also on intracortical and endosteal surfaces, it seems improper to define SSBT solely based on the examination of cancellous bone. The purpose of this study was an attempt to provide a novel criterion for the determination of SSBT.

Iliac bone biopsies from 43 healthy premenopausal white women and 12 white women with either complete (n = 5) or incomplete (n = 7) atypical femoral fracture (AFF) after long-term (>5 years) BP treatment were examined. The different bone surfaces (cancellous, intracortical and endosteal) were combined as one, and the parameters of erosion surface (ES/BS, %), osteoid surface (OS/BS, %), osteoid thickness (O.Th, μm), mineralizing surface (MS/BS, %), mineral apposition rate (MAR, $\mu\text{m}/\text{day}$) and bone formation rate (BFR/BS, $\mu\text{m}^3/\mu\text{m}^2/\text{year}$) were obtained on the combined bone surface. Compared to the healthy premenopausal women, all parameters were significantly reduced in AFF patients ($p < 0.05-0.001$; Table 1). The reference range for each parameter is shown in Table 1 and the lower limit of BFR/BS was 0.736. In 12 patients with AFF, 8 (67%) had BFR/BS < 0.736 , in which 3 patients had no tetracycline labeling in the whole biopsy. In the other 4 patients, BFR/BS remained at lower levels of the reference range.

The current study provided a threshold value of BFR/BS (~ 0.74) on the combined bone surface for the determination of SSBT. In this study, 2/3rd of the patients had BFR/BS below this threshold. Because the value of BFR/BS obtained from the combined bone surface appears to show the remodeling status in whole bone, it may be reasonable to use this variable for the definition of SSBT.

Table 1. The changes in bone turnover on the combined bone surface in AFF patients

| | AFF | Normal | p | Reference Range | Below Range |
|--------|--------------|--------------|--------|-----------------|-------------|
| ES/BS | 3.50(2.95) | 6.28(2.63) | 0.003 | 2.49-11.0 | 5/12 |
| OS/BS | 2.60(2.37) | 13.6(6.75) | <0.001 | 4.80-29.6 | 11/12 |
| O.Th | 5.06(1.44) | 9.32(1.74) | <0.001 | 6.77-13.8 | 11/12 |
| MS/BS | 1.21(1.73) | 6.59(3.17) | <0.001 | 1.41-12.5 | 7/12 |
| MAR | 0.123(0.108) | 0.553(0.174) | <0.001 | 0.146-0.829 | 7/12 |
| BFR/BS | 0.972(1.71) | 14.1(7.77) | <0.001 | 0.736-27.5 | 8/12 |

Disclosures: *Shijing Qiu, None.*

SU0009

Effects of Eldecalcitol on Inflammatory Markers in Patients with Rheumatoid Arthritis. Hayato Kinoshita¹, Naohisa Miyakoshi¹, Seiya Miyamoto², Yuji Kasukawa¹, Yusuke Sugimura³, Yoichi Shimada¹. ¹Department of Orthopedic Surgery, Akita University Graduate School of Medicine, Japan, ²Division of Orthopedic Surgery, Nakadori General Hospital, Jarvis island, ³Division of Orthopedics, Minamiakita Orthopedic Clinic, Japan

Rheumatoid arthritis (RA) is caused by upregulation of proinflammatory cytokines such as interleukin (IL)-2, IL-6 and tumor necrosis factor (TNF)- α . Furthermore, the rheumatic synovial membrane overexpresses receptor activator of nuclear factor kappa-B ligand (RANKL), which promotes differentiation of osteoclast precursors into osteoclasts, thus increasing bone resorption. Conversely, long term treatment with activated vitamin D3 is reported to suppress RANKL production, thus decreasing bone resorption. This study aimed to investigate whether activated vitamin D3 could prevent inflammation caused by excessive bone resorption in RA patients. From 490 RA patients registered to our Akita Orthopedic Group on Rheumatoid Arthritis (AORA) database, those treated with biological agents or who changed medication during observation period were excluded. Twenty-eight patients (4 male; 24 female; average age 67 years) were enrolled in this study. Patients were classified into the following groups: 1) control group (n=11), no activated vitamin D3 administration; 2) E group (n=9), treatment with eldecalcitol (0.75 $\mu\text{g}/\text{day}$); and 3) switch group (n=8), treatment with alfacalcidol (1.0 $\mu\text{g}/\text{day}$) then eldecalcitol (0.75 $\mu\text{g}/\text{day}$). White blood cells (WBC), C-reactive protein (CRP) and matrix metalloproteinase 3 (MMP-3) were measured pre-treatment, and at first (113rd days post-treatment) and second (216th days post-treatment) time points post-treatment with activated vitamin D3. Percentage (%) changes were determined for each parameter between pre- and post- (first and second) treatment time points. Although the WBC % changes in the control group at first (2.0th24%) and second (12th40%) time points were higher than those of the E group at first (-5.0th9.0%) and second (5.0th26%) and switch group at first (2.0th21%) and second (8.6th17%) time points, these were not significantly different. Additionally, there were no significant differences in CRP % changes at first and second time points between the control (180th312% and 191th336%, respectively), E (36th119% and -7.1th75%, respectively), and switch (33th157% and 3.7th29%, respectively) groups. Finally, there were no significant differences in MMP-3 % changes at first and second time points between the control (6.3th20% and 16th21%, respectively), E (11th18% and 25th33%, respectively), and switch (-19th30% and -3.6th7.6%, respectively) groups. In this study, activated vitamin D3 did not decrease inflammatory markers in RA patients.

Disclosures: *Hayato Kinoshita, None.*

SU0010

Indole sulfate as a metabolite in CKD patients regulates low turnover of bone metabolisms through OAT-3 transporter. Michiko Hirata, Tsukasa Tominari, Masaki Inada, Chisato Miyaura*. Tokyo University of Agriculture & Technology, Japan

Kidney is sole organ that regulates calcium and phosphorus level in blood to maintain body homeostasis. In CKD patients, the mineral levels in blood are altered in many cases of symptom that is resulted in low turnover bone remodeling. One of major toxic metabolites in blood of CKD patients is indoxyl sulfate (IS), a uremic toxins, which causes uremia such as vertigo, loss of appetite, and muscle atrophy. However, the regulations of bone metabolism by IS is still not known. In this study, we investigated the effects of IS on bone metabolism including bone resorption and formation that underlies the mechanisms on CKD patients. IS suppressed osteoclast differentiation in cocultures of primary osteoblast (POB) and bone marrow cells in dose dependent manner. To investigate the direct effect of IS on macrophage lineage cells, we used Raw264.7 and bone marrow macrophages (BMM) with soluble RANKL. IS inhibited RANKL induced osteoclast differentiation from Raw264.7 and BMM. To analyze mRNA expression in osteoclasts, real time PCR was performed. IS significantly suppressed the expression of NFATc1, TRAP and RANK in osteoclasts. In osteoblasts, the expression of RANKL was suppressed by IS treatment. The expression of OAT-3, a possible receptor of IS, was detected in both osteoclasts and osteoblasts, suggesting IS suppressed osteoclast differentiation in macrophage lineage cells directly and osteoblast lineage cells indirectly. These data suggest that IS may be incorporated into these cells via OAT, and inhibits osteoclast differentiation. We next examined the effects of IS on bone formation. IS significantly suppressed the bone formation in cultures of POBs, and the mRNA expression of bmp2, colla1, osterix and osteocalcin was down-regulated in osteoblasts. In conclusion, we showed that IS is incorporated into cells via OAT-3, resulting in inhibition of osteoclast differentiation and survival through down-regulation of NFATc1 gene expression and osteoclastic bone resorption. IS also suppressed bone formation through down-regulation of osterix and osteocalcin. Since, IS inhibited both bone resorption and bone formation. IS might be involved in the abnormality of bone remodeling with low bone turnover in CKD patients. Neutralization of uremic toxin IS may apply a possible approach to prevent low-turnover bone loss in CKD patients.

Disclosures: *Chisato Miyaura, None.*

SU0011

Exploration of associations between air pollutants and Paget's disease of bone. Mohamed Saber Numan¹, Sonia Jean², Jeannette Dumont¹, Jacques P. Brown³, Laetitia Michou⁴. ¹CHU de Québec Research Centre, Canada, ²Institut national de santé publique du Québec & Department of Medicine, Laval University, Canada, ³CHU de Québec Research Centre; Department of Medicine, Laval University; Department of Rheumatology, CHU de Québec, Canada, ⁴Université Laval, Canada

Background: Although genetic factors play an important role in Paget's disease of bone (PDB) pathogenesis, environmental factors such as rural residency have also been reported. We have previously shown an association between PDB and tobacco exposure in French families, and wood heating exposure in French-Canadians.

Purpose: To explore the associations between outdoor and indoor air pollutants and PDB.

Methods: We recruited 141 patients with PDB and 114 healthy controls from our French-Canadian cohort. Exposure was estimated using a questionnaire on the history of residence and proximity to sources of outdoor air pollutants such as highways, bus, train or airport stations, and gas stations. Regarding indoor air pollutants, questions on heating combustibles (carbon, wood, oil) used in past residences and tobacco exposure were also used. Associations between air pollutant exposures and PDB were assessed with Chi-squared, Fisher and t tests. Odds ratio (OR) and 95% confidence intervals were calculated. In a subgroup of patients (n=15 to 46) and controls (n=12 to 48), urinary concentration of 17 heavy metals and 11 polycyclic aromatic hydrocarbons were measured by mass spectrometry. A linear regression analysis with adjustment for PDB status, wood heating exposure, sex and tobacco exposure was performed.

Results: After adjustment for gender, PDB patients were less frequently exposed to outdoor air pollutants than controls during childhood: residence close to highways (32% of patients versus 80% of controls, OR=0.09 [0.04-0.19], $p < 0.0001$), residency close to bus, train or airport stations (6% versus 19%, OR=0.25 [0.09-0.72], $p = 0.01$) and residence close to gas stations (15% versus 25%, OR=0.37 [0.16-0.84], $p = 0.02$). Wood heating exposure during childhood was the only indoor air pollutant positively associated with PDB: 90% of patients versus 80% of healthy controls, OR=2.52 [1.03-6.20], $p = 0.04$). Higher levels of lead ($p = 0.0007$), zinc ($p = 0.02$), bismuth ($p = 0.03$), mercury ($p = 0.05$) and copper ($p = 0.06$) were associated with PDB, whereas higher levels of cadmium were associated with tobacco exposure ($p = 0.07$).

Conclusions: Patients with PDB were less frequently exposed to outdoor air pollutants during childhood, which is consistent with the known association with rural residency, whereas they were more frequently exposed to wood heating during childhood. Higher levels of urinary heavy metals in patients with PDB may support some role for air pollutants in PDB.

Disclosures: *Mohamed Saber Numan, None.*

SU0012

Association between normocalcemic primary hyperparathyroidism and blood pressure. Gang Chen¹, Junping Wen*². ¹Fujian Provincial Hospital, Peoples republic of china, ²Fujian Provincial Hospital, China

Objective: Primary hyperparathyroidism (PHPT) is reported to be associated with an increased frequency of hypertension, however, information in this regard is sparse in relation to normocalcemic primary hyperparathyroidism (NPHPT). The aim of this study was to determine the association between NCHPT and blood pressure. **Methods:** We retrospectively enrolled 940 patients who visited at Fujian Provincial Hospital between September 2010 and December 2013 with a measured serum parathyroid hormone (PTH) and calcium level. Among them, 11 patients were diagnosed with NPHPT, while 296 cases with normal PTH and albumin-adjusted serum calcium. Systolic blood pressure (SBP), diastolic blood pressure (DBP), intact serum PTH and serum calcium were recorded. **Results:** There were no significant differences between subjects identified with NPHPT and those with normal PTH in terms of age, sex, BMI, serum calcium, 25-Hydroxyvitamin D, serum creatinine, FPG, TG, TC, HDL and LDL. The subjects with a diagnosis of NPHPT had higher levels of SBP (141.9±20.2 vs 131.2±16.5, P = 0.041) and DBP (85.2±12.4 vs 76.8±10.3, P = 0.026) than the subjects in the cohort with normal PTH. After adjustment for all potential confounders, risks (odds ratios and 95% confidence interval) of SBP and DBP in NPHPT patients were 1.035 (1.000, 1.071) and 1.063 (1.004, 1.125), respectively (P < 0.05). **Conclusions:** The NPHPT had higher risk of high blood pressure than subjects with normal PTH. It is worth considering the necessity of more aggressive therapeutic intervention aimed to normalize PTH even if patients with NPHPT continue to be normocalcemic.

Disclosures: Junping Wen, None.

SU0013

Blood pressure and obesity in healthy postmenopausal women relationship with PTH, retinol, vitamin E and vitamin D endocrine system. Cristina Navarro Valverde¹, Aura Dulcinea Herrera Martínez*², Maria Dolores Luque de Castro³, Rafael Cuenca-Acebedo⁴, María Concepción Muñoz Jiménez⁵, José Manuel Quesada Gómez⁶. ¹Unidad de Gestión Clínica de Cardiología, HU Virgen de Valme, Spain, ²Unidad de Gestión Clínica de Endocrinología y Nutrición IMIBIC . Hospital Universitario Reina Sofía, Spain, ³Departamento de Analítica Química, Annex C-3, Campus of Rabanales, University of Córdoba, Spain, ⁴Servicio de Medicina Interna Hospital Alto Guadalquivir SEIOMM RETICEF, Spain, ⁵Unidad de Gestión Clínica de Endocrinología y Nutrición. IMIBIC Hospital Universitario Reina Sofía de Córdoba., Spain, ⁶Unidad de Gestión Clínica de Endocrinología y Nutrición. IMIBIC. Hospital Universitario Reina Sofía. RETICEF, Spain

Obesity is linked to depressed 25-hydroxyvitamin D (25OHD) and elevated parathyroid hormone (PTH). Observational data also link low 25OHD to both prevalent Blood Pressure (BP) and incident hypertension. The aim of this study was to evaluate the relationship between fat soluble vitamins and obesity in healthy postmenopausal women of Cordoba who ranged from normal weight to morbid obesity as well as the effects of fat soluble vitamins on BP.

Patients and Methods: Anthropometric data, BP, fat soluble vitamins serum levels and others serum parameters which may influence fat soluble vitamins levels were analyzed in a cross-sectional study in 232 healthy postmenopausal women. Age, age of menarche, age of menopause, Body Mass Index (BMI), HDL-cholesterol, LDL-cholesterol, triglycerides, calcium, 1,25(OH)₂D, 25(OH)D, alkaline phosphatase, PTH, osteocalcin, calcium, vitamin E:lipids ratio, vitamin A and β-crosslap were modeled by a partial least squares for systolic and diastolic blood pressure multivariate logistic regression. **Results:** Prevalence of vitamin D deficiency (< 50 nmol/l) in non-obese population was 47.2%, whereas in obese people increased up to 65%. Vitamin D serum levels were significantly higher in normal weight women (BMI < 25 Kg/m²) than in obese women (BMI > 35 Kg/m²), meanwhile PTH and vitamin E:lipids ratio were significantly higher in obese than non-obese women. Partial least squares (PLS) regression model for Systolic Blood Pressure (SBP) showed that age, BMI, LDL cholesterol, alkaline phosphatase and PTH were positive correlated with SBP. However, age of menopause, HDL-cholesterol and vitamin D were negative correlated with it. Age of menopause, HDL cholesterol, vitamin D (25OHD and calcitriol) and osteocalcin showed a negative effect on Diastolic Blood Pressure (DBP). On the other hand, BMI, triglycerides, alkaline phosphatase and PTH showed a positive correlation with DBP. Our results showed that vitamin D insufficiency is highly prevalent in the population of healthy postmenopausal women. Low 25OHD levels correlated with high body fat and BP. We conclude that vitamin D deficiency is a potential risk factor for obesity and hypertension in postmenopausal women

Disclosures: Aura Dulcinea Herrera Martínez, None.

SU0014

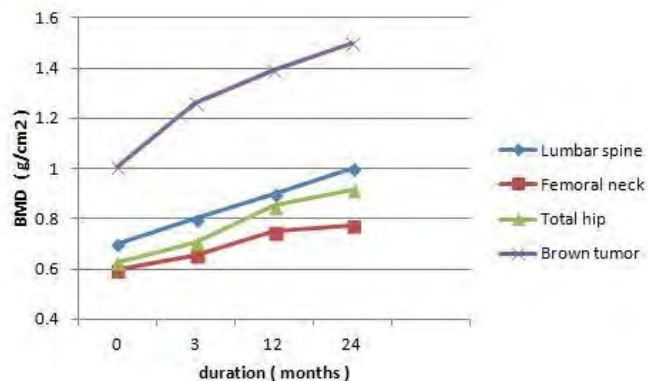
Brown Tumor of the Femur with Changes after Parathyroidectomy. Mohammed Almohaya*¹, Mohammed Almelthel¹, Qun Yang², Stephen Robertson³, David Kendler¹. ¹University of British Columbia, Canada, ²prohealth research center, Canada, ³Prohealth clinical research, Canada

Hyperparathyroidism of longstanding duration or greater severity can result in excess osteoclast activity with increased vascularity, hemorrhage and hemosiderin deposits in bone, so-called "Brown Tumor" (BT) of bone. Rarely, such lesions can result in pathologic fracture. The response of BT to parathyroidectomy has been inadequately documented; some surgical literature recommend excising BT lesions or internal fixation to prevent later complications.

We report a 34 year-old Indian woman presenting with a spontaneous atypical right mid-shaft femoral fracture. Femoral radiographs showed cortical thinning at the mid femoral diaphysis. She underwent intramedullary nailing; curettings from the femoral medullary canal showed giant cell rich pathology with no evidence of fibrous dysplasia or malignancy. An isotope bone scan showed multiple bony lesions that involved both the axial and peripheral skeleton. Serum parathyroid hormone was markedly elevated at 160 pmol/L (normal <6.4) and calcium elevated at 3.79 mmol/L (normal 2.10-2.55). Phosphate was low at 0.72 mmol/L (normal 0.80-1.40) and 25-hydroxy vitamin D was low at 23 nmol/L (normal 75-150). She underwent surgical removal of a left inferior parathyroid adenoma with restoration of normal levels of parathyroid, calcium and phosphate. Calcium intake of 1200 mg/day with supplemental Vitamin D 2000 IU/day was recommended. Six months later, radiographs of the left femur showed multiple sclerotic lesions along the length of the femur reported by the radiologist as suspicious for metastatic malignancy. Isotope bone scan 10 months later showed stable or diminished isotope uptake in these lesions. Baseline bone density lumbar spine Z-score was -3.5, femoral neck Z-score was -2.1 and 1/3 radius Z-score was -3.6.

The figure illustrates the anticipated increases in BMD after parathyroidectomy over 24 months. Placement of a region of interest over the trochanteric BT lesion allowed us to quantitate increases over the lesion of 48.6% after 24 months.

This case and its long-term follow-up document clearly the natural evolution of BT post parathyroidectomy with recovery of BMD, densitometric and radiographic sclerotic BT change after calcium and vitamin D supplementation alone. In the absence of imminent pathologic fracture risk, no other intervention is likely required for these patients.



BMD changes after parathyroidectomy

Disclosures: Mohammed Almohaya, None.

SU0015

FGF23 in patients with hypoparathyroidism. Larissa Savi¹, Maicon Lopes², Victoria Borba², Tatiana Costa², Carolina Moreira*². ¹Serviço de Endocrinologia e Metabologia do Hospital de Clínicas da UFPR (SEMPR), Brazil, ²Serviço de Endocrinologia e Metabologia do Hospital de Clínicas da UFPR (SEMPR), Brazil, Brazil

Introduction: Parathyroid hormone (PTH) and FGF23 have some overlapping effects, both inhibit renal phosphorus reabsorption but both have potentially counter-regulating effects, above all vitamin D metabolism. PTH acts to increase 1,25-hydroxy vitamin D (actively) synthesis and FGF23 increases 24,25-hydroxy vitamin D (not actively). It is not know if the hyperphosphatemia of hypoparathyroidism is sufficient to increase the synthesis of FGF23 in the absence of PTH.

Purpose: to evaluate the clinical parameters and FGF23 levels in patients with permanent hypoparathyroidism and connect the findings to the etiology of the hypoparathyroidism.

Methods: patients were selected from the Service of Endocrinology and Metabology (SEMPR) of the Federal University of Paraná, in Brazil, who had a diagnosis of hypoparathyroidism. A detailed chart review was performed in order to confirm etiology and evaluate the follow up of the laboratory exams. Serum FGF23 was measured using a commercially available two-site immunoassay for the FGF23

intact (Immunotopics, San Clemente, CA), in which the intra-assay coefficient of variation is 4.4% and inter-assay coefficient is 6.5%.

Results: Our study population comprises 55 patients, 50 diagnosed with hypoparathyroidism and 5 patients with pseudohypoparathyroidism (resistance to PTH). The main etiology was postoperative, 75% of patients. The laboratory parameters were: median serum calcium 7.9 ± 1.0 mg/dl; serum phosphorus 5.2 ± 1.3 mg/dl; 136.5 ± 102.5 mg 24-h urine calcium; 2.0 ± 1.7 mg urinary calcium per kilogram; Vitamin D 35.8 ± 28.1 ng/ml; eGFR 36.2 ± 94 mL/min; PTH 63.2 ± 5.7 pg/ml. The median FGF23 was 29.9 ± 93.8 pg/ml.

An inverse relationship between the levels of FGF23 and eGFR, lower glomerular filtration rate, higher the levels of FGF23 ($p < 0.05$).

In general, levels of FGF23 were less than 30 pg/ml in patients with primary hypoparathyroidism ($p: 0.002$) and greater than 30 pg/ml in the cases of postoperative hypoparathyroidism. Conclusion: The overall median FGF 23 of this study was low, suggesting that hyperphosphatemia of hypoparathyroidism does not stimulate FGF23. Patients with postoperative hypoparathyroidism had higher FGF23, lower phosphorus and PTH greater than the group's primary hypoparathyroidism, suggesting that even at low levels, PTH influences the increase in FGF23.

Disclosures: Carolina Moreira, None.

SU0016

Impaired Trabecular Bone Score (TBS) in patients with primary hyperparathyroidism. Manuel Munoz-Torres*¹, Rossana Manzanares Cordova², Beatriz Garcia Fontana³, Antonia Garcia Martin⁴, Rebeca Reyes Garcia⁴, Rafael Nieto Serrano⁵, Sonia Morales Santana³, Fernando Escobar Jimenez⁴. ¹Hospital Universitario San Cecilio, Spain, ²Endocrinology Unit, Hospital Universitario San Cecilio, Spain, ³RETICEF, Hospital Universitario San Cecilio, Spain, ⁴Endocrinology Unit, Hospital Universitario San Cecilio, Spain, ⁵Nuclear Medicine Unit, Hospital Universitario San Cecilio, Spain

Patients with primary HPT exhibit increased bone fragility which is an indication for surgical treatment. The trabecular bone score (TBS) is a grey-level texture measurement based on the use of experimental variograms acquired during a dual-energy X-ray absorptiometry (DXA) of lumbar spine (LS). Several studies show that TBS can be an independent predictor of fragility fractures. However, the usefulness of this new technique in patients with PHPT is not well established. Our study was aimed to investigate TBS in patients with PHPT. Patients and methods: We studied 86 patients with PHPT (mean age 64.9 ± 9.9 years, 82% females, 85% postmenopausal. In all patients bone mineral density by DXA and TBS indices derived from LS DXA was assessed (TBS iNsiteU software). Results: TBS in PHPT was low (1.21 ± 0.13), representing abnormal trabecular microstructure (normal = 1.35). Males showed TBS values significantly lower than the women (1.15 ± 0.14 vs 1.23 ± 0.12 ; $p = 0.028$). PHPT patients with densitometric criteria of osteoporosis T score ($= 2.5$ SD) showed lower values of TBS (1.16 ± 0.13 vs 1.24 ± 0.13 ; $p = 0.019$). However, we found no significant correlation between the values of TBS and DXA. We did not find any correlation between values of TBS and PTH levels and bone turnover markers. Patients with symptomatic and asymptomatic PHPT showed similar values of TBS. We found significant differences when comparing postmenopausal women vs. premenopausal (1.22 ± 0.11 vs 1.30 ± 0.11 ; $p = 0.028$). Conclusion: TBS measurements show that PHPT patients exhibit a degraded trabecular microstructure. If this technique can identify patients with increased bone fragility should be investigated.

Disclosures: Manuel Munoz-Torres, None.

SU0017

Protein Expressions of GABA_B receptor 1 and Vitamin D Receptor Are Decreased in Human Parathyroid Adenoma. A Ram Hong*¹, Jiyeon Lee², Jihyun Lee³, Young A Kim⁴, Hye Sook Min⁴, Jung Hee Kim², Chan Soo Shin², Sang Wan Kim². ¹Seoul National University Hospital, South Korea, ²Department of Internal Medicine, Seoul National University College of Medicine, South Korea, ³Department of Internal Medicine, Seoul National University College of Medicine, South Korea, ⁴Department of Pathology, Seoul National University College of Medicine, South Korea

Objective: We are to examine the protein expression of GABA_BR1 in parathyroid tissue in patients with parathyroid adenoma using tissue microarray. In addition, we are to evaluate the proteins expression of various factors involved in PTH secretion, i.e., FGFR, α -klotho, CaSR, GABA B R1, VDR, CYP24A1, and CYP27B1, and we are to analyze relationship between the proteins expression and biochemical parameters in patients with parathyroid adenoma.

Methods: We retrospectively included 66 patients who underwent parathyroidectomy for PHPT and 29 control patients with normal parathyroid in Seoul National University Hospital from January 2001 to December 2011. All patients diagnosed with PHPT had parathyroid adenomas. We examined the expression of FGFR, α -klotho, VDR, CaSR, GABA_BR1, CYP24A1, and CYP27B1 in parathyroid using immunohistochemistry.

Results: Nuclear and overall VDR expressions were significantly reduced in PHPT compared with the control group ($P < 0.001$ and $P = 0.006$, respectively). In PHPT

group, GABA_BR1 expression was significantly reduced ($P < 0.001$). There were no significant differences in expressions of FGFR, α -klotho (nuclear, cytoplasmic, and overall), CaSR, CYP24A1, and CYP27B1 between the PHPT and control group. Nuclear and overall VDR expression was not correlated with serum PTH in patients with PHPT, however, there was a significantly negative correlation between α -klotho expression and serum levels of PTH ($r = -0.461$, $P < 0.001$). Both serum calcium and phosphorus levels were not correlated with protein expressions of CaSR and GABA_BR1.

Conclusion: The protein expressions of GABA_BR1 as well as VDR were decreased in patients with parathyroid adenoma. This result suggests that hypercalcemia in patients with parathyroid adenoma can affect the expression of GABA_B receptor in parathyroid gland.

Disclosures: A Ram Hong, None.

SU0018

Recombinant Human Parathyroid Hormone (rhPTH [1-84]) Therapy in Hypoparathyroidism and Improvement in Quality of Life. Tamara Vokes*¹, Michael Mannstadt², Michael A. Levine³, Bart L. Clarke⁴, John P. Bilezikian⁵, Hjalmar Lagast⁶, Dolores M. Shoback⁷. ¹University of Chicago, USA, ²Massachusetts General Hospital & Harvard Medical School, Boston, MA, USA, ³Children's Hospital of Philadelphia, Philadelphia, PA, USA, ⁴Mayo Clinic Division of Endocrinology, Diabetes, Metabolism, & Nutrition, Rochester, MN, USA, ⁵College of Physicians & Surgeons, Columbia University, New York, NY, USA, ⁶NPS Pharmaceuticals, Inc., Bedminster, NJ, USA, ⁷SF Department of Veterans Affairs Medical Center, University of California, San Francisco, CA, USA

Many patients (pts) with hypoparathyroidism who are treated with calcium (Ca) and active vitamin D (Vit D) experience a reduced quality of life (QoL). Previous studies of the effects of parathyroid hormone (PTH) on QoL in hypoparathyroidism have yielded inconsistent results. We examined QoL in REPLACE, a randomized, double-blind, placebo (PBO)-controlled, multicenter international study to assess efficacy of rhPTH(1-84) in hypoparathyroidism. During the optimization period (2-16 wks), oral Ca and active Vit D doses were adjusted to achieve and maintain serum Ca level of 8.0-9.0 mg/dL for 2 wks. Pts were then randomized to receive daily subcutaneous injections of PBO or rhPTH(1-84) 50 μ g, which could be increased to 75 μ g and then to 100 μ g only during a 12-wk period according to a titration algorithm. The primary endpoint was the percentage of pts whose need for oral Ca and active Vit D decreased by $\geq 50\%$ at Wk 24 while maintaining serum Ca level at or above baseline. Pts completed a QoL questionnaire (SF-36) at randomization and at Wks 4, 12, and 24. Pre-specified analysis for this exploratory endpoint compared QoL scores between baseline and Wk 24 within each group, and between the groups at Wk 24.

A total of 124 pts were randomized to rhPTH(1-84) (n=84) and PBO (n=40), with 54.8% of rhPTH(1-84) and 2.5% of PBO pts achieving the primary endpoint ($P < 0.001$). The incidence of adverse events was similar between the groups. At 24 wks, there were no differences in serum Ca levels between the rhPTH(1-84) and PBO groups despite a significantly greater reduction from baseline in the number of Ca tablets (54% vs 3%) and active Vit D tablets (74% vs 36%) taken by the rhPTH(1-84) group. There were no changes in any QoL score within the PBO-treated group at Wk 24 compared with baseline; however, pts in the rhPTH(1-84)-treated group showed improved QoL scores in 6 of 10 domains: Role-Physical ($P = 0.033$), Bodily Pain ($P = 0.014$), General Health ($P = 0.002$), Vitality ($P = 0.001$), Mental Health ($P = 0.016$), and Physical Component Score ($P = 0.004$). A comparison between the rhPTH(1-84)-treated and PBO-treated groups showed numerically higher mean QoL scores in the rhPTH(1-84) vs PBO group at Wk 24, but the differences were small and not statistically significant.

This study suggests that rhPTH(1-84) therapy for hypoparathyroidism may improve QoL.

Disclosures: Tamara Vokes, NPS Pharmaceuticals, Inc. This study received funding from: NPS Pharmaceuticals, Inc.

SU0019

Surgery versus no Surgery: What works best for the kidneys in Primary Hyperparathyroidism? A retrospective study on a multi-ethnic patient population. Donovan Tay*¹, Joan Khoo², Manju Chandran³. ¹Singapore General Hospital, Singapore, ²Changi General Hospital, Singapore, ³Osteoporosis & Bone Metabolism Unit Department of Endocrinology Singapore General Hospital, Singapore

Introduction: Guidelines consistently list renal impairment as an indication for surgery in asymptomatic primary hyperparathyroidism. However, studies exploring whether parathyroidectomy is superior to medical therapy or simple surveillance with respect to long term renal function in patients with primary hyperparathyroidism are scanty and conflicting. We sought to determine if treatment modalities affect renal outcomes in a multi-ethnic South East Asian population of patients with primary hyperparathyroidism.

Method: 121 patients who presented with primary hyperparathyroidism and had follow up for up to 9 years at a large teaching hospital in Singapore were

respectively evaluated. Intervention was classified as surgical (parathyroidectomy), medical (treated with bisphosphonates or cinacalcet) or observation (observed without any treatment). One-way analysis of variance (ANOVA) was used for within group comparisons. In case of statistically significant difference in ANOVA, Bonferroni post hoc adjustment was used for multiple pairwise comparisons. One-way analysis of covariance (ANCOVA) was used to adjust within group comparisons for potential confounders. Statistical tests were 2 tailed and a P<.05 was considered as significant.

Results: The study population had 68.6% Chinese, 14.9% Malays, 9.1% Indians, 3.3% Eurasians and 4.1% others. Table 1 shows the baseline characteristics of the study group. Mean duration of follow was 2.4 ± 2.4 years. At last follow up, eGFR in the surgical group (80 ± 30 ml/min) was higher as compared to the medical (52 ± 32 ml/min) or observation group (48 ± 32 ml/min) (p<0.01). Compared to those in the medical or observation group, patients in the surgical group continued to have better eGFR at last follow up after adjustments for pre-intervention eGFR levels (p = 0.010). The between group interaction by treatment modality remained significant after adjusting for age, gender, ethnicity, presence of renal stones, serum corrected calcium, serum phosphate and 24hr urinary calcium excretion (p = 0.025).

Conclusion: Our study provides compelling evidence to support the premise that surgery for primary hyperparathyroidism may be better than a non-surgical approach with respect to long term renal function. Whether parathyroidectomy halts progression of renal impairment in patients with primary hyperparathyroidism and coexisting moderate to severe renal disease needs to be studied through prospective, randomized, controlled trials.

Table 1: Comparative baseline characteristics of the study groups. (Primary hyperparathyroidism identified using ICD-9-CM diagnosis coding)

| | Surgery (n = 34) | Medical (n = 42) | Observation (n = 45) | P value |
|---|------------------|------------------|----------------------|---------|
| Age (yr) | 57 ± 16 | 76 ± 11 | 74 ± 16 | .000 |
| Female (%) | 79.4 | 69.0 | 68.9 | .517 |
| Height (m) | 1.56 ± 0.09 | 1.56 ± 0.11 | 1.61 ± 0.12 | .336 |
| Weight (kg) | 58.2 ± 10.1 | 54.1 ± 13.4 | 57.6 ± 15.3 | .409 |
| BMI (kg/m ²) | 23.8 ± 4.2 | 24.4 ± 4.8 | 24.5 ± 6.6 | .862 |
| Asymptomatic (%) | 64.7 | 71.4 | 80.0 | .311 |
| Renal Stone (%) | 17.6 | 7.1 | 2.2 | .046 |
| 25OHD (ng/ml) | 19.7 ± 16.9 | 22.6 ± 18.9 | 16.7 ± 10.4 | .480 |
| Serum corrected Calcium (mmol/L) | 2.87 ± 0.32 | 2.97 ± 0.29 | 2.78 ± 0.27 | .004 |
| Serum PTH (pmol/L) | 18.76 ± 13.97 | 16.16 ± 15.92 | 19.97 ± 22.03 | .609 |
| Serum Alkaline phosphatase (mmol/L) | 98.5 ± 46.0 | 90.1 ± 38.8 | 103.3 ± 50.3 | .393 |
| Phosphate (mmol/L) | 0.94 ± 0.34 | 0.82 ± 0.27 | 1.06 ± 0.39 | .005 |
| Albumin (g/L) | 35.4 ± 7.5 | 31.2 ± 7.3 | 29.8 ± 5.4 | .002 |
| HbA1c (%) | 6.6 ± 1.3 | 6.8 ± 1.3 | 6.7 ± 2.0 | .929 |
| LDL (mmol/L) | 3.15 ± 1.47 | 2.75 ± 0.96 | 2.76 ± 1.02 | .308 |
| 24hr Urine calcium (mmol/day) | 5.06 ± 5.01 | 3.65 ± 4.89 | 1.28 ± 2.56 | .000 |
| Cr at presentation (μmol/L) | 76.5 ± 21.6 | 102.6 ± 56.1 | 139.4 ± 110.0 | .001 |
| eGFR at presentation (ml/min/1.73m ²) | 82 ± 24 | 62 ± 25 | 56 ± 29 | .000 |
| Hypertension (%) | 55.9 | 78.6 | 68.9 | .106 |
| SBP (mmHg) | 132 ± 26 | 131 ± 19 | 139 ± 27 | .267 |
| DBP (mmHg) | 73 ± 19 | 68 ± 11 | 73 ± 14 | .095 |
| ACE inhibitors or ARB (%) | 20.6 | 38.1 | 44.4 | .082 |
| Diabetes Mellitus (%) | 29.4 | 47.6 | 48.9 | .168 |
| Hyperlipidaemia (%) | 50.0 | 52.4 | 60.0 | .637 |

Table 1: Baseline Characteristics of the study population

Disclosures: Donovan Tay, None.

SU0020

Vitamin D Deficiency and Insufficiency in Primary Hyperparathyroidism: Effects on the Volumetric BMD and Bone Strength at the Lumbar Spine. Marcella Walker¹, Elaine Cong¹, Melissa Sum^{*1}, Isra Saeed², James Lee¹, Anna Kepley¹, Chengchen Zhang¹, Thomas Lang², Shonni Silverberg¹. ¹Columbia University, USA, ²University of California at San Francisco, USA

Data regarding the skeletal effects of vitamin D (25OHD) deficiency and insufficiency in primary hyperparathyroidism (PHPT) are limited. We have shown that lower 25OHD in PHPT is associated with higher PTH levels, which we hypothesized might affect trabecular lumbar spine (LS) volumetric BMD (vBMD) and strength (VSTR) by central quantitative computed tomography (cQCT). Participants were mostly postmenopausal women (n=53; 84.9% women; mean ± SD age 62.3 ± 0.6yrs) and had mild PHPT (calcium 10.6 ± 0.6mg/dl, PTH 82 ± 49pg/ml, 25OHD 31 ± 11ng/ml). 25OHD deficiency (18.9% <20ng/ml, mean 14 ± 2ng/ml) and insufficiency (28.3% 25OHD 20-29ng/ml, 26 ± 2ng/ml) were common, but the majority were replete (52.8% 25OHD ≥30ng/ml, 40 ± 7ng/ml) and severe deficiency was uncommon (1.9% <10ng/ml). Those with lower 25OD (<20 vs. 20-29 vs. ≥30ng/ml) were younger (59.4 ± 12.4 vs. 58.0 ± 9.6 vs. 65.7 ± 8.6yrs, p=0.03) and less likely to be taking vitamin D supplements (20 vs. 73 vs. 86%, p<0.01) but did not differ by sex, race, ethnicity, height, weight, PHPT duration, history of osteoporosis, fragility fracture, nephrolithiasis or meeting 2008 surgical criteria. Those with lower 25OHD had higher PTH (140 ± 74 vs. 78 ± 30 vs. 64 ± 28pg/ml, p<0.0001) and lower PO4 (2.7 ± 0.4 vs. 3.0 ± 0.4 vs. 3.2 ± 0.4mg/dl, p=0.003) levels but serum and urine calcium and 1,25-dihydroxyvitamin D did not differ. GFR was worse in those with 25OHD ≥30ng/ml vs. other groups (p=0.02). DXA T-scores were normal (-1.0 ± 1.7) and did not differ by vitamin D status (-1.0 ± 1.8 vs. -1.3 ± 1.3 vs. -0.8 ± 1.8, p=0.71). Neither PTH nor 25OHD levels correlated with L1&L2 trabecular vBMD (25OHD: r=-0.07, p=0.60; PTH: r=-0.04, p=0.78) or VSTR (25OHD: r=-0.06, p=0.66; PTH: r=-0.05, p=0.71). Prior to adjusting for covariates, there were no differences in trabecular or intertrabecular vBMD or strength by vitamin D status (<20 vs. 20-29 vs. ≥30ng/ml). After adjusting for age, weight and GFR, L1&L2 trabecular vBMD (0.125 ± 0.040 vs. 0.090 ± 0.041g/cm³, p=0.03) and VSTR (0.214 ± 0.112 vs. 0.135 ± 0.84, p=0.04) were higher in those with 25OHD 20-29 vs. ≥30ng/ml. There were no differences vs. those

with 25OHD <20ng/ml. Results were similar in women only. Comparing those with 25OHD <20 vs. ≥20 and <30 vs. ≥30ng/ml, there were no differences before or after adjusting for covariates. While low 25OHD levels are associated with higher PTH levels in PHPT, neither 25OHD deficiency or insufficiency appeared to adversely affect vBMD or VSTR in a cohort in whom 25OD deficiency was uncommon.

Disclosures: Melissa Sum, None.

SU0021

3D Atlas-based Modeling of the Spine using MDCT images for Detecting Local Density Variations in an Age-matched Cohort. Alexander Valentinitich^{*1}, Stefano Trebeschi¹, Eva Alarcón¹, Thomas Baum¹, Cristian Lorenz², Jan S. Bauer¹. ¹Klinikum rechts der Isar, Technische Universität München, Germany, ²Philips Research Hamburg, Germany

DEXA is considered the standard assessment of osteoporosis, providing a global T-score that poorly correlates with fracture risk and neglects local variations in bone density. As these local variations in density of each individual vertebra could provide more insights for fracture prediction, we present a 3D atlas of the complete spine, based on voxel density (BMD) of each individual vertebral body. The purpose of this study was to evaluate local variations of normal, age-related differences among different age groups using this 3D atlas of the complete spine. Non-contrast MDCT scans of 18 patients under the age of 40 (28yrs) without spinal pathology were used for modeling the atlas. Each vertebra ranging from T1-L5 was used individually for calculations. For comparison, we defined 4 cohorts, of 10 patients each: forties (41-50yrs), fifties (51-60yrs), sixties (61-70yrs) and seventies (71-80yrs). We used voxel-based morphometry (VBM), which allows a voxel-wise comparison of the local BMD among each vertebra and groups. The procedure included an automatic spine segmentation and detection, non-rigid registration for spatial normalized vertebral bodies and statistical parametric mapping using a standard t-test, which was corrected for multiple comparisons by the random field method. We additionally calculated a voxel-based T-score map for each of the groups to highlight local density differences in comparison to the young population. As expected, highest global T-scores were found in the forties cohort (-0.15 ± 0.16), followed by the fifties (-1.25 ± 0.27), sixties (-2.01 ± 0.37) and seventies (-2.51 ± 0.37). All global comparisons showed statistical significance (p<0.001). VBM showed no significantly different local BMD areas in the forties cohort compared to the young population. In the fifties cohort, L4 and L5 started to highlight small local changes among the BMD distribution within the vertebra. The affected (significant) lumbar regions had a fraction 4.0% and 5.4% respectively, which grew 2-5 fold in the fifties cohort. Regions in T9-L5 also had significantly different fractions, ranging 3.6-25.2%. In the seventies cohort almost all vertebrae had significant differences in the local BMD distributions in 50% of all voxels, which was more severe around T6 and L1. We demonstrated that a local T-score of the spine, assessed by a 3D VBM-based atlas, shows local variations in an aging healthy population that correspond to known areas of increased fracture incidence.

SU0023

Characterization of Collagen Fiber Orientation in Bone with Chronic Kidney Disease Using FTIR Imaging. Tepei Ito^{*1}, Kyosuke Kanazawa², Yuva Kanehira¹, Hiroimi Kimura-Suda¹. ¹Chitose Institute of Science & Technology, Japan, ²Chitose Institute of Science & Technology, Japan

Secondary hyperparathyroidism (2HPT) due to chronic kidney disease (CKD) decreases both the bone mineral density (BMD) and bone quality leading to increase a risk of bone fractures. BMD is a relatively good barometer of bone strength and reflects the risk of bone fracture; however, it is difficult to identify which factors associated with bone quality affect bone fragility. In our previous works, we characterized bone quality in the femurs in rats with primary or secondary osteoporosis using Fourier transform infrared (FTIR) imaging and demonstrated that collagen fiber orientation was a good marker of bone strength. In this work, the mineral-to-collagen matrix ratio, carbonate-to-phosphate ratio, crystallinity, collagen maturity, and collagen fiber orientation in the femurs of rats with 2HPT due to CKD were characterized by FTIR imaging. Eleven-week-old male Sprague-Dawley rats underwent 5/6 subtotal nephrectomy to replicate 2HPT due to CKD or sham surgery to prepare controls and were thereafter kept for 16 weeks. After sacrifice, the femurs were removed, embedded in PMMA, and were sliced into 3- μ m longitudinal sections by a microtome in preparation for FTIR imaging. Collagen fiber orientation was assessed with IR dichroism images of the amide I band, and the other bone quality parameters were calculated based on FTIR spectra. Both the thickness and the amount of the trabecular bone were decreased in the CKD rat femurs, and these bone conditions are typical of secondary osteoporosis due to 2HPT. The carbonate-to-phosphate ratio was reduced in both the cortical and trabecular bone of the CKD rat femurs; however, there was no significant difference in the mineral-to-collagen matrix ratio, crystallinity or collagen maturity between the sham and CKD rats. Collagen fibers in the cortical bone in the sham and CKD rats were aligned longitudinally, and the degree of collagen fiber orientation was lower in metaphysis than in the diaphysis. The carbonate-to-phosphate ratio and mineral-to-collagen matrix ratio were also lower in metaphysis than in the diaphysis. Bone quality in cases of 2HPT due to CKD can be characterized as having reduced trabecular bone thickness and decrease the amount of trabecular bone, reduced carbonate-to-phosphate ratio in both the cortical and trabecular bone, and a lower degree of collagen fiber orientation, carbonate-to-phosphate ratio and mineral-to-collagen matrix ratio in metaphysis than in the diaphysis in the cortical bone.

Disclosures: Tepei Ito, None.

This study received funding from: JSPS KAKENHI Grant Number 24591237

SU0024

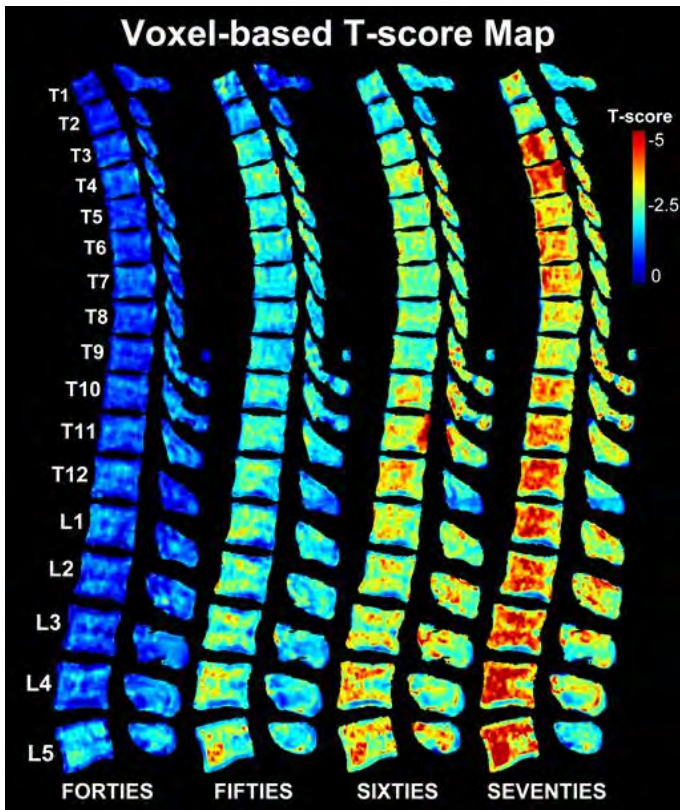
Cortical Bone Thickness Measurements from CT in the Presence of Metalwork. Tristan Whitmarsh, Graham Treece^{*}, Andrew Gee, Kenneth Poole. University of Cambridge, United Kingdom

Purpose: Measuring bone thickness can be an important tool in assessing fracture healing and investigating other bony pathological processes after hip replacement surgery. Measurements from CT near metallic implants or fixation devices are difficult to obtain due to the high attenuation coefficient of metal. This study therefore proposes and evaluates a method for the measurement of cortical bone thickness in the presence of metal components.

Methods: Four cases with distinct metallic implants at the proximal femur were examined. These include a post-operative CT scan of a hemi-arthroplasty, a dynamic hip screw fixation, a bipolar hemi-arthroplasty and a fixation with cannulated screws. All CT scans were processed using metal artefact removal software (Boas, Radiology 2011). A previously validated technique based on the fitting of a cortical model was used to measure the cortical thickness over selected regions, which results in a colour coded cortical thickness map (Treece, Med Image Anal 2015). This method was adapted to also model metal structures when required. The measurements were compared with the corresponding sections on the un-fractured contralateral bone segment whereby point-to-point correspondences were obtained through the registration of the two cortical maps.

Results: For the proximal femoral sections of the aforementioned cases, the cortical thickness was measured with a mean absolute difference of 0.57, 0.37, 0.44 and 0.52 mm with respect to the contralateral femur. The hemi-pelvis produced thickness differences of 0.47, 0.49, 0.51 and 0.46 mm respectively. There was no noticeable structural over- or under-estimation of the thickness measurements. Cortical thickness maps indicate a reduction of noise by applying metal artefact removal software and more valid cortical measurements with a greater accuracy when modelling metal structures.

Conclusion: A method is proposed for the measurement of cortical bone thickness in the presence of metalwork, with results indicating sub-millimetre accuracy. This new technique might be helpful in assessing fracture healing near implants, and improve the evaluation of periprosthetic bone after hip replacement surgery.



Voxel-based T-score map for each of the four cohorts

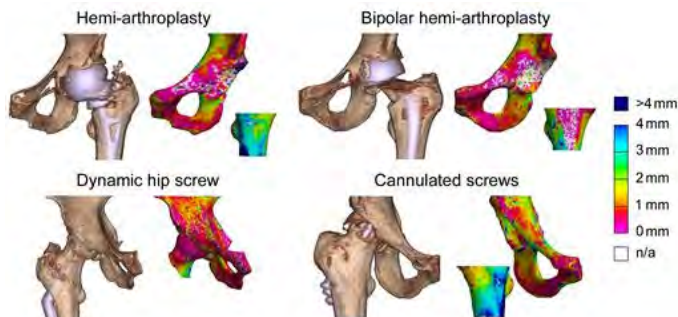
Disclosures: Alexander Valentinitsh, None.

SU0022

Bone quality of ovariectomized rats after combination therapy with bisphosphonate and eldcalcitol. Hiroimi Kimura-Suda^{*1}, Tepei Ito¹, Hirohata Wagatsuma², Tetsuo Yano², Daisuke Inoue³. ¹Chitose Institute of Science & Technology, Japan, ²Ajinomoto Pharmaceuticals Co., Ltd., Japan, ³Teikyo University School of Medicine, Japan

Both bisphosphonate (BIS) and eldcalcitol (ELD; a vitamin D analog) act against bone loss due to osteoporosis. We have demonstrated that combination therapy with BIS and ELD improves bone mineral density (BMD) and bone structure in ovariectomized (OVX) rats, and that three kinds of BIS, risendronate (RIS), alendronate (ALN) and minodronate (MIN), have comparable effects when used in combination with ELD. In this work, we characterized the bone quality of the femur and vertebral body in OVX rats after combination therapy with BIS and ELD using FTIR imaging. Thirteen-week-old female Sprague-Dawley rats underwent ovariectomy (OVX) or sham operation (sham). The OVX group was divided into 8 subgroups treated with Vehicle, RIS (0.7 μ g/kg/day s.c.), ALN (1.4 μ g/kg/day s.c.), MIN (0.14 μ g/kg/day s.c.), ELD (0.04 μ g/kg/day p.o.), RIS+ELD, ALN+ELD or MIN+ELD. The various forms of BIS and ELD were administered to rats five times a week for 16 weeks. The rats were sacrificed at 29 weeks of age, and the femurs and vertebrae were then removed and embedded in PMMA. Sagittal sections (3 μ m) were prepared for FTIR imaging. The mineral-to-collagen matrix ratio (the degree of calcification), carbonate-to-phosphate ratio, crystallinity, and collagen maturity in the bone were assessed based on the FTIR images. The degree of calcification was reduced in both trabecular and cortical bone of the femurs as well as in the trabecular bone of the vertebral body in the vehicle group, but was improved in all the drug-treated subgroups. The degree of calcification in trabecular bone in all BIS+ELD subgroups was higher than that of the BIS or ELD subgroups. However, the increase in calcification in cortical bone of the femur was not reflected in improved mechanical properties in the three-point bending testing of the femur. Comparisons among the three forms of BIS revealed that, RIS and MIN had almost identical effects on calcification, whereas ALN was less effective than RIS and MIN. The carbonate-to-phosphate ratio in the cortical bone of the vertebral body was increased in the vehicle subgroup and was improved in all the drug-treated subgroups. However, no significant differences from the vehicle subgroup in terms of crystallinity or collagen maturity were observed for the rats undergoing combination therapy. In conclusion, combination therapy with BIS and ELD further increased calcification of the trabecular bone in OVX rats in comparison to single treatment regimens.

Disclosures: Hiroimi Kimura-Suda, Ajinomoto Pharmaceuticals Co., Ltd.
This study received funding from: Ajinomoto Pharmaceuticals Co., Ltd.



The four test cases with volume renderings and cortical thickness maps of the selected bone regions

Disclosures: *Graham Treece, None.*
This study received funding from: *Eli Lilly*

SU0025

Development of a strongly simplified method for determination of bone quality within joint near regions of long bones. *Volker Kuhn*¹, *Spaska Kovacheva*², *Nikola Ivanovic*¹, *Wolfgang Recheis*¹. ¹Medical University Innsbruck, Austria, ²University of Applied Sciences Wiener Neustadt, Austria

According to World Health Organization (WHO) osteoporosis is defined as a disease characterized by lessening the strength of bones, especially trabecular structures and increased proclivity of fractures. There is variety of reasons for osteoporosis - hormonal, medicinal and gastroenterological. The trend shows high morbidity and mortality. It affects mostly elderly women. The probability of a fracture in Caucasian man is up to 20%, in woman - twice as much. Within Austria/EU 700.000 people, which is 45% of all women over 50, suffer from severe osteoporosis. The main diagnostic methods - Dual Energy X-ray Absorptiometry (DXA) and Quantitative Computed Tomography (QCT) have different limitations.

The purpose of this research is the development of strongly simplified method to determine bone quality within joint near regions of long bones. This method is based on analysis of CT datasets with the image processing software ImageJ, ITK Snap and VolView and setting a relation between non-bone and bone volumes. The basic achievement of this study are several equations which after setting correct input data calculates [non-bone/bone] volume ratio and [non-bone/total] volume ratio.

This project includes various types of statistical analyzes which prove that these ratios are influenced by many factors including age and gender, associate with the disease of osteoporosis. This research should be a starting point of various studies which analyze other factors related to the disease. Patient's health history may be essential in order to improve this method and might give an opportunity for an easy and quick diagnosis of osteoporosis.

Disclosures: *Volker Kuhn, None.*

SU0026

Effect of Teriparatide Treatment on Trabecular Microstructure in Postmenopausal Women with Osteoporosis Assessed with High Resolution Quantitative Computed Tomography. *Daniel J Blackwell*¹, *Margaret A Paggiosi*¹, *Eugene V McCloskey*¹, *Nicola FA Peel*², *Jennifer S Walsh*¹, *Richard Eastell*¹, *Lang Yang*^{*1}. ¹University of Sheffield, United Kingdom, ²Sheffield Teaching Hospitals NHS Foundation Trust, United Kingdom

Teriparatide (TPTD) treatment given for one year has been shown to significantly improve the microstructural integrity of the vertebral trabecular bone assessed with high resolution quantitative computed tomography (HRQCT) [1]. Since the treatment is now licensed for 2 years, the aim of this study was to develop and apply a HRQCT based structural analysis tool, to analyse in vivo, the microstructural changes associated with TPTD treatment over 2 years of treatment. In an open-label single-centre study, 20 postmenopausal women (age 64.4 ± 15.4 years) with osteoporosis (BMD T score < -2.5 at spine or hip) were treated with TPTD (FORSTEO, 20 micrograms daily) for 104 weeks. HRQCT scans of vertebra T12 (resolution $0.188 \times 0.188 \times 0.625$ mm³) were acquired at baseline, 26, 52 and 104 weeks. The Mindways density calibration phantom was used to calibrate HRQCT scans to volumetric bone mineral density. The vertebral body was segmented semi-automatically slice by slice and rotated to standardise the orientation between each scan. The endplates and 1.5 mm thick cortex were excluded, leaving only trabecular volume (Figure 1). The vertebrae were matched slice by slice, allowing the analysis of a constant region from baseline to 104 weeks. A threshold of 100 and 200 mg/ml was used to separate bone from marrow for bone density and structure analysis, respectively. Microstructural variables were calculated based on a 3D adaptation of the parallel plate model [2] and the mean intercept length method. Variables studied

included apparent trabecular bone density (appTbD), bone volume fraction (appBV/TV), trabecular number (appTbN), thickness (appTbTh) and separation (appTbSp). Intra-operator precision was assessed by analysing baseline scans 3 times. Effects of treatment was examined by comparing group means at follow up against baseline. The intra-operator %CV ranged from 0.9 to 3.4% (Table 1). By the end of 104 weeks therapy, TPTD treatment resulted in significant increases in mean appBV/TV, appTb.N and appTb.Th with a non-significant trend to reduce appTbSp (Table 1). In conclusion, effects of TPTD treatment on the T12 trabecular microstructure can be measured by HRQCT. [1] Graeff et al (2007) J Bone Miner Res 22: 1426-1433. [2] Parfitt et al (1983) J Clin Invest 72: 1396-1409.

Table 1. Mean (SD) of the apparent trabecular microstructural variables

| | Baseline | Week 26 | Week 52 | Week 104 | %CV |
|----------------|-------------|-------------|-------------|--------------|-----|
| appTbD (mg/ml) | 180 (13) | 171 (20) | 179 (16) | 190 (22) | 0.9 |
| appBV/TV (%) | 15 (7) | 13 (7) | 20 (9) | 24 (12)* | 3.4 |
| appTbN (1/mm) | 2.3 (0.7) | 2.09 (0.80) | 2.69 (0.90) | 3.03 (0.90)* | 1.8 |
| appTbTh (mm) | 0.25 (0.03) | 0.25 (0.03) | 0.28 (0.50) | 0.31 (0.07)* | 1.8 |
| appTbSp (mm) | 1.65 (0.76) | 2.07 (1.27) | 1.51 (1.07) | 1.16 (0.64) | 2.5 |

Intra-operator precision in %CV was assessed by analysing baseline scans 3 times
* indicates that the mean is significantly different from the baseline value at P<0.05

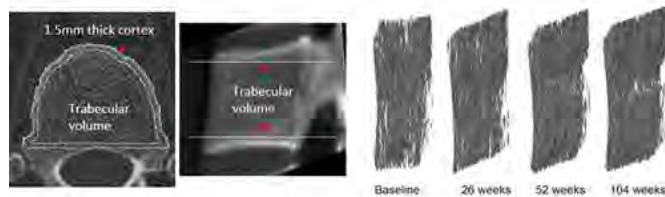


Figure 1. Trabecular volume definition and typical rendered trabecular bone images at each visit

Table 1 and Figure 1

Disclosures: *Lang Yang, None.*

SU0027

Effects of Disuse and Estrogen Deficiency on the Bone Microarchitecture and Biomechanical Properties. *Melise Peres Ueno*^{*}, *Mário Jefferson Louzada*. Unesp, Brazil

Our goal was to determine whether the different causes of osteopenia have the same effects on trabecular and cortical bone structure and on the biomechanical parameters. For this study, 30 female Wistar rats of 19 weeks old, were distributed on the groups: control (CON), hindlimb unloading (HLU) and ovariectomized (OVX). The unloading of the hindlimbs was conducted by tail suspension for 21 days at 24 weeks of age and euthanasia was performed at 27 weeks of age. Femur and tibia were removed to determine the microstructure of trabecular and cortical bone by micro-computed tomography and also the mechanical properties by 3 points bending tests for the femoral and tibial diaphysis, and mechanical testing to failure to the neck of the femur. After OVX, there was a deterioration in the microstructure of the trabecular bone in the femoral neck, with a reduction in bone volume ($p = 0.034$) and an increase in porosity ($p = 0.048$) compared to CON (Table 1, Figure 1). In tibia OVX showed greater bone changes with a change in bone volume, trabecular number, connectivity density, struture model index and porosity (all $p < 0.05$) compared to group CON, and an increase in trabecular spacing compared to HLU group ($p = 0.042$). In the cortical bone of the femur diaphysis, the disuse showed a greater change in microstructure with high total porosity ($p = 0.000$). In the tibial diaphysis, there was an increase in the total area and medullary area in the OVX group compared to the HLU group ($p = 0.0137$ and $p = 0.0194$, respectively). The three point bending test of the femur diaphysis showed a lower maximum force in HLU group compared to the OVX group ($p = 0.036$) (Table 2), the absorbed energy was higher in OVX ($p = 0.001$). However, in the diaphysis of the tibia, biomechanical parameters analyzed did not obtain statistically significant differences between groups. Femoral neck, HLU showed higher stiffness compared to OVX ($p = 0.014$), and the absorbed energy was higher in OVX ($p = 0.016$). Animals suspended by the tail had the most affected femurs, with a further deterioration in the cortical region leading to a decrease in mechanical properties. Already estrogen deficiency showed higher trabecular deterioration in the tibia without mechanical properties change. Taken together, the results suggest that different stimuli, either mechanical or hormones may affect different bones in different site, besides presenting different biomechanical responses.

SU0028

Fibroin particle supported cationic lipid-layers (Fibroplex) as a high efficient intracellular protein delivery system for osteoinductive treatment. Woo Jin Kim*¹, WON-JOON YOON², HYUN-MO RYOO². ¹Seoul National University, South Korea, ²Seoul National University school of dentistry, South Korea

An average cell contains thousands of proteins that participate in normal cellular functions, and most diseases are somehow related to the malfunctioning of one or more of these proteins. Protein therapy, which delivers proteins into the cell to replace the dysfunctional protein, is considered the most direct and safe approach for treating disease like bone tissue regenerations which required long-term treatment. However, the effectiveness of this method has been limited by its low delivery efficiency and poor stability against proteases in the cell, which digest or change 3D-structure of the protein. Here we report Fibroin particle supported cationic lipid-layers (Fibroplex) that synergistically combine intracellular delivery ability of cationic liposomes and bio-mechanical advantages of natural polymer particles. Fibroplex was able to load a large amount of target proteins without chemical modifications and showed stable and proper releasing profiles for more than 90 days with sheltered target proteins from environment factors such as pH, temp changes or serum factors. Furthermore, Fibroplex achieved cytosolic delivery in several cell lines (including primary MEF cells and preosteoblasts) with high efficiency represented a 32-folds improvement over comparable delivery platforms remained protein stability over 4 weeks in vitro/vivo and observed only a relatively small amount of material remained trapped inside endosome. Fibroplex mediated delivery did not noticeably affect cell viability or immune response. Also, multiple molecules could be delivered simultaneously. The scope of application of fibroplex was extended to osteogenesis control by direct introduce intracellular regulatory factor Pin1, a cis-trans isomerase which recently reported playing critical role in osteogenesis via regulation of intracellular Runx2 protein stability. Fibroplex mediated Pin1 protein delivery enable to promoted differentiation of Pin1 KO MEF driven into osteogenic lineage caused by maintained proper protein concentration within the cell for a long period, suggesting potential therapeutic strategy for bone tissue regenerative treatment.

Disclosures: *Woo Jin Kim, None.*

SU0029

From material to structural properties. Density, mass and size. Arne Hoiseth*¹, Knut Strømsoe². ¹Univeristy of Oslo, Akershus University Hospital, Norway, ²University of Oslo, Norway

Bone parameters were assessed by computed tomography (CT) in patients having had a proximal femoral fracture and in controls. By employing a semiautomatic approach, CT densities were used to differentiate cortical (CT values >200) from cancellous bone (CT values 60-199). The amount of cortical, cancellous and total calcified bone (g) and area (cm) were assessed in CT slices in the middle of lumbar vertebral bodies, at right angle to the femoral necks, at cross section through the trochanteric regions and the femoral condyles. Bone density (g/cm³) was assessed in cortical bone only. In the femoral necks the mechanical parameters compressive and bending strength and buckling ratio were calculated. For buckling ratios mean cortical thickness, area of cortex and calcium mass in the cortex were employed. Morphological parameters were measured manually in the necks (diameters, cortical thickness and hip axis length). 95% confidence intervals were used for testing statistical significance. We found statistically significant gender differences for all mass and area parameters and for morphological parameters except for cortical thickness. The gender differences were found for all cases combined and for separate fracture and control cases. For some parameters there were no difference between non-fractured females and fractured men. There were statistically significant differences between fractured and non-fractured cases for all cortical and integrated cortical/cancellous area and bone mass parameters, but not for morphological parameters, nor for any of the density parameters. Of the biomechanical parameters only buckling ratios, using cortical area and mass for cortical thickness, significantly differentiated between fractured non-fractured cases. Importantly, cortical densities did not differentiate between genders or between fractured and non-fractured cases. Body weight was associated to area and mass parameters and to morphological parameters, except for cortical thickness. After adjusting for weight by calculating standardized residuals, differences between genders as well as between fractured cases and controls became less, with some loss of statistical significance. Our findings suggest that, as a structural parameter, the amount of calcified bone, particularly in the cortex, is important for fracture risk prediction. Material properties, such as cortical density and porosity and trabecular bone index are essential for appreciation of bone biology.

Disclosures: *Arne Hoiseth, None.*

| | CON | HLU | OVX | ANOVA |
|----------------------------|-----------------------------|-----------------------------|----------------------------|-------|
| <i>Femoral neck</i> | | | | |
| BV/TV (%) | 82,53 ± 3,13 ^d | 58,73 ± 8,42 ^{bc} | 44 ± 18,21 ^c | 0,049 |
| Tb.N (mm ²) | 3,73 ± 0,26 | 3,61 ± 0,00 | 3,01 ± 1,53 | 1,000 |
| Tb.Th (mm) | 0,15 ± 0,00 ^d | 0,14 ± 0,01 ^{bc} | 0,13 ± 0,005 ^b | 0,048 |
| Tb.Sp (mm) | 0,16 ± 0,01 | 0,15 ± 0,02 | 0,29 ± 0,22 | 0,223 |
| Conn.Dn (mm ²) | 73,89 ± 4,20 | 90,94 ± 20,31 | 77,39 ± 35,17 | 0,241 |
| SMI | -0,18 ± 0,28 | 0,17 ± 0,80 | 0,61 ± 0,58 | 0,075 |
| Po total (%) | 37,44 ± 3,096 ^d | 41,26 ± 8,41 ^{bc} | 55,99 ± 18,21 ^c | 0,049 |
| <i>Tibial Metaphyseal</i> | | | | |
| BV/TV (%) | 37,46 ± 11,97 ^a | 36,37 ± 10,27 ^{bc} | 13,02 ± 6,52 ^b | 0,013 |
| Tb.N (mm ²) | 3,019 ± 0,68 ^d | 3,019 ± 0,6801 ^d | 0,994 ± 0,505 ^c | 0,013 |
| Tb.Th (mm) | 0,11 ± 11,97 | 0,10 ± 0,009 | 0,10 ± 0,009 | 0,511 |
| Tb.Sp (mm) | 0,20 ± 0,05 ^{bc} | 0,19 ± 0,04 ^d | 0,450 ± 0,12 ^b | 0,013 |
| Conn.Dn (mm ²) | 103,1 ± 37,75 ^{cd} | 106,6 ± 26,40 ^d | 25,99 ± 14,45 ^c | 0,013 |
| SMI | 1,41 ± 0,66 ^d | 1,47 ± 0,48 ^c | 2,38 ± 0,16 ^b | 0,003 |
| Po total (%) | 62,53 ± 11,97 ^a | 63,62 ± 10,27 ^{bc} | 86,97 ± 6,52 ^b | 0,013 |

Table 1 - microarchitecture of trabecular bone of the femur and tibia.

| | CON | HLU | OVX | ANOVA |
|--------------------------|-----------------------------|----------------------------|----------------------------|-------|
| <i>Femoral diaphysis</i> | | | | |
| Maximum force (N) | 99,38 ± 10,5 ^{bc} | 94,26 ± 16,46 ^a | 113,3 ± 13,97 ^b | 0,036 |
| Stiffness (N/mm) | 228,2 ± 26,02 | 232 ± 49,42 | 226 ± 33,98 | 0,952 |
| Energy (mJ) | 33,25 ± 6,02 ^d | 34,81 ± 7,71 ^d | 48,94 ± 9,51 ^b | 0,001 |
| <i>Tibial diaphysis</i> | | | | |
| Maximum force (N) | 61,01 ± 9,17 | 64,12 ± 9,61 | 65,97 ± 8,97 | 0,600 |
| Stiffness (N/mm) | 99,34 ± 15,2 | 101 ± 17,49 | 100,6 ± 11,63 | 0,979 |
| Energy (mJ) | 26,71 ± 5,93 | 31,9 ± 4,53 | 31,42 ± 5,19 | 0,180 |
| <i>Femoral neck</i> | | | | |
| Maximum force (N) | 104,3 ± 16,83 | 99,08 ± 8,89 | 107 ± 7,99 | 0,389 |
| Stiffness (N/mm) | 200,1 ± 136,6 ^{bc} | 302 ± 132,9 ^a | 127,3 ± 64,52 ^b | 0,019 |
| Energy (mJ) | 48,29 ± 22,34 ^{bc} | 33,66 ± 13,47 ^a | 60,26 ± 15,33 ^b | 0,016 |

Table 2 - Parameters biomechanical: 3 points bending test and mechanical testing to failure.

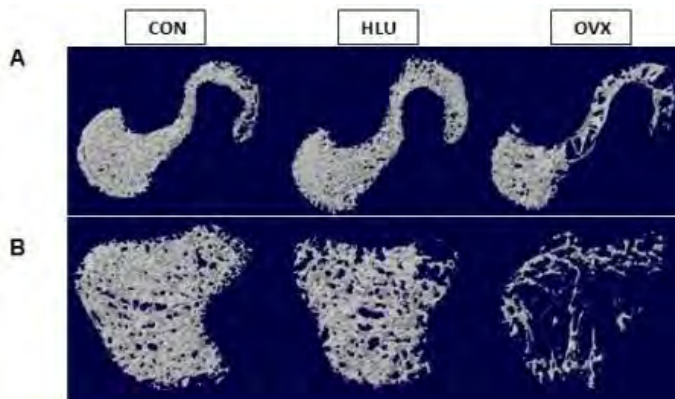


Figure 1 - 3D Reconstruction of 50 slices microtomography the trabecular bone.

Disclosures: *Melise Peres Ueno, None.*

SU0030

Improving Cortical Bone Measurements through the Inclusion of an Endocortical Parameter. Rose Pearson*¹, Graham Treece*². ¹Cambridge University PhD student, United Kingdom, ²University of Cambridge, United Kingdom

Introduction: recent advances in cortical bone measurement using model based approaches have allowed the evaluation of bone strength determinates from QCT scans in studies assessing fracture risk (Poole PLoS1 12) and osteoporosis treatments (Damm ACR 14, Allison JBMR 15). All techniques capable of measuring cortical bone morphology are limited by their inability to distinguish between the trabecularised cortical bone and the endocortical extremity of the medullary cavity (Zebaze 15). To address this weakness, we propose a new model of cortical bone that incorporates an endocortical measure.

Methods: the quality of a new 'ramp' model was investigated through direct comparison with a previously validated 'rectangular' model (Treece MedIA 15). In both cases the density variation was modelled perpendicular to the cortex; the model parameters were optimised to provide the best fit to the underlying data. In contrast to the rectangular model, the ramp model includes a gradual linear transition across the endocortical edge as illustrated in Fig. 1. Both models were fit to QCT data and compared with the equivalent profile in an HR-pQCT scan. Spatial alignment was achieved by registering the same periosteal surface to both scans. Calibration between the QCT Hounsfield units (HU) and the HR-pQCT HU was achieved with a quadratic calibration curve. The evaluation used data from 70 cadaveric femurs, 18 female and 17 male with a mean age of 77, scanned using both QCT and HR-pQCT (Dall'Ara Bone 13). Measurements were made at approximately 10,000 sites per femur.

Results: the stability and quality-of-fit of each model was assessed. In each case the comparisons were grouped into thickness ranges measured over HR-pQCT data using the Full Width Half Max technique, see Table 1. The model stabilities are comparable, with each producing a valid result at more than 98% of measurement sites. The quality-of-fit of each model was assessed using the root mean square (RMS) error between the model and the corresponding HR-pQCT profiles. The ramp model provided a highly significant reduction in the RMS error across each thickness grouping as shown in Table 1.

Conclusions: the ramp model results in a better fit to the cortical bone in HR-pQCT; the physical meaning of the additional endocortical measure merits more investigation. This measure has the potential to disentangle the effects of endocortical trabecularisation and intracortical remodelling from both cortical and trabecular bone.

Table 1: The stability and RMS errors (Mean \pm SD) for the ramp and rectangular models.

| Cortical Thickness: | < 1 mm | 1 to 3 mm | > 3 mm |
|---|--------------------|--------------------|---------------------|
| Rectangular Model Stability (%)* | 99.07 \pm 0.01 | 99.36 \pm 0.01 | 98.52 \pm 0.01 |
| Ramp Model Stability (%)* | 99.09 \pm 0.01 | 99.34 \pm 0.01 | 98.59 \pm 0.01 |
| Rectangular RMS Error (QCT HU) [†] | 263.22 \pm 75.91 | 372.87 \pm 99.45 | 398.61 \pm 112.89 |
| Ramp RMS Error (QCT HU) [†] | 241.52 \pm 68.00 | 326.61 \pm 97.18 | 363.57 \pm 144.77 |

* SD reported between profiles, irrespective of femur

[†] SD reported between femurs

Table 1

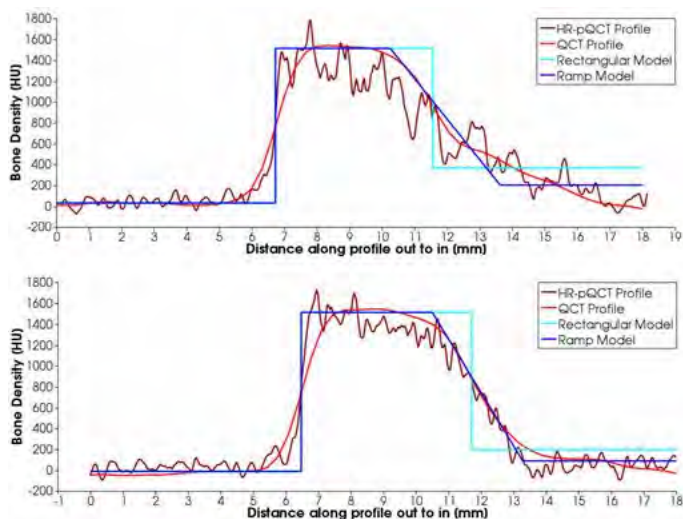


Figure 1: Two image profiles with associated ramp and rectangle models.

Figure 1

Disclosures: Rose Pearson, None.

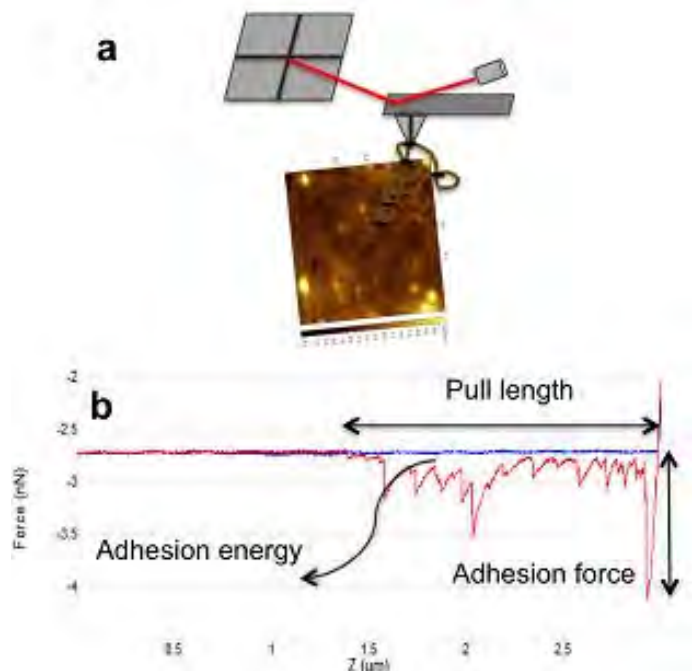
SU0031

Investigation of the Effect of Fluoride Ions on the Molecular Interaction between Bone-minerals and Non-collagenous Proteins using Single Molecule Force Spectroscopy. Soma Biswas*¹, Georg Fantner*². ¹École Polytechnique Fédérale de Lausanne (EPFL), Switzerland, ²EPFL, Switzerland

The key to understanding the remarkable mechanical toughness of bone is to explore the interfacial molecular interactions between the organic and inorganic components of bone. Some non-collagenous proteins (NCPs) in bone can act as molecular shock absorbers, dissipating large amounts of energy and preventing micro-crack formation. The adhesion of the NCP molecules to the inorganic components is essential for this mechanism to function properly. It is as yet unclear how the chemical composition of the mineral affects this molecular adhesion. Related studies have also reported that Fluoride (F-) treatment of bone resulted in a disturbance of the normal protein/mineral interaction (mostly visible at the nanometer level), which might further lead to a reduction in material quality. Given this, the effect of F- on the interaction between organic and inorganic matrix of bone needs to be studied further.

We therefore aim to elucidate the molecular interactive forces and strengths between bone minerals and NCPs, both in the presence and absence of F- ions, by utilizing atomic force microscope (AFM) analysis between synthetic hydroxyapatite (HA) and adsorbed Osteopontin molecules. AFM-based single molecule force spectroscopy has become a powerful tool to study the rupture of molecular bonds, unfolding of proteins and nucleic acids; because of its very high force sensitivity in the order of piconewton. We observed that the adhesion force and energy increased significantly while taking the pulling curves on a layer of Osteopontin deposited on HA surface instead of mica, which was used before as a crude model for bone mineral. We further found that the interaction between HA and Osteopontin did not change while replacing the monovalent ions (Na+) containing buffer with the bivalent ions (Ca2+) containing buffer solution. Finally, we show that the presence of F- ions change the molecular interaction between the synthetic HA and Osteopontin by pretreating the HA with NaF solution.

We believe that the above results will contribute towards the knowledge base for treating bone related diseases by providing quantitative information that is necessary to properly understand and model the fracture toughness of bone.



(a) an artist's conception of molecules pulled by AFM (b) a typical force spectroscopy curve

Disclosures: Soma Biswas, None.

SU0032

Mechanical and biochemical assessment of bone quality in men with type 2 diabetes. Heather Hunt*¹, Stephen Warner*², Ashley Torres¹, Jonathan Jo², Joseph Lane², Christopher Hernandez¹, Eve Donnelly. ¹Cornell University, USA, ²Hospital for Special Surgery, USA

Patients with type 2 diabetes mellitus (T2DM) have an increased risk of fracture, despite having normal or above average bone mineral densities (BMD). This suggests that the T2DM disease state affects the quality of bone, independently of variations in the quantity of bone. One proposed mechanism for the altered bone quality in T2DM is the posttranslational modifications of collagen that take place in the presence of

sugars and culminate in the formation of advanced glycation endproducts (AGEs). Our objective was to compare the mechanical and biochemical properties of bone from T2DM and non-DM patients.

Specimens were retrieved from the femoral necks of men undergoing total hip arthroplasties. Pre-operative serum glycated hemoglobin (HbA1c) was measured to assess glycemic control (Table 1). Patients with an HbA1c ≥ 6 and a previous T2DM diagnosis were allocated to the T2DM group (n=13), and patients with an HbA1c < 6 and no T2DM diagnosis were designated as non-T2DM controls (n=13). Cancellous cores were retrieved and analyzed with micro CT to determine morphological parameters. Ten age-matched specimens (n=5 T2DM, n=5 non-DM) were designated for mechanical testing and tested in compression to 3% strain to assess mechanical properties. Sixteen age-matched specimens (n=8 T2DM, n=8 non-DM) were designated for biochemical analyses. A fluorescence assay was used to determine AGE concentration.

Study groups were similar in BMI and bone volume fraction (BV/TV) (Table 1). As expected, HbA1c levels were 24% greater in the T2DM cohort vs the non-DM cohort ($p < 0.001$, Table 1). Tissue from T2DM patients compared to non-DM controls did not differ in apparent elastic modulus, apparent elastic modulus normalized by BV/TV, yield strain, or yield stress. Also, no correlations were found between HbA1c and these mechanical properties. For the biochemical analysis, AGEs in T2DM patients were 19% greater compared to those in non-DM patients ($p > 0.05$).

Bone tissue AGEs correlated positively with HbA1c for T2DM patients ($R^2 = 0.83$, $p = 0.001$), but not for non-DM patients ($R^2 = 0.22$, $p > 0.05$) (Figure 1) suggesting a relationship between glycemic control and bone tissue AGEs in T2DM. Direct assessment of mechanical properties and AGEs within the same specimens is required to discern the functional relationships among glycemic control, AGE accumulation, and mechanical properties.

| Characteristic | Non-DM (n=13) | T2DM (n=13) | % Difference vs non-DM | p |
|--|-------------------|-------------------|------------------------|--------|
| Age (years) | 63.2 \pm 2.9 | 68.3 \pm 3.3 | 8 | 0.498 |
| Mechanical Testing Cohort (n=5/group) | 61.8 \pm 4.4 | 62.8 \pm 5.5 | 2 | 0.896 |
| Biochemical Composition Cohort (n=8/group) | 64.0 \pm 3.9 | 68.3 \pm 3.9 | 7 | 0.462 |
| Height (cm) | 181.3 \pm 2.8 | 177.2 \pm 2.3 | -2 | 0.200 |
| Mechanical Testing Cohort | 181.9 \pm 5.9 | 175.3 \pm 3.7 | -4 | 0.378 |
| Biochemical Composition Cohort | 180.9 \pm 3.3 | 177.2 \pm 3.2 | -2 | 0.432 |
| Weight (kg) | 99.7 \pm 5.7 | 96.8 \pm 5.0 | -3 | 0.844 |
| Mechanical Testing Cohort | 94.6 \pm 11.9 | 100.3 \pm 7.8 | 6 | 0.706 |
| Biochemical Composition Cohort | 102.2 \pm 6.6 | 96.9 \pm 6.9 | -5 | 0.581 |
| BMI (kg/m ²) | 30.7 \pm 1.2 | 30.2 \pm 1.4 | -2 | 0.536 |
| Mechanical Testing Cohort | 28.1 \pm 1.9 | 32.4 \pm 1.6 | 15 | 0.135 |
| Biochemical Composition Cohort | 31.2 \pm 1.9 | 30.7 \pm 1.6 | -2 | 0.833 |
| HbA1c | 5.60 \pm 0.06 | 6.92 \pm 0.21 | 24 | <0.001 |
| Mechanical Testing Cohort | 5.53 \pm 0.12 | 6.57 \pm 0.20 | 19 | <0.005 |
| Biochemical Composition Cohort | 5.64 \pm 0.08 | 6.92 \pm 0.05 | 23 | <0.005 |
| Bone Volume Fraction (BV/TV) | 0.193 \pm 0.032 | 0.187 \pm 0.024 | -3 | 0.887 |
| Mechanical Testing Cohort | 0.175 \pm 0.034 | 0.217 \pm 0.035 | 24 | 0.372 |
| Biochemical Composition Cohort | 0.197 \pm 0.044 | 0.187 \pm 0.037 | -5 | 0.875 |

Values shown as means \pm SEM. A two-sample t-test was used for p values.

Table 1: Patient Characteristics

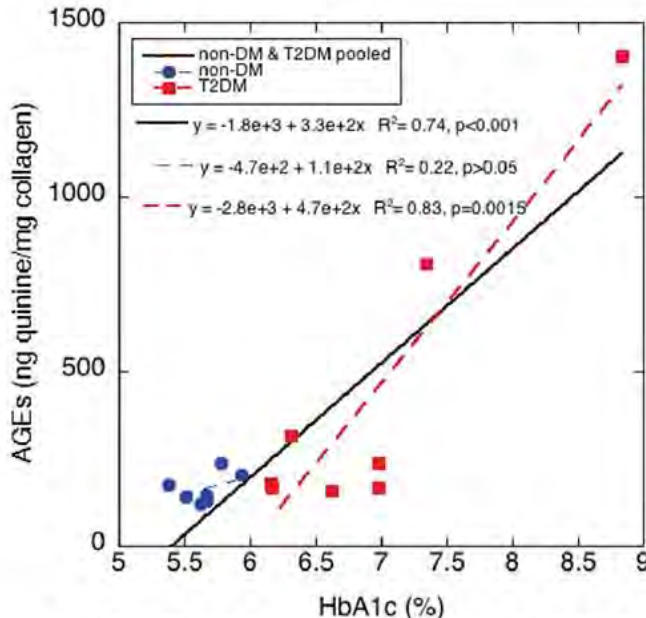


Figure 1: Concentration of bone tissue advanced glycation endproducts (AGEs) vs. preoperative serum glycated hemoglobin (HbA1c).

Figure 1: AGEs vs HbA1c

Disclosures: Heather Hunt, None.

SU0033

Microstructural and Strength Changes in Trabecular Bone in Patients with Type 2 Diabetes Mellitus. Merce Giner^{*1}, M Jose Montoya², Cristina Miranda³, M Angeles Vazquez², J Ramon Caiero⁴, David Guede⁵, Ramon Perez-Canó⁶. ¹Bone Metabolism Unit, "Virgen Macarena" University Hospital, Spain, ²University of Seville, Spain, ³Bone Metabolism Unit, Department of Internal Medicine, "Virgen Macarena" University Hospital, Spain, ⁴Department of Orthopaedic Surgery, Complejo Hospitalario Universitario de Santiago de Compostela, Spain, ⁵Trabeculae, Parque Tecnológico de Galicia, 32900 San Cibrao das Viñas, Spain, ⁶Bone Metabolism Unit, Department of Internal Medicine, "Virgen Macarena" University Hospital university os Seville, Spain

Type 2 Diabetes Mellitus (T2DM) is one of the most common chronic diseases worldwide. Bone is one of the many organs affected by T2DM, and T2DM is associated with an increased risk of osteoporosis and fragility fractures.

This study analyses trabecular microstructural and bone material strength (BMS), markers of bone turnover (BTM) and bone mineral density (BMD) in patients with T2DM with or without recent fragility fractures.

Subjects and Methods: We recruited 23 patients, aged 65-80 years: 5 patients with osteoporotic hip fracture without T2DM (OP); 7 patients with osteoporotic hip fracture with T2DM (OP-T2DM); 6 patients with hip osteoarthritis without T2DM (OA) or osteoporotic fractures during their lifetime; and 5 patients with hip osteoarthritis and T2DM (OA-T2DM). We measured serum levels of β -CrossLaps, aminoterminal propeptide of type I procollagen (PINP), parathyroid hormone (PTH) and 25-hydroxyvitamin D (25(OH)D). We also tested BMD (by dual-energy-X-ray absorptiometry), microstructural and bone material strength from femoral heads by micro-CT. We estimated the 10-year risk of major osteoporotic and hip fracture, using the FRAX[®] tool calibrated for Spain. Variables were compared using the Student's *t* test or chi-square test, depending on the type and distribution. Correlations were examined using the Spearman correlation. All hypotheses were two-tailed. *p* value < 0.05 was considered statistically significant (IBM SPSS Statistics 22.0).

Results: We found OP and OP-T2DM patients had lower BMD values at the femoral neck and total hip than the OA and OA-T2D groups. Microstructural and BMS parameters confirm a worse quality and lower strength of the trabecular bone in T2DM patients (OA-T2DM and OP-T2DM) and OP compared with OA patients. β -CrossLaps and PINP were lower in OA-T2DM patients than in the other groups. The probability of major and hip fracture (FRAX) were higher in OP and OP-T2D patients than in OA patients with or without DM ($p < 0.006$). However, there were not differences in FRAX 10-year risk of major and hip fracture between OP and OP-T2DM nor OA and OA-T2DM.

Conclusion: Our results show the negative effect of T2DM on trabecular bone structure and mechanical properties. These results emphasize the importance of evaluating diabetic bones using not only bone markers and bone mass, but also bone quality parameters.

Therefore, diabetes should be included as a risk factor for osteoporotic fracture in daily clinical practice and in the FRAX tool.

Disclosures: Merce Giner, None.

SU0034

Mineral and collagen maturity in a polygenetic murine model of type 2 diabetes point to complex effects of sustained hyperglycemia on bone tissue composition. David Diaz^{*1}, Michelle Chin¹, Dan Weinreb¹, Tarryn Tertulien¹, Ida Adjivon¹, Karen King², Eve Donnelly¹. ¹Cornell University, USA, ²University of Colorado School of Medicine, USA

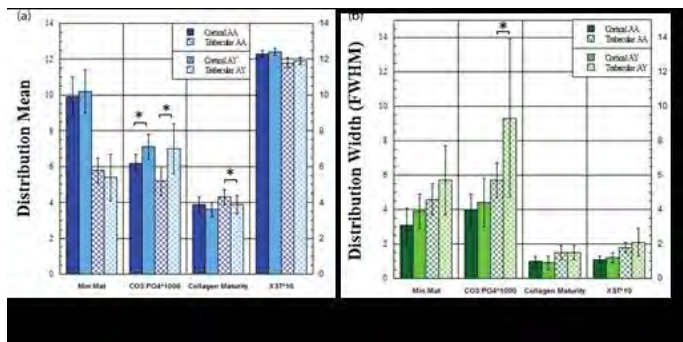
Type 2 diabetes mellitus (T2DM) increases fracture risk independently of bone mineral density. This suggests that hyperglycemia contributes to bone tissue embrittlement. However, the effects of T2DM on bone matrix properties are incompletely understood. The objective of this work is to compare bone tissue compositional properties between T2DM mice and their non-DM siblings.

With IACUC approval, proximal femora were collected after euthanasia from 20-week-old T2DM KKAy/KKAA (Ay, n=11) and non-DM KKAy/KKAA (AA, n=8) male mice. Fourier transform infrared imaging (FTIRI) was used to characterize the pixel distribution mean and full width at half maximum for 4 parameters per image: mineral:matrix ratio, carbonate:phosphate ratio (CO₃:PO₄), collagen maturity, and mineral crystallinity.

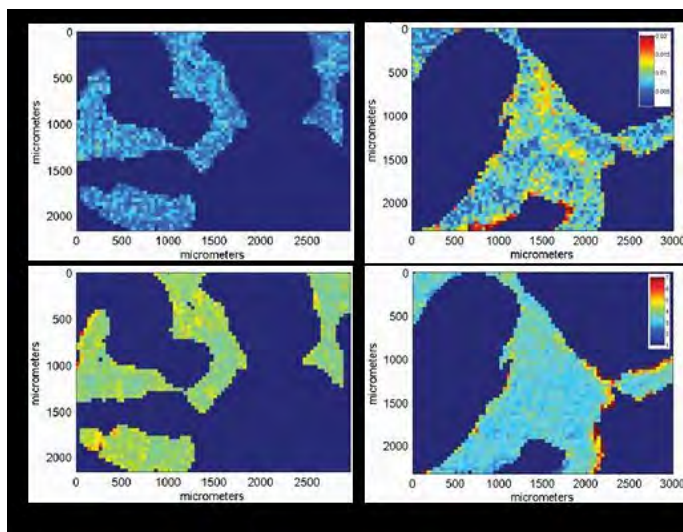
At euthanasia, T2DM mice were 8% heavier (Ay: 40 \pm 2.3 g vs. AA: 37 \pm 1.3 g, $p = 0.005$) and had 15% higher blood glucose levels than non-DM controls (Ay: 415 \pm 79 mg/dl vs. AA: 360 \pm 106 mg/dL, $p > 0.05$). The mean CO₃:PO₄ was 14% greater in T2DM cortical bone (Ay: 7.1 vs. AA: 6.2, $p = 0.011$) and 34% greater in T2DM trabecular bone (Ay: 7.0 vs. AA: 5.2, $p = 0.006$) (Fig. 1a, Fig. 2). Mean collagen maturity was 11% lower in T2DM trabecular bone than in non-DM bone (Ay: 3.9 vs. AA: 4.3, $p = 0.038$) (Fig. 1a, Fig. 2). The distribution of the CO₃:PO₄ ratio was 61% wider in T2DM trabecular bone than in non-DM bone (Ay: 9.3 vs. AA: 5.7, $p = 0.052$) (Fig. 1b).

One limitation of the study is that only end-point glucose levels were measured. Blood glucose levels in mice vary over time, and biweekly measurements would have given a clearer picture of the DM state. Because Ay male mice attain hyperglycemia

(glucose > 300 mg/dL) by ~10 weeks of age, we conclude that the observed effects on bone properties were due to sustained hyperglycemia. The greater mean CO₃:PO₄ in the Ay mice indicates increased substitution of carbonate for phosphate in the hydroxyapatite lattice with hyperglycemia. It suggests that greater mineral maturity may occur with diabetes, which is consistent with increased fracture risk. In contrast, the 11% decrease in trabecular collagen maturity would be expected to reduce fracture risk. Direct assessment of mechanical properties is required to discern the functional effects of these complex concomitant changes in mineral and collagen maturity on fracture behavior.



Distribution Mean and Width of Parameters



Mineral and Collagen Maturity Comparison

Disclosures: David Diaz, None.

SU0035

Removal of Proteoglycans from Bone Matrix Significantly Reduce its *In Situ* Toughness. Haoran Xu¹, Yehong Huang², Sumin Gu³, Jean Jiang³, Xiaodu Wang⁴. ¹Mechanical Engineering, University of Texas at San Antonio, Texas, USA, ²Biomedical Engineering, University of Texas at San Antonio, Texas, USA, ³Biochemistry, University of Texas Health Science Center at San Antonio, Texas, USA, ⁴Mechanical & Biomedical Engineering, University of Texas at San Antonio, Texas, USA

Introduction: Proteoglycans are present in the extracellular space between collagen fibrils. The highly negatively charged glycosaminoglycans (GAGs) in proteoglycans tend to attract water molecules for charge equilibrium. We hypothesized here that coupled with water proteoglycans play a significant role in toughening bone. To test the hypothesis, we used a novel nanoscratch test to access the effect of removal of GAGs by PNGase F on the *in situ* toughness of bone under dry/wet conditions. In addition, the efficacy of PNGase F in removing GAGs from bone matrix was verified.

Methods & Materials: 18 cubes (91mm³) were prepared from 6 middle-aged male human femurs, with 3 samples from each donor. Among the 3 samples, one served as baseline control without any treatments, one served as control with heating but without enzyme treatments, and the remaining one was heated first to unfold the proteins and then treated for 48 hours in PNGase F (8mg/mol), which cleaves N-linked oligosaccharides. After the treatments, nanoscratch tests were performed to measure the *in situ* toughness of bone. Two-factor ANOVA and Turkey *post hoc* tests were performed to analyze the experimental data. In addition, bone whole lysate extracted from mouse femurs was treated with PNGase F to confirm its efficacy in removal of GAGs in bone matrix and analyzed using SDS-PAGE gel.

Results and Discussion: The results indicated that the *in situ* toughness of bone was 2.048±0.133 GJ/m² for baseline control, 1.528±0.161 GJ/m² for control, and 1.151±0.177 GJ/m² for treated group, respectively, under wet condition. However, under dry condition the bone toughness changed to 1.418±0.059 GJ/m² for baseline control, 1.270±0.154 GJ/m² for control, and 1.142±0.260 GJ/m² for the treated group, respectively. The two-way ANOVA showed that both dehydration and partial removal of GAGs had significant effects on the *in situ* toughness of bone. In addition, a strong cross-effect was observed between the two factors (Table 1 & 2). The Turkey *post hoc* analyses indicate that removal of GAGs is significantly correlated with bone toughness only when water is present (*p*=0.02), suggesting that water functions as a plasticizer when GAGs are present. In SDS-PAGE gel profile (Fig. 1), the protein band between 70-100 kd in control (lane C) was shifted downwards after PNGase F treatment (lane D), thus suggesting that GAGs are removed.

Conclusion: The result of this study supports the hypothesis of this study.

Table 1 Nanoscratch toughness of bone

| | Wet (GJ/m ²) | Dry (GJ/m ²) |
|------------------|--------------------------|--------------------------|
| Baseline Control | 2.048±0.133 | 1.418±0.059 |
| Control | 1.528±0.161 | 1.270±0.154 |
| Treated | 1.151±0.177 | 1.142±0.260 |

Table 2 ANOVA analysis

| Factors | P-Value |
|--------------------|-----------|
| Dehydration | < 0.00001 |
| PNGase F treatment | < 0.00001 |
| Cross-Interaction | < 0.0004 |

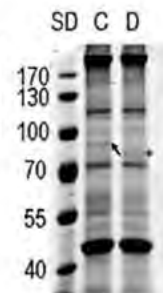


Fig. 1, SDS-PAGE profile of control (C) and PNGase F treated

SDS-PAGE, nanoscratch result and ANOVA analysis

Disclosures: Haoran Xu, None.

This study received funding from: NIH

SU0036

Reproduction Differentially Affects Cortical and Trabecular Bone and Alters Cortical Bone Stiffness and Trabecular Structure towards a Male Phenotype. Chantal De Bakker¹, Allison R. Altman¹, Connie Li¹, Youwen Yang¹, Chih-Chiang Chang¹, Wei-Ju Tseng¹, Yong-Hoon Jeong², Do-Gyoon Kim², X. Sherry Liu¹. ¹University of Pennsylvania, USA, ²The Ohio State University, USA

Despite significant bone loss during pregnancy and lactation, no adverse effects on future fracture risk have been reported. However, our recent study demonstrated a persistent, cumulative trabecular (Tb) bone loss in rat tibiae after 3 reproductive cycles, which resulted in 52% lower Tb bone volume than age-matched virgin rats. We hypothesized that better cortical (Ct) bone mechanical competence after reproduction may explain this paradox. Therefore we compared bone quality at multiple skeletal sites in 6-mo-old rats (n=4-6/group) euthanized at parturition (PAR), after 2 wks lactation (LAC), and 6 wks post-weaning (WEA), with virgin females (VIRG) and males (MALE) as controls.

At the femur, PAR, LAC, and WEA had 10-12% lower Ct area than VIRG. However, 3-point bending indicated that reproduction increased Young's modulus (E) by 34-61%, resulting in 21% greater bone stiffness in WEA than VIRG (Fig1A). Despite 31% lower Ct area in WEA vs. MALE, greater E in WEA (104%) compensated for the structure difference, resulting in similar whole bone stiffness in WEA and MALE.

LAC rats had 84% and 67% lower BV/TV at the tibia and vertebra (L4), respectively, than VIRG. BV/TV remained 40% and 21% lower in WEA compared to VIRG (Fig1 C,D). Conn.D was unchanged and Tb.N was 14% lower in WEA than VIRG at L4, while at the tibia, these differences were 57% and 32%, respectively. Interestingly, WEA had similar Tb structure as MALE rats, which also had inferior Tb structure (53% and 28% lower BV/TV at the tibia and L4, respectively) than VIRG. Nanoindentation of the vertebra indicated a reversible decrease in E at the inner region of the trabeculae (Fig1B). At the edges, E remained 14% lower after weaning, likely due to incomplete new bone mineralization. Results suggest that the mechanical integrity of the highly load-bearing regions of bone, such as Ct bone in the femur and Tb bone at L4, were preserved either through improved material properties (femur), or maintenance of structural integrity (L4). Skeletal calcium release during pregnancy and lactation is highly selective, resulting in an adapted skeletal composition where bone quality is optimized at the more load-bearing regions. This may account for the low fracture risk observed in parous women. Furthermore, the post-weaning Tb phenotype was more similar to male rats than virgin females, suggesting that the female skeleton may initially contain more Tb bone than needed to compensate for reproductive bone loss.

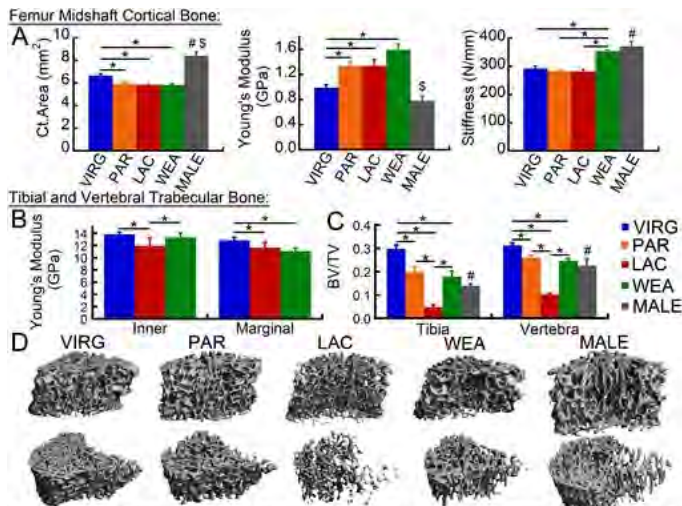


Fig 1. Effects of reproduction on (A) cortical bone at the femur, (B) material properties of vertebral trabeculae, (C) trabecular BV/TV, and (D) trabecular architecture at the vertebra (top), and tibia (bottom). *: p<0.05 among reproductive groups. In a separate analysis, MALE compared to VIRG and WEA: #MALE ≠ VIRG, \$:MALE ≠ WEA (p<0.05).

Figure 1

Disclosures: Chantal De Bakker, None.

SU0037

The initial slope of the variogram, foundation of the trabecular bone score, does not predict vertebral strength in three distinct biomechanical tests.

Ghislain Maquer¹, Enrico Dall'Ara², Yan Chevalier³, Yongtao Lu⁴, Lang Yang⁵, Matthias Krause⁶, Richard Eastell⁵, Kurt Lippuner⁷, Philippe Zysset¹. ¹Institute for Surgical Technology & Biomechanics, University of Bern, Switzerland, ²Department of Mechanical Engineering & INSIGNEO Institute for in silico Medicine, University of Sheffield, United Kingdom, ³Klinikum Großhadern, Orthopaedic Department, Laboratory for Biomechanics & Experimental Orthopaedics, Germany, ⁴Institute of Biomechanics, TUHH Hamburg University of Technology, Germany, ⁵Academic Unit of Bone Metabolism, Mellanby Centre for Bone Research, University of Sheffield, United Kingdom, ⁶Department of osteology & biomechanics, University Medical Center Hamburg-Eppendorf, Germany, ⁷Osteoporosis Clinic, Inselspital, University Hospital & University of Bern, Switzerland

Degradation of bone architecture characterises osteoporosis, but dual energy X-ray absorptiometry (DXA), the clinical tool to evaluate fracture risk, does not capture the 3D trabecular microstructure. Trabecular bone score (TBS) may recover the missing data via texture analysis of DXA images. Yet, in vitro biomechanical tests by Roux et al. demonstrated a lack of correlation between TBS and vertebral strength[1], leaving unclear the reasons for its discriminative power in fracture studies. Our hypothesis is that the biomechanical testing set-up could affect this surprising result. The initial slope of the variogram (ISV) was derived from the description of TBS as a purely textural index[2]. Simulated DXA, as previously used to test the robustness of TBS[3], was used to evaluate areal bone mineral density (aBMD) and ISV. HR-pQCT scans acquired for 62 vertebral samples were coarsened to DXA resolution and projected in a frontal plane. Failure loads of the samples (Fexp) were measured via three biomechanical testing set-ups. To overcome disc degeneration and distribute the load on the vertebral body, the endplates of 37 vertebral bodies (T12-L4; 7 males and 3 females; 64±12 yrs) were trimmed before compression (vertebral section). Alternatively, the endplates of 12 vertebral bodies (L1-L5; male; 66±15 yrs) were embedded in PMMA (vertebral body). Thirdly, spinous processes (except facet joints) were kept and loads were transmitted to 13 vertebrae (T12; female; 80±8 yrs) via intervertebral discs to mimic the in vivo situation (vertebra). The relation of aBMD and ISV with Fexp was assessed and their relative contribution to a multi-linear model quantified via ANOVA. On clinical DXA, ISV compared well with TBS (n=16, r²=0.745, p<0.001). Significant correlations were found between aBMD and all Fexp (0.587< r²<0.694, p<0.05). In comparison, relations of ISV with Fexp were non-significant, except in the vertebral body case (r²=0.396, p=0.028). Combined with aBMD, ISV brought no significant improvement for any of the experiments (Fig. 1). Independently of the testing set-up, ISV is not related to vertebral strength. This result brings a strong confirmation to those by Roux et al.[1] They also relaunch the question of the deterministic factors underlying the statistical relationship between TBS and vertebral fracture risk.1 Roux et al. Osteoporos Int. 2013;24(9):2455-602 Pothuaud et al. Bone. 2008; 42(4):775-7873 Winzenrieth et al. J Clin Densitom. 2013;16(3):287-296

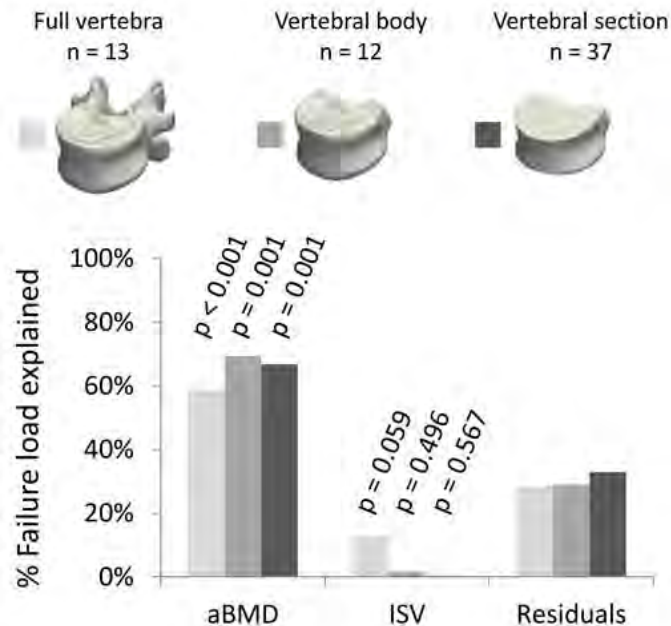


Fig. 1. Contribution of aBMD and ISV to the variance of failure load explained by their combination

Disclosures: Ghislain Maquer, None.

SU0038

Validation of High-Resolution Peripheral Quantitative Computed Tomography for Measurement of Bone Quality in Monkeys. Aurore Varela*, Gabrielle Boyd, Susan Y. Smith. Charles River Laboratories, Canada

Accurate quantification of bone micro-architecture is important in understanding bone mechanics and response to disease or treatment. High-resolution peripheral quantitative computed tomography (HR-pQCT) can scan extremities within a few minutes at a 30 µm voxel size, allowing for the quantification of trabecular and cortical BMD and micro-architecture. The purpose of this study was to evaluate the precision and reproducibility of the HR-pQCT (XtremeCT II, Scanco Medical AG) when scanning in vivo and ex vivo radii in Cynomolgus monkeys. Two radii were scanned ex vivo 5 times without repositioning to assess precision and reproducibility at a resolution of 30 µm. In vivo, the radius diaphysis and distal metaphysis from 7 monkeys were scanned 4 times with repositioning between each scan, at a resolution of 61 µm and 30 µm respectively.

Machine precision and reproducibility was good for all ex vivo radius diaphysis parameters (BV/TV, apparent density BMD, material density TMD and cortical thickness), with %CV between 0.04% and 0.54%. For the ex vivo metaphysis, %CV for the trabecular region (BV/TV, TMD, Tb.N and Tb.Th) were between 0.10% and 3.96%. For the cortical region, %CV, vBMD, TMD and Ct.Th, were between 0.20% and 1.32%. The cortical porosity had the highest variability, with a mean %CV of 7.16%.

For all in vivo radius diaphysis parameters: BV/TV, vBMD, vTMD and cortical thickness, %CV obtained were between 0.02% and 1.04%.

For the in vivo radius metaphysis site, %CV for the trabecular region, BV/TV, TMD, Tb.N and Tb.Th, were between 0.15% and 3.40%. %CV for the cortical region, vBMD, TMD and Ct.Th, were between 0.09% and 1.91%. The cortical porosity had the highest variability, with a mean %CV of 12.7%, consistent with the ex vivo variability.

HR-pQCT provided precise, reproducible non-invasive measurements of bone mass and micro-architecture in monkeys. HR-pQCT scans can be used for FEA as part of a comprehensive evaluation of bone quality, including bone mass, micro-architecture and estimated bone strength, and is an important translational tool in osteoporosis drug research.

Disclosures: Aurore Varela, None.

SU0039

Comparison of Alendronate and Zoledronate Effects on Bone Turnover and Mechanical Properties for Two Successive Periods of Simulated Microgravity Unloading. Scott Lenfest^{*1}, Harry Hogan², Susan Bloomfield³, Corinne Metzger³, Jon Elizondo², Matthew Allen⁴. ¹Texas A&M University, USA, ²Texas A&M University Department of Mechanical Engineering, USA, ³Texas A&M University Department of Health & Kinesiology, USA, ⁴Indiana University School of Medicine Department of Anatomy & Cell Biology, USA

Bisphosphonates (BP) are being tested by a limited number of International Space Station crew as part of countermeasures against bone loss. The anti-resorptive effects of BPs persist well beyond treatment withdrawal. This study used the adult hindlimb unloaded (HU) rat model to simulate two successive missions and test whether beneficial effects of BP treatment given for an initial HU period extend to a second HU period, and also to compare two BPs (Alendronate (AL) and Zoledronate (ZA)).

Adult male rats (6 mo.) were block assigned to aging control (AC) and HU groups by body weight. HU animals were exposed to 28d of HU, followed by 56d of recovery, and then a second 28d HU exposure. Subsets of HU animals were administered AL (HU+A), ZA (HU+Z), or no drug (HUC). AL (2.4 µg/kg) was given 3x/week for 5 weeks, starting the week before the first HU. ZA (60 µg/kg) was given in a single dose just prior to the first HU. Fluorochrome label injections were given 7d apart after 28d of recovery (Rec28) and after 56d of recovery (Rec56), just before the 2nd HU period. Dynamic cortical histomorphometry was performed on the tibia mid-diaphysis at these two time points. Analyses conducted at the endpoint of the study, after the 2nd HU period, included static cancellous histomorphometry (at the distal femur metaphysis), and reduced platen compression (RPC) mechanical testing (performed on a 2mm slice specimen from the proximal tibia metaphysis).

Periosteal bone formation rate (BFR) for the tibia mid-diaphysis was significantly higher ($p < 0.05$) for HUC compared to AC, HU+Z, and HU+A at Rec28, and BFR was significantly higher for HUC and HU+A compared to AC and HU+Z at Rec56. HU+Z animals had significantly lower trabecular bone osteoclast surface compared to AC (-75%) and HUC (-76%), and higher trabecular thickness compared to HU+A (+33%). Max compressive stress from RPC testing was significantly higher compared to AC (+69%), HUC (+67%), and HU+A (+66%).

Both BPs delayed recovery of BFR at Rec28, but by Rec56, BFR remained suppressed for ZA and not for AL. On balance, however, ZA proved more beneficial in giving rise to improved mechanical strength and trabecular architecture due to vastly reduced osteoclast surface. These results are consistent with the greater potency of ZA we have found for femoral neck strength and trabecular architecture from microCT, and they also provide insights into the relative effects on formation and resorption.

Disclosures: Scott Lenfest, None.

SU0040

Associations of Fluoride Intake with Adolescents' pQCT-derived Bone Outcome Measures at Age 17. Reem Oweis^{*1}, Steven Levy², John Warren², Julie Eichenberger Gilmore², Trudy Burns², Punam Saha², Kathleen Janz², James Torner², Elena Letuchy², Barbara Broffitt². ¹University of Iowa, USA, ²The University of Iowa, USA

Purpose: To investigate associations between period-specific and cumulative fluoride (F) intakes from birth to age 17 years and pQCT bone measures. **Methods:** Subjects are members of the Iowa Bone Development Study (IBDS) that grew out of the longitudinal Iowa Fluoride Study (IFS) that investigates fluoride and dietary exposures, dental fluorosis and dental caries. IFS subjects were recruited from 8 Iowa hospital postpartum wards in 1992-95, with detailed questionnaires sent every 1.5-6 months. Data on combined F intakes from water, other beverages, selected foods, dietary supplements and dentifrice were determined from the questionnaires and F assay of the products. Subjects underwent peripheral quantitative computed tomography (pQCT) of the radius and tibia (XCT-2000/3000) at age 17. pQCT cortical and trabecular bone outcomes (bone mineral content (BMC), bone mineral density (BMD), and strength) were related to F intake in bivariate and multivariable analyses adjusted for height, weight, years since peak height velocity, average daily time in moderate-to-vigorous intensity physical activity, and daily calcium and protein intake. **Results:** Mean daily F area-under-the-curve (AUC) intake from birth to age 17 was 0.79 mg (SD = 0.32) for males and 0.70 mg (SD = 0.25) for females. Unadjusted Spearman correlations between daily F intake and bone measures were weak (females $r = -0.01$ to 0.15 for radius, -0.001 to 0.23 for tibia; males $r = 0.03$ to 0.24 for radius, -0.008 to 0.27 for tibia). From partially adjusted (for height, weight, and years since peak height velocity) linear regression models for females, there was a significant negative association ($p < 0.05$) between F AUC (birth-8.5 years) and radial bending strength ($n = 179$) and significant positive association between F AUC (14-17 years) and tibial cortical content ($n = 154$). For males ($n = 137$), there were significant positive associations ($p < 0.05$) between F AUC (14-17 years) and radial compression strength and tibial cortical content and bending strength. In fully-adjusted models (physical activity, protein and calcium added), there were significant negative associations for females ($n = 140$) between F AUC (birth-8.5 years) and radial bending strength and positive associations for males ($n = 115$) between F AUC (14-17 years) and tibial bending strength at age 17. **Conclusion:** Findings suggest that life-long F intakes from

combined sources for U.S. adolescents in fluoridated areas are weakly associated with radius and tibia pQCT measures.

Disclosures: Reem Oweis, None.

SU0041

Fully Automated Bone Detection, Segmentation, Axis Extraction, Trabecular Labeling, and ASBMR Morphometric Analysis in Small Animal Micro-computed Tomography. Ali Behrooz¹, Peet Kask², Jeff Meganck^{*3}, Josh Kempner³, Wael Yared³. ¹PerkinElmer, Us, ²PerkinElmer, Estonia, ³PerkinElmer, USA

In vivo micro-computed tomography (micro-CT) imaging of small animals provides 3D anatomical images that are useful for study and analysis of skeletal bone structures, formation, and diseases. Detecting the bone voxels in raw micro-CT images is necessary for enabling such studies and analyses. While micro-CT images provide contrast between bone and soft tissue components, detecting the bone voxels in micro-CT volumes can be challenging considering noise and partial volume effects which result in low voxel density in thin bones such as the pelvis. Also, automated separation of individual bones is necessary for bone analysis when manual segmentation is impractical. In this work, a fully automated optimized framework is presented for robust detection, segmentation, and analysis of bones from micro-CT images. The imaging platforms used in this work consist of stand-alone Quantum FX and GX micro-CT systems. Data from mice and rats are acquired in vivo and postmortem at different fields of view (5 to 30 mm) and voxel resolutions of 10 to 58 microns. For bone detection, after conversion to Hounsfield units, a hybrid thresholding algorithm is employed which combines the benefits of histogram-based global thresholding with local thresholding. This algorithm offers significant improvements over existing auto-thresholding techniques. After bone detection, a watershed-based algorithm is used for individual bone splitting. Despite differences in shapes of bones and partial volume effects, especially at low resolutions, the segmentation algorithm can robustly separate individual bones. The robustness in the segmentation is secured by applying splitting filters to the bone mask prior to marker-controlled watershed. Additionally, a morphological algorithm is used to separate the cortical and trabecular compartments of each bone. Results of bone segmentation and trabecular labeling for a dataset with 10 micron voxel resolution are shown in Figure 1. For shape and structural analysis of the bone, a framework is presented for obtaining the principal and 3D medial axes of each bone. Also, 3D morphometric ASBMR and structural parameters are computed for cortical and trabecular components of individual bones. In this work, we present results for various ASBMR parameters including volume, thickness, porosity, density, and anisotropy. Results of bone segmentation, axis extraction, and ASBMR thickness for a dataset with 20 micron voxel resolution are presented in Figure 2.

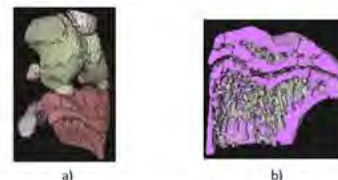


Figure 1. Bone detection, segmentation, and trabecular cortical separation for the knee joint of a mouse imaged in an in vivo micro-CT platform at 10 micron voxel resolution. a) Bones comprising the knee joint are segmented and labeled (femur, tibia, patella, and partially in-view fibula). b) The trabecular and cortical compartments of the tibia are separated and labeled.

Figure 1

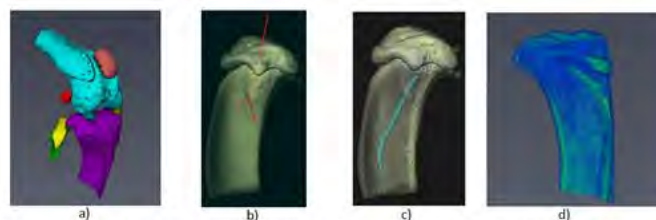


Figure 2. Bone detection, segmentation, axis extraction, and local thickness analysis for the knee joint of a mouse imaged in an in vivo micro-CT platform at 20 micron voxel resolution. a) Bones comprising the knee joint are segmented and labeled (femur, tibia, patella, and fibula). b) The principal axes of tibia are calculated and plotted overlaid with the tibia mask. c) The medial axis of tibia is extracted and visualized overlaid with the tibia mask. d) The local thickness of the cortical shell of tibia is calculated and visualized.

Figure 2

Disclosures: Jeff Meganck, PerkinElmer

This study received funding from: PerkinElmer

SU0042

Intrinsic Material Property Differences in Bone Tissue from Fracturing vs Non-fracturing Women. Severine Vennin¹, Anastasia Desyatova¹, Joseph Turner¹, Robert Recker², Mohammed Akhter^{*3}. ¹University of Nebraska-Lincoln, USA, ²Creighton University, USA, ³Creighton University Osteoporosis Research Center, USA

Osteoporotic (low-trauma) fractures are a significant public health problem. Up to 50% of those over 50 yrs of age are at high risk of osteoporotic fracture. While current therapies reduce the skeletal fracture risk, additional information concerning the intrinsic material strength properties of bone tissue is needed to develop better treatments, since measurements of bone density account for no more than ~50% of fracture risk. The hypothesis is that postmenopausal women who have sustained osteoporotic fractures will have reduced bone quality as indicated by measures of intrinsic material strength properties, compared to those with who have not fractured. 120 iliac biopsies were collected from fracturing (n=60, cases) and non-fracturing postmenopausal women (n=60, matching controls) to measure intrinsic strength properties using the nano-indentation (NI) technique. Each biopsy specimen was embedded in epoxy resin, then ground and polished, and used for the NI testing. After calibration, multiple indentations were made with a target force of 6 mN (milli-newtons) at a constant loading rate of 400 µN/s (micro-newtons per second). The indentation procedure included a linear loading period of 15s, a holding period at a maximum load of 10s and a linear unloading period of 15s. In addition, dynamic testing was done using standard protocols to quantify storage and loss moduli. The load-displacement data from each indentation were used to calculate reduced indentation modulus (Er, GPa) and hardness (H, GPa) for both cortical and trabecular bone tissue. The descriptive statistics and t-tests for the NI data set are shown in Table-1. While cortical hardness was significantly greater (P=0.04), the cortical modulus showed an increased trend in controls as compared to the cases. The standard deviation (St Dev) of the measured variance in the majority of the variables, for both cortical and trabecular bone tissue (hardness/modulus, storage modulus), was reduced in controls compared to the cases. This result suggests that the cases had less heterogeneous material properties as compared to the controls, and therefore, were more prone to fracture. The higher variation in loss modulus for the cases suggests there was existing damage in bone tissue that could propagate more easily in the relatively homogenous material, and therefore, is responsible for the increased risk of fracture.

| Table-1 Variable | Cases | | Controls | | p(t) |
|-----------------------------|--------|-------|----------|-------|------|
| | Mean | Std | Mean | Std | |
| Cort Hardness-H (GPa) | 0.448 | 0.184 | 0.543 | 0.297 | 0.04 |
| St Dev Cort Hardness | 0.096 | 0.051 | 0.118 | 0.073 | 0.08 |
| Cort Modulus-Ec (GPa) | 13.572 | 4.320 | 14.974 | 4.589 | 0.10 |
| St Dev Cort Modulus | 1.638 | 0.782 | 2.075 | 0.918 | 0.00 |
| St Dev Cort Storage Modulus | 1.668 | 0.744 | 2.062 | 0.746 | 0.00 |
| St Dev Cort Loss Modulus | 0.214 | 0.180 | 0.166 | 0.096 | 0.04 |
| St Dev Trab Hardness | 0.070 | 0.027 | 0.083 | 0.033 | 0.02 |
| St Dev Trab Modulus | 1.727 | 0.895 | 1.969 | 0.725 | 0.03 |
| St Dev Trab Loss Modulus | 0.183 | 0.104 | 0.142 | 0.098 | 0.01 |

Cases-fracturing; Controls-non fracturing; Cort-Cortical; Trab-trabecular; Std and St Dev-standard deviations.

Table-1. Nano data for Bone Quality study

Disclosures: Mohammed Akhter, None.

SU0043

Osteogenesis on Nanoparticulate Mineralized Collagen Scaffolds via Auto-genous Activation of the Canonical BMP Receptor Signaling Pathway. Xiaoyan Ren^{*1}, David Bischoff², Daniel Weisgerber³, Michael Lewis⁴, Victor Tu⁵, Dean Yamaguchi⁶, Timothy Miller⁵, Brendan Harley⁷, Justine Lee⁵. ¹Division of Plastic & Reconstructive Surgery, UCLA David Geffen School of Medicine & VA Greater Los Angeles Healthcare System, USA, ²VA Greater Los Angeles Healthcare System, USA, ³Department of Chemical & Biomolecular Engineering, Institute for Genomic Biology, University of Illinois at Urbana Champaign, USA, ⁴Department of Pathology, VA Greater Los Angeles Healthcare System, USA, ⁵Division of Plastic & Reconstructive Surgery, UCLA David Geffen School of Medicine & Division of Plastic & Reconstructive Surgery, VA Greater Los Angeles Healthcare System, USA, ⁶VA Greater Los Angeles Healthcare System & UCLA David Geffen School of Medicine, USA, ⁷Department of Chemical & Biomolecular Engineering, Institute for Genomic Biology, University of Illinois at Urbana Champaign, USA

Skeletal regenerative medicine frequently incorporates deliverable growth factors to stimulate osteogenesis. However, the cost and side effects secondary to supraphysiologic dosages of growth factors warrant investigation of alternative methods of stimulating osteogenesis for clinical utilization. In this work, we describe growth factor independent

osteogenic induction of human mesenchymal stem cells (hMSCs) on a novel nanoparticulate mineralized collagen glycosaminoglycan scaffold (MC-GAG).

hMSCs were plated on scaffolds and treated with osteogenic medium for up to 12 weeks. Markers of osteogenic differentiation were assessed by real time RT-PCR. Mineralization and bone formation was followed by histology and microCT. Signal transduction was analyzed by western blot and immunohistochemistry.

hMSCs demonstrated elevated osteogenic gene expression and mineralization on MC-GAG with minimal to no effect upon addition of BMP-2 when compared to non-mineralized scaffolds (Col-GAG). To investigate the intracellular pathways responsible for the increase in osteogenesis, we examined the canonical and non-canonical pathways downstream from BMP receptor activation. Constitutive Smad1/5 phosphorylation with nuclear translocation occurred on MC-GAG independent of BMP-2, whereas Smad1/5 phosphorylation depended on BMP-2 stimulation on Col-GAG. When non-canonical BMPR signaling molecules were examined, ERK1/2 phosphorylation was found to be decreased in MC-GAG but elevated in Col-GAG. No differences in Smad2/3 or p38 activation were detected.

Collectively, these results demonstrated that MC-GAG scaffolds induce osteogenesis without exogenous BMP-2 addition via endogenous activation of the canonical BMP receptor signaling pathway.

Disclosures: Xiaoyan Ren, None.

SU0044

Trabecular bone microdamage, microarchitecture and resorption in whole human vertebrae are regionally distributed and distinctly related to intervertebral disc properties. Vincent T. Carpentier^{*}, Helen Tsangari, Nicola L. Fazzalari, Julia S. Kuliwaba. Bone & Joint Research Laboratory, Anatomical Pathology, SA Pathology, Australia

Study aim: Vertebral strength is determined by bone size, shape, bone mineral density (BMD), microarchitecture, and bone material properties. Despite its importance to vertebral mechanics, no studies have reported on the variation of bone microdamage present in the human vertebra and its association with intervertebral disc (IVD) properties.

Methods: L2-L3 lumbar functional units were obtained from 15 human cadaveric spines (8 males; 7 females; 16-87 years). L2 vertebra BMD status and L2-L3 IVD thickness (IVD.Th) were respectively measured with DXA and X-rays. L2-L3 IVD degenerative grade (IVD.Gr) was determined with a phantom-based T2 weighted MRI technique. Parasagittal slices were then cut from each L2 vertebral body, en bloc-stained in basic fuchsin and resin embedded. Histomorphometric assessment of trabecular bone microarchitecture, in vivo bone microdamage, and extent of bone resorption was undertaken following the antero-posterior and cranio-caudal axes.

Results: No association was found between IVD.Th and IVD.Gr. Concerning the whole L2 vertebra, IVD.Th was negatively correlated with BMD Z-score (r=-0.55, p<0.04) and IVD.Gr was correlated with microcrack length (r=0.71, p<0.01) and surface density (r=0.66, p<0.02). No differences were found between regions following the antero-posterior axis. For the cranio-caudal axis, the bone volume fraction (BV/TV) was the highest in the cranial region (p<0.04) and negatively correlated with IVD.Th (r=-0.55, p<0.05). In this region, bone resorption was the highest (p<0.02), and microcrack length (Cr.Le) (r=0.69, p<0.01), density (Cr.Dn) (r=0.69, p<0.01) and surface density (Cr.S.Dn) (r=0.80, p<0.005) were correlated with IVD.Gr. In contrast, the mid-vertebral region had the lowest BV/TV and the highest Cr.S.Dn (p<0.04). In addition, bone resorption was the lowest (p<0.02) and correlated to IVD.Gr (r=0.59; p<0.02). The caudal region had the lowest Cr.S.Dn (p<0.04). Diffuse microdamage was minimal or absent within vertebrae.

Conclusions: For the cranio-caudal axis of the L2 human vertebra, the mid-vertebral region may be biomechanically compromised due to reduced bone volume being accompanied by an increased microcrack burden. The distinctive correlations between bone microdamage, microarchitecture and resorption with either IVD.Th or IVD.Gr suggest a heterogeneous adaptive response within the human vertebra to intervertebral disc degeneration.

Disclosures: Vincent T. Carpentier, None.

SU0045

Effects of Hind Limb Unloading on Wild Type and Osteocalcin Knockout Mice. Patricia Buckendahl^{*}, JAYANTH Watson, Matthew Flanagan, Aedan Hannah. Rutgers University, USA

Purpose: To evaluate the lack of osteocalcin on response to hind limb unloading (HLU). Skeletal unloading, whether due to prolonged bed rest, paralysis, or microgravity of space flight, causes physiological changes affecting not only bone, but also immune function. Male 8-week old C57Bl/6 wild type (WT) and osteocalcin null mutant (KO) mice, progeny of homozygous WT or KO mothers, were subjected to hind limb unloading or control conditions in similar cages, 6 mice per group, for 1 week. Technical difficulties forced the elimination of 2 KO controls and 2 KO HLU subjects. Weights were recorded daily. All mice tolerated the procedure well. After 1 week, mice were killed and dissected to obtain adrenals, spleen, lumbar spinal cord, lumbar vertebrae, humerus and hind limb bones. Soft tissues were quickly frozen, while tibial metaphysis and L2 were stored in RNAlater for later analysis of gene expression by RT-PCR. One femur, L3-5 vertebrae and humeri were stored in 70% ethanol for microCT analysis. The other femur was wrapped in saline soaked gauze and frozen pending breaking strength measurements. To evaluate possible stress

responses, we analyzed adrenal gene expression of tyrosine hydroxylase and NPY, which did not differ among treatment groups indicating minimal effects of the procedures. Because HLU is known to induce inflammatory responses, we examined expression of a spectrum of cytokines. There were no significant differences in gene expression among these factors in spleen. In spinal cord, NFkB and NOS2 decreased significantly with treatment, but not genotype, while BDNF was significantly lower in both KO groups relative to WT control. The involvement of BDNF with sensory transduction in the cord and the lower expression of this factor in KO mice may help explain sensory latencies that we have observed in KO mice. The lack of differences in ALP and Col1A1 in lumbar vertebrae were surprising, but may have begun to adapt to the altered loading by 1 wk. The marginal decrease in expression of OG1 (bglap1) is consistent with data from HLU and spaceflight rats. MicroCT imaging of femurs revealed lower Tb.Th. in WT HLU, but no effect of HLU on KO. This plus the marginal difference in cortical thickness between WT and KO controls is consistent with that obtained from older WT and KO mice subjected to spinal cord injury. Analyses of microCT data for humeri and vertebra are ongoing.

Disclosures: Patricia Buckendahl, None.

SU0046

Moderate Elevations in Iron Stores Improves Skeletal Integrity in Mice Even During Disuse. Corinne Metzger¹, Matthew Allen², Scott Lenfest³, Harry Hogan³, Nancy D. Turner⁴, Sara Zwart⁵, Susan A. Bloomfield³, Rihana Bokhari³. ¹Texas A&M University Dept. Health & Kinesiology, USA, ²Indiana University School of Medicine, USA, ³Texas A&M University, USA, ⁴Texas A&M University Dept. Nutrition & Food Science, USA, ⁵NASA Johnson Space Center - Universities Space Research Association, USA

International Space Station crewmembers experience moderate elevations in iron stores early during flight that are associated with greater in-flight declines in bone mineral density (BMD). Preliminary data from our lab demonstrated oxidative stress induced by iron loading in adult rats was associated with high bone resorption and bone loss. The objective of this study was to test the hypothesis that increasing iron stores would aggravate bone loss during hindlimb unloading (HU). Male C57BL/6 mice (n=44; age 16 wks) were acclimated to AIN93-G purified diet with normal (45 mg Fe/kg) or high (650 mg Fe/kg, Fe) iron content for 4 wks. Mice were randomly assigned to 4 groups: weight bearing cage controls (CC), HU, CC+Fe, and HU+Fe. Liver iron in Fe groups was 28% higher than in normal diet groups after 8 weeks on the diet. PIXImus (DEXA) scans revealed HU+Fe mice did not have statistically different hindlimb and total body BMD than CC+Fe mice. Total body lean and fat mass were lower in all HU mice compared to cage controls with no dietary differences. SkyScan µ-CT of distal femurs revealed higher cancellous bone volume (BV/TV), elevated trabecular thickness and number and lower trabecular separation with high Fe. HU induced an approximately 30% lower cancellous BV/TV within both diet groups, but Fe diet led to a higher cancellous BV/TV in both groups. In all cases µCT trabecular microarchitecture measures in HU+Fe mice were equivalent to those of CC. Three-point bending to failure on mid-shaft femur demonstrated higher ultimate load values in high Fe compared to controls. Ultimate load in femoral neck axial loading to failure was greater in CC+Fe but was not different between CC, HU and HU+Fe. Contrary to our hypothesis, high dietary iron intake led to higher BMD, improved trabecular microarchitecture and bone strength in both CC and HU mice. Although most bone measures were lower in high iron mice subjected to HU compared to their diet controls, the overall bone status at the end of 4 wks of HU was equivalent to that of weight bearing mice on the control diet. These findings contrast with our previous data in adult rats and may represent a species difference in response to moderate increase in dietary iron levels. Future studies will focus on gender comparisons and the impact of constant low dose radiation-induced oxidative damage on mice during HU with elevated dietary iron intake.

Disclosures: Rihana Bokhari, None.

SU0047

Physical strenuousness of occupation is risk factor for intervertebral disc degeneration. Sami Salo^{*1}, Ville Leinonen², Toni Rikkinen³, Pauli Vainio⁴, Jarkko Marttila⁴, Risto Honkanen³, Marjo Tuppurainen⁵, Heikki Kröger⁶, Joonas Sirola⁶. ¹Kuopio Muskuloskeletal Research Unit (KMRU), University of Eastern Finland, Finland, ²Department of Neurosurgery, Kuopio University Hospital, Kuopio, Finland, Finland, ³Kuopio Muskuloskeletal Research Unit, KMRU, Surgery, Institute of Clinical Medicine, University of Eastern Finland, Kuopio, Finland, Finland, ⁴Department of Radiology, Kuopio University Hospital, Kuopio, Finland, Finland, ⁵Department of Obstetrics & Gynecology, Kuopio University Hospital, Finland, Finland, ⁶Kuopio Muskuloskeletal Research Unit, KMRU, Surgery, Institute of Clinical Medicine, University of Eastern Finland & Department of Orthopedics, Traumatology & Hand Surgery, Kuopio University Hospital, Finland

Introduction: Occupational lumbar spine load has been linked to intervertebral disc degeneration in the lumbar spine. The aim was to study the relationship between

physical strenuousness of occupation (PSO) and intervertebral disc degeneration (IDD) in postmenopausal women.

Materials and methods: The study population consisted of 160 postmenopausal women (aged 61.9 – 78.0 years, mean 70.22 years) from the OSTPRE and OSTPRE-FPS study cohorts. Information on PSO was based on self-report questionnaires and it was divided into three groups: 1) heavy, 2) moderate and 3) sedentary or light. Severity of IDD was graded from T2-weighted MRI images using 5-grade Pfirrmann classification. Five intervertebral levels (L1-L2 to L5-S1) were studied. A mean IDD grade of all five discs was calculated for each woman separately. It was categorized into three groups: slight (mean grade less than 3), moderate (mean grade 3 or more, but less than 4) and severe (mean grade 4 or more). Logistic regression was used in the analysis to calculate odds ratios (OR). Potential confounders including height, weight, age, smoking duration in years, use of postmenopausal hormone therapy, L2-L4 BMD and femoral neck BMD were used as covariates in the analysis.

Results: The heavy PSO group had higher odds for severe disc degeneration (OR = 5.07, 95% CI: 1.37-18.79, p=0.015) in comparison to slight IDD. Adjustment strengthened this association (OR = 15.31, 95% CI: 2.97-78.97, p=0.001). Age (OR = 1.33, 95% CI: 1.14-1.56, p<0.001), L2-L4 BMD (OR = 36.50, 95% CI: 1.41-947.10, p=0.030) and smoking history in years (OR = 1.08, 95% CI: 1.01-1.15, p=0.035) were statistically significant covariates in the analysis.

Conclusions: Physical strenuousness of work seems to be a significant risk factor for intervertebral disc degeneration in postmenopausal women.

Disclosures: Sami Salo, None.

SU0048

Comparison of Accelerometer Processing Data for Bone-Related Physical Activity Studies: Iowa Bone Development Study. Shelby Francis, Kathleen Janz*, Elena Letuchy, Rick Paulos, Kristen Metcalf, Trudy Burns, Steven Levy. University of Iowa, USA

BACKGROUND: To more precisely understand how bone adapts to mechanical loading outside of laboratory settings, measurement methods must unobtrusively capture the dimensions of physical activity (intensity, frequency, time, intensity rate of change, and non-repetitiveness of loading). Accelerometers with their small packaging, relative stability over time, minimum user interface, good dynamic g-force ranges, and long monitoring time are well suited for this task. Currently, micro electro mechanical system (MEMS) accelerometers are the principal class of motion sensors used in epidemiologic studies of bone-related physical activity. This study used the ActiGraph GT3X+ MEMS accelerometer (Pensacola, FL) to compare new triaxial accelerometer output that includes g-force output (Hildebrand, 2014) and 1-second data summary with traditional movement count approaches.

METHODS: Three hundred and sixty-two young adults (mean age 19 y) from the Iowa Bone Development Study cohort wore the ActiGraph GT3X+ for at least 3 days and for at least 8 hours per day. Raw acceleration data (30 Hz) were processed using Freedson 1998 (F98), Freedson 2011 (F11), and Hildebrand 2014 (H14), and reduced to minutes per day in moderate-and-vigorous intensity PA (MVPA), and minutes per day in vigorous intensity PA (VPA). These variables were compared to pQCT-derived tibia bone strength outcomes (Stratec, Pforzheim, Germany; Bone Strength Index (BSI) and polar Stress Strain Index (pSSI)) in 254 (142 females) participants. Spearman correlation coefficients were estimated to investigate the associations among the PA measures and between the PA measures and bone strength outcomes.

RESULTS: Associations among the three MVPA/VPA measures were strong, consistent, and of similar magnitude (e.g., MVPA r = 0.81 to 0.96, VPA r = 0.76 to 0.96). While those between the acceleration data and bone strength indices (sex-specific, adjusted for weight and height) were low-to-moderate, consistent, and of similar magnitude (r = 0.04 to 0.39).

CONCLUSIONS: The use of different algorithms to summarize ActiGraph accelerometer outputs, including a new raw data approach, yielded comparable results for predicting bone strength based on MVPA/VPA. Therefore, general conclusions drawn from studies using different approaches to reduce accelerometer data are likely to be comparable.

Spearman Correlation Coefficients for pQCT Tibial Bone Outcomes vs. MVPA/VPA Measures, by Sex, Adjusted by Weight and Height (n = 254)

| SEX | pQCT Bone Outcomes | MVPA F98 | VPA F98 | MVPA F11 | VPA F11 | MVPA H14 | VPA H14 |
|-----|---|----------|---------|----------|---------|----------|---------|
| M | BSI, 4%, mg ³ /mm ⁴ | 0.18 | 0.12 | 0.19 | 0.16 | 0.12 | 0.22 |
| | pSSI, 38% tibia, mm ³ | 0.17 | 0.15 | 0.17 | 0.15 | 0.07 | 0.17 |
| | Cortical thickness, 38% tibia, mm | 0.39 | 0.23 | 0.38 | 0.23 | 0.38 | 0.29 |
| F | BSI, 4%, mg ³ /mm ⁴ | 0.24 | 0.33 | 0.25 | 0.30 | 0.21 | 0.17 |
| | pSSI, 38% tibia, mm ³ | 0.17 | 0.26 | 0.20 | 0.27 | 0.04 | 0.18 |
| | Cortical thickness, 38% tibia, mm | 0.19 | 0.19 | 0.23 | 0.22 | 0.08 | 0.12 |

Table 1

Disclosures: Kathleen Janz, None.

SU0049

Current Physical Activity Is Independently Associated with Cortical Bone Size in Older Swedish Women. Martin Nilsson*¹, Daniel Sundh², Dan Mellström², Mattias Lorentzon². ¹Centre for Bone & Arthritis Research At the Sahlgrenska Academy, Sweden, ²Geriatric Medicine, Centre for Bone & Arthritis Research, The Sahlgrenska Academy, University of Gothenburg, Sweden, Sweden

Purpose: We have previously reported that exercise during growth and young adulthood was independently associated with increased cortical bone size via periosteal expansion, whereas physical activity at old age was related to decreased endosteal bone loss in weight-bearing bone in old men (Nilsson, M. et al. JBMR. Aug, 2014).

The aim of this study was to investigate if physical activity during growth or at old age was associated with cortical geometry and trabecular microarchitecture in weight-bearing bone in older women.

Methods: In this population-based study 964 women, 78.2±1.6 (mean±SD) years old, were included. Cortical geometry and trabecular microstructure were measured at the distal (14 % level) and ultra distal tibia, respectively, using a high-resolution 3D pQCT device (XtremeCT, Scanco Medical AG). Areal bone mineral density (aBMD) was assessed using DXA (Discovery A, Hologic). A standardized questionnaire was used to collect information about previous circumference and current physical activity (Physical Activity Scale for the Elderly (PASE)).

Results: Current level of physical activity (PASE-score) was associated with cortical cross-sectional area (CSA) at the distal tibia (Fig.1). A linear regression model (including age, height, weight, calcium intake, smoking, levels of exercise during growth, and PASE-score) revealed that level of current physical activity was independently associated with CSA ($\beta=0.21$, $p<0.001$), cortical thickness ($\beta=0.17$, $p<0.001$), and bone volume fraction ($\beta=0.09$, $p=0.004$) at the distal tibia, and total hip aBMD ($\beta=0.10$, $p<0.001$). Exercise during growth and young adulthood was independently associated with periosteal circumference at the distal tibia ($\beta=0.06$, $p<0.05$) but not with any other bone measurements.

Conclusion: In this large cohort of older women, current physical activity was independently associated with cortical bone size, in terms of thicker cortex but not larger periosteal circumference, at the distal tibia. These findings indicate that physical activity at old age may decrease cortical bone loss in weight-bearing bone in older women. In contrast to our previous findings in older men, physical activity during growth and young adulthood is not the strongest determinant of cortical bone size in older women, suggesting sex-specific mechanisms.

Figure 1 MEAN CORTICAL CROSS-SECTIONAL AREA AT THE DISTAL TIBIA (mm²)

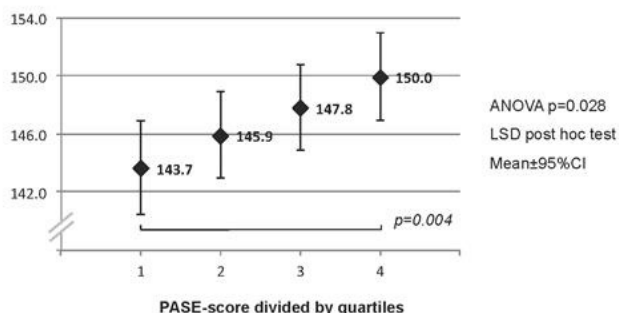


Figure 1

Disclosures: Martin Nilsson, None.

SU0050

The Use of Accelerometers to Measure Lower Limb Loading During Activity: Sampling Rate and Operating Range Considerations. Christina Ziebart*, Jenna C Gibbs, Iris Levine, Andrew Laing, James Tung, Lora Giangregorio. University of Waterloo, Canada

Background: It has been suggested that bone response to loading varies with the frequency and intensity of impact loads. While wearable accelerometers have been suggested as a tool for measuring impact loading in daily activities, it is not known how variations in sensor characteristics might affect measurement accuracy. The purpose of this study was: 1) to characterize the peak vertical acceleration achieved during a variety of activities, and 2) to compare peak acceleration values measured across three accelerometers (differing in sampling rate and operating range) during a range of activities. **Methods:** Twelve healthy young adults performed nine activities while simultaneously wearing three triaxial accelerometers. Two accelerometers designed for monitoring daily activities employed lower sampling rates and operating ranges (Actigraph GT3X: 100Hz sampling rate, ~6g range; X6-2mini: 320Hz, ~6g) were compared with a criterion standard accelerometer (Endevco 2707A: 1000Hz, ~20g) using Bland-Altman and correlation analyses. **Findings:** Box drop, vertical jump, heel drop and left single leg lateral jump resulted in the highest measured impacts. The correlation between the criterion standard accelerometer and the others was low-moderate for the majority of activities (Actigraph: R²= 0.587, X6-2mini: R²= 0.398),

but improved when the range was limited to the activity monitoring accelerometers' ~6 g operating range (Actigraph: R²= 0.831, X6-2mini: R²= 0.863). **Interpretation:** This study found that activity monitoring accelerometers under-estimated peak accelerations compared to the criterion standard accelerometer. There was variation in the magnitude of impact load detected by the different devices and studies employing these devices should take sensor characteristics into account.

Disclosures: Christina Ziebart, None.

SU0051

Trabecular Bone Score is Related to Physical Function in Adults. Diane Krueger*¹, Ellen Fidler², Jessie Libber², Neil Binkley², Bjoern Buehring². ¹University of Wisconsin, Madison, USA, ²University of Wisconsin, USA

Background: Muscle force alters bone structure. Thus, it is not surprising that physical function and trabecular bone score (TBS; a surrogate for bone micro-structure) are related to fracture risk. It has been reported that physical performance is positively correlated with TBS in young women. This observation is plausible, as greater load application should improve bone microarchitecture. As such, we hypothesized that TBS would be positively correlated with physical function not only in young adults, but across the lifespan. This study evaluated the relationship of TBS with physical function parameters in adult men and women.

Methods: Subjects (n = 221, 90 M/131 F) from 4 studies that collected physical function measures and spine DXA were used for this analysis. The sample was limited to those with a BMI of 15-38 kg/m² to meet TBS requirements. Functional assessments included grip strength, chair rise, gait speed and relative force and power determined by jumping mechanography. Univariate and multivariate regressions were performed with each physical function test to explore the correlation of function tests with TBS and BMD using XLSTAT (New York, NY).

Results: Mean (±SD, range) age, BMI and T-score were 65.1 (±19.0, 27 to 96.5) years, 26.8 (±4.7, 15.1 to 37.3) kg/m² and +0.25 (±1.9, -4.3 to +7.0) respectively. TBS was positively correlated with all functional tests (p < 0.01) in univariate analyses. Spine and/or hip BMD was positively correlated (p < 0.01) with all functional tests except gait speed. In multivariate modeling including TBS and BMD, TBS remained independently correlated with all functional tests (p < 0.01) except grip strength. In subsequent age (< 45, < 65 and > 65 years) and sex-stratified analyses, TBS remained positively correlated with all functional parameters in men and in women younger than age 65, but not in women age > 65.

Conclusion: TBS is positively correlated with function suggesting that muscle performance affects bone microarchitecture reinforcing the paradigm that muscle is vital in fracture prevention. Loss of the relationship between TBS and function in older women may imply that estrogen depletion driven microarchitectural deterioration supersedes the role of function on bone microarchitecture. Further studies evaluating whether measures to improve physical performance alter TBS are indicated.

Disclosures: Diane Krueger, None.

SU0052

Bone quality and quantity in Duchenne Muscular Dystrophy patients. Renaud Winzenrieth*¹, Luis Del Rio², Silvana Di Gregorio². ¹Med-imaps, Hôpital X. Arnoz, PTIB, Pessac, France, France, ²Cetir Group Medic, Spain

It is well known that subjects with Duchenne Muscular Dystrophy (DMD) have low areal bone mineral density (aBMD) and are at higher risk for fractures. However, no data exist concerning bone microarchitecture status. The aim of the study is to evaluate bone quantity (aBMD) and bone quality as assessed by TBS in DMD subjects.

Forty three boys and girls suffering from DMD with a mean age 10.5±3.7 years and Height and Weight z-score medians of -0.67 and 0.25 SD were included in the study. Spine DXA scans were obtained using a GE Lunar Prodigy with software v13.31. Lumbar spine TBS was determined using Med-Imaps custom software to calculate raw values that were subsequently adjusted for tissue thickness based on a normative population (from birth to 19 years old) of healthy Spanish boys (n=1468) and girls (n=2659). Subjects were stratified based on tertile approach for TBS and aBMD.

Overall, the mean aBMD Z-score of the population was moderate (-1.19±1.19 SD) while TBS Z-score was normal for age (-0.08±1.32 SD). Negative associations were observed between aBMD, Height and weight Z-scores and age (r=-0.56, -0.43 and -0.51, p<0.001) whereas no association was obtained with TBS Z-score (r<0.1, p=0.9). aBMD explained 25% (r²) of TBS values. Considering subjects in the lowest tertile (LT), 14 subjects were in this tertile based on aBMD or TBS. No differences in terms of age, height and weight Z-scores, lumbar tissue thickness or fat percent (all p>0.7) were observed between these two group of subjects. The LT cut-off values were 0.582 g/cm² for aBMD (z-score=-0.84SD) and 1.188 for TBS. Subjects in the aBMD LT have a TBS value normal for age (Z-score=-0.04SD) while subjects in the TBS LT have a low aBMD for age (Z-score=-0.95SD). Interestingly, considering the minimum of TBS or aBMD LT values, 21 subjects were classified as low bone status.

As expected, low aBMD was observed in DMD subjects. Interestingly, a normal trabecular bone texture (TBS) for age was observed in those patients. aBMD and TBS identified similar number of subjects with low bone status. One striking finding concerns the cut-off value of TBS LT which is similar to that obtain for adults and

link to a high risk for fracture (1.188 vs 1.200). In addition, it seems that the combination of aBMD and TBS allows to identify more subjects with low bone status. Further researches are needed to evaluate parameters associated with a low TBS value as well as TBS changes during growth in DMD subjects.

Disclosures: Renaud Winzenrieth, Med-Imaps

SU0053

Evolution of bone quality and quantity in patients suffering from Duchenne Muscular Dystrophy. Luis Del Rio¹, Silvana Di Gregorio¹, Renaud Winzenrieth^{*2}. ¹Cetir Group Medic, Spain, ²R&D department, Med-Imaps, France

The aim of the study is to evaluate, across time, if a bone microarchitectural texture modification exists or not and to evaluate its associations with other bone and body composition parameters.

Sixteen Spanish boys (n=15) and girls (n=1) suffering from DMD with a mean age 9.7 ± 3.0 years and Height and Weight z-score of -0.76 and 0.16 SD were included in the study. Spine DXA scans and body composition scans were obtained using a GE Lunar iDXA (GE-Lunar, Madison) at baseline, 12 and 24 months of follow-up. Lumbar spine TBS was determined using Med-Imaps custom software to calculate raw values that were subsequently adjusted for tissue thickness based on a normative population of healthy Spanish boys and girls (n=4127). Z-score TBS were evaluated using the same normative population. Variations of mean BMD and TBS during the follow-up were expressed in SD. Z-scores variations of BMD, TBS, height and weight were also assessed.

At baseline, BMD and TBS Z-scores were -1.1SD and -0.2SD respectively. Both TBS and BMD increased significantly during the follow-up with more marked increase for TBS as expressed in SD (see figure 1). A weak correlation between TBS and BMD variations has been observed ($r=0.51$). BMD and TBS Z-score decreased along the follow-up as expressed by Z-score Changes presented figure 1. Similarly, height and weight Z-score still decreased during the follow-up. This Z-score decreases seems to be more marked on TBS (ΔZ -score=-0.78SD), Height (ΔZ -score=-1.04SD) and Weight (ΔZ -score=-1.39SD) than on Spine BMD (ΔZ -score=-0.34SD) after 24 months of follow-up. At baseline and 12 months, TBS was associated positively with total fat mass ($r^2=0.46$, $p=0.01$ and $r^2=0.64$, $p<0.001$) while lean mass, BMD at spine, age, BMI, height were excluded from the model. No association was calculated at 24 months due to a small number of patients.

As expected, both BMD and TBS increase during growth with a weak correlation between BMD and TBS changes ($r^2=26\%$). Although these physiological increases, these values remained below normal values for age. Interestingly, TBS seemed to be associated with the total fat mass while BMD was not. These results suggest that a bone texture impairment exists in DMD and that this impairment varies with growth.

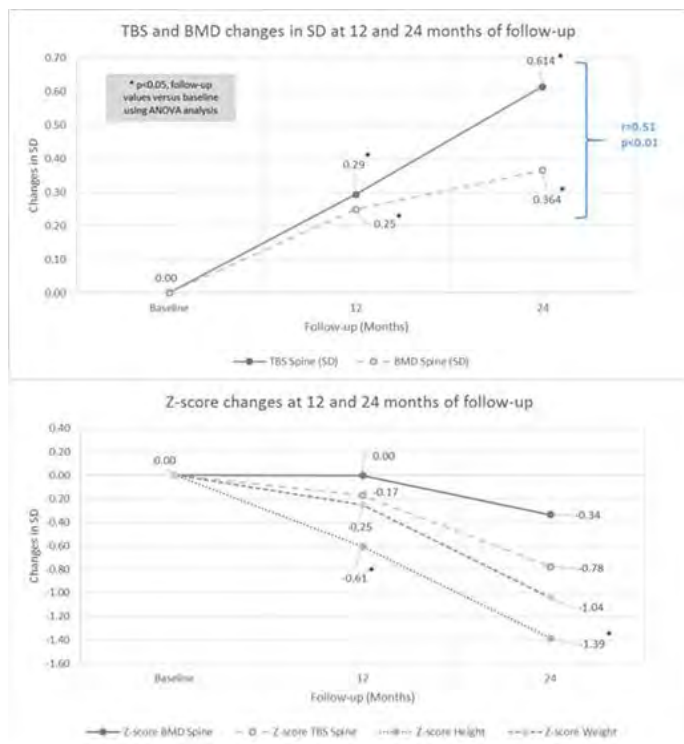


Figure 1

Disclosures: Renaud Winzenrieth, None.

SU0054

Early Bone Deficits Measured by pQCT in the Mucopolysaccharidoses Despite Current Therapies. Lynda E. Polgreen^{*1}, Anna Petryk², Aaron S. Kelly², Lesley Scibora³, Bradley S. Miller², Chester B. Whitley², Ellen B. Fung⁴. ¹Los Angeles Biomedical Research Institute at Harbor-UCLA, USA, ²University of Minnesota, USA, ³St. Thomas University, USA, ⁴UCSF Benioff Children's Hospital Oakland, USA

With the development of enzyme replacement therapy (ERT) and hematopoietic cell transplantation (HCT), children with mucopolysaccharidoses (MPS) types I, II and VI are now living into adulthood and long-term disease complications need to be considered. We have previously identified deficits in areal bone mineral density (aBMD) and content measured by dual-energy x-ray absorptiometry (DXA) in children and adolescents with MPS. However, severe short stature is characteristic of these MPS diseases, which complicates interpretation of DXA measures. In addition, abnormal bone geometry has been suggested by radiographic analysis, but has never before been evaluated by peripheral quantitative computed tomography (pQCT). Therefore, we have obtained pQCT measurements to test our hypothesis that children and adolescents with MPS have bone deficits compared to healthy controls. A cross-sectional analysis was performed on 38 MPS (age 5-20 years, 29% female) and 36 healthy control (age 8-16 years, 33% female) subjects. Mean age and body mass index percentile (BMI%) were not significantly different between groups. Tibia pQCT outcomes [3% (metaphyseal) and 38% (diaphyseal) sites] were compared between groups using linear regression with adjustment for tibia length; secondary analysis evaluated the impact of age and BMI% on the group differences. At the 3% site MPS subjects had 24% lower trabecular volumetric (vBMD) ($p<0.001$). At the 38% site MPS subjects had 10-27% lower total vBMD, bone area, polar section modulus, strength strain index, periosteal circumference and cortical thickness (all $p<0.01$). There was no difference in cortical vBMD at the 38% site. These differences were unchanged with the addition of age and BMI% to our model. These results confirm our previous findings of low aBMD by DXA. In addition, with this study we were able to further show that decreased density and abnormalities in bone apposition combine leading to decreased strength measures independent of stature and despite current therapies. These abnormalities suggest that as young patients with MPS are living into adulthood they will be at risk for early osteoporosis and increased risk of fracture. Determination of underlying etiology of bone deficits is needed to direct future therapies.

Disclosures: Lynda E. Polgreen, None.

SU0055

A Genetic Variant in the Gamma Glutamyl Carboxylase Gene Affects Bone Quality in a Pediatric African American Cohort. Jacqueline McKesey^{*1}, Courtney Sproue², Heather Gordish-Dressman², Elizabeth Dominic³, Elizabeth Hedges³, Zachary Kendrick⁴, Michael Liu⁴, Leticia Ryan⁵, Joseph Devaney⁶, Laura Tosi⁷. ¹Georgetown University School of Medicine, USA, ²Center for Genetic Medicine Children's National Medical Center, USA, ³The School of Medicine & Health Sciences George Washington University, USA, ⁴School of Medicine & Health Sciences George Washington University, USA, ⁵John's Hopkins Children's Center, USA, ⁶Department of Laboratory Medicine Children's National Medical Center, USA, ⁷Department of Orthopaedics & Sports Medicine Children's National Medical Center, USA

Objective: To explore whether a single nucleotide polymorphism (SNP), rs699644, located in the GGX gene and recently demonstrated to be associated with bone quality, is associated with bone mineral density (BMD) and bone mineral content (BMC) in a population of African American children.

Methods: The Bone Health cohort included 142 African-American children (ages 5 to 9) previously recruited for a study on forearm fractures. Measures of bone quality were collected using Dual Energy X-ray Absorptiometry. Phenotypes included total body minus head (tBMD) and lumbar (lBMD) height and age adjusted BMD z-scores, total body minus head BMC (tBMC) and lumbar BMC (lBMC). Z-scores were obtained using the Bone Mineral Density in Childhood Study Z-score calculator. The SNP was genotyped using a TaqMan allelic discrimination assay. Statistical Analysis was performed using ANOVA on z-scores and ANCOVA on all other phenotypes with covariates of age and gender. Analyses used the dominant genetic model. The SNP was in Hardy-Weinberg equilibrium.

Results: A significant association was discovered between tBMD z-score and genotype (GA/GG[n=59]: -0.507 ± 0.120 ; AA[n=38]: -0.111 ± 0.151 ; $p=0.04$). The association approached statistical significance with tBMC (GA/GG [n=75]: $942 \pm 19g$; AA [n=43]: $999 \pm 25g$; $p=0.07$) and lumbar BMD z-score (GA/GG [n=76]: 0.013 ± 0.122 ; AA [n=44]: 0.362 ± 0.160 ; $p=0.08$). See Table 1.

Discussion: Analysis of the cohort revealed an association between variants in the GGX gene and BMD. This suggests that the SNP,rs699644, influences bone quality in children. Our results show individuals with at least one copy of the G allele display lower BMD values. Further studies with increased statistical power and ethnically diverse participants should be conducted to further determine an association between osteocalcin activity and bone quality across the lifespan.

Conclusion: This study demonstrated that a SNP in the GGX gene is associated with BMD in a pediatric African American cohort. Osteocalcin activity, whose

mineralizing properties are affected by the GGCX protein carboxylase activity, has been demonstrated to play a role in the maturation and turnover of bone as well as BMD and fracture risk in the elderly. This study demonstrated that this may also be true for the young. Literature has suggested that bone health and the achievement of peak mass is correlated with bone health in adulthood. Therefore, demonstrating the modulators of childhood BMD is essential.

| Phenotype | Genotype | | p value |
|-----------------------------------|-----------------------|-----------------------|---------|
| | GG/GA (325R) | AA (325Q) | |
| Total body (less head)BMD z-score | (N=59) -0.507 ± 0.120 | (N=38) -0.111 ± 0.151 | 0.04 |
| Lumbar BMD z-score | (N=76) 0.013 ± 0.122 | (N=44) 0.362 ± 0.160 | 0.08 |
| Total body mean BMC (g) | (N=75) 942 ± 19 | (N=43) 999 ± 25 | 0.07 |

Table 1

Disclosures: *Jacqueline McKesey, None.*

SU0056

Bone health status and associated factors in the adolescents in Taiwan. Yi-Chin Lin^{*1}, Wen-Harn Pan². ¹Chung Shan Medical University, Taiwan, ²Institute of Biomedical Sciences, Academia Sinica, Taiwan

Adolescence is critical for the development of peak bone mass, which may in turn affect the risk for osteoporosis in later life. This preliminary analysis is based on the data collected from high school subjects recruited during the Nutrition and Health Survey in Taiwan (NAHSIT) 2010-2011. A total of 1098 male and 1124 female adolescents, aged 12-19 years, have completed bone scan by DXA. The results showed that for both genders, age and body weight significantly predicted bone mineral content (BMC, in gram) at total body, lumbar spine 2-4, and femoral neck in a non-linear manner. The results of multiple regression showed that age, height and body weight explained 82.06% and 74.93% of the variation in total body BMC in adolescent boys and girls, respectively. Grip strength was significantly correlated to BMC and BMD at all sites in both genders. For girls, post-menarcheal age predicted BMC at all sites slightly better than the chronological age. In the adolescent boys, there was a significant correlation (partialled for age) between dietary intake of calcium by calories (calcium density, in mg/kcal) and bone mineral density (BMD, in g/cm³), but not BMC, at lumbar spine 2-4 ($r=0.071$). Dietary intake of protein, as the absolute amount or as percent of daily total calories, was not significant predictors for BMC or BMD at all sites. The amount of protein per kilogram of body weight (0.09 – 5.82, mean=1.62±0.82 for boys and 0.18 – 5.91, mean=1.68±0.85 for girls), however, significantly related to BMC at all site in a negative manner, although the statistical significance slightly decreased in the multivariate models. On the other hand, there was significant correlation between the stories of stairs climbed per day, the number of days per week engaged in intensive exercise and BMC at all sites, respectively, in the adolescent boys, and the significance remained in the multivariate models. The results of our current analyses showed that dietary intake and the level of physical activity may play some roles in bone health in Taiwanese adolescents.

Disclosures: *Yi-Chin Lin, None.*

SU0057

Vitamin D levels in Swedish Children Over the Past 30 years. Diana Swolin-Eide^{*1}, Bjorn Andersson², Per Magnusson³, kerstin Albertsson-Wikland⁴. ¹Queen Silvia Children's Hospital, Sweden, ²Department of Pediatrics, The Sahlgrenska Academy at the University of Gothenburg, Sweden, ³Division of Clinical Chemistry, Linköping University, Sweden, ⁴Department of Physiology/Division of Endocrinology, The Sahlgrenska Academy at the University of Gothenburg, Sweden

Background: The importance of vitamin D for skeletal health is well established and its potential role for extraskeletal health has generated much hype in recent years, since many reports indicate that vitamin D deficiency is linked to chronic diseases. Vitamin D status is defined by serum 25-hydroxyvitamin D (25(OH)D), and although there is no consensus on optimal levels of 25(OH)D, the Institute of Medicine stated that 25(OH)D concentrations of 50 nmol/L (20 ng/mL) meet the requirements in 97.5% of the population. During infancy vitamin D supplementation is recommended in Sweden. We hypothesized that increased indoor activities and obesity would contribute to decreased vitamin D levels in children and adolescents during the three last decades. Methods: We analysed serum collected during the years 1982 to 2013 from 2048 Swedish children (mean age ± SD, 8.59 ± 3.68 years; 1197 boys). 25(OH)D was determined with the IDS-iSYS 25-Hydroxy Vitamin DS automated chemiluminescence immunoassay. Studies of decades-old sera have revealed that 25(OH)D is a stable analyte and can thus be used to explore long-term trends of vitamin D-related issues. Results: Seven hundred and four (34.4%) subjects had serum 25(OH)D levels below the recommended level of 50 nmol/L over the entire study period of 32 years. Interestingly, only 3.1% of the children had 25(OH)D levels below 25 nmol/L defined as vitamin D deficiency. We found a significant association with age, i.e., younger

children had higher levels of 25(OH)D, possibly due to the general supplementation of vitamin D recommended for Swedish children. Conclusion: We found no trend for decreased vitamin D levels over time in this study population. These results provide a unique long-term follow-up over 30 years of vitamin D levels in a large group of children. This will be of high value for future cost-benefit analyses in preventive health care.

Disclosures: *Diana Swolin-Eide, None.*

SU0058

A Subtrochanteric Femoral Stress Fracture Following Bisphosphonate Treatment in an Adolescent Girl. Alison Boyce^{*1}, Michael Collins², Laura Tosi³, Rachel Gafni⁴. ¹National Institutes of Health, USA, ²CDSB, NIDCR, NIH, USA, ³Children's National Health System, USA, ⁴CDSB, NIDCR, NIH, USA

Bisphosphonates are increasingly used to treat low bone mineral density (BMD) in children and adolescents. Long-term bisphosphonate use in adults has been associated with atypical subtrochanteric and diaphyseal femoral fractures (AFFs). Bisphosphonate-related AFFs have not been reported in children or adolescents. Case: A 16-year-old girl presented with left thigh pain. Her history was significant for idiopathic juvenile osteoporosis diagnosed at age 11 after presenting with back pain and thoracic compression fractures. A DXA scan at that time showed a lumbar spine Z-score -3.9 and total body less head -2.0. An extensive workup including vertebral biopsy and COL1A1/1A2 testing did not reveal an etiology for her low BMD. She was treated with pamidronate for a 2-year period, receiving a cumulative dose of 12 mg/kg. During treatment she had partial reconstitution of her vertebral bodies and no additional fractures. At pamidronate discontinuation (age 14), her lumbar spine Z-score improved to -1.6 and total body less head to -0.6. Just prior to the onset of thigh pain she had joined a cross-country team after several years of limited sports activity. Plain films showed diffuse cortical thickening of the bilateral femoral diaphysis, and a localized periosteal reaction at the medial cortex of the proximal left femur. A bone scan showed focal tracer uptake in this location, consistent with a stress fracture. Management: The patient was treated with relative rest and physical therapy. After a protracted 16-week course her pain improved and she was able to resume regular activities. Plain films 8-months after initial presentation with thigh pain showed resolution of the periosteal reaction. Discussion: This adolescent's presentation with a femoral stress fracture following high-dose pamidronate treatment shares several features in common with AFFs, including subtrochanteric location, localized periosteal reaction, and generalized cortical thickening of the femoral diaphysis. However unlike bisphosphonate-associated AFFs in adults, which typically develop on the lateral tensile cortical surface, this patient's stress fracture occurred at the medial cortex. Thus while suggestive, the contribution of bisphosphonates to this patient's stress fracture is not known. Nevertheless practitioners should evaluate thigh pain in children and adolescents with a history of bisphosphonate treatment, and include AFFs and other femoral stress fractures in the differential.



Arrows indicate proximal femoral stress fracture.
Stars indicate thickened femoral cortices.

Figure 1

Disclosures: *Alison Boyce, None.*

This study received funding from: NIDCR, NIH

SU0059

Withdrawn.

SU0060

Differential Behavioral and Skeletal Responses to Methylphenidate in Male and Female. Sardar Uddin¹, Lisa Robison², Melissa Vitale², Junho Lee², Michalis Michaelos², Jason Gandhi³, Soyeh Paeng³, Panayotis Thanos³, Michael Hadjiargyrou⁴, David Komatsu¹. ¹Department of Orthopaedics, Stony Brook University, USA, ²Department of Psychology, Stony Brook University, Stony Brook, NY, USA, ³Department of Psychology, Stony Brook University, USA, ⁴Department of Life Sciences, New York Institute of Technology, USA

Methylphenidate (MP) is widely used to treat Attention Deficit Hyperactivity Disorder (ADHD), the most commonly diagnosed adolescent psychological disorder with a US incidence of ~9.5%. We previously showed that MP treatment in adolescent female rats resulted in mild effects during skeletal development. The current study was conducted to examine the differential response of male and female rats to MP. Four-week old Sprague-Dawley rats were randomized to 5 groups (n=12/T_x): Water, Low-Dose MP (LD, 10mg/Kg MP), High-Dose MP (HD, 60mg/Kg MP), Water Pair-Fed to LD MP (Water LD PF), and Water Pair-Fed to HD MP (Water HD PF). Water groups received no MP. LD and HD received MP via their drinking water. Pair-fed groups had food restricted to their corresponding treatment groups' ad-lib consumption. After 13 weeks of treatment, both male and female rats showed significant decrease in body weight. HD MP treated rats were more active than water and LD MP treated rats during the dark cycle, and this was significant for both males and females (p<0.05). Within HD MP treated rats, females were more active than males during the dark cycle (p<0.001). There were no differences between any groups during the light cycle. Femora were assessed by microCT at cortical (mid-diaphysis) and trabecular (distal metaphysis) regions. No significant differences were observed during female skeletal development. Male rates showed significant decreases in trabecular thickness between LD MP vs HD MP (6%, p=0.007), Water HD-PF vs. HD MP (7%, p=0.027) and bone mineral density between LD MP vs HD MP (1%, p=0.022). Endosteal volume and surface significantly decreased in LD MP (13%) treated rats relative to water controls. Three-point bending revealed no differences in female rats but showed significant decrease energy to failure (23%), energy to ultimate force (17.5%), and ultimate force (11%) in HD MP compare to Water fed rats (Fig. 1). Overall female rats displayed hyperactivity but no effects on skeletal development while males had little behavioral difference with significant decrease in bone quality and quantity. Pair-feeding removed body weight as a confounding variable at the low dose, but not at the high dose. This is likely due to the tremendous increases in physical activity seen in the high dose rats. We speculate that increase activity in female rats protects bone from the detrimental effects of MP on skeletal development, which were apparent in less active male rats.

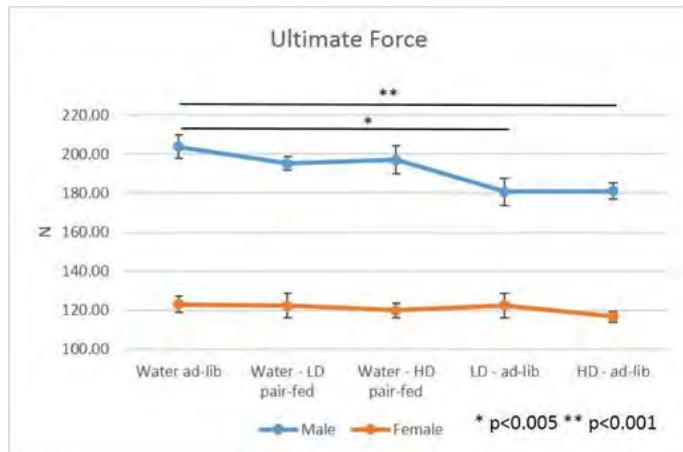


Figure 1: Three point bending Ultimate Force. No difference were observed in female rats. Male rat

Disclosures: Sardar Uddin, None.

SU0061

Physiologic PTH Signaling in Osteocytes Restrains Long-Term Hematopoietic Stem Cells in the Niche. Benjamin Frisch¹, Alexandra Goodman¹, Olga Bromberg¹, Xiaolin Tu², Teresita Bellido³, Laura Calvi¹. ¹University of Rochester School of Medicine & Dentistry, USA, ²University of Indiana Department of Anatomy & Cell Biology, USA, ³Indiana University Department of Anatomy & Cell Biology, USA

The bone marrow microenvironment, including osteolineage cells, regulates hematopoietic stem cell (HSC) fate choices. Pharmacologic treatment of mice with parathyroid hormone, PTH (1-34), increases HSCs through their niche, as HSCs do not express the PTH receptor (PTH1R). However, it is not known if PTH plays a physiologic role in HSC regulation. Osteocytes, the most abundant osteolineage cells in bone, coordinate multiple cell types that are components of the HSC niche including osteoblasts, osteoclasts and resident macrophages. While osteocytes express the PTH1R, the role of osteocytes in HSC regulation is unclear. Therefore, we studied

the physiologic role of osteocyte-mediated PTH regulation of HSCs, using cre recombinase driven by the 8kb-DMP1 promoter to conditionally delete PTH1R in osteocytes (OCyPTH1Rko mice). Targeted deletion of PTH1R was demonstrated. OCyPTH1Rko mice were viable, fertile, and did not exhibit any significant skeletal defect as juveniles or at 6 months of age, and had no significant difference in PTH levels compared to WT mice. In juvenile OCyPTH1Rko mice there was a subtle, but significant decrease in long-term HSCs as measured by flow cytometric analysis (0.0029 ± 0.00028 vs. 0.0021 ± 0.00021 % of cells, WT vs. OCyPTH1Rko p ≤ 0.05 N ≥ 19 mice/group). OCyPTH1Rko mice had a dramatic functional loss of long-term engraftment capacity as measured by secondary competitive transplantation over 22 weeks (WT vs. OCyPTH1Rko donors, 2-way ANOVA p ≤ 0.001 , N ≥ 10 mice/group) that was evident in all hematopoietic lineages. Short-term engraftment however was increased in OCyPTH1Rko mice as measured by primary competitive transplantation (WT vs. OCyPTH1Rko donors, 2-way ANOVA p ≤ 0.01 , N ≥ 9 mice/group). These data demonstrate that physiologic PTH signaling in osteocytes regulates the balance of long-term and short-term HSC potential in juvenile, growing mice. Adult OCyPTH1Rko mice also had a dramatic decrease in long-term engraftment (WT vs. OCyPTH1Rko donors, 2-way ANOVA p ≤ 0.001 , N ≥ 15 mice/group). Our findings demonstrate a previously unrecognized physiologic role of PTH signaling in HSC regulation. Moreover, these data identify osteocytes as a critical constituent of the HSC niche that, either directly or indirectly, contribute to maintenance of the long-term repopulating HSC pool.

Disclosures: Benjamin Frisch, None.

SU0062

Erythropoietin and bone remodeling. Sukanya Suresh¹, Luis Fernandez De Castro Diaz², Soumyadeep Dey¹, Pamela Robey², Constance Noguchi¹. ¹Molecular Medicine Branch, Molecular Cell Biology Section, NIDDK, NIH, USA, ²Skeletal Biology Section, Craniofacial & Skeletal Diseases Branch, NIDCR, NIH, USA

Erythropoietin (EPO) is best known for its role as a hematopoietic hormone essential for red blood cell (RBC) production. Recombinant forms of EPO are widely used in the clinic to treat patients suffering from anemia resulting from low EPO such as chronic kidney failure, chemotherapy and antiviral treatment for Human Immunodeficiency Virus (HIV). Bone marrow is the primary site of EPO activity and EPO effects on bone remodeling have been reported to be associated with both improved bone healing as well as with bone resorption. Here we find that EPO treatment of wild type mice (1200 IU/kg daily dose of EPO for ten days) increased hematocrit (70%) and bone marrow cellularity, and resulted in decreased trabecular bone mineral density, decreased trabecular number, and increased trabecular spacing. This observed difference with EPO treatment could result from the direct or indirect EPO response of the cells that are involved in bone remodeling namely osteoblasts (bone forming) and osteoclasts (bone resorbing). Cultures of bone marrow cells for osteoclast differentiation and of osteogenic calvarial cells both express EPO receptor. However, EPO treatment did not show a change in osteoclast or osteoblast differentiation, respectively, or increased mineralization. This raises the possibility that indirect mechanisms such as the proposed EPO stimulated production of BMPs by hematopoietic stem cells may contribute to EPO induced bone resorption or that the culture conditions for wild type osteoclastic or osteogenic cells do not sufficiently mimic the in vivo microenvironment that promotes bone resorption with EPO treatment. These data provide evidence for the direct or indirect effects of EPO on bone remodeling and decreased trabecular bone mineral density associated with EPO treatment in mice in addition to the known increase in erythropoiesis and bone marrow cellularity.

Disclosures: Sukanya Suresh, None.

SU0063

Bone marrow blood vessels are further away from trabecular bone with age and short-term intermittent PTH 1-34 administration augmented bone perfusion in young Fischer-344 rats. Rhonda Prisby^{*}, Sophie Guderian, James Cirone, Shaopeng Pei, Liyun Wang, Seungyong Lee. University of Delaware, USA

Spatial closeness of bone marrow blood vessels to sites of new bone formation with intermittent parathyroid (PTH) 1-84 administration may have aided in bone accrual (Prisby et al., 2011). Under this paradigm, age-related bone loss may be partially attributed to an increased separation between blood vessels and bone. We sought to assess age- and PTH-related changes in blood vessel location and bone perfusion. Male Fischer-344 rats were divided into the following groups: 1) young control (CON; 4-6 mon; n=16), young PTH (n=16), 3) old CON (22-24 mon; n=16) and old PTH (n=16). Rats were given either PTH 1-34 (43 mg/kg/d) or a placebo (PBS; 100 μ l/d) s.c. for 5 d/wk for 2 weeks. At sacrifice, half the rats were perfused with barium sulfate and right femora analyzed by bone histomorphometry. Distances of vessels 1-29 μ m, 30-100 μ m and 101-200 μ m in diameter were analyzed in relation to quiescent trabeculae and osteoid. In the other half of rats, fluorescent microspheres were injected into the left ventricle to determine perfusion in the proximal and distal femur, marrow and femoral diaphysis. Perfusion was expressed as tissue fluorescent density (TDF [AU/g] = tissue fluorescence \div tissue mass). Left femora were scanned via μ CT. As anticipated, BV/TV was lower (p<0.05) in old ($18.48 \pm 0.01\%$) vs. young

(26.23±0.02%) CON rats via reduced Tb.N (2.7±0.5/mm² vs. 4.1±0.2/mm², respectively). BV/TV was unaltered by PTH treatment in young rats (28.89±0.02%) but tended (p=0.08) to augment BV/TV in old rats (22.41±0.01%) via thicker trabeculae. Bone static properties (i.e., OS/BS, Obs/BS and Ocs/BS) did not differ among groups. Marrow perfusion was reduced (p<0.05) in old (5769±1444AU/g) vs. young (14726±2387AU/g) CON rats. Further, perfusion in the distal (p=0.06) and proximal (p=0.08) femur tended to reduce with age. Perfusion was higher (p<0.05) in the proximal femur (6407±1020AU/g vs. 4683±406AU/g, respectively) and tended (p=0.08) to increase in the marrow (21361±4433AU/g vs. 14726±2387AU/g) in young PTH vs. CON rats. Vessels 1-29µm (110±22µm vs. 170±22µm, p=0.07) and 30-100µm (209±23µm vs. 284±23µm, p<0.05) were further away from trabeculae in old vs. young rats (main effect) and vessels 101-200µm were closer (p<0.05) to osteoid in PTH-treated (320±31µm) vs. CON (418±31µm) rats (main effect). Blood vessel distance from bone is greater and bone perfusion lower in old age and short-term (15 days), intermittent PTH 1-34 administration augmented bone perfusion in young rats.

Disclosures: Rhonda Prisby, None.

SU0064

Short-Term Intermittent PTH (1-34) Administration Augments Skeletal Blood Flow and Perfusion in Mice as Assessed with Fluorescent Microspheres. SEUNGYONG LEE*, Rhonda Prisby. University of Delaware, USA

Bone loss and fracture risk is prevalent in old age. Further, reduced bone vascular function and blood flow occur in senescence (Prisby et al., 2007). Intermittent parathyroid hormone (PTH) administration augmented bone volume and enhanced vasodilation of bone arteries in young (Prisby et al., 2013) and old (Lee et al., 2014) rats. Additionally, intermittent PTH 1-84 administration increased tibial perfusion (Roche, et al., 2014) in mice. We sought to kinetically determine the rapidity by which PTH influences bone perfusion following 5 and 10 days of intermittent PTH 1-34 administration. Secondly, we compared perfusion expressed as absolute blood flow rate vs. tissue fluorescent density (TFD). Male and female C57BL/6 mice (6-8 mon) were divided equally into three groups (CON, 5dPTH, 10dPTH) and given either PTH 1-34 (43 µg/kg/d) or PBS (50 µl) for 5 and 10 consecutive days. Under anesthesia, fluorescent microspheres (Life Technologies) were injected directly to the left ventricle. Subsequently, a left ventricular reference blood sample was collected. Following sacrifice, the vertebral column, left and right tibiae and right femora were collected, decalcified and dissolved. Blood flow rate was calculated in ml/min/100 grams of tissue by use of the reference blood sample and TFD (AU/g) was determined as tissue fluorescence ÷ tissue weight. Data were excluded if kidney flow rates differed by >20% or if there were <400 beads per tissue. Femora were sectioned into the distal and proximal ends, marrow and cortical shell. Body mass and tissue weights did not differ among conditions. Blood flow to all bones, except the left tibia, was higher (p<0.05) in the 10dPTH vs. 5dPTH and CON groups. There were tendencies for higher blood flows to the marrow (p=0.09; 10dPTH, 5.3±1.9 ml/min/100g vs. 5dPTH, 0.6±0.2 ml/min/100g and CON, 2.9±1.0 ml/min/100g, respectively) and left tibia (p=0.068; 10dPTH, 1.0±0.2 ml/min/100g vs. 5dPTH, 0.3±0.2 ml/min/100g and CON, 0.5±0.2 ml/min/100g, respectively). In contrast, left tibial TFD was higher (p<0.05) in the 5dPTH vs. 10dPTH group. Further, cortical shell TFD tended (p=0.1) to be higher in the 5dPTH vs. 10dPTH and CON groups. Short-term intermittent PTH 1-34 administration improves bone blood flow in as short as 10 days and may alleviate the age-related declines observed in skeletal perfusion. Moreover, these data suggest that blood flow rate may be a more sensitive determination of skeletal perfusion in comparison to TFD.

Disclosures: SEUNGYONG LEE, None.

SU0065

Inflammatory Cytokines Cause a Shift in the Haematopoietic Microenvironment Modulating the Development of Osteoclasts. Nina Ruef*, Silvia Dolder¹, Mark Siegrist¹, Deepak Balani², Daniel Aeberli³, Michael Seitz³, Willy Hofstetter¹. ¹Bone Biology, Department Clinical Research, University of Bern, Switzerland, ²Endocrine Unit, Massachusetts General Hospital & Harvard Medical School, USA, ³Department of Rheumatology, Clinical Immunology & Allergology, Bern University Hospital, Switzerland

Levels of circulating inflammatory cytokines (Tumor Necrosis Factor-α (TNFα), Interleukins (IL)-1 and -17) are increased in inflammatory diseases. TNFα and IL-17A induce the release of Granulocyte-Macrophage Colony-Stimulating Factor (GM-CSF) by murine osteoblasts (OB), leading to a change in the haematopoietic microenvironment of osteoclasts (OC) and osteoclast progenitor cells (OPC). Herein, the effects of IL-17A on OC development *in vitro* were further investigated.

OC development was investigated in co-cultures of primary calvarial OB from *DDY* or *C57BL/6J* mice and of OPC in the presence of 1,25(OH)₂D₃, w/o TNFα, and in cultures of OPC suppl. with Macrophage Colony-Stimulating Factor (M-CSF) and Receptor Activator of NF-κB Ligand (RANKL). IL-17A was added to the cultures and OC formation, as well as the release and function of cytokines and their transcript levels, were assessed.

In co-cultures with *DDY* OB, IL-17A dose dependently inhibited OC development, leading to a reduction of the number of OC by 90% at 50 ng/ml. In co-cultures with

C57BL/6J OB, IL-17A dose-dependently increased OC number. In cultures of OPC with M-CSF/ RANKL, IL-17A did not affect osteoclastogenesis. Addition of neutralizing antibodies against GM-CSF attenuated the inhibitory effect of IL-17A in co-cultures. Neutralizing antibodies against TNFα fully restored osteoclastogenesis mediated by IL-17A in co-cultures with *C57BL/6J* OB. *C57BL/6J* and *DDY* OB released GM-CSF in response to treatment with IL-17A/ 1,25(OH)₂D₃/ TNFα. *DDY* OB, however, released higher levels of GM-CSF independently of TNFα. In co-cultures, transcripts encoding RANKL, OPG, IL-6, GM-CSF and NHA2 were regulated by IL-17A, 1,25(OH)₂D₃ and TNFα. Levels of transcripts for RANKL were upregulated and those for OPG were downregulated by 1,25(OH)₂D₃/ IL-17A. Levels of transcripts encoding GM-CSF and IL-6 were upregulated by IL-17A and further increased in the presence of 1,25(OH)₂D₃ and TNFα.

In summary, OB release GM-CSF in response to an exposure to IL-17A and TNFα, generating an inflammatory microenvironment inhibiting osteoclastogenesis. The effects of IL-17A, TNFα, and 1,25(OH)₂D₃ were found to depend on the genetic background of the mice. This mechanism leads to changes in OPC pools in bone, bone marrow and blood in systemic inflammatory diseases. Upon homing to bone, with its specific inflammation driven microenvironment, the increase in OPC numbers stimulates osteoclastogenesis, causing accelerated bone resorption.

Disclosures: Nina Ruef, None.

SU0066

Hedgehog signaling in jawbone invasion of oral squamous cell carcinoma. Tsuyoshi Shimo*, Kenichi Matsumoto², Eriko Aoyama³, Tatsuo Okui², Naito Kurio², Akira Sasaki². ¹Okayama University Graduate School of Medicine, Dentistry & Pharmaceutical Sci, Japan, ²Department of Oral & Maxillofacial Surgery, Okayama University Graduate School of Medicine, Dentistry, & Pharmaceutical Sciences, Japan, ³Advanced Research Center for Oral & Craniofacial Sciences, Okayama University Graduate School of Medicine, Dentistry, & Pharmaceutical Sciences, Japan

INTRODUCTION: Oral squamous cell carcinoma invasion into the maxilla and the mandible is a frequent events which action is associated with a worse prognosis. Previously, we have reported that Sonic Hedgehog (SHH) stimulated the osteoclasts differentiation and activation by upregulating RANKL expression in bone stromal cells. In this study, we examined the expression of Hedgehog signaling in the oral squamous cell carcinoma at bone invasion sites, and defined the molecular changes that occur when osteoclasts are exposed to smoothened agonist. **METHODS:** From surgically resected lower gingival squamous cell carcinoma mandible samples, decalcified, immunohistochemical staining was performed. RAW264.7 cells were treated with 50 ng/ml RANKL for 3days, and then cultured with or without smoothened agonist 5 µM SAG for 24h. After the treatment of SAG, total RNAs were isolated, genome-wide gene expression analysis was performed using SuperPrint G3 Mouse GE 8x60K 2 color, and the data was analyzed by GeneSpring GX v.13. **RESULTS:** We found that SHH was highly expressed in tumor cell that had invaded bone matrix. On the other hand, Patched and Gli-2 was highly expressed in the preosteoclasts and mature osteoclasts. When comparing vehicle sample, SAG treated samples showed elevated mostly G protein-coupled receptor (GPCR) pathways. The expression of Tachykinin receptor 3 was highest upregulated in 9.8 times more than control in Non-odorant GPCRs pathways. **DISCUSSION:** Our results suggest that tumor derived SHH regulate osteoclast formation and bone resorption in the tumor bone microenvironment.

Disclosures: Tsuyoshi Shimo, None.

SU0067

MMP13-induced type I collagen degradation plays a key role in the prostate cancer dependent bone metabolism. Kenta Watanabe, Michiko Hirata, Chisato Miyaura, Masaki Inada*. Tokyo University of Agriculture & Technology, Japan

Matrix metalloproteinases (MMPs) are involved in the degradation of extra-cellular matrix (ECM) during the invasion and the metastasis of cancer cells. When prostate cancer cells invade to bone, the cells interact with type I collagen as the major ECM in bone tissue. However, the relationship between type I collagen degradation and prostate cancer dependent bone resorption is still unclear. In this study, we first examined the mRNA expression of MMP-2, MMP-8, MMP-9, MMP-13 and MMP-14 in mouse prostate cancer cell line TRAMP. TRAMP cells expressed MMP-13 and MMP-14 mRNAs. We analyzed the invasive activity of TRAMP using type I and type IV collagen chamber migration system with or without MMP-13 specific inhibitor and general MMPs inhibitor. Both MMP inhibitors suppressed TRAMP invasive activity, and the inhibition effects was higher in MMP-13 specific inhibitor than that of general MMPs inhibitor. For the tracking precise image of the TRAMP growth, the real time culture imaging system was used during 3 days. When TRAMP cells cultured on the type I collagen coated surface, the proliferation was observed by the degradation of type I collagen by collagenases, but the growth was dramatically suppressed by the treatment of MMP-13 specific inhibitor. Next we generated MMP-13 knockdown TRAMP (TRAMP13mi) by the transfection of MMP-13 miRNA expressing vector. When TRAMP13mi cells were cultured on type I collagen surface, the collagen-induced proliferation was attenuated to compare by the control TRAMP. Finally, we cultured TRAMP on cross-linked type I collagen surface that is resistant to the

degradation by collagenase. When TRAMP cells were cultured on cross-linked type I collagen, the growth was inhibited. When TRAMP cells were cultured on mouse calvaria, we detected bone resorbing activity compared with control calvaria, and the treatment of MMP13 specific inhibitor abrogated TRAMP induced bone resorption. These results suggest that prostate cancer degrades type I collagen by MMP13 for its proliferation and bone resorption. MMP13 specific inhibitor might be a candidate for the treatment of bone metastasis of prostate cancer accompanied proliferation and bone resorption.

Disclosures: Masaki Inada, None.

SU0068

Novel 3D model mimics the physical properties of bone to allow for detailed studies of interactions between tumor and bone. Ushashi Dadwal¹, Ruijing Guo², Alyssa Merkel³, Shanik Fernando⁴, Denise Buenostro¹, Scott Guelcher⁵, Julie Sterling^{*6}. ¹Vanderbilt Center for Bone Biology, USA, ²Vanderbilt University, Department of Chemical & Biomolecular Engineering, USA, ³Department of Veterans Affairs (TVHS)/ Vanderbilt Center for Bone Biology, USA, ⁴Vanderbilt Department of Chemical & Biomolecular Engineering, USA, ⁵Vanderbilt University Department of Chemical & Biomolecular Engineering, USA, ⁶Department of Veterans Affairs (TVHS)/Vanderbilt University Medical Center, USA

Unique properties of the bone microenvironment influence the behavior of tumor cells. In order to study these dynamic and complex interactions, we developed novel 3D polyurethane (PUR) scaffolds that approximate the mechanical and topological characteristics of bone. Scaffolds were fabricated using 3D-printed molds with uniform pore size and pore spacing ($423 \pm 34 \mu\text{m}$ to $557 \pm 44 \mu\text{m}$) based on the average trabecular separation and thickness of a mouse tibia. Molds were filled with PUR from 10 MPa (compliant) to 2600 MPa (rigid) and coated with adhesion molecules to allow for cell attachment. Fibronectin had the highest percentage of cell attachment and gene expression compared to vitronectin, type I collagen, poly-L-lysine in tumor cells and osteoblasts. In 3D scaffolds seeded with osteoblasts, markers of differentiation (Runx2, Collagen-I and OPN) and mineralization (Alizarin Red S staining) increased significantly with increasing rigidity and decreasing pore size, suggesting that the physical bone microenvironment can alter the host cells. In scaffolds seeded with tumor cells, Gli2 and parathyroid hormone related protein (PTHrP) expression (QPCR) increased with increasing rigidity, decreasing pore size, and increasing flow rate using a perfusion based bioreactor, suggesting that gene expression and tumor cell behavior depend on tissue rigidity. Tumor seeded scaffolds implanted onto the mammary fat pad of mice demonstrated increased Gli2 (18-fold), Integrin $\beta 3$ (20-fold), and PTHrP (26-fold) expression on rigid (bone) versus compliant (tumorigenic breast) scaffolds, and contained abundant infiltrating host cells after 28 days. Flow cytometry and immunohistochemistry analyses indicated an increase in C11b+ cells (2.5-fold) and F4/80+ cells (10-fold) in the rigid scaffolds. These findings suggest that the mechanical and topological properties of the matrix regulate the response of osteoblast, inflammatory, and tumor cells, which may contribute to the uniqueness of tumors growing in the bone microenvironment. Ongoing studies are focused on investigating cellular interactions between the host and tumor cells by seeding combinations of cell types into the 3D scaffolds. Taken together, these data demonstrate the potential of this 3D model system as a unique approach for studying the dynamic and complex interactions between tumor cells and the bone microenvironment.

Disclosures: Julie Sterling, None.

SU0069

Anti Urokinase Receptor (uPAR) Antibody (ATN-658) Blocks Breast Cancer Growth and Skeletal Metastasis *in vitro* and *in vivo*; Effects which are Potentiated in Combination with Zometa. Shafaat Rabbani^{*1}, Ani Arakelian², Surabhi Parashar³, Haseeb Khan⁴, Imrana Tanvir⁴, Andrew P. Mazar⁵. ¹McGill University, Ca, ²McGill University Health Centre, Canada, ³McGill University, Canada, ⁴Fatima Memorial Hospital System, Pakistan, ⁵Northwestern University, USA

The proteolytic effects of urokinase (uPA) are localized within the tumor cell environment by the uPA receptor (uPAR) promoting tumor growth and metastasis resulting in the identification of uPAR as an attractive diagnostic and therapeutic target. Towards these goals we developed an anti-uPAR antibody (ATN-658) and examined its ability alone and in combination with bisphosphonate Zometa on breast cancer growth and skeletal metastasis.

Human breast cancer cells, MDA-MB-231, which express high levels of uPA and uPAR were treated with different doses of ATN-658 and Zometa alone and in combination to monitor their effect on tumor progression. In *in vitro* studies treatment with ATN-658 resulted in a dose dependent decrease in tumor cell invasion and increased apoptosis without affecting cell doubling time. Zometa decreased cell proliferation and increased apoptosis. This effect was significantly more pronounced when cells were treated in combination setting. For *in vivo* studies, MDA-MB-231 cells were inoculated via mammary fat pad (5×10^5) into female Balb c nude mice and after staging to 50 mm³ treated with control IgG or ATN-658 (10.0 mg/kg) for 5

weeks. In other studies at day three following intratibial injection of 2×10^5 of tumor cells mice were treated with vehicle alone, ATN-658 Zometa (100 $\mu\text{g}/\text{kg}$) or ATN-658 plus Zometa in combination for 4 weeks. Tumor volume and skeletal lesions were determined by calipers and X-ray using Faxitron. Treatment with ATN-658 caused a significant decrease in primary tumor volume. Both ATN-658 and Zometa were equally effective in causing a marked decrease in skeletal lesions or blocking them in >57% of experimental animals in the combination group. Following combination therapy the area of skeletal lesions was significantly smaller as compared to animals treated with either ATN-658 or Zometa alone. Results of change in the markers of tumor cell proliferation (Ki67), angiogenesis (CD31), osteoclastic activity (TRAP), intracellular signalling pathways and tumor promoting growth factors and proteases of which are regulated by uPAR signalling will be discussed. ATN-658 has now been humanized (huATN-658) and is advancing toward a phase I trial. Results from these studies provide compelling evidence for the continued development of huATN-658 as a potential therapeutic agent for the treatment of breast cancer patients as monotherapy and combined with currently available agents for blocking skeletal metastasis.

Disclosures: Shafaat Rabbani, None.

SU0070

Effect of Type 1 Diabetes in Prostate Cancer Model. Sherry Abboud Werner^{*1}, Kathleen Woodruff², Diane Horn², Hanes Martha², Chung Song², Fermin Tio³, Julie Foley⁴, Robert Maronpot⁵, Bandana Chatterjee². ¹University of Texas Health Science Center at San Antonio, USA, ²University of Texas Health Science Center, USA, ³VIA Medical Center, USA, ⁴National Institute of Environmental Health Sciences, USA, ⁵Maronpot Consulting LLC, USA

Prostate cancer is a leading cause of cancer deaths worldwide. Adenocarcinomas of the prostate frequently metastasize and many patients suffer from bone metastasis. High grade tumors, extraprostatic extension and metastasis are associated with a poor prognosis. Diabetes mellitus (DM) has been linked to prostate cancer risk and high grade prostate cancer. However, the precise role of type 1 and type 2 DM in prostate cancer has not been well-defined. Studies to determine whether DM influences prostate cancer have been hampered by the lack of animal models. To examine the effect of type 1 DM in prostate cancer, we performed genetic crosses between transgenic adenocarcinoma of mouse prostate (TRAMP) mice and type 1 diabetic Akita mice. TRAMP mice show carcinoma of the prostate by 24 weeks and develop metastasis with age. At 32 weeks of age, we examined the phenotype of wild type (WT) (n=4), TRAMP (TR) (n=6), heterozygous Akita (AK) (n=3) and TRAMP/heterozygous AK mice (TR/AK) (n=7). Body weight and fasting blood glucose levels were measured. Prostate glands were excised and histologic sections of lateral, dorsal, ventral and anterior lobes were graded for epithelial-stromal/epithelial proliferation, and for the presence of carcinoma. AK and TR/AK mice showed decreased body weight and hyperglycemia compared to TR and WT controls. AK prostates showed normal glandular and stromal elements similar to WT, whereas prostates in TR and AK/TR mice showed increased epithelial proliferation in the lateral, dorsal and anterior lobes. Notably, the degree of epithelial proliferation in prostates from AK/TR mice was significantly reduced compared to that in TR prostates. Moreover, 5 of 6 TR prostates (83.3%) showed carcinoma with two tumors having anaplastic morphology, whereas only 2 of 7 AK/TR mice (28.6%) showed prostate carcinoma. These findings indicate that prolonged exposure to high glucose levels in type 1 DM may act to suppress epithelial proliferation and development of prostate cancer. Results in AK mice provide the first evidence that prostate morphology remains normal under hyperglycemic conditions. Importantly, the AK/TR mouse provides a useful preclinical model for elucidating mechanisms by which type 1 DM regulates local prostate cancer growth and metastasis. Further studies may lead to therapeutic strategies to prevent prostate cancer and improve urologic health.

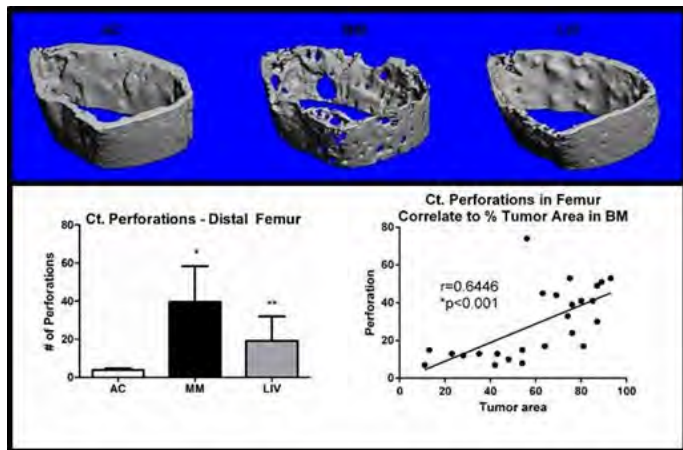
Disclosures: Sherry Abboud Werner, None.

SU0071

Low Intensity Mechanical Signals Slow Tumor Progression and Osteolysis in a Murine Model of Multiple Myeloma. Gabriel Pagnotti^{*1}, Benjamin J. Adler¹, M. Ete Chan¹, Kenneth R. Shroyer², Janet E. Rubin³, Clinton T. Rubin¹. ¹Stony Brook University, USA, ²Stony Brook Medicine, USA, ³University of North Carolina, Chapel Hill, USA

Multiple myeloma (MM), a primary bone cancer, is associated with the rapid and extensive destruction of bone and marrow. Interventions aimed at mitigating this damage fall short due to comorbid outcomes. Mechanical stimuli have been extensively shown to have influence both bone and marrow phenotype. Here we evaluated the ability of low-intensity vibrations (LIV) to protect the quantity and quality of bone morphology and the marrow phenotype in the presence of MM. 25 7w-old immunocompromised mice (NSG, Jackson Laboratory, Bar Harbour, ME) were tail vein-injected with a human MM cell line. 8 mice (AC) were injected with saline for vehicle control. Of the MM-engrafted mice, 13 were subject to mechanical loading (LIV) (15m/d; 0.3g @ 90Hz), while 12 were sham handled (MM). At 8w post-injection, micro-CT quantification of the distal femur showed a 86% (p<0.04) decrease in trabecular bone volume fraction in MM as compared to AC, while Tb.BV/

TV of LIV femurs was only 23% less than AC and 48% greater than MM ($p < 0.05$). Cortical BV/TV of the femoral metaphysis was 16% ($p < 0.03$) lower in MM as compared to AC, as compared to 8% (NSD) lower in LIV than AC. Perforations of the cortex at the distal femur resulting from MM osteolysis, were 52% ($p < 0.002$) fewer in LIV as compared to MM. Histological examination revealed plasmacytoma infiltration throughout both MM (72%) and LIV (50%) femurs; a tumor burden that was 30% lower in LIV from that of MM. The extent of the infiltration of plasmacytoma throughout the marrow correlated to marked reductions in bone quality and integrity ($r = 0.645$; $p < 0.001$). Tartrate-resistant acid phosphatase (TRACP5b), a serum biomarker of osteoclast-mediated resorption, was significantly elevated in MM (60%; $p < 0.001$) and LIV (34%; $p < 0.05$) as compared to AC. However, TRACP5b measured from LIV was 16% ($p < 0.06$) lower than from MM serum. Quantification of skeletal and histological endpoints demonstrate the destructive capability of MM cells as they propagate, significantly and negatively impacting bone quality, and markedly elevating bone resorption of the trabecular and cortical compartments. LIV also appears to slow progression of the disease itself, perhaps reflecting some salutary benefit of mechanical signals on cell activity and/or fate. These data provide some early evidence for the introduction of mechanical signals as a means of ameliorating cancer-induced damage to bone and protecting the marrow microenvironment.



LIV Slows Resorption of Cortical Bone

Disclosures: Gabriel Pagnotti, None.

SU0072

Characterizing Prostate Cancer Bone Metastasis Using Tissue Engineered Matrices. Sum Ying Chiu^{*1}, Damian Genetos². ¹Anatomy, Physiology & Cell Biology, School of Veterinary Medicine, UC Davis, USA, ²Anatomy, Physiology, & Cell Biology, School of Veterinary Medicine, UC Davis, USA

Purpose:

The American Cancer Society estimates ~28,000 men will die mostly from advanced prostate cancer (PCa) bone metastasis in 2015. The preferential localization of PCa to the skeleton indicates that metastasis is enhanced by PCa cellular response to chemical cues from the bone microenvironment (bone organic matrix). The molecular mechanism of this process is unclear. We propose using tissue engineering with cell and molecular biology assays to identify novel factors critical for PCa cell migration, osteomimicry and secondary tumor formation.

Methods:

To mimic the organic matrix, we created de-cellularized matrices (DM) from human BM-MSCs and treated DM with enzymes (eDM) to abolish growth factor binding sites. The matrices were characterized with staining and protein analysis. Cell response towards DM and eDM was measured in non-osteotropic LNCaP, osteoblastic C4-2B and osteolytic PC-3 PCa cell lines. Migration to DM or eDM was measured through Boyden chamber assays, and gene expression was analyzed *via* qPCR to examine osteomimicry in PCa cells seeded on DM or eDM. DM and eDM were profiled by LC-MS/MS to identify differential matrix components.

Results:

PCa cells showed heterogeneous migration to DM or eDM (Fig. 1). Non-osteotropic LNCaP cells did not specially migrate to DM, and revealed modest migratory capacity to eDM. Osteotropic C4-2B cells revealed significant migration to DM, and this was attenuated with eDM. PC-3 cells did not reveal migration to DM or eDM. Expression of osteogenic genes *RUNX2* and *BGLAP*, and indices of Wnt, BMP and TGF- β signaling, were neither temporally nor matrix-type dependent in all PCa cells.

Coomassie Blue staining and microBCA protein assay showed no qualitative or quantitative difference in homogeneity or total protein in DM vs. eDM; Alcian Blue staining showed reduced growth factor-binding glycosaminoglycans (GAGs) in eDM compared to DM. These data suggest DM and eDM only differ in growth factor presence and not overall matrix deposition (Fig. 2).

Proteomic analysis of DM and eDM identified differential expression of potential metastasis-promoting candidates in matrix proteins associated with TGF- β /BMP/Wnt signaling, including biglycan, decorin and periostin. These continuing studies and future *in vivo* work will expose details on how PCa invades into the bone. This knowledge can lead to metastasis-inhibiting therapies that when combined with treatments targeting primary tumors will finally eradicate PCa.

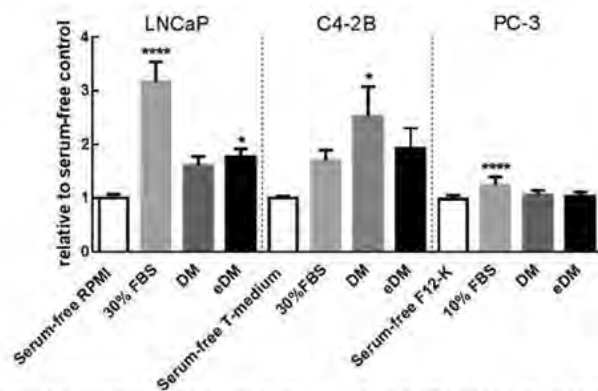


Figure 1. Comparison of DM vs. eDM as chemoattractants for PCa cell lines LNCaP, C4-2B, and PC-3. Migration of LNCaP, C4-2B and PC-3 cells towards DM and eDM were determined using Boyden chamber assay and quantified by detection of fluorescence after Calcein AM staining. All conditions were normalized to migration towards their respective serum-free media control. Bars shows mean (+SEM). White bars, serum-free media; light grey bars, FBS; dark grey bars, DM; black bars, eDM. * $P < 0.05$, **** $P < 0.0001$

Figure 1. Comparison of DM vs. eDM as chemoattractants for PCa cell lines LNCaP, C4-2B, and PC-3

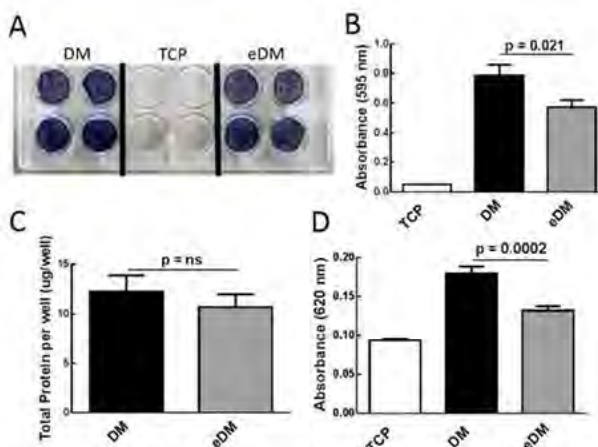


Figure 2. Characterization of decellularized matrices (DM) and enzyme modified DM (eDM). (A) Visual representation of Coomassie Blue staining for total protein in DM and eDM. (B) Quantification of Coomassie Blue staining in (A) via absorbance measurement at 595nm. (C) Total protein analysis measuring total protein per well for DM and eDM using the microBCA protein assay kit. (D) Quantification of Alcian Blue staining for GAGs in DM and eDM via absorbance measurement at 620nm. Bars show mean (+SEM). White bars, tissue culture plastic (TCP); black bars, DM; grey bars, eDM.

Figure 2. Characterization of decellularized matrices (DM) and enzyme modified DM (eDM)

Disclosures: Sum Ying Chiu, None.

This study funding from: University of California, Cancer Research Coordinating Committee award A23

SU0073

The tumor suppressor miRs-30-5p family in the control of metastatic bone disease. Martine Croset^{*1}, Casina Kan¹, Edith Bonnelly², Fransecco Pantano³, Françoise Descotes⁴, Catherine Alix-Panabières⁵, Charles Lecellier⁶, Saw See Hong⁷, Philippe Clézardin¹. ¹INSERM, UMR_S1033, UFR de médecine Lyon-Est, University of Lyon, France, ²INSERM, UMR_S1033, UFR de médecine Lyon-Est university of Lyon, France, ³Medical Oncology Dept.\Translational Oncology Laboratory, Italy, ⁴Service de Biochimie Biologie Moléculaire, Hospices Civils de Lyon, France, ⁵Department of Cellular & Tissular LCCRH Biopathology of Tumors, University Medical Centre, France, ⁶Université Montpellier 1, France, ⁷Université Lyon 1, UCBL-INRA-EPHE UMR-754, France

Bone metastasis is a common complication of advanced breast cancer. Breast tumor cells that escape the primary tumor to invade the bone marrow (BM) express a

set of deregulated genes and/or microRNAs (miRs) that facilitate BM engraftment which may lead to the formation of overt osteolytic lesions. Comparative expression of miRs in human breast cancer cell lines, MDA-MB-231 (non-osteotropic), MDA-B02 (an osteotropic subpopulation of MDA-MB-231) and micrometastases from BM aspirate (BC-M1) identified the miR-30 family (miR-30s) as being down-regulated in osteotropic cell lines MDA-B02 and BC-M1. The role of miR-30s in the formation of bone micrometastases and subsequent development of overt osteolytic lesions was therefore investigated.

MDA-B02 cells were transduced with a retroviral vector containing the genomic sequences for miR-30s (MDA-B02-miR-30s) and injected in the tail artery of immunodeficient mice. X-ray and histomorphometric analyses showed that mice bearing MDA-B02-miR-30 tumors developed osteolytic lesions that were significantly smaller than those of mice bearing MDA-B02. The inhibitory effect of miR-30s on tumor-induced bone destruction was confirmed by the significant increase of bone volume/tissue volume ratio in tibias from mice injected with MDA-B02-miR-30 (14.1% \pm 1.7 vs 26.6% \pm 2.7 p<0.01). This was associated with a decrease in tumor burden/tissue volume ratio (45.2% \pm 5.4 vs 21.7% \pm 6.1 p<0.01) and a decrease of TRAP-positive osteoclast surface at the bone/tumor cell interface (77.4% \pm 8.1 vs 41.7% \pm 16.5 p<0.05). Consistent with these *in-vivo* data, conditioned medium from MDA-B02-miR-30s (CM-miR-30s) decreased the formation of TRAP-positive multinucleated osteoclasts and IL-11 and IL-8 concentration in CM. The mineralization of bone nodules induced by MC3T3-E1 osteoblastic cells was inhibited in the presence of CM from MDA-B02 cells and this inhibitory effect was repressed by miR-30s through a decreased production of the Wnt inhibitor *Dkk1* in the CM. Osteotropic and osteomimetic gene expression (*ITGbb3*, *ITGa5*, *CDH11*, *RUNX2*, *CTGF*, *CX43*) was down-regulated in MDA-B02-miR-30s cells. The invasiveness of MDA-B02-miR30s cells was also decreased *in-vitro*. In the clinic, low miR-30s expression in primary tumors from patients with breast cancer was associated with poor relapse-free survival. We conclude that miR-30s control breast cancer cell invasion in the BM and the formation of overt skeletal lesions in tumor-bearing animals.

Disclosures: Martine Croset, None.

SU0074

Effects of ONO-5334, a Cathepsin K Inhibitor, on Bone Volume and Bone Turnover Markers in a Rabbit VX2 Carcinoma Induced Bone Osteolysis Model. YASUO OCHI*, YASUTOMO NAKANISHI, YASUAKI HASHIMOTO, SATOSHI NISHIKAWA, HIROYUKI YAMADA, HIROSHI MORI, SHINSEI FUJIMURA, MAKOTO TANAKA, KAZUHIITO KAWABATA, ONO Pharmaceutical Co., LTD., Japan

Osteolytic bone metastasis can cause a broad range of symptoms that could impair a quality of life in cancer patients. ONO-5334 is a small molecule and an orally-active inhibitor of cathepsin K. In this study, we evaluated the effect of ONO-5334 on bone volume and bone turnover markers in a rabbit bone osteolysis model induced by VX2 carcinoma. VX2 carcinoma cells or phosphate buffered saline (PBS) was intratibially transplanted in female New Zealand White rabbits. Seven days after the transplantation (day 7), VX2-transplanted rabbits were assigned to one of the following 5 groups (8-9 animals/group): vehicle-treated (Cont), ONO-5334 (1.2, 6 or 30 mg/kg) or zoledronic acid (ZOL, 0.06 mg/kg), based on a value of plasma tartrate-resistant acid phosphatase (TRAP) activity. ONO-5334 or vehicle was orally administered once daily from day 8 to 20, and ZOL was administered intravenously in a single dose on day 8. Osteolysis in the isolated proximal tibia was evaluated by peripheral quantitative computed tomography (total and cortical bone mineral content (BMC) at 5 and 10% of total tibia length from the proximal end) and χ CT (trabecular bone volume, number, thickness and separation, measurement area: 2.5 - 6% of total tibia length from the proximal end) on day 21, and urine helical peptide (HP) concentration and plasma TRAP activity were measured. Transplantation of VX2 carcinoma caused a significant decrease in total and cortical BMC and also caused a significant deterioration in trabecular architectures (all parameters, p<0.05 vs PBS). ONO-5334 significantly increased total and cortical BMC (1.2, 6 and 30 mg/kg), and significantly improved trabecular bone volume (1.2 and 30 mg/kg), number (30 mg/kg), thickness (1.2 and 6 mg/kg) and separation (30 mg/kg) compared to Cont (p<0.05). ZOL significantly improved all of the parameters except for the trabecular separation (p<0.05 vs Cont). In bone turnover markers, transplantation of VX2 carcinoma caused a significant increase in TRAP activity (p<0.01 vs PBS). ONO-5334 significantly decreased HP (all doses, p<0.01 vs Cont) but did not affect TRAP activity. ZOL significantly decreased both HP and TRAP activity (p<0.01 vs Cont). These results suggest that ONO-5334, unlike ZOL, inhibited a bone resorption without influence on osteoclast survival and improved both trabecular and cortical osteolysis induced by VX2 carcinoma. Thus, ONO-5334 may become a novel oral therapy for treatment of osteolytic bone metastasis.

Disclosures: YASUO OCHI, None.

SU0075

Elevated and persistent cAMP-Creb1 pathway activation is essential for the maintenance of osteosarcoma. Mannu Walia*¹, Patricia Ho², Alvin Ng², Ankita Gupte², Alistair M. Chalk², T. John Martin², Carl Walkley². ¹St Vincents Institute of medical research, Australia, ²St Vincents Institute of Medical Research, Australia

Osteosarcoma (OS) is the most common primary tumor of bone. Several studies highlight that alterations in the cyclic AMP (cAMP)/protein kinase A (PKA) pathway are important in OS, although this has not been functionally evaluated. There are three main subtypes of osteosarcoma (OS) (osteoblastic, fibroblastic and chondroblastic). We have generated the fibroblastic subtype in mice using deletion of p53 and pRb from the osteoblast-lineage, and the osteoblastic subtype by shRNA-mediated knockdown of p53 within the lineage. All the primary and metastatic tumors from either subtype express PTHR1, and PTHrP. Elevated generation of cAMP and persistent downstream signaling through Creb1 are characteristics of these OS, with the activation pathway greater in osteoblastic OS than in fibroblastic OS. Creb1 was phosphorylated more prominently in the osteoblastic than in either the fibroblastic OS or primary osteoblasts, and the mean expression of Creb1 mRNA was 2-3 fold higher in osteoblastic OS compared to fibroblastic OS and primary osteoblasts. Greater than 95% knockdown of Creb1 using shRNAs greatly increased apoptosis and reduced OS proliferation, as did similar knockdown of PTHrP (proliferation reduced by 40-60%), revealing that OS requires sustained PTHrP-cAMP-Creb1 activity for proliferation and survival. Loss of Creb1 in fibroblastic OS cells resulted in significantly reduced proliferation. Knockdown of Creb1 in osteoblastic OS caused a profound proliferation arrest and loss of viability, thus showing the dependence of osteoblastic OS on Creb1 is greater than that of fibroblastic OS, revealing a genetic difference between the OS subtypes. In order to test for autocrine regulation via PTHrP, cyclic AMP was assayed after OS cells were incubated without agonist, in the presence of IBMX. Cyclic AMP accumulation was ablated when either PTHrP or PTHR1 were knocked down by shRNA, and was inhibited by 80% when a neutralizing antibody against PTHrP was included in incubations. Furthermore knockdown of PTHrP resulted in 50% inhibition of growth of each of two explanted fibroblastic OS cell lines, as shown previously with PTHR1 knockdown in these cells. These findings identify an autocrine/paracrine circuit of PTHrP-PTHr1-cAMP-Creb1 as a critical proliferation and survival pathway in OS, with PTHrP as the autocrine/paracrine driver. These results demonstrate that constitutively active and enhanced cAMP signaling is oncogenic in OS

Disclosures: Mannu Walia, None.

SU0076

Human Breast Cancer Cell Derived PTHrP Reduces Osteoblast Cell Death and Apoptosis Induced by Potential Anticancer Compounds. Sahiti Chukkappalli¹, Magesh Muthu², Arun Rishi³, Nabanita Datta^{*1}. ¹Wayne State University School of Medicine, USA, ²Karmanos Cancer Institute, USA, ³Wayne State University, USA

Breast cancers with advanced disease metastasize to the skeleton. Although osteoclasts are largely responsible for osteolytic metastatic lesions, osteoblasts themselves are negatively affected by metastatic breast cancer. Current clinical strategies are primarily focused on inhibiting the tumor-induced osteoclastic osteolysis. There is a critical need to minimize chemotherapy associated side effects in bone by restoring osteoblast function while preventing osteolysis, and reduce the risk of worsening the disease. Therefore development of new anti-cancer agents that have superior efficacy and minimal toxicity is warranted. Cell cycle and apoptosis regulatory protein (CARP)-1 (aka CCAR1) is a novel regulator of signaling by diverse agents including cell growth and differentiation factors, and chemotherapy-dependent apoptosis. The therapeutic potential of CARP-1 functional mimetics (CFMs)-4 and -5 for triple negative human breast cancer (TNBC) cells has been recently shown in vitro and in xenograft studies. Our in vitro and in vivo studies revealed that CARP-1 is present in osteoblasts and CFM-4 and -5 cause osteoblast cell death and apoptosis correlated with caspase-3 activation and cyclin D1 down-regulation. Parathyroid hormone-related peptide (PTHrP) is a secretory protein associated with many tumors including breast cancer. In this study we investigated the role of MDA-MB-231 TNBC cell-derived PTHrP on MC3T3-E1 (MC-4) osteoblast with CFM-4 and -5 treatments. MC-4 cells, either in normal differentiation media, or in condition media (CM) derived from serum starved MDA-MB-231 cells, were treated with or without 10 μ M dose of respective CFMs overnight. ApoAlert caspase profiling indicates that CFM-4 or -5 dependent caspase-3 activation was reduced by 1.6- 3-fold in the presence of CM. Neutralizing CM with anti PTHrP antibody failed to attenuate caspase-3 activation. The QPCR and/or Western blot analysis revealed a 2-4 fold down-regulation of cyclin D1, but not CARP-1 expression by CFMs in the CM with or without PTHrP neutralization. These data indicate that PTHrP from TNBC cells likely antagonizes osteoblast apoptosis by CFMs. On the other hand, regulation of cyclin D1 by CFMs maintains G1-phase arrest of mature osteoblasts that permits continued extracellular matrix production. The present study provides the first proof-of-principle evidence that PTHrP regulates signaling by potential anticancer agents to benefit osteoblast survival.

Disclosures: Nabanita Datta, None.

SU0077

Discoidin Receptor 2 is Necessary for In Vitro TMJ Chondrocyte Differentiation While Its Absence is Associated with Aging Related TMJ Degeneration. Chunxi Ge^{*1}, Yan Li², Hanshi Sun², Sunil Kapila², Renny Franceschi². ¹Pom Univ of Michigan School of Dentistry, USA, ²University of Michigan, USA

Temporomandibular joint disorder (TMJD), a relatively common condition, is associated with development of osteoarthritis (OA)-like degenerative changes in the mandibular condyle. Discoidin Receptors 1 and 2 (DDR1/2), are associated with OA formation in hyaline cartilage and may also be similarly relevant in TMJD. As recently reported, the selective development of TMJ-OA in Ddr1 knockout mice is accompanied by compensatory up-regulation of DDR2 (Schminke et al Cell Mol Life Sci 71:1081, 2014).

To test whether DDR2 can drive OA-like hypertrophic differentiation/mineralization of TMJ fibrocartilage, DDR2 levels were modified in established TMJ chondrocyte cell lines using lentivirus-mediated shRNA knockdown of DDR1 or overexpression of DDR2. Cells were cultured in chondrogenesis medium for 15 days and differentiation was measured by Alcian Blue and Alizarin Red staining. Expression of chondrocyte differentiation marker and OA associated gene mRNAs were measured by quantitative RT/PCR. The spontaneous development of TMJ degeneration in 10 month-old smallie (slie) mice harboring a spontaneous 150 kb deletion in Ddr2 gene was analyzed by microCT.

Ddr1 shRNA was shown to knockdown DDR1 levels by more than 50%. DDR1 knockdown was associated with up-regulation of DDR2, MMP13 and VEGF mRNA. Lentivirus-mediated DDR2 overexpression in TMJ cells resulted in dramatically increased DDR2 protein levels as compared to very low levels of endogenous DDR2 in control cells. DDR2 overexpressing cells had an enlarged chondrocyte-like appearance after 5 days of chondrogenesis induction. After 15 days, these cells formed increased numbers of mineralizing nodules and expressed hypertrophic cartilage marker genes (Collagen X and MMP13) as well as RUNX2 and osteocalcin. Paradoxically, 100% of 10 month-old Ddr2(slie/slie) mice developed severe spontaneous TMJ degeneration while only 12% of wild type mice showed slight TMJ degeneration. MicroCT analysis showed dramatic bone loss in the TMJ of Ddr2(slie/slie) mice compared to wild type litter mates. Three dimensional reconstruction of the mandibular condyles of Ddr2(slie/slie) mice showed a rough, flattened bone surface and increased TMJ joint space. The bone mineral density of mandibular condyle surface was greatly decreased in Ddr2(slie/slie) mice compared to wild type littermates.

These studies indicate that appropriate expression of DDR2 is required for normal TMJ chondrocyte differentiation and maintenance of an intact TMJ.

Disclosures: Chunxi Ge, None.

SU0078

High fat diet compromises articular cartilage thickness relative to body weight, while low intensity mechanical signals protects this relationship, building cartilage relative to body size. Tee Pamon^{*}, Vincent Bhandal, Mei Lin Chan, Patryk Krzesaj, Clinton Rubin. Stony Brook University, USA

Obesity is a risk factor for osteoarthritis, a degenerative joint disease characterized by joint pain and immobility. The elevated risk has been attributed to higher joint loading due to body weight. Since obesity has been associated with the disruption of bone formation, it is possible that cartilage formation is also impeded. Recent evidence has shown that low intensity vibration (LIV) protects mesenchymal stem cell (MSC) lineage selection towards the formation of higher order connective tissues, and we sought to determine if these signals could protect the formation of AC in spite of the obese phenotype. C57BL/6 male, 5w mice were separated into 3 groups (n=10): Regular diet (RD), High fat diet (HF), and High fat diet + LIV (HFv). 2w of high fat diet were given to HF and HFv. LIV (90Hz, 0.2g, 30 min/d, 5 d/w) was then administered to HFv for 6 wks, with all groups continuing their respective diets. The R tibias were extracted, and the AC and subchondral bone (SB) of the tibial plateau were visualized using contrast agent enhanced μ CT. AC and SB thickness were measured within a 480um ROI, centered at the midpoint of the medial condyle. Means reported, and the one-way ANOVA was used to detect differences between groups; a p-value<0.05 was considered statistically significant. After 8 wks of high fat diet, AC thickness between RD and HF animals was not statistically different. However, these similarities in thickness reflect a failure of AC to adapt to increased mechanical demands relative to the 17.2% increase in body weight in HF (p=0.006), a weight gain similar to LIV. More specifically, HF exhibited a lower thickness/weight ratio compared to RD (-27.0%, p=0.03). In contrast, LIV stimulated a 46% increase in AC thickness as compared to HF (p=0.001), as well as a 51% higher thickness/weight ratio (p=0.002), levels n.s.d. from RD. SB thickness and mineralization were not different between groups, however, the medial condyle width of the HF group increased compared to RD and LIV groups (~3%, p<0.05). Resisting loading challenges is a major function of cartilage, a goal that seemingly was not achieved in the obese controls. Introducing dynamic mechanical signals, however, appears to have 'activated' the adaptive goals of the musculoskeletal system, with LIV driving AC thickness towards a more suitable support structure.

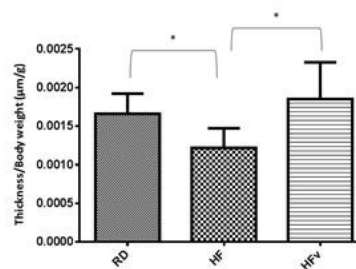


Figure 1: When AC thickness is normalized to body weight, HF has a significantly lower ratio compared to RD, and the relationship is protected with LIV.

AC Thickness normalized to body weight

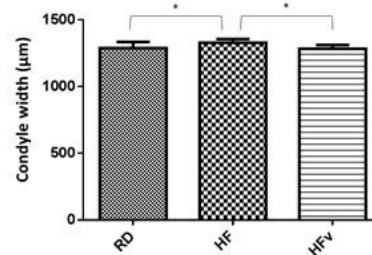


Figure 2: The medial condyle is wider in HF compared to both RD and HFv groups.

Medial Condyle Width

Disclosures: Tee Pamon, None.

SU0079

In Vivo Identification and Induction of Articular Cartilage Stem cells by Inhibiting NF- κ B Signaling in osteoarthritis. Xiaoling Zhang¹, Wenxue Tong^{*2}, Yiyun Geng². ¹Institute of Health Sciences, Peoples republic of china, ²The Key Laboratory of Stem Cell Biology, Institute of Health Sciences, Shanghai Jiao Tong University School of Medicine (SJTUSM) & Shanghai Institutes for Biological Sciences (SIBS), Chinese Academy of Sciences (CAS), Shanghai 200025, China, China

Abstract

Osteoarthritis (OA) is a highly prevalent and debilitating joint disorder characterized by the degeneration of articular cartilage. However, no effective medical therapy has been found yet for such condition. In this study, we directly confirmed the existence of articular cartilage stem cells (ACSCs) in vivo and in situ for the first time both in normal and OA articular cartilage, and explored their chondrogenesis in Interleukin-1 β induced inflammation environment and disclose whether the inhibition of NF- κ B signaling can induce ACSCs activation thus improve the progression of experimental OA. We found an interesting phenomenon that ACSCs were activated and exhibited a transient proliferative response in early OA as an initial attempt for self-repair. During the in vitro mechanism study, we discovered IL-1 β can efficiently activate the NF- κ B pathway and potently impair the responsiveness of ACSCs, whereas the NF- κ B pathway inhibitor rescued the ACSCs chondrogenesis. The final in vivo experiments further confirmed ACSCs' activation were maintained by NF- κ B pathway inhibitor, which induced cartilage regeneration, and protected articular cartilage from injury in an OA animal model. Our results provided in vivo evidence of the presence of ACSCs, and disclosed their action in the early OA stage and gradual quiet as OA process, presented a potential mechanism for both cartilage intrinsic repair and its final degradation, and demonstrated the feasibility of inducing endogenous adult tissue-specific mesenchymal stem cells for articular cartilage repair and OA therapy.

Acknowledgements. This work was supported by grants from National Natural Science Foundation of China (No. 81190133), Chinese Academy of Sciences (No. XDA01030502), Science and Technology Commission of Shanghai Municipality (No. 12411951100 & No. 13430710700), Shanghai Municipal Commission of Health and Family Planning (No. 2013ZYJB0501) and Shanghai Jiao Tong University (No.2013SMC-A-6).

Key words. Articular Cartilage Stem cells, identification, induction, NF- κ B Signaling, osteoarthritis

Disclosures: Wenxue Tong, None.

SU0080

Male Estrogen Receptor Beta KO mice Develop TMJ Degeneration. Sunil Wadhwa, Jing chen, Manshan Xu*, Jennifer Robinson, Alina O'Brien, Thomas Choi. Columbia University, USA

Introduction-Temporomandibular joint diseases (TMD) are a collection of diseases that afflict over 20 million Americans. One form of chronic TMD is TMJ joint degeneration. TMJ degeneration occurs in an older age group (mean age 55) than other TMD diseases and accounts for 35-50% of the people who seek treatment. Women most often seek treatment suggesting a role of estrogen in the disease process. However, conflicting reports indicate the role of estrogen either in potentiating or inhibiting the degenerative process. It is known that WT mice develop mild age related TMJ degeneration at 12 months of age. Therefore, the goal of this project was to evaluate the effect of estrogen through estrogen receptor β (ER β) on TMJ degeneration at 12 months.

Material and Methods- TMJ condyle was dissected and sectioned from male C57Bl/6 WT and ER β KO 4-month old (n=12) and 12-month old (n=6) mice. Histomorphometry was conducted to determine cartilage thickness and cell numbers. Cell proliferation was measured by BrdU labelling and quantification. Histopathology of TMJ degeneration was conducted using OARSJ scoring.

Results- No significant difference was observed in any of the parameters comparing 4-month old ER β KO mice to age-matched WT controls. At 12 months of age, a significant increase in histopathological scoring of TMJ degeneration was observed in 12-month old male ER β KO mice (4 +/- 1) compared to male WT mice (2 +/- 1).

Conclusion- These results may suggest that ER β signaling delays TMJ degeneration in older mice.

Disclosures: Manshan Xu, None.
This study received funding from: NIH

SU0081

The change of UCHL1/PGP 9.5 expression in initial progressive of rat temporomandibular joint osteoarthritis cartilage induced by unilateral traumatic occlusion. Di Liu*¹, Xiao Zhao², Ping Ji³. ¹Shandong University; Shandong Provincial Key Laboratory of Oral Biomedicine, Peoples republic of china, ²Shandong Provincial Key Laboratory of Oral Biomedicine, China, ³Shandong University; Shandong Provincial Key Laboratory of Oral Biomedicine, China

Objective: As one of the pathological changes of temporomandibular disorders (TMD), Osteoarthritis (OA) lesion can be caused in many molecular pathways by mechanical loading, especially the traumatic occlusion. Ubiquitin Carboxy Hydro-lase-L1/ protein Gene Product 9.5 (UCHL1/PGP 9.5) is an enzyme with both ubiquitin hydrolase and ubiquitin ligase activity, and plays a pivotal role in the complex mechanism protein metabolism. In the present study, we want to determine the mechanotransduction response of UCHL1/PGP 9.5 in TMJ-OA condylar cartilage induced by unilateral traumatic occlusion. Methods: To establish a unilateral traumatic occlusion rat model by the right bite-raised. The animals were randomised into experimental (Exp) groups received unilateral bite-raised and control (Con) groups received no treatment. Hematoxylin-eosin and immunohistochemical staining were performed on the condylar cartilage at the end of 1, 3, 7, 14 and 28 days, and evaluate histopathological changes and immunohistochemical staining by Colombo scores and average optical density (OD) value respectively. Gene expression was analyzed by SYBR green real-time PCR (RT-PCR). Results: Osteoarthritis-like lesions were detected in Exp groups. The UCHL1/PGP 9.5-positive chondrocytes were mainly located in hypertrophic layer. After exposure, Colombo scores showed increased and significantly higher than those in the Con groups at the end of 3, 7, 14 and 28 days (p<0.05); The average OD-value of UCHL1/PGP 9.5 was increased with peak at the end of 7 days before decreasing, and significantly higher than those in the Con groups at the end of 3 and 7 days (P<0.05); And UCHL1/PGP 9.5 mRNA expression had a transient increasing and significantly higher relative to the Con groups in the first 3 days (P<0.05). Pearson's correlation analysis indicated that the histological scores of condylar cartilage had significantly positive correlations to the average OD-value of UCHL1/PGP 9.5 (r=0.8785, p<0.05), and had significantly negative correlations to the UCHL1/PGP 9.5 mRNA expression (r=-0.8796, p<0.05). Conclusion: Experimentally created unilateral bite-raised can lead to temporomandibular joint OA-like changes. UCHL1/PGP 9.5 is the first to specifically identify involved in initial progressive TMJ-OA induced by traumatic occlusion in condylar cartilage.

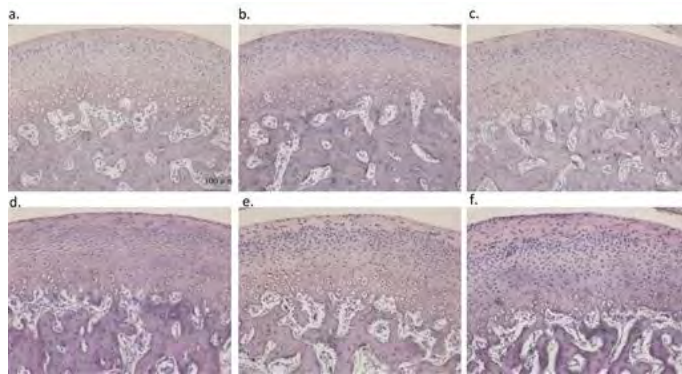


Fig. 1 The HE stain in the right condylar cartilage

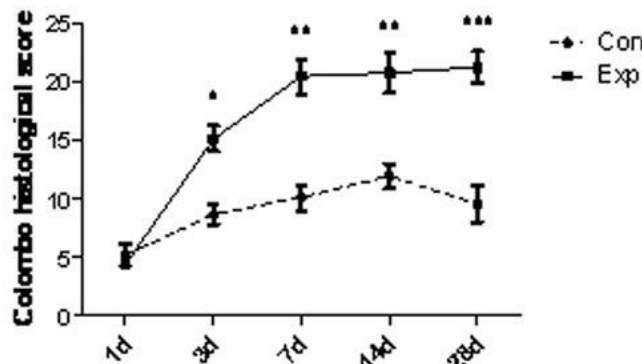


Fig. 2 The Colombo histological scores of the right condylar cartilage

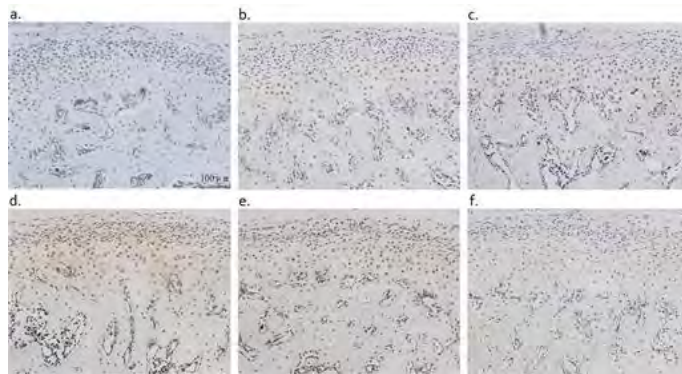


Fig. 3 The immunohistochemistry stain in the right condylar cartilage

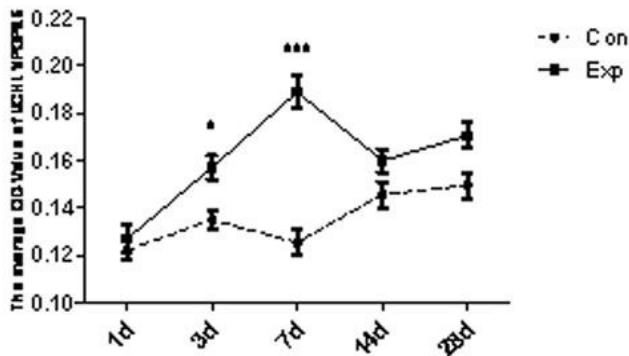


Fig. 4 The mean OD-value of UCHL1/PGP 9.5 in the right condylar cartilage

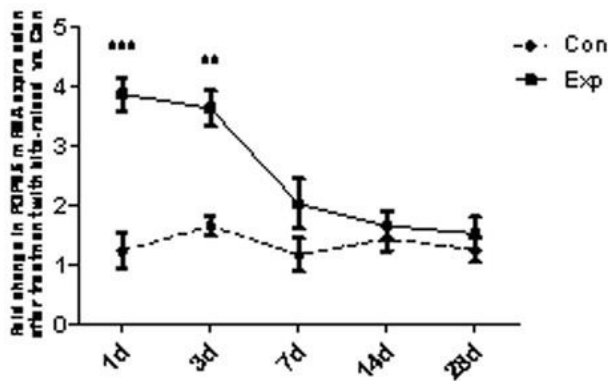


Fig. 5 PGP9.5 mRNA in the right condylar cartilage

Disclosures: Di Liu, None.

SU0082

Smurf2-Deficient Chondrocytes Exhibit Enhanced Chondrogenic Potential. Henry Huang*, Hong Zhang, David Avers, Jie Song. University of Massachusetts Medical School, USA

Background: Osteoarthritis (OA) is a degenerative joint disease leading to articular cartilage loss, osteophyte formation and subchondral bone thickening. OA is a leading cause of disability and a significant socioeconomic burden. There are no effective disease modifying drugs for OA. Smad ubiquitin regulatory factor 2 (Smurf2) is expressed in human OA cartilage and overexpression of Smurf2 in mouse chondrocytes leads to OA-like changes[1]. We previously[2] showed that Smurf2-deficient mice had similar age-dependent skeletal phenotype as WT. However, after surgical destabilization of the medial meniscus (DMM), Smurf2-deficient mice developed milder OA symptoms than WT. Here, we isolated primary chondrocytes from MT and WT mice and performed in vitro experiments to evaluate their chondrogenic potential.

Methods: A previously reported[3] C57BL/6 Smurf2-deficient MT and WT mice were used. Immature primary articular chondrocytes were isolated from 5-6 day old litters as previously described[4]. Chondrogenesis was evaluated by culturing cells for 4 days and treating them with a combination of TGF- β 3 (10ng/mL) and IL-1 β (5ng/mL). RNA was extracted after 24-hour treatment and RT-PCR was performed to compare the relative gene expression of anabolic (COL2, ACN) and catabolic (MMPs) markers. Dedifferentiation was also evaluated by changes in COL1, COL2 and ACN expression. Changes in growth curves with each passage were also assayed using cell counting kit-8 (CCK-8).

Results: Smurf2-deficient chondrocytes expressed statistically significant higher levels of COL2 and ACN genes than WT. These differences were maintained after treatment with TGF- β 3. Addition of IL-1 β drastically suppressed anabolic gene expression but the level of COL2 expression was still higher in the MT chondrocytes. Upregulation of catabolic genes in response to IL-1 β , including MMP3, were comparable between WT and MT chondrocytes. Smurf2-deficient chondrocytes also showed slower dedifferentiation on 2D TCPS culture, where COL2 and ACN levels remained higher and COL1 expression remained lower in later passages. Impaired metabolic activity (by CCK8) associated with later passages was also less severe in Smurf2-deficient chondrocytes than WT.

Conclusion: Smurf2-deficient chondrocytes express higher levels of chondrogenic markers than WT and undergo slower dedifferentiation during passaging on 2D culture. Future work will evaluate whether and how this difference in chondrogenic potential may contribute to the observed joint articular cartilage phenotype *in vivo* after DMM.

[1] Wu Q, et al. Arthritis & Rheumatism. 2008

[2] Huang H, et al. ASBMR Abstract SA0203. 2014

[3] Ramkumar C, et al. Cancer Research. 2012[4] Gosset M, et al. Nature Protocols. 2008

Disclosures: Henry Huang, None.

SU0083

The cell cycle regulation of chondrocyte development. HIROYUKI INOSE¹, MASANORI SAITO², PHILIPP KALDIS³, ATSUSHI OKAWA². ¹Tokyo Medical & Dental University, Japan, ²Department of Orthopedics, Tokyo Medical & Dental University, Japan, ³Institute of Molecular & Cell Biology, A*STAR, Singapore

Cell cycle regulation is known to be important for cell development; however, its importance on chondrocyte development remains unknown. Thus we chose to focus

on the role of cell cycle regulator on chondrocyte development. The regulator we chose was cyclin dependent kinases.

Reverse transcription PCR (RT-PCR) confirmed mRNA expression of Cdk1, Cdk2, Cdk4 and Cdk6 in murine primary chondrocytes. Previously, conventional knockout mice of Cdk2, Cdk4 and Cdk6 were reported to be viable, and do not display any overt skeletal phenotypes. However, the deletion of Cdk1 resulted in embryonic lethality. This led us to generate chondrocyte specific Cdk1 knock out mice using type 2a1 collagen promoter. Unfortunately, these mice died within one day after birth. The spines and hind limbs of Cdk1 cKO were markedly shorter than their Cre-negative littermates. Histological analysis revealed proliferative zone of Cdk1 cKO embryos was significantly reduced with disorganized columnar chondrocyte structure. BrdU labelling revealed that the proliferation on peri-articular chondrocytes was dramatically reduced in Cdk1 cKO. In situ hybridization showed lower expression of chondrocyte marker genes in Cdk1 cKO, which indicated impaired chondrocyte differentiation. In vitro analysis further revealed that knockdown of Cdk1 in ATDC5 cells inhibited chondrocyte proliferation. In addition, over-expression of Cdk1 in ATDC5 cells promoted chondrocyte proliferation. Collectively, our findings suggest that Cdk1 is indispensable for chondrocyte development and further investigations might lead to better understanding of cell cycle regulation of chondrocyte development.

Disclosures: HIROYUKI INOSE, None.

SU0084

Failed Vertebral Bone Formation in Mucopolysaccharidosis VII is Associated with Aberrant Sox9 Regulation and Altered Wnt Signaling. Sun Peck^{*1}, Eileen Shore¹, Neil Malhotra¹, George Dodge¹, Margret Casal¹, Maurizio Pacifici², Mark Haskins¹, Lachlan Smith¹. ¹University of Pennsylvania, USA, ²Children's Hospital of Philadelphia, USA

Mucopolysaccharidosis (MPS) VII is a lysosomal storage disorder defined by deficient β -glucuronidase activity that results in abnormal accumulation of glycosaminoglycans. MPS VII presents with severe spine disease associated with failed vertebral cartilage-to-bone conversion during postnatal growth. Progressive kyphoscoliosis significantly increases mortality. Our objective was to establish the molecular basis of failed vertebral endochondral bone formation in MPS VII using the naturally-occurring canine model, which exhibits a similar disease phenotype to humans. Our specific aims were to identify 1) the stage of failed chondrocyte differentiation in MPS VII vertebral epiphyses and 2) dysregulation of relevant biological pathways using RNA-Seq.

Previously, we identified the developmental window when failed vertebral bone formation first manifests (between 9 and 14-days of age) in MPS VII dogs. For this study, we collected vertebral epiphyseal cartilage from unaffected control and MPS VII dogs at both ages (n=5, all groups) and measured mRNA levels of chondrocyte differentiation markers using qPCR, and Sox9 protein levels using immunoblotting. RNA-Seq was performed for 14-day samples.

SOX9 mRNA was downregulated at 14 days compared to 9 days in both control and MPS VII dogs, but Sox9 protein expression decreased only in controls (Fig). Expected mRNA increases for subsequent differentiation stage markers (RUNX2, PTH1R, MEF2C, COL10A1) at 14 days were seen only in controls. RNA-Seq identified Wnt/ β -catenin signaling as the top dysregulated bone formation pathway at 14 days, revealing significant downregulation of key inhibitory elements and activating signaling molecules in MPS VII compared to controls. Our data suggest that both unaffected and MPS VII chondrocytes receive regulatory signals to exit the proliferative stage as indicated by downregulation of SOX9 mRNA at 14 days. However, aberrant persistence of Sox9 protein in conjunction with low expression of late-differentiation stage markers in MPS VII suggests that aberrant Sox9 protein processing may contribute to abnormal chondrocyte differentiation. Downregulation of both inhibitory and activating molecules in the Wnt pathway suggests MPS VII cells experience decreased Wnt signaling but are unable upregulate compensatory responses. These results provide the basis for further mechanistic investigations of bone disease in MPS and implicate the Wnt/ β -catenin pathway as a potential therapeutic target.

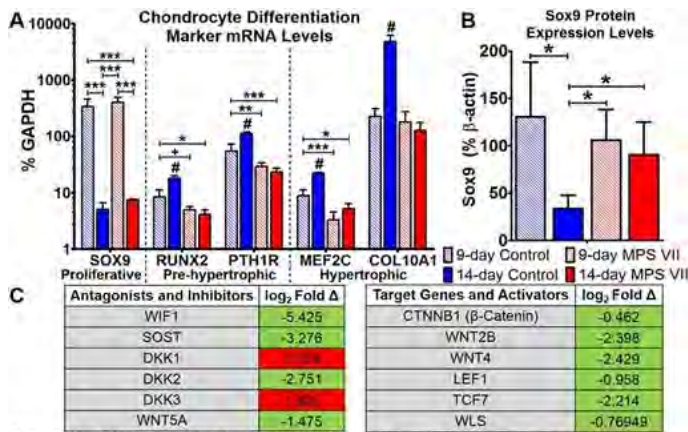


Figure. A) mRNA expression levels of chondrocyte differentiation markers in vertebral epiphyseal cartilage of unaffacted control and MPS VII dogs at 9 and 14-days of age. **B)** Sox9 protein levels in vertebral epiphyseal cartilage of control and MPS VII dogs at 9 and 14-days of age. **C)** Gene expression log₂ fold changes (all $p < 0.05$) of key antagonists and activators of Wnt/ β -catenin pathway in MPS VII vertebral epiphyseal cartilage compared to controls at 14 days, identified by RNA-Seq. (Green: downregulated in MPS VII; Red: upregulated in MPS VII). (N=5 for all groups. Statistical analyses with 2-way ANOVA and post-hoc Tukey's test. # $p < 0.001$ for 14-day controls compared to all other groups, *** $p < 0.001$, ** $p < 0.01$, * $p < 0.05$, + $p < 0.1$.)

Sun Peck 2015 ASBMR Abstract Figure

Disclosures: Sun Peck, None.

SU0085

Regulation of IL36 α by TBRII Signaling in Articular Chondrocytes: Potential Role in the Osteoarthritic Process. Tieshi Li^{1*}, Joseph temple¹, Alessandra Esposito¹, Arnavaz Hakimiyan², Susan Chubinskaya², Yiwen Zhao³, Richard Loeser³, Daniel Del Gaizo⁴, Christopher Olcott⁴, Anna Spagnoli¹. ¹Department of Pediatrics, Rush University Medical Center, USA, ²Department of Biochemistry, Rush University Medical Center, USA, ³Department of Medicine, University of North Carolina at Chapel Hill, USA, ⁴Department of Orthopedics, University of North Carolina at Chapel Hill, USA

Osteoarthritis (OA) is the most common form of arthritis, affecting millions of people around the world. TGF β signaling and proinflammatory cytokines play essential roles in the pathophysiology of OA. In a mouse model, we have previously reported that the induced conditional postnatal inactivation of TGF β type II receptor, TBRII, (TBRII-ER-Prx1KO) in chondro-progenitors led to OA and demonstrated a functional role for IL36 α and IL36R up-regulation in the process. Increased levels of IL36 α are found in synovial tissues of patients with different forms of arthritis. The present study is aimed at determining whether the TBRII/IL36 α axis is involved in the OA process in humans. To this purpose, chondrocytes were freshly isolated from articular cartilage of human donors (cadavers) that had no documented history or histological signs of OA (normal chondrocytes) and from subjects with histologically proven OA. Cells were treated with either TBRII inhibitor (SB-505124), or IL36 α or IL36 receptor antagonist (IL36Ra). Conditioned medium (CM) or cell lysates were collected for immunoblotting analyses. Isolated mRNA was subjected to qRT-PCR. Untreated cells were used as negative control. We found that in normal chondrocytes, inhibition of TGF β signaling with SB-505124 (5-10 μ M for 24 hrs) induced increases of Mmp13 (28.3 \pm 2.12 fold increase), IL36 α (80.6 \pm 9.04 fold increase) and IL36R (2.68 \pm 0.194 fold increase) mRNA expression ($p < 0.001$; SB-505124 at 10 μ M). An increase of Mmp13 protein was also detected in CM of SB-505124 treated cells. These results suggested that in human normal chondrocytes, TGF β signaling maintains the expression of IL36 α , IL36R at low levels. Next, we found that in normal human chondrocytes, IL36 α treatment (2-200ng/ml) induced a dose-dependent increase of Mmp13 at both mRNA (17.4 \pm 7.23 fold increase, $P < 0.05$; IL36 α at 200ng/ml) and protein levels. Furthermore, in normal chondrocytes, IL36 α treatment (2-200ng/ml for 30 minutes) induced a dose-dependent increase in phosphorylation of ERK1/2, P65, P38, and JNK1/2. These results suggested that IL36 α may regulate articular cartilage homeostasis by regulating Mmp13 expression via NF κ B and MAP kinase signaling pathways. Lastly, treatment of chondrocytes from subjects with histologically proven OA, with IL36Ra (2-10ng/ml) inhibited Mmp13 expressions at both mRNA (0.35 \pm 0.013 fold decrease; $P < 0.01$; IL36Ra at 10ng/ml) and protein levels. Our findings indicate that a TBRII/IL36 α axis is involved in maintaining chondrocyte homeostasis and promotes the development of OA when altered. Our studies provide a novel approach to alter the progression of OA by manipulating the TBRII/IL36 α axis.

Disclosures: Tieshi Li, None.

SU0086

Smad3 deficiency leads to mandibular condyle degradation via the Sphingosine 1-phosphate (S1P) /S1P3 signaling axis. Hiroki Mori^{*}, Takashi Izawa, Eiji Tanaka. Tokushima University Grad Sch, Japan

Temporomandibular joint osteoarthritis (TMJ-OA) is a degenerative disease that is characterized by permanent cartilage destruction. Transforming growth factor- β (TGF- β) is one of the most abundant cytokines in the bone matrix and has been shown to regulate the migration of osteoprogenitor cells. It is hypothesized that TGF- β /Smad3 signaling influences cartilage homeostasis by influencing S1P/S1P receptor signaling and chondrocyte migration. Therefore, the molecular mechanisms by which signaling crosstalk could occur between TGF- β /Smad3 and S1P/S1P receptors to maintain condylar cartilage and prevent TMJ-OA were investigated. Abnormalities in the condylar subchondral bone, including dynamic changes in bone mineral density and microstructure, were observed in Smad3^{-/-} mice by micro-computed tomography. Cell-free regions and proteoglycan loss characterized the cartilage degradation present, and increased numbers of apoptotic chondrocytes and MMP-13-positive chondrocytes were also detected in the condylar cartilage of the Smad3^{-/-} mice. Furthermore, expression of S1P receptor 3 (S1P3), and not S1P1 or S1P2 was significantly downregulated in the condylar cartilage of Smad3^{-/-} mice. By employing RNA interference technology and pharmacological tools, S1P was found to transactivate Smad3 in an S1P3/TGF- β type II receptor-dependent manner, and S1P3 was found to be required for TGF- β -induced migration of chondrocyte cells and downstream signal transduction via Rac1, RhoA, and Cdc42. Taken together, these results demonstrate that the Smad3/S1P3 signaling pathway plays an important role in the pathogenesis of TMJ-OA.

Disclosures: Hiroki Mori, None.

SU0087

Transcriptome landscape of Notch signaling reveals novel canonical and non-canonical targets during chondrogenesis. Yangjin Bae^{*}, Shan Chen, Abhirami Rajagopal, Feng Wang, Hui Wang, Huan-Chang Zeng, Huan-Chang Zeng, Brian Dawson, Terry Bertin, Rui Chen, Brendan Lee. Baylor College of Medicine, USA

Notch signaling, a well conserved pathway across many species, plays critical roles in embryonic development, stem cell maintenance, fate-specification and adult tissue homeostasis. It is activated by direct cell-to-cell physical interaction via Notch receptors and ligands. While Notch signaling pathway has been extensively studied in various cell and tissue types, the mechanism by which Notch governs chondrogenesis in the axial skeleton remains to be elucidated. Our previous studies showed that cartilage specific Notch gain-of-function (Notch GOF) mice exhibited chondrodysplasia and the deletion of *Rbpj* in Notch GOF mice did not fully rescue the axial skeletal deformities. This observation not only demonstrates the importance of canonical *Rbpj*-dependent Notch signaling but also provide interesting evidence for the regulation of Notch targets in a non-canonical (*Rbpj*-independent) manner during chondrogenesis. To further understand the significance of the *Rbpj*-dependent and *Rbpj*-independent Notch signaling during chondrogenesis, we performed ChIP-seq and RNA-seq experiments in chondrocyte cell lines (ATDC5) engineered to overexpress *Notch* alone or both *Notch* and *Rbpj*. These experiments have led to the identification of putative novel *Rbpj*-dependent and *Rbpj*-independent Notch target genes. We have also identified regulatory factors such as Runx1, Nfatc2 and Kid3 that form complex *in silico* and potentially occupy cis-regulatory regions of downstream non-canonical targets in chondrocytes. The functional interactions among these putative regulatory partners during chondrogenesis and novel non-canonical Notch candidate genes are currently under validation. Findings from our study will provide a genome-wide transcriptional network for Notch signaling during chondrocyte differentiation.

Disclosures: Yangjin Bae, None.

SU0088

The Effects of Endurance Training and Dietary Methionine Restriction on Energy Metabolism, Bone Histomorphometry and Bone Densitometry in Adult Male Rats. Tsang-hai Huang^{*}, Gene Ables², Ming-shi Chang³, Rong-sen Yang⁴. ¹National Cheng-Kung University, Taiwan, ²Orentreich Foundation for the Advancement of Science, USA, ³National Cheng Kung University, Taiwan, ⁴National Taiwan University Hospital, Taiwan

Dietary methionine restriction (MetR) and endurance exercise (EE) have been well-proven in their benefits to metabolic sensitivity and body weight (BW) loss. Simultaneously, MetR and EE also cause reduction in bone mass. The current study aimed to investigate the effects of MetR and EE on energy metabolic and bone quality indices of adult male rats. Animals (26-wk-old male SD rats) were BW matched and assigned to groups subjected to the following interventions: non-treatment baseline group (BA), non-treatment age-matched control (CON) group, dietary methionine restriction (MetR) group, endurance exercise (EE) group, and pioglitazone (PIO) treatment group. By the end of the 10-week intervention, the EE group had lower BW than the CON and PIO group, while the MetR group was lighter than the PIO group ($p < 0.05$). The MetR and PIO groups showed the most efficient performance in

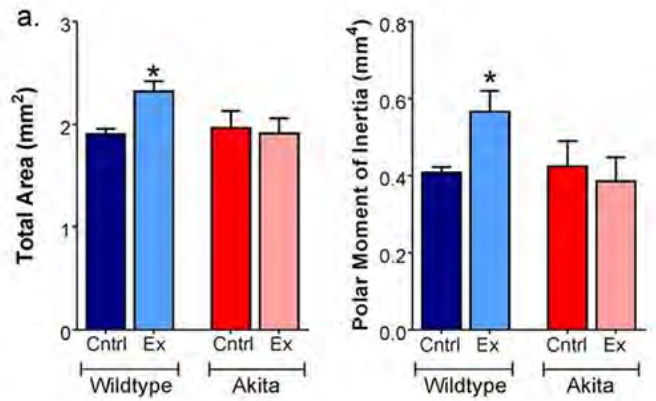
intraperitoneal glucose tolerance test (IPGTT) performance followed by the EE group as compared to the CON group. In serum marker assays, except for a significantly higher procollagen type I amino-terminal propeptide (PINP) and lower leptin, respectively, shown in the BA group, no difference was shown among four experiment groups. In densitometric measurement, a lower total bone mineral density (BMD) was shown in the BA group ($p < 0.05$). In spongy BMD, the CON group was higher as compared to the BA group, MetR and PIO groups, while the EE and MetR groups were higher than the PIO groups ($p < 0.05$). In spongy BMC, the MetR and PIO groups were lower than other groups ($p < 0.05$). In histomorphometry of metaphysis, the BA group showed higher Tb.N and Conn.Dn as compared to other 4 groups. The PIO group showed significantly lower BV/TV and Tb.Th as compared to most of other groups ($p < 0.05$). And, the BA and MetR group had lower Tb.Th compared to the CON group. In summary, EE, MetR and pioglitazone showed benefits to glucose regulation and/or BW control. However, MetR and pioglitazone showed minor or major compromised effects to indices of bone histomorphometry and densitometry. Therefore, in terms of whole body health as well as bone quality, EE might be a better option than diet manipulation or medical intervention.

Disclosures: Tsang-hai Huang, None.

SU0089

Type I diabetes altered bone cell purinergic mechanosignaling and anabolic bone response to exercise. Zeynep Seref-Ferlengez¹, Herb B. Sun¹, Mitchell B. Schaffler², Sylvia Suadican¹, Mia M. Thi¹. ¹Albert Einstein College of Medicine, USA, ²City College of New York, USA

Patients with Type 1 diabetes (T1D) exhibit decreased bone density and volume, increased risk for fragility fractures and defective bone healing. Our previous studies demonstrated that the expression of mechanosignaling mediators [purinergic receptors (P2Rs) and pannexin 1 (Panx1) channels] are altered (i) in bone cells exposed to high extracellular glucose levels *in vitro*, and (ii) in bone cells from a T1D mouse model *in vivo*. Given that maintenance of skeletal integrity in response to daily physical activity relies on ability of bone cells to perceive and respond to mechanical loading, we hypothesized that response/sensitivity to mechanical loading is impaired in T1D. In this study we used the Akita (C57BL/6J-Ins2^{Akita}) mouse model of T1D. Young Akita and wildtype (WT) mice (8 wk old, male, n=10/group) were divided into treadmill exercise and cage control groups. The exercise group was subjected to treadmill running for 4 weeks (5 days/wk, 300 m/day, speed up to 10 m/min). All animals were euthanized immediately after the last running exercise. Right hindlimbs were used for histomorphometric study, and lefts were used to examine protein expression. Mid-diaphyseal crosssections from PMMA embedded femurs were used to measure the bone area parameters. Expression level of Panx1 and P2R subtypes (P2Y₁, P2Y₂, P2Y₄, P2X₇) were quantified by Western blotting of osteocytes enriched samples (left femur and tibia diaphyses were cleaned from soft tissues and marrow, pulverized, protein extracted). All experiments were performed under IACUC approval. Histomorphometry studies showed that 4 wks exercise caused radial expansion in femur (increased in Bone Area (~25%) and moments of inertia (~40%), ($p < 0.05$; Fig. 1) in WT mice compared to their cage controls. In contrary, Akita T1D animals did not show anabolic response with exercise. There was no significant difference in bone area parameters between exercised and cage control Akita mice. Western blot analyses showed that mechanosignaling mediators (specifically Panx1, P2X₇R, $p < 0.05$; Fig. 2) were significantly altered in exercised diabetic mice compared to control and exercised WT mice. Our current findings demonstrate that exercise-induced anabolic response of bone is impaired in T1D and likely related to T1D-induced changes in bone cell purinergic mechanosignaling, which is essential for proper response to mechanical loading and maintenance of bone health.



| Parameter | Wildtype | | Akita | |
|-----------------------------------|-------------|--------------|-------------|--------------|
| | Control | Exercise | Control | Exercise |
| Blood Glucose(mg/dL) | 194±42 | 187±27 | 550->600* | 550->600* |
| Body Weight (g) | 26.1±0.7 | 26.0±2.5 | 24.7±2.9 | 23.6±1.1 |
| Bone Length (mm) | 15.0±0.2 | 14.9±0.9 | 15.1±0.2 | 14.4±0.2 |
| Cortical Area (mm ²) | 0.81 ± 0.1 | 0.93 ± 0.1 | 0.80 ± 0.1 | 0.73 ± 0.1 |
| Cortical Ar./Total.Ar. | 0.43 ± 0.02 | 0.39 ± 0.05 | 0.40 ± 0.02 | 0.37 ± 0.02* |
| Marrow Area (mm ²) | 1.1 ± 0.1 | 1.4 ± 0.2 | 1.2 ± 0.1 | 1.2 ± 0.1 |
| Cortical Thickness (µm) | 185 ± 10 | 186 ± 24 | 175 ± 8 | 163 ± 13* |
| I _x (mm ⁴) | 0.13 ± 0.01 | 0.17 ± 0.05 | 0.14 ± 0.02 | 0.13 ± 0.02 |
| I _y (mm ⁴) | 0.28 ± 0.02 | 0.39 ± 0.07* | 0.28 ± 0.04 | 0.26 ± 0.04 |

Figure 1. Body weights, blood glucose levels, histological bone (mid-femur) area parameters from cage control and exercised 12-week-old Akita and age-matched wildtype, expressed as Mean±S.D. (* $p < 0.05$, vs. wildtype control; n = 4-5).

Figure 1

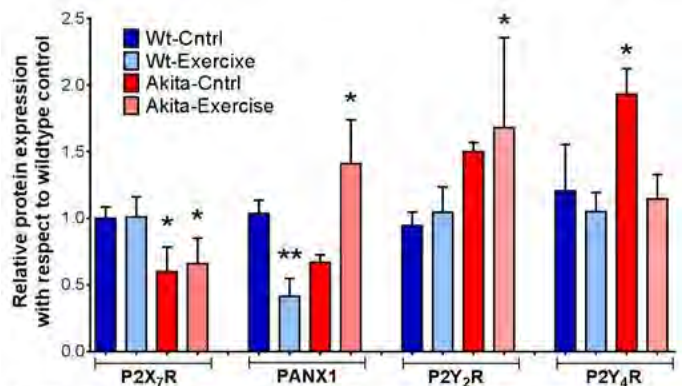


Figure 2. Representative Western blots and expression levels of P2Y₂R, P2Y₄R, P2X₇R subtypes and Panx1 measured in long bone of control and exercised 12-week-old Akita and age-matched wildtype mice. Samples were first normalized with loading control (β -actin) and subsequently normalized with non-exercised wildtype control values of the protein of interest. (mean±SD, * $p < 0.05$, ** $p < 0.05$ vs. wildtype control; n = 4-5).

Figure 2

Disclosures: Zeynep Seref-Ferlengez, None.

SU0090

VEGF Expression Levels in Human Diabetic and Non-Diabetic Vertebral Bone Tissue. Roberto Fajardo*¹, Jesus Hernandez², Trevor Wait², Ammar Saigal², Elena Geraymovych², Zachary Child². ¹UT Health Science Center, San Antonio, USA, ²The UT Health Science Center at San Antonio, USA

Adults with type 2 diabetes mellitus (DM2) are at increased risk for fractures compared to non-diabetics. Diabetic patients with a prior fracture have increased cortical porosity compared to diabetic subjects without fracture. The porosity suggests a locally acting resorptive process that is independent of hyperglycemia, but so far no mechanisms have been identified.

Micro- and macro-vascular problems are common complications in DM2. Ocular microvascular pathology leads to ischemia that stimulates a neoangiogenic response to restore perfusion. This response is driven by increased vascular endothelial growth factor (VEGF) expression in the diabetic eye. In contrast, in cardiac tissue neoangiogenesis is inhibited in response to ischemia because local cells are unable to secrete VEGF. It is currently unknown what roles ischemia and micro-vascular complications play in diabetic bone.

Spine tissue was collected from human subjects undergoing surgery. Subjects were 50 yrs of age or older and either diabetic or non-diabetic. Exclusion criteria included previous lumbar or thoracic surgeries, use of anti-osteoporosis medications, bone metastases, and other exclusion criteria. Standard of care procedures were used at all times during surgeries. The Institutional Review Board of the University of Texas Health Science Center at San Antonio approved the study.

Bone tissue was harvested and fixed for 5 days under vacuum. Samples were then decalcified and embedded in paraffin. After antigen retrieval sections were treated with 3% hydrogen peroxide treatment to inhibit endogenous peroxidases. Following treatment with a blocking buffer, they were incubated overnight in primary anti-VEGF antibody (Santa Cruz). The tissues were then treated with a secondary antibody (Chicken IgG) and Streptavidin-HRP complex. Sections were stained with a DAB substrate. Figure 1 shows representative images of (A) non-diabetic and (B) diabetic sections. Vascular tissues were intensely stained for VEGF in the non-diabetic sections, with a positive signal focused in cortical bone vascular channels. Evidence indicated that VEGF expression was suppressed in diabetic bone tissue compared to the non-diabetic samples. This decrease in VEGF expression suggests that its protective actions of maintaining the integrity, antithrombotic, anti-inflammatory properties of the endothelium and suppressing apoptotic pathways in endothelial cells and bone cells may be compromised.

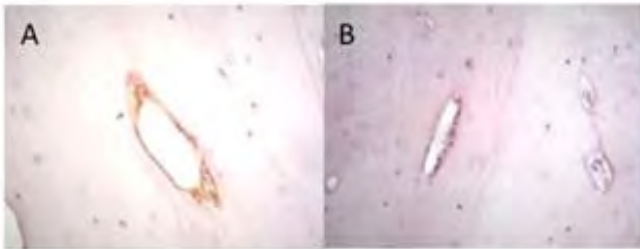


Figure 1

Disclosures: Roberto Fajardo, None.

SU0091

Adiponectin Contributes to Bone Marrow Adipose Tissue Expansion but Not Bone Loss in Calorie Restricted Mice. Theresa Roth¹, Rebecca Hayden², Carolynn Roth³, Linh Ho*², Liping Wang¹, Robert Nissenson¹. ¹UCSF / VA, USA, ²UCSF / NCIRE, USA, ³UCSF, USA

Anorexia nervosa affects up to 1% of American women and is associated with increased fracture risk. Peripheral adipose tissue is reduced in anorexia and bone marrow adipose tissue (BMAT) is increased, but it is unclear why this occurs or whether increased BMAT is responsible for decreased bone density. As circulating adiponectin (APN) levels are known to increase with caloric restriction (CR), we hypothesized that APN may drive increases in BMAT. APN levels are also positively correlated with fracture, suggesting that APN null mice may be resistant to CR-induced bone loss. We subjected male wild type (WT) and global APN null mice to 30% CR from 4 weeks of age until sacrifice at 10 weeks of age and compared these mice with age-matched controls fed ad libitum (AL). Total body fat averages and standard deviations by nuclear magnetic resonance at sacrifice were 1.93 +/- 0.41 grams in AL APN null mice, 1.32 +/- 0.29 grams in AL WT mice, 0.83 +/- 0.30 grams in CR APN null mice, and 0.22 +/- 0.13 grams in CR WT mice. These results demonstrate that endogenous adiponectin limits total body fat in mice maintained on either a normal or a restricted diet. Lean mass was decreased by about 25% in CR mice regardless of genotype ($p < 0.001$). BMAT in the proximal tibia was assessed by osmium tetroxide staining. In AL animals, there was a weak trend towards lower BMAT with deletion of APN. As expected, CR resulted in increased BMAT in WT mice, ($p < 0.05$), and this effect was inhibited in APN null mice. BMAT volume in CR WT mice was approximately twice that of CR APN null mice ($p < 0.05$), indicating a

significant contribution of APN to the increase in BMAT seen with CR. Micro-CT revealed that CR resulted in a 13% decrease in trabecular thickness at the distal femur ($p < 0.01$) and a 14% decrease at the proximal tibia ($p < 0.001$), and a 12% decrease in cortical thickness at the tibiofibular junction ($p < 0.001$) in WT animals. APN deletion did not alter these effects, suggesting that bone loss seen with CR is not dependent on APN. While literature reports on the effect of APN deletion on bone have been varied, we found a trend towards decreased trabecular thickness in APN null mice under AL conditions. Additionally, cortical bone volume was lower in APN null mice than WT mice on either diet ($p < 0.01$). These results indicate that APN contributes to the increase in BMAT that occurs with caloric restriction. However, APN is not required for the negative effects of CR on bone.

Disclosures: Linh Ho, None.

SU0092

Aging B6 mice are protected from the deleterious effects of calorie restriction on trabecular bone. Casey Doucette*¹, Mark Horowitz², Clifford Rosen¹. ¹Maine Medical Center Research Institute, USA, ²Department of Orthopaedics & Rehabilitation, Yale University School of Medicine, USA

In humans, anorexia nervosa causes a dramatic reduction in bone mineral density (BMD) and visceral adipose tissue with a paradoxical increase in marrow adipose tissue volume. In mice, 30% caloric restriction (CR) during adolescence has similar effects, but studies have also suggested that a CR diet can increase longevity, which could indicate a protective role for CR against age-related bone loss. Here, we investigated the effects of a 30% CR diet on bone in both adolescent and aging mice from two strains with distinct bone phenotypes; one with high bone mass (C3H/HeJ, C3H) and one with low bone mass (C57BL/6J, B6). Male mice from each strain were administered a 30% CR diet daily for a period of 12 weeks from 3-15 weeks of age (adolescent) or 40-52 weeks of age (aging); littermate controls from each strain were fed control diet *ad libitum*. In adolescent mice, areal BMD and bone mineral content (BMC) were reduced in CR mice as compared to controls, which was supported by μ CT analysis demonstrating significant reductions in trabecular BV/TV and cortical BA/TA with CR. Reductions in cortical parameters and femoral length also indicated inhibition of appositional and interstitial growth, respectively, in CR-fed mice. Interestingly, osteoblast numbers (N.Ob/TAR) were significantly increased in CR versus control animals; coupled with μ CT data, these results imply that osteoblast function is reduced during CR in adolescent mice. In aging mice, areal BMD and BMC were significantly reduced in CR-fed C3H mice as compared to controls, but this difference was not observed in CR-fed B6 mice. Analysis of bone microarchitecture by μ CT also indicated that aging B6 mice were protected from the CR-induced reductions in trabecular BV/TV observed in C3H mice. In aging CR mice from both strains, N.Ob/TAR and osteoid volume fraction (OV/BV) were increased as compared to controls, and in calorie-restricted C3H mice, osteoclast numbers were also increased. This increase in osteoblast activity in B6 CR mice without an increase in osteoclast activity may be indicative of the mechanism by which they are protected from CR-induced trabecular bone loss. We conclude that the negative effects of CR on aBMD, BMC, bone microarchitecture, and interstitial and appositional growth during adolescence may be a result of reduced osteoblast function. On the other hand, aging B6 mice may be protected from the effects of CR on trabecular bone through increased osteoblast activity.

Disclosures: Casey Doucette, None.

SU0093

Can Magnetic Resonance Spectroscopy Measure Bone Marrow Adipose Tissue Fraction? Ingvild Hogestol*¹, Maziar Shabestari², Hanne Gulseth¹, Tom Mala³, Erik Rud⁴, Erik Eriksen¹. ¹Department of Endocrinology, Morbid Obesity & Preventive Medicine, Medical Clinic at Oslo University Hospital, University of Oslo., Norway, ²Department of Biomaterials, Institute of Clinical Dentistry., Norway, ³Department of Endocrinology, Morbid Obesity & Preventive Medicine, Medical Clinic & Department of Gastrointestinal Surgery, Surgical Clinic at Oslo University Hospital., Norway, ⁴Department of Radiology & Nuclear Medicine, Oslo University Hospital, University of Oslo., Norway

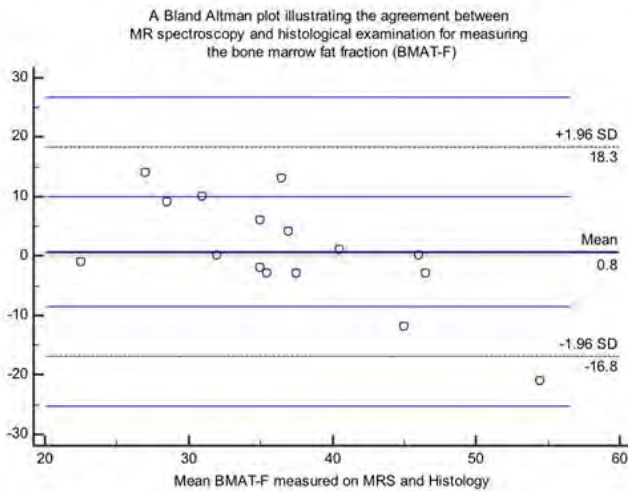
Purpose: Measurement of bone marrow adipose tissue fraction (BMAT-F) may be of prognostic value in a variety of conditions such as osteoporosis, obesity and diabetes. We compared measurement of BMAT-F using bone marrow biopsy (reference) and magnetic resonance spectroscopy (MRS).

Material and methods: Participants were part of a study where we examined bone marrow adipose tissue before and after gastric bypass surgery. The BMAT-F was assessed in trephine needle samples from the posterior iliac crest. Bone marrow biopsies were embedded in methyl methacrylate at -20°C. Subsequently, paired 7 μ m thick sections were stained with Hematoxylin and Eosin. Mosaic images of the sections were analyzed by bone histomorphometric software (BioQuant Osteo). The MRS was performed over the same region using a pelvic phased array with a 1.5 T magnetic resonance imaging scanner (Siemens, Erlangen). MRS values were corrected using the coefficient of variance of duplicate measurements between the two methods. Correlation was evaluated using a Pearson's coefficient. The variability between histology and MRS was estimated as 1.96 x SD of the mean arithmetic difference

according to Bland and Altman. The range between ± 1.96 SD of the mean difference is referred to as 95% limits of agreement. All patient gave informed consent, and the study was approved by the Regional Ethical Committee.

Results: Sixteen patients were included, 8 patients were eligible for gastric bypass surgery and 8 patients had received gastric bypass surgery 1 year prior to study inclusion; mean (\pm SD) age was 41 (\pm 9.1) years, BMI 33.9 (\pm 7.2) kg/m² and 13 (81%) were women. The coefficient of variance of duplicate measurements was 50%. The mean BMAT-F (95% CI) as assessed by histology and MRS was 36.5% (30 to 43%) and 37.2% (34 to 40%), respectively. The two methods correlated positively ($R=0.669$, $p=0.005$). The mean difference and variability was 0.8% (-4 to 5) and 18%, respectively. The 95% limits of agreement ranged from -17 to 18%.

Conclusion: A significant positive correlation between measurements of BMAT-F in bone marrow biopsies and MRS was observed. Significant variability between the two methods was observed and assessment by MRS overestimates BMAT-F. Further studies are needed to assess the clinical utility of MRS in the measurement of BMAT-F.



Bland Altman plot illustrating the agreement between histology and MRS measurements of BMAT-F

Disclosures: Ingvild Hogestol, None.

SU0094

Fate Determination and the Bioenergetics of Osteoblastogenesis and Adipogenesis. Anyonya Guntur*, Victoria DeMambro, Clifford Rosen. Maine medical center research institute, USA

Osteoblastogenesis is an energy consuming process. Signaling mechanisms that control the substrates utilized by osteoblasts during bone formation and the bioenergetic pathways that are employed during mineralization are currently understudied in skeletal biology. To better understand the substrates and the catabolic pathways through which these fuels are metabolized we utilized C3H^{smi/smi} mice which have a loss in IRS1 phenotypically resulting in low bone and fat mass. We isolated calvarial osteoblasts from Wildtype (Wt) and C3H^{smi/smi} mice and compared their bioenergetic response to addition of pyruvate and glucose as substrates. Wt osteoblasts cultured in osteoblast differentiation media for 7 days (ODM) upregulated Oxidative Phosphorylation (OxPhos) compared to Non differentiating osteoblasts and the IRS1 mutant cells showed an attenuated response to differentiation, with 1) decreased basal respiration and 2) decreased spare respiratory capacity compared to differentiating Wt cells, suggesting that loss of IRS1 compromises mitochondrial respiration. Furthermore, Wt calvarial osteoblasts differentiated for 21 days and tested for utilization of pyruvate and glucose showed engagement of both OxPhos and Glycolysis (Glyc) for catabolism compared to Non differentiated cells which were highly OxPhos dependent. Next we wanted to contrast this with the bioenergetic profile of cells undergoing adipogenesis, so we utilized primary ear mesenchymal stem cells (EMSC's) from Wt and C3H^{smi/smi} mice and compared the response of these cells to pyruvate and glucose during adipogenic differentiation. Wt cells after 7 days in differentiation media upregulated OxPhos compared to C3H^{smi/smi} cells and Non differentiating controls, but Glyc compared to Non differentiating cells was lower. This is in contrast to what we observed in differentiated osteoblasts, suggesting that cells of different lineage utilize different catabolic pathways during differentiation. Interestingly, the C3H^{smi/smi} EMSC's undergoing differentiation in contrast to calvarial osteoblasts showed 1) higher spare respiratory capacity compared to Wt cells undergoing differentiation even though they had 2) lower basal respiration, suggesting an important role for IRS1 in modulating adipogenesis. In sum these data suggest that osteoblasts and adipocytes during differentiation utilize different metabolic pathways to generate energy.

Disclosures: Anyonya Guntur, None.

SU0095

Increased Osteocalcin Levels and Bone Mineral Content During Rapid Weight Gain Therapy in Anorexia Nervosa Patients. Bojan Tubic*¹, Cecilia Pettersson², Anna Svedlund³, Heléne Bertéus Forslund⁴, Per Magnusson⁵, Diana Swolin-Eide³. ¹Gothenburg University, Se, ²Department of Internal Medicine & Clinical Nutrition, Sahlgrenska Academy, Gothenburg University, Sweden, ³Department of Pediatrics, Institute of Clinical Sciences, The Queen Silvia Children's Hospital, Sahlgrenska Academy, Gothenburg University, Sweden, ⁴Department of Internal Medicine & Clinical Nutrition, Sahlgrenska Academy, Gothenburg University, Göteborg, Sweden, ⁵Department of Clinical Chemistry & Department of Clinical & Experimental Medicine, Linköping University, Sweden

Purpose: Patients with anorexia nervosa (AN) are at high risk of reduced bone mass. Osteocalcin (OC) reflects bone formation but has also been proposed to act as a link between bone and energy metabolism in mice, however, human data are inconclusive. We investigated how the various forms of OC respond during a 12-week novel intensive nutrition therapy in AN patients during a short period of large changes in energy metabolism. The potential influence of the fat mass and obesity-associated gene (FTO), SNP rs9939609, was also investigated in relation to study parameters.

Methods: Twenty-two female AN patients, mean 20.9 years of age, with a mean body mass index (BMI) 15.5 kg/m² completed the study. Biochemical markers, body composition, bone mass by dual-energy X-ray absorptiometry (DXA) and peripheral quantitative computed tomography (pQCT) were assessed.

Results: Subjects gained in median (minimum-maximum) 9.9 kg (5.5-17.0 kg), and BMI increased from median 15.4 kg/m² to 19.0 kg/m², $p<0.0001$. Fat mass increased from median 11.4% to 26.7%. Total OC, carboxylated OC (cOC), undercarboxylated OC (ucOC) and bone-specific alkaline phosphatase (BALP) increased during the study period. No change was observed for the resorption marker carboxy-terminal cross-linking telopeptide of type I collagen (CTX). Total body bone mineral content increased, but no changes were found for whole body, lumbar spine or femoral neck bone mineral density (BMD). Tibial trabecular density measured by pQCT decreased. Total OC, cOC, ucOC were not associated with BMI, delta BMI or body composition parameters at any time point.

Conclusion: In conclusion, although a small study, this is the first clinical study that contributes to the knowledge how the different forms of OC respond to rapid weight gain. Total OC, cOC, ucOC and BALP increased, but the resorption marker CTX did not change. These biochemical findings corroborate with the findings of increased total body BMC. No associations were found with the measured body composition fat and muscle parameters.

Disclosures: Bojan Tubic, None.

SU0096

ApoE deficiency in osteoblasts leads to a low bone mass phenotype in mice. Brigitte Müller, Alexander Bartelt, Timo Beil, Till Köhne, Thorsten Schinke, Andreas Niemeier*. University Medical Center Hamburg-Eppendorf, Germany

Objective

Apolipoprotein E (apoE) is an important component of lipoproteins. As a ligand for members of the LDL receptor family, it mediates the endocytosis of these lipoproteins. ApoE deficiency in mice causes an accumulation of remnant lipoproteins but also results in a high-bone mass phenotype with increased bone formation while bone resorption is unaffected. Up to now it is unknown from which cell type the apoE that regulates bone remodeling is derived from. The objective of this study was to explore the role of osteoblast-apoE in the regulation of bone mass in vivo.

Methods

In order to specifically analyze the function of osteoblast-apoE in vivo we generated a conditional ApoE knockout-mouse (Cre-loxP). Runx2-Cre mice were crossed to ApoE^{fl/fl} mice to generate mice lacking ApoE in the osteoblast lineage. Histomorphometry and μ CT was performed on trabecular vertebral and femoral bone of three and six months old females. Bone turnover makers alkaline phosphatase, osteocalcin and DPD/creatinine were measured in the serum and urine by ELISA.

Results

Interestingly, the specific deletion of ApoE in the osteoblast lineage results in an age-dependent bone phenotype which does not reflect the global ApoE knock-out phenotype. Hence, three months old ApoE^{fl/fl}/Runx2-Cre⁺ female mice do not display an altered bone mass phenotype yet, whereas the trabecular bone mass of six months old ApoE^{fl/fl}/Runx2-Cre⁺ females is significantly reduced compared to ApoE^{fl/fl}/Runx2-Cre⁻ littermates. This reduction is caused by an increased number of osteoclasts and increased bone resorption, while the bone formation rate remains unchanged. In addition, these mice exhibit an elevated osteocalcin concentration in the serum.

Conclusion

These findings confirm that apoE has a powerful regulatory function in bone remodeling. The effects of osteoblast apoE and systemic (mostly liver-derived) apoE on the regulation of trabecular bone mass appear to be diverging. The lack of apoE in

osteoblasts triggers a yet to be identified signal that stimulates osteoclastic bone resorption. It is conceivable that apoE, via its effect on osteocalcin production by osteoblasts, plays a relay function in the postprandial energy metabolism at the interface of lipid and glucose metabolism in the osteoblast.

Disclosures: *Andreas Niemeier, None.*

SU0097

Estrogen Loss Impairs Osteocyte Mitochondrial Electron Transport Chain Activity (oxidative phosphorylation) In Vivo. Dorra Frikha-Benayed^{*1}, Jelena Basta-Plajkic², Robert J. Majeska², Mitchell B. Schaffler². ¹The City University of New York, USA, ²CCNY, USA

Recently we showed that estrogen (E2) loss acutely leads to dramatic accumulation of NADH in osteocytes, indicating oxidative stress. Because E2 has been suggested to directly alter mitochondrial oxidative functions (1), we tested whether E2 loss impairs mitochondrial electron transport chain activity (i.e. oxidative phosphorylation) of osteocytes in vivo. Following IACUC-approved procedures, groups of 17 wk old C57BL/6J mice that had undergone OVX or SHAM surgery were treated either with Methylene Blue (MB, 0.2% in cage water supply) or with normal water beginning at the time of surgery. Methylene Blue is an alternative mitochondrial electron carrier that bridges complexes I and III and has been shown to be neuroprotective against ischemic injury and Parkinson's disease (2). Osteocyte NADH accumulation was monitored in situ by multiphoton microscopy (MPM) at 2 days post-OVX in metatarsal diaphyses of anesthetized mice (3). NADH fluorescence intensities were measured using ImageJ and differences among groups were tested using one-way ANOVA followed by post-hoc testing using the Mann-Whitney U-test. We found that OVX markedly increased osteocyte NADH levels and that this increase was completely prevented by Methylene Blue treatment (Fig 1,2). How E2 loss produces oxidative stress in osteocytes remains obscure. Estrogen depletion is associated with increased ROS (4), but it is not clear how the absence of estrogen's antioxidant effects would so dramatically alter osteocyte NADH levels. Similarly, absence of estrogen's antioxidant effects also would not be expected to alter osteocyte NADH levels (5). In any case, oxidative stresses like those resulting from E2 loss can lead to osteocyte apoptosis or autophagy that trigger and regulate resorption. The present finding that Methylene blue treatment in OVX mice effectively abrogated the increases in osteocyte oxidative stress suggests that E2 loss acts directly on mitochondria. Moreover, since Methylene Blue appears to normalize osteocyte oxidative metabolism after OVX, it may limit some or all of the downstream consequences of estrogen depletion.

REFERENCES: 1) Chen et al. *Biochim Biophys* 2009; 2) Xie et al. *Cellular neuroscience* 2013; 3) Frikha-Benayed et al. *Trans Orthop Res*, 2013; 4) Almeida. *IBMS BoneKey*, 5) Emerton et al *Bone*, 2010.

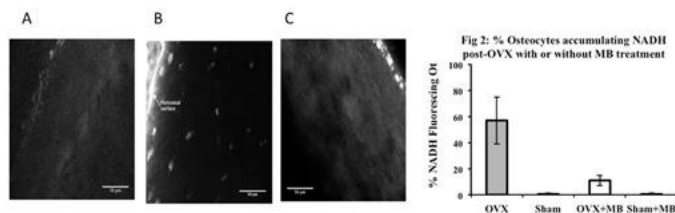


Figure1: (A) In vivo imaging of metatarsal cortex of Sham operated animal shows no NADH fluorescence in osteocytes. **(B)** Strong NADH fluorescence seen in osteocytes at 48 hours post OVX. **(C)** NADH fluorescence is absent in osteocyte 48 hours post OVX + Methylene blue treated animals.

Figures

Disclosures: *Dorra Frikha-Benayed, None.*

SU0098

NGF-BDNF-Osteocalcin and oxytocin genes interaction in brain, bone, fat stores and reproductive organs. Claudia Camerino^{*1}, Maria Cannone², Elena Conte², Domenico Tricarico². ¹School of Medicine, University of Bari, Italy & ²University of Cincinnati, USA, ²Dept. of Pharmacy – Drug Sciences, University of Bari, Italy

Bone mass, metabolism and reproduction require a coordinated regulation. The bone-derived osteocalcin (Ost) favors insulin sensitivity, male fertility and neurogenesis. The neurotrophins BDNF/NGF and oxytocin(Oxt) are involved in energy and bone metabolism. NGF regulates fertility elevating LH in female, *Ost*^{-/-} mice show obesity and high LH in spite of decreased testosterone. To investigate the NGF-osteocalcin- BDNF-Oxt interaction we analyzed by RT-PCR the mRNA levels of NGF, BDNF, Oxt, Ost and their receptors p75NTR/NTRK1, TRKb, OxtR and Gprc6a in brain and bone, adipose WAT/BAT and reproductive organs, of 3 months old female and male mice. Brain and bone were used as positive controls respectively.

The mRNA levels of NGF and p75NTR are 50% higher in BAT than brain. NGF and its receptors are downregulated in WAT and bone in both genders. Ost and Gprc6a are upregulated in bone and brain, down-regulated in BAT/WAT. BDNF and TRKb expression in bone is higher than brain, but lower in BAT/WAT; TRKb is downregulated in bone and up-regulated in adipose tissue. NGF is up-regulated in ovaries/uterus, but down-regulated in the testes. The mRNA levels of p75NTR is respectively 300%, 100% and 50% higher in testis, ovaries and uterus than brain. NTRK1 is downregulated in all tissues. The Gprc6a is expressed in testes, not in ovaries and uterus. BDNF and TRKb are downregulated in the sexual organs. The Oxt gene is markedly expressed in brain and with minor extend in bone in either genders, while the OxtR in ovaries although a significant level of expression is observed in adipose tissues and bone. The up-regulation of NGF and related-receptors in fat are consistent with NGF as an energy regulator. The inverse correlation of NGF and BDNF in fat and bone, shows these exerting opposite effects on leptin with BDNF regulating bone. The up-regulation of p75NTR in testes match the Gprc6a expression, and may be responsible for the higher LH in the *Ost*^{-/-} mice. The pattern of expression of these molecules and their receptors show a similar trend with Ost, NGF, Oxt and BDNF genes highly expressed in brain of both male and female mice, while their receptors were instead expressed in the reproductive organs showing a gender expression profile. This is consistent with the fact that these molecules have limited or no access through the blood brain barrier and add evidences that the signalling of bone metabolism and fertility are released from CNS to act on peripheral tissues.

Disclosures: *Claudia Camerino, None.*

SU0099

Peripheral Leptin Stimulates Bone Formation at Very Low Circulating Levels. Russell T. Turner^{*}, Kenneth Philbrick, Carmen Wong, Amida Kuah, Dawn Olson, Adam Branscum, Urszula Iwaniec. Oregon State University, USA

Leptin is produced by adipocytes and enters peripheral circulation where it may act directly on bone cells. Leptin is also transported across the blood brain barrier via a saturable transport system where, in addition to regulating appetite and thermogenesis, it may indirectly regulate bone metabolism. Leptin levels in peripheral circulation greatly exceed those in the central nervous system. Thus, the direct peripheral actions of leptin should be evident at lower concentrations than the hormone's centrally mediated actions. We performed a dose response study in which leptin was continuously infused (0, 4, 12, 40, 140, and 400 ng/hr) for 12 days into 6-week-old leptin-deficient female *ob/ob* mice (n=8/group) using s.c. implanted osmotic pumps. Additional controls consisted of *ob/ob* and wild type (WT) mice sacrificed at the start of leptin infusion and WT mice sacrificed at study termination. Changes in energy metabolism in response to leptin administration were evaluated by measurement of food consumption, body composition, blood glucose, uterine weight, and UCP-1 gene expression in brown adipose tissue. Bone response to leptin was evaluated by imaging, dynamic histomorphometry, gene profiling and biochemical markers of bone turnover. As expected, longitudinal bone growth, osteoblast-lined bone perimeter, mineralizing perimeter and bone formation rate were depressed in distal femur in *ob/ob* mice. Subcutaneous infusion of leptin into *ob/ob* mice resulted in a dose-dependent increase in serum leptin levels, with WT levels achieved at 140 ng/hr. Leptin treatment increased osteoblast-lined bone perimeter, mineralizing perimeter and bone formation rate at the exceptionally low level of 4 ng/hr and longitudinal growth rate and mineral apposition rate at 12 ng/hr. Leptin replacement in *ob/ob* mice increased mRNA levels for bone matrix proteins and BMP signaling in tibia. Higher dose rates of leptin (40 to 140 ng/hr) were required for leptin to increase UCP-1 gene expression in brown adipose tissue, and to decrease food consumption, blood glucose levels, body weight and adipose tissue weight. These findings suggest that the bone anabolic effects of leptin are primarily mediated through peripheral leptin signaling. The exquisite sensitivity of the skeleton to peripheral leptin suggests caution should be made in interpreting results obtained by direct administration of the hormone into the hypothalamus because of efflux from the brain into peripheral circulation.

Disclosures: *Russell T. Turner, None.*

SU0100

Phosphate Restriction Leads to Global Inhibition of Mitochondrial Oxidative Function in Fracture Healing. Amira Hussein^{*1}, Serkalem Demissie², Kyle Lybrand¹, Heather Matheny¹, Brenna Hogue¹, Anthony DeGiacomo¹, Louis Gerstenfeld¹. ¹Orthopaedic Surgery, Boston University School of Medicine, USA, ²School of Public Health, Boston University, USA

Introduction: Phosphate is essential for healthy bone development and fracture repair. Although phosphate deficiency has been shown to impair fracture healing, the mechanisms involved in impaired healing are unknown. The goal of this study was to determine the effects of phosphate restriction on the biologic functions identified from the transcriptomic analysis of fracture calluses.

Methods: Closed stabilized fractures were generated in the femora of three strains of male mice: A/J, C57BL/6J, and C3H/HeJ. Phosphate deficiency was initiated 2 days prior to fracture and maintained for 15 days by supplying the mice with a low phosphate diet. Matching control groups were given a normal diet. Microarray analyses of the exomic transcriptome were performed using total RNAs isolated from fracture calluses across the 35 day time course. Gene expression values were compared

between Pi and control groups using analyses of covariance with strain and time-point as covariates to examine the effect of diet. The biologic functions of genes with FDR q-value ≤ 0.005 were assessed.

Results: Many biologic functions were affected by phosphate deficiency. Metabolic-related functions such as oxidative phosphorylation and mitochondrial dysfunction were the top pathways affected by the phosphate deficiency. Mice with phosphate deficient diet had significantly lower expression levels compared to controls, indicating impairment in the metabolic functions ($p < 0.0001$).

Discussion: Oxidative metabolic functions were those most affected by phosphate deficiency within all strains of mice. The effect of phosphate deficiency was more pronounced in the C57BL/6J strain of mice, which interestingly, is the most sensitive to dietary oxidative stress, which is associated with obesity and diabetic condition. Comparative studies with cardiac tissue microarray data using hearts obtained from diet induced cardio-myopathies showed similar alterations in oxidative functions. These findings provide a crucial link between genetic variability or life style factors that affect system wide metabolic activity and fracture healing outcome.

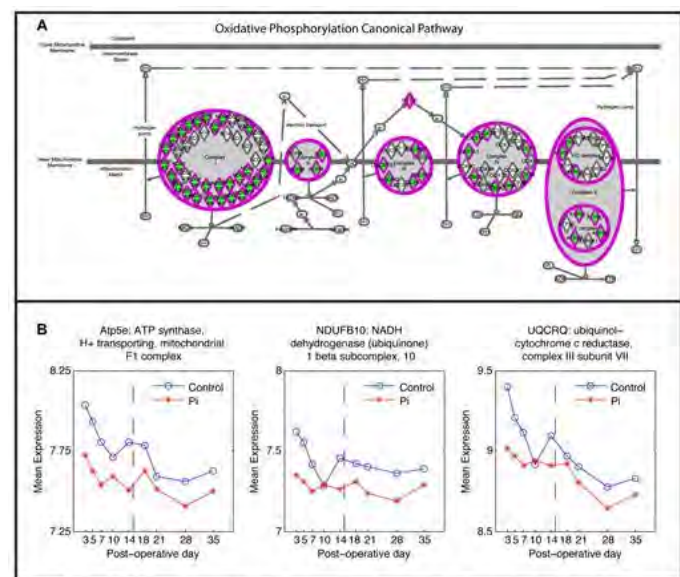


Figure 1. For Oxidative phosphorylation canonical pathway: (A) The canonical pathway for Oxidative phosphorylation, where green indicates down-regulation of gene expression in Pi Deficient fracture calluses tissues. (B) Time profiles for three genes; the dashed line indicates when Pi mice were put back on normal diet.

Figure1

Disclosures: Amira Hussein, None.

SU0101

The Phosphate Hypothesis: Thyroid Disease and the Skeleton. Robert Fredericks¹, Ilka Nemere². ¹Endocrine Associates, USA, ²Utah State University, USA

Translation of basic science to clinical care is dependent upon understanding the nature of variance in the expression of human disease. Anticipation that the human genome project would clarify this question has been a dominant influence on healthcare policy. It is now recognized that all human beings are compound mutants, including those considered healthy. This discovery explains the dissonance between observations made in inbred animals and clinical care. Personalization of healthcare delivery will require recognition that each individual is profoundly unique. Based on the assumption that phosphate is a primary signal in the organization of heat and that calcium serves as an organizing signal for phenotypic expression, highly influenced by the calcium sensing receptor, we have developed physiologic/metabolic models based on existing data from both animal and human studies, in the context of practice, engaging oral calcium challenge and immersion in water (gravitational subtraction) to explore the nature of human variance. The intestinal MARRS 1-25 D receptor appears to interface with the T3 alpha/beta receptor signaling and the models predict that paricalcitol would have a favorable effect on hyperthyroidism when pathogenically influenced by a T3alpha receptor gain of function, mediated by an antagonistic effect on the 1-25D MARRS receptor. Ten consecutive cases of refractory hyperthyroidism, considered obligate candidates for radioactive iodine or surgical intervention, have been managed with paricalcitol resulting in either complete remission or effective management with concomitant thioamides. In addition an association with spinal BMD and the balance between T3 alpha and beta receptor function as predicted by the models is readily demonstrated. The physiologic/metabolic models serve as a template for understanding the phenotypic expression of compound mutant influences on the heterostatic organization of heat that is the foundation of the general theory of metabolism and serves to clarify fundamental organizational principles operative in the organization of biology and healthcare.

Disclosures: Robert Fredericks, None.

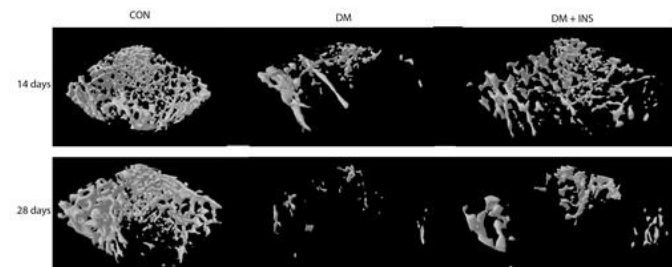
SU0102

Uncontrolled glucose significantly impairs trabecular and cortical micro-architecture and delays bone callus formation in type 1 diabetic rats, which are ameliorated by insulin administration. Ariane Zamarioli¹, Maysa Campos², Ana Paula Frantini², Mariana Butezloff², Francisco de Paula², José Volpon². ¹School of Medicine of Ribeirao Preto, University of Sao Paulo, Brazil, ²University of São Paulo, Brazil

We assessed the microstructural changes in the bone tissue and in the bone callus in both uncontrolled and controlled glucose level of diabetic rats. Sixty female Wistar rats weighing approximately 200g were given single intravenous injection with streptozotocin to induce diabetes (DM). Control rats (CON, n=12) were injected with citrate buffer alone. Diabetes was diagnosed on the basis of blood glucose concentrations (≥ 250 mg/dL on two consecutive days). Rats from groups DM+INS received daily insulin treatment. Thirty days after diabetes induction (or buffer injection), half of the animals were anesthetized and a closed bone fracture was produced in the right mid-femur (CON+FRA, DM+FRA and DM+INS+FRA, n=16/group). Then a surgical procedure with a 1-mm-diameter Kirschner wire was conducted for bone fragments stabilization. The status of the fracture was radiographically confirmed immediately after surgery and then followed-up weekly. On both days 14 and 28 post-surgery, eight rats from each group, respectively, were killed and the femurs harvested in preparation for three-dimensional analysis, where a micro-CT system was used to quantify the BMD and the 3D microarchitecture parameters in the femurs. In the non-fractured bone, two regions of interest were made, one at the femoral distal metaphysis, which mainly contains trabecular bone and, another at the mid-diaphysis, which mainly contains cortical bone. Callus was analyzed by calculating the volume. Uncontrolled glucose (DM rats without treatment) significantly impaired trabecular and cortical micro-architecture and mass and, delayed bone callus formation in type 1 diabetic rats. On the other hand, these deleterious changes were ameliorated by insulin administration. We concluded that uncontrolled diabetes leads to dramatic changes in both trabecular and cortical bone mass and microstructure. Additionally, bone healing was negatively affected by uncontrolled diabetes; with deficit of 80% in callus volume and mineralization. On the other hand, the administration of insulin mitigates the deleterious effects of diabetes not only on the bone tissue (trabecular and cortical), but also on the bone healing process.



MicroCT images of bone callus, both in sagittal and axial planes



Trabecular bone microstructures of femoral metaphysis

SU0103

Conserved Dynamics in Genes Associated with Human BMD and Bone Disorders During Zebrafish and Rat Bone Formation. Leah Worton¹, Arden Chew¹, Claire Watson¹, Edith Gardiner¹, Dobrawa Napierala², Amarjit Virdi³, D. Rick Sumner³, Cole Trapnell¹, Yi-Hsiang Hsu⁴, Ronald Kwon^{*1}. ¹University of Washington, USA, ²University of Alabama at Birmingham, USA, ³Rush University Medical Center, USA, ⁴Harvard Medical School & BROAD Institute of MIT & Harvard, USA

Zebrafish have emerged as a valuable model for human disease modeling due to their genetic tractability, optical properties, and amenability to *in vivo* screening. While zebrafish hold potential to open novel avenues for bone genetic research including rapid gene function mapping, mutant allele testing, and prioritization of candidate GWAS genes, the degree to which zebrafish and mammalian bone physiologies transcriptionally resemble each other is unknown. In this study, our goals were to 1) develop a cross-species framework for comparative analysis of zebrafish and rat gene expression, and 2) identify genes whose temporal dynamics are conserved during osteogenesis in both systems. For this, we used a custom meta-analysis pipeline [1] to analyze two microarray datasets: zebrafish fin regeneration (a model of intramembranous ossification that we have found to exhibit the physiochemical hallmarks of mammalian bone formation, Fig 1A), and rat marrow ablation-induced bone regeneration. To align profiles across species, we developed a three-step strategy in which we ordered the zebrafish and rat datasets within a principal component basis (adapting an approach based on [2]) (Fig 1B), correlated each pair of zebrafish and rat profiles (Fig 1C), and identified the rat ordering subset whose endpoints had the highest correlation with the endpoints of the zebrafish ordering. Using a L2 norm-based distance measure *q* (Fig 1D), we identified orthologs exhibiting similar (and differential) dynamics in zebrafish and rat (Fig 1E). Within this analysis, we isolated a number of genes with low *q* values (i.e., similar in both species) that have previously been implicated in human bone disorders [3] (Fig 1F). Using qPCR we analyzed genes previously identified in BMD GWAS studies, and identified two genes (*trps1* and *wnt16*) significantly elevated during zebrafish fin regeneration (Fig 1G). Similar patterns of expression were found during rat bone regeneration (Fig 1H), validating the predictive potential of this system. Collectively, this study develops a novel framework for cross-species gene expression analysis, identifies clinically-relevant genes conserved during rat and zebrafish bone formation, and advances zebrafish fin regeneration as a functional testbed for skeletal gene analysis.

[1] Kwon RY, Virdi A, Sumner DR, Trans ORS 2015.

[2] Trapnell C, Cacchiarelli D, et al., Rinn JL, Nat Biotechnol, 2014.

[3] Bais MV, et al., Gerstenfeld LC, PLoS One 2009.

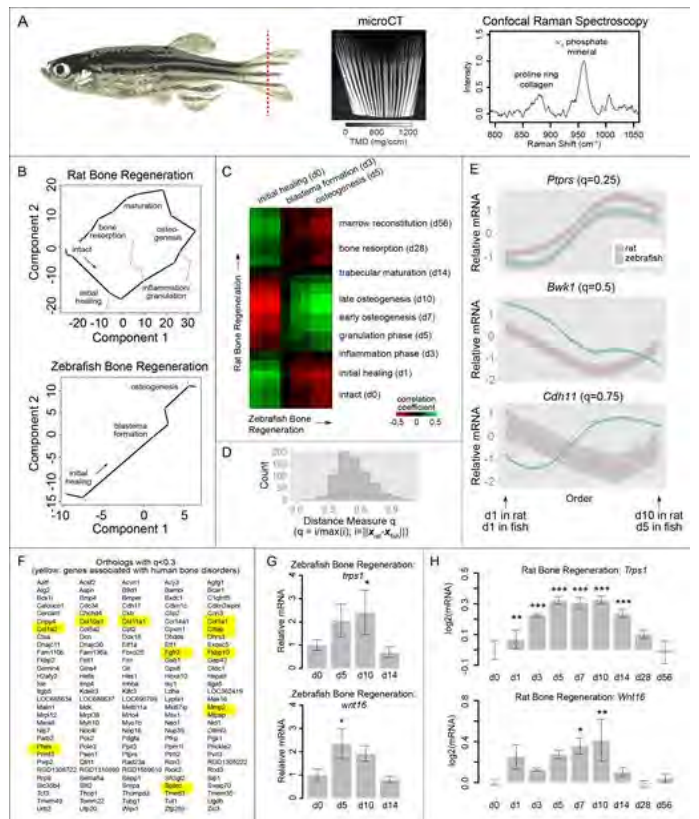
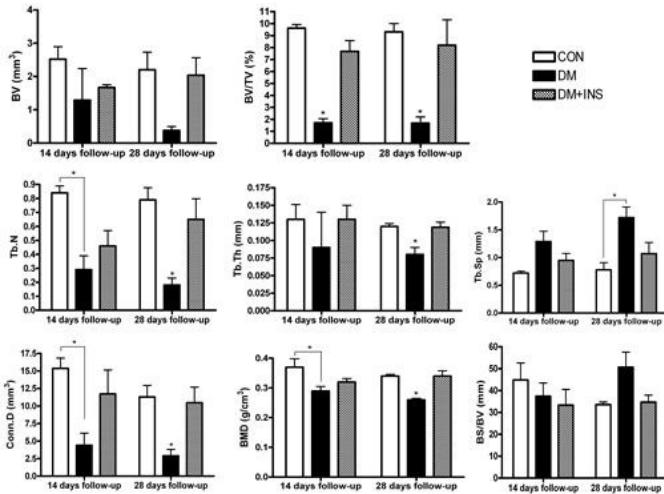
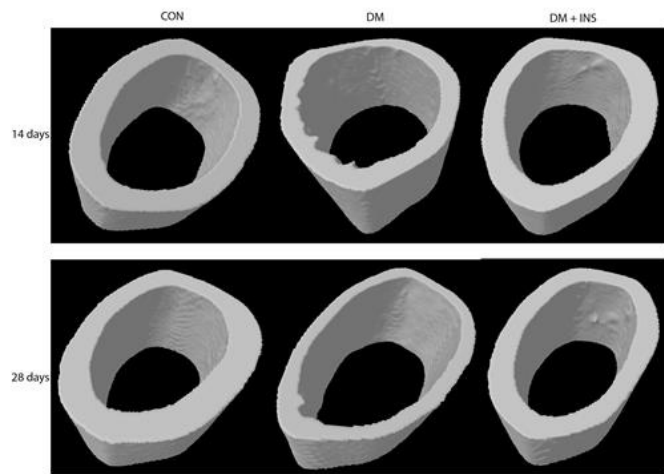


Fig 1

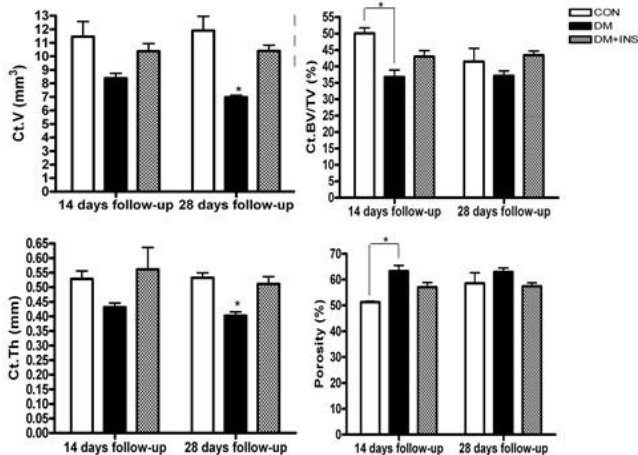
Disclosures: Ronald Kwon, None.



Quantitative analysis of trabecular bone microstructure.



Cortical bone microstructures of femoral diaphysis



Quantitative analysis of cortical bone microstructure.

Disclosures: Ariane Zamarioli, None.

SU0104

Cortical bone phenotypes observed in *Mmp8* and *Prokr1* null mice produced by the Knock Out Mouse Project. Douglas Adams¹, Renata Ryzdik¹, Li Chen¹, Zhihua Wu¹, Seung-Hyun Hong¹, Gaven Garland², Pujan Joshi¹, Caibin Zhang¹, John Sundberg², Dong Guk Shin¹, David Rowe¹, Cheryl Ackert-Bicknell³. ¹The University of Connecticut, USA, ²The Jackson Laboratory, USA, ³University of Rochester, USA

The Knockout Mouse Program (KOMP) is part of a larger effort to generate transgenic mice carrying a null mutation for every gene, and many of the targeted genes are uncharacterized. We are examining the bone phenotype of approximately 80 KOMP lines per year. We have implemented a comprehensive, high-throughput, high-resolution phenotyping pipeline based on 3-D X-ray microtomography (μ CT) and dynamic histomorphometry of frozen sections to quantify bone physiology within the peripheral (femur) and axial (lumbar vertebrae) skeleton of knockout mice. All transgenic mice are homozygous global knockouts on a C57BL/6NJ (B6/N) strain background with B6/N mice serving as controls. Groups of 8-10 male and female null and control mice are raised to 12 weeks of age for phenotyping. Some genes, but not all, affect bone in one sex. Herein we present 2 new lines that exhibit a cortical bone phenotype, but do not have an impact on the trabecular compartment. The first of these is matrix metalloproteinase 8 (*Mmp8*), a gene highly expressed by the osteoclast, which has been studied for its role in periodontal disease and osteoarthritis. While *Mmp8* null male mice had a lower body weight than controls, femur length was equivalent ($P = 1.00$). Male mice had a lower cortical bone area fraction (Ct.Ar/Tt.Ar) (null = 37.9 ± 1.4 vs control = $40.6 \pm 1.7\%$, $P=0.007$) and this is driven primarily by a decrease in cortical area (Ct.Ar). No phenotype was observed in females. Mice lacking prokineticin receptor 1 (*Prokr1*) presented with a reduction in cortical bone area fraction in both males (null = 37.3 ± 1.4 vs control = $40.6 \pm 1.7\%$, $P=0.002$) and females (null = 37.6 ± 0.8 vs control = $40.8 \pm 1.4\%$, $P<0.001$), due to a concomitant increase in total area (Tt.Ar) and decrease in Ct.Ar. This gene is expressed in both osteoblasts and osteoclasts, but is otherwise unstudied in the skeleton. In total, approximately 25% of the genes that we have studied have an impact on at least one compartment of bone (trabecular versus cortical). These 2 strains represent two manners in which cortical bone mass can be impacted, emphasizing the benefit of careful and comprehensive phenotyping to determine the role of genes in bone. A greater understanding of all genes that impact skeletal disease, and the degree and manner in which they do so, is a current gap in knowledge that our project seeks to fill. Additional findings from this study can be found at bonebase.org.

Disclosures: Douglas Adams, None.

SU0105

Exercise Capacity of Mice with Genetically Induced Hypophosphatemia. Daniel Caballero¹, Dominik Pesta², John Sterpka¹, Ali Nasiri¹, Michael Jurczak¹, Gerald Shulman³, Clemens Bergwitz¹. ¹Yale School of Medicine, USA, ²University of Innsbruck, Austria, ³Yale School of Medicine/HHMI, USA

Mutations in the sodium phosphate co-transporters, NPT2a and NPT2c, have been reported in kindreds with hypophosphatemic rickets. In addition to a mineralization defect of their bone matrix, growth plate abnormalities and renal calcifications due to high circulating levels of 1,25(OH)₂D and hypercalciuria, hypophosphatemia causes muscle weakness in these individuals. In this study we examined the potential role of blood phosphate on muscle function in *Npt2a* knockout mice. These mice become hypophosphatemic on a diet containing 0.02% phosphate (LP-diet) because they are unable to conserve phosphate in their kidneys. Normophosphatemia is restored when these mice are fed a diet containing 1.2% phosphate (HP-diet). Spontaneous activity monitored in metabolic cages over 72 hrs. of mice maintained on LP-diet for 8 weeks was reduced, when compared to mice maintained on HP-diet. Likewise, forced exercise capacity in a metabolic treadmill assembly was reduced in these mice, when compared to HP-diet. However, HP-diet was unable to restore critical speed and anaerobic exercise capacity to values previously reported for wild-type C57Bl6 mice. Oxygen consumption and carbon dioxide production was reduced in *Npt2a* knockout mice on LP-diet when compared to HP-diet during spontaneous and forced exercise, albeit not significantly. These *in vivo* findings parallel our observation *in vitro* that the oxygen consumption rate (OCR) is stimulated by phosphate in cultured 3T3 fibroblast cells using a Seahorse XFe24 analyzer and previous observations by us indicating that myocyte and isolated mitochondrial ATP-flux is dependent on cellular and mitochondrial phosphate uptake (Pesta et al. in preparation). In conclusion, exercise capacity of hypophosphatemic mice is decreased, which may be due to decreased mitochondrial respiration.

Disclosures: Daniel Caballero, None.

SU0106

Identification of sub-populations within Diversity Outbred mice representing differing states of bone turnover. Cheryl Ackert-Bicknell¹, Douglas Adams², Seung-Hyun Hong³, Renata Ryzdik³, Li Chen², Zhihua Wu², Laura Mello⁴, Caibin Zhang², Shin Dong Guk², David Rowe². ¹University of Rochester, USA, ²The University of Connecticut, USA, ³University of Connecticut, USA, ⁴The Jackson Laboratory, USA

The majority of genetic studies for bone have focused on bone mineral density (BMD). At its simplest, BMD is the sum of formation and resorption, yet even limited to these two processes, there are multiple ways that high bone mass can be achieved. The complex nature of BMD has impeded the transition from identification of a genetic locus to an understanding of the biological implications of a locus. To explore the genetic regulation of bone turnover, we are using the Diversity Outbred (DO) population of mice. The DO was generated by interbreeding 8 strains of inbred mice, such that each DO mouse is genetically unique from all other DO mice. We phenotyped femurs from 65 male and 54 female 6 month old DO mice. After splitting the population by gender, we conducted bottom-up Unweighted Pair Group Method with Arithmetic Mean (UPGMA) hierarchical clustering. After iterative modeling multiple combinations of formation and resorption phenotypes, the combination of trabecular bone mass (BV/TV), mineralizing surface (MS/BS) and TRAP over bone surface (TRAP/BS) yielded the most robust clustering. This allowed us to identify 4 male and 4 female sub-populations within this DO cohort, with each subpopulation containing 7 or more mice. For the males, 2 clusters with low BV/TV were identified (cluster1 mean = 11.8 ± 4.4 and cluster 2 mean = $11.9 \pm 7.0\%$, male mean = $16.4 \pm 8.9\%$), but these clusters did not differ for BV/TV ($P = 1.00$). However, these clusters did differ for MS/BS (cluster1 = 15.3 ± 5.3 vs cluster 2 = $24.4 \pm 4.5\%$, $P<0.0001$, male mean = $20.4 \pm 7.6\%$) and TRAP/BS (cluster1 = 8.7 ± 4.4 vs cluster2 = $17.7 \pm 5.5\%$, $P=0.0002$, male mean = $18.0 \pm 10.3\%$). Similarly, 2 of the clusters for females had low BV/TV (6.2 ± 4.4 , $8.5 \pm 3.7\%$, population mean BV/TV = $9.4 \pm 7.4\%$) and were not different from each other ($P=0.91$). The 1st cluster presented with high TRAP/BS ($27.2 \pm 3.3\%$ vs female mean = $21.6 \pm 6.8\%$) and normal MS/BS ($23.0 \pm 3.9\%$ vs female mean = $23.0 \pm 9.3\%$). In contrast, the 2nd presented with low TRAP/BS ($18.4 \pm 3.9\%$ vs female mean = $21.6 \pm 6.8\%$) and high MS/BS ($30.3 \pm 1.8\%$ vs female mean = $23.0 \pm 9.3\%$). These sub-populations appear to represent different states of bone turnover. These data highlight that within a population, individuals presenting with similar bone mass may have differing statuses of formation or resorption. Moving forward, we will use clustering to map genes for states of bone turnover to improve identification of important genes controlling bone physiology.

Disclosures: Cheryl Ackert-Bicknell, None.

SU0107

Mouse with substitution of type I collagen 3-hydroxylation site has altered ECM but does not recapitulate the bone dysplasia of types VII/VIII Osteogenesis Imperfecta. Wayne Cabral¹, Nadja Fratzi-Zelman², Joseph Perosky³, Adrienne Alimasa³, Rachel Harris³, Peter Backlund⁴, Paul Roschger², Klaus Klaushofer², Antonella Forlino⁵, Kenneth Kozloff³, Joan Marini¹. ¹Bone & Extracellular Matrix Branch, NICHD, NIH, USA, ²Ludwig Boltzmann Institute of Osteology at Hanusch Hospital of WGKK & AUVA Trauma Centre Meidling, 1st Med. Dept. Hanusch Hospital, Austria, ³Orthopaedic Research Laboratories, Department of Orthopaedic Surgery, University of Michigan, USA, ⁴Biomedical Mass Spectrometry Facility, NICHD, NIH, USA, ⁵Department of Molecular Medicine, Biochemistry Unit, University of Pavia, Italy

Recessive types VII and VIII osteogenesis imperfecta (OI) are severe bone dysplasias caused by null mutations in the genes that encode prolyl 3-hydroxylase 1 (P3H1) or cartilage-associated protein (CRTAP), two mutually supportive components of the prolyl 3-hydroxylase (P3H) complex expressed in bone and cartilage. Individuals with types VII or VIII OI lack both the P3H complex components and post-translational hydroxylation of its collagen substrate at residue a1(I)P986. This primary modification defect leads to increased post-translational lysine hydroxylation of the type I collagen helix, consistent with delayed folding and loss of complex chaperone function. Several potential functions of the substrate modification have been proposed, including modulating collagen helical stability, fine-tuning the alignment of collagen monomers within fibrils, and regulating bone matrix mineralization. We therefore sought to clarify the role of the P986 substrate modification in bone dysplasia and collagen overmodification by generating a knock-in mouse model with an a1(I)P986A substitution that cannot be 3-hydroxylated. Exclusive expression of a1(I)A986 collagen in murine-derived tissues and cellular transcripts and protein was confirmed by cDNA sequencing and mass spectrometry. Neither heterozygous (986P/A) nor homozygous (986A/A) mice recapitulate critical features of types VII and VIII OI. Mutant mice exhibited normal growth rates, femoral mechanical properties (stiffness, ultimate load, brittleness) and collagen folding kinetics. However, the P986A substitution affected collagen biochemistry, matrix organization and mineralization. Despite normal P3H complex levels in cell lysates, 986P/A and 986A/A osteoblast type I collagen was moderately overmodified on PAGE analysis. Dermal fibrils of 986A/A displayed decreased diameters and heterogeneity. Skeletal staining and radiographs revealed flared rib cages, delayed

calvarial mineralization and kyphosis by 2 months in 986A/A pups. Interestingly, although femoral aBMD and TMD was reduced in 986A/A versus WT femora, bone matrix mineral density distribution assessed by qBEI was normal. Together, these data suggest that 3-hydroxylation of a1(I)P986 is important for regulating type I collagen modification, crosslinking and mineral organization in bone, but does not cause the severe bone pathology of collagen 3-hydroxylation defects, which likely result from absence of the ER complex and cartilage a1(II)P986 3-hydroxylation.

Disclosures: Wayne Cabral, None.

SU0108

Positive Effects of Pamidronate on Bone and Muscle in a Mouse Model of Duchenne Muscular Dystrophy. Sung-Hee Yoon^{*1}, Kim Sugamori¹, Marc Grynblas², Jane Mitchell¹. ¹University of Toronto, Canada, ²Samuel Lunenfeld Research Institute, Mount Sinai Hospital, Canada

Patients with Duchenne muscular dystrophy (DMD) often present with decreased bone mineral density and are at increased risk of peripheral fractures while ambulatory. Bisphosphonates have been used to treat bone pain and recurrent fractures in patients with DMD with positive outcomes. In this study we used a well characterized mouse model of DMD, the Mdx mouse, to assess the effects of early and brief treatment with the bisphosphonate pamidronate during a period of rapid bone growth from 5 to 13 weeks of age.

Mdx mice were injected subcutaneously with pamidronate at a dose of 2mg/kg body weight twice per week at 5 and 6 weeks of age to give a total dose of 8mg/kg body weight. Control and pamidronate-treated mice were assessed for muscle strength by weekly grip strength tests from 5-13 weeks. At 13 weeks of age, serum, bone and muscle tissue was assessed. Mice treated with pamidronate had increased cortical bone volume, architecture and strength with increased resistance to fracture in femurs. While overall long bone growth was not affected by pamidronate, there was significant inhibition of remodeling in metaphyseal trabecular bone with evidence of residual calcified cartilage. There were no effects of pamidronate on osteoclast, osteoblast or osteocyte numbers on trabecular bone, however, dynamic histomorphometry showed 80-90% reduction in bone formation. In vitro assessment of bone marrow derived osteoclasts showed 90% reduction in TRAP-stained multinucleated cells suggesting that pamidronate significantly depleted osteoclast precursors from the bone marrow.

Pamidronate treatment had positive effects on skeletal muscle in the Mdx mice with decreased serum creatine kinase, decreased mRNA encoding brain-type creatine kinase in muscle and evidence of improved muscle histology, however, muscle function measured by grip strength was not altered by pamidronate.

These results suggest that early use of bisphosphonates may have positive effects on cortical bone strength and decrease peripheral bone fractures in patients with DMD and has the potential to improve some aspects of dystrophic muscle pathology.

Disclosures: Sung-Hee Yoon, None.

SU0109

Tissue-Nonspecific Alkaline Phosphatase Enzyme Deficient Mice Reveal Cellular Mechanisms Leading to Craniosynostosis in Murine Hypophosphatasia. Hwa Kyung Nam¹, Jin Liu¹, Cassandra Campbell¹, Manisha Yadav², Jose Luis Millan², Nan Hatch^{*1}. ¹University of Michigan, USA, ²Sanford Burnham Medical Research Institute, USA

Hypophosphatasia (HPP) is a rare metabolic disorder that occurs due to loss-of function mutations in the gene (Alpl) encoding tissue-nonspecific alkaline phosphatase (TNAP). Alpl^{-/-} mice exhibit many characteristics seen in infantile HPP including long bone, tooth and craniofacial skeletal defects. Approximately 40% of infants affected with HPP develop craniosynostosis but it is unknown how premature cranial bone fusion occurs in this rachitic disorder. To investigate the etiology of HPP-associated craniosynostosis, we assessed pathogenic changes that occur prior to the onset of craniosynostosis in Alpl^{-/-} mice +/- daily postnatal subcutaneous injection with mineral-targeted TNAP. Craniosynostosis, cranial bone volume and density, and craniofacial skeletal shape abnormalities were assessed by histology, digital caliper measurements and micro CT. The influence of TNAP deficiency on cranial bone and suture cell proliferation and differentiation was assessed by immunohistochemistry, and in vitro studies of cells isolated from Alpl^{-/-} and Alpl^{+/+} mice. As expected, treatment with mineral-targeted TNAP prevented the cranial bone hypomineralization seen in Alpl^{-/-} mice. TNAP enzyme replacement also prevented a localized and transient cranial bone hypermineralization seen in untreated Alpl^{-/-} mice prior to the onset of craniosynostosis, and prevented craniosynostosis. Further analysis indicated that TNAP deficiency leads to aberrant osteoblastic gene expression and diminished proliferation in cranial bone cells and tissues. Some but not all of these cellular abnormalities were rescued by treatment with inorganic phosphate (Pi). Together, these results confirm an essential role for TNAP in craniofacial skeletal development and demonstrate the efficacy of TNAP enzyme replacement for preventing craniofacial abnormalities leading to craniosynostosis in murine infantile HPP. Future studies are required to determine if mineralization, differentiation and/or proliferation changes caused by TNAP deficiency cause craniosynostosis, and establish the degree to which TNAP influences other forms of craniosynostosis.

Disclosures: Nan Hatch, None.

This study received funding from: Alexion Pharmaceuticals International

SU0110

Towards the identification of the genetic defect underlying the osteopetrosis (op/op) rat. Eveline Boudin^{*1}, Hanna Witwicka², Geert Vandeweyer¹, Paul Odgren², Wim Van Hul¹. ¹Department of Medical Genetics, University & University Hospital of Antwerp, Belgium, ²Department of Cell Biology, University of Massachusetts Medical School, USA

The osteopetroses are rare genetic disorders characterized by increased bone mass resulting from a defect in bone resorption by osteoclasts. The group of osteopetroses is genetically, radiologically, and clinically very heterogeneous. So far, mutations in several genes have been identified which have increased the understanding of osteoclast differentiation and function. The osteopetrosis (op/op) rat is a severe osteopetrosis mutation spontaneously developed on a LEW/SsN background. The phenotype is inherited in an autosomal recessive manner and affected mutants show generalized sclerosis, fail to develop bone marrow cavities in the long bones, and the bones have a typical club-shaped appearance due to the impaired resorption. The osteoclasts of the op/op rats are larger, reduced in number, and their activity is greatly impaired, although, they still can form the ruffled borders and clear zones essential for the function of osteoclasts. Linkage studies demonstrated that the responsible gene is localized in a 1.36Mb region on chromosome 10. We previously reported the exclusion by Sanger sequencing of mutations in the coding regions of candidate genes such as Cln7 and Atp6v0c, located in the linked region. To identify the disease causing mutation in the op rat, the complete linked region (rn5, chr10: 13365691-14721326) was sequenced using sequencing-by-synthesis technology (HiSeq, Illumina Inc.). Sample preparation and enrichment of the selected region was performed using the KAPA library preparation kit combined with the NimbleGen SeqCap EZ choice technology. Sequence data of the complete region were generated for DNA from an op/op and two wild type (Lewis and BN/SsN background) rats. Next, the raw data were analyzed using the web-based platform Galaxy. Subsequently, all datasets were compared, and variants homozygous in the op/op rat sample and absent from the wild type samples and from the dbSNP database were selected and annotated using snpEFF. Using this strategy, we identified 77 unknown homozygous variants in the op/op rat sample. None of the variants are located in exonic regions. The majority of the variants, 28, are located in gene introns, while 21 and 9 variants are located respectively upstream or downstream of a gene, and the remaining 19 variants are located in between two genes. The conservation of the identified variants and the effect of the variants on splicing will be investigated in order to identify the disease causing variant.

Disclosures: Eveline Boudin, None.

SU0111

V-ATPase $\alpha 3$ R740S Mutation Affects Enamel Development in Osteopetrotic Mice. Lisa Johnson^{*1}, Bernhard Ganss¹, Celeste Owen², Grace Bradley¹, Irina Voronov¹. ¹University of Toronto, Canada, ²The Toronto Centre for Phenogenomics, Canada

Osteopetrosis is a disease characterized by sclerotic bone due to deficient osteoclast function. Over 50% of the cases of autosomal recessive osteopetrosis are associated with mutations in the vacuolar H⁺-ATPase (V-ATPase) $\alpha 3$ subunit. This multisubunit proton pump is highly enriched in osteoclasts and is responsible for extracellular acidification necessary for proper bone resorption. Patients with osteopetrosis also develop dental anomalies, such as delayed tooth eruption and enamel defects. Bone marrow transplantation at an early age corrects bone and tooth eruption abnormalities, but does not appear to rescue the enamel defects. We hypothesized that $\alpha 3$ -containing V-ATPases are also expressed in ameloblasts and play an important role in enamel formation. To test this hypothesis we investigated enamel mineralization and spatiotemporal expression of enamel matrix proteins using a mouse model with an $\alpha 3$ mutation. This mutation replaces evolutionary conserved arginine responsible for proton translocation with serine (R740S), resulting in a nonfunctional proton pump. Mice with this mutation have mild osteopetrosis in the heterozygous (+/R740S) and severe disease in the homozygous (R740S/R740S) animals. Histological and μ CT data showed that R740S/R740S mice displayed aberrations in both crown and root development, likely due to bony constraints created by the overabundant sclerotic mandibular bone. Enamel thickness and mineralization were significantly decreased in R740S/R740S mice compared to +/R740S and wild type (+/+) animals as measured by μ CT. Delayed enamel mineralization in R740S/R740S was confirmed by scanning electron microscopy. Immunohistochemistry showed that the expression pattern of secretory stage protein amelogenin was comparable in all three genotypes at postnatal day 5, but displayed heavier cytoplasmic staining in R740S/R740S ameloblasts at a later (day 9) time point, suggesting delayed transition to the maturation stage. The expression of maturation stage proteins amelotin and odontogenic ameloblast-associated protein (ODAM) had lighter and more diffuse staining patterns in R740S/R740S ameloblasts compared to other genotypes, confirming delayed transition to the maturation stage. $\alpha 3$ protein was expressed at low levels in the ameloblasts, with higher expression during the secretory stage. Our results suggest that $\alpha 3$ -containing V-ATPases may play a role in enamel protein secretion, contributing to enamel defects observed in R740S/R740S mice.

Disclosures: Lisa Johnson, None.

SU0112

Generation of human bone from a subject with osteogenesis imperfecta (OI) using iPSC-induced MSCs. Xiaonan Xin^{*1}, Xi Jiang¹, Liping Wang¹, Li Chen¹, Kyle Shin¹, Mark Kronenberg¹, Nathaniel Dyment¹, Jianping Huang¹, Benjamin Lerner¹, Keiichi Fukuda², Noemi Fusaki², Akihiro Iida², Mamoru Hasegawa², David Rowe¹, Alexander Lichtler¹. ¹University of Connecticut Health Center, USA, ²DNAVEC Corporation, Japan

Previously we reported our EB-EGM protocol for differentiation of hESC or iPSC into MSC-like cells, which form human cartilage and bone in a murine in vivo calvarial defect model. Histological analysis suggested that the implanted cells undergo endochondral-like bone formation, which was further confirmed by RT-PCR demonstrating expression of lineage specific human genes. Here we present the generation of human OI-iPSC and transplantation of the OI-iPSC derived MSC into a calvarial defect of the NSG/Col3.6GFP mouse. The OI iPSC were derived from the subject's fibroblasts harboring a COL1A1 Gly313Ala mutation utilizing Sendai viral vectors. This transplantation protocol resulted in better in vivo skeletogenic potential than iPSC produced with Yamanaka retroviral vectors. The transplanted mice were injected with calcein and tetracycline at 7 and 1 day prior to sacrifice, and the tissue within the defect was harvested at 12 weeks. The tissue formed by OI iPSC derived MSCs showed distinctly different morphology compared with tissue formed by control iPSC. In the control, the majority of the tissue was composed of chondrocytes, and bone was formed around invading blood vessels. In contrast, OI cells only formed bone near the edges of the defects. The bone tissue produced an actively mineralizing matrix that was forming in an appositional manner but without osteoclastic remodeling. It contained a marrow cavity and was separated from the rest of the implants by fibrous tissue. Human specific BSP antibody staining demonstrated accumulation of human bone matrix. Cells resembling hypertrophic cartilage cells were also seen, suggesting that the implanted OI iPSC derived MSCs underwent endochondral bone formation. However, the center of the defects showed no evidence of bone formation; instead, the majority of cells, which were human nuclear antigen positive, contained large vacuoles, with some having a signet ring appearance resembling adipocytes. Further analysis of specific markers will be done to determine whether these cells are adipocytes. The fact that human bone was only found next to the mouse bone at the edges of the defects suggests that the mouse bone may be facilitating production of bone by the human cells. We plan to use laser capture microscopy (LCM) to better understand the tissues formed by the OI iPSC cells and to probe the molecular consequences of the OI mutation on osteogenic differentiation and matrix production.

Disclosures: Xiaonan Xin, None.

SU0113

Serotonin Measured in Platelet Poor Plasma is Normal in OPPG Patients. Myrto Eliades¹, Sara Schwab^{*2}, Christine Simpson³, Karl Insogna³, Mary Pavlovich², Elizabeth Streeten². ¹University of Maryland School of Medicine, Us, ²University of Maryland School of Medicine, USA, ³Yale School of Medicine, USA

Purpose: Osteoporosis-pseudoglioma (OPPG) is a rare autosomal recessive disorder of childhood-onset osteoporosis and congenital blindness due to inactivating mutations of *LRP5*. Conflicting data in mice have been reported on the involvement of duodenal serotonin in the pathogenesis of OPPG. We previously found that serum serotonin was elevated in OPPG. However, platelet leakage of serotonin can cause spuriously high serum serotonin. The aim of this study was to measure serotonin in platelet poor plasma (PPP) and platelet pellet (PP) in OPPG patients compared to unaffected controls.

Methods: Eleven patients with OPPG (aged 15.0 ± 7.0 yrs) and known *LRP5* mutations and 16 unaffected first degree relatives (aged 25.5 ± 17.1 yrs) were recruited from our Old Order Mennonite kindred. This kindred consists of 3 nuclear families, all sharing common ancestors. Fasting blood was collected in tubes containing EDTA and ascorbic acid (5mg), immediately placed on ice and processed within 3 hours. An ELISA and ultrasensitive ELISA were used to measure PP and PPP serotonin respectively. Samples were blinded before being sent for analysis to the Yale Mineral Metabolism laboratory.

Results: The mean PPP serotonin level in subjects with OPPG was not different from that in controls (13.00 ± 6.93 vs. 10.86 ± 6.97 ng/mL; affected vs. control; $p=0.31$). There was no effect of age on PPP serotonin. The mean PP serotonin level was higher in OPPG (543.28 ± 174.67 vs. 403.25 ± 163.65 ng/mL; affected versus control; $p=0.04$). Since PP serotonin tended to decline with age the analysis was repeated using only closely age-matched affected and control subjects (11 affected vs. 9 controls; mean age 15 vs. 12 yrs respectively). In this analysis mean PPP serotonin levels remained the same in the two groups (13.00 ± 6.93 vs. 10.16 ± 6.78 ng/mL; affected vs. control; $p=0.22$), but mean PP serotonin levels were no longer significantly different (543.28 ± 174.67 ng/mL vs. 450.39 ± 155.27 ng/ml; affected vs. control; $p=0.40$).

Conclusions: Contrary to our previous results measuring serum serotonin, we found no significant differences in PPP and PP serotonin levels between 11 individuals with OPPG and 16 unaffected controls. Our results do not support the notion that circulating serotonin levels mediate the low bone mass resulting from loss-of-function mutations in *LRP5* in humans.

Disclosures: Sara Schwab, None.

SU0114

Characterization of Bone Phenotypes in Sickle Cell Trait and Sickle Cell Disease Mice. Liping Xiao^{*1}, Biree Andemariam¹, Pam Taxel¹, William T Zempsky², Douglas J Adams¹, Marja Marie Hurley¹. ¹University of Connecticut Health Center, USA, ²Connecticut Children's Medical Center, USA

The molecular mechanisms of bone loss in Sickle cell disease (SCD) have not been fully investigated. Sickle cell trait (SCT) is clinically silent; however, its effect on BMD or fracture risk is unknown. DXA of BMD and BMC was performed on 6 month-old female Control, SCT, and SCD mice. Micro-CT of vertebrae and femurs, and femur mechanical integrity testing (3-point flexure) was performed. Body weight was significantly decreased in SCT and SCD. Total body BMD was significantly decreased by 12% in SCD, and BMC significantly decreased by 20% and 19% in SCT and SCD, respectively. Tibial BMD was significantly decreased by 11% in SCD, and BMC significantly decreased by 12% and 11% in SCT and SCD, respectively. There was a 7% and 17% significant decrease in BMD and 10% and 19% decrease in excised femur BMC in SCT and SCD, respectively. Vertebral BMC of SCT and SCD were significantly decreased by 6 and 13%, respectively. Micro-CT revealed no differences in SCD or SCT femur trabecular bone: however, mid-diaphyseal cortical mass (Table 1) was significantly reduced in SCT and SCD. Cortical thickness was significantly decreased in SCD versus Control. Diaphysis structural stiffness and strength was significantly reduced in SCT and SCD (Table 2). Trabecular and cortical matrix mineralization density of SCD was reduced by 3.5% relative to Control and SCT mice. Histomorphometry (Table 3) of cortical femur showed a significant increase in N.Oc/B.Pm in SCD versus Control. Ir.L.Th, MAR, BFR/BS were significantly decreased in SCD compared with Control and SCT. BFR/BS was lower in SCT compared to Control. Trabecular analysis showed increased OC.S/BS but decreased Ir.L.Th, MAR, BFR/BS in SCD compared with Control.

Quantitative PCR of femur mRNA (Table 4) revealed decreased Runx2, osteocalcin and Dmp1 in SCD vs. Control and SCT. Trap was decreased in SCT vs. Control, and further decreased in SCD. Serum calcium, phosphorus, PTH, 25(OH)VitaminD, CTX-1 were normal. However serum osteocalcin and IGF-1 were decreased in SCD mice compared with Control and SCT. In addition IGF-1 was decreased in SCT mice compared with Control (Table 5).

We conclude that reduced bone mass in SCD and SCT mice carries architectural consequences that are detrimental to the mechanical integrity of femoral diaphysis, and may include deficits in cortical matrix integrity and/or mineral content. Furthermore reduced osteoblast terminal differentiation could contribute to reduced bone formation in SCD mice.

Table 1. Micro-CT analysis of Femur diaphysis of Control, SCT and SCD Mice

| | Control | SCT | SCD |
|----------------------------------|--------------|--------------|----------------|
| Length (mm) | 15.8 ± 0.14 | 15.1 ± 0.12* | 15.8 ± 0.01# |
| Total Area (mm ²) | 1.64 ± 0.04 | 1.48 ± 0.01* | 1.67 ± 0.03# |
| Cortical Area (mm ²) | 0.78 ± 0.03 | 0.68 ± 0.02* | 0.61 ± 0.02*# |
| Marrow Area (mm ²) | 0.86 ± 0.03 | 0.80 ± 0.02 | 1.06 ± 0.04*# |
| Cortical Thickness (mm) | 0.19 ± 0.01 | 0.18 ± 0.01 | 0.14 ± 0.01*# |
| Periosteal Perimeter (mm) | 4.44 ± 0.06 | 4.26 ± 0.04* | 4.68 ± 0.02*# |
| Endosteal Perimeter (mm) | 3.28 ± 0.06 | 3.17 ± 0.04 | 3.66 ± 0.02*# |
| Cortical Porosity (%) | 0.008 ± 0.00 | 0.007 ± 0.00 | 0.010 ± 0.05*# |
| Tissue Density (mg/ccm HA) | 1278 ± 13 | 1271 ± 13 | 1231 ± 0*# |

*: Compared with Control $p<0.05$; #: compared with SCT $p<0.05$, $n=5-8$

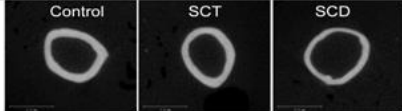


Table1

Table 2. Femur 3-point flexure tests of Control, SCT and SCD Mice

| | Control | SCT | SCD |
|--|-------------|--------------|--------------|
| Fracture Force (N) | 18 ± 1.3 | 14 ± 0.9* | 15 ± 0.7 |
| Fracture Moment (N-mm; force x 2.5) | 45 ± 3.3 | 35 ± 2.2* | 37 ± 1.7 |
| Bending Stiffness (N/mm) | 93 ± 9.1 | 77 ± 4.4 | 66 ± 1.6*# |
| Geometric prediction of stiffness (mm ³) | 0.13 ± 0.01 | 0.10 ± 0.00* | 0.11 ± 0.01 |
| Geometric prediction of strength (mm ³) | 0.19 ± 0.01 | 0.16 ± 0.00* | 0.16 ± 0.01* |
| Estimated matrix stiffness (MPa) | 233 ± 11 | 225 ± 11 | 232 ± 16 |
| Estimated matrix strength (GPa) | 14 ± 0.71 | 16 ± 0.64 | 12 ± 1.05# |

*: Compared with Control $p<0.05$; #: compared with SCT $p<0.05$, $n=5$

Table2

Table 3. Bone histomorphometric analysis of femur from Control, SCT and SCD Mice

| Cortical Endosteum | Control | SCT | SCD |
|--|--------------|--------------|---------------|
| OC.S/BS (%) | 25.06 ± 3.44 | 23.21 ± 3.12 | 31.00 ± 6.24 |
| N.Oc/B.Pm (1/mm) | 3.99 ± 0.42 | 4.61 ± 0.54 | 5.61 ± 0.80* |
| MS/BS (%) | 21.06 ± 1.76 | 16.94 ± 1.60 | 11.23 ± 3.11* |
| Ir.L.Th (um) | 8.25 ± 0.74 | 6.14 ± 0.80 | 3.56 ± 0.32*# |
| MAR (um/day) | 1.65 ± 0.15 | 1.23 ± 0.16 | 0.71 ± 0.06*# |
| BFR/BS (µm ³ /µm ² /day) | 0.34 ± 0.03 | 0.22 ± 0.04* | 0.09 ± 0.03*# |
| Trabecular | Control | SCT | SCD |
| OC.S/BS (%) | 50.02 ± 3.38 | 46.93 ± 4.64 | 46.87 ± 1.55 |
| N.Oc/B.Pm (1/mm) | 7.71 ± 0.52 | 8.69 ± 1.03 | 11.45 ± 1.98* |
| Ob.S/BS (%) | 23.20 ± 1.69 | 25.61 ± 0.90 | 22.69 ± 1.75 |
| MS/BS (%) | 28.10 ± 0.96 | 27.51 ± 1.50 | 23.97 ± 1.75* |
| Ir.L.Th (um) | 12.85 ± 2.45 | 8.32 ± 0.69 | 6.62 ± 0.64* |
| MAR (um/day) | 2.57 ± 0.49 | 1.66 ± 0.14 | 1.32 ± 0.13* |
| BFR/BS (µm ³ /µm ² /day) | 0.73 ± 0.15 | 0.46 ± 0.04 | 0.32 ± 0.05* |

* : Compared with Control p<0.05; #: compared with SCT p<0.05, n=6-8

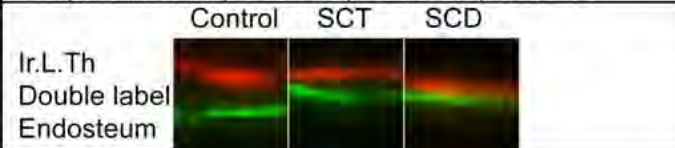


Table3

Table 4. qPCR of mRNA extracted from femurs of Control, SCT and SCD Mice

| | Control | SCT | SCD |
|-----------|-------------|--------------|---------------|
| Opg/Rankl | 0.73 ± 0.06 | 1.03 ± 0.14 | 0.73 ± 0.18 |
| Trap | 0.84 ± 0.05 | 0.30 ± 0.04* | 0.19 ± 0.03*# |
| Osterix | 1.17 ± 0.10 | 1.43 ± 0.22 | 0.91 ± 0.09# |
| Runx2 | 1.33 ± 0.10 | 1.46 ± 0.16 | 0.70 ± 0.08*# |
| Ocn | 0.93 ± 0.07 | 0.91 ± 0.12 | 0.22 ± 0.03*# |
| Dmp1 | 0.90 ± 0.06 | 1.12 ± 0.13 | 0.55 ± 0.06*# |

* : Compared with Control p<0.05; #: compared with SCT p<0.05, n=7-8

Table4

Table 5. Serum biochemistry markers of Control, SCT and SCD Mice

| | Control | SCT | SCD |
|--------------------------|--------------|---------------|----------------|
| Ca (mg/dL) | 10.68 ± 0.26 | 11.20 ± 0.34 | 10.50 ± 0.12 |
| P (mg/dL) | 7.11 ± 0.55 | 6.96 ± 0.74* | 7.35 ± 0.37 |
| PTH (pg/mL) | 125.4 ± 31.8 | 117.9 ± 23.1 | 104.2 ± 12.8 |
| CTX-1 (ng/ml) | 11.39 ± 0.44 | 12.09 ± 1.16 | 11.49 ± 1.33 |
| OCN (ng/ml) | 43.67 ± 3.64 | 34.17 ± 4.09 | 7.77 ± 2.58*# |
| IGF-1 (ng/ml) | 333.8 ± 22.0 | 254.9 ± 13.1* | 199.2 ± 10.2*# |
| 25(OH) Vitamin D (ng/ml) | 38.57 ± 1.49 | 38.84 ± 2.16 | 40.75 ± 1.21 |

* : Compared with Control p<0.05; #: compared with SCT p<0.05, n=7-8

Table5

Disclosures: Liping Xiao, None.

SU0115

Reduction of p27 expression correlates with somatic *MEN1* gene mutations in sporadic parathyroid adenomas. Filomena Cetani¹, Simona Borsari², Elena Pardi², Federica Saponaro², Liborio Torregrossa³, Fulvio Basolo³, Paolo Miccoli³, Claudio Marcocci². ¹University Hospital of Pisa Endocrine Unit 2, Italy, ²Department of Clinical & Experimental Medicine University of Pisa, Italy, ³Department of Surgical, Medical & Molecular Pathology & Critical Area University of Pisa, Italy

MEN1 is the main gene responsible for tumorigenesis of syndromic and sporadic primary hyperparathyroidism (PHPT). Up to date somatic mutations of the *MEN1* gene (20-35%) represent the main molecular defects of sporadic PHPT. Germline mutations of the Cyclin-Dependent Kinase Inhibitor 1B (*CDKN1B*) gene encoding p27 have been associated with multiple endocrine tumors in rats and humans. Menin, as a component of a Histone Methyltransferase Complex, directly regulates the expression of the *CDKN1B* binding to transcriptional regulatory elements of its promoter. P27 is mainly localized in the nucleus in quiescent cells, where negatively regulates the progression of G1 to S phase of the cell cycle, whereas in proliferating cells a fraction translocate to the cytoplasm where it can be degraded by proteolysis. Loss or reduced nuclear expression of p27 have been frequently detected in various

human malignancies, while *CDKN1B* somatic mutations are rarely involved in tumorigenesis.

We evaluated the expression of p27 protein in a group of 50 sporadic parathyroid adenomas *CDKN1B* mutation-negative and its statistic correlation with *MEN1* gene mutations.

Immunohistochemistry was performed using the Ventana Benchmark immunostaining system. A monoclonal anti-p27 antibody was used to detect p27 expression. Nuclear and cytoplasmic p27 expression was scored as "negative" in case of no staining in any cell, or ≤20-10%, respectively, of positive cells. In addition, *MEN1* gene alterations were studied by automatic sequencing the tumor DNA and performing Loss of Heterozygosity (LOH) analysis at *MEN1* locus. Fifty-four percent (27/50) of the sporadic adenomas had negative p27 nuclear staining. Positive cytoplasmic staining was detected in 12 adenomas (24%). Somatic *MEN1* mutations (associated with LOH in all, but one sample) were identified in 15 of 50 (30%) samples. Twelve of 15 *MEN1* mutation-positive adenomas (80%) had a negative nuclear p27 staining. Moreover, we observed that no *MEN1* mutation was detected in samples with positive p27 cytoplasmic staining.

The occurrence of *MEN1* gene mutations in our cohort is in agreement with the percentage previously reported in the literature in sporadic parathyroid adenomas. Herein we found that *MEN1* mutations significantly segregated in tumors negative for p27 nuclear and cytoplasmic staining, suggesting that menin inactivation may be directly related to the downregulation of p27 expression through the inhibition of *CDKN1B* transcription rates.

Disclosures: Filomena Cetani, None.

SU0116

Anti-inflammatory role of Vitamin D in IL-1β-mediated inflammatory chemokine, IL-8 synthesis in Osteoarthritis. Aparna Maiti¹, William A Jiranek². ¹Virginia Commonwealth University, USA, ²Virginia Commonwealth University School Medicine, USA

Osteoarthritis (OA), is one of the most common form of arthritis, and the leading cause of chronic disability in the United States. The common risk factors for OA include obesity, previous joint injury, genetics, epigenetics and anatomical factors. Additional factors include gender, race, and nutritional factors, such as vitamin D deficiency. There are various pro-inflammatory mediators found to be increased in OA patients, including interleukin-1β (IL-1β), interleukin-6 (IL-6), interleukin-8 (IL-8), and tumor necrosis factor-α (TNF-α). IL-1β production is markedly increased, and has the capability to induce several pro-inflammatory mediators including IL-8, TNF-α, angiogenic factors, and proteolytic enzymes involved in the recruitment of local hematopoietic cells during OA. These catabolic effects of IL-1β are exerted through the activation of several signaling pathways including the activation of master transcription factor NF-κB, which regulates several genes including IL-8, and TNF-α. Vitamin D has many immunomodulatory actions and deficiency is linked to the development of arthritis although the mechanism is unclear. Severe vitamin D deficiency is also associated with methylation changes in immune cells DNA. We observed that high level of IL-8 induction in low serum vitamin D human synovial tissue samples which suggests that serum vitamin D deficiency may enhance the development of OA. However, whether Histone methylation (H3K9me3), a repressor histone mark of transcription, is also involved in vitamin D-mediated IL-1β activated IL-8 mRNA synthesis regulation remains mostly unknown in OA. In our study, we explored the molecular basis of IL-1β mediated IL-8 regulation and anti-inflammatory role of vitamin D associated with OA progression in humans. Adult human mesenchymal stem cells (hMSCs) have the ability to differentiate into different bone cells lineage. We used hMSCs as our cell model to explore our hypothesis. We found that IL-1β treatment to hMSCs or IL-1β treated human monocytes (U937) conditioned medium enhanced NFκB activation and its several target genes including IL-8, and TNF-α mRNA synthesis in hMSCs. Furthermore, vitamin D pre-treatment with hMSCs inhibits IL-1β-mediated NFκB activation and IL-8 mRNA synthesis. Interestingly, vitamin D pre-treatment followed by IL-1β treatment in hMSCs, dramatically enhanced nuclear bulk histone H3 methylation (H3K9me3), a repressor mark of transcription. Our data suggested that vitamin D is playing an important anti-inflammatory role via inhibition of NFκB and enhancing promoter histone H3 methylation (H3K9me3) for transcription repression of inflammatory mediators such as IL-8 in OA.

Disclosures: Aparna Maiti, None.

SU0117

Fibroblast growth factor 23 (FGF23) increases cardiac contractility and induces cardiac mechanical alternans which are eliminated by FGFR4 antibody treatment. Matthew Hendrix¹, Chelsea Shapland¹, Chad Touchberry², Alexander Grabner³, Christian Faul³, Michael Wacker¹. ¹University of Missouri-Kansas City School of Medicine, USA, ²University of Memphis, USA, ³University of Miami School of Medicine, USA

FGF23 is released by osteocytes and is an important hormone in bone-kidney crosstalk in the regulation of phosphate. During chronic kidney disease (CKD), as kidney function declines, plasma levels of FGF23 increase significantly in order to maintain phosphate homeostasis. This increase in FGF23 has been correlated with

cardiac pathologies. Recently, we have shown that acute FGF23 increases intracellular calcium in isolated adult primary cardiomyocytes as well as increases cardiac contractility in left ventricular cardiac muscle strips. While FGFR1-4 are expressed in the heart, it is currently unknown which receptor mediates the acute effects of FGF23 on cardiac muscle contractility. Therefore, in this study we utilized adult male CD1 mouse hearts and dissected out left ventricular muscle strips to test the effects of FGF23 on contractility in the presence of an isoform specific FGFR4 blocking antibody (U3 Pharma/Daiichi-Sankyo). In addition, to determine if our results translated to a whole heart preparation, the aortas of isolated hearts were cannulated and we reverse perfused the coronary circulation by a modified Langendorff system. Both muscle strip and whole heart preparations were hung in an oxygenated organ bath containing stimulating electrodes, pacing was set between 1 and 1.5 Hz, and contraction was measured. FGF23 treatment (9000 pg/ml) of paced left ventricular muscle strips increased contractility 1.6 ± 0.1 fold over control contraction ($P < 0.01$; $n = 5$) and pretreatment with anti-FGFR4 eliminated this increase ($P > 0.05$ compared to control; $n = 5$). Interestingly, FGF23 treatment of paced Langendorff perfused hearts caused contraction abnormalities predominantly in the form of mechanical alternans (17 ± 6 alternans/min) followed by transient increases in cardiac contractions (1.4 ± 0.1 fold over control; $P < 0.01$; $n = 4$). Anti-FGFR4 pretreatment of perfused hearts prevented both the FGF23-induction of alternans as well as the change in contraction ($P > 0.05$ compared to control; $n = 4$). These results suggest that FGF23 works via FGFR4 to alter cardiomyocyte calcium levels which affects cardiac contractility and promotes abnormal ventricular rhythms. Previously, it has been shown that pathological hypertrophy induced by chronic FGF23 administration was also mediated by FGFR4 (Faul et al. 2014) and thus the cardiac contractility, calcium homeostasis, and hypertrophy effects may be linked. In conclusion, cardiac FGFR4 is an important target for preventing the cardiac effects of FGF23 on the heart during CKD.

Disclosures: Matthew Hendrix, None.

SU0118

Metabolic Acidosis Stimulates MEPE Expression Regulating Fibroblast Growth Factor 23 in Osteoblasts. Nancy Krieger^{*1}, Min Ho Kim², David Bushinsky². ¹University of Rochester, USA, ²University of Rochester School of Medicine, USA

Serum fibroblast growth factor 23 (FGF23) increases significantly with progressive chronic kidney disease (CKD), leading to reduced renal tubular phosphate (Pi) reabsorption and decreased serum 1,25(OH)₂D₃. Increased FGF23 is associated with increased mortality. FGF23 is synthesized in osteoblasts and osteocytes; however, the primary factors regulating its production are not clear. Patients with CKD have decreased renal net acid excretion leading to metabolic acidosis (MET). During MET, acid is buffered by bone with release of mineral calcium (Ca) and Pi. MET increases intracellular Ca signaling and cyclooxygenase 2 (COX2)-induced prostaglandin production in the osteoblast leading to decreased osteoblastic bone formation and increased osteoclastic bone resorption. We recently found that MET directly stimulates FGF23 in mouse bone and primary osteoblastic cells utilizing the same signaling pathways. To further characterize the regulation of FGF23 by MET we have studied gene expression pathways upstream of FGF23 production in primary cells isolated from neonatal mouse calvariae. Confluent osteoblastic cells were incubated in neutral (NTL, pH=7.44, Pco₂=38 mmHg, [HCO₃]=27 mM) or acid (MET, pH=7.18, Pco₂=37 mmHg, [HCO₃]=13 mM) medium. The major extracellular phosphoglycoprotein, MEPE, has been shown to stimulate FGF23. We observed a significant stimulation of MEPE RNA expression as early as 3h after changing to MET medium compared to NTL (relative expression = 1.47 ± 0.30 , MET vs 0.76 ± 0.12 , NTL, $p < 0.05$). Significant stimulation increased further at 6 and 24h. This early increase in MEPE precedes any significant stimulation of FGF23 RNA expression by MET in the osteoblast which first becomes significant by 6h. No significant changes in PHEX expression were observed in response to MET compared to NTL. Thus, the stimulation of MEPE by MET appears to be an initial step in the regulation of FGF23 by MET in mouse osteoblasts. By better understanding the MET regulation of FGF23 in bone, therapeutic interventions directed toward correction of MET, especially in CKD patients, can be devised and have the potential to not only prevent bone resorption but also lower FGF23 and perhaps decrease mortality.

Disclosures: Nancy Krieger, None.

SU0119

Ablation of maternal Gnas exon Nesp (Nesp^{m-/p+}) in mice dramatically reduces Gsa expression in brown adipose tissue. Olta Tafaj^{*1}, Harald Juppner². ¹Massachusetts General Hospital, Harvard Medical Sc¹, USA, ²MGH, USA

The *Gnas* locus gives rise to *Gsz* and several splice variants, including 1A, Xlas, Nespas and Nesp. The promoters for 1A, XI, and Nespas are methylated on the maternal allele and transcripts are thus derived exclusively from the paternal allele; the converse is observed for Nesp. The promoter for *Gsz* does not undergo parent-specific methylation. However, in some tissues, like proximal renal tubules (PRT), *Gsz* is derived mainly from the maternal allele, while expression from the paternal allele is silenced through unknown mechanisms. PTH-responsive PRT cells are difficult to isolate, thus precluding their use for mechanistic studies. Brown adipose tissue (BAT), which also shows predominantly maternal *Gsz* expression, can be readily

isolated from mice of different ages. Using RT-qPCR, *Gsz* expression in WT-BAT was maximal at E17.5 and then declined after birth. XI, 1A, and Nesp transcript levels were maximal at E16.5 and showed a pronounced decline by P20. To distinguish between maternal and paternal RT-PCR products, we took advantage of a SNP in exon 11 (G in Sv129; C in BL6). Matings between WT-Sv129 females and WT-BL6 males resulted in offspring that are heterozygous for the SNP thus allowing assessment of the parental contribution by BanII enzyme digestion of the PCR products. Densitometric gel analysis of RT-PCR digests revealed that *Gsz* in BAT is predominantly transcribed from the maternal allele at all developmental time points (E16.5 to P60). To investigate the genomic elements that potentially contribute to *Gsz* allelic silencing, BAT from mice with maternal ablation of *Gnas* exons Nesp/Nespas2-4 (Nesp^{m-/p+}) and XI (XI^{p-/m+}) were studied. At E18.5, BAT from Nesp^{m-/p+} mice, which show decreased methylation at *Gnas* exons 1A, XI, and Nespas, revealed a >3-fold decrease in overall *Gsz* transcript levels. This decrease in *Gsz* expression occurred primarily because of reduced transcription from the maternal allele; surprisingly, however, transcripts appeared to be derived from both parental alleles. Conversely, BAT from mice with ablation of the paternal exon XI (XI^{m+/p-}) revealed on day P2 an $\approx 30\%$ increase in *Gsz* mRNA level that could be attributed to enhanced paternal expression. Taken together, our data indicate that *Gsz* expression in BAT is strongly affected by *Gnas* methylation and that a non-methylated *Gnas* region comprising exon XI and possibly exon 1A may contribute *in cis* to the reduction of paternal *Gsz* expression in BAT and possibly other tissues, such as PRT cells.

Disclosures: Olta Tafaj, None.

SU0120

Intermittent PTH treatment induces bone anabolism through regulatory T cells. Mingcan Yu^{*1}, Lindsey Walker¹, Jerid Robinson¹, Abdul Malik Tyagi¹, Jau-Yi Li¹, Jonathan Adams¹, Richard DiPaolo², Roberto Pacifici³. ¹Emory University, USA, ²St. Louis University, USA, ³Emory University School of Medicine, USA

Intermittent PTH (iPTH) treatment stimulates bone formation and increases bone mass in mice and humans. iPTH stimulates bone marrow (BM) CD8+ T cells to release Wnt10b, an osteogenic Wnt ligand essential for inducing Wnt signaling in osteoblastic cells and bone formation. In this study we have found that iPTH treatment at 80µg/kg/day for 4 weeks increases the production of Wnt10b by CD8+ T cells by increasing the differentiation of BM naïve CD4+ cells into CD25+Foxp3+ regulatory T cells (Tregs), an effect which results in a >2 fold increase in the number of BM Tregs. iPTH directly targets CD4+ cells and increases their sensitivity to the Treg-inducing factor TGFβ, via a dual effect on notch signaling. iPTH upregulates the Notch ligand Jagged1 in osteoblasts (OBs) and increases the sensitivity of CD4+ cells to Jagged1. The resulting upregulation of Notch-1c leads to recruitment of Smad3 and RBPJ to the Foxp3 promoter to activate Foxp3 transcription. B cells are the most abundant antigen presenting cells in the BM. Tregs down regulate the costimulatory molecules CD80/86 on B cells via their surface receptor CTLA4, thus preventing the activation of CD28 on CD8+ cells. Stimulation of CD8+ cells by iPTH in conditions of blunted CD28 signaling stimulates Wnt10b gene expression. This is because repression of CD28 signaling leads to inhibition of a β-arrestin-phosphodiesterase complex, resulting in up-regulation of cAMP levels in T cells. The Wnt10b promoter contains two essential CREB binding sites and cAMP is a critical inducer of Wnt10b transcription. To demonstrate relevance, Tregs were depleted *in vivo* by either treatment of WT mice with anti CD25 Ab, or by treating DEREK mice with diphtheria toxin (DT). DEREK mice express DT receptor under control of the FoxP3 promoter. Thus, FoxP3+ Tregs are selectively depleted in DEREK mice upon DT administration. In both models *in vivo* depletion of Tregs prevents the capacity of iPTH to expand Tregs, induce Wnt10b production, activate Wnt signaling, stimulate bone formation and increase bone mass. In summary these findings demonstrate a novel effect of PTH on the differentiation of naïve CD4+ cells into Tregs. Expansion of Tregs is a critical, previously unknown mechanism by which iPTH exerts its bone anabolic activity.

Disclosures: Mingcan Yu, None.

SU0121

PTEN is a novel mediator of the anti-proliferative effects of (1-34) PTH in osteoblastic cells. Andrew Sunters¹, Imelda McGonnell², Robert Fowkes², Gabriel Galea², Lance Lanyon³, Joanna Price^{*4}. ¹Royal Veterinary College, United Kingdom, ²The Royal Veterinary College, United Kingdom, ³Bristol University, United Kingdom, ⁴University of Bristol, United Kingdom

PTH and mechanical loading are both potent osteogenic stimuli, with intermittent PTH being the only drug licensed to treat osteoporosis. In young mice PTH and mechanical loading also act synergistically to increase cortical bone mass. Here we explore the potential mechanisms underlying this interaction, specifically the role of the phosphatidylinositol 3-kinase (PI3K) pathway that is known to be activated by mechanical strain in osteoblasts. Quiescent UMR-106 osteoblastic cells treated with 10-100pM (1-34) PTH displayed a mitogenic response, but no proliferation was

observed with doses exceeding 1nM. Similarly 10-100pM PTH had no effect on exponential proliferation whilst doses exceeding 1nM blocked proliferation. Mechanical strain-induced proliferation following application of 4-point bending to serum depleted UMR106 cells was unaffected by 100pM PTH, but attenuated by 100nM, which also attenuated the expression of the Wnt inhibitor Sost. Western blotting showed that activation of the AKT/GSK-3 beta/beta-catenin axis by strain was unaffected by 100pM, but blocked by 100nM PTH. PTH induced a dose-dependent increase in the expression of the phosphatase MKP-1, maximally increasing between 1 and 100nM, correlating with reduced AKT phosphorylation. AKT phosphorylation increased following treatment with the PKA inhibitor H89, basally or in response to PTH or by PKA activators di-Br ATP or forskolin, suggesting a dependence of MKP-1 induction on protein kinase A. 100nM PTH treatment or ectopic over-expression of MKP-1 correlated with increased expression of the PI3K inhibitor PTEN and subsequent reduction of AKT phosphorylation. 100nM PTH treatment of ROS17/2.8 cells, which lack PTEN, failed to inhibit AKT phosphorylation or proliferation, despite stimulating MKP-1. Transfection of UMR-106 cells with anti-PTEN siRNA attenuated PTH inhibition of AKT phosphorylation and proliferation, highlighting a key role for PTEN in regulating AKT mediated control of proliferation. 100nM PTH inhibited AKT inhibitory phosphorylation of Foxo3a correlating with increased expression of the cell cycle regulator p27, a Foxo3a and PTH target. The observation that PKA-dependent activation of MKP-1 by PTH stimulates PTEN expression, repression of AKT and subsequent Foxo3a mediated transcription of p27 represents a novel mechanism underlying the anti-proliferative effects of PTH, potentially rendering cells insensitive to the proliferative effects of Sost attenuation.

Disclosures: Joanna Price, None.

SU0122

Dietary Fat Independent of Caloric Intake Impairs Cortical Bone Structure via Glucocorticoid Signaling in Osteoblasts and Osteocytes. Sarah Kim^{*1}, Holger Henneicke², Sylvia Gasparini², Markus Seibel³, Hong Zhou². ¹ANZAC Research Institute, Australia, ²Bone Research Program, ANZAC Research Institute, The University of Sydney, Australia, ³Department of Endocrinology & Metabolism, Concord Hospital, The University of Sydney, Australia

High-fat diets adversely affect bone morphology, strength and development while simultaneously increasing systemic glucocorticoid levels. We hypothesized that a mechanistic link exists between high dietary fat content, increased glucocorticoid signaling in osteoblasts and osteocytes and structural bone changes.

We tested this hypothesis in a transgenic (tg) mouse model in which glucocorticoid signaling has been selectively disrupted in osteoblasts and osteocytes via targeted overexpression of the glucocorticoid-inactivating enzyme, 11 β -hydroxysteroid dehydrogenase type 2. Seven-week-old male tg mice and their wild type (WT) littermates (n=12-15/group) were fed *ad libitum* a control diet (13.8kJ/g total energy (TE), 14% TE as fat, 26% TE as protein) or an isocaloric high-fat diet (iHFD; 13.8kJ/g TE, 43% of TE as fat, 26% TE as protein) for 18 weeks. Body weight and food intake were measured weekly and serum corticosterone (CS) levels were quantified after 10 weeks of feeding. At endpoint, body composition was assessed by DXA, and both the tibia and L3-vertebra were analyzed by micro-CT.

As animals were fed an isocaloric diet, changes in body weight, lean mass and fat mass did not differ between groups. Mice fed the iHFD had higher serum CS concentrations than mice on the control diet (iHFD: 365 \pm 24nM CS vs. control: 291 \pm 33nM CS; p=0.07). Serum CS levels in WT and tg mice fed the same diets were similar (control: WT 288 \pm 32nM CS, Tg 295 \pm 56nM CS; iHFD: WT 352 \pm 36nM CS, Tg 378 \pm 33nM). Isocaloric high-fat feeding resulted in significant loss of tibial cortical volume (WT: -14% vs. tg: -1%, p<0.01), cortical thickness (WT: -15% vs. tg: -1%, p<0.05) and area (WT: -14% vs. tg: -1%, p<0.01) in WT but not tg mice when compared to their respective controls. Similarly, WT iHFD mice exhibited loss of tibial trabecular bone mass when compared to WT controls (BV/TV: -23%, p=0.07). This difference was due to a decrease in trabecular number and a corresponding increase in trabecular separation, while trabecular thickness remained unaffected. In iHFD tg mice, tibial trabecular bone was not significantly affected compared to control fed tg mice (BV/TV: -15%, p=0.54). Trabecular bone in the vertebra was unaffected in both WT and tg iHFD mice.

We conclude that high dietary fat intake, independent of overall caloric intake and obesity induces severe loss of cortical bone via glucocorticoid signaling in osteoblasts and osteocytes.

Disclosures: Sarah Kim, None.

SU0123

Estrogens protect against endocortical bone resorption in both female and male mice; likely via ER α -mediated suppression of SDF1/CXCL12 in uncommitted mesenchymal progenitors. Srividhya Iyer^{*1}, Serra Semahat Ucer², Ha-Neui Kim², Li Han², Aaron Warren², Julie Crawford², Maria Almeida², Stavros Manolagas². ¹Central Arkansas VA Healthcare System, Univ of Arkansas for Medical Sciences, USA, ²Center for Osteoporosis & Metabolic Bone Diseases, Central Arkansas Veterans Healthcare System, University of Arkansas for Medical Sciences, USA, USA

Estrogens in women and both androgens and estrogens in men contribute to the maintenance of bone mass. Evidence from mice with conditional deletion of the estrogen (ER) or androgen (AR) receptors has revealed that in cortical, but not cancellous, bone ER α signaling in uncommitted mesenchymal progenitors targeted by Prx1-Cre attenuates endocortical resorption in females. The effects of androgens, on the other hand, do not require AR signaling in any cell type of the mesenchymal lineage, nor do they require ER α signaling downstream of committed osteoblast progenitors targeted by Osx1-Cre, or AR or ER α signaling in the osteoclast lineage. We investigated the possibility that ER α signaling in uncommitted mesenchymal progenitors protects against endocortical resorption in both sexes. We report that estrogens (E2), but not androgens (DHT), prevented the ORX-induced loss of cortical bone mass in C57BL/6 mice; DHT, nonetheless, prevented the loss of cancellous bone. We next performed microarray analysis of FACS preparations of GFP:Osx1-Cre targeted ER α null cells and identical cell preparations from mice with intact ER α . The mRNA for stromal cell-derived factor1 (SDF1) a.k.a CXCL12 – a chemotactic cytokine that is abundantly expressed in Prx1-Cre targeted cells and promotes osteoclast generation – was increased by 3.7-fold. Similarly, the mRNA and secreted protein levels of SDF1 were higher (5- and 100- fold, respectively) in bone marrow cell cultures from female ER α ^{fl/fl}:Prx1-Cre mice as compared to identical cultures from littermate controls. More strikingly, both OVX and ORX increased the levels of SDF1 in the bone marrow plasma; and E2 administration to ORX mice prevented it. Bone marrow macrophages co-cultured with ER α ^{fl/fl}:Prx1-Cre bone marrow stromal cells developed twice as many TRAP+ osteoclasts as compared to similar cultures of ER α ^{fl/fl} cells. Finally, the protein levels of SDF1 in the supernatant of bone marrow cell cultures from wild type C57BL/6 mice was decreased in the presence of E2; and the SDF1 mRNA in the same cells was also decreased by E2, but not DHT. These data suggest that estrogens protect against endocortical resorption in both males and females, at least in part, via ER α -mediated actions (upon aromatization of androgens to estrogens in males) on Prx1-Cre targeted uncommitted mesenchymal progenitors. These actions repress SDF1 production, thereby attenuating osteoclast formation (and perhaps homing) at the endosteal surface.

Disclosures: Srividhya Iyer, None.

SU0124

Female Mice are Resilient to Glucocorticoid-Induced Bone Loss. Sylvia Gasparini^{*1}, Holger Henneicke², Sarah Kim², Lee Thai², Hong Zhou², Markus Seibel³. ¹ANZAC Research Institute, Australia, ²Bone Research Program, ANZAC Research Institute, The University of Sydney, Sydney, NSW, Australia, Australia, ³Department of Endocrinology & Metabolism, Concord Hospital, The University of Sydney, Sydney, NSW, Australia, Australia

Glucocorticoid induced osteoporosis (GIO) is the most common form of secondary osteoporosis (1). However, to date, most mechanistic studies of GIO have been performed in male mice. We compared the effect of exogenous glucocorticoid (GC) administration on bone in male and female mice, while concurrently examining the main cellular target of GCs in the skeleton.

We made use of a transgenic (tg) mouse model in which GC signaling has been selectively disrupted in osteoblasts and osteocytes via targeted overexpression of the glucocorticoid-inactivating enzyme, 11 β -hydroxysteroid dehydrogenase type 2. Eight-week-old male (M) and female (F) wild-type (wt) and tg mice received either placebo (plc) or corticosterone (CS) at a dose of 50 μ g/ml or 75 μ g/ml dissolved in the drinking water for 4 weeks. Body weight and water intake were measured weekly, while body composition as well as bone mineral content (BMC) and density (BMD) were assessed by DXA at baseline and endpoint.

Male and female mice consumed the same amount of water irrespective of treatment (~4ml/mouse/day). The physiological increase in BMC (Fig 1.; M-plc-wt +17%, M-plc-tg +24%, F-plc-wt +23%, F-plc-tg +29%) was dose dependently diminished by CS administration in male wt mice while tg mice increased their BMC despite CS exposure, particularly at a lower CS dose (M-50 μ g-wt +5.6% vs. M-50 μ g-tg +14%, p<0.05 & M-75 μ g-wt +0.4% vs. M-75 μ g-tg +8.8%, p<0.05). Surprisingly BMC in female mice was unaffected by CS treatment even at the higher CS dose (F-50 μ g-wt +17.7% vs. F-50 μ g-tg +24.3%, p=ns & F-75 μ g-wt +18.4% vs. F-75 μ g-tg +22.4%, p=ns). Similar observations were made for BMD, where CS treatment adversely affected wt males while wt females remained resilient to CS (M-50 μ g-wt +6.7% vs. F-50 μ g-wt +10.1%, p=0.06 & M-75 μ g-wt +6.1% vs. F-75 μ g-wt +12.7%, p<0.01).

Disruption of glucocorticoid signalling in the osteoblast partially protects male mice from the deleterious effects of GCs on bone. Interestingly, young female mice are less sensitive than their male littermates to the negative impact of high dose exogenous GCs on bone.

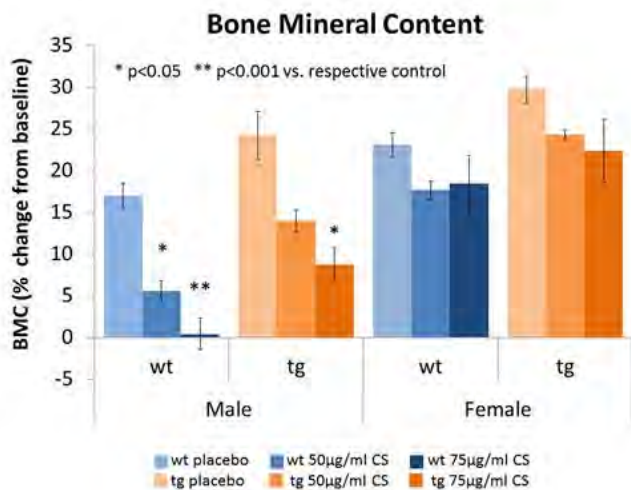


Figure 1

Disclosures: Sylvia Gasparini, None.

SU0125

The Adipokines and Estradiol in Relation to Bone Mineral Density and Carotid Atherosclerosis in Postmenopausal Women – The OSTPRE-BBA Study. Miika Värri*¹, Leo Niskanen², Tomi-Pekka Tuomainen³, Risto Honkanen⁴, Heikki Kröger⁵, Marjo Tuppurainen⁶. ¹University of Eastern Finland, Finland, ²Endocrinology, Helsinki University Hospital & University of Helsinki, Finland, ³Institute of Public Health & Clinical Nutrition, University of Eastern Finland, Finland, ⁴Kuopio Musculoskeletal Research Unit (KMRU), Surgery, Institute of Clinical Medicine, University of Eastern Finland, Finland, ⁵Department of Orthopaedics, Traumatology & Hand Surgery, Kuopio University Hospital, Finland, ⁶Department of Obstetrics & Gynaecology, Kuopio University Hospital, Finland

Purpose: Carotid artery calcifications (CAC) and high carotid arteries intima-media thickness (cIMT) are by unknown mechanisms associated with low bone mineral density (BMD) in postmenopausal women. The link between atherosclerotic vascular changes and BMD may be via the adipose tissue, which by secreting adiponectin and leptin and modifying estradiol (E2), may influence these processes. Our aim was to study the relationships of aforementioned factors to bone health (BMD) and carotid atherosclerosis measured with CAC and cIMT. **Methods:** This cross sectional OSTPRE-BBA study (Bone, Brain and Atherosclerosis) is a part of the Kuopio Osteoporosis Risk Factor and Prevention Study (OSTPRE), Finland. The 290 women (mean age 73.6 years, range 69.2 – 79.2) were randomly selected from the OSTPRE cohort in 2009. BMD, total body fat mass (FM) were measured with dual energy x-ray absorptiometry (DXA), cIMT (mm) and CAC (no/yes) were measured with B-type ultrasound. Free estradiol, adiponectin and leptin were measured from serum samples. Correlation, analysis of variance, linear and binary logistic regression were used in analyses between BMD, CAC or cIMT as dependent variable and adipokines or E2 as independent variable. The analyses with BMD were adjusted with total body FM, age, current smoking, and with E2 levels, where appropriate. The analyses with CAC were adjusted with total body FM, age and dietary calcium intake. **Results:** Total body FM was associated with leptin ($r=0.795$, $p<0.001$) and adiponectin ($r=-0.305$, $p<0.001$). E2 levels were associated with leptin ($\hat{O}=0.131$, $p<0.001$), but not with adiponectin (adjusted with FM). There were no significant differences between E2 tertiles and total or femoral neck BMD nor with cIMT and CAC. Serum adiponectin levels were inversely associated with femoral neck ($\hat{O}=-0.142$, $p=0.019$), and total body BMD ($\hat{O}=-0.138$, $p=0.009$), but showed no relationships with CAC. Leptin levels were not associated with BMD. The odd's ratio was 1.6 between CAC and leptin quartiles ($p=0.010$). There were no associations between adipokines and cIMT. **Conclusions:** In conclusion, the loss of the bone mineral and vascular calcification are connected by adipokines secreted by adipose tissue in postmenopausal women. Endogenous E2 levels were not independently associated with BMD or vascular calcifications, but cross-sectional analysis may not reveal the role of E2 in these processes.

Disclosures: Miika Värri, None.

SU0126

1,25-Dihydroxyvitamin D Induces Vitamin D Receptor-Dependent Large-Scale Changes in mRNA Expression in Human Skeletal Muscle Cells. Zachary Ryan¹, Theodore Craig¹, Clifford Folmes², Xuwei Wang³, Ian Lanza⁴, Niccole Schaible⁵, Jeffrey Salisbury⁶, K. Sreekumaran Nair⁴, Andre Terzic², Gary Sieck⁷, Rajiv Kumar*¹. ¹Division of Nephrology & Hypertension, Department of Medicine, USA, ²Division of Cardiovascular Diseases, Department of Medicine, USA, ³Division of Biomedical Statistics & Informatics, Department of Health Sciences Research, USA, ⁴Division of Endocrinology, Department of Medicine, USA, ⁵Mayo Clinic, USA, ⁶Department of Biochemistry & Molecular Biology, USA, ⁷Department of Physiology, Biophysics & Biomedical Engineering, USA

Muscle weakness and myopathy are prominent features of vitamin D deficiency and respond rapidly to therapy with vitamin D3. Treatment with 1-hydroxylated vitamin D analogs reduces falls in humans. The goal of this study was to determine whether 1,25-dihydroxyvitamin D3 (1,25(OH)2D3) alters skeletal muscle function in humans through changes in nuclear gene expression.

Gene expression was assessed using next generation, whole transcriptome sequencing (RNA-seq) following treatment of primary cultures of human skeletal muscle cells with 1,25(OH)2D3, 10-8M or vehicle. Primary cultures of human skeletal muscle cells treated with control siRNA or vitamin D receptor (VDR) anti-sense siRNA prior to treatment with 1,25(OH)2D3 were analyzed by RNA-seq. Human skeletal muscle biopsies and skeletal muscle cells were verified to express the VDR. Over one thousand nine hundred genes were differentially expressed following treatment of VDR-expressing skeletal muscle cells with 1,25(OH)2D3. RNAs encoding proteins involved in 1,25(OH)2D3-metabolism (CYP24A1), muscle relaxation (parvalbumin), cytoskeletal dynamics (IGFN, ARHGAP16), RNA and nucleotide binding (TDRD1), cellular energy metabolism (IGFL3), apoptosis (FAM12) and nucleosome function (HIST1H3J) were significantly up-regulated. The most significantly repressed RNAs encoded calpain 11 (calcium-sensitive cysteine protease), WFDC1 (involved in cellular proliferation) and podocan (involved in cell migration). Eighty three mRNAs encoding mitochondrial proteins were significantly altered by 1,25(OH)2D3. Changes in gene expression are dependent upon cellular VDR expression as only 15 genes are altered following treatment of primary cultures of human skeletal muscle cells treated with a control siRNA compared with the 1947 genes altered when the VDR is silenced by an anti-VDR siRNA. These genes are identical to those altered by 1,25(OH)2D3 in cells expressing normal amounts of the VDR but the changes are quantitatively reduced. We also demonstrated that deletion of the VDR in cells resulted in changes in gene expression that were in the opposite direction of those observed following treatment of VDR expressing cells with 1,25(OH)2D3. In skeletal muscle cells,

1,25(OH)2D3 alters the expression of nuclear mRNAs encoding cellular and mitochondrial proteins that influence energy metabolism, cell proliferation, cytoskeletal dynamics and apoptosis.

Disclosures: Rajiv Kumar, None.

SU0127

1,25-Dihydroxyvitamin D₃ Alleviates Inflammatory Bowel Phenotypes in a Genetic Mouse Model with a High Disease Susceptibility. Savantani Goswami*¹, Shiyan Yu¹, Juan Flores¹, Sylvia Christakos², Nan Gao¹. ¹Department of Biological Sciences, Rutgers University, USA, ²Department of Microbiology, Biochemistry & Molecular Genetics, Rutgers University, USA

The anti-inflammatory function of 1,25-dihydroxyvitamin D₃ (1,25(OH)₂D₃) the hormonally active form of vitamin D, is widely recognized in multiple biological systems, with its protective role against experimental colitis having been established previously. The pathogenesis of chronic inflammatory bowel disease (IBD) attributes to genetic as well as environmental factors. Although various susceptibility loci for Crohn's disease and ulcerative colitis have been identified, their contributions to disease mechanisms remain poorly defined. We show for the first time that genetic ablation specifically in mouse intestinal epithelial cells of a recycling endosome small GTPase, Rab11a, a gene adjacent to a Crohn's disease risk locus, results in increased expression of pro-inflammatory cytokines (e.g., IL-6), enhanced IRF5+ M1 macrophage infiltration into the submucosa, increased crypt cell proliferation, early onset enteritis and IBD phenotypes. Rab11a deficiency was found to alter TLR9 sorting and processing resulting in an inflammatory response. In order to determine whether vitamin D supplementation may be beneficial under conditions of genetic predisposition to IBD, we investigated the effect of 1,25(OH)₂D₃ on the IBD phenotypes in Rab11a intestinal epithelial cell specific knockout mice. 1,25(OH)₂D₃ (50 ng per mouse) was administered by intra-peritoneal injection on day 1 and 3 to Rab11a mutant mice expressing IBD phenotypes. The tissues were analyzed on day 6. 1,25(OH)₂D₃ administration to mutant mice resulted in a significant decrease in intestinal IL-6 mRNA (4 fold ; $p < 0.01$ compared to vehicle treated), decreased expression of NF-κB (p65) in intestine, a reduction of M1 macrophage infiltration, and reduced crypt cell proliferation. Rab11a deficient intestines showed blunted and branched villi with pseudo epithelial layer stratification, whereas 1,25(OH)₂D₃ treatment partially restored the morphology towards normal intestinal villus architecture. These data suggest beneficial effects of vitamin D supplementation in

protecting against disease pathogenesis under conditions of genetic predisposition to IBD.

Disclosures: Sayantani Goswami, None.

SU0128

1,25-Dihydroxyvitamin D₃ treatment of mice infected with *M. tuberculosis* results in increased pathogen burden. Kamlesh Bhatt*¹, Sylvia Christakos², Padmini Salgame¹. ¹NJMS-Medicine-Infectious Diseases, Rutgers University, USA, ²Department of Microbiology, Biochemistry & Molecular Genetics, NJMS, Rutgers University, USA

In vitro studies have shown that 1,25-dihydroxyvitamin D₃ (1,25(OH)₂D₃), the hormonally active form of vitamin D, restricts intracellular Mycobacterium tuberculosis (Mtb) replication via induction of the anti-microbial peptide, cathelicidin. In addition to the induction of cathelicidin, 1,25(OH)₂D₃ also inhibits the production of inflammatory cytokines including IFN γ and IL-17. During primary tuberculosis both IFN γ and IL-17 are induced and play a role in the protective immune response. Thus vitamin D can be a double edged sword in tuberculosis. Despite significant evidence showing the negative effect of 1,25(OH)₂D₃ on Mtb growth in vitro, the impact of the aggregate effect of 1,25(OH)₂D₃ in vivo on host resistance against Mtb has remained undetermined. We therefore examined the effect of 1,25(OH)₂D₃ on the outcome of Mtb infection in the mouse model. C57BL/6 mice were treated with 1,25(OH)₂D₃ (1 ng/g bw) or vehicle one day prior to aerosol infection with Mtb (Erdman strain in a whole body inhalation exposure system) and then every other day via subcutaneous injection during the course of the study (4–6 weeks; at least 5 mice/time point and two individual experiments). At 6 weeks post infection 1,25(OH)₂D₃ treated animals had significantly increased bacterial burden as determined by plating serial dilutions of lung homogenates for colony forming units (CFUs) (vehicle treated, 5.3 Log₁₀ CFUs/Lung vs. 1,25(OH)₂D₃ treated, 6.1 Log₁₀ CFUs/Lung p < 0.01). The development of inflammatory lesions in the lungs of the vehicle and 1,25(OH)₂D₃ treated mice was compared histologically. At 6 weeks post infection in the mice receiving 1,25(OH)₂D₃ there was a significant decrease in the B cell rich lymphocytic clusters in the lungs (vehicle; 21 ± 1 vs. 1,25(OH)₂D₃ treated; 11 ± 1 μ m²; p < 0.01). 1,25(OH)₂D₃ treated mice also exhibited increased expression of IL-10 in lymph nodes and lungs (IL-10 production has previously been shown to promote bacterial growth during Mtb infection, in part, due to poor T cell responses). Our findings indicate for the first time using an in vivo model that the immune-modulatory functions of 1,25(OH)₂D₃ interfere with the establishment in the lungs of the appropriate cytokine axis necessary for generating optimal granulomatous response and anti-Mtb immunity and caution that 1,25(OH)₂D₃ treatment may have adverse effects on the host adaptive immune response to Mtb.

Disclosures: Kamlesh Bhatt, None.

SU0129

Assessment of 24,25-dihydroxyvitamin D as a Marker of Vitamin D Status in Children. Selene Bantz*, Christine Simpson, Jane Zhang, Thomas Carpenter. Yale University School of Medicine, USA

Vitamin D is an important nutrient for skeletal and extraskeletal health. Optimal vitamin D status, reflected by circulating 25-hydroxyvitamin D (25D), is controversial. Most agree that 25D < 20 ng/mL identifies a risk for bone and mineral abnormalities; others suggest that 25D < 40 ng/mL warrants supplementation. 25D is widely accepted as the best measure of vitamin D status, but other derived markers have been proposed. 25D is converted to 1,25(OH)₂D (1,25D) or 24,25(OH)₂D (24,25D). As stores decrease, regulatory mechanisms shift to maximize production of 1,25D with less production of 24,25D.

Employing these homeostatic principles, Kaufmann investigated normal, healthy women with 25D levels < 20 ng/mL. After supplementation with increasing doses of vitamin D, curvilinear increases in serum 25D and 24,25D occurred, with both metabolites reaching plateau values at doses of 4000 IU/day. Marked elevations of the 25D:24,25D ratio occurred as 25D decreased to < 25 ng/mL. Large elevations in this ratio were evident with only modest changes in circulating 25D. The study concluded the 25D:24,25D ratio may serve as a more sensitive marker of vitamin D deficiency than PTH or 25D alone.

We hypothesized this relationship may be evident in children and examined circulating 25D and 24,25D in 364 healthy infants and toddlers, aged 6-36 months. Vitamin D intake was quantified using a 24-hr recall methodology. 24,25D correlated strongly with 25D (R = 0.47; p < 0.00001). Both 24,25D and 25D correlated positively with daily vitamin D intake per body weight (R = 0.18, p < 0.003 and R = 0.36, p < 0.00001, respectively) and total daily vitamin D intake (R = 0.222, p < 0.0002 and R = 0.286, p < 0.00001, respectively). Consistent with Kaufmann's observation, the 25D:24,25D ratio was inversely associated with vitamin D intake (R = -0.117, p < 0.044), but the ratio was a weaker indicator of vitamin D intake than either metabolite alone. Moreover, the 25D:24,25D ratio did not correlate with vitamin D intake corrected for body weight (R = 0.045, p < 0.5).

In our study of young children, the 25D:24,25D ratio did not serve as a more sensitive marker of vitamin D insufficiency than 25D, as was demonstrated in an older female population. This may be due to overall looser regulation of the vitamin hydroxylases in children than in adults. More studies are needed to understand the utility of 24,25D as a biomarker in a variety of populations.

Disclosures: Selene Bantz, None.

SU0130

Calcitriol Is Not Required During Fetal Development to Regulate Serum Minerals or Skeletal Development, Although It May Act Through Non-Genomic Pathways to Stimulate Placental Calcium Transport. Kamal Alhani*¹, Yue Ma¹, Beth J. Kirby¹, René St-Arnaud², Christopher Kovacs¹. ¹Memorial University of Newfoundland, Canada, ²McGill University, Canada

Study of two vitamin D receptor ablation models found that *Vdr* null fetuses have normal serum minerals, PTH, and skeletal morphology/mineralization. But in both models placental calcium transport and placental expression of the calcitriol-dependent channel TRPV6 were increased. These results, and prior studies in severely vitamin D deficient rats, suggest that calcitriol is not required during fetal development. However, *Vdr* null fetuses have high calcitriol levels which conceivably acted through non-classical receptors to increase placental calcium transport and TRPV6 expression.

We used *Cyp27b1* null mice, which do not make calcitriol, to study the role of calcitriol during fetal development. *Cyp27b1*^{+/−} mice were mated to generate pregnancies with WT, *Cyp27b1*^{+/−}, and *Cyp27b1* null fetuses. Pregnant dams were given an intracardiac injection of ⁴⁵Ca and ⁵¹Cr-EDTA to measure placental calcium transport. Fetal serum and amniotic fluid were collected; intact fetuses were reduced to ash; ash mineral content was assessed by atomic absorption spectroscopy; tibiae, placentas, and fetal kidneys were harvested.

As compared to their WT littermates, *Cyp27b1* null fetuses had normal serum calcium (2.2 ± 0.2 vs. 2.2 ± 0.1 mM) and phosphorus (4.3 ± 0.3 vs. 3.9 ± 0.2 mM), and amniotic fluid calcium (1.8 ± 0.1 vs. 1.7 ± 0.1 mM) and phosphorus (1.5 ± 0.1 vs. 1.7 ± 0.2 mM). They also had normal tibial lengths, morphology, and mineral deposition. Skeletal ash weight, and calcium and phosphorus content of the ash, were normal. Placental calcium transport at 5 min was 0.94 ± 0.04% in *Cyp27b1* nulls vs. 1.00 ± 0.03 in *Cyp27b1*^{+/−} and 1.05 ± 0.09 in WT (p = NS). qPCR showed loss of *Cyp27b1* expression but no change in renal or placental expression of calcium or phosphorus transporting genes, including TRPV6, calbindin-D-9k, Ca²⁺ATPase, and NaPi2a/b/c.

In summary, loss of calcitriol in *Cyp27b1* null fetuses did not significantly alter any measured parameter of mineral or bone homeostasis, confirming earlier evidence from mice and rats that calcitriol/vitamin D is not required during fetal development. However, whereas placental calcium transport and *Trpv6* expression were increased in *Vdr* null fetuses, in *Cyp27b1* nulls placental calcium transport was non-significantly reduced and *Trpv6* expression was unaltered. These findings may indicate that high levels of calcitriol are able to act through non-genomic receptors to upregulate placental calcium transport and *Trpv6* expression in *Vdr* null fetuses.

Disclosures: Kamal Alhani, None.

SU0131

Expression of Vitamin D Receptor in Seminal Vesicle of Cholesterol Formula Mice. Dong Won Byun*¹, Tae-Hee Kim², Hae-Hyeog Lee². ¹Soon Chun Hyang University Seoul Hospital, South Korea, ²Department of Obstetrics & Gynecology, Soonchunhyang University Hospital, South Korea

Objective

By VDR stimulation, Vitamin D controls calcium homeostasis and bone health and Genomic function of VDR indicates spermatogenesis that is important for in male reproductive organ. Authors evaluated the VDR expression in seminal vesicle with high cholesterol formula diet rat, because there is no report about relationship or difference in VDR in seminal vesicle between high cholesterol and control.

Methods

Male C57BL/6 mice aged 5 weeks were raised for 13 weeks. After one week of adaptation-period, they were fed different diet on normal AIN-93G diet, or high cholesterol diet containing 2% cholesterol for 12 weeks. The antibodies used were rabbit anti-VDR primary polyclonal.

Result

There was no significant difference in VDR reactivity in seminal vesicle, body weight of rat and weight of seminal vesicle between high cholesterol group and normal control group.

Conclusion

Our data give the no difference in expression of VDR of seminal vesicle rat between high cholesterol formula diet and normal AIN-93G diet. But we confirm the VDR expression in seminal vesicle.

Keywords: Vitamin D receptor, cholesterol, seminal vesicle

Disclosures: Dong Won Byun, None.

SU0132

MATURE OSTEOBLASTS REGULATE VITAMIN D-MEDIATED BONE RESORPTION DURING GROWTH AND DIETARY CALCIUM/PHOSPHORUS RESTRICTION. Jackson Ryan¹, Michele Milne², Rebecca Sawyer¹, Patrisha Russel³, Kate Barratt⁴, Yolandi Starczak¹, Helen Tsangari¹, Gerald Atkins⁵, Howard Morris¹, Rachel Davey³, Paul Anderson⁶. ¹University of South Australia, Australia, ²University of Melbourne, Australia, ³University of Melbourne, Australia, ⁴University of South Australia, Australia, ⁵University of Adelaide, Australia, ⁶Musculoskeletal Biology Research, University of South Australia, Australia

Active vitamin D (1,25D), bound to the vitamin D receptor (VDR), can directly regulate osteoblast activity modulating bone resorption via induction of RANKL. However, it is somewhat unclear as to which cells of the osteoblast lineage are predominantly responsible for this activity. We have generated mature Osteoblast-VDR Knock Out (mOb-VDRKO) mice using an osteocalcin promoter-Cre to demonstrate the role of VDR-mediated bone resorption in mature osteoblasts during growth and under dietary calcium/phosphorus restriction. 6 week old female mOb-VDRKO mice displayed a pronounced reduction in RANKL mRNA expression, metaphyseal osteoclast surface (OcSur/BS) and serum X-laps. As a consequence, trabecular bone volume (BV/TV%) was increased in the femur (19%, p<0.05) and vertebra (21%, p<0.05) in comparison to littermate controls. The increase in trabecular bone in female mOb-VDRKO persisted at 12w of age but was absent by 26w of age. When 3 week old female mOb-VDRKO mice were subjected to a combined low calcium (0.03%) and phosphorus diet (0.08%) (LowCa/P) for 3 weeks, serum PTH levels and X-laps levels were approximately 2-fold greater than LowCa/P fed control mice, resulting in the abrogation of the bone phenotype to levels comparable to control mice. When the LowCa/P diet was continued until 20 weeks of age, higher serum PTH and X-laps levels persisted in mOb-VDRKO mice, which was associated with deleterious effects on bone including a deranged growth plate, cortical spaying and marked intra-cortical porosity. By comparison, 6 week old female Osteocyte-specific-VDRKO mice (deletion driven by Dmp1-Cre), exhibited no structural differences in femoral trabecular BV/TV%, and unchanged OcSur/BS. However, when 3 week old Oy-VDRKO KO mice were fed the LowCa/P diet for the 3 weeks, periosteal and endosteal circumference measure were reduced by 13% and 16% and when compared to levels in LowCa/P diet fed control mice, suggesting impaired bone remodelling specifically in cortical bone. Collectively, these data suggest that mature osteoblasts play a greater role in VDR-mediated bone resorption than osteocytes in young mice fed a normal diet. However, VDR and mature osteoblasts and osteocytes play a role in regulating bone turnover in response to dietary calcium/phosphorus restriction.

Disclosures: Paul Anderson, None.

SU0133

The Vitamin D Receptor Interacts with Peroxisome Proliferator-activated Receptor Gamma and Suppresses Target Gene Expression in Keratinocyte Stem Cells. Vaibhav Saini^{*1}, Francesca Gori², Marie Demay³. ¹MGH, Harvard Medical School, USA, ²Harvard School of Dental Medicine, USA, ³Massachusetts General Hospital, USA

Vitamin D Receptor (VDR) null mice develop hypocalcemia, hyperparathyroidism, osteomalacia, rickets, and alopecia. A calcium and phosphate enriched, lactose supplemented diet prevents all of these abnormalities with the exception of alopecia. Hair follicle morphogenesis is unaffected in VDR null mice; however, they exhibit absence of postmorphogenic hair cycling due to impaired self renewal and lineage progression of keratinocyte stem cells (KSCs), leading to the development of lipid laden dermal cysts.

To identify the molecular pathways dysregulated in the absence of the VDR in KSCs, RNA-Seq analysis was performed on KSCs isolated from 18-day-old VDR null and WT mice. Ingenuity Pathway Analyses identified over 1,900 differentially regulated genes involved in organismal survival, cell death and survival, cell proliferation, organ morphology, and lipid metabolism. Based on the presence of the lipid laden dermal cysts in the VDR null mice we focused on the genes involved in lipid metabolism. A significant increase in peroxisome proliferator-activated receptor gamma (PPARγ), PPARγ coactivator-1 beta (PGC1β), and *Lipoprotein Lipase* (LPL) mRNA expression was observed in the KSCs of VDR null mice compared to those of WT mice. ChIP-Seq analyses of KSCs from WT and VDR null mice identified VDR binding sites in the promoters of *PGC1β*, an established co-activator of PPARγ, and *LPL*, a known downstream target of PPARγ. ChIP analyses of primary murine keratinocytes confirmed VDR recruitment to the promoters of the *PGC1β* and *LPL* genes. Of note, the VDR and PPARγ were recruited to the same regulatory regions of the *LPL* gene, suggesting co-transcriptional regulation of *LPL* by these two nuclear receptors. To address whether the VDR and PPARγ could physically interact, immunoprecipitation analyses were performed. These studies demonstrated that the VDR co-immunoprecipitated PPARγ in transiently transfected COS-7 cells as well as in primary murine keratinocytes.

These data demonstrate that absence of the VDR leads to enhanced expression of PPARγ and its target genes in keratinocyte stem cells. The presence of a physical interaction between the VDR and PPARγ suggests that coordinated regulation of

gene expression by these nuclear receptors is required for normal lineage commitment of KSCs.

Disclosures: Vaibhav Saini, None.

SU0134

Vitamin D and Key Regulators of Bone Turnover during Pregnancy. Bernhard Svejda^{*1}, Astrid Fahrleitner-Pammer². ¹Gynecologist, At, ²Department of Internal Medicine, Medica I University Graz, Austria

Background: In order to develop the fetal skeleton the mineral metabolism of the mother must adapt to meet the fetal calcium demand. Conflicting and few data are available on bone turnover and vitamin D status of pregnant women. The aim of this study was to investigate serum levels of Vitamin D (25-OH Vitamin D), osteoprotegerin (OPG), soluble Receptor Activator of NF-κB Ligand (sRANKL), Dickkopf-related protein 1 (DKK1) during pregnancy in healthy women in order to analyze whether or not these markers change after conception.

Methods: 200 women gave informed consent for additional blood sampling. 178 unselected healthy women were included – pregnant women n=125 first trimester (T1); n=86 second trimester (T2); n=3 third trimester (T3); and n=21 postnatal women within 7-11 weeks postpartum. Blood sampling was performed after an overnight fast between 7 and 10 am in the morning and serum levels of OPG, DKK1 and free sRANKL (Biomedica, Austria) and Vitamin D (Immudiagnostik AG, Germany) were assayed by ELISA.

Results: Median serum OPG levels were significantly higher during pregnancy (Trimenon 1= 4.9, Trimenon 2= 6.75 and T3= 5.25 pmol/l) and postpartum 5.8 pmol/l, compared to 3.8 pmol/l for healthy, non-pregnant women (all except T3 p<0.05). DKK-1 levels were significantly lower during second and third trimester (T1= 27.2, T2= 19.7 and T3= 21.8 pmol/l) (p<0.05), but returned to normal (29.9 pmol/l) post partum = 29.7 pmol/l. Free sRANKL significantly decreased (p<0.05) during pregnancy in all three trimesters (T1= 0.08, T2 & T3= 0.03 pmol/l), but post partum levels were found similar (0.15 pmol/l) to the levels of non-pregnant women. Vitamin D levels significantly decreased (p<0.05) during pregnancy and stayed low post partum (T1= 40.1, T2 = 45.6, T3= 30.3 and postpartum = 34.7 nmol/l) compared to non-pregnant women 58.8 nmol/l.

Conclusions: These preliminary results show significant changes of serum levels of OPG, free sRANKL, DKK-1 and Vitamin D during pregnancy mainly during the first two trimesters. The changes of OPG, sRANKL and DKK1 may play a crucial role in the prevention of maternal bone loss. While maternal vitamin D deficiency may result in several negative outcomes for mother and child indicating an urgent need of an appropriate vitamin D supplementation during pregnancy.

Disclosures: Bernhard Svejda, None.

SU0135

Vitamin D deficiency and CYP27B1 ablation in the mammary epithelium accelerates tumor development in male mice carrying the PYMT oncogene. Jiarong Li^{*1}, René St-Arnaud², Timothy Reinhardt², Richard Kremer⁴. ¹McGill University, Canada, ²Shriners Hospital for Children, Canada, ³Iowa State University, USA, ⁴MUHC, Canada

Breast cancer in men is rare with a lifetime risk of 1 in 1000 compared to 1 in 8 in women. A strong inverse relationship between vitamin D exposure and breast cancer development has been reported in women and vitamin D has been shown to slow breast cancer progression in female mice models. In contrast this relationship has never been investigated in male studies. We previously reported the beneficial effect of vitamin D administration in the pYMT mouse model of breast tumor progression. In this model female mice develop breast cancer rapidly with palpable tumors around 6 weeks rapidly progressing to metastatic carcinoma at around 11 weeks. In contrast the male counterparts develop palpable tumors at around 18-20 weeks and metastatic disease around 30-36 weeks. In order to investigate the mechanistic relationship between vitamin D and breast cancer development in this male model of breast tumor progression, we used two different approaches. First we examined the effect of either a low (25IU/kg) or high (1000 IU/kg) vitamin D diet on tumor progression. Next we ablated CYP27B1, the enzyme responsible for the conversion of 25 hydroxyvitamin D (25OHD) to 1, 25-dihydroxyvitamin D (1, 25(OH)2D, in the mammary epithelium of male pYMT animals using the Cre/LoxP recombination system. Animals fed the low vitamin D diet had very low 25OHD but normal calcium levels and an earlier tumor onset and accelerated tumor growth compared to the high vitamin D diet group (n=4 per group P<0.001). Ablation of CYP27B1 reduced by over 80% 1α hydroxylase expression in the mammary epithelium as shown by confocal microscopy and Western Blot analysis and a similar reduction of 1, 25(OH)2D production in breast tumor extracts. Tumor onset was significantly accelerated with palpable tumors appearance around 14 weeks compared to 20 weeks in control animals (n=39 per group, P<0.001) and accompanied with accelerated tumor growth and of the number and size of lung metastases (P<0.05). Comparative gene array analysis of tumor tissues showed that over 1100 genes were either up or downregulated in CYP27B1 ablated tumors compared to control tumors (FC>2, P<0.05) with the major pathways involving cell death and apoptosis.

In summary our data demonstrate that vitamin D is an important regulator of male breast cancer development in this representative model of human breast cancer

and suggest that human studies are warranted to determine the role of vitamin D in the development male breast cancer.

Disclosures: Jiarong Li, None.

SU0136

CDKN1a/p21 suppresses osteogenesis and regenerative bone remodeling in an age-dependent manner. Elizabeth Blaber*¹, Yasaman Shirazi-Fard², Eduardo Almeida². ¹NASA Ames Research Center, USA, ²Space Biosciences Division, NASA Ames Research Center, USA

CDKN1a/p21 has previously been implicated in cell cycle and tissue regeneration arrest. In this study of the CDKN1a/p21 knock out (KO) mouse, we report a novel phenotype for this molecule in bone, leading to accelerated bone remodeling and aging. Because CDKN1a/p21 is elevated in bone subjected to mechanical unloading in microgravity, we investigated its role in bone formation and in the cellular response to alterations in mechanical load.

In juvenile (11-week old) KO mice, we found increased trabecular bone formation in the distal femur, indicated by increased bone volume fraction (BV/TV, 35.8%) and trabecular number (Tb.N, 34.4%), and decreased trabecular spacing (Tb.S, -17.9%). Cortical bone of the femoral midshaft in juvenile KO mice exhibited decreased periosteal perimeter (Ps.Pm, -3.4%) and a trend for decreased cortical thickness (Ct.Th). Additionally, three-point bending of the tibias from KO mice showed significantly decreased bone stiffness (-19.3%).

In adult (18-week old) mice, BV/TV, Tb.N, Tb.S, and mechanical properties showed no significant differences in KO mice compared to WT, but woven bone structure and increased osteoclast numbers were highly indicative of rapid bone remodeling. In addition, cortical bone in adult KO mice showed typical characteristics of aged bone, including, increased cross-sectional tissue area (T.Ar, 15.6%), Ps.Pm (8.8%), cross-sectional bone perimeter (B.Pm, 10.5%), and marrow area (Ma.Ar, 23.9%) with a corresponding decrease in bone area fraction (B.Ar/T.Ar, -9.1%). However, in vitro, mesenchymal stem cells from KO mice exhibited maintenance of differentiation potential indicated by significantly increased proliferation rates and mineralized nodule formation.

KO mice subjected to hindlimb unloading for 14 days revealed greater sensitivity to mechanical unloading resulting in nearly tripled cortical and trabecular bone loss compared to WT mice. However, in vitro, the ability of mesenchymal stem cells from KO mice to differentiate into mature mineral forming osteoblasts was increased, again indicating maintenance of regenerative potential.

In total, these findings indicate an important role for CDKN1a/p21 in regulating bone formation and bone turnover and suggest a potential target for therapeutic intervention in treating bone formation deficits.

Disclosures: Elizabeth Blaber, None.

SU0137

Effects of Mechanical Unloading on Skeletal Structure and Properties of Connexin 43 Transgenic Mice. Huiyun Xu*¹, ruofei liu², ruixin yang², zhouqi yang², sumin gu³, jean jiang³, peng shang⁴. ¹Northwestern Polytechnical University, Peoples republic of china, ²Key Laboratory for Space Biosciences & Biotechnology, School of Life Sciences, Northwestern Polytechnical University, China, ³Department of Biochemistry, University of Texas Health Science Center at San Antonio, USA, ⁴Key Laboratory for Space Biosciences & Biotechnology, School of Life Sciences, Northwestern Polytechnical University, USA

As the most abundant connexins in bone cells, connexin43 (Cx43) forms gap junctions and hemichannels, which play critical roles in cell-cell communication in bone tissue. Our previous studies have shown that R76W transgenic mouse model blocks gap junction channel, but promotes hemichannel function specifically in osteocytes. In this study, we aim to understand the function of Cx43 mutant in response to mechanical unloading by subjecting 10-week-old R76W and wildtype C57BL/c mice (WT) to hindlimb suspension (HLS) for four weeks. The bone structure, bone material properties and dynamic bone formation of femur were detected by microCT, three-point bending and bone histomorphometry analysis, respectively. Our results showed that mechanical unloading obviously increased bone loss of WT and R76W mice. But the bone mineral density (BMD), bone volume/tissue volume (BV/TV) and trabecular thickness (Tb.Th) of male-R76W mice significantly decreased more than that of WT mice. In cortical bone, male-R76W mice also showed larger changes after HLS treatment, including smaller BMD, BV/TV, cortical thickness (Ct.Th) and larger marrow cavity. The three-point bending analysis showed that mechanical unloading decreased the material properties of both R76W and WT mice, including elastic module, ultimate load and stiffness. The changes of R76W were all less than that of WT mice, but the difference was not significant. Previous studies have shown that inhibition of gap junction function leads to restraining of sensitivity for mechanical unloading. Our results showed an increase of sensitivity in R76W mice to mechanical unloading. We assumed that difference response may be due to the role

of increased hemichannel function in R76W mice. Further studies will be done with ?130-136 transgenic mouse model, which block both gap junctions and hemichannel function. Then we can compare the response of R76W and ?130-136, to distinguish the role of gap junctions and hemichannels. The results of bone histomorphometry analysis showed that the changes of mineral apposition rate (MAR) and bone formation rate (BFR/BS) decreased more in female-R76W mice compared with that of WT mice. However the alternation of BMD and material properties were not different with WT mice. It is likely that bone absorption also decreased along with the inhibition of bone formation.

Disclosures: Huiyun Xu, None.

This study received funding from: NSFC

SU0138

Effects of Simulated Microgravity and Hypergravity on the Matrix Mineralization in Osteoblast MC3T3-E1 and Preosteocyte-like Cell MLO-A5. Zhouqi Yang*¹, Fengtao Hao², Dandan Dong², Peng Shang². ¹Northwestern Polytechnical University, Peoples republic of china, ²Key Laboratory for Space Bioscience & Biotechnology, Institute of Special Environmental Biophysics, Faculty of Life Sciences, Northwestern Polytechnical University, China

The normal 1g-earth gravity is vital for maintaining bone homeostasis. Gravity change may result in the destroy of bone balance *in vivo*, such as weightlessness-induced bone loss, however, its cellular mechanism still remains unclear. In this study, a random positioning machine (RPM) and a 2g centrifuge were employed to investigate the long-term effects of simulated microgravity and hypergravity on matrix mineralization in osteoblast MC3T3-E1 and preosteocyte-like cell MLO-A5 via alizarin red S staining. In addition, the calcium consumption in culture medium and total protein level in osteoblasts and preosteocytes exposed to abnormal gravity environments were detected with atomic absorption spectroscopy and BCA assay. After culturing for 21 days with RPM, osteoblast demonstrated a decrease in the mineralized nodules formation. Similarly, a reduction in matrix mineralization was found in preosteocytes after a 9-day exposure to RPM, while shortly increased in day 6. During culturing period with RPM, total protein level was not altered in osteoblasts, but significantly decreased in preosteocytes. The calcium deposits slowed in day 7 and slightly accelerated in day 14 and day 21 in osteoblasts, and a similar tendency was also found in preosteocyte after being subject to a 9-day exposure to RPM. In contrast, Hypergravity (2g) environment had different impacts on osteoblasts and preosteocytes. After 21-day 2g centrifugation, matrix mineralization in MC3T3-E1 cells was distinctly inhibited, calcium consumption was suppressed and total protein level was increased. For preosteocyte MLO-A5 cells, 9-day 2g centrifugation enhanced mineralized nodule formation and calcium consumption in culture medium, but no evident change was found in cellular total protein. From these results, it is concluded that microgravity inhibited the matrix mineralization in both osteoblast and preosteocyte. Hypergravity (2g) has different influences on the mineralization ability for various differentiation stages of osteoblast-like cells.

Disclosures: Zhouqi Yang, None.

SU0139

Elcatonin Prevents Bone Loss due to Skeletal Unloading by Suppressing Bone Resorption with Unloading-Induced High Expression of Calcitonin Receptors in Bone Marrow Cells. Manabu Tsukamoto*¹, Kunitaka Menuki², Teppei Murai², Akihisa Hatakeyama², Shinichiro Takada², Kayoko Furukawa², Akinori Sakai². ¹University of Occupational & Environmental Health, Japan, ²Dept. of orthopaedic surgery, University of occupational & environmental health, Japan

Introduction: Osteoclasts highly express specific receptors of calcitonin, which acts directly on osteoclasts to reduce their motility and activity. There is no evidence of efficiency of elcatonin for prevention of bone loss due to skeletal unloading in mice. The aim of this study is to investigate the effect of elcatonin on bone loss due to unloading. Materials and Methods: C57BL/6J male 7-week-old mice were assigned to four groups with either ground control (GC) or tail suspension (TS) and either administration of elcatonin 20U/kg (EL) or vehicle (veh) three times per week; GCEL, GCveh, TSEL, TSveh. Mice were sacrificed at 1, 4 and 7 days, and blood samples, bilateral femurs and tibias were obtained for analysis. Results: The expression of calcitonin receptor (Calcr) mRNA at 1 day of TSveh and the number of Calcr-positive cells at 4 days of TSveh were significantly increased more than those of GCveh. After 7 days of unloading, the trabecular bone volume of the proximal tibia and trabecular bone mineral density of distal femur measured by pQCT in TSEL were significantly increased more than those in TSveh. The parameter of bone resorption, the osteoclast surface, the osteoclast number and the serum level of TRACP-5b, were significantly decreased in TSEL. On the other hand, the number of preosteoclasts, which was TRACP-positive mononuclear cells, was significantly increased in TSEL. There was no difference of the parameter of bone formation, the bone formation rate, the mineral apposition rate and the serum level of PINP, between TSveh and TSEL. At 4 days of TSEL, the expression of NFATc1, Cathepsin K and ATP6V0D2 mRNA in bone marrow cells were decreased. At 7 days of TSEL, the expression of Sphk1 mRNA in bone marrow cells was increased. Conclusions: Tail-suspension induces high

expression of calcitonin receptors in bone marrow cells of hindlimb and calcitonin prevents unloading-induced bone loss by suppressing bone resorbing activity.

Disclosures: Manabu Tsukamoto, None.

SU0140

Influence of Mechanical Loading on Alignment of Biological Apatite Crystallites and Lacunar-canalicular System in Rabbits. Muneteru Sasaki¹*, Shinichiro Kuroshima¹, Takayoshi Nakano², Takashi Sawase¹. ¹Nagasaki University, Japan, ²Osaka University, Japan

Introduction

Osteocytes, which reside within bone matrix, are regulator cells that control bone reaction in response to mechanical stimulation. Bone matrix is mainly constituted of collagen and biological apatite. Recently we have indicated that the orientation of biological apatite (BAP) c-axis in bone matrix were associated with mechanical strength of bone. However, relationship between osteocyte network and preferential alignment of BAP c-axis around bone matrix via loaded implants is unclear. The aim of this study was to investigate osteocyte ultrastructural morphology and the alignment of BAP c-axis around loaded implants.

Materials and Methods

Anodized Ti-6Al-4V alloy dental implants were placed in the both sides of proximal tibia metaphysis of each rabbit. Mechanical repetitive loading was randomly applied along the long axis of the implant (50 N, 3 Hz, 1,800 cycles, 2 days/week) for 8 weeks at 12 weeks after implant placement using a custom made loading device (loading group). The implants in remaining side did not received any loading (control group). Tibiae with the implants were dissected, and resin embedded samples were prepared following manufacturer's instructions. Scanning electron microscopy (SEM) and microbeam X-ray diffractometer were used to investigate osteocyte morphology and crystallographic orientation of BAP c-axis, respectively.

Results and Conclusions

The number of osteocytes and cell process in loading group was significantly increased compared with control. Osteocyte dendrite processes in control group evenly aligned, whereas their processes in loading group randomly aligned. Preferential alignment of BAP c-axis in control group was consistent with the longitudinal direction of osteocyte cell bodies, but the consistency was not observed under loaded condition. Our findings suggests that mechanical repetitive loading affected not only the development of lacuno-canalicular system but also the preferential alignment of BAP c-axis.

Disclosures: Muneteru Sasaki, None.

SU0141

Mechanical Vibration Promotes Proliferation and Differentiation of Cementoblasts and its regulation of Osteogenesis via ERK1/2 Signaling Pathway. Dawei Liu, Hua Wang*. Marquette University School of Dentistry, USA

Objective: To study the effect of mechanical vibration on the proliferation and differentiation of cementoblastic OCCM.30 cells and its regulation of osteoblastic mineralization. **Methods and Methods:** OCCM.30 cementoblasts were subjected to low-magnitude (0.3 × g) sinusoidal vibrations at various frequencies (0, 30, 60, 90 Hz) for 1 h every day. For signal transduction studies, cells were pre-incubated with U0126 (20mM) or DMSO for 1 h and then subjected to mechanical vibration for 1 h. Conditioned medium (CM) was collected from OCCM.30 cells 1 h after the completion of 1 h of mechanical vibration at various frequencies. Osteoblastic MC3T3-E1 cells were cultured in a mixture 1:1 (v/v) of growth medium and CM for 7 days and 14 days. **Results:** Mechanical vibration enhanced cementoblastic proliferation and differentiation, most significantly at 60 Hz. Application of an ERK1/2 signaling pathway blocker - U0126 partly blocked this vibration-induced up-regulation. After induced with the CM, there was a significant increase in osteoblastic mineralization in the vibration group as the frequency increased, most significantly after 7 days of culture. **Conclusion:** Mechanical vibration induces and promotes the osteogenesis of cementoblasts via the potentiation of ERK1/2, which is able to enhance the osteoblastic mineralization.

Disclosures: Hua Wang, None.

SU0142

A novel β_3 -integrin based mechanosome structure in bone tissue. Pamela Cabahug-Zuckerman¹, Robert Majeska¹, Mia Thi², Dave Spray², Shledon Weinbaum¹, Mitch Schaffer¹. ¹the City College of New York, USA, ²Albert Einstein College of Medicine, USA

Osteocyte (OCY) processes are 10-100X more sensitive to physiological stimuli than OCY bodies [1-4]. In vitro studies of MLO-Y4 cells show activation of cellular Ca^{2+} signaling when <10pN fluid forces are focused at OCY process attachments, and inhibition of the Ca^{2+} response when either $\alpha_5\beta_3$ integrins (β_3) or ATP are blocked [4]. β_3 found along OCY processes in situ don't colocalize with either vinculin [5] or paxillin [6], suggesting β_3 in bone tissue don't form typical focal adhesion complexes and ruling out classical integrin transduction mechanisms. We test the

hypothesis that in situ β_3 -based foci along OCY processes, sites of high membrane strains during mechanical loading [1], associate with ligand-gated and stretch-activated Ca^{2+} channels. Mice femoral bone sections were double immunostained for β_3 and one of candidate channels: CaV3 Ca^{2+} channel [7], P2X₇R purinergic channel, Panx1 hemichannel and Cx43, found in OCY processes [8,9], but not expected to associate with β_3 . Structured Illumination Microscopy was used to acquire images with resolutions of 100nm [10]. Protein distribution and pair colocalization were quantified from single optical planes of foci on OCY processes, from lacuna margins sampled every 0.5 μ m up to 3.5 μ m away, Fig1a. Manders Coefficients were used to assess overlap of β_3 and candidate channel foci. For each protein pair two coefficients were measured: the 1st tested association between a channel as reference and β_3 ; the 2nd, the reverse. Values >0.4 indicate biologically significant colocalizations [11]. ANOVA & M-W U-test were used to compare values. β_3 , CaV3, P2X₇R, Cav3 and Panx1 were concentrated at the most proximal region of OCY processes and then decreased with distance, unlike Cx43 which had the lowest value, Fig1b. At the proximal region <1.5 μ m from the lacuna margin, association between the CaV3, P2X₇R and Panx1 with β_3 foci were >0.4, indicating biologically significant colocalization; likewise, reverse coefficients show β_3 foci association with CaV3, P2X₇R and Panx1 in the same region, Fig2, although to a lower extent, indicating that a fraction of β_3 sites may be associated with other channels or simply be anchors. Here we show that P2X₇R, critical to OCY cell mechanotransduction in vitro, is present on OCY processes in situ. Moreover, this receptor channel strongly colocalizes with β_3 attachment sites. A similar strong association was also found between β_3 foci and T-type calcium channel CaV3 and hemichannel Panx1, but not with Cx43. β_3 attachment foci are sites of high tension in the cell process membrane during mechanical loading [1]. Our studies suggest that foci found on processes consisting of $\alpha_5\beta_3$ integrins, P2X₇R, CaV3 and Panx1 may function as novel integrin-based mechanosome complexes.

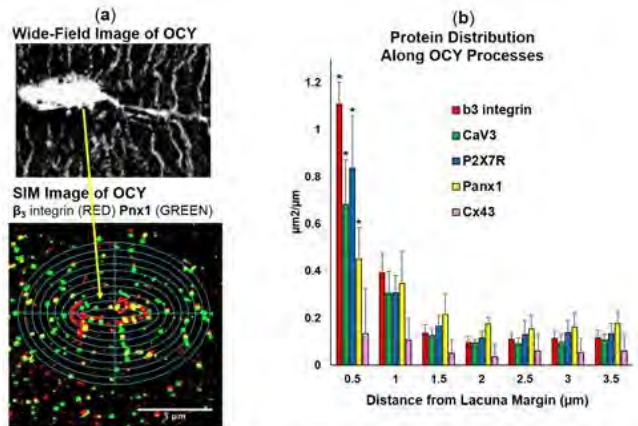


Fig1 (a) Example of a Structured Illumination Microscopy (SIM) image of one optical plane examined, showing the elliptical donut regions of interest in blue, for a β_3 and Panx1 pair; and a Wide-Field image, for comparison. (b) The distribution of all proteins examined along osteocyte processes. * = $p < 0.05$ versus distances $> 0.5 \mu$ m.

Fig1

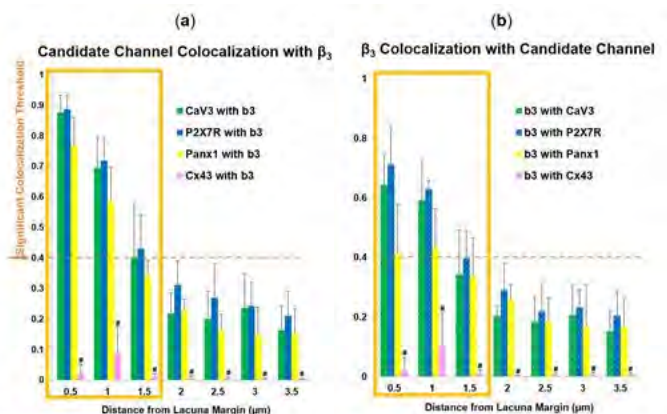


Fig2 Manders Coefficients are shown above, where the 0.4 threshold for biological significance is indicated by the dashed orange line. (a) Colocalization of candidate channels with β_3 , are high at the proximal region of osteocyte processes, within the rectangular orange outline, and also seen (b) in β_3 colocalization with CaV3, P2X₇R and Panx1; not Cx43. # = $p < 0.05$ vs β_3 , CaV3, P2X₇R & Panx1

Fig2

References

[1] Wang *et al.*, Proc Natl Acad Sci USA 2007 Oct 2;104(40):15941-6; [2] McNamara *et al.*, Anat Rec (Hoboken) 2009 Mar;292(3):355-63; [3] Wu *et al.*, Proc Natl Acad Sci USA 2013 Jul 16;110(29):12096-101; [4] Thi *et al.*, Proc Natl Acad Sci USA 2013 Dec 24;110(52):21012-7; [5] Cabahug-Zuckerman *et al.*, Trans ORS 2014; [6] Vatsa *et al.*, Biochem Biophys Res Commun 2008 Dec 26;377(4):1019-24; [7] Thompson *et al.*, J Bone Miner Res. 2011 Sep;26(9):2125-39; [8] Doly, Calcif Tissue Int. 1981;33(5):509-12; [9] Cheng *et al.*, J Bone Miner Res. 2001 Feb;16(2):249-59; [10] Gustafsson *et al.*, Biophys J 2008 Jun;94(12):4957-70; [11] Zrncic *et al.*, Acta Histochem Cytochem. 2007 Aug 30;40(4):101-11.

References

Disclosures: Pamela Cabahug-Zuckerman, None.

SU0143

Pulsed electromagnetic fields (PEMF) enhance osteoblastic differentiation of human bone marrow stromal cells by activation of microRNA21 expression and the TGF- β signaling pathway. Zhiming He*¹, Nagarajan Selvamurugan², Jawed Siddiqui¹, Teruyo Nakatani¹, Erik Waldorff³, Nianli Zhang³, James Ryaby³, Nicola Partridge⁴. ¹New York University, USA, ²SRM University, India, ³Orthofix, Inc., USA, ⁴New York University College of Dentistry, USA

Previously we reported that PEMF stimulates the proliferation, osteoblastic differentiation and mineralization of human bone marrow stromal cells (hBMSCs). Our further studies by Affymetrix microarray analysis suggested the osteogenic effects were through activation of certain signaling pathways and regulation of specific gene expression, notably the TGF- β signaling pathway and microRNA21 (miR21), respectively. In order to verify the role of the TGF- β signaling pathway, we examined phosphorylation of Smad 2/3 proteins, the critical TGF- β intracellular signaling components, in differentiating hBMSCs after PEMF treatment. We found that PEMF causes highly increased phosphorylated Smad2 in human osteoblastic cells in their differentiation phase and lesser but clear activation in their mineralization phase compared to controls. No Smad3 phosphorylation was found in either treatment group. Neutralization with pan-TGF- β antibody blocked the PEMF-induced Smad2 phosphorylation and decreased the stimulatory effect of PEMF on osteoblastic RNAs. MicroRNA21 has been shown to be an osteogenic miRNA and has members of the TGF- β pathway as target genes. RT-qPCR showed miR21 expression is increased by PEMF treatment in differentiating hBMSCs. The significance of miR21 expression was determined by RNA interference with transient transfection of miR21 inhibitor and miR21 mimic. Transient transfection with miR21 inhibitor increased miR21's putative target gene, Smad7, an antagonist of the TGF- β signaling pathway in both control and PEMF-treated hBMSCs. PEMF caused a decrease in expression of Smad7 presumably via stimulation of miR21. Runx2, a bone transcription factor, was increased by PEMF treatment and the miR21 inhibitor prevented the PEMF stimulation of Runx2 expression in differentiating hBMSCs. Increased expression of Runx2 correlated with increased alkaline phosphatase mRNA expression after PEMF treatment and the miR21 mimic further enhanced this effect. It has been shown that Smad7 interacts with Smurf2 (E3 ubiquitin ligase) but it does not interact with Runx2. Thus, based on the results we suggest that PEMF could mediate its effect on bone metabolism by regulating miR21, which leads to a decrease in Smad7 to activate the TGF- β signaling pathway, stimulating Runx2 mRNA expression and stabilizing its protein levels. Therefore, this study identifies that miR21 expression and activation of the TGF- β signaling pathway play important roles in PEMF's effects on hBMSCs.

Disclosures: Zhiming He, Orthofix, Inc.

This study received funding from: Orthofix, Inc.

SU0144

Role of P₂R-ER Ca²⁺ Signaling Pathway in Medium Intensity Focused Ultrasound induced Ca²⁺ Oscillations in *In-Situ* Osteocytes. Minyi Hu*, Jian Jiao, Daniel Gibbons, Yi-Xian Qin. Stony Brook University, USA

Osteocyte mechanotransduction has gained significant research attention for its clinical potential in related dysfunctional bone remodeling. Elevation of [Ca²⁺]_i has been observed as one of the earliest biochemical events in bone cells under external physical signals. Our lab has recently observed *in-situ* Ca²⁺ oscillations in response to Medium Intensity Focused Ultrasound (MIFU). However, the underlying biochemical mechanisms responsible for such Ca²⁺ signaling is unknown. Thus, the current study aimed to investigate the roles of various Ca²⁺ signaling pathways in MIFU-induced Ca²⁺ oscillations *in-situ*. All animal protocols were approved by SBU's IACUC. Fresh calvarias were obtained from 3mo Black6 mice immediately after euthanasia, and were kept in DMEM w/ 5% FBS and 1% penicillin/streptomycin til ready for incubation in specific Ca²⁺ signaling blockers: 1) Amlodipine (L-type VGCC antagonist; n=4), 2) 18 α -glycyrrhetic acid (18 α -GA, reversible intercellular GJ blocker; n=5), 3) thapsigargin (TG, inhibitor of Ca²⁺-ATPase pump of the ER; n=5), 4) NNC 55-0396 (T-type Ca²⁺ channel inhibitor; n=5), 5) pyridoxalphosphate-6-azophenyl-2',4'-disulfonic acid (PPADS, nonselective P₂R blocker; n=2), 6) ICG-001 (antagonist of Wnt/ β -catenin-TCF-mediated transcription; n=3), and control (n=5). The samples were stained w/ Fluo-8 AM for Ca²⁺ fluorescent label, and subjected to 6W of MIFU stimulation for 30sec. Real-time confocal imaging (40X, 488-nm, 2 frames/sec) was performed to capture the Ca²⁺ signals. To analyze, the fluorescent intensity of each cell body was extracted as a function of time. By normalization to the

baseline, the responsive percentage, number of spikes, normalized spike magnitude, and the initiation time were quantified. Results showed that 6W MIFU-induced Ca²⁺ oscillations were completely abandoned by PPADS ($p < 0.01$ vs. control). TG significantly lowered the number of Ca²⁺ spikes and spike initiation time; NNC 55-0396 also significantly lowered the spike initiation time ($p < 0.05$ vs. control). We concluded that the P₂R-ER pathway played a major role in *in-situ* MIFU-induced Ca²⁺ oscillations. This study provided promising findings on the signaling mechanisms involved in the interactions between acoustic mechanical stress and *in-situ* osteocytic Ca²⁺ oscillations, which provides future exploration of the ultrasound triggered mechanosensing mechanism.

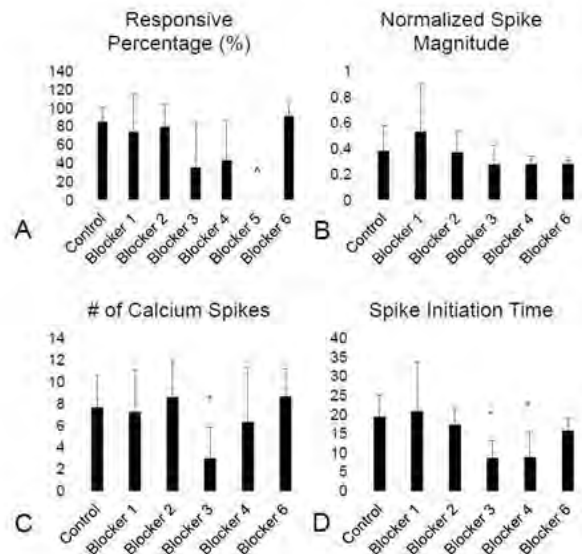


Figure 1. Investigation of the roles of various Ca²⁺ signaling pathways in 6W MIFU-induced Ca²⁺ oscillations. (A) Responsive percentage, (B) normalized spike magnitude, (C) number of spikes, and (D) spike initiation time. Blocker 1 – Amlodipine, Blocker 2 – 18 α -GA, Blocker 3 – TG, Blocker 4 – NNC 55-0396, Blocker 5 – PPADS, Blocker 6 – ICG-001. * $p < 0.01$ vs. control; $p < 0.05$ vs. control.

Figure 1

Disclosures: Minyi Hu, None.

SU0145

Effect of mechanical stimulation on the Hedgehog signaling in osteoblast. Matsumoto Kenichi*¹, Tsuyoshi Shimo¹, Naito Kurio², Tatsuo Okui³, Akira Sasaki². ¹Okayama University, Japan, ²Department of Oral & Maxillofacial Surgery, Okayama University Graduate School of Medicine, Dentistry, & Pharmaceutical Sciences, Japan, ³Department of Oral & Maxillofacial Surgery, Okayama University Graduate School of Medicine, Dentistry, & Pharmaceutical Sciences, Okayama, Japan

INTRODUCTION: Previously, we have reported that Sonic Hedgehog (SHH) signaling was activated in osteoblasts at the dynamic remodeling site of a bone fracture. Mechanical stimulation is one of the crucial factor in bone remodeling and speculated the involvement of the primary cilia as a sensor of Hedgehog signaling. In this study, we examined the effect of mechanical stimulation on the Hedgehog signaling and primary cilia. **METHODS:** The right eighth ribs of 8-week-old male ICR mice were fractured, resected, decalcified, and immunofluorescence staining were performed. To evaluate the effects of mechanical stimulation on the osteoblasts, MC3T3-E1 cells were stimulated by low-intensity pulsed ultrasound (LIPUS). Expression of primary cilia was examined by anti-gamma tubulin and anti-acetylated tubulin antibody. **RESULTS:** SHH was expressed in bone marrow cells at the fracture site on day 3 and the number of primary cilia in MC3T3-E1 cells were increased in the osteoblasts. The number and the length of primary cilia were increased by LIPUS stimulation for 24 and 48 hours. LIPUS upregulated the expression of Patched, Gli1 and Gli2 protein and stimulated the differentiation in MC3T3-E1 cells. **CONCLUSION:** Our results suggested that mechanical stimulation mediate the primary cilia and upregulate the osteoblast differentiation through Hedgehog signaling.

Disclosures: Matsumoto Kenichi, None.

SU0146

Withdrawn.

SU0147

Orthodontic Force-Induced Nociception Stimulates Sympathetic Nervous Signaling Centrally, which Accelerates Tooth Movement through Osteoclast Activation. Hisataka Kondo*¹, Mayo Kondo², Ken Miyazawa², Shigemitsu Goto², Akifumi Togari². ¹Aichi-Gakuin University, Japan, ²Aichi Gakuin University, Japan

Orthodontic force changes bone architecture through stimulation of bone remodeling. Recent we reported that experimental tooth movement (ETM) induced osteoclast activation in periodontal ligament through stimulation of the sympathetic nervous system (Kondo et al. Bone. 2013;52(1):39-47). However, it is unknown how orthodontic force stimulates the sympathetic nervous system. ETM changes the distribution of sensory and sympathetic nerve fibers in periodontal ligament, so we compared the effects of sympathectomy and sensory lesion on ETM. Sensory neuron lesion produced by capsaicin (CAP) showed similar results to sympathectomy by 6-hydroxydopamine (6-OHDA), which suppressed tooth movement and the proportion of osteoclast-covered surface on bone (alveolar socket) (Oc.S/BS) in periodontal ligament. CAP treatment also inhibited ETM-induced increase in a sensory neuromarker, calcitonin gene-related peptide (CGRP)-immunoreactive (IR) neurons, and a sympathetic neuromarker, tyrosine hydroxylase (TH)-IR neurons, in periodontal ligament. On the other hand, 6-OHDA treatment did not suppress ETM-induced increase in CGRP-IR neurons, but did suppress TH-IR neurons in periodontal ligament. Furthermore, treatment with β -agonist, isoproterenol (ISO), masked CAP-induced inhibitions of tooth movement and Oc.S/BS. Destruction of ventromedial hypothalamus (VMH) by gold thioglucose (GTG) treatment suppressed the ETM-induced increases of tooth movement, Oc.S/BS and CGRP-IR. These data suggest that ETM activates osteoclasts through the neural loop of the sensory-central-sympathetic nervous system.

Disclosures: Hisataka Kondo, None.

SU0148

Strain Determination in Finite Element Models of the Mouse Forearm under Dynamic Loading. Mark Begonia*, Mark Dallas, Mark L. Johnson, Ganesh Thiagarajan. University of Missouri-Kansas City, USA

Whole bone strain leads to heterogeneous gene expression, which is believed to be linked to strains experienced by individual osteocytes and their lacuna. Bone strain can be predicted with numerical finite element (FE) models, but their accuracy relies on the anatomical and material properties of a specimen. Previously, we measured forearm strains via strain gaging and a non-contact method known as Digital Image Correlation (DIC) to quantify the bone stiffness induced by gage attachment, and we found that DIC values exceeded gage values in the ulna (148%) and radius (221%). In this study, we simulated cyclic axial compression in FE models of 3 different TOPGAL mouse forearms and analyzed strains after including the interosseous membrane (IOM) and mouse-specific material properties. FE strains were then compared to strain gage and DIC values to assess the true strain response. The goal of this research is to apply a multiscale FE modeling scheme where the strain fields observed in these macro FE models are used to find activated osteocytes in micro FE models of the bone.

FE models were created in the Mimics® Innovation Suite and modified in the FEBio Software Suite to incorporate the IOM. The 1st iteration FE models used Young's moduli (E) and densities (ρ) from literature for the ulna (E_u : 20 GPa; ρ_u : 1168 kg/m³) and radius (E_r : 18 GPa; ρ_r : 1172 kg/m³). The 2nd iteration used moduli from 3-point bending (E_u : 19.1-21.9 GPa; E_r : 12.1-15.4 GPa), densities from μ CT (ρ_u : 1052-1077 kg/m³; ρ_r : 1023-1092 kg/m³), and an IOM stiffness from tension tests (15 N/mm). Peak strains were higher in the ulnae (6%) and radii (10.7%) of the 2nd iteration FE models vs. the 1st iteration. Compared to DIC and gage values, Forearm #1 had a peak ulna strain (4185 $\mu\epsilon$) that was closer to the DIC value (3887 $\mu\epsilon$) than gage value (1565 $\mu\epsilon$) while the peak radius strain (1736 $\mu\epsilon$) ranged between the DIC value (2845 $\mu\epsilon$) and gage value (884 $\mu\epsilon$). In Forearm #2, the peak strains in the ulna (2528 $\mu\epsilon$) and radius (1626 $\mu\epsilon$) were both lower than DIC values yet higher than gage values. The variation in peak ulna strains between Forearm #1 and #2 are due to differences in bone geometry and Young's modulus (E_1 : 19.4 GPa; E_2 : 21.9 GPa), and ongoing work on the third mouse specific FE model could elucidate this finding. Ultimately, this study shows that due to the IOM and individualized material properties, our FE models accurately predict bone strains ranging between strain gage and DIC values.

Disclosures: Mark Begonia, None.

SU0149

CaMKK2 inhibition enhances bone fracture healing. Uma Sankar*¹, Justin Williams², Mariah Hassert², Jianying Liu², Yinghua Cheng², Alexander Robling², Melissa Kacena², Yong Li². ¹Indiana University Purdue University Indianapolis, USA, ²Indiana University School of Medicine, USA

Fractures associated with osteoporosis and acute trauma result in significant medical costs, loss of productivity and loss of patient quality of life. Prolonged healing time and non-union occur in 5-10% of fractures, contributing to further medical costs and patient morbidity. Established therapies such as bisphosphonates only reduce the risk of fractures by an average of 20% and do not promote efficient bone growth and

fracture healing. Consequently, there are no current pharmacological treatment options available to promote efficient bone fracture healing.

We recently identified Ca²⁺/calmodulin (CaM)-dependent protein kinase kinase 2 (CaMKK2) to have roles in the anabolic and catabolic pathways of bone remodeling. Pharmacological inhibition of CaMKK2 in female mice using its selective cell-permeable inhibitor STO-609 protects from ovariectomy-induced osteoporosis. Moreover, treatment of 32 week old male mice with STO-609 reverses age-associated decline in bone volume and strength. Based on these studies, we hypothesized that targeting CaMKK2 will result in accelerated fracture healing. To test this hypothesis, we generated unilateral mid-shaft fractures will be using the three-point bending method (first described for use in rats by Bonnarens and Einhorn, 1986) in the right femurs of 10-week old anesthetized male mice after first inserting an intramedullary pin (25 gauge needle, approx. 0.5 mm) retrograde through the distal condyle of the femur. Radiographic analyses were performed to confirm the location and quality of the fractures. Fractured animals were divided into three groups: (a) saline only (n=15), (b) STO-609 from day 0 (n=15) and (c) STO-609 from day 7 (n=15). Tri-weekly intraperitoneal (i.p.) injections of saline or STO-609 (10 μ mol/kg) were performed for 6 weeks. Progression of fracture healing was monitored through weekly radiographic examination. Fractured callus and non-fractured contralateral femur diaphysis were analyzed by micro computed tomography, histology, immunohistochemistry and histomorphometry. Preliminary results indicate that treatment with STO-609 results in the formation of a robust callus at the fracture site, as well as a 43% increase in total bone volume, 50% increase in trabecular thickness, 9% increase in trabecular number and a 10% decrease in trabecular separation. These data indicate accelerated healing of femoral fractures following the pharmacological inhibition of CaMKK2.

Disclosures: Uma Sankar, None.

SU0150

Effect of intermittent administration of teriparatide (PTH1-34) on BMP induced bone regeneration in a rat critical-sized femoral defect model. Sadaaki Kanayama*, Takashi Kaito, Masafumi Kashii, Takahiro Makino, Tokimitsu Morimoto, Masayuki Furuya, Kazuma Kitaguchi, Yusuke Sakai, Hideki Yoshikawa. Osaka University Graduate School of Medicine, Japan

Introduction

Although clinical bone morphogenetic protein (BMP) therapy is effective, required doses are very high. The uncontrolled release of high concentrations of BMPs can cause inflammation and unintended bone formation. Intermittent administration of PTH1-34 results in osteoblastic proliferation and differentiation, thereby leading to an increase in bone mass. Recently, up-regulation of BMP and Wnt signaling by PTH have been reported. These mechanisms indicate the possibility of synergistic bone regeneration by the co-administration of BMP and PTH. The aim of this study is to elucidate the effect of intermittent administration of PTH1-34 on BMP-induced new bone in a rat critical-sized femoral defect (7mm) model.

Materials and methods

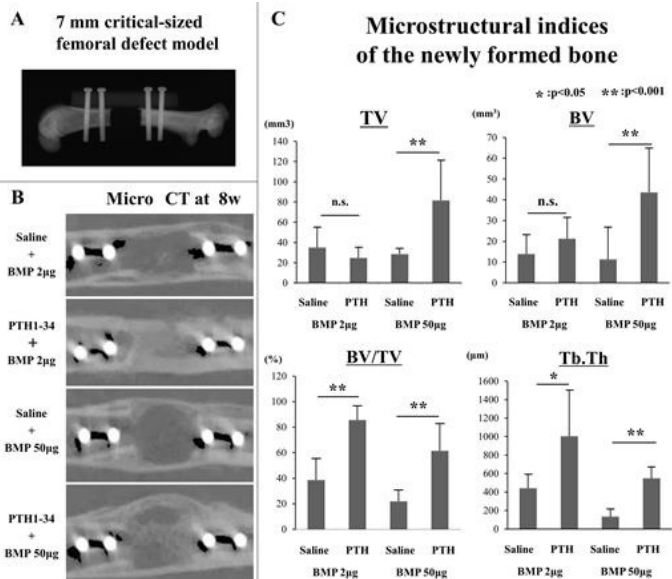
A total of 32 SD rats (10w) were operated (Fig.A) by two different BMP-2 treatments; 1) 2 μ g (low dose), 2) 50 μ g (high dose). Each of the BMP treatments was studied in combination of intermittent PTH1-34(180 μ g/kg/w) or saline injection since 2w before the operation to 8w after operation. Microstructural indices of the newly formed bone and the contralateral femur were evaluated by micro CT (0, 1, 2, 4, 6, 8w). Bony fusion at femoral defects was evaluated using micro CT.

Results

Micro CT demonstrated bone formation since post-op. 2w and bony fusion since post-op. 4w in all groups. Fusion rates at post-op. 8w were not significantly different w/ or w/o PTH (PTH/Saline: BMP; 2 μ g 100%/75%, 50 μ g; 100%/100%). Microstructural indices of the newly formed bone (BV/TV, Tb.Th) were significantly improved by PTH in both BMP low and high dose groups. BV/TV of the contralateral femur was also significantly increased at post-o. 8w (PTH 38.3%; saline 15.7%, $p < 0.001$) (Fig.B,C). Though the TV of newly formed bone in BMP low dose group did not significantly changed by PTH, the TV in BMP high dose group significantly increased by PTH ($p < 0.01$).

Discussion and Conclusions

Intermittent PTH1-34 administration significantly improved the quality of the newly formed bone in this model. However, the remodeling process of the newly formed bone in this model was sluggish or devoid compared to that in our previous rat spinal fusion model. Stress shielding by internal fixation may inhibit the osteocyte-mediated remodeling process where PTH can work through PTH/PTH-related peptide type 1 receptor (PPR). These results suggest that mechanical stress which works through PPR in osteocyte may play a critical role in the remodeling of BMP-induced new bone.



Intermittent PTH1-34 administration improved the quality of the BMP-induced new bone

Disclosures: Sadaaki Kanayama, None.

SU0151

Effects of Sclerostin Antibody in Attenuation of Cortical Bone Loss in Ovariectomized Rats with Concurrent Mechanical Unloading. Dongye Zhang*¹, Mariana Miranda¹, Minyi Hu¹, Liangjun Lin¹, Xiaodong Li², Hua Zhu Ke³, Yi-Xian Qin¹. ¹Stony Brook University, USA, ²Amgen Inc., USA, ³UCB Pharma, United Kingdom

Osteoporosis is a skeletal disease characterized by low bone mass and microarchitectural deterioration of cortical and trabecular bone with a consequent increase in bone fragility and susceptibility to fracture. Sclerostin antibody (Scl-Ab) increased bone formation and bone mass, and decreased bone resorption in animal models of bone loss due to estrogen deficiency (OVX) or immobilization. The current study was undertaken to examine the effect of Scl-Ab on cortical bone in OVX rats with concurrent hindlimb suspension (HLS). Four-month-old virgin female SD rats were divided into 7 groups (n=11 per group). HLS was performed 2 weeks after sham or OVX; and treatment was initiated at the time of HLS. Scl-Ab (25 mg/kg) or vehicle was injected sc twice per week for 5 weeks. The femoral diaphyses were analyzed with μ CT, four-pt bending and histomorphometry for cortical thickness (Ct.Th), mechanical properties and bone formation parameters. Ct.Th was significantly lower in HLS alone, OVX alone and OVX+HLS groups (-13.7%, -14.2% and -15.4%, respectively) than sham control. Scl-Ab significantly preserved Ct.Th in all three conditions, (Fig.1). Scl-Ab prevented the decrease in stiffness associated with HLS or OVX+HLS. Ultimate load was not significantly lower in HLS, OVX or OVX+HLS as compared with Sham controls, but it was significantly greater in Scl-Ab-treated HLS or OVX rats (Fig.2). Scl-Ab-treated HLS, OVX and HLS+OVX showed significant increases in mineralizing surface (MS/BS) as compared to respective controls at both endosteum (Ec) and periosteum (Ps) sites. Ps. bone formation rate (BFR/BS) was elevated in HLS, OVX and HLS+OVX groups treated with Scl-Ab (721%, 55% and 460%, respectively). Similarly, Ec.BFR/BS increased by 636%, 42% and 312%, respectively, in Scl-Ab-treated groups compared with respective control, indicating the thickening of the cortical bone was associated with dynamic bone formation events at both Ec. and Ps. sites (Fig.3., 4.). In summary, Scl-Ab increased Ps. and Ec. bone formation and prevented cortical bone thinning condition in HLS-, OVX- as well as HLS+OVX rats. The data suggested that sclerostin antibody represents a promising therapeutic approach for bone loss induced by estrogen deficiency with concurrent mechanical unloading.

Femur Midshaft Cortical Thickness

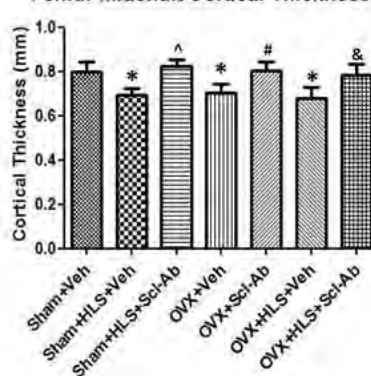


Fig. 1. Mean±SD values for cortical thickness at femur midshaft. HLS, OVX and HLS+OVX showed significant cortical bone thinning vs. sham control (*). Scl-Ab increased cortical bone thickness against the respective controls, i.e., vs. HLS alone (*), OVX alone (#), and HLS+OVX (Overall, *p<0.05 vs. Sham+Veh; *p<0.05 vs. Sham+HLS+Veh; #p<0.05 vs. OVX+Veh; &p<0.05 vs. OVX+HLS+Veh)

Fig. 1.

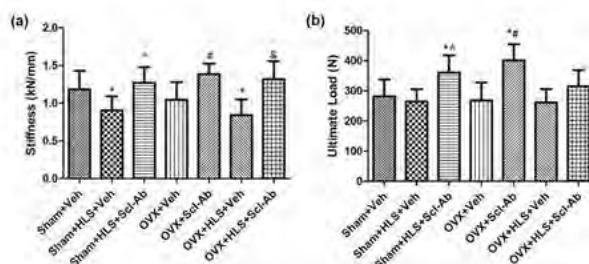


Fig. 2. (a) Mean±SD values for 4-pt bending stiffness. HLS and HLS+OVX showed significant bone stiffness loss vs. sham control (*). Scl-Ab maintained and increased bone strength against the respective controls, i.e., vs. HLS alone (*), OVX alone (#), and HLS+OVX (&). (b) Mean±SD values for 4-pt bending ultimate load. (Overall, *p<0.05 vs. Sham+Veh; #p<0.05 vs. Sham+HLS+Veh; &p<0.05 vs. OVX+Veh; &p<0.05 vs. OVX+HLS+Veh)

Fig. 2.

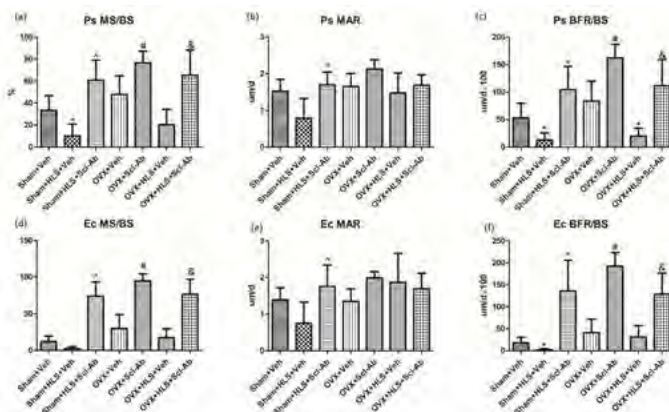


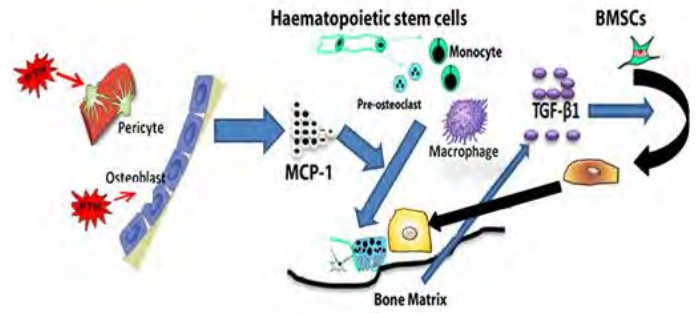
Fig. 3. (a), (b), (c) mean±SD values for histomorphometry: Ps. MS/BS, MAR, BFR/BS respectively. (d), (e), (f) mean±SD values for histomorphometry: Ec. MS/BS, MAR, BFR/BS respectively. Scl-Ab increased bone formation rate against respective controls, i.e., vs. HLS alone (*), OVX alone (#), and HLS+OVX (&). (Overall, *p<0.05 vs. Sham+Veh; *p<0.05 vs. Sham+HLS+Veh; #p<0.05 vs. OVX+Veh; &p<0.05 vs. OVX+HLS+Veh)

Fig. 3.

SU0153

Osteoblastic Monocyte Chemoattractant Protein-1 (MCP-1) Mediates Parathyroid Hormone's Anabolic Actions in Bone: Role of TGF- β Signaling. Jawed Siddiqui¹, Joshua Johnson², Joseph Tamasi³, Nicola Partridge². ¹New York University, USA, ²Department of Basic Science & Craniofacial Biology, New York University College of Dentistry, USA, ³Bristol-Myers Squibb, USA

Parathyroid hormone is now the only osteoanabolic hormone available for treating osteoporosis. The precise mechanisms behind the PTH's anabolic effects are still not completely clarified. Microarrays of bone from rats injected with hPTH-(1-34) daily for 14 days showed that the chemokine, MCP-1, was the most highly stimulated gene. Recently, we have shown that PTH's anabolic effects are abolished in MCP-1^{-/-} mice. In addition, MCP-1 increases multinucleated osteoclasts in culture and MCP-1^{-/-} mice do not recruit osteoclasts after PTH injection, suggesting these cells are implicated in PTH's actions through MCP-1. To identify the cells expressing MCP-1, we performed *in situ* hybridization of MCP-1 mRNA in rat tibiae. Daily hPTH injection to 4 month old male rats showed increased expression of MCP-1 in bone lining osteoblasts and in cells surrounding blood vessels compared to saline-injected animals. To determine the role of MCP-1 in PTH's actions, 4 month old male wild type (WT) and MCP-1^{-/-} mice were injected daily with hPTH (8 μ g/100g/day) or saline for 6 weeks. Immunohistochemistry of tibiae showed very little staining for phosphorylated Smad2 in marrows of MCP-1^{-/-} mice, especially after PTH treatment, whereas pSmad2 staining was enhanced in marrows of WT mice. Similarly, Western blot analyses of bone marrows showed enhanced pSmad2 expression in WT mice after hPTH treatment whereas MCP-1^{-/-} mice showed no PTH-mediated increase in Smad2 phosphorylation. These data show that MCP-1 is necessary for PTH-mediated TGF- β signaling in bone marrow. In addition, mRNA analysis of the distal femurs of hPTH-injected mice showed that PTH induced the expression of ALP, c-fos, CCR2, Coll (α 1) and TGF- β 1 in WT mice but failed to demonstrate such changes in MCP-1^{-/-} mice. Alizarin Red-S staining of bone marrows from these mice, cultured for 21d in osteoblast differentiation medium, showed enhanced mineralized nodule formation from WT mice treated with PTH while marrows from MCP-1^{-/-} mice showed no effect of PTH treatment. Together we conclude that, MCP-1, secreted by cells of the osteoblast lineage in response to PTH stimulation, is necessary for the recruitment of monocytes and pre-osteoclastic cells towards remodeling sites and assists in the formation of mature osteoclasts. Subsequently, latent TGF- β 1 released from bone matrix enhances the recruitment of BMSCs towards the remodeling sites and facilitates osteoblast differentiation and bone formation.



Schematic Mode of PTH's Action through MCP-1 activation

Disclosures: Jawed Siddiqui, None.

SU0154

Bisphosphonate treatment differentially affects bone mechanical properties of mice with robust and slender bone. Drew Brown¹, Erin McNerny¹, Jason Organ¹, Chris Newman¹, Karl Jepsen², Matthew Allen¹. ¹Indiana University School of Medicine, USA, ²University of Michigan, USA

Although currently used anti-osteoporosis drugs, such as bisphosphonates, are highly effective in reducing fractures, there are individuals who adversely respond to these drugs and experience atypical femoral fractures (AFFs). The goal of this study was to test the hypothesis that bisphosphonates exert differential effects on bone mechanical properties of animals that have a robust (high total cross-sectional area / bone length) versus a slender (low total cross-sectional area / bone length) bone morphology. Skeletally mature male A/J (slender; n=16) and B6 (robust; n=16) mice were dosed with zoledronic acid (ZOL; 0.08 mg/kg) or vehicle (VEH) at 14 and 18 weeks of age and at 22 weeks of age femora were collected and frozen in saline-soaked PBS. High-resolution microCT scans of the femora were taken to examine trabecular bone morphology of the distal metaphysis region and mid-diaphysis cortical bone geometry. Mechanical properties were assessed using four-point bending to failure. Confirming previous work, VEH-treated animals with robust bones had significantly higher cortical bone mechanical properties and cross-sectional area, and lower tissue mineral density, compared to VEH-treated slender animals. ZOL significantly increased ultimate load (+26% versus +7%) and stiffness (+23% vs no effect) to a greater degree in robust mice compared to slender. Pre-yield displacement tended to be higher in ZOL-treated slender bones (+11%) and lower in robust bones (-14%)

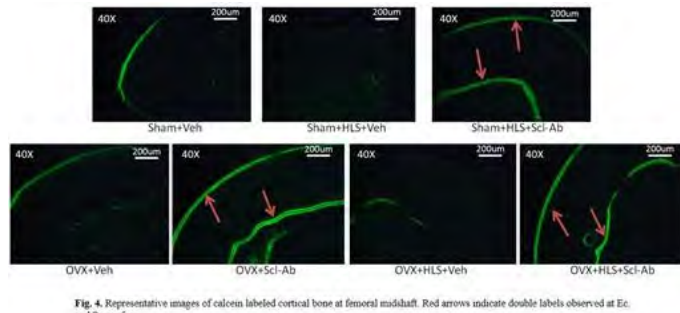


Fig. 4. Representative images of calcein labeled cortical bone at femoral midshaft. Red arrows indicate double labels observed at Et and Ps surface

Fig. 4

Disclosures: Dongye Zhang, None.

This study received funding from: Amgen Inc.

SU0152

Improving PTH/Raloxifene Combination Osteoporosis Therapy in a Preclinical Model. Joseph Bidwell¹, Yu Shao², Selene Hernandez-Buquer³, Paul Childress⁴, Drew Brown³, Yongzheng He⁵, Marta Alvarez⁶, Feng-chun Yang⁷, Stuart Warden⁸, Matthew Allen³. ¹Indiana University School of Medicine, USA, ²Medical & Molecular Genetics, Indiana University School of Medicine, USA, ³Anatomy & Cell Biology, Indiana University School of Medicine, USA, ⁴Microbiology & Immunology, USA, ⁵Pediatrics Neonatal Basic Research, Indiana University School of Medicine, USA, ⁶Orthopaedic Surgery, Indiana University School of Medicine, USA, ⁷Biochemistry & Molecular Biology, Miller School of Medicine, University of Miami, USA, ⁸Health & Rehabilitation Science, Indiana University School of Medicine, USA

The bone-forming potency of parathyroid hormone (PTH) wanes during osteoporosis therapy. Adding an anti-catabolic with PTH to enhance anabolism has yielded mixed clinical results. Disabling the transcription factor Nmp4 enhanced PTH anabolism in mice likely by increasing the number of bone marrow (BM) osteoprogenitors and BM CD8⁺ T cells. Here we addressed whether various PTH+anti-catabolic therapies are more efficacious in osteoporotic Nmp4^{-/-} mice than wild type (WT). Mice were ovariectomized at 12wks of age. Therapies were initiated at 16wks and included PTH only (30 μ g/kg/day), the bisphosphonates alendronate (ALN) only (1 μ g/kg/day), zoledronate (ZOL) only (80 μ g/kg 1x dose), the selective estrogen receptor modulator (SERM) raloxifene (RAL) only (1mg/kg/day), PTH+ALN, PTH+RAL, PTH+ZOL and a vehicle control comprised of all the carriers. Dual energy X-ray absorptiometry was used to record total bone mineral density (BMD) throughout the experiment. At 24wks of age mice were euthanized and the cancellous and cortical bone of the distal femur and L5 vertebra were analyzed by micro-computed tomography. Fluorescence-activated cell sorting of the BM was used to profile osteoprogenitors and T cells. Expanded cultures of mesenchymal stem/progenitor cells (MSPCs) were established for *in vitro* studies. Statistical analyses used either a series of 2W ANOVAs, 1W ANOVA, or the Kruskal-Wallis ANOVA by ranks. Post hoc tests included the Tukey-Kramer HSD and the Student's t tests. PTH+RAL therapy was the most effective at augmenting PTH mono-therapy in both genotypes and disabling Nmp4 significantly improved response to PTH+RAL but had no effect on the PTH+bisphosphonate treatments. The PTH+RAL-treated Nmp4^{-/-} mice exhibited a significantly larger increase in femoral and L5 BV/TV. This therapy increased the Nmp4^{-/-} but not WT mouse % change total body BMD over PTH mono-therapy. The PTH+RAL treatment further elevated the number of BM Nmp4^{-/-} osteoprogenitors. Raloxifene enhanced mineralization of WT MSPCs but did not further augment the precocious Nmp4^{-/-} MSPC mineralization. PTH+RAL increased the percentage of WT BM CD8⁺ T cells to equal that of the already expanded Nmp4^{-/-} pool. We conclude that Nmp4 suppresses the combined actions of PTH and the SERM raloxifene on osteoprogenitors, osteoblasts, and perhaps CD8⁺ T cells but does not regulate bisphosphonate activity. Nmp4 and its associated pathways may be novel targets for adjuvant anabolic osteoporosis therapy.

Disclosures: Joseph Bidwell, Eli Lilly

while displacement to fracture was significantly reduced in both strains (-15 and -26% for A/J and B6, respectively). After accounting for differences in bone size, there was no significant effect of treatment on ultimate stress or modulus in either strain. Modulus of toughness in ZOL-treated animals was lower in both strains (-16% for A/J and -27% for B6) due in part to divergent effects on pre-yield toughness (+18% in A/J and -23% for B6). These data suggest that bones with slender and robust morphologies are differentially affected by bisphosphonates, with robust bones showing a significantly greater benefit to whole bone stiffness and strength but appearing to be more negatively affected with respect to differences in both pre-yield displacement and post-yield properties. Future work will aim to understand the tissue-level basis for differential responses of these two divergent morphologies through study of remodeling suppression in a model with intracortical remodeling.

Disclosures: Drew Brown, None.

SU0155

Bortezomib inhibits *P. gingivalis* LPS-induced alveolar bone loss in mice. Youngkyun Lee*. Kyungpook National University School of Dentistry, South Korea

Healthy bone is maintained by the coordinated activities of the osteoblast-mediated bone formation and osteoclast-dependent bone resorption. Pathologic conditions such as hormonal imbalance and inflammation cause increased osteoclastogenesis resulting in the osteoporosis, rheumatoid arthritis, and periodontitis. Bortezomib is novel anti-myeloma agent that also has direct beneficial effect on bone formation. However, the role of bortezomib in osteoclastogenesis and underlying mechanisms still remain fully comprehended. In the present study, we show that bortezomib directly inhibited the receptor activator of nuclear factor κ B ligand (RANKL)- and lipopolysaccharide (LPS)-dependent osteoclast differentiation. Interestingly, the bortezomib-mediated inhibition of osteoclastogenesis was transient, since the removal of bortezomib from culture completely restored osteoclast differentiation. Bortezomib impeded the induction and nuclear localization of nuclear factor of activated T-cells, cytoplasmic 1 (NFATc1) and reduced both macrophage colony-stimulating factor (M-CSF)- and RANKL-induced ERK phosphorylation. In a mouse model of periodontitis, bortezomib prevented alveolar bone erosion induced by *P. gingivalis* LPS. These data not only suggest previously unappreciated mechanism by which bortezomib regulates bone resorption, but also propose novel applications of bortezomib beyond its use as an anti-myeloma agent.

Disclosures: Youngkyun Lee, None.

SU0156

Differential effects of OPG, alendronate and a Cathepsin K inhibitor on load adaptation in mice. Nicolas Bonnet¹, Le Duong², Serge Ferrari³. ¹University Geneva Hospital (HUG), Switzerland, ²Merck & Co, USA, ³Service des Maladies Osseuses, Hôpitaux Universitaires, Genève, Switzerland

We previously reported that osteopetrotic Cathepsin K (CatK) knock-out mice have an increased long bone adaptation to mechanical loading, suggesting an interaction between CatK inhibition and biomechanical stimulation. Here we tested whether pharmacological inhibition of CatK improves the long bone response to axial compression and how it compares to other antiresorptives. Adult male mice were treated with the CatK inhibitor L235 (30mg/kg twice a day), alendronate (ALN, 25 μ g/kg/d sc, twice a week), OPG-Fc (4mg/kg sc, twice per week) or PBS (Veh) for 3 weeks. Axial compression (12N, 2Hz, 7min) was applied to the tibia for 1 week after initiating treatment for two weeks (n=5 per group). Bone turnover markers were measured at baseline and sacrifice. BMD, microstructure and cortical strength by 3-points bending of tibia were evaluated at sacrifice.

Compared to the non-loaded site (NL), axial compression increased BMD in all treatments groups (from +19.4% to +22.2%, all p<0.05). However, loading significantly increased cortical bone volume and mineralized perimeter both at the periosteal and endosteal vs those from non-loaded (NL) tibia only in Veh (+4.5%, +43% and +15% vs NL, respectively all p<0.1) and even more prominently in L235 group (+8.5%, +72% and +109% vs NL, respectively, all p<0.05) but not in ALN or OPG-Fc groups. However, OPG-Fc maximally increase bone mass, trabecular and cortical parameters independently of loading, so that trabecular and cortical bone parameters were ultimately similar in OPG-Fc and loaded L235-treated groups. CTX and osteocalcin reflected the differential mechanism of action of the various treatments. Indeed, both markers were decreased by OPG-Fc and to a lesser extent by ALN. In contrast, during the experiment L235 treatment reduced CTX, similar to ALN, but maintained osteocalcin levels as in Veh (+24.8% and +42.8%, respectively).

In this study, while inhibiting bone resorption less than OPG-Fc, the CatK inhibitor maintained bone formation and allowed a better bone adaptation to loading. This also suggests that a certain level of load must be applied to reach the optimal skeletal strength during treatment with a CatK inhibitor. The molecular mechanisms of CatK inhibition in mediating the adaptive response of the skeleton to loading are currently under investigation.

Disclosures: Nicolas Bonnet, None.
This study received funding from: Merck & Co

SU0157

Effect of IL-18 on mechanical loading-induced osteoclastogenesis and bone resorption solely, and in synergy with IL-12. Yumiko Ochi¹*, Hideki Kitaura², Keisuke Kimura², Masahiko Ishida², Haruki Sugisawa², Jafari Saeed², Akiko Kishikawa², Teruko Takano-Yamamoto². ¹Tohoku University, Japan, ²Division of Orthodontics & Dentofacial Orthopedics, Department of Translational Medicine, Tohoku University Graduate School of Dentistry, Japan

In mechanical loading-induced osteoclastogenesis, cellular responses are mediated by interactions between various factors such as cytokines. It has been reported that TNF- α was recognized one of the important factor for osteoclastogenesis. It has also been reported that TNF- α plays an important role in mechanical loading-induced osteoclastogenesis and bone resorption. We previously reported that the proinflammatory cytokine interleukin-18 (IL-18) inhibited TNF- α -mediates osteoclastogenesis *in vitro* and *in vivo*. However, its influence on mechanical loading-induced osteoclastogenesis and bone resorption is still unknown. We established mechanical loading-induced osteoclastogenesis in mice for exploring the mechanism underlying the mechanical loading-induced bone changes. Thus, the purpose of this study was to investigate the effect of IL-18 and combination of IL-18 and IL-12 on orthodontic tooth movement and associated root resorption in mice model. Mouse orthodontic tooth movement model was established, and investigated whether IL-18 inhibits osteoclastogenesis and bone resorption on mechanical loading. The maxillary first molars of male mice were subjected to mesial force by a Ni-Ti coil spring. IL-18 was injected locally adjacent to the first molar every other day. After 12 days of experimental tooth movement, the amounts of orthodontic tooth movement and the number of tartrate-resistant acid phosphatase (TRAP)-positive cells along the loaded alveolar bone and root surface was counted as osteoclasts and odontoclasts, respectively, in histological sections. Orthodontic tooth movement and the number of osteoclasts were significantly decreased in IL-18 treated mice. IL-18 significantly suppressed the mechanical loading-induced odontoclast formation and root resorption. Furthermore, IL-12 and IL-18 synergistically inhibited the mechanical loading-induced osteoclast formation and odontoclast formation. Our results suggested that IL-18 might be a useful adjunct for regulation of the extent of orthodontic tooth movement and control of root resorption.

Disclosures: Yumiko Ochi, None.

SU0158

Effects of alendronate and low-intensity pulsed ultrasound therapies on bone mineral density at cancellous osteotomy sites in the proximal tibia of ovariectomized rats. Chie Sato*, Naohisa Miyakoshi, Yuji Kasukawa, Hayato Kinoshita, Kentaro Ouchi, Masashi Fujii, Tetsuya Kawano, Masazumi Suzuki, Michio Hongo, Yoichi Shimada. Dept. of Orthopedic Surgery, Akita University Graduate School of Medicine, Japan

Purpose We previously reported that alendronate (ALN) increased the bone mineral density (BMD) at cancellous bone osteotomy sites. In contrast, low-intensity pulsed ultrasound (LIPUS) improved cancellous bone healing after osteotomy, but did not affect the BMD. However, the effects of ALN and/or LIPUS on the BMD at cancellous bone osteotomy sites in an osteoporotic animal model remained unclear. Thus, we aimed to evaluate the effects of ALN and/or LIPUS on the BMD at cancellous bone osteotomy sites in ovariectomized (OVX) rats.

Methods Six-month-old female Sprague-Dawley rats underwent OVX or sham surgery, and then underwent osteotomy at the right proximal tibia and tying with non-resorbing thread at seven-month. We created five groups: 1) Sham (n=15), sham operation plus treatment with ALN vehicle and sham LIPUS (SEFHS; Teijin, Japan); 2) OVX-Control (n=11), OVX plus treatment with ALN vehicle and sham LIPUS; 3) OVX-ALN (n=10), OVX plus treatment with ALN (1 μ g/kg/day) and sham LIPUS; 4) OVX-LIPUS (n=12), OVX plus treatment with ALN vehicle and LIPUS (20 min/day); and 5) OVX-Combined (n=11), OVX plus treatment with ALN and LIPUS. BMD was assessed by dual-energy x-ray absorptiometry (Hologic QDR-4500; Hologic, MA, USA) at 20 mm proximal to the cancellous osteotomy site at the right tibia after 2 and 4 weeks of treatment with ALN and/or LIPUS.

Results The BMD in the OVX-Control and OVX-LIPUS groups was not significantly lower than that in the Sham group after 2 weeks. After 4 weeks, the BMD in the OVX-Control and OVX-LIPUS groups was significantly lower (p<0.05, respectively) than that in the Sham group. ALN without LIPUS for 4 weeks, but not 2 weeks, significantly increased the BMD compared with that in the OVX-Control group (p=0.0252). Combined ALN and LIPUS for 4 weeks, but not 2 weeks, significantly increased the BMD compared with that in the OVX-Control group (p<0.01) and OVX-LIPUS group (p<0.01).

Conclusion ALN with or without LIPUS for 4 weeks, but not 2 weeks, recovered the BMD of the proximal tibia after cancellous bone osteotomy in OVX rats. However, there were no significant effects of LIPUS on BMD at the proximal tibia after osteotomy in OVX rats.

Disclosures: Chie Sato, None.

SU0159**Effects of Long-Term Odanacatib Treatment on Bone Gene Expression in Ovariectomized Adult Rhesus Monkeys: Differentiation from Alendronate.**

Eric Muise^{1*}, Maureen Pickarski², Alexei Podtelezhnikov¹, Andrey Loboda¹, Yejun Tan¹, Guanghui Hu¹, John Thompson¹, Le Duong¹.
¹Merck & Co., Inc, USA, ²Merck & Co., Inc., USA

Odanacatib (ODN) is a selective and reversible Cathepsin K (CatK) inhibitor, currently in late stage development for postmenopausal osteoporosis. We previously reported efficacy of ODN versus alendronate (ALN) on bone turnover, DXA-based BMD in ovariectomized rhesus monkeys treated for 20 months. The study consisted of 4 groups: VEH (vehicle), L-ODN (2mg/kg), H-ODN (4mg/kg) daily p.o., and ALN (15µg/kg, twice-weekly, s.c.). L-ODN and ALN doses were selected to approximate the clinical exposures of ODN 50-mg and ALN 70-mg once-weekly, respectively. Both doses of ODN and ALN effectively reduced bone resorption markers vs VEH. Conversely, ODN reduced formation markers to a significantly lesser degree than ALN. L-ODN increased lumbar spine and hip BMD to levels similar to ALN, supporting the efficacy of ODN in protection of bone loss. Here, we profiled the RNA from tibial metaphysis and diaphysis of monkeys treated with VEH, L-ODN or ALN using Affymetrix microarrays. The H-ODN group was not included in this study. L-ODN and ALN produced strikingly different effects on known bone-related genes and pathways at the transcriptional level. ALN generally reduced the expression of known osteoblast/bone formation-related genes (N=34), including TGFBR1, SPP1, and PTH1R (-1.3, -1.4, and -1.4 fold change, respectively), while ODN either increased or showed no change. Conversely, ODN treatment resulted in an increase in the expression of osteoclast-related genes (N=45), including genes involved in osteoclast differentiation (NFATC1 (1.7 fold) and TM7SF4 (2.6 fold)) or activity (CTSK, ACP5, CALCR; 1.6, 1.7, and 1.9 fold change, respectively). ALN showed either no change or reduced the expression of these same osteoclastic genes. Interestingly, ODN and ALN also differentially regulated genes participating in osteoclast-osteoblast bidirectional communications, including RANKL, SEMA4D or CTHRC1 (2.6/no change, 1.3/-1.5, and no change/-1.9 fold change for ODN/ALN, respectively). Effects on gene expression levels of these bone resorption- and formation-related genes were confirmed by RT-PCR. The molecular profiling results are consistent with the observed differential mechanisms of these two therapies on bone remodeling in monkeys as previously delineated by histomorphometry. Long-term treatment with ALN decreases bone remodeling while ODN maintains osteoclast-derived signals in mediating subsequent bone formation.

Disclosures: Eric Muise, Merck & Co., Inc
 This study received funding from: Merck & Co., Inc

SU0160**Generation and characterization of a humanized cathepsin K mouse model.**

Maureen Pickarski^{1*}, Myung Kyun Shin², Michael Gentile², Le Duong².
¹Merck & Co., Inc., USA, ²Merck & Co., Inc, USA

Odanacatib (ODN), a selective, reversible inhibitor of human cathepsin K (CatK), is in development for treatment of osteoporosis. Human versus rodent CatK exhibit ~86% amino acid similarity and even less around the enzyme active site. Due to interspecies differences, potency of selective human CatK inhibitors is significantly reduced against the rodent enzymes. To take advantage of the range of well characterized disease models in rodent, we attempted to generate a humanized CatK mouse for direct evaluation of human CatK inhibitors. The mouse *ctsk* exon/intron region downstream of the signal peptide (aa.1-14, exon2) to the stop codon (exon8) was replaced with orthologous ~9.5kb human *ctsk* genomic region in C57Bl/6N ES cells. The Neo cassette from targeted ES cells was removed and then injected to establish the humanized *ctsk* mouse line. Wild-type (^{m/m}*ctsk*, WT), heterozygous (^{m/h}*ctsk*) and homozygous (^{h/h}*ctsk*) mice were tested for CatK mRNA levels, bone mineral density (BMD) and resorption marker (CTX). RT-PCR analysis showed only mouse or human CatK mRNA in WT or ^{h/h}*ctsk* tibia, respectively; whereas mRNA from both species was detected in ^{m/h}*ctsk*. DEXA-based BMD of total femur revealed no differences in WT (0.057±0.001 g/cm²), ^{m/h}*ctsk* (0.057±0.001 g/cm²) and ^{h/h}*ctsk* (0.058±0.001 g/cm²). Serum CTx was previously shown to be significantly higher in global CatK^{-/-} vs. WT mice. Here, CTx levels from age-matched WT, ^{h/m}*ctsk* and ^{h/h}*ctsk* animals were comparable, yet lower than that of CatK^{-/-} mice. BMD and CTx results suggested ^{h/h}*ctsk* fully replaced ^{m/m}*ctsk* gene and was sufficiently active to maintain bone mass comparably to WT level. Next, bone marrow derived osteoclasts (OC) from WT, ^{m/h}*ctsk* and ^{h/h}*ctsk* mice were cultured on bovine cortical bone slices; resorption activity was determined by CTx in the media. ^{h/h}*ctsk*-OC vigorously resorbed bone (234nM CTx), compared to OC from ^{h/m}*ctsk* (89nM) or WT (54nM). The different resorptive activities of humanized vs. murine OC are likely due to species differences of CatK in degradation of bovine collagen. Treatment with ODN inhibited ^{h/h}*ctsk*-OC resorption at a potency (IC₅₀~39nM) similar to human OC (IC₅₀~20nM), without displaying significant activity against murine OC (3µM). Taken together, the *in vivo* and *in vitro* assessments of OC resorption activity in ^{h/h}*ctsk* mice demonstrated successful development of a humanized CatK mouse line suitable for further validation by a pharmacological approach in a disease model of bone loss.

Disclosures: Maureen Pickarski, Merck & Co., Inc
 This study received funding from: Merck & Co., Inc

SU0161**Herbacetin inhibits osteoclast differentiation through downregulating NFATc1 signaling and suppresses bone loss in LPS-induced mouse model.**

Yunjo Soh^{1*}, Liang Li¹, Mahesh Sapkota¹, Se woong Kim².
¹School of Dentistry, Chonbuk National University, South Korea, ²School of Dentistry, Chonbuk National University, South Korea

A constant balance between osteoclast-induced bone resorption and osteoblast-induced bone formation are a dynamic process for bone remodeling. Inhibition of osteoclast differentiation in a certain extent can play a significant role in treating bone resorption-associated diseases such as osteoporosis. Herbacetin, an active flavonoid belonging to flavonoid, has various biological effects such as antioxidant, antitumor, and anti-inflammatory activities. However, the novel biological activity of Herbacetin in osteoclast differentiation still has not been studied. Therefore, we tried to reveal the effect and mechanism of Herbacetin on osteoclastogenesis in RANKL-treated RAW264.7 cells and LPS-induced mouse model. Herbacetin significantly inhibited the RANKL-induced osteoclast formation and differentiation in a concentration dependent manner. Additionally, the suppressive effect of Herbacetin resulted in the decrease of osteoclast-related genes including RANK, TRAP, cathepsin K, MMP2 and MMP-9. Herbacetin also decreased the expression of c-Fos and NFAT-c1, blocked the activation of JNK, and significantly inhibited the bone resorption activity in pit formation assay. Furthermore, the *in vivo* suppressive effect on bone loss was assessed quantitatively in a LPS-induced mouse model using micro-computational tomography and histochemical analyses. Taken together, this study identifies Herbacetin as a potent inhibitor of osteoclastogenesis and bone resorption and provides evidence for its therapeutic potential to treat diseases involving abnormal bone lysis.

Disclosures: Yunjo Soh, None.

SU0162**Compensatory Mechanisms in Mouse Offspring with Inherently Weak Bones Suggest a Genome-by-Environment Interaction *in utero*.**

Maria Raygorodskaya¹, Arkady Torchinsky², Yankel Gabet², Chen Shochat¹, Eugene Kobylansky², David Karasik^{1*}.
¹Faculty of medicine in the Galilee, Bar Ilan University, Israel, ²Sackler school of Medicine, Tel Aviv University, Israel

Establishment of normal structure and functioning of bones begins early in life. An exposure of embryo to different adverse environmental factors can detrimentally affect offspring's bones later in life. Our purpose was to investigate to what extent the genetic differences between mouse strains translate into variable response to teratogen 5-deoxy-2'-cytidine (5-AZA).

Two inbred strains, C3H/HeJ (C3H, with inherently stronger bones) and C57Bl/6J (C57, with weaker bones), were studied. Females were injected with diluted 5-AZA or saline (control) at day 10 of pregnancy (dpf). Five mice offspring from each strain/sex groups (C3H males and females, C57 males and females) at two ages (3- and 6-month-old) were studied. We compared left femora of treated and untreated mice within each group using micro-CT analysis and calculated the change in bone parameters between 3 and 6-month old and strain-by-environment interactions, using two-way ANOVA. We tested expression of 84 osteogenic genes in limb buds of embryos from each group at age 11 dpf.

At age 3 mo, treated C57 female offspring demonstrated decrease of cortical volumetric bone mineral density (p<0.05). Treated females from both strains demonstrated loss of cortical thickness (p<0.05). Loss of trabecular thickness was observed in treated C3H females (p<0.01). At age 6 mo, treated C3H males demonstrated loss of cortical thickness (p<0.01), had lower trabecular number and higher trabecular separation (p<0.05; Fig.1). Treated C57 males and females demonstrated increase of trabecular thickness (p<0.05; Fig.2). Furthermore, we revealed significant (p<0.05) strain-by-treatment interactions for several measurements, such as change in trabecular thickness in male groups (Fig.3).

Analysis of gene expression revealed 10 genes that differed (at least 2-fold) between control and treated samples. Two of them, *Csf2* and *Tnfa*, were upregulated in treated C57 but downregulated in treated C3H embryos.

Ultimately, this study demonstrates that the exposure to a sub-teratogenic dose of 5-AZA *in-utero* affects bone structure in young adult offspring. In 3-month-old mice, teratogenic exposure caused bone loss in both strains. At the age of 6 mo, bone loss was observed in the strain with strong bones (C3H), while, on the contrary, in the strain with weak bones (C57) there was gain (thickening of bone trabeculae) which might be an evidence of genome-by-environment interaction. Genes such as *Csf2* and *Tnfa* may be involved in this process.

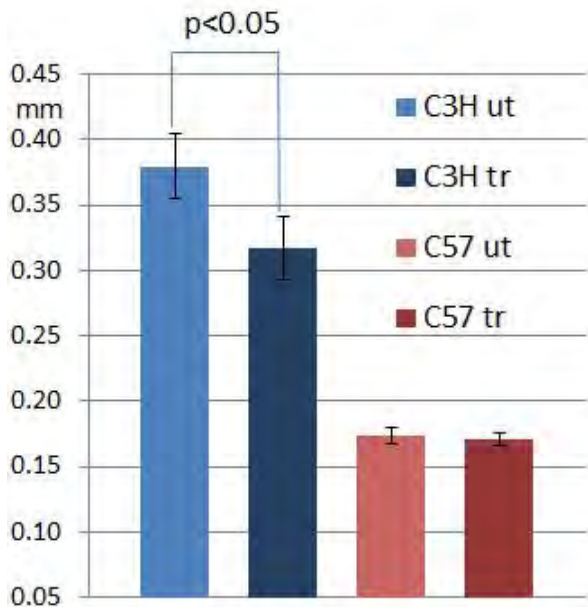


Figure 1. Cortical thickness, 6-month-old males (ut - untreated, tr - treated)

Figure 1. Cortical thickness, 6-month-old males (ut - untreated, tr - treated)

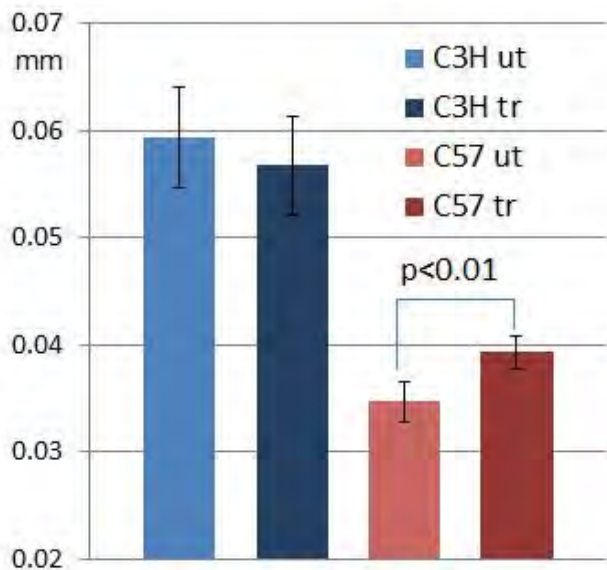


Figure 2. Trabecular thickness, 6-month-old males (ut - untreated, tr - treated)

Figure 2. Trabecular thickness, 6-month-old males (ut - untreated, tr - treated)

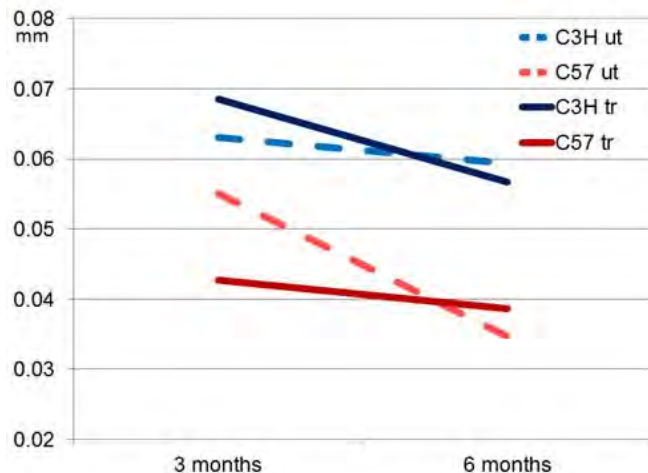


Figure 3. Example of significant strain-by-treatment interaction: trajectories of change of trabecular thickness between 3 months and 6 months of age, males (ut - untreated, tr - treated)

Figure 3. Trajectories of change of trabecular thickness between 3 and 6 months of age, males

Disclosures: David Karasik, None.

SU0163

Effects of Activin Receptor Type IIB Fusion Protein (ActRIIB-mFc) on Serum Biomarkers and Bone Remodeling in Osteogenesis Imperfecta Model (*oim/oim*) Mice. Young Jeong¹, Molly Hulbert², Mark Dallas², Yixia Xie², Scott Pearsall³, Sarah Dallas⁴, Charlotte Phillips⁵. ¹University of Missouri, USA, ²University of Missouri Kansas City, USA, ³Accelaron Pharma Inc, USA, ⁴University of Missouri Kansas City, USA, ⁵University of Missouri Columbia, USA

Osteogenesis imperfecta (OI) is a heritable connective tissue disorder characterized by compromised biomechanical properties of type I collagen containing tissues such as bone. The transforming growth factor- β superfamily (TGF- β) comprises diverse cytokines, including TGF- β , activins, bone morphogenic proteins (BMPs), and growth and differentiation factors (GDFs). Activin A is highly expressed in bone cells to regulate osteoblastogenesis and osteoclastogenesis, whereas GDF-8 (myostatin) regulates muscle growth and differentiation. These two cytokines control cellular processes by signaling through activin receptor type IIs. Recent studies have shown improved bone quality and increased muscle mass and force production in mature rodents treated with soluble activin receptor type IIB fusion protein [ActRIIB-Fc(RAP-031), Accelaron Pharma]. We therefore investigated whether RAP-031 would increase bone mass in the osteogenesis imperfecta mouse (*oim/oim*) model. At 2 months of age, bi-weekly injections (10mg/kg) of RAP-031 were given for 8 weeks to *oim/oim* mice and WT littermate controls. Previously, we showed that the overall body weights and hindlimb skeletal muscle weights were increased with RAP-031 treatment regardless of genotype. By μ CT analyses, female WT femora showed increases in several geometric parameters, while *oim/oim* mice femora showed a gain in cortical bone thickness and trabecular BV/TV with RAP-031 treatment. Serum levels of the bone formation biomarker, procollagen type I N-terminal propeptide, were unchanged in Wt and *oim/oim* mice with RAP-031 treatment. In contrast, levels of the bone resorption serum biomarker, C-terminal telopeptide, were increased with RAP-031 treatment in *oim/oim* mice. By histomorphometric analyses, femora from female Wt mice exhibited an increase in periosteal bone formation rate, mineral apposition rate and mineralizing surface with RAP-031 treatment. The *oim/oim* mice exhibited similar trends although they did not reach significance. Our findings suggest that systemic administration of RAP-031 in Wt mice induced gains in both muscle size and cortical and trabecular bone geometry. *Oim/oim* mice exhibited increased muscle mass and increased femoral trabecular bone geometry with RAP-031 treatment, suggesting ActRIIB receptor fusion protein may provide a new therapeutic approach to enhance bone and muscle function in osteogenesis imperfecta.

Disclosures: Young Jeong, None.

SU0164

Interplay between the adaptive immune and bone system in fracture healing: Friend or foe? Claudia Schlundt*¹, Hanna Schell¹, Hans-Dieter Volk², Georg Duda¹, Katharina Schmidt-Bleek¹. ¹Julius Wolff Institute & Center for Musculoskeletal Surgery; Berlin Brandenburg Center for Regenerative Therapies, Charité-Universitätsmedizin Berlin, Germany, ²Institute for Medical Immunology; Berlin Brandenburg Center for Regenerative Therapies, Charité-Universitätsmedizin Berlin, Germany

The bone and the immune system (IS) are interdependent on each other. During bone fracture, homeostasis is disturbed. Bone fracture healing starts with a hematoma formation that is accompanied by an inflammatory reaction. This is an indispensable step for the initiation and regulation of the regenerative healing process. T cells seem to play a key role in regulating the healing process by determining the local cytokine milieu in the fractured area. In our well established mouse osteotomy model, we could already show that a specific depletion of CD8+ T cells leads to a better healing outcome compared to an untreated wild type (WT) group (higher BV/TV). CD4+ CD25+ regulatory T cells (Tregs) are another promising candidate playing a crucial role in bone fracture healing. In studies with sheep, we already observed a higher amount of Tregs in an osteotomy hematoma compared to a soft tissue hematoma. We hypothesize that Tregs have a positive modulating effect on the bone fracture healing process as well as outcome.

To evaluate the impact of Tregs in fracture healing, freshly isolated murine Tregs were adoptively transferred prior to surgery in our mouse osteotomy model (C57BL/6). Animals with different immune competence were compared: SPF (specific pathogen free; less activation of the IS) (Treg+ SPF) and semi sterile housing (activation of the IS) (Treg+). An osteotomy was performed in the left femur after stabilization by an external fixator. By μ CT analysis, the healing outcome was analyzed 21d post-surgery in comparison to an untreated WT group. In the Treg+ animals, half of the mice healed significantly better (BV: $p=0.01$; TV: $p=0.01$) compared to the control mice. However, the other half showed a significantly poorer healing outcome (BV: $p=0.01$; TV: $p=0.01$) in comparison to the WT. In contrast, in the Treg+ SPF mice, all animals had a higher TV ($p=0.065$) as well as BV ($p=0.015$) with regard to the WT group. The consistent healing outcome in the Treg+ SPF mice confirmed our assumption of the partially negative impact of the adaptive IS in fracture healing. Semi sterile housing conditions lead to a higher activation of the IS. The controversial healing outcome in the Treg+ animals clearly shows the impact of the individual immune status of an animal in immunological research approaches. This brings our model closer to the clinical situation and shows the importance of evaluating the individual status of the patient's immune system prior to immunotherapy.

Disclosures: Claudia Schlundt, None.

SU0165

Live imaging of osteoblast-osteoclast coupling in a medaka fish model for osteoporosis. Christoph Winkler*¹, Tingsheng Yu¹, Manish Dasrani¹, Sudha Sundaram¹, Wen Hui Tan¹, Anita Buettner¹, Ann Huvssseune², Paul Eckhard Witten². ¹National University of Singapore, Singapore, ²Ghent University, Belgium

Small laboratory fish, such as zebrafish and medaka, have become powerful vertebrate models for biomedical research and to model human diseases. Bone homeostasis in humans and fish requires the controlled activity of bone forming osteoblasts and bone resorbing osteoclasts. Interfering with the concerted interplay between bone cell types leads to bone diseases, such as osteoporosis. In order to generate an animal model for osteoporosis that is suitable for live imaging and drug screening, we produced transgenic medaka fish that allow the ectopic formation of osteoclasts, as well as conditional ablation of osteoblasts. Using reporter lines, we are able to follow the behaviour of osteoblasts and osteoclasts at various differentiation stages during bone resorption and repair in vivo in living specimen. We show that inducible expression of receptor activator of nuclear factor kappa-B ligand (RANKL) in transgenic medaka fish results in ectopic osteoclast formation, which leads to severe osteoporosis-like phenotypes. Interestingly, the induced osteoporotic lesions stimulate recruitment of osteoblast progenitors that accumulate at the lesion sites and contribute to bone repair. In this medaka model, osteoclast activity can be blocked by treatment with Etidronate and Alendronate, two bisphosphonates commonly used in human osteoporosis therapy. Both drugs efficiently ameliorate induced skeletal defects by blocking bone resorption and permitting bone repair by recruited osteoblast progenitors. We developed protocols to isolate distinct bone cell populations from medaka larvae during bone degeneration and repair by fluorescence activated cell sorting (FACS). Transcriptome sequencing was performed to identify novel molecular pathways implicated in recruitment of osteoblast progenitors to osteoporotic lesion sites. This project is supported by funds from the Singapore Ministry of Education (MOE2013-T2-2-126).

Disclosures: Christoph Winkler, None.

SU0166

Seasonality in Bone Mineralization of Auditory Ossicles and Long Bones in the Primate *Macaca fuscata*. Makoto Morikawa¹, Porrawee Pomchote², Tadashi Sankai³, Yuzuru Hamada², Koichi Matsuo*¹. ¹Keio University School of Medicine, Japan, ²Primate Research Institute, Kyoto University, Japan, ³National Institute of Biomedical Innovation, Japan

Bones of adult mammals undergo continuous change due to dynamic bone remodeling and secondary mineralization processes. In humans, bone mass decreases with sex hormone levels, while mineralization increases with aging. However, seasonal variations in non-human primate bones are incompletely characterized. To address these activities, we analyzed bones in Japanese macaques (*Macaca fuscata*), primates exhibiting strong seasonality in breeding behavior. We first isolated the largest and smallest bones, femur and auditory ossicles, respectively, from dried specimens of 52 male monkeys that had died over the past 30 years, assuming that specimens reflected bone mass and mineralization status at time of death. We then analyzed bone volume and tissue mineral density (TMD, mg/cm³) using micro-CT. We also measured TMD of distal radii of 14 living macaques, as well as serum testosterone levels of 8 living monkeys in both breeding (autumn/spring) and non-breeding (spring/autumn) seasons. Intriguingly, average rates of change in radial trabecular TMD (Δ TMD, mg/cm³/day) as well as testosterone levels (ng/dl/day), increased to the maximum positive value at the mid-breeding season, and decreased to the maximum negative value at mid-non-breeding season. TMD seasonality was further confirmed by analysis of dried femur and malleus specimens. Such seasonal changes may counteract yearly effects of aging on bone in non-human primates.

Disclosures: Koichi Matsuo, None.

SU0167

The impact of reducing osteal macrophages and their efferocytotic function on bone turnover and bone mass. Benjamin Sinder*¹, Amy Koh¹, Megan Michalski¹, Lorenz Hofbauer², Hernan Roca¹, Laurie McCauley¹. ¹University of Michigan, USA, ²Technische Universität Dresden, Germany

Osteal macrophages are critical cells that support bone mass and bone healing. An important macrophage function is efferocytosis (phagocytosis of apoptotic cells), a process critical for wound healing and associated with the production of anti-inflammatory factors, Wnts, and chemoattractants in non-skeletal tissues. Trabectedin is an anti-cancer treatment approved in Europe for soft-tissue sarcomas that also reduces mononuclear phagocytes and tumor-associated macrophages. The purpose of this study was to use trabectedin to examine the role of osteal macrophages, and their efferocytosis function, on bone. Two trabectedin regimes included short-(1wk) and long-(6wk) term treatments followed by microCT, histology, serum, complete blood counts, bone marrow flow cytometry, RT-PCR, and efferocytosis outcomes. The initial cellular response was assessed in 16wk old male C57/B6 mice administered trabectedin (0.15mg/kg) or vehicle (veh) for 1wk, n=8/group. Flow cytometric analysis of bone marrow confirmed trabectedin altered the macrophage and mononuclear phagocytic populations, with reduced M1 F4/80⁺CD86⁺ (-33%), M2 F4/80⁺CD206⁺ (-19%), and CD68⁺ (-39%) cells. The shift in macrophages by trabectedin corresponded with reduced serum P1NP (-27%), a marker of bone formation, and TRAcP5b (-38%), a marker of bone resorption. The whole bone phenotype was assessed in a separate cohort of mice administered trabectedin (0.15mg/kg, bi-weekly for 6wks) or veh, n=11/group. Trabectedin significantly reduced trabecular BV/TV (-56%) in the tibia, evidenced with reduced trabecular number (-38%). To examine functional changes in efferocytosis with trabectedin, fresh bone marrow cells from mice treated for 1wk were co-cultured with FITC⁺ carboxylated apoptotic-mimicry beads. Trabectedin significantly decreased F4/80⁺ macrophages (-28%) that were engulfing, or attached to, FITC⁺ beads, indicating reduced efferocytotic capability. These data suggest that trabectedin effects on bone are due to reductions in the macrophage population as well as their individual efferocytotic capacity. In conclusion, trabectedin significantly inhibits mononuclear phagocytes and macrophages, decreases efferocytosis, and reduces bone turnover and bone mass.

Disclosures: Benjamin Sinder, None.

SU0168

Active vitamin D possesses beneficial effects on the interaction between muscle and bone. Ippei Kanazawa*¹, Ken-ichiro Tanaka¹, Toru Yamaguchi¹, Shozo Yano¹, Hiroshi Kai², Toshitsugu Sugimoto¹. ¹Shimane University Faculty of Medicine, Japan, ²Kinki University Faculty of Medicine, Japan

Background and aims: Vitamin D deficiency and advanced glycation end products (AGEs) are involved in the pathogenesis of osteoporosis and sarcopenia. However, the effects of vitamin Ds and AGEs on myogenesis and the interaction between muscle and bone remains still unclear. We previously showed that osteoglycin (OGN) is secreted from myoblasts and stimulates osteoblastic differentiation, suggesting that it plays important roles in the interaction between muscle and bone. The aim of this study is thus to examine the effects of vitamin Ds and AGEs on myoblastic

differentiation of C2C12 cells and osteoblastic differentiation through OGN expression. Materials and Methods: Mouse myoblastic C2C12 cells (ATCC) were used. AGE2 and AGE3 were prepared by incubating 50 mg/mL BSA with 0.1 M DL-glyceraldehyde and 0.1 M glycolaldehyde, respectively, at 37 °C for 7 days. After reached cell confluent, C2C12 cells were incubated with or without 1,25D for 2 days. After that, the cells were washed and incubated in DMEM without FBS and 1,25D for 24 hours. Then, the medium was collected. Results: 1,25-dihydroxyvitamin D3 (1,25D) induced the expression of MyoD, myogenin and OGN, and these effects were abolished by vitamin D receptor (VDR) suppression by siRNA in C2C12 cells. Moreover, conditioned medium from 1,25D-pretreated C2C12 cells stimulated the expression of type I collagen and alkaline phosphatase in osteoblastic MC3T3-E1 cells, compared to control medium from 1,25D-untreated C2C12 cells. In contrast, conditioned medium from VDR-suppressed and 1,25D-pretreated C2C12 cells showed no effects. Although AGE2 and AGE3 suppressed the expression of MyoD, myogenin and OGN, 1,25D blunted the AGEs' effects. Conclusion: These findings showed for the first time that active vitamin D plays important roles in myogenesis and muscle-induced osteoblastogenesis through OGN expression. Active vitamin D treatment may rescue the AGEs-induced sarcopenia as well as -suppressed osteoblastic differentiation via OGN expression in myoblasts.

Disclosures: Ipeei Kanazawa, None.

This study received funding from: Uehara Memorial Foundation

SU0169

FGF9 is highly expressed in an osteocyte-like "mini-bone" cell line and inhibits C2C12 myogenesis via overexpression of myostatin. Jian Huang*, Jeanha Choi, David Robbles, Seth Evans, Lora McCormick, Sarah Dallas, Marco Brotto. University of Missouri Kansas city, USA

We previously reported that PGE₂ is a secreted factor from osteocytes that significantly accelerates myogenesis and Ca²⁺ release from the sarcoplasmic reticulum of muscle cells. We recently communicated that another osteocyte factor, Wnt3a, also exerts similar effects on myogenesis. After performing a qPCR gene array, we found that FGF9 was upregulated in a cell line, OmGFP66, which differentiates in vitro to form "mini-bone" structures containing embedded osteocytes within mineralized lacunae. FGF9 is strongly expressed in neurons, and has roles in regulating embryonic development, cell proliferation, differentiation, and migration. To investigate the potential effects of FGF9 as a bone to muscle signaling factor, C2C12 myoblasts were treated with 2, 10, and 50ng/ml FGF9 recombinant protein. Myogenesis was monitored by myosin heavy chain and myonuclei staining at day 3 of differentiation. The control Fusion Index was 47.6% ± 2.6 compared to 38.2 ± 4.8 (*p* > 0.05) for the 2ng/ml; 34.6% ± 6.99 for 10ng/ml (*p* < 0.05), and 17.0% ± 2.1 for 50ng/ml *p* < 0.0001 (*n*=3). These results suggest that FGF9 may work as an inhibitory signaling factor from bone to muscle. To study molecular mechanisms underlying the inhibitory effects of FGF9 on C2C12 differentiation, the expression of myogenic markers (*MyoD*, *MyoG*, *MHC* and *Myostatin*) were analyzed by qRT-PCR. No significant changes in *MyoD* expression were found in FGF9 treated groups compared to controls. In the 2ng/ml FGF9 group, there was no significant change in the expression of *MyoG*, *MHC* and *Myostatin*. In the 10ng/ml group there was a significant 29.1% decrease in expression of *MHC*. In the 50ng/ml group, *MHC* expression was decreased significantly by 58%. Also, in 10ng/ml and 50ng/ml FGF9 treated C2C12 cells, *MyoG* expression was decreased significantly by 21.1% and 20.5%, respectively. Interestingly, expression of the myogenic inhibitor *myostatin* was increased significantly in 10ng/ml and 50ng/ml FGF9 treated C2C12 cells by 135.3% and 185.8%, respectively. These results suggest that FGF9 inhibition of C2C12 cell differentiation may be mediated by the overexpression of *myostatin*. These results could potentially imply that bone cells function as major regulators of muscle homeostasis by secreting both stimulatory and inhibitory factors for the fine-tuning of myogenesis. This could have important applications to a range of musculoskeletal pathological conditions, including the twin diseases of aging osteo-sarcopenia.

Disclosures: Jian Huang, None.

SU0170

Acute Marrow Inflammation Induced by Muscle Paralysis Does Not Directly Mediate Rapid Bone Resorption. Brandon Ausk*, Leah Worton, Ronald Kwon, Sundar Srinivasan, Edith Gardiner, Steven Bain, Ted Gross. University of Washington, USA

Transient muscle paralysis induced by a single injection of Botulinum Toxin A (BTxA) precipitates extremely rapid and predominantly focal bone loss in adjacent bones. Acute trabecular bone resorption (beginning within 3 d and completed by 12 d post-paralysis) arises via RANKL mediated osteoclastic resorption. At 3 d post-paralysis, bone marrow gene expression reflects the presence of an inflammatory response with TNF-alpha upregulated 4-fold vs naïve mice. Cell sorting data from proximal tibia bone marrow supports this thesis as acute CD4+ T-cell infiltration occurs within 24 hr of calf paralysis. We therefore hypothesized that inhibition of the marrow inflammatory response would mitigate BTxA induced bone resorption. We tested this thesis by assessing acute bone loss following calf paralysis in three mouse KO models of inflammatory signaling deficiency: 1) TNF-alpha (germ deletion of TNF-alpha), 2) Toll-Like Receptors (MyD88 KO), and 3) T-Cells (TCR δ KO). A fourth group of C57 mice served as WT controls (*n*=6 to 8/grp). All mice received high-resolution μ CT imaging of the proximal tibia metaphysis on d 0, d 5, and d 12.

Outcomes measures included standard trabecular morphology analyses, normalized as percent change from baseline (i.e., d 0) for each mouse to account for any baseline differences in trabecular morphology across mice strains. One-way ANOVAs were performed on d 5 and d 12 datasets to determine the effect of each inflammatory deficiency upon on BTxA induced osteoclastogenesis. Consistent with historical data, muscle paralysis induced significant trabecular degeneration in WT mice by d.5 (39.2 ± 1.8%) with loss reaching (76.8 ± 2.5%) at d 12. When compared to WT controls, the same temporal osteoclastogenic response following muscle paralysis was observed in the TNF-alpha KO (d.5: 30.5 ± 4.6%, *p*>0.59; d.12: 75.7 ± 1.9%, *p*=1.00), MyD88 KO (d.5: 45.6 ± 3.6%; d.12: 77.3 ± 0.8%, both *p*=1.00) and TCR δ KO mice (d.5: 39.8 ± 2.8% on d.5, d.12: 78.9 ± 1.5%, both *p*=1.00). We conclude that interruption of three critical aspects of inflammatory signaling does not alter the rate or extent of osteoclastic trabecular resorption induced by transient muscle paralysis. However, these data do not preclude the possibility that an acute neurogenic inflammatory event could induce osteoclastogenesis upstream of bone marrow inflammation.

Disclosures: Brandon Ausk, None.

SU0171

Exogenous IGF-1 Fails to Increase Muscle Fiber Cross-Sectional Area After Severe Burns. Lucas Sansevero¹, Amina El Ayadi², Yi-Xian Qin¹, Celeste C Finnerty³, Minyi Hu⁴, Sachin Hegde³, Anesh Prasai⁵, Laura Porro³, Noe Rodriguez⁶, David Herndon³, Gordon Klein^{*7}. ¹Department of Bioengineering, State University of New York at Stony Brook, USA, ²Shriners Hospitals for Children & University of Texas Medical Branch, USA, ³Shriners Hospital for Children & University of Texas Medical Branch, USA, ⁴Department of Bioengineering, State University of New York at Stony Brook, USA, ⁵Shriners Hospitals for Children, Galveston Texas, USA, ⁶Shriners Hospital for Children & University of Texas Medical Branch, USA, ⁷University of Texas Medical Branch, USA

Severe burn injury is associated with muscle wasting and negative nitrogen balance. During disuse muscle atrophy ectopic expression of IGF-1 within the gastrocnemius attenuates the reduction of muscle fiber cross-sectional area, muscle mass and density (Alzghoul et al FASEB J 2004) while overexpression of human IGF-1 in mouse muscle is associated with an increase in muscle mass (Banu et al Calcif Tissue Int 2003). The aim of our study was to determine whether continuous infusion of IGF-1 in rats following severe burn could increase muscle cross-sectional area. To that end we continuously infused IGF-1, 3.8 mg/kg/d via an implanted Alzet minipump in rats following a 60% surface area scald burn under anesthesia and evaluated gastrocnemius cross-sectional area in microns squared following sacrifice at 1 (n=6) or 4 (n=7) weeks post-burn compared to specimens from identically burned rats with no intervention (n=7) and normal ratw undergoing sham burn (n=8 at 1 wk, n=7 at 4 wk). Specimens of muscle were subject to cryosection followed by hematoxylin and eosin staining and analysis of muscle fiber cross-sectional area using Photoshop and Image J. Results indicated that one-way ANOVA failed to demonstrate a significant rise in muscle fiber cross-sectional area with IGF-1 infusion (*p*=0.175), an analysis confirmed by use of unpaired *t* tests. Possible explanations include loss of IGF binding proteins to attach IGF-1 to its receptor in muscle, or to down-regulation of the IGF-1 receptor itself due to the burn injury, or to a dose of IGF-1 that was inadequate for the extent of catabolic injury resulting from the burn.

Disclosures: Gordon Klein, None.

SU0172

Investigation for the Protecting Effects and Molecular Mechanisms of Exercise on Glucosamine-induced Insulin Resistance in Ovariectomized Rats. Chung-Hwan Chen^{*1}, Lin Kang², Shih-Tse Chen³, Tsang-Hai Huang⁴. ¹Kaohsiung Medical University Hospital & Kaohsiung Medical University, Taiwan, ²National Cheng Kung University Hospital, Taiwan, ³National Taiwan University Hospital Hsin-Chu Branch, Taiwan, ⁴National Cheng-Kung University, Taiwan

Objective:

Glucosamine (GlcN), which had been reported to cause insulin resistance (IR), is a popular nutritional supplement used to treat osteoarthritis in menopausal women, who are exposed to the risk of type 2 diabetes mellitus (T2DM) and metabolic syndrome due to ovarian hormone deficiency. We previously found female rats do not develop IR upon GlcN treatment except after ovariectomy (OVX) and the underlying mechanisms are relevant to decreasing the expression of glucose transport protein subtype 4 (GLUT4) in skeletal muscle and increasing the size of pancreatic islets. Herein, we used ovariectomized (OVX) rats and add exercise regimen to investigate whether exercise can reverse GlcN-induced IR.

Materials and methods:

The female rats were divided into 5 groups: (1) Sham-operated group (SHAM), (2) SHAM with 750 mg/kg/day GlcN intraperitoneally (i.p.) injected for 14 days, (3) OVX group, (4) OVX with 750 mg/kg/day GlcN i.p. injected for 14 days, (5) OVX with GlcN 750 mg/kg/day intraperitoneally injected for 14 days and then receiving exercise regimen (running program) for 8 weeks. Intraperitoneal glucose tolerance test

(IPGTT) was performed to measure plasma glucose and insulin, and calculate clinical homeostasis model assessment-insulin resistance (HOMA-IR) and glucose-insulin index.

Results and conclusions

Fasting plasma glucose increased in the OVX + GlcN group, and fasting plasma insulin and HOMA-IR were elevated more significantly in this group. After receiving exercise regimen (running program) for 8 weeks, no increase in fasting plasma glucose, insulin, and HOMA-IR were found. In IPGTT, plasma glucose, plasma insulin, HOMA-IR, and glucose-insulin index were significantly elevated only in the OVX with GlcN group after IP glucose injection, implying that IR was induced by GlcN only in female rats without the protection of ovarian hormone. However, the elevated plasma glucose, plasma insulin, HOMA-IR, and glucose-insulin index disappeared after exercise regimen (running program) for 8 weeks, implying the GlcN-induced IR in OVX rats could be reversed by exercise.

The results demonstrate that female rats do not develop IR upon GlcN treatment except after ovariectomy. Those who take GlcN after menopause or bilateral oophorectomy should watch their blood glucose level closely, especially after meals. Exercise had the protecting effect for GlcN-induced IR in female rats and investigation for the underlying mechanisms is ongoing in our present studies.

Disclosures: Chung-Hwan Chen, None.

SU0173

Vestibular System Is Involved in Changes of Muscle and Bone Induced by Hypergravity in Mice. Naoyuki Kawao*¹, Hironobu Morita², Koji Obata², Yukinori Tamura¹, Katsumi Okumoto³, Hiroshi Kaij¹. ¹Kinki University Faculty of Medicine, Japan, ²Gifu University Graduate School of Medicine, Japan, ³Life Science Research Institute, Kinki University, Japan

Linkage between muscle and bone has recently noted. Gravity change in a space flight concurrently affects muscle and bone with changes in vestibular signals and sympathetic outflow. However, the roles of vestibular signals in the gravity-dependent muscle and bone changes remain unknown. We therefore investigated the involvement of vestibular system in hypergravity-induced muscle and bone changes in mice. Bilateral inner vestibules were surgically lesioned (VL) in male C57/BL6 mice, 6 weeks old. After a recovery period for 14 days, the mice were kept in 1 g or 3 g environment for 4 weeks by using a centrifuge. The tibial muscle and bone mass were analyzed by quantitative computed tomography (QCT) and evaluated by adjusting with body weight, since hypergravity or VL itself significantly reduced body weight. QCT analysis revealed that VL blunted the increases in tibial muscle mass and trabecular bone mass induced by hypergravity, although hypergravity did not affect cortical bone and fat mass. Histological analysis showed that VL antagonized the increase in cross sectional area of muscle fiber induced by hypergravity in soleus, but not in gastrocnemius. Although hypergravity did not affect number of Pax7-positive cells (muscle satellite cells) and mRNA levels of Pax7, atrogene-1 and MuRF1 in soleus, VL suppressed mRNA levels of myogenic genes (MyoD, Myf6 and myogenin) enhanced by hypergravity, suggesting that vestibular system contributes to the hypergravity-induced muscle hypertrophy partly through an enhancement of myogenic differentiation. As for muscle-derived humoral factor affecting bone, VL blunted the increase in the levels of FAM5C and follistatin, a myostatin inhibitor, enhanced by hypergravity in soleus, although hypergravity did not affect the mRNA levels of myostatin, IGF-1, FGF2, TGF- β , osteoglycin and irisin. On the other hand, propranolol, a blocker of beta-adrenergic receptors, antagonized the increases in muscle and bone mass induced by hypergravity, suggesting the involvement of sympathetic tones in the effects of hypergravity on muscle and bone. In conclusion, the present study indicates that gravity change affects muscle and trabecular bone through vestibular signals and the subsequent sympathetic outflow in mice. The control of vestibular system might be important for the management of osteopenia and muscle wasting in space flight and bed rest state.

Disclosures: Naoyuki Kawao, None.

SU0174

ZIP4 Silencing Improves Bone Loss in Pancreatic Cancer. Qiang Zhang¹, Xiaotian Sun², Jingxuan Yang³, Hao Ding¹, Catherine Ambros⁴, Xiaohong Bi*⁵, Min Li³. ¹University of Texas Health Science Center, USA, ²University of Oklahoma Health Sciences Center, USA, ³The University of Oklahoma Health Sciences Center, USA, ⁴University of Texas Health Science Center at Houston, USA, ⁵University of Texas Health Science Center at Houston, USA

Pancreatic cancer (PC) patients usually suffer severe nutrition deficiency, muscle wasting, and loss of bone mass. While muscle wasting has been extensively investigated, bone loss and its related molecular mechanism in PC is poorly understood. Effective prevention and treatment of bone loss in these patients can improve their life quality, reduce both direct and indirect medical costs, and enhance the therapeutic efficacy of the primary disease. We have previously found that silencing of a zinc transporter ZIP4 prolongs the survival and reduces the severity of PC-associated cachexia in vivo. However, the role of ZIP4 in the pancreatic cancer-related bone loss remains unknown. In this study we investigated the effect of ZIP4

knockdown on the bone structure, composition and mechanical properties of femurs in an orthotopic xenograft mouse model using microCT and Raman spectroscopic imaging and whole bone testing. Our data showed silencing ZIP4 restored the bone tissue mineral density values to the control group levels which were significantly increased compared to the untreated PC animals. Bone mineral crystallinity significantly decreased and collagen content significantly increased with the treatment of ZIP4 knockdown, indicating the presence of smaller or less crystalline mineral crystallites and elevated new bone formation in the treatment group. Significant differences were observed among groups in elastic and plastic energy, plastic displacement, elastic and plastic toughness, and plastic strain. The improved mechanical properties in the ZIP4 silencing group suggest that the bones from these animals demonstrated higher ductility and could absorb more energy before failure when compared to the untreated PC animals. Western blot showed that RANKL in control PC cells was higher than that in ZIP4 knockdown cells under zinc-deficient environment. Coculture in the medium from ZIP4 knockdown cells increased the average osteoclast count per high-power field and upregulated the RANK and TRAP mRNA levels in differentiated murine macrophages, suggesting that RANK/RANKL pathway may be involved in the ZIP4 mediated bone loss seen in PC patients. These combined results further support that the participation of ZIP4 in the development and progression of pancreatic cancer may be an important event, and also verify its potential significance as a therapeutic target for treating patients with such devastating disease and cancer related disorders.

Disclosures: Xiaohong Bi, None.

SU0175

Clinical Features and HLA-B loci of Japanese Patients with Ankylosing Spondylitis (2nd report). Tsuyoshi Kobashigawa*, Yuki Nanke, Hisashi Yamanaka, Shigeru Kotake. Tokyo Women's Medical University, Japan

Background: The pathogenesis of AS remains to be elucidated. Despite the strong association between HLA-B27 and susceptibility to AS, the exact pathogenic role of HLA-B27 in AS and other spondyloarthropathies has yet to be determined [1].

Objective: To elucidate the clinical features of Japanese AS patients visited our clinic and the relationships between AS and HLA-B loci. Our hypothesis is other HLA-B loci except for B27 related to AS.

Methods: Sixty-three AS patients visited our clinic in 2 years (2007 to 2008). We enrolled 32 AS patients (male: 27, mean age (SD): 37.4 (13.0) year-old) whose HLA were measured. HLA data of the registered donors in the Japanese unrelated bone marrow donor registry [2] were used as a healthy control group data. We analyzed the relationships between AS and HLA using Chi square test.

Results: In the present study, the frequency of patients fulfilled the ESSG [3] criteria was 31 (96.9%) patients and 1 male patient unfulfilled without experience of inflammatory spinal pain (ISP) and synovitis, but he had some histories of alternate buttock pain (ABP), enthesopathy and sacroiliitis. The frequency of symptoms of ESSG criteria were as follows; ISP: 5 patients (15.6%), synovitis: 22 (68.8%), positive family history: 3 (9.4%), psoriasis: 3 (9.4%), IBD: 1 (9.4%), enthesopathy: 12 (37.5%), ABP: 8 (25.0%) and sacroiliitis: 22 (68.8%), and that of definite AS patients fulfilled the modified New York criteria (MNYC) [4] was 21 (65.6%). On the other hand, 11 (34.4%) probable AS with radiographs finding of sacroiliitis were without clinical symptoms. The frequency of MNYC's symptoms were as follows; low back pain: 13 (96.9%), limitation of lumbar spine: 12 (40.6%), chest expansion: 12 (37.5%), and sacroiliitis: 22 (68.8%). Moreover, we detected 14 HLA-B loci: HLA-B27 ($p=2.3 \times 10^{-317}$) was strongly related to development of AS, and HLA-B52 ($p=0.017$) was possibly related to that.

Conclusion: The present findings supported our hypotheses because there was a tendency that HLA-B52, except for B27, showed a relation to AS.

References: [1] Primer on the Rheumatic Diseases 2007. [2] MHC 2007. [3] A&R 1991. [4] A&R 1984.

Disclosures: Tsuyoshi Kobashigawa, None.

SU0176

Epiphyseal Bone, Subchondral Bone Plate and Epiphyseal Trabecular Bone in Surgically and Chemically Induced Rat Models of Osteoarthritis. Jukka Morko*, ZhiQi Peng, Jukka Vääräniemi, Katja M Fagerlund, Jukka P Rissanen, Jenni Bernoulli, Jussi M Halleen. Pharmatest Services Ltd, Finland

Several experimental animal models have been developed for human osteoarthritis (OA) and used to study the preclinical efficacy of disease and symptom modifying OA drug candidates. Recently, the histopathology initiative of Osteoarthritis Research Society International (OARSI) has presented recommendations for histological OA assessment. These recommendations focus on articular cartilage, synovium, joint capsule, and growth plate. When studying treatment effects on bone, the histological OA assessment should be completed with the analysis of epiphyseal bone, subchondral bone plate and epiphyseal trabecular bone. In this study, we performed a systemic characterization of these bone compartments together with knee joint discomfort, pain and degenerative changes in four rat OA models. Unilateral OA was induced in knee joints of male Lewis rats at 3 months of age using the following OA models: intra-articular moniodoacetate (MIA, 1 mg), medial meniscal tear and medial collateral ligament transection (MMT+MCLT), anterior cruciate ligament transection and partial medial meniscectomy (ACLT+pMMx), and ACLT. Body

weight, static weight bearing and static secondary mechanical allodynia were followed during the in-life phase of the study. Knee joints were harvested at the end of the in-life phase, and histological OA assessment was performed following the OARSI recommendations and by analyzing the amount of epiphyseal, subchondral and trabecular bone in medial tibial plateau. Knee joint discomfort was observed in operated hind limbs during the first week, and knee joint pain in operated and MIA-injected hind limbs during the first week and at the end of the in-life phase. Knee joint pain was associated with cartilage degeneration down to intermediate layer and mild synovial inflammation in the rat MIA model, with marked cartilage loss down to tidemark, large osteophytes and synovial inflammation in the rat MMT+MCLT and ACLT+pMMx models, and with cartilage loss down to deep layer, osteophytes and mild synovial inflammation in the rat ACLT model. These OA changes were observed together with decreased amount of epiphyseal and/or subchondral bone in the rat MIA and ACLT models and with increased amount of epiphyseal and subchondral bone in the rat MMT+MCLT model. These results can be used to design studies for testing the preclinical efficacy of OA drug candidates on bone in association with articular cartilage, synovium and knee joint discomfort and pain.

Disclosures: *Jukka Morko, Pharmatest Services Ltd, Employee*

SU0177

HIGH PREVALENCE OF VARIOUS UPPER LIMB MUSCULOSKELETAL DISORDERS IN KOREAN ORCHARDISTS. Sang-Hyon Kim^{*1}, Sang-Il Lee², Sang-Heon Lee³, Young-Il Seo⁴, Jinseok Kim⁵, Jung Soo Song⁶. ¹Div. of Rheumatology, South Korea, ²Division of Rheumatology, Department of Internal Medicine, ²Department of Preventive Medicine, Gyeongsang National University School of Medicine, ³Clinical Research Institute, Gyeongsang National University Hospital, Jinju, Republic of Korea, South Korea, ³Division of Rheumatology, Konkuk University School of Medicine, Seoul, Republic of Korea, South Korea, ⁴Division of Rheumatology, Hallym University Medical Center, Ahnyang, Republic of Korea, South Korea, ⁵Department of Internal Medicine, Jeju National University Hospital, Jeju, Republic of Korea, South Korea, ⁶Division of Rheumatology, Department of Internal Medicine, Chung-Ang University Medical school, Seoul, Republic of Korea, South Korea

Background: Orchardists are expected to show high prevalence of upper limb musculoskeletal disorders (MSDs) due to their heavy works and working postures. However, there are no systematic studies relating upper limb MSDs in Korean orchardists. **Objectives:** To evaluate the prevalence and characteristics of upper limb MSDs among orchardists in rural areas of Korea. **Methods:** The study was carried out from June 2013 to May 2014 in a tertiary medical center. The physical examinations of upper extremities were performed by rheumatologists, orthopedists, and rehabilitation medicine specialists. The plain radiographs of shoulder, elbow, and hand, nerve conduction examination of upper extremities, and MRI of both shoulder were taken. The Disabilities of the Arm, Shoulder, and Hand (DASH) questionnaire was used to assess symptoms and function of upper extremities. **Results:** Five hundred and fifty orchardists were included. Participants comprised of 49.5% female and 50.5% male with mean age of 59.5 ± 8.1 years. The mean farming duration was 31.3 ± 13.2 years. A total of 34 different types of upper limb MSDs were detected. The most frequent disorder was myofascial pain syndrome (80.5%) followed by rotator cuff syndrome (58.9%), hand osteoarthritis (58.0%), carpal tunnel syndrome (42.9%), and lateral epicondylitis (39.5%). Prevalence of any form of MSD was 98.5% and of three and more of MSDs was 77.3%. Participants with longer duration of farming had higher numbers of MSDs. Almost part of pruning and harvesting postures in orchard farming were loaded works for musculoskeletal systems. Total DASH score was relatively high (14.9 ± 14.4). **Conclusions:** Almost orchardists have upper limb MSDs. Our results suggest the need to implement interventions in orchardists to prevent MSDs.

Disclosures: *Sang-Hyon Kim, None.*

SU0178

Assessment of Notch Activation Status in Bone Cells in Inflammatory Arthritis using Hes1-GFP Reporter Mice. Wen Sun^{*1}, Hengwei Zhang¹, Xing Li¹, Brendan Boyce¹, Matthew Hilton², Lianping Xing¹. ¹University of Rochester Medical Center, USA, ²Duke University School of Medicine, USA

Notch signaling plays a critical role in maintenance of bone homeostasis in part via HES-mediated suppression of mesenchymal stem cell (MSC) differentiation toward the osteoblast lineage. Notch is activated in MSCs in TNF transgenic (TNF-Tg) mice, a model of chronic inflammatory arthritis, and thus inhibits osteoblast differentiation. However, the distribution of cells with active Notch signaling in bone, bone marrow (BM) and synovium, and changes in expression levels under normal and arthritic conditions have not been reported. Here, we used Hes1-GFP reporter and Hes1-GFP/TNF-Tg mice and found that Hes1-GFP+ cells, including MSCs, hematopoietic and endothelial cells, have a heterogeneous distribution in normal BM. CD45-/GFP+ cells expressed high levels of mesenchymal surface markers and formed CFU-F and CFU-

ALP colonies. Expansion of CFU-F colonies was associated with a rapid increase in Hes1-GFP+ cells and GFP intensity. In Hes1-GFP/TNF-Tg mice with established arthritis, the numbers of Hes1-GFP+ cells, including CD45-/Hes1-GFP+ MSC-enriched cells and CD45+/CD11b+/Hes1-GFP+ myeloid precursors were increased significantly in BM. Hes1-GFP+ cells that were osteocalcin-, some of which expressed the endothelial cell marker CD31, localized mainly near the endosteal surface and small blood vessels. Compared to the moderate increase within the BM, the numbers of GFP+ cells in synovium were markedly increased (fold over Hes1-GFP mice: 1.5±0.4 in BM vs. 13.5±1.7 in synovium). About 70% of synovial GFP+ cells were F4/80+ macrophages, 15% were B220+ B cells, and 5% were CD31+ endothelial cells. Further analysis indicated that most of F4/80+/GFP+ macrophages expressed the M1 macrophage marker iNOS, but not the M2 marker CD206+ (74.8±5.9% M1 vs. 25.2±5.9% M2). Treatment of BM macrophages from Hes1-GFP mice with the M1 inducers, LPS or TNF, promoted GFP+/iNOS+ M1 macrophage formation, while the M2 inducer, IL4, promoted CD206+ M2 macrophage formation, but these cells were GFP-. Thus, the majority of cells with active Notch signaling in the inflamed synovium are M1 macrophages. Currently, we are in the process of treating Hes1-GFP/TNF-Tg mice with Thapsigargin, a Notch inhibitor and M2 macrophage inducer, to determine its effect on joint inflammation, Notch activation and macrophage polarization. Hes1-GFP mice represent a useful tool for assessment of the distribution and activation status of Notch in bone cells using *in vivo*, *ex vivo*, and *in vitro* assays.

Disclosures: *Wen Sun, None.*

SU0179

Comparative Study between Denosumab and Minodronate with Eldecalcitol as the Treatment after 2-Year Daily Teriparatide in Osteoporosis in Patients with Rheumatoid Arthritis. Yuji Hirano^{*}, Shinya Hirabara, Masaaki Isono. Rheumatology, Toyohashi Municipal Hospital, Japan

Background: Although daily teriparatide (dTPTD) treatment greatly increases bone mineral density (BMD), increase of BMD is not enough after 2-year dTPTD treatment in some patients with osteoporosis (OP). It is known that no treatment after dTPTD treatment results in decrease of BMD. Although effective treatment strategy after 2-year dTPTD treatment is necessary, it is controversial. This prospective study compared minodronate with eldecalcitol (MIN/ELD) and denosumab (DMB) as the treatment after 2-year dTPTD treatment in OP in patients with rheumatoid arthritis (RA-OP).

Methods: Female RA-OP patients treated with MIN/ELD (n=21) or DMB (n=10) after dTPTD were used. Patients' characteristics, change of BMD (lumbar spine and total hip: LSBMD and THBMD) measured by DEXA at every 6 month from the initiation of dTPTD and change of bone turnover markers (BTM) (PINP and TRACP-5b) at every 6 month from the initiation of dTPTD were compared between two groups. DMB (60mg) was injected every 6 month with prescribing of native vitamin D and calcium. MIN (50mg) was administered every 4 weeks and ELD (0.75µg) was administered every day. MIN is a bisphosphonate drug and ELD is activated vitamin D.

Results: Patients' characteristics (MIN/ELD: DMB): Mean age (70.2: 70.8). Body mass index (20.8: 21.3). FRAX (39.6%: 33.8%). PSL use (71.4%: 70.0%). No significant differences in patients' characteristics were observed between two groups. % increase of LSBMD (dTPTD6m/12m/18m/24m/AfterTPTD6m): 7.0/11.7/12.3/12.0/16.8 in MIN/ELD and 10.3/13.7/15.2/16.1/18.4 in DMB. % increase of LSBMD after dTPTD treatment was 4.4% in MIN/ELD and 1.8% in DMB, respectively. No significant differences were observed at all time-points. % increase of THBMD: 1.2/3.1/4.3/5.3/5.9 in MIN/ELD and 1.5/4.4/4.7/4.7/6.5 in DMB. % increase of THBMD after dTPTD treatment was 0.6% in MIN/ELD and 1.1% in DMB, respectively. No significant differences were observed at all time-points. % change of BTM was expressed as the value at the initiation of dTPTD was 100. PINP: 100/413.9/355.7/258.5/219.2/44.5 in MIN/ELD. 100/407.4/380.5/272.8/228.6/56.9 in DMB. TRACP: 100/148.9/157.4/139.8/144.7/51.2 in MIN/ELD. 100/188.0/209.7/178.5/178.6/91.9 in DMB. There were no significant differences in BTM between two groups.

Conclusions: This study shows that short-term efficacy of MIN/ELD equals to that of DMB as the treatment option after 2-year TPTD in RA-OP. Long-term results are necessary in the future.

Disclosures: *Yuji Hirano, None.*

SU0180

Effects of Monosodium Urate (MSU) Crystals on MLO-Y4 Cell Viability; Is There a Role for Osteocytes in Bone Erosion in Gout? . Ashika Chhana^{*}, David Musson, Karen Callon, Dorit Naot, Greg Gamble, Jill Cornish, Nicola Dalbeth. University of Auckland, New Zealand

Purpose: Gout is the most common form of inflammatory arthritis. It is characterised by the deposition of monosodium urate (MSU) crystals within joints. MSU crystals are found within subchondral bone. We have previously shown that patients with advanced gout have enhanced osteoclast-mediated bone resorption and impaired osteoblast-mediated bone formation, leading to focal bone erosion. Given that the osteocyte has been shown to be a master regulator of bone

remodelling, the aim of this study was to investigate the effects of MSU crystals on osteocyte-like cell viability.

Methods: MSU crystals were prepared by recrystallization of uric acid. MLO-Y4 osteocyte-like cells were cultured on plastic (2D) or in 3mg/mL type I collagen gels and cultured with 0.01-0.5mg/mL MSU crystals or soluble urate for 24 hours. Cells were then washed and MSU crystals or urate completely removed. Cell viability was assessed 24 hours and 48 hours after the addition of MSU crystals using MTT and alamarBlue assays. BCP, CPPD and aluminium crystals were tested using the same methods. Live-dead staining was also performed 24 and 48 hours after the addition of MSU crystals to cells cultured in collagen gels with MSU crystals for 24 hours.

Results: In 2D cultures, 0.1-0.5mg/mL MSU crystals significantly reduced MLO-Y4 cell viability by ~70% 24 hours after the addition of MSU crystals ($P<0.05$). In collagen gels, higher concentrations of MSU crystals (0.3-0.5mg/mL) reduced MLO-Y4 cell viability by ~30-40% 24 hours after the addition of MSU crystals ($P<0.01$); whereas lower concentrations of MSU crystals (0.01-0.1mg/mL) had no effect ($P>0.05$). However, 48 hours after the addition of MSU crystals, culture with the higher concentrations (0.3-0.5mg/mL) of MSU crystals resulted in a 100% reduction of MLO-Y4 cell viability ($P<0.01$). The inhibitory effect on cell viability was specific to MSU crystals, as soluble urate and other types of crystals did not reduce MLO-Y4 viability. Live-dead staining demonstrated that there was a spatial-dependent effect of MSU crystals on MLO-Y4 cell death. Greater cell death was observed at the top of the gel (closer to the site of crystal deposition) compared to the bottom of the gel (further away from the site of crystal deposition) 48 hours after the addition of MSU crystals for 24 hours. A further 24 hours of culture (72 hours after the addition of MSU crystals) revealed dead cells through all layers of the collagen gel. Conclusion: These results indicate that MSU crystals are toxic to osteocyte-like cells and that direct crystal-cell interactions are not necessarily required to reduce osteocyte viability. The interactions between MSU crystals and osteocytes may contribute to bone erosion in gout.

Disclosures: Ashika Chhana, None.

SU0181

Crosstalk Between BMSCs and Regulatory T Cells Through A GILZ/Del-1-Dependent Mechanism. Nianlan Yang*, Babak Baban, Carlos Isales, Xing-Ming Shi. Georgia Regents University, USA

Background: Bone marrow mesenchymal stem cells (BMSCs) have potent modulatory effects on T-cells either through direct cell-cell contact or through releasing soluble factors such as indoleamine-2,3-dioxygenase, interleukin-27 and transforming growth factor beta etc. However, studies on the interaction or crosstalk between the bone cells and immune cells in the bone marrow are sparse. We showed previously that glucocorticoid induced leucine zipper (GILZ) inhibits pro-inflammatory cytokine TNF-alpha-induced COX-2 expression and antagonizes TNF-alpha inhibition of osteogenic differentiation. Recently, we found that GILZ can induce the expression of developmental endothelial locus-1 (Del-1), a secreted protein which has been implicated in the regulation of neutrophil recruitment and inflammatory bone loss, in bone tissues. Thus, in this current study, we seek to exploit whether the induction of Del-1 by GILZ in BMSCs is involved in bone and immune system communication. Methods: Bone marrow and peripheral blood cells were collected from GILZ transgenic mice, in which the expression of GILZ is under the control of a 3.6kb type I collagen promoter fragment (Col3.6-GILZ). Lymphocyte profiles were analyzed by using flow cytometry assay. Del-1 expression in bone tissues was determined by real time RT-PCR and histochemistry analysis. Cytokine production was measured using ELISA. Mixed lymphocyte reaction was performed to determine the regulator effect of GILZ on T lymphocytes. Results: Del-1 expression is increased 3-9 fold ($p<0.05$) in the bone tissues of GILZ transgenic mice and this is coupled with significant increase of IL-10 (2.8 \pm 1.7, $p<0.1$) and decrease of IL-6 (0.1 \pm 0.01, $p<0.01$) and IL-12 (0.47 \pm 0.06, $p<0.05$). FACS results showed that the percentages of FOXP3+ and CD25+ cells are increased significantly in both blood (4.44% vs. 11%, $p<0.1$ and 1% vs. 3.5%, $p<0.1$) and bone marrow (1.35% vs. 6.5%, $p<0.05$ and 1.75% vs. 5.25%, $p<0.05$) of the GILZ Tg mice, which is also confirmed by immunohistochemistry study. Mixed lymphocyte reaction show that compared to control BMSCs, GILZ-expressing BMSCs (MSC-GILZ) induce less allogenic lymphocytes to proliferate (4% vs. 16%); however, the induction activity of MSC-GILZ on Treg cells population is 2-fold higher than the control cells. Conclusion: GILZ expressed in BMSCs upregulates Treg cells by inducing Del-1 expression and altering cytokines profile, thus plays a critical role mediating the crosstalk between BMSCs and Tregs in the bone marrow microenvironment. This data, together with our previous findings that overexpression of GILZ in BMSCs antagonizes TNF-alpha-elicited inflammatory responses suggest that GILZ plays important roles in bone-immune cell communication and BMSC immune suppressive functions.

Disclosures: Nianlan Yang, None.

SU0182

Development and characterization of two polyclonal antibodies directed against human periostin. Philippe Vergnaud¹, Aurélie Pagnon-Minot², Cindy Bertholon³, Yannick Lhoste¹, Emeric Chassaigne¹, Olivier Borel³, Evelyne Ginevts³, Tanja Schubert¹, Philippe Clezardin³, Roland Chapurlat⁴, Jean-Charles Rousseau^{*3}. ¹BioClinicaLab, Lyon, France, ²Novotec, France, ³INSERM UMR 1033, Lyon, France, ⁴INSERM UMR 1033 & Hospices Civils de Lyon, Lyon, France

Purpose: Matricellular protein periostin (PN) is mainly expressed in the periosteum. PN regulates Notch1 signaling, activates lysyl-oxylidase and mediates cancer cell adhesion, survival and invasion in different tissues. The aim of this study was to develop two polyclonal antibodies against the Fas-1 region of human PN and determine their specificity in human serum and bone tissue specimens.

Methods: *In silico* analysis of the total protein sequence of human PN led us to identify two amino acid sequences that are suitable for antibody generation (Patent n° 13/375870) in the second and fourth Fascilin-like domains [ETLEGNTIEIGCDGDSI (Ab-34) and KGFEPGVTNLIKTTQGSK (Ab-12), respectively]. These two peptides were injected in rabbits following a standard protocol of 10 weeks of immunization. Specific polyclonal antibodies Ab12 and Ab34 were purified by immunoaffinity chromatography. We assessed the specificity of these antibodies for PN by immunohistochemistry (IHC) and western blotting (WB) using, respectively, human bone tissue and human sera previously depleted for albumin, IgG and transferrin.

Results: Ab-12 and Ab-34 antibodies did not have the same pattern of recognition of PN. WB analysis of the serum showed that, under non-reducing conditions, Ab-12 recognized two bands, a high molecular weight band around 200 kDa and a second one at 75 kDa. After treatment of the serum with dithiothreitol to reduce disulfide bonds, the 200 and 75kDa bands disappeared and 3 new bands were detected at 70, 50 and 25 kDa. On the other hand, under non-reducing conditions, Ab-34 recognized a single band at 75 kDa in the serum. After dithiothreitol reduction, this band at 75 kDa migrated at a molecular weight of 100 kDa, indicating that the reduction of intradisulfide bonds in PN leads to a more extended conformation of the molecule and makes it run more slowly in the gel. By IHC, Ab-12 stained the cytoplasm of osteoblasts, lining the endosteal surface between cortical bone and the bone marrow, and the cytoplasm of osteoblasts present within the Haversian canals. Ab-34 stained the periosteum and the Haversian canals.

Conclusion: We have generated two polyclonal antibodies against the Fas-like domains of human PN. Our preliminary results suggest that they bind at least two forms of PN molecules in the serum and bone.

Disclosures: Jean-Charles Rousseau, None.

SU0183

A Dynamic Anesthesia System for Long-Term Imaging in the Adult Zebrafish Skeleton. Brenen Wynd*¹, Karuna Patil², Claire Watson³, George Sanders², Ronald Kwon³. ¹Department of Orthopaedics & Sports Medicine, USA, ²Department of Comparative Medicine, University of Washington, USA, ³Department of Orthopaedics & Sports Medicine, University of Washington, USA

Zebrafish (*Danio rerio*) represent a potentially powerful model for bone biomedical research due to their unique optical properties and amenability to *in vivo* imaging strategies. However, to date application of such strategies to study zebrafish bone physiology has been hindered by two challenges: most of the zebrafish skeleton ossifies post-embryonically, and established anesthetic regimens for long-term imaging (i.e., 1-24hrs) in zebrafish embryos are ineffective in adults (with mortality occurring within 20-40 minutes [1]). To overcome this challenge, the goal of the project was to develop an anesthesia system for long-term *in vivo* imaging in the adult zebrafish. For this, we constructed a computer-controlled anesthetic system consisting of a 3D-printed imaging chamber coupled to programmable peristaltic pumps. The pumps intermittently replenished the chamber with anesthetic and fresh water to avoid respiratory arrest (RA). Using 0.0035% benzocaine, we found that statically administering this solution resulted in a mean time to RA of 4.9 \pm 2.9hrs, roughly 3-12 times longer than sedation times previously reported using MS-222/isofluorane cocktails [1]. Next, we examined the potential to use an intermittent dosing regimen (15min of anesthetic water followed by 5min of fresh water) to extend this sedation period. Over an 8hr testing period, we found that dynamic administration successfully maintained the fish between stage 2 and 3 anesthesia while significantly increasing the percent of survival at 8hrs compared to static controls (S: 14%, D:75%, $p<0.05$, Fig 1). As proof of concept, we subjected a single fish to 24hr sedation; the system was able to successfully keep the fish sedated with normal respiratory rates (140-198 breaths/min) for the entire trial period. In summary, we have shown the potential for a dynamic anesthesia protocol utilizing benzocaine to achieve sedation in adult zebrafish for up to 24 hours, a period of time sufficient to observe *de novo* bone formation during fin regeneration [2]. Given the large number of transgenic zebrafish reporter lines and new imaging practices for examination of fluorescence and mineralization [3], this study opens new opportunities to reveal the molecular and cellular events mediating osteogenesis in the adult zebrafish skeleton.

References:

- [1] Huang WC, et al, Chuang YJ. Zebrafish 7(3):297-304, 2010.
 [2] Recidoro AM, et al Kwon RY. JBMR 29(11):2346-2356, 2014.
 [3] Watson CJ and Kwon RY. BoneKEy, In Review.

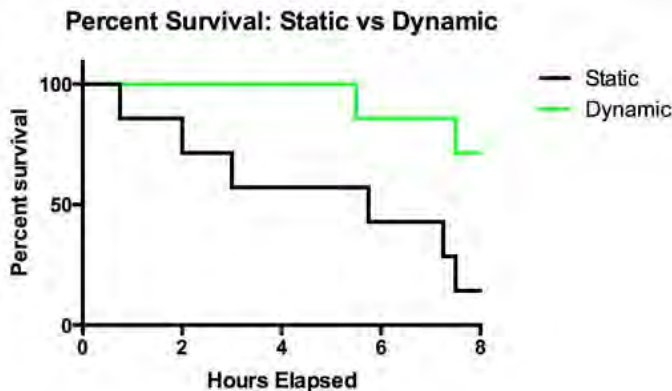


Figure 1

Disclosures: Brenen Wynd, None.

SU0184

Analysis of Osteoactivin in Reamer-Irrigator-Aspirator (RIA) Wastewater as an Osteogenic Factor for Bone Regeneration. Gregory Sondag¹, Lucas Upperman^{*2}, Douglas Crowder¹, Derek Klaus¹, Ethan Scott³, Eric Miller¹, Favez Safadi¹. ¹NEOMED, USA, ²Northeast Ohio Medical University, USA, ³Rootstown, USA

Non-unions and critical-size bone defects are challenging problems that can be successfully treated with a combination of rigid fixation and autologous bone graft. Historically, harvesting iliac crest bone graft (ICBG) has been the gold standard for massive bone grafting procedures; however, ICBG harvest is limited by the amount of graft available as well as a relatively high complication rate. Recently, the Reamer-Irrigator-Aspirator (RIA) device has become a popular method to obtain large amounts of autologous bone graft, with less donor site morbidity compared to ICBG. The RIA is an intramedullary reaming device capable of retrieving finely morselized cortical cancellous bone in excess of 90 cm³ that has osteogenic properties comparable to ICBG. The aspirated femoral contents are passed through a filter to collect and separate the desired bone graft from the remaining filtrate or wastewater (WW). Traditionally, the WW is discarded; however, recent studies have demonstrated the presence of growth factors and viable cells within WW. In this study we examined the presence of osteogenic factors in the WW and tested their effects on RIA-derived growth factors on mesenchymal stem cell (MSC) differentiation *in vitro* and *in vivo*. We also show the presence of the osteogenic factor osteoactivin (OA) – a downstream mediator of BMP-2 discovered by our lab – in the WW. Our results indicate that OA can be found in greater concentrations in the concentrated WW than in the platelet rich plasma (PRP-control). To demonstrate the multipotency effect of MSCs extracted from the wastewater, we differentiated these cells into the osteogenic and adipogenic lineages confirmed by ALP and Oil Red Staining respectively. In order to determine the effects of WW supplement on MSC proliferation and survival, we added concentrated WW to MSCs over 72 hours. MSC's treated with WW demonstrated 80% increased proliferation and survival rates over untreated controls. Furthermore to assess the osteogenic potential of the WW *in vivo*, 5-mm critical-size defects were made in the calvaria of immunodeficient mice. The defects were either left untreated or packed with a collagen sponge. The sponge was loaded with either PBS, PRP, or WW. Four weeks post-surgery, the calvaria and were harvested and assessed by microCT analysis. WW showed dramatic in bone regeneration compared to controls. These data suggest that WW has an osteogenic potential to stimulate bone regeneration in large bony defects and fracture repair.

Disclosures: Lucas Upperman, None.

SU0185

Beta-Aminopropionitrile Treatment Effects on MC3T3-E1 Osteoblast Gene Expression and Type I Collagen Production. SILVIA CANELON^{*1}, Joseph Wallace². ¹Purdue University, USA, ²Indiana University-Purdue University at Indianapolis, USA

Type I collagen morphology can be characterized using fibril D-spacing, a metric that is sensitive to differences in collagen structure across tissue types and disease states. D-spacing describes repeating bands of gap and overlap regions of collagen molecules arranged in a quarter-staggered array. This fibrillar structure is stabilized by enzymatic crosslinks initiated by lysyl oxidase (LOX), a step which can be disrupted using beta-aminopropionitrile (BAPN). Murine *in vivo* studies have confirmed effects of BAPN on collagen nanostructure and the objective of this study

was to evaluate the mechanisms of these effects *in vitro* by measuring D-spacing and quantifying gene expression of type I collagen and LOX. Osteoblastic cells were cultured and differentiated in dishes in the presence or absence of 0.25mM BAPN (n=4/group). Cells proliferated in complete α -MEM media for 7 days then differentiated for 7 days using ascorbic acid. Media was removed from the dishes and cells dissociated from the matrix with an EDTA buffer. The matrix was allowed to dry and imaged in air using atomic force microscopy (AFM) in 5 locations/dish. A 2D Fast Fourier transform was performed on 10 fibrils/location to extract D-spacing (50 fibrils/dish, ~200 fibrils/group). The experiment was repeated for qRT-PCR analysis (n=5). Following RNA isolation and RT, qRT-PCR was performed using SYBR Green primers and master mix (coll1a1, coll1a2, LOX, and β -actin as reference) and gene expression levels analyzed using the comparative C_T method. The D-spacing distribution of collagen produced in the presence of BAPN was shifted toward significantly higher D-spacing values, indicating that BAPN affects the morphology of collagen produced *in vitro*, supporting aforementioned *in vivo* experiments. In contrast, no difference in gene expression was found for any target gene in BAPN-treated samples relative to controls suggesting that inhibition of LOX does not upregulate the LOX gene to compensate for the reduction in aldehyde formation, nor does it regulate expression of genes encoding type I collagen. To understand how inhibition of LOX affects collagen stability, Fourier Transform Infrared (FTIR) spectroscopy has been used in a preliminary study to indirectly measure enzymatic crosslinks by determining the area ratio of two bands in the amide I region of type I collagen produced *in vitro*. Studies are underway to fully characterize the impact of BAPN-treatment on this measure of collagen crosslinking.

Disclosures: SILVIA CANELON, None.

SU0186

Characterization of Mineralization-Competent Matrix Vesicles During Odontoblast-supported Mineralization. Sandeep Chaudhary^{*1}, Maria Kuzynski¹, Morgan Goss¹, Callie Mobley¹, Anne Poliard², Odile Kellermann³, Jose-Luis Millan⁴, Dobrawa Napierala⁵. ¹University of Alabama at Birmingham, USA, ²UFR d'Odontologie Université Paris Descartes 1 rue Maurice Arnoux, France, ³INSERM UMR-S 1124, Université René Descartes Paris 5, Centre Universitaire des Saints-Pères, France, ⁴Sanford Children's Health Research Center, Sanford-Burnham, Medical Research Institute, USA, ⁵Oral & Maxillofacial Surgery, Institute of Oral Health Research, School of Dentistry, University of Alabama at Birmingham, USA

The process of mineralization is initiated by membranous vesicles, called matrix vesicles (MVs), which are released by bone, dentin, and cartilage cells into fibrous extracellular matrix (ECM). Mineralization-competent MVs are enriched in tissue-nonspecific alkaline phosphatase (TNAP), PHOSPHO1 phosphatase, and PO₄³⁻ and Ca²⁺ transporters, which facilitate initial hydroxyapatite crystal formation and thus mineralization. The regulation of MVs formation is not yet clear. Here, we investigated the role of cytoskeletal organization and Rho/Rac1/Cdc42 GTP-ases in the biogenesis of mineralization-competent MVs. We used preodontoblast-derived 17IIA11 cell line as a model of MV-initiated mineralization in osteogenic medium containing 10mM sodium phosphate and 50mg/ml ascorbic acid. MVs were analyzed by Nanosight NS300 and Western blot. Remodeling of cytoskeleton components was inhibited by cytochalasin D, nocodazole, forchlorfenuron and dynasore. We determined that osteogenic conditions induce rapid production of MVs. The number of MVs/cell significantly increased by 5 fold within the 12h and 11 fold within 24h of osteogenic differentiation in comparison with untreated cells. This was associated with activation of Rac1 and Cdc42 GTP-ases but not RhoA. MVs release was increased by non-cytotoxic levels of inhibitors of cytoskeletal organization, with the strongest effect of nocodazole, which inhibits polymerization of microtubules. Comparative protein analyses revealed differential distribution of TNAP and PHOSPHO1 isoforms between MVs and cells in osteogenic and non-osteogenic conditions. Furthermore, we determined that molecular markers of MVs released by 17IIA11 cells were different than proteins in exosomes from serum and cancer cell lines. Earlier, we demonstrated that 17A111 cell lines deficient for the Trps1 transcription factor showed impaired MVs production and mineralization. In this study, we observed that Trps1 deficiency results in impaired activation of Rac1 and Cdc42 in osteogenic conditions. Taken together, our results suggest that osteogenic properties of 17IIA11 cell line rely in MVs released by cells and cytoskeletal modelling along with activation of Rac1 and Cdc42 play a role in MVs biogenesis during odontoblast-supported mineralization.

Disclosures: Sandeep Chaudhary, None.

SU0187

Withdrawn.

SU0188

EDA and EDB Containing Fibronectin Stimulate Osteoblast Differentiation by Acting on $\alpha 4\beta 1$ and $\beta 3$ Integrins Respectively. Carla Sens*¹, Katrin Rau¹, Verena Klemis¹, Inaam Nakchbandi². ¹University of Heidelberg & Max-Planck Institute of Biochemistry, Germany, ²Max-Planck Institute of Biochemistry & University of Heidelberg, Germany

Fibronectin is an extracellular matrix protein produced by many cell types. It modulates the behavior of adjacent cells by binding to cell surface receptors called integrins. Several isoforms have been described. In contrast to the circulating Isoform, the EDA isoform contains an extra domain A and the EDB isoform an extra domain B. Deletion of fibronectin in osteoblasts results in decreased bone mineral density. This effect is mediated by diminished osteoblast differentiation that cannot be corrected by the circulating isoform of fibronectin, suggesting a role for EDA and/or EDB in modulating osteoblast differentiation.

We first evaluated the role of EDA. Transient transfection of a construct of EDA in wildtype newborn murine calvarial osteoblasts enhanced osteoblast differentiation (von Kossa staining, alkaline phosphatase and osteocalcin). In contrast, using siRNA directed against EDA suppressed differentiation. Addition of EDA increased pFAK suggesting that integrins mediate the enhanced differentiation. EDA binds to either $\alpha 4\beta 1$, $\alpha 9\beta 1$ or enhance binding to $\alpha 5\beta 1$ integrins. Deletion of $\beta 1$ integrin in osteoblasts prevented EDA-mediated differentiation. Stimulating $\alpha 4$ or $\alpha 9$ by culturing on VCAM enhanced differentiation. In contrast, inhibiting $\alpha 4\beta 1$ diminished pFAK and osteoblast differentiation. Taken together these data suggest that $\alpha 4\beta 1$ integrin mediates osteoblast differentiation. In line with these findings, a peptide called CS1 that activates $\alpha 4\beta 1$ increased total BMD in treated mice. This effect was mediated via racl and enhancement of wnt signaling.

Similar studies were performed for EDB. EDB enhanced differentiation and its silencing using siRNA inhibited differentiation. However, EDB effects are mediated by $\beta 3$ integrin, because the absence of $\beta 3$ prevented EDB effects. Adding echistatin activated $\beta 3$ in osteoblasts and enhanced differentiation. This was mediated by the RGD sequence because transfecting EDB without RGD into osteoblasts prevented stimulation by EDB, even in the presence of $\beta 3$ integrin. Further, knockout of $\beta 3$ in one allele only is associated with a decrease in BMD in 5-week-old $\beta 3^{+/-}$ heterozygote mice, while homozygote loss is not, because $\beta 3$ integrin is critical for osteoclastic resorption.

In summary, EDA activates $\alpha 4\beta 1$ integrin, while EDB in cooperation with RGD activates $\beta 3$ integrin. Both effects result in enhanced osteoblast differentiation. Furthermore, pharmacologic stimulation of $\alpha 4\beta 1$ increases bone formation and density *in vivo*.

Disclosures: *Carla Sens, None.*

SU0189

Human micro-RNAs miR-29b, miR-30c2 and miR-125b and their target genes are important modulators of bone metabolism. Andreas Kindmark*¹, Navya Laxman², Carl-Johan Rubin³, Hans Mallmin⁴, Olle Nilsson⁴, Elin Grundberg⁵, Tomi Pastinen⁵. ¹Uppsala University Hospital, Sweden, ²Department of Medical Sciences, Uppsala University, Sweden, ³Department of Medical Biochemistry & Microbiology, Uppsala University, Sweden, ⁴Department of Surgical Sciences, Uppsala University, Sweden, ⁵Department of Human Genetics, McGill University & Genome Quebec Innovation Centre, McGill University, Montreal, Quebec, Canada, Canada

Background: MicroRNAs (miRNAs) are important post-transcriptional regulators that have recently introduced an additional level of intricacy to our understanding of gene regulation. We have investigated miRNA-mRNA interactions that may be relevant for bone metabolism by assessing correlations and interindividual variability in miRNA levels and global correlations between miRNA and mRNA levels in a large cohort of primary human osteoblasts (HOBs) obtained during orthopedic surgery in otherwise healthy individuals.

Materials and methods: miRNA levels were assessed by LNA arrays and qPCR. mRNA levels were assessed using Illumina arrays in bone cells from a total of 95 subjects undergoing orthopedic surgery for osteoarthritis. We used an integrated analysis of global miRNA - mRNA correlations, mRNA expression profiling, DE, bioinformatics analysis and functional studies to identify novel target genes for miRNAs with the potential to regulate osteoblast differentiation and extracellular matrix production. We also performed functional studies by overexpression and knockdown of miRNAs

Results: We identified differential expression (DE) of 24 miRNAs, and found 9 miRNAs exhibiting DE between males and females. In functional assays, the differentially expressed miRNAs hsa-miR-29b, hsa-miR-30c2 and hsa-miR-125b were found to target genes highly relevant to bone metabolism, e.g. Collagen, type I, alpha 1 (COL1A1), Osteonectin (SPARC), Runt-related transcription factor 2 (RUNX2), Osteocalcin (BGLAP) and Frizzled-Related Protein (FRZB). Overexpression or knock-down of the miRNAs also affected mineralization. **Conclusion:** hsa-miR-29b, hsa-miR-30c2 and hsa-miR-125b are involved in orchestrating the activities of key regulators of human osteoblast differentiation and extracellular matrix proteins by their convergent action on target genes and pathways to control skeletal gene expression.

Disclosures: *Andreas Kindmark, None.*

SU0190

Leukotrienes B₄ and C₄ play a role on the osteogenic differentiation by mechanism dependent on their receptors binding. Flávia Oliveira*¹, Amanda Pereira¹, Marília Buzalaf¹, Camila Peres-Buzalaf², Rodrigo Oliveira¹. ¹Bauru Dental School - University of São Paulo, Brazil, ²Universidade Sagrado Coração, Brazil

Leukotrienes (LTs) are lipid mediators derived from arachidonic acid metabolism via 5-lipoxygenase (5-LO) and they are shown to modulate bone remodeling. Although osteoblasts present LT receptors, little is known about their effects on these cells. Therefore, we hypothesized to study the role of exogenous LTB₄ and LTC₄ on proliferation and differentiation of preosteoblast lineage cells. To accomplish this, we have used LTB₄, LTC₄ as well as BLT1 and CysLT1 receptors antagonists on MC3T3-E1 cells. *In vitro* data have demonstrated that LTB₄ at 10⁻¹⁰ M increased cell proliferation while at higher doses (10⁻⁸ and 10⁻⁹ M) decreased it when compared to untreated cells. On day 10, exogenous LTB₄ significantly increased preosteoblast proliferation, regardless the tested dose (p<0.05). Also, the treatment of cells with 10⁻⁷, 10⁻⁸ and 10⁻⁹ M LTC₄ increased the cell density on day 1, compared to control cells. On the other hand, on 7 and 10 days, only lower doses of LTC₄ (10⁻⁸ and 10⁻⁹ M) have enhanced it (p<0.05). Thus, we clearly have shown that LTs alter the proliferation of preosteoblasts in a time- and dose- dependent manners. In addition, the pretreatment of cells with BLT1 or CysLT1 receptor antagonists have impaired the increased LTB₄ and LTC₄-induced proliferation, respectively. Osteoblast differentiation was assessed by alkaline phosphatase (ALP) activity, alizarin red-staining bone nodule formation and type 1 collagen and 5-LO expression in osteogenic medium cultured MC3T3-E1 cells. The data have showed that exogenous LTC₄ or LTB₄ increased the ALP activity on day 7, but decreased on day 14, suggesting that LTs modulate ALP activity in a time-dependent manner. Also, the mineralized bone nodules were increased when cells were treated with LTB₄ or LTC₄, compared to untreated cells (p<0.05). While 5-LO expression was up-modulated in differentiated cells on 7 and 14 days (p<0.05), the expression of type 1 collagen was unaltered by both LTs. We conclude that exogenous LTB₄ and LTC₄ affect osteogenic differentiation, judged by increased proliferation and bone formation markers. Importantly, they act through BLT1 or CysLT1 receptors specific binding, respectively and thus they may serve as a therapeutic target for bone diseases in the future.

Disclosures: *Flávia Oliveira, None.*

SU0191

MicroRNAs Involved in Bone Metabolism Are Transported into Matrix Vesicles during Bone Formation. Yuko Nakao*¹, Yuichiro Takei², Tomoko Minamizaki², Hirotaaka Yoshioka², Faisal Ahmed¹, Kotaro Tanimoto², Shumpei Niida³, Yui Yoshiko². ¹Hiroshima University Graduate School of Biomedical & Health Sciences, Japan, ²Hiroshima University Institute of Biomedical & Health Sciences, Japan, ³Biobank, National Center of Geriatrics & Gerontology, Japan

MicroRNAs (miRs) coordinate a broad spectrum of biological processes via epigenetic machinery to regulate gene expression, and growing evidence suggests the roles of miRs in bone and its related diseases. Exosomes have been of great interest in recent years, especially in the context of miRs in the vesicles as cell-to-cell signaling molecules. Exosomes are secreted by most cell types from multivesicular endosomes and present in biological fluids, including blood and urine, while matrix vesicles (MVs) are extracellular organelles budding from osteoblasts and resided in the premineralized matrix of bone. MVs play a pivotal role in bone mineralization and contain a number of biological molecules including tissue non-specific alkaline phosphatase, annexins and growth factors involved in osteoblastogenesis. We hypothesized that, as the proper assembly "bone," MVs provide a protective and enriched source of miRs involved in bone formation and resorption. We prepared MVs from the mouse osteoblastic cell line MC3T3-E1 using ultracentrifugation methods. To evaluate miR expression profiling, we performed microarray analysis on MVs (SurePrint Mouse miRNA Microarrays). Of 1,881 mouse miRs listed, 194 were identified in MVs, and 74 shared homology with human counterparts. To further analysis, we chose 10 miRs of interest, based on the concept that target gene(s) of miRs were established or predicted to be involved in bone resorption and formation. We also confirmed these miRs in primary human and rodent osteoblasts and corresponding MVs. Among miRs tested, miR-125b and let-7c were more abundant in MVs, compared with cells. To determine whether miRs in cells versus MVs are involved in matrix mineralization, we treated MC3T3-E1 cells with U0126, an inhibitor MEK1/2, to enhance matrix mineralization. Eighty-one miRs, including miR-125b and let-7c, were significantly down-regulated, while none of miRs identified in MVs were up-regulated.

Disclosures: *Yuko Nakao, None.*

SU0192

Mineralization in MC3T3-E1 Osteoblast Cultures: A Comparison with Bone. William Addison¹, Valentin Nelea², Florencia Chicatun², Yung-Ching Chien³, Nicolas Tran-Khanh⁴, Michael Buschmann⁴, Showan Nazhat², Mari Kaartinen², Hojatollah Vali², Mary Tecklenburg⁵, Renny Franceschi⁶, Marc McKee^{*2}. ¹Harvard University, USA, ²McGill University, Canada, ³University of California at San Francisco, USA, ⁴Ecole Polytechnique, Canada, ⁵Central Michigan University, USA, ⁶University of Michigan, USA

MC3T3-E1 osteoblast cell cultures are the most commonly used in vitro model of bone matrix mineralization. Despite the widespread use of this cell line to study biomineralization, there is as yet no systematic characterization of the mineral phase produced in these cultures. Our aim was to provide a comprehensive, multi-technique biophysical characterization of this cell culture mineral, and compare it to mouse bone mineral, to determine the suitability of MC3T3-E1 cultures for biomineralization studies. Energy-dispersive X-ray spectroscopy (EDS), X-ray diffraction (XRD), electron diffraction, Fourier-transform infrared spectroscopy (FTIR), confocal microscopy, and transmission (TEM) and scanning (SEM) electron microscopy were used to characterize the mineral phase of MC3T3-E1 osteoblast cultures and mouse calvarial bone. Elemental compositional analysis by EDS showed calcium and phosphorus, and trace amounts of sodium and magnesium, in both samples. XRD on intact resin-embedded cultures indicated that similar to mouse bone, apatite crystals grew with preferential orientations along the (100), (101) and (111) mineral planes indicative of guided biogenic growth as opposed to dystrophic calcification. XRD of crystals isolated from the cultures revealed that the mineral phase was poorly crystalline hydroxyapatite with 10-20 nm-sized nanocrystallites. Consistent with the XRD observations, electron diffraction patterns indicated that culture mineral had low crystallinity typical of biological apatites. FTIR confirmed apatitic carbonate and phosphate. With all techniques utilized, cell culture mineral and mouse bone mineral were remarkably similar. SEM and TEM showed that the cultures had a dense, fibrillar collagen matrix with small 100-nm collagen fibril-associated mineralization foci which coalesced to form larger mineral aggregates. Confocal imaging showed that some cells had dendritic processes and became embedded within the mineral in an osteocyte-like manner. In conclusion, we have documented the characteristics of the mineral phase of MC3T3-E1 osteoblast cultures, and determined that this mineral is highly similar to that of mouse bone.

Disclosures: Marc McKee, None.

SU0193

Murine MicroRNA 126-3p is Upregulated by Endothelin-1 Signaling and Mediates some of Its Pro-Mineralization Effects. Michael Johnson^{*1}, Robert D. Blank². ¹University of Wisconsin, USA, ²Medical College of Milwaukee-Endocrinology, USA

Ecel, encoding endothelin converting enzyme 1 (ECE1), is a positional candidate for a pleiotropic quantitative trait locus affecting femoral size, shape, mineralization, and biomechanical performance and is responsible for 40% of the variation in bone biomechanical performance between HCB8 and HCB 23 congenic mice. ECE1 is a membrane bound protease that converts the inert big endothelin¹ (big ET1) to active endothelin-1 (ET1). Previously, we demonstrated that treatment of TMOB osteoblasts with big ET1 increases mineralization and secretion of IGF1 while decreasing secretion of DKK1 and SOST. Big ET1 exposure also caused significant changes in miRNA expression, suggesting interaction of ET1 with multiple signaling pathways. To further test the hypothesis that ET1 signaling is vital for normal bone physiology we pharmacologically inhibited EDNRA and ECE1 in TMOB osteoblasts. Inhibition of either EDNRA (BQ-123) or ECE1 (phosphoramidon) reduced mineralization ($p < 0.001$). Blockade of EDNRA showed the expected decrease in IGF1 ($p < 0.001$) secretion and increase in DKK1 ($p < 0.001$) and SOST ($p < 0.001$) secretion. However, ECE1 blockade decreased IGF1 signaling ($p < 0.001$) but led to an unexpected decrease in SOST and DKK1. To confirm that this result was not due to non-specific protease inhibition by phosphoramidon, we used *Ecel* siRNA to knockdown *Ecel*. We confirmed knockdown by qPCR and saw similar results in mineralization ($p < 0.001$), and decreased secretion of IGF1, and DKK1 and SOST ($p < 0.05$ respectively). We previously demonstrated that big ET1 treatment increased expression of miRNA 126-3p, a miRNA that is predicted to target murine SOST and decrease its expression, during mineralization by 121X. To test the hypothesis that ET1 signaling partially works through miRNA regulation we transfected TMOB cells with the miRNA 126-3p mimic, a miRNA a 126-3p inhibitor, and a negative control in the presence and absence of big ET1. We found that transfection of the mimic in the absence of big ET1 increased mineralization ($p < 0.01$) and decreased secretion of SOST ($p < 0.05$). We found that transfection of the inhibitor decreased mineralization ($p < 0.01$) and increased secretion of SOST ($p < 0.05$). Our data suggest that the finely balanced process of mineralization is critically influenced by ET1 signaling and that part of influence is mediated through control of miRNA 126-3p expression.

Disclosures: Michael Johnson, None.

SU0194

Parafibromin, a transcriptional repressor, is required in early development but not in mature osteoblasts, where its loss results in increased bone mass. Casey Droscha^{*}, Diegel Cassandra, Bart Williams, Van Andel Institute, USA

Inactivating mutations that lead to loss of heterozygosity within the HRPT2 gene are directly linked to the development of primary hyperparathyroidism, parathyroid adenomas, and ossifying fibromas of the jaw (HPT-JT). The protein product of the HRPT2 gene, parafibromin, is a core member of the polymerase-associated factors (PAF) complex, and also binds to a plethora of transcriptional and chromatin remodeling complexes such as RNAPII, histone methyltransferases and β -catenin. Several lines of evidence in both yeast and mammalian cells have demonstrated that parafibromin is a requisite link between the PAF complex and the transiting RNAPII complex coordinating chromatin remodeling to establish and maintain active from inactive chromatin. Developmentally, parafibromin expression is required for mesenchymal precursor survival and proliferation as deletion results in embryonic lethality at E11.5. Hrpt2 cKO mutant embryos lack organ development due to extensive apoptosis evaluated by cleaved caspase-3 immunohistochemical staining. Further work in our lab has shown that conditional loss of parafibromin within mature osteoblasts results in significantly increased cortical bone volume and thickness, reducing cortical porosity. Trabecular thickness and spacing was also significantly higher in Hrpt2 cKO femurs. Biomechanically, Hrpt2 cKO femurs exhibited increased stiffness and maximum load assessed via four-point bending analysis. Interestingly, bone histomorphometry of WT and Hrpt2 cKO femurs display a reduction in osteoblast surface. Further investigations into osteoblast/osteoclast populations to contribute to the Hrpt2 cKO bone phenotype are underway. To assess transcriptional changes upon loss of Hrpt2 expression with mature osteoblasts, calvarial osteoblasts, identified by Cre-mediated GFP expression, from wildtype and cKO neonatal pups were isolated via flow cytometry and RNA was isolated and subjected to RNA-sequence analysis. These results aid in our understanding of the role parafibromin plays within transcriptional regulation, terminal differentiation, and bone homeostasis. Taken together, the roles of parafibromin and the PAF complex are numerous and essential within differentiating or proliferating cells, yet expendable within terminal, post-mitotic cells.

Disclosures: Casey Droscha, None.

SU0195

Contrasting Effects of Parathyroid Hormone on PHOSPHO1 and Alkaline Phosphatase Expression During Osteoblast Mineralization. Dean Houston^{*1}, Katherine Myers¹, Vicky MacRae¹, Jose Luis Millan², Katherine Staines¹, Colin Farquharson¹. ¹The Roslin Institute, The University of Edinburgh, United Kingdom, ²Sanford Burnham Medical Research Institute, USA

Intermittent parathyroid hormone (PTH) is widely used in the treatment of osteoporosis. The anabolic effects of intermittent PTH on bone are attributed to a number of mechanisms including: stimulation of osteoblast differentiation and inhibition of sclerostin. Despite this, there exists a hiatus in the knowledge surrounding the effects of PTH on key phosphatases required for skeletal mineralization. *Phosphol* and *Alpl*, encoding PHOSPHO1 and tissue-nonspecific alkaline phosphatase (TNAP) respectively, are required for bone mineralization and ablation of either leads to hyperosteooidosis with combined ablation completely abolishing the initiation and progression of skeletal mineralization.

This study sought to investigate the effects of bovine (b)PTH 1-34 on the expression of PHOSPHO1 and TNAP. The osteoblast-like cell line MC3T3-E1 (clone 14) displays profound matrix mineralization over a 10-day period with temporal increases in *Phosphol* and *Alpl* expression (150-fold and 60-fold respectively compared to day 0; $p < 0.001$). Treatment of these cells with 50nM bPTH every 2-days caused a reduction in matrix mineralization at day 10 (42%, $p < 0.05$). At day 10, *Phosphol* mRNA was significantly reduced after a 15 min exposure to bPTH (50nM; 80% decrease, $p < 0.001$). This inhibition was more profound after 1 and 6 hour bPTH exposures (96% & 93% decrease respectively, $p < 0.001$) and persisted to 24 hours (48% decrease, $p < 0.05$). A marked reduction in PHOSPHO1 protein was observed after 24 and 48 hour bPTH treatment. In contrast, the expression of *Alpl* increased after 1 (2.8-fold, $p < 0.05$) and 6 hour (3.6-fold, $p < 0.001$) bPTH exposure which was consistent with increased TNAP protein after 24 and 48 hours of bPTH treatment. The response of *Phosphol* and *Alpl* to 24 hours of bPTH exposure was dose dependent (0.05nM-50nM). Indeed, a 50% reduction ($p < 0.001$) in *Phosphol* expression was achieved by the addition of 0.5nM bPTH with comparable changes at the protein level. Induction of TNAP mRNA and protein was achieved with 5nM bPTH. Further analyses revealed that the cAMP activator forskolin was capable of inducing a suppression of *Phosphol* comparable to the effects of bPTH (93% & 96% respectively). Forskolin induced *Alpl* expression (2.4-fold, $p < 0.05$). In summary, bPTH had differential effects on PHOSPHO1 and TNAP expression during *in vitro* osteoblast mineralization. Initial studies implicate the cAMP/PKA signalling pathway as the mechanism of PTH-induced *Phosphol* inhibition and *Alpl* stimulation.

Disclosures: Dean Houston, None.

SU0196

β -adrenergic blockade suppresses pancreatic lipase expression via osteocalcin in obese mice. Kyunghwa Baek*¹, HyoRin Hwang², Jiho Kang², Danbi Park³, Yewon Kwon³, Heesu Lee³, Sunghee Ko³, Jeong-Hwa Baek².

¹Gangneung-Wonju national university, School of dentistry, South Korea, ²Department of Molecular Genetics, School of Dentistry & Dental Research Institute, Seoul National University, South Korea, ³Department of Pharmacology, College of Dentistry & Research Institute of Oral Science, Gangneung-Wonju National University, South Korea

Obesity is known to be associated with increased sympathetic nervous system (SNS) activation. We previously elucidated β -adrenergic blockade attenuates dietary fat absorption and obesity development and such an effect is associated with downregulation of pancreatic lipase (PNLIP) expressions in pancreatic acinar cells. In the present study, we tested whether β -adrenergic blockade downregulates bioactive osteocalcin secretion in osteoblasts, thereby reduces PNLIP expressions in pancreatic acinar cells.

Forty of male 6wk old C57BL/6 mice were assigned into control diet (CON) and a high calorie diet (HIGH) group. In each diet group, mice were treated with vehicle (VEH) or with propranolol, a β -adrenergic antagonist (BB; 0.5 g/L in drinking water) over 12 wks. Over 12 weeks, increase in body weight observed in the HIGHVEH group was mitigated in HIGHBB mice. Increase in fecal fat amount observed in HIGHVEH mice was mitigated in HIGHBB mice. Increase in PNLIP mRNA and protein levels observed in HIGHVEH mice pancreatic tissues was abolished in HIGHBB mice. Expression levels of *Esp* in HIGHVEH mice femur was higher vs. in CONVEH mice, but this increment was attenuated by propranolol in HIGHBB animals. Reduction in serum undercarboxylated osteocalcin (ucOC) level in HIGHVEH mice was mitigated in HIGHBB mice. In MC3T3E1 osteoblasts, upregulated *Esp* expression, followed by downregulated ucOC secretion observed in isoproterenol treated cells, was attenuated by propranolol treatment. In 266-6 cells, mouse pancreatic acinar cell line, PNLIP expression decreased when the cells were treated with ucOC. Luciferase assay showed that ucOC attenuated isoproterenol induced mouse PNLIP promoter activity. G protein-coupled receptor (GPCR6A) was highly expressed in mouse pancreatic tissue and in 266-6 cells. Knockdown of GPCR6A by siRNA suppressed downregulating effect of ucOC on PNLIP expressions, proposing that GPCR6A mediates responses to osteocalcin in pancreatic acinar cells.

In summary, β -adrenergic blockade mitigated body weight increase and dietary fat absorption during high fat diet feeding and attenuated increment in PNLIP expression. In the context of SNS stimulation, β -adrenergic blockade rescued bioactive osteocalcin secretion in osteoblasts, thereby suppressed PNLIP secretion in pancreatic acinar cells. These data suggest an important role for β -adrenergic signaling pathway in bone and pancreas response to excessive energy metabolism.

Disclosures: Kyunghwa Baek, None.

SU0197

Homer-1b/c is required for calcium-sensing receptor-mediated signaling in osteoblasts. Mark Rybchyn¹, Tara Brennan-Speranza¹, Arthur Conigrave¹, Rebecca Mason*². ¹Sydney University, Australia, ²University of Sydney, Australia

Homer proteins are known to interact with G-protein coupled receptors such as Group 1 metabotropic glutamate receptors type 1 and type 5 and with calcium-signaling proteins in the brain and some other tissues. In human osteoblasts, we show for the first time that the scaffolding protein Homer-1b/c binds to the calcium sensing receptor (CaSR), in a calcium (Ca^{2+})-dependent manner. RNAi studies showed that Homer-1b/c was required for CaSR expression, whereas CaSR knockdown enhanced Homer-1b/c expression. We also show for the first time, that Homer-1b/c mediates extracellular Ca^{2+} - and CaSR-dependent activation of Akt via the protein kinase mammalian target of Rapamycin complex 2 (mTORC2). RNAi and western blot studies showed that this process results in stimulation of key downstream signaling pathways, such as Akt-dependent canonical Wnt signaling, along with resistance to apoptosis. Homer-1b/c and CaSR are highly expressed in osteosarcoma cells, thereby contributing to a high survival phenotype. Since the CaSR is essential for skeletal development, these new findings reveal Homer-1b/c as a key physiological component of functional and survival pathways in bone-forming cells.

Disclosures: Rebecca Mason, None.

SU0198

Hydrogen sulfide protects osteoblastic cells against homocysteine-induced oxidative damage: Implications for the treatment of osteoporosis. Neetu Tyagi, Anuradha Kalani*, Suresh Tyagi. University of Louisville, USA

Clinical studies report that children born with severe hyperhomocysteinemia (HHcy), due to deficiency in cystathionine- β -synthase (CBS) gene, resulting in an elevation in plasma homocysteine (Hcy) levels, develop skeletal malformations with

weaker bone. However, pathogenic mechanisms that increase oxidative stress, DNA damage, the triggering of apoptosis and excitotoxicity by homocysteine (Hcy) are unsubstantiated. Interestingly, all these important factors may be involved in the development of osteoporosis. Osteoporosis is a bone disease that leads to an increased risk of fracture. Hydrogen sulfide is a gaseous signaling molecule; produced endogenously in the body has been demonstrated protective in various diseases. However, the effect of H_2S has not been explored in Hcy induced oxidative damage in MC3T3-E1 (osteoblastic) cells. Therefore, the present study was designed to investigate whether H_2S ameliorated Hcy-induced redox stress in MC3T3-E1 cells. The MC3T3-E1 cells were exposed to Hcy treatment in the presence or absence of NaHS (donor of H_2S). Our results demonstrate that Hcy-induced cell toxicity, increased the levels of free radicals which leads to apoptosis. Hcy also increased NADPH-oxidase-4 (NOX-4) expression and mitigated thioredoxin-1 (Trx-1) expression. NaHS increased cell viability and stimulates osteoblast proliferation by enhancing both transcription and activity of alkaline phosphatase in MC3T3-E1 cells that was decreased by Hcy. Additionally, treatment with NaHS stimulated the transcriptional level of osteocalcin. NaHS reversed the reduced superoxide dismutase activity, decreased reactive oxygen species production, and suppressed NADPH oxidase activity in Hcy treated cells. NaHS treatment also produced anti-inflammatory effect of H_2S . Western blotting analysis demonstrated that the protective effects of H_2S were facilitated by ERK1/2 MAPKs. In conclusion, H_2S protects osteoblastic cells against oxidative stress-induced cell injury via an MAPK-dependent mechanism. Our findings suggest that H_2S may have a therapeutic potential for osteoporosis.

Disclosures: Anuradha Kalani, None.

SU0199

RBPJK Deficient Mesenchymal Stem Cell Enhances Osteogenesis by Up-regulation of BMP Signaling. Bo Tian*¹, Junkui Sun¹, Xifu Shang², John Marymont¹, Yufeng Dong³. ¹Department of Orthopedic Surgery, LSUHSC-Shreveport, LA, USA, ²Anhui provincial Hospital, China, ³Louisiana State University, USA

Recently we have demonstrated the importance of RBPJK-dependent Notch signaling in the regulation of mesenchymal stem cell (MSC) differentiation during skeletogenesis both in vivo and in vitro. Here we further performed RBPJK loss-of-function experiments to demonstrate for the first time that RBPJK deficient MSC shows enhanced differentiation and osteogenesis acts via up-regulation of the BMP signaling. It was found that RBPJK highly expressed in fresh isolated human bone marrow MSCs and its expression was progressively down-regulated during spontaneous differentiation and even greater in osteogenic media induced differentiation. Deletion of RBPJK in MSCs not only enhances alkaline phosphatase (ALP) activity and cell spontaneous differentiation, but also significantly accelerates condition media induced osteogenic differentiation by showing enhanced Alizarin red staining, gene expression of Runx2, Osteopontin (OPN), Type I collagen (COL1a1) in culture (Fig. 1). Furthermore, luciferase assays demonstrate that deletion of RBPJK in MSCs significantly enhanced BMP signaling reporter 12XSBE activity. Additionally, phosphor-smad1/5/8 expression was also significantly increased upon removal of RBPJK in MSCs (Fig. 2). Taken together, our results proved that inhibition of Notch signaling in MSCs promotes cell osteogenic differentiation by up-regulation of BMP signaling, and RBPJK deficient MSC maybe a better cell population for cell-based bone tissue engineering. These data provide novel insights into our understanding of the molecular mechanisms underlying Notch regulation of osteogenesis.

Fig. 1

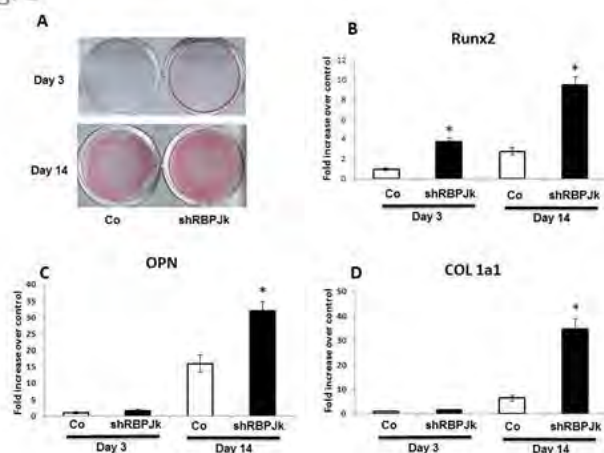


Figure 1

Fig. 2

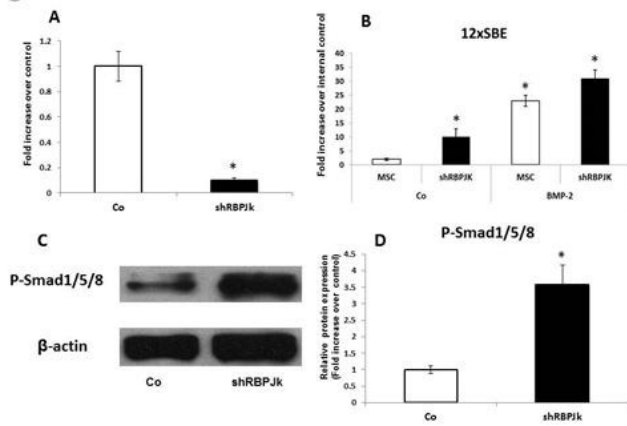


Figure 2

Disclosures: *Bo Tian, None.*

SU0200

Discovery of Long Noncoding RNAs During Osteoblast Differentiation of Pluripotent Mesenchymal Stromal Cells. [Coralee Tye*](#), [Jonathan Gordon](#), [Hai Wu](#), [Janet Stein](#), [Jane Lian](#), [Gary Stein](#). University of Vermont College of Medicine, USA

Long noncoding RNAs (lncRNAs) recently emerged as novel regulators of gene expression. These molecules are critical for lineage commitment, differentiation, development, disease progression and organism viability. lncRNAs have these diverse regulatory roles by facilitating epigenetic mechanisms including chromatin looping, histone post-translational modification, directly regulating mRNA splicing, transcription, protein translation, as well as functioning as microRNA sponges. Thus, lncRNAs have tremendous potential for regulating the “bone” genome. Because there are few studies of lncRNAs in bone tissue, we initiated characterization of lncRNAs in osteoblast lineage cells by global expression analysis. We performed next-generation sequencing (RNA-Seq) on primary mesenchymal stromal cells (MSCs) undergoing osteoblastic differentiation to 4 specific stages of maturation: day0 (proliferation), day7 (commitment), day14 (extracellular matrix deposition) and day21 (mineralization). Results from human MSCs (hMSCs; Adult Mesenchymal Stem Cell Resource, Texas A&M IRM) and mouse bone marrow derived MSCs (mMSCs) were compared and we found 22% of mouse lncRNAs had conserved expression in human, compared to 97% conserved expression of mRNAs. This suggests unique functions for lncRNAs within species, but also demonstrates that mouse models can be used for functional evaluation of a subset of lncRNAs relevant to human disease. We identified 1912 annotated lncRNAs expressed during mMSC differentiation and 5363 lncRNAs in hMSCs. During mMSC differentiation, 198 lncRNAs are differentially expressed (FDR adjusted p-value <0.05). To validate their expression, expression profiles were correlated with ChIP-Seq analysis of epigenetic modifications associated with transcriptional activation, elongation and repression (H3K4me³, H3K27ac, H3K36me³, H3K27me). As with mRNAs, changes in lncRNA expression are reflected at the chromatin level by changes in histone marks. Dynamic changes were observed in a subset of lncRNAs; others were constitutively expressed. Intersection of lncRNAs with enrichment profiles of Runx2 revealed >40% of lncRNAs genomic loci were bound by Runx2. Our comprehensive dataset identifies over a hundred lncRNAs that are dynamically expressed during osteogenesis, many of which are potentially regulated by Runx2. These findings open novel dimensions for exploring lncRNAs in regulating normal bone formation and their deregulated expression in skeletal disorders.

Disclosures: *Coralee Tye, None.*

SU0201

Identification of novel enhancer regions in mesenchymal stromal cells that regulate osteogenic differentiation. [Jonathan Gordon*](#)¹, [Hai Wu](#)², [Coralee Tye](#)², [Joesph Boyd](#)², [Andre van Wijnen](#)³, [Janet Stein](#)², [Gary Stein](#)², [Jane Lian](#)². ¹University of Vermont, USA, ²University of Vermont, Department of Biochemistry, USA, ³Mayo Clinic, Department of Orthopedic Surgery, USA

Adult bone formation requires a highly regulated program of differentiation from a mesenchymal-derived osteoprogenitor to a mature osteocyte. Epigenetic mechanisms control mesenchymal stromal cell (MSC) commitment to a mature osteoblast through facilitating of binding of transcriptional regulators to promoter regions of

genes, however less well understood are inter- and intra-genic regulatory regions that control cell-type-specific gene expression programs. These regulatory elements called enhancers, are bound by transcription factors (TFs) and specific post-translationally modified histones, and play key roles in the control of tissue morphogenesis. To define novel regulatory regions during osteogenesis, pluripotent CD45-/Ter119-/SCA1+/CD29+/Nestin+/CD146+/aSMA+ MSCs were isolated by FACS to obtain a homogenous population of cells that were differentiated to mature osteoblasts (defined by expression of late-stage marker genes (e.g. Ibsp, Dmp1 and Mepe)). We then used ChIP-seq to develop genome-wide enrichment profiles of intergenic genomic regions of occupied by TFs, cofactors, chromatin regulators, and transcription apparatus occupying osteogenic-specific enhancers in MSCs. Supervised pattern discovery was performed using ChromHMM to segment genomic regions into active, quiescent, TF-bound, transcribed and super-enhancer regions. From this analysis, we identified novel enhancers near genes involved in osteogenesis and novel enhancers for bone formation were predicted in intragenic regions of several osteoblast-related genes. Several novel enhancers were identified within the HoxA cluster (chr6: 52,151,599-52,268,229), as well as intragenic enhancers in the osteoblast regulators Znf521 (chr18: 52,151,599-52,268,229), Runx2 (chr17:44,603,989-44,814,627) and Sp7 (chr15:102,357,177-102,366,271). In addition we identified new regulatory regions proximal to VISTA-defined enhancers near the Fgfr1 gene, previously identified to regulate bone formation. Ongoing functional evaluation of these regions will provide new information on the regulation of osteoblast gene function and MSC commitment.

In conclusion, we have defined novel regulatory regions, denoted by histone modifications and transcription factor binding sites that function as enhancers critical for osteogenic differentiation. This comprehensive epigenetic signature of lineage commitment and osteoblast differentiation is clinically relevant to pathogenic conditions involving bone loss and repair.

Disclosures: *Jonathan Gordon, None.*

SU0202

Inhibition of c-src activity in primary bone marrow cells mimics the decreased expression of the osteoblast phenotype seen in tumor cells. [Ashley Dinkel*](#), [Joseph Tarr](#), [Dana Branch](#), [Joshua Luster](#), [Thomas Owen](#). Ramapo College of New Jersey, USA

Deletion of the c-src gene results in decreased osteoclast and increased osteoblast activity resulting in osteopetrosis. PP2 is a commonly used c-src inhibitor and PP3 is a structurally similar inactive compound. Previous work showed that PP2 treatment of primary rat calvarial osteoblasts (ROB) increases their differentiation as demonstrated by increased mineralized nodule formation. We tested PP2 and PP3 on ROS 17/2.8 osteosarcoma cells in order to further investigate the mechanisms through which c-src inhibition drives differentiation. C-src inhibition by PP2 beginning at plating decreased alkaline phosphatase (AP) activity at days 4 and 8 as compared to cells treated with PP3, in contrast to the ROB cells. In order to address whether this unexpected observation was due to the tumor-derived nature of ROS cells, rat bone marrow cells (BMC) were chosen as a second osteoblastic differentiation system. BMCs were treated with PP2 or PP3 by a single application or by continuous treatment. For single applications, cells were treated with PP2 or PP3 at plating or with the first or second media change (days 3 or 7). Continuous treatment involved adding PP2 or PP3 beginning at plating or at the first or second media change and continuing until harvest. BMCs were fixed on day 25 and stained for AP activity and mineralized nodules. BMC differentiation was quantitated by image analysis for both AP positive and mineralized nodule area. Our results in BMCs mirrored those found in the ROS cells, not those found in the primary rat calvarial cells; the application of PP2 resulted in less differentiation. Addition of a single dose of PP2 at plating resulted in a 50-70% decrease in AP positive and mineralized nodule area, whereas addition of a single dose of PP2 at days 3 or 7 had no effect as compared to PP3-treated cells. With continuous treatment, a similar decrease was seen when cells were dosed beginning at plating or day 3, however, if dosing was initiated at day 7, a smaller decrease of ~25% was seen in AP activity. These data suggest that c-src is involved in the commitment of bone marrow stem cells to becoming osteoblasts as well as in their initial differentiation. ROS 17/2.8 cells are thought to represent early stage osteoblasts potentially equivalent to the BMCs several days after attachment. In contrast, the increased differentiation seen in ROB cells following PP2 treatment may be due to the calvarial osteoblasts' different developmental origin.

Disclosures: *Ashley Dinkel, None.*

SU0203

Neuropeptide-Receptor expression during Osteoblastic Differentiation of Mouse iPS cells. [Tetsuya Goto*](#). Kagoshima University Graduate School of Medical & Dental Sciences, Japan

Recent evidence suggests that both sensory and autonomic nerves affect bone metabolism; however, it has been unclear how neuropeptides are associated with the differentiation of pluripotent stem cells into osteoblastic cells. To evaluate the putative effects of neuropeptides during the differentiation of mouse induced pluripotent stem (iPS) cells into calcified tissue-forming osteoblastic cells, we investigated the expression patterns of neuropeptide receptors at each differentiation stage; iPS, Embryoid body, early osteoblast, and late osteoblast stages. Mouse iPS cells were seeded onto feeder cells and then transferred to low-attachment culture dishes to form

embryoid bodies. Embryoid bodies were cultured for 4 weeks in osteoblastic differentiation medium. The expression of α 1-adrenergic receptor (AR), α 2-AR, β 2-AR, neuropeptide Y1 receptor (NPY1-R), neuropeptide Y2 receptor (NPY2-R), calcitonin gene-related protein receptor (CGRP-R), and neurokinin 1-R (NK1-R) was assessed by reverse transcription-polymerase chain reaction (RT-PCR) and real-time PCR. Among these neuropeptide receptors, CGRP-R and β 2-AR were expressed at all stages of cell differentiation, including the iPS cell stage, with peak expression occurring at the early osteoblast-differentiation stage. Another sensory nervous system receptor, NK1-R, was expressed mainly in the late osteoblast-differentiation stage. Furthermore, CGRP-R mRNA showed an additional small peak corresponding to embryoid bodies cultured for 3 days, suggesting that embryoid bodies may be affected by serum CGRP. These data suggest that the sensory nervous system receptor CGRP-R and the autonomic nervous system receptor β 2-AR may be involved in the differentiation of iPS cells into the osteoblastic lineage. It follows from these findings that CGRP and β 2-AR may regulate cell differentiation in the iPS and embryoid body stages, and that each neuropeptide has an optimal period of influences during the osteoblast-differentiation process.

Disclosures: Tetsuya Goto, None.

SU0204

Pin1-mediated modification prolongs the nuclear retention of β -catenin in wnt3a-induced osteoblast differentiation. Hea-rim SHIN¹, Taegyung Lee¹, Han-sol BAE¹, Rabia ISLAM¹, Won-joon YOON¹, Young-dan CHO², Bong-su KIM¹, Kyung-mi WOO¹, Hyun-mo RYOO¹. ¹Seoul National University, South Korea, ²Seoul National University, South Korea

The canonical Wnt signaling pathway plays an important role in osteoblast differentiation and cancer development. β -catenin nuclear localization is a crucial step in the pathway as it functions as a transcription factor with LEF/TCF. Pin1 plays a key role in the post-phosphorylational conformational change of β -catenin by cis/trans isomerization and Pin1 is known as a regulator of turnover and subcellular localization of β -catenin in cancer. However, the association of Pin1 in Wnt-induced osteoblast differentiation is poorly understood and the detailed molecular mechanism that promotes β -catenin nuclear localization has yet to be revealed. Therefore, we investigated whether Pin1 functions in bone formation by regulating β -catenin. Proximal tibial osteoblasts of Pin1 knock-out (KO) mice showed a reduction in β -catenin levels, and Pin1 controls Wnt-induced TOP Flash activity in Pin1 WT/KO mouse embryonic fibroblast (MEF) cells. Pin1 knockdown repressed Wnt3a-induced osteoblast differentiation and bone marker gene expression in MC3T3E1 cells. In contrast, overexpression of Pin1 enhanced osteoblast differentiation stimulated by Wnt3a administration. In addition, the transcriptional synergy of Wnt3a with Pin1 was observed in TOP Flash and alkaline phosphatase gene promoter activity. In this study, we demonstrate that Pin1 binds to β -catenin in the nucleus and Pin1 activity increases the nuclear retention of β -catenin, while it does not stimulate translocation of β -catenin into the nucleus. Isomerized β -catenin did not bind to nuclear adenomatous polyposis coli (APC), a tumor suppressor and nuclear β -catenin chaperone, which consequently increases retention of β -catenin in the nucleus. These results provide great insight into the importance of Pin1 in β -catenin-mediated osteogenesis and tumorigenesis.

Disclosures: Hea-rim SHIN, None.

SU0205

A murine model of acute and chronic long bone segmental defect repair. David Rowe^{*}, Liping Wang, Jianping Huang. University of Connecticut Health Center, USA

The functional repair of a critical-size long bone segmental defect implies the reconstitution of the cortical bone and the ability of the animal to ambulate free of orthopedic support. Here we report a model in both the tibia and femur of mice that are immune tolerate to all cell sources and carry a Col3.6GFPtpz reporter to mark host derived bone cells. In either long bone, a 3.5 mm defect is created and supported by either a rigid or compliant fixation device. Each device is designed to be removed or released in the living animal to test the functionality of the repair. The test material can be either cells or scaffold and can be introduced at the time of surgery, or 4-6 weeks after the initial surgery when end-capping of the bone has developed. In the chronic non-union model, a second surgery is performed in which the ends of the bones are freshened followed by introduction of the test cells or scaffold. Primary BMSCs derived from a mouse carrying a Col3.6GFPcyan reporter were plated in MEM/5% O2 and expanded for 5-6 days without passage. Approximately 1x10⁶ cells were added to a commercial collagen scaffold (Healos) placed within the defect space. The mice are followed by serial digital X-rays and the support structure are removed when the cortical bone has developed (5-6 weeks). The animals are injected with alizarine complexone 1 day prior to sacrifice, which is usually 4-6 weeks after the supports are removed.

The histology demonstrates that the regenerated bone comes almost exclusively from the donor cells. Within the defect space, the bone lining cells carry the Col3.6GFPcyan reporter, are AP positive and actively depositing a mineralization label. Host osteogenic activity is limited to the site where the support structures were applied. A striking feature is the distribution of the osteoclastic activity. In the compliant repair, osteoclasts are located on the periosteal surface and resemble the inward movement of the outer cortical shell of a fracture. In a rigid fixation, the

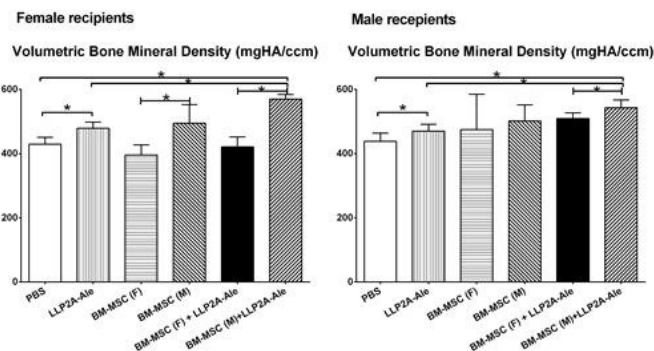
osteoclasts are restricted to the marrow and endocortical surface. Despite the regeneration of the cortex, the matrix still contains regions of unresorbed proteins and the endochondral->periosteal conversion to lamellar bone remains incomplete. We believe that this model will be an informative and relatively low cost platform for characterizing intrinsic donor cells capacity and host environmental factors that contribute to a successful repair outcome.

Disclosures: David Rowe, None.

SU0206

Bone targeted delivery of mesenchymal stem cells for fracture healing and sex difference. Wei Yao^{*1}, Evan Lay², Hongliang Zhang², Haiyan Chen², Nancy Lane². ¹University of California, Davis Medical Center, USA, ²Center for Musculoskeletal Health, Internal Medicine, University of California at Davis Medical Center, USA

Introduction. Traumatic fractures can require hospitalization, surgery, frequent physician visits, and lost time from work. Exogenous mesenchymal stem cells (MSCs) transplantations have been tested in animal models and human fractures. Whether these transplanted MSCs would directly home to fracture sites and participate in the healing process, or indirectly influence the healing process via paracrine mechanisms are under investigations. We have developed a bone-seeking compound, LLP2A-Alendronate (LLP2A-Ale) that selectively targets the integrin α 4 β 1, and increases exogenous MSCs homing to bone. The purpose of this study was to determine if treatment with the LLP2A-Ale or combination of LLP2A-Ale and MSCs would accelerate healing in a closed fracture model and if the effects would differ by sex. **Methods.** The right femurs from were fractured in 2-month-old osterix-mCherry (Ox-mCherry) reporter mice of both sexes. The mice were subsequently treated with placebo (PL), LLP2A-Ale (500 μ g/kg, IM), bone marrow derived MSCs (BM+ MSCs) obtained from either Col1-2.3kb-GFP or the wild-type Ox-mCherry mice from both sexes (BM-MSC (F) & BM-MSC (M), 5 x 10⁵, IM), alone or in combination with LLP2A-Ale. The study endpoints included exogenous MSC bone engraftment assessed at days 7, 14 and 21 post-fracture and callus volumetric mineralization (BMD) assessed at day 21 and 42. **Results.** Initially, LLP2A-Ale increased homing of exogenous MSCs to the fracture callus, located at the periosteum, incorporated into callus and contributed to the endochondral bone formation. At day 42, LLP2A-Ale significantly increased callus BMD compared to PL in both sexes ($p < 0.05$). Treatment with only BM-MSCs derived from males ([M-MSCs (M)]) induced greater callus BMD than BM-MSCs (F). LLP2A-Ale + BM-MSCs (M) had a greater increase in callus BMD both females and males treatment groups compared to either treatment alone (Figure).



Yao-LLP2AMSC-FX

Disclosures: Wei Yao, None.

SU0207

Effects of combination melatonin, strontium citrate, vitamin D3 and vitamin K2 on osteoblast and osteoclast differentiation grown as co-cultures. Sifat Maria^{*1}, Larry Enderby², Holly Lassila¹, Christine O'Neil¹, Mark Swanson³, Paula Witt-Enderby⁴. ¹Duquesne University, USA, ²Enderby Healthcare/Legal Consulting, LLC, USA, ³Private practice, Heart Preventions, LLC, USA, ⁴Duquesne University, School of Pharmacy, USA

A translational research study, *Melatonin-micronutrients Osteopenia Treatment Study (MOTS)*, was designed to assess the efficacy of combination natural bone tropic agents: melatonin, strontium citrate, vitamin D₃ and vitamin K₂ (MSDK) on bone health and quality of life in post-menopausal osteopenic women. As part of this study, mechanisms underlying MSDK's effects on bone-forming osteoblasts and bone-resorbing osteoclasts was evaluated using a unique co-culture system containing human bone marrow stem cells (hMSCs) and human peripheral blood monocytes (hPBMCs). Using a novel *in vitro* treatment paradigm that closely mimics the *in vivo* condition, hMSCs/hPBMCs were co-cultured either by seeding hPBMCs directly on top of differentiating hMSCs (layered co-culture) or separately using transwell

(transwell co-culture). Co-cultures were exposed to vehicle, each component (M, S, D or K) alone or combination (MSDK) in either osteogenic (Os+) or growth medium (Os-) for 21 days. Effects of M, S, D and K either alone or in combination on osteoblast and osteoclast differentiation and activity were measured by alizarin red or TRAP staining, respectively. In transwell co-culture, combination MSDK enhanced osteoblast differentiation and mineralization to the greatest extent (30-fold) vs. Os-/V. Layered co-culture study demonstrated similar patterns of osteoblast induction (50-fold vs Os-/V). Interestingly, osteoblast induction occurred at a greater extent in all Os+ treated culture vs Os-/V, suggesting that cell-to-cell contact was important for modulating osteoblast differentiation. In both cases, M and S alone showed a significant increase in osteoblast mineralization suggesting the possible contribution of these two agents in bone formation by MSDK treatment. Parallel assessment of the treatment's effect on osteoclast differentiation showed that combination MSDK inhibited osteoclast differentiation to the greatest extent vs Os-/V cells even though exposure to M, S or K alone also inhibited osteoclast differentiation. Measurement of the ratio of RANKL; an osteoclast inducer and OPG; a RANKL decoy receptor in transwell co-culture further revealed the potential underlying root of MSDK's effect, which involved induction of membrane bound OPG: RANKL ratio by MSDK treatment as a result of both increasing membrane bound OPG level and decreasing membrane bound RANKL level.

Disclosures: Sifat Maria, None.

SU0208

Ethanol Exposure Increases FoxO Activation in Cultured Primary Rat Mesenchymal Stem Cells. Philip Roper*. Loyola University, USA

The process of fracture healing is complex, and poor or incomplete healing remains a significant health problem. During normal healing, resident mesenchymal stem cells (MSCs) at the fracture site differentiate into osteoblasts and chondrocytes, which are the necessary cell types for callus formation. MSC differentiation relies on canonical Wnt signaling activation of the transcription factor β -catenin within MSCs. β -catenin drives the expression of pro-osteogenic and pro-chondrogenic genes. Alcohol abuse is a major factor associated with increased incidence of poor or delayed healing. Although it is unknown how alcohol actuates perturbed fracture healing, a contributing factor could be alcohol's ability to induce oxidative stress. The family of FoxO transcription factors are activated by oxidative stress, and FoxOs are known to inhibit Wnt signaling by competing for β -catenin, a necessary FoxO cofactor. We have previously shown that FoxO expression, as well as markers of activation, are increased in the fracture callus of alcohol-treated animals exhibiting delays in fracture healing. Also, these alcohol-induced fracture repair deficiencies were attenuated by antioxidant therapy. Therefore, we hypothesize that ethanol exposure inhibits proper MSC differentiation by increasing oxidative stress and FoxO activation within MSCs, which will inhibit Wnt/ β -catenin signaling. To test this, we have cultured primary rat MSCs, and exposed them to either media alone, 50mM ethanol, or 50uM hydrogen peroxide, as a positive control of oxidative stress, for 24 hours. Exposure to either ethanol or hydrogen peroxide in culture increased intracellular oxidative stress by measuring DNA damage. This coincided with an increase in FoxO nuclear localization, by western blotting, and association with β -catenin, as measured by co-immunoprecipitation. We also found ethanol was able to increase FoxO activity, as measured by DNA binding, using a DNA-binding assay. This study shows that alcohol, by increasing oxidative stress, shifts intracellular MSC signaling away from Wnt/ β -catenin signaling and towards FoxO signaling, potentially perturbing the overall MSC differentiation capability. This highlights a potential mechanism behind alcohol-induced impaired healing, thereby elucidating potential methods of intervention while bolstering our overall understanding of fracture healing.

Disclosures: Philip Roper, None.

SU0209

GATA4 Regulates Mesenchymal Stem Cell Differentiation. Aysha Khalid*¹, Miriam Guemes², Gustavo Miranda-Carboni³, Susan Miranda³.
¹University of Tennessee, USA, ²UCLA, USA, ³UTHSC, USA

GATA4 is a zinc-finger transcription factor that is essential in various tissues, such as heart, kidneys, intestine and more recent studies showed that it also has a role in osteoblasts and it is essential for bone mineralization. Total *Gata4* knockout mice or conditional knockout mice, both exhibit embryonic lethality, which suggests that *Gata4* not only is important for bone development but also for mice survival. However, it is not known if GATA4 plays a role in mesenchymal stem cells (MSC) commitment to osteoblasts. MSCs are multipotent cells that can give rise to a range of different lineages, including osteoblasts and adipocytes. This study investigates the expression and function of GATA4 in MSCs, adipocytes and osteoblasts. qPCR analysis of the cDNA of pericytes, bone marrow MSCs, and primary calvarial cells differentiated for 14 days in osteogenic media demonstrated a significant decrease in *Gata4* expression levels as compared to undifferentiated cells. This suggests that GATA4 regulates bone mineralization early in the differentiation process. Cell proliferation rates were also reduced in primary calvarial cells infected with lentivirus expressing shRNA directed to *Gata4* (shGATA4) as compared to GFP (shGFP), as determined by WST-1 assay. Bone marrow stromal cells differentiated for 14 days showed reduced fat accumulation and mineralization, as visualized by Oil red O and

Alizarin Red staining, respectively. This indicates that the knockouts have less bone and less fat which indirectly suggests a cellular defect in MSCs. This defect was confirmed *in vivo* by performing immunohistochemistry on GATA4 knockout and wildtype femurs. The knockouts showed fewer nestin positive stem cells as compared to wildtypes. Together this data suggest that *Gata4* knockouts have fewer and slower proliferating MSCs, which in turn leads to reduced bone mineral density in *GATA4* knockout bones, as compared to wildtype bones.

Disclosures: Aysha Khalid, None.

SU0210

Localized SOX9 Expression Delineates Regions of Cartilage and Bone Formation in a Tissue-Engineered Construct. Pieter-Jan Stiers*, Nick van Gastel, Riet Van Looveren, Sophie Torrekens, Geert Carmeliet. Laboratory of Clinical & Experimental Endocrinology, KU Leuven, Belgium

Bone tissue engineering is a promising therapy for non-healing bone defects and generally consists of a scaffold, skeletal progenitor cells and/or growth factors. To improve clinical outcome, a better understanding of the behavior of implanted cells, especially during the early stages, is required.

We have previously shown that ectopic implantation of FGF2-pretreated mouse periosteum-derived cells (mPDC^{FGF2}) embedded in a collagen gel resulted in manifest bone formation via endochondral ossification, whereas non-treated mPDC (mPDC^{control}) did not. We now investigated the behavior and fate of the implanted cells as well as the host response during the early phases using intravital imaging together with histology.

One day after implantation numerous mPDC^{FGF2}, but not control cells, were SOX9-positive, whereas SOX9 expression was decreased in mPDC^{FGF2} prior to implantation. Apoptosis, proliferation and migration were hardly detected in both conditions. After 3 days, the organization of the mPDC^{FGF2} implant was completely changed: mPDC in the outer layers were highly proliferative but mostly SOX9 negative, whereas in the center most mPDC expressed SOX9, showed limited proliferation but differentiated to collagen 2-positive chondrocytes. These changes were not observed with mPDC^{control}, although a comparable angiogenic host response was noticed. At day 7, only mPDC^{FGF2} implants had increased in size and contained hypertrophic chondrocytes, although blood vessel invasion at the periphery of the implant was present in both conditions. Close to blood vessels mPDC^{FGF2} differentiated to osteoblasts, analyzed using Col1-dsRed mPDC. The number of donor osteoblasts increased over the following days, especially at sites of invasion into the cartilage, concomitant with the appearance of small numbers of host cells. At day 14, mainly donor cells were found lining the bone trabeculae that had formed, while after 21 days both donor- and host-derived osteoblasts were observed.

Our results show that early after implantation, mPDC with bone-forming potential do not elicit an increased angiogenic response but diverge into distinct populations that form cartilage and bone, both of which derive from a common SOX9-positive progenitor. These insights can help in the development of new, more robust therapies for non-healing bone defects.

Disclosures: Pieter-Jan Stiers, None.

SU0211

Single CD271 marker identifies mesenchymal stem cells from human dental pulp with high osteogenic potential. Christine Hong*, Ruth Alvarez, Hyelim Lee, Cun-yu Wang. UCLA School of Dentistry, USA

Mesenchymal stem cells (MSCs) are a promising tool in regenerative medicine due to their capacity to differentiate into multiple lineages. In addition to MSCs isolated from bone marrow (BMSCs), adult MSCs are isolated from craniofacial tissues including dental pulp tissues (DP) using various stem cell surface markers. However, there has been a lack of consensus on a set of surface makers that are reproducibly effective at isolating putative multipotent dental mesenchymal stem cells (DMSCs). In this study, we used different combinations of surface markers (CD51/CD140a, CD271, and STRO-1/CD146) to isolate homogeneous populations of DMSCs from heterogeneous dental pulp cells (DPCs) obtained from DP and compared their capacity to undergo multilineage differentiation. Fluorescence-Activated Cell Sorting (FACS) revealed that 27.3% of DPCs were CD51+/CD140a+, 10.6% were CD271+, and 0.3% were STRO-1+/CD146+. Under osteogenic conditions, all three subsets of isolated DMSCs exhibited differentiation capacity into osteogenic lineages. Among these isolated subsets of DMSCs, CD271+ DMSCs demonstrated the greatest osteogenic potential. While all three combinations of surface markers in this study successfully isolated DMSCs from DPCs, single CD271 marker presents the most effective stem cell surface marker for identification of DMSCs with high osteogenic potential. Isolated CD271+ DMSCs could potentially be utilized for future clinical applications in dentistry and regenerative medicine.

Disclosures: Christine Hong, None.

SU0212

Analysis of contribution of marrow stromal cells and bone marrow macrophages to mechanical loading-induced osteoclastogenesis and bone resorption. Hideki Kitaura¹, Keisuke Kimura², Masahiko Ishida², Yumiko Ochi², Haruki Sugisawa², Jafari Saeed², Akiko Kishikawa², Teruko Takano-Yamamoto². ¹Tohoku University, Japan, ²Division of Orthodontics & Dentofacial Orthopedics, Department of Translational Medicine, Tohoku University Graduate School of Dentistry, Japan

Mechanical stress such as orthodontic tooth movement induces osteoclastogenesis *in vivo*. It has been reported that TNF- α plays an important role in mechanical loading-induced osteoclastogenesis and bone resorption. *In vitro* studies suggested three cell types, marrow stromal cells, macrophages and T-cells, participate in TNF- α -induced osteoclastogenesis. Our purpose is to determine the *in vivo* contribution of each above mentioned cell types, as direct or indirect TNF- α target cell type to mechanical loading-induced osteoclastogenesis. We established mechanical stress-induced osteoclastogenesis model in mice using orthodontic tooth movement in which an Ni-Ti coil spring was inserted between the upper incisors and the upper first molar. Using TNF receptor 1- and 2-deficient mice (KO), we showed that orthodontic tooth movement and mechanical loading-induced osteoclastogenesis was mediated by TNF- α . We applied orthodontic tooth movement to chimeric mice which wild type mice (WT) marrow was transplanted into lethally irradiated WT (WT>WT), WT marrow was transplanted into lethally irradiated KO (WT>KO), KO marrow was transplanted into lethally irradiated WT (KO>WT) and KO marrow was transplanted into lethally irradiated KO (KO>KO). In those mice, T cells were blocked by anti-CD4 and anti-CD8 antibodies. After 12 days of experimental tooth movement, the amounts of orthodontic tooth movement were measured and the number of tartrate-resistant acid phosphatase (TRAP)-positive cells along the loaded alveolar bone and root surface were counted as osteoclasts and odontoclasts, respectively, in histological sections. The amount of orthodontic tooth movement, the number of osteoclasts and odontoclasts in WT>KO and KO>KO were significantly lower than that in WT>WT and KO>WT mice. These findings suggested that stromal cells were more contributed than bone marrow macrophage in mechanical loading-induced osteoclastogenesis.

Disclosures: Hideki Kitaura, None.

SU0213

Bone Active Nitrogen-containing Bisphosphonates with a Near Infrared Fluorescent Label for Potential Use in Arthritis Models. Shuting Sun¹, Frank Ebetino¹, Kim Nguven², Boris Kashemirov², Charles McKenna², Mark Lundy¹, Xiaodong Hou³, Zhenqiang Yao³, Brendan Boyce³. ¹BioVinc LLC, USA, ²University of Southern California, USA, ³University of Rochester, USA

Rheumatoid arthritis (RA) is characterized by synovial inflammation and articular cartilage and bone erosion. Although there is no cure for RA, disease modifying anti-rheumatic drugs, including anti-TNF agents, significantly improve the clinical course of RA. However, it is still difficult to detect early erosion. A noninvasive tool for diagnosis of erosions and evaluation of the response to therapies is therefore an unmet need. Bisphosphonates (BPs) including risedronate (RIS) and zoledronate (ZOL) have high affinity for bone, particularly at active turnover sites. Thus, BPs could be ideal carriers to deliver imaging probes to sites of bone erosion in RA patients. Near infrared (NIR)-BP conjugates may be used to noninvasively identify bone erosions because of higher penetration depth and attenuation of light scattering. Interestingly, the 5,6-carboxyfluorescein (FAM)-conjugated BPs (FAM-RIS and FAM-ZOL) retain anti-prenylation/antiresorptive activity in J774 macrophages and in osteoclasts, but, no significant anti-prenylation activity is observed with the NIR-BP conjugates based on Alexa fluor 647 (AF647), Cy5 and IRDye 800CW. To expand the utility of these NIR agents, we have prepared a series of AF647-RIS conjugates in order to reduce fluorophore interference on cellular activity. Linker lengths were extended between the AF647 fluorescent label and the pyridyl moiety to increase the distance of the fluorescent component from the BP binding site. To determine if these AF-BP structural modifications improved the osteoclast (OC) inhibitory activity, we tested them *in vitro* using mouse bone marrow cells. We found that while the control probe AF647-RIS had little effect on OC numbers (221+/-37, 241+/-21 and 230+/-36 for 0.1, 1 and 10 μ M AF647-RIS), two linker extensions significantly decreased OC numbers: 218+/-24, 208+/-21 and 19+/-5 for 0.1, 1 and 10 μ M AF647-RIS-v1 (a 3 carbon extension), and 205+/-22, 221+/-19 and 43+/-10 for 0.1, 1 and 10 μ M AF647-RIS-v2 (a 15-atom poly(ethylene glycol) linker), compared to vehicle (239+/-17) and RIS (214+/-37, 220+/-28 and 143+/-21 for 0.1, 1 and 10 μ M). These data suggest that increasing the linker chain length of an AF647-BP conjugate can dramatically increase its inhibitory effects. Thus, while the pharmacologically inactive AF647-RIS may be a useful tool to detect bone erosion in RA, longer linked antiresorptive conjugates (AF647-RIS-V1/V2) may be used to study the location and therapeutic effect of N-BPs.

Disclosures: Charles McKenna, BioVinc LLC
This study received funding from: BioVinc LLC

SU0214

C-C chemokine receptor 5, a co-receptor of HIV, -mediated signalregulates bone resorption via locomotion of osteoclasts. Ji-Won Lee¹, Akiyoshi Hoshino², Takashi Saitou³, Kazuki Inoue⁴, Shunsuke Uehara⁵, Yasuhiro Kobayashi⁶, Satoshi Ueha⁷, Kouji Matsushima⁷, Masako Ito⁸, Akira Yamaguchi⁹, Yuuki Imai¹⁰, Tadahiro Iimura¹¹. ¹Division of Bio-Imaging, Protea-Science Center (PROS), Ehime University, Japan, ²Department of Pathology, Nagoya University Graduate School of Medicine, Japan, ³Translational Research Center & Artificial Joint Integrated Center, Ehime University, Japan, ⁴Department of Biological Resources, Integrated Center for Sciences, Ehime University, Japan, ⁵Department of Biochemistry, Matsumoto Dental University, Japan, ⁶Institute for Oral Science, Matsumoto Dental University, Japan, ⁷Department of Molecular Preventive Medicine, Graduate School of Medicine, The University of Tokyo, Japan, ⁸Medical Work-Life-Balance Center, Nagasaki University Hospital, Japan, ⁹Department of Pathology, Nagoya University Graduate School of Medicine, Nagoya, Japan, Japan, ¹⁰Division of Integrative Pathophysiology, Proteo-Science Center, Graduate School of Medicine, Japan, ¹¹Division of Bio-Imaging, Proteo-Science Center (PROS), Ehime University, Japan

The lifespan of patients who have HIV infection has increased significantly with global HIV epidemic treatment in last few decades, and simultaneously low bone mass has emerged as a significant comorbidity. C-C chemokine receptor 5 (CCR5) is a co-receptor of macrophage-tropic viruses including HIV. Epidemiological and pathological findings have reported that functional changes in CCR5 correlate with HIV transmission and bone destruction diseases. However, physiological roles of CCR5 in bone metabolism have not been well documented. Live imaging and super-resolution microscopy analyses revealed that *Ccr5*-deficient osteoclasts showed larger in size and disorganized motility, cytoskeletal rearrangement and cell-attachment machineries including integrins, thus leading decreased bone resorption activity. Our further molecular and cellular analyses suggested that CCR5-mediated signal was associated with c-Src and small GTPase activation that was required for proper osteoclasts function. *Ccr5*-deficient mice had significantly increased number and size of osteoclasts, although they did not show significant difference in BMD compared to their wild-type littermates. Interestingly, *Ccr5*-deficient mice were less susceptible to RANKL-induced bone loss, suggesting functional impairment of osteoclasts. Moreover, blockades of human CCR5 by anti-hCCR5 neutralizing antibody obviously inhibited human osteoclastogenesis in dose-dependent manner, without affect to osteoblast differentiation. These data unveil unique and essential roles of CCR5 in bone metabolism and bone destruction diseases, and have implications concerning bone physiopathology for the HIV therapy targeting CCR5.

Disclosures: Ji-Won Lee, None.

SU0215

G Protein-Coupled Receptor 120 Signaling Negatively Regulates Osteoclast Differentiation, Survival, and Function. Hyun Ju Kim¹, Hye-Jin Yoon², Bo Kyung Kim², Sook Jin Seong², Shin-Yoon Kim², Young-Ran Yoon². ¹Kyungpook National University Hospital, South Korea, ²Kyungpook National University, South Korea

G protein-coupled receptor 120 (GPR120) plays an important role in the regulation of inflammation and lipid metabolism. In this study, we investigated the role of GPR120 in osteoclast development and found that GPR120 regulates osteoclast differentiation, survival and function. We observed that GPR120 was highly expressed in osteoclasts compared to their precursors, bone marrow-derived macrophages (BMMs). Activation of GPR120 by its ligand GW9508 suppressed receptor activator of NF- κ B ligand (RANKL)-induced osteoclast differentiation and the expression of nuclear factor of activated T cells c1 (NFATc1), a key modulator of osteoclastogenesis. GPR120 activation inhibited the RANKL-stimulated phosphorylation of I κ B α and JNK without affecting p38. In addition to osteoclast differentiation, GPR120 activation increased the apoptosis of mature osteoclasts by inducing caspase-3 and Bim expression. Activation of GPR120 also interfered with cell spreading and actin cytoskeletal organization mediated by M-CSF but not by RANKL. Coincident with the impaired cytoskeletal organization, GPR120 activation blocked osteoclast bone resorbing activity. Furthermore, knockdown of GPR120 using small hairpin RNA abrogated all these inhibitory effects on osteoclast differentiation, survival, and function. Together, our findings identify GPR120 as a negative modulator of osteoclast development that may be an attractive therapeutic target for bone-destructive diseases.

Disclosures: Hyun Ju Kim, None.

SU0216

Inhibition of CysLTR1 Suppresses RANKL-induced Osteoclast Formation and Bone Loss in vivo. Ju-Hee Kang*¹, Mijung Yim². ¹Sookmyung Women's University, South Korea, ²Sookmyung women's university, South Korea

Leukotrienes are inflammatory lipid mediators derived from arachidonic acid through the involvement of the 5-lipoxygenase (5-LO) pathway. They are divided into two groups, LTB4 and Cysteinyl leukotrienes (CysLTs), namely LTC4, LTD4, LTE4. Especially, LTC4 is formed by LTC4 synthase (LTC4S), and it converted to LTD4, and further into LTE4. CysLTs are well known for a cause of many diseases such as asthma, allergic rhinitis, coronary artery, and immune disorder by binding on 2 types of receptor (CysLTR1 or CysLTR2). It has been implicated as a promising drug target to treat various inflammatory diseases. Since little is known about the role of CysLTR1 on osteoclastogenesis, we investigated its functions and intracellular signaling pathways in osteoclast differentiation using CysLTR1 antagonist. In this study, we showed that CysLTR1 antagonist suppressed RANKL-induced osteoclast formation at late (day2-4) stage without cytotoxicity. Real-time PCR analysis revealed that the mRNA levels of osteoclastogenic markers were decreased by CysLTR1 antagonist. In addition, CysLTR1 antagonist reduced RANKL-induced pit formation on dentin slices. Inhibition of CysLTR1 was attributable to reduction in the expression of NFATc1, an essential transcription factor for osteoclast differentiation. It is also associated with impaired activation of multiple signaling events downstream of RANK, including ERK, Akt, CREB, PLC β 2 phosphorylation and I κ B degradation. Ectopic overexpression of a constitutively active form of NFATc1 partly rescued the anti-osteoclastogenic effect of CysLTR1 antagonist. The knockdown of LTC4S in BMMs also resulted in a significant reduction in RANKL-induced osteoclast formation, accompanied by decreased expression of NFATc1. Finally, we evaluated the effect of CysLTR1 antagonist using LPS-calvaria mouse model and ovariectomy mouse model in vivo. CysLTR1 antagonist decreased lipopolysaccharide (LPS)-induced osteoclast formation in vivo. Furthermore, inhibition of CysLTR1 reduced ovariectomy (OVX)-induced bone loss. Our findings suggest that the CysLTR1 can be a therapeutic target for the treatment of bone resorption diseases.

Disclosures: Ju-Hee Kang, None.

SU0217

Inhibitory effects of KP-A159, a thiazolopyridine derivative, on osteoclast differentiation, function, and inflammatory bone loss via suppression of RANKL-induced MAP kinase signaling pathway. Hye Jung Ihn*¹, Taeho Lee², Sang-Hyun Kim¹, Hong-In Shin³, Yong Chul Bae⁴, Eui Kyun Park⁵. ¹Department of Pharmacology, School of Medicine, Kyungpook National University, South Korea, ²College of Pharmacy, Research Institute of Pharmaceutical Sciences, Kyungpook National University, South Korea, ³Department of Oral Pathology & Regenerative Medicine, School of Dentistry, IHBR, Kyungpook National University, South Korea, ⁴Department of Oral Anatomy, School of Dentistry, Kyungpook National University, South Korea, ⁵Kyungpook National University, South Korea

Abnormally elevated formation and activation of osteoclasts are primary causes for a majority of skeletal diseases. In this study, we found that KP-A159, a thiazolopyridine derivative, inhibited osteoclast differentiation and function in vitro, and inflammatory bone loss in vivo. KP-A159 did not cause a cytotoxic response in bone marrow macrophages (BMMs), but significantly inhibited the formation of multinucleated tartrate-resistant acid phosphatase (TRAP)-positive osteoclasts induced by macrophage colony-stimulating factor (M-CSF) and receptor activator of nuclear factor- κ B ligand (RANKL). KP-A159 also dramatically inhibited the expression of marker genes related to osteoclast differentiation, including TRAP (Acp5), cathepsin K (Ctsk), dendritic cell-specific transmembrane protein (Dcstamp), matrix metalloproteinase 9 (Mmp9), and nuclear factor of activated T-cells, cytoplasmic 1 (Nfatc1). Moreover, actin ring and resorption pit formation were inhibited by KP-A159. Analysis of the signaling pathway involved showed that KP-A159 inhibited RANKL-induced activation of extracellular signal-regulated kinase (ERK), c-Jun N-terminal kinase (JNK), and mitogen-activated protein kinase kinase1/2 (MEK1/2). In a mouse inflammatory bone loss model, KP-A159 significantly rescued lipopolysaccharide (LPS)-induced bone loss by suppressing osteoclast numbers. Therefore, KP-A159 targets osteoclasts, and may be a potential candidate compound for prevention and/or treatment of inflammatory bone loss.

Disclosures: Hye Jung Ihn, None.

This study received funding from: National Research Foundation of Korea

SU0218

Phosphorylation of the Actin Bundling Protein L-Plastin Regulates the Early Phase of Sealing Ring Formation. Meenakshi Chellaiah*¹, Tao Ma. University of Maryland, Dental School, USA

Background: L-plastin (LPL), also known as fimbrin is a cytoskeleton-associated protein or Plastin-2. This was initially detected in leukocytes, and subsequently in cancer cells derived from solid tumors. LPL consists of phosphorylation sites at serine 5 and serine 7 at the amino-terminal region (NT) and two actin binding domains (ABDs). LPL phosphorylation on Ser 5 and/or 7 increases LPL's F-actin binding and bundling capacity. In addition, LPL stabilizes actin filaments and protects them from depolymerization. The process of sealing ring formation in osteoclasts (OCs) requires major actin filament reorganization; indeed bundling and stability of actin filaments is a fundamental step in sealing ring formation allowing OCs to tightly adhere to the bone surface. Our previous studies presented compelling evidence demonstrating that LPL, in the presence of TNF- α or RANKL, plays a key role in the formation of nascent sealing zones (NSZs) which are precursor zones for mature and fully functional sealing rings. Here, our aim is to identify by structure function analysis, the elements of LPL that are critical to NSZs formation.

Methods: OCs were transduced with TAT-fused full-length (FL) - or elements of LPL in the presence of TNF- α and native bone particles (100 μ m size) for 3-5h to determine their effects on LPL phosphorylation, NSZs formation, and actin content. OCs treated for 12-18h were used to determine mature sealing ring formation and bone resorption level. Vector protein and/or non-specific (NS) TAT-fused HSV-TK proteins were used as controls

Results: Transduction of TAT-fused FL- LPL not only increases the number of NSZs but also increased mature sealing rings, actin content and bone resorption in OCs plated on dentine slices in the presence of TNF- α . OCs transduced with the amino-terminal LPL fragment containing Ser5 and 7 aa demonstrated the following: a) reduced endogenous LPL phosphorylation; b) a significant decrease in the number of NSZs and mature sealing rings in a time-dependent manner; c) punctate podosome-like structures on dentine; d) a decrease in actin content; e) reduced capacity of bone resorption in vitro. There was no change with the LPL peptide containing ABDs alone.

Conclusions: Structure-function analyses with NT-LPL fragments demonstrated that phosphorylation of LPL at Ser5 and 7 regulates the formation of NSZs. Cooperativity between serine phosphorylation and actin-binding to ABDs is required for actin bundling process mediated by LPL. We suggest that inhibiting LPL phosphorylation will attenuate mature sealing ring formation and bone resorption. Therefore, LPL may be a potential therapeutic target for OC mediated bone loss (Supported by NIH-NIAMS 5 R01 AR066044-02).

Disclosures: Meenakshi Chellaiah, None.

SU0219

Regulation of tartrate-resistant acid phosphatase in osteoclasts by tetraspanin CD82. Alexis Bergsma*¹, Cindy Miranti. Van Andel Institute, USA

The tetraspanin CD82 is a metastasis suppressor protein known to be involved in cell adhesion and regulation of tyrosine kinases, integrins, proteases, and Src. However, the normal function of CD82 in development and homeostasis remains elusive. To address this gap in knowledge, our lab generated CD82^{-/-} mice, which are healthy and fertile. Recently, CD82 was identified as being upregulated 9.4-fold during osteoclast differentiation when plated on bone (Crotti, T.N., et al., J Cell Physiol, 2011.). To determine if loss of CD82 impacts bone homeostasis, I evaluated bone parameters in WT and CD82^{-/-} mice using microCT. My preliminary data show that CD82^{-/-} mice have increased bone mineral density, suggesting a possible defect in osteoclasts. In ex-vivo differentiation assays of osteoclasts isolated from CD82^{-/-} mice, the multinucleated osteoclasts displayed a significant reduction in TRAP (tartrate-resistant acid phosphatase) activity. TRAP is a metalloenzyme in osteoclasts that assists in the process of bone resorption. Activation of TRAP requires proteolytic cleavage by the protease Cathepsin K. Because tetraspanins can regulate proteases, I hypothesize that CD82 expression is required for normal differentiation of osteoclasts into fully functional, TRAP-positive cells, and that CD82 is important for Cathepsin K activation of TRAP. Preliminary immunoblotting experiments from the ex vivo differentiated osteoclasts demonstrated that both Cathepsin K and active TRAP protein are decreased in CD82^{-/-} osteoclasts. These observations validate that CD82 is important for osteoclast differentiation and suggest that CD82 is either working to assist in complex assembly of Cathepsin K and TRAP or in their processing into functional proteins. To address this, I am currently working to delineate the localization and processing of Cathepsin K and TRAP between the ER, endosome, and lysosome by confocal microscopy.

Disclosures: Alexis Bergsma, None.

SU0220

Role of the iRhom2/TACE/TNF α pathway in the pathogenesis of haemophilic arthropathy. Coline Haxaire^{*1}, Narine Hakobyan², Jane Salmon¹, Carl Blobel¹. ¹Hospital for Special Surgery, USA, ²Rush University, USA

A major manifestation of Hemophilia A, an X-linked bleeding disorder, is hemophilic arthropathy (HA), a debilitating degenerative joint disease that is caused by intraarticular bleeding. HA typically begins with haemophilic synovitis (HS), a hypertrophy of synoviocytes with inflammation of the synovium and a neovascular response, followed by joint erosion and ultimately arthropathy with cartilage destruction and erosion of the underlying bone. HS has features in common with inflammatory arthritides such as Rheumatoid arthritis (RA). The pro-inflammatory cytokine tumor necrosis factor α (TNF α) is a major target for treatment of RA. TNF α is synthesized as a membrane-anchored precursor that is released by the TNF α convertase (TACE, also referred to as ADAM17). We have recently uncovered a crucial role for TACE and its regulator, iRhom2, in the pathogenesis of inflammatory arthritis in mice. Since RA is caused, at least in part, by inappropriate release of TNF α , we hypothesize that iRhom2/TACE/TNF α also have a pivotal role in promoting HA.

Here, we show that treatment of macrophages with blood *in vitro* activated TNF α shedding, but not from macrophages lacking iRhom2. We then studied the role of TNF α in HA/HS *in vivo* using *Fviii*-deficient mice (*Fviii*^{-/-} mice), using a joint puncture model. *Fviii*^{-/-} developed a severe hemarthrosis one day after knee puncture, and had a synovial invasion with an increase in neovascularisation in the joint space and cortical thickening of the bone two weeks after the puncture. μ CT analysis showed a significant decrease in trabecular bone volume (BV/TV; -74%), number of trabeculae (Tb.N; -41%) and a significant increase in trabecular separation (Tb.Sp; +52%) in the punctured knee compared to the contralateral control. Inactivation of TNF α in *Fviii*^{-/-} mice significantly reduced the osteopenia in the HA/HS model, with improved bone trabecular parameters compared to *Fviii*^{-/-} mice (BV/TV; -57%, Tb.N; -18%; Tb.Sp; +23%). TRAP staining demonstrated that the bone loss in *Fviii*^{-/-} mice was mainly caused by a significant local increase in osteoclast number and osteoclast surface per bone surface compared to *Fviii*^{-/-}Tnf α ^{-/-} mice. Taken together, these preliminary results support the hypothesis that the iRhom2/ADAM17/TNF α signaling pathway contributes to osteopenia observed in HA/HS patients. Further studies are in progress to analyze whether or not this pathway also has role in synovitis and cartilage destruction in HA/HS.

Disclosures: Coline Haxaire, None.
This study received funding from: Bayer

SU0221

Tensin 3 activates Dock5 to drive podosome organization in osteoclasts and efficient bone resorption. Anne Blangy^{*1}, Heiani Touaitahuata², Nabila Mansouri², Anne Morel². ¹CNRS Montpellier University, France, France, ²CNRS Montpellier University, France

Osteoclasts resorb the bone matrix through a specific adhesion structure called the sealing zone, which is based on a belt of podosome. Whereas the architecture of individual podosomes is getting well understood, a lot remains to be uncovered regarding the molecular mechanisms driving podosome organization into super-structures such as the osteoclast podosome belt. We showed that Dock5, an exchange factor for the small GTPase Rac, is essential for podosome organization in osteoclasts and then for bone resorption *in vitro* and *in vivo* (Vives et al, JBM, 2011; Touaitahuata et al., Dev Biol 2014). We also demonstrated that systemic administration of a small chemical compound inhibitor of Dock5 protects the mice against pathological bone loss while preserving bone formation (Vives, Cres et al., Nature Communications, 2015).

To understand how Dock5 signaling pathways control podosome belt formation, we performed proteomic analyses and identified Tensin 3 as a partner of Dock5 in osteoclasts. As that of Dock5, the expression of Tensin 3 increases during osteoclast differentiation. Confocal and 3D-SIM super-resolution microscopy revealed that Dock5 and Tensin 3 are not associated with individual podosomes. By contrast, they colocalize in the podosome cloud region when these assemble into a belt. Suppression of Tensin 3 in osteoclasts destabilizes podosome organization and severely impairs bone resorption. At the molecular level, we found that binding to Tensin 3 to Dock5 increases its exchange activity towards Rac.

Our results identify Tensin 3 as a novel regulator of osteoclast bone resorbing activity. They further suggest that binding of Dock5 to Tensin 3 allows efficient activation of Rac to ensure the assembly of podosomes into a belt, the basal architecture of the bone resorbing apparatus of osteoclasts.

Disclosures: Anne Blangy, None.

SU0222

Bach1 nuclear export attenuates osteoclastogenesis and osteoclast activation via inhibition of intracellular ROS signaling. Hiroyuki Kanzaki^{*1}, Shinohara Fumiaki², Masazumi Matsuzawa³, Yoshiki Nakamura³. ¹Tsurumi University School of Dental Medicine, Japan, ²Tohoku University Graduate School of Dentistry, Oral Microbiology, Japan, ³Department of orthodontics, School of Dental Medicine, Tsurumi University, Japan

Objectives: It was reported that reactive oxygen species (ROS) play a role in osteoclast differentiation as intra-cellular signaling molecule. Previously we reported that transcriptional factor nuclear factor E2-related factor 2 (Nrf2) negatively regulate osteoclastogenesis via anti-oxidative enzyme expression and thereby ROS scavenging. However, it is still remain unknown Bach1, the competitor for Nrf2 in transcriptional regulation of anti-oxidative enzymes can be therapeutic target for bone destructive disease. We hypothesized that Bach1 nuclear export activates Nrf2-dependent anti-oxidative enzyme expression, diminish intracellular ROS signaling, and thereby attenuates osteoclastogenesis. Methods: Mouse monocyte cell-line RAW264.7 were stimulated with sRANKL with or without the induction of Bach1 nuclear export by sodium ferrous citrate (SFC) and 5-Aminolevulinic acid (ALA). Localization of Bach1 was examined with immuno-cyto staining. Expressions of Nrf2, Bach1, and anti-oxidative enzymes such as heme oxygenase 1, were examined by realtime PCR and western blot. Intracellular ROS signaling was examined by flowcytometry using fluorescent ROS probe. sRANKL-dependent osteoclastogenesis were observed, and marker genes for osteoclast differentiation were examined by realtime PCR. Results: SFC and ALA treatment resulted in the Bach1 nuclear export, and induced Nrf2 nuclear import. Bach1 nuclear export increased anti-oxidative stress enzyme expression. Furthermore, Also bach1 nuclear export diminished RANKL-mediated intracellular ROS signaling. Finally, RANKL-mediated osteoclastogenesis was inhibited by bach1 nuclear export. Conclusion: Bach1 nuclear export activates Nrf2-dependent anti-oxidative enzyme expression, and thereby attenuates osteoclastogenesis. Bach1 nuclear export could be therapeutic target for bone destructive disease.

Disclosures: Hiroyuki Kanzaki, None.

SU0223

Bone Parameters Are Unchanged by Activation or Deletion of TGF- β Signaling in Mature Osteoclasts. Jenna Regan^{*}, Sutha K. John, Maria Niewolna, Yun She, Khalid S. Mohammad, Theresa A. Guise. Indiana University School of Medicine, USA

Calcified bone matrix is the most abundant source of transforming growth factor beta (TGF- β) in the body. TGF- β that is released and activated during osteoclast-mediated bone resorption can act locally to influence bone remodeling or enter the circulation to exert systemic effects. In the setting of cancer bone metastasis, high TGF- β levels induced by increased osteolysis play a key role in the feed-forward cycle of tumor progression in bone. In addition to its activity on tumor cells, TGF- β in the microenvironment may also signal directly to bone cells to modulate their differentiation and activity. TGF- β has been shown to increase osteoclast differentiation, but whether TGF- β signals directly to mature osteoclasts to modulate their activity or survival, and thus impact bone mass *in vivo*, is not known. To test the importance of TGF- β signaling in mature osteoclasts, we targeted the pathway using transgenic cathepsin K (CatK)-cre mice to either delete TGF β R2 (CatK-cre; T β R2 flox/flox) or induce the expression of constitutively active TGF β R1-T204D (CatK-cre; T β R1-T204D). We monitored the bone phenotype of both male and female mice (N = 11 per group) *in vivo* using micro-computed tomography and dual-energy X-ray absorptiometry at regular intervals from 6 weeks to 6 months of age. Neither deletion nor activation of canonical TGF- β signaling in mature CatK-positive osteoclasts had any profound effect on trabecular or cortical bone parameters or bone mineral density *in vivo*. Likewise, *ex vivo* analyses, including bone marrow cell differentiation assays, failed to indicate any differences between control mice and those with altered TGF- β signaling in mature osteoclasts. Therefore, we conclude that any direct effects of TGF- β signaling in the osteoclast lineage likely occur earlier during the differentiation process and that normal bone homeostasis may not rely on TGF- β signaling in mature osteoclasts.

Disclosures: Jenna Regan, None.

SU0224

Sialylated Glycans of MMP-9 Mark Bone Resorption Lacunae. Yukiko Kuroda*¹, Atsushi Kuno², Hisashi Narimatsu³, Koichi Matsuo⁴.
¹Laboratory of Cell & Tissue Biology, Keio University School of Medicine, Japan, ²Research Center for Medical Glycoscience (RCMG), National Institute of Advanced Industrial Science & Technology (AIST), Japan, ³Research Center for Medical Glycoscience (RCMG), National Institute of Advanced Industrial Science & Technology (AIST), Japan, ⁴Laboratory of Cell & Tissue Biology, Keio University School of Medicine, Japan

Wheat germ agglutinin (WGA) is a plant lectin that selectively binds to bone resorption pits formed by osteoclasts on dentine or bone slices (Selander et al., 1994). However, WGA-binding proteins are broadly distributed *in vivo*, and the identities of WGA target glycoproteins on pits/lacunae are unknown. We hypothesized that mature osteoclasts, but not preosteoclasts, produce WGA-binding glycoproteins that stick to the surface of resorption pits. Using a lectin microarray, we searched for lectins with carbohydrate specificity narrower than WGA that differentially recognized mature osteoclast-derived and preosteoclast-derived glycoproteins. Among 45 lectins tested, we identified *Maackia amurensis* hemagglutinin (MAH), which binds to sialylated O-linked carbohydrate chains. MAH stained bone resorption pits formed *in vitro* and specifically bound osteoclasts and blood vessels in the mouse tibial metaphysis. We then affinity purified MAH target glycoproteins from culture media of mature osteoclasts using biotinylated MAH and streptavidin-immobilized magnetic beads. A major MAH-binding protein of 90 kD was further analyzed by MALDI-TOF mass spectrometry and identified as matrix metalloproteinase 9 (MMP-9, also known as gelatinase B). Double-staining of mouse tibial sections with MAH and anti-MMP-9 antibodies revealed overlapping immunostaining in most osteoclasts, suggesting that osteoclast-derived MMP-9 is a MAH target glycoprotein *in vivo*. Interestingly, while MMP-9 signals were distributed along the transverse septum at the chondro-osseous junction, MAH-signals were not. These results suggest that sialylated MMP-9 exists in osteoclastic resorption lacunae, while non-sialylated MMP-9 is present in chondroclastic resorption lacunae at the transverse septum, potentially accounting for differential regulation of bone filling at these lacunae.

Disclosures: Yukiko Kuroda, None.

SU0225

Zinc-induced effects on osteoclastogenesis involves activation of HCN channels via changes in membrane potential. Takuya Notomi*¹, Miyuki Kuno², Akiko Hiyama³, Kiyoshi Ohura³, Masaki Noda⁴, Timothy Skerry⁵.
¹Department of Pharmacology, Osaka Dental University, Japan, ²Osaka City University, Japan, ³Osaka Dental University, Japan, ⁴Tokyo Medical & Dental University, Japan, ⁵University of Sheffield, United Kingdom

Zinc is a trace element in the mammalian body, and increasing evidence shows its critical role in bone development and osteoclastogenesis. The relationships between zinc and voltage-gated ion channels have been reported; however, the effects of zinc on membrane potential and the related ion channels remain unknown. In this study, we found that zinc-induced hyperpolarization in RAW264.7 cells (RAW) was promoted by inhibition of hyperpolarization-activated cyclic nucleotide modulated channels (HCNs). In electrophysiological experiments with RAW-derived osteoclasts, HCNs were functional and generated hyperpolarization-activated inward currents (I_h) with properties similar to the I_h recorded in excitable cells such as neurons and cardiomyocytes. Quantitative PCR of HCN subunits HCN1 and HCN4 in RAW cells and bone marrow-derived osteoclasts showed detectable levels of HCN1 mRNA and HCN4 expression was the highest of all four subunits. HCN4 knockdown decreased osteoclastic I_h and promoted osteoclastogenesis in the presence of zinc, but not in the absence of zinc. To determine the effect of membrane hyperpolarization on osteoclastogenesis, we developed a light-controllable membrane potential system in RAW cells by stably expressing the light-driven outward proton pump, Archaeorhodopsin3 (Arch). Arch activation by yellow-green light hyperpolarizes the cell membrane by -11 ± 1.5 mV upon the onset of light stimulation and returned to pre-stimulus potential after termination of the stimulus. Light-induced hyperpolarization accelerated osteoclast differentiation in the presence of RANKL. Thus, HCN activation reduced the hyperpolarization-related promotion of osteoclast differentiation in the presence of zinc. This study revealed the novel role of HCN and membrane potential in non-excitable osteoclasts. Light-induced hyperpolarization may facilitate investigations of changes in membrane potential generated by ligands and chemicals in the search for novel drug candidates to treat bone disorders.

Disclosures: Takuya Notomi, None.

SU0226

Human scaphoid non-unions exhibit increased TNF-α and osteoclast activity compared to adjacent cancellous bone. Björn Behr*¹, Marcus Lehnhardt², Christoph Wallner³, Stephanie Abraham², Jessica Schira².
¹Ruhr-University of Bochum, Germany, ²Ruhr-University Bochum, Germany, ³Ruhr-University Bochum, Germany

Scaphoid bones have a high prevalence for non-union. Even with adequate treatment, bone regeneration may not occur in certain instances. Although this condition is well described, the molecular pathology of scaphoid non-unions is still poorly defined.

The purpose of the study was an intraindividual gene expression comparison of osteogenic, inflammatory and angiogenic growth and transcription factors between human scaphoid non-unions and adjacent autologous cancellous bone from the distal radius. In addition, histology and immunohistochemical stainings were performed to verify qRT-PCR data.

Gene expression analysis revealed a significant upregulation of TNF-α, RANKL, ALP, CYCLIN D1, MMP-13, OPG, NFATc1, TGF-β and WNT5A in scaphoid non-unions. Interestingly, TNF-α was highly upregulated in all non-union samples (mean: 24 fold increase). Moreover, RANKL, a marker for osteoclastogenesis was increased by 19 fold in non-unions. TRAP staining confirmed this observation. Other inflammatory markers such as IL-1β or IFN-γ were not detectable in both tissues. With respect to genes related to osteogenesis, alkaline phosphatase was significantly upregulated in scaphoid non-unions. No differences were detectable for other osteogenic genes such as RUNX-2 or BMP-2. Importantly, we did not detect differences in angiogenesis between scaphoid non-unions and control in both gene expression and immunohistochemistry.

Summarized, our data indicate chronic inflammation and increased osteoclast activity in scaphoid non-unions. Moreover, scaphoid non-unions still have a partial osteogenic and angiogenic potential which obviously does not lead to sufficient bone healing. These data increase our understanding for the reduced bone regeneration capacity present in scaphoid non-unions and may translate into identification of new therapeutic targets in order to avoid secondary damages and prevent occurrence of non-unions to scaphoid bones.

Disclosures: Björn Behr, None.

SU0227

Titanium Particles and Mechanical Instability of Implants Induce Osteoclast Differentiation Through Indistinguishable Inflammatory Pathways. Mehdi Amirhosseini*¹, Göran Andersson², Per Aspenberg³, Anna Fahlgren⁴.
¹Faculty of Health Sciences, Linköping University, Linköping, Sweden, ²Division of Pathology, Department of Laboratory Medicine, Karolinska University Hospital, Sweden, ³Division of Orthopedics, Department of Clinical & Experimental Medicine, Faculty of Health Sciences, Linköping University, Sweden, ⁴Division of Cell Biology, Department of Clinical & Experimental Medicine, Faculty of Health Sciences, Linköping University, Sweden

Peri-prosthetic bone loss can be due to an inflammatory response to wear debris particles, but clinical (Anthony et al 1990) and experimental (Fahlgren et al 2010) data support additional role of mechanical factors in osteoclast differentiation of periprosthetic loosening. In an established animal model for aseptic loosening (Skripitz et al 2000), mechanical instability differed quantitatively in mRNA expression of inflammatory cytokines compared to titanium particles (Nilsson et al 2012). Therefore, we tested the hypothesis that mechanical instability and titanium particles induce osteoclast differentiation via different pathways, using microarray analysis. Male SD rats with a validated implant for aseptic loosening were exposed either to mechanical instability or titanium particles. The bone tissue underneath the implant was harvested after 0 hrs (control), 3, 48 and 120 hrs for RNA extraction and microarray analysis with RaGene-2:1st Affymetrix array (n=3-4/group). Top 1000 genes that reached the cut-off levels of 1.5 fold-change with a FDR-adjusted p-value below 0.05 were used for pathway analysis using Ingenuity Pathway Analysis software. Compared to controls, both treatments regulated about 300 genes at 3 hrs, 1900 genes at 48 hrs and 900 genes at 120 hrs. Of all the genes regulated significantly, there were no significant differences when mechanical instability was compared with titanium particles at any time point. Pathway analysis showed that mechanical instability and titanium particles shared similar canonical pathways for acute phase response signaling, IL-6 signaling and MIF regulation of innate immunity at 3 and 48 hrs. iNOS signaling and Wnt/β-catenin signaling pathway were shared at 48 hrs and leukocyte extravasation signaling pathway at 120 hrs. Macrophage- and osteoclastogenesis-associated genes showed similar patterns of change. However, a higher RANKL/OPG ratio with titanium particles than with mechanical instability was detected at 48 hrs, suggesting a more rapid osteoclastogenic response induced by particles (Table 1). These data suggest that despite some differences in biologic responses driven by wear debris particles and mechanical loading, the main processes leading to osteoclastogenesis are regulated through similar pathways. However, although key genes showed similar changes in our data, differences in the genes responsible for triggering the inflammatory processes might hide in the cloud of statistical uncertainty.

Table 1: Fold-change of osteoclast-related genes, and statistically significant changes from base-line.

| Gene | 3 hrs | | 48 hrs | | 120 hrs | |
|------------------------------|-------|-------|--------|--------|---------|-------|
| | Ti | MeIn | Ti | MeIn | Ti | MeIn |
| Macrophage/Osteoclast | | | | | | |
| CD14 | 3.5 * | 3.4 * | 2.6 ** | 3.4 ** | 2 * | 2.9 |
| Csfl | 2.1 | 2.1 * | 1.9 ** | 2 ** | 1.6 * | 2 * |
| Csflr | -1.2 | -1.2 | 1.5 ** | 1.3 * | 1.2 | 1.3 * |
| c-Fos | 4.2 * | 4.5 * | 3.4 ** | 4.5 ** | 2.2 * | 2.5 |
| IL-6 | 74 * | 75 * | 26 ** | 7 * | 3.7 * | 9.6 |
| IL-1 α | 2.9 * | 4.2 | 2 ** | -1.0 | 1.4 | 11.7 |
| MMP-9 | 1.1 | 1.2 | 1.6 ** | 1.3 * | 1.7 * | 1.9 * |
| RANK | -1.1 | -1.2 | 3.3 ** | 2.5 ** | 2 | 2.8 |
| RANKL | 1.3 | 1.3 | 5.8 ** | 3.4 ** | 2.5 * | 4.6 |
| OPG | 2.6 * | 3.8 * | 1.8 * | 3.4 * | 1.4 | 1.3 |
| RANKL/OPG | 0.52 | 0.34 | 3.2 | 1.0 | 1.7 | 3.4 |

Ti: Titanium particles, MeIn: Mechanically Instability. * = adjusted p-value<0.05, ** = adjusted p-value<0.01

Table 1: Fold-change of osteoclast-related genes and statistically significant changes from baseline

Disclosures: Mehdi Amirhosseini, None.

SU0228

A RANKL-binding peptide W9 inhibits human osteoclast differentiation and stimulates human osteoblast differentiation. Midori Nakamura¹, Yuko Nakamichi¹, Teruhito Yamashita¹, Yuriko Furuya², Hisataka Yasuda², Nobuyuki Udagawa³. ¹Department of Biochemistry, Institute for Oral Science, Matsumoto Dental University, Japan, ²Nagahama Institute for Biochemical Science, Biochemical Production & Development Center, Oriental Yeast Co., Ltd., Japan, ³Matsumoto Dental University, Japan

A RANKL-binding peptide WP9QY (W9) is known to inhibit mouse osteoclastogenesis. In addition, W9 showed an anabolic effect on cortical bone in mice in vivo. W9 bound RANKL and differentiated osteoblasts with production of autocrine factors like BMP. In this experiment, we examined the effects of W9 on differentiation of osteoblasts, osteoclasts and dendritic cells in human culture system. Osteoclasts and dendritic cells are derived from common progenitors, such as bone marrow-derived macrophages. W9 strongly inhibited multinucleated osteoclast formation in human peripheral blood mononuclear cell cultures in the presence of RANKL and M-CSF for 14 days as well as strikingly stimulated alkaline phosphatase (ALP)-positive osteoblast differentiation in human bone marrow stromal cells for 12 days. In contrast, W9 have no effect on dendritic cell differentiation in human peripheral blood mononuclear cell cultures in the presence of GM-CSF and IL-4 for 10 days. These experimental results indicate that W9 inhibited human osteoclast formation but not dendritic cell differentiation and directly stimulated osteoblast differentiation via RANKL signaling-mediated autocrine factors. Our findings suggest that the reverse signal from RANK on osteoclasts to RANKL on osteoblasts, and the forward signal from RANKL to RANK, could play an important role in the coupling between bone-formation and bone resorption.

Disclosures: Midori Nakamura, None.

SU0229

Effect of FTY720 on osteoclast formation in rats with periodontitis. Dong-Eun Lee¹, Eun-Jung Bak^{2*}, Ji-Hye Kim¹, Gye-Hyeong Woo³, Yun-Jung Yoo¹. ¹Yonsei University Dental college, South Korea, ²Yonsei University Health System, South Korea, ³Department of Clinical Science, Semyung University, South Korea

Osteoclast precursors (OPs) re-migrate from the bone surface into blood vessels through sphingosine-1-phosphate receptor 1 (S1PR1) expression. T cells also express S1PR1, mediating their migration from the lymph nodes into blood vessels. OP and T cell migration is one of the sequential steps related to osteoclast formation. To characterize the role of S1PR1 in osteoclast formation induced by periodontitis, we investigated effect of S1PR1-binding molecule FTY720 (FTY) on the number of OPs and T cells in periodontal tissue and peripheral blood of rats with ligature-induced periodontitis. Rats were divided into four groups: control (C), FTY (F), periodontitis (P), and periodontitis + FTY (PF) groups. Ligatures were placed around the first molars in the left and right mandibles. The rats were intraperitoneally injected with vehicle or 3 mg/kg FTY daily until they were sacrificed. The number of osteoclasts

and cluster of differentiation (CD)11b, CD3, and receptor activator of NF- κ B ligand (RANKL)-positive cells in first molar furcation were counted by tartrate-resistant acid phosphatase (TRAP) or immunohistochemistry staining. The number of CD11b-positive and CD3-positive cells in peripheral blood was estimated by flow cytometry. The number of osteoclasts in P group was higher than C, PF, and F groups and CD11b, CD3, and RANKL-positive cells were also higher in P group than other groups in furcation. While CD11b-positive cells in furcation of PF group were lower than the P group, they were higher in peripheral blood. Dissimilar to CD11b-positive cells, CD3-positive cells in the PF group were lower in peripheral blood as well as furcation than the P group. RANKL-positive cells in furcation of the PF group were also lower than P group. These results indicate that FTY may facilitate re-migration of OPs from the alveolar bone surface into blood vessels, blocking T cell migration from the lymph nodes into blood vessels and subsequently reducing osteoclast formation induced by periodontitis. This suggests that S1PR1-S1P binding may play a role in osteoclast formation of periodontitis by modulating OP and T cell migration.

Disclosures: Eun-Jung Bak, None.

SU0230

Mef2C Targets Energy Metabolism Genes in Bone. Aimy Sebastian¹, Deepa K. Murugesu², Sarah Hatsell³, Aris N. Economides³, Gabriela G. Loots⁴. ¹University of California, Merced, USA, ²Lawrence Livermore National Laboratories, USA, ³Regeneron Pharmaceuticals, USA, ⁴Lawrence Livermore National Laboratories; University of California, Merced, USA

Mef2C is a member of the myocyte enhancer factor-2 (MEF2) family of transcription factors which plays a pivotal role in myogenesis. We have previously shown that Mef2C regulates *Sost* expression and *Mef2C^{CKO};Coll1-Cre* mice have high bone mass (HBM). Recently, we found that Mef2C is expressed in osteoclasts and *Ctsk-Cre* mediated deletion of Mef2C also results in HBM. To understand the mechanisms by which Mef2C regulates bone metabolism we isolated RNA from femurs of *Mef2C^{CKO};Coll1-Cre* and *Mef2C^{CKO};Ctsk-Cre* mice and profiled gene expression using RNA-seq. We found 164 genes up- and 977 genes down-regulated in *Mef2C^{CKO};Coll1-Cre* mice compared to controls while 269 genes were up- and 1292 were down-regulated in *Mef2C^{CKO};Ctsk-Cre* mice. *Sost* was 2.46 fold reduced in *Mef2C^{CKO};Coll1-Cre* mice while *Mef2C^{CKO};Ctsk-Cre* femurs had unaltered levels of *Sost* mRNA. Several bone metabolism related genes such as *Ibsp*, *Mgp* and *Bglap* were down-regulated in *Mef2C^{CKO};Coll1-Cre* mice but were unchanged in *Mef2C^{CKO};Ctsk-Cre* mice, suggesting that osteoblast function is molecularly unaltered in *Mef2C^{CKO};Ctsk-Cre* mice. We found 208 energy metabolism genes [regulators of glycolysis; TCA cycle; oxidative phosphorylation; fatty acid metabolism] down-regulated in *Mef2C^{CKO};Ctsk-Cre* mice, including PGC1 α and PGC1 β , two transcriptional co-activators that have been previously shown to regulate mitochondrial biogenesis and energy metabolism. To identify direct transcriptional targets of Mef2C we mapped publicly available Mef2C ChIP-seq data to the nearest genes and found that 43/208 energy metabolism genes including PGC1 β harbor Mef2C binding sites. Analysis of the energy metabolism gene promoters with HOMER motif finding software identified estrogen-related receptors (ERRs) as the most enriched transcription factors with binding sites in 161/208 promoters. We also found that ERR α and ERR γ are significantly down-regulated in *Mef2C^{CKO};Ctsk-Cre*. It has previously been shown that ERR α coordinates with PGC1 β to regulate mitochondrial function in osteoclasts and both ERR α and PGC1 β gene deletions cause osteoclast defects. Our findings suggest that Mef2C regulates a large number of energy metabolism genes in bone which may have a direct effect on osteoclast and osteoblast function. Further studies will elucidate whether the energy metabolism genes are direct transcriptional targets of Mef2C or whether Mef2C indirectly regulates these genes by modulating the expression of other factors such as PGC1 β or ERR α .

Disclosures: Aimy Sebastian, None.

SU0231

Microgravity Induction of TRAIL in Preosteoclast Cells Enhances Osteoclastogenesis. Yuvaraj Sambandam¹, Kelsey Baird¹, Maxwell Stroebel¹, William Ries², Sakamuri Reddy². ¹Medical University of South Carolina, USA, ²MUSC, USA

Evidence indicates that astronauts experience significant bone loss in space. We previously showed that simulated microgravity (μ Xg) using the NASA developed rotary cell culture system (RCCS) enhanced bone resorbing osteoclast differentiation. However, the mechanism by which μ Xg increases osteoclast formation is unclear. RANK/RANKL signaling pathway is critical for osteoclast differentiation/activity. Tumor necrosis factor-related apoptosis inducing ligand (TRAIL) has been shown to increase osteoclastogenesis. We hypothesize that TRAIL may play an important role in μ Xg enhanced osteoclast differentiation. In the present study, we identified by RT profiler PCR array screening that μ Xg induces high levels (10-fold) of TRAIL expression in mouse bone marrow derived preosteoclast cells compared to ground based (Xg) cultures. Western blot analysis of total cell lysates obtained from μ Xg subjected preosteoclast cells further demonstrated increased (5-fold) levels of TRAIL protein expression. Also, real-time PCR analysis showed a significant increase (12-fold) in TRAIL mRNA expression in these cells. We further identified that μ Xg elevated TRAF-6 protein and mRNA expression in preosteoclast cells. Also, tartrate

resistant acid phosphatase (TRAP) expression levels were increased in these cells without RANKL stimulation. We further identified that addition of TRAIL to RAW 264.7 cells cultured in the presence of RANKL and MCSF potentiated osteoclast differentiation. Interestingly, neutralizing antibody against TRAIL significantly reduced μ Xg induced osteoclast formation. These results indicate that TRAIL signaling plays an important role in the μ Xg increased osteoclast differentiation. Therefore, inhibition of TRAIL expression could be an effective countermeasure for μ Xg induced bone loss.

Disclosures: Yuvaraj Sambandam, None.

SU0232

Morinda citrifolia (Noni) inhibits inflammation-induced osteoclastogenesis. Jeong-Hwa Baek^{*1}, Kanitsak Boonantanasarn², Hanna Gu², Gwan-Shik Kim². ¹Seoul National University, School of Dentistry, South Korea, ²Seoul National University School of Dentistry, South Korea

The primary indigenous use of the Noni plant (*Morinda citrifolia*) is to apply the leaf as a traditional topical treatment for bone fractures or dislocation to promote bone remodeling and reduce inflammation. However, the experimental study of Noni leaves, which have been supported the traditional use is still limited. In this study, we examined the inhibitory effect of Noni on osteoclastogenesis and its molecular mechanisms. Noni ethanol extract was prepared. Osteoclastogenesis was induced by treating RAW264.7 murine monocyte cells with lipopolysaccharide (LPS), TNF- α , or RANKL. In the concentration range that did not show cytotoxicity, Noni significantly decreased the expression levels of osteoclastogenesis-related transcription factors (NFATc1, c-Fos, Fra1, and Fra2) and osteoclast differentiation marker genes (integrin B3, SRC, cathepsinK, and TRAP), and reduced tartrate resistant acid phosphatase activity in all osteoclastogenesis models used in this study. Noni also inhibited expression levels of LPS-induced inflammatory cytokines (IL-6, TNF- α , IL-1 β) and COX2/PGE2 in both RAW264.7 and MC3T3E1 cells. In addition, Noni significantly down-regulated LPS and TNF- α -induced RANKL expression in MC3T3E1 cells. In defining signaling pathways, Noni was shown to significantly suppress LPS-mediated activation of NF- κ B activation and ERK phosphorylation with moderate inhibitory effect on p38, but not on JNK. In conclusion, we demonstrated that Noni leaf has *in vitro* inhibitory effects on inflammatory responses and osteoclast differentiation, suggesting the therapeutic potential of Noni leaf for prevention and treatment of inflammatory bone loss.

Disclosures: Jeong-Hwa Baek, None.

SU0233

PU.1 and HDAC7 Interact to Regulate Osteoclast Differentiation. Nick Blixt^{*1}, Rajaram Gopalakrishnan², Eric D. Jensen², Kim Manskv¹. ¹University of Minnesota, USA, ²Contributing Author, USA

Osteoporosis is a widespread disease caused by increased bone resorption relative to bone formation, resulting in reduced bone density and higher incidence of fractures. Elucidating molecular mechanisms that regulate osteoclast differentiation and activation will lead to improved therapies for osteoporosis and other bone-related diseases caused by increased osteoclastic activity. Our lab has previously shown by both *in vitro* and *in vivo* experiments that Histone Deacetylase 7 (HDAC7) is an inhibitor of osteoclast differentiation through repression of the activity of the MTF transcription factor. MTF binds DNA and functionally interacts with another transcription factor, PU.1, to regulate osteoclast genes. To further characterize the molecular mechanism behind HDAC7's repression of osteoclast differentiation, we asked whether HDAC7 interacts with PU.1. By co-immunoprecipitation, we demonstrated that HDAC7 and PU.1 could physically interact. Reporter assays showed that HDAC7 repressed PU.1's transcriptional activity. We have mapped the amino acids in HDAC7 and PU.1 necessary for their interaction and for HDAC7's repression of PU.1-activated gene expression. Currently we are determining if HDAC7's deacetylase activity is required for HDAC7 to repress PU.1 and seeking to identify osteoclast promoters at which PU.1 and HDAC7 are found together. Based on our data, we conclude that HDAC7 is a potent negative regulator of osteoclast differentiation, acting by repressing both PU.1 and MTF to prevent transcription of osteoclast genes necessary for differentiation and survival.

Disclosures: Nick Blixt, None.

SU0234

Signaling interactions of myeloid DC precursors on osteoclastogenesis and bone remodeling: an alternative insight. Yen-Chun Grace Liu¹, Andy Yen-Tung Teng^{*2}. ¹Koahsiung Medical University, Taiwan, ²Center for Osteoimmunology & Biotechnology Research, College of Dental Medicine, Kaohsiung Medical University & KMU-Hospital, Taiwan

Background: Dendritic cells (DC) are immune effectors, involved in T-cell immunity where DC/T-cell interactions play a central role in normal & inflammatory conditions, associated with disorders such as rheumatoid arthritis, osteoporosis & periodontitis. Besides being professional antigen presenting cells, DC share common

precursors with osteoclast (OC). Inflammation-associated bone loss is a poorly understood osteo-immune interactions, whose frequency & activity of OC are elevated in response to various stimuli, including osteotropic cytokines & growth factors. Methods: We have developed a working model, where immature myeloid DC subsets (CD11c⁺ MHC-II^{low} CD11b⁺ F4/80⁺ CD31⁻ Ly-6C⁺ CT-R⁻ Cath-K⁻) act as OC precursor in response to RANKL plus stimuli on activation signals (Infect Immun. 2009). Herein, the signal interactions between mDCp/T-cells (e.g., Treg & Th17 cells) and osteotropic cytokines (i.e., IL-17, TGF- β , etc.) that modulate the innate-vs.-adaptive immunity for osteoclastogenesis were investigated using established *in-vitro*/*in-vivo* models. Results: Our data showed that: i) neutralization of TGF- β activity by Mab (or si-RNA) abolished mDDOC development in co-cultures (p<0.03) & *in-vivo* adoptive transfers (p<0.02), based on TRAP & resorptive-pit assays; ii) transfection of SOCS3 or TGF β -R2 lentiviral vectors containing sh-RNA into CD11c⁺ mDCp resulted in a significant inhibition of osteoclastogenesis & bone resorption *in-vitro* & adoptive transfer *in-vivo* (p<0.05); iii) added TGF- β signaling was able to rescuing the reduced TRAP vs. bone resorption upon using TRAF6-KO CD11c⁺ mDCp/T-cells *in-vitro* & *in-vivo* (p<0.05); iv) addition of Foxp3⁺ CD4⁺Treg cells in co-cultures resulted in strongly reduced TRAP expression on osteoclastogenesis vs. bone resorption *in-vitro*, and in calvarias of NOD/SCID mice (p<0.05); whereas, such effects were significantly reversed by IL-17 administered (p<0.05). Summary: The results suggest that: i) immature mCD11c⁺DcP and CD4⁺T-cell interactions is intriguing, which may serve as a unique model to study the links between immunity and inflammation-associated osteoclastogenesis on bone remodeling; ii) TGF- β II & IL-17 (Th17 cells) can interactively signal with RANKL via TRAF6 or unclear novel pathway in mDCp & OCp to modulate osteoclastogenesis, where such alternative signals may be promiscuous, depending on which vital environmental factors interplay for activity at the osteo-immune interface for disease pathogenesis.

Disclosures: Andy Yen-Tung Teng, None.

This study received funding from: University of Rochester & NIH-DE018356

SU0235

Blocking P2X7 receptor prevents the bystander osteocyte RANKL signaling normally triggered by osteocyte apoptosis at microdamage sites. Wing-Yee Cheung^{*1}, Mitchell Schaffler¹, Robert Majeska¹, David Spray², Eliana Scemes². ¹City College of New York, USA, ²Albert Einstein School of Medicine, USA

Osteocyte apoptosis around bone microdamage sites is required to trigger osteoclastogenesis and intracortical remodeling (Cardoso et al., JBMR 2009). Dying osteocytes trigger viable neighboring (bystander) osteocytes to upregulate osteoclastogenic cytokines like RANKL, but how this occurs is unknown. During apoptosis, activated caspase-3 has been shown to open Pannexin 1 (Panx1) membrane hemichannels, releasing a bolus of ATP (Chekeni et al, 2010 Nature). This ATP release is a major 'find-me' signal to bystander cells to call for recruitment of phagocytic cells. We previously showed that osteocytes in Panx1-deficient mice undergo apoptosis as expected in response to microdamage (Mdx); however, the bystander osteocytes do not upregulate RANKL (Cheung et al, 2014 ORS Trans. #0034). These data prompt the hypothesis that bolus ATP released may be an essential signal through which apoptotic osteocytes trigger their intact neighbors to produce RANKL. In the current studies, we tested whether pharmacologically blocking the P2X7 receptor – a major target for ATP signaling – would suppress Mdx-induced RANKL expression in osteocytes. Under IACUC approval, C57Bl/6 mice (14 week old, n=5 each group) were treated with the P2X7R antagonist brilliant blue G (BBG, 50 mg/kg) or PBS vehicle daily for 3 days. Mdx was induced in right ulnae on Day 0 by *in vivo* fatigue loading, after which mice were allowed unrestricted cage activity. On day 3, mice were sacrificed and tissues were processed for IHC analysis. Sections were reacted with antibodies against cleaved caspase-3 (casp3) or RANKL to detect apoptotic osteocytes and osteoclastogenic signaling, respectively. % Casp3⁺ and % RANKL⁺ osteocytes were measured in damaged (Mdx) and non-damaged (non-Mdx) bone regions within the ulnar cortex. BBG treatment did not alter osteocyte apoptosis in Mdx regions. However, BBG completely blocked increases in RANKL⁺ osteocytes in Mdx zones (P<0.05). BBG had no effect on osteocyte Casp-3 or RANKL expression in non-damaged cortical bone regions. These results show that purinergic signaling via P2X7 receptors is an essential component for triggering RANKL upregulation in bystander osteocytes at microdamage sites, thus suggesting a key role of ATP in the activation and targeting of bone resorption.

SU0237

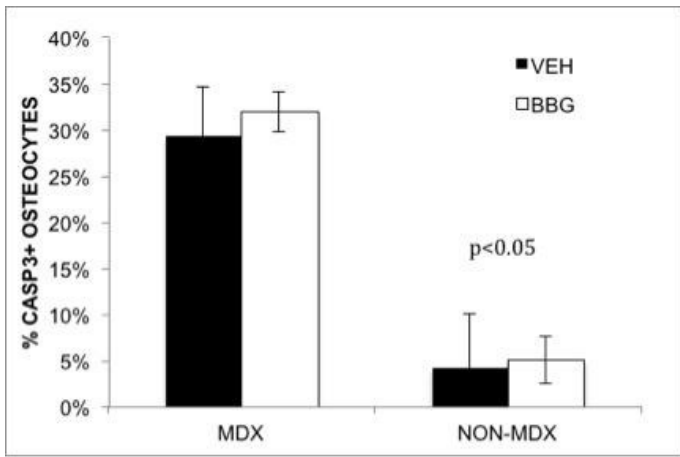
Ex Vivo Preservation of Phenotypic State of Primary Osteocytes via Microbeads-Guided Microfluidic Perfusion Culture. Qiaoling Sun^{*1}, Yexin Gu¹, Wenting Zhang¹, Leah Dziopa², Jenny Zilberberg², Woo Lee¹.
¹Stevens Institute of Technology, USA, ²Research Department, Hackensack University Medical Center, USA

Introduction: Considerable challenges exist for in vitro studies of osteocytes because: (1) current cell lines do not sufficiently represent the phenotypic state of mature osteocytes and (2) primary cells differentiate to osteoblasts upon isolation from bone. In this study, we used a 3D perfusion culture approach to: (1) reconstruct the 3D cellular network of primary murine osteocytes by biomimetic assembly with microbeads and (2) preserve ex vivo the phenotypic state of the osteocytes.

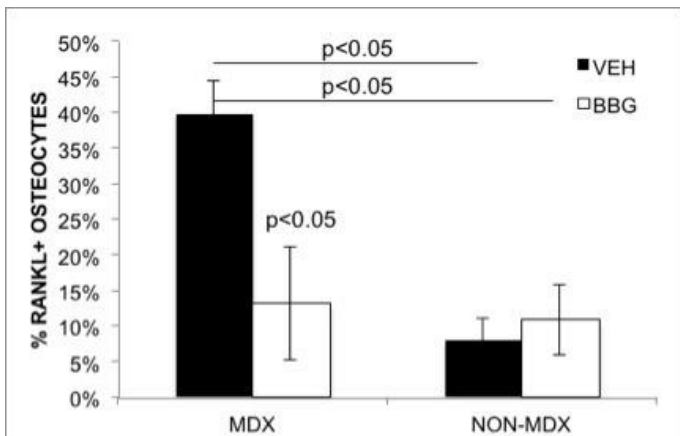
Methods: Primary osteocytes were isolated from long bones of 20-weeks old B10.BR mice by collagenase digestion. For 3D reconstruction with a sufficient number of viable cells, we used cells proliferated from a small population of healthy osteocytes migrated out of digested bone chips. The cells and microbeads (biphasic calcium phosphate) were mixed at a 1:1 ratio and injected into microfluidic chambers to form 3D tissues (Fig. 1a) and cultured for 21 days. The effects of culture time on the viability, differentiation, and proliferation of 3D-reconstructed cells.

Results and Discussion: Mechanically integrated 3D tissues could be produced after 14 days of culture (Fig. 1b). Cells were well distributed in the interstitial spaces between microbeads, and did not proliferate due to the physical confinement within the interstitial sites (Figs. 1c and 1d). The entrapped cells were able to form a 3D cellular network by extending their processes through openings between the microbeads. Because cells began osteoblastic differentiation prior to 3D culture, SOST gene expression was not initially detected, but became significant after 14 days (Fig. 1e). In contrast, SOST expression remained undetectable in 2D culture. FGF23 gene expression was initially detected in both 2D and 3D (Fig. 1f). FGF23 gene expression was significantly increased in 3D after 14 days, but remained at a similar level in 2D.

Conclusions: The results show that the 3D approach was effective in: (1) distributing and entrapping cells within the interstitial spaces between the microbeads, (2) inhibiting proliferation of the entrapped cells, and (3) maintaining cell-to-cell distance to be 20-25 μ m as observed in murine bones. Although cells began osteoblastic differentiation prior to 3D culture, they were able to restore osteocyte gene expressions during 3D culture. The 3D approach is expected to provide a new means of studying the biology of 3D-networked osteocytes and developing bone disease models.



%CASP3



%RANKL

Disclosures: Wing-Yee Cheung, None.

SU0236

Evidence for the novel role of Dynamin in regulating osteocyte dendrite elongation, and genes critical for bone remodeling. Pierre Eleniste^{*}. Indiana University School of Dentistry, USA

Osteocytes orchestrate bone remodeling by regulating the activity of osteoblasts (OB) and osteoclasts (OC). Osteocytes contain membrane extensions known as dendrites, which allow cell-to-cell coupling with osteocytes, OBs and OCs. However, the mechanisms for dendrite elongation are uncertain. The Dynamin GTPase is involved in various cellular activities, such as endocytosis and actin remodeling. Previously, we demonstrated that Dynamin regulates OB migration and differentiation, as well as OC bone resorbing activity. In the current study, we examined the role of dynamin in osteocyte dendrite elongation and function. MLO-Y4 osteocytic cells were treated with increasing concentrations of dynasore, a chemical inhibitor of Dynamin, for 1-3 days. The cells were imaged and dendrite length quantified. Dynasore-treated MLO-Y4 cells exhibited a significant increase in dendrite length of 162% (day 2) and 171% (day 3) compared to controls. Moreover, dynasore-treated cells exhibited an increase in filamentous actin, suggesting dynamin may be involved in actin remodeling. To examine the role of dynamin on osteocyte gene expression, long-bones were collagenase digested to remove OBs and then treated with dynasore for 3 days, followed by QPCR analysis. Dynasore-treated long bones exhibited a significant >20-fold increase in mRNA expression of Wnt3a, which is known to promote OB differentiation. In addition, dynasore-treated long-bones and MLO-Y4 cells exhibited a 6-fold increase in OPG mRNA levels, suggesting dynamin may regulate osteocyte-mediated OC differentiation. OPG expression is regulated by β -catenin/Tcf4 pathway. Our studies also demonstrate that dynamin regulates β -catenin and GSK-3 β levels and dynamin forms a protein complex with nuclear β -catenin, suggesting it may regulate OPG gene transcription. Together, these studies suggest a novel role for Dynamin in regulating osteocyte dendrite elongation as well as signaling to OCs and OBs to control bone remodeling.

Disclosures: Pierre Eleniste, None.

Approximately 60% of the osteocytes in the bone chips were alive at day 7. Osteocytes in bone chips did express mRNA for the osteocyte markers sclerostin, FGF23, DMP1, and MEPE, and the cytokines IL-1 β , IL-6, and TNF α at day 0 and 7. Osteocytes in bone chips were positive for sclerostin immuno-staining. RA-serum, IL-1 β , TNF α , and the combination of IL-1 β , TNF α , and IL-6 enhanced IL-1 β gene expression (3.3 to 80-fold). RA-serum, IL-8, CCL20, IL-1 β , IL-6, TNF α , and the combination of IL-1 β , TNF α , and IL-6 enhanced TNF α gene expression (2 to 3.5-fold). CCL20, IL-17, IL-1 β , TNF α , and the combination of IL-1 β , TNF α , and IL-6 enhanced IL-6 expression (3 to 87-fold). IL-8, CCL20, IL-1 β , TNF α , and the combination of IL-1 β , TNF α , and IL-6 enhanced IL-8 expression (5 to 233-fold). IL-8, CCL20, IL-1 β , TNF α , and the combination of IL-1 β , TNF α , and IL-6 enhanced FGF23 gene expression (2.3 to 3.9-fold). RA-serum, IL-1 β , and the combination of IL-1 β , TNF α , and IL-6 enhanced SOST gene expression (2.5 to 8.5-fold). RA-serum enhanced DKK1 expression (2-fold).

Active RA-serum, individual exogenous recombinant cytokines, chemokines, and a combination of cytokines modulated gene expression of cytokines, phosphate homeostasis-related signaling molecules, and Wnt inhibitors in human osteocytes cultured in their native matrix. These results suggests that osteocytes could be a new target in the prevention of bone loss in inflammatory diseases.

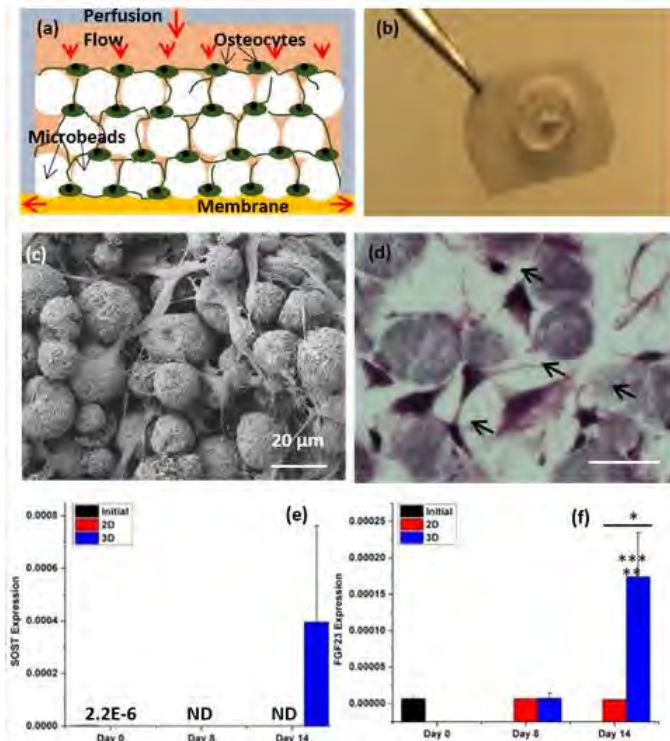
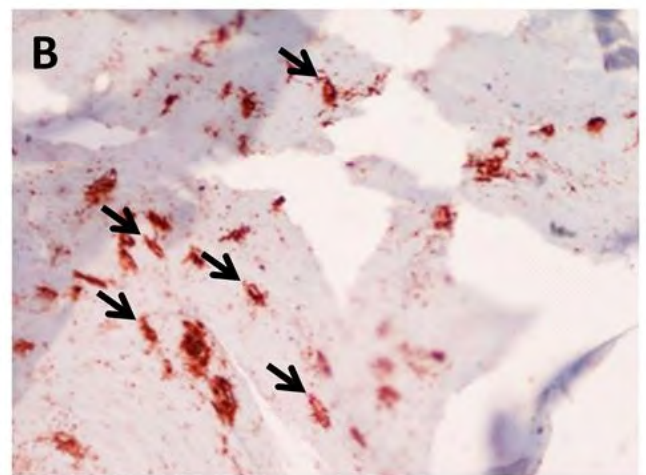
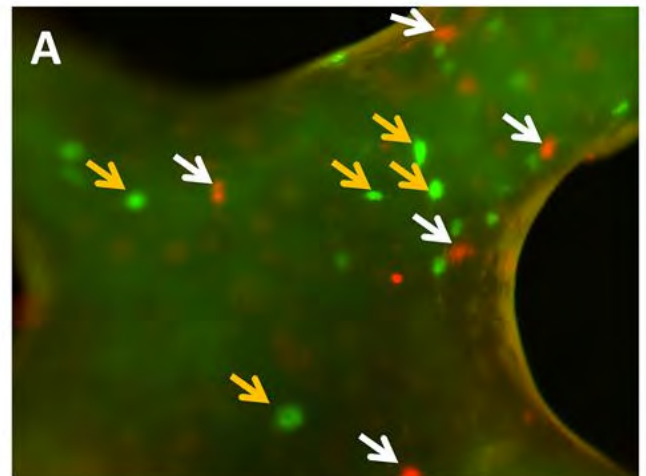


Fig. 1. (a) Schematic illustration of microbeads-guided 3D-network formation of osteocytes under perfusion culture, (b) Picture of a reconstructed tissue sample harvested at Day 14, (c) SEM image showing 3D network formation at Day 14, (d) H&E-stained histologic image showing cell distribution, entrapment, and inhibited proliferation, (e) and (f) SOST and FGF23 gene expressions, respectively, measured by RT-PCR. *Significant difference between 2D and 3D. **Significant difference compared to Day 0. ***Significant difference compared to previous time point. $P < 0.05$.



Live human osteocytes (A, yellow arrows; dead: white arrows) expressing sclerostin (B, black arrows)

Abstract Figures

Disclosures: Qiaoling Sun, None.

SU0238

Inflammatory Cytokines Alter Gene Expression of Osteocyte Signaling Molecules by Human Osteocytes Cultured in Their Native Matrix. Janak L. Pathak*¹, Astrid D. Bakker¹, Frank P. Luyten², Patrick Verschuere², Willem F. Lems³, Jenneke Klein-Nulend⁴, Nathalie Bravenboer⁵.

¹Department of Oral Cell Biology, Academic Centre for Dentistry Amsterdam (ACTA), University of Amsterdam & VU University Amsterdam, MOVE Research Institute Amsterdam, Netherlands, ²Skeletal Biology & Engineering Research Center, KU Leuven, Belgium, ³Department of Rheumatology, VU University Medical Center, MOVE Research Institute Amsterdam, Netherlands, ⁴ACTA-VU University Amsterdam Dept Oral Cell Biology (Rm # 11N-63), The Netherlands, ⁵Department of Clinical Chemistry, VU University Medical Center, MOVE Research Institute Amsterdam, Belgium

Bone remodeling is disturbed in rheumatoid arthritis (RA), leading to bone loss, possibly as a result of elevated levels of circulating inflammatory cytokines. Osteocyte signaling plays a vital role in bone mass regulation by orchestrating bone formation and/or bone resorption, but the effect of inflammatory cytokines on osteocyte signaling remains to be elucidated. Therefore we aimed to investigate the effect of RA-serum or exogenous recombinant inflammatory cytokines and chemokines on human osteocyte signaling molecule production.

Human trabecular bone chips were denuded by collagenase-2 treatment for 2 h. Then bone chips, containing osteocytes embedded in their native matrix, were cultured \pm 10% active RA-serum, or \pm 10 ng/ml recombinant IL-1 β , IL-6, IL-17, or TNF α , 200 pg/ml IL-8, 500 pg/ml CCL20, or a combination of IL-1 β , TNF α , and IL-6 for 7 days. Live-dead staining was performed to assess cell viability. Gene expression of cytokines and osteocyte signaling proteins was analyzed by qPCR. Immunostaining was performed for sclerostin.

SU0240

Osteocyte response to mechanical loading is reduced upon exposure to cobalt and chromium ions. Karan Shah*, Peter Orton, Mark Wilkinson, Alison Gartland. The University of Sheffield, United Kingdom

Elevated levels of cobalt (Co) and chromium (Cr) in patients following metal-on-metal hip replacements and modular total hip arthroplasty directly affect osteoclast and osteoblast cell viability and function *in-vitro*¹, with implications for patient bone health. In this study, we provide evidence that Co and Cr compound these direct effects by altering osteocytes' regulation of bone remodelling following mechanical stimuli.

Fluid shear-stress induced changes in intracellular Ca²⁺ were observed in real-time in murine osteocyte cell-line (MLO-Y4) following 30 minute or 24 hours exposure to 50µg/L or 500µg/L combinations of Co²⁺ and Cr³⁺. Time-lapse fluorescence images were analysed using ImageJ and the data expressed relative to control as area under the curve (AUC) and peak intensity. The effect of fluid shear-stress on osteocyte gene expression (RANKL, Dkk-1, CX43 and Gp38) in absence and presence of metal ions was assessed using real time RT-PCR.

Following 30 minute and 24 hour exposure to Co and Cr, a reduction in cellular response (AUC) to mechanical stimuli was observed for 50µg/L (p<0.0001) and 500µg/L (p<0.0001) compared to untreated controls. A reduction in peak response was also observed for both 50µg/L (p<0.0001) and 500µg/L (p<0.0001) at both time-points. MLO-Y4 cells robustly expressed all the genes with the rank order of expression Cx43>Gp38>RANKL>Dkk-1. Application of fluid shear-stress upregulated Gp38 and RANKL expression and reduced Dkk-1 expression. Cells exposed to Co and Cr prior to loading had a blunted increase in Gp38 and RANKL expression following fluid shear-stress, with the effect being dose-dependent, whilst the reduction in Dkk-1 expression was unaffected. CX43 gene expression was unaffected by either loading alone or loading following Co and Cr treatment.

The data suggests that Co and Cr at concentrations observed in patient serum and hip aspirate following hip replacement may impair osteocyte response to mechanical stimuli and reduce the intensity of their response. Alterations in osteocyte-mediated regulation of bone remodelling in response to mechanical loading by metal ions will have significant detrimental effects on bone health.

References: 1. Andrews, RL et al. Bone (2011), 49; 717-723

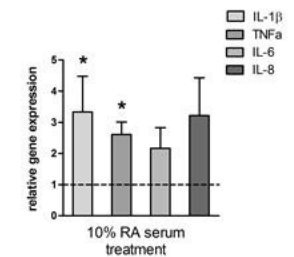
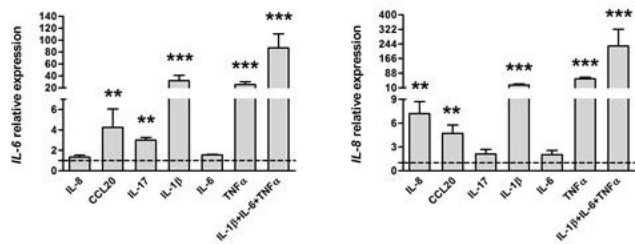
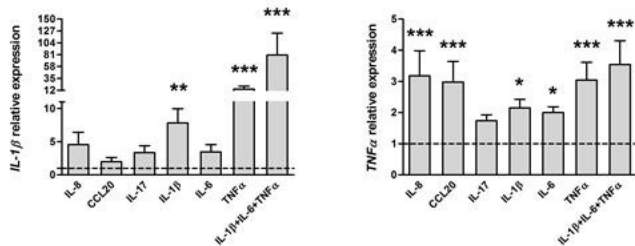
Disclosures: Karan Shah, None.

SU0241

RANKL Expressed by Osteocytes is Required for the Increase in Bone Marrow B lymphocytes and Bone Loss Caused by Estrogen Deficiency. Yuko Fujiwara*¹, Marilina Piemontese¹, Jinhu Xiong¹, Yu Liu¹, Priscilla Baltz¹, Stavros Manolagas¹, Charles O'Brien². ¹University of Arkansas for Medical Sciences & Central Arkansas Veterans Healthcare System, USA, ²Central Arkansas VA Healthcare System, Univ of Arkansas for Medical Sciences, USA

Cancellous bone loss caused by estrogen deficiency requires RANKL produced by B lymphocytes and is mimicked by estrogen-receptor alpha deletion from osteoclast precursors. These studies demonstrate that estrogen controls cancellous bone resorption via diverse mechanisms. Under physiological conditions, RANKL produced by osteocytes is essential for osteoclast formation in remodeling cancellous bone. Here we examined whether RANKL produced by osteocytes is also required for the bone loss caused by estrogen deficiency. Mice lacking RANKL in osteocytes, hereafter referred as conditional knockout (KO) mice, were generated by crossing mice harboring a RANKL conditional allele with Dmp1-Cre transgenic mice, which causes Cre-mediated recombination in mature osteoblasts and osteocytes. Ovariectomy and sham operations were performed on 6-month-old conditional KO mice and control littermates and tissues were harvested 6 weeks later. Uterine weight was decreased by ovariectomy in both control and conditional KO mice. As expected, ovariectomy caused bone loss in the spine of control mice as measured by DXA but this did not occur in conditional KO mice. Micro-CT analysis revealed that ovariectomy caused loss of vertebral cancellous bone and femoral cortical bone in control mice but these changes were prevented in conditional KO mice. Consistent with previous studies, ovariectomy increased the number of B lymphocytes in the bone marrow. However, this change was also abrogated in the conditional KO mice. In a separate experiment, estrogen receptor alpha was deleted from the entire B cell lineage using the CD19-Cre driver strain. However, this maneuver did not alter B cell number in intact mice and had no effect on the increase in B cell number caused by ovariectomy. Taken together, these results demonstrate that RANKL expressed by osteocytes is required for the cancellous and cortical bone loss, as well as the increase in B cell number, caused by estrogen deficiency. Moreover, they suggest that estrogen control of B cell number is indirect via osteocytes and that the increase in bone marrow B cell number may be a necessary component of the cascade of events that lead to cancellous bone loss during estrogen deficiency.

Disclosures: Yuko Fujiwara, None.



RA-serum, cytokines or chemokines enhanced cytokine gene expression by human osteocytes

Disclosures: Janak L. Pathak, None.

SU0239

Isolating osteocytes from human trabecular bone. Matthew Prideaux*, Christine Schutz, David Findlay, Lucian Solomon, Gerald Atkins. University of Adelaide, Australia

While several murine osteocyte-like cell lines are available and techniques for isolating osteocytes from mouse bone have been described, few models exist for studying human osteocytes *in vitro*. We have developed a method for isolating osteocytes from bone taken from patients undergoing knee arthroplasty. Trabecular bone was dissected and washed to remove marrow and subjected to sequential digestions in collagenase/EDTA. Cells were harvested after each digest, plated on collagen coated wells and cultured over a 5 day time course. Osteocyte gene expression was analysed by RT-PCR and cell morphology examined by phalloidin staining. Cells harvested from digests 1 and 2 expressed low levels of the osteocyte markers *SOST* and *DMP1*, with increased levels observed in digests 3 and 4. The highest levels of these markers were observed in digests 5 and 6, with a 20-fold increase in *DMP1* and a 9-fold increase in *SOST* mRNA compared to digest 1. *FGF23* mRNA expression was absent in the early digests but was observed from digest 3 onwards, increasing up to 150-fold in expression in digest 6. The osteocyte markers *PHEX* and *MEPE* were also expressed in the isolated cells and were increased in the later digests. The cells isolated in digests 1 and 2 displayed a mixed morphology, with osteoblast-like cells and some dendritic osteocyte-like cells after 5 days of culture. Digests 3-6 contained many highly dendritic cells, which were initially observed after 2 days of culture and increased in number and dendricity after 5 days. Treatment of isolated cells from digests 3-6 with PTH or 1,25(OH)₂vitaminD₃ for 24 hours resulted in the downregulation of *SOST* and upregulation of *FGF23* mRNA levels, respectively, similar to osteocytes *in vivo*. In conclusion, we have developed a reproducible method of isolating osteocytes from human bone. Such cells will be invaluable for furthering osteocyte research.

Disclosures: Matthew Prideaux, None.

SU0242

Sclerostin expression in osteocytes of alveolar bone in streptozotocin-induced diabetic rats with ligature-induced periodontitis. Ji-Hye Kim^{*1}, Dong-Eun Lee², Eun-Jung Bak², Yun-Jung Yoo². ¹College of Dentistry, South Korea, ²Yonsei University Dental college, South Korea

Osteocytic sclerostin inhibits bone formation and its expression is stimulated by tumor necrosis factor (TNF)- α . We investigated sclerostin and TNF- α expression in diabetic rats with periodontitis. Rats were divided into control (C), periodontitis (P), and diabetes + periodontitis (DP) groups. After induction of diabetes by streptozotocin, periodontitis was induced by ligature. At day 0 (control) and at days 3 and 20 after induction of periodontitis, alveolar bone, osteoclasts, osteoid, and TNF- α and sclerostin expression were evaluated. The cementoalveolar junction-alveolar bone crest distance of the DP group was longer than that of the P group at day 20 after induction of periodontitis, but the number of osteoclasts was not different. Osteoid area decreased in both the P and DP groups by day 3, but while sustained osteoid suppression was observed in the DP group at day 20, osteoid formation was increased in the P group. The number of sclerostin-positive osteocytes increased in both groups at day 3, but, the increased number of sclerostin-positive osteocytes was maintained only in the DP group through day 20. The number of TNF- α positive cells increased more in the DP group than in the P group. Enhanced alveolar bone loss, suppressed bone formation, and prevalent TNF- α expression were characteristic of the DP group compared to the P group. Suppressed bone formation in the DP was observed simultaneously with increased sclerostin and TNF- α expression. These results suggest that up-regulated osteocytic sclerostin expression in periodontitis with diabetes may play a role in suppressed bone formation.

Disclosures: Ji-Hye Kim, None.

SU0243

Bidirectional Notch Signaling Activated by Interactions Between Multiple Myeloma Cells and Osteocytes Drives Tumor Cell Proliferation and Osteoclast Recruitment. Jesus Delgado-Calle^{*}, Judith Anderson, Meloney D. Cregor, Khalid S. Mohammad, Lilian I. Plotkin, Teresita Bellido, G. David Roodman. Indiana University School of Medicine, USA

Multiple Myeloma (MM) is characterized by growth of monoclonal plasma cells in the bone marrow, increased bone resorption, concomitant reduced bone formation, and increased osteocyte apoptosis. The role in MM of matrix-embedded osteocytes, which comprise more than 95% of bone cells and are major regulators of osteoclast and osteoblast activity, is unclear. We investigated the mechanism(s) that trigger osteocyte apoptosis and its significance for MM cell growth and associated bone disease. We found that apoptosis of murine osteocytic MLO-A5 cells is induced by interactions with MM cells lines of murine and human origin as well as with primary CD138+ plasma cells from MM patients, and is blocked by the caspase3 inhibitor DEVD. In addition, apoptosis measured at 8h-24h is abolished by the Notch inhibitor GSIXX, whereas apoptosis measured at 48h is only fully inhibited with a combination of GSIXX and a neutralizing anti-TNF α antibody. These findings demonstrate that osteocyte apoptosis induced by MM is triggered by Notch activation and sustained by MM-derived TNF α . Further, interactions with MM cells increased osteocytic RANKL expression (3-fold) and increase the recruitment of osteoclast precursors by 50% compared to osteocytes cultured alone. These effects were inhibited by blocking osteocyte apoptosis with DEVD or by the combination of GSIXX and anti-TNF α . CD138+ cells from MM patients also increased osteocytic RANKL expression. Further, the percentage of apoptotic and RANKL-positive osteocytes increased by 100% and 53%, respectively, in tumor bearing bones of a mouse model of human MM. Importantly, interactions with osteocytes reciprocally activated Notch signaling in MM cells and in CD138+ cells from patients. Osteocytic cells increased MM cell proliferation by 50% and cyclinD1 expression by 8-fold, and these effects were blocked in a time- and dose-dependent manner by GSIXX. Moreover, osteocytes upregulated Notch receptor 1-4 in MM cells by 4-8-fold. This altered Notch receptor repertoire could impact tumor growth that is dependent on autocrine and paracrine Notch signaling. Thus, bidirectional Notch signaling between MM cells and osteocytes stimulates MM cell proliferation and induces osteocyte apoptosis, which enhances the osteoclastogenic potential of osteocytes. This study emphasizes the ability of osteocytes to impact the MM niche within the bone marrow and supports development of novel approaches to treat MM bone disease by targeting osteocytes.

Disclosures: Jesus Delgado-Calle, None.

SU0244

Mechanisms of Palmitate-Induced Lipotoxicity in Osteocytes. Krishanthi Gunaratnam^{*1}, Christopher Vidal¹, Gustavo Duque². ¹Musculoskeletal Ageing Research Program, Sydney Medical School Nepean, The University of Sydney, Australia, ²Musculoskeletal Ageing Research Program, University of Sydney, Australia

BACKGROUND: Although apoptosis and autophagy play an important role in the regulation of bone metabolism, the mechanisms triggering these two processes in osteocytes (Ocy) remain poorly understood. We have previously demonstrated that

osteoblasts lose their function and undergo autophagy and apoptosis after exposure to palmitic acid (PA), which is the most prevalent fatty acid within the human bone marrow. Here we hypothesized that, as in osteoblasts, PA has a lipotoxic effect on Ocy affecting their function and survival

METHODS: Wild type MLO-Y4 osteocytic cells derived from murine long bones were plated on 0.01% collagen type I-coated plates and cultured in α -MEM in the presence of either PA (250 and 500mM) or vehicle for 48 hrs. Cell viability was measured using MTS-Formazan. Apoptosis was identified by TUNEL and Annexin V assays. Autophagy was quantified using western blotting for LC3 II and flow cytometry analysis of punctate formation using lysoTracker red fluorescence. Finally, changes in Ocy-secreted proteins (sclerostin [Sost], Dickkopf-related protein 1 [Dkk1] and receptor activator of nuclear factor kappa-B ligand [RANKL]) were determined by western blot.

RESULTS: Treatment with PA induced significantly higher levels of cell death (~40%, $p < 0.001$) in a time- and dose-dependent manner. PA induced high levels of apoptosis in MLO-Y4 cells (~35%, $p < 0.001$), with PA-treated cells showing a significantly higher percentage of cytoplasmic area occupied by cytochrome C after 48h of treatment ($p < 0.001$). In addition, we found a dose-dependent failure in autophagy in PA-treated Ocy ($p < 0.01$). Finally, PA treatment induced higher levels of Sost, Dkk1 and RANKL expression in a dose-dependent manner.

CONCLUSION: In summary, we have identified a previously unknown effect of PA on Ocy, which not only corresponds to lipotoxicity but also could explain the high levels of apoptosis and failure in autophagy observed in aged and osteoporotic bone. In addition, PA had an effect on Ocy-secreted factors, which could have a significant effect on bone metabolism *in vivo* that deserves further exploration. In conclusion, the regulation of fatty acid secretion and the inhibition of lipopoptosis would protect Ocy against fat and could become a potential therapeutic target for osteoporosis in the future.

Disclosures: Krishanthi Gunaratnam, None.

SU0245

Association between plasma sphingosine 1-phosphate levels and incident fractures in postmenopausal women: A 3-year follow-up observation study. Seung Hun Lee^{*1}, Sung Jin Bae², Hyeonmok Kim³, Seong Hee Ahn³, Beom-Jun Kim³, Jae Suk Chang⁴, Jung-Min Koh³. ¹Asan Medical Center, University of Ulsan College of Medicine, South Korea, ²Health Screening & Promotion Center, Asan Medical Center, University of Ulsan College of Medicine, South Korea, ³Division of Endocrinology & Metabolism, Asan Medical Center, University of Ulsan College of Medicine, South Korea, ⁴Department of Orthopedic Surgery, Asan Medical Center, University of Ulsan College of Medicine, South Korea

Sphingosine 1-phosphate (S1P) has been recognized as a significant regulator of bone metabolism. Recently we found that higher plasma S1P levels were associated with lower bone mineral density (BMD), higher bone resorption marker, and higher risk of prevalent vertebral fracture in postmenopausal women. The objective of the study was to investigate the possibility of S1P as a biomarker for incident fracture risk and insufficient response to bisphosphonate therapy. A total 263 postmenopausal women participated in this 3-year longitudinal study conducted in a clinical unit in Korea. Postmenopausal women were untreated (n = 79) and treated with bisphosphonate, hormone-treated, or selective estrogen receptor modulator (n = 184) with a mean 3.5 years follow-up. Vertebral fracture and non-vertebral fractures were assessed at both baseline and follow-up visits. BMD and bone turnover markers were measured at both baseline and follow-up visits. Plasma S1P levels were obtained from all subjects at the baseline visits. Prevalent fractures were identified in 57 of 263 (21.7%) in this study. Higher plasma S1P levels were significantly associated with higher rate of prevalent fracture after adjustment for femur neck (FN) BMD and potential confounders [Odds ratio (OR): 2.13, 95% confidence interval (CI): 1.08 - 4.22]. A total of 9 (3.4%) incident fractures occurred during the follow-up periods. The fracture-event rate was 95.1 per 10,000 person-years. Subjects with incident fracture had higher plasma S1P levels (mean: 5.87 $\mu\text{mol/L}$, 95%CI: 3.82 - 8.94 $\mu\text{mol/L}$) compared with those without incident fracture (mean: 3.63 $\mu\text{mol/L}$, 95%CI: 3.36 - 3.94 $\mu\text{mol/L}$) even after adjusted for prevalent fracture, FN BMD, anti-osteoporotic medication, annualized changes in FN BMD, and potential confounders ($P = 0.034$). Incident fracture more frequently occurred in the highest plasma S1P tertile group than in the lower two tertile groups [hazard ratio (HR): 5.12, 95% CI: 1.02 - 34.48]. Even after adjustments with confounders including baseline FN BMD, prevalent fracture, anti-osteoporotic medication, annualized changes in FN BMD, and potential confounders, incident fracture more frequently occurred in the highest S1P tertile group (HR: 7.30, 95% CI: 1.05 - 75.75). The OR for insufficient response to bisphosphonate therapy in the highest S1P tertile was 5.03 (95% CI: 1.03 - 24.47), compared with those in the lower two tertile groups. These findings suggest that plasma S1P may be a potential biomarker for the risk of osteoporotic fracture and insufficient response to bisphosphonate therapy in postmenopausal women.

Disclosures: Seung Hun Lee, None.

SU0246

Profiling C3-Epi-25-Hydroxyvitamin D₃ concentrations in paediatric populations as determined by LC-MS/MS. Jonathan Tang^{*1}, Holly Nicholls², Milka Budnik-Zawilska², Paul Brookes³, John Dutton², Isabelle Picc², Christopher Washbourne², William Fraser². ¹University of East Anglia, Norwich, UK, United Kingdom, ²University of East Anglia, United Kingdom, ³Norfolk & Norwich University Hospitals, United Kingdom

Background: The C-3 Epimer of 25 Hydroxyvitamin D₃ (3-epi-25OHD₃) is produced in the liver by the epimerisation pathway of 25-hydroxy vitamin D₃. It differs from 25OHD₃ in configuration of the hydroxyl group at the third carbon (C-3) position. Despite the fact that little is known regarding its clinical significance, higher concentrations 3-epi-25OHD₃ have been reported in paediatric populations than in adults, and that concentration decreases with age.

Objective: This study profiled the concentrations of 3-epi-25OHD₃ in samples from patients of age 0-12 years. A LC-MS/MS technique was developed to resolve and quantify 3-epi-25OHD₃ from 25OHD₃. Commercially available NIST (SRM972a) traceable 3-epi-25OHD commercial standards were used to ensure assay accuracy.

Method: Serum was precipitated with zinc sulphate and acetonitrile containing [³H]-3-epi-25OHD₃ as internal standard. The extract was chromatographed using a 2.6µm 100 x 2.1mm I.D. solid core pentafluorophenyl bonded phase column. Mass detection and quantification were performed by positive electrospray ionization with MS/MS in multiple reaction monitoring mode.

Results: The method was able to fully resolved 3-Epi-25OHD₃ from 25OHD₃. The intra-assay and inter-assay CVs were the epimer were within 8% across the analytical range. In our sample cohort with 25OHD₃ ranged between 7.4 – 185 nmol/L, mean 73 nmol/L. C3-epi-25OHD₃ was detected in 89.7% of samples, mean 3.8 nmol/L ranged between 0.8 - 50.8 nmol/L. Relative percentage of 3-epi-25OHD₃ to 25OHD₃ was averaged at 12%. **Conclusion:** We observed a two fold increase in average concentration of 3-epi-25OHD₃ in paediatric population compare to our previous study on adult population (poster SA0004, ASBMR 2014) and higher concentration was found in neonates than in older children. Our findings showed the level of 3-epi-25OHD₃ in infant contributed to the overestimation of 25OHD₃ that could potentially result in misinterpretation of total vitamin D status. Measurement of 3-epi-25OHD₃ should be included clinical investigations and epidemiological studies of paediatric and infant populations.

Disclosures: Jonathan Tang, None.

SU0247

Surgery Alters Laboratory Results: Implications for Fracture Liaison Services. Neil Binkley^{*1}, Gretta Borchardt², Ellen Fidler², Jessie Libber², Diane Krueger², Paul Iglar², Joan Lappe³, John Heiner⁴, Richard Illgen⁴, Matthew Squire⁴, Douglas Coursin⁵, Kirk Hogan⁵. ¹University of Wisconsin, Madison, USA, ²University of Wisconsin, USA, ³Creighton University, USA, ⁴University of Wisconsin Department of Orthopedics, USA, ⁵University of Wisconsin Department of Anesthesiology, USA

Background: Fracture liaison services (FLS) are advocated internationally to improve osteoporosis care. As secondary causes of osteoporosis are common, FLS programs often perform laboratory testing. Indeed, a proposed Joint Commission quality measure will require fragility fracture patients to have specified lab tests “ordered or performed” prior to hospital discharge. We hypothesize that lab tests obtained immediately after surgery, e.g., post hip fracture repair, do not accurately indicate an individual’s baseline status.

Methods: Individuals having elective hip total arthroplasty were studied as a surrogate for hip fracture patients. In this ongoing study, 26 adults; 18 women/8 men (mean age 65.0 [8.0] range 53 to 82 years) had blood obtained ~2 wks before surgery, the morning of surgery before anesthesia, at post-op day 1 (POD#1) and at a 6 wk follow-up visit. Hemoglobin (Hgb), serum 25(OH)D, creatinine, calcium, albumin (Alb) and alkaline phosphatase (ALP) were measured at all timepoints.

Results: Of 26 subjects having surgery; 19 had regional, 4 general and 3 combined anesthesia. Mean (SD) estimated blood loss and IV fluid administration during surgery and in the recovery room were 298 (142) mL and 1757 (652) mL respectively. Pre-operative lab results were stable from 2 wks pre-op to day of surgery. Serum calcium, creatinine, ALP, 25(OH)D, Alb and Hgb declined by 11-27% (p < 0.0001) at POD#1 (Table). Calcium, albumin, 25(OH)D and Hgb declined in 100% of subjects. Lab values returned to normal in the 10 subjects with data available at 6 weeks.

Conclusion: Laboratory tests proposed for FLS quality metrics are uniformly and significantly reduced after elective total hip arthroplasty. Similar decrements after fragility fracture surgery are likely. Accordingly, lab test results immediately following surgery do not ascertain a patient’s baseline status; this may lead to incorrect diagnoses/interventions and inappropriately consumes limited healthcare resources. Evaluation for secondary causes of osteoporosis should not be performed immediately post-operatively but rather should be done at a subsequent follow-up visit.

Table 1: Laboratory values (n = 26)

| Timepoint | Analyte | Hgb (g/dL) | Calcium (mg/dL) | Creatinine (mg/dL) | ALP U/L | Alb (mg/dL) | 25(OH)D (ng/mL) |
|----------------|---------|------------|-----------------|--------------------|-------------|-------------|-----------------|
| 2 weeks pre-op | | 13.7 (1.2) | 9.5 (0.4) | 0.84 (0.16) | 80.5 (19.2) | 4.1 (0.3) | 34.9 (15.3) |
| Day of surgery | | 13.5 (1.3) | 9.2 (0.5) | 0.86 (0.17) | 79.4 (19.3) | 3.8 (0.3) | 34.9 (14.7) |
| POD#1 | | 10.8 (1.2) | 8.3 (0.3) | 0.76 (0.16) | 55.7 (14.0) | 3.0 (0.2) | 27.0 (12.3) |

Data as mean (SD)

Table

Disclosures: Neil Binkley, None.

SU0248

Characteristics of mandibular cortical layer between osteoporotic and normal patients : 3D volumetric analysis with CBCT. Jin-Sun Jeong^{*1}, Yumie Rhee², Jisun Huh³, Kyeong-Mee Park⁴, Yu Gu⁵, Kee-Deog Kim⁴, Wonse Park³. ¹Department of Advanced General Dentistry, Yonsei University College of Dentistry, South Korea, ²Department of Internal Medicine, Endocrine Research Institute, Yonsei University College of Medicine, South Korea, ³Department of Advanced General Dentistry, Yonsei University College of Dentistry, South Korea, ⁴Department of Advanced General Dentistry, College of Dentistry, Yonsei University, South Korea, ⁵Department of Conservative Dentistry, Seoul National University, South Korea

Background: Early detection of osteoporosis is very important for patient’s prognosis. Panoramic radiography is common diagnostic aids not only for general dental evaluation but also for the detection of osteoporosis using inferior cortical layer. However, it is 2D measurement of 3D structure so the errors between inter and intra observer is a problem. Recently, dental cone beam computed tomography (CBCT) is widely used in dental clinic to get 3D skeletal structure of jaw bones with low radiation dose. In this study, we tried to find regional characteristics of mandibular cortical bone with 3D volumetric analysis using CBCT.

Methodology: 20 osteoporotic and normal female patients were included this study. Five parameters using CBCT for RCT (Ramus Cortical bone Thickness), ACT (Angular cortical bone thickness), AI (Antegonial index), and MCW (mandibular cortical width) of mandible were measured using a ROI (region of interest) tool of CTan program at both grayscale 80-120 and 120-200. The t-test was used to determine significance. (P < .05)

Results: Significant differences were found in RCT and ACT through grayscale 120-200 and ACT and AI through grayscale 80-120 from the CBCT images between the patients with and without osteoporosis.

Conclusions: Cortical bone analysis of mandible with CBCT might be effective for early detection of osteoporosis, but site specific evaluation is mandatory.

Disclosures: Jin-Sun Jeong, None.

SU0249

Examining the Calcaneus Using HRpQCT: Method Reproducibility and Regional Trabecular Variation. Louis Metcalf^{*1}, John Rochester², Nicolas Vilayphiou³, Margaret Paggiosi², Eugene McCloskey². ¹University of Sheffield, United Kingdom, ²University of Sheffield, United Kingdom, ³SCANCO Medical AG, Switzerland

High resolution peripheral quantitative computer tomography (HR-pQCT) assesses volumetric bone density (vBMD) and microstructure at distal sites in the radius and tibia. The calcaneus is equally accessible, has a thinner cortex, is rich in trabecular bone and calcaneal measurements (e.g. quantitative ultrasound) can assess fracture risk. We wished to develop a technique for HR-pQCT scanning of the calcaneus.

The calcanei of 21 cadaveric leg/foot specimens (tibia present=15, tibia absent=6) were each scanned twice in situ, with repositioning, using the XtremeCT (SCANCO Medical AG). All specimens were scanned at an integration time of 100ms and a subset (n=11) also at 200ms. Scans were obtained in the transverse plane centred on the midpoint of the calcaneus (Figure) between the Achilles tendon attachment and flexor digitorum brevis attachment (defined as the height of the calcaneus). This central region was divided into 3 equal 110-slice sections (inferior, middle and superior) and underwent a standard evaluation analysis using a 12.25 x 12.25 x 9.02mm volume of interest (excluding cortical bone). Parameters included vBMD, trabecular number (Tb.N), trabecular spacing (Tb.Sp) and trabecular thickness (Tb.Th).

The mean repositioning error for height measurements was 2.50% but was lower in specimens with the tibia present (0.51% [95% CI: 0.21%, 0.80%]) rather than the foot alone (5.83% [95% CI: 0.74%, 10.92%]). All of the measured parameters showed good reproducibility between scans (R²>0.867, p<0.001). The vBMD and Tb.Th was significantly higher in the superior section compared to the middle and inferior sections (Table), with no significant differences between the latter sections. Increasing the scan integration time from 100ms to 200ms led to an apparent decrease in Tb.N

(-19%, p=0.013) and an increase in Tb.Sp (+34%, p=0.033), with no effect on vBMD or Tb.Th.

Reproducibility has been demonstrated for measurements of density and trabecular morphology in cadaveric calcanei using HR-pQCT. Future studies will compare our findings with micro-CT and examine reproducibility in vivo. Examining specific regions of the calcaneus may prove useful in assessing response to treatment and mechanical loading, as well as fracture risk prediction.

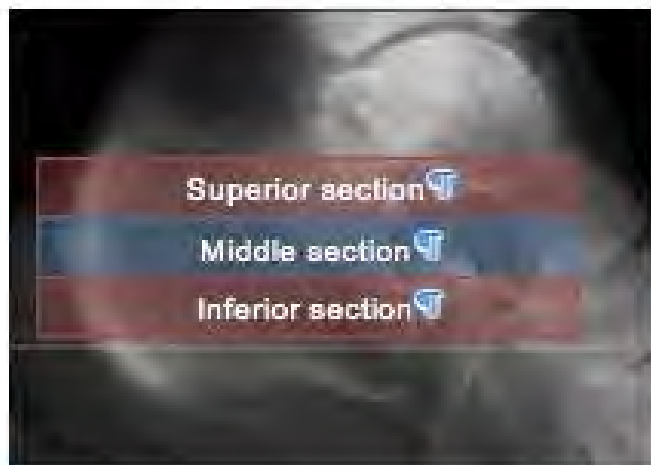


Figure. HR-pQCT scan region and slice section positioning on the calcanei

Figure. HR-pQCT scan region and slice section positioning on the calcanei

Table. HR-pQCT measurements for the three different slice sections in cadaveric calcanei (n=21 at 100ms integration time)

| Parameters | Inferior section | Middle section | Superior section |
|-------------------------------|---------------------|----------------------|---------------------|
| vBMD (mg HA/cm ³) | 70 (43.4-96.5) | 82.5 (67.1-117.9)* | 168.9 (137.8-200) |
| Tb.N (mm ⁻¹) | 2.54 (2.27-3.60) | 2.78 (2.47-3.53) | 2.72 (2.45-3.49) |
| Tb.Th (mm) | 0.015 (0.007-0.024) | 0.022 (0.013-0.031)* | 0.046 (0.040-0.053) |
| Tb.Sp (mm) | 0.372 (0.252-0.422) | 0.324 (0.254-0.383) | 0.314 (0.234-0.362) |

vBMD and Tb.Th as mean (95% CI). Tb.N and Tb.Sp as median (IQR).
*Differs from the superior section using ANOVA with Bonferroni correction (p<0.001)

Table. HR-pQCT measurements for the three different slice sections in cadaveric calcanei (n=21 at 10

Disclosures: Louis Metcalf, None.

SU0250

Microindentation Assessed Bone Material Strength Is Associated with Cortical Porosity and Subcutaneous Fat in Older Women. Daniel Sundh^{1*}, Robert Rudäng², Michail Zoulakis², Anna Darelid², Mattias Lorentzon². ¹Institute of Medicine, Sahlgrenska Academy, Sweden, ²GERIATRIC MEDICINE, INSTITUTE OF MEDICINE, Sweden

Microindentation is a novel method to measure actual bone material strength (BMS) in vivo in humans. The association between cortical microstructure and BMS in vivo has not previously been reported.

The aim of this study was to investigate if BMS was associated with cortical bone geometry and microstructure in a population based cohort of 211 women (78.3 ± 1.1 years (mean ± SD)). Bone parameters were measured at the radius and tibia with a High Resolution pQCT (XtremeCT, Scanco Medical). Images were obtained using the manufacturer's recommended standard program (ultradistal site) and at an additional measuring site, at 14% of the bone length. BMS was assessed by four operators using the Osteoprobe® (Active Life Scientific) device, and calculated as the mean of at least 11 valid reference point indentations performed at the midtibia of the non-dominant leg. The coefficient of variation for the method was 3.2%, calculated by duplicate measurements performed on 30 study subjects.

BMS was not associated with age or height, but an inverse association was found for body weight (r=-0.14, p=0.04) and BMS differed by operator (Anova p<0.01). BMS, adjusted for body weight and operator, was correlated to cortical porosity, cortical volumetric BMD and cortical area at the proximal tibial section but not with bone parameters at any other bone site (Table 1). A negative correlation was seen between operator adjusted BMS and total body fat (r=-0.18, p=0.01) but not with total body lean mass (r=-0.10, p=0.15). BMS was associated with DXA-derived fat mass (r=-0.18, p=0.01) rather than lean mass (r=-0.13, p=0.07) at the measured leg. The strongest association between BMS and adipose tissue (r=-0.31, p<0.001) was observed for subcutaneous (s.c) fat (measured using the HR-pQCT images). S.c. fat

was also associated with cortical porosity (r=0.21, p<0.01) and cortical vBMD (r=0.20, p<0.01) at the proximal tibial site.

In a population-based sample of older women, low BMS was associated with reduced cortical vBMD and high porosity, but the associations were apparent only at CT-measurements performed in close proximity to the indentation site, indicating that BMS does not reflect cortical bone microstructure in general. Furthermore, s.c. fat near the indentation site was most strongly associated with BMS and also with cortical porosity and density, indicating a possible adverse effect of adipose tissue on bone material properties and bone microstructure.

Table 1. Correlations between adjusted BMS and bone parameters

| | Tibia | Tibia | Radius | Radius |
|---------------------------------|--------------|---------------------|--------------|--------------|
| | ultradistal* | proximal* | ultradistal* | proximal* |
| Cortical porosity | -0.02 (0.77) | -0.14 (0.04) | -0.02 (0.85) | 0.02 (0.83) |
| Cortical volumetric BMD | 0.10 (0.16) | 0.17 (0.02) | 0.04 (0.65) | 0.004 (0.96) |
| Cortical area | 0.10 (0.16) | 0.16 (0.03) | 0.11 (0.17) | 0.12 (0.11) |
| Trabecular bone volume fraction | 0.12 (0.08) | 0.03 (0.67) | 0.08 (0.29) | 0.04 (0.60) |

Results presented as correlation factors together with a p-value within the parenthesis.

p-value < 0.05 was regarded significant and illustrated in bold numbers.

BMS was adjusted for operator and weight.

*202 measurements with adequate quality for the tibia measurements

*170 measurements with adequate quality for the radius measurements

Table 1. Correlations between adjusted BMS and bone parameters

Disclosures: Daniel Sundh, None.

SU0251

The Canadian Multicentre Osteoporosis Bone Quality Study (CaMos BQS): Baseline Comparison of HR-pQCT and pQCT and Fracture Associations.

Andy Kin On Wong^{1*}, Claudie Berger², George Ioannidis³, Karen Beattie³, Christopher Gordon³, Laura Pickard³, Alexandra Papaioannou⁴, David Goltzman², Jerilynn Prior⁵, Heather Macdonald², Maureen Ashe⁵, Leigh Gabel⁵, Danmei Liu⁶, Steve Boyd⁷, Lauren Burt⁷, Michelle Kan⁷, Kyle Nishiyama⁸, Saija Kontulainen⁹, Andrew Frank-Wilson⁹, Chantal Kawalilak⁹, Wojciech Olszynski⁹, K. Shawn Davison¹⁰, Lora Giangregorio¹¹, Robert Josse¹², Eva Szabo¹³, Marta Erlandson⁹, Tassos Anastassiades¹⁴, Norma MacIntyre³, Angela M. Cheung¹³, Jonathan D. Adachi³. ¹University Health Network, Ca, ²McGill university, Canada, ³McMaster University, Canada, ⁴Hamilton Health Sciences, Canada, ⁵UBC, Canada, ⁶CHHM, Canada, ⁷University of Calgary, Canada, ⁸Columbia University, USA, ⁹University of Saskatchewan, Canada, ¹⁰University of Victoria, Canada, ¹¹University of Waterloo, Canada, ¹²St. Michael's Hospital, Canada, ¹³UHN, Canada, ¹⁴Queens University, Canada

Objectives: 1) to validate pQCT bone measures against HR-pQCT; 2) to compare pQCT and HR-pQCT bone measures in their association with fractures. Study design: cross-sectional analyses of a population-based cohort study. Inclusion: Women 60-85 within 6 CaMos centres were approached (N=1066). pQCT: A 2.3 ± 0.5mm thick slice was prescribed at 4% distal radius and tibia (200 µm in-plane resolution). HR-pQCT: 110 slices were acquired at the ultradistal radius and tibia (82 µm isotropic). Image processing: Bone from pQCT slices was segmented using region-growing (OsteoQ, ISS). Bone from HR-pQCT images was segmented using a dual-threshold algorithm (ScanCo). Clinical data: Fractures (low trauma, all trauma, and ever fracture) in the last 15 years were obtained from CaMos. Data analyses: Linear regression analysis determined slopes and intercepts regressing HR-pQCT on pQCT bone measures. Binary logistic regression models examined the association between bone measures from each modality and fractures. Odds ratios were reported with 95% confidence intervals. Analyses were performed for each modality separately. Alternatively, bone measures from pQCT were pooled with HR-pQCT measures after cross-calibration. All models adjusted for age and BMI. Results: In 644 women (mean age: 72 ± 7 years and BMI: 27.68 ± 5.33 kg/m²), linear regression analyses showed significant associations between all pQCT-derived bone parameters and corresponding outcomes on HR-pQCT (R²=0.122-0.908). Bone volume fraction (BTVF) from pQCT images explained the largest variance (R²=0.908) in HR-pQCT images. A larger number of pQCT and HR-pQCT bone parameters associated with fractures by including those who have ever had a fracture as compared to all or low trauma (ORs ranged: 1.28-1.92). At both anatomical sites, HR-pQCT yielded a larger number of parameters that associated with fractures than pQCT. When cross-calibrated pQCT parameters were pooled with HR-pQCT data (Table 1), effect sizes remained similar to that prior to pooling. Smaller fracture numbers for all and low trauma fractures precluded the observation of significant findings. However, by pooling cross-calibrated data, Ct.Th at the radius (2.76(1.16,6.57)) and Tb.Th at the tibia (2.23(1.07,4.63)) were associated with low trauma fractures. Conclusions: Pooling HR-pQCT and cross-calibrated pQCT data yielded stronger associations with fractures. Study centres with poor access to HR-pQCT technology could use pQCT as a valid alternative.

Table I. Comparison of significant associations with fractures (ever) observed at the tibia versus the radius based on pooled sample of HR-pQCT and cross-calibrated pQCT bone parameters.

| Variable | TIBIA | | | | RADIUS | | | |
|----------|---------|-------|--------|--------|--------|-------|--------|--------|
| | UNIT | OR | 95%Low | 95%Upp | UNIT | OR | 95%Low | 95%Upp |
| vBMDi | -119.90 | 1.067 | 0.907 | 1.256 | -77.50 | 1.3 | 1.085 | 1.557 |
| vBMDtr | -78.00 | 1.076 | 0.909 | 1.274 | -75.06 | 1.133 | 0.948 | 1.355 |
| vBMDc | -115.40 | 1.181 | 0.982 | 1.421 | -96.87 | 1.401 | 1.146 | 1.713 |
| BVTv | -0.029 | 1.348 | 1.133 | 1.603 | -0.031 | 1.4 | 1.162 | 1.688 |
| CTTh | -0.271 | 1.297 | 1.074 | 1.567 | -0.199 | 1.363 | 1.115 | 1.666 |
| TbSp | 0.134 | 1.203 | 0.999 | 1.448 | 0.191 | 1.447 | 1.143 | 1.832 |
| TbN | -0.346 | 1.119 | 0.944 | 1.326 | -0.347 | 1.315 | 1.087 | 1.59 |
| TbTh | -0.014 | 1.242 | 1.048 | 1.472 | -0.011 | 1.179 | 0.982 | 1.415 |

Table I

Disclosures: *Andy Kin On Wong, None.*

SU0252

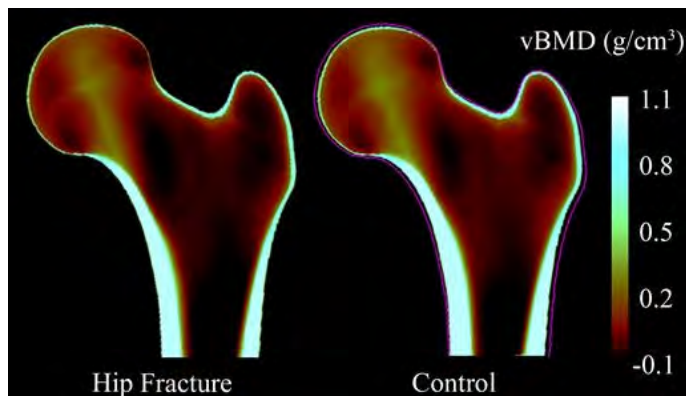
Cortical and Trabecular Bone Analysis of Hip Fracture Patients using 3D-DXA. Alexis Bague¹, Luis Del Rio Barquero², Silvia Di Gregorio², Yves Martelli³, Miguel A. González Ballester⁴, Ludovic Humbert*³. ¹SIMBioSys – Simulation, Imaging & Modelling for Biomedical Systems, Universitat Pompeu Fabra, Spain, ²CETIR Grup Medic, Spain, ³Galgo Medical, Spain, ⁴SIMBioSys – Simulation, Imaging & Modelling for Biomedical Systems, Universitat Pompeu Fabra - ICREA, Spain

The purpose of this study is to analyze the cortical and trabecular bone of hip fracture patients and controls using 3D-DXA.

A retrospective study was carried out to collect 128 DXA scans of post-menopausal Caucasian women (CETIR Grup Medic, Barcelona), including 64 patients with a hip fracture event occurring between one and 6 years from baseline and 64 age-matched controls without any osteoporotic fracture during at least a 6 years follow-up. None of the patients had osteoporotic fracture at baseline. 3D-DXA was used to obtain patient-specific models from the baseline DXA projections. The 3D-DXA technology provides a three dimensional analysis of the femoral shape and bone density distribution from a single Dual energy X-ray Absorptiometry (DXA) scan, allowing for a separate assessment of cortical and trabecular bone. The algorithm performs the registration of a 3D appearance model incorporating statistical information about the femoral shape and density onto the 2D DXA image. From the resulting patient-specific models, the volumetric BMD (vBMD), BMC, volume (for trabecular and cortical regions) and cortical thickness distribution can be automatically quantified. The clinical parameters were compared over both groups using the Student's t-test.

No statistically significant differences were found between the average age, weight, height and BMI of both groups. Fracture group femurs were bigger than controls (p = 0.007), and had a lower vBMD in both cortical (p = 0.001) and trabecular (p < 0.001) compartments. The average cortical thickness was also lower for fracture group (1.49 mm) than for controls (1.63 mm, p < 0.001).

By providing a detailed analysis of cortical and trabecular bone in 3D using DXA modality, 3D-DXA could potentially improve the management of osteoporosis in clinical routine.



E:\Presentations - Publications - Congres\Journal Papers\3D-DXA Alexis\Figures

Disclosures: *Ludovic Humbert, None.*

SU0253

Dynamically Filtered Control of X-ray Flux Maintains Precision and Accuracy Over Wide Tissue Thicknesses in the Norland DXA System. Pat Cunniff¹, Joe Joyce¹, Jing Mei Wang², Tom Sanchez*³. ¹Bone Health Division, Norland at Swissray, USA, ²Bone Health Division, Norland at Swissray, China, ³Norland at Swissray, USA

As in any x-ray assessment, precision and accuracy of measured tissue content can suffer with varying tissue thicknesses as the study is compromised by beam hardening or detector saturation or starvation. The current study examined the performance of a dynamically filtered Norland DXA system evaluating known materials under widely ranging tissue thickness.

A Norland XR-46 fitted with dynamic filtration and calibrated over a 77-step range to adjust for varying thicknesses of material was used to evaluate a known bone mineral content in tissue ranging between 5cm and 30cm of thickness. Evaluations carried out 25 studies of the known bone material in six thickness level starting at 5cm and advancing in 5cm increments to 30cm. Studies were done at seven scan speeds ranging from 65mm/s to 260mm/s. Studies were evaluated for precision of bone mineral density, lean content and fat content and for accuracy in measured bone mineral density in all scan sets.

Independent of scan speed, the Norland XR-46 studies indicate consistent repeatability (2%) and accuracy (2%) in bone density assessments for studies going up to 25cm in thickness. The table below indicates repeatability as a %CV and accuracy as a ratio of measured bone density to true bone density at evaluated scan speeds and tissue thicknesses.

| | 5cm | 10cm | 15cm | 20cm | 25cm | 30cm |
|---------|-----------|-----------|-----------|-----------|-----------|-----------|
| 65mm/s | 0.3/100.6 | 0.3/99.4 | 0.2/100.8 | 0.6/101.2 | 0.4/102.7 | 0.7/105.7 |
| 97mm/s | 0.4/100.5 | 0.5/99.2 | 0.5/101.0 | 0.6/101.2 | 0.7/103.2 | 0.7/104.5 |
| 130mm/s | 0.4/100.6 | 0.3/99.0 | 0.6/100.8 | 0.5/101.4 | 0.9/103.5 | 0.9/102.4 |
| 162mm/s | 0.5/100.7 | 0.6/100.2 | 0.8/100.8 | 0.7/102.3 | 0.9/104.0 | 0.7/104.5 |
| 195mm/s | 0.5/101.0 | 0.8/100.5 | 0.6/100.6 | 0.8/102.0 | 0.8/103.7 | 1.3/104.0 |
| 227mm/s | 0.5/101.0 | 0.7/100.5 | 0.7/101.2 | 0.7/102.6 | 0.9/103.8 | 1.2/104.2 |
| 260mm/s | 0.5/101.0 | 0.8/100.7 | 0.7/100.6 | 0.9/102.1 | 1.1/103.6 | 1.3/103.8 |

Evaluating the repeatability of lean or fat content over the various tissue thicknesses and scan speeds indicates results are generally within 2.0% of the average measured results.

In conclusion, these studies of a well defined bone phantom demonstrate that when fitted with dynamic filtration the Norland scanner is able to deliver results with good precision and accuracy in studies with tissue thickness up to 30cm thick.

Disclosures: *Tom Sanchez, None.*

SU0254

Reliability and validity of lower extremity computed tomography as a screening tool for osteoporosis. Ki Hyuk Sung*¹, Soon-Sun Kwon², Seung Jun Mun¹, Seung Yeol Lee³. ¹Myongji Hospital, South Korea, ²National University Bundang Hospital, South Korea, ³Ewha Womans University Mokdong Hospital, South Korea

Introduction: This study aimed to evaluate the reliability and validity of CT as a screening tool for osteoporosis and to estimate the correlation between central BMD and peripheral bone attenuation using lower extremity CT. Methods: In total, 292 patients who underwent a lower extremity, lumbar spine, or abdomen and pelvic CT scan within a 3-month interval of a dual-energy X-ray absorptiometry (DEXA) examination were included. Following reliability testing, bone attenuation of the L1, L2, L3, L4, femoral head, femoral neck, greater trochanter, distal femur, proximal tibia, distal tibia, and talus was measured by placing a circular region of interest on the central part of each bony region on a coronal CT image. Partial correlation was used to assess the correlation between CT and DEXA after adjusting for age and body mass index. Results: In terms of reliability, all bone attenuation measurements, except the femoral neck, showed good to excellent interobserver reliability (intraclass correlation coefficients, 0.691–0.941). In terms of validity, bone attenuation of the L1 to L4, femoral neck, and greater trochanter on CT showed significant correlations with BMD of each area on DEXA (correlation coefficients, 0.399–0.613). Bone attenuation of the distal tibia and talus on CT showed significant correlations with BMD of all parts on DEXA (correlation coefficients, 0.493–0.581 for distal tibia, 0.396–0.579 for talus). Conclusion: Lower extremity CT is a useful screening tool for osteoporosis, and peripheral bone attenuation on lower extremity CT adequately reflects central BMD on DEXA.

Disclosures: *Ki Hyuk Sung, None.*

SU0255

Stochastic Predictors from DXA Scans of Human Lumbar Vertebrae Are Correlated with Microarchitecture Parameters of Trabecular Bone. Neil Dong*¹, Rajeshwar Pinninti¹, Amy Twinnereim², Timothy Lowe¹, David Di Paolo¹, Mukul Shirvaikar¹. ¹The University of Texas at Tyler, USA, ²UT Health Northeast, USA

The purpose of this study was to provide a novel stochastic assessment of inhomogeneous distribution of bone mineral density (BMD) from the Dual-energy X-ray Absorptiometry (DXA) scans of human lumbar vertebrae and identify the stochastic predictors that were correlated with the microarchitecture parameters of trabecular bone.

Eighteen human lumbar vertebrae with intact posterior elements from cadaveric spines were scanned in the posterior-anterior projection using a Hologic densitometer (Fig.1a). The BMD map of human vertebrae was obtained from the raw data of DXA scans by directly operating on the transmission measurements of low- and high-energy X-ray beams (Fig.1b). Stochastic predictors, including correlation length, sill variance, and nugget variance, were calculated by fitting a theoretical model onto the experimental variogram of the BMD map (Fig.1c), rather than grayscale images, from DXA scans. The theoretical model represented a comprehensive view, rather than an initial trend, of the experimental variogram. In addition, microarchitecture parameters of trabecular bone in the vertebral body were measured from the 3D images of human vertebrae (Fig.1d) acquired using a Micro-CT scanner.

Significant correlations were observed between stochastic predictors and microarchitecture parameters (Fig.2). The sill variance, to some extent, representing the standard deviation of the BMD map, had significant positive correlations with bone volume fraction ($r=0.621, p=0.006$), trabecular thickness ($r=0.484, p=0.042$), trabecular number ($r=0.611, p=0.007$) and connectivity density ($r=0.515, p=0.029$). The sill variance was also negatively correlated with bone surface to volume ratio ($r=-0.473, p=0.048$) and trabecular separation ($r=-0.614, p=0.007$).

This study demonstrates that the stochastic assessment of the inhomogeneous distribution of bone mineral density from DXA scans of human lumbar vertebrae can reveal microarchitecture information of trabecular bone. In addition, the sill variance observed in this study may represent the point-to-point variations of bone mineral density due to local bone remodeling. A previous study indicated that the standard deviation of vertebral regional bone mineral density values was a good predictor of fracture load. Therefore, stochastic predictors from routine clinical DXA scans of human lumbar spine may have the potential to become an economical and effective tool for providing bone fragility information complementary to BMD.

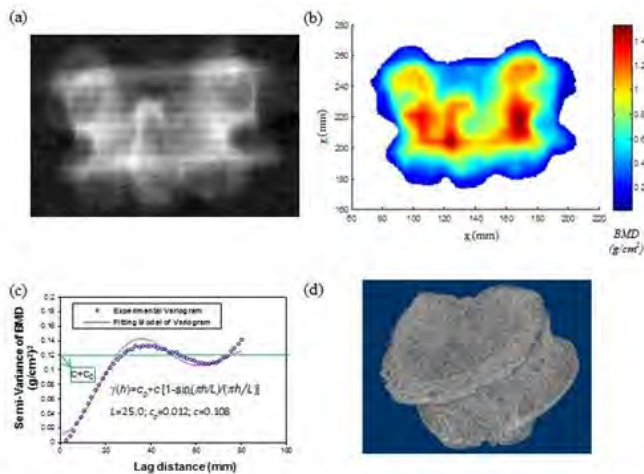


Figure 1. Calculation of stochastic predictors from the BMD map of human vertebrae. (a) A DXA image of human vertebrae in the posterior-anterior projection from a Hologic densitometer; (b) A typical BMD map obtained from the raw data of DXA scans of human vertebrae; (c) A hole-effect fitting model of the experimental variogram of the BMD map. The stochastic predictors, correlation length (L), sill variance (c) and nugget variance (c_0), were extracted from the hole-effect model; and (d) Three-dimensional Micro-CT image of the vertebral body.

Figure 1

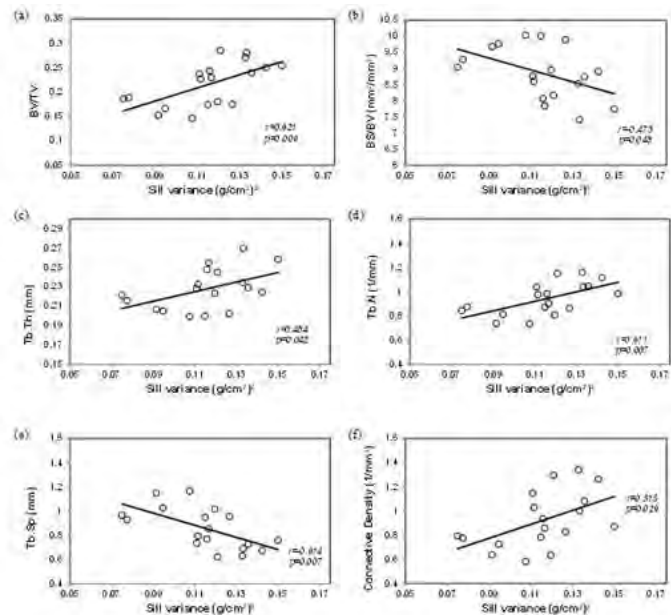


Figure 2. Sill variance of the BMD map from the DXA scans of human vertebrae had significant relationships with microarchitecture parameters of trabecular bone within the vertebral body. (a) bone volume fraction (BV/TV); (b) bone surface-to-volume ratio (BSBV); (c) trabecular thickness (Tb.Th); (d) trabecular number (Tb.N); (e) trabecular separation (Tb.Sp); and (f) connectivity density.

Figure 2

Disclosures: Neil Dong, None.

SU0256

A New System for Ultrasonic Assessment of the Calcaneus. Emily Stein¹, Fernando Rosete¹, Mariana Bucovsky¹, Gangming Luo², Jonathan Kaufman*², Alfred Rosenbaum³, Elizabeth Shane¹, Robert Sifferl⁴. ¹Columbia University College of Physicians & Surgeons, USA, ²CyberLogic, Inc., USA, ³Computerized Scanning Associates, USA, ⁴The Mount Sinai School of Medicine, USA

The objective of this study was to evaluate a new clinical ultrasound device (*QRT 250*, CyberLogic, Inc., NY, USA, Fig. 1) in terms of its ability to estimate bone mineral density (BMD) at the calcaneus, as well as to investigate its short-term precision. The device (Fig. 1) rests on the floor and permits real-time evaluation of the calcaneal BMD. The *QRT 250* employs a novel heel positioning system that relies on an individual's foot size to locate a specific region-of-interest (ROI) in the calcaneus. The device measures in thru-transmission net time delay (NTD) and mean time duration (MTD) parameters. NTD is defined as the difference between the transit time of an ultrasound pulse through overlying soft-tissues and calcaneus, and the transit time through soft tissue only of equal overall distance. MTD is a measure of the time duration of an initial temporal cycle of the received waveform. A linear regression of the product of $NTD \cdot MTD$ is used to provide an estimate of calcaneal BMD that would be measured by DXA. A clinical IRB-approved study was carried out in which 67 adults (age range 21-83, 55% female) were measured at the calcaneus using ultrasound and DXA (Lunar GE PIXI, Madison, WI). In addition, ten (10) subjects were each ultrasonically measured five (5) times with full foot repositioning, and the short term precision was evaluated. BMD_{DXA} ranged from a low of 0.45 g/cm^2 to a high of 0.92 g/cm^2 . A linear regression showed that $BMD_{US} = 0.48 \cdot [NTD \cdot MTD] + 0.071$ and that the linear correlation between BMD_{DXA} and BMD_{US} was 0.92 ($P < 0.0001$, Fig. 2). We found that calcaneal ultrasound measurements yield results that are very closely associated with those from DXA. These results are consistent with previous computer simulation and *in vitro* studies, in terms of the ability to ultrasonically estimate calcaneal bone mass. In the short-term precision study, we found a mean percent precision of 1.21%. This is similar to the short-term reproducibility of DXA scanners. In conclusion, although x-ray methods can estimate BMD, osteoporosis remains one of the world's most undiagnosed diseases. This research should enable significant expansion of the identification of bone loss as occurs in osteoporosis using an inexpensive radiation-free ultrasonic device that can serve as a proxy for BMD_{DXA} at the calcaneus.

SU0257

Age dependent sensitivity and specificity of osteoporosis diagnostics at primary healthcare with Bindex. Janne Karjalainen^{*1}, Ossi Riekkinen², John Schousboe³, Heikki Kröger⁴. ¹Bone Index Finland Ltd., Finland, ²Bone Index Finland Ltd, Finland, ³Park Nicollet Institute, USA, ⁴Kuopio University Hospital, Finland

Objectives

An ultrasound based device (Bindex[®]) has been recently introduced to address the challenges in osteoporosis diagnostics at primary care (1). Bindex measures cortical thickness and determines parameter called density index (DI). Thresholds for DI in osteoporosis assessment have been determined in Finnish Caucasian population (n= 448) along the International Society of Clinical Densitometry (ISCD) guidelines (2). In this study, the sensitivity and specificity in different age groups was assessed.

Materials and Methods

A total of 1316 Caucasian females participated the study (age 68.0 ± 9.5 years). Subjects were measured with dual energy x-ray absorptiometry (DXA) to determine bone mineral density (BMD) at proximal femur. Further, the cortical thickness was measured at three locations (distal radius, distal and proximal tibia) with Bindex[®]. Subjects were diagnosed with OP when T-score at femoral neck or total proximal femur was below -2.5 (NHANES III reference database). A subgroup of 865 subjects was formed in which the subjects with T-score -2.1 - -2.9 were removed due to the precision error in T-score values and uncertainty of osteoporosis/healthy status (3). In this subgroup, OP was diagnosed when T-score was below -2.9. The subjects were healthy when T-score was over -2.1. Density index was calculated either by using measurement at one location (DI₁, proximal tibia) or all three locations (DI₃).

Results

The sensitivity of density index showed increasing trend with increasing age and specificity a decreasing trend with increasing age (Table 1 and Table 2). Within the total population of 1316 the negative predictive values ranged from 93.2% to 94.7% with DI₃ and from 91.3% to 92.5% with DI₁ in different age decades.

Conclusions

The trends observed in the sensitivity and specificity of DI for osteoporosis in different age groups suggests that the thresholds values should be adjusted with age. However, the high negative predictive value in all age groups shows very efficient discrimination of healthy individuals and highlights the potential of the technique as a first line screening tool.

- (1) Karjalainen JP, ASBMR, Baltimore, 2013,
- (2) Hans, J Clin Densitom., 2008,
- (3) Kiebzak, J Clin Densitom., 2007

Table 1. Sensitivity and specificity in study population of 1316 subjects in different age decades.

| Parameter | AGE (years) | | | | All |
|---|-------------|-------|-------|-------|------|
| | 50-59 | 60-69 | 70-79 | 80-89 | |
| n | 303 | 453 | 389 | 171 | 1316 |
| Osteoporotic | 61 | 105 | 113 | 75 | 354 |
| Sensitivity DI ₁ | 78.3 | 75.2 | 86.7 | 94.6 | 84.5 |
| Specificity DI ₁ | 95.4 | 87.5 | 81.5 | 65.6 | 85.5 |
| Sensitivity DI ₃ | 68.9 | 71.4 | 87.6 | 93.3 | 80.8 |
| Specificity DI ₃ | 96.7 | 90.5 | 81.2 | 58.3 | 86.2 |
| % subjects between DI ₁ thresholds | 21.6 | 27.9 | 31.1 | 27.8 | 31.8 |
| % subjects between DI ₃ thresholds | 23.1 | 30.2 | 35.2 | 30.0 | 29.8 |

Table 2

Table 2. Sub-group of 865 subjects. The negative predictive values ranged from 97.7% to 99.0% with DI₁ and from 94.9% to 98.5% with DI₃ in different age decades.

| Parameter | AGE (years) | | | | All |
|---|-------------|-------|-------|-------|------|
| | 50-59 | 60-69 | 70-79 | 80-89 | |
| n | 221 | 313 | 231 | 109 | 865 |
| Osteoporotic | 17 | 31 | 35 | 41 | 124 |
| Sensitivity DI ₁ | 87.5 | 86.2 | 94.3 | 97.6 | 92.5 |
| Specificity DI ₁ | 96.5 | 89.6 | 86.7 | 72.9 | 89.4 |
| Sensitivity DI ₃ | 82.3 | 83.9 | 88.6 | 95.1 | 88.7 |
| Specificity DI ₃ | 98.0 | 92.9 | 86.7 | 62.7 | 90.3 |
| % subjects between DI ₁ thresholds | 16.0 | 23.4 | 31.2 | 34.0 | 24.5 |
| % subjects between DI ₃ thresholds | 18.1 | 28.4 | 37.2 | 27.0 | 28.0 |

Table 2

Disclosures: Janne Karjalainen, Bone Index Finland Ltd. This study received funding from: Bone Index Finland Ltd



Fig. 1

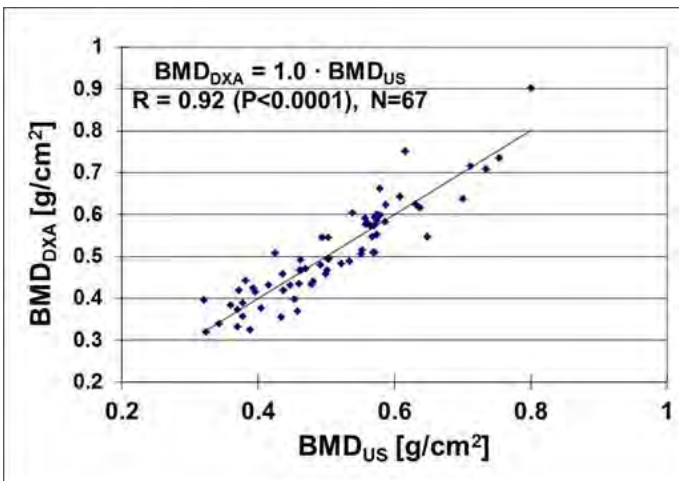


Fig. 2

Disclosures: Jonathan Kaufman, None. This study received funding from: CyberLogic, Inc.

SU0258

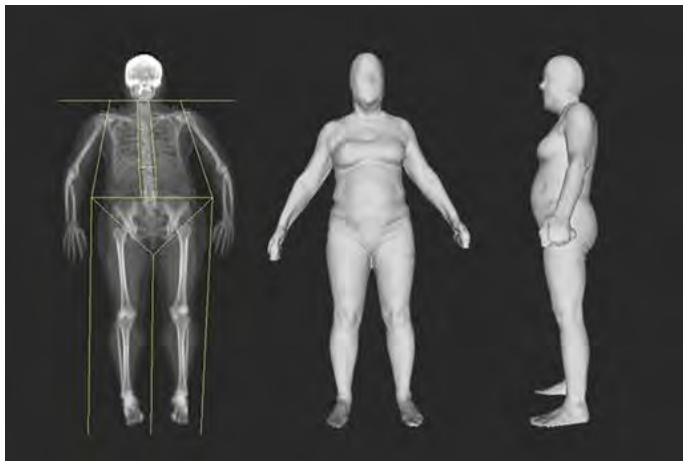
Association of Body Habitus to Bone Density and Mass in Adults. John Shepherd¹, Bennett Ng², Alka Kanaya², Kathy Mulligan², Louise Marquino², Bo Fan². ¹University of California, San Francisco, USA, ²UCSF, USA

There is a need to identify men and women at high fracture risk. The current worldwide paradigm of quantifying fracture risk using DXA is woefully underutilized for reasons of cost, x-ray exposure, and accessibility. The FRAX risk model can be used without a BMD assessment but with lower sensitivity. We explore a new low-cost, radiation-free, and highly accessible technology, 3-dimensional whole body optical scanning, to estimate BMD and BMC measures.

Methods: We had a target to recruit healthy ambulatory adult volunteers stratified by sex, and tertiles of age and BMI. Each participant received a whole body DXA using a Hologic Discovery/W and a 3-D optical whole body scan using a Fit3D system. The Fit3D creates 470 anthropomorphic measures (lengths, circumferences, diameters.) To control for covariance, we derived the principal components (PCA) of body shape. We estimated whole body BMD and BMC as well as subregional spine BMD and BMC using step forward linear regression from demographic (DEMO) measures alone (height, weight, age, sex, $1/\text{height}^2$, and BMI), PCA components alone, and DEMO+PCA measures.

Results: To date, 29 individuals (13 men) have been recruited with an average age of 40 +/- 14 years, and BMI of 27.0 +/- 5.6 g/cm². Only 14 PCA modes were required to explain 95% of the variance in body shape. Using DEMO alone, we found correlations of $r^2 = 0.76$ and 0.34 for whole body BMC and subregional spine BMC respectively. Using PCA alone, the r^2 values were substantially higher at $r^2 = 0.88$ and 0.41 for the same measures. Combining DEMO and PCA did not improve the r^2 values beyond PCA alone. Similar results were seen for BMD values: DEMO alone $r^2 = 0.52$ and 0.1 for whole body and spine; PCA alone $r^2 = 0.67$ and 0.33 respectively.

Conclusions: We conclude that whole body and regional measures of bone, but especially whole body BMC, can be well estimated from whole body 3D optical scans. Future studies are needed with populations at risk of osteoporosis with comparisons to hip and spine BMD measures from dedicated scans.



Comparative images of optical to DXA

Disclosures: John Shepherd, None.

SU0259

Clinical efficacy of a simplified hip structure analysis method for the prediction of incident hip fracture events. Ben Khoo¹, Joshua Lewis², Keenan Brown³, Richard Prince². ¹Western Australian Health Department, Australia, ²University of Western Australia, Australia, ³Mindways Software, Inc, USA

Non-invasive two dimensional Dual Energy X-ray (DXA) imaging of the proximal femur to produce an areal bone density (aBMD) is a clinically useful predictor of future fracture risk. Recently a four measurements assumption free algorithm, derived from the currently used eight HSA variables, has been used to capture population variation in bone structure at the narrow femoral neck (NN), trochanter (TR) and shaft (S). These parameters include two previously used variables, the localised areal bone mineral density (aBMD) and sub-periosteal width (W) applying to the 0.5 cm wide box at the three sites and two new variables, the standard deviation of a normalised mineral-mass projection profile distribution (s), and the displacement between centre-of-mineral-mass and geometric centre-of-mineral-mass of the projection profile (d). Using a cohort study of 1159 women mean age 75 at baseline who sustained 140 hip fractures over 15 years we determined whether these measures significantly improved 15-year hip fracture prediction compared to the current approach utilising age and total hip BMD. There were strong correlations between the variables. To describe the most parsimonious model for hip fracture risk prediction the 12 base measures (4 from each site), total hip BMD and age were evaluated in stepwise logistic regression models. The final model included TR_s, total

hip BMD and age and provided improved utility for hip fracture prediction compared to total hip BMD and age alone (C-statistic 0.73 and 0.69 respectively, $P = 0.007$, net reclassification improvement 0.166, $P < 0.001$). Many attempts have been made to improve on the predictive ability of aBMD which integrates bone mass and bone area. The addition of one HSA derived variable TR_s which describes the distribution of mass within the scanned area of the trochanter, substantially improved the prediction of 15-year hip fracture probability in elderly women.

Disclosures: Keenan Brown, None.

SU0260

Comparison of MRI Measures versus DXA Hip Structural Analysis Narrow Neck Geometric Indices in a Limited Sample of Adolescent Females. Jodi Dowthwaite¹, Tomas Cervinka², Paula Rosenbaum³, Tamara Scerpella⁴. ¹SUNY Upstate Medical University; Syracuse University, USA, ²Tampere University of Technology, Finland, ³SUNY Upstate Medical University, USA, ⁴University of Wisconsin, USA

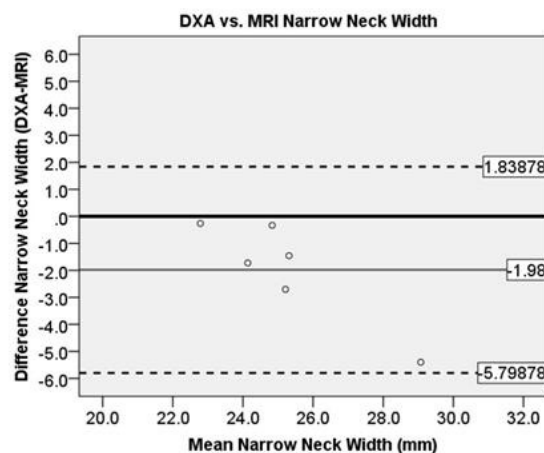
Purpose: Hip structural analysis (HSA) derives proximal femur bone geometric and strength indices from postero-anterior dual energy X-ray absorptiometry (DXA) scans, generating limited radiation exposure. Magnetic resonance imaging (MRI) provides an opportunity to evaluate correlation between 3-dimensional indices of bone geometry and 2-dimensional DXA output, without additional X-ray exposure. In the current analysis, we compared DXA HSA results against output from proximal femur MRI scans in a pilot sample of adolescent females.

Methods: In 6 female subjects, informed assent with parental consent (or informed consent) was obtained for postero-anterior DXA scans (Hologic Discovery A; Waltham, MA) and MRI scans (3.0 T Siemens Magnetom Tim Trio; Malvern, PA) of the left proximal femur. The longest inter-scan interval was 5 weeks. DXA hip positioning was used for both scans. MRI scans used a region-specific coil. MRI images were segmented manually. Anthropometrics were performed. Semi-annual records were used to calculate annual mean weight-bearing organized activity participation. MRI and DXA HSA Narrow Neck assessments of periosteal width, mean cortical thickness, mean endosteal diameter and section modulus were evaluated. Pearson correlations evaluated effect sizes for inter-method associations. Bland-Altman plots evaluated inter-method agreement.

Results: Subject chronological age ranged from 11.1 to 23.6 years (mean 16.0, sd 4.2), and biological age relative to menarche ranged from -0.8 years to 9.2 years (mean 2.9, sd 4.1). Anthropometric means were as follows: height 161.6 cm (sd 7.4); weight 54.0kg (sd 9.7); body mass index 20.5 kg/m² (sd 2.4). Prior year organized weight-bearing physical activity ranged from 1.6 to 18.3 hours per week (mean 8.3, sd 6.0).

Narrow Neck bone index correlations were as follows: mean cortical thickness $r = 0.62$ ($p = 0.15$); endosteal diameter $r = 0.66$ ($p = 0.18$), superior-inferior periosteal width $r = 0.90$ ($p = 0.01$) and section modulus $r = 0.42$ ($p = 0.40$). A Bland-Altman plot indicates underestimation of Narrow Neck periosteal width using HSA that increases with increasing bone width.

Conclusions: Although small available sample size limited statistical significance of results, Pearson r effect sizes for correlations were moderate (> 0.3) to large (> 0.5) for all outcomes, but inter-method agreement was variable. These pilot analyses indicate that HSA geometric and bone strength index parameters should be validated in growing children.



Bland-Altman Plot

Disclosures: Jodi Dowthwaite, None.

SU0261

Guided wave-based ultrasound biomarkers of cortical bone discriminate fractured from non-fractured post-menopausal women. Quentin Vallet^{1*}, Jean-Gabriel Minonzio¹, Nicolas Bochud¹, Adrien Etchet², Karine Briot², Sami Kolta², Christian Roux², Pascal Laugier³. ¹Sorbonne Universités, UPMC Univ Paris 06, CNRS, INSERM, Laboratoire d'Imagerie Biomédicale, France, ²INSERM, U 1153, Rheumatology Department, Cochin Hospital, Paris Descartes University, France, ³Université Pierre et Marie Curie-Paris 6, France

Structural decay of bone is not fully assessed by current X-ray methods, and there is an unmet need in identifying women at risk of fracture who should receive a treatment. The last decade has seen the emergence of ultrasound (US) axial transmission (AT) techniques to assess cortical bone. Recent AT techniques exploit the multimode waveguide response of long bones such as the radius. Guided wave (GW)-based approaches would be expected to provide estimates of bone strength-related factors, such as cortical thickness and porosity, which cannot easily be captured by X-ray densitometry techniques. The objective of this cross sectional study was to evaluate if a new GW-based prototype device can discriminate between fractured and non-fractured postmenopausal women. One hundred and nineteen postmenopausal women were included, among whom 78 were non fractured (NF, mean age 61 ± 8 years), and 41 with a non-traumatic fractures (F, mean age 71 ± 10 years). Measurements were performed at the distal radius using a prototype device (Azalée, Paris, France) consisting of 1-MHz multi-transmitter multi-receiver probe. In addition to the fundamental wave (FW) velocity, the cortical thickness (C.Th) and a cortical porosity index (C.PI) were estimated by fitting a homogenized free plate model to the experimental frequency-dependent wavenumbers measured in the 0.5-1.5 MHz frequency bandwidth. The total femur areal bone mineral density (BMD) was obtained using DXA at the proximal femur. The measured characteristics in both groups were as follows: BMD 0.82 ± 0.11 g.cm² T-score=-1.47 ± 0.83 (NF), 0.72 ± 0.12 g.cm² T-score=-2.17 ± 0.79 (F); FW 1681 ± 56 m/s, (NF) 1646 ± 50 m/s (F); C.PI, 10 ± 4%, (NF) 12 ± 3% (F). Discrimination of fractures with ultrasound variables (except for the C.Th) and with BMD was statistically significant (p < 0.05) (US: odds ratios [ORs] = 1.8–2.1, area under the ROC curve [AUCs] 65–68%; BMD: OR = 2.5, AUC 73%). However, after adjustments on age, the differences were no more significant (p>0.05), as expected due to the large difference in age of the two groups. A weak but significant correlation was found between BMD and FW (R=0.26, p<0.005) and BMD and C.PI (R=0.19, p<0.05). In multiple logistic regression analysis, several combinations of US variables and BMD (C.PI and BMD; FW and BMD) were found to be discriminant with AUC of 76%, which improved the AUC by 3% in comparison with BMD alone. These preliminary results suggest that ultrasound GW-based technologies have the potential to yield cortical bone biomarkers to predict fracture risk in postmenopausal women. The study will be completed in the next future by the inclusion of a larger population. This work received financial support from the Fondation pour la Recherche Médicale (FRM DBS201311228444) and was supported in part by a research grant from investigator-initiated studies program of Merck Sharp & Dohme Corp. The opinions expressed in this paper are those of the authors and do not necessarily represent those of Merck Sharp & Dohme Corp.

Table 1. Unadjusted odds ratios (uOR) and unadjusted areas under the curve (uAUC) for ultrasound and DXA measurements.

| | uOR [95%] | uAUC [95%] |
|--|-----------------------|-----------------------|
| <i>Ultrasound variables and BMD</i> | | |
| FW | 2.071 [1.311 - 3.272] | 0.680 [0.579 - 0.782] |
| C.PI | 1.790 [1.178 - 2.722] | 0.659 [0.559 - 0.759] |
| C.Th | 1.336 [0.909 - 1.962] | 0.588 [0.497 - 0.697] |
| BMD | 2.554 [1.568 - 4.159] | 0.730 [0.636 - 0.826] |
| <i>Combination of ultrasonic variables and BMD</i> | | |
| FW | 1.562 [1.066 - 2.289] | 0.760 [0.667 - 0.853] |
| BMD | 2.411 [1.587 - 3.662] | |
| C.PI | 1.609 [1.032 - 2.506] | 0.755 [0.661 - 0.848] |
| BMD | 2.382 [1.450 - 3.912] | |

Table I: Logistic regression and area under ROC

Disclosures: Quentin Vallet, None.

This study received funding from: Azalée (Paris, France)

SU0262

Inter-Operator Precision and Monitoring Time Intervals for Bone Strength and BMD as Measured from CT Scans — A Comparison of Phantom and Phantomless Calibrations. David Lee^{1*}, Paul Hoffmann¹, Kwang Lee¹, David Kopperdahl¹, Tony Keaveny². ¹O.N. Diagnostics, USA, ²University of California Berkeley, USA

Clinical computed tomography (CT) scans can be analyzed to measure BMD, and, when coupled with finite element analysis, bone strength. The use of a phantomless calibration scheme can expand the availability of CT by not requiring an external calibration phantom. However, precision must be maintained, and the monitoring time interval should be as good as with DXA, the clinical standard. Addressing these issues, we sought to compare the precision and the monitoring time interval of CT-based estimates of BMD and strength in the hip and spine, measured with phantom versus phantomless calibration. VirtuOst (O.N. Diagnostics, Berkeley CA) was used for all analyses, and utilized measurements of blood, fat and air for phantomless calibration. We analyzed CT scans of 56 women (mean age ± SD 62 ± 17 years) and 44 men (59 ± 16 years), acquired on 27 CT scanners. Each scan was processed by two analysts and was calibrated using both calibration techniques. Inter-operator precision was calculated as the percent coefficient of variation. Monitoring time interval for an individual patient was calculated as 2.77 times the clinical precision divided by the annual rate of change. Since repeated CT scans were unavailable, clinical precision was calculated as 0.5% points worse than interoperator precision [1]; annual rates of changes were estimated for a 70-year old Caucasian woman using data from population studies. We found that interoperator precision ranged from 0.49–0.69% across all measured CT parameters, and was similar for phantom and phantomless calibration (Table). The lowest monitoring time intervals occurred for femoral strength at the hip (1.4 years) and trabecular BMD at the spine (1.5 years). Monitoring time interval for vertebral trabecular BMD and vertebral strength were similar to each other, and appreciably shorter than for total spine areal BMD based on the reported precision for DXA [2]. The monitoring time interval for femoral strength was also shorter than for areal BMD, whether measured by CT or DXA. Because the precision was similar for strength and areal BMD, these lower monitoring time intervals were due primarily to the larger annual changes for strength compared to areal BMD. We conclude that, using VirtuOst, precision for CT-based BMD and bone strength were similar for both phantom and phantomless calibration and the monitoring time interval was shorter than for DXA.

[1] Engelke et al Bone 44:566, 2009 [2] Fan et al Osteoporos Int 19:1597, 2008

Table: Inter-operator precision and monitoring time interval, measured for 56 women and 44 men, using 27 different CT scanners.

| Measured Parameter (Units) | Inter-Operator Precision (% coefficient of variation) | | Annual Change* (%) | Monitoring Time Interval (Years) | | |
|---------------------------------------|---|------------|--------------------|----------------------------------|------------|-------|
| | Phantomless CT | Phantom CT | | Phantomless CT | Phantom CT | DXA** |
| <i>Hip</i> | | | | | | |
| Femoral neck BMD (g/cm ²) | 0.49 | 0.51 | -0.7 | 3.9 | 4.0 | 5.9 |
| Total hip BMD (g/cm ²) | 0.23 | 0.33 | -0.7 | 2.9 | 3.3 | 3.6 |
| Femoral strength (N) | 0.51 | 0.57 | -2.0 | 1.4 | 1.5 | — |
| <i>Spine</i> | | | | | | |
| Trabecular BMD (g/cm ³) | 0.57 | 0.52 | -2.0 | 1.5 | 1.4 | — |
| Total spine BMD (g/cm ²) | — | — | -0.8 | — | — | 3.3 |
| Vertebral strength (N) | 0.69 | 0.64 | -1.8 | 1.8 | 1.7 | — |

* calculated for a 70-year old Caucasian woman; ** precision from [2]; — not measured or not applicable.

Table

Disclosures: David Lee, O.N. Diagnostics

This study received funding from: O.N. Diagnostics

SU0263

Investigating the effects of motion streaks on the association between pQCT-derived leg muscle density and fractures in older adults. Adrian Chan^{*}, Jonathan D. Adachi, Alexandra Papaioannou, Laura Pickard, Andy Kin On Wong. McMaster University, Canada

Objectives: 1) to assess the degree of difference in pQCT-derived leg muscle density computed with versus without motion streaks, and 2) to determine how motion streaks affect the relationship between leg muscle density and fractures, and how they are related to fractures.

Method: Women 60-85 years of age from the Canadian Multicentre Osteoporosis Bone Quality Study participated in this cross-sectional analysis of the population-based cohort. Trans-axial leg scans at 66% of the tibial length were obtained using pQCT and motion was graded on a scale of 1-5 according to motion streak severity. Muscle and motion streak areas were segmented using a semi-automated method (sliceOmatic) incorporating a watershed algorithm with manual refinements. The same scans were analyzed by an automated threshold-based algorithm (Stratec) (Figure 1). Bland-Altman analyses and Student's paired *t*-tests determined the degree of difference in muscle densities before versus after removing motion streaks from

both segmentation methods. The same tests were used to find the degree of difference of motion-corrected muscle densities and motion surface areas computed via sliceOmatic versus Stratec. A binary logistic regression ascertained how motion streak removal or adjustment as a covariate affects the relationship between leg muscle density and fractures for both methods.

Results: The majority (84.5%) of the 439 visually graded scans did not warrant repetition due to the minor presence of motion (<grade 3). Out of 95 women examined (age: 74.12 ± 6.94 years, BMI: 27.85 ± 4.92 kg/m², 47.37% ≥ 1 prior fracture, 28.26% ≥ 1 prior fall), significant differences were found for motion-corrected muscle density for sliceOmatic versus Stratec (p<0.01), motion streak area for both methods (p<0.001), and adjusted versus unadjusted muscle density for sliceOmatic (p=0.001). Motion-adjusted muscle density values were similar between sliceOmatic and Stratec, though sliceOmatic yielded lower values. There were slightly larger associations between motion streak-adjusted leg muscle density and fractures after controlling for age, BMI, and falls compared to unadjusted muscle density (Table I).

Conclusions: Using a semi-automated algorithm to remove motion streaks from pQCT leg scans exhibited a statistically significant decrease in computed muscle density. This change resulted in a larger association between motion streak-adjusted muscle density and fractures after controlling for age, BMI, and falls.

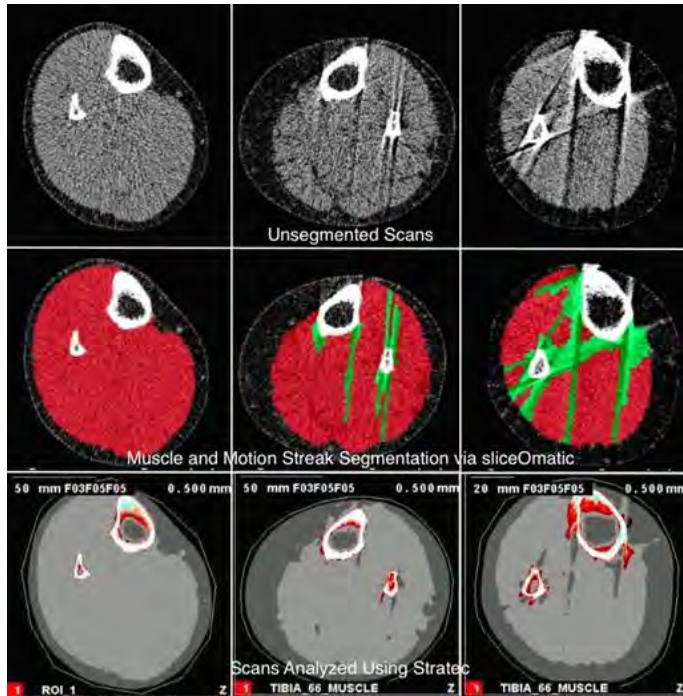


Figure 1: pQCT Leg Scan Segmentations

| Independent Variable | Odds Ratio Adjusted for Age, BMI (95% CI) | Odds Ratio Adjusted for Age, BMI, Falls (95% CI) |
|---|---|--|
| Motion-corrected Muscle Density (sliceOmatic) | 1.226 (1.066 – 1.409) | 1.230 (1.066 – 1.418) |
| Uncorrected Muscle Density (sliceOmatic) | 1.196 (1.051 – 1.361) | 1.190 (1.044 – 1.356) |
| Motion-adjusted Muscle Density (Stratec) | 1.175 (1.006 – 1.373) | 1.167 (0.996 – 1.367) |
| Unadjusted Muscle Density (Stratec) | 1.106 (0.993 – 1.233) | 1.108 (0.996 – 1.234) |

Table I: Odds Ratios between Leg Muscle Density and Fractures in Older Adults

Disclosures: Adrian Chan, None.

SU0264

Searching for side to side difference within the same vertebral body - The preliminary QCT study of trabecular bone density in intact lumbar vertebra of elderly patients with back pain. Wojciech Glinkowski¹, Jerzy Narloch^{*2}. ¹Medical University of Warsaw, Poland, ²Chair & Department of Orthopaedics & Traumatology of Locomotor System, Center of Excellence "TeleOrto", Medical University of Warsaw, Poland, Poland

Searching for side to side difference within the same vertebral body - The preliminary QCT study of trabecular bone density in intact lumbar vertebra of elderly patients with back pain

Introduction

Adult scoliosis in elderly group may show up with the vertebral bodies lateral deformities. The research hypothesis concerns in the question whether an intact vertebral bodies may present differences of mineral density trabecular bone from side to side of the same vertebra.

Methods

In a group of 17 female patients (mean, 68.35 ± 3.4 years) with back pain, but no history of osteoporotic fracture 45 intact vertebra were analyzed. Patients average height was 160,4 cm; and weight 65,71 kg. Nine mm-thick ROI's were selected for finding differences between left and right side of the vertebral body. Patients underwent CT scan due to the history of low back pain after minor trauma. The BMD protocol and phantom for each CT examination of the lumbar spine. The data were used for analysis of vertebral bone mineral density using QCTPro Software (Mindways Software Inc., Austin, TX).

Results

Twenty seven percent of vertebrae revealed a substantial difference between left and right sides of the vertebral bodies. The differences in BMD reached approximately 20 mg/cm³. The overall vertebral body density was 72,16 mg/cm³. The density in the right trabecular bone of vertebra was 74,54 but left side was 71,36 72,16 mg/cm³. The average t-score value was -3,73 SD, and z-score was -0,77 SD.

The average difference of side to side comparison of examined vertebra was approximately 10 mg/cm³. All patients met densitometric, QCT criteria of osteoporosis. No case of vertebral compression fracture was detected.

Conclusions

It is expected that approximate difference of 20 mg/cm³ may produce the side to side deformity and produce consequent scoliosis. This preliminary study may show the path for further investigation.

Acknowledgement: Grant N404 695940 National Science Center, POLAND

Disclosures: Jerzy Narloch, None.

SU0265

TBS reflects trabecular microarchitecture in premenopausal women and similarly aged men with low traumatic fractures. Christian Muschitz^{*1}, Roland Kocijan², Judith Haschka², Dieter Pahr³, Alexandra Kaider⁴, Didier Hans⁵, Astrid Fahrleitner-Pammer⁶, Heinrich Resch². ¹St. Vincent's Hospital, Austria, ²St. Vincent Hospital Vienna - Medical Department II, Austria, ³Institute of Lightweight Design & Structural Biomechanics, Vienna University of Technology, Austria, ⁴Center for Medical Statistics, Informatics & Intelligent Systems, Medical University of Vienna, Austria, ⁵Center of Bone Diseases, Lausanne University Hospital, Switzerland, ⁶Department of Internal Medicine, Division of Endocrinology & Metabolism, Medical University of Graz, Austria

Purpose: Transiliac bone biopsies are still considered to be the gold standard for the analysis of bone microstructure, but limited to specialized centers. The benefit of Trabecular Bone Score (TBS) in addition to areal bone mineral density (aBMD) for fracture risk assessment has been documented in cross-sectional and prospective studies. The aim of this study was to test if TBS may be useful as a surrogate to histomorphometric trabecular parameters of transiliac bone biopsies. Methods: Transiliac bone biopsies from 80 female patients (median age 39.9 years - interquartile range, IQR 34.7; 44.3) and 43 male patients (median age 42.7 years - IQR 38.9; 49.0) with low traumatic fractures and without any comorbidities known to affect bone metabolism were included. Bone volume fraction (BV/TV), trabecular thickness (Tb.Th), trabecular number (Tb.N), trabecular separation (Tb.Sp), structural model index (SMI) as well as serum bone turnover markers (BTMs) sclerostin, intact N-terminal type 1 procollagen propeptide (PINP) and cross-linked C-telopeptide (CTX) were investigated. Results: Median SMI, Tb.Th and sclerostin levels (45.5 vs 33.4 pmol/L, p< 0.0001) were higher in males. Multiple regression models including gender, aBMD and BTMs revealed TBS as an independent discriminative variable with adjusted R² values of 69.1% for SMI, 79.5% for Tb.N, 68.4% for Tb.Sp, and 83.3% for BV/TV. In univariate regression models BTMs showed statistically significant findings, but in the multiple models only PINP and CTX were significant for Tb.N. Conclusions: TBS is a feasible non-invasive surrogate technique for the assessment of cancellous bone microarchitecture and should be implemented as an additional tool for the estimation of trabecular bone properties.

Disclosures: Christian Muschitz, None.

SU0266

The Fracturing Phenotype: What Can We Learn from Examining Cross-sectional Geometry with pQCT? Timo Rantalainen¹, Daniel Belavý², Rachel Duckham^{*2}, Tilo Blenk³, Franziska Luhn³, Rainer Rawer⁴, Johannes Willnecker⁴, Gabriele Armbrecht³, Dieter Felsenberg³. ¹Centre for Physical Activity & Nutrition Research, Deakin University, Finland, ²Centre for Physical Activity & Nutrition Research, School of Exercise & Nutrition Sciences, Deakin University, 221 Burwood Highway, Burwood, Victoria, 3125, Australia, Australia, ³Centre for Muscle & Bone Research, Charité Universitätsmedizin Berlin, Hindenburgdamm 30, 12203 Berlin, Germany., Germany, ⁴Stratec Medizintechnik GmbH, Durlacher Str. 35, 75172 Pforzheim, Germany, Germany

Over 50% of fracture cases in women are non-osteoporotic, and are not treated preventatively. Therefore exploring supplementary fracture risk screening methods is prudent. Although evidence suggests that some fractures unrelated to aBMD are possibly due to the deterioration in bone size, structure, and strength, it remains scarcely explored whether a bone phenotype susceptible to fragility fractures exists. Therefore, from a data set of 535 postmenopausal women aged 60 to 94 years, 29 individuals who had suffered a low-energy fracture within the last 10 years (age = 72 (SD 7) years, height = 160 (4) cm, weight = 69.6 (9.6)) were identified and matched for age, height weight and total FN t-score with randomly selected non-fracture individuals. Data from DXA (femoral neck, FN) and pQCT scans (at 38% tibia length and 60% radius length, density and material distribution analysed with BoneJ) along with grip strength, low-intensity fracture history, a history of bisphosphonate use, physical activity, falls within the last year, age at menopause, and timed up and go performance were available. MANOVA indicated no difference between the fracture and matched non-fracture groups (P=0.36) for age, height, weight, FN t-score, age at menopause, bisphosphonate use, falls within the last year, physical activity, grip strength, or up and go time. Whole bone pQCT analysis (total and cortical area, medullary area [Me.Ar], cortical volumetric bone mineral density [Ct.Dn], strength indices) showed 14% larger tibia Me.Ar, and 4.8% lower radius Ct.Dn for the fracture compared to the non-fracture group (P<0.039). Radii, and vBMD distribution analysis showed 6.5%, and 9.9% wider tibia and radius endocortical radii (P<0.043) for the fracture group compared to the non-fracture group, respectively (FIG 1). In further exploration of fracture sites it was observed that the upper limb fracture cases (N = 13) did not differ from other fracture cases while lower limb fracture cases (N = 6) had lower FN t-score, and larger tibial Me.Ar than other fracture cases. In conclusion, the fracture group differed from the matched non-fracture group only based on pQCT-measured bone characteristics. Specifically, enlarged medullary cavity was observed in the fracture history group compared to the non-fracture history group (FIG 1). This indicates that a fragility fracture phenotype may be characterised by an enlarged marrow cavity.

Disclosures: Rachel Duckham, None.

SU0267

Quantitative proteomics and integrative network analysis identified novel genes and pathways related to osteoporosis. YONG ZENG^{*1}, Lan Zhang¹, Wei Zhu¹, Chao Xu¹, Hao He¹, Yu Zhou¹, Qing Tian¹, Ji-Gang Zhang¹, Fei-Yan Deng², Yao-Zhong Liu¹, Hong-Wen Deng¹. ¹Tulane University, USA, ²Hunan Normal University, China

Osteoporosis is characterized by low bone mineral density (BMD), and can be attributed to excessive bone resorption by osteoclasts. Migration of circulating monocytes from blood to bone is fundamental for subsequent osteoclast differentiation and bone resorption. Osteoimmunology studies suggested a close and complex interaction between immune system and bone metabolism. Identification of those genes and pathways related to osteoclast differentiation and BMD will contribute to a better understanding of the pathophysiological mechanisms of osteoporosis. In this study, we applied the LC-nano-ESI-MSE for quantitative proteomic profiling in 33 female Caucasians with discordant BMD levels, with 16 high vs. 17 low BMD subjects. Comparison of protein expression in high vs. low BMD subjects showed that ITGA2B (p=0.0063) and GSN (p=0.019) were up-regulated in the high BMD group. Additionally, our protein-RNA integrative analysis showed that RHOA (p=0.00062) differentially expressed between high vs. low BMD groups. Network analysis based on multiple tools revealed two pathways: "Regulation of actin cytoskeleton" (p=1.13E-5, FDR=3.34E-4) and "Leukocyte transendothelial migration" (p=2.76E-4, FDR=4.71E-3) that are functionally relevant to osteoporosis. Consistently, ITGA2B, GSN and RHOA played crucial roles in these two pathways respectively. All together, our study strongly supported the contribution of the genes ITGA2B, GSN and RHOA and two pathways to osteoporosis risk.

Disclosures: YONG ZENG, None.

This study received funding from: Edward G. Schlieder Endowment

SU0268

The Effect of Chronic Hyponatremia on Bone Mineral Loss Evaluated by Retrospective National Danish Patient Data. Christian Kruse^{*1}, Pia Eiken², Joseph G. Verbalis³, Peter Vestergaard⁴. ¹Aalborg University, Dk, ²Department of Cardiology, Nephrology & Endocrinology, Nordsjællands Hospital Hilleroed, Hilleroed, Denmark, Denmark, ³Division on Endocrinology & Metabolism at Georgetown University, USA, ⁴Department of Endocrinology, Denmark

CONTEXT: Hyponatremia is associated with increased risk of osteoporosis in retrospective data. The effect of chronic hyponatremia has been studied sparsely. OBJECTIVE: Evaluating the effect of different severities of chronic hyponatremia on bone mineral content (BMC) and bone mineral density (BMD) loss through serial dual-energy X-ray absorptiometry (DXA) scans. DESIGN: Retrospective cohort study. SETTING: Two regional Danish databases of biochemical and hip and lumbar spine DXA scan data. National Danish patient diagnosis and prescription reimbursement databases. PATIENTS: All patients having undergone serial DXA scans at Aarhus and Aalborg University Hospitals between 2004 and 2011. INTERVENTIONS: Stratification into "normonatremia" ([Na+] = [137.00-147.00] mmol/L), "mild hyponatremia" ([Na+] = [130.00-137.00] mmol/L) and moderate hyponatremia ([Na+] = [120.00-130.00] mmol/L) based on mean and confidence interval (CI) values between the first and last DXA scan. MAIN OUTCOME MEASURE: Baseline, follow-up and delta values for BMC and BMD between groups. Adjustment for comorbidity and medication use. RESULTS: Hip and lumbar spine groups had 884 and 1,069 patients with "normonatremia", 58 and 58 patients with "mild hyponatremia", and 3 and 3 patients with "moderate hyponatremia". Mild hyponatremia was associated with lower BMC and BMD in nearly all regions of the hip, and with worse losses in the trochanteric, femoral neck and total hip regions. Mild hyponatremia had limited effect on the lumbar spine. CONCLUSIONS: Chronic mild hyponatremia seems to greatly affect bone in the hip, while the effect is limited in the lumbar spine. We suggest prospective studies to further examine the association.

Disclosures: Christian Kruse, None.

The Obel Family Foundation is sponsoring the PhD Fellowship with an unrestricted grant.

SU0269

Time to Osteoporosis and Incidence of Major Osteoporotic Fracture in Older Men: the MrOS Study. Margaret Gourlay^{*1}, Robert Overman¹, Jason Fine¹, Guillaume Filteau¹, Peggy Cawthon², John Schousboe³, Eric Orwoll⁴, Timothy Wilt⁵, Tuan Nguyen⁶, Nancy Lane⁷, Pawel Szulc⁸, Brent Taylor⁵, Thuy-Tien Dam⁹, Carrie Nielson⁴, Jane Cauley¹⁰, Elizabeth Barrett-Connor¹¹, Howard Fink⁵, Jodi Lapidus⁴, Deborah Kado¹¹, Susan Diem³, Kristine Ensrud⁵. ¹University of North Carolina, USA, ²Research Institute, California Pacific Medical Center, USA, ³University of Minnesota, USA, ⁴Oregon Health & Science University, USA, ⁵University of Minnesota, Minneapolis VA Health Care System, USA, ⁶Garvan Institute of Medical Research, Australia, ⁷University of California, Davis, USA, ⁸University of Lyon, France, ⁹Columbia University, USA, ¹⁰University of Pittsburgh, USA, ¹¹University of California, San Diego, USA

Rationale: No standard of care exists for osteoporosis screening in older men. To guide bone mineral density (BMD) testing interval recommendations, we estimated the time to incident osteoporosis and fracture incidence according to baseline BMD in older men participating in MrOS.

Methods: We conducted a competing risk analysis of 5415 community-dwelling men aged 65 years and older who were without a history of hip or clinical vertebral fracture or antifracture treatment and had up to 8.7 years of concurrent BMD (2 to 5 DXA measurements) and fracture follow-up. We estimated the time for 10% of men with higher baseline BMD (T-scores >-1.50 at the femoral neck, total hip and lumbar spine calculated using young white female norms; n=4203), moderate osteopenia (lowest T-score -1.50 to -1.99; n=680) or advanced osteopenia (lowest T-score -2.00 to -2.49; n=352) to develop osteoporosis by World Health Organization diagnostic criteria (lowest T-score ≤-2.50). Parametric cumulative incidence curves for the time to osteoporosis were estimated from log logistic cumulative incidence models for interval censored data, adjusting for race, baseline age and body mass index. Initiation of antifracture treatment, incident hip or clinical vertebral fracture and death were competing risks. Incident major osteoporotic fractures between the baseline visit and end of follow-up were tabulated.

Results: Only nine men (0.2% of 4203) with higher BMD at baseline developed osteoporosis during follow-up; their time to osteoporosis could not be estimated due to the very small number of endpoint events. The adjusted time for 10% to develop osteoporosis was 8.5 years for those with moderate osteopenia and 2.7 years for those with advanced osteopenia (table). Most men who sustained a major osteoporotic fracture had T-scores >-2.50; in fact, 29% of the hip and clinical vertebral fractures occurred in men with normal BMD at baseline.

Conclusions: These results indicate that older men with baseline BMD T-scores >-1.50 have a very low likelihood of developing osteoporosis in the subsequent 8

years, and suggest that repeat BMD measurements may not be warranted in this group. In contrast, BMD testing intervals as short as 2.5 years may be considered for men with advanced osteopenia. Many men without osteoporosis will experience major osteoporotic fractures, suggesting that risk factors other than BMD must be addressed to prevent fractures in older men.

| Baseline T-score range | Incident osteoporosis by WHO criteria, ³ N (%) | Time interval for 10% of participants to develop osteoporosis, ² years (95% CI) | |
|------------------------------------|---|--|-------------------|
| | | Unadjusted | Adjusted |
| Higher BMD >-1.50 | 9/4203 (0.21) | | |
| Moderate osteopenia -1.50 to -1.99 | 35/680 (5.15) | 8.57 (6.67-10.99) | 8.51 (6.67-10.86) |
| Advanced osteopenia -2.00 to -2.49 | 73/352 (20.74) | 2.59 (2.03-3.30) | 2.68 (2.12-3.40) |

³ osteoporosis defined as lowest T-score \leq -2.50 at femoral neck, total hip or lumbar spine, calculated using BMD norms for young white women

² time estimates adjusted for race and mean-centered age and BMI

table

Disclosures: Margaret Gourlay, None.

SU0270

Does DNA Methylation Underpin the Social Gradient of Osteoporotic Fracture? A Conceptual Model. [Sharon Brennan-Olsen](#)^{*1}, [Richard Page](#)¹, [Michael Berk](#)¹, [Jose Riancho](#)², [William Leslie](#)³, [Karen Saban](#)⁴, [Julie Pasco](#)¹, [Shae Quirk](#)¹, [Natalie Hyde](#)¹, [Sarah Hosking](#)¹, [Lana Williams](#)¹.
¹Deakin University, Australia, ²University of Cantabria, IDIVAL, Spain, ³University of Manitoba, St Boniface Hospital, Canada, ⁴Loyola University Chicago, USA

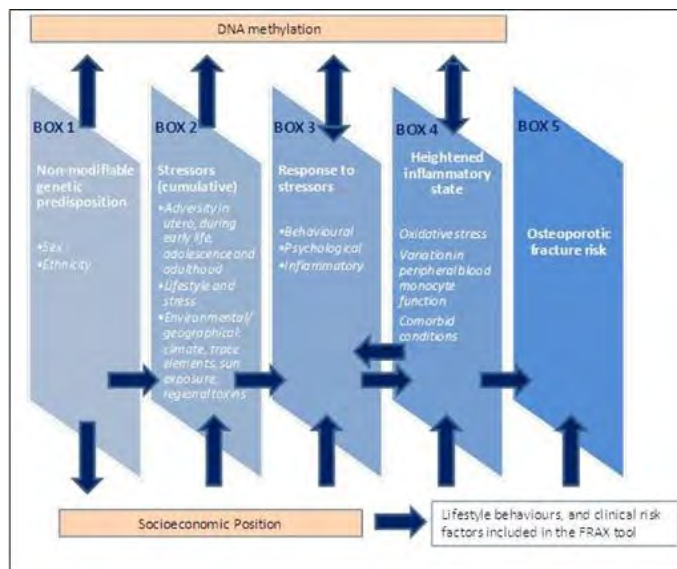
Purpose: Although a social gradient for osteoporosis is documented, the underlying mechanisms for that gradient remain unknown. To advance our understanding of the aetiology and pathogenesis of osteoporosis, there are now large-scale efforts to identify genes associated with fracture risk via genome-wide association studies of bone mineral density. We propose a conceptual model based upon Saban et al's (1) allostatic load theory model, to suggest how DNA methylation (DNAm) may underpin the social gradient in osteoporosis and fracture. We hypothesise that socioeconomic position (SEP) is associated with sensitisation of immune signalling pathways mediated by epigenetic modification that leads to an enhanced state of immune reactivity and oxidative stress and thus places socially disadvantaged individuals at greater risk of osteoporotic fracture.

Methods/Results: Based on a review of the literature, we present a conceptual model (Figure) in which social disadvantage and stress during all stages of life engender a proinflammatory epigenetic signature, leading to a heightened inflammatory state that increases risk for osteoporotic fracture in disadvantaged groups. Despite a paucity of data, the available studies suggest that plasticity in molecular responses in stress response pathways that may be related to the influence of SEP on the epigenetic pathway. Given that the epigenetic signature is influenced by many environmental factors across the lifespan, the epigenome appears to function as a vital conduit that transduces exposures into phenotypic expression and disease risk.

Conclusions: DNAm is a dynamic modulator of gene expression with considerable relevance to the field of osteoporosis. Elucidating the extent to which this epigenetic mechanism mediates the psycho-social environment and risk of osteoporotic fracture may yield novel entry points for intervention that can be used to reduce individual and population-wide risks for osteoporotic fracture. Specifically, an epigenetic evidence-base may enhance the importance of lifestyle modification and stress reduction programs, and help to reduce health inequities across social groups.

Reference

1. Saban KL, Mathews HL, DeVon HA, Janusek LW 2014 Epigenetics and social context: Implications for disparity in cardiovascular disease. *Aging and Disease* 5(5):346-355.



Conceptual model: DNA methylation and the social gradient of osteoporotic fracture

Disclosures: Sharon Brennan-Olsen, None.

SU0271

Prospective study of kyphosis and lower extremity function in women and men: The Framingham Study. [Amanda Lorbergs](#)^{*1}, [Yanhua Zhou](#)², [Ching-An Meng](#)³, [Brochin Elana](#)³, [Douglas P. Kiel](#)⁴, [L. Adrienne Cupples](#)², [Joanne Murabito](#)², [Dennis E. Anderson](#)⁵, [Brett Allaire](#)⁵, [Mary B. Bouxsein](#)⁶, [Thomas G. Travison](#)⁷, [Elizabeth J. Samelson](#)⁷.
¹Institute for Aging Research, Hebrew SeniorLife & Harvard Medical School, USA, ²School of Public Health, Boston University, USA, ³Institute for Aging Research, Hebrew SeniorLife, USA, ⁴Institute for Aging Research, Hebrew SeniorLife & Harvard Medical School, USA, ⁵Beth Israel Deaconess Medical Center, USA, ⁶Beth Israel Deaconess Medical Center, Harvard Medical School, USA, ⁷Institute for Aging Research, Hebrew SeniorLife & Harvard Medical School, USA

Background: Increased thoracic kyphosis is a spinal disfigurement manifested as a hunched posture. In older women, greater kyphosis is associated with mobility deficits, yet the effect on risk of poor mobility in men is not known.

Objective: We conducted a prospective study to determine the contribution of baseline kyphosis angle (KA) on performance-based measures of physical function at 6y follow-up in a community-based population of women and men.

Methods: Participants included 808 cohort members (447 women, 361 men) with mean age 64y (range, 50-85y) of the Framingham Offspring Study. Baseline (2002-2005) lateral CT images were used to measure kyphosis (T4-T12 Cobb angle, degrees), where greater KA indicates greater forward curvature. At 6y follow-up, participants performed 5 chair stands without using arms and a fast 4m walk. We used linear models to estimate mean chair stand time (s) and gait speed (m/s) at follow-up by sex-specific quartiles of baseline KA. We conducted stratified analysis to evaluate whether the contribution of greater KA to performance measures differed by age (<65, ≥65y).

Results: Mean (SD) baseline KA, chair stand time, and gait speed were 33(9)°, 5.9(1.5) s, and 1.6(0.3) m/s for women and 30(9)°, 6.0(1.5) s, and 1.8(0.4) m/s for men, respectively. Women with greater KA at baseline took longer to perform 5 chair stands (Table; trend, $p=0.009$) and had slower gait speed (trend, $p=0.038$) at follow-up. After adjusting for baseline age, height, weight, and smoking, the association between greater KA and longer chair stand time remained significant (trend, $p=0.024$), whereas the association with gait speed was no longer significant (trend, $p=0.52$). In men, greater KA at baseline was not associated with poor physical function at follow-up. Finally, the results were similar in age <65 and ≥65y (not shown).

Conclusion: Women with greater kyphosis performed chair stands more slowly at 6y follow-up (0.3s slower per 10° increase in KA). Sit-to-stand transitions require a high rate of knee extensor torque development; thus, greater kyphosis may be associated with reduced muscle power. Functional limitations are observed at older ages in men than women. The relatively young age of older adults in our sample may have limited the ability of our study to detect associations in men. Alternatively, accentuated forward curvature may pose greater challenges for women during rapid shifting of the center of mass due to weaker lower extremity muscles.

SU0273

Both High and Low serum Serotonin levels Predicts Incident Non-vertebral Fractures. Dan Mellstrom^{*1}, Ewa Waern², Catharina Lewerin³, Östen Ljunggren⁴, Claes Ohlsson⁵, Daniel Sundh⁶, Mattias Lorentzon⁵, Magnus Karlsson⁷, Steven Cummings⁸, Helena Johansson⁹, Henrik Zetterberg¹⁰, Ulf Lerner⁵. ¹Sahlgrenska University Hospital, Sweden, ²Department of Geriatrics, University of Gothenburg, Sweden, ³Section of Hematology & coagulation, department of internal medicine & clinical nutrition, institute of medicine, Sahlgrenska Academy, University of Gothenburg, Sweden, ⁴Department of Medical Sciences, University of Uppsala, Sweden, Sweden, ⁵Centre for Bone & Arthritis Research, Institute of Medicine, Sahlgrenska Academy, University of Gothenburg, Sweden, ⁶Geriatric Medicine, Institute of Medicine, Sahlgrenska Academy, University of Gothenburg, Sweden, ⁷Clinical & Molecular Osteoporosis Research Unit, Department of Clinical Sciences, Lund University, & department of Orthopedics, Skåne University Hospital, Sweden, ⁸San Francisco Coordinating Center, California Pacific Medical Center Research Institute, USA, ⁹Geriatric Medicine, Institute of Medicine, Sahlgrenska Academy, University of Gothenburg, Sweden, Centre for Bone & Arthritis Research, Institute of Medicine, Sahlgrenska Academy, University of Gothenburg, Sweden, ¹⁰Department of Psychiatry & Neurochemistry, University of Gothenburg, Sweden

Experimental studies indicate that Lrp5 regulates serotonin synthesis in the gut and through this regulate bone formation. A study of women showed that serum serotonin was inversely related to bone density (BMD). The aim of this study was to examine the predictive value of serum serotonin for incident fractures. Elderly men in the Gothenburg part of the Swedish MrOS study (n=1010) (aged 69-81 years) had baseline analysis by Elisa of serum serotonin. 248 incident fractures, of which 61 hip fractures, were observed in radiographic registers up to 10 years from baseline. The probability of incident fracture was determined by Cox proportional hazards models. Serum serotonin levels were associated with hand grip strength (r=0.11, p<0.002) and inversely with hip total BMD (r=-0.08, p<0.01) but not with lumbar spine BMD. Serotonin levels were inversely associated to body mass index (BMI; r=-0.09, p<0.01). Smokers had higher and men with serotonin reuptake inhibitors (SSRI) and falls during the last year had lower serotonin levels (p<0.01). Serotonin levels were not associated to incident fractures in linear models. However, analyzing all fractures there was a u-shaped relationship between fracture risk and quintiles of serotonin. The Hazard ratio (HR 95% CI) for all fractures when comparing quintile 1 to quintiles 2-4 (referent group) was 1.54 (1.14-2.16) and quintile 5 vs. referent group 1.64 (1.20-2.23). The HR for hip fracture was for quintile 1 vs. referent group 1.74 (0.89-3.41) and for quintile 5 vs. referent group 2.95 (1.67-5.20). The HR for non-vertebral fractures was for quintile 1 vs. referent group 1.67 (1.19-2.36) and for quintile 5 vs. referent group 1.70 (1.22-2.38). Serotonin levels did not predict risk for vertebral fracture. Multivariable models adjusting for age, BMI, hip BMD, falls, SSRI and smoking had small impact on the models. HR for hip fracture for quintile 5 vs. referent group in a multivariable model was 2.62 (1.45-4.74). Serum serotonin levels were also associated with plasma osteocalcin (r=0.08, p<0.01) and inversely with serum leptin (r=-0.15, p<0.001). The HR for falls during the last year in quintile 1 of serotonin vs. referent group was 1.79 (1.18-2.71) and in quintile 5 vs. referent group 0.84 (0.51-1.38) adjusted for age, BMI, hip BMD, SSRI and smoking. We conclude that both low and high circulating serotonin predicts non vertebral fractures indicating a relation between cortical bone and serotonin.

Disclosures: Dan Mellstrom, None.

SU0274

Elevated Fasting Triglyceride Levels Are Associated With Risk of Subsequent Fracture in Midlife Women: Study of Women's Health Across the Nation (SWAN). Po-Yin Chang^{*1}, Jennifer S. Lee², Ellen B. Gold³, Wesley Johnson⁴, Carrie Karvonen-Gutierrez⁵, Kristine Ruppert⁶, Elizabeth A. Jackson⁷, Jane A. Cauley⁶. ¹Stanford University, USA, ²Stanford University School of Medicine, USA, ³Department of Public Health Sciences, University of California, Davis, USA, ⁴Department of Statistics, University of California, Irvine, USA, ⁵Department of Epidemiology, University of Michigan School of Public Health, USA, ⁶Department of Epidemiology, University of Pittsburgh School of Public Health, USA, ⁷Division of Cardiovascular Medicine University of Michigan Health Systems, USA

Background: Cardiovascular disease increases risk of osteoporotic fracture. The mechanism is unclear; unfavorable lipid levels could be related. Mice with hyperlipidemia had inhibited osteoblast differentiation, reduced bone mineralization and stimulated osteoclast activity. Atherosclerosis of arteries supplying bone may lead to bone ischemia. We tested the hypothesis that elevated lipid levels were associated with subsequent fracture in midlife women.

| Association between baseline kyphosis angle (KA) and physical performance at 6y follow-up in women and men in the Framingham Study | | | | |
|--|------------------|----------------|------------------|----------------|
| Baseline KA** | WOMEN (N=447) | | MEN (N=361) | |
| | Unadjusted Mean | Adjusted* Mean | Unadjusted Mean | Adjusted* Mean |
| | Chair Stands (s) | | Chair Stands (s) | |
| Quartile 1 (least) | 5.61 | 5.61 | 6.08 | 6.08 |
| Quartile 2 | 5.77 | 5.91 | 5.72 | 5.76 |
| Quartile 3 | 6.06 | 6.03 | 6.09 | 6.12 |
| Quartile 4 (most) | 6.15 | 6.04 | 6.16 | 6.09 |
| Trend | p=0.009 | p=0.036 | p=0.42 | p=0.62 |
| | Gait Speed (m/s) | | Gait Speed (m/s) | |
| Quartile 1 (least) | 1.62 | 1.60 | 1.82 | 1.80 |
| Quartile 2 | 1.63 | 1.52 | 1.73 | 1.73 |
| Quartile 3 | 1.65 | 1.54 | 1.71 | 1.70 |
| Quartile 4 (most) | 1.62 | 1.57 | 1.74 | 1.78 |
| Trend | p=0.038 | p=0.52 | p=0.18 | p=0.55 |

* Adjusted for baseline age, height, weight, and smoking

** Mean (min-max) of quartiles

Women Q1=22 (8-27) Q2=30 (27-34) Q3=38 (34-41) Q4=48 (42-65)

Men Q1=23 (12-27) Q2=31 (28-33) Q3=36 (33-40) Q4=46 (40-65)

Association between baseline KA and physical performance_Lorbergs2015

Disclosures: Amanda Lorbergs, None.

SU0272

Associations of spinal inclination and vertebral deformities with difficulties in activities of daily living. Yasuyo Abe^{*}, Kiyoshi Aovagi. Nagasaki University, Japan

Vertebral deformities are the most frequent form of osteoporotic fractures, which lead to difficulties in activities of daily living (ADLs) and worsening of quality of life. We have previously reported that vertebral deformities are associated with spinal kyphotic change, and forward spinal inclination is associated with impairment in various physical functioning measurements. In this study, we explored associations of spinal inclination and vertebral deformities with selected ADLs among 109 Japanese women ages 40 year and over. Spinal posture was assessed as inclination to a perpendicular line by using computer-assisted device (SpinalmouseU). Greater inclination value means forward inclination of the spine. Lateral spine radiographs were obtained and radiographic vertebral deformities were assessed by quantitative morphometry. A self-administered questionnaire was used to survey participants about low back pain and difficulty in performing selected ADLs. Mean age of the participants was 66.2 years and median value of spinal inclination was 3 degrees. Of the participants, 14.7% had at least one vertebral deformity and 38.5% reported back pain. Number of vertebral deformities had significant positive correlation with spinal inclination (r=0.25). Univariate analysis showed that difficulties in bending- and spine-extended- and walking-related ADLs were associated with older age, greater spinal inclination, and higher prevalence of vertebral deformities. Multiple logistic regression analysis showed that increase in spinal inclination was associated with difficulties in walking related ADLs: "walking 100m on a level surface", "climbing 10 steps", and "walking down 10 steps." On the other hand, vertebral deformities were associated with difficulties in bending- and spine-extended-related ADLs: "bending over or picking up a lightweight object", "lifting a 5 kg object from the floor", and "reaching an object above your head." Back pain was associated with difficulties in walking related ADLs: "climbing 10 steps", and "walking down 10 steps." In conclusion, forward inclination of the spine was associated with walking-related ADLs, part of which might be mediated by back pain, while vertebral deformities were associated with bending- or spine-extension-related ADLs. Associated factors for difficulty might differ in different ADLs.

Disclosures: Yasuyo Abe, None.

Method: From SWAN, 2413 midlife women ages 42-53 years (50% White, 28% Black, 12% Japanese, and 10% Chinese) were at baseline either premenopausal (54%) or early perimenopausal (46%) and had bone mineral density (BMD) measured by DXA. Self-reported fractures (at skeletal sites other than skull or digits) at each near-annual visit from visits 2 to 12 were counted as incident fractures. Fasting blood lipid panel, high-sensitivity C-reactive protein (CRP) and endogenous sex hormones were measured at baseline. We estimated hazard ratios (HR) and 95% confidence intervals (CI) in discrete-time Cox models, adjusting for age, race/ethnicity, study site, menopausal status, body mass index (BMI), fracture history, and smoking (model 1), and also for baseline lumbar spine BMD, diabetes, hormone use, estradiol, sex hormone binding globulin, and CRP (full model).

Results: Median (interquartile range, IQR) levels for baseline triglycerides (TG), total cholesterol, HDL-C, and LDL-C were 89 (67-129) mg/dL, 192 (171-215) mg/dL, 55 (46-65) mg/dL, and 114 (94-135) mg/dL, respectively. At visit 12, retention was 65% (1576 of 2413) and 266 women ever reported fractures. Every 50 mg/dL increase in TG level was associated with an HR of 1.11 (95% CI: 1.05-1.17, model 1) for fractures; per 25mg/dL increase in TG level, HR 1.05 (95% CI: 1.03-1.08). Associations remained in the full model, with HRs of 1.09 (95% CI: 1.03-1.16) per 50 mg/dL change and 1.05 (95% CI: 1.02-1.08) per 25 mg/dL change. Notably, an HR of 1.24 (95% CI: 1.06-1.44) was observed for every 50 mg/dL increase in TG level in Black women (*P* for interaction = 0.057). Women who had a TG/HDL-C ratio ≥ 3 (vs TG/HDL-C < 3) also had an increased hazard for fractures (HR 1.14, 95% CI: 1.03-1.26, full model). Other lipids were not associated.

Conclusion: Pre- and early peri-menopausal women, particularly Black women, with elevated fasting triglycerides had an increased risk of fracture after multivariable adjustment. Further understanding of this relation is warranted.

Disclosures: Po-Yin Chang, None.

SU0275

Fractures from Same-Level Falls in the Workplace: A Descriptive Study of Workers' Compensation Claims in Ontario, Canada. Chamila Adhithetty¹, Dorcas Beaton², Sheilah Hogg-Johnson³, Susan Jaglal¹. ¹University of Toronto, Canada, ²St. Michael's Hospital, Canada, ³Institute for Work & Health, Canada

Background/Purpose: Same-level falls (falls from standing height or less, e.g. slips, trips) account for a significant portion of workplace injuries, and fractures are one of the most disabling outcomes. In 2012 fractures accounted for about 15% of workplace same-level fall injuries in the US, and same-level falls was the leading cause of work-related fractures. Further evidence is required to determine where efforts should be targeted to prevent fractures from same-level falls. The objective of this study was to use Ontario workers' compensation claims data to describe fractures from same-level falls at work in terms of i) the proportion of total claims and ii) worker, employment and circumstance characteristics (demographics; industry; when, where and how fractures occurred).

Methods: Using a descriptive quantitative analysis, this study examined allowed lost-time (LTA) workers' compensation claims from 2002-2011 for workers aged 20-80 years. The analyses focused on LTA claims coded as "fracture" resulting from "fall on same level", but comparisons were also made with non-fracture injuries from same-level falls (e.g. sprains, strains).

Results: There were 828,704 LTA claims over the 10 year period, and 12.4% (n=103,167) were for same-level falls among workers 20-80 years old. The data indicated that 15.3% of LTA claims for fall on same level resulted in fracture (n=15,800). The overall age and gender distribution for fractures indicated that older females (50-80 years) had sustained the greatest proportion of fractures (37.0%) followed by older males (27.7%), younger males (20-49 years) (20.3%) and younger females (14.9%). Fracture and non-fracture claims appeared to affect different regions of the body, with the most common specific fracture sites being wrist and ankle. There were similar proportions of fracture and non-fracture injuries among workers in different industries. The highest proportions of injuries were found among people employed in Services (25.6% of fractures) and Schedule 2 (government and related entities) (21.4% of fractures) industries. Various patterns emerged in the proportions of fractures when industries were analyzed in terms of age and gender differences. Fracture and non-fracture claims were both most prevalent in the winter and during the morning.

Conclusion: These findings will inform efforts to prevent fractures from same-level falls such as interventions directed toward particular industries and/or worker demographics.

Disclosures: Chamila Adhithetty, None.

SU0276

High incidence of typical osteoporotic fractures following an atypical femoral fracture. Emmanuel Biver¹, Marie Claude Audet¹, René Rizzoli¹, Raphael Meier², Robin Peter³, Serge Ferrari¹. ¹Division of Bone Diseases, Geneva University Hospitals & Faculty of Medicine, Switzerland, ²Division of Visceral & Transplant Surgery, Geneva University Hospitals & Faculty of Medicine, Switzerland, ³Division of Orthopedic Surgery, Geneva University Hospitals & Faculty of Medicine, Switzerland

Atypical femoral fractures (AFF) are well recognized stress or insufficiency fractures frequently associated with long-term anti-resorptive therapies. Clinical management of patients who sustained an AFF, despite the context of bone fragility, generally includes cessation of bisphosphonates or denosumab treatment. Fracture outcome and fractures incidence following AFF remains however unknown. We previously reported 39 cases of AFF based on retrospective analysis of radiographs and medical records between 2000 and 2010 in Geneva University Hospitals (1). From 2010 to March 2015, all incident AFF were prospectively recorded, in addition to patients follow-up, to complete an observational study of subjects who sustained an AFF between 2000 and 2015. Sixty five subjects (94% women, age 74 ± 9yrs) sustained a subtrochanteric or diaphyseal femoral stress fracture between 2000 and March 2015, including 62 (95%) meeting the ASBMR Task Force 2013 criteria, and 3 sub-prosthetic fractures with morphological characteristics of AFF. Fifty five subjects (85%) had received bisphosphonate or denosumab, whilst 9 (14%) had no exposure to these drugs (one undetermined). Sixty three AFF (97%) were complete and 2 (3%) were incomplete fractures. One subject sustained bilateral complete fractures at once, and 2 subjects had concomitant fragility fractures (humerus and ankle). Nineteen (29%) had concomitant contralateral incomplete fracture on X-ray, needing prophylactic nail for 10 (53%) of them. Longitudinal follow up after AFF was obtained for 50 subjects (77%, range 3 months-12 years). Delayed fracture healing or non-union was observed in 11 patients (22%). Eight (16%) developed a contralateral AFF, including 6 complete AFF. Eighteen (36%) sustained at least one non atypical fragility fracture after AFF (incidence 123/1000 patients-years). Ten subjects (20%) died during the follow-up period. In this observational study of 65 cases of AFF (85% in subjects under antiresorptive drugs), the high incidence of osteoporotic fractures following AFF supports the concept of bone fragility in these patients. These data, in addition to frequent delayed fracture healing, highlight the interest to consider alternative treatments such as bone anabolic agents after AFF. Ref: (1) Meier RP et al. Increasing occurrence of atypical femoral fractures associated with bisphosphonate use. Arch Intern Med. 2012 Jun 25;172(12):930-6.

Disclosures: Emmanuel Biver, None.

SU0277

High Serum SHBG Predicts Incident Vertebral Fractures in Elderly Men. Liesbeth Vandenput¹, Dan Mellström², Östen Ljunggren³, Andreas Kindmark³, Helena Johansson⁴, Mattias Lorentzon⁵, Jason Leung⁶, Inga Redlund-Johnell⁷, Björn Rosengren⁷, Magnus Karlsson⁷, Timothy Kwok⁶, Claes Ohlsson⁴. ¹University of Gothenburg, Sweden, ²Center for Bone & Arthritis Research & Geriatric Medicine at the Sahlgrenska Academy, University of Gothenburg, Sweden, ³Department of Medical Sciences, University of Uppsala, Sweden, ⁴Centre for Bone & Arthritis Research at the Sahlgrenska Academy, University of Gothenburg, Sweden, ⁵Centre for Bone & Arthritis Research & Geriatric Medicine at the Sahlgrenska Academy, University of Gothenburg, Sweden, ⁶Jockey Club Centre for Osteoporosis Care & Control, The Chinese University of Hong Kong, Hong Kong, ⁷Clinical & Molecular Osteoporosis Research Unit, Lund University, & Department of Orthopaedics, Skåne University Hospital, Sweden

Previous prospective cohort studies have shown that serum sex steroid levels associate with non-vertebral fracture risk in men. The predictive value of sex hormones for vertebral fracture risk is, however, less studied.

Elderly men (aged ≥ 65 yrs) from Sweden and Hong Kong participating in the MrOS study had baseline estradiol (E2) and testosterone (T) analyzed by GC-MS and sex hormone-binding globulin (SHBG) by IRMA. Incident clinical vertebral fractures (n=242 cases) were evaluated in as many as 4,324 men during an average follow-up of 9.1 yrs (MrOS Sweden, n=2,847/n=221 cases; MrOS Hong Kong, n=1477/n=21 cases). In a subsample of these men (n=2,256), spine X-rays were obtained at baseline and after an average follow-up of 4.3 yrs to identify incident radiographic vertebral fractures (n=157 cases) (MrOS Sweden, n=1108/n=91 cases; MrOS Hong Kong, n=1148/n=66 cases). The likelihood of incident clinical and radiographic vertebral fractures was estimated by Cox proportional hazards models and logistic regression models, respectively. Discrimination was determined using C-statistics while net reclassification improvement (NRI) was used for reclassification analyses.

Neither serum E2 (HR per SD increase (95% CI): 0.93 (0.80-1.08), p=0.34) nor T (1.05 (0.91-1.21), p=0.51) predicted incident clinical vertebral fractures in age-adjusted models in the combined data set. High serum SHBG, however, associated with increased clinical vertebral fracture risk (1.24 (1.12-1.37), p<0.0001). This association remained significant after further adjustment for FRAX[®] without BMD (1.26 (1.14-1.39), p<0.0001) and FRAX[®] with BMD (1.25 (1.13-1.38), p<0.0001). SHBG slightly

improved clinical vertebral fracture risk classification (AUC) from a model adjusted for age ($p < 0.05$) when examined in MrOS Sweden. When evaluated with the more sensitive NRI, SHBG significantly improved clinical vertebral fracture reclassification models adjusted for age (20%, $p < 0.01$), for FRAX[®] without BMD (19%, $p < 0.01$) and for FRAX[®] with BMD (18%, $p < 0.05$). Similar as for the incident clinical vertebral fractures, neither E2 nor T predicted fracture risk in age-adjusted models in the subsample with incident radiographic vertebral fractures available. Again, high SHBG associated with increased radiographic vertebral fracture risk (combined data set; OR per SD increase (95% CI): 1.22 (1.05-1.43), $p < 0.05$). This association also remained significant after adjustment for FRAX[®] without BMD (1.24 (1.06-1.44), $p < 0.01$) and FRAX[®] with BMD (1.23 (1.05-1.43), $p = 0.01$).

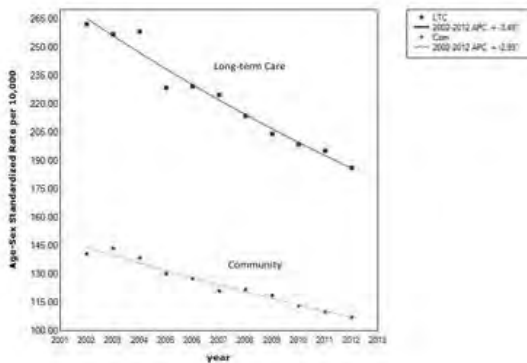
In conclusion, high SHBG predicts incident clinical and radiographic vertebral fractures in elderly men and adds information beyond FRAX[®] with BMD for vertebral fracture risk prediction. The mechanism by which SHBG affects vertebral fracture risk warrants further investigation.

Disclosures: Liesbeth Vandenput, None.

SU0278

Hip Fracture Rates in Long-term Care Residents Declining Faster than in the Community. Alexandra Papaioannou¹, Courtney Kennedy¹, George Ioannidis¹, Ruth Croxford², Cathy Cameron³, Sara Mursleen¹, Jonathan Adachi¹, Susan Jaglal³. ¹McMaster University, Canada, ²Institute for Clinical Evaluative Sciences, Canada, ³University of Toronto, Canada

Background: Reported hip fracture rates are stable or declining in the last two decades both in Canada and internationally. Fracture incidence trends in institutionalized versus community-dwelling seniors have not been considered, yet long-term care (LTC) cohorts are older, frailer, and at increased risk for falls and fractures. **Purpose:** To compare temporal trends in incident hip fracture rates for LTC versus community-dwelling residents. **Methods:** A retrospective cohort was defined using population-level health administrative data for all individuals aged 65 years and older living in Ontario, Canada between 2002 and 2012. The LTC cohort was defined based on records indicating an LTC admission or a physician visit or prescription filled while residing in LTC. In Ontario, approximately 620 LTC facilities (nursing homes) are funded by the provincial health ministry and provide residential care for older adults who need access to 24-hour nursing, supervision, or higher levels of personal care assistance. Fractures were identified (ICD-10-CA diagnosis codes) from emergency department, inpatient records, and physician claims. To compare overall incidence rates among different years and cohorts, rates were age-sex standardized using the 2002 population of LTC residents as the standard population. Join point regression analyses (Joinpoint Regression Program, Version 4.1.1.5) were used to examine temporal trends in osteoporotic fracture rates. **Results:** Hip fracture rates declined for both LTC and community cohorts during the years 2002-2012 (figure). Rates decreased faster among individuals living in LTC than in the community ($p < 0.05$ for difference in slopes). The annual percent change in hip fracture rates was -3.49 (95% CI: -3.97, -3.01) in LTC and -2.93 (95% CI: -3.28, -2.57) in the community. There was no evidence that the trend changed during the study period for either LTC or the community during (i.e. indicating constant slopes). Although women had higher overall hip fracture rates, there was a similar rate of decline for men and women during the study years. **Conclusions:** Between 2002 and 2012, hip fracture rates in Ontario, Canada decreased more rapidly in LTC versus community-dwelling residents. Initiatives to decrease falls and improve osteoporosis and fracture care have been ongoing by LTC providers and the government-funded Ontario Osteoporosis Strategy which may, in part, have contributed to the decline in hip fracture rates.



Figure

Disclosures: Alexandra Papaioannou, Amgen, Eli Lilly, Merck Canada Inc., Werner Chilcott; Amgen, Eli Lilly

SU0279

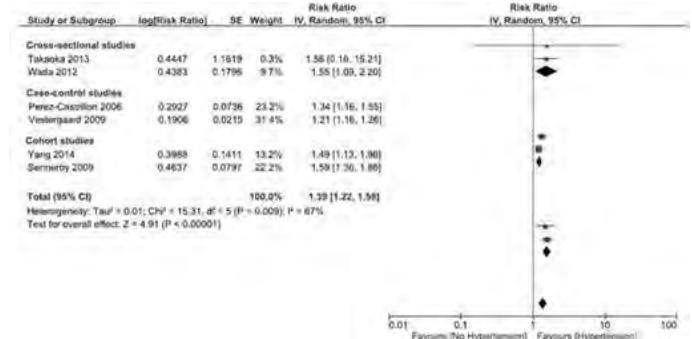
Hypertension as a Risk Factor for Fractures: a Systematic and Meta-analysis of Observational Studies. Raghad Alharthy¹, Debra A. Butt², Jeevitha Sriganthan³, George Tomlinson², Angela M. Cheung⁴. ¹University Health Network, Canada, ²University of Toronto Departments of Family & Community Medicine & Medicine, Canada, ³University Health Network Osteoporosis Program, Canada, ⁴University Health Network Osteoporosis Program; University of Toronto Departments of Family & Community Medicine & Medicine, Canada

Background: Two of the most prevalent co-morbidities in the elderly population are hypertension and osteoporosis. Complications from these two conditions account for significant morbidity, mortality and health-care costs. There are no systematic reviews/meta-analyses published to date that examine the association of hypertension as a risk factor for osteoporotic fractures in the elderly.

Methods: We searched Medline, EMBASE, Cochrane, CINAHL and Web of Science from inception to March 11, 2015 without language restriction for all studies assessing the effect of hypertension on fracture risk. We also reviewed the reference lists of qualifying articles and reviews. Two independent reviewers extracted the data and assessed study quality. Using a random-effects model weighted by inverse variance of the effect size, we determined the pooled adjusted and unadjusted risk ratios (RR) and their 95% CIs. Statistical heterogeneity was tested using the I² statistic. Publication bias was assessed using funnel plots comparing standard error and effect size.

Results: Of the 885 citations identified by the search strategy, 6 studies met the inclusion criteria and 2 additional studies were retrieved from the reference lists of included articles. Eight observational studies with a total of 549,181 participants (52% female, average age 66.4 years old) were included in the systematic review: 6 of these had summary estimates adjusted for covariates such as age, sex, BMD, history of falls and use of antihypertensives. Studies evaluated one of three primary outcomes: hip (4 studies), vertebral (4 studies), or any fracture (3 studies). Elderly with hypertension had a significant increase in fracture risk (RR 1.39, 95% CI 1.22-1.58, $p < 0.001$) (See figure). Pooling unadjusted risk ratios from 7 studies resulted in a similar pooled estimate but with wider confidence intervals and greater heterogeneity. These results are not sensitive to the quality of the studies [good and fair studies (RR 1.40, 95% CI 1.13-1.73) versus poor studies (RR 1.37, 95% CI 1.20-1.56)].

Conclusion: This systematic review and meta-analysis of observational studies suggests that having a diagnosis of hypertension may increase the risk of fragility fractures in the elderly by 39%. Further work is needed to examine whether these findings are due to hypertension itself or the effects of the drugs that treat it.



Forest Plot of adjusted RRs- HTN and Fx meta-analysis

Disclosures: Raghad Alharthy, None.

SU0280

Identification of bone and fall-related patient phenotypes based on hierarchical cluster analysis in patients with a recent fracture. Lisanne Vranken¹, Joop van den Bergh², Piet Geusens³, Caroline Wyers², Robert van der Velde². ¹Maastricht University Medical Centre & VieCuri Medical Centre, NL, ²VieCuri Medical Center, Venlo, The Netherlands, Netherlands, ³Maastricht University Medical Center, Maastricht, The Netherlands, Netherlands

Purpose

Bone mineral density (BMD), bone-related risk factors and fall-related risk factors are independently related to fracture risk. In patients over 50 years of age with a recent fracture, these risk factors are overlapping, heterogeneous, and found in multiple combinations. We evaluated the prevalence of bone and fall-related risk factors in patients visiting the Fracture Liaison Service (FLS) to identify clusters of fracture patients based on bone and fall-related risk factors.

Methods

A retrospective chart review was performed in consecutive patients with a recent fracture visiting the FLS for fracture risk evaluation between January 2009 and June

2011. Cluster analyses were performed using SPSS (version 21.0) to identify clusters of patients.

Results

Out of 3057 patients aged 50-90 years, 1111 consecutive patients, who were willing and able to be evaluated at the FLS, were included (71% women, mean age 65 ± 10 years), 8% presented with a hip, 29% with a major, 57% with a minor and 6% with a finger or toe fracture. Osteoporosis was diagnosed in 29%, osteopenia in 48% and 23% had a normal BMD. A fall in the past year was reported by 25% of patients. At least one bone-related risk factor was present in 90%, and at least one fall-related risk factor was present in 82% of patients. Based on 35 risk factors and using hierarchical cluster analysis a Pearson correlations, 3 variables (BMD, falls past year and ≥5 fall risks) were identified that were representative for each cluster. Based on these 3 variables, the program built five patient phenotypes. The frequency of past fractures was significantly different between the clusters. It was highest in elderly patients (mean 72 ± 11 years) with ≥5 fall risks and in 44% osteoporosis (45%), younger patients (mean 64 ± 9 years) with falls during last year and in 29% osteoporosis (41%) or with osteoporosis (42%). Patients with osteopenia and <5 fall risks or normal BMD with <5 fall risks had less past fractures (25-28%, p<.001 between all clusters).

Conclusion

Detailed evaluation of bone and fall-related risks using cluster analyses in patients at the FLS helps to identify patient phenotypes with different bone and fall characteristics. These clusters were associated with a significant difference in the history of fractures. These results indicate the potential value to use cluster analyses in identifying patients at the FLS at risk of further fractures based on a combination of bone and fall-related risk factors.

Disclosures: Lisanne Vranken, None.

SU0281

Incidence, Skeletal Site of, and Risk Factors for Clinical Fractures in Older Men by Baseline BMD Category. Howard Fink*¹, Terri Blackwell², Brent Taylor³, Eric Orwoll⁴, Kristine Ensrud⁵. ¹GRECC, Minneapolis VA Medical Center, USA, ²California Pacific Medical Center, USA, ³Center for Chronic Disease Outcomes Research, VA Healthcare System, USA, ⁴Oregon Health Sciences University, USA, ⁵Center for Chronic Disease Outcomes Research, VA Health Care System, USA

Older men with osteoporotic BMD are at high fracture risk. However, most men with fractures are not osteoporotic, and characteristics of older men with higher BMD who fracture are uncertain. Therefore, we used data from MrOS, a prospective study in men >=65 yr, to examine whether rates, sites, and risk factors for incident clinical fractures differ in older men by BMD category. Baseline BMD of total hip, femoral neck, and lumbar spine, and a young female reference database were used to categorize 5984 men as normal (T-score >=-1 all sites), low bone mass (-2.5 > T < -1 all sites), or osteoporotic (T < -2.5 any site). Baseline participant characteristics were ascertained by questionnaire and clinic exam. Self-reported incident fractures were collected every 4 months and centrally confirmed by radiology reports. Participant characteristics with age-adjusted associations with incident clinical fracture (p<0.05) were selected for assessment of age-adjusted associations with major osteoporotic fracture (hip, wrist, proximal humerus, or clinical spine; MOF) in analyses stratified by BMD category. We used a test of interaction to evaluate whether association of risk factors with incident MOF differed by BMD category. 54% of men had normal BMD, 40% had low bone mass, and 5% had osteoporosis. Over 10.5 +/- 3.6 yr of follow-up, 9% of men (532) had a MOF. Age-adjusted MOF incidence was 4.4, 11.4, and 26.2 per 1000 person-yr in men with normal BMD, low bone mass, and osteoporosis, respectively (p-trend <0.001). Among men with a MOF, 28% had normal baseline BMD, 56% had low bone mass, and 17% were osteoporotic. Among men with clinical fractures, the percent with a MOF was 34%, 52%, and 68% in those with normal BMD, low bone mass, and osteoporosis, respectively. Age-adjusted associations of risk factors for MOF appeared similar between men with normal BMD, low bone mass, and osteoporosis (Table). In summary, the rate of MOF was 6-fold higher in older men with osteoporosis compared to those with normal BMD. However, >80% of men with MOF were not osteoporotic, and clinical fracture sites were only half as likely to be MOF in men with normal BMD vs. those with osteoporosis. The strength of age-adjusted associations of individual risk factors with MOF appeared similar between men regardless of BMD category. These results suggest that intervention strategies to address modifiable non-BMD risk factors may be essential to reduce the population burden of fractures in older men.

Table. Association of participant characteristics with risk of incident MOF as a function of baseline BMD category

| | Risk for incident clinical fx, HR (95%CI) | | | P for interaction |
|---|---|----------------------|--------------------|-------------------|
| | Normal BMD (3251) | Low Bone Mass (2419) | Osteoporotic (314) | |
| Age (SD) | 1.7 (1.4-2.0) | 1.7 (1.5-1.9) | 1.6 (1.3-2.0) | 0.92 |
| Race, nonwhite | 0.7 (0.4-1.4) | 0.6 (0.4-1.1) | 0.5 (0.2-1.1) | 0.75 |
| BMI (SD) | 1.0 (0.8-1.1) | 0.9 (0.8-1.0) | 0.9 (0.7-1.1) | 0.69 |
| Height change from age 25 (SD) | 1.1 (1.0-1.3) | 1.2 (1.1-1.4) | 1.4 (1.1-1.7) | 0.22 |
| Smoking pk-yr (SD) | 1.1 (0.9-1.3) | 1.2 (1.1-1.3) | 1.1 (0.9-1.4) | 0.76 |
| Walk daily for exercise | 0.9 (0.6-1.2) | 0.9 (0.7-1.1) | 1.0 (0.7-1.6) | 0.86 |
| Moderate or strenuous exercise, sometimes/often | 0.7 (0.5-1.1) | 0.7 (0.5-0.9) | 1.1 (0.6-1.8) | 0.55 |
| Fell past 12 mo | 1.5 (1.0-2.1) | 1.4 (1.1-1.9) | 1.6 (1.0-2.4) | 0.91 |
| Fracture after age 50 | 1.6 (1.4-1.8) | 1.7 (1.3-2.1) | 1.8 (1.2-2.8) | 0.86 |
| Parental fracture | 1.2 (0.8-1.7) | 1.3 (0.9-1.7) | 1.1 (0.6-2.0) | 0.84 |
| Comorbidity score* | 1.4 (1.2-1.7) | 1.4 (1.3-1.6) | 1.3 (1.0-1.6) | 0.60 |
| Self-reported health, G-EX | 0.8 (0.4-1.0) | 0.7 (0.5-1.0) | 1.2 (0.7-2.1) | 0.51 |
| IADL impairment, any | 1.5 (1.1-2.2) | 1.7 (1.3-2.2) | 2.1 (1.4-3.4) | 0.36 |
| CNS-active meds use† | 1.6 (1.0-2.4) | 1.6 (1.1-2.1) | 1.3 (0.7-2.2) | 0.99 |
| Anti-ulcer med use‡ | 1.7 (1.1-2.5) | 1.5 (1.1-2.0) | 1.4 (0.8-2.4) | 0.82 |
| Trails B, total time (SD) | 1.1 (0.9-1.3) | 1.3 (1.1-1.4) | 1.1 (0.9-1.4) | 0.38 |
| Grip strength, mean both hands (SD) | 1.3 (1.1-1.5) | 1.3 (1.1-1.4) | 1.2 (0.9-1.5) | 0.97 |
| Walk speed, m/s (SD) | 1.1 (0.9-1.3) | 1.3 (1.1-1.4) | 1.3 (1.0-1.7) | 0.32 |
| Use arms to stand | 2.2 (1.0-4.8) | 2.7 (1.7-4.5) | 1.7 (0.7-3.9) | 0.70 |

*Co-morbidity score is the number of 8 self-reported physician-diagnosed conditions: COPD, heart attack, stroke, CHF, surgical removal of stomach or intestine, Parkinson's, rheumatoid arthritis, diabetes.

†CNS-active medications defined as urinary antispasmodics, Alzheimer's medications, benzodiazepines, tricyclic antidepressants, trazodone, SSRI, anticonvulsants, or opioids.

‡Anti-ulcer medications defined as a proton-pump inhibitor or H2 blocker.

Table

Disclosures: Howard Fink, None.

SU0282

Loss in Health Related Quality of Life Following Low-Trauma Fractures in Frail Elderly. Jean-Eric Tarride¹, Robert B. Hopkins¹, Louis Bessette², Natasha Burke¹, Jacques Brown², William D Leslie³, Suzanne Morin⁴, Alexandra Papaioannou¹, Louisa Pericleous⁵, Jonathan D. (Rick) Adachi*¹. ¹McMaster University, Canada, ²Laval University, Canada, ³University of Manitoba, Canada, ⁴McGill University, Canada, ⁵Amgen Canada Inc., Canada

Purpose: To estimate the change in health related quality of life (HRQoL) following low trauma fractures using healthcare administrative data from Ontario, Canada.

Methods: HRQoL was estimated using the Health Utility Index (HUI) with the InterRai Minimum Data Set (MDS), a mandatory questionnaire for long term care (LTC) and home care in Ontario (population 14 million). The HUI, a validated HRQoL instrument, allows the calculation of health utility where 0 represents death and 1 the best imaginable health state. For reference, the HUI utility value for Canadians aged 80-84 years is 0.61 and the minimal clinically important difference is 0.03. The MDS was linked to Ontario acute care databases for years 2007-2011 to identify low trauma fractures using ICD-10-CA codes. As the MDS is administered every quarter, changes in HRQoL were estimated over 2 intervals: prior to and 1 month post-fracture, and prior to and 3 years post-fracture. Regressions were used to identify the predictors of the differences in HRQoL over time (e.g. age, sex, fracture type, comorbidities).

Results: 23,382 unique patients with low-trauma fractures were identified with pre-and post- HRQoL assessments; of which 5,057 fractures had at least 3 years of follow-up (39% were hip fractures). The mean age was 83 (SD 10) years, 81% were women, 35% resided in LTC prior to fracture, and 53% had a heart/circulation comorbidity and 43% had a neurological disorder. HRQoL decreased significantly from 0.491 (SD 0.188) pre-fracture to 0.334 (SD 0.166) 1 month post-fracture (p<0.001). Although HRQoL then increased over time, the mean utility value 3 years post-fracture was 0.406 (SD 0.182), a clinically significant reduction from pre-fracture (p<0.001). Similar temporal patterns were seen for all types of fractures (Figure). Regression analyses indicated that older age, living in a LTC facility compared to receiving assistive care at home, having a hip versus other fractures and living with neurological disorders were associated with additional decrements in utility. For example, the difference between baseline and 3-year utility values was statistically greater for individuals with a neurological condition (-0.126) compared to those without (-0.075) (p<0.001).

Conclusion: Among individuals living with non-acute institutional care, fractures have a significant impact on HRQoL up to 3 years following fracture. Although improvement is seen over time, HRQoL never returns to pre-fracture levels.

SU0284

Mortality risk associated with fractures, The 45 and Up study, a population based cohort study of 238,673 Australians. Weiwien Chen^{*1}, Lyn March², Fiona Blyth³, Judy Simpson⁴, Jacqueline Center⁵. ¹Garvan Institute, Australia, ²Kolling Institute of Medical Research, University of Sydney, Australia, ³Sax Institute, University of Sydney, Australia, ⁴University of Sydney, Australia, ⁵Garvan Institute of Medical Research, University of New South Wales, Australia

Background: Mortality post fractures is well accepted for hip and vertebral fractures. However there is less data available for non-hip, non-vertebral fractures. The 45 and Up study is a population based cohort study of community dwelling women and men in the state of New South Wales (NSW), Australia.

Objectives: To examine mortality risk in men and women following all fractures.

Methods: Baseline questionnaire data from the 45 and Up Study were linked to the Emergency Department Data Collection (EDDC), Admitted Patient Data Collection (APDC-including all hospital admissions, procedures and diagnoses within NSW), Registry of Births, Deaths and Marriages (RBDM) and Pharmaceutical Benefits Scheme (PBS-medication dataset). Fractures were identified from the EDDC and APDC using the ICD 9, 10, SNOMED and procedure codes. Death data was obtained from the RBDM dataset. Participants were followed from recruitment (2006-2008) till either death or 31 December 2013. Cox proportional hazards models were used to calculate mortality hazard ratios (HR) between participants who fractured and those who did not.

Results: 113499 men and 125174 women were included for analysis. The mean age of the cohort was 62.6 years (SD: 11.1) in women and 5.6 years (SD: 1.2) in men. The mean length of follow-up was 5.7 years (SD: 1.0) in women and 5.6 years (SD: 1.2) in men. Women had 8414 fractures and men had 5216 fractures. There were 5604 deaths in women and 10017 deaths in men. In the whole cohort, absolute mortality rate was higher in men (15.7/1000 person years) compared to women (7.9/1000 person years). Having a fracture increased mortality by approximately two-fold in both men (33.9/1000 person years) and women (18.6/1000 person years). However this differed for different fracture types as demonstrated by age and Charlson comorbidity index adjusted HRs in the table below. HRs were increased following proximal site but not distal site fractures (see Table). In general, relative risk of mortality was higher in the younger participants.

Conclusion: In a large sample of community dwelling men and women, proximal but not distal fractures were associated with an increased mortality risk after adjustment for Charlson comorbidity index. The cause of this increased mortality needs to be explored.

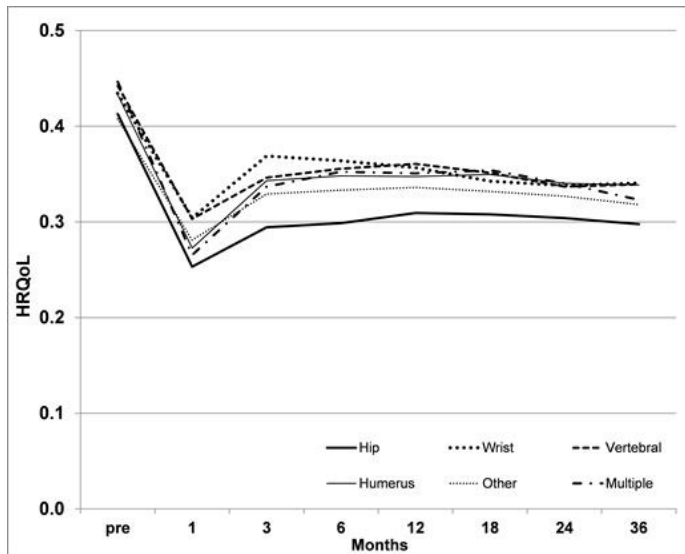
Table: Age and Charlson comorbidity index adjusted hazard ratios

| Fracture | Women | | Men | |
|-----------------------|---------------------|--------------------|---------------------|--------------------|
| | Number of fractures | HR (95% CI) | Number of fractures | HR (95% CI) |
| Proximal sites | | | | |
| • Pelvis | 373 | 2.33 (1.83, 2.97)* | 253 | 3.17 (2.47, 4.06)* |
| • Hip | 1110 | 2.48 (2.16, 2.85)* | 848 | 3.26 (2.86, 3.71)* |
| • Femur | 191 | 2.08 (1.46, 2.97)* | 167 | 2.85 (1.72, 3.49)* |
| • Humerus | 711 | 1.90 (1.46, 2.47)* | 307 | 2.01 (1.52, 2.68)* |
| • Vertebral | 415 | 2.84 (2.20, 3.66)* | 443 | 2.95 (2.38, 3.66)* |
| • Rib | 394 | 2.83 (2.13, 3.76)* | 718 | 2.33 (1.90, 2.85)* |
| Distal sites | | | | |
| • Forearm | 1544 | 1.24 (0.99, 1.25) | 401 | 1.53 (1.06, 2.22)* |
| • Wrist | 1014 | 1.12 (0.80, 1.57) | 340 | 1.30 (0.82, 2.07) |
| • Hand | 166 | 1.00 (0.41, 2.39) | 163 | 1.63 (0.88, 3.03) |
| • Ankle | 865 | 1.27 (0.84, 1.93) | 421 | 1.20 (0.78, 1.85) |
| • Foot | 478 | 1.17 (0.68, 2.01) | 194 | 1.41 (0.74, 2.72) |

*Significance: P < 0.05

Table: Age and Charlson comorbidity index adjusted hazard ratios

Disclosures: Weiwien Chen, None.



Health Related Quality of Life (HRQoL) Pre- and Post-Fracture, by Type of Fracture

Disclosures: Jonathan D. (Rick) Adachi, None.

This study received funding from: Amgen Canada Inc

SU0283

Low level of thoracic bone mineral density and low doses of glucocorticoid use are risk factors for clinical fractures in patients with rheumatoid arthritis: fourth-year results of the TOMORROW study. Tatsuya Koike^{*1}, Kenji Mamoto², Tadashi Okano³, Yuko Sugioka⁴, Masahiro Tada⁵, Kentaro Inui⁶. ¹Search Institute for Bone & Arthritis Disease (SINBAD), Japan, ²Department of Orthopaedic Surgery, Osaka City University Medical School, Japan, ³Department of Orthopedic Surgery, Osaka City University Medical School, Japan, ⁴Center for Senile Degenerative Disorders, Osaka City University Medical School, Japan, ⁵Department of Orthopedic Surgery, Osaka City General Hospital, Japan, ⁶Department of Rheumatology, Osaka City University Medical School, Japan

[Objectives]

Patients with rheumatoid arthritis (RA) who have muscle weakness and stiff or painful joints might be at increased risk of fall and fracture. The present study prospectively determined the incidence of fracture and risk factors in patients with RA who participated in the TOMORROW study (UMIN000003876) that began in 2010.

[Methods]

We evaluated anthropometric parameters, bone mineral density, disease activity and the incidence of clinical fractures for a period of 4 years in 202 patients with RA (mean age, 58.6 years; medication with biological agents, 54.9%) and 202 age- and sex-matched healthy volunteers (Controls; mean age, 57.4 years). The study successful execution rate for 4 years was 91.3 % in RA group and 93.2% in Control group, respectively.

[Results]

The incidence of clinical fractures did not differ significantly between patients with RA (n = 30, 14.9%) and Controls (n = 21, 10.4%) within the 4-year period (p=0.23). Furthermore, there was no difference among the sites of fractures between two groups. After adjusting for risk factors for fractures, including age, sex, smoking and body mass index, logistic regression analysis revealed previous vertebral fracture, past history of clinical fracture and low bone mineral density (BMD) at thoracic vertebrae as the parameters significantly associated with incidence of fractures (odds ratio [OR], 2.60; 95% confidence interval [CI], 1.36-4.98; p = 0.004, OR, 2.03; 95%CI, 1.11-3.71, p=0.022, OR, 3.35; 95%CI, 1.66-6.76, p=0.001, respectively) in whole group. Although the use of glucocorticoid (GC) was also a significant risk factor for fractures (OR, 2.59; 95%CI, 1.31-5.12, p=0.006), being RA was not a risk factor for fracture throughout subjects. Among patients with RA, low BMD at thoracic vertebrae was the most prominent risk factor for fracture (OR, 6.29; 95%CI, 2.29-17.2, p<0.001). Additionally, the use of GC at the entry (2010) (OR, 2.80; 95%CI, 1.23-6.40, p=0.014) was a significant risk factor for fracture in RA patients. Surprisingly, the use of GC more than an average of only 2 mg/day for four years increased OR for fracture in patients with RA (OR, 4.61; 95%CT, 1.87-11.34, p<0.001).

[Conclusion]

Incidence of clinical fractures did not differ significantly between patients with RA and Controls during a 4-year period. Low levels of BMD at thoracic vertebrae and low doses of GC appear significantly associated with an increased frequency of fractures among patients with RA.

Disclosures: Tatsuya Koike, None.

SU0285

Rest-activity patterns and their relation to falls and fractures in older men: The Osteoporotic Fractures in Men (MrOS) Study. Peggy Cawthon^{*1}, Terri Blackwell², Greg Tranah², Douglas Bauer³, Eric Orwoll⁴, Dan Evans², Jane Cauley⁵, Sonia Ancoli-Israel⁶, Katie Stone², Steven Cummings². ¹San Francisco Coordinating Center, USA, ²California Pacific Medical Center Research Institute, USA, ³University of California, San Francisco, USA, ⁴Oregon Health & Science University, USA, ⁵University of Pittsburgh, USA, ⁶University of California, San Diego, USA

Rest-activity levels follow a diurnal pattern in humans, and deficits in these patterns have been associated with increased risk of mortality and cardiovascular disease in older adults. The relation between rest-activity patterns and risk of falls and fractures has not been evaluated. MrOS is a prospective cohort study of 5,994 ambulatory men free of bilateral hip replacements, aged =65 years at enrollment in 2000-2. Using data from a follow-up visit of a subset of the MrOS cohort (2002-3, N for analysis: 3,001), we determined rest-activity patterns. We fit the extended cosine model to activity count values from wrist-worn actigraphy data initially collected to measure sleep characteristics over 4.8*0.8 24-hr periods (SleepWatch-O; Ambulatory Monitoring, Inc., Ardsley, NY). We determined amplitude, mesor, acrophase, and the pseudo-F statistic (Table 1). Following the visit, men reported falls and fractures via mailed questionnaires every four months. Recurrent fallers were classified as men with =2 falls in the year after the visit (versus men with 0-1 fall). Fractures were centrally adjudicated by physician review of radiology reports. Rest-activity components were evaluated as continuous variables with associations reported per SD increase or decrease in models adjusted for potential confounders (footnote, Table 2). Logistic regression was used to estimate the likelihood of recurrent falls; proportional hazards models were used to estimate the risk of non-spine fractures. In the year after the visit, 417 men (14.0%) had =2 falls. Later acrophase (indicating later phase shift of activity) and lower pseudo F-statistic values (indicating greater disorganization of activity), but not mesor or amplitude, were associated with a greater likelihood of falls. In 8.0 years (SD: 3.0) after the visit, 488 men (16.3%) had at least one non-spine fracture. None of the rest-activity patterns were associated with risk of non-spine fractures. No consistent associations were observed between rest-activity patterns and fractures analyzed by anatomical location (that is, spine, hip, wrist, upper arm, ankle/foot/toe). Minimally adjusted models were similar for all outcomes. In summary, later timing of activity and disorganization of activity patterns were independently associated with risk of falls in older men, but this did not translate into higher fracture risk. Future research should evaluate whether interventions that alter circadian patterns affect fall risk.

Table 1. Circadian patterns assessed in MrOS

| Rest-activity component | Definition |
|--|---|
| Amplitude (counts per minute) | Difference between peak & nadir in activity; higher values indicate greater difference in activity |
| Mesor (counts per minute) | Mean level of activity; higher values indicate greater activity |
| Pseudo F-statistic (unit less measure) | Measure of how well the activity fits the extended cosine model; higher values indicate better fit/less disorganization |
| Acrophase (time of day) | Time of day when peak activity (used in amplitude) occurs. Earlier/later indicates phase shift. |

Table 1. Circadian Patterns assessed in MrOS

Table 2. Rest-activity patterns and falls and fractures in older men

| Rest-activity component (SD unit) | Likelihood of recurrent falls (OR per SD, 95% CI)* | Risk of non-spine fractures (HR per SD, 95% CI)* |
|--|--|--|
| Amplitude (-1090 counts/min) | 1.11 (0.95, 1.31) | 1.00 (0.88, 1.12) |
| Mesor (-502 counts/min) | 1.02 (0.88, 1.19) | 0.99 (0.88, 1.12) |
| Pseudo F-statistic (- 512.9) | 1.23 (1.04, 1.46) | 1.04 (0.91, 1.19) |
| Acrophase (1 hour, 12 min) | 1.18 (1.06, 1.32) | 0.99 (0.90, 1.08) |

*adjusted for age, clinic site, race, body mass index, any medical condition (diabetes mellitus, coronary heart disease, hypertension, stroke), smoking, alcohol use, caffeine use, depression, use of benzodiazepines, use of prescription sleep medications, presence of an IADL, walking speed, activity count and nocturia. Fracture models additionally adjusted for femoral neck BMD.

Table 2. Rest-activity patterns and falls and fractures in older men

Disclosures: Peggy Cawthon, None.

SU0286

Short Term Functional Outcomes in Elderly Patients Sustaining Fragility Hip Fractures. Jordan Villa^{*1}, Joseph Koresse², Joaquin Moya¹, Arianna Gianakos³, Joseph Lane¹. ¹Hospital for Special Surgery, USA, ²Weill Cornell Medical College, USA, ³Hospital for Special Surgery, USA

Introduction: Hip fracture (HF) is one of the most common fractures in the elderly population with in-hospital mortality ranging from 3% to 9% and higher mortality at 6 months with increase in immobility after the fracture. Guidelines for management after HF surgery recommend first walk within 48 hours. Early ambulation (EA) reduces the negative effects of immobilization, improves functional recovery and is associated with an increased number of discharges directly home. Delay of getting a patient out of bed after this period is associated with poor function at 2 months. Although HF outcomes in elderly women have been established there has been little investigation about short term outcomes in males. We hypothesize that male sex is a predictor of worse short term functional outcome. The aim of this study was to evaluate the difference in time to standing and ambulation in men vs women and other factors associated with short term functional outcomes following HF surgery. **Methods:** A total of 443 patients older than 50 years with fragility HF admitted to the New York Presbyterian Hospital from 2013 to 2014 were included in this retrospective study. Information was collected from medical records. Cox proportional hazards modeling was used to compare time to stand and time to walk between sexes. **Results:** After adjustment for epidemiologic and operative care variables, there was no evidence of an association between sex and time to stand or time to walk ($P = 0.277$ and 0.681). The strongest predictors of a delayed time to stand were dementia and depression ($P = 0.010$ and 0.042). The strongest predictors of a delayed time until first walking were higher ASA, anemia, and higher age ($P=0.002$, 0.016 , and 0.038 , respectively). **Discussion:** The results show that gender is not a variable that can predict short term functional outcomes after surgical stabilization of HF. Results are different from previous studies that report no significant influence of either cognitive impairment or high comorbidity in EA. Although the time to surgery and the type of anesthesia were associated with 30 days outcomes, there has been no association with time to standing or ambulation 5 days after the surgery. **Conclusion:** There is no association between gender and time to stand or time to walk after surgical stabilization of a HF. Instead dementia, depression, ASA, anemia and age predict a longer time to stand and walk in the post-operative course.

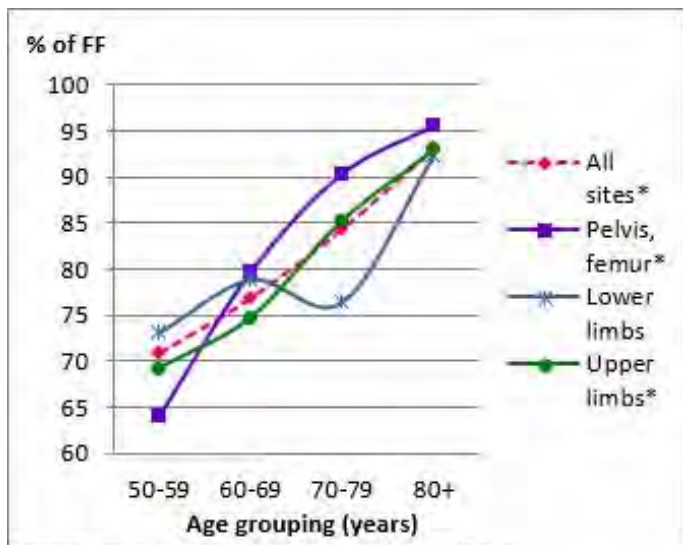
Disclosures: Jordan Villa, None.

SU0287

A Clinical Definition of Fragility Fracture. Claudia Beaudoin^{*1}, Sonia Jean², Louis Bessette³, Louis-Georges Ste-Marie⁴, Jacques P. Brown³. ¹CHU de Quebec Research Centre, Canada, ²Institut national de santé publique du Québec, Canada, ³CHU de Québec Research Centre, Canada, ⁴Université de Montréal, Canada

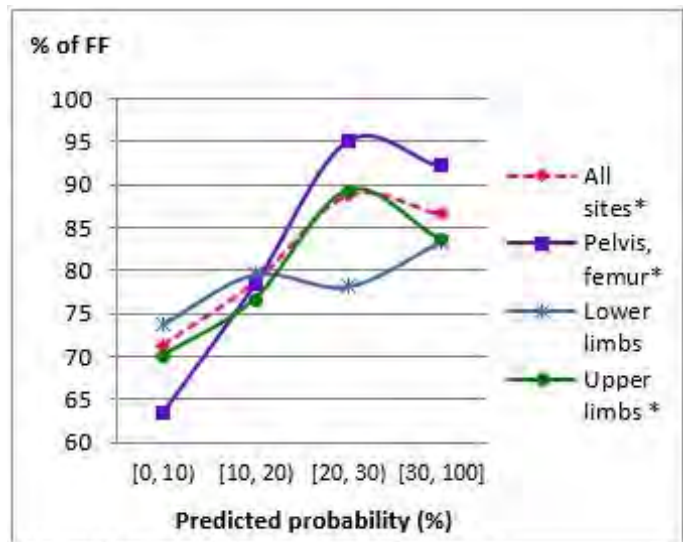
Background: Fractures at a given skeletal site are traditionally considered osteoporotic when fracture risk at this site increases with decreasing BMD and increasing age. **Objective:** The aim of this study was to assess if a simple clinical definition of fragility fracture (FF) based on circumstances of fracture satisfies the classical criteria defining an osteoporotic fracture and correlates with the FRAX risk

of major osteoporotic fracture (MOF). Methods: Women aged 50 and older who suffered a peripheral fracture were recruited in the ROCQ programme. Fractures were classified as FF based on the following definition: occurring spontaneously, from a fall from standing height, sitting, lying, missing 3 or fewer steps, coughing, sneezing or from a movement outside of the normal range of motion. All other fractures were classified as traumatic fractures. Six to eight months following fracture, women completed a questionnaire detailing personal and clinical characteristics. Femoral neck BMD (FN-BMD) were collected for participants who had a BMD measurement within 2 years of the fracture event. BMD data was imputed for about 50% of women who did not have a FN-BMD result available. The FRAX 10-year risk of MOF was calculated with and without BMD. Only fractures that happened before the programme were considered to estimate the risk. Mantel-Haenszel Chi-Square tests for trend were performed to determine whether the proportion of FFs increases significantly with age and FRAX risk and decreases significantly with increasing FN-BMD t-score, both globally and by fracture sites. Results: A total of 2712 women were included in the analyses and provided data on 294 fracture events at the hip or femur, 838 at the lower limbs and 1597 at the upper limbs. Overall, 77% of the fractures were FFs and the proportion of FF increased significantly with age (Fig. 1) and FRAX without and with BMD risk (Fig. 2) at all sites except lower limbs. The proportion of FF decreased significantly with increasing FN-BMD t-score at all sites except lower limbs (Fig. 3). Conclusion: We have shown that a simple clinical definition of FF based on the cause and circumstances of fracture satisfies the classical criteria defining an osteoporotic fracture and correlates with the FRAX predicted risk. These findings provide support to the validity of our definition of FF. A subsequent analysis assessing the ability of the proposed definition to predict a future fracture is planned.



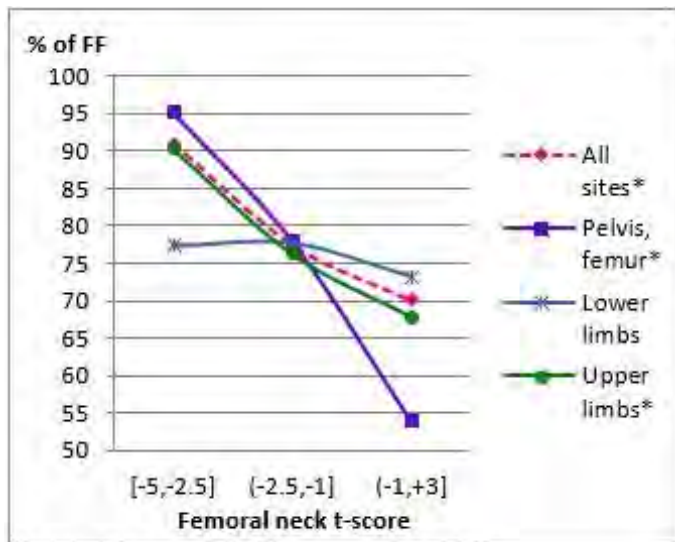
* Mantel-Haenszel Chi-Square p-value < 0.05

Fig. 1: Proportion (%) of fragility fracture (FF) by fracture site according to age



* Mantel-Haenszel Chi-Square p-value < 0.05

Fig. 2: Proportion (%) of fragility fracture (FF) by fracture site according to FRAX with BMD risk



* Mantel-Haenszel Chi-Square p-value < 0.05

Fig. 3: Proportion (%) of fragility fracture (FF) by fracture site according to femoral neck t-score

Disclosures: Claudia Beaudoin, Merck, Actavis, sanofi-aventis, Amgen, Eli Lilly, Novartis
 This study received funding from: Merck, Actavis, sanofi-aventis, Amgen, Eli Lilly, Novartis

SU0288

Are Fragility Fractures Associated With Frailty Prior to Fracture? Healthcare Utilisation In Older Women Prior to Fracture Compared With Those Without Subsequent Fracture. Kerrie Sanders¹, Jenny Watts², Lucy Busija¹, Amanda Stuart², David Scott³, Geoff Nicholson¹. ¹Australian Catholic University, Australia, ²Deakin University, Australia, ³Monash University, Australia

To examine the association between frailty and risk of fracture in older women we investigated total healthcare utilisation for one year prior to longitudinal fracture ascertainment in women aged at least 70 years at recruitment. Australia provides universal health coverage through Medicare for all health services except public hospitals. Medicines are subsidized by pharm benefits scheme PBS). Free public hospital care is widely accessible.

Women at higher risk of falls and fracture were recruited. Participants' total PBS scripts and health service use for the year prior to fracture ascertainment, was obtained from Medicare/PBS. These data stratified by age and subsequent fracture (yes/no) were used to calculate the average number of services and scripts per participant in each group. The regional public hospital provided patient level data on all hospital services used. Binominal regression was used to analyse hospital service use.

Healthcare use, scripts and hospital data were obtained from 590 consented women who were then contacted monthly for fracture ascertainment for the next 3 years. All fractures were radiologically confirmed. 68 women sustained fracture(s) and 512 did not.

The average health service and script use for women with and without subsequent fracture was 15.7 vs 18.9 items and 34.4 vs 39.6 scripts, respectively (table). Although the study was only powered to detect a 30% difference in hospital services, the data adjusted for age and self-reported prior fracture (since 50 y.o) suggests number of hospital services was not predictive of subsequent fracture (odds ratio; 95%CI: 1.14; 0.60, 2.17; p=0.7).

The findings suggest older women who fracture are not less healthy prior to the fracture event.

Healthcare services expressed per person per annum*

| Age group (years) | Subsequent fracture Medicare | No fracture Medicare | Subsequent fracture PBS | No fracture PBS |
|-------------------|------------------------------|----------------------|-------------------------|-----------------|
| 70-74 | 10.6 | 15.5 | 29.0 | 32.4 |
| 75-79 | 20.5 | 20.9 | 33.0 | 41.5 |
| 80+ | 14.4 | 21.1 | 41.3 | 47.6 |

*p values not reported as variance not calculated as data were de-identified.

Disclosures: Kerrie Sanders, None.

SU0289

Differences In Pain Experience Between Women With And Without Vertebral Fractures: Novel Independent Descriptors Identified. Emma Clark*, Rachael Goberman-Hill, Tim Peters, University of Bristol, United Kingdom

Background: Osteoporotic vertebral fractures (VFs) are present in approximately 12% of the postmenopausal population, but less than a third come to clinical attention. One reason for this is lack of clear clinical triggers for referral for radiographs, including a lack of evidence about which characteristics of back pain may indicate presence of VF. **Aim:** To investigate whether the quality or type of back pain in people with VFs is different to those with back pain but no VFs, and if so to develop a simple back pain questionnaire for discrimination. **Methods:** A case-control study was undertaken. Digital radiological archives were used to identify a population of potential participants who had a thoracic radiograph for back pain. Inclusion criteria were >60 years, female and thoracic spinal radiograph performed in the previous 3 months. 683 potential participants were approached, and all who agreed to take part self-completed a questionnaire assembled from domains and scales taken from questionnaires previously validated in UK populations including the McGill Pain Questionnaire and the Keele STarT back pain score as well as demographics. Cases were defined at the end of the study as those with a VF identified from spinal radiographs by the PI using the ABQ method. Chi-squared tests were used to assess univariable associations and logistic regression to identify independent predictors of VFs. Receiver Operating Characteristic (ROC) curves were used to evaluate the ability of the combined independent predictors to differentiate between women with and without VFs via Area Under Curve (AUC). **Results:** 64 cases and 135 controls completed questionnaires. Those with VFs were older (77.9 years vs 73.2, $P < 0.001$), more likely to have previously fractured a bone (70.8% vs 42.5%, $P = 0.001$) and more likely to have taken steroids (27.7% vs 10.4%, $P = 0.007$). History of previous fracture, reduced walking distance, poor vision, pain described as crushing, pain not described as taut and pain not spreading down legs were independent predictors of VFs. ROC analysis showed the AUC was 0.81 for these questions. **Conclusion:** We identify novel predictors of VFs in older women based on descriptions of back pain. These could be combined to produce a simple questionnaire that has the potential to discriminate between women who are likely to have a VF and should therefore have diagnostic spinal radiographs, and women who have degenerative spinal disease instead.

ROC curve to evaluate the ability of the combined independent predictors to differentiate between women with and without VFs

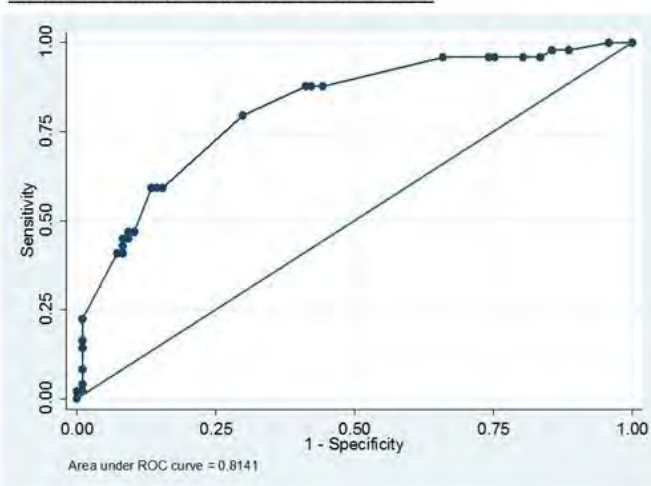


Figure1: ROC

Disclosures: Emma Clark, None.

This work was funded by the Elizabeth Blackwell Institute and the Wellcome Trust Institutional Strategic Support Fund to the University of Bristol

SU0290

Muscle Mass Predicts Incident Fracture in Postmenopausal Women: The OFELY Study. Elisabeth Sornay-Rendu¹, Francois Duboeuf², Stéphanie Boutroy², Roland Chapurlat^{*2}, ¹INSERM UMR1033, Université de Lyon, France, ²INSERM UMR1033 & Université de Lyon, France

The relationships between body composition and bone mineral density are well established but the independent contribution of body composition to the risk of fracture (Fx) has rarely been evaluated prospectively. The aim of this study was to prospectively investigate the prediction of fragility Fx by fat, lean and muscle mass in postmenopausal women. We measured body composition at the 9th annual follow-up of the OFELY study in 595 postmenopausal women, mean age 66.8 yrs. Whole body DXA (HologicÜ, QDR4500) exams were analyzed using the APEX version 4.0.2 to get visceral (VFAT) and subcutaneous fat mass (SFAT) in an abdominal region of interest along with measurement of total body fat mass (FM), lean mass (LM),

appendicular skeletal muscle mass (ASM) and Femoral Neck BMD (FNBM). The LM (LMI) and ASM indexes (ASMI) were obtained by dividing by height squared. During a median [IQR] 13.1 [1.9] yrs of follow-up, 138 women sustained a first incident fragility Fx, including 85 women with a major osteoporotic Fx (MOP Fx: hip, clinical spine, shoulder or wrist). After adjustment for age, women who sustained Fx had lower BMI (-4%, $p = 0.01$), VFAT (-4%, $p = 0.07$), SFAT (-6%, $p = 0.06$), LMI (-6%, $p = 0.002$) and ASMI (-3%, $p = 0.003$), compared with women without Fx ($n = 457$). The differences were more pronounced for women who sustained MOP Fx ($p < 0.01$ for all). After adjustment for age, prevalent Fx, physical activity, incident falls (during the whole follow-up in women without Fx and until the first incident Fx in fractured women) and FNBM, each SD increase of baseline values of LMI and ASMI were associated with significant decreased fracture risk with adjusted hazard ratios [HR(95%CI)] of 0.76(0.61-0.95) and 0.76(0.62-0.94), $p < 0.02$. Those associations remained significant after adding body weight in the multivariate model ($p = 0.02$). For all Fx, FM, VFAT and SFAT were not independently associated with fracture risk in the multivariate model with or without adding body weight. For MOP Fx, FM, VFAT and SFAT, were associated with fracture risk in the multivariate model without ($p < 0.05$), but not with body weight in the model. We conclude that both visceral and subcutaneous fat mass are associated with fracture risk but not independently of BMD and body weight. In contrast, lean mass and appendicular muscle mass indexes predict the risk of fracture in postmenopausal women independently of BMD and clinical risk factors.

Disclosures: Roland Chapurlat, None.

SU0291

Nonsteroidal Anti-Inflammatory Drug Prescriptions are Associated with Increased Stress Fracture Risk in U.S. Army Soldiers. Julie Hughes*¹, Craig McKinnon¹, Lakmini Bulathsinghala², Katelyn Guerriere¹, Mary Bouxsein³, Joseph Kardouni¹, Ronald Matheny, Jr.¹, ¹US Army Research Institute of Environmental Medicine, USA, ²DoD-VA Extremity Trauma & Amputation Center of Excellence, USA, ³Endocrine Unit, Massachusetts General Hospital, Center for Advanced Orthopedic Studies, Beth Israel Deaconess Medical Center, Department of Orthopaedic Surgery, Harvard Medical School, USA

Use of nonsteroidal anti-inflammatory drugs (NSAIDs) is widespread in the U.S. Army and in civilian populations. NSAIDs inhibit prostaglandin synthesis, which is necessary for adaptive bone formation in response to mechanical loading. Further, animal models have shown that adaptive bone formation inhibits development of stress fracture. Whether NSAID use increases risk of stress fractures is not known. Therefore, the purpose of this study was to determine the stress fracture risk among U.S. Army soldiers prescribed NSAIDs. A retrospective cohort study was conducted using data from the Total Army Injury and Health Outcomes Database from 2002 to 2011. We identified soldiers who had stress fractures at the lower extremity and pelvis ($n = 55,162$; 3.1% of male soldiers, 9.1% of female soldiers). Soldiers prescribed NSAIDs between 180 and 21 days prior to injury ($n = 31,463$) were compared with four randomly selected controls from the population at risk ($n = 1,261,297$) after matching on date of stress fracture diagnosis. Conditional logistic regression was used to calculate the odds ratios (OR) for stress fracture. In the unadjusted model, soldiers prescribed NSAIDs were twice as likely to suffer a stress fracture compared to controls (OR = 1.98 [95% CI 1.94-2.02]). A model adjusting for age, race, ethnicity, and length of military service yielded an OR of 2.87 (2.80-2.94) for NSAID use. To account for potential sex-based differences in stress fracture risk with NSAID prescription, a sex-stratified adjusted analysis was performed, yielding an OR of 2.79 (2.68-2.91) for females and 2.84 (2.76-2.92) for males. This retrospective study showed that in both men and women, NSAID prescriptions are associated with a nearly 3-fold increased risk of stress fracture in soldiers.

The views expressed in this abstract are those of the authors and do not reflect the official policy of the Department of Army, Department of Defense, or the U.S. Government.

Disclosures: Julie Hughes, None.

SU0292

Osteoporosis markers and atherosclerosis: higher bone density is associated with greater carotid intima-media thickness in middle-aged women. Monika Frvz*¹, Kevin Deere², Debbie A Lawlor³, William D Fraser⁴, L-L Benfield¹, Jon H Tobias², Celia Gregson⁵, ¹School of Social & Community Medicine, University of Bristol, United Kingdom, ²Musculoskeletal Research Unit, School of Clinical Sciences, University of Bristol, United Kingdom, ³MRC Integrative Epidemiology Unit at the University of Bristol, United Kingdom, ⁴Faculty of Medicine & Health Sciences, University of East Anglia, United Kingdom, ⁵University of Bristol, United Kingdom

Aims

Osteoporosis and cardiovascular disease (CVD) are common age-related diseases which have frequently been found to be associated. We aimed to explore the relationship between osteoporosis markers and preclinical atherosclerosis measured

by carotid intima-media thickness (cIMT) in mid-aged, predominantly pre-menopausal women.

Methods

Data from 2933 mothers from the Avon Longitudinal Study of Parents and Children were used. Total body (TB) bone mineral density (BMD), bone mineral content (BMC), bone area (BA) and hip BMD were measured by DXA scanning, bone turnover (a further marker of osteoporosis) was assessed by serum beta-carboxyterminal cross linking telopeptide (CTX) levels. cIMT was measured by high-resolution B ultrasound. We used multivariable linear regression to examine the association between both CTX and DXA-derived variables and cIMT, adjusting for a range of confounders. Results are expressed as partial correlation coefficients with 95% confidence intervals.

Results

Mean (SD) participant age was 48 (4.0) years, BMI 26.2 (5.0) kg/m², and 70% were premenopausal. CTX was positively associated with cIMT (0.064 [0.027, 0.101] p=0.001), but this association attenuated to the null with adjustment for age (0.003 [-0.034, 0.040] p=0.8). Total hip BMD was positively associated with cIMT (0.060 [0.024, 0.097] p=0.001), and this association persisted after adjustment for age, height, lean & fat mass, smoking, education level, estrogen replacement and menopausal status (0.057 [0.017, 0.097] p=0.005). There were also positive (confounder adjusted) associations of TB BMD and TB BA with cIMT, though the latter had 95% confidence intervals that included the null. A positive association was also seen between bone area-adjusted BMC and cIMT. There was no evidence that associations differed between pre- and post-menopausal women (e.g. partial correlation coefficients for association of hip BMD with cIMT were 0.062 [0.016, 0.108] and 0.042 [0.039, 0.122] in pre- and post-menopausal women respectively (interaction p=0.8)).

Conclusion Contrary to previous studies, mostly performed in older populations, which suggest that osteoporosis is associated with greater CVD risk, we found weak positive associations of BMD with cIMT, in a predominantly premenopausal group, which appeared to reflect an association with bone size and volumetric density and was not related to bone turnover. These findings require further replication and exploration in large prospective studies.

Disclosures: *Monika Frysz, None.*

SU0293

Parental Hip Fracture is an Independent Risk Factor for Fracture: A Population-Based Parent-Offspring Linkage Analysis. Shuman Yang^{*1}, William Leslie¹, Lin Yan¹, Randy Walld¹, Leslie Roos¹, Suzanne Morin², Sumit Majumdar³, Lisa Lix¹. ¹University of Manitoba, Canada, ²McGill University, Canada, ³University of Alberta, Canada

Background: A meta-analysis of cohort studies suggests that parental hip fracture (HF) independently predicts fractures in their offspring. However, parental HF information from these studies was self-reported and may be subject to recall bias. We examined the association of parental HF, ascertained from population-based administrative data and parent-offspring record linkage, with major osteoporotic fracture (MOF) and HF.

Methods: We identified 263,368 women and men (age ≥ 40 years) with continuous health coverage in Manitoba, Canada who were able to successfully link to their parental healthcare information (possible for offspring born after 1951). Parental HF was derived from hospital discharge abstracts dating back to 1970 (6.0% maternal, 2.9% paternal and 8.6% either parent). Incident MOF and HF events in the offspring were ascertained from hospital and physician claims data using validated algorithms. Cox proportional hazards models (with time-varying covariates updated annually) were used to estimate the association between parental HF and offspring MOF and HF, adjusted for age, sex, prolonged glucocorticoid use, rheumatoid arthritis, osteoporosis treatment, prior major fracture, and proxies for smoking and high alcohol use.

Results: During 2,827,772 person-years of offspring follow-up, we identified 7,207 incident MOFs (4.3% and 2.6% for those with and without either parent HF, p<0.001) and 374 incident HF (0.3% and 0.1% for those with and without either parent HF, p<0.001). Either parent HF was significantly and independently associated with increased risk of MOF in fully adjusted model (HR: 1.29; 95% CI: 1.19-1.40; Table). Results were similar for women (HR: 1.36; 95% CI: 1.22-1.51) and men (HR: 1.21; 95% CI: 1.07-1.37), without significant interaction between sexes (p=0.16). HRs of MOF associated with a maternal HF (HR: 1.30; 95% CI: 1.18-1.43) or a paternal HF (HR: 1.24; 95% CI: 1.09-1.42) were similar to that seen in either parent analysis. The relationship between either parent HF and offspring HF was even stronger (HR: 1.67; 95% CI: 1.25-2.21), and again there was no significant interaction according to offspring's sex (p=0.29).

Summary: Using population-based data with parent-offspring linkage, we have confirmed parental HF to be an independent risk factor for both MOF and HF. Our findings support a previous meta-analysis based on self-reported parental hip fracture and justify the use of this variable in fracture risk prediction.

Table. Fully adjusted hazard ratios (95% CI) for incident major osteoporotic fracture (MOF) and hip fracture (HF) associated with parental HF.

| | MOF | HF |
|------------------|------------------|------------------|
| Maternal HF | 1.30 (1.18-1.43) | 1.63 (1.17-2.28) |
| Paternal HF | 1.24 (1.09-1.42) | 1.67 (1.05-2.67) |
| Either parent HF | 1.29 (1.19-1.40) | 1.67 (1.25-2.21) |

Table. Fully adjusted hazard ratios (95% CI) for incident MOF and HF

Disclosures: *Shuman Yang, None.*

SU0294

The Relationship between Smoking Duration, Pulmonary Function and Bone Mineral Density in Korean Men: KNHANES 2008-2011. Ji Hyun Lee^{*1}, Jung Hee Kim², A Ram Hong³, Chan Soo Shin³, Sang Wan Kim³. ¹Seoul national university hospital, South Korea, ²Department of Internal Medicine, Seoul National University College of Medicine, Seoul, South Korea, ³Department of Internal Medicine, Seoul National University College of Medicine, South Korea

Smoking is one of well established risk factors that induce bone loss, however, data on the amount a person has smoked over a long period of time are lacking. We investigated the relationships between pack-years smoked, pulmonary function and bone mineral density (BMD) among Korean men. This cross sectional study was performed using data from the 2008-2011 Korean National Health and Nutrition Examination Survey, including men aged 50 to 64 years. All subjects underwent bone mineral density measurements using dual energy X-ray absorptiometry and pulmonary function tests using standardised spirometry. A total of 1,476 subjects were classified into groups with regard to their pack-years smoked included <1 (n=301), 1-30 (n=693), and greater than 30 pack years (n=482). Forced expiratory volume in 1 second (FEV1) values were decreased according to pack-years smoked (3.17 ± 0.53; 3.16 ± 0.51; 3.02 ± 0.56; p<0.001). The mean BMD at total hip was decreased according to pack-years smoked groups with < 1, 1-30, and greater than 30 pack years adjusted for age, body mass index, alcohol consumption, physical activity, socioeconomic status, and vitamin D level which might affect bone metabolism (1.131 ± 0.142; 1.128 ± 0.156; 1.102 ± 0.143 g/cm³; p<0.05). The mean BMD at femur neck was increased according to forced vital capacity (FVC) quartile and was independent of covariates mentioned above (0.770 ± 0.110; 0.782 ± 0.107; 0.783 ± 0.112; 0.796 ± 0.113 g/cm³; p<0.05). In conclusion, smoking over 30 pack years and low FVC were associated significantly with low hip BMD. They should be considered to be risk factors associated with bone loss in men aged 50-64 years.

Disclosures: *Ji Hyun Lee, None.*

SU0295

Upper Body Center of Mass Location Affects the Factor of Risk for Vertebral Fracture. Julie Choise¹, Celia Amabile², Agathe Nérot², Christophe Travert², Hélène Pillet², Wafa Skalli^{*2}. ¹Arts et Metiers ParisTech, France, ²Arts et Metiers ParisTech, LBM/Institut de Biomecanique Humaine Georges Charpak, France

The factor of risk for vertebral fracture (Φ) is defined as the ratio of spinal loading to vertebral strength and was demonstrated to change depending on the age and gender's population. Another factor to consider in the vertebral fracture risk assessment is the location of the upper body center of mass (COM) situated above the lumbar spine. Previous studies assumed that the upper body COM is located directly over the center of the vertebral column but this location may vary depending on each one posture. The purpose of this study was to determine the change in upper body COM depending on age and gender and its effect on Φ for vertebral fracture calculation.

32 asymptomatic adults were considered (15 male, 17 female, age: 53 yo [21-85]). Head to feet low dose bi-planar X-Rays were acquired in standing position using the EOS system (EOS Imaging, Paris, France). 3D reconstructions of the external body shape and L1 were performed (Figure 1). The upper body weight and COM situated above L1 were calculated with the head, neck and thorax personalized volume and generic densities, and arms mass determined as a percentage of total body mass for each participant. A finite element model of L1 was built with subject-specific 3D geometry and a generic bone mineral density distribution converted in elastic modulus for material properties attribution. Antero-posterior distance between L1 upper plate's center and the upper body COM was determined. Φ was determined with 1) the load applied to the center of L1 and 2) the load applied at the upper body COM location. To assess age specific differences, participants were divided in 3 groups; 12 participants in group 1 (20-40), 10 in group 2 (41-65) and 10 in group 3 (>65). Differences between groups were assessed with a t-test.

The upper body COM was located 13 mm (± 19) anterior to L1 for group 1, 37 mm (± 16) for group 2 and 44 mm (± 27) for group 3. Significant changes in distances were found between group 1 and 2 ($p=0.005$) and between group 1 and 3 ($p=0.005$). Φ significantly increased (worsened) with age when the load was applied at the upper body COM location (Figure 2).

Even though at this step muscle forces were not modeled, the upper body has the tendency to shift forward with age and therefore apply higher forces to the lumbar spine which increases the factor of risk for vertebral fracture. Future factor risk calculation should incorporate the upper body COM location.



Figure 1: Upper body 3D reconstruction with L1 in yellow, L1 center in blue and gravity line in red

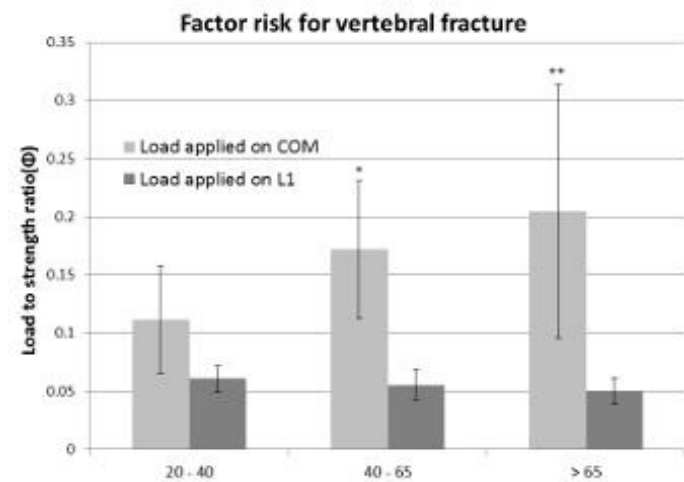


Figure 2: Factor risk for each group; * ($p<0.05$) and ** ($p<0.01$) compared to group 1
Disclosures: Wafa Skalli, None.

SU0296

Weight Change and Risk of Central Body Fractures in Older Community-Dwelling Men. Kristine Ensrud¹, Stephanie Harrison², Jane Cauley³, Deborah Kado⁴, Cora Lewis⁵, Andrew Hoffman⁶, Eric Orwoll⁷, Carolyn Crandall⁸, Marcia Stefanick⁶, Peggy Cawthon². ¹University of Minnesota & Minneapolis VA Health Care System, USA, ²California Pacific Medical Center Research Institute, USA, ³University of Pittsburgh, USA, ⁴University of California - San Diego, USA, ⁵University of Alabama at Birmingham, USA, ⁶Stanford University, USA, ⁷Oregon Health & Science University, USA, ⁸University of California - Los Angeles, USA

Purpose: Determine associations of weight loss and weight gain in late life on risk of central body (hip, clinical vertebral, or pelvis) fractures in older men.

Methods: We used data from 4523 men attending Visit 2 of the prospective MrOS study. Weight change from baseline to Visit 2 an average of 4.5 years later was classified as moderate weight loss (loss $\geq 10\%$), mild weight loss (loss 5% to $<10\%$), stable weight ($<5\%$ change) or weight gain (gain $\geq 5\%$). At Visit 2, men were asked if they were trying or not trying to lose weight. Men were contacted tri-annually after Visit 2 to ascertain incident fractures confirmed by radiographic reports.

Results: Mean age was 77.5; 283 men (6%) had moderate weight loss, 742 (16%) had mild weight loss, 3076 (68%) had stable weight and 422 (9%) gained weight. During an average follow-up of 7.4 years, 313 men (7%) experienced ≥ 1 central body fracture including 156 hip fractures, 128 clinical vertebral fractures and 47 pelvis fractures. Age-adjusted rates of central body fractures per 1000 person years were higher among men with moderate weight loss (15.5) and men with mild weight loss (10.4) and similarly lower among men with stable weight (8.8) and men with weight gain (8.4). An analogous pattern was seen for hip and clinical vertebral fractures. After adjustment for age, race, smoking and comorbidities, greater weight loss was associated with a higher risk of central body fracture (p trend 0.02) (Table). Men with moderate weight loss had 1.5-fold (HR 1.54 95%CI 1.01-2.33) higher risk compared with those with stable weight or weight gain (referent group); men with mild weight loss had a modest increase in risk that was not significant. Associations of weight loss with fracture risk did not vary by BMI or intention to lose weight (p interaction term ≥ 0.54). Inclusion of potential mediators including physical activity, fall history, gait speed or femoral neck BMD in the model attenuated the association between moderate weight loss and central body fracture by 6 to 13%, with BMD having the greatest impact.

Conclusion: Among community-dwelling older men, men with moderate weight loss compared to those with stable weight or weight gain had an increased risk of central body fractures irrespective of body weight or intention to lose weight. While fall propensity, lower physical activity and mobility play minor roles as mediators, our findings suggest that this association is due in part to lower hip BMD among men with weight loss.

Table: Association between Weight Change and Risk of Central Body Fracture

| Weight Change Category | Fracture Risk Hazard Ratio (95% CI) | | | | |
|--------------------------------------|-------------------------------------|----------------------|-------------------------|----------------------|----------------------|
| | Base Model ¹ * | Model 2 ¹ | Model 3 ¹ ** | Model 4 ¹ | Model 5 ¹ |
| Stable weight or weight gain | 1.00 (reference) | 1.00 (reference) | 1.00 (reference) | 1.00 (reference) | 1.00 (reference) |
| Mild weight loss (5% to $<10\%$) | 1.23 (0.93, 1.64) | 1.23 (0.93, 1.64) | 1.23 (0.93, 1.64) | 1.17 (0.87, 1.57) | 1.10 (0.82, 1.46) |
| Moderate weight loss ($\geq 10\%$) | 1.54 (1.01, 2.33) | 1.52 (1.00, 2.31) | 1.48 (0.97, 2.25) | 1.44 (0.93, 2.23) | 1.33 (0.87, 2.03) |
| p-trend | 0.02 | 0.02 | 0.03 | 0.07 | 0.18 |

¹adjusted for age, race, smoking and comorbidity index

*Base model = PASE

**Base model = fall history

³Base model = gait speed

⁵Base model = femoral neck BMD

Table. Association between Weight Change and Risk of Central Body Fracture

Disclosures: Kristine Ensrud, None.

SU0297

Withdrawn.

SU0298

Applying the Health Action Process Approach to Develop Educational Videos to Improve Vitamin D Adherence in Older Adult with Osteoporosis-A Pilot Knowledge Translation Study. AHMED NEGM¹, Jonathan D. Adachi², Arthur Lau³, Norma J. MacIntyre⁴. ¹McMaster University, Canada, ²St. Joseph's Healthcare/McMaster University, Canada, ³Division of Rheumatology, McMaster University, Canada, ⁴School of Rehabilitation Science, Faculty of Health Sciences, McMaster University, Canada

Purpose: Despite high level evidence that vitamin D is effective in osteoporosis (OP) fracture prevention, adherence to vitamin D supplementation is low. The Health Action Process Approach (HAPA) is a theoretical model used to change health behaviors. This study aimed to pilot four educational videos developed using the HAPA to address self-efficacy, OP fracture risk perception, outcome expectancy and action planning related to vitamin D adherence in people with OP.

Methods: Eligible participants were recruited through OP specialty clinics (≥ 50 years, diagnosed with OP, not taking vitamin D for the last 3 months regularly, fluent

in English and with no cognitive diseases or mal-absorption syndromes). Participants were instructed to select the number and order of videos to watch and reported the following: knowledge gained on a scale from 1 to 7, the most important information and what else they would like to know related to each topic. Descriptive data were summarized.

Results: Fourteen participants (mean age (SD) = 68.4 (8.7) years; 12 females) were recruited during one winter month. The OP fracture risk perception and action planning videos were watched first or second. In contrast, the outcome expectancy video tended to be watched third and the self-efficacy video fourth (F=21.98; P = 0.0001). Figure 1 shows that participants learned significantly more from the OP fracture risk perception video than the self-efficacy video (P = 0.05) and from the outcome expectancy video than the self-efficacy (P = 0.04) and action planning (P = 0.006) videos. The most important knowledge gained in each video was: 'risk of death and disability after hip fracture' (fracture risk perception); 'take vitamin D in the same time and place' (action planning) 'falls prevention' (outcome expectancy); and 'take vitamin D regularly' (self-efficacy).

Conclusion: Most participants watched all four videos. This study supports the administration of all four videos rather than tailoring to assessed phase of the HAPA model. Less was learned from the self-efficacy and action planning videos. Feedback from these knowledge users will be used in revision. Further study will determine if viewing the videos increases vitamin D adherence, as assessed by serum levels, compared to a control group who do not view the videos.

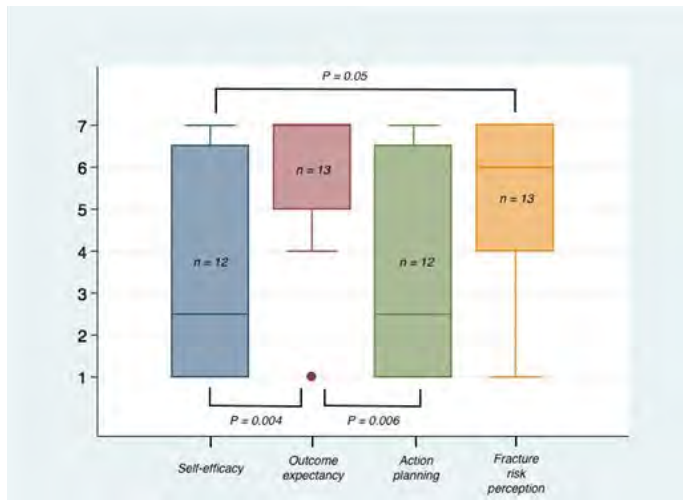


Figure 1 Box plot of knowledge gained in each video

Disclosures: AHMED NEGM, None.

SU0299

Comparing Agreement of Osteoporosis Treatment Guidelines Using Data from the Patient Activation after DXA Receipt Notification (PAADRN) Study. Nicole Wright^{*1}, Peter Cram², Fred Wolinsky³, Douglas Roblin⁴, Stephanie Edmonds³, Kenneth Saag¹. ¹University of Alabama at Birmingham, USA, ²University of Toronto, Canada, ³University of Iowa, USA, ⁴Georgia State University, USA

Purpose: To compare the osteoporosis (OP) treatment guideline concordance in participants of the PAADRN study using the US National Osteoporosis Foundation (NOF) and the International Osteoporosis Foundation (IOF) guidelines.

Methods: We used the control arm (n=2711) of the PAADRN study, a randomized, controlled trial aimed to activate patients around OP treatments, to evaluate guideline concordance in a usual care setting. We defined NOF guideline concordant therapy as either receipt of OP therapy at the 12-week post-DXA survey if the participant had a fracture after age 40, a T-score at or below the OP threshold, or a T-score within the low bone mass range and a FRAX score ≥20%. Instead of one FRAX threshold, the IOF guidelines include aged-based FRAX thresholds. We used the UK thresholds for this study. We used descriptive statistics to compare and contrast the characteristics of participants for whom the treatment indications from the NOF and IOF guidelines did not agree.

Results: Our sample was 85% female, 20% from minority backgrounds, and 60% ≥65 years of age. At baseline, 760 (28%) reported having a fracture after age 40, 576 (21%) had DXA-defined OP, 188 (7%) had low bone mass with a FRAX ≥20%, and 949 (35%) had FRAX scores above the UK age-based thresholds. Using NOF guidelines, OP therapy was indicated for 1,170 and not indicated for 1,541 participants. Using IOF guidelines, OP therapy was indicated for 1,395 and not indicated for 1,316 participants. At the 12-week survey, 38.2% and 35.8% of patients with NOF and IOF based indications for OP therapy reported medication use. Among patients without indications for OP therapy, 15.4% of NOF and 14.0% of IOF patients reported medication use. Two hundred and thirty-five participants who were indicated for therapy using IOF guidelines were not indicated for therapy using NOF guidelines, whereas 10 participants were not indicated for therapy using IOF guidelines but were indicated for therapy using NOF guidelines. These discordant participants differed on a few characteristics (Table).

Conclusion: We found significant overlap in treatment indications when using either NOF or IOF guidelines; however, for a small number of participants, the treatment indications differed based on guideline used. Although, both guidelines are based on cost-effectiveness of OP treatment, clinical judgment takes precedent for treating individuals, which may explain guideline discordance.

Table. Characteristics of Discordant Participants Based on IOF and NOF Treatment Guidelines

| | IOF Treatment Indicated/ NOF Treatment Not Indicated (n=236) | | IOF Treatment Not Indicated/ NOF Treatment Indicated (n=10) | | p-value |
|----------------------------|--|------|---|------|---------|
| | N/Mean | %/SD | N/Mean | %/SD | |
| Age Category | | | | | <0.001 |
| <60 | 110 | 46.8 | 0 | 0.0 | |
| 60-69 | 121 | 51.5 | 0 | 0.0 | |
| 70-79 | 4 | 1.7 | 2 | 20.0 | |
| 80+ | 0 | 0.0 | 8 | 80.0 | |
| FRAX Score | 12.5 | 3.8 | 22.7 | 3.1 | <0.001 |
| Public Insurance | 78 | 33.2 | 8 | 80.0 | 0.002 |
| History of Crohn's Disease | 11 | 4.7 | 2 | 20.0 | 0.034 |

Table

Disclosures: Nicole Wright, Amgen

SU0300

Healthcare costs of osteoporotic fracture in South Korea. Ha Young Kim^{*1}, Deog-Yoon Kim², Sunmee Jang³, Yong Chan Ha⁴, Tae Young Kim⁵. ¹Wonkwang University Sanbon Hospital, South Korea, ²Kyung Hee University, South Korea, ³Gachon University, South Korea, ⁴Chung-Ang University, South Korea, ⁵Hallym University, South Korea

Background: Although many studies have been reporting cost of osteoporotic fractures, study of cost of osteoporotic fracture in South Korea was rarely reported. The present study was to estimate healthcare costs of osteoporotic fractures including spine, hip, distal radius and humerus in Korean people over 50 years of age using national claim data from 2008 to 2011.

Methods: With using KNHI data, we identified all claims records of outpatient visits or hospital admissions of patients who were fifty years of age or older between January 1, 2008 and December 31, 2011. To identify osteoporosis-related fractures, we used certain ICD-10 codes and a patient age cut-off value of 50 years. The healthcare costs were included that acute phase costs accounting for medical care given immediately after osteoporotic fracture was sustained, which includes an emergency room visit and the expected costs due to further hospitalization and surgical procedures, physiotherapy sessions according to the site of the fracture, and outpatient visits after discharge over a one year.

Results: Total number of osteoporosis related fractures among those aged 50 years or older was increased 32% from 192,986 in 2008 to 254,794 in 2011. Total healthcare cost of osteoporotic fracture was increased 41.2% from 2008 to 2011 and portion of total healthcare cost was increased from 3.41% in 2008 to 3.52% in 2011. The average healthcare cost in each person was increased 6.2% from 2,823,324 won in 2008 to 3,013,620 won in 2011. The mean healthcare costs were highest in hip fracture, and followed by humerus fracture, spine fracture, and distal radius fractures.

Conclusion: This study presents increasing trend of total healthcare costs of osteoporotic fractures using the Korean National Health Insurance data and must be acknowledged as an important health problem in elderly population.

Disclosures: Ha Young Kim, None.

SU0301

Online Linkage of FRAX Fracture Risk Assessment to Management Guidance is Used by Clinical Practitioners. An Analysis of Access to National Osteoporosis Guideline Group Guidance in the UK (July 2013-June 2014). Eugene McCloskey^{*1}, Helena Johansson², Nicholas Harvey³, Juliet Compston⁴, John Kanis⁵. ¹University of Sheffield, United Kingdom, ²Centre for Metabolic Bone Diseases, University of Sheffield, United Kingdom, ³MRC Lifecourse Epidemiology Unit, University of Southampton, United Kingdom, ⁴Dept. of Medicine, Cambridge Biomedical Campus, United Kingdom

In several countries, the online output of FRAX is linked to independent country-specific guidelines (e.g. UK, Lebanon, and Finland) which facilitates treatment decisions according to local assessment guidelines. In the UK, guidance provided by the National Osteoporosis Guideline Group (www.shef.ac.uk/NOGG) was made available in 2008. The aim of this study was to determine the uptake of this facility by exploring website activity using GoogleAnalytics software. We have undertaken an analysis of FRAX and NOGG website usage for the year between 1st July 2013 and 30th June 2014 (GoogleAnalytic reports 8th August 2014). During this period, there was a total of 1,774,812 sessions (a user interaction with the website) on the FRAX website with 348,964 of these from UK-based users. Over the same time, 253,530 sessions were recorded on the NOGG website. Of the latter, two-thirds were returning

users, one-third new users and the vast majority (208,766, 82%) arose from users in the UK. The remainder of users were from other countries with the US comprising approximately half of the non-UK use, demonstrating that some users of FRAX in other countries make use of the NOGG guidance. Of the UK-sourced sessions, the majority were from England, but the session rate (adjusted for population) was highest for Scotland (Table 1). Almost all (95.7%) of the UK sessions arose from calculations being passed through from the FRAX tool (www.shef.ac.uk/FRAX) to the NOGG website, comprising FRAX calculations in patients without a BMD measurement (155K, 74.5%) or FRAX calculations with a BMD result (44K, 21.2%). A minority of sessions were conducted for other reasons (manual calculations, document downloads, FAQs etc.). National Health Service (NHS) sites were identified as the major source of visits to the NOGG website, comprising 64% of the identifiable visiting locations, but this is an underestimate as many sites from within the NHS are not classified as such. The study shows that the facilitated interaction between web based fracture risk assessment and clinical guidelines is widely accepted by clinical users. The approach could usefully be adopted in all countries for which a FRAX model is available.

Table 1. Usage of the NOGG website within the UK.

| Country | Total sessions | Population | Session rate/ 100, 000 |
|------------------|----------------|------------|---------------------------|
| England | 163,749 | 53012456 | 309 |
| Scotland | 32,740 | 5295000 | 618 |
| Wales | 7,677 | 3063456 | 251 |
| Northern Ireland | 4,586 | 1810863 | 253 |

Table

Disclosures: Eugene McCloskey, None.

SU0302

Osteoporosis Patients Assessed by Telemedicine: A Unique High Risk Cohort. Rachel Johnston^{*1}, Sarah Munce¹, Sonya Allin¹, Alexandra Pearce², Arlene Silverstein², Shelley Bouchard², Tarik Berekat¹, Gillian Hawker¹, Susan Jaglal¹, Sandra A. Kim³. ¹University of Toronto, Canada, ²Women's College Hospital, Canada, ³Women's College Hospital, University of Toronto, Canada

Background:

Evidence in support of telemedicine (TM) for rural populations for chronic conditions has been well described. However, there is limited literature on the role of TM in osteoporosis. In 2005, a multidisciplinary osteoporosis TM program, based on an existing outpatient program, was developed at Women's College Hospital (Toronto, Canada) in conjunction with the Ontario Telemedicine Network, to improve access to specialized osteoporosis care in remote areas of Ontario. The purpose of this study was to describe the demographic and clinical characteristics of osteoporosis patients assessed by TM and to compare them to those assessed in the outpatient clinic (clinic patients).

Methods:

A retrospective chart review of 57 TM patients and 880 clinic patients first seen between February 2013 to August 2014 was performed. T-tests and chi-square analyses were used to compare parametric data for the two groups, and Mann-Whitney U tests were used for non-parametric data.

Findings:

The mean age of TM and clinic patients were 64 and 63 years, respectively ($p=0.639$); patients were 90% female and 10% male in both cohorts. Forty-two percent of TM patients were at high-fracture risk as per the Canadian Association of Radiologists and Osteoporosis Canada tool, compared to 19% of clinic patients (Likelihood ratio (LR) 16.80, $p<0.0001$). Thirty-nine percent of TM patients had sustained a prior fragility fracture, compared to 20% of clinic patients (LR 10.07, $p=0.001$). TM patients were more likely to have co-morbidities (LR 6.946, $p=0.002$), more likely to be smokers (LR 3.49, $p=0.036$), and less likely to have completed post-secondary education (LR 9.71, $p=0.009$). TM patients were referred to allied health professionals more frequently: dietician (LR 12.646, $p=0.000$), pharmacist (LR 10.883, $p=0.000$), occupational therapist (LR 7.866, $p=0.004$), clinical nurse specialist (LR 7.074, $p=0.005$), and physical therapist (LR 1.913, $p=0.163$).

Conclusion:

Significant differences in baseline clinical and demographic characteristics were observed in TM patients, as compared to clinic patients. TM patients were observed to have a higher fracture risk profile, prevalence of fragility fractures, co-morbidities, and greater use of allied health resources. These data enable future research to better understand the financial and social costs associated with osteoporosis care delivered by TM.

Disclosures: Rachel Johnston, None.

SU0303

Osteoporosis screening and treatment among Veterans with recent low-trauma fracture after implementation of a centralized, interdisciplinary Bone Health Service. Richard Lee^{*1}, Megan Pearson², Patricia Jenkins², Kenneth Lyles², Cathleen Colon-Emeric². ¹Duke University, USA, ²Durham VAMC, USA

Background: In the 2010 Office of the Inspector General report, less than 24 percent of Veterans received appropriate evaluation and/or treatment for osteoporosis within 6 months of an index fracture. While Fracture Liaison Services have been shown to significantly improve osteoporosis treatment, they require timely identification of recent fracture patients by a specialty team, which may be less feasible for patients residing in remote areas and small medical centers with lower fracture volume. **Objective:** To evaluate the effect of a regional post-fracture Bone Health Service through a single, centralized Veterans Affairs Medical Center (VAMC) on osteoporosis evaluation and management, among Veterans with recent low-trauma fracture at 5 VAMCs and affiliated outpatient clinics in North Carolina, Virginia, and West Virginia. **Method:** The Bone Health Service identified Veterans with potential osteoporotic fractures using an automated query of inpatient and outpatient encounters, based on ICD9 diagnosis codes (800-829). The medical record of an eligible patient was reviewed remotely by a bone health physician at the central VAMC, and a consult note was sent to the patient's primary care provider, through the electronic medical record, that specified guideline-based recommendations for further evaluation and management. In 3 of the 5 VAMCs, a bone health nurse liaison then coordinated the ordering and follow-up of laboratory and bone density assessment, osteoporosis education (e.g. medication administration and side effects, calcium and vitamin D supplementation, falls prevention, and exercise), and adherence follow-up via telephone. **Results:** Between Oct 2013 and Dec 2014, the Bone Health Service identified 482 patients with a low-trauma fracture who were not already on osteoporosis treatment. 113 (27%) consults recommended immediate bisphosphonate treatment and 316 (66%) recommended bone density assessments. Bisphosphonates were prescribed in 65 patients (50%) and bone density testing was ordered in 245 (78%) patients. A bone health nurse liaison significantly improved bisphosphonate ordering (from 39 to 70%) and BMD testing completion rates (from 42 to 69%), $P<0.01$. **Conclusion:** A centralized, interdisciplinary Bone Health Service, including a nurse liaison to coordinate care and provide patient education, significantly improved the rate of osteoporosis evaluation and treatment among patients with a recent low-trauma fracture.

Disclosures: Richard Lee, None.

SU0304

Patients Undergoing Their First DXA Receive NOF Guideline Discordant Osteoporosis Pharmacotherapy. Stephanie Edmonds^{*1}, Yiyue Lou¹, Peter Cram², Douglas Roblin³, Nicole Wright⁴, Kenneth Saag⁴, Fredric Wolinsky¹. ¹University of Iowa, USA, ²University of Toronto, Canada, ³Georgia State University, USA, ⁴University of Alabama at Birmingham, USA

Purpose: To examine treatment concordance with NOF guidelines among healthcare providers ordering their patients' first DXA tests, and differences between physician and non-physician providers.

Methods: 7,749 participants were enrolled in a randomized control trial of adults 50 years old or older presenting for DXA at three US institutions from February 2012 to August 2014. Our analyses focused on 2,018 participants who were DXA naive and had never taken OP medications. Treatment indications were based on NOF guidelines using self-reported fracture history, DXA T-scores, and 10-year major osteoporotic and hip FRAX score. At 12 weeks post-DXA, we asked patients if their provider recommended a bone medication and used this data to determine concordance with NOF guidelines. We used Fisher's exact test for crude differences and random effects models to adjust for clustering, site, and percent of provider's patients undergoing their first DXA in concordant and discordant treatment between patients of physician vs. non-physician providers.

Results: The DXA scans for the 2,018 patients were ordered by 515 healthcare providers, with the numbers of providers split evenly among the three study sites. Most providers (78.5%) ordered DXAs for five or fewer DXA naive patients over the course of the study, and most providers were physicians (88.9%). Most patients were either concordantly not recommended for treatment per NOF guidelines (61.9%; Table 1, cell B), or concordantly recommended for treatment (9.1%, cell A). However, 26.9% of patients (cell D) were not recommended for treatment when NOF guidelines recommended pharmacotherapy, and 2.1% of patients (cell C) were recommended for treatment when they not indicated for treatment. Non-physicians were marginally more likely to be guideline concordant than physicians ($p=0.06$). After accounting for clustering of patients within provider, site, and percent of DXA naive patients, non-physicians were significantly more likely to provide guideline concordant recommendations ($p=0.049$).

Conclusion: We found that 29.0% of patients (cells C & D) undergoing their first DXA had providers whose decisions to recommend treatment were not concordant with NOF treatment guidelines. Because NOF guidelines are based on cost-effectiveness, individual treatment plans may be discordant. Further research needs to examine reasons why providers do not follow NOF guidelines and how to improve provider-training in OP-related care.

Table 1: Guideline Concordance of Treatment Recommendations among PAADR N Ordering Providers for Patients Undergoing First DXA Screening, n(%)

| N=2,018 | Treatment Recommended by Provider at 12 weeks | Treatment Not Recommended by Provider at 12 weeks | Total |
|----------------|---|---|---------------|
| NOF Concordant | CELL A 183 (9.1%) | CELL B 1,250 (61.9%) | 1,433 (71.0%) |
| NOF Discordant | CELL C 42 (2.1%) | CELL D 543 (26.9%) | 585 (29.0%) |
| Total | 225 (11.1%) | 1,793 (88.9%) | |

Table 1

Disclosures: *Stephanie Edmonds, None.*

SU0305

Physicians' Prescribing Considerations and Perceptions of Osteoporosis Patients' Compliance of Oral Bisphosphonate. Tao Gu¹, Debra Eisenberg², Jingbo Yu³. ¹HealthCore, USA, ²healthcore Inc, USA, ³Merck, USA

Objective: To assess physicians' prescribing considerations/preference for osteoporosis and perceptions of patients' compliance with oral bisphosphonates. Methods: This was an online survey of physicians identified in the HealthCore Integrated Research US claims database, as prescribing oral bisphosphonates to women aged ≥ 55 . The survey consisted of 22 questions gauging physicians' prescribing patterns and preferences for various types of osteoporosis medications, predicted patient persistence and compliance, and identified reasons for oral bisphosphonate non-compliance. Physician's demographic and clinical practice characteristics were also queried.

Results: Among the 158 physicians completing the survey, 77.7% were male, 67.5% were aged 45-60, 58.6% had 20 or more years in clinical practice, and on average had 263 (191) osteoporosis patients in clinic. Most were specialists from internal medicine (44.0%) or general practice (34.4%). Bone mineral density, long-term medication use, and a history of fracture were ranked as major considerations by 94.9%, 88.6%, 86.7% of physicians, respectively, when deciding whether to treat an osteoporosis patient. Most physicians expressed a preference of weekly or monthly oral bisphosphonates, for newly diagnosed patients (54.4% and 34.2%, respectively) and for long-term users of oral bisphosphonates (40.5% and 36.1%, respectively). Most physicians (23.4% always, 58.9% sometimes) incorporated a drug holiday into their prescribing patterns. Majority of physicians (N=131; 82.9%) estimated that patients would rate the acceptability of oral bisphosphonates as osteoporosis therapy as 5-8 on a 0-10-point scale. Although most physicians predicted that more than half of patients would comply with the prescribed medication for at least a year, 17.7% predicted that less than half of patients would be compliant in the first year, and 29.7% predicted the same result for compliance beyond 1 year. The major reasons for non-compliance of oral bisphosphonates were gastrointestinal intolerance (71.5%) and experience of medication side effects (69.6%).

Conclusions: US physicians who regularly prescribe oral bisphosphonates consider several relevant risk factors when prescribing and have a preference for weekly or monthly regimens. These physicians estimated a substantial minority of patients to be non-compliant of oral bisphosphonates, for reasons including primarily gastrointestinal intolerance and medication-related side effects.

Disclosures: *Tao Gu, HealthCore Inc*

This study received funding from: *Merck and company*

SU0306

Risk Factors that are Associated with Osteoporosis Treatment in High Risk Residents Living in Long Term Care (LTC) Homes? The Gaining Optimal Osteoporosis Assessments in Long-Term Care (GOAL) Study. George Ioannidis¹, Alexandra Papaioannou², Denis O'Donnell³, Courtney Kennedy², Hrishikesh Navare³, Lora Giangregorio⁴, Sharon Marr², Angela Cheung⁵, Richard Crilly⁶, Sid Feldman⁷, Ravi Jain⁸, Sophie Jamal⁵, Robert Josse⁵, Sadhana Prasad¹, Lehana Thabane¹, Jonathan Adachi¹. ¹McMaster University, Canada, ²McMaster University & GERAS Centre, Canada, ³Medical Pharmacies Group Limited, Canada, ⁴University of Waterloo, Canada, ⁵University of Toronto, Canada, ⁶University of Western Ontario, Canada, ⁷Baycrest Geriatric Health Care System, Canada, ⁸Osteoporosis Canada, Canada

Background: The GOAL initiative was developed to assess high risk residents and recommend appropriate pharmacotherapy to reduce fractures by utilizing multifaceted knowledge translation strategies.

Methods: GOAL is a delayed-entry stepped-wedge cluster randomized controlled trial in 50 long term care homes in Ontario. Information sources for the study included de-identified clinical/prescribing data from the database of a large pharmacy

provider that services all study homes, chart audits, and the Resident Assessment Instrument Minimum Data Set (RAI-MDS). These data were entered into a pharmacist's electronic decision support tool that generated individual management recommendations and calculated the number of high risk residents living in long term care. High risk was based on the osteoporosis guidelines and was defined as those individuals who had at least one spine/hip fracture, 2 or more non-hip/non-spine fractures, or were currently taking corticosteroids ($>7.5\text{mg/d}$ prednisone equivalent). Residents with previous diagnoses of osteoporosis were also considered at high risk. We determined whether there were associations among risk factors and osteoporosis treatment at baseline using the generalized estimating equations technique with an exchangeable correlation structure. The analysis was adjusted for risk factors and age. Values are expressed as odds ratios and 95% confidence intervals (CI).

Results: Of the 6862 residents from 50 long term care homes who were evaluated, a total of 2949 (43.0%) were considered at high risk. High risk residents had a mean age (SD) of 85.9 (9.0) years, weighed 64 (17.1) kg and were 158.5 (10) cm tall. Overall, osteoporosis medications were taken by 37% (1101/2949) of high risk residents. Adjusted odds ratios indicated that a diagnosis of osteoporosis (3.2; 95% CI: 2.5, 4.0), prior spine fracture (1.9; 95% CI: 1.5, 2.5), and those currently taking corticosteroids (1.9; 95% CI: 1.2, 3.0) were factors associated with the use of osteoporosis treatment.

Conclusion: A total of 43% of residents, living in long term care homes, are at high risk for fracture. Of these individuals, a diagnosis of osteoporosis, a prior spine fracture and those currently taking corticosteroids were characteristics that were found to be related with the use of osteoporosis treatment. Prior hip fractures did not appear to trigger the use of osteoporosis therapy.

Disclosures: *George Ioannidis, None.*

This study received funding from: *Amgen*

SU0307

Association between Teriparatide Treatment Duration and Fracture Incidence in Taiwan: Analysis Using the National Health Insurance Research Database.

Ding-Cheng CHAN¹, Cecile Hsiao-Chun CHANG², Lay-Chin LIM³, Alan BRNABIC⁴, Jau-Yih TSAU⁵, Russel BURGE⁶, Fei-Yuan HSIAO⁷, Ling JIN⁸, Sirel GURBUZ⁹, Rong-Sen YANG¹⁰.

¹Superintendent Office, Jin-Shan Branch, National Taiwan University Hospital, Taipei, Taiwan; ²Department of Geriatrics & Gerontology, & Department of Internal Medicine, National Taiwan University Hospital, Taipei, Taiwan, Taiwan, ³Eli Lilly & Company, Taipei, Taiwan, ⁴Department of Orthopaedics & Department of Geriatrics & Gerontology, National Taiwan University Hospital, Taipei, Taiwan, ⁵Real World Analytics, Eli Lilly Australia Pty Ltd, Sydney, Australia, ⁶School & Graduate Institute of Physical Therapy, National Taiwan University, Taipei, Taiwan, ⁷Global Health Outcomes, Eli Lilly & Company, Indianapolis, USA, ⁸Graduate Institute of Clinical Pharmacy, College of Medicine, National Taiwan University, Taipei, Taiwan, ⁹Lilly Research Laboratories, Eli Lilly & Company, Indianapolis, USA, ¹⁰Emerging Markets, Eli Lilly & Company, Indianapolis, USA, ¹⁰Department of Orthopaedics, National Taiwan University Hospital, Taipei, Taiwan

Purpose: Teriparatide is approved for treatment of men and women with osteoporosis at high risk of fracture. This study examined the associations between persistence and adherence with teriparatide treatment and the incidence of new-onset non-vertebral and hip fractures in Taiwanese patients with osteoporotic fractures.

Methods: This retrospective, cohort study included patients from Taiwan who were prescribed teriparatide 20 μg daily between 2005 and 2008, were ≥ 50 years, and were diagnosed with a prevalent fracture. Patient data were collected using the Taiwan National Health Insurance Research Database. All patients were followed for 24 months after index teriparatide prescription. Persistence was determined as the time from the start of treatment to the first 90-day gap between 2 teriparatide prescriptions. Patients were classified as persisting with teriparatide for ≤ 12 months or >12 months. Adherence was measured using a medication possession ratio (MPR), determined as the proportion of prescriptions filled over 24 months. The effect of persistence and adherence with teriparatide on fracture incidence was assessed using Kaplan-Meier and Cox proportional hazard models after adjusting for baseline demographics (age, sex, and previous fractures), concomitant medications for osteoporosis, other confounding medications, and comorbidities.

Results: A total of 4,624 patients were included in the study. Of these, 85.0% were female and 65.5% were ≥ 75 years old. Previous hip and vertebral fractures were reported in 20.3% and 87.7% of patients, respectively. Only 1 in 4 (24.9%) patients persisted with teriparatide for >12 months and only 1 in 3 (33.9%) had an MPR $>50\%$. Persistence with teriparatide for >12 months was associated with lower incidence of hip (hazard ratio [HR], 0.61 [95% confidence interval (CI), 0.40-0.93], $p=0.023$) and non-vertebral fractures (HR, 0.79 [95% CI, 0.63-0.99], $p=0.046$) when compared with patients persisting with teriparatide for ≤ 12 months. After adjusting for other covariates, high adherence to teriparatide (MPR $\geq 50\%$) was associated with lower incidence of hip (HR, 0.66 [95% CI, 0.46-0.96], $p=0.029$) and non-vertebral (HR, 0.81 [95% CI, 0.66-0.99], $p=0.038$) fractures compared with low adherence to teriparatide (MPR $\leq 50\%$).

Conclusions: Our results demonstrate that higher persistence and adherence to teriparatide are associated with reduced risk of hip and non-vertebral fractures in Taiwanese patients who had previous fractures.

Disclosures: *Ding-Cheng CHAN, Lilly. MSD, Harvester, GSK, TCM biotech international*
This study was sponsored by Eli Lilly and Company, manufacturer/licensee of teriparatide (Forteo®).

SU0308

Characteristics of Patients Classified as Low or Moderate Risk Based on Fracture Risk Assessment (FRAX) After a Fragility Fracture. *Louis Rodrigue*¹, Francois Cabana¹, Marie-Claude Beaulieu¹, Nathalie Carrier², Joanna Sale³, Sophie Roux¹, Gilles Boire².* ¹Université de Sherbrooke, Canada, ²Centre hospitalier universitaire de Sherbrooke, Canada, ³St. Michael's Hospital, University of Toronto, Canada

BACKGROUND. Canadian osteoporosis (OP) guidelines recommend an individual's 10-year fragility fracture (FF) risk is determined as Low, Moderate or High by using either FRAX or Canadian Association of Radiologists and OP Canada (CAROC) tools. While treatment decisions for patients at High risk are quite clear, the management of patients at Moderate risk is subject to a number of risk modifiers, which complicate the decision-making process, particularly in the context of a recent FF. **OBJECTIVE.** To describe characteristics and outcomes of patients FRAX-classified as Low or Moderate risk despite a recent FF. **METHODS.** The OPTIMUS program is a program implemented at the Centre hospitalier universitaire de Sherbrooke (CHUS) fracture clinics to educate patients and to empower primary care physicians to diagnose and treat OP after a FF. Women and men over 50 were screened for incident FF, and 1410 patients with a FF were followed by phone calls for a mean period of 4 years. FRAX-BMI scores were calculated at time of the incident FF, defining High ($\geq 20\%$ for major or $\geq 3\%$ for hip FF), Moderate (10 to 20% for major and $< 3\%$ for hip FF), and Low ($< 10\%$ for major and $< 3\%$ for hip FF) risks. **RESULTS.** Prior to the incident FF, 64 patients had at least 1 previous FF (29 Low and 35 Moderate) and did not change risk category. Including the incident FF event increased FRAX scores for major FF from 0 to 18% [median (IQR): 7.1% (4.7-11)], but 337 (23.9%) patients remained classified as Low and 279 (19.8%) as Moderate risk. Recurrent FF occurred in 14.1 and 18.2/1000 patient-years in Low and Moderate risk categories (not significant, NS); mortality rates were 7.9 and 4.3/1000 patient-years in Low and Moderate risk categories, respectively (NS). In comparison, recurrent FF and mortality rates were 35.8 and 35.4/1000 patient-years in our High risk population. Relative to patients at Low risk, those at Moderate risk after a FF were older [mean age (years) 61 vs 55], more frequently female (94.2% vs 62.9%) and already treated for OP (22.3% vs 10.7%) ($p < 0.001$ for all). No FRAX item enabled us to identify those patients at Low or Moderate risk who sustained a recurrent FF over follow up (Low: 4.7%; Moderate: 6.2%). **CONCLUSIONS.** More than 40% of the patients with incident FF are still classified at Low or Moderate 10 year-risk after a FF, with similar rates of recurrent FF and mortality rates. Parameters not yet included in FRAX calculation are required to improve the prediction of recurrent FF risk in patients estimated at Low or Moderate risk after a FF.

Disclosures: *Louis Rodrigue, None.*

SU0309

Improving the Rate of Bone Mineral Density Testing After Fracture. *Sabita Challagulla*, Veronica Pizjak.* Baylor Scott & white, USA

This study describes a successful quality initiative to improve bone mineral density (BMD) testing compliance in a population of post fracture patients using a team consisting of the BSW Health Plan, Endocrinology, the Emergency department and the Radiology department.

Methods: A monthly list of Baylor Scott and White Health Plan (BSWHP) members age 65 and over presenting to the Emergency Department with fractures between October 2013 and May of 2014 was sent to the BSWHP and forwarded to Endocrinology. Letters were sent informing these patients that the BSWHP would order a bone density scan and explaining the importance of the scan to assess their risk of future fractures and diagnose osteoporosis. An endocrinologist then ordered DXA scans on patients whose scans had not already been obtained and radiology called the patients to schedule promptly. The PCP was sent a copy of the results and patients were sent another letter telling them to contact their PCP for the results to determine if therapy was needed. The percent of patients obtaining a BMD within one year of fracture was obtained after the intervention. The percent of the population obtaining DXA scans ordered by the team was compared to the percent of patients who had the BMD ordered by their primary provider during that time.

Results: The baseline value for BMD compliance for the system in 2014 was 14.9%. 197 patients were included in the quality initiative group and a total of 57 patients (29%) obtained DXA scans, 8 (14%) ordered by a PCP and the 49 (85%) ordered by the team. 32.8% of the patients contacted by Radiology initially agreed to have the DXA scheduled. The reasons given for declining were: patient did not want 11.5%, deceased 5.7% and nursing home 4.1%.

Conclusion: A team approach to post fracture BMD testing was able to increase the number of patients obtaining a BMD from the 8 obtained by their PCPs to 49 obtained by the team because scans were consistently ordered and the patients were contacted at least twice by team members emphasizing the importance of obtaining

the scans. We feel that enlarging this initiative to include lists of fractures from casting rooms for patients who do not go to the emergency room would enhance the collection of post fracture BMD data even more.

Disclosures: *Sabita Challagulla, None.*

SU0310

Dietary potassium intake is beneficial to bone mineral density: Korean National Health and Nutrition Examination Survey 2008 - 2011 (KNHANES IV-V). *Jung Hee Kim*¹, Sung Hye Kong², A Ram Hong³, Jee Hyun Lee³, Kyoung Min Kim⁴, Sang Wan Kim⁴, Seong Yeon Kim⁴, Chan Soo Shin³.*

¹Seoul National University College of Medicine, South Korea, ²Department of Internal Medicine, Seoul National University Hospital, South Korea, ³Department of Internal Medicine, Seoul National University Hospital, South Korea, ⁴Department of Internal Medicine Seoul National University Hospital, South Korea

Potassium intake has been suggested to be beneficial to bone through the neutralization of the endogenous metabolic acid and the reduction urinary calcium loss. We aimed to evaluate the association between daily potassium intake and the bone mineral density (BMD) in Korean population.

We included 3208 men aged over 50 years and 4067 postmenopausal women from the 2008 - 2011 Korea National Health and Nutrition Examination Survey (KNHANES). Subjects were divided into tertiles according to dietary potassium intake (< 2443 , $2443-3616$, > 3616 mg/day for men, < 1833 , $1833 - 2888$, > 2888 mg/day for women). Lumbar spine, total hip, and femur neck BMDs were measured by dual energy X-ray absorptiometry.

Mean age was 63.88 ± 8.66 , and BMI was 23.98 ± 3.08 . In correlation analyses, dietary potassium intake was not associated with lumbar spine BMD, but positively correlated with femur neck and total hip BMDs in men. In women, dietary potassium intake was positively correlated with lumbar spine, femur neck and total hip BMDs. In men, total hip (0.913 ± 0.004 for 1st, 0.926 ± 0.003 for 2nd, 0.927 ± 0.004 or 3rd tertile, p -trend = 0.016) and femur neck BMDs (0.734 ± 0.001 , 0.746 ± 0.003 , 0.751 ± 0.004 , p -trend = 0.004) were highest in the 3rd tertile of dietary potassium intake among groups after adjusting for age, body mass index, serum creatinine, 25[OH]vitamin-D level, total daily food intake, calcium intake, and physical activity. Postmenopausal women in the highest tertile of potassium intake had significantly higher lumbar spine (0.791 ± 0.003 , 0.794 ± 0.003 , 0.806 ± 0.003 across the tertiles), total hip (0.764 ± 0.002 , 0.774 ± 0.003 , 0.781 ± 0.003 across the tertiles) and femur neck BMDs (0.614 ± 0.002 , 0.621 ± 0.002 , 0.630 ± 0.003 across the tertiles).

Dietary potassium intake was positively associated with BMD in men over 50 years old and postmenopausal women, suggesting the beneficial effect of dietary potassium intake on bone health.

Disclosures: *Jung Hee Kim, None.*

SU0311

Effect of Young Coconut Juice Supplementation on Bone Metabolism in Ovariectomized Rats. *Hiroshi Matsushita*¹, Akira Minami², Yuriko Ohyama³, Hiroaki Kanazawa⁴, Takashi Suzuki², Sanan Subhadhirasakul⁵, Kazushi Watanabe³, Akihiko Wakatsuki³.* ¹Aichi Medical University, Japan, ²Department of Biochemistry, School of Pharmaceutical Sciences, University of Shizuoka, Japan, ³Department of Obstetrics & Gynecology, School of Medicine, Aichi Medical University, Japan, ⁴Department of Functional Anatomy, School of Nursing, University of Shizuoka, Japan, ⁵Department of Pharmacognosy & Pharmaceutical Botany, Faculty of Pharmaceutical Sciences, Prince of Songkla University, Thailand

Estrogen deficiency after menopause is strongly associated with rapid resorption and loss of bone density in women. Hormone replacement therapy (HRT) has been regarded as one treatment option for the prevention of postmenopausal bone loss and fracture. However, whether the benefits associated with HRT outweigh the risks remains controversial, which has heightened interest in dietary and lifestyle factors that may minimize postmenopausal bone loss. *Cocos nucifera* Linn. (Arecaceae), also known as coconut, has many uses in traditional medicine. Young coconut juice (YJC), defined as the juice extracted from the fruit of a 6-month-old coconut, has traditionally been consumed by women in Thailand to alleviate symptoms associated with menopause. The aim of this study was to determine the effects of YJC on bone metabolism in ovariectomized rats. Ten-week-old female Wistar rats were randomized to the following 4 groups: Baseline, Sham, OVX, and OVX/YJC ($n = 8-10$ per group). Rats in the Baseline group were sacrificed immediately, and those in the other groups were subjected to either sham operation (Sham) or bilateral ovariectomy (OVX and OVX/YJC). The rats in the OVX/YJC group were administered YJC at a dose of 50 mL/kg body weight (BW)/day for 6 weeks in experiment 1, and 75 mL/kg BW/day for 12 weeks in experiment 2. After supplementation of YJC, the rats were sacrificed, and indices of bone mass and bone histomorphometry were measured. In experiment 1, the bone mineral content and bone mineral density of the femur were significantly higher in the OVX/YJC group than in the OVX group ($p < 0.05$, respectively). The OVX/YJC group showed significantly higher measurements for mineralizing surface,

mineral apposition rate, and bone formation rate in the proximal tibial metaphyseal cancellous bone than the OVX group ($p < 0.05$, respectively). In contrast, there were no significant differences in parameters examined between the OVX and OVX/YCJ groups in experiment 2. These findings suggest that YCJ supplementation may be helpful in slowing the bone loss observed following menopause, but it may not be able to prevent the development of osteoporosis, even when supplemented at higher doses.

Disclosures: Hiroshi Matsushita, None.

SU0312

Long-term green tea polyphenols supplementation improves bone micro-structure of middle-aged ovariectomized rats: a dose-response study. Chwan-Li Shen^{*1}, Xiao Song², Jia-Sheng Wang², Kylie Corry³, Jiliang Li³. ¹Texas Tech University Health Sciences Center, USA, ²University of Georgia, USA, ³Indiana University-Purdue University Indianapolis, USA

Our previous studies have shown that the osteo-protective effects of green tea polyphenols (GTP) in middle-aged female rats, because of GTP's antioxidant capacity. The project is further to evaluate bone microstructure properties in middle-aged OVX rats supplemented with different dosages of GTP in drinking water. 182 SD female rats were sham (n=39) or ovariectomy (OVX, n=143). Both sham and OVX-control animals receiving no GTP were assigned for sample collection at baseline, 3, and 6 months. The remaining OVX animals were randomized into 0.15%, 0.5%, 1%, and 1.5% (wt/vol) GTP for 3 and 6 months. Bone microstructure was assessed by static and dynamic histomorphometric analysis in proximal tibia and endocortical bone of tibia, respectively. At 3 months, trabecular mineralizing surface/bone surface (MS/BS) and bone formation rate/bone surface (BFR/BS) were elevated in the OVX-control animals compared to the Sham-control animals, resulting in a decrease in trabecular bone volume (BV/TV). Except for the OVX+0.15% GTP group, GTP supplementation suppressed the OVX-induced increase in trabecular MS/BS and BFR/BS relative to the OVX-control. Inhibitory effects of GTP supplementation on the OVX-treated animals was also observed in trabecular bone resorption parameters, such as osteoclast surface/bone surface (OCs/BS), number osteoclasts/bone perimeter (N.Oc/B.Pm), and number osteoclasts/osteoclast perimeter (N.Oc/Oc.Pm). Thus, an increase in BV/TV among GTP supplemented groups was the result of suppression of bone formation and resorption. Both periosteal and endocortical BFR were higher in the OVX-control group compared to the Sham-control group. At 3 months, BV/TV data in OVX+1% GTP and OVX+GTP 1.5% groups were higher than OVX-control, while periosteal mineral apposition rate (MAR) and BFR/BS (OVX+0.5% GTP, OVX+1% GTP, and OVX+1.5% GTP), endocortical MS/BS (OVX+1% GTP and OVX+1.5% GTP), endocortical MAR and BFR (OVX+0.5% GTP, OVX+1% GTP, and OVX+1.5% GTP) were all lower relative to the OVX-control group. The similar impacts of GTP on both trabecular and cortical parameters were also observed at 6 months. This study demonstrates that the osteo-protective benefits of GTP supplementation in OVX-treated animals were mostly observed at high GTP doses (1% and 1.5%), and not at low doses (0.15% and 0.5%); and there is no significant difference in most bone parameters among the OVX-control, OVX+0.15% GTP, and OVX+0.5% GTP groups. Supported by NIH/NCCAM AT006691.

Disclosures: Chwan-Li Shen, None.

SU0313

Nutritional status of calcium and other bone-related nutrients in Type 2 Diabetes Mellitus patients. Sahoko Sekiguchi-Ueda^{*1}, Eri Ninomiya², Eisuke Tomatsu³, Mizuho Ando³, Izumi Hiratsuka³, Yasumasa Yoshino³, Takeshi Takavanagi³, Avako Kakita³, Megumi Shibata³, Masaki Makino³, Akemi Ito², Tadashi Kinoshita², Kazuhiro Uenishi⁴, Atsushi Suzuki³. ¹Fujita Health University, Division of Endocrinology, Japan, ²Food & Nutrition Service, Fujita Health University Hospital, Japan, ³Division of Endocrinology & Metabolism, Department of Internal Medicine, Fujita Health University, Japan, ⁴Laboratory of Physiological Nutrition, Kagawa Nutrition University, Japan

Background: Enough daily intakes of nutrients including Ca and vitamin D are considered to be necessary for both prevention and treatment of osteoporosis. Traditional Japanese foods seem to be good for health, but seems to contain less milk products compared with occidental ones. Type 2 Diabetes Mellitus patients (T2DM patients) commonly reduce their calorie intake in order to control their blood glucose level. On the other hand, the strict control of food intake leads to the reduction of their Ca intake, which could deteriorate bone strength in T2DM patients. The aim of this study is to estimate nutritional status of Ca and other nutrients which could affect bone and Ca metabolism in T2DM patients.

Subjects and Methods: T2DM patients of Fujita Health University Hospital were recruited (n=103, M/F=56/47, age 61.0 ± 13.4 years old). We estimate intake of nutrients including Ca, vitamin D and other nutrients by simple food frequency questionnaire by Uenishi et al (J Nutr Sci Vitaminol 2008). Data are expressed as median with interquartile range.

Results: Median total energy in T2DM patients was 1816 kcal/day (1686-1945). Their daily intake of Ca, vitamin D and vitamin K were 451 mg (416-485), 10.2 µg (9.6-10.7), and 204 µg (172-235), respectively. Only 14.6 % of study subjects were found to take more than 600 mg/day Ca. Protein and salt intake were 62.7 g/day (59-

66.3) and 10.6 g/day (10.2-11), respectively. **Discussion:** Our findings suggest that Japanese T2DM patients seem to restrict well their calorie intake for the prevention of their overweight and metabolic disorder. On the contrary, their daily Ca intake was insufficient, and their median Ca intake was below those in non-diabetic Japanese population. The most of them could take vitamin D and K more than recommended adequate intake (vitamin D, 5.5 µg/day and vitamin K, 65-75µg/day), but the vitamin D intake did not reach the level for the prevention and treatment of osteoporosis.

Conclusion: It seems likely that more Ca and vitamin D intake or supplementation should be recommended to Japanese T2DM patients as well as diabetic diet therapy.

Disclosures: Sahoko Sekiguchi-Ueda, None.

SU0314

Soluble Corn Fiber Increases Bone-Calcium Retention in Postmenopausal Women in a Dose-Dependent Manner. Steven Jakeman^{*1}, Courtney Henry², Berdine Martin³, George McCabe², Linda McCabe², George Jackson⁴, Munro Peacock⁵, Connie Weaver³. ¹Department of Food Science, Purdue University, USA, ²Department of Statistics, Purdue University, USA, ³Department of Nutrition Science, Purdue University, USA, ⁴Department of Physics & Astronomy, Purdue University, USA, ⁵Department of Medicine, Indiana University, USA

Soluble corn fiber (SCF) significantly improves calcium absorption in adolescents and bone strength and architecture in rodent models. In this study, we aimed to see if PROMITOR® SCF 85, which provides 85% dietary fiber, would also benefit bone retention in postmenopausal women. We used novel technology to determine bone calcium retention—by measuring urinary appearance of ⁴¹Ca from pre-labeled bone—to rapidly and sensitively evaluate the effectiveness of SCF to reduce bone loss. A randomized-order, crossover, double-blinded trial was performed in 14 healthy postmenopausal women to compare 0 g/d, 10 g/d, and 20 g/d fiber from SCF for 50 days. A dose-response effect was demonstrated with 10 g/d SCF and 20 g/d SCF improving bone retention by 4.8% (P = 0.013) and 7% (P = 0.007) respectively. A significant increase in bone-specific alkaline phosphatase was detected between 0 g/d SCF and 20 g/d SCF levels (8%, P = 0.035). There was no change in N-terminal telopeptide and osteocalcin. Daily PROMITOR® SCF consumption significantly increased bone calcium retention in postmenopausal women, improving bone balance by an estimated 50 mg/d, or 2.5% total body bone mineral content per year if the effect persists.

Disclosures: Steven Jakeman, None.

This study received funding from: Tate & Lyle Health & Nutrition Sciences

SU0315

Low bone mass is associated with low vitamin D levels in young healthy Korean adults. Hee-Jeong Choi^{*1}, Byeong Yeon Yu², Han Jin Oh³, Bom Taek Kim⁴, Hyuk Jung Kweon⁵. ¹Department of Family Medicine, Eulji University School of Medicine, South Korea, ²Department of Family Medicine, Konyang University School of Medicine, Korea, democratic people's republic of, ³Department of Family Medicine, Hansoo University, Korea, democratic people's republic of, ⁴Department of Family Medicine, Ajou University School of Medicine, Korea, democratic people's republic of, ⁵Department of Family Medicine, Konkuk University School of Medicine, Korea, democratic people's republic of

Background Although osteoporosis treatment involves the use of pharmacologic agents, it must be considered as the main strategies for prevention of osteoporosis consist of maximizing peak bone mass (PBM) and minimizing the rate of bone loss. Lifestyle habits including nutrition and physical activity during adolescence and early adulthood contribute up to 20% of the observed variation in the attainment of PBM as well as to the rate of bone loss later in life. The aims of this study were to identify the determinants of bone mineral density (BMD) in young healthy adults. **Methods** Data was gathered from 2,673 males and females aged 20 to 49 years after excluding subjects who had history of cancer including breast cancer; taking medications for diabetes; menopause or hysterectomy. Lumbar spinal BMD (L1-4) was measured by dual-energy X-ray absorptiometry. Multivariate linear regression analysis was done to identify the major determinants of the spinal BMD. **Results** The mean age of the 947 males and 1,726 females were 40.6 years and 38.9.6 years, respectively. The mean spinal BMD was 1.178±0.142 g/cm² in males and 1.165±0.128 g/cm² in females. Spinal BMD was correlated with height, weight, eGFR, alkaline phosphatase (ALP), 25(OH)D and insulin levels after adjusting for age, gender, and body mass index (BMI) (P<0.05). In the linear regression models, 25(OH)D levels had significant association with spinal BMD after adjusting for age, gender, BMI, alcohol, smoking, exercise, eGFR, ALP, and insulin levels. Also, gender, BMI, eGFR, ALP, and insulin levels were significantly associated with the spinal BMD. The odds ratio of low BMD (T-score <-1.0) in vitamin D deficiency group (25(OH)D <10 ng/mL) was 1.39 (95% CI, 1.084-1.790, P=0.01) after adjustment for age, gender and BMI. **Conclusions** In young healthy adult males and females, 25(OH)D levels were significantly associated with spinal BMD. These results suggest that the prevention of vitamin D deficiency in young adults must be considered as the main strategies for prevention of osteoporosis.

Disclosures: Hee-Jeong Choi, None.

SU0316

Peptide analysis of racially linked vitamin D binding protein isoforms in older men. Carrie Nielson^{*1}, Jon Jacobs², Jodi Lapidus¹, Joseph Zmuda³, Tujin Shi², Yuqian Gao², Richard Smith², Eric Orwoll¹. ¹Oregon Health & Science University, USA, ²Pacific Northwest National Laboratory, USA, ³University of Pittsburgh, USA

Introduction: Vitamin D binding protein (DBP) affects circulating concentrations of free and bioavailable 25OHD, which may be more relevant to skeletal outcomes than total 25OHD concentration. DBP has 3 major genetic isoforms whose frequencies differ by race. That is, GC-1F alleles are more common in those of African descent than are GC-1S and GC-2 isoforms, and this difference may contribute to racial differences in DBP detection in serum. In particular, in several studies a monoclonal ELISA has demonstrated lower DBP concentrations in GC-1F individuals, while polyclonal assays have not. We sought to determine the concentrations of DBP peptides representing both non-variant regions of DBP and genetically variant regions.

Methods: In men from the Osteoporotic Fractures in Men (MrOS) study, we determined the relevant GC-genotypes, rs4588 (Thr436Lys) and rs7041 (Asp432Glu), and selected a total of 116 men to represent each of the six GC diplotypes. Selected reaction monitoring (SRM) MS based assays were used to analyze 5 variant DBP peptides from the genetically variant region and 3 non-variant DBP peptides. Associations between GC diplotype and abundance of each peptide were tested by ANOVA, followed by post-hoc pairwise tests.

Results: The serum concentration of nonvariant peptides was similar in all genotypes, including GC-1F. The concentration of one of the nonvariant peptides (THLPEVFLSK, Figure 1 center panel), was slightly lower in participants with GC-22 than in those with 1F1F and 1F1S (both pairwise $p \leq 0.01$). The GC-1F variant peptide was detected in all men whose GC genotypes predicted the presence of the GC-1F isoform (Figure 2).

Conclusions: In contrast with previous reports of low circulating DBP in GC-1F carriers, DBP peptides did not circulate at lower serum concentration in men with GC-1F genotypes than in men with other genotypes. These results support the conclusion that DBP assays yielding lower concentrations of serum DBP in GC-1F individuals are more likely due to lack sensitivity to GC-1F variant proteins than to be a reflection of truly lower DBP concentration.

Figure 1. SRM results for three non-variant peptides per GC genotype (n=116). The distribution of nonvariant peptides showed similar peptide abundance for all genotypes, including for GC-1F. For only one of the peptides (THLPEVFLSK, right panel), participants with GC-22 had lower abundance than 1F1F and 1F1S ($p \leq 0.01$). Box and whisker plots show the 25th and 75th percentiles and median. Whiskers represent 1.5 times the interquartile range.

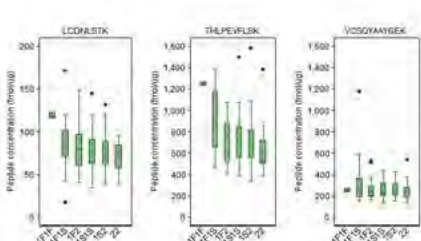


Figure 1

Figure 2. Peptide concentration by GC genotype (x axis) for GC-1F (left), GC-1S (middle), and GC-2 (right) variant peptide sequences. E416D and 1420K substitutions, which define the GC categories are highlighted in each peptide sequence.

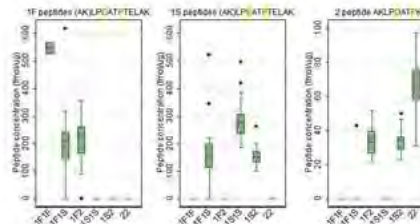


Figure 2

Disclosures: Carrie Nielson, None.

SU0317

Relationships of resting energy expenditure and bone metabolism in postmenopausal Japanese women with type 2 diabetes: 6-month follow-up with vitamin D supplementation. Makiko Ogata^{*1}, Risa Ide², Miho Takizawa², Naoko Iwasaki², Yasuko Uchigata². ¹Tokyo Women's Medical University, Japan, ²Diabetes Center, Tokyo Women's Medical University, Japan

Objective: Bone and glucose metabolisms have a close correlation. Interestingly, despite a high bone mineral density in most type 2 diabetes (T2D) patients, the fracture risk is particularly high in this population. Especially, postmenopausal women have high risks of fracture; among them, the risk is higher in T2D patients. Further, although the resting energy expenditure (REE) increases after menopause, it conversely decreases in women with T2D, indicating that the pathophysiology of bone metabolism in postmenopausal women differs between patients with and without T2D. Various biomarkers for bone metabolism have been reported to correlate with the fracture risk in T2D. This study examined the relationships of REE, respiratory quotient (RQ), and diabetic neuropathy with bone metabolism in postmenopausal Japanese women with T2D in a stable state of diabetic therapy. **Methods:** Postmenopausal women with T2D (n=46) who were not taking any supplements and had no other severe disease except hypertension and dyslipidemia, and without proteinuria and severe obesity (body mass index <30 kg/m²) were included. The procollagen type 1 N-terminal propeptide (PINP) and carboxy-terminal collagen crosslinks-1 (CTX-1) levels were evaluated, along with intact parathyroid hormone, 25-hydroxyvitamin D (25[OH]D), urine microalbumin, motor and sensory nerve conduction velocities, R-R interval, body composition, REE, RQ, and bone mineral density at the non-dominant distal radius. After the first examination, 14 patients with low 25(OH)D were administered alphacalcidol. All patients were reexamined after 6 months. **Results:** The mean T-score was low, with high variance (1.7 ~ 1.6; Mean ~ SD), and 18 patients (39%) met the osteoporosis criteria. At baseline, REE positively correlated with body mass index, serum calcium, mean glycated hemoglobin (prior 6 months, 7.6 ~ 1.2%), and the serum PINP/CTX-1 ratio. RQ positively correlated with serum 25(OH)D only. The motor and sensory nerve conduction velocities did not correlate with the bone markers. At the 6-month follow-up, the changes in REE and PINP/CTX-1 were found to positively correlate. The change in RQ did not correlate with 25(OH)D after vitamin D supplementation, but correlated with the mean glycated hemoglobin in the prior 6 months. **Conclusion:** REE and RQ are useful indices of basal metabolic function and bone metabolism in postmenopausal Japanese women with T2D. Calculating REE may help in the treatment of osteoporosis in such women.

Disclosures: Makiko Ogata, None.

This study received funding from: Japan osteoporosis foundation; Lilly research grant program

SU0318

The Association of Vitamin D with Femoral Neck Strength: an Additional Evidence of Vitamin D on Bone Health. HyeonMok Kim*, Seung Hun Lee, JinJu Kim, Kyeong-Hye Lim, Seong Hee Ahn, Beom-Jun Kim, Jae Suk Chang, Jung-Min Koh, Asan Medical Center, University of Ulsan College of Medicine, South Korea

Although bone mineral density (BMD) is a strong predictor of fracture risk, additional parameters, such as bone strength, are needed to predict future fracture risk because of the low sensitivity of BMD for predicting the fracture risk. We aimed to investigate the association of vitamin D with femoral neck (FN) strength in a representative community cohort in South Korea. This cross-sectional study was based on data acquired in the Fourth Korean National Health and Nutrition Examination Surveys (KNHANES IV), which were conducted from 2007 to 2009. This study included 1,209 Koreans (586 men and 623 women) aged 50 years or older. We calculated composite indices of FN strength, such as indices of compression strength (CSI), bending strength (BSI), and impact strength (ISI), by combining BMD, body weight, and height with the femoral axis length and width which were measured by dual-energy X-ray absorptiometry. Multiple regression analysis demonstrated that serum 25-hydroxyvitamin D [25(OH)D] levels were associated with CSI, BSI, and ISI in both genders. When women were categorized into four quartiles of 25(OH)D, FN BMD and composite indices, except for BSI, significantly increased from the lowest (Q1) to the highest quartile (Q4) (P for trend = 0.001–0.004). In contrast, there is no significant association of quartiles with composite indices in men. When women were divided into two groups according to their serum 25(OH)D levels, the composite indices as well as the FN BMD were markedly higher in subjects with higher 25(OH)D levels (more than 51.5 nmol/L). These findings provide the first clinical evidence that high serum 25(OH)D levels exhibit higher composite indices of FN strength in a dose-dependent manner, especially in women.

Disclosures: HyeonMok Kim, None.

SU0319

The effectiveness of Siriraj orthopaedic vitamin D2 supplementation protocol to achieve sufficient vitamin D level. Aasis Unnanuntana, Pojchong Chotiyarnwong*, Wachirapan Narktang, Siriraj Hospital, Thailand

Objective: The objective of this study was to assess the effectiveness of our vitamin D2 supplementation protocol to achieve normal vitamin D status in orthopaedic patients who presented at the metabolic bone disease clinic. **Methods:** After our institutional review board approval, we retrospectively reviewed medical records of patients enrolled in the metabolic bone disease clinic. We included all patients who aged more than 18 years and had serum 25-hydroxyvitamin D (25(OH)D) levels available at both baseline and post-treatment visits. Exclusion criteria were patients who received vitamin D3 supplementation or took calcium formulation that contained some amount of vitamin D; those with medical problems that affect vitamin D absorption and metabolism such as short bowel syndrome, chronic kidney disease, granulomatous disorders; and patients who received anticonvulsants, rifampicin, cholestyramine, or antiretroviral drug. The protocol used to correct low vitamin D level was showed in table 1. In general, serum 25(OH)D level was repeated at an approximately 3 months after treatment. The goal is to keep serum 25(OH)D level in a range of 30-50 ng/mL. **Results:** From a total of 513 patients, 243 patients passed the inclusion/exclusion criteria and were analyzed for this study. Most patients were female with an average age of 72 years. The prevalence of hypovitaminosis D (25(OH)D <30 ng/mL) was approximately 60%. After applying our vitamin D2 supplementation protocol, 187 patients (77.0%) had serum 25(OH)D level > 30 ng/mL. There were 4 patients who had 25(OH)D level >50 ng/ml after treatment; however, these patients were asymptomatic. Fifty six patients (23.0%) still had 25(OH)D level < 30 ng/ml at the latest visit (Table 2). If 20 ng/mL was used as a cut-off value for adequate vitamin D status, our protocol was able to restore serum vitamin D up to 98.4% of the patients. **Conclusion:** Low serum vitamin D status can be treated by using both D2 and D3 formulation. This study showed that our vitamin D2 supplementation protocol was able to restore 25(OH)D levels to more than 20 and 30 ng/mL in 98.4% and 77% of the patients, respectively. Given the high prevalence of hypovitaminosis D, the importance of evaluation and subsequent treatment is necessary to prevent complications that are arisen from low vitamin D levels. Vitamin D2 is cheap, easy to use and can be administered safely by using our protocol.

Table 1. Siriraj vitamin D2 supplementation protocol to achieve normal vitamin D level

| Baseline serum 25-hydroxyvitamin D level* (ng/mL) | Dosage of vitamin D2 supplementation (International Unit, IU) |
|---|---|
| < 20 ng/mL | 60,000 IU/week |
| 20-30 ng/mL | 40,000 IU/week |
| 30-40 ng/mL | 20,000 IU/week |
| >40 ng/mL | No additional D supplementation |

The baseline serum 25-hydroxyvitamin D level was defined as serum vitamin D level without any other vitamin D supplementation.

table 1

Table 2. Serum vitamin D levels after treatment using Siriraj vitamin D2 supplementation protocol

| Serum vitamin D level after treatment | Number of patients (%) |
|---------------------------------------|------------------------|
| <20 ng/mL | 4 (1.6) |
| 20-30 ng/mL | 52 (21.4) |
| 30-50 ng/mL | 183 (75.3) |
| >50 ng/mL | 4 (1.6) |

table 2

Disclosures: Pojchong Chotiyarnwong, None.

SU0320

Vitamin D Status, Bone Health and Depressive Symptoms in Young Women. Emma Callegari*¹, Nicola Reavley¹, Suzanne M. Garland², Alexandra Gorelik³, John D. Wark⁴. ¹The University of Melbourne, Australia, ²The University of Melbourne. Royal Women's Hospital, Murdoch Childrens Research Institute, Australia, ³Melbourne Epi Centre, Royal Melbourne Hospital, Australia, ⁴The University of Melbourne, Bone & Mineral Medicine, Royal Melbourne Hospital, Australia

Vitamin D deficiency has been associated with poor musculoskeletal and mental health outcomes but the interplay between these indices remains uncertain. The Safe-D study is a comprehensive study of vitamin D status and a range of clinical, behavioural and lifestyle factors in young women, an understudied demographic. The aim of this analysis was to investigate the associations between serum 25-hydroxyvitamin D (25OHD), bone mineral density (BMD) and depressive symptoms in young women. Female participants aged 16-25 years living in Victoria, Australia, were recruited through Facebook. Participants completed an extensive online health survey and attended a site visit. Dual-energy X-ray absorptiometry was used to measure BMD at the lumbar spine, total hip and femoral neck. Osteopenia and osteoporosis were defined using WHO criteria (Z-score was used in participants aged <20). Serum 25OHD was measured using liquid chromatography tandem mass spectrometry (LC-MS/MS). The Patient Health Questionnaire (PHQ-9) was used to measure depressive symptoms. To date, 197 participants have been fully evaluated. The mean serum (± SD) 25OHD concentration was 74.3±28.8 nmol/L: 41 (20.8%) participants were vitamin D-deficient (25OHD <50 nmol/L). One hundred and twenty-eight (66%) participants had normal BMD; 59 (30%) had osteopenia and 8 (4%) had osteoporosis at one or more skeletal sites. Serum 25OHD of <50 nmol/L was significantly associated with a diagnosis of osteopenia or osteoporosis when compared to 50 nmol/L or above (39% vs. 27%, p=0.041). There was no association found between serum 25OHD and depressive symptoms nor between BMD and depressive symptoms. Serum 25OHD was associated with BMD at the total hip (β=0.0050, 95% CI 0.0003-0.0096, p=0.036) and femoral neck (β=0.0046, 95% CI 0.0004-0.0087, p=0.033) and approached significance at the lumbar spine (β=0.0036, 95% CI -0.00003-0.0073, p=0.052) in participants with serum 25OHD <50 nmol/L. This association remained significant at the total hip (p=0.035) and femoral neck (p=0.028) after adjusting for body mass index, years since menarche, PHQ score and melanin density at the upper, inner arm. Analysis revealed significant associations between vitamin D deficiency and BMD in vitamin D-deficient young women. The Safe-D study will recruit up to 500 participants to further investigate the associations between vitamin D status, musculoskeletal health and mental health in young women, aiming to optimise their health and wellbeing.

Disclosures: Emma Callegari, None.

SU0321

Leptin is a Key Regulator of Bone Turnover and Bone Density in Obese Adults. Amy L Evans¹, Fatma Gossiel¹, Margaret A Paggioli¹, Richard Eastell¹, Jennifer Walsh*². ¹Academic Unit of Bone Metabolism, University of Sheffield, United Kingdom, ²University of Sheffield, United Kingdom

Background: Obese (OB) adults have greater BMD and more favourable bone microarchitecture than normal weight (NW) adults and the difference is greater in older adults. The mechanisms of association of obesity with BMD and microarchitecture are unclear. We aimed to identify relationships between fat distribution, biochemical factors, BMD and bone microstructure.

Methods: 200 healthy men and women age 25-40 or 55-75 years were recruited in individually-matched OB (BMI ≥ 30) and NW (BMI 18.5-24.9) pairs. Whole body, total hip and lumbar spine aBMD were determined by DXA. vBMD and microarchitecture at the radius and tibia were determined by HR-pQCT. Total, trunk, android, gynoid and appendicular fat masses (FM) were determined from whole body DXA. Abdominal subcutaneous (SAT) and visceral (VAT) fat volumes were determined by computed tomography. Bone turnover and regulation was assessed by CTX, PINP, OC, bone ALP, OPG and sclerostin. Potential mechanistic mediators assessed were: PTH, 25OHD, calcium, albumin, oestradiol (totE2), SHBG, free E2 (fE2), bioavailable E2 (bioE2), glucose, insulin, leptin and adiponectin.

Results: All measures of adiposity were higher in OB than NW ($p < 0.001$). Age did not affect BMI or total FM. OB had lower CTX, PINP and OC than NW (all $p < 0.01$). CTX predicted aBMD and vBMD. OB had higher leptin ($p < 0.001$), PTH ($p < 0.05$), glucose ($p < 0.001$) and insulin ($p < 0.001$), and lower adiponectin ($p < 0.001$), IGF-1 ($p < 0.05$), 25OHD ($p < 0.001$), SHBG ($p < 0.001$) and albumin ($p < 0.01$) than NW. TotE2, fE2 or bioE2, calcium, bone ALP, OPG or sclerostin did not differ between OB and NW. BMI had a greater effect on leptin, totE2 and fE2 in older than younger adults ($p < 0.05$). aBMD was best predicted by SAT, gynoid and appendicular FM; vBMD was best predicted by SAT, android and trunk FM; and microarchitecture was best predicted by SAT. SAT negatively predicted CTX ($p < 0.001$). When leptin was added to this model, SAT no longer predicted, but leptin negatively predicted CTX ($p < 0.05$). When leptin and totE2 were added, SAT no longer predicted, but both leptin ($p < 0.05$) and totE2 ($p < 0.01$) negatively predicted CTX.

Discussion: SAT is the key determinant of lower resorption in obese adults, probably acting through greater leptin production. The greater effect of BMI on leptin in older adults may contribute to a greater effect of obesity on BMD and microstructure in older adulthood.

Disclosures: Jennifer Walsh, None.

SU0322

Absence of hypophosphatasia mutations in atypical femur fractures. Timothy Bhattacharyya*¹, Smita Jha², Nicholas Laucis¹, Hongying Wang³, Daniel Kastner³, Elaine Remmers³. ¹NIH/NIAMS, USA, ²NIH/NICHD, USA, ³NIH/NHGRI, USA

Case reports have linked adult hypophosphatasia as a possible cause of atypical femur fractures (AFF) associated with bisphosphonate use. Hypophosphatasia is caused by a mutation in the tissue non-specific alkaline phosphatase (TNSALP) gene resulting in low alkaline phosphatase activity and a buildup in inorganic pyrophosphate (measured through pyridoxal phosphate levels) which further inhibits bone mineralization. We performed a prospective study to identify whether hypophosphatasia is associated with atypical femur fracture.

We recruited 15 control patients who took long term bisphosphonates without complication and 10 patients who sustained atypical femur fractures (9 years mean bisphosphonate use both cohorts). Patients underwent clinical exam and measurement of alkaline phosphatase and pyridoxal phosphate (PLP) levels. In addition, DNA was extracted and the TNSALP gene sequenced in both cohorts.

The AFF cohort satisfied 5/5 Major Criteria and 2 or more Minor Criteria as defined by ASBMR. Low alkaline phosphatase levels (< 55 U/L) were seen in 5/5 AFF patients and 5/7 control patients. One patient in each group demonstrated low alkaline phosphatase levels and elevated PLP. The TNSALP genes and intron splice sites in the atypical femur fracture cohort were sequenced and no coding mutations were identified in any subjects.

In conclusion, we found no evidence of mutations in the TNSALP gene in patients with atypical femur fractures. Laboratory findings of mildly low alkaline phosphatase activity were equally common in atypical and control cohorts and may be due to long term bisphosphonate use.

Disclosures: Timothy Bhattacharyya, None.

SU0323

Cytosolic Proteome Profiling of Monocytes for Male Osteoporosis. Wei Zhu*¹, Hong-Wen Deng¹, Lan Zhang¹, Yao-Zhong Liu¹, Qing Tian¹, Fei-Yan Deng², Yong Zeng¹, Yin-Chun Zhao³, Hua-Lin Huang¹, Ji-Gang Zhang¹. ¹Tulane University, USA, ²Soochow University, China, ³none, USA

Male osteoporosis is a serious public health problem, leading to significant mortality in aging males. Peripheral blood monocytes (PBMs) play important roles in bone metabolism by acting as precursors of osteoclasts and producing cytokines important for osteoclast development. Cytosolic proteins have important functions on bone cells and so far few proteomics studies have been focused on cytosolic proteome. Here, we conducted 2D-nanoLC-ESI-MS/MSE to profile PBMs cytosolic proteome in Caucasian male subjects with extremely discordant hip BMD (29 low BMD vs. 30 high BMD). We successfully identified 15 significant ($P < 0.05$) and additional 17 suggestive ($P < 0.1$) differentially expressed proteins (DEPs) (Fold change > 1.5 or < 0.67) out of a total of 3193 detected proteins. Combining evidence from our other proteomics data (from 34 Caucasian female subjects), PBMs microarray analyses (from ~ 100 Caucasian females) and SNPs association analyses (e.g., the deCODE and GEFOS2 datasets), we identified Ezrin, Gelsolin, Vinculin and Filamin A as potential functional genes for hip BMD variation. In addition, by utilizing bioinformatics tools of The Database for Annotation, Visualization and Integrated Discovery (DAVID) and Search Tool for the Retrieval of Interacting Gene (STRING) for pathways and networks analyses, we identified the enrichment of DEPs in the pathways of actin cytoskeleton regulation ($P = 2.71E-10$) and leukocyte trans-endothelial migration ($P = 4.07E-07$) and functional terms for monocyte proliferation, differentiation and apoptosis. This study represents a pioneering effort in comprehensive characterization of PBMs cytosolic proteome and may shed light on the monocyte-mediated pathogenesis of male osteoporosis.

Disclosures: Wei Zhu, None.

This study received funding from: Edward G. Schlieder Endowment

SU0324

MicroRNA miR-30e-5p discriminates patients with idiopathic osteoporosis and low-traumatic fractures. Roland Kocjan*¹, Christian Muschitz², Fabian Plachel², Rainer Dormann², Elisabeth Geiger³, Susanna Skalicky³, Heinrich Resch², Patrick Heimerl⁴, Astrid Fahrleitner-Pammer⁵, Johannes Grillari⁶, Heinz Redl⁷, Matthias Hackl³. ¹St. Vincent Hospital Vienna, Austria, ²St. Vincent Hospital – Medical Department II, The VINFORCE Study Group, Academic Teaching Hospital of Medical University of Vienna, Austria, ³TAmiRNA GmbH, Muthgasse 18, 1190 Vienna, Austria, ⁴Ludwig Boltzmann Institute for Experimental & Clinical Traumatology Donaueschingenstraße 13, A-1200 Vienna, Austria, ⁵Department of Internal Medicine, Division of Endocrinology & Metabolism, Medical University of Graz, Austria, ⁶Department of Biotechnology, University of Natural Resources & Life Sciences Vienna, Austria, ⁷Ludwig Boltzmann Institute for Experimental & Clinical Traumatology Austrian Cluster of Tissue Regeneration, Austria

Purpose: Bone turnover markers (BTMs) are proteins or peptides that are meant to reflect the metabolic activity of bone, but which are not involved in the regulation of bone metabolism. In contrast, circulating microRNAs (miRNAs) have been recently reported as a novel class of biomarkers, which can control and reflect the activity of a specific tissue based on their active release from tissues within microvesicles. A number of studies have reported on the intracellular expression and function of miRNAs in bone metabolism, and therefore, circulating miRNAs might have clinical utility for the management of bone disease. **Methods:** We analyzed 187 circulating miRNAs in in otherwise healthy pre-menopausal (n=10), post-menopausal (n=10) and male patients (n=15) with idiopathic osteoporosis and at least one low-traumatic fracture (FX). Secondary causes for osteoporosis were excluded by clinical investigation. Data were compared to respective healthy age-matched control groups (CO) of equal size. **Results:** For each cohort, differential expression analysis was performed using non-parametric tests and p-values were adjusted for multiple testing using BH false-discovery rate ($q < 0.05$). In case of pre-menopausal women, 36 miRNAs were found to be differentially expressed in comparison to healthy controls, 53 in case of post-menopausal women and 56 in case of males. An overlap of 18 regulated miRNAs (4 down-regulated, 14 up-regulated in FX) in all three cohorts was observed and subject to further analysis: classification performance of individual miRNAs was assessed by ROC analysis to find that miR-30e-5p was more than 2-fold up-regulated in serum of idiopathic fracture patients and was able to differentiate FX from controls with AUC-values ranging between 0.92 and 1.00. In order to assess the potential biological impact of all 18 commonly regulated miRNAs, target prediction was performed and KEGG-pathway enrichments were calculated using public bioinformatic tools. Based on this analysis we found that target genes were significantly enriched ($p < 0.05$) in pathways such as WNT-signaling and energy metabolism (Insulin signaling, mTOR signaling). **Conclusion:** Our data provide evidence that patients with idiopathic osteoporosis show distinct profiles of circulating miRNAs. miR-30e-5p in particular discriminates patients with low-traumatic

fractures. This miRNA was previously reported to suppress osteogenic differentiation via IGF2 in vitro and in vivo.

Disclosures: Roland Kocijan, None.

SU0325

Nrf2 mediates gender specific mechanisms on bone accrual and maintenance.

Gretel G Pellegrini¹, Meloney Cregor¹, Kevin McAndrews¹, Jesus Delgado-Calle¹, Amy Y Sato¹, Hannah M Davis¹, Lilian I Plotkin¹, David Burr¹, Connie M Weaver², Teresita Bellido³. ¹Department of Anatomy & Cell Biology Indiana University School of Medicine, Indianapolis, IN, USA, ²Department of Nutrition, Purdue University, West Lafayette, IN., USA, ³Department of Anatomy & Cell Biology, Department of Medicine, Division of Endocrinology, Indiana University School of Medicine, Indianapolis, IN, Roudebush Veterans Administration Medical Center, Indianapolis, IN, USA

Mice lacking the transcription factor nuclear factor erythroid 2-related factor2 (Nrf2) are prone to develop diseases associated with elevated oxidative stress, suggesting its critical role in endogenous antioxidant responses. However, conflicting results have been published regarding the skeletal phenotype of these mice likely due to differences in genetic background, age, or gender among the studies. Here, we performed a longitudinal analysis of bone mineral density (BMD) and circulating markers of bone remodeling in a cohort of littermates Nrf2+/+ (WT) and Nrf2-/- (KO) mice (10 males and 10 females per genotype) between 2 and 15 months of age. KO mice were generated by injection of targeted I29X1/SvJ-derived JM-1 embryonic stem cells into blastocysts, followed by breeding to C57BL6 mice. Similar to WT littermates, male and female KO mice reached adult peak BMD at ~5 months of age. However, female KO mice attained lower BMD whereas male KO mice reached higher BMD than WT littermates, particularly in the spine (-6.62 for female and +5.33% for male mice). After 5 months of age, both male and female WT mice began to lose spinal BMD (-19.57 and -18.69%, for male and female WT mice, respectively, between 5 and 15 months of age). However, KO mice lost much less BMD (-9.69 and -5.04%, for male and female KO mice, respectively). The higher adult peak BMD in KO male mice was accompanied by higher circulating PINP at 2 and 5 months of age, suggesting that increased bone accrual was a consequence of elevated bone formation. Further, collagen1 expression was increased ~300% vs WT in 15 month old male KO mice, without changes in other osteoblast or osteoclast markers. In contrast, osteoblast (collagen1, osterix, Runx2, and osteocalcin) as well as osteoclast (cathepsin K and TRAPase) markers were markedly reduced to ~10% of WT littermates in 15 month old female KO mice, potentially reflecting a reduction in both osteoblasts and osteoclasts. These results suggest that bone maintenance with aging in male KO mice results from increased collagen accumulation whereas in female KO mice is due to decreased bone remodeling rate. We conclude that Nrf2 is required for full bone acquisition in the female skeleton and has the opposite effect on the male skeleton. Further, the absence of Nrf2 similarly protects both male and female skeletons from bone loss with aging, although by different mechanisms. Thus, Nrf2 regulates bone accrual and maintenance by gender specific mechanisms.

Disclosures: Gretel G Pellegrini, None.

SU0326

Pathogenesis of Atypical Femur Fractures: Recruitment and Preliminary Results. Sudhaker Rao¹, Shijing Qiu², Elizabeth Warner², Heather Remtema², Mahalakshmi Honasoge², George Divine². ¹Henry Ford Hospital, USA, ²Henry Ford Health System, USA

Background and Purpose: Atypical femur fractures (AFF) are an established complication of long term bisphosphonate (BP) therapy, but considered rare based on retrospective database analyses. However, the true prevalence remains unknown. Accordingly, we initiated a prospective study to determine the prevalence and pathogenesis of AFF. We report preliminary results of recruitment and AFF prevalence.

Methods: In the first 10 months of the study we recruited 108 patients; 50 BP-unexposed and 58 BP-exposed (at least >2 years) with a mean age of 67.1 ± 7.9y. AFFs were diagnosed using Hologic software designed to detect AFF in both femurs in AP projection. Incomplete AFFs were confirmed as cracks by x-ray tomosynthesis. **Results:** BP-exposed patients were about 4y older (69.1 ± 8.4y vs. 64.8 ± 6.6y; p=0.003). The mean duration of BP-exposure was 6.1 ± 3.5y (range 2-18y). Ethnic composition was similar in the 2 groups. Most patients were on one of the three approved oral BPs.

We identified several barriers to recruitment. These included fear of bone biopsy even if AFF were to be detected and needle sticks for blood draw, concerns about transportation arrangements and associated costs, busy schedule, perception that participation would not benefit them, variability in BP exposure or the gap since discontinuation, and previous anabolic therapy (an exclusion criterion). Despite these limitations, we recruited the expected number of subjects during the 10 months.

The prevalence of AFF was 4/65 (or 6%), much higher than previously reported based on retrospective database analyses, but lower than our preliminary estimate of 12% (3/25), and about the same as our predicted estimate of 5% before the study began. Four patients had 6 femur AFFs: one patient had bilateral AFF, one patient

had AFF in one femur and incomplete AFF in the other femur, two patients had incomplete AFF in one femur each. The patient with AFF in one femur had multiple cracks in the other femur (or incomplete AFF), hitherto unreported.

Conclusion: The prevalence of AFF may be higher than previously estimated. There are a few barriers to recruitment, which we plan to overcome. Continued surveillance and research is needed both to determine the true prevalence and pathogenesis of AFF

Disclosures: Sudhaker Rao, None.

SU0327

A Clinical Used Antidepressant Drug Reduces Bone Volume by Increasing Osteoclastogenesis via Ubiquitin E3 Ligase ITCH. Xing Li^{1*}, Wen Sun², Mengmeng Wang², Hengwei Zhang², Zhiyu Wang³, Lingpeng Pei², Brendan Boyce⁴, Lianping Xing¹. ¹University of Rochester Medical Center, USA, ²U of Rochester, USA, ³Hebei Medical University, China, ⁴University of Rochester, USA

Clinical studies report that patients taking antidepressants including Clomipramine (CLP) have a high risk of osteoporotic fracture. CLP belongs to the tricyclic family of antidepressants whose influence on bone has not been studied. Here we investigated the effect of CLP on bone and bone cell functions in mice and molecular mechanisms involved. WT mice were treated CLP (10mg/kg/day, similar to doses given to humans) or vehicle (Veh) for 2 wks, and bones were examined by μ CT and histology. CLP significantly decreased trabecular bone volume (BV/TV: 19.3 vs. 25.3% in Veh) and cortical bone thickness (0.202*0.01 vs. 0.224*0.01mm in Veh) of tibiae, associated with increased osteoclasts (OCs) (OC surface/bone surface: 15*1.5 vs. 12*1.5% in Veh; OC#/mm bone surface: 13*3 vs. 7*1 in Veh), but no change in osteoblasts or bone formation rate. Bone marrow cells from CLP-treated mice formed significantly more OCs in the presence of RANKL/M-CSF (7*0.8 vs. 2.5*0.6/mm2 in Veh). CLP significantly increased OC formation (14*0.5 vs. 6*0.7/mm2 in Veh), resorption pit area (0.24*0.04 vs. 0.10*0.02 mm2 in Veh), and expression of OC-associated genes in vitro. To test if the bisphosphonate, Zoledronic acid (ZA), could prevent CLP-induced bone loss, WT mice were pre-treated with ZA (0.25mg/kg, 2x/wk) for 2 wks (a standard murine regimen), followed by CLP for an additional 2 wks. ZA markedly increased bone volume of CLP-treated mice (BV/TV: 28*3 vs. 20*2% in CLP) and cortical bone thickness (0.230*0.0 vs. 0.209*0.01 mm in CLP), which was associated with decreased OC numbers (OC#/mm bone surface: 8.5*2 vs. 16*1.5 in Veh). A recent study indicated that CLP has a specific inhibitory effect on the ubiquitin E3 ligase, ITCH, which we previously reported negatively regulates OC formation by promoting deubiquitination of TRAF6. To examine if ITCH is involved in CLP-induced OC formation, we treated bone marrow cells from ITCH KO or WT mice with CLP in OC formation assays. ITCH KO cells formed more OCs than WT cells (8*1.4 vs. 3*0.7/mm2). CLP increased OC formation from WT cells (6*0.75 vs. 3*0.65/mm2 in Veh), but not from ITCH KO cells (9*1.4 vs. 8*1.4/mm2 in Veh). Furthermore, CLP did not cause bone loss in ITCH KO mice. Thus, CLP reduces bone volume by increasing OC formation via E3 ligase ITCH. CLP-induced bone loss could be rescued by ZA. Our preclinical study suggests that anti-resorptive medication may have beneficial effects on patients who take antidepressants.

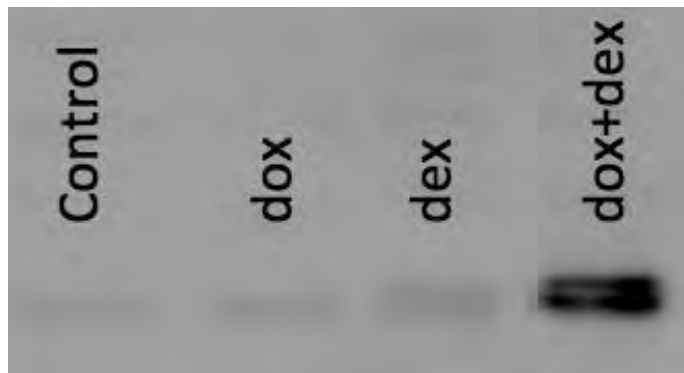
Disclosures: Xing Li, None.

SU0328

Hijack of RUNX2 in Glucocorticoid-Induced Osteoporosis. Eri Morimoto, Nyam-Osor Chimgé, Baruch Frenkel*. University of Southern California, USA

Glucocorticoid (GC)-Induced Osteoporosis (GIO), the most prevalent drug-induced bone disease, is attributable to myriad mechanisms. Most significantly, GCs attenuate cell replication, differentiation, function, and survival in the osteoblast lineage through deleterious effects on membrane receptor signaling (e.g., Wnt, Notch, RTKs), kinase cascades (e.g., ERK, Akt, Pyk) and downstream transcription factors (e.g., AP1, FoxO, RUNX2). Additionally, GCs stimulate osteoclast function through both cell autonomous and cell non-autonomous mechanisms. Regardless of how bone mass and strength are initially compromised, a perplexing question remains unanswered: given biomechanical feedback loops known to trigger bone formation in response to compromised bone strength, how is it that such loops do not result in increased osteoblastogenesis during GIO development, not even in young patients with a robust osteogenic potential? Because such feedback loop(s) likely entail activation of RUNX2, and because RUNX2 interacts with the GC receptor (GR) physically and functionally, we hypothesized that homeostatic feedback loops that normally compensate for bone weakening by triggering osteoblastogenesis are broken in GIO, and that the GR hijacks RUNX2 to synergistically stimulate genes with deleterious effects on osteoblasts. To address this hypothesis, we profiled mRNA expression in ST2/Rx2dox pluripotent mesenchymal stem cells (MSCs) treated with doxycycline (dox), to induce RUNX2 and/or 1 μ M dexamethasone (dex). Although GCs generally attenuated RUNX2-driven gene expression, there were some exceptional cases of synergism between RUNX2 and GCs. Among them was Wnt-inhibitory factor 1 (WIF1). RT-qPCR analysis confirmed 200-fold stimulation of WIF1 expression by dex+dox compared with 4- to 8-fold by the individual treatments, and Western blot analysis showed robust biosynthesis and secretion of WIF1 by cells treated with dex+dox versus hardly detectable levels in cultures treated with dex or

dox alone. Finally, dex-mediated cell death was dramatically augmented in cultures co-treated with dox, and this did was prevented by two independent shRNAs targeting WIF1. These results support a working model whereby GCs hijack RUNX2 to inhibit Wnt signaling in MSCs that turn on RUNX2 to drive osteoblast differentiation and bone formation. Thus, in the presence of GCs, upregulation of RUNX2 through homeostatic feedback loops might not result in the desirable enhancement of osteoblast differentiation and bone formation, but might instead lead to WIF1-mediated inhibition of Wnt signaling and exacerbation of GIO.



WIF1 Western blot analysis

Disclosures: Baruch Frenkel, None.

SU0329

Osteocyte-Derived RANKL Is Required for the Detrimental Effects of Glucocorticoids on Murine Cortical Bone. Marilyna Piemontese^{*1}, Jinhu Xiong¹, Yuko Fujiwara¹, Priscilla Baltz¹, Stuart Berryhill¹, Stavros Manolagas¹, Charles O'Brien². ¹University of Arkansas for Medical Sciences & Central Arkansas Veterans Healthcare System, USA, ²Central Arkansas VA Healthcare System, Univ of Arkansas for Medical Sciences, USA

Therapeutic administration of glucocorticoids causes bone loss and previous studies have shown that administration of prednisolone to adult C57BL/6 female mice for 28 days increases bone resorption at the endocortical surface and decreases cortical thickness. Moreover, blockade of glucocorticoid action on osteoblast-lineage cells prevents these changes. Osteocytes are an essential source of the RANKL involved in cancellous bone remodeling as well as the cortical bone resorption caused by mechanical unloading or dietary calcium deficiency. However, whether osteocyte-derived RANKL participates in the bone loss caused by glucocorticoid excess is unknown. To address this question, we generated mice lacking RANKL in mature osteoblasts and osteocytes, designated as conditional knockout (CKO) mice, by crossing RANKL-*fl/fl* mice with Dmp1-Cre transgenic mice. Six-month-old male CKO mice and RANKL-*fl/fl* littermates were then implanted with placebo pellets or pellets releasing prednisolone at a dose of 2.1 mg/kg/day for 28 days. Consistent with previous studies, femoral and vertebral cancellous bone was much higher in placebo-treated CKO mice compared with placebo-treated RANKL-*fl/fl* mice. However, prednisolone had no effect on cancellous bone volume of the femur or vertebra in either genotype. In contrast, prednisolone reduced femoral bone mineral density as well as cortical thickness and bone strength in RANKL-*fl/fl* mice. These changes were associated with increased osteoclast number at the endocortical surface of the femur. Similarly, prednisolone also reduced cortical thickness in vertebral bone of RANKL-*fl/fl* mice. Consistent with the histological results, prednisolone elevated osteoclast-specific gene expression in cortical bone of RANKL-*fl/fl* littermates. However, all of the effects of prednisolone observed in RANKL-*fl/fl* mice were completely prevented in CKO mice. Prednisolone administration significantly reduced osteoprotegerin (OPG) mRNA in osteocyte-enriched cortical bone of both genotypes. As expected, deletion of RANKL from DMP1-Cre expressing cells decreased RANKL mRNA abundance compared to RANKL-*fl/fl* mice but prednisolone did not change RANKL mRNA abundance in either genotype. These results suggest that glucocorticoid suppression of OPG in mature osteoblasts or osteocytes may be one of the molecular mechanisms driving the increase in osteoclast number at the endocortical surface. However, this increase also depends on RANKL produced by osteocytes.

Disclosures: Marilyn Piemontese, None.

SU0330

Estrogen Regulates Bone Turnover by Targeting RANKL Expression in Bone Lining Cells. Carmen Streicher¹, Alexandra Heyny¹, Olena Andrukhova¹, Christiane Schüller¹, Karoline Kollmann¹, Ingrid Kantner¹, Veronika Sexl¹, Miriam Kleiter¹, Lorenz Hofbauer², Paul Kostenuik³, Reinhold Erben^{*1}. ¹University of Veterinary Medicine, Austria, ²Technische Universität Dresden, Germany, ³Phylon Pharma Services, USA

Estrogen is critical for skeletal homeostasis and regulates bone remodeling, in part, by modulating the expression of receptor activator of NF- κ B ligand (RANKL), an essential cytokine for bone resorption by osteoclasts. RANKL can be produced by a variety of hematopoietic (e.g. T and B-cell) and mesenchymal (osteoblast lineage, chondrocyte) cell types. The cellular mechanisms by which estrogen acts on bone are still a matter of controversy. Here, we established reconstitution models that allow for selective deletion of estrogen receptor- α (ER α) or selective inhibition of RANKL in hematopoietic vs. mesenchymal cells. We first showed in irradiated wildtype (WT) mice reconstituted with WT bone marrow that irradiation and bone marrow transplantation *per se* are not associated with bone loss. To selectively delete ER α in hematopoietic or mesenchymal cells, we lethally irradiated female WT and global ER α knockout mice (α ERKO), and reconstituted them with sex-matched bone marrow from α ERKO or WT mice, respectively. To selectively inhibit RANKL in hematopoietic or mesenchymal cells, we lethally irradiated female WT and human RANKL knock-in (huRANKL-KI) mice, and reconstituted them with sex-matched bone marrow from hRANKL-KI or WT mice, respectively. huRANKL-KI mice express a chimeric RANKL protein which, unlike murine RANKL, is inhibited by the anti-huRANKL antibody AMG161, and thus AMG161 treatment of the respective reconstituted mice results in selective inhibition of RANKL produced from hematopoietic or mesenchymal cells. All mice were ovariectomized (OVX) 4 weeks after irradiation, and were treated with vehicle, estradiol, or AMG161 over 4 weeks. Both reconstitution models showed that OVX-induced bone loss was only prevented by estrogen stimulation of ER α or inhibition of RANKL expression in mesenchymal, but not in hematopoietic cells. To further refine the mesenchymal cell compartment, we analyzed RANKL expression by immunohistochemistry and by *in situ* mRNA expression profiling using laser capture microdissection. OVX profoundly upregulated RANKL expression in bone lining cells, but not in osteoblasts, and only marginally in osteocytes, indicating that the increase in bone resorption observed in states of estrogen deficiency in mice is mainly caused by lack of ER α -mediated suppression of RANKL expression in bone lining cells. In conclusion, we identified bone lining cells as important gatekeepers of estrogen-controlled bone resorption.

Disclosures: Reinhold Erben, None.

SU0331

Role of Antiretroviral therapy (ART) on bone mass and bone texture. Esteban Martinez^{*1}, Polyana Monteiro¹, Luis Del Rio². ¹Infectious Diseases Unit, Hospital Clinic, Barcelona, Spain, Spain, ²CETIR Grup Mèdic, Barcelona, Spain, Spain

Rational: The aim of the study is to evaluate effects of different ART on areal bone mineral density (aBMD) and bone microarchitectural texture (TBS) of HIV infected patients.

Methods: 245 men and 80 women aged 45 and older were analyzed. Among them 44 HIV-infected patients are free from antiretroviral therapy (Naive group). Other subjects received either therapy containing Tenofovir plus Ritonavir-boosted protease inhibitor (TeRiPi, n=35) or Ritonavir-boosted protease inhibitor (RiPi, n=51) or Tenofovir (Te, n=141) or therapy not containing Te or RiPi (NoTeRiPi, n=54). Lumbar aBMD were measured by dual energy X-ray absorptiometry using a QDR 4500 device (Hologic, Madison, USA). TBS was computed using TBS iNsight® (v2.1, Med-Imaps, France).

Results: No differences in terms of age was observed between groups (all $p > 0.08$). Subjects in the naive group had mean viral charge of 127215 particles per milliliter of blood whereas those under TeRiPi, RiPi, Te and NoTeRiPi had a viral charge of 37 or lower. Subjects in the naive group had significant lower number of T4 in comparison with subjects under therapies (all $p < 0.001$). Those under TeRiPi and RiPi had a significant decrease in both TBS (all $p < 0.0001$) and aBMD (all $p < 0.03$) when compared to the naive group. Interestingly, those under Te and NoTeRiPi therapies exhibited a significant decrease on TBS (all $p < 0.02$) while aBMD seems to be similar (all $p > 0.33$). We observed a trend to the TeRiPi therapy be the most impacting TBS when compared to other therapies ($0.001 < p < 0.07$). When considering subjects with a low bone mass (T-score ≤ -1 ; n=176), those under TeRiPi, RiPi and NoTeRiPi have a significant lower TBS than the naive group (all $p < 0.01$) while no differences were observed in BMD (all $p > 0.3$) and thus without differences for age or BMI between groups. In multivariate analysis, a low TBS value (lowest tertile) was best explained ($r^2 = 31\%$) by a model combining age, T4basal, BMI (negative association, all $p < 0.02$) and aBMD and T8 (positive association, all $p < 0.05$).

Conclusions: For the first time we observed an impairment on bone micro-architectural texture at spine linked to the ART and thus for all studied therapies while an impairment on aBMD has been observed only for TeRiPi and RiPi. It seems that TeRiPi exhibited the worse effect on TBS but further studies are needed to confirm these preliminary results. TBS could be used in addition to aBMD to monitor effect of ART on bone in HIV infected patients.

Disclosures: Esteban Martinez, None.

SU0332

Cortisol Circadian Rhythm Changes are associated with low trabecular bone score (TBS) and increased fracture risk, without any influence on bone mineral density (BMD): The OsteoLaus Cohort. Elena Gonzalez Rodriguez¹, Bérenère Aubry-Rozier¹, Delphine Stoll¹, Olivier Lamy¹, Didier Hans². ¹Center of Bone Diseases, Rheumatology Unit, Bone & Joint Department, Lausanne University Hospital, Switzerland, ²Lausanne University Hospital, Switzerland

Aim: In glucocorticoid (GC)-induced osteoporosis, fracture risk is poorly correlated with BMD. TBS is a bone texture analysis which correlates with micro-architecture parameters. It independently correlates to fracture risk. Lower TBS but normal BMD are found in patients with high GC levels, even in subclinical hypercortisolism. Cortisol production and bone turnover exhibit a circadian cycle. Cortisol circadian rhythm changes with age, with globally a greater area under the curve mainly due to an increase of the nadir levels during the 1st half of the night. Bone turnover circadian pattern is inversely correlated to cortisol one with a time lag of 4h. Changes in cortisol circadian cycle with aging could be at the origin of BMD loss. No study has addressed its role on TBS alteration or fracture risk.

Method: OsteoLaus is a population-based cohort of 1500 randomly selected Caucasian women (50 to 80 y old) living in Lausanne. Bone parameters include BMD, TBS and VFA. 754 women also had salivary cortisol circadian rhythm measures (wake-up, 30 min after wake-up, 11 am and 8 pm). Women with more than 3 months of GC therapy were excluded. They were split in tertiles of age, and in tertiles of salivary cortisol values at 11 am and at 8 pm.

Results: Salivary cortisol concentration at 11 am and 8 pm increased with age. On the contrary, hip BMD and spine TBS decreased with age (there was no difference in spine BMD). Comparison between lowest versus highest tertiles of salivary cortisol concentration at 8 pm showed: a) Significantly lower TBS values (1.31 vs 1.27) (but not spine or hip BMD) with highest cortisol concentration, independently of age, BMI or BMD (spine or hip) ($p < 0.0001$); b) Significantly higher number of prevalent vertebral fractures (15.0% versus 8.4%) in the tertile showing the highest concentration of salivary cortisol as well as in the tertile having the lowest TBS values ($p < 0.03$). No statistical difference was found for any of the BMD parameters. These associations were not found when using salivary cortisol at 11 am.

Conclusions: Highest cortisol values at 8 pm are associated with altered microarchitecture, but not BMD decrease, independently of age and BMI. Moreover, highest cortisol values and lowest TBS values are both associated with an increased prevalence of vertebral fractures. If these results are confirmed in other studies, the measurement of cortisol at 8 pm may play a role in the assessment of fracture risk.

Disclosures: Elena Gonzalez Rodriguez, None.

SU0333

Obstructive Sleep Apnea is Associated with Deterioration in Bone Mass and Quality in Type 2 Diabetes. Hataikarn Nimitphong¹, Nantaporn Siwarasanond¹, Chanika Sritara², Sunee Saetung¹, Boonsong Ongphiphadhanakul¹, Sirimon Reutrakul¹. ¹Medicine department, Ramathibodi hospital, Mahidol university, Thailand, ²Radiology Department, Ramathibodi Hospital, Mahidol University, Thailand

Background: Type 2 diabetes (T2D) adversely affects the skeleton and is associated with an increased risk of osteoporosis and fragility fractures despite normal or slightly elevated bone mineral density (BMD). Growing evidence suggests obstructive sleep apnea (OSA) may affect bone biology and cause secondary osteoporosis. The effect of OSA in T2D patients on bone quality and metabolism is less explored. We investigated the impact of OSA on bone markers, BMD, and Trabecular Bone Score (TBS; a bone quality assessment) in T2D subjects. **Methods:** Eighty-nine T2D patients without history of metabolic bone disease were included. OSA was diagnosed using an overnight in-home monitoring device (WatchPAT200). N-terminal propeptides of type I procollagen (PINP) and C-terminal cross-linking telopeptides of type I collagen (CTX-I) were measured. L1-4 lumbar spine and femoral BMD were measured using dual-energy X-ray absorptiometry (DXA) and TBS was computed from DXA images. **Results:** Seventy one patients (80%) were diagnosed with OSA [apnea hypopnea index (AHI) ≥ 5]. There were no differences in PINP and CTX-I between those with or without OSA. Those with OSA had higher L1-4 BMD than those without. The prevalence of low bone mass/osteoporosis was similar between groups. In patients with OSA, bone markers and sleep parameters were not correlated. However, TBS L1-4 negatively correlated with respiratory disturbance index during rapid eye movement (REM) phase of sleep (REM RDI; $r = -0.33$, $p = 0.011$) and REM AHI ($r = -0.28$, $p = 0.031$), while there were no associations between L1-4 BMD and sleep parameters. Femoral neck (FN) BMD negatively correlated with time spent under the oxygen saturation of 90% (T90) ($r = -0.30$, $p = 0.018$) and a trend emerged for REM AHI ($r = -0.26$, $p = 0.05$). In addition, total hip (TH) BMD negatively correlated with T90 ($r = -0.25$, $p = 0.045$). Multiple regression analyses adjusting for age, sex and body mass index revealed that REM RDI significantly correlated to TBS L1-4 and BMD with the hierarchy as follow; FN BMD: $r = -0.35$, $p = 0.003$, TBS L1-4: $r = -0.33$, $p = 0.008$, TH BMD: $r = -0.28$, $p = 0.026$, L1-4 BMD: $r = -0.27$, $p = 0.047$. Furthermore, both FN BMD and TBS L1-4 negatively correlated with AHI REM, and FN BMD negatively correlated with T90. **Conclusions:** In subjects with T2D and OSA, there is a relationship between OSA severity and deterioration of bone mass and

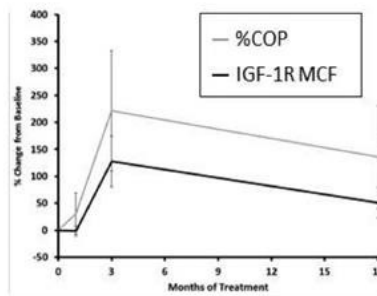
quality. Further studies to investigate the causal relationship of OSA and bone metabolism in T2D are warranted.

Disclosures: Hataikarn Nimitphong, None.

SU0334

Circulating osteogenic progenitors (COPs) and COP surface IGF-1 receptor density predict tissue-based bone formation rate and response to teriparatide (TPTD) in premenopausal women with idiopathic osteoporosis (IOP). Adi Cohen¹, J. Sanil Manavalan², Stavroula Kousteni², Robert Recker³, Joan Lappe³, David Dempster², Hua Zhou⁴, Donald McMahon², Mariana Bucovsky², Mafo Kamanda-Kosseh², Julie Stubby³, Elizabeth Shane². ¹Columbia University Medical Center, USA, ²Columbia University, USA, ³Creighton University, USA, ⁴Helen Hayes Hospital, USA

In premenopausal women with IOP, those with low bone formation rate (BFR) on transiliac bone biopsy have the most substantial microarchitectural deficits and respond less well to TPTD. IGF-1 stimulates bone formation and is critical for TPTD action on osteoblasts (OB). Therefore, we measured IGF-1 receptor (IGF-1R) density on COP cells from 25 premenopausal women with IOP (age 38 ± 7), of whom 11 subsequently participated in an open-label study of TPTD. COP cells were isolated by flow cytometry from peripheral blood mononuclear cells (PBMCs) as osteocalcin+ Runx2+ cells after excluding hematopoietic lineage cells. IGF-1R density on COPs was measured by mean channel fluorescence (MCF) of antibodies to IGF-1R. We show that the percentage of COPs in PBMCs correlates directly with cancellous BFR ($r = 0.41$, $p = 0.04$), mineral apposition rate (0.75, < 0.0001) and wall width (0.51, 0.01) on transiliac biopsies of all 25 women. IGF-1R density also correlated with BFR ($r = 0.57$, $p = 0.003$) and was significantly lower on COPs from women with low turnover (LT) than high turnover (HT) IOP (MCF: 863 ± 217 vs 1547 ± 806 ; $p = 0.04$). Compared to the HT group, the LT IOP group also had significantly lower OB number on biopsies (0.7 ± 0.3 vs 1.5 ± 1.1 #/mm; $p = 0.002$) and %COPs (13.3 ± 8.0 vs 29.0 ± 8.8 %; $p = 0.004$). COPs and IGF-1R expression were also investigated at baseline and after 1, 3 and 18 months (M) of TPTD (20 mcg qd) in 11 IOP women (age 38 ± 7). The %COPs increased with TPTD, peaking at 3M by 221% ($p = 0.02$) and remained above baseline at 18M. Similarly, IGF-1R MCF peaked at 3M by 128% ($p < 0.01$). There were substantial 12M increases in BMD (LS: 12.9 ± 5.7 %; FN: 6.9 ± 4.6 %) but response was quite variable. Neither baseline %COP nor 3M increase in %COP predicted BMD response to TPTD. In contrast, the % increase in IGF-1R MCF in COPs at 3M correlated directly and significantly with the 6M increase in BMD in response to TPTD at the spine ($r = 0.70$; $p = 0.02$) and femoral neck ($r = 0.67$; $p = 0.02$), with trends at 12M: spine ($r = 0.55$; $p = 0.08$) and femoral neck ($r = 0.49$; $p = 0.1$). We conclude that %COP and IGF-1R density on COPs are directly associated with indices of bone formation measured on biopsies in the same subjects. Both measures rise markedly in IOP women in response to TPTD and the increase in IGF-1R density on COPs correlates directly with BMD response to TPTD. An early increase in IGF-1R density may both predict and play an important role in the osteoanabolic response to TPTD.



COPFig

Disclosures: Adi Cohen, Eli Lilly

This study received funding from: Eli Lilly

SU0335

Comparative effect of alendronate and teriparatide on bone mineral density and bone turnover among Japanese postmenopausal women with history of fragility fractures: A clinical practice-based observational study. Jun Iwamoto^{*1}, Mitsuyoshi Uzawa². ¹Keio University School of Medicine, Japan, ²Keiyu Orthopaedic Hospital, Japan

A clinical practice-based observational study was performed to compare the outcome of alendronate (ALN) and teriparatide (TPTD) treatment among Japanese postmenopausal women with a history of fragility fractures. Sixty-one Japanese postmenopausal women with a history of fragility fractures were treated with ALN (35 mg weekly, n = 32) or TPTD (20 µg daily, n = 29) for 2 years in our outpatient clinic. Alfacalcidol (1 µg daily) was combined with ALN. The lumbar spine or total hip bone mineral density (BMD) was measured using dual energy X-ray absorptiometry, and bone turnover markers were monitored. ALN decreased the urinary levels of cross-linked N-terminal telopeptides of type I collagen (NTX) (38.3% after 3 months) and the serum levels of alkaline phosphatase (ALP) (25.7% at 24 months), whereas TPTD increased the serum levels of intact procollagen type I N-terminal propeptide (PINP) and ALP (79% and 14.1%, respectively at 24 months). Both ALN and TPTD increased the lumbar spine BMD (8.8% and 15.9%, respectively) and sustained the total hip BMD at 24 months. One patient treated with ALN experienced vertebral fractures, and one patient treated with TPTD experienced a nonvertebral fracture. These results confirmed the differential effects of ALN and TPTD on bone turnover and the greater effect of TPTD on the BMD among Japanese postmenopausal women with a history of fragility fractures.

Disclosures: Jun Iwamoto, None.

SU0336

Rapid, High Dose vs. Slower, Low Dose Accrual of Bone Mass Following Sclerostin Antibody Treatment in Ovariectomized Rats: Comparison of Effects on Bone Strength. Henry Bryant^{*1}, Matthew Hamang¹, Guilherme V Rocha¹, Qianqiang Zeng¹, Jonathan Lucchesi¹, Sarah E Raines¹, Stuart A Kuhstoss¹, Victor Obungu¹, Venkatesh Krishnan², Yanfei Ma¹. ¹Eli Lilly & Company, USA, ²Eli Lilly & Company, USA

Osteoporotic patients who have experienced a fracture are the highest risk population for future fractures and are ideal patients for bone anabolic therapies that rapidly stimulate new bone formation. Currently in clinical trials for osteoporosis, sclerostin (SOST) antibodies show a robust and rapid gain in vertebral bone mineral density (BMD). Similar effects can be observed in animal models. The speed at which bone can be built by SOST antibodies raises the question: Is bone built rapidly at a higher dose level by this mechanism as biomechanically sound as bone accrued over a longer period of time by a lower dose of the SOST antibody? To address this we compared bone quality in ovariectomized rats given a high or low dose of SOST antibody over a shorter or longer time period, respectively. Athymic nude rats were ovariectomized (OVX) at 4 months of age and allowed to lose bone for 2 months. The animals were then treated with blosozumab (Bmab), a humanized SOST antibody at 3 or 10 mg/kg (sc) once per week. Animals given 10 mg/kg were sacrificed after 6 weeks and the 3 mg/kg group was sacrificed after 10 weeks of Bmab treatment. The 10 week time point was specifically selected as this was the time interval required for the lower dose group to attain a BMD level (as measured by in vivo CT) comparable to that attained by the higher dose Bmab group with the 6 week dosing period. BMD was reduced at both the lumbar vertebrae (LV, 16%) and proximal femur (PF, 14%) at the start of Bmab treatment. As depicted in the table below, the higher Bmab dose given for only 6 weeks produced comparable BMD gain to the lower dose given for 10 weeks in both LV and mid-femur. These effects on BMD translated to comparable effects on peak load, or slightly favorable for the more rapid, high dose Bmab group. Interestingly, the PF responded more robustly (relative to LV) to the shorter, higher dosing regimen than to the longer, lower Bmab treatment, both in terms of BMD and bone strength. This study suggests that even with a shorter treatment period and time to accrue bone mass, a high dose of SOST antibody produces comparable, or possibly, superior effects on BMD and bone strength when compared to a lower dose given for a longer period of time.

BMD and strength changes with Bmab 10mg/kg for 6 weeks vs Bmab 3mg/kg for 10 weeks (% OVX vehicle)

| Endpoint | BMD | BMD | Peak Load | Peak Load |
|--------------------|----------|----------|-----------|-----------|
| Bmab Dose/duration | 10mg/6wk | 3mg/10wk | 10mg/6wk | 3mg/10wk |
| Lumbar vertebra | 23% | 18% | 61% | 62% |
| Mid femur | 5% | 6% | 17% | 11% |
| Proximal femur | 18% | 10% | 43% | 28% |

BMD and strength changes with Bmab 10mg/kg for 6 weeks vs Bmab 3mg/kg for 10 weeks (% OVX vehicle)

Disclosures: Henry Bryant, Eli Lilly and Company
This study received funding from: Eli Lilly Company

SU0337

Can We Use Bone Turnover Markers as Targets for Antiresorptive Treatment in Postmenopausal Osteoporosis? An Analysis From the DECIDE and STAND Clinical Trials. JP Brown^{*1}, P Dakin², P Hadji³, MR McClung⁴, PD Miller⁵, JY Reginster⁶, RB Wagman², A Wang², E McCloskey⁷. ¹Laval University & CHU de Quebec-(CHUL) Research Centre, Canada, ²Amgen Inc., USA, ³Philips-University of Marburg, Germany, ⁴Oregon Osteoporosis Center, USA, ⁵Colorado Center for Bone Research, USA, ⁶University of Liège, Belgium, ⁷University of Sheffield, United Kingdom

Purpose: Bone turnover markers (BTMs) respond much quicker than BMD as an indicator of response to therapy in osteoporotic patients; however, it remains unclear when and how best to evaluate treatment response using BTMs. Denosumab (DMAB) has a dynamic BTM profile over the 6-mo dosing period (ie, reduction in turnover with release of inhibition at the end of the dosing interval). This analysis assessed the use of potential target values for serum C-telopeptide of type I collagen (CTX) and serum procollagen type I N-terminal propeptide (PINP) to explore guidance to clinicians for monitoring postmenopausal women with osteoporosis (PMO) during treatment.

Methods: BTMs measured at baseline in treatment-naïve PMO entering FREEDOM, a large randomized, placebo-controlled study of DMAB (Cummings *NEJM* 2009), were used to derive threshold values at the 5th percentiles of the observed distributions. The relevant values for serum CTX (N=7594) and PINP (N=1023) were 0.2 ng/mL and 25.8 ng/mL, respectively. These BTM target values were applied to the study populations of DECIDE (Brown *JBMR* 2009) and STAND (Kendler *JBMR* 2010) enabling evaluation of a population-based assessment of BTM target values. DECIDE (N=1189) and STAND (N=504) were phase 3, randomized, double-blind, double-dummy studies to compare the efficacy and safety of DMAB (60 mg SC Q6M) with alendronate (ALN) (70 mg PO QW) in treatment-naïve PMO or PMO already receiving ALN, respectively. The percentage of subjects in each treatment group with BTMs below the predefined target values was evaluated mid-cycle at mo 3 after the 1st dose of DMAB, which also enabled trough values for ALN, and then re-evaluated at mo 9. Subjects with BTM values below the predefined targets at baseline were excluded from the analysis.

Results: A total of 1112 women in DECIDE and 155 women in STAND had CTX values ≥ 0.2 ng/mL and PINP values ≥ 25.8 ng/mL at baseline. Table 1 reports the percentage of subjects with CTX and PINP values below the respective targets at mo 3 and 9. The predefined target values were almost universally achieved at 3 and 9 mo on DMAB, whereas the target for CTX, for example, on ALN was only achieved in 49.1% and 19% of treatment-naïve and ALN-pretreated PMO, respectively, at mo 3.

Conclusion: In this population-based analysis, in both treatment-naïve and pretreated PMO, BTMs have utility in determining response, and awareness of failure to reach a treatment target may help improve clinical management.

Table 1 Percentage of Subjects With CTX <0.2 ng/mL or PINP <25.8 ng/mL at Follow-up

| DECIDE | CTX <0.2 ng/mL | | PINP <25.8 ng/mL | |
|---------|---------------------|-------------------|---------------------|-------------------|
| | Alendronate (N=544) | Denosumab (N=568) | Alendronate (N=544) | Denosumab (N=568) |
| Month 3 | 49.1 | 95.1* | 65.6 | 98.0* |
| Month 9 | 66.5 | 96.4* | 80.7 | 97.0* |

| STAND | CTX <0.2 ng/mL | | PINP <25.8 ng/mL | |
|---------|--------------------|------------------|--------------------|------------------|
| | Alendronate (N=83) | Denosumab (N=72) | Alendronate (N=83) | Denosumab (N=72) |
| Month 3 | 19.0 | 97.1* | 41.0 | 98.5* |
| Month 9 | 15.6 | 100.0* | 52.0 | 100.0* |

N=total number of subjects with baseline CTX ≥ 0.2 ng/mL and PINP ≥ 25.8 ng/mL.

CTX, serum C-telopeptide of type I collagen; PINP, serum procollagen type I N-terminal propeptide. *p<0.0001; Pearson's chi-square test for between-group comparisons.

Table

Disclosures: JP Brown, Amgen, Eli Lilly, Novartis; Amgen, Eli Lilly; Amgen, Eli Lilly
This study received funding from: Amgen Inc.

SU0338

Changes in Bone Metabolic Markers During Long-Term (>3 Years) Bisphosphonate Treatment. Yuji Kasukawa^{*1}, Naohisa Miyakoshi², Michio Hongo³, Koji Nozaka³, Yoshinori Ishikawa³, Daisuke Kudo³, Toshihito Ebina⁴, Hiroshi Aonuma⁴, Kimio Saito⁴, Yoichi Shimada³. ¹Akita University Graduate School of Medicine, Japan, ²Department of Orthopedic Surgery, Akita University Graduate School of Medicine, Japan, ³Department of Orthopedic Surgery, Akita University Graduate School of Medicine, Japan, ⁴Department of Orthopedic Surgery, Kakunodate General Hospital, Japan

Although bisphosphonates (BPs) suppress bone resorption markers, these markers sometimes become over-suppressed or show re-elevation during long-term treatment with BPs. At present, the precise changes of bone metabolic markers during long-term

treatment with BPs remain unclear. The purpose of this study was to evaluate changes of bone resorption and formation markers during treatment with BPs, including minodronate, for longer than 3 years. We enrolled 55 osteoporotic women to the study who had been treated with BPs for longer than 3 years since 2005. The average age at the beginning of treatment was 73 years. BP types included alendronate (ALN) in 22 cases (monotherapy in 13 cases, combined therapy with calcium [Ca] and activated vitamin D [Vit.D] in 9 cases), and risedronate (RIS) in 33 cases (monotherapy in 20 cases, combined therapy with Ca and Vit.D in 4 cases, and combined therapy with menatrenone in 9 cases). BP treatments were switched in 6 cases, from ALN to RIS in 3 cases and from ALN to minodronate in 5 cases. Serum cross-linked N-telopeptide of type-1 collagen (NTX) and bone alkaline phosphatase (BAP) were measured at the beginning of treatment and 1, 2, 3, and 5 years post-treatment. Average levels of NTX (nmol of bone collagen equivalent [BCE]/L) and BAP (units [U]/L) at the beginning of treatment were 19.5 and 21.7, respectively. After treatment with BPs, the average levels of NTX and BAP, which were 14.1 ($p < 0.0001$) and 12.8 ($p < 0.0001$) at 1 year ($n = 45$), 13.8 ($p < 0.0001$) and 10.6 ($p < 0.0001$) at 2 years ($n = 37$), 15.9 ($p < 0.0001$) and 12.6 ($p < 0.0001$) at 3 years ($n = 42$), and 15.2 ($p = 0.02$) and 12.2 ($p = 0.0004$) at 5 years ($n = 18$), respectively, were significantly lower than those at the beginning of treatment at all time points post-treatment. The percentage decreases of NTX and BAP were not significantly different between ALN and RIS BP treatments. BP treatment for longer than 3 years significantly decreased serum levels of NTX and BAP in the study patients.

Disclosures: Yuji Kasukawa, None.

SU0339

Characteristics Associated with Bone Mineral Density Increase by 1-Year ALN/D5600 Treatment in a Randomized, Controlled Study on Postmenopausal Osteoporosis in Chinese Women. Zhen Lin Zhang¹, Er Yuan Liao², Wei Bo Xia³, Hua Lin⁴, Qun Cheng⁵, Li Wang⁶, Yong Qiang Hao⁷, De Cai Chen⁸, Hai Tang⁹, Yong De Peng¹⁰, Li You¹⁰, Liang He¹¹, Zhao Heng Hu¹², Chun Li Song¹³, Fang Wei¹⁴, Jue Wang¹⁴, Lei Zhang¹⁴, Arthur C Santora^{*15}. ¹Shanghai Sixth People's Hospital, Shanghai Jiaotong University, China, ²The Second Xiangya Hospital, Central South University, China, ³Peking Union Medical College Hospital, China, ⁴Nanjing Drum Tower Hospital, China, ⁵Huadong Hospital Affiliated to Fudan University, China, ⁶Tianjin Hospital, China, ⁷Shanghai Ninth People's Hospital, China, ⁸West China Hospital, West China School of Medicine, Sichuan University, China, ⁹Beijing Friendship Hospital, Capital Medical University, China, ¹⁰Shanghai First People's Hospital, China, ¹¹Beijing Jishuitan Hospital, China, ¹²Peking University People's Hospital, China, ¹³Peking University Third Hospital, China, ¹⁴Global Medical Affairs, Merck Sharp & Dohme China, China, ¹⁵Merck Research Laboratories, Rahway, NJ, USA, USA

Purpose: Little is known about the characteristics of Chinese postmenopausal women who gain greater bone mineral density (BMD) on antiresorptive therapy. We explored characteristics associated with changes in 1-year lumbar spine (LS) BMD in a 12-month randomized controlled study comparing the efficacy of weekly alendronate 70 mg/vitamin D3 5600 IU (ALN/D5600) versus calcitriol 0.25µg daily in Chinese patients.

Methods: patients who had on-treatment BTM (PINP/s-CTX) and 1-year LS-BMD measurements were eligible for the analysis. Baseline characteristics [age, weight, LS-BMD, vertebral fracture, dietary calcium, 25(OH)D, BTMs] and BTM changes at Month 6 were selected for univariate analysis based on clinical discretion. Continuous or categorical variables with a p value < 0.25 in a linear regression or a general linear model were included in multivariate analysis. A multiple regression model by least squares method was constructed to explore variables significantly correlated with 1-year LS BMD change. Hierarchical forward selection with switching was applied for variable elimination until all remained in the model had a p -value < 0.1 for a standardized coefficient (β).

Results: In the ALN/D5600 group ($n=96$), mean change in 1-year LS-BMD was 0.03 g/cm². Age, weight, dietary calcium, baseline BTMs and 25(OH)D, and changes of BTMs at Month 6 entered into multivariate model. LS-BMD change at 1 year was negatively associated with age ($\beta=-0.27$, $p<0.01$), baseline s-CTX ($\beta=-0.66$, $p<0.01$), and dietary calcium ($\beta=-0.17$, $p=NS$). An increase in 1-year LS-BMD was correlated with s-CTX decrease at Month 6 ($\beta=-0.62$, $p=0.001$). Baseline PINP was positively associated with the BMD change ($\beta=0.25$, $p=NS$). In calcitriol treated group ($n=104$), mean change in LS-BMD at the end of 1 year was 0.01 g/cm². Age, baseline BTMs, baseline 25(OH)D, prior vertebral fracture(s), and s-CTX change at Month 6 were analyzed in the multivariate model. One-year LS-BMD change was negatively correlated with baseline 25(OH)D ($\beta=-0.23$, $p=0.01$). Patients had more increases in the LS-BMD at 1 year if they had prior vertebral fracture(s) ($\beta=0.37$, $p<0.001$).

Conclusion: In this exploratory analysis, Chinese patients in the ALN/D5600 group with lower baseline s-CTX or greater on-treatment s-CTX decreases had larger increases in the spine BMD at 1 year. On the other hand, lower baseline vitamin D or prior vertebral fracture significantly predicted 1-year spine BMD increases by calcitriol treatment.

Disclosures: Arthur C Santora, Merck; Merck

This study received funding from: MSD China Holding Co., Ltd., China

SU0340

Denosumab Compared With Zoledronic Acid in Postmenopausal Women With Osteoporosis Previously Treated With Oral Bisphosphonates: Efficacy and Safety Results From a Randomized Double-blind Study. PD Miller^{*1}, N Pannacciulli², JP Brown³, E Czerwinski⁴, BS Nedergaard⁵, MA Bolognese⁶, J Malouf⁷, HG Bone⁸, JY Reginster⁹, A Singer¹⁰, C Wang², RB Wagman², SR Cummings¹¹. ¹Colorado Center for Bone Research, USA, ²Amgen Inc., USA, ³Laval University & CHU de Québec (CHUL) Research Centre, Canada, ⁴Krakow Medical Center, Poland, ⁵Center for Clinical & Basic Research, Denmark, ⁶Bethesda Health Research Center, USA, ⁷Hospital de la Santa Creu i Sant Pau, Spain, ⁸Michigan Bone & Mineral Clinic, USA, ⁹University of Liège, Belgium, ¹⁰Georgetown University Medical Center, USA, ¹¹San Francisco Coordinating Center, CPMC Research Institute, USA

Purpose

Oral bisphosphonates (BP) are the most common osteoporosis (OP) treatment, but inconvenient dosing regimens and side effects lead to low adherence. Less frequently dosed BP, eg, once yearly zoledronic acid (ZOL), are part of the treatment algorithm for patients who have failed or are intolerant to oral BP. Yet there is no evidence that cycling through BP offers therapeutic benefit. Denosumab (DMAB) has shown BMD increases in subjects previously treated with oral BP, in contrast to ZOL (McClung, 2007). This study evaluated DMAB compared with ZOL in postmenopausal women with OP previously treated with oral BP.

Methods

This was a 12-month, multicenter, randomized, double-blind, double-dummy study in postmenopausal women ≥ 55 years who had received oral BP for ≥ 2 years; had a BMD T-score ≤ -2.5 at the lumbar spine, total hip, or femoral neck; and a serum C-telopeptide of type 1 collagen (sCTX) ≤ 0.5 ng/mL. Subjects were randomized 1:1 to DMAB 60mg every 6 months (Q6M) + placebo (IV once yearly) or ZOL 5mg IV once yearly + placebo (SC Q6M), and received calcium and vitamin D daily. Endpoints included percentage change from baseline in BMD at the lumbar spine (primary endpoint), total hip, femoral neck, and 1/3 radius at month 12. sCTX and procollagen type 1 N-terminal propeptide (PINP) were measured post baseline in a subset of subjects. Safety was also assessed.

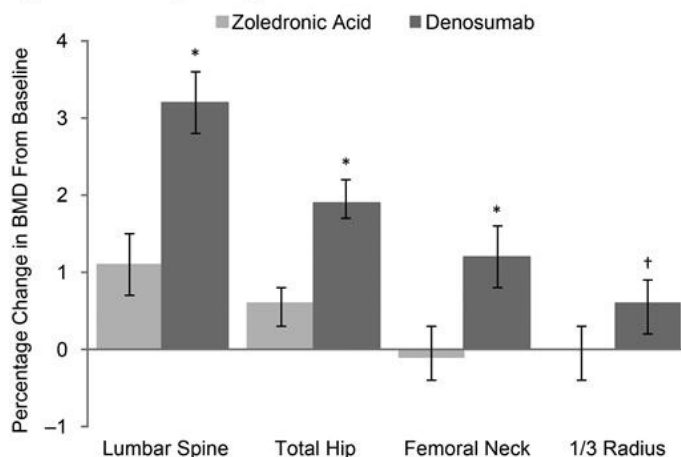
Results

643 subjects were randomized (321 DMAB; 322 ZOL). Mean (SD) age was 69 (7) years, mean (SD) lumbar spine BMD T-score was -2.7 (0.8), and mean (SD) duration of prior oral BP use was 6.3 (3.8) years. BMD change from baseline at month 12 was significantly greater with DMAB compared with ZOL at the lumbar spine (3.2% vs 1.1%; $p<0.0001$; Figure) and all other measured skeletal sites (Figure). Median decrease from baseline was greater with DMAB compared with ZOL for sCTX at months 1 (-78% vs -68%), 6 (-63% vs -22%), and 12 (-63% vs 2%; all $p<0.01$), and for PINP at months 6 (-48% vs -30%) and 12 (-50% vs 4%; both $p<0.01$). Overall and serious adverse events were similar between groups. There were no cases of osteonecrosis of the jaw, hypocalcemia, or delayed fracture healing. Three events consistent with the definition of atypical femoral fracture were observed (2 DMAB vs 1 ZOL).

Conclusions

In postmenopausal women with OP previously treated with oral BP, DMAB treatment increased BMD at all measured skeletal sites and reduced bone remodeling more than ZOL. No new safety risks were identified.

Figure. Percentage Change From Baseline in BMD at Month 12



* $p < 0.0001$ and † $p < 0.02$ denosumab vs zoledronic acid.

Data displayed are least-squared means and 95% CIs based on an ANCOVA model adjusting for treatment, sCTX stratification variable (< 0.3 ng/mL vs 0.3 to 0.5 ng/mL), baseline BMD, DXA machine type, and baseline value by DXA machine-type interaction.

Figure

Disclosures: PD Miller, Alexion, Lilly, Amgen, Novartis, NBHA, Pfizer, University of Alabama, Boehringer Ingelheim, Merck, Merck Serono, Radius; Grünenthal, Shionogi, Radius, Amgen, Lilly; Radius, Alexion, Amgen
This study received funding from: Amgen Inc.

SU0341

Ectosteric inhibitors of cathepsin K prevent bone resorption. PREETY PANWAR*¹, Liming Xu², Kent Soe³, Simon Law², Jean-Marie Delaisse³, Dieter Bromme⁴. ¹University of British Columbia, Canada, ²UBC, Canada, ³Vejle Hospital, University of Southern Denmark, Denmark, ⁴University of British Columbia, Canada

The potent collagenase activity of cathepsin K (CatK) in osteoclasts is of major interest for the development of anti-osteoporosis drugs. In this study, we evaluated low molecular weight ectosteric inhibitors that specifically block the collagenase activity of CatK without interfering with its catalytic site. Ectosteric inhibitors prevent the formation of collagenolytically active oligomers of CatK. Two compounds (T01 and T06) that differentially inhibit the *in vitro* CatK-mediated degradation of soluble and fibrillar collagen were analyzed for their antiresorptive efficacy in human osteoclasts. In addition, T06 efficacy was tested in ovariectomized (OVX) mice. Here, we demonstrate that T06 is the most potent ectosteric inhibitor of CatK for both soluble and fiber collagen degradation whereas T01 primarily inhibits soluble collagen degradation. Neither of the compounds affected the metabolic activity and viability of osteoclasts. T01 and T06 strongly inhibited the overall bone resorption in osteoclast pit formation assays by about 55 %, reduced the release of C-terminal telopeptide of type I collagen (CTX) fragments by more than 60%, and abolished the formation of trenches. μ CT analysis of femur and vertebra of OVX mice revealed a significant reduction in bone mineral density loss and an improvement of trabecular bone parameters by oral treatment with T06.

This study indicates that ectosteric inhibitors effectively prevent osteoclast-mediated bone resorption in cellular and in *in vivo* disease models. This opens a therapeutic window for the potential treatment in osteoporosis with a novel class of drugs which selectively block the collagenase activity of CatK without inferring with other functions of the multifunctional target protease.

Disclosures: PREETY PANWAR, None.

SU0342

Effects of weekly risedronate with cholecalciferol on bone mineral density in Korean patients with osteoporosis. Ho-Yeon Chung*¹, Hyoung-Moo Park². ¹Kyung Hee University, South Korea, ²Chung-ang University, South Korea

Introduction: We have previously reported that a single pill of risedronate combined with cholecalciferol demonstrated efficacy in correction of 25-hydroxyvitamin D(25OHD) and reducing bone markers. However, the short duration of previous study prevented meaningful evaluation of bone mineral density (BMD). Therefore, we performed a phase 4, randomized, open, prospective, 12-month clinical trial to evaluate the efficacy and safety of weekly risedronate with and without cholecalciferol on 25OHD levels and BMD in Korean patients with osteoporosis. **Methods:** we randomly assigned 1076 adults with osteoporosis to one of two treatment groups: RSD+ (weekly risedronate 35 mg and cholecalciferol 5,600 IU combined in a single pill, n=820) or RSD (weekly risedronate 35 mg alone, n=256). We measured serum levels of 25(OH)D, parathyroid hormone (PTH), and BMD at baseline and after 12 months of treatment. **Results:** After 12 months of treatment, mean serum 25(OH)D increased significantly from 18.3 to 30.4 ng/mL in the RSD+ group and increased from 17.8 to 18.6 ng/mL in the RSD group. The RSD+ groups had decreases in serum PTH from 40.6 to 39.4 pg/mL during the study, but the RSD group showed significant increase of PTH from 38.7 to 44.6 pg/mL. At 12-months, BMD at lumbar spine, femoral neck and femur total increased by 4.9%, 2.5%, 1.9% in the RSD+ group and 4%, 2.1%, 2.1% in the RSD group, respectively. The overall incidence of clinical adverse events was not significantly different between groups. **Conclusion:** In patients with osteoporosis, a once-weekly pill of risedronate and cholecalciferol significantly increased BMD and efficiently improved 25(OH)D level over a 12-month treatment period without significant adverse events.

Disclosures: Ho-Yeon Chung, None.

SU0343

Lasofloxifene 0,25 mg compared with raloxifene 60 mg for effects on bone mineral density and markers of bone turnover. Results from the Phase III Comparison of Raloxifene and Lasofloxifene (CORAL) Trial. Michael McClung*¹, Andrea LaCroix², James Simon³, James Symons⁴, David Portman⁵. ¹Oregon Osteoporosis Center, USA, ²UCSD, USA, ³James Simons Associates, USA, ⁴James Symons, USA, ⁵Pfizer, USA

There are few comparator trials between different selective estrogen receptor modulators (SERMs) for osteoporosis. The Phase 3 CORAL clinical trial is a head-to-head comparison of the SERMs lasofloxifene, a potent 3rd generation SERM, and raloxifene for osteoporosis prevention. The study was prospective, double-blind, randomized, placebo- and active-controlled, and multicenter. Subjects were women, ages 48-75 years inclusive, at least 3 years from last menses with baseline bone mineral density (BMD) T-score values by dual energy X-ray absorptiometry of the lumbar spine L1-L4 (LS) between <0.0 and >-2.5.

Subjects received lasofloxifene 0.25 mg/d, raloxifene 60 mg/d, or matching placebo for 2 years and were provided a daily supplement of approximately 1000 mg calcium

and 400 IU Vitamin D. The primary endpoint compared the effects on LS-BMD (% change from baseline and % of responders at Month 24); a secondary endpoint compared change in total hip (TH) BMD. For the primary endpoint, Bonferroni's method and a 1-sided a priori fixed sequence procedure were used to control the type I error rate at 5%.

A total of 540 subjects were enrolled (218 lasofloxifene, 215 raloxifene, and 107 placebo). Baseline demographics were similar across treatment groups. Mean baseline LS-BMD T-scores were -1.4, -1.3, and -1.3 in the lasofloxifene, raloxifene, and placebo treatment groups, respectively.

The LS-BMD and TH-BMD responses to lasofloxifene 0.25 mg/d were significantly greater than with raloxifene 60 mg/d or placebo at Month 24; % change LS-BMD from baseline vs raloxifene: least squares mean (LSM) difference 0.896 (95% CI: 0.26, 1.53), p-value=0.003; vs placebo: LSM difference 3.16% (95% CI: 2.38, 3.94), p-value <0.00001. Superiority of BMD changes was observed by Month 6 and sustained over time.

Logistic regression analysis of proportion of responders (no decrease from baseline in LS-BMD at a given time point) indicated the odds of subjects treated with lasofloxifene 0.25 mg/d responding positively were 1.9 times (95% CI: 1.2, 2.9) higher compared with those treated with raloxifene (p-value=0.003). Lasofloxifene 0.25 mg/d was superior to placebo and raloxifene in reducing markers of bone resorption and formation.

In the CORAL trial, lasofloxifene was effective and superior to raloxifene in preventing bone loss, reducing bone turnover, and for responder rates in postmenopausal women at risk for osteoporosis.

Disclosures: Michael McClung, None.

This study received funding from: Pfizer

SU0344

Monthly Oral Ibandronate 100mg Is as Effective as Monthly Intravenous Ibandronate 1mg in Japanese Patients with Primary Osteoporosis: the Phase III MOVEST Study. Toshitaka Nakamura*¹, Masako Ito², Junko Hashimoto³, Kenji Shinomiyama³, Yoshihiro Asao³, Hiroshi Hagino⁴, Tomoyuki Inoue⁵, Tetsuo Nakano⁶, Hideki Mizunuma⁷. ¹National Center for Global Health & Medicine, Japan, ²Nagasaki University Hospital, Japan, ³Chugai Pharmaceutical Co. Ltd., Japan, ⁴Tottori University Faculty of Medicine, Japan, ⁵Taisho Pharmaceutical Co. Ltd., Japan, ⁶Tamana Central Hospital, Japan, ⁷Hiroshima University School of Medicine, Japan

Purpose: The randomized, double-blind MOVEST (Monthly Oral Versus intravenous ibandronate) study compared the efficacy and safety of monthly oral ibandronate (IBN) with the licensed monthly intravenous (IV) dose in Japanese patients (pts) with primary osteoporosis. We present efficacy and safety data after 12 months of treatment and conclude the optimal dose of monthly oral IBN in Japanese osteoporotic pts. **Methods:** Ambulatory pts aged \geq 55 years with primary osteoporosis were randomized to receive monthly oral IBN 100mg + monthly IV placebo, or monthly IV IBN 1mg + monthly oral placebo. The primary endpoint was the non-inferiority of oral versus IV IBN with respect to bone mineral density (BMD) gains at the lumbar spine (L2-L4) after 12 months. **Results:** 422 pts were randomized. The per-protocol set comprised 372 pts: 183 and 189 in the oral and IV IBN groups, respectively. Baseline characteristics were balanced across the treatment groups. Over 12 months, BMD gains were substantial at all sites and significantly improved from baseline with all treatments after just 4 months. The mean relative changes from baseline in lumbar spine BMD at 12 months were 5.22% (95% CI 4.65-5.80) with oral IBN and 5.34% (95% CI 4.78-5.90) with IV IBN. The least squares mean difference between the two groups was -0.23% (95% CI -0.97-0.51), showing the non-inferiority of oral to IV IBN (non-inferiority limit -1.60). BMD gains at the total hip and femoral neck were also evident throughout the study. The proportion of responders at all sites was comparable between the two groups. Reductions in bone turnover markers were substantial with both treatments after 4 months. There were no apparent differences in the safety profiles of the two treatment groups. The incidence of acute phase reaction (APR) was comparable with oral (11.2%) and IV (11.8%) IBN; most APRs were mild in intensity and transient, and decreased with each subsequent dose of medication. No renal function-related adverse events, hypocalcemia, osteonecrosis of the jaw, or atypical fracture of the femur were reported. **Conclusions:** Monthly oral IBN 100mg demonstrated non-inferiority to monthly IV IBN 1mg in terms of lumbar spine BMD gains in Japanese pts with primary osteoporosis. These data suggest that two different monthly regimens of one agent are effective alternative treatment options for pts with osteoporosis in Japan, in accordance with their lifestyle and disease conditions.

Disclosures: Toshitaka Nakamura, Asahi Kasei Pharma Corp; Japan Ministry of Health, Welfare and Labor as a councillor for hospital administration and social medical insurance.

This study received funding from: Chugai Pharmaceutical Co. Ltd and Taisho Pharmaceutical Co. Ltd.

SU0345

Retrospective Study of the Safety of Intravenous Bisphosphonate (Zoledronic Acid) in Patients with Chronic Kidney Disease. Ali Achira*, Wael Taha, Dania Abushanab, Maria Diab, Bayan Chaker, Krishna Chalasani. Wayne State University, USA

Background

Bisphosphonates are anti-resorptive bone agents that effectively treat cancer related hypercalcemia, Paget's disease and osteoporosis. However, their usage is restricted due to the prevailing concern regarding their nephrotoxicity.

Objectives

To study the safety of intravenous zoledronic acid (ZOL) in patients with Chronic Kidney Disease (CKD) with estimated Glomerular Filtration Rate (eGFR) ≤ 50

Methods

Our study is a retrospective review of patients, aged 18 to 80 years, with chronic kidney disease with eGFR ≤ 50 mL/min/1.73m² based on the MDRD formula, who were treated in Detroit Medical Center with IV ZOL between 2010 to 2014. We excluded patients who were on dialysis before the treatment, who had nephrotoxic treatment and who had insufficient data to analyze. We compared creatinines at up to 12 months before and up to 6 months after treatment with ZOL. The baseline renal function is defined as average of at the most recent two eGFRs in two different periods before date. Periods defined are three before, and three after admissions: 1-3 months, 3-6, 6-12 months before, and 0-3, 3-6 and 6-12 months after admission. The creatinine is considered the average in each period. The patient should have at least 2 eGFRs in 2 occasions after ZOL infusion. We considered a minimum of 10 mL/min/1.73m² change in eGFR between average before and average to be significant. We considered acute kidney injury (AKI) on admission if Cr is ≥ 15% from baseline.

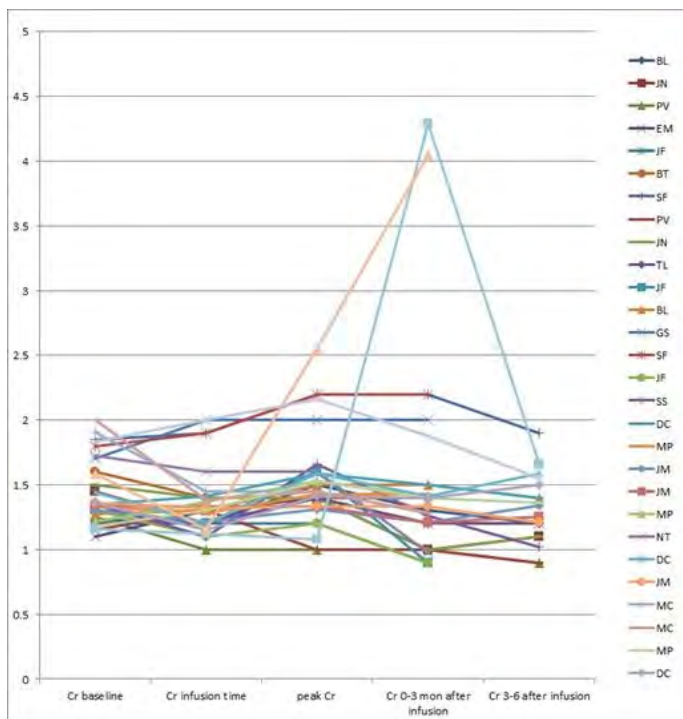
Results

We found 3742 patient who were treated with Zoledronic acid. So far we reviewed 912 charts, of which, 108 patients had eGFR of < 50 (average eGFR 36.5). None of which had significant decrease in eGFR in the 6 month period before the infusion. The rest were excluded due to eGFR > 50, or not enough data before infusion. Further only 31 patients had enough data after infusion and were included. Six of 31 had hypercalcemia.

The average eGFR was 42.25 mL/min/1.73m² (n=31). 28 of 31 (90.3 %) had maintained stable, or had some improvement of eGFR up to 6 month after ZOL infusion. Three patients (9.6 %) had a drop of eGFR at 0-3 month after infusion. Two of the 3 had improvement of renal function in period 3-6 month after. One of 3 had no data of renal function after. One of the two who had renal failure improved to his baseline eGFR. Therefore, two of 31 patients (6.5%) possibly had permanent drop of eGFR after ZOL infusion

Conclusion

IV ZOL caused no renal harm in 90.3%, reversible renal impairment in 3.2% and permanent renal impairment in 6.5% of the patients. Therefore, we believe ZOL treatment has good safety data in CKD and should be given if indicated.



Graph

Disclosures: Ali Achira, None.

SU0346

Safety Observations With Three Years of Denosumab Exposure: Comparison Between Subjects Who Received Denosumab During FREEDOM and Subjects Who Crossed Over to Denosumab During the FREEDOM Extension. NB Watts*¹, JP Brown², S Papapoulos³, EM Lewiecki⁴, DL Kendler⁵, P Dakin⁶, RB Wagman⁶, A Wang⁶, NS Daizadeh⁶, S Smith⁶, HG Bone⁷. ¹Mercy Health, USA, ²Laval University & CHU de Québec Research Centre, Canada, ³Leiden University Medical Center, Netherlands, ⁴New Mexico Clinical Research & Osteoporosis Center, USA, ⁵University of British Columbia, Canada, ⁶Amgen Inc., USA, ⁷Michigan Bone & Mineral Clinic, USA

Purpose: Denosumab (DMAb) is approved for the treatment of postmenopausal women with osteoporosis at increased risk for fracture. In the 3-year FREEDOM trial comparing placebo (Pbo) and DMAb, questions arose regarding imbalances of low-frequency adverse events and some common adverse reactions. Here, we examined the incidences of these events in women who originally received Pbo during FREEDOM and then received DMAb for 3 years during the FREEDOM Extension (cross-over group). This provided a unique opportunity for comparison with the original 3-year Pbo and DMAb FREEDOM observations.

Methods: In FREEDOM, postmenopausal women with osteoporosis received Pbo or DMAb for 3 years. Women were eligible for the Extension if they completed the 3-year FREEDOM visit, missed no more than 1 dose of investigational product (IP) during FREEDOM, and agreed to enroll. During the Extension, all women received DMAb. Three-year cumulative incidences of selected adverse events of interest observed during FREEDOM for the Pbo and DMAb groups also were determined for the first 3 years of DMAb exposure during the Extension for the cross-over group. For each of these 3 groups, the safety analyses included women who received ≥ 1 dose of IP during the respective 3-year periods (FREEDOM Pbo: N=3883; FREEDOM DMAb: N=3879; Extension cross-over DMAb: N=2206). Selected safety events of interest included malignancy, pancreatitis, endocarditis, delayed fracture healing, serious infections, serious opportunistic infections, and serious cellulitis or erysipelas, in addition to the top 5 most frequent adverse events in the US prescribing information (USPI; back pain, pain in extremity, musculoskeletal pain, hypercholesterolemia, and cystitis).

Results: The incidences of these adverse events in the cross-over DMAb group during the first 3 years of the Extension were similar to or lower than the incidences reported in FREEDOM and did not show a trend for increasing risk of any of these events (Table). For example, the incidence of serious adverse events of cellulitis or erysipelas observed in FREEDOM DMAb subjects (0.31%) was not observed in the FREEDOM Pbo subjects who crossed-over to DMAb (0.05%) in the Extension.

Conclusions: Analyses of 3-year safety data from FREEDOM (Pbo and DMAb groups) and 3-year safety data from the Extension (cross-over DMAb group) did not show an increasing trend regarding the imbalances of low-frequency events and some common adverse reactions observed in FREEDOM.

Table. Incidences of Events of Interest

| Event of interest - n (%) | FREEDOM (3 years) | | Extension (3 years) |
|---|---------------------|-----------------------|-------------------------------------|
| | Placebo N = 3883 | Denosumab N = 3879 | Cross-over Denosumab N = 2206 |
| Adverse Events | | | |
| Malignancy* | 167 (4.30) | 187 (4.82) | 108 (4.90) |
| Pancreatitis [‡] | 3 (0.08) | 7 (0.18) | 2 (0.09) |
| Endocarditis | 0 (0.00) | 3 [†] (0.08) | 0 (0.00) |
| Delayed fracture healing [§] | 5 (0.13) | 2 (0.05) | NA |
| Delayed fracture healing [¶] | 1 (0.03) | 0 (0.00) | 1 (0.05) |
| Serious Adverse Events | | | |
| Infections | 134 (3.45) | 160 (4.12) | 81 (3.67) |
| Opportunistic infections* | 3 (0.08) | 4 (0.10) | 2 (0.09) |
| Cellulitis or erysipelas | 1 (0.03) | 12 (0.31) | 1 (0.05) |
| Top 5 Most Frequent Events in USPI | | | |
| Back pain | 1343 (34.59) | 1344 (34.65) | 318 (14.42) |
| Pain in extremity | 432 (11.13) | 451 (11.63) | 171 (7.75) |
| Musculoskeletal pain | 291 (7.49) | 297 (7.66) | 118 (5.35) |
| Hypercholesterolemia | 236 (6.08) | 280 (7.22) | 145 (6.57) |
| Cystitis | 225 (5.79) | 228 (5.88) | 125 (5.67) |

Treatment groups are the original randomized assignments in FREEDOM. Seven placebo subjects received one dose of denosumab in FREEDOM were analyzed in the denosumab column in US PI.
 N = Number of subjects who received ≥ 1 dose of investigational product.
 Includes only treatment-emergent adverse events; based on MedDRA version 13.0.
 * Based on neoplasms benign, malignant and unspecified (including cysts and polyps) system organ class excluding benign events used in the FREEDOM Extension
[‡] Based on acute pancreatitis event of interest search strategy
[§] Based on delayed fracture healing response collected on Clinical Fracture Summary CRF II in FREEDOM
[¶] Based on AE reporting of delayed fracture healing events and subsequently selected by search strategy
[†] Includes aspergillosis, herpes zoster, pulmonary tuberculosis, and tuberculosis
[‡] No causative pathogen was identified in any of the 3 cases reported as endocarditis. One subject was hospitalized for treatment with antibiotics. One had endocarditis listed as a consideration in a fatal event of multi-organ failure due to sepsis; however, no treatment details from the case were available. The third case was listed as "non-serious," and the patient did well without long-term antibiotic therapy. Further information is not available.

Table

Disclosures: NB Watts, NPS, Merck; OsteoDynamics; Abbvie, Amgen, Merck, Radius, Sanofi, Sprout; Amgen, Merck
This study received funding from: Amgen Inc.

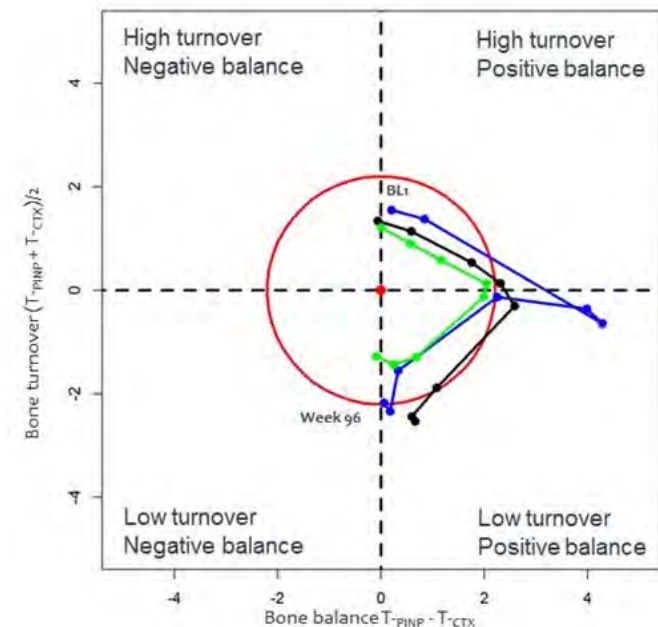
SU0347

The Effect of Bisphosphonate Treatment on Bone Turnover and Bone Balance in Postmenopausal Women with Osteoporosis. Fatma Gossiel¹, Richard Jacques², Kim Naylor², Eugene McCloskey², Nicola Peel², Jennifer Walsh², Richard Eastell². ¹The University of Sheffield, United Kingdom, ²University of Sheffield, United Kingdom

Postmenopausal osteoporosis is characterised by increased bone turnover, a negative balance (resorption>formation) and increased fracture risk. Bisphosphonates reduces bone turnover and fracture risk but their effect on bone balance is yet to be fully investigated. We have compared the effects of bisphosphonates on turnover and balance in postmenopausal women with osteoporosis using a T-score bone marker plot. 165 postmenopausal women (hip and spine BMD T-score ≤ -2.5 or < -1 with a prior fracture) were recruited, mean age 67 years. They were provided with calcium and vitamin D supplements and randomised to receive ibandronate (n=55, 150mg/month), alendronate (n=54, 70mg/week) or risedronate (n=56, 35mg/week). A fasting serum sample was collected at baseline and weeks 1,2,4,12,13, 48 and 96 on treatment. A control group of 200 healthy premenopausal women received no treatment. PINP and CTX were measured using the iSYS-IDS analyser. Values were log₁₀-transformed and normalised. The T-scores for PINP and CTX value were calculated for each postmenopausal woman using the mean and standard deviation values from the premenopausal group.

By week 96 bisphosphonates reduced mean levels of turnover to -2.1SD units (95% CI: -2.322, -1.848) below the mean of the premenopausal women $p < 0.001$. Bone balance was positive for all agents in the early phase of treatment. At week 96, mean levels of balance were positive in all treatments combined, (0.3SD units, 95% CI: 0.145, 0.559), $p < 0.01$ but bone balance was more positive with alendronate only, $p < 0.01$, (Figure).

In postmenopausal osteoporosis treatment with bisphosphonates improves bone balance by making it more positive and reduces bone turnover, relative to healthy premenopausal women. Bisphosphonates have differing effects on turnover and balance.



IBN (blue line), ALN (black line) and RIS (green). Circle is the premenopausal group

Disclosures: Fatma Gossiel, None.

This study received funding from: Warner-Chilcott

SU0348

The concept of ectosteric cathepsin inhibitors. Dieter Bromme^{*}. The University of British Columbia, Canada

Cathepsins K, V, and S are potent extracellular matrix protein-degrading proteases exhibiting either elastase and/or collagenase activities. The collagenase activity of cathepsin K is a major anti-resorptive drug target in skeletal diseases, whereas the elastase activities are considered detrimental in cardiovascular, respiratory, and potentially skin diseases. Substantial efforts have been invested to design highly

potent and selective active site-directed cathepsin K inhibitors for the treatment of osteoporosis which all showed efficacy in preclinical and/or clinical studies but were plagued with serious side effects leading either to the termination of clinical studies or ongoing delays in the regulatory approval process. To our opinion, side effects are not only due to off-target problems but also due to the inhibition of non-matrix protein degradation functions of the drug target cathepsin. All active site-directed inhibitors developed to date will affect these regulatory activities as well and thus a different concept of inhibition is needed if matrix degradation is the target.

We have identified specific ectosteric sites associated with matrix protein degradation in cathepsins. These sites are needed for the binding to substrates such as elastin and collagen, for the binding of ligands or for protease oligomerization. In contrast to allosteric sites, they do not affect the active site. For example, cathepsin K requires glycosaminoglycans (GAGs) as ligand for the formation of oligomeric protease complexes. Only these complexes are collagenolytically active whereas the monomer exhibits all other proteolytic functions. Preventing oligomerization, GAG binding or non-active site-based interactions with matrix proteins allows for the selective inhibition of the therapeutically relevant elastase and collagenase activities of cathepsins without interfering with their other functions. These inhibitors represent a new class of drugs which specifically block only the disease-relevant activity of a target enzyme and thus avoid potential side effects intrinsic to a multifunctional drug target.

Disclosures: Dieter Bromme, None.

SU0349

Adherence to Osteoporosis Medications in Japanese Patients after Hospitalization for Acute Osteoporotic Fracture. Shusuke Ota^{*}, Yoshiaki Tsuboi, Yasuyoshi Okamoto, Takanobu Doi. Shizuoka Medical Center, Japan

PURPOSE: Osteoporosis Medications are reduced osteoporotic fracture risk and increased of bone mineral density in elderly patients. The aim of this study were (1) to investigate the baseline demographics in hospitalized patients with osteoporotic hip fracture (HF) compared with vertebral fracture (VF) and upper extremity fracture (UEF), including distal radius fracture and proximal humeral fracture, and (2) to quantify the use of and adherence to osteoporotic medications following the osteoporotic fractures. **METHODS:** A retrospective chart review was conducted of 384 hospitalized Japanese patients (97 males and 288 females) with acute HF, VF or UEF (221 patients with HF, 80 patients with VF, and 97 patients with UEF) between January 2011 and December 2012. We calculated the proportion receiving more than one osteoporosis drug after discharge. Adherence to the osteoporosis treatment was measured as the proportion of days covered (PDC) during the second year following the osteoporotic fracture. **RESULTS:** The patients with HF were significantly older age and longer length of hospital stay than that with VF or UEF (mean age, HF; 85.0 \pm 10.0 years, VF; 81.0 \pm 9.0 years, UEF; 76.0 \pm 11.2 years, length of hospital stay, HF; 29.0 \pm 30.0 days, VF; 16.6 \pm 11.1 days, UEF; 14.5 \pm 13.2 days). The percentage of patients taking an osteoporosis medication at the time of discharge and 2 years after the discharge was 69.2% and 25.3% in HF group, 75.0% and 35.0% in VF group, and 24.7% and 22.7% in UEF group, respectively. The mean PDC in 2-year following the fracture was 0.25 (HF), 0.35 (VF), and 0.23 (UEF). The second fracture occurred at the rate of 7.2% in HF group, 22.5% in VF group, and 0% in UEF group over the 2-year period following the initial fracture. **CONCLUSIONS:** While the adherence rate of osteoporosis treatment was decreased over time in HF and VF groups, the low compliance in VF group was an increased risk of secondary osteoporotic fracture. Despite of lower rates of initiation of osteoporosis medications at the discharge, the UEF group was not occurred secondary osteoporotic fracture for 2 years after the initial fracture.

Disclosures: Shusuke Ota, None.

SU0350

NHS Lanarkshire Osteoporosis Therapeutic Review Project. Eamonn Brankin^{*}¹, Wendy Feeney², Robin Munro². ¹NHS Lanarkshire / University of Glasgow, United Kingdom, ²NHS Lanarkshire, United Kingdom

From 2013 to 2014 NHS Lanarkshire worked with an independent pharmacy service to undertake osteoporosis therapeutic reviews on patients in general practices in the county. 59 of 109 practices took part in ongoing annual review. Parameters measured included diagnosis, residential status (own home vs in care), current treatment with calcium & vitamin D, (Ca & D3) bisphosphonates and oral steroids, prevalent fragility fracture, (age 50-74) (+/- subsequent diagnosis of osteoporosis), and concordance with oral therapy. 15203 patients were identified as being at risk and 4621 patients had a case note review by a pharmacist. Therapeutic interventions (therapy initiation, change and/or information and concordance advice) were made in 1900 cases. 3971 patients had a diagnosis of osteoporosis. Of these 3517 were on Ca & D3. 4675 were on bisphosphonates (including those with osteopenia) 394 (8%) of these were not on concurrent Ca & D3. 428 were on steroids of whom 90 (21%) were not on Ca & D3. Of those with prevalent fragility fracture (2719) only 2216 were on Ca&D3. 1726 were found to be non compliant with Ca & D3 therapy and 1025 had appropriate medication started. 77 new diagnoses of osteoporosis were made & 164 patients were started on a bisphosphonate. Concordance with osteoporosis therapies, particularly with Ca & D3 is known to be very variable. Of those who underwent case note review, 1619 patients were identified as likely to benefit from therapeutic intervention but were clinically contraindicated. 1794 patients were identified as having had a possible

fragility fracture (age 50-74) but who had not been subsequently investigated and managed according to current national guidelines to confirm that the fracture was fragility in nature, indicating potential significant inadequacies in clinical coding. Current gaps in coding practice leave open the possibility of a significant shortfall in clinical care. Multidisciplinary working, including therapeutic review by a pharmacist was found to be helpful in identifying diagnostic code gaps and concordance issues in at risk patients. This data allowed targeted pilot concordance clinics to be run by an osteoporosis specialist nurse (OSN) & offered more cost effective use of her time. As a result a large number of patients received better, more focused disease education and support & therapeutic advice in an attempt to increase patient awareness and education, with subsequent benefits in medication concordance.

Disclosures: *Eamonn Brankin, Prostrakan*

This study received funding from: Prostrakan Ltd

SU0351

Persistence and Compliance with Subcutaneous Denosumab in Routine Practice. Richard Pikner^{*1}, Zlata Fejfarkova², Michaela Heidenreichova³. ¹Klatovska Hospital, Czech republic, ²Dept. of Clinical Laboratories, Klatovska Hospital, Czech republic, ³Dept. of Bone Metabolism, Klatovska Hospital, Czech republic

We evaluated all women that received denosumab during the period from August 2011 to March 2015 in our center. We evaluated 320 women, that represents 1174 denosumab applications. Women received first dose of denosumab within the period from September 2014 to March 2015 were excluded. We evaluated persistence and compliance with denosumab used according to approved reimbursement criteria in the Czech Republic (T-score $>2.5SD$ and osteoporotic fracture, or intolerance to other osteoporosis treatment).

From 320 treated women, 79.1 % were older than 75 years at the start of denosumab administration. 100 women of them discontinued the denosumab administration (non-persistent group), represents persistence 68.75%. The average number of doses in non-persistent patients was 2.7 doses and 4.12 in persistent group. Compliance was estimated as a percentage of doses administered within the interval of 6 months \pm 4weeks between doses. In persistent group the compliance was 93.1 %, in non-persistent group 94.8 % respectively. We analyzed reasons for therapy discontinuation in non-persistent group. From 100 non-persistent women, 24 died (23 were older 70 years), 35 women do not continue with therapy and in 41 women denosumab was stopped due to clinician decision.

Denosumab is medication having high compliance over 90 % even in routine practice. Persistence is highly influenced by age, comorbidities and reimbursement criteria and will be detailed discussed in presented work.

Disclosures: *Richard Pikner, None.*

SU0352

Effect of Teriparatide or Risedronate on Pertrochanteric Hip Fractures Recovery: 26-Week Results of a Randomized Clinical Trial. Per Aspenberg^{*1}, Jorge Malouf², Umberto Tarantino³, Pedro A. Garcia-Hernandez⁴, Costantino Corradini⁵, Soeren Overgaard⁶, Jan Stepan⁷, Lars Borris⁸, Eric Lespessailles⁹, Frede Frihagen¹⁰, Kyriakos Papavasiliou¹¹, Helmut Petto¹², José Ramón Caero¹³, Fernando Marin¹⁴. ¹Orthopaedic Surgery, Linköping University, Sweden, ²Internal Medicine, Hospital San Pablo, Spain, ³Orthopaedic Surgery, Univeristy Tor Vergata, Italy, ⁴Osteoporosis Centre, University Hospital, Mexico, ⁵Orthopaedic Institute; University of Milan, Italy, ⁶Orthopaedic Surgery, University of Southern Denmark, Denmark, ⁷Institute of Rheumatology, Charles University, Czech republic, ⁸Orthopaedic Surgery, University Hospital, Denmark, ⁹IPROS Unit, Hospital Porte Madeleine, France, ¹⁰Orthopaedic Surgery, University Hospital, Norway, ¹¹Orthopaedic Surgery, Aristotle University, Greece, ¹²Eli Lilly & Company, Austria, ¹³Orthopaedic Surgery, University Hospital, Spain, ¹⁴Eli Lilly & Company, Spain

There is few data on the effect of anti-osteoporosis drugs on fracture healing in weight-bearing bones. We present 26-wk interim results of an ongoing, prospective, randomized, multicenter, active-control trial of 78-wk duration, comparing the effect of teriparatide (TPTD:20 μ g/d) and risedronate (RIS:35 mg QW) initiated within 2 weeks after the surgical treatment of a pertrochanteric hip fracture. Methods: 224 patients were randomized and 171 (TPTD: 86, RIS: 85) contributed to the efficacy analysis. Main inclusion criteria were BMD T-score $<-2.0SD$, 25-OH-vitamin D (>9.2 ng/mL) and a recent low-trauma pertrochanteric hip fracture (AO/OTA 31-A1 or A2) treated with osteosynthesis. During the first 26-wk, patients received double-dummy study medication with either an oral or injected placebo plus Ca+vitD3 supplements. We here report secondary and exploratory endpoints related with function, hip pain, quality of life (QoL), radiology outcomes and safety. Results: Mean (SD) age was 77 (8) yr, 77% were women, and 26% had a history of a prior low-trauma fracture after the age of 50. There were no significant between-group differences in the SF-36 QoL questionnaire, Charnley's scale hip pain, ability to walk or the use of walking aids during follow-up. A significantly shorter time to complete

the timed up-and-go (TUG) test was recorded in the TPTD group at all the post-randomization visits (6, 12, 18 and 26 wk) (range: -3.1 to -5.7 seconds; $p<0.05$ full-adjusted Mixed Model for Repeated Measures). The 100 mm hip pain Visual Analog Scale during the TUG test also showed statistically significant lower values (adjusted absolute difference range: -10.6 to -11.9 mm) in the TPTD group at 12 and 18 wk, with a trend at 26 wk (-10.1 mm; $p=0.053$). There were no significant between-group differences in radiographic fracture healing at 6 or 26 wk, mechanical failure of the implant (TPTD:7, RIS:8), loss of reduction (TPTD:2, RIS:4) or non-union (0 cases). AEs were similar between groups. Seven deaths unrelated to treatment were reported. Hypercalcemia and hyperuricemia were more frequently observed in the TPTD group. There were 3 and 8 non-vertebral fractures in the TPTD and RIS group respectively ($p=0.14$). Conclusions: TPTD or RIS showed similar results in several fracture-related outcomes. TPTD-treated subjects reported significantly less pain and a shorter time to complete the TUG test. These results should be interpreted with caution given the exploratory nature of the data.

Disclosures: *Per Aspenberg, Lilly; Addbio AB; Amgen; Biologics MD Inc.*

This study received funding from: Eli Lilly and Company

SU0353

Histochemical examination on bone of postmenopausal model rats with switched administration from PTH to eldcalcitol. Hiroshi Hongo^{*1}, Sadaiki Sakai², Tomomaya Yamamoto³, Tomoka Hasegawa³, Satoshi Takeda², Koichi Endo², Hitoshi Saito⁴, Norio Amizuka³. ¹Hokkaido University, Japan, ²Product Research Dept., Chugai Pharmaceutical CO., LTD., Japan, ³Department of Developmental Biology of Hard Tissue, Hokkaido University, Japan, ⁴Medical Science Dept., Chugai Pharmaceutical CO., LTD., Japan

Introduction: Parathyroid hormone (PTH) has been shown to accelerate bone formation accompanying with the increased proliferation of preosteoblasts, while eldcalcitol (ELD) induces bone formation by mini-modeling and inhibits osteoclast differentiation and bone resorption. However, there is a limitation of administration period of PTH, so that, it seems of interest to investigate whether ELD would show the biological effects after the PTH administration. In this study, we have attempted to histologically examine the bone tissue of postmenopausal model rats with switched administration from PTH to ELD. Materials and Methods: Six months old Wister female rats were ovariectomized, and after two months later, we administered human PTH (1-34; 10 μ g/kg, 5 days/week) during 4 weeks, and then, continuously administered hPTH in the same manner, switched to administer ELD (20ng/kg, 5 days/week) or discontinue for medication. After 4 weeks or 8 weeks administration, the treated rats were fixed, and the femurs were processed for paraffin or MMA embedding in order for histochemical examination and Villanueva bone staining. Result and Discussion: The rats administered with PTH for 4 weeks showed an elevated bone mineral density (BMD) and increased trabecular thickness, compared with those of the vehicle group. The specimens which continuously had the PTH administration or switched from PTH to ELD administration revealed a tendency to increase or keep the same level of BMD and trabecular thickness as the ones administered with PTH for 4 weeks. In the rats switched to ELD administration, bone deposition seemed to be mediated by mini-modeling, featuring convex calcein labeling and focal budding of bone matrix. In contrast, the specimens with drug discontinuation displayed attenuated trabecular thickness and BMD. Taken together, it seems likely that ELD is a strong candidate to induce bone formation by means of mini-modeling after the PTH administration.

Disclosures: *Hiroshi Hongo, Chugai Pharmaceutical CO., LTD*

This study received funding from: Chugai Pharmaceutical CO., LTD

SU0354

Small molecules targeting the NXI-motif-binding pocket abrogate suppression of wnt-beta-catenin signaling by sclerostin. Myengmo Kang^{*1}, Eunjin Kim², Jiwon Choi², Sungkil Lim². ¹College of Medicine, Yonsei University, Seoul Korea, South Korea, ²50 Yonsei Seodeamungu, South Korea

Wnt-b catenin signaling has been reported to play an important role for bone homeostasis. Both sclerostin and DKK1 can bind to LRP5/6 and inhibit the canonical Wnt signaling. Recently, clinical trial of monoclonal antibodies against sclerostin revealed a significant increase in bone mineral density remarkably. Sclerostin binds to LRP5/6 through NXI motif of the loop 2 region. To identify the small compounds which can inhibit binding of sclerostin to LRP5/6 and abrogate Wnt3a mediated b catenin signaling suppressed by sclerostin in MC3T3E1 stable cell lines, we screened small compounds library through the high throughput put system. Further SPR analysis, Alp assay and ex vivo calvarial bone formation assay were also performed. Here we show that Chromen-4-one derivative could abrogate the suppression of Wnt3 mediated b catenin signaling by sclerostin and DKK1. It bound to the E1-E2 domain of LRP5/6 in SPR analysis and stimulated ex vivo calvarial bone formation. In vitro cytotoxicity was low in both MC3T3E1 cells and 293 cells. Consequently, these results suggest that Chromen-4-one derivatives can antagonize the endogenous inhibitor, sclerostin and DKK1 in bone, and thereby have the beneficial effects on management of fracture healing and metabolic disease such as osteoporosis.

Disclosures: *Myengmo Kang, None.*

SU0355

Modeling and Simulation to Link Concentration of Urinary C-terminal Telopeptide of Type I Collagen and Percent Change in Hip Bone Mineral Density with Fracture Risk: MOVER Study with Monthly Intravenous Ibandronate. Kiyohiko Nakai^{*1}, Masato Tobinai², Masayuki Matsunaga², Masao Yamamoto², Junko Hashimoto², Satofumi Iida², Takehiko Kawanishi². ¹Chugai Pharmaceutical Co., Japan, ²CHUGAI PHARMACEUTICAL CO., LTD., Japan

Purpose: Modeling & simulation (M&S) using the results of population pharmacokinetics and pharmacodynamics analyses can accelerate the efficient development of new drugs. By predicting efficacy and safety, MS using data from the MOVER study showed links between ibandronate (IBN) dosage, urinary concentration of C-terminal telopeptide of type I collagen (uCTX), and lumbar spine bone mineral density (BMD). In this study, in addition to IBN dosage, uCTX, and BMD, the modeling of relationships between IBN dosage, uCTX, and BMD, the modeling of relationships was extended to include the prevention of fractures regarded as the primary endpoint for the osteoporosis treatment. Methods: IBN (0.5 or 1.0 mg) was administered intravenously to Japanese osteoporosis patients once a month for 3 years in the MOVER study. uCTX, percentage change in hip BMD, and fracture data obtained from 758 patients (per protocol set) in the MOVER study were used to develop the mathematical model to link these data. To develop this mathematical model, statistical analysis software TIBCO Spotfire S+ version 8.2J and nonlinear mixed effects modeling software NONMEM version 7.2 were utilized. Results: As before, a K-PD model was used to link IBN dosage and uCTX. Next, an indirect model was used to link uCTX with the percentage change in hip BMD (which was a newly employed marker used as a representative value of BMD instead of the lumbar spine BMD used previously). This procedure resulted in good agreement between observations and predictions. Finally, percentage change in hip BMD and fracture risk were connected by a logistic regression model represented by the following equations 1 and 2 using both percentage change in hip BMD and fracture data at 3 years after initiation of IBN treatment. $\text{Logit} = \text{Baseline} + \text{Slope} \times \% \text{ change in hip BMD} \dots$ Equation 1 $\text{Fracture risk} = \exp(\text{Logit}) / (1 + \exp(\text{Logit})) \dots$ Equation 2 Conclusions: We successfully developed a mathematical model to describe the relationships between IBN dosage, uCTX, percentage change in hip BMD, and fracture risk. This mathematical model quantitatively connected uCTX with fracture risk. It also suggests that the degree of reduction in uCTX by treatment with IBN has great potential to predict the decrease of future fractures.

Disclosures: Kiyohiko Nakai, None.

SU0356

Health Related QoL of Osteoporosis Patients with Daily Teriparatide in the Japan Fracture Observational Study (JFOS): Interim Report. Hiroyuki Enomoto^{*1}, Saeko Fujiwara², Ryoichi Takayanagi³, Masayo Sato¹, Mika Tsujimoto⁴, Takanori Yamamoto⁴, Satoshi Soen⁵. ¹Medicines Development Unit Japan, Eli Lilly Japan K.K., Japan, ²Health Management & Promotion Center, Hiroshima Atomic Bomb Casualty Council, Japan, ³Department of Medicine & Bioregulatory Science, Graduate School of Medical Sciences, Kyushu University, Japan, ⁴Medicines Development Unit Japan, Eli Lilly Japan K.K., Japan, ⁵Department of Orthopaedic Surgery & Rheumatology, Nara Hospital, Kinki University Faculty of Medicine, Japan

Background: In addition to reducing the risk of fragility fractures, the improvement of health related quality of life (HRQoL) is also important for osteoporosis treatment. The Japan Fracture Observational Study (JFOS) was conducted to investigate the impact of teriparatide 20 µg/day (TPTD) on clinical fractures and HRQoL in osteoporosis patients in a daily clinical setting. We report an interim analysis of results of 12-month observation. Methods: JFOS is a 24-month, multicenter, prospective, observational study in Japan. TPTD-naïve patients with osteoporosis at high risk of fracture were included. The cumulative incidence of clinical fracture at 12 month was reported. Change in back pain was assessed by visual analogue scale (VAS). Changes in HRQoL were assessed by European quality of life questionnaire-5 dimensions (EQ-5D) and Japanese osteoporosis quality of life questionnaire (JOQOL; maximum total score of 152). Instrumental activities of daily living (IADL) scale was also used to assess independent living skills. Results: A total of 1810 (90.1% women) patients were analyzed at baseline. Mean age (SD) was 76.9 (7.9) years. Two-thirds of patients had prevalent vertebral fractures and 34.3% of patients had 2 or more fractures. One-third of patients received bisphosphonates prior to TPTD. Cumulative incidences of any clinical fractures, mean VAS scores, mean EQ-5D Index scores, mean total scores of JOQOL, and mean IADL scales for 12 months are shown in Table 1. Conclusion: JFOS is the first large observational study to investigate the effectiveness of TPTD as a primary objective in osteoporosis patients in Japan. TPTD treatment resulted in a reduction of back pain over time and improvement of HRQoL and IADL at 6 months. These findings are consistent with the results of previous studies.

Table 1 Cumulative incidences of any clinical fractures, and mean scores of VAS, EQ-5D Index, JOQOL (total score), and IADL

| | Baseline | 3 months | 6 months | 12 months |
|---|----------|----------|----------|-----------|
| Cumulative incidences of any clinical fractures (%) | - | - | 2.9 | 3.7 |
| VAS | 51.1 | 33.0 | 31.6 | 29.3 |
| EQ-5D Index | 0.55 | 0.68 | 0.69 | 0.70 |
| JOQOL (total score) | 78.3 | - | 91.0 | 93.9 |
| IADL | | | | |
| Men | 3.4 | - | 3.6 | 3.9 |
| Women | 5.9 | - | 6.4 | 6.4 |

Table 1

Disclosures: Hiroyuki Enomoto, Eli Lilly Japan K.K. This study received funding from: Eli Lilly Japan K.K.

SU0357

Improvement of Spinal Alignment and Quality of Life after Corrective Spinal Instrumentation for Spinal Kyphosis in Patients with Osteoporosis. Naohisa Miyakoshi^{*1}, Michio Hongo¹, Takashi Kobayashi², Toshiki Abe², Eiji Abe², Yoichi Shimada¹. ¹Akita University Graduate School of Medicine, Japan, ²Akita Kousei Medical Center, Japan

Introduction: With the increased aging of society, the demand for corrective spinal instrumentation for spinal kyphosis in osteoporotic patients is increasing. However, previous studies have not focused on the improvement of quality of life (QOL) after corrective spinal surgery in patients with osteoporosis, compared to non-operated control patients. This study evaluated changes in spinal sagittal alignment and QOL after corrective spinal instrumentation for patients with postmenopausal osteoporosis and spinal kyphosis, and to compare these results with non-operated patients with postmenopausal osteoporosis. Methods: Participants comprised 39 patients with postmenopausal osteoporosis >50 years old who underwent corrective spinal surgery using multilevel posterior lumbar interbody fusion (PLIF) for symptomatic thoracolumbar or lumbar kyphosis, and 82 age-matched patients with postmenopausal osteoporosis with no prevalent vertebral fractures. Spinopelvic parameters were evaluated with standing lateral spine radiography, and QOL was evaluated with the Japanese Osteoporosis QOL Questionnaire (JOQOL), SF-36, and Roland-Morris Disability Questionnaire (RDQ). Results: Lumbar kyphosis angle, sagittal vertical axis, and pelvic tilt were significantly improved postoperatively ($p < 0.05$). QOL evaluated with all three questionnaires also significantly improved after 6 months postoperatively, particularly in domain and subscale scores for pain and general/mental health ($p < 0.05$). However, these radiographic parameters, total JOQOL score, SF-36 physical component summary score, and RDQ score were significantly inferior compared with non-operated controls ($p < 0.05$). Conclusions: The results indicate that corrective spinal surgery using multilevel PLIF for patients with osteoporosis and spinal kyphosis significantly improved spinal global alignment and QOL after surgery, but did not reach the level of non-operated controls.

Disclosures: Naohisa Miyakoshi, None.

SU0358

Bone Resorption Assessed by Serum Type I Collagen C-terminal Telopeptide (Crosslaps) is Inversely Associated with Bone Mineral Density and Change in BMD but Not with Change in Calcified Atherosclerotic Plaque in African Americans with Diabetes (AA-DHS). Thomas C. Register^{*1}, J. Jeffrey Carr², Leon Lenchik¹, Jasmin Divers¹, Gregory B. Russell¹, Nicholette D. Palmer¹, Lynne E. Wagenknecht¹, S. Carrie Smith¹, Jianzhao Xu¹, Donald W. Bowden¹, Barry I. Freedman¹. ¹Wake Forest School of Medicine, USA, ²Vanderbilt, USA

Background: Age independent inverse relationships between the degree of calcified atherosclerotic plaque (CP) and bone mineral density (BMD) suggest that there is a mechanistic relationship between the two phenotypes. In order to explore the relationships between bone resorption, bone density, and calcified plaque, we

assessed the levels of serum C-terminal cross-link of type I collagen (Crosslaps) in relation to bone and atherosclerosis phenotypes in 545 unrelated African Americans with type 2 diabetes (T2D). We also assessed associations of Crosslaps with change over time in CP and BMD.

Methods: Computed tomography (CT) was used to measure aorta, coronary and carotid artery CP, as well as thoracic (T-) and lumbar (L-) vertebral trabecular volumetric bone mineral density (vBMD). Associations between serum Crosslaps and bone and CP phenotypes were assessed.

Results: At baseline, participants were 56.9% female with mean±SD age 55.7±9.6 years, T2D duration 10.3±8.2 years; 288 subjects had follow-up CT scans after 5.1±0.9 years. Serum Crosslaps, 25-hydroxy vitamin D, and bioavailable vitamin D (BAVD) were associated ($p<0.05$) with aortic and carotid CP and T-vBMD and L-vBMD before but not after adjustment for age, sex, BMI, duration of diabetes, and smoking. Crosslaps was associated with baseline T-vBMD and L-vBMD in unadjusted and fully adjusted models which included the above plus % African ancestry, use of HRT, steroids, bisphosphonates, and calcium supplements, smoking, and change in eGFR, BMI, HbA1c and systolic BP. There was no association between baseline serum Crosslaps and change in CP in the aorta, carotid, or coronary arteries before or after adjustment for age, sex, diabetes duration, and other variables (all $p>0.3$). In contrast, baseline Crosslaps was significantly associated with future change in BMD in the lumbar but not thoracic spine.

Conclusions: Bone resorption activity, as estimated by serum Crosslaps, was associated with change in L-vBMD but not with change in T-vBMD or change in calcified plaque. Additional exploration of potential links between the two phenotypes is required for mechanistic explanations for the age independent inverse relationships between BMD and CP.

Disclosures: Thomas C. Register, None.

SU0359

Effects of Uncontrolled Type II Diabetes on Vertebral Bone Marrow Fat Distribution. Mona Al Mukaddam*, Chamith Rajapakse, Mahdieh Bashoor Zadeh, Jeremy Magland, Wenli Sun, Helen Peachey, Peter Snyder, Felix Wehrli. University of Pennsylvania, USA

Purpose: Osteoporosis and increased risk of fractures are newly-recognized complications of Type 2 diabetes mellitus (T2DM). Paradoxically, bone mineral density (BMD) by DXA is higher in T2DM, so BMD underestimates the risk of fractures. Osteoblasts and adipocytes are derived from the same precursor mesenchymal stem cell in the bone marrow. Prior studies suggest that higher marrow fat is associated with impaired bone quality independent of BMD (1, 2), and poor control of diabetes is strongly correlated with mean vertebral bone marrow fat (BMF) (3). The aim of this cross-sectional pilot study was to determine if vertebral BMF measured by MRI is higher in diabetics than nondiabetics.

Methods: We selected 16 post-menopausal women with poorly controlled T2DM (DM) and 16 age-, race- and BMI- matched non diabetic (non-DM) post-menopausal women (table 1). BMF content of the lumbar vertebrae (L1-L5) was assessed using a clinical 3-Tesla MRI scanner (Siemens). A 2D interleaved multiple-gradient-echo chemical-shift imaging (IMGE-CST) sequence was implemented using the manufacturer's spine and body matrix coils. At each 2.5 mm² voxel a full spectrum with relative contributions from fat and water was obtained. The BMF was calculated as the ratio of these two signal values averaged across nine central voxels in each of five lumbar vertebrae(4).

Results: In non-diabetic women, BMF significantly increased from L1 to L5 ($R=0.31$, $p<0.005$, Figure 1a), which is similar to what has been reported (5). However, in women with poorly controlled diabetes, BMF did not change across the vertebrae ($R=0.09$, $p=0.49$, Figure 1b). There was a trend towards a higher bone marrow fat at L1 in subjects with poorly controlled diabetes than in nondiabetics (DM: $63.5 \pm 6.7\%$ vs non-DM: $58.8 \pm 8.0\%$; $p=0.08$). There was no significant difference in the average L1-L5 BMF (DM: $63.8 \pm 9.1\%$ vs non-DM: $61.2 \pm 7.5\%$; $p=0.39$).

Conclusion: This pilot study suggests that diabetes could affect the bone-fat-axis in L1 more than L5. That data highlights the need to evaluate different vertebral sites when monitoring effects of disease/treatment on bone. A potential explanation for the difference in the fat fraction gradient across L1-L5 could be the differences in the loading mechanics at L5 compared to L1, so that the effects of diabetes are blunted by the higher mechanical loading observed at the lower vertebrae. A study in larger patient cohort is needed to confirm these findings.

| Mean (SD) | DM (N=16) | Non-DM (N=16) | p |
|--------------------------|-------------------------------|-------------------------------|------------|
| Age (yrs) (range) | 60.9 (55-68) | 60.4 (55-68) | 0.75 |
| Race | 8 Black 7 White 1 Asian | 8 Black 7 White 1 Asian | N/A |
| Height (cm) | 161.8 (6.4) | 161.6 (7.8) | 0.92 |
| Weight (kg) | 86.5 (13.8) | 86.5 (13.6) | 0.99 |
| BMI (kg/m ²) | 33.0 (4.9) | 33.1 (4.5) | 0.97 |
| Duration of DM (yr) | 17.1 (7.1) | N/A | N/A |
| HbA1c (%) | 9.9 (1.4) | 5.7 (0.4) | $p<0.0001$ |

Table 1

Figure 1. Bivariate linear fit of bone marrow fat (%) by lumbar vertebrae in subjects without diabetes (A) and poorly controlled type 2 diabetes (B).

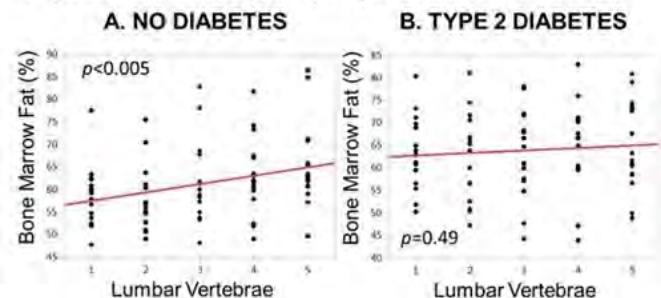


Figure 1

Disclosures: Mona Al Mukaddam, None.

SU0360

Microalbuminuria has additional negative impact on trabecular bone score and bone mineral density in postmenopausal women with longstanding type 2 diabetes. Tomaz Kocjan*¹, Moica Jensterle¹, Gaj Vidmar², Andrej Janez³. ¹University Medical Centre Ljubljana, Slovenia, ²University Rehabilitation Institute, Slovenia, ³University Medical Centre Ljubljana, Slovenia

Objective: Microalbuminuria (MA), a marker of renal microvascular disease, is associated with fracture risk. Our aim was to examine the impact of MA on trabecular bone score (TBS), bone mineral density (BMD) and bone turnover markers in postmenopausal women with longstanding type 2 diabetes (T2D).

Methods: A cross-sectional study included a total of 27 T2D subjects (mean age 63.4 years, BMI 28.0 kg/m², duration of T2D 10.1 years, HbA1c 7.4%) treated with oral antihyperglycemic agents. They were divided into normoalbuminuric group (n=11) and microalbuminuric group (n=16) according to urinary albumin excretion rate (UAER; threshold > 2.2 mg/mmol). BMD at lumbar spine, total hip, femoral neck and distal radius was measured by DXA and trabecular bone microarchitecture was assessed by TBS. Procollagen type 1 N-terminal propeptide (PINP) and C terminal cross-linked telopeptide of type-I collagen (CTX) were determined. The association of MA with all variables was tested using regression models, adjusting for the effect of BMI.

Results: The average serum HbA1c in study subjects did not differ between normo- and microalbuminuric group. There were also no statistically significant differences in other baseline characteristics (age, years since menopause, BMI, waist circumference, duration of T2D) between the two groups (all $p > 0.10$ from exact Mann-Whitney test). The observed associations of MA were negative with TBS and the four standard BMD measurements, and positive with CTX and PINP values (Pearson and Spearman correlations, as well as corresponding coefficients in the regression models). However, statistical significance could only be verified for lumbar spine BMD (logistic regression model for predicting MA from BMI and BMD: estimated adjusted odds ratio 0.57 with 95% CI 0.33-0.98 per 0.1 g/cm² increase in BMD, $p=0.044$). Multivariate testing (using MANOVA with BMI as numerical covariate) of the

combined four BMD measurements confirmed the effect of MA ($p=0.049$ for the difference between normo- and microalbuminuric group). Conclusions: Our results suggest that presence of MA in T2D has additional negative effect on bone.

Disclosures: Tomaz Kocjan, None.

SU0361

RISK FACTORS FOR FRAGILITY FRACTURES IN TYPE 1 DIABETES. Giulia Leanza^{*1}, Dario Pitocco², Concetta Suraci³, Anna Maria Altomare³, Andrea Palermo¹, Claudio Pedone¹, Roberto Sacco¹, Simone Alfieri¹, Sergio Leotta³, Paolo Pozzilli¹, Ann Schwartz⁴, Nicola Napoli¹. ¹Campus Bio-Medico university, Italy, ²Università Cattolica Sacro Cuore, Italy, ³Ospedale Pertini, Italy, ⁴University of California, San Francisco, USA

Type 1 diabetes (T1D) is an autoimmune disease characterized by chronic hyperglycemic state, which incidence has been globally rising during the past decades. Besides the well-known diabetic complications, poor bone health has been reported as a clinical concern, leading to an increased risk of fractures. Although some factors like hypoinsulinemia, low levels of insulin-like growth factor-1 and vitamin D have been reported as possible causes, clinical risk factors for fracture risk in T1D patients are still unknown.

Aim of this study was to evaluate the effect of glycaemic control, complications and diseases duration on fracture risk in T1D patients.

We have enrolled 247 T1D patients (116 males) referring to the IMDIAB group clinical network (Rome, Italy). All recruited patients underwent clinical evaluation and screening for bone fragility risk factors. Glucose control was assessed through the average of HbA1c levels measured in the last 5 years. Fractures were assessed through a validated questionnaire. Vitamin D levels were analyzed by RIA while calcium intake by a weekly evaluation form.

Patients were 43.47 ± 12.87 years old (range 18-76), had a BMI of 24.13 ± 4.21 kg/m² (15.6-44) and disease duration of 20.28 ± 12.49 years (1-63). The mean of HbA1c of the last five years was $7.54 \pm 1.08\%$ (5.31-12.87). HbA1c was $< 7\%$ in 31.5%, $\geq 7\%$ $< 9\%$ in 60% and $\geq 9\%$ in 8%. Insulin requirement was 19 ± 8.98 IU/daily for fast-acting and 19.17 ± 9.65 IU for long-acting.

Patients had in average low 25(OH)Vitamin D serum levels (16.38 ± 2.74 ng/mL) and low daily calcium intake (634.84 ± 159.97 mg). 56 patients (22.6%) reported at least one fracture after the diagnosis, whom 14.6% had only 1 fracture, 6.1% 2 fractures and 1.2% had 3 or more. Most common fractures sites were: hand (18.6%), foot (17.1%), tibia/fibula (10.5%), wrist (9.3%) and ribs (8%).

T1D related complications were more common in patients with fractures than in patients without ($p=0.03$). Disease duration was associated to an increased risk of any fractures (OR 1.2, 95% CI: 1.02-1.42). Insulin requirement and glycaemic control were not associated to risk of fractures. In conclusion, our data confirm that T1D patients should be carefully screened for fracture risk. Glycaemic control over the last 5 years did not influence risk of fractures. Prevention of complications may be crucial to preserve bone health in T1D. Calcium and vitamin D intake should be adequately replaced.

Disclosures: Giulia Leanza, None.

SU0362

Site Specific Prevalence of Fragility Fractures and their Relationship with Body Mass Index in Patients with Type 1 Diabetes. Tayyab Khan^{*1}, Lisa-Ann Fraser². ¹Department of Medicine, Western University, Canada, ²Western University, Canada

Background: The increased risk of fragility fractures associated with type 1 diabetes (T1DM) is thought to be mediated by mechanisms different from those of primary osteoporosis. However the effects of these mechanisms on fracture risk at different bone sites, and the relationship between BMI and fracture site, is unknown. We aimed to study the relative prevalence of fragility fractures at different sites, and their relationship with Body Mass Index (BMI), among patients with T1DM followed at a tertiary care center.

Methods: Consecutive patients, over age 40 years, with T1DM completed a bone health questionnaire during their appointment with their Endocrinologist between May to December 2013. Fragility fractures were defined as fractures occurring from standing height or less, and excluded fractures of the skull, fingers or toes. Characteristics of patients with a prior fragility fracture were reviewed using descriptive statistics. For BMI analysis, only patients whose fractures occurred within 5 years of BMI measurement were included.

Results: Among 201 patients with T1DM, median age 52 (range 40 – 82), who were included in the study, 52 fragility fractures were identified. Of these, most occurred at the ankle/metatarsal (13/52; 25.0%), followed by the hip (11/52; 21.1%), and wrist (10/52, 19.2%). No association between BMI and fracture site was identified. However, we noted that the BMI of most patients who experienced a fragility fracture was high (average 28.3 ± 4.8), with 5.9% of patients in the overweight, and 52.9% in the obese category. The average age of patients with fragility fractures was 42.1 (± 14.7) years for the ankle, 57.2 (± 7.1) years for the hip, and 49.2 (± 13.7) years for the wrist.

Conclusions: In this cohort of patients with T1DM, fragility fractures occurred at younger ages than expected. Similarly, although low BMI is thought to be important

in the pathophysiology of fracture in T1DM, we found patients were more likely to be overweight/obese. This study confirms that the characteristics of patients with T1DM who fracture are different from those of other populations and need further evaluation to facilitate appropriate preventative care and treatment.

Disclosures: Tayyab Khan, None.

This study received funding from: No funding was received any sources

SU0363

FES-Rowing Attenuates Bone Loss Following Spinal Cord Injury as Assessed by HR-pQCT. Robin Gibbons¹, Gary Beaupre², Galateia Kazakia^{*3}. ¹Brunel University, United Kingdom, ²VA Palo Alto Health Care System, USA, ³University of California, San Francisco, USA

Introduction: Motor complete spinal cord injury (SCI) leads to rapid bone loss in the lower limbs and individuals with chronic SCI are at high risk of fragility fracture in the tibia and femur. We recently demonstrated the potential for attenuation of bone loss using Functional Electrical Stimulation (FES)-rowing, a hybrid exercise that combines voluntary upper limb movement concurrent with FES-assisted lower limb actions [1]. To test the hypothesis that FES-rowing attenuates bone loss post-SCI, we used high resolution peripheral quantitative computed tomography (HR-pQCT) to: (1) characterise the density, microstructure, and strength of the ultradistal radius and tibia in an FES-rower with chronic SCI, and (2) compare these to previously published data on a group of FES-untrained individuals with chronic SCI [2] and two normative groups [3,4,5]. **Materials and methods:** Individual and group characteristics are presented in Table 1. Over the previous 24-months, the FES-rower performed an average of three weekly 30-min rows at 30 strokes/min, exposing the lower limbs to ~2,700 loading cycles/wk. The FES-rower was imaged using an HR-pQCT scanner (XtremeCT I, Scanco Medical AG) and analyzed using established protocols [6]. **Results:** At the tibia, the FES-rower metrics were 0.7 to 2.4 SD better than the untrained group means (Table 2). FES-rower densitometric and trabecular parameters were within 1 SD of normative control group means, while cortical porosity was 4.6 SD higher and biomechanical indices were 1.2 to 3.5 SD lower compared to normative means. At the radius, FES-rower densitometric and trabecular metrics were 0.9 to 2.0 SD better than the normative group means, while cortical and biomechanical indices were within 1 SD of normative group means. **Discussion:** Based on a single FES-rower, we speculate that: (1) in the tibia there is evidence that bone loss has been mediated compared to an FES-untrained group; (2) in the radius of the rower the superiority of key bone metrics compared to controls reflects a greater daily bone stimulus for an active manual wheelchair user; and (3) the positive effects on bone from FES-rowing have the potential to reduce fracture risk in individuals with chronic SCI. **References:** [1] Gibbons et al, 2014; [2] Wuermser et al, 2015; [3] Burghardt et al, 2010; [4] Sode et al, 2010; [5] UCSF Normative Cohort; unpublished data; [6] Kazakia et al, 2014.

SU0365

Grip Strength and Mortality in Osteoporotic Hip Fractures Among Latin American Elderly Patients. Hugo Gutierrez Hermosillo¹, ENRIQUE DIAZ DE LEON GONZALEZ². ¹Hospital aranda de la parraConacyt.IMSS, UMAE I CMN BAJIO, Mexico, ²IMSS, Mexico

Most of hip fractures in the upcoming years will occur in developing countries, but the risk for these fractures has not been studied in many of those countries. Therefore we carried out a cohort study; our general objective was to evaluate the low hand grip strength (HGS) as a risk for death among elderly patients with osteoporotic hip fracture in a tertiary hospital in Monterrey, Mexico.

Material and Methods

This is a prospective cohort study, we included patients older than 69 years old, admitted to a tertiary hospital in Monterrey, Mexico, with the diagnoses of osteoporotic hip fracture and were taken to surgery repair. The study was approved by the local Ethics and Research Committee.

Data such as age, gender, and education were asked. Medical history including chronic diseases. Clinimetric variables that were asked include: Barthel's index Score, Folstein's test, Mini Nutritional Assessment scale and the Charlson's Co morbidity Index. HGS measurement was performed by a trained physician using a Jamar® Hydraulic Hand Dynamometer, with standard method. The average result was recorded; the data was clustered in tertiles according to the HGS of the non-dominant using the standard method.

Statistical Analysis

All data was analyzed using the IBM SPSS version 21 software.

Results

A total of 644 patients were included, after one year of follow up there were 112 deaths (17.4%), mean age 83 for those dead and 81 for those alive (p=0.002), according to their tertile distribution, 61 in the first tertile (27.5%), 37 in the second tertile (17.1%) and 14 in the third (6.8%), died (p=0.021).

In the multivariate analysis the low HGS remained significant, tertile 2 p=0.021, HR 2.10 (CI95 1.21-3.95), tertile 1 p=0.006, HR 2.58(CI95 1.35-5.67), Charlson's Co morbidity Index p=0.031, HR 1.23 (CI95 1.01-1.22), age p=0.022 HR 1.032 (CI95 1.005-1.059), and Barthel's index Score p=0.029 HR0.98 (CI95 0.967-0.998). None of the rest of the variables seen on table 1 remained significant.

Conclusions

In elderly patients with osteoporotic hip fracture, low HGS is a risk factor for death one year after the fracture, as well as being older, poorer performance in ADL prior the fracture and having more comorbidities.

Table 1 Comparison of subject characteristics of FES-rower to normative cohort and FES-untrained groups

| | Normative Cohort (ref 3,4,5) | FES-untrained (ref 2) | FES-rower |
|------------------------|------------------------------|---------------------------|------------------|
| Age (yrs) | 45.5 ± 16.4 (20-79) | 55.3 ± 2.6 (50-59) | 41.8 ± 7.8 |
| Gender | male (n=55)* | male (n=28)** | 59 male |
| Injury (yrs) | non-SCI | non-SCI | T3-T12 AIS A & B |
| Time post injury (yrs) | n/a | n/a | 11.4 ± 8.8 |
| | *Radius n=55, tibia n=53 | **Radius n=28, tibia n=22 | 14 |

Table 2 Comparison of radius and tibia metrics of FES-rower to normative cohort and FES-untrained groups

| Variable | Normative Cohort | | FES-untrained | FES-rower |
|-----------------------------------|-----------------------|---------------------|---------------|--------------|
| | 20-79 yrs mean ± SD | 50-59 yrs mean ± SD | mean ± SD | |
| HR-pQCT ultradistal radius | | | | |
| Total vBMD | mg HA/cm ³ | 332.6 ± 51.0 | 329.7 ± 42.9 | 416.2 |
| Tb.vBMD | mg HA/cm ³ | 183.8 ± 36.5 | 178.6 ± 30.9 | 233.7 |
| Tb.N | 1/mm | 1.98 ± 0.29 | 2.01 ± 0.27 | 2.28 |
| Tb.Sp | mm | 0.440 ± 0.082 | 0.434 ± 0.074 | 0.353 |
| Tb.Th | mm | 0.078 ± 0.015 | 0.075 ± 0.010 | 0.085 |
| CT.vBMD | mg HA/cm ³ | 850.0 ± 50.0 | 898.1 ± 56.5 | 961.7 |
| CT.TMD | mg HA/cm ³ | 971.1 ± 35.1 | 978.3 ± 30.0 | 994.0 |
| CT.Po | % | 1.0 ± 0.5 | 2.0 ± 1.3 | 2.4 |
| CT.Po.Dm | mm | 0.165 ± 0.018 | 0.168 ± 0.015 | 0.164 |
| CT.Th | mm | 0.85 ± 0.18 | 1.02 ± 0.14 | 1.15 |
| CT.Ar | mm ² | 67.7 ± 13.8 | 73.6 ± 10.5 | 84.6 |
| FEA radius | | | | |
| Stiffness (K) | kN/mm | 101.9 ± 19.4 | 84.2 ± 16.0 | 76.4 |
| App Modulus (E) | N/mm ² | 2013 ± 388 | 1609 ± 402 | 1530 |
| Predicted failure load | N | 5138 ± 941 | 4578 ± 614 | 4442 |
| Cortical load fraction (distal) % | | 77.2 ± 6.7 | 41.7 ± 6.3 | 40.8 |
| HR-pQCT ultradistal tibia | | | | |
| Total vBMD | mg HA/cm ³ | 317.9 ± 55.5 | 326.3 ± 54.1 | 168.4 ± 69.2 |
| Tb.vBMD | mg HA/cm ³ | 184.6 ± 42.1 | 179.0 ± 36.7 | 69.1 ± 58.1 |
| Tb.N | 1/mm | 1.97 ± 0.41 | 1.90 ± 0.39 | 1.10 ± 0.54 |
| Tb.Sp | mm | 0.450 ± 0.108 | 0.468 ± 0.109 | 1.18 ± 0.87 |
| Tb.Th | mm | 0.079 ± 0.015 | 0.079 ± 0.013 | 0.04 ± 0.03 |
| CT.vBMD | mg HA/cm ³ | 860.0 ± 40.0 | 890.2 ± 64.8 | 811.2 ± 56.4 |
| CT.TMD | mg HA/cm ³ | 976.4 ± 30.4 | 984.1 ± 29.6 | 997.4 |
| CT.Po | % | 3.3 ± 1.2 | 4.2 ± 1.5 | 11.1 |
| CT.Po.Dm | mm | 0.185 ± 0.026 | 0.187 ± 0.021 | 0.264 |
| CT.Th | mm | 1.38 ± 0.28 | 1.51 ± 0.26 | 1.52 |
| CT.Ar | mm ² | 156.8 ± 33.2 | 148.0 ± 27.9 | 83.4 ± 31.1 |
| FEA tibia | | | | |
| Stiffness (K) | kN/mm | 260.2 ± 50.9 | 209.3 ± 30.1 | 118.6 |
| App Modulus (E) | N/mm ² | 2506 ± 468 | 2099 ± 468 | 1554 |
| Predicted failure load | N | 13050 ± 2491 | 11177 ± 1257 | 6744 |
| Cortical load fraction (distal) % | | 62.8 ± 7.2 | 45.5 ± 8.5 | 56.0 |

Tables 1 & 2

Disclosures: Galatea Kazakia, None.

SU0364

Fracture Diagnosis in Women compared with Men Veterans. Jennifer Lee^{*1}, Po-Yin Chang², Jimmy Lee³, Fay Saechao³, Susan Frayne⁴. ¹Stanford University Medical Center Palo Alto Veteran Affairs Health Care System, USA, ²Department of Medicine, Stanford Medical Center, USA, ³Veterans Affairs Palo Alto Health Care System, USA, ⁴Veterans Affairs Palo Alto Health Care System & Stanford Medical Center, USA

Purpose: Impact of fractures is not well known in women veterans (WV) and men veterans (MV). We aimed to characterize the prevalence and risk of fracture diagnosis in WV and MV within the Veterans Health Administration (VHA) nationally.

Methods: 355,352 WV and 5,021,151 MV who used VHA in FY2012 were examined cross-sectionally. Veterans with a fracture diagnosis were identified if ICD-9 code for fracture was included in inpatient/outpatient records in VHA or fee-basis services. Logistic regression models estimated sex-specific odds ratios (OR) and 95% confidence intervals (CI) for having a fracture diagnosis and included age (18-44, 45-64, and 65+ years), race/ethnicity (non-Hispanic White (NHW), Black, Hispanic, Native American, and Asian/Pacific Islander), number of primary care visits, number of mental health visits, urban/rural residence, and service-connected disability.

Results: Prevalence of any fracture diagnosis and hip fracture diagnosis were, respectively, 2.65% and 0.15% in all WV and 2.11% and 0.18% in all MV. For WV ages 18-44, 45-64, or 65+ years, prevalence of any fracture diagnosis were 1.81%, 3.06% and 4.09%, respectively, whereas for MV, 2.70%, 2.46%, and 1.62%. Hip fracture diagnosis was 1.3-fold greater in MV than WV ages 45-64 years (0.10% vs 0.13%, P<0.001), particularly in Black (0.05% vs 0.13%, P<0.001) and Hispanic (0.09% vs 0.17%, P=0.005); yet prevalence was 2.6-fold higher in WV than MV ages 65+ years (0.66% vs 0.26%, P<0.0001). In women and men, 2+ primary care visits or any mental health visit (versus none) was associated with greater odds of any fracture diagnosis (for 5+ primary care visits: WV OR 3.34, CI: 2.99-3.72; MV, 2.81, CI: 2.73-2.89). Among WV and MV, those with 5+ mental health visits had higher odds of fracture diagnosis (WV OR 1.55, CI: 1.46-1.64; MV, 1.63, CI: 1.60-1.66). **Conclusions:** Having a fracture diagnosis differed by age and race/ethnicity. Hip fracture diagnosis was more common in middle-aged MV than WV but not in the 65+ group. Veterans with any fracture diagnosis had more primary care and mental health visits. Primary care and mental health clinics may provide windows of opportunity for age-, race/ethnic-, and sex-specific interventions against fracture risk factors.

Disclosures: Jennifer Lee, None.

Table 1. Mortality

| Variables | Dead n=112 | Alive N=532 | P |
|---------------------------------------|-------------|-------------|--------|
| Age (years) | 83 ± 7 | 81 ± 7 | 0.002 |
| Gender | | | 0.21 |
| | Male | Female | |
| | 40 35.70% | 158 29.70% | |
| | 72 64.30% | 374 70.30% | |
| Charlson's Co morbidity index | 1.79 ± 2.06 | 1.19 ± 1.66 | 0.004 |
| Diabetes mellitus | 41 36.60% | 174 32.70% | 0.426 |
| High Blood pressure | 54 48.20% | 313 58.80% | 0.039 |
| Cancer | 6 5.40% | 15 2.80% | 0.169 |
| Chronic obstructive pulmonary disease | 13 11.60% | 35 6.60% | 0.066 |
| Stroke | 10 8.90% | 40 7.50% | 0.612 |
| Depression | 21 18.80% | 80 15.00% | 0.326 |
| Dementia | 45 40.20% | 114 21.40% | <0.001 |
| Parkinsons disease | 9 8.00% | 40 7.50% | 0.851 |
| Barthel's index Score | 70 ± 28 | 84 ± 21 | <0.001 |
| Folstein's test | 14 ± 11 | 19 ± 10 | <0.001 |
| Nortons test | 10 ± 3 | 12 ± 3 | <0.001 |
| Mini Nutritional Assessment scale | 17 ± 5.3 | 20.1 ± 5.0 | <0.001 |

The data represent mean standard deviation, absolute frequencies (%) and were compared with ANOVAs and Squared Chi tests respectively to obtain p values

TABLE 1

SU0367

Table 2. Multivariate analysis

| Variables | P ^a | HR (CI 95%) |
|--|----------------|---------------------|
| Hand grip strength in Tertil 3 | 0.021 | 1.000 |
| Hand grip strength in Tertil 2 | 0.021 | 2.107 (1.121-3.959) |
| Hand grip strength in Tertil 1 | 0.006 | 2.581 (1.315-5.067) |
| Age | 0.022 | 1.032 (1.005-1.059) |
| Male gender | 0.313 | 1.23 (0.823-1.839) |
| Charlson's Co morbidity Index ^b | 0.031 | 1.11 (1.01-1.221) |
| Barthel's index Score ^b | 0.029 | 0.983 (0.967-0.998) |
| Folstein's test ^b | 0.234 | 0.985 (0.961-1.010) |
| Norton's test ^b | 0.253 | 1.059 (0.96-1.168) |
| Mini Nutritional Assessment scale ^b | 0.071 | 0.959 (0.917-1.004) |

^a: p was obtained Through Logistic Regression analysis.
^b: Denotes scores in its respective scale
 HR: Hazard ratio.
 CI: Confidence Interval

High prevalence of reduced bone mineral density and undertreatment of osteoporosis in patients with systemic sclerosis. Moon J Spanjer¹, Alexandre E Voskuyl¹, Willem F Lems², Irene EM Bultink*². ¹Department of Rheumatology, Amsterdam Rheumatology & immunology Center, location VU University Medical Center, Netherlands, ²Amsterdam Rheumatology & immunology Center, location VU University Medical Center, Netherlands

Purpose: Systemic sclerosis is a systemic inflammatory rheumatic disease with a very low prevalence (10-275/million persons), which has been associated with an increased risk of low bone mineral density (BMD)(1), but data on risk factors associated with bone loss in systemic sclerosis are scarce. The objective of this study was to investigate the prevalence of and risk factors for low BMD in patients with systemic sclerosis.

Methods: Demographic and clinical data of 61 patients with systemic sclerosis were collected. BMD measurements of the lumbar spine, total hip and femoral neck were performed using DXA. Osteoporosis was defined as a T score less than -2.5 SD and osteopenia as a T-score between -1.0 and -2.5 SD, according to WHO definitions. Systemic sclerosis disease severity was defined by the Rodnan skin score and by the Medsger disease severity score (2). Multiple linear regression analyses was used to assess factors associated with BMD. Results: Patient characteristics are shown in table 1. BMD measurements revealed osteopenia or osteoporosis in at least one measurement site in 67% of the patients, of whom 30% had osteoporosis. Low body mass index (BMI) and postmenopausal state were significantly associated with low BMD in all skeletal sites (table 2). No significant associations were found between age, Rodnan skin score, Medsger disease severity score, glucocorticoid treatment and BMD. Of the 30% of patients who had an indication for anti-osteoporosis treatment, 91% did not receive anti-osteoporosis medication.

Conclusions: The results of this cross-sectional study demonstrate a high frequency of osteoporosis or osteopenia in 67% of our patients with systemic sclerosis. Low BMI and postmenopausal state were identified as the most important risk factors. No relationship between disease severity and BMD was found, which finding could be related to the sample size, although it can be argued that low BMI is, at least partly, a marker of disease severity. This study also shows a high frequency (91%) of undertreatment of osteoporosis in this patient group. These results underline the importance of monitoring and treatment of low BMD in systemic sclerosis.

(1) Omair MA, et al. Low bone density in systemic sclerosis: a systematic review. J Rheumatol 2013;40:1881-90.

(2) Medsger TA jr, et al. Assessment of disease severity and prognosis. Clin Exp Rheumatol 2003;21:S42-6.

Table 1 Patient characteristics

| | n = 61 |
|-------------------------------------|--------------|
| Age, in years, mean ± SD | 56.7±12.4 |
| Female/male, n | 44/17 |
| Female, postmenopausal state, n (%) | 34/44 (77.3) |
| LcSSc/dcSSc, n | 41/20 |
| mRSS, mean ± SD | 14.5±9.2 |
| BMI, mean ± SD | 24.6±4.1 |
| Corticosteroid use, ever: | |
| LcSSc, n (%) | 14/41 (34.1) |
| DcSSc, n (%) | 14/20 (70.0) |

LcSSc= limited cutaneous systemic sclerosis, DcSSc = diffuse cutaneous systemic sclerosis, mRSS = modified Rodnan skin score, BMI = body mass index

Table 1

Table 2 Multiple linear regression analysis of BMD in the total hip, femoral neck and lumbar spine

| | Covariates | β | p-value | r ² |
|--------------|-----------------------|--------|---------|----------------|
| Total Hip | Postmenopausal state | -0.326 | 0.003 | 43% |
| | BMI | 0.406 | <0.001 | |
| | Medsger score general | -0.150 | 0.251 | |
| | Proteinuria | -0.229 | 0.085 | |
| Femoral Neck | Postmenopausal state | -0.280 | 0.02 | 33% |
| | BMI | 0.351 | 0.004 | |
| | Medsger score general | -1.06 | 0.461 | |
| | Proteinuria | -0.146 | 0.342 | |
| | Physical activity | 0.146 | 0.247 | |
| Lumbar Spine | Postmenopausal state | -0.301 | 0.015 | 37% |
| | BMI | 0.391 | 0.003 | |
| | Medsger score general | -0.07 | 0.640 | |
| | DcSSc subtype | -0.226 | 0.165 | |
| | Rodnan skin score | 0.204 | 0.199 | |
| | ESR | -0.152 | 0.282 | |

BMI = body mass index, DcSSc = diffuse cutaneous systemic sclerosis, ESR = erythrocyte sedimentation rate, β = standardized regression coefficient

Table 2

Disclosures: Irene EM Bultink, None.

TABLE 2

Disclosures: Hugo Gutierrez Hermosillo, None.

SU0366

High Bone Turnover is Independently Related with Left Ventricular Stiffness in Primary Hyperparathyroidism – the EPATH Trial. Nicolas Verheyen*¹, Astrid Fahrleitner-Pammer², Cristiana Catena³, Evgeny Belvavkiy⁴, Johann Martensen², Julia Wetzel², Martin Gaksch², Martin Grüberl², Jakob Voelkl⁵, Florian Lang⁵, Elisabeth Kraigher-Kraimer⁴, Andreas Meinitzer², Burkert Pieske⁴, Stefan Pilz², Andreas Tomaschitz². ¹Medical University Graz, Austria, ²Medical University of Graz, Austria, ³University of Udine, Italy, ⁴Charite Universitaetsmedizin Berlin, Germany, ⁵University of Tübingen, Germany

Purpose: Accumulating evidence suggests a direct link between bone metabolism and cardiovascular stiffening which may be clinically pronounced in hyperparathyroid state. We therefore hypothesized that markers of bone turnover are associated with left ventricular (LV) stiffening in a large cohort of patients with primary hyperparathyroidism (pHPT).

Methods

We analyzed patients with pHPT who participated in the “Eplerenone in Primary Hyperparathyroidism” (EPATH) Trial. Blood sampling was performed after overnight fasting and standard laboratory parameters were determined immediately. Markers of bone formation (osteocalcin, bone-specific alkaline phosphatase [BALP] and procollagen type 1 [P1NP]) and resorption (beta-crosslaps [b-CTX]) were measured in serum that had been stored at -80°C. Transthoracic echocardiography was performed applying tissue Doppler imaging. Following international recommendations average of both septal and lateral early diastolic peak velocity of the mitral annulus (e') was used to quantify LV stiffening (lower e' indicates a higher degree of LV stiffening).

Results

We enrolled 131 patients with pHPT (mean age: 67 +/- 10 years, 107 were females [79%]). Median parathyroid hormone (PTH) (IQR) was 99 pg/mL (83 – 124), mean calcium was 2.63 +/- 0.15 mmol/L, 61 (45%) had a diagnosis of osteoporosis and mean e' was 7.1 +/- 2.3 (reference range: >7). e' was directly correlated with P1NP (r=0.154, P=0.07), osteocalcin (r=0.205, P=0.02), BALP (r=0.147, p=0.09) and b-CTX (r=0.149, P=0.09). We performed four separate multivariate linear regression analyses with e' as the dependent variable, with adjustment for age, sex, diabetes mellitus, smoking status, body mass index, systolic nocturnal blood pressure, GFR, PTH, calcium and treatment for osteoporosis. Markers of bone formation were independently and directly related with e' (osteocalcin: adjusted beta=0.243, P=0.01; BALP: beta=0.234, P=0.01; P1NP: beta=0.215, P=0.03), respectively, and b-CTX with borderline significance (beta=0.165, P=0.09).

Conclusions

We found that stimulated bone turnover in the setting of pHPT was independently and inversely related with LV stiffening and, thus, with a favorable cardiac phenotype. These data warrant further experimental studies on the effects of osteoblast or osteoclast activation on cardiac function.

Disclosures: Nicolas Verheyen, None.

SU0368

Increased body weight as a risk factor of intertrochanteric fracture severity in elderly women. Hyung Min Ji¹, Jun Han¹, Dong San Jin², Ye-Yeon Won¹. ¹Ajou University Hospital, South Korea, ²Mary's Orthopedics Hospital, China

Purpose

Risk factors for intertrochanteric fracture severity were not studied thoroughly despite the high failure rate of osteosynthesis previously reported. The purpose of this study was to identify the risk factor for each fracture type using AO/OTA classification in female patients who experienced intertrochanteric fractures.

Materials and Methods

This cross-sectional study identified 240 women over 50 years old with an incident intertrochanteric fracture in whom dual-energy x-ray absorptiometry (DEXA) was obtained. Two independent orthopaedic specialists graded the fracture severity by AO/OTA classification. Age, body weight, height, BMI and trochanteric T-score were used in univariate and multivariate logistic regression analysis to identify risk factor for each fracture type, and unstable intertrochanteric fracture.

Results

44.4% (106 hips) were graded as unstable intertrochanteric fracture. Lower BMD (OR 0.743, p=0.049), body weight (OR 0.970, p=0.031) and BMI (OR 0.927, p=0.045) predicted AO/OTA 31 A1 fracture while higher BMD (OR 1.443, p=0.010), body weight (OR 1.036, p=0.010), and BMI (OR 1.089, p=0.023) predicted 31 A2 fracture after univariate logistic regression. Increased body weight (OR 1.027, p=0.044) was the only independent risk factor for unstable intertrochanteric fracture after multiple logistic regression.

Conclusion

The higher the body weight, the greater the likelihood of experiencing an intertrochanteric fracture that is more unstable and displaced.

Disclosures: Hyung Min Ji, None.

SU0369

Progressive Cortical and Trabecular Bone Loss Four Years After Bariatric Surgery. Emily Stein^{*}, Angela Carrelli, Mariana Bucovsky, Nientara Anderson, Chengchen Zhang, Melissa Bagloo, Marc Bessler, Beth Schroppe, Elizabeth Shane, Shonni Silverberg. Columbia University College of Physicians & Surgeons, USA

Recent data suggest that fracture rates increase after bariatric surgery, particularly after procedures associated with the most weight loss. These emerging fracture data highlight the importance of understanding the long-term skeletal consequences of these procedures. Substantial skeletal changes are known to occur in the first year after surgery, but data are limited thereafter. To our knowledge, this 4-year study of 22 women represents the longest duration of follow-up of BMD and skeletal microarchitecture in the bariatric population. We hypothesized that bone loss at all sites would cease after weight loss stabilized.

At baseline and annually after surgery, we measured calcitropic hormones, bone turnover markers, areal BMD (aBMD) by DXA at the lumbar spine (LS), total hip (TH), femoral neck (FN) and 1/3 radius (1/3R), volumetric BMD (vBMD) and cortical (Ct) and trabecular (Tb) microstructure at the distal radius (RAD) and tibia (TIB) by high resolution peripheral quantitative CT (HRpQCT). Subjects (age 44±12; 65% Latina; mean BMI: 44±5 kg/m²) had normal baseline Z-scores. After Roux-en-Y gastric bypass (n=15), sleeve gastrectomy (n=2) and gastric banding (n=5) weight declined by 25% the 1st year and then remained stable (Table). All women received supplemental calcium and vitamin D and 25OHD was stable. However, PTH increased through year 3 (46%; p<0.01). CTX increased over the first 2 years (135%; p<0.01) and then trended toward baseline. aBMD at the TH and FN declined progressively over the 4 years. Declines at the LS and 1/3R BMD only became significant in years 3 (LS) and 4 (1/3R). HRpQCT did not change in the 1st year, but over the next 3 years, there were progressive declines in Ct bone (density, area and thickness), total and Tb density at both radius and tibia. Tb microarchitecture did not significantly change except for Tb thickness, which declined between years 2 and 4 at both sites.

In summary, after early declines in hip aBMD, we find significant progressive deterioration of cortical and trabecular microarchitecture. We conclude that while the initial bone loss at the hip may reflect skeletal unloading, pathologic changes affecting both cortical and trabecular bone continue long after cessation of weight loss. These findings suggest a structural mechanism for fracture in this population. Given the burgeoning number of bariatric procedures, additional studies are critical to further investigate the extent and sequelae of these changes.

Four-Year Changes in DXA and HRpQCT Following Bariatric Surgery (% Δ from baseline)

| | Yr 1 | Yr 2 | Yr 3 | Yr 4 |
|----------------|--------|--------|--------|---------|
| Weight | -25** | -25** | -25** | -22** |
| aBMD LS | -0.9 | -0.9 | -3.2* | -4.3** |
| aBMD TH | -5.3** | -6.1** | -9.1** | -10.1** |
| aBMD 1/3R | 1.0 | -1.4 | -2.5 | -3.8* |
| RAD Total vBMD | -0.9 | -4.9** | -7.6** | -8.0** |
| RAD Ct.vBMD | -0.2 | -1.6† | -3.0** | -3.3** |
| RAD Ct.Th | -1.6 | -4.3* | -6.2** | -6.8** |
| RAD Tb vBMD | 0.9 | -5.9** | -9.4** | -10.9** |
| RAD TbTh | 0.8 | -3.7 | -9.7** | -10.6** |
| TIB Total vBMD | -0.3 | -4.8** | -7.3** | -7.6** |
| TIB Ct vBMD | -1.0 | -3.5** | -4.1** | -5.5** |
| TIB Ct Th | -0.8 | -6.0* | -8.8** | -8.7** |
| TIB Tb vBMD | 0.6 | -3.5** | -6.7** | -6.4** |
| TIB Tb.Th | 1.5 | -0.5 | -3.9† | -5.2* |

†p<0.10, *p<0.05, **p<0.01 vs baseline

Table. Bariatric 4 Yr Change in DXA and HRpQCT

Disclosures: Emily Stein, None.

SU0370

Withdrawn.

SU0371

Transient Regional Osteoporosis of the Hip: Case study with use of bisphosphonate as a treatment option. Susan Williams-Judge, MN, CNS, ARNP^{*}, Julie Carkin, M.D.¹, Yuli Son, M.D.², Camelia Whitten, M.D.³. ¹University of Washington/Northwest Hospital, USA, ²University of Washington, USA, ³Via Radiology, USA

Abstract:

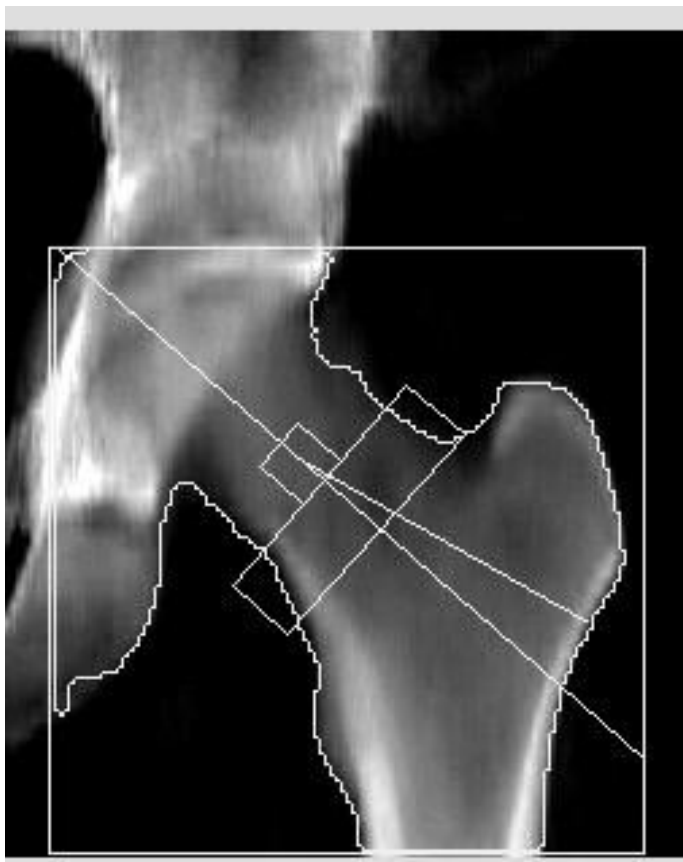
Transient regional osteoporosis is an uncommon, self-limited, transient disease resulting in osteoporosis at one site predisposing one to fragility fractures. Identification of this disorder is often difficult with MRI being the gold standard to differentiate it from other disorders such as avascular necrosis, stress fracture, infection, malignancy, and reflex sympathetic dystrophy. It generally affects middle aged men in a M:F 3:1 distribution, and is seen predominantly in women during the third trimester of pregnancy. Etiology is unknown, but thought to represent a vascular disease possibly driven by the sympathetic nervous system. Treatment options can range from conservative therapy with non-weightbearing, NSAIDs, and tincture of time to treatment with bisphosphonates which can prevent further fracture, and treat pain. Using this case study we hope to provide recognition of a rare disease, and the measures taken to make the diagnosis which is essentially a diagnosis of exclusion.

Case study A 45 year old male presented to the Sports Medicine Clinic with three weeks of acute onset left hip pain without prior trauma. He had prophylactically tried NSAIDs, and his primary care physician had performed x-ray imaging which was normal, and had placed the patient on steroids with referral to the sports medicine clinic. Medical history was significant for brain aneurysm rupture age 18, no past history of fracture, smoking or alcohol use. Remote history of marijuana and cocaine use 20 years prior. Clinical exam, laboratory and imaging studies will be included in the case study including normal baseline x-ray results with further imaging showing changes consistent with transient osteoporosis of the left hip. Subsequent arthrogram MRI findings, and DEXA scan, again supporting a diagnosis of transient osteoporosis, are also included.

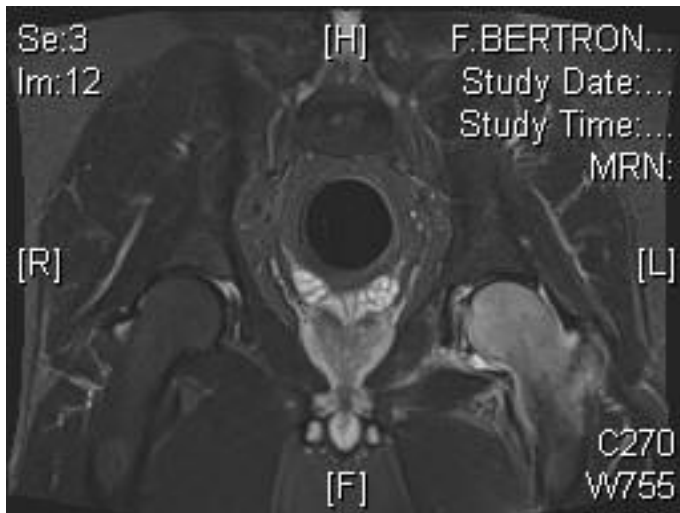
IV bisphosphonates were used in this case to decrease fracture risk, and help with pain control. Decision-making strategy will be included in the case study.

Relevant references will be included in the case study.

** I have additional MRI, and xray images to include



DEXA hip



left hip MRI



mri series 12



lateral hip



pelvis

Disclosures: Susan Williams-Judge, MN, CNS, ARNP, None.

SU0372

Efficacy and Safety of Denosumab for the Treatment of Patients With Low Bone Mineral Density Post Renal Transplantation: An Investigator-Initiated Pilot Study. Medi Aloosh^{*1}, Anthony A. Karaplis², Mark Lipman², Andrew C. Karaplis¹. ¹Lady Davis Institute for Medical Research, & Division of Endocrinology, Jewish General Hospital, McGill University, Canada, ²Lady Davis Institute for Medical Research, & Division of Nephrology, Jewish General Hospital, McGill University, Canada

BACKGROUND: Renal transplant recipients are at particular risk of fractures (vertebral greater than lower extremity). The overall fracture risk after kidney transplantation is 3.6–3.8-fold higher than in healthy individuals, and is 30% higher during the first 3 years after transplantation than in patients on dialysis. In bone biopsy studies, the main alteration in bone remodeling after renal transplantation is decrease in bone formation and mineralization in face of persistent bone resorption, which may lead to an imbalance in remodeling favoring resorption. The KDIGO guidelines recommend treatment with bisphosphonates in patients with estimated GFR >30 mL/min/1.73 m² and low BMD.

The development of a human monoclonal antibody to RANKL, denosumab, constitutes a novel approach to prevent fragility fractures in osteoporosis. Denosumab reduces osteoclastic resorption and, hence, could be beneficial in the treatment of osteoporosis in renal transplant recipients. This agent however has not been studied in this patient population. Although in a number of published clinical trials the overall rate of infections was similar with denosumab and placebo, the risk of severe infections in immunocompromised patients remains to be carefully scrutinized.

OBJECTIVE: Evaluate denosumab therapy in patients with low BMD post kidney transplantation.

METHOD: This was an investigator-initiated open-label pilot study conducted in the osteoporosis clinic at our hospital. The participants included 3 women and 2 men (mean age 64 ± 9 years) post renal transplantation (median time 10 years) who received denosumab 60 mg SC every 6 months (mean observation time 2.9 ± 0.6 years). All patients were on calcium and vitamin D. The main outcome measures were changes in BMD and safety.

RESULTS: During treatment, BMD increases occurred with denosumab administration (8.6% lumbar spine; 1.9% femoral neck; 2.7% total hip). There was no discontinuation of study treatment because of adverse events. One patient sustained a new vertebral fracture while off treatment. No serious adverse events such as infection or deteriorating renal function were reported.

LIMITATIONS: This was a short period, open-label pilot study with small sample size.

CONCLUSIONS: Denosumab treatment in a small number of patients with low BMD following kidney transplantation increased BMD and was well tolerated. No new safety signals were identified.

Disclosures: Medi Aloosh, None.

SU0373

Adipokines Visfatin and Adiponectin Promote Inflammatory Phenotype for Human Nucleus Nulposus Cells. Stephanie Miller^{*1}, Rachel Willardson², Dezba Coughlin², Jeffrey Lotz². ¹University of California, San Francisco, USA, ²UC San Francisco, USA

Inflammation is a potential unifying clinical feature of intervertebral disc (IVD) degeneration and low back pain (LBP). Human nucleus pulposus (NP) cells have been shown to have direct inflammatogenic properties, separate from an immunologic mechanism. Adipokines, a class of cytokines produced by adipose tissue, have been implicated as active proinflammatory molecules in a variety of inflammatory conditions, including those correlated with LBP. We hypothesized that adipokines drive human NP cells towards an inflammatory phenotype, and we aimed to quantify the effects of various adipokines on human NP expression of genes associated with inflammation. Human NP cells were suspended in alginate beads and treated with low and high doses (2-100 ng/mL range) of the adipokines adiponectin, visfatin, resistin, leptin, fibroblast growth factor 21, or fatty acid binding protein 4 for seven days. The cells were collected and mRNA expression of markers of inflammation and remodeling were quantified via PCR analysis: including interleukin 1B (IL1B), IL 6, IL 8, IL 10, transforming growth factor β , matrix metalloproteinase 1 (MMP1), MMP3, collagen type 1a1, and aggrecan. Visfatin treatment (100 ng/mL) resulted in significant upregulation of the widest array of genes, including a 60-fold increase in IL1B expression, a 19-fold increase in IL8 expression, and four-fold increase in IL6, MMP1, and MMP3 expression. Treatment with 10 ng/mL adiponectin resulted in a three-fold increase in MMP3 expression. None of the tested treatments resulted in significant downregulation of any of the evaluated genes. These results suggest a potential role for the adipokines visfatin and adiponectin in NP-associated IVD inflammation. Additionally, MMPs 1 and 3 may play a central role in translating the effects of these two adipokines on disc degeneration.

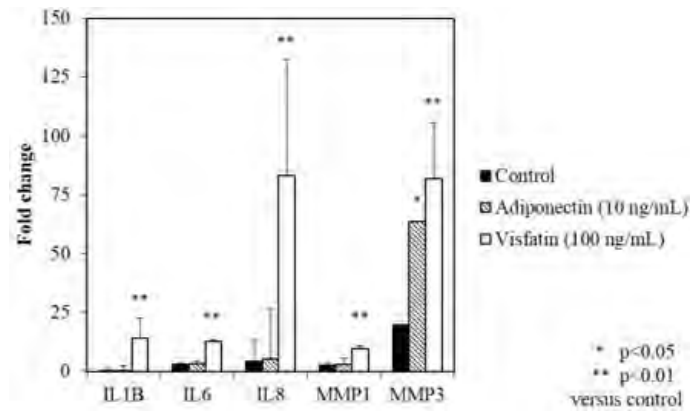


Figure 1

Disclosures: Stephanie Miller, None.

SU0374

Interleukin-1 β Suppresses Expression of Osteoblastic Genes as well as the Regulators of Ecto-nucleotides and Pyrophosphate That Negatively Regulate Bio-mineralization in Mouse Bone Marrow Stromal Cells. Yoichi Ezura^{*1}, Arina Hatta², Shin Lin², Yayoi Izu², Tadayoshi Hayata³, Masaki Noda². ¹Tokyo Medical & Dental University, Medical Research Institute, Japan, ²Tokyo Medical & Dental University, Japan, ³University of Tsukuba, Japan

Heterotopic ossification (HO) in arterial walls, cardiac valves, peri-articular tissues and spinal ligaments can cause serious clinical symptoms depending on the situations. The mechanisms involved in bio-mineralization and pathology of HO in various diseases indicate that inflammatory responses of the host individuals could be an important aspect. However, such responses of stromal progenitor cells residing in the host tissues has not been fully investigated on its possible contribution to HO. Recently in 2013, Ferreira et al., reported that pro-inflammatory cytokines including IL-1 β suppresses the expression of the negative regulator of the soft-tissue calcification, ectonucleotide pyrophosphatase/ phosphodiesterase-1 gene (*ENPP1*) in bone marrow derived mesenchymal stem cells of human, suggesting the involvement of this mechanism in the pathogenesis of HO. However, possible contribution of other regulators on soft-tissue calcification including *ANKH*, *NT5E*, *SLC29A1* and *ENTPDs* were not investigated in multiple cell sources. Therefore in this study, we investigated the effects of IL-1 β on the mouse bone marrow stromal cells (BMSCs) for the expression of such genes. As a reference, expression of various osteoblastic marker genes including alkaline-phosphatase, type I collagen, osteopontin, bone-sialoprotein, and osteocalcin was monitored by RT-PCR for BMSCs culture in osteogenic medium periodically for three weeks. Consistent with previous studies, such characteristic expression was suppressed by IL-1 β . In addition, we observed a reduction of *Enpp1*, *Nt5e*, *Ank* and *Slc29a1*. Reduction of extracellular pyrophosphate in the medium was confirmed. Our results suggest that IL-1 β suppresses osteoblastic gene expression as

well as negative regulators of soft-tissue calcification in BMSCs both in human and mouse, and may contribute to the mechanisms of HO in non-skeletal and skeletal soft-tissues.

Disclosures: Yoichi Ezura, None.

SU0375

Loss of TIEG expression results in severe colitis-mediated bone loss. Malayannan Subramaniam*, James Krempski, Kevin Pitel, Konstantinos Papadakis, John R. Hawse, Mayo Clinic, USA

Nearly 1.5 million Americans are afflicted with inflammatory bowel diseases (IBD) such as ulcerative colitis or Crohn's disease and approximately 30,000 new cases are diagnosed in the United States annually. A common consequence of IBD is bone loss and more than 30% of patients with IBD ultimately develop osteoporosis. A number of factors are thought to contribute to bone loss in patients with IBD including increased levels of inflammatory cytokines; however, the cellular and molecular basis for this phenomenon is not understood. Recently, multiple lines of evidence have linked a critical role for TGF β Inducible Early Gene-1 (TIEG) in mediating immune system function and loss of TIEG expression in mice has been shown to result in an enhanced susceptibility to the development of colitis. Therefore, we sought to determine the effects of colitis on the skeleton of wild-type (WT) and TIEG knockout (KO) mice. To induce colitis, male mice were administered 2% dextran sulfate sodium salt (DSS) for 3 cycles on days 1-8, 23-29, and 43-50. Following treatment, mice were monitored for weight loss and disease activity, and colon length and histology were used to assess inflammation between WT and TIEG KO animals. Additionally, tibiae were collected and used for pQCT analysis. In the absence of DSS treatment, TIEG KO mice do not exhibit any skeletal phenotype compared to WT littermates as determined by DXA, pQCT and micro-CT analyses. Following treatment of mice with DSS, TIEG KO animals developed more severe colitis relative to WT mice as indicated by decreased colon length, higher disease activity index and histological score. Interestingly, DSS treatment of TIEG KO mice also resulted in substantial decreases in multiple bone parameters compared to treated WT controls. Specifically, within the tibial metaphysis, significant decreases in total content (21%), trabecular content (30%), trabecular density (9%) and trabecular area (22%) were observed. At the tibial diaphysis, significant decreases in total content (15%), cortical content (15%), cortical area (13%), cortical thickness (5%) and periosteal circumference (8%) were detected in DSS treated KO animals relative to WT mice. These data demonstrate that loss of TIEG expression leads to the development of severe colitis-mediated bone loss in mice and provide a novel model system through which the cellular and molecular basis of IBD associated osteoporosis can be explored.

Disclosures: Malayannan Subramaniam, None.

SU0376

RANKL Induction of Cytokines in Pre-Osteoclasts In Vitro: Dependence on Cyclooxygenase-2 (Cox2). Trisha Kwarko*, Shilpa Choudhary, Thomas Estus, Carol Pilbeam, University of Connecticut Health Center, USA

Prior to stimulating differentiation of M-CSF-treated bone marrow macrophages (BMMs) into osteoclast-like cells, RANKL induces expression of multiple genes that can potentially mediate effects of inflammation or autoinflammatory diseases on bone. We are interested in the role of prostaglandins (PGs) in this induction. To determine if RANKL induces *Cox2* expression, the major enzyme controlling PG production, we cultured murine BMMs with M-CSF (30 ng/ml) \pm RANKL (30 ng/ml) for 24 h. RANKL induced *Cox2* expression by 30 min and expression peaked at 6 h. Prostaglandin E synthase, *Ptges*, which converts products of *Cox2* to PGE₂, was induced by RANKL at 1.5 h and peaked at 6 h. To examine the effects of *Cox2* absence on cytokine induction by RANKL, we performed a microarray on BMMs from wild type (WT) and *Cox2* knockout (KO) mice, treated for 24 h and 3 d with M-CSF + RANKL. At both time points the most highly differentially expressed genes in WT BMMs compared to KO BMMs were serum amyloid A 3 (*Saa3*) and interleukin-1 β (*Il-1 β*). Both *Saa3* and *Il-1 β* are involved in innate immunity and can mediate local and systemic inflammation. The RANKL induction of *Saa3* was 207-fold greater in WT BMMs compared to KO BMMs at 24 h and 30-fold greater at 3 d. The RANKL induction of *Il-1 β* was 108-fold greater in WT BMMs compared to KO BMMs at 24 h and 26-fold greater at 3 d. We confirmed the microarray results in a 24 h time course study of WT and *Cox2* KO BMMs. *Il-1 β* and *Saa3* were induced by RANKL in WT, but not KO, BMMs at 30 min and 3 h, respectively, and both peaked at 6 h. NS398, an inhibitor of *Cox2* activity, prevented the induction by RANKL in WT BMMs, and addition of PGE₂ restored the induction. To determine if *Saa3* and *Il-1 β* were secreted from RANKL-stimulated BMMs, we cultured WT BMMs with M-CSF \pm RANKL for 24 h and performed ELISAs. *Saa3* protein was not measurable in the culture medium from M-CSF-treated cultures but was secreted by cultures treated with M-CSF + RANKL. *Il-1 β* secreted protein was not detectable, with or without RANKL, suggesting that another factor is needed to activate caspase-driven cleavage and release of *Il-1 β* . We conclude that RANKL induces *Cox2* and *Ptges* in BMMs and that *Cox2*-produced PGs are required for the RANKL induction of *Il-1 β* expression and *Saa3* expression in BMMs. This is an example of how factors that induce both RANKL and *Cox2*, such as parathyroid hormone, could stimulate not only osteoclastogenesis but enhance inflammation.

Disclosures: Trisha Kwarko, None.

SU0377

Gender-Specific Effects of Insulin-like Growth Factor Binding Protein 4 in Body Composition and Skeletal Maturation. David Maridas*¹, Victoria DeMambro¹, Phuong Le¹, Casey Doucette¹, Subburaman Mohan², Clifford Rosen¹. ¹Maine Medical Center Research Institute, USA, ²Loma Linda University, USA

Insulin-like Growth Factor Binding Protein 4 (IGFBP4) is highly expressed in human adipose tissue and in osteoblasts. *In vitro* models have revealed IGFBP4 as an inhibitor of IGF-I signaling. However, previous reports showed that systemic injections of IGFBP4 in mice induced bone formation while local injections inhibited IGF-I actions making it unclear whether IGFBP4 enhances or inhibits IGF-I signaling *in vivo*. Our purpose was to determine how IGFBP4 mediates adipose differentiation and if this impacts skeletal acquisition *in vivo*. Thus, we investigated the skeletal and adipose phenotypes of IGFBP4 null (IGFBP4^{-/-}) mice at 8 and 16 wks. Whole body DXA revealed a significant decrease of fat proportion and lean mass in IGFBP4^{-/-} males and females (p<0.05). At 16 weeks, IGFBP4^{-/-} females had a reduction (p<0.04) of areal and femoral BMD and BMC while males were unaffected. Reductions in femur length, inguinal (iWAT), gonadal white adipose tissues, and interscapular brown fat were observed in IGFBP4^{-/-} mice. MicroCT of femurs showed reductions in BV/TV (p=0.06) and trabecular and cortical thicknesses (p=0.05) in IGFBP4^{-/-} females. Surprisingly, males had higher connectivity density (p=0.02) and trabecular number (p=0.005). Gene expression analysis showed that femoral *Sost* expression was decreased in IGFBP4^{-/-} males but not females. *Ppar γ* expression was reduced in iWAT of both genders. When challenged with a high fat diet (HFD, 60%kcal) or a control diet (10%kcal), IGFBP4^{-/-} mice were protected against HFD-induced obesity. Histology of iWAT revealed a hypertrophy of adipocytes in HFD-fed control mice that was not observed in IGFBP4^{-/-} females. To measure adipogenesis, outer ear mesenchymal stem cells (eMSCs) were isolated from 3-wk-old mice and differentiated into adipocytes. IGFBP4^{-/-} eMSC showed a significant decrease in adipogenesis compared to control cells (p<0.001). In summary, our data suggest that IGFBP4 is an important modulator of bone and fat development, but there is clear gender and tissue specificity. Indeed, males appeared to be protected against the reduction in bone parameters observed in females. Reduction of *Sost* expression in males but not in females may contribute to this gender-specific phenotype. Impaired adipocyte differentiation and function may contribute to reduction of adipose tissue and the resistance to HFD-induced obesity. Taken together, our results support the hypothesis that IGFBP4 regulates fat and bone tissues *in vivo*.

Disclosures: David Maridas, None.

SU0378

Bone Mineral Density in Hypophosphatasia. Franca Genest*, Franz Jakob, Nicole Luksche, Michael Schneider, Lothar Seefried, Musculoskeletal Center Wuerzburg, Germany

Hypophosphatasia (HPP) is a rare inherited metabolic disease caused by inactivating mutations in the ALPL gene, coding for the Tissue-nonspecific alkaline phosphatase (TNAP). Clinical manifestation is associated with a broad range of symptoms with increased risk of insufficiency fractures and bone marrow edema being a well-known hallmark of the disease especially in adult patients. Little is known as to how Bone Mineral Density is altered in adult patients and about the clinical significance of BMD measurement in HPP.

From November 2014 to March 2015, in total 60 adult HPP patients were examined at our department. DXA was performed in 56 Pat. using Hologic Discovery A. Lumbar spine BMD was valid in all patients, total hip BMD could be determined in 52 patients.

Mean age of the 56 patients (45 female) with available DXA was 43.6 years (SD 10.8, range 24-72). Mean T-Score was -0.49 (SD 1.2) for lumbar spine and -1.06 (SD 1.0) for total hip. Comparing BMD with age/gender matched reference groups using Z-Scores revealed normal results for lumbar spine BMD (Z-Score 0.0, SD 1.2) and a slight decrease (Z-Score -0.64, SD 1.0) for total hip. In total 29 patients reported at least one fracture in their medical history with 9 patients having experienced 5 or more fractures. Differential analysis of DXA results pertaining to fracture history displayed lumbar spine BMD at Z=-0.02/T=-0.57 and Z=0.02/T=-0.4 for the fractured (n=29) and unfractured (n=27) group, respectively. Similarly, total hip BMD did not reveal substantial between-group differences. Mean levels of residual ALP activity were 21.7 U/I (SD 8.65) and 28.6 U/I (SD 14.24) for the fractured and unfractured group, respectively. So far we were not able to identify an association between ALP activity and BMD.

HPP is commonly reflected to be associated with deficient bone mineralization. According to our cross-sectional analysis, HPP in adults is not generally associated with reduced BMD as compared to age/gender matched reference cohort as measured by Z-Score. Basically, BMD values were lower in total hip as compared to lumbar spine. Comparing subgroups of patients with/out fractures did not find differences in their T- and Z-Score, suggesting that BMD is not a good predictor of fracture risk in HPP. Accordingly, BMD in moderate adult HPP seems not to be a function of residual ALP activity, while the latter might be associated with fracture risk. Examinations are ongoing and more substantiated data with higher patient numbers can be expected by the time of data presentation in October.

Disclosures: Franca Genest, None.

SU0379

Establishing Reference Intervals for Pyridoxal 5'-Phosphate: the National Health and Nutrition Examination Survey 2007-2008 Data. Philip Nicklin*¹, Richard Eastell², Kim Naylor². ¹University of Sheffield, United Kingdom, ²Academic Unit of Bone Metabolism, United Kingdom

Diagnosis of adult-onset Hypophosphatasia (HPP) is particularly important in patients with osteoporosis, as treatment with bisphosphonates may result in atypical femur fractures. Pyridoxal 5'-phosphate (PLP) is a substrate for alkaline phosphatase (ALP) and so it is high in HPP and thus it is useful in the diagnosis of HPP. It is important to establish reference intervals for PLP that take into account confounding factors that affect PLP measurement. We determined the factors which influenced PLP results and calculated race and gender specific reference intervals for serum PLP in adults using the National Health and Nutrition Examination Survey (NHANES) 2007-2008 data. We selected adults ages 20 to 80 years (n=4496).

Serum PLP was measured by reversed-phase HPLC with post-column derivatization and fluorometric detection. The 95% reference intervals were calculated for PLP using the Robust method (CLSI Guidelines C28-A3), skewed data was back transformed after logarithmic transformation.

The factors which influenced PLP results included: inflammation (C-reactive protein >5.0mg/L) which was associated with lower PLP (median, 44nmol/L; IQR, 24-77nmol/L; compared to median, 64nmol/L; IQR, 37-114nmol/L; P<0.001), people with low ALP (<36.0 U/L) had higher PLP (median, 107nmol/L; IQR, 59-240nmol/L) compared to normal (median, 58nmol/L; IQR, 33-105nmol/L; P<0.001) and those taking vitamin B6 supplements had higher PLP (median, 73nmol/L; IQR, 47-123nmol/L; compared to no supplement, median, 47nmol/L; IQR, 28-89nmol/L; P<0.001). There was no effect of reduced kidney function (eGFR <60 ml/min) on PLP (median, 62nmol/L; IQR, 32-120nmol/L; compared to median, 58nmol/L; IQR, 34-105nmol/L; P=0.68).

Reference intervals were calculated after excluding the identified confounding factors. Subjects were categorised by race/ethnicity into the following groups: Mexican American, Non-Hispanic white, and Non-Hispanic black. The Kruskal-Wallis test showed a significant effect of race and gender on PLP (P=0.014, P=0.002), but not age (P=0.49) (Kruskal-Wallis). Serum PLP reference intervals for race and gender specific populations are shown in the table. We have established gender specific reference intervals for serum PLP in three race/ethnicity categories after excluding factors that affect PLP measurements. These reference intervals provide useful information for the diagnosis of adult-onset HPP.

| Race/ethnicity | n | Geometric Mean | Lower Limit (90% CI) | Upper Limit (90% CI) |
|----------------------------|-----|----------------|----------------------|----------------------|
| Mexican American Males | 68 | 53 | 13 (10 – 17) | 195 (147 – 253) |
| Mexican American Females | 88 | 45 | 12 (10 – 15) | 147 (119 – 183) |
| Non-Hispanic White Males | 305 | 63 | 10 (9 – 12) | 344 (290 – 402) |
| Non-Hispanic White Females | 361 | 55 | 8 (7 – 9) | 310 (264 – 364) |
| Non-Hispanic Black Males | 73 | 55 | 9 (6 – 12) | 336 (248 – 447) |
| Non-Hispanic Black Females | 84 | 44 | 6 (5 – 8) | 235 (167 – 324) |

Table 1. Reference intervals for serum PLP (nmol/L) in US adults (age 20-80).

Table 1

Disclosures: Philip Nicklin, None.

SU0380

Exposure-Response Modeling and Simulation to Support Evaluation of Efficacious and Safe Exposure and Dose Range for Asfotase alfa in Patients with Hypophosphatasia. Rajendra S Pradhan*¹, Marc R Gastonguay², Xiang Gao¹, Jonathon Monteleone¹, Jeannine Fisher³, CJ Godfrey³, Nathanael L Dirks³, Augustin Melian¹, David Thompson¹, Chetan D Lathia¹. ¹Alexion Pharmaceuticals, USA, ²The Metrum Research Group, USA, ³Metrum Research Group LLC, USA

Asfotase alfa is a human recombinant tissue-nonspecific alkaline phosphatase-Fc-deca-aspartate fusion protein in development as a subcutaneous (SC) treatment for hypophosphatasia (HPP). HPP is a rare, serious, and potentially fatal, genetic disorder caused by loss-of-function mutation(s) in the gene encoding the tissue-nonspecific isoenzyme of alkaline phosphatase (TNSALP).

Sparse, repeated-measures, pharmacokinetic (PK), pharmacodynamic (PD) and immunogenicity data were collected from 5 interventional studies. The PD data selected for analysis covered the continuum of mechanistic biomarkers to clinical efficacy endpoints, starting with the reduction of TNSALP substrate levels (plasma inorganic pyrophosphate or P_i and Pyridoxal-5'-phosphate or PLP), and leading to improvements in bone mineralization, [Radiographic Global Impression of Change (RGI-C) and Rickets severity scale (RSS)], skeletal morphology and musculoskeletal function, [6-minute walk test (6MWT)], Bruininks-Oseretsky Test of Motor Proficiency, Second Edition (BOT-2) and Modified Performance-Oriented Mobility Assessment – Gait subtest (MPOMA-G)]. Safety data selected for analysis included ectopic calcification, injection/infusion associated reactions, and injection site reactions.

The serum asfotase alfa activity-time profiles were described adequately by a linear two-compartment population PK model. The PD-time profiles were described adequately by indirect PD response models linking time-continuous patient-specific predicted serum asfotase alfa activity to each of the PD endpoints. The safety

variables of interest were assessed for relationship between asfotase alfa exposure and safety findings across the clinical program. Model-based simulations were conducted to explore the dose-exposure-response relationships for all endpoints, across a range of possible dosing regimens. The integrated view of the simulated dose/exposure - response relationships for PD efficacy endpoints revealed that all PD endpoints approached a plateau around a weekly dose of 6 mg/kg administered SC as 3 or 6 times a week. This dose regimen showed normalization of TNSALP substrates from elevated levels prior to treatment, clinically meaningful improvement in bone mineralization and substantial improvement in skeletal morphology and musculoskeletal function. There was no apparent relationship between PK and any safety variables of interest.

Disclosures: Rajendra S Pradhan, Employee of Alexion Pharmaceuticals
This study received funding from: Alexion Pharmaceuticals

SU0381

Manifestations of Hypophosphatasia in Adults with Pediatric Onset of Symptoms: a Review of the Case Literature. Eileen K Sawyer*, Karen Anderson. Alexion Pharmaceuticals, USA

Purpose. Hypophosphatasia (HPP) is the rare inherited metabolic disease resulting from loss-of-function mutations in the tissue-nonspecific alkaline phosphatase (TNSALP) gene. The natural history in adult patients who first presented with symptoms of HPP as children (i.e. <18 years of age) is not well characterized. We sought to better understand the clinical presentation of HPP in these patients through a comprehensive review of the case literature.

Methods. Cases were identified through searches of PubMed using the keywords “hypophosphatasia” AND (“case report” OR “case study”) and reference lists of identified articles, and filtered for those reporting patients over age 18 with pediatric onset of symptoms. Available information captured for each case included: age of patient, presenting features, pre-specified systemic manifestations of interest including nephrocalcinosis, fractures, and muscle pain, and age at death if applicable.

Results. 293 publications were identified, dating from 1939; 28 publications described a total of 32 adults with pediatric onset of HPP (median age 42.5 years, ranging from 21 to 75 years). Two patients were reported as deceased (1 at age 23 of renal failure; 1 at age 57 of sepsis). Half of the patients were first diagnosed in adulthood, presenting most commonly with fractures and pain. Overall, the systemic manifestations of interest most frequently reported were fractures (24 patients), pain (22 patients), and early tooth loss (17 patients). Other common complications included limited mobility/function (9 patients), and short stature or loss of height (6 patients). Of note, few patients reported current or past characteristic pediatric symptoms such as nephrocalcinosis, respiratory complications, seizures (1 patient each), and craniosynostosis (5 patients).

Conclusions. Pain and fractures are prominent features of HPP in patients with pediatric-onset HPP surviving to adulthood. All symptoms of HPP should be queried in adult patients presenting with these symptoms. Missed diagnosis of pediatric-onset HPP is common in these patients, and highlights the need for increased recognition of HPP symptoms in childhood.

Disclosures: Eileen K Sawyer, Employee of Alexion Pharmaceuticals
This study received funding from: Alexion Pharmaceuticals

SU0382

PHEX 3'-UTR c.*321A>G demonstrates X-linked recessive inheritance in a large American family. Gary S. Gottesman*¹, Katherine L. Madson¹, Valerie Wollberg¹, Steven Mumm², William H. McAlister³, Michael P. Whyte¹. ¹Center for Metabolic Bone Disease & Molecular Research, Shriners Hospitals for Children - St Louis, USA, ²Division of Bone & Mineral Diseases, Washington University School of Medicine, USA, ³Department of Pediatric Radiology, Mallinckrodt Institute of Radiology at St. Louis Children's Hospital, Washington University School of Medicine, USA

X-linked hypophosphatemia (XLH) is considered an X-linked dominant disorder. This year we reported (*JBMR*, 2015; 30:138-43) six American children (5 boys, 1 girl) diagnosed with sporadic XLH who carried a mutation (c.*231A>G 3'-UTR) in *PHEX* three base pairs upstream of the putative polyadenylation signal. Therefore, we found this mutation in ~12% of the 52 patients with “sporadic” XLH in our previous report. Further study revealed that four of these boys' mothers harbored the mutation, yet were considered unaffected by their families and we verified their lack of physical findings of XLH (e.g. short stature, bowed lower limbs, scapulocephaly, disproportionately long arms). For this *PHEX* mutation, we established a mild biochemical phenotype that could masquerade as sporadic or X-linked recessive hypophosphatemic rickets (HR).

Subsequently, we documented this *PHEX* mutation in 4-generations of an American kindred with HR spanning 7 generations who we followed for ~30 years. The proband presented at age 2 years with HR in 1985. His maternal grandfather had hypophosphatemic bone disease, but this boy's mother and the mother's three sisters were normal in stature without physical features of XLH. Here, we document the X-linked recessive inheritance pattern of HR in this kindred (including two additional branches), evaluating a total of 9 affected boys for whom we prescribed therapy, and 6

obligate "carrier" women of normal stature and appearance. In addition to the carrier women's normal stature, sequential measurements of fasting serum phosphate, in the five women who were tested, averaged 2.64 and 2.48 (NL: 2.5 – 4.5 mg/dL) at 2 hours and 4 hours, respectively. Four of these six women had TmP/GFR results, which averaged 2.28 and 2.43 (NL: 2.5 - 4.2) at 2 and 4 hours, respectively. Arm spans were commensurate with height in these women. FGF23 levels have not yet been measured, but were normal in a mother and daughter carrying this *PHEX* mutation in our previous report. Hence, this kindred demonstrates an X-linked recessive inheritance pattern resulting from this unique *PHEX* 3'-UTR mutation.

Disclosures: Gary S. Gottesman, None.

SU0383

Modification of hydroxyapatite involves carbonate ion substitution in both patients with XLH and HYP mice. Eva Amenta^{*1}, Helen King², Catherine Skinner³, Steven Tommasini⁴, Carolyn Macica¹. ¹Department of Medical Sciences, Frank H. Netter, M.D., School of Medicine at Quinnipiac University, USA, ²Department of Earth Sciences, Utrecht University, Netherlands, ³Department of Geology & Geophysics, Yale University, USA, ⁴Department of Orthopaedics & Rehabilitation, Yale University School of Medicine, USA

X-linked hypophosphatemia (XLH) is the most common form of the familial phosphate-wasting disorders, arising as a consequence of an inactivating mutation in the phosphate-regulating neutral endopeptidase, X-linked (*PHEX*) gene. While persistent osteomalacia characterizes this disorder, the impact of insufficient phosphate on hydroxyapatite composition, the major inorganic component of bone, is unknown in patients with XLH. We previously showed that the ratio of phosphate to carbonate in cortical bone mineral matrix is increased in HYP mice, a murine model of XLH, compared to wild type mice (Tommasini et al., ASBMR 2014). To determine if this phenomenon is reproduced in human mineralized tissues, tooth dentin was studied as a human proxy for bone. Dentin is deposited by odontoblasts, a cell of neural crest origin that appears in the 17-18th week of gestation and exists throughout the lifespan. We hypothesized that there would be an increase in carbonate ion substitution in permanent teeth as a consequence of the hypophosphatemia associated with the osteomalacia of XLH. We measured and compared the phosphate to carbonate ion ratio in both primary and permanent teeth from patients with XLH to those who are not affected using Raman spectroscopy. The carbonate ion substitution levels were higher in permanent teeth (0.39 ± 0.11 vs. 0.19 ± 0.01 $p = .5E-9$), but not statistically significant between the primary teeth (0.28 ± 0.11 vs. 0.24 ± 0.01 $p = .05$). These preliminary data suggest that, during early development, the fetus has sufficient phosphate mineral available for normal dentin mineralization to occur. However, in permanent tooth dentin deposition during the 2nd through 5th year of life, accelerated carbonate ion substitution occurs due to the phosphate-poor environment. Consistent with our previous data that showed bone mineral carbonate content increased during pregnancy and lactation in both wild type and HYP mice, the substitution of carbonate ions into the hydroxyapatite may be a means of compensating for increased mineral demand and hypophosphatemia. However, although carbonate ion substitution appears to provide adequate mineral for permanent tooth formation, calcium carbonate is more easily resorbable than hydroxyapatite. Thus, the increase in carbonate content may contribute to the clinical sequelae of multiple dental caries and abscesses that XLH patients experience throughout their lifetime.

Disclosures: Eva Amenta, None.

SU0384

Mouse Model with Uncleavable Type I Collagen C-propeptide Processing Site has Extremely Brittle Bones. Aileen Barnes^{*1}, Joseph Perosky², M. Helen Rajpar¹, Kenneth Kozloff², Joan C. Marini¹. ¹NICHD/NIH, USA, ²University of Michigan, USA

Classical osteogenesis imperfecta (OI) is caused by mutations in type I collagen. Mutations in the C-propeptide cleavage site of both *COL1A1* and *COL1A2* cause high bone mass OI, characterized by bone hypermineralization and normal to increased DXA Z-scores. To elucidate the role of type I procollagen C-propeptide processing in bone formation, we generated a mouse with a heterozygous C-propeptide cleavage site defect (high bone mass, HBM) in which both residues of the *COL1A1* cleavage site were mutated to prevent cleavage by BMP1. Procollagen processing by HBM calvarial osteoblasts was severely decreased, with a 75% reduction in fully cleaved trimeric C-propeptide. Western blots of HBM long bone extracts revealed the presence of pC-collagen, in which the C-propeptide is attached to the collagen helix, and an increased amount of cleaved C-propeptide. Dermal collagen fibril diameters were smaller and more homogeneous in HBM than WT, consistent with uncleaved C-propeptide in fibroblast matrix. Fibroblast secretion of collagen into media was reduced 40% in HBM vs WT cells, consistent with HBM osteoblasts depositing half the normal amount of matrix. Multiple osteoblast (*Runx2*, *Alpl*, *Spp1*, *Bglap*) and osteocyte (*Mepe*, *Phex*, *Sost*) markers were decreased in differentiated HBM osteoblasts. In vitro mineralization by HBM osteoblasts was decreased ~20% ($p < 0.001$); direct assays of tissue mineralization are ongoing. Impaired C-propeptide processing affects skeletal size and biomechanics. At 2 months, male HBM mice are

significantly smaller in weight and length and have shorter femurs (92%). Femoral areal BMD in HBM mice is decreased 25% ($p < 0.001$), but vertebral BMD is normal. All 2 month HBM mice have pelvic deformities, and 40% have kyphosis. On μ CT, HBM femora have a thinner cortex with decreased cortical area. Four point bending revealed an extremely brittle phenotype; post-yield displacement is only ~10% of WT (0.03 vs 0.23, $p < 0.001$). HBM femoral stiffness, yield load, and ultimate load are also significantly decreased. At 1 year, male HBM mice remain smaller overall. However, femoral length is normalized and femoral aBMD is improved to 93.5% of WT. Vertebral aBMD remains normal. The HBM mouse phenotype demonstrates that the skeletal elements of *Bmp1/1111* deficiency are reproduced by a substrate defect in type I C-propeptide cleavage. Processing of the type I procollagen C-propeptide influences collagenous, cellular and mineral properties of bone.

Disclosures: Aileen Barnes, None.

SU0385

A Case of Progressive Bony and Soft Tissue Overgrowth. Doriel Pearson¹, Manish Butte², Joy Wu^{*3}. ¹Lucille Packard Children's Hospital, USA, ²Stanford University School of Medicine, USA, ³Stanford University School of Medicine, Us

A 14 year-old female was referred to the metabolic bone disease clinic for bony and soft tissue overgrowth. Her early childhood history has previously been reported (Am J Med Genet Part A 146A:543, 2008) and is briefly summarized here. The patient was born at term following an uneventful pregnancy, with weight, length and head circumference all approximately 50th percentile. At 3 months of age she developed symmetric and progressive overgrowth of supraorbital ridges, followed at 6 months by enlargement of bilateral posterior neck masses, biopsy of which demonstrated normal muscle and fat tissue. By 22 months growth parameters were above 90th percentile. At 33 months she underwent decompression for spinal cord impingement. Excision of excess supraorbital bone revealed normal-appearing bone, but regrowth occurred within 3 months. Motor and cognitive development was normal. Her parents are from Ethiopia, there was no familial consanguinity, and family history was unremarkable. Since age 6 her clinical course has been notable for continued bony overgrowth in the skull and facial bones, complicated by frontal sinusitis and osteomyelitis, as well as marked overgrowth involving the upper cervical spine and 3rd and 4th digits of her hands and feet. Menarche occurred at age 13, and since then her scoliosis has significantly worsened. In addition, since puberty she has developed massive bulbous hypertrophy of areolar tissue. She has not experienced any fractures. She suffered severe respiratory failure following influenza A infection, but has shown no other susceptibility to infections or autoimmunity. Immunological testing of adaptive immune cells and function was normal. Exome sequencing of the patient and her parents did not detect any deleterious mutations in disease genes related to clinical phenotype. Several variants of unknown significance were identified, including a heterozygous c.1348C>T (p.R450W) variant in TNFRSF11A (encodes RANK), a heterozygous c.578G>C (p. R193P) variant in SOST (encodes sclerostin), and a heterozygous c.4589T>C (p.V1530A) variant in FLNA (encodes filamin A); however, the patient's mother is also heterozygous for these variants. In summary, we report on a female of Ethiopian descent with progressive symmetric bony and soft tissue overgrowth involving the skull, facial bones, cervical spine, 3rd and 4th digits with severe scoliosis and areolar hyperplasia, of unknown etiology.

Disclosures: Joy Wu, None.

SU0386

A novel *GNAS* deletion identified among 58 patients affected by the sporadic form of pseudohypoparathyroidism type Ib (PHP1B). Rieko Takatani^{*1}, Angelo Molinaro², Monica Reyes², Lucy Raymond³, Harald Jüppner². ¹Massachusetts General Hospital & Harvard Medical School, USA, ²Endocrine Unit, Massachusetts General Hospital & Harvard Medical School, USA, ³Medical Genetics Department, Addenbrooke's Hospital, United Kingdom

Introduction: Pseudohypoparathyroidism type Ib (PHP1B) is caused by proximal tubular resistance to parathyroid hormone (PTH) that occurs in most cases in the absence of Albright's Hereditary Osteodystrophy (AHO). Patients affected by PHP1B have epigenetic changes that involve one or multiple differentially methylated regions (DMRs) in *GNAS*, the gene encoding Gsx and several splice variants thereof. Maternally inherited microdeletions within *STX16* (encoding syntaxin 16), or within *GNAS* cause familial forms of PHP1B. Most sporadic cases of PHP1B show broad *GNAS* methylation abnormalities, but the underlying molecular mechanism remains unknown.

Objective: To determine whether maternally inherited deletions can cause sporadic PHP1B.

Methods: We investigated 58 sporadic PHP1B cases, who had presented with PTH-resistant hypocalcemia and hyperphosphatemia, some of whom had mild AHO features. The *GNAS* methylation status was evaluated by different methods including Methylation-Specific Multiplex Ligation-dependent Probe Amplification (MS-MLPA), copy number was determined by Multiplex Ligation-dependent Probe Amplification (MLPA); the *GNAS* region was furthermore analyzed with micro-satellite markers.

Results: DNA from all investigated sporadic PHP1B patients (n=58) showed broad *GNAS* methylation changes. Their mothers revealed no evidence for *GNAS* methylation changes and microsatellite analysis for this chromosomal region provided no evidence for discordance thus excluding paternal uniparental isodisomy of large portions of chromosome 20q. Furthermore, none of the 74 siblings of sporadic PHP1B patients were affected, and none of the 19 children of the adult patients were affected. Only one patient showed evidence for an allelic loss within the *GNAS* region as determined by MLPA, which resulted in the discovery of two adjacent novel deletions (37,597 and 1,427bp, respectively) removing exon NESP55 and two noncoding *GNAS* antisense exons. The same deletion was identified in the healthy mother, who therefore showed a complete loss of NESP55 methylation, indicating that she had inherited the deletion from her father.

Conclusion: Our findings confirm that the *GNAS* region comprising antisense exons 3 and 4 is required for establishing all maternal *GNAS* methylation imprints. Some "sporadic" PHP1B cases can be carriers of an inherited *GNAS* microdeletion that had not led to symptomatic disease in other family members, possibly because it was transmitted only through males in earlier generations. The genetic defects leading to PTH-resistance in the other investigated sporadic PHP1B patients remains unknown.

Disclosures: Rieko Takatani, None.

SU0387

Activating Calcium Sensing Receptor Mutations Result in Abnormal Bone Quality Indices Independently of Parathyroid Hormone (PTH) Deficiency.

Diana Ovejero^{*1}, Barbara Misof², Rachel Gafni³, Beth Brillante⁴, Hua Zhou⁵, David Dempster⁶, James Reynolds⁷, Jaime S. Brahimi⁸, Paul Roschger⁹, Klaus Klaushofer², Michael T Collins³. ¹National Institutes of Health, USA, ²Ludwig Boltzmann Institute of Osteology at the Hanusch Hospital of WGKK & AUVA Trauma Centre Meidling, Austria, ³National Institute of Dental & Craniofacial Research, National Institutes of Health, USA, ⁴National Institutes of Dental & Craniofacial Research, National Institutes of Health, USA, ⁵Regional Bone Center, Helen Hayes Hospital, USA, ⁶Columbia University College of P&S, USA, ⁷National Institute of Child Health & Human Development, National Institutes of Health, USA, ⁸University of Maryland Medical Center, USA, ⁹Ludwig Boltzmann Institute of Osteology, Austria

The role of the calcium sensing receptor (CaSR) as a regulator of PTH secretion is well-established, but its function at the bone is less well-defined. Autosomal dominant hypocalcemia (ADH) is a genetic form of primary hypoparathyroidism (HPTH) caused by activating mutations in the *CASR* gene. Thus, ADH bone analysis could offer insight into the CaSR's skeletal function. Iliac crest biopsies from 6 ADH patients (2 male, 4 female, ages 11-48 years, duration of HPTH 11-48 years) and 10 postsurgical (PS) HPTH patients (10 women, ages 25-47 years, duration of HPTH 2-11 years) were evaluated by histomorphometry and backscattered electron microscopy (qBEI). BMD was also measured by DXA at the time of the biopsy. Only patients that had been hypoparathyroid for ≥ 2 years and had never received PTH therapy were included. To normalize for age and gender all values were transformed to Z-scores. The association of length of disease with all outcomes was analyzed through linear regression. T-tests were used to compare groups (mean \pm SEM). Structural parameters (bone volume/trabecular volume, trabecular width, number and separation, and cortical width) were not statistically different. Of dynamic parameters (mineral apposition rate (MAR); mineralized, osteoid and eroded perimeters; bone formation; and adjusted apposition rate), only MAR was significantly different between the ADH vs PS group (2.15 ± 1.07 vs -2.78 ± 0.78 , respectively, $p < 0.01$). Bone mineral density distribution assessed by qBEI revealed that ADH bone had lower calcium content than PS bone: CaMean (mean calcium concentration): -1.6 ± 0.56 vs 0.83 ± 0.4 , $p < 0.01$; CaPeak (the mode calcium concentration): -1.78 ± 0.6 vs 0.68 ± 0.55 , $p = 0.01$; CaLow (% of bone with low mineral content): 3.5 ± 1 vs -0.45 ± 0.15 , $p = 0.01$. Further, mineral distribution was more heterogeneous in ADH bone: CaWidth (variation in mineral density): 3.37 ± 0.7 vs 0.24 ± 0.2 , $p < 0.01$. The % of areas of highly mineralized bone (CaHigh) was not significantly different. Mean BMD was lower at all sites (spine, femoral neck, total hip, forearm) in the ADH vs PS group, but only mean forearm BMD yielded a significant difference (ADH: -0.48 ± 0.3 vs PS: 0.69 ± 0.3 , $p = 0.03$). Length of disease was not associated with any of the observed differences between groups. These results indicate that despite the structural similarities between groups, ADH bone is less mineralized and more heterogeneous than PS bone, suggesting a direct role of bone CaSRs in skeletal mineralization.

Disclosures: Diana Ovejero, None.

SU0388

Biochemical evidence for increased bone formation in patients with osteopetrosis. Christine Simpson^{*1}, Lisa Basso², Anna Maria Cusano¹, Paul Orchard², Karl Inosona¹. ¹Yale University School of Medicine, USA, ²University of Minnesota, USA

Osteopetrosis (OPT) is characterized by defective osteoclast formation or function resulting in high bone mass. In autosomal recessive (AR) OPT, hematopoiesis is

severely impaired and perinatal lethality occurs unless bone marrow transplantation is performed. The most common molecular defects in AR OPT are loss of function mutations in the *TCIRG1* gene, which encodes the α_3 subunit of the vacuolar H^+ -ATPase proton pump. In the autosomal dominant (AD) intermediate forms of OPT, patients can survive into young adulthood but suffer a variety of complications including osteomyelitis and optic nerve compromise due to bony encroachment. Common molecular defects in AD OPT include loss of function mutations in *CLCN7*, which encodes a H^+/Cl^- exchange transporter. Most patients with AR and AD OPT have increased numbers of osteoclasts in bone perhaps representing a compensatory response to the defect in resorption. Recent evidence suggests an important paracrine role for osteoclasts in bone formation and is consistent with the notion that in osteoclast-rich osteopetrosis, an increase in bone formation in vivo further compounds the defect in bone resorption leading to a progressive increase in bone mass. There are very few histomorphometric data available to evaluate this hypothesis and limited data on biochemical markers of bone formation, particularly P1NP. We therefore measured bone turnover markers in 9 patients with AR OPT, 7 of whom had mutations in *TCIRG1*, one patient with a mutation *CLCN7* and one in whom a genotype was not identified. We also measured bone markers in 7 patients with AD OPT, 2 of whom had mutations in *CLCN7*, 2 with mutations in *TCIRG1* and three in whom a genetic mutation was not identified. The table summarizes the findings in these individuals. The exaggerated increase in P1NP with relatively low CTX values is consistent with an "uncoupling" of bone turnover in favor of formation, consistent with the common clinical course of a progressive increase in bone mass over time in OPT. Interdicting anabolic signals from osteoclasts to osteoblasts may ameliorate symptoms in some forms of OPT.

| | Age (M/F) | Normal Range | CTX (pg/mL) | P1NP (ng/mL) | Ocn (ng/mL) | Sclerostin (pmol/L) | BSAP (ng/mL) | PTH (nLEq/mL) |
|--------------|------------------|--------------|-----------------------------------|----------------------------------|-------------|---------------------|---|---------------|
| | | | <1yrs: 146-818 >25yrs: 100-700 | <1yrs: 277-824 >25yrs: 28-128 | 10-46 | 12-48 | <2yrs: 28-221 13-15yrs: 28-211 >25yrs: 7-20 | 10-25 |
| Infantile | 8±3 months (6/5) | MaSEM (N) | 327±100 (8) | 1632±367 (7) | 41±6 (8) | 24±4 (9) | 747±135 (9) | 64±9 (7) |
| Intermediate | 29±3 years (5/2) | MaSEM (N) | 210±128 (7) | 223±73 (7) | 12±3 (7) | 97±26 (7) | 532±112 (7) | 21±3 (7) |

Simpson C

Disclosures: Christine Simpson, None.

SU0389

Case Report: Clinical and genetic analysis in a unique systemic skeletal disorder characterised by high bone turnover and bone expansion.

Huilin Jin¹, Alison Meynert², Martin Williams³, Jon H Tobias⁴, Stuart Ralston¹, Celia Gregson^{*5}. ¹Centre for Genomic & Experimental Medicine, University of Edinburgh, United Kingdom, ²MRC Human Genetics Unit, University of Edinburgh, United Kingdom, ³Department of Radiology, North Bristol NHS Trust, United Kingdom, ⁴Musculoskeletal Research Unit, School of Clinical Sciences, University of Bristol, United Kingdom, ⁵University of Bristol, United Kingdom

Background

Major advances have been made in understanding the molecular basis of rare bone diseases over recent years. Here we describe the results of clinical and genetic analysis of a patient with unique bone dysplasia characterised by high bone turnover, with radiological features of generalised osteosclerosis and bone expansion alternating with areas of osteolysis with features that overlap with but were distinct from those in Paget's disease of bone (PDB).

Case

A 34 year old man presented with generalized weakness, an inability to squat, and lower limb pain on persistent exertion since his mid-teens. He reported limb fractures aged 2, 7, 15 and 21. Sensory neural hearing loss required hearing aids from aged 28. After delayed primary tooth eruption, he experienced normal puberty, skeletal growth and schooling. He has mildly shortened terminal phalanges, quadriceps wasting and BMI 18kg/m². He is the eldest of two sons from a non-consanguineous healthy family. Routine biochemistry was normal except that alkaline phosphatase was raised (134U/L; normal 30-130). Levels of serum β CTX 1.7 μ g/L (0.1-0.5) and P1NP 179 μ g/L (20-76) were both raised. Radiographs showed abnormal bone architecture throughout the skeleton, with areas of osteosclerosis alternating with osteolysis, coarse trabecular markings and cortical thickening. Bone density as assessed by DXA was high at the spine and hip (T-score $>+4.0$). Nerve conduction studies and EMG were normal. Muscle biopsy showed mild non-specific myopathic changes.

Genetic analysis

We performed whole-exome sequencing on the index patient and three unaffected family members on an Ion Proton™ Sequencer using standard techniques. On average, each exome generated 42 million mapped reads and 90% were covered more than 20x. We identified 64 damaging variants that might have been responsible for the disorder but were unable to narrow the list down further to conclusively define the

responsible variant(s). Of note, the exome analysis excluded mutations in known candidate genes for PDB (*TNFRSF11A*, *TNFRSF11B*, *TNFSF11*, *SQSTM1*, *VCP*, *TM7SF4*, *CSF1*, *RIN3*, *OPTN*) and high bone mass syndromes (*TCIRG1*, *CLCN7*, *PLEKHM1*, *OSTM1*, *CA2*, *IKBKG*, *ITGB3*, *LRP5*).

Conclusion

We describe a novel skeletal disorder, presumed to be genetic in origin with features overlapping with, but distinct from, PDB which appears to have a novel molecular basis. Further investigations are in progress to define the cause.

Fig. 1: Pelvis X-ray

Table 1: Exome variant metrics



Figure 1

| Genetic Model | Autosomal recessive | X-linked (male) | De novo* |
|--|---------------------|-----------------|----------|
| Original variants | 2110 | 122 | 895 |
| Missense, nonsense and splicing variants | 194 | 21 | 357 |
| In conserved regions from 46-species alignment | 105 | 8 | 150 |
| Remove variants in segmental duplication regions | 94 | 7 | 137 |
| Remove variants in known databases** with MAF > 0.01 | 68 | 2 | 18 |
| Remove variants in dbSNP138 (excluding clinically associated SNPs) | 66 | 0 | 18 |
| Variants with predicted damaging or deleterious effects*** | 48 | 0 | 16 |

*de novo variants are heterozygous or homozygous alternate in patient, missing or homozygous reference in sibling and parents

**known databases include: 1000Genomes Projects, NHLBI-ESP 6500 exomes and ExAC 65000 exomes

***predicted SIFT score < 0.05 and PolyPhen2 score > 0.9

Table 1

Disclosures: Celia Gregson, None.

SU0390

Characterization of Biological Interaction between Steroid and Palvarotene. Savantani Sinha^{*1}, Kenta Uchibe², Haruna Shimizu², Jiveon Son², Arima Naoko², Maurizio Pacifici², Masahiro Iwamoto². ¹Children's Hospital Of Philadelphia, USA, ²Divison Of Orthopedic Surgery, USA

Heterotopic Ossification (HO) is a multifaceted pathological condition that leads to the formation of excess endochondral bone at extraskelatal sites. Fibrodysplasia Ossificans Progressiva (FOP) is a severe form of HO caused by mutations in *ALK2* and is characterized by intermittent flare-ups. Prednisone is thus used as a standard-of-care anti-inflammatory agent for FOP patients since there is no effective treatment to prevent HO itself. Previous studies from our group showed that the retinoic acid receptor gamma agonist Palovarotene inhibited HO in injury and genetic mouse models. Though promising, those studies did not determine whether a combination therapy involving Palovarotene plus prednisone may be more effective or whether the two drugs would actually negatively impact each other. To this end, we used our

standard HO model in which rhBMP-2 mixed in Matrigel is implanted subcutaneously in 8 weeks old CD-1 female mice, eliciting HO in about 2 weeks. Freshly implanted mice were treated by gavage with pre-established doses of Palovarotene, prednisone or combination at different times/regimens. For comparison, companion mice received vehicle. Micro-CT scans showed that prednisone and dexamethasone given singly reduced HO, but co-treatment with Palovarotene was more effective. Early treatment appeared to be important for effectiveness of steroid action. To exclude non-specific systemic drug effects, mice were subjected to body weight measurements and blood analyses showed no obvious detrimental effects. To uncover mechanisms of drug action, we analyzed signaling pathways in mesenchymal progenitor cells in vitro. Cells were reverse-transfected with various reporter plasmids and quantified for activity with or without drug treatment. Treatment with dexamethasone increased glucocorticoid-response elements/GRE-Luc activity within 24hrs, while co-treatment with dexamethasone and palovarotene did not further increase or decrease GRE-Luc activity. Similar results were obtained with a retinoic acid receptor reporter plasmid (RARE) in response to palovarotene or in combination. Interestingly, co-treatment did result in appreciable decreases in NFkB activity. In sum, our data indicate that there is no major negative interactions of palovarotene and steroids against HO and a combination therapy may in fact offer alternative regimens, possibly making the therapy as effective and safe as possible for FOP patients.

Disclosures: Savantani Sinha, None.

SU0391

Dysregulated TGF-β signaling and oxidative DNA damage as the cause for osteoporosis in the progeroid disorder geroderma osteodysplastica. Magdalena Steiner^{*1}, Hardy Chan², Thorsten Schinke³, Michael Amling³, Danny Chan⁴, Stefan Mundlos², Uwe Kornak⁵. ¹Charité, Germany, ²Charité Universitätsmedizin, Germany, ³Universitätsklinikum Hamburg Eppendorf, Germany, ⁴The University of Hong Kong, China, ⁵Charité Universitätsmedizin, Germany

Geroderma Osteodysplastica (GO) is a premature ageing disorder characterized by wrinkled, lax skin and infantile osteoporosis. It is caused by loss-of-function mutations in *GORAB*, encoding a golgin with poorly understood function. A conditional Gorab mouse model was created and crossed with *Px1cre* to inactivate Gorab starting in the limb mesenchyme. The *Gorab^{Px1cre}* mutants showed mild growth retardation, a reduction of trabecular and cortical bone volume, mineralization defects, and spontaneous long bone fractures. Further analysis revealed a significant increase in osteoblast and osteocyte numbers with a delay in terminal osteoblast differentiation. *Gorab^{Px1cre}* mutant bone cells and GORAB-deficient fibroblasts exhibited increased levels of reactive oxygen species (ROS) leading to an accumulation of DNA damage and subsequently to cellular senescence. In mutant cells as well as bone tissue upregulated TGF-β signaling and expression of the ROS-producing enzyme Nox4 were evident. Enhanced TGF-β levels in Gorab-deficient tissues were correlated with a striking decrease in decorin glycosylation known to regulate the bioavailability of TGF-β. Finally, treatment with the antioxidant N-acetyl cysteine (NAC) not only rescued the accumulation of DNA damage in Gorab-deficient cells, but also improved the trabecular bone volume as well as the organization of collagen fibers in the cortical bone of *Gorab^{Px1cre}* mice. Taken together, our results demonstrate that oxidative DNA damage and cellular senescence secondary to elevated TGF-β signaling caused by abnormal glycosylation of extracellular matrix components plays a pivotal role for the pathomechanism of GO.

Disclosures: Magdalena Steiner, Österreichische Akademie der Wissenschaften

SU0392

Improvement in Giant Cell Tumor of the Jaw treated with Denosumab. Jessica Abramowitz^{*1}, Stuart Weinerman², Salvatore Ruggiero³. ¹Hofstra North Shore LIJ, US, ²Hofstra North Shore LIJ, USA, ³Long Island Jewish Medical Center, USA

Introduction: Giant cell tumors of the bone are known to express RANK ligand which contributes to the osteoclastic nature of these lesions. Traditional treatment for giant cell tumors of the jaw are: surgical, intralesional steroid injections, subcutaneous calcitonin, and alpha interferon. Denosumab a monoclonal antibody against RANK ligand, inhibits osteoclast formation and thereby decreases bone resorption. Denosumab has been studied and used successfully in treating giant cell tumors of bones of the extremities. We report the use of denosumab in a patient with giant cell tumor of the jaw.

Case presentation: An 18 year old female with Noonan's syndrome was referred to our clinic for management of benign giant cell tumor of the jaw. Giant cell tumors of the jaw were initially noted 12 years prior and confirmed on multiple biopsies. 9 years after initial diagnosis she was treated with subcutaneous calcitonin injections for an expansile jaw lesion. The lesion initially responded to calcitonin but then re-growth occurred. Initial laboratory testing included a bone specific alkaline phosphatase of 13 mcg/L, urine N telopeptides of 71 nmol BCE/mmol creatinine. Treatment was initiated with denosumab 60mg/mL. 4 months after the initial dose her urine N telopeptides decreased to 9 nmol BCE/mmol creatinine, bone specific

alkaline phosphatase decreased to 7.7 mcg/L. 7 months after the initial dose of denosumab bone specific alkaline phosphatase increased to 9.4 mcg/L, urine N telopeptides increased to 46 nmol BCE/mmol creatinine. A second dose of denosumab 60mg/mL was given at that time. 3 months following the second dose of denosumab bone specific alkaline phosphatase decreased to 6.1 mcg/L and urine N telopeptides decreased to 12 nmol BCE/mmol creatinine. Panoramic jaw x-rays performed 6 months after the initial denosumab showed some resolution of the jaw lesion and repeat x-ray 1 year after treatment showed complete resolution of the giant cell tumor.

Conclusions: We report clinical and radiologic improvement in a patient with giant cell tumor of the jaw following treatment with denosumab. Denosumab is a targeted therapy for treatment of giant cell tumor of the bone. It is a potential agent for use in patients with giant cell tumor of the jaw given the over expression of RANK ligand in giant cells. Evidence of response in this patient includes a decrease in bone turnover markers and resolution of the lesion on imaging following treatment.

Disclosures: Jessica Abramowitz, None.

SU0393

New protocol to optimize iPS cells for genome analysis of fibrodysplasia ossificans progressiva. Yoshihisa Matsumoto^{*1}, Makoto Ikeya², Makoto Fukuta¹, Takanobu Otsuka¹, Junya Toguchida². ¹Nagoya city university, Japan, ²Center for iPS Cell Research & Application, Kyoto University, Japan

Fibrodysplasia Ossificans Progressiva (FOP) is a rare genetic disease characterized by progressive ectopic ossifications, which are often initiated after physiological stimuli. The responsible gene for FOP is the ACVR1 gene, which is one of type I receptors for BMP. The replacement of one amino acid in ACVR1 seems to activate downstream genes regulating bone formation, although the precise mechanisms are still to be investigated. Application of patient-derived iPS cells will be useful for the research of this disease, because harvesting target tissues from patients is strictly prohibited because tissue damage accelerates the ectopic ossification. Recently we have reported that iPSCs derived from FOP patients showed enhanced osteogenic and chondrogenic differentiation properties. Here we addressed this issue by a new approach using the differentiation system through the neural-crest cell lineage. Multi-potent neural crest cells (NCCs) were efficiently induced from iPSCs, from which multipotential mesenchymal stromal cell (MSC)-like cell (iMSCs) population can be obtained. Therefore we are able to analyse the signal pathway at each of iPSC, NCC, iMSC, and terminally differentiated stage. In addition, to minimize the effect of genetic background other than ACVR1 mutation, we established genetically rescued cell lines from parental FOP-iPSCs by the homologous recombination. FOP-iMSCs possessing enhanced chondrogenic ability were transcriptionally distinguishable from reFOP-iMSCs and activated the SMAD1/5/8 and SMAD2/3 pathways at steady state. Using this method, we identified responsible genes for accelerating the chondrogenesis of FOP-iMSCs. This indicates that iMSCs through NCC lineage are useful for investigating the molecular mechanism of FOP and corresponding drug discovery.

Disclosures: Yoshihisa Matsumoto, None.

SU0394

Non-osteoporotic post-menopausal women do not have elevated concentrations of autoantibodies against osteoprotegerin. Isabelle Picc^{*1}, Christopher Washbourne², Jonathan Tang², Julie Greeves³, Sarah Jackson³, Stuart Ralston⁴, Philip Riches⁵, Helen MacDonald⁶, William D Fraser⁷.

¹BioAnalytical Facility, University of East Anglia, United Kingdom, ²University of East Anglia-Bioanalytical Facility, United Kingdom, ³HQ Army Recruiting & Training Division, United Kingdom, ⁴University of Edinburgh, United Kingdom, ⁵Rheumatic Disease Unit, Institute of Genetics & Molecular Medicine, United Kingdom, ⁶University of Aberdeen, United Kingdom, ⁷University of East Anglia- Bioanalytical facility, United Kingdom

Introduction: Osteoprotegerin (OPG) plays a protective role in bone remodelling as it provides a "decoy" site for RANKL, modifying the stimulation of osteoclasts. Autoantibodies to OPG allow a sustained reaction between RANKL and RANK which in turn will increase bone resorption. Autoantibodies against OPG (α -OPGAb), first isolated in patients with autoimmune conditions associated with high bone turnover, have been shown to be present in 14% of an apparently healthy young adult population. Bone resorption is increased in the elderly, particularly in women who may demonstrate increased α -OPGAb.

Objective: To define a reference range for OPG autoantibodies in non-osteoporotic post-menopausal women.

Method: Using a previously developed sandwich ELISA assay we were able to detect α -OPGAb in serum samples taken from non-osteoporotic post-menopausal women (ANSAVID study - 60-65yrs). Briefly, α -OPGAb are captured by the use of an immobilized full-length human recombinant OPG and detected by the sequential addition of a biotinylated antibody and a horseradish-peroxydase-labelled streptavidin. The concentration of human α -OPGAb in the samples is determined directly from a 4PL-fit standard curve.

Results : We established that the population of normal post-menopausal women who do not have osteoporosis also do not have elevated concentrations of α -OPGAb when compared to a younger female population (17-32yrs). The reference ranges obtained were 134-190ng/mL and 131-184ng/mL for control and post-menopausal women, respectively. This suggests that α -OPGAb is not positively associated with increasing age suggesting that the increased production of α -OPGAb is mainly related to pathologic conditions which can result in significant bone resorption.

Conclusion: Comparison of osteoporotic patient samples to non-osteoporotic post-menopausal women would be interesting to determine whether α -OPGAb can be used to detect patients at high risk of bone resorption and identify appropriate treatment for this particular subgroup of patients.

Disclosures: Isabelle Picc, None.

SU0395

Pathophysiology of Melorheostosis: A Theoretical Framework. Smita Jha^{*1}, Nicholas Laucis², Timothy Bhattacharyya². ¹National Institutes of Health, USA, ²NIH, USA

Melorheostosis is a rare sclerosing bone disease with a prevalence of "one in a million." We report on five subjects with melorheostosis seen at National Institutes of Health, Maryland. All subjects were adult females. Subjects reported an average Patient Reported Outcome Measurement Information System (PROMIS) score of: pain - 60; physical function - 40; depression - 50 (norm: 50 ± 2 SD; 1 SD = 10) All subjects described the pain as neuropathic. No subject had other relatives affected with the disease. One subject showed evidence of bilateral disease. Three subjects had the disease affecting lower extremity while the remaining two had melorheostosis in the upper extremity. Physical exam revealed limb thickening in all subjects. No skin lesions associated with melorheostosis was noted in any subject. The distribution of the disease was limited to long bones affecting the appendicular skeleton. All subjects had normal serum calcium, phosphorus, magnesium, Vitamin D 25-hydroxy, 24 hour calcium excretion and tubular reabsorption of phosphorus. Imaging studies showed the classing "candle-wax" appearance described by Leri and Joanny. MRI showed evidence of soft tissue extension in three subjects. Lesion in all subjects was noted to be metabolically active on a ¹⁸FNa bone scan. All subjects showed progressive disease on comparison with prior images. None of these subjects described any successful intervention thus far.

It has been proposed that the distribution of the disease can be explained by sclerotomes. Sclerotomes are zones of skeleton supplied by an individual spinal sensory nerve. The existence of sclerotome remains controversial. We propose that the disease distribution can be better explained by clonal expansion of a somatic mutation in the limb bud. The somatic mutation hypothesis is supported by equal gender preponderance, sporadic occurrence and asymmetrical distribution. We suspect this is likely a disease of the osteoblast given its origin from the mesenchymal stem cell which can better explain the disease distribution. In the future, we plan to study the affected bone tissue with whole exome sequencing to identify the genetic cause of the disease. A better understanding of melorheostosis will help enhance our knowledge of bone biology and develop therapeutic agents not only for melorheostosis but for other common bone diseases.

Disclosures: Smita Jha, None.

SU0396

Distribution of body composition parameters and sarcopenia in Finnish female population – comparison of two geographically comparable cohorts. Samu Sjöblom^{*}, Juha Suuronen, Toni Rikkinen, Risto Honkanen, Heikki Kröger, Joonas Sirola. University of Eastern Finland, Finland

Purpose: The aim of the study was to examine the differences of body composition and muscle strength between young and elderly women and also changes during aging. **METHODS:** The present study was based on 1) Young reference population (YRP), 400 healthy women aged 20 to 40 years (mean 30.4, SD 6.0) and 2) Postmenopausal women from the population-based OSTPRE study (N=397), aged 63 to 75 years (mean 68.6 years, SD 2.9) in 15-year follow-up point. The same subjects were remeasured 5 years later, (aged 68 to 80 years mean 73.6, SD 2.7) at 20-year follow-up visit. Both samples underwent weight, height, grip strength (GS), quadriceps strength (QS) and total body DXA (TB-DXA) measurements including RSMI i.e relative skeletal muscle index (The appendicular lean mass divided by the square of their height) and fat percent (FP). Based on the distributions (SD) of the indices in the YRP, the distributions of GS, QS, FP and RSMI were determined in the OSTPRE sample. Both study populations were divided into three groups (A < -2SD, -2SD-1SD C > -1SD) based on the distribution of the measures in the YRP. Results In the YRP sample, the mean (SD) values were: RSMI 6.7 (0.8) kg/m², GS 37.6 (5.6) kPa, QS 49.8 (10.0) kg, FP 29.6 (7.1), while at the OSTPRE 15-year follow-up point sample these were: RSMI 6.7 (0.8), GS 26.3 (6.3), QS 30.5 (7.8), FP 40.4, respectively. At the 20-year follow-up point sample these were: RSMI 6.6 (0.9) kg/m², GS 27.6 (5.6) kPa, QS not measured, FP 39.7 (6.5). The cut-off points, based on the YRP data (A: -2sd and B: -1sd) were for RSMI; A: 5.1 and B: 5.9 kg/m², for GS; A: 26.4 kPa and B: 32 kPa, for QS; A: 29.8 kg and B: 39.8, for FP; A: 15.4 and B: 22.5. **CONCLUSIONS:** Among postmenopausal women, muscle strength i.e grip strength and quadriceps strength are mostly deteriorated. The decreasing of RSMI during aging is quite minimal. The study will provide new cut-off points for diagnostics of sarcopenia in

Western European women. Acknowledgements The study was supported by Kuopio University Hospital EVO-grants and Ministry of Education and Culture and Finnish Cultural Foundation.

Disclosures: *Samu Sjöblom, None.*

SU0397

Effects of life-style factors on body composition in healthy Finnish women aged 20-40 years. *Juha Suuronen*¹, *Samu Sjöblom*², *Marjo Tuppurainen*³, *Risto Honkanen*², *Toni Rikkinen*², *Heikki Kröger*⁴, *Joonas Sirola*⁴.

¹University of Eastern-Finland, Kuopio Musculoskeletal Research Unit (KMRU), Finland, ²Kuopio Musculoskeletal Research Unit (KMRU), Finland, ³Kuopio Musculoskeletal Research Unit (KMRU) & Departments of Obstetrics & Gynaecology, Kuopio, Finland, Finland, ⁴Kuopio Musculoskeletal Research Unit (KMRU) & Surgery/Orthopaedics, University of Eastern Finland, Kuopio, Finland, Finland

Purpose:

The aim of the study was to investigate the effects of life-style factors on body composition and muscle strength in healthy female population.

Methods:

400 Finnish women (aged 20-40) were measured with DXA, hand-held dynamometer and knee extension bench between 2011-2014. Inclusion criteria for the study were: no chronic diseases or permanent medication. Life-style factors were assessed with inquiries parallel with the measurements and included: alcohol consumption, pregnancies, hormonal contraception, smoking, self-rated health and physical activity. Body composition variables (lean and fat mass) were measured with DXA. Effects of life-style factors on body composition and muscle strength were investigated with AN(C)OVA.

Results:

Women aged 35-40 had higher appendicular skeletal muscle mass (ASM), BMI, relative skeletal muscle index (RSMI), fat-%, grip (GS) and quadriceps strength (QS) and total lean mass (TLM) compared to women aged 20-25 (p<0.001). They also had lower skeletal muscle index (SMI) (p<0.01). Significance prevailed after adjustment for multiple variables (p<0.01). Women using oral contraception (progesterone + ethinyl estradiol) had lower GS (p<0.001), ASM, RSMI and TLM (p<0.01) compared to the women without hormonal contraception. After adjustment ASM, SMI and GS remained lower (p<0.05) as well as RSMI and TLM (p<0.01). Women who exercised 4 ≤ times/week had significantly higher ASM, RSMI, SMI and TLM (p<0.001) and lower fat-% (p<0.001) compared to women exercising once a week or less. In addition women exercising 4-6 times/week had higher GS (p<0.01) and QS (p<0.001) while in women who exercised daily QS was higher (p<0.01) but GS was not significantly different in comparison. After adjustment, women exercising 4 ≤ times/week had higher ASM, RSMI, SMI, QS and TLM as well as lower fat-% (p<0.001) while women exercising 4-6 times/week had higher GS (p<0.01) after adjustment. There were no significant difference in BMI according to amount of exercise/week. Those who self-rated their health as "very good" had lower BMI and fat-% and higher SMI (p<0.001) and TLM (p<0.05) compared to women with moderate health. After adjustment BMI (p<0.01) and fat-% was lower and SMI higher (p<0.001).

Conclusions:

Muscle and fat mass increases between 20-40 years. Hormonal oral contraception has negative effect on muscle mass. Higher self-rated health has connection to lower fat-% and BMI. Exercise increases muscle mass and strength and lowers fat mass.

Disclosures: *Juha Suuronen, None.*

SU0398

Forearm Bone Density is Not Related to Lean Body Mass in Postmenarcheal Girls Who Habitually Consume Less Than 2 Servings of Dairy per Day: Preliminary Results of the FAMILY Study. *May Slim*^{*1}, *Catherine Vanstone*¹, *Suzanne Morin*¹, *Elham Rahme*², *Hope Weiler*¹. ¹McGill University, Canada, ²McGill University Health Center, Canada

Humans achieve peak skeletal muscle mass and bone density in young adulthood. Data on how measures of bone health relate to lean body mass (LMI) in adolescent girls are lacking. Dietary Reference Intakes for calcium range from 1100 to 1300 mg/d for adolescent girls. In Canada, more than 50% of females 14 to 18 y of age do not meet these targets with usual intakes of 917 (SE 21) mg/d and < 2 dairy servings/d. Our objective was to examine the relationship between lean tissue and bone health indicators at multiple skeletal sites in postmenarcheal (PM) girls participating in the Family Milk product 2-Year (FAMILY) dose response study to enhance bone health in youth. We present a preliminary cross sectional analysis of baseline data on healthy white girls 14 to 18 y (n=16) recruited from Montreal (Canada). We measured weight and height to calculate body mass index (BMI, kg/m²) and WHO z-scores. Bone area (BA, cm²), bone mineral content (BMC, g) and bone mineral density (BMD, g/cm²) of the whole body (WB), non-dominant forearm (FA), femoral neck (FN), total hip (TH) and lumbar spine (LS) as well as LBM (kg) and lean mass index (LMI, kg/m²) were measured using DXA (Hologic Discovery, Apex software version 13.5). The LMS method was used to compute LMI Z scores (LMIZ) based on NHANES reference data (2008) which were stratified into tertiles. Differences in LMIZ tertiles

were tested using mixed model ANOVA adjusting for covariates. The participants, aged 15.5 ± 1.6 y, showed healthy mean BMI z-scores of 0.35 ± 0.94. LBM positively correlated to all bone parameters at all sites except TH area (table 1). Participants in LMIZ Tertile 1 had significantly lower BMC and BMD at LS, FN, TH, WB and lower BA at WB only compared to tertile 2 and 3, whereas tertile 2 and 3 were comparable (table 2). Interestingly, there were no differences among tertiles in any of the FA parameters, which could be attributed to the fact that FA is a non-weight-bearing site and the non-dominant side was assessed. Age at menarche was greater in tertile 1 compared to tertile 2 and 3 (table 2) suggesting that late maturing girls display lower muscle mass, as surrogated by LMIZ, in association with lower BMD. Lean tissue relative to height had a significant beneficial relationship to BMD in PM girls especially at weight-bearing sites. Further research using computed tomography would be of interest to examine the relationship of lean mass to cortical and trabecular bone, particularly at the FA site.

Table 1: Correlation between Bone Measurements at WB, FN, TH, LS and FA and Whole Lean Body Mass, Lean Mass Index, Appendicular Lean Mass Index, and Height

| | WB Lean mass (kg) | LMI (kg/m ²) | Appendicular LMI (kg/m ²) | Height (cm) |
|---------------------|-------------------|--------------------------|---------------------------------------|-------------|
| Whole body | | | | |
| BA | 0.91* | 0.53* | 0.41 | 0.85* |
| BMC | 0.86* | 0.61* | 0.55* | 0.71* |
| BMD | 0.65* | 0.63* | 0.64* | 0.42 |
| BMD Z-score | 0.64* | 0.66* | 0.70* | 0.38 |
| Femoral Neck | | | | |
| BA | 0.63* | 0.16 | 0.08 | 0.78* |
| BMC | 0.85* | 0.49 | 0.46 | 0.80* |
| BMD | 0.78* | 0.63* | 0.64* | 0.58* |
| BMD Z-score | 0.78* | 0.66* | 0.67* | 0.56* |
| Total Hip | | | | |
| BA | 0.45 | -0.001 | -0.06 | 0.67* |
| BMC | 0.86* | 0.55* | 0.51* | 0.76* |
| BMD | 0.84* | 0.69* | 0.68* | 0.62* |
| BMD Z-score | 0.84* | 0.70* | 0.69* | 0.60* |
| Lumbar Spine | | | | |
| BA | 0.65* | 0.27 | 0.25 | 0.72* |
| BMC | 0.75* | 0.45 | 0.40 | 0.68* |
| BMD | 0.73* | 0.58* | 0.50* | 0.56* |
| BMD Z-score | 0.69* | 0.59* | 0.54* | 0.49* |
| Forearm | | | | |
| BA | 0.69* | 0.24 | 0.28 | 0.75* |
| BMC | 0.82* | 0.50* | 0.49 | 0.71* |
| BMD | 0.70* | 0.38 | 0.30 | 0.66* |

* P < 0.05

Table 2: Baseline Characteristics According to Lean Mass Index Z-score Tertiles

| Characteristics | Tertile 1 (n=5) | Tertile 2 (n=5) | Tertile 3 (n=6) |
|----------------------------|----------------------|----------------------|-----------------------|
| Age (y) | 15.4 ± 1.5 | 16.0 ± 1.9 | 15.3 ± 1.6 |
| Age at menarche (y) | 13.2 ± 0.8 | 12.2 ± 1.1 | 12.5 ± 1.9 |
| Years since menarche (y) | 2.3 ± 1.8 | 3.8 ± 1.3 | 2.8 ± 1.1 |
| Weight (kg) | 49.7 ± 5.9 | 69.6 ± 9.7 | 64.4 ± 11.4 |
| Height (cm) | 162.7 ± 7.9 | 171.8 ± 5.2 | 165.9 ± 10.8 |
| Height Z score | 0.06 ± 1.26 | 1.42 ± 0.75 | 0.46 ± 1.39 |
| BMI (kg/m ²) | 18.7 ± 1.5 | 23.5 ± 2.1 | 23.3 ± 2.0 |
| BMI Z-score | -0.73 ± 0.58 | 0.83 ± 0.60 | 0.87 ± 0.63 |
| Fat mass (%) | 22.5 ± 5.2 | 31.3 ± 6.3 | 25.1 ± 3.5 |
| Lean body mass (kg) | 36.4 ± 5.5 | 44.8 ± 2.4 | 45.9 ± 5.9 |
| Lean mass index Z score | 0.03 ± 0.34 | 0.74 ± 0.09 | 1.32 ± 0.27 |
| Calcium intake (mg/day) | 686.2 (515.9, 864.3) | 522.8 (367.8, 709.8) | 814.0 (279.7, 1533.6) |
| Vitamin D intake (IU/day) | 73.1 (56.9, 86.3) | 29.5 (20.9, 125.9) | 171.8 (40.2, 320.3) |
| Physical Activity (h/week) | 9.5 (4.9, 12.0) | 10.6 (6.5, 16.8) | 6.3 (5.2, 7.4) |

Values are mean ± SD except for calcium and vitamin D intake and physical activity in median and interquartile

Tables-ASBMR 2015

Disclosures: *May Slim, None.*

This study received funding from: Supported by a contribution from the Dairy Research Cluster Initiative (Dairy Farmers of Canada, Agriculture and Agri-Food Canada, the Canadian Dairy Network and the Canadian Dairy Commission

SU0399

High Prevalence of Muscle-Skeletal Abnormalities in Patients with Chronic Obstructive Pulmonary Disease. *Tatiana Costa*¹, *Fabio Costa*², *Carolina Moreira*¹, *Thaís Jonasson*¹, *Leda Rabelo*², *César Boguszewski*¹, *Victoria Borba*^{*1}. ¹Serviço de Endocrinologia do Hospital de Clínicas da UFPR (SEMPR), Brazil, ²Serviço de Pneumologia da UFPR, Brazil

Introduction: Loss of fat free mass (sarcopenia), is associated with reduced exercise capacity and poor quality of life in patients with COPD. Besides, in conjunction with the bone loss, contributes to the bone fragility and increased fractures prevalence.

Purpose: To evaluate the relationship between the severity and prognosis of COPD with the prevalence of morphometric vertebral fractures (MVF), bone mineral density (BMD) and body composition data compared with two control groups.

Methods: A group of COPD patients (DG) and two control groups, smokers without COPD (SG) and a healthy group (HG) underwent a body composition, VFA (Vertebral Fracture Assessment) and BMD evaluation by DXA. DG patients were classified by BODE prognosis index (B-body mass index, O-airway obstruction, D-dyspnea and E-exercise capacity); the clinical stage GOLD and the degree of obstruction (FEV1). The diagnosis criterion of densitometric sarcopenia (DS) was based, for the low weight patients on Baumgartner method, and all the others were adjusted for fat mass based on Newman reference. The groups consisted of 91 patients (50 females), 67.4 ± 8.7 years old in DG; 72 patients (38 females) 63.7 ± 9.80 years in

SG and 86 patients (47 females) 69.5±7.15 years in HG (p=0.11). DG showed a reduction in lumbar spine (LS), total femur (TF) and femoral neck (FN) BMD that was associated to an increase in the disease severity and prognosis, p<0.05. A correlation between lower lean mass and lower BMD was found in all bone sites p<0.001 (LS r=0.339, TF r=0.465 and FN r=0.459) in DG. The DG mean BMD was low in all sites compared to SG (p=0.007) and the HG (p=0.003). DS was present in 40.6% of DG, 29.7% of SG and 26.9% of HG. In DG, the quartiles of best prognosis were different from those of worst prognosis (p=0.009) and, the multivariate analysis showed that regardless of age, gender and clinical stage, the BODE index was associated with DS, OR = 3,12 (95% CI 1,04 - 9,38). MVF were seen in 62,6% of the DG patients and was associated with the FN BMD (p=0,022).

Conclusions: Patients with COPD had higher prevalence of DS and low BMD compared to controls groups, the low BMD was correlated with lower fat free-mass, disease severity and prognosis. The DS was associated with BODE that may suffer great influence of lean mass, since it is considered a parameter of physical capacity. MVF was also highly prevalent.

Disclosures: Victoria Borba, None.

SU0400

Perceptions of Elderly Women with Osteoporosis and Back Pain by Using a Spinal Orthosis. Helena Salminen*¹, Nathalie Frisendahl², Ann-Charlotte Grahn Kronhed³, Christina Kaijser Alin¹. ¹Karolinska Institutet, Sweden, ²Umea university, Sweden, ³Linköping University, Sweden

Purpose: The aim of this study was to explore the perceptions of elderly women with osteoporosis and back pain, with or without vertebral fractures, by using a spinal orthosis. Methods: A qualitative study with five focus group interviews using a semi-structured interview guide, with a total of 18 women (mean age 78 years) who had all used the Spinomed spinal orthosis during six months in a RCT. The interviews were analyzed using qualitative content analysis with an inductive approach. Results: One overall theme was found: The spinal orthosis could be perceived as an integrated part of everyday life, if it met the needs of the individual woman. The four main categories found under this theme were: 1) The meaning of the spinal orthosis; the orthosis being an integrated part of the woman and giving support 2) The perceived physical changes in posture, decreased pain and increased mobility and increased muscle strength 3) Possibilities in everyday life with increased autonomy and facilitating daily activities 4) The importance of the individual shaping of the spinal orthosis, to be easy to use and not to attract too much attention. Conclusions: The spinal orthosis showed perceived positive effects on the participants' everyday life by supporting the woman's autonomy. It was perceived to facilitate performing daily activities and to relieve back pain, to increase mobility and positively affect the woman's posture. Because the orthosis was perceived as an integrated part of the woman, it was of utmost importance for the orthosis to fit well.

Disclosures: Helena Salminen, None.

SU0401

Sarcopenia – prevalence, incidence, and association with osteoporosis: A four-year follow-up of the ROAD study. Noriko Yoshimura*¹, Shigeyuki Muraki², Hirovuki Oka³, Sakae Tanaka⁴, Hiroshi Kawaguchi⁵, Kozo Nakamura⁶, Toru Akune⁶. ¹22nd Century Medical & Research Center, The University of Tokyo, Japan, ²Department of Clinical Motor System Medicine, 22nd Century Medical & Research Center, The University of Tokyo, Japan, ³Department of Medical Research & Management for Musculoskeletal Pain, 22nd Century Medical & Research Center, The University of Tokyo, Japan, ⁴Department of Orthopaedic Surgery, Sensory & Motor System Medicine, Graduate School of Medicine, The University of Tokyo, Japan, ⁵JCHO Tokyo Shinjuku Medical Center, Japan, ⁶National Rehabilitation Center for Persons with Disabilities, Japan

The present 4-year follow-up study was performed to clarify the prevalence of sarcopenia (SP), coexistence of SP and osteoporosis (OP), and contribution of SP to the occurrence of OP in the general population. The second survey of the Research on Osteoarthritis/Osteoporosis Against Disability (ROAD) study—a large-scale population-based cohort study—was conducted between 2008 and 2010. We enrolled 1,099 participants (aged >=60 years, 377 men, 722 women) from the second survey of the ROAD study who had completed assessments of handgrip strength, gait speed, skeletal muscle mass measured by bioimpedance analysis, and bone mineral density measured by dual X-ray absorptiometry (DXA). The third survey was conducted between 2012 and 2013; 767 of the 1,099 individuals who were enrolled from the second survey (69.8%, 253 men, 514 women) had completed assessments identical to those in the second survey. SP was defined as per the algorithm of the Asian Working Group for Sarcopenia, whereas OP was defined based on the World Health Organization criteria. The prevalence of SP in the second survey was found to be 8.2% (men, 8.5%; women, 8.0%). The co-existing rate of SP and OP at the lumbar spine L2-L4 and/or the femoral neck was 57.8%. The cumulative incidence of SP during the 4-year period between the second and third visits was 2.0%/yr (men, 2.2%/yr; women, 1.9%/yr). There were no gender differences in the prevalence or incidence of SP. After adjustment for age (yrs), gender (0:men, 1:women), regional differences (0:mountainous area, 1:coastal area), and emaciation (0:body mass index (BMI) >=18.5 kg/m2,

1:BMI <18.5 kg/m2), a logistic regression analysis using the occurrence of SP as the objective variable and the presence of OP as the explanatory variable indicated that the presence of OP was significantly associated with the occurrence of SP in the near future (odds ratio, 2.86; 95% confidence interval, 1.41-5.79; p = 0.003). This prospective study suggests that the presence of OP might predict the incidence of SP in the near future. The treatment of the OP might reduce the risk not only of osteoporotic fracture but also that of SP.

Disclosures: Noriko Yoshimura, None.

This study received funding from: Japan Osteoporosis Society, Japan Osteoporosis Foundation, and Japanese Orthopaedic Association

SU0402

SARCOPENIA IN UKRAINIAN WOMEN: ASSESSMENT AND DETERMINATION OF LEAN BODY MASS DEFICIENCY. Vladyslav Povorozyuk*¹, Dzerovych Nataliia², Povorozyuk Roksolana². ¹Institute of Gerontology AMS Ukraine, Ukraine, ²D.F. Chebotarev Institute of gerontology NAMS Ukraine, Ukraine

The aim of this study was to evaluate the normative data of lean mass in the healthy Ukrainian women.

Materials and methods. 301 women aged 20-87 years (mean age – 57.6±0.9 yrs; mean height – 1.62±0.004 m; mean weight – 63.5±0.5 kg, body mass index – 24.2±0.2 kg/m2) were examined. No subject had any systemic disorders (endocrine, renal, hepatic et al.) or took medications known to affect the skeletal and muscle metabolism. The women were divided into the following age-dependent groups: 20-29 yrs (n=25), 30-39 yrs (n=27), 40-49 yrs (n=22), 50-59 yrs (n=62), 60-69 yrs (n=91), 70-79 yrs (n=59), 80-87 yrs (n=15). The lean and fat masses, bone mineral density (BMD) were measured by the DXA method (Prodigy, GEHC Lunar, Madison, WI, USA). Appendicular skeletal mass (ASM) was measured at all the four limbs with DXA. We've also calculated the appendicular skeletal mass index (ASMI) according to the formula: ASM/height (kg/m2). Low muscle mass values conform to the following definitions: European guidelines (ASMI <5.5 kg/m2) [Cruz-Jentoft A.J. et al., 2010], less than 20% of sex-specific normal population and two SD below the mean of the young adult Ukrainian females (20-39 yrs).

Results. We observed a significant decrease of ASM with age (20-29 yrs – 16.5±0.4 kg, 30-39 yrs – 16.4±0.3 kg, 40-49 yrs – 17.0±0.5 kg, 50-59 yrs – 16.9±0.3 kg; 60-69 yrs – 16.5±0.2; 70-79 yrs – 15.8±0.3; 80-87 yrs – 15.3±0.3; F=2.7; p=0.01). The ASMI values corresponding to a cutoff of low muscle mass by the definitions used were as follows: <5.5 kg/m2 (European guidelines), <5.7 kg/m2 (<20th percentile of sex specific population), <4.8 kg/m2 (two SD below the mean of young Ukrainian females aged 20-39 yrs). The prevalence of low muscle mass in women aged 65 yrs and older based on the above three criteria was 12%, 16% and 1.7%, respectively. ASM was positively correlated with the total fat mass (r=0.20, p=0.0006) and BMD at all sites (p<0.0001).

Conclusion. Peak muscle mass among the Ukrainian women is achieved in the fifth decade. The cutoff value of ASMI (<4.8 kg/m2) defined as two SD below the mean of reference young population was lower in this study compared with the Rosetta Study (<5.5 kg/m2). As for the sex specific cutoff (ASMI <5.7 kg/m2), this index was similar to the data of the Health ABC study (<5.67 kg/m2) [Cruz-Jentoft A.J. et al., 2010]. Appendicular skeletal mass was positively correlated with total fat mass and BMD at all sites.

Disclosures: Vladyslav Povorozyuk, None.

SU0403

The Effects of Vitamin D and Sarcopenia on Bone Mineral Density in Korean women. Sung Won Yang*¹, Duck Joo Lee, Bom Taek Kim. Ajou University School of Medicine, South Korea

A osteoporotic fracture has become a global health issue that causes tremendous impact on mortality as well as heavy socioeconomic burden. Previous studies suggested that vitamin D may prevent fractures by improving muscle mass as well as via increasing bone density directly. The purpose of the study is to determine that the influence of vitamin D on bone mineral density depends on its effects on muscle mass.

We analyzed the data from Korean National Health and Nutritional Survey IV in 2009. Women older than age 20 were included for the analyses. Bone mineral density and muscle mass were measured by DXA. serum vitamin D concentration was tested.

Vitamin D and muscle mass affected BMD at proximal femur, but not at lumbar spine. Vitamin D deficiency and sarcopenia increased odd ratio for osteoporosis before and after adjusted for multiple variables. The effects of vitamin D deficiency on BMD still remained significant after adjustment for sarcopenia, which was vice versa.

Though vitamin D deficiency and sarcopenia shared common effects on BMD, they their own effects on BMD independent from each other.

Disclosures: Sung Won Yang, None.

SU0404

Using the European Working Group of Sarcopenia in Older People (EWGSOP) criteria for identifying sarcopenia and sarcopenic obesity in a group of community dwelling Seniors. Angela Juby*, Christopher Davis, Suglo Minimaana, Marilyn Cree. University of Alberta, Canada

Purpose

Sarcopenia prevalence increases with age, and is associated with increased risk for frailty, drug side effects, worsening chronic disease, falls/fractures, and dependence. Sarcopenia and sarcopenic subtypes have been defined by the European Working Group of Sarcopenia in Older People (EWGSOP). This classification is based on presence or absence of low muscle mass, plus/minus low muscle strength or low performance. This is baseline data from participants in a twelve month study evaluating the impact of exercise.

Methods

All are > 65 years, mobile, and community dwelling in Edmonton, Alberta, Canada. All had baseline assessments including dual energy Xray absorptiometry (DXA) body composition (BC) analysis, grip strength measurement (dynamometer) and gait speed (10 metre walk test). BC allowed calculation of appendicular lean mass/height² (aLM/ht²) and body percentage fat. Data was evaluated as per EWGSOP guidelines, using the following cut offs: aLM/ht² of <5.67 (women) <7.26 (men); grip strength of <20 (women), <30 (men); and gait speed <1m/s for both. Based on these each participant was classified into a body type. (Low grip strength and gait speed, with normal aLM/ht² were classified as "weak" for want of a better description, to differentiate them from normal). Presarcopenics had only low aLM/ht², sarcopenics had low aLM/ht² plus one abnormal level in one of the other parameters, and severe sarcopenics were defined as those having abnormal levels in all the parameters. Obesity was defined by DXA BC percentage fat of >40% (women), >28% (men).

Results

39 participants were evaluated, 32 women and 7 men, with an average age of 75.9 years (67-90 years), and an average MOCA 25.5/30. All were independently mobile (with or without walking aids) and community dwelling. EWGSOP classification of the women: 9 normal; 2 presarcopenia; 2 sarcopenic obesity; 1 sarcopenia; 1 severe sarcopenia; 1 severe sarcopenic obesity; 3 sarcopenic obesity; 10 obese; 1 normal "weak"; 2 obese "weak", for a total of 32. Of the 7 men: 2 normal; 1 sarcopenia; 3 sarcopenic obesity; and 1 obese. The groups were comparable for age. Baseline BMI was 27.5 (18.8 – 37.5) and BMI did not discriminate the body types.

Conclusions

In these independently living, highly functioning Seniors, there was a surprising diversity of body composition. BMI alone was of limited use in classifying body type. The EWGSOP classification is useful to stratify an outwardly homogenous group of Seniors.

Disclosures: Angela Juby, None.

SU0405

Effect of Aging on Bone Properties in Male and Female Transgenic Mice Carrying the Human LRP5^{G171V} (HBM) Mutation. Nuria Lara*¹, Mark Begonia², Mark Dallas², Ganesh Thiagarajan², Mark L. Johnson². ¹University of Missouri - Kansas City, USA, ²University of Missouri-Kansas City, USA

We have previously shown that a single point mutation in the human LDL receptor-related protein 5 (LRP5) results in a high bone mass trait. It has been published that transgenic mice expressing this same mutation under the expression of 3.6-kb type I collagen promoter results in high bone mass and maintains this phenotype up to 52 weeks of age. In this current study we sought to determine the effect of aging on maintaining bone properties in this animal model. We sought to determine whether aging would result in parallel declines in HBMtg mice compared to C57Bl/6 control littermates or if the high bone mass trait would be maintained.

MicroCT analysis of femurs from 88 week old female transgenic mice (n=4) demonstrated increased cortical compartment parameters compared to wild type or littermate controls (n=5). Cortical BMD (mgHA) (1237.8±17.4 vs 1196.3±26.8, p<0.05), cortical thickness (mm) (0.24±0.04 vs 0.18±0.01 p<0.001) and cortical bone area (mm²) (1.3±0.2 vs 0.9±0.13, p<0.05) were all higher in HBMtg mice. In the trabecular compartment, female HBM transgenic mice had increased BV/TV (%) (4.6±2.4 vs 0.3±0.2, p<0.05), and trabecular thickness (mm) (0.071±0.015 vs 0.043±0.008, p<0.05). Biomechanical studies showed transgenic female bones had higher work to failure (mJ) (4.6±1.1 vs 2.4±0.9, p<0.05), ultimate load (N) (25.4±6.3 vs 16.02±4.21, p<0.05) and elastic stiffness (N/mm) (154.6±26.0 vs 86.4±34.6, p<0.01) compared to controls. In the male group, no significant differences were observed in the cortical and trabecular material parameters or biomechanical properties of HBMtg (n=8) mice vs littermate controls (n=4). In both male and female, bone parameters of control and HBMtg mice were lower compared to previously published data from younger mice.

These studies demonstrate that aging results in a reduction in cortical and trabecular bone properties in both male and female HBMtg mice. However, the female HBMtg mice appear to retain their enhanced properties to a greater extent. Given that the HBM transgene is driven by the 3.6-kb type I collagen promoter, studies are currently underway to determine if this sex difference is due to differential

regulation of the promoter or reflects general differences in male vs female mice as they age. These data support a central role for the LRP5/Wnt/β-catenin in bone mass maintenance across aging.

Disclosures: Nuria Lara, None.

SU0406

Vascular Endothelial Growth Factor: Relationship to Bone Mineral Density (BMD), Size and Strength: The Osteoporotic Fractures in Men Study (MrOS). Jane Cauley*¹, Stephanie Harrison², Joseph Zmuda³, Elizabeth Barrett-Connor⁴, Jodi Lapidus⁵, Eric Orwoll⁵. ¹University of Pittsburgh Graduate School of Public Health, USA, ²California Pacific Medical Center Research Institute, USA, ³University of Pittsburgh, USA, ⁴University of California, USA, ⁵Oregon Health & Science University, USA

Vascular endothelial growth factor (VEGF) is a major coupling factor for the osteogenic-angiogenic interface. Activation of angiogenesis mediated via VEGF leads to increased bone mass. However, little is known about circulating VEGF and skeletal strength in humans.

To test the hypothesis that levels of VEGF are positively correlated to areal (a) and volumetric (v) BMD, bone size and skeletal strength, we chose a random sample of 500 men enrolled in MrOS who had QCT scans of the proximal femur and lumbar spine. The first 650 participants at each clinic and all minority men were referred for QCT. Of the 5,994 men enrolled in MrOS, 3,563 men had usable QCT scans. VEGF was measured in baseline serum by enzyme linked immunoassay; minimum detectable concentration, 5pg/ml; intra-assay CV%, 5.4%; inter-assay CV%, 7.3%. aBMD was measured by DXA and remaining bone parameters, by QCT. QCT scans were acquired using standardized protocols (Black DM, JBMR 2008;23(8):1326). Image processing was performed using the methods of Lang et al (Lang TF, JBMR 2006;21:1224). We examined the characteristics of men and bone parameters across quartiles of VEGF.

Men with highest VEGF (Quartile 4, > 444.4 - < 1563 pg/ml were more likely to report difficulty with at least one instrumental activity of daily living (IADL) compared to Quartile 1 (< 129pg/ml) but other characteristics e.g., age, BMI, health status, smoking, fall history or comorbidities did not differ across quartiles of VEGF. There was no association between VEGF and hip or spine aBMD. There was no association between VEGF and lumbar spine vBMD (integral, or trabecular), trabecular bone volume or vertebral strength or femoral neck vBMD (integral, trabecular, or cortical) and cross-sectional area (CSA). However, we found significant interactions between VEGF and IADL impairment for femoral shaft medullary area, CSA and cortical bone area (Table). Among men with > 1 IADL impairment, shaft medullary area, CSA and cortical bone area increased with increasing VEGF. Among men with no IADL impairment medullary area and CSA decreased with increasing VEGF. There was no association with femoral shaft BMD. We found no relationship between VEGF and either aBMD or vBMD. There was some suggestion that the association between VEGF and femoral shaft size differs by whether or not a man reported an IADL impairment but this may have occurred by chance. Future research will need to confirm these results.

Table: Femoral Shaft Parameters by VEGF Quartiles Stratified by IADL Impairment (age adjusted) (All P Interaction <0.05)

| | At least one IADL Impairment | |
|--------------------------------|------------------------------|------------|
| | Yes (n=103) | No (n=385) |
| Medullary Area (cm) | | |
| VEGF Quartile 1 | 3.05 | 3.19 |
| Quartile 2 | 2.96 | 3.15 |
| Quartile 3 | 3.04 | 2.99 |
| Quartile 4 | 3.45 | 2.76 |
| p trend | 0.13 | 0.004 |
| CSA (cm) | | |
| VEGF Quartile 1 | 8.92 | 9.39 |
| Quartile 2 | 8.91 | 9.59 |
| Quartile 3 | 9.31 | 9.06 |
| Quartile 4 | 9.83 | 8.97 |
| p trend | 0.005 | 0.007 |
| Cortical Bone Area (cm) | | |
| VEGF Quartile 1 | 5.86 | 6.20 |
| Quartile 2 | 5.95 | 6.45 |
| Quartile 3 | 6.28 | 6.07 |
| Quartile 4 | 6.38 | 6.21 |
| p trend | 0.03 | 0.44 |

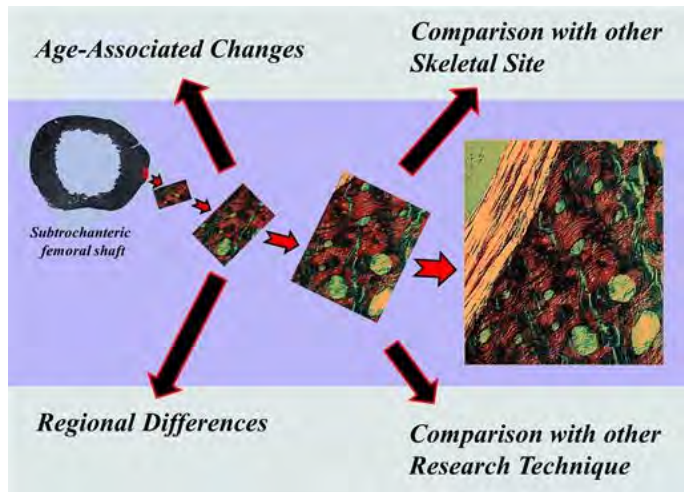
Table

Disclosures: Jane Cauley, None.

SU0407

Histomorphometrical Characteristics of Cortical Bone in Male Subtrochanteric Femoral Shaft. Xiaoyu Tong*¹, Markus Malo², Inari Burton³, Hanna Isaksson⁴, Jukka Jurvelin², Heikki Kröger⁵. ¹Kuopio Musculoskeletal Research Unit (KMRU), Finland, ²Department of Applied Physics, University of Eastern Finland, Finland, ³Kuopio Musculoskeletal Research Unit (KMRU), Institute of Clinical Medicine, University of Eastern Finland, Finland, ⁴Department of Biomedical Engineering, Department of Orthopaedics, Lund University, Sweden, ⁵Department of Orthopaedics, Traumatology, & Hand Surgery, Kuopio University Hospital, Finland

The underlying morphometric changes at the proximal femur that might predispose for subtrochanteric fractures are poorly understood. The aim of this study was to investigate the age-dependent variations and regional differences of histomorphometric properties in the cortical bone of subtrochanteric femoral shaft, and to compare the histological characteristics with those in the femoral neck, as well as to cortical characteristics found with scanning acoustic microscopy. Undecalcified histological sections of the subtrochanteric femoral shaft (n=20, aged 18-82 years, males) were cut (15µm) and stained using modified Masson-Goldner stain. Histomorphometrical parameters of cortical bone were analysed with low (x50) and high magnification (x100), after identifying cortical bone boundaries with our previously validated method. The cortical widths of the medial and lateral quadrants were significantly higher than those measured for the anterior and posterior quadrants (p<0.01). Osteonal area/cortical area and porosity in the posterior quadrant were significantly lower and higher than the other quadrants (p<0.05). Several cortical bone parameters (e.g. osteonal area/cortical area, erosion perimeter/endocortical perimeter) of the middle aged group (40-60 years) were significantly different from the younger and older subjects (< 40 years and >60 years) (p<0.05). Compared to the femoral neck, each osteonal parameter (e.g. osteonal area/cortical area, osteon number) was significantly higher in the femoral shaft (p<0.01). The values of porosity were significantly lower in the anterior and lateral, and higher in the posterior femoral shaft compared to the corresponding quadrants of the femoral neck. When comparing to cortical bone parameters measured by using the scanning acoustic microscopy, the values measured by both techniques were strongly correlated (0.73 ≤ R² ≤ 0.97, p<0.001). However, the histomorphometrically measured parameters were generally lower (p<0.001). This study describes the changes in cortical bone of the subtrochanteric femoral shaft during ageing in healthy males, which may aid to reveal the underlying morphometric changes that might predispose to subtrochanteric fractures.

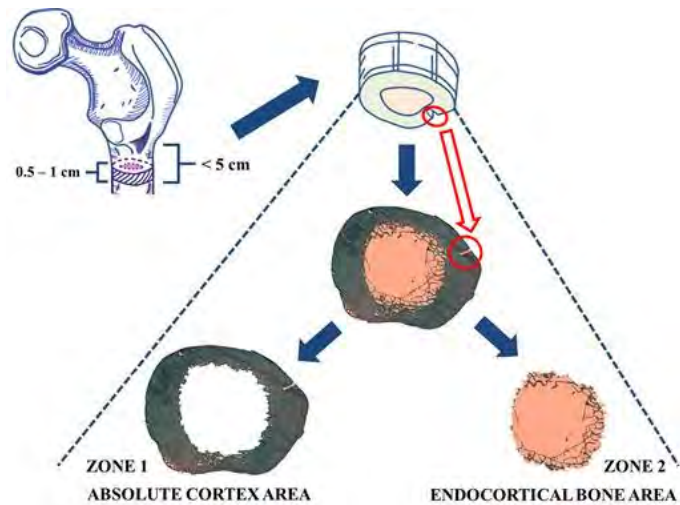


Graphic Abstract

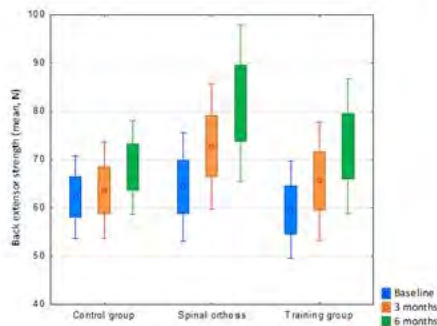
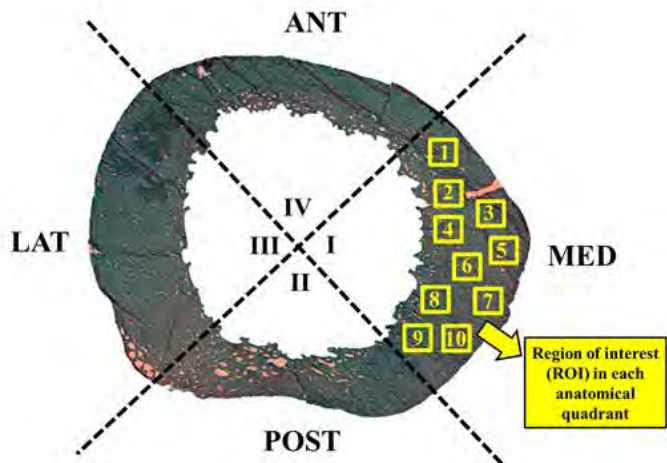
Basic anthropometric data of the cadavers. Individual values and the mean ± SD are shown.

| Age [years] | Age Group | Height [cm] | Weight [kg] |
|-------------|-----------|-------------|-------------|
| 17 | 1 | 178 | 74 |
| 22 | 1 | 186 | 106 |
| 29 | 1 | 184 | 105 |
| 32 | 1 | 171 | 69 |
| 34 | 1 | 187 | 102 |
| 36 | 1 | 177 | 74 |
| 39 | 1 | 185 | 84 |
| 43 | 2 | 171 | 98 |
| 44 | 2 | 179 | 96 |
| 46 | 2 | 185 | 85 |
| 48 | 2 | 178 | 85 |
| 50 | 2 | 185 | 108 |
| 52 | 2 | 180 | 136 |
| 53 | 2 | 176 | 73 |
| 58 | 2 | 175 | 73 |
| 58 | 2 | 169 | 96 |
| 62 | 3 | 170 | 68 |
| 74 | 3 | 166 | 64 |
| 77 | 3 | 177 | 72 |
| 82 | 3 | 165 | 53 |
| 47 ± 18.2 | - | 177 ± 6.9 | 84 ± 20.4 |

Basic information of subjects



Separation of the cross-sectional subtrochanteric femoral shaft



Back extensor strenght

Disclosures: Christina Kaijser Alin, None.

The company Medi sponsored the with free spinal orthosis to the study participants in the spinal orthosis group

SU0409

The Association between Spinal Curvature and Balance in Elderly Women at High Risk of Osteoporotic Fractures in Primary Healthcare. Helena Salminen¹, Ann-Charlotte Grahn Kronhed^{*2}, Christina Kaijser Alin¹. ¹Karolinska Institutet, Sweden, ²Linköping University, Sweden

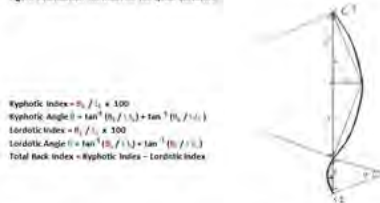
Purpose: The aim was to study the associations between kyphotic and lordotic measurements and balance in elderly women at high risk of osteoporotic fractures. Further, the associations of vertebral fractures to balance and spinal curvature were studied.

Methods: The population in this study, 88 women (mean age 84 years), survivors from the population based cohort PRIMOS of 351 women, originally included in 1999-2000, were re-examined in a follow-up study in 2011-2013. Static timed standing and dynamic balance tests were performed and spinal curvature was measured by using the Flexicurve ruler and X-ray data on vertebral fractures were gathered. Several calculation methods were used to describe the spinal curvature (see Figure 1).

Results: Positive correlations between the presence of hyperkyphosis and tandem standing eyes open ($r_s = 0.24, p < 0.05$) and standing on right leg eyes closed ($r_s = 0.27, p < 0.05$), tandem gait forwards ($r_s = 0.24, p < 0.05$), and also tandem gait backwards ($r_s = 0.30, p < 0.01$) were found. Lordotic Index and Lordotic Angle were positively associated to one leg standing eyes closed, to right leg eyes closed and left leg eyes closed. The Total Back Index was negatively related to left leg standing eyes open ($\beta = -0.3, p < 0.05$). However, there were no associations between the Kyphotic Index or Angle and balance. Presence of vertebral fractures had no associations to balance.

Conclusions: A larger lumbar lordosis was associated with better balance performance. Both thoracic kyphosis and lumbar lordosis should be calculated to describe spinal curvature.

Figure 1 Calculation methods for the spinal curvature

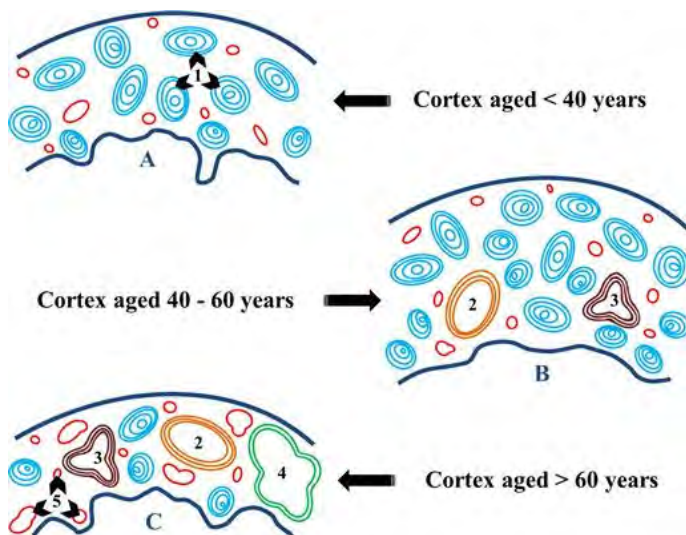


The Kyphotic Index, the Kyphotic Angle, the Lordotic Index, the Lordotic Angle, and the new method "Total Back Index" were used. A reference line through the traced curves between the points of C7 and S1 was drawn and measured the lengths of the kyphosis and, if present also the lordosis. The width of both curves at the widest point and the lengths of the halves of the curves were measured and divided through their widest point. Cut-off values for the presence of hyperkyphosis was set to 15. Since it was desirable to take the lengths of both curves into account, a new measurement the "Total Back Index" was constructed, subtracting the Lordotic index from the Kyphotic Index.

Kyphosis measurements

Disclosures: Ann-Charlotte Grahn Kronhed, None.

Anatomical quadrants and regions of interest



Schematic cortex of the subtrochanteric femoral shaft with respect to age

Disclosures: Xiaoyu Tong, None.

SU0408

Effect of Treatment on Back Pain and Back Extensor Strength with a Spinal Orthosis in Elderly Women with Osteoporosis; a Randomized Controlled Trial. Helena Salminen¹, Christina Kaijser Alin^{*1}, Ann-Charlotte Grahn Kronhed², Hans Lundin¹. ¹Karolinska Institutet, Sweden, ²Linköping University, Sweden

Purpose: The aim of the study was to evaluate effect of treatment with the spinal orthosis Spinomed on pain and back extensor strength, compared to a physiotherapy equipment training group and a control group, in elderly women with osteoporosis and back pain.

Methods: A randomized controlled trial of six months duration with a total of 113 women (46 with vertebral fractures), randomized in three arms: 1. Training in spinal orthosis Spinomed. 2. Training in a physiotherapy equipment training group and a home exercise training program. 3. Control group. Inclusion criteria: Women > 60 years old with back pain, osteoporosis and/or vertebral fractures. Exclusion criteria: Spinal stenosis. Difficulty to follow the study program. The RCT started in spring 2011 and was completed in December 2014. Main outcome was back extensor strength measured with ISO-Check, Digimax (Messtechnik).

Results: A total of 96 women, mean age 76 years, completed the RCT at the six months follow-up. Back extensor muscle strength increased with 27% in the spinal orthosis group, 22% in the exercise training group and 10% in the control group.

Conclusions: Treatment with the spinal orthosis Spinomed increased the back extensor muscle strength to the same degree as training with a physiotherapist group. Treatment with the spinal orthosis may be a good alternative method to strengthen the back extensor muscles in elderly women with osteoporosis.

SU0410

3D scaffold with VEGF/FGF9 conjugated fibrin, nano calcium sulfate and BMP2 genetically engineered mesenchymal stem cells promotes vascularized bone formation. Xue Yuan*¹, Randall J Smith Jr², Huiyan Guan³, Zunpeng Liu¹, Stelio T. Andreadis⁴, Ciprian N Ionita⁵, Parag Khobragade², Manhui Pan⁶, Changdong Wang¹, Guoqiang Guan³, Shuving Yang⁷. ¹Department of Oral Biology, State University of New York at Buffalo, USA, ²Department of Biomedical Engineering, State University of New York at Buffalo, USA, ³Department of Orthodontics, State University of New York at Buffalo, USA, ⁴Department of Biomedical Engineering; Department of Chemical & Biological Engineering; Center of Excellence in Bioinformatics & Life Sciences, State University of New York at Buffalo, USA, ⁵Toshiba Stroke & Vascular Research Center; Department of Biomedical Engineering, State University of New York at Buffalo, USA, ⁶Clinical & Translational Research Center, State University of New York at Buffalo, USA, ⁷Department of Oral Biology; Center of Excellence in Bioinformatics & Life Sciences, State University of New York at Buffalo, USA

Bone defects including bone fractures are increasing social and medical problems in the world, which dramatically decreased overall health and quality of life and caused huge medical costs of nearly \$20 billion per year in United State. Therefore, there is an urgent need for bone reconstruction. Bone tissue engineering has been extensively studied as an alternative to overcome clinical disadvantages of current bone grafts. In our previous study, we developed an injectable nano-scale calcium sulfate and alginate paste (nCS) to support the delivery and growth of BMP2 genetically engineered mesenchymal stem cells (nCS+M/B2), which significantly repaired bone defects. Because effective bone formation, especially for critical size bone defects, also requires vascular intervention, in this study, we developed a new fibrin gel system, in which angiogenic factor VEGF, FGF9 or both were conjugated to fibrin to increase their stability meanwhile control the release. To investigate whether this system combined with nCS+M/B2 would synergistically promote vascularized bone regeneration, nCS+M/B2 was coated with VEGF- or/and FGF9- conjugated fibrin to form a sandwich-like 3D scaffold, and then subcutaneously implanted into mice to test the osteogenic and angiogenic activity. MicroCT, alkaline phosphatase activity assay and histological analysis were used to evaluate bone formation while immunostaining were employed to indicate newly formed blood vessels. Coating with fibrin greatly preserved the nCS+M/B2 scaffold structure and also promoted de novo bone formation. Conjugated FGF9 alone did not significantly elevate ectopic bone formation, however, FGF9 combined with VEGF significantly promoted vascularized bone formation. We also compared different ways to load M/B2 and found that the group equally loaded M/B2 to fibrin gel and nCS showed best bone formation compared with the groups loaded a same amount of M/B2 to fibrin or nCS only, suggesting M/B2 may have different functions in nCS and fibrin. Overall, our results suggested that integration of nCS+M/B2 (support bone formation) with fibrin-based VEGF/FGF9 release system (support vascular formation) is an innovative strategy to improve bone regeneration.

Disclosures: Xue Yuan, None.

SU0411

Mesenchymal Cell-Based Biological Enhancement of Porous Titanium Orthopedic Implants. Eric Lewallen*¹, Dakota Jones¹, Amel Dudakovic¹, Carolina Bonin¹, Matthew Getzlaf¹, Roman Thaler¹, Scott Riester¹, Emily Camilleri¹, Jennifer Westendorf¹, Allan Dietz¹, Robert Cohen², David Lewallen¹, Andre van Wijnen¹. ¹Mayo Clinic, USA, ²Stryker Orthopedics, USA

More than 4 million yearly hip and knee replacements are expected by 2030 in the US. A small percentage of these implants fail, yet these failures are often catastrophically detrimental to limb function (e.g., major bone loss, infection) and result in a significant clinical challenge and health care burden. Motivated by this pressing clinical need, we address the central hypothesis that autologous cell transplants onto porous metallic implants can favorably alter the microenvironment of the bone-implant interface to improve osseointegration. Mesenchymal stromal cells (MSCs) are recognized for their potential to restore bone loss or damage, because of their ability to differentiate into osteoblastic precursors. Specifically, we focus on clinical-grade MSCs derived from the stromal vascular fraction of adipose tissue that are expanded in human platelet lysate and can be obtained in large quantities. High resolution comparisons using mRNASeq, microRNASeq, scanning electron microscopy, and histomorphometry were used to compare MSCs from four patients cultured on porous structured titanium (psTi) disc inserts in osteogenic medium vs. controls. Differential expression analysis on mRNASeq data revealed 55 genes of special interest, which were further investigated via RT-qPCR. Significant differences in gene expression between culture plastic and titanium substrate were confirmed for twelve biomarkers: *ATF4*, *BGLAP*, *CD44*, *COL3A1*, *DCN*, *DLX3*, *DLX5*, *EZH1*, *KLF10*, *PRRX1*, *RUNX3*, *TRPS1* ($p < 0.05$). Expression of the epigenetic regulator *EZH2* exhibited a decreasing trend in psTi-attached cells, a pattern consistent with

our recent demonstration that pharmaceutical inhibition of *EZH2* improves bone formation. Imaging of MSCs revealed distinct adhesive properties as they attach, proliferate and differentiate into osteoblast-like cells on psTi. This behavior varies among MSCs from different patients and may be modifiable by changing the physical properties of psTi, or conditions and duration of autologous cell culture.

Disclosures: Eric Lewallen, None.

SU0412

Bone Loss in C57BL/6J-OlaHsd Mice, a Substrain of C57BL/6J Carrying Mutated Alpha-Synuclein and Multimerin-1 Genes. Tamar Liron*¹, Bitva Raphael², Itai Bab³, Yankel Gabet¹. ¹Tel Aviv University, Israel, ²Tel Aviv University, Israel, ³Hebrew University, Israel

The inbred mouse strain C57BL/6 is commonly used for the generation of transgenic and knockout mice and is a well-established strain in bone research. Different vendors supply different sub-strains of C57BL/6J as wild-type animals when genetic drift did not incur any noticeable phenotype. However, we sporadically observed drastic differences in the bone phenotype of the WT C57BL/6J controls originating from different labs and speculated that these variations are attributable at least in part to the variation between C57BL/6J sub-strains, which is often overlooked. C57BL/6J-OlaHsd is a commonly used sub-strain that despite a well-defined deletion in the alpha-synuclein (*Snc*) and multimerin-1 (*Mm1*) genes, was reported to display no obvious phenotype and is still commonly used as WT control. Here we compared the bone phenotype of C57BL/6J-OlaHsd (6J-Ola) to C57BL/6J-RccHsd (6J-Rcc), the parent strain of the 6J-Ola lacking the deletion and closest genetically to the original 6J sub-strain developed by the Jackson labs. Both sub-strains are supplied by Harlan Laboratories. Using micro-CT analysis, we found that 6J-Ola mice display a significantly lower trabecular BV/TV, Conn.D, Tb.N, and Tb.Th. 6J-Ola mice also demonstrate reduced cortical thickness and a general cortical expansion. PCR analysis revealed that both the *Snc* and *Mm1* genes are detectable in RNA derived from bone marrow cells and bone tissue of 6J-Rcc animals but not of 6J-Ola mutants. Up to date, there is no data in the literature linking *Snc* and/or *Mm1* to bone remodeling but our data implies that either or both genes may play a role. Our findings not only highlight the potential new role of these genes in bone biology but they further emphasize the critical importance of sub-strain unity. The use of littermate controls may also be questioned in the case of cross breeding between different sub-strains. Our data may help elucidating some of the unexplained differences in basal bone measurements between different research centers and reiterate the need of specifying the exact sub-strain type.

Disclosures: Tamar Liron, None.

SU0413

Bone Mineral Density of the Bottlenose Dolphin: Establishing a Definitive Region of Interest and Clinical Reference Dataset. James Powell*¹, Wayne McFee², Gangming Luo³, Jonathan Kaufman³. ¹Portland State University, USA, ²National Ocean Service, USA, ³CyberLogic, Inc., USA

The study reported herein has been developed to overcome a knowledge gap in anatomy of the common bottlenose dolphin, *Tursiops truncatus*, through examination of bone mineral density (BMD) of the radius in the dolphin pectoral flipper. The critical necessity to comprehensively define a target skeletal site for osteodensitometric assessment is addressed, and a normative bone density distribution curve is proposed for the species. Statistical support for the use of the available specimens as a normative reference dataset is provided by tests to examine differences within the dataset based on sex, age, total body length, handedness, nutritional status, and geographical affinity. Radii from 280 bottlenose dolphins were analyzed using dual energy x-ray absorptiometry (DXA), the accepted gold-standard in human medical studies. Bone density increases with age and total body length but not with enough statistical accuracy to use bone density to estimate age ($R^2=0.58$, $p<0.05$) as suggested in previous studies. No statistically significant differences were observed in BMD measurements for subsets of male vs female dolphins ($t=-1.60$; $p>0.05$) or right vs left flipper ($t=-1.76$, $p>0.05$). BMD was corrected for age and total body length using Principle Component Analysis to collapse these three variables into a synthetic variable, Principle Component I (PCI). PCI accounts for 88% of the variance in BMD, age, and total body length in the dataset. No statistically significant differences were observed in age- and length- corrected BMD within the subsets examined, including nutritional status ($F=0.83$, $p>0.05$) and geographical region ($t=-0.190$, $p>0.05$). These results support the total inclusion of all specimens as a normative reference dataset for bone density values in bottlenose dolphins.

Disclosures: James Powell, None.

SU0414

Development of Peak Bone Traits in Young Men – Estimations by pQCT and DXA. Erik Lindgren^{*1}, Magnus Karlsson¹, Mattias Lorentzon², Jan Åke Nilsson¹, Bjorn Rosengren¹. ¹Skåne University Hospital Malmö, Lund University, Sweden, ²Geriatric Medicine, Institute of Medicine, Sahlgrenska University Hospital & Gothenburg University, Sweden, Sweden

Introduction

Studies with DXA, gold standard when determining bone mass, have defined peak bone mass for areal BMD (aBMD) in hip to age 17-18, in spine to age 25-30 and in distal forearm as late as age 35-40 years. DXA however provides a combined measure of both the amount of mineral and bone size, does not separate cortical and trabecular bone and cannot estimate volumetric BMD (vBMD) or structural bone parameters separately. These estimations are possible by pQCT, but data in a broad age span around the time of peak bone mass is not available. We aimed to identify peak values for pQCT traits in young men and their relation to peak values in DXA traits.

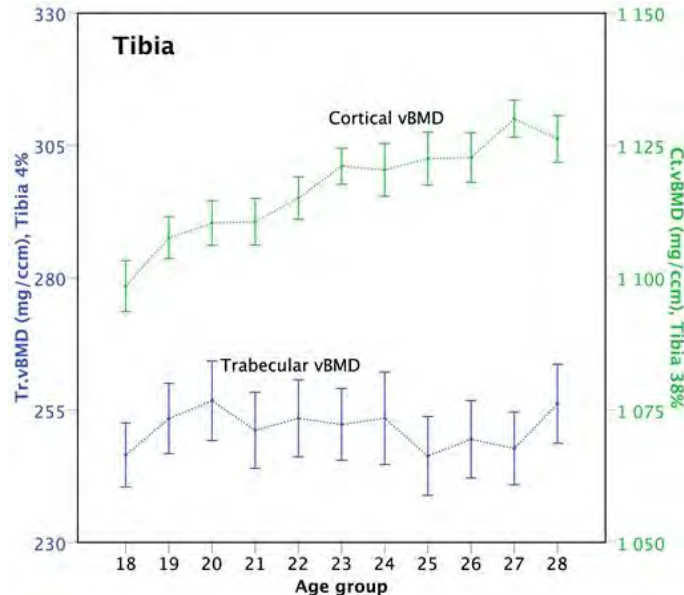
Methodology

We recruited a population based random sample age stratified (in 1-year age classes) that included 1083 young men aged 18-28 years and assessed trabecular vBMD (g/cm³), cortical vBMD, cortical thickness (mm) and cortical cross sectional area (CSA, mm²) by pQCT-scans (Stratec XCT2000) at *radius and tibia* in an *ultra-distal site*, where trabecular bone largely dominates, and at a *diaphyseal site*, where cortical bone dominates. We also assessed aBMD (g/cm²) by DXA-scans (Lunar Prodigy) at the hip [femoral neck (FN)], the spine and total body (TB).

Results

At *ultra-distal sites* we found no statistically significant differences in trabecular vBMD between age groups in either of the extremities (Tibia 4% shown in Figure). At *diaphyseal sites* cortical (Ct) vBMD, Ct CSA and geometrical variables showed increment by age throughout the examined age span (Tibia 38% in Figure). With DXA we found another pattern in that FN aBMD diminished by 6.7% from the highest (age 19 years) to the lowest (age 26 years) value ($p < 0.05$) and the opposite was found for TB.aBMD which increased 4.9% between the lowest value at age 18 years to the highest at age 28 years ($p < 0.01$). No statistically significant differences between age groups were found for spine aBMD.

Conclusions This study shows that the peaks of different bone traits (estimated by pQCT) are reached at different ages. This has important implications for inferences from previous research as it indicates that DXA, that reflects a combination of bone size and amount of mineral, may confer a biased estimate of peak bone mass.



Figure

Disclosures: Erik Lindgren, None.

SU0415

Different regulation of limb development by p63 transcript variants. Manabu Kawata^{*1}, Daisuke Mori², Yuki Taniguchi¹, Fumiko Yano², Keita Okada¹, Song Ho Chang¹, Kosuke Kanke³, Sakae Tanaka¹, Taku Saito². ¹Department of Orthopaedic Surgery, Graduate School of Medicine, The University of Tokyo, Japan, ²Department of Bone & Cartilage Regenerative Medicine, The University of Tokyo, Japan, ³Center for Disease Biology & Integrative Medicine, The University of Tokyo, Japan

Mutations in p63 gene cause genetic disorders with split hand-foot malformations in humans, such as Ectrodactyly-ectodermal dysplasia-cleft (EEC) syndrome and Ankyloblepharon-ectodermal defects-cleft lip/palate (AEC) syndrome. Meanwhile, p63-null mice show severely truncated limbs. Previous studies indicate that these phenotypes are mainly caused by hypoplasia of apical ectodermal ridge (AER) where p63 is abundantly expressed; however, the underlying molecular mechanisms and specific roles of p63 transcript variants are not fully understood. In the present study, we investigated expression of TA and deltaN (dN) isoforms of p63 during limb development, and their functions using p63-flox mice and mouse ES cells. FACS analysis of limb bud cells obtained from mouse E11.5 embryos showed that dNp63 was expressed more abundantly in ectodermal cells than in mesenchymal cells, while TAp63 was also expressed in both cells at about one-tenth level of dNp63. In AER-specific p63 knockout mice, forelimb autopod was truncated, and hindlimb zeugopod and autopod were hypoplastic. mRNA expression levels of Fgf8 and Jag2, essential molecules in AER, were decreased in the limb buds of E11.5 AER-specific p63 knockout embryos. When we introduced dNp63 and TAp63 into mouse ES cells in feeder-free condition, Fgf8 and Jag2 were induced, respectively. Luciferase assay using B16 melanoma cells showed that dNp63 enhanced promoter activity of Fgf8, while TAp63 enhanced that of Jag2. Deletion of p63 consensus sequences in these regions significantly decreased both promoter activities, and chromatin immunoprecipitation assay using mouse ES cells confirmed the binding of p63 protein to the responsive elements identified in Fgf8 and Jag2 promoters. Considering that Fgf8 is essential for maintenance of AER and that Jag2/Notch signaling negatively regulates growth and function of AER through apoptosis induction, dNp63 and TAp63 may regulate limb development in different ways through transcriptional induction of different target genes in AER.

Disclosures: Manabu Kawata, None.

SU0416

Effects of vivarium temperature on body composition and bone architecture in young, growing male C57Bl/6J mice. Maureen Devlin^{*}, Katarina Alajbegovic, University of Michigan, USA

Mouse models of human skeletal biology and metabolism require experimental conditions that are physiologically relevant to humans. There is a recent lack of consensus about whether the standard vivarium temperature of 22°C creates an inadvertent cold stress for laboratory rodents, with some data suggesting the thermoneutral temperature for mice is as high as 30°C, but other studies concluding that 22°C is an appropriate model for the thermal environment of clothed humans. If vivarium temperature perturbs mouse physiology, this finding would have important implications for interpreting experimental data. Thus here we test the hypothesis that skeletal acquisition and body composition vary in mice raised at different temperatures. To test this hypothesis, male C57Bl/6J mice were housed in pairs from 3 wks of age to 6 or 12 wks of age at 26°C (WARM) or 22°C (STD, standard vivarium temperature), with access to food and water ad libitum (N=4-6/group). Outcomes included body mass, food intake, body and tail length, femur and tibia length, %body fat and whole body bone mineral density (BMD) via pDXA, and cortical and trabecular microarchitecture via μ CT. Overall, there were no differences between STD and WARM in body mass, body length, or limb length between groups. STD mice ate more than WARM mice at 6-7 wks of age (GLM; $p < 0.05$). Housing temperature altered body composition throughout the experiment. In STD vs. WARM, %body fat increased more from 3-6 wks of age (+86% vs. +58%, GLM; $p = 0.02$), decreased more from 6-9 wks of age (-33 vs. -26%, GLM; $p = 0.05$), and increased more from 9-12 wks of age (+27% vs. +8%, GLM; $p = 0.05$). There were no differences in BMD between STD and WARM from 3-12 wks of age. At 6 wks of age, trabecular bone in the distal femur and proximal tibia showed no significant differences in bone volume fraction, trabecular number or thickness, and cortical bone from the midshaft femur and tibia showed no significant differences in cross-sectional geometry or bone area fraction. Thus, our results indicate that housing mice at 26°C vs. 22°C does not alter cortical or trabecular microarchitecture at 6 wks of age. However, increasing housing temperature from 22°C to 26°C significantly decreases food intake and has complex effects on body composition from 3-12 wks of age in male C57Bl/6J mice, potentially confounding the results of metabolic studies.

Disclosures: Maureen Devlin, None.

SU0417

MicroRNA Profiling of the Early Phases of Fracture Repair. Michael Hadjiargyrou*¹, David Komatsu², Jizu Zhi². ¹New York Institute of Technology, USA, ²Stony Brook University, USA

Fracture repair is a complex tissue regeneration process that involves multiple biological processes requiring the temporal and spatial expression of thousands of genes within multiple cell types and tissues. Although the regulation of many of these genes is known at the DNA level, our knowledge at the mRNA/protein level is extremely limited. Recently, microRNAs (miRNAs) have emerged as potent regulators of gene expression by binding to their target mRNAs and promoting their degradation or blocking translation. Thus, knowledge of which miRNAs are expressed during the early phases of fracture repair is essential in our complete understanding of the molecular mechanisms controlling the regulation of this regenerative process. In an effort to identify the expression of all known miRNAs during fracture repair, we generated transverse femoral fractures in mice and isolated miRNA-enriched RNA from Intact (IN) and post fracture day (PFD) 1, 3, 5, 7, 11, and 14. RNA from each time point (n=3) was hybridized to Mouse miRNA Microarrays (n=3, Agilent Release 21, containing 1881 miRNAs). Following hybridization, background subtraction and normalization, 959 (51%) genes were absent across all samples and were removed from further analysis. 922 (49%) displayed expression in at least one sample and were further characterized. Of these 922 miRNAs, 306 (33.2%) were up-regulated and 374 (40.6%) were down-regulated in the PFD calluses in comparison to IN bone. In addition, 20 (2.2%) miRNAs displayed differential expression (up/down, down/up, up/down/up and down/up/down) among the PFD calluses, also in comparison to IN. The remaining 222 (24%) miRNAs did not exhibit any changes between PFD and IN. To explore the biological significance of the up and down-regulated miRNAs, we first identified the target genes of these miRNAs using miRDB. 2048 target genes were unique to the up-regulated miRNAs and 4782 target genes were unique to the down-regulated miRNAs. Next, gene ontology and pathway enrichment analyses on the two target gene lists were conducted using the Database for Annotation, Visualization and Integrated Discovery (DAVID) Bioinformatics Resources and indicated several relevant biological processes (i.e. wound response; various signaling pathways). Moreover, about 15 target genes of the down-regulated miRNAs were identified as members of the PPAR signaling pathway which has been implicated as a major catabolic regulator of bone mass. These and additional analyses are still on-going. Taken together, these data provide the first complete analysis of miRNA expression during fracture repair and will aid in deciphering some of the molecular mechanisms responsible for the early phases of this tissue regenerative process. In addition, the results will reveal regulatory miRNAs as potential therapeutic targets for treating delayed or nonunions as well as accelerating normal repair.

Disclosures: Michael Hadjiargyrou, None.

SU0418

Specific deletion of Ebf1 within the kidney mesangium results in renal osteodystrophy, growth reduction, and premature death. Jackie Fretz*¹, Li Li², Rose Webb², Tracy Nelson², Ben-hua Sun², Nancy Troiano². ¹Yale University School of Medicine, USA, ²Yale University School of Medicine, USA

Globally deficient mice lacking the transcription factor Ebf1 (Ebf1 KO) are extremely sick owing to the multiple functions of Ebf1 across the body. While Ebf1 is present in osteoblast-lineage cells, specific deletion of Ebf1 using Osterix-cre and Runx2-cre resulted in a normal bone phenotype. We recently described a novel role for Ebf1 in kidney development and function. Within the kidney Ebf1 is present within multiple cell types including distinct tubular epithelium, interstitial pericytes, glomerular mesangium, and podocytes. In this study we made a specific deletion of Ebf1 within the Foxd1+ lineage using a cre-driver that targets the progenitors of the kidney glomerular mesangium and interstitial pericytes. Restricted deletion of Ebf1 from these cells resulted in development of hypoplastic kidneys and renal insufficiency at P21 (one week later than Ebf1 KO mice), with the appearance of proteinuria and 2+ leukocytes in urine. Growth is normal until P25. Approximately half of the Foxd1+, Ebf1fl/fl mice die before they are 3 months old. Mechanistic investigation of the pathways involved in Ebf1-directed renal development identified impaired Cox2 signaling within both the Ebf1-KO mice and targeted Foxd1+, Ebf1fl/fl animals have. Bone quality, assessed by micro-CT on femur, shows no differences between genotypes at 1 month, but significant reductions in connective density, trabecular thickness, and SMI and increased BS/BV within trabecular bone at 3 months. Cortical bone was more severely affected. Targeted Ebf1-deletion correlated to decreases in TV, BV, BV/TV, CtTh, apparent density, bone tissue density and pMOI, while BS/BV increased here as well. Taken together these results suggest that the renal insufficiency imposed on mice deficient for Ebf1-mediated signaling within the renal Foxd1-lineage accounts for significant reductions in bone quality as a secondary outcome of impaired renal mineral homeostasis. Furthermore, the delayed onset of the kidney phenotype in this model, compared with global Ebf1 KO mice, suggests a significant second role for Ebf1 in another cell type that influences renal development.

Disclosures: Jackie Fretz, None.

SU0419

Study of a PLGA film / Titanium Nanotubes Compound Growth Factor Sustained Releasing System. Sun Shengjun*¹, Yu Weiqiang², Zhang Yilin³, Zhang Fuqiang². ¹Shandong University, Peoples republic of china, ²Shanghai 9th People's Hospital, China, ³Shandong Province Hospital, China

Purpose: The application of growth factors around the implants is an effective method to improve osseointegration. TiO₂ nanotube array can improve the biocompatibility of titanium implants and anti-corrosion. Polymerized α -polyester type lactic acid - glycolic acid copolymer (PLGA) by the poly(lactic acid - polyglycolic acid) is a biodegradable organic compound, which have good biocompatibility and film-forming ability. It is possible to become an ideal carrier material to build up a drug delivery system. The purpose of this research is to build a bone growth factor delivery system with anodized TiO₂ nanotube arrays and PLGA film on the surface of the titanium implant surface, and study its biological efficacy both in vivo and in vitro, to provide evidence for the development of new implanting system.

Methods: (1). TiO₂ nanotube array was prepared and filled with recombinant human bone morphogenetic protein -2 (rhBMP-2) growth factors, then PLGA was deposited on the surface of this material. Scanning electron microscopy (SEM), atomic force microscopy (AFM) was used to study the characterization, and ELISA assay was used to detect the pharmacokinetic release rate in vitro. (2). The osteoblast cells were cultured on the surface of the material, SEM, MTT and alkaline phosphatase activity test was used to study the behavior of osteoblasts. (3). The method was applied to titanium implant screws, and embedded in rabbits on tibia. After implantation, the experimental animals were killed and samples were taken out and evaluated.

Results: (1). When the PLGA solution is certain concentration, PLGA membranes of different thickness can be deposited on the surface of TiO₂ nanotube layer. A certain thickness PLGA membrane can sustain release rhBMP-2 during four weeks' time, and have a more suitable surface of nano-roughness. (2). In vitro, PLGA film / TiO₂ nanotube sustained release system can promote the adhesion of MC3T3-E1 osteoblasts, and can improve the osteogenesis of osteoblasts. (3). In vivo, PLGA film / TiO₂ nanotube sustained release system has the ability of promoting osteogenic for a long time in experimental animals.

Conclusion: The PLGA film / TiO₂ nanotube growth factor delivery system can be effectively sustained release the bone growth factor rhBMP-2, the delivery system can promote osteoblast adhesion and osteoblast function in vitro and promote bone integration in vivo. It can be used as a good surface material of implants.

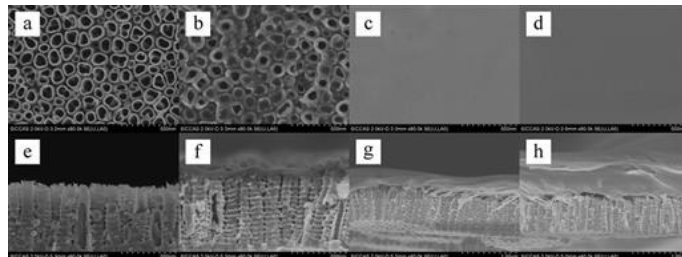


Figure 1: SEM micrographs of the samples' surface and section

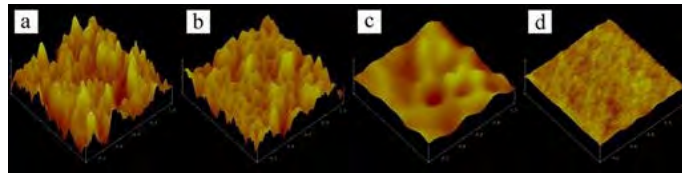


Figure 2: AFM images of the samples' surface

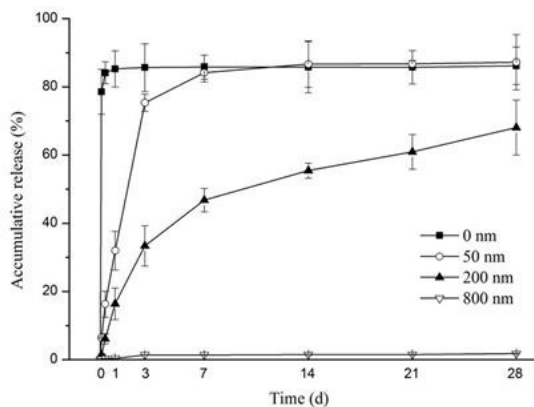


Figure 3: Sustained release curve of the samples

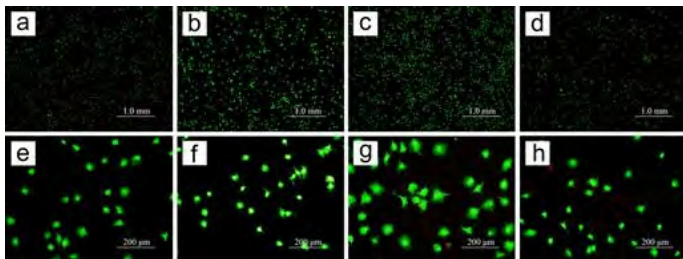


Figure 5: Live/dead staining of MC3T3-E1 cells on the samples

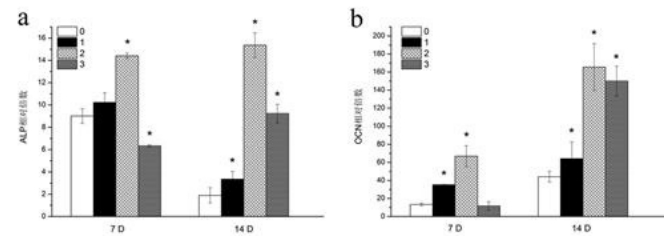


Figure 4: Osteogenesis genes expression level

Disclosures: Sun Shengjun, None.

This study received funding from: National Natural Science Foundation of China (81070866)

SU0420

Study of Body Composition and Bone Measures Acquired from Osteoporotic Measurement Sites using Regional DXA Scans. Louise Marquino¹, Bo Fan², Bennett Ng², Vicente Gilsanz³, Heidi Kalkwarf⁴, Joan Lappe⁵, Sharon Oberfield⁶, Karen Winer⁷, Babette Zemel⁸, John Shepherd².
¹University of California, San Francisco, USA, ²UCSF, USA, ³USC, USA, ⁴CCHMC, USA, ⁵Creighton Univ, USA, ⁶CUMC Columbia, USA, ⁷NICHD, USA, ⁸CHOP, USA

Background: Accurately measuring body composition at regional locations is a useful measurement when studying mechanical loading and development of the skeleton. DXA is increasingly being used as a safe, low-cost tool for body composition measurement across the lifespan. Currently body composition data is only available from adult and infant whole body scans for GE and Hologic DXA systems. We are investigating methods to derive fat and fat-free masses from dedicated forearm and femur scans. The purpose of this study was to derive methods and present pilot findings of body composition measures derived from forearm DXA scans.

Methods: We retrospectively analyzed forearm and whole body DXA scans acquired on 34 participants from the Bone Mineral Density in Children Study (BMDCS). The participants' forearm scans were analyzed to mimic infant whole body scans. Fat, fat-free, and percent fat masses were quantified within a 1.0-cm wide region located at the 4/10th distal forearm. This region was picked because it was the most proximal region that could be analyzed on all standardly acquired forearm scans and maximized muscle cross-sectional area. A similar region was defined on the whole body scans. All scans were acquired on Hologic DXA systems and analyzed using Hologic, Apex 5.5.

Results: Of the 34 participants (18 male), the average age, height, weight, and BMI was 10.8, 143.4 cm, 39.9 kg, and 18.5 kg/m². The correlation between the forearm and whole body percent fat was R² 0.63 and RMSE of 4.1 %. Including age and BMI improved the R² values to 0.61 and 0.64 respectively.

Conclusions: In this pilot, we demonstrated a method to assess body composition from dedicated forearm scans that agree well with similar measures from whole body scans. Further work will be to include more participants and to quantify the association of our measures to forearm pQCT muscle cross sectional area measures available in this population.

Disclosures: Louise Marquino, None.

SU0421

The Essential Role of Connective Tissue Growth Factor (CTGF/CCN2) in Palatogenesis. Joseph Tarr^{*}, Honey Hendsi, Alex Lambi, James Bradley, Steven Popoff. Temple University School of Medicine, USA

Nonsyndromic cleft palate is a common craniofacial birth defect with an incidence of 1 in 700 live births. Connective tissue growth factor (CTGF/CCN2) has emerged as an essential player in normal craniofacial skeletal formation. Recent studies suggest that CTGF acts as a necessary downstream mediator of TGF- β -dependent mesenchymal stem cell proliferation in palatogenesis. Previous work in our laboratory identified numerous craniofacial defects such as failure of formation of the bony palate in CTGF knockout (KO) mice. In this study, microCT and histological analyses showed that in the absence of CTGF, the growth of the palatal shelves is arrested at an early stage in the process of palatogenesis. We isolated mesenchyme-derived pre-osteoblasts from crania of WT and CTGF KO mice for in vitro studies. CTGF KO cells exhibited decreased proliferation with a significant reduction in the number of cells in the S phase and a concomitant increase in the number of cells accumulating on the G0/G1 phase compared to WT cells. CTGF KO cells exhibited decreased ability to adhere to extracellular matrices, reduced spreading, altered cytoskeletal organization, and reduced levels of total and activated Rac1 compared to WT cells. The reduction in Rac1 resulted in decreased focal adhesion formation in CTGF KO cells. Since all of these cell functions are necessary for proper formation of the secondary palate during craniofacial development, we conclude that these defects contribute to the failure of the palatal shelves to form and grow in CTGF KO mice. Future studies will focus on elucidating how CTGF regulates the activity of other factors (e.g. TGF β /BMPs, SHH/IHH, Wnt-5a), known to play key roles in palatal development.

Disclosures: Joseph Tarr, None.

MO0001

CKD effects on cortical bone are age-independent. Karl Foley, Emily Stein, Natalia Cortez, Kyle Nishiyama, Donald McMahon, Elizabeth Shane, Thomas Nickolas*. Columbia University, USA

Chronic kidney disease (CKD) and aging are common causes of osteoporosis. However, the skeletal effects of these processes differ. This is relevant because highest fracture risk in CKD patients occurs after age 65 and the joint effects of CKD and aging on cortical (Ct) and trabecular (Tb) compartments are poorly described. In CKD high levels of parathyroid hormone are catabolic for Ct bone and may be anabolic for Tb bone. In contrast, in aging hypogonadism is associated with Ct and Tb loss. Thus, strategies to prevent fractures in older CKD patients may require a multifaceted approach that targets several pathogenetic mechanisms of bone loss. In a cross-sectional cohort of patients with and without CKD between 50 and 85 years, we used high-resolution peripheral computed tomography (HRpQCT, XtremeCT, Scanco, 82µm³) to assess the effects of CKD and age on Ct and Tb geometry, volumetric bone mineral density (vBMD) and microarchitecture at the distal radius and tibia. We hypothesized that compared to an age, race and sex matched healthy reference group without CKD or diabetes that: (1) older age would modify the effect of CKD on the severity of Ct defects; and (2) Older age alone would account for the severity of Tb defects. We enrolled 180 CKD patients from the renal clinics. A reference group of 73 patients was enrolled from the General Medicine clinics. eGFR was assessed by MDRD. Linear regression models were used to assess relationships between CKD status, age and their first-order interaction; all models were adjusted for sex and race. CKD and Reference groups were well matched for age, sex and race, and between-group differences were not significant (Table 1). Contrary to our hypothesis, there was no effect modification of age on CKD for radius and tibia Ct measures. Thus, CKD and age had independent effects on Ct bone. CKD status and each 10-year increase in age were associated with less dense and thinner cortices (Table 2). Consistent with our hypothesis Tb vBMD and microarchitecture did not differ by CKD status. Surprisingly older age had no effect on Tb measures. These findings suggest that CKD and age independently drive Ct defects, which may have broad implications for preventing bone loss and fractures in older CKD patients. Pathogenetic mechanisms for these relationships are currently being explored.

Table 1: Demographics of CKD patients and an age, race and sex matched healthy Reference Group

| | CKD (N=180) | Reference Group (N=73) |
|---|-------------|------------------------|
| Age (mean±SD yrs) | 69±9 | 64±9 |
| Women % (N) | 46 (82) | 58 (46) |
| White % (N) | 55 (99) | 49 (39) |
| HD % (N) | 27 (49) | NA |
| eGFR for non-dilaysis patients (mean±SD mL/min) | 34±17 | 82±15 |

Table 1

Table 2: Linear regression models for radius and tibia Ct and Tb measures by HRpQCT in CKD patients compared to an age, race and sex matched healthy Reference Group

| | β-coefficient for CKD Effect | β-coefficient for Age Effect (per 10-year increment) | Interaction p-value between CKD and Age |
|---|------------------------------|--|---|
| Radius | | | |
| Total Area (mm ²) | 7±7 | -9.0±3.2 † | NS |
| Ct Area (mm ²) | -6.5±2.0 † | -4.8±0.9 ‡ | NS |
| Tb Area (mm ²) | 13.5±7.2 | -4.2±3.3 | NS |
| Total vBMD (mgHA/cm ³) | -36.3±9.9 † | -14.4±4.6 † | NS |
| Ct vBMD (mgHA/cm ³) | -40.7±10.1 ‡ | -29.2±4.7 ‡ | NS |
| Ct Thickness (mm) | -0.1±0.03 † | -0.1±0.01 ‡ | NS |
| Tb vBMD (mgHA/cm ³) | -11.9±6.4 | -4.7±3.0 | NS |
| Tb Number (1/mm) | -0.1±0.1 | -0.03±0.03 | NS |
| Tb Heterogeneity (SD) | 0.06±0.04 | 0.01±0.02 | NS |
| Tibia | | | |
| Total Area (mm ²) | 0.6±16.9 | -1.8±7.8 | NS |
| Ct Area (mm ²) | -10.6±4.4 * | -11.5±2.0 ‡ | NS |
| Tb Area (mm ²) | 11.2±17.6 | 9.6±8.2 | NS |
| Total vBMD (mgHA/cm ³) | -24.4±8.3 † | -15.0±3.8 † | NS |
| Ct vBMD (mgHA/cm ³) | -44.3±9.8 ‡ | -40.6±4.5 ‡ | NS |
| Ct Thickness (mm) | -0.12±0.4 † | -0.1±0.02 ‡ | NS |
| Tb vBMD (mgHA/cm ³) | -10.6±6.1 | -2.6±2.8 | NS |
| Tb Number (1/mm) | -0.1±0.1 | -0.01±0.03 | NS |
| Tb Heterogeneity (SD) | 0.04±0.03 | 0.001±0.01 | NS |
| Comparison of CKD to the Reference Group: *<0.05; †<0.01; ‡<0.001 | | | |
| All models are adjusted for race and sex | | | |

Table 2

Disclosures: Thomas Nickolas, None.

MO0002

Diminished bone quality in tissue formed following the onset of moderate Chronic Kidney Disease in C57BL/6 mice. Chelsea Heveran*¹, Moshe Levi², Karen King², Virginia Ferguson¹. ¹University of Colorado, USA, ²University of Colorado School of Medicine, USA

Chronic Kidney Disease (CKD) increases fracture risk, yet fragility in human CKD is not explained by decreased bone mass. CKD disrupts systemic mineral homeostasis and is characterized by abnormal osteocyte activity. Thus we hypothesize that skeletal fragility in CKD results primarily from impaired bone material quality. In this study, 10-week-old male C57BL/6 mice were subjected to 5/6th Nephrectomy (5/6Nx) to establish CKD, or Sham surgeries (n = 6 / group). Mice were fed a standard chow diet and euthanized after 11 weeks post surgery.

Elevated BUN (83%, p < 0.05) and creatinine (26% p < 0.05) confirmed moderate CKD status in 5/6Nx. Bone material quality was evaluated in cortical bone at the tibia mid-diaphysis in “New” bone, determined to be formed following Sham or 5/6 Nx surgeries, and “Extant” bone deposited prior to surgery. Tibiae were embedded in PMMA, sectioned at the mid-diaphysis, polished (0.05 µm finish), carbon coated, and evaluated using quantitative backscattered electron microscopy with calibrated glass reference standards. Nanoindentation (5mm spherical tip; Hysitron TI-950) evaluated indentation modulus (E) in arrays extending through New bone and Extant bone; mineral volume fraction (minVf) measurements were collected at matched sites.

In Sham, E increased in New bone with distance from the periosteal surface and plateaued in Extant bone - a pattern indicative of expected tissue maturation. The minVf did not change with distance in Sham. Analysis of mean E and minVf showed no significant difference between New and Extant bone in Sham. Conversely, for 5/6Nx, both mean E and minVf were reduced in New vs. Extant bone (-10.3%, -5.5%; respectively, p < 0.01). Regression analysis showed E in New 5/6Nx bone at the periosteal surface is lower than in Sham (-13.5%, p < 0.01); however, E increased more rapidly with distance in 5/6Nx (+52.6%, p < 0.01) to achieve equal E values in Extant bone in both groups. Preliminary observations via Raman spectroscopy imply that altered mineral chemistry is a contributor to diminished bone quality with 5/6Nx. In summary, cortical bone material formed following the onset of moderate CKD in skeletally mature mice has diminished minVf and E. These results suggest that deleterious bone material changes may impart skeletal fragility in human CKD.

Disclosures: Chelsea Heveran, None.

MO0003

Nanomechanical properties of cortical bone in dialysis patients. Yoshiko Iwasaki¹, Ryota Kawamata², Yuko Mikuni-Takagaki², Junichiro Kazama³, Masafumi Fukagawa⁴. ¹Oita University of Nursing & Health Sciences, Japan, ²Division of Biochemistry & Molecular Biology, Kanagawa Dental University, Japan, ³Dialysis center, Niigata University Medical & Dental Hospital, Japan, ⁴Division of Nephrology, Endocrinology, & Metabolism, Tokai University School of Medicine, Japan

Bone histology in dialysis patients is conventionally classified into three types based on bone histomorphometry with tetracycline labeling i.e., mild change type (M), osteitis fibrosa (OF), and adynamic bone disease (ABD). Although mineralization and bone turnover varies in dialysis patients, common abnormality is increasing bone fragility. Recent report demonstrates that reducing mechanical properties accompanied with chemical composition changes are observed in trabecular bone biopsy samples from dialysis patients, which have not been examined with cortical bone. In this study, we analyzed biopsy samples of cortical bone from dialysis patients. Double tetracycline-labeled bone specimens were obtained by iliac crest bone biopsies from dialysis patients. As controls, we obtained control bone specimens from healthy volunteers with normal kidney function. Bone turnover was assessed by conventional bone histomorphometry using the section from bone specimens. The remaining tissue blocks were analyzed by direct raman spectroscopy measurement, nanoindentation assessment, and microfocus computed tomography (MCT). Although the ratio of carbonate to phosphate seemed higher in OF group, significant differences were not confirmed among three groups. The level of crystallinity in ABD group was tended to be low. Young's modulus (shape-independent material stiffness) in cortical bone was 26% and 17% less in bone with OF compared with bone with normal or Mild change type. Hardness (the ability of resistance) of bone in OF was 30% less compared with ABD. In addition, wider variations in ten indentation data were observed in OF and ABD groups compared with normal group. The degree of porosity in cortical bone increased in both OF and ABD groups. These results suggest that nanomechanical property of cortical bone in dialysis patients is affected by microarchitecture changes, but not by alterations of chemical composition, mineralization or bone turnover.

Disclosures: Yoshiko Iwasaki, None.

MO0004

The impact of dementia in hip fractures in patients receiving dialysis therapy. Milka Maravic¹, Agnes Ostertag², Pablo Urena Torres³, Martine Cohen-Solal⁴. ¹department of rheumatology, hopital Lariboisiere, France, ²Inserm U1132, hopital Lariboisiere, France, ³Unité de nephrologie et de dialyse, clinique du Landy, France, ⁴Centre Viggo Petersen, France

Objectives: Hip fractures (HF) are associated with significant morbidity and the incidence is further increased in patients with chronic kidney disease (CKD). Higher morbidity in dialysis patients is related to several risk factors. We have shown that proportion of dementia is significantly higher in CKD patients. We here aimed to investigate 1) the impact of dementia in FH in patients on dialysis therapy and 2) to assess if the risk of HF in demented patients is increased CKD patients compared to non CDK patients. **Methods:** Data are obtained from the National Database of Hospitalizations over the period 2011-2013. Three populations of subjects aged 60 and over were extracted and analyzed: population with hip fracture, population in dialysis and population of demented patients (whatever the reason for hospitalization in connection or not with dementia). These populations were crossed to estimate fracture risk based on the presence of dementia or dialysis, adjusted for age and sex. The fracture risk was calculated using a multiple logistic regression model.

Results: Over the period 2011-2013, 213 180 patients had a HF (70% women), 660 434 patients were diagnosed for dementia (64% women) and 47 430 patients were on dialysis (39% women). There was a strong effect of age and gender in the incidence of fractures and dementia in CKD and non CKD patients. In dialysis patients, the risk of HF was higher in patients with dementia than without dementia: OR 1.99 [95% CI: 1.66-2.38], this being the same for men OR 2.37 [1.81-3.05] and women OR 2.56 [1.97-3.29] at any age. In patients with dementia, the fracture risk is independent of dialysis OR: 1.25 [0.99-1.59] in each sex and age categories. However, the risk of dementia is not increased by dialysis therapy in the population with HF: OR 1.52 [0.77-3] after adjustment for age and gender.

Conclusion: Dementia significantly increases the risk of hip fracture in dialysis patients, but this risk in demented patients is equally high whether receiving dialysis therapy or not. These results highlight dementia as a major risk factor for FH in dialysis therapy and suggest that attention should be paid to dementia in order to prevent hip fracture.

Disclosures: Martine Cohen-Solal, None.

MO0005

The Role of Activin in the Pathogenesis of the CKD-MBD. Toshifumi Sugatani¹, Olga Agapova¹, Yifu Fang¹, William Smith², Hartmut Malluche³, Keith Hruska⁴. ¹Washington University, USA, ²Celgene Corporation, USA, ³University of Kentucky, USA, ⁴Washington University in St. Louis School of Medicine, USA

Introduction: At its inception the CKD-MBD includes vascular calcification, osteodystrophy, loss of klotho and stimulation of FGF23, and its pathogenesis is unknown. Here we report the role of activin in the pathogenesis of renal osteodystrophy in a model of type 2 diabetes with a low turnover osteodystrophy prior to the induction of CKD equivalent to stage 3-4 human CKD.

Methods: CKD with hyperphosphatemia, elevated FGF-23 and PTH, and 60% reduction in GFR (CKD-3) was induced at 14 weeks of age in the *ldlr*^{-/-} high fat fed model of atherosclerotic vascular calcification. CKD mice were treated with RAP-011, an ActRIIA ligand trap, 10mg/kg (n=15) or VEH, (n=13), IP twice weekly beginning at 22 weeks of age and studied at 28 weeks by skeletal histomorphometry and microCT.

Results: Relative to CKD-3 mice receiving vehicle, microCT of long bones revealed that RAP-011 significantly increased cortical bone volume and cortical thickness. Induction of CKD caused high turnover bone disease in VEH mice, that also demonstrated a reduction in TBV (11.22%) that was reversed by six weeks of RAP-011 treatment (13.28%). Histomorphometry revealed that relative to SHAM, CKD caused an increase in erosion surface/bone surface (1.05 & 1.83% respectively) and osteoclast number/100mm bone length (33.40 & 62.32/100mm respectively), that were reduced by RAP-011(1.23% and 38.37/100mm). Relative to SHAM, CKD caused an increase in osteoblast surface/bone surface (0.76 & 1.58% respectively) and osteoblast number/100mm bone length (45.03 & 110.63/100mm respectively, p<0.05 WT vs SHAM and SHAM vs VEH). RAP-011 significantly reduced, relative to VEH, both osteoblast surface/bone surface and osteoblast number/100mm bone length (0.68% and 43.18/100mm, p<0.05). Despite the significant reduction in osteoblast number relative to VEH, the mineral apposition rate in RAP-011 was maintained (0.42 and 0.40 $\mu\text{m}^3/\text{day}$, respectively), with a significant increase in the bone formation rate/osteoblast (0.17 and 0.48 $\mu\text{m}^3/100$ cell/year, respectively, p<0.05), to a rate similar to wild type (0.42 $\mu\text{m}^3/100$ cell/year).

Conclusion: Increased circulating Activin during CKD contributes to the high turnover osteodystrophy produced by CKD-3, and its inhibition through an ActRIIA ligand trap increased bone volume by inhibiting bone resorption and counteracting the negative effects of CKD, at the cellular level, on osteoblasts normalizing the mineral apposition rate and bone formation rate/osteoblast.

Disclosures: Toshifumi Sugatani, None.

This study received funding from: Celgene corporation

MO0006

LIM-Domain Protein AJUBA Is A Required Co-Factor For Gfi1 Suppression Of Runx2 In Pre-Osteoblasts In Multiple Myeloma. Juraj Adamik¹, Jixin Ding², Peng Zhang¹, Sun Quanhong¹, G. David Roodman³, Deborah L. Galson¹. ¹University of Pittsburgh, USA, ²Indiana University, USA, ³Indiana University & Veterans Administration Medical Centre, USA

We previously reported that the transcriptional repressor Gfi1 is increased in multiple myeloma (MM) exposed bone marrow stromal cells (BMSC) and represses the *Runx2* gene. Gfi1 directly binds to the *Runx2* promoter and recruits various chromatin modifiers causing long-term epigenetic inactivation of *Runx2* expression, which results in impaired osteoblast (OB) differentiation. In this study, we explored if the LIM-domain protein family member AJUBA plays a role in MM-induced Gfi1 repression of *Runx2*. AJUBA, which doesn't bind DNA directly, is known to act as a co-repressor of SNAI1 and SNAI2/SLUG-dependent repression and as an HDAC-dependent co-repressor for a subset of Gfi1 target genes in myeloid cells. We hypothesized that AJUBA functions as a corepressor of Gfi1 to epigenetically repress the *Runx2* gene in MM-exposed pre-OB. To address this question we co-cultured pre-OB (MC4) with 5TGM1 MM cells and used ChIP to assay for the presence of AJUBA on the *Runx2* promoter. After 36-48h MM exposure of MC4 cells, enrichment of AJUBA occupancy was co-localized to the previously mapped Gfi1 binding site in the *Runx2* promoter concurrently with the recruitment of Gfi1. Biotin-oligo pulldown of Gfi1 brought down AJUBA as well. Further, cotransfection of AJUBA and Gfi1 revealed that AJUBA enhanced repression by suboptimal doses of Gfi1 of both a *Runx2*-luciferase reporter as well as the endogenous *Runx2* gene in pre-OB. Studies using deletion constructs showed that the LIM region of AJUBA in conjunction with Gfi1 is necessary and sufficient for *Runx2* repression, and the pre-LIM portion of AJUBA does not affect *Runx2* luciferase expression. Transfected AJUBA exhibits cytoplasmic localization in MC4 cells unless co-expressed with full-length Gfi1, which brings it into the nucleus. Nuclear co-localization of AJUBA with Gfi1 was uncoupled in MC4 cells when transfected with Gfi1 containing only the DNA binding region (aa 239-423). Transfected 239-423 Gfi1 binds the endogenous *Runx2* promoter, but fails to repress transcription, likely due to impaired recruitment of AJUBA. Importantly, knockdown of AJUBA caused decreased recruitment of Gfi1 to the *Runx2* gene in pre-OB and prevented the Gfi1 repression of a *Runx2* reporter. Consistent with these observations, lack of AJUBA in MC4 pre-OB prevented the MM-induced sustained repression of *Runx2* mRNA. Our study reveals that AJUBA functions as a required Gfi1 co-factor for *Runx2* suppression in OB lineage cells in MM bone disease.

Disclosures: Juraj Adamik, None.

MO0007

Knee Loading Enhances Vessel Remodeling and Bone Healing in a Rat Femoral Head Osteonecrosis Model. Daquan Liu¹, Jie Li¹, Xinle Li¹, Hiroki Yokota², Ping Zhang^{*1}. ¹School of Basic Medical Sciences, Tianjin Medical University, China, ²Department of Biomedical Engineering, Indiana University Purdue University Indianapolis, USA

Osteonecrosis of the femoral head is a serious orthopedic problem. Moderate loads with knee loading promote bone formation, but its effects on the healing of osteonecrosis have not yet been investigated. Using a rat model, we examined a hypothesis that knee loading enhances vessel remodeling and bone healing through the modulation of the fate of bone marrow-derived cells.

Eighteen male SD rats (~12 wks) were divided into 3 groups such as the sham-operated control, osteonecrosis, and loaded osteonecrosis (n=6). Osteonecrosis was induced by transecting the ligamentum teres followed by a tight ligature around the femoral neck. For knee loading, 5 N loads were laterally applied to the knee at 15 Hz for 5 min/day for 35 days. Changes in bone mineral density (BMD) and bone mineral content (BMC) of the femur were measured by pDEXA, and ink infusion was performed to evaluate vessel remodeling. Femoral head were harvested for histomorphometry, and bone marrow-derived cells were isolated to examine osteoclast development and osteoblast differentiation.

Osteonecrosis induced a significantly bone loss, and knee loading stimulated vessel remodeling and bone healing. Among these 3 groups, osteonecrosis exhibited a shorter height of the femoral head ($p<0.01$), lower trabecular BV/TV ($p<0.001$) in femoral head, and lower femoral BMD ($p<0.05$) and BMC ($p<0.01$). However, knee loading restored femoral head BMD/BMC (both $p<0.05$) and trabecular BV/TV ($p<0.001$). Osteonecrosis decreased the vessel volume and vessel number (both $p<0.001$), while knee loading increased them (both $p<0.001$). A significant positive correlation was observed between bone quality (BMD/BMC and BV/TV) and vessel remodeling (vessel volume and vessel number) ($r=0.89-0.92$, $p<0.001$). Osteonecrosis activated osteoclast development, and knee loading reduced its formation, migration and adhesion (all $p<0.001$). In addition, knee loading attenuated the level of "pit" formation to base level. Furthermore, knee loading significantly increased CFU-F and CFU-OBL (both $p<0.01$).

The results indicate that in response to knee loading vessel remodeling is associated with bone healing. Further studies are needed to clarify the molecular mechanism underlying the vessel remodeling and bone remodeling, and the role of bone marrow-derived cells. The current study suggests that knee loading can non-invasively enhance the healing of osteonecrosis through vessel remodeling.

Disclosures: Ping Zhang, None.

MO0008

acromegaly and bone health: combined effects of disease activity and gonadal status. giuseppe guglielmi¹, claudia battista², francesca di chio¹, antonio salcuni³, michelangelo nasuto¹, renaud winzenrieth^{*4}, doris tran⁴, alfredo scillitani³. ¹Department of Radiology, University of Foggia, Italy, ²Unit of Endocrinology, "Casa Sollievo della Sofferenza" IRCCS, Italy, ³Unit of Endocrinology, "Casa Sollievo della Sofferenza" IRCCS, Italy, ⁴Department of Clinical Research, Medimaps Group, France

The effects of GH excess on bone architecture and strength are still unclear. Vertebral fractures have been observed in acromegalic patients with areal Bone Mineral Density (BMD) T-score > -2.5 . Previous study also reported unclear effects of disease activity and gonadal status on bone parameters at spine. The aim of this study was to assess in acromegalic patients the effects of disease activity and gonadal status on bone health assessed by bone mineral density (BMD) and Trabecular Bone Score (TBS), respectively.

This cross-sectional study involved 47 acromegalic patients (27 women and 20 men; mean age and BMI of 54.9 ± 11.5 years and 29.6 ± 4.5 kg/m² respectively). Subjects were stratified in respect to disease activity (active, ACT, or controlled, CTR) and gonadal status (hypogonadal, HYP, or eugonadal, EUG). Thirty-two patients were hypogonadal (22 female and 10 male). Among 22 hypogonadal female, 9 patients had an active disease and 13 patients had a controlled disease. Among 10 hypogonadal male, 4 patients had an active disease and 6 patients had a controlled disease.

BMD and TBS were evaluated at PA Spine (L1-L4) using a iDXA GE encore 13.60 device and TBS iNsight® (v2.1, Med-Imaps, France).

In respect to normative data, TBS Z-score of patients with controlled disease and hypogonadism (CTRL/HYP) was significantly lower ($p<0.001$), while TBS Z-score of the other 3 subgroups were not different. Regarding BMD Z scores, there was not any difference between each subgroup and the normative data. Moreover, BMD Z-scores were not different among the 4 groups, while TBS Z-score of patients with controlled disease and hypogonadism (CTRL/HYP) was significantly lower than the other 3 groups.

The prevalence of vertebral fractures (VFs) in our population of acromegalic patients was 21.3%. In an univariate analysis TBS associated with the presence of VFs (OR=2.69 [1.13-6.41]), and among the variable evaluated, only TBS associated with VFs in multiple regression analysis.

In conclusion, bone microarchitectural texture at lumbar spine is impaired in acromegalic patients with controlled disease and hypogonadism.

Disclosures: renaud winzenrieth, None.

MO0009

Clinical and Biochemical Features of Adults with Hypercalcemia, Hypercalciuria, Elevated Calcitriol and Nephrolithiasis due to CYP24A1 Mutations in a Single Family. Derek O'Keeffe^{*}, Peter Tebben, Rajiv Kumar, Ravinder Singh, Yanhong Wu, Robert Wermers. Mayo Clinic, USA

Background: We identified a 60 year old male (proband) with intermittent hypercalcemia, hypercalciuria, elevated 1,25-OH₂D (calcitriol), undetectable 24,25-OHD, chronic nephrolithiasis and osteopenia. His family history was significant for several family members with a similar clinical phenotype. Genetic analysis revealed two mutations in the *CYP24A1* gene: (A) p.R396W and (B) c.428_430delAAG which encodes 1,25-OH₂D 24-hydroxylase, the key enzyme of 1,25-OH₂D inactivation. **Objective:** To identify the clinical, biochemical and genetic features of *CYP24A1* mutations in a single family. **Methods:** After Institutional Review Board approval 4 siblings, 2 nieces and the daughter of the proband consented to take part in the study, which included measurement of calcium biomarkers, CYP24A1 gene analysis, and a review of their medical history. **Results:** The pedigree of the syndrome was autosomal recessive, with subjects either inheriting, A, B, A/B or none (Table 1). Clinically, including the proband (subject 1), 4 subjects had a history of symptomatic nephrolithiasis (passed kidney stones) while 4 did not. Two subjects were compound heterozygous (A/B) and had more severe clinical features (Table 1). One subject without stone passage had no evidence of a mutation. Of the remaining 4 subjects with a single heterozygous mutation (either A or B), 2 had nephrolithiasis. Four subjects had hypercalciuria (> 300 mg/spec) but only 2 had hypercalcemia (> 10.1 mg/dl). Six subjects had 1,25 Vit D > 60 pg/ml. The 25-OHD / 24,25 OH₂D ratio, in the 2 subjects with A/B mutations was > 100 . **Conclusion:** Adult familial *CYP24A1* mutations have a heterogeneous clinical and biochemical spectrum. A gene dose effect is apparent given that subjects with compound heterozygous mutations (A/B) have more severe clinical and biochemical patterns. However, subjects with a single heterozygous mutations (A or B) also developed clinical disease (2 subjects), likely influenced by environmental factors such as hydration, 25 OHD levels, and calcium intake.

| Subject | Mutation | Symptomatic Nephrolithiasis | 25-OHD / 24,25 OH ₂ D | Urinary Calcium (mg/24 hours) |
|---------|----------|-----------------------------|----------------------------------|-------------------------------|
| 1 | A/B* | Yes | 477 | 493 |
| 2 | None | No | 13 | 289 |
| 3 | A | No | 17 | 311 |
| 4 | A/B | Yes | 104 | 672 |
| 5 | A | Yes | 30 | 229 |
| 6 | B | No | 13 | 139 |
| 7 | A | No | 23 | 359 |
| 8 | A | Yes | 16 | 289 |

* (A) p.R396W and (B) c.428_430delAAG mutation in CYP24A1 gene

Table 1 Clinical and Laboratory Features of CYP24A1 Mutations in a Single Family

Disclosures: Derek O'Keeffe, None.

MO0010

Withdrawn.

MO0011

Increased MicroRNA-34a Expression Levels in Paget's Disease of Bone. Daniela Merlotti^{*1}, Guido Sebastiani², Simone Bianciardi², Marco Valentini², Stefano Gonnelli², Carla Caffarelli², Isabella Evangelista², Simone Cenclì³, Ranuccio Nuti², Francesco Dotta², Luigi Gennari². ¹University of Siena, Italy, ²Department of Medicine, Surgery & Neurosciences University of Siena, Italy, Italy, ³Division of Genetics & Cell Biology, San Raffaele Scientific Institute, Milan, Italy, Italy

MicroRNAs (miRs) have recently emerged as important regulatory factors involved in the developmental processes and in the regulation of bone cell activity. Despite different miRs have been associated with modulation of osteoblast activity, two miRs have been mainly associated with osteoclast activity and bone resorption, miR-21 and miR-34a. While the former (miR-21) is up-regulated during RANKL-induced osteoclastogenesis and seems to be essential for osteoclast activity (Blood 2011;117:3648-57), the latter (miR-34a) is a suppressor of osteoclastogenesis and its overexpression attenuated ovariectomy-induced bone loss as well as the development of bone metastases in mice models (Nature 2014;512:431-5). Here, we analysed the expression levels of miR-21 and miR-34a in peripheral blood mononuclear cells from patients with Paget's disease of bone (PDB), a disease characterized by a marked increase in osteoclast activity and bone turnover at affected skeletal sites. Peripheral blood mononuclear cells were obtained from 30 patients with active PDB (10 with SQSTM1 mutation) and 20 age-matched controls. Quantitative analysis of miR-21 and miR-34a was performed using specific stem-loop primers followed by real-time

polymerase chain reaction. All values were normalized to endogenous control U6. Expression levels of miR-34a were 4.4¹.7-fold increased in peripheral blood mononuclear cells from patients with PDB with respect to controls (p<0.0001). A similar but not significant trend was observed concerning miR-21, which was 2-fold increased in PDB cases than controls. A statistically significant inverse correlation was observed between bone turnover markers and miR-34a levels in controls but not in patients with PDB. Moreover, miR-34a expression did not significantly differ between monostotic and polyostotic PDB cases or in relation to SQSTM1 mutation status. Taken together these results show for the first time an inverse relationship between miR-34a expression and bone turnover, *in vivo*, in elderly individuals. However, miR-34a expression levels were unexpectedly increased in patients with active PDB (despite the increase in bone turnover markers typically observed in this condition) and this might account, at least in part, for the delayed time to bone metastases and the improved overall survival of patients with prostate cancer and PDB than patients with prostate cancer alone, recently reported in a large retrospective analysis (Br J Cancer 2012;107:646-51).

Disclosures: Daniela Merlotti, None.

MO0012

MVNP Alters The Balance Of TBK1 And Optineurin In Osteoclast Lineage Cells To Generate Pagetic Osteoclasts. Quanhong Sun^{*1}, Peng Zhang¹, Juraj Adamik¹, Jolene J Windle², Laëtiti Michou³, Jacques P Brown³, Noriyoshi Kurihara⁴, G. David Roodman⁵, Deborah Galson¹. ¹University of Pittsburgh, USA, ²Virginia Commonwealth University, USA, ³Laval University, CHU de Quebec Research Centre & CHU de Quebec, Canada, ⁴Indiana University, USA, ⁵Indiana University & Veterans Administration Medical Center, USA

Paget's disease of bone (PDB) is characterized by abnormal osteoclasts (OCL) with increased nuclei/OCL. Measles virus nucleocapsid protein (MVNP) was reported to play a key role in the development of pagetic OCL. Additionally, MVNP expression targeted to OCL in mice (Tg-MVNP) induces pagetic bone lesions *in vivo* and aberrant OCL *in vitro*. MVNP's upregulation of IL-6 is essential for the pagetic phenotype. We recently reported that MVNP activation of TBK1, an IKK family member, is a critical mediator of MVNP-dependent generation of pagetic OCL. We also reported that another IKK family member, optineurin (OPTN), is a novel negative regulator of OCL formation that also blocks MVNP and TBK1 induction of IL-6. We demonstrated that Tg-MVNP pre-OCLs and MVNP^{p62^{P392L}}-Paget's patient OCLs had increased TBK1 and decreased OPTN protein levels, resulting in an increased TBK1:OPTN ratio. Further, MVNP transduced into normal human CFU-GM also increased TBK1 and decreased OPTN in both pre-OCLs and mature OCLs.

We demonstrate here that endogenous OPTN and TBK1 interact in the pre-OCL cell line 4B12 by co-IP. IP of OPTN also pulls down MVNP in cotransfected cells. Immunohistochemistry of Tg-MVNP pre-OCL revealed that MVNP colocalized with both endogenous TBK1 and OPTN in large perinuclear puncta. Lentiviral transduced TBK1-GFP and dsRed-OPTN were almost entirely colocalized with MVNP in Tg-MVNP pre-OCL. Ectopic TBK1 increased OCL formation and IL-6, whereas ectopic OPTN decreased OCL formation and IL-6. MVNP's interaction with OPTN may be how MVNP activates TBK1, by preventing OPTN from repressing TBK1 activity. In turn, TBK1 phosphorylation of OPTN induces its degradation. Inhibition of TBK1 in pre-OCL with BX795 elevated OPTN mRNA and protein. We recently generated a new mouse model with TBK1 targeted to the OCL lineage (Tg-TBK1). Tg-TBK1 pre-OCL from 3 founder lines displayed a pagetic phenotype *in vitro* with increased OCL, IL-6, and nuclei/OCL. Further, Tg-TBK1 pre-OCL have higher activated TBK1 and lower OPTN levels. OPTN knockdown increased OCL formation by WT and Tg-MVNP pre-OCL 2-3 fold, but only increased Tg-TBK1 OCL formation slightly since ectopic TBK1 already repressed OPTN levels. However, ectopic OPTN in Tg-TBK1 pre-OCL decreased OCL formation. These results confirm OPTN as a negative OCL regulator and reveal that MVNP's interaction with the TBK1-OPTN complex in pre-OCL decreases OPTN and plays an important role in generating pagetic OCL.

Disclosures: Quanhong Sun, None.

MO0013

Paget's disease of Bone in Thai: Clinical Characteristics and Genetic Studies of Three Sporadic Cases. Lalita Wattanachanya^{*1}, Sumittra Charoenhirunyingyos², Voranuch Thanakit³, Weerapan Khovichunkit². ¹Kingchulalongkorn memorial hospital, Thailand, ²Division of Endocrinology & Metabolism, Departments of Medicine, Faculty of Medicine, Chulalongkorn University & King Chulalongkorn Memorial Hospital, Thai Red Cross Society, Bangkok, 10330 Thailand, Thailand, ³Departments of Pathology, Faculty of Medicine, Chulalongkorn University, & King Chulalongkorn Memorial Hospital, Thai Red Cross Society, Bangkok, 10330 Thailand, Thailand

Paget's disease of bone (PDB) is considered rare in Asians and there are scant published studies regarding genetic basis of PDB in this population. Here, we reported clinical features and genetic studies of three Thai patients with PDB. The first case was a 35-year-old man who presented with progressive low back pain, left hip tenderness

and generalized muscle weakness. Serum alkaline phosphatase (ALP) level was elevated. Bone surveys revealed generalized lytic and blastic lesions at skull, clavicles, lumbar spines and femurs corresponding to the increased uptake on bone scans. PDB was confirmed by an iliac bone biopsy showing a mosaic-like pattern with increased number of cement lines of bone matrix, prominent osteoclasts, foci of new bone formation with osteoblastic rimming and vascular-intervening stroma. The second case was a 59-years-old man presented with low back pain and right leg weakness with elevated ALP level. Radiographs demonstrated lytic lesions at the 5th lumbar vertebra. Bone metastasis was initially considered, however, extensive investigations failed to show any evidence of malignancy. Thoracic and abdominal CT scans demonstrated mixed expansile blastic and lytic lesions at left acetabulum, left iliac bone, and the 5th lumbar vertebra. Bone scans showed increased uptake at sacrum and left pelvis. The iliac bone biopsy result was compatible with the diagnosis of PDB. The two patients responded well to oral bisphosphonate treatment and achieved normalized ALP levels and pain relief. The third case was a 79-year-old woman who was asymptomatic and presented with an isolated raised ALP level during routine testing. Bone surveys found a sclerotic change at occipital bone with thickening of the diploic space. The mixed regions of sclerosis and lucency were seen at the temporal bone, left iliac bone and acetabulum. Bone scans showed increased uptake at skull and left pelvis. She denied bone biopsy; however, the investigations suggested the diagnosis of PDB. Mutational analysis of the sequestosome1 gene was performed in our patients; however, no mutation was detected. In conclusion, we reported three cases of PDB in Thai. Although it is rare in Asian, PDB should be considered in the differential diagnosis in Asian patients with isolated elevation in ALP level or with bone lesions resembling bone metastasis. Further studies regarding clinical features and genetics of PDB in Asian population could provide important insights into its pathogenesis and could explain the ethnic disparity in PDB.

Disclosures: Lalita Wattanachanya, None.

MO0014

Changes in BMD and TBS up to 2 years after Surgical or Medical Management of Primary Hyperparathyroidism. Alice Abraham^{*1}, Cristiana Cipriani², Zhang Chengchen³, Didier Hans⁴, Bilezikian John⁵. ¹Endocrinology fellow, USA, ²Sapienza University of Rome, Italy, ³Columbia College of Physicians & Surgeons, Division of Endocrinology, USA, ⁴University of Lausanne, Switzerland, ⁵Columbia University College of Physicians & Surgeons, Division of Endocrinology, USA

It is well known that BMD improves after parathyroidectomy (PTX) in primary hyperparathyroidism (PHPT) but little is known about post-PTX changes in skeletal microstructure. We report post-PTX results in 15 subjects (10 women and 5 men) two years after surgery and compare these with 5 female subjects with PHPT observed without surgery for two years. We compared BMD and TBS between surgical and non-surgical patients at baseline, 1 and 2 years.

There were no significant between group differences in patient age (64 ± 14 vs 68 ± 8 years; p=0.54), BMI (31 ± 6 vs 29 ± 3 ; p=0.25), TBS scores, BMD at lumbar spine, femoral neck, total hip or 1/3 radius at baseline.

After one year, the non-surgery patients had no significant changes in TBS, BMD at lumbar spine, femoral neck, and total hip. After two years, there were no significant differences from baseline in BMD at the lumbar spine, radius, femoral neck and TBS.

At one year post PTX, patients had a significant gain in BMD at the lumbar spine ($+4.96\% \pm 1.31\%$; p=0.002), as well as at the femoral neck ($+3.00\% \pm 1.20\%$; p=0.02) and total hip ($+3.11\% \pm 0.82\%$; p=0.002). There were no significant differences at one year follow up in 1/3 radius and TBS among post-surgical patients. Two years after PTX, patients had sustained gains in BMD from baseline at the lumbar spine ($+4.23\% \pm 1.52\%$; p=0.01), as well as at the femoral neck ($+4.13\% \pm 1.09\%$; p=0.002) and total hip ($+4.12\% \pm 1.21\%$; p=0.004).

At one year of follow up, there were no significant differences in BMD and TBS scores between surgery and non-surgery subjects. At two years, post-PTX patients had greater gains in BMD at the lumbar spine ($+4.234\% \pm 1.518\%$ vs $-0.433 \pm 0.493\%$; p=0.01) and femoral neck ($+4.128\% \pm 1.089\%$ vs $-0.483 \pm 1.284\%$; p=0.03). There were no significant differences at two years of follow up in BMD at the radius, total hip and TBS among post-PTX patients and controls. Although not significant, there were positive changes in TBS in the medical group ($+1.4\%$) and surgical group ($+1.7\%$) at 24 months.

In the present study, we demonstrate there are significant gains in BMD at the lumbar spine and femoral neck two years after PTX in patients with hyperparathyroidism compared with nonsurgical controls. However, there were no significant differences in TBS after two years of observation. Postoperative changes in skeletal microstructure may take longer than 2 years to be appreciated by TBS.

MO0016

Table. Percent Change From Baseline

| | | 12 months* | 24 months* |
|------------------|------------|--------------------|---------------------|
| Lumbar spine BMD | Surgery | 4.96 (0.11) | 4.23 (0.001) |
| | Nonsurgery | 0.65 | -0.43 |
| Femoral neck BMD | Surgery | 3.0 (0.46) | 4.13 (0.04) |
| | Nonsurgery | 1.2 | -0.48 |
| Total Hip BMD | Surgery | 3.11 (0.28) | 4.12 (0.23) |
| | Nonsurgery | 0.01 | 1.35 |
| 1/3 Radius | Surgery | -0.28 (0.18) | 0.47 (0.40) |
| | Nonsurgery | -2.87 | -1.29 |
| TBS | Surgery | 2.8 (0.35) | 1.71 (0.92) |
| | Nonsurgery | 6.56 | 1.42 |

* p-value in parentheses for comparison between groups at specific month; bolded values are statistically different from baseline within-group

Table

Disclosures: Alice Abraham, None.

MO0015

Comparative Effect of PTH(1-84) on Bone Mineral Density and Trabecular Bone Score (TBS) in Hypoparathyroidism and Osteoporosis. Cristiana Cipriani^{*1}, Barbara Silva², Mishaela Rubin³, Natalie Cusano³, Donald J. McMahon³, Jessica Pepe⁴, Sara Piemonte⁵, Wen-Wei Fan³, Juviza K. Rodriguez³, Federica De Lucia⁵, Federica Biamonte⁴, Salvatore Minisola⁵, John P. Bilezikian³. ¹"Sapienza", University of Rome, Italy, ²Santa Casa de Belo Horizonte & Felicio Rocho Hospital, Division of Endocrinology, Brazil, ³Metabolic Bone Diseases Unit, Division of Endocrinology, Department of Medicine, College of Physicians & Surgeons, Columbia University, USA, ⁴Department of Internal Medicine & Medical Disciplines, "Sapienza" University of Rome, Italy, ⁵Department of Internal Medicine & Medical Disciplines, "Sapienza" University of Rome, Italy

We have shown previously in hypoparathyroidism (hypoPT), a disorder associated with above average BMD, that PTH(1-84) improves lumbar spine (LS) BMD and TBS over a 5-year treatment period. Studies in osteoporosis, a disorder associated with low BMD, have shown with PTH(1-34) a significant increase also in LS BMD and TBS. No data are yet available on the effects of PTH(1-84) on TBS in osteoporosis and no study has compared the two populations each treated with PTH(1-84). In this report, we provide data on the effects of PTH(1-84) on BMD and TBS in HypoPT and osteoporosis patients over an 18-month treatment period.

We studied 35 HypoPT women (19 PreM and 16 PostM; mean age 48.2 ± 13.4 yrs) and 40 women with post-menopausal osteoporosis (71 ± 8.3 yrs) treated with PTH(1-84) for 18 months. 3-site DXA (Hologic) [LS, femoral neck, total hip and distal 1/3 radius (Rad)] were assessed. Site-matched LS TBS data were extracted from the DXA image using TBS iNsite software. Within group comparison of % change in BMD and TBS relative to baseline and between-group comparison adjusting for age, BMI, baseline values and average monthly PTH(1-84) dose were assessed.

We observed a significant increase in LS BMD in hypoPT (3.3 ± 0.9%, p < 0.001) and osteoporosis (6.7 ± 1.1%, p < 0.002) patients after 18 months. There was a tendency towards an increase (1.9 ± 1.1%, p = 0.09) in TBS in hypoPT patients, while no difference in TBS was observed in osteoporosis patients. Rad BMD significantly declined in hypoparathyroid (-1.6 ± 0.7%, p < 0.02) and osteoporosis (-6.3 ± 1.2%, p < 0.0001) patients. The between-group comparison showed a significantly greater increase in TBS in hypoPT (1.9 ± 1.1%) compared to osteoporosis (0.3 ± 0.9%) patients (p < 0.001). No association was found between TBS and LS BMD in both groups. Similar results were obtained comparing postmenopausal hypoparathyroid and postmenopausal osteoporosis patients.

Our data show significant and similar increases in LS BMD in hypoparathyroid and osteoporosis patients treated with PTH(1-84) for 18 months. As shown by TBS, PTH(1-84) seems to stimulate a greater improvement in trabecular microstructure in hypoparathyroid patients (low bone turnover) than in osteoporosis patients (normal bone turnover). Mechanisms associated with gains in LS-BMD in hypoparathyroid and osteoporosis patients, however, are not significantly associated with changes in bone microarchitecture as captured by TBS, confirming that changes in TBS and BMD are independent of each other.

Disclosures: Cristiana Cipriani, None.

This study received funding from: NPS Pharma

Prevalence of Normocalcemic Primary Hyperparathyroidism among Blood Donors. Federica De Lucia^{*1}, Federica Ferrone¹, Vittoria Danese¹, Valeria Fassino¹, Giancarlo Ferrazza², Enrico Panzini³, Jessica Pepe¹, Cristiana Cipriani¹, Frank Block⁴, Salvatore Minisola¹. ¹Department of Internal Medicine & Medical Disciplines University of Rome 'Sapienza', Policlinico Umberto I, Viale del Policlinico, 155, 00161 Rome, Italy, ²Department of Immunohematology & Transfusion Medicine, University of Rome 'Sapienza', Policlinico Umberto I, Viale del Policlinico, 155, 00161 Rome, Italy, ³Department of Immunohematology & Transfusion Medicine, University of Rome 'Sapienza', Policlinico Umberto I, Viale del Policlinico, 155, Italy, ⁴DiaSorin, 1951 Northwestern Avenue, Stillwater, MN, USA, USA

Normocalcemic primary hyperparathyroidism (NPHPT) is a variant of the traditional hypercalcemic presentation of PHPT; it is characterized by consistently elevated PTH concentrations with normal total and ionized serum calcium concentration in the absence of secondary causes for elevated PTH concentrations. Few studies have addressed the issue of its prevalence. Here we report the results of an ongoing study aimed at evaluating the prevalence of NPHPT in blood donors volunteers.

MATERIAL AND METHODS. We enrolled 1053 normal blood donors aged 18-66 (40 ± 12) years (781 males and 272 females). After informed consent was obtained, a blood sample was taken for measuring serum ionized calcium (Nova 8; Nova Biochemical, Waltham, MA), 25(OH)vitamin D and serum immunoreactive, N-terminal specific-PTH (DiaSorin, LIAISON, PTH 1-84).

RESULTS. We found that there were 113 patients with serum PTH levels above normal range (88 males and 25 females, 10.7% of the total). Serum 25(OH)D levels were below 20 ng/ml in 69 of 113 subjects and below 30 ng/ml in 100 of 113 individuals. Forty-one of these patients volunteered to be studied again after vitamin D supplementation (50,000 UI cholecalciferol weekly for one month), for the determination of serum ionized and total calcium, phosphorus, 25(OH)vitaminD, 1-84 PTH, anti-transglutaminase antibodies, 24-hour urine calcium and creatinine clearance. In 35 of the subjects studied (including one with positive anti-transglutaminase antibodies) PTH normalized after vitamin D supplementation. In one of the remaining six patients, the increased serum PTH was due to renal hypercalciuria (24hours Ca/Cr ratio > 0.20). No other biochemical abnormalities were found in the remaining five subjects.

CONCLUSIONS. This study demonstrates that hypovitaminosis D in normal blood donors is the most frequent cause of raised serum PTH levels. Even though the study is ongoing, there is an unexpected high prevalence of increased PTH levels in the face of normocalcemia (12%), not related to identifiable causes. These subjects with PTH values above the normal range, are being followed prospectively in order to evaluate the long term natural history of this disease.

Disclosures: Federica De Lucia, None.

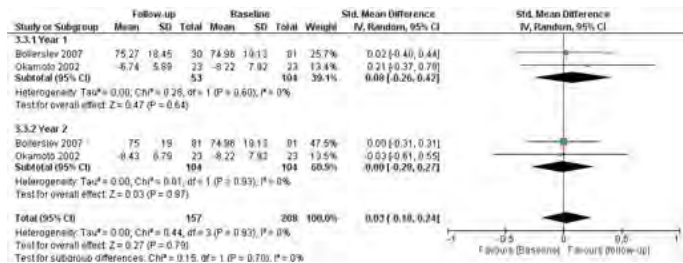
This study received funding from: DiaSorin

MO0017

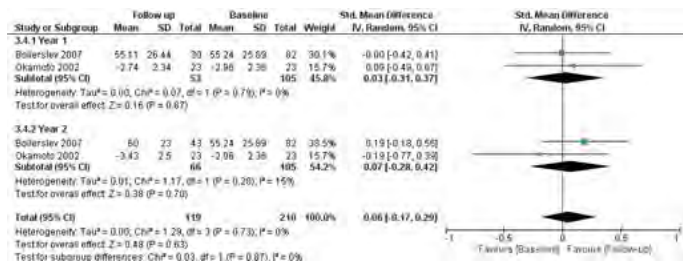
Quality of Life Changes in Patients with Asymptomatic Primary Hyperparathyroidism. Systematic Review and Meta-analysis. Navkky Singh Ospina^{*1}, Spyridoula Maraka², Ana E Espinosa De Ycaza³, Rene Rodriguez Gutierrez⁴, Sina Jasmin⁵, Michael Gionfriddo⁴, Ana Castaneda-Guarderas⁴, Alaa Al Nofal⁶, Victor Montori², Robert Wermers⁷. ¹Mayo Clinic, Rochester, MN, USA, ²Endocrinology, Mayo Clinic, USA, ³Mayo Clinic, USA, ⁴Knowledge Evaluation Research Unit, Mayo Clinic, USA, ⁵Endocrinology, Mayo Clinic, ⁶Pediatric Endocrinology, Mayo Clinic, USA, ⁷Endocrinology, Mayo Clinic, USA

Patients with primary hyperparathyroidism (PHPT) without strong clinical indications for surgery face a treatment decision between active surveillance and parathyroidectomy. The aim of this study was to identify the literature for quality of life (QOL) and neuropsychiatric symptoms (NPS) changes in patients with asymptomatic PHPT treated with active surveillance or parathyroidectomy. A literature search was performed by a medical librarian. We included randomized (RCT) and observational studies of patients with asymptomatic PHPT without strong indications for surgery managed with parathyroidectomy or active surveillance where changes in QOL or NPS were reported. Screening for eligible studies, assessment of risk of bias and data extraction was performed in duplicate by trained reviewers. The random effect model was used for statistical analysis. We standardized to the mean to combine different scales measuring the same construct. A clinically important difference is defined as 0.5 SD. The search yielded 3141 articles of which 6 studies using 17 scales for different constructs of QOL and NPS were included for qualitative assessment (3 RCTs, 3 observational studies of surgical patients). In surgical patients there was a standard mean difference (SMD) of 0.08 (95%CI: -0.26, 0.42) and 0.00 (95%CI: -0.28, 0.27) in the mental health construct at 1 and 2 years of follow up as compared to baseline. For the vitality construct in surgical patients there was a SMD of 0.03 (95%CI: -0.31, 0.37) and 0.07 (95%CI: -0.28, 0.42) at 1 and 2 years of follow up as compared to baseline. The studies had moderate risk of bias due to unclear allocation, follow up and patient selection. Three RCTs (262 patients) showed a

statistical significant change favoring those who had surgery in specific domains of the included scales but the effect size was unavailable in 2. Two observational studies following 163 surgical patients found a statistical significant improvement in non specific symptoms at 1-2 years of follow up. The available comparative evidence suggests a statistically significant improvement in subdomains of QOL/NPS scales in surgical patients with asymptomatic PHPT. However, the magnitude of this effect in surgical patients appears to be minimal. Overall, the confidence in these estimates is decreased due to imprecision and indirectness. The use of disease specific QOL tools in RCTs is needed to clarify the magnitude of potential benefits in this otherwise low risk population.



Mental Health Meta-analysis



Vitality Meta-analysis

Table 1. Summary of included studies of patients with asymptomatic PHPT without strong indications for surgical intervention.

| Author | Year | Type of study | Inclusion Criteria | Scale Used | Patients with Surgery | Patients with Observation | Last follow up (months) |
|-----------|------|---------------|---|---|-----------------------|---------------------------|-------------------------|
| Blanchard | 2013 | Observational | Mild PHPT schedule for parathyroidectomy. Calcium levels between 2.6 – 2.85 mmol/L with a PTH level ≥ 25 ng/L and serum creatinine < 160 umol/L or serum calcium between 2.5 and 2.6 mmol/L and a PTH of > 35 ng/L. Patients with serum calcium > 2.85 mmol/L, calcitriol > 10 pmol/24 h, creatinine clearance decreased by > 10% and age < 50 years | Questionnaire that evaluated presence and severity of 22 frequently observed symptoms in patients with PHPT | 116 | | 12 |
| Perrier | 2009 | RCT | Patients aged ≥ 50 years with mild PHPT who did not meet criteria for operative intervention (kidney stones, fractures, neuromuscular syndrome, calcium > 11.2 mg/dL, peak bone mineral density < 2.5 SD of T score, creatinine clearance < 30%, urinary calcium excretion >400 mg/hours), Myocardial infarction, cerebrovascular accident in the preceding 3 months, neurologic or psychiatric conditions | Digit Span and Digit Symbol subtests of the Wechsler Adult Intelligence Scale, Controlled Oral Word Association test, Grooved Pegboard test, Trail Making Test (A and B), Hopkins Verbal Learning Test, Revised Paced Auditory Serial Addition Task, State/Trait Anxiety Inventory Trait, Beck Depression Index, Stroop Color and Word Test | 9 | 9 | 6 |

Included Studies 1

Table 1. Summary of included studies of patients with asymptomatic PHPT without strong indications for surgical intervention.

| Author | Year | Study Type | Inclusion Criteria | Scale Used | Patients with Surgery | Patients with Observation | Last follow up (months) |
|------------|------|---------------|---|--|-----------------------|---------------------------|-------------------------|
| Bollerslev | 2007 | RCT | Untreated, asymptomatic PHPT; serum calcium 2.6-2.85 mmol/L Age 50-80 years No medications interfering with calcium metabolism | Short Form-36 general health survey (SF-36) Comprehensive Psychopathological Rating Scale (CPRS) | 96 | 95 | 24 |
| Edwards | 2006 | Observational | Mild PHPT defined as absence of National Institute of Health (NIH) surgical criteria | Health Outcomes Institute Health Status Questionnaire | 47 | | 24 months or greater |
| Rao | 2004 | RCT | Age 50-75 years, mean albumin adjusted serum calcium between 10.1-11.5 mg/dL; intact PTH > 20 ng/L, normal renal function, serum creatinine less than 1.5 mg/dL, forearm bone mineral density within 2 SD adjusted for age, sex, race, absence of symptoms and complications from hypercalcaemia or excess PTH, living 150 miles from the institution | SF-36 Symptom checklist revised (SCL-90R) | 25 | 28 | At least 24 months |
| Okamoto | 2002 | Observational | Albumin-corrected serum calcium less than 12 mg/dL, no evidence of osteitis fibrosa cystica on x-ray films of the hand, no history or evidence of nephrolithiasis | General Health Questionnaire (GHQ) | 23 | | 24 |

Included Studies 2

Disclosures: Naykky Singh Ospina, None.

MO0018

Spontaneous Remission of Primary Hyperparathyroidism - A Case Report.

Barbara Silva^{*1}, Jessica Fleischer², Zachary Lenane², Wen-Wei Fan², Donald McMahon², John Bilezikian². ¹Uni-BH, Santa Casa de Belo Horizonte & Felicio Rocho Hospital, Brazil, Brazil, ²Columbia University, USA

Natural history studies of Primary Hyperparathyroidism (PHPT) have shown that in patients who do not have parathyroid surgery the disease persists and complications can ensue. Spontaneous remissions are rare and usually related to parathyroid infarction or hemorrhage. Another possible explanation for spontaneous remission of PHPT would be the onset of an autoimmune process. We report an unusual case of a woman with unequivocal PHPT for 13 years who experienced spontaneous remission of her disease in association with the diagnosis of psoriatic arthritis.

A 42-yr-old woman was referred for evaluation of persistent hypercalcemia 2 months after unsuccessful parathyroid surgery for PHPT, in which a single, hyperplastic parathyroid gland was removed. Further evaluation confirmed persistent PHPT evidenced by hypercalcemia (12.1 mg/dL), elevated PTH level (118 pg/mL), normal calcium urinary excretion and increased bone turnover markers. During the first 11 years of follow up, she remained hypercalcemic, with serum calcium values ranging between 10.3 and 12.5 mg/dL. Serum PTH levels continued to be above normal, ranging from 63 to 125 pg/mL. Approximately 5 years following the parathyroidectomy, the patient experienced a downward trend of her serum calcium and PTH, while the phosphorus followed an upward trend. She reported no neck trauma, further neck surgery, general anesthesia, nor any episodes of hypotension. Six years later (11 years after surgery), serum calcium and PTH had become normal for the first time, which coincided, remarkably, with the development of psoriatic arthritis. Since the patient was diagnosed with an immune disease, we considered the possibility that the remission was due to the development of antibodies interfering with parathyroid gland function. However, measurements of anti calcium-sensing receptor (anti-CaSR) and the NACT leucine-rich-repeat protein 5 (NALP5) antibodies were negative. Since return to normal of the serum calcium and PTH level, the PHPT has remained in remission for 10 years without any signs of recurrent disease. During this time, the psoriatic arthritis remained active.

Spontaneous remission of PHPT is exceedingly rare. The patient's clinical course was not characteristic of parathyroid hemorrhage or infarction. The concomitant appearance of psoriatic arthritis, an immune disease, raises the possibility of an immune-mediated process accounting for spontaneous long-term remission of PHPT in this patient.

Disclosures: Barbara Silva, None.

MO0019

Vitamin D Deficiency and Insufficiency in Primary Hyperparathyroidism: Effects on the Trabecular Bone Score. Marcella Walker¹, Elaine Cong¹, Melissa Sum^{*1}, James Lee¹, Anna Kepley¹, Chengchen Zhang¹, Didier Hans², Shonni Silverberg¹. ¹Columbia University, USA, ²Lausanne University, Switzerland

Data regarding the skeletal effects of vitamin D (25OHD) deficiency and insufficiency in primary hyperparathyroidism (PHPT) are limited. We have shown that lower 25OHD in PHPT is associated with higher PTH levels and modestly lower 1/3 radius BMD by DXA, but no BMD differences at the lumbar spine (LS) and hip. We compared the trabecular bone score (TBS) at the LS in PHPT patients with 25OHD deficiency (<20ng/ml), insufficiency (20-29ng/ml) or sufficiency (≥30ng/ml). Participants were mostly women (n=88; 81% women; mean±SD age 62±13yrs) with mild PHPT (calcium 10.7±0.6mg/dl, PTH 86±51pg/ml). Mean 25OHD was 29±10ng/ml (3.4% <10ng/ml; 19.3% <20ng/ml, mean 14±3ng/ml; 37.5% 25OHD 20-29ng/ml, mean 25±3ng/ml; and 43.2% 25OHD≥30ng/ml, mean 38±7ng/ml). Those with lower vitamin D were younger (<20: 57±14 vs. 20-29: 59±14 vs. ≥30: 67±9yrs, p=0.006) but did not differ by sex, race/ethnicity, height, weight, PHPT duration, history of osteoporosis, fragility fracture, nephrolithiasis or meeting 2008 surgical criteria except for age <50yrs (p=0.03). Those with lower 25OHD had higher PTH (130±64 vs. 81±43 vs. 71±39pg/ml, p=0.0001) and lower PO4 (2.8±0.4 vs. 3.0±0.4 vs. 3.2±0.4mg/dl, p=0.003) levels but serum and urine calcium and 1,25-dihydroxyvitamin D did not differ. Renal function was worse in those with 25OHD ≥30 vs. <20ng/ml (77±17 vs. 92±18ml/min, p=0.04). LS T-Score was normal (-1.0±1.7) and did not differ by 25OHD level (-0.9±1.5 vs. -1.0±1.8 vs. -1.0±1.7, p=0.96). TBS (1.302±0.124) was in the partially degraded range. Neither PTH (r=-0.14, p=0.21) nor 25OHD (r=-0.12, p=0.27) levels correlated with TBS. TBS did not differ by vitamin D status before (<20ng/ml: 1.306±0.134 vs. 20-29: 1.221±0.105 vs. ≥30: 1.274±0.132, p=0.15) or after adjusting for age, weight, GFR (p=0.24). TBS did not differ in those with 25OHD <20 vs. ≥20ng/ml (1.306±0.134 vs. 1.301±0.123, p=0.87) or <30 vs. ≥30 (1.323±0.115 vs. 1.274±0.132, p=0.07) before or after adjusting for covariates (p=0.81 and 0.10). TBS results were similar in the subset of women only: partially degraded (1.293±0.121), not associated with 25OHD levels (r=-0.04, p=0.73), and no between-group differences in adjusted (p=0.55) or unadjusted (p=0.81) TBS by vitamin D status. In conclusion, TBS values were in the partially degraded range in PHPT. While 25OHD deficiency and insufficiency were associated with higher PTH levels in PHPT, vitamin D status did not affect TBS in a cohort in whom severe 25OHD deficiency was uncommon.

Disclosures: *Melissa Sum, None.*

MO0020

Primary Hyperparathyroidism: Investigating Mechanisms of Cognitive Dysfunction. Elaine Cong, Marcella D. Walker, Melissa Sum*, Ronald M. Lazar, Yunglin Gazes, Anna Kepley, Kevin Slane, Chen Cheng Zhang, Donald J. McMahon, Randolph S. Marshall, Shonni J. Silverberg. College of Physicians & Surgeons, Columbia University, USA

We previously reported cognitive dysfunction in primary hyperparathyroidism (PHPT) reversible with cure (PTX). We have also shown that the extent of PTH elevation in PHPT positively correlates with aortic/carotid vascular stiffness. We hypothesized that PTH-dependent intracerebral vascular dysfunction may impair blood flow and cognition in PHPT. Pre- and 6 mos. post-PTX, postmenopausal women with PHPT underwent cognitive testing, functional magnetic resonance imaging (fMRI) and transcranial Doppler to measure intracerebral vasomotor reactivity (VMR). Patients (n=10; age±SD 65±7yrs) had mild PHPT (calcium 10.5±0.3mg/dl, PTH 78±22pg/ml) and normal vitamin D (37±17ng/ml), renal and thyroid function. Age-, gender- and education-adjusted Z-scores for visuospatial memory, verbal memory and motor speed were slightly below average but not abnormal. VMR was worse in 8 PHPT vs. 9 controls (3.2±0.9 vs. 4.2±1.1%, p=0.02). VMR did not correlate with PTH (r=0.35, p=0.35) or calcium (r=0.46, p=0.21) levels, but higher (better) VMR tended to be positively associated with better verbal (Hopkins Verbal Learning Test total recall: r=0.67, p=0.07) and symbolic memory (r=0.64, p=0.09). On fMRI, PHPT (n=9) had reduced activation in the cerebellum during non-verbal abstraction (t(25)=4, k=29 voxels, p<0.001) vs. 21 controls. In PHPT, activation was inversely correlated with PTH but not calcium level in several areas involved in decision-making and executive function [anterior cingulate BA 25 (r=-0.97, t(7)=10, k=61), inferior frontal area (r=-0.95, t(9)=8, k=65), claustrum (r=-0.99, t(7)=8, k=62), all p<0.0001]. Post-PTX (n=5 to date), only depressive symptoms improved (23±7 vs. 9±4, p=0.02), while verbal fluency (0.0±1.2 vs. 0.5±1.4, p=0.07) and motor speed tended to improve (dominant/non-dominant hand: -0.9±1.2 vs. 0.2±1.4, p=0.07; -0.9±1.2 vs. 0.2±1.4, p=0.08). VMR (3.1±1.4 vs. 3.3±0.8, p=0.81) and fMRI task-related activation did not change. In summary, very preliminary data suggest that PHPT may be associated with lower VMR. In PHPT, brain activation in areas controlling executive function was worse in those with highest PTH levels. Post-PTX, depressive symptoms and some aspects of cognition tended to improve. Further work is needed to determine if VMR improves post-PTX. If extended and confirmed, these results could suggest that reduced intracerebral vascular reactivity may underlie cognitive dysfunction in PHPT and that elevated PTH may play a role in executive function.

Disclosures: *Melissa Sum, None.*

MO0021

In vivo RPI by BioDent, but not OsteoProbe, Correlates with Bone Tissue-Level Mechanical Properties. Erin McNerny*¹, Jason Organ¹, Christopher Newman¹, Drew Brown¹, Joseph M. Wallace², Matthew R. Allen¹. ¹Indiana University School of Medicine, USA, ²Indiana University-Purdue University Indianapolis, USA

In vivo measures of bone material properties could significantly improve estimates of patient fracture risk. Two reference point indentation (RPI) devices, BioDent and OsteoProbe, were developed to address this issue. BioDent is a reference probe-based device that cyclically indents the bone surface to yield several measures of tissue properties (indentation depth [ID], ID increase [IDI], unloading slope, energy dissipation [ED]). OsteoProbe lacks a reference probe, using a pre-load reference force followed by a single high-force impact to test the depth of indentation. It yields a single variable, bone material strength index (BMSi), which is inversely related to indentation depth. The goal of this study was to test the hypothesis that RPI measures, obtained in vivo, would correlate with measures of whole bone mechanical properties. Skeletally mature female beagle dogs (n=48) were treated daily with oral raloxifene (RAL; 0.5 mg/kg/day), alendronate (ALN; 0.2mg/kg/day), both RAL and ALN, or saline vehicle (VEH; 1.0 mL/kg/day). After 1 year of treatment, cortical bone properties were measured in vivo at the tibia mid-diaphysis using BioDent (right tibia, 3 tests per bone) and OsteoProbe (contralateral tibia, 5 tests per bone). Ex vivo pQCT imaging and 3 point bending mechanical tests were performed on the right femur mid-diaphysis. Associations between tissue mineral density (TMD), BioDent & OsteoProbe measures, and tissue level mechanical properties calculated from 3-pt bending using beam theory to account for differences in bone size were evaluated by Pearson correlation. OsteoProbe BMSi did not correlate with TMD, mechanical properties, or any BioDent outcome. In contrast, the BioDent measures of 1st cycle ID (ID 1st), 1st cycle ED (ED 1st), 1st cycle unloading slope, total ID (TID), and total ED (Tot ED) were significantly correlated to TMD (Table 1). Excluding unloading slope, these measures, as well as 1st cycle creep ID (CID) and IDI, significantly correlated with femur toughness. Stepwise linear regression was used to test the hypothesis that combined with TMD and bone size, RPI would improve predictions of whole bone mechanical properties. The best model (adjR²=0.274, p=0.001) to predict work to fracture included cortical area (β=0.399, p=0.004) and ED 1st (β=0.394, p=0.005). These data demonstrate the ability of in vivo BioDent, but not OsteoProbe, to provide insight into bone tissue quality at a remote site.

| Pearson r p value | Ultimate | | | |
|-----------------------|------------------------|------------------------|-----------------------|-----------------------|
| | TMD | Stress | Modulus | Toughness |
| TMD | | 0.429 0.007 | 0.412 0.01 | -0.043 0.796 |
| OsteoProbe | | | | |
| BMSi | -0.013 0.938 | 0.120 0.474 | -0.018 0.917 | -0.130 0.438 |
| BioDent | | | | |
| ID 1 st | -0.516 0.001 | 0.04 0.812 | 0.089 0.596 | 0.313 0.056 |
| ED 1 st | -0.478 0.002 | 0.050 0.766 | 0.106 0.528 | 0.387 0.016 |
| Unloading | 0.307 | 0.010 | 0.062 | -0.144 |
| Slope 1 st | 0.060 | 0.953 | 0.713 | 0.388 |
| CID 1 st | -0.249 0.132 | 0.079 0.637 | 0.130 0.436 | 0.386 0.017 |
| IDI | -0.192 0.249 | 0.184 0.268 | 0.184 0.268 | 0.362 0.026 |
| TID | -0.511 0.001 | 0.047 0.779 | 0.094 0.577 | 0.316 0.053 |
| Tot ED | -0.383 0.018 | -0.076 0.651 | 0.020 0.903 | 0.334 0.041 |

Table 1 - RPI Correlations

Disclosures: *Erin McNerny, None.*

MO0022

Age and Sex Dependence of Human Vertebral Body Composite Traits Determined Using Statistical Shape and Density Modeling. Jessica Coogan¹, Travis Eliason¹, Donald Moravits¹, Arthur Nicholls¹, Ellen Quillen², Daniel Nicoletta¹, Todd Bredbenner*¹. ¹Southwest Research Institute, USA, ²Texas Biomedical Research Institute, USA

The structural integrity of bone under mechanical load is a complex function of interrelated characteristics, including macroscopic bone morphology and bone density. We hypothesize that combinations of vertebral traits are dependent on both age and sex. Using quantitative CT, we imaged 29 human L1 vertebrae (15 male 14 female, age range 25-88 years), along with a density calibration phantom, in order to

investigate composite variation in geometry and bone mineral density (BMD) distribution with sex and age. Vertebral body models describing geometry and spatial BMD distribution were created, each consisting of 115,084 variables (i.e. spatial location and density at mesh nodes located at corresponding anatomic positions for all vertebrae). Variation in 3D bone geometry and BMD distribution within the set of 29 vertebral bodies was described using statistical shape and density modeling (SSDM) [1]. The ~115,000 highly correlated variables for each model were reduced to a set of 28 uncorrelated and independent principal components (e.g. composite geometry and BMD traits) without loss of information. In addition, discrete vertebral body measures (i.e. minimum cross-sectional area, anterior height, posterior height, volumetric BMD) were determined. Two-way unbalanced ANOVAs were used to test composite trait weighting factors and discrete measurements for dependence on sex and age, where subjects were grouped into young (age < 45 years), old (> 65 years), and middle-aged (others). Three weighting factors were significantly associated with sex, one with age grouping, and 2 with age x sex interaction, while discrete measures were not significantly associated with age, sex, or age x sex interaction. Sex and age-based differences in geometry (Fig. 1) and density (Fig. 2) were observed, with a general decrease in vertebral body size and increase in BMD for females with age and converse changes for males. Age- and sex- based variations in structural bone traits are complex and were not detected with simple measures; however, variation in complex patterns of traits were identified using SSDM. Previous studies have related structural bone traits to vertebral fracture risk [2-3], supporting the notion that age and sex differences in structural bone traits contribute to vertebral fracture risk.[1] Bredbenner TL, et al. J. Bone Miner Res, 29(9):2090-2100, 2014. [2] Ruysen-Witrand A, et al. Osteoporos Int, 18:1271-1278, 2007. [3] Bruno AG, et al. J. Bone Miner Res, 29(3):562-569, 2014.

MO0023

Assessment Of A Finite Element Model To Reproduce An Ex-Vivo Forward Fall Protocol Leading To Fractured And Non-Fractured Radii. Helene Follet¹, Edison Zapata^{*2}, Francois Duboeuf³, Jean-Baptiste Pialat⁴, David Mitton⁵. ¹INSERM, UMR1033 ; Universite De Lyon, France, ²Universite de Lyon, F-69622; IFSTTAR, LBMC, UMR_T9406. INSERM UMR1033, Universite de Lyon, France, ³INSERM UMR1033, Universite de Lyon, France, ⁴INSERM UMR1033, Universite de Lyon, Department of radiology, Hospital E. Herriot, Hospices Civils de Lyon, France, ⁵Universite de Lyon, F-69622 ; IFSTTAR, LBMC, UMR_T9406., France

Forward falls represent a risk of injury for the elderly, in particular those suffering from bone diseases, such as osteoporosis. Finite element models (FEM) have been proposed to improve the bone strength prediction. However, these models have considered quasi-static loadings and a loading orientation along the distal radius. The aim of this study was then to design an ex vivo protocol on radii with a non-axial loadings and a loading speed of 2m/s in average and compare to FE model. Results attempt to assess the predictive capability of finite element models (FEM).

Six distal radii from elderly donors (50 to 96 y.o.) were cut and cleaned of soft tissues. They were placed with an alignment of 15° between the frontal anatomical plane and the anterior face and then potted in a polyurethane resin on a steel cylinder, reproducing the most common forward fall¹. The load was applied using a mold, specifically done for each radius, at 2m/s (LF technologies, France). Loads, acceleration and displacement were recorded. Previously acquired cone beam CT scans (NewTom 5G, QR, Italy) were used to create the specimen-specific FEM. Dicom was segmented using an adaptive threshold in CTAn (Bruker, Belgium). Bone was meshed using an in-house software in hexahedral of 450µm element size and exported to Hypermesh (Altair Engineering, USA) in order to reproduce all experiment conditions (linear and isotropic behaviour law, Young's moduli: 10 GPa, Poisson ratio: 0.3). Simulations were performed using LS-dyna (LSTC, Usa). Fig. A.

Reaction loads from the experiment were compared with the results from the simulation. Among the 6 radii, 4 fractured and 2 did not. Experimental peak forces are in agreement with those reported in the literature². Comparison between model and experiment is shown in Fig. B. Peak forces are overestimated in a 2.2 factor. Nevertheless, there is a good correlation (R²=0.91) between predicted and experimental load.

Experimental data shown that one impact, in same loading conditions, will not systematically end in bone fracture. The high predicted load might be due to the resolution of the model, which overestimate the trabecular bone. Compromise has to be done between resolution and number of elements. Further tests are in process to refine the model (law, heterogeneity...) on 24 more oncoming samples. These models will be useful to identify factors affecting fracture during a forward fall. Ref: 1. Greenwald et al, 1998. 2. Burkhart et al, 2014.

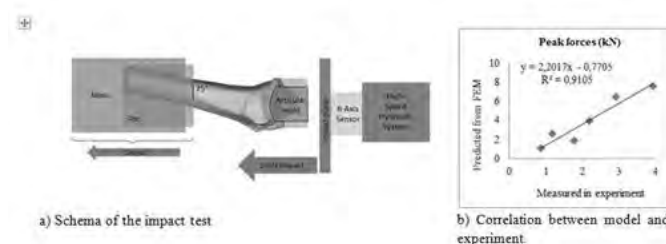


Figure 1: Variation in vertebral bone geometry

Zapata_Fig

Disclosures: Edison Zapata, None.

MO0024

Combining Microindentation and Monotonic Macroscopic Testing to Bridge Scales in Human Osteonal Bone. Mohammad Mirzaali, Jakob Schwiedrzik, Suwanwadee Thaiwichai, Philippe Zysset^{*}, Uwe Wolfram. Institute for Surgical Technology & Biomechanics, University of Bern, Switzerland

The growing incidence of skeletal fractures poses a significant challenge to ageing societies. Since a major part of physiological loading in the lower limbs is carried by cortical bone, it would be desirable to better understand the structure-mechanical property relationships and scale effects in this tissue. This study aims at assessing whether micro-mechanical properties measured by microindentation combined with morphological information may be used to predict macroscopic elastic and strength properties in a donor- and site-matched manner.

Specimens for microindentation and quasi-static macroscopic tests in tension, compression, and torsion were prepared from a cohort of 19 male and 20 female donors (46 to 99 years of age). All tests were performed under fully hydrated conditions. The results of the micro-mechanical tests were combined with

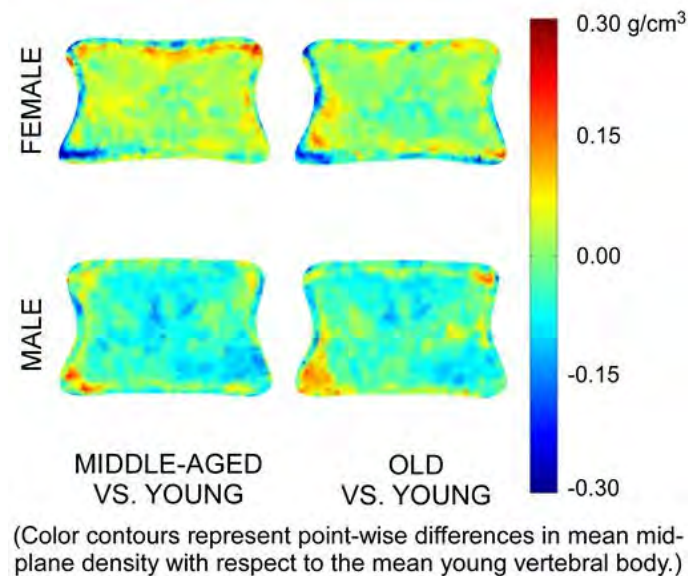


Figure 2: Variation in mid-plane vertebral body density

Disclosures: Todd Bredbenner, None.

morphological properties such as porosity and cement line density using a power law relationship to predict the macroscopic properties.

Microindentation properties were not gender dependent, remarkably constant over age, and showed an overall small variation with standard deviations of approximately 10%. Macro-mechanical stiffness and strength were significantly related to porosity for all load cases ($p < 0.05$). In cases of macroscopic yield strain and work-to-failure this was only true in torsion and compression, respectively. The correlations of macro-mechanical with micro-mechanical and morphological properties showed no significance for cement line density or variations in the microindentation results and were dominated by porosity with a moderate explanatory power of most often less than 50%.

The results confirm that gender and age have negligible effect on the tissue microindentation properties of human lamellar bone. Furthermore, our findings suggest that a microindentation experiment is not suitable to predict macroscopic mechanical properties. The presented data may help to form a better understanding of the mechanisms of ageing in bone tissue and of the length scale at which they are active. This may be used for prediction of fracture risk in the elderly in the future.

Disclosures: Philippe Zysset, None.

MO0025

Effects of vitamin C and teriparatide on bone mineral density, quality, and strength in vitamin C-deficient rats. Masashi Fujii¹, Naohisa Miyakoshi², Yuji Kasukawa², Koji Nozaka², Tovahito Segawa², Kentaro Ouchi², Hayato Kinoshita², Chie Sato², Yoichi Shimada². ¹Akita University, Japan, ²Akita university graduate school of medicine, Japan

Introduction

A deficiency of vitamin C (ascorbic acid, AA) has been considered to be one reason for reduced bone quality and bone strength in elderly individuals with severe osteoporosis. AA-deficient rats (Osteogenic Disorder Shionogi Rats) showed decreased bone strength in our previous study. Teriparatide (TPTD) promotes osteoblast formation and improves bone strength, particularly in terms of bone quality. However, the efficacy of TPTD on bone strength under AA-deficient conditions remains unclear. The objective of this study was thus to evaluate the efficacy of AA and TPTD administration on bone mineral density (BMD) and bone strength in AA-deficient rats.

Materials and Methods

AA-deficient rats were bred with normal-concentration AA water (2 mg/mL) until 4 months of age and with low-concentration AA water (0.5 mg/mL) thereafter until 8 weeks to develop vitamin C-deficient rats ($n = 40$). After that, rats were assigned to one of the following four groups: 1) AA-deficient (AA-) group receiving a low concentration of AA water, 2) AA-supplementation (AA+) group receiving a normal concentration of AA water, 3) AA-deficient and TPTD (30 µg/kg body weight, three times a week subcutaneous injection) administration (AA-T) group, and 4) AA-supplementation and TPTD administration (AA+T) group ($n = 10$ for each group). After 12 weeks of experiment, bilateral femora were harvested. The left femur was used for BMD measurement, and the right femur was evaluated for bone strength by a three-point bending test of the diaphysis and a condyle compression test. These examinations were also performed for Wistar rats of the same age ($n = 10$) as a control group.

Results

BMD was significantly lower in the AA- group than in other groups ($p < 0.05$). BMD in the AA-T and AA+T groups was comparable to that in controls. Parameters of bone strength indices including bone breaking force, breaking energy, and maximum load in the three-point bending test showed no significant difference among experimental groups. In the condyle compression test, maximum load was significantly higher in the AA+T group than in the AA- and AA+ groups ($p < 0.05$ each).

Discussion and Conclusion

BMD was decreased by AA deficiency. AA supplementation and TPTD administration with and without AA recovered BMD to the same level as controls. TPTD treatment with AA supplementation significantly improved bone strength at the epiphysis, but not at the diaphysis, which contained a higher proportion of cancellous bone.

Disclosures: Masashi Fujii, None.

MO0026

Finite Element Methods on Multi-Row Detector CT Imaging to Estimate Elastic Modulus of Human Trabecular Bone. Cheng Chen*, Elena Letuchy, Ryan Amelon, Anneliese Heiner, Kathleen Janz, Trudy Burns, James Torner, Steven Levy, Punam Saha. The University of Iowa, USA

Multi-row detector computed tomographic (MD-CT) imaging generates unique bone quality information, such as volumetric bone mineral density (vBMD), isolation of trabeculae from cortical bone, and characterization of trabecular bone (TB) micro-architecture. Novel image processing algorithms and finite element methods (FEM) were applied to MD-CT images to estimate the elastic modulus (EM) of human TB.

Twenty-two cadaveric ankle specimens and a pilot sample of young (age 19) healthy participants from the Iowa Bone Development Study (IBDS) cohort (12 males and 13 females) were included in this study. MD-CT scans of the distal tibia were

acquired on a 128 slice Siemens Flash scanner at 120kV, 200mAs, pitch: 1, 0.3mm slice-thickness and 10cm scan-length. A Gammex phantom was used to transform CT Hounsfield units into BMD (mg/cc). Space-variant thresholding and hysteresis algorithms were applied to preserve TB connectivity for mesh generation, which was used in FEM to estimate EM. For the *in vivo* study, 30%, 45%, and 60% peels at 6-8% distal tibia were applied to generate ROIs. For the cadaveric study, the actual EM was determined using compressive mechanical testing and the ROIs for FEM were matched with the recorded location of the test volume.

The observed intra-class correlation coefficient of MD-CT-based EM from three-repeat scans of cadaveric specimens was 98.4%, and the estimates EM demonstrated a stronger linear association with the actual EM (correlation coefficient $r=0.95$) (Figure 1) than did vBMD ($r=0.89$). Analysis of pilot sample data suggested a higher mean EM for the TB of young males vs. females over the 45% peel ROI ($p=0.053$ two-sample t-test; effect size=0.82) (Table 1). Height differences explained most of the EM difference, as EM showed a strong positive association with height in IBDS participants, with a mean increase in EM of 292MPa for every 5cm increase in height ($p<0.001$ for height in a simple regression model) at the 45% peel. Sex was not statistically significant in models that included height.

Together with advanced image processing algorithms, FEM is applicable to MD-CT imaging for determining the EM of human TB. MD-CT-based computed EM is reproducible and strongly associated with actual bone strength. Our preliminary finding that the male-female difference in TB EM may be largely due to height differences requires confirmation in a larger sample.

This study was funded by NIH grants: R01-AR054439, R01-DE012101, and UL1-TR044206.

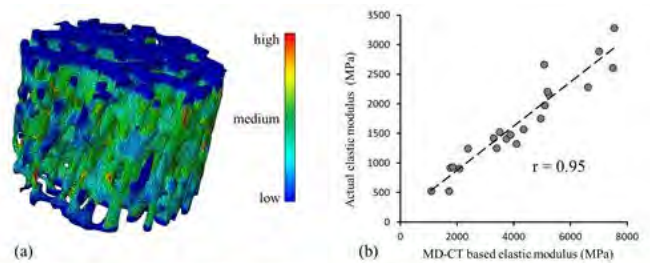


Figure 1. Finite element methods (FEM) on MD-CT imaging of human trabecular bone (TB) at distal tibia. (a) Color-coded strain distribution. (b) Ability of MD-CT-based FEM together with advanced image processing algorithms to estimate elastic modulus of TB.

Figure 1. Finite element methods on MD-CT imaging of human trabecular bone at distal tibia

| ROI | Males (Mean±SD) | Females (Mean±SD) | Effect size | p-value* |
|-----|-----------------|-------------------|-------------|----------|
| 30p | 7279.3 ± 1032.9 | 6616.0 ± 912.8 | 0.68 | 0.1017 |
| 45p | 6461.0 ± 997.9 | 5614.0 ± 1068.6 | 0.82 | 0.0526 |
| 60p | 5497.9 ± 1080.5 | 4579.0 ± 1265.6 | 0.78 | 0.0642 |

Table 1. Comparison of MD-CT based elastic modulus for males (N=12) and females (N=13)

Disclosures: Cheng Chen, None.

MO0027

Genetic Variability in Fracture Healing Under Phosphate Deficiency. Amira Hussein*, Alexander Wulff¹, Heather Matheny¹, Brenna Hogue¹, Kyle Lybrand¹, Anthony DeGiacomo¹, Louis Gerstenfeld¹, Elise Morgan². ¹Orthopaedic Surgery, Boston University School of Medicine, USA, ²Mechanical Engineering, Boston University, USA

Introduction: Phosphate deficiency leads to osteomalacia in adults and affects many systemic and local physiological processes, including fracture healing. This study's goal was to determine how the genetic variability that controls the structural and biomechanical phenotypes of bone interacts with phosphate deficiency to affect fracture healing. **Methods:** Closed, stabilized fractures were generated in the femora of three strains [A/J (AJ), C57BL/6J (B6), and C3H/HeJ (C3)] of male 8- to 12-week-old mice. Phosphate deficiency (Pi) was initiated 2 days prior to fracture and was maintained for 17 days, after which a normal diet was resumed. Control groups were given a normal diet throughout. Fracture calluses were harvested at post-operative days 14, 21, 35, and 42 ($n=12$ per time-point/strain/diet). Micro-computed tomography (μ CT) was used to evaluate the structural and material properties of the calluses. Mechanical properties of the calluses were assessed by torsion testing. Outcomes were compared among strains, between diets, and among time-points using three-factor analyses of variance with Tukey *post hoc* tests. **Results:** μ CT evaluations showed that Pi calluses had lower volume fraction (BV/TV), bone mineral density (BMD) and tissue mineral density (TMD) than control calluses ($p<0.0001$) (Table 1). Yet, Pi calluses had higher strength (maximum torque), toughness (work to failure), and ductility (twist to failure), and lower rigidity, compared to control calluses ($p<0.0015$). Although neither callus strength nor toughness was dependent on the interaction between diet and strain ($p>0.174$), an effect of diet was seen in some strains at some time-points ($p<0.0068$): both toughness and strength were higher in

C3 Pi vs. C3 control calluses at day 35; and toughness was higher, and callus rigidity lower, in B6 Pi vs. B6 control calluses at day 14. Discussion: The results indicate that phosphate deficiency affects the strength and mineralization of calluses at different stages of healing depending on the strain of mice. Despite Pi-induced reductions in callus volume fraction and mineral density, callus strength and toughness were higher with Pi. These data suggest that an overall compensatory response to the early phosphate deficiency occurs during the later stages of bone formation when phosphate was replenished in the diet. This compensation was most pronounced in the C3 strain, which heals through more osteogenic versus chondrogenic mechanisms.

Table 1. p-values for model effects in the ANOVA for microstructural and mechanical properties measures of the callus

| | BV/TV [-] | BMD [mgHA/cm ³] | TMD [mgHA/cm ³] | Maximum Torque [Nm] | Work to Failure [Nm-rad] | Twist at Failure [rad] | Rigidity [Nm ² /rad] |
|-------------------|-----------|-----------------------------|-----------------------------|---------------------|--------------------------|------------------------|---------------------------------|
| Strain | <0.0001 | <0.0001 | <0.0001 | <0.0001 | <0.0001 | 0.144 | <0.0001 |
| POD | <0.0001 | <0.0001 | <0.0001 | 0.0016 | <0.0001 | <0.0001 | <0.0001 |
| Strain *POD | <0.0001 | <0.0001 | 0.0012 | 0.0202 | 0.0002 | 0.0006 | <0.0001 |
| Diet | <0.0001 | <0.0001 | <0.0001 | 0.0015 | <0.0001 | <0.0001 | <0.0001 |
| Strain *Diet | 0.0156 | 0.528 | 0.8577 | 0.1746 | 0.9174 | 0.4525 | <0.0001 |
| POD *Diet | <0.0001 | <0.0001 | <0.0001 | 0.1352 | 0.0039 | <0.0001 | 0.0124 |
| Strain *POD *Diet | 0.0001 | 0.0012 | <0.0001 | 0.0068 | 0.0003 | 0.0151 | <0.0001 |

Table 1

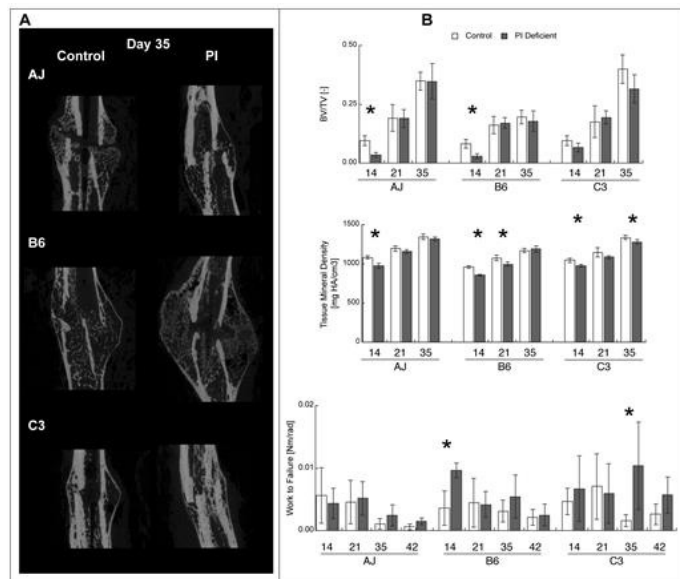


Figure 1. For each strain of mice: (A) Representative micro-computed tomography images of calluses at day 35; (B) Callus volume fraction, Tissue mineral density, and Work to failure (* indicates significant difference between Pi and control calluses p<0.05)

Figure 1

Disclosures: Amira Hussein, None.

MO0028

Glucose-dependent insulinotropic polypeptide (GIP) is required for an optimal bone strength and quality. Benoît Gobron¹, Béatrice Bouvard¹, Satoko Kuwahara², Sheng Zhang³, Norio Harada², Burton Wice³, Nobuya Inagaki², Erick Legrand¹, Daniel Chappard¹, Guillaume Mabiliau¹. ¹GEROM-LHEA, LUNAM University, France, ²Department of Diabetes, Endocrinology & Nutrition, Graduate School of Medicine, Kyoto University, Japan, ³Department of Internal Medicine, Washington University School of Medicine, USA

After a meal ingestion, gut hormones are secreted in the blood stream and induce a response in cells expressing gut hormone receptors. A role for the glucose-dependent insulinotropic polypeptide receptor (GIPr) in controlling bone strength and quality has previously been reported. GIPr KO animals presented with higher trabecular bone mass and reduction. Nevertheless tissue mineral density and extent of collagen cross-linking were altered in trabecular and cortical bone. However, a second animal model of GIPr deletion exists in which the opposite bone phenotype has been reported. The

aims of the present study were to decipher the role of GIP in bone physiology by using an animal model of GIP deletion (GIP-GFP KI) and animals deprived in GIP-producing cells (GIP-DT). Eight GIP-GFP KI and GIP-DT mice (16-week old) were age- and sex-matched with eight wild-type (WT) littermates. Trabecular bone microarchitecture was studied by high resolution microCT in long bones. Osteoclast and osteoblast activities were assessed in undecalcified bone sections. Bone strength was investigated at the organ level by three-point bending and at the tissue level by nanoindentation. The composition of the matrix was assessed with quantitative electron backscattering imaging and Fourier transform infrared microspectroscopy. Non-parametric Mann-Whitney U-test was used to compare differences between groups. As compared with control mice, GIP-GFP KI animals exhibited significant reductions in BV/TV (-22%), trabecular number (-19%) and higher values for trabecular separation (14%). GIP-GFP KI mice had a higher bone remodelling with significant higher values for Oc.S/BS and BFR/BS. These modifications of trabecular microarchitecture were not seen in GIP-DT animals, lacking K-cell-produced gut hormone, including GIP. Furthermore, bone strength at the organ level presented with a 10% reduction in stiffness in GIP-GFP KI mice that was not mirrored in GIP-DT animals. Bone strength at the tissue level was altered in GIP-GFP KI animals with a significant drop in ultimate load. These results support a role for the GIP/GIPr pathway in controlling bone strength and quality. However, these data also suggest that GIP-DT animal have a compensatory mechanism to maintain bone quality in the absence of GIP, that will require further investigation. This might open a new therapeutical approach to prevent fragility fracture.

Disclosures: Benoît Gobron, None.

MO0029

HIV infection is associated with reduced bone material properties independently of bone mineral density. Robert Güerri-Fernández¹, Daniel Prieto-Alhambra², Judit Villar-García¹, Xavier Nogués³, Leonardo Mellibovsky⁴, Ana Guelar⁵, Natalia Garcia-Giral⁶, Anna March¹, Maria Rodríguez-Sanz⁷, Juan Pablo Horcajada⁵, Hernando Knobel⁵, Adolfo Díez-Pérez⁴. ¹Infectious Diseases. Hospital del Mar., Spain, ²NIHR Clinician Scientist NDORMS, University of Oxford, United Kingdom, ³Internal Medicine. Hospital del Mar, Spain, ⁴Internal Medicine. Hospital del Mar., Spain, ⁵Infectious Diseases. Hospital del Mar, Spain, ⁶URFOA. IMIM, Spain, ⁷URFOA. IMIM, Spain

Introduction: Both HIV infection and anti-retroviral therapies are associated with an increased risk of fragility fracture, partially independent of BMD changes. Bone microindentation allows to measure in vivo the mechanical properties of bone at a tissue level. Resulting measurements (BMSi = Bone Material Strength index) have been shown to correlate better than BMD with fracture risk in several studies. We aimed to study the association between treatment-naïve HIV infection and BMSi.

Methods: A group of treatment naïve HIV-infected patients were compared to HIV infection-free controls. Measurements: Bone mineral density (DXA Hologic QDR4500SL), high sensitivity CRP, 25-hydroxy-Vitamin D, bone turnover (PINP, bone-specific alkaline phosphatase, C-telopeptide), and BMSi (Osteoprobe, Active Life Sci). Characteristics of the infection were recorded in the HIV participants. Multivariable linear regression modelling was used to compare groups adjusted for age, sex, body mass index, BMD, vitamin D, and CRP levels.

Results: A total of 49 HIV patients (37 men, 75.5%) and 33 controls (21 men, 63.6%) were analyzed. HIV patients had been diagnosed for a median of 1.56 years; their mean (SD) CD4 nadir concentration was 501.6/mm³ (368.1) and viral load 230,524 copies (694,936). HIV-infected participants presented a significantly reduced BMSi compared to controls (85.034 vs 90.995, p < 0.001), which stood for multivariable adjustment (adjusted beta -5.87 [95%CI -8.63 to -3.10]; p < 0.001). Conversely, no differences were observed in BMD (at any of the studied sites) nor in bone formation or resorption markers.

Conclusions: HIV infection has direct bone toxicity independently of antiretroviral treatment, patient characteristics, and systemic inflammation markers. Bone microindentation identifies a bone material strength deterioration that occurs in the early stages of HIV infection, not detectable by either densitometry or bone turnover markers.

Founded FIS PI13/00589

| | CONTROLS | HIV-INFECTED | p VALUE |
|---|---------------|---------------|---------|
| BMSi | 90.995 (6,3) | 85.034(5,2) | 0.0001 |
| BMD lumbar spine (g/cm ² (SD)) | 0.9858(0,2) | 0.9802 (0,3) | 0.861 |
| BMD femoral neck (g/cm ² (SD)) | 0.825 (0,2) | 0.825 (0,13) | 0.936 |
| BMD total hip (g/cm ² (SD)) | 0.939 (0,14) | 0.954 (0,16) | 0.336 |
| C-Telopeptide (ng/dl (SD)) | 0.329 (0,177) | 0.311 (0,136) | 0.765 |
| P1NP (ng/ml (SD)) | 57.47 (32,5) | 57,05 (25,16) | 0.97 |
| 25OH Vitamin D (ng/ml (SD)) | 30.218 (17,9) | 22.6 (12,2) | 0.049 |

Table 1. comparison of the main clinical measurements.

Table 1

Disclosures: Robert Güerri-Fernández, None.

MO0030

Impaired Bone Material Properties are associated with increased fracture risk and severity of vertebral fractures in osteoporosis. Erik Fink Eriksen^{*1}, Daysi Duarte Sosa². ¹Dept. of Clinical Endocrinology, Morbid Obesity & Preventive Medicine, Oslo University Hospital, Norway, ²Dept. of Endocrinology, Morbid Obesity & Preventive Medicine, Oslo University Hospital, Norway

Bone mass, bone architecture and bone material properties are the principal determinants of bone strength. In this study we tested how bone material properties relate to overall risk of fracture and severity of vertebral fractures in osteoporosis.

Bone material strength of the thick cortex of the anterior tibia was assessed using a bioindentation device (Osteo Probe III, ActiveLife Scientific, Santa Barbara, CA) in 40 controls and 72 patients with postmenopausal osteoporosis, (23 cases with hip fracture, 29 cases with vertebral fracture and 23 patients with non-vertebral non-hip fracture). The penetration into bone (indentation distance increase) measured by the device was standardized towards a calibration phantom made from methylmethacrylate yielding a Bone Material Strength Index (BMSi). Bone mineral density (BMD) was measured by dual x-ray absorptiometry at the hip and spine and vertebral fracture severity was determined by semi-quantitative (SQ) grading of compression fractures on lateral X-rays from the DXA-scanner. Bone turnover markers were measured using commercially available assays.

BMSi was found to be significantly lower in subjects with osteoporotic fractures than in controls (77 ± 6.1 vs 71.2 ± 6.1 $p < 0.001$) and each incremental decrease of one unit in BMSi was associated with increased risk of fracture, after adjustment for age, height and weight (OR 4.45, 95% CI 1.07, 19.21 $p = 0.04$). Moreover, a significant negative correlation was observed for BMSi on vertebral fracture severity ($r^2 = 0.14$, $p = 0.012$), which remained significant after adjusting for age and lumbar spine BMD ($r^2 = 0.19$, $p = 0.008$). Fracture cases exhibited higher PINP- and CTX-levels and lower BMD at the total hip than controls ($p = 0.03$, $p = 0.01$ and $p < 0.05$, respectively). Regression analysis revealed that BMSi did not vary with BMD, age, or markers of bone turnover.

Conclusion: Bone material strength constitutes an independent risk factor for osteoporotic fractures and also determines severity of vertebral fractures. Moreover, BMSi does not vary with age, BMD or bone turnover.

Disclosures: Erik Fink Eriksen, Got the micro indentation device and probe for free from ActiveLife Scientific

MO0031

Is it time to say goodbye to SMI? Michael Doube¹, Phil Salmon^{*2}, Ava Tivesten³. ¹Royal Veterinary College, United Kingdom, ²Bruker-microCT, Belgium, ³Sahlgrenska Institute

Osteoporotic deterioration of trabecular bone involves a transition from plate-like to rod-like architecture. The structure model index (SMI) measures convex curvature and has long been used to quantify this transition. But it has a significant shortcoming: it is confounded by porosity. Both porosity and high percent volume result in extensive concave curvature, whose existence is ignored in the standard narrative of the shape-dependence of SMI. Traditionally SMI ranges from 0 (plate) to 3 (rod); however in real bone samples negative SMI routinely arises from high trabecular BV/TV or from porosity. To improve upon SMI two alternatives are presented.

The first is the Ellipsoid Factor (EF), a development of the 3D local thickness algorithm, but with fitted ellipsoids in place of spheres [1]. The ellipsoid has freedom to assume a range of shapes from oblate (flat disc shaped, $EF = -1$) to prolate (long javelin shaped, $EF = 1$). EF ranges from -1 (ideal plate) to +1 (ideal rod). The EF algorithm calculates both a mean value of EF and a 3D spatial map of local EF values.

The second alternative to SMI is a simpler parameter; the unplate index (uPi) which is the ratio of the trabecular direct thickness measured in 3D by sphere-fitting, $Th(d)$, to that calculated from the plate model ($2BV/BS$). Thus $uPi = Th(d) \times BS/2BV$. For an ideal plate $uPi = 1$ and with departure from plate shape the value increases above 1.

MicroCT morphometric data of rat femoral trabecular bone from an OVX study into efficacy of sex steroids [2] is reanalysed to compare values of SMI, EF and uPi. This study is a case where high BV/TV from anabolic drug treatment resulted in negative SMI. The unplate index uPi followed both trabecular SMI and BV/TV in showing weaker than sham amelioration of OVX osteopenia from administered testosterone (DHT) and stronger than sham architecture in both estradiol (E2) and E2 + DHT treatment groups, with the strongest response in the latter, combined treatment. The EF results however depart from this pattern in that, while E2 gives a stronger response than DHT, the E2 + DHT group gives the weakest, not strongest, reversal of OVX changes. Both EF and uPi are free of the problem of out-of-range values, unlike SMI. Also unlike SMI, both uPi and especially EF have nonlinear regression with BV/TV indicating that they bring new information beyond BV/TV.

1. Doube M (2015) *Frontiers in Endocrinol / Bone Res.* Vol. 6: 15
2. Tivesten A et al. (2004) *JBMR* 19 (11): 1833

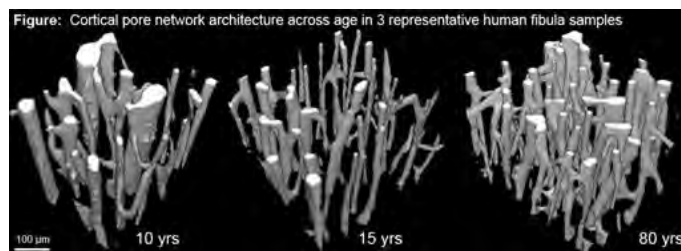
Disclosures: Phil Salmon, None.

This study received funding from: Bruker Inc, employer of P Salmon

MO0032

Pore Network Architecture Determines Cortical Bone Elasticity During Growth and Aging. Yohann Bala^{*1}, Emmanuelle Lefèvre², Jean-Paul Roux¹, Cécile Baron², Philippe Lasaygues³, Martine Pithieux², Valérie Kaftandjian⁴, Hélène Follet⁵. ¹INSERM U1033, Université de Lyon, France, ²Aix-Marseille Université, CNRS, ISM UMR 7287, 13288 Marseille Cedex 09, France / APHM, Hôpital Sainte Marguerite, IML, Marseille Cedex 09, France, France, ³Laboratory of Mechanics & Acoustics, UPR CNRS 7051, Aix-Marseille University, Centrale Marseille, 13009 Marseille, France, France, ⁴Laboratoire Vibrations Acoustique, INSA Lyon, Campus LyonTech la Doua, 69621 Villeurbanne Cedex, France, France, ⁵INSERM UMR 1033, Université de Lyon, France

Cortical porosity is a major determinant of bone strength. Haversian and Volkmann's canals are 'seen' as pores in 2D cross-section but fashion a dynamic network of interconnected channels in 3D, a quantifiable footprint of intracortical remodeling. Given the changes in bone remodeling across life, we hypothesized that the 3D architecture of the cortical pore network is age-dependent and influences its stiffness. Cubes of cortical bone of 2 mm side-length harvested in the distal 1/3 of the fibula in 13 growing children (9M, 4F, mean age \pm SD: 12.4 yrs) and 16 adults (7M, 9F, 74.12 yrs) were imaged using desktop micro-CT (8 μ m isotropic voxel size). Pores were segmented as a solid to assess pore volume fraction (Po.V/TV, %), number (Po.N, 1/mm), diameter (Po.Dm, μ m), separation (Po.Sp, μ m) and connectivity ConnD, 1/mm³). Compression (C33) and shear (C66) elastic coefficients were derived by assessing waves velocity using ultrasonic measurements. Spearman correlation coefficients (r) are reported when statistical significance reached ($p < 0.05$). Pore volume fraction (Po.V/TV) did not differ between growing children and adults groups but originated from different architectural pattern (Figure). Relative to children, adults had 46% higher Po.N, 17% lower Po.Sp, 250% higher ConnD, 14% and 13% higher compressive (C33) and shear (C66) stiffness, respectively (All $p < 0.02$). In growing children, age was associated with a decrease in Po.V/TV ($r^2 = -0.6$) due to decreasing Po.N ($r^2 = -0.5$), Po.Dm ($r^2 = -0.4$) and increasing Po.Sp ($r^2 = 0.6$). C33 and C66 were inversely correlated with Po.V/TV, Po.N and Po.Dm (r ranging from -0.56 to -0.82), none of the correlations remained significant after adjustment for Po.V/TV contribution. Among adults, age was associated with higher Po.V/TV ($r^2 = 0.7$) originating from an increase in Po.N ($r^2 = 0.8$), Po.Dm ($r^2 = 0.5$) and a decrease in Po.Sp ($r^2 = -0.8$). C33 was inversely correlated with Po.V/TV ($r^2 = -0.6$), Po.N ($r^2 = -0.6$) and positively with Po.Sp ($r^2 = 0.7$). Po.Sp remained correlated with C33 after accounting for Po.V/TV contribution ($r^2 = 0.6$). No correlation was found between C66, Po.V/TV or pore network architecture. We infer that changes in intracortical remodeling across life alter the distribution, size and connectedness of the channels forming cortical porosity. These alterations in pore network architecture participate in compressive stiffness impairments with aging, independently of the age-related increase in porosity.



Figure

Disclosures: Yohann Bala, None.

MO0033

Precision Assessment of Biomechanical Testing of the Distal Radius in Cynomolgus Monkeys. Gabrielle Boyd, Aurore Varela^{*}, Susan Y. Smith. Charles River Laboratories, Canada

Biomechanical strength testing of bones, considered the ultimate test of bone quality, is a key end-point in the safety testing and efficacy evaluation of test compounds in nonclinical studies. In humans, distal radius fractures are an early and sensitive marker of skeletal fragility and represent a high risk for subsequent spine or hip fracture. The purpose of this study was to assess the adequate procedures to obtain appropriate precision for biomechanical testing of the distal radius in Cynomolgus monkeys.

Twenty radii were collected from female Cynomolgus monkeys aged 5 to 9 years old. A disc with plano-parallel ends was prepared from the distal metaphysis region, 6 mm distal from the styloid process. Densitometry and morphology parameters were measured by HR-pQCT (Xtreme-CT II, Scanco Medical) for the prepared specimens, and height was measured by caliper (5.60 \pm 0.05 mm). All discs underwent axial compression using a MTS MiniBionix Testing System (model 358.02C). The load was applied on the distal surface at a rate of 20 mm/min. Load and displacement data were collected using TestSuite with TWE software version 1.1, along with derived biomechanical parameters.

Results for the compression test were: peak load 1267-2517 N, CV 17%; stiffness 9451-19693 N/mm, CV 25%; yield load 1177-2410 N, CV 18%; area under the curve at peak load (AUC) 243-584 N-mm, CV 22%. Results for the respective intrinsic parameters normalized for specimen size were: apparent strength 30-58 MPa, CV 17%; modulus 856-2276 MPa, CV 24%; yield stress 24-54 MPa, CV 17%; toughness 0.9-2.2 MPa, CV 30%.

It was noted that peak load, yield load, apparent strength and yield stress were the least variable. Linear regression analysis showed a positive relationship between HR-pQCT area BMC and peak load: $r=0.7413$. With respect to precision, these results were similar to tests performed for vertebral body compression, confirming that the current procedures used for specimen preparation and compression testing of the distal radius were adequate. Compression testing of the distal radius in addition to established procedures to assess strength at the spine and proximal femur (hip) will be important to provide a comprehensive assessment of the effects of drug treatment on biomechanical strength in nonclinical studies.

Disclosures: *Aurore Varela, None.*

MO0034

QCT Intra- and Inter-Scanner Precision In Estimation Of Proximal Femur Strength. SERENA BONARETTI¹, JULIO CARBALLIDO-GAMIO², JOYCE KEYAK³, ISRA SAEED⁴, LIFENG YU⁵, MICHAEL BRUESEWITZ⁵, ANDREW J. BURGHARDT², SUNDEEP KHOSLA⁶, THOMAS F. LANG². ¹University of California, San Francisco, USA, ²Musculoskeletal Quantitative Imaging Research Group, Department of Radiology & Biomedical Imaging, University of California, San Francisco, CA, USA, ³University of California, Irvine, Irvine, CA, USA, ⁴Musculoskeletal Quantitative Imaging Research Group, Department of Radiology & Biomedical Imaging, University of California, San Francisco, CA, USA, ⁵Division of Medical Physics, Department of Radiology, College of Medicine, Mayo Clinic, Rochester, MN, USA, ⁶Division of Endocrinology, Metabolism & Nutrition, Department of Internal Medicine, College of Medicine, Mayo Clinic, Rochester, MN, USA

Quantitative Computed Tomography (QCT) is increasingly used to assess proximal femur strength in epidemiologic and drug studies using finite element analysis (FEA). Bone material properties are derived from image intensities, which strongly depend on QCT scanners. Inter-scanner differences are critical in multicenter studies where multiple scanners are used, and in longitudinal studies where scanner upgrades or substitutions frequently occur. Inter-scanner corrections can be applied to reduce inter-scanner variability to intra-scanner precision. However, standardized scanner cross-calibration procedures are still an open challenge. The aim of this study was to compare single scanner precision to inter-scanner reproducibility for FEA calculations of proximal femur strength.

We scanned proximal femurs of 60 subjects at UCSF and 60 subjects at Mayo Clinic using QCT. At each site, we scanned 30 subjects on the same scanner for intra-scanner precision measurements (scan/rescan with subject repositioning), and 30 subjects on two different scanners for inter-scanner precision measurements. We processed images automatically, using a novel pipeline constituted of segmentation¹, image calibration and creation of FE mesh with QCT-based mechanical properties and boundary conditions. We computed FEA for stance and posterolateral fall loading conditions, both for intra-scanner and inter-scanner precision measurements.

Intra-scanner precision was in the range 2.26-4.41% for stance and fall configurations (Table1). Although the mean values for the subject on the different scanners were not significantly different, inter-scanner variability was more than two-fold greater than intra-scanner precision error.

In this study we found that inter-scanner precision errors of bone strength for stance and fall conditions were considerably higher than intra-scanner precision errors. We are currently working on reducing inter-scanner precision errors to intra-scanner precision errors using scanner cross-calibration corrections. We will calculate corrections using a novel anthropomorphic hip phantom, which contains a calibration hip to calculate inter-scanner corrections, and a test hip to test the corrections². Corrections will be applied to bone mineral density, from which mechanical properties derive, and will take into account body size.

¹Carballido Gamio et al. Bone. Submitted. 2015

²Bonaretti et al. Phys. Med. Biol. 2014

Table 1. Intra-scanner precision vs. inter-scanner variability for proximal femur strength in stance and fall configurations. Precision was measured as root mean square of percentage coefficients of variation.

| | Siemens Biograph / GE VCT 64 system (UCSF) [RMSCV%] | Siemens Definition Flash / GE VCT 64 system (Mayo Clinic) [RMSCV%] |
|----------------------------------|---|--|
| Precision | | |
| Stance | 2.26 | 4.14* / 3.28** |
| Fall | 4.21 | 3.95 |
| Inter-scanner variability | | |
| Stance | 8.00 (9982/10287)*** | 7.27 (11142/11128)*** |
| Fall | 9.43 (3875/3652)*** | 4.76 (3999/3931)*** |

*Precision affected by 2 outliers (under current investigation)

** Precision without outliers

*** Mean strengths per scanner (values in [N])

Table1

Disclosures: *SERENA BONARETTI, None.*

MO0035

Significant Alterations in Gene Expression Within the Wnt Pathway Contribute to the Natural Variation in Bone Mechanical Function. Stephen Schlecht^{1*}, Lauren Smith¹, Erin Bigelow¹, Yueqin Yang², Amber Cathey¹, Bonnie Nolan¹, Eugene Manley¹, Melissa Ramcharan¹, Maureen Devlin³, Joseph Nadeau⁴, Karl Jepsen¹. ¹University of Michigan, USA, ²Tsinghua University, China, ³Department of Anthropology, USA, ⁴Pacific Northwest Research Institute, USA

Targeted perturbations within the Wnt pathway identified genes that alter bone strength and thus contribute to mechanical homeostasis. However, it remains unclear how genes and their interactions within the Wnt pathway contribute to normal bone mechanical function. We tested the hypothesis that two inbred mouse strains (*A/J*, C57BL/6J (B6)) that achieve similar whole bone mechanical function, albeit via different morphological and compositional traits (Fig.1), will show significant differences in gene expression. *A/J* and B6 mice have slender (narrow) and robust (wide) femora, respectively, similar to the natural variation seen in humans.

cDNA from femoral diaphyses of 4 week old male B6 (n=18) and *A/J* (n=18) mice was analyzed using a TaqManTM gene array of 87 osteogenic genes. Several genes were differentially expressed (> 2-fold) between the two strains, including *SOST* and several *BMPs*. We then examined the Wnt pathway using a TaqManTM gene array of 46 involved genes, testing for differential gene expression between male *A/J* and B6 femurs at critical ages in long bone growth (n=18/strain/age). The array showed that 25%, 17%, 61%, 69%, and 78% of the genes were significantly differentially expressed at 2, 4, 6, 8, and 12 weeks of age, respectively. Importantly, *SOST* was upregulated 1.7-7.6 fold in *A/J* across all ages, with *SOSTDC1*, *DKK1*, and *DKK2* also upregulated in *A/J* for all but one age. *A/J* femurs had significantly lower total cross-sectional area (29-40%) and cortical area (10-19%) than B6 at most ages (Fig 1), suggesting the increased *SOST* expression may contribute to these morphological differences. Finally, femora from *A/J* females increased in cortical area with exercise compared to controls (GLM ANOVA; p=0.04), whereas B6 femora became more slender with exercise (p=0.0004), confirming a differential response to increased loading.

The differential gene expression provided evidence that the Wnt pathway, in particular *SOST*, is involved in bone homeostasis, as expected. However, we showed that the relative expression of many genes in the Wnt pathway differ significantly between two normal inbred mouse strains that achieve similar bone strength but in different ways. Further work testing for differences in gene networks using RNAseq will provide context to how the Wnt pathway is being differentially regulated in these strains. Additional studies will test if this model is clinically meaningful by testing for a differential response to *SOST* inhibition.

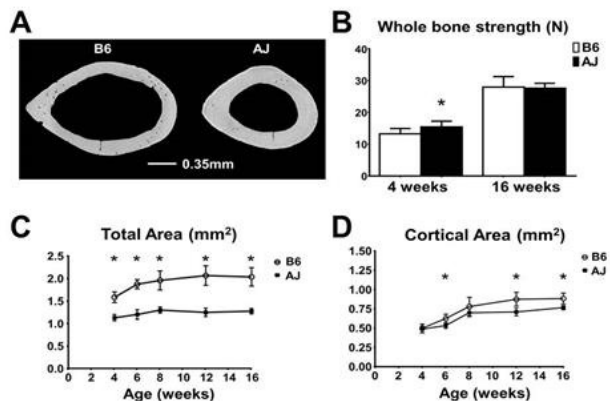


Figure 1. Phenotypic differences between B6 (wide) and AJ (narrow). A) Typical mid-diaphyseal cross sections of both strains at 16 weeks of age, nanoCT images at 1.5µm voxel size. B) Whole bone strength derived from 4-point bending of both strains at 4 and 16 weeks of age. Morphological traits C) total cross sectional area and D) cortical area for B6 and AJ at 4, 8, 12 and 16 weeks of age, measurements derived from nanoCT images at 1µm voxel size. AJ has significantly lower total cross sectional area throughout the time sequence and tends to also have lower cortical area after 4 weeks of age. * signifies $p < 0.01$.

Figure 1

Disclosures: Stephen Schlecht, None.

MO0036

The Effect of Age on Cortical Bone Crack Initiation and Crack Growth Toughness. Travis Eliason¹, Todd Bredbenner¹, Lorena Havill², Daniel Nicoletta¹. ¹Southwest Research Institute, USA, ²Texas Biomedical Research Institute, USA

Humans experience an age-related increase in the risk of skeletal fractures due to changes in a variety of bone properties. Of particularly high interest is the change in the fracture toughness of bone and its resistance to crack initiation and propagation. In order to compare the fracture toughness of cortical bone, fracture toughness arch-shaped tension specimens (ASTM E399) were machined from the femoral shaft of 10 young (< 15 years) and 10 old (>22 years) female baboons. Specimen geometries were chosen for each animal to minimize the amount of machining needed to match the prescribed ASTM standard geometry. Specimens were loaded in tension under a Keyence digital optical microscope using a custom microscopy test frame to directly measure force vs crack length. The stress intensity factor K was calculated from the geometry, force, and crack length measures according to the ASTM standard and used to approximate the K-resistance (K vs. change in crack length) curves for each animal. Crack initiation toughness and the R curve slope were determined from the least squares linear regression of K given change in crack length. One way analysis of variance was used to compare crack initiation toughness and slope between old and young animals. Both crack initiation toughness and R curve slope were significantly different between the old and young animals (p-values of .048 and .0396 respectively). Older animals had both lower crack initiation toughness (4504 vs .5892 MPa (m)^{1/2}) and a lower R curve slope (2.216 vs 3.218 MPa(m)^{1/2}/mm). These results show that the femoral cortical bone has experience fundamental material changes during the aging process which results in a lower resistance to fracture. In ongoing work we are characterizing these bones with a comprehensive suite of bone traits to investigate the combinations of traits which lead to strong vs weak bones along with the associated age and sex effects.

Disclosures: Travis Eliason, None.

MO0037

Tumor necrosis factor negative regulation on the bone mineral density and trabecular bone architecture texture in chickens. Lixian Liu¹, Hua Rong¹, Qihua Li¹, Dahai Gu¹, Zhiqiang Xu¹, Tengfei Dou¹, Ying Huang¹, Limei Huang¹, Hongyong Zhang², Marinus F.W.te Pas³, Changrong Ge¹, Junjing Jia⁴. ¹Yunnan Provincial Key Laboratory of Animal Nutrition & Feed Technology, Yunnan Agricultural University, China, ²Department of Medicine, University of California at Davis Medical Center Sacramento, USA, ³ Animal Breeding & Genetics Centre, Wageningen UR Livestock Science, Wageningen, Netherlands, ⁴Faculty of Animal Science & Technology, Yunnan Agricultural University, Peoples republic of china

The bone mineral density (BMD) and strength are most important economical traits for poultry production. It has been caused huge economic losses in poultry industry due to bone defects, osteoporosis, rickets and other bone diseases. Tumor necrosis factor- α (TNF- α) is a key cytokine regulator of bone and mediates inflammatory bone loss. In our previous studies, we found that slow growing small chicken with 1.2 kg of adult body weight (Daweishan mini chicken) showed higher bone strength and association with lower expression of TNF- α mRNA in tibia bone,

compare to slow growing large chicken with 2.5 kg of adult body weight (Wuding chicken) and fast growing large avian broilers. TNF- α may plays important role effect on the BMD and trabecular bone architecture in chicken. The objective of this study was to investigate the effect of expression of TNF- α mRNA on the BMD and trabecular bone architecture. A total of 180 1-day-old chicks from Daweishan mini chickens, Wuding chicken and avian broiler were fed in an environmentally controlled room. All chickens from 1-21 days were fed a starter diet, older chickens received a full diet. The chickens had free access to feed and water. Twenty chickens from each breed were scarified at 4, 8 and 12 weeks and samples from cartilage and distal tibia were taken to detect the expression of TNF- α mRNA. The femur and tibia in each time point were used to scan mineral density and trabecular bone microarchitecture by using MicroCT, and then to determine the mechanical properties via by 3-point bending test.

Results: Daweishan mini chickens showed the highest femur and tibia bone strength ($P < 0.01$); BMD, BV/TV, trabecular thickness (Tb Th) and number (Tb N) ($P < 0.05$) while converse case were observed in broilers that showed the lowest these parameters and with the highest trabecular space (Tb Sp) among the thress breed in all time points. It is interesting to find that broilers showed the highest expression of TNF- α mRNA in cartilage and distal tibia in all time points while converse case were observed in mini chickens ($P < 0.05$).

In conclusion, TNF- α gene expression is negative association with femur and tibia bone strength, BMD and trabecular score in chickens. Acknowledgments: This work was funded by National 863 Proposal of P. R. China (2011AA100305); National and Yunnan Provincial Natural Science foundation Research Projects of China (31260532; 2009CD060; 2011FA015).

Disclosures: Lixian Liu, None.

MO0038

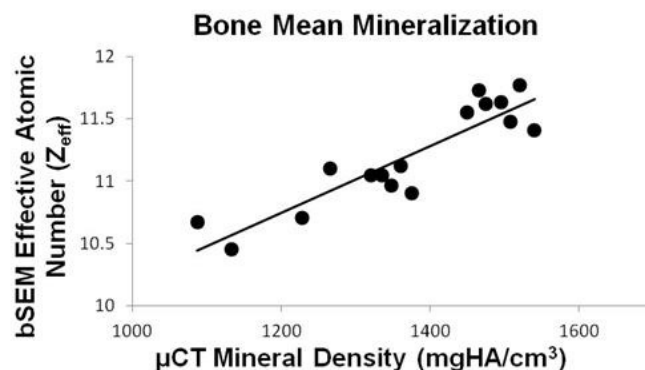
Validation of CT-based Assessment of Bone Mineralization and Heterogeneity. Maleeha Mashiatulla*, Ryan D. Ross, D. Rick Sumner, Rush Medical University, USA

A number of studies indicate the importance of bone quality for bone strength. Bone quality covers a wide range of parameters, including matrix mineralization and geometry. Micro-computed tomography (μ CT) has been extensively used to quantify bone geometry, but recently tissue mineral density (TMD) has been reported, which has been validated with ash density. TMD has not been validated against backscatter scanning electron microscopy (bSEM), which has the advantage of anatomic specificity. The aim of the present study was to validate μ CT-based TMD assessment against bSEM and to explore if mineralization heterogeneity can also be evaluated by μ CT, analogous to the bone mineral density distribution (BMDD) assessed in bSEM.

Phantoms between 0-1860mgHA/cm³ were used for calibration and to select scanner settings. One set of phantoms was prepared for bSEM and a second set was used for μ CT imaging. Results with μ CT (70kVp, 200 μ A, 2 μ m voxel size and 1500ms integration time; Scanco μ CT50) were strongly correlated with bSEM-derived mineralization levels ($R^2=0.99$, $p < 0.001$). A cohort of animal samples ($n=16$) were obtained from several species and assessed with both μ CT and bSEM. The mean TMD from μ CT was strongly correlated with the mean effective atomic number obtained with bSEM (Fig.1, $R^2=0.81$; $p < 0.001$).

To determine if μ CT can also be used to measure BMDD, TMD frequency distributions were analyzed to measure the full width at half maximum (FWHM-mineralization heterogeneity) and the lower 5% and upper 5% cutoffs for the frequency distribution. Significant correlations were found for the upper 5% cutoff ($R^2=0.57$; $p < 0.001$) and the lower 5% cutoff ($R^2=0.34$, $p=0.01$). However, no correlation was found for FWHM ($R^2=0.01$; $p=0.66$). Since porosity is a potential confounding factor, pore number, diameter and area fraction were determined using bSEM sample images. The μ CT FWHM measurements were weakly correlated with mean pore diameter ($R^2=0.07$, $p=0.039$), %pore area ($R^2=0.25$, $p=0.032$) and total number of pores ($R^2=0.29$, $p=0.031$). None of the pore characteristics were correlated with bSEM-based FWHM.

In this study, we have shown that μ CT can be utilized to accurately measure mean mineralization of bone with anatomic specificity. Although some of the BMDD characteristics can be measured with μ CT, it is likely that porosity may be a confounding variable. Further investigation is needed to determine if mineralization heterogeneity can be accurately assessed by μ CT.



Correlation of mean mineralization of different animal species measured by bSEM and μ CT, $R^2=0.81$

Disclosures: Malecha Mashiattulla, None.

MO0039

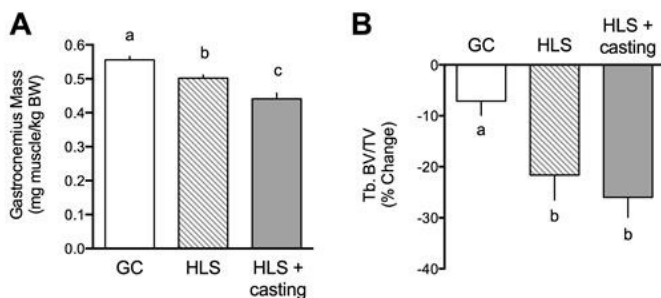
Hindlimb Suspension Plus Immobilization Exaggerates Sarcopenia but not Osteopenia. Toni Speacht^{*1}, Andrew Krause¹, Jennifer Steiner², Charles Lang³, Henry Donahue⁴. ¹Division of Musculoskeletal Sciences, Department of Orthopaedics & Rehabilitation, Penn State College of Medicine, USA, ²Department of Cellular & Molecular Physiology, Penn State College of Medicine, USA, ³Department of Cellular & Molecular Physiology, Department of Surgery, Penn State College of Medicine, USA, ⁴Division of Musculoskeletal Sciences, Department of Orthopaedics & Rehabilitation, Department of Cellular & Molecular Physiology, Penn State College of Medicine, USA

Astronauts in space experience a unique environment that causes both bone and muscle loss. However the interaction between these two tissues and how osteopenia and sarcopenia affect each other is unclear. We used a hindlimb suspension (HLS) model to study the effects of microgravity experienced by astronauts during space travel. This model is also appropriate to study the effects of age-related muscle and bone loss, including osteoporosis, as the mechanisms of loss are similar. To explore the relationship between bone and muscle, we examined the hypothesis that exaggerating unloading-induced muscle loss via HLS + casting, will also exaggerate unloading-induced bone loss.

Twenty C57Bl/6J mice (5m, male) were exposed to HLS with one limb unrestrained (HLS) and one limb casted (HLS+Cast), or maintained as ground controls (GC) for 2 weeks (2 groups, n=10/group). Mice were subjected to baseline and endpoint microCT scans to assess bone micro-architectural changes. Quadriceps and gastrocnemius muscles were excised, weighed, and assessed for protein synthesis and protein degradation.

Gastrocnemius and quadriceps weight was decreased 10% in HLS limbs and 20% in HLS+Cast mice compared to GC ($p<0.05$). The rate of in vivo protein synthesis was decreased in both HLS and HLS+Cast groups compared to GC ($p<0.05$), however, HLS+Cast limbs had a 15% increase in protein synthesis compared to the HLS limbs ($p<0.05$). Measurements of mTOR signaling (S6K1 and 4E-BP1 phosphorylation) correlated with our in vivo protein synthesis measurements. We also evaluated markers for protein degradation. There was no difference in ubiquitin-E3 ligases (Atrogin-1 and MuRF1) mRNA between any groups. There was, however, an increase in autophagy associated proteins LC3-II/I, Atg7, and Atg5-12 in the HLS+Cast limb compared to both HLS and GC ($p<0.05$). Bone volume/total volume (BV/TV) decreased significantly in HLS and HLS+Cast limbs compared to GC mice ($p<0.01$), however, unlike muscle, there was no difference in HLS and HLS+Cast limbs, suggesting a disconnect between bone and muscle loss.

Our data suggest that casting exacerbates the muscle loss attributed to unloading and the mechanism of this response includes activation of the autophagy degradation pathway. Surprisingly, casting did not cause an exacerbation of bone loss, suggesting that muscle and bone loss, in response to unloading, are uncoupled. Thus, countermeasures to prevent muscle loss will not necessarily affect bone loss.



Effect of HLS and HLS+Casting for 2 weeks on gastrocnemius mass (A) and tibia trabecular BV/TV (B)

Disclosures: Toni Speacht, None.

MO0040

Pre-Treatment with Bisphosphonates Mitigates Bone Loss at the Tibia Metaphysis and Femoral Neck During Subsequent Hindlimb Unloading and Recovery. Jessica Brezicha^{*1}, Scott Lenfest², Jennifer Kosniowski², Coleman Leach¹, Jeremy Black¹, Susan Bloomfield¹, Matthew Allen³, Harry Hogan¹. ¹Texas A&M University, USA, ²Texas A&M, USA, ³Indiana University School of Medicine, USA

Disuse during long-duration space flight is a potent down-regulator of bone mass and density. We have used the rat hindlimb unloading (HU) model previously to

demonstrate that bisphosphonates (BPs) given during HU can mitigate negative effects of simulated microgravity. In this study, we compared two BPs, alendronate (ALN) and risedronate (RIS), given prior to HU on bone properties during HU and a recovery period. Since ALN has a higher binding affinity than RIS, we hypothesized that ALN would protect bone more than RIS.

Adult Sprague-Dawley male rats (6 mo.) were assigned by initial body weight and cancellous vBMD to 1 of 4 groups: AC (aging control), HU, ALN+HU, and RIS+HU. ALN (2.4 μ g/kg) and RIS (1.2 μ g/kg) were administered 3x/wk for a 28d pre-treatment period prior to HU. After 28d of HU, animals returned to normal weight bearing for 56d of recovery. *In vivo* peripheral quantitative computed tomography (pQCT) scans were made of the proximal tibia metaphysis (PTM) at baseline (BL) and every 28d. Femurs were collected from a subset of animals at the end of HU and from the remaining animals at the end of recovery. *Ex vivo* pQCT scans were made of the femoral neck (FN), and then the FN was mechanical tested to failure.

Disuse caused significant total BMC loss (-9%) at the PTM vs. AC after 28d HU, and this was prevented by pre-treatment with either RIS or ALN. PTM cancellous BMC was higher vs. AC (+38% for ALN, $p<0.05$; and +22% RIS, n.s.), and cancellous vBMD was significantly higher for both BPs (+30% for ALN, +25% for RIS). After the full 56d recovery, results were similar, with cancellous BMC significantly higher for both BPs (+58% for ALN, +37% for RIS) vs. AC and cancellous vBMD also higher for both (+39% for ALN, +32% for RIS). At the FN, both BPs were protective after HU, with cancellous vBMD higher than HU (+6% for ALN, +12% for RIS) and HU lower than AC (-12%). There were no differences after 56d recovery. FN fracture force was higher for ALN (+28%) and RIS (+32%) vs. HU at 28d, with no differences for either BP vs. AC.

In conclusion, beneficial effects of BP pre-treatment not only mitigated losses during a period of disuse but also enhanced cancellous bone properties during recovery at the PTM. Protective effects at the FN were less dramatic (lower %) for densitometric variables but similar in magnitude for mechanical properties. Contrary to our hypothesis, there were no major differences between ALN and RIS effects.

Disclosures: Jessica Brezicha, None.

MO0041

Age Matters: Correlating Age with Spectroscopic Markers of Fragility Risk. Adele Boskey^{*1}, Lyudmila Spevak¹, Elizabeth Boskey², Robert Recker³. ¹Hospital for Special Surgery, USA, ²Boston University, USA, ³Creighton University, USA

Bone mineral density (BMD) is routinely used to predict fragility fracture risk. However women with equivalent BMDs may show a different fracture incidence due to differences in "bone quality". Bone quality refers to architecture, morphology, extent of mineralization, mineral crystal properties and collagen structure. All but architecture and morphology can be determined by Fourier transform infrared spectroscopic imaging (FTIRI). In a previously published random population of otherwise healthy women with and without fractures (Gourion-Arsiquaud et al, 2009), increased collagen maturity and crystal size in both cortical and cancellous bone within iliac crest bone biopsies were associated with risk of fragility fracture. In a larger population of iliac crest bone biopsies from women with and without fragility fractures, paired by age and BMD (Boskey et al, 2015), collagen maturity was no longer predictive, implying that this variable might be a biological mechanism or marker for patient age related fracture risk. Knowing that bone matrix composition varies with age (Cleland & Vasishth, 2015) and that risk of fragility fracture also increases with age (Ensrud, 2013), we queried whether enzymatic cross-links measured by FTIRI in these earlier reports was age dependent. Linear-regression (Prism 3.03) was used to determine whether collagen maturity and other FTIRI variables were correlated with age at the time of biopsy, analyzing cortical and cancellous variables separately, in those patients from the first study for which age was known (n=31), all patients from the second study (n=120) and the combined studies (n=151). There was a significant positive correlation (Figure 1) between cancellous collagen maturity and age ($r^2=0.88$) in all data sets, and between crystallinity and age in the fracture group alone ($r^2=0.66$). This suggests that some of the fracture risk associated with aging may be related to age-related changes in crystallinity, but that collagen maturity is likely a marker for age-related changes in bone rather than directly associated with excess fracture risk.

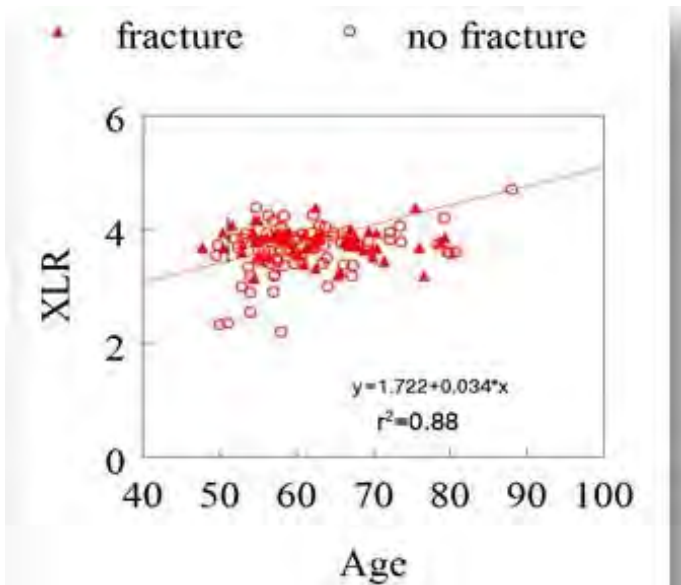


Fig 1: Collagen cross-links (XLR) determined by FTIRI increase with increasing age

Disclosures: Adele Boskey, None.

MO0042

Global Phosphorylation of Bone Matrix and Bone Fragility. Grazyna Sroga*, Deepak Vashishth, Rensselaer Polytechnic Institute, USA

It has been proposed that posttranslational modifications (PTMs) of bone matrix proteins play a significant role in controlling biomineralization [1]. Despite years of studies, the precise roles of different matrix phosphoproteins in the context of their levels of phosphorylation remain elusive.

Mechanically tested specimens (18) from male and female cadavers (age range 19 to 97) cadavers were used to isolate bone matrix proteins using methods published previously [2]. Detection of protein phosphorylation was based on the addition of the pIMAGO reagent (Tymora Analytical, West Lafayette, IN). The pIMAGO is the water-soluble nanopolymer that attaches only to phosphoproteins. This nanopolymer contains biotin groups that allow enzyme-linked spectrophotometric detection using a microtiter plate reader. The normalized values of triplicate assays were then averaged and tested for correlation with fracture toughness of bone using crack propagation test [2].

The level of global protein phosphorylation in human posterior cortex bone was inversely related to the age ($p < 0.001$, $R^2 = 0.46$) and was on average about 1.5-fold lower in the tenth than the third decade of human life. Positive and highly correlated relationship between phosphorylation of bone matrix measured “in bulk” and propagation toughness of bone was observed ($R^2 = 0.26$, $p < 0.03$).

To our knowledge, this is the first study on the relationship between the global bone matrix phosphorylation levels, age and bone quality. Further studies should be conducted to investigate the role of phosphorylation in bone fracture.

[1] Glimher MJ, Phys Trans Roy Soc Soc Trans London B, 304 (1984) 479-508.
 [2] Sroga et al, PLoS ONE (2015) 10(1): e0117046.doi:10.1371/journal.pone.0117046

Acknowledgement: NIH grant R01AR49635 (Vashishth).

Disclosures: Grazyna Sroga, None.

MO0043

Hip Fracture Risk during Simulated Falls: Influence of Pelvis Impact Angle and Hip Muscle Forces. Woochol Joseph Choi*¹, Stephen Robinovitch², ¹Chapman University, USA, ²Simon Fraser University, Canada

Over 90% of hip fractures in older adults are caused by falls (Grisso et al., 1991). Risk for hip fracture depends on bone strength, and on the impact force and stress applied to the proximal femur during the fall (Bouxsein et al., 2007). In the current study, we used a mechanical model to examine how peak stresses at the femoral neck during simulated falls are affected by (1) the angle of the pelvis at impact, and (2) the forces in the muscles spanning the hip. We also examined how pelvis impact angle influences the protective benefit of wearable hip protectors. Using the SFU hip impact simulator (Choi et al., 2015), we measured 3D forces at the femoral neck under various levels of gluteus maximus and medius muscle forces, and pelvis impact angles. Hip abductor muscle forces were set to either 300 or 700 N. Seven impact configurations of the pelvis were examined, ranging in 5 deg increments between -15 degrees and +15 degrees (Figure 1). Measures were conducted with no hip protector, and two commercially available protectors (HipSaver and SafeHip). Outcome variables (Figure 2) included peak values at the femoral neck of: (a) axial

force, (b) shear force, (c) bending moment, (d) shear stress, (e) compressive stress and (f) tensile stress, and (g) percent attenuation in peak compressive stress provided by hip protectors. ANOVA was used to test whether each outcome variables associated with our testing conditions at $\alpha = 0.05$. All of our outcome variables were associated with pelvis impact angle ($p < 0.0005$), hip abductor muscle force ($p < 0.018$) (Table 1), and padding device ($p < 0.0005$). On average, peak compressive and tensile stresses decreased 27% and 68%, respectively, when the pelvis impact angle changed from 15° posterior to 15° anterior, and were 8% and 73% lower, respectively, in the 700 N than 300 N muscle force condition when the pelvis impact angle was zero. Furthermore, the force attenuation provided by hip protectors peaked between zero and 10° anterior, and declined rapidly for posterior impacts (Figure 3). Our results indicate that activation of the hip abductors is protective (caused a reduction in bending moment, and peak compressive and tensile stress) at zero degree and anterior impact angles, and dangerous (caused an increase in bending moment and peak stresses) for posterior impact angles (Figure 4). Furthermore, the protective benefit of common hip padding devices depends strongly on pelvis impact configuration during falls.

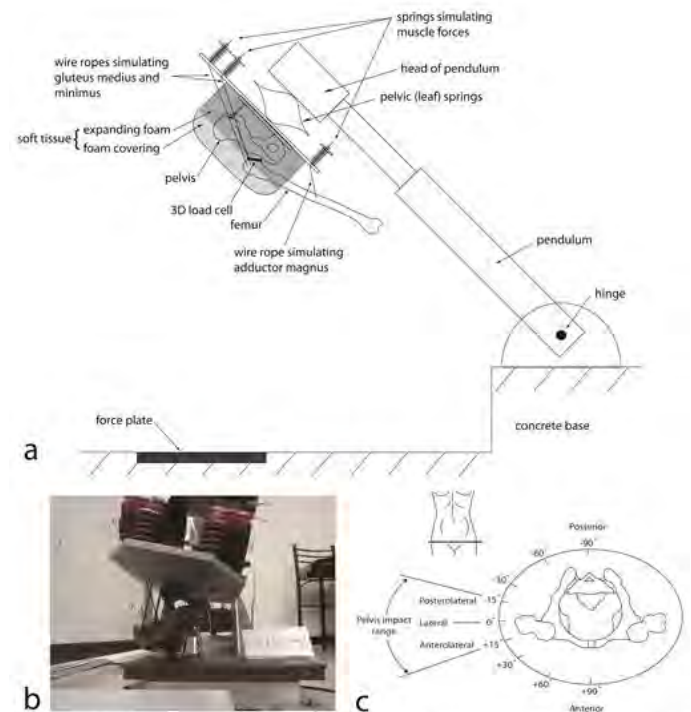


Figure 1. SFU Hip impact simulator, showing (a) schematic of the system, and (b) snapshot of surrogate pelvis (soft tissue covering removed) before impact with a pelvis rotation of 15° posterior along with (c) range of pelvis impact angle tested.

Figure 1

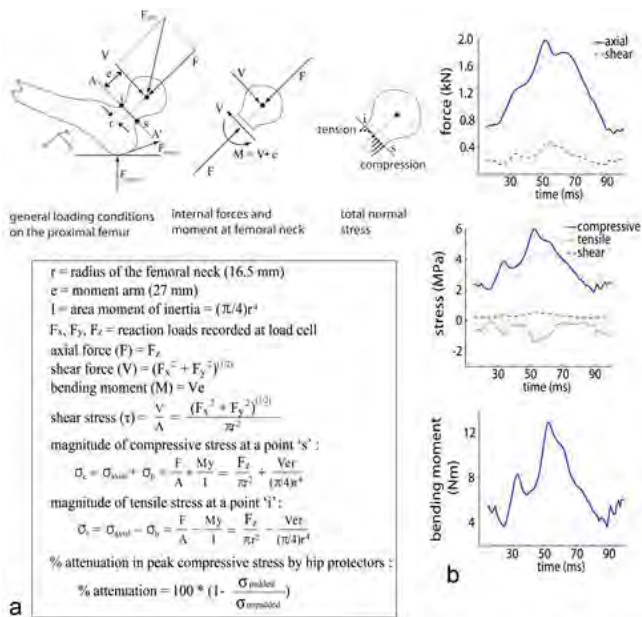


Figure 2. Experimental measures and calculated outcome variables. (a) Free body diagram and stress analysis at the proximal femur at impact from a fall. (b) Sample force and stress traces for 300 N with zero degree of pelvis rotation (lateral impact).

Figure 2

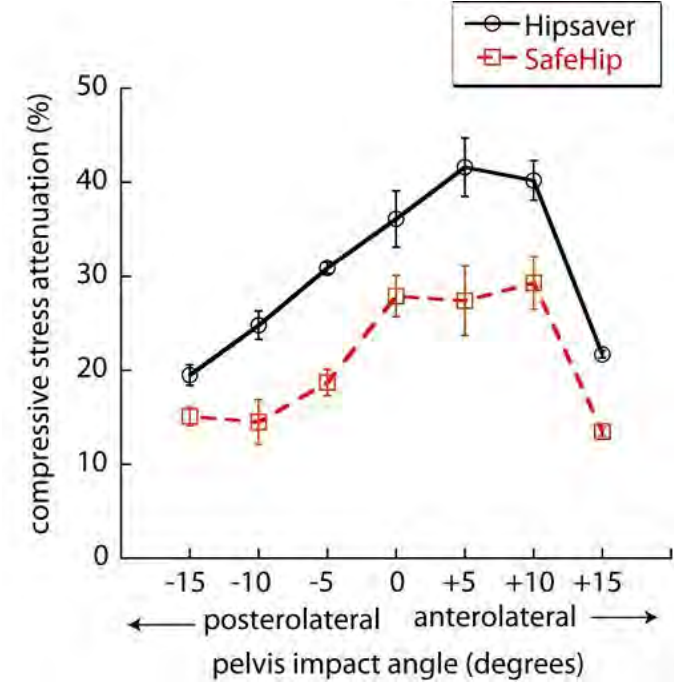


Figure 3. Effect of pelvis impact angle on percent compressive stress attenuation.

Figure 3

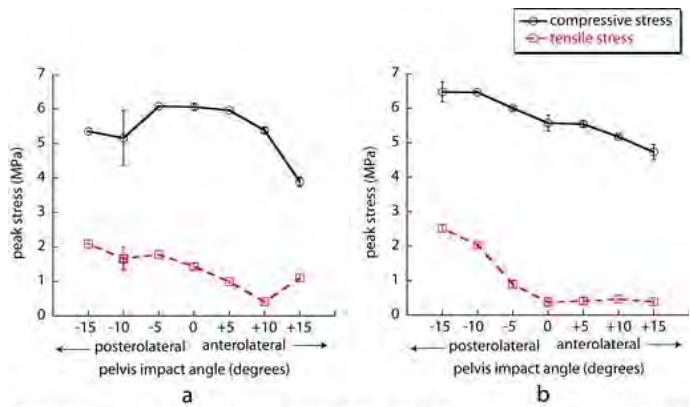


Figure 4. Effect of pelvis impact angle on peak stresses at the femoral neck with hip abductor muscle force of (a) 300 N and (b) 700 N.

Figure 4

| muscle force (N) | 300 N | | | | | | 700 N | | | | | |
|-------------------------------|--------------|--------------|--------------|--------------|--------------|--------------|--------------|--------------|--------------|--------------|--------------|--------------|
| | posterior | lateral | zero | lateral | anterior | anterior | posterior | lateral | zero | lateral | anterior | |
| peak axial force (N) | 1418 (11) | 1515 (12) | 1850 (15) | 2004 (17) | 2138 (18) | 1899 (19) | 1709 (20) | 1906 (21) | 2177 (22) | 2284 (23) | 2134 (24) | 2025 (25) |
| peak shear force (N) | 484 (1) | 445 (2) | 511 (3) | 489 (4) | 454 (5) | 378 (6) | 384 (7) | 545 (8) | 451 (9) | 388 (10) | 355 (11) | 112 (12) |
| peak bending moment (Nm) | 12.1 (0.0) | 12.3 (0.0) | 13.8 (0.1) | 12.7 (0.1) | 10.2 (0.2) | 8.8 (0.4) | 15.9 (0.7) | 14.6 (0.8) | 12.1 (0.2) | 10.5 (0.6) | 9.6 (0.2) | 7.7 (0.3) |
| peak shear stress (MPa) | 0.56 (0.00) | 0.52 (0.00) | 0.60 (0.01) | 0.57 (0.01) | 0.44 (0.01) | 0.38 (0.02) | 0.68 (0.02) | 0.63 (0.01) | 0.52 (0.01) | 0.45 (0.02) | 0.41 (0.01) | 0.33 (0.01) |
| peak compressive stress (MPa) | 5.35 (0.01) | 5.16 (0.01) | 6.08 (0.01) | 6.06 (0.01) | 5.96 (0.01) | 5.38 (0.01) | 3.89 (0.01) | 6.47 (0.01) | 6.46 (0.01) | 6.00 (0.01) | 5.54 (0.01) | 5.17 (0.01) |
| peak tensile stress (MPa) | -2.00 (0.01) | -1.66 (0.01) | -1.78 (0.01) | -1.48 (0.01) | -0.99 (0.01) | -0.41 (0.01) | -1.10 (0.01) | -2.52 (0.01) | -2.03 (0.01) | -0.90 (0.01) | -0.38 (0.01) | -0.45 (0.01) |

Table 1: Average values of outcome variables (with SD shown in parentheses).

Table 1

Disclosures: Woochol Joseph Choi, None.

MO0044

Optimizing Pulsed Electromagnetic Field (PEMF) Signals to Reduce Bone Loss in the Ovariectomized (OVX) Rat. Caroline Androjina^{*1}, Erik I. Waldorff², Nianli Zhang², James T. Ryaby², Maciej Z. Zborowski³, Ronald J. Midura³. ¹Lerner Research Institute/Cleveland Clinic, USA, ²Orthofix Inc., USA, ³Cleveland Clinic, USA

PEMF treatments have been shown to exhibit anabolic effects on bone tissue specifically by enhancing the metabolic activities of osteoblastic cells. However the efficacy to significantly block bone loss has been shown to be variable and it is unclear what parameters may result in an optimal PEMF dosage regimen for osteoporosis treatment. This study focused on signal slew rate (SR) variations of a commercially available FDA approved PEMF waveform (PhysioStimU, Orthofix, Lewesville, TX). We hypothesized that exposure to PEMF at higher SRs, and thus higher energy dosage, would more effectively reduce trabecular bone losses in osteoporotic rats. In this study 6-7 month-old OVX female Sprague-Dawley rats underwent 4 weeks (wks) of estrogen-depletion to achieve a state of menopausal bone loss. Five groups were followed (n = 10/group): CON (OVX control, no PEMF); ALN (alendronate); PS10 (PEMF SR 10 T/s, PhysioStim); PS100 (PEMF SR 100 T/s) and PS300 (PEMF SR 300 T/s). All treatments began 4 wks after OVX surgery for a period of 6 wks. ALN treated animals received sc injections of ALN, 3 days/wk (10 µg/kg BW per wk). All PEMF-treated rats received daily 3-h whole body treatments, 7-days per week. Using in vivo microCT imaging (20 µm) at 3 time-points (baseline, 4-wks post-OVX and 10-wks post-OVX) trabecular (proximal tibia) bone volume fraction (BV/TV), bone mineral content, and bone mineral density were examined. Injections of Alizarin Red and Calcein were done at 8 and 10-wks post-OVX, respectively, for end-point dynamic histomorphometry assessment of endosteal cortical bone formation rates (BFR) at the proximal tibia. Results (Fig. 1) show that treatment with the PS10 and PS300 do not mitigate trabecular bone losses, while treatment with the PS100 is trending towards a sizeable mitigation of OVX bone loss. BFR in the PS100 and PS300 groups were comparable to that of the ALN group, and both of these treatments showed BFR roughly 1/3 of that shown for the CON group (Fig. 2). In contrast, BFR for the PS10 were significantly different from the ALN group, and found to be comparable to the CON group. It appears that PEMFs of various SRs exhibit a variable range of biological effects on trabecular bone loss in osteoporotic rats. Interestingly, treatment with the PS100 partially mitigated trabecular loss supporting the rationale that PEMF treatment merits further investigation as a possible alternate treatment modality for the mitigation of osteoporotic bone loss.

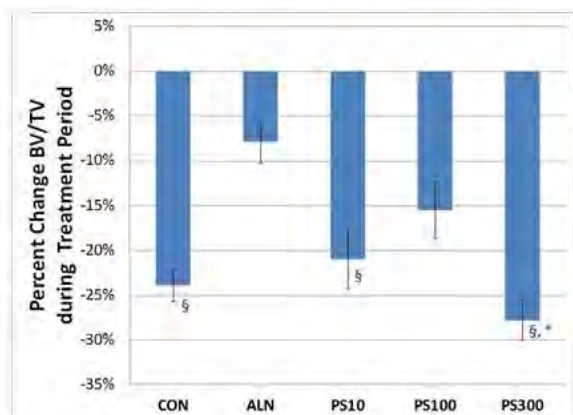


Figure 1: Percent change in bone volume fraction (BV/TV) during the 6-week treatment period. Values presented as mean \pm SE; \S $p < 0.05$ vs ALN and * $p < 0.05$ vs CON.

Fig1

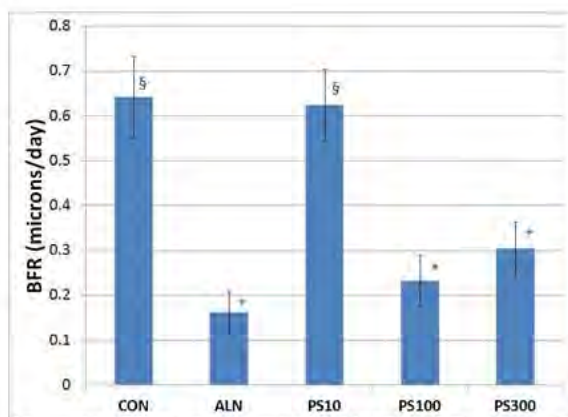


Figure 2: Bone formation rates (BFR) during the 6-week treatment period. Values presented as mean \pm SE; \S $p < 0.01$ vs ALN and * $p < 0.01$ vs CON.

Fig2

Disclosures: Caroline Androjna, Orthofix Inc
This study received funding from: Orthofix Inc.

MO0045

Low-Impact Multi-Directional Mechanical Loading Using a Fine-Wire Climbing Substrate Enhances Mechanical Properties of the Mouse Femur. Jason Organ^{*1}, Benjamin Vickery¹, Jeffery Joll¹, Kelly Biro¹, Craig Byron², Joseph Wallace³, Matthew Allen¹. ¹Indiana University School of Medicine, USA, ²Mercer University, USA, ³Indiana University-Purdue University at Indianapolis, USA

High-impact exercise (running/jumping) during childhood has been shown to be a potent osteogenic stimulus to augment the growing skeleton. However, physical activity of this nature is associated with an increased incidence of skeletal fracture, and therefore may not be an appropriate recommendation for children with already elevated risk of fracture. Multi-directional off-axis loading events, having low magnitude forces, can elicit osteogenic responses and therefore may represent a potential alternative to high-impact exercise for improving skeletal mechanical properties. We examined the effect of low-impact, multi-directional mechanical loading using a novel fine-wire climbing exercise regimen. We raised 19 weanling female C57BL/6 mice to skeletal maturity (4 months) in custom enclosures that prevent (control) or require (experimental) manual and pedal grasping while balancing and climbing above fine wire substrates. At sacrifice, we measured whole body bone density (DEXA) and performed geometric/architectural (μ CT) and mechanical (4-pt bending) analyses of the femur. Body mass was similar between groups, although experimental mice were significantly leaner (-34% fat mass). Bone mineral density and bone mineral content were similar between the groups. Femoral midshaft polar moment of inertia, cortical area, and cortical thickness were also similar between groups, but experimental mice had significantly lower BV/TV (-24.1%) of the distal femur as a result of having significantly lower trabecular number (-27%). Experimental mouse femora experienced significantly higher ultimate force (+17%), post yield displacement (+67%) and post yield work (+82%) prior to failure

than controls, while stiffness was non-significantly higher (+22%). Calculation of material properties showed that experimental mouse femora were non-significantly tougher (+33%) and experienced non-significantly lower strain to yield (-28%) than controls. These data suggest that the low-impact, multi-directional mechanical loading model improve whole bone mechanical properties by affecting aspects of the material. Future work will focus on understanding the specific aspects of the material-level properties that are responsible for these positive changes.

Disclosures: Jason Organ, None.

MO0046

Structural and Mechanical Improvements to Bone are Strain Dependent in a Targeted Tibial Loading Model of Young Female C57BL/6 Mice. Alycia Berman^{*1}, Creasy Clauser², Caitlin Wunderlin², Max Hammond³, Joseph Wallace⁴. ¹Indiana University - Purdue University Indianapolis, USA, ²Indiana University Purdue University Indianapolis, USA, ³Purdue University, USA, ⁴Indiana University Purdue University Indianapolis (IUPUI), USA

The targeted tibial loading murine model has been used extensively to assess the adaption of bone to external loading. However, most studies only explore alterations in bone morphology. Doing so provides useful information as to the adaptive response, but does not consider the broader functional implications of those changes. For example, analysis of bone architecture only measures bone quantity, even though bone quality also plays an integral role in overall bone integrity. For that reason, we studied the morphological and the mechanical adaption of bone to three levels of strain using the targeted tibial loading model. The right tibiae of female C57BL/6 mice (8 week old) were compressively loaded to one of three strain levels (1700 ue, 2050 ue, and 2400 ue as determined by a strain calibration), while the contralateral limb served as a non-loaded control. Mice were loaded for 3 days, followed by 1 day of rest, repeated 3 times over a 12 day period. Each day of loading consisted of 4 cycles of compression at 2 Hz, followed by 3 seconds of rest. This block (load then rest) was repeated 55 times, yielding a total of 220 cycles of compression per day. Two days following the last loading cycle, mice were euthanized and the tibiae were harvested for analysis. Ex vivo analyses consisted of micro-computed tomography to assess cortical and cancellous bone architecture, and 4-point bending to assess structural and tissue level mechanical integrity. Results indicated that loading improved bone architecture in a dose-dependent manner. At the lowest strain level (1700 ue), loading had little effect on bone morphology or mechanical integrity. In contrast, significant changes in bone architecture of the mid-strain group (2050 ue) indicated a formation response in both cortical and cancellous regions (Figure 1 and 2). In addition, significantly increased structural and tissue level strength and energy dissipation indicated improved mechanical integrity (figure 3). The highest strain group (2400 ue) also showed an increased formation response, but to the point of woven bone formation in half of the animals. These results indicate that loading to 2050 ue provided the greatest improvement in bone architecture and mechanical function, while not inducing a woven bone response. Future work will use these results to explore mechanical stimulation as a therapeutic means to recover bone functional quality in diseased mouse models.

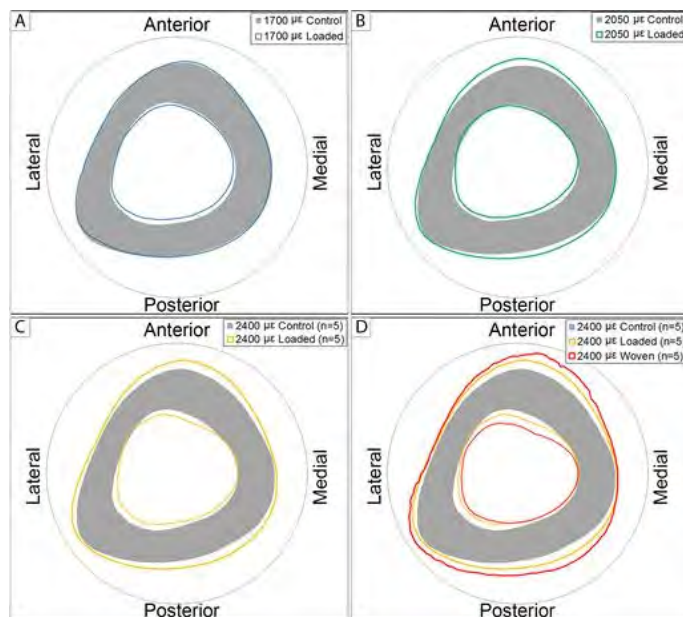


Figure 1: Cortical Geometry

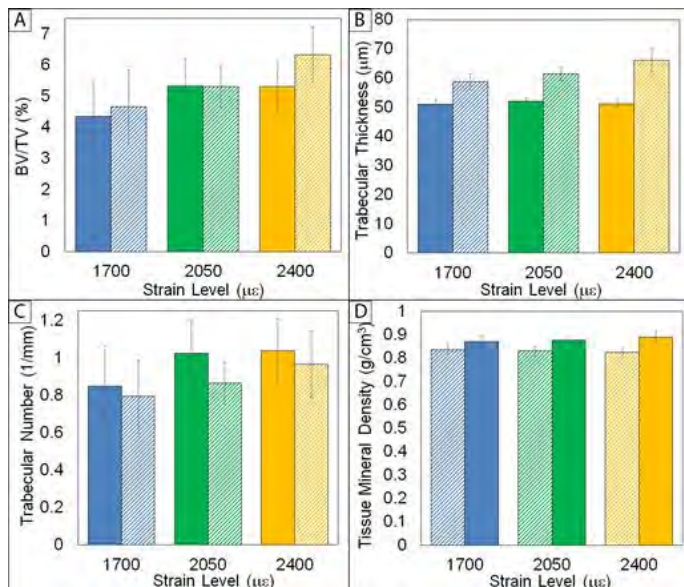


Figure 2: Cancellous morphology

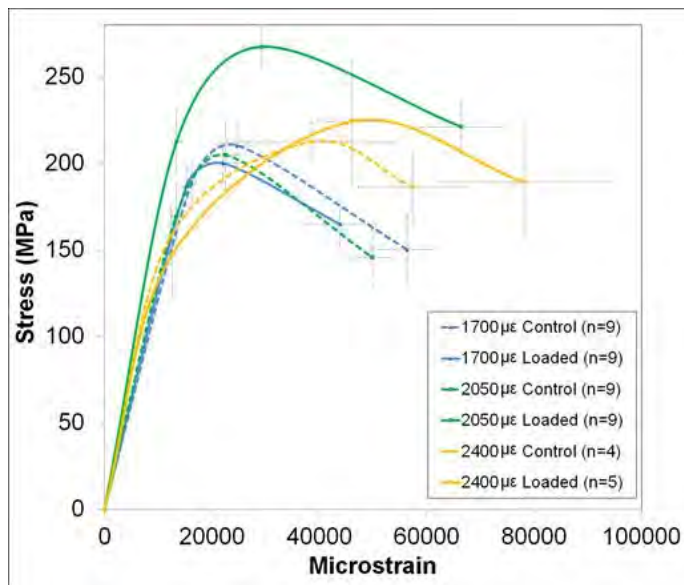


Figure 3: Mechanical Profiles

Disclosures: Alycia Berman, None.

MO0047

A 7-Year School-Based Exercise Intervention Improves Musculoskeletal Traits in Both Genders and Reduces in Girls with Each Year with the Program the Fracture Risk. Jesper Fritz¹, Björn Rosengren², Magnus Dencker², Caroline Karlsson², Magnus Karlsson². ¹Skane University Hospital, Sweden, ²Clinical & Molecular Osteoporosis Research Unit, Departments of Orthopedics & Clinical Sciences, Lund University, Sweden

Purpose: Short-term childhood physical activity programs seem to improve musculoskeletal development but it is unclear if they continue to be beneficial in puberty and more importantly, decrease the fracture risk. **Methods:** In a prospective cluster randomized controlled trial (RCT) we increased school physical education (PE) to 200 minutes per week in one school as intervention and closely monitored 72 girls and 100 boys from mean age 7 to mean age 14 years. 45 girls and 47 boys, in three other schools continued with the Swedish standard of 60 PE minutes per week. They were followed in the same manner and were thus used as controls. Before study start and after 7 years we measured bone mineral content (BMC), bone mineral density (BMD) by DXA and muscle strength by a computerized dynamometer (Biodex[®]). At follow-up we also measured tibia with pQCT. In all 3534 children who in the four schools were included in the program (1339 in the intervention and 2195 in the control group) we registered incident fractures and estimated fracture incidences and risk ratios (RR). Data are presented as mean differences (95% CI). **Results:** Girls in the intervention group gained more total spine BMD [+0.04 g/cm² (+0.01, +0.08)] and

knee flexion strength [+6.2 Nm (+1.6, +10.7)] than control girls. They also had a greater tibial cortical thickness [+0.1 mm (+0.0, +0.3)] at follow-up. Boys in the intervention group gained more knee extension [+7.3 Nm (+0.4, +14.2)] and knee flexion strength [+7.4 Nm (+2.3, +12.4)] than control boys. In girls there was also a statistically significant inverse relationship between years with extra PE and the RR of fracture [$r = -0.86$; 95% CI -0.98 to -0.23] not evident in boys ($r = -0.64$ [95% CI -0.93 to +0.26]). **Conclusion:** A 7-year pediatric school-based moderate exercise intervention program enhances bone mass, muscle strength and reduces the fracture risk in girls and enhances the gain in muscle strength in boys. 74% of the variance in the diminished fracture risk during the study period could in the girls be explained by the intervention.

Disclosures: Jesper Fritz, None.

MO0048

Peri-menarcheal Upper Extremity Bone Loading Index Reflects Post-menarcheal DXA Outcomes. Jodi Dowthwaite^{*1}, Kristen Dunsmore², Paula Rosenbaum³, Carol Sames³, Tamara Scerpella⁴. ¹SUNY Upstate Medical University, Syracuse University, USA, ²SUNY Upstate Medical University, USA, ³SUNY Upstate Medical University, USA, ⁴University of Wisconsin, USA

Purpose: Mechanical loading is believed to provide a potent osteogenic stimulus during growth. However, the extent to which different organized physical activities (sports) promote site-specific osteogenesis has not been determined. The current analysis refined and tested a novel sport-specific bone loading index for the non-dominant upper extremity in 2 samples of post-menarcheal girls with detailed records of sport exposure for 3 years prior to the focal DXA scans.

Methods: Cohort A was recruited between 1998 and 2003 (n=55); Cohort B was recruited between 2008 and 2011 (n=48). For inclusion in analyses, subjects provided whole body and radius DXA scans at 1.0-2.6 years post-menarche, with semi-annual sport records for 36 months prior. DXA outcomes were Area, bone mineral content (BMC) and areal bone mineral density (aBMD) for the non-dominant distal radius (1/3, ultradistal) and Arm regions of interest, as well as Arm non-bone lean mass (nbFFM). The bone loading index is based on sport-specific loading factors as follows: velocity (non-loaded, static load, non/low/high impact), magnitude (load mass), frequency (impulses per session) and non-dominant arm loading (non/low/high). Sport-specific bone loading indices were multiplied by 3-year cumulative exposure hours to yield 3 year total BLI (totBLI). Separate regression analyses were performed for Cohorts A&B, with years post-menarche, height, whole body nbFFM and totBLI as independent variables and bone outcomes as dependent variables. Squared semi-partial correlation coefficients (SSPCCs) were evaluated as metrics of explanatory value.

Results: After accounting for years post-menarche, height and nbFFM, totBLI explained 7%-34% of variance for all outcomes ($p < 0.05$), except Arm Area. In comparison, nbFFM explained 6%-31% of variance for all outcomes ($p < 0.05$), except 1/3 aBMD (Cohorts A&B), UD Area (A). Comparing the 2 Cohorts, totBLI SSPCCs were within 10% of each other for BMC (1/3, UD, arm), arm aBMD and arm nbFFM.

Conclusions: Peri-menarcheal 3-year bone loading index was significantly correlated with post-menarcheal arm lean mass and all bone outcomes except non-dominant arm Area, demonstrating similar explanatory value to that of whole body lean mass. These results support the consistent utility of the BLI algorithm as an index of site- and sport-specific loading for the upper extremity.

Disclosures: Jodi Dowthwaite, None.

MO0049

Restoring Standing Height: Yet Another Benefit of Exercise for Osteoporosis. Belinda Beck^{*}, Benjamin Weeks, Amy Harding, Sean Horan, Steven Watson. Griffith University, Australia

Purpose: The utility of exercise for improving or maintaining bone mass is well-recognized. The ability of exercise to maintain or restore lost stature however has rarely been reported. Such a finding would have considerable clinical significance in light of the known relationships between stature, function and quality of life. We hypothesized a targeted heavy progressive resistance training program would increase back muscle strength and prevent loss of height in postmenopausal women with low bone mass.

Methods: Fifty postmenopausal women (66.3 ± 5.1 y) with low bone mass (FN or LS t-score: ≥ 1) who undertook twice weekly progressive heavy resistance training (EX) or a very low intensity home exercise program (CON) for 8 months were tested for height, LS BMD, WB lean mass (DXA, XR-800, Norland) and back extensor strength (BES) at baseline and follow-up. Between-group difference in change in height over time was examined by repeated measures ANOVA. Multiple regression analysis was used to determine the degree to which baseline values and change in BES, lean mass and LS BMD predicted variance in change in height.

Results: Change in height over the 8 month period differed significantly between groups (CON, -0.41 ± 0.28 vs EX, 0.60 ± 0.27 cm, $P = 0.001$). Change in BES ($R^2 = 0.637$, $P = 0.032$) and change in WB lean mass ($R^2 = 0.310$, $P = 0.039$) together accounted for almost three quarters of the variance in change in height ($R^2 = 0.707$, $P = 0.038$). The correlation of change in LS BMD with change in height approached significance ($r = 0.518$, $P = 0.058$), but did not contribute significantly to the regression model, $P = 0.074$.

Conclusion: Heavy progressive resistance training induced a mean net benefit of 1 cm in stature over the course of an 8 month training program in comparison with very lightly exercising controls. The clear relationship of changes in back extensor strength and lean mass to changes in height suggest heavy resistance training is a powerful therapy for the maintenance or restoration of height in postmenopausal women.

Disclosures: *Belinda Beck, None.*

MO0050

Sclerostin Serum Level Immediate Variation After Physical Activity in Young Females. Marie-Eva Pickering¹, Marie Simon², Karim Chikh³, Marie Christine Carlier³, Cyrille Confavreux^{*4}. ¹Université de Lyon-INSERM UMR1033-Hospices Civils de Lyon, France, ²Hospices Civils de Lyon, France, ³Université de Lyon - Department of Biochemistry, Hospices Civils de Lyon, France, ⁴Université de Lyon-INSERM U1033- Department of Rheumatology Hospices Civils de Lyon, France

Objectives: Osteoporosis is characterized by low bone mass and poor bone quality leading to a reduction in bone strength and an increase risk of fracture. Osteoporosis prevention is of major interest for public health. In addition to vitamin D supplementation, prevention relies on regular loading physical activity such as a 30mn daily walk to favor bone formation. Wnt pathway is the main anabolic pathway in osteoblasts. It is regulated by sclerostin which is secreted by osteocytes, a bone cell harboring mechanoreceptors. Thus we assayed sclerostin serum level variation after physical activity. Patients and methods: After ethical comity approval and sample size calculation, we recruited young healthy female volunteers with a body mass index (BMI) between 18 and 25 kg/m². Participants practicing more than 90 mn physical activity per week or having any cardiac medical history or any chronic diseases were excluded. We submitted participants to a 45mn run on a treadmill. After 5 mn warm-up, participants ran at the established speed of 7.5 km/h. Blood withdrawal was performed before and 5mn after the end of physical activity. Sclerostin was assessed using ELISA kit (Teco médical®). Results: We enrolled 23 young females and all completed the whole protocol. Mean age of participants was 22 ± 1.5 years with a mean BMI of 21.9 ± 2.4 kg/m². Mean strength of participants, assessed by a dynamometer, was 35.2 ± 5.7 kg. Mean vitamin D serum level was 75 ± 18 nmol/L. Sclerostin serum level significantly increased by 44.6 ± 26.4% (mean gain) after physical activity with 290 ± 90 ng/L at rest and 410 ± 130 ng/L after activity (p<0.001). CTX variations were not significant and bone specific alkaline phosphatase variations remained below the CV (8.1%) of the method. Conclusion: We observed a sharp increase of serum sclerostin levels immediately after physical activity in a homogenous group of young healthy females. Our study shows a high reactivity of osteocytes in response to physical activity.

Disclosures: *Cyrille Confavreux, None.*

MO0051

Vitamin C and E supplementation reduces the beneficial skeletal effects of strength training in elderly men. Astrid Kamilla Stunes^{*1}, Unni Syversen², Sveinung Berntsen³, Göran Paulsen⁴, Tonje H. Stea³, Ken J. Hetlelid³, Hilde Lohne-Seiler³, Thomas Bjørnsen³, Glenn Haugeberg⁵. ¹Norwegian University of Science & Technology, Norway, ²Department of Cancer Research & Molecular Medicine, Norwegian University of Science & Technology, (NTNU), Trondheim, Norway & Department of Endocrinology, St Olav's University Hospital, Trondheim, Norway, ³Department of Public Health, Sport & Nutrition, University of Agder, Norway, ⁴Department of Physical Performance, Norwegian School of Sport Sciences, Oslo, Norway & Norwegian Olympic Sport Center, Oslo, Norway, ⁵Department of Rheumatology, Hospital of Southern Norway Trust, Kristiansand, Norway & Department of Neuroscience, Division of Rheumatology, Norwegian University of Science & Technology (NTNU), Trondheim, Norway, Norway

Resistance training and impact-loading activities are considered beneficial for maintaining bone mass and preventing osteoporosis in elderly men. The musculoskeletal effects of dietary intake of high doses of antioxidants, such as vitamin C and E, have been disputed. We wanted to study possible additive effects of strength training and supplements with antioxidants on bone health.

The skeletal effects of vitamin C and E were examined in a double-blinded randomized placebo-controlled study during a 12 weeks supervised strength training program in healthy, elderly men. All participants followed an undulating training program: 2/wk 8-10RM (1 min inter-set rest periods), 1/wk between 3-5RM (2 min rest) and 13-15RM (45 sec rest). The load was weekly adjusted, and the volume increased progressively. The control group (CTR), (N=17, 67 ± 5 years old) received daily placebo pills, and the antioxidant group (AO), (N=16, 70 ± 7 years old) received 1000 mg vitamin C and 235 mg vitamin E daily. Fasting blood samples were drawn for analyses of bone turnover and sclerostin. BMD and lean mass at whole body and BMD at hip and lumbar spine (L1-L4) were measured by DXA, and muscle strength was assessed by one repetition maximum (1RM), at baseline and post-intervention.

After the intervention significant increases were observed in total lean mass and muscle strength in both the CTR and AO groups. Both groups displayed significantly increased total hip BMD, while whole body and femoral neck BMD remained unchanged. The CTR group had a significant increase in L1-L4 BMD when compared to the AO group. A significant decrease in serum sclerostin levels in the CTR group compared to the AO group was also observed. The serum levels of the bone formation markers PINP and osteocalcin were significantly increased in both groups, while the bone resorption marker CTX remained unchanged. Data (mean±SD) are presented in the table below.

In conclusion, 12 weeks of supervised strength training increased total hip BMD and serum bone formation markers in elderly men. The CTR group also displayed an increased BMD at the lumbar spine and a decrease in serum sclerostin, indicating a favoring of bone formation. This was not observed in the AO group, indicating a blunting of some of the positive effects of strength training. High doses of vitamin C and E during strength training have no beneficial or probably negative skeletal effects in healthy, elderly men.

| | Control group (placebo, N=17) | | Antioxidant group (vitamin C and E, N=16) | | |
|--------------------------|-------------------------------|----------------|---|---------------|--------------|
| | pretest | Posttest | pretest | posttest | |
| Age (years) | 66.89±5.00 | 67.18±5.00 | 69.65±6.77 | 69.94±6.76 | |
| Body weight (kg) | 84.1±14.9 | 84.7±15.2 | 80.3±11.2 | 80.5±11.5 | |
| Whole body | BMD (g/cm ²) | 1.267±0.082 | 1.261±0.076 | 1.251±0.084 | 1.239±0.084 |
| | T-score | 0.588±1.025 | 0.500±0.961 | 0.400±1.049 | 0.238±1.054 |
| Total hip | BMD (g/cm ²) | 0.995±0.108 | 1.004±0.106** | 1.051±0.104 | 1.055±0.102* |
| | T-score | -0.724±0.748 | -0.671±0.735* | -0.344±0.726 | -0.269±0.689 |
| Femoral neck | BMD (g/cm ²) | 0.929±0.110 | 0.934±0.107 | 0.967±0.118 | 0.963±0.122 |
| | T-score | -1.076±0.849 | -1.047±0.819 | -0.794±0.912 | -0.837±0.934 |
| Spine L1-L4 | BMD (g/cm ²) | 1.285±0.170 | 1.295±0.164# | 1.260±0.202 | 1.247±0.197 |
| | T-score | 0.547±1.404 | 0.629±1.363# | 0.344±1.679 | 0.225±1.627 |
| Serum P1NP (µg/L) | 43.96±14.14 | 51.54±20.40** | 41.47±12.48 | 46.02±12.04* | |
| Serum osteocalcin (µg/L) | 5.723±2.552 | 9.883±11.58* | 5.673±2.341 | 8.362±4.503** | |
| Serum CTX (µg/L) | 0.389±0.129 | 0.379±0.122 | 0.374±0.133 | 0.379±0.167 | |
| Serum sclerostin (µg/L) | 4.962±1.393 | 4.429±0.871*** | 4.985±0.871 | 4.873±1.032 | |

Data are presented as mean±SD

**p<0.05, p<0.01 significantly different versus pretests within same group (Wilcoxon Signed Rank Test)

#p<0.05 significantly different changes in pre-post values between groups (ANCOVA)

Table

Disclosures: *Astrid Kamilla Stunes, None.*

MO0052

Adenine based mouse model of juvenile chronic kidney disease: preliminary bone and mineral findings. Oleh Akchuric^{*1}, Sara Gardenghi², Paraskevi Rea Oikonomidou², Adele Boskey³, Stefano Rivella². ¹Cornell University, USA, ²Weill Cornell Medical College, USA, ³Hospital for Special Surgery, USA

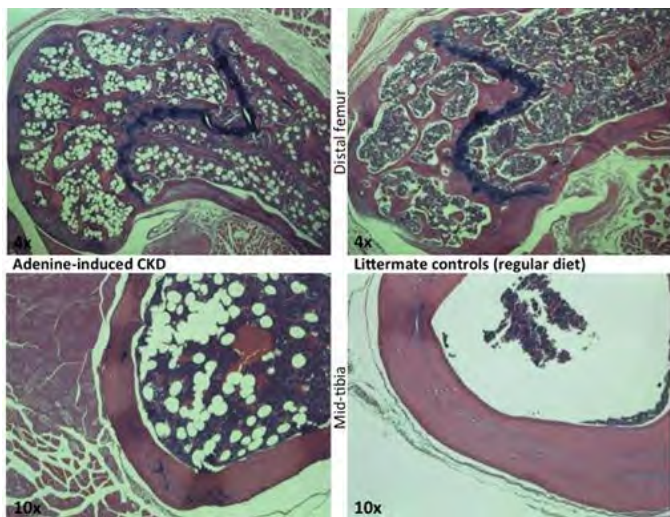
Chronic kidney disease (CKD) in children has a number of differences from CKD in adults, such as development of growth failure. However, no convenient mouse model is available to address numerous knowledge gaps related to pediatric CKD, such as, for example, the role of CKD mineral and bone disease in growth retardation.

High adenine diet has been shown to induce CKD in adult mice. The purpose of this study was to test whether 0.2% adenine diet would also induce CKD in growing mice resembling CKD in children, including CKD - mineral and bone disease and growth delay.

C57Bl6 mice were started on 0.2% adenine diet (Harlan) at weaning (3 weeks) and sacrificed in 8 weeks. Littermate controls were fed a regular diet. Weekly measurements of nose-to-tip-of-tail length were used for tracking linear growth.

Adenine fed juvenile mice had statistically significant elevation of BUN (87.0 vs. 29.5 mg/dL in controls), creatinine (0.57 vs. 0.19 mg/dL) and phosphorus (14.6 mg/dL vs. 5.3 mg/dL) at sacrifice. Adenine fed mice had slower rate of weight gain compared with controls and by 3 weeks they stopped gaining and / or started to loose weight. Linear growth was also significantly slower in adenine fed mice. At sacrifice, adenine fed mice had about 40% deficit in body weight and 10-15% deficit in body length, as compared with controls (both differences are statistically significant). In addition, adenine fed mice developed anemia, increased neutrophil count and relative lymphopenia. Bone histology revealed extensive marrow adiposity and cortical thinning in adenine fed mice (figure).

In conclusion, this study demonstrated for the first time that 0.2% adenine diet reliably induces CKD-related growth failure and cachexia in juvenile mice, resembling those seen in children with CKD. Adenine induced CKD in juvenile mice is also characterized by distinct changes of bone histology. Our ongoing experiments are directed towards further characterization of the bone and mineral phenotype and eliciting the mechanisms of the described findings, as well as utilizing this model to characterize the contribution of disordered phosphorus homeostasis to growth delay in pediatric CKD.



Disclosures: Oleh Akchurin, None.

MO0053

Low Bone Mineral Density and Fractures are Prevalent in Children with Spinal Muscular Atrophy. Halley Wasserman*, Lindsey Hornung, Peggy Stenger, Meilan Rutter, Brenda Wong, Irina Rybalsky, Jane Khoury, Heidi Kalkwarf. Cincinnati Children's Hospital Medical Center, USA

Background: Spinal Muscular Atrophy (SMA), an autosomal recessive disease of the spinal motor neurons, results in varying degrees of hypotonic immobility. Lack of weight-bearing activity and low muscle mass lead to poor bone accrual. Prior reports demonstrate an increased risk of fracture and a trend toward low bone mineral density (BMD). However, no studies report the prevalence of fractures or low BMD (Z-score ≤ -2.0) by SMA subtype, low BMD of the lateral distal femur (an important fracture location in non-ambulatory children), nor the prevalence of osteoporosis according to 2013 ISCD criteria, in this population. **Methods:** A retrospective chart review was conducted of 86 patients, ages 12 months to 25 years, with confirmed diagnosis of SMA, seen at our institution between January 2005 and January 2015 (Table 1). Lumbar spine (LS), total body (TB), and lateral distal femur (LDF) DXA scans (Hologic 4500) were obtained as part of routine clinical care, and patients' initial DXA scans results were reported for this study. All DXA scans were reviewed for image quality. Fracture history was reported at annual clinic visits and confirmed when possible by review of radiographs. Cumulative fracture frequencies from patients' last encounters were reported for this study. Kruskal Wallis, Chi-square and Fisher's exact tests were utilized to compare groups.

Results: Median age at initial SMA visit was 1.8 years, but differed by SMA subtype. DXA data were available on 69% of the sample: of these, 90% had a BMD Z-score ≤ -2.0 SD at time of first DXA. In those with missing DXA data, 63% of patients were <3 years of age at time of last encounter. BMD of all sites was lower with worsening SMA severity. Fractures occurred in 36% of patients with the femur being the most common location (25 of 53 total fractures). Median age at first fracture was significantly younger with worsening SMA severity. 13% of patients had multiple fractures.

Conclusion: Low BMD is highly prevalent in SMA patients at the time of first DXA. Fracture frequency is also high with a predominance of femur fractures in all subtypes. However, few patients met ISCD diagnostic criteria for osteoporosis. Our data suggests poor bone health is a significant concern for SMA patients, but may be underestimated using the 2013 ISCD criteria for diagnosis of osteoporosis in children.

| | SMA 1 (most severe) | SMA 2 (moderate) | SMA 3 (mild) | p-value |
|--|-----------------------------|-----------------------------|-----------------------------|-----------|
| Number (n) | 24 | 44 | 18 | |
| Female (%) | 15 (63%) | 23 (52%) | 8 (44%) | 0.50 |
| Age (y) at initial neuromuscular visit | 0.6 (0.3, 1.1) [n=24] | 2.0 (0.9, 4.4) [n=44] | 3.9 (2.1, 8.7) [n=18] | 0.0003 |
| Age (y) at last encounter | 7.6 (2.2, 12.4) [n=24] | 6.2 (3.5, 12.2) [n=44] | 12.9 (7.7, 17.9) [n=18] | 0.01 |
| Age (y) at 1 st reported fracture | 3.0 (1.9, 6.0) [n=11] | 6.6 (3.3, 11.1) [n=12] | 10.4 (9.2, 11.5) [n=8] | 0.004 |
| Patients ≥ 1 fracture | 11 (46%) | 12 (27%) | 8 (44%) | 0.22 |
| Fractures at femur | 13/22 (59%) | 7/19 (37%) | 5/12 (42%) | 0.33 |
| Age (y) at 1 st DXA | 3.9 (2.8, 4.8) [n=14] | 5.4 (4.1, 6.6) [n=28] | 8.1 (5.1, 11.3) [n=17] | 0.007 |
| LS BMD Z-score | -4.7 (-5.7, -3.6) [n=14] | -2.5 (-3.3, -0.7) [n=22] | -0.2 (-1.8, 0.2) [n=13] | <0.0001 |
| TB BMD Z-score | -2.8 (-2.9, -2.2) [n=7] | -1.8 (-2.7, -0.5) [n=16] | -1.9 (-2.8, -1.6) [n=10] | 0.25 |
| LDF BMD Z-scores | [n=6] | [n=22] | [n=13] | |
| Region 1 | -4.5 (-5.1, -3.6) | -3.5 (-4.3, -2.9) | -2.7 (-3.7, -1.1) | 0.01 |
| Region 2 | -4.6 (-5.8, -3.6) | -3.8 (-4.2, -3.1) | -2.3 (-4.1, -1.4) | 0.02 |
| Region 3 | -3.9 (-5.1, -3.1) | -2.9 (-3.5, -2.1) | -1.6 (-3.5, -1.3) | 0.06 |
| Prevalence of BMD ≤ -2.0 SD at 1 st DXA (any site) | 14/14 (100%) | 25/28 (89%) | 14/17 (82%) | 0.34 |
| Osteoporosis by ISCD criteria at last encounter | 2/14 (14%) | 1/28 (4%) | 2/17 (12%) | 0.07 |

Data expressed as n (%) and median (25th, 75th percentile).

Table 1: Demographics and Bone Health Indices in Pediatric Spinal Muscular Atrophy Patients

Disclosures: Halley Wasserman, None.

MO0054

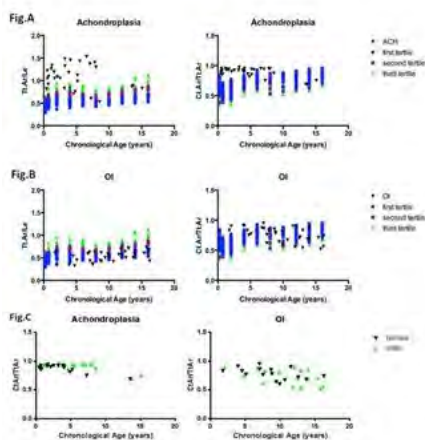
Bone Robusticity in Two Distinct Skeletal Dysplasias: an Evaluation of the Second Metacarpal, a Surrogate for Bone Strength. Josephine Marino¹, Karl Jepsen², Erin Carter³, Cathleen Raggio^{*4}. ¹Hospital for Special Surgery, USA, ²Department of Orthopaedic Surgery, University of Michigan, USA, ³Kathryn O. & Alan C. Greenberg Center for Skeletal Dysplasias, Hospital for Special Surgery, USA, ⁴Pediatric Orthopaedics, Hospital for Special Surgery, USA

Radiographs of the second metacarpal are used to assess bone strength development in pediatric populations. Children with achondroplasia and osteogenesis imperfecta (OI) have known differences in bone strength. Details of how bone strength develops and compares within these populations to unaffected children are lacking. A data set for patients with achondroplasia and OI was established.

A retrospective IRB-approved review of bone-age films (n=67; 1-11 films/patient) from patients (5mos to 16yrs+3mos old) with achondroplasia (6 males; 10 females) or OI (9 males; 11 females) was conducted. A sample of modern controls (diagnosis: leg-length discrepancy) matched historical measurements from Bolton-Brush collection (6mos-16yrs). Metacarpal length (Le) was measured from the proximal end to the most distal ossified end along the midshaft axis. Outer and inner diameters were measured at 50% and 60% of the length, averaged, and used to calculate total cross-sectional area (Tt.Ar) and cortical area (Ct.Ar) using a circular approximation. To adjust for differences in body size, we compared robustness (Tt.Ar/Le) and relative cortical area (RCA=Ct.Ar/Tt.Ar) among groups.

Achondroplasia patients tend to have both robusticity and RCA values above the most robust Bolton-Brush tertile (Fig. A). This robust phenotype was consistent with the reduced longitudinal growth seen in achondroplasia patients. Increased RCA values were unexpected and may indicate deregulated mass-accumulation. In contrast, OI patients followed the Bolton-Brush pattern of decreased robusticity and increased RCA, but not the distribution. OI patients all fell in the most slender tertile (Fig. B). No sexual dimorphism was noted in this study (Fig. C).

The lack of sexual dimorphism in the dysplasia populations is in contrast to that reported in the unaffected population. We suggest that the underlying dysplasia overrides the sex-specific effects on bone strength development. The contribution of the specific mutation is unknown and needs to be further studied.



Composite Figure

Disclosures: Cathleen Raggio, None.

MO0055

Decreased Vertebral Dimensions and Increased Spine Flexibility in Girls And Patients With Adolescent Idiopathic Scoliosis. Tishya Wren¹, Skorn Ponrartana², Carissa Fisher¹, Patricia Aggabao¹, Vicente Gilsanz¹. ¹Children's Hospital Los Angeles, USA, ²Children's Hospital Los Angeles, USA

Adolescent idiopathic scoliosis (AIS) affects girls more than boys and has an unknown etiology. We hypothesized that AIS is promoted by decreased vertebral size and increased spine flexibility, which would accentuate differential loading of the vertebrae during bending. MRI and CT were used to measure vertebral height, anterior-posterior and lateral width, and cross-sectional area of the L1, L2, and L3 vertebrae and height of the inferior intervertebral discs (IVD) in 80 adolescents (61 girls, 19 boys) with AIS and 229 adolescents (122 girls, 107 boys) without spinal deformity ages 10-15 years. Maximum rotation of each vertebral body was estimated from the ratio of IVD height to vertebral width using a simple biomechanical model. Two-way ANOVA was used to examine the effects of sex and scoliosis on outcome measures. Boys had greater height, weight, and BMI than girls (all $p \leq 0.03$), but scoliosis did not affect these measures (all $p > 0.2$ for scoliosis, $p > 0.1$ for interaction). All vertebral cross-sectional dimensions were significantly smaller for females compared with males (all $p < 0.0001$) and for adolescents with AIS compared with controls (all $p < 0.0001$) at all vertebral levels examined. In many cases, there was also a significant interaction between sex and scoliosis reflecting a larger difference between AIS and controls in boys than in girls. Vertebral height was larger in controls (all $p \leq 0.003$), but IVD height was larger in AIS (all $p < 0.0001$) with no significant differences due to sex (all $p > 0.06$). Consequently, predicted spine motion was significantly greater for females and adolescents with AIS (all $p < 0.0001$). The increased spine flexibility would increase asymmetric loading on the vertebrae during anterior and lateral bending, promoting differential longitudinal growth. Growth would be accelerated on the convex side of the curve by increased tensile stresses and inhibited on the concave side by increased compressive stresses, leading to vertebral wedging. Decreased vertebral size and increased flexibility may therefore help to explain the greater prevalence of AIS in females. If these relationships can be confirmed in future prospective longitudinal studies, multi-planar imaging of vertebral morphology may contribute to improved prognosis for adolescents with early AIS and development of treatments to prevent AIS progression.

Disclosures: Tishya Wren, None.

MO0056

Side-to-side Differences in Bone Strength and Microstructure in Children and Adolescents with a Distal Radius Fracture. Mikko Maatta¹, Heather Macdonald², Douglas Race², Lindsay Nettlefold², Kishore Mulpuri³, Heather McKay². ¹University of British Columbia, Canada, ²Centre for Hip Health & Mobility, Canada, ³British Columbia Children's Hospital, Canada

We recently reported⁽¹⁾ associations between impaired bone strength, microstructure and forearm fractures (Fx) in children and adolescents. Here we aimed to determine if similar bone strength deficits were apparent on the contralateral non-fractured (NF) limb.

Participants were 173 youth with a recent distal radius Fx [61 girls, 112 boys (12.1 ± 1.8y)]. We assessed bone strength and microstructure of the distal radius (7%

site) on both the Fx and NF arm using high-resolution pQCT (Scanco Medical). The average time between injury and the HR-pQCT scan was 2.6 ± 0.9 mo. We excluded 40 participants due to motion during scan acquisition, previous distal radius Fx, Fx due to high energy trauma or missing trauma degree. We also excluded 63 participants for whom a Fx line was visible throughout the region of interest (ROI), which resulted in a final sample of 70 [26 girls, 44 boys (11.8 ± 1.8y)]. In cases where the Fx was visible in part of the ROI (n=46), we excluded slices (48 ± 17) with a visible Fx line. We assessed total area (Tt.Ar) and bone mineral density (Tt.BMD), trabecular bone volume ratio (BV/TV), trabecular thickness (Tb.Th) and number (Tb.N), cortical area (Ct.Ar), BMD (Ct.BMD), thickness (Ct.Th) and porosity (Ct.Po), and used finite element analysis to estimate bone strength (failure load and ultimate stress). We calculated the mean difference (95% confidence intervals) in bone outcomes between the Fx and NF arms, adjusting for hand dominance and used paired samples *t*-tests to estimate statistical significance.

40% of fractures occurred on dominant arm. We found higher Tt.Ar on the Fx radius compared with the NF radius (250.8 vs. 236.3 mm²; mean difference 14.5 (95% CI 8.5-20.5) mm²). Compared with the NF radius, Fx radii also showed higher Ct.Po (4.8 vs. 4.0%; 0.8 (0.5-1.1)%), smaller Ct.Th (0.47 vs. 0.49 mm; 0.03 (0.01-0.04) mm) and Ct.Ar (25.7 vs. 27.4 mm², 1.7 (0.8-2.6) mm²) and lower Ct.BMD (504.4 vs. 539.9 mgHA/cm³; 35.4 (24.9-46.0) mg HA/cm³, $p < 0.01$ for all). Fx radii had higher BV/TV (0.155 vs. 0.145; 0.010 (0.002-0.017)) and higher Tb.Th (0.070 vs. 0.067 mm; 0.003 (0.001-0.006) mm) than NF radii ($p < 0.02$). Bone strength did not differ between sides.

Deficits in cortical bone structure and BMD were only apparent on the Fx limb and thus may predispose growing bone to Fx. Greater bone volume and thicker trabeculae in the trabecular compartment may compensate for these cortical bone deficits.

References

1. Määttä et al. Osteoporos Int 26:1163-1174

Disclosures: Mikko Maatta, None.

MO0057

Underdevelopment in trabecular bone microarchitecture is dictated by level of motor function in children with cerebral palsy. Christopher Modlesky¹, Harshvardhan Singh¹, Daniel Whitney¹, Freeman Miller². ¹University of Delaware, USA, ²Nemours AI duPont Hospital for Children, USA

Nonambulatory children with cerebral palsy (CP) have a severely underdeveloped trabecular bone microarchitecture; however, whether children with milder forms of the disorder have a similar profile or whether the degree of underdevelopment is related to the degree of motor function has not been determined. Nonambulatory children (n = 13) and ambulatory children (n = 13) with spastic CP and typically developing children (n = 50) between 5 and 13 years of age participated in the study. Twenty six axial magnetic resonance images (175 x 175 x 700 μm³) of the distal femur were collected from the more affected limb in children with CP and the nondominant limb in controls. Measures of trabecular bone microarchitecture [apparent trabecular bone volume to total volume (appBV/TV), trabecular number (appTb.N), trabecular thickness (appTb.Th) and trabecular separation (appTb.Sp)] were estimated using the 20 most central images and custom software (Interactive Data Language, Boulder, CO). Level of gross motor function was assessed using the gross motor function classification system (GMFCS) with levels I and II representing children able to ambulate independently, and levels III to V representing children unable to ambulate independently. Compared to controls, nonambulatory and ambulatory children with CP had lower appBV/TV by 28% (Cohen's d (d) = 2.4, $p < 0.001$) and 11% (d = 1.0, $p = 0.007$), lower appTb.N by 18% (d = 2.5, $p < 0.001$) and 9% (d = 1.3, $p = 0.001$), and higher appTb.Sp by 31% (d = 2.6, $p < 0.001$) and 15% (d = 1.2, $p = 0.004$), respectively. Additionally, compared to controls, nonambulatory children with CP had lower appTb.Th by 11% (d = 1.6, $p < 0.001$). GMFCS was negatively correlated with appBV/TV, appTb.N, and appTb.Th ($r = -0.45$ to -0.56 , $p < 0.05$) in children with CP; on the other hand, GMFCS was positively related to appTb.Sp ($r = 0.48$, $p = 0.014$). The findings suggest that the degree of underdevelopment in trabecular bone microarchitecture in children CP is dictated by the level of compromise in motor function. Although the degree of underdevelopment in ambulatory children with milder forms of CP is not as large as that observed in nonambulatory children with more severe forms of CP, it is substantial with measures of trabecular bone microarchitecture deviating from control values by ≥ 1 SD. Treatments that enhance the development of trabecular bone microarchitecture in children with CP, irrespective of motor function, are needed.

Disclosures: Christopher Modlesky, None.

MO0058

Denosumab treatment of severe disuse osteoporosis in a boy with Werdnig-Hoffmann disease. Stepan Kutilek^{*}. Klatovy Hospital, Czech republic

Denosumab is a fully human recombinant monoclonal antibody to the receptor activator of nuclear factor-κB ligand (RANKL). In postmenopausal osteoporotic women subcutaneous denosumab administration every 6 months increases bone mineral density (BMD) at the lumbar spine, total hip, and/or femoral neck, and significantly reduces markers of bone turnover, thus reducing the risk of vertebral, nonvertebral, and hip fractures. There are only scarce data about denosumab treatment in children and adolescents.

Case report: 14-year old boy presented with severe disuse osteoporosis due to muscular atrophy in Werdnig-Hoffmann disease.(SMA type 2). The boy was wheelchair-bound with muscle weakness, severe joint contractures, quadraparesis, kyphoskoliosis, difficult swallowing and had recurrent respiratory infections. In the past 6 months he experienced 2 low-energy trauma fractures of the right femur and left tibia. L1-L4 BMD was low: 0.406 g/cm²(-6.2 SD Z-score;DXA Lunar). Serum levels of Ca, P, ALP and PTH were normal. Osteoporosis treatment was clearly indicated, however intravenous bisphosphonates were out of question due to history of convulsions triggered by fever including low-grade fever. Neither oral bisphosphonates could be used due to difficult swallowing and risk of consequent oesophageal ulceration. Therefore, denosumab treatment (60 mg s.c.) was started with the patients and parents consent. He also received 1000 mg calcium/day and 1000 IU cholecalciferol/day p.o. The denosumab injection was well tolerated and there were no adverse reactions. Six months later upon check-up his L1-L4 BMD increased by 19% to 0.485 g/cm² (Z-score -5.8 SD). S-Ca, P, ALP and PTH were normal. Unfortunately the same day he fell from the wheelchair and broke his right femur. This fracture could be attributed to the high-energy trauma mechanism and still very low BMD. He received his second denosumab injection one month later (i.e on month 7), without any complications. Third denosumab injection was scheduled 6 months later. Prior to the planned visit and third injection, the boy died from respiratory failure due to pneumonia. This should be considered as not related to the denosumab treatment, as respiratory failure is a frequent cause of death in patients with WHD. Conclusion: One dose of s.c. denosumab significantly increased BMD in a child with severe disuse osteoporosis. Denosumab might present a suitable treatment option in children with bone fragility.

Disclosures: Stepan Kutilek, None.

MO0059

Improved Functional Mobility with Asfotase alfa Treatment in Childhood Hypophosphatasia. Katherine L Madson¹, Dawn Phillips², Cheryl Rockman-Greenberg³, Amy Reeves¹, Kenji P Fujita⁴, Scott Moseley⁴, David Thompson⁴, Michael P Whyte¹. ¹Shriners Hospital for Children, USA, ²University of North Carolina Division of Physical Therapy, USA, ³University of Manitoba, Canada, ⁴Alexion Pharmaceuticals, USA

Purpose. Hypophosphatasia (HPP) is the rare inborn-error-of-metabolism caused by loss-of-function mutation(s) within the gene that encodes the tissue nonspecific isoenzyme of alkaline phosphatase (TNSALP) gene. The biochemical hallmark is hypophosphatasemia (low serum alkaline phosphatase activity). Children with HPP may experience compromised physical function, including gait impairments, secondary to skeletal deformities and muscle weakness. We report significant gait improvements in children with HPP treated with asfotase alfa, an investigational, bone-targeted human TNSALP replacement, compared with untreated historical control (HC) patients (pts).

Methods. Videos of basic mobility of treated and HC pts ages 5–15 years were assessed using the 12-point Modified Performance-Oriented Mobility Assessment – Gait subscale (MPOMA-G; 12=no impairment.) The MPOMA-G, an adaptation of the POMA-G, provides improved sensitivity for HPP-related impairments. Results were compared between pts participating in a Phase II, open-label, ongoing study of asfotase alfa¹ (n=8) and those in a HC gait substudy² (n=6) from a retrospective natural history study of pts matched for age and HPP severity. Enrollment criteria for these analyses included: onset of HPP symptoms from age ≥6 months, HPP-related skeletal abnormalities, and ≥2 gait assessments between 5 and 15 years of age. Rate of change per year was calculated as MPOMA-G change from Baseline (BL) to Last Assessment (LA) divided by intervening time. For treated pts with a pre-treatment video (n=5), rates of change (Pre-treatment to BL assessment) were compared with untreated rates.

Results. Group ages were not significantly different at BL or LA (Table 1). BL characteristics were also generally similar. All pts showed deficits in gait as assessed by MPOMA-G at BL (Table 1). Treated pts had a significantly greater rate of improvement in MPOMA-G scores compared to HC (p=0.03), and a greater absolute increase in MPOMA-G score from BL. Of note, gait had deteriorated prior to BL in pts who later received asfotase alfa (Table 1). Significance was retained in sensitivity analyses controlling for assessment interval and BL gait score.

Conclusion. Children with impaired gait due to HPP demonstrated clinically significant improvement in functional mobility when treated with asfotase alfa compared to both pretreatment history and historical controls.

Table 1

| | Untreated historical controls (n=6) | Treated patients | |
|--|-------------------------------------|------------------|---|
| | | Overall (n=8) | With available pre-treatment videos (n=5) |
| Male, % | 100% | 75% | 80% |
| Ethnicity, % | | | |
| Hispanic/Latino | 33% | 13% | 0% |
| Not Hispanic/Latino | 67% | 88% | 100% |
| Age, years | Median (min, max) | | |
| Pre-treatment Assessment | — | — | 6 (4, 9) |
| Baseline | 6 (5, 11) | 8 (6, 12) | 9 (6, 12) |
| Last Assessment | 11 (8, 15) | 10 (8, 14) | 10 (8, 14) |
| Pre-treatment MPOMA-G ¹ | Median (min, max) | | |
| Pre-treatment Assessment | — | — | 5 (4, 11) |
| Change from Pre-treatment Assessment to Baseline | — | — | -2 (-2, 0) |
| Rate of change per year | — | — | -0.7 (-1, 0) |
| Historical Control and On-treatment MPOMA-G ¹ | Median (min, max) | | |
| Baseline | 6 (3, 11) | 4 (2, 9) | 4 (2, 9) |
| Change from Baseline to Last Assessment | 1.5 (0, 2) | 3 (0, 7) | 5 (0, 7) |
| Rate of change per year | 0.3 (0, 0.9) | 2.5 (0, 4.6) | 3 (0, 3.6) |

—, not applicable. MPOMA-G, Modified Performance Oriented Mobility Assessment – Gait.
¹MPOMA-G: 12=no impairment.

Table 1

Disclosures: Katherine L Madson, Honoraria from Alexion Pharmaceuticals
 This study received funding from: Alexion Pharmaceuticals

MO0060

Treating Low Bone Mass with Calcium and Vitamin D Supplementation in Girls with Adolescent Idiopathic Scoliosis (AIS) – A Randomized Double-blinded Placebo-controlled Trial. Tsz Ping Lam¹, Benjamin Hon Kei Yip¹, Echo Ka Ling Tsang¹, Fiona Wai Ping Yu¹, Kenneth Kin Wah To², Yuk Wai Lee¹, Kwong Man Lee³, Bobby Kin Wah Ng¹, Jack Chun Yiu Cheng¹. ¹Department of Orthopaedics & Traumatology, The Chinese University of Hong Kong, Hong kong, ²School of Pharmacy, The Chinese University of Hong Kong, Hong kong, ³Lee Hysan Clinical Research Laboratories, The Chinese University of Hong Kong, Hong kong

Purposes AIS is a prevalent three-dimensional spinal deformity associated with low bone mass which has been reported to be a significant prognostic factor for curve progression in AIS. If left untreated, low bone mass in AIS could persist into adulthood thus leading to subsequent health problems. This study aimed at evaluating the therapeutic effect of oral calcium plus Vit-D supplementation for low bone mass in skeletally immature AIS girls. **Methods** This was a randomized double-blinded placebo-controlled trial recruiting AIS girls (11-14 years old, Tanner < IV) with BMD Z-scores <0 and Cobb angle >15°. 330 subjects were randomly allocated to Group1 (placebo), Group2 (600mg Calcium + 400 IU Vit-D3/day) and Group3 (600mg Calcium + 800 IU Vit-D3/day). The study period was two years. At baseline (T0) and 24-month (T1) time-point, aBMD and BMC at bilateral femoral necks were measured with Dual-Energy X-ray Absorptiometry (DXA); and serum 25(OH)Vit-D level was measured with liquid chromatography tandem mass spectrometry. Intention-to-Treat principle was followed. ANOVA and Generalized Estimating Equations were used for analyses. Results The baseline data at T0 are shown in Table 1. The corresponding mean % increases at T1 are shown in Table 2. The gain in right and left aBMD and BMC were significantly greater in the treatment group than the placebo group (Table 2) **Conclusions** The results provided strong evidences that treatment with 600mg calcium + 400/800 IU Vit-D3 was effective for treating low bone mass in AIS subjects having Z-score <0. Given the suboptimal 25(OH)Vit-D levels detected in this study and the association between AIS and low bone mass, Vit-D status and bone mineral density should be assessed and be followed as indicated by calcium+Vit-D supplementation for all AIS subjects.

Table 1 Baseline data on Age, 25(OH)VitD and DXA parameters

| | mean \pm SD at T0 | | | P* |
|------------|---------------------|-------------------|-------------------|-------|
| | Gp 1 N=110 | Gp 2 N=110 | Gp 3 N=110 | |
| Age | 13.0 \pm 0.86 | 12.9 \pm 0.91 | 12.7 \pm 0.88 | 0.142 |
| 25(OH)VitD | 41.4 \pm 13.3 | 42.3 \pm 14.3 | 39.4 \pm 15.4 | 0.306 |
| Left BMD | 0.683 \pm 0.059 | 0.677 \pm 0.071 | 0.673 \pm 0.066 | 0.500 |
| Right BMD | 0.694 \pm 0.064 | 0.681 \pm 0.068 | 0.677 \pm 0.065 | 0.126 |
| Left BMC | 1.917 \pm 0.221 | 1.924 \pm 0.237 | 1.904 \pm 0.232 | 0.810 |
| Right BMC | 1.960 \pm 0.254 | 1.940 \pm 0.244 | 1.928 \pm 0.217 | 0.601 |

*P-value from one-way ANOVA

primarily due to the compromised BM shown here and interventions to alleviate and recover BM are critical to preserving bone health.

Disclosures: Divya Krishnamoorthy, None.

MO0062

EPO Attenuation of Bone Formation Is Mediated by the Plexin B1-Sema4D Pathway. Sahar Hiram-Bab¹, Tamar Liron¹, Namit Deshet-Unger¹, Moshe Mittelman¹, Max Gassmann², Martina Rauner³, Ben Wielockx⁴, Drorit Neumann¹, Yankel Gabet¹. ¹Tel Aviv University, Israel, ²Institute of Veterinary Physiology, Vetsuisse Faculty, & Zurich Center for Integrative Human Physiology (ZIHP), University of Zurich, Switzerland, ³Department of Medicine III, Dresden University Medical Center, Germany, ⁴Institute of Clinical Chemistry and Laboratory Medicine, Department of Clinical Pathobiochemistry, University of Technology, Dresden, Germany

In addition to the pivotal erythropoietic role of erythropoietin (EPO), recent publications underline EPO's non-erythropoietic functions, occurring *via* non-erythroid cells. We recently reported on the dramatic effect of EPO on bone metabolism. High EPO levels were associated with reduced bone formation (number and activity of osteoblasts) and increased bone resorption. While EPO's catabolic effect is attributable - at least in part - to EPO receptor (EPO-R) signaling in preosteoclasts, the effect on bone formation remains elusive. Here we tested whether EPO-R signaling acts directly on osteoblasts and/or indirectly via non-osteoblastic cells to suppress bone formation. Previous studies, including our own, showed that EPO administration at high doses on isolated osteoblasts resulted in no response (1 to 10 U/ml) or in enhanced osteogenesis (>50 U/ml). We therefore tested lower doses of EPO *in vitro*. Doses between 1 and 10 mU/ml EPO inhibited mineralization of primary osteoblasts, in line with the *in vivo* observation, thus demonstrating a direct effect of EPO-R signaling in these cells. We then tested whether EPO-R signaling renders the osteoblasts more sensitive to inhibitory signals from other cells. The Plexin B1-Sema4D axis is one of the few identified osteoblasts' inhibiting pathways involving osteoclast-to-osteoblast communication. Expression levels of Plexin B1, the osteoblastic receptor of Sema4D, were increased in total bone marrow (BM) RNA from EPO-injected mice as well as in EPO-treated (1 to 10 mU/ml, versus vehicle) isolated primary osteoblasts. To test indirect mechanisms, we also examined BM total mRNA expression of Sema4D. In EPO-treated mice as well as in constitutively EPO-overexpressing Tg6 animals, high levels of EPO were associated with a ~2-fold increase in Sema4D expression. Moreover, EPO administration (10 U/ml) in differentiating preosteoclasts in cultures (treated with RANKL and M-CSF), induced a 1.4-fold increase in Sema4D transcript levels. Here we present a dual direct and indirect pathway of EPO action in bone cells in the inhibition of bone formation. These findings support the notion that EPO-R signaling in both osteoblasts and osteoclasts affects bone turnover via direct effects as well as through the regulation of paracrine signals.

Disclosures: Sahar Hiram-Bab, None.

MO0063

Bone Marrow Blood Vessel Ossification is Present in 1-month-old Fischer-344 rats and Coincides with Altered Bone and Hematological Parameters in Advanced Age. Sophie Guderian¹, Mary Ann McLane², Rhonda Prisby³. ¹The University of Delaware, USA, ²The University of Delaware Department of Medical Laboratory Sciences, USA, ³The University of Delaware Bone & Microcirculation Lab, USA

Advanced age corresponds with reduced bone mass and blood flow, diminished hematopoiesis, vascular rarefaction, and augmented marrow adiposity and ischemia (Prisby et al., 2007; Burkhardt et al., 1987; Kita et al., 1987). Further, we discovered ossification of bone marrow blood vessels (BMBV) in 6- and 24-month old rats (Prisby, 2014). Since, bone marrow is the site for erythrocyte and lymphocyte production and blood cells access the peripheral circulation via blood vessels, we sought to assess whether ossification coincides with age-related declines in red and white blood cell count. We kinetically examined the development and progression of BMBV ossification and hematological parameters as a function of advancing age. Left femora and whole blood samples were collected from young (1 mon; n=4), middle-aged (12 mon; n=5) and aged (24 mon; n=6) male Fischer-344 rats. Bone microarchitecture (BV/TV, %; Tb.N, /mm²; Tb.Th, μ m & Tb.Sp, μ m) in distal femora and ossified vessel volume (OsVV) in femoral shafts were assessed by μ CT (Scanco Medical). Density (g/cm³) and SMI were compared between bone and ossified vessels. Complete blood counts were determined with a Coulter[®] AcT diffTM Analyzer (Beckman Coulter). Body mass (p<0.05) increased with age. BV/TV was higher in middle-aged (25.9 \pm 1.1%) vs. young (17.4 \pm 0.26%) and aged (13.9 \pm 1.6%) rats, resulting from an augmented Tb.N and Tb.Th. Tb.Sp was greater (p<0.05) in young (2098 \pm 203 μ m) vs. middle-aged (237 \pm 9 μ m) and aged (463 \pm 42 μ m) rats. OsVV increased (p<0.05) across the lifespan (young, 0.075 \pm 0.02%; middle-aged, 0.57 \pm 0.18% and aged, 2.00 \pm 0.41%) and coincided with SMI values indicative of cylindrical (range: 3.0-4.0) vs. plate-like shapes of middle-aged (range: 0.7-1.2) and aged (range: 0.9-2.1) trabecular bone. Bone was denser

Table 1

Table 2 Percentage increase on 25(OH)VitD and DXA parameters from T0 to T1 for Group 1, Group 2 and Group 3

| | Percentage increase at T1 mean \pm SD | | | P* | | |
|------------|--|-----------------|-----------------|-----------------|-----------------|-----------------|
| | Gp 1 N=91 | Gp 2 N=91 | Gp 3 N=88 | Gp 1 Vs Gp 2 | Gp 1 Vs Gp 3 | Gp 2 Vs Gp 3 |
| 25(OH)VitD | 22.3 \pm 47.0 | 62.4 \pm 65.1 | 97.0 \pm 88.0 | <0.001 | <0.001 | <0.001 |
| Left BMD | 10.7 \pm 6.7 | 13.0 \pm 7.0 | 13.6 \pm 8.3 | 0.0237 | 0.0055 | >0.20 |
| Right BMD | 10.3 \pm 6.7 | 12.8 \pm 7.0 | 13.4 \pm 8.3 | 0.029 | 0.020 | >0.20 |
| Left BMC | 13.8 \pm 8.8 | 16.0 \pm 8.6 | 17.9 \pm 11.3 | 0.0421 | 0.0013 | >0.20 |
| Right BMC | 12.5 \pm 8.5 | 15.5 \pm 10.0 | 16.8 \pm 10.4 | 0.0366 | 0.0018 | >0.20 |

*P-value from analysis using Generalized Estimating Equations

Table 2

Disclosures: Tsz Ping Lam, None.

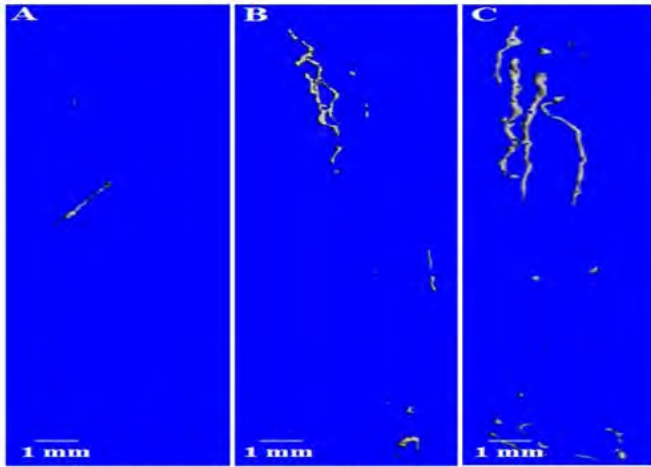
This study was partially funded by an Investigator Initiated Research grant from Pfizer Inc (IIR Grant No. WI 174540).

MO0061

Bone marrow niche crippled by obesity is dependent on potent bone marrow HSC transplants for repopulation. Divya Krishnamoorthy¹, Benjamin J. Adler², Tee Pamon², Jayant Srinivas Sankaran², Danielle M. Frechette³, Clinton T. Rubin². ¹SUNY Stony Brook University, USA, ²Stony Brook University, USA, ³Stony Brook, USA

Obesity is associated with systemic complications that are realized not only in the skeleton but also within bone marrow (BM) niches. Understanding obesity driven disruptions to BM hematopoietic (HSC) and mesenchymal stem cell fate can help elucidate the mechanisms by which musculoskeletal and immune systems are compromised by adipose invasion into the BM. Using a high-fat diet model of obesity, *in vivo* HSC function was first analyzed by their ability to repopulate a system following bone marrow transplantation (BMT). 6w old male B6 mice were pre-fattened with either a 60% fat (HF, n=5) or 10% fat (RD, n=5) diet for 7w in order to establish an obese or lean phenotype, respectively. Mice were lethally irradiated (6+6 Gy), rescued by BMT consisting of equal doses of enriched cd45.1 tagged HSCs (LSK⁺). Control animals (n=6) were on a lean diet, received no irradiation and saline BMT. By 1w post-irradiation, RD and HF mice lost 8 & 12% of body weight, respectively. However, while RD recovered their weights by 8w, HF had not reestablished body weight by 16w, suggesting the extent to which obesity hinders the rate of tissue recovery. Interestingly, flow cytometric analysis showed that HF mice had an overall increased engraftment of donor cd45.1 cells in bone marrow, peripheral blood as well as visceral fat depots compared to RD, with +149% (p=0.068), +260% (p<0.05) and +55% (p=0.08) increase. Indicating that in spite of significant bone loss that results from radiation and HF, there was successful engraftment and repopulation into multiple tissues as cd45.1 leukocytes were also quantified. Further, the contribution of donor cd45.1 cells to total BM leukocytes in HF was +53% (p>0.05) greater than those contributed by recipient non cd45.1 cells, while there was an opposite trend of -211% (p<0.05) fewer donor cell contribution in RD mice. From these finding we hypothesize that HF recipient BM HSC stores were either more sensitive to radiation than those in RD, or more severely compromised by the HF diet thus repopulation of the immune system was more dependent on the donor cd45.1 HSCs. In conclusion, the results from this competitive repopulation assay, where a pre-established marrow niche was competing with potent donor HSCs, may be indicative of a failing marrow in HF where donor cd45.1 HSCs proved to be dominant and more relevant to recovery. In effect, skeletal deterioration following HF maybe

($p < 0.05$) but similar to the densities of ossified vessels at all ages. Red blood cell (RBC; $8.0 \pm 0.1 \times 10^6/\mu\text{L}$ vs. $6.2 \pm 0.1 \times 10^6/\mu\text{L}$ & $6.6 \pm 0.9 \times 10^6/\mu\text{L}$), hemoglobin (Hgb; $14.1 \pm 0.3 \text{ g/dL}$ vs. $11.8 \pm 0.3 \text{ g/dL}$ & $12.7 \pm 0.8 \text{ g/dL}$) and hematocrit (Hct; $41.5 \pm 0.7\%$ vs. $35.7 \pm 0.8\%$ & $37.6 \pm 2.0\%$) were higher in middle-aged vs. young and aged rats, respectively. Percent lymphocyte (%LY) declined with age (young, $84 \pm 2\%$; middle-aged, $77 \pm 2\%$ & aged, $60 \pm 2\%$) and was negatively correlated ($r^2 = -0.81$, $p = 0.00$) with OsVV. Ossified vessels were prevalent as early as 1 month and OsVV progressively worsened with advancing age. This vascular pathology coincided with reduced bone mass, RBC, Hgb, Hct and %LY from 12- to 24-months.



Ossified bone marrow blood vessels in the femoral shafts of 1-mon-old (A), 12-mon-old (B) and 24-mon-old (C) male Fischer-344 rats.

Ossified Blood Vessels

Disclosures: *Sophie Guderian, None.*

MO0064

Bone marrow mesenchymal stem cells are recruited towards expansion of fat depots, a migration accelerated by high fat diet and disrupted by mechanical signals. Danielle Frechette*, Divya Krishnamoorthy, Vihitaben Patel, Meilin Chan, Clinton Rubin. Stony Brook University, USA

Obesity, an expanding epidemic, involves significant adipose accumulation that may depend in part on the recruitment of mesenchymal stem cells (MSC) from bone marrow (BM). Using GFP+ cell tracking, we hypothesized that high fat diet would enhance the migration of bone marrow cells to extra-BM fat depots, while low intensity vibration (LIV) would interrupt this fate by biasing differentiation towards forming higher order tissues such as bone. Following (6+6) Gy of ^{137}Cs γ -irradiation, 8w male C57BL/6 mice received intravenous GFP+ bone marrow transplants (BMT). Irradiated mice were fed a 45% high fat (HD, $n=20$) or 10% regular (RD, $n=20$) diet for 10w. Age-matched controls were sham irradiated and given saline injections (AC, $n=10$). At 2w, 50% of mice from each diet group were vibrated (RDV, HDV) (0.25g, 90Hz) for 30min/d and 5d/w. FACS quantification of MSC (Sca1+/C-Kit+/CD44+/CD90.2+/CD105+) was performed from either pooled BM of femur and tibia or epididymal fat pad. After 10w, transplanted bone marrow cells (GFP+) were detected in the fat pads of all BMT groups (between 26-30% of total fat cell population excluding adipocytes), demonstrating that bone marrow cells contribute to formation of extra-BM fat depots and/or function. Further, transplanted MSC proportions were higher in only HD compared to AC (+51.5%, $p < 0.05$), showing acceleration of MSC fate to extra-BM tissues due to diet. The proportion of total transplanted bone marrow cells in the epididymal fat pad was higher in both HD and HDV groups compared RD (+55%, +60%, respectively; $p < 0.05$) despite no differences in visceral fat pad weights, likely due to an increase in adipose inflammation. In the BM cavity, MSC proportions were decreased in LIV compared to AC (RDV: -24%, $p \leq 0.05$; HDV: -27%; $p = 0.07$) while non-vibrated groups did not see similar declines. Differentiation markers of fat (PPAR γ) and bone (Runx2) showed no differences in the BM, suggesting the noted changes with LIV may be due to stem cell migration or differentiation at an earlier time point. Together, these data demonstrate that bone marrow cells contribute to extra-BM fat depots and possibly the fat pad inflammatory response, while high fat diet specifically accelerates BM MSC recruitment to abdominal fat depots.

Disclosures: *Danielle Frechette, None.*

MO0065

Alternative activation of macrophages by IL-10 promotes efferocytosis of osteoblasts. Megan Michalski*, Amy Koh, Hernan Roca, Laurie McCauley. University of Michigan School of Dentistry, USA

Macrophages play a key role in the inflammatory and resolution phases of wound healing and promote intramembranous bone healing in animal models of osseous injury. Apoptotic cells are increased in the early phases of wound healing and are engulfed by alternatively activated (M2) macrophages, a process termed efferocytosis. The role of efferocytosis during the process of osseous wound healing has not been examined. The objective of this study was to define the role of macrophages in clearing apoptotic bone cells. Bone marrow macrophages harvested from 4-8wk C57BL/6, IL-10KO or BALB/c mice were differentiated *in vitro* with M-CSF for 6-7d and treated with rIL-10 (0.1-100ng/mL) or vehicle for 24h. Bone marrow stromal cells (BMSCs) harvested from 4-8wk C57BL/6 mice or MC3T3-E1 (subclone 4, MC4) pre-osteoblastic cells were grown to confluency, stained with cell tracking dye, and apoptosis (ap) induced with UV light. Macrophages were incubated with apBMSCs or apMC4 cells for 0.5-6.0hrs. Efferocytosis was assessed via fluorescence-activated cell sorting (FACS) for cells exhibiting double-positive immunofluorescence for F4/80 and cell tracker, reflecting internalized apBMSCs within macrophages. Double positive gates were confirmed using ImageStream analysis and IDEAS software for imaging of gated populations. Bone marrow macrophages treated with rIL-10 (10ng/mL; 24h) were analyzed for the M2 phenotype via double positive staining for F4/80 and CD206 (mannose receptor). FACS analysis showed a significant increase in double-positive immunofluorescent cells in cultures pre-treated with 1-100ng/mL rIL-10 compared to vehicle, with 10ng/mL showing the largest increase ($p < 0.01$). The greatest change in efferocytosis between vehicle and treatment groups was apparent at 0.5-1hr of co-culture. Additionally, IL-10 promoted alternatively activated macrophages, detected by increased CD206-antibody staining ($p < 0.01$). Efferocytosis of MC4 cells by IL-10KO vs. BALB/c macrophages was not different, and both displayed increased efferocytosis and M2 polarization with IL-10 treatment ($p < 0.05$). Efferocytosis of apoptotic bone cells by macrophages is enhanced with IL-10 treatment and M2 polarization. Upregulation of IL-10 in bone may enhance effective clearing of apoptotic bone cells and other debris in an osseous wound environment, promoting optimal healing.

Disclosures: *Megan Michalski, None.*

MO0066

A Novel Sequestosome-1 / p62-ZZ Domain Inhibitor Prevents Gfi1-Mediated Epigenetic Suppression of Runx2 in Myeloma Exposed Preosteoblasts. Rebecca Silbermann*¹, Juraj Adamik², Dan Zhou³, Xiang-Qun Xie², Noriyoshi Kurihara³, Deborah Galson², G. David Roodman³. ¹Indiana University School of Medicine, USA, ²University of Pittsburgh, USA, ³Indiana University, USA

Myeloma bone disease (MMBD) is a paradigm for uncoupled bone remodeling, with increased bone destruction and persistent osteoblast (OB) suppression in the absence of MM cells. As the mechanisms mediating long term OB suppression in MMBD are unclear, we hypothesized that MM cells induce epigenetic changes to the Runx2 promoter, the key regulator of OB differentiation, in bone marrow stromal cells (BMSC), which are preOB. We found that the transcriptional repressor Gfi1 directly binds and recruits the chromatin corepressor HDAC1 to Runx2 in MM exposed preOB, reducing euchromatin marks such as H3K9ac. Importantly, this reduction persists in the absence of MM cells, suggesting these epigenetic changes result in long term OB suppression.

We recently showed that p62 (sequestosome-1) in BMSC is a platform for the formation of signaling complexes critical to MMBD and that XRK3F2, an inhibitor of the p62-ZZ domain, induced new bone formation in mice with established MMBD, but did not affect bones without MM. Interestingly, osteoclasts were noted in the new bone, suggesting that XRK3F2 restores coupled bone remodeling in the presence of MM. These data suggest that p62 is critical to the persistent OB suppression of MMBD. We hypothesized that XRK3F2 prevents Gfi1-induced epigenetic suppression of Runx2 and showed that XRK3F2 blunted MM cell induction of Gfi1 expression and Runx2 repression in preOB. We then performed ChIP analyses of MM exposed preOB treated with XRK3F2 and found that XRK3F2 decreases both MM induced Gfi1 occupancy and prevents the decrease of H3K9ac at the Runx2 promoter, consistent with a lack of Runx2 mRNA suppression. As we found that TNF α is a major suppressor of OB in MMBD that reduces Runx2 levels and induces Gfi1 in preOBs, we compared the epigenetic changes at Runx2 induced by TNF α to those in MM exposed preOB and found them similar. To determine how XRK3F2 alters MM effects on OB, we tested if XRK3F2 blocked TNF α -induced signaling or changed TNF α production in the MM marrow microenvironment. XRK3F2 blocked TNF α -induced NF κ B signaling in preOB and in MM cells. Interestingly, adding XRK3F2 to cocultures of MM cells with murine BMSC blunted the upregulation of TNF α observed in both MM and BMSCs after coculture, but did not alter TNF α production in cocultures of p62^{-/-} BMSC and MM cells. These results suggest that targeting the p62-ZZ domain in MMBD may restore coupled bone remodeling in MM.

Disclosures: *Rebecca Silbermann, Celgene*

MO0067

Etoposide directs apoptosis and myeloid driven cell clearance with net negative impacts on bone. Amy Koh*, Megan Michalski, Benjamin Sinder, James Rhee, Laurie McCauley. University of Michigan, USA

Chemotherapy is widely used for the treatment of various cancers and has often been attributed for negative effects in bone. Etoposide, is a chemotherapy which targets rapidly dividing cells, inducing them to undergo apoptosis. While tumor cells are the intended target, normal cells are affected as well. The aim of this study was to determine the impact of etoposide on bone and the bone marrow microenvironment. Sixteen week old female C57B6 mice were injected i.p. with etoposide (20mg/kg) or vehicle in two different regimes: 1) daily for 5d or 9d, or 2) daily for 5d then 3x/wk for 6wks. Skeletal phenotyping, flow cytometry, serum bone markers, and marrow gene expression were analyzed. After 5 days of treatment, etoposide significantly reduced RBC and WBC populations, reducing neutrophil, lymphocyte and monocyte numbers by 50% and increasing platelet numbers. In the bone marrow, etoposide increased early apoptotic cells (AnnexinV⁺PI⁻), Lin⁻CD29⁺sca1⁺ (mesenchymal stem cells, MSCs) and CD45⁺ leukocytes. Myeloid CD11b⁺, and phagocyte CD68⁺ cells in combination with the expression of MER (an apoptotic bridge receptor tyrosine kinase) were also increased. Etoposide had noted bone effects as early as 9 days resulting in a significant decrease in tibial bone area (via histomorphometry) and femoral bone volume (via microCT). In the longer treatment regime, flow cytometry of the bone marrow cellular population revealed increased CD68⁺, monocyte Gr1⁺, CD11b⁺, F4/80⁺, CD45⁺ and MSCs. MicroCT and histomorphometry revealed etoposide decreased tibial bone volume and bone area, with decreases in both trabecular thickness and cortical bone volume. Serum TRAcP5b was increased with etoposide, while PINP levels were unchanged. Functionally, flow cytometry revealed that CD68⁺ cells in the bone marrow were significantly increased and were significantly more effective at phagocytosing carboxylated beads which suggested instigation of the cell clearance program. Gene expression studies revealed that etoposide increased CCL2 (MCP-1) expression in the bone marrow which could explain the increased myeloid cell population and the bone resorptive phenotype. These data indicate that induction of apoptosis via the chemotherapeutic agent etoposide skews normal bone marrow in favor of monocyte/macrophage populations as well as MSCs, yet ultimately has deleterious effects on bone.

Disclosures: Amy Koh, None.

MO0068

Osteocytes are an Important Mediator of Bone Pain in Myeloma. Masahiro Hiasa*¹, Tatsuo Okui², Yuki Nagata², Yohance M Allette³, Matthew S Ripsch³, Jesús Delgado-Calle⁴, Teresita Bellido⁴, G David Roodman², Lilian Plotkin⁴, Fletcher White³, Toshiyuki Yoneda². ¹Indiana University School of Medicine, USA, ²Department of Medicine, Hematology Oncology, Indiana University School of Medicine, USA, ³Department of Anesthesia, Paul & Carole Stark Neurosciences Research Institute, USA, ⁴Department Anatomy & Cell Biology, Indiana University School of Medicine, USA

Bone pain is one of the most prevalent and devastating complications of multiple myeloma (MM). Although the mechanisms of MM-associated bone pain (MABP) remain unclear, complex interactions between cancer cells and bone cells in the bone microenvironment are likely critical to the pathophysiology of MABP. Several studies have reported that calcitonin gene-related peptide-positive (CGRP+) sensory neurons (SN) deeply innervate mineralized bone where numerous osteocytes (OCy) reside and develop cell-cell networks, suggesting that OCy and SN may interact. We propose that these interactions occur and play an important role in the pathophysiology of MABP. To test this hypothesis, we examined whether OCy and SN fibers are in physical contact in bone, and if they could exchange small molecules via these connections. We found that CGRP+ SN fibers in bone were in direct physical contact with OCy, predominantly via connexin 43 (Cx43) on OCy. Further, co-culture of MLO-A5 osteocytic cells with F11 SN cells demonstrated that F11 cells contacted with dendritic processes of MLO-A5 cells by extending their neurites and exchanged small soluble molecules with MLO-A5 cells, as determined by transfer of permeable dye calcein. Using Ca²⁺ influx imaging assays, we also found that co-culture with MLO-A5 cells enhanced F11 cell excitation induced by acid (pH 6.5), which, we showed, corresponds to the acidic microenvironment developed in MM-bearing bone. Importantly, addition of GAP27, a selective inhibitor of Cx43, or knockdown of Cx43 in MLO-A5 cells abolished the enhanced F11 cell excitation seen in the co-culture. To confirm that blocking Cx43 also affected bone pain in vivo, mice injected intratibially with human MM JN3 cells were treated with GAP27 and assessed for MABP by measuring tactile hypersensitivity and thermal hyperalgesia in JN3-bearing tibiae and expression of p-ERK, a molecular marker of pain, in the dorsal root ganglia. We found marked suppression of MABP and p-ERK in mice treated with GAP27 compared with vehicle-treated control mice. These data demonstrate that OCy and SN are in intimate physical contact in mineralized bone, and that they exchange small molecules via Cx43 gap junctions or hemi-channels to induce SN excitation that results in severe MABP. These results further suggest that targeting Cx43-mediated OCy-CGRP+ SN fiber contacts may provide a new potent approach for treating the devastating bone pain seen in patients with MM.

Disclosures: Masahiro Hiasa, None.

MO0069

Curcumin promoting osteosarcoma cell death by activating miR-125a/ ERRA/ ROS pathway. Peng Chen*¹, Haibing Wang², Junjian Wang³, Wei He². ¹First School of Clinical Medicine of Guangzhou University of Chinese Medicine, USA, ²First Affiliated Hospital of Guangzhou University of Chinese Medicine, China, ³Cancer Center, UC Davis, USA

Curcumin (CUR) shows valuable therapeutic potential against a variety of cancers. However, the molecular mechanism underlying antitumor remains unclear. By RNA sequence profiling, we found that curcumin effectively suppressed ERRA and its target gene expression. Employing ERRA ectopic stable cell line, we found that ERRA overexpression blocked CUR-induced cell death through down-regulating CUR induced ROS production, and ERRA silencing sensitized osteosarcoma cells to CUR-induced cell death. Furthermore, our results also revealed that CUR suppressed ERRA expression through enhancing miR-125a level. In conclusion, our results revealed a novel mechanism for CUR induced cell death, which involves tumor cell killing via activating miR-125a/ ERRA/ROS pathway and provide further support for targeting ERRA only or combine with CUR in the potential cancer therapy.

Disclosures: Peng Chen, None.

MO0070

Enhanced sensitivity of bone seeking breast cancer cells to Metformin by targeting Runx2-IGF-1R β and AMPK-Erk pathway. Manish Tandon*, Ahmad Othman, Zujian Chen, Jitesh Pratap. Rush University Medical Center, USA

The breast cancer metastasis is a major cause of skeletal-related events and patient mortality due to lack of effective targeting strategies against tumor survival in bones. The breast cancer cells preferentially survive in hypoxic and growth factor rich bone microenvironment, however, the underlying molecular mechanisms are not clear. Here we show that bone-derived breast cancer cells can be sensitized to Metformin by targeting Runx2-related transcription factor (Runx2) regulatory network. Since Runx2 regulates osteoblast differentiation, growth factor and metabolic signaling, mammary gland morphogenesis, invasive properties and cell survival during stressful conditions, we investigated its role in invasive breast cancer survival in bones. We performed systemic inoculation of control or Runx2 knockdown invasive MDA-MB-231 cells in NOD/SCID mice, and compared parental and bone-derived variants for phenotypic and molecular alterations. Both control and Runx2 knockdown cells showed tumor growth in bone coupled with osteolysis. Notably, the Runx2 knockdown cells showed early (0-2 weeks) delay but late (4-6 weeks) aggressive metastatic outgrowth in bones suggesting Runx2-dependent bi-phasic response and reprogramming of survival pathways. The late-stage tumor growth and bone loss in Runx2 knockdown cells associated with increased IGF-1-induced pIGF-1R β and pAkt signaling. Interestingly, glucose uptake and glycolysis were reduced in the Runx2 knockdown cells due to reduced extracellular-regulated protein kinase (Erk1/2) activity leading to the activation of AMP activated protein kinase (AMPK), the sensor of cellular metabolism. Therefore, we tested if Runx2 expression alters the sensitivity towards pharmacological compounds targeting IGF-1R β , AMPK and Erk1/2 signaling pathway. The Runx2 knockdown increased the sensitivity towards both Erk1/2 inhibition and AMPK activation by PD184161 and Metformin, respectively. The growth inhibitory effects were increased in bone-derived Runx2 knockdown cells compared to controls as indicated by cellular rounding, cytoskeletal condensation and reduced metabolism. In addition to increased pAMPK levels, p70S6K were significantly downregulated in Metformin treated Runx2 knockdown cells. Collectively, our results reveal a critical link between de-regulated energy metabolism and cell survival via Runx2, AMPK-Erk1/2 and IGF-1R β -Akt signaling crosstalk, and support repositioning Metformin treatment for breast cancer bone metastasis.

Disclosures: Manish Tandon, None.

MO0071

P38 MAPK regulates the Wnt-inhibitor Dickkopf-1 in osteolytic prostate cancer cells. Andrew Browne¹, Andy Göbel¹, Martina Rauner¹, Lorenz Hofbauer¹, Tilman Rachner^{*2}. ¹Technische Universität Dresden, Department of Medicine III, Germany, ²University Hospital Dresden, Germany

Prostate cancer (PCa) is the most common cancer in men above 50 years of age with a predilection to metastasize to bone in advanced stages.

The Wnt-inhibitor Dickkopf-1 (DKK-1) has been described to be highly expressed in bone metastasizing cancers and is thought to inhibit osteoblast function thereby enhancing the osteolytic process. P38 MAPK (p38) activity is also dysregulated in patients with advanced stages of cancer and has previously been shown to regulate DKK-1 in multiple myeloma. This study aimed to clarify the regulatory function of DKK-1 by p38 in PCa.

DKK-1 was barely expressed in MDA-Pca2b and C4-2B cell lines which are known to induce osteoblastic and mixed lesions in vivo respectively. In contrast, the osteolytic PC3 cells had a high level of DKK-1 expression as measured by qPCR and by ELISA (p<0.005). Treatment of the osteoblastic cell line C2C12 with supernatants

of PC3 cells, but not MDA-PCa2b supernatants, led to a significant suppression of Wnt3a inducible osteoblastic markers including alkaline phosphatase and osteopontin. This inhibition could be reversed by adding a neutralizing DKK-1 antibody or by knocking down DKK-1 expression in PC3 cells using siRNA. The expression and secretion of DKK-1 was significantly decreased by the p38 inhibitors LY2228820 and SB202190 ($p < 0.001$). Vice versa, treatment of PC3 cells with anisomycin, which activates the MAPK pathway, increased DKK-1 ($p < 0.01$). Knockdown of p38 in PC3 cells using siRNA further confirmed the link between p38 and DKK-1 expression ($p < 0.001$).

Assessment of DKK-1 expression and p38 isoforms (MAPK11, MAPK12 and MAPK14) in prostate cancer samples using a cDNA array containing samples from 48 patients revealed an increased DKK-1 expression in prostate cancer compared to benign tissue and a significant positive correlation between DKK-1 and MAPK11 and MAPK14.

These results indicate that DKK-1 is regulated by p38 in osteolytic PCa cells. Future investigations may strengthen the role of both DKK-1 and p38 activity as novel therapeutic targets in PCa-induced osteolytic bone lesions.

Disclosures: Tilman Rachner, None.

MO0072

Runx2 is associated with poor survival in dogs with malignant mammary tumors. Kristi Milley*¹, Eman Saad², Syu Mi Sam², Barbara Bacci³, Judith Nimmo⁴, Samantha Richardson², Janine Danks⁵. ¹RMIT University, Australia, ²School of Medical Sciences, RMIT University, Australia, ³School of Veterinary Science, The University of Melbourne, Australia, ⁴Australian Specialised Animal Pathology Laboratories, Australia, ⁵School of Medical Science, RMIT University, Australia

Runx2 is a master-regulator of bone development and is essential for osteoblast differentiation. Recent data has outlined a potential role for Runx2 in breast cancer development. The loss of Runx2 expression, in transgenic mouse models, resulted in increased tumor latency and increased overall survival. As canine mammary tumors (CMTs) are a good natural model for human breast cancer, our aim was to evaluate the potential of Runx2 as a prognostic marker using these companion animals. Samples were prospectively collected by the Australian Veterinary Cancer BioBank and follow-up data on recurrence and survival was collected until death. Runx2 was localized in benign (n=21) and malignant (n=69) CMTs as well as in adjacent normal mammary tissue (n=37) by immunohistochemistry. In addition, malignant samples were also subtyped using a five antibody panel (ER, HER2, p63, CK5 and Vimentin). Finally, Runx2 gene expression was quantified in both normal and CMT samples from animals which had corresponding RNA-stabilized frozen tissue available. Runx2 protein was localized in the nuclei of 92% of normal mammary samples, 81% of benign CMTs and 78% malignant CMTs. A subset of Runx2 positive malignant CMTs (15/54) demonstrated significantly stronger staining compared to normal samples. This increased Runx2 staining was associated with poor survival ($p < 0.0001$). The median survival of dogs with increased Runx2 was only 258 days compared to 724 days for Runx2 negative tumours. Runx2 was not associated with a specific subtype but was more common in basal-like and HER2+ subtypes. Our study is the first to demonstrate and link the presence of Runx2 in CMTs to survival. Overall, our results support the potential use of Runx2 as a prognostic marker for breast cancer.

Disclosures: Kristi Milley, None.

MO0073

CD44 and RUNX2 Peptides Prevents Osteoclastogenesis by Suppressing RANKL Expression in Prostate Cancer PC3 cells. Meenakshi Chellaiiah*¹, Aditi Gupta². ¹University of MarylandDental School, Us, ²University of Maryland, USA

Background: Pathological skeletal fractures develop in prostate cancer patients as a result of bone loss induced by androgen deprivation therapy and bone metastases. In this regard, bone-resorbing osteoclasts are essential in mediating bone loss induced by metastatic prostate cancer cells homing to the skeleton. Therefore, there is a critical need for novel pharmacotherapeutic approaches to control this debilitating disease. We have previously demonstrated that prostate cancer cells secrete receptor activator of NF- κ B ligand (RANKL), a protein essential for osteoclast differentiation and activation. The objective of our study is to inhibit the expression and function of RANKL in metastatic prostate cancer cells.

Results: We used prostate cancer cells lines derived from a variety of anatomic metastases. We found a significant increase in the expression of CD44, a cell surface receptor in prostate cancer cells derived from human bone metastases (PC3) as compared with those derived from brain (DU 145) or lymph node (LNCaP) metastases. CD44 expression is very negligible or not observed in LNCaP cells. We find that RUNX2 and Smad 5 are involved in the regulation of expression of RANKL. CD44 and α v β 3 signaling pathways support RANKL expression by phosphorylation of RUNX2 and Smad 5 proteins, respectively. RUNX2-Smad 5 complex formation and intranuclear targeting of RUNX2 are functionally required for this process. An inhibitor to integrin α v and siRNA to CD44 attenuated the expression of RANKL in PC3 cells. Immunohistochemistry analysis of tissue microarray sections containing primary prostatic tumor (grade2-4) detected pre-

dominant localization of RUNX2 and phosphorylated Smad 5 in the nuclei. Small molecular weight peptides to CD44 and RUNX2 have the potential to block localization of RUNX2 in nuclei and RANKL expression/secretion. As a consequence of these peptide-based approaches, conditioned media from these cells failed to support osteoclast formation in vitro.

Conclusions/Future Perspectives: We found that CD44 and RUNX2 peptides have the potential to block RANKL expression by PC3 cells. Studies are under way to test for the efficacy of these peptides in the inhibition of metastasis to bone and subsequently bone loss by osteoclast differentiation in animal models. We envision that peptide-based therapeutics will greatly impact cancer treatment in the near future. Ultimately, these peptides could be useful for the development of novel therapies for the treatment of prostate cancer bone metastases (Supported by NIH-NIAMS 5 R01 AR066044-02).

Disclosures: Meenakshi Chellaiiah, None.

MO0074

Withdrawn.

MO0075

TRAIL is not a proapoptotic but rather anti-apoptotic mediator for osteoclasts to stimulate their differentiation and survival. Hirofumi Tenshin*¹, Jumpei Teramachi², Asuka Oda³, Ryota Amachi¹, Masahiro Hiasa⁴, Keiichiro Watanabe¹, Shingen Nakamura³, Hirokazu Miki⁵, Itsuro Endo³, Eiji Tanaka¹, Toshio Matsumoto⁶, Masahiro Abe³. ¹Department of Orthodontics & Dentofacial Orthopedics, Institute of Biomedical Sciences, Tokushima University Graduate School, Japan, ²Department of Histology & Oral Histology, Institute of Biomedical Sciences, Tokushima University Graduate School, Japan, ³Department of hematology, endocrinology & metabolism, Institute of Biomedical Sciences, Tokushima University Graduate School, Japan, ⁴Department of Biomaterials & Bioengineering, Institute of Biomedical Sciences, Tokushima University Graduate School, Japan, ⁵Division of Transfusion Medicine & Cell Therapy, Tokushima University Hospital, Japan, ⁶Fujii Memorial Institute of Medical Sciences, Tokushima University, Japan

Myeloma (MM) cells preferentially reside in the bone marrow, and develop extensive osteolytic lesions. TNF-related apoptosis-inducing ligand (TRAIL) selectively induces apoptosis in various cancers including MM. Although TRAIL agonists are considered as an attractive anti-MM agent, the impact of TRAIL-mediated immunotherapy on osteoclast (OC) formation and function is unclear. The present study was undertaken to clarify the role of TRAIL-mediated signaling in OC differentiation and survival. RANK ligand time-dependently induced the expression of death receptor5 (DR5), a TRAIL receptor in mice, along with NFATc1 and cathepsin K in mouse RAW264.7 preosteoclastic cells or bone marrow cells during their osteoclastogenesis. Treatment with rTRAIL promptly induced RANK in a dose-dependent manner at 10 to 500 ng/ml to facilitate RANK ligand-mediated expression of c-fos, NFATc1 and DC-STAMP and osteoclastogenesis in RAW264.7 cells. Although DR5 expression was up-regulated in mature osteoclasts, treatment with rTRAIL at concentrations up to 500 ng/ml neither induced apoptotic cell death with caspase8 cleavage nor impaired actin ring formation in them, while rTRAIL at concentrations as low as 10 ng/ml was able to induce cell death in a portion of MM cell lines, including MM.1S. Interestingly, rTRAIL induced the degradation of I κ B α in RAW264.7 cells and OCs, suggesting deflection of DR-mediated signaling towards activation of the NF- κ B pathway while sparing the extrinsic caspase-dependent apoptotic pathway. We also found increase of TGF-beta-activated kinase-1 (TAK-1), an up-stream mediator of the NF- κ B pathway, during osteoclastogenesis. The TAK-1 inhibitor LLZ1640-2 abrogated the NF- κ B activation by rTRAIL in OCs, and impaired RANK ligand-mediated osteoclastogenesis, and triggered cell death in OCs in the presence of rTRAIL, suggesting a role of TAK-1 in the NF- κ B activation and survival by rTRAIL in OCs. Collectively, these results demonstrate that osteoclastic lineage cells efficaciously utilize TRAIL for their differentiation and activation, and that TAK-1 may play a critical role in skewing DR-mediated signaling to be anti-apoptotic but not pro-apoptotic in OCs. Caution on bone resorption should be taken in TRAIL-mediated immunotherapy especially for cancers with enhanced bone resorption such as MM.

Disclosures: Hirofumi Tenshin, None.

MO0076

$\alpha_v\beta_3$ -Fumagillin-prodrug Nanoparticles and Zoledronic Acid Additively Reduce Tumor Angiogenesis Through Differential Effects on Endothelial and Myeloid Cells. Alison Esser¹, Anne Schmieder¹, Michael Ross¹, Jingyu Xiang¹, Xinming Su¹, Grace Cui¹, Huiving Zhang¹, Xiaoxia Yang¹, John S. Allen¹, Chidananda Mudalagiriappa¹, Samual Wickline¹, Rebecca Aft¹, Dipanjan Pan², Gregory Lanza¹, Kathy Weilbaecher¹.
¹Washington University in St. Louis, USA, ²University of Illinois at Urbana-Champaign, USA

Innate and acquired resistance to VEGF targeted therapies is a significant problem of angiogenesis blockade for breast cancer. Effective treatments require novel non-cancer resistant strategies. This project elucidated the potential of a dual-therapy anti-angiogenic approach using $\alpha_v\beta_3$ -targeted fumagillin nanoparticles in combination with zoledronic acid. Zoledronic acid (ZA), a long acting osteoclast and macrophage inhibitor used in breast cancer patients, has anti-angiogenic properties in mouse tumors through an unknown mechanism. In a cohort of breast cancer patients receiving chemotherapy, ZA treatment decreased vascularity (CD31) relative to those without ZA ($p < 0.05$). ZA improved survival in those patients with pre-chemotherapy gene expression profiles indicative of high levels of inflammatory macrophages (CD163+) and VEGF. *In vitro*, ZA reduced macrophage viability ($p < 0.05$) without effects on endothelial cell viability or tube formation. Fumagillin (Fum), a methionine aminopeptidase-2 inhibitor, elicits anti-angiogenesis via neoendothelial apoptosis rather than by VEGF suppression. Fumagillin-prodrug (Fum-PD), a photochemically stable drug form, alone and incorporated into $\alpha_v\beta_3$ -targeted nanoparticles (NP) reduced ($p < 0.05$) endothelial cell viability and tube formation, but did not have an impact on macrophage viability. Rabbits with popliteal Vx2 tumors were given serial control, ZA, $\alpha_v\beta_3$ -Fum-PD NP, or ZA plus $\alpha_v\beta_3$ -Fum-PD NP treatment to assess the benefit of dual complementary anti-angiogenesis therapy. On day 17, tumor MR neovascular molecular imaging revealed that Fum-PD NP alone and with ZA decreased ($p < 0.05$) angiogenesis, while ZA alone did not. Microscopically, tumor vascularity (CD31) was reduced ($p < 0.05$) by both ZA and Fum-PD NP independently and further decreased ($p < 0.05$) by the dual-therapy. These data suggest a complementary role for ZA and $\alpha_v\beta_3$ -Fum-PD NPs to accelerate anti-angiogenesis benefits in aggressive tumors characterized by increased angiogenesis and inflammatory macrophages.

The purpose of this study was to elucidate the potential of a dual-therapy anti-angiogenic approach using $\alpha_v\beta_3$ -targeted fumagillin nanoparticles in combination with zoledronic acid.

Disclosures: Alison Esser, None.

MO0077

A high-throughput screening identified flucinolone acetonide as a potent synergistic factor of TGF- β 3-mediated chondrogenesis of BMSCs for articular surface repair. Emilio Hara^{*1}, Takuo Kuboki², ¹Department of Oral Rehabilitation & Regenerative Medicine, Graduate School of Medicine, Dentistry & Pharmaceutical Sciences, Japan

In this study, we performed a high-throughput screening of 640 FDA-approved drugs for compounds that can enhance chondrogenesis and interact synergistically with major growth factors (TGF- β , BMP) regulating chondrogenesis. We found that the combination of flucinolone acetonide (FA) and TGF- β 3 strongly potentiated chondrogenic differentiation of human bone marrow-derived mesenchymal stem cells (hBMSCs). In contrast, FA repressed BMP-2-mediated chondrogenesis of hBMSCs. In a newly-generated full-thickness articular cartilage defect model in knee joints of immunocompromised mice, transplantation of FA/TGF- β 3-treated hBMSCs could clearly regenerate the articular surface. However, cartilage repair could not be observed in groups that received hBMSCs treated with other glucocorticoids (dexamethasone (DEX) and triamcinolone acetonide (TA)) in association with TGF- β 3. Analysis of intracellular pathways revealed that FA enhanced TGF- β 3-induced phosphorylation of Smad2 and Smad3. Additionally, we performed a pathway array and found that FA activates mTORC1/AKT pathway. Chemical inhibition of mTORC1 with rapamycin substantially suppressed FA effect. Furthermore, activation of glucocorticoid receptor (GR) was evidently highly with FA and TA, but to a less extent with DEX. Since glucocorticoids are known to bind to GR, inhibition assays with rapamycin also suppressed FA effect, suggesting that FA action involves binding to GR. In summary, these results show a unique ability of FA to strongly enhance TGF- β 3-associated chondrogenesis, and suggest that FA/TGF- β 3 may be used as major inducers of chondrogenesis of stem cells to improve clinical outcomes for cartilage regeneration.

Disclosures: Emilio Hara, None.

MO0078

Involvement of Core binding factor β in maintenance of the articular cartilage through interaction with Runx. Xiangguo Che^{*}, Clara Yongjoo Park, Na-Rae Park, Yu-Ra Choi, Da-In Yeo, Je-Yong Choi. Kyungpook National University, School of Medicine, South Korea

The function of core binding factor β (Cbfb), a partner protein of the Runx family transcription factor, has not been determined in articular cartilage. To explore the *in vivo* function of Cbfb in articular cartilage, we generated articular cartilage-specific Cbfb-deleted mice (Cbfb^{Δac/Δac}) by crossing Gdf5 promoter-driven Cre mice with Cbfb floxed mice. Osteoarthritis (OA) was induced through destabilization of the medial meniscus (DMM) surgery in 12 week-old mice. At 8 weeks, OA phenotypes were exacerbated in Cbfb^{Δac/Δac} mice compared to wild type mice. Type II collagen and Runx1 decreased and MMP13 increased in Cbfb^{Δac/Δac} OA mice compared to wild type OA mice. In addition, sham Cbfb^{Δac/Δac} mice had less Runx1 and type II collagen, and more MMP13 than wild type sham mice, though no difference was detected in joint and skeletal tissue formation. Cbfb^{Δac/Δac} mice naturally acquired phenotypes similar to mild OA from 8 months of age in which Runx1 and type II collagen diminished and MMP13 increased. Messenger RNA levels of early chondrogenic markers, including *Aggrecan* and *Col2*, decreased and late chondrogenic markers, such as *collagen X*, *Vegf* and *Mmp13*, increased in Cbfb^{Δac/Δac} mice compared to wild type mice at 1 year. Rescue of Cbfb in Cbfb-deficient primary articular chondrocytes increased Runx1 and decreased MMP13 expression. The formation of a Runx1/Cbfb complex, stabilizing Runx1 from proteosomal degradation, was detected in primary cultured articular chondrocytes as well as in ATDC5 cells *in vitro*.

Collectively, these results indicate that Cbfb is required for Runx1 stability as a partner protein in articular cartilage and that the formation of the Cbfb-Runx1 complex plays an essential role in maintaining articular cartilage integrity.

Disclosures: Xiangguo Che, None.

MO0079

Long-Acting Parathyroid Hormone Analog as a Therapy for Osteoarthritis in mice. Tomoyuki Watanabe^{*}, Thomas Gardella, Tatsuya Kobayashi, Braden Corbin, Monica Reves, Henry Kronenberg, John Potts. Massachusetts General Hospital, USA

The parathyroid hormone receptor-1 (PTH1R) plays a key role in regulating the proliferation and differentiation of chondrocytes in growth plate cartilage, but its role in regulating chondrocytes in articular cartilage is less well understood. Evidence suggesting that the PTH1R plays a role in maintaining the integrity of articular cartilage is provided by a recent study showing that the receptor is up-regulated in articular chondrocytes in patients with osteoarthritis (OA), as well as in rodents with surgically induced OA. Indeed, this same study showed that articular cartilage degeneration in mice with surgically induced OA can be inhibited by daily injection with PTH (1-34). We have recently developed a new high affinity, long-acting PTH analog, called LA-PTH, as a potential PTH1R-based therapeutic, and assess it here for the capacity to inhibit OA development in mice with surgical destabilization of the medial meniscus (DMM). Sham or DMM surgery was performed on the right knee of wild-type mice (C57/BL6, female, 11-weeks old), and the mice were then treated by subcutaneous injection with either vehicle, PTH (1-34) at 10 nmol/kg, or LA-PTH at 2 nmol/kg, for eight weeks at five days per week. We used LA-PTH at a five-fold lower dose versus PTH(1-34) to avoid risk of excessive bone turnover and hypercalcemia that can occur with this long-acting PTH ligand. At the end of the eight-week treatment, right knee joints were isolated and processed for histopathology. Safranin-O-stained sections were scored according to the OARSI (Osteoarthritis Research Society International) Histopathology Initiatives. In addition, the left distal femurs (non-DMM) were isolated and processed for micro-computed tomography (micro-CT) analysis of bone-mineral density (BMD).

At the end of the study, basal blood calcium levels were normal in all animal groups. Micro-CT results showed that both PTH (1-34) and LA-PTH induced modest increases in BMD in the distal femur region. The OARSI scoring results showed that articular cartilage degeneration was reduced significantly ($P < 0.05$) in both the PTH (1-34)- and LA-PTH-treated groups, as compared to the vehicle-treated group. Thus, LA-PTH, even at a five-fold lower dose, was at least as effective as PTH (1-34) in preventing OA progression in DMM mice. These results support the hypothesis that the PTH1R is a valid target for OA therapy, and that long-acting PTH analogs might provide improved efficacy.

Disclosures: Tomoyuki Watanabe, Chugai Pharmaceutical Co.Ltd.

MO0080

Mechanical responsive miR-365 contributes to osteoarthritis development. Xu Yang^{*1}, Yuanhe Wang¹, Yingjie Guan², Qian Chen², Kang Sun¹.
¹Affiliated Hospital of Medical College of Qingdao University, China, ²Alpert Medical School of Brown University, USA

Purpose: Joint tissues are exquisitely sensitive to their mechanical environment. Mechanical overload is an important pathogenic factor to osteoarthritis, which is the major cause of traumatic osteoarthritis (OA). We aim to characterize the role of

mechanical responsive miR-365 in OA development by using human articular chondrocytes, animal model and OA patients. Methods: Human articular chondrocytes isolated from cartilage were seeded into 3D collagen sponges and subjected to cyclic loading. Surgically induced OA model in rats was created by anterior cruciate ligament transection and medial meniscal tear with approval from institutional animal care and use committee. Human articular cartilages were aseptically obtained from OA patients at the time of total knee replacement which have been approved by the institutional human research committee. The OA patients were divided into primary arthritis group and traumatic arthritis group according to their clinical, radiographic feature and history of trauma. The control cartilage was harvested from normal looking cartilage in non-weight bearing area from same patient. Total RNA was extracted then reverse transcribed and analyzed for expression of collagen type 2(Col2) and MMP13 by real-time PCR. miR - 365 expression level was determined by using TaqMan miRNA assay. Results: The expression of miR-365 in OA chondrocytes was significantly higher than the control as well as up-regulated in surgically induced OA cartilage compared with sham control. Overexpression of miR-365 in chondrocytes significantly reduced the mRNA level of Col2 and up-regulated MMP13. Furthermore, miR-365 expression was also significantly up-regulated by treatment with pro-inflammatory cytokine IL-1 β . Moreover, In OA patients, the miR-365 expression levels of lesion area were significantly higher than the non-lesion control both in primary osteoarthritis group as well as traumatic osteoarthritis group. Conclusions: miR-365 expression is induced by both biophysical and biochemical factors in human articular chondrocytes which constitute one of the key factors of osteoarthritic cartilage destruction. miR-365 inhibitor may be one of mechanosensitive chondroprotective molecule and a novel target in preventing cartilage degeneration.

Disclosures: Xu Yang, None.

MO0081

P34HB film promote cell adhesion and proliferation in vitro and cartilage repair in vivo. Na Fu^{*1}, Yunfeng Lin². ¹Sichuan University, Peoples republic of china, ²Sichuan University, China

A. Objective The management of chondral defects is a challenging topic of current actuality for scientists and surgeons, and resultantly has an important impact on human costs. For several centuries after its first observation, this problem has not yet found a satisfactory and definitive answer. Cartilage tissue engineering, which involves novel natural scaffolds, has emerged as a promising strategy for cartilage regeneration and repair. In our previous study, the results had indicated that P34HB was a good material for tissue engineering. Therefore, in the present study, in order to further mimic the native ECM microenvironment of articular cartilage and improve the biomechanical strength of scaffold microarchitecture, P34HB film were fabricated and characterized. B. Materials and Methods In the study, the bioplastic poly(3-hydroxybutyrate-co-4-hydroxybutyrate) (P34HB) film was first fabricated. The characteristics of P34HB film were tested by using SEM and AFM, and the contact and mechanical properties of P34HB film were all tested. Cell morphologies on P34HB film were obtained by SEM and fluorescence microscopy after cell seeding. The tests of cell adhesion and proliferation on P34HB film were conducted by the MTT and CCK-8 assay, respectively. Furthermore, the full cartilage defects in rats were created and P34HB films were implanted to evaluate the healing effects within 8 weeks. C. Results By AFM, contact angle and tension test, we found P34HB film suitable for implantation for cartilage defect as a relatively favorable natural biomaterial, especially for its intrinsic hydrophilicity. RASCs seeded and green fluorescent mASCs 1 day, 3 days, 5 days and 7 days P34HB film SEM showed apparent morphological and quantity differences. Through the observation of the SEM, fluorescence microscopy we could only draw that the ASCs grow well in the P34HB film. The MTT and CCK-8 results showed that, after 3 day, the rASCs on the P34HB film had a significantly higher proliferation rate than on the petri dish group (up to ~ 81%). P34HB has been shown to have a wide range of physical properties ranging from high crystalline to elastic character depending on mol (%) of 4HB monomer. The samples from the repair sites of cartilage defects at 4 and 8 week post-surgery were evaluated by HE, Toluidine Blue O, Alcian blue and type-II collagen stains. Among the implant groups, the interfaces at 4 week were more distinct compared with those at 8 week post-surgery. At 4 week, the layers of P34HB film were clearly shown, but the newly formed tissue (NT) was gradually covered at the top of cartilage defect indentation. At this time, the original tissue (OT), newly formed tissue (NT), and P34HB film (F) were all clearly observed at the site of cartilage defects. At 8 week, a better repaired new-formed tissue gradually covered the P34HB film to form integral cartilage-like tissue. D. Conclusion In the study, the P34HB film was fabricated and the mechanical properties were characterized. The adipose-derived stem cells (ASCs) were seeded onto the films to evaluate their abilities of adhesion, and proliferation. It was found that cells seeded onto the films had better abilities of adhesion, and proliferation in vitro. Next the full thickness cartilage defects were created at the site of the femoropatellar groove of rat knee and the P34HB film scaffold were immediately implanted. After 8 weeks post-surgery, a new cartilage-like tissue was formed at the site of defects. By evaluation from histological staining to immunohistochemistry, a better integration between native tissues and scaffolds were confirmed. These results demonstrated that P34HB film scaffold has a great potential in the field of tissue engineering and may lead to better repair of cartilage defect.

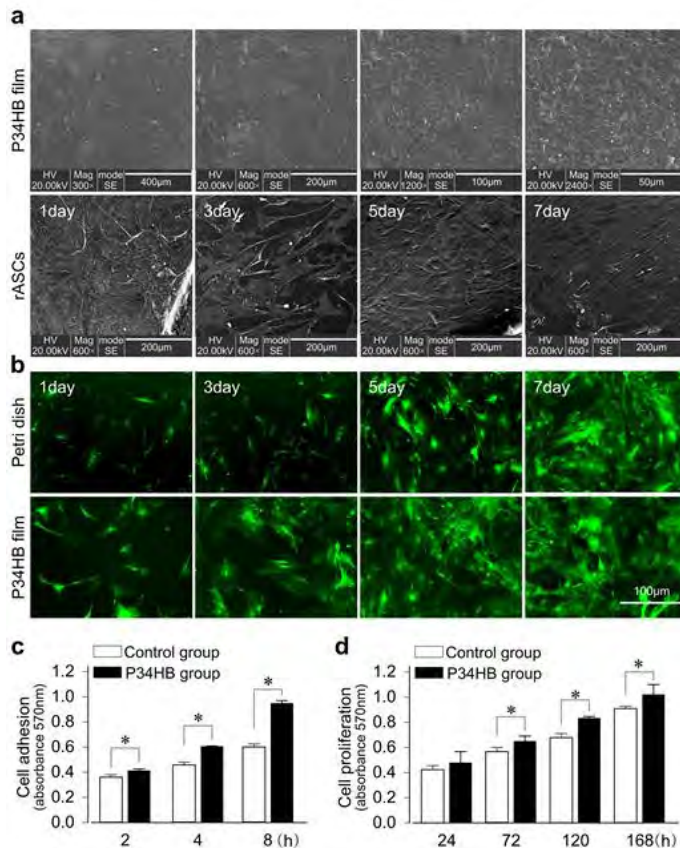


Figure.2



Figure.3

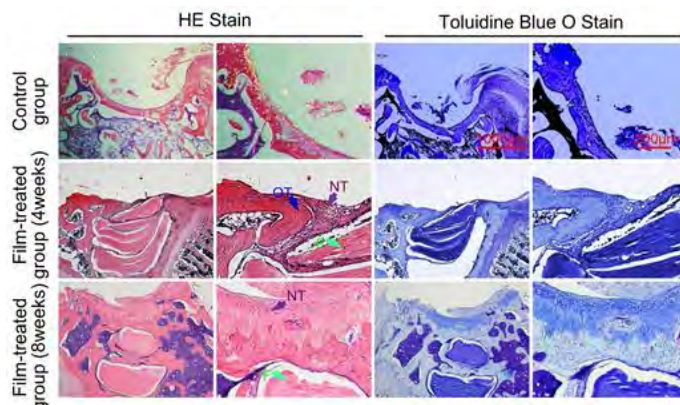


Figure.4

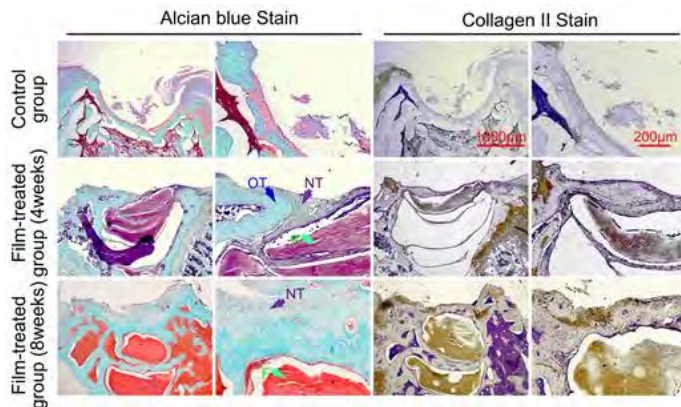


Figure.5

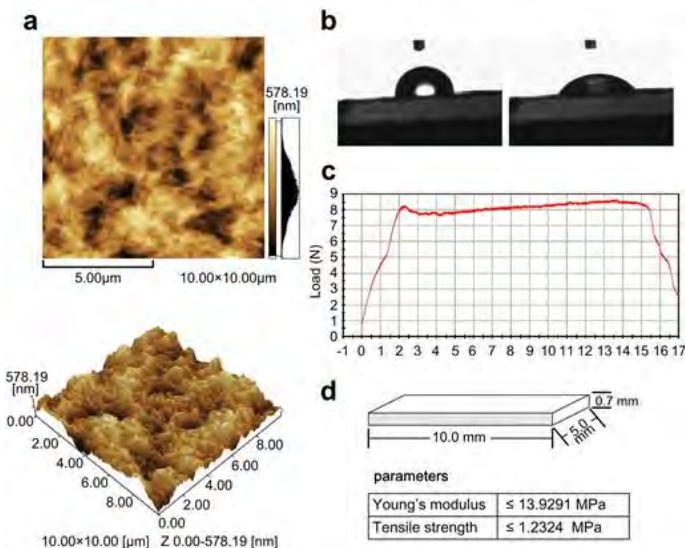


Figure.1

Disclosures: Na Fu, None.

MO0082

Protein Malnutrition affects cartilage quality and could contribute to osteoarthritis development. CEDRIC LAVET^{*1}, Patrick AMMANN². ¹Division of Bone Diseases, Switzerland, ²Division of Bone Diseases, Department of Internal Medicine Specialties, Geneva University Hospital & Faculty of Medicine., Switzerland

IGF-I is a major anabolic agent for cartilage homeostasis. Protein malnutrition results in major alteration of the somatotrophic axis as well as IGF-I local production and thus may contribute to osteoarthritis (OA) development. Such malnutrition could also be implicated in subchondral bone (SB) alterations described in early OA. We hypothesizes that protein malnutrition could alter cartilage metabolism and predispose to OA.

To address this question, 9 months old rats were pair fed a normal or an isocaloric low protein diet (LP, 2.5% casein) for 2 months (n=6/group). Contrast enhanced computed tomography (Hexabrix) of distal femur allowed to assess cortical and trabecular SB architecture, thickness of hyaline and calcified cartilage as well as an estimation of hyaline cartilage proteoglycan (PG) density. Since early OA is characterized by PG loss and collagen network disorganization which could alter cartilage biomechanical properties we set up a novel bio-indentation technique to assess hyaline cartilage material level properties. Indentation tests corresponding to 35-40% of hyaline cartilage thickness were performed with an accuracy of 8%.

Systemic IGF-I was 18% decreased in LP group (p<.001). Hyaline cartilage biomechanical properties (force, elastic modulus and working energy) were respectively decreased by 47, 58 and 41% (p<.01) in the medial condyle of the LP group as well as SB cortical thickness (-12%, p<.05). These parameters remained unaltered in the lateral condyle. Trabecular SB mass was 10% decreased (p<.01) in LP. Medial and lateral hyaline cartilage thicknesses tended to decrease by 8-10% but not significantly without alterations of PG density, thickness of calcified cartilage and SB cortical density in LP group.

We identified alteration of hyaline cartilage biomechanical properties and SB cortical thickening at the most frequently affected condyle in OA (ie. medial condyle) as well as trabecular SB deterioration with only mild alteration of hyaline and

calcified cartilage. Since these parameters have been documented in early OA, alteration of the somatotrophic axis by LP could predispose to OA. In the medial condyle, cortical SB alteration could alter pattern of joint loads distribution and initiate OA. However, crosstalk between modulated cellular activities in LP SB and cartilage and/or alteration of the cartilage collagen synthesis could also onset OA. Since protein malnutrition is frequent in elderly this mechanism could be relevant in human.

Disclosures: CEDRIC LAVET, None.

MO0083

Delayed bone fracture healing in mice due to the knockout of CaSR gene in chondrocytes. Zhiqiang Cheng^{*1}, Alfred Li², fuqing song², Hanson Ho², dolores shoback², Chia-ling Tu², wenhan chang². ¹University of California, San Francisco, USA, ²Department of Veterans Affairs Medical Center, NCIRE, University of California, San Francisco, CA, USA., USA

Bone fracture repair recapitulates key steps of endochondral bone formation. Studies of mice with extracellular calcium-sensing receptor (CaSR) gene knockout (KO) targeted specifically to chondrocytes confirmed non-redundant roles of the receptor in mediating terminal differentiation and mineralizing functions of chondrocyte, and growth delay in the mice. We now investigate the role of chondrocyte CaSR in modulating bone fracture healing by studying the repair of unfixed tibial mid-shaft fractures (created by 3-point bending) in 3-month-old Tamoxifen-inducible cartilage-specific CaSR KO (Tam-CartCaSR-KO) mice and control (Cont) littermates. Calluses were analyzed at day 10 and 28 post-fracture by histomorphometry and uCT. At day 10 post-fracture, the sizes of Tam-CartCaSR-KO calluses were significantly (p<0.05) increased by >54% when compared to Cont, as indicated by the increased tissue/callus volume (TV) by micro-computed tomography (uCT) analyses. Ablation of the CaSR gene in the cartilage of the Tam-CartCaSR-KO callus was confirmed after by genomic DNA analyses. Changes in callus size were accompanied by a 12% increase (p>0.05) in cartilage fraction (cartilage volume over TV, CV/TV) in the Tam-CartCaSR-KO calluses, as determined by von Kossa and Safranin O staining and histomorphometry. However, the ratio of mineralized cartilage volume (MCV) over CV (MCV/CV) was reduced by 38% (p<0.01) in Tam-CartCaSR-KO calluses vs Cont, indicating a delay in chondrocyte terminal differentiation and/or reduced mineralizing function. At day 28 post-fracture and in the osteogenic phase of fracture repair, TVs of Tam-CartCaSR-KO and Cont calluses were not different. However, the Tam-CartCaSR-KO calluses showed smaller bone fraction (BV/TV) by >13% (p<0.05) mainly due to decreased trabecular thickness by 21% (p<0.05) and lower bone mineral density (BMD) in the Tam-CartCaSR-KO calluses (p<0.05), as determined by histomorphometry and µCT, respectively. Our data indicate a critical role for the CaSR in promoting terminal differentiation of chondrocyte and subsequent osteogenic activity in the fracture calluses and present a novel molecular target for fracture repair.

Disclosures: Zhiqiang Cheng, None.

MO0084

Estrogen via Estrogen Receptor α Promotes Mandibular Condylar Chondrogenesis. Jennifer Robinson^{*1}, Jing Chen¹, Manshan Xu¹, Thomas Choi¹, Kenneth Korach², Helen H. Lu¹, Sunil Wadhwa¹. ¹Columbia University, USA, ²National Institutes of Health, USA

Purpose: Temporomandibular joint pain afflicts approximately 10% of the population. Of those affected, 30-50% experience degeneration-related diseases of the joint (TMJ-DD). Among TMJ-DD patients, the majority are women 44-65 years of age. These clinical statistics suggest the role of female sex hormones, namely loss of estrogen, in TMJ degeneration. The biological effects of estradiol are predominantly mediated by the nuclear estrogen receptors (ERs) ER α and ER β . Previously, we have illustrated the role of estrogen through ER β in inhibiting cell proliferation and estrogen independent of ER β in mediating mandibular condylar chondrogenesis. Thus, the role of estrogen through ER α on the condylar cartilage is necessary to determine the mechanism of estrogen signaling in TMJ growth and degeneration. This work details the phenotypic characterization of the condylar cartilage of 49-day old ER α KO mice.

Methods: Breeding pairs of heterozygous C57Bl/6 ER α KO +/- mice were obtained from Dr. Ken Korach. Genotyping utilizing PCR methods was done to identify homozygous female KO (n=6 for each analysis technique) and WT (n=6) mice for evaluation. Mice were euthanized at 49 days and condyles extracted for analysis. Sections were stained with hematoxylin/eosin to assess cell and matrix structure and Safranin O to observe glycosaminoglycan content. Histomorphometry was conducted to determine cartilage thickness and cell numbers. Cell proliferation was measured by BrdU labelling and quantification.

Results: No significant difference in cartilage thickness, cell numbers, or proliferation was found in the ER α KO mice compared to age-matched WT controls. A significant decrease in Safranin O-positive matrix thickness was observed in the ER α KO condylar cartilage compared to WT.

Conclusions: We have previously found that estradiol treatment caused increased chondrogenesis in both WT and ER β KO mice. In this study, despite having reported increased endogenous estradiol levels, the ER α KO mice had decreased Safranin O staining compared to age- and gender-matched WT mice. Together these results

suggest a role of ER α in mediating mandibular condylar chondrogenesis warranting further investigation.

Disclosures: Jennifer Robinson, None.

MO0085

Halofuginone Attenuates Osteoarthritis by Inhibition of TGF- β activity and H-type Vessel Formation in Subchondral Bone. Zhuang Cui^{*1}, Janet Crane¹, Hui Xie¹, Xin Jin¹, Gehua Zhen¹, Changjun Li¹, Liang Xie¹, Long Wang¹, Qin Bian¹, Tao Qiu¹, Mei Wan¹, Sheng Ding², Bin Yu³, Xu Cao¹. ¹Johns Hopkins University School of Medicine, USA, ²University of California, San Francisco, USA, ³Nanfeng Hospital, Southern Medical University, China

Osteoarthritis (OA) is the most common degenerative joint disease and major cause of physical disability. Abnormal vascular congestion in subchondral bone has long been recognized as a pathologic feature of OA. A specific subtype of vessels, termed H-type vessels as defined by high co-staining for CD31 and endomucin (CD31hiEmcnhi), have been identified in the murine skeletal system to couple angiogenesis and osteogenesis. Our recent study demonstrated that the formation of subchondral bone "osteoid islet" induced by aberrant TGF- β signaling promotes OA development. In the present study, we investigated whether the increased vessels along with "osteoid islet" during the onset of OA were H-type vessels; and whether a small molecule isolated from ancient Chinese herb Chang Shan, halofuginone (HF), could attenuate OA development by inhibition of TGF- β signaling and the formation of H-type vessels. We found that HF, delivered either systemically or locally, effectively attenuates OA progression in an anterior cruciate ligament transaction (ACLT) rodent model. HF protected articular cartilage from degeneration by normalizing subchondral bone microarchitecture and prevented proteoglycan loss and calcification of articular cartilage relative to vehicle-treated ACLT control mice. HF reduced levels of collagen X and matrix metalloproteinase-13, increased expression of lubricin and resulted in substantially lower OARSI scores for cartilage degradation. In parallel, HF normalized subchondral bone microarchitecture defined by reduced subchondral bone tissue volume (TV), lower trabecular pattern factor (Tb.pf) and increased thickness of subchondral bone plate (SBP) relative to vehicle-treated ACLT controls. Furthermore, we found the underlying molecular mechanisms for the protective effect of HF on the articular cartilage rely on the inhibition of TGF- β signaling by reducing the Th17-induced TGF- β release and directly suppressing TGF- β -dependent Smad2/3 signaling in MSC/osteoprogenitor cells, as well as the attenuation of H-type vessel formation along the "osteoid islet" in subchondral bone. Therefore, halofuginone attenuates OA progression and is a potential therapeutic agent for OA.

Disclosures: Zhuang Cui, None.

MO0086

A bioactive perlecan/HSPG2 IV-3 subdomain promotes chondrocyte condensation. Jerahme Martinez^{*}, Mary C. Farach-Carson, Brian Grindel, Jose Olmos. Rice University, USA

Perlecan/HSPG2, a large heparan sulfate proteoglycan (HSPG), is instrumental in the development and maintenance of musculoskeletal tissue including cartilage and bone. Perlecan is deposited within the pericellular matrix (PCM) of chondrocytes and turns over at the chondro-osseous junction (COJ) of developing long bones. A reduction in perlecan secretion is associated with chondrodysplasia with widespread musculoskeletal and joint defects, including the disruption of epiphyseal cartilage and bone. This work sought to elucidate novel signaling roles of perlecan and to identify cell surface receptors that initiate perlecan signaling during development. To examine the core protein of perlecan exclusively, we produced purified recombinant fragments of perlecan and tested bioactivity in a chondrogenic cell line, ATDC5. Our findings showed that a subfragment (IV-3) within domain IV of perlecan has anti-adhesive properties and promotes cell-cell adhesion and chondrocyte clustering. Furthermore, the perlecan induced cell cluster phenotype is significantly enhanced when domain IV-3 is partially unfolded by mild heating into an intermediate conformation. We tested a mutant IV-3 fragment, harboring a single residue change that is associated with the human skeletal disorder Schwartz-Jampel syndrome, and found that cell clustering activity was reduced. Through solid phase binding assays we found that perlecan domain IV-3 binds to various cell adhesion molecules (CAMs) expressed by cartilage and bone cells. We believe the ectodomains of these CAMs serve as binding partners of perlecan and initiate signal transduction associated with chondrocyte clustering. Preliminary results indicate that both FAK and Src activation are involved in the perlecan IV-3 induced phenotype. Together, these results point to a key role for perlecan in chondrocyte condensation in the developing growth plate, which is disrupted in certain chondrodysplasias.

Disclosures: Jerahme Martinez, None.

MO0087

Regulation of Chondrocyte Differentiation by miR-483. Britta Anderson^{*}, Audrey McAlinden. Washington University in St. Louis, Department of Orthopaedic Surgery, USA

Purpose: MicroRNAs (miRNAs) are important regulators of diverse cellular processes and regulate multiple genes simultaneously, typically resulting in destabilization of target mRNAs and suppression of protein synthesis. To gain insight into miRNA-mediated regulation during chondrogenesis, we recently described miRNA expression patterns in precursor, differentiated, and hypertrophic chondrocytes during human embryonic cartilage development. Among those differentially-expressed miRNAs, we discovered miR-483 to be more highly expressed in precursor and differentiated chondrocytes. We hypothesize a potential pro-chondrogenic role for miR-483. To address this, we aim to determine the effects of miR-483 on stem cell chondrogenic differentiation and whether co-regulation with its host gene, IGF2, is important.

Methods: Human bone marrow mesenchymal stem cells (BM-MSCs - Lonza) were transduced with lentivirus overexpressing miR-483 or a non-silencing (NS) control miRNA. BM-MSCs (passage 3) were seeded in Transwell inserts and cultured as three-dimensional discs for 28 days in chondrogenic medium containing 10 ng/mL TGF- β 3. RNA from two discs was pooled at each time point for gene expression analysis by TaqMan miRNA assay, SYBR Green qRT-PCR, or TaqMan gene expression quantitative RT-PCR arrays (Life Technologies).

Results: During BM-MSC chondrogenesis, miR-483-5p and miR-483-3p increase as differentiation proceeds and are upregulated approximately 30-fold by day 14. A similar trend was observed for IGF2 (~100-fold increase by day 14). Stable overexpression of miR-483 did not affect IGF2 expression during differentiation, but it did result in increased chondrogenic gene expression compared to NS control cultures. Examination of several signaling pathways known to regulate chondrogenesis revealed increased TGF β 3 and IGF1 mRNA levels and upregulation of the Wnt antagonists DKK2, SFRP1, and SFRP2, as well as the Wnt pathway transcriptional mediator LEM1 at day 4 of differentiation.

Conclusions: miR-483 promotes chondrogenesis in the BM-MSC model of differentiation, possibly by exaggerating responses to the pro-chondrogenic growth factors TGF- β 3 and IGF1 and/or by altering Wnt signaling. miR-483 does not appear to participate in a feedback loop with its host gene, IGF2 in this system. Further studies will decipher the apparent pro-anabolic effects of miR-483 in chondroprogenitor cells as well as in primary human chondrocytes.

Disclosures: Britta Anderson, None.

MO0088

Bone density and strength are significantly compromised in the db/db mouse model of diabetes. Rana Samadfam^{*1}, Erik C. Rocheford², Joe Cornicelli², Gabrielle Boyd¹, Susan Y. Smith¹. ¹Charles River Laboratories, Canada, ²Charles River Laboratories, USA

Cardiovascular disease, renal impairment, neuropathy, inflammation, ocular changes and impaired wound healing are well recognized complications of diabetes, sometimes even in the presence of reasonably well-controlled blood glucose. Recently osteoporosis and increased fracture risk have also been added to this long list. To complicate matters, some therapies that provide good glycemic control have adverse effects on the skeletal system, further compromising already fragile bones in diabetic patients.

db/db mice are commonly used for diabetes research. The goal of this work was to first investigate the skeletal integrity of this model. In addition, as PPAR gamma agonists reportedly decreases bone mass, our other objective was to assess the effects of pioglitazone (PIO) on bone density and strength in a disease model. The diabetes status in db/db mice were characterized by fasted glucose levels and by oral glucose tolerance test (OGTT). Body weight and soft tissue composition were performed prior to necropsy. At necropsy, bones were collected from db/db mice following 1 month of treatment. Wild type littermates (same age group) were used as controls. Collected femurs were scanned using pQCT and BMC, BMD and bone geometry parameters were obtained at the metaphysis and diaphysis sites. Femur bone strength was measured using three point bending. Marked increases in body weight were noted for db/db mice compared to controls. These increases were for the most part attributed to marked increases in fat tissue. Marked increases in OGTT and glucose levels were noted for db/db mice compared to controls, confirming the diabetic status of the db/db mice. The bone evaluations revealed that db/db mice have smaller bones with lower bone density and reduced bone strength compared to wild type controls. Pioglitazone slightly increased the body weight associated with slight increases in fat. Pioglitazone treatment partially corrected the changes in OGTT and glucose levels and showed no effect on bone density or bone strength in this model. The bone density and bone strength data from db/db mice were in line with the reported data in clinic for diabetic patients. In addition, the lack of effect on bone for PIO highlights the importance of the model selection in safety studies to monitor for diabetic complications.

Disclosures: Rana Samadfam, None.

MO0089

Disruption of Glucocorticoid Signaling in Osteoblasts Prevents Diet-induced Obesity and Metabolic Dysregulation. Sarah Kim^{*1}, Holger Henneicke², Sylvia Gasparini², Lee Thai², Markus Seibel³, Hong Zhou². ¹ANZAC Research Institute, Australia, ²Bone Research Program, ANZAC Research Institute, The University of Sydney, Australia, ³Department of Endocrinology & Metabolism, Concord Hospital, The University of Sydney, Australia

Hypercaloric diets are causally associated with obesity and diabetes. Increased glucocorticoid action has been described as a central feature of metabolic dysregulation. Since osteoblasts are involved in the regulation of overall energy balance, this study aims to examine the contribution of glucocorticoid action in osteoblasts to whole-body energy metabolism during high-calorie feeding.

To this end, we utilized a transgenic (tg) mouse model in which glucocorticoid signaling has been selectively disrupted in osteoblasts and osteocytes via targeted overexpression of the glucocorticoid-inactivating enzyme, 11 β -hydroxysteroid dehydrogenase type 2. Seven-week-old male tg mice and their wild type (WT) littermates (n=6-15/group) were fed *ad libitum* a control diet (13.8kJ/g total energy (TE), 14% TE as fat, 26% TE as protein) or a high-calorie, high-fat (HC-HF) diet (16.3kJ/g TE, 43% TE as fat, 26% TE as protein) for 18 weeks. To delineate the effects of high caloric intake and high fat intake, a high-calorie, normal-fat (HC-NF) diet group was also included (16.3kJ/g TE, 14% TE as fat, 26% TE as protein). Body weight and composition, insulin sensitivity and glucose tolerance, as well as serum osteocalcin (OCN) levels were measured.

High-calorie feeding, regardless of dietary fat composition resulted in significantly increased fat mass in WT mice compared to mice fed the control diet (HC-NF: +88%, p<0.01, HC-HF: +73%, p<0.01, Fig 1A). Furthermore, WT mice fed either high-calorie diet exhibited elevated fasting glucose levels and reduced insulin sensitivity, with HC-HF mice displaying pronounced insulin resistance (Fig 1B). Correspondingly, WT mice fed the HC-HF diet showed marked glucose intolerance (Fig 1D). Interestingly, tg mice on high-calorie diets were not only protected from excessive fat accrual (HC-NF: +5%, HC-HF: +35%, Fig 1A) but also revealed healthy insulin sensitivity and glucose tolerance (Fig 1C&E). While serum OCN levels were reduced in WT HC-NF mice relative to WT control mice, they remained unchanged in WT HC-HF, despite marked obesity and glucose intolerance. Moreover, there was no difference in OCN levels of tg mice on either diet.

We conclude that glucocorticoid signaling in osteoblasts and osteocytes plays a central role in the pathogenesis of diet-induced obesity and impaired glucose tolerance through an OCN-independent mechanism.

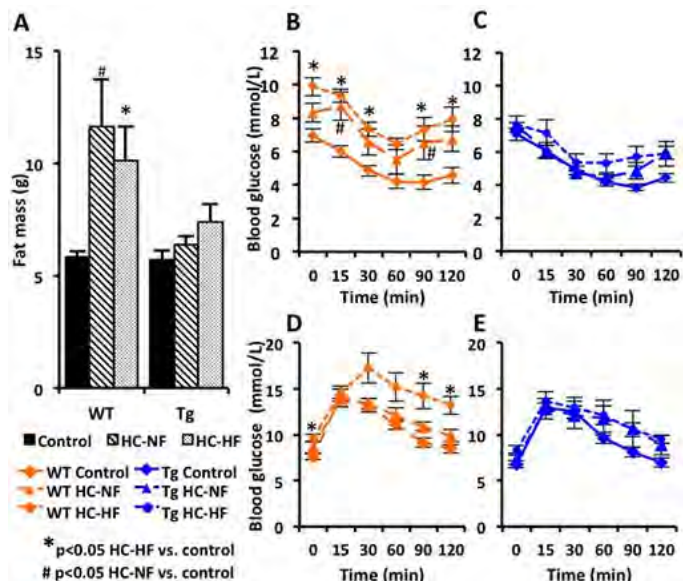


Figure 1

Disclosures: Sarah Kim, None.

MO0090

Effect of Hydrogenated Coconut Oil High Fat Diet on Bone Mass in Streptozotocin-induced Type 1 Diabetic Mice. Adriana Carvalho^{*1}, Katherine Motyl², Francisco De Paula¹, Clifford Rosen². ¹University of Sao Paulo, Brazil, ²Maine Medical Center Research Institute (MMCRI), USA

Bone loss is a well described feature of type 1 diabetes mellitus (T1DM) and bone marrow adipose tissue (BMAT) has been investigated as a biomarker of bone health may play a key role. We hypothesized that nutritional status has a major protective

effect on T1DM bone mass. This study aims to evaluate the effect of high-fat diet (HFD) on bone mass and BMAT in streptozotocin (STZ)-induced T1DM mice. Eight week-old male C57BL/6J mice were submitted to a 5-day STZ (50mg/kg) or vehicle IP injections (0.1M citrate buffer pH 4.5). Mice were considered diabetic when glucose levels were > 300 mg/dL. Mice were then fed with HFD (58% kcal from fat: hydrogenated coconut oil) or low-fat diet (LFD) (11% kcal from fat) for 6 weeks after diabetes confirmation. Mice were placed in 4 different groups: STZ-HFD group (n=10), STZ-LFD group (n=8), Vehicle-HFD group (n=7), and Vehicle-LFD (n=7). Bone mass was measured by DXA (baseline, 2 weeks after baseline, and endpoint) and also by micro-computed tomography (μ CT) at endpoint. Energy expenditure (EE), food and water consumption were also measured at the end of the study. There were no differences in BMD or body composition between groups at baseline (p>0.05). STZ mice exhibited a significant fat mass loss 2 weeks after baseline (p<0.05) but there was no change in BMD (p>0.05) at this time point. STZ-HFD mice tended to have less weight loss when compared to STZ-LFD group. At the endpoint, all STZ mice presented with a significantly lower femur BMD regardless of the diet treatment. However, non-fasting glucose levels in STZ-HFD mice were lower than STZ-LFD (447 \pm 36 vs >600 mg/dL, respectively). Yet, STZ-HFD mice exhibited a lower EE when compared to STZ-LFD and Vehicle-HFD. STZ-LFD mice had marked diabetic symptoms such as polydipsia, polyphagia, and ketoacidosis condition (respiratory quotient = 0.61) and these symptoms were ameliorated in STZ-HFD mice. Our preliminary μ CT data showed a lower BV/TV in both STZ groups but also that STZ-HFD (n=3) tended to have higher BV/TV and Tb.N and a lower Tb.Sp compared to STZ-LFD (n=3) mice. Thus, although coconut oil HFD did not have an effect on diabetic BMD, preliminary μ CT indicates that it did shield against trabecular bone loss. Ongoing studies are investigating the role of HFD and nutritional status in bone marrow adipose tissue in this diabetes mouse model.

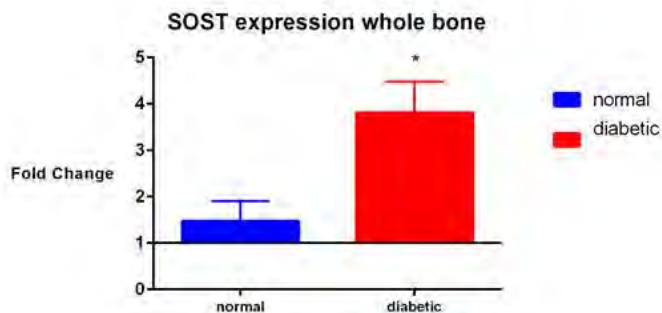
Disclosures: Adriana Carvalho, None.

MO0091

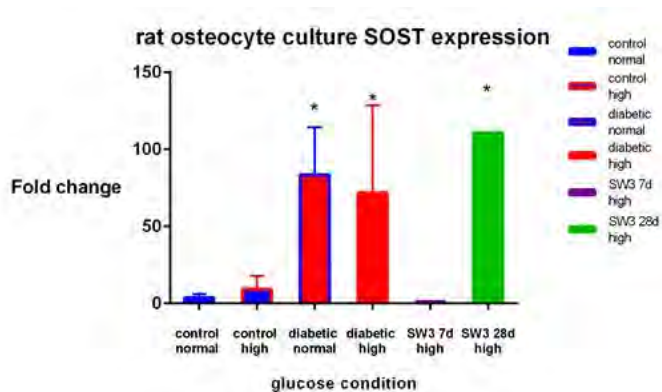
Glucose Fluctuations in Diabetes Have Targeted Effects on the Osteocyte *In Vitro* and *In Vivo*. Donna Pacicca^{*1}, Tammy Brown¹, Josh Wirtz¹, Karen Kover¹, Yun Yan¹, Dara Watkins¹, Pei Tong¹, Lynda Bonewald². ¹Children's Mercy Hospital, USA, ²University of Missouri - Kansas City, USA

Diabetic patients have increased fracture risk, but the effect of glucose fluctuation on bone cells has not been well-studied. We have previously shown few effects of high and low glucose on osteoblast function, but dramatic effects on sclerostin production in osteocytes. In this study we compared these *in vitro* data with *in vivo* results using the streptozotocin (STZ)-induced diabetic rat model. We hypothesized that elevated glucose and increased glucose variation would result in increased SOST/sclerostin expression in osteocytes and increased circulating serum sclerostin. Male Sprague-Dawley rats were divided into diabetic (n=8) and control groups (n=8). Diabetic animals were given one dose of STZ (70 mg/kg), resulting in elevated blood glucose within 2 days and were subsequently treated with insulin via osmotic pumps. We recorded blood glucose measurements. At 8 weeks, serum samples were taken and long bones harvested for qPCR and osteocyte isolation. Isolated rat osteocytes were cultured under 5.5mM and 25mM glucose conditions. SOST qPCR was performed on whole bone and cultured osteocytes. Sclerostin protein ELISA was performed on serum samples and culture media.

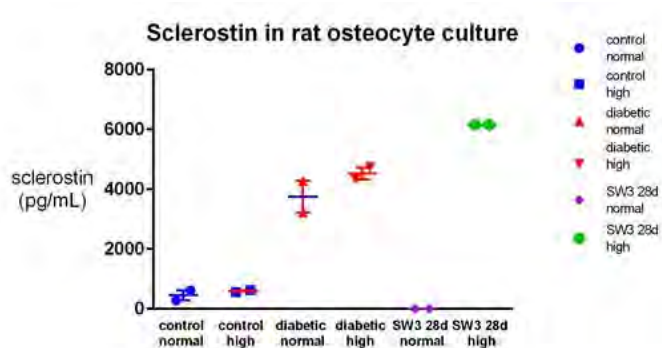
Glucose variability and maximum glucose were significantly increased in the diabetic vs. control animals (670/796 vs. 102/142 mg/dL). Relative SOST expression was increased 4 fold in the long bones of diabetic animals, with no difference in osteocalcin. SOST and sclerostin were elevated in cultured osteocytes from diabetic animals compared to normal regardless of whether cultured in normal or high glucose. These levels (60+ fold increase) were comparable to response of the IDG-SW3 osteocyte cell to high glucose. However, serum sclerostin from the rats was decreased in diabetics (300 pg/ml vs. 450 pg/ml controls). Diabetic rats express higher levels of SOST in bone, correlating with both high glucose levels and increased variability. Cultured osteocytes from diabetic animals continue to express higher levels of SOST and sclerostin in culture even under normal glucose, showing retention of the *in vivo* phenotype. Despite this, the diabetic animals have lower serum sclerostin, which may reflect retention of sclerostin in bone matrix. These data suggest that high glucose and glucose variability have a detrimental effect on bone through a dramatic increase in sclerostin production by osteocytes. Local elevation in sclerostin may be responsible for increased fractures in diabetics.



SOST expression whole bone



SOST expression in rat osteocyte culture



Sclerostin expression in rat osteocyte culture

Disclosures: Donna Pacicca, None.

MO0092

Metformin Increases Bone Mass, Reduces Adipocyte Size and Significantly Changes Circulating Metabolites in B6 Mice Only During States of Energy Excess. [Michaela Reagan](#)¹, [Michele Moschetta](#)², [Yawara Kawano](#)², [Mark Horowitz](#)³, [Karla Salem](#)², [Mary Bouxsein](#)⁴, [Daisy Huynh](#)², [Juliette Bouyssou](#)², [Aldo Roccaro](#)², [Clifford Rosen](#)⁵, [Irene Ghobrial](#)². ¹Dana-Farber Cancer Institute/ Harvard Medical School, Us, ²Dana-Farber Cancer Institute, USA, ³Yale University, USA, ⁴Beth Israel Deaconess Medical Center, USA, ⁵Maine Medical Center Research Institute, USA

Patients with type 2 diabetes mellitus (T2DM) have an increased risk of fracture, despite normal BMD. Factors contributing to increased fracture risk in T2DM are not well understood. Metformin (*met*) is the most frequently prescribed treatment for T2DM. In retrospective studies of T2DM patients, *met* has variable effects on BMD and a very modest reduction in fractures. However, its effects on bone mass and adipocytes are not well defined, and differential effects of *met* in obese vs normal weight patients are unknown. We hypothesized that *met* would have both local and systemic actions that positively affect bone mass in obese, pre-diabetic mice. Hence we performed an analysis of diet by drug interactions in female B6 mice. Female B6 mice fed a high fat diet (HFD:60% fat) or low fat diet (LFD:4% fat) for 16 weeks were then administered *met* (300 mg/kg per day in drinking water) or no *met*, for 6.5 weeks. Bone structure was measured by μ CT, circulating metabolomics by LC-MS, inguinal (iWAT) and visceral adipocyte (VAT) size by histology, and marrow adiposity by

histology and osmium μ CT. HFD alone had no effect on trabecular or cortical bone, but HFD mice with *met* had higher trabecular BV/TV, greater trabecular thickness and lower SMI than LFD+*met* (drug x diet interaction, $p=0.02$). Cortical thickness and BV/TV were higher in HFD+ *met* mice vs LFD+*met* mice ($p<0.05$). *Met* significantly improved glucose uptake ($p=0.04$) in the HFD group. Although *met* had no significant effect on weight, it significantly reduced marrow adiposity in the HFD+*met* vs HFD groups ($p=0.01$). Adipocyte size was significantly greater in HFD vs LFD mice in VAT and iWAT, and HFD vs HFD+*met* in iWAT but not VAT ($p=0.0036$). Many metabolites were significantly different between groups. Interestingly, a HFD, independent of *met*, induced a profound suppression in serum shikimate, a metabolite only produced by gut microbiome. *Met* significantly suppressed the microbial metabolite citraconic acid, but only in HFDs. Serine, associated with glycolysis, and 3 other metabolites were increased in HFD, independent of metformin. In summary, *met*'s positive effects on bone may depend on the degree of substrate availability (e.g. fatty acids). Drug and diet-induced changes in the gut microbiome, quantified with sequencing, may also impact bone mass and contribute to the skeletal effects of *met* in T2D. In conclusion, effects of *met* on bone and other tissues may be different in obese vs normal weight individuals.

Disclosures: Michaela Reagan, None.

MO0093

Arachidonic Acid Reduces Bone Mass Without Influencing Visceral Adiposity in Growing Obese Rats. [Ivy Mak](#)^{*}, [Krystyna Wang](#), [Paula Lavery](#), [Sherry Agellon](#), [Hope Weiler](#). McGill University, Canada

Visceral (VAT) and subcutaneous (SAT) adipose tissues exert differential effects on bone density. Long-chain polyunsaturated fatty acids such as arachidonic acid (AA, C20:4 n6) modulate bone mass and adiposity. AA is elevated in obesity and fatty marrow; whether AA status affects the two fat compartments and bone growth in obrogenic states is not clear. This study aims to determine the effect of AA on bone and adipose mass acquisition in diet-induced obesity during growth. Male Sprague-Dawley rats $n=42$, 4 wk, 89.8 ± 1.1 g) were randomized to one of the following diets: CTRL, high-fat (HFD, 16.7% fat w/w), HFD + AA (1% w/w) for 6 wk. Body composition and bone mass were measured by *in vivo* micro-computed tomography (μ CT, Aloka LCT-200) at baseline and end-point. VAT and SAT were quantified from CT scans of the abdominal region (L3–5). Fatty acid composition was measured in red blood cells (RBC) using gas chromatography. Group differences were tested by repeated-measures 2-way ANOVA with post-hoc Tukey's HSD and relationships assessed by a general linear model. No differences in body weight, bone parameters, body composition or RBC fatty acids were observed at baseline. High fat feeding led to 28-45% lower RBC α -linolenic acid (ALA, C18:3 n3) incorporation; whereas reductions in linoleic acid (LA, C18:2 n6, -38%), eicosapentaenoic acid (EPA, C20:5 n3, -70%) and docosahexaenoic acid (DHA, C22:6 n3, -70%) was observed in HFD + AA only. HFD + AA had significantly lower bone mineral content of the whole body and L2-4, along with lower lumbar bone volume relative to HFD and CTRL (Table 1). Despite greater % total fat and body weight gain in HFD + AA ($504 \pm 12\%$) vs HFD ($495 \pm 13\%$) and CTRL ($484 \pm 11\%$), addition of AA in the diet did not lead to greater gains in abdominal fat mass, VAT or % VAT than high-fat feeding alone (Table 2). In addition, RBC ALA status negatively related to total abdominal fat mass ($\beta=-85.3 \pm 35.5$, $p=0.02$) and % VAT ($\beta=-45.1 \pm 21.1$, $p=0.04$), while an inverse relationship between LA and % VAT ($\beta=0.5 \pm 0.3$, $p=0.04$) was observed. RBC AA, EPA and DHA were not related with abdominal adiposity. These results suggest potential adverse effects of elevated AA status on bone in obese states is independent of the influence on regional fat distribution, and could be mediated indirectly through influencing the balance of other fatty acids that share common metabolic pathways.

Table 1. Whole-body and LS bone mass after 6 wk of diet intervention (10 wk of age)

| | CTRL | HFD | HFD + AA |
|---------------------------|--------------------------------|-------------------------------|-------------------------------|
| Whole body | | | |
| Total BMC (mg) | 6828.95 ± 101.80 ^{ab} | 6819.38 ± 101.80 ^a | 6671.70 ± 105.64 ^b |
| Trab BMC (mg) | 2151.83 ± 49.05 ^{ab} | 2201.17 ± 49.05 ^a | 2118.49 ± 50.90 ^b |
| Lumbar spine 2-4 | | | |
| Total BMC (mg) | 331.38 ± 7.13 ^{ab} | 336.58 ± 7.58 ^a | 308.55 ± 7.89 ^b |
| Volume (cm ³) | 0.84 ± 0.02 ^a | 0.83 ± 0.02 ^{ab} | 0.77 ± 0.02 ^b |
| vBMD (g/cm ³) | 394.34 ± 6.84 | 411.58 ± 7.31 | 407.11 ± 7.10 |
| Trab BMC (mg) | 140.33 ± 4.97 ^{ab} | 144.86 ± 5.31 ^a | 124.25 ± 5.36 ^b |
| Volume (cm ³) | 0.43 ± 0.01 ^a | 0.42 ± 0.01 ^{ab} | 0.39 ± 0.01 ^b |
| vBMD (g/cm ³) | 331.76 ± 5.23 | 344.26 ± 5.54 | 331.92 ± 5.51 |

Mean ± SE. Within rows different superscripts indicates, p < 0.05, n=42.

Table 2. Whole-body and abdominal fat mass after 6 wk of diet intervention (10 wk of age)

| | CTRL | HFD | HFD + AA |
|--------------------|--------------------------|--------------------------|-------------------------|
| Whole body | | | |
| % total fat | 29.0 ± 0.9 ^a | 31.1 ± 0.8 ^{ab} | 32.0 ± 0.9 ^b |
| Abdominal (L3 – 5) | | | |
| Fat mass (g) | 26.5 ± 1.7 ^{ab} | 30.0 ± 1.7 ^{ab} | 30.5 ± 1.8 ^b |
| VAT (g) | 21.6 ± 1.3 ^a | 24.8 ± 1.3 ^b | 24.8 ± 1.3 ^b |
| % VAT ¹ | 31.0 ± 1.0 ^a | 33.7 ± 1.0 ^b | 33.3 ± 1.0 ^b |

¹ %VAT = VAT (g) / abdominal lean + fat mass (g)

Mean ± SE. Within rows different superscripts indicates, p < 0.05, n=42.

MO0095

Exercise diminishes obesity-associated Marrow Fat as quantified by Magnetic Resonance Imaging (MRI). Maya Styner¹, Martin Styner², Gabriel Pagnotti³, Xin Wu⁴, Buer Sen⁴, Gunes Uzer⁵, Zhihui Xie⁴, Mark Horowitz⁶, Clinton Rubin³, Janet Rubin⁴. ¹University of North Carolina, Chapel Hill, School of Medicine, USA, ²Departments of Computer Science & Psychiatry, University of North Carolina at Chapel Hill, USA, ³Department of Biomedical Engineering, State University of New York, Stony Brook, NY, USA, ⁴Department of Medicine, University of North Carolina at Chapel Hill, USA, ⁵University of North Carolina at Chapel Hill, USA, ⁶Department of Orthopedics & Rehabilitation, Yale University, New Haven, CT, USA

The effect of marrow adipose tissue (MAT) on bone remains poorly understood. Using a μ CT measure of osmium to visualize and quantify MAT, we found that 6 wk of high fat diet (HFD) increased MAT prior to attaining obesity. Here we asked whether MAT would respond to running exercise in the setting of diet-induced obesity (DIO). 4-wk old female C57BL/6 mice were fed low fat diet (LFD) or HFD. After 12 wk, mice were divided into control (LFD, DIO) or exercise groups (LFD-E, DIO-E) with voluntary running wheels (n=7/group). Running distances were equivalent in LFD and DIO mice. After 3 wks running, total body fat mass was double in DIO compared to DIO-E (p<0.05). Lean mass was also higher in DIO vs. LFD (p<0.01). Respiratory quotients were lower in DIO (p<0.01) suggesting use of fat energy. After 6 wks running, mice were significantly heavier in DIO vs LFD (p<0.001). Femoral MAT (osmium- μ CT) and μ CT tibial bone quantity were assessed^{1,2}. To increase reproducibility and prepare for future *in-vivo* studies, femoral MAT was also assessed via 9.4 Tesla MR resulting in fat and water intensity normalized image maps. Total femur MAT (osmium volume/femoral volume) was 6.2 ± 2.8 in LFD, 4.7 ± 2.1 in LFD-E, 9.0 ± 4.2 in DIO and 4.7 ± 2.9 in DIO-E (p<0.05 for an exercise). MAT quantified by MRI (fat signal/femoral volume) was 2.5 ± 1.1 in LFD, 1.2 ± 0.8 in LFD-E, 3.3 ± 1.5 in DIO and 0.5 ± 0.4 in DIO-E (p<0.001 for exercise, p<0.01 for DIO vs. DIO-E). Pearson correlation coefficient showed an appropriate correlation of MAT quantification between osmium- μ CT and MRI of 0.65 (95% CI 0.31-0.84, p-value=0.0012). Obese mice had similar relative amount of MAT to the controls, likely due to increased femoral volume in DIO (14% higher in DIO compared to LFD, p<0.01). Trabecular BV/TV increased with exercise by 20% in both LFD and DIO groups, p<0.001. DIO did not affect BV/TV or cortical parameters. In conclusion, MAT normalized to femoral volume as assessed by either osmium- μ CT or MRI was significantly attenuated by exercise in obese mice as well as mice on LFD. Both measures are relativized to bone volume, which as DIO mice have increased femoral volume, shows MAT is increased in DIO. In summary, diet and exercise effect on bone quantity and marrow fat are maintained in the setting of obesity. In addition, we present a quantitative MRI image tool, which should allow longitudinal study of MAT during behavioral, pharmacologic and genetic modification.

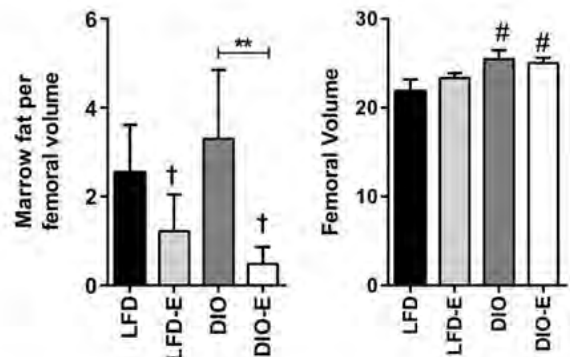


Figure 1. Volumetric MRI fat quantification normalized to total femoral volume. Obese or lean C57BL/6 +/- exercise for 6 weeks. # Denotes a significant effect due to diet by 2-way ANOVA. † Denotes a significant effect due to exercise by 2-way ANOVA.

Figure 1

Disclosures: Maya Styner, None.

MO0096

High fat diet mediated inflammation contributes to the development of osteoarthritis: Role of the innate immune system. Evangelia Kalaitzoglou¹, MaryBeth Humphrey², Jacquelyn Herron². ¹University of Kentucky, Us, ²OHSU, USA

Obesity increases the risk of developing osteoarthritis (OA) in weight-bearing and non-weight-bearing joints suggesting that both mechanical and non-mechanical factors associated with obesity increase the risk of OA. Abnormal innate immune responses in obesity, mediated via free fatty acid (FFA) activation of Toll-Like

Tables

Disclosures: Ivy Mak, None.

MO0094

Bone Marrow Adipose Tissue (BMAT) in Short Bowel Syndrome (SBS).

Francisco Jose De Paula^{*1}, Luciana Parreiras-e-Silva², Jessica Bonella², Iana Araújo², Carlos Salmon³, Júlio Marchini², Vivian Suen², Marcello Nogueira-Barbosa², Jorge Elias Jr.². ¹School of Medicine of Ribeirão Preto - USP, Brazil, ²Ribeirão Preto Medical School, USP, Brazil, ³Faculty of Philosophy, Sciences & Arts of Ribeirão Preto, USP, Brazil

Introduction: The SBS is a complex disease marked by severe impairment in nutrient absorption consequent to extensive bowel resection. The initial hallmark of this disease is loss of gut function leading to malnutrition. No previous study evaluated the role of adipose tissue distribution, particularly BMAT, in bone mass of patients with SBS.

Objective: Investigate the influence of BMAT, visceral adipose tissue (VAT) and intrahepatic lipids (IHL) in bone mass in SBS.

Material and Methods: The study comprised 12 controls (8M and 4F) and 13 patients with SBS (7M and 6F). Nuclear magnetic resonance (NMR) was used to assess BMAT in L3 (1H spectroscopy), VAT and IHL. We also assessed biochemical parameters in serum: calcium, phosphorus, alkaline phosphatase (AP), 25-OHD, PTH and IGF-1.

Results: The mean time of SBS diagnosis was 5.8±3.0 years. There was no difference between the groups in age (C=57±11 vs SBS=55.4±12 years), height, weight (C=65±6.7 vs SBS=56.5±14.7 Kg) and BMI (C=24±1.6 vs SBS=21±5 Kg/m²). Unexpectedly, only 30.7% of the SBS group was underweight, while 46.1% had normal IMC and 23.2% were overweight. The SBS group showed serum levels of albumin (C=4.4±0.2 vs SBS=3.7±0.6 g/dL;p<0.005) and calcium (C=9.8±0.4 vs SBS=9±0.7 mg/dL;p<0.01) lower and AP (C=180±50 vs SBS=313±137 U/L;p<0.01) higher than the C group. The T-score in 1/3 radius (C=-1.4±1.3 vs SBS=-2.2±0.7) and in total hip (C=0.8±0.8 vs SBS=-1.7±1.3) were lower in SBS group;p<0.05. There was no difference in BMAT between groups (C=34.6±10.8 vs SBS=36.8±12.1%). It should be highlighted that the patient with lowest BMI (10.2 Kg/m²) also had the lowest BMAT (19.1%). The amount of fat in the subcutaneous (C=21,382±6,004 vs SBS=7,104±4,210 mm²) and VAT (C=8,646±4,226 vs SBS=3,197±2,678 mm²) was lower in SBS group; p<0.05, whereas the IHL (C=3.2±2.6 vs SBS=13±11%; p<0.05) was higher in SBS group. BMD of total hip was positively correlated with body weight in SBS group (r=0.59;p<0.05). There was no correlation between lumbar spine BMD and BMAT.

Conclusion: Our results support previous studies showing the detrimental effects of SBS on the skeleton. In addition the present study shows that BMAT is not increased in SBS, suggesting that bone loss mechanisms in these patients differ from other conditions associated with weight loss, namely anorexia nervosa. These results encourage further studies about the effects of incretins and central nervous system in the modulation of bone remodeling.

Disclosures: Francisco Jose De Paula, None.

Receptor 4 (TLR4), increase pro-inflammatory mediators and contribute to the development of OA. TREM2, paired with DAP12, inhibits TLR-induced cytokine responses in macrophages and therefore may provide protection from high-fat diet induced OA. Our in vitro studies show that palmitic and lauric acid induce dose and time-dependent ERK and NF κ B activation as well as tumor necrosis factor- α (TNF α) production in WT macrophages. DAP12 KO macrophages have increased ERK and NF κ B activation and TNF α production indicating that DAP12 negatively regulates FFA-induced responses in macrophages, while TLR4 KO macrophages show no TNF- α production in response to FFA stimulation. We hypothesize that high fat diet-induced OA is partly mediated by dysregulation of innate immune responses to FFA leading to increased pro-inflammatory cytokines driving abnormal cellular responses within joints resulting in OA. To test our hypothesis, WT, DAP12 KO and TLR4 KO mice were placed on high fat (HF) or control diet (Con) for 12 weeks and knee joints collected for histological OA analysis and gene expression analysis. All three groups of mice gained significant fat mass on high fat diet (60% fat). HF diet induced significant glucose intolerance in WT and TLR4 KO mice but minimal glucose intolerance was seen in DAP12 KO mice. HF diet lead to the development of more osteophytes in medial and lateral compartments of knee in DAP12 KO mice compared to WT and TLR4 KO mice. Histological analysis of knee joints and qPCR results from joint specific domains including the subchondral bone, subchondral bone marrow, long bone marrow, infrapatellar fat pads are being processed. Results from these studies will provide new insight into the role of innate immunoreceptor regulation of high fat diet induced inflammation and osteoarthritis.

Disclosures: Evangelia Kalaitzoglou, None.

MO0097

Male, But Not Female, *Trpm8*^{-/-} Mice Have Impaired Core Temperature Regulation, Altered Body Composition, and Low Bone Mass With Age. Katherine Motyl^{1*}, Daniel Brooks², Mary Bouxsein², Clifford Rosen¹. ¹Maine Medical Center Research Institute, USA, ²Beth Israel Deaconess Medical Center, Harvard Medical School, USA

TRPM8 (the transient receptor potential cation channel, subfamily M, member 8) is expressed in several tissues and is the principal detector of environmental cold. TRPM8 activation in brown adipose tissue (BAT) can induce UCP-1 dependent thermogenesis. With age, BAT function declines concomitantly with loss of bone. We hypothesized that TRPM8 was involved in the co-regulation of bone mass and temperature during aging. At 52 weeks, male C57BL/6J mice with a global deletion of TRPM8 (*Trpm8*^{-/-}) had significantly reduced core temperature (T), total body mass, fat mass and fat-free mass compared to male wildtype littermates (+/+). Although female *Trpm8*^{-/-} mice had reduced body mass and fat mass, they did not have significantly altered lean mass or core T compared to +/+ females. The absence of TRPM8 also significantly reduced total body bone mineral density (BMD, $p=0.02$), content (BMC, $p<0.001$), and femur length ($p=0.003$) in male *Trpm8*^{-/-} mice. However, female *Trpm8*^{-/-} mice had no difference in BMD, BMC or femur length compared to +/+. Despite the differences in BMD and BMC in male mice, μ CT revealed no significant differences in trabecular bone parameters in the femur of *Trpm8*^{-/-} male or female mice compared to +/+. However, total area (bone + marrow) and marrow area at the cortical midshaft were both reduced in male *Trpm8*^{-/-}, consistent with reduced femur length and body weight. When challenged at 18°C and 4°C, male *Trpm8*^{-/-} mouse core T decreased significantly compared to +/+ mice at the same environmental temperatures, while female mice had no genotype-specific alterations in core T. Both +/+ and *Trpm8*^{-/-} mice lost bone similarly after 3 weeks at 4°C (male mice lost trabecular bone and female mice lost cortical bone). To summarize, male *Trpm8*^{-/-} mice, which have impaired temperature regulation, also have reduced BMD and growth during the first year of life. Surprisingly, female *Trpm8*^{-/-} mice had normal thermoregulation and bone parameters, despite reduced body mass. Investigations are underway to determine (1) the cell-specific role of TRPM8 in the skeleton and in thermoregulation and (2) the mechanism of compensation for loss of TRPM8 in female mice, which could be through other thermosensitive TRP channels. In conclusion, these findings support the concept that functional brown fat and normal temperature homeostasis is necessary for bone acquisition and maintenance and demonstrate that TRPM8 is a critical regulator of these processes in male mice.

Disclosures: Katherine Motyl, None.

MO0098

Aromatic Amino Acids Restore the Impaired Anabolic Effect to PTH Associated With A Low Protein Diet. Mona El Refaey, Mark Hamrick, Ke-Hong Ding, Qing Zhong, William Hill, Xing-ming Shi, Mohammed Elsalanty, Nicole Howie, Monte Hunter, Meghan McGee-Lawrence, Jianrui Xu, Wendy Bollag, Carlos Isales*. Georgia Regents University, USA

Aging is associated with a gradual loss of bone mass. Anabolic agents such as parathyroid hormone (PTH) are commonly used to reduce fracture risk. However, it has recently been reported that PTH therapy is not effective in increasing bone mass in 6 month-old female rats on a low protein diet (Ammann P, et al. *Endocrinology* 2015). We previously reported that addition of aromatic amino acids to a low protein diet for eight weeks in aged (approximately 2-year-old) C57BL/6 mice prevented the bone loss

associated with low protein diets. The aromatic amino acids supplemented were tyrosine, tryptophan and phenylalanine equivalent to that of an 18% diet. The dietary benefits of aromatic amino acids on bone mineral density was not observed at time points earlier than eight weeks. Further, we had also previously shown that the bone mass of C57BL/6 mice peaks around 12 months, followed by a subsequent marked decline in bone mass and density by 24 months of age. We wished to study whether the loss of PTH anabolic effects were also seen in 24-month-old male mice on a low protein diet as well as what impact the addition of aromatic amino acids to the diet had on PTH effects. Twenty four-month-old, male C57BL/6 mice were divided into one of five treatment groups; 18% protein diet (normal protein diet); 8% protein diet (low protein diet); 8% protein diet + aromatic amino acids, 8% protein diet + PTH (20 μ g/kg) or 8% protein diet + aromatic amino acids + PTH (20 μ g/kg) for 4 wks. Bone densitometry and micro-CT analyses demonstrated bone loss with the low protein diet, which was not prevented by either the addition of PTH or aromatic amino acids. However the combination of both PTH + aromatic amino acids completely prevented any bone loss associated with a low protein diet. Bone mineralization is associated with the generation of reactive oxygen species while aromatic amino acids are natural antioxidants. Measurement of oxidized amino acids (kynurenine) in the bone marrow of these mice demonstrated a large and significant drop of oxidation products in those mice fed the diet enriched in aromatic amino acids. Thus, these data demonstrate that specific amino acid supplements can restore PTH's anabolic effects on bone in the setting of a low protein diet and we propose that part of the beneficial effects on bone mass might be through changes in the levels of reactive oxygen species.

Disclosures: Carlos Isales, None.

MO0099

Dietary restriction of methionine affects bone structure differently in young male and female mice. Jason Plummer¹, Frantz Perodin¹, Mark Horowitz², David Orentreich¹, Julie Hens^{1*}. ¹Orentreich Foundation for the Advancement of Science, USA, ²Yale Medical School, USA

Dietary methionine (met) restriction (MR) increases longevity and improves healthspan, by reducing adiposity and improving insulin sensitivity in rodent models. We placed young male (3 wk) and female (8 wk) C57BL/6J mice on MR to assess effects on bone structure, growth, and formation. Mice were fed diets containing 0.86% or 0.12% met for 5 weeks. Fasting blood plasma was analyzed for metabolic and bone-related biomarkers. Tibiae were analyzed by histology and histomorphometry, while femurs were analyzed by micro-CT and biomechanically using 4-point bending. Marrow fat was measured by osmium staining with micro-CT. MR mice had reduced plasma glucose and insulin, while FGF21 increased; FGF23 increased only in males. Plasma levels of osteocalcin and osteoprotegerin were unaffected, but sclerostin and procollagen I intact N-terminal decreased. Female mice were more resistant to MR effects on bone than younger males. In cortical bone, μ CT analysis showed significant decreases in Bone Tissue Density (BTD) (CF: 971 ± 28 mg HA/cm³ vs. MR: 929 ± 34 mg HA/cm³) and Apparent Density (CF: 895 ± 31 mg HA/cm³ vs. MR: 845 ± 33 mg HA/cm³) in males, but increased BTD in females (CF: 1020 ± 24 mg HA/cm³ vs. MR: 1035 ± 31 mg HA/cm³). In trabecular bone, males had decreased BTD, bone surface, trabecula and bone volume, and trabecular thickness (CF: 0.033 ± 0.008 mm vs. MR: 0.027 ± 0.0012 mm), while in females only trabecular thickness decreased (CF: 0.039 ± 0.0046 mm vs. MR: 0.035 ± 0.0033 mm). Histomorphometry confirmed reduced trabecular thickness. Bone formation rate (BFR/BV) and index for bone remodeling (DLS/BS) increased in MR males, but in females BFR/BV and SLS/BS were decreased and DLS/BS was not different between CF and MR. Biomechanical testing showed in both MR females and males bones were significantly less stiff and had reduced maximum load and total work, suggesting greater fragility. Reduced expression of RUNX2, DMP1, and osteocalcin occurred in bone marrow from MR mice. MR induced bone marrow fat accretion in both sexes, antithetical to the reduced fat depots seen throughout the body. These results suggest that MR alters bone remodeling and apposition differently in young male and female mice. MR reduction of RUNX2 may alter osteoblast function and lower sclerostin levels may change anabolic activity of osteocytes. Therefore, use of dietary MR to promote improved healthspan should be limited to adults, who appear to be more refractory to MR effects on bone.

Disclosures: Julie Hens, None.

MO0100

Down-regulation of Sirtuin type 1 (Sirt 1) expression in bone marrow of anorexia nervosa mouse model: potential involvement in osteoporotic phenotype. OLFA GHALI^{1*}, DAMIEN LETERME², ANNE RESONET², SEVERINE DELPLACE², PIERRE MARCHANDISE², FLORE MIELLOT², PIERRE HARDOUIN², CHRISTOPHE CHAUVEAU². ¹Laboratory of bone diseases inflammatory (PMOI) EA 4490, France, ²PMOI-EA 4490, France

Background: Osteoblasts and adipocytes share a common mesenchymal stem cell (MSC) origin. Marrow adipocyte accumulation observed in osteoporosis is caused by a shift in MSCs commitment from osteogenic to adipogenic pathway. Sirt1 is implicated in the regulation of osteoblast/adipocyte differentiation. Its activation by resveratrol increases osteoblastogenesis and reduces adipogenesis in vitro. At present, no study focused on the link between sirt1 and osteoporosis related to Anorexia

Nervosa (AN). Thus the aim of this work is to determine if sirt1 alterations could be linked to bone loss observed in AN. Methods: A mouse model mimicking numerous consequences of severe AN (SBA) was used to obtain female mice with significant bone alterations [Zgheib S et al. Plos One 2014]. Determination of the effect of sirt1 on osteoblastic/adipogenic differentiation was performed in the co-differentiation medium [Ghali O et al. BMC cell Biol 2015] after treatment of bone marrow stromal cells (BMSCs) from control (CT) and SBA mice with resveratrol and sirtinol, an activator and an inhibitor of sirt1 respectively. Bone marrow adipocytes number and microarchitecture were performed by histological and μ CT analysis respectively. Results: After 48 h of adhesion, BMSCs of SBA mice presented a decrease of 80% and 50% in mRNA expression of sirt1 and runx2 respectively and an increase of 50% in PPAR γ 2 expression. BMSCs from SBA mice showed earlier and higher adipogenic capacities than those from CT mice in the co-differentiation medium while osteoblast functions were decreased. Interestingly, partial correction of sirt1 expression by resveratrol in BMSCs from SBA mice induced an increase in early osteoblastic markers expression (Runx2, ALP and Osterix/SP7) but failed to enhance osteocalcin expression. Accordingly, high adipocyte number/mm² of tibias of SBA mice was also accompanied by a decrease in cortical and trabecular parameters. Conclusion and Perspective: These data demonstrate for the first time that down-regulation of sirt1 in BMSCs of SBA mice is associated with a rise in adipogenesis and a decrease in osteoblastogenesis which may partly explain its involvement in osteoporosis related to AN. This study will be completed by analyzing the effects of sirt1 on bone marrow adiposity and microarchitecture on sirt1 transgenic mice and organotypic culture of tibias treated with sirtinol and resveratrol for 10 days.

Disclosures: OLFA GHALI, None.

MO0101

LCN2 knock out mice have an unexpected osteopenic phenotype. Association with altered energy metabolism. Nadia Rucci*¹, Mattia Capulli², Sara Gemini-Piperni², Antonio Maurizi², Anna Teti². ¹University of L'Aquila, Italy, ²Department of Biotechnological & Applied Clinical Sciences, University of L'Aquila, Italy

Lipocalin 2 (LCN2) is an adipokine that carries out a variety of functions in different organs. We previously demonstrated that increased LCN2 expression impairs osteoblast differentiation and enhances bone resorption in response to bone mechanical unloading. To in-depth characterize the role of LCN2 in bone metabolism, we investigated the bone phenotype of LCN2 knock out (LCN2KO) mice. Unexpectedly, microCT analysis revealed 40% less bone volume/total volume in LCN2KO mice compared to WT littermates ($p=0.02$, Student's t test), paralleled by 50% and 21% lower trabecular number ($p=0.02$) and thickness ($p=0.019$), respectively, and 20% higher trabecular separation ($p=0.053$). Consistently, histomorphometry showed 43% lower osteoblast surface/bone surface ($p=0.045$), while osteoclast parameters were unremarkable. Despite this overt in vivo osteoblast deficiency, LCN2 expression in WT osteoblasts was almost undetectable and osteoblast primary cultures from calvariae of 7 day-old WT and LCN2KO mice revealed no difference in alkaline phosphatase activity and nodule mineralization, suggesting that the osteopenic phenotype in LCN2KO mice was not osteoblast autonomous. Of note, LCN2KO mice presented with higher body weight and gonadal fat weight compared to WT mice. Therefore, we hypothesized that the low bone mass in LCN2KO mice was due to an altered energy metabolism. Accordingly, we observed significant lower levels of fasted glucose (60.58 \pm 7.48 vs 83.10 \pm 18.9, $p=0.008$) and higher levels of insulin (3.67 \pm 0.7 vs 2.25 \pm 0.7, ng/ml, $p=0.036$) in LCN2KO mouse sera compared to WT. Furthermore, the insulin tolerance test (ITT) showed normal response, confirmed by the glucose tolerance test (GTT) that revealed 20% lower glycaemia ($P=0.003$, area under the curve test) in LCN2KO mice. These results suggest that the sensitivity of peripheral tissues to insulin was normal. However, the mRNA expression of the insulin receptor (InsR) in LCN2KO osteoblasts was 30% lower compared to WT, indicating that there was an osteoblast-specific insulin resistance in the LCN2KO mice. Consequently, the InsR signal was impaired in LCN2KO osteoblasts, as demonstrated by the reduced transcriptional expression of the InsR downstream gene, osteocalcin. In conclusion, our data underscore a systemic role of LCN2 in bone homeostasis and point to this adipokine as an important linker between bone and energy metabolism.

Disclosures: Nadia Rucci, None.

MO0102

Thermoneutral Housing Prevents Premature Age-Related Cancellous Bone Loss in Mice. Urszula T. Iwaniec*¹, Kenneth Philbrick¹, Carmen Wong¹, Dawn Olson¹, Arianna Kahler-Quesada¹, Adam Branscum¹, Russell Turner². ¹Oregon State University, USA, ²Oregon State University, USA

Mice housed at room temperature exhibit age-related cancellous bone loss prior to achieving peak bone mass at approximately 4 months of age. Sympathetic-mediated non-shivering thermogenesis is induced in mice housed at room temperature as an adaptive response to cold stress. Increased sympathetic tone has been implicated as having a negative influence on the skeleton. The purpose of this study was to assess the efficacy of thermoneutral housing (temperature range where the basal rate of energy production is at equilibrium with heat loss) in preventing premature cancellous bone loss in mice. Female C57BL/6J (B6) mice were housed at room temperature

(22 \pm 3 \circ C) or at thermoneutral (32 \pm 3 \circ C) from 2 to 4 months of age. Cancellous bone was evaluated by microcomputed tomography and histomorphometry. Mice housed at room temperature exhibited dramatic cancellous bone loss from the distal femur metaphysis and lesser bone loss from other skeletal sites, whereas cancellous bone volume fraction in thermoneutral-housed mice, depending on the skeletal site, either remained the same or increased. This phenomenon was not limited to B6 mice because C3H/He mice housed at room temperature also exhibited lower cancellous bone volume fraction than mice housed at thermoneutral. The sparing effect of thermoneutral housing on cancellous bone in B6 mice was associated with increased bone marrow adiposity and higher rates of bone formation. Mice housed at room temperature consumed more food but did not differ in weight from mice housed at thermoneutral. However, the room temperature-housed mice had lower abdominal white adipose tissue mass and lower serum leptin levels. Gene profiling revealed that housing temperature had a major effect on expression of osteogenic genes in tibia. Specifically, room temperature-housed mice had lower expression levels of genes for bone matrix proteins (type I collagen and osteocalcin) and genes associated with BMP signaling (BMPs, BMP receptors and SMADs). Our findings support the conclusion that mild cold stress has a major negative impact on cancellous bone mass in mice and that early onset cancellous bone loss in this species is due, in part, to cold adaptation. The findings also suggest that studies using mice as a preclinical model to investigate interactions between energy homeostasis and bone or the etiology of age-related bone loss need to account for confounding species differences in thermoregulation and energy metabolism.

Disclosures: Urszula T. Iwaniec, None.

MO0103

Fkbp10 deletion in osteoblast and joint tissues leads respectively to qualitative but not quantitative defects in bone, and a postnatal contracture phenotype seen in Bruck syndrome. Caressa Lietman*¹, Zhechao Ruan¹, Ingo Grafe¹, Elda Munivez¹, Yuqing Chen¹, Hao Ding², Xiaohong Bi², Catherine Ambrose², Nadia Fratzl-Zelman³, Paul Roschger³, MaryAnn Weis⁴, David Eyre⁴, Deborah Krakow⁵, Brendan Lee¹. ¹Baylor College of Medicine, USA, ²University of Texas Health Science Center at Houston, USA, ³Ludwig Boltzmann Institute of Osteology, Austria, ⁴University of Washington, USA, ⁵University of California at Los Angeles, USA

Osteogenesis Imperfecta (OI) is the most commonly inherited form of brittle bone disease and displays a spectrum of clinical severity from mild (OI type I) to severe early lethality (OI type II). Mutations in FKBP5 Binding Protein 10 (*FKBP10*), encoding the FKBP65 protein, causes a recessive form of OI and Bruck Syndrome, the latter being characterized by congenital joint contractures in addition to the low bone mass. We have shown that *Fkbp10* expression is limited to bone, tendon and ligaments in postnatal tissues. Furthermore, in both patients and *Fkbp10* knockout mice, collagen telopeptide crosslinking has been shown to be dramatically reduced. To further characterize the tissue specific contribution of *Fkbp10* to bone and joint tissues, we conditionally ablated FKBP65 in *Fkbp10*^{fl/fl} mice using the osteoblast specific *Coll1a1* 2.3kb Cre and Scleraxis Cre. Using μ CT, histomorphometry and quantitative backscattered electron imaging, we find only minimal alterations in the quantity of bone and no differences in bone matrix mineralization in this model. However, mass spectroscopy of bone collagen demonstrated reduction of telopeptide collagen crosslinking. Furthermore, collagen and matrix components are altered as shown by Raman spectroscopy, and mutant bone is weaker and less stiff than that from wild type littermates on 3-point bending experiments. Taken together, these data suggest that the reduction of collagen crosslinking through *Fkbp10* ablation in osteoblasts leads to qualitative, rather than quantitative changes in the skeleton. Similarly, loss of *Fkbp10* in presumptive tendons and ligaments led to a progressive contracture phenotype in mutant mice, evidenced through radiography, histology, and biomechanical testing. As such, this model represents the first one characterized by postnatal joint contractures. Together, loss of *Fkbp10* leads to altered collagen crosslinking that leads to qualitative defect in bone, tendon, and ligaments.

Disclosures: Caressa Lietman, None.

MO0104

Gnas Inactivation Adversely Affects Cortical Bone Quality by Altering Osteoclast and Osteocyte Activity During Bone Remodeling. Girish Ramaswamy*¹, Hyunsoo Kim, Deyu Zhang, Yongwon Choi, Frederick Kaplan, Robert Pignolo, Eileen Shore. University of Pennsylvania, USA

The *GNAS* gene encodes multiple transcripts, including the α -subunit of the stimulatory G-protein ($G_{\alpha s}$) of adenylyl cyclase, and shows genomic imprinting, with paternal but not maternal *GNAS* inactivation associated with Progressive Osseous Heteroplasia, a rare disorder of extraskelatal (heterotopic) ossification. We previously showed that paternal *Gnas* inactivation enhances osteoblastogenesis and inhibits adipogenesis. This study examined whether heterozygous *Gnas* inactivation also enhances bone formation during skeletal development and bone remodeling.

Trabecular BV/TV and architecture were unaffected in both *PatGnas*^{+/-} and *MatGnas*^{+/-} mice at all ages. However, compared to WT, 2-week-old *PatGnas*^{+/-} and *MatGnas*^{+/-} mice showed cortical BV/TV reduced by 15% and cortical thickness by

20% by μ CT. At 3 and 9 months of age when bone remodeling occurs, *PatGnas*^{+/-} showed persistent reductions in BV/TV and cortical thickness, while *MatGnas*^{+/-} were similar to WT. Cortical porosity was elevated by ~10% in *PatGnas*^{+/-} mice at all ages. Femurs from *PatGnas*^{+/-} mice were weaker by >25% by 3-pt bending at all ages while *MatGnas*^{+/-} femurs had reduced strength only at 2 weeks of age, consistent with μ CT data.

TRAP staining revealed dramatically increased numbers of multinucleated endosteal osteoclasts in 9-month-old *PatGnas*^{+/-} but not in *MatGnas*^{+/-} mice. Differentiation of bone marrow macrophages (BMM) from *PatGnas*^{+/-} mice formed more multinucleated osteoclasts and increased TRAP activity compared to WT BMMs indicating that $G_{\alpha s}$ regulates osteoclast differentiation. In addition, cortical bone from 9-month-old *PatGnas*^{+/-} mice showed higher fraction of TRAP+ osteocytes and elevated *Acp5*, *Sost* and *Pthrp* mRNA levels by qPCR. Osteoblast number and mineral apposition rate were similar between 2-week-old WT and *PatGnas*^{+/-} mice supporting that changes in bone formation did not contribute to the cortical bone defects.

Overall our results indicate that paternal inheritance of *Gnas* inactivation in mice adversely affects cortical bone quality by altering osteoclast and osteocyte activity during bone remodeling. Studies are ongoing to investigate the effects of $G_{\alpha s}$ mutation on osteoclast progenitors and signaling mechanisms driving the differential effects between *PatGnas*^{+/-} and *MatGnas*^{+/-} mice. Thus *Gnas* regulates multiple cell types within the normal skeleton and extraskeletal tissues in age and inheritance dependent manner to impact skeletal development and heterotopic ossification.

Disclosures: Girish Ramaswamy, None.

MO0105

An Optimized In Vivo Chemical Screening Regimen For Osteoactive Compound Discovery in the Regenerating Zebrafish Tail Fin. Adrian Monstad-Rios*, Ronald Kwon. University of Washington, USA

Though *in vivo* chemical screens represent a powerful strategy for bone pathway discovery, such screens are largely inaccessible in traditional animal models. In this project, we seek to utilize the regenerating zebrafish tail fin, a rapid, genetically tractable, and optically transparent model of intramembranous ossification, for osteoactive compound discovery. Given that adult zebrafish require a relatively large water volume for housing, this makes chemical screening costly due to the large compound quantities necessary to achieve an active concentration in the water. To overcome this hurdle, we previously developed a 3D printed screening system that enabled rapid, efficient, and cost-effective chemical administration in adult zebrafish [1]. Further, we demonstrated its potential to detect clinically-relevant inhibitors of bone formation during tail fin regeneration. In this study, our objective was to define optimal dosing and imaging regimens to maximize chemical screening efficiency. Zebrafish were subjected to 50% tail fin amputation and dosed each day for 1 hr/day. Fin area was measured periodically following amputation. We computed the coefficient of variation (COV) of fin regrowth at different days post amputation (dpa). Analysis revealed decreasing COV with time, with values plateauing by 8 dpa. The COV was not decreased when area of regrowth was normalized by pre-amputation area. Administration of 10, 50, and 100 μ M cyclopamine for 8 days resulted in a characteristic dose-response curve in percent regrowth (0 μ M:50.2%, 10 μ M:53.5%, 50 μ M:24.8%, 100 μ M:17.2%), demonstrating the fidelity of our system. Previously, we found that administration of dorsomorphin (an inhibitor of type I BMP receptors and AMPK currently in therapeutic development) impaired mineralizing activity during fin regeneration as indicated by decreased calcein labeling [1]. To examine the potential to measure mineralization using label-free methods, we imaged bone ray birefringence in dorsomorphin-treated fish using Rotopol microscopy [2]. We observed a 20.2% decrease in birefringence in dorsomorphin-treated animals relative to vehicle controls, suggesting the utility of this approach. Collectively, this study develops optimized parameters for efficient chemical screening during zebrafish fin regeneration, an essential step towards *in vivo* osteoactive compound discovery in this system.

[1] Monstad-Rios AT, Kwon RY. Trans ORS 2015

[2] Recidoro AM, Roof AC, et al., Kwon RY. JBMR 2014

Disclosures: Adrian Monstad-Rios, None.

MO0106

Cause of Abnormal Bone Mineralization in X-Linked Hypophosphatemia. Baozhi Yuan*¹, Abigail Radcliff², Ryley Zastrow³, Ying Liu⁴, Jian Feng⁵, Robert Blank⁶, Marc Drezner⁷. ¹Department of Medicine, University of Wisconsin-Madison & GRECC, William S. Middleton Memorial Veterans Hospital, USA, ²Department of Medicine, University of Wisconsin-Madison & GRECC, William S. Middleton Veterans Hospital, USA, ³University of Wisconsin-Madison, USA, ⁴Baylor College of Dentistry, Texas A&M Health Science Center, USA, ⁵Baylor College of Dentistry, Texas A&M Health Science Center, USA, ⁶Medical College of Wisconsin & Clement J Zablocki Veterans Administration Hospital, USA, ⁷University of Wisconsin, USA

Loss of function PHEX mutations lead to increased serum FGF-23, which underlies the biochemical abnormalities in patients with X linked hypophosphatemic rickets (XLH) and *hyp* mice: renal phosphate (P) wasting and hypophosphatemia. Whether abnormal bone mineralization is due to direct effects of FGF-23 and/or hypophosphatemia is less certain. To explore the cause of osteomalacia, we compared the phenotype of *hyp*-mice to that in mice with *Phex* deletion in osteoblasts (*Ocn-Cre-Phex*^{Afloxly}) and in osteocytes (*Dmp1-Cre-Phex*^{Afloxly}). Although *Ocn-Cre-Phex*^{Afloxly}- and *Dmp1-Cre-Phex*^{Afloxly}-mice had biochemistries no different from *hyp*-mice, the mineralization defect in *Dmp1-Cre-Phex*^{Afloxly}-mice was mild compared to severe osteomalacia present in *Ocn-Cre-Phex*^{Afloxly}- and *hyp*-mice. Moreover, while treatment with high P diet normalized serum P in each model, osteomalacia persisted in *hyp*-mice, but normal bone mineralization ensued in *Dmp1-Cre-Phex*^{Afloxly}-mice (mineral apposition rate 1.4 ± 0.2 vs 3.1 ± 0.4 μ m/day). Thus the mild mineralization defect in *Dmp1-Cre-Phex*^{Afloxly}-mice is a P dependent abnormality, whereas the profound osteomalacia in *Ocn-Cre-Phex*^{Afloxly}- and *hyp*-mice is due to hypophosphatemia and an additional unidentified factor(s). In this regard, we found that *hyp*-mouse bone exhibited decreased *Dkk1* mRNA expression (0.35 ± 0.2 vs 1.2 ± 0.4 relative expression [re], $p < 0.05$) and an increase in β -catenin mRNA (6.6 ± 0.5 vs 1.4 ± 0.7 re, $p < 0.0001$), whereas *Dmp1-Cre-Phex*^{Afloxly}-mouse bone had normal *Dkk1* and β -catenin mRNA levels. In parallel experiments, we observed that constitutively expressed β -catenin in osteoblasts results in osteomalacia. Thus, we compared treatment of *hyp*-mice with Hexa-D-Arginine (D6R), a curative therapy for the osteomalacia, vs saline control. Five weeks of D6R (1.5 μ M/kg/day, ip) increased serum P in *hyp*-mice (6.2 ± 0.1 vs 3.2 ± 0.2 mg/dl, $p < 0.001$) to levels no different from D6R treated normals (6.8 ± 0.3). D6R also significantly increased *Dkk1* mRNA in *hyp*-mouse bone (2.3 ± 1.0 vs 0.31 ± 0.2 re, $p < 0.05$) to levels greater than in D6R treated normals and decreased β -catenin mRNA (4.4 ± 0.7 vs 2.0 ± 0.3 re, $p < 0.05$) to levels no different than in D6R treated normals. The *Dkk1* change occurred due to normalization of miRNA-217 (6.6 ± 0.5 vs 1.4 ± 0.7 re, $p < 0.001$). Our data indicate that osteomalacia in *hyp*-mice results from both hypophosphatemia and increased bone β -catenin, indicating successful treatment of XLH requires normalization of both abnormalities.

Disclosures: Baozhi Yuan, None.

MO0107

Collaborative cross Mice in a GWA Study Reveal New Candidate Genes for Bone Microarchitecture. Roei Levy*¹, Richard Mott², Fuad Iraqi¹, Yankel Gabet¹. ¹Tel Aviv University, Israel, ²Oxford University, United Kingdom

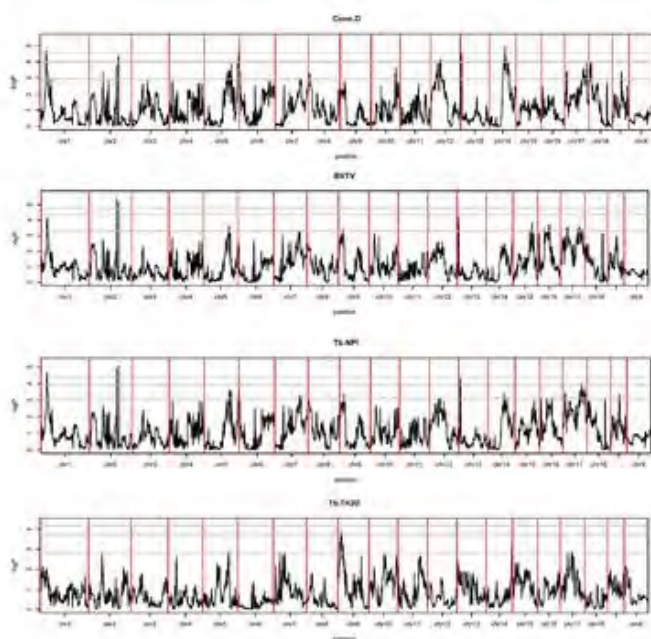
Purpose To identify new causative genetic determinants of bone microarchitecture.

Background The microstructure of trabecular bone is a composite trait governed by a complex interaction of multiple genetic determinants. Comprehensive mapping of their full expression spectra can drastically improve our ability to predict the risk of osteoporosis and other bone pathologies. The inclusion of the widely-varied collaborative cross (CC) - the latest recombinantly inbred mouse reference panel - in GWA studies enables reproducible experiments at a resolution of one mega base-pairs and below, with a relatively small cohort size. Here we utilized 30 CC lines (160 individuals in total) of both genders to perform a detailed haplotype mapping across 170K genome-wide SNPs. Samples were collected over a period of two years that spanned a near-complete seasonal cycle. Femurs were scanned at a resolution of 10 μ m to morphometrically analyze the trabecular bone compartment in the distal femur. We carried out our bioinformatics analyses on the trabecular bone volume fraction (BV/TV), trabecular number (Tb.N), trabecular thickness (Tb.Th), and trabecular connectivity density (Conn.D). Thorough refinement of the initial haplotype scan was done by merging the full genomic sequence of the CC founders to pinpoint specific genes.

Results With heritability of 0.7-0.8 for the morphometric parameters we noted a cardinal ($P < 0.01$) sex-specific effect in all but Tb.Th. Our haplotype scan yielded three QTL; BV/TV, Tb.N and Conn.D yielded one at chromosome 2 ($-\log P > 5$; $CI_{95} = 4.4$) and another at chromosome 1 ($-\log P > 4.7$; $CI_{95} = 4.5$) while Conn.D has contributed an extra QTL at chromosome 14 ($-\log P > 4.9$; $CI_{95} = 4.5$). Using eight-way merge analysis we located two adjacent genes, namely *AVP* and *OXT*, near the peak of the first QTL. *AVP* encodes for vasopressin and *OXT* encodes for a precursor of oxytocin. Recent articles attributed a role for both vasopressin and oxytocin in bone biology. However, to the best of our knowledge, genome-wide significance has not yet been demonstrated for either gene. The third QTL yielded *Lrch2*, which was previously found to be associated with knee osteoarthritis. Lastly, the candidate genes

for Conn.D are *C4bp* and *Zp3r* for which a role in bone biology has yet to be documented.

Conclusion These data demonstrate for the first time genome-wide significant association between OXT and AVP and trabecular microstructural parameters, which support previously reported experimental observations. In addition, these data validate our approach and its ability to reveal new determinants of bone microarchitecture.



Association plots

Disclosures: *Roei Levy, None.*

MO0108

Development of a database and web portal for murine models of skeletal variation. Caibin Zhang¹, Pujan Joshi², Seung-Hyun Hong², Cheryl Ackert-Bicknell³, John Sundberg⁴, Douglas Adams¹, Dong-Guk Shin², David Rowe^{*1}. ¹University of Connecticut Health Center, USA, ²University of Connecticut, USA, ³University of Rochester, USA, ⁴The Jackson Laboratory, USA

The mouse genetics community has built a number of modeling systems for identifying genetic loci that contribute to phenotypic variation in every organ system. The mouse knock out project (KOMP) produces lines with inactivation of genes in a C57BL/6NJ background. In contrast, the diversity outbred population (DO) is a random distribution of genetic segments from 8 inbred mouse lines. These populations demonstrate extreme phenotypic variation that can be associated with strain specific SNPs. Additional inbred lines derived from the 8 same strains provide a stable phenotype are called the collaborative cross (CC) lines. The essential element for using these tools is the ability to perform high throughput, digital and objective phenotyping such that the data can be retrieved and linked to genomic data through web-accessible databases.

We have developed a μ CT screening \rightarrow histomorphometric pipeline that is being used to study unselected KOMP lines, DO populations and CC lines. Here we introduce a website (bonebase.org) that is an evolving effort to present this information. The site is populated with measurements from an internal database that captures all the data streams, calculates statistics and flags measures that exceed the control values. The flagged items are grouped into biological categories (bone architecture, cellular activity) to provide an overview of analysis. The database also distinguishes if the abnormality is present in both genders and within appendicular and axial bone to identify dimorphic phenotypes.

From the bonebase.org website, the user selects which type of model system to be queried (KOMP, DO, CC, investigator initiated). The list of lines is presented and indicates which lines contain information that was flagged. The next level (analysis) lists all the biological categories in which an abnormality was found and whether it had any dimorphic properties. The next (summary) level presents the group means for each measurement within each biological category and it is followed by the individual mouse values for each measurement (detail level). The final level presents the images of the μ CT and histology from which the measurements were made. All of these features can be found by searches and have been marked with terms listed in the Mouse Phenotype Ontology database. We welcome suggestions and contributions to what we hope will become a common resource for the skeletal biology community.

Disclosures: *David Rowe, None.*

MO0109

MicroCT-Based Barcoding Reveals Novel High Bone Mass Mutations in Zebrafish. Philippe Huber, Jane Lee, Claire Watson, Marjorie Thompson, Sarah McMenamin, David Parichy, Ronald Kwon^{*}. University of Washington, USA

Zebrafish have emerged as an indispensable system for human disease modeling due to their genetic tractability, optical properties, and amenability to in vivo screening. However, their use as a model for bone biomedical research has been hindered by the lack of quantitative strategies for skeletal imaging in zebrafish, as well as the unknown degree to which zebrafish and mammalian bone physiologies are regulated by similar genetic and cellular networks. In this project, our goal was to 1) develop a microCT-based platform for systems-level bone phenotyping in adult zebrafish, and 2) identify coordinated patterns of altered bone mass/mineralization following mutagenesis. For this, we integrated whole-body (21 μ m resolution) microCT scanning in multiple fish with a custom image processing pipeline to compute 288 different measures (24 vertebral bodies x 3 vertebral elements x 4 quantities per fish) of axial bone morphology and mineralization in a process we call "skeletal barcoding" (Fig 1A). Using this pipeline, we barcoded zebrafish mutants previously isolated from genetic screens (Fig 1B), and identified two mutants with abnormal skeletal phenotypes: *puma* and *opallus* (which harbors a mutation in thyroid stimulating hormone receptor (*tshr*) identical to a human mutation causing constitutive TSHR activity and hyperthyroidism [1]) exhibited significantly elevated TMD across all centra (Fig 1C). *puma* (which harbors a mutation in the alpha tubulin gene *tuba8/3a* [2]) exhibited increased volume in anterior haemal arch/rib elements only (Fig 1D), suggesting the potential to detect both global and regional shifts in mass/mineral accrual. In humans, hyperthyroidism is associated with low BMD [3], whereas TSHR gain-of-function has been associated with high BMD [4]. Thus, this study suggests the potential for the zebrafish skeleton to predict a complex phenotype integrating competing influences at both systemic (hyperthyroidism) and local (e.g., Tshr activity in bone cells) levels. Together, this study develops quantitative technologies for bone imaging in zebrafish, advances novel approaches to systems-level bone phenotyping, and provides new evidence supporting the translational value of zebrafish as a model of human genetic bone disorders.

[1] McMenamin SK, et al., Parichy DM. *Science*, 2010.

[2] Larson TA, et al., Parichy DM. *Zebrafish*, 2010.

[3] Greenspan SL, Greenspan FS. *Ann Int Med*, 1999

[4] de Lloyd A, et al., Ludgate M. *J Endocrinol*, 2010

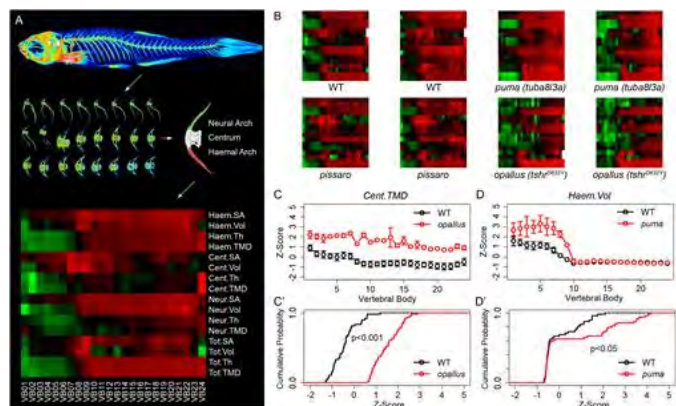


Fig 1

Disclosures: *Ronald Kwon, None.*

MO0110

Mutations in *Lrp5* Improve Bone Properties and Osteoblast Function In Mice with Osteogenesis Imperfecta. Christina Jacobsen^{*1}, Erin Spiller², Kyung-Eun Lim³, Alexander Robling³, Matthew Warman⁴. ¹Boston Children's Hospital/Harvard Medical School, USA, ²Keck School of Medicine, University of Southern California, USA, ³Indiana University, USA, ⁴Boston Children's Hospital, Harvard University School of Medicine, Howard Hughes Medical Institute, USA

Heterozygous missense mutations in the cell surface receptor, low-density lipoprotein receptor-related protein 5 (LRP5) increase bone mass and strength in humans and mice. Osteogenesis Imperfecta (OI), a disorder most frequently caused by mutations in Type I collagen, is characterized by increased skeletal fragility which can lead to deformity, pain and disability. Therapies are needed that can reduce fractures and improve bone health in patients with OI. Our previous work demonstrated that increased LRP5 signaling from either a high bone mass (HBM) mutation or a monoclonal antibody targeting an inhibitor of LRP5 improves bone density and strength in a mouse model of moderate OI by increasing the amount of type I collagen incorporated into the bone matrix.

We mated mice with a dominant *Lrp5* HBM-causing knockin allele to a mouse model of severe OI (*Colla1⁴⁸⁰*) that carries a mutation causing retention of type I collagen in the ER and subsequent osteoblast apoptosis. We analyzed bone density at 12 weeks of age by DEXA and measured the number of long bone fractures by Faxitron. As expected, offspring with OI alone have lower bone density and more fractures than wild-type siblings. Compared to siblings with OI alone, siblings with OI and a HBM allele have significantly increased bone density ($p < 0.05$). More importantly, more fractures were seen in the mice with OI alone (9/14) than the mice with OI and a HBM allele (2/13). This suggests that *Lrp5* HBM mutations improve bone properties even in a mouse model of OI with compromised collagen secretion.

To further determine the effects of *Lrp5* HBM mutations on collagen secretion in osteoblasts, we examined osteoblasts from femurs of 3-week old mice with both a moderately severe OI allele (*Colla2^{6610C}*) and a *Lrp5* HBM allele as well as siblings with an OI allele alone by electron microscopy ($n = 3$ per genotype). The mice with an OI allele alone had disordered, swollen ER. The appearance of the ER improved in mice with both an OI allele and a *Lrp5* HBM allele, suggesting that the HBM allele may improve mutant type I collagen processing and/or secretion in osteoblasts.

These results indicate that therapies targeting the LRP5 pathway may improve bone properties in mice with OI even if the causative mutation affects collagen production by osteoblasts. This suggests that most human patients with OI may benefit from these therapies, even if their mutation affects collagen processing and/or secretion.

Disclosures: Christina Jacobsen, None.

MO0111

Osteogenesis Imperfecta Causes Splenomegaly and Elevated Osteoclast Progenitor Numbers in OIM Mice. Brya Matthews^{*1}, Emilie Roeder¹, Mara O'Brien¹, Danka Grcevic², Ivo Kalajzic¹. ¹University of Connecticut Health Center, USA, ²University of Zagreb, Croatia

Osteogenesis imperfecta (OI) is caused by insufficient or improper type I collagen synthesis, and is characterized by bone fragility. However, in children with severe OI and a number of mouse models of OI, high bone turnover is observed with elevated osteoclast numbers. While this phenotype is likely to be influenced by osteoblast dysfunction, *in vitro* studies suggest that there is also a defect in the osteoclast compartment. Therefore, in this study we sought to evaluate osteoclast progenitor (OCP) numbers and their differentiation potential in the well-characterized OIM mouse model.

OIM mice and their wild-type (WT) sex-matched littermates were analyzed at 7-9 weeks of age. Peripheral blood was collected, whole spleens were weighed, then processed, and bone marrow was flushed from the tibias and femurs. Identification of OCPs was achieved using established antibody cocktails for flow cytometry. Mice were processed individually and at least 4 animals per group were including in each experiment.

Serum CTx levels are 5-6x WT levels in both male and female OIM animals indicating elevated resorption, consistent with previous results showing increased osteoclast surface. OIM mice consistently showed lower bodyweight than WT controls. OIM mice had enlarged spleens, and therefore higher spleen cell numbers up to at least 13 weeks of age, particularly when corrected for bodyweight. OCPs in peripheral tissues like spleen reside in the lymphocyte(CD3/B220/NK1.1)CD11b^{hi} fraction. Male OIM mice showed a significantly higher proportion (50-100% increase) of CD11b^{hi}CD115⁺ cells, and CD11b^{hi}CD115⁺Ly6C^{hi} cells, which have been shown to be most enriched for OCPs. Similar trends were seen in females, although these did not reach significance. Unsorted OIM spleen cells formed around 2.5x more osteoclasts in culture, however, we did not observe changes in osteoclast differentiation from sorted CD11b^{hi} progenitors. We did not find any consistent changes in OCP fractions in peripheral blood, and have been unable to identify consistent changes in bone marrow OCP frequencies or their differentiation.

In conclusion, young adult OIM mice show enlarged spleens and increased numbers of spleen-resident OCPs suggesting a systemic effect of the disease on the hematopoietic system.

Disclosures: Brya Matthews, None.

MO0112

Identification of the mutations in the prostaglandin transporter gene, *SLCO2A1* and clinical characterization in Korean patients with pachydermoperiostosis. Sihoon Lee^{*1}, So Young Park², Yumie Rhee³. ¹Gachon University School of Medicine, South Korea, ²Cheil General Hospital, South Korea, ³Yonsei University College of Medicine, South Korea

Objective: Pachydermoperiostosis (PDP), or primary hypertrophic osteoarthropathy, is a rare genetic disease affecting both skin and bones. Both autosomal dominant with incomplete penetrance and recessive inheritance of PDP have previously been confirmed. Recently, hydroxyprostaglandin dehydrogenase (HPGD) and solute carrier organic anion transporter family member 2A1 (*SLCO2A1*) were reported to be pathogenic genes responsible for PDP. Both genes are involved in the PGE2 degradation. We aimed to identify responsible genes for PDP and the clinical features in Korean patients with PDP.

Methods: We studied six affected individuals and their available healthy family members from three unrelated Korean families with PDP. The *SLCO2A1* and HPGD genes were screened and analyzed.

Results: We identified two different *SLCO2A1* mutations in the PDP patients from two unrelated families; homozygous for c.940+1G>A and compound heterozygous for c.940+1G>A and p.Arg603* (c.1807C>T). In a third family, we found a novel heterozygous mutation in the *SLCO2A1* gene at nucleotide 302 causing a substitution of the amino acid isoleucine to serine at codon 101 (p.Ile101Ser) in affected individuals. Genetic analyses of the PDP patients showed no abnormality in HPGD gene. Mutated patients displayed characteristic phenotypes of PDP with various degrees of pachydermia and bone abnormality.

Conclusion: Our study further supports the role of mutations in *SLCO2A1* gene in the pathogenesis of PDP and could provide extended clues to the genotype-phenotype relations of PDP.

Supported by the Basic Science Research Program, National Research Foundation of Korea (NRF-2013R1A1A1A05005629 to S.L.).

Disclosures: Sihoon Lee, None.

MO0113

Mild bone phenotype in a young adult man with homozygous p.Val667Met mutation in LRP5 gene: the culprit gene. Corinne Collet^{*1}, Agnes Ostertag², Thomas Funck-Brentano³, Jean-Louis Laplanche¹, Marie-Christine de Vernejoul³, Martine Cohen-Solal⁴. ¹Department of biochemistry & Genetics, hospital Lariboisiere, France, ²Inserm U1132, hospital Lariboisiere, France, ³Inserm U1132 & university Paris 7, hospital Lariboisiere, France, ⁴Centre Viggo Petersen, France

Purpose: Osteoporosis is characterized by low bone mineral density (BMD) and susceptibility to fracture. Genetic determinants are major factors of low bone mass with a high heritability. Polymorphisms in fifty genes have been reported to be associated with osteoporosis. Among them, LRP5 mutation has been described in osteoporosis pseudoglioma (OPGG), a rare recessive disease characterized by severe osteoporosis with fractures in infancy associated with a congenital blindness. Moreover, heterozygous mutations of p.Val667Met in LRP5 are associated with idiopathic osteoporosis and risk of fractures in young adults. Interestingly, this mutation is classified as a conflict variant in databases and described as a polymorphism with heterozygous frequency of 1-4% according to the analysed ethnic population.

Method: This study was performed to investigate the prevalence of LRP5 heterozygous mutations of p.Val667Met in a young adult idiopathic osteoporosis cohort.

Results: Among the 60 patients with T-score below 2.5 SD, 14 displayed heterozygous mutations and one carried the p.Val667Met variant at homozygous level. The patient was 35 year-old, had a T-score of -3.2 SD and a mild vertebral deformity, but no ophthalmologic signs. No mutation was found in other genes such as SOST. The mild phenotype revealed at mid-age raised the question of the severity of bone signs in the first description and that OPGG cannot be attributed to homozygous p.Val667Met alone. This observation suggests that another LRP5 variant or another gene was could have been responsible for OPGG.

Conclusion: This report showed that homozygous mutation in p.Val667Met LRP5 variant does not fully explain the OPGG phenotype and suggest the need to investigate mutations of other genes in severe osteoporosis.

Disclosures: Corinne Collet, None.

MO0114

Identification of Novel BMD Associated Genes Using Integrated Genome-Wide Analyses Employing DNA Methylations and Transcript Levels in Bone Biopsies from Postmenopausal Women. Sjur Reppe^{*1}, Tonje G. Lien², Ole K. Olstad³, Vigdis T. Gautvik⁴, Ingrid K. Glad², Kaare M. Gautvik⁵. ¹Oslo University Hospital, Ullevaal, Norway, ²Department of Mathematics, University of Oslo, Norway, ³Oslo University Hospital, Department of Medical Biochemistry, Norway, ⁴University of Oslo, Institute of Basic Medical Sciences, Norway, ⁵Lovisenber Diakonale Hospital, Norway

While 60-80% of the BMD variation has been shown to be heritable, genome wide analyses have so far been able to explain only a fraction. This study attempts to dissect information from global transcription and DNA methylation analyses obtained from bone biopsies of postmenopausal women of varying BMD to identify novel BMD associated genes using the statistical method weighted lasso.

Eighty trans-iliacal bone biopsies, containing cortical and trabecular bone have been collected, and bone DNA and RNA have been isolated from the same samples. For RNA expression analysis HG-U133 plus 2.0 chips (Affymetrix) were used, and for DNA methylation analysis we used the Infinium HumanMethylation450 BeadChip, with about 17 CpG sites per gene region present in the promoter, 5'UTR, first exon, gene body, and 3'UTR.

We use the statistical method lasso, which is based on multiple linear regression, but contains a penalty part to reduce the number of influencing variables/covariates. In a weighted lasso approach we reduce the penalty part for methylations that are highly associated to one or more transcript levels. Thus, the methylation sites

which best explain BMD and are highly associated with gene expression will be slightly favored, while methylations with no association to gene expression will be weighted down. The output of lasso is a short list of DNA methylations that together explain a large part of BMD variation.

The R package glmnet is used to fit the weighted lasso, and use of weighted lasso leads to a 17% reduction in the prediction error as compared to un-weighted Lasso. Using this method, methylations in 22 genes are selected, including COL11A2, PCDH9, MKL1, SPI1 and ALDH3B1. For 14 of these, the degree of methylation is inversely correlated to BMD. Functional analysis of the 22 genes using DAVID Bioinformatics Resources 6.7 and applying 5% FDR, results in enrichment favoring: "collagen fibril organization", "alternative splicing" and "splice variant". Our novel statistical approach to map DNA methylations which correlate to BMD and favors methylations associated with gene expression shows the presence of mitochondrial, muscle and bone related genes, of which most have previously not been associated with BMD. The 22 methylations explain 62% of the variation in BMD, while a set of 22 randomly chosen methylations explain on average 22%, indicating that DNA methylation contribute significantly to BMD variation in postmenopausal women.

Disclosures: *Sjur Reppe, None.*

MO0115

Osteoblasts from Type V OI patients demonstrate gain-of-function for mineralization despite decreased COL1A1 expression. ADI REICH*¹, Alison Bae², Aileen Barnes², Wayne Cabral², Aleksander Hinek³, Jennifer Stimec⁴, Suvmil Hill⁵, David Chitavat⁶, Joan Marini². ¹NIH, USA, ²Bone & Extracellular Matrix Branch, NICHD, NIH, USA, ³Physiology & Experimental Medicine Program, Heart Center, Hospital for Sick Children, University of Toronto, Canada, ⁴Division of Diagnostic Imaging, Department of Pediatrics, Hospital for Sick Children, University of Toronto, Canada, ⁵Diagnostic Radiology Department, NIH Clinical Center, NIH, USA, ⁶The Prenatal Diagnosis & Medical Genetics Program, Department of Obstetrics & Gynecology, Mount Sinai Hospital, University of Toronto, Canada

Osteogenesis imperfecta (OI) is a genetically heterogeneous disorder characterized by bone fragility. Most cases result from dominant mutations in type I collagen, while recessive OI is caused by defects in genes whose products interact with type I collagen. Type V OI has dominant inheritance, with characteristic skeletal findings including ossification of the forearm interosseous membrane, radiodense metaphyseal bands, propensity for hyperplastic callus formation, and mesh-like lamellation on bone histology. It is caused by a unique heterozygous mutation in *IFITM5* (c.-14C>T), which encodes BRIL, a transmembrane protein expressed in osteoblasts. The mutation generates a start codon in the 5'-UTR, adding five residues to the BRIL N-terminus. However, the mechanism of type V OI and its relationship with type I collagen is unknown. We identified 8 patients with the *IFITM5* (c.-14C>T) mutation. Using cultured primary osteoblasts from patients with type V OI, we verified that *IFITM5* expression and BRIL protein level were comparable to control during osteoblast differentiation. Type V OI osteoblast function was most consistent with a gain-of-function mutation. Both early (*ALPL* and *IBSP*) and late (osteopontin and osteocalcin) markers of osteoblast differentiation are increased in type V OI osteoblasts; as are *SERPINF1* expression and PEDF secretion during differentiation. *SOST*, a marker of mature osteocytes, was also increased, although in-vitro mineralization by type V OI osteoblast was increased on alizarin red stain compared to control. In contrast, *RANKL/OPG* ratio was decreased due to increased *OPG* expression. This result supports prior histomorphometry reports on type V OI patients, who do not have high turnover bone. In addition, *COL1A1* is not activated in type V OI osteoblasts, which have less than half the level of *COL1A1* transcripts found in control in mid to late differentiation, with concomitantly decreased collagen protein secretion. Decreased secreted type I collagen underlies decreased crosslinked collagen in matrix, and altered appearance of fibrils deposited in culture. The increased mineralization and advanced differentiation of type V OI osteoblasts likely underlie the overactive tissue calcification and hypertrophic callus formation seen in affected individuals and demonstrates that type V OI has a gain-of-function mechanism. Decreased type I collagen expression, secretion and matrix incorporation establish type V OI as a collagen-related defect

Disclosures: *ADI REICH, None.*

MO0116

The Role of Wnt10b in Antiresorptive Therapy for Ovariectomy-Induced Osteoporotic Rats. Jia-Fwu Shyu*¹, Hung-Shu Ma², Jung-Tzu Cheng², Tzu-Hui Chu², Wei-Yu Chen², Yen-Nien Ting². ¹National Defense Medical Center, Taiwan, ²Department of Biology & Anatomy, National Defense Medical Center, Taiwan

Osteoporosis is characterized by a marked decrease in bone mineral density and strength, resulting in fragility fractures associated with high morbidity and mortality. Uncoupling antiresorptives, such as calcitonin, odanacatib, and saracatinib, are better drugs because they inhibit osteoclast bone resorbing activity while maintaining the communication between osteoclasts and osteoblasts that promotes bone formation.

Our recent results indicated that calcitonin inhibited bisphosphonate-induced osteoclast apoptosis and combined usage of calcitonin and bisphosphonate increases its efficacy in a rat model of osteoporosis. This suggests that different kinds of antiresorptives may induce different bone formation-stimulating osteoclast-derived factors (clastokines). Wnt10b is a recent identified clastokine and potential novel therapeutic target of postmenopausal osteoporosis. The role of Wnt ligands involved in skeletal physiology and disease is not fully understood yet. We hypothesize that uncoupling antiresorptive increase bone formation by inducing Wnt10b expression in osteoclasts. Bone marrow hematopoietic mononuclear cells were isolated from femur and tibia of Sprague-Dawley rats. They were induced into osteoclasts by M-CSF and RANKL treatments. In these cells, calcitonin induced a decrease of TRAP stain-positive reaction. However, ELISA analysis showed increase of Wnt10b expression in supernatant collected from the calcitonin-treated osteoclasts. Pretreatment of Wnt10b secretion inhibitor, C-59, blocked the increase of Wnt10b induced by calcitonin. Western blot analysis showed increase of Wnt10b in the calcitonin-treated osteoclasts. Culture of osteoblasts isolated from neonatal rat calvarias with the calcitonin-treated osteoclasts supernatant showed increase of mineralization as indicated by alizarin red staining. In vivo, microCT analysis showed calcitonin and alendronate treatment recover bone loss in ovariectomized rats. In these animals, immunohistochemistry showed calcitonin increases level of Wnt10b in femur as compared to saline- and alendronate-treated groups. In conclusion, the present study provides more information of calcitonin on the molecular level of bone remodeling which will help in future potential therapeutic studies on postmenopausal osteoporosis.

Disclosures: *Jia-Fwu Shyu, None.*

MO0117

Effects of genetic ablation of parathyroid hormone on the induction of FGF23 by dietary phosphate. Sherrri-Ann Burnett-Bowie*, Marie Demay. Massachusetts General Hospital, USA

Both parathyroid hormone (PTH) and fibroblast growth factor 23 (FGF23) increase in response to a dietary phosphate load in humans and mice. Because PTH promotes production of 1,25-dihydroxyvitamin D, a known inducer of FGF23 expression, it is not known whether PTH induces FGF23 directly or indirectly through its actions on 1,25-dihydroxyvitamin D or circulating calcium levels.

To determine if PTH is required for induction of FGF23 in response to dietary phosphate loading, male and female PTH-knockout (*PTHKO*) mice and their wildtype (*WT*) littermates were weaned onto chow d18 and transitioned to a 0.6% calcium, 1.25% phosphate diet d28 with terminal bleeding on d35. To determine the contributions of PTH to basal FGF23 levels, *WT* and *PTHKO* littermates were treated with the calcimimetic R568 at 10 mcg/g (Amgen, Inc) from d28 to 35 while being maintained on standard chow (1.0% calcium and 0.4% phosphate). FGF23 was measured using the Immotopics C-terminal assay.

Chow fed *PTHKO* mice were hypocalcemic and hyperphosphatemic d28 as compared with *WT* littermates. Despite this hyperphosphatemia, *PTHKO* mice had significantly lower circulating FGF23 levels than *WT* littermates. In response to 7 days of dietary phosphate loading, (d28- 35) circulating FGF23 increased significantly, in both the *PTHKO* mice and *WT* littermates, suggesting that PTH is not required for the induction of FGF23 by a dietary phosphate load. Ionized calcium decreased with dietary phosphate loading in the *PTHKO* mice, but not in *WT* littermates. Administration of R568 to chow-fed *PTHKO* and *WT* littermates from d28-35 decreased circulating ionized calcium and increased circulating FGF23 levels, though there was no difference in these levels between *WT* and *PTH gene* ablated mice.

Thus, PTH is not required to maintain basal circulating FGF23 levels, nor is PTH required for induction of FGF23 in response to dietary phosphate loading. The induction of FGF23 observed with the administration of a calcimimetic suggests that the parathyroid or renal calcium sensor may be involved in the regulation of circulating FGF23.

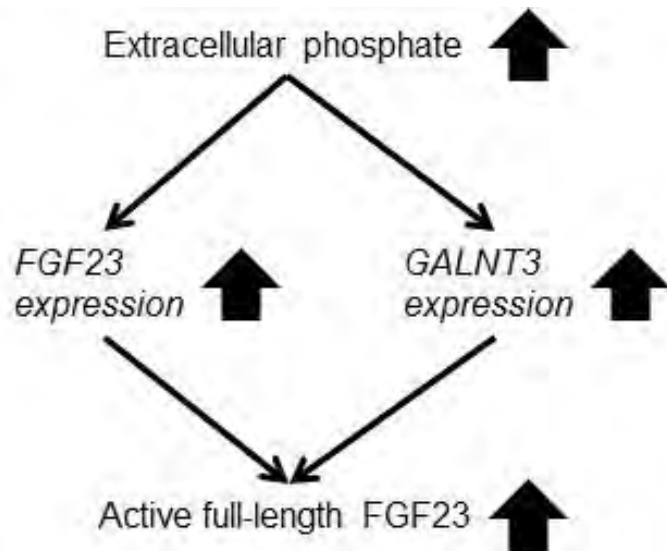
Disclosures: *Sherrri-Ann Burnett-Bowie, None.*

MO0118

Phosphate Regulates Production and Post-Translational Modification of FGF23. Yuichi Takashi*¹, Yuka Kinoshita², Nobuaki Ito³, Michiko Hori³, Manabu Taguchi³, Seiji Fukumoto¹. ¹Fujii Memorial Institute of Medical Sciences, Tokushima University, Japan, ²Division of Nephrology & Endocrinology, The University of Tokyo Hospital, Jordan, ³Division of Nephrology & Endocrinology, The University of Tokyo Hospital, Japan

Purpose: Hormonal function is regulated not only by the production but also by post-translational modification. Fibroblast growth factor 23 (FGF23) is a hormone produced by bone. FGF23 affects serum phosphate levels by suppressing the expression of sodium-phosphate co-transporters in the proximal tubules. In addition, FGF23 suppresses the production of 1,25-dihydroxyvitamin D and decreases intestinal phosphate absorption. A part of FGF23 protein is cleaved into inactive fragments. It was previously shown that O-glycosylation of FGF23 protein by GalNac-T3, a gene product of *GALNT3*, inhibits this cleavage. However, the regulatory mechanisms of this processing remain to be clarified. Methods: Human *FGF23* was overexpressed in UMR106 cells and the processing of FGF23 protein was analyzed by Western blotting of conditioned media using an antibody recognizing C-

terminal portion of FGF23. We also analyzed the expression of *Fgf23* and *Galnt3* by real-time PCR. Results: Western blotting detected both intact full-length and C-terminal fragment of FGF23. Increase of extracellular phosphate enhanced *Fgf23* expression and also increased full-length / C-terminal fragment ratio of FGF23 protein indicating that phosphate prevented the processing of FGF23 protein. Extracellular phosphate also enhanced *Galnt3* expression. Overexpression of both *FGF23* and *GALNT3* in UMR106 cells increased full-length / C-terminal fragment ratio of FGF23 protein in the conditioned media compared to cells with *FGF23* alone. Conclusions: It is well known that the increase of calcium concentration inhibits parathyroid hormone (PTH) production and enhances PTH degradation in parathyroid glands. In this study, the increase of extracellular phosphate not only promoted *Fgf23* production but also inhibited the cleavage of FGF23 protein possibly through enhancing expression of *Galnt3* (Fig.). Therefore, the activity of FGF23 is regulated by both its production and post-translational processing. These results confirm that FGF23 functions as a phosphotropic hormone.



Fig

Disclosures: Yuichi Takashi, None.

MO0119

Calorie restriction changes bone metabolism by a pathway both GH-IGF-1 axis and others in rat. Seichiro Shimauchi^{1*}, Masato Tomita¹, Isao Shimokawa², Makoto Osaki¹. ¹Department of Orthopaedic Surgery, Graduate School of Biomedical Sciences, Nagasaki University, Japan, ²Investigative Pathology, Graduate School of Biomedical Sciences, Nagasaki University, Japan

Objective: Previous studies elucidated the effect of caloric restriction on life extension in different kinds of experimental animal; however, the effect on bone metabolism has not been sufficiently clarified. Growth hormone-insulin-like growth factor (GH-IGF-1) axis, greatly associated with the effect of caloric restriction on life extension, may have an effect on bone metabolism. In this study, we investigated the effect of caloric restriction on bone metabolism and the role of GH-IGF-1 axis by comparing the bone metabolism of calorie-restricted rats with that of GH-suppressed rats.

Methods: We divided male Wistar rats into a WT AL group (wild-type, fed *ad libitum* from 6 weeks old) and WT CR group (wild-type, fed a calorie-restricted diet [30%]) and sacrificed them at the age of 10 months. Similarly, GH-antisense transgenic (Tg) rats, the first filial hybrid rats fed *ad libitum* (F1 AL) until the age of 10 months, were sacrificed. Their femurs and blood were collected. While bone microstructural analysis of the femurs was conducted by micro CT, IGF-1 and bone metabolism markers were measured in blood; thereby, we compared the differences among the groups.

Results: The body weight was significantly higher in the WT AL group than WT CR and F1 AL groups, and was the second highest in the WT CR group. Blood IGF-1 level was significantly higher in the WT AL group than F1 AL groups, but there were no significant differences in blood IGF-1 level between WT AL and WT CR groups. On bone microstructural measurement by micro CT, the bone density (bone volume over total volume [BV/TV]) was significantly higher in the WT AL group than WT CR ($P < 0.05$). There were no significant differences in BV/TV between WT AL and F1 AL groups, but values were lower in the F1 group. No significant differences were observed in bone alkaline phosphatase, a type of osteogenic marker, among the groups.

Discussion: From the results of this study, the effect of caloric restriction on bone metabolism is likely to be due to GH-IGF-1 axis, but it is suggested that there is another pathway other than GH-IGF-1.

Disclosures: Seichiro Shimauchi, None.

MO0120

Diphtheria Toxin- and GFP-PTX-based mouse models of acquired hypoparathyroidism and treatment with a long-acting parathyroid hormone analog. Ruiye Bi^{1*}, Tomoyuki Watanabe¹, Yi Fan², Thomas Gardella¹, Michael Mannstadt¹. ¹Massachusetts general hospital, USA, ²Harvard School of Dental Medicine, USA

Background: Hypoparathyroidism (HP) is caused by inadequate levels of PTH and is characterized by hypocalcemia, hyperphosphatemia, and low bone turnover. The most common form of HP is post-surgical, caused by damage or removal of the parathyroid glands during neck surgery. Treatment with oral calcium and active vitamin D can lead to hypercalciuria and renal complications. More effective therapies are needed, but development of these requires reliable animal models.

Methods: PTHcre-iDTR mouse were generated by crossing mice carrying an inducible diphtheria toxin receptor (iDTR) allele with mice carrying a PTH-Cre allele, such that DTR is expressed specifically in the parathyroid glands. Parathyroid cells can thus be selectively destroyed by injecting mice with diphtheria toxin (DT). GFP-PTX mice were generated using mice that specifically express GFP in the parathyroid glands, such that surgical removal of the glands is greatly facilitated by the localized green fluorescence.

Results: Optimizing the dosing regimen of DT in PTHcre-iDTR mice revealed that two repetitive injections of DT at 5ug/kg, i.p. yielded the greatest reductions in serum PTH and blood Ca^{++} levels, as compared to vehicle injections (PTH = 251 ± 83 vs. 580 ± 53 pg/mL; Ca^{++} = 1.12 ± 0.03 vs. 1.26 ± 0.06 mmol/L; $p < 0.05$; $n=8$). More pronounced reductions in serum PTH and blood Ca^{++} levels were observed in the GFP-PTX mice (PTH = 32 ± 21 pg/mL; Ca^{++} = 1.05 ± 0.05 mmol/L measured 3 days after PTX surgery).

We then evaluated the efficacy of a long-acting PTH analog, LA-PTH, in correcting the hypoparathyroidism in these two mouse models. In each model, a single s.c. injection of LA-PTH (10 nmol/kg) elevated blood Ca^{++} to approximately the normal range, and the calcemic effects persisted for up to ~48 hours. In contrast, a single injection of PTH(1-34) at a five-fold higher dose (50 nmol/kg) elevated blood Ca^{++} levels for no longer than 6 hours. Importantly, LA-PTH did not increase urinary calcium excretion.

Conclusions: We present two new mouse models of acquired hypoparathyroidism: a PTHcre-iDTR mouse, which eliminates the need for surgery, and a GFP-PTX mouse, which greatly facilitates parathyroid surgery and provides for a more severe HP phenotype. The utility of these models is highlighted by the rescue effects observed with a long-acting PTH analog.

Disclosures: Ruiye Bi, None.

MO0121

Effects of Abaloparatide on the Expression of Bone Resorption- and Formation-related Factors in Osteoblastic Cells; a Comparison with Teriparatide. Akito Makino^{*}, Hideko Takagi, Hiroyuki Sugiyama, Tsunefumi Kobayashi, Yoshinori Kasahara. Teijin Institute for Bio-Medical Research, Teijin Pharma Limited, Japan

Abaloparatide (ABL), a novel synthetic analog of human parathyroid hormone-related peptide, is currently under clinical development for severe osteoporosis in United States, Europe and Japan. In these clinical studies, the intermittent administration of ABL showed robust increase in bone mineral density (BMD) while its calcemic effect was limited as compared with teriparatide (TPD). Analysis of bone turnover markers suggested that both ABL and TPD increased bone formation and resorption, but bone resorption by ABL was lower than that by TPD.

In this study, to address the difference in the mechanism of action of ABL and TPD, effects on the expression of bone formation- and resorption-related factors were examined in human osteoblastic cell line, SaOS. Cells were treated with ABL or TPD transiently by mimicking clinical dosing regimen. Then, the expression of RANKL and M-CSF as bone resorption-related factors, and SOST and DKK1 as bone formation-related factors was measured by quantitative PCR and ELISA. ABL and TPD increased RANKL and M-CSF mRNA expression level, but these effects were rapidly reversed after removal of ABL from the culture media, while those in TPD-treated cells were sustained. Similarly, increased expression of M-CSF declined more rapidly after removal of ABL than TPD.

Next, to assess the influence on bone formation, expression of Wnt signaling inhibitors, SOST and DKK1, were measured. Cells were differentiated into post-osteoblast/pre-osteocyte state where the higher expression levels of SOST and DKK1 were confirmed. Both ABL and TPD suppressed the expression of SOST and DKK1. These effects continued after removal of the compounds and no difference was seen between ABL and TPD, suggesting comparable efficacy of ABL and TPD on Wnt-mediated bone formation.

These results suggest that ABL stimulates bone resorption less than TPD, while bone formation is similarly enhanced. The difference between ABL and TPD obtained in this study strongly supports the results of the clinical studies. ABL has a more potent effect on BMD increase and lower risk of hypercalcemia based on the preferable balance of bone formation to bone resorption as compared with TPD.

Disclosures: Akito Makino, Teijin Pharma Limited

MO0122

The Calcium-Sensing Receptor Supports the Growth and Survival of Breast Cancer Cells By Stimulating Parathyroid Hormone-related Protein Production in Calcium Rich Environments. Wonnam Kim*, Pamela Dann, Karena Swan, John Wysolmerski. Yale School of Medicine, USA

Bone metastases from breast cancer cause pain, hypercalcemia, pathologic fractures and, ultimately, death. In order for breast cancer cells to grow in the bone microenvironment, they must adapt to high levels of extracellular calcium. Cells respond to extracellular calcium by activating the calcium-sensing receptor (CaSR), a G protein-coupled receptor that binds and signals in response to calcium and other cations. The CaSR is expressed in many breast cancer cell lines and its expression has been shown to be higher in bone metastases than in primary tumors in patients. Therefore, we studied the role of the CaSR in breast cancer cell behavior. First, we identified that activation of the CaSR with high extracellular calcium stimulated proliferation in human BT474 breast cancer cells. Knocking down expression of the CaSR inhibited proliferation in response to extracellular calcium. BT474 cells treated with the CaSR antagonist, NPS2143, showed decreased proliferation in a dose dependent manner. Activation of the CaSR also increased the production of parathyroid hormone-related protein (PTHrP). Since PTHrP has been reported to increase proliferation in some breast cancer cell lines, we also knocked down PTHrP expression in BT474 cells, which reduced proliferation in response to increasing doses of calcium. The proliferation was not mediated by PTH receptor signaling but by nuclear translocation of PTHrP, which inhibited the cell cycle inhibitor p27. Knocking down either the CaSR or PTHrP, or treatment with NPS2143 also dramatically induced apoptosis in response to increasing doses of extracellular calcium. Apoptosis was mediated through the nuclear translocation of apoptosis-inducing factor (AIF). In order to determine whether these findings were relevant in vivo, we knocked out the CaSR in breast tumors in MMTV-PyMT transgenic mice. These mice showed decreased tumor PTHrP expression, slower tumor growth and prolonged survival. CaSR knockout tumors showed lower rates of BrdU incorporation and increased p27 levels. However, at normal calcium levels, rates of apoptosis were negligible in both knockout and control tumors. These data suggest that the CaSR promotes the survival and proliferation of breast cancer cells under calcium-rich conditions such as those found in the bone microenvironment, and that PTHrP acts as an important mediator of these effects.

Disclosures: Wonnam Kim, None.

MO0123

Cyp11a1 Expression In Bone Is Associated With Aromatase Inhibitor-Related Bone Loss. MARIA RODRIGUEZ SANZ*¹, NATALIA GARCIA-GIRALT¹, DANIEL PRIETO-ALHAMBRA², SONIA SERVITJA³, SUSANA BALCELLS⁴, ROSANGELA PECORELLI⁵, ADOLFO DÍEZ-PÉREZ⁵, DANIEL GRINBERG⁴, IGNASI TUSQUETS³, XAVIER NOGUES⁵. ¹IMIM (Hospital del Mar Research Institute), Red Temática de Investigación Cooperativa en Envejecimiento y Fragilidad (RETICEF), ISCIII, Barcelona, Spain., Spain, ²Nuffield Department of Orthopaedics, Rheumatology & Musculoskeletal Sciences, Oxford. NIHR Musculoskeletal Biomedical Research Unit, University of Oxford, Oxford, UK., United Kingdom, ³Medical Oncology Department, Hospital del Mar, Universitat Autònoma de Barcelona, IMIM (Hospital del Mar Research Institute), Barcelona, Spain., Spain, ⁴Departament de Genètica, Universitat de Barcelona, IBUB, Centro de Investigación Biomédica en Red de Enfermedades Raras (CIBERER), ISCIII, Barcelona, Spain., Spain, ⁵Internal Medicine Department, Hospital del Mar, Universitat Autònoma de Barcelona, Barcelona, Spain., Spain

Aromatase inhibitors (AIs) used as adjuvant therapy in postmenopausal women with hormone receptor-positive breast cancer cause diverse musculoskeletal side effects that include bone loss and its associated fracture. The present study aimed to determine the genetic basis for the bone loss variability observed among women receiving AI treatment. B-ABLE is a prospective cohort of 531 women recruited at the time they initiate AI therapy in a bone metabolism unit. Bisphosphonate users were excluded, and finally 391 patients were selected for these analyses. SNPs in candidate genes involved in vitamin D and estrogen hormone-response pathways (CYP11A1, CYP17A1, HSD3B2, HSD17B3, CYP19A1, CYP2C19, CYP2C9, ESR1, DHCR7, GC, CYP2R1, CYP27B1, VDR and CYP24A1) were genotyped for association analysis with AI-related bone loss (AIBL). Multivariate linear regression was used to test their association with relative lumbar spine (LS) and femoral neck (FN) BMD loss after 1 and 2 years of follow-up. All models were adjusted for age, body mass index, previous tamoxifen and chemotherapy. Further, potential confounding for baseline 25(OH)-VITD concentrations and AI used was assessed. Next, CYP11A1 and expression in human fresh bone tissue and primary osteoblasts was assessed by RT-PCR. Western blot was used to detect the human cholesterol side-chain cleavage enzyme (encoded by CYP11A1 gene) in osteoblasts. After 2 years on AI treatment, 80.3% and 61.6% patients suffered a significant bone loss at lumbar spine (LS) and femoral neck (FN), respectively. In contrast, up to one third (19.6% LS, 38.6% FN) showed no decline or even increased bone density. After multiple testing correction, 3 tag-SNPs (rs4077581, rs11632698 and rs900798) located in the gene CYP11A1 were

significantly associated ($p < 0.005$) with FN AIBL at 2 years of treatment. CYP11A1 and CYP17A1 mRNA were detected in primary osteoblasts and total bone tissue. Both common isoforms of cholesterol side-chain cleavage enzyme were identified in osteoblasts. In conclusion, the genetic association of CYP11A1 gene with AIBL and its expression in bone tissue reveals a potential local function of this enzyme in bone metabolism regulation, offering a new vision of the steroidogenic ability of this tissue and new understanding of aromatase inhibitor-induced bone loss.

Disclosures: MARIA RODRIGUEZ SANZ, None.

MO0124

Enzalutamide Reduces the Bone Mass in the Axial but not the Appendicular Skeleton in Male Mice. Jianyao Wu*¹, Sofia Movérare-Skrtic¹, Anna E Börjesson¹, Marie K Lagerquist², Klara Sjögren¹, Sara H Windahl¹, Antti Koskela³, Louise Grahne², Ulrika Islander², Anna S Wilhelmson⁴, Åsa Tivesten⁴, Juha Tuukkanen³, Claes Ohlsson¹. ¹Centre for Bone & Arthritis Research, Institute of Medicine, Sahlgrenska Academy, University of Gothenburg, Sweden, ²Centre for Bone & Arthritis Research, Institute of Medicine, Sahlgrenska Academy, University of Gothenburg, Gothenburg, Sweden, ³Department of Anatomy & Cell Biology, Medical Research Center, University of Oulu, Finland, ⁴The Wallenberg Laboratory for Cardiovascular & Metabolic Research, Institute of Medicine, Sahlgrenska Academy, University of Gothenburg, Sweden

Testosterone is a crucial regulator of the male skeleton and its skeletal effects are at least partly mediated via estrogen receptors as a result of aromatization of testosterone into estradiol. In addition, lifelong global androgen receptor (AR) inactivation results in reduced bone mass in both the axial and appendicular skeleton of male mice. In the present study, the role of the AR for adult bone metabolism was evaluated by means of the drug enzalutamide, which is a new efficient and specific AR antagonist used in the treatment of prostate cancer patients.

Nine-week-old male mice were treated with 10 mg/kg/day, 30 mg/kg/day, or 100 mg/kg/day of enzalutamide for 21 days or were surgically castrated and compared with vehicle-treated gonadal-intact mice.

Enzalutamide treatment markedly reduced the weights of the seminal vesicles and the levator ani muscle, confirming an AR antagonistic effect of enzalutamide. Although orchidectomy (orx) substantially reduced the cortical bone thickness and trabecular bone volume fraction (BV/TV) in the appendicular skeleton, these parameters were unaffected by enzalutamide. In contrast, both enzalutamide and orx reduced the trabecular bone mass in the axial skeleton as revealed by reduced lumbar spine areal bone mineral density (enzalutamide 100 mg/kg/day $-10.1 \pm 1.1\%$; orx $-7.7 \pm 0.9\%$, $p < 0.001$) and trabecular BV/TV in L₅ vertebrae (enzalutamide 100 mg/kg/day $-11.8 \pm 1.9\%$; orx $-20.5 \pm 2.7\%$, $p < 0.001$) compared with vehicle-treated gonadal intact mice. A compression test of the L₅ vertebrae revealed that the mechanical strength in the axial skeleton was significantly reduced by enzalutamide treatment (maximal load at failure, $-15.3 \pm 3.5\%$; $p < 0.01$). The effects of enzalutamide in the axial skeleton were associated with a high bone turnover supported by elevated serum levels of the bone resorption marker C-terminal collagen cross-links ($+40.7 \pm 8.4\%$; $p < 0.01$) and the bone formation marker osteocalcin ($+55.0 \pm 10.1\%$; $p < 0.01$) as well as increased bone formation rate as measured by dynamic histomorphometry in the L₄ vertebrae.

In conclusion, enzalutamide reduces the bone mass in the axial but not the appendicular skeleton in male mice. Castration, affecting both estrogenic and androgenic pathways, increases the risk of both vertebral and non-vertebral fractures while our findings suggest that anti-androgen monotherapy with enzalutamide may increase vertebral but not non-vertebral fracture risk.

Disclosures: Jianyao Wu, None.

MO0125

Estrogen and Androgen Differentially regulate RUNX2: Genome-wide analysis with implications to gender-dependent control of bone formation and resorption. Anthony Martin¹, Jiali Yu¹, Jian Xiong¹, Jie Ji¹, Anna Börjesson², Sara Windahl², Paul Kostenuik³, Yankel Gabel⁴, Nyam-Osor Chimgé¹, Dustin Schones⁵, Claes Ohlsson², Baruch Frenkel^{*1}. ¹University of Southern California, USA, ²Gothenburg University, Sweden, ³Phylon Pharma Services, USA, ⁴Tel Aviv University, Israel, ⁵City of Hope, USA

The master transcription factor RUNX2 promotes both osteoblast differentiation and osteoblast-driven osteoclastogenesis. Receptors for steroid hormones, including estrogens and the androgens, physically interact with RUNX2 and generally attenuate stimulation of its target genes. Loss of these interactions may therefore contribute to increased bone turnover upon loss of sex steroids. To investigate the RUNX2-related regulatory gene network mediating skeletal effects of estradiol (E2) and dihydrotestosterone (DHT), we employed the NeMCO/Rx2dox primary culture system, in which doxycycline (dox) induces premature RUNX2 expression in Newborn Mouse Calvarial Osteoblasts. As expected, dox induced, and both E2 and DHT counteracted, expression of osteoblast marker genes (e.g., *Ibsp*, *Sparc*). Additionally, RUNX2 induced, and sex steroids antagonized osteoclastogenic genes (e.g., *Ltc4s*), as well as association of RANKL with the osteoblast membrane, likely contributing to

osteoblast-driven osteoclastogenesis and the anti-resorptive properties of sex steroids, respectively. Because loss of sex steroids increases bone resorption more than it increases bone formation, we hypothesized that it has differential effects on the activity of RUNX2 upon different target genes. Furthermore, because the bone-sparing effects of androgens go beyond those mediated through aromatization to estrogens, we also hypothesized that the locus-specific hormonal responses of RUNX2 target genes differ between estrogens and androgens. To test these hypotheses, we compared the influence of E2 and DHT on RUNX2-driven gene expression in NeMCO/Rx2dox cells using microarray hybridization. Whereas both sex hormones generally attenuated RUNX2-driven expression of its target genes, each of E2 and DHT displayed locus-specific interactions. Thus, the magnitude of attenuation varied considerably among RUNX2 target genes. Furthermore, exceptional gene sets were defined, which were resistant to steroid-mediated RUNX2 attenuation, and these gene sets varied considerably between E2 and DHT. Finally, we identified genes displaying uncommon additive and even synergistic interactions between RUNX2 and sex steroids, and again these gene differed considerably between E2 and DHT. In summary, RUNX2 may play a pivotal role in the skeletal response to loss of sex steroids. First, the general upregulation of RUNX2-driven transcription may contribute to increased bone turnover. Second, locus-specific effects of estrogens and androgens may contribute to shifting the balance between bone resorption and bone formation towards the former. Third, differential modulation of the responses to RUNX2 by androgens versus estrogens may contribute to gender differences in adult bone metabolism.

Disclosures: Baruch Frenkel, None.

MO0126

High-fat diet can elicit diverse effects on bone in relation with different sex hormone status. Shinya Tanaka¹, Takuto Tsuchiya², Akinori Sakai³, Hiroshi Odd¹. ¹Saitama Medical University, Japan, ²University of Occupational & Environmental Health, Japan, ³University of Occupational & Environmental Health, Japan

(Background and Objective) High-fat diets also decreased bone volume, what we clearly demonstrated in our recent study using male mice given high-fat diet due to increases in bone resorption and decreases of bone formation. On the other hand, weight losses in women are one of independent risk factors of osteoporotic fracture. Thus high-calorie diet can elicit diverse effects on bone in relation with different sex hormone status. The objective of this study is to clarify the difference of effects of high-fat diet on bone between ovariectomized (OVX) mice and sham operated female mice.

(Materials and Methods) Seven weeks old, female, C57BL/6J mice were purchased and subjected to 4 groups, sham operated mice given standard chow (SS), OVX mice given standard chow (OS), sham operated mice given high-fat diet (SH), and OVX mice given high-fat (OH). After 1 week of acclimatization, mice were operated sham or OVX, and were given standard or high-fat diets from 8 weeks age to 20 weeks age. At 6 and 12 weeks of experiment, bone mineral density (BMD) in the lumbar spine and the femur of mice were detected under anesthesia. At the end of experiment, mice were sacrificed and the left tibia was harvested for bone histomorphometry.

(Results) Decreases in BMD were observed in the lumbar spine of OVX mice and what was more apparent in OH mice, while the lumbar BMD did not decrease in SH mice. In the femur, although decreases in BMD was not observed OS mice or SH mice, while decreased in BMD in OH mice was apparent. Increasing in bone volume (BV/TV) were observed in SH mice insignificantly, while decreased of BV/TV were observed in OH mice significantly. Although mineralizing surface (MS/BS) and bone formation rate (BFR/BS) increased insignificantly in SH mice compared with SS mice, MS/BS and BFR/BS in OH mice decreased compared with OS mice insignificantly. (-Conclusion) High-fat diet increases in bone formation and in bone volume in sham operated mice, but facilitates decreases of bone formation and of bone volume in ovariectomized mice.

Disclosures: Shinya Tanaka, None.

MO0127

Broader Transcriptional Activity of Vitamin D Receptor (VDR) in the Absence of 1,25-dihydroxyvitamin D in Human Cells. Bruno Ferraz-de-Souza¹, Pedro L F Costa², Eduardo C Teodoro², Maria L Katayama³, Maria A K Folgueira³, Monica M Franca². ¹Univ of Sao Paulo School of Medicine (FMUSP), Brazil, ²Endocrinology/LIM-18, Univ of Sao Paulo School of Medicine, Brazil, ³Oncology/LIM-24, Univ of Sao Paulo School of Medicine, Brazil

The vitamin D receptor (VDR) is expressed in several cell types beyond those involved in vitamin D-mediated mineral homeostasis, prompting the investigation of its actions in general human health. VDR activation by 1,25-dihydroxyvitamin D (1,25D) leads to transcriptional regulation of numerous targets, and the unliganded VDR is believed to mainly silence target gene transcription. Understanding human VDR actions in the absence of 1,25D may shed light on the transcriptional outcome of 1,25D dosage variation and the molecular consequences of vitamin D insufficiency.

We have established skin fibroblast cultures from a patient bearing a severe homozygous p.Arg30* VDR mutation (MUT), leading to ablation of VDR expression, and from a healthy control individual (CO). Absence of VDR expression

and resistance to 1,25D in MUT cells were confirmed by immunoblotting and RTPCR. Total RNA was extracted from MUT and CO cells after 24-h treatment with vehicle or 10 nM 1,25D, and global gene expression was analyzed with Affymetrix Human Gene 2.0 ST arrays. A Benjamini-Hochberg $p < 0.05$ was set for significance. For subsets of targets, relative gene expression was confirmed by TaqMan qRT-PCR and direct VDR binding to DNA was confirmed by chromatin immunoprecipitation.

In CO fibroblasts with intact VDR, expression of 1,161 target genes was regulated by 1,25D. Confirming the extreme insensitivity of MUT cells, 1,25D treatment led to differential expression of 2 genes only. Surprisingly, 4,051 genes were differentially expressed in CO and MUT cells treated with vehicle, reflecting basal VDR regulation. A bioinformatics approach was undertaken to correct for putative genetic background variability, rendering the identification of 2,164 genes regulated by VDR in the absence of 1,25D (71% up-, 29% down-regulated). Of these, 268 genes were also 1,25D targets, and an antagonistic effect in absence vs presence of ligand was seen. Strikingly, 194 genes (73%) were basally upregulated by VDR and downregulated by 1,25D stimulus. In conclusion, we report broader transcriptional output induced by VDR in the absence of 1,25D in human fibroblasts. Approximately a quarter of 1,25D targets in these cells are also basally regulated by VDR. Furthermore, an antagonistic transcriptional activity of the VDR is seen in basal vs 1,25D-activated states, mainly in the form of basal upregulation and ligand-induced downregulation of target genes, challenging the current paradigm for VDR activity.

Disclosures: Bruno Ferraz-de-Souza, None.

MO0128

CKD induces intrinsic alterations in osteoblast response to 1,25D. Renata Pereira¹, Nadine Khouzam¹, Richard Bowen¹, Earl Freymiller², Isidro Salusky¹, Katherine Wesseling-Perry³. ¹David Geffen School of Medicine at UCLA, USA, ²School of Dentistry, UCLA, USA, ³UCLA Medical Center, USA

Chronic kidney disease (CKD) increases expression of osteocyte-specific regulators of bone metabolism, including FGF23. 1,25D is used to control bone turnover in children with CKD but increases osteocytic FGF23 expression. We have demonstrated that primary osteoblasts obtained from patients with CKD have altered proliferation and mineralization characteristics, suggesting CKD-mediated intrinsic changes to osteoblast biology. The direct effect of 1,25D and FGF23 on osteoblast maturation and mineralization in the context of CKD remains unknown. Thus, primary human osteoblasts from 3 healthy controls, 3 pediatric dialysis patients with low bone turnover (adynamic bone) and 3 pediatric patients with high bone turnover (2°HPT) were cultured under pro-mineralizing conditions consisting of 10mM β -glycerolphosphate and 100 μ g/ml ascorbic acid in the presence of 1,25D at 1, 10, and 100 nM. After 2, 3, and 4 weeks of growth, cells were washed, fixed with 10% formalin, and stained with 2% Alizarin Red S. Mineral content was assessed by measuring absorption of acetic acid-extracted Alizarin Red S dye (at 405 nm) normalized by live cell concentration (as assessed by absorption (at 570 nm) of methanol-extracted Crystal Violet staining obtained from parallel cultures. 1,25D treatment decreased proliferation and increased mineralization; however, high concentrations were required in CKD cells, suggesting osteoblast resistance to 1,25D in CKD. (Figure 1)

To assess whether FGF23 modifies the effects of CKD and 1,25D on osteoblast maturation and mineralization, cells from 3 healthy controls and 3 pediatric CKD patients with normal rates of bone turnover were induced to mineralize by culturing for 2 weeks under pro-mineralizing conditions (as above). 1,25D (10nM) and/or FGF23 (10 nM) were then added to the media for an additional 2 weeks. Mineralized nodule formation was compared to cells from the same individuals grown for 4 weeks in the presence of 1,25D, FGF23, or both. 1,25D alone increased mineralization in control and CKD cells already entering a mineralized state while the addition of FGF23 to 1,25D increased mineralization in CKD but not in control cells already starting to mineralize. By contrast, the addition of FGF23 and 1,25D before the onset of mineralization inhibited mineralization in control, although not in CKD, cells, suggesting an interaction between the effects of 1,25D, FGF23, and CKD in osteoblast maturation and mineralization. (Figure 2)

between D2 and D3 mice ($193 \text{ pg/ml} \pm 9.0$ vs. $196 \text{ pg/ml} \pm 6.2$) at wk 8. Using two-way ANOVA to assess the impact of diet independent of sex, bone histomorphometric analysis showed that wk8 mice fed D2 only had significantly higher values for osteoclast surface/bone surface (Oc.S/BS), eroded surface/bone surface ES/BS), and mineral apposition rate (MAR) compared to D3 mice. By Mann-Whitney, osteoblast surface/bone surface (Ob.S/BS) was higher in wk 8 female but not wk 8 males. At wk16, D2 animals had significantly higher bone volume/total volume (BV/TV) and trabecular number (Tr.N) compared to D3 mice. Differences in bone phenotype were observed despite D2 fed mice reaching similar serum 25D levels and lower 1,25D levels compared to D3 fed animals. This suggests that D2 is less well bound to DBP, with the resulting higher levels of free 25D2 relative to 25D3 promoting differential effects on bone.

Disclosures: Rene Chun, None.

This study received funding from: Merck

MO0130

Examination of VDR/RXR/DRIP205 interaction, intranuclear kinetic and DNA binding in ras-transformed keratinocytes and its implication for designing optimal vitamin D therapy in cancer. Sylvester Jusu^{*1}, John Presley², Richard Kremer³. ¹Royal Victoria Hospital, Canada, ²McGill University, Canada, ³Supervisor, Canada

We previously reported that the malignant human keratinocyte HPK1Aras cell line is resistant to the growth inhibitory action of $1, 25(\text{OH})_2\text{D}_3$, compared to its normal counterpart immortalized HPK1A cells. We further demonstrated that this resistance was due to phosphorylation of the vitamin D receptor (VDR) heterodimeric partner, human retinoid X receptor alpha (hRXR α) on a critical amino acid, serine 260 located in close spatial proximity to regions of coactivators and corepressors interactions. We next demonstrated that subcellular localization of the hRXR α was impaired in HPK1Aras cells but could be restored using either the MAPK inhibitor UO126 or a non-phosphorylatable mutant of hRXR α (hRXR α ala260 mutant). In order to examine further the mechanisms of $1, 25(\text{OH})_2\text{D}_3$ resistance we looked at VDR/RXR and DRIP 205(a critical coactivator required for downstream signaling of $1, 25(\text{OH})_2\text{D}_3$) interactions, intranuclear kinetic in live cells and DNA binding in fixed cells using FRET (Fluorescence Resonance Energy Transfer), FLIP (Fluorescence Loss In Photobleaching), FRAP (Fluorescence Recovery After Photobleaching) and Hoechst staining. We used VDR-GFP, hRXR α wt-GFP, hRXR α mutant-GFP, VDR-mCherry, hRXR α wt-mCherry, hRXR α mutant-mCherry and DRIP205-GFP fluorescent receptors transfected into either HPK1A or HPK1A ras cells and treated with $1, 25(\text{OH})_2\text{D}_3$, 9-cis-Retinoic Acid or vehicle in the presence or absence of UO126.

Using FRET we showed that $1, 25(\text{OH})_2\text{D}_3$ addition increases their interaction in HPK1A cell but only in HPK1Aras cells treated with either UO126 or transfected with the hRXR α mutant. Furthermore, we demonstrated using FLIP that the half time of dissociation of hRXR α in the nucleus and residence time of the receptor within the nuclear compartments are significantly increased in HPK1Aras cells transfected with the non-phosphorylatable hRXR α mutant or treated with the MAPK inhibitor UO126.

Finally we demonstrated with Hoechst staining impaired VDR/ hRXR α /DRIP205 complex binding to chromatin in HPK1A-ras cells that was restored with UO126 treatment or transfection of the hRXR α mutant.

In summary we have demonstrated using highly specific intra-cellular tagging methods in live cells important alterations of the vitamin D signaling system in cancer cells in which the ras-raf-MAP kinase system is activated suggesting that specific inhibition of this commonly activated pathway could be targeted therapeutically to enhance vitamin D efficacy.

Disclosures: Sylvester Jusu, None.

MO0131

Gender Differences in Vitamin D Metabolism in MSCs from Pre-Pubertal Subjects. Julie Glowacki^{*1}, Brian Ruggiero¹, Kristina Christoph¹, Bonnie Padwa². ¹Brigham & Women's Hospital, USA, ²Boston Children's Hospital, USA

Vitamin D is crucial for mineral homeostasis and contributes to bone metabolism by inducing osteoblast differentiation of marrow stromal cells (MSCs). We recently reported that MSCs from adults demonstrate 1α -hydroxylase activity *in vitro* and express vitamin D-related genes; this raises a possible autocrine/paracrine role for D activation in pre-osteoblasts. Because nothing is known about vitamin D metabolism in MSCs from children, we tested the hypotheses that pre-pubertal MSCs have 1α -hydroxylase activity and express vitamin D-related genes. With IRB approval, we isolated MSCs from discarded excess iliac marrow graft from 6 male and 6 female subjects (age 8-12 yrs) undergoing alveolar cleft repair. There was a small difference in mean age (male: 10.3 yrs; female: 8.7 yrs; $p=0.01$). 1α -hydroxylation of substrate $25(\text{OH})\text{D}$ ($1 \mu\text{M}$, 24hr) was measured by ELISA for $1\alpha, 25(\text{OH})_2\text{D}$. RT-PCR was used for expression of D-related genes. Pediatric MSCs showed 1α -hydroxylase enzyme activity *in vitro* (68.7 - $160.3 \text{ fmol/mg protein/hr}$). There was constitutive expression of D receptor (VDR) and D-hydroxylases ($1\alpha/\text{CYP27B1}$, CYP27A1 , CYP2R1 , and CYP24A1). The constitutive expression of $1\alpha/\text{CYP27B1}$ paralleled the level of 1α -hydroxylase enzyme activity. There was 2.6-fold greater expression of $1\alpha/\text{CYP27B1}$ in

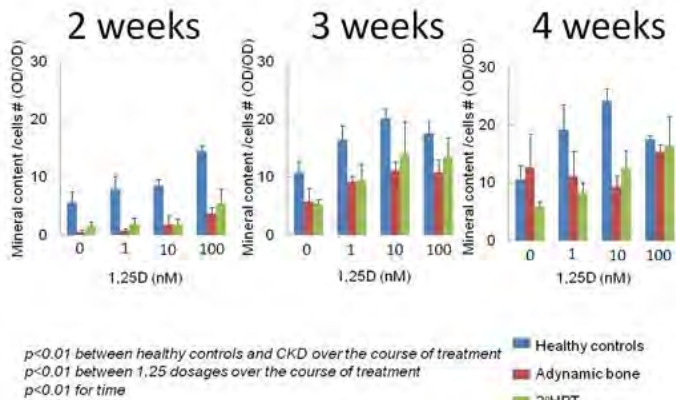


figure 1

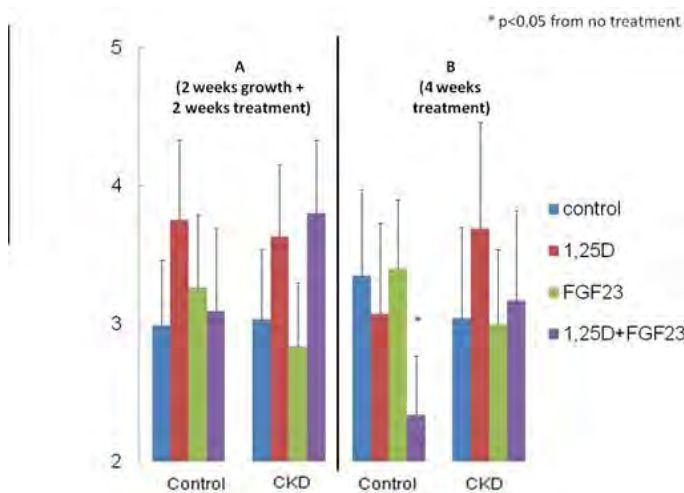


Figure 2

Disclosures: Renata Pereira, None.

MO0129

Differential Effects of Vitamin D2 vs. Vitamin D3 on Bone are Associated with Variations in Free 25-Hydroxyvitamin D. Rene Chun^{*1}, Renata Pereira², Tonnie Huijs³, Leon Swinkels³, Ivan Hernandez⁴, Rui Zhou⁵, Nancy Liu⁵, John Adams⁵, Martin Hewison⁴. ¹Dept of Orthopaedic Surgery, UCLA-Orthopaedic Hospital Research Center, Us, ²Dept of Pediatric Nephrology, David Geffen School of Medicine at UCLA, USA, ³Future Diagnostics, Netherlands, ⁴Centre for Endocrinology, Diabetes & Metabolism, The University of Birmingham, United Kingdom, ⁵Dept of Orthopaedic Surgery, UCLA-Orthopaedic Hospital Research Center, USA

Pro-hormone 25-hydroxyvitamin D (25D) circulates bound primarily to the serum vitamin D binding protein (DBP). For some target tissues DBP facilitates receptor-mediated uptake of 25D by cells, but 25D may also access target cells in a free, non-DBP-bound, form. To assess the importance of 'free' versus DBP-bound 25D for bone health, we compared the effects of vitamin D2 (D2) and vitamin D3 (D3) diets in mice. Both forms of vitamin D show similar 25-hydroxylation (to 25D2 and 25D3 respectively), but the 25D3 metabolite shows higher binding affinity for DBP than 25D2, so that free 25D may be higher for D2 relative to D3. Male and female mice were placed on diets containing equal amounts (1000 IU/kg) of D2 or D3 beginning at wk3 of age. At wk8 of age mice fed D2 diet had only 25D2 in circulation ($26.6 \text{ ng/ml} \pm 1.9$), and mice fed D3 mice had only 25D3 ($28.3 \text{ ng/ml} \pm 2.0$). Similar results were obtained at wk16 ($33.3 \text{ ng/ml} \pm 4.4$ for 25D2 vs. $31.7 \text{ ng/ml} \pm 2.1$ for 25D3). D2 fed mice had significantly ($p<0.05$) lower total $1, 25(\text{OH})_2\text{D}$ compared to D3 diet at both wk8 ($44.5 \text{ pg/ml} \pm 6.4$ vs. $62.4 \text{ pg/ml} \pm 11.6$) and wk16 ($78.4 \text{ pg/ml} \pm 12.6$ vs. $95.5 \text{ pg/ml} \pm 11.6$). By contrast, measured 'free' 25D was significantly ($p<0.001$) higher in D2 animals at wk8 ($16.8 \text{ pg/ml} \pm 0.65$ vs. $8.4 \text{ pg/ml} \pm 0.63$) and wk16 ($17.4 \text{ pg/ml} \pm 0.43$ vs. $8.4 \text{ pg/ml} \pm 0.44$). There was no significant difference in serum PTH

MSCs from boys compared with girls ($p=0.04$) and 3.5-fold greater expression of CYP24A1 in boys compared with girls ($p<0.0001$). There was 2.4-fold greater expression of ER α in MSCs from prepubertal boys than girls ($p<0.02$). *In vitro* treatment of female prepubertal MSCs with 10 nM 25(OH)D upregulated 1 α /CYP27B1 (4.8-fold), VDR (6.4-fold), and ER α (4.4-fold); and 10 nM 17 β -estradiol upregulated 1 α /CYP27B1 (5-fold) and CYP24A1, as well as VDR (2.6-fold), ER α (2.0-fold), and ER β , with no change in CYP27A1 or CYP2R1. These data show ranges of 1 α -hydroxylase activity and D-related genes in pre-pubertal hMSCs. The unexpected pre-pubertal gender differences in D metabolism in MSCs, not found for adults, suggest a possible metabolic insufficiency in prepubertal girls. Expression and regulation of vitamin D related genes in pre-pubertal hMSCs reinforce an autocrine/paracrine role for vitamin D in hMSCs. Finding striking gender differences in D-related genes in MSCs from prepubertal subjects adds insight to the metabolic environment of bone and presents a research approach for investigating and optimizing pediatric bone health.

Disclosures: Julie Glowacki, None.

MO0132

Mouse and Human Bacterial Artificial Chromosomes Encoding the CYP24A1 Loci Rescue the Ability of Cyp24a1 Null Mice to Catabolize 25-Hydroxyvitamin D₃ to 24,25-Dihydroxyvitamin D₃ and 25-Hydroxyvitamin D₃-26,23-Lactone. Alex Carlson^{*1}, Martin Kaufmann², Rene St-Arnaud³, Glenville Jones², J. Wesley Pike¹. ¹University of Wisconsin-Madison, USA, ²Queen's University, Canada, ³McGill University, Canada

Serum 25-hydroxyvitamin D₃ and 1,25-dihydroxyvitamin D₃ (1,25(OH)₂D₃) levels are maintained in part through CYP24A1 activity. Produced in the kidney, CYP24A1 expression is also found in all cellular targets of vitamin D action and is rapidly upregulated in response to 1,25(OH)₂D₃. Traditional approaches and more recent ChIP-seq analyses have identified 1,25(OH)₂D₃-inducible vitamin D receptor binding to both the promoter proximal region of CYP24A1 and to a cluster of elements downstream as well. Analyses of cell lines with stably integrated recombinant mouse and human BAC clones spanning the CYP24A1 loci and containing luciferase reporters within the 3' UTRs of each gene have shown that these constructs recapitulate the expression profile of endogenous CYP24A1 and that both the proximal and distal enhancer elements are involved in CYP24A1 regulation. To study this regulation further, we utilized these two mouse and human constructs as transgenes in mice. Two strains for each transgene were selected for their high basal, yet 1,25(OH)₂D₃-inducible renal luciferase activity as well as for inducible activity in other 1,25(OH)₂D₃ target tissues such as intestine, but not liver or muscle. Importantly, when crossed into a Cyp24a1 null background, both transgenes rescued the 24,25(OH)₂D₃ deficiency seen in the absence of Cyp24a1, producing somewhat higher levels of the metabolite than in wildtype mice. Interestingly, while 24,25(OH)₂D₃ was produced from both transgenes, the mouse version made significantly higher levels of the 25-hydroxyvitamin D₃-26,23-lactone than in human, supporting previous studies suggesting that utilization of this pathway is more prevalent in mice. Finally, examination of transgene expression revealed that all strains of mice expressed lower basal levels of renal CYP24A1 than seen for endogenous Cyp24a1. Coincident with this finding, the higher levels of circulating 24,25(OH)₂D₃ suggest either that the enzyme produced is incapable of fully catabolizing 24,25(OH)₂D₃ to water soluble products or that post transcriptional regulation of Cyp24a1 enzyme activity exists independently of low transcript production. Our current studies demonstrate that both mouse and human CYP24A1 gene loci are similarly expressed and regulated by 1,25(OH)₂D₃ in mice and are capable of rescuing the Cyp24a1 null phenotype. Nevertheless, these two transgenes continue to display both similar and unique features consistent with the species from which they were obtained.

Disclosures: Alex Carlson, None.

MO0133

Optimization of an Elisa for the Direct Measurement of Free 25OH Vitamin D. Nicolas Heuereux^{*1}, Leon Swinkels², Fabienne Mathieu¹, Tonnie Huijs², Ernst Lindhout², Gregg Mayer², Mike Martens². ¹DIAsource Immunoassays, Belgium, ²Future Diagnostics Solutions, Netherlands

The objective of this project was to optimize and characterize a simple immunoassay for the quantification of free 25-hydroxyvitamin D (25OH Vit D). Recent studies suggest that the concentration and genotype of Vitamin D binding protein (DBP) are important factors that determine the bioavailability of 25OH Vit D in blood. It has been suggested that measurement of free, non-protein bound 25OH Vit D in serum, may provide more relevant diagnostic information than the measurement of total 25OH Vit D, for instance in critically ill patients, statin treated patients, chronic kidney disease, liver failure, bladder cancer, pregnant women, or in hemodialysis patients. Following the first laboratory evaluation phase, a two-step enzyme-linked immunosorbent assay (ELISA) was optimized for the quantification of free 25OH Vit D assay. Modifications were made in the protocol for the coating of the monoclonal anti-25OH Vit D in the microtiter plates as well as in the formulation of the sample diluent and of the biotinylated Vitamin D conjugate. The optimized assay was validated against the first version of the assay and the calibration and sample values remained equivalent. The following performances were obtained: the calibrator

range was 0.2-35 pg/ml. The LoB was 1.9 pg/ml; the LoD was 2.8 pg/ml. Total assay precision was 10.2% at 6.0 pg/ml, 7.6% at 10.9 pg/ml and 5.5% at 24.9 pg/ml. The cross-reactivity of the antibody towards 25OH Vitamin D₂ was 77% and the influence of interfering hemoglobin, bilirubin and triglycerides was also verified. Finally the shelf life of the assay was extended to over one year when stored at 2-8°C. The evaluation of plasma samples and of the stability of free 25OH Vit D in serum samples stored at room temperature and at 2-8°C were also performed. The assay was recently compared to the calculation method for the determination of free 25OH Vit D levels in clinical populations and showed better results, i.e. in relationship with iPTH. (J.B. Schwartz, J. Clin. Endocrinol. Metab. 2014). The assay was optimized so that it reproducibly determines the level of free 25OH Vit D in human serum or plasma samples. The assay can be used as a valuable tool in studies to establish the clinical relevance of free 25OH Vit D.

Disclosures: Nicolas Heuereux, DIAsource Immunoassays
This study received funding from: DIAsource Immunoassays

MO0134

RNA- and ChIP-sequencing Analyses Identify Gene Networks Modulated by 1,25-Dihydroxyvitamin D₃ in Mouse Intestine and Directly Regulated by the Hormone-activated Vitamin D Receptor. Seong Min Lee^{*}, Mark Meyer, Nancy Benkusky, Lori Plum, Hector DeLuca, J. Wesley Pike. University of Wisconsin-Madison, USA

The vitamin D receptor (VDR) is a nuclear factor that mediates the process of mineral regulation by 1,25-dihydroxyvitamin D₃ (1,25(OH)₂D₃) through actions in intestine, kidney and bone. In the intestine, various genetic deletion studies suggest that calcium absorption is a prerequisite for normal calcium/phosphorus homeostasis. To understand the gene networks modulated by the 1,25(OH)₂D₃/VDR system in the intestine, we have identified through RNA-sequencing analysis a subset of 45 genes that are regulated by 1,25(OH)₂D₃ in duodena of Cyp27b1 null mice under both hypocalcemic and normocalcemic conditions. This gene network includes previously identified calcium regulators such as Trpv6, Atp2b1, S100g and Cldn2. Importantly, 1,25(OH)₂D₃-responsive genes were similarly regulated by 1,25(OH)₂D₃ in the duodena of wildtype mice, and many were expressed in more distal portions of the intestinal track as well. To explore the molecular mechanisms associated with the regulation of 1,25(OH)₂D₃ target genes, we performed in vivo ChIP-sequencing analysis using intestinal epithelial cells obtained from the proximal small intestine of vehicle- or 1,25(OH)₂D₃-treated vitamin D sufficient wildtype mice to identify VDR binding sites. The results reveal a striking VDR cistrome in the absence of added 1,25(OH)₂D₃ and a dramatic increase in VDR binding sites following treatment with 1,25(OH)₂D₃. VDR action was confirmed at sites previously identified as regulatory for Cyp24a1, Trpv6 and Pllim2 and newly identified for genes such as S100g, Atp2b1, Pllim2 and Slc37a2 known to be VDR targets. Further bioinformatic analysis of the ChIP-sequencing data revealed that VDR binding sites were located predominantly within intronic and intergenic regions that contained a high frequency of classic VDREs which were associated with adjacent motifs for HNF4 and GATA4. Most importantly, almost all of the 1,25(OH)₂D₃ regulated genes that were identified by RNA-sequencing analysis and linked to calcium absorption and metabolism contained VDR binding activity within their loci. In conclusion, we have identified a gene network that is regulated directly by 1,25(OH)₂D₃ in a spatially-dependent manner throughout the intestinal track through enhancers that are occupied by the VDR in both vitamin D sufficient and 1,25(OH)₂D₃ treated mice. These studies provide a foundation for understanding the molecular mechanisms of target gene regulation and calcium absorption by 1,25(OH)₂D₃ in the intestine.

Disclosures: Seong Min Lee, None.

MO0135

Up-regulation of CYP24A1 splicing variants (CYP24A1-SV) expression is associated with vitamin D metabolic abnormality in insulin deficient diabetes mellitus. Hironori Yamamoto^{*1}, Mari Tajiri², Otoki Nakahashi², Mariko Ishiguro³, Eiji Takeda², Yutaka Taketani². ¹University of Jin-ai, Japan, ²University of Tokushima, Japan, ³Jin-ai University, Japan

Decrease of blood vitamin D concentration has been reported in patients with type 1 and 2 diabetes. However, the molecular reason behind this decrease is unclear. The aim of this study was to investigate the molecular mechanism of vitamin D metabolic abnormality in insulin deficient diabetes rats which were injured pancreatic beta cell by injection of streptozotocin (STZ). Sprague-Dawley rats were injected with STZ (65 mg/kg BW), and sacrificed after 9 or 29 days. Plasma activated vitamin D [1,25(OH)₂D₃], calcium and osteocalcin levels were significantly lower in STZ rats than control rats, however, there were no difference in plasma 25(OH)D₃, iFGF23 and TRAP5b levels. On the other hand, plasma levels of phosphate, iPTH and corticosterone were higher in STZ rats than control rats. Quantitative real-time PCR analysis showed that vitamin D catabolic enzyme CYP24A1 mRNA expression was significantly higher in kidney of STZ rats compared with control rats. In addition, the treatment of insulin recovered the high CYP24A1 mRNA expression levels in STZ rats. Interestingly, western blotting analysis found a strong expressed 40 kDa CYP24A1 which is differ from the reported 50-55kDa CYP24A1 in the kidney of STZ rats. And, we observed the up-regulation of CYP24A1-splicing variant (CYP24A1-SV) which lacked exon 1, 2 and N-terminal region was reported in human and chick

CYP24A1 gene in kidney of STZ rats. Finally, we confirmed the transcriptional up-regulation of endogenous CYP24A1 mRNA expression by glucocorticoid and glucocorticoid receptor in renal proximal tubular cells. These results suggest that the transcriptional up-regulation of renal CYP24A1-SV gene expression by corticosterone may cause to decrease plasma 1,25(OH)₂D level in STZ induced diabetic rats.

Disclosures: Hironori Yamamoto, None.

MO0136

A Novel Mechanically-Induced Osteocyte/Th17 Cell Signaling Mechanism.
Travis McCumber*, Kristen Drescher, Diane Cullen. Creighton University, USA

Mechanical loading of bone triggers bone formation, via osteocyte signaling. However, when mechanical loads of extreme force or repetition create tissue damage, osteocytes stimulate the remodeling of the damaged bone matrix. We have previously reported an up regulation of the pro-inflammatory cytokine GRO/KC, T cell recruiting cytokines (IL-2, MCP-1), and an increase in osteoclast number within fatigue loaded bone. This suggests a relationship between bone fatigue and the recruitment of both T cells and osteoclasts. We examined a novel, mechanically-induced signaling pathway between osteocytes and T cells, and hypothesized that repetitive fluid shear stress (FSS) would induce osteocyte production of cytokines that stimulate Th17 cell development and IL-17 and RANKL production. MLO-Y4 osteocyte-like cells were exposed to FSS (7 ± 3 dynes and 10 ± 3 dynes, at 1Hz) or Static control. The cells and medium were collected after 15, 30, 60, or 180 minutes. ELISA analysis of MLO-Y4 medium revealed greater IL-6 and TGF- β 1 in FSS versus Static groups ($p < 0.01$). IL-6 and TGF- β 1 levels were greater after 10 ± 3 dynes than 7 ± 3 dynes ($p = 0.02$ and 0.01). MLO-Y4 medium also revealed greater RANKL in Static than FSS groups ($p < 0.01$), which increased with exposure time ($p < 0.02$). Murine splenocytes were cultured in T cell growth medium and treated with FSS or Static medium for 96 hours. ELISA analysis of splenocyte culture medium revealed greater IL-17 and RANKL in cultures treated with FSS versus Static medium ($p < 0.01$). IL-17 and RANKL were greater after 10 ± 3 dynes than 7 ± 3 dynes ($p < 0.01$ and $p = 0.02$). To our knowledge these data are the first to support a novel, mechanically-induced osteocyte/Th17 cell signaling mechanism. Our data illustrates that mechanically-stimulated MLO-Y4 cells secrete cytokines (IL-6, TGF- β 1) known to induce murine Th17 cell development, and that splenocyte cultures treated with MLO-Y4 FSS medium produce Th17 cell products (IL-17, RANKL). IL-6, TGF- β 1 (MLO-Y4) and IL-17, RANKL (Th17) were expressed in a dose dependent manner with the greatest levels seen at 10 ± 3 dynes. These results suggest that greater osteocyte mechanical stress potentiates greater Th17 cell development and activity. Th17 cells, through the secretion of IL-17 and RANKL, can stimulate osteoclast formation. Future research on the osteoclast response to our osteocyte/Th 17 cell signaling model would provide a new paradigm for bone remodeling in response to mechanical stress.

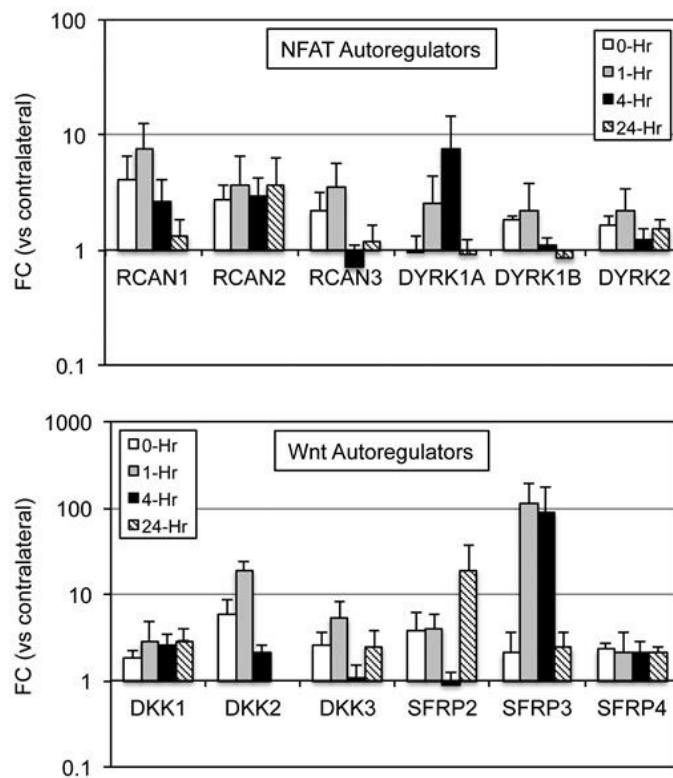
Disclosures: Travis McCumber, None.

MO0137

Acute Negative Feedback Autoregulation During Bone Mechanotransduction.
Leah Worton, Dewayne Threet, Brandon Ausk, Edith Gardiner, Steven Bain, Ronald Kwon, Ted Gross, Sundar Srinivasan*. University of Washington, USA

Bone tissue adapts its structure to its imposed loading environment. In theory, adaptation of bone's structure should proceed until the strain environment post adaptation approaches that prior to the imposition of external loading. In practice however, bone's anabolic response rapidly saturates, and subsequently declines to baseline within 2-4 wks despite continued loading. We estimate that bone's anabolic response (amplitude or duration) would have to be ~6-fold larger than observed in order to attain the strain-equilibrated, functionally adapted state. Given these data, we speculate that while mechanical loading activates anabolic pathways, it also activates repressive mechanisms that ultimately result in the premature cessation of the anabolic response. Here, we hypothesize that mechanical loading rapidly induces autoregulatory feedback that functions to inhibit the sustained activation of anabolic pathways. To test this hypothesis, we examined the expression of negative autoregulators of the Wnt and NFAT pathways. Briefly, the right tibiae of female C57BL6 mice ($n = 12$) underwent a single, 10-min bout of cantilever bending ($2350 \mu\text{e}$ peak strain, 50 cycles, 10-s rest). Animals ($n = 3/\text{grp}$) were sacrificed at 0, 1, 4 or 24 hrs post-loading, and the expression of Wnt and NFAT pathway autoregulators were determined via qRT-PCR at the tibia mid-shaft. We found that gene expression of a number of autoregulators of the Wnt (e.g., DKK1) and NFAT pathways (e.g., RCAN1) were elevated 2 to 5 fold (vs contralateral) immediately post-loading (i.e., 0 hr; Fig 1). Autoregulatory gene expression also followed distinct temporal patterns: a) immediate (0 hr) activation followed by a decline by 24-hrs (e.g., RCAN1, DKK2), b) late activation (peak at 4 hrs) followed by decline by 24 hrs (e.g., DYRK1A), c) sustained expression from 0 to 24 hrs (e.g., RCAN2, sFRP4), and d) oscillatory (e.g., DKK3, sFRP2). While preliminary, negative autoregulators of both NFAT and Wnt pathways were rapidly induced and displayed varied expression patterns. Given that autoregulators serve to inhibit the pathways responsible for their synthesis, sustained anabolism is not likely to be achieved via protocols that repeatedly load bone. We

propose that understanding and accounting for autoregulatory dynamics will yield novel loading strategies that robustly enhance and sustain bone's response such that a strain-equilibrated, functionally adapted state is ultimately achieved.



Fold change (FC) in NFAT and Wnt autoregulators

Disclosures: Sundar Srinivasan, None.

MO0138

Application of Mechanical Vibration to Enhance Orthodontic Tooth Movement – The Science Behind It. Dawei Liu*. Marquette University School of Dentistry, USA

Objective: To review and present the current evidence on the application of mechanical vibration to enhance orthodontic tooth movement. **Materials and Methods:** Using mechanical vibration to enhance orthodontic tooth movement seems to become one of the promising new technologies in orthodontics. Although several papers have been published, the scientific evidence behind it is largely unknown. Through searching engines such as PubMed, the current literature on this topic was reviewed. With the funding support of NIDCR, the author's group has been conducting a series of experiments on this topic, using study models of animal (*in vivo*), tissue and organ culture (*ex vivo*) and cell culture (*in vitro*). In addition to the biologic effect, the role of vibration in reducing the friction in the fixed orthodontic appliance system was also investigated. These new findings were presented. **Results:** Among the very limited amount of publications on this topic, current findings are of controversy and no conclusion can be made. Using a mouse model, we applied mechanical vibration to the orthodontically moved upper 1st molars for 4 weeks. As results, the vibrated molar moved 35% faster than the control molar, with more bone resorption found on the compression side and more newly formed bone presented on the tension side. To minimize variation of the animals, we further developed a tissue (organ) culture model in which the rat mandibular slices were preloaded with an orthodontic force then subjected to vibration for 7 days. The histologic findings in this tissue model supported our findings in the animal experiment. To investigate the cellular and molecular mechanism, we subjected human PDL cells to fluid shear stress with and without vibration. Interestingly, vibration enhanced the shear stress induced decrease of OPG/RANKL (mRNA) ratio. As practically vibration imposes on orthodontic fixed appliance system, we investigated the impact of vibration on the friction in the fixed appliance system and found that vibration significantly reduces 23% of friction between the orthodontic bracket and arch wire. **Conclusion:** In summary, mechanical vibration potentially impacts both biologic and mechanic aspects of orthodontic tooth movement. However, the science behind it is still not absolutely solid, which asks for more future endeavors on this topic.

Disclosures: Dawei Liu, None.

MO0139

Interpretation of Gene Expression During Immobilization – Don't Miss the Boat. Jens Bay Vegger*, Annemarie Brüel, Jesper Skovhus Thomsen, Department of Biomedicine, Health, Aarhus University, Denmark

Botulinum toxin (BTX) is widely used to paralyze a rodent's hind limb in order to study immobilization induced bone loss. Many studies have characterized the BTX model, but it remains unclear how gene expression correlates to dynamic histomorphometry, microarchitecture, and biomechanical properties as a function of time.

Thirty 16-week-old C57BL/6 female mice were randomized into 6 groups: Ctrl1, BTX1, Ctrl2, BTX2, Ctrl3, and BTX3. The mice in the BTX groups were injected with 2 IU/100 g BW BTX in the right hind limb musculature. Ctrl1 and BTX1, Ctrl2 and BTX2, and Ctrl3 and BTX3 were killed after 1, 2, and 3 weeks, respectively. The analysis included RT-qPCR of the distal tibia, μ CT of the femoral mid-diaphysis, distal metaphysis and epiphysis, dynamic histomorphometry of the distal femoral metaphysis and epiphysis, and mechanical testing of the femoral mid-diaphysis and neck. BTX groups were compared with their respective Ctrl groups with a Mann-Whitney Rank Sum test and results were defined significant when $p < 0.05$.

Genes related to osteoclasts (Ctsk and Acp5) were significantly up-regulated after one (+375% and +276%) and two weeks (+437% and +318%) of immobilization, but not after three weeks. Genes related to osteoblasts (Bglap and Col1a1) were significantly down-regulated after one week (-79% and -68%), Bglap was significantly down-regulated after two weeks (-56%), while it was significantly up-regulated after three weeks (+65%). BFR/BS was significantly decreased in the first week (-29%) and significantly increased in the third week (+54%) at the distal femoral epiphysis. B.Ar of the femoral mid-diaphysis was significantly decreased after one (-4%), two (-8%), and three weeks (-15%), BV/TV was significantly decreased at the distal femoral epiphysis after one week (-33%) and at both the distal femoral epiphysis and metaphysis after two (-58% and -33%) and three weeks (-62% and -37%). Tb.Th was significantly decreased at both the distal femoral epiphysis and metaphysis after one (-28% and -24%), two (-46% and -33%), and three weeks (-42% and -29%). Bone strength was significantly decreased at the femoral neck after two weeks (-40%) and at both the femoral neck and mid-diaphysis after three weeks (-57% and -24%).

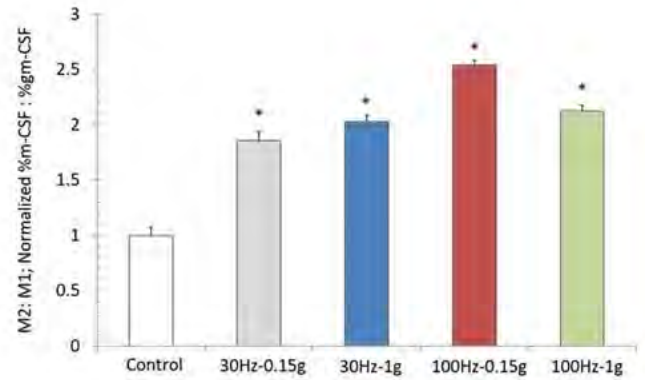
This study shows that changes in gene expression and dynamic histomorphometry takes place already during week one, whereas changes in microarchitecture and mechanical strength occur mostly during week three.

Disclosures: Jens Bay Vegger, None.

MO0140

Low Intensity Vibrations Alter Macrophage Phenotype. Suphanee Pongkitwittoon¹, Eileen Weinheimer-Haus², Timothy Koh², Stefan Judex*¹. ¹Stony Brook University, USA, ²University of Illinois at Chicago, USA

Macrophages play ubiquitous roles in human physiology. Their sensitivity to mechanical signals is largely unexplored but could open up an array of opportunities from manipulating bone resorption to enhancing healing. Here, we applied low intensity vibrations (LIV) to macrophages to test their influence on cell proliferation and polarization. Two different LIV signal frequencies (30Hz or 100Hz) were combined with two acceleration magnitudes (0.15g or 1g) to generate four distinct LIV signals. Murine macrophages (J774.1) were exposed to each of the four different LIV signals for 20min per session, 2x/d. We monitored cell viability, proliferation, polarization, as well as VEGF and TGF- β gene expression. Cell viability was unaffected by LIV. Macrophage proliferation was increased significantly (1.5x-2.5x, $p < 0.05$) by each of the four LIV signals on days 1, 2, and 3. The 100Hz/0.15g was consistently the most effective signal for all three days. Flow cytometry showed that the ratio of pro-healing to inflammatory phenotypes was significantly greater (2x-2.5x, $p < 0.05$) in LIV groups than in controls, with a preference of 100Hz signals over 30Hz signals. IL-10 was up-regulated up to 2-fold with LIV ($p < 0.05$). Transcriptional levels of VEGF were 2.6x greater ($p < 0.05$) in the 100Hz/0.15g group with smaller increases for the other LIV signals. LIV also increased gene expression of TGF- β , albeit to a lesser extent, and there were no significant differences between individual LIV groups. These data demonstrate the sensitivity of macrophages to high-frequency oscillations applied at low intensities. Interestingly, LIV not only enhanced macrophage proliferation but also modulated a change in phenotype from pro-inflammatory to pro-healing macrophages. Increased VEGF expression induced by LIV may contribute towards angiogenesis and ultimately facilitate healing and survival of the pro-healing macrophages. Future studies will test whether low intensity vibrations may directly attenuate macrophage induced osteoclastogenesis and whether enhanced healing associated with LIV is driven by changes to macrophage phenotype.



Upregulation of pro-healing macrophages with four different LIV signals

Disclosures: Stefan Judex, None.

MO0141

“Static” Osteoblasts Placed in Contact with Osteoblasts Previously Subject to Low Intensity Vibration Increases Proliferation, Gap Junction Based Cell-to-Cell Communication and Mineralization. M. Ete Chan*, Michael Lopez, Dorothy Yuan, Clinton T. Rubin, Stony Brook University, USA

Low intensity vibration (LIV), acting as a surrogate for the mechanical components of exercise, has been shown as a potential non-invasive, non-drug treatment to improve bone quality. LIV exerts its salutary effect, in part, by promoting the anabolic response of osteoblast (OB) to form new bone. However, the mechanotransduction pathway of OB in response to LIV is unclear, or even if direct mechanical stimulation of the cell is required. In this study, we hypothesize that cell-to-cell communication via gap junction between OBs plays a role in mechanotransduction. Using a parachute assay, this study examines if proliferation and mineralization of OBs *not directly subject to* LIV could be enhanced simply by being exposed to OB previously subject to LIV. OB-like MC3T3 cells were used in this study (n=3): (1)OBs stimulated with LIV were parachuted onto recipient “static” OBs and compared to (2)static OBs placed in contact only with OBs which had received no mechanical stimulation. LIV was delivered via a vertically oscillating platform (90Hz, <1g, where $g=9.8ms^{-2}$) for 30min. While parachuted OBs were stained with a red membrane-bound dye DiI, recipient static OBs were stained with a green calcein dye which can be transferred to adjacent cells when gap junction intercellular communication (GJIC) is established. Following 24h, OBs exposed to LIV-OBs increased overall cell proliferation by 116% compared to OB in contact only to non-LIV OB ($p \leq 0.05$). Further, flow cytometry revealed that GJIC, as shown by dual colors in recipient OBs, was 73% higher in those in contact with LIV-OBs ($p \leq 0.05$), indicating that LIV promotes intercellular communication even in those cells isolated from mechanical signals. Mineralization assay showed that the OB group exposed to LIV-OBs was 16% ($p \leq 0.05$) more mineralized than control. This study demonstrated that cell-to-cell communication can be enhanced even in ‘static’ cells when in contact with cells subject to mechanical stimulation, emphasizing a ripple effect of mechanical stimulation to remote responsive cell populations. Future experiments can help elucidate what biochemical factors (e.g., nitric oxide) are being communicated through this GJIC that may foster mechanically mediated responses in bone cells, and roles of other bone marrow cell types (e.g., osteoclasts, adipocytes, mesenchymal and hematopoietic stem cells) to further expand our understanding of the working mechanism of mechanical signals to improve bone health.

Disclosures: M. Ete Chan, None.

MO0142

Mechanobiological Modulation of Ca^{2+} Oscillations in Osteocytes of Intact Mouse Calvaria by Medium Intensity Focused Ultrasound. Minyi Hu*, Daniel Gibbons, Jian Jiao, Yi-Xian Qin, Stony Brook University, USA

Current clinical evidences have shown that mechanotransduction is critical in bone remodeling related to tissue regeneration. While the biological effect of ultrasound on bone healing has been well documented, the underlying mechanism is currently unknown. Our previous study elucidated the mechanobiological modulation of cytoskeleton and Ca^{2+} influx in *in-vitro* osteoblastic cells by short-term focused acoustic radiation force. In greater relation to physiological setting, our current study aimed to visualize and quantify Ca^{2+} oscillations of *in-situ* osteocytes in real-time response to Medium Intensity Focused Ultrasound (MIFU). All animal protocols were approved by Stony Brook University IACUC. Three-month-old Black6 mice were used to obtain fresh calvaria samples immediately after euthanasia by CO_2 inhalation. The bone samples were incubated in DMEM with 5% FBS and 1% penicillin/streptomycin til ready for Ca^{2+} fluorescent label using Fluo-8 AM (Santa

Cruz Biotechnology, Inc., Santa Cruz, CA). The stimulation pattern of MIFU with 1W (n=5), 3W (n=8), 6W (n=5), 9W (n=9) and 12W (n=7) energy powers with 2sec intervals was 10sec baseline – 30sec stimulation – 10sec post stimulation. Real-time confocal imaging (Zeiss LSM 510 META NLO Two-Photon Laser Scanning Confocal Microscope System) with 40X objective, 488-nm laser excitation, and 2 frames/sec was performed to capture the Ca²⁺ signals of the osteocyte cell bodies within each bone that was subjected to MIFU stimulation. For data analysis, the fluorescent intensity of each cell body was extracted as a function of time using the microscope software. By normalization to the baseline intensity, the percentage of response cells, number of Ca²⁺ spikes, spike magnitude, and the time to the first spike were quantified. MIFU stimulation at 6W, 9W and 12W lead to significant Ca²⁺ oscillations - 85 ± 16% (p<0.01 vs. 1W; p<0.05 vs. 3W), 80 ± 18% (p<0.01 vs. 1W; p<0.05 vs. 3W) and 84 ± 17% (p<0.01 vs. 1W; p<0.05 vs. 3W) of responsive cells, respectively. MIFU at >6W energies lead to higher number of Ca²⁺ spikes and larger spike magnitudes compared to lower energies. The initiation time to the first Ca²⁺ spike seemed to be relatively the same for all energy levels (~18sec). In conclusion, this study provided insights into the interactions between acoustic mechanical stress and *in-situ* osteocytic Ca²⁺ oscillations, which aids further exploration of the mechanosensing mechanism triggered by noninvasive acoustic radiation force.

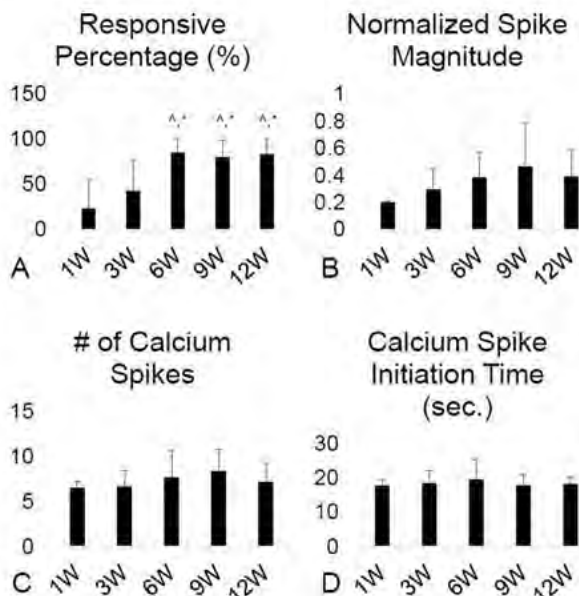


Figure 1. Responsive percentage (A), normalized spike magnitude (B), number of spikes (C), and spike initiation time (D) of osteocyte Ca²⁺ responses to MIFU at various energy powers. *p<0.01 vs. 1W; *p<0.05 vs. 3W.

Figure 1

Disclosures: Minyi Hu, None.

MO0143

Strain Derived Fluid Flow Explains Observed Alignment of New Osteons towards the Main Direction of Loading in the Compact Bone. Majid Nazemi*, James D. Johnston, David M. L. Cooper. University of Saskatchewan, Canada

Introduction: In cortical bone, basic multicellular units (BMUs) proceed by tunneling in which osteoclasts dig a resorption space that is refilled by osteoblasts, creating a new secondary osteon with a central vascular canal. Osteocytes are hypothesized to sense mechanical stimuli, including interstitial bone fluid flow caused by bone tissue strain, and coordinate BMU activities accordingly. To investigate this hypothesis, the objective of this study was to assess patterns of fluid flow around a newly forming osteon ‘breaking out’ of an existing canal using 3D biphasic poroelastic finite element (FE) modeling.

Methods: A biphasic poroelastic FE model was developed and consisted of a cylindrical space with 200µm diameter (representing BMU-created resorption space) modeled in a cube with 1000 µm side length (representing cortical bone). Required inputs for the model were adopted from literature: elastic modulus = 15.8 GPa; Poisson’s ratio = 0.33; 5% lacuno-canalicular porosity; bone bulk modulus = 17.7 GPa; fluid bulk modulus = 2.3 GPa and hydraulic permeability = 2.2 × 10⁻⁷ mm⁴/Ns. The analysis was based on an assumption of bone being fully saturated with interconnected porosity. The canal pressure was neglected against the pressure in the lacuno-canalicular porosity. A resorption space was sequentially simulated as breaking out of an existing canal wall at an initial angle of 90°, propagating straight for 200µm and then redirecting towards the longitudinal loading direction in steps of 30° (Fig 1 to 4). Fluid velocity was calculated in the cortical bone under physiologic loading conditions; mimicking a walking cycle with a peak compressive micro-strain of 1500.

Results: Lower fluid velocity was observed at the superior-inferior region of the resorption space compared to other regions, including the lateral walls at the initial breaking out phase (Fig 1 to 4). Following re-routing towards the main direction of loading, fluid velocity reduced at the resorption space tip and increased in all regions of the space’s wall except superior-anterior regions of the initial breaking out zone (Fig 1 to 4).

Conclusion: Our results support the hypothesis that reduced fluid velocity may be a stimulus for directing osteoclasts and further resorption in longitudinal directions (i.e., superior-inferior regions of the resorption space). This may explain the predominance of longitudinal osteonal canals despite many generations of remodeling activity.

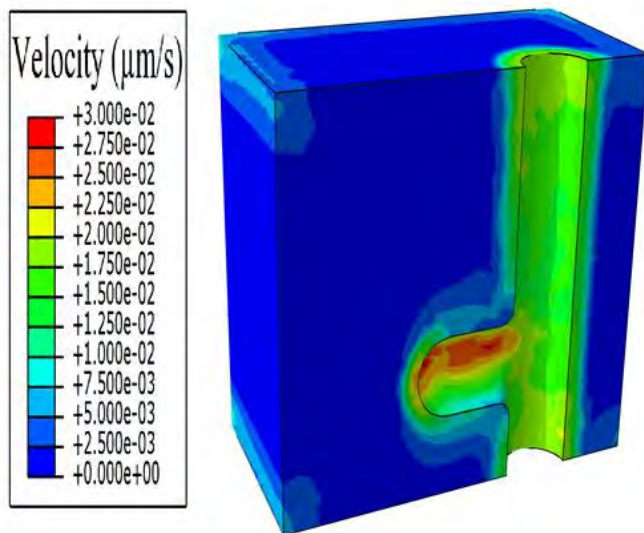


Fig 1. Pattern of fluid velocity around the newly forming osteon

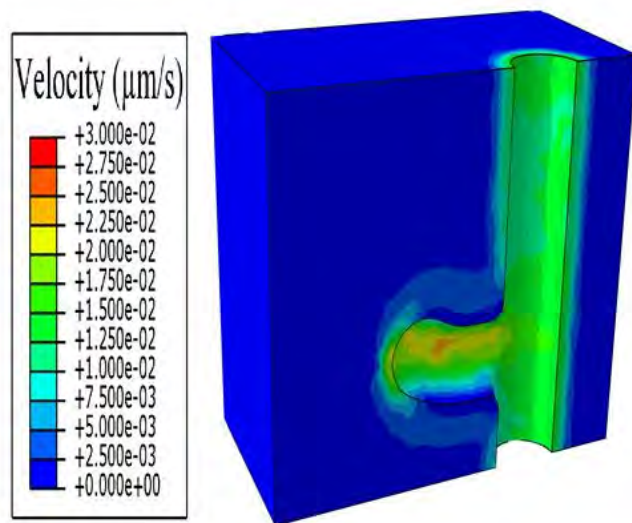


Fig 2. Pattern of fluid velocity around the osteon after 30 degrees of re-routing

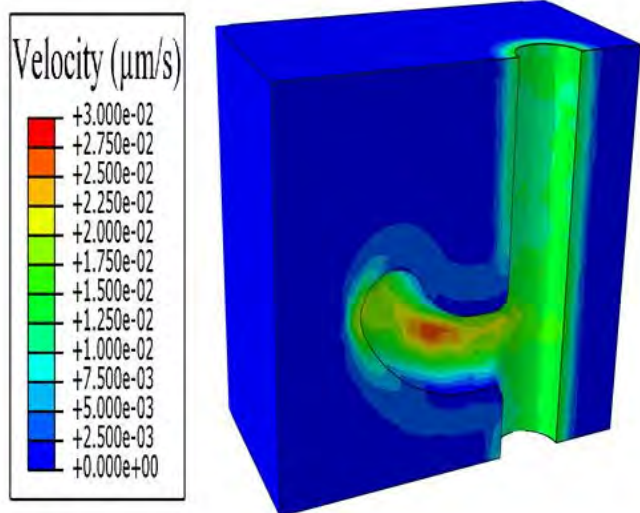


Fig 3. Pattern of fluid velocity around the osteon after 60 degrees of re-routing

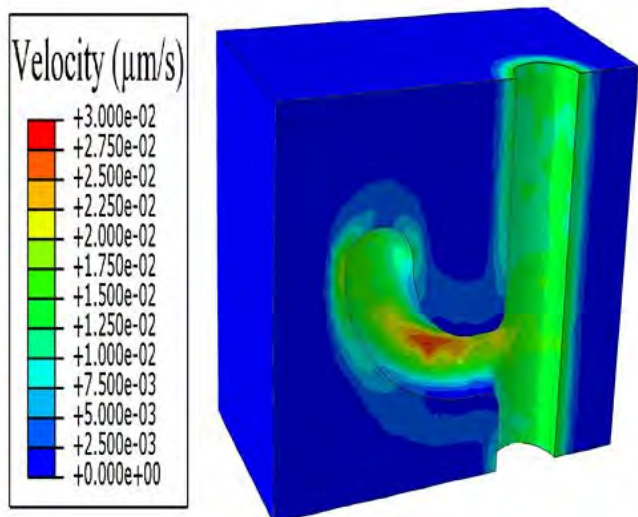


Fig 4. Pattern of fluid velocity around the osteon after 90 degrees of re-routing

Disclosures: Majid Nazemi, None.

MO0144

T-type Voltage-Sensitive Calcium Channels Mediate Mechanically Induced Intracellular Calcium Oscillations by Regulating Intracellular and Endoplasmic Reticulum Calcium Dynamics in Osteocytes. Genevieve Brown*, Prajesh Desai, X. Edward Guo. Columbia University, USA

Osteocytes (OCY) are highly mechanosensitive, exhibiting robust oscillations in intracellular calcium ($[Ca^{2+}]_i$) in response to mechanical stimuli, whereas osteoblasts (OB) demonstrate fewer, weaker responses. The release of Ca^{2+} from endoplasmic reticulum (ER) stores is critical to these multiple responses. Thus, the mechanisms of Ca^{2+} release and reuptake by the ER are important to OCY mechanotransduction. The differentiation of OB to OCY is characterized by many phenotypic changes, including expression of membrane Ca^{2+} channels. OB express both T- and L-type voltage-sensitive Ca^{2+} channels (VSCC), whereas L-type VSCC are barely detectable in OCY. We hypothesized that the predominant expression of T-type channels in OCY may contribute to their unique $[Ca^{2+}]_i$ patterns and further speculated that T-type VSCC in OCY may interact with ER stores.

We sought to simultaneously visualize the dynamics of Ca^{2+} in the cytosol ($[Ca^{2+}]_i$) using the calcium indicator Fura Red-AM and endoplasmic reticulum ($[Ca^{2+}]_{ER}$) by transfection with the DIER fluorescence resonance energy transfer (FRET) biosensor (Palmer 2006) within bone cells under loading. The osteocyte-like MLO-Y4 and osteoblastic MC3T3-E1 cell lines were grown to confluency, and single cells were imaged at 60x under fluid flow stimulation in the presence/absence of VSCC

inhibitors. Fluorescence emissions of YFP, CFP and Fura Red were captured separately and simultaneously using a quadview beamsplitter under single excitation. The FRET ratio was calculated on a pixel-by-pixel basis using image registration.

In OCY, elevations of $[Ca^{2+}]_i$ coincided with depression of $[Ca^{2+}]_{ER}$, with subsequent peaks occurring after recovery of $[Ca^{2+}]_{ER}$ levels (Fig 1A). Treatment with an L-type VSCC inhibitor had no effect on this behavior (Fig 1C), consistent with its lack of expression in OCY. The T-type inhibitor significantly reduced the number of $[Ca^{2+}]_i$ responses in OCY (Fig 1E, 2A) and disrupted synchrony between $[Ca^{2+}]_i$ and $[Ca^{2+}]_{ER}$ responses (Fig 2B). In OB, few $[Ca^{2+}]_i$ responses were observed in all groups (Fig 1 left, Fig 2A) and ER contribution was minimal (Fig 2B). By observing Ca^{2+} dynamics in both cytosolic and ER spaces, this study indicates that OCY generate multiple responses by an ability to refill ER stores. Our data suggests that T-type VSCC facilitate the recovery of $[Ca^{2+}]_{ER}$ in OCY to effect this behavior. We uncovered a new mechanism involving T-type VSCC underlying the unique behavior of OCY as mechanosensors.

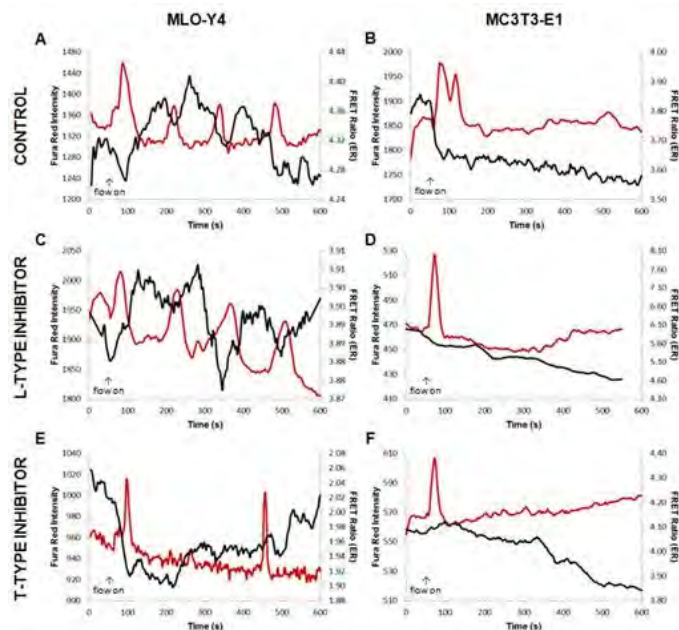


Figure 1. Simultaneous measurement of cytosolic (red) and ER (black) Ca^{2+} levels in bone cells under fluid flow. Representative time courses are shown for osteocyte-like MLO-Y4 (A) and osteoblastic MC3T3-E1 (B) control cells subjected to 35 dyne/cm² fluid flow stimulation. The effects of treatment with the L-type VSCC inhibitor nifedipine on MLO-Y4 (C) and MC3T3-E1 (D). The effects of the T-type inhibitor NNC 55-0396 on MLO-Y4 (E) and MC3T3-E1 (F).

Figure 1

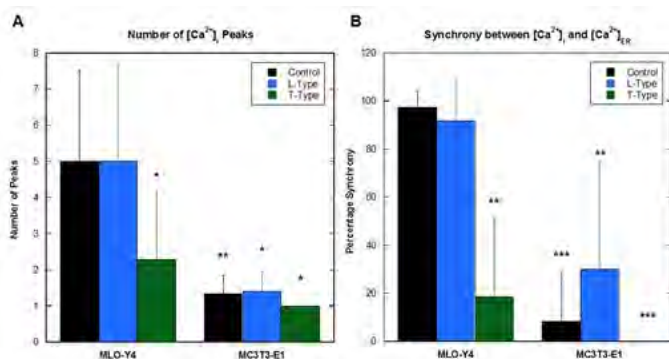


Figure 2. Effect of VSCC inhibitors on bone cell Ca^{2+} responses. (A) The number of $[Ca^{2+}]_i$ peaks. (B) Synchrony between $[Ca^{2+}]_i$ peaks and $[Ca^{2+}]_{ER}$ depressions. Synchrony was defined as the percentage of ER depressions over cytosolic peaks. Student t-test: * $p < 0.05$, ** $p < 0.01$, *** $p < 0.001$ compared to MLO-Y4 control.

Figure 2

Disclosures: Genevieve Brown, None.

MO0145

BIPHASIC BEHAVIOR AND SITE- AND GENDER-SPECIFICITY OF pQCT-ASSESSED “DISTRIBUTION/QUALITY” RELATIONSHIPS CONCERNING TORSION STRENGTH THROUGHOUT THE HUMAN TIBIA. Gustavo Cointry¹, Laura Nocciolino¹, Jörn Rittweger², Jose Ferretti^{*3}, Ricardo Capozza¹. ¹Centro de Estudios de Metabolismo Fosfo-Cálcico, Argentina, ²German Space Agency (DLR), Germany, ³National University of Rosario, Argentina

“Distribution/quality” (d/q) curves describe the negative, hyperbolic relationships between pQCT-assessed indicators of the efficiency of cross-sectional design concerning bending or torsion (CSMI’s, y) and of the bone tissue stiffness (cortical vBMD, vCtD, x) in long bones [Capozza *et al*, *JMNI* 2013]. The slopes and significances of d/c curves would reflect the modeling-dependent ability of bone *mechanostat* to distribute cortical tissue as an inverse function of its stiffness. We have shown that the significance of d/q relationships for *bending* of the tibia, higher in men than women, is also higher toward the midshaft than at both bone ends. This should cope with tibia bending stresses (maximal at midshaft), but not with torsion stress which can be high toward the heel, where cortical mass is the lowest throughout the bone. To search for a possible homeostatic compensation of that inadequacy, this study describes the evolution of d/q relationships calculated for *torsion* in serial slices taken at every 5% of the tibia length from heel (S5) to knee (S95) in 17/21 men/women untrained (10/12) or chronically trained (7/9) in long-distance running.

The d/q curves showed the typical hyperbolic shape from S10 to S85. The distribution of correlation coefficients r of the d/c curves throughout that tibia region was biphasic (“V”- shaped). Values were minimal at S25-S35 (-0.050 to -0.330, non-significant), increased homogeneously to maximal values toward both bone ends (up to about -0.700 at S10 and S70, all significant) and were higher by average 0.200 in men than women. The ordinates of the curves were significantly higher in men than in women ($p < 0.001$). Running tended to enhance pCSMI and reduce vCtD values (probably by increasing microdamage-induced remodeling), but it did not affect the d/c relationships. In this study, a higher r value of a d/q relationship does not indicate a higher bone strength, but just a higher efficiency of bone *mechanostat* to spatially orient the available cortical mass to resist torsion. The progressively increasing r values from S25 to the knee would have reflected what had been previously observed concerning bending, just as a parallel effect. However, the rapid distal r increase from S25 to S10 (not observed in the bending analysis), where bone section tends to be circular, would confirm the proposed homeostatic control of tibia torsion strength toward the heel as a compensation for the naturally low bone mass at that level.

Disclosures: Jose Ferretti, None.

MO0146

Early Stage of Osteoarthritis Development is Associated with Substantial Weakening in Cartilage Nanomechanical Properties. Wei Tong^{*1}, Basak Doyran², Qing Li³, Haoruo Jia⁴, Xianrong Zhang⁵, Ling Qin⁴, Lin Han³. ¹Perelman school of medicine, USA, ²School of Biomedical Engineering, Science & Health Systems, Drexel University, PA, United States, USA, ³School of Biomedical Engineering, Science & Health Systems, Drexel University, USA, ⁴Department of Orthopaedic Surgery, University of Pennsylvania, USA, ⁵Department of Physiology, School of Basic Medical Sciences, Wuhan University, China

Osteoarthritis (OA) is the most common degenerative joint disease in adults with no early detection method available, which is one main reason of unsatisfactory treatment up to now. Current evaluation of murine OA relies on semi-quantitative histological assay that mainly relies on structural or biochemical symptoms noticeable at intermediate or late stages. To find a sensitive and function-relevant indicator of OA, we applied atomic force microscopy (AFM)-based nanoindentation to detect mechanical changes of articular cartilage in a post-traumatic osteoarthritis murine model. To do so, we first performed destabilization of the medial meniscus (DMM) surgery on right knees and sham surgery on left knees of skeletally mature 12-week-old male C57BL/6J mice. The joints were then harvested at different time points ($n \geq 10$ /time point) for nanoindentation and histology. Each femoral condyle cartilage was indented at more than 10 locations by a borosilicate colloidal spherical tip ($R = 5 \mu\text{m}$, nominal spring constant $k = 7.4 \text{ N/m}$) with maximum indentation depth of $\sim 1 \mu\text{m}$ at $10 \mu\text{m/s}$ indentation rate. Effective indentation modulus, E_{ind} (MPa), was calculated from the loading portion of indentation force-depth curves using the Hertz model. Interestingly, E_{ind} of the medial side of femoral condyle cartilage started to decrease significantly ($61.2 \pm 2.3\%$ of sham, mean \pm SEM) at 7 days, very shortly after DMM, reached the lowest level ($27.3 \pm 2.9\%$ of sham) at 2 weeks, maintained at this low level until 8 weeks, and increased to normal value at 12 weeks. At the lateral side, E_{ind} was unchanged at 2 weeks, which is consistent with our observation that OA only develops at medial side but not lateral side in this DMM model. In contrast, there was no significant morphological change in cartilage up to 4 weeks after DMM. Mankin score increased only at 8 (7.7 ± 0.9) and 12 weeks (10.0 ± 0.5) after. Hence, this study provided direct experimental evidence that the early decrease in E_{ind} (7-14 days) of cartilage can serve as a more sensitive and functional-relevant indicator of early OA than gross-level signs measured by histology (8-12 weeks). The increase in E_{ind} in DMM femur at 12 weeks was due to a substantial loss of uncalcified cartilage, suggesting that at this stage E_{ind} of cartilage after DMM reflects the mechanical

properties of the stiffer middle/deep zone cartilage. A comprehensive understanding of nanomechanical symptoms will shed new light on the diagnosis and treatment of OA.

Disclosures: Wei Tong, None.

MO0147

IL-36 inhibits TGF- β -mediated collagen expression by suppressing nuclear localization of Smad2 and causes development of BRONJ-like lesions in mice. Sol Kim^{*1}, Reuben Kim¹, Drake Williams¹, Cindy Lee¹, Teresa Kim¹, Ki-Hyuk Shin¹, Mo Kang¹, No-Hee Park¹, Songtao Shi², Jennifer Towne³. ¹UCLA School of Dentistry, USA, ²University of Pennsylvania School of Dental Medicine, USA, ³Amgen Inc, USA

Objective: Long-term users of Bisphosphonates (BPs), anti-resorptive drugs commonly prescribed to treat bone disorders, are at higher risk of developing bisphosphonate-related osteonecrosis of the jaw (BRONJ), but the pathophysiology of BRONJ remains unclear. The purpose of this study are to identify molecular determinants of BRONJ with microarray analysis using osteomucosal tissues obtained from mice and to elucidate the role of the identified gene in vivo and in vitro.

Methods: An Affymetrix-based microarray assay was used to identify differentially regulated genes in BRONJ-like lesions in 11 week-old female C57BL/6 mice. Expression of IL-36 was validated using qRT-PCR, immunohistochemical staining and ELISA. IL-36 receptor (IL-1Rrp2) neutralizing antibody was used to inhibit the IL-36 signaling pathway in vivo, and bone necrotic lesions were evaluated using uCT scans and bone morphometric analysis. Gingival mesenchymal stromal cells (GMSCs) were isolated from the oral cavity of the mice and treated with IL-36 and TNF- β in vitro to examine expression of Col1a1, Col1a2, a-Sma using qRT-PCR, Western, and ELISA. Phosphorylation status and nuclear localization of p-Smad2 was examined using Western blots, and binding of p-Smad2 on the promoter of Col1a1 and a-Sma was determined using the CHIP assay. Nuclear localization of p-Smad2 in the presence of TGF- β and IL-36 was also examined in GMSCs isolated from IL-36 knockout mice.

Results: The Microarray analysis identified IL-36 family members among the upregulated genes. IL-36 was up-regulated both locally and systemically in a ONJ-specific manner. IL-1Rrp2 neutralizing antibody ameliorated BRONJ lesions in mice. Mechanistically, IL-36 treatment inhibited TGF- β -mediated collagen expression in GMSCs in vitro. IL-36 suppressed TGF- β -mediated nuclear localization of p-Smad2 and occupancy of Smad2 in the Col1a1 and a-Sma promoter regions. GMSCs isolated from IL-1Rrp2 KO mice nullified suppressive effect of IL-36 on nuclear localization of p-Smad2. Conclusion: IL-36 may induce BRONJ development by inhibiting wound healing processes via suppression of TGF- β -mediated collagen synthesis, suggesting that the IL-36 signaling pathway may be a potential target for managing/preventing ONJ development.

Keywords: bisphosphonate, osteonecrosis of the jaw, IL-36, collagen, TGF-beta

Disclosures: Sol Kim, None.

MO0148

The Effects of Decellularisation on the Mechanical Properties of Bone, and Subsequent Recellularisation of the Samples. MOHD RIDUAN MOHAMAD^{*}, Philip Riches, M. Helen Grant. University of Strathclyde, United Kingdom

Regenerative medicine strategies involving decellularised extracellular matrix scaffolds are developing fast and, in particular, decellularized bone has been proposed for bone tissue engineering. This study aimed to establish decellularisation and recellularisation protocols and to measure the Young’s modulus and pore size of the decellularised trabecular bone samples. Twelve bovine cancellous proximal femur samples (7mm x 7mm x 2mm) were decellularised by six cycles of overnight incubation at 37 C using two protocols: A – 10mM Tris, 1mM EDTA, 0.1% v/v Triton X-100 and B – method A plus 0.5% w/v trypsin. Decellularisation was confirmed by the absence of DNA staining with DAPI both by detecting any DNA remaining on the bone matrix spectrofluorometrically, and by microscopic examination. Young’s modulus was determined before and after incubation through compression testing at 1 mm/s up to 400N (8.16MPa). The porosity of the bone samples before and after decellularisation was measured using a mercury porosimeter. Recellularisation using HOS cells (seeded at 5×10^5 cells per cm^2 bone) progressed for up to 3 weeks in DMEM supplemented with L-ascorbic acid, β -glycerophosphate, dexamethasone, FCS, PEST, and NEAA. Bone samples were placed onto non-adherent dishes and adherent dishes. The extent of recellularisation was compared in static and dynamic culture conditions using a roller incubator set at 15 rpm to effect dynamic conditions. DAPI staining revealed that protocol B removed all measurable DNA from the bone samples (Figure 1). Decellularisation did not affect Young’s modulus (Figure 2). Pore diameters did not differ with decellularisation and were in the ideal range for cell growth. Mean ALP activity (Figure 3A) and MTT reduction (Figure 3C) was greater on the adherent surface than on non-adherent surface albeit non-significantly. There was no significant difference between static and dynamic conditions in ALP activities between 3 and 7 days (Figure 3B). Data suggests that cells proliferated more readily when samples were placed in adherent dishes (Figure 3D). This work has established appropriate protocols to make donor bone scaffolds with appropriate porosity to allow reseeding with human bone cells. These could be used to repair bone defects in recipient patients.

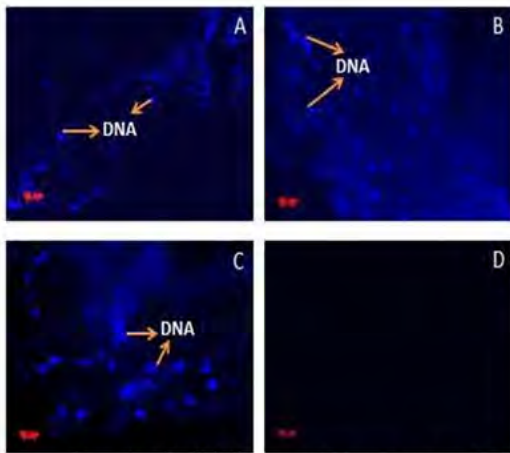


Figure 1: Bone sample tested in 0.6 nM DAPI agent A) before any treatment. B) after incubation with protocol A and B for 10 minutes. C) after overnight incubation with protocol A. D) after incubation with protocol B overnight. Protocol A – 10mM Tris, 1mM EDTA, 0.1% v/v Triton X-100; and B – method A plus 0.5% w/v trypsin. All images were taken at the surface.

Figure 1

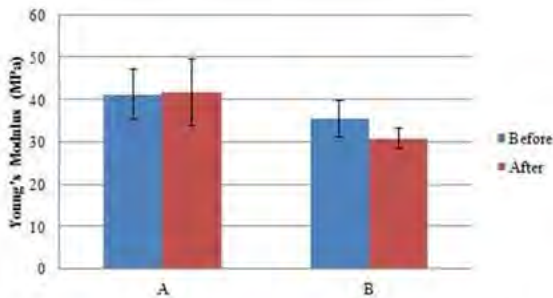


Figure 2: Young's modulus before and after six cycles of incubations with protocol A and B. A – 10mM Tris, 1mM EDTA, 0.1% v/v Triton X-100; and B – method A plus 0.5% w/v trypsin. Results are the mean ± SEM of n = 6. p > 0.05 compared with the control (ANOVA for repeated measures).

Figure 2

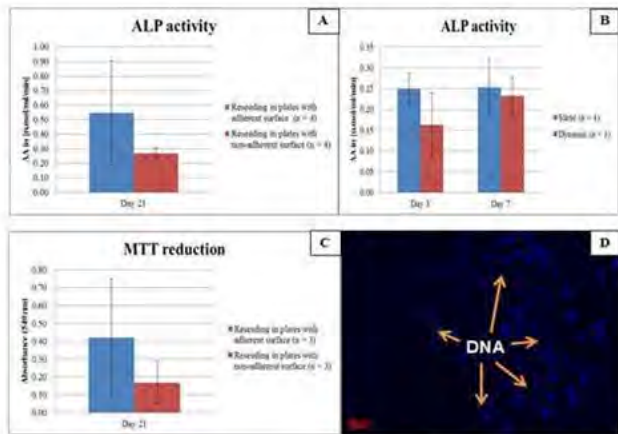


Figure 3: ALP activity of HOS cells reseeded at 5x10³ cells per cm² onto bone in A) adherent and non-adherent surface for 3 weeks, B) static and dynamic environment on day 3 and day 7. C) MTT reduction of HOS cells growing on bone seeded at 5x10³ cells per cm² in adherent and non-adherent surface for 3 weeks. Results are the mean ± SEM. p > 0.05 for all values by unpaired student's t-test. D) Bone samples were stained in 400ul of 0.6nM DAPI on bone pieces on an adherent surface after 21 days.

Figure 3

Disclosures: MOHD RIDUAN MOHAMAD, None.

MO0149

A Novel Vitamin D Receptor Modulator, VS-105, Improves Bone Mineral Density in an Estrogen-deficient Rat Model of Osteoporosis. J. Ruth Wu-Wong*¹, Yung-wu Chen², Jerry L. Wessale², Theresa Chen², Maysaa Oubaidin³, Phimon Atsawasuwan³. ¹University of Illinois at Chicago, USA, ²Vidasym, USA, ³University of Illinois, USA

Vitamin D is essential for bone health. Not surprisingly, vitamin D receptor modulators (VDRMs) such as calcitriol have been used as therapeutic agents for osteoporosis since 1983 in some countries outside of the US. VDRMs increase bone mineral density (BMD) and reduce the incidence of bone fracture in patients with osteoporosis. However, the fact that VDRMs are not more widely used for treating osteoporosis is in part due to the hypercalcemic side effects of current VDRMs. It is not well studied whether VDRMs at non-hypercalcemic doses have effects on bone mineral density (BMD). VS-105, a novel VDRM with an exceptionally wide therapeutic index (TI) at >50-fold (vs. TI of calcitriol at 1-fold) offers a unique opportunity for answering the aforementioned question. In this study, the effect of VS-105 on BMD was evaluated in an ovariectomized (OVX) rat model of osteoporosis. Treatment of OVX rats by VS-105 at three doses (0.1, 0.2 or 0.5 µg/kg, i.p., 3x/week, for 12 weeks, n=8-12 per group) significantly improved BMD in the L3 lumbar vertebra in a dose-dependent manner (sham: 324 ± 14 mg/cm²; OVX/vehicle: 279 ± 10 mg/cm²; VS-105 at 0.1, 0.2 and 0.5 µg/kg: 306 ± 9, 329 ± 12, and 327 ± 10 mg/cm², respectively) without affecting serum calcium (Ca). In comparison, calcitriol at 0.1 µg/kg significantly increased BMD, but it also increased serum Ca (13.8 ± 0.3 mg/dL vs. sham at 11.3 ± 0.5 mg/dL). VS-105 significantly suppressed serum PTH without affecting serum Ca at all doses tested, results attributable to its lack of effects on inducing the expression of intestinal Ca transporter genes such as Calb3 and TRPV6, and on stimulating intestinal Ca transport. VS-105 increased serum osteocalcin (a marker for osteoblast activity) in a dose-dependent manner, and reduced the expression of receptor activator of nuclear factor kappa-B ligand (RANKL) in tibia. In a mouse calvaria bone primary organ culture system, VS-105 was ~2-fold less effective than calcitriol in stimulating net Ca release from calvaria (a measurement of osteoclast activity). These results demonstrate that VS-105 is effective in improving BMD in a dose range that does not affect serum Ca in OVX rats; the improvement in BMD by VS-105 is likely attributable to increased osteoblast activity and reduced osteoclastic bone resorption, but not related to enhanced intestinal Ca absorption. The overall preclinical profile of VS-105 supports future clinical development for its use in treating osteoporosis.

Disclosures: J. Ruth Wu-Wong, Vidasym
This study received funding from: Vidasym

MO0150

Effects of osteoporosis on the osteoinductivity of rhBMP-2 in the healing of segmental long-bone defect models. Jae Hyup Lee*¹, Hae-Ri Baek², Kyung Mee Lee², Guang Bin Zheng², Sung Joon Shin², Hee-Jong Shim². ¹Seoul National University, College of Medicine, South Korea, ²Department of Orthopedic Surgery, Seoul National University, College of Medicine, SMG-SNU Boramae Medical Center, South Korea

This study used the segmental long-bone defect model to assess the effects of osteoporosis on the formation of new bones and the osteoinductivity of recombinant human bone morphogenetic protein-2 (rhBMP-2). Seventy-two female Sprague-Dawley rats were divided into two groups: an osteoporosis group with ovariectomies and dexamethasone intramuscular injections and a sham group. When they reached 22 weeks in age, each group was further divided into two groups and a 5-mm defect was made in both fibular mid-shafts of each rat. One fibula in each rat was picked randomly and was injected with 0.05 ml of hydrogel carrier; the opposite fibula was injected with the same carrier mixed with rhBMP-2 (10 µg). After rearing for a further 5 and 9 weeks, the ratios of the lengths of the newly formed bones in the fibular defects were determined using micro-CT. The micro-CT parameters of the newly formed bones were analyzed and their undecalcified histologies were compared. The sham rhBMP-2-injected group—in all of the 5- and 9-week-kept groups—showed a significantly higher bridging bone formation ratio than the other three groups. The osteoporosis rhBMP-2-injected group showed a significantly higher ratio than both the non-rhBMP-2-injected sham hydrogel and the osteoporosis hydrogel groups. More than 50% of the ratios of the bridging bone formation in the sham rhBMP-2 group at 5 and 9 weeks were 100%, whereas the ratios of the osteoporosis rhBMP-2 group were 55.6% and 72.7% at 5 and 9 weeks, respectively. The comparison of the micro-CT parameters of the newly formed bones showed that the sham rhBMP-2 group at both 5 and 9 weeks compared with the osteoporosis rhBMP-2 group had significantly higher percentage bone volumes, trabecular thicknesses, and trabecular numbers, as well as significantly lower specific surfaces, trabecular pattern factors, and structural model indices. The histology results showed that the sham-rhBMP-2 group began forming bridging bones in the defect areas in the fifth week, and at 9 weeks, they formed trabecula and marrow spaces. However, the osteoporosis rhBMP-2 group exhibited a relatively minor level of new bone and trabecula formation. Consequently, the rhBMP-2 group showed significantly increased bone formation in the osteoporosis rat fibular defect model compared with the hydrogel group, whereas the new bone quantities, qualities, and remodeling in the osteoporosis rhBMP-2 group were less effective than those in the sham-rhBMP-2 group, signaling that osteoporosis significantly undermines rhBMP-2 osteoinductivity.

Disclosures: Jae Hyup Lee, None.

MO0151

EP4 Agonist in Combination with Autograft Accelerated the Bone Fusion Time on Posterolateral Spinal Fusion in Canines. YASUTOMO NAKANISHI*, AKINA SAITOH, RYOHEI MIYATA, YUSUKE ETO, SATOSHI NISHIKAWA, HIROSHI MORI, SHINSEI FUJIMURA, KAZUYA ABE, AKIO NISHIURA, YASUO OCHI, YASUSHI HIROTA, ONO Pharmaceutical Co., LTD., Japan

In spinal fusion surgery, autografts are commonly used to obtain bone fusion. However, the successful fusion often takes quite long time and a prolonged period of bone fusion leads to potential problems with quality of life in the patients. Prostaglandin (PG) E2 receptor subtype EP4 is known to involve in an osteogenic action of PGE2. Moreover, EP4 agonist enhanced bone formation by bone morphogenic protein (BMP)-2 in vitro and in vivo. Since an autograft bone contains several growth factors including BMP-2, in this study, we investigated the effect of a small molecule, specific EP4 receptor agonist (EP4a) in combination with iliac crest autograft on posterolateral spinal fusion in canines. Eight male beagle dogs (14 - 16 months of age) underwent bilateral posterolateral lumbar spinal fusion at the fourth and fifth lumbar vertebrae (L4 and L5). After decortication of the posterior aspect of the transverse processes was performed, iliac crest bone was harvested as an autograft bone and placed on bilateral transverse processes. EP4a with gel formulation was administered at one side, and the other side was without treatment (autograft only). Fusion was evaluated by four grades fusion score (0: no osteogenesis, 3: continuous osteogenesis) every 2 or 4 weeks radiographically. Dogs were sacrificed at 8 (n=4) or 24 weeks (n=4) after the surgery, the L4-L5 vertebral segments were removed and analyzed by plain radiographs, peripheral quantitative computed tomography (pQCT) and micro (c) CT. Compared to autograft only, EP4a + autograft improved the fusion score from 4 weeks after surgery, and the score was 1.3 ± 1.0 (autograft only) and 2.8 ± 0.5 (EP4a + autograft) at 8 weeks, 2.0 ± 0.8 (autograft only) and 2.5 ± 0.7 (EP4a + autograft) at 24 weeks. EP4a + autograft significantly increased bone mass of grafted area at 8 weeks in pQCT and cCT analysis (both: $p < 0.05$ vs autograft only), and tended to increase bone mass measured by pQCT at 24 weeks ($p = 0.074$ vs autograft only). The values of bone mass in EP4a + autograft at 8 weeks was almost double compared to autograft only in pQCT and cCT. These results suggest that EP4 agonist improves the fusion score by enhancing autograft-induced new bone production. Thus, EP4 agonist is considered to shorten the time to bone fusion after spinal fusion surgery in combination with an autograft, and reduce surgery-related complications such as pseudoarthrosis.

Disclosures: YASUTOMO NAKANISHI, None.

MO0152

Integrin beta 3 is required for the skeletal response to loading in mice. Nicholas Heiniger*¹, Candice Tahimic², Yongmei Wang³, Alicia Menendez³, Katherine Weilbaecher⁴, Daniel Bikle³. ¹University of California, San Francisco, USA, ²Space Biosciences Division NASA Ames Research Center, USA, ³University of California, San Francisco VA Medical Center, USA, ⁴Washington University School of Medicine, Division of Oncology, USA

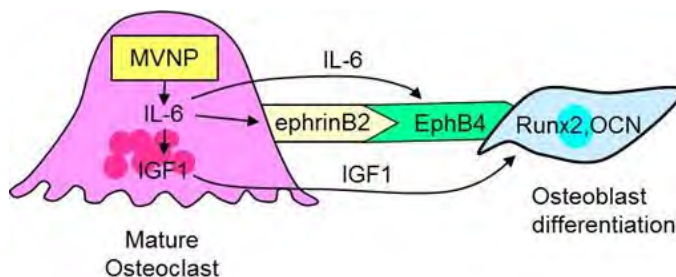
IGF1 signaling pathways are inhibited in conditions of skeletal unloading, with decreased activation of IGF1R, proliferation of bone marrow osteoprogenitor cells, and expression of α V (ITGAV) and β 3 (ITGB3) subunits of integrin in osteoblasts, associated with decreased bone formation and increased bone resorption. Applying echistatin, an inhibitor of ITGAV/ITGB3, showed similar inhibition of IGF1 signaling pathways. As neither unloading nor echistatin altered IGF1 binding to IGF1R, we hypothesized that these effects were not via interference of binding, but via a post-receptor mechanism. In further studies we observed that knock down of ITGB1 and/or ITGB3 prevented IGF1 from activating IGF1R, that ITGB3 coimmunoprecipitated with IGF1R, and that ligands for ITGB1 & ITGB3 potentiated the activation of IGF1R by IGF1. These results lead us to hypothesize that integrins such as ITGB3 are an important component of the post-receptor mechanism by which bone responds to load. We used osteocalcin-cre to selectively knock out ITGB3 from mature osteoblasts in mice. When these mice, and matched wild-type controls, were 3 months old, the femurs and tibias were harvested in 3 sets: at baseline, after 3 weeks of hind limb unloading, and after 3 weeks of hind limb unloading followed by 2 weeks of reambulation (reloading). Fourteen days prior to harvest, the mice received injections of calcein, followed 12 days later by demeclocycline. After harvest the bones were analyzed using micro-CT and histomorphometry to evaluate bone structure and formation. In males, structural parameters between ITGB3 and controls were only significantly different in trabecular number (Tb.N), bone mineral density (BV/TV), and connectivity density in unload only mice, and trabecular thickness (Tb.Th) in baseline mice, while cortical studies showed significant differences in BV/TV of reload and baseline mice, and cortical thickness of baseline mice. In females only trabecular studies revealed significant differences, seen in Tb.N of reload mice, and Tb.Th of unload only mice. Bone formation rate (BFR) and mineralizing surface (MS) of ITGB3 knockout mice were decreased compared to control after unloading followed by reloading. Further, while MS of control mice were able to recover to baseline with reloading, this did not occur in the knockout mice. These results suggest that in mice integrin β 3 is an important means through which mechanical loading is translated to osteoblast activity and bone growth.

Disclosures: Nicholas Heiniger, None.

MO0153

Measles Virus Nucleocapsid Protein Increases IL-6 and IGF1 in Osteoclasts to Enhance Osteoblast Differentiation in Paget's Disease. Jumpei Teramachi¹, Yuji Inagaki¹, Khalid Mohammad², Theresa Guise², Laëtitia Michou³, Jacques P. Brown³, Jolene J. Windle⁴, Noriyoshi Kurihara^{*1}, G. David Roodman⁵. ¹Indiana University, Medicine/Hematology-Oncology, USA, ²Indiana University, Medicine/Endocrinology, USA, ³Department of Medicine, Laval University, CHU de Quebec Research Center, Canada, ⁴Human & Molecular Genetics, Virginia Commonwealth University, USA, ⁵Indiana University, Medicine/Hematology-Oncology, Roudebush VA Medical Center, USA

Paget's Disease (PD) is characterized by focal dramatic bone resorption and formation. Since treatments targeting osteoclasts (OCLs) block both pagetic bone resorption and formation, PD offers key insights into resorption/formation coupling. However, the mechanisms responsible are unclear. We reported that OCLs from 70% of PD patients express measles virus nucleocapsid protein (MVNP), and transgenic mice with MVNP targeted to OCLs (MVNP mice) develop PD-like bone lesions that are dependent on MVNP's induction of high IL-6 in OCLs. In contrast, mice with knock-in of p62P394L (p62KI mice), the most frequent mutation linked to PD, have increased bone resorption but not formation. Since PD represents the most exaggerated form of coupled bone formation, we determined expression levels of coupling factors, ephrins and their receptors, on OCLs and osteoblasts (OBs) from MVNP, p62KI/MVNP, p62KI and WT mice. Only MVNP or p62KI/MVNP, but not p62KI mice, had high ephrinB2 levels on OCLs and EphB4 on OBs compared to WT mice. We then performed a preliminary gene expression profiling study of highly purified OCLs from MVNP, p62KI and WT mice to assess if additional factors produced by MVNP expressing OCLs (MVNP-OCLs) could be involved. It showed that OCLs from MVNP but not from p62KI mice expressed elevated levels of IGF1 mRNA compared to WT mice. We further found that IL-6 increased IGF1 protein expression in MVNP-OCLs, and IL-6 and IGF1 in turn increased ephrinB2 on OCLs. IL-6 also increased EphB4 on OBs, while IGF1 enhanced OB differentiation. To confirm these results, we measured IGF1 protein levels in total bone lysates from tibia and OCLs formed from CD11b+ cells from MVNP mice and in OCLs from normals and PD patients. OCLs and bones from MVNP but not p62KI mice expressed increased levels of IGF1 compared to WT. IGF1 expression was also markedly increased in MVNP-OCLs from PD patients, but not in OCLs from a MVNP-negative patient. Immunohistochemical analysis confirmed that IGF1 expression was elevated in OCLs of MVNP mice. IGF1 was not elevated in OBs from MVNP or p62KI mice. Further, MVNP-OCLs (200k/ml) secreted 1000 pg/ml of soluble IGF1 compared to 100-200 pg/ml secreted by WT OCLs. Importantly, anti-IGF1 or anti-IGF1R blocked Runx2 and osteocalcin upregulation in OBs co-cultured with MVNP-OCLs. These results suggest that enhanced coupling factor expression and increased IGF1 production by pagetic OCLs are major contributors to the rapid bone formation in PD.



Model of OCL/OB coupling in PD

Disclosures: Noriyoshi Kurihara, None.

MO0154

Stereological Analysis Reveals Differential Effects of Sclerostin Antibody and Parathyroid Hormone on the Osteoblast Lineage in Young Female Rats. Michael S Ominsky*¹, Danielle Brown², Gwyneth Van¹, David Cordover¹, Efrain Pacheco¹, Emily Frazier¹, Linda Cherepow¹, Marnie Higgins-Garn¹, J Ignacio Aguirre³, Thomas J Wronski³, Marina Stolina¹, Lei Zhou¹, Ian Pvrach¹, Rogely W Boyce¹. ¹Amgen Inc., USA, ²WIL Research Laboratories, USA, ³Department of Physiological Sciences, University of Florida, USA

Romosozumab, a sclerostin antibody (Scl-Ab), and parathyroid hormone (PTH) are bone-forming agents that have different modes of action on bone hypothesized to lead to quantitative differences in the osteoblast (OB) lineage at the tissue level. To compare the temporal effects of these agents on the OB lineage, 8-week-old female rats were administered vehicle (Veh), Scl-Ab (romosozumab, 3 or 50 mg/kg/week sc) or human PTH (1-34) (75 µg/kg/day sc) for 4 or 26 weeks. The high doses of Scl-Ab and PTH were also used in the respective rat lifetime studies and were the basis of these comparative assessments. At week 4, Scl-Ab effected greater increases in lumbar

vertebrae (LV) 4 cancellous bone mass compared with PTH, consistent with a higher bone formation rate (BFR/BS). In contrast to PTH, Scl-Ab did not increase osteoclastic surface. After 26 weeks, BFR/BS was similar with both agents. Using RUNX2 or nestin immunostaining, the total number of osteoprogenitor (OP) subpopulations, OBs, and lining cells was estimated across the entire LV6 body using the fractionator or proportionator stereological estimators. Density estimates referent to total bone surface, OB surface, or marrow volume were also calculated. At week 4, both Scl-Ab and PTH increased OB number, with no significant effect on OB density (Ob.N/Ob.S). After 26 weeks, in Veh-treated rats, OB surface was greatly reduced; however, total OB number was maintained, resulting in increased Ob.N/Ob.S and a reduced OB footprint (Ob.Fp; the area of bone surface covered by an OB). In contrast, in Scl-Ab-treated rats, Ob.Fp was similar to young Veh-treated rats and significantly greater than in PTH-treated rats, with fewer total OBs and a lower Ob.N/Ob.S required to provide equivalent mineralizing surface and greater mineral apposition rate (Fig.). The lower OB number at week 26 was associated with a coordinated reduction in OP number with Scl-Ab vs Veh and PTH (Fig.), with these endpoints generally positively correlated across groups and timepoints. These time-dependent reductions in subpopulations of the OB lineage may be integral to the greater attenuation of bone formation observed at the vertebra with Scl-Ab. The observation that PTH results in more OBs at the formative site, with correlative increases in progenitors compared with Scl-Ab, indicates a potentially greater stimulus for progenitor pool proliferation or differentiation with PTH, an effect that could increase carcinogenic risk in bone in the rat.

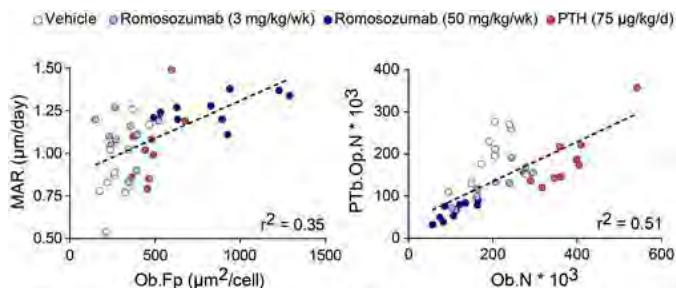


Fig. Correlations of (left) osteoblast footprint (Ob.Fp; inverse of Ob.N/Ob.S) with mineral apposition rate (MAR) and (right) osteoblast number (Ob.N) with RUNX2+ peritrabecular osteoprogenitor number (PTb.Op.N) from female rat vertebrae after treatment with vehicle, romosozumab, or parathyroid hormone (PTH) for 26 weeks.

Figure

Disclosures: Michael S Ominsky, Amgen Inc.

This study received funding from: Amgen Inc. and UCB Pharma

MO0155

Attenuation of antiresorptive action in withdrawal of minodronic acid for three months after treatment for twelve months in ovariectomized rats. Makoto Tanaka^{*1}, Hiroshi Mori², Kazuhito Kawabata². ¹ONO Pharmaceutical Co., Ltd., Japan, ²Discovery Research Laboratories, Ono Pharmaceutical Co., Ltd., Japan

The purpose of the study was to assess the effects of withdrawal of minodronic acid for 3 months after 12 months of treatment on bone mineral density (BMD), bone strength, bone turnover markers, histomorphometry and minodronic acid concentration in a rat ovariectomized (OVX) osteoporosis model. Female F344 rats were treated orally with minodronic acid (0.006, 0.03 and 0.15 mg/kg/day) for 12 months from the day after OVX, and necropsied on the day after the last dosing or following 3 months of withdrawal. Lumbar and femoral BMD were decreased in OVX controls. Minodronic acid dose-dependently increased lumbar and femoral BMD. Withdrawal eliminated the effect of minodronic acid on BMD loss after treatment at low dose, but not after treatment at middle and high doses. Trabecular microstructural changes, decrease of bone volume and trabecular elimination progressed during the withdrawal period in OVX controls. In minodronic acid-treated rats, trabecular thinning occurred during withdrawal after treatment at low dose, but the trabecular microstructure was maintained after treatment at middle and high doses. In a mechanical test of the femoral diaphysis in OVX controls, stiffness was decreased but maximal load was similar to that in sham rats after withdrawal. Minodronic acid increased maximal load and stiffness, but endosteal length at the femoral diaphysis decreased after withdrawal. Suppression of bone turnover by minodronic acid based on bone turnover markers and histomorphometrical indices was attenuated by withdrawal after treatment at low and middle doses, and partially after treatment at high dose. The minodronic acid concentration in the humerus decreased during withdrawal, and the half-life at middle dose was shorter than that at high dose. These results show that the antiresorptive action of minodronic acid was attenuated by 3 months withdrawal in a rat OVX model. An absence of BMD increase was only observed at a low dose, but decreases in antiresorptive activity occurred over a wide dose range. The rate of elimination of minodronic acid from bone was dependent on antiresorptive action by the minodronic acid dose.

Disclosures: Makoto Tanaka, None.

This study received funding from: Ono Pharmaceutical Co.,Ltd

MO0156

In vivo MRI and RPI measures reveal the positive effects of raloxifene on bone properties. Mohammad Aref^{*1}, Drew Brown¹, Erin McNerny¹, Jason Organ², Chris Newman¹, Paul Territo¹, Matthew Allen¹. ¹Indiana University School of Medicine, USA, ²Indianan University School of Medicine, USA

Raloxifene affects mechanical properties of bone through both cellular and non-cellular mechanisms. Our laboratory has shown that exposure to raloxifene, both in vivo and in vitro, increases matrix bound water and this is associated with improvements in bone mechanical properties. The goal of the current work was to utilize novel in vivo methods to assess both bone hydration and mechanical properties of raloxifene-treated animals. Skeletally mature female beagle dogs (n=12/group) were treated daily for one year with oral raloxifene (RAL; 0.5 mg/kg/day) or oral saline vehicle (VEH; 1.0 mL/kg/day). All animals underwent in vivo mechanical property assessment of the tibial cortex using reference point indentation (RPI) at 6 and 12 months. One half of each group underwent MRI scans of the proximal tibia at 6 and 12 months to assess bound water. Additional MRI diffusion-weighted imaging scans at the 12-month time point were used to measure molecular diffusion of water. RAL-treated animals had significantly lower indentation distance increase (IDI), reflective of higher mechanical properties, at 6 months and a trend toward lower values at 12 months (p=0.08) compared to VEH-treated animals. Matrix bound water was significantly higher in the tibia cortex of RAL-treated animals at both time points (p < 0.05) compared to VEH-treated animals. Additional assessments at the 12-month time point reveal higher bound water in subchondral bone and lower bound water in articular cartilage of RAL-treated animals. Raloxifene significantly increased the molecular diffusion of water, after 12 months of treatment, in cortical bone, subchondral bone, and cartilage regions of interest. Taken together these results show that the positive effects of raloxifene on mechanical properties and hydration can be measured using in vivo technologies.

Disclosures: Mohammad Aref, None.

MO0157

Local Reduction in Iron Promotes Bone Formation and Reduces Osteoclast Mediated Resorption. Justin Drager^{*1}, Zeeshan Sheikh², Yu Ling Zhang², Abhishek Kumar², Jake Barralet², Edward Harvey². ¹McGill University, Canada, ²McGill University, Canada

Purpose: Local delivery of the widely available iron chelator, Deferoxamine (DFO) has recently been shown to augment osteogenesis through activation of Hypoxia Inducible Factor (HIF) regulated angiogenesis. HIF may also induce osteoclast differentiation and function; however mimicking this effect with chelators has shown contradicting in vitro results. We aimed to determine the effect of DFO on bone growth and graft integration in a rabbit long bone defect bridged by a calcium phosphate bone graft substitute. Additionally, we aimed to quantify its effect on osteoclast mediated graft resorption using a non-weight bearing cranial onlay model. Methods: In 6 rabbits, 3D-printed Monetite (CaHPO₄) grafts were implanted into bilateral 10mm ulnar defects. Starting on day 4 post-op, DFO (600ul/200uM) was injected into one graft every 48hrs x 6 doses, with the contralateral receiving saline. In 10 rabbits, 2 circular grafts (9mm d / 4mm thick) were fixed subperiosteally onto the cranium. Four rabbits had DFO injected into both grafts and 4 had saline. Two rabbits were injected with another chelator, 1,10-Phenanthroline (PHT). At 8 weeks, micro-CT and histology were used to assess bone growth and graft resorption. TRAP stain identified osteoclast density at the bone-graft interface. Results: Ulnar defect: New bone growth was significantly higher in the DFO group compared to the saline group (Bv/Tv: 19.6% vs 13.5%; p<0.05) (fig1) and histological analysis showed more bone integrated at the graft surface. Cranial Model: A marked decrease in graft resorption and vertical bone growth was evident in the DFO and PHT group as compared to saline controls (fig2). Osteoclast density decreased 3-fold in the chelation groups compared to controls (p<0.05). Conclusion: In the long bone model, where cellular resorption of the graft is not required for bone formation as graft dissolution is predominant, bone growth was enhanced by DFO. In the static onlay model, bone growth was actually decreased by iron chelators and this correlated to a reduction in osteoclast number and graft resorption. We propose a second mechanism in addition to HIF induced angiogenesis, by which iron chelators may function as bone anabolic agents - they may also reduce osteoclast mediated resorption by targeting iron requirements during differentiation. This previously unreported in vivo finding has exciting potential applications for implant integration, improving bone quality, and limiting bone destruction.

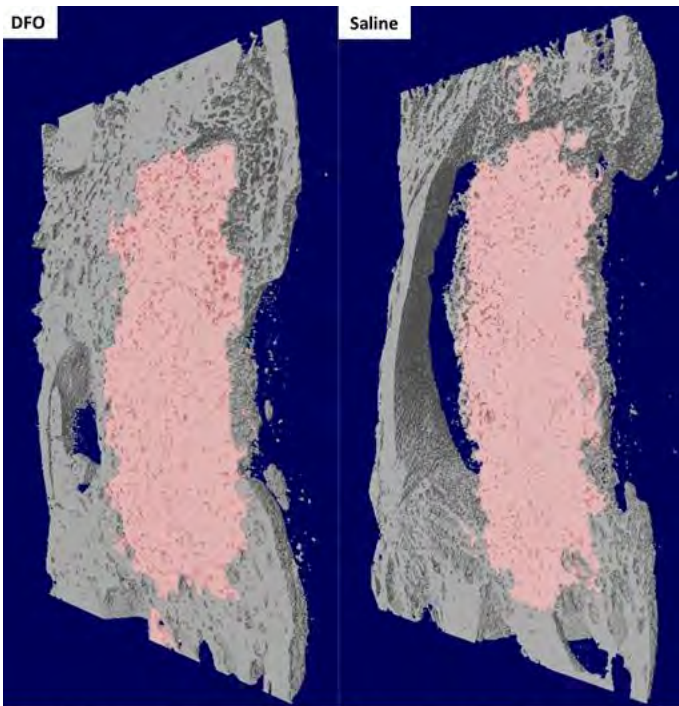


Figure 1: Representative 3D coronal cuts of the osteotomy site. Grey represents new bone and pink represents the remaining graft material.

Figure 1

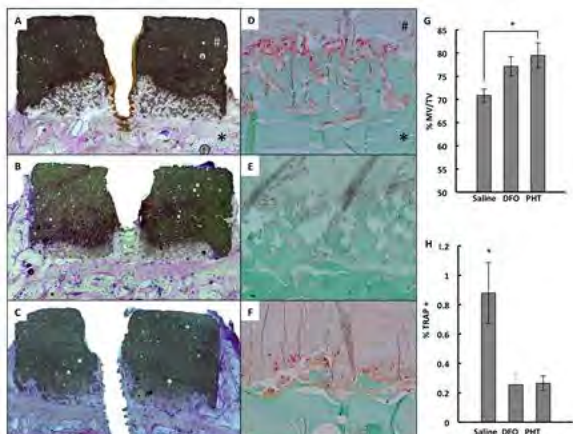


Figure 2: (A-C) Coronal sections through the center of the graft demonstrating the resorptive fronts of the grafts. A: Saline, B: DFO, C: PHT. (D-F) representative sections of the bone/graft interface stained with TRAP and fast green. D: Saline, E: DFO, F: PHT. (G) average micro-CT metric MV/TV calculated for each cranial graft post explanation. (H) average quantification of TRAP+ stain normalized per interface.

Figure 2

Disclosures: Justin Drager, None.

MO0158

Odanacatib Inhibits Bone Resorption and Reverses Glucocorticoid-Induced Bone Loss in Adult Rabbits. Brenda Pennypacker¹, Peter Szczerba², Marc Washington², Maureen Pickarski², Le Duong². ¹Merck Research Laboratories, USA, ²Merck & Co., USA

Long-term glucocorticoid (GC) therapy is a common cause of secondary osteoporosis leading to an increased fracture risk. The cathepsin K inhibitor odanacatib (ODN) has been shown to effectively restore bone loss in preclinical models and in postmenopausal osteoporosis. Here, we compare efficacy of ODN versus alendronate (ALN) on bone mass and remodeling in a GC-induced osteoporosis study in rabbits in treatment mode. Adult female (7 mo.) NZW rabbits were allocated to either untreated control (CTRL) or pre-treatment with methyl-prednisolone (MP, 0.6 mg/kg IM wkly). After 3 mo., rabbits on MP were randomized by body weight and lumbar vertebral bone mineral density (LV.BMD) into 4 groups receiving: MP +Veh, MP+ALN (150µg/kg, 2x/wk), MP+ODN (1.5mg/kg/d in food), or MP+ODN (6mg/kg/d in food) for an additional 9 mo. Note, ODN 1.5mg/kg/d dosed in food provided daily drug exposures approximating the 50-mg once-wkly clinical dose. LV.BMD measurements, bone resorption marker urinary helical

peptide (uHP) and bone formation marker serum bone specific alkaline phosphatase (sBSAP) were performed at -3, baseline, 3, 6, and 9 mo. At baseline, LV.BMD in MP-pretreated rabbits decreased by 16% ($p < 0.001$), uHP elevated 3-fold ($p < 0.001$), and body weight decreased by 9% compared to rabbits not treated with MP. After 3-mo. of treatment, ODN at both doses and ALN significantly reduced uHP by 57-90% below MP+Veh (all $p < 0.001$). In addition, uHP levels remained lower in the ODN groups compared to ALN at 3 and 9 mo. uHP in the MP+Veh remained 3-4 fold higher than CTRL throughout the study ($p < 0.001$). Measurements of sBSAP were not different across all treatment groups. LV.BMD in the MP+Veh group remained 14-16% below that in CTRL at mo. 3, 6, and 9 ($p < 0.001$). ODN 6mg/kg increased LV.BMD by 16% at mo. 6 and by 20% at mo. 9 vs. MP+Veh (all $p < 0.001$). By mo.9, LV.BMD of ODN 6mg/kg was not different from CTRL. ODN 1.5mg/kg and ALN treatment gradually increased LV.BMD, achieving 12% and 10% gains respectively vs. MP+Veh by mo. 9 ($p < 0.05$). In conclusion, GC treatment accelerated bone loss accompanied with elevated bone resorption in adult rabbits. In treatment mode, ODN and ALN reversed GC-induced BMD loss similarly, with ODN achieving greater reduction of bone resorption marker than that by ALN. These results provide preclinical evidence to support the evaluation of ODN for the treatment of GC-induced osteoporosis in humans.

Disclosures: Brenda Pennypacker, Merck and Co., Inc. -employee
This study received funding from: Merck and Co., Inc.

MO0159

Osteoclast-induced TcREG limit bone loss but cannot suppress innate immune response in Serum-transfer induced arthritis. Reggie Aurora¹, Anna Cline-Smith², Elena Shashkova². ¹Saint Louis University University, USA, ²St. Louis University School of Medicine, USA

We have recently shown that osteoclast-induced FoxP3+ CD25+ CD8 T-cells (OC-iTcREG) suppress osteoclasts, effector T-cells and have an anabolic effect on bone volume in ovariectomy induced osteoporosis in mice. Here we tested these cells in a murine model of rheumatoid arthritis. We used serum-transfer induced arthritis because inflammation in this disease model is primarily through activated neutrophils and macrophages as compared to ovariectomy where proinflammatory cytokines are produced primarily by T-cells. OC-iTcREG were either induced in vivo or ex vivo induced CD8 T-cells were adoptively transferred prior to injection of arthritogenic serum. In parallel, we also used TGFβ-induced FoxP3+ CD25+ CD4 T-cells that were adoptively transferred. Our results show that while transferred OC-iTcREG limit bone and cartilage loss, they do not suppress inflammation as measured by cytokine production of cells isolated from the joint. In contrast, TREG were effectively able to suppress inflammation and limit bone loss. These results show that TcREG and TREG have overlapping yet distinct functions in vivo: while OC-iTcREG act as a buffer to limit bone loss, TREG are able to suppress the activation of the innate immune system. The implications and alternate explanations of these observations will also be discussed.

Disclosures: Reggie Aurora, None.

MO0160

Zoledronate prevents lactation induced loss of bone strength and micro-architecture in mice. Mette Høegh Wendelboe, Jesper Skovhus Thomsen, Annemarie Brüel*. University of Aarhus, Denmark

Purpose: In rodents, lactation is associated with a considerable and very rapid bone loss, which almost completely recovers after weaning. The aim of the present study was to investigate whether the bisphosphonate Zoledronate (Zln) could inhibit bone loss during lactation. In addition, to study whether Zln interfered with recovery of bone mass after lactation has ceased. **Materials and methods:** Seventy NMRI mice, 10-weeks-old, were divided into the following groups: baseline, pregnant, lactation, lactation + Zln, recovery, recovery + Zln, and recovery control (virgin). The lactation period was 12 days, then the pups were removed, and thereafter recovery took place for 28 days. Zln, 100 µg/kg sc, was given at the day of delivery, and again 4 and 8 days after delivery. The experiment was approved by the Danish Animal Experiments Inspectorate. Mechanical testing and χ CT of femur, tibia and L4 were performed. **Results:** In L4, lactation resulted in a substantial loss of trabecular BV/TV (-40% vs. pregnant, $p < 0.001$), trabecular thickness (Tb.Th) (-29% vs. pregnant, $p < 0.001$), bone material density (-4% vs. pregnant, $p < 0.001$), and bone strength (-55% vs. pregnant, $p < 0.001$). Zln completely prevented lactation induced changes in L4: BV/TV (+10% vs. pregnant, NS), Tb.Th (+0.03% vs. pregnant, NS), bone material density (+1.2% vs. pregnant, NS), and bone strength (+11% vs. pregnant, NS). Similar results were found in the proximal tibia. Full recovery of microarchitectural and biomechanical properties was found 4 weeks after weaning. Interestingly, in the recovery group treated with Zln during the lactation period L4 had higher BV/TV (+45%, $p < 0.05$), Tb.Th (+16%, $p < 0.05$), and bone strength (+38%, $p < 0.05$) compared with recovery controls. This indicates that Zln did not interfere with the substantial anabolic response, which takes place during recovery. **Conclusion:** Zln fully prevented lactation induced loss of bone strength and microarchitecture, and did not inhibit the anabolic response taking place after weaning.

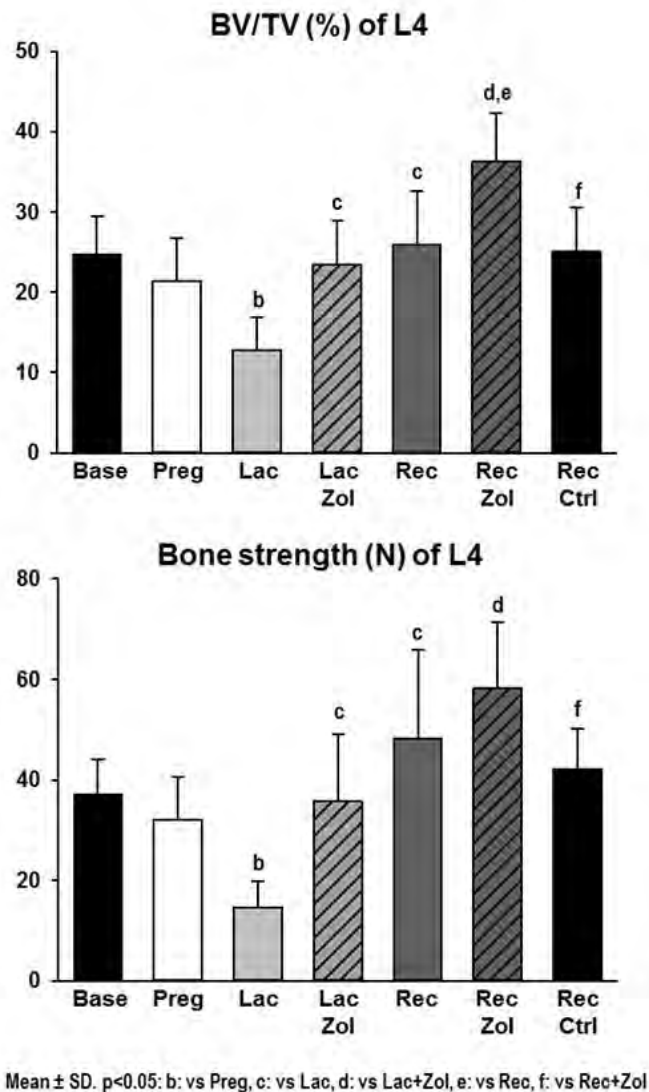


Figure 1

Disclosures: Annemarie Brüel, None.

MO0161

S. aureus infection causes aberrant bone healing. Brandon Romero*, Nisreen Akef, Larry Suva, Allister Loughran, Mark Smeltzer, Dana Gaddy, University of Arkansas for Medical Sciences, USA

Osteomyelitis is a serious bone infection typically caused by *Staphylococcus aureus*, the pathogenesis of which is poorly understood. The details of the cellular host responses of bone to the infection are especially lacking. We sought to determine the time course and extent of the host bone response to infection using a contemporary clinical *S. aureus* isolate (UAMS1), and measuring reactive bone formation and the temporal changes in markers of bone resorption and bone formation during the development of osteomyelitis *in vivo*. A unicortical femoral diaphyseal defect was created in 8 week old female mice that were infected with either vehicle control or UAMS1. On days 3, 7 and 14, serum was collected and infected limbs harvested and formalin fixed. As expected during healing of the unicortical bone defect, serum PINP levels increased in sham, uninfected animals across the time course of the entire bone healing response, whereas serum CTX levels were unchanged, confirming the bone formation phase of direct bone healing. In controls, the bone defect was completely healed within 14 days, whereas in UAMS1-infected bones defect healing was not observed, yet progressive and inappropriate reactive bone formation occurred over 14 days. Despite the dramatic increases in reactive bone formation in UAMS1 infected bones, serum PINP levels were diminished compared with the uninfected bones across the time course of bone healing. To determine the cellular effects of *S. aureus* products, *ex vivo* bone marrow cultures were grown toward osteoblast (OB) or osteoclast (OCL) differentiation for 4 days, and exposed to increasing concentrations (10, 25, 50%) of UAMS1 conditioned medium (CM). Cultures were then evaluated for proliferation and cytotoxicity at 24hr. UAMS1 50% CM suppressed cell survival and proliferation of OB and OCL, whereas 10 and 25% had no effect. Recruitment into the

OB lineage was unaffected by 25% CM (indicated by % AP+ CFU-AP), although exposure of cultured calvarial OBs to 25% CM significantly reduced cell survival. Thus, secreted products from a clinically relevant *S. aureus* strain has suppressive effects on the survival of OB, OCL, and their precursors, with the virulence mediated by its cytotoxic effects on more differentiated cells. Collectively, these data demonstrate that an abnormal bone response occurs in the presence of *S. aureus*, which inhibits normal bone healing, yet is not predicted by serum markers of bone turnover.

Disclosures: Brandon Romero, None.

MO0162

Chronic Antibiotic Treatment Causes Gender Specific Bone Loss. Jonathan Schepper*, Fraser Collins, Regina Irwin, Sandi Raetz, Nara Parameswaran, Laura McCabe, Michigan State University, USA

Chronic antibiotic therapy for recurring gastrointestinal infections significantly reduces intestinal bacteria levels. Recent studies link the intestinal microbiome and bone health. However, the effect of chronic antibiotic use on bone health is still unknown. To examine this, we treated 12-week-old healthy male and female BALB/c mice with commonly used antibiotics (1g/L ampicillin and 0.5g/L neomycin) for 4 weeks. Fecal bacterial counts were significantly decreased throughout the experiment in antibiotic treated male and female mice. MicroCT analysis of femur trabecular bone demonstrated a significant reduction in bone volume fraction (BVf) in male and a downward trend in female mice treated with antibiotics compared to gender matched controls. Interestingly the degree of bone loss was significantly greater in males compared to females (35 vs 22%). Similarly, antibiotic treated males, but not females, displayed a decrease in vertebral trabecular BVf. Consistent with the CT parameters, analysis of serum bone remodeling markers revealed significantly reduced levels of osteocalcin (osteoblast marker) and TRAP5b (osteoclast marker) in the treated males (by 50% and 12%, respectively), whereas in female mice the markers trended to decrease but were not significant. Taken together our data demonstrate that long-term antibiotic treatment could have an adverse effect on trabecular bone volume by modulating bone remodeling. The results also identify gender related differences in response to antibiotic treatment.

Disclosures: Jonathan Schepper, None.

MO0163

Effects of dietary iron and intermittent adriamycin administration on FGF23 and Fetuin A levels of C57BL/6J mice. Masanori Takaiwa*¹, Kosei Hasegawa², Hirovuki Tanaka³, Hirokazu Tsukahara². ¹Dept. of Pediatrics, Matsuyama Red Cross Hosp., Japan, ²Okayama University Graduate Department of Pediatrics, School of Medicine, Dentistry & Pharmaceutical Sciences, Japan, ³Department of Pediatrics, Okayama Saiseikai General Hospital, Japan

FGF23 plays significant role in the pathogenesis of Chronic Kidney Disease-Mineral and Bone Disorder (CKD-MBD). FGF23 shows elevation during the early CKD, and was associated with insulin resistance and cardiovascular mortality risk of CKD. Fetuin A is also related to the pathogenesis of insulin resistance, cardiovascular disease and CKD. Iron (Fe) supplementation is commonly initiated from the early CKD. Since Fe deficiency exacerbates FGF23 elevation, we created an early CKD model by intermittent administration of adriamycin (ADR) to C57BL/6J mice (C57) and examined the effect of dietary Fe on FGF23 and Fetuin A during the early CKD. Using 6 groups (2%-Fe and 2%-Fe-AN groups - fed a 2.0% Fe diet; 0.6%-Fe and 0.6%-Fe-AN groups - fed a 0.6% Fe diet and 0.02%-Fe-AN groups - fed a 0.02% Fe diet), 10-week-old male C57 were administered serine (2%-Fe, 0.6%-Fe and 0.02%-Fe) or ADR weekly (2%-Fe-AN, 0.6%-Fe-AN and 0.02%-Fe-AN) for 28 days. After treatment, Fe for 2%-Fe and 2%-Fe-AN were higher, and that of 0.02%-Fe-AN was lower than 0.6%-Fe. The kidneys of three ADR treated groups were significantly smaller in size. Although there was no statistical difference, Cr levels of ADR treated groups were higher than the groups without ADR treatment. There was no significant difference in Ca, Pi and PTH levels among all experimental groups. Oral Fe supplementation mildly suppressed intact FGF23 levels of animals without ADR treatment in dose dependent manner. Markedly this negative regulatory effect of oral Fe loading on FGF23 concentration was significantly enhanced in ADR treated groups. 0.02%-Fe-AN showed significant elevation (670 ± 134pg/ml) compared with 0.6%-Fe-AN (284 ± 10pg/ml) and 2%-Fe-AN (106 ± 10pg/ml). Oral Fe deprivation increased Fetuin A in 0.02%-Fe (149 ± 3ng/ml) compared with 0.6%-Fe (137 ± 5ng/ml) and 2%-Fe (124 ± 5pg/ml). Fetuin A was highest in 0.02%-Fe-AN (158 ± 6ng/ml) and the negative correlation between diet Fe content and Fetuin A was not observed among three ADR treated groups. The ADR treatment caused small kidney, mild increase in FGF23 without affecting Pi and PTH, serving as a reasonable early CKD model. Both FGF23 and Fetuin A levels were elevated in the Fe depleted early CKD model. Since negative regulatory effect of Fe on FGF23 was significant, it was suggested that the initiation of oral Fe during early CKD suppresses FGF23 level and has a favorable effect on progression of CKD.

Disclosures: Masanori Takaiwa, None.

MO0164

Healing of large-scale bone defects in a mouse model involves hybrid cartilage/bone progenitors. Nikita Tripuraneni, Sandeep Paul, Simone Schindler, Helen Chou, Jason Hsieh, Gage Crump, Francesca Mariani*. University of Southern California, USA

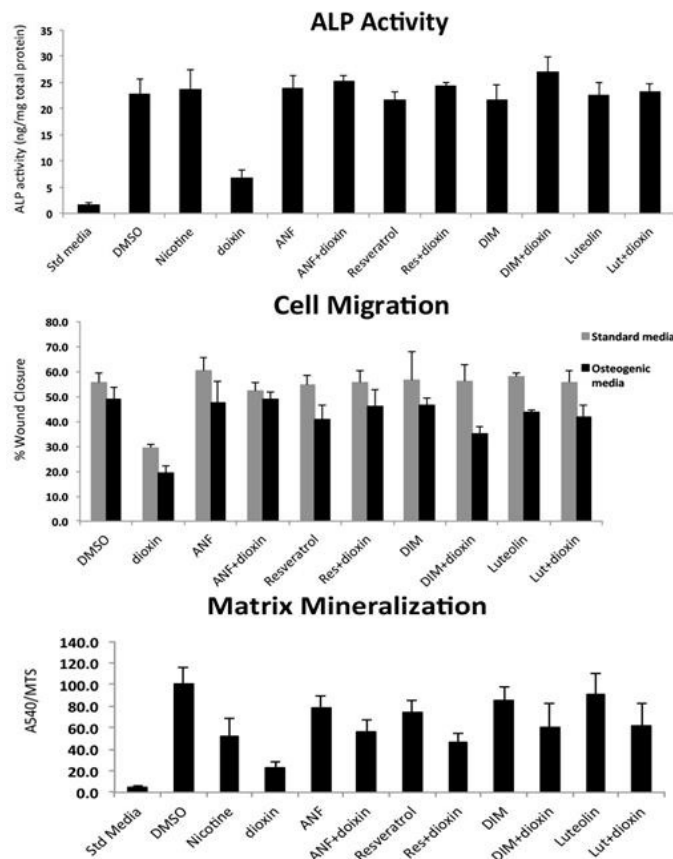
The treatment of significant bone loss remains an unresolved problem. Autogenous bone graft material is limited in supply and the biological activity of synthetic substitutes requires further refinement. Thus, new strategies stimulating the repair of large-scale bone defects are needed. We have found that, as has been anecdotally reported in humans, large resections of the adult rib of the mouse can fully repair. We believe full repair depends on skeletal progenitors emerging from the periosteum since repair fails to occur when it is removed. In addition, ectopic placement of rib periosteum into muscle supports new bone deposition. We are also testing a novel hypothesis that repair chondrocytes are distinct from growth plate chondrocytes because they have hybrid properties of both cartilage and bone cells. Our hypothesis is supported by gene expression analysis and other assays which indicate that these repair cells rapidly and actively build a stabilizing bone matrix rather than simply acting as a template for invading osteoprogenitors. Current studies in our laboratories are determining the molecular signature of these repair cells and developing ways to generate them in large numbers for augmenting repair in other parts of the skeleton.

Disclosures: Francesca Mariani, None.

MO0165

Mechanistic insight into the adverse effects of Aryl hydrocarbon receptor activation on osteogenic differentiation. Erin Hsu*, Chawon Yun, Sean Mitchell, Abhishhek Kannan, Kevin Sonn, Sharath Bellary, Christian Park, Jonghwa Yun, Ryan Freshman, Danielle Chun, Ami Parekh, Wellington Hsu. Northwestern University, USA

Cigarette smoking is associated with increased rates of pseudarthrosis after spine fusion procedures. Numerous toxic ligands for Aryl hydrocarbon receptor are present in cigarette smoke, and recent evidence suggests that Ahr activation may inhibit osteogenic differentiation. We showed previously that activation of the Aryl hydrocarbon receptor by dioxin treatment inhibits bone regeneration and spine fusion in the rat. The purpose of this study was to elucidate downstream mechanisms of dioxin action, and to identify therapeutics that might mitigate the effects of dioxin on bone. Bone marrow stromal cells were isolated from rat femurs and tibiae and cultured under standard or osteogenic conditions. Factors that are critical to osteogenesis were evaluated after exposure to vehicle control, dioxin, Ahr antagonists, or antagonists + dioxin. Antagonists evaluated were: alpha-naphthoflavone (ANF; a synthetic antagonist), resveratrol (Res; a stilbenoid found in grapes and present in red wine), 3,3'-diindolylmethane (DIM; a flavonoid product of cruciferous vegetables), and luteolin (Lut; a flavonoid present in celery, broccoli, and other sources). We found that dioxin inhibits ALP activity, BMSC migratory capacity, and matrix mineralization. Co-treatment with each of the 4 antagonists mitigates these effects. Dioxin was also found to inhibit BMSC chemotaxis towards various chemoattractants. Co-treatment with ANF and Res generally rescued the anti-chemotactic effects of dioxin to a greater degree than DIM and Lut. RNA and protein expression studies showed that dioxin down-regulates numerous pro-osteogenic genes. Co-treatment of BMSC with Ahr antagonists prevented dioxin-induced expression changes of Col2, Col12, Phex, MMP-3, and MMP-13 proteins to varying degrees. Our results suggest that Ahr activation may play a critical role in the adverse effects of cigarette smoke on bone healing. Dietary supplementation with Ahr antagonists should be investigated as therapeutic option to combat these inhibitory effects.



abstract figure

Disclosures: Erin Hsu, None.

MO0166

The fate and distribution of autologous bone marrow mesenchymal stem cells with intra-arterial infusion in osteonecrosis of the femoral head in dogs. Hongting Jin*¹, Taotao Xu², Qiqing Chen², Chengliang Wu², Pinger Wang², Qiang Mao³, Shanxing Zhang², Jiavi Shen², Peijian Tong³. ¹Zhejiang Chinese Medical University, Peoples republic of china, ²Zhejiang Chinese Medical University, China, ³Department of Orthopaedic Surgery, The First Affiliated Hospital of Zhejiang Chinese Medical University, China

Objectives: To observe the fate and distribution of autologous bone marrow mesenchymal stem cells (MSCs) with intra-arterial infusion in treatment of osteonecrosis of the femoral head (ONFH) in dogs. **Methods:** Twelve Beagle dogs were randomly divided into two groups: MSCs group and control group. ONFH models were established by a liquid nitrogen freezing method. After three weeks, dogs in MSCs group were injected with 1 ml autologous MSCs ($5 \times 10^6 - 1 \times 10^7$ /ml) and 0.9% normal saline were used in control group. Necrotic lesions were evaluated by MRI and changes in general architecture of the femoral heads were determined by hematoxylin and eosin stain after eight weeks. The differentiation of grafted cells in the femoral heads was observed by immunofluorescence, and distribution of grafted cells in vital organs was observed through immunohistochemistry and histomorphometry. **Results:** The rate of radiological progression in MSCs group was statistically lower than that in the control group. Trabecular bone volume was increased and empty lacunae rate was decreased in MSCs group ($p < 0.05$). Most of BrdU-positive MSCs in necrotic region co-stained together with osteocalcin in MSCs group. It means that MSCs with intra-arterial infusion migrating into the necrotic field of femoral head directionally differentiated into osteoblasts and improved the necrosis of femoral head. Simultaneously, the BrdU-positive MSCs were nonuniformly distributed in vital organs and the number of BrdU-positive cells in kidney (IOD/Area = 0.050 ± 0.0013), gallbladder (IOD/Area = 0.032 ± 0.0020) and liver (IOD/Area = 0.023 ± 0.0026) were obviously higher than those in small bowel (IOD/Area = 0.005 ± 0.0009), prostate (IOD/Area = 0.005 ± 0.0006). MSCs differentiated into normal cells in corresponding organs. **Conclusions:** autologous MSCs with intra-arterial infusion may be a feasible and safe avenue for the treatment of femoral head necrosis.

Figure 1. Evaluation of MSCs and BrdU-labeling efficacy.

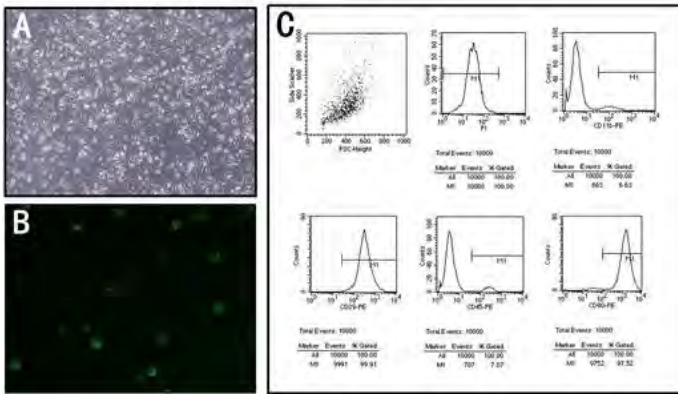


Figure 1

Figure 2. Homing and osteogenic differentiation of MSCs with intra-arterial infusion in necrotic field of femoral head may be an important mechanism to improve the signs of ONFH in imaging and histopathology.

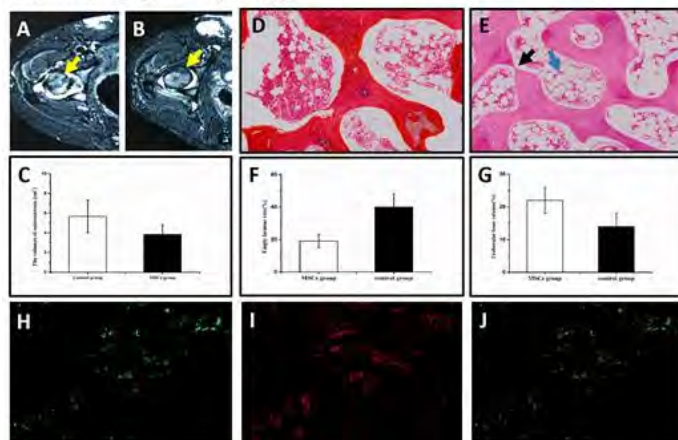


Figure 2

Figure 3. The safety and distribution of MSCs with intra-arterial infusion in vital organs.

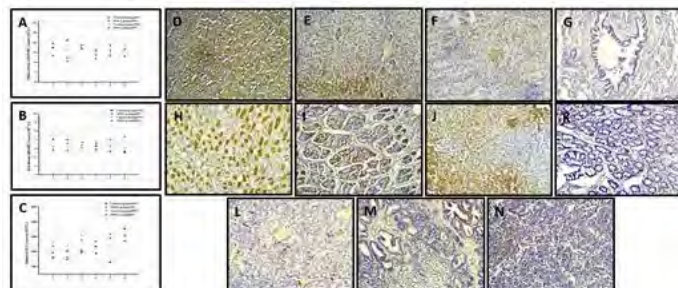


Figure 3

Table 2. Mean volume of IOD/Area of BrdU express in different tissues at eight weeks after intra-arterial infusion of MSCs

| Tissues | IOD/Area |
|-------------|-----------------|
| Heart | 0.016 ± 0.001* |
| Liver | 0.023 ± 0.0026* |
| Spleen | 0.003 ± 0.0002^ |
| Lung | 0.012 ± 0.0008 |
| Kidney | 0.05 ± 0.0013* |
| Stomach | 0.015 ± 0.0014 |
| Gallbladder | 0.032 ± 0.002* |
| Intestine | 0.005 ± 0.0009^ |
| Pancreas | 0.007 ± 0.0007 |
| Testicle | 0.003 ± 0.0004^ |
| Prostate | 0.005 ± 0.0006^ |

*: Significantly higher
 ^: Significantly lower

Table

Disclosures: Hongting Jin, None.

MO0167

α2-Antiplasmin Deficiency Protects from Bone Loss Induced in Ovariectomized Mice. Naoyuki Kawao^{*1}, Akihito Shiomi¹, Kiyotaka Okada¹, Yukinori Tamura¹, Katsumi Okumoto², Osamu Matsuo¹, Masao Akagi³, Hiroshi Kajii¹. ¹Kinki University Faculty of Medicine, Japan, ²Life Science Research Institute, Kinki University, Japan, ³Department of Orthopaedic Surgery, Kinki University Faculty of Medicine, Japan

The production of bone resorptive cytokines, such as IL-10 and TNF-α, was increased in patients with postmenopausal osteoporosis. α2-antiplasmin (α2-AP) is the primary inhibitor of plasmin in fibrinolytic system, and tissue fibrinolytic system is involved in bone metabolism and bone repair. However, its various functions other than fibrinolysis inhibition have been shown. We therefore investigated the roles of α2-AP in bone loss induced by ovariectomy using α2-AP-deficient and counterpart wild-type mice. Bone mineral density (BMD) in femur and indices of bone metabolism were analyzed at 8 weeks after ovariectomy. The levels of plasma α2-AP were elevated in wild-type mice with ovariectomy, compared to those with sham operation. Quantitative computed tomography analysis revealed that α2-AP deficiency blunted the trabecular bone loss induced by ovariectomy. α2-AP deficiency attenuated the increases in serum levels of bone-specific alkaline phosphatase, cross linked C-telopeptide of type I collagen and IL-10 induced by ovariectomy. α2-AP elevated the mRNA levels of IL-10 and TNF-α in mouse monocytic RAW 264.7 cells. Although α2-AP did not affect the mRNA levels of Runx2, Osterix, alkaline phosphatase and osteocalcin in mouse osteoblastic MC3T3-E1 cells, it attenuated RANKL-induced osteoclast formation in RAW 264.7 cells. Plasmin did not affect the mRNA levels of IL-10 and TNF-α in RAW 264.7 cells, suggesting that the effects of α2-AP on IL-10 and TNF-α in monocytes are blood fibrinolysis inhibition-independent. On the other hand, α2-AP induced the phosphorylation of ERK1/2 and p38 MAPK in RAW 264.7 cells, and PD98059, an inhibitor of ERK1/2, and SB203580, an inhibitor of p38 MAPK, antagonized IL-10 mRNA levels enhanced by α2-AP in RAW 264.7 cells, indicating that the enhancement of α2-AP on IL-10 expression in monocytes is via the activations of ERK1/2 and p38MAPK pathways. In conclusion, the present study indicates that α2-AP is involved in bone loss induced by ovariectomy through the expression of IL-10 and TNF-α from monocytes in mice.

Disclosures: Naoyuki Kawao, None.

MO0168

BMP2 Regulates Both Osteogenesis and Angiogenesis. Beth Bragdon^{*1}, Thomas Cheng², Elise F. Morgan³, Ivo Kalajic⁴, Stephen E. Harris⁵, Louis C. Gerstenfeld². ¹Boston University School of Medicine Department of Orthopaedics, USA, ²Department of Orthopaedic Surgery, Boston University School of Medicine, USA, ³Department of Mechanical Engineering, Boston University College of Engineering, USA, ⁴Center for Regenerative Medicine & Skeletal Development, University of Connecticut Health Center, USA, ⁵Department of Periodontics, University of Texas Health Science Center at San Antonio, USA

Introduction: Angiogenesis is required for successful skeletal tissue repair which is highlighted during distraction ossification (DO), a procedure in which bone is regenerated by mechanical strain due to the slow lengthening of bone. Vessels formed during DO are sites where Bone Morphogenetic Protein 2 (BMP2) is predominately expressed, both in endothelial and smooth muscle cells. Although it is known that BMP2 is osteogenic and is involved with angiogenesis, it remains unclear as to

functional role that BMP2 expressed in vessels carries out in bone development as well as angiogenesis.

Methods: A transgenic mouse containing a tamoxifen inducible Cre recombinase driven by the α -SMA (Smooth Muscle Actin) promoter was crossed with a BMP2 Floxed transgenic mouse resulting in a mouse (BMP2 cKO) that upon tamoxifen treatment, BMP2 was conditionally knocked out in α -SMA positive cells. The DO surgery was performed on male mice (10-15 weeks old) and starting at post-operative day six received vehicle or tamoxifen. Distraction began at day seven and continued for 10 days resulting in a 1.5mm gain of length. The regenerating skeletal tissue within the gap and surrounding tissue was analyzed molecularly across time using RT-qPCR analysis. Bone and vessel formation was characterized with micro-CT by perfusing the vasculature with a contrasting agent followed by micro-CT scan.

Results: The expression of *BMP2* and *Id1* (Figure 1) direct targets of BMP signaling were decreased in the surrounding tissue of the BMP2 cKO. The micro-CT results suggest the BMP2 cKO has decreased bone formation, although gene expression for osteogenesis (*RUNX2* and *Osteocalcin*) was increased. Strikingly, these studies showed that the loss of BMP2 within the surrounding soft tissues led to diminished vessel formation at d31 which is supported by the expression of markers for angiogenesis, *VEGFR2*, *Pecam1*, and *Ve-Cadherin* and microCT findings (Figure 2).

Discussion: The conditional BMP2 cKO in vascular tissues decreased both osteogenesis and angiogenesis. Although osteogenic gene expression was increased in the BMP2cKO, it did not result in more mineralized tissue. Most striking was the angiogenic phenotype that occurred within the surrounding tissue where BMP2 cKO showed decreased angiogenesis. These results suggest BMP2 provides a critical mechanistic link in the morphogenetic signals that promote skeletal and vascular tissue formation.

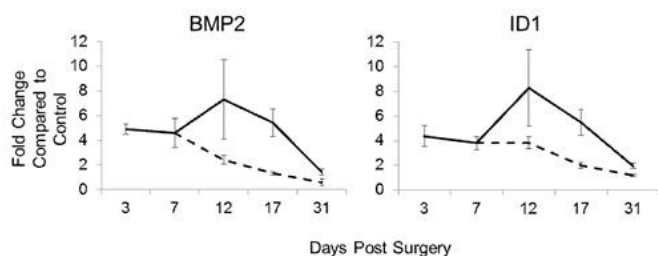


Figure 1. Relative gene expression for BMP2 and ID1 within the surrounding tissue. Control is shown in solid line and BMP2cKO is shown by dash line. Expression was determined by quantitative RT-PCR. n=3-4.

Figure 1

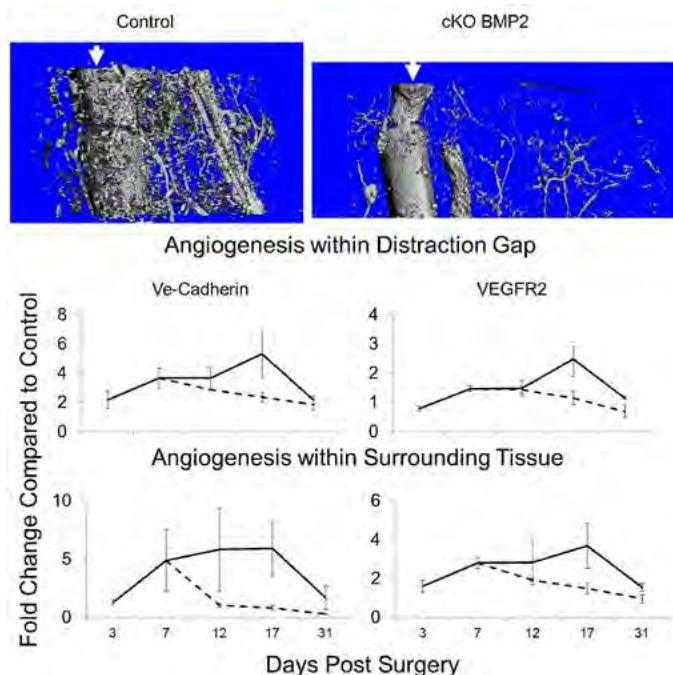


Figure 2. Top panels. 3D rendering of the micro-CT scan before decalcification showing both femur (arrow) and vasculature. Lower panels. Relative gene expression for angiogenic markers within the distraction gap and surrounding tissue. Control is shown in solid line and BMP2cKO is shown by dash line. Expression was determined by quantitative RT-PCR. n=3-4.

Figure 2

Disclosures: Beth Bragdon, None.

MO0169

A selective androgen receptor modulator that prevents disused muscle atrophy in rats. Kyohei Horie*, Masanobu Kanou, Kenichirou Takagi, Shinnosuke Hosoda, Hidekazu Watanabe, Motoko Hamada, Naoki Hase, Hiroimichi Sugiyama, Kei Yamana. TEIJIN PHARMA LIMITED, Japan

Muscle atrophy is caused by inactivity such as unloading and immobilization after fracture. Hip fracture is one of the most serious consequences of osteoporosis and is associated with increased mortality in older adults. Therefore, prevention of muscle atrophy after hip fracture is significant unmet medical needs and a key success factor for rehabilitation and reduction of mortality.

Selective androgen receptor modulator, SARM is one of the promising candidates for treatment of muscle atrophy due to its anabolic activity in muscle. Recently, we identified a novel non-steroidal orally available SARM, TEI-SARM2 with unique characteristics. TEI-SARM2 has strong ability to AR binding and AR-dependent transcriptional activity same as ostarine, the most advanced SARM in clinical studies. Interestingly, TEI-SARM2 showed strong activity of N/C interaction same as DHT and nandrolone (ND), a clinically available anabolic steroid while ostarine has minimal activity of it. In addition, TEI-SARM2 has longer half-life and higher AUC in blood than that of ostarine in pharmacokinetic study in rats.

To evaluate the potential values of TEI-SARM2 as a pharmaceutical candidate for muscle atrophy, we compared in vivo activity of TEI-SARM2 with ostarine and ND. In orchidectomized (ORX) rats, once-weekly oral treatment of TEI-SARM2 for 2 weeks increased muscle weight significantly stronger than ostarine and similar extent as ND. Moreover, in normal male rats, once-weekly treatment of TEI-SARM2 for 6 weeks significantly increased muscle weight same as ND treatment but did not change prostate and testis weights which were significantly reduced by ND treatment. Furthermore, in hindlimb-unloading female rats, oral treatment of TEI-SARM2 for 2 weeks almost completely prevented rapid loss of muscle weight same as ND treatment while TEI-SARM2 has no effect in ovary and uterus weights which were significantly affected by ND treatment.

In summary, TEI-SARM2 has tissue selective activity with strong anabolism in muscle and minimal adverse effects in reproductive tissues and can prevent rapid loss of unloading-induced muscle atrophy. Taken together our results suggest that TEI-SARM2 is a promising therapeutic candidate for muscle atrophy after hip fracture.

Disclosures: Kyohei Horie, TEIJIN PHARMA LIMITED

MO0170

Considerations for Intramuscular Injections in Rodents. Melanie Felix*, Annie Martin, Solomon Haile, Susan Y. Smith, Charles River Laboratories, Canada

Purpose: The intramuscular route is frequently used for compound administration for nonclinical efficacy/toxicology testing, including juvenile studies. Selection of appropriate muscle to inject and tolerable limit of injection volume need careful consideration. The objective of this study was to determine the maximum volume for intramuscular injection in mice and rats at selected sites.

Method: Different volumes of diluted India ink (10%) were injected into the tibialis anterior of mouse pups weighing 1 to 7g. The outcome was assessed by visual inspection of the injection site in the live animal and following euthanasia. At the site of the India ink injection, the skin was removed and the spread of the ink within the muscle and extent of leakage outside of the muscle, were evaluated. In albino rats weighing 200-250g, different volumes of India ink and a contrast agent (Omnipaque™) were injected into the rectus femoris. Faxitron radiographs were taken immediately post, 15 minutes post and 5 hours post injection. The spread of the ink was also evaluated macroscopically.

Results: For mice weighing less than 4g, a single injection of India ink at a dose volume of ≥ 1 mL/kg caused severe swelling of the muscle and was considered unacceptable. Repeat dosing of 5 μ L in mice ≤ 4 g over 2 consecutive days, corresponding to a total dose volume of 5 mL/kg, was considered too high based on observed swelling, limb stiffness, impaired movement and abnormal posture. Two consecutive daily doses of 5 μ L in older/heavier mice of ≥ 5 g, corresponding to a dose volume of 3 mL/kg, was well tolerated. For rats, faxitron radiographs indicated that single injections of ≥ 0.20 mL resulted in leakage outside of the muscle and showed distal expansion cranially to the patella and patellar ligament. Gross observations supported these observations.

Conclusion: A single intramuscular injection in the anterior tibial muscle region at 0.5 mL/kg in mouse pups weighing 2.17 to 3.25 g did not cause any adverse local clinical observations. For mouse pups weighing at least 5g, a maximum dose volume of 3 mL/kg was considered acceptable, when administered over 2 days. For rats, a fixed volume of 0.10 mL (equal to 0.5 mL/kg) was determined as the optimal volume for injection in the rectus femoris of 200-250 g rats based on minimal spread to the neighboring muscles and limited leakage into the subcutaneous tissue.

Disclosures: Melanie Felix, None.

MO0171

CRTAP, the causative protein in type VII OI, may be tethered to the ER membrane. Simone Smith*¹, Joan C. Marini². ¹National Institutes of Health, USA, ²NIH, USA

Cartilage associated protein (CRTAP) is a component of the ER-resident procollagen prolyl 3-hydroxylation complex, which also contains prolyl 3-hydroxylase 1 (P3H1) and cyclophilin B and 3-hydroxylates the $\alpha 1(I)$ Pro986 residue of types I and II collagen. The components of this complex were the first proteins shown to cause recessive OI. CRTAP is the helper protein of the complex. It shares 55% homology with the amino half of P3H1, but lacks carboxy terminal sequences harboring enzymatic activity. CRTAP deficiency causes type VII OI, with absent $\alpha 1$ Pro986 hydroxylation and over-modification of collagen α -chains. We noted hydrophobic, putative transmembrane motifs in CRTAP (Gly4-Ser32) and P3H1, but it is unknown whether components of the 3-hydroxylation complex reside at the ER membrane. We also noted 2 potential N-glycosylation sites (N⁸⁶X⁸⁷S⁸⁸, N³¹²X³¹³T³¹⁴) in CRTAP C-terminal to the hydrophobic motif. After subcellular HEPES/sucrose fractionation, CRTAP was found in ER fractions (mean 71%, range 62-88%) containing the luminal marker PDI, with a smaller but consistent portion (mean 29%, range 12-38%) co-fractionating with the ER membrane marker calnexin. P3H1, with similar putative hydrophobic domains as CRTAP, fractionated to the luminal fraction, with values similar to PDI (>90% luminal). On immunofluorescence microscopy, we observed perinuclear reticular staining of calnexin at the ER membrane, with colocalization of CRTAP; more precise localization will be performed by EM immunogold labeling. Enzymatic deglycosylation further resolved CRTAP into a smaller band consistent in size with a doubly-deglycosylated form; presence of sugars indicates the C-terminal glycosylation sites orient towards the lumen with the N-terminus towards the cytosol. In cells from a patient lacking P3H1, the residual CRTAP was detected in the ER membrane fraction. Therefore, membrane tethering of a pool of CRTAP might explain the residual CRTAP seen when its mutually stabilizing 3-hydroxylation partner, P3H1, is absent (type VIII OI), although P3H1 is totally absent when CRTAP is null. Tethering of CRTAP might improve access of the modifying complex to collagen chains during coordinated translation and folding of the collagen helix, while disruption of ER-tethering might underlie the collagen overmodification seen in types VII and VIII OI. Experiments are ongoing to obtain genetic corroboration using CRTAP constructs from which the putative transmembrane domain is deleted.

Disclosures: Simone Smith, None.

MO0172

Elucidating the Antifibrosis Effects of rPTH Therapy on Critical Defect Healing in the Murine Cranial Window Model. Longze Zhang*¹, Claire Kaiser¹, Matthew Todd², Ryan Gao¹, Xinping Zhang¹, Edward Schwarz¹.

¹Center for Musculoskeletal Research, University of Rochester Medical Center, School of Medicine & Dentistry, USA, ²Center for Musculoskeletal Research, University of Rochester Medical Center, USA

Background: Reconstruction of critical bone defects remains a major clinical challenge. To address this, we aim to elucidate the molecular and cellular differences between healing and non-healing critical defects, and assess novel interventions. Previously we found that intermittent teriparatide (rPTH) therapy facilitates structural femoral and calvarial allograft healing in mice via increased osteogenesis and decreased fibrosis, which results in significantly increase host-allograft bone union. We also discovered that rPTH significantly decreased large vessel arteriogenesis and the accumulation of mast cells in the interfacial tissue between the host and allograft bone. In the current study we utilized a chronic cranial defect window chamber model for in vivo multiphoton laser scanning microscopy (MPLSM) and longitudinal micro-CT to test the hypothesis that rPTH therapy: 1) increases small vessel (<30um) angiogenesis, and 2) decreases large vessel (>30um) arteriogenesis and mast cell numbers, to 3) significantly increase critical defect closure. To assess the direct role of mast cells on angiogenesis and bone healing, we also evaluated the effects of cromolyn sodium in our model. **Methods:** 8-week-old female C57B/6 mice received a cranial defect window, and were randomized into three groups: 1) placebo (saline), 2) rPTH treated (40cg/kg/day), and 3) cromolyn sodium (24cg/kg/day). Co-visualization of blood vessels and mast cells was achieved with i.v. administration of Texas Red-dextran and FITC-conjugated anti-Mcpt-5 antibody respectively. In vivo micro-CT and MPLSM imaging were performed every two weeks, and 3D-reconstruction of the z-stack images with Amira and Visiopharm software was used to quantify % defect closure and vascularity within the defect. We also quantified Mcpt-5+ cell numbers and determined their mean distance from large vessels (>30um) vs. small (<30um) blood vessels. **Results & Discussion:** At 4-weeks post-op the percentage of small (<30um) vs. large (>30um) vessels for the placebo group was 19.7% vs. 80.3%. rPTH therapy significantly increase small vessels to 40.4%, and decreased large vessels to 59.6% (p<0.05). Remarkably, cromolyn sodium had similar significant effects (43.1% vs. 56.9%; p<0.05). However, only rPTH significantly increased the mean % critical defect closure vs. placebo (p<0.01), which was 17.9%, 45.8% and 25.5% respectively for the 3 Groups. We also found that Mcpt-5+ cells were significantly closer to large vs. small vessels (26.9 +/- 14.6 um vs. 61 +/- 3.7 um; p < 0.05), and more Mcpt-5+ cells were found in placebo group vs. the rPTH and cromolyn treatment groups. These novel findings suggest that coupled osteogenesis and angiogenesis at the healing edge of a critical defect is opposed by arteriogenesis, mast cell accumulation and fibrosis within the defect, and that rPTH efficacy includes inhibitory effects on arteriogenesis and mast cell-induced fibrosis. However, the synergistic anabolic effects of rPTH are also required for critical defect healing, as alteration of vascularity and mast cell numbers with cromolyn is insufficient to heal critical defects.

Disclosures: Longze Zhang, None.

MO0173

Phosphate overload via type III Na-dependent Pi transporter deteriorates elastic fiber formation in vascular wall in Pit-1-overexpressing transgenic rats. Yasumasa Yoshino*¹, Tomoka Hasegawa², Shukei Sugita³, Eisuke Tomatsu⁴, Sahoko Sekiguchi-Ueda¹, Megumi Shibata¹, Takeo Matsumoto³, Norio Amizuka², Atsushi Suzuki¹.

¹Division of Endocrinology & Metabolism, Fujita Health University, Japan, ²Department of Developmental Biology of Hard Tissue, Division of Oral Health Science, Graduate School of Dental Medicine, Hokkaido University, Japan, ³Biomechanics Laboratory, Nagoya Institute of Technology, Japan, ⁴Division of Endocrinology & Metabolism, Fujita Health University, Japan

Phosphate (Pi) has been reported to change arterial smooth muscle cells (ASMC) to osteoblastic phenotype through the induction of type III Na-dependent Pi transporter, Pit-1. We have previously shown that extracellular Pi overload via Pit-1 induces its osteoblastic trans-differentiation, but also keeps ASMC from the terminal differentiation as mature osteoblasts, and limits the progress of further aortic calcification in Pit-1-overexpressing transgenic (TG) rats. In the present study, we investigated the role of extracellular Pi in microstructural change of arterial wall of Pit-1 TG rats. **Methods:** Aorta of TG and its wild-type littermates (WT) were obtained 8 weeks after birth. Descending aorta from both WT and TG rats were used for measurement of wall thickness and uniaxial tensile test. Breaking stress was calculated as force/(initial thickness x initial width), while breaking strain was as (length - initial length)/initial length. Elastic moduli in low and high strain regions were calculated as slopes of stress-strain relationship by fitting a linear line in each region. Structural and ultrastructural analyses were performed by using light microscopy and transmission electron microscopy (TEM). Expression of the components of connective tissue in aorta was quantified by qRT-PCR. **Results:** Aortic wall thickness in TG rats was same as that in WT. Uniaxial tensile test showed that the circumferential breaking stress in TG was significantly lower than that in WT (p<0.05), though longitudinal

breaking stress was not different. On the other hand, breaking strain in TG was same as that in WT. However, elastic moduli in TG were not different from those in WT. Ultrastructural analysis of TG rat aorta by TEM showed damaged formation of elastic fiber in aortic wall. qRT-PCR showed significant decrease of fibrillin-1 expression in aorta in TG rats. In conclusion, Pi overload via Pit-1 transporter on arterial wall weakened circumferential strength through malformation of elastic fibers including the decrease of fibrillin-1.

Disclosures: Yasumasa Yoshino, None.

MO0174

Variants in regulatory regions of *SREBF1*, a Lamin A interaction factor exert pleiotropic effects on BMD and lean mass in children. Carolina Medina-Gomez*¹, John P. Kemp², Eskil Kreiner-Møller³, Alessandra Chesì⁴, Denise H.M. Heppè⁵, Babette S. Zemel⁶, Klaus Bønnelykke³, Hans Bisgaard³, Vincent W.V. Jaddoe⁵, André G Uitterlinden⁷, Jon H Tobias⁸, Gustavo Duque⁹, Struan F.A. Grant⁴, David M. Evans², Fernando Rivadeneira¹⁰. ¹Erasmus Medical Center, The Netherlands, ²University of Queensland Diamantina Institute, Translational Research Institute, Brisbane, Queensland, Australia, ³Copenhagen Prospective Studies on Asthma in Childhood, Health Sciences, University of Copenhagen, Danish Pediatric Asthma Center, Copenhagen University Hospital, Gentofte, Denmark, ⁴Division of Human Genetics, Children's Hospital of Philadelphia, Philadelphia, PA 19104, USA, ⁵The Generation R Study Group, Erasmus University Medical Center, 3015GE, Rotterdam, Netherlands, ⁶Division of GI, Hepatology, & Nutrition, Children's Hospital of Philadelphia, Philadelphia, PA 19104, USA, ⁷Department of Internal Medicine, Erasmus University Medical Center, 3015GE, Rotterdam, Netherlands, ⁸School of Clinical Sciences, University of Bristol, Bristol, United Kingdom, ⁹Musculoskeletal Ageing Research Program, Sydney Medical School Nepean, The University of Sydney., Australia, ¹⁰Department of Internal Medicine, Erasmus University Medical Center, Rotterdam, Netherlands

Background: Lean and bone mass are heritable traits with high phenotypic correlation ($\rho=0.44$), likely reflecting the underlying mechanical and biochemical interactions between tissues. **Aim:** Estimate the shared SNP-heritability (genetic correlation) of both traits in children and identify genetic determinants displaying pleiotropic effects on lean mass and bone mass accrual. **Methods:** Participants make part of three prospective birth cohorts, the Generation R Study (GenR) and the Avon Longitudinal Study of Parents and Children (ALSPAC) and the Copenhagen Studies on Asthma in Childhood (COPSAC). GenR children ($n=4,071$) born in Rotterdam, Netherlands are of multiethnic background with mean age=6.2, SD=0.37 years. ALSPAC children ($n=4,820$) born in Avon, UK had mean age=9.9, SD=0.32 years. COPSAC children ($n=273$) born in Copenhagen from asthmatic mothers had mean age=6.9, SD=0.61. Lean mass and BMD were measured with DXA (GE-Lunar iDXA/ Prodigy) and genome-wide genotyping (II 660K-III 550K) imputed to HapMap. Shared heritability estimates derived from array data of GenR were obtained using GCTA (with modified admixed-aware relatedness estimates using REAP). GWAS in GenR, ALSPAC and COPSAC were run using PLINK multivariate. Meta-analysis was performed by Fisher's method. All analyses were adjusted for age, sex, height, fat percent (and 20 genomic principal components in GenR). $P<5\times 10^{-8}$ was considered genome-wide significant. **Results:** SNP-heritability estimates were 0.31 for BMD and 0.40 for lean mass, with a genetic correlation of 0.3. The bivariate GWAS meta-analysis identified six established BMD loci with concordant effects on lean mass and BMD including: *WNT4* ($P<10^{-9}$), *GALNT3* ($P<10^{-8}$), *CPED1/WNT16* ($P<10^{-20}$), *TNFSF11* ($P<10^{-9}$), *RIN3* ($P<10^{-10}$) and *PPP6R3/LRP5* ($P<10^{-8}$). Another signal ($P<10^{-10}$) with opposite effects on lean mass and BMD mapped to the *TOM1L2/SREBF1* locus. ENCODE analyses identified enhancers for *SREBF1* in the same haplotype block. **Conclusion:** Several variants at BMD loci exert pleiotropic effects on lean mass. Bivariate analysis is a powerful method for identifying novel pleiotropic effects. *SREBF1*, an adipocyte differentiation factor, is a regulator of muscle protein synthesis regulating *MYO1D*, *MYOG* and *MEF2C* factors, which interacts with the C-terminal of *Lamin A* (*LMNA*). *LMNA* is the cause of different muscular dystrophies and has been proposed as a determinant factor in the pathogenesis and potential treatment of both sarcopenia and osteopenia.

Disclosures: Carolina Medina-Gomez, None.

MO0175

Comparison of Hyaluronic Acid and Placebo in Patients with Knee Osteoarthritis. A Simulated Meta-Analysis Study. Abdulhafez Selim¹, Sahar Ghoname*². ¹Center for Chronic Disorders of Aging, PCOM, USA, ²Ain Shams University School of Medicine, Egypt

Although acknowledged as a conservative treatment choice for knee osteoarthritis, hyaluronic acid (HA) is still not universally embraced due to conflicting results with

respect to its efficacy in clinical studies. Several randomized clinical trials (RCTs) found significant improvement in pain after treatment as compared with the baseline, but found no significant improvement when the efficacy of HA was compared with placebo (saline). In this systematic review simulation, we compared the effects of intra-articular administration of HA with similarly administered placebo as well as, more specifically, the effects of individual HA products as compared to placebo.

A systematic review of RCTs was conducted using databases including MEDLINE, Cochrane Database of Systematic Reviews, Cochrane Clinical Trial Register, and EMBASE. Summarized data was then simulated using a Bayesian analytical approach.

Seventy-four RCTs were included in this review. Based on simulated data, HA improved pain by a mean of 79.6% (SD= 7.6%) as compared with baseline levels, while placebo improved pain by a mean of approximately 56.3% (SD= 15.6%). When HA was compared with saline, however, the difference in efficacy was only 23.3%. By testing several superiority margins (10%, 15%, 20%, and 25%), the superiority of HA performance compared to placebo could not be established beyond the 20% margin, which may not represent a clinically meaningful difference. Furthermore, when various HA products, differing in molecular weight, concentration, and volume of HA, were compared, we were not able to determine that any one brand had better efficacy than another. In addition, neither the molecular weight (MW) of the HA, its dosing, or its concentration effected efficacy outcomes. This could be explained by the wide heterogeneity of the study population as well as the high SDs that characterized the data.

This study highlighted several critical variables with potential impact on study design approaches evaluating HA effectiveness. The following variables may be considered in future studies: more objective endpoint(s), an overall success composite index (with objective as well as subjective outcomes), and the selection of more homogeneous population. Due to the limitations of this analysis (follow-up of just 3 months and the heterogeneity of the included studies), evaluation of different HA products in order to determine which product(s) as well as which MW range, concentration, and/or volume of HA are optimal in the treatment of specific population(s) of osteoarthritic patients is still needed.

Disclosures: Sahar Ghoname, None.

MO0176

Pre-operative pre-albumin: Relation to 30-day risk of complication in elective spine surgical patients. Erin Coburn*¹, Jung Yoo², Jackie Shannon², Sabina Blizzard², Lizzy Boshears², Lynn Marshall². ¹Oregon Health & Science University, USA, ²OHSU, USA

Protein malnutrition assessed by serum pre-albumin is associated with increased risk of post-operative morbidity and mortality in adult spine surgery patients. However, whether the risk of post-operative complications also varies across the range of serum pre-albumin in this patient group has not been established. We determined the association of pre-operative serum pre-albumin with 30-day risk of complication. Medical records were reviewed for adult patients age ≥ 50 years who underwent elective cervical, thoracic, thoracolumbar, or lumbar spine surgery for painful spinal degenerative conditions between June 2013 and June 2014. For the pre-operative visit just prior to surgery, we obtained serum pre-albumin level (mg/dL), serum transferrin (mg/dL), demographic factors, and health measures (such as blood pressure). Surgical information was obtained from the operative note. The primary outcome was 30-day risk of medical complication, such as deep vein thrombosis, wound problems, or infections. The relation between pre-albumin level and complications was estimated with risk ratios (RR) and 95% confidence intervals (CI) from log-binomial regression. In the final model, RRs were adjusted for transferrin, body mass index, number of levels fused, age, sex, and American Society for Anesthesiology (ASA) score, an indicator of fitness prior to surgery. During model building, factors found not to be confounders were blood pressure, previous spine surgery, and total anesthesia time. The analytic cohort included 275 adults with mean (SD) pre-albumin of 27.5 mg/dL (± 5.6 mg/dL), and median serum pre-albumin (inter-quartile range) was 27.4 (23.8, 30.8) mg/dL, and was largely within the normal range. Those in the lowest pre-albumin quartile tended to be male, heavier, have a higher ASA score, and have more levels fused compared to those in the highest quartile. The 30-day cumulative incidence of complication was 12.7% (95% CI: 10.0%-17.3%). Risk of complication was not associated with decreasing pre-albumin level. The RR per 1 mg/dl decrease in pre-albumin was 1.00 (95% CI: 0.94-1.07, p-trend=0.98). Pre-albumin below the median (vs above the median) also was not associated with risk of complications (adjusted RR=1.1, 95% CI: 0.8-1.5) (Table). Among adults undergoing surgery for degenerative spine conditions, the 30-day risk of complication was not associated with serum pre-albumin. Other biomarkers should be explored as possible risk factors for surgical complications.

Table. Risk Ratios (RR) and 95% confidence intervals (CI) of complications within 30 days among adults undergoing elective spine surgery according to pre-surgical level of pre-albumin

| Median (mg/dl) | Pre-Albumin Level | |
|--------------------------|-------------------|---------------|
| | <27.4 | ≥27.4 |
| Minimum, Maximum (mg/dl) | (12.9-27.3) | (27.4-47.9) |
| Total N | 137 | 138 |
| No. Complications (%) | 18 (13%) | 17 (12%) |
| Model | RR (95% CI) | |
| Unadjusted | 1.0 (Referent) | 0.9 (0.5-1.7) |
| *Model 1 | 1.0 | 1.1 (0.8-1.5) |
| **Model 2 | 1.0 | 1.1 (0.8-1.5) |

* Variables modeled are pre-albumin level, transferrin level, body mass index (<30 kg/m², ≥30 kg/m²) and number of levels fused (no fusion, 1 level fused, 2-3 levels fused, ≥4 levels fused)

** Variables modeled include those in model 1 plus age group (50-59 years, 60-69 years, ≥70 years), sex (female, male), and ASA score (1-2 points, 3-4 points)

Table

Disclosures: Erin Coburn, None.

MO0177

Prevalence of Hand Osteoarthritis and Factors associated with Pain in Korean Farmers. Sang-Hyon Kim¹, Sang-Il Lee^{*2}, Sang-Heon Lee³, Young-Il Seo⁴, Jinseok Kim⁵, Jung Soo Song⁶. ¹Div. of Rheumatology, South Korea, ²Division of Rheumatology, Department of Internal Medicine, ²Department of Preventive Medicine, Gyeongsang National University School of Medicine, ³Clinical Research Institute, Gyeongsang National University Hospital, Jinju, Republic of Korea, South Korea, ³Division of Rheumatology, Konkuk University School of Medicine, Seoul, Republic of Korea, South Korea, ⁴Division of Rheumatology, Hallym University Medical Center, Ahnyang, Republic of Korea, South Korea, ⁵Department of Internal Medicine, Jeju National University Hospital, Jeju, Republic of Korea, South Korea, ⁶Division of Rheumatology, Department of Internal Medicine, Chung-Ang University Medical school, Seoul, Republic of Korea, South Korea

Background: A few studies investigated the prevalence of hand osteoarthritis (HOA) and associating factors of hand pain in Korean farmers. Objectives: To investigate the prevalence of HOA and to identify factors that influence hand pain among farmers in rural areas of Korea. Methods: The study was conducted from June 2013 to Dec 2014 with 700 farmers in Gyeong-nam Province of Korea. Clinical evaluation for hand joints was performed and the plain radiographs of both hands were taken. The Australian/Canadian Osteoarthritis Hand Index (AUSCAN) was used to assess pain severity of hand joints. Radiographic HOA was defined as Kellgren-Lawrence (KL) grade=2 on plain radiographs and symptomatic HOA as KL grade=2 with pain at the same joints. Presence of HOA at individual level was defined as =1 affected joint. Depressive symptoms were assessed using the Patient Health Questionnaire. Results: Participants comprised of 371 (53%) women and 329 (47%) men with mean age of 59.7±8.6 years. The mean farming duration was 30.0±14.3 years. The overall prevalence of radiographic and symptomatic HOA was 59.1%, and 13.9%, respectively. The prevalence rates of radiographic HOA for women and men were 62.3 and 55.6% (p=0.077), and symptomatic HOA for women and men were 14.8% and 12.8% (p=0.445), respectively, not significantly different. However, AUSCAN pain scores were higher in women (99.9±106.8) than men (68.0±99.9, p=0.002) among participants with radiographic HOA. Linear regression analysis showed that women and depressive symptoms were associated with AUSCAN pain scores after adjustment for radiographic severity of HOA, total numbers of affected joints, frequently repetitive hand use and pinch grip working during harvest. Conclusions: The AUSCAN pain scores were higher in women with HOA compared to men, and associated with depressive symptoms after controlling other factors. Therefore, our results show the need for depression care management in female farmers to reduce hand pain.

Disclosures: Sang-Il Lee, None.

MO0178

Ultrasound-Guided intra-articular injection of platelet-rich plasma in treating knee osteoarthritis in short-term follow-up: a prospective, randomized, controlled trial. Peijian Tong*. Zhejiang Provincial Hospital of TCM, Peoples republic of china

Purpose: To compare the clinical efficacy of platelet-rich plasma (PRP) and hyaluronic acid (HA) treatment in 2 groups of Knee osteoarthritis (KOA) patients and evaluate if the age, body mass index (BMI) and grade of gonarthrosis are associated with the outcomes on the PRP injection. Methods: A total of 100 consecutive patients were enrolled between December 2013 and November 2014. The gonarthrosis was graded according to the Kellgren-Lawrence radiographic classification. The 100 patients were randomized into 2 groups in accordance with the random

number table in a 1:1 ratio: 50 patients (50 knees) in Group A were given 3 injections of HA, and 50 patients (50 knees) in Group B received 3 injections of PRP at an interval of 3 weeks. Patients were assessed on the WOMAC, VAS and Cartilage Lesions Score (CaLS) for clinical evaluation before and after the treatment. Meanwhile we calculated the effective rate, as defined by at least 36% improvement from baseline WOMAC score at the follow-up. Results: The results had significant difference in each period (VAS: HA, P<0.01; PRP, P<0.01. WOMAC: HA, P<0.01; PRP, P<0.01) comparing with the baseline except the result at 6 months in VAS score of Group A (VAS: HA, P>0.05). The patients in Group B had better clinical outcomes than those in Group A at the 6 months follow-up (P<0.05) in Grade I, 3 months (P<0.05) and 6 months (P<0.01) in Grade II, and each period (P<0.01) as well as VAS score (P<0.05) at the 6 months follow up in Grade III. In addition, we found older patients who receives PRP injections obtained worse VAS Score and WOMAC Score at the final follow-up. In addition, we found older patients who receives PRP injections obtained worse VAS and WOMAC at 6 months' follow-up, and higher KL grade connected with lower effective rate. However, the BMI had no certain positive or negative correlation to the outcomes on the Group B. The depth and shape scores of the CaLS from different lesion location in 7 patients had no significant difference in Group B at the 6 months follow-up. As time goes on, the efficacy in both groups wore off, and the trend of recurrence rate of clinical symptom was seemingly more pronounced in Group A. Overall, the effective rate was 68% after the last treatment and 36% at the final follow-up in group A, and 84%, 60% in group B. Conclusions: The short-term efficacy of PRP injection was associated with age and level of joint degeneration. Meanwhile the PRP injection had a better clinical outcome than HA injection in providing better functional results at the final follow-up.

Disclosures: Peijian Tong, None.

MO0179

Efficacy and Safety of Undenatured Type II Collagen Supplement in Modulating Knee Joint Function in Osteoarthritic Subjects. James Lugo¹, Zainulabedin Saived¹, Nancy Lane^{*2}. ¹InterHealth Nutraceuticals, USA, ²University of California, USA

Background: Preclinical and clinical studies support the safety and efficacy of undenatured type II collagen (UC-II) in promoting joint comfort, mobility and flexibility in healthy as well as osteoarthritic (OA) populations. Herein we report the combined results of two recently completed, similarly designed, randomized, double-blind, placebo-controlled clinical trials in OA subjects.

Objective: To evaluate the efficacy and safety of the UC-II® supplement in comparison to placebo and glucosamine hydrochloride plus chondroitin sulfate (GC) in modulating knee joint function in OA subjects.

Methods: One hundred ninety one eligible subjects were randomized into three groups receiving a daily dose of UC-II (40 mg), GC (1500 mg G & 1200 mg C), or placebo over a 180-day period. The primary endpoint was defined as the change in total Western Ontario McMaster Universities Osteoarthritis Index (WOMAC) from baseline to day 180 for the UC-II group versus placebo. Secondary endpoints encompassed reductions in the Lequesne Functional Index (LFI), the Visual Analog Scale (VAS) for pain and the WOMAC subscales for pain, stiffness and physical function. One hundred sixty-four subjects completed the trials.

Results: At study conclusion (180 days), statistically significant reductions in the overall WOMAC score was observed in the UC-II supplemented cohort compared to placebo (p=0.0023) and GC (p=0.0404). The change in overall WOMAC score for the UC-II group resulted from statistically significant reductions in the WOMAC pain (p=0.0003 vs. placebo; p=0.0162 vs. GC), stiffness (p=0.0041 vs. placebo; p=0.0443 vs. GC) and physical function (p=0.0065 vs. placebo) subscales. The UC-II cohort also demonstrated a significant reduction in total LFI and mean VAS scores versus both placebo (p=0.0085 and 0.0021, respectively) and GC (p=0.0084 and 0.0246, respectively). No significant change in any of these clinical outcomes were observed in the GC cohort versus placebo during the study period. No major adverse events associated with supplementation were reported. Conclusions: Supplementation with UC-II was well-tolerated and led to improved knee joint function, suggesting that additional studies are warranted to better define these observations.

Disclosures: Nancy Lane, InterHealth Nutraceuticals
This study received funding from: InterHealth Nutraceuticals

MO0180

The Short-Term Efficacy of Denosumab in Osteoporosis in Patients with Rheumatoid Arthritis from a Japanese Multicenter Registry. Yuji Hirano^{*1}, Yasuhide Kanayama², Shinya Hirabara³, Syuji Asai⁴, Nobunori Takahashi⁴, Takavasu Ito⁵, Naoki Ishiguro⁴, Toshihisa Kojima⁴. ¹Toyohashi Municipal Hospital, Japan, ²Orthopaedic Surgery & Rheumatology, Toyota Kosei Hospital, Japan, ³Rheumatology, Toyohashi Municipal Hospital, Japan, ⁴Orthopaedic Surgery, Nagoya University Graduate School of Medicine, Japan, ⁵Ito Orthopaedic Hospital, Japan

Purpose: Osteoporosis (OP) is one of the important comorbidities in rheumatoid arthritis (RA). Pathogenesis of RA-OP is composed from multiple factors, such as hyper cytokine, concomitant drugs and disuse. Although denosumab (DMB), a fully-

human anti-RANKL antibody, is expected to be a good treatment option for RA-OP, clinical data from real-world is limited. This study investigated the effects of DMB on RA-OP from a multicenter registry data in Japan (TBCR-BONE).

Methods: 53 RA-OP cases were included. (1) %increase of bone mineral density (BMD) in lumbar spine (LSBMD) and total hip (THBMD) at 6month, (2) %change of bone turnover markers (PINP and TRACP-5b) at 6m, (3) correlation between change of BMD and change of BTM, (4) results until 12m (n=16), (5) the influence of concomitant use of biological agents (BIO) for the treatment of RA and (6) adverse events were investigated.

Results: Patients' characteristics: 50 females and 3 males. Mean age: 69.7 years old. RA duration: 14.2 years. Mean body mass index: 19.8. FRAX: 27.1%. Prednisolone use: 45.3% (mean doses: 4.3mg/day). BIO for the treatment of RA was concomitant in 34.0%. Treatment naïve of OP was 35.8%. Cases after teriparatide (TPTD) treatment were 11 cases. (1) LSBMD (g/cm²) was significantly increased from 0.825 at baseline to 0.857 at 6m (mean %increase: 3.9%). THBMD (g/cm²) was significantly increased from 0.598 at baseline to 0.611 at 6m (3.1%). (2) Both PINP and TRACP-5b were significantly decreased at 6m (41.4% and 34.8% decrease, respectively). (3) There were no significant correlation between %change of BMD at 6m and %change of BTM at 6m. (4) %increase of LSBMD was 5.1% at 6m and 6.3% at 12m. %increase of THBMD was 2.4% at 6m and 5.6% at 12m. BTMs were decreased at 6m and unchanged at 12m. (5) Baseline THBMD of BIO group was significantly low compared with that of NonBIO group. TRACP-5b of BIO group was significantly high compared with that of NonBIO group. %increase of LSBMD at 6m was 4.7% in BIO group and 3.0% in NonBIO group. %increase of THBMD at 6m was 3.4% in BIO group and 3.0% in NonBIO group. No significant differences were observed. (6) Hypocalcemia was occurred in 2 and pelvis fracture was occurred in one. Pelvis fracture was healed.

Conclusions: The short-term results of DMB in RA-OP was good especially in THBMD. This study showed that %change of BTMs were not the predictor for efficacy of DMB on BMD increase at 6m. BIO did not affect the efficacy of DMB.

Disclosures: Yuji Hirano, None.

MO0181

A Novel Optogenetic Approach To Elucidate Spatial Regulation Of Semaphorin-Plexin Signaling In Osteoblasts. Abhijit Deb Roy*¹, Taofei Yin², Yi Wu². ¹University of Connecticut Health Centre, USA, ²University of Connecticut Health Center, USA

Osteoclasts express Semaphorin 4D (Sema4D), a transmembrane ligand for the receptor Plexin-B1, expressed by osteoblasts. Osteoblasts and osteoclasts are spatially segregated on the bone surface *in vivo*. In mice deficient in either Sema4D or Plexin-B1, osteoclasts and osteoblasts no longer display spatial segregation and have increased cell-cell contact. Previous studies provide limited understanding of how intracellular signaling events downstream of Plexin-B1 are spatially regulated to mediate directional migration of osteoblasts. Here we developed a novel optogenetic tool, optoPlexin, to specifically activate Plexin-B1 in a ligand-independent manner, at precise subcellular locations using light.

In osteoblastic MC3T3-E1 cells, activation of optoPlexin in lamellipodial protrusions led to rapid, local recruitment of RhoGEFs, PDZ-RhoGEF and Leukemia Associated RhoGEF, necessary for RhoA activation. We observed subsequent accumulation of myosin, leading to collapse of these protrusions. Such collapse repolarized the cell to migrate away from the site of optoPlexin activation. Biosensors of Rho GTPases identified the specific induction of RhoA activity upon optoPlexin activation, which required the interaction of optoPlexin with Rnd1 or Rac1 on the membrane. Rac1/Rnd1 and RhoA are generally mutually inhibitory. However, our data demonstrate that activation of PlexinB1 converts Rac1 from an inhibitor of RhoA activity to a stimulator, initiating a rapid negative feedback loop that inhibits Rac1 at protrusions.

Local activation of optoPlexin caused local depletion and distal accumulation of beta-Pix, an activator of Rac1 and Cdc42. These distal regions of beta-Pix accumulation correlate with high Cdc42 and Rac1 activity, as well as formation of new protrusions. OptoPlexin-induced coordination among Rho GTPases was dependent on ROCK kinase activity and myosin-dependent contractility. Local perfusion of soluble Sema4D induced similar local retractions and distal protrusions in primary calvarial osteoblasts. The coordination of local suppression and distal promotion of protrusions by Plexin-B1 signaling is consistent with contact repulsion between osteoclasts and osteoblasts, which could explain their spatial segregation *in vivo*. These results revealed spatially distinct effects of Plexin-B1 signaling in regulating Rho GTPases and osteoblast migration, and highlight the utility of optogenetic approaches in studying spatiotemporal regulation of cellular signaling.

Disclosures: Abhijit Deb Roy, None.

MO0182

Antiarrhythmic peptide GAP-134 promote osteoblastic differentiation and function in association with upregulation of Cx43 *in vitro*. Dong Jin Chung*, Nam Hee Lee, Jin Ook Chung, Dong Hyeok Cho, Min Young Chung, Chonnam National University Medical School, South Korea

Bone-forming cells are highly coupled by gap junctions formed primarily by connexin43 (Cx43). The biological importance of Cx43 in skeletal development has been established by work in human and mouse genetics. Selective Cx43 gene deletion

in osteoblasts results in adult osteopenia, delayed osteoblast differentiation, and greatly attenuated osteoanabolic response to PTH. Recently, we demonstrated that aminobisphosphonate promote osteoblastic differentiation and function in association with upregulation of Cx43 *in vitro*. Another gap junction modulator, the antiarrhythmic peptides, stimulate gap junction communication between cardiomyocytes. Furthermore, the prototype compound had been shown to prevent deterioration of bone biomechanical properties in estrogen dependent bone loss in rats. In this study, we investigated the effect of other antiarrhythmic peptide GAP-134 on osteoblast differentiation and Cx43 expression using the cell line C2C12 and HEK293. Alkaline phosphatase (ALP) activity was increased by GAP-134 dose-dependently. When GAP-134 and 5 ng/ml of BMP2 were used in combination, ALP activity increased to a larger extent than when BMP2 was used alone. These results suggest that GAP-134 may facilitate the differentiation of osteoblasts, synergizing with BMP-2. In our previous study, co-transfection of expression vectors and luciferase-reporter constructs revealed that Runx2, Dlx5 and Osterix increased Cx43-promoter activity in a concentration-dependent manner. As the concentration of GAP-134 was increased, Cx43-promoter activity was increased by 2.5 fold. Furthermore, the combination of Dlx5 (0.5 µg) and GAP-134 up-regulated Cx43 promoter activity to a far larger extent than did Dlx5 or GAP-134 alone, suggesting an interaction between the GAP-134 and Dlx5 in activating the Cx43 promoter. These results suggest that GAP-134 promotes osteoblast differentiation and regulates Cx43 expression in C2C12 cells.

Disclosures: Dong Jin Chung, None.

MO0183

Collagens VI and XII Matrix Bridges Mediate Osteoblast Cell Communicating Networks During Bone Formation. Yayoi Izu*¹, Yoichi Ezura², Manuel Koch³, David Birk⁴, Masaki Noda⁷. ¹Tokyo Medical & Dental University, Medical Research Institute, Japan, ²Tokyo Medical & Dental University, Japan, ³University of Cologne, Germany, ⁴University of South Florida, USA

Ullrich congenital muscular dystrophy (UCMD) and Bethlem myopathy (BM) are diseases representing overlapping phenotypes of connective tissue and muscle. Both diseases are caused by genetic mutations in the genes encoding collagen VI. Recently COL12A1 gene mutations were identified in UCMD and BM-like patients harboring no COL6 mutations, indicating shared functions of these collagens for connective tissue homeostasis. We have previously demonstrated that the genetic deletion of Col6a1 or Col2a1 in mice cause altered osteoblast arrangement at bone forming sites that result in bone mass reduction and fragility. During bone formation, osteoblasts migrate toward appropriate bone forming sites where osteoblasts form well-organized cell communicating networks that is essential for healthy, strong bone formation. Therefore, we hypothesize that collagens VI and XII function together on the formation of osteoblast cell communicating networks at the site of bone formation. Because extracellular matrix proteins are accumulated in extracellular environment, it is hard to detect the initial localization *in vivo*. Thus, to elucidate the hypothesis, we examined collagens VI and XII localization in the process of cell-cell contact formation *in vitro*. Primary osteoblasts were obtained from neonatal mouse calvariae and were cultured in a medium supplemented with 10% FBS or osteogenic medium. The cells were harvested on day 2, 4, and 11 and then analyzed based on immunofluorescence microscopy using antibodies against collagen I, VI, and XII. The double staining analysis revealed that co-localization of collagen VI and XII was detected in the matrix bridges between adjacent cells on day 2 and 4 when initial cell-cell connections were detected. On the other hand, collagen I was localized in a region close to the cell surface where it was colocalized with collagen XII. However no clear localization of collagen I was detected in between adjacent cells on day 2 and 4. All the collagens were detected as a filamentous network surrounding osteoblasts on day 11. The percentage of the cells harboring collagens bridges was analyzed based on the immunostaining on day 2 and 4, demonstrating that matrix bridges were made via collagen VI and XII but not via collagen I. Our data indicate that collagen VI and XII have a novel coordinate function in the formation of cell communicating networks during bone formation.

Disclosures: Yayoi Izu, None.

MO0184

A Novel Role of MACF1: Positively Regulates Osteoblast Differentiation. Lifang Hu*¹, Peihong Su², Runzhi Li², Chong Yin², Kun Yan², Ge Zhang³, Peng Shang², Airong Qian². ¹Northwestern Polytechnical University, Peoples republic of china, ²Key Laboratory for Space Bioscience & Biotechnology, Institute of Special Environmental Biophysics, School of Life Sciences, Northwestern Polytechnical University, China, ³Institute for Advancing Translational Medicine in Bone & Joint Diseases, School of Chinese Medicine, Hong Kong Baptist University, China

Microtubule-actin crosslinking factor 1 (MACF1), also referred to as actin crosslinking factor 7 (ACF7), plays a key role in cell migration by regulating dynamics of microtubules and F-actins. Besides, MACF1 plays critical role in Wnt/β-catenin signaling activation through translocating Axin complex. We previously found that mechanical unloading inhibited osteoblast differentiation and bone formation, and

down-regulated MACF1 expression. Therefore, we propose a hypothesis that MACF1 may play an important role in regulating osteoblast differentiation. MACF1 knockdown pre-osteoblasts were constructed using MC3T3-E1 cells transfected with shRNA-MACF1 lentivirus vector and the MACF1 expression level was detected by real time PCR and western blot. After induction of osteoblast differentiation with osteogenic medium, alizarin red staining was applied to detect mineralized nodules formation and real time PCR was used to detect the mRNA expression of osteogenic genes including alkaline phosphatase (ALP) and runt-related transcription factor 2 (Runx2). Immunocytochemistry and western blot were used to examine β -catenin localization and nuclear translocation. In order to determine if MACF1 functions upstream of GSK-3 β and β -catenin signaling, lithium chloride (LiCl, 30 mM) was used to treat cells to inhibit GSK-3 β activation. The results showed that the expression of MACF1 was dramatically down-regulated after transfection with LV3-shRNA-MACF1 (Figure 1). MACF1 deficiency significantly inhibited the mineralized nodules formation and osteogenic gene expression (Figure 2). Besides, the translocation of β -catenin into nuclear was decreased by MACF1 knockdown (Figure 3A). However, 6 h treatment of 30 mM LiCl induced β -catenin nuclear translocation (Figure 3B) and inhibits GSK-3 β activation in MACF1 knockdown cells (Figure 4). The western blot detection of β -catenin expression in cytosol and nuclear confirmed the above findings (Figure 5). These findings showed that MACF1 deficiency inhibited osteoblast differentiation and the nuclear translocation of β -catenin, suggesting that MACF1 positively regulates osteoblast differentiation and may act through activating β -catenin signaling.

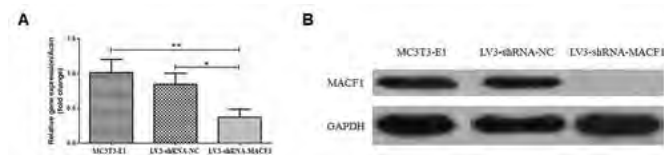


Figure 1

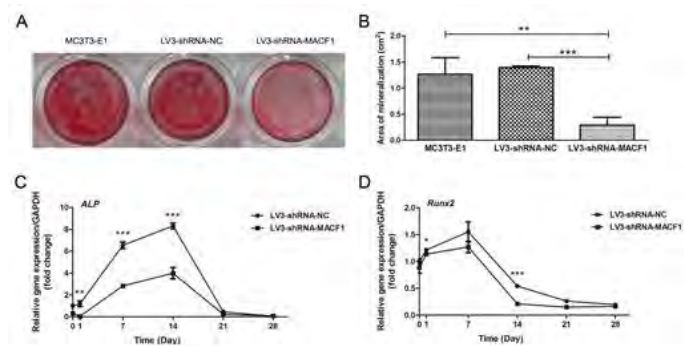


Figure 2

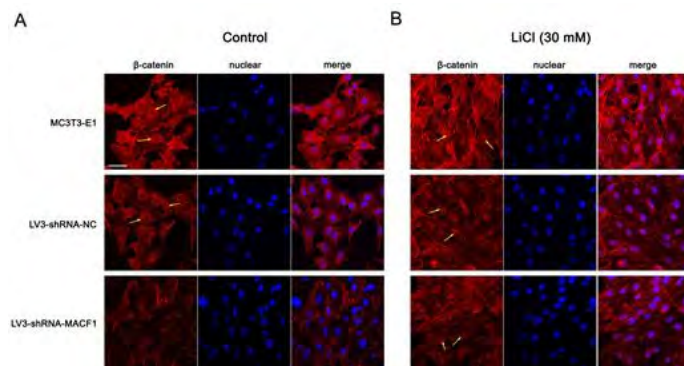


Figure 3

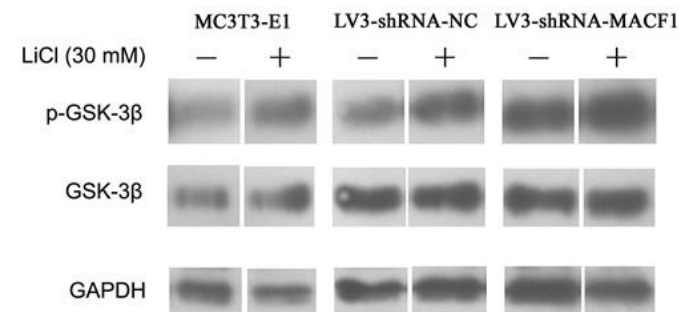


Figure 4

Figure 4

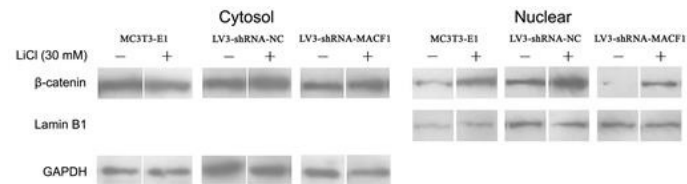


Figure 5

Disclosures: Lifang Hu, None.

MO0185

Effects of Bone Morphogenetic Protein-4 (BMP-4) on Adipocyte Differentiation from mouse Adipose-derived Stem Cells. Xueqin Wei*¹, Xiaoxiao Cai². ¹Sichuan University, Peoples republic of china, ²Sichuan University, China

Objectives: Mesenchymal stem cells (MSCs) could be easily isolated from adipose tissues and keep self-renewal and multipotent differentiation capacities, they hold promising possibilities to be extensively applied in tissue engineering. Bone morphogenetic protein (BMP) family members have been reported to provide instructive signals to MSCs to differentiate into several cell lineages. This study aims to investigate whether BMP-4 could promote Adipose-derived stem cells (ASCs) differentiation into adipocytes under various concentrations.

Materials and methods: ASCs were isolated from mouse inguinal adipose pads and cultured in vitro. 10 ng/ml and 50 ng/ml BMP-4 were added into adipogenic media for 8 days. Oil red-O staining, reverse transcription/polymerase chain reaction and immunofluorescent staining were performed to examine the differentiation of ASCs.

Results: As indicated by increased expressions of adipogenic and lipogenic genes (PPAR- γ , APN and LPL) and proteins, 50 ng/ml BMP-4 seems to induce mASCs to differentiate into adipocyte lineage compared to 10 ng/ml BMP-4 and control groups. In addition, lipid droplets accumulated within the adipocytes under 50 ng/ml BMP-4 stimulation, shown by oil red-O staining.

Conclusions: Our present study suggested that BMP-4, as an adipogenic inducing factor, could promote adipogenesis of ASCs at higher concentrations (50 ng/ml) and may be considered as a candidate for adipose tissue engineering.

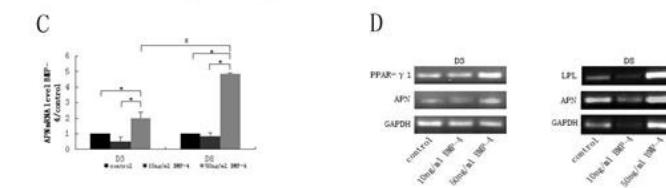
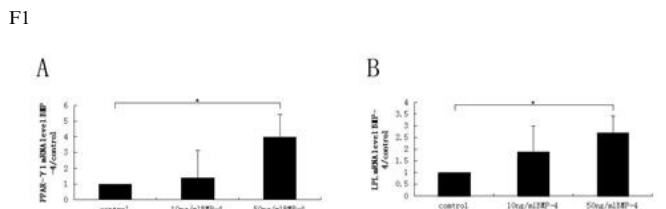
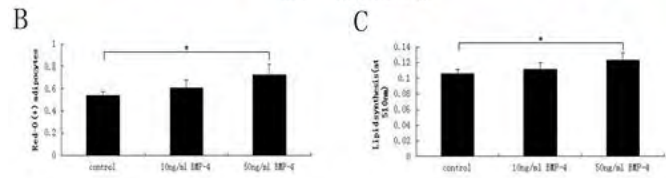
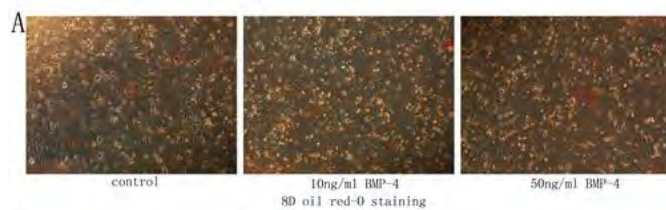
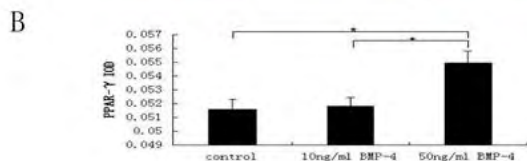
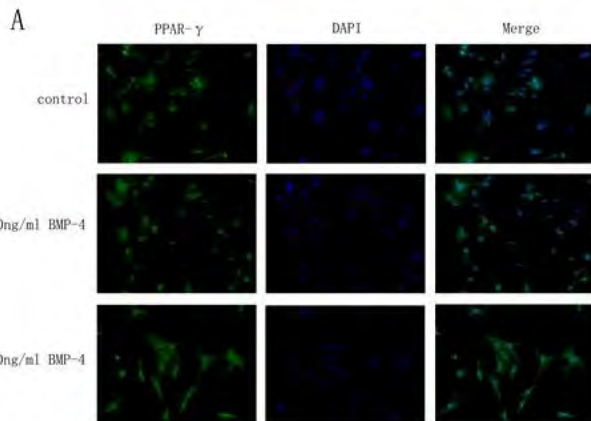
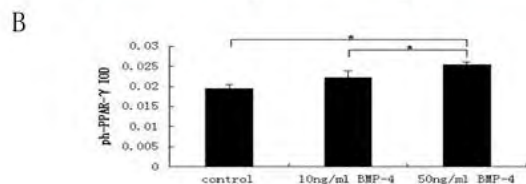
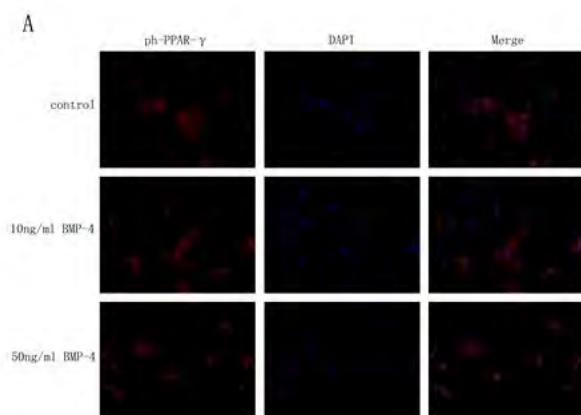


Figure 5



F3



F4

Disclosures: Xueqin Wei, None.

MO0186

Functionalized self-assembling nano-peptides promote osteogenic differentiation of human Mesenchymal Stem Cells (hMSCs) in vitro. Shaun Peggrem¹, Baichuan Wang², James Triffitt³, Zhidao Xia*¹. ¹Swansea University, United Kingdom, ²Union Hospital Affiliated to Huazhong University of Science & Technology, China, ³University of Oxford, United Kingdom

Self-assembling nanopeptides are of great interest in the field of regenerative medicine for their unique characteristics that help support tissue repair and regeneration. The aim of this study was to assess a functionalized self-assembling nano-peptide hydrogel for its osteogenic potential when used with either Coralline Hydroxyapatite/Calcium Carbonate (CHACC) or cuttlefish bone powder. We designed a new functionalized self-assembling nanopeptide (AcN-RADARADAR-ADARADAGGRGDARGDA-COHN2) with the functional group RGDA (The amino acid sequence for multiple calcium-binding sites were selected from the glycoprotein Thrombospondin). An additional group was created using RADA16

only (Puramatrix), the nano-fibres of which were coated in Bone Morphogenic Protein-2 (BMP-2) and the control group was composed of RADA-16 only. These self-assembling nano-peptide hydrogels were then integrated with either CHACC or cuttlefish bone particles in addition to human Mesenchymal Stem Cells (hMSCs) and cultured in alpha-MEM containing 10% FCS before testing for cytotoxicity and osteogenic potential. The functionalized nano-fibre scaffolds exhibited no cytotoxicity in comparison to the control group. hMSCs adhesion and differentiation in three-dimensional cell culture was prominent. AlamarBlue assay confirmed cell proliferation was statistically significant within each group comparing day 7 to day 1. Confocal microscopy was used to observe cell viability and cytochemical staining of alkaline phosphatase was used to assess osteogenic potential. Alizarin Red staining confirmed calcification had occurred significantly more in the functionalized peptide groups than in the RADA16 alone group. The functionalised nano-fibre scaffolds had excellent biocompatibility in vitro and showed improved osteogenic potential with hMSCs. These scaffolds could be very valuable for future use in the field of bone regeneration.

Disclosures: Zhidao Xia, None.

MO0187

How Do Heavy Metal Ions Uncouple Bone Formation from Bone Resorption.

J. Edward Puzas*¹, Tzong-jen Sheu², Catherine A. Muzytchuk², Eric E. Beier². ¹University of Rochester School of Medicine, USA, ²University of Rochester School of Medicine & Dentistry, USA

Purpose

We have investigated the effects of heavy metal ions (lead and cobalt) on skeletal metabolism. With exposure to either of these agents we find a low bone mass phenotype resembling osteoporosis in mice. The studies with lead are clinically relevant in that mounting evidence shows that exposure to this metal ion decreases bone density and increases fracture risk. The studies with cobalt are also clinically relevant because of the observed high incidence of permanent bone loss and "metalosis" in patients receiving a metal-on-metal orthopaedic cobalt-chromium implant.

Our hypothesis is that lead and cobalt uncouple bone formation from bone resorption and lead to a permanent loss of bone. The mechanism for the uncoupling is through up-regulation of the expression of the formation inhibitor, sclerostin.

Methods

Mice were exposed to lead in their drinking water or gavaged with cobalt salts to achieve concentrations seen in the humans. In vitro experiments were also performed with lead and cobalt ions in the culture medium.

DXA and microCT imaging were used to measure bone density and bone quality. Sclerostin levels were measured in vivo and in vitro using ELISA assays and western blotting. Sclerostin null mice (SOST^{-/-}) were used as control animals for both in vivo experiments and from which to isolate cells for in vitro experiments. TGF β reporter activity was measured using P3TPLuc. Immunohistochemistry analyses were performed using standard methods.

Results

We have found an osteoporosis-like phenotype with DXA and microCT analyses in mice exposed to lead over a 3-6 week period. At the same time we found that sclerostin levels increased dramatically (over 7-fold) in both serum and bone tissue. We observed the same effect when osteoblasts were exposed to lead and cobalt ions in cell culture. We have also found that lead and cobalt block TGF β signaling through the p-Smad3 pathway. Blockade of this pathway up-regulates sclerostin production, implying repressor function for this transcription factor.

Conclusion

Our findings show that exposure of osteoblasts to lead and cobalt ions markedly depresses bone formation. This occurs, in part, through heavy metal ion up-regulation of sclerostin. Our data also support that the mechanism by which this occurs is through lead and cobalt inhibition of TGF β signaling, thereby de-repressing SOST gene expression. These findings point to new ways to combat this bone loss clinically.

Disclosures: J. Edward Puzas, None.

MO0188

Inhibition of histone deacetylases enhances the osteogenic differentiation of human periodontal ligament cells. Nam Cong-Nhat Huvnh*¹, Vincent

Everts², Prasit Pavasant³, Ruchanee Salingcarnboriboon Ampornaramveth⁴. ¹Mineralized Tissue Research Unit, Faculty of Dentistry, Chulalongkorn University, Thailand, ²Department of Oral Cell Biology, Academic Centre for Dentistry Amsterdam (ACTA), University of Amsterdam & VU University Amsterdam, Research Institute MOVE, Netherlands, ³Department of anatomy, Faculty of Dentistry, Chulalongkorn University, Thailand, ⁴DRU in Oral Microbiology, Microbiology department, Faculty of Dentistry, Chulalongkorn University, Thailand

When appropriately triggered, periodontal ligament (PDL) cells can differentiate into mineralized tissue, thus make it be a good candidate for autologous bone graft. However, the underlying mechanisms responsible for the plasticity of PDL cells are unknown. One possible mechanism might be related to epigenetics, since histone

deacetylases (HDACs) have been shown to play a role in osteoblast differentiation. This study was aimed to investigate the role of histone deacetylases (HDACs) in osteogenic differentiation of human periodontal ligament (hPDL) cells. Methods: hPDL cells were isolated from teeth subjected to be extracted from healthy volunteers. Activity of HDACs was blocked using the inhibitor trichostatin A (TSA). Effect of TSA on proliferation and cytotoxicity of primary hPDL cells was tested by MTT assay. Osteogenic and adipogenic differentiations were induced in the presence of TSA. Gene expression was assessed by semi-quantitative and real time RT-PCR. ALP activity and mineral deposition assays were used to assess osteoblast phenotype. Histone acetylation and the expression of different HDACs were also observed by WB. Co-polymer scaffold (PCL/PEG) was used to perform 3D culture and mineralization level was verified by Von Kossa and Alizarin red staining. Results: During the course of osteogenic differentiation in the presence of the HDAC inhibitor, osteoblast-related genes expression were accelerated in hPDL cells. ALP activity as well as bone nodule formation were also enhanced under these conditions. Inhibition of HDACs was quite specific to osteoblast lineage since it did not induce the differentiation into adipocyte lineage. hPDL highly expressed HDACs of both class I (HDAC 1, 2, 3) and class II (HDAC 4, 6). During osteogenic differentiation, HDAC 3 expression gradually decreased. This was apparent in the absence and presence of the inhibitor. The level of acetylated histone H3 was increased during osteogenic differentiation. Inhibition of HDAC activity also induced hyperacetylation of Histone H3. These data, therefore, post an important role of HDAC3 and histone H3 as a candidate target molecules for HDAC inhibition. The effect of TSA was also consistent when bone formation in 3D culture model was performed. In conclusion, hPDL cells express a distinguished series of HDACs and these enzymes appear to involve in the osteogenic differentiation. Inhibition of HDACs activity in hPDL cells might make it more applicable for bone regeneration therapy.

Disclosures: Nam Cong-Nhat Huynh, None.

MO0189

Osteoblastogenesis increases through up-regulation of RUNX2, CX43 and beta-catenin after treatment with human serum collected 1 hour and 2 hour post dried plum ingestion. Paulina Cuenca*, Shirin Hooshmand. San Diego State University, USA

Recent studies showed that treatment with dried plum (*Prunus domestica* L.) polyphenols increased osteoblast alkaline phosphatase (ALP) activity, mineralization and increased the expression of bone marker genes RUNX2 and osterix. The purpose of this study was to determine if human serum collected 1 hour (1h) and 2 hour (2h) after dried plum ingestion influenced osteoblast cell activity and gene expression. Five healthy women were asked to consume 100g dried plum and serum samples were collected at baseline (before dried plum ingestion), and 1h, and 2h post-dried plum ingestion. MC3T3-E1 osteoblast cells were treated with 2% of the baseline, 1h and 2h post-dried plum ingestion serum for three and nine days. Treatment with human serum 1h and 2h post-dried plum ingestion for three and nine days significantly increased intracellular and extracellular ALP activity. Also, treatment with human serum 1h and 2h post-dried plum ingestion for three and nine days significantly increased the mRNA level of bone markers RUNX2 and CX43. Finally, treatment with human serum 1h and 2h post-dried plum ingestion for nine days increased the expression of beta-catenin. We concluded that treatment with human serum 1h and 2h post-dried plum ingestion for three and nine days increased osteoblast activity and function by up-regulating RUNX2, CX43 and beta-catenin.

Disclosures: Paulina Cuenca, None.

MO0190

Transgenic Expression of Dentin Phosphoprotein (DPP) Inhibits Long Bone Growth. Hua Zhang*¹, Peihong Liu², Chao Liu¹, Privam Jani¹, Xiaohua Xie¹, Yongbo Lu¹, Chunlin Qin¹. ¹Texas A&M University Baylor College of Dentistry, USA, ²Harbin Medical University School of Stomatology, China

Objectives: Dentin sialophosphoprotein (DSPP), the most prominent non-collagenous protein expressed by odontoblasts, plays an essential role in dentin formation. DSPP is expressed in the long bone at a much lower level. Previous studies have indicated a role of DSPP in bone turnover, however, the exact mechanism by which DSPP functions in the bone mineralization and remodeling remains largely unknown. DSPP is proteolytically processed into an N-terminal fragment called dentin sialoprotein (DSP) and a C-terminal fragment known as dentin phosphoprotein (DPP). These two fragments are believed to perform distinct roles in the formation and mineralization of mineralized tissues. The goal of this study was to investigate the functions of DPP in skeletal development. Methods: Transgenic mice were generated to overexpress the hemagglutinin (HA)-tagged DPP under control of a 3.6 kb type I collagen (Col1a1) promoter (referred to as "Col1a1-HA-DPP"). Combined approaches of Real-time PCR, Western immunoblotting and immunohistochemistry were used to validate overexpression of HA-DPP in the mineralized tissue of Col1a1-HA-DPP transgenic mice. Plain x-ray radiography, skeleton staining, histology and immunohistochemistry analyses were performed to characterize the skeletal phenotype in these transgenic mice. Results: Fifteen Col1a1-HA-DPP founder mice were obtained and were bred with C57BL/J mice to establish the transgenic lines. Transgenic expression of HA-DPP was confirmed at both mRNA and protein levels.

The Col1a1-HA-DPP transgenic mice were significantly smaller by weight, and they had smaller skeletons and shorter femurs than their wild-type littermates, as demonstrated by plain x-ray radiography. Histology analysis showed that the Col1a1-HA-DPP transgenic mice had narrower zones of the proliferative and hypertrophic chondrocytes in the growth plates of the long bones. Consistently, BrdU labeling revealed a reduction in the number of proliferating chondrocytes. In addition, the transgenic mice with high level of transgene expression displayed malformed joints and spontaneous long bone fracture. Conclusions: Overexpression of DPP inhibits long bone growth, suggesting that the balanced actions of both DSP and DPP may be required for normal skeletal development.

Disclosures: Hua Zhang, None.

MO0191

A gram positive bacterial toxin lipoteichoic acid induces inflammatory bone resorption through PGE2 production. Tsukasa Tominari, Michiko Hirata, Chisato Mivaura, Masaki Inada*. Tokyo University of Agriculture & Technology, Japan

Toll-like receptors (TLRs) are the mold receptors play a critical role in innate immunity, and various ligands for TLRs regulate the host defense against the pathogens. Lipopolysaccharide (LPS) is a potent toxin for inflammatory bone resorption such as periodontitis, that is an outer membrane component of gram-negative bacteria binds to TLR4. The other TLRs, TLR1/2 heterodimer recognizes triacylated lipopeptides from gram-negative bacteria, whereas TLR2/6 heterodimer recognizes diacylated lipopeptides from gram-positive bacteria. We have reported that synthetic ligands for TLR1/2 and TLR2/6 induced prostaglandin (PG) E₂-mediated and receptor activator of NFκB ligand (RANKL)-mediated osteoclast differentiation, and that TLR2 heterodimer signaling induced mouse experimental periodontitis in vivo. In this study, we examined the effects of a gram-positive bacteria originated lipoteichoic acid (LTA), a natural ligand for TLR2/6 heterodimer on inflammatory bone resorption. In cocultures of mouse primary osteoblast (POB) and bone marrow cell, LTA significantly induced osteoclast differentiation. In cultures of POB, LTA increased PGE₂ production in conditioned medium and up-regulated the mRNA expression of membrane bound PGE synthase (mPGES)-1, cyclooxygenase (COX)-2 and RANKL. Both osteoblasts and osteoclasts expressed TLR2 and TLR6 mRNAs. To compare the LTA induced NFκB inducing activity, the degradation of IκBα was measured. LTA promoted degradation of IκBα, suggesting RANKL production was increased by NFκB nuclear translocation in osteoblasts. Furthermore, to examine the direct actions of LTA on the survival in mature osteoclasts, RANKL treated RAW264.7 cells were treated with LTA. LTA enhanced the life span and cell survival in mature osteoclasts. In the organ culture of mouse calvaria, LTA induced bone resorbing activity in dose-dependent manner, and the effect was less than that of LPS. In conclusion, LTA induced TLR2/6 signaling to promote RANKL expression via mPGES-1 and COX2 mediated PGE₂ production and stimulate inflammatory bone resorption. TLR4 recognizes LPS from gram-negative bacteria and TLR2/6 recognizes LTA from gram-positive bacteria, and both signals simultaneously enhance the inflammatory activity at the sites of bacterial infection in periodontitis.

Disclosures: Masaki Inada, None.

MO0192

Expression of Collagen-Modifier Genes in the Gonads: Another Link between Bone and Reproduction. Sarah Zimmerman*¹, Roberta Besio², Milena Dimori¹, Melissa Heard¹, Frances Swain¹, Dana Gaddy¹, Larry Suva¹, Alberto Ferlin³, Patrizio Castagnola⁴, Roy Morello¹. ¹University of Arkansas for Medical Sciences, USA, ²University of Pavia, Italy, ³University of Padova, Italy, ⁴IRCCS, Italy

Sc65 (Synaptonemal complex 65, aka LEPREL4) is a poorly characterized member of the Leprecan gene family. Three members of this family are prolyl 3-hydroxylase enzymes (P3H1, P3H2, and P3H3) which hydroxylate certain proline residues on fibrillar collagens. The family also includes cartilage-associated protein (Crtap), and mutations in CRTAP and LEPREL1 (encoding P3H1) cause recessive osteogenesis imperfecta (OI). While Sc65 was first identified as a synaptonemal complex protein, we demonstrated that Sc65-null mice have a low bone mass phenotype, albeit milder than Crtap or P3H1 knockout mice. Since both Crtap and Sc65 are non-enzymatic proteins we hypothesized that similar to Crtap, Sc65 potentially interacts with fibrillar procollagen chains and collagen modifiers. To identify candidate Sc65 interacting proteins, a yeast 2-hybrid approach was utilized. Surprisingly, the most robust interactions occurred with spermatogenesis-associated proteins and included spermatogenesis-associated 4 (Spata4), Spata3 and spermatogenesis-associated serine-rich protein 1 (Spats1). Spata4 was further investigated since it had been shown by others to promote osteoblast differentiation. Indeed, Spata4 is expressed in mouse primary osteoblasts and a murine fibroblast cell line although preliminary co-immunoprecipitation results did not confirm that Sc65 and Spata4 interact. Immunofluorescence (IF) for Sc65 and Spata4 appeared to show no colocalization. Nonetheless, Sc65 gene expression was confirmed in mouse testis by RT-PCR and western blot analysis revealed higher levels of Sc65 expression in prepubertal versus adult testis, with even higher protein expression in ovarian tissue. Immunohistochemistry detected Sc65 protein in spermatogonia, spermatocytes, and developing spermatids and in the granulosa and theca cells of the ovary. Interestingly,

Crtap was also expressed in mouse testis and ovary in a pattern similar to Sc65. Despite this, neither Sc65 nor Crtap knockout mice have infertility issues. Conversely, IF detection of Sc65 and Crtap in adult human testis biopsies revealed a very different expression pattern with staining only in the interstitial cells and not the seminiferous tubules. Sirius-red collagen staining of adult murine testis sections showed no overt differences. Thus, Sc65 and Crtap do not appear to play a role in collagen modification in the gonads, or in spermatogenesis. A potential role in the synaptonemal complex is currently being investigated.

Disclosures: Sarah Zimmerman, None.

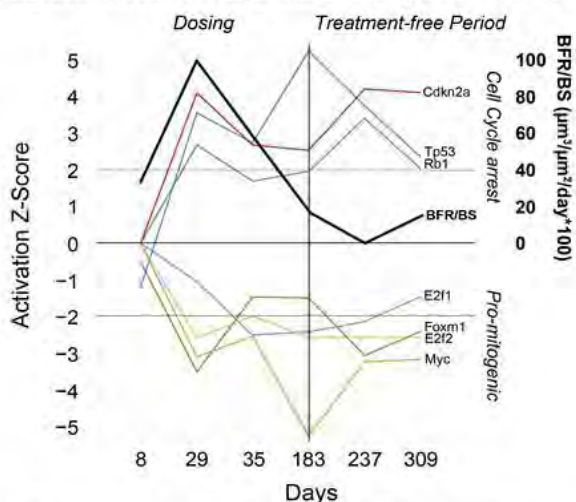
MO0193

Analysis of the Osteoblast Lineage Reveals Inhibition of Mitogenesis and Cell Cycle Progression Associated With Attenuation of Bone Formation in Response to Sclerostin Antibody in Ovariectomized Rats. Scott Taylor*, Paul Nioi, Rong Hu, Efrain Pacheco, Yudong He, Cynthia A Afshari, Ian Pyrah, Michael S Ominsky, Rogely W Boyce. Amgen Inc., USA

In aged ovariectomized (OVX) rats, sclerostin antibody (Scl-AbVI) rapidly increased vertebral bone formation rate (BFR/BS), which attenuated toward control values by 26 weeks. To gain insight into the signaling pathways that may be involved in self-regulation of BFR/BS, the transcriptional response of subpopulations of the osteoblast (OB) lineage was assessed. Microarray analysis of mRNA isolated from laser capture microdissection-enriched samples of lining cells (LC), OB, and osteocytes (OCy) from the vertebrae of OVX rats was evaluated following exposure to Scl-AbVI for 26 weeks and during a treatment-free period (TFP).

Six-month-old rats were OVX and after 8 weeks received vehicle or Scl-AbVI (3 or 50 mg/kg/wk) up to Day (D) 183. Animals were euthanized on D8, 29, 85, and 183 and during the TFP at intervals up to D309. In L4 vertebrae, progressive increases in bone volume (BV/TV) were observed through D183 (end of treatment) and gradually declined thereafter, while BFR/BS peaked at D29 before normalizing to control during the TFP. Co-expression analysis of differentially expressed genes (DEGs) from the 3 cell types collected from L3 vertebrae demonstrated that OCy displayed unique patterns of temporally regulated genes, with distinct gene modules split on D29 correlating to BFR/BS and BV/TV. Wnt target genes (*Wisp1/Twist* cluster) were similar in LC, OB, and OCy at D8. The OCy pattern changed at D29–183, with a sustained increase of *Wisp1* but not *Twist1*, coupled with upregulation of different Wnt targets including *Irx3*, *Id2*, and *Tcf4*. Furthermore, DEGs consistent with cell cycle arrest, such as increased *Cdkn1a* and decreased *Foxm1*, *Cdk1*, and *Ccnb1* were observed beginning on D29. DEGs were analyzed to predict activation or inhibition of upstream molecules based on downstream expression changes. The most significant effects were observed in OCy from D29–183 for the 50 mg/kg/wk Scl-AbVI group, with predicted activation of transcription factors (TFs), which are known tumor suppressors and inhibitors of cell cycle progression, and coincident inhibition of pro-mitogenic TFs (Figure). The onset of these TF changes mirrored the changes in BFR/BS. In the TFP, the status of these TFs trended toward control values. The temporal relationship between these transcriptional changes and changes in BFR/BS suggests that suppression of mitogenesis and cell cycle progression may contribute to the attenuation of bone formation observed with chronic Scl-AbVI treatment.

Figure. Predicted Transcription Factor Activation in OCy-enriched Cell Population From Rats Treated With 50 mg/kg/wk of Scl-AbVI



BFR/BS, bone formation rate; OCy, osteocytes; Scl-Ab, sclerostin antibody.

Figure

Disclosures: Scott Taylor, Amgen

This study received funding from: Amgen Inc. & UCB Pharma

MO0194

Ascorbic acid drives Tet-mediated methylcytosine hydroxylation to induce osteoblastogenesis in vitro. Casey Droscha*, Bart Williams, Van Andel Institute, USA

Ascorbic acid (AA) is a common supplement added to cell culture medium due to its functions both as an anti-oxidant and its ability to promote cell proliferation. AA is also an essential component of osteogenic media required to induce *in vitro* osteoblast differentiation. AA has long been known to facilitate prolyl-hydroxylation of nascent procollagen polypeptides required for extracellular collagen fibrillation, a marker of osteoblast differentiation. This function of AA has been assumed to underlie its role in promoting osteoblast differentiation. However, recent evidence demonstrates that AA is also a co-factor for the Ten-eleven-translocation (Tet) methylcytosine dioxygenase family responsible for hydroxylating methylcytosine (5mC to 5hmC) within the CpG moiety. The hydroxylation of methylated CpGs initiates active DNA de-methylation, which allows for a cascade of chromatin remodeling occurring within distal regulatory elements. This leads to substantial reprogramming of cells resulting in significant, epigenetically heritable changes in gene expression. We hypothesize that the role of AA in initiating demethylation of cytosine residues may also contribute to its function in inducing osteoblast differentiation. To address the requirement of active demethylation during AA-induced osteoblast differentiation, MC3T3-E1 cells lacking either Tet1 or both Tet1 and Tet2 were generated via CRISPR/Cas9 technology and differentiated for 0, 4, and 7 days in the presence of 50ug/mL ascorbic acid. As predicted, AA exposure resulted in a time dependent increase in global 5hmC. Currently, *in vitro* osteoblast differentiation assays are being performed on Tet single- and double-KO MC3T3-E1 to assess the necessity of Tet1/2 expression for differentiation. Osteoblast-specific gene enhancer activation and remodeling is assessed by global changes of 5mC to 5hmC via DNA Immunoprecipitation-sequence (meDIP-seq) in combination with ChIP-sequence analysis of the enhancer signature. Furthermore, identification of differentially methylated regions corresponding to enhancer signatures will be assessed by Nucleosome Occupancy Methylation-sequence (NOME-Seq) analysis to determine, at base pair resolution, both DNA methylation changes and nucleosome remodeling. This work aims to elucidate the role of Tet methylcytosine hydroxylases to regulate epigenetic remodeling and control developmental gene transcription during osteoblast differentiation.

Disclosures: Casey Droscha, Amgen

MO0195

Carbamazepine and Phenytoin Inhibit Native Sodium Currents in Murine Osteoblasts. Sandra Petty*¹, Carol J Milligan², Marian Todaro³, Kay L Richards², Pamu Kularathna⁴, Charles Pagel⁴, Elisa L Hill-Yardin⁵, Chris French⁶, Terence J O'Brien⁶, John D Wark⁷, Eleanor J Mackie⁴, Steven Petrou². ¹The University of Melbourne, Australia, ²The Florey Institute of Neuroscience & Mental Health, Australia, ³Melbourne Brain Centre at The Royal Melbourne Hospital, Australia, ⁴Faculty of Veterinary & Agricultural Sciences, The University of Melbourne, Australia, ⁵Department of Physiology, University of Melbourne, Australia, ⁶Melbourne Brain Centre at The Royal Melbourne Hospital, The University of Melbourne, Australia, ⁷Department of Medicine, The Royal Melbourne Hospital, The University of Melbourne, Australia

Purpose: Fracture risk is increased in epilepsy, however, understanding of the mechanism is limited. Osteoblasts express ion channels, which we hypothesized would be inhibited by anti-epileptic medication (AED), potentially altering signaling during bone remodeling. We aimed to investigate whether: (1) mouse primary calvarial osteoblasts express voltage-activated sodium current (NaV), and (2) carbamazepine (CBZ) and phenytoin (PHT) inhibit this current.

Methods: Immunocytochemistry, RNA-Seq (Illumina USA) and Patchliner (Nanion, Germany) recordings were performed on primary calvarial osteoblasts extracted from neonatal C57BL/6J mice. Cell samples were stained for alkaline phosphatase to confirm osteoblastic characteristics. The impact of AED on whole-cell current recordings was examined using the Patchliner. Currents were elicited using a range of voltage protocols designed to examine sodium channel biophysical and pharmacological properties. CBZ (50 μM) or PHT (50 μM) was applied to the cells in continued presence of internal and external tetraethylammonium (10 mM) and internal Cs⁺. Following washout of AED, 10 μM tetrodotoxin (TTX), a known NaV blocker was applied.

Results: NaV expression was demonstrated with immunocytochemistry and RNASeq. Robust voltage-activated inward currents were elicited. External application of AED resulted in significant inhibition of current amplitude: for CBZ $31.6 \pm 5.9\%$ ($n = 9$; $p < 0.001$), and for PHT $35.5 \pm 6.9\%$ ($n = 7$; $p < 0.001$), which was partially reversed upon washout. Subsequent application of TTX (10 μM) produced almost complete inhibition of current amplitude.

Conclusion: Mouse osteoblasts express native NaV which are sensitive to CBZ and PHT. Further study is required to determine whether these effects translate to alterations in osteoblast effector function producing clinically-important changes in bone signaling and bone quality.

Disclosures: Sandra Petty, None.

MO0196

Integrative Analysis of RNA-seq and ChIP-seq Data Identifies Wnt3a Inducible Genes and Regulatory Elements in Osteoblasts. Aimy Sebastian*¹, Nicholas R. Hum², Deepa K. Muruges², Sarah Hatsell³, Aris N. Economides³, Gabriela G. Loots⁴. ¹University of California, Merced, USA, ²Lawrence Livermore National Laboratories, USA, ³Regeneron Pharmaceuticals, USA, ⁴Lawrence Livermore National Laboratories; University of California, Merced, USA

Wnt3a is a canonical Wnt ligand that has been shown to promote bone formation, yet very few of its target genes are known in osteoblasts. To identify new Wnt3a target genes and regulatory elements, neonatal osteoblasts isolated from *C57Bl/6 (WT)* calvaria were treated with Wnt3a for 24 hrs and the transcripts were quantified by RNA-Seq analysis. In total, 452 genes including many Wnt pathway members such as *Porcn*, *Fzd1*, *Lef1*, *Tcf7* and *Axin2* were significantly differentially expressed between Wnt3a and sham treated osteoblasts. A gene ontology analysis with DAVID showed that Wnt3a regulates the expression of many major regulators of differentiation, proliferation, growth, apoptosis, ossification and extracellular matrix organization. We conducted the same experiment in Wnt3a treated *Lrp5^{KO}* osteoblasts and found 405/452 genes significantly changed in Wnt3a treated *WT* osteoblasts to overlap with the Wnt3a treated *Lrp5^{KO}* osteoblasts, suggesting that Wnt3a gene activation in osteoblasts is *Lrp5* independent. Next, we downloaded 21 TCF/LEF ChIP-Seq datasets from ENCODE and GEO, aligned them to the reference genome and identified 804,156 TCF/LEF binding peaks. Subsequently, we identified 56,854 putative regulatory elements in osteoblasts by computationally identifying regions with overlapping H3K4me1/2 and H3K27ac ChIP-Seq peaks (H3K4me1/2+, H3K27ac+) that are also enriched for DNase hypersensitive sites. To identify Wnt3a inducible regulatory elements, we mapped all the TCF/LEF binding sites to the putative regulatory elements in osteoblasts and identified 1,621 Wnt3a inducible distal regulatory elements near up-regulated genes. Of 212 genes up-regulated by Wnt3a administration, 162 (76%) had TCF/LEF binding sites in their promoter and/or a distal noncoding region. Transcription factor binding site analysis of the putative Wnt3a-inducible regulatory elements with HOMER identified several transcription factors, including *Fos2*, *Runx2* and *Foxo1*, with enriched binding motifs in these regions. This study identified 452 genes regulated by Wnt3a in osteoblasts, 1,621 putative Wnt3a inducible distal regulatory elements and transcription factors that may cooperate with TCF/LEFs to regulate the expression of these genes. Ongoing validation of these regulatory elements *in vitro* and *in vivo* will allow the characterization and modeling of Wnt3a-regulatory pathways in osteoblasts, and predict the role of transcription factors, enhancers and proteins in bone metabolic functions.

Disclosures: *Aimy Sebastian, None.*

MO0197

Pigment Epithelium Derived Factor Activates Wnt/b-Catenin Signaling Pathway in Mesenchymal Stem Cells via cross-talk with ERK Signaling Pathway. Christopher Niyibizi¹, Feng Li*², Joyce Tombran-Tink³. ¹The Pennsylvania State University College of Medicine, USA, ²Penn State College of Medicine, USA, ³Penn State College of Medicine, USA

Pigment epithelium-derived factor (PEDF) encoded by *Serpinf1* is found in a wide variety of fetal and adult tissues. Mutations in *Serpinf1* have been shown to be the cause of osteogenesis imperfecta type VI whose hallmark is defective mineralization. In these patients, there is excessive osteoid buildup and failure to mineralize the matrix. Mechanisms by which PEDF regulates matrix mineralization remain undefined. We and others reported that PEDF enhances human and mouse mesenchymal stem cell (MSCs) differentiation and increased osteoblastic mineralization *in vitro*. To begin to understand mechanisms by which PEDF plays a role in osteoblast differentiation and matrix mineralization, we determined signaling pathways activated by PEDF to enhance MSCs-osteoblastic differentiation. Human MSCs exposed to PEDF activated ERK signaling within 5 min to 48h of analysis. Erk activation led to increased phosphorylation of GSK-3beta and increased accumulation of LRP6 and beta-catenin. Exposure of human MSCs to PEDF in presence of ERK inhibitor prevented ERK activation and phosphorylation of GSK-3beta. Inhibition of ERK activation also reduced LRP6 and beta-catenin accumulation suggesting that Wnt/beta-catenin activation in human MSCs by PEDF occurs via a cross-talk with ERK signaling pathway. Examination of osteoblastic gene expression by MSCs exposed to PEDF for 48h showed increase in ALP, *Col1A1*, *Runx2* and *osterix* genes. Human MSCs exposed to PEDF in presence of ERK inhibitor reduced expression of all these genes. These data taken together strongly indicate that PEDF activates Wnt/beta-catenin in human MSCs via cross-talk with ERK signaling to enhance expression of osteoblastic genes that play a role in MSCs-osteoblastic differentiation.

Disclosures: *Feng Li, None.*

MO0198

SIT (SHP2-Interacting Transmembrane Adaptor) - A Novel Regulator of Bone Mass. Joseph Tarr*¹, Sarah Carrante², Lev Blekher², Brooke Marks², Samantha Dyckman², Elizabeth Figueiredo², Kaitlin Reilly², Luca Simeoni³, Thomas Owen², Steven Popoff¹. ¹Temple University School of Medicine, USA, ²Ramapo College of New Jersey, USA, ³Otto von Guericke University, Germany

SIT (SHP2-interacting transmembrane adaptor) is a member of the family of transmembrane adapter proteins which have tyrosine signaling motifs in their intracellular tails through which they are phosphorylated by kinases of the src and syk families. This allows them to subsequently recruit SH2 domain containing signaling molecules to the membrane and influence signaling pathways. SIT has been well studied in the immune system where it has been shown to be an important regulator of T-cell receptor signaling and T-cell activation. SIT was identified as being potentially involved in regulating bone mass in a study comparing gene expression changes between the bones of normal and osteopetrotic (op/op) mutant rats. On the RNA level, the expression of SIT was found to be lower in the bones of the op/op mutant rats than those of their wild-type littermates. SIT is expressed in cultures of primary rat calvarial osteoblasts where its RNA increases concurrently with the expression of alkaline phosphatase and peaks during the maturation phase prior to mineralization. Similarly in ROS 17/2.8 osteosarcoma cells SIT RNA increases with the rise in alkaline phosphatase activity. Overexpression of SIT in ROS 17/2.8 cells results in a delayed increase in alkaline phosphatase activity. Analysis of the bones from SIT knockout (KO) mice shows that deletion of SIT significantly altered a number of trabecular bone parameters. Sit KO mice exhibited increased trabecular bone volume fraction (BV/TV), number (Tb.N), connectivity (Conn) and connectivity density (Conn.Dn), and decreased trabecular thickness (Tb.Th) and spacing (Tb.Sp) compared to age-matched wild-type littermates. We are exploring the localization of SIT in bone by immunohistochemistry and are developing additional reagents through which to further explore the role of SIT in bone metabolism. It is possible that SIT is an integral part of signaling through many of the receptors which influence the development and activity of both osteoblasts and osteoclasts, and could also be intimately linked with the actions of c-src kinase in both cell types.

Disclosures: *Joseph Tarr, None.*

MO0199

Trps1 Affects Signaling and Expression of Mineralization Genes in Response to Phosphate. Maria Kuzynski*¹, Sandeep Chaudhary², Morgan Goss², Callie Mobley², Dobrawa Napierala². ¹University of Alabama at Birmingham, USA, ²UAB, USA

Phosphate availability is critical for the initiation and progression of mineralization. When genes regulating phosphate are mutated, defective mineralization results. Besides being a component of hydroxyapatite crystals, phosphate is also able to act as a signaling molecule by mediating biphasic Erk1/2 activation and regulating expression of mineralization-related genes. *Trps1* is a transcriptional repressor identified to play a role in the mineralization process. In our previous studies identifying the molecular role of *Trps1* during mineralization, we uncovered a link between *Trps1* and phosphate. Specifically, *Trps1*-deficient cells had decreased levels of phosphatases (Phospho1 and Tissue non-specific alkaline phosphatase) and *Trps1*-overexpressing cells were unable upregulate genes involved in phosphate regulation (Phex and Vitamin D receptor) during the later stages of mineralization. To clarify the role of *Trps1* in phosphate signaling, we analyzed whether deficiency or upregulation of *Trps1* affects cellular response to phosphate by comparing Erk1/2 activation and phosphate-regulated gene expression. In pre-odontoblastic mineralizing cells deficient for *Trps1*, we observed a delayed second activation of Erk1/2 upon phosphate treatment. In contrast, cells overexpressing *Trps1* displayed an accelerated second activation of Erk1/2 in response to phosphate. To further understand *Trps1* function during phosphate signaling, we analyzed changes in the expression of mineralization-related genes in response to phosphate and uncovered that *Trps1* affects the expression of several of these genes. *Trps1*-deficient cells displayed a delayed response in the upregulation of Osteopontin and Dentin matrix protein 1 twelve hours after phosphate treatment. *Trps1*-overexpressing cells had a significantly greater decrease in the expression of *Runx2*, Vitamin D receptor, and Tissue non-specific alkaline phosphatase 48 hours after phosphate treatment. Altogether, these data suggest that *Trps1* participates in the phosphate-mediated signaling cascade by specifically affecting the second activation of Erk1/2 and regulating the expression of mineralization-related genes.

Disclosures: *Maria Kuzynski, None.*

MO0200

BCL11B a Transcriptional Regulator of Sutural Patency. Kenneth Philbrick*, Kateryna Kyrylkova, Urszula Iwaniec, Mark Leid, Oregon State University, USA

One in every 2,500 babies develops craniosynostosis. Untreated, craniosynostosis increases risk of deafness, blindness, developmental delay, and learning disabilities. Calvaria forms through primary intramembranous ossification. BCL11B is a transcription factor that plays a key role in the development of numerous tissues including skin, teeth, and the immune system. Data we report here provide evidence that BCL11B regulates intramembranous ossification and suggests that it may play a role in the etiology of craniosynostosis.

BCL11B expression was studied throughout mouse craniofacial development and in the perinatal period. Within osteogenic, calvarial tissues BCL11B expression was primarily detected within sutures and in mesenchymal cell condensates surrounding, but not immediately adjacent to the calvaria. In contrast, cells expressing Runx2, the master osteogenic transcription factor, were found immediately adjacent to and within the calvaria. BCL11B⁺ cells were found to form a halo around Runx2⁺ cells with only a minimal number of cells co-expressing these two transcription factors.

Microcomputed tomography analyses of newborn mice lacking BCL11B in the germline revealed that these mice exhibited synostoses of the facial and calvarial skeleton that were accompanied by mid-facial hypoplasia and malocclusion (Figure 1). Mice lacking BCL11B in tissues derived from neural crest and mesoderm exhibited loss of sutural patency in facial and calvarial sutures, respectively, with accompanying distortions of craniofacial structures (Figure 1).

These findings provide evidence that BCL11B is a top-level regulator of sutural patency and osteogenesis in the craniofacial skeleton. Further studies are ongoing to determine the molecular mechanism(s) through which BCL11B contributes to osteogenesis and maintenance of sutural patency. Manipulation of BCL11B expression and/or activity may provide an avenue for therapeutic manipulation of sutural patency in the treatment of craniosynostosis.

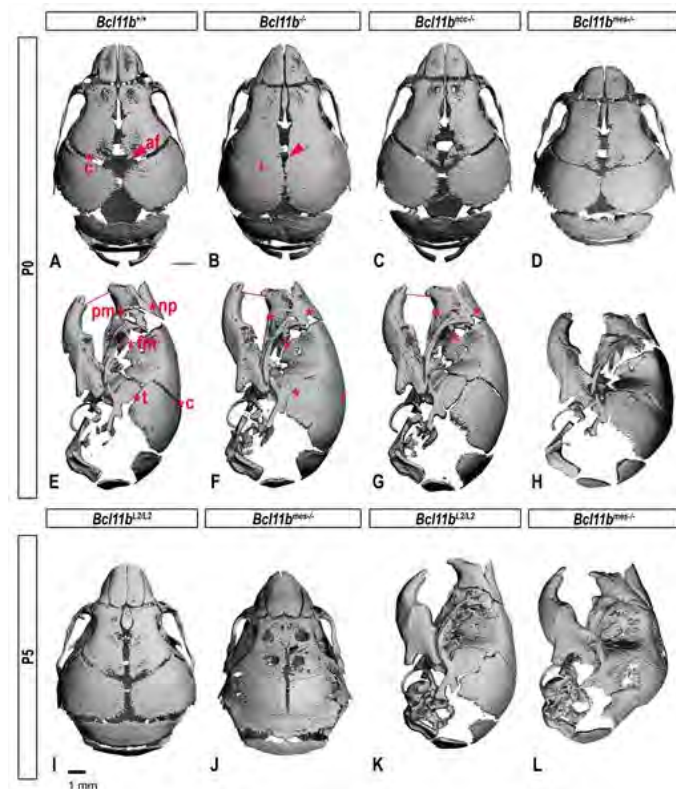


Fig 1: UCT imaging of P0 & P5 WT (+/+), P0 Total KO (-/-), P0 neural crest KO (nc -/-), P0 & P5 mesoderm KO (mes-/-)

Disclosures: Kenneth Philbrick, None.

MO0201

Ectoderm neural cortex 1 isoforms have disparate effects on MC3T3 osteoblast differentiation and mineralization. Leah Worton*¹, Yanchuan Shi², Elisabeth Smith², David Little³, Jon Whitehead⁴, Edith Gardiner¹. ¹University of Washington, USA, ²Garvan Institute, Australia, ³The University of Sydney, Australia, ⁴The University of Queensland, Australia

In recent years the importance of Wnt signaling in the skeleton has been repeatedly demonstrated but Wnt pathway mechanisms in bone cells are far from understood.

We previously found expression of a Wnt target gene, ENC1 (ectoderm neural cortex 1), in osteoblasts of mouse distal femur and *in vitro* during osteoblast differentiation, so we investigated its role in these cells. We first observed two ENC1 protein isoforms of 57 and 67kDa throughout MC3T3 (MC) cell differentiation (21 days). MC cell lines stably transduced with doxycycline-inducible shRNA lentiviral expression constructs were established. Simultaneous shRNA knockdown of both 57 and 67kDa ENC1 proteins from d 1 of culture reduced alkaline phosphatase staining and virtually abolished MC culture mineralization whereas selective targeting of only the 67kDa isoform had the opposite effect, increasing mineralized nodule formation above the level in a control scrambled GFP shRNA cell line (Fig.1). The distinctive mineralization patterns of the general 57/67kDa and the 67kDa-selective ENC1 knockdown cell lines both declined as initiation of doxycycline treatments was progressively delayed, but the effects of ENC1 shRNA remained significant even with induction as late as d 9. At confluence (d 3) with general 57/67kDa knockdown begun at d 1, there was a 68% reduction in *Osx* mRNA compared to the scGFP control. In these cells *Tnap* expression was also markedly reduced (10% of scGFP level) and there was significant and coordinated alteration of other genes involved in cellular phosphate biochemistry including *Phospho1*, *Ank*, *Enpp1* and *Opn*. At mineralization onset (d 13), expression of osteoblast marker genes reflected the reduced and enhanced mineralization phenotypes for the general 57/67kDa and 67kDa-selective ENC1 knockdown lines respectively. At this time point expression of the Wnt antagonist *Sfrp2* was up-regulated 2-fold with general 57/67kDa knockdown but reduced by 50% with 67kDa-selective knockdown compared to scGFP control. These results are the first to demonstrate a role for ENC1 in control of osteoblast differentiation and mineralization. In addition, the contrasting mineralization phenotypes and transcriptional patterns seen with coordinate knockdown of both 57kDa and 67kDa ENC1 vs the isoform-selective knockdown of 67kDa ENC1, suggest opposing roles for the isoforms in regulation of osteoblastic mineralized nodule formation through effects on phosphate cellular biochemistry and the Wnt pathway.

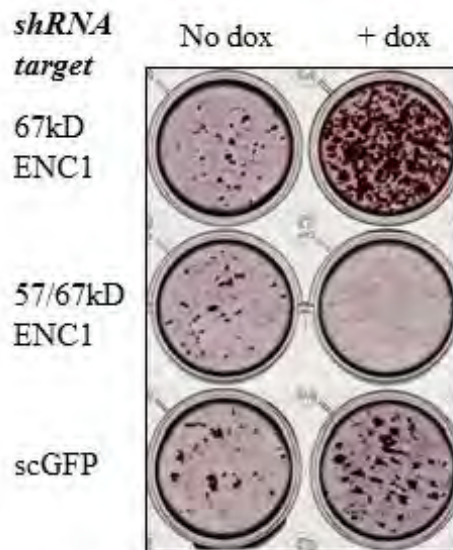


Figure 1. Knockdown of ENC1 isoforms alters MC cell differentiation. Cell lines expressing inducible shRNA sequences targeted to ENC1 isoforms or a scrambled GFP were differentiated in the absence or presence of doxycycline for 21 days and then stained with Alizarin Red.

Fig.1

Disclosures: Leah Worton, None.

MO0202

Modulation of the extracellular matrix environment and epigenetic DNA methylation improves osteogenicity of human mesenchymal stromal cells. Roman Thaler*¹, Markus Schreiner¹, Eric A. Lewallen¹, Dakota L. Jones¹, David R. Deyle¹, Allan B. Dietz², David G. Lewallen¹, Andre J. van Wijnen². ¹Mayo Clinic, USA, ²Mayo Clinic, USA

Bone degeneration and nonunion of bone upon fracture in elderly patients may be reversed using bone regenerative therapies with human mesenchymal stromal cells (MSCs). We have shown that clinical-grade MSCs derived from adipose tissue

(AMSCs) and grown in human platelet lysate have the potential to differentiate into osteoblasts with a mineralizing extracellular matrix (ECM), which is known to mediate epigenetic feed-back control of gene expression in osteoblasts. Yet, expression of principal osteoblast-related transcription factors (TFs) like Sp7/Osterix or Dlx5, remains suppressed in these cells. In this study, we investigated whether the osteogenic effectiveness of AMSCs for skeletal therapies can be improved by manipulating epigenetic mechanisms (e.g., CpG methylation) linked to ECM dependent activation of osteogenic TFs. We first analyzed intact ECMs that were decellularized with deoxycholate and isolated from primary human AMSCs and human osteoblasts (hOBs) or mouse MC3T3-E1 osteoblasts cultured for 1 week in osteogenic media. Examination of ECM deposition by fluorescence spectroscopy and laser scanning microscopy reveals major structural differences between ECMs. While AMSCs produce a wide-meshed network of collagen fibrils, osteoblasts deposit a closed-mesh ECM structure with significantly higher amounts of collagen. When AMSCs cells are cultured on ECMs derived from MC3T3-E1 osteoblast (ost-ECM) or AMSCs (msc-ECM), the pre-deposited ost-ECM but not msc-ECM slows proliferation and marginally enhances osteoblastic differentiation. Neither ECM supported expression of the osteogenic TFs Sp7 or Dlx5. However, co-treatment of AMSCs with the DNA methylation inhibitor 5'Aza-cytidine (AzaC) strongly accelerates osteoblastic differentiation (e.g., alkaline phosphatase (ALP) activity) on ost-ECM compared to msc-ECM or plastic (control). Mechanistically, this osteogenic effect is attributable to both ost-ECM and AzaC-dependent activation of both Sp7/Osterix and Dlx5 (10-20 fold stimulation within 3d after induction of differentiation). We conclude that combinatorial modulation of both the ECM environment and the epigenetic landscape of multi-potent AMSCs promotes osteoblast lineage-commitment and maturation. This combination treatment of clinical grade adipose-tissue derived MSCs may represent a realistic approach for bone regenerative therapies.

Disclosures: Roman Thaler, None.

MO0203

Rorb β , a Negative Regulator of Osteoblast Function, Regulates the Circadian Clock Through Upregulation of Bmal1 and Period Genes. [David Monroe](#)^{*1}, [Joshua Farr](#)², [Sundeep Khosla](#)². ¹Mayo Foundation, USA, ²Mayo Clinic, USA

Circadian rhythms control a wide variety of biological processes involved in virtually all aspects of metabolism. While the hypothalamic central clock regulates general metabolic events (entrained by the light/dark cycle), peripheral clocks located in all tissues, including bone, function to regulate tissue-specific events. These clocks rely on a transcriptional/translational feedback system where the transcriptional activators Bmal1/Clock activate expression of the Per1-3 and Cry1-2 genes, which feedback to inhibit Bmal1/Clock. Previous studies have demonstrated that genetic deletion of these genes in mice results in increased osteoblastic function and/or bone mineral density, suggesting that the clock inhibits bone formation. An additional modulatory loop consisting of the nuclear hormone receptor families Rev-erb and Ror form a fine-tuning loop which regulates Bmal1. We have demonstrated that Rorb β knockout (KO) mice exhibit increased trabecular vBMD, BV/TV and trabecular number, similar to what is observed in other clock KOs. Since Rorb β expression is elevated in osteoprogenitor cells from aged mice and humans, Rorb β may play a role in regulation of the clock. To investigate the role of Rorb β on the osteoblastic clock, we examined the effects of Rorb β on the clock genes in MC3T3-E1 pre-osteoblastic cells. Transient expression of an adenovirally-expressed Rorb β resulted in increased Bmal1 expression. In synchronized MC3T3 cells, Bmal1 and Rorb β expression exhibit identical patterns, with an amplitude maximum at Zeitgeber (ZT) circadian time ZT4. These data establish Rorb β as a regulator of Bmal1 in osteoblasts. In MC3T3 cells stably expressing Rorb β , which exhibit low mineralization potential, the steady-state levels of Per1-3 are significantly enhanced. Finally, Per3 expression is elevated in osteoprogenitors from aged mice (<12-mo), where Rorb β expression is high. Overall, these data are consistent with the notion that increasing clock activity in osteoblasts is associated with impaired osteoblast function. In summary, our data demonstrate that Rorb β affects the circadian clock in osteoblasts by upregulating Bmal1 and Per1-3 expression. This suggests that increased Rorb β expression in pre-osteoblastic cells, as seen in aged mice, would stimulate the clock possibly resulting in compromised bone metabolism. These data reveal a novel mechanism for Rorb β in aged bone and identifies a new pathway for future interventions in the treatment of age-related bone loss.

Disclosures: David Monroe, None.

MO0204

Candidate Enhancer RNA Expression During α SMA+ Progenitor to Mineralizing Osteoblasts-Osteocytes: Exploration of the 'Dark Matter' of the Genome. [Stephen Harris](#)^{*1}, [Marie A Harris](#)², [Coralee Tye](#)³, [Ivo Kalajzic](#)⁴, [Jonathan Gordon](#)³, [Jane Lian](#)³, [Gary Stein](#)³. ¹University of Texas Health Science Center at San Antonio, USA, ²u. of Texas health science center at san antonio, USA, ³U. of Vermont Medical School, USA, ⁴U. of Connecticut Health Center, USA

Deletion of the Bmp2 gene in α SMA+ bone marrow progenitors (MSC) results in a profound decrease in bone formation rate and decrease in the number of expanding MSC to mineralizing osteoblasts-osteocytes, assessed by lineage tracing methods.

Using an α SMA+ MSC to osteoblast-osteocyte differentiation model, we determined the coding and non-coding transcriptome using RNA-seq. Of the coding transcripts, we identified 2968 genes (q value<0.01) that are regulated between the early α SMA+ progenitor/stem cell state to the mineralizing osteoblast-osteocyte state after 7days of in vitro treatment with rBMP2 (653 positive and 2316 negative), with 87 transcription factors (TF) with defined binding motifs. Using this transcriptome data from 2 hr. to 7 days, control and rBMP2 treatment, with ARACNe program, we developed a transcriptional gene network model with a subset of the TFs regulated during differentiation (e.g. Osterix and Egr2). Recently, in cancer biology, muscle cell differentiation, and other systems, enhancer RNAs, or eRNAs, have been shown to be critical for positive transcriptional regulation, acting as 3D scaffolds for complex TF interactions within a given enhancer. These eRNAs are found as a subset of the long-noncoding RNAs. Using the latest annotation file for long-coding RNAs (lncRNAs) thought to be a major component of the 'Dark Matter' of the Genome and transcribed asymmetrically from both Minus and Plus strands (Gencode vM4.long-noncoding_RNAs.gtf), we found 3764 lncRNAs regulated from progenitor state to mineralizing state (2049 Positive and 1750 Negative). We used only Minus strand data, to avoid confusion with Plus strand intronic and exonic regions. We then used H3K27ac Chip-seq data, which marks engaged active enhancers during α SMA cell differentiation to mineralizing osteoblast-osteocyte states, to intersect Minus strand lncRNAs genome dataset. Of the 2049 positively regulated Minus strand lncRNAs, 745 intersect with H3K27ac active enhancers and are activate during differentiation from progenitor state to mineralizing osteoblast-osteocyte state. These experiments define a set of candidate enhancer RNAs (eRNA) for osteoblast differentiation. Data on the Bmp2, Osterix, and Dmp1 genes will be presented as examples, including overlay Chip-seq data with Runx2, TCF/ β -catenin, and repressor-off markers (Ezh2 of the polycomb complex and H3K27me) that intersect with the lncRNA-H3K27ac domains that are modulated during osteoblast-osteocyte differentiation.

Disclosures: Stephen Harris, None.

MO0205

Effect of Tryptophan on the stemness and osteogenesis of bone marrow-derived mesenchymal stromal cells *in vitro* and *in vivo*. [Hai Pham](#)^{*1}, [Mitsuaki Ono](#)², [Emilio Hara](#)², [Yasutaka Oida](#)², [Ha Nguyen](#)², [Kentaro Akiyama](#)², [Takuo Kuboki](#)². ¹Okayama University, Japan, ²Department of Oral Rehabilitation & Regenerative Medicine, Okayama University Graduate School of Medicine, Dentistry & Pharmaceutical Sciences, Okayama, Japan, Japan

Amino acids are essential for life and cell metabolism. We hypothesized that amino acids can regulate the stem cell phenotype and differentiation ability of human bone marrow-derived mesenchymal stem/progenitor cells (hBMSCs). Thus, we performed a screening of 22 standard amino acids and found that D-Tryptophan (10 μ M) increased the number of cells positive for the early stem cell marker SSEA-4, and gene expression levels of *OCT-4*, *NANOG* and *SOX-2* in hBMSCs. Comparison between D- and L-tryptophan showed that the latter presents stronger effect in inducing the mRNA levels of *OCT-4* and *NANOG*, and increasing the osteogenic differentiation of hBMSCs. Additionally, L-tryptophan also enhanced chondrogenesis, but inhibited adipogenesis. Migration and colony forming ability of hBMSCs was also enhanced by L-tryptophan treatment. *In vivo* experiments delivering L-tryptophan (50 mg/kg/day) by intra-peritoneal injections for 3 weeks confirmed that L-tryptophan significantly increased the percentage of cells positive for SSEA-4, mRNA levels of *Nanog* and *Oct-4*, and migration and colony forming ability of BMSCs. Additionally, surgical defects of 1 mm in diameter were created in mouse femur to evaluate bone formation after 2 weeks of L-tryptophan injection. L-tryptophan accelerated bone healing, and increased bone volume and trabecular number compared to PBS-injected group. In summary, L-tryptophan enhances the stemness and osteoblastic differentiation of BMSCs, and may be used as an essential factor to accelerate bone healing and/or prevent bone loss, such as in the case of ageing and osteoporosis.

Disclosures: Hai Pham, None.

This study received funding from: Grant-in-Aid for Scientific Research (KAKEN) for T.K., No.22249064 in Japan

MO0206

Fatty Acids and Energy Metabolism in Mesenchymal Stem Cells. [Laura Shum](#)^{*}, [Roman Eliseev](#). University of Rochester, USA

Purpose: During aging, bone quality declines and fat accumulates in the bone marrow. We hypothesize that the increased presence of fatty acids, such as palmitate, in bone marrow inhibit mesenchymal stem cell (MSC) differentiation towards osteoblasts by disrupting oxidative phosphorylation via induction of the mitochondrial permeability transition (MPT). The MPT is a large, non-selective mitochondrial pore, gated by cyclophilin D. Our goal is to fully characterize the effect of palmitate on the bioenergetic and osteogenic functions of MSCs.

Methods: C3H/10T1/2 cells are a mesenchymal stem-like mouse cell line. Cells were grown in osteogenic media for 14 days for differentiation. Clark electrode was used to measure oxygen consumption as an indicator of oxidative phosphorylation after treatment with 100 μ M palmitate for 24 hours. Mitochondrial Calcium Retention Assay was used to determine mitochondrial calcium buffering capacity, a measure of

sensitivity to the MPT. Mitochondrial uptake of calcium was measured with fluorescent calcium indicator, Calcium Green 5N. Real time RT-PCR was performed on differentiated cells in the presence or absence of palmitate using SYBR Green, and normalized to beta actin.

Results: Palmitate reduced ATP-linked respiration after 24 hour, as compared to control (0.3688 vs 0.7260 nmol/min/10⁶ cells, respectively). Treatment with palmitate for 24 hours reduced mitochondrial ability to buffer calcium by 80%. Osteogenically differentiated cells in the presence of palmitate significantly increased gene expression of alkaline phosphatase 2.7-fold, and increased PPAR-gamma 3.29-fold.

Conclusions: This study demonstrates the effects of palmitate on metabolism and differentiation of MSCs. The increase in alkaline phosphatase gene expression indicates that palmitate may not affect the early stages of osteogenic differentiation, which are less dependent on oxidative phosphorylation. However, the significant increase in the adipogenic marker (PPAR-gamma), indicates a shift away from osteogenic differentiation, and instead toward the adipogenic lineage, which is not dependent on oxidative phosphorylation. Furthermore, palmitate decreases oxygen consumption, and reduces mitochondrial capacity to buffer calcium due to the MPT induction. This indicates that even with short exposure, palmitate can affect metabolism and may uncouple oxidative phosphorylation in MSCs through induction of the MPT, potentially leading to reduced bone quality.

Disclosures: Laura Shum, None.

MO0207

Foxd1 lineage tracing during skeletal development identifies a unique subset of osteogenic precursors. Jackie Fretz¹, Nancy Troiano², Rose Webb², Tracy Nelson². ¹Yale University School of Medicine, USA, ²Yale School of Medicine, USA

The Foxd1-cre is used in kidney research as a marker of the precursors to the glomerular mesangium and interstitial pericytes. While it is known that the Foxd1-cre driver is not specific to this subset of the kidney mesenchyme, its contribution to skeletal development has not been examined in detail. Through mating of the Foxd1-cre Tg with the mT/mG "flip" mouse we investigated the contribution of Foxd1-lineage cells to anabolic bone populations throughout the skeleton. These tracing experiments revealed that the presence or absence of Foxd1 expression during osteocyte and chondrocyte (Chd) development did not uniformly mark or exclude osteogenic populations in all bones. Instead, location-specific contributions of Foxd1+ cells were observed in reproducible patterns throughout the skeleton. Long bones of the hind leg lacked Foxd1-driven recombination, while vertebrae harbored significant GFP+ populations: 50-70% of the osteocytes and Chds in cervical and thoracic vertebrae, 70-90% of these osteogenic cells in the tail, and 20-40% of the osteogenic cells of the lumbar vertebrae. While Foxd1-driven recombination was apparent in approximately 10-15% of the osteoblast (Ob) and Chds within the humerus and ulna, it was rarely seen within the hip, and absent from the scapula. The clavicle, phalanges, carpals, and tarsals had recombination rates of 15-25%. Within the skull the relative contribution of Foxd1-lineage cells to the total Ob population ranged from the occipital bone (100% GFP+ cells) > interparietal bone (75-85%) > frontal bone (60%) > squamosal bone (50%) > parietal bone (40%) > maxillary bone (5%) > mandible (0%). Both fibrocartilage and hyaline cartilage were marked, and traced as complete columns of either RFP or GFP labeled cells suggesting that Foxd1 was expressed in a precursor cell or only in the first stages of cellular differentiation. Overall these results reveal that the promoter driving the Foxd1-cre identifies a unique subset of osteogenic progenitors that vary in their overall contribution to the skeleton in location-specific patterns. It presents the possibility that multiple types of mesenchymal progenitors contribute to the bone not only at different locations throughout the body but within a single bone as well. Furthermore, renal osteodystrophy generated using the Foxd1-cre mouse should be interpreted carefully and restricted to the femur and tibiae to minimize confounding contributions from recombination in the skeleton.

Disclosures: Jackie Fretz, None.

MO0208

Human Platelet Lysate derived Exosomes affect Proliferation and Osteogenic Differentiation of Adipose Stem Cells. Behrouz Zandieh-Doulabi¹, Jenneke Klein-Nulend². ¹Department of Oral Cell Biology, Academic Centre for Dentistry Amsterdam (ACTA), University of Amsterdam & VU University Amsterdam, MOVE Research Institute Amsterdam, Amsterdam, The Netherlands., Netherlands, ²Dept. Oral Cell Biology, Academic Centre for Dentistry Amsterdam (ACTA), University of Amsterdam & VU University Amsterdam, Move Research Institute Amsterdam, Amsterdam, The Netherlands, Netherlands

Platelets contain bioactive substances such as growth factors for the expansion and differentiation of adipose stem cells (ASCs). Almost all cell types including platelets secrete exosomes, i.e. nanovesicles, ranging in size from 50 to 100 nm diameter. Exosomes contain proteins, mRNAs, and microRNAs, thereby providing a novel paracrine signaling mechanism in physiological and pathological processes. This study aimed to evaluate the potential use of platelet-derived exosomes for modulating proliferation and osteogenic differentiation of human ASCs after a short (6 hours)

treatment. To test the effect of exosomes on ASC proliferation and differentiation, ASCs were cultured in medium with exosome-free platelet lysate, and with or without exosomes at two concentrations (5 and 10 µg/ml) for 6 hours followed by an additional cell culture in absence of exosomes up to 7 days. Gene expression of the proliferation marker Ki67 as well as osteogenic differentiation markers RUNX-2, alkaline phosphatase (ALP) and osteonectin (ON), were determined after 6 hours, 3 days, and 7 days. Six hours of treatment with exosomes increased Ki67 gene expression in ASCs by 1.8-fold using 5 µg of exosomes at 6 hours and by 7-fold at day 3, but decreased Ki67 gene expression by 2-fold at day 7. Treatment with exosomes decreased RUNX-2 gene expression by 2-fold using 5 µg of exosomes at 6 hours, but no change was observed at 3 and 7 days in ASCs. Treatment with exosomes resulted in decreased ALP gene expression in ASCs by 0.3-fold using 5 µg exosomes at day 3, while treatment with 10 µg exosomes increased ALP expression by 2.5-fold at day 7. Treatment with 5 µg exosomes increased ON gene expression in ASCs by 2.8-fold after 6 hours, it decreased ON gene expression by 2-fold after 3 days, and increased ON expression by 2.5-fold and 3.9-fold after 7 days when ASCs were treated with 5 µg and 10 µg exosomes respectively. In conclusion our data indicate that platelet-derived exosomes increase ASC proliferation as indicated by enhanced Ki67 gene expression, and can be used as a cell culture additive for ASC expansion. Only 6 hours of treatment with exosomes affected osteogenic cell differentiation even after 7 days. Treatment with exosomes appears to downregulate osteogenic differentiation of ASCs in an early stage, followed by a significant upregulation of osteogenic differentiation at a later stage. This suggests a potential role of exosomes in bone tissue engineering.

Disclosures: Behrouz Zandieh-Doulabi, None.

MO0209

Inhibition of Histone Methyltransferase SMYD2 Attenuates Lineage Commitment of Mesenchymal Stem Cells. Christopher Paradise¹, Amel Dudakovic, Scott Riester, Emily Camilleri, Allan Dietz, Andre van Wijnen. Mayo Clinic, USA

Lineage commitment of mesenchymal stem cells (MSCs) *in vivo* can drive pathogenic processes such as heterotrophic ossification and fatty degeneration of muscle and tendon. Therapies that can inhibit MSC differentiation in patients can be applied to treat these musculoskeletal disorders. Histone lysine methyltransferases (HKMTs) and their gene targets are key players in shaping the epigenetic landscape responsible for activating or silencing of lineage specific transcription factors. Specifically, tri-methylation of Histone 3 Lysine 4 (H3K4) in MSCs has been shown to promote osteogenic differentiation while suppressing the potential for alternative lineage commitment. Thus, small molecule inhibitors targeting HKMTs provide a unique approach to alter the epigenetic landscape and direct differentiation of MSCs. Here, we investigated whether the inhibition of SMYD2, an H3K4/K36 methyltransferase, via a small-molecule inhibitor AZ505 prevents commitment of MSCs to the osteogenic lineage. Human adipose-derived mesenchymal stem cells (AMSCs) as well as primary mouse bone marrow derived stem cells (BMSCs) were treated with AZ505 and cultured in either osteogenic or adipogenic differentiation medium. Expression of osteoblast-specific markers (SP7, RUNX2, BGLAP, ALPL, COL1A1, SPP1) and adipocyte-specific markers (ADIPOQ, FABP4, PPARγ, KLF3) was measured using real-time quantitative PCR (RT-qPCR). Our data demonstrate that expression of both osteoblast and adipocyte specific markers was decreased in AMSCs and BMSCs treated with SMYD2 inhibitor. A decrease in expression of these markers suggests prevention of commitment to both osteogenic and adipogenic lineages. Thus, inhibition of SMYD2 interferes with the differentiation of mesenchymal progenitors into at least osteogenic and adipogenic lineages. These findings suggest that pharmacologic inhibition of SMYD2 may have therapeutic applications for treating an array of orthopedic disorders including heterotrophic ossification and muscle/tendon degeneration.

Disclosures: Christopher Paradise, None.

MO0210

Potential role of Secreted frizzled related protein (Sfrp2) in regulating activity of bone marrow stem/progenitor cells. Luis Fernandez De Castro¹, Brian Sworder², Agnes Berendsen³, Matthew Phillips³, Natasha Cherman³, Sergei Kuznetsov³, Kenn Holmbeck¹, Pamela Robey³. ¹NIDCR (NIH), USA, ²Boston University-NIDCR, USA, ³NIDCR, USA

Bone marrow stromal cells (BMSCs, also known as bone marrow-derived mesenchymal stem cells) are a population of fibroblastic reticular cells, a subset of which is composed of multipotent skeletal stem cells (SSCs). SSCs can recreate bone, marrow adipocytes and hematopoiesis-supportive stroma, upon *in vivo* transplantation with an appropriate scaffold, but more committed BMSCs make only bone or fibrous tissue. In an attempt to find specific genes that would distinguish SSCs from more committed BMSCs, we performed microarray analyses of human single-cell derived lines with known potency based on *in vivo* transplantation. The results identified SFRP2 as being highly represented in human multipotent clones. SFRP2 is thought to inhibit Wnt signaling, but its role in the bone marrow microenvironment is unclear. To assess the function of *Sfrp2* in bone, we analyzed *Sfrp2*-deficient (KO) mice by microCT analysis and found no significant differences between KO and wildtype (WT) mice in any parameter. However, colony forming efficiency, the closest approximation of the number of SSCs in the BMSC population, was reduced

in KO bone marrow by ~40% compared to WT. In addition, *Sfrp2* deficiency in BMSCs (using both KO BMSCs and siRNA knocked down mBMSCs) reduced expression of osteogenic transcription factors (*Runx2* and *Osx*) and reduced calcium accumulation *in vitro*. Moreover, the phosphorylation of the Wnt co-receptor Lrp6 and expression of the Wnt downstream target gene *Axin 2* were also reduced in these cells. These *in vitro* results suggested that *Sfrp2* is a positive regulator of Wnt signaling. However, there was no difference in growth rate between KO and WT BMSCs. Furthermore, no difference between WT and KO was found in ectopic ossicles formed by *in vivo* transplantation of mBMSCs in collagen sponges into immunocompromised mice, as well as those induced by BMP-soaked sponges transplanted into KO and WT recipient mice. Lastly, we assessed the role of *Sfrp2* in bone regeneration by creating a non-critical sized defect in femoral diaphyses of KO and WT mice and no significant differences in healing were noted. In conclusion, although *Sfrp2* appears to be a positive regulator of osteogenic cells *in vitro*, there is little effect caused by its deficiency *in vivo*. These phenomena may be related to redundancies (compensation by other *Sfrp* family members), and control of Wnt signaling by other factors that are present *in vivo*, but not in the *in vitro* setting.

Disclosures: Luis Fernandez, De Castro, None.

MO0211

SWI/SNF-mediated lineage determination in mesenchymal stem cells confers resistance to osteoporosis. Stephen Flowers*¹, Kevin Hong Nguyen¹, Fuhua Xu¹, Eric Himelman¹, Edek AJ Williams¹, J Christopher Fritton¹, Elizabeth Moran². ¹Department of Orthopaedics, New Jersey Medical School, Rutgers, The State University of New Jersey, Newark, NJ 07103., USA, ²Rutgers, The State University of New Jersey, NJMS Cancer Center, USA

The SWI/SNF chromatin-remodeling complex, which contains either brahma-related gene-1 (BRG1) or brahma (BRM) as the catalytic ATPase, functions as a master regulator of gene expression in development and differentiation. BRG1 is required for induction of essentially all tissue specific gene expression, such that BRG1-null mice die as pre-implantation embryos. Comparatively little is known about the role of the alternative ATPase, BRM, as BRM-null mice seem developmentally normal and live a full life span. The studies reported here now indicate that BRM-SWI/SNF represents a sensitive physiological point for control of osteoblast vs adipocyte lineage selection in mesenchymal stem cells. Key osteogenic genes are targeted directly by BRM-SWI/SNF for repression. Depletion of BRM causes dissociation of HDACs and other repressors from these promoters. Simultaneously, BRM-SWI/SNF cooperates with BRG1-SWI/SNF to promote expression of adipogenic genes. These effects are manifested at the earliest stages of stem cell differentiation, upstream of the important osteogenic or adipogenic transcription factors such as Runx2 or PPAR γ 2. BRM can be a precise target for increasing formation of osteoblast progenitors and sustaining osteoblast formation. The bone marrow stromal cell population of BRM-null mice shows an enhanced proportion of cells expressing markers of osteoblast precursors at the expense of cells able to differentiate along the adipocyte lineage. This altered precursor balance has no apparent negative developmental effects, but can have major physiological significance in conditions of osteoblast insufficiency. This is apparent in the BRM-null mouse model as protection against age-related osteoporosis. Scanning by micro-CT shows cortical porosity reaching an average of 7.2% in the femurs of wild type females by 18 months. BRM-null mice lose far less bone, averaging only 1.8% porosity at the same age. Wild type mice also lost more than 11% mineral density in their cortical tissue by 18 months, while BRM-null mice showed no significant loss.

Disclosures: Stephen Flowers, None.

MO0212

Denosumab and Odanacatib as Reference Compounds in Human Osteoclast Cultures. Jussi Halleen*, Jenni Bernoulli, Jukka Rissanen, Katja Fagerlund. Pharmatest Services Ltd, Finland

Human osteoclasts can be generated from bone marrow-derived CD34+ mesenchymal stem cells in the presence of M-CSF and RANKL. In this study we report optimization of separate *in vitro* culture systems for determining osteoclast differentiation and activity, and validation of the RANKL inhibitor denosumab and the cathepsin K inhibitor odanacatib as reference inhibitors of osteoclast differentiation and activity, respectively. CD34+ human osteoclast precursor cells were cultured on bovine bone slices for 7 days. Different concentrations of denosumab (0.01 – 10 μ g/ml) were added in the cultures at day 0, and tartrate-resistant acid phosphatase isoform 5b activity (TRACP 5b) was measured in the culture medium collected at day 7 as an index of the number of formed osteoclasts. Osteoclast activity was studied by allowing the formed mature osteoclasts to resorb bone during an additional 3-day culture period. The culture medium was changed and different concentrations of odanacatib (0.001 – 1.0 μ M) were added into the cultures at day 7, and the amount of C-terminal cross-linked telopeptides of type I collagen (CTX-I) was measured in the culture medium collected at day 10 to quantitate bone resorption during days 7-10. Denosumab and odanacatib showed strong concentration dependent inhibition of osteoclast differentiation and activity, respectively, with EC50 values of 0.124 μ g/ml for denosumab and 0.0433 μ M for odanacatib. We conclude that we have validated denosumab as a reference compound of osteoclast differentiation and odanacatib as a

reference compound of and osteoclast activity in a human *in vitro* osteoclast culture system, and the culture system is a clinically reliable tool for identifying new osteoporosis drug candidates with anti-resorptive activity.

Disclosures: Jussi Halleen, Pharmatest Services Ltd; Pharmatest Services Ltd, employer; IDS plc

MO0213

Elevated miR-214 level within osteoclasts associates with increased bone resorption in both postmenopausal osteoporosis and osteolytic bone metastasis. Defang Li*¹, Jin Liu¹, Baosheng Guo¹, Lei Dang¹, Chao Liang¹, Xiaojuan He¹, Aiping Lu¹, Ge Zhang². ¹Institute for Advancing Translational Medicine in Bone & Joint Diseases, School of Chinese Medicine, Hong Kong Baptist University, Hong Kong SAR, China, ²nstitute for Advancing Translational Medicine in Bone & Joint Diseases, School of Chinese Medicine, Hong Kong Baptist University, Hong Kong SAR, China

Objective and method: The diseases with elevated bone resorption, including postmenopausal osteoporosis and osteolytic bone metastasis, are still great clinical challenges to orthopedic surgeons. Emerging evidences indicate that microRNAs play an important role in regulating osteoclast-mediated bone resorption. Recent studies showed that the phosphatase and tensin homolog (PTEN) plays a unique role in regulating osteoclast differentiation and activities^[1,2]. In addition, miR-214 was shown to target PTEN in various cancer cells^[3,4]. These data prompt us to suppose that miR-214 could target PTEN to regulate osteoclastic bone resorption. So, we examined the expression profile of intraosseous miR-214 in human bone specimens from either postmenopausal osteoporosis or osteolytic bone metastasis and the expression profile of osteoclastic miR-214 in either ovariectomized mice or human breast cancer xenografted nude mice.

Results: We found that the miR-214 and the mRNA expression levels of *TRAP* and *CTSK* were elevated in bone specimens from either post-menopausal (PMO) fractured women or fractured women with breast cancer bone metastasis (Fig a). The correlation analysis showed that the miR-214 level was positively associated with the mRNA expression levels of *TRAP* and *CTSK* in either peripheral menopausal (Peri-MO) and PMO fractured women or the fractured women with and without bone metastasis (Fig b). Consistently, the data from mice model showed that the osteoclastic miR-214 level and the bone resorption-related histomorphometric parameters (Oc.S/BS and Oc.N/Pm) were progressively increased in either ovariectomized mice or human breast cancer xenografted nude mice when compared to their corresponding control group, respectively (Fig c). Further correlation analysis indicated that the level of osteoclastic miR-214 was positively associated with Oc.S/BS and Oc.N/Pm in both mice models, respectively (Fig d).

Conclusions: The elevated miR-214 level in osteoclasts associated with increased bone resorption in both postmenopausal osteoporosis and osteolytic bone metastasis of cancer. It implied a potential role of miR-214 within osteoclasts in regulating bone resorption in in these diseases with elevated bone resorption.

References: 1. Sugatani T, et al. The Journal of biological chemistry 278, 5001-5008 (2003). 2. DeMambro VE, et al. Endocrinology 149, 2051-2061(2008). 3. Zou ZJ, et al. Oncotarget (2014). 4. Yang H, et al. Cancer research 68, 425-433(2008).

MO0215

Leucine Rich Repeat Kinase 1 (Lrrk1) Regulates Osteoclast Function via Modulating RAC1 Serine/Threonine Phosphorylation and Activation.Weirong Xing¹, Subburaman Mohan². ¹Musculoskeletal Disease Center, Jerry L. Pettis Memorial Veteran's Admin., USA, ²Jerry L. Pettis Memorial VA Medical Center, USA

Lrrk1 belongs to the ROCO protein family, and contains ankyrin repeats and leucine-rich repeats, a GTPase-like domain of Roc, a COR domain, and a serine/threonine kinase domain. We recently demonstrated that knockout (KO) of Lrrk1 in mice cause severe osteoporosis due to dysfunction of multinucleated osteoclasts (OCs). Lrrk1 KO mice are healthy and respond to anabolic PTH treatment, but are resistant to ovariectomy-induced bone loss. Mature OCs derived from Lrrk1 KO monocytes exhibited defects in cytoskeletal rearrangement, peripheral sealing zones and ruffled borders. In our previous studies on the mechanism by which Lrrk1 regulates OC functions, we determined that Src pY-416 phosphorylation was significantly reduced while Src pY-526 was increased in Lrrk1 KO cells, thus implicating a role for Src in the Lrrk1 signaling pathway. However, the observed osteoprotective phenotype of Src KO mice was much less severe than the Lrrk1 KO mice, suggesting involvement of additional regulators besides Src in mediating the Lrrk1 effect on OCs. To evaluate this possibility, we identified proteins that are differentially phosphorylated at serine/threonine residues in Lrrk1 KO osteoclasts by Western blot analysis. We found that one phosphorylated peptide of molecular weight 28 kD was dramatically reduced in Lrrk1 deficient OCs as compared to the WT cells. Because RAC/Cdc42 small G proteins run in SDS-PAGE with an estimated mass of 24-28 kD, and because mice with disruption of RAC1/2 exhibit a severe osteoporosis phenotype caused by impaired OC function, we examined the phosphorylation status of RAC/Cdc42 proteins by Western blot analyses, and RAC1 activation by pull down assays in Lrrk1 KO and WT OCs. We found a dramatic reduction in RAC1/Cdc42 serine 71 phosphorylation (28 kD), and more than a 50% reduction in RAC1 binding to the p21 binding domain of p21 activated protein kinase in Lrrk1-deficient OCs. Immunoprecipitation analyses found that RAC1 interacted with Lrrk1 in mature OCs. Our data suggest that Lrrk1 may regulate OC function via modulating RAC1 serine/threonine phosphorylation and activation, and that RAC1 is a key biological substrate of Lrrk1 in OCs.

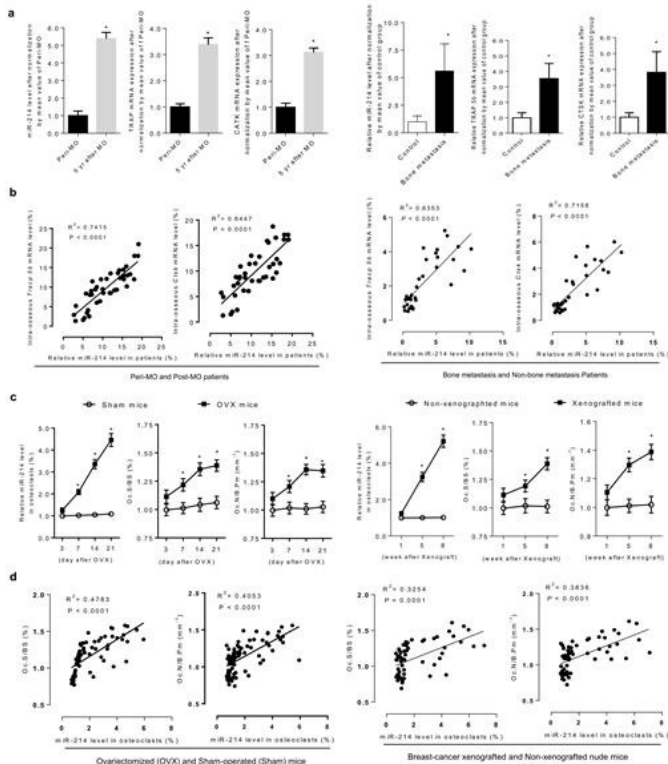
Disclosures: Weirong Xing, None.

MO0216

Loss Of Gfi1 Disorganizes The Podosome Belt And Impairs Osteoclast Migration And Bone Resorption. Peng Zhang*, Quanhong Sun, Juraj Adamik, Deborah L. Galson. University of Pittsburgh, USA

Gfi1 was found to be a novel transcriptional repressor of the critical osteoblast differentiation factor Runx2. BMSC isolated from *Gfi1*^{-/-} mice were resistant to myeloma-induced osteoblast suppression. Gfi1-deficiency studies have revealed that Gfi1 has key regulatory roles in inner ear sensory hair cells, and a wide array of hematopoietic lineage cells (HSC, B cells, T cells, DC cells, and neutrophils). While *Gfi1*^{-/-} mice have roughly normal appearance within 1 week of birth, by 3 weeks postnatal, they have lower body weights and are smaller than WT and *Gfi1*^{+/-} mice, and this difference increases with increasing age. This suggests that Gfi1-deficiency may cause abnormalities in postnatal bone homeostasis. Histomorphometry revealed that the femurs of both male and female *Gfi1*^{-/-} mice at 10 weeks displayed higher trabecular and cortical bone mass (BV/TV) and cortical bone thickness than control mice. Therefore, we investigated the role of Gfi1 in osteoclast (OCL) function and bone resorption. We found that Gfi1 was upregulated by RANKL induction of OCL differentiation of WT mouse bone marrow monocytes (preOCL). Comparison of RANKL-induced OCL formation by preOCL from *Gfi1*^{-/-} and control mice on plastic revealed that *Gfi1*^{-/-} preOCL cells form similar numbers of TRAP+ multinuclear OCL, similar nuclei/OCL, but they are smaller with less cytoplasm and decreased spreading. The *Gfi1*^{-/-} cells on bovine cortical bone slices formed "ball-like" multi-nuclear cells unlike the shape of the WT OCL. Resorption assays revealed that while *Gfi1*^{-/-} OCL generated a similar number of pits as WT OCL, the resorption area was dramatically smaller indicating that *Gfi1*^{-/-} OCLs have reduced resorptive ability. The tiny individual lacunae with no trails generated by *Gfi1*^{-/-} OCL suggested that they might have a migration defect. Using time-lapse video, we confirmed that Gfi1-deficiency inhibits the migration of preOCL. Actin ring visualization demonstrated that Gfi1-deficiency strongly reduced podosome belt formation, which is required for osteoclast migration and resorption. We do not yet know the molecular mechanism by which Gfi1 supports OCL migration and resorption. However, the lack of Gfi1-deficient OCL function in concert with our findings that decreasing Gfi1 in BMSC reduces multiple myeloma suppression of bone formation suggests that Gfi1 is a promising target for treatment of multiple myeloma bone disease since that would decrease OCL function and increase bone formation.

Disclosures: Peng Zhang, None.



Elevated miR-214 level within osteoclasts associates with increased bone resorption in either postmenopausal osteoporosis or osteolytic bone metastasis of cancer. (a) The miR-214 levels and the bone resorption marker genes (tartrate-resistant acid phosphatase 5b, TRAP 5b; cathepsin K, CTSK) mRNA expression levels in bone specimens from either peripheral menopausal (PMO) and post-menopausal (PMO) fractured women or fractured patients with and without bone metastasis were quantified using Q-PCR analysis, respectively. (b) The correlation analysis between miR-214 level and TRAP 5b (or CTSK) mRNA expression level in bone tissue from the groups of indicated patients. (c) The miR-214 levels within osteoclasts, bone resorption-related histomorphometric parameters (osteoclast surface (Oc.S/BS) and osteoclast number (Oc.N/Pm)) in distal femora in either ovariectomized mice and sham-operated mice or breast-cancer xenografted and non-xenografted female nude mice. (d) The correlation analysis between miR-214 levels within osteoclasts and bone resorption-related histomorphometric parameters (osteoclast surface (Oc.S/BS) and osteoclast number (Oc.N/Pm)) in both mice models, respectively.

Results

Disclosures: Defang Li, None.

This study was fund by the Croucher Foundation.

MO0214

Heme Oxygenase-1 Protects Bone Loss via Attenuating Oxidative Stress.KE KE¹, Hye-Seon Choi². ¹University of Ulsan, South Korea, ²Department of Biological Sciences, University of Ulsan, South Korea

Redox status has been shown a crucial role in the pathogenesis of osteoporosis by increasing bone resorption activity. Heme oxygenase-1 (HO-1), known as the enzyme to catalyze heme degradation, was found to play a pivotal role in protecting tissues from oxidative stress. In this study, we have explored the physiological role of HO-1 in bone metabolism using HO-1 knock-out (KO) mice. Compared with its littermate wild type, HO-1 KO mice showed a significant decrease of bone mineral density, bone volume, trabecular number, trabecular thickness, and with an increasing of trabecular space by μ CT. In vivo tartrate-resistant acid phosphatase (TRAP) staining of long bone from HO-1KO mice also exhibited increasing TRAP-positive OC number. Consistently, by investigating serum parameter of bone resorption markers, we found elevated levels of serum C-telopeptide of type 1 collagen and TRACP 5b in the absence of HO-1. While no change was found in bone formation markers, such as N-terminal propeptide of type 1 procollagen and osteocalcin. Additionally, we also observed absence of HO-1 resulted in elevated serum ROS level, indicating increased oxidative stress might contribute to higher bone loss phenomena observed in HO-1KO mice. Our results demonstrated the crucial role of HO-1 in maintaining bone density under physiological conditions, suggesting the therapeutic potential of HO-1 to protect from bone loss.

Disclosures: KE KE, None.

MO0217

Pit And Trench Forming Osteoclasts: a Distinction That Matters?. Ditte MH Merrild¹, Dinisha C Pirapaharan¹, Christina M Andreassen², Per Kjærsgaard-Andersen³, Ming Ding², Jean-Marie Delaisse¹, Kent Soe^{*1}.

¹Dept. of Clinical Cell Biology, Vejle Hospital, University of Southern Denmark, Denmark, ²Dept. of Orthopaedic Surgery & Traumatology, Odense University Hospital, University of Southern Denmark, Denmark, ³Department of Orthopedic Surgery, Vejle Hospital, University of Southern Denmark, Denmark

Osteoclasts (OCs) seeded on bone slices either drill round resorption pits or dig long resorption trenches. Trench-making OCs differ from the pit-forming ones by an asymmetrical organization of their cytoskeleton and sealing zone, a re-arrangement of the exocytosis and endocytosis routes and higher collagenolytic activity. Trenches reflect periods of continuous resorption and thus represent a faster resorption mode compared with the well-investigated pit resorption mode that reflects intermittent resorption. However, it has not yet been investigated whether the distinction between trench and pit resorption modes have any relevance with respect to the natural variation found in human OC populations of different origin, and therefore matter in a clinical context. OCs generated from CD14+ cells isolated from different human blood donors (n=28) show a widespread variation in the prevalence of resorption trenches (3% to 80% of the eroded surface). Male OCs (n=14 donors) made significantly more trenches (mean=41%) than female OCs (n=13)(mean=21%), and male OCs (n=30) also had a 1.6-fold higher gene expression level of CatK than female OCs (n=42). In addition, male OCs showed a positive correlation ($r^2=0.57$, $p=0.003$) between %ES and %trench-surface/ES, whereas female OCs showed a negative correlation ($r^2=0.40$, $p=0.012$). Thus, OCs from male and female donors seem different in vitro. Furthermore, OCs generated from human bone marrow CD14+ cells showed a higher likelihood of generating trenches (57% vs 26%) and a higher collagenolytic activity (2.5-fold higher CTX/ES), compared with OCs obtained from blood. A specific CatK inhibitor abrogated the generation of trenches, even when their prevalence was very high, while it still allowed the generation of pits. This indicates that CatK activity is more stringent for generating trenches than for generating pits. Finally, SEM of bone surfaces eroded in vivo show indeed resorption patterns corresponding to trenches and pits made by OCs in culture. We conclude that the distinction between trench and pit-forming OCs is not merely a laboratory peculiarity, but is relevant to the differences amongst OCs from different skeletal sites, different individuals and gender. We also confirm that the collagenolytic power of OCs determines their resorption mode. Thus, more attention should be given to the mechanism driving trench-making OCs. This is of special interest in the context of CatK inhibitors as anti-osteoporotic drugs.

Disclosures: Kent Soe, None.

MO0218

Protein Kinase D2 (PRKD2) Regulation of the Actin Cytoskeleton during Osteoclast Differentiation. Amanda Leightner^{*}, Eric Jensen, Kim Mansky, Rajaram Gopalakrishnan. University of Minnesota, USA

The activity of osteoclasts and osteoblasts must be tightly balanced to maintain a healthy skeleton. Pathological bone loss in many adult skeletal diseases such as osteoporosis, metastatic bone disease and periodontal disease are caused by excessive osteoclast activity. Better understanding of gene regulatory mechanisms and signal transduction pathways controlling osteoclast differentiation and activity are necessary for development of new therapies. Previous work in our group identified the serine/threonine kinase Protein Kinase D2 (PRKD2) as a key regulator of osteoclast differentiation, necessary for fusion of mononuclear preosteoclasts into multinucleated mature osteoclasts. PRKD2 has many reported cellular functions including coordination of cell migration and invasion through modulation of the actin cytoskeleton and regulation of gene transcription. The goal of the current project is to better understand the mechanism of PRKD2 regulation of osteoclast differentiation and function. We hypothesize that PRKD2 may direct osteoclastogenesis through both control of preosteoclast fusion and regulation of the actin cytoskeleton. We first characterized PRKD2 subcellular localization during osteoclast differentiation from mouse bone marrow monocytes stimulated with RANKL and M-CSF. Active PRKD2 showed weak association with individual podosomes in the cluster or ring stage, but stronger localization to podosomes in the mature actin belt. Treatment of cultures with the PRKD2 inhibitor CID755673 showed that PRKD2 is dispensable for early steps of podosome cluster assembly where its inhibition prevented the transition from podosome clusters to belts and resulted in significant loss of mature podosome belts, confirming a role for PRKD2 in actin dynamics in osteoclasts. Phosphorylated PRKD2 also localized to filipodia where the protein may function in preosteoclast cell fusion. Current data suggest that PRKD2 regulates actin organization through phosphorylation of the actin regulatory protein cofilin. Inhibition of PRKD2 in post-fusion osteoclasts resulted in decreased resorptive activity and impeded cell migration, suggesting a requirement of PRKD2 in basic osteoclast functionality. These data suggest that PRKD2 may affect both progenitor fusion and actin cytoskeletal rearrangements during osteoclast differentiation.

Disclosures: Amanda Leightner, None.

MO0219

Targeted inhibition of miR-214 in osteoclasts suppresses bone resorption in both ovariectomy-induced osteoporosis and osteolytic bone metastasis in vivo: A pilot study. Lei Dang^{*1}, Ge Zhang², Defang Li², Jin Liu², Baosheng Guo², Aiping Lu². ¹Hong Kong Baptist University, Hong kong, ²Hong Kong Baptist University, China

Introduction: Our previous study indicated that elevated osteoclastic miR-214 associated with increased bone resorption in postmenopausal osteoporosis and osteolytic bone metastasis (unpublished data). Recently, we developed an osteoclast-targeting delivery system (Liu et al., 2015), (D-Asp₈)-liposome, which facilitated examining the hypothesis that targeted inhibition of osteoclastic miR-214 could suppress bone resorption in mice with ovariectomy-induced osteoporosis and mice with osteolytic bone metastasis.

Objective: To examine the effect of antagomir-214 delivered by (D-Asp₈)-liposome in both ovariectomized mice and mice with osteolytic bone metastasis.

Methods: 16 6-month-old female mice were OVX or sham-operated. At day 3 after OVX, all mice were administrated intravenously with (D-Asp₈)-liposome-antagomir-214, (D-Asp₈)-liposome-antagomir-NC, Vehicle or PBS weekly for 4 weeks. Antagomir-214 was given at doses of 3, 5, 7 mg/kg body weight. All mice were sacrificed after treatment. The left mice were sacrificed as baseline before treatment. After sacrifice, femurs were dissected for microCT analysis. On the other hand, human breast cancer cells (MM231-LN) were xenografted into 14 female nude mice through intracardial injection. At day 3 after injection, all mice were divided into PBS, Vehicle, (D-Asp₈)-liposome-antagomir NC or (D-Asp₈)-liposome-antagomir-214 according to treatment. All above mice were sacrificed after treatment weekly for 5 weeks. Antagomir-214 was given at doses of 3, 5, 7 mg/kg body weight. The left mice were sacrificed as baseline. Before sacrifice, all mice were detected by biophotonic and X-ray imaging weekly.

Results: In the mouse model of OVX, microCT result showed that impaired trabecular microarchitecture was improved in the mice treated with (D-Asp₈)-liposome-antagomir-214 compared to other treatments. In the mouse xenograft model, biophotonic imaging showed that mice treated with (D-Asp₈)-liposome-antagomir-214 resulted in diminished bone metastasis. X-ray imaging showed that osteolytic lesions in limbs alleviated after treated with (D-Asp₈)-liposome-antagomir-214. In above models, bone resorption was in a dose-dependent inhibitory at doses of 3, 5, 7 mg/kg and the middle dose and high dose groups got similar results.

Conclusion: Targeted inhibition of osteoclastic miR-214 might suppress bone resorption in both ovariectomy-induced osteoporosis and osteolytic bone metastasis. We will increase sample size for further study.

Disclosures: Lei Dang, None.

This study was supported by the Ministry of Science and Technology of China (2013ZX09301307 to A.L.), the Hong Kong General Research Fund (HKBU479111 to G.Z., HKBU478312 to G.Z., HKBU12102914 to G.Z. and HKBU261113 to A.L.).

MO0220

The subcellular distribution of Siglec-15 in bone-resorbing osteoclasts implies complementary roles at the cell surface and ruffled border. Matthew Stuible^{*1}, Annie Fortin², Mario Filion², Gilles B. Tremblay². ¹Alethia Biotherapeutics, Canada, ²Alethia Biotherapeutics Inc., Canada

Siglec-15, a sialic acid-binding receptor, is required for differentiation of precursor cells into mature osteoclasts. In animal models, Siglec-15 can be targeted therapeutically to inhibit bone resorption while maintaining bone formation. Previous studies have reported that Siglec-15 is localized to the cell surface, where, in complex with DAPI2, it generates signals that promote osteoclast differentiation and function. We have found that in addition to its role in osteoclast differentiation, Siglec-15 continues to play a role in resorbing osteoclasts. Here, we report that culturing osteoclasts on bone has a dramatic effect on the subcellular distribution of Siglec-15. In addition to cell-surface staining, Siglec-15 becomes concentrated in punctate structures near the osteoclast ruffled border (RB). The acidic nature of the osteoclast resorption lacuna led us to examine the effect of these conditions on Siglec-15 ligand-binding. Indeed, in vitro binding assays showed that the affinity of Siglec-15 for sialylated substrates is dramatically increased at pH 4.5 vs pH 7. While co-localization of Siglec-15 with DAPI2 was readily observable at the cell surface, it was not observed in the Siglec-15-positive structures in the RB, suggesting a novel function at this location. Siglec-15 does not appear to be involved in the secretion of enzymes into the resorption lacuna; for example, Cathepsin K (CatK) is concentrated at the periphery of the RB while Siglec-15 is more central. The central subdomain of the RB is involved in uptake of hydrolytic enzymes (e.g., CatK) and degraded bone components for transport and secretion from the basolateral membrane (termed "transcytosis"). Specifically in the RB, Siglec-15 exhibits strong co-localization with the endosomal marker Rab9, which has a proposed role in vesicle trafficking between the RB and the transcytotic pathway. Furthermore, treatment of osteoclasts with Siglec-15 mAb AB-25E9 leads to nearly complete inhibition of CatK secretion. Transcytotic vesicles are an important site for continued degradation of bone structural proteins (i.e., collagen) as well as bone-derived growth factors (IGF-1, TGF- β , etc.) by CatK and TRAP. With regards to the maintenance of bone formation upon treatment with AB-25E9, our results suggest that in addition to osteoclast-intrinsic factors that may stimulate osteoblast activity, the reduced degradation of key bone-derived growth factors may also be of central importance.

Disclosures: Matthew Stuible, Alethia Biotherapeutics

This study received funding from: Alethia Biotherapeutics Inc.

MO0221

Autophagy and Phospho-Inositide Dependent Kinase 1 (PDK1) -Related Kinome in Pagetic Osteoclasts. Stephen McManus*, Martine Bisson, Richard Chamberland, Michèle Roy, Shekeba Nazari, Sophie Roux. University of Sherbrooke, Canada

Background. In Paget's Disease of Bone (PDB), part of the pathology is due to osteoclasts (Ocs) that are increased in size and number, overactive and resistant to apoptosis. We have previously shown that PDK1 associates with p62 and PKC ζ , even prior to RANKL stimulation in pagetic Ocs. Given the established role of PDK1 in the Akt/PKB axis, and because we previously showed an increase in pAkt/Akt levels in pagetic Ocs, we hypothesized that PDK1 may play an important role in the Oc-related kinome regulation, from activation to autophagy (ATG) and survival.

Methods. We used an in vitro human Oc model from peripheral blood monocytes of patients with PDB and healthy donors (40 /group, no p62 mutations).

Results. In immunoblot studies of MAP kinase activation (n=4-6 /group), we observed that in Ocs, pERK/ERK levels were significantly increased in PDB vs. controls (p<0.001), but not pp38/p38 levels. The increased phosphorylation of Akt and of its substrate GSK3 β observed in pagetic Ocs was ablated upon treatment with a PDK1-specific inhibitor. Although inhibition of PDK1 did not affect ERK phosphorylation, it reduced that of RSK2. In addition to their roles in cell survival, both PDK1/Akt and ERK are implicated in ATG regulation. The phosphorylation of 4EBP1 and raptor (mTOR-interacting adaptor), which are both related to mTORC1 activation and ATG inhibition, were increased in pagetic Ocs (p<0.01), and both were reduced upon inhibition of PDK1 in normal and pagetic Ocs (p<0.05), suggesting a PDK1-dependent activation of mTORC1 in PDB Ocs. Using IF studies, LC3B puncta numbers per Oc in basal conditions were increased in pagetic Ocs (p<0.001), but did not further increase in the presence of protease inhibitors compared to controls (n=4/group, 15-20 Ocs each condition). Gene expression analyses (n=26/group) did not reveal any increase in several ATG-associated genes (except *ULK1*) in basal conditions. Finally, deprivation of MCSF and RANKL induced a significant increase in LC3B-II/I ratios in control Ocs, but only in the presence of PDK1 inhibitor in pagetic Ocs (p<0.01).

Conclusion. Our findings suggest that the induction of autophagy might be impeded in pagetic Ocs, which also exhibit defects in late autophagosome maturation. The results also indicate a strong potential regulatory role for PDK1 in Oc stimulatory pathways (Akt, ERK) and ATG induction (via mTORC1), which allow for further exploration of several survival and autophagic pathways in pagetic Ocs.

Disclosures: *Stephen McManus, None.*

MO0222

Cathepsin K deficiency suppresses disuse-induced bone loss. Shuichi Moriya*¹, Yoichi Ezura¹, Yayoi Izu¹, Masaki Noda². ¹TMDU, Japan, ²Tokyo Medical & Dental University, Japan

Unloading induces bone loss and causes disuse osteoporosis. This osteopenic condition is seen when patients are subjected to long term bed rest or they are suffering from neurological diseases. However, the mechanism underlying disuse osteoporosis is still incompletely understood. Here we examined the effects of CatK deficiency on disuse osteoporosis induced by using sciatic neurectomy (Nx) model. Male mice were used in the experiments. Cat-K KO and wild type (Wt) mice were anesthetized and a 5 mm segments of left sciatic nerve and femoral nerve were resected. The right sciatic nerve and femoral nerve were exposed surgically but were not resected. After four weeks of surgery, Cat-K KO and Wt mice were sacrificed and subjected to analysis. For cancellous bone rich region, Nx reduced the BMD compared to the sham operated side in Wt mice. In contrast, CatK deficiency suppressed such Nx-induced reduction of BMD in the proximal tibia. Nx also reduced the BMD in the mid shaft compared to sham side in Wt. In contrast, CatK deficiency suppressed such Nx-induced reduction of BMD in the mid shaft. Bone marrow cells were obtained from these mice were cultured for 3 weeks and the calcified nodules were measured. The area of calcified nodules tended to be slightly reduced by Nx. CatK deficiency reduced the levels of calcified nodule formation compared to wild type in the bone marrow cells obtained from loaded side femur. When the bone marrow cells obtained from Nx side femur were cultured, the levels of the calcified area in culture were increased. For osteoclast development, the levels of TRAP+ osteoclastic cell numbers tended to increase in the Nx side of the Wt mice. The levels of TRAP+ cells in culture was reduced in the CatK deficient bone marrow cells obtained from loaded limb. The levels of TRAP+ cell development in culture was also rescued in the cells obtained from femora of Nx side. Further examination of gene expression indicated that Nx suppressed the expression of genes encoding osteoblast-phenotype-related molecules such as Runx2 and alkaline phosphatase in Wt. In contrast, CatK deficiency suppressed such reduction. With respect to bone resorption markers, RANKL and OPG expression was reduced by Nx in Wt, but CatK deficiency suppressed such reduction. These data indicate that CatK is involved in the disuse-induced bone mass reduction.

Disclosures: *Shuichi Moriya, None.*
This study received funding from: MSD

MO0223

C-reactive protein could promote osteoclastogenesis in rheumatoid arthritis. Sang-Hyon Kim¹, Sang-Heon Lee^{*2}, Young-Il Seo³, Sang-Il Lee⁴, Jinseok Kim⁵, Jung Soo Song⁶. ¹Div. of Rheumatology, South Korea, ²Division of Rheumatology, Konkuk University School of Medicine, Seoul, Republic of Korea, South Korea, ³Division of Rheumatology, Hallym University Medical Center, Ahnang, Republic of Korea, South Korea, ⁴Division of Rheumatology, Department of Internal Medicine, ²Department of Preventive Medicine, Gyeongsang National University School of Medicine, ³Clinical Research Institute, Gyeongsang National University Hospital, Jinju, Republic of Korea, South Korea, ⁵Department of Internal Medicine, Jeju National University Hospital, Jeju, Republic of Korea, South Korea, ⁶Division of Rheumatology, Department of Internal Medicine, Chung-Ang University Medical school, Seoul, Republic of Korea, South Korea

Background: C-reactive protein (CRP) is one of the biomarkers for the diagnosis and assessment of disease activity in rheumatoid arthritis (RA). CRP is not only the by-product of inflammatory response, but also plays pro-inflammatory and pro-thrombotic roles. Objectives: This study aims to determine the role of CRP on bone destruction in RA. Methods: CRP levels in RA synovial fluid (SF) and serum were measured using the immunoturbidimetric method. The expression of CRP in RA synovium was assessed using immunohistochemical staining. CD14+ monocytes from peripheral blood were cultured with CRP, and RANKL expression and osteoclast differentiation were evaluated by using real-time PCR, counting TRAP-positive multinucleated cells and assessing bone resorbing function. CRP-induced osteoclast differentiation was also examined after inhibition of Fc γ receptors. Results: There was a significant correlation between CRP levels serum and SF in RA patients. The SF CRP level was correlated with interleukin(IL)-6 levels, but not with RANKL levels. Immunohistochemical staining revealed that CRP was more abundantly expressed in the lining and sublining areas of the RA synovium, compared with the osteoarthritis synovium. CRP promoted RANKL production in monocytes, which in turn, induced osteoclast differentiation from monocytes and increased bone resorption in the absence of RANKL. Conclusions: CRP could play an important role in the bony destructive process in RA through the induction of RANKL expression and direct differentiation of osteoclast precursors into mature osteoclasts. In the treatment of RA, lowering CRP levels is a significant parameter not only for improving disease activity but also for preventing bony destruction.

Disclosures: *Sang-Heon Lee, None.*

MO0224

Molecular Mechanism of Hyponatremia-Induced Osteoporosis. Julia (Julianna) Barsony*¹, Qin Xu², Joseph G Verbalis². ¹Georgetown University Hospital, USA, ²Georgetown University Medical Center, USA

Both animal and human studies have indicated that chronic hyponatremia (CH) increases fracture frequency in patients by inducing excess bone resorption and loss of bone mineral density and by impairing balance and increasing falls. The high prevalence of CH in the aging population due to comorbidities, medication use and the syndrome of inappropriate antidiuretic hormone secretion highlights the public health importance of CH-induced osteoporosis. Prior studies indicated that some of CH effects are mediated by direct signaling of low extracellular sodium concentration ([Na⁺]) to osteoclasts and neuronal cells. However, the [Na⁺] sensing and signaling mechanisms have not yet been elucidated. In these studies, we identified [Na⁺] responses in cultured murine primary osteoclastic cells, RAW264.7 derived osteoclasts, and murine neuroblastoma N2a cells. Rapid effects of [Na⁺] on mature osteoclasts included change of cell shape within one minute, lysosome acidification and shift to the ruffled border membrane within 5 minutes, increased actin ring formation within 2h, increased cell motility in a Boyden chamber, and increased mitochondrial ATP production within 24 hours. Consistent with CH-induced osteoclastogenesis, gene expression changes detected by whole genome microarray and qRT-PCR in osteoclastic cells consistently included upregulated expression of Slc8A1 sodium/calcium exchanger, Igf1, Vnt6, Mmp9, Mmp12, Mmp14, Tnf, Rex2 Apc2, and Myc1 and downregulated expression of the AVP receptor 1. Neuronal cells also responded with rapid gene expression changes to culture in low [Na⁺] media (upregulation of Tgfb1, Dram1, Tnf, Igf1, and downregulation of Sqstm1). Western blot analyses detected protein phosphorylation changes proportional to reduction in media [Na⁺], consistent with immediate activation of osteoclastogenesis. These results indicate that a membrane receptor mediated signaling pathway directly mediates hyponatremia induced target cell responses, leading to increased bone fragility and neurological deficits. Our rat studies indicated that CH also decreases bone formation, and we have observed that patients with CH generally have very low serum osteocalcin levels. However, the lack of effects of low [Na⁺] on cultured osteoblasts suggests that the effects of CH on bone formation may be indirect. These combined results provide a better understanding of the mechanisms that contribute to hyponatremia-induced osteoporosis and fall and fracture risks.

Disclosures: *Julia (Julianna) Barsony, None.*

MO0225

Role of Becn1 ubiquitination in RANKL-mediated osteoclastogenesis. Atsushi Arai¹, Sol Kim¹, Teresa Kim¹, Cindy Lee¹, Cun-Yu Wang¹, No-Hee Park¹, Reuben Kim^{2*}. ¹UCLA School of Dentistry, USA, ²UCLA, USA

Purpose: During osteoclastogenesis, RANKL activates osteoclast precursors to undergo differentiation to form multinucleated osteoclasts. Autophagic process, an important cellular mechanism that becomes activated under stress such as starvation, is recently shown to be involved in osteoclasts. However, the precise role of autophagy in normal physiological process of osteoclastogenesis is not clear. Here, we investigated role of autophagy and Becn1, a protein involved in autophagy initiation, during osteoclastogenesis upon RANKL stimulation. **Methods:** Bone marrow (BM) and RAW 264.7(RAW) cells were used to undergo osteoclastic differentiation upon RANKL treatment. Osteoclastic and autophagic genes were examined in a time-dependent manner using qRT-PCR and Western blotting. Protein expression of LC3B, a marker for autophagy, was monitored using Western blotting and confocal microscope. Bone resorptive functions were evaluated using dentin slices. Becn1 phosphorylation and ubiquitination at S14 and K117, respectively, were examined. Becn1 mutants, S14D, S14A, and K117R, were retrovirally overexpressed in RAW cells, and osteoclast differentiation was evaluated. TRAF6 was knocked down using siRNA, and ubiquitination of Becn1 was examined. **Results:** RANKL-treated BM and RAW cells exhibited significant increases in autophagic genes, LC3B protein expression and punctae in a time-dependent manner. Overexpression of Becn1 in RAW cells increased osteoclast differentiation and functions. Modulating S14 site of Becn1 did not have any effects on osteoclastic differentiation. However, RANKL treatment induced ubiquitination of Becn1. Knockdown of TRAF6 or overexpression of ubiquitination-incompetent Becn1-K117R resulted in suppression of Becn1 ubiquitination and osteoclastogenesis. **Conclusion:** Autophagy is physiologically important process during the RANKL-mediated osteoclastogenesis, and Becn1 may be a potential therapeutic target for managing osteoclast-specific bone-related diseases.

Disclosures: Reuben Kim, None.

MO0226

Smad4 In Osteoclasts Reduce Bone Mass by Inhibiting Osteoclast Differentiation. Mayu Morita^{1*}, Ryotaro Iwasaki², Hiromasa Kawana², Shigevuki Yoshida², Taneaki Nakagawa², Takeshi Miyamoto³. ¹Keio University, Japan, ²Division of Oral & Maxillofacial Surgery, Department of Dentistry & Oral Surgery, Keio University School of Medicine, Tokyo, Japan, ³Department of Orthopedic Surgery, Keio University School of Medicine, Tokyo, Japan, Japan

Background: Bone remodeling maintains constant bone mass by a delicate balance between bone-resorption followed by bone-formation. TGFβ1 is one of the TGFβ superfamily ligands including TGFβ1-5 and bone morphogenetic proteins (BMPs), and transduces their signals by binding to their specific receptors via receptor-regulated Smads (R-Smads), Smad2/3 and Smad1/5/8, respectively, and subsequently R-Smads form oligomers with common-mediator Smad, Smad4. Smad4 was reportedly played pivotal roles for mesenchymal stem cell migration and bone formation, role of Smad4 on osteoclasts remain largely unknown. Thus, objects of our study are to clarify the roles of Smad4 on osteoclasts.

Methods: Osteoclast specific Smad4 conditional knockout mice (*Ctskcrel+Smad4fl*) were generated, and *Ctskcrel+Smad4fl/fl* and control littermates were analyzed. 8 wk old mice were necropsied, and their hind limbs were removed, fixed with 70% ethanol, and subjected to DEXA analysis to measure bone mineral density and to bone histomorphometric analysis.

Results: We found that osteoclast-specific Smad4 conditional knockout mice exhibited significant reduction of bone mass with elevated osteoclast formation compared to controls.

Our data demonstrate that Smad4 in osteoclasts is required to inhibit osteoclastogenesis to maintain bone mass *in vivo*.

Disclosures: Mayu Morita, None.

MO0227

Pentosan Polysulfate Sodium Suppress RANK Ligand Induced Osteoclast Differentiation via IL-1R/TLR Signal Transduction Involving Fos-Jun/AP-1 Transcriptional Regulator Complex Repression. Suranji Wijekoon*, Sangho Kim, Jing Fang, Eugene C. Bwalya, Kenji Hosoya, Masahiro Okumura, Hokkaido University, Japan

One of the most important transcription factor complexes that is activated by RANKL/TRAF signals is Fos-Jun/AP-1 in osteoclastogenesis (OCLG). It is induced in rheumatoid arthritis (RA) by immunoregulatory molecules and provide valuable drug target for RA. It was newly recognized that beech wood derived pentosan polysulfate sodium (PPS) has an effect on osteoarthritis to reduce pain and inflammation. But mechanism of action of PPS over the OCLG and osteoclasts function is not fully understood. The purpose of the current study was to investigate the effect of PPS on inflammatory reaction of osteoclasts. Bone marrow derived

hematopoietic stem cells from five healthy dogs were treated for OCLG. After interleukin (IL)-1β stimulation for the fusion and survival of osteoclast, PPS, polysulfated glycosaminoglycan (PSGAG) and heparin (0.2, 1, 5 μg/ml) were supplemented. Specific genes expression such as carbonic anhydrase, cathepsin-k, MMP9 and c-fos, intracellular incursion of PPS, nuclei/cell and area/cell ratio were examined after completion of the differentiation by quantitative PCR, fluorescence assay and TRAP staining respectively. Even expression of carbonic anhydrase, cathepsin-k and c-fos were significantly (p<0.05) suppressed by PPS, effect of PSGAG and heparin were not significant. The master switch for regulating terminal differentiation of osteoclasts, NFATc1 was significantly down regulated by PPS and heparin at the concentration of 5 μg/ml. In this present study, IL-1 influenced MMP9 synthesis by osteoclasts was certainly reduced in significant (p<0.05) manner by three types of treatments at the concentration of 5 μg/ml. Even there was decline of AP1 gene expression with heparin in concentration dependent pattern, significant (p<0.001) effect were detected from PPS at 5 μg/ml. Comparative to PSGAG and heparin, significant genomic suppression of AP-1 thus altering of nuclei/cell and area/cell ratio in significantly (p<0.05) was perceived with PPS. The fluorescence images of interaction of PPS and c-Jun interface more endorsed that intra-nuclear invasion of PPS and effects on transcription factors. In conclusion, those outcomes have been revealed that the inhibitory effect of PPS on signaling components within the RANKL transduction pathway could moderate Fos-Jun/AP-1 transcriptional regulator complex expression and activation while stimulation of IL-1R/TLR. This manner of suppression of OCLG by PPS would be a novel therapeutic approach for RA.

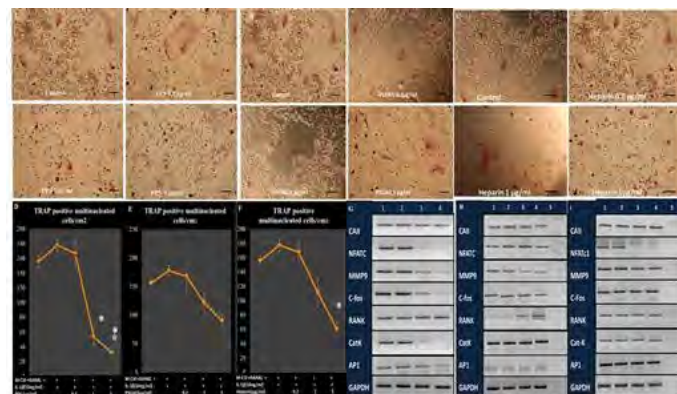


Figure 1: PPS suppresses API, c-Fos, MMP9 and NFATc1 activity but not alter RANK expression in bone marrow differentiated osteoclasts. M-CSF/RANKL induced osteoclasts formation and their morphology was altered in different degree by PPS, PSGAG and heparin treatments. A,B,C- PPS, PSGAG and heparin treatment respectively reduced osteoclasts formation. Bone marrow cells were differentiated in to osteoclasts by M-CSF/RANKL and treated with PPS, PSGAG, heparin for 7 days and then TRAP stained. Scale bar size 50 μm. D, E, F- TRAP stained multinucleated giant cells/cm² after treatment of PPS, PSGAG and heparin concentration of 0.2, 1 and 5 μg/ml. Number of osteoclasts significantly reduced at the concentration of 1 and 5 μg/ml of PPS and 5 μg/ml of heparin. Data expressed as mean ± standard deviation (n=5) for each value. * p<0.05, ** p<0.01 value expression relative to positive control that was stimulated by IL-1 without any treatment. G,H,I- Gel electrophoresis image shows the effect of PPS, PSGAG and heparin treatment on osteoclast specific genes: CAII: carbonic anhydrase, NFATc1, MMP9, c-Fos, RANK, CatK: cathepsin k, API: activator protein 1 and GAPDH housekeeping gene (1: Positive control, 2: 0.2, 3: 1, 4: 5 μg/ml, 5: Negative control)

Morphological and genomic expression of osteoclasts after treatment of PPS, PSGAG and heparin

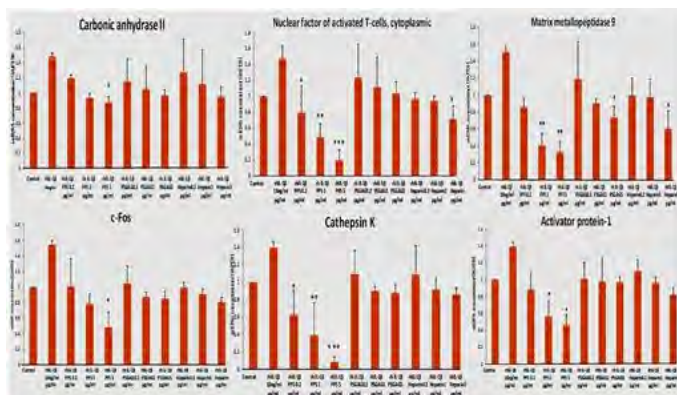


Figure 2: PPS regulates the mRNA level of API, c-Fos, NFATc1 and their target genes during osteoclastogenesis of bone marrow derived monocytes (BMDM). Isolated hematopoietic stem cells after 48 hours culture of BMDM were cultures in the presence of M-CSF (20 ng/ml), RANKL (50 ng/ml) and IL-1β (10 ng/ml) for 10 days with or without PPS, PSGAG and heparin (0.2, 1, 5 μg/ml) separately. mRNA expression of osteoclasts specific genes were quantitatively analyzed by quantitative real-time polymerase chain reaction. MMP9 was significantly down regulated by all treatment groups. When heparin suppresses the activity of NFATc1 at 5 μg/ml PPS is done it by all 3 concentrations. Carbonic anhydrase and cathepsin K genomic expressions are results of activation of transcription factors. Data expressed as mean ± standard deviation (n=5) for each concentration after normalizing for the expression of the housekeeping gene GAPDH. * p<0.05, ** p<0.01, *** p<0.001. Gene expression relative to osteoclasts stimulated with rhIL-1β alone.

Quantitative and comparative assessment of osteoclasts specific genes expression after treatment

| A | Control (n=38) | | PPS (n=46) | | Heparin (n=44) | | PSGAG (n=47) | |
|----------------------|----------------|-------|------------|---------|----------------|---------|--------------|---------|
| | Mean | SEM | Mean | SEM | Mean | SEM | Mean | SEM |
| Nuclei/Cell | 28.18 | 4.2 | 9.10* | 1.87 | 14.11 | 2.09 | 21.06 | 3.5 |
| Area μm^2 | 60800 | 14810 | 18700* | 3887.47 | 26300 | 6058.30 | 37310 | 7310.41 |

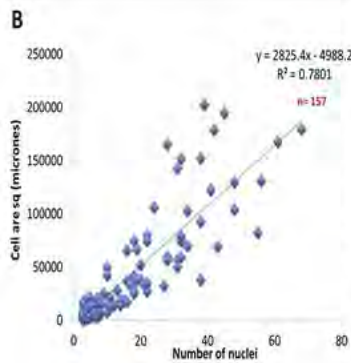


Figure 3: Cell fusion was significantly affected by PPS (5 $\mu\text{g}/\text{ml}$) compared with control where PPS was not added. PPS appears to down-regulate RANKL-induced c-Jun/Fos AP1 transcriptional regulator complex that is one of the most important factors for activating cell fusion and osteoclast differentiation. Hematopoietic stem cells isolated from cultured BMM after 48hours were supplemented with M-CSF, RANKL and IL-1 β and treat with PPS, PSGAG and heparin for 10 days. TRAP stained osteoclasts were analyzed using Image-J software for cell area and nuclei. A- Mean value of nuclei/cell and area of cell after treatment of PPS, PSGAG and heparin in 5 $\mu\text{g}/\text{ml}$ concentration. B- Relationship between nuclei number and cell area of the osteoclasts. There was a positive correlation between those two factors. a: p < 0.05. Values relative to osteoclasts stimulated with rhIL-1 β alone.

| Target gene | Sense and anti-sense (5-3) | Annealing temperature($^{\circ}\text{C}$) | Product (bp) |
|-----------------------|----------------------------|---|--------------|
| Carbonic anhydrase II | AAGGAGCCCATCAGCGTTAG | 59.82 | 104 |
| | GGGCGCCAGTTATCCATCAT | 60.25 | |
| NFATC1 | CACAGGCAAGACTGTCTCCA | 56.9 | 176 |
| | TCCTCCAATGTCTGTCTCC | 67.9 | |
| MMP9 | GGCAAATCCAGACCTTTGA | 56.4 | 166 |
| | TACACGCGAGTGAAGGTGAG | 53.4 | |
| c-Fos | GTCCTACAGACCACAGACC | 59.76 | 192 |
| | CGCTCCACTTCATTGTGCTG | 59.83 | |
| Cathepsin K | ACCCATATGTGGGACAGGAT | 57.79 | 169 |
| | TGGAAAGAGGTCAGGCTTGC | 60.25 | |
| Activator protein I | TCTACGACGATGCCCTCAAC | 59.56 | 159 |
| | TGAGCAGGTCCGAGTTCCTG | 59.65 | |

Table 1: Primes use to polymerize the osteoclast-specific function genes.

Quantitative valuation of morphological changes of osteoclasts after treatment

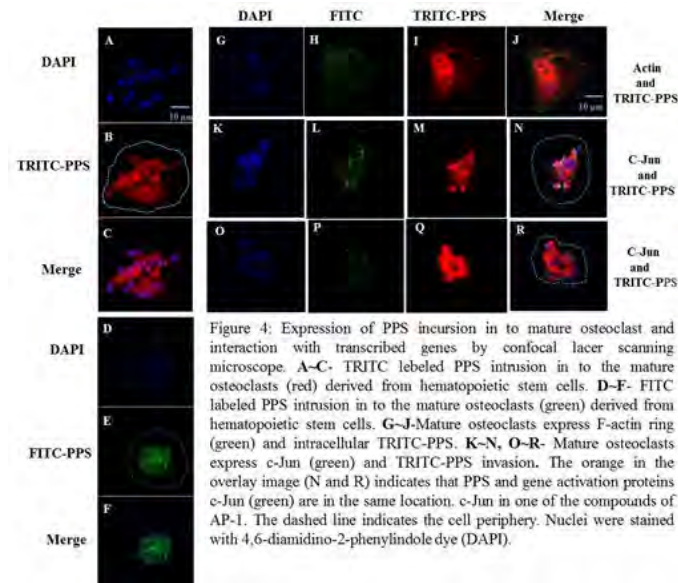


Figure 4: Expression of PPS incursion in to mature osteoclast and interaction with transcribed genes by confocal laser scanning microscope. A-C- TRITC labeled PPS intrusion in to the mature osteoclasts (red) derived from hematopoietic stem cells. D-F- FITC labeled PPS intrusion in to the mature osteoclasts (green) derived from hematopoietic stem cells. G-J-Mature osteoclasts express F-actin ring (green) and intracellular TRITC-PPS. K-N, O-R- Mature osteoclasts express c-Jun (green) and TRITC-PPS invasion. The orange in the overlay image (N and R) indicates that PPS and gene activation proteins c-Jun (green) are in the same location. c-Jun in one of the components of AP-1. The dashed line indicates the cell periphery. Nuclei were stained with 4,6-diamidino-2-phenylindole dye (DAPI).

Fluorescence image of PPS invasion and interaction with transcribed genes in osteoclasts

Primers of osteoclasts specific function genes

Disclosures: Suranji Wijekoon, None.

MO0228

Withdrawn.

MO0229

DICAM attenuates macrophage differentiation via suppression of integrin $\alpha\text{V}\beta\text{3}$ -dependent Akt-Foxo3a-Irf7 pathway. Gunwoo Kim^{*1}, Youn-Kwan Jung², Seung-Woo Han³, Min-Su Han², Eun-Ju Lee², Hye-Ri Park², Ji-Ae Jang², Dong-Ju Shin⁴. ¹Fatima Research Institute & Daegu Fatima Hospital, Daegu, Republic of Korea, South Korea, ²Fatima Research Institute, Daegu Fatima Hospital, South Korea, ³Department of Internal Medicine, Daegu Fatima Hospital, South Korea, ⁴Department of Orthopedics, Daegu Fatima Hospital, South Korea

DICAM, a dual Ig domain containing adhesion molecule, is involved in cell-cell adhesion through a direct interaction with $\alpha\text{V}\beta\text{3}$ integrin. In our previous study showing the inhibitory role in osteoclastogenesis, we found a clue that DICAM also has a suppressive role in macrophage differentiation. To investigate the role of DICAM in macrophage differentiation, we induced the differentiation of macrophage from THP-1 cells by treatment of PMA for 3 days. Also we investigated the gain or loss of function of DICAM during THP-1 macrophage differentiation by infection of adenovirus or lentivirus system respectively. The expression of DICAM was decreased during PMA-induced THP-1 differentiation at day1, and increased time-dependently. The overexpression of DICAM in THP-1 cells suppressed PMA-mediated macrophage differentiation in the number of activated branched macrophage and macrophage marker expression, CD14 and CD68. However, DICAM does not affect the viability and proliferation of PMA-stimulated THP-1 macrophage. Functionally, DICAM attenuated the TNF- α secretion of differentiated THP-1 cells and their phagocytic activity as well. To investigate the molecular mechanisms for DICAM-mediated suppression of macrophage differentiation, we conducted microarray analyses, which revealed that overexpressed DICAM significantly suppressed type 1 interferon system. Among interferon regulatory factors (IRFs) family, IRF7 was most significantly reduced by DICAM. DICAM also attenuated Akt activation and increased a nuclear translocation of FoxO3a that is known to be a critical negative regulator of IRF7. Consistently, DICAM also decreased total integrin β3 level and integrin-linked kinase (ILK) phosphorylation, the major adaptor molecule of integrin β3 . Overexpression of integrin β3 in DICAM-mediated inhibition of THP1 differentiation rescued the expression of macrophage differentiation markers partially. These results show that DICAM potentially reduces differentiation and function of THP-1 macrophage via suppression of integrin $\alpha\text{V}\beta\text{3}$ -dependent Akt-FoxO3a-IRF7 pathway.

Disclosures: Gunwoo Kim, None.

MO0230

Intravenous Immunoglobulin (IVIG) Attenuates TNF-induced Pathologic Bone Resorption and Suppresses Osteoclastogenesis by Inducing A20 Expression. Min Joon Lee*, Elisha Lim, Shwan Mun, Lionel Ivashkevich, Kyung-Hyun Park-Min. Hospital for Special Surgery, USA

Intravenous immunoglobulin (IVIG) treatment is an effective therapy in various autoimmune and chronic inflammatory diseases by suppressing autoantibody- and immune complex-mediated pathogenesis. Several possible mechanisms for the action of IVIG have been suggested, yet the component of IVIG that mediates the suppression of inflammation is not well understood. Many inflammatory diseases such as rheumatoid arthritis are often accompanied by excessive bone resorption but the effect of IVIG on osteoclasts, bone-resorbing cells, has not been studied. Thus, we investigated whether IVIG directly regulates osteoclast differentiation and has therapeutic potential for suppressing osteoclast-mediated pathologic bone resorption. For osteoclast differentiation, receptor activator of nuclear factor-kappa B ligand (RANKL) and macrophage colony-stimulating factor (M-CSF) are essential. IVIG suppressed RANKL-induced osteoclastogenesis and expression of osteoclast-related genes such as integrin $\beta 3$ and cathepsin K in a dose-dependent manner by downregulating RANKL-induced expression of NFATc1, the master regulator of osteoclastogenesis. IVIG functions by interacting with Fc γ Rs (Fc γ RIa, Fc γ RIIa, Fc γ RIb, and Fc γ RIIIa) and we have found that the engagement of Fc γ RIIIa with IVIG is important for the IVIG-mediated suppression of human osteoclastogenesis. Interestingly, unbiased transcriptomic analysis revealed novel negative regulators that are induced by IVIG. A20 is a well-known NF- κ B signaling inhibitor and the expression of A20 is increased by IVIG. Strikingly, the siRNA-mediated deletion of A20 has reversed the suppressive effect of IVIG. Consistent with our observation, IVIG suppressed NFATc1 expression by attenuating RANKL-induced NF- κ B signaling, explained in part by the induction of A20. Our in vitro observation was further corroborated in our in vivo model; IVIG administration attenuated in vivo osteoclastogenesis and suppressed bone resorption in the tumor necrosis factor (TNF)-induced calvarial osteolysis model. Take together, our findings show that, in addition to suppressing inflammation, IVIG directly inhibits osteoclastogenesis through a mechanism involving suppression of RANK signaling. Our results suggest that direct suppression of osteoclast differentiation may provide beneficial effects on preserving bone mass when IVIG is used to treat rheumatic disorders.

Disclosures: Min Joon Lee, None.

MO0231

Proliferation-coupled osteoclast differentiation by RANKL. Sunao Takeshita*, M. Motiur Rahman, Kyoji Ikeda. National Center for Geriatrics & Gerontology, Japan

During a 4-day course of osteoclastogenesis ex vivo from bone marrow macrophages (BMMs) stimulated with M-CSF and RANKL, BMMs proliferate actively during the first half (0-48h), followed by cell-cycle arrest, cell fusion, and formation of multinucleated osteoclasts in the latter half. Although it is generally thought that osteoclast differentiation induced by RANKL is linked to the anti-proliferative activity of the cytokine, we have found that RANKL in the presence of M-CSF actually stimulates DNA synthesis and cell proliferation during the first-half proliferative phase (0-48h), while the same cytokine exerts an anti-proliferative activity in the latter half (48-96h). Inhibition of DNA synthesis with hydroxyurea (HU) during the first half almost completely inhibited osteoclastogenesis, as reported. However, the same HU-treated cells, when re-plated at 48h at increasing cell densities, restored osteoclast formation at 96h, suggesting that a sufficient number of cells, rather than prior DNA synthesis per se, is critical for osteoclast formation. In fact, when BMMs were plated at varying cell densities at 0h, 5×10^3 cells/96-well was optimal for osteoclast formation assessed on day 4, while $10-30 \times 10^3$ cells/96-well had given rise to mature functional osteoclasts already on day 3, most of which died by day 4. Interestingly, this accelerated differentiation with increased cell densities was not associated with up-regulation of osteoclastogenesis-related gene expression, suggesting that cells respond to RANKL with very similar gene expression patterns irrespectively of cell density, and that the accelerated osteoclastogenesis is not ascribed to an acceleration of the intrinsic genetic program. 5×10^3 BMMs are supposed to give rise to 20×10^3 pre-osteoclasts (preOCs) after two rounds of cell cycling for 48h. Evidently, when varying numbers of preOCs were plated on day 2, 20×10^3 cells/96-well, but neither lower or higher cell density, yielded the most osteoclasts on day 4. Taken together, it is suggested that proliferation of BMMs during the first half is important to secure a sufficient number of preOCs, that during the second half, a cell density of preOCs is critical for the formation of multinucleated osteoclasts, in which a stochastic factor, such as increased chances for preOCs to contact each other, is important for cell fusion and generation of multinucleated osteoclasts.

Disclosures: Sunao Takeshita, None.

MO0232

Small leucine-rich proteoglycans may regulate osteoblast-osteoclast coupling through TNF-alpha sequestration. Vardit Kram*, Tina Kilts, Nisan Bhattacharyya, Marian Young. Craniofacial & Skeletal Diseases Branch, NIDCR, NIH, USA

Biglycan (Bgn) and Fibromodulin (Fmod) are two subtypes of the small leucine-rich family of proteoglycans, which are known to be highly expressed in the extracellular matrix (ECM) of bone and cartilage. They are known to regulate osteoblast proliferation and activity. Previously, we have shown that *Bgn/Fmod* double knockout (*Bgn*^{-/-}; *Fmod*^{-/-} DKO) have a low bone mass (LBM) phenotype, mis-articulation of joints, early onset osteoarthritis as well as ectopic bone formation and tendon ossification. In addition, by 5 weeks of age, the *Bgn*^{-/-}; *Fmod*^{-/-} DKO have increased osteoclast number and activity as can be seen by TRAP staining and pit formation assays. Tumor necrosis factor α (TNF- α), a multifunctional proinflammatory cytokine produced by a wide variety of immune and epithelial cells, has been shown to stimulate osteoclastogenesis in a RANKL independent manner by activating nuclear-factor of activated T-cell c1 (NFATc1), the master transcription factor in osteoclast differentiation. Moreover, TNF- α activation suppresses both RUNX2 transcription as well as MAPK-mediated osteoclast expression and its promoter activity in bone marrow stromal cells (BMSCs). Using solid phase binding assays as well as co-immunoprecipitation (co-IP), we show that both Bgn and Fmod directly bind TNF- α in a dose dependent manner. qPCR analysis of RNA extracted from primary osteoclast cultures derived from *Bgn*^{-/-}; *Fmod*^{-/-} DKO mice indicate increased expression of several osteoclast marker genes. Because neither Bgn nor Fmod are expressed by osteoclasts, we extracted RNA from CD45⁺ and CD11b⁻ (macrophage depleted) BMSCs and found elevated levels of TNF- α , DKK1 and RANKL in the RNA derived from *Bgn*^{-/-}; *Fmod*^{-/-} DKO mice. Additionally, increased levels of pDKK1, a NF κ B inhibitor, were found in protein isolated from *Bgn*^{-/-}; *Fmod*^{-/-} DKO BMSCs. Since soluble TNF- α can induce osteoclast differentiation and survival as well as suppress bone formation, we propose that Bgn and Fmod made by the BMSCs are novel coupling ECM components that serve to regulate osteoclast differentiation through TNF- α sequestration and therefore regulation of its bioavailability

Disclosures: Vardit Kram, None.

MO0233

TNF Promotes Osteoclastogenesis by Inducing M1 Macrophage Formation and Limits it through RelB Inhibition of NFATc1 Activity. Xiaodong Hou*¹, Zhijun Zhao², Chunyu Wang³, Xiaoxiang Yin², Yanyun Li¹, Rong Duan¹, Brendan F Boyce¹, Zhenqiang Yao¹. ¹University of Rochester, USA, ²Henan University First Affiliated Hospital, China, ³The First Hospital of Shangqiu City, China

TNF mediates osteoclast (OC) formation directly and indirectly, but it also limits OC formation by inducing expression of the inhibitory NF- κ B protein, p100. OC precursors (OCPs) are derived from cells classified as M1 (inflammatory) and M2 (resident) macrophages (Mac). However the mechanisms whereby TNF stimulates or limits OC formation, if these are through regulation of M1 and M2 differentiation, and if RelB (a partner of p100) is involved are poorly understood. We treated WT mouse bone marrow (BM) cells with M-CSF or M-CSF+TNF to enrich for OCPs, which we called M-OCPs and T-OCPs, resp. TNF inhibited RANKL-induced NFATc1 mRNA expression and OC formation from M-OCPs, but it stimulated OC formation from RANKL-treated T-OCPs. FACS showed that CD11b⁺F4/80⁺Gr1⁻Ly6C⁺ and CD11b⁺F4/80⁺Gr1⁻Ly6C⁻ cells comprised 38% & 68% of M-OCPs and 53% & 30% of T-OCPs, resp. After sorting, Gr1⁻Ly6C⁺, but not Gr1⁻Ly6C⁻, M-OCPs formed OCs in response to RANKL, while both cell types from T-OCPs formed more OCs than from M-OCPs (503 \pm 38 and 360 \pm 12 from T-OCPs vs. 125 \pm 16 and 0 from M-OCPs). Levels of M1 markers, iNOS and TNF, were 7-10-fold higher in Gr1⁻Ly6C⁺ T-OCPs than in Gr1⁻Ly6C⁻ T- and M-OCPs. TNF increased RelB mRNA and protein levels by 9- and 40-fold, while RANKL reduced RelB protein level (it also increased RelB mRNA). The proteasome inhibitor, MG-132, increased RelB protein by 7-fold in RANKL-treated M-OCPs. Importantly, in response to TNF, Gr1⁻Ly6C⁺ and Gr1⁻Ly6C⁻ cells from RelB^{-/-} BM cells comprised 24% and 54%, resp. of the CD11b⁺F4/80⁺ population vs 68% and 31% in WT cells. Overexpression of RelB in M-OCPs reduced RANKL-induced OC# (412 \pm 14 vs. 572 \pm 14 in GFP controls) and NFATc1 mRNA expression, while it increased TNF-induced OC# (412 \pm 24 vs. 17 \pm 5 GFP) without changing low NFATc1 mRNA levels. Transfection of RelB alone or with RelA or p52 reduced NFATc1 luciferase reporter activity. In summary: TNF inhibits RANKL-induced OC formation from M-CSF-primed OCPs, but promotes it from TNF-primed OCPs; TNF switches M-CSF induced Gr1⁻Ly6C⁻ to Gr1⁻Ly6C⁺ M1 Mac, which have enhanced OC forming potential; induction of RelB is required for TNF-induced Gr1⁻Ly6C⁺ M1 cell formation; RelB inhibits NFATc1 activity to inhibit OC formation and RANKL degrades RelB. We conclude that TNF induction of RelB enhances OC formation by promoting M1 Mac differentiation, which is independent of NFATc1, and blocking M1 Mac formation could be a novel strategy to limit OC formation.

Disclosures: Xiaodong Hou, None.

MO0234

Twisted gastrulation-deficient osteoclast precursors are hypersensitive to RANKL and M-CSF due to changes in RANK and C-fms Expression. Melissa Stemig^{*1}, Raphael Huntley², Anna Petryk³, Kim Mansky², Rajaram Gopalakrishnan², Eric Jensen². ¹University of Minnesota School of Dentistry, USA, ²University of MN School of Dentistry, USA, ³University of MN School of Medicine, USA

Mice deficient for the BMP antagonist Twisted gastrulation (*Twsg1*) are osteopenic due to enhanced osteoclastogenesis mediated through increased BMP signaling. Culturing of bone marrow osteoclast precursors from *Twsg1*-deficient mice in RANKL and M-CSF is characterized by larger and increased number of osteoclasts compared to wild type mice. In the current study, we tested whether osteoclast precursors from *Twsg1*-deficient mice are hypersensitive to RANKL and M-CSF. Bone marrow derived osteoclast precursors from *Twsg1*-deficient and wild type mice were cultured with the concentration of M-CSF progressively increased while that of RANKL remained constant. In other cases, RANKL, but not M-CSF was varied. In both circumstances, the level of the invariant cytokine was below that used in our standard osteoclastogenic assays. Osteoclastogenesis was determined by TRAP staining. At all concentrations of RANKL and M-CSF osteoclasts derived from the *Twsg1*-deficient mice were both larger and had more nuclei per cell when compared to wild type cells. This increased sensitivity was more evident at lower concentrations of RANKL and M-CSF. Through immunostaining and flow cytometry, we determined that there was no difference in the proportional subpopulation of osteoclast precursors in *Twsg1*-deficient bone marrow compared to wild type mice. The hypersensitivity could be explained by the increased expression of *RANK* and *c-fms*, receptors for RANKL and M-CSF that we measured in *Twsg1*-deficient osteoclast precursors by real time RT-PCR. The transcription factors MTF and PU.1 have been shown to regulate the expression of *RANK* and *c-fms* in osteoclasts. Experiments are currently underway to determine if the increase in *RANK* and *c-fms* expression in *Twsg1*-deficient osteoclasts is due to changes in activity of MTF or PU.1. Additionally, we are performing starve/stimulate experiments with osteoclast precursors from wild type and *Twsg1*-deficient mice using either M-CSF or RANKL to determine which signaling pathway(s) are responsible for the hypersensitivity we observe in culture.

Disclosures: Melissa Stemig, None.

MO0235

Direct roles of osteocyte in bone mineralization and weightless-caused bone loss: beyond mechanosensors. Yuan Hui^{*1}, Rong Zhang², Yinshi Ren¹, Ying Liu¹, Jingya Wang¹, Lynda Bonewald³, Weiping Qin⁴, Jian.Q Feng². ¹Department of Biomedical Science, Texas A&M Baylor College of Dentistry, USA, ²Department of Biomedical Sciences, Texas A&M Baylor College of Dentistry, USA, ³University of Missouri-Kansas City School of Dentistry, USA, ⁴Medicine, Mount Sinai School of Medicine Researcher, James J. Peters VA Medical Center, USA

For many decades the osteocyte (Ocy) has been considered a "retired" bone builder with limited roles, such as a mechanosensor, despite its ideal anatomic location, huge cell numbers and large surfaces that are perfect for forming mineralized bone matrices. On the other hand, osteoclasts are considered to be responsible for weightless-caused bone loss, but they can't address a very basic fact: surface cells do not penetrate into the deep cortical bone. Using acid-etched and backscattered SEM, we found a close relationship between Ocy maturation and bone mineralization. The mature Ocy volume was reduced by 50% while its surface was >50% more due to increased dendrites, leading to the replacement of the decreased cell volume by minerals present in individual spheres and sheets (Fig 1). Confocal microscopy of DAPI nuclear-stained bone, labeled with calcein and alizarin red, clearly demonstrated the mineral deposition in the matrix surrounding the Ocy and at the mineralization front surrounding the Ocy canaliculi (Fig 1). To address the role of Ocy in weightless-related bone loss (induced by tail suspension for 4 weeks), we analyzed the tail-suspended long bone compared to the control using X-ray and FITC-confocal images. The tail-suspended long bone showed a minor reduction in bone thickness in radiographs but great changes of Ocy morphologies by FITC, in which Ocy lacunae appear much larger. The distribution of the Ocy is less organized, and the canaliculi are crooked and randomly oriented (Fig 2). Quantitative RT-PCR analyses in unloading bone showed: 1) an increase in osteoclast markers as observed in lactated long bone (osteolysis), with ~3 fold increase of *Trap*, ~5 fold increase of cathepsin K and ~3.5 fold increase of *Mmp13*; and 2) changes of Ocy marker, ~4 fold increase of sclerostin (Fig 2). Similar but more severe Ocy changes occurred in a rat model of spinal cord injury-induced bone loss (Fig 3). Finally, we showed demineralization by backscattered SEM images and remineralization by calcein-alizarin red stained confocal images in the same dog long bone slide (Fig 4). Collectively, these data indicate that Ocy is the key cells to maintain bone mineralization and remodeling in cortical bone, and that poorly-maintained bone remodeling due to the defective Ocy plays a key pathological role in weightless-caused bone loss. Thus, we propose that Ocy plays novel roles in bone remodeling beyond merely a simple role as mechanosensors.

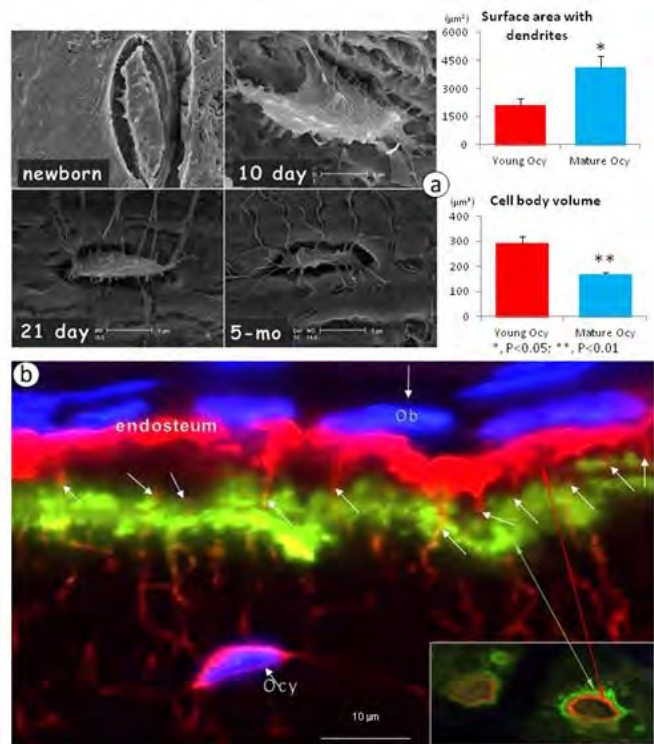


Figure 1. Bone mineralization is directly linked to osteocyte. (a). Acid-etching SEM shows mouse calvaria osteocyte maturation from newborn to 5 months of age. As it matures osteocyte volume was close to 50% reduced, but its surface was >50% increased, due to increased dendrites, leading to replacement of the decreased cell volume by well-defined mineral. (b). Double labeling + Dapi staining by confocal shows mineral deposition in the matrix surrounding the Ocy and at the mineralization front surrounding Ocy canaliculi.

Figure 1.

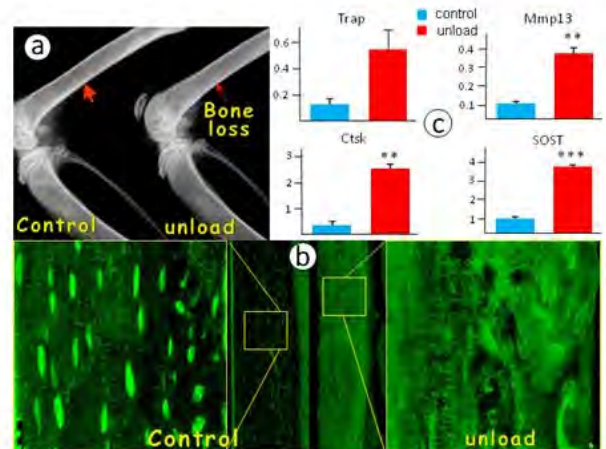


Figure 2. Unloading in mice lead to altered osteocytes morphology and increased bone resorption. (a). X-ray shows thinner cortical bone in unloaded mouse femurs. (b). FITC staining by confocal microscope reveals great changes of osteocyte morphologies, in which osteocyte lacunae appear much larger, the distribution of the osteocytes are less organized and the canaliculi are somewhat crooked and more randomly oriented. In contrast, the osteocyte lacunae in the control cortical bone appear highly organized and regularly spaced apart, generally in linear arrays. Furthermore, the canaliculi are mostly straight and run perpendicular to the long axis of the osteocyte. (c). RT-PCR quantitatively shows significantly higher expression of osteoclast markers by osteocytes like *Trap* and cathepsin K and osteocyte marker like *SOST*.

Figure 2

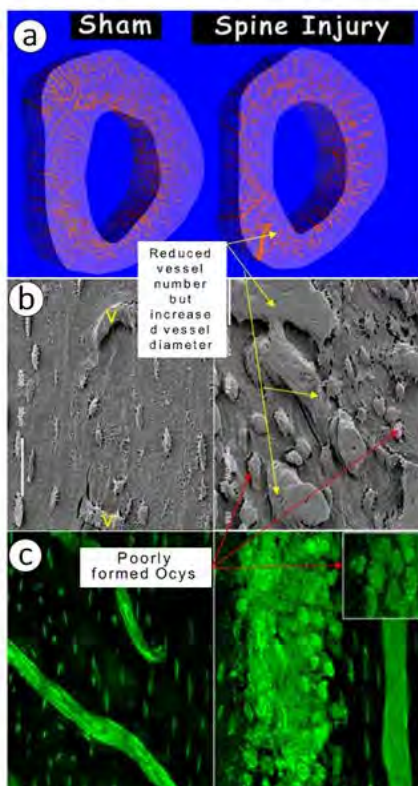


Figure 3. Unexpected changes in vessel number and size in the unloaded rat tibia caused by spinal cord injury (SCI), which is closely associated with sharp changes in osteocytes.

uCT data showed reductions in vessel (v) numbers but increases in vessel diameters, leading to a 11% reduction of vessel surface in SCI bone (Fig 3a). The acid-etched SEM (3b) and FITC (3c) images revealed severe pathological changes in osteocyte shape and organization in the SCI bone, suggesting osteocytes well-being are closely linked to bone quality.

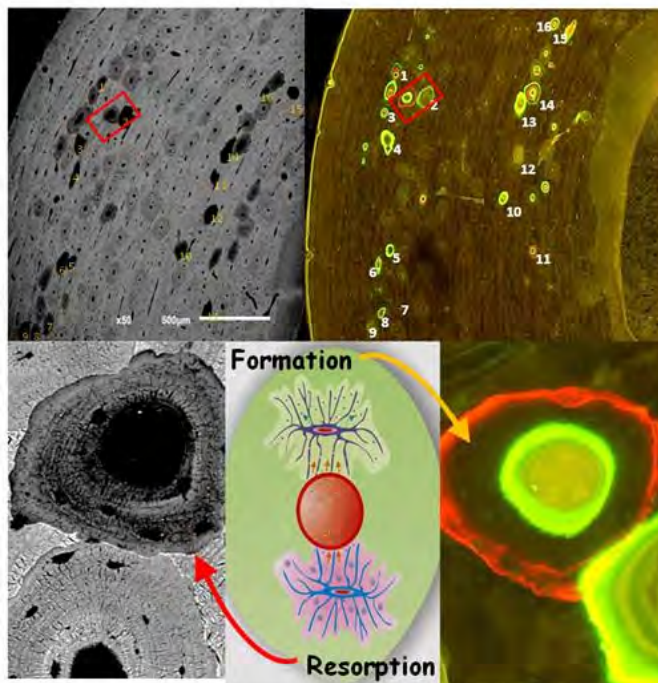


Figure 4. Demineralization by backscattered SEM images and remineralization by calcein-alizarin red stained confocal images in the same dog long bone slide. We used confocal double-labeled images to directly assess mineral deposition from Ocy's, and backscattered SEM images to define mineral resorption. Arrow showed the bone remodeling in the same osteon without cell replacement.

Figure 3.

Figure 4

Disclosures: Yuan Hui, None.

MO0236

Indirect Effects of Factors from Contracted Muscle on Osteoblasts via Osteocytes. Hisataka Kondo*, Ning Zhao, Matt Prideaux, Yukiko Kitase, Julian Vallejo, Sarah Dallas, Marco Brotto, Lynda Bonewald. University of Missouri Kansas City, USA

As exercise has a positive effect on both muscle and bone, we sought to determine if muscle-derived factors have an effect on osteoblasts. Extensor Digitorum Longus (EDL) and Soleus (SOL) muscles isolated from 5 month old C57Bl/6 mice were incubated in Ringer's solution alone (static) or stimulated at a frequency of 90Hz to maintain maximal force for 30 min (contracted) and the muscle conditioned medium (MCM) collected. Pre-osteoblastic MC3T3-E1 and osteoblastic IDG-SW3 (Day0) cells were treated with 10% MCM, however no effects were observed on proliferation, metabolic activity or mineralization. As we have shown previously that muscle factors have potent effects on osteocytes, we hypothesized that MCM may induce osteocytes to produce factors that affect osteoblast function. Day 28 IDG-SW3 cells that express the mature osteocyte phenotype were pretreated with 10% MCM for 24hrs and then the osteocyte conditioned media (OCM) was collected. Pretreatment of osteocytes with static EDL and SOL MCM had no significant effect on MC3T3 or IDG-SW3 (Day0) cell proliferation and metabolic activity compared to control, but contracted MCM significantly increased both proliferation and metabolic activity (ranging from 12 to a 35% increase). As both prostaglandin E2 and sclerostin are made by mature osteocytes, these were quantitated. OCM from day 28 IDG-SW3 cells pretreated with static MCM had approximately 500 pg/ml of PGE₂ which was increased 3-fold by pretreatment with contracted MCM. No PGE₂ was detected in MC3T3 and osteoblastic IDG-SW3 (Day0) cells directly treated with MCM. The effects of muscle-pretreated OCM on proliferation and metabolic activity of osteoblastic cells was inhibited by indomethacin. As PGE₂ has been reported to decrease osteocyte production of sclerostin, the effects of MCM on sclerostin levels in OCM were determined. Contracted MCM decreased Sost mRNA and sclerostin levels in day 28 osteocytic IDG-SW3 cells and this effect was also blocked by indomethacin. These results indicate that contracted muscle secretes factors that have indirect effects on osteoblasts through stimulating PGE₂ production and decreasing sclerostin in osteocytes. Osteocytes appear to be the target bone cells of muscle.

Disclosures: Hisataka Kondo, None.

MO0237

Inflammatory Bowel Disease Alters Osteocyte Protein Levels Controlling Bone Turnover. Corinne Metzger*¹, Anand Narayanan², Tatiana AzZani¹, Walter Cromer², David Zawieja², Susan Bloomfield¹. ¹Texas A&M University, USA, ²Texas A&M Health Science Center, USA

An inflammatory bowel disease (IBD) comorbidity is bone loss leading to elevated fracture risk. Chronic systemic inflammation causes increased bone resorption and decreased bone formation. Tumor necrosis factor- α (TNF- α), a pro-inflammatory cytokine, stimulates osteoclasts and inhibits osteoblasts. In addition, TNF- α is a transcriptional activator of sclerostin (Scl), the osteocyte protein inhibiting Wnt signaling. TNF- α , the receptor activator of nuclear factor κ B ligand (RANKL), and RANKL's decoy receptor osteoprotegerin (OPG) are key proteins controlling osteoclastogenesis. The RANKL:OPG ratio is altered in the serum of IBD patients. However, the *in vivo* response of these proteins in osteocytes, the primary regulators of bone, is unknown. Utilizing an IBD rat model, the goal of this study was to evaluate prevalence of TNF- α ⁺ RANKL⁺, OPG⁺, and Scl⁺ osteocytes in the cortical mid-shaft femur (cort-MSF), distal femur metaphysis (cort-DFM), and DFM cancellous bone (can-DFM) and correlate with markers of bone turnover. Male Sprague Dawley rats (2 months, n=16) were divided into two groups: IBD (induced via TNBS instillation over 4 weeks) and vehicle controls. Statistical difference was determined by p<0.05. Standard cancellous histomorphometry of the proximal tibia and 4th lumbar vertebrae revealed lower bone volume, lower bone formation rate (BFR), lower osteoid surface (OS), and higher osteoclast surface (Oc.S) in IBD. Tibia midshaft BFR was also lower in IBD. Immunohistochemical staining of the distal femur showed %TNF- α ⁺, %RANKL⁺, %OPG⁺, and %Scl⁺ osteocytes were elevated 1.4-2.2 fold in IBD can-DFM. %TNF- α ⁺, %OPG⁺ and %Scl⁺ osteocytes were elevated 1.4-1.7 fold in IBD cort-DFM. %RANKL⁺ and %Scl⁺ osteocytes were elevated 1.3-3.7 fold in IBD cort-MSF. With regression analysis, %RANKL⁺ osteocytes in can-DFM predicted the increase in cancellous Oc.S (R²=0.565). %TNF- α ⁺ osteocytes in can-DFM predicted increased %Scl⁺ (R²=0.588). %Scl⁺ predicted declines in cancellous OS (R²=0.581) as well as BFR in cancellous and cortical bone (R²=0.674, R²=0.908). In conclusion, systemic inflammation caused by IBD altered the prevalence of regulatory proteins in osteocytes that control bone resorption and bone formation contributing to IBD-induced bone loss. These data highlight the deleterious effect of systemic inflammation on bone, while providing a rationale for pharmacological and non-pharmacological treatment options to mitigate inflammatory bone loss.

Disclosures: Corinne Metzger, None.

MO0238

Osteocyte Conditional Deletion of Sirtuin 1 Results in Distinct Alterations in Bone Structure. Elizabeth Rendina-Ruedy*¹, Guillaume Vignaux², Nicole Fleming², Daniel Perrien³. ¹Vanderbilt University Medical Center, VA Tennessee Valley Healthcare System, USA, ²Vanderbilt University Medical Center, USA, ³VA Tennessee Valley Healthcare System, Vanderbilt University Medical Center, USA

Sirtuin1 (Sirt1) is a NAD⁺-dependent deacetylase that exists in the nucleus and cytosol to regulate many cellular functions including energy metabolism, inflammation, and aging. It has previously been reported that conditional deletion of Sirt1 in osteoblast (OB) progenitors (*Osx1-Cre*) or mature osteoblasts (*2.3kbColl1-Cre*) results in a low bone mass phenotype in female, but not male mice. Since these models also delete Sirt1 in osteocytes (OCY), it remained unclear which cell types were contributing to the overall bone phenotype. Therefore, we have characterized the targeted disruption of Sirt1 in OCY using *9.6kbDmp1-Cre:Sirt1^{fl/fl}* mice in which exon 4 of *Sirt1*, encoding the catalytic domain, is deleted rendering a functionally inactive protein (*Sirt1^{Ocy-/-}*). At 14 wks old, tibiae, femora, and vertebrae were harvested and trabecular bone microarchitecture were determined by *ex vivo* μ CT in male (n=9,6) and female (n=5) mice. Interestingly, male *Sirt1^{Ocy-/-}* mice had higher trabecular BV/TV in the proximal tibia compared to *Sirt1^{fl/fl}* mice. While the female phenotype was much more modest, several measures of trabecular structure including connectivity density, trabecular number, and trabecular separation were significantly improved in the femur and tibia of *Sirt1^{Ocy-/-}* vs. *Sirt1^{fl/fl}* mice. Trabecular number and connectivity density were also higher in the tibia, femur, and vertebra of male *Sirt1^{Ocy-/-}* mice. Despite these improvements, tissue mineral density was lower for the *Sirt1^{Ocy-/-}* mice compared to the *Sirt1^{fl/fl}* mice (femur and vertebra in males; tibia and femur in females). Together, these data define a novel role for Sirt1's catalytic activity in OCY, by demonstrating that OCY-conditional deletion of *Sirt1* results in a distinct structural bone phenotype in both genders. Furthermore, this study also suggests that the low bone mass phenotype in OB-conditional *Sirt1* deletion models is due to a distinct role in mature osteoblasts. As we continue to investigate this novel mouse model we will gain insight in to how Sirt1 functions in osteocytes to regulate bone metabolism, which could provide insight into new ways of preventing age-related bone loss.

Disclosures: Elizabeth Rendina-Ruedy, None.

MO0239

Osteocyte-Driven Perilacunar Remodeling is Impaired in Glucocorticoid Induced Osteonecrosis. Tristan Fowler*¹, Faith Hall-Glenn¹, Aaron Fields¹, Hrishkesh Bale¹, Robert Ritchie², Thomas Vail¹, Jeffrey Lotz¹, Tamara Alliston¹. ¹University of California San Francisco, USA, ²Lawrence Berkeley National Laboratory, University of Berkeley, USA

Despite the multitude of therapeutic uses of glucocorticoids (GCs), the side effects on skeletal health can be serious, including bone fragility. The cellular mechanisms underlying GC-dependent regulation of bone mass through osteoblast, osteoclast, and osteocyte (OCY) activity have been widely recognized, however the mechanisms by which GCs compromise bone quality remain unclear. OCYs remodel matrix through a process of perilacunar remodeling (PLR), which is essential for the maintenance of bone quality. OCY-driven PLR involves acidification of the microenvironment and secretion of proteases including cathepsin K and matrix metalloproteases (MMPs). However, the extent to which PLR is involved during GC deregulation of bone quality remains unclear. Therefore, here we test the hypothesis that GCs repress the expression of PLR enzymes, which impairs the ability of OCY to maintain the lacunocanalicular network and bone matrix integrity by PLR. To test this hypothesis, we evaluated the effect of the GC dexamethasone (Dex) on PLR enzyme expression *in vivo* and *in vitro*. RNA was isolated from flushed femoral cortical bone from BALB/cJ mice following 14 days of treatment with Dex (0.1 mg/mL) or vehicle by the drinking water. GC-treatment caused a 2-fold reduction in MMP13 RNA expression, as well as a reduction of the percentage of MMP13-positive OCYs by immunohistochemistry (n>5, p<0.05). GCs also significantly repress the expression of PLR enzymes, MMP2, 13, and 14, in Dex-treated MLO-Y4 cells (1 μ M, 24h, n=4, p<0.05), even in the presence of the apoptosis inhibitor, DEVD. This suggests that GCs regulate PLR independently of apoptosis. To test the effect of GCs on PLR, functional outcomes were assessed in femora of Dex and vehicle-treated mice. Quantitative analyses of silver and picrosirius red stained histological sections showed significant GC-dependent decreases in lacunocanalicular area and collagen alignment, respectively (n=3, p<0.05). Parallel studies of normal and sclerotic bone from GC-treated patients also showed disrupted PLR with sclerosis, including deregulated MMP13 expression, disorganized collagen, hypermineralization, and reduced lacunar size as quantified by X-ray tomographic microscopy. These studies implicate MMP13 and GCs in the regulation of perilacunar bone matrix composition and organization, suggesting that deregulation of PLR may be one mechanism by which GC treatment impairs bone quality independent of apoptosis induction.

Disclosures: Tristan Fowler, None.

MO0240

Variation in systemic human cortical osteocyte lacunar density: relationships with intracortical porosity. Randee Hunter*¹, Amanda Agnew². ¹The Ohio State University, Us, ²The Ohio State University, USA

The objective of this study is to investigate variation in cortical osteocyte cell populations using their lacunae as a proxy. Osteocytes and their lacunocanalicular network have been identified as regulators of bone quality and function by exerting extensive influence over the remodeling process. Recent research has shown that osteocyte malfunction and apoptosis leads to a decrease in bone quality and increase in bone fragility. This study analyzes variation in osteocyte lacunar density and intracortical porosity from three skeletal sites to establish regional and systemic age and sex related trends. Bone samples were recovered from the midshaft femur, distal 1/3 diaphyseal radius, and midshaft 6th rib of 30 modern cadaveric individuals (15 males and 15 females) ranging from 49 to 100 years old. Thin ground histological (80 μ m) cross-sections were made, imaged and analyzed under bright field microscopy. Size measurements (total subperiosteal area Tt.Ar; cortical area Ct.Ar) were collected using ArcGIS for femora and ImageJ for radii and ribs. ImageJ was used to manipulate images to identify and count osteocytic lacunae (Ot.Lc.N) automatically over the entirety of the cross-section. Intracortical porosity area (Po.Ar) was measured using a semi-automatic method with extensive manual verification. Ot.Lc.N and Po.Ar were each normalized for size: osteocyte lacunar density (Ot.Lc.N/B.Ar) and Ot.Lc.N/Ct.Ar) and intracortical porosity (%Po.Ar). Independent samples t-tests indicated no significant sex differences between either variable in any element; thus analyses are performed on males, females and the pooled sample. Pearson correlations demonstrated an overall decrease in osteocyte lacunar density (Ot.Lc.N/B.Ar) and an increase in intracortical porosity (%Po.Ar) with age for each element. Intracortical porosity (%Po.Ar) was significantly negatively correlated with lacunar density (Ot.Lc.N/Ct.Ar) with varying strengths (see Figure 1). A systemic trend in the decrease in osteocyte lacunar density (Ot.Lc.N/B.Ar) with age was identified in males only between the femur and radius (p=0.029) but no relationship between the rib and radius, or rib and femur. These results indicate that although all elements are experiencing systemically influenced declines in osteocyte lacunar density with measurable effects on remodeling, there appears to be a differential effect at each anatomical site.

MO0242

E11 protein stabilization through inhibition of the proteasome promotes osteocyte differentiation in murine *in vitro* models and may protect against osteoarthritis bone pathology. Katherine Staines¹, Matt Prideaux², Peter Hohenstein¹, Mark Hopkinson³, Anish Amin⁴, David Buttle⁵, Andrew Pitsillides³, Colin Farquharson¹. ¹The Roslin Institute & R(D)SVS, The University of Edinburgh, United Kingdom, ²University of Adelaide, Australia, ³Royal Veterinary College, United Kingdom, ⁴The University of Edinburgh, United Kingdom, ⁵The University of Sheffield, United Kingdom

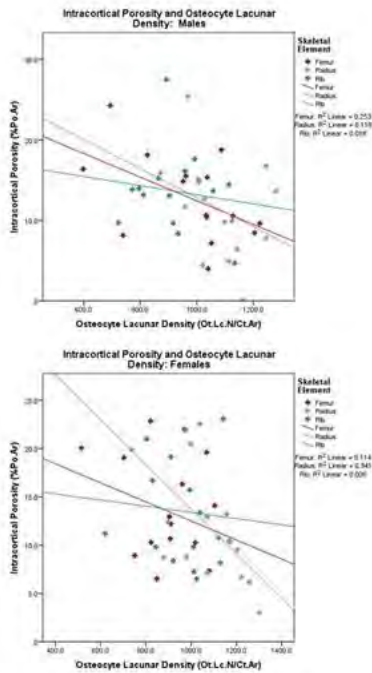


Figure 1: Scatterplot of intracortical porosity versus osteocyte lacunar density per element for males and females separately.

Figure 1: Scatterplot of intracortical porosity versus osteocyte lacunar density per element for male

Disclosures: Rande Hunter, None.

MO0241

Activation of AMP-activated Protein Kinase Protects Against Homocysteine-Induced Apoptosis of Osteocytic MLO-Y4 Cells by Regulating the Expressions of NADPH oxidase 1 (Nox1) and Nox2. Ayumu Takeno*, Ippei Kanazawa, Ken-ichiro Tanaka, Masakazu Notsu, Maki Yokomoto, Toru Yamaguchi, Toshitsugu Sugimoto. Internal Medicine 1, Shimane University Faculty of Medicine, Japan

Background and aims: Elevated plasma homocysteine (Hcy) level is associated with the risk of osteoporotic fracture. Hcy is a potent pro-oxidant, and it has been reported that Hcy induces apoptosis of marrow stromal cells via increasing oxidative stress. On the other hand, AMP-activated protein kinase (AMPK), which plays a pivotal role as an intracellular energy sensor, ameliorates oxidative stress in various cells. However, to our best knowledge, no study has described the effects of Hcy and AMPK on osteocytes. Thus, the aim of our study was to examine the effects of Hcy and AMPK activators on the apoptosis of osteocytic MLO-Y4 cells and on the expressions of oxidant and antioxidant enzymes such as NADPH oxidase (Nox) and superoxide dismutase (SOD) in the cells. Materials and methods: We used MLO-Y4, a murine long bone-derived osteocytic cell line. DNA fragment ELISA assay and TUNEL staining were performed to evaluate apoptosis. To investigate the mRNA expression of AMPK subunits ($\alpha 1$, $\alpha 2$, $\alpha 1$, $\alpha 2$, $r 1$, $r 2$, and $r 3$) in MLO-Y4 cells, we performed reverse transcription (RT) PCR. To examine the expressions of Nox and SOD, quantitative real-time PCR and Western blot were performed. Results: DNA fragment ELISA and TUNEL staining assays showed that Hcy treatments (0.1–5.0 mM) induced apoptosis of MLO-Y4 cells in a dose-dependent manner. The detrimental effect of Hcy was partly but significantly reversed by an antioxidant (N-acetylcysteine) and Nox inhibitors (apocynin and diphenyleneiodonium). In addition, treatment with AICAR (0.05–0.1 mM) and metformin (10–100 μ M) ameliorated Hcy-induced apoptosis of the cells. The favorable effect of metformin on Hcy-induced apoptosis was completely cancelled by an AMPK inhibitor Ara-A. Hcy increased the expression levels of Nox1 and Nox2, while it had no effects on the expressions of Nox4, SOD1 or SOD2. Hcy-induced increases in the expressions of Nox1 and Nox2 were significantly decreased by treatments with AICAR. Conclusion: These findings suggest that Hcy induces apoptosis of osteocytes by increasing the expressions of Nox1 and Nox2, and that AMPK activation by AICAR and metformin effectively prevents the detrimental reactions. Thus, AMPK activation may be a potent therapeutic candidate for preventing Hcy-induced osteocyte apoptosis and the resulting bone fragility.

Disclosures: Ayumu Takeno, None.

The transmembrane glycoprotein E11 is recognized to be critical for early osteocyte commitment. However, its precise role in osteoblast-osteocyte transition (osteocytogenesis) has yet to be established. Here we have explored the regulation and function of E11 expression during osteocytogenesis and bone formation. We have also examined whether these processes are compromised in osteoarthritis (OA) in which abnormal subchondral bone remodelling is observed. Increased expression of E11 protein/mRNA ($P < 0.001$) in MLO-A5 osteoblasts was concomitant with extensive osteocyte dendrite formation and matrix mineralization ($P < 0.001$). Over-expression of E11 exhibited significantly increased mRNA expression ($P < 0.001$) but no changes in protein levels, suggestive of post-translational regulation. Treatment of MLO-A5 cells and osteocytic IDG-SW3 cells with the proteasome inhibitor ALLN induced E11 protein expression and a profound increase in stellate cell morphology (50%, $P < 0.001$). MG132, lactacystin, Bortezomib, and Withaferin-A produced similar dose-dependent increases in E11 protein expression that was also observed in primary osteoblasts. These data implicate proteasome degradation in controlling post-translational E11 expression. We generated mice harbouring a conditional deletion of E11 in late osteoblasts (osteocalcin promoter driven) (*Oc-cre;E11^{fl/fl}*) and analysed its bone phenotype through histology, micro-CT scanning and 3-point bending. Immunohistochemistry and western blotting revealed selective deletion of E11 in *Oc-cre;E11^{fl/fl}* mice, whereas sclerostin expression and localization to osteocytes were normal. MicroCT analyses of 6-week old *Oc-cre;E11^{fl/fl}* mice revealed that cortical and trabecular parameters were normal. Similarly, 3-point bending revealed no significant differences in biomechanical properties at this age. To assess whether E11 dysregulation contributes to OA pathology, we performed immunohistochemistry on joint sections from a natural model of OA, the STR/Ort mouse, and human OA patients. Both revealed decreased E11 protein expression in subchondral bone osteocytes in regions of the joint where OA pathology was observed. Together these data suggest that proteasome-mediated E11 protein degradation limits acquisition of the osteocyte phenotype and that its deregulation may contribute to bone changes observed in OA. The function of E11 in normal bone formation remains, however, elusive.

Disclosures: Katherine Staines, None.

MO0243

Calcitonin modulates the osteocyte S1P signalling pathway and sclerostin expression. Jonathan Gooi*. The University of Melbourne, Australia

Calcitonin (CT) is widely known for its pharmacological role in inhibiting osteoclast bone resorption. Surprisingly however, recent studies utilizing genetically modified mice have suggested a role for CT as an inhibitor of bone formation. Recently, we demonstrated a potential mechanism by which CT could modulate bone formation, with CT treatment significantly increasing sclerostin expression in bone. More recently, it has been suggested that CT controls bone formation by inhibiting the release of sphingosine 1-phosphate (S1P) from osteoclasts. As we have previously reported freshly isolated osteocytes express calcitonin receptor (CTR) mRNA, raising the question of what is the action of CT treatment on osteocyte S1P and sclerostin signaling expression.

To resolve this question we used the Ocy454 cells, a novel murine osteocytic cell line. We have previously reported CTR and sclerostin expression are both lost in long-term cultures of osteocytes. Therefore it was necessary to ensure CTR expression in Ocy454 cells. Here, we report that CTR is expressed in Ocy454 cells and increases throughout differentiation. Furthermore, *Spk1* and *Spk2* mRNA, the two genes required for intracellular S1P production, *Spns2*, the transmembrane exporter protein necessary for the secretion of S1P, and the five receptors for S1P, *S1pr1-5* are expressed at high levels in osteocytes and increase in expression throughout osteocyte differentiation.

Treatment of differentiated (14 days) Ocy454 cells with salmon CT (10nM) for 3 hours significantly increased *Sphk1* (1.4 fold, $P < 0.01$) and *Spns2* (1.5 fold, $P < 0.05$) mRNA. In addition, *Sost* mRNA levels were increased (6.5 fold, $P < 0.01$) in Ocy454 cells.

Taken together, these results demonstrate that CT has significant and contrasting effects on S1P and sclerostin production. It is expected that the increased production of S1P promotes bone formation while conversely; increased sclerostin production promotes inhibition of bone formation. However it seems most likely that the dominant of CT treatment in osteocytes is promoting bone formation based on the increased level of expression of S1P related genes. This has profound implications for CT and osteocyte biology given the predominance of osteocytes throughout the human skeleton.

Further studies are ongoing to determine the mechanism of action by which CT modulates S1P and sclerostin signaling, and to determine the dominant effect of CT treatment on bone formation.

Disclosures: Jonathan Gooi, None.

MO0244

Validation of a novel *in vitro* 3D mineral-collagen model for the study of osteocyte biology. Maxime Gallant^{*1}, Brian Golz¹, Haisheng Yang¹, Jesus Delgado-Calle², Teresita Bellido², Sherry L. Voytik-Harbin¹, Russell P. Main¹. ¹Purdue University, USA, ²Indiana University School of Medicine, USA

In vitro studies of bone cell response to environmental stimuli have traditionally used 2D culture models. However, bone cells, particularly osteocytes, exist in a mineral-collagen matrix *in vivo* and form a 3D syncytium with neighboring cells. The objective of this study is to develop a 3D mineral-collagen tissue culture model to study the influence of physical or pharmacological stimuli on primary osteocytes.

Gt(ROSA)26Sor^{tm4}(ACTB-tdTomato,-EGFP)^{Luo}/J mice (RO/RO) were crossed with DMP1-8kb-Cre mice (Cre^{-/-}). In Cre^{-/-}; RO/RO offspring, all cells express membrane-tdTomato protein except in osteocytes where Cre expression prevents tdTomato expression and induces membrane-eGFP. Osteoblast-enriched cell samples were extracted from long bones of 4-6 wk/old male and female Cre^{-/-}; RO/RO mice using collagenase and EDTA digestion. Isolated cells were cultured for 14 days, and seeded in a 3D matrix prepared from type-I collagen oligomers (2.5 mg/ml) and hydroxyapatite (27 mg/ml) in osteogenic media for up to 28 days. 3D cultures were processed at 14d and 28d to assess gene expression by qPCR and at 3d and 28d to quantitate cell differentiation using confocal microscopy. By confocal microscopy, osteoblast differentiation to osteocytes was quantified by determining the proportion of red (tdTomato = osteoblast), green (eGFP = osteocyte), and yellow cells (co-expression = early osteocyte).

Expression of the osteoblast marker gene *alkaline phosphatase* was reduced 16-fold in 28d cultures compared to 14d cultures and native cortical bone. *El1gp38*, an early marker for osteocyte differentiation, was increased 3-fold in the 14d and 28d cultures compared to native bone samples. Consistent with these gene-level data, we measured a reduction in the proportion of red cells in the 3D cultures from 3d to 28d (-18%) and an increase in both green and yellow cells (+5% and +13%). Taken together, the gene-level and cell fluorescence data indicate differentiation of the primary cells seeded in the 3D cultures from osteoblasts (red) to mature osteoblast/early osteocyte (yellow) to osteocytes (green). Our approach combines a mineral-collagen 3D matrix and cells from a novel genetic reporter mouse model for longitudinal assessment of osteocyte differentiation in 3D culture. Future work with this model will use bone cells from novel transgenic mice to examine the independent and interactive effects of fluid flow-induced shear stress and pharmacological treatments on osteocyte biology.

Disclosures: Maxime Gallant, None.

MO0245

High Bone Turnover is Associated with Hypocalcemia Induced by Denosumab in Women with Postmenopausal Osteoporosis. Koji Ishikawa^{*1}, Takashi Nagai¹, Kenji Ohara², Katsunori Inagaki¹. ¹Showa University School of Medicine, Japan, ²Department of Orthopaedic Surgery, Yamanashi Red Cross Hospital, Japan

Background: Hypocalcemia has been reported as the most common adverse events in patients with osteoporosis receiving denosumab. While close monitoring of calcium concentration is recommended in patients with kidney dysfunction, limited information is available on the risk factor for hypocalcemia. Accordingly, the aim of the present study was to identify the risk factors for hypocalcemia induced by denosumab for osteoporosis.

Methods: We retrospectively reviewed the records of patients who had received initial denosumab with supplementation of activated vitamin-D for osteoporosis at Yamanashi Red Cross Hospital between November 2014 and March 2015. Serum levels of the following bone metabolic markers were measured at baseline: BAP, total-PINP, TRACP-5b, urinary-NTX. Patients with hypocalcemia at baseline, kidney failure requiring hemodialysis, relatively severe hyperparathyroidism were excluded.

Results: Sixty-three patients were analyzed and sixteen patients (25.4 %) had hypocalcemia [corrected Ca levels <8.7 mg/dl, median (IQR): 8.4 (8.3-8.5) mg/dl] after administration of denosumab. All patients experienced hypocalcemia were asymptomatic, grade1 (CTCAG grade), and required daily oral calcium treatment (≥ 1000 mg). As shown in Figure1, levels of the bone metabolic markers at baseline were significantly different between patients without and those with hypocalcemia (BAP, total-PINP, TRACP-5b: all $P < 0.01$, u-NTX: $P < 0.05$). A positive correlation was observed between baseline bone metabolic marker levels and the reductions in calcium levels from baseline (BAP, total-PINP, TRACP-5b: $r=0.34-0.61$, all $P < 0.01$, u-NTX: $r=0.26$, $P < 0.05$). Multivariate logistic regression analysis revealed that the patients who had high level of TRACP-5b at baseline had a higher risk of hypocalcemia after denosumab treatment (OR = 9.64, CI = 1.75-53.11, $P < 0.01$, adjusted for baseline serum Ca levels, eGFR). Other bone metabolic markers showed the similar analysis as well.

Conclusion: Our reports suggest that higher baseline bone turnover sustaining serum calcium levels in patients with postmenopausal osteoporosis, inhibition by denosumab may have a greater impact on serum calcium levels. Routine measurement of bone metabolic markers before denosumab administration, is useful to identify the patients who have the risk of hypocalcemia. Furthermore, close monitoring of serum calcium levels is strongly recommended, especially those with high bone turnover.

Figure1: The levels of the bone metabolic markers at baseline

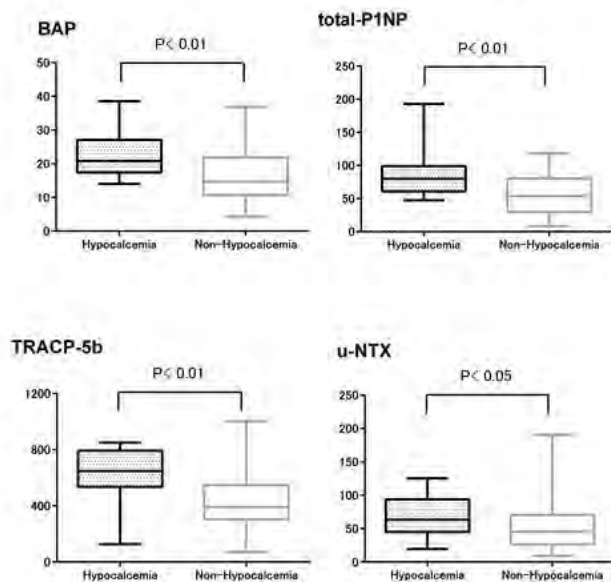


Figure 1

Disclosures: Koji Ishikawa, None.

MO0246

MicroRNAs miR-29b-3p, miR-365a-3p, miR-550a-3p are correlated to histomorphometry and bone turnover markers in idiopathic osteoporosis.

Roland Kocijan^{*1}, Christian Muschitz², Astrid Fahrleitner-Pammer³, Rainer Dormann², Fabian Plachel², Susanna Skalicky⁴, Elisabeth Geiger⁴, Heinrich Resch², Heinz Redl⁵, Patrick Heimel², Johannes Grillari⁶, Matthias Hackl⁴. ¹St. Vincent Hospital Vienna, Austria, ²St. Vincent Hospital – Medical Department II, The VINFORCE Study Group, Academic Teaching Hospital of Medical University of Vienna, Austria, ³Department of Internal Medicine, Division of Endocrinology & Metabolism, Medical University of Graz, Austria, ⁴TAmiRNA GmbH, Muthgasse 18, 1190 Vienna, Austria, ⁵Ludwig Boltzmann Institute for Experimental & Clinical Traumatology Donaueschingenstraße 13, 1200 Vienna, Austria, ⁶Department of Biotechnology, University of Natural Resources & Life Sciences Vienna, Austria

Purpose: MicroRNAs (miRNAs) are small non-coding RNAs that are involved in several biological processes including osteogenesis, bone formation and resorption as well as bone homeostasis. Eighteen miRNAs discriminating pre- and postmenopausal women as well as male patients with idiopathic osteoporosis and low-traumatic fractures have been recently identified. Based on these findings, we tested the correlation between bone specific circulating miRNAs and bone histomorphometry as well as bone turnover markers (BTM).

Methods: Transiliacal bone biopsies were performed in 35 patients (46.6 ± 13.0 years) with idiopathic osteoporosis and low-traumatic fractures to assess bone histomorphometry (BV/TV, BS/BV, OS/BS, ES/BS, QS/BS, Tb.N, Tb.Th, MS/BS, MAR, BFR/BS). Time to last fracture was at least 6 months. Secondary causes for osteoporosis were excluded by careful clinical examination. BTM including iPTH, 25(OH)vitamin D, BALp, osteocalcin, PINP, OPG, RANKL, TRAP5b, CTX were analyzed. MiRNAs were measured by RT-qPCR.

Results: Bone specific miRNAs did not differ between pre-menopausal women, postmenopausal women and men, respectively. MiRNAs did not show any correlation to age. Three miRNAs which were up-regulated in patients with low-traumatic fractures were identified to be associated to histomorphometric parameters and bone turnover markers: miR-29b-3p was significantly correlated to PINP ($r=0.400$, $p=0.021$), RANKL ($r=0.421$, $p=0.021$), CTX ($r=0.415$, $p=0.013$) and by trend to TRAP5b ($r=0.311$, $p=0.078$). Significant correlations were found for miR-29-3p and MAR ($r=0.740$, $p < 0.001$) and BFR/BS ($r=0.536$, $p=0.022$). miR-365-3p was associated to PINP ($r=0.491$, $p=0.004$), osteocalcin ($r=0.368$, $p=0.030$), CTX ($r=0.337$, $p=0.048$), TRAP5b ($r=0.346$, $p=0.049$) and Tb.N ($r=-0.389$, $p=0.037$). No correlations were found between miR-550a-3p and BTMs. However, miR-550a-3p was negatively associated to BV/TV ($r=-0.435$, $p=0.018$) and Tb.Th ($r=-0.429$, $p=0.020$) and positively to BS/BV ($r=0.432$, $p=0.019$) and MAR ($r=0.535$, $p=0.018$). No significant correlations were found between histomorphometry data, BTM and the remaining 15 miRNAs.

Conclusion: This is the first study reporting correlations between miRNAs, BTMs and histomorphometry. Serum levels of miR-29b-3p and miR-365-3p, which

are well-known modulators of bone turnover in vitro, are associated to BTMs in patients with idiopathic osteoporosis.

Disclosures: Roland Kocijan, None.

MO0247

Plasma periostin associates significantly with non-vertebral but not vertebral fracture in postmenopausal women: clinical evidence for the different effect of periostin depending on the skeletal site. Beom-Jun Kim^{*1}, Yumie Rhee², Chong Hwa Kim³, Ki Hyun Baek⁴, Yong-Ki Min⁵, Deog-Yoon Kim⁶, Seong Hee Ahn⁷, Hyeonmok Kim⁷, Seung Hun Lee⁷, Moo-Il Kang⁴, Jung-Min Koh⁷. ¹Asan Medical Center, South Korea, ²Department of Internal Medicine, Severance Hospital, Endocrine Research Institute, Yonsei University College of Medicine, South Korea, ³Department of Internal Medicine, Sejong General Hospital, South Korea, ⁴Division of Endocrinology & Metabolism, Department of Internal Medicine, Seoul St. Mary's Hospital, The Catholic University of Korea College of Medicine, South Korea, ⁵Division of Endocrinology & Metabolism, Department of Internal Medicine, Sungkyunkwan University School of Medicine, South Korea, ⁶Department of Nuclear Medicine, Kyunghee University School of Medicine, South Korea, ⁷Division of Endocrinology & Metabolism, Asan Medical Center, University of Ulsan College of Medicine, South Korea

Context: Periostin is preferentially expressed by the periosteum, which mainly covers the long bones. Therefore, the role of periostin in osteoporotic fracture (OF) may differ depending on bone type. **Objective:** To investigate whether periostin can serve as a predictor of OF risk, especially after dividing OFs into non-vertebral and vertebral fractures. **Design and Setting:** A case-control study conducted in a clinical unit in Korea. **Participants and Main Outcome Measures:** 133 cases having any kind of OF (i.e., non-vertebral and/or vertebral fractures) and age- and body mass index-matched 133 controls were enrolled among 532 consecutive postmenopausal women. Non-vertebral (i.e., wrist, forearm, humerus, hip, and pelvis) and morphological vertebral fractures were identified by an interviewer-assisted questionnaire and lateral thoracolumbar radiographs, respectively. Bone mineral density (BMD) and plasma periostin levels were also measured. **Results:** Plasma periostin was markedly higher in subjects with non-vertebral fracture than in those without this condition even after adjustment for BMD and potential confounders ($P = 0.023$). The odds for non-vertebral fracture were 2.33-fold higher in subjects in the highest periostin quartile compared with those in the lowest periostin quartile (95% CI = 1.06–5.10). However, associations between plasma periostin and vertebral fracture were not observed, regardless of adjustment. Consistently, plasma periostin levels associated inversely with proximal femur BMD ($P = 0.007$ to 0.030) but did not associate with lumbar spine BMD. **Conclusions:** Plasma periostin may be a potential biomarker of the risk of OF, especially in non-spinal skeletal sites, such as the limbs, rather than spine.

Disclosures: Beom-Jun Kim, None.

MO0248

Serial measurement of BMD and bone turnover to detect a treatment response to zoledronic acid: The HORIZON-PFT Trial. Katy J.L. Bell¹, Stephanie Harrison², Paul Glasziou³, Andrew Haven⁴, Les Irwig⁵, Richard Eastell⁶, Dennis M. Black², Douglas Bauer^{*2}. ¹University of Sydney & Bond University, Australia, ²University of California, San Francisco, USA, ³Bond University, Australia, ⁴University of New South Wales, Australia, ⁵University of Sydney, Australia, ⁶University of Sheffield, United Kingdom

Introduction: Bisphosphonate (BP) therapy is often monitored with serial BMD or bone turnover markers (BTMs) to estimate treatment response and adherence. Zoledronic acid (ZOL) is given intravenously once a year, and unlike oral BPs, adherence is known. Differences in the observed effects of ZOL between women are a result of both signal (true differences in response which contribute to variance of the ZOL group) and noise (background random variation due to within-person measurement variability which is reflected in the variance of the placebo group). We were interested in the 'detectability of response' which can be assessed by the ratio of signal (true treatment effects) to noise (random variation).

Methods: We analysed data from the Health Outcomes and Reduced Incidence with Zoledronic Acid Once Yearly Pivotal Fracture Trial (HORIZON-PFT), which compared the effects of 5mg once yearly infusions of ZOL with placebo in 7765 postmenopausal women with osteoporosis, to compare the detectability of response to treatment with the following monitoring tests: hip and spine BMD, serum N-terminal propeptide of type I collagen (PINP, Roche Elecsys) and C-telopeptide of type I collagen (sCTX, Roche Elecsys). The mean and between-person variation in treatment effects (signal) as well as background within-person variation (noise) were estimated by comparing the distributions of change in each monitoring test from baseline to 1 year (BMD and PINP) or 6 months (sCTX) in the ZOL and placebo groups.

Results: Data were available for 7056 women with hip BMD, 520 with spine BMD, 258 with serum PINP, and 484 women with sCTX. Although there was a (placebo adjusted) treatment effect on the mean change for all BMD sites and BTMs (Table), this was larger than random within-person variation only for sCTX

[(treatment - placebo mean)/placebo SD = 2.56]. A treatment effect on the variance was only seen with sCTX [(treatment - placebo variance)/placebo variance = 1.08]. This implies that (i) detection of the expected ZOL effect in an individual is most likely using sCTX, and (ii) between-women differences in treatment effects are negligible on all markers except sCTX where the between-women differences in treatment effect appear to be at least as big as the random within-person differences.

Conclusion: Among the BMD sites, BTMs and time periods we examined, change in sCTX at 6 months appears the most able to detect an individual's true response to ZOL treatment.

| Treatment group | Statistical measure | Hip BMD (g/cm ² , n=7056) [% change from baseline] | Spine BMD (g/cm ² , n=520) [% change from baseline] | PINP (log ng/mL, n=258) [% change from baseline] | sCTX (log ng/mL, n=484) [% change from baseline] |
|-----------------|---------------------|--|---|---|---|
| Placebo | Mean | 0.0014 [0.02%] | 0.0066 [0.8%] | 0.65 [5%] | -0.15 [1.4%] |
| | SD | 0.25 | 0.30 | 0.67 | 0.45 |
| Zoledronic acid | Mean | 0.018 | 0.035 | -0.57 [43%] | -1.30 [73%] |
| | Unadjusted | 0.018 [2.8%] | 0.029 [3.6%] | -0.62 [46%] | -1.15 [68%] |
| | Placebo-adjusted | 0.018 [2.8%] | 0.029 [3.6%] | -0.62 [46%] | -1.15 [68%] |
| Variability | Signal:Noise* | 0.72 | 0.81 | 0.93 | 2.56 |
| | SD | 0.23 | 0.28 | 0.68 | 0.65 |
| | Signal:Noise† | 0† | 0† | 0.04 | 1.08 |

* Signal:noise for mean: indicates detectability of true expected (mean) response to treatment. Signal calculated as difference in mean change between zoledronic acid and placebo groups; noise calculated as SD in placebo group.
† Signal:noise for variance: indicates detectability of true between-person differences in response to treatment. Signal calculated as difference in variance of change between zoledronic acid and placebo groups; noise calculated as variance in placebo group
‡ Signal assumed to be zero as variance lower in treated group than placebo group

Table: Change in BMD and BTMs by treatment group

Disclosures: Douglas Bauer, None.

This study received funding from: Novartis

MO0249

Microindentation Assessed Bone Material Strength is Associated with Areal BMD but not with Prevalent Fractures in Older Women. ROBERT RUDANG¹, MICHAEL ZOULAKIS^{*2}, ANNA DARELID², DANIEL SUNDH², DAN MELLSTROM², MATTIAS LORENTZON², LISA JOHANSSON². ¹INSTITUTE OF MEDICINE, SAHLGRENKA ACADEMY, Sweden, ²GERIATRIC MEDICINE, INSTITUTE OF MEDICINE, SAHLGRENKA ACADEMY, Sweden

Reference point indentation is a novel method for assessment of bone material strength (BMS) in vivo, where a probe is used to make microindentations in the bone surface of the midtibia. The aim of this study was to investigate the associations between BMS and areal bone mineral density (aBMD) and prevalent fractures in older women.

A total of 211 women with the mean age of 78.3 ± 1.1 yrs (range 75.1-80.7) were included in this cross-sectional, population-based study.

BMS was assessed by four operators using the Osteoprobe® (Active Life Scientific, USA), and calculated as the mean of at least 11 reference point indentations performed at the midtibia of the non-dominant leg on each subject. The coefficient of variation for the method was 3.2%, calculated by duplicate measurements performed on 30 study subjects. Areal BMD of the hip, spine and non-dominant radius was assessed by Dual-photon X-ray Absorptiometry (DXA, Discovery A, Hologic). Fracture history was retrieved by a standardized questionnaire, and vertebral fractures were identified using VFA (vertebral fracture assessment) by DXA, where fractures were graded mild, moderate or severe due to the semi-quantitative method of Genant.

A total of 198 previous fractures in 109 subjects were reported. By means of VFA, a total of 106 subjects with vertebral fractures were found, of which 58 subjects had moderate or severe fractures and 42 multiple fractures. Using Pearson correlation we found no correlations between BMS and any of the aBMD measurements, but there was an inverse correlation with weight ($r = -0.14$, $p = 0.04$) and BMS differed according to operator (Anova $p < 0.01$). Adjusting for weight and operator in a linear regression model we found that BMS was positively associated with aBMD of the total hip ($\beta = 0.14$, $p = 0.04$), non-dominant radius ($\beta = 0.17$, $p = 0.02$) and lumbar spine ($\beta = 0.14$, $p < 0.05$). Using independent samples T-test we found no differences in crude or weight- and operator-adjusted BMS between subjects with reported fractures and subjects with no reported fractures (Table 1). Neither could we detect any differences in BMS between subjects with VFA-verified vertebral fractures and non-fractured subjects (Table 1).

We conclude that microindentation assessed BMS is associated with aBMD in a population-based material of 211 older women. In contrast to previous studies we could not demonstrate any associations between reported prevalent fractures of any kind or VFA-verified vertebral fractures and BMS.

Table 1. BMS and prevalent fracture in older women

| Fracture category | BMS | | p ¹ | p ² |
|---|------------|-------------|----------------|----------------|
| | Fracture | No Fracture | | |
| All fractures (n=109) vs. Never fracture (n=102) | 74.9 ± 6.9 | 76.4 ± 8.2 | 0.18 | 0.39 |
| All fractures after age 50 (n=86) vs. Never fracture (n=102) | 75.4 ± 7.2 | 76.4 ± 8.2 | 0.39 | 0.65 |
| Peripheral fractures after age 50 (n=53) vs. Never fracture (n=102) | 75.5 ± 7.0 | 76.4 ± 8.2 | 0.49 | 0.73 |
| Wrist fractures after age 50 (n=40) vs. Never fracture (n=102) | 75.0 ± 7.3 | 76.4 ± 8.2 | 0.35 | 0.84 |
| Osteoporotic fractures after age 50 (n=53) vs. Never fracture (n=102) | 75.8 ± 7.1 | 76.4 ± 8.2 | 0.69 | 0.94 |
| VFA-verified vertebral fractures (n=106) vs. Never fracture (n=55) | 75.3 ± 7.6 | 75.8 ± 8.4 | 0.71 | 0.87 |
| VFA-verified moderate and severe vertebral fractures (n=58) vs. Never fracture (n=55) | 77.1 ± 7.5 | 75.8 ± 8.4 | 0.37 | 0.33 |
| Multiple VFA-verified vertebral fractures (n=42) vs. Never fracture (n=55) | 76.5 ± 7.5 | 75.8 ± 8.4 | 0.65 | 0.55 |
| VFA-verified vertebral fractures and all fractures (n=156) vs. Never fracture (n=55) | 75.6 ± 7.3 | 75.8 ± 8.4 | 0.88 | 0.96 |

¹) Independent samples T-test, presenting p-value for unadjusted BMS

²) Independent samples T-test, presenting p-value for weight- and operator-adjusted BMS

Table 1

Disclosures: MICHAEL ZOULAKIS, None.

MO0250

Osteocalcin detection in human bone extracts by antibody microarray. Corinne Thomas^{*1}, Thao Nguyen², Timothy P. Cleland², Pankaj Karande², Deepak Vashishth². ¹Rensselaer Polytechnic Institute, USA, ²Rensselaer Polytechnic University, USA

Introduction: Osteoporosis is the most common human bone disease, characterized by the increased susceptibility of bone to fracture [1]. Osteoporosis is currently assessed using bone mineral density (BMD); however, recent studies have found normal or high BMD in bones with increased risk of fracture [2-4]. This may be explained by the bone matrix quality, including the concentrations of non-collagenous bone proteins. One of these proteins, osteocalcin, has been shown to contribute to bone structure and enhances the ability of bone to resist fracture through a more effective dissipation of energy [5]. The amount of osteocalcin found in bone has been shown to correlate to fracture properties of bone or clinical fracture [6,7].

The aim of this project is to develop and validate a new high throughput chip ELISA assay to characterize the osteocalcin content of bone as it changes with age and health.

Methods: We developed a high throughput ELISA Chip and optimized various parameters such as antibody concentration and slide type to measure the osteocalcin content of bone at physiological levels. We used the chip to test human cadaveric bone protein extracts from donors over a wide range of ages and from different locations along the same bone surface. We then evaluated these results against commercially available human osteocalcin ELISA.

Results: The chip yields measurable concentrations of osteocalcin from human bone samples as small as 0.4 mg. Measurements taken from multiple locations on the same donor bone establish the consistency of the measurements taken by the chip, and demonstrate the efficacy of chip as a diagnostic tool. The chip offers distinct advantages to current commercial methods as it uses a very small volume of sample for each measurement, is able to perform more measurements per run, and is easily expanded to test multiple antibodies against each sample.

Citations:

1. Bone health and osteoporosis: a report of the Surgeon General. Office of the Surgeon General (US), 2004.
2. Janghorbani, M., et al., Am J Epidemiol, 2007. 166(5): p. 495-505.
3. Nickolas, T.L., et al., Kidney Int, 2008. 74(6): p. 721-31.
4. Saito, M., et al., Osteoporos Int, 2006. 17(10): p. 1514-23.
5. Poundarik, A.A., et al., PNAS, 2012. 109(47): p. 19178-19183.
6. Karim et al. Proc. of the 58th Annual Meeting of the ORS. Vol. 37, p. 0116, 2012
7. Rodrigues, A.M., et al., Bone, 2012. 51(6): p. 981-9.

Disclosures: Corinne Thomas, None.

MO0251

TBS is lower in African American than in Caucasian American women referred for bone density testing. Tamara Vokes^{*1}, Disha Kumar², Rajesh Jain², Hans Didier³. ¹University of Chicago, USA, ²University of Chicago Medicine, USA, ³Lausanne University Hospital, Switzerland

Background: African Americans (AA) have lower fracture rates compared to Caucasians (CA) and this difference is only partly explained by the higher BMD in AA. We wanted to determine whether AA also have higher TBS (stronger bone) than CA.

Methods: In 893 women age 40 and over (48% AA) who were referred for bone densitometry as a part of their routine clinical care, we assessed the BMD, TBS and presence of vertebral fractures (VFX) on VFA using Prodigy. VFX (grade 2 or higher) were present in 18% of CA and 16% of AA women (p=0.4).

Results: AA women were older (69 vs. 64 years, p<0.0001), heavier (74 vs. 68 kg, p<0.0001), and had higher BMI (29 vs. 26, p=0.0001), and BMD T-scores at all skeletal sites (lowest of hip and spine T-score (low T) -1.9 vs. -2.4, p<0.0001). TBS

was lower in AA (1.24 vs. 1.28, p=0.0001), a difference of 0.25 standard deviations (SD). When controlling for age, BMI, and spine BMD, TBS was lower in AA than in CA women by 0.33 SD (p<0.001). Among CA women, TBS was lower in women with compared to those without VFX (1.20 vs. 1.29, p<0.0001). Among AA women the difference was smaller and less significant (1.21 vs. 1.25, p=0.05). In a multivariate model that included the known predictors of VFX, TBS was significantly associated with VFX in CA but not in AA women (table).

Conclusion: TBS is lower in AA than in CA women, at least among those referred for BMD testing as a part of their clinical care. The predictors of fragility may also differ between races: the association between prevalent VFX with BMD and with TBS is less significant while the use of glucocorticoids is more significant in AA.

Limitation: when studying densitometry population there may be a selection bias if clinicians refer AA women for BMD testing if they suspect high fragility and CA women as a matter of routine testing.

Implications: if confirmed, our results suggest that 1. TBS may need to be used differently in different races; and 2. Greater bone strength in AA may be due to cortical rather than trabecular compartment.

Table: Association of prevalent vertebral fractures with TBS and other predictors (multivariate logistic regression)

| Predictor | CA women | | AA women | |
|-----------------------------|------------|---------|------------|---------|
| | Odds ratio | p-value | Odds ratio | p-value |
| TBS/1 SD decrease | 1.50 | 0.011 | 1.11 | 0.49 |
| Age/decade increase | 2.05 | <0.001 | 1.70 | <0.001 |
| Low T/1 unit decrease | 1.61 | 0.004 | 1.30 | 0.057 |
| Glucocorticoid (yes vs. no) | 1.96 | 0.046 | 2.34 | 0.010 |

Table

Disclosures: Tamara Vokes, None.

MO0252

Trabecular bone score improves identification of major osteoporotic and vertebral fractures in Polish postmenopausal women with non-osteoporotic BMD. Magdalena Ignaszak-Szczepaniak^{*1}, Michal Michalak². ¹Poznan University of Medical Science, Poland, ²Department of Computer Science & Statistics, University of Medical Sciences, Poznan, Poland, Poland

Many osteoporotic fractures (OP Fx) occur in patients with BMD outside the WHO-based definition of osteoporosis.

The aim of the study was to assess whether TBS can differentiate osteopenic and normal BMD women with prevalent major and vertebral osteoporotic fractures from those without fractures and to estimate how TBS can improve assessment of fracture risk in these patients.

Material and methods: Retrospective, case-control study on 439 female patients of Osteoporosis Specialty Outpatient Clinic over 50 years. Fracture status was reviewed in medical record and vertebral fractures (VFs) were identified by VFA for each subject. Spine DXA images were evaluated for all subjects (GE-Lunar Prodigy) and then reanalyzed using TBS iNsight version 2.1 (Med-Imaps). Further analysis considered only women with T-scores >-2.5SD, who were compared depending on TBS tertiles and fracture status (separately for major OP Fx and VFs). Statistical analysis was performed using Statistica 10 (StatSoft Inc).

Results: In 218 osteopenic and normal BMD women (mean age 71.7±7.4 y) we identified 72 prevalent major OP Fx and 43 VFs Genant grade 2/3, which are respectively 40% and 38% of all OP Fx observed in whole studied group. Mean TBS in major OP Fx was 1.13 vs 1.20 for non-fractured (p<0.001) and in VFs 1.08 vs 1.19 in women without VFs (p<0.001). 66% of major OP Fx was detected in the lowest (1st) TBS tertile and only 7% were over the highest (3rd) tertile. In group with VFs 81% had TBS <1.200 and only 1 woman had TBS >1.350. The difference was significant. In normal BMD patients 5 VFs were detected in 1st TBS tertile and no one with TBS>1.350 sustained vertebral fracture. Comparing only osteopenic women with and without major OP Fx depending on TBS thresholds, ORs were respectively: 3.3 for 1st vs 3rd tertile (p=0.02) and 2.34 for 1st vs 2nd tertile (p=0.02). Moreover osteopenic subjects whose TBS was in 1st tertile had 10.1 higher risk of VFs as compared to 3rd tertile (p=0.0008) and 4.8 higher when compared to 2nd (p=0.001). There were no differences when compared 2nd and 3rd tertiles for both major OP Fx and VFs.

Conclusions:

TBS better identifies osteoporotic fractures in postmenopausal women whose BMD is in non-osteoporotic range.

The difference between fractured and non-fractured women in TBS level is significant.

TBS improves fracture risk assessment in osteopenic female patients, particularly identification of women prone to vertebral fractures.

In osteopenia TBS<1.200 is related to 10 times higher risk of vertebral fracture as compared to TBS>1.350

TBS>1.350 and normal BMD exclude probability of VFs.

Disclosures: Magdalena Ignaszak-Szczepaniak, None.

MO0253

Trabecular Bone Score (TBS) Predicts Incident Clinical and Radiographic Vertebral Fractures in Older Men: Findings from the Osteoporotic Fractures in Men (MrOS) study. John Schousboe¹, Tien Vo², Brent Taylor³, Peggy Cawthon⁴, Ann Schwartz⁴, Douglas Bauer⁴, Eric Orwoll⁵, Nancy Lane⁶, Elizabeth Barrett-Connor⁷, Kristine Ensrud⁸. ¹Park Nicollet Clinic/University of Minnesota, USA, ²University of Minnesota, USA, ³Center for Chronic Diseases Outcomes Research, Minneapolis VAMC; Department of Medicine, University of Minnesota, USA, ⁴University of California San Francisco, USA, ⁵Oregon Health Sciences University, USA, ⁶University of California Davis, USA, ⁷University of California San Diego, USA, ⁸Division of Epidemiology, University of Minnesota; Department of Medicine, University of Minnesota, USA

Background: TBS predicts fractures in those with body mass index (BMI) < 37 kg/m². It is unknown how well TBS predicts incident vertebral fractures in men independent of prevalent radiographic vertebral fracture (PVF)^{*} and other clinical risk factors. Our purpose was to estimate the associations of TBS with incident clinical vertebral fractures (iCVF) and radiographic vertebral fractures (iRVF) in men after adjustment for age, femoral neck bone mineral density (FNBMD), PVF, and other clinical risk factors. **Methods:** TBS was estimated on AP on baseline visit spine DXA scans for 5,862 men age = 65 years with a BMI < 37 kg/m². Incident clinical vertebral fractures were ascertained by self-report every 4 months and confirmed by centralized review of community acquired clinical images and baseline lateral spine radiographs. Visit 2 lateral spine radiographs were available and evaluable for 4,317 men with BMI < 37 kg/m². We defined an iRVF as an increase of = 1 Genant SQ grade on follow-up compared to baseline radiographs. The associations of TBS with iCVF and iRVF were estimated, respectively, with proportional hazards and logistic regression models. Model discrimination was tested in randomly selected split half samples; models were first run in 50 bootstrapped samples of the first half and model discrimination compared using Harrell's C and area under receiving operating characteristics (AUROC) curves statistics in the second half. **Results:** Mean (SD) TBS was 1.27 (0.12). 186 men had an iCVF over a mean follow-up time of 10.7 years, and 197 men had an iRVF on follow-up radiographs taken a mean 4.7 years after the baseline visit. A one SD decrease in TBS was associated with a 1.44 and 1.26 fold increased risk, respectively, of iCVF and iRVF adjusted for age and FNBMD (Table). These associations were only slightly attenuated with adjustment for PVF, and were even stronger when further adjusted for other clinical risk factors. By Harrell's C statistic, TBS improved discrimination of those with from those without incident clinical vertebral fracture. Results from models substituting lumbar spine BMD for FN BMD were similar, except that the association of TBS with iRVF when adjusted for PVF was attenuated and no longer significant. **Conclusion:** TBS is associated with incident clinical and radiographic vertebral fractures in older men independent of PVF and other clinical risk factors, and improves prediction of incident clinical vertebral fractures.

Table: Associations TBS with Incident Clinical & Radiographic Vertebral Fracture

| Predictors | Clinical Vertebral Fracture (n=5280) | | Radiographic Vertebral Fracture (n=4317) | |
|--|--------------------------------------|--------------------------|--|--------------------------|
| | HR (95% C.I.) | Harrell's C (95% C.I.) | OR (95% C.I.) | AUROC (95% C.I.) |
| Model 1: Age + FNBMD | | 0.72 (0.66 to 0.78) | | 0.60 (0.57 to 0.68) |
| Model 2: TBS (per SD decrease) + Age + FNBMD | 1.52 (1.32-1.75) | 0.75** (0.70 to 0.81) | 1.31 (1.13-1.52) | 0.62** (0.57 to 0.68) |
| Model 3: TBS + Age + FNBMD + PVF* | 1.43 (1.24-1.65) | 0.76** (0.71 to 0.82) | 1.21 (1.04-1.40) | 0.69* (0.64 to 0.75) |
| Model 4: All Predictors ^A | 1.78 (1.48-2.14) | 0.77** (0.72 to 0.83) | 1.29 (1.06-1.56) | 0.69* (0.64 to 0.74) |

*One or more SQ grade 2 or 3 vertebral fracture(s)

^ATBS, Age, FNBMD, PVF, prior fracture, parental history of hip fracture, body mass index

**p-value <0.003 compared to model 1

**p-value 0.06 compared to model 1

[†]p-value<0.001 compared to model 1

Table

Disclosures: John Schousboe, None.

MO0254

Why Are Additional Women with Fracture Identified by Measurement of Cortical Porosity than Identified by FRAX? Marit Osima¹, Rajesh Shigdel², Ragnar M Joakimsen³, Erik F Eriksen⁴, Ashild Bjornerem⁵. ¹Department of Community Medicine, UiT – The Arctic University of Norway, Norway, ²Department of Health & Care Sciences, UiT – The Arctic University of Norway, Norway, ³Department of Clinical Medicine, UiT – The Arctic University of Norway, Norway, ⁴Department of Clinical Endocrinology, Oslo University Hospital, Norway, ⁵UiT The Arctic University of Norway, Norway

The Fracture Risk Assessment Tool (FRAX) is useful to identify persons at risk for fracture but has limitations due to low sensitivity. Moreover FRAX does not take into account the cortical porosity, which is important for bone strength and is associated with fracture independent of FRAX. It is not clear why some women with fracture are identified by FRAX, while others are identified by cortical porosity. We wanted to 1) test the sensitivity and specificity for fracture when cortical porosity was combined with FRAX, and 2) compare the additional fracture cases captured by cortical porosity with those captured by FRAX.

We quantified FRAX score with femoral neck areal bone mineral density (FN aBMD) using dual-energy x-ray absorptiometry, and femoral subtrochanteric architecture using StrAx1.0 software in 211 postmenopausal women aged 54-94 years with non-vertebral fractures and 232 fracture-free controls in Tromsø, Norway.

Of 211 fracture cases, FRAX score >20% identified 45 women; the sensitivity was 21% (95% confidence interval (CI) 16-28) and specificity 93% (89-96), while porosity cut-off >80th percentile identified 61 women; the sensitivity was 29% (23-36) and specificity 88% (83-92). When porosity >80th percentile was combined with FRAX, the sensitivity was 43% (36-50) and specificity 83% (78-88). The additional fracture cases identified by porosity >80th percentile exhibited lower FRAX score (12.3 vs 27.4%) than those identified by FRAX alone, were younger, a smaller proportion had prior fracture (15.9 vs 69.7%), all p < 0.001, and marginally higher FN aBMD (796 vs 753 mg/cm², p = 0.07). They exhibited higher porosity of the total cortex (48.5 vs 41.7%), compact cortex (38.5 vs. 33.9%) and the transitional zone (61.8 vs 57.9%), thinner cortices (3.76 vs 4.17 mm), larger total and medullary cross-sectional areas (649 vs 566 and 231 vs 173 mm²), and lower cortical and total volumetric BMD (946 vs 1059 and 599 vs 722 mg HA/cm³), higher cross-sectional moment of inertia (2528 vs 2247 mm³), but lower buckling ratio (21 vs 28%), all p < 0.001.

Combining cortical porosity with FRAX increased the sensitivity and maintained high specificity for fracture, which is suggesting that cortical porosity capture additional elements of bone strength not captured by FRAX. We infer that the architecture in the additional fracture cases identified by cortical porosity, but not identified by FRAX, offset the positive impact of larger bone size on bone strength.

Disclosures: Ashild Bjornerem, None.

MO0255

Efficacy of Dual Energy Xray Absorptiometry for Evaluation of Biomechanical Properties. Il-Hyung Park¹, Sung Hwa Seo², Joo-Mi Lee³, Wonju Jeong⁴. ¹Kyungpook National University Hospital, South Korea, ²Department of Health & Medical Tourism, Gyeongju University, South Korea, ³Department of Orthopaedic Surgery, Kyungpook National University School of Medicine, South Korea, ⁴Department of Orthopaedic Surgery, Kyungpook National University Hospital, South Korea

Purpose: Bone mineral density (BMD) is an important index in diagnosis of osteoporosis and other metabolic bone diseases, prediction of fractures, and monitoring treatment. This study was to find a more feasible technique for prediction of osteoporotic fracture between DXA and QCT and to reveal the actual change of bone strength when BMD was changed. **Materials and Methods:** Ten of these 20 specimens were used as the demineralized group and the other 10 as the control. Each specimen was immersed in HCl solution at for a period of at least 10 minutes, up to 100 minutes, at an interval of 10 minutes for different levels of demineralization. BMD was measured using DXA and QCT. Uniaxial compression tests were conducted to measure biomechanical parameters. Pearson correlation analysis was used respectively between BMD and biomechanical parameters and between DXA and QCT. **Results:** Elastic modulus ($\gamma=0.87$) and yield stress ($\gamma=0.84$) showed a statistically significant correlation with DXA BMD. Through correlation analysis with QCT BMD and elastic modulus, correlation coefficient showed hemivertebra ($\gamma=0.80$) and trabecular ($\gamma=0.68$). In yield stress, there was a statistically significant correlation in hemivertebra ($\gamma=0.87$) and trabecular bone ($\gamma=0.84$). **Conclusion:** DXA is a current standard technique not only for diagnosis of osteoporosis but also for prediction of fracture risk compared to QCT. Actual decrease of bone strength was much greater than that of BMD by both DXA and QCT.

Disclosures: Il-Hyung Park, None.

MO0256

Functional muscle-bone unit assessed by 3D-DXA: Study in a cohort of post-polio syndrome patients. Luis Del Rio*¹, Silvana Di Gregorio¹, Yves Martelli², Dolors Grados³, Ludovic Humbert². ¹CETIR Grup Medic; RETICEF Instituto Carlos III, Spain, ²Galgo Medical, Spain, ³Reumatologia, Hospital Sant Rafael, Spain

Muscular weakness is the main symptom of post-polio syndrome (PPS) and is related to bone mass status as part of functional muscle-bone unit. Subjects suffering PPS have a low bone mass in the affected extremity and propensity to fall which increases the fracture risk. The aim of this study is to assess the influence of muscle atrophy and weakness on volumetric bone density and cortical thickness using the new 3D-DXA technology. Method: We analyzed the total body composition and hip DXA scans of 29 women (57.12 ± 7.51 years old) suffering PPS. The iDXA bone densitometer (GE Healthcare) was utilized. The 3D-DXA software (Galgo Medical) was used to obtain 3D patients-specific models from hip DXA scans. The algorithm uses a statistical model of shape and BMD distribution obtained from an atlas of quantitative computed tomography scans. The 3D modeling is performed in an intensity based 3D-2D registration process that maximizes the similarity between a projection of the statistical volumetric model and the 2D DXA image. We assessed the lean mass in limbs and bone mass (BMC) of integral bone (trabecular + cortical), Cortical Bone Mineral Content (CBMC), Trabecular Bone Mineral Content (TBMC), Cortical Thickness (CT) and volumetric Bone Mineral Density (vBMD) at total femur area. Comparison between affected and non-affected limb were performed using t-test. A multiple regression approach was used to assess correlations between parameters (3D parameters and lean mass in legs). To categorize the patient's cohort the results were compared with proprietary reference data of Spanish healthy adult young women. Results: Left limb was the most affected side. All parameters were significantly lower in the affected side in comparison with non-affected. Parameters measured at the non-affected side were below reference values. Six patients had a normal areal BMD, but all 3D parameters were lower in the affected side. Cortical volumetric BMD -vBMD-was significantly lower at affected leg when compared with non-affected leg. Limb lean mass had a negative correlation with all 3D parameters, and the correlation was especially high with cortical thickness ($R^2: 0.752$). Conclusion: This study demonstrates that PPS induces a significant decrease in the density of the bones the affected area. The information from the new 3D-DXA software indicates that cortical thickness is the main parameter affected by PPS, and was highly correlated with the decrease of lean mass.

Disclosures: Luis Del Rio, None.

MO0257

Vertebral Fracture Assessment vs X-ray in severe osteoporosis. Peter Schwarz¹, Linn Deleskog*², Barbara Nielsen³. ¹Glostrup Hospital, Denmark, ²Endokrinologisk Klinik PE, Rigshospitalet, Denmark, ³Research Centre of Ageing & Osteoporosis, Denmark

Background and Purpose: Vertebral fracture assessment (VFA) by dual X-ray absorptiometry (DXA) has been under evaluation for many years and its use is still debated. Radiographic imaging (X-Ray) of thoracolumbalis is considered to be gold standard in the assessment of vertebral fracture (VF). In a cross sectional setting we aimed to compare VFA and X-ray in patients with severe osteoporosis. As a second objective we wanted to study VFA as an effect marker in the evaluation of Teriparatide treatment.

Patients and Methods: A total of 23 patients suffering severe osteoporosis, 4 (17%) men and 19 (83%) women with a mean age of 69.2 years, had DXA and VFA performed at baseline and after 18 months of Teriparatide treatment. Of the 23 subjects, 18 patients (78%) were evaluated by X-ray image at baseline. VFs were defined in accordance with the grading system assessed by Genants, subdividing fractures after its deformity into mild (20-24%), moderate (25-39%) and severe ($\geq 40\%$).

Results: At baseline X-ray showed in total 41 VFs of whom 29 fractures were at the Th10 to L4 level: 5 ($\geq 20\%$); 21 (25-39%); and 3 ($\geq 40\%$). These numbers are in contrast to in total 53 vertebral fractures diagnosed by VFA ($p < 0.001$), at Th10 to L4 level: 22 ($\geq 20\%$); 13 (25-39%); and 18 ($\geq 40\%$).

After 18 months of Teriparatide treatment, the VFA showed 77 fractures in 23 participants, which was unchanged from the 77 fractures observed at baseline. Baseline fractures were: 31 ($\geq 20\%$); 19 (25-39%); and 27 ($\geq 40\%$) compared to: 26 ($\geq 20\%$); 22 (25-39%); and 29 ($\geq 40\%$) at 18 months of treatment. Five fractures had progressed one step to the next severity grade, 4 fractures were incident; 3 of them mild and 1 was of grade 3. Four mild fractures at baseline were evaluated normal at 18 month of treatment. However none of these assessments showed a change of vertebral height of more than 1-2 %.

Discussion: A very low specificity was seen using X-ray as reference and almost twice as many fractures appeared with VFA. In our cases evaluation of fractures above Th10 seemed impossible due to risk of misclassification. After 18 months of Teriparatide treatment VFA showed no increase in the total amount of fractures, even though 4 incident fractures were observed; 3 mild and 1 severe fracture.

Conclusion: Our pilot data demonstrates that VFA is inferior to X-ray in the diagnosis of VFs at all levels when using the same grading scale of fractures.

Disclosures: Linn Deleskog, None.

MO0258

Bone Structure and Osteocyte Lacunar Properties in Kidney Patients. Brad Hugenroth¹, Laura Armas¹, Mohammed Akhter*². ¹Creighton University, USA, ²Creighton University Osteoporosis Research Center, USA

Chronic kidney disease (CKD) is a major cause of skeletal fragility and subsequent fractures in patients. While fracture rate has increased, the mechanism and its treatment is still under investigation. This project provides both the qualitative and quantitative assessment of bone structure and unique osteocyte lacunar properties in iliac crest biopsies from stage 4 chronic kidney disease patients on dialysis (CKD4D) compared to data from healthy adults. Using MicroXCT200 system, bone biopsies were scanned at both macro (10 μ m resolution, Figure 1a, b) and submicron (0.6 μ m, Figure 1c) levels to study the trabecular bone structure and osteocyte lacunar characteristics. Five biopsies from CKD4D patients (age range 39 to 72 yrs) were analyzed. For macro scanning, we measured trabecular bone volume fraction (BV/TV). For high resolution scanning a 300 μ m thick section was cut and analyzed for two trabecular (nodes) and one cortical regions of interest. Images from high resolution (0.6 μ m) scans were analyzed for osteocyte lacunar void characteristic (volume and density). Osteocyte lacunar distribution is shown (Figure 1c) in a trabecular node as an example. All analyses were done using Avizo 9.0 software (FEI). Finally, the data were compared to healthy adults (n=8). Trabecular bone volume fraction (were lower in biopsies from the CKD4D patients 28 ± 10 , n=5) as compared to comparable healthy males (32 ± 6 , n=5). In addition, the osteocyte lacunar volume and density were lower (both cortical and trabecular) in CKD4D patients as compared to healthy adults (Figure 2). We note that the majority of biopsies from CKD4D patients show less cortical bone as result of trabecularization (Figure-1b) compared to healthy adults (Figure 1a), which may also be the major source of skeletal fragility. Declining osteocyte lacunar void volume and density (Figure-2) may suggest the filling in of spaces (voids) with mineral (osteopetrosis), thus increasing the brittleness of bone tissue. While these unique data may be helpful in understanding the skeletal fragility, additional work is needed to further investigate bone tissue properties in patients with chronic kidney disease to develop better therapies for fracture prevention.

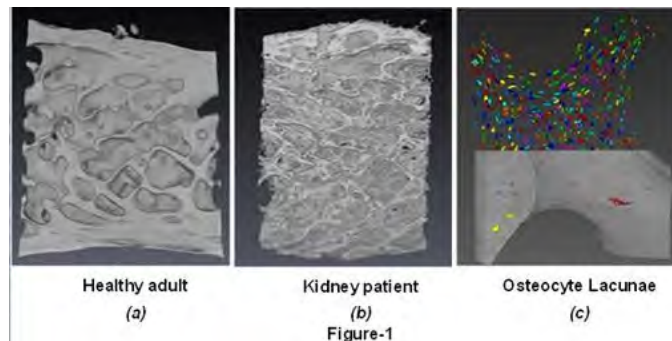


Figure-1. Macro and osteocyte lacunar images

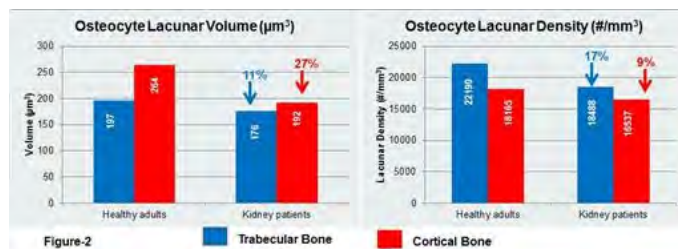


Figure-2. Osteocyte lacunar volume and density data

Disclosures: Mohammed Akhter, None.

MO0259

Comparative Analysis of Human Lumbar and Thoracic Vertebrae Using Micro Computed Tomography (micro-CT) and the Fine Structure Analysis (fineSA®) MRI Technique. Kirk McGilvray, PhD*¹, Samantha Telfer, PhD², James Rafferty, PhD², Amanda Cox², Lance Farr², Mario Mendoza³, Snehal Shetye, PhD¹, Christian Puttlitz, PhD¹. ¹Colorado State University, USA, ²Acuitas Medical Ltd, United Kingdom, ³University of California, Santa Barbara, USA

Introduction There is a need for a clinical in vivo imaging method to examine bone architecture that avoids ionizing radiation exposure; but which delivers detailed information comparable to high resolution CT. MRI avoids radiation exposure but it has traditionally provided relatively poor resolution and low signal-to-noise ratio at central sites. To address these limitations, we have developed a novel Fine Structure Analysis algorithm (fineSAU) based on MRI data that, delivers at selected locations a high resolution (typically =100 μ m depending on acquisition parameters) spatial

frequency spectrum representative of repetitive structure within the region of interest (ROI). fineSA was applied to human cadaveric spine specimens and the resulting structural metrics compared to those obtained from micro-CT structural analyses. Methods Ten vertebral bodies (VB) (T7-L5) from two cadaveric human spines were individually imaged via micro-CT and MRI modalities. Micro-CT scanning was performed with an isotropic voxel size of 37 μm (Scanco USA Inc. Wayne, PA), followed by fineSA MRI data acquisition (Siemens TrioTim 3.0T). fineSA trades the reduction from 2D imaging to a 1D spatial frequency spectrum for higher resolution sampling along the corresponding line of k-space. Features from the fineSA spectrum were extracted and used in linear support vector regression (SVR) against target values of trabecular number (Tb.N) calculated from micro-CT data to produce a fineSA metric. One example of extracted features is the mean spectral intensity calculated for selected frequency ranges. Rigid-body image registration was used to match the position of ROI acquired by MRI to the corresponding location in the micro-CT images. Two ROIs within each VB (anterior section and central) were acquired. Results Strong and statistically significant correlations were found between the fineSA metric and the micro-CT Tb.N data. The best result gave a Pearson correlation coefficient $R=0.98$, $p<0.05$, and showed the linear relationship between the MRI fineSA metric and Tb.N data, Figure 1. Conclusion The data demonstrated close similarity between the information provided by micro-CT and the fineSA analyses on a set of cadaver vertebrae. These data indicate the utility of MRI-based fineSA for extracting a measure strongly correlated to Tb.N for in vivo applications such as the determination of osteoporosis and potential fracture risk. Figure 1: Metrics derived from the FSA application compared to the micro-CT Tb.N data. Strong and statistically significant correlations (Pearson correlation coefficient $R=0.98$, $p<0.05$ and $R^2=0.96$) were observed.

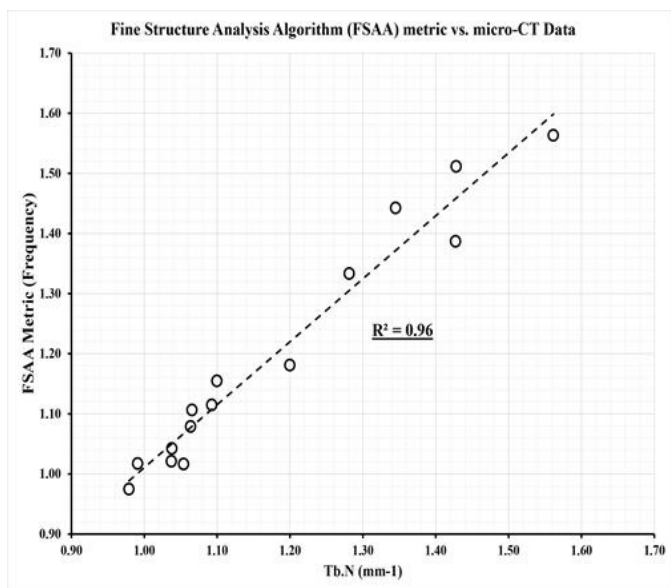


Figure 1

Disclosures: Kirk McGilvray, PhD, None. This study received funding from: Acuitas Medical Ltd

MO0260

Effect Of PTH (1-84) Treatment On Bone Quantity And Quality. Jorge Malouf^{*1}, Berta Magallares¹, Silvia Herrera¹, Ana Marin¹, Silvana DiGregorio², Luis Del Rio². ¹Hospital de la Santa Creu i Sant Pau, Spain, ²Cetir Medical Group, Spain

Objective: It has been demonstrated that PTH (1-84) treatment induced an improvement of both bone quality and quantity. The aim of the study is to assess effect of PTH (1-84) treatment on bone microarchitectural texture at lumbar spine using TBS. Method: A group of 20 osteoporotic women with a mean age and BMI of 70.1 \pm 6.8 yrs and 24.8 \pm 3.5 kg/m² were included in this study. All the patients had PTH (1-84) treatment during 24 months. DXA scans at lumbar spine L1-L4 were obtained using a Discovery densitometer (Hologic, USA) and acquired at baseline, and after roughly 12 and 24 month of treatment. The follow-up changes were analyzed by T-Test. Variation in % and in SD from baseline were assessed and normalized at 12 and 24 months. Responder and agreement analysis were performed. Statistical significance was set at $p<0.05$. Results: After normalization, both BMD and TBS at spine exhibited an increase at 12 and 24 months as presented figure 1. After 12 months and compared to baseline, significant increases ($p<0.05$) of +0.37 SD (+2.6%) and +0.42SD (+6.1%) were observed for TBS and BMD. After 24 months, BMD still increased significantly ($p<0.001$) to reach +0.52SD (+8.9%) while TBS remained stable +0.39SD (+2.7%, $p=0.08$). TBS and BMD changes at 12 and 24 months were not correlated ($r=0$; $p>0.8$). Interestingly, considering subjects who exhibited an increase, TBS exhibited an increase of 4.9% (70% of subjects) and 6.4% (60% of subjects) were observed at 12 and 24 months while increases of 8.4% (80% of subjects) and 10.9% (90% of subjects) were observed for BMD. Finally, agreements

between BMD and TBS in terms of changes were 80% and 70% at 12 and 24 months respectively. Conclusion: This study confirms that PTH (1-84) induces both BMD and TBS increases which is more pronounced in terms of BMD. Mean TBS and BMD increases are consistent with those previously published in the literature. After 12 months, TBS remained stable indicating a possible differentiating effect of the treatment on trabecular and cortical compartments supporting a finite modification of the trabecular structure recently hypothesized by Del Rio et al. (Bone 2015).

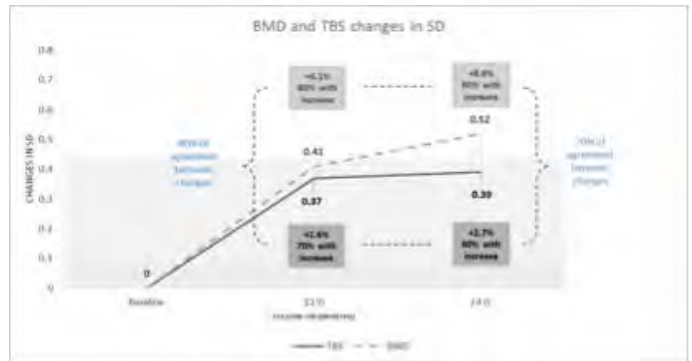


Figure 1: TBS and BMD changes at 12 and 24 months follow-up

Disclosures: Jorge Malouf, None.

MO0261

Establishing Bone Mineral Density Reference Curves for HR-pQCT. Lauren Burt^{*1}, Tolulope Sajobi², David Hanley³, Steven Boyd⁴. ¹University of Calgary, Canada, ²Department of Community Health Sciences & O'Brien Institute for Public Health, University of Calgary, Canada, ³CaMos Centre Director, Departments of Medicine, Community Health Sciences, & Oncology, University of Calgary, Canada, ⁴McCaig Institute for Bone & Joint Health, Department of Radiology, Faculty of Medicine, University of Calgary, Canada

High-resolution peripheral quantitative computed tomography (HR-pQCT) provides volumetric information on bone density and microarchitecture. For HR-pQCT to be used as a clinical assessment tool, used to identify individuals with osteoporosis or poor bone quality, normative reference data must be established. In our population-based cohort we aimed to define sex-specific reference intervals for bone mineral density and microarchitecture at the radius and tibia from 16 to 80+ years of age.

Participants from the Calgary cohort of the Canadian Multicentre Osteoporosis Study (CaMos) received a HR-pQCT scan of their non-dominant radius and left tibia (Scanco Medical, Switzerland). Total volumetric BMD (Tt.BMD), cortical BMD (Ct.BMD), trabecular BMD (Tb.BMD) and cortical porosity (Ct.Po) were assessed. Centile curves were generated for males and females at the tibia and radius using the Box-Cox power exponential (BCPE) method in the generalized additive models for location, scale and shape (GAMLSS) statistical package in R.

The study cohort consisted of 468 participants (308 females) with a median age of 53 (range 16 to 85) years. Sex-specific centile curves for age were created at the distal radius and tibia. Similar trends are observed for males and females. At the radius, Tt.BMD declines from 50 years onwards for both males and females. The percentage of cases below the 25th centile for Tt.BMD at the radius is 24% for females and 26% for males. The percentage of cases above the 75th centile for Tt.BMD at the radius is 26% for females and 25% for males. Ct.BMD increases up to 50 years, and then begins to decrease. As Ct.BMD decreases with age, Ct.Po increases substantially (50+ years). Similar curves were detected at the tibia.

We have developed sex-specific reference curves using HR-pQCT for the assessment of bone density and microarchitectural parameters at the distal radius and tibia. These data are valuable normative reference data for assessing bone health with HR-pQCT.

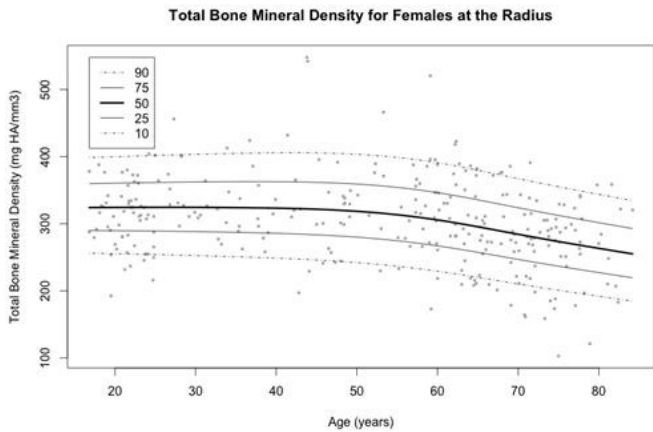


Figure 1
Disclosures: Lauren Burt, None.

MO0262

Factors causing curved femur in elderly women. Hiroyuki Tsuchie¹, Naohisa Miyakoshi¹, Yuji Kasukawa², Yoichi Shimada². ¹Akita university graduate school of medicine, Japan, ²Akita University Graduate School of Medicine, Japan

Purpose: Multiple factors are involved in the development of atypical femoral fracture (AFF), and excessive curvature of the femur is thought to be one of the factors. However, the pathogenesis of femoral curvature in elderly women is unknown. Therefore, we evaluated the influence of factors related to bone metabolism and posture on the development of femoral curvature in elderly women. Methods: One hundred and thirty-nine women who consented (mean age: 75 years) participated in the present study. Curvatures were measured using antero-posterior and lateral radiography of the femur, as within a previous report (mean angle: lateral curvature: 3.0°±3.3 degrees, anterior curvature: 9.8°±2.5 degrees). We divided the women into 2 groups, curved and non-curved groups, based on the average plus standard deviation at the cut-off between the groups (lateral curvature: 6.3 degrees, anterior curvature: 12.3 degrees). We compared the age, some laboratory examination items, such as alkaline phosphatase (ALP), calcium (Ca), inorganic phosphorus (IP), intact parathyroid hormone (PTH), 1,25-hydroxyvitamin D3 (1,25(OH)2D), 25-hydroxyvitamin D (25(OH)D), pentosidine, homocysteine, intact procollagen I N-terminal propeptide (PINP), and tartarate-resistant acid phosphatase 5b (TRACP5b), the bone mineral density (BMD) of the lumbar spine and proximal femur, lumbar lordosis angle, lumbo-sacral angle, and steroid usage. Results: On comparing the curved (n=25) and non-curved (n=114) groups with respect to the lateral curvature, age, intact PTH, pentosidine, and homocysteine level in the curved group were significantly higher than in the non-curved group (P<0.01, p<0.05, p<0.05, and P<0.05, respectively), and the Ca, 25(OH)D level, and proximal femur BMD in the curved group were significantly lower than in the non-curved group (P<0.05, P<0.01, and p<0.01, respectively). In a further comparison of the curved (n=19) and non-curved (n=120) groups with respect to the anterior curvature, age, intact-PTH level, and pentosidine in the curved group were significantly higher than in the non-curved group (P<0.01, p<0.05, and P<0.05, respectively), and the 25(OH)D level and proximal femur BMD in the curved group were significantly lower than in the non-curved group (P<0.01 and p<0.01, respectively). Conclusion: Femoral curvature in elderly women was strongly influenced by the age, presence of osteomalacia, a low BMD, and deterioration of bone quality.

Disclosures: Hiroyuki Tsuchie, None.

MO0263

Intravertebral Heterogeneity of Lumbar Vertebral Trabecular Bone Density is Associated with Vertebral Fracture Independently of Average BMD. Elise Morgan^{*1}, Brett Allaire², Paul Fein³, Darlene Lu⁴, Alexander Adams³, Douglas Kiel⁵, Serkalem Demissie⁴, Elizabeth Samelson⁶, Mary Bouxsein⁷. ¹Boston University, USA, ²Beth Israel Deaconess Medical Center, Harvard Medical School, USA, ³Department of Mechanical Engineering, Boston University, USA, ⁴Department of Biostatistics, Boston University, USA, ⁵Department of Medicine, Harvard Medical School, USA, ⁶Institute for Aging Research, Hebrew SeniorLife, USA, ⁷Beth Israel Deaconess Medical Center, Harvard Medical Center, USA

Purpose: The spatial variation, or heterogeneity, in bone density within the vertebral centrum has been proposed as a major reason why measures of the average BMD in the vertebra explain only 60-80% of the variation in bone strength and exhibit low sensitivity in identifying fracture risk. *In vitro* studies using CT scans of

cadaveric spine segments have identified measures of the intravertebral heterogeneity in trabecular density that are associated with vertebral strength, independent of average BMD [1,2]. The present study evaluated whether these heterogeneity measures are associated with prevalent vertebral fracture.

Methods: We conducted a case-control study from 148 subjects enrolled in the Framingham Heart Study Multidetector CT study. Cases included individuals (16 women, 21 men, ages 50-81) with moderate or severe prevalent vertebral fracture (VFX) in a level other than L3. Three age- and sex-matched controls (48 women, 63 men) with no VFX were selected for each case. Volumetric QCT scans of L3 were analyzed to determine integral BMD (iBMD) and to quantify the intravertebral heterogeneity in trabecular density. For heterogeneity measures, we first subdivided the trabecular centrum into 5mm contiguous cubic regions and then calculated the BMD for each cube. Two measures of heterogeneity were calculated from the cube BMD values for a given vertebra: 1) the interquartile range (IQR); and 2) the quartile coefficient of variation (QCV) in cube BMD values [2]. iBMD, IQR, and QCV were compared between cases and controls using Wilcoxon Rank Sum tests. Conditional logistic regression was used to test for associations with prevalent fracture.

Results: Individuals with prevalent VFX had higher QCV (0.19 vs. 0.15, p=0.003), similar IQR (28.6 vs. 32.7 mg/cm³, p=0.145), and lower iBMD (0.13 vs. 0.17 g/cm³, p<0.001) than controls. Increased QCV was associated with increased odds of VFX both with (p=0.014) and without (p=0.004) adjustment for iBMD and weight. After adjusting for iBMD and weight, individuals in the highest tertile of QCV had more than six-fold increased odds of VFX as compared to those in the lowest tertile (OR=6.47; 95% CI: 1.63-25.78) (Table 1).

Conclusions: Increased intravertebral heterogeneity in trabecular density, as measured by QCV in QCT scans of the lumbar spine, was associated with prevalent VFX, independent of average BMD.

References: [1] Hussein et al, Osteop Int, 24:979-89, 2013. [2] Hussein et al, Osteop Int, 24:3021-30, 2013.

Table 1. Odds ratios (and 95% confidence interval) for association between heterogeneity and prevalent vertebral fracture with adjustment for iBMD and weight in N=148 individuals (37 cases, 111 controls)

| Tertile | IQR | QCV |
|-----------|-------------------|-------------------|
| Tertile 1 | 1.00 (ref) | 1.00 (ref) |
| Tertile 2 | 1.07 (0.34-3.29) | 1.39 (0.40-4.84) |
| Tertile 3 | 3.14 (0.84-11.69) | 6.47 (1.63-25.78) |
| p-value | 0.183 | 0.014 |

Table 1
Disclosures: Elise Morgan, None.

MO0264

QCT-based hip structural analysis: comparison between osteoporotic and non- osteoporotic patients. Wojciech Glinkowski¹, Jerzy Narloch^{*2}. ¹Medical University of Warsaw, Poland, ²Chair & Department of Orthopaedics & Traumatology of Locomotor System, Center of Excellence "TeleOrto", Medical University of Warsaw, Poland, Poland

Introduction: Fracture risk of the femoral neck can be determined by the geometry of the proximal femur. Quantitative computed tomography (QCT) offers thorough 3D analysis with high spatial resolution. It provides information regarding bone geometry separately for cortical and trabecular bone. The aim of the present study was to investigate hip structural analysis differences between patients with diagnosed osteoporosis and those not.

Methods: In a preliminary study 24 patients aged 53-88 years (mean, 71.95 ± 9.12 years), diagnosed and treated in our department, underwent CT scan due to the history of low back pain after minor trauma. The patient's height ranged from 151 to 170 cm (Avg 161,6cm). The weight ranged from 41 to 88 kg (Avg. 63,35). T scores were utilized for analysis of proximal femoral geometry using QCTPro Software (Mindways Software Inc., Austin, TX). Patients were divided into two groups, based on T-score - osteoporotic (below -2,5 SD) and non-osteoporotic (above -2,5 SD). We compared 20 structural indices between the groups. Furthermore, correlations between selected bone density and morphometric variables were evaluated. Statistical analysis was performed using SAS 9.3 (SAS Inc., Cary, NC).

Results: Wilcoxon two-sample test revealed there were significant differences (p<0.05) between the groups concerning cortical indices: femoral neck BMD, intertrochanteric BMD, total BMD. Similarly for trabecular parameters, though there was the additional significant difference regarding trochanteric BMD. No significant differences were found for neck-trochanter angle (p=0.4), femoral neck width (p=0.23), height or weight. Patients meeting the densitometric criteria of osteoporosis were significantly older than the other group (p=0.02). Pearson correlation coefficients revealed strongest correlations of femoral neck cortical perimeter and area with femoral neck cortical BMD. Femoral neck cortical analysis showed that 42% of patients with no osteoporosis have a consistent distribution of cortical bone, compared to 8% in another group. The average results for the group are provided in the table:

| | Min. | Max. | Avg |
|-----------|-------|--------|---------|
| fnCBMD | 672,2 | 2147,9 | 1142,02 |
| itrCBMD | 809 | 975,3 | 884,37 |
| itrTBMD | 74,6 | 173,1 | 105,69 |
| totTBMD | 79,1 | 158 | 107,69 |
| FNTrangle | 34,7 | 51,6 | 43,35 |
| FNwidth | 25,7 | 41,8 | 30,19 |
| TOTscore | -4,2 | 0,54 | -2,3825 |

Conclusions

The fracture risk assessment determination in osteoporosis of the femoral neck can be determined by the geometry of the proximal femur. The study showed that structural, morphological and densitometric differences can be observed between patients with or without diagnosed osteoporosis when Quantitative computed tomography (QCT) was employed for thorough 3D analysis with high spatial resolution.

Acknowledgment: Project supported by N404 695940, National Science Center, POLAND.

Disclosures: Jerzy Narloch, None.

MO0265

Racial and Sexual Dimorphism in Cortical Porosity Requires Appropriately Positioned Regions of Interest (ROI). Ali Ghasem-Zadeh¹, Xiao-Fang Wang², Afrodite Zendeli², Ashild Bjørnerem³, Andrew Burghardt⁴, Roger Zebaze², Ego Seeman². ¹Austin Health, University of Melbourne, Australia, ²Depts Medicine & Endocrinology Austin Health, University of Melbourne, Australia, ³Dept of Health & Care Sciences, UiT The Arctic University of Norway, Norway, ⁴Department of Radiology & Biomedical Imaging, University of California, USA

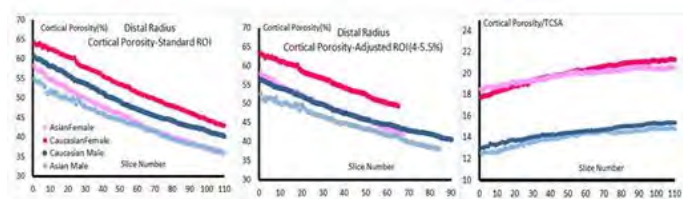
Rational Several studies report higher cortical porosity in men than women, and higher cortical thickness and lower cortical porosity in Asians than Caucasians [1,2]. Similarly, taller persons are reported to have relatively thinner and more porous cortices [3].

Men and Caucasians have a longer and wider radius and tibia compared with women and Asians respectively. When comparing, the automatically selected ROI is more distal in taller than shorter individuals; features that may partly account for some of these observations. The ROI selected scanning using by HR-pQCT is 9.5 mm and 22.5 mm proximal to the mid-joint line for distal radius and tibia, respectively in all individuals regardless of bone length which may over or underestimate traits being quantified.

Methods We imaged the non-dominant distal radius of 80Caucasian and Asian females and males, age range (25-46 yrs) using HR-pQCT the standard ROI and analysed slice by slice using StrAx 1.0 [4]. The ROI and number of slices were positioned at 4-5.5% forearm length and porosity was quantified comparing the Standard ROI vs ROI Adjusted for length alone and then length and total cross sectional area.

Results Biologically and statistically significant sex and racial differences in cortical porosity resulted after adjusting the ROI for length and total CSA such that only sex differences remain with high porosity in females than males in each race. However, after adjustments, neither males of different race, nor females of difference race differed in porosity [Fig 1-3].Conclusion Failure to correctly position the ROI produces misleading information concerning cortical porosity; erroneously suggesting men have higher porosity than women and that racial differences are present when they are not. Differences in appendicular length and total CSA need to be considered in the study of morphology in growth, aging, disease and drug therapy.

I-Walker, M.D.et al.,JBMR 2011 2-Wang, X.F. et al., JBMR 2009 3-Bjørnerem, Å. et al.,JBMR 2013 4-Zebaze, R., et al. Bone 2013



Disclosures: Ali Ghasem-Zadeh, None.

MO0266

The Reliability of Peripheral Quantitative Computed Tomography-Derived Marrow Fat Density and Area Measures Using Three Analysis Techniques. Zachary Brown¹, Jenna Gibbs¹, Andy Kin On Wong², Beverley Catharine Craven³, Jonathan D Adachi⁴, Lora Giangregorio⁵. ¹University of Waterloo, Canada, ²University Health Network, Canada, ³University Health Network - Toronto Rehabilitation Institute, Canada, ⁴McMaster University - St. Joseph's Health Care, Canada, ⁵University of Waterloo -Toronto Rehabilitation Institute, Canada

Purpose: To compare the precision for peripheral quantitative computed tomography (pQCT)-derived bone marrow density (MaD) and cross-sectional area (MaA) segmentation using three analysis techniques. Methods: Secondary data analysis of pQCT scans collected in 85 participants: young adults, n=18; mean age (SD): 25.4±3.2yr; older adults, n=48; mean age (SD): 71.9±8.2yr; and individuals

with spinal cord injury (SCI) (American Spinal Injury Association Impairment Scale categories A-C) (n=19; mean age (SD): 43.5±8.6yr) were completed. Repeat scans of the tibial shaft (66%) were performed using pQCT (Stratec XCT2000). Comparisons of test-retest precision error for MaD (mg/cc) and MaA (mm²) using a watershed algorithm (WS) method (Sliceomatic version 4.3) and two threshold-based edge detection methods (Stratec version 6.0 (S-TB) and BoneJ version 1.3.14 (BJ-TB)) were conducted. Intra-rater reliability calculations of the WS method were performed. Root mean square standard deviation (RMSSD) and root mean square coefficient of variation (RMSCV; root mean square coefficient of variation percent [RMSCV%]) were calculated to determine interrater and intrarater reliability. Results: RMSCV% for segmentation of MaD was ≥10% for all techniques (S-TB: 11.81-12.83%; BJ-TB: 14.46-24.58%; WS: 13.69-20.16%), RMSCV% for MaA were <5% for all techniques, except in the older adults group using the BJ-TB and WS methods (S-TB: 1.96-4.35%; BJ-TB: 2.37-5.09%, and WS: 2.25-6.65%). RMSCV% and RMSSD for MaD were similar between the young adult (12.83-14.83% and 2.61-2.82 mg/cc) and SCI groups (12.08-15.63% and 2.32-2.78 mg/cc), respectively. In the older adult group, RMSCV% and RMSSD were lower using S-TB (11.81% and 2.72 mg/cc) compared to BJ-TB (24.58% and 3.18 mg/cc) and WS (20.16% and 2.98 mg/cc). The lowest RMSCV% and RMSSD of MaA were achieved using S-TB (1.96-4.35 and 3.26-6.91 mg/cc) compared to BJ-TB and WS techniques (2.60-5.09% and 3.49-7.30 mg/cc; 2.25-6.65% and 3.81-12.63 mg/cc). Intra-rater RMSCV% for MaD using the WS method was lowest in younger adults (7.35%) followed by SCI (7.43%) and by older adults (11.23%) subgroups. Conclusion: The precision error for segmentation of pQCT-derived MaD using all three techniques exceeded 10%; whereas the precision for MaA using all three techniques ranged from 2.0% to 6.7%. Further investigation is necessary to determine alternative analysis methods with improved precision error for pQCT-derived MaD and MaA segmentation.

Table 1. Comparison of the reliability of peripheral quantitative computed tomography marrow fat measures, obtained using S-TB and BJ-TB and WS in study participants organized by subgroup.

| Reliability Data Variable and Method | Precision Error for Test-Retest Imaging Compared Between Methods | | | | | |
|---|--|--------------|------|-----------------|--------------|-------|
| | RMSSD (units) | | | RMSCV (% error) | | |
| | Young Adults | Older Adults | SCI | Young Adults | Older Adults | SCI |
| Marrow Density (mg/cc) | | | | | | |
| S-TB | 2.61 | 2.72 | 2.32 | 12.83 | 11.81 | 12.08 |
| BJ-TB | 2.69 | 3.18 | 2.78 | 14.46 | 24.58 | 15.63 |
| WS | 2.82 | 2.98 | 2.44 | 14.83 | 20.16 | 13.69 |
| Marrow Area (mm²) | | | | | | |
| S-TB | 3.26 | 6.91 | 3.80 | 1.96 | 4.35 | 2.05 |
| BJ-TB | 3.98 | 7.30 | 3.49 | 2.60 | 5.09 | 2.37 |
| WS | 3.81 | 12.63 | 5.75 | 2.25 | 6.65 | 2.44 |

BJ-TB – BoneJ Threshold Based Segmentation Method; MaA – Bone Marrow Cross-sectional Area; MaD – Bone Marrow Density; RMSSD – Root Mean Squared Standard Deviation; RMSCV – Root Mean Squared Coefficient of Variation; SCI – Spinal Cord Injury; S-TB – Stratec Threshold Based Segmentation Method; WS – Watershed-guided Manual Segmentation Method

Precision Table

Disclosures: Jenna Gibbs, None.

This study received funding from: CIHR New Investigator, Ontario Ministry of Research and Innovation- Early Researcher Award, Canadian Foundation for Innovation (L. Giangregorio)

MO0267

Genetic Risk Score Based on the Lifetime Prevalence of Femoral Fracture in 924 Consecutive Autopsies of Japanese Males. Heying Zhou¹, Seiji Mori¹, Tatsuro Ishizaki², Masashi Tanaka², Kumpei Tanisawa³, Makiko Mieno⁴, Motoji Sawabe⁵, Tomio Arai¹, Masaaki Muramatsu⁵, Yoshiji Yamada⁶, Hideki Ito¹. ¹Tokyo Metropolitan Geriatric Hospital, Japan, ²Tokyo Metropolitan Institute of Gerontology, Japan, ³Waseda University, Japan, ⁴Jichi Medical University, Japan, ⁵Tokyo Medical & Dental University, Japan, ⁶Mie University, Japan

Purpose: Recent large-scale meta-analyses of genome-wide association studies have identified a number of single nucleotide polymorphisms (SNPs) associated with low bone mineral density (BMD) or increased risk of fracture. However, the clinical utility of these SNPs for identifying individuals who are at increased risk of osteoporosis has been limited owing to relatively low odds ratios (ORs) for single SNPs to predict disease occurrence. The aim of this study was to develop a genetic risk score (GRS) by including multiple SNP profiles for predicting fracture risk based on lifetime prevalence of femoral fractures in 924 consecutive autopsies of Japanese males. Methods: A total of 922 non-synonymous SNPs located in 62 osteoporosis susceptibility genes were genotyped and evaluated for their association with the prevalence of femoral fracture in autopsy cases. GRS values were calculated as the sum of risk allele counts (unweighted GRS) or the sum of weighted scores estimated from logistic regression coefficients (weighted GRS). Results: Five SNPs (a-L-iduronidase rs3755955, C7orf58 rs190543052, homeobox C4 rs75256744, G patch domain-containing gene 1 rs2287679, and Werner syndrome rs2230009) showed a significant association (P < 0.05) with the prevalence of femoral fracture in 924 male subjects. The receiver-operating characteristic curves show that both the unweighted and weighted GRS adequately predicted femoral fracture; for the model predicted by the unweighted GRS with and without the effect of age at autopsy, areas under curves

(AUCs) were 0.750 (95% CI: 0.660–0.840) and 0.808 (95% CI: 0.728–0.887), respectively; for the model predicted by the weighted GRS with and without the effect of age at autopsy, AUCs were 0.770 (95% CI: 0.681–0.859) and 0.816 (95% CI: 0.736–0.895), respectively. The unweighted and weighted AUCs did not differ significantly. Multiple logistic regression analysis revealed that the OR for the association between fracture prevalence and unweighted GRS = 3 (n = 124) was 8.39 (95% CI: 4.22–16.69, P < 0.001) relative to a score < 3 (n = 797). Likewise, the OR for a weighted GRS of 6–15 (n = 135) was 7.73 (95% CI: 3.89–15.36, P < 0.001) relative to scores of 0–5 (n = 786). Conclusions: The GRS based on risk allele profiles of the five SNPs could help identify at-risk individuals and enable implementation of preventive measures for femoral fracture.

Disclosures: Heying Zhou, None.

MO0268

A Reduction in Kidney Function is Associated with Bone Mineral Density and Bone Loss in Elderly Swedish Women aged 75-85 years. Linnea Malmgren*, Fiona McGuigan, Anders Christensson, Kristina Åkesson, Lund University, Sweden

Introduction: Chronic Kidney Disease (CKD) is associated with bone mineral density and bone loss, but longitudinal studies in elderly women are scarce. Most studies estimate kidney function (estimated GFR, eGFR) from serum creatinine which is affected by muscle mass and diet while most eGFR equations were not developed in the elderly. Cystatin C (CysC), a GFR-marker which is relatively independent of body size, may be more appropriate in the elderly who typically have low muscle mass.

We estimated kidney function using CysC in the population based OPRA cohort of Swedish women (n=1044), all aged 75 years at baseline and followed for 10 years. We investigated the association between kidney function and BMD and specifically, how BMD, bone loss and bone markers differ between stages of CKD.

Methods: Plasma CysC was measured at age 75 (n=981), 80 (n=685) and 85 (n=365). Estimated GFR was calculated using the Chronic Kidney Disease Epidemiology Collaboration (CKD-EPI). At each visit, BMD was measured by DXA and biochemical bone markers were assayed. Multi-linear regression adjusted for weight, smoking and serum vitamin D was performed with kidney function as a continuous variable at ages 75-85. Women were stratified by CKD stage (1-2, 3A or 3B-5) to determine association between kidney function, BMD, bone loss and bone markers.

Results: Kidney function was associated with femoral neck (FN) BMD at age 75 and 80 (p=0.028; p=0.001). FN BMD did not differ with CKD stage, but women with stage 3A or 3B-5 had higher total body (TB) BMD (p<0.05 for age 75, 80 and 85). Stage 3A or 3B-5 lost more bone between age 75-80 at FN compared to stage 1-2 (p=0.016 and p=0.007) and stage 3B-5 lost more bone at TB (p=0.030). Apart from increased bone loss, women in CKD stage 3B-5 had higher PTH, phosphate, osteocalcin and ALP levels at baseline (all p<0.001). There was no association between kidney function and TB BMD or FN BMD at age 85 and the association between kidney function and bone loss was not significant from 80-85y.

Conclusion: Kidney function estimated by cystatin C is associated with BMD at the femoral neck in elderly women. Women with the worst kidney function have a higher rate of bone loss and increased levels of bone markers. The association between kidney function, BMD and bone loss is not seen in women >80 years, suggesting that in the very elderly the general decline in health outweighs the kidney specific decline with increasing age.

Disclosures: Linnea Malmgren, None.

MO0269

Differences in the Trajectory of Change in BMD Measured at the Total Hip and Femoral Neck between Men and Women Following Hip Fracture. Alan Rathbun*, Michelle Shardell², Denise Orwig¹, Richard Hebel¹, Gregory Hicks³, Thomas Beck⁴, Marc Hochberg¹, Jay Magaziner¹. ¹University of Maryland School of Medicine, USA, ²National Institutes on Aging, USA, ³University of Delaware, USA, ⁴Beck Radiological Innovations, USA

Approximately 260,000 older adults per year experience a hip fracture in the US, an event associated with increased morbidity and mortality. However, few studies have assessed sex differences in the sequelae of hip fracture. Women experiencing hip fracture have excess decline in bone mineral density (BMD) in the year following fracture compared to normal decrements due to aging. This study examined differences in BMD change between older men and women in the year after hip fracture. The sample (n=286) included persons enrolled in the Baltimore Hip Studies 7th cohort, a study that frequency matched (1:1) men and women on calendar time of fracture and hospital, who underwent dual-energy x-ray absorptiometry (DXA) measurement. DXA assessments occurred at study enrollment and two, six, and twelve months after hip fracture. Inverse-probability weighted independence estimating equations with robust standard error estimators, which accounted for missing data, selective survival, and within-patient clustering, were used to estimate sex differences in femoral neck and total hip BMD changes (g/cm²). Estimates were adjusted for baseline covariates selected a priori: age, race, weight, height, smoking, alcohol use, comorbidity, functional disability, depressive symptoms, bisphosphonates, hormone replacement therapy, and calcium supplements. Crude femoral neck

and total hip baseline BMD was significantly higher in men. Men also had larger average annual adjusted percent decline in BMD at both sites. There was a statistically significant adjusted twelve months percent decrease at the femoral neck of -4.8% (95% CI: -7.9%, -1.7%) in men and a statistically insignificant decline of -1.8% (95% CI: -4.7%, 1.0%) in women (Table 1). However, the difference (3%) in femoral neck change by sex did not reach statistical significance (P=0.16). Men had increasing prospective BMD decrements, while women had a decreasing rate of BMD decline. The differences in total hip BMD decline by sex were lower in magnitude and more similar between men and women (Table 2). The results suggest that men experience greater decrements in BMD compared to women after hip fracture, even after adjustment for age, body size, and use of bone-active treatments. Previous research has indicated that men and women have different patterns of bone loss associated with aging. Thus, these findings are likely due to sex differences in bone turnover or structural geometry following hip fracture.

Table 1. Unadjusted and adjusted percent change in femoral neck BMD between men and women following hip fracture at 2, 6, and 12 months.

| Time Point | Percent BMD Change | | | | P Value |
|------------|--------------------|----------------|----------|---------------|---------|
| | Males | | Females | | |
| Baseline | REF | REF | REF | REF | *0.32 |
| Δ T2 | 0.03 | [-2.51, 2.55] | -0.53 | [-3.52, 2.43] | 0.78 |
| Δ T6 | 0.04 | [-3.14, 3.22] | 1.08 | [-2.87, 5.05] | 0.69 |
| Δ T12 | -4.41 | [-8.15, -0.69] | -0.19 | [-4.45, 4.07] | 0.12 |
| Time Point | *Males | | *Females | | P Value |
| Baseline | REF | REF | REF | REF | *0.27 |
| Δ T2 | -0.24 | [-2.40, 1.90] | -1.08 | [-3.09, 0.91] | 0.56 |
| Δ T6 | -2.24 | [-4.95, 0.47] | -1.23 | [-3.65, 1.19] | 0.58 |
| Δ T12 | -4.79 | [-7.91, -1.68] | -1.83 | [-4.68, 1.01] | 0.16 |

*P value for the global test of the sex by time interaction.

* Adjusted for potential confounders: race, age, weight, height, smoking, alcohol use, bisphosphonates, hormone replacement therapy, calcium supplements, comorbidity count, instrumental activities of daily living, center for epidemiologic studies depression scale, and clinical site.

Table 1

Table 2. Unadjusted and adjusted percent change in total hip BMD between men and women following hip fracture at 2, 6, and 12 months.

| Time Point | Percent BMD Change | | | | P Value |
|------------|--------------------|---------------|----------|---------------|---------|
| | Males | | Females | | |
| Baseline | REF | REF | REF | REF | *0.92 |
| Δ T2 | 0.04 | [-2.50, 2.59] | -0.25 | [-3.09, 2.57] | 0.88 |
| Δ T6 | 0.51 | [-2.91, 3.93] | -0.17 | [-3.61, 3.26] | 0.77 |
| Δ T12 | -2.16 | [-5.71, 1.38] | -1.27 | [-4.84, 2.28] | 0.66 |
| Time Point | *Males | | *Females | | P Value |
| Baseline | REF | REF | REF | REF | *0.97 |
| Δ T2 | -0.37 | [-2.58, 1.83] | -0.53 | [-2.67, 1.60] | 0.93 |
| Δ T6 | -1.26 | [-4.05, 1.54] | -1.43 | [-3.83, 0.96] | 0.95 |
| Δ T12 | -2.13 | [-5.31, 1.04] | -1.47 | [-4.07, 1.12] | 0.71 |

*P value for the global test of the sex by time interaction.

* Adjusted for potential confounders: race, age, weight, height, smoking, alcohol use, bisphosphonates, hormone replacement therapy, calcium supplements, comorbidity count, instrumental activities of daily living, center for epidemiologic studies depression scale, and clinical site.

Table 2

Disclosures: Alan Rathbun, None.

MO0270

Femoral Neck Cortical and Trabecular bone and Mortality: The AGES-Reykjavik Study. Elisa Marques¹, Vilundur Gudnason², Gunnar Sigurdsson³, Thomas Lang⁴, Osório Meirelles⁵, Fjola Johannesdottir⁶, Kristin Siggeirsdottir⁷, Lenore Launer⁵, Gudny Eiriksdottir⁸, Tamara Harris⁵. ¹National Institute on Aging, USA, ²Icelandic Heart Association Research Institute, Kópavogur, Iceland; University of Iceland, Reykjavik, Iceland, ³Icelandic Heart Association Research Institute, Kópavogur, Iceland; University of Iceland, Reykjavik, Iceland; Landspítalinn University Hospital, Reykjavik, Iceland, ⁴Department of Radiology & Biomedical Imaging, University of California, San Francisco, CA, USA, ⁵Laboratory of Epidemiology & Population Science, Intramural Research Program, National Institute on Aging, National Institutes of Health, Bethesda, MD, USA, ⁶Faculty of Industrial Engineering, Mechanical Engineering & Computer Science, University of Iceland, Reykjavik, Iceland, ⁷Icelandic Heart Association Research Institute, Kópavogur, Iceland, ⁸Icelandic Heart Association Research Institute, Kópavogur, Iceland, USA

Objective: This study examined associations of femoral neck trabecular and cortical volumetric bone mineral density (vBMD) with all-cause mortality over 12 years of follow-up.

Methods: We conducted a prospective study in the Age Gene/Environment Susceptibility (AGES) –Reykjavik cohort. A total of 4,777 participants (2,091 men

and 2,686 women), aged 66-96 years were included in the present analyses. Femoral neck trabecular and cortical vBMD (g/cm^3) and minimal cross-sectional area (cm^2) of the femoral neck were calculated from quantitative computed tomography data. A Cox proportional hazard model was used to examine independent associations between trabecular and cortical BMD and total mortality.

Results: At baseline, men had significantly more cortical and trabecular bone in the femoral neck than women. Men also had larger femoral necks than women. During 12 years of follow-up with an average follow-up time of 10 years, 990 (47.3%) men and 917 (34.1%) women died. In men, every standard deviation (SD) increment in femoral neck trabecular vBMD was related to a significantly lower mortality risk (HR=0.92, $p=0.011$) and femoral neck cortical vBMD (per SD increment) was also associated to a significantly lower mortality risk (HR=0.91, $p=0.006$) after adjustment for age, body mass index, education, history of osteoporosis or medication known to affect bone health and femoral neck minimal cross-sectional area. In women, no significant associations were observed.

Conclusions: Trabecular and cortical bone density of the femoral neck is associated with mortality over 12 years of follow-up independent of bone size. Preventive strategies should be considered to increase and maintain high bone mass at both cortical and trabecular compartments at the femoral neck in older adults, particularly in men, to reduce mortality risk. The divergent results between men and women suggest complex relationships between the possible factors (such as vascular calcification and diabetes) associated with the mechanisms explaining the causal relationship between BMD and mortality risk.

Disclosures: Elisa Marques, None.

MO0271

Withdrawn.

MO0272

Physical exercise and vitamin D level improve BMD independently of each other and sex in Young Adults. Rune Tønnesen^{*1}, Lars Thorbjørn Jensen², Peter Hambak Hovind³, Peter Schwarz⁴, ¹Center of ageing & osteoporosis, Denmark, ²Department of Clinical Physiology & Nuclear Medicine, Herlev University Hospital, Denmark, ³Clinical Physiology & Nuclear Medicine, Righospitalet Glostrup University Hospital, Denmark, ⁴Research Centre of Ageing & Osteoporosis, Departments of Medicine & Diagnostics, Glostrup University Hospital, Denmark

Background & Purpose: Vitamin D in various forms has a very important role in bone health. Bone mineral density and exercise have an acknowledged positive association, both in short and long-term. Young men and women accrue the majority of their bone mass in the teens and twenties. Rarely investigated is the effect of exercise on BMD in late skeletal maturation.

We comparatively examine the effect of physical exercise and S-25[OH]D level on aBMD (areal BMD) measured at the femoral neck, total hip, (both sides) and the lumbar spine (L2-L4) in both sex.

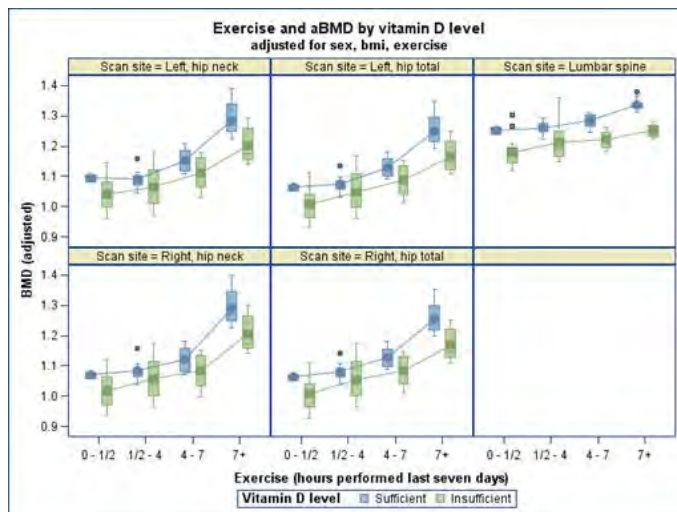
Material & Methods: We present data from a cross-sectional study examining exercise, aBMD measured with DXA and vitamin D level in a population of healthy young adults age 18 to 25 years. We grouped participants based on their Vitamin D levels into two groups; insufficient S-25[OH]D < 50 nmol/L and sufficient S-25[OH]D > 80 nmol/L. We grouped exercise (hours the last seven days) into four levels; 0-1/2, 1/2-2, 2-4, 4-7, or 7 hours or more

Results: The group with insufficient S-25[OH]D level had a systematic lower aBMD -0.080 (-0.138, -0.021) g/cm^2 ($p=0.008$) at all DXA-scan sites compared to the group with sufficient S-25[OH]D level.

We found a positive association between exercise and aBMD at all DXA-scan sites ($p_{trend}=0.0001$). All DXA-scan sites benefitted equally on aBMD from exercise, as there was no interaction between exercise and DXA-scan site ($p=0.09$).

Gender and DXA-scan site interacts ($p=0.002$) as men do not systematically have higher aBMD than women for all scan sites. The effect of gender on aBMD was only present at the hips, both total and femoral neck while it was absent at lumbar spine.

Conclusion: We conclude that aBMD in young healthy adults is influenced by physical activity independently of gender and S-25[OH]D status. Sufficient S-25[OH]D does not improve the effect of exercise; the group with sufficient S-25[OH]D had a systematically higher aBMD for all levels of exercise. Both genders had the equal effect of exercise.



BMD and Exercise for Vitamin D levels

Disclosures: Rune Tønnesen, None.

MO0273

Loneliness and Osteoporotic Fractures in Older Adults. Meltem Zeytinoglu^{*1}, Elbert Huang², Megan Huisinigh-Scheetz³, Diane Lauderdale⁴, Tamara Vokes⁵. ¹University of Chicago, USA, ²University of Chicago, Department of Medicine, Section of General Internal Medicine, USA, ³University of Chicago, Department of Medicine, Section of Geriatric & Palliative Medicine, USA, ⁴Department of Public Health Sciences, USA, ⁵University of Chicago, Department of Medicine, Section of Endocrinology, Diabetes, & Metabolism, USA

Objective: To determine whether osteoporotic fractures are associated with loneliness and other dimensions of psychological wellbeing, all of which have been shown to influence health domains in the elderly.

Methods: We used data from Wave 2 of the National Social Health and Aging Project (NSHAP), a study of social life and health in a nationally-representative cohort of older adults. Our main outcome of interest was osteoporotic fracture (Fx). Predictors of interest were subjective loneliness, depression, and anxiety. In multivariable analyses, we adjusted for age and gender.

Results: Among 2724 adults aged 57-89, 124 (4.5%) reported Fx in the past 5 years: 31 hip, 37 leg, 43 wrist, and 13 vertebrae. Compared to subjects without osteoporotic fractures, those with fracture were older (73.8 years vs 72.0, $p=0.017$), were higher percentage female (68% vs 54%, $p=0.002$), and had higher 12-month history of falls (18.9% vs 11.9%, $p=0.001$). There were no differences by Fx status in race ($p=0.98$), weight ($p=0.40$), or BMI ($p=0.50$). While self-reported physical activity was lower in Fx patients, the contrast was not statistically significant ($p=0.07$). We used the Center for Epidemiologic Studies Depression Scale to examine the association of depressive symptoms with Fx. When controlling for age and gender, subjects' report of "was lonely" was the only component associated with Fx [Odds Ratio (OR) 1.29, $p=0.023$]; overall depression score was not. In a separate analysis using the Hospital Anxiety and Depression Scale, anxiety and depression were associated with Fx ($p=0.043$), but this significance was lost when adjusting for loneliness ($p=0.167$). In a third independent analysis using questions from the UCLA loneliness scale, and controlling for age and gender, there was an association between Fx and "feel isolated" (OR 1.62, $p=0.002$), and "feel left-out" (OR 1.42, $p=0.024$), but not "lack companionship" (OR 1.11, $p=0.438$). The UCLA loneliness scale composite trended towards, but did not reach a statistical significance (OR 1.45, $p=0.062$).

Limitations: The small number of incident Fx within survey population. The cross-sectional nature of the survey data does not allow for determination of whether feelings of loneliness occurred prior to or following the Fx.

Conclusions: Feelings of loneliness, but not other indicators of emotional wellbeing, are associated with Fx. Further research is needed to understand whether loneliness is a cause or consequence of Fx.

Disclosures: Meltem Zeytinoglu, None.

MO0274

Total Protein and Dietary Protein Food Pattern are Not Associated with Bone Mineral Density (BMD) Among Protein Replete Middle-Aged Adults. Kelsey Mangano¹, Shivani Sahni², Robert McLean², Alyssa Dufour², Douglas Kiel², Katherine Tucker³, Marian Hannan⁴. ¹Institute for Aging Research/Hebrew SeniorLife/Harvard Medical School, USA, ²Institute for Aging Research, Hebrew Senior Life, Harvard Medical School, BIDMC, USA, ³Department of Clinical Laboratory & Nutritional Sciences, University of Massachusetts, USA, ⁴Institute for Aging Research, Hebrew SeniorLife, Harvard Medical School, BIDMC, USA

Total protein intake has been shown to be positively associated with BMD in adults, yet little is known about the influence of protein food source on bone health. It is advantageous to examine protein from a dietary pattern perspective due to nutrient-nutrient and food-food interactions within the diet, which may affect bone differentially. We examined the cross-sectional association of total protein and dietary protein patterns with BMD in a wide age range of men and women. BMD of the hip (n=2,921) and spine (n=2,840) were measured in Framingham 3rd Generation Study participants (2008-2011; GE Lunar Prodigy). Dietary intakes were estimated using the Willett food frequency questionnaire (2002-2005). Cluster analysis (SAS FASTCLUS) by the k-means method classified participants into clusters (protein patterns), determined by major source of dietary protein. First, multivariable linear regression was used to assess the relation between total protein and BMD. Next, analysis of covariance was used to compare crude and adjusted mean BMD among protein patterns. Models adjusted for age, sex, estrogen status, BMI, physical activity (PASE), supplemental use of calcium and/or vitamin D, current smoking, total energy and total protein (cluster models only). Average age 41 ± 9y (range: 19-72y; 85% <50y); 46% men; mean total protein intake 96 ± 18g/d (approximately 1.2g/kg/d on average; well above the recommended daily allowance [RDA] for protein 0.8g/kg/d). Total protein was not significantly associated with BMD at any site (p-range: 0.19-0.51). Five dietary protein patterns were identified based on the top food contributors to overall protein intakes (Table). Crude models showed significantly greater femoral neck BMD in the chicken pattern (1.008 ± 0.006g/cm²) compared to the red meat pattern (0.986 ± 0.006g/cm², p=0.03); no other statistically significant associations were observed at any other bone site. Following multivariable adjustment, no significant differences were observed across the protein patterns at any BMD site (p-range: 0.25-1.0). Results were similar when men and women were analyzed separately. Overall, in this cohort of men and women across a wide age range, dietary protein patterns were not associated with BMD of the hip or spine following adjustment for other factors associated with bone. These results suggest that among young to middle aged adults with protein intakes above the RDA, variation in protein intake is not associated with bone health.

| Least squares means ± SD ¹ bone mineral density by dietary protein pattern ² | | | | | |
|--|----------------------------|-----------------|---------------|---------------------------|---------------|
| Variable | Fish, plant & whole grains | Processed foods | Low fat milk | Red meat & processed meat | Chicken |
| | n=418 | n=1003 | n=408 | n=466 | n=626 |
| Total protein (g/d) | 91 | 92 | 96 | 92 | 105 |
| Bone sites³ | | | | | |
| Femoral neck | 1.003 ± 0.006 | 0.994 ± 0.007 | 0.993 ± 0.005 | 0.985 ± 0.006 | 1.005 ± 0.007 |
| Trochanter | 0.808 ± 0.005 | 0.801 ± 0.007 | 0.799 ± 0.004 | 0.796 ± 0.005 | 0.807 ± 0.007 |
| Total femur | 1.020 ± 0.006 | 1.014 ± 0.007 | 1.014 ± 0.005 | 1.009 ± 0.005 | 1.024 ± 0.007 |
| Lumbar spine | 1.236 ± 0.009 | 1.231 ± 0.011 | 1.222 ± 0.008 | 1.226 ± 0.009 | 1.234 ± 0.011 |

¹ The analyses were adjusted for multiple comparisons using Tukey's test (no significant difference observed).
² Protein food pattern named by top food contributors to overall protein intake on average
³ Adjusted for: age, sex, estrogen status, total energy, physical activity, body mass index, height, calcium supplement use, vitamin D supplement use, current smoking, total protein intake

Bone mineral density by dietary protein pattern in Framingham 3rd Generation participants

Disclosures: Kelsey Mangano, None.

MO0275

A Useful Clinical Model to Predict Hip Fracture in U.S. Nursing Home (NH) Residents: the first step in developing a screening tool in the nursing home. Sarah Berry¹, Zullo Andrew R², Yoojin Lee², Vincent Mor², Ralph D'Agostino³, David Dosa², Jeffrey Hiris², Geetanjali Banerjee², Douglas P Kiel⁴. ¹Hebrew SeniorLife/Beth Israel Deaconess Medical Center, USA, ²Brown University, USA, ³Boston University, USA, ⁴Hebrew SeniorLife & Beth Israel Deaconess Medical Center, USA

Purpose: Strategies used to screen community dwellers for fracture (fx) risk are unlikely to be useful in the NH setting because they fail to account for the variable functional status and life expectancy of NH residents. The purpose of our study was to use readily available clinical characteristics of NH residents to develop a model to predict 2-year risk of hip fx.

Methods: Medicare claims data was linked with the Minimum Data Set (MDS), a federally mandated needs assessment performed on all U.S. NH residents at least quarterly. We identified 1,461,909 long-stay residents with ≥ 100 days in the same

facility in 2007. We restricted the sample to residents aged ≥ 65 years with Medicare Parts A and D, not enrolled in Medicare Advantage or Hospice, and not prescribed an osteoporosis drug (n=784,779). A 2/3 random sample was selected to develop our model. Hip fx was defined using Medicare Part A diagnostic codes. Information on 40 characteristics from 8 domains (demographics, cognitive/function, neuropsychiatric, pain, falls, nutrition, sensory, and co-morbidities) was obtained using the baseline MDS assessment closest to the date the resident qualified as long-stay. Residents were followed until the first event of hip fx, death, or 2-yr follow-up. Competing risk regression was used to model univariate associations. An interaction with cognition and transfer ability was considered given observed differences in univariate and multivariate results. Characteristics associated with hip fx (p≤0.05) in the univariate models were entered into 8, domain-specific stepwise models. Characteristics from each domain that remained significant were entered into a final model.

Results: Among 523,169 residents, mean age was 84 yrs and 72% were female. During a mean follow-up of 1.5 yrs, 3.3% of residents experienced a hip fx, whereas 46.1% died without a hip fx. The association between characteristics and hip fx that remained in the final model are shown in the Table.

Conclusions: Using readily available clinical characteristics, we developed a useful model to predict hip fx in NH residents. In contrast to community based tools where age and prior fracture are strong predictors of fx, an interaction between cognition and transfer ability was the strongest predictor of hip fx. We will refine our model and validate it in the remaining 1/3 sample. If validated, this tool could identify a clinically meaningful risk threshold to guide osteoporosis treatment in the NH.

| | Final adjusted model HR (95%CI) |
|--|---------------------------------|
| Demographics | |
| Age (per year) | 1.00 (1.00, 1.01) |
| Male | 0.77 (0.74, 0.80) |
| Race | |
| Black (vs white) | 0.55 (0.51, 0.59) |
| Hispanic (vs white) | 0.87 (0.77, 1.00) |
| Asian (vs white) | 0.74 (0.62, 0.89) |
| Cognitive/Functional | |
| Bed mobility* | 1.28 (1.12, 1.46) |
| Walking* | 1.31 (1.22, 1.42) |
| Dressing* | 1.29 (1.17, 1.42) |
| Eating* | 1.35 (1.26, 1.53) |
| Urinary continence* | 1.35 (1.28, 1.43) |
| Interaction with cognition & transfer ability | |
| Severe dementia*transfer independence vs severe dementia*transfer dependence | 3.67 (2.97, 4.55) |
| Falls | |
| Recent fall | 1.30 (1.26, 1.34) |
| Neuropsychiatric | |
| New onset mental status change | 1.10 (0.94, 1.30) |
| Wandering | 1.34 (1.27, 1.40) |
| Psychotropic drug use | 1.01 (1.01, 1.02) |
| Pain | |
| No pain (vs daily pain) | 0.93 (0.88, 0.99) |
| Arthritis | 0.95 (0.92, 0.98) |
| Nutrition | |
| BMI (per kg/m ²) | 0.95 (0.94, 0.95) |
| Comorbidities | |
| Anemia | 0.93 (0.90, 0.97) |

Table: Results from a clinical model to predict the 2 yr risk of hip fx in NH residents

Disclosures: Sarah Berry, Amgen

MO0276

atypical femoral fractures: Radiographic features in 40 patients and Histomorphometric features in 11 patients. Waleed Hashem¹, aliya khan², zohair rahman², angela cheung³, ken pritzker³, brain lentle⁴. ¹McMaster University, Saudi arabia, ²McMaster University, Canada, ³university of toronto, Canada, ⁴british columbia university, Canada

This study describes characteristics, histomorphometric in 11 patients and radiographic features in 40 patients with AFF referred for evaluation. Methods: All patients referred for evaluation of AFF were reviewed. Patients meeting the ASBMR criteria were further evaluated and tetracycline labeled bone biopsies were completed. Radiographs were reviewed by musculoskeletal radiologists. Results: All fracture lines were transverse or short oblique and cortices were thickened. 12 patients had bilateral fractures. 72% of the fractures occurred spontaneously with 28% occurring after a fall. All patients were female except 2 men; average age was 67.5 years. 4 were Chinese, 9 were East Indian and the rest being Caucasian. We report 40 cases of AFF in patients on long term bisphosphonate (BP) therapy. Average BP duration of use was 10.5 years. 20 patients were on ALN alone, 3 patients were on RIS alone, 8 patients were on ALN and RIS sequentially, one of them intravenous ZOL was given for three years later and another one received two doses of Dmab. 2 patients were on PAM, 1 for 15 years then received ALN for 3 years for OI and the other one for 16 years as a part of MM protocol. 4 patients were treated by ALN then by Dmab. After they received ALN, 2 years of Teriparatide, and Dmab. 2 patients had AFF. 1 patient was on ALN for 3 years followed by Strontium Ranelate for 4 years. Thigh pain was seen in 26 patients for 1 to 15 months. PPI use was present in 14 patients and 12 women used HRT. 3 patients were on prednisone for RA and 1 patient for MS and 3 patients on inhaled steroid for asthma. All patients had 25OH Vit D > 50 nmol/L. 7 patients had CKD, however renal osteodystrophy was not evident. 1 patient had PHPT developed AFF while she was on Dmab. BMD T-score at any site, FN, TH, LS or 1/3R, was as following: 18 patients T-score ≤ -2.5, 19 patients T-score > -2.5 but < -1.0 and 3 patients had normal BMD. Conclusion: There was an evidence of tetracycline label in all of the biopsy specimens with the exception of 1 patient with necrotic biopsy. This indicates that bone mineralization is not impaired. Bone remodeling was variable

based on the static parameter, OS/BS. The majority of subjects had low OS/BS consistent with the MoA of BPs. Receiving Dmab after prolonged use of BP may increase the risk of AFF. Improved understanding of the pathophysiology leading to these fractures may be gained with further histomorphometric data, particularly from the site of AFFs, in large numbers of patients.

Disclosures: *Waleed Hashem, None.*

MO0277

Characteristics of Prevalent Vertebral Fractures Enhance Prediction of Prevalent Osteoporosis and Incident Fractures. Magnus Karlsson*¹, Mehrsa Kherad², Ralph Hasseri², Jan-Åke Nilsson², Inga Redlund-Johnell³, Caroline Karlsson⁴, Claes Ohlsson⁵, Dan Mellström⁶, Mattias Lorentzon⁶, Björn Rosengren⁷. ¹Skåne University Hospital Malmö, Lund University, Sweden, ²Departments of Orthopedics & Clinical Sciences, Lund University, Skåne University Hospital, Malmö, Sweden, ³Departments of Radiology & Clinical Sciences, Lund University, Skåne University Hospital, Malmö, Sweden, ⁴Departments of Orthopedics & Clinical Sciences, Lund University, Skåne University Hospital, Malmö, Sweden, ⁵Center for Bone & Arthritis Research, Institute of Medicine, Gothenburg University, Sahlgrenska University Hospital, Sweden, ⁶Department of Geriatric Medicine, Gothenburg University, Sahlgrenska University Hospital, Sweden, ⁷Departments of Orthopedics & Clinical Sciences, Lund University, Skåne University Hospital, Sweden

Purpose: Prevalent vertebral fractures are associated with low BMD and high fracture risk. We evaluated if characteristics of prevalent vertebral fractures enhance prediction of osteoporosis and new fractures. **Methods:** MrOS Sweden is a population based prospective observational study of 3014 community living men aged 69-81 years. 1453 underwent at baseline a lateral thoracic and lumbar spine radiograph (1427 readable) in which prevalent vertebral fractures were characterized according to the Genant semi-quantitative method. Total hip (TH) BMD was measured by DXA. During the 5-year follow-up, all incident fractures were objectively registered through radiographs. **Results:** 15% of the men had at baseline at least one prevalent vertebral fracture. Men with a prevalent vertebral fracture had lower TH BMD than men without (0.85±0.14 vs 0.94±0.14 g/cm²; p<0.001) (mean±SD). The lowest BMD was found in men with 3 or more vertebral fractures, biconcave vertebral fractures and fractures with vertebral body compression in the worst quartile (all p<0.05 compared to men with other vertebral fractures). The OR [mean (95% CI)] for prevalent osteoporosis with any type of prevalent vertebral fracture was 6.1 (3.9, 9.5) 3 or more vertebral fractures 21.2 (7.1, 63.6), a biconcave vertebral fracture 8.5 (2.5, 28.8) and a vertebral body compression in the worst quartile 22.2 (8.3, 58.8) compared to men with no baseline fracture. Men with a prevalent vertebral fracture had during the 5 year follow-up a relative risk (RR) [mean (95% CI)] of 3.3 (2.6, 4.3) to sustain incident fractures, 4.7 (3.5, 6.3) osteoporotic fracture and 2.9 (1.5, 5.5) hip fractures. The RR to sustain new fractures with one prevalent vertebral fracture at baseline was 2.0 (1.4, 3.0) with 2 or more fractures 5.5 (3.7, 7.8), with different types 5.7 (3.6, 8.5), with fractures in both thoracic and lumbar region 6.4 (4.5, 8.8) and with fracture in the worst compression quartile 4.0 (2.6, 5.9). Results remained after adjustment for number of prevalent fractures at baseline. **Conclusions:** Old men with a prevalent vertebral fracture have 6 times higher risk of having prevalent osteoporosis and during the next 5 year 3 times higher risk of sustaining fractures than men without prevalent vertebral fractures. Old men with 2 or more prevalent vertebral fractures, different types, fractures in both the thoracic and lumbar region and/or a vertebral body compression in the worst quartile are at especially high risk to sustain new fractures.

Disclosures: *Magnus Karlsson, None.*

MO0278

Development of models for predicting fracture-associated outcomes. Tuan Nguyen*¹, Steve Frost², Jacqueline Center³, John Eisman⁴. ¹Garvan Institute of Medical Research; University of Technology, Sydney, Australia, ²University of Western Sydney, Australia, ³Garvan Institute of Medical Research, Australia, ⁴Garvan Institute of Medical Research; University of Notre Dame School of Medicine, Australia

Background and Aim — A fragility fracture signals a series of adverse events, including recurrent fracture and mortality. Existing predictive models in osteoporosis have been developed to predict the risk of an initial fracture only, and do not predict the risk of subsequent fractures. In this study, we sought to examine the inter-relationships between an initial fracture, subsequent fracture, and mortality.

Methods — This study was based on a population-based cohort consisting of 757 men and 1224 women, aged 60 years and older, whose fracture status and health outcomes had been continuously monitored for up to 24 years. Fragility fractures were ascertained using X-ray report and circumstance of fracture. The incidence of mortality was obtained from individual participant during the follow-up period. Femoral neck bone mineral density and risk factors (eg lifestyle factors, physical activity, and concomitant illnesses and medications) were also ascertained at the initial visit as well as during the study period. A multistate Markov style of the Cox's

proportional hazards model was used to estimate the transition probabilities between three statuses (ie initial fracture, refracture, and mortality).

Results — The average age of participants was 70 years (range: 60 to 101). Approximately 25% of women and 12% of men had osteoporosis (BMD T-scores <-2.5). Among women without a fracture, approximately 37% would remain fracture-free during the subsequent 10-year follow-up; 24% would suffer a fracture, and 8% went on to refracture, and another 32% would die during this 10-year period. Among women with an initial fracture, 56% died after within 10 years, and 60% died after a recurrent fracture. Among men without a fracture, 38% would remain fracture-free, 14% would sustain a fracture, and 45% would die during the next 10 years. Among men with an initial fracture, the risk of a recurrent fracture was 16%, and the risk of death was 76%. However, in both genders, the risks of subsequent fracture and mortality were increased with advancing age and reduced BMD.

Conclusions — Individuals with an initial fracture have an increased risks of subsequent fracture and mortality, and the risk of fracture-associated mortality in men is greater than in women. The strong effects of advancing age and reduced BMD on the three related events of fracture, refracture, and mortality allow an individualized approach to the risk assessment for a man and woman. Such an assessment can aid patients and doctors to reach an informed decision concerning treatment in individuals with an initial fracture to reduce fracture and mortality in the general population.

Disclosures: *Tuan Nguyen, None.*

MO0279

Falls predict death differentially by type of fall in postmenopausal women. Risto Honkanen*¹, Nadia Afrin¹, Heli Koivumaa-honkanen¹, Toni Rikkonen¹, Joonas Sirola², Marjo Tuppurainen², Heikki Kröger¹. ¹University of Eastern Finland, Finland, ²Kuopio University Hospital, Finland

Fragility fractures are usually sustained in falls. We found that falls are related to morbidity differentially by type of fall and that falls also predict fractures differentially by type of fall. The purpose of this study was to estimate if and how a fall history predicts death in postmenopausal women before old age.

Methods: The study population was selected from the population-based Kuopio Osteoporosis Risk Factor and Prevention (OSTPRE) Study cohort, Eastern Finland by including all women aged 57-66 (N=10210) who responded to the fall question of the 10-year follow-up enquiry in 1999. Falls were classified into slip falls and nonslip falls. Information on deaths in 1999-2009 was obtained from the national population register. Kaplan-Meier and Cox regression were used as statistical methods.

Results: A total of 1962 women reported a fall during the preceding 12 months in 1999: 1069 women reported a single fall and 893 women reported two or more falls (frequent faller). A fall due to a slip was reported by 921 women and a fall due to other mechanism (nonslip) by 781 women.

A total of 722 women died during the 10-year follow-up: 152 out of 1962 fallers (7.7 %) and 570 out of 8248 non-fallers (6.9 %) (log rank p=0.179). Mortality in women who fell due to a slip was similar (6.6%) to that of non-fallers (p=0.741), while it was 9.3 % for women with a non-slip fall (p=0.009). In Cox regression, the hazard ratio (HR) for risk of death related to non-slip fall was 1.38 (p=0.009). Adjusting for strong predictors of death – smoking, self-rated health, No. of prescribed drugs, waist circumference and life (dis)satisfaction – weakened the HR of history of nonslip fall to 1.28 (p=0.077).

In conclusion, nonslip falls are a moderate predictor of death in women before old age, while slip falls are not. Apparently, nonslip falls are more related to health status but slip falls more to environmental factors.

Disclosures: *Risto Honkanen, None.*

This study received funding from: Academy of Finland

MO0280

Incidence and mortality after distal radius fractures over 50 years of age in South Korea. Tak Kim¹, Hyung Moo Park*², Yongchan Ha². ¹Korea University Anam Hospital, South Korea, ²Chung-ang University, South Korea

Abstract

Purpose: The purpose of this study was to assess the incidence and mortality of distal radius fracture in Koreans over 50-years-of-age using a nationwide claims database from 2008 to 2012.

Methods: This study was performed on patients ≥50-years-of-age treated for distal radius fractures with diagnosis code (ICD10; S52.5, S52.6). All patients were followed using patient identification code to identify deaths. The standardized mortality ratios (SMR; observed/expected deaths) of distal radius fracture were calculated based on age and gender-specific rates in the entire Korean population.

Results: The number of distal radius fractures increased by 48.1% over the 5-year study period (55,243 in 2008 and 82,230 in 2012). The incidence of distal radius fractures was 161.6/100,000 for men and 643.7/100,000 for women in 2008, and 187.7/100,000 for men and 818.2/100,000 for women in 2012. The cumulative mortality rate over the first 12 months after distal radius fracture was steady at 1.9% (1,052/55,243) in 2008 and 1.5% (1,206/82,230) in 2012. The mean year mortality over 5 years in men (3%, 1,497/59,835) over the first 12 months was 1.5-times higher than in woman (2%,

4,457/291,369). The mean of SMR of distal radius fracture at 1 year post-fracture was 1.24 in man and 0.99 in woman.

Conclusions: The nationwide data demonstrate that distal radius fractures are increasing, as is fracture-related mortality in South Korea. A public health strategy to prevent the distal radius fracture is necessary to minimize secondary osteoporotic fractures, reduce the economic burden, and improve public health.

Keywords: Distal radius fracture, Incidence, Mortality, Osteoporotic fracture

Disclosures: *Hyung Moo Park, None.*

MO0281

Mortality Risk, Cause of Death and Hip Fracture: A Prospective Study Over Two Decades of Hip Fracture Patients and Their Background Controls. My von von Friesendorff¹, Alicja Wizert², Jonas Ranstam², Fiona McGuigan³, Cecilia Rogmark⁴, Anna Holmberg¹, Anthony Woolf⁵, Kristina Åkesson¹. ¹Clinical Sciences Malmö, Lund University & Dept Orthopedics Malmö, Skåne University Hospital, Sweden, ²Lund University, RCSI, Skane University Hospital, Lund, Sweden, ³Lund University, Sweden, ⁴Dept of Clinical Sciences Malmö, Lund University & Dept Orthopedics Malmö, Skåne University Hospital, Sweden, ⁵Dept of Rheumatology, Royal Cornwall Hospital, Truro, United Kingdom

Background: The association between hip fractures in the elderly and mortality, particularly in the first year post fracture is well documented. But we still lack a clear picture if hip fracture is associated with higher mortality over the remaining lifetime and to which extent post-fracture mortality risk is influenced by age and sex over many years. We address these questions and identify the leading causes of death in hip fracture patients against the perspective of the background population.

Methods: The cohort consists of prospectively followed low-trauma hip fracture cases (757 women; 256 men) and 2026 individually matched community controls, from Malmö, Sweden who were followed for 22 years. Cause of death was obtained from the National Board of Health and Welfare, Sweden. Mortality risk within specific time windows (0-3 months, 3 months-1 year, 1-5 years, 5-10 years and 10-22 years) was analysed using Cox survival models. Fine and Gray models were used to determine short- and long term cause of death in a competing risks setting.

Results: Men were younger than women when they fractured (76 vs. 81). For both sexes and at all ages, excess mortality in hip fracture patients was evident across the study period. Men lost more life years than women ($p < 0.001$) and life expectancy was shorter, particularly after age 85. Among women, mortality risk was 2-times higher for up to 15 years post-fracture (RR 2.0 [95% CI 1.8-2.3]) and continued to be 50% higher for the 7 years until the end of the study (RR 1.6 [1.4-1.7]). For the same time periods, among men mortality risk was ~3-times (RR 2.7 [2.2-3.4]) and 2-times higher (RR 1.9 [1.6-2.2]). CVD, pneumonia, neurological diseases and musculoskeletal trauma were the most common causes of death among hip fracture patients and incidence was higher than in the background population. In the first 12 months post fracture, the highest risk of mortality was from CVD (RR 3.8 [2.0-7.2]); women RR 3.6 [2.5-5.1] and pneumonia (men RR 4.7 [1.9-11.3]; women RR 3.4 [1.6-7.1]). Men continued to be at risk of pneumonia in the long term (RR 2.1 [1.2-3.7]).

Conclusions: Patients who sustain a hip fracture and survive the first year continue to have a higher mortality rate than the background population for up to 20 years. These findings may be valuable in developing multi-disciplinary strategies that are specific to age and risk to improve outcome not just in the immediate post-fracture period, but thereafter.

Disclosures: *My von von Friesendorff, None.*

MO0282

Peri-Aortic Fat Is Associated with a Higher Risk of Vertebral Fracture and Negatively Associated with Volumetric Bone Mineral Density, Cross-Sectional Area and Compressive Strength of Lumbar Vertebrae: The Framingham Osteoporosis Study. Yi-Hsiang Hsu¹, Mary Bouxsein², Udo Hoffmann³, David Karasik⁴, L. Adrienne Cupples⁵, Caroline Fox⁶, Douglas Kiel⁷. ¹HSL Institute for Aging Research, Harvard Medical School, USA, ²Center for Advanced Orthopedic Studies, Beth Israel Deaconess Medical Center, USA, ³Massachusetts General Hospital, Department MR PET CT & Harvard Medical School, USA, ⁴Hebrew SeniorLife Institute for Aging Research, USA, ⁵Dept of Biostatistics, Boston Univ. Sch. of Public Health, Boston, USA, ⁶Brigham & Women's Hospital, Division of Endocrinology & Harvard Medical School, USA, ⁷Hebrew SeniorLife Institute for Aging Research & Harvard Medical School, USA

Both obesity and osteoporotic fracture are increasingly recognized as major health problems worldwide. The long prevailing view that BMI defined obesity is associated with beneficial effects on the skeleton has recently been challenged by contrasting studies demonstrating that visceral fat is associated with lower bone density. Peri-aortic adipose tissue volume (PAAT) is the adipose tissue surrounding the aorta, which is anatomically adjacent to the spine. Excess fat deposits at peri-aorta has been

found to be associated with a higher risk of CVD and CHD. We hypothesized that PAAT is associated with vertebral fracture risk and bone measures; and it may be due to its local paracrine effect on the adjacent lumbar vertebrae. Methods: To determine the association between PAAT and vertebral fracture risk as well as, volumetric integral BMD (In.vBMD); volumetric trabecular BMD (Tb.vBMD); and cross-sectional area (CSA), L3 lumbar vertebrae were measured by qCT on 3,138 men and women from the Framingham Study. The Compress Strength (CS) of vertebrae body was calculated. Subcutaneous abdominal tissue volume (SAT) and visceral abdominal tissue volume (VAT) were also estimated from the same qCT scans. Multivariable regression models were used to calculate least-squares means and to assess regression coefficients for the vertebral fracture risk and bone measures across PAAT quartiles. Results: Significantly negative correlations between PAAT and the bone measures were found in both men and women after adjusting for age, height, BMI and menopause status (women only). The magnitude of the correlations was stronger than that between BMI and the bone measures, and was in the opposite direction. PAAT was associated with a higher risk of vertebral fractures. Participants in the highest PAAT quartile had 2.2 times higher risk (OR=2.2; 95%CI=1.4~3.3) comparing to the participants in the lowest PAAT quartile. This association is not mediated by Tb.vBMD and independent from the effect of VAT, BMI and diabetes status, suggesting that excess fat deposits adjacent to vertebrae may have a detrimental paracrine effect on bone mass and strength of the adjacent lumbar vertebrae. To identify potential factors that may mediate the relation between high PAAT and a higher risk of vertebral fracture, we screen ~300 metabolites and lipids as well as ~180 protein biomarkers via proteomics on the same Framingham participants. These results will be presented at the ASBMR annual meeting.

Disclosures: *Yi-Hsiang Hsu, None.*

MO0283

Post-Fracture Care: Do we need to educate the patients rather than the doctors? The PREVOST Randomized Control Trial. Blandine Merle¹, Roland Chapurlat², Emmanuelle Vignot³, Thierry Thomas⁴, Julie Haesebaert⁵, Anne-Marie Schott³. ¹INSERM, France, ²Hospices Civils Lyon, France, ³Hospices Civils de Lyon, France, ⁴Hospital Bellevue, France, ⁵PIMER Hospices Civils de Lyon, France

Osteoporotic fractures predispose to future fractures and related morbi-mortality, but so far only a minority of patients with recent osteoporotic fracture receives adequate therapy. Therefore, we implemented a patient-centered post-fracture care program, Prevost (PREvention of OSTeoporosis) and evaluated its impact on BMD prescription and/or anti-osteoporotic treatment prescription. We enrolled 436 women aged 50 to 85 years in a multicenter, randomized controlled trial, while visiting emergency and orthopaedic departments of 21 hospitals from Region Rhône-Alpes, France, for a low-energy fracture of the radius/ulna or humerus, between march 2012 and december 2013. The randomization was stratified on age, hospital department type and site of fracture. The intervention was performed by a centralized coordinator who provided information solely to the patient about fragility fractures and osteoporosis, and encouraged her to contact her primary care physician for a follow-up concerning prevention of fragility fractures and osteoporosis. Patients from control group received usual care. All patients completed a standard questionnaire at baseline and 6 months later. Data were analyzed in intention to treat. At 6 months of follow-up, we found a significant increase in the primary endpoint, ie the proportion of women who initiated a post-fracture care, with 53% in the intervention group versus 33% for usual care (OR:2.3, 95%CI [1.54-3.36], $p < 0.001$). Post-fracture management was more frequent after wrist than humerus fracture (46% versus 31%, $p = 0.009$), and for women aged 50 to 69 than for those aged 70 and older, in both arms (48% versus 36%, $p = 0.01$). The intervention resulted in 50% of Bone Mineral Density (BMD) prescription versus 33% in usual care (OR:2.0, 95% CI [1.35-2.94], $p < 0.001$), and 41% of BMD test performed versus 25 % for usual care (OR:2.1, 95%CI [1.37-3.10], $p < 0.0005$). BMD results showed that 87% of women had a low BMD: 28% had a t-score $< -2.5SD$, 59% had a $-2.5 < t\text{-score} < -1SD$. Having performed a BMD test significantly increased the set-up of a pharmacological treatment: +22% (OR:3.3, 95%CI [4.08-16.8], $p < 0.001$) and Calcium/vitamin D supplementation: +38% (OR:5.1, 95%CI [3.26-8.12], $p < 0.001$). However, only 24% of women with humerus fracture were treated at 6-months post-fracture. In conclusion, our trial showed that a patient-centered care program with a dedicated coordinator can significantly improve post-fracture BMD testing and treatment initiation

Disclosures: *Blandine Merle, None.*

MO0284

Potential Years of Life Lost Following Low-Trauma Fractures in Canada. Robert B. Hopkins¹, Jonathan D. (Rick) Adachi¹, Louis Bessette², Natasha Burke¹, Jacques Brown², William D Leslie^{3,4}, Suzanne Morin⁴, Alexandra Papaioannou¹, Louisa Pericleous⁵, Jean-Eric Tarride¹. ¹McMaster University, Canada, ²Laval University, Canada, ³University of Manitoba, Canada, ⁴McGill University, Canada, ⁵Amgen Canada Inc., Canada

Purpose: To estimate the potential years of life lost (PYLL) due to low-trauma fractures in Canada.

Methods: Two national administrative databases from the Canadian Institute for Health Information were used to identify a cohort of Canadians age 50 years and

older with low-trauma fractures for years 2007 to 2011. Low-trauma fractures were categorized using ICD-10-CA codes as hip, humerus, vertebral, distal forearm, other sites (ribs/sternum, pelvis, trunk, clavicle, scapula, femur, patella, tibia/fibula), and multiple sites fractures (more than 1 of the preceding). PYLLs were calculated for each age group, sex and fracture type by adjusting the provincial and sex-based standard life tables estimate of life expectancy for the increased risk of death associated with a fracture. Results were compared with PYLL estimates due to other diseases reported by Statistics Canada in 2007.

Results: Based on an estimated 133,500 low-trauma fractures in Canada in 2011, the PYLL due to low-trauma fractures was 89,247 years (52,131 years for women, 37,116 years for men). While being only 23% of fractures hip fractures accounted for 43% of all PYLL. Specifically, a hip fracture at ages 50 to 59 years decreases life expectancy by 4.0 years for women and 3.9 years for men, which corresponds to a loss of 15% of life expectancy relative to the national average life expectancy. While the percent loss of years for hip fracture versus typical life expectancy was constant across age groups for women, it increased with age for men (up to 24% by age 90 to 99). After hip fracture, fractures at 'other sites' and vertebral fractures were the two other types of fractures contributing the most to PYLL (28% and 12% of the total PYLL, respectively). Although women have more fractures, the PYLL was on average 1.57 times higher per fracture for men than for women. When compared to other diseases, the PYLL for low-trauma fractures (89,247 years) is less than the PYLL for all respiratory diseases (159,117), breast cancer (138,808), colorectal cancer (127,560), and cerebrovascular diseases (104,971) but higher than the PYLL associated with other conditions such as pneumonia and influenza (44,462), HIV (36,312), and prostate cancer (21,812).

Conclusion: Low-trauma fractures are associated with a significant loss of life expectancy and burden of illness. Strategies to reduce the risk of fracture and improve post-fracture care should be implemented and optimized.

Disclosures: William D Leslie, None.

This study received funding from: Amgen Canada Inc

MO0285

Presence of low bone mass and osteoporosis and cognitive impairment contribute to an increased risk for falls and fractures in older cancer patients. Beatrice Edwards*, Holly Holmes, Juhee Song, Ming Sun, MD Anderson Cancer Center, USA

Background: Chemotherapy associated cognitive impairment has been recently described. This study aimed to typify the baseline bone health status and cognitive function in older adults prior to allogeneic stem cell transplant (HSCT), and during the care of solid tumors such as breast and prostate cancer.

Methods: This is a retrospective study at the Program for Healthy Aging at MD Anderson Cancer Center between January 1, 2013 and June 30, 2014. Patients with hematologic malignancies and solid tumors were assessed. Functional and cognitive status were determined with the Lawton instrumental activities of daily living, the Katz activities of daily living, and the Montreal cognitive status exam. Bone health status was determined by bone densitometry and risk factor analysis. Montreal cognitive testing was considered normal if score was >26/30, mild (19-25), moderate (12-18), and severe (<12/30). Patients with bone loss or osteoporosis and patients with normal bone density were compared utilizing Wilcoxon rank-sum test for continuous variables and Chi-square test or Fisher's exact test for categorical variables. Univariate logistic regression analysis was performed to identify factors associated with increased risk of bone disease. A p-value of less than 0.05 indicated statistical significance. SAS 9.4 (SAS Institute INC, Cary, NC) was used for data analysis.

Results: Fifty two patients, 24 with hematologic malignancies (myeloma, lymphoma, leukemia, and myelodysplastic syndrome), and 28 with solid tumors (breast and prostate cancer) were assessed. The mean age was 76 ± 5.6 years, 55% were female, 66% White, 27% African American, and 4% Latinos, 38 patients had low bone mass or osteoporosis (73%). Cognitive impairment was evident in 57% of patients of which 22 were mild (58%), 7 were moderate (19%) and one case was severe. Age predicted low bone mass with an OR of 1.139 per additional year of life, (95% CI, 1.019-1.274, $p=0.0223$). When the age at the time of bone test was dichotomized as ≥ 72 vs. < 72 , OR of age ≥ 72 comparing to age < 72 is 5.905 (95% CI, 1.548-22.530) and showed a significant association ($p=0.0093$). Coexistence of low bone mass/osteoporosis and cognitive impairment was evident in 55% of cases.

Conclusions: Cognitive impairment and bone loss/osteoporosis are common in cancer patients. Their co-existence likely contribute to falls and fractures in this population. Greater research in this area is needed.

Disclosures: Beatrice Edwards, None.

MO0286

Prospective study of C-reactive protein and risk of hip fracture. Junjuan Li*¹, Shouling Wu¹, Shivani Sahni², Chunpeng Ji¹, Xiang Gao³, Katherine Tucker⁴. ¹Kailuan Hospital, China, ²Institute for Aging Research, Hebrew SeniorLife, Harvard Medical School, USA, ³The Pennsylvania State University, USA, ⁴University of Massachusetts, Lowell, USA

Inflammation has been hypothesized to have a role in pathogenesis of bone fracture. However, few prospective studies have examined this hypothesis to date. We,

thus, investigated whether higher high-sensitivity C-reactive protein (CRP), a marker of chronic systemic inflammation, was associated with risk of developing hip fracture in ~ 100,000 Chinese adults from the Kailun cohort.

We included 96,689 Chinese participants (76,890 men and 19,799 women), aged 18 years or older, who were free of hip fracture, cardiovascular diseases, and cancer, and had available information on CRP at baseline (2008). Plasma CRP concentrations were determined using a high-sensitivity particle-enhanced immunonephelometry assay with the detection limit of 0.1 mg/L. Incident hip fracture cases over the follow-up (from 2008 to 2013) were identified by reviewing medical records. We used Cox proportional hazard models to assess the hazard ratio (HR) of hip fracture during follow-up, by baseline CRP status (< 0.5 mg/L, 0.5-0.99 mg/L, 1-2.99 mg/L, or 3+ mg/L), adjusting for age, sex, body mass index, physical activity, smoking status, alcohol intake, diabetes, and menopausal status (for women only).

The mean age was 52 y (range: 18-98). During 5.4 years of follow-up, we documented 187 new hip fracture cases. Participants with higher baseline CRP concentration had higher risk of hip fracture (P-trend < 0.0001). The adjusted HRs were 1(ref), 1.55, 1.98, and 1.89 (95%CI: 1.11, 3.22), for CRP concentration < 0.5 mg/L, 0.5-0.99 mg/L, 1-2.99 mg/L, and 3+ mg/L, respectively (Figure). We did not observe significant interaction between CRP and sex (P-interaction=0.54).

In conclusion, we observed a significant dose-response relation between higher CRP and increased hip fracture risk. This finding suggests that inflammation may be an important risk factor for hip fracture.

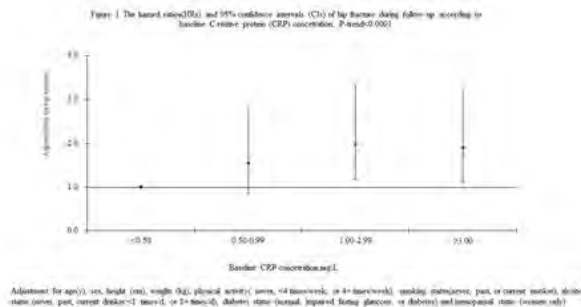


Fig. Adjusted HRs for hip fracture, according to baseline CRP status

Disclosures: Junjuan Li, None.

MO0287

Risk for Hip Fracture Ten Years Before and After Total Knee Replacement Surgery in the Entire Swedish Population. CECILIE HONGSLO VALA*¹, Johan Kärrholm², Sabine Sten³, Magnus Karlsson⁴, Valter Sundh², Mattias Lorentzon², Dan Mellström². ¹University of Gothenburg, Sweden, ²Goteborgs Universitet, Sweden, ³Uppsala Universitet, Sweden, ⁴Skåne University Hospital Malmö, Lund University, Sweden, ⁵Sahlgrenska University Hospital, Sweden

13,328 primary arthroplasties were 2013 reported in Sweden and from the literature it is known that osteoarthritis (OA) in the knee is associated with high bone mass. We therefore studied the risk of having a hip or vertebral fracture during the ten years before and after total knee replacement (TKR), in addition with mortality rates after surgery.

We followed the total Swedish population born 1902-1952 (n=4 546 820) during the period 1987-2002. We identified from the patient register coordinated by the Swedish National Board of Health patients with diagnosis and surgical code for TKR due to primary OA (n= 51 631), for hip fracture (n= 200 522) and vertebral fracture (n= 33 351). These data were linked with information from national census registers (Statistics Sweden) on mortality, marital status, migration, living place, professional occupation, income and education level. The risk time analyses were based on a Poisson regression models. Patients with total hip replacement were excluded. Data is reported as mean with 95% confidence interval within brackets.

A total of 3719 patients had both a TKR and a hip fracture. The relative risk (RR) for patients with knee OA to have sustained a hip fracture during the ten years preceding TKR was 0.59 (0.55-0.64) and during the ten year after the surgery 1.06 (1.01-1.11). The RR for patients with knee OA to have sustained a vertebral fracture during the ten years preceding TKR was 0.49 (0.42-0.58) and during the ten year after the surgery 1.21 (1.07-1.32). The lower risk of hip or vertebral fracture before and the higher risk of hip or vertebral fracture after TKR remained after adjustment for income, education, occupation and latitude. The RR for mortality the first five years after TKR was 0.26 (0.25-0.27) and after 10 years after TKR 0.99 (0.95-1.04).

Individuals with TKR due to primary OA had a low risk for hip or vertebral fracture the decade before surgery. This might be explained by the association between OA and high bone mass, but also by decreased physical activity level due to pain. After TKR the risk for hip and vertebral fracture increased. This might be explained by pain, increase of physical activity due to rehabilitation, and other biomechanical factors. The mortality rate was low after TKR, probably due to a selection bias for surgery.

Disclosures: *CECILIE HONGSLO VALA, None.*

MO0288

The Predictive Value of Falls History for Incident Fracture Decreases With Time: MrOs Sweden. Helena Johansson*¹, Nicholas Harvey², Anders Odén³, Magnus Karlsson⁴, Björn Rosengren⁴, Östen Ljunggren⁵, Cyrus Cooper⁶, Eugene McCloskey⁷, John Kanis⁷, Claes Ohlsson⁸, Dan Mellström⁸. ¹Centre for Metabolic Bone Diseases, University of Sheffield Medical School, Sweden, ²MRC Lifecourse Epidemiology Unit, University of Southampton, Southampton, UK; NIHR Southampton Biomedical Research Centre, University of Southampton & University Hospital Southampton NHS Foundation Trust, Tremona Road, Southampton, UK, United Kingdom, ³Centre for Bone & Arthritis Research (CBAR), Sahlgrenska Academy, University of Gothenburg, Gothenburg, Sweden; Centre for Metabolic Bone Diseases, University of Sheffield, Sheffield, UK, Sweden, ⁴Clinical & Molecular Osteoporosis Research Unit, Department of Clinical Sciences, Lund University & Department of Orthopedics, Skane University Hospital, Malmö, Sweden, Sweden, ⁵Department of Medical Sciences, University of Uppsala, Uppsala, Sweden, Sweden, ⁶NIHR Musculoskeletal Biomedical Research Unit, University of Oxford, Oxford, UK, United Kingdom, ⁷Centre for Metabolic Bone Diseases, University of Sheffield, Sheffield, UK, United Kingdom, ⁸Centre for Bone & Arthritis Research (CBAR), Sahlgrenska Academy, University of Gothenburg, Gothenburg, Sweden, Sweden

A history of falls is a strong risk factor for future falls but its predictive value wanes with time. The aim of the present study was to determine whether the predictive value of past falls for fracture remained stable with increasing follow-up time.

1836 elderly men recruited from the Swedish population to the MrOs study was studied. Baseline data included falls history, clinical risk factors, BMD at the femoral neck and calculated FRAX probabilities. 187 men experienced one or more incident major osteoporotic fracture during an average of 5.5 years follow-up. An extension of Poisson regression was used to investigate the relationship between falls history and FRAX to the risk of incident fracture. All associations were adjusted for age and time since baseline. To enable comparison with past falls, FRAX probability (without BMD) was dichotomised to above (high FRAX) and below (low FRAX) 15% for major osteoporotic fracture, which equalised the prevalences of high risk categories.

At enrolment 15.5% of the men had fallen during the preceding 12 months (past falls). Overall the HR of past falls vs no past falls was 1.61 (95% CI: 1.14-2.28) for incident osteoporotic fracture. The overall HR of high FRAX vs low FRAX was for incident osteoporotic fracture was 1.53 (95% CI: 1.07-2.17). After one year follow-up the HR of past falls for incident osteoporotic fracture was 2.21 (95% CI: 1.37-3.56) and after 5 years was 1.11 (95% CI: 0.63-1.96), with $p=0.081$ for the interaction between past falls and follow-up time. In contrast, after one year the HR for osteoporotic fracture for high FRAX above vs low FRAX was 1.58 (95% CI: 0.95-2.64) and after 5 years was 1.47 (95% CI: 0.88, 1.46). Thus the predictive ability of high versus low FRAX probability at baseline appeared to be stable with time (p for interaction between fracture probability and time > 0.30).

Although a history of falls is predictive of future osteoporotic fracture, the magnitude of this risk wanes with time, suggesting that inclusion of falls history in algorithms for calculation of long-term fracture risk may have limited utility.

Disclosures: *Helena Johansson, None.*

MO0289

Wrist Fracture and Risk of Subsequent Fracture: Post-hoc Findings from the Women's Health Initiative Study. Carolyn Crandall*¹, Kathleen Hovey², Jane Cauley³, Christopher Andrews⁴, Jeffrey Curtis⁵, Jean Wactawski-Wende⁴, Nicole Wright⁵, Wenjun Li⁶, Meryl LeBoff⁷. ¹University of California, Los Angeles, USA, ²State University of NY at Buffalo, USA, ³University of Pittsburgh, Graduate School of Public Health, USA, ⁴State University of NY at Buffalo, Buffalo, NY, USA, ⁵University of Alabama at Birmingham, USA, ⁶University of Massachusetts Medical School, USA, ⁷Brigham & Women's Hospital, Harvard Medical School, USA

Purpose. Wrist fractures are common in postmenopausal women and are associated with functional decline. Fracture patterns after wrist fracture are unclear. The goal of this study was to determine the frequency and types of fractures that occur after a wrist fracture among postmenopausal women.

Methods. We carried out a post-hoc analysis of data from the Women's Health Initiative Observational Study and Clinical Trials (1993-2010) carried out at 40 U.S. clinical centers with a mean follow-up duration 11.8 years. Participants were postmenopausal women aged 50-79 at baseline. Main measures included incident wrist, clinical spine, humerus, upper extremity, lower extremity, hip, and total non-wrist fractures and bone mineral density (BMD) in a subset.

Results. Among women who experienced wrist fracture, 15.5% subsequently experienced non-wrist fracture. The hazard for non-wrist fractures was higher among women who had experienced previous wrist fracture than among women who had not experienced wrist fracture: non-wrist fracture overall (hazard ratio [HR] 1.40, 95% confidence interval [CI] 1.33-1.48), spine (HR 1.48, 95% CI 1.32-1.66), humerus (HR 1.78, 95% CI 1.57-2.02), upper extremity (non-wrist) (HR 1.88, 95% CI 1.70-2.07), lower extremity (non-hip) (HR 1.36, 95% CI 1.26-1.48), and hip (HR 1.50, 95% CI 1.32-1.71) fracture (Table 1). Associations persisted after adjustment for BMD, physical activity, and other risk factors. Risk of non-wrist fracture was higher in women who were younger when they experienced wrist fracture (interaction p -value 0.02). Associations between incident wrist fracture and subsequent non-wrist fracture did not vary by baseline BMD category (normal, low bone density, osteoporosis).

Conclusions. A wrist fracture is associated with increased risk of subsequent hip, vertebral, upper extremity, and lower extremity fractures. There may be substantial missed opportunity for intervention in the large number of women who present with wrist fractures. The WHI program is funded by the National Heart, Lung, and Blood Institute, National Institutes of Health, U.S. Department of Health and Human Services through contracts HHSN268201100046C, HHSN268201100001C, HHSN268201100002C, HHSN268201100003C, HHSN268201100004C, and HHSN271201100004C.

Table 1. Associations between Incident Wrist Fracture and Subsequent Fracture

| | Total N | Event | Wrist Fracture | |
|---|---------|--------|----------------|--------------------|
| | | | No | Yes HR (95% CI) |
| Any non-wrist fracture | | | | |
| Crude | 160,930 | 33,979 | 1 (ref) | 1.54 (1.46-1.62) |
| Model 1 | 159,118 | 33,596 | 1 (ref) | 1.40 (1.33-1.48) |
| Model 2 | 139,790 | 29,540 | 1 (ref) | 1.40 (1.32-1.49) |
| Model 3 | 136,017 | 28,790 | 1 (ref) | 1.37 (1.29-1.46) |
| Spine Fracture | | | | |
| Crude | 160,930 | 5,373 | 1 (ref) | 1.75 (1.57-1.96) |
| Model 1 | 159,118 | 5,301 | 1 (ref) | 1.48 (1.32-1.66) |
| Model 2 | 139,790 | 4,658 | 1 (ref) | 1.51 (1.34-1.70) |
| Model 3 | 136,017 | 4,544 | 1 (ref) | 1.46 (1.29-1.65) |
| Humerus Fracture | | | | |
| Crude | 160,930 | 4,361 | 1 (ref) | 1.99 (1.76-2.26) |
| Model 1 | 159,118 | 4,309 | 1 (ref) | 1.78 (1.57-2.02) |
| Model 2 | 139,790 | 3,793 | 1 (ref) | 1.72 (1.50-1.96) |
| Model 3 | 136,017 | 3,676 | 1 (ref) | 1.67 (1.46-1.92) |
| Upper extremity (non-wrist) fracture¹ | | | | |
| Crude | 160,930 | 7,312 | 1 (ref) | 2.06 (1.87-2.27) |
| Model 1 | 159,118 | 7,228 | 1 (ref) | 1.88 (1.70-2.07) |
| Model 2 | 139,790 | 6,360 | 1 (ref) | 1.85 (1.67-2.06) |
| Model 3 | 136,017 | 6,184 | 1 (ref) | 1.80 (1.62-2.01) |
| Lower extremity Fracture² | | | | |
| Crude | 160,930 | 15,034 | 1 (ref) | 1.41 (1.30-1.53) |
| Model 1 | 159,118 | 14,867 | 1 (ref) | 1.36 (1.26-1.48) |
| Model 2 | 139,790 | 13,051 | 1 (ref) | 1.35 (1.24-1.48) |
| Model 3 | 136,017 | 12,718 | 1 (ref) | 1.30 (1.19-1.43) |

Model 1 adjusted for age, race, and BMI
 Model 2 is adjusted for covariates in Model 1 plus education, income, cigarette smoking status, pack-years of cigarette smoking, total metabolic equivalent of task hours/week, dietary calcium intake, calcium supplement intake, dietary vitamin D intake, vitamin D supplement intake, WHI-Hormone Therapy Trials treatment assignment, and WHI Dietary Modification Trial treatment assignment
 Model 3 is adjusted for covariates in Model 2 plus number of falls, alcohol intake, history of cancer, and physical function score
¹ Includes elbow, hand, upper arm/humerus, and shoulder fractures, excludes finger fractures
² Includes foot, knee/patella, upper leg, and lower leg/ankle fractures, excludes hip fractures

Table 1

Disclosures: *Carolyn Crandall, None.*

MO0290

Determining interdependency structure of contributors to bone microarchitecture: The Framingham Osteoporosis Study. Roby Joehanes*¹, Kerry Broe², David Karasik¹, Shivani Sahni¹, Robert McLean¹, Kelsey Mangan¹, Ching-An Meng², Yi-Hsiang Hsu¹, L. Adrienne Cupples³, Elizabeth Samelson¹, Marian Hannan¹, Mary Bouxsein⁴, Douglas Kiel¹. ¹Harvard Medical School, USA, ²Hebrew SeniorLife, USA, ³Boston University School of Public Health, USA, ⁴BIDMC & Harvard Medical School, USA

Previous studies of risk factors for BMD have largely focused on areal BMD measured using DXA. There have been very few studies looking across multiple risk factors for bone microarchitecture. Since some of these risk factors may exhibit interdependency structure, deciphering such structure may reveal the underlying pathways associated with bone microarchitecture. Here we present a study to investigate such structure.

Distal radius cortical porosity percent (CtPo) from high-resolution peripheral quantitative computed tomography (HR-pQCT) was measured in men and women in the Framingham Offspring cohort (2012-2014; n = 1,109; 43.2% male;

age=70.2 ± 7.7y, range: 46-92y). Based on previous studies of DXA-derived BMD, the contributing factors in our study included sex, age, height, weight, body mass index (BMI), smoking status, physical activity (assessed using the Physical Activity Scale for the Elderly), fasting blood glucose, type 2 diabetes, alcohol, and total intake of vitamin D and calcium. Structural Equation Modeling (SEM) using Onyx was used to confirm and explore the interdependency structure. Three latent variables, metabolic (from BMI, weight, physical activity, diabetes, and fasting blood glucose), nutritional (from vitamin D and calcium intakes), and behavioral (from smoking and alcohol intake) factors, were created as surrogate measurements inferred from observed variables.

Figure 1 shows the interdependency structure. Age, weight, and alcohol intake were directly positively associated with CtPo. Physical activity, height and the latent metabolic factor were significantly negatively associated with CtPo. Type 2 diabetes, after adjusting for fasting blood glucose, was not significantly associated with metabolic factor or CtPo. Smoking status is not significantly associated with CtPo (either directly or indirectly), and hence, behavior factor was dropped. Nutritional factors (vitamin D and calcium intakes) were indirectly associated with CtPo acting through the metabolic factor.

Significant associations between the latent metabolic factor and CtPo suggests that radius cortical porosity reflects a long-term metabolic status. Significant associations between CtPo and other factors, such as physical activity, age, height, weight, and alcohol intake, suggest additional pathways may influence cortical porosity.

Figure 1 note: Each edge is statistically significant (p<0.05). B refers to the beta coefficients.

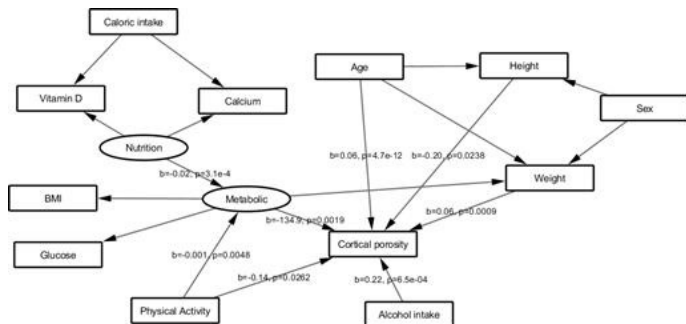


Figure 1. Interdependency structure of risk factors contributing to radius cortical porosity

Disclosures: Roby Joehanes, None.

This study received funding from: Friends of Hebrew SeniorLife and Investigator-Initiated Studies Program of Merck Sharp & Dohme

MO0291

Fracture Risk is Increased in Middle-aged Persons with Lower but Normal Range Serum Sodium Concentration: Results from the NEO study. Chantal Wiepjes¹, Renée de Mutsert², Anne de Boer², Natasia Appelman², Frits Rosendaal², Martin Den Heijer³. ¹VUMC / LUMC, Netherlands, ²LUMC, Netherlands, ³VU Medical Center Pb 70571007 MB Amsterdam, The Netherlands

Background Hyponatremia is the most common electrolyte disorder and sodium plays a role in the mineralisation of bone. Recent studies indicate that mild hyponatremia is associated with fractures in the elderly, but most studies were retrospective. The aim of this study was to prospectively investigate the association between serum sodium concentration with the occurrence of fractures in middle-aged men and women. Methods The Netherlands Epidemiology of Obesity (NEO) study is a population-based cohort of 6,671 men and women aged 45 to 65 years. At the baseline visit several measurements were performed including fasting blood sampling and anthropometry. Fractures during follow-up were obtained through the medical records of the general practitioners of the participants using the International Classification of Primary Care (ICPC) codes and search terms. We performed logistic regression analysis to calculate the odds ratio and 95% confidence intervals for a first fracture after the baseline visit associated with serum sodium, adjusted for age, sex, total body fat, waist circumference, physical activity, alcohol use, diuretic use, prevalent diabetes mellitus, and for menopausal status in women. Results After exclusion of participants with a fasting glucose concentration higher than 15 mmol/L (because of pseudohyponatremia, n=28) and missing values of serum sodium concentration (n=38), 6256 participants (43.8% men) were analyzed, with a mean and standard deviation (SD) of age: 56 (6) years, BMI: 26.3 (4.4) kg/m², serum sodium concentration: 142.3 (2.0) mmol/L. At baseline, 0.2% of the participants had hyponatremia (<135 mmol/L). During a mean follow-up of 2.5 years, 2.3% of the participants had at least one fracture. In the crude model, per mmol/L higher serum sodium concentration the odds ratio for fractures was 0.86 (95% CI: 0.78, 0.95). The odds ratio remained similar after adjustment for age, sex, total body fat, waist circumference, physical activity, alcohol use, diuretic use, prevalent diabetes mellitus, and menopausal status in women (OR 0.89, 95% CI: 0.81, 0.99). Conclusion Even within a normal range of serum sodium concentration, lower serum sodium concentration was associated with an increased risk of fractures in middle-aged persons.

Disclosures: Chantal Wiepjes, None.

MO0292

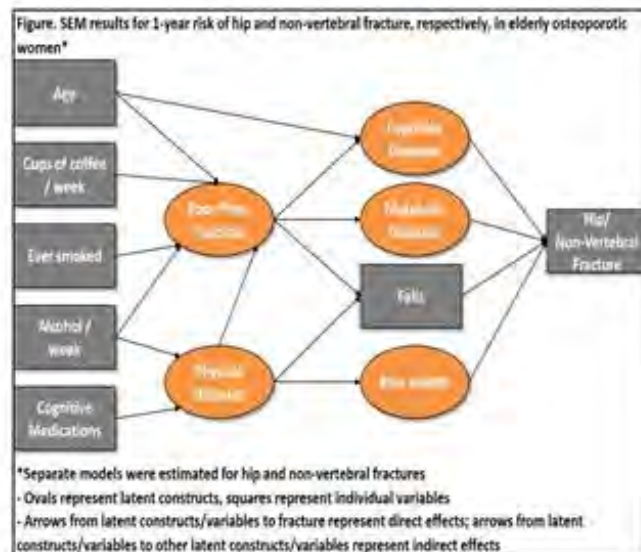
Imminent Fracture Risk in Elderly Osteoporotic Women: Underlying Relationships Between Risk Factors and Outcome. Rich Barron¹, Derek Weycker², John Edelsberg³, Alex Kartashov³, Barry Crittenden¹, Andreas Grauer¹, James Lani⁴. ¹Amgen Inc., USA, ²Policy Analysis Inc. (PAI), USA, ³Policy Analysis Inc., USA, ⁴Statistics Solutions Inc., USA

Background: Evidence on factors contributing to imminent risk for fracture within the next year among elderly women with osteoporosis is sparse. Moreover, data are limited about the underlying relationships between risk factors and the nature of their relationship with fracture.

Methods: A retrospective cohort design and data from the Study of Osteoporotic Fractures (SOF)—which includes 20 years of prospectively collected data on osteoporosis care and outcomes—were employed. The study population comprised all women aged ≥ 65 years with osteoporosis (T-score ≤ -2.5 at total hip) in the Caucasian cohort. Hip and other non-vertebral fractures were ascertained over a 1-year follow-up period. Potential predictors of fracture included anthropometric measures, BMD, cognitive function, comorbidities, drug use, fracture/fall history, lifestyle variables, medical symptoms, physical function/performance, quality of life, and vision status. Latent constructs (i.e., combinations of predictors that measure the same domain [e.g., physical function]), and inter-relationships between candidate risk factors and outcomes, were evaluated using factor analysis and structural equation modeling (SEM).

Results: The study population included 2,499 women who contributed 6,811 observations. During the 1-year follow-up, 2.2% had a hip fracture and 6.6% had a non-vertebral fracture. Latent constructs that were measured by factors with good model fit included: poor physical function (e.g., impairment in activities of daily living [ADL], physical activity), physical diseases (e.g., stroke, Parkinson's), cognitive diseases (e.g., Alzheimer's), metabolic diseases (e.g., BMD, prior fracture), and poor health (e.g., self-reported health). Direct and indirect predictors of hip and non-vertebral fractures—including individual variables and latent constructs—are reported in the Figure.

Conclusions: Indirect predictors of imminent fracture risk among elderly women with osteoporosis include age, physical function, physical diseases, and cognitive medications, which were related to each other and contributed to fall risk, cognitive function, overall health status, and metabolic diseases. Assessment of fracture risk for patients should be individualized considering the full picture of their health status, risk factors, and relationships between risk factors and fracture.



Figure

Disclosures: Rich Barron, Amgen Inc.

This study received funding from: Amgen Inc.

MO0293

Insulin Resistance Independently Had the Negative Association with the Bone Mineral Density in Korean young women. Sangmo Hong^{*1}, Woong Hwan Choi². ¹Hanyang University, South Korea, ²Department of Internal Medicine, Hanyang University College of Medicine, South Korea

Abstract Body The relationships between insulin resistance and BMD are not clear. Therefore, we conducted a cross-sectional study to examine the relationship between insulin resistance and BMD among Korean young adult population. This study is based on the Korea National Health and Nutrition Examination Survey (KNHANES) from 2008-2010. BMD and body composition were measured by DXA method. Insulin resistances were obtained by HOMA-IR equation. The relationship between BMD and HOMA-IR were analyzed with multiple regression models, which were adjusted with age, body weight, alcohol drink, exercise level and 25(OH) vitamin D level. We analyzed 1936 persons who were aged between 20-39 years old. HOMA-IR showed positive correlations with lumbar BMD and femur BMD in men and all BMD in women. However we adjusted with age body weight, alcohol drink, exercise level and 25(OH) vitamin D level, insulin resistance had negative relationship with Lumbar BMD (B=-0.123, p<0.001), femur neck BMD (B=-0.057, p=0.01). In this study, BMD were decreased with the increase of insulin resistance in Korean young adult.

Disclosures: Sangmo Hong, None.

MO0294

Serum phosphate levels are related to all-cause, cardiovascular and COPD mortality in men: the Rotterdam Study. Natalia Campos^{*1}, Lies Lahousse², Guy G Brusselle³, Bruno H Stricker⁴, Albert Hofman⁴, Henning Tiemeier⁵, Oscar H Franco⁴, André G Uitterlinden⁶, M Carola Zillikens⁶. ¹Erasmus MC, The Netherlands, ²Department of Respiratory Medicine, Ghent University, Belgium, ³Department of Respiratory Medicine, Ghent University Hospital, Belgium, ⁴Department of Epidemiology, Erasmus Medical Center, Netherlands, ⁵Department of Psychiatric Epidemiology, Erasmus Medical Center, Netherlands, ⁶Department of Internal Medicine, Erasmus Medical Center, Netherlands

High serum phosphate levels have been associated with increased mortality risk in chronic kidney disease (CKD) but the nature of such a relation in the general population is unclear. In two cohorts from the Rotterdam Study (RS-I and RS-II) we assessed the relation between phosphate levels and all-cause and cause-specific mortality divided into 7 groups, using ICD-10: cardiovascular diseases (CVD), cancer, external causes, infectious diseases, dementia, chronic lung diseases and other causes. In 3732 elderly participants from RS-I and 2494 from RS-II serum phosphate levels were measured in the fasting state and assessed with same technique. Cox and competing risk regression models were applied, adjusted for age, BMI and smoking; results from both cohorts were meta-analyzed applying fixed-effect model. Pooled HRs (95% CI) are expressed for each 1 mg/dL increase in serum phosphate levels. Due to interaction by gender, we performed sex-stratified analyses. Average follow-up was 14.5 y (RS-I) and 10.9 y (RS-II). A significant positive association was found between phosphate and all-cause mortality in men 1.46 (1.27-1.69) but not in women (0.90 (0.77-1.04)). In men, higher phosphate increased the risk for CVD mortality (1.66 (1.29-2.14)), other causes (1.67 (1.16-2.41)) and chronic lung disease mortality (1.96 (1.02-3.76)), the latter driven by mortality due to Chronic Obstructive Pulmonary Disease (COPD) (4.39 (2.12-9.07)). No significant relations were found for mortality due to infections, cancer, dementia or external causes in men. Analyses restricted to male subjects with phosphate levels within normal range yielded essentially same results. Our findings were not essentially modified after adjustments for calcium and 25-hydroxyvitamin D levels; further adjustment for eGFR produced only slight attenuation: CVD 1.62 (1.27-2.08), other causes (1.82 (1.26-2.62)), lung diseases 1.94 (1.03-3.64), COPD 3.70 (1.89-7.27). We observed no associations between phosphate levels and cause-specific mortality in women. In conclusion, even within normal range serum phosphate levels are associated with increased all-cause, cardiovascular and COPD mortality in men but not women not explained by calcium, 25-hydroxyvitamin D levels or kidney function. Our results suggest that the concept of phosphotoxicity beyond CKD population deserves further attention. The novel finding of an association of phosphate levels with COPD mortality needs further research on underlying mechanisms.

Disclosures: Natalia Campos, None.

MO0295

The Association Between Inflammatory Markers and Measures of Hip Bone Density, Geometry, and Strength in Older Men: the Osteoporotic Fractures in Men Study. Kamil Barbour^{*1}, Stephanie Harrison², Eric Orwoll³, Jane Cauley⁴. ¹University of Pittsburgh, USA, ² California Pacific Medical Center Research Institute, San Francisco, CA, USA, USA, ³Portland VA Medical Center, & Oregon Health Sciences University, Portland, Oregon, U.S.A, USA, ⁴Department of Epidemiology, University of Pittsburgh, Pittsburgh, PA, USA, USA

Introduction: Despite compelling evidence linking inflammation and fractures, the mechanism by which inflammatory markers influence bone biology is not well understood. The relatively weak association between inflammatory markers (IM) and bone mineral density (BMD), has led investigators to hypothesize that inflammation may increase fracture risk through other mechanisms (e.g., geometry, and strength).

Methods: To test this hypothesis, we examined the association between IM and measures of bone density, geometry, and strength in 239 men (mean age= 73.7 ± 5.8 years) from the Osteoporotic Fractures in Men Study (MrOS). Interleukin-6 (IL-6), tumor necrosis factor alpha (TNF-α), and soluble receptors (SR) for IL-6 (IL-6 SR) and TNF-α (TNF SR1 and TNF SR2) were measured using enzyme-linked (ELISA). C-reactive protein (CRP) was measured with an immunoturbidimetric assay. All bone measures were assessed using quantitative computed tomography (QCT) of the proximal femur. Linear regression models were used to determine the association between inflammatory marker levels and the bone measures. Multivariate models were adjusted for age, race, BMI, clinic site, fracture history, diabetes, heart disease, rheumatoid arthritis, areal BMD (aBMD), smoking, physical activity, health status, total calcium and vitamin D intake , and use of non-steroidal anti-inflammatory drugs, statins, corticosteroids, and selective serotonin reuptake inhibitors.

Results: Levels of IL-6, TNF-α, TNF SR1 and TNF SR2 were not associated with hip vBMD or structure. Higher levels of CRP were associated with greater trabecular volumetric BMD (vBMD) of the total hip and trochanter, but lower cross-sectional area (for both trochanter and femoral neck) and proximal femoral strength. Moreover, men with 2 or 3-6 inflammatory markers in the highest quartile compared with men who had 0 or 1 inflammatory marker(s) in the highest quartile had significantly lower trochanteric cross-sectional area (32.3 and 32.8 vs. 34.0 cm², respectively), p-trend=0.03. Conversely, higher IL-6 SR was associated with increased cortical volume of the total hip, femoral neck and trochanter, and higher proximal femoral strength.

Conclusions: Higher levels of inflammatory markers were not associated with lower vBMD, but a high inflammatory burden was associated with lower trochanteric cross-sectional area, and higher CRP was associated with lower cross-sectional area and proximal femoral strength. On the other hand, men with higher IL-6-SR levels had greater cortical volume and bone strength. Our findings suggest that inflammation may play a larger role for bone geometry as opposed to bone density.

Table: The association between inflammatory markers and measures of hip bone density, geometry, and strength in older men: the Osteoporotic Fractures in Men Study (MrOS)

| Bone Measures | IL-6 SR | | | | | CRP | | | | | Number of Inflammatory Markers in the Top Quartile | | | | |
|--|---------|---------|---------|---------|----------------------|---------|---------|---------|---------|----------------------|--|-------|-------|-------|-----|
| | Q1 Mean | Q2 Mean | Q3 Mean | Q4 Mean | P [†] Trend | Q1 Mean | Q2 Mean | Q3 Mean | Q4 Mean | P [†] Trend | 0 | 1 | 2 | 3-6 | |
| Density | | | | | | | | | | | | | | | |
| Total hip cortical vBMD (g/cm ³) | .32 | .32 | .32 | .32 | .87 | .32 | .32 | .32 | .32 | .68 | .32 | .32 | .32 | .32 | .28 |
| Total hip trabecular vBMD (g/cm ³) | .39 | .39 | .39 | .39 | .22 | .39 | .39 | .39 | .39 | .40 | .39 | .39 | .39 | .39 | .25 |
| Femoral neck cortical vBMD (g/cm ³) | .32 | .31 | .31 | .32 | .97 | .32 | .31 | .32 | .32 | .52 | .32 | .32 | .32 | .32 | .30 |
| Femoral neck trabecular vBMD (g/cm ³) | .47 | .47 | .47 | .47 | .37 | .47 | .47 | .47 | .47 | .68 | .47 | .47 | .47 | .47 | .39 |
| Trochanter cortical vBMD (g/cm ³) | .54 | .54 | .54 | .54 | .69 | .54 | .53 | .54 | .54 | .43 | .53 | .53 | .53 | .54 | .13 |
| Trochanter trabecular vBMD (g/cm ³) | .39 | .39 | .39 | .39 | .22 | .39 | .39 | .39 | .39 | .40 | .39 | .39 | .39 | .39 | .28 |
| Geometry | | | | | | | | | | | | | | | |
| Total hip cortical volume (cm ³) | 44.9 | 47.3 | 47.4 | 48.9 | .482 | 43.3 | 46.2 | 46.4 | 48.0 | .30 | 46.7 | 47.4 | 47.9 | 47.9 | .41 |
| Femoral neck cross-sectional area (cm ²) | 12.7 | 12.9 | 12.7 | 12.8 | .56 | 13.2 | 12.8 | 12.7 | 12.7 | -.48 | 12.7 | 12.5 | 12.4 | 12.4 | .56 |
| Femoral neck cortical area (cm ²) | 9.3 | 9.2 | 9.3 | 9.4 | .84 | 8.8 | 8.8 | 9.3 | 9.4 | 0.17 | 9.2 | 9.3 | 9.3 | 9.3 | .31 |
| Trochanter cross-sectional area (cm ²) | 33.5 | 32.8 | 34.3 | 33.3 | .39 | 34.1 | 34.3 | 33.3 | 32.5 | .49 | 34.0 | 32.3 | 32.8 | 32.8 | .40 |
| Trochanter cortical volume (cm ³) | 32.3 | 34.4 | 34.3 | 33.3 | .482 | 32.4 | 34.9 | 33.8 | 34.9 | .22 | 33.7 | 33.9 | 34.6 | 34.6 | .44 |
| Strength | | | | | | | | | | | | | | | |
| Proximal femur strength under reference BMI loading conditions | 5166 | 5740 | 5751 | 5781 | .48 | 5781 | 5634 | 5551 | 5453 | .47 | 5544 | 5293 | 5382 | 5382 | .48 |
| Proximal femur strength under a static load condition | 11367 | 12128 | 12474 | 12902 | .48 | 12733 | 12319 | 11880 | 11957 | .69 | 12002 | 11843 | 11974 | 11974 | .39 |
| Femoral neck strength after control of all BMD effects | 1363 | 1326 | 1363 | 1349 | .29 | 1390 | 1417 | 1264 | 1350 | .42 | 1333 | 1275 | 1329 | 1329 | .24 |

Abbreviations: IL-6 SR=Soluble Receptors for Interleukin-6; CRP=C-reactive Protein; Q1-Q4=Quartiles 1-4; vBMD=trabecular bone mineral density; vBMD=areal BMD.
[†]Only results for IL-6 SR, CRP, and the Inflammatory Markers variables are shown. All other inflammatory markers were not associated with any of the bone measures.
 All measurements were adjusted for the age, race, BMI, clinic site, fracture history, diabetes, heart disease, rheumatoid arthritis, smoking, physical activity, health status, non-steroidal anti-inflammatory drugs, statins, corticosteroids, selective serotonin reuptake inhibitors, and total calcium.

Table

Disclosures: Kamil Barbour, None.

MO0296**The Saudi Central Osteoporosis Registry (T-Score): A Kingdom-Wide Observational and Longitudinal Registry for Saudis with Osteoporosis.** Nasser Al-Daghri*. King Saud University, Saudi Arabia

Background: Epidemiologic evidence points to increased incidence of osteoporosis in KSA. The aim of this research registry is to obtain the incidence, prevalence and patterns of osteoporosis and risk factors in KSA. Methods: The registry was launched last July 2014 after the completion of the registry website and ethical approval from the College of Science, King Saud University in Riyadh, KSA. Data collection started in several hospitals in Riyadh (central region) but encompasses several regions in KSA as well to enrol Saudi patients with osteoporosis and related diseases based on bone mineral density (BMD) assessment. The follow-up part of the registry are to be completed at specified times in-line with the patient's treatment. A general and validated questionnaire is to be administered to all enrolled patients which contains demographic and anthropometric measurements, family history, medications taken and results from imaging and several bone-related markers. As of January 2015, a total of 325 cases have been registered (excluding males) and is expected to increase since it is on-going. Pilot results will be presented based on the aims of the registry, including FRAX assessment specific to KSA patients. Results: Preliminary data revealed that women with osteoporosis had a significantly higher percentage of illiteracy than controls, with a significantly higher prevalence of divorcees and widows (p-values<0.01). In the clinical category however, the control group had a significantly higher waist circumference and circulating levels of total cholesterol than the osteoporosis group (p-values<0.01). The control group also had a higher prevalence of mild activity and a lower prevalence of allergy to medicines (p-values<0.01). Conclusion: Pilot data reveals marked differences in demographic and metabolic indices between patients with and without osteoporosis. Prospective evaluation is necessary to include medications that will account for a more accurate picture of osteoporosis burden in KSA.

Disclosures: Nasser Al-Daghri, None.

MO0297**Catch-a-Break: A novel approach to detect osteoporosis after an incident fracture.** Angela Juby¹, Liz Evens², David Hanley³, Lara Osterreicher⁴, Members Bone Joint Health Strategic Clinical Network⁵. ¹University of Alberta, Canada, ²Alberta Bone & Joint Health Institute, Canada, ³University of Calgary, Canada, ⁴Health Link Alberta, Alberta Health Services, Canada, ⁵Alberta Health Services, Canada**Purpose**

In Alberta, 80% of fragility fractures over age 50, are not assessed or treated for osteoporosis (OP). This project addresses that care gap with a phone-out approach, utilizing a pre-existing phone-in health information service (Healthlink).

Methods

Patients are identified from Emergency Department, Urgent Care Centre, Cast Clinic, or Ortho/Fracture Clinic with the following criteria: age >49; Alberta resident; ICD code for fracture (includes vertebrae, ribs, pelvis, shoulder, arm, wrist, lower leg, ankle, and any pathological fracture associated with osteoporosis); ICD code for mechanism of fracture conducive to a fragility fracture (e.g., unspecified fall). Identified patients are called at home by the Health Link Alberta team. Screening questions identify those at high risk of having had a fragility fracture. If high-risk patients have not seen their Family Physician (FP), they are followed-up every 3 months to ensure they visit their physician. All high-risk patients will be followed up at 12 months to complete an evaluation survey. In high risk patients, their FP is sent a letter reinforcing a low impact fracture is a risk for osteoporosis; and both the FP and patient receive educational materials about osteoporosis and links to Osteoporosis Canada guidelines

Results

Catch-a-Break launched in June 2014. Currently, Alberta-wide, of 8,135 patients called: 19% were not reached, 1% had died and 5% are in progress. Of those contacted (6,166), 65% were high risk, 17% low risk, and 18% chose not to participate. Results from the initial call, indicated 24% of high risk patients already had a diagnosis of OP, and 71% had seen their FP about their recent fracture. In September 2014, 3 month follow up calls were made to those patients indicating they had not seen their FP at the time of the initial call (1012 patients): 12% were not reached, 2% refused, and 33% are in progress. Of those contacted to date (525), 73% of patients had seen their FP since the initial call, and indicated it was a due to the Health Link Alberta contact. Upcoming 12 month (June 2015) data, will allow further evaluation, including OP investigations and therapy for those at high risk, and a full economic evaluation (qualitative and quantitative).

Conclusion

Using a pre-existing phone in service, for call-out screening, resulted in an increased identification of suspected OP fractures and led to increased FP follow up.

Disclosures: Angela Juby, None.

MO0298**Decline in BMD testing: a nation-wide study in France.** Eric Lespessailles^{*1}, Pierre Gabach², Daniel Buchon³, Maryline Douge², Jean Marc Feron⁴, Laurent Grange⁵, Claire Leboucher², Erick Legrand⁶, Gabrielle PEYRE-LANQUAR², Eleonore Ronfle², Pascal Guggenbuhl⁶, Thomas Thierry⁶. ¹Centre Hospitalier Regional Orleans, France, ²CNAMTS, France, ³Universitary Limoges, France, ⁴Saint Antoine Hospital, France, ⁵CHU Grenoble, France, ⁶CHU, France**Background**

The assessment of bone mineral density (BMD) remains crucial for the general management of osteoporosis (OP). Since 2006, French national health insurance provides conditional reimbursement for bone density testing by dual-energy x-ray absorptiometry (DXA).

Methods

We aimed to evaluate the evolution of the number of BMD testing between 2011 and 2013 using the sources of national health insurance information system (SNIRAM). In addition, we sought to describe in the population of patients hospitalized for fragility fracture in 2012 the dispensation of BMD testing in the following year.

Results The total number of BMD testing went down by 13%, essentially in private activity which represents 90% of the BMD measurements in France (table).

Among patients hospitalized for a fragility fracture, only 0.8 % of patients had a BMD testing in the month following their fracture hospitalization. This percentage slightly increased to 6% and 8.5% at 6 and 12 months respectively.

Only 25% of the patients having a BMD testing, received an anti-osteoporotic treatment within 6 months following the exam.

Discussion

These data showed that there is a declining number of BMD testing from 2011 to 2013 with a 6.4% annual decrease. While the number of BMD testing plateaued in men, the downward trend of BMD testing was the most prominent in women. There is a substantial post-fracture BMD testing and treatment gap. These worrying findings underlined important undertreatment of patients with osteoporosis, especially after the fracture. Procedures that will improve post-fracture coordination between health care professionals are needed for a better management of these patients with the objective of reducing future fracture risk.

Number of BMD testing realized in the private sector

| Year | 2011 | 2012 | 2013 |
|-----------------|---------|---------|---------|
| Male | 32 942 | 32 883 | 32 043 |
| Female | 552 710 | 511 665 | 474 964 |
| Badly filled in | 189 | 173 | 111 |
| Total | 585 841 | 544 721 | 507 118 |

Source: DCIR, 2011-2013

Number of BMD testing realized in the public sector

| Year | 2011 | 2012 | 2013 |
|-----------------|--------|--------|--------|
| Male | 8 380 | 8 648 | 9 632 |
| Female | 54 224 | 53 677 | 54 157 |
| Badly filled in | 4 811 | 4 269 | 518 |
| Total | 67 415 | 66 594 | 64 307 |

Source: French hospital national database, 2011-2013

Table

Disclosures: Eric Lespessailles, None.

MO0299

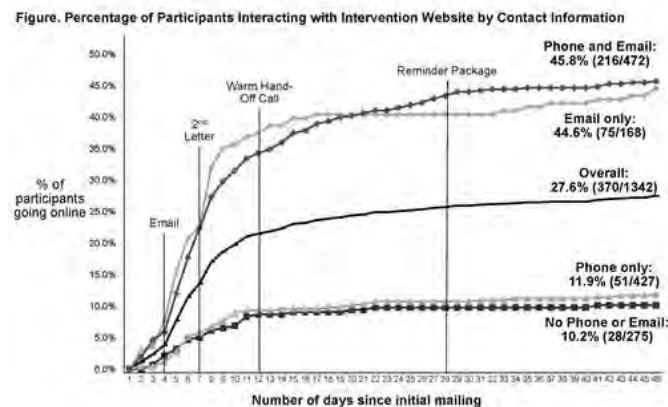
Design and Uptake of a Multi-modal Intervention for the Activating Patients at Risk for Osteoporosis (APROPOS) Study: a Cluster-randomized Trial within the GLOW Cohort. Maria Danila¹, Ryan Outman¹, Tammi Thomas¹, Jeroan Allison², Fred Anderson², Jeffrey Curtis¹, Susan Greenspan³, Andrea LaCroix⁴, Michael Miller⁵, Jeri Nieves⁶, Monika Safford¹, Stuart Silverman⁷, Ethel Siris⁶, Amy Warriner⁸, Nelson Watts⁹, Kenneth Saag¹. ¹University of Alabama at Birmingham, USA, ²University of Massachusetts Medical School, USA, ³University of Pittsburgh, USA, ⁴University of California at San Diego, USA, ⁵University of Oklahoma, USA, ⁶Columbia University, USA, ⁷Cedars-Sinai Center of Excellence, USA, ⁸University of Alabama at Birmingham, USA, ⁹Mercy Health Osteoporosis & Bone Health Services, USA

Purpose: Initiation of osteoporosis treatment is suboptimal, even among older women with history of a prior fracture. We designed a tailored intervention to increase use of osteoporosis medications in the GLOW cohort, a prospective cohort study of women aged 55 years and older at risk for fractures.

Methods: US GLOW women with a prior fracture and not currently using anti-osteoporosis therapy were eligible. Four nominal groups including 41 racially/ethnically diverse women identified osteoporosis treatment barriers. We used the Information, Motivation, Behavior Skills model to develop a direct-to-patient intervention to mitigate potentially modifiable barriers. The intervention included videos tailored by race/ethnicity, barriers, and stage of change and grounded in "story telling" narratives, based on stories from osteoporosis patients and portrayed by actresses of different race/ethnicity. Other videos addressed fracture risk awareness and patient-provider communication. Participants were randomized to either intervention or usual care. The intervention group was sequentially sent a letter and email (if an email address was provided) with a web link and a "code" to access the personalized videos online and a DVD. Those who provided phone numbers were called by staff members a week after the DVD was mailed followed a week later by an interactive voice response technology call.

Results: 2684 GLOW women met eligibility criteria with 1342 randomly assigned to the intervention. 860 women did not rank a barrier to treatment, 364 ranked 3 or more, and 118 noted 4 or more barriers. For those that ranked a barrier, preference for natural treatments was ranked highest (n=130, 27%) and concerns about osteonecrosis of the jaw was the most commonly ranked barrier (n=322, 67%). Overall, 28% (n=370) viewed the educational videos online. Of those who provided an email address, 45% (291/640) viewed the videos online versus 11% (79/702) of those who did not provide an address. Uptake of the DVD component is not yet available.

Conclusion: We describe implementation science methods used to develop a multi-modal patient activation intervention within the GLOW cohort. A large proportion of women assigned to the intervention arm viewed the videos online, particularly those with email addresses, reflecting the growing proportion of older women who access the Internet. Low cost, generalizable web-based interventions have potential to address osteoporosis treatment barriers.



Percentage of Participants Interacting with Intervention Website by Contact Information

Disclosures: Maria Danila, None.

MO0300

Electronic Decision Support for the Investigation and Management of Osteoporosis. Yvonne Selecki¹, Tuan Nguyen¹, Jackie Center¹, John Eisman². ¹Garvan Institute of Medical Research, Australia, ²Garvan Institute of Medical Research, Australia

The increasing use of computerised patient records has opened new opportunities to use this virtual database to improve health outcomes.

Clinical decision support systems have been designed and tested with the aim of closing the gap between evidence based guidelines and daily practise.

We have developed clinical decision support software to assist doctors and patients in the investigation and treatment of Osteoporosis.

The software expands from the Garvan Fracture Risk Calculator to provide individualised risk calculations and recommendations for treatment.

Graphic displays of fracture risk and how this risk changes with treatment are provided.

Uniquely this software connects with patient records so the software self populates enabling seamless use during a consultation.

The development of clinical software requires unique collaborations between doctors and IT professionals. Early utility testing in rural Australia is described.

Disclosures: Yvonne Selecki, None.

MO0301

Integrated Osteoporosis, Sarcopenia, Fall Related Screening, Education, and Health Promotion Program for High Risk Population in Taiwan. Rong-Sen Yang¹, Ding-Cheng Chan¹, Chih-Hwa Chen², Hung-Yi Chiou³, Jaw-Shan Hwang⁴, Shih-Te Tu⁵, Kuang-Hung Hsu⁶, Fang-Ping Chen⁷, Jung-Fu Chen⁸, Chung-Yhu Yang⁹, Lay-Chin Lim¹. ¹National Taiwan University Hospital, Taiwan, ²Taipei Medical University Hospital, Taiwan, ³Taipei Medical University, Taiwan, ⁴Chang Gung Memorial Hospital, Taiwan, ⁵Changhua Christian Hospital, Taiwan, ⁶Chang Gung University, Taiwan, ⁷Keelung Chang Gung Memorial Hospital, Taiwan, ⁸Kaohsiung Chang Gung Memorial Hospital, Taiwan, ⁹Kaohsiung Medical University, Taiwan

Purpose

To determine the effects of 4 independent but integrated programs for intervention of osteoporosis, sarcopenia, fall related screening, education, and health promotion in Taiwan.

Methods

Sponsored by the Wang Jhan-Yang Charitable Trust Fund (WJYCTF), and the Taiwanese Osteoporosis Association (TOA), the study included 4 programs with 8 sub-programs targeting community adults with high risks for fall/osteoporosis/fracture/sarcopenia. Core assessments include demographics, osteoporosis/fracture/fall risks, sarcopenia indices, and nutrition. Interventions include combinations of educations to improve awareness, screening and referral, exercise programs, nutrition evaluation and consultation, and post-fracture care management.

Results

In total 3,911 subjects were enrolled. Program #1 found that 70% of subjects had low bone mineral density (BMD) and 15% with osteoporosis. Less exercise, higher fat mass, and lower muscle mass were associated with lower BMD ($p < 0.05$). The exercise intervention improved muscle strength but not muscle mass. Program #2 found that 3 exercise interventions for 3 months resulted in significant and similar improvements in sarcopenic indices including walking speed (+8.3%), hand grip strength (+8.7%) and knee extensor strength (+24.9%). Program #3 found that group health promotion improved medication adherence rate to >80%. The basic muscle exercise improved grip muscle strength (+18.2%). Advanced core body muscle exercise significantly increased muscle mass (+1%), decreased fat mass (-3.2%), and increased grip strength (+20.4%) (all, $p < 0.05$). One sub-program using commercial X-box exercise program for 3 months improved physical performance ($p < 0.05$). Program #4 found that individualized exercise specialist program showed improvements in muscle endurance (standing-up repetitions from sitting position (+55.3%), lifting weight in 1-minute (+38.4%)), walking speed (+17.2%), heart beats after step on-the-spot (-9.3%) (all, $p < 0.05$). One sub-program #4 showed an average of 1.2 falling episodes/year, 80% occurred at home (bathrooms, 60%). Fracture liaison service program significantly improved on osteoporosis and medication knowledge.

Conclusions

This national integrated education and screening campaign were highly appreciated and showed significant results in improving osteoporosis awareness, most sarcopenic indices through short-term muscle exercises programs. Further efforts will be made to show their effects on the decreasing the falling episodes and fragility fractures.

Disclosures: Ding-Cheng Chan, None.

This study received funding from: Wang Jhan-Yang Charitable Trust Fund

MO0302

Mortality and re-fracture benefits of Orthogeriatric and Fracture Liaison Service Models of Care: A UK Population Based Study. Muhammad Javaid¹, Samuel Hawley², Jose Leal¹, Daniel Prieto-Alhambra², Alastair Gray¹, Nigel Arden², Janet Lippett³, Sally Sheard¹, Cyrus Cooper⁴, Andrew Judge². ¹University of Oxford, United Kingdom, ²NIHR Musculoskeletal Biomedical Research Unit, University of Oxford, United Kingdom, ³Royal Berkshire Hospital, United Kingdom, ⁴MSc Lifecourse Epidemiology Unit, University of Southampton, United Kingdom

Purpose: a) To evaluate the clinical and cost-effectiveness of specialist orthogeriatric (OG) and nurse-led fracture liaison service (FLS) care for patients presenting with a hip fracture; b) To estimate UK hospital costs of hip fracture up to two years post fracture.

Methods: Using routine administrative data, a cohort of patients with hip fracture between 2003 and 2011 were identified from 11 secondary care centres in a region of England, UK. For each centre, the time when an OG or FLS was introduced/expanded was identified. The effect of these interventions on subsequent mortality (using multivariable Cox regression) and second hip fracture rates (using competing risks survival models accounting for death) was determined within a before and after study design. For estimation of hospital costs, non-parametric censoring methods were used for estimating average annual costs and generalised linear models for the determinants of cost.

Results: 33,152 patients (mean age 83yrs, 75% women) were identified as having a hip fracture. 3033 (9.5%) and 9662 (29.8%) died within 30-days and 1-year respectively. 1288 (4.2%) sustained a second hip fracture within 2-years. The pooled estimated impact of OG and FLS models demonstrated clinically significant reductions in mortality but not re-fracture (table). Mean censor-adjusted 1-year hospital costs after index hip fracture were £14,163 (95%CI: £14,008 to £14,317) giving a UK estimate hospital cost of £1.1 billion / year for hip fractures. Only 60% of the first year costs were due to the index admission and were significantly higher for men and those with complications including re-fracture.

Conclusions: The data demonstrate that OG and FLS models of post-hip fracture care have large beneficial effect on subsequent mortality rates with no evidence for a reduction of second hip fracture rate. Secondary care costs following hip fracture are high and provide a strong economic incentive for effective FLSs that reduce the risk of the index and subsequent hip fractures.

| | Orthogeriatrician | | Osteoporosis Nurse Specialist | |
|--------------------------|-------------------|-------------------------|-------------------------------|-------------------------|
| | Hazard Ratio | 95% Confidence Interval | Hazard Ratio | 95% Confidence Interval |
| Mortality (30-days) | 0.73 | 0.65-0.82 | 0.80 | 0.71-0.91 |
| Mortality (1-year) | 0.81 | 0.75-0.87 | 0.84 | 0.77-0.93 |
| Hip re-fracture (2-year) | 0.95 | 0.79-1.15 | 1.03 | 0.82-1.31 |

Table 1: Hazard ratios for mortality and second hip fracture risk

Disclosures: Muhammad Javaid, Merck; Consilient Health; Jarrow Formulas; Lilly UK; Medtronic; Amgen; Servier; Internis

MO0303

Real-world Persistence to Injectable Osteoporosis Therapy. Ankita Modi¹, Shiva Sajjan^{*2}, Ralph Insinga², Jessica Weaver². ¹Merck & Co., Inc., USA, ²Merck & Company, USA

Background: Relatively poor persistence to oral bisphosphonate therapy for osteoporosis (OP) is well known in the US. Little research has been conducted regarding real-world persistence to injectable (IV) OP therapies. It is important to understand real-world and long term persistence to IV OP therapies in order to understand their long term value.

Objectives: This study was designed to describe treatment persistence among patients who initiate IV OP therapies and to examine predictors of persistence among OP patients who started on IV OP therapies.

Materials and Methods: This retrospective, observational study utilized an administrative claims database from a large US managed care plan to measure persistence to IV OP therapy at 6 month intervals over 2 years. Patients included were ≥55 years of age, and had newly initiated IV OP therapy between January 2008 and June 2012. Eligible patients were continuously enrolled in the health plan for 1 year prior to the index date (date of start of first OP medication) and for 1.5 years after the index date, although patients that had data for up to 2 years were also followed. IV OP treatments included in the analysis were ibandronate (IBN), zoledronic acid (ZOL), teriparatide (TER) and denosumab (DEN). Patients receiving IV OP therapy prior to the index period, patients with Paget's disease or neoplasms, and patients on chemotherapy were excluded. Persistence to treatment was assessed for each drug using Kaplan-Meier survival analysis. A 90 day grace period after the date of the next indicated time point for administration was allowed for flexibility in scheduling of re-administrations.

Results: 4,756 patients met the inclusion criteria for the study, with 233 on IBN, 3,128 on ZOL, 778 on TER and 617 on DEN. Depending on treatment type, the mean age of patients at index date ranged from 71.5 years (IBN) to 73.5 years (DEN). 9.4% (IBN) to 31.2% (TER) had a history of recent osteoporotic fracture, and mean Charlson comorbidity scores ranged from 0.51 (ZOL) to 0.61 (TER). At 12 months, persistence was 51.2% among patients using DEN, followed by ZOL (40.6%),

TER (32.9%) and IBN (31.8%). By 24 months, persistence was lower for each treatment, at 36.4% for DEN, followed by ZOL (24.2%) IBN (14.3%) and TER (14.1%). Conclusion: For the majority of patients, real world persistence with IV OP treatment beyond 1 year is lacking, as has previously been observed for patients initiating oral bisphosphonates.

Disclosures: Shiva Sajjan, Merck and Company
This study received funding from: Merck and Company

MO0304

Specialty Care Increases Odds of Osteoporosis Screening and Diagnosis in Postmenopausal Women Medically Homed in an Academic Multispecialty Practice. Clare O'Connor^{*}, Christie Bartels, Karen Hansen. University of Wisconsin School of Medicine & Public Health, USA

Half of postmenopausal white women sustain an osteoporotic fracture, causing significant morbidity and mortality. The US Preventive Services Task Force recommends bone mineral density (BMD) screening for women = 65 years old yet screening remains suboptimal. We assessed predictors of screening and diagnosis of low BMD in postmenopausal women receiving care in an academic multispecialty practice. We hypothesized that specialty care would increase odds of screening, as reported by others. We studied 8,217 women age =65 years old who were medically homed (=2 primary care visits in 2010-2011) at an academic health center. We calculated multivariate odds ratio and 95% confidence intervals for BMD screening and/or diagnosis of osteopenia or osteoporosis since age 60. Covariates included sociodemographic factors (age, marital status, race, language), health habits (body mass index, tobacco use), comorbid conditions (29 conditions, Elixhauser score), and healthcare utilization (number of primary and specialty visits). Subjects were 72.6 years old, predominantly white (97%) and English-speaking (99%). In the cohort, 86% were screened for and/or diagnosed with low BMD. Women seeing specialists had higher screening/diagnosis rates than women without specialty care (86% versus 78%, p<0.001). A dose-response relationship between specialty visits and screening/diagnosis was observed (Table). Other factors associated with greater odds of screening/diagnosis were English language (2.87, 95% CI 1.72-4.67), marriage (1.29, 95% CI 1.13-1.47), hypothyroidism (1.23, 95% CI 1.03-1.48) and Elixhauser score =4 (1.41, 95% CI 1.10-1.82). Women 70-80 years old were more likely to be screened or diagnosed than those younger or older (Table). Factors associated with reduced screening and diagnosis included primary care visits (0.90, 95% CI 0.86-0.95), tobacco use (0.58, 95% CI 0.46-0.74), obesity (0.55, 95% CI 0.48-0.63), heart failure (0.53, 95% CI 0.37-0.75) and diabetes (0.75, 95% CI 0.63-0.91). In our study, specialty visits increased, while primary visits reduced, the odds of osteoporosis screening and diagnosis. Such findings might reflect specialist adherence to guidelines, indication bias and/or competing demands in primary care. Although tobacco use increases fracture risk, tobacco users had reduced odds of screening and diagnosis. Remaining gaps support the need for systems-based interventions such as primary care nurse orders to further improve osteoporosis screening.

| Characteristic | Odds Ratio | 95% CI |
|------------------------|---------------------------|------------------|
| Specialty Care | referent | |
| No Visits | 1.36 | 1.14, 1.63 |
| 1 Visit | 1.52 | 1.24, 1.87 |
| ≥2 Visits | | |
| Age | referent | |
| 65-69 | 1.62 | 1.37, 1.92 |
| 70-74 | 1.43 | 1.19, 1.72 |
| 75-79 | 1.09 | 0.91, 1.32 |
| ≥80 | | |
| Language | English | 2.87, 1.72, 4.67 |
| Married | Yes | 1.29, 1.13, 1.47 |
| Tobacco | Current | 0.58, 0.46, 0.74 |
| Obesity | BMI ≥30 kg/m ² | 0.55, 0.48, 0.63 |
| Comorbid Conditions | Congestive Heart Failure | 0.53, 0.37, 0.75 |
| | Diabetes Mellitus | 0.75, 0.63, 0.91 |
| | Hypothyroid | 1.23, 1.03, 1.48 |
| | Elixhauser Score ≥4 | 1.41, 1.10, 1.82 |
| Healthcare Utilization | Any ambulatory visit | 1.09, 1.05, 1.13 |
| | PCP Visit | 0.90, 0.86, 0.95 |

An odds ratio >1 indicates higher odds of screening or diagnosis of low bone mineral density. 95% CI denotes the 95% confidence interval for the odds ratio. "PCP" indicates primary care provider. The multivariate model was highly significant (p<0.0001) and provided an area under the curve of 0.67 to predict testing.

Table

Disclosures: Clare O'Connor, None.

MO0305

The Ethics of Treating Osteopenia: What are we Preventing?. Loren Greene^{*}. New York University School of Medicine, USA

First you have a drug. Then you have a test for a disease, then you need to treat people who become patients with a drug. Furthermore, you market the test and then create a perception of need for treatment. In 1995, a drug was approved, and simultaneously, the disease could be diagnosed by bone density testing. This led to

treatment for a new class of disease, that could be prevented and treated. BMD itself became an indication for treatment and the improvement in BMD became a standard measure of drug efficacy, rather than the harder to achieve true clinical outcome, the reduction in fracture. The marketing problem was solved by expanding testing, and expanding awareness by medical professionals and the public.

The use of bone density criteria greatly expanded the number of people who might be diagnosed to have osteoporosis or low bone density and therefore requiring or requesting medication to treat or prevent osteoporosis. Marketing to and by the medical community, as well as to the general public created a huge demand for medication to treat osteoporosis and low bone density. Susceptible to influences from pharmaceutical companies and device manufacturers, physicians helped to expand the market for these drugs through consultant meetings for "thought leaders", "education (including dinner meetings and CME, and provisions for inexpensive (though not precise) bone density testing at "alternative sites" or loans for bone density machines. Direct-to-consumer marketing served to increase patient awareness and understanding, but also the acceptance by new "patients" who "needed" pharmacologic prevention as well as treatment of osteoporosis, with questionable medical and economic and even psychological results..

Disclosures: Loren Greene, None.

MO0306

Why patients still untreated 1 year after a Fragility Fracture refuse an intervention to treat osteoporosis?. Noémie Gionet Landry*¹, François Cabana², Isabelle Gaboury¹, Gilles Boire², Sophie Roux², Nathalie Carrier², Marie-Claude Beaulieu¹. ¹Université de Sherbrooke, Canada, ²CHUS, Canada

OBJECTIVE: To determine the reasons underlying refusal or acceptance of an intensive intervention to improve bone health 1 year after a fragility fracture (FF). **METHODS:** The OPTIMUS program is a strategy implemented in fracture clinics to educate patients and empower primary care physicians (PCPs) to treat osteoporosis (OP) after a FF. Women and men over 50 with an incident FF were randomly assigned to Standard Care (SC) or to either minimal (MIN) or intensive (INT) interventions and followed up (FU) by phone calls (up to 4 yrs). Interventions consisted in information letters to PCPs at baseline and when patients remained untreated during the first year FU. Relative to MIN, INT patients had a prescription for baseline laboratory tests and more frequent FU phone calls. At year 1, untreated patients in SC and MIN groups were offered an INT intervention. **RESULTS:** We included 563 patients in SC (n=192) and in MIN (n=371) groups, of which 531 had a 12-month FU. At year 1, 267 patients (50.3%) remained untreated (SC 113/184 (61.4%) vs MIN 154/347 (44.4%), p<0.001). Only 69 (25.8%) of these patients accepted the INT intervention. Untreated patients who agreed to switch from SC or MIN to INT were more likely to have a family history of OP (43.2% vs 24.1%, p=0.035); lower FRAX for major FF [med (EIQ) 9.7 (7.6-14.5) vs 12.0 (8.7-20.3), p=0.003] or for hip FF [1.3 (0.8-2.9) vs 2.2 (1-7.2), p=0.002]; were younger (61.3 ± 8.9 vs 66.1 ± 11.9, p=0.006); and more physically active (= 1 day/week) (31.3% vs 16.0%, p=0.012). In patients accepting an INT intervention, the main reason given to explain absence of treatment at 1 year was that they had not seen their PCP yet (65%). Most patients declining the INT intervention while untreated (58.8%) stated no need for treatment. Qualitative interviews were conducted to further explore the reasons for declining the intervention to treat OP. **CONCLUSION:** One year after a FF, patients have little interest to investigate and potentially treat underlying OP. Those patients who did accept the intervention were younger, more physically fit and at lower risk than those who refused. The major hurdles explaining the absence of treatment in those willing to be investigated appeared to be the lack of an evaluation by their PCP, knowledge problems and wrong beliefs from both patients and PCPs. Our data further support the concept of a window of opportunity closing within the first year after a FF.

Disclosures: Noémie Gionet Landry, None.

This study received funding from: Merck Canada, Eli Lilly Canada, Amgen Canada, Alliance for a Better Bone Health (Procter&Gamble and sanofi-aventis), Warner Chilcott Pharma Canada, Servier Canada, Novartis Canada

MO0307

Change in Physical Function Following Hip Fracture among Elderly Osteoporotic Women. Derek Weycker*¹, Rich Barron², John Edelsberg³, Alex Kartashov³, Barry Crittenden², Andreas Grauer². ¹Policy Analysis Inc. (PAI), USA, ²Amgen Inc., USA, ³Policy Analysis Inc., USA

Background: While hip fractures among elderly women with osteoporosis are known to lead to a decline in functional status, the extent of short-term and long-term functional loss that is attributable to hip fracture is not well established.

Methods: A retrospective matched-cohort design and data from the Study of Osteoporotic Fractures (SOF)—which includes 20 years of prospectively collected data on osteoporosis care and outcomes at periodic exams—were employed. The source population included all women in the SOF Caucasian cohort. From the source population, each woman who had an adjudicated fracture of the hip ("Fx subject") between exams was matched to a woman who did not have a hip fracture between

those exams ("comparison subject"); matching was implemented based on age, baseline physical function, and propensity score (fixed 1:1 ratio). Change in physical function from the pre-fracture exam to each post-fracture exam was measured using the Total Functional Difficulty (TFD) score, and was defined dichotomously by a clinically meaningful functional deficit (increase ≥5 vs. <5 units). The TFD score is the sum of responses (range, 0 [no difficulty] to 3 [unable to perform]) to five activities of daily living including meal preparation, heavy housekeeping, ability to climb ten stairs, shopping, and getting in/out of a car.

Results: A total of 334 Fx subjects were matched to comparison subjects; mean (SD) age was 80 (5) years and mean (SD) pre-fracture TFD score was 1.8 (2.7) and 1.7 (2.6), respectively. Between the pre-fracture exam and first post-fracture exam (~3 years), 37% (95%CI 32-43) of Fx subjects had ≥ 5-unit increase in TFD score, versus 13% (95%CI 10-18) of comparison subjects; differences between cohorts decreased but generally persisted over time (up to ~7 years) (Figure).

Conclusions: While apparent age-related decline in functional status was observed in the fracture and non-fracture subjects, hip fractures among elderly women with osteoporosis worsened this decline during the period from 2-3 years post-fracture up to 7 years post-fracture. Further research is needed to confirm the specific ways in which hip fracture impacts physical function, as well as the relative contribution of fractures versus other age-related comorbidities to declining functional status in this population.

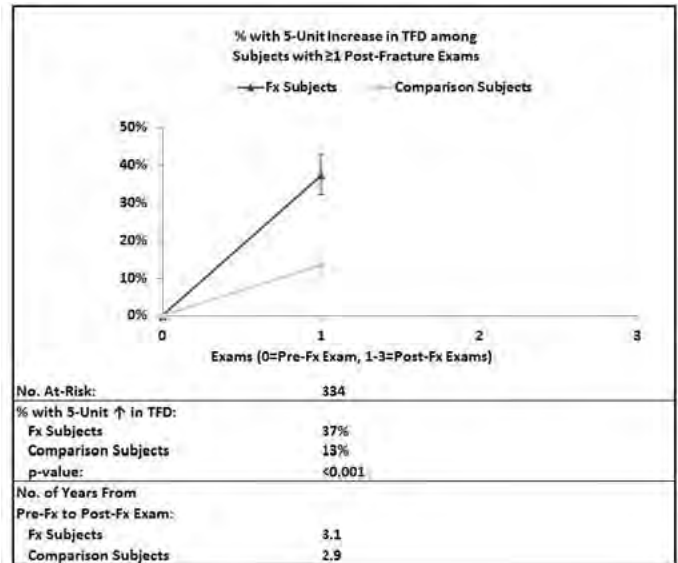


Figure 1

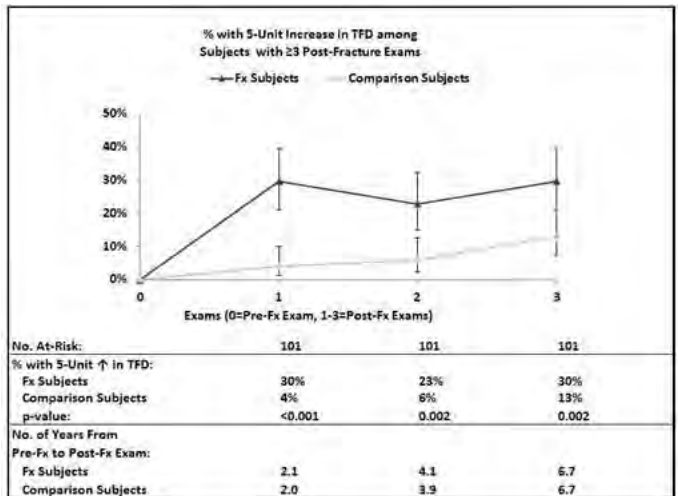


Figure 2

Disclosures: Derek Weycker, Amgen Inc.

This study received funding from: Amgen Inc.

MO0308

Health Utility Following Osteoporotic Fracture Using SF6D: Results from ICUROS US. Stuart Silverman*¹, Deborah T Gold², John T Schousboe³, Loretta H Pearson⁴, Mackenzie R Bronson⁴, Fergus E McKiernan⁵, Robert A Yood⁶, John I Reed⁶, Daniel H Solomon⁷, Chad Deal⁸, William Griffith⁹, Michael B Nichol¹⁰, Susan Gallagher⁴, Kristin Anton⁴, Anna NA Tosteson⁴. ¹Cedars-Sinai/UCLA, USA, ²Duke University, USA, ³Park Nicollet Clinic, HealthPartners, USA, ⁴Geisel School of Medicine at Dartmouth, USA, ⁵Marshfield Clinic, USA, ⁶Reliant Medical Group, USA, ⁷Brigham & Women's Hospital, USA, ⁸Cleveland Clinic, USA, ⁹University of Wisconsin, USA, ¹⁰USC Pharmacy, USA

Introduction: Osteoporotic fractures result in loss of quality of life, which can be measured as health utility (HU) using EQ5D and SF6D. ICUROS (International Costs and Utilities Related to Osteoporotic Fractures Study) is a global study of medical costs and HU following osteoporotic fractures. Although all ICUROS participants completed EQ5D, only U.S. participants completed SF6D and these data are presented here.

Methods: We report HU using SF6D for hip, wrist, humerus, and vertebral fracture. Vertebral fracture is described by type of management: vertebral augmentation or non-operative care. At the time of enrollment, post-fracture HU was collected along with pre-fracture HU (retrospectively by recall). Subsequently, HU was prospectively measured at 4, 12, and 18 months post-fracture. Mean HU changes from pre-fracture (Δ post-fx - pre-fx) and standard deviations (SD) are reported for each post-fracture time point. Regression analyses were undertaken to assess changes in HU by fracture type over time after adjusting for age and gender.

Results: Mean pre-fracture SF6D HU was lowest for vertebral fracture patients. All patients had significant HU losses post-fracture, which lessened over time (Table). Mean HU changes for vertebral fracture patients were comparable for those treated with augmentation vs. non-operative care; while non-operatively treated patients had a smaller loss of HU at 18 months compared to baseline (-0.040 vs. -0.083, p-value=0.13). For all fracture types, improvements in HU (changes that became smaller with time since fracture) were seen. By 18 months post-fracture, only wrist fracture patients had attained pre-fracture HU levels. Hip, humerus and vertebral fracture patients had persistent loss of HU relative to pre-fracture through 18 months.

Conclusions: We conclude that health utility measured using SF6D decreases significantly following fracture but improves with time. The loss in HU and gains over time vary between fracture types.

| Mean pre-fracture SF-6D HU and mean changes (Δ) from pre-fracture. | Hip n=58 mean (SD) | Wrist n=47 mean (SD) | Humerus n=31 mean (SD) | Vertebral: non-operative n=109 mean(SD) | Vertebral: augmentation n=35 mean (SD) |
|---|--------------------------|----------------------------|------------------------------|---|--|
| Pre-fracture (fx) | 0.795 (.15) | 0.846 (.15) | 0.842 (.14) | 0.752 (.16) | 0.756 (.18) |
| Δ Initial Post-fx | -0.186 (.17) | -0.188 (.16) | -0.250 (.15) | -0.131 (.15) | -0.145 (.15) |
| Δ 4-mths Post-fx | -0.110 (.15) | -0.087 (.14) | -0.127 (.12) | -0.085 (.15) | -0.093 (.13) |
| Δ 12-mths Post-fx | -0.094 (.16) | -0.069 (.13) | -0.064 (.12) | -0.037 (.15) | -0.076 (.13) |
| Δ 18-mths Post-fx | -0.096 (.13) | -0.034 (.12) | -0.065 (.13) | -0.040 (.12) | -0.083 (.12) |

Table: Mean pre-fracture SF-6D HU and mean changes from pre-fracture at each time point

Disclosures: Stuart Silverman, None. This study received funding from: None

MO0309

The Osteoporosis Care Gap: Evaluation of Solutions for Remote and Rural Communities. Rosemary Hollick*¹, Alison Black², Lorna McKee³, David Reid³. ¹Aberdeen Royal Infirmary, United Kingdom, ²NHS Grampian, United Kingdom, ³University of Aberdeen, United Kingdom

A significant care gap exists between evidence based management of osteoporosis and clinical practice. In Scotland a significant proportion of the population live in remote and rural communities, posing challenges to the delivery of healthcare. The ageing population is increasing faster in rural communities, who are also disadvantaged by geographical access to services with an associated cost premium. Local experience suggests significant unmet need in access to DXA in rural areas where populations are older. Mobile DXA services were proposed to address inequalities in access to care for those living rurally. Similar UK interventions have failed, having only outcome evaluation and excluding evaluation of process implementation, or factors influencing sustainability.

We undertook an implementation and outcome evaluation of the new service at multiple levels; macro, meso and micro to explain 'how and why' innovations are translated into practice. Specifically we performed an implementation process evaluation with comparison of local service implementation to similar successful/unsuccessful mobile services in England, using a participatory action research (PAR) framework. The implementation process and outcome evaluation involves three local case studies; two island communities and one rural mainland community, using a real-time, before and after approach. We use mixed methods with both quantitative

(surveys, fracture risk assessment tool) and qualitative (in-depth interviews, ethnography) and secondary data. Quantitative data is analysed using descriptive statistics. Qualitative data is analysed thematically using a conceptual framework derived from organisational and implementation theory, with triangulation of data from different sources.

Pre-implementation, referrals from islands are younger than those from the mainland, Table 1, with significantly more subjects <65 yrs referred for DXA in the islands. Survey data showed that age, frailty and travel distance were significant barriers to referral. Journey length/complexity and accessibility to public transport also influenced access to DXA. Data 6 months post implementation reveals a 53% increase in referrals, with a 4 fold increase in referrals > 75 yrs. Early data indicates that multiple interactions of political, sociocultural, educational and contextual factors influence service implementation.

In summary we report the first service implementation evaluation in osteoporosis using a PAR framework.

| Age at time of DXA scan | City | Rural mainland | Island 1 | Island 2 |
|-------------------------|-----------------|-----------------|-----------------|-----------------|
| Mean (yrs) | 63.75 (14.8) | 63.51 (14.3) | 60.22 (12.1) | 58.82 (12.9) |
| Range (yrs) | 6 - 93 | 9 - 93 | 28 - 79 | 19 - 86 |

Table 1. Mean age of referrals, pre-implementation of mobile DXA service

Table 1. Mean age of referrals, pre-implementation of mobile DXA service

Disclosures: Rosemary Hollick, None.

MO0310

A low dietary calcium intake is a major health problem in Hong Kong postmenopausal Chinese women. Rick Chung*¹, Connie Au², Gabrielle Lee², Ivy Wong², Selegne Wong², Novem Lam², Edith Lau². ¹Center for Clinical & Basic Research (CCBR) (Hong Kong), Hong kong, ²CCBR Hong Kong, Hong kong

Background and objectives

Osteoporosis is a major and increasingly important public health problem in Hong Kong. Previous studies showed 1/3 of Hong Kong postmenopausal women have osteoporosis. Adequate calcium intake has been found to prevent bone loss and osteoporotic fractures. The objective of current study is to investigate the updated dietary calcium intake of Hong Kong postmenopausal Chinese women in order to provide a basis for future public health recommendations.

Method

The dietary calcium intake was carried out using a food frequency questionnaire (FFQ). The FFQ contained 133 food which are calcium rich and commonly eaten in the Hong Kong Chinese diet. A total of 620 Hong Kong Chinese postmenopausal women aged 50-86 were recruited from the community and interviewed with the FFQ from Jul 2014 to Mar 2015.

Subjects were required to answer the number of times they consumed each food item daily or weekly with the serving sizes based on their usual diet for the last three month period. The total daily dietary calcium intake was calculated by multiplying the consumption frequency, portion sizes and calcium contents of the foods. The subjects also provide the data that if they are on calcium supplement.

Results

The results showed that the mean calcium intake from the dietary record was 649.2 \pm 354.8 mg/day. 91.5% of the subjects failed to meet the RDA for calcium (1,200 mg/day), while only 45.6% had intakes above 600 mg/day (Figure 1). Figure 2 demonstrated that most of the calcium for Hong Kong Chinese women was from dairy product (28.7%) and vegetable/fruit (24.5%). There were 40.2% of subjects did not consume dairy product regularly and 22.1% of subjects took dairy product daily. 77.3% of subjects were not on calcium supplement, while only 6.6% and 16.1% took calcium supplement daily and occasionally, respectively.

Conclusions

The dietary calcium intake of Hong Kong Chinese postmenopausal women is low, the mean value is only around half of the RDA. It is a major health issue in Hong Kong.

In the common Hong Kong diet, most of the calcium is from dairy product and vegetable/fruit.

Dairy product is one of the main source of dietary calcium intake, however, 77.9% of subjects did not consume dairy product regularly.

There were 77.3% of subject not on calcium supplement.

Encouragements for high calcium diet and calcium supplementation are important for Hong Kong women, in order to prevent osteoporotic fracture.

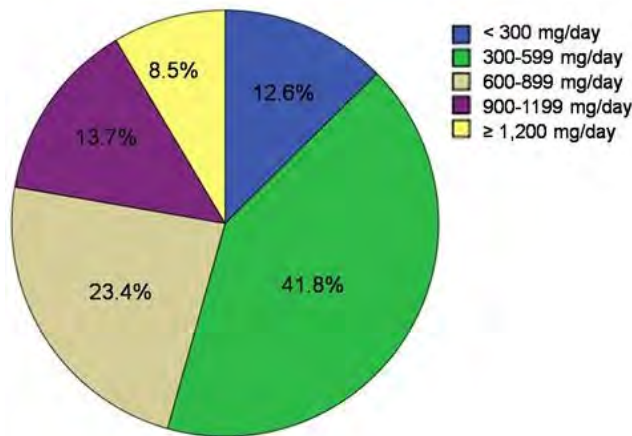


Figure 1. The percent distribution of subjects' calcium intake

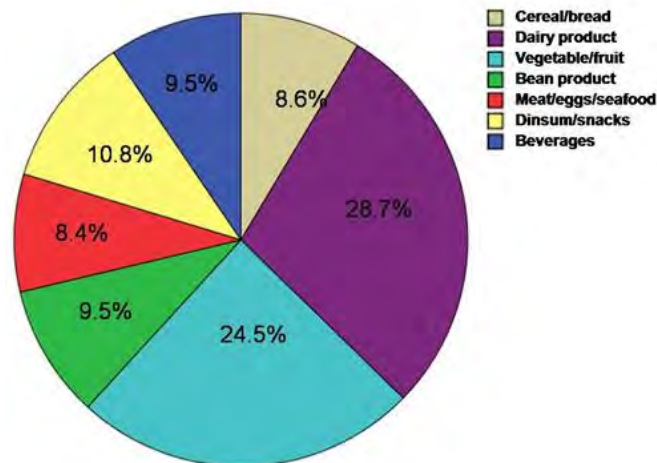


Figure 2. Percentage of calcium intake from various food sources

Disclosures: Rick Chung, None.

MO0311

A Short, Quick, and Easy Questionnaire to Estimate Daily Dietary Calcium Intake of Osteoporosis Patients. Linda Rasch¹, Marian de van der Schueren², Irene Bultink³, Lilian van Tuyl³, Willem Lems^{*3}. ¹Amsterdam Rheumatology & immunology Center, VU University Medical Center, The Netherlands, ²Department of Nutrition & Dietetics, VU University Medical Center, Netherlands, ³Amsterdam Rheumatology & immunology Center, VU University Medical Center, Netherlands

Background: Calcium supplements are widely used for the prevention and treatment of osteoporosis. However, recent literature suggests that too much calcium supplementation may be associated with cardiovascular events (1). For this reason, calcium supplementation should be based on actual and adequate dietary calcium intake. A previously designed calcium intake list appeared to be invalid (2) and other alternatives are too time consuming for clinical practice. Therefore, we developed a new calcium intake list, to accurately estimate dietary calcium intake, which was validated in this study.

Objectives: The aim of this study is to validate a short, quick, and easy calcium intake list, to be able to estimate dietary calcium intake, with an extensive dietary history (DH) as a reference method.

Methods: This cross-sectional study included consecutive patients attending the outpatient rheumatology department at the VUmc in Amsterdam, the Netherlands, for the treatment of primary or secondary osteoporosis. Based on the food groups which contribute most to daily dietary calcium intake and portion sizes determined from our earlier validation study (2), a short three-item calcium intake list was designed. As a reference method, an extensive DH with specific focus on calcium products and extra attention for portion sizes was performed. Before starting the study, a difference of 250 mg calcium or more between both methods was determined as clinically relevant. Performing the short calcium intake list took about 3 minutes, performing the DH took 60 minutes.

Results: In this study, 66 patients with primary (n=40) and secondary (n=26) osteoporosis were included. The three-item calcium intake list showed a small, clinically

non-relevant, difference with the DH of 25 ± 350 mg calcium per day (p=0.568), see table 1. Sensitivity and specificity of the short calcium intake list, compared to the DH, were respectively 73% and 80%. In 50% of the individuals, a clinically relevant difference of 250 mg calcium or more was observed between the calcium intake list and the DH, while in 17% a difference of 500 mg or more was observed.

Conclusions: The short calcium intake list is a three-item, quick and easy questionnaire to accurately estimate dietary calcium intake of osteoporosis patients at a group level, and thus very helpful for clinical studies. The mean calcium intake is within the currently advocated recommendation of 1000-1200 mg calcium per day. Since calcium supplements are prescribed in patients with an adequate intake in approximately 30% of patients, this indicates that a large proportion of the osteoporosis patients are "over-supplemented". In contrast, clinicians should be aware of not identifying a deficient calcium intake in approximately 20% of the patients.

References: (1) Bolland MJ, et al. BMJ 2010. (2) Rasch LA, et al. Austin J Nutri Food Sci 2014.

Table 1. Mean ± SD daily calcium intake of patients with osteoporosis

estimated by the calcium intake list versus dietary history

| Calcium intake (mg/day) | | Difference (mg) | P-value |
|---------------------------|-----------------|-----------------|---------|
| Short calcium intake list | Dietary History | | |
| 1148 ± 440 | 1170 ± 485 | 25 ± 350 | 0.568 |

Table 1

Disclosures: Willem Lems, None.

MO0312

High serum uric acid concentration show different association between vitamin C intake and spine Quantitative Computed Tomography (QCT) bone measures in women. Shivani Sahni^{*1}, Katherine Tucker², Caroline Fox³, Douglas Kiel¹, Marian Hannan¹. ¹Hebrew SeniorLife, Institute for Aging Research & Harvard Medical School, USA, ²University of Massachusetts, USA, ³Framingham Heart Study, NHLBI, Harvard Medical School, USA

Higher Vitamin C intake has been associated with lower serum uric acid (sUA) concentration and less bone mineral density (BMD) loss over time. sUA (an antioxidant within normal range: 3-7mg/dL) has been associated with higher BMD. However, at elevated concentration, sUA can act as a pro-oxidant, contributing to inflammation. Given the inter-relation between vitamin C and sUA, it is unclear if the association of vitamin C and bone varies by uric acid concentration. The trabecular bone compartment may be a sensitive indicator of change due to inflammation-mediated bone loss. Thus, we examined the association of vitamin C intake with QCT volumetric measures of bone [vBMD (g/cm³), integral and trabecular vBMD], cross-sectional area (CSA, cm²) and vertebral compressive strength (VCS, N) at the L3 level of the spine in men and women from the Framingham 3rd Generation Cohort. Associations were further examined within categories of sUA [normal physiological levels =7 men; =6mg/dL women) and high sUA].

In this cross-sectional analysis, 802 women and 965 men (ages 32-72y) had measures of vitamin C intake (mg/d) from the food frequency questionnaire, and sUA (mg/dL) and QCT spine measures (2002-05). VCS was estimated from the QCT data. Sex-specific multivariable linear regression was used to calculate the association of vitamin C with each QCT measure, adjusting for covariates. Interactions of vitamin C intake and sUA were tested. If significant (P<0.10), associations were examined by sUA sub-group.

Mean ages were 44 (± 6) y in men and 46 (± 6) y in women. Mean vitamin C intakes (mg/d) were 240 (men) and 271 (women). Mean UA concentrations (mg/dL) were 6.28 (± 1.24) (men) and 4.44 (± 1.09) (women). Significant interactions of sUA and vitamin C intake were seen for CSA (men, P=0.06; women, P=0.005) but not for other QCT measures (P range: 0.56-0.90). Among women with sUA>6 mg/dL, higher vitamin C was associated with higher integral vBMD (P=0.005), trabecular vBMD (P=0.02) and VCS (P=0.01) but these were not significant in women with lower sUA concentration (Table). No significant associations were seen in men.

Although the sample size was limited in women with high sUA (n=53), these findings suggest that higher vitamin C intake may be protective of bone in women with high sUA (pro-oxidative state). The sex differences observed could be due to higher vitamin C intake in women compared to men. Future work should examine vitamin C and sUA (as an antioxidant and pro-oxidant) in relation to QCT bone changes over time.

Table. Association of vitamin C intake with spine QCT bone measures by serum uric acid levels.

| WOMEN | NORMAL UA ≤6 mg/dL (Range: 1.5-6 mg/dL, (n=749)) | | HIGH UA >6 mg/dL (Range: 6.1-9.1 mg/dL, (n=53)) | |
|------------------|---|---------|--|---------|
| | Mean vitamin C (mg/d) | | | |
| | 268 ± 287 | | 330 ± 353 | |
| | $\beta \pm SE$ | P value | $\beta \pm SE$ | P value |
| CSA ^a | 0.0493 ± 0.056 | 0.37 | 0.1509 ± 0.247 | 0.54 |
| Integral vBMD | 0.0011 ± 0.001 | 0.37 | 0.0123 ± 0.004 | 0.005* |
| Trabecular vBMD | 0.0013 ± 0.001 | 0.34 | 0.0093 ± 0.004 | 0.02* |
| VCS | 30.18 ± 38.97 | 0.43 | 302.39 ± 116.08 | 0.01* |

| MEN | NORMAL UA ≤7 mg/dL (Range: 3-7 mg/dL, (n=722)) | | HIGH UA >7 mg/dL (Range: 7.1-10.8 mg/dL, (n=243)) | |
|------------------|---|---------|--|---------|
| | Mean vitamin C (mg/d) | | | |
| | 247 ± 342 | | 218 ± 269 | |
| | $\beta \pm SE$ | P value | $\beta \pm SE$ | P value |
| CSA ^a | -0.0072 ± 0.048 | 0.88 | -0.0311 ± 0.083 | 0.71 |
| Integral vBMD | 0.0011 ± 0.001 | 0.37 | 0.0003 ± 0.002 | 0.90 |
| Trabecular vBMD | 0.0014 ± 0.001 | 0.30 | -0.0003 ± 0.002 | 0.91 |
| VCS | 20.30 ± 40.05 | 0.61 | 2.86 ± 75.11 | 0.97 |

^aModels for CSA were adjusted for age, weight, smoking, total energy intake and physical activity. Models for other QCT bone measures were additionally adjusted for height. *P<0.05

Table

Disclosures: Shivani Sahni, PAI, Inc.; General Mills Bell Institute of Health and Nutrition
 This study received funding from: The ASBMR JFOR201314 Award

MO0313

Hypophosphatemia Associated with Elemental Formula Use in Children with Feeding Problems. Luisa Gonzalez Ballesteros^{*1}, Nina Ma², Leanne Ward³, Philippe Backeljauw⁴, David Weber⁵, Linda DiMeglio⁶, Julie Gagne⁷, Robert Stein⁸, Declan Cody⁹, Kimber Simmons¹⁰, Paul Zimakas¹¹, Linda Casey¹², Erik Imel⁶, Thomas Carpenter¹³. ¹Yale University, USA, ²Boston Children's Hospital, USA, ³Children's Hospital of Eastern Ontario, Canada, ⁴Cincinnati Children's Hospital, USA, ⁵University of Rochester, USA, ⁶Indiana University, USA, ⁷Centre hospitalier de l'Université Laval, Canada, ⁸Children's Hospital of Western Ontario, Canada, ⁹Our Lady's Children's Hospital, Crumlin, Ireland, ¹⁰Children's Hospital Colorado, USA, ¹¹University of Vermont Medical Center, USA, ¹²British Columbia Children's Hospital, Canada, ¹³Yale University School of Medicine, USA

We encountered 18 cases of hypophosphatemia occurring in children receiving elemental formula feeds at 7 US and 3 Canadian sites, as well as one case in Ireland. Due to a variety of underlying diagnoses, all patients had feeding difficulties and were fed Neocate or the related products (Neocate Infant, Junior). Hypophosphatemia was severe and, usually occurred in association with overt rickets disease. Elevation in serum alkaline phosphatase activity and appropriate renal conservation of phosphate (P) were evident in all cases where examined. Tubular reabsorption of P was >99% in 3 cases, and 90% in 1 case, and not calculable due to undetectable urine P in 10 cases. No urine P data is available in the remaining 4 cases. P levels corrected with either P supplementation or a change in formula. Age, sex, biochemistry, and treatment responses are summarized in the table.

Neocate may be associated with hypophosphatemic rickets due to impaired intestinal absorption of P in certain children with feeding difficulties. The mechanism for this phenomenon is unclear, however considerations include altered P absorption due to GI pH alteration particular to the product, an inhibitor or binder of P, or inclusion of a phosphate species in the formula composition that is not readily absorbed. Genetic predisposition to impaired P absorption may also be possible.

These cases emphasize the need to consider nutritional etiologies in the evaluation of children with metabolic bone disease, even in a controlled hospital setting. Specifically, we raise the consideration that the bioavailability of phosphate in Neocate may be compromised in certain children and recommend monitoring of serum phosphate and for the development of bone disease during the use of elemental formulas.

| Age | Sex | Bone Dz | Ca (mg/dl) | P (mg/dl) | Alk Phos (IU/L) | Treatment | Response |
|-------|-----|---------|------------|-----------|-----------------|--|----------|
| 3.5 y | M | Y | 9.0 | 1.7 | 459 | P | Improved |
| 1.5 y | M | Y | 8.9 | 1.3 | 1137 | P, New Formula | Improved |
| 0.8 y | M | Y | 10.2 | 2.6 | 1321 | P, New Formula | Improved |
| 1.5 y | F | Y | ? | 2.5 | 736 | P | ? |
| 3 y | F | Y | iCa 4.96 | 1.6 | 1626 | P + Calcitriol | Improved |
| 0.8 y | F | Y | ? | 2.2 | 1977 | P | Improved |
| 0.2 y | F | Y | 9.8 | 4.6 | 215 (bone) | P, TPN | Improved |
| 2 y | F | Y | 9.9 | 1.8 | 3777 | P, New Formula | Improved |
| 7.5 y | F | Y | 9.8 | 2.2 | 831 | P, New Formula | Improved |
| 2 y | M | Y | 9.0 | 0.3 | 1134 | P | Improved |
| 2 y | F | Y | 7.0 | 1.0 | 754 | Ca + P, New formula | Improved |
| 3.5 y | F | Y | 9.4 | 2.3 | ? | P | Improved |
| 2 y | M | N | 8.2 | 2.4 | ? | New formula | ? |
| 3 y | F | Y | 9.7 | 1.7 | 1590 | P | Improved |
| 0.2 y | F | N | 7.9 | 2.4 | 1190 | P | Improved |
| 0.3 y | M | N | 10.2 | 1.7 | 1030 | P | Improved |
| 14 y | M | Y | 9.1 | 1.6 | 742 | P | Improved |
| 0.2 y | F | N | 11.1 | 2.6 | 774 | D/C Neocate fortification of breast milk | Improved |

TABLE

Disclosures: Luisa Gonzalez Ballesteros, None.

MO0314

Low ingestion of calcium and magnesium and high odds of hip fracture: a cross-sectional study. Juliana Brondani, Raisa Bringhenti, Felipe Langer, Giovanni Sartori, Adnan de Vieira, Antonio Codevilla, Fabio Comim, Melissa Premaor*. Federal University of Santa Maria, Brazil

Background: A health nutrition represents an important role in bone formation. A balanced alimentation, both in quality and quantity, probably will supply the necessary nutrients to maintain, at least in part, bone health during the aging. Furthermore, it could be a possible protection factor for the main consequences of the osteoporosis in elderly. Objectives: the aim of our study was to compare the alimentary consumption of calcium, phosphorus, magnesium, and proteins in hospitalized women with hip fracture with outpatient women without fractures. Methods: We carried out a cross-sectional study at the Santa Maria University Hospital, Santa Maria - Brazil. All women, 55 or older with hip fractures were invited to participate. The outpatient women were recruited from an ongoing cohort study (1). Sixty-two women were recruited (42 women with fractures and 20 women without fractures). Information about clinical data and social history were recorded. An anthropometric evaluation was performed. A Questionnaire Quantitative of the Frequency of Foods (QQFA) to evaluate the ingestion of calcium, phosphorus, magnesium and proteins was applied. Results: the ingestion of calcium and magnesium was significant lower in women with fractures [446.9 mg/day vs. 689.90 mg/day and 135.49 mg/day vs. 188.92 mg/day, respectively]. In the logistic regression analysis of fractures, high ingestion of calcium and magnesium were associated with a low odds of fracture. This result was adjusted for age and BMI. There were no differences in the protein intake between the groups. Conclusion: a high dietetic ingestion of calcium and magnesium evaluated by QQFA was protective against hip fractures in our study. 1) Copós RM, et al. Obesity and Fractures in Postmenopausal Women: A Primary-care Cross-Sectional Study at Santa Maria, Brazil. J Clin Densitom. 2014 Dec 17

Disclosures: Melissa Premaor, None.

MO0315

Calgary Vitamin D Trial: Safety of Supplementation up to 10,000 IU Vitamin D Daily, 12 Month Pilot Data. Erin Hildebrandt*, David Hanley, Steven Boyd. University of Calgary, Canada

The beneficial effects of vitamin D have been widely investigated, including its role bone health. The 2011 Institute of Medicine report identified a Recommended Dietary Intake for skeletal health of 600 IU vitamin D/day (from all sources) and a Tolerable Upper Limit (TUL) of 4,000 IU/day for adults under 70 years. Benefits of higher doses of vitamin D have not been systematically explored or identified, perhaps because of safety concerns. Very high doses of vitamin D have been associated with hypercalciuria and hypercalcemia, although Vitamin D toxicity is usually associated with doses above 40,000 IU/day. The present study was designed to evaluate the safety of taking daily doses of up to 10,000 IU of vitamin D daily as part of an ongoing controlled trial in Calgary by assessing markers of calcium and bone metabolism after 12 months of supplementation in a small pilot cohort.

Healthy men and women with normal parameters of calcium metabolism between 55-70 years (N=362) were recruited for a three year, randomized, double blind trial of 400, 4,000 or 10,000 IU vitamin D daily. The primary outcome of this study is to assess the relationship between vitamin D dose and bone health. Participants had baseline 25(OH)D levels between 30-120 nmol/L and were excluded if they had osteoporosis or medications or other conditions affecting calcium metabolism. A subset of participants (N=62; 18 M, 44 F; age 63.2 ± 4.1 yrs) formed a pilot cohort, for which we report first year parameters of calcium metabolism.

Safety parameters measured are depicted in Table 1. Four participants withdrew from the study for reasons unrelated to vitamin D supplementation (2 diagnosed with malignancy, 2 withdrew for non-medical reasons). We remain blinded to supplementation levels, but tested serum 25(OH)D. At 12M average 25(OH)D was 144.4 ± 69.3 nmol/L (min: 61.1 nmol/L, max: 325 nmol/L). There was no relationship between 25(OH)D and serum calcium or urinary calcium excretion. One high serum calcium was detected at 6 months, but normalized on re-testing. All urine calcium/creatinine ratios were below the upper normal limit (<1.0 mmol/L).

In this small study, there were no safety concerns with taking doses of Vitamin D at or above Health Canada's TUL Level of 4,000 IU/day for one year. We are also currently completing analysis of bone remodeling biomarkers CTX and PINP for this cohort.

Table 1: Biomarker safety data from pilot cohort at baseline (0M) and one year (12M). Healthy ranges are presented below each biomarker, with males and females split for liver enzymes.

| | 0M | 12M |
|---|--------------|---------------|
| 25(OH)D (nmol/L) | 76.2 (±17.4) | 144.4 (±69.3) |
| Serum Ca (mmol/L) (2.10-2.55) | 2.38 (±0.06) | 2.35 (±0.06) |
| 24Hr Urine Ca (mmol/day) (2.50-7.50) | 4.23 (±1.81) | 4.88 (±2.38) |
| Urine Ca/Crea (mmol/L) (<1.0) | 0.22 (±0.13) | 0.24 (±0.14) |
| PTH (ng/L) (13-54) | 23.6 (±6.3) | 20.5 (±5.6) |
| AST (U/L) (Male: 8-40) (Female: 8-32) | 21.3 (±7.3) | 21.8 (±4.4) |
| ALT (U/L) (Male: 1-60) (Female: 1-40) | 20.2 (±6.9) | 21.7 (±7.7) |
| | 17.8 (±6.5) | 17.1 (±7.4) |

Values are represented as mean (±SD).

*Biomarkers: 25-hydroxyvitamin D (25(OH)D), serum calcium (Ca), urine calcium creatinine ratio (Ca/Crea), parathyroid hormone (PTH), aspartate aminotransferase (AST) and alanine aminotransferase (ALT).

Table 1

Disclosures: Erin Hildebrandt, None.

This study received funding from: Pure North Synergy Foundation

MO0316

Relationship of Directly Measured Free 25(OH) Vitamin D and Total 25(OH) Vitamin D: Effect of Daily Vitamin D Supplementation in Postmenopausal Women. Gretta Borchardt*, Ellen Fidler, Diane Krueger, Neil Binkley, University of Wisconsin, USA

Background: The free hormone hypothesis holds that biological activity of a hormone is due to its unbound (free) rather than protein-bound concentration. As such, it is plausible that free 25(OH)D concentration is a better measure of an individual's vitamin D status than is total 25(OH)D. Free 25(OH)D measurement has previously faced technical challenges; direct measurement by immunoassay has recently become available, but data are limited regarding the relationship of free to total 25(OH)D. This study evaluated the effect of daily vitamin D supplementation on total and free 25(OH)D in postmenopausal women.

Methods: Sixty-two postmenopausal women were randomly assigned to receive daily vitamin D₃ 2,000 IU or matching placebo for 4 months. Their mean (SD) age and BMI was 67.8 (9.1) years and 28.5 (6.1) kg/m² respectively. Blood was drawn at baseline and following 1 and 4 months of supplementation. Total and free 25(OH)D were measured by ELISA using kits from Diasource (Louvain-La-Neuve, BE). Repeated measures ANOVA and regression analyses were performed.

Results: Overall, baseline 25(OH)D and free 25(OH)D mean (SD) were 35.2 (11.0) ng/mL and 5.1 (1.8) pg/mL respectively; both total and free 25(OH)D were higher at baseline in the vitamin D₃ supplemented group (Table). Supplement compliance was 98%. With daily supplementation, both free and total 25(OH)D increased ($p < 0.0001$) while neither changed in the placebo group (Table). Free and total 25(OH)D were highly correlated (R^2 0.35-0.55) at all timepoints. After 4 months of supplementation the increase in free 25(OH)D was highly correlated with the increase in total 25(OH)D; $R^2 = 0.58$; $p < 0.001$

Conclusion: In this study the circulating concentration of free 25(OH)D was less than 0.02% of the total 25(OH)D concentration. Free and total 25(OH)D levels were highly correlated and both increased with supplementation. Further research is needed to define the utility of free 25(OH)D measurement.

Table: Effect of daily vitamin D₃ supplementation on total and free 25(OH)D

| Group | Total 25(OH)D (ng/mL) | | | Free 25(OH)D (pg/mL) | | |
|-------------------------------|-----------------------|-------------|-------------|----------------------|-----------|-----------|
| | Baseline | 1 mo | 4 mo | Baseline | 1 mo | 4 mo |
| Daily D ₃ 2,000 IU | 38.5 (11.0) | 45.6 (10.5) | 52.1 (13.7) | 5.8 (1.9) | 7.1 (1.7) | 8.0 (2.1) |
| Placebo | 32.0 (10.2) | 33.3 (11.1) | 33.4 (13.2) | 4.4 (1.4) | 4.3 (1.3) | 4.5 (1.8) |

Data as mean (SD)

Table

Disclosures: Gretta Borchardt, None.

This study received funding from: Merck

MO0317

Relationship of Serum 25-Hydroxyvitamin D Measured by Liquid Chromatography-Mass Spectrometry to Bone Turnover Markers and Parathyroid Hormone and Bone Mineral Density in Korean Adult Males with Low Bone Mass. Da Young LEE*¹, Ju Young Jang², Tae Yang Yu², Won Jung Hong², Yong Joo Hong², Yong-Ki Min², Jae Hoon Chung², Jae Hyeon Kim², Kyu Yeon Hur³, Moon Kyu Lee², Sun Wook Kim². ¹Samsung Medical Center, South Korea, ²Division of Endocrinology & Metabolism, Department of Medicine, Samsung Medical Center, Sungkyunkwan University School of Medicine, South Korea, ³Division of Endocrinology & Metabolism, Department of Medicine, Samsung Medical Center, South Korea

1. Objective

Vitamin D is involved in bone and mineral metabolism, and its deficiency is associated with metabolic bone disease such as osteoporosis. Measurement of serum 25-hydroxyvitamin D [25(OH)D] is the best approach to assess an individual's vitamin D status. However, there is no consensus on the optimal level of serum 25(OH)D. Liquid chromatography-mass spectrometry (LC-MS/MS) is the method of choice for the analysis of 25(OH)D. Nevertheless, previous studies were based on 25(OH)D measured by immunoassay, and focused on postmenopausal women rather than men. The aim of this study is to assess vitamin D status measured by LC-MS/MS in adult men with low bone mass and its relationship to bone turnover markers, parathyroid function, and bone mineral density.

2. Method

We investigated medical record of 258 adult men newly diagnosed with osteopenia or osteoporosis whose serum 25(OH)D were measured by LC-MS/MS (Agilent Technologies, Inc.) in Samsung Medical Center from July 2009 to February 2014. Subjects were divided into 3 groups by serum 25(OH)D concentration: <10 (group A), 10-20 (group B), and >20 ng/mL (group C). Serum concentrations of bone-specific alkaline phosphatase (BS-ALP), C-telopeptide (CTX), intact parathyroid hormone (iPTH) and bone mineral density (BMD) were compared. All patients underwent BMD using dual-energy X-ray absorptiometry.

3. Result

The age of the subjects was 56.8 ± 12.2 years, 93.4% of them were diagnosed with osteoporosis. The mean of 25(OH)D was 20.4 ± 8.9 ng/mL. The concentrations of BS-ALP in group A, B and C were 23.6 ± 12.7, 20.2 ± 12.2 and 18.8 ± 13.8 μg/L, respectively. The concentrations of CTX were 0.528 ± 0.249, 0.464 ± 0.310, 0.409 ± 0.312 ng/mL and those of iPTH were 70.5 ± 95.3, 36.7 ± 20.8, 34.9 ± 25.5 pg/mL, respectively. The concentration of 25(OH)D was negatively correlated with those of BS-ALP, CTX and iPTH significantly. The concentrations of BS-ALP and CTX in group A were higher than group C, not group B. In case of iPTH, that in group A was higher than other groups.

The femur neck BMD in group A, B and C were 0.659 ± 0.114, 0.733 ± 0.122 and 0.722 ± 0.084 g/cm², respectively. And total femur BMD were 0.710 ± 0.122, 0.795 ± 0.116, 0.794 ± 0.094 g/cm², respectively. In femur neck and total femur BMD, group A was significantly lower than group B and C.

4. Conclusion

In Korean adult males with low bone mass, the serum concentration of 25(OH)D above 20 ng/mL would not be able to give further benefits in bone health markers such as BS-ALP, CTX, iPTH and BMD.

Disclosures: Da Young LEE, None.

MO0318

The effects of vitamin D on bone mineral density in rheumatoid arthritis and systemic lupus erythematosus. Chang-Hee Suh¹, Ju-Yang Jung^{*2}, Hyoun-Ah Kim². ¹Ajou University School of Medicine, South Korea, ²Ajou University Hospital, South Korea

Introduction: Vitamin D has been revealed to involve immunologic pathogenesis in rheumatoid arthritis (RA) and systemic lupus erythematosus (SLE). Moreover, vitamin D plays a pivotal role in bone formation, which tends to be vulnerable in RA and SLE. We studied the effects of vitamin D on bone mineral densities (BMD) in RA and SLE.

Materials and Methods: Age matched 94 female patients with SLE and 92 female patients with RA were recruited. The medical data including levels of 25-OH-vitD

from March to May, and T-scores on BMD which were measured by Dual energy X-ray absorptiometry were collected.

Results: The L-spine and hip T-scores were not different between RA and SLE patients, and the T-scores were not different between the patients with vitamin D deficiency and patients without it. In SLE, the patients with osteoporosis had higher ESR than those without osteoporosis did (31.4 ± 23.9 vs 16.4 ± 11.9 , $p=0.008$). Among the patients taking vitamin D replacement, RA patients had lower levels of 25-OH-vitD than SLE patients (19.83 ± 8.07 vs 24.33 ± 10.45 , $p=0.011$), and L-spine and hip T-scores in RA patients were lower than those in SLE patients. On multiple regression analysis, age, duration, vitamin D replacement, and steroid dose were shown to contribute to BMD in RA patients, while nothing contributed to BMD in SLE patients. Conclusions: There was no difference of BMD between RA and SLE, and there was no difference in BMD in the presence or absence of vitamin D deficiency. Only in RA, age, disease duration, vitamin replacement, and steroid dose were shown to contribute on BMD.

Disclosures: *Ju-Yang Jung, None.*

MO0319

The effects of vitamin D3 versus 25-hydroxyvitamin D3 on serum vitamin D metabolites and markers of calcium balance in a multi-ethnic cohort of healthy adults. Albert Shieh^{*1}, Christina Ma², Emily Sondergaard², Yang Shen², Kathryn Zavala², Philip Liu², John Adams². ¹University of California, Los Angeles, USA, ²UCLA, USA

Purpose: Vitamin D deficiency is associated with multiple adverse health outcomes, and disproportionately affects minority U.S. populations. Pharmacologic 25-hydroxyvitamin D3 (25D3) has a smaller volume of distribution than parent vitamin D3 (D3); 25D3 may therefore more quickly and robustly restore serum levels of 25-hydroxyvitamin D (25D). The aim of this study is to examine the effects of D3 versus 25D3 on serum vitamin D metabolites and markers of calcium balance in a multi-ethnic cohort of healthy adults.

Methods: Study participants will include a multi-ethnic cohort of 48 healthy adults >18 years of age (12 White, 12 Asian, 12 Black, 12 Latino) who have baseline 25D levels <20 ng/ml. Subjects are being randomized to receive 60 mcg/day of D3 or 20 mcg/day of 25D3. Serum and urine are collected at baseline and 4, 8, and 16 weeks follow-up to assess changes in serum vitamin D metabolites and markers of calcium balance.

Results: To date, 20 subjects have been randomized (2 White, 8 Asian, 5 Black, 5 Hispanic) with 11 receiving D3 and 9 receiving 25D3. As only 5 subjects have completed all study visits at present time, no statistical tests of significance for within-group changes and between-group differences were performed beyond 4 weeks. At baseline, 25D (16.1 ± 1.2 v. 17.8 ± 0.5 ng/ml), 1,25-dihydroxyvitamin D (1,25D) ($53. \pm 5.6$ v. 65.3 ± 7.4 pg/ml), serum calcium (Ca) (9.5 ± 0.1 v. 9.5 ± 0.2 mg/dl), urinary calcium:creatinine (U/Ca/Cr) (0.06 ± 0.01 v. 0.06 ± 0.01), and immunoreactive parathyroid hormone (iPTH) (39.4 ± 4.7 v. 30.9 ± 3.8 pg/ml) levels were similar between D3 v. 25D3 groups. By four weeks, 25D levels had increased significantly in D3 (mean within-group change 10.0 ng/mg; $p=0.02$) and 25D3 (mean within-group change 20.2 ng/ml; $p=0.001$) groups, but mean 25D level at this time point was significantly higher in those taking 25D3 (38.0 v. 27.3 ng/ml; $p=0.02$). Within-group changes in 1,25D, Ca, U/Ca/Cr, and PTH from baseline to 4 weeks were not statistically significant. Between-group differences in each parameter at 4 weeks were also not statistically significant.

Conclusions: Preliminary data from our pilot study demonstrates that subjects with baseline vitamin D deficiency experienced faster and more robust increases in 25D level taking 20 mcg/day of 25D3 v. 60 mcg/day of D3. There was no hypercalcemia or hypercalciuria in either group. We continue to collect data on the effects of completing both regimens on free 25D and markers of calcium balance.

Disclosures: *Albert Shieh, None.*

MO0320

Vitamin D Replacement in Bariatric Surgery: A Critical Appraisal of Current Guidelines. Marlene Chakhtoura^{*1}, Ghada El Hajj Fuleihan², Nancy Nakhoul², Elie Akl¹, Christos Mantzoros³. ¹American University of Beirut, Lebanon, ²American University of Beirut - Lebanon, Lebanon, ³Harvard Medical School, USA

Introduction:

Bariatric surgery is the most effective therapeutic option to reduce weight in morbidly obese individuals, but it results in a number of mineral and vitamin deficiencies. Clinical Practice Guidelines (CPGs) attempt to balance those benefits and harms to provide guidance to patients and to their physicians.

Objectives:

The objectives of this paper are to compare and evaluate the quality of the development process, and of the evidence of current CPGs providing recommendations on vitamin D replacement in patients undergoing bariatric surgery.

Methods:

We searched 3 databases, with no time restriction, to identify relevant and current CPGs. Two reviewers assessed eligibility and abstracted data, in duplicate. They evaluated the quality of CPGs development process using the Appraisal of Guidelines, Research, and Evaluation II (AGREE II) tool that consists of 6 domains. A content expert verified those assessments.

Results:

We identified 3 eligible CPGs: (1) the Endocrine Society (ES) Guidelines (2010); (2) the American Association of Clinical Endocrinologists (AAACE), The Obesity Society (TOS), and the American Society for Metabolic & Bariatric Surgery (ASBMS) Guidelines (update 2013); and (3) the Interdisciplinary European (IE) Guidelines (IEG) on Metabolic and Bariatric Surgery (latest update 2014).

The ES and the AAACE/TOS/ASBMS guidelines recommend high doses of vitamin D, varying from 3,000 IU daily to 50,000 IU 1-3 times weekly. Vitamin D doses were not mentioned in the IE guidelines.

In terms of quality, only the IE guidelines described their search methodology but none of the CPGs provided details on evidence selection and appraisal. None of the three CPGs rigorously assessed the preferences of the target population, resource implications, and the applicability of these guidelines. According to the AGREE tool, we rated the ES guidelines as average in quality, while the other two as low in quality.

The recommendations were based on a low quality of evidence, if any, or limited to a single high quality trial, for some outcomes.

Conclusion:

Current CPGs recommendations on vitamin D supplementation in bariatric surgery differ between societies. They do not fulfill criteria for optimal guideline development, possibly due to limited resources, and are based on expert opinion. Thus, the pressing need for high quality randomized trials to inform CPGs, ideally developed using commonly accepted standards.

Disclosures: *Marlene Chakhtoura, None.*

MO0321

Higher Body Fat Mass is Associated with Reduced Serum 1,25-dihydroxyvitamin D Levels in Healthy Postmenopausal Women. Magaly Hars, Andrea Trombetti, Mélyny Hars, Claire Durosier, Emmanuel Biver, Thierry Chevalley, Serge Ferrari, René Rizzoli^{*}. Division of Bone Diseases, Geneva University Hospitals & Faculty of Medicine, Switzerland

It is well established that higher body fat mass and obesity are associated with lower 25-hydroxyvitamin D (25(OH)D) and higher parathormone (PTH) levels. However, the relation between 1,25-dihydroxyvitamin D (1,25(OH)2D) and adiposity is much less recognized, though it has been suggested that 1,25(OH)2D may favor the development of fat tissue. The present study aimed at assessing the association between serum 1,25(OH)2D levels and body fat mass in a homogeneous cohort of 65-year old healthy women.

Cross-sectional data of 728 healthy postmenopausal women (age 65.0 ± 1.4 years), enrolled in the Geneva Retirees Cohort (GERICO) study, were analyzed. Fat mass was assessed using dual X-ray absorptiometry (Hologic Discovery W). Serum concentrations of 1,25(OH)2D were ascertained by a chemiluminescence immunoassay (IDS) and IGF-I was measured with an automated chemiluminescence-based immunoassay using two monoclonal antibodies. 25(OH)D and PTH were determined using Roche Diagnostics reagents. Univariate and multivariate regression analyses were performed.

The mean concentration of 25(OH)D was 67.5 ± 27.7 nmol/L. Three percent of participants had serum 25(OH)D below 25 nmol/L and 30% serum levels below 50 nmol/L. Univariate regression analyses showed that serum 1,25(OH)2D and 25(OH)D levels were negatively associated with total body fat mass ($P < 0.004$ and $P < 0.001$, respectively) while a positive association was found between 1,25(OH)2D and PTH ($P < 0.004$), but not with IGF-I. The negative association between 1,25(OH)2D and total body fat mass remained significant in a multivariate stepwise regression model with 25(OH)D, PTH, calcium intakes, dietary protein intakes retained in the final model ($P < 0.004$). It was not related to renal function.

Our results showed a strong inverse association between serum 1,25(OH)2D levels and body fat mass in 65-year old healthy postmenopausal women, despite higher PTH levels. These findings do not support the hypothesis of 1,25(OH)2D favoring body fat mass accumulation.

Disclosures: *René Rizzoli, None.*

MO0322

Changes in Gene Expression in Osteoblastic cell line SCP1 after Stimulation with Adult Crohn's Disease Patient Serum. Martina Blaschke¹, Regine Koepf², Marina Komrakova², Matthias Schieker³, Heide Siggelkow^{*2}. ¹Georg-August Universität, Germany, ²University Medical Center, Germany, ³Ludwig-Maximilians-Universität, Germany

Introduction: Crohn's disease (CD) is associated with a higher prevalence of osteoporosis, a complication that is recognized as a significant cause of morbidity. Its pathogenesis is still controversial, but the activity of CD is thought to be one contributing factor.

Methods: Serum levels of inflammatory cytokines IL-6, IL-1 beta, and TNF alpha were measured in CD patients during acute phase. A combination of these cytokines and CD-patient sera were evaluated using the human cell line SCP-1 (osteoblastic cell model). SCP1 cells were stimulated for 14 days with CD patient sera or control sera supplemented with cytokines. The gene expression of osteogenic marker genes and the RANKL/OPG ratio were determined using RT-PCR 48 hours or 14 days after stimulation.

Results: The combination of cytokines, but not the individual cytokines IL-6, IL-1 beta nor TNF alpha at relevant concentrations, increased the receptor activator of NF-kappaB ligand/osteoprotegerin (RANKL/OPG) ratio. None of other bone gene expressions were affected (COL1A1, OC, PPARg, RUNX2, SPP1, bAP, SP7) Application of serum obtained from male CD patients to SCP-1 cells resulted in increased RANKL expression. This effect was not present when applying serum obtained from female CD patients.

Discussion: Our results show that factors in serum from adult patients with acute CD are involved in bone remodeling and that gender specific factors might contribute to development to osteoporosis.

Disclosures: Heide Siggelkow, None.

MO0323

Circulating levels and liver protein and gene expression of sclerostin in patients with primary biliary cirrhosis. Correlation with hepatic histological features. Silvia Ruiz-Gaspa¹, Laia Gifre¹, Rosa Miquel², Marta Dubreuil¹, Pilar Peris¹, Ana Monegal¹, Ana Arias¹, Albert Pares³, Nuria Guanabens⁴. ¹Metabolic Bone Diseases Unit, CIBERehd, Hospital Clinic, University of Barcelona, Spain, ²Department of Pathology, Hospital Clinic, University of Barcelona, Spain, ³Liver Unit, CIBERehd, IDIBAPS, Hospital Clinic, University of Barcelona, Spain, ⁴Metabolic Bone Diseases Unit, Hospital Clinic, IDIBAPS, CIBERehd, University of Barcelona, Spain

Sclerostin is involved in the regulation of osteoblastogenesis and little is known about its role in the development of bone disease in primary biliary cirrhosis (PBC), characterized by low bone formation. Therefore, we have assessed the circulating levels and the liver expression of sclerostin in this cholestatic disease. Serum sclerostin levels were measured in 83 women with PBC (mean age: 60 ± 12 years) and 101 control women. Lumbar and femoral BMD as well as parameters of mineral metabolism and bone remodeling were measured. Moreover, sclerostin gene expression in the liver was assessed by real time PCR in samples of liver tissue taken by biopsy in 11 PBC patients and in 5 normal liver specimens. Presence and distribution of sclerostin was evaluated in liver slices from 11 patients by immunohistochemistry. The severity of histologic lesions was assessed semiquantitatively in the same liver samples. 77% of patients had low BMD (22% osteoporosis and 55% osteopenia). PBC patients had higher sclerostin levels than controls (76.7±38.6 vs. 32.5±14.7 pmol/L, $p < 0.001$). Serum sclerostin correlated inversely with markers of bone formation and resorption. Sclerostin mRNA in the liver was overexpressed as compared with control samples (2.7±0.3 fold vs healthy liver). Sclerostin was detected by immunohistochemistry in 7 of the 11 liver samples and mainly located in the bile ducts. Liver sclerostin was associated with the severity of cholangitis ($p=0.02$) and indirectly with the degree of lobular inflammation ($p=0.03$). Sclerostin mRNA expression was higher in samples positive by immunohistochemistry (2.9±0.4 vs 2.5±0.3, $p.n.s.$), and particularly in those with lobular granuloma (3.6±0.6 vs 2.4±0.2, $p=0.02$). The increased expression of sclerostin in the liver and the association with histologic cholangitis may explain the high serum levels of this protein in patients with PBC, thus suggesting that sclerostin influences the decreased bone formation in this cholestatic disease.

Disclosures: Silvia Ruiz-Gaspa, None.

MO0324

Deficiency of C/EBP Homologous Protein Enhances Bone Mineral Density Loss in Female Mice. Shing-Hwa Liu^{*}, Cheng-Tien Wu, Rong-Sen Yang. National Taiwan University, Taiwan

Introduction: Endoplasmic reticulum (ER) stress has been shown to be involved in the imbalanced bone remodeling that leads to osteopenia or osteoporosis. Expression of CCAAT/enhancer binding protein (C/EBP) homologous protein (CHOP) is induced during ER stress, which is related to apoptosis in several cell types. CHOP null mice have been exhibited to decrease bone formation. However, a study of transgenic mice overexpressing CHOP in the bone microenvironment showed that CHOP overexpression impairs the osteoblastic function leading to osteopenia. The regulatory role of CHOP in bone formation is controversial and still remains to be clarified. Here, we investigate the alterations in bone structure of CHOP knockout mice using a micro-computed tomography (μ CT).

Methods: Mice lacking the *Chop* gene (C57BL/6 background) were purchased from Jackson Laboratories. Adult female and male mice of wild type (C57BL/6) and CHOP knockout (*Chop*^{-/-}), weighing 18-25 g, were used in this study. Bone mass and microarchitecture analysis in wild-type and CHOP knockout mice were determined by μ CT. The bone marrow stromal cells (BMSCs) were also isolated and cultured. The animal study was approved by institutional animal research committee.

Results: CHOP genome typing experiment demonstrated the gene knockout in the CHOP knockout mice. The results of μ CT analysis showed that bone mineral density (BMD), bone volume ratio (BV/TV), trabecular number, and trabecular thickness were significantly decreased and trabecular space was significantly increased in *chop*^{-/-} mice as compared with wild type control ($p < 0.05$, $n=6$, Figure 1). The BMD, bone volume ratio, trabecular number, and trabecular thickness of trabecular bones were significantly decreased more for female than for male *chop*^{-/-} mice ($p < 0.05$, $n=6$, Figure 1). Similarly, the cortical mineral density of cortical bone was also decreased

more for female than for male *chop*^{-/-} mice ($p < 0.05$, $n=6$). Moreover, the activities of alkaline phosphatase and mineralized nodule formation were significantly decreased in BMSCs isolated from female *chop*^{-/-} mice ($p < 0.05$, $n=6$, Figure 2).

Conclusion: These results indicate that ER stress-related CHOP signaling may play an important role in bone formation especially in females. Proper regulation of CHOP signaling may be a clue to further target for treatment of osteoporosis.

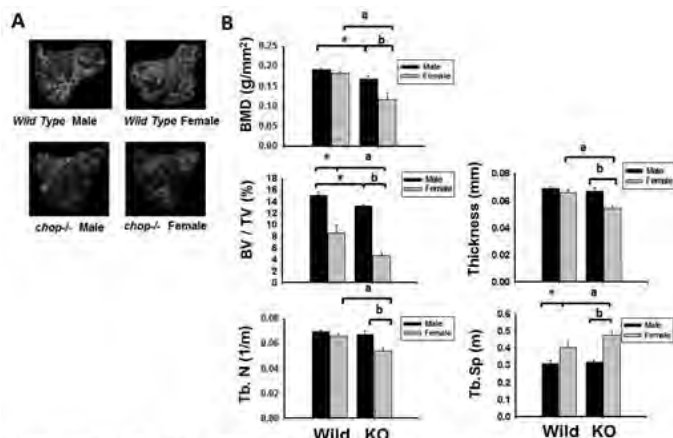


Figure 1. Changes of trabecular microarchitecture in wild type and *chop*^{-/-} (KO) mice. (A) Representative photomicrographs of trabecular bone of the proximal tibia by μ CT. (B) Morphometric results for trabecular bone (BMD, BV/TV, number (Tb.N), thickness and space (Tb.Sp)). Data are mean \pm SD ($n = 6$ mice/group). * $p < 0.05$, vs female wild type. † $p < 0.05$, vs male KO. ‡ $p < 0.05$, vs male wild type.

μ CT analysis

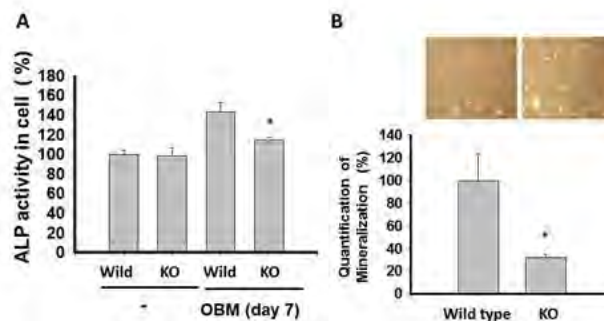


Figure 2. The activities of alkaline phosphatase (A) and mineralized nodule formation (B) were decreased in bone marrow stromal cells (BMSCs) isolated from female *chop*^{-/-} (KO) mice. OBM: osteoblast differentiation medium. Data are mean \pm SD ($n = 6$). * $p < 0.05$, vs wild type.

osteoblast differentiation

Disclosures: Shing-Hwa Liu, None.

MO0325

Discovery of Small Molecules to Promote BMP Signaling and Bone Formation. Chao Liang^{*1}, Mengyang Xu², Xin Zhou³, Kavan Wang⁴, Jun Xu², Baoting Zhang⁴, Aiping Lu³, Ge Zhang³. ¹Hong Kong Baptist University, Hong kong, ²Research Center for Drug Discovery & Institute of Human Virology, School of Pharmaceutical Sciences, Sun Yat-Sen University, China, ³Institute for Advancing Translational Medicine in Bone & Joint Diseases, School of Chinese Medicine, Hong Kong Baptist University, Hong kong, ⁴School of Chinese Medicine, The Chinese University of Hong Kong, Hong kong

Objective: Metabolic skeletal diseases with impaired bone formation are public health issues. The only FDA-approved bone anabolic agent is parathyroid hormone. However, the dominant bone resorption after 2-year use is of serious concern¹. BMP signaling plays a significant role in bone formation and Smurf1 negatively regulates BMP signaling by ubiquitinating critical factors (Smad1/5) for degradation². Thus, Smurf1 could be a promising pharmacological target for developing bone anabolic agents. Here, we aim to discover small molecules to block the interaction between Smurf1 and Smad1/5 by high-throughput in silico screening and test the effect of the most likely hits on BMP signaling and bone formation.

Methods: We defined a potential ligandable pocket on WW domains of Smurf1 as a docking site for more than 100,000 compounds in virtual screening. We incubated mouse osteoblast MC3T3-E1 with the most likely hits in differentiation medium and

evaluated the protein level of phosphorylated Smad1/5 (p-Smad1/5), cell viability, mRNA expression of differentiation markers (ALP, Osterix and Osteocalcin) and ALP activity by western blot, MTT assay, real-time PCR and ALP staining, respectively. We established drill-hole defect mouse model³ and examined the effects of the most likely hits on bone formation and bone healing by bone histomorphometry and microCT, respectively.

Results: Based on Smurf1-Smad1 interaction, an area on the WW domains, surrounded by R214, Y247, L245 and W251, was defined as a hydrophobic pocket to satisfy the requirement of accommodating small molecules in the concave groove and a chalcone derivative exhibited the most preferable binding model (Fig. 1). Furthermore, *in vitro* data from western blot showed that the chalcone derivative elevated the protein level of p-Smad1/5 in dose dependent manner (Fig. 2). MTT assay, real-time-PCR and ALP staining demonstrated that chalcone derivative had no cytotoxicity (Fig. 3) and promoted the mRNA expression of ALP, Osterix and Osteocalcin and ALP activity, respectively (Fig. 4, 5). After local administration, bone histomorphometry and microCT analysis indicated that chalcone derivative improved MAR, BFR/BS (Fig. 6) and bone healing of the defect region on mid-diaphyseal femur at 21 d (Fig. 7).

Conclusion: Chalcone derivative could be a promising agent to promote BMP signaling and bone formation.

Reference1. Kroll MH, Bull Math Biol 2000. 2. Lu K, et al. Nat Cell Biol 2008. 3. He Y, et al. Bone 2011.

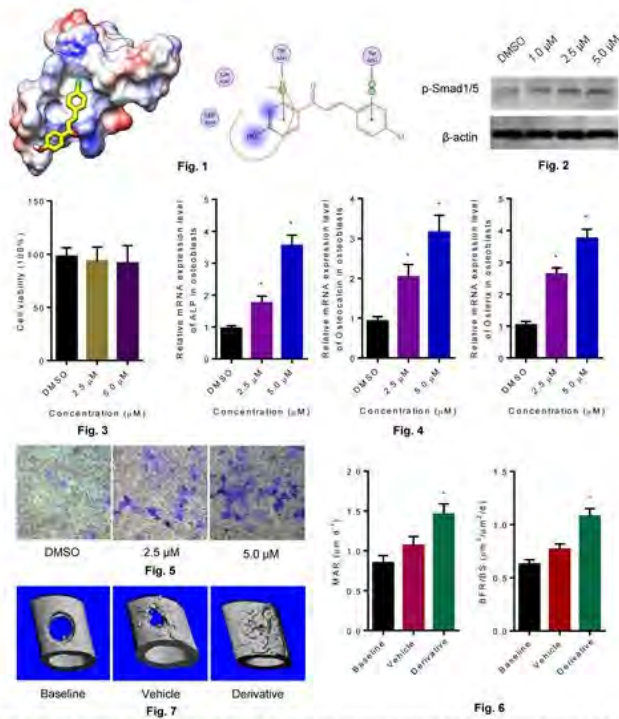


Fig. 1 Refined structure of the Smurf1 WW domain bound to the Chalcone derivative and Key residues in Smurf1. Fig. 2 Effect of chalcone derivative on protein level of phosphorylated Smad1/5 (p-Smad1/5) in 3E3-E1 cells. Fig. 3 Effect of chalcone derivative on cell viability. Fig. 4 Effect of chalcone derivative on mRNA expression level of differentiation markers (ALP, Osterix and Osteocalcin) in differentiation medium (supplemented with 50 mg/ml ascorbic acid and 10 mM β-glycerophosphate). **P* < 0.05 for a comparison of chalcone derivative (2.5 and 5.0 μM) with DMSO, *n* = 3 per group. Fig. 5 Effect of chalcone derivative on ALP activity. Fig. 6 Effect of chalcone derivative on mineral apposition rate (MAR), bone formation rate (BFR/BS). **P* < 0.05 for a comparison of chalcone derivative with Vehicle, *n* = 6 per group. The data are presented as the mean ± sd. Student's *t* test was used to determine the significance. Fig. 7 Effect of chalcone derivative on bone healing pattern.

Figure

Disclosures: *Chao Liang, None.*

MO0326

GPR120 As a Molecular Target For Inflammatory Bone Diseases. Md Rahman*¹, Stephen Harris², Wasim Chowdhury². ¹University of Texas Health Science Center, USA, ²UTHSCSA, USA

Bone homeostasis is maintained by a balance between bone resorption by osteoclasts and bone formation by osteoblasts. Chronic inflammation in bone microenvironment can increase bone resorption, decrease bone formation resulting in an uncoupling of bone formation from resorption. As such chronic inflammation can favor excessive resorption leading to osteoporosis. Activation of NF-κB and MAPK, two key pro-inflammatory signaling pathways are directly linked to reduced bone formation and accelerated bone resorption in inflammatory bone diseases. Activation of G protein coupled receptor (GPR)120 signaling pathway has been shown to be associated with down-regulation NF-κB and MAPK signaling activation. GPR120, also known as free fatty acid receptor (FFR)4 is a ligand for long chain polyunsaturated fatty acids (PUFAs). We have previously demonstrated the anti-bone resorbing and anti-osteoporotic effect of omega-3 PUFAs. Therefore, GPR120

could be a potential target for the drug development for the prevention and treatment of inflammatory bone diseases. Interestingly, osteoclast precursors, osteoclasts, osteoblast precursors, osteoblasts and chondrocytes are reported to express GPR120. Our gene array data from *ex vivo* mouse long bone osteocyte enriched bone tubes and calvarial osteoblast cells reveals that both osteoblasts and osteocytes express GPR120, however, the expression level of GPR120 in long bone osteocytes is 190 times higher than calvarial osteoblasts. On the other hand, GPR40, another omega-3 FFR4 was not expressed in our system. Osteocytes are now believed to be the master regulator of both osteoblastogenesis and osteoclastogenesis. Our cell culture data further reveals that knock-down of GPR120 by shRNA augments RANKL-induced osteoclast differentiation of RAW264.7 cells. Moreover, GPR120 knocked-down cells generate giant osteoclasts. Knock-down of GPR120 by siRNA also partially abrogated the anti-osteoclastogenic effect of GPR120 agonists. Our preliminary studies suggest that activation of GPR120 signaling pathway by GPR120 specific agonist may have a potential preventive/therapeutic effect in inflammatory bone diseases. Further studies with cell specific culture models and tissue specific knockout animal models with specific pharmacological agonists and antagonists of GPR120 are warranted to determine the utility of GPR120 as a molecular target to treat inflammatory bone diseases.

Disclosures: *Md Rahman, None.*

MO0327

Relation of serum serotonin levels and rates of bone loss in men. Kihyun Baek*, Mooil Kang, Jeho Han. The Catholic University of Korea, South Korea

Background: Recent genetic studies in rodents have demonstrated a key role for circulating serotonin (5-hydroxytryptamine, 5-HT) in regulating bone formation and skeletal mass.

Further support for an important role for serotonin in bone metabolism comes from studies in patients treated with selective serotonin reuptake inhibitors (SSRIs), which increase extracellular serotonin levels. This study assessed the impact of serum serotonin on bone loss rates in an elderly population-based cohort of 180 healthy (or ambulatory) men, aged 56-70 years and followed up for a median of 3.7 years.

Method: Serum serotonin, serum creatinine, and mobility test were assessed at baseline. Bone mass at the lumbar spine, femoral neck and total hip was measured at baseline and at follow up by dual energy X-ray absorptiometry.

Results: Serotonin levels were inversely associated with lumbar spine BMD ($r = -0.174, P=0.028$). No associations were found between femur neck & total hip BMD and serotonin levels. The annual rates of bone loss in the lumbar spine, femoral neck and total hip was $-0.07, -0.5$ and -0.49% , respectively. Serum serotonin at baseline did not predict bone loss rates at all skeletal sites. Lower limb disability (Get Up and Go test) at baseline predicted bone loss at the lumbar spine and total hip.

Conclusions: Serum serotonin (circulating serotonin) is not associated with loss rate of bone density in elderly men.

Disclosures: *Kihyun Baek, None.*

MO0328

Relationship between acetylcholine levels and bone loss in the early stages of Alzheimer disease: a mouse study. Yun Ma*¹, Randy Blakely², Florent Elefteriou³. ¹Vanderbilt University, USA, ²Department of Pharmacology, Vanderbilt University, USA, ³Department of Medicine, Department of Pharmacology, Department of cancer biology, Vanderbilt Center for Bone Biology, Vanderbilt University, USA

Alzheimer disease (AD) is characterized by central nervous system atrophy and memory decline. It is also associated with low parasympathetic nervous system (PSNS) and high sympathetic nervous system (SNS) outflow, low bone mineral density and increased fracture risk at early stages of the disease, prior to plaque development, reduced locomotor activity and skeletal unloading typical of later-stage AD. In mice, high peripheral SNS and low central acetylcholine signaling, due to deletion of the muscarinic acetylcholine receptor 3, both cause low bone mass. Because early stages of AD are characterized by reduced central acetylcholine levels (generated by parasympathetic neurons), acetylcholine esterase inhibitors (AChEIs) are used to treat these patients. Interestingly, the use of AChEIs is associated with reduced fracture risk in AD patients. These observations led us to ask if and how changes in PSNS activity contribute to the early bone loss observed in patients with AD.

To address this question, we used both gain and loss of function approaches to alter acetylcholine levels in mice and measure consequences on the skeleton. Acetylcholine levels were increased globally or peripherally by using AChEIs that pass or do not pass the blood brain barrier (BBB) in adult wildtype (WT) mice. *ChT*^{+/-} mice with reduced level of the choline transporter, which is necessary for neurons to generate acetylcholine, were used as a model of low PSNS outflow. Microcomputed tomographic and histomorphometric analyses were used to quantify treatment or gene deficiency impact on the skeleton.

ChT was not detected in MSC, osteoblast, osteocyte, chondrocyte or osteoclast cultures, regardless of their differentiation stage, whereas *AchE* was detected in osteoblast cultures, suggesting that osteoblasts can catabolize acetylcholine released by PSNS nerves but cannot synthesize it. Treatment of 3 month-old C57BL6 mice for

6 weeks with galantamine or donepezil, two AChEIs that pass the BBB, significantly increased bone turnover (increased osteoblast and osteoclast number/bone surface) and bone volume/tissue volume, whereas pyridostigmine, an AChEI that does not cross the BBB, increased osteoclast number and reduced bone volume. On the other hand, 3 month-old *ChT+/-* mice displayed a low bone mass phenotype compared to WT littermates.

These results support a model by which reduced central PSNS signaling contributes to the bone loss observed in early-stage AD patients.

Disclosures: Yun Ma, None.

MO0329

Highly expressed CKIP-1 inhibits BMP signaling pathway to suppress osteogenic differentiation and mineral deposition in osteoblast during glucocorticoid treatment *in vitro*. Jin Liu^{*1}, Changwei Lv², Baosheng Guo³, Defang Li⁴, Chao Liang⁴, Xiaohua Pan⁵, Lingqiang Zhang⁶, Baoting Zhang⁷, Aiping Lu⁴, Ge Zhang¹.¹ Hong kong, ²Institute for Advancing Translational Medicine in Bone & Joint Diseases, Hong Kong Baptist University, Hong Kong, Department of Orthopedics, Xijing Hospital, The Fourth Military Medical University, Hong kong, ³Institute for Advancing Translational Medicine in Bone & Joint Diseases, Hong Kong Baptist University, Hong Kong, Hong kong, ⁴Institute for Advancing Translational Medicine in Bone & Joint Diseases, Hong Kong Baptist University, Hong kong, ⁵Department of Orthopedics in Second Hospital of Medical College (Shenzhen), Jinan University, China, ⁶State Key Laboratory of Proteomics, Beijing Proteome Research Center, Beijing Institute of Radiation Medicine, Beijing, China, ⁷School of Chinese Medicine, The Chinese University of Hong Kong, Hong kong

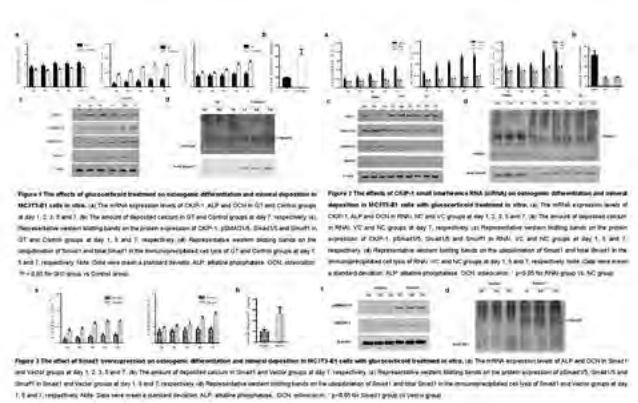
Introduction: The molecular mechanism for bone formation reduction during glucocorticoid-induced osteoporosis (GIO) remains unclear. It has been documented that the BMP pathway, a critical intercellular pathway responsible for osteoblastic bone formation, was repressed in osteoblast after glucocorticoid (GC) treatment. We have identified CKIP-1 as a novel negative regulator of BMP pathway, which specifically targets the linker region of Smurf1 to promote ubiquitin-mediated degradation of Smad1/5 (Lu et al. 2008). In our preliminary study, we found increased CKIP-1 expression and decreased Smad1/5 phosphorylation within osteoblast during bone formation reduction in rodent model with GIO. In this study, we tested the hypothesis that highly expressed CKIP-1 could inhibit BMP pathway to suppress osteogenic differentiation and mineral deposition in osteoblast during GC treatment *in vitro*.

Aim: To investigate the role of CKIP-1 in osteoblastic MC3T3-E1 cells during GC treatment *in vitro*.

Methods: We performed qPCR, Alizarin Red-S staining and immunoblotting to examine: (1) the effect of GC treatment on CKIP-1 expression, osteogenic differentiation, mineral deposition and BMP pathway activity in MC3T3-E1 cells *in vitro*; (2) the effect of CKIP-1 siRNA on osteogenic differentiation, mineral deposition and BMP pathway activity in MC3T3-E1 cells treated with GC *in vitro*; (3) the effect of Smad1 overexpression on osteogenic differentiation, mineral deposition and BMP pathway activity in MC3T3-E1 cells treated with GC *in vitro*.

Results: The CKIP-1 mRNA expression was higher, whereas the mRNA expression of osteoblastic genes was lower in GT group than Control group during GC treatment (Fig 1a). The amount of deposited calcium was lower in GT group than Control group at day 7 during GC treatment (Fig 1b). The CKIP-1 protein level was higher, while the protein level of phosphorylated Smad1/5 and total Smad1/5 were both lower in GT group than Control group during GC treatment (Fig 1c). The ubiquitination level of Smad1 was higher in GT group than Control group during GC treatment (Fig 1d). Impressively, the above inhibitory effect of GC on MC3T3-E1 cells could be either reversed after CKIP-1 siRNA treatment (Fig 2) or attenuated after transfection with Smad1 lentivirus vector (Fig 3).

Conclusion: Highly expressed CKIP-1 could inhibit BMP signaling pathway to suppress osteogenic differentiation and mineral deposition in osteoblast during GC treatment *in vitro*.



Figures

Disclosures: Jin Liu, None.

MO0330

Modulation of Apolipoprotein E on Estrogen Mediated Bone Metabolism. Ling Wang^{*1}, Yu-Yan Gui², Xue-Min Qiu². ¹Fudan University, Institute of Obstetrics & Gynecology, Obstetrics & Gynecology, Peoples republic of china, ²Laboratory for Reproductive Immunology, Hospital & Institute of Obstetrics & Gynecology, IBS, Fudan University Shanghai Medical College, Shanghai 200011, China, China

Osteoporosis and atherosclerosis are among the most frequent morbidities in postmenopausal women because of the disorder occurred in lipid metabolism and bone metabolism due to estrogen deprivation. Apolipoprotein E (ApoE), which plays a major role in the transport and metabolism of lipids by acting as a ligand for low density lipoprotein receptors, was induced strongly during osteoblastogenesis *in vivo*. Estrogen could up-regulate the ApoE level in peripheral blood. Mice lacking ApoE raised by chow displayed a high bone mass phenotype, while by high-fat diet presented decreased bone mass accounted for increased osteoblast apoptosis. To investigate the underlying mechanism, we isolated the osteoblast from the skull of ApoE^{-/-} and WT newborn mice respectively. Afterwards, ALP staining and ALP activity assay were conducted to detect the osteoblast activity. Bone formation *in vitro* was performed then confirmed by alizarin red staining and von kossa staining. Cell proliferation and apoptosis were detected by flow cytometry. Co-culture of ApoE^{-/-} or WT osteoblast with ApoE^{-/-} or WT osteoclast was done respectively to observe the direct and indirect effects of osteoblast on osteoclastogenesis. Expression of type I collagen, Runx2, osterix, RANKL and OPG were measured by real-time PCR, and these proteins were identified with ELISA or western blot. Our results showed that ApoE gene deficiency attenuated the osteoblast activity and osteoblastogenesis via down-regulating the osterix. Moreover, ApoE gene deficiency enhanced the osteoclastogenesis indirectly through decreasing the OPG secretion without affecting RANKL. Further study need to be done to investigate the related molecular mechanism and signaling pathway. We will treat WT osteoblast with serial concentrations of estrogen during osteogenesis *in vitro*, then the expression and translation of ApoE would be detected by real-time PCR as well as western blot. Selective estrogen receptor antagonist would be used to explore the molecular mechanism of estrogen regulating ApoE. Moreover, we will build animal model of postmenopausal osteoporosis with ovariectomized mice to observe ApoE's effects on bone phenotype after estrogen deprivation. In conclusion, ApoE gene plays an important role in osteoblastic differentiation and function through regulating the expression of osterix and OPG, might modulate bone mass on estrogen mediated bone metabolism.

Disclosures: Ling Wang, None.

MO0331

Longitudinal changes of trabecular bone score during aromatase inhibitor treatment in Korean breast cancer patients. A Ram Hong^{*1}, Jung Hee Kim², Sang Wan Kim², Chan Soo Shin². ¹Seoul National University Hospital, South Korea, ²Department of Internal Medicine, Seoul National University College of Medicine, South Korea

Objective: We were to examine the effects of treatment with aromatase inhibitor (AI) on bone mineral density (BMD) measured by dual-energy X-ray absorptiometry (DXA) and trabecular bone score (TBS), a novel grey-level index of bone microarchitecture based on DXA images in postmenopausal women with hormone receptor-positive early breast cancer.

Methods: We retrospectively included 190 patients who were treated with AI at least 3 years and baseline T-score > -2.5 from January 2006 to March 2015 at Seoul National University Hospital. Patients who were taking anti-osteoporosis medications including bisphosphonate, selective estrogen receptor modulator, or estrogen therapy at baseline or during treatment with AI were excluded. Patients with prior treatments with tamoxifen or other hormone replacement, and disease progression during follow-up were further excluded. Lumbar spine TBS and lumbar spine, femur neck, and total hip BMD were measured annually.

Results: Mean age of patients was 58.8 years and mean duration of follow-up was 4.27 years. Ninety-nine patients (47.9%) had osteopenia at baseline. Lumbar spine BMD was significantly decreased during follow-up (From baseline, 1, 2, 3, 4, 5 year; 1.068 ± 0.010 , 1.038 ± 0.011 , 1.030 ± 0.011 , 0.999 ± 0.009 , 1.013 ± 0.011 , 0.991 ± 0.013 ; $P < 0.001$) after adjusting for age, and body mass index (BMI). Femur neck and total hip BMD were also significantly decreased (0.860 ± 0.007 , 0.840 ± 0.008 , 0.833 ± 0.008 , 0.813 ± 0.008 , 0.804 ± 0.007 , 0.796 ± 0.011 in femur neck; 0.921 ± 0.007 , 0.895 ± 0.008 , 0.887 ± 0.008 , 0.871 ± 0.008 , 0.866 ± 0.007 , 0.862 ± 0.010 in total hip; both $P < 0.001$). Lumbar spine TBS was significantly decreased from baseline after adjusting for age, BMI, and baseline lumbar spine BMD (1.330 ± 0.006 , 1.321 ± 0.008 , 1.304 ± 0.007 , 1.292 ± 0.007 , 1.291 ± 0.007 , 1.296 ± 0.009 ; $P < 0.001$).

Conclusion: Lumbar spine TBS was significantly decreased during treatment with AI independent of BMD in Korean early breast cancer patients.

Disclosures: A Ram Hong, None.

MO0332

Use of ibuprofen before, but not after, exercise blunts the serum IL-6 response in older women and men. Sarah Wherry*, Catherine Jankowski, Pamela Wolfe, Robert Schwartz, Wendy Kohrt. University of Colorado, USA

Prostaglandin E2 (PGE2) is involved in the signaling pathway by which mechanical loading stimulates bone formation. Inhibition of PGE2 synthesis with non-steroidal anti-inflammatory drugs (NSAIDs) impairs the bone formation response to mechanical loading in animals when the NSAID is present before loading but not when it is introduced after. However, NSAIDs also have the potential to have anti-resorptive effects in bone by suppressing inflammatory cytokines, such as interleukin-6 [IL-6], that have pro-resorptive effects. The aim of this study was to determine if the timing of ibuprofen use two hours before versus immediately after an exercise bout has acute effects on serum IL-6 and markers of bone resorption (C-terminal telopeptide; CTX) and formation (bone-specific alkaline phosphatase; BAP). **Methods:** This was a sub-study of a larger trial involving exercise training and ibuprofen use in which participants were randomized to 3 drug treatment groups: placebo before and placebo after exercise (PP), ibuprofen before and placebo after exercise (IP), or placebo before and ibuprofen after exercise (PI). A subgroup of 42 participants (12 PP, 17 IP, 13 PI) participated in the current study. At week 8 of the 36-week exercise intervention, blood was sampled before and immediately, 30 minutes, and 60 minutes after an exercise bout for the measurement of IL-6, BAP, and CTX. Participant characteristics at baseline were compared across groups by one-way ANOVA for continuous measures and by a chi square test for categorical variables. The effects of ibuprofen and the timing of ibuprofen relative to exercise were evaluated by maximum likelihood estimates in a repeated measures model regressing each outcome measure on the baseline value of the outcome measure, sex, and an indicator for treatment group by time. **Results:** Increases in IL-6 were blunted in response to IP when compared to PI 60 minutes after exercise ($p < 0.001$). There were no significant differences in the change in IL-6 between the PI and PP or the IP and PP groups (all $p > 0.05$). There were no significant differences among the groups in the BAP or CTX responses. **Conclusion:** Taking ibuprofen prior to exercise dampened the IL-6 response to exercise in older adults, whereas taking ibuprofen after exercise did not. Although there was no apparent effect of ibuprofen use on markers of bone turnover, it may be necessary to track changes for a longer duration of time after exercise.

Disclosures: Sarah Wherry, None.

MO0333

Trabecular Bone Score (TBS) is associated with pulmonary function and severe vertebral fractures in chronic obstructive pulmonary disease(COPD). Reiko Watanabe*¹, Takeshi Tanaka¹, Keisuke Aita¹, Masaaki Hagiva¹, Hiroaki Masaki¹, Nobuyuki Tai¹, Jvunko Hirano¹, Kyoko Yokosuka², Hisami Yamakawa², Toshiaki Homma¹, Tsutomu Yaritha², Daisuke Inoue¹, Ryo Okazaki¹. ¹Teikyo University Chiba Medical Center, Japan, ²Yarita Hospital, Japan

Background&Aim: Chronic obstructive pulmonary disease (COPD) has recently been recognized as a major secondary cause of osteoporosis. We also reported a high prevalence of vertebral fractures and osteoporosis in Japanese male patients with COPD. The mechanism of COPD-associated osteoporosis however remains elusive. A population-based study in Manitoba has suggested that COPD is associated with reduced Trabecular Bone Score (TBS), a novel measure of bone microarchitecture. Thus, the aim of the present study is to investigate bone status including TBS and relationship between pulmonary function in COPD.

Subjects&Methods: In this cross-sectional study, 61 Japanese male COPD subjects (age, 70.0 ± 8.2 ; BMI, 21.7 ± 3.9 kg/m²) were enrolled. They were 19,23,13, and 6 subjects in each of GOLD 1-4 stage. The number and severity of existing vertebral fractures(VFx) were assessed by lateral spine x-rays, and bone mineral density (BMD) was measured by DXA scan. Bone metabolic markers and parameters of calcium metabolism were measured by standard assays.

Results: We found prevalent VFx in 46 (75.4%), SQ Grade 2 or 3 VFx in 12 (19.7%), and multiple VFx in 34 (55.7%), mean number of VFx per person was 2.1 ± 1.8 . Lumbar spine and femoral neck BMD T scores were -1.005 ± 1.46 and -1.87 ± 1.27 , respectively. In severe VFx group (Grade 2 or 3 fracture), FEV_{1.0}, BMI, BMD, TBS and serum Ca levels were significantly lower, whereas intact PTH and hsCRP were higher compared to non- or Grade1 VFx group by student t-test. Osteoporosis defined as BMD T score < -2.5 was found 23 subjects (37.7%). BMD was significantly decreased with advanced GOLD stage while the number of VFx was not. Interestingly, TBS was correlated positively with BMD and pulmonary function parameters including FEV_{1.0} and %VC, and negatively with height loss, SQ grade, levels of intact PTH, Tracp-5b, and hsCRP. Among these correlates, intact PTH, Tracp-5b and hsCRP were not correlated with BMD. In multilogistic regression analysis, BMD, FEV_{1.0}, and hsCRP were independent determinants of TBS after adjustment for age, height, BMI. In addition, when osteoporotic subjects were divided into 3 groups according to the levels of TBS, the lowest TBS tertile had more severe VFx.

Conclusions: We demonstrated the first time pulmonary function is associated with pulmonary function in COPD subjects. Decreased TBS may be a critical component of bone fragility associated with pulmonary dysfunction and can be a predictor of severe VFx in COPD.

Disclosures: Reiko Watanabe, None.

MO0334

Acceleration of Fracture Healing and Improvement of Quality of Life with Teriparatide: about 16 Cases. Delphine Stoll¹, Bérengère Aubry-Rozier*², Elena Gonzalez Rodriguez², Didier Hans², Olivier Lamy². ¹Centre a bone diseases, Switzerland, ²Center of Bone Diseases, Bone & Joint Department, Lausanne University Hospital, Lausanne, Switzerland, Switzerland

Introduction: A non-healing fracture (Fx) may affect severely the quality of life. It is defined by a non-union after > 3-6 months or a pseudoarthrosis > 9 months after the Fx occurrence. This raises the question of increasing the bone formation and of accelerating the Fx healing by medical intervention with an anabolic treatment. Some cases reports suggest that Teriparatide (TP) improve bone healing and functional state.

Method: We used TP in complex cases of non-healing Fx based on the surgeons' judgment. The delay between Fx and non-union was > 6 months. The surgeons estimated that the clinical and radiological (RX) evolution was not successful and a new surgery was too risky. Some patients had already had 2 or 3 previous orthopaedic interventions. Every patient received calcium and vitamin D. Between 01.2013 and 12.2014, 16 patients fulfilled these criteria.

Results: 12 women and 4 men, mean age 64.5 y. (min. 26, max. 89), mean vitamin D 53.5 ± 24.3 nmol/l, received TP for > 2 months. The Fxs were: humerus (5), pelvis (5), tibia (4), femur (2). The median time between the Fx and the beginning of TP was 9.5 months (min 6, max.108). The mean duration of TP treatment at the time of RX evaluation was 4.7 months (min. 2, max. 12). Rx evolution was excellent (mean follow-up 8 months) or good (mean follow-up 8 months) in 73% of cases. In the 4 cases without Rx consolidation, the follow-up was 3 months. The clinical evolution was excellent or good in 69% and partially good in 13% of cases (patients' judgments). For three patients with instable and complex Fx, the consolidation obtained allowed a new conclusive surgical intervention while still on TP. Two patients who had lived in wheel chairs for several months because of instability due to the Fx (femur or tibia) could walk again (with or without stick) after TP treatment. Two patients with humeral Fx and severe functional deficits could use their arms nearly normally again after TP treatment.

Conclusions: This series has several limitations. It is not a randomized controlled study. We don't know what would have been the natural evolution without TP treatment. There were no selection criteria in terms of age, fracture localization, underlying osteoporosis or duration of evolution from the fracture. The clinical severity and the lack of alternative guided the decision of treatment with TP. Nevertheless as far as fracture healing was concerned the results were generally spectacular.

Disclosures: Bérengère Aubry-Rozier, None.

MO0335

Biochemical Markers of Bone Turnover and the Prediction of the BMD Response to Teriparatide, Denosumab or Both in Postmenopausal Women in the DATA Study. Joy Tsai¹, Paul Wallace¹, Sherri-Ann Burnett-Bowie¹, Alexander Uihlein², Robert Neer², Hang Lee³, Benjamin Leder⁴.
¹Endocrine Unit, Massachusetts General Hospital, USA, ²MGH Endocrine Unit, USA, ³Biostatistics Center, Massachusetts General Hospital, USA, ⁴Massachusetts General Hospital Harvard Medical School, USA

Background: Baseline and early changes in the levels of serum markers of bone turnover (BTMs) predict the long-term bone mineral density (BMD) response in patients treated with anabolic and antiresorptive medications. In the DATA study, we reported that the combination of denosumab (DMAB) and teriparatide (TPTD) increased BMD more than the individual agents. We now report the relationship between BTMs and BMD in each of the treatment groups. Methods: 94 postmenopausal osteoporotic women (age 51-91) with no recent bisphosphonate use were randomized to receive TPTD (20 mcg SC daily), DMAB (60 mg SC every 6 months), or both for 2 years. BMD (DXA) of the hip, spine and 1/3 distal radius and serum osteocalcin (OC) and C-telopeptide (CTX) were measured at 3, 6, 12, 18, and 24 months. Pearson's correlation coefficients (r) were calculated to determine the relationship between BTMs (baseline levels and changes) and 2-year BMD changes. Significance was determined by Fisher's z-transformed normal approximation. Results: In women receiving TPTD, baseline BTMs did not correlate with 2-year BMD changes at any site while the 12-month increase in OC was positively associated with the 2-year increase in spine BMD (r=0.43, P=0.029). In women receiving denosumab, baseline levels of OC were positively associated with 2-year spine BMD increases (r=0.51, P=0.02), while the changes in OC and CTX at 3, 6, and 12 months negatively correlated with the 2-year change in spine BMD (all r values between -0.44 and -0.51, P<0.05). Similar negative associations were found between BTMs and 2-year BMD changes at the total hip. In women receiving both drugs, there were no significant associations between BMD and baseline BTMs. The 2-year increase in distal radius BMD, however, was positively associated with the 12-month change in CTX (r=0.53, P=0.03) with a trend towards similar relationship with 3-month changes in OC (r=0.44, P=0.075) and CTX (r=0.48, P=0.052). Summary and Conclusions: In women treated with either teriparatide or denosumab, early changes in BTMs (increases and decreases, respectively) predict 2-year BMD gains, especially at the spine. In women treated with combination therapy, greater increases in radius BMD are associated with less suppression of bone turnover. These results suggest that the superior efficacy of combination therapy at cortical sites such as the radius may depend on persistent bone turnover despite RANKL inhibition.

Disclosures: Benjamin Leder, None.
 This study received funding from: Lilly, Amgen

MO0336

Genome-Wide Analysis Identifies Significant Predictors of Therapeutic Response to Teriparatide in Severe Osteoporosis. Nerea Alonso¹, Philip Riches², Bente Langdahl³, Stuart Ralston².
¹University of Edinburgh, United Kingdom, ²Rheumatic Diseases Unit, CGEM-IGMM, University of Edinburgh, United Kingdom, ³Department of Endocrinology & Internal Medicine THG, Aarhus University Hospital, Denmark

Osteoporosis is a common disease associated with low bone mass and an increased risk of fragility fractures. Teriparatide, an anabolic agent, is the preferred treatment for severe osteoporosis, since substantial bone loss has already occurred by the time osteoporosis first presents. Studies have demonstrated superiority to oral bisphosphonates in preventing vertebral fractures, but treatment costs for TPTD are high and the response is variable. Identifying markers to response to TPTD is crucial to target treatment more effectively, but there are no established means of doing this at present. We performed a genome wide association study (GWAS) of 162 patients from UK and Denmark, using an Illumina Omni Express array. Standard quality control tests were applied. Statistical analysis tested the percentage of change in lumbar spine BMD following treatment with TPTD, adjusted by duration of treatment (18-24 months). The data from the two cohorts were analysed separately and results were combined using an inverse-variance meta-analysis. No evidence of inflation was found ($\lambda=1.001-1.003$). Adjusting for gender, age, smoking, alcohol intake, dietary calcium intake, age at menopause and previous bisphosphonate therapy was also performed with similar results to the unadjusted test. We identified a genome wide significant association between changes in spine BMD following TPTD therapy and a SNP on chromosome 3, within the neuroigin 1 gene (p=8x10⁻⁹), with a substantial effect size (beta=0.654 [95%CI=0.43-0.87]); heterozygote carriers of the rare A allele (good responders) had a 28% gain in BMD over 24 months compared with a 11.7% gain in GG homozygotes - a clinically significant difference over 11 standard deviations. Besides, five separate signals in chromosomes 2, 15, 13, 1 and 9 were found suggestively associated to the trait (p=1x10⁻⁷-1x10⁻⁶). We combined information from these six hits finding a highly significant association with the number of response alleles carried and change in BMD (24 month change in BMD in those who carried < 2 responder alleles was 8.8% compared with 33.8% for those who carried five or more responder alleles (p=4.95x10⁻¹¹)). Our results will help to gain greater understanding of the genes and pathways responsible for the bone formation. Furthermore, we have established an allelic score in response to TPTD that could be

used to improve treatment decisions in clinical practice. An extended study and replication are currently in progress.

Disclosures: Nerea Alonso, None.

MO0337

A Retrospective Cohort Study Assessing the Incidence of Non-Vertebral and Hip Fractures in Women Receiving Treatment for Postmenopausal Osteoporosis in Routine Clinical Practice. Maurille Feudjo Tepie¹, Lung-I Cheng², Paula Dakin², Leslie Spanger², Brad Stolshek², Rachel Wagman², J. Michael Sprafka².
¹Amgen Ltd, United Kingdom, ²Amgen Inc., USA

Purpose

There are few fracture outcomes studies of therapies for postmenopausal osteoporosis (PMO) in the community setting. This study used MarketScan data to assess the effectiveness of antiresorptive agents in women with PMO in routine practice by assessing non-vertebral fracture (NVFX) and hip fracture (HPFX) rates.

Methods

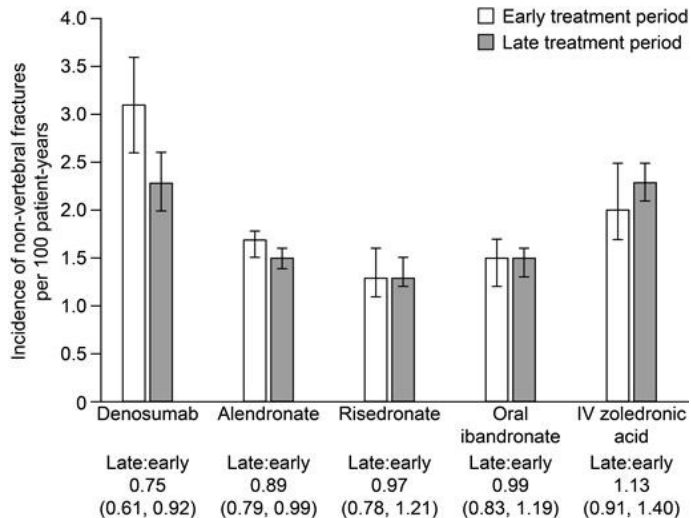
Eligible women were ≥50 years, had initiated treatment for PMO (index event) between 1 Jan 2010 and 31 Dec 2012, and had data available for ≥12 months prior to, and ≥4 months after, the index date. Women were considered independent of their persistence or compliance with therapy, to reflect routine clinical practice. Primary outcomes included incidence of NVFX and HPFX. To control for differences in baseline fracture risk, patients were their own controls: the ratio of fracture rate in the late treatment period (12 months after the first 90 days of antiresorptive therapy) to fracture rate in early treatment period (first 90 days of therapy, during which medication effect is assumed absent) was calculated for each treatment.

Results

A total of 213 102 patients were included: denosumab (DMAB; 17 561 women), intravenous (IV) zoledronic acid (ZA; 20 223), IV ibandronate (IBAN; 1230), oral IBAN (40 739), risedronate (RIS; 31 651) and alendronate (ALN; 101 698). Women who initiated DMAB, IV ZA and IV IBAN were older (mean age 67.1-69.2 vs 63.6-65.2 years) and more likely to have had a prior fracture (5.9-7.5% vs 3.2-4.7%) than those receiving oral agents. Despite DMAB patients having the highest fracture risk in the early treatment period (3.1 NVFX and 0.8 HPFX per 100 patient-years), in the year following the early treatment period DMAB reduced NVFX by 25% compared with the early treatment period (Fig). ALN was the only other agent to reduce NVFX incidence (11%). These agents prevented 8 and 2 NVFX per 1000 patient-years, respectively. No agent reduced HPFX incidence in this assessment. Sensitivity analyses showed that changing the length of the early and late treatment periods and censoring patients at first fracture during follow-up did not affect the results.

Conclusions

DMAB produced the greatest reduction in NVFX in this large, community cohort, although the fracture rate remained high, reflecting the baseline characteristics of patients initiating DMAB. The results for ALN and IBAN are consistent with Abelson *et al.* (Osteoporos Int 2010). The lack of effect of RIS is surprising and warrants further research.



IV ibandronate not included because of small sample size
 Numbers annotated are fracture rate ratio between late and early treatment periods and 95% confidence interval

Incidence of non-vertebral fractures after starting therapy

Disclosures: Maurille Feudjo Tepie, Amgen
 This study received funding from: Amgen Inc.

MO0338

Denosumab Compared to Other Treatments to Prevent or Treat Osteoporosis: a Systematic Review and Meta-analysis. Claudia Beaudoin*¹, Sonia Jean², Louis Bessette³, Louis-Georges Ste-Marie⁴, Jacques P. Brown³.¹CHU de Québec Research Centre, Canada, ²Institut national de santé publique du Québec, Canada, ³CHU de Québec Research Centre, Canada, ⁴Université de Montréal, Canada

Background: Denosumab is a new pharmacological treatment for osteoporosis which acts by a different mechanism than bisphosphonates, the most commonly used drugs. **Objective:** To compare the efficacy and safety of denosumab over other pharmacological treatments for osteoporosis in individuals at high risk of fracture or suffering from osteoporosis. **Methods:** Randomized controlled trials comparing the effect of denosumab with another pharmacological treatment for osteoporosis were searched in MEDLINE, EMBASE and CENTRAL. Identified articles (1763) were screened by two independent reviewers and assessed for inclusion. Studies including only individuals with a specific condition other than osteoporosis were excluded. Data from included studies were extracted and meta-analyses were conducted using Mantel-Haenszel, generic inverse variance or Peto method. Results (preliminary): Nine studies conducted on a maximum follow-up period of 24 months were found and included 4339 participants (Table 1). All participants were post-menopausal women. None of the individual studies were powered and designed to evaluate the comparative effectiveness of denosumab to decrease the fracture risk. There was no statistically significant difference between patients receiving denosumab and those receiving another treatment in terms of fracture risk (RR [95% CI] = 1.31 [0.94; 1.84]), number of adverse events (RR [95% CI] = 0.98 [0.95; 1.02]), withdrawals due to adverse events (OR [95% CI] = 0.73 [0.47; 1.16]) or deaths (OR [95% CI] = 0.75 [0.14; 4.05]). The percent change in bone mineral density was higher in participants who received denosumab (mean difference [95% CI] at the total hip: 1.12[0.88;1.36], lumbar spine: 1.34[0.79;1.89], femoral neck: 0.99[0.71;1.28], one-third radius: 1.31[0.31;2.31]). **Conclusion:** The results of this meta-analysis suggest that the safety and efficacy of denosumab to reduce fractures is not significantly different from other osteoporosis medications. A recent review from Institut national d'excellence en santé et en services sociaux (INESSS, Quebec, Canada) has shown that, in a clinical setting, persistence and compliance with denosumab is significantly better than with oral bisphosphonate. In the real-world clinical practice, denosumab may have an increased effectiveness. Other studies conducted over a longer period and specifically designed to evaluate the comparative effectiveness of denosumab to decrease the incidence of fractures should be performed.

| Study | Denosumab | Other treatment | Duration (months) |
|---------------------|--------------------------------|-----------------|-------------------|
| AMG 162 Bone Loss | DENO1 (n=129) DENO2 (n=190) | ALEN (n=47) | 24 |
| DECIDE | DENO3 (n=594) | ALEN (n=595) | 12 |
| STAND | DENO3 (n=253) | ALEN (n=251) | 12 |
| DAPS | DENO3 (n=124) | ALEN (n=126) | 12 |
| DenoZol | DENO3 (n=46) | ZOL (n=46) | 3 |
| DATA | DENO3 (n=34) | TERI (n=36) | 24 |
| Roux et al. 2014 | DENO3 (n=435) | RISE (n=435) | 12 |
| Recknor et al. 2013 | DENO3 (n=417) | IBAN (n=416) | 12 |
| Seeman et al. 2010 | DENO3 (n=83) | ALEN (n=82) | 12 |

DENO1: Subcutaneous injection of denosumab, 6-30 mg Q3M

DENO2: Subcutaneous injection of denosumab, 14-210 mg Q6M

DENO3: Subcutaneous injection of denosumab, 60 mg Q6M

ALEN: Oral alendronate, 70 mg Q1W

ZOL: Single intravenous infusion of zoledronic acid, 5 mg

TERI: Subcutaneous injection of teriparatide, 20 mcg Q1D

RISE: Oral risedronate, 150 mg Q1M

IBAN: Oral ibandronate, 150 mg Q1M

Table 1: Studies comparing the effect of denosumab with another treatment for osteoporosis

Disclosures: Claudia Beaudoin, Merck, Actavis, sanofi-aventis, Amgen, Eli Lilly, Novartis

MO0339

Difference and similarity between alendronate oral jelly therapy and alendronate weekly tablet therapy in the treatment of osteoporosis in Japanese clinical settings. Nobukazu Okimoto*¹, Satoshi IKeda², Hidehiro Matsumoto³, Akinori Sakai⁴. ¹Okimoto Clinic, Japan, ²Ken-Ai memorial Hospital, Japan, ³Sanzai Hospital, Japan, ⁴University of Occupational & Environmental Health Japan, Japan

Purpose: We conducted the comparative trial of alendronate oral jelly (ALN-J, 35mg) versus alendronate weekly tablet (ALN-T, 35mg) to clarify the effect of

alendronate oral jelly in the treatment of osteoporosis in Japanese clinical settings. **Methods:** We allocated ALN-J or ALN-T to the patients in accordance with their preferences in each institution. The patients took ALN-J or ALN-T weekly and were observed for 6 months. Bone turnover marker (TRACP-5b, PINP) was measured at baseline, 3 months and 6 months and bone mineral density was measured at baseline and 6 months. Upper gastrointestinal symptoms were assessed using Izumo scale questionnaire with nine questions in three domains. Compliance with medical treatment and intention of continuing allocated therapy were periodically confirmed. **Results:** A total of 94 patients were enrolled in this trial from ten institutions. Of 94 patients, 65 patients (female, 62; male, 3) assigned to the ALN-J group and 29 patients (female, 27; male, 2) to the ALN-T group. Mean [SD] of age was 77.5 [7.6] in the ALN-J group and 76.0 [6.6] in ALN-T group, and proportion of history of fracture was over 70 % in each group. TRACP-5 decreased by 38.8 % in the ALN-J group and 36.8 % in the ALN-T group at 3 months and 44.0 % in both groups at 6 months. PINP decreased by 44.2 % in the ALN-J group and 45.9 % in the ALN-T group at 3 months, and 51.6 % and 57.8 % at 6 months, respectively. The scores of upper gastrointestinal symptoms such as heartburn, epigastralgia and epigastric fullness increased in ALN-T therapy group during the period of treatment, however, that of ALN-J group was stable. The compliance of medical treatment was similar and good in both groups. **Conclusions:** The patients preferred ALN-J to ALN-T therapy. ALN-J has equal effectiveness to ALN-T, however, ALN-J therapy has the potential to alleviate upper gastrointestinal symptoms compared with ALN-T therapy.

Disclosures: Nobukazu Okimoto, None.

MO0340

Difference in Bone Mineral Density Change at the Lateral Femoral Cortices According to Administration of Different Bisphosphonate Agents. Kyu Hyun Yang*¹, Sungjun Kim¹, IL Hyung Park². ¹Gangnam Severance Hospital, South Korea, ²Kyungbook National University, South Korea

Purpose: Even though the effect of bisphosphonate (BP) agents in preventing osteoporotic fracture is eminent, their strong association with atypical femoral fracture (AFF) has recently been suspected after long-term administration. The purpose of this study was to retrospectively assess whether the response in the subtrochanteric lateral cortex (STLC) was different in BPs. **Material and Methods:** 1) Subject collection: A total of 149 individuals who underwent serial DXA examinations during the 2 or more years to trace bone mineral density during bisphosphonate administration (alendronate or risedronate) as naïve users or who simply underwent health check-up were included. Among them, 48 were naïve alendronate users (alendronate group), 63 were naïve risedronate users (risedronate group) and 38 did not take bisphosphonate medications (control group). 2) DXA examination and BMD measurement: For each subject, serial DXA examinations were performed by a technician at the same scanner of Lunar Prodigy (GE-healthcare Lunar, Madison, WI) without system change of the DXA scanner during the study interval. The PA spine and unilateral hip (right hip in all patients) DXA examination were performed. To validate whether the medication compliance was acceptable, BMD measurement for spine and hip was performed. BMD was measured at STLC and subtrochanteric medial cortex (STMC) for each patient at the level just distal to the lesser trochanter. Rectangular region of interest (ROI) was drawn at the cortex. As for the width, ROIs were drawn not violating the boundary of the cortices. The proximal to distal length of the ROI was unified as 1 cm. All measured BMD data were recorded as g/cm². 3) Measurement of BMD change and its assessment: Percent change (% change) = (BMD from the second DXA examination - BMD from the first DXA examination) x 100 / BMD from the first DXA examination. The % changes were calculated for STLC, STMC, spine, and total hip and were assessed statistically as stated below in the following two aspects: 1) to compare % change of total hip and spine BMD between medication and control groups to test the compliance of the patients who took the medication; 2) to test difference of later cortex % change according to agents. 4) Statistical analysis: To test whether there is difference of % change of BMD in hip, spine, and STLC among the agents, ANCOVA (analysis of covariance) model was adopted to control five independent variables assessed in this study including age, BMI, STMC % change, hip axis length, time interval between DXA examinations concurrently assessing whether any of the variables other than medication affect the % change of BMD in hip, spine, and STLC. Using the ANCOVA model, the least square means of % change for hip BMD, spine BMD, and STLC BMD were obtained for each medication group, and multiple comparisons were done to assess between group differences. Subsequent post-hoc comparison t-tests with Bonferroni correction were used. **Results:** Subject's age, interval between the first and the second DXA examinations, BMI, HAL, mean % change values of spine, hip, medial and lateral subtrochanteric cortices are summarized in Table 1. Difference of BMD % change among the medication groups in the analysis of covariance, % change of spine BMD was affected by medication (p<0.001) and time interval between DXA examination (=0.026). Similarly, % change of hip BMD was affected by medication (p<0.001) and time interval between DXA examination (=0.029). In the assessment of difference of BMD % change of STLC according to the given medication after controlling of the dependent variables, risedronate group showed higher % change with statistical significance than did control (adjusted p=0.012) and alendronate (adjusted p=0.016) groups (Figure 1). **Conclusion:** We traced and confirmed that increase in BMD on the STLC was significant after risedronate administration even though the implication of these changes must be qualified in the future.

| | Control | Risedronate | Alendronate |
|--|-----------------------|----------------------|-----------------------|
| Age (years) at the first DXA examination | 67.9±3.0 (63-74) | 69.9±2.9 (65-75) | 69.8±3.1 (62-75) |
| DXA interval (months) | 42.3±9.8 (27-69) | 43.1±11.7 (25-71) | 40.9±12.9 (13-70) |
| Body mass index | 24.8±2.8 (20.2-31.0) | 22.6±3.2 (16.3-30.5) | 23.4±3.2 (17.2-33.1) |
| Hip axis length | 10.1±0.5 (9.4-11.1) | 10.0±0.5 (8.8-11.3) | 10.0±0.5 (9.1-11.7) |
| BMD % change, hip | -1.5±4.9 (-12.7-14.9) | 1.6±3.9 (-8.0-11.8) | 1.1±5.0 (-11.1-13.0) |
| BMD % change, spine | 0.1±6.0 (-19.5-12.2) | 4.7±7.4 (-30.1-18.8) | 6.2±7.5 (-5.9-26.5) |
| BMD % change, MC | 0.5±8.5 (-23.0-16.9) | 3.3±6.1 (-12.0-25.5) | 4.0±10.8 (-15.3-42.6) |
| BMD % change, LC | 1.2±6.5 (-14.0-15.1) | 6.9±9.8 (-6.8-41.0) | 2.5±9.5 (-21.9-21.9) |

Table 1

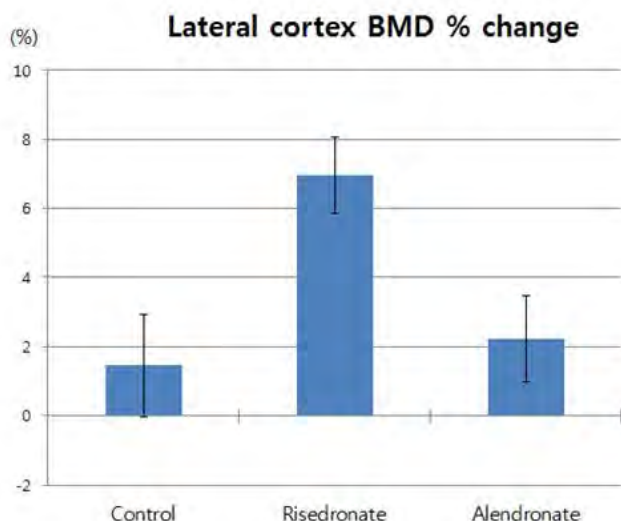


Figure 1

Disclosures: Kyu Hyun Yang, None.

MO0341

Different BMD gains after denosumab compared to zoledronate following teriparatide in women with postmenopausal osteoporosis – a case-control study. Albrecht Popp*, Schaefer Silke, Helene Buffat, Piera Rossi, Christoph Senn, Kurt Lippuner. Department of Osteoporosis, University Hospital Bern, Switzerland

Background: Treatment with parathyroid hormone (PTH) or its 1-34 derivate teriparatide (TPTD) increases bone mineral density (BMD) and reduces fracture risk by anabolic mode of action. Antiresorptives after PTH preserve the gains in BMD achieved with PTH (Black DM 2005). It is unknown whether highly potent antiresorptives such as the bisphosphonate zoledronate (ZOL) or the monoclonal antibody denosumab (Dmab) lead to different BMD changes after TPTD.

Methods: A case-control study was performed in women with postmenopausal osteoporosis who were treated with TPTD at the Department of Osteoporosis, University Hospital Bern, Switzerland. Baseline BMD was measured at the end of the treatment period with TPTD at the lumbar spine (LS), femoral neck (FN), total hip (TH) as well as distal tibial epiphysis (T-EPI) and diaphysis (T-DIA), the last two according to a previously validated method (Casez JP1994; Popp AW 2009) using cross calibrated Hologic QDR 4500 A und Discovery™ scanner. Antiresorptive therapy was initiated with either ZOL (control group) or Dmab (cases). Follow-up BMD was measured 24 months later. Of ninety-two women, 23 pairs could be matched for age, TH T-scores, and treatment duration with TPTD. Changes in BMD were compared using Mann-Whitney U test. Values are indicated as means ± SEM.

Results: Baseline characteristics (mean ± SD) were similar between groups in terms of age, 74.7 ± 8.5 years; TH T-score, -1.8 ± 1.0 and treatment duration with TPTD 21.4 ± 3.1 months. Consistent with reimbursement restrictions for the usage of TPTD in Switzerland, almost all women were treated with bisphosphonates and switched to TPTD. The percentual changes in BMD vs. baseline after 24 months of ZOL or Dmab following TPTD were:

| | Dmab | ZOL | p |
|----|-------------|-------------|-------|
| LS | +6.8 ± 0.8% | +2.3 ± 0.9% | 0.001 |
| FN | +5.7 ± 1.5% | +1.3 ± 1.0% | 0.024 |

| | | | |
|-------|-------------|-------------|-------|
| TH | +3.2 ± 1.1% | +2.0 ± 0.9% | 0.69 |
| T-DIA | +2.2 ± 1.1% | +0.7 ± 0.9% | 0.337 |
| T-EPI | +2.9 ± 0.9% | +3.0 ± 1.2% | 0.663 |

Conclusion: In this case-control study, Dmab led to significantly higher gains in LS and FN BMD in women previously treated with TPTD compared to ZOL, while differences at the total hip and the tibial sites did not reach statistical significance.

Disclosures: Albrecht Popp, Amgen Switzerland

MO0342

Discontinuation of Denosumab is associated with a severe increase risk of spontaneous vertebral fractures: 3 case reports. Olivier Lamy¹, Delphine Stoll², Elena Gonzalez Rodriguez³, Didier Hans², Bérengrère Aubry-Rozier^{*2}. ¹Chief of the Bone Unit, Switzerland, ²Center of Bone Diseases, Lausanne University Hospital, Switzerland, ³Center of Bone Disease, Lausanne University Hospital, Switzerland

Introduction : The discontinuation of bisphosphonates is associated with a prolonged reduction in bone turnover markers (BTMs), a slow decrease of bone mineral density (BMD) and no increase of fracture risk (FxR). In contrast, the discontinuation of other antiresorptive agents, is associated with a BTMs rebound and a rapid decrease of BMD to above pretreatment values. FxR is increased after the discontinuation of oestrogens. The discontinuation of Denosumab (Dmab) is associated with a severe rebound effect on BTMs and BMD. It is not known whether this rebound effect is associated with an increase of FxR. Method: We report the cases of 3 women with postmenopausal osteoporosis without any prior fracture. They received Dmab 60mg every 6 months for 4 to 6 doses. The 3 women were on calcium and vitamin D during and after the discontinuation of Dmab. A wide biological assessment, performed at the time of fracture, was strictly normal. A secondary cause of osteoporosis was excluded.

Results : A 77y old women (BMD -4.1 DS at lumbar spine (LS) and -3.4 DS at total hip (TH)) received 5 doses of Dmab between Feb. 2011 and June 2013. The BMD changes were +6.7% and -5.0%, respectively. At the end of 2014, She presented 9 symptomatic spontaneous vertebral fractures (SSVFx) (D5, D6, D7, D8, D9, D11, D12, L1, L2) and one costal Fx.

A 56y old women (BMD -3.1 DS at LS and -2.5 DS at TH) received 4 doses of Dmab between Oct. 2011 and Nov. 2013. The BMD changes were +12% and +6.5%, respectively. She presented 5 SSVFx (D11, D12, L2, L3, L4) between August and Sept. 2014.

A 55y old women (BMD -3.1 DS at LS and -2.0 DS at TH) received 6 doses of Dmab between Dec. 2010 and Nov. 2013. The BMD changes were +11.1% and +13.5% respectively. She presented 1 SSVFx (D12) in Sept. 2014

Conclusion : These 3 cases show an increased risk of vertebral fractures in the 9 to 16 months after the last injection of Dmab. This raises several questions. Can we identify patients at risk of fracture after discontinuation of Dmab? Can we reduce this risk with a bisphosphonate for 6 to 12 months after Dmab discontinuation?

Disclosures: Bérengrère Aubry-Rozier, None.

MO0343

Ectosteric inhibitors of cathepsin K from *Salvia miltiorrhiza*. Simon Law*, Preeti Panwar, Nham Nguyen, Gary Braver, Dieter Bromme. University of British Columbia, Canada

Cathepsin K is a lysosomal cysteine protease highly expressed in osteoclasts and macrophages which has been implicated in musculoskeletal and cardiovascular diseases. It displays potent collagenase and elastase activity and has become a target for bone diseases. However, existing drugs are active-site inhibitors, which block the entire protease activity and have been implicated in side effects. Our strategy is to identify compounds that selectively block the collagenase activity without interfering with other regulatory functions of cathepsin K. We call these drugs ectosteric inhibitors which in contrast to allosteric inhibitors have no effect on the active site.

Natural products are a great source of chemical diversity and some have been used for millennia to treat diseases. *Salvia miltiorrhiza* is a widely used Chinese herb for the treatment of musculoskeletal and cardiovascular diseases and produces a unique pool of diterpenoids, called tanshinones. We identified these compounds as ectosteric inhibitors for cathepsin K. From 37 tanshinones about half of them revealed a selective anticollagenase activity without blocking the active site of cathepsin K. Some of the compounds can differentiate between the degradation of soluble and fibrous collagen and thus provide ideal tools for studying the mechanism of collagen degradation by osteoclasts. The most potent tanshinone identified was Tanshinone IIA Sulfonic Sodium with an IC₅₀ value of approximately 2µM for soluble collagen degradation and was highly potent in inhibiting insoluble collagen degradation at the same concentrations. Molecular modeling has identified an ectosteric site on cathepsin K which is required to form collagenolytically active protease oligomers. Crystallization experiments are in progress which will define the exact binding mode of Tanshinone IIA Sulfonic Sodium. The inhibitor-cathepsin K complex structure will provide structural information that will assist in designing high affine and selective ectosteric inhibitors of cathepsin K.

Disclosures: Simon Law, None.

MO0344

Factors Affecting Persistence With Denosumab (Prolia®) in Postmenopausal Women With Osteoporosis: Results From a Prospective Observational Study. SL Silverman*¹, E Siris², DL Kendler³, D Belazi⁴, JP Brown⁵, DT Gold⁶, EM Lewiecki⁷, A Papaioannou⁸, C Simonelli⁹, G Quinn¹⁰, S Yue¹¹, LI Cheng¹¹, B Stolshek¹¹, C Recknor¹². ¹Cedars-Sinai Medical Center, UCLA School of Medicine, & OMC Clinical Research, USA, ²Columbia University Medical Center, USA, ³University of British Columbia, Canada, ⁴AlchemiPharma LLC, USA, ⁵Laval University & CHU de Québec (CHUL) Research Centre, Canada, ⁶Duke University Medical Center, USA, ⁷New Mexico Clinical Research & Osteoporosis Center & University of New Mexico School of Medicine, USA, ⁸McMaster University, Canada, ⁹Health East Osteoporosis Care, USA, ¹⁰Sarnia Statistics Ltd, United Kingdom, ¹¹Amgen Inc., USA, ¹²United Osteoporosis Centers, USA

Purpose
Osteoporosis therapy is effective in reducing fracture risk. Evidence has shown that low persistence with therapy in the community setting is associated with suboptimal patient outcomes. This analysis evaluated whether factors affecting persistence with denosumab at 24 months were different from those at 12 months in the United States (US).

Methods
In this multicenter, single-arm study, postmenopausal women were enrolled within 4 weeks of initiating treatment with denosumab for osteoporosis. No clinical procedures, assessments, or changes in routine management of patients were required. Persistence with denosumab was assessed at 12 and 24 months, defined as receiving ≥2 injections and ≥4 injections, respectively, and no 2 consecutive injections more than 6 months + 8 weeks apart. Persistence rates were based on total patient count at enrollment. Univariate analysis was performed to assess factors associated with persistence with no adjustment for multiplicity, and we report the US results.

Results
Of the 935 patients enrolled, 632 were from the US. These patients had a mean (SD) age of 72 (10) years, mean (SD) lumbar spine BMD T-score of -1.9 (1.4), and 95% were white. Persistence with denosumab was 81% at 12 months and 50% at 24 months. Of >60 factors assessed, 23 were associated with persistence at either time point (Table). Six factors were associated with persistence at both time points, including geographic, socioeconomic, patient, and healthcare system-related factors. Differences were observed in factors associated with persistence at 12 and 24 months. Of the additional 17 factors identified as associated with persistence, 3 factors influenced persistence at 12 months only: patients' beliefs about medication (assessed using the Beliefs and Medicines Questionnaire), intolerance to previous osteoporosis therapies, and prior insurance authorization required for denosumab treatment. Considerably more factors (n=14) affected persistence at 24 months than at 12 months; several of these factors were patient related (Table).

Conclusions
Many factors influenced persistence with denosumab at 12 and 24 months, although several factors that influenced persistence at 24 months did not affect persistence at 12 months. Awareness of these factors may assist in the identification of patients who may become nonpersistent with therapy, and some factors may be modifiable, such as the use of a reminder program, and could be incorporated in clinical practice.

Table. Factors Associated With Denosumab Persistence in the US

| Category | Factor | Association | |
|-------------------|--|-------------|-----------|
| | | 12 Months | 24 Months |
| Geography | Region | * | ** |
| Socioeconomic | Marital status | * | *** |
| | Household income | NS | *** |
| | Education level | NS | ** |
| Patient | OP therapy for >5 years prior to enrollment | ** | *** |
| | Mental illness at baseline | * | *** |
| | Modified-Wolfe comorbidity index at baseline | NS | *** |
| | SF-12 MCS score at baseline | * | ** |
| | Number of comorbidities at baseline | NS | ** |
| | Stopped OP medications in 12 months before denosumab | NS | ** |
| | Age | NS | ** |
| | Ethnicity | NS | * |
| | Number of prescriptions at baseline | NS | * |
| | SF-12 PCS score at baseline | NS | * |
| Physician | BMQ-S11NCD score at baseline | * | NS |
| | Physician gender | NS | ** |
| | Type of practice | NS | * |
| | Reimbursement benefit (medical/pharmacy) | NS | * |
| Condition | Reason for prescribing: intolerant to other OP therapies | * | NS |
| | Time since most recent previous fracture | NS | * |
| Therapy | Participation in denosumab reminder program | NS | ** |
| Healthcare system | Insurance requirement: full cash payment for denosumab | ** | * |
| | Prior authorization needed | ** | NS |

*p < 0.05; **p < 0.01; ***p < 0.001.
BMQ, Beliefs about Medicines Questionnaire; MCS, mental component summary; NCD, necessity-concerns differential; NS, not significant; OP, osteoporosis; PCS, physical component summary; SF-12, 12-item Short Form Health Survey.

Table

Disclosures: SL Silverman, Lilly, Amgen, Pfizer; Lilly, Amgen, Pfizer; Amgen
This study received funding from: Amgen Inc.

MO0345

Incidence Rate of Osteonecrosis of the Jaw among Women with Postmenopausal Osteoporosis Treated with Prolia or Bisphosphonate. Fei Xue*¹, Rachel Wagman², Susan Yue², Shawna Smith³, Violeta Hennessey⁴, Tarun Arora⁵, Jeffrey Curtis⁵, Vera Ehrenstein⁶, Henrik Sorensen⁶, Grethe Tell⁷, Helle Kieler⁸, Florence Wang⁹, David Dore⁹, J. Michael Sprafka¹⁰. ¹Amgen Inc., USA, ²Global Development, Amgen Inc., USA, ³Global Safety, Amgen Inc., USA, ⁴Global Biostatistics, Amgen Inc., USA, ⁵Division of Clinical Immunology & Rheumatology, University of Alabama at Birmingham, USA, ⁶Department of Clinical Epidemiology, Aarhus University, Denmark, ⁷Department of Global Public Health & Primary Care, University of Bergen, Norway, ⁸Center for Pharmacoepidemiology, Karolinska Institute, Sweden, ⁹Optum Epidemiology, USA, ¹⁰Center for Observational Research, Amgen Inc., USA

Purpose: To estimate the incidence rate (IR) of osteonecrosis of the jaw (ONJ) in recipients of Prolia (denosumab 60 mg) or bisphosphonate (BP) for postmenopausal osteoporosis (PMO) in multiple administrative databases.

Methods: Using administrative data from US Medicare, Optum and Scandinavian national medical registries (Denmark, Norway and Sweden), postmenopausal women with a diagnosis of osteoporosis or osteoporotic fracture, or osteoporosis medications were identified from May 2010 to Dec 2011 (Medicare and Scandinavian national registries) or Mar 2013 (Optum). The women were followed for incident event of potential ONJ defined by ICD codes. Prolia and BP (oral and IV) exposure was updated in a time-varying manner and characterized "as treated", with and without a 1 year extension following the on-treatment period defined as the days supplied plus 60 days. The age-standardized IR of ONJ was computed for each exposure cohort.

Results: A total of 2,561,119 women with PMO were identified from Medicare (1,995,915), Optum (193,003), Denmark (106,691), Norway (95,628) and Sweden (169,882). The IR (95% CI) per 100,000 person-years of ONJ in women with PMO was 40 (38 - 42) in Medicare, 27 (20 - 34) in Optum, 37 (27 - 50) in Denmark, 17 (11 - 26) in Norway and 25 (17 - 38) in Sweden. In Medicare, when exposure cohorts were classified only by the on-treatment period, the IR (95% CI) was 70 (28 - 145) in the Prolia only cohort and 90 (11 - 328) in the Prolia + BP cohort, and ranged from 45 (41 - 49) to 77 (7 - 310) in cohorts exposed to BP only (Table 1). When exposure cohorts were classified by on-treatment + 1-year post-treatment period, the IR (95% CI) was numerically lower in the Prolia only cohort [59 (11 - 180)] and the Prolia + BP cohort [76 (30 - 160)], and remained similar in cohorts exposed to BP only [ranging from 45 (42 - 48) to 84 (53 - 125)] relative to the corresponding on-treatment only cohorts (Table 2). The number of ONJ cases in the other data systems was too low (0 - 2) in Prolia recipients to allow a robust estimation of the IR.

Conclusion: The descriptive analysis based on Medicare suggested the IR of ONJ was low in the PMO population and did not differ substantially by treatment. The number of cases in other data systems was low and precluded meaningful interpretation of the ONJ IR, especially in Prolia recipients. To confirm these results, further analysis based on medically confirmed cases and adjustment for confounders is warranted.

Disclosures: Fei Xue, Amgen Inc.; Amgen Inc.
This study received funding from: Amgen Inc.

ASBMR 2015 Annual Meeting Abstract
April 15 deadline
2498 of 2500 characters: including spaces but not including the title, authors or attachments

Incidence Rate of Osteonecrosis of the Jaw among Women with Postmenopausal Osteoporosis Treated with Prolia or Bisphosphonates

Fei Xue¹, Rachel B Wagman², Susan Yue³, Shawna Smith³, Violeta Hennessey⁴, Tarun Arora⁵, Jeffrey R. Curtis⁵, Vera Ehrenstein⁶, Henrik T. Sorensen⁶, Grethe Tell⁷, Helle Kieler⁸, Florence T Wang⁹, David D Dore⁹, J Michael Sprafka¹

Attachment:

Tables:

Table 1. Distribution of cases and age-standardized incidence rates (95% CI) of osteonecrosis of the jaw (ONJ) identified by ICD codes in women with postmenopausal osteoporosis during time on-treatment with Prolia or Bisphosphonates.

| Exposure Cohorts | US Medicare | United Healthcare | Scandinavian National Medical Registries | | |
|--|-----------------|-------------------|--|-------------|-------------|
| | | | Denmark | Norway | Sweden |
| | | | Number of Cases | | |
| BP only ^a | 659 | 32 | 30 | 18 | 30 |
| Oral BP only ^a | 563 | 30 | 29 | 17 | 30 |
| IV BP only ^a | <1 ^f | 2 | 1 | 1 | 0 |
| IV BP + oral BP ^b | <1 ^f | 0 | 0 | 0 | 0 |
| Prolia only ^a | <1 ^f | 2 | 1 | 0 | 0 |
| Prolia + BP ^a | <1 ^f | 0 | 0 | 0 | 0 |
| Age-Standardized Incidence Rate (95% CI)/100,000 pys | | | | | |
| BP only ^a | 48 (44, 52) | 30 (19, 45) | 40 (26, 66) | 31 (17, 75) | 23 (15, 36) |
| Oral BP only ^a | 46 (41, 49) | 29 (19, 44) | 39 (25, 67) | 32 (16, 80) | 24 (16, 37) |
| IV BP only ^a | 66 (53, 81) | 44 (4, 183) | 87 (0, 528) | 32 (0, 195) | NA |
| IV BP + oral BP ^b | 77 (7, 310) | NA | NA | NA | NA |
| Prolia only ^a | 70 (28, 145) | 434 (27, 1935) | 72 (0, 437) | NA | NA |
| Prolia + BP ^a | 90 (11, 328) | NA | NA | NA | NA |

^a Exposed to any BP (oral and/or IV) without concomitant Prolia treatment
^b Exposed to any oral BP without concomitant treatment with Prolia or IV BP
^c Exposed to any IV BP without concomitant treatment with Prolia or oral BP
^d Exposed to both IV BP and oral BP without concomitant treatment with Prolia
^e Exposed to Prolia without concomitant BP treatment (oral or IV)
^f Exposed to both Prolia and BP (oral and/or IV)
^g Data Use Agreement with CMS prohibits cell size of 10 or less to be displayed

1

ASBMR 2015_Prolia PV Study on ONJ_Revised3_attachment_Page_1

ASBMR 2015 Annual Meeting Abstract
April 15 deadline
2498 of 2500 characters: including spaces but not including the title, authors or attachments

Table 2. Distribution of cases and age-standardized incidence rates (95% CI) of osteonecrosis of the jaw (ONJ) identified by ICD codes in women with postmenopausal osteoporosis during time on-treatment plus 1-year post-treatment with Prolia or Bisphosphonates.

| Exposure Cohorts | US Medicare | United Healthcare | Scandinavian National Medical Registries | | |
|--|-----------------|-------------------|--|-------------|-------------|
| | | | Denmark | Norway | Sweden |
| | | | Number of Cases | | |
| BP only ^a | 912 | 45 | 36 | 27 | 36 |
| Oral BP only ^a | 778 | 43 | 34 | 26 | 36 |
| IV BP only ^a | 108 | 1 | 2 | 0 | 0 |
| IV BP + oral BP ^b | 26 | 1 | 0 | 1 | 0 |
| Prolia only ^a | <1 ^f | 1 | 0 | 0 | 0 |
| Prolia + BP ^a | <1 ^f | 1 | 1 | 0 | 0 |
| Age-Standardized Incidence Rate (95% CI)/100,000 pys | | | | | |
| BP only ^a | 47 (44, 50) | 27 (19, 38) | 41 (28, 65) | 44 (27, 80) | 22 (15, 32) |
| Oral BP only ^a | 46 (42, 48) | 27 (18, 38) | 40 (27, 64) | 45 (27, 83) | 22 (15, 33) |
| IV BP only ^a | 65 (52, 79) | 10 (0, 53) | 163 (20, 583) | NA | NA |
| IV BP + oral BP ^b | 84 (53, 125) | 189 (5, 1,054) | NA | 87 (0, 530) | NA |
| Prolia only ^a | 59 (11, 180) | 81 (2, 453) | NA | NA | NA |
| Prolia + BP ^a | 76 (30, 160) | 906 (23, 5,050) | 169 (0, 1,032) | NA | NA |

^a Exposed to any BP (oral and/or IV) without concomitant Prolia treatment
^b Exposed to any oral BP without concomitant treatment with Prolia or IV BP
^c Exposed to any IV BP without concomitant treatment with Prolia or oral BP
^d Exposed to both IV BP and oral BP without concomitant treatment with Prolia
^e Exposed to Prolia without concomitant BP treatment (oral or IV)
^f Exposed to both Prolia and BP (oral and/or IV)
^g Data Use Agreement with CMS prohibits cell size of 10 or less to be displayed

2

ASBMR 2015_Prolia PV Study on ONJ_Revised3_attachment_Page_2

MO0346

Relationship Between Suppression of Bone Turnover Markers (TRACP-5b, BAP) and Future Increases in Bone Mineral Density in Risedronate Treatment- Sub-analysis of Japanese Phase III Study of Risedronate 75 mg - Taro Mawatari¹, Ryoichi Muraoka², Yukihide Iwamoto³.
¹Hamanomachi Hospital, Japan, ²Ajinomoto Pharmaceuticals Co., Ltd., Japan, ³Department of Orthopaedic Surgery, Graduate School of Medical Sciences, Kyushu University, Japan

While bone turnover markers (BTMs) are useful to monitor response and adherence to osteoporosis treatment, the relationship between risedronate-related suppression of BTMs and future increase in bone mineral density (BMD) is not fully established. This study further explored the nature of this relationship.

Sub-analysis included 800 subjects included in the Japanese phase III study of patients treated with risedronate 75 mg once a month for 12 months, whose vertebral BMD, serum TRACP-5b (tartrate-resistant acid phosphatase 5b), and serum BAP (bone alkaline phosphatase) were measured sequentially. The minimal significant change (MSC) was defined as 12.4% for TRACP-5b, and 23.1% for BAP. The upper limit of normal (ULN) was defined as 420 mU/dL for TRACP-5b, and 29.0 U/L for BAP. The subjects were divided into three subgroups according to the change in BTMs at 3 months: Group L (reduction more than MSC), Group N (change within MSC), and Group H (elevation more than MSC). Alternatively, the subjects were divided into two groups, depending on whether the BTMs at 3 months were less than ULN. Percent change in BMD at 12 months was compared among these subgroups.

Vertebral BMD gain in Group L was significantly greater than that in the other groups, for both TRACP-5b and BAP analyses (TRACP-5b: Group L [N = 661] 6.24 ± 4.11%, Group N [N = 99] 4.38 ± 4.50%, Group H [N = 33] 2.15 ± 4.21%, one-way analysis of variance (ANOVA): P < 0.0001; BAP: Group L [N = 463] 6.52 ± 4.02%, Group N [N = 332] 4.97 ± 4.47%, Group H [N = 7] 2.26 ± 3.13%, one-way ANOVA: P < 0.0001). With regard to suppression in BTMs less than ULN, TRACP-5b at 3 months was related to a future increase in BMD (TRACP-5b ≤ ULN [N = 678] 5.99 ± 4.03%, TRACP-5b > ULN [N = 115] 4.94 ± 5.43%, P < 0.0150), but this was not seen in BAP.

In summary, BMD gain at 12 months was greater (more than 6% on average) in the subgroups showing reduction more than MSC in serum TRACP-5b or BAP at 3 months, while BMD gain was attenuated when reduction in BTMs was less than MSC. Furthermore, BMD gain at 12 months was greater when the value of serum TRACP-5b at 3 months was less than ULN, compared with cases with a value higher than ULN. These results suggest that monitoring patients with BTMs may be useful in predicting future BMD gain with risedronate treatment.

Disclosures: Taro Mawatari, None.

MO0347

Spaceflight Bone Atrophy-Problem Solved?. Adrian LeBlanc¹, Toshio Matsumoto², Jeffrey Jones³, Jay Shapiro⁴, Thomas Lang⁵, Linda Shackelford⁶, Scott M. Smith⁶, Scott M. Smith⁶, Harlan Evans⁷, Elisabeth Spector⁸, Robert Ploutz-Snyder⁹, Jean Sibonga⁶, Joyce Kevak¹⁰, Toshitaka Nakamura¹¹, Kenjiro Kohri¹², Hiroshi Ohshima¹³, Gilbert Moralez¹⁴.
¹Universities Space Research Association (USRA), USA, ²Fujii Memorial Institute of Medical Sciences, University of Tokushima, Japan, ³Baylor College of Medicine- Center for Space Medicine, USA, ⁴Kennedy Krieger Institute, USA, ⁵UC San Francisco, USA, ⁶NASA, USA, ⁷Wyle Houston, USA, ⁸Wyle Science, Technology & Engineering Group, USA, ⁹USRA, USA, ¹⁰UC Irvine, USA, ¹¹National Center for Global Health & Medicine Center Hospital, Japan, ¹²Nagoya City U, Japan, ¹³Space Biomedical Research Group, JAXA, Japan, ¹⁴The University of North Texas Health Science Center (UNTHSC), USA

The NASA Human Research Program (HRP) has explored bone loss countermeasures for long duration spaceflight since the 1970's. Three main strategies have emerged: exercise, nutrition, pharmacological. During Skylab and subsequent Soviet Mir and Shuttle/Mir missions, aerobic exercises with limited amounts of resistive exercise were employed. Following the Mir era, NASA and space partners (Russia, Japan, Europe Canada) launched the International Space Station (ISS) with a new resistive exercise device called the IRED (interim resistive exercise device). Implementation of this device met with limited success partly because of engineering problems. This was followed in 2008 by the Advanced Resistive Exercise Device (ARED) with significantly improved capability. In addition to exercise, the diet has been improved over the years with the use of Vitamin D and improved energy intake. Other dietary improvements are being explored, e.g., lowering Na content of the diet. A third option is pharmacological-an antiresorptive drug, oral alendronate, 70 mg/week, was tested on ISS. Current status: while the exercise protocol using the ARED device alone appears partially effective, BMD loss continues (fig1) and urinary Ca and resorption markers remain elevated (p<0.05). Still under investigation is whether bone strength is preserved or if there is a redistribution of bone targeted by resistive

exercise. Exercise plus an antiresorptive drug appears to preserve bone mass (fig1) and bone strength without elevation of bone resorption markers or urinary calcium excretion ($p > 0.05$). This third option allows for a more robust countermeasure for long duration flight in case exercise is precluded, e.g., equipment failure or crew injury. Related to this issue, bed rest studies have shown that antiresorptive treatment would be effective without exercise. The question posed: is the problem solved? Conclusion: NASA Human Systems Risk Board has changed the status of bone loss in space from high risk to manageable risk. Exercise or exercise plus a pharmacological intervention appear effective but additional investigations are needed to optimize the ultimate prescription. Newer medications such as RANKL, Sclerostin or Cathepsin-K inhibitors which might offer similar protection with a better tolerability profile should be investigated. The combination of various exercise prescriptions and drug combinations to improve countermeasure efficiency warrant further investigation.

Figure 1. Percent change in DXA BMD after 6 months of flight

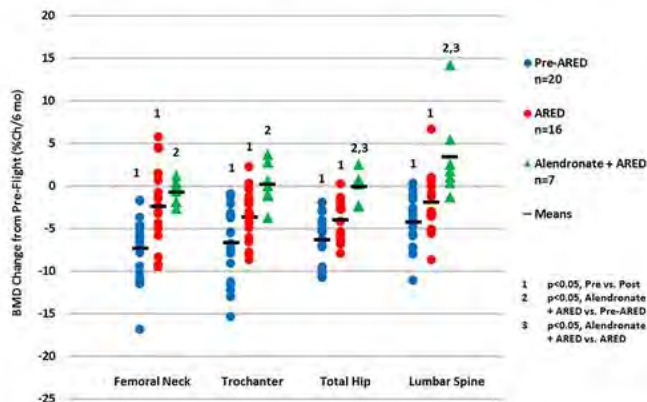


figure 1 for poster A LeBlanc

Disclosures: Adrian LeBlanc, None.

MO0348

The Effects of a Novel Selective Estrogen Receptor Modulator (SERM) pERD on Bone Health in Intact Female Rats. Jukka Morko¹, Arndt Schmitz², ZhiQi Peng¹, Katja M Fagerlund¹, Yvonne Konkol¹, Mari I Suominen¹, Jenni Bernoulli¹, Jukka P Rissanen¹, Jussi M Halleen¹, Andrea Wagenfeld². ¹Pharmatest Services Ltd, Finland, ²Bayer Pharma AG, Finland

Selective estrogen receptor modulators (SERMs) are a diverse class of compounds that bind to estrogen receptors (ERs) and agonize or antagonize estrogen action in different tissue types. Due to a broad spectrum of physiological and pathological processes contributed by ERs, SERMs provide a potential therapeutic benefit for a variety of diseases exhibiting modulated estrogen action. In this study, we characterized the effects of a novel SERM pERD on bone health in intact female rats, and we compared the effects of pERD treatment with the effects of ovariectomy (OVX), fulvestrant (FUL), raloxifene (RAL) and tamoxifen (TAM). FUL was used as a complete antagonist and RAL and TAM as reference SERMs exhibiting agonist activity on bone and being used in clinical practice. Treatment of female Sprague-Dawley rats was started at 3 months of age and continued once a day for 8 weeks. Intact rats were treated with pERD at 3, 10 and 30 mg/kg/d *p.o.*, FUL at 3 mg/kg/d *s.c.*, RAL at 1 mg/kg/d *p.o.*, TAM at 10 mg/kg/d *p.o.* or with vehicle, and OVX rats were treated with vehicle. Treatment effects on bone were studied by peripheral quantitative computed tomography (pQCT) and measuring serum levels of bone turnover biomarkers. In metaphyseal trabecular bone, treatment with pERD at 3 mg/kg/d decreased bone mineral density (BMD) and bone mineral content (BMC) slightly. These pERD effects were only minor when compared with the effects of OVX and FUL. In diaphyseal cortical bone, treatment with pERD at 3 mg/kg/d decreased cortical bone area and cortical thickness slightly as well. These pERD effects were opposite to the effects of OVX and similar with the effects of RAL. Treatment with pERD at 10 and 30 mg/kg/d did not affect metaphyseal trabecular bone and diaphyseal cortical bone significantly. In circulation, treatment with pERD decreased serum levels of N-terminal mid-fragment of osteocalcin (OC) at 30 mg/kg/d and serum activity of tartrate-resistant acid phosphatase isoform 5b (TRACP 5b) at 3, 10 and 30 mg/kg/d. These effects of pERD treatment indicate a minor antagonist activity in metaphyseal trabecular bone and an agonist activity in diaphyseal cortical bone at 3 mg/kg/d. Therefore, this study presents pERD as a novel mixed partial antagonist and agonist in bone at the dose of 3 mg/kg/d, and as novel SERM without agonist and antagonist activities in metaphyseal trabecular bone and diaphyseal cortical bone at the doses of 10-30 mg/kg/d in young adult female rats.

Disclosures: Jukka Morko, Pharmatest Services Ltd, Employee

MO0349

The Effects of Teriparatide and Zoledronic Acid Differ Across Different Bones Sites. A Study at the Femoral Neck, Vertebra and Iliac Crest in Ewes. Nathalie R Portero-Muzy, Pascale Chavassieux*, Evelyne Gineyts, Roland D Chapurlat. INSERM UMR1033, Université de Lyon, France

Iliac crest (IC) bone biopsies are used to assess the mechanism of action of therapeutic agents, yet there is little data comparing this site to sites prone to fracture. Zoledronic acid (ZOL) and teriparatide (TPTD) have different mechanism of action. We have previously shown in ewes that the magnitude and time to response to ZOL and TPTD differed between the 1st lumbar vertebra (LV1) and iliac crest (1). In the present experimental study in ewes, we distinguish their respective effects on 2D-microarchitecture, collagen crosslinks composition and bone remodeling in the femoral neck (FN) compared to IC and LV1. Three groups of 24 aged ewes received either vehicle (CTRL; 8.4±0.4 yrs, n = 8) or a single injection of 10 mg of ZOL (8.1±0.4 yrs, n = 8) or daily injection of 20µg/d of TPTD (8.1±0.4 yrs, n = 8). After 3 months, ewes received a double tetracycline labeling before slaughtering and IC, LV1 and FN were collected. In CTRL, BV/TV was 2 times lower at IC than at FN and LV1 ($p < 0.0001$). FN was characterized by a significantly lower bone formation (OS/BS: 3.2±2.1, 17.8±12.7 and 5.9±3.8 % in FN, IC and LV1 respectively, $p < 0.0001$) and resorption (ES/BS: 0.5±0.1, 1.5±0.7 and 3.9±1.6% in FN, IC and LV1 respectively, $p < 0.0001$). The bone turnover was the lowest at FN: BFR/BS was 4 and 2.5 times lower in FN than in IC and LV1 respectively ($p < 0.0001$). This was associated with significantly lower pyridinoline (PYR) and deoxypyridinoline (DPD) contents at FN than at other sites ($p < 0.0001$). After 3 months, ZOL induced a marked decrease of bone turnover at all sites but the magnitude was the lowest at FN. MS/BS, BFR/BS and MAR were significantly decreased by 72.4, 93.3 and 97.8% ($p < 0.001$), 75, 93.2 and 95.3% ($p < 0.001$) and 13, 58.4 and 52.9% ($p < 0.05$) respectively at FN, LV1 and IC when compared to CTRL. This was associated with a lower PYR/DPD ratio at FN than at IC ($p < 0.02$). After 3 months of TPTD the augmentations of ES/BS and BFR/BS were significantly higher at FN than at the other sites ($p < 0.01$ and 0.03 respectively) but the crosslinks contents were not changed. In conclusion, in ewes, the early effects of ZOL and TPTD on bone are observed at FN, LV1 and IC, but with a different magnitude according to the skeletal site. To fully understand the mechanisms underlying the anti-fracture efficacy of osteoporosis therapies, the distinction of bone sites is important.1 - Portero-Muzy N.R. et al., Bone 51:714-719, 2012.

Disclosures: Pascale Chavassieux, None.

MO0350

Utilization of osteoporosis medication after a fragility fracture among elderly Medicare beneficiaries. Akeem Yusuf¹, Tom Matlon¹, Andreas Grauer², Rich Barron², David Chandler², Yi Peng¹. ¹Chronic Disease Research Group, USA, ²Amgen Inc., USA

Osteoporosis (OP) medications are recommended for elderly patients after a fragility fracture, but under-treatment is common. In this study of elderly Medicare beneficiaries after a fragility fracture, we 1) determined the incidence of OP medication prescription, and 2) examined factors associated with OP medication use.

Our cohort included elderly (age ≥ 66 years) Medicare-enrolled patients who sustained a fragility fracture between January 1, 2008, and December 31, 2011. OP medication prescriptions were determined in the 12 months after the index fracture (follow-up period). Proportions of treated patients overall and by fracture site were examined. Using multivariate logistic models, we examined the association between post-fracture OP medication use and predictors (demographics, clinical conditions, bone mineral density [BMD] tests).

We identified 145,185 patients with fragility fractures (mean age 80.9 ± 7.8 years; 91.2% white; 81.3% female). Hip, vertebral, and non-hip-non-vertebral (NHNV) fractures accounted for 29.9%, 31.8%, and 38.3%, respectively, of identified index fracture events. Overall, 30.4% of the cohort received an OP medication in the follow-up period. Proportions receiving bisphosphonates, calcitonin, raloxifene, teriparatide, and denosumab were 25.3%, 4.1%, 2.0%, 1.3%, and 0.3%, respectively. Of patients on OP pharmacotherapy before an index fragility fracture, 23.8% did not receive an OP medication in the follow-up period. Of those with index hip, vertebral, and NHNV fractures, proportions receiving OP medications were 23.3%, 43.2%, and 25.4%, respectively ($P < 0.0001$). Odds of post-fracture OP medication use were 68% higher for women than for men. Osteoporosis diagnosis (odds ratio, 1.55; $P < 0.0001$) and BMD tests before an index fracture (odds ratio, 1.24; $P < 0.001$) were significantly associated with OP medication use after fracture.

In a large cohort of nearly 150,000 elderly US Medicare beneficiaries with a fragility fracture, less than a third received an OP medication in the year after the fracture, when risk of a second fragility fracture is highest. This study confirms results of previous smaller studies on a larger scale, and demonstrates dramatic under-treatment. These findings are a call to action for improved monitoring, patient identification, and treatment with OP therapy of elderly patients experiencing fragility fractures.

| Characteristics | Fracture site | | | | | | | |
|-------------------------------|---------------|---------|------------|---------|------------|---------|-----------------------|---------|
| | All | | Hip | | Vertebral | | Non-Hip-Non-Vertebral | |
| | Odds ratio | P-value | Odds ratio | P-value | Odds ratio | P-value | Odds ratio | P-value |
| Age (75+ vs. 66-75yrs) | 0.91 | <.0001 | 0.78 | <.0001 | 0.92 | 0.002 | 0.99 | 0.9 |
| Female vs. male | 1.68 | <.0001 | 1.61 | <.0001 | 1.60 | <.0001 | 2.20 | <.0001 |
| Race | | | | | | | | |
| Black vs. white | 0.81 | <.0001 | 0.83 | 0.03 | 0.83 | <.0001 | 0.80 | <.0001 |
| Hispanic vs. white | 1.20 | <.001 | 1.26 | 0.03 | 1.05 | 0.7 | 1.42 | 0.01 |
| Other vs. white | 1.52 | <.0001 | 1.41 | <.0001 | 1.51 | <.0001 | 1.69 | <.0001 |
| Index fracture year | | | | | | | | |
| 2009 vs. 2008 | 0.87 | <.0001 | 0.87 | <.001 | 0.89 | <.0001 | 0.85 | <.001 |
| 2010 vs. 2008 | 0.69 | <.0001 | 0.70 | <.0001 | 0.70 | <.0001 | 0.65 | <.0001 |
| 2011 vs. 2008 | 0.55 | <.0001 | 0.52 | <.0001 | 0.57 | <.0001 | 0.56 | <.0001 |
| Atherosclerotic heart disease | 0.91 | <.0001 | 0.93 | 0.03 | 0.90 | 0.0001 | 0.93 | 0.03 |
| CHF | 0.86 | <.0001 | 0.79 | <.0001 | 0.93 | 0.02 | 0.88 | 0.001 |
| CVA/TIA | 0.87 | <.0001 | 0.85 | <.0001 | 0.84 | <.0001 | 0.93 | 0.08 |
| Peripheral vascular disease | 0.92 | <.0001 | 0.92 | 0.02 | 0.95 | 0.08 | 0.90 | 0.003 |
| Dyslipidemia | 0.96 | 0.01 | 0.93 | 0.03 | 1.00 | 0.9 | 0.93 | 0.02 |
| Other cardiovascular disease | 1.00 | 0.8 | 1.02 | 0.6 | 1.00 | 0.9 | 0.94 | 0.1 |
| Diabetes mellitus | 0.93 | <.0001 | 0.94 | 0.06 | 0.89 | <.0001 | 0.97 | 0.4 |
| COPD | 1.04 | 0.02 | 1.02 | 0.5 | 1.06 | 0.04 | 1.03 | 0.3 |
| Malignancy | 1.19 | <.0001 | 1.16 | 0.001 | 1.14 | <.0001 | 1.25 | <.0001 |
| Gastrointestinal disorders | 0.89 | 0.003 | 0.77 | <.0001 | 0.91 | 0.1 | 1.00 | 0.9 |
| Liver disease | 1.01 | 0.9 | 1.08 | 0.6 | 1.03 | 0.8 | 0.93 | 0.5 |
| CKD | 0.87 | <.0001 | 0.88 | <.01 | 0.90 | 0.003 | 0.82 | <.0001 |
| Anemia | 1.00 | 0.8 | 1.03 | 0.3 | 0.99 | 0.8 | 0.98 | 0.5 |
| Thyroid disease | 1.02 | 0.3 | 1.04 | 0.2 | 0.99 | 0.9 | 1.03 | 0.4 |
| Rheumatoid arthritis | 1.3 | <.0001 | 1.2 | <.01 | 1.29 | <.0001 | 1.44 | <.0001 |
| Ankylosing spondylitis | 1.01 | 0.9 | 1.05 | <.01 | 0.87 | 0.2 | 1.01 | 0.9 |
| Osteoporosis | 1.55 | <.0001 | 1.60 | <.0001 | 1.50 | <.0001 | 1.61 | <.0001 |
| Any treatment during baseline | 13.42 | <.0001 | 12.77 | <.0001 | 8.70 | <.0001 | 21.84 | <.0001 |
| Chococorticoid use | 1.14 | <.0001 | 1.13 | 0.0001 | 1.15 | <.0001 | 1.09 | 0.004 |
| Infectious hospitalization | 0.87 | <.0001 | 0.44 | 0.1 | 0.79 | <.0001 | 1.03 | 0.3 |
| Bone mineral density test | 1.24 | <.0001 | 1.32 | <.0001 | 1.29 | <.0001 | 1.09 | 0.02 |

Table: Predictors of osteoporosis medication utilization in the 12 months following a fracture event

Predictors of osteoporosis medication utilization within 12 months following a fracture event

Disclosures: Akeem Yusuf, None.
This study received funding from: Amgen Inc.

MO0351

Bone Union rate of PLIF using local bone graft in long term bisphosphonates users. Si Young Park^{*1}, Seung Wo Suh², Jae Young Hong², Hyun Min Lee², Hwan Mo Lee³, Hwan Mo Lee². ¹Korea University, College of Medicine, South Korea, ²Korea University Hospital, South Korea, ³Yonsei University Severance Hospital, South Korea

Introduction

Bisphosphonates are the most popular drugs for treatment of postmenopausal osteoporosis. However, long-term use of bisphosphonates (BPs) may cause several complications such as atypical fracture of hip, osteonecrosis of jaw and delayed fracture healing. PLIF is a typical surgical technique for treatment of degenerative spinal disorders. Long-term use of BPs may also inhibit spinal fusion process after PLIF. We compared bony union rates of long-term BPs users and non-users after undergoing PLIF.

Methods

The subject were 81 postmenopausal women whose course could be observed for at least 2 years after surgery. Single interbody PLIF was done using local bone graft from laminectomy. Participants were divided into two groups; there were 46 patients in long-term BPs users group and 35 in non-users group. Serum C-terminal cross linking telopeptide levels were checked for bone resorption marker which could be extremely decreased in long-term BPs users. Bone fusion rates were calculated, 2 years after the surgery using plain radiographs and computed tomographic scans. Clinical outcomes were measured using ODI and VAS.

Results

Serum CTX level was extremely decreased in long-term BPs user group (p<.05). However, fusion rates turned out to be 82% in long-term BPs users group and 87% in non-users group (p>.05, not significant). There was no significant difference between two groups in ODI and VAS.

Discussion

At the two-year postoperative follow-up, there was no significant difference in bone fusion rate between two groups. Long-term BPs users showed fusion rates greater than 80% and clinical outcome improvement that were compatible to those in non-users. No significant effect was found after long-term BPs use on fusion rate of PLIF.

Disclosures: Si Young Park, None.

MO0352

Can combined therapy with teriparatide and low-intensity pulsed ultrasound accelerate fracture healing with an Ilizarov external fixator?. Koji Nozaka^{*}, Yoichi Shimada, Naohisa Miyakoshi, Shin Yamada, Michio Hongo, Yuji Kasukawa, Hidetomo Saito, Hiroaki Kijima, Tsuchie Hiroyuki. Akita University Graduate School of Medicine, Japan

Background: Ilizarov external fixators have many advantages in the treatment of fractures. However, a disadvantage of the Ilizarov system is the relatively frequent incidence of pin infection. It is an advantage for orthopedic surgeons to remove an Ilizarov external fixator as early as possible after surgery. Although both teriparatide

and low-intensity pulsed ultrasound (LIPUS) have been found to accelerate fracture-healing processes, the effect of the combination of teriparatide and LIPUS in clinical bone fracture management remains unclear. Therefore, a retrospective study comparing the treatment effects of use of an Ilizarov external fixator alone and that of an Ilizarov external fixator combined with teriparatide and LIPUS was performed among elderly patients with lower limb fractures. Subjects: From among 721 patients with a lower limb fracture on admission to our department who underwent surgical treatment for a lower limb fracture with an Ilizarov external fixator, 38 patients >60 years old were investigated. Patients were either treated with an Ilizarov external fixator alone (IEF alone, n=20) or an Ilizarov external fixator combined with teriparatide and LIPUS (IEF combination, n=18). The patients' mean age was 64.1 years (range, 60-79 years) in the IEF alone group and 67.2 years (range, 60-83 years) in the IEF combination group. Teriparatide (20 µg subcutaneous injection daily or 56.5 µg subcutaneous injection once-weekly) and LIPUS (20 min/day) were started immediately after surgery for IEF combination group in an attempt to accelerate healing of the lower limb fracture with the Ilizarov external fixator. Results: The mean duration of union was 111.9 days (range, 94-175 days) for IEF alone and 72.1 days (range, 68-141 days) for the IEF combination; it was significantly shorter with the IEF combination (p<.05). Bone density (relative to young adult mean, YAM) was 61.3% (range, 38-82%) for IEF alone and 52.1% (range, 30-79%) for the IEF combination. The mean AOFAS score was 86.2 (range, 72-100) for IEF alone and 91.2 (range, 82-100) for the IEF combination. Discussion: In elderly patients with lower limb fractures, combined therapy (teriparatide and LIPUS) showed a shorter mean duration of union than the Ilizarov external fixator alone. Combined therapy with teriparatide and LIPUS may become a useful option in the treatment of elderly patients with lower limb fractures.

Disclosures: Koji Nozaka, None.

MO0353

The bone union promoting effect of intermittent administrated Teriparatides daily or weekly in the treatment of vertebral fractures. Yoichi Kishikawa^{*}. Kishikawa Orthopedics, Japan

Background: Intermittent administrated teriparatide has an excellent bone formation promoting effect, but its bone union promoting effect in the treatment of vertebral fracture has not yet proven. Patient's rest level could be a major bias in the evaluation of therapeutic effect of drugs in the conservative management of vertebral fractures. In the past we reported the non-weight-bearing rest (: NWB rest, patient's are never allowed to sit up until the pain aboished when rolling on the bed) in the initial phase of treatment of vertebral fractures could prevent a vertebral collapse. We also reported the difference of changing in serum bone metabolism markers that took place after 4 months , between daily teriparatide (Forteo20µ/day : FOR) and weekly one (Teribone56.5µ/week : TRB, chemically synthesized and available only in Japan) in the treatment of vertebral fractures. We have found a difference in bone union promoting effect of the two teriparatides , when compaired under the same initial NWB rest level. Methods: 129 subjects (115female, 14male) who have recent vertebral fractures in thoracic or lumbar spine, all recieved conservative treatment with soft corset, then were divided into four subgroups, according to both the rest level and the administrated teriparatides, daily or weekly. Administrated teriparatides were as follows, FOR 73 (including 42 NWB rest), TRB 56 (including 26 NWB rest). Vertebral collapse rate was calculated as a ratio of anterior vertebral height to posterior vertebral height. We also measured the weight bearing change in anterior vertebral height by comparing the lateral X-ray examination standing and lying in supine position, this indicates the instability of the vertebral fracture. The bone union of vertebral fractures wre confirmed by comparing standing and lying in supine position as well. We also checked the number of previous vertebral fractures, posterior vertebral hight collapse score, local alignment score , and bone mineral density of proxymal femur . These are factors that may influence the bone union that would be found from X-ray examination. Results: Comparing in the same rest level , initial NWB rest subgroup (FOR 42, TRB 26), weekly teriparatide seemed to take a better advantage rather than the daily teriparatide with regard to fracture healing. The time it took for the bone union from the start of treatment were 12.4weeks in FOR subgroup and 9.2weeks in TRB subgroup . The time was statistically shorter in the later one (Student's T test P=0.034). In daily teriparatide subgroup, the vertebral collapse rate and the age might be major factors that influence to the time that was needed for the bone union. On the other hand, in weekly teriparatide no factor was found that prevent the bone union. Although there were no statistical difference between FOR and TRB subgroups in the vertebral collapse rate (Mann-Whitney U test P=0.148) and the age (Mann-Whitney U test P=0.071) at the baseline. Discussion: When teriparatide was used in the treatment of vertebral fracture, two types of teriparatides might have different effects on healing process of vertebral fracture according to their different change in bone metabolism. Daily teriparatide showed very high change in bone absorption as much as bone formation (4months after/ before: TRACP5b205%, uOC313%, uOC858%), while weekly teriparatide showed no change in bone absorption and mild changing in bone formation (4months after/ before: TRACP5b96%, OC129%, uOC237%) as we reported in ASBMR 2013.

Disclosures: Yoichi Kishikawa, None.

MO0354**Effects of Mineralocorticoid Receptor Antagonism on Markers of Bone Turnover in Patients with Primary Hyperparathyroidism – the EPATH Trial.**

Nicolas Verheyen^{*1}, Astrid Fahrleitner-Pammer², Cristiana Catena³, Evgeny Belyavkiy⁴, Johann Martensen², Julia Wetzel², Martin Gaksch², Martin Grüber², Elisabeth Kraigher-Krainer⁵, Jakob Voelkl⁴, Florian Lang⁶, Andreas Meinitzer², Burkert Pieske⁵, Stefan Pilz², Andreas Tomaschitz². ¹Medical University Graz, Austria, ²Medical University of Graz, Austria, ³University of Udine, Italy, ⁴Medical University of Graz, Germany, ⁵Charite Universitaetsmedizin Berlin, Germany, ⁶University of Tübingen, Germany

Purpose

Animal and human studies indicated that mineralocorticoid receptor (MR) antagonism affects bone metabolism. We therefore aimed to test in a randomized, placebo-controlled trial whether the MR-blocker eplerenone affects markers of bone turnover in patients with primary hyperparathyroidism.

Methods

The present study analysed the pre-specified secondary endpoint change in levels of bone turnover markers of the “Effect of Eplerenone on Parathyroid Hormone Levels in Patients with Primary Hyperparathyroidism” (EPATH) Trial (ISCRN 33941607). Patients with primary hyperparathyroidism (pHPT; n=110), 25-hydroxy vitamin D >= 20ng/mL, GFR > 50mL/min/1.73m² and plasma potassium <= 5.0 mmol/L were randomly 1:1 assigned to treatment with 25mg eplerenone (escalation to 50mg after 4 weeks) or matching placebo for 8 weeks. Markers of bone formation (osteocalcin [OC], bone-specific alkaline phosphatase [BALP] and procollagen type 1 [P1NP]) and beta-crosslaps [beta-CTX]) from before and after 8 weeks of intervention were measured in serum that had been frozen and stored at -80°C immediately after blood sampling.

Results

The trial was completed by 97 (88.2%) participants (mean age 68 +/- 10 years, 76 (78%) females). Median PTH was 102 (83 – 127) pg/mL, mean calcium was 2.62 +/- 0.14 mmol/L and 48 (49.5%) had osteoporosis. Median OC at baseline was 22.5 (16.2 – 36.4) ng/mL, median BALP was 19.9 (15.5 – 26.5) µg/mL, median P1NP was 52.9 (34.7 – 75.6) ng/mL, median TRAP was 3.84 (3.25 – 4.74) U/L and median b-CTX was 0.435 (0.242 – 0.770) ng/mL. In analysis of covariance with adjustment for baseline values eplerenone had a mean treatment effect on OC of 1.507 ng/mL (95% CI (-1.205 – 4.219), P=0.38), on BALP of 0.775 µg/mL ((-0.627 – 2.177), P=0.32), on P1NP of -4.092 ng/mL (-9.879 – 1.796), P=0.21) and on beta-CTX of 0.003 ng/mL (-0.68 – 0.74), P=0.97).

Conclusions

MR antagonism for 8 weeks had no significant effects on serum levels of bone turnover markers in patients with pHPT. These data are contrasting previous observational studies. Further interventional trials should evaluate whether MR antagonism affects bone turnover after intermediate- or long-term treatment and in patients without PTH excess.

Disclosures: Nicolas Verheyen, None.

MO0355**Inhibition of Osteoclastogenesis by Poly - γ - glutamic acid. Tae-Hwan Kim^{*1}, Bitnara Lee¹, Eunji Kwon¹, Jong Dae Ji², Sang-Hyon Kim³.**

¹Hanyang University Hospital for Rheumatic Diseases, South Korea, ²College of Medicine, Korea University, South Korea, ³Keimyung University Dongsan Medical Center, South Korea

Background : We examined whether Poly - γ - glutamic acid(γ -PGA) inhibited RANKL-induced osteoclast differentiation via the Toll-like receptor 4(TLR4) signaling pathway in human and mice.

Methods : We tested the inhibitory effects of γ -PGA on osteoclastogenesis in healthy human peripheral blood monocytes and mice bone marrow macrophages (BMMs). The osteoclastogenesis was assessed by generation of *Tartrate-resistant acid phosphatase (TRAP)* + multinucleated cells and actin ring formation. Also we analyzed essential genes and proteins expression for osteoclast differentiation by real-time PCR and Western blot analysis. And we observed whether the treatment of mice with γ -PGA significantly reduce *in vivo* the TRAP-stained osteoclasts of the joint. To investigate the regulatory mechanism of γ -PGA through a *TLR4*-dependent pathway, we tested effects of LPS which is a *TLR4* ligand on osteoclastogenesis in human and mice. Also the inhibitory effects of γ -PGA was evaluated by osteoclast formation in BMMs which were obtained from *TLR4*^{-/-} mice, and compared with wild type (WT) mice.

Results : γ -PGA strongly inhibited human osteoclastogenesis as assessed by generation of TRAP+ multinucleated cells and suppressed expression of osteoclast specific gene such as cathepsin K, Integrin β 3, ATP6v0d2. Also primary transcript analysis showed that γ -PGA inhibited RANK gene expression but not protein. Treatment with γ -PGA acted on mouse osteoclast precursors to suppress differentiation of TRAP+ multinucleated cells. However, the expression of genes and proteins much less inhibited or did not show a significant change in BMMs compared with human.

In contrast to γ -PGA, we confirmed LPS suppressed osteoclast formation and expression of osteoclast specific genes, RANK mRNA and protein in both species. But we observed that many more TRAP+ single cells created by γ -PGA in

osteoclastogenesis than by LPS. TRAP staining of osteoclasts showed that the number of osteoclast was increased on osteoclast differentiation with γ -PGA in the *TLR4*^{-/-} mice compared to in the WT mice. γ -PGA in *IL-10*KO mice with arthritis decreased joint osteoclast in joint sections compared to controls *IL-10*KO with arthritis mice.

Conclusions : γ -PGA can be a good therapeutic approach to prevent selectively osteoclast differentiation and to reduce bony destruction and can be used to be a drug for prevention of chronic destructive joint disease like Rheumatoid arthritis.

Disclosures: Tae-Hwan Kim, None.

MO0356**The importance of vitamin D on mineralization by the osteocyte in CKD subjects with renal hyperparathyroidism. Aiji Yajima^{*}. Otsuki Municipal Central Hospital, Japan**

The importance of vitamin D on mineralization by the osteocyte in CKD subjects with renal hyperparathyroidism

Aiji Yajima M.D., Ph.D.

Bone mineral recovery in Basic Multicellular Unit (BMU) and Bone Structural Unit (BSU) following the treatment of hyperparathyroid bone disease has not been discussed. Vitamin D receptor on the osteocyte is important in thinking about poorly mineralized bone area because the volume and texture of bone in both BMU and BSU depend on mineralization in the osteocytic perilacunar/canalicular system.

The patients with renal hyperparathyroidism were treated with cinacalcet hydrochloride, vitamin D sterols, and parathyroidectomy.

The eighteen hemodialysis (HD) patients underwent parathyroidectomy, followed by 2.0 µg/day of alfacalcidol administration (Group I). The four HD patients also underwent parathyroidectomy, without following vitamin D administration (Group II). Plasma 1.25(OH)₂D₃ level was significantly increased, but lower than the upper limit (Group I), however 1.25(OH)₂D₃ was below 10 pg/mL (Group II) after the surgery.

Poorly mineralized bone volume in BMU (PM.BV(BMU)/BV) and BSU (PM.BV(BSU)/BV) were evaluated before and after parathyroidectomy. PM.BV(BMU)/BV was significantly decreased from 20.2 ± 16.2 to 3.1 ± 4.2 %, and PM.BV(BSU)/BV was also decreased from 16.7 ± 15.2 to 2.6 ± 3.0 % at 4 weeks after the surgery (Group I), however both PM.BV(BMU)/BV and PM.BV(BSU)/BV were increased (Group II).

In addition, the seven HD patients were treated with cinacalcet hydrochloride and low doses (0.25 or 0.5 µg/day) of alfacalcidol (Group III) and the seven HD patients were treated with cinacalcet hydrochloride and low doses of alfacalcidol + low doses of intravenous maxacalcitol (Group IV). PM.BV(BMU)/BV and PM.BV(BSU)/BV were not changed (Group III), but both of them were decreased in Group IV after 1 year of the treatment.

As a conclusion, vitamin D plays an important role in mineralization by osteocytes, resulting in the reduction of poorly mineralized bone volume and improvement in bone stability.

Disclosures: Aiji Yajima, None.

MO0357**Patient Perspectives on Participating in the Effectiveness of Discontinuing Bisphosphonates (EDGE) Study. Nicole Wright^{*1}, Phillip Foster¹, Sally Fullman², Susan Randall³, Mary Melton¹, Wilson Pace⁴, Walter Calmbach⁵, Kenneth Saag¹.**

¹University of Alabama at Birmingham, USA, ²Project Healthy Bones, USA, ³National Osteoporosis Foundation, USA, ⁴University of Colorado Denver, USA, ⁵University of Texas Health Science Center at San Antonio, USA

Purpose: Patient engagement during the design of clinical trials is important, particularly to select outcomes of highest interest to patients and to identify issues affecting recruitment. We designed a web-based survey to gain patient insight on potential study outcomes, randomization, and consequences of participating in the EDGE study, a pragmatic clinical trial examining the long-term effectiveness and safety of alendronate (ALN).

Methods: Our survey, posted on the National Osteoporosis Foundation website, focused on: 1) optimal study outcomes, including quality of life, and physical and mental health, 2) willingness to be randomized either to discontinue or continue ALN, and 3) the effect of trial participation on physical activity.

Results: We received 311 survey responses from 12/30/14 to 02/26/15. Our sample included 215 women with 25% reporting current ALN use. The table below shows the outcome categories reported by patients from the entire population and ≥3 years ALN users (n=25). Overall, quality of life was the top category. Among those with ≥3 years of use, medication effectiveness, specifically fracture reduction, was the outcome category of greatest interest. Willingness to be randomized to discontinue ALN was indicated by 38% of respondents. An additional 11% were willing to discontinue ALN after a discussion with their doctor or if the study/physician provided additional monitoring. Nearly 22% reported concern about being randomized to discontinue ALN, and some patients were not willing to be randomized to discontinue ALN (Overall: 9%; ≥3 years ALN users: 22%). Willingness to be randomized to continue

ALN was indicated by 49% of patients, but 22% indicated they would not want to continue ALN. The majority of respondents indicated that they would continue their current level of physical activity, regardless of randomized study arm. Concern about physical activity was indicated by 13% of respondents when considering stopping ALN, and only 3% of respondents when considering continuing ALN.

Conclusion: Engaging patients during the design of EDGE provided insight into the outcomes patients are interested in and their willingness to participate in the study. Patients were equally interested in quality of life and effectiveness outcomes, such as fractures. The majority of patients were willing to be randomized, although a small number had concerns that would warrant additional attention during recruitment efforts.

Table. Proposed Study Outcomes Categories for the EDGE Study Indicated on the EDGE National Osteoporosis Foundation Patient Survey

| | Overall (N=215)* | | =3 Years ALN Use (N=25) | |
|---------------------------------|------------------|-------------|-------------------------|-------------|
| | | | | |
| Quality of life | 86 | 33.2 | 8 | 32.0 |
| Mental Health | 19 | 22.1 | 1 | 12.5 |
| Physical Health | 34 | 39.5 | 3 | 37.5 |
| Medication Effectiveness | 85 | 32.8 | 13 | 52.0 |
| Fractures | 35 | 41.2 | 8 | 61.5 |
| Retaining bone mass/strength | 12 | 14.1 | 3 | 23.1 |
| Safety | 67 | 25.9 | 4 | 16.0 |
| ONJ | 10 | 14.9 | - | - |
| Atypical Fractures | 5 | 7.5 | - | - |
| Medication duration | 12 | 4.6 | - | - |

ALN – alendronate; ONJ – osteonecrosis of the jaw
*Indicates totals study sample; however, each person may have contributed more than one response.

Table

Disclosures: Nicole Wright, Amgen

MO0358

Accelerated tooth loss in HIV-infected women. Grace Kim^{*1}, Elizabeth Shane², Kyle Nishiyama², Sunil Wadhwa¹, Michael Yin². ¹Columbia College of Dental Medicine, USA, ²Columbia University Medical Center, USA

Introduction: The advent of effective antiretroviral therapy (ART) has dramatically increased the lifespan of HIV-infected individuals. However, the effect of ART on dentition is largely unknown. Initiation of ART is associated with decreased bone mineral density (BMD) at the spine and hip, and fracture rates are higher in HIV-infected than uninfected women especially after menopause. The goal of this study is to evaluate number of teeth in relation to mandibular cortical width in HIV-infected women before and after the menopausal transition.

Material and Methods: A retrospective chart review of existing panoramic dental x-rays and dental records was performed to compare number of teeth and inferior mandibular cortical width at the mental region in 40-60 year old HIV-infected women (n=39) and age and race/ethnicity matched uninfected controls (n=89) from the same dental clinic in New York City.

Results: HIV-infected and uninfected controls were similar in age (53+7 vs 53+7), race/ethnicity (41% black, 38% Hispanic), and history of diabetes (30% vs 20%, p=0.23). Cigarette use was greater among HIV-infected women (27% vs 12%, p=0.03). Mean CD4+ T cell count was 653 cells/ul and 87% of women were on ART. Number of teeth decreased in both groups after age 50 (Table). Although HIV-infected women had 2-3 less teeth than controls, the differences were not statistically significant. Further, the proportion of HIV-infected women who were edentulous increased from 5% to 18% after age 50. In comparison, the mean number of teeth in women age 50-64 from NHANES was 22, and only 10% were edentulous. Mandibular cortical width did not differ between HIV-infected women and controls before or after menopause. Conclusion: HIV-infected women appear to have accelerated age-related tooth loss, which is unrelated to mandibular cortical width. Further research using more sensitive imaging modalities such as cone beam CT is necessary to determine effects of HIV and ART on alveolar bone density and trabecular microarchitecture, and their associations with tooth loss.

| Table | Age 40-50 | | P value | Age 50-60 | | P value |
|--------------------------------|-------------|-----------------|---------|-------------|-----------------|---------|
| | HIV+ (N=22) | controls (N=48) | | HIV+ (N=17) | controls (N=41) | |
| Number of teeth | 18±4 | 20±7 | 0.34 | 13±9 | 16±8 | 0.16 |
| % edentulous | 5% | 0% | 0.31 | 18% | 5% | 0.13 |
| Mandibular cortical width (mm) | 4.5±1.0 | 4.4±1.0 | 0.82 | 4.7±1.1 | 4.3±1.0 | 0.15 |

Table

Disclosures: Grace Kim, None.

MO0359

Age at first Major Osteoporotic Fracture in Danes aged 50 and over: Influence of diabetes on mean age at fracture and one year mortality. Bo Abrahamsen^{*1}, Björn Rosengren², Daniel Prieto-Alhambra³, Nicola Napoli⁴, Cooper Cyrus⁵. ¹University of Southern Denmark, Denmark, ²Clinical & Molecular Osteoporosis Research Unit, Department of Orthopedics, Sweden, ³Oxford NIHR Musculoskeletal Biomedical Research Unit, Nuffield Department of Orthopaedics, United Kingdom, ⁴Division of Endocrinology & Diabetes, Università Campus Bio-Medico di Roma, Italy, ⁵MRC Lifecourse Epidemiology Unit, University of Southampton, United Kingdom

Diabetes mellitus (DM) is associated with an increased risk of fractures in excess of what would be expected from age and BMD. Further, DM is associated with increased risk of mortality in patients with hip fractures and possibly also other osteoporotic fractures. Study population and methods: Patients aged 50+ who were treated for fractures of the hip, forearm, humerus and spine over six years (2004-2009, N=146,256) not coded as road traffic accidents were tracked in national registers for one year post fracture mortality and for a history of DM by ICD-10 code, with a look-back to 1/1/2000. Results: Patients with DM sustained their first major osteoporotic fracture at a slightly younger age at the hip only (78.1 vs 80.5, p<0.001). By contrast, forearm (71.8 vs 69.8, p<0.001), and spine fractures (73.2 vs 72.0, p=0.005) occurred at a higher age in patients with DM, with no difference in age for humerus fractures (p=0.34). Patients with DM had poorer ly survival after fracture than fracture patients without DM, with the only exception being spine fractures in the very old (age 90-99), fig. Conclusions: The increased risk of fractures in patients with DM does not manifest itself in a clinically significant earlier age a first major osteoporotic fracture. Patients with DM have poorer short term post fracture survival than patients w/o DM irrespective of fracture site.

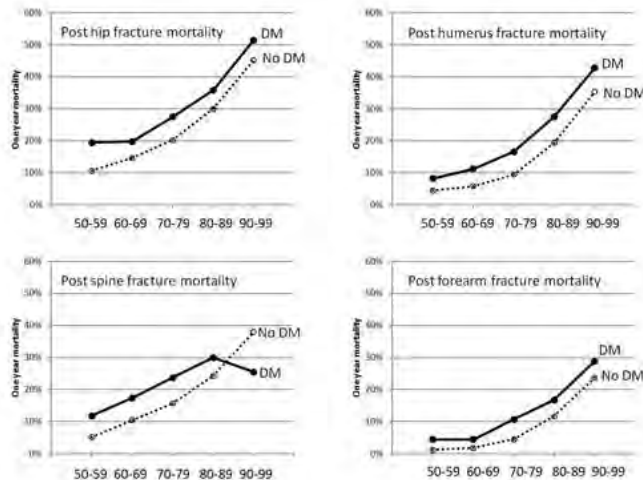


Fig 1

Disclosures: Bo Abrahamsen, Novartis

MO0360

Serum Sclerostin and Bone Turnover Markers in Patients with Type 2 Diabetes or LADA. Nicola Napoli¹, Rocky Strollo^{*1}, Giuseppe Defeudis¹, Mohammed Hawa², Gaetano Leto³, Luca D'Onofrio³, Andrea Palermo¹, Giuseppe Campagna³, Richard David Leslie⁴, Paolo Pozzilli¹, Raffaella Buzzetti³. ¹University Campus Bio-Medico, Italy, ²Queen Mary University of London, United Kingdom, ³University Sapienza of Rome, Italy, ⁴Queen Mary University of London, Italy

Diabetic patients may suffer of a low bone turnover condition. Several factors, including insulin deficiency and suppression of Wnt signaling may be involved. Sclerostin, a circulating Wnt antagonist, has been shown to be increased in patients with type 2 diabetes (T2D) but not in type 1 autoimmune diabetes (T1D). However, no data are available on bone turnover or sclerostin levels in patients with latent autoimmune diabetes of adults (LADA), an autoimmune type of diabetes often confused with T2D because of the late onset and the presence of metabolic syndrome (MS).

The aim of this study was to evaluate serum sclerostin levels and bone turnover in subjects with T2D or LADA in relation to MS. Subjects with LADA were defined as non-insulin-requiring patients with GAD-autoantibodies who had not received insulin therapy for at least 6 months after diagnosis.

This was a cross-sectional study including 95 subjects with T2D and 89 with LADA with similar age (51.08 ± 10.80 years), disease duration (2.65 ± 1.94 years) and BMI, recruited through the ACTION LADA and NIRAD cohorts and further

divided according to diagnosis of MS (NCEP criteria). Serum sclerostin, serum markers of bone formation (PINP) and bone resorption (serum CTx) were analyzed by ELISA.

Serum sclerostin was significantly higher in T2D compared with LADA (30.9 ± 1.8 vs 23.8 ± 1.8 pmol/l, $P < 0.001$) also after adjustment for age and BMI ($P = 0.008$). For each type of diabetes, there was no difference in serum sclerostin between patients with or without MS ($P > 0.139$) (Fig.1). T2D with MS had almost double levels of sclerostin in comparison with LADA without MS (33.6 ± 2.3 vs 19.7 ± 1.8 pmol/l, $P < 0.001$). In patients without MS, serum sclerostin was higher in T2D than LADA (29.4 ± 2.4 vs 19.7 ± 1.8 pmol/l, $P = 0.04$), but this difference was lost after adjustment for BMI. PINP levels were lower in T2D compared to LADA ($P = 0.038$) while CTx levels were similar between the two groups. In the all groups of subjects, sclerostin levels were significantly correlated with BMI ($r = 0.28$; $P = 0.003$).

In conclusion, our findings indicate that T2D patients present higher levels of sclerostin than LADA ones which may cause low bone formation. MS may not play a crucial role, but power to detect modest association was limited. Although T2D and LADA share similar clinical features, specific pathophysiological elements linked to the type of diabetes may determine differences in sclerostin levels and bone turnover.

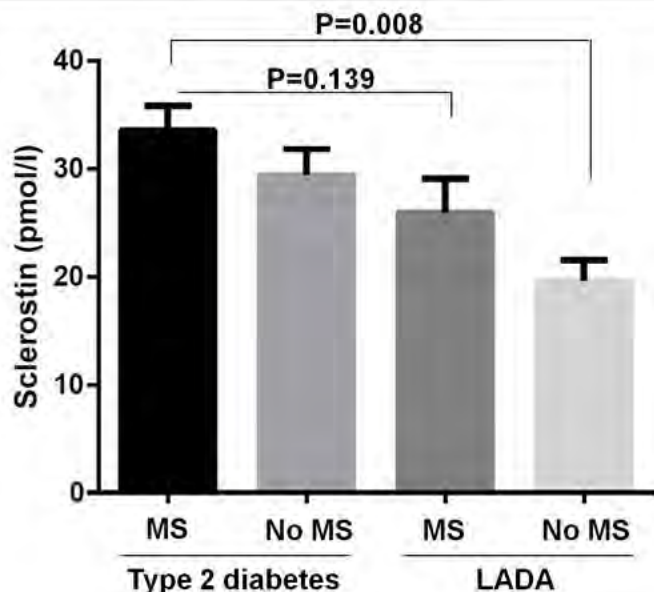


Fig. 1

Disclosures: Rocky Strollo, None.

MO0361

Parkin, A link between Parkinson's disease and bone homeostasis. Thomas Mbimba^{*1}, Kimberly Novack², Fouad M. Moussa², Gregory Songdag², Li Lin³, Christine Dengler-Criss³, Werner J Geldenhuys³, Favez Safady⁴. ¹Kent State University, USA, ²Biomedical Science Department, Kent State University/ Anatomy & Neuroscience Department NEOMED, USA, ³NEOMED, USA, ⁴NEOMED - KENT STATE, USA

Parkinson's Disease (PD) is a neurodegenerative disease characterized by a loss of dopaminergic neurons in the nigrostriatal pathway, which causes movement disorder distinguished by resting tremor, bradykinesia, rigidity, postural instability and gait disturbance. PD patients show a high risk of fracture incidents compare to age- and gender-matched controls. Mutation in the Parkin (PARK2) gene has been associated patients with PD. PARK2 is an E3 ubiquitin protein ligase that plays a role in the regulation of mitochondrial function. To date, various models of PARK2 dysfunction have been generated in an effort to understand the underlying mechanism of the disease. Human mutation in Parkin showed mitochondrial dysfunction in dopamine-producing nerve cells that plays an important role in causing signs and symptoms of Parkinson disease. In this study, we sought to examine the relationship between PD and skeletogenesis. First, we examined the expression of PARK2 in bone cells and observed that PARK2 mRNA expression is increased during osteoclast and osteoblast differentiation. Next, we examined the skeletal phenotype of transgenic mice expressing the mutant form of PARK2. These mice are carrying the human Q311X truncation associated with Turkish early-onset Parkinson's disease. Micro-CT analysis of 6-month old Parkin mutant mice have decreased bone mass associated with decreased trabecular number and thickness. DEXA showed significant reduction in bone mineral density in Parkin mutants. qPCR analysis of bone related markers showed significant reduction in the Parkin mutants compared to WT mice. Next, we examined the effects of Parkin mutant on bone cell differentiation and function *ex vivo*. There was significant decrease in bone marrow-derived osteoblast differentiation associated with decreased matrix production and osteoblast-related gene expression. RANKL-induced osteoclast differentiation was dramatically reduced in Parkin mutants compared to controls. Osteoclast-mediated bone resorption

determined by Osteologic assays showed significant decrease in Parkin mutants compared to WT mice. Taken together, these data suggest possible relationship between PD-associated protein and bone loss. Currently, studies are underway to determine the mechanism of Parkin on bone cell differentiation and function. These studies are the first to report a link between PD and bone homeostasis.

Disclosures: Thomas Mbimba, None.

This study received funding from: OHIO Department of Development

MO0362

A Testosterone Deficit Precedes Bone Loss in a Rodent Contusion Spinal Cord Injury Model. Joshua Yarrow^{*1}, Fan Ye¹, Christine Conover², Dana Otzel², Thomas Wronski³, J. Ignacio Aguirre³, Stephen Borst¹. ¹VA Medical Center, University of Florida, USA, ²VA Medical Center, USA, ³University of Florida, USA

Disuse resulting from a neurologic insult induces bone loss after spinal cord injury (SCI). However, SCI-induced bone loss occurs more quickly and is more severe than in other disuse models, suggesting that additional factors influence bone loss after SCI. Interestingly, a large proportion of men with SCI exhibit severe testosterone (T) deficits that persist for several years after injury, coinciding with the time frame of the most severe bone loss. Our purpose was to determine the time course for T deficits in relation to cancellous/cortical bone loss in a rodent SCI model. Forty-five 20-week old male Sprague-Dawley rats received SHAM surgery or T9 laminectomy plus moderate/severe contusion SCI and were euthanized 1-, 2-, or 3-months post-surgery. Expected sublesional functional deficits persisted in SCI animals throughout the study duration. Following SCI, T was reduced 40-45% at 1-week and 1-month post-SCI, 37% at 2-months, and restored to SHAM levels by 3-months. Cancellous bone deficits were observable 1-month post SCI at the distal femur (assessed via microCT) and proximal tibia (assessed via histology), but did not reach a level of significance due to high variability. At 2-months and 3-months post-SCI, cancellous bone mineral density was 32-35% lower than respective SHAMs, and was characterized by a 51-66% lower cancellous bone volume ($p < 0.05$, 2-month; $p < 0.01$, 3-month) that primarily resulted from reduced trabecular number. Trabecular pattern factor (an inverse measure of trabecular connectivity) and structure model index (a measure of plate-/rod-like trabecular structures) were also elevated by SCI at 2-months ($p < 0.05$) and 3-months ($p < 0.01$). At the femoral diaphysis, 2- and 3-month SCI animals exhibited 10% lower cortical thickness ($p < 0.01$), 8% lower total bone area ($p < 0.05$, 3-month only), 12-13% lower cortical area ($p < 0.01$), and 5-6% lower cortical bone volume ($p < 0.05$) compared with SHAMs. Our data indicates that T deficits occur early after SCI in our rodent model, preceding the time frame in which the vast majority of bone losses occur, and persist for 2 month after SCI. The deleterious morphological and microarchitectural alterations we observed indicate compromised lower-limb skeletal integrity exists, similar to what is observed clinically. These findings suggest that our rodent model is clinically-relevant and can be used to test therapeutic interventions designed to prevent bone loss and/or regenerate bone after SCI.

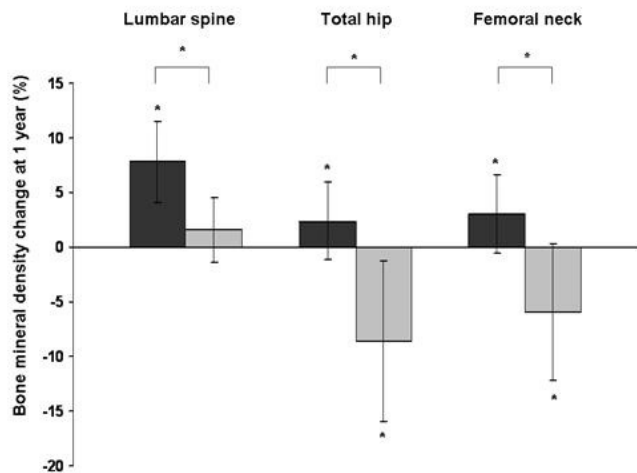
Disclosures: Joshua Yarrow, None.

MO0363

Denosumab Increases Sublesional Bone Mass In Osteoporotic Patients With Recent Spinal Cord Injury. Laia Gifre^{*1}, Joan Vidal², Josep Lluís Carrasco³, Africa Muxi⁴, Enric Portell², Ana Monegal⁵, Núria Guañabens⁵, Pilar Peris⁵. ¹Hospital Clinic Barcelona, Spain, ²Guttmann Neurorehabilitation Institute, Universitat Autònoma de Barcelona, Spain, ³Public Health Department, University of Barcelona, Spain, ⁴Nuclear Medicine Department, Hospital Clínic of Barcelona, Spain, ⁵Rheumatology Department, Hospital Clinic of Barcelona, Spain

Background: Osteoporosis development is a frequent complication related to spinal cord injury (SCI), especially at the sublesional level. However, although treatment with bisphosphonates may attenuate bone loss after SCI, no effective treatment has been reported to treat this clinical complication. Thus, the aim of this study was to analyze the efficacy of denosumab, a potent antiresorptive agent, in the treatment of patients with SCI-related osteoporosis. Methods: 14 patients aged 39-75 years with osteoporosis secondary to recent complete SCI (13 ASIA A-B; mean injury duration: 15.4 months) were treated with denosumab 60mg every 6 months for 12 months. Bone turnover markers (BTMs) (PINP, bone ALP and sCTX), 25-OH vitamin D (25OHD) levels and bone mineral density (BMD) at lumbar spine (LS), total hip (TH) and femoral neck (FN) were assessed at baseline and at 12 months. Results were compared with a control group of 9 SCI-patients with similar clinical characteristics (age, gender, duration and severity of SCI) without osteoporosis. All patients received calcium and vitamin D supplementation. Results: At 12 months, SCI patients treated with denosumab showed a significant increase in BMD at TH (+2.4-3.6%, $p = 0.042$), FN (+3.3.6%, $p = 0.006$) and LS (+7.8-3.7%, $p < 0.001$) compared to baseline values, whereas non-treated SCI patients showed a significant maintained BMD decrease at sublesional sites (TH: -8.6-7.4%, $p = 0.013$; FN: -5.9-6.2%, $p = 0.03$). In addition, denosumab treatment was associated with a significant decrease in BTMs (bone ALP -42%, $p < 0.001$; PINP -58%, $p < 0.001$, sCTX -57%, $p = 0.002$) at 12 months, with significantly greater changes compared to non-treated patients. BMD evolution was not related to BTM changes or to 25OHD

serum levels. No skeletal fractures were observed during follow-up and no treatment-related adverse events were noted. Conclusions: Treatment with denosumab increases lumbar and femoral BMD and decreases bone turnover markers in SCI-patients with secondary osteoporosis. This drug may be a promising therapeutic option in patients with SCI-related osteoporosis.



Percent changes in BMD in patients treated (black bars) and not treated (grey bars) with denosumab

Disclosures: Laia Gifre, None.

This study received funding from: Work funded by a grant from Fundació La Marató de TV3.

MO0364

A semi-automatic algorithm to assess bone attenuation and thoracic kyphosis on chest CT scans of patients with chronic obstructive pulmonary disease.

Mayke J. van Dort^{*1}, Erica P.A. Rutten², Bert van Rietbergen³, Elisabeth A.P.M. Romme⁴, Frank W.J.M. Smeenk⁴, Piet P.M.M. Geusens⁵, Emiel F.M. Wouters⁶, Joop P.W. van den Bergh⁷. ¹Department of Internal Medicine, NUTRIM School of Nutrition & Translational Research in Metabolism, Maastricht University Medical Center+ (MUMC+), Netherlands, ²Research & Education, Centre of expertise for chronic organ failure + (CIRO+), Netherlands, ³Department of Medical Engineering, Eindhoven University of Technology, Netherlands, ⁴Department of Respiratory Medicine, Catharina Hospital, Netherlands, ⁵Department of Internal Medicine, Rheumatology, Maastricht University Medical Center+ (MUMC+), Netherlands, ⁶Department of Respiratory Medicine, Maastricht University Medical Centre + (MUMC+), Netherlands, ⁷Department of Internal Medicine, VieCuri Medical Centre, Venlo & Department of Internal Medicine, NUTRIM School of Nutrition & Translational Research in Metabolism, Maastricht University Medical Center+ (MUMC+), Netherlands

Chronic obstructive pulmonary disease (COPD) is associated with osteoporosis and vertebral fractures (VFs). We developed a semi-automatic algorithm to assess bone attenuation (a measure of bone density) and kyphosis on regular chest CT scans in a pilot study in COPD patients and control subjects.

We investigated chest CT scans of a subgroup of the ECLIPSE cohort (a non-interventional, observational, multicenter, three-year study): 25 COPD subjects (COPDs), 25 non-COPD smoking (SC) and 25 non-smoking controls (NSC). A semi-automatic algorithm was created in Matlab (MathWorks) to assess thoracic kyphosis and 3D bone attenuation. Bone attenuation was measured in a region of 275 mm³ centered in T4, T7 and T10. Kyphosis was measured calculating the angle between two lines (above T4 and below T12) perpendicular to the tangents to a 3rd order polynomial fit through the spine. VFs were evaluated according Genant's method using SpineAnalyzerTM (OptasiaMedical) software. Age, gender and body mass index (BMI, kg/m²) were available.

Intraclass correlation coefficients (ICC) and coefficients of variation (CV) were calculated to examine reproducibility of the algorithm based on triple measurements of 25 scans by one reader.

We calculated ICCs and CVs of the semi-automatic assessment of bone attenuation (ICC: 0.994, CI [0.988;0.997], p<0.001; CV: 2.21%) and kyphosis angle measurements (ICC: 0.994, CI [0.988;0.997], p<0.001; CV: 3.21%).

A significant difference in bone attenuation was found between COPDs and NSC (172 and 228 Hounsfield Units resp., p=0.005) but not between COPDs and SC (p=0.815), and SC and NSC (p=0.104). However, after correction for age the difference was no longer significant. Gender nor BMI influenced the model significantly.

The prevalence of VFs and degree of thoracic kyphosis were not significantly different between the groups. Thoracic kyphosis was significantly related to the presence of VFs (p=0.001), but bone attenuation was not.

Our semi-automatic algorithm for assessment of bone attenuation and kyphosis angle on chest CT has a high reproducibility and CV of 2.21% and 3.21%, respectively.

In this pilot study, bone attenuation (after correction for age), thoracic kyphosis and presence of VFs were not significantly different between COPDs, SC and NSC. ICCs and CVs showed that our algorithm is reproducible and allow further investigation of associations between COPD, bone attenuation, thoracic kyphosis and VFs in larger and longitudinal studies.

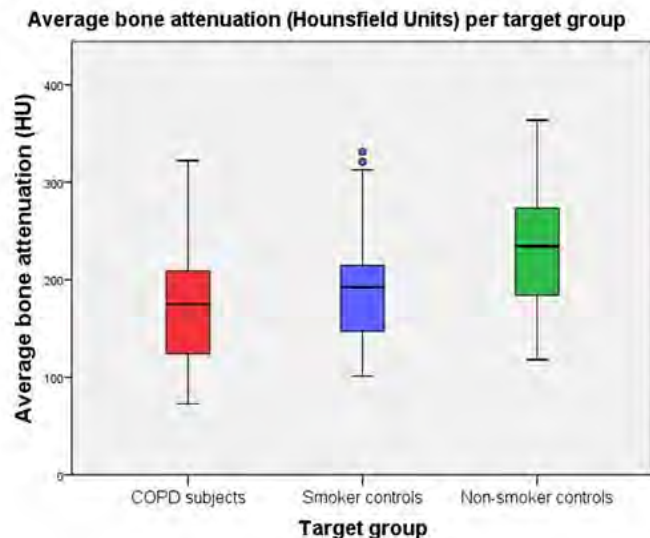


Figure 1. Average bone attenuation per group

Table 1. Characteristics of the three groups

| | COPD subjects | Smoker controls | Non-smoker controls | |
|---------------------------------------|---------------|-----------------|---------------------|---------|
| n | 25 | 25 | 25 | |
| Age, mean (sd), years | 62,72 (7,31) | 55,16 (9,08) | 53,28 (8,06) | p<0,001 |
| Sex, male (%) | 14 (56) | 15 (60) | 7 (28) | p=0,009 |
| BMI, mean (sd), kg/m ² | 25,27 (3,94) | 26,03 (4,96) | 30,09 (6,51) | p=0,004 |
| Bone attenuation, mean (sd), HU | 171,9 (61,35) | 191,0 (60,95) | 228,2 (60,86) | p=0,006 |
| VFs, Genant grade 1-3 (%) | 6 (24) | 4 (16) | 8 (32) | p=0,175 |
| Thoracic kyphosis, mean (sd), degrees | 34,49 (10,27) | 29,13 (13,31) | 35,83 (12,81) | p=0,128 |

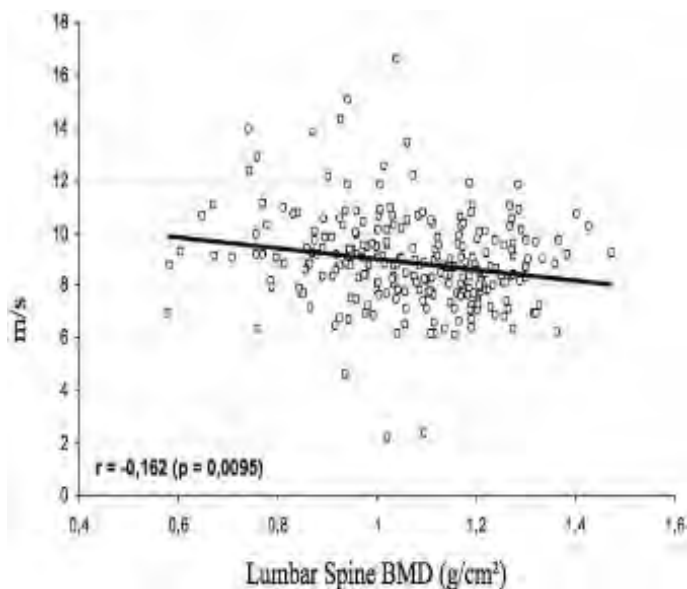
Table 1. Characteristics per group

Disclosures: Mayke J. van Dort, None.

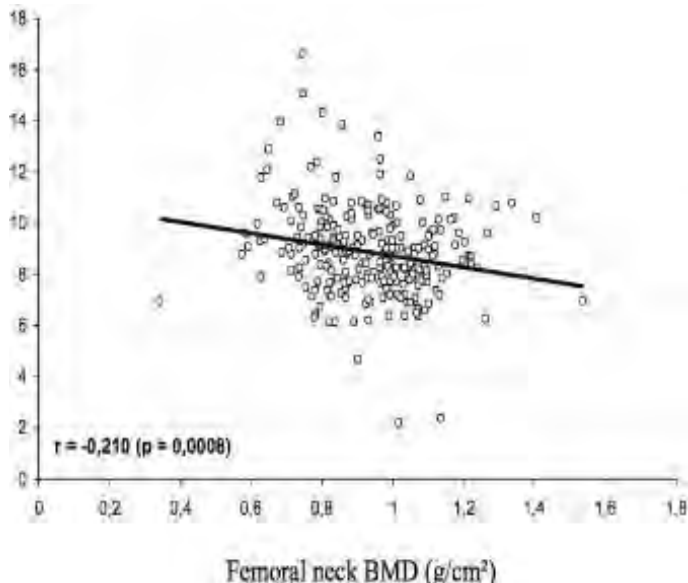
MO0365

Arterial Stiffness is Associated with Low Bone Mineral Density in Women Living with Human Immunodeficiency Virus. Zoraya Barros¹, Francisco Bandeira², Érico Carvalho³, Democrito Miranda Filho⁴, Heloisa Melo¹, Nathalia Brito³, Maria Albuquerque⁶, Ulisses Montarroyos⁷, Ricardo Ximenes⁷. ¹Departamento de Medicina Clínica, Universidade de Pernambuco, Brazil, ²Serviço de Endocrinologia, Hospital Agamenon Magalhães, SUS/Universidade de Pernambuco, Brazil, ³Serviço de Infectologia, Universidade de Pernambuco, Brazil, ⁴Departamento de Medicina Clínica, Universidade de Pernambuco, Brazil, ⁵Hospital Maternidade Sao Vicente De Paulo, Brazil, ⁶Centro de Pesquisa Aggeu Magalhães, Brazil, ⁷Departamento de Medicina Tropical, Universidade Federal de Pernambuco, Brazil

Introduction: Osteoporosis and cardiovascular disease are major causes of morbidity and mortality in people living with the human immunodeficiency virus (PLHIV). An independent relationship was found between the BMD, which represents the low BMD values and vascular calcification, as a risk factor for cardiovascular disease, but most data so far are derived from the male population and the link between those two conditions remains elusive. **Methods:** We investigated the association between BMD and aortic stiffness in 254 women living with HIV, aged 37-55 years; mean 45,8 ± 9,0; BMI (kg/m²) 25,0 ± 6,7; WC (cm) 89,1 ± 11,5; SBP(mmHg) 131 ± 22,2; DBP(mmHg) 83,2 ± 13,9. BMD was measured by dual energy x-ray absorptiometry (DXA) in the lumbar spine, femoral neck and total femur, and aortic stiffness was measured by aortic pulse wave velocity (aPWV). **Results:** There was a high frequency of low bone mass (63,4%), arterial hypertension (50%), and metabolic syndrome (43,2%). In multiple linear regression analysis there was a negative correlation between femoral neck BMD (Coefficient β=-2,191, p = 0,001), total femur (Coefficient β=-1,940, p = 0,004) and the aPWV, which remained significant after adjustment for age, long menstrual intervals, body mass index (BMI), metabolic syndrome, non-HDL cholesterol, mean arterial pressure and heart rate. **Conclusion:** Our data demonstrate an independent association between arterial stiffness and low BMD in women living with HIV suggesting common mechanisms on the development of both atherosclerosis and bone fragility. **Keyword:** osteoporosis, aortic stiffness, aortic pulse wave velocity, HIV.



GRAPHIC 1



GRAPHIC 2

Table 3. Multiple linear regression for an association between bone mineral density (BMD) and aortic pulse wave velocity (aPWV) in 254 women living with HIV/AIDS

| Variable | aPWV | | | | | |
|--|-------------------|----------|-------------------|----------|-------------------|----------|
| | Coefficientβ (EP) | p-value | Coefficientβ (EP) | p-value | Coefficientβ (EP) | p-value |
| Lumbar spine BMD (g/cm ³) | -1.155 (0.697) | 0.099 | - | - | - | - |
| Femoral neck BMD (g/cm ³) | - | - | -2.191 (0.679) | 0.001* | - | - |
| Total femur BMD(g/cm ³) | - | - | - | - | -1.940 (0.662) | 0.004* |
| Age group> 50 anos | 0.833 (0.274) | 0.003* | 0.758 (0.261) | 0.004* | 0.841 (0.258) | 0.001* |
| More than three delayed menstrual cycles | 0.194 (0.254) | 0.445 | 0.147 (0.248) | 0.554 | 0.137 (0.250) | 0.585 |
| BMI (kg/m ²) | -0.005 (0.016) | 0.769 | -0.011 (0.024) | 0.659 | -0.010 (0,024) | 0.682 |
| Metabolic syndrome | 0.376 (0,232) | 0.107 | 0.486 (0,235) | 0.040* | 0.481 (0,236) | 0.043* |
| Non-HDL cholesterol (mg/dL) | -0.001 (0,002) | 0.546 | 0.00003 (0,002) | 0.985 | 0.0002 (0,002) | 0.920 |
| Mean blood pressure (mmHg) | 0.037 (0,007) | <0.0001* | 0.039 (0,007) | <0.0001* | 0.039 (0,007) | <0.0001* |
| Heart rate (bpm) | 0.020 (0,010) | 0.052 | 0.015 (0,010) | 0.129 | 0.014 (0,010) | 0.142 |

*Statistically significant association (p < 0.05)

TABLE 1

Disclosures: Nathalia Brito, None.

MO0366

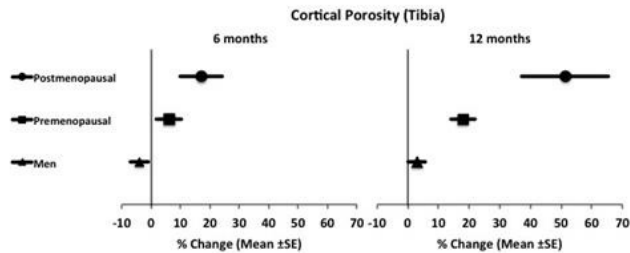
Effects of Gastric Bypass Surgery on Bone Mass and Microarchitecture Occur Early and Particularly Impact Postmenopausal Women. Anne Schafer^{*1}, Galateia Kazakia², Lygia Stewart³, Stanley Rogers², Jonathan Carter², Andrew Posselt², Courtney Pasco², Dolores Shoback³, Dennis Black². ¹University of California, San Francisco & the San Francisco VA Medical Center, USA, ²University of California, San Francisco, USA, ³San Francisco VA Medical Center & University of California, San Francisco, USA

Roux-en-Y gastric bypass (RYGB) surgery has negative effects on the skeleton. Skeletal effects may begin very early in the postoperative period, but no studies using advanced quantitative computed tomography (QCT) in addition to standard dual-energy X-ray absorptiometry (DXA) have included that imaging as early as 6 months after surgery. Also, as a result of modestly sized samples of mostly premenopausal women and very few men, the relative skeletal effects of RYGB by sex and menopausal status are uncertain. We conducted a prospective cohort study of RYGB and skeletal health, the largest to date to examine changes in axial and appendicular volumetric bone mineral density (vBMD) and appendicular bone microarchitecture.

Obese adults (N=47; 37 premenopausal and 10 postmenopausal women, 10 men) with BMI 44 ± 7 kg/m² were assessed before and 6 and 12 months after RYGB. Participants underwent hip and spine DXA, spine QCT, and high-resolution peripheral QCT (HR-pQCT) (radius and tibia).

Mean weight loss 6 and 12 months postoperatively was 31 and 37 kg. Femoral neck BMD by DXA decreased by mean 5.0% and 8.0% at 6 and 12 months postoperatively. Spine vBMD by QCT declined 6.6% and 8.1% after 6 and 12 months; declines were statistically significant among premenopausal and postmenopausal women and men, with a greater decline among postmenopausal vs. premenopausal women (-11.6% vs. -6.0% at 12 months, p=0.02). At the tibia, detrimental changes in trabecular (Tb) microarchitecture (decreased number, increased spacing and heterogeneity) occurred at 6 and 12 months. At the radius, changes in Tb number and spacing were not significant vs. baseline but were more detrimental for women than men (p≤0.03 for difference). Cortical porosity increased at the radius and tibia, with more dramatic 12-month increases among postmenopausal than premenopausal women at the tibia (+51.4% vs. +18.0%, p<0.01, Figure); increases among men were not detected (p≤0.02 for difference vs. the other groups). At 12 months, decline in Tb vBMD was larger at radius than tibia, while decline in cortical vBMD was larger at tibia than radius (p=0.02 for site comparisons). Cortical vBMD decline was greater in postmenopausal than premenopausal women (-4.4% vs. -0.7%, p<0.01).

Detrimental effects of RYGB on axial and appendicular vBMD and on bone microarchitecture are detectable as early as 6 months postoperatively and progress thereafter. Postmenopausal women are at highest risk for skeletal complications.



Figure

Disclosures: Anne Schafer, None.

MO0367

Osteoporosis: What Is the Burden of Disease in Psoriatic Arthritis?. Glenn Haugeberg^{*1}, Berit Helen Grandaunet², Hege Høiberg³, Andreas P Diamantopoulos⁴, Arthur Kavanaugh⁵. ¹Hospital of Southern Norway, Norway, ²St. Olavs Hospital, Norway, ³Sørlandet sykehus, Norway, ⁴Sshf Kristiansand, Norway, ⁵UC San Diego School of Medicine, USA

Bone damage, including localized as well as generalized osteoporosis is a well known consequence of the inflammatory arthritides such as rheumatoid arthritis (RA). Psoriatic arthritis (PsA) can be characterized by bone destruction but also new bone formation. In PsA, the literature on osteoporosis is inconclusive and scarcer than in RA. The aim of the study was to explore if PsA patients are at increased risk of having reduced bone mineral density (BMD) at hip and/or lumbar spine. Consecutive patients from an outpatient clinic fulfilling CASPAR criteria for PsA were enrolled. We excluded PsA patients with only axial manifestation without peripheral arthritis. All patients underwent a thorough examination according to an extensive protocol. Data collection included demographics, clinical and laboratory disease measures, treatments, and previous fracture history. BMD was measured at spine (L1-4) and hip (femoral neck and total hip) by dual energy X-ray absorptiometry (DXA, Lunar Prodigy). Calibration of the DXA machine was stable during the whole measurement period. BMD was expressed as g/cm², Z-score and T-score. The percentage of patients with T-score = -2.5 SD (WHO osteoporosis definition) and with Z-score = -1.0 SD was calculated. Appropriate descriptive statistics was applied for continuous and categorical variables. Patient characteristics among the 141 examined PsA patients (men 50.4%): mean (SD) age 52.5 (9.9) years, body mass index (BMI) 28.3 (4.4) kg/m², disease duration 8.9 years (6.8) and current smoker 17.0%. Median (range) 68 tender joint count was 6.0 [0-55], 66 swollen joint count 0 [0-6] and CRP 2.0 [0-63] mg/dl. Mean (SD) DAS28 was 3.2 (1.2), ESR 15.9 (11.9) mm/hr, MHAQ 0.44 (0.40) and pain and fatigue on visual analogue scale 35.1 (23.5) and 45.7 (32.4) mm respectively. Biologic DMARDs were used by 33.3%, synthetic DMARDs by 56.7% and glucocorticosteroids by 9.9%. Only 11.3% of patients were using calcium and vitamin D supplementation and 2.1 % antiresorptive osteoporosis treatment. Low energy fracture was reported in 8.9% of the patients. In the table below mean (SD or 95%CI) bone density values expressed as BMD, Z-score and T-score and percentage of patients with T-score = -2.5 SD and Z-score = -1.0 SD (by definition 16% in the reference population) is displayed. As shown the proportion of patients with Z-score = -1.0 SD was comparable with the 16% seen in the reference population database. In conclusion the proportion of PsA patients with osteoporosis in our study was low. Overall BMD was comparable to that from normative bone density reference values.

| | Femoral neck left | Femoral neck right | Total hip left | Total hip right | Spine L1-4 |
|-------------------------------|-------------------------|-------------------------|-------------------------|-------------------------|-----------------------|
| BMD (g/cm²) | 0.97 (0.14) | 0.97 (0.14) | 1.02 (0.15) | 1.01 (0.15) | 1.21 (0.17) |
| T-score (SD) | -0.66 (-0.86, -0.47) | -0.70 (-0.88, -0.51) | -0.23 (-0.42, -0.03) | -0.33 (-0.52, -0.13) | 0.13 (-0.11, 0.36) |
| Z-score (SD) | -0.09 (-0.26, 0.08) | -0.13 (-0.29, 0.04) | -0.03 (-0.20, 0.15) | -0.10 (-0.28, 0.07) | 0.16 (-0.05, 0.38) |
| Z ≤ -1.0 SD | 19.4% | 19.1% | 16.5% | 17.6% | 17.4% |
| T ≤ -2.5 SD | 4.5% | 2.9% | 1.5% | 2.2% | 1.4% |

Table

Disclosures: Glenn Haugeberg, None.

MO0368

Serum carboxy-terminal telopeptide of type 1 collagen (ICTP) is a prognostic factor in a cohort of Japanese male patients undergoing coronary angiography: CHIBA (Coronary Heart Disease of Ischemia and Bone Association) Study. Nobuyuki Tai^{*1}, Reiko Watanabe², Junko Hirano², Hiroaki Masaki², Toshihiro Amaki², Fumitaka Nakamura², Ryo Okazaki², Daisuke Inoue². ¹Teikyo University School of Medicine, Japan, ²Third Department of Medicine, Teikyo University School of Medicine, Japan

Background: Evidence suggests a link between atherosclerotic diseases and osteoporosis. Some resorption markers have been shown to be associated with cardiovascular diseases and related mortality, but relationship between bone metabolic abnormalities and such events has not been established. We previously reported that an MMP-dependent marker, ICTP, was strongly correlated with cardiac dysfunction in a cross-sectional study.

Aim: To evaluate the ability for bone metabolic markers to predict cardiovascular events and mortality.

Methods: Subjects undergoing coronary angiography (CAG) was consecutively recruited to this cohort study in our hospital. Baseline levels of various parameters of bone, heart, glucose and lipid metabolism were measured. A survey using mail questionnaires and medical records was conducted in 2014 targeting 577 subjects recruited from Jan 2006-Jan 2007, excluding females and those with serum Cr level of 2 mg/dl or more. Primary end points are cerebro-cardiovascular events and all-cause deaths.

Results: Out of 362 eligible subjects, 215 responded and were included in the analysis. Mean age and observation period were 65.3 ± 10.7 years old and 78.8 ± 20.6 months. Ninety patients had the history of intervention (PCI or CABG). Cerebro-cardiovascular events and all cause deaths occurred 17.1 % and 19.0 %, respectively. At baseline, ICTP was correlated with NT-proBNP and left ventricular ejection fraction. Kaplan-Meier analysis showed that the survival was significantly shorter in the highest ICTP quartile (log-rank, p<0.001). Cox regression analysis revealed that age, ICTP, NTX and NT-proBNP were independent predictors of all-cause death after correction for eGFR and the past history of PCI or CABG. Interestingly, TRACP-5b, a non-collagen resorption marker, was also an independent determinant of survival together with age and NT-proBNP, demonstrating a definite link to bone metabolic abnormalities, not just an abnormal collagen metabolism in the cardiovascular tissues. As for cerebro-cardiovascular events, age, 25(OH)D and the number of significant coronary artery stenosis were independent predictors.

Conclusions: ICTP was found to be a strong predictor of all-cause death in male subjects undergoing CAG, and thus may be a useful prognostic marker in the context of coexistent cardiovascular and bone metabolic abnormalities.

Disclosures: Nobuyuki Tai, None.

MO0369

Using electronic health records and machine learning to develop a fracture prediction tool in end stage renal disease patients. Kyle Nishiyama^{*1}, Chengchen Zhang¹, Jianhua Li¹, Donald McMahon¹, Jonathan Lorch², Elizabeth Shane¹, Jeri Nieves¹, Herbert Chase¹, Thomas Nickolas¹. ¹Columbia University, USA, ²Rogosin Institute, USA

Fractures in end stage renal disease (ESRD) patients are 14-fold greater than in the general population. Unfortunately we lack tools to adequately identify these individual ESRD patients who are at risk. Only recently was bone mineral density (BMD) shown to predict fractures, and the World Health Organization's Fracture Risk Assessment (FRAX) tool was shown to have no predictive value in ESRD. Thus, while tools to predict fracture in ESRD are needed, their development has been impeded by the lack of large prospective ESRD cohorts with fracture outcomes. To address these significant limitations, we leveraged the data-rich content of electronic health records (EHR) to build a cohort of ESRD patients and then used machine-learning methods to develop an ESRD-specific fracture prediction models. We

evaluated the ability of clinical risk factors available to clinicians on the first day of dialysis to predict fracture. This retrospective study with prospective follow-up included 7191 ESRD patients with (n=809) and without (n=6382) fracture from New York-Presbyterian Hospital. Clinical predictors included, but were not limited to, demographics (age, sex, race), labs (serum creatinine, PTH, hemoglobin, total alkaline phosphatase, phosphate), secondary causes of osteoporosis (glucocorticoids, diabetes) and BMD. We used feature selection and machine learning (Naïve Bayes) to classify fracture cases and controls. To determine whether BMD contributed to fracture prediction above clinical risk factors, we repeated these analyses in a subset of subjects with BMD (cases n=173; controls n=589) representative of the full dataset. Sensitivity, specificity, accuracy and area under the ROC curve (AUC) are presented (Table). In the full dataset, we achieved moderate prediction (AUC=0.67) with clinical data alone. In patients with BMD, performance significantly improved in models with BMD compared to without BMD (AUC=0.67 vs. AUC=0.59, $p<0.05$). These preliminary findings suggest that using large-scale datasets from EHR combined with machine learning methods has potential to build fracture risk prediction tools in understudied populations. They suggest that BMD, which is not assessed routinely in ESRD patients, may improve fracture prediction above that of clinical risk factors. Future work will include model refinement using other machine learning methods as well as using natural language processing to extract additional information from text written notes in the EHR.

Table: Results using machine learning to classify subjects with and without fractures.

| | Model | AUC | Accuracy (%) | Sensitivity (%) | Specificity (%) |
|----------------------------|-------------|------|--------------|-----------------|-----------------|
| Full Dataset (n=7179) | Naïve Bayes | 0.67 | 85 | 24 | 90 |
| Subset with DXA (n=762) | Naïve Bayes | 0.67 | 69 | 32 | 80 |
| Subset without DXA (n=762) | Naïve Bayes | 0.59 | 74 | 30 | 78 |

Table

Disclosures: Kyle Nishiyama, None.

MO0370

Advanced Glycation End-products are Higher in Trabecular Bone from Premenopausal Women with Idiopathic Osteoporosis. Timothy Cleland¹, Adi Cohen², David Dempster², Robert Recker³, Joan Lappe³, Hua Zhou⁴, Elizabeth Shane², Deepak Vashishth¹. ¹Rensselaer Polytechnic Institute, USA, ²Columbia University, USA, ³Creighton University, USA, ⁴Helen Hayes Hospital, USA

The pathogenesis of fragility fractures (FX) in premenopausal women with idiopathic osteoporosis (IOP) is unclear. Our prior studies found no differences in clinical characteristics, key hormones, turnover markers, and bone microarchitecture in women with IOP who have had fragility FX (IOP-FX) and those with idiopathic low bone mineral density (ILBMD) but no FX [1]. IOP-FX and ILBMD have differences in matrix mineralization compared to age-matched controls with normal BMD (CON), but also show significant between-groups differences in newly formed organic matrix suggesting osteoblast dysfunction as one possible reason for fragility fracture [2]. Because accumulation of Advanced Glycation End-products (AGEs) in the organic matrix has been shown to reduce osteoblastic differentiation and activity, osteoclastic resorption, and material properties of cancellous bone tissue [3], we measured fluorescent AGE content in cortical and cancellous bone in transiliac biopsies from premenopausal women with IOP, 45 IOP-FX, 19 ILBMD, and 40 CON, using a fluorescent AGE assay. By Student-Newman-Keuls one-way ANOVA, we found trabecular AGE concentrations were higher in the ILBMD than the CON group (228.14 ± 415.08 versus 52.48 ± 97.44 ng quinine/mg collagen; $p<0.05$), a non-significant trend for higher AGE concentrations in the ILBMD than the IOP-FX group (228.14 ± 415.08 versus 99.42 ± 255.74 ng quinine/mg collagen; $p=0.064$) and no difference between CON and IOP groups ($p>0.05$). In contrast to trabecular bone, we detected no group differences in cortical bone ($p > 0.05$ for ANOVA). A trend for presence of higher AGEs between the combined IOP-FX and ILBMD groups than CON ($p=0.099$) may translate into higher risk of fragility fracture, as accumulation of AGEs is associated with poorer material properties of bone. Furthermore, these results suggest that IOP in premenopausal women is associated with more glycated and, hence, older tissue that is resistant to complete resorption and promotes osteoblast dysfunction. Alteration in both these key processes would render bone deficient in key matrix proteins and modify the proteins that are present. Analyzing the proteomic profile of tissue from the IOP-FX and ILBMD groups may further elucidate the pathogenesis of fragility fractures associated with IOP.

References: (1) Cohen et al. 2011 J. Clin. Endocrinol. Metab. 96:3095-105. (2) Misof et al. 2012 JBMR:27, 2552-61. (3) Vashishth 2007 Curr Osteoporosis Rep. 5:62-6.

Disclosures: Timothy Cleland, None.

MO0371

Pregnancy and Lactation Associated Osteoporosis (PLO): Similar Bone Structure and Lower Bone Remodeling than Idiopathic Osteoporosis. Adi Cohen¹, Mafo Kamanda-Kosse², Hua Zhou³, David Dempster², Mariana Bucovsky², Julie Stubby⁴, Robert Recker⁴, Joan Lappe⁴, Elizabeth Shane². ¹Columbia University Medical Center, USA, ²Columbia University, USA, ³Helen Hayes Hospital, USA, ⁴Creighton University, USA

Pregnancy and lactation (P/L) are associated with rapid decreases in lumbar spine (LS) and femoral neck (FN) BMD followed by recovery. Rarely, young women present with fragility fractures that occur during P/L, and, in the absence of a secondary cause, are said to have P/L associated osteoporosis (PLO). Whether clinical, structural or metabolic characteristics of women with PLO differ from those with premenopausal idiopathic osteoporosis (IOP) is unknown and bone biopsy data are lacking in PLO. We compared 10 women with PLO to 56 women with IOP and 40 premenopausal normal controls. All women were otherwise healthy, and normally menstruating at the time of the evaluation. All had a complete history, physical exam, biochemistries to exclude secondary osteoporosis, BMD by DXA and transiliac crest bone biopsy after double tetracycline labeling. Subjects were evaluated ≥ 12 months after delivery or weaning and > 3 months after fracture. Two with PLO, 7 with IOP, and 0 Controls were using estrogen-based hormonal contraception. Parity, months of breastfeeding, and age at first pregnancy did not differ between the groups. Vertebral fractures were more common in PLO than IOP (70% versus 25%; $p = 0.005$). Non-vertebral fractures were comparable; PLO: 2 had rib, 3 had hip and 8 had extremity fractures. IOP: 12 had rib, 12 had hip and 41 had extremity fractures. A family history of osteoporosis was similar in both groups ($\sim 50\%$). More PLO women had a history of multiple fractures (100% vs 75%) and of childhood fracture (70% vs 30%), suggesting that bone fragility may antedate the presentation with PLO. PLO women tended to be younger (33 ± 6 vs 37 ± 8 yrs; $p=0.1$). Height, weight, BMI and DXA body fat did not differ between IOP and PLO. Serum and urine calcium, PTH and 25-OHD were normal in all and did not differ between groups. LS BMD tended to be lower in PLO than IOP, but trabecular microstructure did not differ on biopsies. Cortical width tended to be lower in PLO than IOP, but cortical porosity was similar. Cancellous bone remodeling was lower in those with PLO vs both IOP and Controls, tended to be lower at the endocortical surface, but did not differ in cortical bone (data not shown); 56% of women with PLO had cancellous bone formation rate (BFR) < 0.006 mm³/mm²/yr, a cutoff we previously used to define low turnover IOP, compared to 29% with IOP. Further research is needed to determine whether low bone formation contributes to the risk of PLO.

| Table: Bone Structure and Remodeling in PLO and IOP | PLO N=10 | IOP N=56 | Controls N=40 | P: PLO vs IOP | P: PLO vs Control |
|---|---------------|---------------|---------------|---------------|-------------------|
| DXA BMD Z score | | | | | |
| Lumbar Spine | -2.14 ± 0.71 | -1.46 ± 1.29 | 0.74 ± 0.88 | 0.1 | <0.001 |
| Total Hip | -1.54 ± 0.79 | -1.05 ± 1.07 | 0.48 ± 0.65 | 0.2 | <0.001 |
| Femoral Neck | -1.66 ± 0.76 | -1.31 ± 1.07 | 0.39 ± 0.74 | 0.3 | <0.001 |
| Distal Radius | -0.04 ± 0.69 | 0.24 ± 0.84 | 0.68 ± 0.89 | 0.3 | 0.004 |
| Transiliac Bone Biopsy: Available for 9 with PLO, 52 with IOP, 40 Controls | | | | | |
| Trabecular Structure | | | | | |
| BV/TV (%) | 17.5 ± 3.1 | 18.2 ± 4.7 | 21.6 ± 5.4 | 0.7 | 0.06 |
| Trabecular Width (µm) | 123 ± 37 | 116 ± 25 | 133 ± 24 | 0.5 | 0.4 |
| Trabecular Number (#/mm ²) | 1.48 ± 0.31 | 1.59 ± 0.34 | 1.62 ± 0.26 | 0.4 | 0.2 |
| Trabecular Separation (µm) | 693 ± 169 | 652 ± 172 | 621 ± 110 | 0.6 | 0.1 |
| Cortical Structure | | | | | |
| Cortical Width (µm) | 547 ± 219 | 689 ± 230 | 866 ± 212 | 0.1 | <0.001 |
| Cortical Pore Area (%) | 6.29 ± 3.93 | 5.78 ± 2.95 | 7.45 ± 3.11 | 0.7 | 0.4 |
| Pore #/Cortical Area (#/mm ²) | 5.72 ± 1.20 | 5.80 ± 2.38 | 5.39 ± 1.70 | 0.9 | 0.6 |
| Cancellous Remodeling | | | | | |
| Mineralizing Surface (%) | 2.49 ± 2.21 | 4.57 ± 3.58 | 3.25 ± 2.56 | 0.1 | 0.4 |
| Mineral Apposition Rate (µm/d) | 0.501 ± 0.074 | 0.620 ± 0.102 | 0.642 ± 0.091 | 0.003 | <0.001 |
| Bone Formation Rate (mm ³ /mm ² /yr) | 0.005 ± 0.004 | 0.010 ± 0.009 | 0.008 ± 0.007 | 0.01 | 0.2 |

PLOtable

Disclosures: Adi Cohen, None.

MO0372

Are fractures and bone loss to be inevitably expected after renal transplantation? Results of up to 5 year follow up in a South East Asian population of renal transplant patients. Manju Chandran¹, Matthew Tan². ¹Singapore General Hospital, Singapore, ²Osteoporosis & Bone Metabolism Unit, Department of Endocrinology, Singapore General Hospital, Singapore

Introduction: The risk of bone loss and fractures is reportedly very high during the first year of follow-up after kidney transplantation and this risk apparently remains high even in the long term. We have previously reported on the prevalence and predictors of bone loss in the first year after renal transplantation amongst Singaporean patients¹. We now aimed to evaluate the baseline bone health

and to examine factors correlating with BMD changes and fractures if any in patients followed up to five years after renal transplantation.

Method: 164 patients who underwent renal transplant between 2008 and 2014 were studied retrospectively. Baseline bone parameters evaluated were BMD, parathyroid status, and 25(OH)D level. In post-menopausal women and in men over the age of 50, osteoporosis was diagnosed if the lowest T score at any axial site was ≤ -2.5 . In premenopausal women and in men under the age of 50, a diagnosis of low bone mass was made if the Z score was ≤ 2 . BMD changes at 6 months, 1 year, 2 years, and 5 years were compared using paired T-tests. $P < 0.05$ was considered significant. Pearson's correlation coefficient was used to measure correlations between changes in BMD and the different covariates.

Results: At baseline, 80.9% of patients had secondary and 4.5% had tertiary hyperparathyroidism. 14.5% had parathyroidectomy. The median 25(OH)D level was 14.6 ng/ml (11.7-22.8). 46% of the patients had osteoporosis or low bone mass. PTH level correlated negatively with the BMD at the femoral neck ($r = -0.169$, $p = 0.032$). BMD decreased significantly at 6 months compared to baseline at all 3 axial sites ($p = .000$). Subsequent to this there was no significant change in BMD in the patients who had follow-up over the next 4.5 years. During the 5 year follow up period, 6 patients had a low trauma metatarsal fracture each and 1 patient had an ankle fracture. No other atraumatic clinical fractures were noted in the patient population. BMD was not significantly correlated with the peripheral fractures.

Conclusion: Unlike reported in the western literature, we did not find an increased incidence of typical osteoporotic fractures during follow up, nor did we see a continued and significant bone mass loss after the first 6 months following transplant. This raises very intriguing questions about possible differences in the bone biology and genetic make up of SE Asian renal transplant patients as compared to Caucasian populations. Further studies are needed to elucidate these differences.

References

1. Lim D et al. Transplantation 2011; 92(5)

Disclosures: Manju Chandran, None.

MO0373

PDGF and BMP2 Enhance Proliferation, Migration and Differentiation of Periosteal Progenitor Cells. Xi Wang*, Brya Matthews, Ivo Kalajzic. University of Connecticut Health Center, USA

The periosteum contains multipotent skeletal progenitor cells and plays an essential role in bone repair. Understanding factors that regulate cell behavior and differentiation in the periosteum is important for future therapeutic applications. BMP2 has been widely used in orthopaedics but supraphysiological doses lead to side effects. A growth factor which could potentially reduce BMP2 doses is Platelet Derived Growth Factor-BB (PDGF-BB). It is involved in the early stages of bone repair but its effect on periosteal cells is unknown. We aimed to evaluate the effects of PDGF-BB and BMP2 on periosteal progenitor cells (PPCs).

To isolate PPCs, we scraped the periosteum from femurs and tibias of 6-8 week old mice and enzymatically digested for 1 hour. Primary cells were cultured in 5% oxygen for the first 4 days. For differentiation, cells were treated with 10ng/ml rhPDGF-BB and/or 100 ng/ml BMP2 beginning on Day 3, and cultured in osteogenic medium from Day 7-21. Gene expression and mineralized nodule formation was evaluated by expression of Col2.3GFP transgene and von Kossa staining. EdU and TUNEL assay was completed to evaluate the effects of PDGF-BB and BMP2 on the proliferation and apoptosis of PPCs. Migration was evaluated by measuring closure of a scratch wound.

Flow cytometric analysis showed that a large proportion of CD45- PPCs express mesenchymal stem cell markers: 81.3% are Sca-1+ and 75.6% express CD105. 30.5% PPCs express PDGF Receptor- α , 71.8% cells are PDGFR- β +. During osteogenic differentiation, continuous PDGF-BB treatment inhibited the formation of mineralized nodules while pretreatment with PDGF-BB at days 3-7 of culture promoted mineralization. Sequential combination of PDGF-BB and BMP2 resulted in the highest level of mineralization and expression of osteocalcin and bone sialoprotein. In addition, PDGF-BB significantly increased the proportion of EdU+ cells from 3.7% to 20.5% and prevented apoptosis of periosteal cells. PDGF also accelerated the migration of PPCs in a scratch assay, while the combination of PDGF-BB and BMP2 further increased speed of scratch healing in vitro.

In conclusion, our data show that under temporal control, PDGF-BB and BMP-2 can significantly promote osteogenic differentiation of PPCs. They also jointly accelerate in vitro wound healing, suggesting therapeutic potential for combination treatment. We are currently evaluating the effects of combinatorial treatment in models of bone repair in vivo.

Disclosures: Xi Wang, None.

MO0374

Release of Titanium particle by Ultrasonic Cleaning of dental implants may aggravate the peri-implant inflammatory response. Yankel Gabet, Michal Eger*, Tamar Liron, Nir Sterer, David Kochavi. Tel Aviv University, Israel

Titanium (Ti) and its alloys are widely used as dental implants due to their biocompatibility, mechanical strength, corrosion resistance and osseointegration. To

date, virtually all-available implants undergo surface roughening in order to accelerate osseointegration and shorten healing time. Peri-implantitis is a major clinical concern and main cause of long term implant failure. Triggered by specific oral bacteria, it consists of an inflammatory process that leads to bone resorption around dental implants. Once the process starts it can hardly be controlled and often results in implant loss. Treatment includes mechanical cleaning of the surrounding oral flora by ultrasonic scaling (US). We hypothesize that the scaling process releases Ti particles into the implant microenvironment and that these particles aggravate or even trigger the inflammatory response. To test this hypothesis, we performed US of Ti discs with various surface types. The released particles were then added to bone marrow-derived mouse macrophages (BMDM) cultures. Bacterial lipopolysaccharides (LPS) were added to parallel cultures as positive control and in addition to Ti particles to assess additive/synergistic effects in the RNA expression of inflammatory cytokines. Atomic force microscopy and electron scanning microscopy were used for profilometry of the released particle and post-cleaning titanium surface. RT-qPCR indicated that Ti particles originating from sand-blasted/acid etched (SLA) implants stimulated gene expression of pro-inflammatory cytokines (TNF α , IL1 β , IL6) to a greater extent than LPS. Using SEM we then compared the profile, size and quantity of Ti particles obtained from all 3 different surface types, namely machined, SLA and sand-blasted (SB). BMDM were then cultured with the particles released from each surface type. In general, particles originating from SB implants yielded the most severe inflammatory response, while particles from machined implants induced the mildest response. Our results showed that both the amount and the shape of particles have an effect on the inflammatory response. These data suggest that scaling of Ti implants, intended at preventing peri-implantitis, may in fact aggravate the osteolytic inflammatory response by causing an accumulation of Ti particles in the peri-implant environment. This adverse reaction is likely to be even more severe around roughened Ti implants.

Disclosures: Michal Eger, None.

MO0375

The Role of EphrinB2 Signaling during Endochondral Bone Formation. Yongmei Wang*¹, Alicia Menendez², Chak Fong³, Nicholas Heiniger³, Daniel Bikle⁴. ¹Endocrine Unit, University of California, San Francisco/VA Medical Center, USA, ²Endocrine Unit, University of California, San Francisco/ San Francisco VA Medical Center, USA, ³Endocrine Unit, University of California, San Francisco/San Francisco VA Medical Center, USA, ⁴Endocrine Unit, University of California, San Francisco/San Francisco VA Medical Center, USA

EphrinB2 (ENF2) and its receptor EphB4 are critical in regulating chondrocyte, osteoblast (OB), and osteoclast differentiation, the communication between these cells and the skeletal actions of parathyroid hormone and insulin-like growth factor (IGF-I). However, whether and how ENF2/EphB4 regulates endochondral bone formation remains unknown. To address these issues, we generated mice with specific ENF2 null mutation in their type II collagen (Col.II) expressing chondrocytes (Col.II.ENF2KO) (floxed ENF2 X Col.II promoter driven Cre-recombinase) to investigate the role of ENF2 during endochondral bone formation. The deletion of ENF2 was confirmed by immunohistochemistry in the proliferating chondrocytes and in the OBs of the trabecular bone surface in the Col.II.ENF2KO. At P7, the Col.II.ENF2KOs showed shorter proliferating zone and hypertrophic zone with fewer PCNA positive cells in the proliferating zone of the growth plate and the cells lining the trabecular bone surface when compared to the controls. As determined by μ CT, at 6 weeks, trabecular bone volume (BV/TV, 30%) and number (Tb.N, 28%) were significantly lower in the female Col.II.ENF2KOs than in the female controls. Quantitative PCR revealed that mRNA levels of Col.II and Indian Hedgehog were decreased by 56% and 40%, respectively in the Col.II.ENF2KOs compared to the controls. To determine the role of ENF2 in mediating skeletal stimulation of IGF-I during endochondral bone formation, metatarsals (MTs) from the P0 controls and the Col.II.ENF2KOs (KOs) were cultured with or without IGF-I treatment (100 ng/ml). At day 7, IGF-I treatment significantly increased the total bone (30%) and cartilage (32%) length in the control MTs, but not in the KO MTs. IGF-I increased the number of PCNA positive cells and phosphorylated ERK (pERK) expression in growth plate chondrocytes of the control MTs, but these effects were abolished in the KO MTs. Our data indicate that ENF2 in Col.II expressing cells promotes chondrocyte proliferation and differentiation and is required for IGF-I stimulated endochondral bone formation.

Disclosures: Yongmei Wang, None.

MO0376

Localization of parathyroid hormone-related protein and its receptor in different pancreatic tumor types. Syu Mi Sam*¹, Kristi Milley¹, John Slavin², Peter Little¹, Mathis Grossmann³, Jeffrey Zajac³, Janine Danks¹. ¹School of Medical Sciences, RMIT University, Australia, ²Department of Pathology, St Vincent's Hospital, Melbourne, Australia, ³Department of Medicine, The University of Melbourne, Austin Health, Australia

PTHrP has been demonstrated to be involved in calcium homeostasis, smooth muscle relaxation and cellular proliferation, survival and differentiation in tissues such as skin, mammary gland and bone in physiological conditions. In pathological conditions, PTHrP has been shown to be expressed in common malignancies such as

breast and prostate cancer. There is limited data on the expression and secretion of PTHrP in pancreatic tumors, most literature has only focused on adenocarcinomas. Little is known about the role or presence of PTHrP in other pancreatic tumors such as in benign or premalignant tumors. To date no studies have examined the presence of PTHrP and PTH1R in other pancreatic tumor histopathological types. The aim of this study was to establish if PTHrP and PTH1R are present in different pancreatic tumor histopathological types. Using WHO classification, PTHrP and PTH1R was localized using immunohistochemistry in six benign, four premalignant and 27 malignant formalin-fixed paraffin-embedded archival samples. Slides were digitally scanned using Aperio ScanScope and both the tumor and adjacent normal tissue were analyzed using the ImageScope cytoplasmic algorithm. Cytoplasmic localization patterns were observed in the pancreatic islets and staining intensity was varied depending on their location to the tumor. Overall, the result of this study is the first to demonstrate both PTHrP and its receptor using immunohistochemistry in benign, premalignant and malignant pancreatic tumors.

Disclosures: *Syu Mi Sam, None.*

MO0377

PTH Stimulation of RANKL in Primary Osteoblasts Is Independent of PTH-Stimulated cAMP. Thomas Estus*, Shilpa Choudhary, Carol Pilbeam, University of Connecticut, USA

Parathyroid hormone (PTH) can stimulate both bone formation and resorption. When PTH is given continuously, resorption is greater than formation and bone is lost. We showed that the osteogenic actions of continuous PTH *in vitro* are suppressed by a factor that blocks PTH-stimulated cAMP production in osteoblastic cells. The production of this factor is dependent on the expression of cyclooxygenase 2 (Cox2), the major enzyme regulating prostaglandin production. When we treated wild type (WT) and Cox2 knockout (KO) mice with PTH infusion for 12-21 days, we found that anabolic actions of PTH were suppressed in WT, but not KO mice. However, the PTH stimulation of bone resorption was the same in both WT and KO mice. We have identified the inhibitory factor *in vitro* as serum amyloid A 3 (Saa3) and shown that Saa3 is secreted by bone marrow macrophages (BMMs) treated with RANKL. In this study we use the conditioned media (CM) from RANKL-treated WT BMMs or a recombinant, human-homolog of murine Saa3 (SAA) to study the involvement of cAMP-activated signaling in the PTH induction of *Rankl*. We cultured primary osteoblasts (POBs) from neonatal calvaria to confluence (5 days), treated with PTH (10 nM) in the presence or absence of CM or SAA (10 µg/mL) for 3 h and measured gene expression by qPCR. SAA concentration was determined by dose response as measured by cAMP signaling inhibition. As expected, both CM and SAA blocked the PTH-stimulated gene expression of cAMP-regulated receptor activity modifying protein 3 (*Ramp3*). However, PTH stimulated *Rankl* expression was not decreased by CM or SAA. The protein kinase A (PKA) inhibitor, H-89, blocked PTH-stimulated *Ramp3* expression but had no effect on PTH-stimulated *Rankl* expression. PTH has also been shown to activate the protein kinase C (PKC) pathway, which subsequently signals via extracellular-signal-regulated kinases (ERKs). The PKC inhibitor GF109203X and the ERK inhibitor PD98059 both blocked PTH-stimulated *Rankl* expression but did not decrease PTH-stimulated *Ramp3*. The calcium chelation agent BAPTA also blocked PTH-stimulated *Rankl* expression. In conclusion, our results indicate that PTH-stimulated *Rankl* in POBs is independent of cAMP signaling and likely to depend upon the PKC pathway. These data support our PTH infusion study, which indicated that the anabolic and catabolic effects of PTH occur via different signaling pathways.

Disclosures: *Thomas Estus, None.*

MO0378

Osteogenic potential of FOP iPSC cell-derived endothelial cells. Emilie Barruet*¹, Marcela Morales¹, Iris Pennings², Debby Gawlitta³, Hannah Kim¹, Ashley Urrutia¹, Wint Lwin¹, Mark P. White⁴, Christina Theodoris⁴, Deepak Srivastava⁴, Edward C Hsiao¹. ¹University of California, San Francisco, USA, ²Department of Orthopaedics, University Medical Center Utrecht, Netherlands, ³Department of Orthopaedics, University Medical Center Utrecht, Utrecht, The Netherlands, ⁴Gladstone Institute of Cardiovascular Disease & University of California, San Francisco, USA, USA

Patients with mutations in the Activin A Type I receptor (ACVR1), a bone morphogenetic protein (BMP) receptor, develop the debilitating disease fibrodysplasia ossificans progressiva (FOP) with massive heterotopic ossification. Several studies have suggested that stem cells or osteoprogenitors from different tissues may be responsible for the heterotopic ossification, and that human endothelial cells (ECs) carrying the ACVR1 R206H mutation may contribute to the formation of FOP lesions. Our overall hypothesis is that activated BMP signaling caused by the ACVR1 R206H mutation in ECs increases heterotopic bone formation by activating osteogenesis. The recent advent of human induced pluripotent stem cells (iPSCs) provides an ideal opportunity to create human-specific models for FOP, particularly as primary cells are extremely difficult to isolate from FOP patients. Using a series of human iPSCs created from normal control and FOP donors, we previously showed that FOP iPSCs demonstrated increased mineralization and enhanced chondrogenesis. Here we show that the mineralizing FOP cultures have increased numbers of ECs

but no differences in mesenchymal stem cells (MSCs). To determine if the ACVR1 R206H mutation could lead to increased ECs formation we created iPSC-derived endothelial progenitor cells (iECs). CD31⁺/KDR⁺ iECs formed at equal yields of 20% from both control and FOP iPSC lines in standard culture conditions. However, we found that FOP iPSCs could form iECs at lower BMP4 concentrations compared to control iPSCs, even in conditions lacking BMP4 (1% FOP vs 0.1% WT yield). FOP iECs also expressed increased level of fibroblastic (FSP-1), chondrogenic (COL1A1 and COL2A1), and osteogenic (ALPL) markers. When cultured in osteogenic conditions, FOP iECs showed significantly increased alkaline phosphatase staining. Despite these signs of increased early cell fates favoring osteogenesis, FOP iECs showed little difference in mineralization using 2D or 3D assays to recapitulate endochondral bone formation. These studies show that the FOP ACVR1 activating mutation can activate two potential mechanisms for inducing heterotopic ossification: increasing EC formation and increasing expression of early osteogenic genes. The insights gained from these studies will help identify cellular targets for treating FOP and related diseases, while potentially identifying endogenous skeletal stem cells that could be activated for regenerative medicine.

Disclosures: *Emilie Barruet, None.*

MO0379

Response to treatment with bisphosphonates in McCune-Albright Syndrome: A case series. Natasha Appelman-Dijkstra*¹, Bas Majoor², Sander Dijkstra³, Neveen Hamdy³. ¹Leiden University Medical Center Netherlands, Netherlands, ²Leiden University Medical Center in the Netherlands, , ³Leiden University Medical Center, Netherlands

Introduction McCune-Albright syndrome (MAS) is a rare bone dysplasia due to a postzygotic mutation of the GNAS1-gene, characterized by a classical triad of polyostotic fibrous dysplasia (FD), café-au-lait patches and precocious puberty. Other endocrinopathies may be present. Patients with FD favourably respond to treatment with bisphosphonates, with decrease in bone pain associated with decreases in bone turnover and arrest of progression of bone lesions. Whether patients with MAS respond similarly to treatment with these agents remains to be established.

Patients & Methods We studied the effect of treatment with bisphosphonates in twelve patients with MAS (10 female) and aged 7-51 yrs, all of whom had precocious puberty (mean age 4.6yrs ± 3.6 SD) & 9 had café-au-lait patches. Mean duration of follow-up was 11.8 yrs (0.3-22yrs). Therapeutic objective was normalization of bone turnover and evaluation of the effect of this on pain symptoms.

Results Median age at time of diagnosis was 3.5 years ± 13.8 SD. Endocrinopathies included hyperthyroidism (n=3), growth hormone (GH) excess (n=3) and hyperprolactinemia (n=3). Ten patients (83%) had hypophosphatemia. Nine patients (75%) had at least one fracture (median 2/patient). GH-excess was adequately controlled before starting treatment. Dimethyl-APD (olpadronate) was administered in 11 patients (maximum dose 200 mg/d po or iv 4-8 mg for 3-5 days 3 monthly), and intermittent iv zoledronate in one patient, for variable duration of time aiming at normalization of bone turnover. After longer duration of treatment and use of higher cumulative doses of bisphosphonates, this was achieved in 7 patients (58%), 2 (17%) demonstrated a moderate decrease in bone-turnover, and there was no significant effect on bone-turnover in the 3 patients with GH-excess (27%). There was no adverse effect of treatment, and decreases in bone turnover were associated with corresponding improvement in bone pain.

Conclusion Our data demonstrate that patients with MAS require higher cumulative doses of bisphosphonates to achieve a clinical and biochemical response, and that those with GH-excess respond poorly to treatment, possibly because of the effect of GH-excess on the extent and severity of the skeletal manifestations. These findings suggest that GH-excess should be identified and treated early after the disease is diagnosed, and that bone-modifying treatment other than bisphosphonates may be required to control disease activity in these patients.

Disclosures: *Natasha Appelman-Dijkstra, None.*

MO0380

Clinical, Biochemical and Radiographic Spectrum of gene diagnosed X-linked Hypophosphatemia in Adults. Bo Wu*, Yan Jiang, Lijun Xu, Zhen Zhao, Ou Wang, Mei Li, Xiaoping Xing, Wei Yu, Weibo Xia. Peking Union Medical College Hospital Department of Endocrinology, China

X-linked hypophosphatemic rickets or osteomalacia (XLH) is congenital disease, characterized by renal phosphate wasting induced hypophosphatemia and defective mineralization of bones. Few studies focus on phenotype of XLH in adulthood. Therefore, this cross-sectional study systematically described anthropometric, clinical, biochemical and radiological features in 47 adult XLH patients. Similar to previous studies, adult XLH patients were characterized by short stature and disproportioned body proportion, as well as hypophosphatemia, elevated ALP, increased PTH concentration. The radiological spectrum illustrated more severe, prevalent and influential degenerative joint disease in hip than knee, the distribution of vertebral fracture and enthesopathy, both were rarely mentioned in previous study. Patients also showed elevated vertebra BMD, negatively affect by OPG and PTH, and decreased femur BMD, positively impacted by serum phosphate, and negatively affected by ALP and PTH. There is no genotype and phenotype association in adult XLH patients. Male patients presented with less osteoarthritis, higher calcium, ALP

and sclerostin than female. Lower upper body measurements and sitting height, higher PTH may indicate higher fracture risk. In a word, this is the largest study investigating clinical spectrum of adult XLH patients, proposed rarely reported radiologic characters and the biochemical factors affect BMD.

Disclosures: Bo Wu, None.

MO0381

Searching for Hypophosphatasia: Conditions Associated with Low Serum Alkaline Phosphatase in Children. Linda Dimeglio¹, Erik Imel², Marc Rosenman². ¹Indiana University School of Medicine, USA, ²Indiana University, USA

Hypophosphatasia (HPP) is a rare, inherited metabolic bone disorder caused by mutations in the *ALPL* gene and characterized by low serum alkaline phosphatase (ALP) activity. HPP can present clinically as mild to severe forms and is associated with five recognized phenotypes: perinatal, infantile, childhood, adult, and odontohypophosphatasia. The variety of phenotypic expression as well as low awareness of the disease among physicians can make diagnosing HPP difficult and nosology relatively subjective. Given the wide variety of presentations of HPP, many cases may be missed or misdiagnosed. We used a large multi-health system electronic medical record (EMR) database (through the Indiana Network for Patient Care) to identify children with low serum ALP values, in order to examine causes of persistent low ALP and to search for undiagnosed cases of HPP.

After IRB approval, we queried the database for children aged ≤ 18 years with available records from 1/1980-12/2012. 896,473 children had at least one ALP result. We then looked for those who had at least 2 low ALP levels (>10 U/L below the lower normal limit for age) separated by at least 6 months with records at our children's hospital or county hospital. 50 subjects met these criteria. 34 subjects (85% female, mean age 12.2 years, range 0-18 years) had EMRs with ICD-9 codes available for review. Four of these children had been diagnosed with HPP. Two additional cases had clinical characteristics suggestive of HPP (hypercalcemia, fracture, scoliosis) without evidence of prior or subsequent normal ALP values. The remaining 28 had other identifiable associated medical conditions including congenital heart disease (N=5, 1 post-transplant); gastrointestinal disease (N=3); end-stage renal disease (N=3, 2 post-transplant); acute lymphocytic leukemia (N=3); lupus (N=3), pregnancy (N=2, 1 with hyperemesis), cerebral palsy (N=2), anorexia (N=2), fatigue (N=1), Behcet's (N=1), histiocytosis (N=1, post-transplant), Marfan's (N=1), and hepatitis C (1). Several of these children had documentation of steroid use at the time the ALP was obtained.

When age-specific normal ranges are used, persistently low ALP is a relatively uncommon finding in the pediatric setting. Prior reports have identified early puberty, hypothyroidism, malnutrition, pernicious anemia, vitamin D toxicity, Wilson disease and zinc deficiency as causes of low ALP in addition to the diagnoses of HPP and malnutrition which we identified. Our investigation, therefore, adds to the list of conditions associated with persistently low serum ALP in children.

Disclosures: Linda Dimeglio, Alexion Pharmaceuticals
This study received funding from: Alexion Pharmaceuticals

MO0382

Validation of a Novel Scoring System, the Radiographic Global Impression of Change (RGI-C) Scale, for Assessing Skeletal Manifestations of Hypophosphatasia in Infants and Children. Michael P Whyte¹, Kenji P Fujita², Scott Moseley², David Thompson², William H McAlister³. ¹Shriners Hospital for Children, USA, ²Alexion Pharmaceuticals, USA, ³Department of Pediatric Radiology, Mallinckrodt Institute of Radiology, St. Louis Children's Hospital, USA

Purpose: Hypophosphatasia (HPP) is the rare inherited metabolic bone disease caused by loss-of-function mutations in the tissue nonspecific alkaline phosphatase (TNSALP) gene. Resultant TNSALP deficiency leads to extracellular excess of inorganic pyrophosphate, an inhibitor of bone mineralization. The rickets in infants and children has distinctive radiographic features. Here, we report the validity and reproducibility of a novel scoring system to quantify HPP-specific radiographic changes in pediatric patients (pts).

Methods: The Radiographic Global Impression of Change (RGI-C) is a 7-point ordinal scale (-3=severe worsening; 0=no change; +3=near/complete healing) designed to provide a comprehensive evaluation of skeletal health in pediatric pts with HPP. Sequential radiographic studies (chest [<5 years only], knees, and wrists) are assessed for improvement or worsening using age-specific ($<$ or ≥ 5 years of age) hallmarks of HPP developed by expert consensus. Features common to both age groups include metadiaphyseal sclerosis, apparent physeal widening, and metaphyseal radiolucencies and/or fraying. Age-specific features include gracile and/or absent bones and chest deformity for pts <5 years, and osteopenia, "popcorn calcification", and physeal corner defects for pts ≥ 5 years. Inter- and intra-rater agreements for 6 raters across 3 treatment studies were assessed using intraclass correlation coefficients (ICC) and weighted kappa coefficients (KC). Concurrent validity was assessed via correlation between RGI-C scores and simultaneous changes from baseline in: 1) Rickets Severity Scale (RSS)¹; 2) Pediatric Outcomes Data Collection Instrument (PODCI) Global Function scale; 3) Child Health Assessment Questionnaire (CHAQ)

Disability Index; 4) 6 Minute Walk Test (6MWT); and 5) height z-scores, in children ≥ 5 years.

Results: ICC revealed moderate-to-good inter-rater agreement for pts <5 years (0.65, 227 radiographs; $p<0.0001$) and pts ≥ 5 years (0.57, 136 radiographs; $p<0.0001$). Most raters achieved substantial ($n=4$, KC >0.6) or almost perfect ($n=4$, KC >0.8) intra-rater agreement ($n=1$, moderate agreement, KC >0.5). The linear regressions revealed significant correlations with RSS, PODCI Global Function, CHAQ Disability Index, 6MWT, and height z-scores (Table 1).

Conclusion: The RGI-C scale is a reproducible and valid measure for assessing over time clinically important changes in skeletal manifestations of HPP in pediatric patients.1. Thacher, *J Trop Ped* 2000

Table 1. Correlations between RGI-C and changes from baseline in other clinical outcomes in patients with HPP

| Measure | Number of data points | Pearson correlation (r) | p-value |
|------------------------|-----------------------|-------------------------|-----------|
| Rickets Severity Scale | 135 | -0.664 | <0.0001 |
| PODCI Global Function | 84 | 0.595 | <0.0001 |
| CHAQ Disability Index | 84 | -0.589 | <0.0001 |
| 6-Minute Walk Test | 100 | 0.284 | 0.0043 |
| Height Z-score | 108 | 0.261 | 0.0065 |

Correlations between RGI-C and changes from baseline in other clinical outcomes in patients with HPP

Disclosures: Michael P Whyte, Honoraria, research grant, travel support
This study received funding from: Alexion Pharmaceuticals

MO0383

⁶⁸Ga-DOTATATE for tumor localization in Tumor-induced Osteomalacia. Diala El-Maouche¹, Samira Sadowski², Lori Guthrie³, Candice Cottle-Delisle², Roxanne Merkel², Corina Millo⁴, Clara Chen⁴, Electron Kebebew², Michael Collins⁵. ¹University of Miami/ National Institutes of Health/NIDCR, USA, ²NIH/NCI, USA, ³NIH/NIDCR, USA, ⁴NIH/CC, USA, ⁵NIH/NIDCR, USA

Purpose:

Evaluate the use of ⁶⁸Ga-DOTATATE for tumor localization in Tumor-induced osteomalacia (TIO).

Background:

Tumor-induced osteomalacia (TIO) is a paraneoplastic disorder caused by small mesenchymal tumors that produce high levels of the hormone fibroblast-growth-factor 23 (FGF23). Complete surgical resection leads to cure, however these tumors are notoriously difficult to locate, often due to their small size.

In a recent NIH series, successful localization was achieved in only 61% of patients even with a combination of localization studies that included two functional imaging modalities (¹¹¹In- pentetreotide -SPECT/CT (octreotide) and FDG-PET/CT), anatomical localization studies, and as needed, selective venous sampling¹. Recent case reports and a small series suggest ⁶⁸Ga-DOTANOC or DOTATATE may be useful at identifying tumors, but these have not been compared to conventional studies^{2,3}. In this series, we compared ⁶⁸Ga-DOTATATE PET/CT vs. octreotide SPECT/CT and FDG-PET/CT scan in a series of 12 patients with presumed TIO.

Methods and Results:

Twelve patients (7 female, 5 males) with TIO diagnosed on clinical and biochemical presentation and who had previously failed localization elsewhere were enrolled in an NIH IRB-approved study and underwent imaging for tumor localization (Table 1). The tumor was successfully localized and resected in 4/12 (33.3%) patients, not localized in 6/12 (50%), localized and pending surgical resection in 1/12, and found to be metastatic in 1/12. ⁶⁸Ga-DOTATATE imaging correlated with octreotide imaging in 10/12 (83.3%), and was more sensitive than octreotide in 2/12. However in these 2 subjects in whom results were confirmed upon surgical resection, the tumors were visualized on FDG-PET.

Conclusion:

In two cases, ⁶⁸Ga-DOTATATE found the lesions not seen on octreotide, but no tumors were localized on ⁶⁸Ga-DOTATATE scanning that were not localized on a combination of octreotide and FDG-PET scans. Limitations of this study include small sample size. Future studies, including larger patient sample, and possibly DOTANOC, are needed to assess the utility of DOTATATE or DOTANOC compared to existing imaging modalities.

References:

- Chong WH, Andreopoulou P, Chen CC, et al. Tumor localization and biochemical response to cure in tumor-induced osteomalacia. *J Bone Miner Res* 2013;28:1386-98.
- Clifton-Bligh RJ, Hofman MS, Duncan E, et al. Improving diagnosis of tumor-induced osteomalacia with Gallium-68 DOTATATE PET/CT. *The Journal of clinical endocrinology and metabolism* 2013;98:687-94.
- Naswa N, Sharma P, Kumar R, Malhotra A, Bal C. Successful localization of residual culprit tumor in a case of tumor-induced osteomalacia using ⁶⁸Ga-DOTANOC PET/CT. *Clinical nuclear medicine* 2013;38:639-40

MO0385

Muscle Function in Osteogenesis Imperfecta Type IV. Louis-Nicolas Veilleux*¹, Francis H. Glorieux², Frank Rauch². ¹McGill University/Shriners Hospital for Children-Canada, Canada, ²Shriners Hospital for Children-Canada, Canada

Context: Osteogenesis imperfecta (OI) is a heritable bone fragility disorder that is caused by mutations affecting collagen type I. In addition to bone fragility, we recently showed that patients with the mildest form of OI (OI type I) have muscle weakness. However, there is presently little information on muscle function in more severe forms of OI, such as OI type IV. Objective: The objective of the current study was to investigate upper- and lower-limbs muscle function in children and adolescents with OI type IV and to compare it to OI type I and healthy age- and sex-matched controls. Patients and Other Participants: Forty-four patients with OI type IV (21 females; mean age [SD]: 12.7 years [3.8]) were compared to 42 patients with OI type I (mean age [SD]: 12.6 years [3.8]) and 42 healthy age- and gender-matched controls (mean age [SD]: 12.6 years [3.9]). Main Outcome Measures: Upper-limbs muscle force was tested with grip strength dynamometer. Lower extremity muscle force and power were measured by five mechanography tests. Results: Patients with OI type IV had an average grip strength Z-score of -1.2 for the left hand and -1.6 for the right hand, compared to healthy age and sex reference data. Lower limb muscle power was 20% lower in patients with OI type IV compared to patients with OI type I ($p < 0.001$) and 25% lower compared to age- and sex-matched controls ($p < 0.001$). Lower limb muscle force was 5% lower in patients with OI type IV compared to patients with OI type I ($p = 0.45$) and 25% lower compared to age- and sex-matched controls ($p = 0.01$). Conclusions: Patients with OI type IV have a generalized muscle function deficit compared to healthy controls. Such patients might benefit from a physical training intervention as an adjunct therapy.

Disclosures: Louis-Nicolas Veilleux, None.

MO0386

A heterozygous missense mutation p.His381Arg identified in a patient with a childhood form of hypophosphatasia. Anna Petryk*¹, Lynda Polgreen², Kenneth Beckman³, Amy Calhoun⁴. ¹University of Minnesota, USA, ²Division of Pediatric Endocrinology & Metabolism, Los Angeles Biomedical Research Institute at Harbor-UCLA Medical Center, USA, ³University of Minnesota Genomics Center, USA, ⁴Department of Pediatrics, Division of Genetics & Metabolism, University of Minnesota Masonic Children's Hospital, USA

Background: Hypophosphatasia (HPP) is a rare inherited disorder characterized by low level of tissue-nonspecific alkaline phosphatase (ALP) due to loss-of-function mutations in the ALPL gene. The disease has a wide spectrum of clinical presentation, including the perinatal (usually lethal), infantile, childhood and adult forms. Much remains to be learned about the types of pathogenic mutations in patients with various forms of HPP and their clinical implications. Objective: To describe the clinical course in a patient with childhood HPP and to identify the underlying mutation. Methods: Targeted next generation sequencing of ALPL was performed. Genomic DNA was extracted from the blood sample. Sequencing libraries were prepared and sequence capture performed according to Illumina protocols utilizing the TruSight One Sequencing Panel. The enriched DNA libraries were sequenced on an Illumina HiSeq 2500 instrument. Raw sequencing reads were mapped to the reference genome using Burrows-Wheeler Alignment. Point mutation and indel calls in exons and adjoining intronic regions were made using the GATK Unified Genotyper. Results: The patient is a 3.9 years old boy who presented with premature loss of primary teeth starting at 2.5 years of age. His growth has been normal (height and growth velocity at the 49th percentile). He began walking at 14 months; has had no history of fractures, gait abnormalities, bone pain, or poor muscle tone. His mother also has a low ALP level, but has no history of fractures, bone pain, or premature loss of teeth. His father has a normal ALP level. Maternal great-grandmother had rickets in her youth. Paternal grandmother started wearing dentures in her 40s. He had low ALP level (59 U/L, normal range 110-320), elevated urine phosphoethanolamine, markedly elevated vitamin B6, normal calcium, phosphorus, and vitamin D levels, low PTH level, and no evidence of rickets on a hand radiograph. A heterozygous missense mutation c.1142A>G (p.His381Arg) was identified in ALPL. This mutation (previously reported as p.H364R) has been reported in conjunction with a second missense ALPL mutation in one case of a lethal autosomal recessive hypophosphatasia. Conclusion: p.His381Arg mutation can occur not only in a lethal autosomal recessive HPP, but also a mild, presumably autosomal dominant, form due to haploinsufficiency. Molecular analysis of other family members may help to clarify the inheritance pattern and clinical presentation of this mutation.

Disclosures: Anna Petryk, None.

Table 1. Characteristics and Imaging Results of 12 Patients with Tumor-induced Osteomalacia

| Sex (age of onset) | ⁶⁷ Ga-DOTATATE | Ocetreotide | FDG-PET | Outcome | Intact PTH ²³ (pg/mL)* |
|--------------------|---------------------------|-----------------------|-----------------------------|-----------------|-----------------------------------|
| 1. Male (60) | Negative | Negative | Negative | Not found | - |
| 2. Male (19) | Right acetabulum | Negative | Right acetabulum | Cured | 1787 |
| 3. Male (43) | Right hip | Right hip | Right hip | Cured | 1063 |
| 4. Male (38) | Metastatic | Metastatic | Metastatic | Widespread | 5939 |
| 5. Female (21) | Negative | Negative | Right foot (false positive) | Not found | 860 |
| 6. Female (52) | Left femur | Negative | Left femur | Cured | 1156 |
| 7. Female (44) | Negative | Negative | Negative | Not found | 218 |
| 8. Male (47) | Right inferior pelvis | Right inferior pelvis | Negative | Cured | 1515 |
| 9. Female (27) | Left maxilla | Left maxilla | Negative | Pending surgery | 105 |
| 10. Female (56) | Negative | Negative | N/A | Not found | 83 |
| 11. Female (17) | Negative | Negative | Negative | Not found | 353 |
| 12. Female (48) | Non-specific | Negative | Negative | Not found | 286 |

*Reference range in normal subjects using a similar assay established as 10-60 pg/mL. Shaded area denotes discrepant result between ⁶⁷Ga-DOTATATE and ocetreotide

Table 1. Characteristics and Imaging Results of 12 Patients with Tumor-induced Osteomalacia

Disclosures: Djalal El-Maouche, None.

MO0384

Pain Resulting from Unresolved Skeletal Disease has a Significant Impact on the Daily Function of Adults with X-linked Hypophosphatemia (XLH). Alison Skrinar, PhD*¹, Ayla Marshall², Javier San Martin, MD², Melita Dvorak-Ewell, PhD², Carolyn Macica, M.S., PhD³. ¹Ultragenyx Pharmaceutical, USA, ²Ultragenyx Pharmaceutical Inc., USA, ³Frank H. Netter School of Medicine Quinnipiac University, USA

Background: X-linked Hypophosphatemia (XLH) is a disorder of renal phosphate wasting and defective bone mineralization caused by high circulating levels of fibroblast growth factor 23 that impair normal phosphate reabsorption in the kidney. The disorder presents in childhood with hypophosphatemia leading to rickets and bowing of the legs that is treated with oral phosphate and vitamin D metabolites. Despite treatment, many skeletal defects remain unresolved and lead to significant complications in adulthood. Progressive osteomalacia with associated pseudofractures and bone and joint pain are common, particularly in the lower extremities. Objective: The primary objective of the study was to characterize disease burden in adults with XLH. Methods: An IRB-approved, web-based questionnaire was completed by adults with XLH to evaluate disease history, current clinical conditions and resulting symptoms and complications. Patient-reported pain and disability were assessed using the Brief Pain Inventory (BPI), Western Ontario and McMaster Osteoarthritis Index (WOMAC), and SF-36v2 Health Survey. Results: 195 responders from 16 countries, primarily the US (70%), with a mean age of 46 years (range: 18 – 74) completed the survey. Gait disturbance was common (86%) with 31% using a walking device. A history of fractures was reported by 86/195 (44%) of responders with the most common fracture locations being the femur (18%), feet (14%) and tibia/fibula (14%), which is likely due to the stress of weight bearing. The majority of responders had experienced joint pain (89%) and bone pain (73%) in the lower extremities in the past year that led to regular pain medication use by 69%, including 20% taking opiates. BPI Pain Severity and Pain Interference were measured using an 11-point VAS with 10 as the maximum possible score. Mean BPI Pain Severity and Pain Interference scores were 3.6 and 4.1, respectively, indicating bone pain in the moderate range that interferes with daily activities, such as walking and working. BPI findings were supported by WOMAC Pain and Physical Function scores, as well as SF-36 Physical Component Summary (PCS) and Bodily Pain (BP) scores which indicated significant pain and burden relative to US general population norms. Conclusion: Adults with XLH experience lower extremity bone and joint pain that is readily detectable on various validated measures and significant enough to interfere with daily function.

Disclosures: Alison Skrinar, PhD, Ultragenyx Pharmaceutical Inc. This study received funding from: Ultragenyx Pharmaceutical Inc.

MO0387

Analysis of classical and non-classical Fibrodysplasia Ossificans Progressiva mutations using human induced pluripotent stem cells. Laura Hildebrand^{*1}, Bella Rossbach², Andreas Kurtz³, Manfred Gossen⁴, Harald Stachelscheid⁵, Petra Seemann². ¹Charité - Universitätsmedizin Berlin, Germany, ²Charité- Universitätsmedizin Berlin, Berlin-Brandenburg Center for Regenerative Therapies (BCRT), Berlin, Germany, Germany, ³Seoul National University, College of Veterinary Medicine & Research Institute for Veterinary Science, Seoul, Republic of Korea, Charité – Universitätsmedizin Berlin, Berlin-Brandenburg Center for Regenerative Therapies (BCRT), Berlin, Germany, Germany, ⁴Berlin-Brandenburg Center for Regenerative Therapies (BCRT) Berlin, Helmholtz-Zentrum Geesthacht (HZG), Institute of Biomaterial Science, Teltow, Germany, Germany, ⁵Charité- Universitätsmedizin Berlin, Berlin-Brandenburg Center for Regenerative Therapies (BCRT), Berlin, Germany, Berlin Institute of Health, Berlin, Germany, Germany

Fibrodysplasia Ossificans Progressiva (FOP) is a rare autosomal dominant disorder. Patients appear to be healthy at birth, except for malformed big toes. Starting in childhood, they develop endochondral bone replacing skeletal muscles, tendons and ligaments. This heterotopic ossification can be triggered by viral illnesses, accidents, surgical interventions or even might start spontaneously.

FOP is caused by different gain-of-function mutations in the Bone Morphogenetic Protein (BMP) receptor ACVR1, which lead to constant downstream signaling. The majority of FOP patients carry the R206H mutation located in the GS domain of the receptor. But also other FOP mutations in ACVR1 are described that are predominantly located in the kinase domain. It seems that the different mutations have distinct activation mechanisms. Establishing induced pluripotent stem cells (iPSC) for every FOP mutation is difficult, as some mutations are very rare and patient samples are not always readily available. Furthermore, the genetic backgrounds vary, complicating a direct comparison.

In this study, we apply a newly established stem cell tool, which uses an avian receptor to transduce iPSC with an avian leucosis virus carrying the ACVR1 variants. The avian receptor was introduced via a PiggyBac transposon, leading to a new hiPSC line stably expressing the avian receptor gene, while retaining pluripotency. These iPSC⁺ are infected with ACVR1 variants, carrying FOP mutations in the GS domain (R206H, Q207D) and kinase domain (G356D, G328E, G328W, G328R), respectively. This strategy allows the analysis and comparison of different ACVR1 mutations on the common genetic background of hiPSC⁺.

The functionality of this new stem cell tool will be validated with two FOP patient derived iPSC cell lines, carrying the classical R206H mutation, generated in our laboratory. To this end, a primary cell culture isolated from urine was reprogrammed using Sendai virus technology. We conclude that our iPSC⁺ tool will enable a more reliable biochemical characterization and comparison of different disease-causing mutations in ACVR1. Notably, this novel strategy can also be applied to other monogenetic diseases, as the viral gene delivery system enables an efficient overexpression of the genes of interest generating pluripotent cells with a common genetic background.

Disclosures: Laura Hildebrand, None.

MO0388

Cranial base defects in a mouse model of Hereditary Multiple Exostoses are associated with ectopic hedgehog signaling. Federica Sgariglia^{*1}, Paul Billings², Hyo-Bin Um², Kevin Jones³, Eiki Koyama², Maurizio Pacifici². ¹Children's Hospital of Philadelphia, USA, ²CHOP, USA, ³University of Utah, USA

Hereditary Multiple Exostoses (HME) is a pediatric autosomal-dominant disorder caused by mutations in the heparan sulfate (HS) synthesizing enzymes EXT1 or EXT2. Thus, HME patients are HS-deficient and characterized by the presence of numerous benign cartilaginous tumors –exostoses- forming next to the growth plates of axial and appendicular skeletal elements, including long bones and ribs. However, exostoses have not been described in the craniofacial skeleton, despite the fact that it contains several endochondral structures. Hence, we focused on the cranial base and in particular its synchondroses. These structures contain dual mirror-image growth plates, responsible for antero-posterior cranial base elongation and are flanked by intracranial and sub-cranial perichondrium. Indeed, several exostosis-like masses formed along the sphenoidal and occipital synchondroses of conditional Ext1-deficient mice (Ext1^{fl/fl};Col2CreER) injected with tamoxifen at P10. In the mutants, the occipital bone also was deformed, the cranial base was shorter and thinner, and the synchondrosis growth plates exhibited fewer resting and proliferative chondrocytes and an irregular columnar organization. These events were accompanied by deranged expression of typical growth plate chondrocyte markers including Sox9 and aggrecan as well as reduced expression of two HS-rich proteoglycans: Perlecan and Syndecan 3. To uncover additional mechanisms, we examined hedgehog signaling in Ext1-deficient mice in a Gli1LacZ reporter background. LacZ activity was stronger and widespread along mutant synchondrosis perichondrium and within growth plate at early stages and thus, preceded exostosis formation at later time points. Ectopic hedgehog signaling occurred also in mutant growth plates of limb and trunk elements

and was thus systemic. Treatment with a Smoothed inhibitor partially rescued the mutant phenotype, confirming involvement and active role of Hh signaling. Levels of immuno-detectable Noggin were significantly decreased in mutant perichondrium and growth plates as well, particularly in perichondrial cells facing the intracranial space. In sum, our data reveal that the skull is also affected by Ext1 deficiency and displays large exostosis-like masses whose formation appears to be linked to aberrant Hh and BMP signaling. We are currently re-examining radiographic skull scans from HME patients to determine whether analogous craniofacial skeletal defects are present.

Disclosures: Federica Sgariglia, None.

MO0389

Deformed cranial morphologies are caused by the combined roles of the maldevelopment of calvarias, cranial base and brain in FGFR2-P253R mice. Yangli Xie¹, Xiaolan Du^{*2}, Fengtao Luo², Wei Xu², Junlan Huang², Siru Zhou², Zuqiang Wang², Wanling Jiang², Lin Chen². ¹Third Military Medical University, Peoples republic of china, ²Center of Bone Metabolism & Repair, Department of Rehabilitation Medicine, State Key Laboratory of Trauma, Burns & Combined Injury, Trauma Center, Institute of Surgery Research, Daping Hospital, Third Military Medical University, China

Apert syndrome(AS) is a most common genetic craniosynostosis syndrome in humans. Apert mouse model (Fgfr2+P253R) showed abnormalities in sutures, cranial base synchondroses and cerebrum. They may all be involved in the pathogenesis of skull malformation in AS. In this study, to distinguish the differential roles of these components of head in the pathogenesis of abnormal skull morphology of AS, we generated mouse models with specific expression of mutant FGFR2 in chondrocytes, osteoblasts, and central nerve cells by breeding FGFR2-P253R-neo mice with Col2a1-Cre, Osteocalcin-Cre (OC-Cre), and Nestin-Cre mice, and quantitatively compared the skull morphologies of these mutant mice with their littermates using EDMA (Euclidean distance matrix analysis) analysis. Col2a1-Fgfr2+/P253R mouse skulls showed shortened skull dimensions along the rostrocaudal axis, and craniofacial malformation with shortened nasal, as well as evidently advanced ossification of cranial base synchondroses. In OC-Fgfr2+/P253R mice, their skulls showed malformation in orbit and front of face. Nestin-Fgfr2+/P253R mice showed increased height on the posterior of neurocranium. Our study indicates that the abnormal skull morphologies of AS are caused by the combined results of the maldevelopment in cranial sutures, and the endochondral growth of cranial base, and central nervous system. These findings further deepen our knowledge about the pathogenesis of skull morphologies of AS, and provide some new clues for the future analyses of skull phenotypes and clinical management of AS.

Disclosures: Xiaolan Du, None.

MO0390

Evaluation of FGF23 Levels and Related Factors in a Patient with Hereditary Vitamin D Resistant Rickets. Keiko Yamamoto^{*1}, Makoto Fujiwara², Yasuhisa Ohata², Taichi Kitaoka², Takuo Kubota², Noriyuki Namba², Toshimi Michigami³, Sachiko Kitanaka⁴, Takehisa Yamamoto⁵, Keiichi Ozono². ¹Osaka University, Japan, ²Department of Pediatrics, Osaka University Graduate School of Medicine, Japan, ³Department of Bone & Mineral Research, Osaka Medical Center & Research Institute for Maternal & Child Health, Japan, ⁴Department of Pediatrics, The University of Tokyo, Japan, ⁵Department of Pediatrics, Minoh City Hospital, Japan

1, 25(OH)₂D is a critical inducer of FGF23 expression, but several other factors such as serum Ca and intact PTH are also suggested to have effects on FGF23 levels. Hereditary vitamin D resistant rickets (HVDRR) is a rare disease caused by loss-of-function mutations in the VDR gene. Here we evaluated the change in levels of FGF23 and the other factors in a HVDRR patient with no functional VDR. The patient was a two-year-old girl, when her serum alkaline phosphatase was found to be elevated by chance. The further examination revealed hypocalcemia and secondary hyperparathyroidism without vitamin D deficiency: serum calcium (Ca) 7.7 mg/dl, phosphate (P) 3.0 mg/dl, intact PTH 576 pg/ml, 25(OH)₂D 20.1 ng/ml, 1, 25(OH)₂D 137 pg/ml. She had alopecia and radiographical signs of rickets. A homozygous p.R73X mutation in the DNA-binding domain of the VDR was detected. Initial treatment with oral active vitamin D and calcium had little effects. By increasing the dose of oral calcium without vitamin D, first her serum Ca became normal, and then intact PTH and Pi levels became normal and intact FGF23 levels started to increase. Rachitic change was improved and her IGF-1 level increased with accelerated height velocity. Her renal function was normal throughout our observation. We analyzed the correlation of intact FGF23 with serum Ca, Pi, intact PTH, 1, 25(OH)₂D, IGF-1 (evaluated by standard deviation score), Kaup index and uremic acid because their correlation were previously reported. We analyzed the data from 3y3m to 4y4m using the intact FGF23 level of 3y3m as 10 pg/ml, which is the resolution threshold. We evaluated the correlation of intact FGF23 with the parameters by parametric analysis (Pearson correlation test) and non-parametric analysis (Spearman's rank correlation coefficient), and found significant correlation with IGF1 (SD) and Kaup index (p<0.05). Then, we performed multiple regression analysis by the stepwise procedure

to evaluate the association of intact FGF23 with them, using IGF1, Kaup index and one more parameter; serum Ca, P, intact PTH, 1,25(OH)₂D and uremic acid. The result showed that IGF1 and serum P were the significant parameter (p=0.043, p=0.0384, respectively) and their partial regression coefficient levels were 0.932 and 0.304, respectively. These results suggested that FGF23 can be produced without VDR function and that IGF1 has some correlation with intact FGF23 as well as serum P.

<Laboratory data>

| Age | 2y7m | 2y8m | 2y10m | 3y | 3y1m | 3y3m | 3y6m | 3y8m | 4y1m | 4y4m |
|--|-------|-------|-------|-------|-------|-------|-------|-------|-------|-------|
| FGF23 (pg/ml) | <10 | <10 | <10 | <10 | <10 | <10 | 12 | 25 | 45 | 49 |
| Ca (mg/dl) | 7.4 | 8.2 | 9.3 | 8.7 | 9.1 | 9.5 | 9.3 | 9.8 | 9.4 | 9.8 |
| P (mg/dl) | 2.8 | 2.3 | 3 | 2.9 | 3.6 | 3.6 | 5.5 | 5.4 | 5.1 | 5.1 |
| PTH (pg/ml) | 792.3 | 340.2 | 119.2 | 79 | 103.3 | 75.9 | 35.5 | 21.4 | 27.8 | 20.2 |
| 1,25(OH) ₂ D ₃ (pg/ml) | 1380 | 1860 | 2150 | 1370 | 629 | 72 | 20 | 6 | 6 | 6 |
| ALP (U/L) | 7788 | 5463 | 5924 | 3866 | 2863 | 2298 | 1365 | 1101 | 1403 | 1217 |
| IGF1 (SD) | -1.47 | -1.73 | -1.27 | -2 | -1.49 | -1.16 | -1.52 | -1.12 | -0.43 | -0.16 |
| Kaup index | 17.3 | | 16.9 | 17.8 | 17.4 | 17.6 | 17 | 16.5 | 16.2 | 15.7 |
| Uremic acid (mg/dl) | 2.1 | 3.5 | 3.3 | 3.6 | 3.6 | 3 | 2.9 | 4.3 | 3.8 | 3.8 |
| serum Cre (mg/dl) | 0.13 | 0.18 | 0.19 | 0.17 | 0.18 | 0.2 | 0.2 | 0.24 | 0.27 | 0.29 |
| eGFR (ml/min/1.73m ²) | 316 | | 224.6 | 247.8 | 240.1 | 217.2 | 227.1 | 195.7 | 182.1 | 175.4 |
| cystatin C (mg/l) | 0.66 | | 0.66 | 0.68 | 0.66 | 0.77 | 0.66 | 0.79 | 0.89 | 0.85 |

laboratory data

Disclosures: Keiko Yamamoto, None.

MO0391

Fracturing Without Apparent Skeletal Pathobiology In Congenital Insensitivity to Pain Caused By A Second Heterozygous Mutation in *SCN11A*. Voraluck Phatarakijirund*¹, Steven Mumm¹, William H McAlister², Deborah Novack¹, Deborah Wenkert³, Karen L. Clements³, Michael P Whyte³. ¹Washington University School of Medicine, USA, ²Department of Pediatric Radiology, Mallinckrodt Institute of Radiology at St. Louis Children's Hospital, Washington University School of Medicine, USA, ³Center for Metabolic Bone Disease & Molecular Research Shriners Hospitals for Children - St Louis, USA

Congenital insensitivity to pain (CIP) refers to the rare heritable disorders that feature inability to feel pain and no evidence of peripheral neuropathy. Although bone and joint complications are common in CIP, detailed biochemical studies of mineral and skeletal homeostasis and bone histopathology have not been reported. In 2013, a first and specific heterozygous gain-of-function mutation in *SCN11A* encoding voltage-gated sodium channel 1.9 (Nav1.9) was identified in three unrelated sporadic cases, thereby establishing a distinctive type of CIP. Each individual suffered multiple painless fractures, self-inflicted injuries, repeated self-mutilation causing un-healing wounds, chronic diarrhea, and hyperhidrosis. We studied CIP in a family (mother and her two children) including physical examination, biochemical studies, and radiological imaging with dual-energy X-ray absorptiometry (DXA). Genomic DNA from whole blood was PCR-amplified and sequenced in the children (mother's DNA unavailable) at each of the 26 coding exons and adjacent mRNA splice sites of *SCN11A*. The mother, first evaluated at age 10 years, had multiple fractures (primarily of her lower extremities) beginning at age two years, Charcot deformity of both ankles, and hypermobility of all joints. Her nerve conduction velocity and electromyography were normal. Her children were first studied at 1.5 and 3.5 years-of-age for recurrent major fractures and joint hypermobility. All three individuals had chronic diarrhea. The mother had excoriated right external nares, and both children had severe excoriation and hypertrophic scars of the posterior neck from repeated scratching. The daughter had hyperhidrosis. Skin collagen studies of the son showed normal results. Radiographs of each person revealed old fractures and deformities. However, BMD Z-scores for lumbar spine and total hip, biochemical parameters of mineral and skeletal homeostasis, and iliac crest histopathology of the mother (after *in vivo* tetracycline labeling) all were normal. Mutation analysis revealed a unique heterozygous missense mutation in exon 23 (c.3904C>T, p.Leu1302Phe) of *SCN11A*. This variant was absent in the SNP database, and is evolutionarily conserved. Our report is the first autosomal dominant CIP confirmed by mutation analysis. We discovered in the family the second mutation in *SCN11A*. Joint hypermobility is a novel manifestation. How mutation of Nav1.9 leads to significant skeletal disease remains unexplained. Lack of awareness of injury is typically offered as an explanation for the fractures. Indeed, normal biochemical, radiological, and histological studies in this family fail to indicate intrinsic skeletal pathobiology. We, however, hold open the possibility for intrinsic skeletal disease with poor bone quality underlying the skeletal complications of CIP.

Disclosures: Voraluck Phatarakijirund, None.

MO0392

Induced Pluripotent Stem Cell (iPSC) Derived Mesenchymal Stem Cells (MSCs) for Studying Pathogenic Bone Formation in Spondyloarthritis (SpA). Gerlinde Layh-Schmitt*¹, Shajia Lu², Stephen R. Brooks², Emily Lazowick³, Massimo Gadinà², Robert A. Colbert³. ¹National Institutes of Health, USA, ²Translational Immunology Section, Office of Science & Technology, NIAMS, NIH, USA, ³Pediatric Translational Research Branch, NIAMS, NIH, USA

Many genes and cell types contribute to the axial inflammation, trabecular bone loss, and aberrant bone formation that result in ankylosing spondylitis (AS). However, the functional consequences of genetic variants may be manifest in certain cell types that are not readily accessible. Therefore, we generated iPSCs by reprogramming fibroblasts from SpA patients and healthy controls (HC) and differentiated them into MSCs and osteoblasts (OB) with the goal of identifying disease-related differences. MSCs were generated from iPSCs using a TGFB inhibitor. Gene expression patterns and expression of AS risk genes were compared by RNA-Seq in iPSCs, MSCs and blood. Expression of selected genes involved in bone formation and inflammation was determined in MSCs after treatment with IFN γ (I), TNF α (T) or both (I&T) using Nanostring. Expression of osteogenic genes during OB differentiation was also measured by Nanostring, while mineralizing capacity was determined by Alizarin staining. iPSCs, MSCs and blood cells showed cell type-specific gene expression patterns. Many AS risk genes were robustly expressed in blood (e.g. HLA-B, ERAP1 and ERAP2) and MSCs (e.g. ANTXR2, EDIL3). Patient derived MSCs exhibited up to 10 fold higher expression levels of IL-1 α and IL-6 at baseline compared to HC. MSCs were treated with pro-inflammatory cytokines known to be involved in AS pathogenesis. After T or I&T treatments, IL-1 α was 10-16-fold higher, and IL-1 β and IL-6 5-10-fold higher in patient cells compared to HC. OBs from patients exhibited a 3-fold higher mineralization capacity than the HC and 10-20 times higher expression levels of alkaline phosphatase (ALP) during osteoblastogenesis.

In summary, we have differentiated SpA-patient-derived MSCs, and OBs from iPSCs. Notably, MSCs from patients expressed higher levels of IL-1, IL-6 and ALP mRNA at baseline and in response to T or I&T compared to HC. Patient OBs demonstrated greater mineralization capacity, correlating with higher levels of ALP. These experiments were conducted with two patient derived lines (one derived twice in two independent laboratories) and one healthy control (derived twice). We are presently generating more lines in order to determine if this effect is generalizable, and can be used to unravel the underlying mechanisms. Expression of certain AS risk genes predominantly in MSCs underscores the potential for iPSC-derived cells as a powerful system to examine functional consequences of predisposing genes in AS.

Disclosures: Gerlinde Layh-Schmitt, None.

MO0393

Inflammatory Cytokines are Potent Mediators of Ectopic Ossification Caused by a Novel Sca-1+CD73+ Cell Type in Tissue Engineered Skeletal Muscle. Owen Davies*¹, Mark Lewis¹, Liam Grover², Yang Liu¹. ¹Loughborough University, United Kingdom, ²University of Birmingham, United Kingdom

Heterotopic ossification (HO) is a debilitating condition defined by the de novo formation of bone within non-osseous soft tissues following trauma. Currently, the underlying mechanisms of pathogenesis remain elusive. However, identifying the role of cytokines up-regulated during the initial stages of trauma is likely to be important for HO prediction and the development of future therapies. Our study utilised a novel *in vitro* model of skeletal muscle to define the relationship between post-traumatic inflammation and ectopic ossification. A muscle model was developed by seeding C2C12 myoblasts within a type-I collagen gel. Uniaxial tension was produced by anchoring the gel at opposing ends of a well plate using polyethylene flotation bars. The model was cultured with high glucose DMEM and 20% FBS for 4 days, after which FBS was replaced with 2% horse serum to facilitate myoblast fusion along the axis of tension. After myotube formation the model was exposed to combinations of osteogenic factors and inflammatory cytokines previously identified following trauma. Cytokine combinations were established using Minitab design of experiment. Cells were released from constructs using 0.1% collagenase, and phenotypic reversion analysed using flow cytometry for stem/progenitor markers Sca-1, CD73, CD90 and CD105. Cells were plated at 10x10⁵ per cm² in growth medium, and ossification visualised using alizarin red staining. We identified a population of skeletal muscle cells that did not contribute to myogenesis, and showed that exposure of these cells to PDGF led to ectopic ossification. In fact, exposure to PDGF led to significantly (P<0.05) more mineral deposition than BMP-2. The presence of osteogenic inducers caused phenotypic reversion to a novel Sca-1+CD73+ cell type capable of ossification after just 24hrs. However, we present novel data showing that ectopic ossification was mediated in the presence of an inflammatory environment. In conclusion, our study identified the presence of a novel osteogenic/non-myogenic population of skeletal muscle cells. This cell type has never before been identified, and may have a pathological role in HO. Additionally, we identified that the local inflammatory environment may act to modulate the response of this particular cell population in

skeletal muscle in the presence of osteogenic inducers. This has highly important implications when considering the current use of non-steroidal anti-inflammatories in HO prophylaxis.

Disclosures: Owen Davies, None.

MO0394

Next Generation Sequencing for Hypophosphatasia and X-Linked Hypophosphatemia. Steven Mumm^{*1}, Margaret Huskey¹, Shenghui Duan¹, Valerie Wollberg², Karen E Mack², C. Charles Gu¹, Katherine L Madson², Gary Gottesman², Michael P Whyte². ¹Washington University School of Medicine, USA, ²Center for Metabolic Bone Disease & Molecular Research Shriners Hospitals for Children - St Louis, USA

Hypophosphatasia (HPP) and X-linked hypophosphatemia (XLH), heritable disorders that typically manifest as rickets, are caused by mutations in the tissue non-specific alkaline phosphatase (*TNSALP*) gene and phosphate-regulating gene with homologies to endopeptidases on the X chromosome (*PHEX*), respectively. Both diseases feature a wide range of severity, sometimes with considerable variation among affected family members. We are taking a next generation sequencing (NGS) approach to fully understand the variable expressivity of HPP and XLH encountered among our ~ 200 HPP and ~ 300 XLH patients. We have designed an NGS gene panel, using the Life Technologies Ion Torrent platform, to identify in these patients the primary defects in *TNSALP* and *PHEX*, but also secondary changes in a total of 13 potential modifier genes that regulate pyrophosphate and phosphate homeostasis. All coding exons plus the 5' and 3' UTRs of *TNSALP* and *PHEX* are included. To date, mutations in *TNSALP* were identified in all 5 probands sequenced; 3 were heterozygous for missense mutations, and 2 were compound heterozygous for missense defects. *PHEX* defects were identified in 26 of 52 XLH probands. Mutations (all heterozygous or hemizygous) included missense, nonsense, and

splice-site defects. For the XLH probands, including sporadic and familial cases, without identified *PHEX* mutations, further defects were not detected in *DMP1*, *FGF23*, or the multiple other genes involved in Mendelian hypophosphatemic rickets (e.g. *SLC34A3*). To identify modifier gene effects, we have studied 5 XLH sibling pairs with known *PHEX* mutations and variable clinical severity by looking at SNPs and rare variants in all 15 genes. One sibling pair harbors different heterozygous, non-synonymous, *DMP1* SNPs. Another pair is discordant for *SLC34A3* non-synonymous SNPs. A third sib pair is discordant for non-synonymous SNPs in both *DMP1* and *MEPE*. Thus, identification of modifier gene effects in HPP and XLH may help to explain their variation in disease severity and to guide treatment.

Disclosures: Steven Mumm, None.

MO0395

Twist and Turns in Anthrax 1-Dependent Regulation of Bone Tissue Maintenance. Tatiana Besschetnova^{*1}, Negin Katebi². ¹Harvard School of dental Medicine, USA, ²HSDM, USA

The GAPO syndrome is a progressive condition with dramatically reduced quality of life and reduced life expectancy. The main manifestations of the syndrome include growth retardation, alopecia and failure of primary and permanent tooth eruption. In addition to excessive extracellular matrix accumulation in all organs and interstitial tissues, skeletal tissues are severely affected. Reduced bone density, osteolysis, and delayed osteoid maturation in long bones are other hallmarks of this painful and devastating disease. Recent genetic studies of GAPO patients identified loss of function causative mutations in the surface receptor Anthrax 1 (ANTXR1), also known as TEM8. Expression in different cell types and the existence of at least 5 different splice variants, both with and without transmembrane domains, suggest flexible regulatory functions in different tissues. However, little is known about the mechanisms of TEM8 functions. Our studies of Antxr1 knockout mice provide mechanistic explanations for skin and vascular abnormalities in GAPO syndrome and suggest that fibrotic skin abnormalities in the syndrome are, at least partly, the consequence of increased VEGF signaling. The Antxr1 null mouse phenocopies the human GAPO syndrome. A remarkable feature of the bone phenotype in GAPO patients and Antxr1 null mice is progressive postnatal bone loss. Tem8 is widely expressed both during embryonic development and postnatally, including strong expression in osteoblasts/osteocytes, osteoclasts and in blood vessels. The osteoclast number is dramatically increased in mutant mice. Furthermore, loss of TEM8 results in failure of osteoclast reversal and uncouples bone resorption from bone formation. The increased levels of non-collagenous components, osteocalcin, osteopontin and bone sialoprotein are contrasted with reduced bone mineralization. In addition, MMP2 activity, shown to be an important factor in osteoid mineralization, is reduced in mutants. TEM8-dependent reduction of MMP2 activity suggests that some phenotypic characteristics of GAPO may be the result of pathophysiological mechanisms similar to those underlying syndromes with Multicentric skin Nodulosis and Osteolysis and Arthropathy (MONA) caused by homozygous loss-of-function mutations in MMP2. The results of the work are providing understanding of cellular and molecular regulatory mechanisms of TEM8-dependent bone maintenance. Furthermore, the studies provide novel insights into the reversal phase of bone remodeling. Deeper understanding of this process will help to advance the development of strategies to treat rare (GAPO, MONA) and common (osteoporosis) diseases.

Disclosures: Tatiana Besschetnova, None.

MO0396

Calciphylaxis In a Patient with Liver disease and Prior Gastric bypass: Case Report of an unusual combination. Goral Panchal^{*1}, Catherine Anastasopoulou². ¹Albert Einstein Medical Center, USA, ²Division of Endocrinology, Albert Einstein Medical Center, USA

Background: Calciphylaxis is a microvascular occlusion syndrome of mural calcification, intimal proliferation, fibrosis and thrombosis leading to target organ hypoperfusion. It is mostly known as an important manifestation of disordered calcium homeostasis in end stage renal disease (ESRD) patients. Calciphylaxis in non-ESRD patients is a case reportable phenomenon with only 36 cases described so far. Risk factors associated include hypoalbuminemia, corticosteroid use, neoplasms, anticoagulation, chemotherapy, systemic inflammation, protein C & S deficiency, alcoholic liver disease, obesity and rapid weight loss.

Clinical Case: 37 year old Caucasian female presented with worsening rash on both lower extremities, mainly thighs and buttocks. The lesions initially started as a small nodule about 2 months ago, which gradually progressed to large lesions on both lower limbs with uncontrolled pain and skin discoloration. Her past medical history included alcoholic hepatitis, morbid obesity with gastric bypass surgery in 2003 and chronic thrombocytopenia.

The patient was on spironolactone, rifaximin, furosemide, gabapentin, pantoprazole and multivitamin. On admission Ca 9.7 mg/dL(8.4-10.3), albumin 2.4 gm/dL(3.5-5), Corrected Ca 11.0 mg/dL, PO4 5.2 mg/dL(2.3-4.7), Mg 1.4 mg/dL(1.6-2.6), PTH 19.2 pg/ml(9-73), 25 OH Vit D 16.6 ng/ml, TSH 5.99 mIU/ml(0.35-4.94), Free T4 0.93 ng/dL(0.78-1.48), ALP 167 U/L(40-150), ALT 42 U/L(0-55), AST 129 U/L(5-34), Creat 0.7 mg/dL(0.6-1.0).

Punch biopsy of the lesions revealed calciphylaxis and thrombotic vasculopathy. She was started on Sevelamer, Vit D 1000 U/day and given 30 mg IV Pamidronate once. Repeat chemistries after 3 weeks showed Corrected Ca 9.64, PO4 3 mg/dL, Mg 2.0 mg/dL.

Conclusion: Our patient's risk factors for development of calciphylaxis were liver disease and prior gastric bypass surgery- of which only 2 prior cases have been reported. Some of the proposed mechanisms include osteochondrogenic differentiation of vascular cells in presence of cytokines and inflammation, failed anticalcific process due to loss of inhibitors like cMGP, pOPN, fetuin, pyrophosphate, and also apoptosis induced by altered phosphorus metabolism and remodeling of bone due to above mechanisms causing altered calcium homeostasis in presence of normal parathyroid function.

Purpose: As the exact mechanism of calciphylaxis in such patients have yet to be determined, presentation of these cases will help in future research.

Disclosures: Goral Panchal, None.

MO0397

Dietary Protein Intake is Associated with Better Physical Function and Muscle Strength Among Elderly Women. Masoud Isanejad^{*1}, Arja Erkkilä², Joonas Sirola³, Jaakko Mursu⁴, Heikki Kröger³, Toni Rikkinen³, Marjo Tuppurainen⁵. ¹University of Eastern Finland, Finland, ²Institute of Public Health & Clinical Nutrition, Finland, ³Department of Orthopaedics & Traumatology, Kuopio University Hospital, Kuopio Finland, Finland, ⁴Institute of Public Health & Clinical Nutrition, University of Eastern Finland, Finland, ⁵Department of Obstetrics & Gynaecology, Kuopio University Hospital, Kuopio, Finland

Higher protein intake than RDA (0.8 g/kg/body weight (BW)) might be beneficial to physical performance in elderly. This study evaluated the association of protein intake (g/kg BW) with physical function in non-sarcopenic and sarcopenic elderly women. In total 554 women aged 65.3- 71.6 yr in the OSTPRE-FPS study, filled a questionnaire on lifestyle factors and 3-d food record in 2002. Body composition was measured by dual energy X-ray absorptiometry and physical function tests were performed at baseline and in a 3 yr follow-up. A sarcopenic woman were belonged to lowest quartile of relative skeletal muscle index (RSMI) (5.3-6.3 kg/m²) and the lowest quartile of either grip strength (9-22.3 kPa) or gait speed 10 m (<0.51 m/s) or lowest quartile of RSMI but not the lowest quartile of any other measurement. A non-sarcopenic woman did not belong to the lowest quartile of any measurement (RSMI, grip strength or gait speed 10 m) or lowest quartile of either grip strength or walking speed or both, but not to that of RSMI. At baseline the women with higher protein intake (comparing categories of = 0.8 vs. 0.81-1.19 vs. = 1.2 g/ kg BW) had better performance in one leg stance (P<0.001), chair rise (P=0.042), standing with eyes closed for 10 s (P=0.050) and squat (P=0.027) and squat to the ground tests (P<0.001). They had also faster gait speed 10 m (P<0.001) and greater short physical performance battery score (SPPB) (P<0.001) at the baseline (Table 1). Prospective results showed that higher protein intake was associated with less decline in one leg stance (P=0.007) and squat test (P=0.012) as well as increased chair rises (P=0.001) over 3 yr of follow-up. Aforementioned results were attenuated but remained significant after adjustment for confounders, including age, energy intake, smoking status, alcohol consumption (portions/week), reported physical activity (hours/ week), hormone therapy use, diagnosed osteoporosis, baseline height and lean mass.

However, after controlling for fat mass significances were lost. Further, in non-sarcopenic women the associations between high protein intake and physical performance tests were detected but in sarcopenic women only the grip strength and high protein intake was significantly associated ($\beta=0.06$ and $P=0.043$) (Table 2). In conclusion higher protein intake than current RDA was positively associated with physical function measures in elderly women (namely in non-sarcopenic women as compared to their sarcopenic counterparts).

Table 1. Association of protein intake categories (g/kg body weight) with physical function tests.

| Physical functions tests | ≤ 0.8 g/kg BW (n=171) | | | 0.81-1.19 g/kg BW (n=269) | | | ≥ 1.2 g/kg BW (n=112) | | | P was - value | | |
|---|-----------------------|---------------|---------------|---------------------------|----------|----------|-----------------------|----------|----------|---------------|----------|----------|
| | Mean ± SD | Mean ± SD | Mean ± SD | Model 1* | Model 2* | Model 3† | Model 1* | Model 2* | Model 3† | Model 1* | Model 2* | Model 3† |
| Hand grip strength (kPa) | | | | | | | | | | | | |
| Baseline | 25.96 ± 7.04 | 26.23 ± 4.88 | 24.53 ± 4.56 | 0.029 | 0.657 | 0.135 | | | | | | |
| Change‡ | -1.51 ± 6.70 | -0.79 ± 3.68 | -0.68 ± 3.43 | 0.538 | 0.358 | 0.967 | | | | | | |
| One leg stance 30 s | | | | | | | | | | | | |
| Baseline | 15.79 ± 10.90 | 19.31 ± 10.28 | 21.54 ± 9.42 | <0.001 | 0.047 | 0.804 | | | | | | |
| Change | -1.64 ± 10.02 | -1.50 ± 10.89 | -0.96 ± 10.48 | 0.007 | 0.931 | 0.024 | | | | | | |
| Chair rises | | | | | | | | | | | | |
| Baseline | 7.87 ± 6.97 | 7.84 ± 2.86 | 8.41 ± 2.20 | 0.042 | 0.063 | 0.720 | | | | | | |
| Change | 0.12 ± 6.07 | 0.83 ± 2.82 | 1.15 ± 2.68 | 0.001 | 0.725 | 0.111 | | | | | | |
| Gait speed 10 m (m/s) | | | | | | | | | | | | |
| Baseline | 1.53 ± 0.31 | 1.67 ± 0.32 | 1.70 ± 0.28 | <0.001 | 0.005 | 0.668 | | | | | | |
| Change | -0.11 ± 0.24 | -0.10 ± 0.33 | -0.11 ± 0.29 | 0.505 | 0.486 | 0.712 | | | | | | |
| Standing with eyes closed 10 s (%) | | | | | | | | | | | | |
| Baseline | 94.1 | 95.6 | 97.6 | 0.050 | 0.381 | 0.412 | | | | | | |
| Change | -5.54 ± 2.08 | -5.19 ± 1.73 | -4.94 ± 1.25 | 0.646 | 0.873 | 0.100 | | | | | | |
| Ability to squat (%) | | | | | | | | | | | | |
| Baseline | 91.1 | 94.3 | 97.0 | 0.027 | 0.019 | 0.191 | | | | | | |
| Change | -0.08 ± 0.45 | -0.06 ± 0.32 | -0.02 ± 0.21 | 0.012 | 0.100 | 0.503 | | | | | | |
| Ability to squat to the ground (%) | | | | | | | | | | | | |
| Baseline | 58.0 | 69.8 | 78.7 | <0.001 | 0.001 | 0.080 | | | | | | |
| Change | -0.02 ± 0.53 | -0.01 ± 0.52 | -0.06 ± 0.50 | 0.202 | 0.309 | 0.690 | | | | | | |
| SPPB score | | | | | | | | | | | | |
| Baseline | 5.52 ± 1.82 | 6.28 ± 1.87 | 6.51 ± 1.77 | <0.001 | 0.004 | 0.586 | | | | | | |
| Change | 7.69 ± 2.04 | 7.69 ± 1.98 | 7.80 ± 1.85 | 0.172 | 0.908 | 0.845 | | | | | | |

BW = Body weight. SPPB = Short physical performance battery, calculated by scoring gait speed 10 m (m/s), chair rises in 30 s and one leg stance, which scored to 12 with higher scores indicating better performance.
 *Model 1 was adjusted for age, total energy intake.
 †Model 2 was adjusted for variables in model 1 plus smoking status, alcohol consumption (portions/week), physical activity status, hormone therapy use, osteoporosis and study group, and also for baseline height and lean mass.
 ‡Model 3 was adjusted for variables in model 2 and lean mass was replaced by fat mass.
 § Prospective analysis were adjusted also for baseline variables.

Table 1

Table 2. Association of protein intake ≥ g/kg body weight and physical function tests according to sarcopenia status.

| Physical functions tests | Non-sarcopenic (n=269) | | | | Sarcopenic (n=127) | | | |
|---|---------------------------------|----------|----------|----------|---------------------------------|----------|----------|----------|
| | regression coefficient (95% CI) | Model 1* | Model 2† | Model 3‡ | regression coefficient (95% CI) | Model 1* | Model 2† | Model 3‡ |
| Hand grip strength (kPa) | | | | | | | | |
| Baseline | -0.13 (-4.22, 0.17) | 0.069 | 0.520 | 0.113 | -0.23 (-4.22, 0.17) | 0.114 | 0.850 | 0.334 |
| Change§ | 0.18 (-1.49, 1.94) | 0.018 | 0.430 | 0.406 | 0.06 (-3.14, 5.07) | 0.043 | 0.257 | 0.690 |
| Knee extension (kPa) | | | | | | | | |
| Baseline | -0.04 (-6.17, 17.03) | 0.613 | 0.683 | 0.562 | -0.07 (-4.81, 70.81) | 0.642 | 0.552 | 0.562 |
| One leg stance 30 s | | | | | | | | |
| Baseline | 0.26 (5.62, 15.17) | <0.001 | 0.001 | 0.974 | 0.45 (-2.40, 14.20) | 0.762 | 0.545 | 0.948 |
| Change | 0.14 (0.44, 9.60) | 0.032 | 0.087 | 0.658 | -0.48 (-10.0, 5.64) | 0.718 | 0.489 | 0.055 |
| Chair rises | | | | | | | | |
| Baseline | 0.15 (0.65, 4.13) | 0.038 | 0.059 | 0.658 | 0.01 (-8.15, 1.82) | 0.987 | 0.235 | 0.486 |
| Change | 0.20 (1.02, 3.59) | <0.001 | 0.182 | 0.653 | 0.27 (0.02, 5.22) | 0.064 | 0.126 | 0.228 |
| Tandem walk 6 m speed (m/s) | | | | | | | | |
| Baseline | 0.31 (-0.05, 0.09) | 0.687 | 0.560 | 0.989 | -0.23 (-0.62, 0.20) | 0.133 | 0.667 | 0.972 |
| Change | 0.02 (-0.05, 0.06) | 0.682 | 0.692 | 0.793 | -0.13 (-0.04, 0.11) | 0.616 | 0.844 | 0.728 |
| Gait speed 10 m (m/s) | | | | | | | | |
| Baseline | 0.30 (0.17, 0.48) | <0.001 | <0.001 | 0.161 | 0.11 (-0.11, 0.36) | 0.769 | 0.267 | 0.429 |
| Change | 0.23 (-0.02, 0.24) | 0.119 | 0.854 | 0.324 | -0.01 (-0.28, 0.24) | 0.784 | 0.608 | 0.978 |
| Standing with eyes closed 10 s (%) | | | | | | | | |
| Baseline | 0.04 (-0.06, 0.13) | 0.514 | 0.305 | 0.850 | -0.11 (-0.14, 0.05) | 0.383 | 0.564 | 0.650 |
| Change | 0.23 (0.62, 2.17) | 0.001 | 0.001 | 0.096 | 0.13 (-0.47, 1.54) | 0.297 | 0.246 | 0.557 |
| Ability to squat (%) | | | | | | | | |
| Baseline | 0.18 (0.04, 0.25) | 0.006 | 0.003 | 0.964 | 0.08 (-0.05, 0.09) | 0.536 | 0.309 | 0.545 |
| Change | 0.09 (-0.05, 0.26) | 0.134 | 0.190 | 0.528 | 0.15 (-0.10, 0.40) | 0.256 | 0.123 | 0.578 |
| Ability to squat to the ground (%) | | | | | | | | |
| Baseline | 0.29 (0.26, 0.68) | 0.001 | 0.001 | 0.852 | 0.10 (-0.22, 0.52) | 0.432 | 0.652 | 0.333 |
| Change | 0.59 (-0.11, 0.359) | 0.340 | 0.389 | 0.224 | 0.04 (-0.30, 0.45) | 0.682 | 0.381 | 0.677 |
| SPPB score | | | | | | | | |
| Baseline | 0.32 (1.15, 2.86) | <0.001 | <0.001 | 0.177 | -0.05 (-1.89, 1.23) | 0.722 | 0.214 | 0.132 |
| Change | 0.15 (0.09, 2.11) | 0.052 | 0.301 | 0.919 | -0.02 (-1.80, 1.59) | 0.880 | 0.876 | 0.983 |

SPPB = Short physical performance battery.
 *Model 1 was adjusted for age, total energy intake.
 †Model 2 was adjusted for variables in model 1 plus smoking status, alcohol consumption (portions/week), physical activity level, hormone therapy use, osteoporosis and study group and also for baseline height.
 ‡Model 3 was adjusted for variables in model 2 plus fat mass.

Table 2

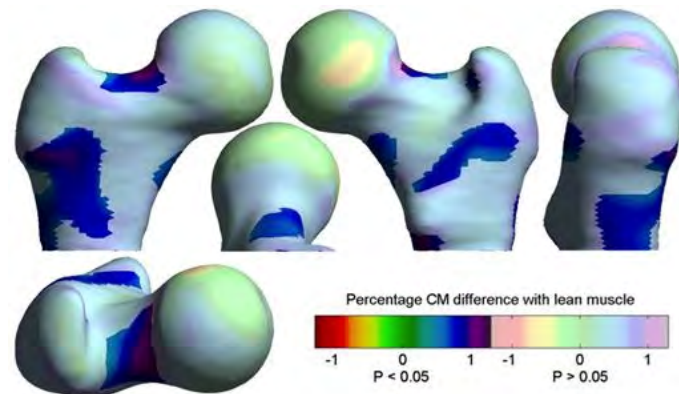
Disclosures: Masoud Isanejad, None.

MO0398

Focal cortical thinning is associated with lower thigh muscle area in hip fractures and controls. Toni Rikkinen¹, Graham Treece², Fjola Johannesdottir³, Kenneth Poole³. ¹Department of Medicine, University of Cambridge, Finland, ²Engineering Division of the Department of Engineering, University of Cambridge, United Kingdom, ³Department of Medicine, United Kingdom

Low muscle strength and focal osteoporosis are known risk factors for hip fracture. However, associations between thigh muscle compartment size and proximal femur 3D bone mass distribution in hip fracture are less clear. SUBJECTS AND METHODS. A total of 84 CT scans consisting of age matched hip fractured patients (n=40) and non-hip fracture controls (n=43) were analyzed (Mean age 78 years, range 61-92). Fracture cases were age matched with patients undergoing routine CT. Age, height and weight were recorded. The thigh muscle compartment was determined just below lesser trochanter using 10 x 1mm slice mean tissue values. Muscle and fat tissue separation and areal bone density (BMD) analysis were done using QCT Pro (5.1.3). Proximal femur bone mass characteristics were measured with Stradwin 5.0 software. Significant associations between muscle cross sectional area and bone parameters, including cortical mass (CM) and endocortical trabecular density (ECTD), were color mapped using SurfStat Matlab toolbox. An independent-samples t-test was conducted to compare the groups. RESULTS. A lower thigh muscle cross-sectional area (cm²) was seen in fractures (Mean=91.7, Standard deviation=13.9) compared to controls (97.8, 12.7); t(81)=-2.1, p<0.05. Across all patients, higher thigh muscle area was

associated with more cortical mass in patches of bone known to associate with hip fracture (Picture). Fracture patients had lower body mass index (22.8, 4.4) than control (26.1, 4.9) group; t(81)=-3.21, p<0.01. A lower areal BMD (g/cm²) was seen in fractures (0.624, 0.162) versus controls (0.698, 0.10) in total hip; t(81)=-2.57, p=0.01 and in femoral neck ((0.539, 0.120) vs. (0.651, 0.81)), respectively; t(81)=-5.0, p<0.001. There was no difference in the amount of intramuscular fat between the groups. Adjusting muscle and fat areas for height², did not change the results. The association persisted after adjusting for age and volumetric bone size. CONCLUSION. Femoral cortical bone distribution is associated with thigh muscle cross-sectional area, in fracture critical zones. In addition, the muscle compartment size and bone mass are significantly lower in hip fracture patients. Smaller muscle area is a modifiable risk factor suggested to contribute towards weaker bone characteristics and hip fractures.



Percentage increase in cortical mass (CM)

Disclosures: Toni Rikkinen, None.

MO0399

Higher Amounts of Calf Inter- and Intra-muscular Adipose Tissue Determined by pQCT are Associated with Poorer Musculoskeletal Health in Older Adults. David Scott¹, Elizabeth Skinner², Ross Clark³, Pazit Levinger⁴, Terry Haines¹, Kerrie Sanders³, Peter Ebeling¹. ¹Monash University, Australia, ²Western Health, Australia, ³Australian Catholic University, Australia, ⁴Victoria University, Australia

Purpose: Age-related increases in inter- and intra-muscular adipose tissue (IMAT) occur concurrently with declines in skeletal muscle mass (sarcopenia). Peripheral quantitative computed tomography (pQCT) can quantify IMAT non-invasively with low radiation doses. We investigated associations of pQCT-determined calf IMAT with indicators of musculoskeletal health in community-dwelling older adults. Methods: 48 volunteers aged 65 years and older (mean 71.6±4.8 years; 52% female) underwent pQCT at 66% tibial length of the dominant leg to assess cortical volumetric bone mineral density (cBMD; mg/cm³), area (mm²), and thickness (mm), and calf muscle IMAT area (cm²). Whole-body DXA determined appendicular lean mass (ALM), and fasting serum samples for glucose, lipids, and wide-range C-reactive protein (wr-CRP), were obtained. Knee extension strength (KES; dominant leg), sit-to-stand (STS), timed up-and-go (TUG), postural sway (computerized posturography; N=41), and gait (GAITrite System; N=40) were assessed. Recurrent falls status in the past 12 months was self-reported. Results: Calf IMAT was negatively associated with high-density lipoprotein cholesterol, and positively associated with glucose and wr-CRP (all P<0.03), but only wr-CRP remained significantly associated with IMAT, after adjusting for age, sex and ALM normalised to BMI. Absolute IMAT levels were not associated with cortical bone parameters, but IMAT normalised to leg lean mass had a borderline negative association with cBMD (r=-0.29, P=0.06). Higher IMAT was not associated with KES (P>0.05), but was significantly associated with slower performance of the STS and TUG (both P<0.05), greater postural sway (anteroposterior amplitude r=0.55, P<0.01; mediolateral amplitude r=0.33, P=0.04), slower gait speed (r=-0.36, P=0.03) and cadence (r=-0.39, P=0.02), and greater step time (r=0.42, P=0.01) and width (r=0.37, P=0.02), after adjusting for confounders. There was a significantly higher likelihood of self-reported falls in the previous 12 months per unit increase in IMAT (OR 1.08, 95%CI 1.02-1.14). Conclusions: pQCT-determined calf IMAT is associated with poorer balance and mobility in community-dwelling older adults, independent of muscle mass, and this may contribute to an increased likelihood of recurrent falls. A trend towards poorer tibial cBMD in participants with high IMAT relative to muscle mass was observed, suggesting IMAT may also influence age-related declines in bone health.

Disclosures: David Scott, None.

MO0400

HPLC-MS-MS 25OHvitaminD levels are associated with prognosis markers of Heart Failure. Federica Saponaro^{*1}, Claudio Passino², Alessandro Saba³, Riccardo Zucchi⁴, Elena Pardi⁵, Simona Borsari⁶, Filomena Cetani⁵, Claudio Marcocci⁵. ¹University of Pisa, Italy, ²Unit of Cardiology, Fondazione Toscana Gabriele Monasterio, Italy, ³ Unit of Biochemistry, University of Pisa, Italy, ⁴Unit of Biochemistry, University of Pisa, Italy, ⁵Unit of Endocrinology 2, Pisa, Italy, ⁶U.O. Endocrinology 2, Pisa, Italy

Introduction

Heart failure (HF) is a health problem with poor prognosis, despite many treatments available. Vitamin D is the prehormone of the active calcitriol (1,25(OH)₂D₃). It is involved in bone homeostasis, but recent studies suggest extraskeletal functions, including pleiotropic effects on cardiovascular system and a relationship between low levels of 25OHvitamin D and worse HF prognosis. The aim of this study was to detect 25OHvitaminD in HF patients and correlate with HF instrumental markers.

Materials and Methods

We performed a retrospective study on 70 consecutive HF patients (NHYA 1-3), collecting clinical, biochemical and instrumental data (echocardiography and cardiopulmonary exercise test – CPET). We retrieved stored blood samples collected at the baseline and developed a fast isotope dilution Mass Spectrometry coupled with Liquid Chromatography (HPLC-MS-MS) method for accurate measurement of 25OHvitaminD levels.

Results

Patients (13 females and 57 males) had stable HF disease (prevalent NYHA 2), with age of 65 ± 11 years, FE of 32 ± 8% and mild kidney failure (creatinine 1.3 ± 0.5 mg/dl). Levels of 25OHvitaminD ranged 2-45 ng/ml with mean of 17 ± 9 ng/ml: 23% (n=16) patients had vitamin D deficiency (<10ng/ml), 67% (n=47) had vitamin insufficiency (between 10 and 20 ng/ml) and 10% (n=7) had vitamin >30 ng/ml, without any supplementation. The linear regression analysis showed that 25OHvitaminD levels were positively correlated with CPET parameters VO₂ peak and VO₂/HR (p<0.01) and negatively mortality Meckel score (p<0.1).

Conclusion

Our study revealed a strong association between variables from CPET, a well recognized valuable tool for HF prognosis and 25OHvitaminD levels, detected with a new and accurate method HPLC-MS-MS.

Disclosures: *Federica Saponaro, None.*

MO0401

Increased Body Weight and Sarcopenic Obesity: Causes of Intertrochanteric Fracture in Non-Osteoporotic Female Patients. Hyung Min Ji^{*1}, Jun Han², Dong San Jin³, Ye-Yeon Won¹. ¹Ajou University Hospital, South Korea, ²Naver Corporation, South Korea, ³Mary Orthopedic Hospital of Beijing, China

Purpose

The purpose of this study was to determine if there were any differences between women diagnosed with an intertrochanteric fracture who were categorized into a low BMD group (T-score ≤ -2.5) and a high BMD group (T-score > -2.5). Additionally, we examined the correlation between T-score and intermuscular adipose tissue (IMAT) in different thigh muscles.

Methods

This cross-sectional study identified 117 women with intertrochanteric fracture in whom both preoperative computed tomography (CT) scan of the pelvis and dual-energy x-ray absorptiometry (DEXA) were obtained. The patients were divided into high BMD (49 patients) and a low BMD (68 patients) groups. Attenuation of the gluteus maximus, abductor, quadriceps, and hamstring muscles were measured from CT scans of the hip and thigh cross-sectional area. The cross-sectional area of normalized IMAT of the muscles was also measured. All variables were compared between the two groups.

Results

Patients with a high BMD were significantly younger, taller, and heavier. IMAT of the quadriceps was significantly higher in these patients (Table 1). A moderate correlation was observed between T-score and weight and a weak correlation was detected between T-score and the IMAT ratio of the quadriceps. Body mass index (BMI) was moderately correlated with IMAT of all muscles (Table 1). T-score was moderately correlated with abductor and quadriceps IMAT ratios in 55–60 kg patients.

Conclusion

BMI and body weight were higher and IMAT of the quadriceps increased in non-osteoporotic women with a T-score > -2.5 who sustained an intertrochanteric fracture when compared with those of patients with osteoporosis. This result indicates that increases in body weight and sarcopenic obesity play a role generating fractures in this population.

Disclosures: *Hyung Min Ji, None.*

MO0402

Prevalence of Sarcopenia and Classification Agreement According to Different Operational Definitions. Andrea Trombetti^{*}, Mélany Hars, Emmanuel Biver, Thierry Chevalley, Serge Ferrari, René Rizzoli. Division of Bone Diseases, Geneva University Hospitals & Faculty of Medicine, Switzerland

Sarcopenia is a devastating feature of aging associated with extensive burden. However, consensus on an operational definition, combining or not muscle mass and function diagnostic criteria, has not been reached yet. Indeed, markedly different criteria and cutpoints for low muscle mass and function have been proposed, with potential different disease prevalence and outcomes. In a homogenous cohort of 68-year old community-dwellers, we applied different criteria and cutpoints to evaluate disease prevalence and classification agreement according to various operational diagnostic criteria, as proposed by the European Working Group on Sarcopenia in Older People (EWGSOP), the International Working Group on Sarcopenia (IWG), and the Foundation for the National Institutes of Health Sarcopenia Project (FNIH). Seven hundred sixty-seven subjects (608 women; age 67.9 ± 1.5 years), enrolled in the Geneva Retirees Cohort (GERICO), were studied. Appendicular lean mass (ALM), ALM/height² and ALM/BMI ratios were determined by DXA (Hologic Discovery W). Gait speed was measured over a 4-m distance and grip strength using a digital handheld dynamometer. Sarcopenia prevalence was estimated using EWGSOP, IWG and FNIH proposed criteria, and degree of agreement assessed using kappa statistics. Low lean mass prevalence ranged from 3.8% (FNIH) to 16.0% (EWGSOP). Weakness (i.e., low grip strength) prevalence ranged from 0.7% (FNIH) to 3.9% (EWGSOP). Prevalence of low lean mass combined with either weakness or low gait speed fulfilling various proposed sarcopenia definitions was the lowest for FNIH (0.3%) compared with IWG (1.2%) and EWGSOP (1.6%) criteria, with higher prevalence in women across all definitions. There was poor agreement between the groups identified according to the different definitions, with kappa values below 0.3. Our results obtained in a large cohort of healthy 68-year old subjects indicate that the prevalence of sarcopenia is low at that age independently of the definition. They also suggest that muscle weakness, slowness and low lean mass prevalence widely vary depending on the criteria and cutpoints applied. Similarly, sarcopenia prevalence considerably varies according to the definitions, with poor agreement between classifications. Further studies should compare the predictive ability of candidate sarcopenia criteria for hard outcomes, like incident falls, fractures, activities of daily living and quality of life.

Disclosures: *Andrea Trombetti, None.*

MO0403

Prevalence of Sarcopenia and Sarcopenic Obesity in Germany using established definitions: Baseline data of the FORMOSA-study. Wolfgang Kemmler, Klaus Engelke^{*}, Simon von Stengel, Ellen Freiburger. University of Erlangen-Nuremberg, Germany

Purpose: The primary aim of the study was to determine the prevalence of Sarcopenia and Sarcopenic Obesity in community-dwelling (CD) older females in Germany. The secondary aim was to assess whether these females really live independently and autonomously.

Methods: 1325 CD females 70 years and older living in the area of Northern Bavaria, Germany were assessed. Sarcopenia as defined by (a) the European Working Group on Sarcopenia in older people (EWGSOP) and (b) the International working group on Sarcopenia (IWGS) were identified. In order to determine Sarcopenic Obesity additionally Obesity defined as (a) BMI ≥ 30 kg/m² (according to NIH) or (b) body-fat ≥ 35% (according to WHO) was determined. In participants with Sarcopenia, Barthel Index, care level, and social network were retrospectively evaluated via personal interview.

Results: Based on anthropometric data, family, education and social status, lifestyle, number and distribution of diseases and medication the present cohort can be considered as representative for the corresponding German population. Sarcopenia prevalence was 4.5% according to EWGSOP (Fig. 1) and 3.3% according to the IWGS criteria.

Obesity prevalence in our cohort averaged 19.8% (BMI ≥ 30 kg/m², NIH) and 63.8% (total body-fat ≥ 35%, WHO). The overlap between both factors (i.e. SO) range from 0% (EWGSOP+NIH criteria) to 2.3% (EWGSOP+WHO criteria). Factors that may represent limited autonomy or independence were very rarely identified in subjects with Sarcopenia.

Conclusion: The prevalence of Sarcopenic Obesity in the CD (female) German population 70 years and older is relatively low. With respect to our second research aim, the hypothesis that Sarcopenia and Sarcopenic Obesity was incompatible with independent life was rejected. However, the latter finding should be addressed with more dedicated study designs.

MO0405

Hydroxytyrosol Relieves Age-related Bone Formation Reduction Through Reversing of Adipogenesis Towards Osteogenesis. [Fan Zhao](#)^{*1}, [Zhihao Chen](#)², [Peihong Su](#)², [Wuxia Qiu](#)², [Xiaoli Ma](#)², [Dijie Li](#)², [Airong Qian](#)².
¹Northwestern Polytechnical University, Peoples republic of china, ²Key Laboratory for Space Bioscience & Biotechnology, Institute of Special Environmental Biophysics, School of Life Sciences, Northwestern Polytechnical University, China

Mediterranean diets have been long reported in disease prevention. Hydroxytyrosol, a kind of polyphenol compound highly abundant in such diets, has significant biological effects on some age-related degenerative diseases like cardiovascular diseases and cancer. However, the effects of hydroxytyrosol on skeletal aging were less understood and required deep-going researches. In order to study the effects of hydroxytyrosol on age-related bone loss and bone formation reduction, and to investigate the biological mechanisms, we used two groups of 3-month old C57BL/6 male mice (Young groups, n=15, respectively) and two groups of 16-month old natural aged C57BL/6 male mice (Aged groups, n=17, respectively), and treated them with Hydroxytyrosol Acetate solution (50mg/kg) or distilled water respectively for consecutively 3 months by intragastric administration. Results showed that after gavage for 3 months, aged mice administered with Hydroxytyrosol Acetate solution showed higher femur BMD and improved trabecular microarchitecture as compared to same age untreated mice, while no significant effect was detected between treated and untreated young mice. Red oil O stained femur FFPE sections showed that in aged mice, less fat was deposited in Hydroxytyrosol Acetate treated group than that in untreated group. Moreover, protein carbonylation level, tissue oxidation/anti-oxidation level, senescence-related gene expression, and some microRNAs expression changed as well, suggesting its antioxidant and anti-senescence role during aging. *In vitro* culture of mouse BMSCs (B6-msc) under induction medium supplemented with Hydroxytyrosol Acetate showed that adipogenesis was inhibited while osteogenesis was promoted in regard to cell proliferation, differentiation, and PPAR γ 2, Adiponectin, FABP4, ALP, Osteocalcin, Runx2 gene expression. Taken together all results reached so far, we have successfully recorded an anti-aging effect of hydroxytyrosol during skeletal aging. Fat accumulation in bone tissue and *in vitro* osteogenesis/adipogenesis induction experiments indicated its role to reverse adipogenesis towards osteogenesis. The results suggest hydroxytyrosol as an effective precaution countermeasure for age-related osteoporosis and bone metabolic diseases.

Disclosures: Fan Zhao, None.

MO0406

Modification of Systemic SDF-1 Levels or CXCR4 Signaling Alters Bone Formation with Age. [Alexandra Aguilar](#)^{*1}, [Sudharsan Periyasamy-Thandavan](#)², [Samuel Herberg](#)³, [Brian Volkman](#)⁴, [Galina Kondrikova](#)², [Mark Hamrick](#)², [Carlos Isales](#)², [William Hil](#)².
¹UCC School of Medicine Georgia Regents University, USA, ²Georgia Regernts University, USA, ³Case Western University, USA, ⁴Medical college of Wisconsin, USA

The rapid increase in the ageing of the population creates new challenges to battle aging-related bone loss. In the United States, there are more than 40 million individuals with low bone mass, or frank osteoporosis. Mechanisms involved in aging-related bone loss and osteoporosis remain poorly understood, but are thought to be mediated, in large part, by the fate of bone marrow mesenchymal stem cells (BMSCs). We demonstrate that bone marrow cell expression, and microenvironmental levels, of SDF-1 change with age and alterations of its signaling pathway leads to bone loss. We hypothesize that with aged there is an increased of SDF-1/CXCL-12 in circulation and a decrease in bone marrow, causing changes in MSC survival, migration and bone formation. Osmotic minipumps with saline, human-SDF-1a, AMD3100 (SDF-1/CXCL12 receptor CXCR4 inhibitor, but a CXCR7 (ACKR3) agonist), 5uM or 100uM human-SDF-1a locked ligand dimers were implanted subcutaneously in three and twenty two month old C57BL/6 mice for 28 days. SDF-1a levels in plasma and bone marrow interstitial fluid were analyzed by ELISA. We performed transwell BMSC migration assays to assess the bioactivity of SDF-1 in BM interstitial fluid. Proximal tibia bone mass content (BMC) and density (BMD) was measured using mCT. Young mice treated with AMD3100 and SDF-1a significantly (p<0.0001) decreased proximal tibia BMC/D. Levels of SDF-1a in three-month-old mice interstitial fluid and bone marrow cells were comparable. In contrast, twenty two month old groups treated with SDF-1a significantly (p<0.001) increased SDF-1a in plasma. Both, AMD3100 and SDF-1a groups decreased SDF-1a levels in bone marrow interstitial fluid. Low dose (5uM) of human-SDF-1a dimer significantly (p<0.05) increased SDF-1a levels in bone marrow cells. Migration of bone marrow cells increased toward interstitial fluid of mice treated with systemic AMD3100 and SDF-1a suggesting increased SDF-1 bioactivity and mediation of bone formation by the alternative SDF-1 receptor CXCR7 (ACKR3). Proximal tibia BMC/D significantly (p<0.0052) increased with AMD3100, SDF-1a, 5uM and 100uM human-SDF-1a dimers. This suggests that MSC engraftment and survival may also be mediated by biased switching of the CXCR4 signaling pathway from G-coupled receptor signaling to b-Arrestin mediated signaling of CXCR4 and possibly CXCR7 (ACKR3). Our data suggest that SDF-1 has a distinct role of in MSC mediated bone homeostasis with age.

Disclosures: Alexandra Aguilar, None.

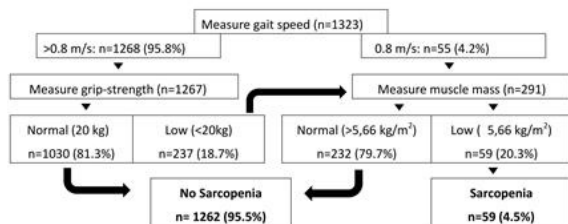


Figure 1: Flow-chart when applying the EWGSOP algorithm on 1325 community-dwelling females 70 years

Disclosures: Klaus Engelke, None.

MO0404

Sarcopenia is independently associated with knee pain. [Shigeyuki Muraki](#)^{*1}, [Toru Akune](#)², [Hiroyuki Oka](#)³, [Sakae Tanaka](#)⁴, [Hiroshi Kawaguchi](#)⁵, [Kozo Nakamura](#)², [Noriko Yoshimura](#)⁶.
¹22nd Century Medical & Research Center, University of Tokyo, Japan, ²National Rehabilitation Center for Persons with Disabilities, Japan, ³22nd Century Medical & Research Center, Faculty of Medicine, The University of Tokyo, Japan, ⁴Department of Orthopaedic Surgery, Faculty of Medicine, The University of Tokyo, Japan, ⁵Department of Orthopaedic Surgery, Japan Community Health care Organization Tokyo Shinjuku Medical Center, Japan, ⁶22nd Century Medical & Research Center, The University of Tokyo, Japan

To clarify the effect of sarcopenia in knee pain by using data from the large-scale population-based cohort ROAD study. Among the 2,566 subjects who participated in the third visit of the ROAD study, 2,152 subjects who underwent X-ray examination of the knee and measurement of muscle strength and mass were enrolled in the present study. Knee osteoarthritis (OA) was graded according to the Kellgren-Lawrence (KL) grade. Knee pain was assessed by well experienced orthopedists. Grip strength was measured on the right and left sides using a TOEI LIGHT handgrip dynamometer (TOEI LIGHT CO. LTD., Saitama, Japan). Isometric knee extension muscle was estimated by using a quadriceps training machine (QTM) (QTM-05F; Alcare Co., Ltd., Tokyo, Japan). Skeletal muscle mass was measured via bioimpedance analysis by using a body composition analyzer (MC-190; Tanita Corp., Tokyo, Japan). The QTM and MC-190 have been validated. Grip strength and quadriceps muscle strength were significantly different between subjects with and without pain in men (grip strength, 37.5 ± 9.5 kgf and 35.1 ± 9.0 kgf, respectively, p < 0.05; quadriceps muscle strength, 32.9 ± 12.5 kgf and 26.4 ± 12.0 kgf, respectively, p < 0.05) and women (grip strength, 24.1 ± 5.8 kgf and 22.5 ± 5.8 kgf, respectively, p < 0.05; quadriceps muscle strength, 27.2 ± 9.9 kgf and 23.2 ± 9.5 kgf, respectively, p < 0.05). After adjustment for age, sex, and BMI, the significant association with quadriceps muscle strength remained (p < 0.05), while that of grip strength disappeared (p = 0.31 and 0.10 in men and women, respectively). Muscle mass (kg)/height (m²) at the lower limbs was not significantly associated with knee pain (men: 2.95 ± 0.44 kg/m² and 3.03 ± 0.47 kg/m², respectively, p = 0.89; women: 2.41 ± 0.27 kg/m² and 2.45 ± 0.32 kg/m², respectively, p = 0.14). After adjustment for age, BMI, sex and KL grade, quadriceps muscle strength were significantly associated with knee pain (5 kgf increase; OR, 0.87; 95% CI, 0.82–0.92), indicating that the significant association of quadriceps muscle strength with knee pain is independent of obesity and knee OA. Next, to determine the prevalence of knee pain according to muscle strength, subjects were classified by quadriceps muscle strength (<10 kgf, =10 to <20 kgf, =20 to <30 kgf, =30 to <40 kgf, and =40 kgf). The prevalence of knee pain was 53.9%, 27.0%, 14.4%, 11.6%, and 9.8% in men and 41.0%, 31.0%, 23.7%, 16.3%, and 12.5% in women with muscle strength <10 kgf, =10 to <20 kgf, =20 to <30 kgf, =30 to <40 kgf, and =40 kgf, respectively. After the adjustment for age, BMI, and KL grade, the prevalence of knee pain was significantly higher in subjects with muscle strength < 10 kgf and =10 to <20 kgf (p<0.05) compared to those with muscle strength = 40 kgf. The present study revealed that muscle strength had a stronger association with knee pain than grip strength or muscle mass.

Disclosures: Shigeyuki Muraki, None.

MO0407

Hyperkyphosis and mortality risk in older men: the Osteoporotic Fractures in Men Study. Deborah Kado*¹, Mei-Hua Huang², Peggy Cawthon³, Kristine Ensrud⁴, Wendy Katzman⁵, Nancy Lane⁶, Diane Schneider⁷, John Schousboe⁸, Eric Orwoll⁹. ¹University of California, San Diego, USA, ²UCLA, USA, ³CPMC, USA, ⁴U. Minnesota, USA, ⁵UCSF, USA, ⁶UC Davis, USA, ⁷4BoneHealth, USA, ⁸Univ Minnesota, USA, ⁹OHSU, USA

Background: Hyperkyphosis (HK), or increased thoracic curvature, commonly affects older people and is associated with poor health. A few studies suggest that older persons with worse kyphosis are at risk of earlier mortality, but most have not accounted for underlying vertebral fractures that are also associated with shortened survival.

Methods: Using data from the Osteoporotic Fractures in Men Study, we evaluated the association between worse kyphosis (measured both clinically and via x-rays) and mortality risk. During the 1st clinic visit in 2000-2, 2,320 men aged ≥ 65 years (mean age 72.7) had supine lateral spine x-rays from which the Cobb angle of kyphosis was calculated from the superior edge of T4 and inferior edge of T12. During the 3rd clinic visit in 2007-09, 2,892 men had a clinical measure of kyphosis measured while lying on the DXA table, where 1.7 cm blocks were placed underneath the participant's neck until he achieved a neutral head position (range 0 to 10). For the Cobb angle analyses, average follow-up was 10.2 years (SD = 3.5) during which 931 died. For the blocks analyses, the average follow-up was 5 years (SD = 1.5) during which 607 died.

Results: The mean Cobb angle was 38.6° (SD = 11.4). In crude analyses, per SD increase in Cobb angle, there was an 8% risk of mortality that was no longer significant after adjustment for age and clinic (RH: 0.98; 95% CI: 0.92, 1.05). Using the top quartile or quintile of kyphosis to define HK did not change the results. For the clinical measure, in age and clinic adjusted models, men who required ≥ 2 blocks were 1.38 times more likely to die than men with 0-1 blocks (95% CI: 1.09 – 1.76). In a model adjusted for baseline prevalent vertebral fracture, hip BMD, BMI, weight, weight loss between the 1st & 3rd visit, smoking and history of stroke, the relative hazard was 1.44 (95% CI: 1.06 – 1.97). However, further adjustment for either timed chair stand (RH: 1.21, 95% CI: 0.93, 1.58) or self-reported physical activity (RH: 1.18, 95% CI: 0.90, 1.53) significantly diminished the effect of blocks kyphosis on mortality.

Conclusions: We found that a clinical assessment of kyphosis using the blocks method was associated with mortality risk while the radiologic measure of Cobb angle kyphosis was not once adjusted for age. In summary, our study confirms previous reports that a clinical measure of kyphosis is associated with mortality risk, yet this association is largely confounded by poor physical function.

Disclosures: Deborah Kado, None.

MO0408

Diffuse Idiopathic Skeletal Hyperostosis (DISH) as a Predictor of Kyphosis in the Osteoporotic Fractures in Men Study (MrOS). Wendy Katzman*¹, Neeta Parimi², Ziba Mansoori³, Lorenzo Nardo³, Deborah Kado⁴, Peggy Cawthon², Lynn Marshall⁵, John Schousboe⁶, Nancy Lane⁷. ¹University of California, San Francisco, USA, ²San Francisco Coordinating Center, USA, ³University of California, USA, ⁴University of California San Diego, USA, ⁵Oregon Health Science University, USA, ⁶University of Minnesota, USA, ⁷University of California Davis, USA

Background. DISH and thoracic kyphosis are well-defined radiographic findings in the spines of older individuals. Characteristics of DISH (ossifications between vertebral segments) reflect changes in spine anatomy and physiology that have previously been associated with Cobb angle of kyphosis. Since the prevalence of these two disorders is high in older adults and can lead to physical disabilities, this study examined the association of DISH with prevalent and worsening kyphosis in older men. **Methods.** 1500 subjects from the MrOS cohort of community-dwelling, ambulatory men aged ≥ 65 years, mean age 72 (5.5 SD), with Cobb angle measurements of kyphosis obtained at year 1 and 4.7 years, measured from supine lateral spine radiographs, were selected for the study. DISH was assessed in the baseline radiographs using the Resnick criteria requiring the presence of ossification of the anterior longitudinal ligament of at least 4 contiguous vertebral bodies (3 intervertebral disc levels) and the absence of severe degenerative disc disease in the involved vertebral segment(s). Characteristics of participants with and without DISH were assessed using chi-square and t tests. Linear regression was used to analyze the association between prevalent DISH and Cobb angle at baseline and percent annualized change in Cobb angle. **Results.** DISH was identified on baseline radiographs in 222 (15%) participants. Participants with DISH were older, had higher BMI and total hip BMD, and higher baseline Cobb angle compared to those without DISH ($p < 0.05$). DISH was not associated with morphometric prevalent vertebral fractures, history of gout or diabetes ($p > 0.1$). The mean baseline Cobb angle in the analytic sample was 38.5 degrees (SD=11.3). There was a 7.9% greater baseline Cobb angle (95% CI: 3.7-12.2) in those with DISH compared to those with no DISH adjusted for age, race, clinic site, and BMI. Further adjustment for total hip BMD and prevalent vertebral fractures slightly strengthened the association (9%, 95%CI: 4.4-13.0). The percent change in Cobb angle from baseline to 4.7 years later was 3.2% with DISH and 4.8% without DISH ($p = 0.2$). There was no association of annualized percent change in Cobb angle with prevalent DISH in age-adjusted models. **Conclusions.** Greater Cobb angle of kyphosis is associated with DISH, and the presence of DISH did not worsen the kyphosis over this 4.7-year interval in older men.

Disclosures: Wendy Katzman, None.

MO0409

Sedentary Behaviour, Sitting and Mortality in the Canadian Multicentre Osteoporosis Study (CaMOS)—cross-sectional and 10-year prospective data. Jerilynn Prior*¹, Adrian Bauman², Ding Ding², Sarah Pont², Claudie Berger³, Heather Macdonald⁴, Jonathan D. Adachi⁵, Wilma M. Hopman⁶, Stephanie M. Kaiser⁷, Christopher S. Kovacs⁸, K. Shawn Davison⁹, Lisa Langsetmo³, David Goltzman¹⁰, CaMOS Research Group¹¹. ¹University of British Columbia, Canada, ²University of Sydney, Epidemiology, Australia, ³CaMOS Methods Centre, Canada, ⁴Orthopedics, University of British Columbia, Canada, ⁵Rheumatology, McMaster University, Canada, ⁶Queens University, Canada, ⁷Endocrinology, Dalhousie University, Canada, ⁸Endocrinology, Memorial University, Canada, ⁹University of Victoria, Canada, ¹⁰Medicine/Endocrinology, McGill University, Canada, ¹¹McGill University, Canada

Prolonged sitting during leisure and work may relate to increased risks for cardiovascular diseases and osteoporosis. This sedentary behaviour, despite moderate-to-high physical activity, is also postulated to cause an increase in mortality. Since baseline, CaMOS has collected detailed sitting data. To date there are no published prospective data on multivariate adjusted changes in sitting over time. Thus, we aimed to describe baseline and longitudinal (baseline to 10 year) sitting behaviour, its predictors and adjusted mortality risks. We used multivariate logistic regression for this preliminary analysis; all-cause mortality was the primary outcome. We adjusted for baseline age (continuous), and categorical data on sex, current smoking, BMI, education, employment, living with an adult, general self-rated health, physical activity and sleep. Low sitting (< 7 hrs/day) and high sitting (≥ 7 hrs/day) were categories used for descriptive outputs. Odds ratios (OR) and their 95% confidence intervals (95%CI) were calculated. The CaMOS sitting analysis cohort included 5,406 women and men with 10-year data (Figure). Those analyzed vs excluded did not differ in categorical sitting ($P = 0.639$). At baseline, women versus (vs) men and those who were part-time/retired vs fulltime were less likely to be high sitters after adjustment for age, BMI, education, and physical activity. Those with a university education vs only high school, those with low vs high physical activity and who were obese vs normal weight were more likely to be high sitters. In 10-year follow-up, those who changed from obese to non-obese (vs always non-obese) or whose physical activity went from low to high still remained higher sitters. But those who changed from full-time to retired became less likely to be high sitters. Mortality considered exposures to total sitting as well as sitting related to work, transit/car, eating and TV-watching. Work-related sitting of 5-6 hrs/day was associated with a decreased mortality, OR 0.51 (0.27 to 0.95), but TV watching of > 10 hours/day related to markedly increased, OR 5.81 (1.96 to 17.26), mortality. Prolonged total sitting of 12-13.5 hrs/day related to increased mortality risk, OR 1.96 (1.30 to 2.95). In summary, these population-based prospective, preliminary Canadian data suggest that normal work-related sitting is not a risk but that prolonged hours of TV-related or total sitting are independently associated with risks for higher adjusted mortality.

Figure. Selecting the Analytical Sample for Canadian Multicentre Osteoporosis Study (CaMOS) 10-Year Prospective Sitting Evaluation and All-Cause Mortality

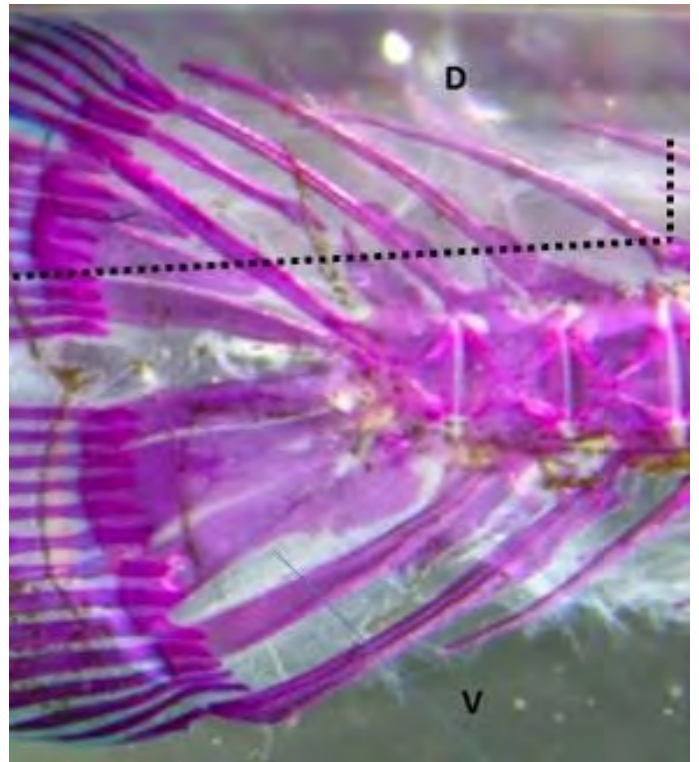
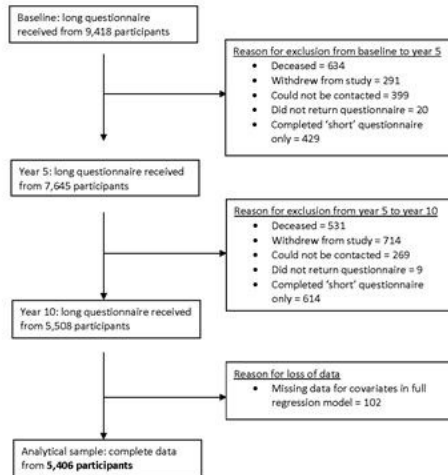


Fig. 1. Skeleton of an adult non-injured fish: dashed lines indicate the plane of amputation

Figure. Selecting the Analytical Sample

Disclosures: Jerilynn Prior, None.

MO0410

Partial Tail Amputation in Zebrafish: A Model of Chondral Bone Regeneration? Yael Govezensky*, Dalia David, Dafna Ben-Yosef, Chen Shochat, David Karasik. Faculty of Medicine in the Galilee, Bar Ilan University, Israel

Purpose: The aim of this research was to develop an *in vivo* platform for conveniently examining the potential of various factors to augment chondral bone regeneration. For this purpose, we have established a *de novo* partial tail amputation model in adult zebrafish, which includes the resection of cartilage-temple based bones from the endoskeletal caudal complex. Endoskeletal amputations were rarely studied, as opposed to those of the distal caudal fin rays, which are a well-established regenerative model of membranous bone regeneration.

Methods: Dorsal (D) hemi-amputations were performed with a sterile scalpel from the proximal 2–3mm of the tail that has scales and musculature, and proceeded distally towards the fin rays (Fig.1). In order to observe regenerative properties, fish skeletons were vitally labeled with two Ca^{2+} -binding chromophores: calcein, and 20 days later, alizarin red s. In order to overcome the potential artifacts of autofluorescence, and the spectral overlap between both chromophores, we employed spectral imaging coupled with image analysis using the linear unmixing algorithm.

Results: After the caudal complex' partial amputation fish were vital, and normal activities such as eating and swimming were not compromised. The labeling method, which was validated in the distal caudal fin model, exhibited newly formed bone (Fig. 2), mainly some broadening at the tip of the stump in neural spines (A), but hypurals (B) did not regenerate. Interestingly, unamputated ventral hypurals (C) showed signs of active bone remodeling, which most probably can be attributed to increased muscle activity. None of the caudal complex bones regrew to form a structure similar to the original one, even 7 months post amputation.

Conclusions: We have acquired the ability to distinguish newly formed and pre-existing bone in our new model. We suggest that neural spines undergo a progressive widening at the tip of the stump, which resembles hypertrophic nonunion fracture in humans. However, hypurals do not seem to regenerate. Thus, our model is appropriate for the investigation of potential therapeutic factors for augmenting chondral bone regeneration, either for the induction of *de-novo* regeneration or for examination of treatments for abnormal regrowth: both of major importance in several clinical conditions and aspects of regenerative medicine.

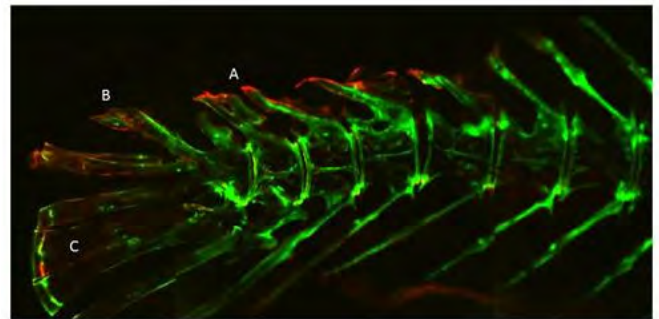


Fig. 2. Example of a double-labeled caudal skeleton of an experimental fish 18 days post amputation

Disclosures: Yael Govezensky, None.

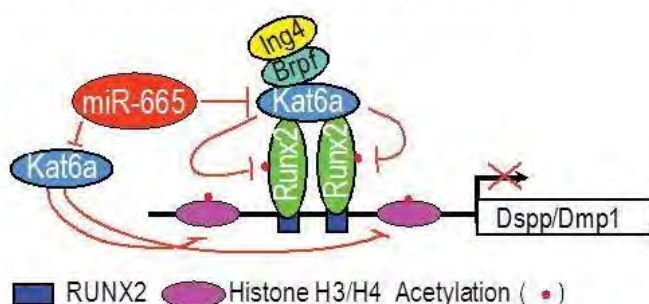
MO0411

A network connecting KAT6A and the miR-665 regulates the odontoblast differentiation program. Mohammad Hassan*. University of Alabama, USA

Dentinogenesis is the process by which dentin, the major mineralized tissue of teeth, is formed through progressive cytodifferentiation of progenitor cells to mature odontoblasts. Multiple layers of gene regulation, including those by microRNA (miRNA or miR), orchestrate the physiologic process of dentinogenesis in a stage-specific manner. Studies of proteins involved in microRNA (miRNA) processing, maturation, and silencing have indicated the importance of miRNAs in skeletogenesis, but the specific miRNAs involved in this process are incompletely defined. Here, we identified miRNA-665 (miR-665) as a potential repressor of odontoblast maturation. Studies with cultured cell lines and primary embryonic cells showed that miR-665 represses the expression of early and late odontoblast marker genes and stage-specific proteases involved in dentin maturation. K (lysine) acetyltransferase 6a (KAT6A) is a founding member of the MYST family of lysine acetyltransferases, acetylates lysine

residues on histones H2B, H3, and H4. Kat6a deletion is embryonic lethal and haploinsufficiency for Kat6a demonstrated craniofacial abnormalities. RISC-complex-immunoprecipitation studies identified Kat6a as a potential target of miR-665. Notably, miR-665 directly targeted Kat6a mRNA, repressed Kat6a translation and increased mRNA degradation. The expression of miR-665 is temporal and reciprocal to KAT6A and RUNX2 during in vitro odontoblast differentiation. KAT6A interacted physically and functionally with RUNX2, activating tissue-specific promoter activity and prompting odontoblast differentiation. MiR-665 prevents KAT6A-induced chromatin remodeling, and promotes the switch from acetylation to methylation of histone H3K9 in the tooth-specific Dsp and Dmp1 promoters. By reducing KAT6A expression, miR-665 hinders the formation of activating complexes to promote epigenetic activation of Dsp and Dmp1 chromatin, impairing odontoblast differentiation. Overall, the linkage of miR-665 to epigenetic factor KAT6A, and transcription factor RUNX2, all of which regulate tooth biology supports the developing concept that miRNAs link genetic and epigenetic events that are requisite for maintaining a normal tissue environment. The involvement of miR-665 at multiple levels of odontoblast differentiation suggests diverse functions for miR-665 that include physiologic tooth formation and homeostasis, and may inform the design of therapeutics for dental disorders.

miR-665 mediated epigenetic mechanism



ASBMR 2015

Disclosures: *Mohammad Hassan, None.*

MO0412

Correlation between the Mineral Compositions and Bone Strength of Tibia bone in poultry. Tengfei Dou¹, Lixian Liu¹, Hua Rong¹, Qihua Li¹, Dahai Gu¹, Zhiqiang Xu¹, Limei Huang¹, Ying Huang², Sumei Zhao¹, Hongyong Zhang³, Marinus F.W.te Pas⁴, Changrong Ge^{*5}, Junjing Jia¹. ¹Yunnan Provincial Key Laboratory of Animal Nutrition & Feed Technology, Yunnan Agricultural University, China, ²Yunnan Provincial Key Laboratory of Animal Nutrition & Feed Technology, China, ³Department of Medicine, University of California at Davis Medical Center Sacramento, USA, ⁴Animal Breeding & Genetics Centre, Wageningen UR Livestock Science, Netherlands, ⁵Yunnan Agricultural University, China, Cn

The bone growth and development are most important factors affecting on the broilers and layer production in poultry. Indigenous Chinese chicken breeds comprise a wide variety of phenotypes, including large and small, and fast and slow growing chicken. Compare with commercial broilers, Wuding chicken breed is a slow growing large chicken breed with 2.5 kg of average body weight in 4 months old and the Daweishan mini chicken breed is a slow growing small chicken breed with 0.8-1.0 kg of average body weight in 4 months old. We had demonstrated that the Daweishan mini chicken showed higher bone strength compared with other local breeds and broilers. It has been hypothesized that the breed and age might affecting on the bone mineral composition and association with bone strength. The objective of this study was to investigate the effects of breed and age on the bone mineral compositions (BMC), and BMC association with bone strength in poultry.

A total of 180 1-day-old chicks from Daweishan mini chicken, Wuding chicken and Avian broilers were fed in an environmentally controlled room to 12 weeks. All chickens from 1-21 days were fed a starter diet, older chicken received a full diet. The chickens had free access to feed and water. Twenty chickens from each group were sacrificed at 4, 8 and 12 weeks to measure tibia minerals composition using Inductively Coupled Plasma - Mass Spectrometry. A 3-point bending test was used to determine the mechanical properties of the left tibia bone in each time point. Results: Daweishan Mini chicken had significantly higher tibia bone strength parameters which are including modulus of elasticity, yield stress and bending stress ($P < 0.01$), and tibia bone strontium content at three time points ($P < 0.01$), and higher magnesium and copper contents ($P < 0.05$) from 8-12 weeks and lower phosphorus, potassium and sodium contents ($P < 0.05$) while converse case were observed for the broilers in all time points. No breed and age effect on the other mineral contents were observed in three time points ($P > 0.05$). The contents of strontium, magnesium and copper in tibia bone were positive correlation with bone strength ($P < 0.01$). In contrast, the contents of phosphorus, potassium and sodium in tibia bone were negative correlation with tibia bone strength ($P < 0.01$).

In conclusion, we found that slow growing small chicken breed had higher bone strength and association with higher tibia bone strontium, magnesium and copper content compare with other two breeds. Our results implicated that supplement appropriate strontium in diet may improve the bone strength and health in broiler and layer.

Acknowledgments: This work was funded by National 863 Proposal of P. R. China (2011AA100305); National and Yunnan Provincial Natural Science foundation Research Projects (31260532; 2009CD060; 2011FA015).

Disclosures: *Changrong Ge, None.*

MO0413

Deletion of the Prolyl Hydroxylase Domain-containing Protein 2 (Phd2) Gene in Chondrocytes but not Osteoblasts Promotes Secondary Ossification at the Epiphysis. Shaohong Cheng^{*1}, Chandrasekhar Kesavan², Sheila Pourteymoor³, Catrina Alarcon³, Subburaman Mohan³. ¹VA Loma Linda Health Care Systems, USA, ²Jerry L Pettis VA Medical Center, USA, ³Pourteymoor, USA

Hypoxia has been shown to induce survival and differentiation of chondrocytes via modulation of the hypoxia-inducible factor (HIF) signaling pathway. HIF signaling in osteoblasts has also been established to play an important role in bone formation. The hypoxia effect on HIF1a signaling is mainly mediated via a direct oxygen sensor, prolyl hydroxylase domain (Phd) enzyme, Phd2. We, therefore, evaluated the role of Phd2 expressed in chondrocytes and osteoblasts on secondary ossification of the epiphysis. The Phd2 gene was conditionally disrupted in osteoblasts or chondrocytes by two generations of breeding of Phd2 floxed mice crossed with Col1a2-Cre or Col2a1-Cre mice. The amount of bone in the proximal tibial epiphysis was quantitated by micro-CT analyses. There was no significant difference in trabecular BV/TV (98.4% of control mice) or any other trabecular parameter comparing osteoblast-specific Phd2 conditional knockout (cKO) and littermate control mice at 5 wks of age. By contrast, chondrocyte-specific disruption of the Phd2 gene caused a 20% ($P = 0.01$) increase in trabecular bone mass as a consequence of the increase in trabecular number (8%, $P < 0.05$) and reduction in trabecular separation (12%, $P < 0.05$). To determine the mechanism for increased bone formation, we measured expression levels of genes involved in osteoblast and chondrocyte differentiation using total RNA extracted from the proximal tibial epiphysis. As expected, Phd2 expression was decreased by 44% ($P < 0.05$) while expression levels of HIF1a target genes, VEGF (59%, $P < 0.05$) and EPO (141%, $P < 0.05$) were increased in the cKO mice compared to control mice. Expression levels of osterix but not ATF4 was significantly increased in the cKO epiphysis. Of the chondrocyte markers, expression level of Col10 was increased by 245% while Col2 was unaffected in the cKO mice. The expression levels of osteoblast specific markers, BSP and ALP were increased by 95% and 80% respectively (both $P < 0.05$) in the cKO tibial epiphyses. Conclusions: 1) Phd2 expressed in chondrocytes inhibits osteoblast formation and secondary ossification at the epiphysis via regulation of HIF1 signaling; 2) the role of Phd2 in chondrocytes and osteoblasts is different.

Disclosures: *Shaohong Cheng, None.*

MO0414

Identifying growth factors for improving the healing of the tendon-bone interface. David Musson^{*1}, Mei Lin Tay², Karen Callon², Dorit Naoit², Jillian Cornish². ¹University of Auckland, New Zealand, New Zealand, ²University of Auckland, New Zealand

Purpose

Injuries to tendon-bone interfaces are a significant clinical problem occurring in otherwise healthy, active people. Primarily caused by overuse or trauma, these injuries significantly affect patient quality of life and are a substantial financial burden to the healthcare economy. While there are currently no clinically accepted biological treatments for improving healing of these soft-hard tissue interfaces, much research has attempted to identify growth factors capable of aiding this challenging process.

In this study, a number of factors (IGF-1, lactoferrin, PTH, TGF- β) that are known to be important in bone biology have been evaluated for their ability to be anabolic to tendon. We compare these factors to those that are important in tendon repair, such as PDGF.

Methods

Primary tenocytes harvested from rat tails or human bicep tendons were treated with a range of factors for 48 hours. Cell growth was determined using alamarBlue[®] assays and collagen deposition was measured by Sirius red dye release. Gene expression analysis using real-time PCR was used to study tenocyte differentiation.

Results

IGF-1 significantly increased tenocyte cell numbers ($< 30\%$, $p < 0.05$), while both IGF-1 and TGF- β increased collagen production *in vitro* ($p < 0.05$). IGF-1 increased the expression of tenascin-C and tenomodulin genes (both $p < 0.05$), both important factors in the early response to tendon healing. TGF- β meanwhile, increased the expression of tenomodulin and tenascin-C ($p < 0.05$) as well as scleraxis ($p < 0.05$), a transcription factor important in tendon development. Both lactoferrin and PTH slightly decreased tenocyte number ($\sim 10\%$, $p < 0.05$) and collagen production, but increased the expression of IGF-1 (lactoferrin ~ 2.5 -fold and PTH ~ 10 -fold). Interestingly, while PDGF greatly increased tenocyte cell number and collagen

production, it significantly decreased the expression of a number of genes important in tendon cell biology, such as decorin, biglycan, scleraxis and tenomodulin (all $p < 0.05$).

Conclusions

Here we have shown that both IGF-1 and TGF- β have the potential to improve healing outcomes of the tendon-bone interface, due to their role in bone biology and their anabolic effects on tendon cells, while it appears that lactoferrin and PTH hold less promise in this regard. Interestingly, it appears that although PDGF is much studied in tendon healing, it may actually result in a de-differentiation away from the tenocytic lineage.

Disclosures: David Musson, None.

MO0415

Inactivation of the progesterone receptor in Mx1+ cells potentiates osteogenesis in vitro but not in vivo. Zhendong Zhong¹, Weihua Sun², Haiyan Chen¹, Hongliang Zhang², Nancy Lane², Wei Yao³. ¹University of California Davis Medical Center, USA, ²University of California Davis Medical Center, USA, ³University of California, Davis Medical Center, USA

Sex hormones are intricately involved in the regulation of bone turnover. The effect of progesterone on bone remains elusive. Global progesterone receptor (PR) knockout mice display high bone mass phenotype suggesting that PR influences bone growth and modeling. Recently, Mx1+ cells were reported to differentiate into osteoblastic lineages. The aim of this study was to evaluate whether the PR in Mx1+ cells regulates osteogenesis. Methods We first evaluated the specificity and induction efficacy of Mx1-Cre by crossing it with the mT/mG reporter mouse strain and characterizing the Cre activity by GFP expression in bone tissue and in primary osteoblast cultures. Next, Mx1-Cre was crossed with PR-flox to generate an inducible PR knockout mouse model. Calvarial cells and calvariae from the Mx1-Cre;PR-flox pups were treated with interferon alpha (IFN α) to activate the Cre expression and delete the PR gene in the Mx1+ cells, and the osteogenic potential was then evaluated. The in-vivo skeletal phenotype of Mx1-Cre;PR-flox mice was evaluated. Results Using the Mx1-Cre;mT/mG reporter mouse model, we found that the calvarial cells exhibited minimal background Mx1-Cre activity prior to Cre activation compared with the bone marrow stromal cells. IFN α treatment significantly activated Mx1-Cre in the calvarial cells. After the PR gene was deleted in the Mx1-Cre;PR-flox calvarial cells in vitro, significantly higher levels of expression of osteoblast maturation marker genes and osteogenic potential were detected. The PR-deficient calvariae also exhibited greater RUNX2 protein expression. Although Mx1-Cre activity could be induced on the bone surface in vivo, the Mx1+ cells did not differentiate into osteocytes in long bones. Bone volumes at the distal femurs and the bone turnover marker serum Osteocalcin were similar between the Mx1-Cre;PR-flox mutant mice and the corresponding wild types. Conclusions Blocking progesterone signaling via PRs in calvarial Mx1+ cells promoted osteoblast differentiation in vitro. Mx1+ progenitor cells did not contribute to osteocyte differentiations during long bone development in vivo. Selectively inactivating the PR gene in Mx1+ cells did not affect peripheral skeletal homeostasis.

Disclosures: Wei Yao, None.

MO0416

Low Dose IGF-I Augments the Bone-Lengthening Effect of Targeted Heat in the Mouse Hindlimb. Maria Serrat^{*}, Gabriela Ion, Kaitlynn Hughes. Marshall University School of Medicine, USA

Introduction: Linear growth deficiencies can result from injury, illness or genetic disease. These conditions can lead to limb length inequality and chronic disability. Delivering therapeutics to avascular growth plates is challenging, and treatments are often limited to invasive surgeries that are only partially effective. We previously developed a unilateral heating model to increase extremity length in mice using targeted heat exposure on one side of the body. We demonstrated that femora were significantly longer and tibial elongation rate was >12% greater on the heat-treated side. The purpose of this study was to combine heat with the growth-stimulating drug IGF-I. We tested the hypothesis that low dose IGF-I augments the bone-lengthening effect of intermittent heat application on hindlimbs of growing mice.

Methods: 3-week old female C57BL/6 mice (N=6) were injected each morning with IGF-I (2.5mg/kg SQ) and treated with 40C unilateral heat for 40 minutes/day for 14 days. Non-injected, heat-treated mice from our prior study (N=14) served as controls for the temperature effect. Body mass and tail length were recorded. Mice were given oxytetracycline (7.5 mg/kg IP) to quantify growth rate. Bones were measured at the 5-week endpoint.

Results: Tibial elongation rate was ~19% greater on the heat-treated side (40C) of IGF-I injected mice compared to their non-treated contralateral side (30C) (Fig. 1). The growth acceleration averaged 18.5 μ m/day (paired $t = 4.89$, $p = 0.003$), 23% faster than mice that received heat alone (15 μ m/day). Femoral length increased over 1.7% ($t = 7.97$, $p < 0.001$). When compared to heat-treated controls (1.3% increase in femoral length), there was a significant heat by drug interaction (ANOVA, $F = 3.06$, $p = 0.05$), indicating that heat had greater lengthening effects when combined with IGF-I. Controlling for variation in starting mass and tail length, IGF-I mice were not significantly larger than controls ($F = 2.63$, $p = 0.123$), but they had longer tails ($F = 16.84$, $p < 0.001$), suggesting that IGF-I increased extremity size without affecting

overall body mass. **Conclusion:** These data support the hypothesis that low dose IGF-I enhances the bone-lengthening effects of heat in growing mice. This research has practical relevance for treating a spectrum of linear growth disorders in children. Results could lead to new, noninvasive approaches with better outcomes by reducing costs and side effects of surgeries and high-dose pharmaceuticals.

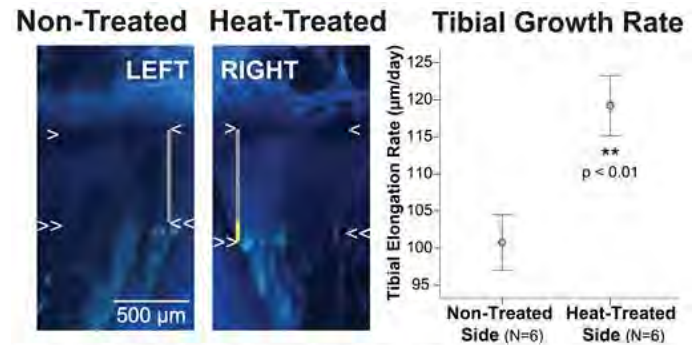


Figure 1. Left-right tibial slab sections from the same mouse labeled with oxytetracycline (OTC) show increased lengthening on the heat-treated side. The metaphyseal chondro-osseous junction is indicated by single arrowheads. Double arrowheads show OTC band in metaphyseal bone. Growth rate was measured as the vertical distance between the arrowheads (gray lines). Yellow segment of vertical line on the heat-treated side shows total difference in length measured over 7-days. Error bar plot (right) illustrates that growth rate was nearly 19% greater on the heat-treated side (18.5 μ m/day). Mean \pm 1 SE.

Figure 1. Increased tibial elongation rate on heat-treated side

Disclosures: Maria Serrat, None.

MO0417

Motor Ability in Early Childhood is Positively Associated with Bone Strength in Late Adolescence. Alex Ireland¹, Adrian Sayers², Kevin Deere², Alan Emond³, Jon Tobias^{1,2}. ¹Manchester Metropolitan University, United Kingdom, ²School of Clinical Sciences, University of Bristol, United Kingdom, ³School of Social & Community Medicine, University of Bristol, United Kingdom

Early life motor milestones (standing, walking, etc.) represent the first exposure of the skeleton to large reaction and muscular forces associated with locomotion. Recent work has shown a strong link between walking onset age and early childhood bone strength. However, it is unknown whether these relationships continue into later life. Therefore data from 2,327 children enrolled in the Avon Longitudinal Study of Children and Adolescents (ALSPAC) was examined. Early life motor ability was measured using Gross Motor Score (GMS) assessed by questionnaire at 18 months, and by the ALSPAC Coordination Test (ACT) conducted in a clinic visit at 7 years. Bone outcomes at 17 years were total hip bone mineral density (BMD) and hip cross-sectional moment of inertia (CSMI) assessed by dual-energy X-ray absorptiometry (DXA) and tibial periosteal circumference (PC), cortical thickness (CT), cortical bone area (CBA), cortical BMD (BMD_C) and CSMI assessed by peripheral quantitative computed tomography (pQCT) at 66% distal-proximal tibia length. When adjusted for sex, maternal social class and age at outcome and exposure GMS and ACT were positively associated with hip BMD [0.086(0.067,0.105) and 0.089(0.07,0.108)], hip CSMI [0.072(0.057,0.087) and 0.074(0.059,0.089)], PC [0.089(0.074,0.104) and 0.083(0.068,0.098)], CT [0.089(0.07,0.108) and 0.061(0.042,0.08)], CBA [0.097(0.081,0.113) and 0.083(0.067,0.099)] and CSMI [0.084(0.069,0.099) and 0.09(0.075,0.105)] (all $P < 0.001$) but not BMD_C ($P > 0.2$). Adjustment for perinatal factors (gestational age and birthweight) did not substantially attenuate regression coefficients. Adjustment for adolescent body size (height, lean mass and fat mass) resulted in 18-75% decrease in coefficients suggesting a mediating pathway. There was evidence of gender interaction for all variables such that associations with motor score were greater in males e.g. total hip BMD and PC regression coefficients for ACT and GMS were twice as large in males. In conclusion, early childhood motor ability is positively associated with skeletal development in late adolescence, most markedly in males. This results from greater periosteal expansion and reduced endosteal expansion, leading to greater cortical area and predicted bone strength. Body size and composition (particularly lean mass) appear to partly mediate these relationships and may reflect differences in physical activity.

Disclosures: Jon Tobias, None.

MO0418

Physiological oxygen tension modulates the profiles of soluble growth factors in chondrocytes after co-culture with osteoblasts. Tao Zhang^{*}, Jing Xie. West China School of Stomatology; State Key Laboratory of Oral Disease, China

Objective: Physiological oxygen tension plays a critical role in the homeostatic maintenance and development of endochondral bone. Based on the adjacent location

between uncalcified cartilage and subchondral bone and the microchannels served as message delivery between them, we aim to explore the influence of low oxygen tension on the soluble factor secretion in both chondrocytes and osteoblasts after co-culture. **Material and methods:** Non-contact co-culture was achieved by transwell chamber; Semi-quantitative polymerase chain reaction was used to screen the gene variation of growth factor profile of chondrocytes and osteoblasts including HIF-1 α , IGF-1, TGF- β ₁, FGF-1, FGF-2, EGF, VEGF-A/B, VE-cadherin, BMP-2/-4/-5/-6/-7 and the respective phenotype markers of these two cells. **Results:** Hypoxia regulates the marker genes in both chondrocytes and osteoblasts in the co-culture system. The physiological oxygen tension activates its sensitive transcription factor HIF-1 α and up-regulates angiogenesis-related growth factors including VEGF-A, VEGF-B and VE-cadherin. Additionally, BMP family is also modulated by oxygen tension after co-culture. **Conclusions:** These results not only indicate the importance of crosstalk between chondrocytes and osteoblasts, but also reveal the change of soluble growth factors modulated by physiological oxygen tension in this crosstalk. The changes of these factors can help to increase understanding of the mechanism underlying homeostatic maintenance of endochondral bone.

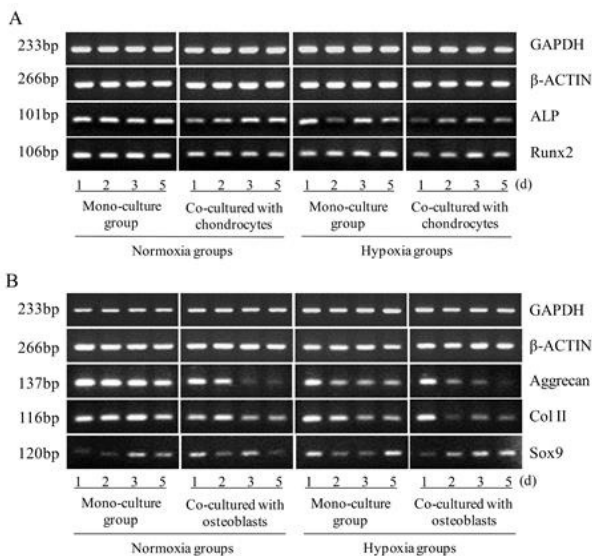


Figure 1

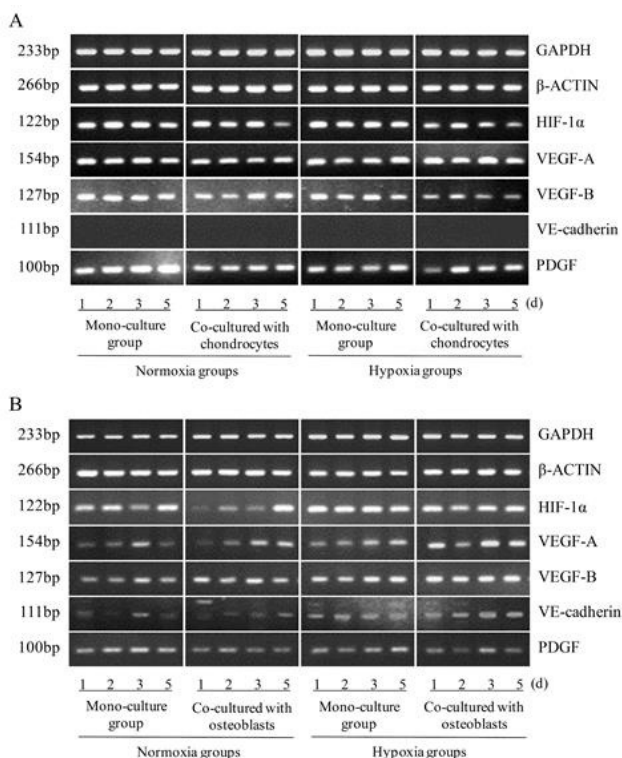


Figure 2

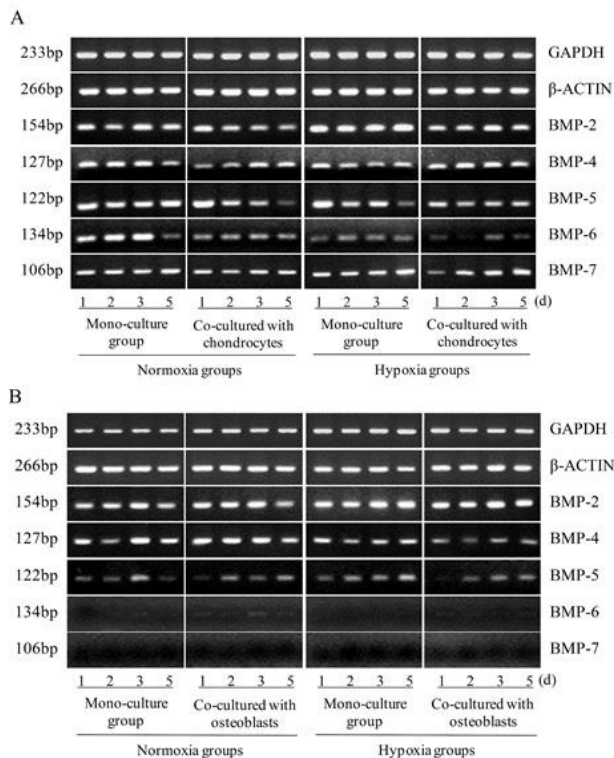


Figure 3

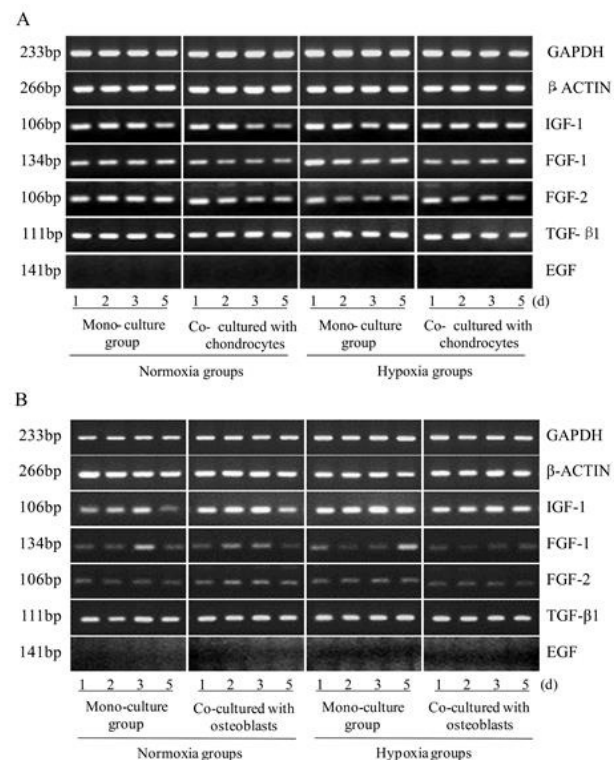


Figure 4

Disclosures: Tao Zhang, None.

MO0419

Raf Kinases regulate growth plate maturation. Garyfallia Papaioannou*¹, Eva Liu², Adalbert Raimann³, Byongsoo Timothy Chae⁴, Marie Demay¹.

¹Massachusetts General Hospital & Harvard Medical School, USA, ²Brigham & Women's Hospital, Massachusetts General Hospital & Harvard Medical School, USA, ³Medical University Vienna & Massachusetts General Hospital, Austria, ⁴Massachusetts General Hospital, USA

During endochondral ossification chondrocytes form an organized structure which, following vascular invasion, is progressively replaced by bone. The growth plate is comprised of three zones, resting, proliferating and hypertrophic chondrocytes which undergo coordinated proliferation, differentiation and apoptosis. MAPKs play a significant role in growth plate maturation. The Raf kinases A-Raf, B-Raf and C-Raf activate MEK1/2 that activates Erk1/2. A- and B-Raf are mainly expressed in proliferative chondrocytes whereas C-Raf is predominantly expressed in hypertrophic chondrocytes. While activation of MEK1/2 by phosphate is required for ERK1/2 phosphorylation and phosphate-induced hypertrophic chondrocyte apoptosis, a role for the Raf kinases in growth plate maturation has not been defined.

Mice with chondrocyte-specific ablation of C-Raf were generated by crossing mice expressing Cre recombinase driven by the Col2 promoter with mice bearing C-Raf alleles floxed at exon 3 (C-Raf^{fl/Col2-Cre+}). These mice were crossed with germline A-Raf knockout mice (A-Raf X^{KO}Y) to create mice with deletion of both A- and C-Raf in chondrocytes. Growth plates were analyzed postnatally.

Chondrocyte-specific C-Raf deletion led to an expansion of the hypertrophic layer, accompanied by decreased p-Erk1/2 and impaired chondrocyte apoptosis. However, in cultured primary chondrocytes, phosphate-induced pERK1/2 was not impaired by C-Raf ablation, suggesting other factors were responsible for the *in vivo* phenotype. Impaired function of VEGF, an inducer of vascular invasion, leads to expansion of the hypertrophic chondrocyte layer in growing mice. While VEGF mRNA was not altered by C-Raf ablation, VEGF protein was reduced in cultured chondrocytes and in the growth plates of C-Raf^{fl/Col2-Cre+} mice. This was accompanied by a decrease in vasculature assessed by CD31 IHC, suggesting that a reduction in metaphyseal angiogenesis underlies the observed phenotype. Mice lacking both A- and C-Raf exhibited a more marked expansion of the hypertrophic zone compared to mice with C-Raf deletion alone.

These data suggest that A-Raf and C-Raf coordinately regulate growth plate maturation. While C-Raf expression in hypertrophic chondrocytes promotes vascular invasion and hypertrophic chondrocyte apoptosis, concomitant ablation of A-Raf, leads to a more significant phenotype, suggesting that A-Raf may play a compensatory role or activate pathways that synergistically regulate growth plate maturation.

Disclosures: Garyfallia Papaioannou, None.

MO0420

Runx2 is required for the osteo-anabolic effects of Sost-deficiency. Meghan McGee-Lawrence*¹, Zachary Ryan², Rajiv Kumar², Jennifer Westendorf².

¹Georgia Regents University, USA, ²Mayo Clinic, USA

Sost deficiency is responsible for high bone mass disorders, Sclerosteosis and van Buchem's disease, and sclerostin neutralizing antibodies are in late-stage clinical trials as novel anabolic therapies for osteoporosis. Sclerostin, the Sost gene product, is highly expressed in osteocytes and inhibits multiple signaling pathways, most notably canonical Wnt signaling via Lrp5/6. Runx2 is an essential transcription factor during skeletal development, as Runx2^{-/-} mice lack a mineralized skeleton and die immediately after birth. Runx2^{+/-} mice are viable but develop cleidocranial dysplasia (CCD), characterized by low bone mass and persistent cranial fontanels. The role of Runx2 in the bone phenotype of Sost-deficient mice is not yet known. The goal of the current study was to determine if the high bone mass phenotype caused by Sost deficiency requires Runx2, and in turn, if modifying Wnt signaling through inducing Sost deficiency would correct the CCD phenotype of Runx2^{+/-} mice. A novel Sost deficient mouse model, which develops high bone mass and has increased Wnt signaling, was crossed with Runx2^{+/-} animals. Parietal bones of double mutant Sost^{-/-}:Runx2^{+/-} mice demonstrated increased calvarial thickness as compared to WT or Runx2^{+/-} mice but had thinner calvarial bones than Sost^{-/-} mice. Genetic dominance of Runx2 was apparent in the calvarial fontanel and clavicle phenotype, where Runx2^{+/-} and Sost^{-/-}:Runx2^{+/-} mice presented with comparable skeletal morphology. No exacerbation or rescue of the fontanel or clavicle phenotypes was found in the Sost^{-/-}:Runx2^{+/-} animals. In intramembranous fracture healing studies, double mutant Sost^{-/-}:Runx2^{+/-} mice presented with an intermediate bone volume fraction in healing bone defects as compared to Runx2^{+/-} or Sost^{-/-} mice. Endochondral bone formation phenotypes (long bone mass, trabecular bone remodeling, fontanel and clavicle morphology) were also quantified. Trabecular bone properties, trabecular bone remodeling indices, cortical bone thickness, and cortical bone mineral density generally demonstrated an intermediate phenotype in Sost^{-/-}:Runx2^{+/-} mice between that of Sost^{-/-} and Runx2^{+/-} single mutants. Interestingly, cortical bone periosteal area and cortical bone area were greatest in Sost^{-/-}:Runx2^{+/-} animals as compared to either Sost^{-/-} or Runx2^{+/-} mice. Taken together, these data suggest that the osteo-anabolic effects of Sost deficiency require Runx2.

Disclosures: Meghan McGee-Lawrence, None.

MO0421

Trabecular Bone Parameters in the Distal Femur and L5 Spine are Differentially Influenced by Genetics and Dietary Calcium Restriction in Growing Mice. James Fleet*, Perla Reyes Fernandez, Sarah Mace, Rebecca Replogle, Xu Lan. Purdue University, USA

Purpose: Attaining peak bone mass is an important osteoporosis prevention goal that is influenced by diet and genetics. We studied if gene-by-diet (GxD) interactions influence distal femur and L5 spine trabecular bone (Tb) parameters in a genetically diverse population of mice. We also examined whether genetic, diet, or GxD effects are different at the two sites. **Methods:** 51 BXD recombinant inbred mouse lines were fed diets with 0.5% (reference) or 0.25% calcium (Ca) from 4 to 12 wks of age (n=8/diet/line). At termination, the right femur and L5 spine were removed, cleaned, fixed, and Tb was analyzed by high-throughput micro computed tomography (uCT). Means were adjusted for the confounding influence of body size by ANCOVA. The response of uCT parameters to dietary Ca restriction (RCR) was calculated: 0.25% value – line mean for 0.5% value.

Results: BV/TV, Tb.N, and Tb.Th were higher, and Tb.Sp. was lower in spine than femur. Structural model index (SMI) showed a rod-like structure in femur and a plate-like structure in spine. Dietary Ca restriction significantly reduced BV/TV and Tb.Th. at both sites and changed SMI to a more rod-like structure. However, the total loss was significantly greater in spine than femur (for BV/TV, -0.023 and -0.015, respectively). Phenotypic diversity was seen across lines for all parameters and a significant line effect was seen for all femur and spine uCT endpoints. This indicates that genetics influences the development of Tb mass and structure. Consistent with this, narrow sense heritability was high at both sites (e.g. 0.5% Ca; femur BV/TV = 0.52; spine BV/TV = 0.56). For each femur and spine parameter, the RCR was significantly influenced by line indicating the existence of GxD interactions. Basal phenotypes and the RCR were negatively correlated, demonstrating that lines with high Tb mass on the reference diet were more sensitive to the consequences of low Ca diets. Compared to basal phenotypes, the heritability of the RCR was moderate (e.g. femur BV/TV = 0.37; spine BV/TV = 0.22). Finally, there was a significant site x line interaction affecting the RCR of BV/TV suggesting the existence of site-specific genetic effects for the impact of dietary Ca on Tb mass.

Conclusions: Our data demonstrates that a complex interaction exists between dietary Ca intake and genetics to influence development of peak Tb mass during growth. There is also evidence that this interaction is different by bone site.

Disclosures: James Fleet, None.

Late-Breaking Abstracts

LB-1153

Reduced Mortality and Subsequent Fracture Risk with Oral Bisphosphonate Treatment in Secondary Fracture Prevention: an Observational 8-Year Follow-Up Study. Tineke van Geel¹, Dana Bliuc², Piet Geusens³, Jacqueline Center⁴, Geert-Jan Dinant⁵, Joop van den Bergh⁶, Alastair McLellan⁷, John A Eisman². ¹Maastricht University, NL, ²Garvan Institute of Medical Research, ³Maastricht University Medical Center, ⁴+61 (02) 9295 8100, ⁵Maastricht University, ⁶VieCuri Medical Centre of Noord-Limburg, ⁷NHS Education for Scotland

Purpose: To analyze the effect of oral bisphosphonate therapy on subsequent fracture and mortality over 8-years of follow-up.

Methods: Between 1999 and 2007, 5011 of 9439 men and women aged ≥ 50 years who had sustained a clinical fracture accepted an invitation to attend the Glasgow Fracture Liaison Service. Mortality and subsequent fracture risk were the pre-defined outcomes. Cox proportional hazard models compared outcomes between patients who were or were not prescribed bisphosphonates.

Results: Of the 9439 patients, 53.1% (n=5011) attended the service and were fully assessed; 22.2% declined assessment, 19.3% were too frail to be assessed and 5.4% were already on treatment. All 5011 patients received calcium and vitamin D and of these, 2534 (50.7%) were prescribed oral bisphosphonates, based on pre-defined fracture history and age-defined bone mineral density cut-offs.

After 8-years of follow-up, absolute subsequent fracture risks for patients who were prescribed bisphosphonates was 13.3% vs 11.8% (p = 0.126) for those on calcium and vitamin D alone. The absolute mortality risks were 15.0% vs. 9.5%, respectively (p < 0.001). These differences related to the treatment selection criteria. Hence, although those prescribed bisphosphonates were more likely to be female (82.9 vs. 72.4%), they were older (73.4 vs. 64.4 years), had lower bone mineral density (T-score: -3.1 vs. -1.5) and had more hip fractures (21.7 vs. 6.2%; p < 0.001).

In the two groups, analysed separately, the predictors of fracture and mortality were age, gender, bone mineral density, fracture location, alcohol, glucocorticoid use and smoking and were similar. After adjustment for these characteristics, patients prescribed bisphosphonates had lower subsequent fracture risk (Hazard Ratio (HR): 0.59; 95%CI: 0.48-0.73) and lower mortality risk (HR: 0.79: 0.64-0.96); the latter not attributable to fewer subsequent fractures.

Conclusions: Amongst patients, fully assessed after a fragility fracture, those with higher fracture risk and prescribed bisphosphonates had worse baseline characteristics. After adjusting for these differences, those prescribed bisphosphonate treatment had a substantially lower hazard for subsequent fragility fracture (0.59) and lower hazard (0.79) for mortality. These long-term community-based data indicate a clear benefit of bisphosphonate therapy for both subsequent fracture and mortality outcomes.

Disclosures: Tineke van Geel, None.

LB-1154

Vosoritide (BMN 111) in children with achondroplasia: Results from a Phase 2, open-label, sequential cohort, dose-escalation study. Melita Irving¹, Carlos Bacino², Xiaofan Cao³, Joel Charrow⁴, Valerie Cormier-Daire⁵, Paul Harmatz⁶, Leonid Katz³, John Phillips⁷, Sagar Vaidya³, Julie Hoover-Fong⁸, Ravi Savarirayan⁹. ¹Guy's & St. Thomas' NHS Foundation Trust, ²Evelina Children's Hospital, ³Baylor College of Medicine, ⁴BioMarin Pharmaceutical Inc., ⁵Ann & Robert H. Lurie Children's Hospital of Chicago, ⁶Institut Imagine, Université Paris Descartes, Hôpital Necker - Enfants Malades, ⁷UCSF Benioff Children's Hospital Oakland, ⁸Vanderbilt University Medical Center, ⁹Johns Hopkins University School of Medicine, ⁹Royal Children's Hospital Victoria, University of Melbourne

Background and objectives. Achondroplasia, the most common form of human dwarfism, is caused by a gain-of-function mutation in the fibroblast growth factor receptor 3 gene (*FGFR3*) and is characterized by abnormal endochondral bone formation. C-type natriuretic peptide (CNP) is a potent stimulator of endochondral bone growth. This phase 2, multi-center, open-label, sequential cohort, dose-escalation study evaluated the safety, tolerability and efficacy of daily subcutaneous injections of vosoritide (BMN 111), a CNP analog, in children with achondroplasia aged 5-14 years.

Design and methods. Subjects were required to complete at least 6 months of pretreatment growth assessment in a natural history study prior to enrollment. 26 children with achondroplasia (12 male, 14 female, mean age 7.8 ± 1.8 years) were assigned to one of three dose cohorts: 2.5 $\mu\text{g}/\text{kg}/\text{day}$ (n = 8), 7.5 $\mu\text{g}/\text{kg}/\text{day}$ (n = 8), and 15.0 $\mu\text{g}/\text{kg}/\text{day}$ (n=10). Subjects remained on a fixed dose for 6 months. Safety was assessed by measures including incidence of adverse events (AEs) and changes in vital signs and clinical laboratory parameters. Efficacy was measured by changes in annualized growth velocity, absolute growth, and body proportions.

Results. Vosoritide was well tolerated across all dose cohorts. The majority of AEs were mild and included injection site reactions, asymptomatic hypotension, and

headache. No serious AEs were reported, and no AEs led to permanent discontinuation of study drug. Mean (SD) baseline annualized growth velocity based on the last 6 month natural history growth measurements was 3.8 ± 1.1 cm/year in the 2.5 $\mu\text{g}/\text{kg}/\text{day}$ dose group, 2.9 ± 1.4 cm/year in the 7.5 $\mu\text{g}/\text{kg}/\text{day}$ dose cohort, and 4.0 ± 2.3 cm/year in the 15.0 $\mu\text{g}/\text{kg}/\text{day}$ dose cohort. Post-treatment mean annualized growth velocity was 3.4 ± 0.9 cm/year in the 2.5 $\mu\text{g}/\text{kg}/\text{day}$ dose cohort, 4.2 ± 1.3 cm/year in the 7.5 $\mu\text{g}/\text{kg}/\text{day}$ dose cohort, and 6.1 ± 1.1 cm/year in the 15.0 $\mu\text{g}/\text{kg}/\text{day}$ dose cohort. A mean increase of 2.0 ± 2.0 cm/year (95% CI 0.6, 3.4; p = 0.0111), which represents a 50% increase from mean baseline annualized growth velocity, was observed in the 15.0 $\mu\text{g}/\text{kg}/\text{day}$ dose cohort. Changes from baseline in body proportionality were not observed after 6 months of treatment.

Conclusions. These data support the further development of vosoritide for the treatment of children with achondroplasia with open growth plates.

Disclosures: Melita Irving, BioMarin Pharmaceutical Inc.

This study received funding from: BioMarin Pharmaceutical Inc.

LB-1155

The *ACVRI*^{R206H} mutant receptor causes Fibrodysplasia Ossificans Progressiva by gaining responsiveness to Activin A. Aris Economides¹, Sarah Hatsell², Vincent Idone², Dana Alessi Wolken², Lily Huang², Hyon Kim², Lili Wang², Xialing Wen², Kalyan Nannuru², Johanna Jimenez², LiQin Xie², Genevieve Makhoul², Rostislav Chernomorsky², David D'Ambrosio³, Richard Corpin², Christopher Schoenherr², Kieran Feeley⁴, Paul Yu⁵, Harikiran Nistala⁶, George Yancopoulos², Andrew Murphy². ¹Regeneron Pharmaceuticals, Inc., USA, ²Regeneron Pharmaceuticals, Inc., ³R, ⁴Ohio State University College of Medicine, ⁵Brigham & Women's Hospital, ⁶Regeneron Genetics Center

Fibrodysplasia Ossificans Progressiva (FOP) is a rare genetic disorder characterized by episodic exuberant heterotopic ossification (HO), whereby certain skeletal muscles, fascia, ligaments, and tendons are abnormally converted into histologically "normal" bone. The HO process may be preceded by "flare-ups", characterized by painful swelling of connective tissue; however, HO can also occur in the absence of obvious flare-ups. Episodes of HO can be spontaneous or may result from trauma or other insults that trigger inflammation. More importantly, the HO that forms in FOP patients is effectively permanent, as attempts to resect it almost invariably trigger additional episodes of HO. Hence, the cumulative effect is progressive immobility with catastrophic consequences. FOP results from mutations in the intracellular domain of the type I BMP receptor ACVRI (also known as ALK2). The most common mutation alters arginine 206 to histidine (*ACVRI*^{R206H}) that has been thought to drive HO as a result of receptor hyperactivity. In contrast to what has been described in the literature, we unexpectedly found that this mutation rendered ACVRI responsive to Activin A, AB, AC, and B, a set of ligands that normally antagonize BMP signaling mediated through ACVRI, and which normally do not induce bone formation. To test the implications of this finding in vivo, we engineered a genetically accurate mouse model of FOP that carries the *Acvri*^{R206H} mutation. As mice that constitutively express *Acvri*[R206H] die perinatally, we generated a Cre/lox-based conditional-on knock-in model of *ACVRI*^{R206H}. When *Acvri*[R206H] expression was induced, mice developed HO mirroring that observed in FOP, whether spontaneously or in response to trauma. Administration of Activin A (using collagen sponges) also triggered HO in the *Acvri*^{R206H/+} mice but not in wild-type controls; mice treated with vehicle did not develop HO irrespective of their *Acvri* genotype. Importantly, the development of both spontaneous and trauma-induced HO in *Acvri*^{R206H/+} mice could be blocked by a fully human neutralizing antibody specific to Activin A. Our results indicate that *ACVRI*^{R206H} causes FOP by gaining responsiveness to Activin A, a ligand that is normally antagonistic to ACVRI-mediated BMP signaling. Furthermore, Activin A is necessary and sufficient for driving HO in our model of FOP; hence, inhibition of Activin A (e.g. by neutralizing antibodies) presents a new potential therapeutic option for FOP.

Disclosures: Aris Economides, Regeneron Pharmaceuticals

LB-1156

The Association of Race Ethnicity and Risk of Atypical Femur Fracture in Women Treated with Oral Bisphosphonate Drugs. Joan Lo¹, Rita Hui², Christopher Grimsrud³, Malini Chandra³, Romain Neugebauer³, Joel Gonzalez³, Amer Budavr³, Gene Lau³, Bruce Ettlinger³. ¹Kaiser Permanente, ²Kaiser Permanente California, ³Kaiser Permanente Northern California

Purpose: Several epidemiologic studies suggest that compared to white women, Asians have a propensity to suffer an atypical femur fracture (AFF) while taking bisphosphonate (BP) drugs. This study examines the relative risk of AFF following BP initiation for Asian compared to white women. **Methods:** Using data from a large northern California healthcare delivery system, we examined diaphyseal femur fractures among women age ≥ 50 years who initiated oral BP therapy during 2002-2007. Demographic and clinical characteristics at baseline, including prior fracture history, diabetes mellitus, rheumatoid arthritis and treatment with glucocorticoids (≥ 1825 mg prednisone equivalent in prior year), aromatase inhibitors and

pharmacologic proton pump inhibitors were examined using health plan and pharmacy databases. Radiographs of diaphyseal fractures were reviewed and classified as AFF or not based on 2013 American Society of Bone and Mineral Research Task Force criteria. The risk of AFF for Asian compared to white women was examined using Cox proportional hazard analyses, adjusting for differences in BP exposure and other potential risk factors. Results: We identified 48,390 women (mean age 69.5 ± 10.0 years) who initiated BP therapy and had at least three years of follow-up. The cohort was diverse, including 65.3% white, 17.1% Asian, 9.5% Hispanic, 4.1% black and 4.0% other/unknown race. During a median follow-up of 7.7 years, 68 women experienced an AFF. The rate of AFF was 18.7 per 100,000 person-years overall, and eight-fold higher among Asian compared to white women (64.2 vs 7.6 per 100,000 person-years, respectively). The median duration of BP use was greater among Asian women (3.8 years) versus whites (2.7 years). In unadjusted analyses, prior fracture, diabetes, rheumatoid arthritis and baseline glucocorticoid, aromatase inhibitor and proton pump inhibitor therapy were not associated with AFF. However, race/ethnicity was strongly associated with risk of AFF, with an age-adjusted relative hazard of 8.5 (95% confidence interval, CI 4.9-14.9) comparing Asian to white women, that was only modestly reduced to 6.6 (CI 3.7-11.5) after adjusting for BP duration and current use. Conclusion: Our study confirms marked racial disparity in AFF risk that should be further examined, particularly the mechanisms accounting for this difference. In the interim, counseling of Asian women about osteoporosis drug continuation should include consideration of their higher AFF risk.

Disclosures: Joan Lo, Sanofi; Amgen

LB-1157

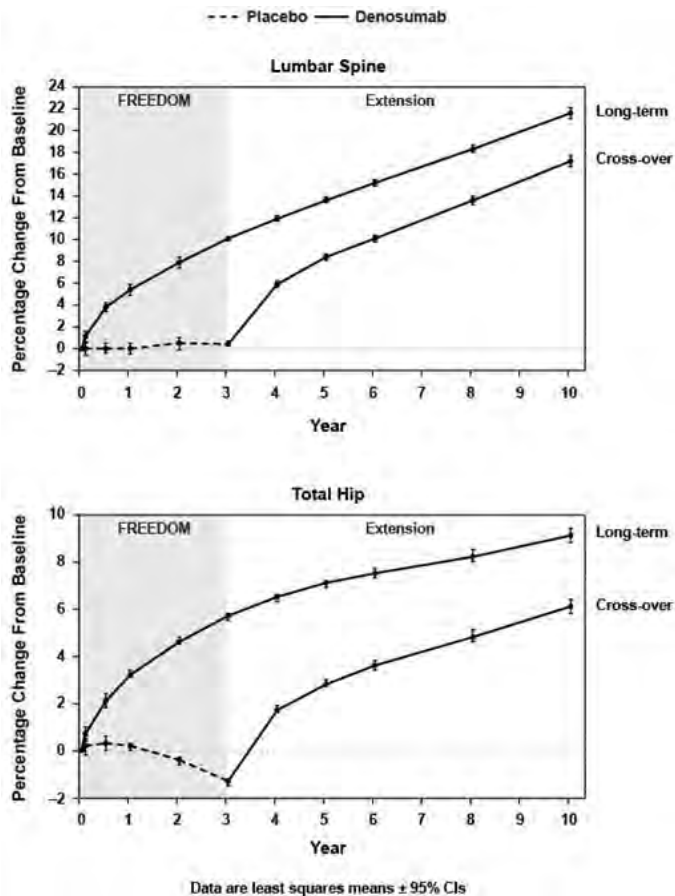
Ten Years of Denosumab Treatment in Postmenopausal Women With Osteoporosis: Results From the FREEDOM Extension Trial. HG Bone^{*1}, ML Brandi², JP Brown³, R Chapurlat⁴, SR Cummings⁵, E Czerwinski⁶, A Fahrleitner-Pammer⁷, DL Kendler⁸, K Lippuner⁹, J-Y Reginster¹⁰, C Roux¹¹, E Vittinghoff¹², NS Daizadeh¹³, A Wang¹³, P Dakin¹³, RB Wagman¹³, S Papapoulos¹⁴. ¹Michigan Bone & Mineral Clinic, ²University of Florence, ³Laval University & CHU de Québec Research Centre, ⁴Hôpital Edouard Herriot, ⁵San Francisco Coordinating Center, CPMC Research Institute, & UCSF, ⁶Krakow Medical Centre, ⁷Medical University Graz, ⁸University of British Columbia, ⁹Bern University Hospital, ¹⁰University of Liège, ¹¹Paris Descartes University, ¹²UCSF, ¹³Amgen Inc., ¹⁴Leiden University Medical Center

Purpose: Osteoporosis is an important chronic disease, requiring prolonged treatment. Long-term efficacy and safety data are therefore of great importance. Denosumab (DMAB) is used in over 80 countries or administrative districts worldwide for the treatment of postmenopausal women with osteoporosis. The effects of DMAB treatment for up to 10 years have been evaluated in the 3-year FREEDOM study and its 7-year extension. Here, we report results through the final year of the extension, representing up to 10 years of continued DMAB treatment.

Methods: During the extension, all subjects were to receive 60 mg DMAB every 6 months and calcium and vitamin D daily. In this analysis, the long-term group received 10 years of DMAB treatment (3 years in FREEDOM and 7 years in the extension), and the cross-over group received 7 years of DMAB treatment (3 years of placebo in FREEDOM and 7 years of DMAB in the extension).

Results: Of the 4,550 subjects who entered the extension, 2,784 (61%) continued to participate at the beginning of year 10. Of these, 2,212 (80%) have completed their final 10-year visit, 120 (4%) discontinued, and 452 (16%) were ongoing at the time of this submission. In the long-term group, further significant increases in BMD occurred with mean cumulative 10-year gains from FREEDOM baseline of 21.6% (lumbar spine) and 9.1% (total hip). The cross-over group had mean cumulative 7-year gains of 16.3% (lumbar spine) and 7.3% (total hip) from the extension baseline (Figure; all $P < 0.0001$ compared with FREEDOM baseline, extension baseline, and previous measurement). Similar and sustained reductions in bone turnover markers were observed in both groups, with the characteristic attenuation of effect at the end of the dosing period. Yearly rates of new vertebral and nonvertebral fractures remained low. Overall incidence rates of adverse events (AEs) and serious AEs were consistent with data reported previously in the extension study.

Conclusions: DMAB treatment for up to 10 years was associated with persistent reduction of bone turnover, continued increases in BMD without therapeutic plateau, and low fracture incidence. The benefit/risk profile for DMAB in an aging population of postmenopausal women remains favorable.



Figure

Disclosures: HG Bone, Amgen, Merck, Grunenthaler; Amgen; Amgen, Merck
This study received funding from: Amgen Inc.

LB-SA0001

Marrow Adiposity is Associated With Low Bone Turnover and Sclerostin Levels in Peritoneal Dialysis Patients. Fellype Barreto¹, Carolina Moreira^{*2}, Rodrigo de Oliveira³, Luciene dos Reis⁴, Vanda Jorgetti⁴, Aluizio Carvalho⁵, Rosa Moyses⁶. ¹Pontificia Universidade Católica do Paraná; Laboratório P.R.O, Fundação Pro Renal, Brazil, ²Federal University of Parana, Brazil, ³Universidade Federal do Rio Grande do Norte, ⁴Universidade de São Paulo, Brazil, ⁵Universidade Federal de São Paulo, Brazil, ⁶Universidade de São Paulo, Universidade Nove de Julho, Brazil

Background: Marrow adiposity has been implicated in the pathogenesis of bone disorders, such as osteoporosis and bone fragility. Diabetes mellitus (DM) is very prevalent among peritoneal dialysis patients. The aim of this study is to investigate the relationship between marrow adiposity, bone turnover and sclerostin levels in patients with renal osteodystrophy with and without diabetes who undergoing peritoneal dialysis.

Methods: Transiliac bone biopsy specimens from 41 peritoneal dialysis patients (age: 50.3 ± 10.2 yrs, 56 % male and 43% with DM) were analyzed by quantitative histomorphometry. Bone and marrow adipocyte parameters were assessed and correlated to biochemical markers of bone turnover and sclerostin.

Results: Adipocyte area (Ad.Ar), perimeter (Ad.Pm) and percentage of adipocyte volume per marrow volume (Ad.V/Ma.V) correlated positively with age. Diabetic patients had higher marrow adiposity than non diabetic (Ad.V/Ma.V = 50 ± 14 vs 39 ± 12 ; $P=0.009$; Ad.Ar = 0.19 ± 0.06 vs 0.15 ± 0.05 mm²; $P=0.02$). An inverse association between Ad.V/Ma.V and bone specific alkaline phosphatase (BSAP) ($r = -0.32$; $P=0.04$) and direct relationship with sclerostin ($r=0.38$; $P=0.01$) was observed. Patients with Ad.V/TV > 41% (median) presented higher percentage of low turnover bone disease seen by histomorphometry dynamic parameters ($P=0.04$) as well as lower BSAP (39.5 ± 27.3 vs 65.3 ± 28.9 U/L; $P=0.006$) and higher sclerostin levels (2.3 ± 0.97 vs 1.6 ± 0.97 ; $P=0.02$) than patients below the median.

Conclusion: Increased marrow adiposity seems to be associated to high sclerostin and to low bone turnover disease in peritoneal dialysis patients. Further studies are required to understand the role of marrow adiposity to the pathogenesis of renal osteodystrophy.

Disclosures: Carolina Moreira, None.

LB-SA0002

Treatment of Autosomal Dominant Hypocalcemia with the Calcilytic NPS795. Mary Ramnitz¹, Rachel Gafni², Beth Brillante², Lori Guthrie², David Gash³, Jeffrey Gelb³, Eva Krusinska³, Sarah Brennan⁴, Daniela Riccardi⁴, Mohd Ezuan Bin Khayat⁵, Donald Ward⁵, Edward Nemeth⁶, Ralf Rosskamp³, Michael Collins². ¹National Institutes of Health, USA, ²Skeletal Clinical Studies Unit, Craniofacial & Skeletal Diseases Branch (CSDB), National Institute of Dental & Craniofacial Research (NIDCR), National Institutes of Health (NIH), United Kingdom, ³NPS Pharmaceuticals, Inc., United Kingdom, ⁴School of Biosciences, Cardiff University, United Kingdom, ⁵Faculty of Life Sciences, University of Manchester, United Kingdom, ⁶MetisMedica, Canada

Autosomal dominant hypocalcemia type 1 (ADH1) is a rare form of hypoparathyroidism caused by heterozygous activating mutations of the calcium-sensing receptor (CaR) gene. Mutant CaRs are more sensitive to activation by extracellular ionized calcium (Ca), resulting in a shift in the set-point for blood Ca homeostasis to a lower level. Affected individuals are hypocalcemic and have inappropriately low levels of parathyroid hormone (PTH) and renal Ca reabsorption. Conventional therapy with Ca and vitamin D analogs raises blood Ca, but exacerbates hypercalciuria, often causing renal complications. Calcilytic compounds directly inhibit CaRs, and by increasing PTH secretion and renal Ca reabsorption, have the potential to restore eucalcemia.

Five adults with ADH1 (aged 24-55 y; 2 women) due to 4 different CaR gene mutations (A840V, Q245R, E228K, and a novel E228A mutation) were studied. After an overnight fast, subjects received escalating doses of NPS795 by iv infusion (5mg/10min, 15mg/3.5h, and 30 mg/3.5h; 2 received 50mg/3.5h). Calcitriol was discontinued 48h and Ca supplements 9-10h prior to infusion. Pharmacokinetics and pharmacodynamics were assessed via serial sampling. Mixed model repeated measures analysis was conducted to assess percent changes in PTH, fractional excretion of Ca (FECa), and blood Ca. Wild type (wt) CaR and the 4 mutant CaR were stably expressed in HEK 293 cells and intracellular responses (cytoplasmic Ca, ERK and p38^{MAPK} phosphorylation) to changes in extracellular Ca concentration were assessed in the presence or absence of NPS795.

Plasma PTH levels increased, and FECa decreased from baseline in a dose-dependent manner. Blood Ca levels remained stable during NPS795 infusion, despite fasting and no Ca or vitamin D supplementation. NPS795 was generally safe and well tolerated. In HEK cells, all mutant CaRs were half-maximally activated (EC₅₀) at lower concentrations of extracellular Ca compared to wt CaR, and exposure to NPS795 increased the EC₅₀ for all CaR activity readouts.

NPS795 increased plasma PTH levels and decreased FECa in subjects with ADH1 in an apparent dose-dependent manner, while maintaining blood calcium levels during fasting. While the optimal dose and dosing regimen are not yet determined, NPS795 appears to represent a potential treatment for ADH.

Disclosures: *Mary Ramnitz, NPS Pharmaceuticals, Inc. This study received funding from: NPS Pharmaceuticals, Inc.*

LB-SA0003

Effect of Density on the Creep Response of Human Cortical Bone. Gavriel Feuer^{*}, Mariane Espalitie, Subrata Saha. SUNY Downstate, USA.

The time-dependent mechanical properties of cortical bone, or creep, have been shown to contribute to etiologies of vertebral compression fractures and subsidence of press fit implants. This type of mechanical loading causes diffuse damage that may repair itself through mechanisms other than remodeling and has also been shown to induce woven bone formation. The purpose of this study was to characterize the creep response of diseased and healthy bone tissue in bending without neglecting variations that can arise from differences in density and porosity.

Cortical bone beams were harvested from the tibias of three separate donors (55 y/o male, 86 y/o female, 95 y/o female, N=28). Wet apparent density of the samples were measured. Multi-step creep tests were conducted on each sample for a ten minute duration per test. The holding stress for the first step was 50 MPa and after each step the stress was increased by 10 MPa. This process continued until the 130 MPa stress level was completed or the sample failed. Following mechanical testing the samples were embedded and polished to measure the 2D porosity. Using a multiple linear regression the secondary creep phase, the region in the creep versus time curve with a constant strain-rate (de/dt), was fit to a power model and included variables for density (ρ) and normalized stress (σ/E), the stress normalized to the initial elastic modulus (E).

The equation that resulted from the power fit was $de/dt = 104(\sigma/E)^{3.26}(\rho)^{-3.77}$ (R=0.9159) All estimated coefficients in the power model were highly significant (P<0.001). This model was found to fit better than using normalized stress alone. Moreover, when using normalized stress as opposed to stress the influence of porosity became insignificant.

Damage accumulation in human cortical bone due to creep bending may have role in orthopedic problems by reducing the overall strength of the bone. The steady-state creep rate for human cortical bone was strongly correlated to the applied normalized stress level by power relationship. In addition, the inclusion of wet apparent density significantly improved the model prediction. Using normalized stress as a variable instead of stress eliminated the need to include porosity in the model. This information may be useful for simulating the creep response of various states of cortical bone.

Disclosures: *Gavriel Feuer, None.*

LB-SA0004

Repeated Scanning of Mouse Hind Limbs Using In Vivo Micro-Computed Tomography Does Not Alter Bone Structure and Muscle Contractile Function in CD-1 Mice. Sandra Sacco^{*}, Caitlin Saint², William Gitting¹, Amanda Longo¹, Jordan Bunda¹, Rene Vandenoorn¹, Phil Salmon³, Wendy Ward⁴. ¹Department of Kinesiology, Faculty of Applied Health Sciences, Brock University; Centre for Bone & Muscle Health, Brock University, ²Department of Health Sciences, Faculty of Applied Health Sciences, Brock University; Centre for Bone & Muscle Health, Brock University, ³Bruker-MicroCT, ⁴Department of Kinesiology, Faculty of Applied Health Sciences, Brock University; Department of Health Sciences, Faculty of Applied Health Sciences, Brock University; Centre for Bone & Muscle Health, Brock University

Background: In vivo micro-computed tomography (μ CT) is a powerful imaging tool for measuring longitudinal changes in three-dimensional bone structure in rodents. New applications in μ CT scanning may include parallel assessments of bone and muscle structures for examining associations between these tissues. While one to nine weeks of repeated exposure to low doses of x-ray radiation from μ CT scanning does not impact trabecular bone structure in mice, its long-term effects on the mouse skeleton when scanned through development and at key stages of the lifespan (representing early, mid and later adulthood) are not known. Moreover, it is unknown whether repetitive scanning of the hind limb affects muscle form and contractile performance. Objective: Determine the structural and functional impact of repetitive μ CT scanning on bone and muscle tissues. Methods: At 2, 4 and 6 months of age, mouse hind limbs were scanned using in vivo μ CT (Skyscan 1176) at 9 μ m isotropic resolution with 1 mmAl filter and at one of three scanning parameters: 1) 50kV, 100mA, 1.0° rotation step, 3300 ms; 2) 50kV, 100mA, 0.8° rotation step, 3300 ms; and 3) 40kV, 300mA, 0.8° rotation step, 3350ms providing radiation doses of 222, 261, and 460 mGy, respectively (MOSFET, Best Medical Canada). Contralateral hind limbs were scanned at 6 months to serve as non-irradiated internal controls to determine whether recurrent radiation exposure alters proximal tibia trabecular bone structure. In vitro contractile performance of representative slow (soleus) and fast (extensor digitorum longus) muscles of the radiated and non-radiated hind limbs were also measured at age 6 months (1200A in vitro System, Aurora Scientific Inc.). Results: Trabecular bone volume fraction, thickness, number and separation at the proximal tibia were similar between radiated and non-radiated mice regardless of level of radiation exposure. No differences (radiated vs. non-radiated) with respect to muscle form (i.e. mass, length, cross-sectional area) or function (i.e. peak isometric twitch, tetanic force) were observed. Conclusion: Radiation exposure from repeated μ CT scanning at early, mid and later adulthood did not alter proximal tibia trabecular bone structure and multiple measures of muscle form and function in the hind limbs of CD-1 mice. These findings can be applied to future studies that investigate lifelong responses of both bone and muscle structures from early life exposure to various intervention strategies.

Disclosures: *Sandra Sacco, None.*

LB-SA0005

Three-dimensional analysis of chin bone for secondary bone graft with beta-TCP in unilateral cleft patients. Kazuaki Miyagawa^{*}, Sachie Hiroishi, Yutaka Matsushita, Susumu Tanaka, Mikihiko Kogo.

Autogenous bone grafting with chin for the reconstruction of alveolar cleft was more noninvasive than iliac crest. We thereby proactively use chin bone as a donor site for secondary bone graft in those with patients with unilateral alveolar cleft. In general, chin bone is not employed as harvesting area because the amount of bone is small compare to other site such as ilium and is restricted because of surgical risk to damage the dental root or mental nerve. It has also a problem of the contour change in the chin area. To resolve these problems, we use beta-tricalcium phosphate, beta-TCP in mixture with chin bone. Thereby, we can increase the amount of donor bone and enable to apply for some extent of wide cleft case. In the present study, we evaluated the usefulness of the secondary bone grafting by chin bone in the mixture with beta-TCP in the patients with unilateral alveolar cleft, the biomechanical properties of alveolar grafted bone and regenerated bone at harvested site are analyzed using cone-beam computed tomography images. This study comprised 34 non syndromic case of unilateral cleft lip (CLA) and cleft lip palate (CLP) Japanese patients. Eight of these were underwent bone grafting without beta-TCP and the rest of them were operated with beta-TCP at the mean age of 9.5 and 9.6 years old, respectively. Furthermore, beta-TCP group was also classified into two subdivisions

by cleft volume. Three-dimensional built images before and after the surgery of each patient were overlaid by several landmarks on facial bone and newly formed (or regenerated) bone could be extracted by subtraction the images using three-dimensional analysis software (Ratoc, Japan). In the formed bone bridge at alveolar cleft site, BV/TV showed no significant difference among three groups, but in the case of CLA, beta-TCP group showed high mean rate in the comparison with the control (without beta-TCP) group. Tb.th, Tb.N and Tb.sp exhibited no statistically significant. As for the regenerated bone at donor site. BV/TV, Tb.Th, Tb.N, Tb.sp, TBPf and SMI were superior in the beta-TCP group compared to those of control group. These results suggested that alveolar bone graft by chin bone in the mixture with beta-TCP is useful for sufficient bone bridge in some degree of wider unilateral alveolar cleft. Also, especially in the case of cleft lip and alveolus, the trabecular bone quality of grafted and regenerated bone could show favorable results in the presence of beta-TCP.

Disclosures: Kazuaki Miyagawa, None.

LB-SA0006

Early developmental effects of Bisphenol-A (BPA) on bone structure and function are sex dependent. Karl Jepsen¹, Lauren Smith^{*2}, Martha Susiarjo³, Marisa Bartolomei³. ¹University of Michigan, USA, ²The University of Michigan, USA, ³University of Pennsylvania Perelman School of Medicine, USA

BPA is a widely used synthetic compound (e.g., plastics, receipts, can-linings, water supply pipes). BPA, which leaches from products and is found ubiquitously in the environment, is associated with estrogenic disrupting effects and can induce metabolic changes across multiple generations. Sex hormones, both in concentration and in timing, are critical to bone growth and development. Effects on bone via direct exposure have been shown but to our knowledge data of trans-placental effects are lacking. We hypothesized that exposure of a filial (F1) generation to BPA during prenatal development and through weaning would lead to detectable changes in bone morphology and/or function. To test this, female C57BL/6 (B6) mice (F0) were assigned to 1 of 3 diets (control (C), lower dose (LD) BPA (10µg/kg/d), or upper dose (UD) BPA (10mg/kg/d)) two weeks prior to mating and through gestation and lactation. F1 mice were placed on control diets upon weaning. Male and female femurs were analyzed as adults (4-13months of age, n=8-29/group) for bone morphology and composition via nanoCT (8µm voxel size) and mechanical properties via 4-point bending. Student's t-test was used for unadjusted comparisons and general linear model ANOVAs for adjusted comparisons, significance of p<0.05. Each dose-group was compared back to the control, and sexes were analyzed independently. We found no significant difference in body mass (BM) across groups, but body composition was altered in both LD and UD males 5% (p=0.04) and 6% (p=0.03), respectively. After BM adjustment both UD and LD males, but not females, showed 6.5% (p=0.01) and 10% (p<0.01) reduced robustness (total cross sectional area (Tt.Ar)/femur length), respectively, compared to controls. BM adjusted Tt.Ar was significantly decreased in UD and LD (p<0.01 and p=0.04, respectively), while femoral length was similar, indicating that the decreased robustness was due to altered periosteal expansion. Only the males, both UD and LD, showed a reduction in maximum load, 13.5% (p<0.02) and 13.7% (p=0.06), respectively after adjustment for BM. The only altered traits in female F1 mice was decreased cortical area and tissue mineral density, 3.5% (p=0.03) and 1.7% (p<0.01), respectively, for the UD group, after adjusting for BM and robustness. This data indicated that exposure of a F0 pregnant female to BPA leads to more slender and weaker bones in F1 males and only minor effects on F1 females with no change in bone strength.

Disclosures: Lauren Smith, None.

LB-SA0007

Bone-specific underdevelopment of trabecular bone microarchitecture in ambulatory children with mild cerebral palsy. Daniel Whitney^{*1}, Harshvardhan Singh¹, Freeman Miller², Keri DiAlessandro², Nancy Lennon², Christopher Modlesky¹. ¹University of Delaware, USA, ²AI duPont Hospital for Children, USA

Nonambulatory children with more severe forms of cerebral palsy (CP) have underdeveloped trabecular bone microarchitecture at the distal femur, their primary fracture site. However, whether ambulatory children with mild CP also have underdeveloped trabecular bone microarchitecture has not been determined. Ten ambulatory children with mild spastic CP and 10 typically developing control children between 5 and 12 years of age participated in this study. Twenty-six axial magnetic resonance images (175 x 175 x 700 µm³) of the distal tibia and the distal femur were collected from the more affected limb in children with CP and the nondominant limb in controls. Measures of trabecular bone microarchitecture [apparent trabecular bone volume to total volume (appBV/TV), trabecular number (appTb.N), trabecular thickness (appTb.Th) and trabecular separation (appTb.Sp)] were estimated using the 20 most central images at each site and custom software (Interactive Data Language, Boulder, CO). Dual-energy X-ray absorptiometry was used to assess bone mineral content (BMC) and areal bone mineral density (aBMD) at the distal tibia and the distal femur. Compared to controls, the distal tibia and the distal femur in ambulatory children with CP had lower appBV/TV by 22% (d = 2.32, p < 0.05) and 13% (d = 1.15, p < 0.05), lower appTb.N by 15% (d = 2.32, p < 0.05) and 10%

(d = 1.66, p < 0.05), and higher appTb.Sp by 32% (d = 2.10, p < 0.05) and 19% (d = 1.5, p < 0.05), respectively. Additionally, compared to controls, children with CP had lower appTb.Th by 8% (d = 1.36, p < 0.05) at the distal tibia, but there was no significant difference between groups at the distal femur. Moreover, the difference in appTb.Sp between children with CP and controls was greater at the distal tibia than at the distal femur (p < 0.05). Compared to controls, children with CP also had lower BMC and aBMD at the distal tibia by 31% (d = 1.25, p < 0.05) and 26% (d = 1.55, p < 0.05) and at the distal femur by 25% (d = 1.12, p < 0.05) and 21% (d = 1.23, p < 0.05), but the degree of the difference was similar (p > 0.25). The findings suggest that, relative to typically developing children, ambulatory children with mild CP have an underdeveloped trabecular bone microarchitecture and lower aBMD and BMC in the distal tibia and the distal femur. However, the degree of compromise in trabecular bone microarchitecture is more pronounced in the distal tibia than the distal femur.

Disclosures: Daniel Whitney, None.

LB-SA0008

Simulating Tumor Induced Bone Disease using a population dynamic model. Ushashi Dadwal^{*}, Mathilde Granke, Junhwan Jeon, Alyssa Merkel, Peter Cummings, Julie Sterling, Scott Guelcher. Vanderbilt University Medical Center, USA

Bone is a frequent site of metastasis of primary breast, prostate, and lung cancer. Upon establishment of tumor cells in the bone, bone remodeling is disrupted which causes clinical morbidities that lead to a decrease in patient quality of life. There are no clinical therapeutics that target tumor in the bone. Despite years of research, the temporal dynamic interactions between tumor cells and bone cells are still not understood. Integrating information from basic studies examining how each cell type behaves is challenging, and restricts our ability, to combine information into a comprehensive understanding of the complexities of tumor-induced bone disease (TIBD), and limits our ability to predict how potential therapeutics may perform. Recent studies have highlighted the potential of mathematical models of tumor progression, but none have been developed to model TIBD. Additionally, the use of experimental data to predict bone destruction and tumor burden using computational modelling has not been reported. We hypothesize that using a fundamental mathematical model to simulate progression of TIBD would allow us predict responses to novel therapeutics. We report the development and validation of a time dependent mathematical model using ordinary differential equations based on Komarova et al(1), to predict rate of bone resorption and tumor burden. Our model takes into account the cellular interaction between osteoclasts, osteoblasts and tumor cells and predicts bone resorption and tumor progression using experimental data over a four week time course by approximating power law relations. We injected bone tropic MDA GFP 231 cells (triple negative breast cancer cell line), using intratibial injections in athymic mice and sacrificed mice every week to input data to parameterize the computational model. We measured bone and tumor cell populations via histomorphometry and bone quality and loss using radiography and µCT imaging. In conclusion, this model fits experimental data, and describes the key events in the vicious cycle and will allow us to predict the effects of novel drug therapies on tumor burden and bone resorption which may aid in the development of clinical strategies for the treatment of metastatic bone disease.

1. Komarova SV (2005) Mathematical model of paracrine interactions between osteoclasts and osteoblasts predicts anabolic action of parathyroid hormone on bone. *Endocrinology* 146(8):3589-3595.

Disclosures: Ushashi Dadwal, None.

LB-SA0009

Validation of Marrow Fat Quantification using HRpQCT: A Pilot Study. Tiffany Butler^{*}, Joshua Johnson, Karen Troy. Worcester Polytechnic Institute, USA

Novel imaging techniques like high resolution peripheral quantitative computed tomography (HRpQCT) accurately quantify bone microarchitecture and volumetric bone mineral density in vivo. Marrow adipose tissue (MAT) has been linked with decreases in bone mineral density negatively regulating bone formation (1, 2). No studies to date have investigated changes in long bone MAT using HRpQCT, which could provide a noninvasive clinical tool to examine changes in marrow adipose tissue.

We set out to determine if MAT could accurately be quantified using HRpQCT. Twenty bovine femurs transversely cut in 5.5-7.5cm pieces were obtained from a local butcher and frozen. Computed tomography (CT) scans were taken (XtremeCT, Scanco, Switzerland) at 246µm isotropic voxel size. Images were analyzed in Mimics v18.0 (Materialise, Belgium). Fat voxels were identified by thresholding the volume located inside the endosteal envelope (Figure 1). Three Hounsfield unit (Hu) ranges that overlapped with typical CT fat values were tested: [-200 to -50, -300 to 50, and -400 to 50]. CT-MAT volume was calculated by multiplying the number of fat voxels by the volume of each voxel. Next, medullary tissue, marrow and fat, was removed and placed in 50 ml tubes filled with 20 ml of water. Tubes were inverted 5 times and centrifuged at 2000 RPM for 5 minutes twice for fat isolation. Fat was removed from the tubes and weighed. Gross MAT volume was calculated by dividing gross MAT mass by fat density (assumed to be 0.9196 g/cm³ (3)). Pearson correlations were used to determine relationships between gross MAT volume and CT-MAT volume (mm³).

Significance was set at $p \leq 0.05$. All statistical analyses were performed in SPSS 17.0 (SPSS Inc, Chicago, Illinois, USA).

No significant correlations were found between gross MAT and CT-MAT volumes within the specified threshold ranges: [-200 to 50 Hu] ($r = .374$, $p = .104$); [-300 to 50 Hu] ($r = .369$, $p = .110$) and [-400 to 50 Hu] ($r = .254$, $p = .280$).

Currently, no studies have investigated MAT quantification using HRpQCT. Although the simple thresholding technique utilized here was not able to accurately delineate MAT, lower resolution CT has been used to measure fat volumes (4,5). Adjusting CT acquisition settings, additional image processing and filtering may be needed to reduce noise and identify fat voxels more reliably and repeatably. Noninvasive *in vivo* quantification of MAT could lead to a better understanding of the role MAT plays in bone health.

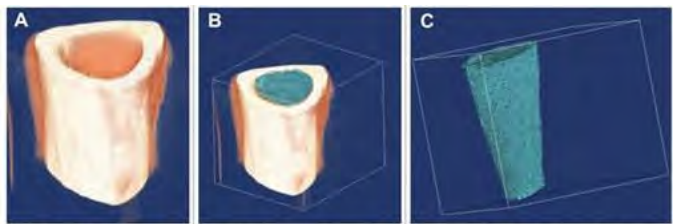


Figure 1: (A) Volume rendering of bone and all other tissues (B) MAT volume thresholded inside the medullary cavity (C) MAT volume threshold isolated

ASBMR_2015_Figure 1_Final

Disclosures: *Tiffany Butler, None.*

LB-SA0010

Zoledronic Acid: A Novel Treatment for Langerhans Cell Histiocytosis Bone Lesions in Children. Karine Bourdet, Melissa Fisceletti*, Anne-Sophie Carret, Sophie Turpin, Nathalie Alos. University of Montreal, Canada

Background:

Langerhans cell histiocytosis (LCH) is a rare disease characterized by proliferation of Langerhans cells in various organs. In children, bone lesions are frequent in up to 80% of cases, leading to pain and functional disabilities. High doses of zoledronic acid were shown to relieve the bone pain and seemed to stabilize the disease in a few adult patients.

Case report :

A 4-month-old boy diagnosed with systemic LCH, including multifocal bone lesions, was treated with chemotherapy. He presented two bone relapses despite second line treatment. Zoledronic acid was added (3 doses of 0.025 mg/kg at 0, 3 and 6 months). Patient is in remission one year post-treatment.

A 5-year-old boy presented with focal bone lesions and progression after six months of chemotherapy. He received 3 doses of zoledronic acid (0.025 mg/kg initially and 0.05 mg/kg at 3 and 6 months) in combination with chemotherapy.

A 10-year-old girl was diagnosed with multifocal bone LCH, including vertebral fracture. She responded well to a combination of chemotherapy and zoledronic acid.

In all 3 patients, F18-FDG PET/CT was used to follow the treatment response and showed rapid normalization of the metabolic activity after one month. Alternatively to Tc99m-MDP bone scintigraphy, F18-FDG biodistribution is not affected by zoledronic acid.

Low dose bisphosphonates was well tolerated and was able to control bone disease.

Results:

Zoledronic acid showed beneficial effects in 3 children with LCH bone lesions. F18-FDG PET/CT could be useful to monitor response to therapy.

Disclosures: *Melissa Fisceletti, None.*

LB-SA0011

Inhibition of epigenetic factor Dnmt3b within articular chondrocytes coordinates cellular metabolic response during the development of osteoarthritis. Jie Shen*¹, Cuicui Wang², Jason Myers³, John Ashton³, Audrey McAlinden², Regis O'Keefe². ¹Washington University in St Louis, USA, ²Washington University in St Louis, ³University of Rochester, USA

Osteoarthritis (OA) is a degenerative joint disease that will affect 67 million people in the US by 2030. Recent genome-wide association screens have implicated a distinct DNA methylation signature in OA patients, indicating DNA methyltransferases (*Dnmt*) may play a role in regulating cartilage homeostasis. We found intense expression of *Dnmt3b* in murine and human articular cartilage. We observed a marked decrease in *Dnmt3b* expression in murine cartilage with aging as well as following meniscal ligament injury (MLI). An IHC array of 14 OA cartilage and 11 healthy cartilage showed that DNMT3b expression was similarly reduced in human OA tissues compared to healthy cartilage.

To define a direct role of *Dnmt3b* in chondrocytes, we treated primary articular chondrocytes with *Dnmt3b* siRNA and found that loss of *Dnmt3b* stimulated cell hypertrophy by reducing TGF β signaling and increasing BMP signaling. To further investigate the role of *Dnmt3b* during OA development, we generated *Dnmt3b* loss-of-function (LOF) mice (*Dnmt3b*^{Age1ER}) and showed that ablation of *Dnmt3b* in articular chondrocytes led to a progressive OA-like pathology in adult mice. Changes in gene expression and methylation profiles were investigated in *Dnmt3b* LOF chondrocytes by integrative analysis of RNA-Seq and Methyl-Seq data. Gene ontology analysis revealed cellular metabolism was primarily affected in LOF cells and 4-aminobutyrate aminotransferase (*Abat*) was further identified as a potential target of *Dnmt3b*. In agreement with elevated *Abat* level, HPLC-MS reviewed an increase of succinate, the product of *Abat*, as well as other downstream TCA metabolites in *Dnmt3b* LOF cells. Mitochondria function was also affected, the basal respiration and ATP production were increased due to accelerated TCA inflow. Notably, inhibition of *Abat* with vigabatrin led to attenuation of hypertrophic gene expression induced in *Dnmt3b* LOF chondrocytes and over-expression of *Abat* stimulated chondrocyte hypertrophy *in vitro*, indicating *Dnmt3b*/*Abat* axis regulates chondrocyte homeostasis. *Dnmt3b* and *Abat* expression were regulated by inflammatory factors in primary murine and human articular chondrocytes. Finally, *Dnmt3b* gain-of-function mice were protected against cartilage breakdown and subchondral bone sclerosis induced by MLI surgery. Therefore, *Dnmt3b*/*Abat* axis is required for appropriate cartilage metabolism during postnatal joint homeostasis and *Dnmt3b*/*Abat* may serve as a novel and important therapeutic target for OA.

Disclosures: *Jie Shen, None.*

LB-SA0012

Bone marrow adipocytes selectively resist lipolysis in response to fasting and β -adrenergic stimulation. Erica Scheller*¹, William Cawthorn², Brian Learman³, Brent Wu⁴, Lindsay Andersen³, Hoai An Pham³, Shaima Khandaker³, Aaron Burr³, Sebastian Parlee³, Becky Simon³, Hirovuki Mori³, Adam Bree³, Benjamin Schell³, Ormond MacDougald³. ¹University of Michigan, USA, ²University of Edinburgh, ³University of Michigan, USA, ⁴University of Illinois, USA

Marrow adipose tissue (MAT) is a functionally distinct adipose depot with the potential to contribute to both local and systemic metabolism [1]. We recently reported that MAT exists in two forms, regulated and constitutive, with underlying differences in development, regulation, adipocyte size, lipid composition, gene expression and genetic determinants [2] (Figure 1). We herein report that unlike adipocytes within regulated MAT (rMAT) and white adipose tissue (WAT), constitutive MAT (cMAT) adipocytes do not decrease in size after a 48-hour fast in rats. Similarly, cMAT remains unchanged after a 72-hour treatment with β 3-agonist CL316,243 in mice. Ingenuity pathway analysis[®] suggests that global MAT gene expression patterns are consistent with resistance to insulin and β -adrenergic agonists. Functionally, β -adrenergic-stimulated phosphorylation of hormone sensitive lipase (HSL) and perilipin (PLIN) is blunted in distal tibial MAT from rats *in vivo*, though phosphorylation of ERK1/2 is maintained. Expression of *Cav1* is decreased in MAT at the gene and protein level. Mice with knock-out of *Cav1* have decreased CL316-243-stimulated phosphorylation of HSL and PLIN in WAT. However, in mice with transgenic overexpression of *Cav1*, rMAT is depleted in response to CL316,243 but cMAT remains unchanged. When stimulated *ex vivo*, purified rMAT, but not cMAT adipocytes, undergo lipolysis and glycerol release in response to β 3-agonist CL316,243. Impaired cMAT lipolysis is rescued by downstream agonists forskolin, dibutyryl cyclic-AMP, and IBMX. These data define cell-autonomous pathways driving the selective resistance of marrow adipose tissue to lipolysis, contributing to the resistance of cMAT to both fasting and β -adrenergic stimulation.

1. Cawthorn WP, Scheller EL, Learman BS, Parlee SD, Simon BR, Mori H, Ning X, Bree AJ, Schell B, Broome DT, et al. Bone Marrow Adipose Tissue Is an Endocrine Organ that Contributes to Increased Circulating Adiponectin during Caloric Restriction. *Cell Metabolism*. 2014;20(2):368-75.

2. Scheller EL, Doucette CR, Learman BS, Cawthorn WP, Khandaker S, Schell B, Wu B, Ding SY, Bredella MA, Fazeli PK, et al. Region-specific variation in the properties of skeletal adipocytes reveals regulated and constitutive marrow adipose tissues *Nature Communications*. 2015 (accepted).

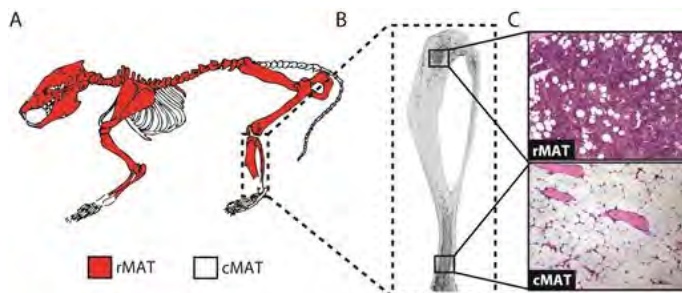


Figure 1. Regulated (rMAT) and constitutive (cMAT) marrow adipose tissue (MAT) in the rodent.

Disclosures: *Erica Scheller, None.*

LB-SA0013**Novel Metabolic Pathways Controlled by Metformin in Diabetic Mouse Bone Marrow.** Yuqi Guo, Xin Li^{*}. NYU

Metformin is the leading drug used to treat diabetic patients, who often experience many symptoms including bone loss. However, both the molecular targets and the biological pathways affected by metformin in bone are poorly understood. We used a metabolomics approach to investigate the biological pathways affected by metformin in bone marrow cells of mice. Metabolite levels were examined in bone marrow samples extracted from metformin-treated healthy and hyperglycemic (diabetic) mice using LC-MS-based metabolomics. A total of 346 unique metabolites were identified, and they are grouped into distinctive clusters that reflected general and diabetes-specific responses to metformin. As evidenced by changes in the TCA and urea cycles, increased catabolism and nitrogen waste that are commonly associated with diabetes were rebalanced upon treatment with metformin. In particular, we found succinate levels which were drastically elevated in diabetic animals are reduced to normal levels by metformin. We demonstrated that succinate stimulated osteoclastogenesis *in vitro*, which was suppressed by metformin. Overall our study revealed the metabolic pathways modulated by metformin in bones and identified a novel molecular target of metformin in osteoclastogenesis. These results have broad implication in our understanding of enhanced osteoclastogenesis with hyperglycemia and its control in mammals.

Disclosures: Xin Li, None.

LB-SA0014**Tibial Geomorphometry Indicate Stronger Bones in *mdx* Mice at 10 and 20 Weeks of Age.** Caitlin Saint^{*}¹, Maral Zibamanzarmofrad², Sandra Sacco², William Gittings², Rene Vandenboom², Wendy Ward², Paul LeBlanc². ¹Canada, ²Brock University

Background: Duchenne muscular dystrophy (DMD) is a recessive x-linked form of muscular dystrophy characterized by muscle weakness, muscle fiber degeneration, and premature death of the individual. An often overlooked phenotype of DMD is fragile bones that occurs in parallel with the advancement of the disease. The *mdx* mouse is a common rodent model of DMD, demonstrating similar muscle fiber degeneration and declines in muscle function. However, due to their efficient muscle regenerative capacity, the *mdx* model demonstrates a slow-progressing phenotype that does not impact lifespan. The trajectory of bone health also differs in the *mdx* model compared to DMD, where *mdx* bone quality has shown to not change or improve with age. Others have hypothesized that repeated degeneration-regeneration of *mdx* muscle may stimulate bone formation early on and this effect is lost after the regenerative capacity of muscle peaks at 16 weeks of age. However, no studies have examined *mdx* bone quality between 7 and 96 weeks of age. Objective: Thus, the purpose of this study was to determine the influence of age on *mdx* bone geomorphometry using micro-computed tomography (μ CT) at 10 and 20 weeks of age compared to wild-type. Methods: Ten 8 week old wild-type (C57BL/10) and *mdx* (C57BL/10ScSn-Dmdmdx/J) male mice were obtained from Jackson's Laboratory (Bar Harbour, Maine, USA). At 10 and 20 weeks of age, tibia were removed and cortical (mid-diaphysis) and trabecular (proximal metaphysis) were scanned using *in vivo* μ CT (Skyscan 1176) with the following parameters: 45 kV, 545 μ A, 0.2° rotation step, 9 μ m resolution, and 0.25 mm Al filter. Results: Cortical cross-sectional area and wall thickness did not differ with age or phenotype. Trabecular bone volume fraction ($p=0.02$) and number ($p=0.01$) were higher in *mdx* but did not differ with age. Trabecular thickness ($p=0.05$) increased with age but did not differ with phenotype. Finally, trabecular spacing increased with age in both phenotypes, more so in wild-type ($p<0.05$). Conclusion: Improved bone quality, as measured by higher trabecular bone volume and number and lower trabecular spacing, occurs in *mdx* tibia at ages 10 and 20 weeks. These findings support the hypothesis that repeated degeneration-regeneration cycles before and shortly after peak regenerative capacity of *mdx* muscle provides an environment that stimulates bone formation. Future work should examine putative osteogenic factors found in the *mdx* model at these ages.

Disclosures: Caitlin Saint, None.

LB-SA0015**LIAISON XL Assay for the Measurement & Monitoring of Active Vitamin D Analogs.** Frank Blocki^{*}¹, Greg Olson¹, John Wall¹, Jeremy Seeman¹, Fabrizio Bonelli¹, J.Ruth Wu-Wong². ¹DiaSorin Incorporated, USA, ²VidaSym

Background: Despite years of vitamin D analogs (for vitamin D receptor agonist, VDRA) research, currently VDRA are indicated mainly for managing secondary hyperparathyroidism in chronic kidney disease, and to a lesser degree are used to treat osteoporosis and psoriasis. The fact that on-the market VDRA are not more widely used for treating osteoporosis is in part due to their narrow therapeutic index, which presents at least two significant, albeit related, challenges. First, the need to frequently monitor serum Ca^{2+} levels to avoid hypercalcemia, which leads secondly, to the need for frequent titration of VDRA dosing. Clearly, emergent VDRA such as VS-105 and VS-110 with a wider therapeutic index will allow expanded utility in

osteoporosis and also into new indications including left ventricular hypertrophy, endothelial-dependent aortic relaxation and fibrosis without the pall of impending hypercalcemia.

Methods: The DiaSorin LIAISON assay was initially designed to specifically detect the complexed form of the nuclear receptor's ligand binding domain (LBD) with 1,25(OH)₂D (calcitriol) for the measurement of serum 1,25(OH)₂D levels, and can be potentially used to measure serum samples of subjects treated with Zemplar, Hecetrol and calcitriol. The assay was further characterized for its broader applicability to measure four novel VDRA with significantly wider therapeutic indices. Real time kinetic (ForteBio *Octer*) binding constants for each LBD-VDRA complex using a specific monoclonal antibody against LBD-1,25(OH)₂D were generated.

Results: 125 normal adults assessed with the DiaSorin LIAISON 1,25(OH)₂D assay had a mean of 49.6 pg/mL (95% CI: 19.9 – 79.3pg/mL). Standard curves constructed from VS-104, VS-105, VS-110 & VS-411 were all linear ($R^2>0.999$ for each) with slopes relative to the 1,25(OH)₂D standard curve of 16%, 69%, 79% and 93%. In the presence of a mean endogenous 1,25(OH)₂D level of 50pg/mL, the assay had sufficient capacity to accurately and precisely detect Zemplar across a linear range of up to 200pg/mL with complete linearity $R^2=0.997$ and a recovery of 93%. Similar results were obtained for VS-105, VS-104, VS-110 & VS-411. Conclusion: The DiaSorin LIAISON assay has potential to provide a convenient and extremely accurate and precise method for the confident clinical management of novel VDRA with a wider therapeutic index as they become cleared for clinical use.

Disclosures: Frank Blocki, DiaSorin Inc

LB-SA0016**Timing of Indomethacin Administration Causes Differential PGE₂ Response in Fluid Shear Stress Stimulated MLO-Y4 Cells.** Cheryl Drucho^{*}¹, Lidan You², Gregory Wohl³. ¹McMaster University, Canada, ²Department of Biomechanical & Industrial Engineering, Institute of Biomaterials & Biomedical Engineering, University of Toronto, Canada, ³Department of Mechanical Engineering, McMaster School of Biomedical Engineering, McMaster University, Canada

Background: Prostaglandins (PGs) are important signaling factors for bone mechanotransduction. Non-steroidal anti-inflammatory drugs (NSAIDs) have been shown to inhibit PG production of bone cells subjected to fluid shear stress *in vitro*. The purpose of this study was to assess the effects of indomethacin and its timing on the PGE₂ response of fluid shear stress stimulated MLO-Y4 cells.

Methods: MLO-Y4 cells were seeded on collagen coated 6-well culture plates 48hrs prior to loading, at 20,000 cells per well to ensure 70–80% confluence at the time of experiment. Plates were placed on an orbital shaker rotating at 200rpm to generate a fluid shear stress of approximately 1.9Pa for 2hrs. The shaker was placed in an incubator at 37°C and 5% CO₂. The media in the control (CON) group contained no NSAID. Media containing indomethacin (1×10^{-5} M) was added 30mins prior to loading in the PRE group and was present during the loading and 30mins after. Media containing indomethacin was added 30mins after loading in the POST group and was present for 3hrs. Plates subjected to shear stress (CON-F, PRE-F, POST-F) were left to sit for 30mins, loaded for 2hrs and then left to sit for 30mins before the media was sampled. Stationary non-loaded plates (CON-S, PRE-S, POST-S) were placed on a shelf in the incubator for 3hrs. Media samples were collected 30mins and 24hrs after loading. Fresh media was added 30mins prior to loading and 30mins, 3.5hrs and 6.5hrs after loading. Medium PGE₂ concentrations were determined by enzyme immunoassay. Groups were compared by 2-way ANOVA.

Results: Fluid shear stress increased the PGE₂ production of MLO-Y4 cells at 30mins in the CON-F and POST-F groups (Figure 1). At 24hrs PGE₂ concentration was similar in the CON-S and CON-F groups. Indomethacin inhibited PGE₂ production in the PRE-S and PRE-F groups at 30mins. At 24hrs, PGE₂ concentration in the PRE group was similar to that of the CON group. Indomethacin administration after loading resulted in lower PGE₂ concentrations in the POST group at 24hrs compared to the CON group.

Discussion: The PGE₂ response of MLO-Y4 cells to fluid shear stress is inhibited by indomethacin administration and varies depending upon its timing. This altered PGE₂ response may affect subsequent downstream events in the mechanotransductive process. Future studies will further examine how NSAIDs affect osteocyte signaling in response to fluid shear stress and how that in turn influences osteoblast activity.

LB-SA0018

Conditional Deletion of Protein Kinase D1 in Osteoprogenitor Cells Results in Decreased Osteogenesis *in vitro* and Decreased Bone Mineral Density *in vivo*. Wendy Bollag^{*1}, Vivek Choudhary², Qing Zhong³, Kehong Ding³, Jianrui Xu³, Lakiea Bailey³, Maribeth Johnson³, Yun Su³, Meghan McGee-Lawrence³, Xingming Shi³, Carlos Isaacs³. ¹Charlie Norwood VA Medical Center & Georgia Regents University, USA, ²Charlie Norwood VA Medical Center & Georgia Regents University, USA, ³Georgia Regents University, USA

Protein kinase D1 (PKD1), a protein kinase possessing homology to the protein kinase C and calcium/calmodulin-dependent kinase families, has been reported to play a role in a number of cellular functions, including proliferation and differentiation, cell survival, autophagy, Golgi trafficking and migration. A recent report has shown that heterozygous transgenic mice expressing a knocked in dominant-negative PKD1 mutant allele show reduced pubertal bone mass. However, the dominant-negative mutant used in these studies is known to inhibit both PKD1 and PKD2; furthermore, these investigators found the mutant to exert effects in several bone cell types including bone marrow stromal cells, osteoblasts and osteoclasts, making identification of the exact mechanism of the low bone mass difficult. PKD1 has been shown to protect cells against mitochondrially generated reactive oxygen species (ROS) and apoptosis by upregulating antioxidant systems. Our preliminary data indicate that PKD1 is expressed in bone marrow-derived mesenchymal stem cells (BMMSC) and can be activated in response to agents that trigger oxidative stress, such as hydrogen peroxide. Since PKD1 is known to protect against damage induced by oxidative stress, we hypothesized that PKD1 would be essential for the ability of osteoprogenitor cells to form bone, an ROS-generating process, *in vitro* and *in vivo*. Using BMMSCs isolated from floxed PKD1 mice, we found that PKD1 ablation upon adenovirus-mediated expression of Cre recombinase inhibited BMMSC differentiation (by alizarin red staining) in an osteogenic medium *in vitro*. Furthermore, conditional knockout mice in which PKD1 was ablated in osteoprogenitor cells by osterix promoter-driven Cre recombinase were generated. By DXA adult (3-month-old) conditional knockout (cKO) mice exhibited a significantly reduced femoral and tibial bone mineral content and bone mineral density (BMD) *in vivo* in comparison with littermate controls, with a femur BMD for control of 0.0588 ± 0.0022 (mean \pm SD; n=6) and for cKO of 0.0547 ± 0.0033 g/cm² (n=8). Micro-CT analysis showed a significant decrease in bone volume and bone surface in the cKO mice compared to controls. Histomorphometric analyses are in progress to further characterize the bone phenotype of the cKO mouse model. Taken together, our results suggest an important role for PKD1 in bone formation through modulation of stem cell/osteoprogenitor cell function.

Disclosures: Wendy Bollag, None.

LB-SA0019

Performance evaluation of the first fully automated immunoassay for Sclerostin detection and measurement. Jennifer Woodley^{*}, Frank Blocki, Kim Hilgers, Christa Klatt, Pete Voth, John Wall, Greg Olson, James Wassenberg, Fabrizio Bonelli, DiaSorin, USA

Background

Sclerostin is an emerging biomarker with an important role in the regulation of bone formation and remodeling. Sclerostin levels have also been implicated in chronic diseases such as kidney disease, diabetes and osteoporosis. However, clinical studies to establish the importance of sclerostin as a diagnostic marker have been hampered by conflicting results about the reliability of the currently available manual Sclerostin assays. Automation can improve the performance and reliability of Sclerostin testing as described herein.

Methods

The LIAISON Sclerostin assay utilizes monoclonal capture antibodies coupled to paramagnetic particles followed by polyclonal antibodies in a "sandwich" format with chemiluminescent detection. The assay is performed on the LIAISON family of analyzers to deliver highly sensitive, precise and fully automated quantitation of Sclerostin from 50 uL of human serum and plasma in 65 minutes.

Results

The LIAISON Sclerostin assay demonstrates linearity over its measuring range from 50 to 6000 pg/mL as standardized to a pure preparation of recombinant human Sclerostin. The within-run imprecision coefficients of variation (CV) calculated on 8 serum samples were between 1.0% and 3.9%. Between run imprecision results were between 2.1% and 8.9%. Limit of detection (LoD) and limit of quantitation (LoQ) were 19.7 pg/mL and 39.2 pg/mL respectively. Analytical recovery of patient samples was between 90% and 104%. Though the Sclerostin protein is subject to thermal degradation, patient samples tested with the LIAISON Sclerostin assay continue to produce reliable results after short term ambient storage, repeated freeze thaw cycles, or long term frozen storage.

Conclusions

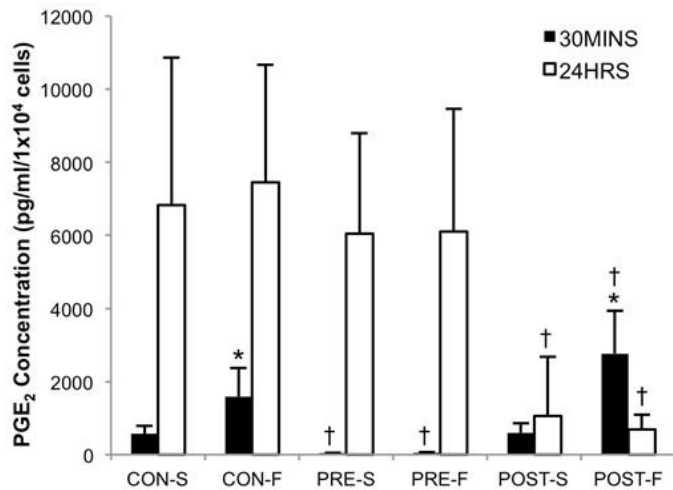


Figure 1. Medium PGE₂ concentration (pg/ml/1x10⁴ cells). Values are mean \pm STD. *Different from static, $p < 0.05$. †Different from CON, $p < 0.05$. S = static; F = flow.

Figure 1

Disclosures: Cheryl Druchok, None.

LB-SA0017

Reversal of *Sost* Deficiency-Induced Sclerosing Bone Gain by Inhibition of Wnt Ligand Secretion. Ina Kramer^{*1}, Sabine Guth-Gundel², Christine Halleux², Shea Carter², Jun Liu³, Jennifer L. Harris³, Michaela Kneissel². ¹Novartis Institutes for Biomedical Research, Switzerland, ²Musculoskeletal Disease Area, Novartis Institutes for BioMedical Research, Switzerland, ³Genomics Institute of the Novartis Research Foundation, Switzerland

Loss-of-function of the bone formation inhibitor sclerostin encoded by the *Sost*/SOST gene results in life-long sclerosing bone growth in mice and humans. Currently, there are no therapeutic treatment options available for patients with rare sclerosing disorders related to *SOST* deficiency, such as sclerosteosis (MIM269500), van Buchem disease (MIM239100) and craniodiaphyseal dysplasia (MIM122860).

Sclerostin has been shown to exert its function as a bone formation inhibitor by blocking canonical Wnt signaling downstream of the Wnt co-receptors low density lipoprotein receptor-related proteins (LRP) 5/6. To test whether the abnormal bone gain in *Sost* deficient mice can be reversed by inhibition of Wnt ligand secretion, we subjected 3-month-old wild-type C57BL/6J and *Sost* deficient female mice to six weeks oral treatment with a novel, potent small-molecule inhibitor of porcupine. Porcupine is an endoplasmic-reticulum-resident acyltransferase that palmitoylates Wnt ligands, a modification required for Wnt secretion.

Porcupine inhibitor treatment decreased femoral and tibial total bone mass and density in a dose-dependent manner in wild-type and *Sost* mutant mice as measured longitudinally by pQCT. Bone gain was similarly suppressed in the cancellous and cortical bone compartment. In contrast, long bone length was not affected by porcupine inhibitor treatment. *Ex vivo* microstructural analyses of the femur and lumbar spine by high-resolution micro-CT confirmed dose-dependent reductions of trabecular bone/tissue volume, cortical bone thickness and total bone mineral density at both skeletal sites. Analysis of serum bone turnover biomarkers osteocalcin and TRACP5b revealed treatment-related combined suppression of osteoblastic bone formation and enhanced osteoclastic bone resorption in line with broad suppression of Wnt signaling activity independent of genotype. Moreover, there was a dose-dependent suppression of circulating sclerostin levels in wild-type mice suggesting feedback-regulation to modulate Wnt pathway activity and maintain skeletal homeostasis. Together, we demonstrate that porcupine function is required for normal bone gain during late-stage skeletal growth in mice. Importantly, porcupine inhibition restores bone growth in *Sost* deficient mice to normal levels present in wild-type mice suggesting that porcupine inhibitors might be a novel treatment strategy for rare sclerosing bone disorders related to *SOST* deficiency.

Disclosures: Ina Kramer, Novartis Pharma AG

This study received funding from: Novartis Pharma AG

The LIAISON® Sclerostin assay offers an automated, precise and sensitive alternative to the currently available manual ELISA Sclerostin assays. The LIAISON® Sclerostin assay represents a valuable tool in determining the clinical relevance of Sclerostin in health and disease.

This assay is available for Research Use Only, not for use in diagnostic procedures

Disclosures: Jennifer Woodley, None.

This study received funding from: DiaSorin, Inc

LB-SA0020

A Novel Bone Graft with an Osteoinductive Surface: Fortigen has rhBMP-2-like characteristics in vitro. Helen Newman*¹, Larry Shimp². ¹VTS & Progenica Therapeutics, ²Progenica Therapeutics & CaP Biomaterials

In order to enhance bone healing, it is important to engineer grafts with enhanced osteoinductive (OI) features. A commercially available example of a manufactured OI growth factor is Infuse®. It contains recombinant human Bone Morphogenetic Protein-2 (rhBMP-2). The veterinary version is known as Truscent®. rhBMP-2 can cause a dramatic increase in bone formation, but it is not bound to the carrier scaffold, and so is free to migrate away after implantation. This has led to extraskelatal bone growth and other adverse effects including inflammation, swelling and radiculopathy. Although bone allograft naturally contains many growth factor types, including BMP-2, it contains relatively low concentrations of the growth factors, so healing is not as robust as with Infuse/Truscent. This study evaluates a novel approach to solving the problem of provision of effective concentrations of osteoinductive growth factors that will remain in a site. We refer to the most osteoinductive versions as Fortigen™.

Both control and investigational particles (synthetic and natural bone grafts) were tested for inductivity using an Alkaline Phosphatase Assay (ALP) (Han et al., 2003). This *in vitro* ALP method is a validated model for assessment of OI. It is based on the ability of inductive agents to transform mesenchymal stem cells into osteoblasts. Controls included positive and negative conditions: a known positive reference lot of rhBMP-2 was used for positive controls; negative controls were graft materials without surface modifications. Cell viability studies were also conducted to determine if the modifications had any adverse impact on cell survival. ALP activity was normalized to cell survival data.

Some versions of surface-modified particles (Fortigen™-S2 and Fortigen™-P) had significantly higher OI when compared to the negative controls (p-values=0.000; n=3). The OI of some of the investigational particles (Fortigen-V2) was similar to the OI of positive control cultures (p-value=0.102 at a non-inferiority margin of 15%; n=3). The data show that these surface modifications can result in substantial increases in standard markers of OI *in vitro*; in some cases comparable to rhBMP-2. Additionally, the modifications did not have an adverse impact on the viability of the cells in culture or their ability to adhere to the particles. These data are very promising. The design has the potential benefit of accelerating bone healing locally without the risk of signaling molecules leaving the site.

Disclosures: Helen Newman, None.

LB-SA0021

Increased bone mass and biomechanical properties in mice deficient for FIAT (Factor Inhibiting ATF4-mediated Transcription). Bahareh Hekmatnejad*¹, Vionnie W.C. Yu², Vice Mandic², Martin Pellicelli¹, Alice Arabian², Rene St-Arnaud³. ¹Dept of Human Genetics, McGill University, ²Shriners Hospitals for Children - Canada, ³Shriners Hospital for Children & McGill University, Canada

We previously reported that FIAT (Factor Inhibiting ATF4-mediated Transcription) interacts with ATF4 to repress its transcriptional activity. Transgenic mice overexpressing FIAT exhibit osteopenia while silencing FIAT in osteoblasts by RNA interference enhanced all ATF4 functions tested. This study reports the first bone phenotype of *Fiat* KO mice at 8- and 16-week of age and the impact of the mutation on the response to functional loading. RT-qPCR and Western blot analysis confirmed efficient *Fiat* gene inactivation with undetectable mRNA or protein levels. *Fiat* mutant mice appeared normal at birth and weight gain was identical between wild type and knock-out animals. Expression of the ATF4 transcriptional target Osteocalcin (*Bglap1*) was significantly increased in *Fiat*-deficient bone. Microcomputed tomography analysis of proximal femur demonstrated an age-dependent increase in trabecular bone volume and thickness in *Fiat* KO mice compared with their wild-type littermates. In addition, cortical bone measurements at the femoral midshaft revealed a significant increase in cortical thickness in older *Fiat* KO mice and consequently a significant increase in stiffness and strength was measured. FIAT protein expression is strongly detected in osteocytes; we thus compared the response to mechanical loading *in vivo* between 16-week-old wild-type and *Fiat*-deficient mice. We measured a difference in baseline BFR of cortical bone between control and *Fiat* KO mice as assessed by calcein double labeling in the unloaded ulna. We observed a robust bone formation response in the loaded bones that was not significantly different between wild-type and *Fiat*-deficient mice. Our results confirm that FIAT is a negative regulator of bone biology contributing to both trabecular and cortical bone homeostasis *in vivo*.

Disclosures: Bahareh Hekmatnejad, None.

LB-SA0022

Insulin Receptor Substrate 1 Time-dependently Regulates Bone Formation by Controlling Collagen I Alpha 2 Expression Through miR-342. Hou-De Zhou*¹, Yue Guo², Chen-Yi Tang², Xiao-Fei Man², She-Wen Tan², Hao-Neng Tang², Fang Wang², Jun Tang², Ci-La Zhou². ¹The 2nd Xiangya Hospital of Central South University, China, ²Institute of Endocrinology & Metabolism, the Second Xiangya Hospital of Central South University, China

Insulin promotes bone formation through canonical insulin signal pathway, the repaired insulin signal was found to be correlated to the diabetic osteopathy. Insulin receptor substrate 1 (IRS-1) is an important signal molecule in insulin signal pathway, which was attenuated in many tissues such as bone and adipose tissue of patients with diabetic osteopathy. As adipocytes and osteoblasts are derived from the same progenitor-mesenchymal stem cells (MSC), and bone marrow stem cells (BMSC) are the primitive source for MSC, we supposed that IRS-1 could regulate differentiation of BMSC and function of osteoblast. So we identified an IRS-1 deficiency mice (IRS-1^{smia/smia}) with a spontaneous mutation at position 57 (S57X) which resulting in complete loss of IRS1 protein expression. We found that the bone mineral density and trabecular number were increased in 3-month of IRS-1^{smia/smia} mice, but were decreased in 12-month of IRS-1^{smia/smia} mice. We then compared the differential expressed genes and miRNAs by osteogenesis PCR array and miRNA array respectively in 3-month of wild type and IRS-1^{smia/smia} mice. We identified 72 differential expressed miRNAs and 39 differential expressed osteogenesis related genes. We then predicted all the target genes of differential miRNAs and compared them with the differentially expressed osteogenesis related genes, and found that collagen type I alpha 2 (Col1a2), one of the target genes of miR-342, were up-regulated in IRS-1^{smia/smia} mice, while miR-342 was down-regulated. Transfection of miR-342 inhibits the collagen 1 alpha 2 expression in primary cultured osteoblast, while antagonist for miR-342 increases Col1a2 expression. Further study *in situ* showed that Col1a2 in osteoblast and bone marrow of 3-month old IRS1^{smia/smia} mice were higher than that of wild type mice, but decreased in 12-month old mice. During *in vitro* induction of bone marrow cells (BMCs) into matured osteoblast and osteocytes, Col1a2 expression gradually increased and reached the peak at the 8th day, and then reduced. While miR-342 expression showed an obvious negative relation with the expression of Col1a2. Col1a2 siRNA decreased the ALP activity, while miR-342 inhibitor can increase the ALP activity and Col1a2 expression of BMCs. Thus our researches showed that IRS-1 can time-dependently regulate bone formation by regulating Col1a2 expression through miR-342, and disclosed a new mechanism for insulin signal involved in the bone formation.

Disclosures: Hou-De Zhou, None.

LB-SA0023

Loss of the nutrient sensor Tas1R3 leads to reduced bone resorption. Michael Eaton¹, Jordan Newby², Maggie Plattes³, Hannah Foster³, Brian Dewar³, Eric Wauson⁴, Jon Arthur⁵, Jonathan Lowery*⁵. ¹Department of Biomedical Science, Marian University College of Osteopathic Medicine, ²Department of Biomedical Science, Marian University College of Osteopathic Medicine & Department of Biology, Freed-Hardeman University, ³Department of Biology, Taylor University, ⁴Department of Physiology & Pharmacology, ⁵Department of Biomedical Science

The TAS1R family of heterotrimeric G protein-coupled receptors participates in monitoring energy and nutrient needs. TAS1R3 is a bi-functional protein that either recognizes amino acids such as glycine and L-glutamate or sweet molecules such as sucrose and fructose when dimerized with TAS1R1 or TAS1R2, respectively. Loss of TAS1R3 expression leads to impaired mTORC1 signaling and increased autophagy, indicating that signaling through this receptor is critical for assessing nutrient needs. Recently, it was reported that global deletion of TAS1R3 expression in mice (*Tas1R3* mutant) leads to increased cortical bone mass and trabecular remodeling (Simon et al 2014) but the underlying cellular mechanism leading to this phenotype remains unclear. To address this open question, we quantified bone turnover markers in serum from 20-week-old wild type and *Tas1R3* mutant mice and found that levels of the resorption marker Collagen Type I C-telopeptide (CTX) were reduced on average by >60% in the absence of TAS1R3 expression (wild type: 8.791 ± 0.75 ng/ml, n=3; *Tas1R3* mutant 3.248 ± 1.14 ng/ml, n=4; p<0.02 by unpaired t test). Levels of the bone formation marker Procollagen Type I N-terminal Propeptide (PINP) tend to be higher in *Tas1R3* mutant mice (wild type: 981 ± 407.5 pg/ml, n=3; *Tas1R3* mutant 2009 ± 421.5 pg/ml, n=3) but this finding did not reach statistical significance (p<0.15 by unpaired t test). These preliminary results suggest that high bone mass in *Tas1R3* mutant mice is due to uncoupled bone remodeling with reduced osteoclast function. We examined the skeletal expression profile of *Tas1R3* in order to determine the cellular compartment(s) in which TAS1R3 impacts bone remodeling. Consistent with the observed defect in bone resorption in *Tas1R3* mutant mice, *Tas1R3* mRNA is expressed in primary osteoclasts obtained from wild type mice. However, *Tas1R3* mRNA is also present in marrow-free humeri, primary bone marrow stromal cells,

and several osteoblast-like cell lines, raising the possibility that osteoblast-to-osteoclast communication may be disrupted in *Tas1r3* mutant mice. Collectively, these findings provide the rationale for future experiments examining the cell type-dependent role for TAS1R3 function in nutrient sensing in postnatal bone remodeling and differentiation of osteoclasts and osteoblasts.

Disclosures: Jonathan Lowery, None.

LB-SA0024

Cellular senescence phenotype attributes trigger of bone remodeling to monocyte recruitment. Insun Song*, Yong Jun Choi, Yoon-Sok Chung. Ajou University School of Medicine, South Korea

Aims: To understand the trigger of monocyte recruitment for bone remodeling, we introduced the model of cellular senescence and examined mouse osteocytes and hypertrophic chondrocytes.

Main Methods: To determine whether the cellular senescence phenotype involved in monocyte recruitment, we first performed senescence-associated β -galactosidase (SA- β -gal) assay in osteocytes and hypertrophic chondrocytes. And we introduced immunohistochemistry with anti-F4/80 and tartrate-resistant acid phosphatase (TRAP) assay for detecting monocytes and mature osteoclasts at mouse osteocytes and hypertrophic chondrocytes in femur and tibia of 8-week-old C57b/6 mice.

Key Findings: Generally recruitment of monocytes occurs by chemokines and their receptors during infection and inflammation. However the process of monocyte recruitment for osteoclasts involved in bone remodeling still remained unclear. So, we hypothesize that the cellular senescence phenotype could appear in bone cells and have a role in bone remodeling initiating recruitment of monocytes. Cellular senescence shows some specific characteristics; cell-cycle arrest, positive SA- β -gal, enlarged and flat cell morphology, and senescence-associated secretory phenotype (SASP) including some inflammatory factors and many kinds of cytokines. So we investigated the cellular senescence pattern in osteocytes and hypertrophic chondrocytes associated with bone remodeling and bone formation. Osteocytes and hypertrophic chondrocytes show growth arrest with enlarged and flat cell morphology. We have examined the endogenous SA- β -gal response related recruitment of immune cells for elimination of semi-permanent structures. We found that hypertrophic chondrocytes and some osteocytes show a clear positive SA- β -gal response. Our results also reveal that these locations show positive anti-F4/80 and TRAP in the almost same region.

Significance: Based on the results of positive endogenous SA- β -gal, anti-F4/80 and TRAP response in the same boundary of bone cells, we propose that the cellular senescence phenotype leads to recruitment of monocytes involved in the first step of osteoclast resorption, triggering of bone remodeling.

Disclosures: Insun Song, None.

LB-SA0025

Transgene expression by Dmp1 promoter fragments occurs in various organs. Hiroaki Saito*¹, Hanna Taipaleenmäki², Ahmed Al-Jazzar³, Andreas Gasser¹, Behzad Javaheri³, Cheryl Scudamore³, Teresita Bellido⁴, Andrew A. Pitsillides³, Eric Hesse¹. ¹Heisenberg-Group for Molecular Skeletal Biology, Department of Trauma, Hand & Reconstructive Surgery, University Medical Center Hamburg-Eppendorf, ²Heisenberg-Group for Molecular Skeletal Biology, Department of Trauma, Hand & Reconstructive Surgery, University Medical Center Hamburg-Eppendorf, Germany, ³Comparative Biomedical Sciences, The Royal Veterinary College, ⁴Department of Anatomy & Cell Biology, Indiana University School of Medicine

Osteocytes are key players in regulating bone mass maintenance and thus constitute a major research focus in the field of bone biology. Since analysis of osteocyte function often requires *in vivo* investigations, promoter elements of osteocyte-specific genes i.e. *SOST* or *Dentin-matrix-protein 1* (*Dmp1*) are used to overexpress genes of interest or the Cre-recombinase for conditional deletion studies. While these tools have been very useful, emerging evidence suggests that these promoters may not be osteocyte-specific, which would be critical for subsequent data interpretation. To investigate the selectivity of these proposed osteocyte-specific *in vivo* models, we crossed 8kb-Dmp1-Cre mice (i) with Ai9 tomato reporter mice (Dmp1-Cre⁺;Ai9^{T/wt}), and (ii) with mice, in which the expression of the diphtheria toxin receptor (DTR) is controlled in a Cre-inducible manner (Dmp1-Cre⁺;iDTR^{T/wt}) to ablate Dmp1-positive cells. Furthermore, we explored the effects of diphtheria toxin (DT) in mice harboring the human DTR (hDTR) regulated by a 10kb-Dmp1 promoter fragment (Dmp1-hDTR). Immunohistochemical staining of tibiae harvested from 8-week old Dmp1-Cre⁺;Ai9^{T/wt} mice revealed a strong tomato expression in all osteocytes and osteoblasts covering endocortical and trabecular surfaces. Furthermore, we detected tomato expression in muscle, brain, testis and in vessels in the heart, spleen, lung, and intestine. Consistently, histological analyses of bones seven days after DT administration in Dmp1-Cre⁺;iDTR^{T/wt} and Dmp1-hDTR mice revealed partial, yet significant ablation of not only osteocytes but also osteoblasts and lining cells. In addition, DT injection resulted in liver vacuolation, acute kidney necrosis, splenic atrophy, and disturbance of bone marrow composition in Dmp1-hDTR mice, which is consistent with expression of hDTR mRNA in these tissues. Taken together,

our results indicate that in 8kb-Dmp1-Cre mice as well as in 10kb-Dmp1-hDTR mice, expression of the respective transgene is not restricted to osteocytes, but also takes place in other organs, some of which are known to be functionally involved in the regulation of bone homeostasis. Our findings therefore suggest that despite the great usefulness of these *in vivo* systems, the expression pattern of the gene of interest should be determined carefully and the results need to be interpreted accordingly.

Disclosures: Hiroaki Saito, None.

LB-SA0026

Defined Sets of Transcription Factors Induce the Expression of Functional Sclerostin in Human Dermal Fibroblasts and Its Expression Responds to Parathyroid Hormone, Hypoxia and Prostaglandin E2. Makoto Fujiwara*¹, Wei Wang², Taichi Kitaoka², Takuo Kubota², Yasuji Kitabatake², Noriyuki Namba³, Toshimi Michigami⁴, Keiichi Ozono². ¹Osaka University graduate school of medicine, Japan, ²Department of Pediatrics, Osaka University Graduate School of Medicine, ³Department of Pediatrics, Osaka University Graduate School of Medicine, ⁴Department of Bone & Mineral Research, Osaka Medical Center & Research Institute for Maternal & Child Health, Japan

Background: Sclerostin, encoded by *SOST*, is a secretory protein expressed specifically in osteocytes and suppresses osteogenesis by the inhibition of the WNT signaling. Regulatory mechanism of *SOST* expression remains unclear mainly due to difficulty in using osteocytes *in vitro*. With the aim to establish the method for inducing the *SOST* expression in human fibroblasts as a substitute for osteocytes, we have identified 4 transcription factors, ATF3, KLF4, PAX4 and SP7 and reported at the annual meeting of ASBMR in 2014.

Purpose: In the present study, we aim to elucidate the function of sclerostin and factors which regulate *SOST* expression in this system.

Methods: We introduced ATF3, KLF4, PAX4 and SP7 genes into human dermal fibroblasts (purchased from Lonza) using retrovirus, and analyzed *SOST* expression levels by real time PCR and measured sclerostin concentrations in conditioned medium by ELISA. Functional analysis of induced sclerostin on the WNT/beta-catenin signal was performed using the TOPflash reporter vector. The changes of *SOST* and sclerostin expression by the addition of Parathyroid Hormone (PTH) or prostaglandin E2 (PGE2) and under hypoxia were also analyzed.

Results: Combination of ATF3, KLF4, PAX4 and SP7 induced *SOST* expression 1000 times and sclerostin at concentration 21.2 pmol/L in the conditioned medium in human dermal fibroblasts at 4 weeks after transduction. Functional analysis using TOPflash reporter vector revealed that the induced sclerostin suppressed the WNT10b-induced transcriptional activity. PTH addition significantly suppressed the induced *SOST* (62.3 % compared to vehicle) and sclerostin (addition: 5.7 pmol/L, vehicle: 31.2 pmol/L). Hypoxia culture caused increase of the induced *SOST*, 162 % compared to normoxia. Furthermore, PGE2 enhance the *SOST* expression remarkably, 1630 % compared to vehicle.

Conclusion: Induced sclerostin expression in human dermal fibroblasts achieved by transduction of ATF3, KLF4, PAX4 and SP7 have an activity of suppressing the WNT/ beta-catenin signaling, and its expression was regulated by PTH, hypoxia and PGE2. This method may contribute to elucidation of sclerostin function and drug developments that regulate sclerostin expression in various kinds of bone diseases.

Disclosures: Makoto Fujiwara, None.

LB-SA0027

Bone Turnover Markers in Young Women. Emma Callegari*¹, Alexandra Gorelik², Nicola Reavley¹, Suzanne M. Garland³, Cherie Chiang⁴, John D. Wark⁵. ¹The University of Melbourne, Grattan St, Melbourne, Victoria, Australia, ²Melbourne EpiCentre, Royal Melbourne Hospital, University of Melbourne, Parkville, Victoria, Australia, ³The University of Melbourne, Grattan St, Melbourne, Victoria, Australia; Murdoch Childrens Research Institute, Melbourne, Victoria, Australia; Royal Women's Hospital, Parkville, Melbourne, Victoria, Australia, ⁴Melbourne Health Shared Pathology Services, Royal Melbourne Hospital, Parkville, Melbourne, Victoria, Australia, ⁵The University of Melbourne, Grattan St, Melbourne, Victoria, Australia; Bone & Mineral Medicine, Royal Melbourne Hospital, Parkville, Victoria, Australia

Bone turnover markers (BTMs) may provide insight into bone development and bone health in young women but have been little studied in this demographic and normative data are lacking. The aim of this analysis was to examine the distribution and association of C-terminal telopeptide of type 1 collagen (CTX) and total procollagen type 1 N-propeptide (PINP) with relevant covariates as well as to determine the reference intervals of BTMs in healthy females aged 16-25 years participating in the Safe-D study. Participants were recruited through the social networking site Facebook, completed an extensive, online questionnaire and attended a study site visit. Fasting blood was collected from 255 participants and tested for CTX and PINP using the Roche Elecsys automated analyser. The reference interval was defined as the central 95% of normalized values. After excluding 54 participants

based on medical history, medication use or abnormal pathology (creatinine <45 or >90 $\mu\text{mol/L}$, corrected calcium <2.10 or >2.60 mmol/L , 25-hydroxyvitamin D (25OHD) <25 nmol/L , parathyroid hormone (PTH) >14 pmol/L , thyroid stimulating hormone <0.35 or >4.94 mIU/L , C-reactive protein >10 mg/L), the reference interval was 0.2-1.2 ng/mL for CTX and 15-177 ug/L for P1NP. BTMs were inversely associated with age and years since menarche [for CTX ($r = -0.40$ and $r = -0.41$, respectively) and for P1NP ($r = -0.38$ and $r = -0.44$, respectively); $p < 0.001$ for both variables]. In a multivariate model, CTX and P1NP were significantly lower in subjects who used hormonal contraception (CTX: users 0.5 vs. non-users 0.7 ng/mL , $p < 0.001$; P1NP: users 60 vs. non-users 83 ug/L , $p < 0.001$). CTX and P1NP were not associated with BMI but CTX was negatively associated with body fat percentage ($\beta = -0.005$, 95% CI -0.0093 to -0.0004, $p = 0.035$). CTX and P1NP were associated with PTH ($\beta = 0.027$, 95% CI 0.012 to 0.041, $p < 0.001$ and $\beta = 0.252$, 95% CI 0.056-0.448, $p = 0.012$, respectively). CTX and P1NP were not associated with 25OHD or whole body BMD as continuous variables. In conclusion: age, menarche, PTH and hormonal contraceptive use were all significantly associated with CTX and P1NP concentrations. Body fat percentage was significantly associated with CTX but not P1NP. To our knowledge this is the first study to report BTMs in healthy young women aged 16-25 years; findings will have important application in bone health research and in the generation of age-specific reference intervals in this demographic.

Disclosures: Emma Callegari, None.

LB-SA0028

Bone Microstructure Identifies Women Without Osteoporosis Suffering Fragility Fractures: the prospective OFELY study. Stephanie Boutroy^{1*}, Roger Zebaze², Elisabeth Sornay-Rendu³, Ego Seeman², Roland Chapurlat³. ¹INSERM UMR1033 & Université de Lyon, France, ²Depts. Medicine & Endocrinology, Austin Health, University of Melbourne, & Straxcorp, ³INSERM UMR1033 & Université de Lyon

Introduction: The aim of treatment is to prevent the first, and all subsequent fractures. The bone mineral density (BMD) diagnostic threshold for 'osteoporosis' (T-score ≤ -2.5 SD) lacks sensitivity because more than half of all the fractures in the community, and around 30% of the morbidity and mortality arise in women with osteopenia or normal BMD (1). The challenge is to identify and target therapy to those women with bone fragility among this large low risk group, before they fracture. We hypothesized that women who sustain incident fractures have disrupted microarchitecture which disproportionately compromises bone strength relative to the modest bone lost (because loss of strength is a 7th power function of porosity and a 3rd power function trabecular bone volume (2)).

Methods: To identify these women we monitored 589 women aged 42 to 94 years for a median of 8.1 [0.9] years [interquartile range IQ] in Lyon, France. We measured hip and lumbar spine BMD using Hologic QDR 4500A, microarchitecture of the distal radius using high resolution peripheral quantitative computed tomography, and quantified cortical and trabecular morphology using StrAx1.0 (Straxcorp, Melbourne).

Results: Fractures occurred in 111 women. These women had 0.36 SD lower cortical thickness, 0.38 SD higher porosity, and 0.44 SD fewer trabeculae compared with women without incident fractures (all $p < 0.001$). Porosity predicted fracture independently of hip BMD, hazards ratio [95%CI] = 1.28 [1.03-1.59] per SD increase ($p = 0.027$) and identified 25 (22%) more women sustaining fracture than the BMD T-score of ≤ -2.5 SD.

Only 27% ($n = 30$) of the 111 women who fractured had osteoporosis at baseline; the majority having an incident fracture [$n = 81$ (73%)] had osteopenia [$n = 49$ (44%)] or normal BMD [$n = 32$ (29%)]. In these 81 women, adding a measurement of porosity identified 25 (31%) more women sustaining fractures and identified 16 (20%) more women than using FRAX alone while increasing the false positive rate by 14%.

Conclusion: This is the first prospective study demonstrating that women who sustain fragility fractures can be identified before they fracture by measuring microarchitecture, particularly women with osteopenia or normal BMD who would usually not be investigated further or considered for treatment.

1. Bliuc D et al. J Bone Miner Res 2015; 30:637-46.
2. Schaffler MB, Burr DB. J Biomech 1988;21: 13-6.

Disclosures: Stephanie Boutroy, None.

LB-SA0029

Digital X-ray radiogrammetry in the Study of Osteoporotic Fractures: Comparison to dual energy X-ray absorptiometry and FRAX. Johan Kalvesten^{1*}, Lily Y Lui², Torkel B Brismar³, Steven R Cummings². ¹Linköping University, CMIV & Sectra AB, Sweden, ²San Francisco Coordinating Center, California Pacific Medical Center, San Francisco, CA, USA, ³Karolinska Institutet, Department for Clinical Science, Intervention & Technology, Division of Radiology, Karolinska University Hospital, Sweden

Background: Osteoporosis is often underdiagnosed and undertreated. Bone mineral density (BMD) screening of post-menopausal women has been proposed to overcome this. However, due to cost, workflow and accessibility not all eligible women are evaluated with central dual X-ray absorptiometry (DXA). More accessible and lower cost techniques for identifying individuals who would benefit from anti-

osteoporotic intervention or further evaluation by central DXA, if available, might improve patient care. One such tool that is widely used is the FRAX[®] online tool. Digital X-ray radiogrammetry (DXR) estimates hand BMD from standard hand X-ray images and have shown to predict fractures and osteoporosis. Digital radiology and the internet have opened up the possibility of conducting automated opportunistic screening with DXR in post-fracture care or in combination with mammography. The purpose of the study was to compare the performance of DXR with FRAX and DXA in discriminating major osteoporotic fracture (MOF) (hip, clinical spine, forearm or shoulder), hip fracture and femoral neck osteoporosis.

Methods: The prospective cohort study was conducted on 5,358 women 65 years and older in the Study of Osteoporotic Fractures (SOF) cohort. Hand X-ray images collected at baseline were analyzed and fractures were ascertained during 10 years of follow up. For comparison of the methods area under age adjusted receiver operating characteristic curve (AUC) for MOF and hip fracture and for osteoporotic DXA FN BMD was used.

Results: DXR was similar to FRAX (no BMD) in fracture discrimination performance with an AUC around 0.65 for MOF and 0.70 for hip fractures for both methods, Table 1. As expected fracture discrimination performance by femoral neck DXA BMD was superior to both DXR and to FRAX (no BMD) with AUC of 0.68 for MOF and 0.75 for hip fractures. AUC for selection of patients with femoral neck osteoporosis (femoral neck DXA BMD T-score < -2.5) was higher for DXR-BMD, 0.76 (0.74-0.77), than for FRAX, 0.69 (0.67-0.71), ($p < 0.0001$), Table 1.

Conclusions: DXR-BMD discriminates incident fractures in women to a similar degree as FRAX. DXR-BMD predicts femoral neck osteoporosis to a larger degree than FRAX. In a possible screening scenario DXR shows promise as a selection tool for DXA. Results require confirmation in other studies.

| | AUC MOF fracture ^a 10 years | AUC hip fracture 10 years | AUC DXA FN BMD T-score < -2.5 |
|-------------------------|--|---------------------------|-------------------------------|
| Age alone | 0.59 (0.57, 0.61) | 0.68 (0.65, 0.71) | 0.64 (0.61, 0.65) |
| Age + DXR | 0.65 (0.63, 0.67) | 0.69 (0.66, 0.72) | 0.76 (0.74, 0.77) |
| Age + DXA FN BMD | 0.68 (0.66, 0.70) | 0.75 (0.72, 0.77) | - |
| Age + FRAX (no BMD) | 0.64 (0.61, 0.65) | 0.71 (0.67, 0.73) | 0.69 (0.67, 0.71) |
| Age + DXA FN BMD + FRAX | 0.69 (0.67, 0.70) | 0.76 (0.73, 0.78) | - |

^a Clinical spine, hip, forearm or shoulder fracture.

BMD: bone mineral density; DXA FN: femoral neck BMD by DXA; DXR: metacarpal BMD estimated by digital X-ray radiogrammetry

Table 1. Discrimination of major osteoporotic fracture, hip fracture and femoral neck osteoporosis.

Disclosures: Johan Kalvesten, Sectra AB

This study received funding from: Sectra AB

LB-SA0030

Low Bone Mass Density Is Associated with Tooth Loss in Postmenopausal Women: A Nationwide Representative Study. Jeong Gyu Lee^{*}. Pusan National University Hospital,

Purpose

Both osteoporosis and tooth loss are major health problems that are frequently observed in postmenopausal women in the fast-aging country. A lack of a nationwide, representative study has made the association between low bone mineral density (BMD) and tooth loss still a controversial issue to this day.

Methods

We conducted a cross-sectional study using data from the fifth Korea National Health and Nutrition Examination Survey 2010-2011. A total of 1,938 postmenopausal women (50-75 years) who had undergone BMD measured by dual-energy X-ray absorptiometry were included as study subjects. All participants had dental examination by a dentist and were examined for the number of remaining teeth, dental prosthetics, dental implants, and periodontal diseases. In addition, the participants self-reported their oral health behaviors. Multivariate logistic regression via complex sampling was used to estimate odds ratio (OR) for osteopenia and osteoporosis regarding to eight or more of tooth loss after the adjustment for confound factor including menopausal age.

Results

Age of subjects was 61.3 ± 0.2 years and 529 (27 %) women had osteoporosis and 923 (47.6 %) women had osteopenia. Mean number of tooth loss was 7.1 ± 0.3 in all participants. Compared to the group with normal BMD, the number of tooth loss was significantly higher in the groups with osteopenia and osteoporosis (4.52 ± 0.4 vs. 6.45 ± 0.4 vs. 9.28 ± 0.5 , P value = 0.001). Women with osteoporosis in femur had a higher risk for eight or more of tooth loss [OR, 2.13; 95% confidence interval (CI), 1.70-2.67] compared to the group with normal BMD in femur after the adjustment of confounding factors including age, menopausal age, oral care related behaviors, and chronic diseases. Similarly, the subjects with osteoporosis in spine had a higher risk for eight or more tooth loss (OR, 1.92; 95% CI, 1.53-2.42) in comparison with the group with normal BMD in spine.

Conclusions

We observed a significant relationship between excessive tooth loss and low BMD in postmenopausal women. Our findings suggest persistent dental care and early intervention in prevention for excessive tooth loss in the postmenopausal women with low BMD.

Disclosures: Jeong Gyu Lee, None.

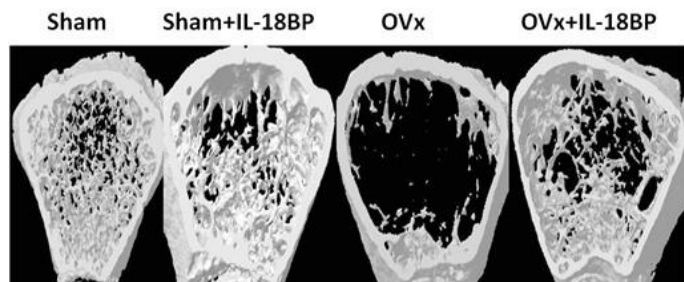
LB-SA0031

Relation between decreased IL-18BP levels and risk of osteoporosis in post menopausal osteoporotic patients: Role of IL-18BP in preventing bone loss by positively regulating Treg/Th17 balance. Mohd Nizam Mansoori^{1*}, Priyanka Shukla¹, Abdul Malik¹, Kamini Srivastava¹, Manisha Kakai², Karam bir Kumar², Manisha Dixit¹, Jyoti Kureel¹, Sushil Kumar Gupta², Divya Singh¹. ¹CDRI, ²SGPGI

Abstract

IL-18BP is a natural antagonist of IL-18 cytokine whose level is increased in several autoimmune disorders. IL-18 promotes IL-17 production and plays important role in autoimmune diseases like rheumatoid arthritis. However its role in Estrogen deficiency induced bone loss is still unknown. In this study we have investigated the effect of mIL-18BP administration to estrogen-deficient mice on T and B cells, Th17/Treg balance and its impact on skeletal parameters. Adult female Balb/c mice were taken for the study. The groups were: sham, sham+mIL-18BP (0.5mg/kg body weight), Ovx, Ovx + mIL-18BP (0.5mg/kg body weight). Treatment was continued for a period of 4 week with s.c. injection twice weekly. After one month, animals were sacrificed; long bones were collected for static and dynamic histomorphometry. Bone marrow was flushed out for peripheral blood mononuclear cell isolation. mIL-18BP robustly inhibited the proliferation of IL-17 secreting Th17 cells with concomitant increase in CD4+CD25+FoxP3 T regulatory cells. mIL-18BP treatment restored trabecular microarchitecture, preserved cortical bone parameters likely attributable to increased number of bone lining cells and reduced osteoclast activity. mIL-18BP treatment restored the levels of proinflammatory and anti inflammatory cytokine to sham level which were altered due to ovariectomy in Balb/c mice. Importantly, these results were corroborated in female human subjects where IL-18BP levels have been evaluated in post menopausal women and serum level of IL-18BP was correlated with BMD data. Based on T score value volunteers were divided in three groups of normal, osteopenic and osteoporotic. Post menopausal females between the age group (55-65yrs) were included in the study. Blood was withdrawn from them and BMD analysis was done using DXA. Serum level of hIL-18BP was found to be decreased to base line level in Osteoporotic patients. BMD data of these groups showed positive correlation with the serum concentration of hIL-18BP. Conclusively we can say that exogenous mIL-18BP administration provides protection against Estrogen deficiency induced bone loss and has the potential as a therapy for postmenopausal osteoporosis.

Key words: Immune system, Bone, Estrogen deficiency, Th17 cells, T regulatory cells, Osteoporotic Patients.



Representative image of micro CT results of in vivo group study.

Disclosures: Mohd Nizam Mansoori, None.

LB-SA0032

Imminent Risk of Fracture after Fracture. Helena Johansson¹, Kristin Siggeirsdottir², Nicholas Harvey³, Anders Odén⁴, Vilmundur Gudnason⁵, Eugene McCloskey⁴, Gunnar Sigurdsson², John Kanis⁴. ¹Centre for Metabolic Bone Diseases, University of Sheffield Medical School, Sweden, ²Icelandic Heart Association, ³MRC Lifecourse Epidemiology Unit, University of Southampton, United Kingdom, ⁴Centre for Metabolic Bone Diseases, University of Sheffield, ⁵Icelandic Heart Association, Kopavogur, University of Iceland

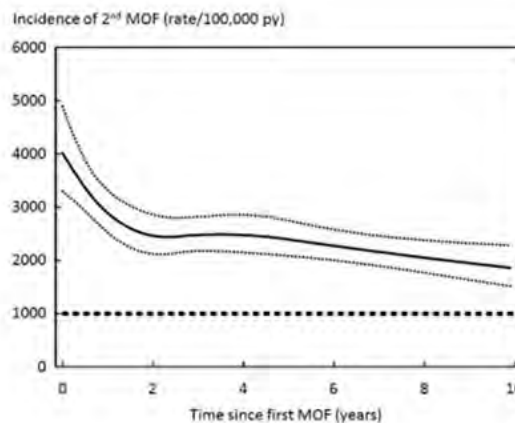
A history of fracture is a strong risk factor for future fractures. The aim of the present study was to determine whether the predictive value of a past major osteoporotic fracture (MOF) for future major fractures changed with time.

The current study was based on a population-based cohort of 18,872 men and women (52% women) born between 1907 and 1935 who attended the Reykjavik Study during the recruitment period in 1967–1991. All fractures from their entry into the study until December 31, 2012 were retrieved and analysed. Where reports contained records of more than one fracture at the same site within 30 days, only the first fracture was included. 5039 patients experienced one or more MOF and could be included in the analysis of a second MOF. An extension of Poisson regression was used to investigate the relationship between the first fracture and the second. All associations were adjusted for age and time since baseline.

During 10 year after the first Following a MOF, 1310 patients experienced a second MOF. The risk of a second MOF after a first increased by 4–5% for each year of age depending on age (95 % CI: 1.02-1.07) and was 25% higher for women than

men (95% CI: 1.09-1.44). The risk of a second MOF was highest immediately after the first fracture and thereafter decreased with time though remained higher than the population risk throughout follow up (Figure). For example, 1 year after the first MOF the risk of a second fracture was 2.9 (95% CI: 2.5-3.3) higher than the population risk. After 10 year this risk ratio was 1.8 (95% CI: 1.5-2.3). The risk of MOF after a first MOF is increased over the whole 10 year follow up but the imminent risk is even higher. If the acute increment in risk in the few years following MOF is amenable to therapeutic, intervention then immediate short-term treatments may provide worthwhile clinical dividends in a very cost-effective manner

Figure Risk of a second major osteoporotic fracture after a first major osteoporotic fracture per 100 000 (95% CI). The knots for the spline function are in 0.5, 2.5 and 5 years of follow up after the first fracture. The dashed line is the risk of first fracture in all patients. The risk of fracture in the figure is for a woman 60 years of age.



Figure

Disclosures: John Kanis, None.

LB-SA0033

Clinically effective PKPD in Post-Menopausal Women after Transdermal hPTH(1-34) Delivery. Bobby Singh^{1*}, Vaeling Miller², ²Corium

Purpose: Forteo[®] [hPTH(1-34)] is approved by FDA for the treatment of osteoporosis as a daily subcutaneous injection. Patient adherence to therapy is poor due to required daily injections. The transdermal delivery of hPTH(1-34) using biodegradable microstructures (MicroCor[®]) is expected to improve adherence by providing a convenient and needle-free alternative to daily injections.

Methods: This Phase 2a study was conducted as a two part study in postmenopausal women aged 50 to 85. Part A was a crossover study, with 18 subjects randomized to either MicroCor PTH 16 mcg, MicroCor PTH 38 mcg or Forteo[®] 20 mcg. The primary objective was to assess the single dose PK of MicroCor PTH compared to Forteo. The secondary objectives were assessment of safety and dose proportionality between the two MicroCor doses. Part B was a 28-day parallel group study, with 21 subjects randomized to either MicroCor PTH 38 mcg or Forteo 20 mcg. The primary objective was to assess the multiple dose PK. The secondary objectives were assessment of safety and changes in concentrations of well characterized bone formation biomarker PINP (procollagen Type 1 N-terminal propeptide) and bone resorption biomarker CTX (collagen type 1 crosslinked C-telopeptide).

Results: All subjects treated with MicroCor PTH completed the trial. Rapid uptake (mean tmax < 10 minutes) and clearance of hPTH(1-34) was observed with the MicroCor PTH. The PK profile of MicroCor PTH was dose proportional across the two doses. Subjects exhibited similar PK profiles at Day 1 compared to Day 28, indicating the absence of drug accumulation. The PINP concentrations increased significantly over baseline and were comparable between MicroCor PTH and Forteo. The CTX concentrations were essentially unchanged compared to baseline for MicroCor PTH and increased above baseline for Forteo starting at day 21. Subjects treated with MicroCor PTH experienced excellent skin tolerability and no systemic adverse events beyond those observed with Forteo. There were no reports of delayed contact sensitization or anti-PTH antibodies.

Conclusions: Rapid and pulsatile PK were demonstrated with MicroCor PTH which is an important factor in stimulating bone formation. This was confirmed by significant and clinically relevant increases in concentrations of PINP. MicroCor PTH showed excellent skin tolerability. Future clinical studies will further establish safety and efficacy of MicroCor PTH transdermal system in osteoporotic patients.

Disclosures: Bobby Singh, None.

LB-SA0034

National Observational Study of Subtrochanteric, Femoral Shaft and Hip Fractures in New Alendronate Users 1996 to 2003. Bo Abrahamsen*¹, Daniel Prieto-Alhambra², Pia Eiken³, Richard Eastell⁴. ¹University of Southern Denmark, Denmark, ²Oxford NIHR Musculoskeletal Biomedical Research Unit, Nuffield Department of Orthopaedics, ³Hillerød Hospital, ⁴Academic Unit of Bone Metabolism, The University of Sheffield

Atypical femur fractures (AFF) are a subset of subtrochanteric and shaft fractures of the femur (ST/FS). Only if rate_{ST/FS} increases during treatment can AFFs be added to the net number of fractures; otherwise any increases must have been offset by prevention of a larger number of conventional ST/FS fractures. Even a net increase in rate_{ST/FS} will allow for an overall risk reduction so long as it is offset by hip fractures saved.

Methods: We used Danish national health registers to track hip and ST/FS fracture events until 31/DEC/2013 in 61,990 men and women aged 50 to 94 who began alendronate treatment between 1/JAN/1996 and 31/DEC/2007. We conducted nested case control (c-c) studies for ST/FS (N=1,428) and hip fractures (neck or IT, N=6,784) against matched controls, and assessed history of cumulative use and refill adherence (Medication Possession Ratio, MPR) of alendronate.

Results: Paralleling the FIT study, alendronate users with optimal adherence (MPR > 80%) had a lower risk of hip fracture (OR 0.73, 95%CI 0.68-0.78), and hip fracture risk was lower with 10+ years of use than with <5 years (OR 0.74, 95%CI 0.56-0.97). The risk of ST/FS fracture was not increased in current (OR 0.91, 95%CI 0.79-1.06) or recent (OR 1.00, 95%CI 0.81-1.23) alendronate users compared with past users. Also, the risk was not higher with 10+ dose years (worth ≥10 years of cumulative use) of alendronate (OR 0.70, 95%CI 0.44-1.11) or with optimal adherence (OR 0.88, 95%CI 0.77-1.01). Including switching to other oral bisphosphonates or dmb in the analysis did not change the results. The risk was higher with diabetes, prior fractures and PPI use.

Conclusions: Long term adherent use of alendronate in excess of 10 dose years was associated with a 25% reduced hip fracture risk but no increase in the risk of ST/FS fractures.

| Dose years | Hip fracture (c-c OR, 95%CI) | ST/FS fracture (c-c OR, 95%CI) |
|--------------------------------------|---------------------------------|-----------------------------------|
| <5 | reference | reference |
| 5-10 | 0.74(0.67-0.83) p<0.001 | 1.04(0.86-1.25) p=0.69 |
| ≥10 | 0.74(0.56-0.97) p=0.031 | 0.70(0.44-1.11) p=0.13 |
| Cohort event rate 1st and 10th yr | 36.2 and 14.3 per 1,000 | 5.1 and 4.6 per 1,000 |

Table 1

Disclosures: Bo Abrahamsen, None.

LB-SA0035

Striking Response of Tumor-Induced Osteomalacia to the FGFR Inhibitor NVP-BGJ398. Michael Collins*¹, Clemens Bergwitz², Gabriella Aitchison¹, Jenny Blau¹, Alison Boyce¹, Rachel Gafni³, Lori Guthrie¹, Flora Miranda⁴, Eric Slosberg⁵, Diana Graus Porta⁶, Christine Hopmann⁶, Karim Welava⁷, Randi Isaacs⁸, Carole Miller⁷. ¹National Institutes of Health, ²Yale School of Medicine, ³National Institutes of Health, USA, ⁴Novartis Pharmaceuticals, ⁵Novartis Institutes for BioMedical Research, ⁶Saint Agnes Cancer Center, ⁷St. Agnes Cancer Center, ⁸Novartis Institute Biomedical Research

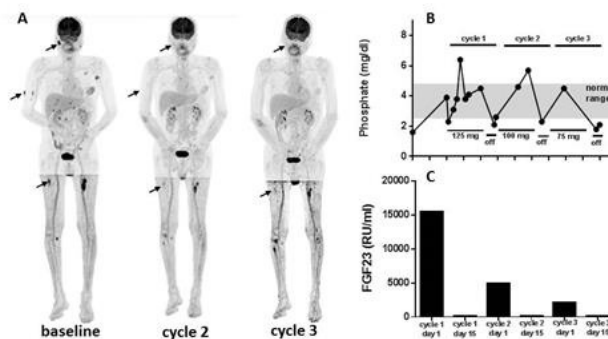
Tumor-induced osteomalacia (TIO) is a paraneoplastic syndrome characterized by bone pain, muscle weakness, and fractures. Symptoms are due to renal phosphate wasting, which results in hypophosphatemia and osteomalacia. TIO is caused by ectopic production of the phosphate- and vitamin D-regulating hormone, FGF23, usually by mixed tissue mesenchymal tumors. Several lines of evidence suggest a role for FGFR signaling in FGF23 regulation and TIO tumorigenesis, especially the recent finding of a fibronectin 1(FN1)/FGFR1 gene fusion in TIO tumors that presumably generates a FN/FGFR chimeric protein with active FGFR signaling. NVP-BGJ398 is a selective pan-FGFR inhibitor that has been shown to have anti-tumor activity in FGFR-driven tumors, and to inhibit the phosphaturic effects of FGF23 in preclinical models. These combined properties suggest a possible role for NVP-BGJ398 in treating TIO.

We identified a FGFR rearrangement in a tumor from a patient with an extremely rare case of widely metastatic TIO, who had previously failed Yttrium-90/Lutetium-177 peptide receptor radionuclide therapy. Based on the FGFR1 rearrangement, the patient enrolled in an IRB-approved phase 2 trial (NVP-BGJ398 Signature Trial; NCT02160041). Through cycles 1, 2, and 3, (1 cycle = 3 weeks on/1 week off drug), doses were 125, 100, and 75mg/day, respectively – adjusted to maintain normal serum phosphate levels.

The major findings are represented in the figure: A) FDG PET scans performed before the 1st, 2nd and 3rd cycles. Treatment resulted in disappearance of pulmonary and hepatic metastases after just one cycle, and progressive shrinkage of multiple

metastatic lesions (arrows). B) serum phosphate increased during treatment and returned to baseline when off, C) plasma FGF23 levels (C-terminal, Immunotopics, San Clemente, CA), which were approximately 100 fold above normal before treatment, decreased to normal on drug and increased when off. Of note, off-drug FGF23 values progressively decreased with each cycle. Treatment was accompanied by hyperuricemia. Side effects included grade 1 stomatitis, hand-foot syndrome, and retinal detachment, which were addressed by dose interruptions and reductions.

The data support: 1) NVP-BGJ398 is tumoricidal to phosphaturic mesenchymal tumors in TIO, and 2) in TIO FGF23 production is FGFR-dependent. While it remains to be proven if these effects will also occur in typical non-malignant TIO, the data support a role for NVP-BGJ398 in the treatment of TIO.



Collins abstract figure

Disclosures: Michael Collins, None.

This study received funding from: Novartis

LB-SA0036

M-CSF is a potential target for Gorham-Stout disease, a disease characterized by lymphatic vessel invasion of bone marrow and massive osteolysis. Lianping Xing*¹, Wensheng Wang, Mengmeng Wang, Li Xing, Sun Wen, Brendan Boyce. University of Rochester, USA

Gorham-Stout disease (GSD) is a rare bone disorder, characterized by proliferation of lymphatic vessels within bone marrow cavities, which is associated with aggressive osteolysis that can lead to complete loss of some bones. The etiology of GSD is poorly understood and there is no effective therapy. The goal of this study is to determine if the GSD osteolytic phenotype occurs because lymphatic endothelial cells (LECs) adversely affect the function of osteoclasts (OCs) or osteoblasts (OBs). We first examined the effect of a mouse LEC line on OC and OB differentiation in cocultures. LECs significantly increased OC formation and bone resorption, but had no clear effect on OBs. We hypothesize that LECs produce factors that promote OC formation and thereby induce osteolysis in GSD. To test this, we examined expression of osteoclastogenic cytokines in LECs by qPCR and found very high levels of M-CSF mRNA compared to other factors (e.g. >1,000, >100 and >60-fold greater than RANKL, TNF, and IL-6, respectively). Conditioned media (CM) from LECs express high levels of M-CSF protein (ng/ml: 2.05 ± 0.02 ng/ml vs 0.018 ± 0.003 in PBS) by ELISA, and LEC CM-mediated OC formation and bone resorption were blocked by a M-CSF neutralizing antibody (OC#/well: 13 ± 1 vs. 218 ± 7 in IgG; pit area/slice: 0 ± 0 vs. 0.61 ± 0.03 mm² in IgG) or by Ki20227, a specific inhibitor of c-fms, the M-CSF receptor, (OC#/well: 0 ± 0 vs. 248 ± 24 in DMSO). To determine if LECs cause the GSD-like phenotype in vivo, we performed intra-tibial injection of LECs in WT mice and examined X-rays of their bones weekly for up to 9 weeks. LECs caused osteolysis of injected tibiae, starting at 2 weeks post-injection. MicroCT analysis confirmed severe bone loss (BV/TV: 1.2 ± 0.5 vs. 30 ± 1% in PBS, N=10 mice/group), and histology showed that LEC-injected tibiae had significantly reduced bone mass, increased OC numbers, and trabecular and cortical bone loss. Furthermore, we detected significantly increased levels of M-CSF in serum and bone marrow plasma of mice that received intra-tibial injection of LECs by ELISA (serum: 1.8 ± 0.3 vs 1.3 ± 0.15 ng/ml in PBS-injected; bone marrow: 59 ± 6 vs 22 ± 4 pg/ml in PBS-injected). Thus, LECs could function as effector cells in GSD to cause bone destruction by producing large amounts of M-CSF. Thus, M-CSF represents a new therapeutic target and perhaps a clinical biomarker for patients suffering from GSD and other lymphatic anomalies that are associated with destruction of bone.

Disclosures: Lianping Xing, None.

This study received funding from: Lymphatic Malformation Institute

LB-SA0037

***Enterococcus faecalis* attenuates both osteoclastogenesis and osteoblastogenesis.** Ok-Jin Park^{*1}, Jiseon Kim², Jihyun Yang³, Cheol-Heui Yun², Seung Hyun Han². ¹Seoul National University School of Dentistry, South Korea, ²Seoul National University, ³Korea Research Institute of Bioscience & Biotechnology

Enterococcus faecalis is closely associated with refractory apical periodontitis often causing apical bone loss and impaired bone regeneration. Despite the fact that *E. faecalis* could contact osteoblast and osteoclast in periapical lesions, little is known about how the bacteria affect osteoclast and osteoblast. In the present study, we investigated the effect of *E. faecalis* on the differentiation of osteoclast and osteoblast. When mouse bone marrow-derived macrophages (BMMs) were treated with heat-killed *E. faecalis* (HKEF), the osteoclast differentiation was remarkably attenuated. HKEF also prevented a reduction in the phagocytic capacity of BMMs after differentiation into osteoclasts, while it induced the expression of inflammatory cytokines and chemokines. HKEF inhibited the RANKL-induced expression of c-Fos and NFATc1, both of which are crucial transcription factors for osteoclast differentiation. On the other hand, when primary osteoblasts derived from mouse calvaria were stimulated with HKEF, there was a substantial decrease in the osteoblast differentiation. Furthermore, HKEF inhibited Runx2 transcriptional activity and the expression of osteogenic marker genes including osterix, β -catenin, osteocalcin, and type I collagen in the osteoblasts. However, it was intriguing that inflammatory chemokines were increased in the cells treated with HKEF. In conclusion, these results suggest that *E. faecalis* attenuates the differentiation of osteoclast and osteoblast but enhances the production of inflammatory cytokines and chemokines, that might contribute to the attenuated bone regeneration.

Disclosures: Ok-Jin Park, None.

LB-SU0001

Oral PTH (1-34) in the Treatment of Hypoparathyroidism. Sofia Ish-Shalom^{*1}, Yoseph Caraco², Nariman Saba Khazen¹, Michal Gershinsky¹, Auryan Szalat², Hillel Galitzer³, Jonathan C. Y. Tang⁴, Gregory Burshtien⁵, Ariel Rothner⁵, Arthur Raskin⁵, Miriam Blum⁵, William D. Fraser⁴. ¹Endocrine Research Center, Lin Medical Center, Clalit Health Services, Haifa, Israel, ²Hebrew University Medical School - Hadassah Medical Center Jerusalem, Israel, ³Entera Bio, IL, ⁴Bioanalytical Facility, Biomedical Research Centre, Norwich Medical School, Faculty of Medicine & Health Sciences, University of East Anglia, Norwich, United Kingdom NR4 7TJ, ⁵Entera Bio Ltd, Hadassah Ein-Kerem, Jerusalem Bio Park, Jerusalem, Israel

Background: Primary hypoparathyroidism (PHP) is a hormone deficiency for which no oral replacement therapy is currently available. Oral PTH administration may allow for more flexibility in providing an adequate therapeutic dose, for achievement of normocalcemia and normophosphatemia in patients with varied severity of hormone deficiency and response to therapy. We present the results of a Phase 2a clinical study.

Objective: A multi-center, open label study to evaluate the safety, tolerability and pharmacokinetics of an oral formulation of PTH (1-34) for treatment of PHP.

Patients and Methods: Patients with established PHP, at least one year on chronic treatment with calcium supplements and alfacalcidol were enrolled for a treatment period of 16 weeks. The first 3 doses of PTH (1-34) 0.75 mg/dose were administered at the research center; subjects were then asked to continue with self-administration 4 times a day (QID). Follow up visits were performed at the end of week 1, 2, 3, 4, 6, 8, 10, 12 and 16. Serum calcium, phosphorus, albumin, creatinine were evaluated on these visits and medication dose adjustments was performed based on albumin adjusted calcium (ACa) levels.

Results: 19 subjects [16(f), 3(m)], mean age 44.5yr (range 20.3-71) were enrolled. 13 subjects had postsurgical hypoparathyroidism (68.4%), 5 autoimmune (26.3%) and 1 hereditary (5.3%). Mean calcium supplement dose at enrollment was 3,640 mg/day (range 1,000- 10,800) and alfacalcidol was 1.1 mcg/day (range 0-2). Mean ACa at enrollment was 7.92 mg/dL, (range 7.2-8.99), mean serum phosphorus was 5.0 mg/dL (range 3.7-7). The calcium supplement dose was gradually and significantly ($P < 0.01$) decreased from the end of week 3 (Figure 1) while maintaining the ACa at a mean level of 8.15 mg/dL (range 6.97-9.14). Serum phosphorus levels were significantly ($P < 0.01$) reduced after each dose and gradually throughout the study (Figure 2) to 4.3 mg/dL (range 2.9-5.2). The study drug was safe and well tolerated - 17 subjects completed with no related adverse events and high adherence ($> 80\%$, average 95.6%). 1 subject withdrew consent on the first day. Another subject was excluded due to hypercalcemia prior to treatment. **Conclusion:** Oral administration of Entera Bio's PTH (1-34) offers a safe and efficient therapeutic option for the treatment of PHP. Further studies are needed for defining the most appropriate treatment regimens for PHP patients with this medication.

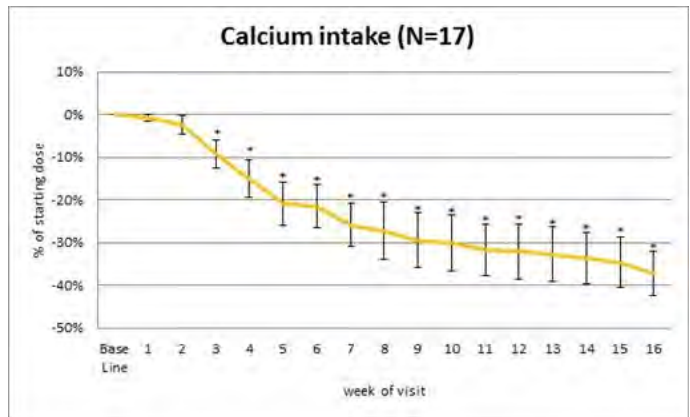


Figure 1: Mean calcium intake as a percent of starting dose at baseline. (* $P < 0.01$)

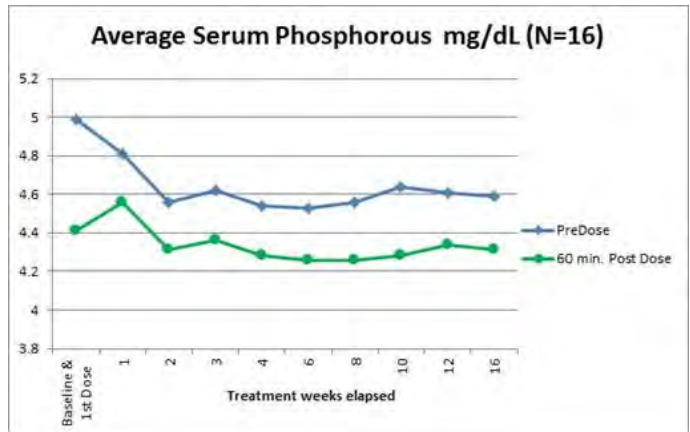


Figure 2: Mean serum phosphorus levels prior to taking the study drug and 60 min. post dose

Disclosures: Sofia Ish-Shalom, Entera Bio
This study received funding from: Entera Bio

LB-SU0002

Bone Material Compositional Properties at Actively Bone Forming Trabecular Surfaces are Able to Discriminate Between Chronic Obstructive Pulmonary Disease (COPD) Patients that Sustain Fragility Fractures vs. Those Who Do Not, Irrespective of Glucocorticoid Therapy. Eleftherios Paschalis^{*1}, Sonja Gamsjaeger², David Dempster³, Vanda Jorgetti⁴, Victoria Borba⁵, Klaus Klaushofer², Carolina Moreira⁵. ¹Ludwig Boltzmann Institute for Osteology, Austria, ²Ludwig Boltzmann Institute of Osteology at the Hanusch Hospital of WGKK & AUVA Trauma Centre Meidling, 1st Medical Department, Hanusch Hospital, Vienna, ³Columbia University, ⁴Department of Nephrology, School of Medicine, University of Sao Paulo, SP, ⁵Endocrine Division (SEMPR), Department of Internal Medicine, Clinical Hospital of the Federal University of Parana, Curitiba, PR

Chronic obstructive pulmonary disease (COPD) is associated with low aBMD by DXA and altered microstructure by bone histomorphometry and microcomputed tomography. Nevertheless, not all of COPD patients sustain fragility fractures. In the present study we used Raman microspectroscopic analysis to determine bone compositional properties at actively forming trabecular surfaces (based on double fluorescent labels) in iliac crest biopsies from 19 postmenopausal COPD patients (62.1 ± 7.3 years of age). Additionally, we also analyzed trabecular geometrical centers, representing tissue much older than the forming surfaces. Eight of the patients had sustained fragility fractures, and 13 had received treatment with inhaled glucocorticoids. None of the patients had taken oral glucocorticoids. The monitored parameters were: mineral / matrix ratio (MM), nanoporosity, and relative glycosaminoglycan (GAG), lipid, and pyridinoline contents (PYD). The data were also compared against previously published values in a group of healthy postmenopausal (POSTM), as well as placebo-receiving postmenopausal osteoporosis patients (POSTMOP). At actively forming surfaces, the COPD patients (N=19) had significantly lower MM values compared to POSTM, while the PYD values were significantly higher than POSTM and lower than the POSTMOP groups. The COPD patients had significantly higher nanoporosity compared to either POSTM or POSTMOP, and higher GAG content compared to POSTMOP. Within the COPD

group, there were no significant differences between the glucocorticoid receiving patients and those who did not receive any. COPD patients sustaining fragility fractures had significantly lower nanoporosity and higher MM and PYD values compared to COPD patients without fragility fractures. To the best of our knowledge, this is the first study identifying differences between COPD patients based on fragility fracture incidence. Given that these bone material compositional differences are evident close to the cement line (a major bone interface), they may contribute to the inferior bone toughness and consequent fragility fractures prevalent in these patients.

Disclosures: Eleftherios Paschalis, None.

LB-SU0003

Differential effects of age and BMI on Trabecular Bone Score and Femur geometry. KyongYoung Kim^{*1}, KyoungMin Kim², Sung Hee Choi², Soo Lim², Sang Wan Kim³, Chan Soo Shin⁴, Hak Chul Jang², ¹Seoul National University Bundang Hospital & Seoul National University College of Medicine, ²Borame Hospital & Seoul National University College of Medicine, ³Seoul National University Hospital & Seoul National University College of Medicine

Bone quality is another major component in determining bone strength together with bone mineral density (BMD). Bone geometry, a spatial distribution of bone, is one of parameters of bone quality. The trabecular bone score (TBS) is a geometric parameter of trabecular bone and it represents the quality of trabecular bone. On the other hand, femur geometry reflects cortical bone quality. The aims of this study were to investigate the correlations between age, BMI and structure measures derived from TBS and femur geometry, and to examine the associations between those measures. This was a cross-sectional study and 263 men and 609 women aged over 50 years (mean age, 64.0 years in male and 67.0 years in female) were included. Subjects with any pathological disorders (such as cancer, hyperthyroidism or renal failure) or using medications (such as corticosteroids, heparin, or anticonvulsants) known to alter calcium and bone metabolism or using antiresorptive agents such as raloxifene, bisphosphonate, or hormone replacement therapies were excluded. Study subjects were divided into 3 age groups; 50-59 years, 60-69 years, and 70 years and older. They were also stratified into 2 groups according to their BMI, less than 23.0 kg/m² or higher than 23.0 kg/m². BMDs at lumbar spine and femur neck were measured from dual-energy X-ray absorptiometry (Hologic Discovery A, Hologic Inc., Waltham, MA), and TBS and femur geometry were further analyzed. The TBS was negatively correlated with age, and the associations were greater in women and age group of 50-59 years both in men and women. On the other hands, femur geometric parameters including cortical thickness, cross-sectional area (CSA) showed negative associations with age, and the relationships were quite similar between genders. Moreover, it showed greater associations in age group of 70 years and older both in men and women. In associations between those geometric measures with BMI, TBS provided negative correlation with BMI only in overweight group (BMI > 23.0 kg/m²), whereas cortical thickness showed positive associations both in overweight group and non-overweight group (BMI ≤ 23.0 kg/m²). TBS and cortical thickness showed strong positive correlations both gender, but it was greater in men (R= 0.435 in men and R= 0.296 in women, P< 0.01 respectively). Although TBS and femur geometric parameters were associated strongly, age and BMI provided differential effects on trabecular bone geometry or cortical bone geometry.

Disclosures: KyongYoung Kim, None.

LB-SU0004

Hypophosphatasemia in Duchenne Muscular Dystrophy. Anna Petryk^{*1}, Peter Karachunski², James Hodges², Michael Whyte³. ¹University of Minnesota, USA, ²University of Minnesota, USA, ³Shriners Hospital for Children & Washington University School of Medicine, USA

Background: Duchenne muscular dystrophy (DMD), an X-linked neuromuscular disorder from loss-of-function mutation within the dystrophin gene, features progressive muscle weakness and wasting, loss of ambulation, and cardiorespiratory compromise with death usually in the third decade of life. Glucocorticoid treatment delays progression, but only temporarily, and is associated with significant morbidity, underscoring the need for new therapies. Hypophosphatasia (HPP) is the inborn-error-of-metabolism characterized by deficient activity of the tissue-nonspecific isoenzyme of alkaline phosphatase (TNSALP) causing low serum ALP activity (hypophosphatasemia), often with muscle weakness and a waddling gait sometimes mistaken for DMD. In HPP, strength and ambulation are improved with treatment using investigational, bone-targeted, recombinant, human TNSALP (asfotase alfa).

Objective: Report hypophosphatasemia in DMD.

Methods: A retrospective chart review of 69 DMD patients (all males) treated at the University of Minnesota. All had DMD mutations. Among them, 31 had serum ALP measured at Fairview Diagnostic Laboratories at least once between 2004 and 2015 using the bichromatic rate methodology applied successively with three different instruments (Vitros 5,1 FS, Vitros 5600, and Siemens Vista). Age- and gender-matched normal ranges were provided for interpretation of patient serum ALP activities.

Results: The average patient age (±SD) at most recent serum ALP measurement was 14.6 (±7.1) yr (range 3.5-29.7 yr). Among the 31 patients, 20 (65%) had at least one low ALP level using the age- and sex-specific reference ranges. For these 20 patients, 3, 8, and 9 children had average serum ALP activities 25-50%, 50-75%, and 75-99% of the lower limit of normal, respectively. The mean age at first reported low ALP was 10.6 ± 4.2

(range 4.9-19.9 yr). Among the 11 patients with more than one low serum ALP value, hypophosphatasemia remained present for the duration of follow up (0.2-6.8 yr).

Conclusion: A large proportion of our DMD patients exhibited hypophosphatasemia. It is currently unknown whether low serum ALP activity is of functional significance in DMD, but in HPP patients it can be associated with notable muscle weakness. While glucocorticoid exposure is common in DMD patients, and may have contributed to low serum ALP, our findings should generate further investigation of DMD hypophosphatasemia, especially since osteoporosis and fractures are common in these patients.

Disclosures: Anna Petryk, None.

LB-SU0005

Withdrawn

LB-SU0006

Atsttrin, an engineered protein derived from progranulin growth factor, is therapeutic in osteoarthritis. Jianlu WEI^{*1}, Qingyun Tian², Brendon Richbrough², chuanju liu². ¹Hospital for Joint Diseases of NYU, USA, ²HJD of NYU

Progranulin (PGRN) is a multifunctional growth factor which is composed of seven-and-a-half repeats directly binds to TNF- α receptors (TNFR), and inhibits TNF- α activity. Atsttrin, an engineered protein composed of three PGRN fragments, exhibited selective TNFR binding, and potentially prevented inflammation in multiple arthritis mouse models (Tang, et al, Science, 2011). In addition, recent studies demonstrated that local injection of PGRN significantly prevented OA progression (Zhao et al, *Annals of the Rheumatic Diseases*, 2015). These previous data promoted us to determine whether Atsttrin also has therapeutic effects in OA, and the molecular mechanism involved. To determine whether Atsttrin can rescue the role of PGRN in PGRN null mice, we established surgically-induced OA model, destabilization of medial meniscus model in PGRN-deficient mice. Safranin O staining showed Atsttrin remarkably prevented loss of proteoglycan and meniscus ossification. In addition, anterior cruciate ligament transection model in wild type mice was established to determine the preventative effect of Atsttrin. Immunohistochemistry staining showed that the Atsttrin decreased the degradation of cartilage matrix molecules, slowing down OA progression. High power photography of HE staining revealed Atsttrin reduced chondrocyte clustering and inhibited migration of the irregular tide mark. Furthermore, Atsttrin dramatically reduced OA-associated pain, measured by open box behavior test, von frey test and inflammatory mediators in the ipsilateral L3-L5 dorsal root ganglion, indicating Atsttrin is a disease- and symptom-modifying drug. Molecular mechanistic studies revealed that Atsttrin significantly inhibited TNF- α -induced catabolic/inflammatory responses. More importantly, Atsttrin stimulated chondrocyte anabolic metabolism through activating Akt and Erk1/2 signaling pathways. To elucidate the contributions of TNFR1 and TNFR2 pathway to Atsttrin-mediated protection in OA, a comparison of Atsttrin's therapeutic effects in OA with ACLT model of wildtype, TNFR1-/-, TNFR2-/- and TNFR1&2 double knockout mice is ongoing. Collectively, Atsttrin has potential to be a novel chondroprotective drug that inhibits OA development through interacting with TNF- α /TNFR signaling pathways. These findings not only provide novel insights into the role of Atsttrin in cartilage homeostasis and arthritis *in vivo*, but may also lead to the development of novel therapeutic intervention strategies for osteoarthritis.

Disclosures: Jianlu WEI, None.

LB-SU0007

Interactive effects of long term high fat high sucrose diet and estrogen deficiency on endothelial function and bone property in 6-month-old female rats. Xiaoli Dong^{*1}, Chunmei Li², Sisi Cao³, Shun Wan Chan³, Man Sau Wong³. ¹The Hong Kong Polytechnic University, Hong kong, ²Guangdong Pharmaceutical College, ³The Hong Kong Polytechnic University

Osteoporosis (OP) and cardiovascular diseases (CVDs) are two multifactorial and degenerative diseases which might co-exist in postmenopausal women. Estrogen deficiency and high fat high sucrose diet (HFS) intake have been recognized as risk factors for OP and CVDs independently. Understanding the combined actions of these two detrimental factors on bone and cardiovascular system is essential for deriving appropriate strategies for simultaneous treatment of OP and CVDs. The present study is designed to determine the interactive actions of estrogen deficiency and HFS on bone properties and endothelial function and to investigate the underlying mechanisms. Six-month-old Sprague Dawley sham or ovariectomized (OVX) rats were fed either a low-fat-low-sucrose (LFS) or a high-fat-high-sucrose (HFS) diet for 12 weeks. The results showed that OVX did not significantly influence endothelium-dependent relaxation in response to acetylcholine (ACh) or sodium nitroprusside (SNP) in the isolated thoracic aorta from LFS fed rats; HFS significantly decreased vasorelaxation in response to ACh (rat aorta gave ~30% maximum relaxation in HFS fed rats and ~50% in LFS fed rats upon ACh challenge; p<0.05) in rats. OVX significantly weakened bone properties as demonstrated by the

reduction of bone property parameters including Tb.BMD, BV/TV, Tb.N, Conn-Des and the increase in Tb.Sp, BS/BV and SMI at femoral metaphysis (FE) of rats ($p < 0.001$). HFS did not result in significant alterations of bone property parameters in sham rats. However, HFS further downregulated Tb.BMD, BV/TV, Tb.N, Tb.Th and Conn-Des; while upregulated Tb.Sp, BS/BV and SMI in the FE of OVX rats ($p < 0.05$). The level of urinary DPD, a bone resorption marker, was significantly upregulated by the interacting actions of HFS and OVX in rats ($p < 0.05$). Mechanistic studies indicated that PPAR γ expressions in the thoracic aorta were induced by HFS to about 1.4-1.7 fold increase ($p < 0.05$) and in the bone by OVX to 1.1-1.7 fold change ($p < 0.05$). In summary, HFS aggravated OVX-induced bone loss. The synergistic detrimental actions of HFS and OVX on bone properties mainly occurred in cancellous bone and were characterized by a high degree of bone resorption. HFS, but not OVX resulted in endothelial dysfunction in rats. Such alterations were associated with PPAR γ expressions in the thoracic aorta and the bone in response to HFS and/or OVX.

Disclosures: Xiaoli Dong, None.

LB-SU0008

Glucose-loading reduces bone remodelling in women and osteoblast function in vitro. Itamar Levinger¹, Ego Seeman², Glenn McConell³, Mark Rybchyn⁴, Samantha Cassar⁵, Elizabeth Byrnes⁶, Steve Selig⁷, Rebecca Mason⁸, Peter Ebeling⁹, Tara Brennan-Speranza⁴. ¹Institute of Sport, Exercise & Active Living (ISEAL), Victoria University, Australia, ²University of Melbourne & the Department of Endocrinology, Austin Health, Melbourne, Australia, ³Clinical Exercise Science Program, Institute of Sport, Exercise & Active Living (ISEAL), Victoria University, Melbourne, Australia, ⁴Department of Physiology, Bosch Institute for Medical Research, University of Sydney, Australia., ⁵Clinical Exercise Science Program, Institute of Sport, Exercise & Active Living (ISEAL), Victoria University, Melbourne, Australia., ⁶PathWest QEII Medical Centre, Perth, Australia, ⁷School of Exercise & Nutrition Sciences, Deakin University, Melbourne, Australia., ⁸Department of Physiology, Bosch Institute for Medical Research, University of Sydney, Australia, ⁹Department of Medicine, School of Clinical Sciences, Faculty of Medicine, Nursing & Health Sciences, Monash University, Australia

Background: Ageing is associated with a reduction in osteoblast life-span and the volume of bone formed by each basic multicellular unit (BMU). Each time bone is resorbed, less is deposited producing microstructural deterioration. Ageing is also associated with insulin resistance and hyperglycaemia, either of which may cause, or be the result of, a decline in undercarboxylated osteocalcin (ucOC), a protein produced by osteoblasts that increases insulin sensitivity. We examined whether glucose loading reduces bone remodelling and ucOC in vivo and osteoblast function in vitro, and so compromises bone formation.

Methods: We administered an oral glucose tolerance test (OGTT) to 18 pre- and post-menopausal, non-diabetic women at rest and following exercise and measured serum levels of bone remodelling markers (BRMs) and ucOC. We also assessed whether increasing glucose concentrations with or without insulin reduced survival and activity of cultured human osteoblasts.

Results: Glucose-loading at rest and following exercise reduced BRMs in pre- and post-menopausal women and reduced ucOC in postmenopausal women. D-glucose (≥ 10 mmol/L) increased osteoblast apoptosis and reduced cell activity compared with 5 mmol/L. Insulin had a protective effect on these parameters.

Conclusions: Circulating glucose reduces osteoblast viability, at least in culture. Suppression of remodelling may preserve bone mineral density by slowing bone loss, but sacrifice bone's material composition. The failure of exercise to attenuate the suppressive effect of glucose on remodelling markers may be due to a direct detrimental effect of glucose on osteoblast survival and function.

Disclosures: Tara Brennan-Speranza, None.

LB-SU0009

Serum citrate is inversely related to bone turnover: findings from a large cross-sectional metabolomic study of adolescents. John Kemp¹, Adrian Sayers², William D. Fraser³, David M. Evans⁴, Jonathan H. Tobias². ¹MRC Centre for Causal Analyses in Translational Epidemiology, Australia, ²School of Clinical Sciences, University of Bristol, Bristol, UK, ³Norwich Medical School, University of East Anglia, Norwich, UK, ⁴MRC Integrative Epidemiology Unit, University of Bristol, Bristol, UK & University of Queensland Diamantina Institute, Translational Research Institute, Queensland, Australia

Aim: Bone mineral density and osteoporosis risk are related to circulating blood metabolites. However, most human studies have only examined a few candidate metabolites at a time. Thus, the relationship between normal serum metabolomic variation and bone development remains largely unstudied. We report findings from a population based study of adolescents in which we investigate the relationships

between blood metabolites [derived by proton nuclear magnetic resonance spectroscopy] and cortical bone parameters [measured by peripheral quantitative computed tomography (pQCT)]. **Methods:** Metabolomic profiles and mid-tibial pQCT scans were available in 1617 subjects (mean age 15.5 years) from the Avon Longitudinal Study of Parents and Children. Pearson correlation was used to quantify the relationships between metabolites (adjusted for age and sex) and pQCT parameters. Metabolites with the strongest relationships were investigated using linear regression, adjusting for potential confounders. **Results:** Citrate showed the largest correlation with cortical bone mineral density [BMDc, ($r = -0.25$, $P = 4 \times 10^{-25}$)]. Sex, Tanner stage, weight and height showed strong inverse relationships with citrate and were included in our model shown here, along with age and time of clinic attendance. Citrate was inversely related to BMDc [$\beta = -0.13$ (-0.16-0.09), coefficient=SD change per SD increase in citrate (95%CI)], and positively associated with periosteal circumference [PC, $\beta = 0.05$ (0.01|0.08)]. Based on a hypothesis that i) lower BMDc reflects greater cortical porosity due to higher bone turnover and ii) higher bone turnover leads to greater periosteal expansion; we investigated if the relationship between citrate, BMDc and PC was explained by increased bone turnover as reflected by serum β -C-telopeptides of type I collagen (CTX). A positive correlation between citrate and CTX was observed ($r = 0.38$, $P = 2 \times 10^{-59}$) and a SD increase in citrate was associated with a 0.21 unit increase in CTX. Adjustment for CTX, attenuated the association between citrate and BMDc [$\beta = -0.03$ (-0.07|0.002)] and PC [$\beta = 0.01$ (-0.02|0.05)] to the null. **Conclusions:** Our results suggest that normal variation in serum citrate levels have unrecognised implications for skeletal metabolism during adolescence, such that higher levels are associated with greater bone resorption with consequent effects on BMDc and periosteal expansion. Further studies are justified to explore the mechanistic basis for these relationships.

Disclosures: John Kemp, None.

LB-SU0010

Targeted Ablation of Macrophages and Mast Cells Impairs Heterotopic Ossification in a Mouse Model of Fibrodysplasia Ossificans Progressiva. Michael Convente¹, EnJun Yang², Salin Chakkalakal², Devu Zhang², Robert Caron², Daniel Perrien³, Taku Kambayashi², Frederick Kaplan², Eileen Shore². ¹University of Pennsylvania School of Medicine, USA, ²University of Pennsylvania, USA, ³Vanderbilt University, USA

Fibrodysplasia Ossificans Progressiva (FOP), a rare and disabling genetic disease characterized by progressive heterotopic ossification (HO), is caused by gain-of-function mutations (most commonly, R206H) in activin A receptor, ACVR1 (also known as ALK2), a bone morphogenetic protein (BMP) type I receptor, resulting in up-regulation of the BMP signaling pathway. BMP signaling amplifies inflammatory pathways, and work from our lab and others has documented the presence of immune cells at pre-ossesous stages of HO formation. HO in FOP can be triggered by soft tissue injury, however the specific role of the immune system in FOP and development of HO remains poorly understood. To investigate the immunological contribution during HO lesion formation, we examined the cellular and molecular response to tissue injury in a knock-in Acvr1^{R206H|FIE/+} mouse FOP model. Following skeletal muscle injury, lesions form and progress through a series of catabolic and anabolic events that forms bone by 14 days. Strikingly, targeted ablation of macrophages via clodronate-encapsulated liposomes or mast cells via a double-transgenic mast cell-deficient Acvr1^{R206H/+}; c-kit^{W-sh/W-sh} mouse each results in ~50% reduction of HO. Further, our preliminary data support an additive decrease in HO when both macrophages and mast cells are ablated. Examination of lesions at early and intermediate stages from Acvr1^{R206H/+} mice shows increased immune cell invasion and protein expression of the inflammatory cytokines TNF α , IL-1 β , and IL-6, predictive biomarkers for non-genetic trauma-induced HO, suggesting common inflammatory-mediated mechanisms during HO formation. We also show that macrophages and mast cells express multiple type I and type II receptors from the TGF- β /BMP superfamily, including Acvr1/Alk2. BMP signaling, assayed by phosphorylated Smad1/5, is substantially up-regulated in Acvr1^{R206H/+} mast cells and macrophages. Consistent with our *in vivo* data, mRNA expression of the pro-inflammatory cytokines TNF α and IL-6 is significantly elevated in mutant cells. Mast cell degranulation, a functional response to inflammatory stimulation, was also significantly increased in mast cells expressing Alk2^{R206H}. Our study identifies key immune cells vital for HO development, as well as dysregulated inflammatory pathways caused by the FOP ACVR1 R206H mutation, providing novel cellular and molecular targets for prophylactic and therapeutic intervention in genetic and non-genetic forms of HO.

Disclosures: Michael Convente, None.

LB-SU0011

“Raine Syndrome”, Caused By Mutations In *FAM20C*, Is “Congenital Sclerosing Osteomalacia With Cerebral Calcification”. Michael P. Whyte^{*1}, William H. McAlister², Vinieth N. Bijancki³, Shenghui Duan⁴, Steven Mum⁵. ¹Center for Metabolic Bone Disease & Molecular Research, Shriners Hospital for Children; ²Department of Pediatric Radiology, Mallinckrodt Institute of Radiology at St. Louis Children’s Hospital, Washington University School of Medicine; St. Louis, MO, USA, 63110, ³Center for Metabolic Bone Disease & Molecular Research, Shriners Hospital for Children, ⁴Division of Bone & Mineral Diseases, Washington University School of Medicine at St. Louis, ⁵Washington University School of Medicine, USA

In 1985, we briefly reported infant sisters with a unique and lethal disorder designated “congenital sclerosing osteomalacia with cerebral calcification” (CSOCC) (Figure). In 1986, CSOCC entered Mendelian Inheritance in Man as a new autosomal recessive entity designated “osteomalacia, sclerosing, with cerebral calcification” (MIM 259660). However, no further citations followed in MIM. Instead, in 1989 Raine and colleagues, apparently unaware of this MIM entry, described the features of CSOCC in a fetus as a new condition. After several additional case reports, this disorder became known in 1992 as “Raine syndrome”, and was included that same year in MIM as “osteosclerotic bone dysplasia, lethal” (259775). In 2007, the etiology was discovered to be loss-of-function mutations within the gene that encodes “family with sequence similarity 20, member C” (*FAM20C*). This advance then enabled characterization of mild variants of the disorder that were associated with hypophosphatemia. *FAM20C* is conserved among mammals, highly expressed in calcified tissues, and importantly involved in the phosphorylation of proteins that regulate skeletal mineralization. *FAM20C* phosphorylates the caseins and several secreted proteins implicated in biomineralization, including the small integrin-binding ligand, N-linked glycoproteins (SIBLINGs).

Here, we detail the clinical, radiological, biochemical, histopathological, and mutational studies of these two patients. The proposita had undergone dual tetracycline labeling just before her death when assessment of her skeletal histopathology became possible at autopsy. Despite no histopathological evidence of rickets, defective bone mineralization (osteomalacia) was a key finding associated with the severe osteosclerosis. Dental radiographs revealed “ghost teeth” consistent with this pathogenesis. Hypophosphatemia had been documented in the affected sister. Using archival DNA from the proposita, an unaffected sibling, and the mother, we found that compound heterozygosity for a unique missense *FAM20C* defect (Gly365Asp, paternal allele) and a deletion of *FAM20C* (maternal allele) explained the disorder. Thus, “Raine syndrome” is “congenital sclerosing osteomalacia with cerebral calcification”.

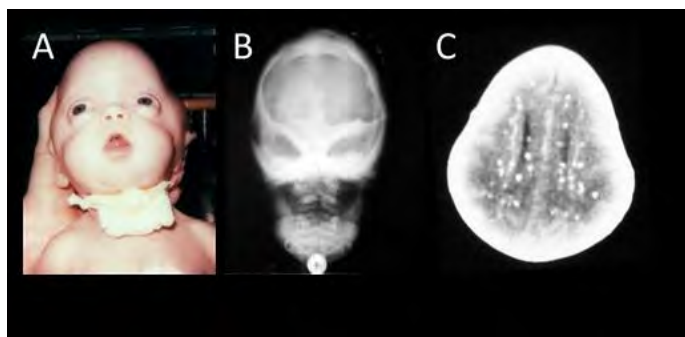


Figure 1

Disclosures: Michael P. Whyte, None.

LB-SU0012

BGJ398, a Pan-specific FGFR Inhibitor, Ameliorates Phosphate Wasting and Impaired Wnt Signaling in FGF2 High Molecular Weight Isoform Transgenic Mice. Erxia Du^{*}, Liping Xiao, Marja Hurley, UCONN Health, USA

High molecular weight FGF2 transgenic (HMWTg) mouse that phenocopies the Hyp mouse homolog of human X-linked hypophosphatemic rickets display dwarfism, hypophosphatemia, osteomalacia, reduced bone mineral density (BMD), increased FGF23 in bone and serum. Hyp mice overexpress HMWFGF2 in bone associated with increased FGF23 and phosphate (Pi) wasting in part via abnormal FGF23/FGFR/Klotho signaling. Since abnormal Wnt signaling was reported in Hyp mice we assessed whether Wnt signaling was impaired in kidneys of HMWTg mice and the effect of blocking FGFR signaling using a novel FGFR inhibitor BGJ398 (Novartis).

Six-7 week old female HMWTg mice were gavaged with one dose of BGJ398 50mg/kg body weight, or Vehicle. Vector/control mice were treated with Vehicle. DXA analysis was performed at baseline. Compared with Vector mice, there were significant reductions in BMD and BMC in HMWTg (Fig.1). Twenty-four hour urine

was collected after gavage. Mice were euthanized at 24 hours post-treatment to collect serum for biochemistry, and kidneys for gene and protein analysis by q-PCR and immunohistochemistry. Serum Pi was significantly reduced in HMWTg (Fig.2) and was partially rescued by BGJ398. Urine Pi was significantly increased and was normalized by BGJ398.

FGFRs and genes important in Pi homeostasis are shown in Fig.3. FGFR2, FGFR4 and Klotho mRNAs were increased and sodium-phosphate co-transporters Npt2a and Npt2c mRNAs were decreased in HMWTg. BGJ398 partially reduced Klotho and significantly increased Npt2a and Npt2c mRNAs in HMWTg. Cyp24 and Cyp27b1, regulated by mitogen activated protein kinases (MAPK/p-ERK) modulates serum Pi via 1,25(OH)2D3 in kidney. Cyp24 was significantly increased in HMWTg while Cyp27b1 was inappropriately decreased. BGJ398 further increased both Cyp24 and Cyp27b1 mRNA. Immunohistochemistry (Fig.4) shows that increased FGFR1, KLOTHO, p-ERK, and decreased NPT2a in HMWTg were rescued by BGJ398.

Wnt signaling studies (Fig.5) revealed that Wnt inhibitors, Sclerostin Domain Containing 1 (Sostdc1) and Engrailed-1 (En-1) mRNA, were significantly increased in HMWTg and were significantly decreased by BGJ398. Beta-catenin mRNA was increased by BGJ398 in HMWTg. Immunohistochemistry showed increased phosphorylated β -catenin in HMWTg which was decreased by BGJ398 and decreased active β -catenin in HMWTg that was increased by BGJ398.

We conclude that blocking FGFR partially rescued serum Pi by regulating FGFR and Wnt signaling in HMWTg.

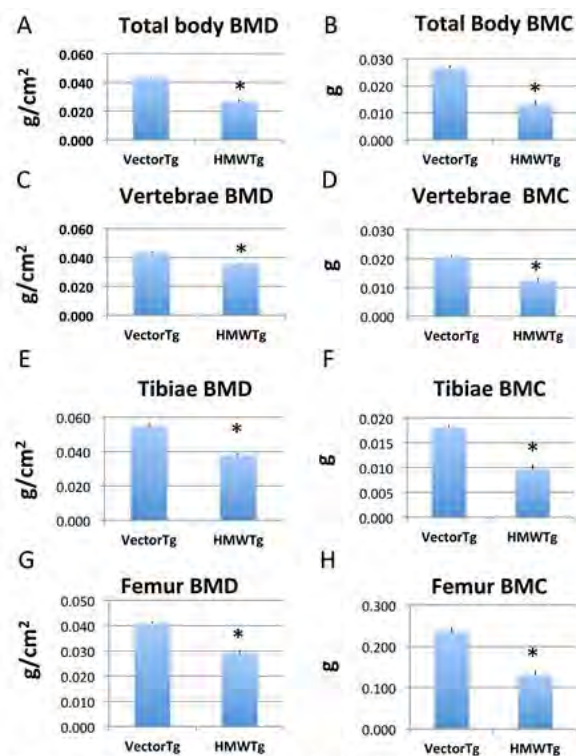


Fig 1. DXA analysis of BMD and BMC in VectorTg and HMWTg mice.

Figure 1

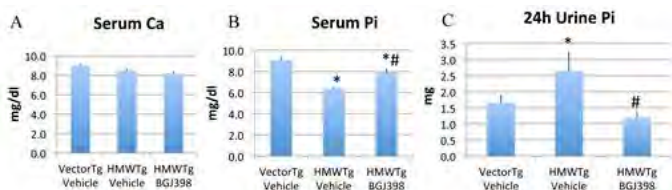


Fig 2. Effect of BGJ398 on biochemical parameters.

Figure 2

LB-SU0013

1-84PTH Amino Terminal Specific Immunoassay Mitigates Sample Instability due to *ex vivo* Processing and Oxidation: A Prevalent Haemodialysis Sample Analysis. Frank Blocki¹, Greg Olson¹, John Wall¹, Angela Podgorski¹, Dawn Vaught¹, Fabrizio Bonelli¹, Gavin Reid², Kevin Martin³. ¹DiaSorin Inc, ²University of Melbourne, ³Saint Louis University

Background: Assay of PTH has been historically problematic due to variable standardization, variable cross reactivity with PTH fragments, and variable correlations with biological parameters. Recent description of endogenous oxidation to PTH peptides further complicates these issues since, aside from lacking biological activity, oxidized PTH is of sufficiently altered structure to significantly impact assay specificity.

Methods: To characterize this issue further, an 'immunocapture LC-MS/MS' assay was developed using stable N15 and C13 isotope labels of both native PTH and 7-84 PTH fragment with each possible permutation of sulfoxide or sulfone at methionine 8 and 18. N15 labels were added to plasma samples just prior to immunocapture (Phases 1 & 2) or coincident with plasma collection (Phase 3) and for C13 internal standards, just prior to LC-MS/MS for all Phases 1-3. Immunoassays with specificity to both native and oxidized PTH were related to LC-MS/MS characterized samples.

Results: Phase 1: Greater than 10% oxidation was detected in 10% and 83% of HD samples collected from site A and B, respectively. Phase 2: Controlled, paired HD plasma samples, collected from site A and processed according to Site A and Site B workflow in parallel, failed to replicate Phase 1; however, overall PTH content of the samples evaluated were significantly lower. Phase 3: HD samples with intact PTH values between 200 and 1400pg/mL, whose workflow mimicked Phase 2, disclosed neither endogenous nor exogenous oxidation.

Conclusion: Extent of sample oxidation exceeding that of N15 standards would indicate in-vivo oxidation. Equivalent percentages of observed oxidation between N15 standards and endogenous PTH indicate oxidation originating with sample collection, environmental exposure / transit and processing. That significant, variable amounts of *ex vivo* oxidation were detected underscores the need for PTH measurement methods that are not impacted by compromised sample integrity due to exposure to widely variable shipping and storage conditions experienced prior to analytical measurement. Only the DiaSorin LIAISON 1-84PTH automated assay returns a measurement of true baseline PTH levels, even from samples of compromised quality, since its N-terminal specificity reports both native and oxidized PTH forms. Since oxidation of PTH peptides was found to vary greatly from sample batch to sample batch, it appears that any PTH oxidation is occurring *ex-vivo*.

Disclosures: Frank Blocki, DiaSorin Inc
This study received funding from: DiaSorin Inc

LB-SU0014

Altered Calcium Homeostasis in the Klotho Mutant Mouse Does Not Reflect Changes in Calcium Homeostasis that Occur with Aging. Vaishali Yeldurthy¹, Puneet Dhawan¹, Leila mady¹, Sylvia Christakos². ¹Department of Microbiology, Biochemistry & Molecular Genetics, NJMS, Rutgers University, ²Rutgers - New Jersey Medical School, USA

Klotho is a multifunctional protein which acts as an obligate coreceptor for FGF23 and is involved in calcium and phosphate homeostasis. Klotho mutant mice show a premature aging phenotype characterized by infertility, atherosclerosis, ectopic calcification, osteoporosis and skin atrophy. To understand the mechanisms of the premature aging phenotype we examined genes and transcription factors involved in calcium homeostasis and the activity of VDR coactivators by *in vivo* ChIP. Klotho mutant mice display elevated serum calcium and 1,25(OH)₂D₃, increased expression of intestinal TRPV6 and calbindin-D_{9k} and intestinal calcium hyperabsorption. In aging 20 month (mo.) old mice there is a marked decline in calbindin-D_{9k} and TRPV6 mRNA expression in all segments of the intestine [3 -5 fold; p < 0.05 compared to young (3 mo. old) and adult (6 mo. old) mice]. mRNA expression of renal CYP24A1, which is involved in the metabolic inactivation of 1,25(OH)₂D₃, increased with aging, suggesting that increased catabolism of 1,25(OH)₂D₃ correlates with the decreased capacity with age to absorb calcium and age related bone loss. Since CARM1 [a methyltransferase that methylates histone 3 at arginine 17] is a coactivator of VDR (vitamin D receptor) mediated CYP24A1 transcription, *in vivo* ChIP assays were done examining VDR binding and H3R17 methylation in response to 1,25(OH)₂D₃. *In vivo* ChIP revealed enhanced H3 arginine methylation and enhanced recruitment of VDR at the CYP24A1 VDREs (vitamin D response elements) in aged 20 mo. old mice (3 h after 1,25(OH)₂D₃ treatment; 10ng/g bw) compared to young and 6 mo. old adult mice. Our findings are the first to address mechanisms contributing to enhanced CYP24A1 and thus increased catabolism of 1,25(OH)₂D₃ with age. In contrast, using klotho mutant mice similarly injected with 1,25(OH)₂D₃. ChIP assays revealed a 2 - 4 fold significant decrease in both VDR binding and histone 3 methylation at the regulatory regions of the CYP24A1 gene (klotho mutant mice compared to WT mice or aging mice respectively; p < 0.05), suggesting that prolonged exposure to high levels of 1,25(OH)₂D₃ results in renal desensitization to 1,25(OH)₂D₃. These findings indicate that altered calcium homeostasis in the klotho mutant mouse is in contrast to changes observed in aging and reflects overproduction of 1,25(OH)₂D₃ and 1,25(OH)₂D₃ toxicity rather than effects on intestinal calcium absorption that contribute to bone loss in aging.

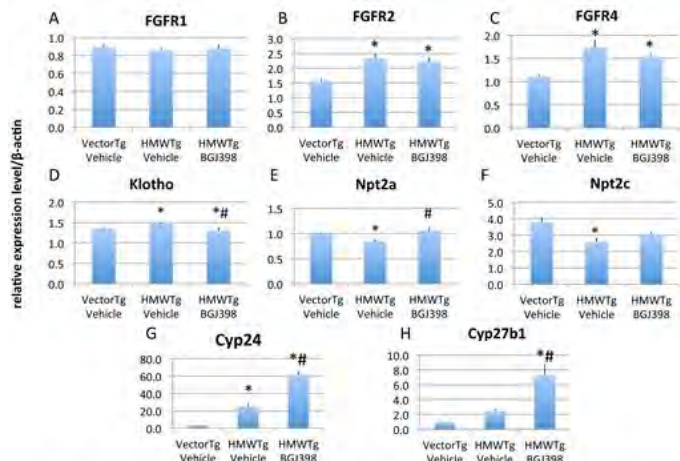


Fig 3. Effect of BGJ398 on mRNA expression in kidneys from 6-7 week old female mice.

Figure 3

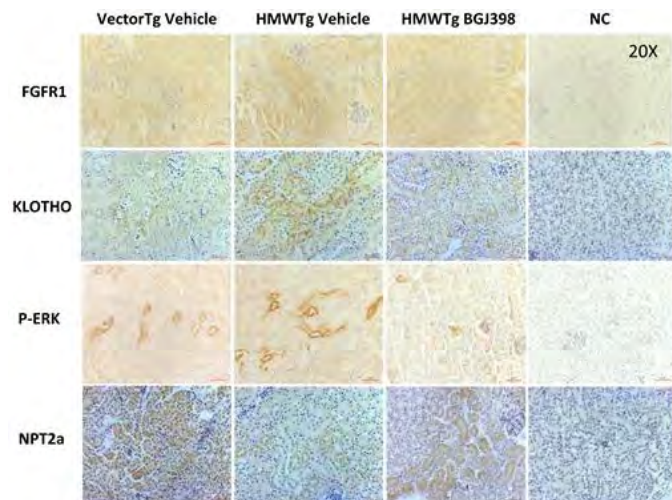


Fig 4. Effect of BGJ398 on protein expression in kidney from 6-7 week old female kidneys.

Figure 4

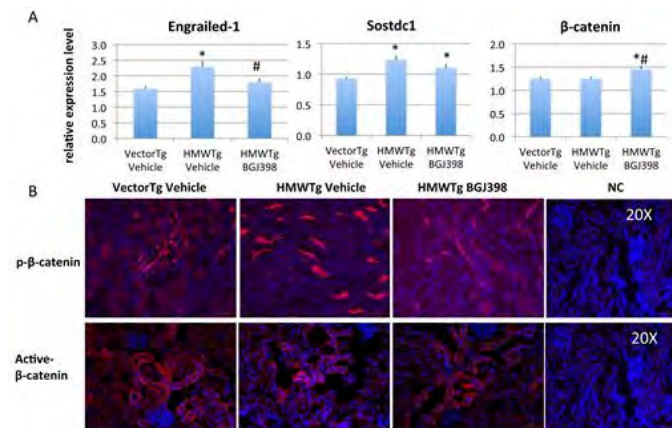


Fig 5. Effect of BGJ398 on gene and protein expression from 6-7 week old female kidneys.

Figure 5

Disclosures: Erxia Du, None.

Disclosures: Vaishali Veldurthy, None.

LB-SU0015

Osteoclasts Exhibit Rheotaxis in Response to Fluid Flow: Crawling Against the Tide. Noelle M. Ochotny¹, Brandon H. Kim¹, David W. Holdsworth², S. Jeffrey Dixon¹, Stephen M. Sims¹. ¹Department of Physiology & Pharmacology, Schulich School of Medicine & Dentistry, Bone & Joint Institute, Western University, ²Department of Surgery, Schulich School of Medicine & Dentistry, Bone & Joint Institute, Western University

Cells display a wide range of directed movements in response to environmental cues. One of these is rheotaxis, the orientation and migration of a cell in response to extracellular fluid flow. Positive rheotaxis, the tendency of a cell to move against the flow, was first reported for spermatozoa. When bone experiences mechanical loading, fluid flows through its canalicular network. The ability of fluid shear stress (FSS) to affect osteoclast behaviour is poorly understood. Our goal was to investigate the effects of FSS on osteoclast migration. Osteoclasts were isolated from the long bones of neonatal Wistar rats. Fluid flow was applied to single osteoclasts using glass micropipettes. The micropipettes, filled with the same medium bathing the cells, were positioned by micromanipulation and fluid flow was directed towards the osteoclast. Osteoclast morphology and motility were monitored using time-lapse phase-contrast microscopy. Migrating osteoclasts were identified by i) a polarized morphology, consisting of a lamellipod at the leading edge and a uropod at the rear (trailing edge), and ii) net displacement of the osteoclast's centroid of at least 50 µm toward the micropipette tip over a 40-minute observation period. In most cases, FSS induced prompt polarization, turning, and migration of osteoclasts toward the flow. As a control, micropipettes were positioned in a similar manner but without flow. To quantify the effect of FSS on osteoclast movement, the net displacement of the osteoclast's centroid from the point of origin was measured over a 40-minute period. The majority of osteoclasts exposed to FSS (28 of the 38 cells tested) migrated at least 50 µm against the flow (toward the micropipette tip). The mean rate of migration was 2.0 ± 0.9 µm/min, markedly greater than during chemotaxis induced by M-CSF or TGF-β. In the absence of FSS, 10 of 10 control osteoclasts showed random movement and no significant orientation toward the micropipette tip. Chi-square analysis revealed statistically significant positive rheotaxis in response to fluid shear ($p < 0.01$). Our data reveal for the first time that osteoclasts exhibit robust positive rheotaxis in response to FSS. This heretofore unrecognized behaviour may play a key role in skeletal mechanotransduction *in vivo*, where osteoclasts are known to accumulate at sites of microcracks. Fluid flow from microcracks may serve to recruit osteoclasts to initiate bone remodeling at these sites.

Disclosures: Noelle M. Ochotny, None.

LB-SU0016

The effects of local and sustained delivery of estrogen conjugated with hydrogel and nanodiamonds on bone formation. Christine Hong^{*1}, Tania Ohebsion¹, Dong Keun Lee², Dean Ho². ¹UCLA School of Dentistry, USA, ²UCLA School of Bioengineering

Estrogen (E2) is a naturally occurring steroid that plays a critical role in bone homeostasis, and it could be utilized as a new anabolic therapy for craniofacial defects. However, E2's clinical application is less appreciated due to its numerous limitations including E2's pleiotropic effects and short half-life. Therefore, new treatment modalities are required to allow E2 to stimulate bone formation via local and sustained release. In order to address this need, we have investigated nanodiamond-estrogen (ND-E2) complexes embedded within gels (G).

NDs are carbon byproducts that have good biocompatibility and chemical stability in solution. Additionally, NDs are excellent drug delivery platforms due to the physical characteristics of the surface of NDs, like their drug retention properties. In preparation of our novel estrogen delivery platform, NDs were loaded with insoluble E2s. The ND-E2 complexes were then delivered via injections into the desired location, where ND-E2 complexes embedded gels formed with the escalating sustained release ability of E2 (Figure 1).

Furthermore, to determine the ND-E2-G drug delivery platform's potential for bone stimulation in the oral cavity within clinical setting, a novel palatal expansion model was established in rats; since following palatal expansion, a strong probability of relapse of the maxilla exists, especially in cleft lip and/or palate (CLP) patients.

A total of 18 female, Sprague Dawley rats underwent 7 days of palatal expansion and were then divided into five groups (Control, E2, E2+ND, E2+G, E2+ND+G) to be injected in the palate. After retaining the expansion for 14 days, expanders were removed and rats were allowed to relapse (Figure 2). Micro-CT analysis demonstrated that the addition of G and ND to E2 (E2+ND+G) significantly reduced relapse ratio by 5.5 fold and increased bone volume and density, compared to all other groups (Figure 3). While the findings of this study are directly useful to craniofacial patients, future applications of local and sustained delivery of estrogen are immeasurable. The long-term goal of this study is to develop this newly established therapeutic model to aid in optimizing the clinical treatment of regenerating craniofacial and bone defects.

Disclosures: Christine Hong, None.

LB-SU0017

Low dose CAPE treatment in a CAIA model of Inflammatory Arthritis. Bonnie Williams¹, Helen Tsangari², Melissa Cantley¹, Victor Marino³, Jiaki Xu⁴, Egon Perilli⁵, A. Kencana Dharmapatri², Tania Crotti^{*6}. ¹Discipline of Anatomy & Pathology, School of Medicine, University of Adelaide, ²Discipline of Anatomy & Pathology, School of Medicine, The University of Adelaide, ³School of Dentistry, University of Adelaide, ⁴School of Pathology & Laboratory Medicine, The University of Western Australia, ⁵Biomedical Engineering Medical Device Research Institute, School of Computer Science, Engineering & Mathematics, Flinders University, ⁶Discipline of Anatomy & Pathology, School of Medicine, University of Adelaide, Australia

Rheumatoid arthritis is a chronic inflammatory disorder resulting in bone and cartilage destruction. Bone loss has been attributed to the relative increase in the number and activity of bone-resorbing osteoclasts and the activation of NF-kappaB: Caffeic acid phenethyl ester (CAPE) is a natural bioactive compound from the propolis of honeybee hives, which inhibits NFkappa B activity (Ang J Cell Physiol 2009) and has anti-inflammatory and immunomodulatory properties. We have shown inhibition of bone resorption with low doses of CAPE (1mg/kg/day) in a wear particle induced calvarial model of osteolysis (Zawawi Cal Tiss Int 2015).

Aims: Given the toxicity concerns with high dose and the effectiveness on bone loss suppression at 1mg/kg, we propose low dose CAPE as a treatment to target inflammation and bone loss in a CAIA model of inflammatory arthritis.

Methods: CAIA model in Balb/c mice (4 groups of 8 mice each: CAIA, CAIA + CAPE, CAPE, Control). CAPE (Sigma) was administered at 1mg/kg/day subcutaneously on day 3, 7 and 10. Local inflammation was assessed by clinical paw scoring. Serum levels of CRP and CTX-1 were measured by ELISA at day 14 to determine systemic inflammation and systemic bone resorption, respectively.

Results: CAIA mice treated with CAPE exhibited significantly greater local inflammation than CAIA mice by day 5 (paw score 5.75 vs 1.75, $p < 0.01$). By day 14, local inflammation reduced in both CAIA and CAPE-treated CAIA mice, with no significant difference between the groups ($p=0.64$); also CRP levels did not significantly differ between the groups ($p=0.89$). At day 14, the CTX-1 levels were higher in the CAIA mice, although not significantly (48.1 vs 28.5 ng/ml, $p=0.16$).

Conclusion: CAIA mice treated with low dose CAPE exhibited earlier onset of inflammation; low dose CAPE did not suppress local inflammation. Systemic inflammation was not evident by day 14 in the CAIA model, with or without CAPE. Systemic bone resorption may be occurring in the CAIA group at day 14.

Disclosures: Tania Crotti, None.

LB-SU0018

Treatment with soluble activin type IIB receptor improves fracture healing in a closed tibial fracture model. Tero Puolakkainen^{*1}, Petri Rummukainen¹, Jemina Lehto¹, Olli Ritvos², Ari Hiltunen³, Anna-Maria Säämänen¹, Riku Kiviranta¹. ¹University of Turku, ²University of Helsinki,

Bone fracture healing is a series of complex events, which happen both simultaneously and in succession aiming to restore the initial form and function of the bone. Despite recent advances in the contemporary treatment methods, bone fractures are still a significant burden to the patients due to pain, disability, long periods of immobility and unproductivity. Extensive research has led to the identification of numerous growth factors and their signaling pathways in bone remodeling. Many of these have also emerged as potential therapeutic agents. Activins are pleiotropic growth factors belonging to the TGF-β superfamily. We and others have recently shown that treatment with recombinant fusion proteins of activin receptors greatly increases bone mass in different animal models by trapping activins and other ligands thus inhibiting their signaling pathways. However, their effects on fracture healing are unknown.

12-week old male C57Bl mice were subjected to a standardized, closed tibial fracture induced by three-point-bending. Animals were divided into control and treatment groups and were administered either PBS control or a soluble activin type IIB receptor (Act-RIIB-Fc) intraperitoneally once a week for a duration of two or four weeks. The calluses were then gathered and analyzed.

There were no significant differences in any of the analyzed parameters between the two-week control and treatment groups but the differences between the four-week groups were robust. As expected, Act-RIIB-Fc treatment resulted in 90-130% higher weight gain during each week compared to controls ($p < 0.001$). Microcomputed tomography imaging results revealed a great increase in callus mineralization in the Act-RIIB-Fc treated animals. Bone volume per tissue volume was 60%, trabecular number 55% and bone mineral density 60% higher in the calluses of the Act-RIIB-Fc treated mice ($p < 0.05$ in all). Biomechanical strength of calluses was also significantly improved by Act-RIIB-Fc treatment as callus stiffness increased by 45% and maximum force by 55% ($p < 0.01$) in the three-point-bending test in treated group compared to PBS-injected controls

These results suggest that Act-RIIB-Fc treatment improves fracture healing in the mineralization and remodeling phases but has little effect on the early endochondral stage. Our findings support the previous reports of activin receptors increasing bone mass but also show a novel approach for using Act-RIIB-Fc to enhance fracture healing.

Disclosures: Tero Puolakkainen, None.

LB-SU0019

Withdrawn

LB-SU0020

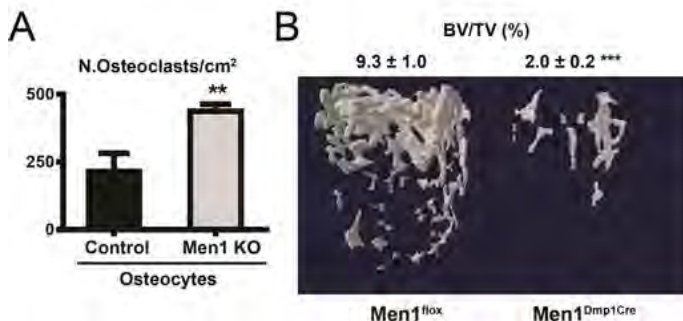
Loss of Multiple Endocrine Neoplasia Type 1 (*Men1*) Gene in Osteocytes Causes Osteoporosis by Increasing Osteoclastogenesis. Peng Liu*¹, Sooyeon Lee², Jeanette Knoll³, Alexander Rauch⁴, Susanne Ostermay³, Mario Zaiss⁵, Nicole Malkusch², Ulf Lerner⁶, Julia Luther⁷, Mona Neven⁷, Martina Rauner⁸, Jean-Pierre David⁷, Philippe Bertolino⁹, Chang Zhang⁹, Jan Tuckermann². ¹University of Ulm, Germany, ²University of Ulm, ³Leibniz Institute for Age Research, Fritz Lipmann Institute (FLI), ⁴University of Southern Denmark, ⁵Swiss Federal Institute of Technology in Lausanne, ⁶University of Gothenburg, ⁷University Medical Center Hamburg-Eppendorf, ⁸TU Dresden, ⁹University of Lyon 1

Multiple endocrine neoplasia type 1 (MEN1) is caused by mutations in the *Men1* gene encoding the protein menin. Many MEN1 patients suffer from osteoporosis, which is primarily attributed to hyperparathyroidism. Recent studies suggested a direct regulatory role of *Men1* in osteoblasts affecting differentiation and apoptosis in aged mice. Our study, however, challenges the role of *Men1* in osteoblasts for bone integrity and demonstrates a critical role of *Men1* in osteocytes.

We demonstrate that elimination of *Men1* in the osteoblast lineage and in osteoblast derived osteocytes using several transgenic osteoblast specific cre expressing mouse strains (*Runx2Cre*, *OsxCre*) caused severe osteoporosis in adolescent and adult mice. Surprisingly, osteoblast differentiation, numbers and bone formation rate were not affected in these mice. Furthermore, the proposed response to BMP2-Smad signaling was not altered in *Men1* ablated primary calvarial osteoblasts.

Instead, we found enhanced osteoclast numbers in mutant mice explaining the bone loss. Strikingly, we found enhanced osteoclastogenesis when osteoclast progenitor cells were cultured with *Men1* deficient osteocytes (Fig. A), but not with osteoblasts. By restricting elimination of *Men1* to late differentiated osteoblasts and osteocytes (*Men1*^{Dmp1Cre} mice), the osteoporosis persisted, demonstrating a major role of *Men1* in osteocytes *in vivo* (Fig. B). We further demonstrated that soluble factors secreted from *Men1* mutant osteocytes could enhance osteoclastogenesis. Cxcl10, a osteoclast-stimulating chemokine, was highly upregulated in primary *Men1* deficient osteocytes and in *Men1*^{Dmp1Cre} mice *in vivo*. Accordingly, neutralizing antibodies decreased the osteoclastogenic potential of *Men1* deficient osteocytes.

Taken together, we discovered here a novel unexpected role of *Men1* in osteocytes to dampen osteoclastogenesis by controlling osteoclastogenic factors and to retain bone integrity. Modulating *Men1* regulated factors in osteocytes might serve as a novel molecular base to develop therapeutical strategies to combat osteoporosis.



(A). Primary cocultures of wild type osteoclast progenitors (bone marrow cells) with control or *Men1* KO primary osteocytes. Cocultures were stained for TRAP activity. Numbers of multinucleated TRAP positive cells were determined (n=3, ** p < 0.01).

(B). Micro CT reconstruction of trabecular bone from femora of 12-week-old female *Men1*^{flax} and *Men1*^{Dmp1Cre} mice (n=4-9, *** p < 0.001).

Figure

Disclosures: Peng Liu, None.

LB-SU0021

Lower leg arterial calcification assessed by high-resolution peripheral quantitative computed tomography is associated with bone microstructure abnormalities in women. Julien Paccou*¹, Mark Edwards¹, Janina Patsch², Karen Jameson¹, Kate Ward³, Charlotte Moss¹, Elaine Dennison¹, Cyrus Cooper⁴. ¹MRC Lifecourse Epidemiology Unit, University of Southampton, Southampton General Hospital, Southampton SO16 6YD, UK, ²Department of Biomedical Imaging & Image-Guided Therapy, Medical University of Vienna, Vienna, Austria, ³MRC Human Nutrition Research, Elsie Widdowson Laboratory, 120 Fulbourn Road, Cambridge CB1 9NL, UK, ⁴University of Southampton, United Kingdom

Purpose: Bone and vascular calcification appear to show overlapping pathogenesis. Here we report the relationships of bone geometry, volumetric BMD, and bone microarchitecture with LLAC as assessed by HR-pQCT.

Methods: We utilised the Hertfordshire Cohort Study, where we were able to study associations between measures obtained from HR-pQCT of the distal radius and distal tibia in 341 participants (162 women and 179 men) aged 72.1-81.4 years with or without LLAC; n=28 (17.3%) vs. n=134 (82.7%) in women; n=83 (46.4%) vs. n=96 (53.6%) in men respectively. Statistical analyses were performed separately for women and men. We used linear regression models to investigate the cross-sectional relationships between LLAC, and bone parameters for men and women, controlling for age, height, weight, smoking status, alcohol intake, diabetes, daily calcium intake, daily vitamin D intake, physical activity, social class and current use of bisphosphonates.

Results: The mean (SD) age of participants was 76.4 (2.6) and 76.1 (2.5) years in women and men, respectively. One hundred and eleven of 341 participants (32.6%) had LLAC (score >1) that were visible and quantifiable by HR-pQCT. The prevalence of LLAC was higher in men than in women (46.4% (n=83) vs. 17.3% (n=28), p<0.001). Women with LLAC had substantially lower cortical area (Ct.area) (p=0.004) and thickness (Ct.Th) (p=0.014) at the distal tibia than those without LLAC. Adjustment for confounding factors did not materially affect the relationship described for Ct.area (p=0.016) at the distal tibia but differences in Ct.Th at the distal tibia were attenuated (p=0.083). Regarding trabecular parameters, trabecular volumetric BMD (Tb.vBMD) and trabecular number (Tb.N) were lower in women with LLAC (p=0.019 and p=0.013, respectively) at the distal tibia while trabecular separation (Tb.Sp) was higher (p=0.008). Adjustment for confounding factors did not materially affect the relationship described for Tb.N (p=0.013) and Tb.Sp (p=0.012) but differences in Tb.vBMD at the distal tibia were attenuated (p=0.087). Similar results were found for Tb.vBMD (p=0.004), Tb.N (p=0.027) and Tb.Sp (p=0.016) at the distal radius with a lower trabecular thickness also observed (Tb.Th) (p=0.009) but results were attenuated after adjustment for confounding factors, with only Tb.Th remaining significant (p=0.027). Distal radial or tibial bone parameters analyses in men according to their LLAC status revealed no significant differences except for Tb.N at the distal tibia when adjusted (p=0.035).

Conclusion: LLAC assessed by HR-pQCT was associated with bone microstructure abnormalities of the distal radius and tibia in women.

Disclosures: Julien Paccou, None.

LB-SU0022

Increased mortality, functional decline and dependency in elderly patients with dementia admitted with Fragility Fracture. Charles Inderjeeth*¹, Noreen Mughal². ¹University of Western Australia, Australia, ²Sir Charles Gairdner Hospital

Background
Patients with cognitive impairment are 2.7 times more likely to sustain a hip fracture when compared with age and sex matched controls without dementia. Patients with dementia continue to be at high risk of worse outcomes including fractures, functional decline, institutionalisation and mortality compared to those without dementia. Elderly patients with hip fracture have a 5 to 8 fold increased risk for all-cause mortality than in age and sex matched control in the first 3 months after a hip fracture. Twenty percent of the patients die in the year following a hip fracture.

Objectives
The primary outcome of the study was to prospectively assess the rate of pre-fracture OP treatment vs OP treatment on discharge from an Orthogeriatric Unit. The secondary outcomes were to evaluate mortality and functional decline.

Results
There were 502 consecutive admissions to the unit. At admission 78% were from home. On discharge only 42% returned to their own home. 30 day mortality was 3 times higher & 90 day 1.5 times higher in patients with a diagnosis of OP with dementia. The 30 and 90 day mortality in those with any fracture was 7% and 27% in those with dementia and 4% and 11% respectively in non-demented patients. This compares to the overall mortality in hip fracture patients of 8% and 22% respectively.

Conclusions
The imperative to treat for OP should be greater in those with dementia to prevent hip fractures and minimise the associated morbidity, mortality, social care burden and health care cost. Hospital admissions of elderly patients should be used as an opportunity for comprehensive assessment and effective management of osteoporosis and comorbidities.

Disclosures: Charles Inderjeeth, None.

LB-SU0023

GWAS meta-analysis for total body BMD unveils 14 new BMD loci and variants exerting age-specific effects. Carolina Medina-Gomez¹, John Kemp², Alessandra Chesi³, Eskil Kreiner-Møller⁴, Tarun Ahluwalia⁴, Dennis Mook⁵, Youfang Liu⁶, Fernando P. Hartwig⁷, Dan Evans⁸, Raimo Joro⁹, Cornelia van Duijn¹⁰, Ivana Nedeljkovic¹¹, Benjamin Mullin¹², Joel Eriksson¹³, Brent Richards¹⁴, Rebecca Jackson¹⁵, David Karasik¹⁶, Nathalie Van der Velde¹⁷, Albert Hofman¹⁰, Babette Zemel¹⁸, Benjamin Mullin¹², Tamara Harris¹⁹, Yanhua Zhou²⁰, John Robins²¹, Ruifang Li²², Bruce Psaty²³, Carrie Nielson²⁴, Wilson Scott²⁵, Bernardo L Horta²⁶, Timo Lakka²⁷, Struan Grant³, Fiona McGuigan²⁸, Jim Wilson²⁹, Unnur Stykkarsdóttir³⁰, Dan Koller³¹, Kun Zhu³², Doug Kiel³³, Claes Ohlsson³⁴, Andre G. Uitterlinden³⁵, Vincent Jaddoe³⁶, Jon H. Tobias³⁷, Dave M. Evans², Fernando Rivadeneira³⁵. ¹Erasmus Medical Center, The Netherlands, ²The University of Queensland Diamantina Institute, The University of Queensland, Translational Research Institute, Brisbane, Australia, MRC Integrative Epidemiology Unit, School of Social & Community Medicine, ³Division of Human Genetics, Children's Hospital of Philadelphia, ⁴COPSAC; Copenhagen Prospective Studies on Asthma in Childhood; Faculty of Health Sciences, University of Copenhagen, Denmark, ⁵Department of Endocrinology & Clinical Epidemiology, Leiden University Medical Centre, Leiden, The Netherlands, ⁶Thurston Arthritis Research Center, University of North Carolina at Chapel Hill, ⁷Postgraduate Program in Epidemiology, Federal University of Pelotas, Brazil, ⁸California Pacific Medical Center Research Institute, ⁹Institute of Biomedicine, Physiology, University of Eastern Finland, ¹⁰Department of Epidemiology, ErasmusMC, ¹¹Department of Epidemiology, Erasmus MC, Rotterdam, The Netherlands, ¹²School of Medicine & Pharmacology, University of Western Australia, ¹³Centre for Bone & Arthritis Research, Institute of Medicine, Sahlgrenska Academy, University of Gothenburg, ¹⁴Centre for Clinical Epidemiology, Lady Davis Institute for Medical Research, Jewish General Hospital, McGill University, ¹⁵Division of Endocrinology, Diabetes & Metabolism, Ohio State University, ¹⁶Hebrew SeniorLife & Harvard Medical School, ¹⁷Department of Internal Medicine-Section Geriatric Medicine, Erasmus MC, ¹⁸Division of GI, Hepatology, & Nutrition, Children's Hospital of Philadelphia, ¹⁹Laboratory for Epidemiology, Demography, & Biometry, National Institutes of Aging, ²⁰Department of Biostatistics, Boston University School of Public Health, ²¹Department of Internal Medicine, University of California at Davis, ²²Department of Clinical Epidemiology, LUMC, ²³Department of Biostatistics, University of Washington, ²⁴School of Medicine, Oregon Health & Science University, ²⁵Department of Twin Research & Genetic Epidemiology, King's College London, ²⁶Postgraduate Program in Epidemiology, Federal University of Pelotas, ²⁷Kuopio Research Institute of Exercise Medicine, Kuopio, Finland; The Department of Clinical Physiology & Nuclear Medicine, University of Eastern Finland, Finland; Department of Physiology, Institute of Biomedicine, University of Eastern Finland., ²⁸Clinical & Molecular Osteoporosis Research Unit, Department of Clinical Sciences Malmö, Lund University, ²⁹Centre for Population Health Sciences at the University of Edinburgh, ³⁰deCODE Genetics/Amgen, ³¹Departments of Medical & Molecular Genetics, Indiana University School of Medicine, ³²Department of Endocrinology & Diabetes, Sir Charles Gairdner Hospital; School of Medicine & Pharmacology, University of Western Australia, ³³Institute for Aging Research, Hebrew SeniorLife, Department of Medicine, Harvard Medical School, ³⁴Department of Internal Medicine & Clinical Nutrition, Center for Bone & Arthritis Research (CBAR), Sahlgrenska Academy, Institute of Medicine, University of Gothenburg, ³⁵Internal Medicine, Erasmus MC University, Rotterdam, The Netherlands, ³⁶The Generation R Study, ErasmusMC, ³⁷School of Clinical Sciences, University of Bristol, Bristol, United Kingdom

Aim: Bone Mineral Density (BMD) is a highly heritable trait used to assess skeletal health in children and risk of osteoporosis later in life. To date >60 loci associated with BMD or bone-related traits measured at different skeletal sites have been identified. We conducted a genome-wide association study (GWAS) meta-analysis of total body (TB)-BMD in children and adults to identify genetic determinants and age specific effects of loci on this trait. **Methods:** We included 24 different study populations comprising ~49,000 individuals with DXA measurements at different age

ranges (0-15 years, n=11,200; 15-45 years, n=9,600; and >45 years, n=28,500) and genetic data imputed to the 1000 Genomes reference panel. Association models were adjusted for sex, age, weight, height and genomic principal components (to control for population stratification). Inverse variance meta-analysis was performed on all the data and within each age strata and comparisons between the two extreme groups leading variants were made. Genome-wide significance (GWS) was set at $P < 5 \times 10^{-8}$. Results: We identified variants associated at GWS level in 45 loci, including both common and less frequent (MAF < 5%) polymorphisms. Of these, 14 loci represent novel associations with variants not clustering within 500kb of previously reported bone loci. Several of the novel signals map in close vicinity of genes with a proven role in bone metabolism such as: *EN1*, *AQPI1*, *RIC8A*, *CSF1*, *SLC8A1-AS1* and *SMAD3*, whereas the other variants, including a missense polymorphism in *NLRP6* are likely to implicate new biology. Loci with previously described skeletal specificity (i.e. *SOX6*, *LIN7C*, *RIN3*, *ABCF2*), age heterogeneity (i.e. *CPED1*, *C17orf53*) and bone compartment specificity (i.e. trabecular volumetric BMD, *FMN2*; or heel ultrasound, *TMEM135*) were all identified by our TB-BMD GWAS meta-analysis. The strongest age specific effects were found for variants in the *RIN3* with GWS effect ($\beta = 0.1$ SD, $P = 1 \times 10^{-8}$) only in children ($P_{\text{het}} = 3 \times 10^{-12}$) and *ESR1* only exerting a GWS effect ($\beta = 0.07$ SD, $P = 9.3 \times 10^{-13}$) in adults ($P_{\text{het}} = 7 \times 10^{-10}$) loci. Conclusion: TB-BMD is a relevant trait for genetic studies of osteoporosis, capable of identifying (novel) variants influencing different bone compartments at different skeletal sites. Applying an age-stratified GWAS approach allowed us to identify loci exerting effects at different stages of the lifespan, helping to unveil further the complex genetic architecture of osteoporosis.

Disclosures: Carolina Medina-Gomez, None.

LB-SU0024

Osteoporotic Fractures in Heart failure; Findings from National Health Insurance Data in Korea. Da Hea Seo¹, Jong-Chan Youn², Jung Wha Hong³, Seok-Min Kang², Yumie Rhee⁴. ¹Department of Internal Medicine, Endocrine Research Institute, Yonsei University College of Medicine, ²Division of Cardiology, Severance Cardiovascular Hospital, Yonsei University College of Medicine, ³Department of Biostatistics, Yonsei University College of Medicine, ⁴Department of Internal Medicine, College of Medicine, Yonsei University, South Korea

Osteoporosis and heart failure are prevalent conditions, particularly among the elderly. Recent findings suggest a role for heart failure in the etiology of osteoporotic fractures, yet the national trends of the incidence and treatment rates of osteoporotic fractures in heart failure patients in Korea is unknown. We investigated osteoporotic fractures in heart failure patients in Korea is unknown. We investigated osteoporotic fractures (spine, hip, humerus, radius and tibia) and their treatment rates with selective estrogen-receptor modulators (SERM) or bisphosphonates in heart failure patients over age 65 during 2009-2013 using the database from the Health Insurance Review and Assessment Service (HIRA), which covers almost 100% of Korean population. Annualized incidence rates for total osteoporotic fractures were 51 per 1000 person-years in heart failure patients (12 hip, 31 spine, 2 humerus, 9 radius and 4 tibia respectively); the annualized incidence rates for total osteoporotic fractures were 27 per 1000 person-years in men and 66 per 1000 person-years, yielding a female to male ratio of 2.41. The annualized incidence rates for osteoporotic fractures were proportional to age until 80 years old when it starts to decline; 8 in 65-70 years, 13 in 70-75 years, 14 in 75-80 years, 10 in 80-85 and 6 in ≥ 85 years. Although higher than general population with osteoporotic fractures, it was estimated that only 24.88% of heart failure patients with osteoporotic fractures are treated with either SERM or bisphosphonate. Our study offers nationwide epidemiological data on osteoporotic fractures in heart failure patients in Korea. Because diagnosis of heart failure predicts a substantial risk of osteoporotic fractures, proper evaluation and treatment for osteoporosis is necessary in heart failure patients.

Disclosures: Da Hea Seo, None.

LB-SU0025

Retrospective Analysis of Osteoporosis Evaluation and Treatment Following Fragility Fracture of the Hip. Sara Heintzman¹, Mitchell Hughes², Tamara Scerpella². ¹University of Wisconsin Hospitals & Clinics, ²University of Wisconsin School of Medicine & Public Health, USA

Purpose: Current practice guidelines recommend evaluation and treatment of osteoporosis in all patients with a fragility fracture. We assessed compliance following operative treatment of hip fractures at an upper Midwest academic medical center.

Methods: This retrospective cohort study reviewed EMR data for all patients, ≥ 65 years, who had surgical treatment of a hip fracture at a single academic medical center, between 2007 and 2013. Subjects were identified via data query, and excluded for failure to meet fragility fracture criteria. The group was refined to patients with an in-network PCP, ensuring maximal data capture. DXA scans were recorded within 1-yr post-fracture. In addition, detailed demographic and treatment outcomes were recorded for the youngest 20% of patients included.

Results: 607 patients were treated during the index period; 6% (38) did not meet fragility fracture criteria, 20% (122) died within 12 months and 35% (214) did not have an in-network PCP. Of the remaining 39% (233), only 16% (38) had a DXA in the 1-yr post-fracture window. Detailed review included the 122 youngest patients; 84% (102) met fragility fracture criteria; average age was 69 yrs. Of these, pre-fracture treatment

included calcium and/or vitamin D in 36% (37) and anti-resorptive therapy in 20% (20). Patients with an in-network PCP were more likely to have been prescribed pre-fracture treatment medication ($p=0.006$); likelihood did not vary based on urban vs. rural residence ($p=NS$). 18% (18) had a change/addition in osteoporosis treatment medication during hospitalization; this did not vary based on residence or PCP ($p=NS$). Vitamin D level was evaluated during hospitalization for 27% (27); likelihood was greater for non-network PCP and rural patients ($p=0.013$, $p=0.021$, respectively). For 52 in-network PCP patients, detailed review over 1-yr post-fracture revealed: 44% (15) had a vitamin D level evaluated, 23% (12) had a DXA, 15% (8) had a medication changed/added, and 12% (6) had a second fracture.

Conclusion: Established guidelines for evaluation of osteoporosis following fragility fracture were met for only 1/6th of patients in this retrospective cohort study. A similarly low rate of treatment was also noted, both during hospitalization and in a 1-yr follow-up period. The status quo for osteoporotic treatment following fragility hip fracture remains inadequate.

Disclosures: Sara Heintzman, None.

LB-SU0026

Enhanced Hip Fracture Management: Use of Sfn System to Evaluate a Fractured Neck of Femur Fast Track Pathway – Pilot Study. Nigel Gilchrist^{*1}, Kris Dalzell², Scott Pearson³, Jeremy Hickling⁴, Kit Hoeben⁵, Ma Yi⁶. ¹Department of Orthopaedic Surgery, Canterbury District Health Board, ²Department of Orthopaedic Surgery, Canterbury District Health Board, ³Emergency Department, Canterbury District Health Board, ⁴Department of Anaesthesia, Canterbury District Health Board, ⁵Planning & Funding, Canterbury District Health Board, ⁶Biosatistician, Canterbury District Health Board, United Kingdom

The purpose of this pilot study was to evaluate the change in management of acute hip fracture patients >65yrs (450/yr) from the time they presented at the Emergency Department of Christchurch Hospital, New Zealand to the time that they were discharged from hospital.

Changes to each facet of the pathway, Emergency Department, peri-operative management, operation, rehabilitation and discharge were agreed by the individual teams and integrated. Data was captured electronically and processed using the sfn toolset to produce statically based performance measurements on all activities in all areas of the Fast Track Fractured Neck of Femur Pathway.

The pilot study began in November 2014, is currently ongoing and the data is shown up to the end of April 2015. Pilot study data was then compared with prior data in a group of similar patients in the preceding 3 years. A Wilcoxon Rank Sum Test was used for statistical comparison.

One hundred and sixty one patients were observed during the pilot study compared to 989 patients from the preceding years. The average time in the Emergency Department reduced significantly from 3.46 +1.46 to 2.87 +1.33 hours ($p<0.0001$), average wait for theatre reduced from 1.62 +1.53 to 1.47 +1.42 days ($p=0.044$), the average wait for rehabilitation reduced from 7.13 +4.49 to 4.29 +2.63 days ($p<0.0001$). Length of stay in the acute hospital with direct discharge home went from 10.44 +8.39 to 7.13 +4.4 days ($p=0.003$). The length of stay in the Orthopaedic Rehabilitation Unit reduced from 24.24 +12.41 to 17.46 +6.68 days ($p<0.0001$) and at another rehabilitation facility (more complex medical co-morbidities) 33.71 +14.2 to 30.43 +14.07 days ($p=0.048$). The overall length of stay for patients reduced from 24.40 +15.06 to 20.48 +13.59 days ($p=0.001$). Total readmissions over this period did not differ significantly from the previous 3 years. Total acute admissions to orthopaedics also did not differ in comparison with the previous years.

We have significantly reduced the time in hospital by a factor of 95 hours in each patient and over the period of the pilot study saved 631 bed days with a projected annual bed day saving of 1,495. Further time could be saved by aiming to get the time from the Emergency Department to Theatre down to 20 hours. This pilot study is ongoing, the immediacy of electronic data to evaluate change in clinical management has shown benefit in reduction in day stay and possible cost savings.

Disclosures: Nigel Gilchrist, None.

LB-SU0027

Falls are increased on Recommended Doses of Vitamin D in Elderly Women.. J. Christopher Gallagher¹, Shervin Yousefian^{*2}, Lynnette Smith³. ¹Creighton University Medical Center, USA, ²Creighton University Medical Center, USA, ³University of Nebraska, USA

Introduction: The effect of vitamin D supplementation on falls and physical performance is controversial. Some studies show a decrease in falls on daily vitamin D 800 IU, others show increased falls on a high annual dose. The American Geriatrics Society consensus statement recommends a daily vitamin D intake from all sources of 4,000 IU daily in the elderly. We analyzed the Fall rate and physical performance tests in our vitamin D dose ranging study.

Design: 163 independent living women entered a 1-year double blind randomized dose ranging study of daily vitamin D 400,800,1600,2400,3200,4,000,4800 IU or placebo together with calcium ~580mg/d (total intake ~1200mg). Diet vitamin D was 114 IU. Inclusion criteria: serum 25OHD \leq 20ng/ml; no known disease or drugs affecting calcium or bone metabolism. Fall history was recorded at baseline and at 3-

monthly visits. Standard physical performance tests included Timed up and Go, Timed walk, Chair Rising test, Grip strength and Balance (Biodex). This was a secondary analysis using Intent to treat and statistical analysis used Chi square and ANOVA

Results: Age range 57-87 years, mean age 66.2 years (SD 7.3), mean BMI 30.3 kg/m² (SD 5.9). Compliance, measured every 3 months, was 94% for vitamin D and 91% calcium. 147 completed study. Fallers: 49% women had falls; the rate was higher 60% in women with a fall history in last year compared to 40% with no fall history. Overall there was no effect of the pooled vitamin D dose on falls. However, when grouped into low dose (400, 800 IU); medium dose (1600-3200 IU) or high dose (4000-4800 IU); the faller rate was reduced by 45% on medium doses compared to placebo and low doses and reduced by 56% compared to the high doses ($p=0.003$). In those with previous fall history 100% of the women on high doses 4,000/4800 IU (serum 25OHD range > 45 ng/ml) suffered a fall. The vitamin D dose and falls followed a U shaped curve. There was a non-significant decline in all physical performance tests on vitamin D in all dose groups.

Conclusions: In this clinical trial Vitamin D 400/800IU had no effect on falls compared to placebo. Vitamin D doses 1600,2400,3200 IU showed a significant decrease in falls. High doses of vitamin D 4,000-4800IU were associated with a marked increase in falls. The American Geriatrics Society recommendation of vitamin D 4,000 IU daily for fall prevention especially in those with fall history should be reconsidered since it may lead to more rather than less falls.

Disclosures: Shervin Yousefian, None.

LB-SU0028

Epigenetic priming confers direct cell trans-differentiation in a transgene-free state. YOUNG DAN CHO^{*}, Han-Sol Bae, Bong-Soo Kim, Kyung-Mi Woo, Jeong-Hwa Baek, Hyun-Mo Ryoo. Seoul National University, South Korea

The bone marrow of healthy individuals is primarily composed of osteoblasts and hematopoietic cells, while that of osteoporosis patients has a larger portion of adipocytes. There is evidence that the epigenetic landscape can strongly influence cell differentiation. We have shown that it is possible to direct the trans-differentiation of adipocytes to osteoblasts, both in vitro and in vivo, by modifying the epigenetic landscape with a DNA methyltransferase inhibitor (DNMTi), 5'-aza-dC, followed by Wnt3a treatment to signal osteogenesis. Gene expression profiles of marker genes (Runx2 and Pparg) of osteoblasts and adipocytes were correlated with epigenetic modifications to their promoter regions. Treating 3T3-L1 adipocytes with 5'-aza-dC induced demethylation in the hypermethylated CpG regions of bone marker genes; subsequent Wnt3a treatment drove the cells to osteogenic differentiation. When 15-month old mice with predominantly adipose marrow, a mouse model for osteoporosis, were treated with both 5'-aza-dC and Wnt3a, histological and micro CT analysis suggested that the fatty tissue decrease and bone volume increased. Together, our results indicate that epigenetic modification permits direct programming of adipocytes into osteoblasts in a mouse model of osteoporosis, suggesting that this approach could be useful in bone tissue-engineering applications.

Disclosures: YOUNG DAN CHO, None.

This study received funding from: National Research Foundation of Korea (NRF) funded by the Ministry of Science, ICT & Future Planning (2013R1A1A3011102)

LB-SU0029

High cardiovascular risk in older men with low sclerostin levels – prospective STRAMBO study. Pawel Szulc^{*1}, Lorenz Hofbauer², Roland Chapurlat³. ¹INSERM UMR 1033, University of Lyon, Hopital E. Herriot, Pavillon F, France, ²Division of Endocrinology, Diabetes, & Bone Diseases, Dresden University Medical Center, ³INSERM UMR 1033, University of Lyon, Hospices Civils de Lyon, France

Data on the association between serum sclerostin levels and cardiovascular risk are scarce, discordant and limited to patients with chronic renal diseases. Our aim was to prospectively assess the association between baseline serum sclerostin levels and risk of incident major cardiovascular event in a cohort of 780 home-dwelling men aged 60 and over. Serum sclerostin levels were measured by ELISA (Biomedica). Incident major cardiovascular event was defined as acute coronary syndrome (myocardial infarction, acute coronary insufficiency with or without ST-T elevation confirmed by angiography), stroke or sudden death. During the median follow-up of 7.8 years, 83 men sustained major cardiovascular events. For the statistical analyses, we used Cox model adjusted for age, weight, professional physical activity, current smoking, comorbidities, abdominal aortic calcification, glomerular filtration rate as well as serum levels of osteoprotegerin, DKK1, FGF23 and parathyroid hormone.

Lower sclerostin levels were associated with higher risk of incident major cardiovascular event (HR= 1.30 per SD decrease, 95%CI: 1.04-1.62, $p<0.05$). The risk of cardiovascular event increased across decreasing sclerostin quintiles ($p<0.05$) and was higher (HR= 3.19, 95%CI: 1.42-7.18, $p=0.005$) in the lowest quintile (<47 pmol/L) vs. the upper quintile (>97 pmol/L). Hypertensive men with low sclerostin (<47 pmol/L) had high cardiovascular risk (HR= 6.92, 95%CI: 2.10-22.8, $p<0.005$) compared to normotensive men with high sclerostin (>97 pmol/L). Men with low sclerostin (<47 pmol/L) and high DKK1 levels (>15 pmol/L, median) had higher

cardiovascular risk (HR= 5.08, 95%CI: 1.54-16.8, p<0.01) compared to men with high sclerostin (>97 pmol/L) and low DKK1 (<15 pmol/L).

In conclusion, our data suggest that low serum sclerostin levels are an independent indicator of cardiovascular risk in older home-dwelling men.

Disclosures: Pawel Szulc, None.

LB-SU0030

Differential changes in bone geometry and microarchitecture in extreme duration type 1 compared to younger type 1's and controls. Ernesto Maddaloni*, Hillary Keenan. Joslin Diabetes Center, USA

Aim. To evaluate the age related changes in bone geometry in a unique population of aging subjects with extreme duration (>50 years) of type 1 diabetes (T1D), the Joslin 50-Year Medalist cohort, and compare to young T1D subjects and controls.

Methods. High-resolution peripheral quantitative computed tomography (HR-pQCT) was used to assess bone geometry, volumetric bone mineral density (vBMD) and microarchitecture of the ultradistal radius and tibia in fourteen subjects with >50 years T1D duration (50% males, mean \pm SD age: 65.7 \pm 8.4yrs; T1D duration 56.3 \pm 6.9yrs, body mass index 26.1 \pm 4.1kg/m²; HbA1c 7.0 \pm 0.8%). Results were compared to values from published data collected from the same system in a cohort of younger T1D subjects (YT1D) (age 45.6 \pm 11.7yrs), and (for the ultradistal radius only, due to data availability) in a population of age and gender matched controls.

Results. Despite the older age, equal trabecular (Tb) vBMD at the radius (166.8 \pm 38.6 vs 158.1 \pm 43.0mgHA/cm³, p=0.43) and increased Tb vBMD at the tibia (192.3 \pm 29.4 vs 172.7 \pm 45.7, p=0.03) in the Medalists vs YT1D were found. No differences were found in Tb vBMD vs control group (p=0.59). Cortical (Ct) vBMD was lower in the Medalist when compared to YT1D at both radius (817.7 \pm 70.2 vs 883.1 \pm 58.3, p=0.006) and tibia (732.6 \pm 109.8 vs 864.1 \pm 58.6, p<0.001). Medalists also showed a decreased Ct vBMD at the radius when compared to controls (862.4 \pm 6.9, p=0.04). In addition, study of the bone microarchitecture showed decreased tibia Ct thickness (th), but increased Tbth amongst Medalists vs YT1D (0.89 \pm 0.38 vs 1.24 \pm 0.29mm, p=0.004; 0.08 \pm 0.02 vs 0.072 \pm 0.014, p=0.04, respectively). The study of bone geometry showed a smaller periosteal perimeter at the radius in the Medalists vs YT1D (75.0 \pm 8.5 vs 81.7 \pm 14.4mm, p=0.01), suggesting decreased periosteal bone apposition.

Conclusions. The association of T1D with increased risk of fragility fractures has been documented. Due to the mean age and the over 50 years of T1D duration, the Joslin Medalist cohort provides a unique opportunity to study the effects of the long exposure to diabetes on bone health, and the interaction of hyperglycemia and aging. In stark contrast to previous reports in people without diabetes, here we show a significant age-related decline in Ct, but not in Tb vBMD. This protection from decline in Tb vBMD may possibly explain the low prevalence of fragility fractures we previously described in the Medalist cohort.

Disclosures: Ernesto Maddaloni, None.

LB-SU0031

MSC therapy for hypophosphatasia. Luke Mortensen*. University of Georgia, USA

Hypophosphatasia (HPP) is a debilitating genetic disease of impaired alkaline phosphatase that limits bone mineralization throughout the skeletal system. Severe infantile cases develop during the first year of life, and often quickly lead to death. Patients that survive exhibit a number of clinical problems, including craniofacial complications like craniosynostosis and tooth loss. Currently there are no approved treatments, and those under investigation have limited craniofacial improvement. We therefore study one potential therapeutic route, administration of mesenchymal stem cells (MSCs), in a mouse model of HPP with a goal of improving mortality and craniofacial mineralization. Several clinical case studies have used MSC or stromal cell administration along with bone marrow transplant under myeloablative conditions, which resulted in improvement of bone mineralization characteristics. This may be due to the presence of alkaline phosphatase-rich stromal cells in the bone, but it remains unclear if MSCs are involved in the observed therapeutic response. Therefore, this work aims to evaluate MSC therapy without myeloablation or bone marrow transplantation for HPP. We hypothesize that MSCs alone will enhance survival in HPP, and that long term cell survival is required for therapy. Our preliminary efforts have isolated and validated an MSC population with inducible apoptosis (CAGCre-ERTM::floxed-DTA) that allow direct evaluation of the need for MSC survival after transplantation in a murine HPP model. Results indicate that cre-induced recombination allows the ablation of cells in vitro, and that cells retain expression of alkaline phosphatase after culture expansion. We determined that intravenously administered MSCs labelled with membrane home to the calvarial bone marrow of mice at a high frequency using our 2-photon imaging strategy and are cleared after apoptosis induction. Ongoing efforts to evaluate the effect of MSC transplantation on HPP therapeutic outcome are ongoing, and future directions will determine the need for long term cell survival in HPP, and develop strategies to enhance cell therapy.

Disclosures: Luke Mortensen, None.

LB-SU0032

DOES AUTOSOMAL DOMINANT OSTEOPETROSIS TYPE 2 (ADO2) HAVE A CENTRAL NERVOUS SYSTEM PHENOTYPE?. Mattia Capulli*¹, Antonio Maurizi², Juliana Cortes², Laura Di Rito², Nadia Rucci², Anna Teti². ¹University of L'Aquila, Italy, ²University of L'Aquila, Italy

ADO2 is a rare genetic disease characterized by high bone density and bone fragility. So far only heterozygous clcn7 gene mutations are reported to trigger the disease. We recently generated an ADO2 mouse model, knocking-in the clcn7 mutation causing the G213R amino acidic substitution in the CIC7 protein. The bone phenotype of our heterozygous mice phenocopied the human disease, while no obvious alterations of the Central Nervous System (CNS) were observed by conventional histological analysis, in agreement with the paucity of information on CNS involvement in human ADO2. However, to our surprise, during the animal handling, we observed ADO2 mice to be more susceptible to strong sounds and uneasy compared to their WT littermates, suggesting a possible unrecognized behavioral phenotype induced by the clcn7 mutation. Consistently, behavioral tests showed that adult (3 month-old) ADO2 mice displayed 46% (p=0.02) lesser time spent in the lit compartment in the dark and light transition test, 48% (p<0.0001) lesser time spent in the center of arena in the open field test, 42% (p=0.04) lesser time spent in the open arm in the elevated plus maze test, and 40% (p=0.01) more time spent immobile in the forced swimming test, demonstrating greater anxiety and depression compared to WT littermates. Conversely, memory and motor abilities were unremarkable. Intriguingly, analyses of 1 year-old ADO2 mice evidenced a worsening of anxiety and depression related parameters (mean worsening 33%), suggesting a progressive degeneration of the brain function, a condition often observed in storage diseases. In agreement with this hypothesis, in-depth histological analyses showed a prominent increase of β -amyloid accumulation in ADO2 brains (+2.1fold; p=0.002). This phenomenon could be due to abnormal protein storage and consequent cellular degeneration, since immunofluorescence sub-cellular localization analysis showed accumulation of mutant CIC7 protein in the Golgi apparatus, which appeared abnormally enlarged. Consequently, lysosomal levels of mutant CIC7 and subsequent acidification were impaired. Finally, real-time RT-PCR analysis of brain mRNAs showed 30% lower expression of the neuron detoxifying enzyme, glyoxalase 1 (p=0.03), in ADO2 mice compared to WT littermates. These results warn about the need to better evaluate the CNS involvement in human ADO2 and could explain some neurological complications in patients, helping the clinician in managing this complex disease.

Disclosures: Mattia Capulli, None.

LB-SU0033

Novel Variant of G α -alpha Associated with Albright's Hereditary Osteodystrophy, Osteolysis, and Syndrome of Inappropriate ADH Secretion. Kelly Wentworth*¹, Edward Hsiao², Murat Bastepe³, Yan Zhu³. ¹University of California- San Francisco, ²Endocrine Unit, Massachusetts General Hospital & Harvard Medical School, USA

G-protein coupled receptors (GPCRs) mediate a wide spectrum of biological activities. The GNAS complex locus encodes the stimulatory α -subunit of the guanine nucleotide binding protein (G α), which stimulates production of the second messenger cyclic AMP (cAMP). Several conditions are associated with loss-of-function GNAS mutations, including Albright's Hereditary Osteodystrophy (AHO) and pseudohypoparathyroidism. Patients with AHO often exhibit short stature, brachydactyly, and subcutaneous ossification. Here, we present the case of a child with some clinical features of AHO as well as osteolysis and neonatal SIADH, in whom we have discovered a novel GNAS mutation causing loss of G α activity.

Our patient is an 11-yo female who was referred to our clinic for frequent fractures and osteolysis. At birth, her right femoral diaphysis was fractured, and a bone survey demonstrated diffuse hypomineralization. She sustained a second right femoral fracture at 14 months and subsequent bone surveys showed osteolysis of the distal phalanges of her hands, feet, and metacarpals/metatarsals with progressive bowing of her femurs, tibiae and fibulae. She was started on bisphosphonate therapy at age 4 to prevent further fractures, but subsequently developed fractures in her right fibula and wrists while on therapy. In addition to her skeletal abnormalities, she was diagnosed with SIADH at birth (Na⁺ =116 mEq/L) which has been managed with fluid restriction. Physical exam at age 11 showed normal craniofacial features, bowing of both legs and normal metacarpals but shortened distal phalanges, small café-au-lait spots on her flank, and labial hyperplasia. The patient did not have short stature or show any evidence of subcutaneous ossification. Exome sequencing revealed a heterozygous c.163A>G (p.T55A) mutation in G α s, which was not detected in her parents' DNA samples. Transfection of G α s-null mouse embryonic fibroblasts with cDNA encoding this mutant showed a 64% reduction in isoproterenol-induced cAMP production compared to wild-type G α s (normalized to forskolin-stimulated cAMP levels). In summary, our patient harbors a novel, de novo missense mutation in the p-loop of the G α GTPase domain, leading to decreased agonist-stimulated cAMP formation. The G α s loss-of-function could account for her presentation with some clinical features of AHO, such as shortened distal phalanges. However, the underlying cause of the osteolysis and neonatal SIADH remains unclear.

Disclosures: Kelly Wentworth, None.

LB-SU0034

Factors Predicting Functional Status, Muscle and Bone Parameters in Long-Term Survivors of Acute Lymphoblastic Leukemia (ALL). Louis-Nicolas Veilleux*¹, Frank Rauch², Daniel Curnier³, Maja Krajinovic⁴, Caroline Laverdière⁴, Daniel Sinnett⁴, Nathalie Alos⁴. ¹McGill University/Shriners Hospital for Children-Canada, Canada, ²McGill University-Shriners Hospital for Children, ³Department of Kinesiology, University of Montreal, ⁴Sainte-Justine University Hospital Center, Canada

Context: Overall cure rates for childhood acute lymphoblastic leukemia (ALL) have improved allowing the cure of over 85% of patients. At least 70% of survivors of childhood ALL cancers have substantial morbidities as a result of their disease and/or their treatment. The goal of this study was to determine the factors susceptible to predict musculoskeletal health status in ALL long term survivors. Patients: 190 long-term ALL survivors were part of this study (52% were females; mean age at recruitment [SD]: 22.7 years [6.6]; mean age at diagnosis [SD]: 5.6 years [4.2]; 57% of patients were classified as high risk at diagnosis; average treatment duration [SD]: 26 months [4.7]). Main outcomes. Functional status was assessed with the 6 minutes' walk test (6MWT). Muscle function was measured using mechanography whereas radius and tibia bones status were assessed using pQCT. Stepwise linear regression was used to identify predictors of muscle and bone parameters. Parameters included in the model were age at diagnosis, risk group (high or standard), effective cumulative dose and radiotherapy (Y/N). Results. Results of the 6MWT showed that the distance walked by the survivors was on average 13% lower than what was expected compared to age and sex-specific reference data. The regression analysis showed that the 'risk group' was negatively related to the performance at the 6MWT ($p=0.003$). For muscle function, none of the predictors entered in the regression model was related to muscle parameters. The 'risk group' was a negative predictor of trabecular BMD ($p=0.02$) at the 4% site and of total BMC ($p=0.04$), cortical CSA ($p=0.04$) and cortical BMD ($p<0.001$) at the 14% site. At this site, the 'age at diagnosis' was positively related to total BMC ($p=0.007$), cortical CSA ($p=0.01$) and cortical thickness ($p=0.02$). At the radius, 'age at diagnosis' was found to be positively related to total BMC ($p=0.04$) at the 4% site and to total CSA ($p=0.03$) at the 65% site. Moreover, 'risk group' was found to be a negative predictor of trabecular BMD at the 4% ($p=0.007$) and cortical BMD at the 65% site ($p=0.001$). Conclusion: 'Risk group' was found to be a negative predictor of bone health whereas 'age at diagnosis' was shown to be a positive predictor of bone health. This was observed at both the radius and tibia bones and for both, trabecular and cortical bone. These two parameters should be taken into account in the long term follow-up of bone health in ALL survivors.

Disclosures: Louis-Nicolas Veilleux, None.

LB-SU0035

Blocking the senescence-associated secretory phenotype (SASP) reduces osteoclastogenesis and prevents age-related bone loss. Ming Xu*, Megan Weivoda, Christine Hachfeld, Merry Jo Oursler, James Kirkland, Mayo Clinic, USA

Age related bone loss occurs in men and women; however the mechanisms for this remain unclear. Senescent cells accumulate in several tissues with age and secrete pro-inflammatory cytokines, defined as the senescence-associated secretory phenotype (SASP). We hypothesized that the SASP increases osteoclastogenesis and contributes to age-related bone loss. Human pre-adipocytes isolated from subcutaneous fat were sham treated or irradiated with 10 Gy to induce senescence. Conditioned media (CM) was collected from control and senescent cultures. Because the JAK signaling pathway has been implicated in senescence, cells were treated with a vehicle or a JAK inhibitor (JAKi) prior to CM collection. Senescence was confirmed by γ H2X staining. Mouse bone marrow was cultured in 50% control or senescent CM, or in the presence of M-CSF overnight. Non-adherent cells were cultured in osteoclast differentiation media and assessed for differentiation. A cytokine array was used to identify senescence induced factors. To assess in vivo responses to JAKi, 22 month male mice were treated with JAKi for 8 weeks. Femurs and vertebrae were assessed by mCT. Bone marrow was assessed for osteoclast and osteoblast progenitor numbers as well as osteoclast differentiation. Irradiated human pre-adipocytes stained positively for senescence markers and CM had increases in numerous inflammatory factors including IL-6, MCP1, and GM-CSF, which were reduced by JAKi treatment. While overnight culture of bone marrow in control CM yielded only minor osteoclast differentiation at day 4, culture in senescent CM yielded osteoclast numbers comparable to bone marrow treated overnight in M-CSF. JAKi treatment of senescent cells prevented senescent cell CM induced osteoclast formation. JAKi did not block M-CSF induced osteoclast differentiation. JAKi treated mice exhibited significantly improved BV/TV in the vertebrae and femur. Vertebral and femur Tb.Th was significantly increased in JAKi treated mice. Tb.N, Tb.Sp, and SMI were not significantly altered. There was no significant difference in total bone marrow colony formation units (CFU) or osteoblast CFU. In contrast, monocyte and granulocyte CFU were significantly reduced in bone marrow isolated from JAKi treated mice. Consistent with this, osteoclast differentiation was significantly reduced in bone marrow derived from JAKi treated mice. Our findings suggest a novel mechanism and therapeutic target for bone loss in aged population.

Disclosures: Ming Xu, None.

LB-SU0036

Targeting CKIP-1 within osteoblast: A potential anabolic strategy for bone formation reduction during aging? Jin Liu*¹, Zongkang Zhang², Jie Li², Baosheng Guo³, Baoting Zhang², Aiping Lu³, Ge Zhang³. ¹Hong Kong Baptist University, Hong Kong, ²School of Chinese Medicine, The Chinese University of Hong Kong, ³Institute for Advancing Translational Medicine in Bone & Joint Diseases, Hong Kong Baptist University

Introduction: The pathophysiological mechanism for the reduction in bone formation during aging is still underexplored. Casein kinase-2 interacting protein-1 (CKIP-1) is an important ubiquitination-related molecule specifically targeting the linker region between the WW domains of Smurf1, thereby augmenting its affinity for and promoting Smad1/5 ubiquitylation (Lu *et al.*, Nat Cell Biol, 2008). In our preliminary study on bone specimens from both aged individuals with fracture and aged ovariectomized (OVX) rat model, we found that aberrantly increased CKIP-1 within osteoblasts was closely associated with suppressed BMP signaling and reduced bone formation during aging. Thus, we hypothesize that CKIP-1 within osteoblasts may participate in the pathological regulation on the bone formation reduction during aging.

Methods: Study 1: We examined the effect of genetic depletion of CKIP-1 gene within osteoblast on bone formation during aging using our established osteoblast-specific *Ckip-1* conditional knockout (CKO) mouse model. Study 2: We evaluated the effect of pharmacological silencing CKIP-1 within osteoblast using CKIP-1 siRNA encapsulated in our recently developed osteoblast-targeting delivery system (CH6-LNPs, Liang *et al.*, Nat Med, 2015) on bone formation in aged rats.

Results: Study 1: The aged CKO mice showed higher BV/TV and improved trabecular micro-architecture than their littermate controls (Fig 1a). The mineral apposition rate (MAR) was also higher in aged CKO mice than that in littermate controls (Fig 1b). In addition, more cells co-expressing ALP and pSmad1/5 were found at the bone sections from aged CKO mice when compared to their littermate controls (Fig 1c). Study 2: The level of CKIP-1 mRNA within osteoblast (ALP+ cells) was remarkably downregulated in the rats received eight consecutive intravenous injection of CKIP-1 siRNA-CH6-LNPs (siRNA group) (Fig 2b). Consequently, the intrasosseous protein levels of CKIP-1 and pSmad1/5 were both elevated in these rats (Fig 2c). In addition, the rats in siRNA group showed improved trabecular micro-architecture at proximal tibiae as well as larger width between xylenol and calcein labeling when compared to the rats in the other groups (Fig 2d&e).

Conclusion: CKIP-1 within osteoblast plays an important role in the pathological regulation on the aging-induced bone formation reduction. Targeting CKIP-1 within osteoblast may be a potential anabolic strategy for the bone formation reduction during aging.

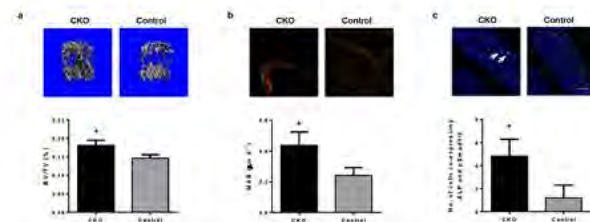


Figure 1 The bone phenotype of the osteoblast-specific *Ckip-1* knockout (CKO) mice. (a) Micro-CT analysis of the trabecular micro-architecture at 5th lumbar vertebra (L5) from the 18-month-old CKO mice and age-matched littermate controls. (b) Dynamic histomorphometric analysis of the trabecular micro-architecture at L5 from the 18-month-old CKO mice and littermate controls. (c) Immunohistochemistry analysis of the L5 bone sections from the 18-month-old CKO mice and age-matched littermate controls showing the number of cells co-expressing ALP (Red, osteoblast marker) and pSmad1/5 (green). Nucleus: Blue. Note: CKO mice: n=4, Control mice: n=6. Female: Male = 1:1. Data are mean \pm sd. * $P<0.05$ vs. Control.

Figure 1

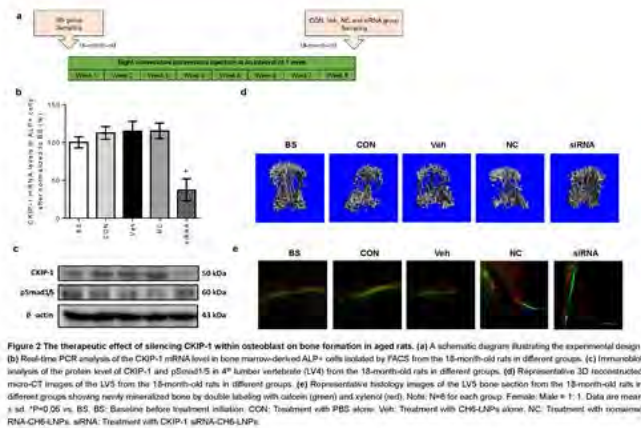


Figure 2
Disclosures: Jin Liu, None.

LB-SU0037

SEN6, a desumoylase, protects osteochondroprogenitors and chondrocytes from senescence and apoptosis. Jianshuang Li¹, Di Lu¹, Kevin Weaver¹, Huadie Liu¹, Hong Dou², Edward Yeh², Bart Williams¹, Tao Yang^{*3}.
¹Van Andel Research Institute, ²MD Anderson Cancer Center, ³Van Andel Research Institute, USA

Sumoylation is a post-translational modification that conjugates small ubiquitin-like modifiers (SUMOs) to the target proteins and alters their functions. In contrast, desumoylation process that is catalyzed by desumoylases removes SUMO modifications from the target proteins. The dynamic balance between sumoylation and desumoylation plays crucial roles in tissue development and homeostasis, and its dysregulation is associated with human disease and aging. A recent GWAS study revealed that a SNP in the upstream sequence of the gene encoding the desumoylase *SEN6* (Sentrin/sumo1 specific peptidase 6), is highly associated with osteoarthritis, providing a tantalizing clue about sumoylation in cartilage development and homeostasis. However, the role of sumoylation/desumoylation in the context of skeletal system is not clear. We have generated mice with osteochondroprogenitor (OCP)-specific *Senp6* deletion using *Prx1-Cre* as well as *Dermo1-Cre*. These mice show distinctively smaller skeletal elements with increased chondrocyte apoptosis and senescence. Moreover, the total level of sumoylated proteins, DNA damage responses, p53 signaling, and expression of genes associated with inflammation are also significantly elevated in *Senp6*-deficient chondrocytes or OCPs. These data suggests that SEN6-mediated desumoylation pathways are pivotal for OCP maintenance and chondrocyte homeostasis, likely through protecting cells from stress-induced apoptosis and senescence during skeletal development. This study will also shed light on the role of sumoylation /desumoylation in osteoarthritis pathogenesis.

Disclosures: Tao Yang, None.

LB-MO0001

Withdrawn

LB-MO0002

Unmasking tumor-induced osteomalacia with bisphosphonate therapy in metastatic prostate cancer, and its management. Tiffany Kim^{*1}, Kelly Wentworth², Jennifer Park-Sigal³, Anne Schafer⁴, Daniel Bikle⁴, Dolores Shoback⁴. ¹University of California, San Francisco, ²University of California, San Francisco, ³San Francisco General Hospital, ⁴San Francisco VA Medical Center, USA

Tumor-induced osteomalacia (TIO) causes profound hypophosphatemia due to renal phosphate wasting and inappropriately normal serum 1,25-dihydroxyvitamin D (1,25 OHD) levels, resulting from excessive fibroblast growth factor 23 (FGF23) production. While mesenchymal tumors typically cause TIO, castration-resistant prostate cancer (CRPC) is also implicated. We describe the course of a 68-year-old man with CRPC and his response to medical therapy. The patient initially had

normal serum phosphate and calcium levels but developed refractory hypophosphatemia while receiving monthly zoledronic acid (ZA) infusions to stabilize bony metastases. ZA had to be intermittently held, due to severe hypophosphatemia and hypocalcemia, from which he was mildly symptomatic with myalgias. Oral phosphate and calcium supplements were started. Initial lab results were notable for hypophosphatemia, hypocalcemia, inappropriately normal 1,25 OHD, secondary hyperparathyroidism, and elevated serum prostate specific antigen (PSA), alkaline phosphatase (AP), C-terminal telopeptide (CTX) and C-terminal FGF23 levels (see Table). PET CT demonstrated diffuse axial sclerotic uptake consistent with osteoblastic metastases. Over the next 2 years, he received daily doses of up to 2 mcg calcitriol, 4 g phosphorus, and 2.4 g elemental calcium. Serum calcium, PTH and CTX levels improved, but there were no changes in serum phosphate or 1,25 OHD levels, and serum PSA, AP and FGF23 levels increased (see Table). Despite therapy, he sustained right radial shaft and left wrist fractures after mechanical falls. TIO in metastatic CRPC is associated with aggressive disease in prior reports. TIO can be unmasked with anti-resorptive therapy or can occur spontaneously. It has been speculated that TIO in the setting of metastatic CRPC is due to FGF23 expression by the prostate cancer, and FGF23 may play a role in progression of this complication. Exogenous FGF23 promotes prostate cancer proliferation *in vitro* and may be produced as a paracrine factor by the tumor or osteocytes adjacent to metastatic deposits (Feng et al, *Oncotarget*, 2015). TIO is difficult to treat with supplements alone. Both cinacalcet, which can decrease FGF23's phosphaturic effects, and FGF23 neutralizing antibodies have therapeutic potential in TIO. This case highlights the importance of recognizing TIO as a potential complication of metastatic CRPC, which may be unmasked with anti-resorptive therapy.

Table

| Laboratory Value | Prior to Treatment* | With Treatment | Normal Range |
|---------------------------|---------------------|----------------|----------------|
| Phosphorus | 1.8 | 1.7 | 2.4-4.5 mg/dL |
| Calcium | 7.4 | 9.1 | 8.5-10.5 mg/dL |
| 25 hydroxyvitamin D | 45 | 43.7 | 20-50 ng/mL |
| 1,25 dihydroxyvitamin D | 38 | 22 | 18-72 pg/mL |
| Parathyroid hormone | 334 | 97.3 | 15-88 pg/mL |
| Alkaline phosphatase | 180 | 914 | 40-125 U/L |
| Prostate specific antigen | 142 | 318 | 0-4 mcg/L |
| C-terminal telopeptide | 1092 | 423 | 87-345 pg/mL |
| C-terminal FGF23 | 398 | 572 | < 181 RU/mL |

* Treatment: calcitriol initiation, titration of oral phosphorus and calcium

TIO Table

Disclosures: Tiffany Kim, None.

LB-MO0003

Optineurin Negatively Regulates Osteoclast Differentiation by Modulating NFκB and Interferon signalling, Implications for Paget's Disease of Bone. Rami Obaid¹, Sachin Wani¹, Asim Azfer¹, Ruth Jones², Philip Cohen², Stuart Ralston¹, Omar Albagha^{*3}. ¹University of Edinburgh, ²University of Dundee, ³University of Edinburgh, United Kingdom

Paget's disease of bone (PDB) is a common skeletal disorder characterised by osteoclast activation which provokes increased but disorganised bone turnover. Genetic factors play an important role in PDB and we have previously shown that susceptibility to PDB is mediated by a common variant (rs1561570) at the *OPTN* locus (Albagha et al, *Nat Genet* 2010) which is associated with reduced levels of mRNA expression although the mechanism by which this causes PDB is unclear. Optineurin is a ubiquitously expressed cytoplasmic protein with multiple cellular functions but its role in bone metabolism is yet unknown. The aim of this study was to investigate the role of OPTN in bone metabolism both *in vitro* by knockdown and over-expression experiments and *in vivo* by analysis of mice with a loss of function mutation (D477N) in OPTN. We found that expression of optineurin increased considerably during osteoclast differentiation from bone marrow cultures. Knockdown of optineurin by shRNA in bone marrow derived macrophages (BMDM) significantly increased osteoclast numbers and size, upon stimulation with M-CSF and RANKL, when compared with a non-targeting shRNA control. Over expression of Optn in Raw 264 cells resulted in a substantial reduction in the number and size of multinucleated TRAP+ cells formed upon stimulation with RANKL. Reduced expression of *OPTN* in BMDM was associated with enhanced RANKL-induced NFκB activation indicating that OPTN acts as a negative regulator of osteoclast differentiation *in vitro* by modulating NFκB signalling. Mice with a loss of function mutation in Optn have osteoclast over-activity and high bone turnover as determined by bone histomorphometric analysis. BMDM derived from mutant mice generated more and larger osteoclasts when compared to wild type cells, consistent with the knockdown data. Furthermore, osteoclasts derived from OPTN mutant mice had increased levels of NFκB activation, reduced levels of interferon beta expression and increased expression of c-fos in response to RANKL, compared with wild type. These data indicate that optineurin acts as a powerful negative regulator of osteoclast differentiation *in vitro* and *in vivo*. Our studies identify OPTN as a novel regulator of bone resorption and are consistent with a model whereby genetically determined reductions in OPTN expression predispose to PDB by modulating RANKL-induced NFκB activation and interferon beta-signaling in a cell lineage specific manner.

Disclosures: Omar Albagha, None.

LB-MO0004

Mechanical consequences of in vivo advanced glycation end-products in aging human bone: comparison of 3-point bending, cyclic reference point indentation, and impact reference point indentation. Simon Tang*, Adam Abraham, Aditya Yadavalli, Avinesh Agarwalla, Jenny Liu. Washington University in St Louis, USA

Advanced glycation end-products (AGEs) accumulate in bone with aging and disease, and are implicated in decreasing bone toughness in diabetics. Reference Point Indentation (RPI) allows the minimally invasive measurement of the mechanical behavior of bone tissue in vivo. Both cyclic and impact RPI, enhance the prediction of bone strength and discriminate between patient cohorts when coupled with DeXA, yet data relating RPI to tissue composition and 3-point bending remain scarce in human bone. Thus this study examines the relationship of bone tissue composition with 3-point bending, cyclic RPI (Biodent), and impact RPI (Osteoprobe) in aging human bone.

Aging female cadaveric limbs were tested (n = 28, Ages: 57-97). Cyclic and impact RPI was performed with soft tissues intact. Cyclic RPI (BioDent 1000) was performed 35 mm above the mid-diaphysis at 5 mm intervals at 15 locations (10 N at 2 Hz x 20). Indentation distance increase is calculated (IDI [μm]; indentation depth change from the 1st and 20th cycle). Impact RPI (Osteoprobe RUO) was performed 5 mm away from the cyclic RPI sites (40 N impact force, 4000 Hz x 1), and Bone Material Strength index (BMSi; 100 x avg PMMA IDI / bone impact IDI) is calculated.

The tibial cortical bone were then sectioned into 50 x 4 x 4 mm planks and tested in 3-point bending to failure (Instron 5866) to determine material properties (40 mm span; 10 N preload; 1 mm/min displacement rate). The RPI-measured cortical bones were scanned using MicroCT (VivaCT 40) to determine the volumetric tissue mineral density (TMD; 30 μm^3 voxel-resolution; 70 keV, 114 mA, 150 ms). Bone from the RPI-sites region were assayed for AGEs.

Cyclic RPI (2 Hz) and impact RPI (4000 Hz) probes bone in dynamic ways that differs from quasi-static 3-point bending. Cyclic RPI ($p = 0.006$, $r = -0.39$) and impact RPI ($p = 0.002$, $r = 0.43$) are more robust than 3-point bending modulus ($p = 0.736$) in predicting TMD variations. Similarly, AGEs were increasingly correlated with cyclic RPI ($p = 0.026$, $r = 0.28$) and impact RPI ($p = 0.001$, $r = -0.61$) but not 3-point bending toughness ($p = 0.126$). As a viscoelastic material, bone protein changes such as AGEs may be most prominent in its time-dependent responses to load. Since fractures are high-frequency, high-energy events, the ability to assess bone in this manner may provide further insight as to how bone may behave under these events.

Disclosures: *Simon Tang, None.*

LB-MO0005

Not only stiffness, but also yield strength of human trabecular bone is best predicted by bone volume fraction and fabric anisotropy. Sarah Musy¹, Ghislain Maquer*², Jarunan Panyasantisuk³, Philippe Zysset⁴. ¹Institute of Nursing Science, University of Basel / Nursing & Midwifery Research Unit, Inselspital Bern University Hospital, ²Institute for Surgical Technology & Biomechanics, University of Bern, Switzerland, ³Institute for Surgical Technology & Biomechanics, University of Bern, ⁴University of Bern, Switzerland

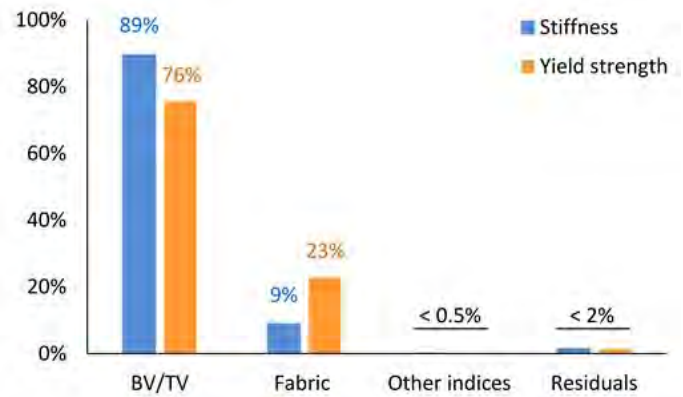
Numerous morphological indices capture the degradation of the trabecular structure characterising osteoporosis. A few even correlate to some extent with the mechanical properties of cancellous bone. Yet, against common belief, bone volume fraction (BV/TV) and fabric anisotropy were shown to determine up to 98% of trabecular bone stiffness variance, a predictive power that no other variables could substantially improve⁽¹⁾. This result remains to be confirmed for yield strength.

The morphology of 126 micro-computed tomography (μCT) scans of trabecular bone cubes extracted from three proximal femora (female, 62-75 years old) was evaluated via 25 indices including standard, individual trabeculae segmentation and textural parameters. Variance inflation factors were computed to evaluate their inter-dependence. Stiffness and yield properties of the samples were determined from independent loadcases performed respectively with linear and non-linear micro finite element analyses (μFEA). Finally, multi-linear regression models for the predictions of either stiffness or yield strength were built upon the independent morphometric indices, which contributions to the predictions were evaluated via ANOVA.

In line with our findings regarding stiffness⁽¹⁾, BV/TV was also the best predictor of yield strength. Accounting for fabric anisotropy had, however, more influence on the yield estimations (stiffness: $r_{\text{iso}}^2 = 0.895$, $r_{\text{aniso}}^2 = 0.985$ vs. yield: $r_{\text{iso}}^2 = 0.755$, $r_{\text{aniso}}^2 = 0.984$). The other independent factors (SMI, Tb.Th.SD, Tb.Sp.SD, pTb.Th, rTb.Th, pTb.S, rTb.l, RR.Junc.D and TBS surrogate) added very little to the models (stiffness & yield: $r_{\text{global}}^2 = 0.986$). Besides, BV/TV and fabric anisotropy explained 76% and 25% of the yield predictions of a global model, the other independent indices less than 1%. Comparatively, fabric anisotropy only described 10% of the variance in stiffness.

Two conclusions can be drawn from this study. First, just as stiffness, trabecular yield strength is best predicted by BV/TV and fabric anisotropy. The lack of influence of the other morphological variables strongly infers that the bone structure remains optimal for load bearing despite bone loss. Second, although stiffness and yield strength are highly correlated, the assessment of trabecular bone anisotropy is even more crucial to ensure accurate simulation of the post-elastic behaviour of whole bones using FEA.

1 Maquer G et al. J. Bone Miner. Res. 2015;30(6):1000-1008.



BV/TV and fabric anisotropy explain most of the stiffness and yield properties of trabecular bone

Disclosures: *Ghislain Maquer, None.*

LB-MO0006

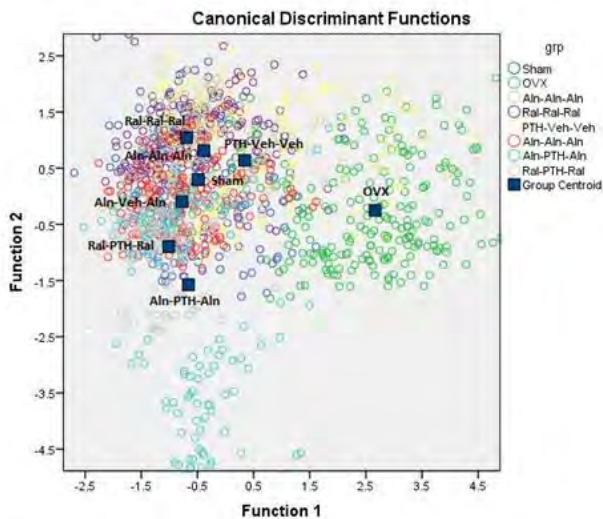
Sequential treatments with alendronate, parathyroid hormone (1-34) and raloxifene alter cortical bone matrix composition and quality in ovariectomized rats by Raman spectroscopy. Xiaomei Yao*¹, Amanuel Berhe², Xinyan Bai², Lucy Wang², Ying Liu², Amber Stern³, Wei Yao⁴, Mark Johnson², Yong Wang², Nancy Lane⁴. ¹University of Missouri-Kansas City, USA, ²University of Missouri-Kansas city, ³Engineering Systems Inc., ⁴University of California Davis Medical Center, USA

Anti-resorptive and anabolic agents are used individually or sequentially in individual patients for the prevention and treatment of osteoporosis. This study evaluated the effect of several of these treatment regimens on cortical bone matrix properties in ovariectomized (OVX) rats using Raman spectroscopy.

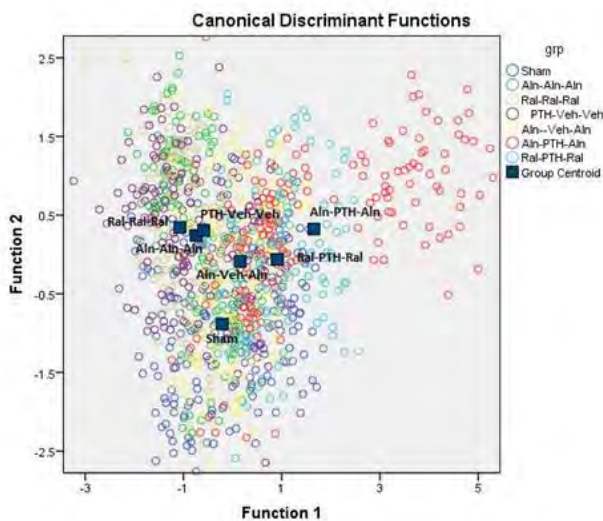
Four-month old female Sprague Dawley rats were either sham operated or OVX, left untreated for two months to develop osteopenia, and then treated with vehicle (Veh), hPTH (1-34) (PTH), alendronate (Aln), or raloxifene (Ral) continuously or sequentially for three, 3-month treatment intervals. Groups included Sham, OVX, Aln-Aln-Aln, Ral-Ral-Ral, PTH-Veh-Veh, Aln-Veh-Aln, Aln-PTH-Aln, and Ral-PTH-Ral (n=5-7/group). A LabRam HR 800 Raman spectrometer with a He-Ne laser (632.8 nm) was used to obtain spectra (700 to 1800 cm^{-1}) from the mid-tibial cortical bone and associated osteocyte perilacunar regions. PO-/amide-I and CO₃/amide-I ratios, mineral crystallinity, and collagen crosslinking were calculated and compared by ANOVA. Principal component analysis (PCA) and discriminant analysis (DA) were used to analyze all spectral data between treatment groups (SPSS v23). The Scree Plot and Analysis of Total Variance Explained functions identified the components that accounted for a threshold of >90% of the total variance in the PCA analysis from the perilacunar (1-4 μm around the lacunae) and the bone matrix (16-20 μm from any lacunae) regions in each of the groups.

Group analyses of the PO-/amide-I and CO₃/amide-I ratios, collagen crosslinking and mineral crystallinity were not different between all groups. 90% of the bone matrix variance was explained by 9 components, while perilacunar matrix included 10 components. PCA/DA analysis indicated that perilacunar and bone matrix regions in OVX were both significantly different from Sham ($p < .001$). Interestingly, single drug treatments clustered separately from the combination treatment groups in both perilacunar and bone matrix regions and were different from the Sham group ($p < .001$).

This study illustrates the power of PCA/DA to identify subtle changes in bone material properties from Raman analysis that are not readily apparent with simple comparison of standard metrics. All therapies restored bone matrix composition in rats with prolonged estrogen deficiency to Sham values. Further analysis is needed to determine which components explain the improvements also observed in bone strength by these sequential therapies.



Discriminant analysis of Bone matrix for all groups



Discriminant analysis of bone matrix for Sham and treatment groups

Disclosures: Xiaomei Yao, None.

LB-MO0007

Neonatal 25(OH)D3 Concentrations at Birth from Archived Dried Blood Spots and Future Risk of Fractures in Childhood - the D-tect study. Mina Händel^{1*}, Peder Frderiksen², Cyrus Cooper³, Berith Lilienthal Heitmann⁴, Bo Abrahamsen⁵. ¹Institute of Clinical Research, OPEN, University of Southern Denmark, Dk, ²Research Unit for Dietary Studies, The Parker Institute & the Institute of Preventive Medicine, ³Medical Research Council Lifecourse Epidemiology Unit, University of Southampton, ⁴Research Unit for Dietary Studies, The Parker Institute & the Institute of Preventive Medicine, Bispebjerg & Frederiksberg Hospital, ⁵Institute of Clinical Research, Odense Patient Data Explorative Network, University of Southern Denmark

Purpose: To examine 25(OH)D3 levels in dried neonatal blood samples (DBS) collected at birth as a predictor of the risk of fractures in childhood.

Methods: Case-cohort study using information on fracture incidence from the Danish National Patient Registry and capillary DBS from the Biological Specimen Bank for Neonatal Screening at *Statens Serum Institut*. Stored blood spots were used to measure neonatal 25(OH)D3 by a highly sensitive liquid chromatography tandem mass spectroscopy coupled with multiple reactant monitoring. A random subcohort of 3,600 individuals born between 1981 and 2002 was selected for analysis. The subcohort was augmented with a random sample of 1,200 fracture cases occurring between ages 6-13 years. The statistical analyses was based on deciles for 25(OH)D3, using Cox regression with Self-Prentice weights. The covariance of the regression coefficients was estimated using the Lin-Ying estimator.

Results: In the entire sample, the distribution of 25(OH)D3 was skewed. The mean (SD) for all subjects was 27.4 (18.7) nmol/L (median, 23.6; IQR, 13.3, 36.8), when corrected for the haematocrit fraction in capillary blood. As expected, 25(OH)D3 showed statistically significant monthly variation ($\chi^2_{11} = 582.36$, $p < 0.001$). The analysis showed that 25(OH)D3 concentrations at birth were not significantly associated with the risk of fractures during childhood. Figure 1 shows the exposure-risk relationship when the 25(OH)D3 concentrations were categorized according to the deciles in the subcohort. Conclusion: While previous studies suggest an association between antenatal maternal vitamin D status and childhood bone mass, our data provide the unique insight that perinatal vitamin D status does not seem to contribute to subsequent fracture risk in childhood. The two sets of findings suggest that intrauterine vitamin D exposure may be the more critical determinant of later offspring skeletal health.

Figure 1. Hazard Ratio (HR) of fractures in offspring at age 6-13 years to the concentration of 25(OH)D3, by the deciles of the distribution of 25(OH)D3 in the subcohort. The HRs are adjusted for season of birth (Nov-Jan, Feb-Apr, May-July, Aug-Oct). Vertical lines indicate 95% confidence intervals (CI). Children in the 70th to 80th percentile of the distribution were chosen as the reference value for the categorical analyses. The HRs are plotted at the median level of 25(OH)D3 within each decile category.

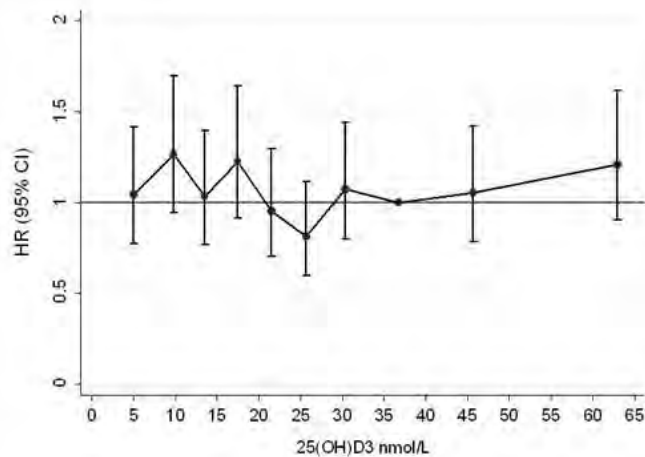


Figure 1

Disclosures: Mina Händel, None.

LB-MO0008

Activation of IKK β in Postnatal Articular Chondrocytes Leads to Catabolism of the Articular Cartilage Matrix. Sarah Catheline^{*}, Martin Chang, Jennifer Jonason. University of Rochester, USA

Osteoarthritis (OA) is a degenerative joint disease that causes degradation and eventual loss of cartilage within the synovial joints. Traumatic injury is known to be an important risk factor for development of OA likely due to the inflammatory environment within the injured joint. Pro-inflammatory cytokines are thought to negatively impact articular chondrocyte function and cartilage metabolism by suppressing production of factors anabolic to, and promoting production of factors catabolic to, the cartilage extracellular matrix (ECM). NF- κ B, a transcriptional regulator of the inflammatory response, has been implicated in regulation of collagenase (i.e., *Mmp13*) and aggrecanase (i.e., *Adamts5*) gene expression, key molecules responsible for the breakdown of the cartilage ECM. The role of NF- κ B in the development and progression of OA, however, is poorly characterized. Here we show evidence of canonical NF- κ B activation in tissues of the knee joint following meniscal/ligamentous injury (MLI) in the mouse. Specifically, we show decreased expression of I κ B α and increased expression of p65/RELA. We, therefore, hypothesize that constitutive activation of the canonical NF- κ B pathway in postnatal articular chondrocytes will be sufficient to drive the onset of an OA-like phenotype. To test this hypothesis, we used a chondrocyte-specific inducible Cre in combination with the *ROSA-Ikk2ca* allele to generate mice that overexpress a constitutively active form of IKK β in chondrocytes. Specifically, *Acan-Cre^{fl}-ER^{T2}*; *ROSA-Ikk2ca^{fl}* and *Acan-Cre^{fl}-ER^{T2}*; *ROSA-Ikk2ca^{fl}* mice were generated and administered tamoxifen at 2 months of age to induce Cre-mediated recombination in postnatal chondrocytes. At 3 months of age, histological analyses of the mutant mice reveal a marked decrease in proteoglycan content of the articular cartilage ECM relative to littermate Cre-negative control mice (Figure 1). Additionally, we detected a decrease in both ACAN and COL2A1, two of the predominant molecules present in the cartilage ECM, in the articular cartilage of the mutant mice by immunohistochemistry. Increased TUNEL staining within the articular cartilage is also observed in these mice. Our results suggest that activation of the canonical NF- κ B pathway can drive both cartilage ECM remodeling as well as chondrocyte apoptosis that, over time, is likely to lead to OA.

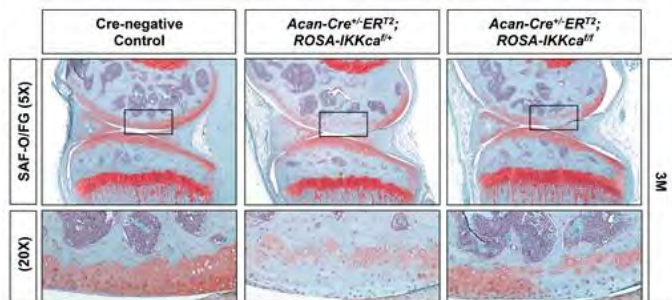


Figure 1

Disclosures: Sarah Catheline, None.

LB-MO0009

Absence of Adiponectin Enhances Exercise Training-Induced Improvements on Bone Structure in Mice. Sandra Sacco^{*1}, Abby Maybee¹, Ian Ritchie², Tara MacDonald², David Wright², David Dyck², Wendy Ward¹. ¹Faculty of Applied Health Sciences & Center for Bone & Muscle Health, Brock University, ²Department of Human Health & Nutritional Sciences, University of Guelph

Background: High-impact exercise such as running improves bone mass and bone structure and stimulates the production of adiponectin. However, human and animal data indicate that adiponectin is associated with negative effects to BMD. Objective: Determine whether the absence of adiponectin potentiates the positive effect of a chronic treadmill running protocol on BMD, bone structure and bone strength. Methods: 12-week-old wild type (WT) and adiponectin knockout (ADKO) mice (n=10 mice per group) received either a progressive treadmill running or a sedentary protocol for 8 weeks. Exercised mice ran 5 days per week for 8 weeks beginning at a speed of 20 m/min for 45 min for the first 3 weeks, with the incline increasing from 5% after week 1 to 15% after week 3. For the remaining 5 weeks, the 15% incline was held constant and the speed increased to 25 m/min by week 5. For the last 3 weeks, exercise duration increased to 60 min and during the last two weeks of training, 30-sec sprints at 32 m/min were performed in 10 min intervals. Tibias and lumbar vertebra (LV3) were scanned *ex vivo* using microcomputed tomography (Skyscan 1176) to measure structural properties of trabecular and cortical bone. BMD of tibias and LV3 were measured using dual energy x-ray absorptiometry (pDEXA[®] SABRETM). Biomechanical strength at the tibia midpoint was determined using a materials testing system (Instron Series IX Automated Materials Tester-Version 8.15.00). Results: WT mice that were exercise trained had higher (p<0.01) bone volume fraction of LV3 compared to sedentary WT mice. In addition, both WT and ADKO mice that were exercise trained had higher (p<0.01) trabecular thickness of LV3 compared to their respective sedentary control group. There was a greater (p<0.05) response to exercise training on bone structure in ADKO mice than in WT mice at both the proximal tibia (i.e. trabecular thickness) and tibia midpoint (i.e. cross-sectional area, cortical thickness). The effect of exercise training on BMD and bone mineral content at the tibia midpoint was dependent on genotype whereby ADKO mice that were exercised trained had higher (p<0.05) BMD and BMC compared to their sedentary counterparts. No other effects of genotype, exercise training or their interaction on bone structure, BMD or biomechanical strength were observed. Conclusion: The absence of adiponectin enhances some improvements to bone structure and BMD, particularly at the tibia, in response to exercise training.

Disclosures: Sandra Sacco, None.

LB-MO0010

Intermittent administration of parathyroid hormone facilitates osteogenesis by different mechanisms in cancellous and cortical bone. Kenji Ogura^{*1}, Tadahiro Iimura², Toshinori Ishizuwa³, Keiji Moriyama⁴, Akira Yamaguchi⁵. ¹Departments of Oral Pathology & Maxillofacial Orthognathics, Tokyo Medical & Dental University, ²Division of Bio-Imaging, Proteo-Science Center, Ehime University, ³Pharmaceuticals Research Center, Asahi Kasei Pharma Corporation, ⁴Department of Maxillofacial Orthognathics, Tokyo Medical & Dental University, ⁵Department of Oral Pathology, Tokyo Medical & Dental University, Oral Health Science center, Tokyo Dental College

Intermittent administration of parathyroid hormone (PTH) induces anabolic action on the bones. To understand the mechanism underlying the early phase of PTH-induced anabolic action, we investigated the expression profiles of osterix and sclerostin after intermittent administration of PTH using immunohistochemistry in adult rats. In the metaphyseal region, daily PTH administration (30 µg/kg) greatly increased the number of osterix-positive cells in the bone marrow, which had been reported as the osteolineage cells of the adult mouse bone marrow, on day 1, but the

cells gradually decreased on days 3 and 5. The number of osterix-positive osteoblasts on the cancellous bone surface showed no significant difference from control group on day 1, but it significantly increased on days 3 and 5 after daily PTH injections. PTH injections induced no significant changes in the number of sclerostin-positive osteocytes in the cancellous bone. In the cortical bone, intermittent administration of PTH induced no changes in the number of osterix-positive osteoblasts on the bone surface, but it significantly reduced the number of sclerostin-positive osteocytes on days 1, 3 and 5 after PTH injection. The effect of PTH on the reduction of sclerostin-positive osteocytes was more prominent at the endosteal region than periosteal region in the cortical bone. The serum sclerostin level was downregulated and the osteocalcin level was upregulated on day 5 after intermittent administration of PTH. Intermittent PTH injections increased osteoblast surface, osteoid thickness, and osteoid surface in cancellous bone, but not in cortical bone. This study provides the first evidence that intermittent PTH administration exerts anabolic action on bone formation through different mechanisms in cancellous and cortical bone during the early phase of PTH-induced anabolic action on osteogenesis. In cancellous bone, the increase in the osterix-positive osteoprogenitors and the subsequent increase in osterix-positive osteoblasts on the bone surface may be a more important function of PTH than the downregulation of sclerostin-positive osteocytes. Conversely, in cortical bone, a dramatic decrease in the number of sclerostin-positive osteocytes may play a critical role in the anabolic action induced by intermittent PTH administration.

Disclosures: Kenji Ogura, None.

LB-MO0011

The Elevation of Renal Renin Production Does Not Necessarily Correlate with Blood Pressure in Vitamin D Receptor Gene Knockout Mice Fed Hypocalcemia Rescue Diet. Naoko Tsugawa^{*1}, Miku Wada², Kisato Kanao², Maya Kamao², Kimie Nakagawa², Toshio Okano². ¹Osaka Shoin Women's University, Japan, ²Kobe Pharmaceutical University, Japan

Introduction: 1,25-Dihydroxyvitamin D₃ is thought to play an important role in controlling cardiovascular functions. In both epidemiological and animal studies, vitamin D deficiency has been reported to induce hypertension. It has been reported that *vitamin D receptor (VDR)* and *CYP27B1* gene knockout mice are hypertensive and both express the elevation of renin production in the kidney in both knockout mice. On the other hand, it has been reported that the increased dietary calcium intake correct the low serum ionized calcium concentration and result in a significant amelioration of the prevailing hypertension in the adult spontaneously hypertensive rat. In present study, we examined the correlation of blood pressure and renal renin production or other blood pressure regulated gene expression in *VDR* knockout mice (*VDR-KO*) fed hypocalcemia rescue diet. Methods: After weaning, wild-type (WT) and *VDR-KO* littermates were fed a normal diet (N-Ca) or a hypocalcemia rescue diet (2% calcium, 1.25% phosphorus, and 20% lactose; H-Ca) for 7 weeks. Blood pressure (BP) was measured using a noninvasive computerized tail-cuff system. The mRNA levels of renal renin and epithelial Na⁺ channel (ENaC) were measured by real-time PCR. Serum renin concentration was measured by ELISA. Results: BP of *VDR-KO* fed N-Ca was significantly higher than that of WT fed same diet. On the other hand, no significant difference in BP was observed between *VDR-KO* and WT fed H-Ca diet. Expression of renal renin mRNA of *VDR-KO* was higher than that of WT in both feeding of N-Ca and H-Ca. Also serum renin concentration of *VDR-KO* was higher than that of WT in both feeding of N-Ca and H-Ca. However, serum renin concentration of *VDR-KO* fed H-Ca was slightly lower than that of *VDR-KO* fed N-Ca diet. Although expression of renal ENaC mRNA of *VDR-KO* was significantly higher than that of WT in both feeding of N-Ca and H-Ca diet, the level of ENaC expression in *VDR-KO* fed H-Ca was lower than that in *VDR-KO* fed N-Ca diet. Conclusion: These results suggest that the elevation of renal renin production led to high gene expression of renal ENaC and elevation of BP in *VDR-KO* fed N-Ca. However, the elevation of renal renin production does not necessarily correlate with BP in *VDR-KO* fed H-Ca diet. There is a possibility that this non-correlation was caused by the suppression of renal ENaC expression via improvement of hypocalcemia.

Disclosures: Naoko Tsugawa, None.

LB-MO0012

Endothelin 1 Signaling is Required for SOST and IGF1 Secretion in Response to Mechanical Load. Everett Smith¹, Michael Johnson^{*2}, Luisa Meyer², Caitlyn Collins², Karen Hansen², Heidi Ploeg², Robert Blank³. ¹University of Wisconsin, USA, ²University of Wisconsin, USA, ³Medical College of Milwaukee, USA

Previously we demonstrated that addition of exogenous big endothelin to *ex vivo* cultured bovine bone or application of -2000 µe elicits similar biochemical and physical responses, change in apparent elastic modulus (E_{app}), mineral apposition rate and secretion of PGE₂. We hypothesized that endothelin (ET1) signaling was required for physical and biochemical responses of bone to mechanical load. To test this hypothesis, we conducted a 2x2 factorial trial of daily mechanical loading (-3000 µe, 120 cycles daily) and 10 mM BQ-123, an endothelin receptor A antagonist. Forty-eight human, trabecular bone cores (5 mm h x 10 mm d) were obtained from 2 male donors undergoing hip replacement. Donor cores and E_{app} were blocked to blocked

to equivalency. The cores were maintained in bioreactors for 25 days post initiation of treatment. There were four groups: control (CC), control+BQ-123 (CB), load+control (LC) and load+BQ-123 (LB). Each specimen was tested quasi-statically with a maximal compression of ~4000 μe on days 0 and 25 of the study to measure E_{app} . Culture medium from each sample was analyzed for secretion of IGF1, SOST and ET1 on days 0, 8, 11, 18, and 25. Biochemical data over time were analyzed by Wilcoxon test, followed by paired analysis by Kruskal-Wallis. There were significant differences in IGF1, SOST and ET1 secretion over time and between the LC and LB groups with the LB group having increased secretion of SOST and ET1 and decreased secretion of IGF1. The percent change in apparent elastic modulus over the duration of the experiment was not significantly different between groups; however, the LC group tended to be higher than the other groups. The increase in ET1 secretion in the CB and LB groups indicates the presence of a feedback loop. The decrease in SOST secretion in the LC group is similar to the change in SOST seen *in vivo* in response to mechanical load. Blockade of ET1 signaling prevents the decrease in SOST secretion in response to mechanical load. The increase in IGF1 secretion in response to mechanical load and the decrease in secretion seen when ET1 signaling is blocked suggest that ET1 signaling interacts with pathways that respond to mechanical load. This is the first study to show that autocrine ET1 signaling is required for response to mechanical load in human trabecular bone cores and that ET1 signaling is required for transduction of mechanical into biochemical signals during the anabolic response of bone to mechanical load.

Disclosures: Michael Johnson, None.

LB-MO0013

Periostin prevents cortical bone loss by increasing OPG levels in response to continuous PTH in mice. Nicolas Bonnet^{*1}, Serge Ferrari². ¹University Geneva Hospital (HUG), Switzerland, ²Division of Bone Diseases, Geneva University Hospital & Faculty of Medicine, Switzerland

Periostin is a matricellular protein expressed in late osteoblasts/osteocytes in response to iPTH. It mediates inhibition of Sost and skeletal bone formation response to iPTH. Interestingly, gene profiling in bones exposed to continuous PTH (cPTH, primary hyperparathyroidism in humans, and mini-pump in rats) have also identified a prominent increase of periostin (Postn) expression. Since cPTH activates osteoclast and induces bone resorption particularly at the endocortical surfaces, we investigated the influence of osteoblastic periostin on osteoclastogenesis and the cortical bone response to cPTH *in vivo* and *in vitro*.

For bone mass and structure evaluations we performed PIXIMUS and microCT after 3 weeks of continuous PTH given by mini-pump (40 $\mu\text{g}/\text{kg}/\text{d}$). To evaluate the role of osteoblastic periostin on osteoclast, we performed co-culture of Postn^{+/+} primary osteoclasts with Postn^{-/-} or Postn^{+/+} primary osteoblasts extracted from long bones of adult mice. We treated cells with recombinant periostin (rPostn, 4 $\mu\text{g}/\text{ml}$, every 2 days for 6 days) or saline (Vehicle, Veh) both containing vitamin D (10^{-6}M). We had 3 wells per group repeated twice. We evaluated the number and activity of osteoclast by TRAP staining and pit resorption assay kit which measure the intensity of fluorescence released from the coated plate into the medium.

In Postn^{-/-}, cPTH decreased femoral BMD (69 ± 1 vs 64 ± 1 mg/cm^2 respectively in Veh, $p < 0.01$), cortical bone volume (-6.2% vs Veh, $p = 0.11$) and increased apparent cortical porosity (+126% vs Veh, $p < 0.05$). No significant changes were observed in Postn^{+/+} in response to cPTH.

In vitro, osteoclast number and activity from Postn^{-/-} was not significantly different than Postn^{+/+}. However co-culture of Postn^{+/+} osteoclasts with Postn^{+/+} or Postn^{-/-} osteoblasts indicate a higher number and activity of osteoclasts in the absence of osteoblast periostin expression (+62% and +50% vs Postn^{+/+}, both $p < 0.01$). Adding rPostn, decreased the number of osteoclasts (-65% vs Veh, $p < 0.001$), as well as their activity (-5.5% vs Veh, $p < 0.001$), in both Postn^{+/+} and Postn^{-/-} osteoblast co-culture. Moreover rPostn increased OPG/RANKL levels in osteoblast conditioned medium by 152% vs Veh ($p = 0.09$). These results highlight the role of periostin not only in bone formation but also in bone resorption. They suggest that PTH-stimulated periostin expression prevents PTH-induced osteoclastogenesis and cortical bone loss by increasing OPG/RANKL levels.

Disclosures: Nicolas Bonnet, None.

LB-MO0014

Alpha-1 antitrypsin (AAT) Gene Delivery by Recombinant Adeno Associated Virus Vector for the Treatment of Osteoporosis. Mohammad Akbar^{*1}, Yuanqing Lu², Ahmed Elshikha², Rubina Ahamed², Mark Brantly², Shannon Holliday², Jay Cao³, Sihong Song². ¹USA, ²University of Florida, ³US Department of Agriculture

Purpose: Osteoporosis, a global public health problem, is characterized by reduced bone mass and poor bone microarchitecture. Although the etiology and pathogenesis of osteoporosis are complex and multifactorial, inflammation is involved in the disease development. Therefore, anti-inflammatory strategy holds great potential for the treatment of this disease. Alpha-1 antitrypsin (AAT) is a multifunctional protein with anti-inflammatory properties. We showed that AAT gene therapy had therapeutic effect in inflammation related disease models including type-1 diabetes

and rheumatoid arthritis. Importantly, we showed that AAT protein therapy reduced bone loss in ovariectomized (OVX) osteoporosis mice. In addition, AAT protein therapy is expensive and requires continuous treatment. Therefore, AAT gene therapy may provide a great advantage for osteoporosis treatment. In this study, we investigated the therapeutic potential of AAT on preventing bone loss in an OVX mouse model using recombinant adeno associated virus (rAAV) as a vector of gene delivery approach. Method: To test the protective effect of AAT on osteoclastogenesis, we generated osteoclast from mouse bone marrow monocyte cells and treated with clinical grade AAT. We also generated recombinant adeno associated virus vector expressing AAT (rAAV8-CB-AAT) as AAT gene delivery vector. In animal study, Ovariectomized mice were i.p. injected with either rAAV8-CB-AAT (1×10^{11} particles/mouse), or phosphate buffer saline (PBS). We used age-matched and sham operated animals as a normal control. Eight weeks after the rAAV-CB-AAT administration, all animals were sacrificed and subjected to μCT scanning for the evaluation of vertebral bone microarchitecture.

Results: *In vitro* studies showed that AAT significantly inhibited osteoclast formation by inhibiting TNF- α production and cell surface Receptor Activator Nuclear Factor κB (RANK) expression. *In vivo* results showed that rAAV-CB-AAT administration significantly increased bone volume density, trabecular number, trabecular thickness and connectivity density, and decreased structural model index (SMI) compared to PBS injection in OVX mice. These results demonstrate that AAT gene delivery by rAAV vector mitigates ovariectomy-induced bone loss in mouse model.

Conclusion: Since rAAV vector has been proven to be safe in humans, AAT gene delivery by rAAV-CB-AAT vector could be a new strategy for the treatment of osteoporosis.

Disclosures: Mohammad Akbar, None.

LB-MO0015

The Oral Commensal Flora, a Dynamic Regulator of Alveolar Bone Remodeling. Chad Novince^{*1}, Keith Kirkwood², Caroline Westwater², Carolyn Whittow². ¹Medical University of South Carolina - College of Dental Medicine, USA, ²Medical University of South Carolina, USA

Recent novel findings published by the applicants, indicate the commensal flora stimulation of the host immune system has catabolic effects in the adult skeleton. Despite recognition that the commensal flora plays a significant role in directing T-cell mediated immunity, the impact of the normal flora on osteoimmunology and coupled osteoclast-osteoblast mediated bone remodeling is currently unclear. The purpose of this study was to define the impact of the commensal flora on physiologic bone remodeling processes in the adult skeleton. Specific-pathogen-free (SPF) vs germ-free (GF) mice were used to elucidate the commensal flora's immunomodulatory effects on marrow CD4⁺/CD8⁺ T-cell hematopoiesis, osteoblastogenesis and osteoclastogenesis. SPF & GF mice were sacrificed, femurs & tibias were harvested, and bone marrow was flushed for assays. Marrow CD4⁺/CD8⁺ T-cell subsets were analyzed via flow cytometry, and marrow gene expression was studied via qRT-PCR. Bone marrow stromal cells (BMSCs) were isolated to assess osteoblast expansion, differentiation & mineralization in culture. Magnetic cell sorting was employed to enrich for defined osteoclast progenitors (dOCs); 3 distinct dOC populations (CD11b^{hi}, dOC^{low}, dOC^{neg}) were plated & treated with control (M-CSF) or Tx media (M-CSF & RANKL) to evaluate osteoclast differentiation. SPF mice had increased marrow T_H17 cells, CD4⁺IL17⁺ cells, and TNF α mRNA levels. GF mice had higher marrow IGF-1 mRNA levels. *In vitro*, GF BMSCs had increased cell expansion over time. RunX2 & col2 mRNA were upregulated in GF BMSC cultures. Mineralization via von Kossa was increased in GF BMSC cultures. *In vitro* dOC TRAP stain studies demonstrated that SPF vs GF CD11b^{hi} and dOC^{low} cultures had increased OC size and nuclei # per OC, while SPF dOC^{neg} cultures inversely had decreased OC size and nuclei # per OC. Gene expression studies paralleled the OC differentiation findings elucidated in the TRAP stain cultures; NFATC1 & RANK mRNA were increased in SPF vs GF CD11b^{hi} and dOC^{low} populations, but inversely decreased in the SPF dOC^{neg} population. DC-STAMP mRNA was decreased in the SPF vs GF dOC^{neg} population, suggesting altered osteoclast fusion. This research defining the commensal flora immunomodulatory effects on skeletal homeostasis is highly relevant in advancing the understanding of physiological osteoimmunological processes, having implications for the prevention of skeletal deterioration in both health & disease.

Disclosures: Chad Novince, None.

LB-MO0016

Withdrawn

LB-MO0017

Intravital Analysis of Neovascularization in Nanofiber-mediated Cranial Bone Defect Repair. Xinping Zhang^{*1}, Xiaochuan Yang², Tao Wang², Honjun Wang³. ¹University of Rochester Medical Center, USA, ²University of Rochester, USA, ³Stevens Institute of Technology

Neovascularization plays a key role in bone tissue engineering. Understanding spatiotemporal regulation of blood vessel formation and regression during bone tissue

engineering represents a critical step toward devising successful strategies aimed at enhancing revascularization and promoting bone tissue repair and reconstruction. Utilizing a chronic cranial defect repair model combined with multiphoton laser scanning microscopy (MPLSM) and live microCT analyses, the goal of our current study is to establish the spatiotemporal regulation of neovasculature during nanofiber-assisted cranial bone defect repair. To this end, nanofibrous matrices were prepared from polycaprolactone (PCL), collagen type I, and hydroxyapatite nanoparticles (nHA) via electrospinning, stacked layer-by-layer to form a 3D tissue construct to repair a 2mm critical defect in cranial bone. To facilitate vascular ingrowth, large pores (~200micron in diameter) were introduced into the constructs using a micro-needle. Compared to acellular fibrous scaffolds which only induced limited mineralization at the site of repair, MicroCT analyses demonstrated that bone marrow stromal cells (BMSCs)-seeded constructs induced progressive mineralization at the defect site over a period of 8 weeks. Quantitative histomorphometric analyses demonstrated a 51% increase of bone formation in BMSC-seeded constructs as compared to the controls (n=4). MPLSM-based analyses of the vasculature showed vigorous small vessel angiogenesis within defect at week 5 post-surgery in BMSC-treated group as compared to the controls. While quantitative analyses demonstrated a similar vascular volume between the two groups, a two-fold increase of total vessel length was recorded in defects treated with BMSCs as compared to the controls (p<0.05). Remarkably, vessels less than 10micron in diameter demonstrated a 3-fold increase over the controls (p<0.05), suggesting that small vessel angiogenesis is associated with BMSC-enhanced new bone formation. Further longitudinal analyses of the regions with or without defect closure demonstrated that regression of the vessels was often seen in regions with osseointegration and defect closure, whereas persistent large-diameter vessels were often associated with non-unions and fibrotic tissue. Taken together, our studies strongly suggest that small vessel angiogenesis is critical for BMSC-mediated repair and engineering functional microvascular networks that support regeneration is essential.

Disclosures: Xiping Zhang, None.

LB-MO0018

Wdfy3 Interacts with TRAF6 and Modulates RANKL-Induced Osteoclastogenesis. Dennis Wu*¹, Ran Gu², Ritu Sarin², Regina Zavodovskaya³, Chia-Pei Chen⁴, Konstantinos S. Zarbalis⁵, Iannis E. Adamopoulos⁶. ¹University of California, Davis, Us, ²Division of Rheumatology, Allergy & Clinical Immunology, University of California at Davis, ³Department of Anatomy, Physiology & Cell Biology, University of California at Davis, ⁴Department of Statistics, University of California at Davis, ⁵Department of Pathology & Laboratory Medicine, University of California at Davis, Institute for Pediatric Regenerative Medicine, Shriners Hospitals for Children, Northern California, ⁶Division of Rheumatology, Allergy & Clinical Immunology, University of California at Davis, Institute for Pediatric Regenerative Medicine, Shriners Hospitals for Children, Northern California

Autophagy and phagocytosis are conserved cellular functions involved in the protein degradation process in immunity. Recently, autophagy-related proteins were shown to regulate osteoclast mediated bone resorption, a critical process in autoimmune diseases such as rheumatoid arthritis. Wdfy3 is a master regulator in selective autophagy for clearing ubiquitinated protein aggregates. In this study, we generated a series Wdfy3 transgenic mice (*Wdfy3^{lacZ}*, and *Wdfy3^{loxP}*) to investigate the function of Wdfy3 in osteoclast development and function. Wdfy3 expression in *Wdfy3^{lacZ}* neonatal mice was analyzed by histology and X-gal staining. Bone marrow-derived macrophages from wild type, *Wdfy3^{lacZ}*, and Wdfy3 conditional knockout (*Wdfy3-cKO*) mice (*Wdfy3^{loxP/loxP}-LysM-Cre⁺*) were differentiated into osteoclasts with macrophage colony-stimulating factor (M-CSF), and receptor activator of NF-κB ligand (RANKL). Wdfy3 expression on osteoclast-like cells was analyzed by X-gal staining and immunohistochemistry. RANKL-induced NF-κB signaling was analyzed by western blot. Osteoclast-related genes *Ctsk*, *Acp5*, *Mmp9* were measured by qPCR. Osteoclasts were characterized by tartrate-resistant acid phosphatase staining and filamentous actin ring formation assay. Osteoclast function was evaluated by dentin resorption assay. Our data showed that Wdfy3 is up regulated in osteoclast in *in vitro* cultures and highly expressed at the growth plate of neonatal mice. Osteoclasts derived from *Wdfy3-cKO*, showed increased osteoclast differentiation and function as evidenced by higher number and enlarged size TRAP⁺ multinucleated cells. Western blot analysis also revealed up-regulation of TRAF6 and an increase in RANKL-induced NF-κB signaling. Consistent with these observations Wdfy3 conditional knockout mice also showed an increase in osteoclast-related genes *Ctsk*, *Acp5*, *Mmp9* and an increase of dentine resorption in *in vitro* assays. Importantly, no difference was observed in autophagic flux in Wdfy3 deficient bone marrow-derived macrophages and control cells at basal level or under starvation. Taken together, our data highlight a novel role for Wdfy3 osteoclast development and function, which can be exploited for the treatment of musculoskeletal diseases.

Disclosures: Dennis Wu, None.

LB-MO0019

TBS change with different spine scan modes on Lunar Prodigy. Weiwen Chen*¹, Anthony Slattery², Jacqueline Center³, Nicholas Pocock³. ¹Garvan Institute, Australia, ²Department of Nuclear Medicine, St Vincent's Hospital, ³Garvan Institute of Medical Research, Australia

Trabecular bone score (TBS) is a measure of grey scale homogeneity which correlates with trabecular microarchitecture and is an independent predictor of fracture risk. TBS is being increasingly used in the assessment of patients at risk of osteoporosis and has recently been incorporated into the FRAX algorithms. Currently, TBS software can be used in Hologic and GE Lunar densitometers. GE Lunar machines acquire spine scans using one of three acquisition modes depending on tissue thickness (thin, standard and thick). As per our Department protocol, 20 patients (mean BMI: 30.8, range 26.2 to 34.1) returning for progress BMD evaluation, who had experienced a significant change in weight, were measured using a Lunar Prodigy (software 14.10) on the manufacturer recommended scanning mode as well as the mode which was recommended and used in the baseline scan. This provided 20 paired spine scans in standard mode and thick mode acquired on the same day with no repositioning. TBS was derived from all paired spine scans. There was no significant difference in lumbar spine BMD between the two scanning modes. There was however significant higher TBS values from the spine scans acquired in thick mode compared to the TBS derived from spine acquisition in standard mode (Mean difference: 20 %, SD ± 9.8). The acquisition parameters of the two modes were reviewed. There is no difference in pixel size (0.6 x1.05mm), X-ray tube current (3.0 mA) or voltage (76 kV) between the Lunar Prodigy standard and thick modes. There is however a significant difference in spine image acquisition times, 28 seconds in standard mode versus 56 seconds in thick mode, which would result in a lower signal-to-noise ratio (SNR) in the standard mode and consequently reduced image quality. Reduced image quality in the standard mode compared to the thick mode would theoretically lead to greater inhomogeneity of the image and consequently lower TBS.

In conclusion these preliminary data suggest that TBS values acquired in the GE-Lunar Prodigy are dependent on the scanning mode used. Further evaluation is required to confirm the cause and develop appropriate protocols.

Disclosures: Weiwen Chen, None.

LB-MO0020

Excessive Bone Loss in Older Men: Effects on Trabecular and Cortical Bone Microarchitecture. Jane Cauley*¹, Andrew Burghardt², Stephanie Harrison³, Peggy Mannen Cawthon³, Andrew Yu⁴, Ann Schwartz³, Elizabeth Barrett Connor⁵, Marcia Stefanick⁶, Sharmila Majumdar⁷, Eric Orwoll⁸. ¹University of Pittsburgh Graduate School of Public Health, USA, ²Department of Radiology & Biomedical Imaging, University of California, San Francisco, ³California Pacific Medical Centre, ⁴Department of Radiology & Biomedical Imaging, University of California, San Francisco, ⁵University of California, San Diego, ⁶School of Medicine, Stanford University, ⁷Department of Radiology & Biomedical Imaging, University of California, San Francisco, ⁸Oregon Health & Science University

Accelerated bone loss has been linked to an increased risk of fracture that was independent of baseline bone mineral density (BMD) perhaps by increasing cortical porosity or decreasing structural or material properties of bone. To test this hypothesis, we used high resolution peripheral quantitative computed tomography (HRpQCT) scans to measure bone microarchitecture in the distal radius and tibia (SCANCO, Inc., Germany). All men who are active in the Osteoporotic Fractures in Men Study (MrOS) are being invited to return for a fourth clinical visit, approximately 14 years since enrolling into MrOS. We defined excessive areal bone loss (EBL) from Visit 3 to Visit 4 (7.1 years) as >10% loss at either the total hip or femoral neck. We used linear regression models to calculate least square mean HRpQCT parameters in men with and without EBL. We adjusted for age, race, clinic, height and weight. To date, 850 men have returned for their visit; of these 84 (10%) have experienced EBL. Their mean percent change in total hip BMD was -14% compared to -2.5% in men without EBL. Compared to men without EBL, men who experienced EBL were older (86.3 vs 83.7 years), had a lower body mass index (25 vs 27 kg/m²) and were more likely to report at least 1 impairment in their instrumental activities of daily living (47% vs 26%). 36% of men with EBL lost >10% body weight since visit 3 compared to 10% of men without EBL (p < 0.0001). As shown (Table), men who experienced EBL had significantly lower trabecular bone volume fraction (BV/TV), fewer trabeculae and greater trabecular separation than men without EBL. Cortical thickness was also significantly lower in men with EBL. However, we found no difference in cortical porosity at either the radius or tibia. Of interest, the mean cortical pore diameter at the radius and cortical pore volume at bone sites were lower among men with EBL. Additional adjustment for weight change had little impact on our results.

In summary, our preliminary data show men with EBL have differences in trabecular microarchitecture and lower cortical thickness than men without EBL. In addition, the changes in cortical bone thickness may reflect endocortical bone loss or trabecularization of cortical bone and not cortical porosity at this time point. Together, these differences in both trabecular and cortical bone architecture may contribute to the increased fracture risk observed with accelerated bone loss.

Keywords: HRpQCT, excessive bone loss, men, oldest old, trabecular microarchitecture, cortical porosity

TABLE: COMPARISON OF BONE MICROARCHITECTURE AMONG MEN WITH AND WITHOUT WITH EXCESSIVE BONE LOSS

| | DISTAL RADIUS (Base + Weight, Height) | DISTAL TIBIA (Base + Weight, Height) |
|--|--|---|
| Trabecular Bone Volume Fraction, mm ³ (BV/TV) | | |
| No | 0.241 (0.237, 0.245) | 0.271 (0.27, 0.27) |
| Yes | 0.219 (0.209, 0.234) | 0.250 (0.24, 0.26) |
| p-value | 0.0044 | 0.00017 |
| Trabecular Number, mm ⁻¹ (Tb.N) | | |
| No | 1.48 (1.47, 1.50) | 1.41 (1.39, 1.42) |
| Yes | 1.39 (1.33, 1.44) | 1.34 (1.30, 1.39) |
| p-value | 0.0008 | 0.0193 |
| Trabecular Thickness, mm (Tb.Th) | | |
| No | 0.243 (0.242, 0.245) | 1.20 (1.18, 1.22) |
| Yes | 0.244 (0.239, 0.249) | 1.05 (0.99, 1.11) |
| p-value | 0.97 | <0.0001 |
| Trabecular Separation, mm (Tb.Sp) ^a | | |
| No | 0.636 (0.626, 0.646) | 0.69 (0.68, 0.70) |
| Yes | 0.708 (0.681, 0.748) | 0.74 (0.71, 0.78) |
| p-value | <0.0001 | 0.0086 |
| Trabecular Bone Volume, mm ³ (Tb.BV) | | |
| No | 792.8 (778, 808) | 2027 (1993, 2061) |
| Yes | 755.6 (708, 805) | 2001 (1894, 2107) |
| p-value | 0.16 | 0.65 |
| Cortical Thickness, mm (Ct.Th) | | |
| No | 0.846 (0.832, 0.860) | 1.24 (1.22, 1.27) |
| Yes | 0.776 (0.731, 0.819) | 1.11 (1.03, 1.20) |
| p-value | 0.0033 | 0.006 |
| Cortical Porosity, (Ct.Po) | | |
| No | 0.025 (0.024, 0.026) | 0.062 (0.060, 0.064) |
| Yes | 0.023 (0.020, 0.026) | 0.059 (0.053, 0.065) |
| p-value | 0.24 | 0.35 |
| Cortical Pore Diameter, mm (Ct, Po,Dm) | | |
| No | 0.204 (0.20, 0.206) | 0.233 (0.231, 0.236) |
| Yes | 0.193 (0.186, 0.201) | 0.225 (0.217, 0.233) |
| p-value | 0.012 | 0.0501 |
| Cortical Pore Volume, mm ³ (Ct.Po.V) ^a | | |
| No | 11.03 (10.5, 11.6) | 75.3 (72.6, 77.9) |
| Yes | 8.81 (7.5, 10.2) | 63.4 (55.1, 71.8) |
| p-value | 0.0067 | 0.0088 |

Base = age, race, clinic.

Table

Disclosures: Jane Cauley, None.

LB-MO0021

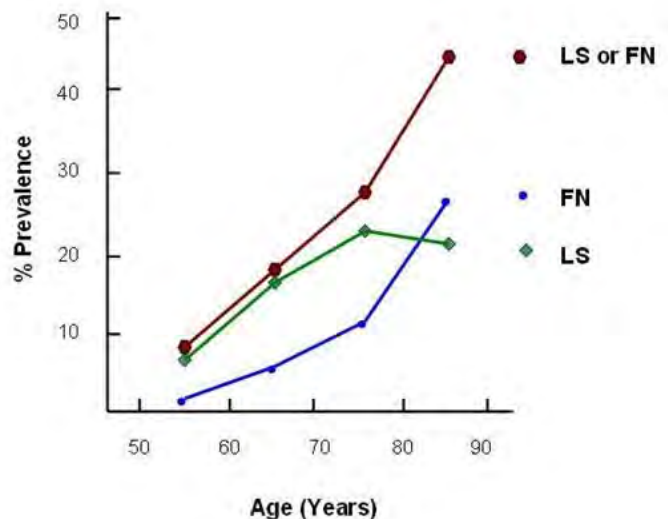
Prevalence and best skeletal areas to diagnose osteoporosis in women in Buenos Aires (Argentina). Carlos Mautalen¹, Silvina Mastaglia^{*2}. ¹Centro de Osteopatías Médicas, Argentina, ²INIGEM, UBA-CONICET

The aim of the study was to report values for osteoporosis (OP) prevalence in Buenos Aires, measuring the bone mineral density (BMD) at three different skeletal sites. From November 2012 to July 2014 a free measurement of the BMD for osteoporosis detection was offered in newspapers for women over 50 y.o. After signing an informed consent, 5448 Caucasian women living in Buenos Aires and surrounding districts were studied. BMD of the lumbar spine L1-L4 (LS), femoral neck (FN) and total hip (TH) was measured (Lunar Prodigy, software Version 12.3). Osteoporosis was defined as a T-Score \leq -2.5.

General prevalence of OP: 1021 women out of 5448 measured (18.7%), had OP at the lumbar spine or femoral neck. Adjusting the age of the sample to that of the general population a moderate increment of the prevalence (+0.5%) was observed. The figure shows the OP prevalence on each area and its combination per decades of age. Up to 70 y.o a low prevalence was observed if only the femoral neck is used. On the contrary the high prevalence up to the 70 y.o at the lumbar spine tended to level off over that age.

The OP prevalence at lumbar spine or femoral neck was similar to the results of the recent NHANES report (1). The total hip only adds a small (0.8 %) and not significant increment. Burden of OP: 346,500 of a total population of 1,853,000 women over 50 y.o in the area had OP, at lumbar spine or femoral neck, while only 163,500 had OP at the upper femur (femoral neck or total hip). Thus, 53% of the women would have been underdiagnosed.

Conclusions: The OP prevalence on the most populated urban area of Argentina has been assessed. The results are similar to those reported on Caucasian population of US and Canada. Since measurement of only the BMD of femoral neck overlooks the diagnosis on half of the women, it is suggested that future studies should include the measurement of the lumbar spine in combination with femoral neck for a more accurate estimation.



Prevalence of OP per decades at lumbar spine (LS), femoral neck (FN) and at LS or FN in this study

Disclosures: Silvina Mastaglia, None.

LB-MO0022

Withdrawn

LB-MO0023

Higher femoral shaft density and thickness as measured using Hip Structural Analysis are risk factors for atypical femur fractures. Andy Kin On Wong^{*1}, Shawn Davison², Jonathan Adachi³, Jacques Brown⁴, Robert Josse⁵, Aliya Khan³, Angela MW Cheung⁶. ¹University Health Network, Canada, ²University of Victoria, ³McMaster University, ⁴Centre Hospitalier de l'Université de Laval, ⁵St. Michael's Hospital, ⁶University Health Network, Canada

Atypical femur fractures (AFF) have been associated with long-term use of antiresorptive therapy. However, in individuals with osteopenia or osteoporosis, it is difficult to know when to stop therapy. Objectives: To determine bone characteristics at the femoral shaft (FS) that can discriminate between those with and without AFFs. Methods: We conducted a cross-sectional analysis combining those with AFFs with individuals from the placebo arm of the Vitamin K Supplementation in Postmenopausal Women with Osteopenia Trial (ECKO) and the Canadian Multicentre Osteoporosis Study (CaMos). X-rays confirmed the diagnosis of AFFs based on ASBMR diagnostic criteria. Hip Structural Analysis (HSA) was completed on total hip dual-energy X-ray absorptiometry (DXA) scans in the three cohorts. Femoral neck bone mineral density (BMD) T-score classified individuals as normal, osteopenic or osteoporotic. Age, body mass index (BMI), prior history of fragility fractures (FFx), parental history of hip fractures (PHFx), use of glucocorticoids (GC), and duration of antiresorptive therapy use were obtained. Data analysis: Histograms of age-adjusted HSA parameters illustrated potential diagnostic thresholds. Fixed effects models determined differences in age-adjusted HSA parameters among osteopenic, osteoporotic and AFF groups, adjusting for covariates: BMI, FFX, PHFx, use of GCs, and duration antiresorptives use. Two standard deviations above the osteopenic distribution was used as a diagnostic threshold for each HSA parameter, which was binarized using these thresholds and examined for associations with AFFs in binary logistic regression models, adjusting for the same covariates. Results: 634 individuals were included in final analyses among which the AFF group was older and used antiresorptives for longer (Table 1). There was a clear separation of distributions for age-adjusted FS BMD, cortical thickness and cross-sectional area across classifications (Figures 1a & b). Fixed effects models showed significant differences between AFF and each of osteopenia and osteoporosis groups for these same variables even after accounting for covariates. Correspondingly, odds for an AFF were two to four-folds higher when FS variables exceeded the given thresholds (Table 2). Conclusions: Femoral shaft density and thickness characteristics may be used to identify individuals with osteopenia or osteoporosis who may be at risk for an AFF, and who may therefore be candidates for a drug holiday.

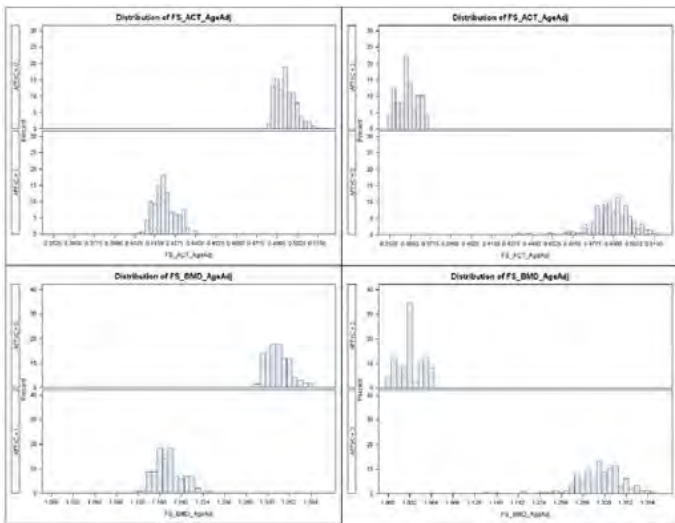


Figure 1a

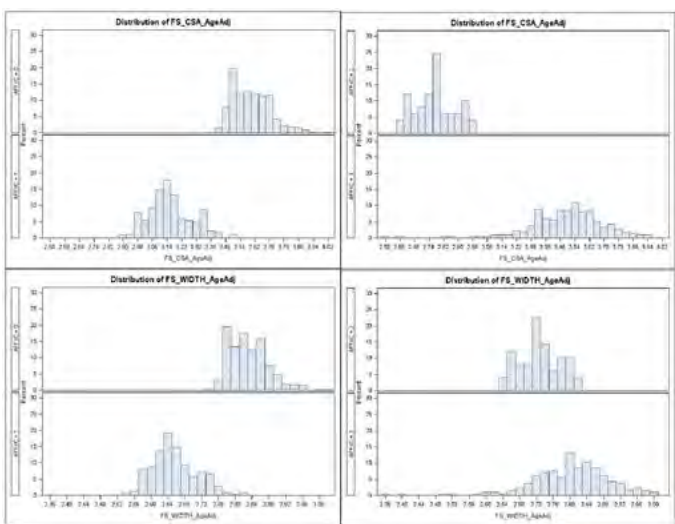


Figure 1b

| Variable | OSTEOPENIA | | | OSTEOPOROSIS | | | AFF | | | P |
|--|------------|-------|------|--------------|-------|------|-----|-------|----------|--------|
| | N | Mean | SD | N | Mean | SD | N | Mean | SD | |
| AGE (years) | 312 | 57.7 | 7.1 | 44 | 59.2 | 5.6 | 198 | 68.6 | 11.49167 | <0.001 |
| BMI (kg/m ²) | 312 | 25.41 | 4.21 | 44 | 25.31 | 6.78 | 198 | 26.64 | 4.380774 | <0.001 |
| Duration Antires (years) | 312 | 2.4 | 3.7 | 44 | 6.2 | 4.1 | 198 | 10.3 | 5.9 | <0.001 |
| FS Average Cortical Thickness (mm) | 312 | 0.42 | 0.08 | 44 | 0.36 | 0.09 | 150 | 0.49 | 0.10 | <0.001 |
| FS Bone Mineral Density [g/cm ²] | 312 | 1.16 | 0.18 | 44 | 1.02 | 0.22 | 150 | 1.32 | 0.20 | <0.001 |
| FS Cross Sectional Area (mm ²) | 312 | 3.10 | 0.52 | 44 | 2.69 | 0.68 | 150 | 3.52 | 0.55 | <0.001 |
| FS Width (mm) | 312 | 2.80 | 0.22 | 44 | 2.76 | 0.22 | 150 | 2.81 | 0.23 | 0.623 |

Table 1

| Age-Adjusted HSA Parameters | Adjust | N | OR | Lower 95 | Upper 95 | Threshold |
|--|--------|-----|------|----------|----------|-----------|
| FS Average Cortical Thickness (mm) | None | 634 | 2.08 | 1.48 | 2.91 | > 0.45 |
| FS BMD (mm) | None | 634 | 2.02 | 1.43 | 2.84 | > 1.27 |
| FS Cross Sectional Area (mm ²) | None | 634 | 1.95 | 1.32 | 2.88 | > 3.70 |
| FS Width (mm) | None | 634 | 0.72 | 0.50 | 1.04 | > 2.90 |
| FS Average Cortical Thickness (mm) | Covars | 620 | 4.61 | 2.02 | 10.50 | > 0.45 |
| FS BMD (mm) | Covars | 620 | 4.02 | 1.78 | 9.04 | > 1.27 |
| FS Cross Sectional Area (mm ²) | Covars | 620 | 3.68 | 1.38 | 9.81 | > 3.72 |
| FS Width (mm) | Covars | 620 | 0.70 | 0.33 | 1.49 | > 2.91 |

Table 2

| Dependent | Adjust | Open | LS5 | URS | OP | LS5 | URS | AFF | LS5 | URS | ptx1 | ptx2 | ptx3 |
|--|--------|------|------|------|------|------|------|------|------|------|--------|--------|--------|
| FS Average Cortical Thickness (mm) | None | 0.42 | 0.39 | 0.45 | 0.36 | 0.28 | 0.44 | 0.49 | 0.45 | 0.53 | <0.001 | <0.001 | <0.001 |
| FS BMD (mm) | None | 1.17 | 1.08 | 1.56 | 1.04 | 0.80 | 1.27 | 1.51 | 1.20 | 1.43 | <0.001 | <0.001 | <0.001 |
| FS Cross Sectional Area (mm ²) | None | 3.17 | 2.84 | 3.89 | 2.78 | 1.38 | 4.18 | 3.50 | 2.84 | 4.18 | <0.001 | <0.001 | <0.001 |
| FS Width (mm) | None | 2.68 | 2.42 | 2.90 | 2.73 | 2.10 | 3.36 | 2.80 | 2.51 | 3.10 | <0.001 | <0.001 | <0.001 |
| FS Average Cortical Thickness (mm) | Covars | 0.42 | 0.39 | 0.45 | 0.36 | 0.28 | 0.44 | 0.46 | 0.42 | 0.55 | <0.001 | <0.001 | <0.001 |
| FS BMD (mm) | Covars | 1.17 | 1.08 | 1.27 | 1.03 | 0.79 | 1.27 | 1.31 | 1.12 | 1.51 | <0.001 | <0.001 | <0.001 |
| FS Cross Sectional Area (mm ²) | Covars | 3.17 | 2.63 | 3.71 | 2.77 | 1.35 | 4.16 | 3.46 | 2.34 | 4.62 | <0.001 | <0.001 | <0.001 |
| FS Width (mm) | Covars | 2.88 | 2.42 | 2.90 | 2.72 | 2.09 | 3.36 | 2.80 | 2.28 | 3.31 | <0.001 | <0.001 | <0.001 |

Table 3

Disclosures: Andy Kin On Wong, None.

LB-MO0024

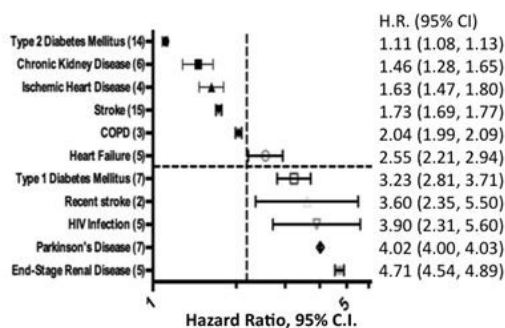
Risk of Hip Fracture in Common Medical Conditions – Meta-Analyses Identify Patients who Warrant Treatment. Steven Cummings¹, Richard Eastell². ¹San Francisco Coordinating Center, USA, ²Sheffield General Hospital, United Kingdom

Background: Many medical conditions have been listed as increasing fracture risk but the magnitudes of those risks have not been quantified. Patients who have some medical diagnoses might have such a high risk of hip fracture that they warrant initiation of osteoporosis, especially in older people. However, the risk of hip fracture with most medical conditions has not been quantified.

Method: We conducted systematic reviews followed by meta-analyses for medical conditions that guidelines list as risk factors for fracture. We took the yardstick of glucocorticoid therapy effects; high-dose glucocorticoids (prednisone >7.5 mg/day) are associated with a 2.2-fold risk of hip fracture, to indicate that a higher risk would be considered to raise concern and perhaps warrant pharmacologic treatment to reduce risk, even without BMD testing.

Results: The Figure shows that the pooled hazard ratio of hip fracture with the broken lines indicating the threshold of 2.2 and above the horizontal broken line, those diseases associated with high risk. The risks ranged from a high of a 4.7-fold increased risk with end stage renal disease (ESRD) down to a 1.1-fold risk of hip fracture for Type 2 Diabetes. Any history of stroke was associated with a 1.7-fold increased risk, however studies found that the risk is about 3.6-fold greater during the 1st 6 months after the stroke.

Conclusions: Patients with ESRD, Parkinson's Disease, HIV infection, recent stroke, Type 1 diabetes, and heart failure have a high risk of hip fracture that warrants treatment to reduce that risk, especially in older women or men. This would extend treatment to numerous patients who are not currently considered for treatment to prevent fractures. On the other hand, patients with COPD, stroke, ischemic heart disease, chronic kidney disease, or Type 2 diabetes have a lesser increase in risk and should be evaluated like any other patient without the disease with FRAX and measurement of BMD to assess fracture risk and make decisions about treatment.



Medical Conditions and Hip Fracture Risk

Disclosures: Steven Cummings, None.

LB-MO0025

National Fracture Risk Screening Finds Majority at High Risk Not Tested or Treated. Kathleen Cody*¹, David Karpf². ¹American Bone Health, USA, ²Stanford University School of Medicine, Division of Endocrinology, Gerontology & Metabolism

OBJECTIVES: To assess the prevalence of DXA screening and osteoporosis treatment in older adults identified as being at high risk of osteoporotic fracture in a community-based setting.

METHODS: We trained and dispatched 90 local peer educators to 9 independent living facilities, 1 short term rehabilitation center and 2 hospitals in six states to screen adults over age 45 for fracture risk using the validated FORE Fracture Risk Calculator™ (FORE FRC). Peer educators queried subjects about twelve clinical risk factors and entered results into the web-based tool. The resulting risk was displayed on a colored graph and explained onsite by the peer educator using companion worksheets “Steps to Take to Reduce Fracture Risk.” A copy of the graphic display was also emailed to participants with email addresses. The 10-year risk of any one of four major osteoporotic fractures was categorized as low (<10%) moderate (10-20%) or high (>20%). Approximately 10 minutes was required for acquisition and discussion of results.

RESULTS:

Table 1: Most of the individuals (69.4%) were over age 65 years. Proportions at moderate or high risk increased with age. 100% of the 314 individuals ≥ age 65 were at moderate to high risk, and 213 of 314 individuals (67.8%) in this age group were at high risk of osteoporotic fracture.

Table 2: Of the 314 adults age 65 and older who were screened, 56.1% reported not having a bone density test, a covered benefit under Medicare.

Table 3: Of the 237 adults at high risk of fracture, only 11.4% were being treated with an FDA-approved osteoporosis medication.

CONCLUSIONS: Fracture risk aligns closely with age. The proportion of the population with high fracture risk was substantial after age 65 (68%), yet less than half (44%) reported having had a bone density test (which is covered under Medicare), and of all the individuals found to be at high risk of fracture, only 11% were being treated. We are not doing a good job of diagnosing or treating osteoporosis to reduce risk of fractures in these older populations. The individuals screened in participating facilities were largely Caucasian and future outreach should attempt to find facilities serving more ethnically diverse adults. Not only did the outreach screening identify residents at risk for fractures, it also served to educate the facility staff who work with them.

Disclosures: Kathleen Cody and David B. Karpf MD report no conflicts of interest

| Distribution of Risk Levels by Age | | | | |
|------------------------------------|------------|-------------|-------------|-------|
| Age | Low | Moderate | High | Total |
| 45-64 | 23 (16.7%) | 91 (65.9%) | 24 (17.4%) | 138 |
| 65-75 | 0 | 50 (54.9%) | 41 (45.1%) | 91 |
| >75 | 0 | 51 (22.9%) | 172 (77.1%) | 223 |
| | 23 (5.1%) | 192 (42.5%) | 237 (52.4%) | 452 |

Table 1

| Have You Had a Bone Density Test? | | | |
|-----------------------------------|-------------|-------------|-------|
| Age | No | Yes | Total |
| 45-64 | 101 (73.2%) | 37 (26.8%) | 138 |
| 65-75 | 45 (49.5%) | 46 (50.5%) | 91 |
| >75 | 131 (58.7%) | 92 (41.3%) | 223 |
| Grand Total | 277 (61.3%) | 175 (38.7%) | 452 |

Table 2

| Taking an Osteoporosis Treatment? | | | |
|-----------------------------------|--------------|--------------|-------|
| Risk Level | No Treatment | On Treatment | Total |
| HIGH | 210 | 27 | 237 |
| MODERATE | 171 | 21 | 192 |
| LOW | 22 | 1 | 23 |
| Total | 403 | 49 | 452 |

Table 3

Disclosures: Kathleen Cody, None.

LB-MO0026

Simultaneous LC-MS/MS measurement of 24,25-dihydroxyvitamin D and 25-hydroxyvitamin D providing a new perspective in the assessment of vitamin D status. Jonathan Tang*¹, Holly Nicholls², John Dutton³, Isabelle Picc³, Christopher Washbourne³, Lanja Saleh⁴, D Nowak⁵, Graeme Close⁶, Helen Macdonald⁷, Sarah Jackson⁸, Julie Greeves⁹, William Fraser³.

¹University of East Anglia, Norwich, UK, ²United Kingdom, ³University of East Anglia, ⁴University of East Anglia, ⁵University Hospital of Zurich, ⁶University Hospital of Zurich, ⁷Liverpool John Moore University, ⁸University of Aberdeen, ⁹HQ Army Recruiting & Training Division, ⁹HQ Army Recruiting & Training Division

Background: 24,25-dihydroxyvitamin D (24,25-d(OH)D) is converted from 25-hydroxyvitamin D (25(OH)D) by 24-hydroxylase. Recent studies suggest the production of 1,25-dihydroxyvitamin D (1,25-d(OH)D) from 25(OH)D is driven by the catabolism of 24,25-d(OH)D. Genetic mutations resulting in loss-of-function of the CYP24A1 gene are associated with hypercalcaemic conditions. We developed a new liquid chromatography tandem mass spectrometry (LC-MS/MS) assay to measure simultaneously 24,25-d(OH)D and 25(OH)D to investigate vitamin D status and metabolism. **Objective:** We describe a LC-MS/MS method used to determine: 1) reference interval of serum 24,25-d(OH)D in healthy individuals; 2) the ratios of serum 25(OH)D to 24,25-d(OH)D and of 1,25-d(OH)D to 24,25-d(OH)D in normals and 3) change in ratios in response to vitamin D supplements. **Method:** Prior to LC-MS/MS analysis 100µL of sample was extracted using [³H]_d-24,25-dihydroxyvitamin D₃ as internal standard, the method involved a derivatisation step to enhance ionisation efficiency. The reference interval of serum 24,25-d(OH)D was determined in samples obtained from 386 healthy unsupplemented individuals, age 17-32 y, mean serum [25(OH)D] 72 nmol/L (range 50-119 nmol/L), 24,25-d(OH)D, 25(OH)D and 1,25-d(OH)D were also measured in serum from three double-blinded randomized controlled studies where participants were given either 400/1000/5000 IU or placebo daily for a minimum of 3 months or a single dose 100,000 IU of vitamin D₃. **Results:** The LC-MS/MS method was able to fully resolve 24,25-d(OH)D₃/D₂ from 25(OH)D₃/D₂. The intra-assay and inter-assay CVs for all analytes were <11% across the analytical range. The reference interval for 24,25-d(OH)D₃ (mean, median, 95% CIs) was 6.5 nmol/L (6.0, 4.6-7.9). In supplement studies, mean (±SD, %CV) ratio of serum 25(OH)D:24,25-d(OH)D in baseline groups were 17.4 (±0.4, 2.6%), mean ratio of serum 1,25d(OH)D (pmol/L):24,25-d(OH)D (nmol/L) was 40.3 (±5.6, 13.9%). Participants who received vitamin D showed a significant increase in serum concentrations of 25(OH)D ($p<0.001$) and 24,25-d(OH)D ($p<0.001$), but showed no significant change in the ratio ($p>0.1$). However, a greater increase in serum 1,25-d(OH)D was observed in individuals with the highest 25(OH)D:24,25-d(OH)D ratio but this resulted in lower 1,25-d(OH)D:24,25-d(OH)D ratios. **Conclusion:** We found remarkable consistency in the ratio of serum 25(OH)D:24,25-d(OH)D. Increasing vitamin D₃ supplementation results in an increase in both metabolites but relative differences in production of 1,25-d(OH)D. The clinical utility of simultaneous measurement of metabolites not only will provide a new assessment tool for indicating loss-of-function mutations of CYP24A1, but can also provide data that may start to explain the lack of “optimal” response to increasing supplementation with vitamin D.

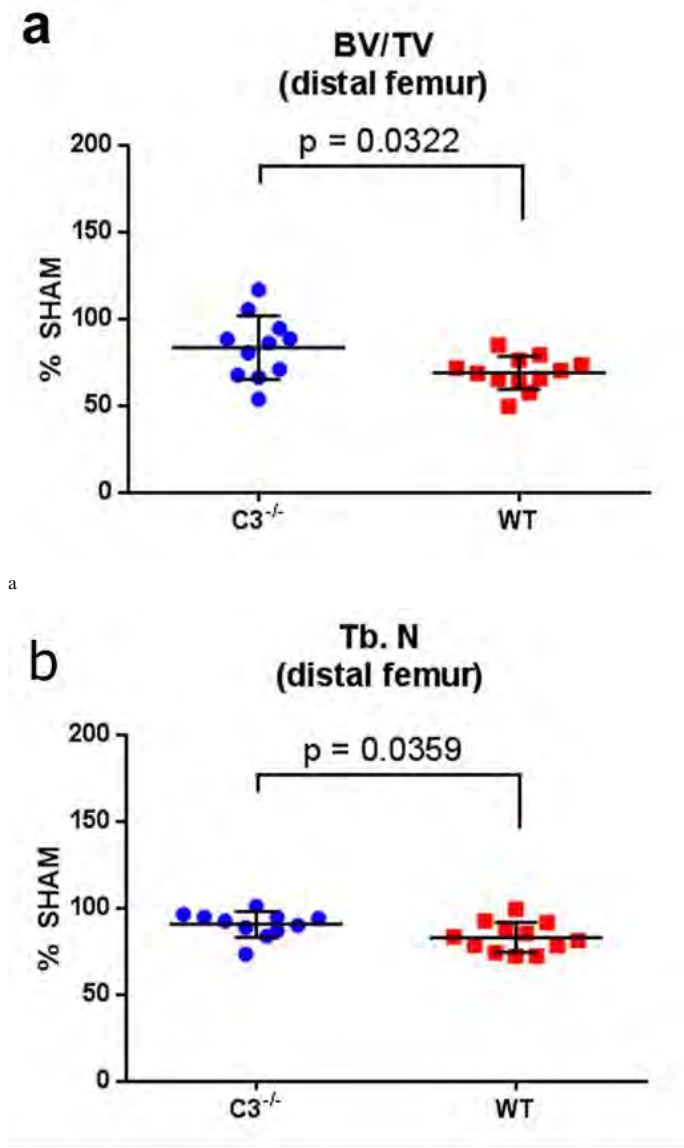
Disclosures: Jonathan Tang, None.

LB-MO0027

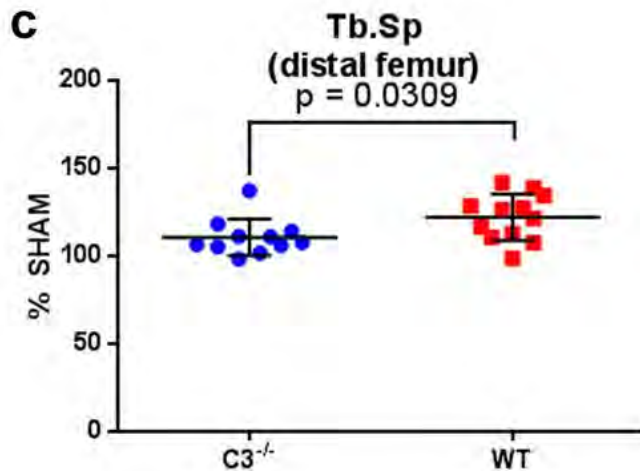
Absence of Complement Component 3 Protects Trabecular Structure and Stiffness of Femora in a Murine Model of Postmenopausal Osteoporosis. Danielle MacKay*¹, Thomas Kean², Kristina Bernardi³, Heather Haerberle⁴, Catherine Ambrose⁵, Feng Lin⁶, James Dennis². ¹Baylor College of Medicine, United States, ²Baylor College of Medicine, ³Seattle Children's, ⁴University of Texas, ⁵University of Texas Health Science Center, ⁶Cleveland Clinic Foundation

The growing field of osteoimmunology seeks to unravel the complex interdependence of the skeletal and immune systems. Notably, we and others have demonstrated that differentiation of osteoblasts and osteoclasts, the two cell types responsible for bone homeostasis, is partially regulated by the complement cascade. It is hypothesized that a deficiency of complement component 3 (C3), a central factor in the three main complement pathways, will reduce bone loss that results from estrogen deprivation in a model of postmenopausal osteoporosis. Wild type and C3^{-/-} mice on a C57BL/6 background were obtained from The Jackson Laboratory and bred and housed in accordance with the guidelines of the ACUC of Benaroya Research Institute. Only mice born on site were used in this study. At 6 weeks of age, ovariectomy or sham surgeries were performed under isoflurane anesthesia. At 12 weeks of age, animals were euthanized, and their uteri and hindlimbs were harvested. Uterine mass validated successful ovariectomies. Hindlimbs were fixed before being processed for microCT, histomorphometry, and/or mechanical testing. MicroCT scans were performed on a Scanco vivaCT 40 desktop scanner with a threshold of 300. Data are presented as a percentage and standard deviation and were normalized by dividing each individual value from ovariectomized mice by the mean value for sham-operated mice. Significance was calculated by unpaired Student's t-test. Micro-computed tomography revealed a 15% increase in the relative trabecular bone volume fraction of ovariectomized C3^{-/-} mice over that of their WT counterparts, an 8% increase in relative trabecular number, and an 11% decrease in relative trabecular separation in

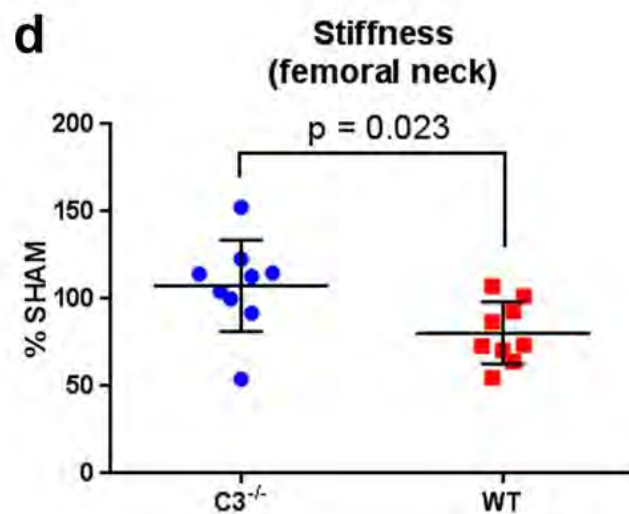
distal femora (a-c). In mechanical testing, the protective effects of the C3 deficiency manifest as a maintenance, compared to a reduction (20% decrease), of stiffness at the femoral neck in estrogen deprivation (d). Using a murine model of postmenopausal osteoporosis, our results demonstrate that the absence of C3 protects against femoral bone loss. In addition to its contribution to our understanding of the role of complement in bone remodeling, this study points to the complement cascade as a potential new target for osteoporosis therapy.



b



c



d

For all graphs, data are presented as % sham, with each data point representing the value for each ovariectomized C3^{-/-} mouse (blue circles) and each ovariectomized wild type mouse (red squares). Horizontal lines indicate the mean ± SD. MicroCT assessment of (a) trabecular bone volume fraction, (b) trabecular number, and (c) trabecular separation of the distal femur are shown. Mechanical testing determined the stiffness at the femoral neck (d).

subtitle

Disclosures: Danielle MacKay, None.

LB-MO0028

The Effects of Vitamin D and Sarcopenia on Bone Mineral Density in Korean women. Bom Taek Kim*¹, Myat Kyi La Thein², Sanghoon Lee², Sungwon Yang², Dukjoo Lee². ¹AJOU University School of Medicine, Kr, ²Ajou University School Of Medicine

A osteoporotic fracture has become a global health issue that causes tremendous impact on mortality as well as heavy socioeconomic burden. Previous studies suggested that vitamin D may prevent fractures by improving muscle mass as well as via increasing bone density directly. The purpose of the study is to determine that the influence of vitamin D on bone mineral density depends on its effects on muscle mass.

We analyzed the data from Korean National Health and Nutritional Survey IV in 2009. Women older than age 20 were included for the analyses. Bone mineral density and muscle mass were measured by DXA. Serum vitamin D concentration was tested.

Vitamin D and muscle mass affected BMD at proximal femur, but not at lumbar spine. Vitamin D deficiency and sarcopenia increased odd ratio for osteoporosis before and after adjusted for multiple variables. The effects of vitamin D deficiency on BMD still remained significant after adjustment for sarcopenia, which was vice versa.

Though vitamin D deficiency and sarcopenia shared common effects on BMD, they have their own effects on BMD independent from each other.

Disclosures: Bom Taek Kim, None.

LB-MO0029

Mice Expressing a Hypersensitive Form of the Glucocorticoid Receptor in Osteocytes Have High Cancellous Bone Mass and Reduced Cortical Thickness. Marilina Piemontese*, Jinhu Xiong, Yuko Fujiwara, Priscilla Baltz, Stuart Berryhill, Charles O'Brien. University of Arkansas for Medical Sciences, USA

Exogenous glucocorticoids act directly on cells of the osteoblast lineage to decrease cancellous bone formation and to increase bone resorption at the endocortical surface. However whether osteoblasts, osteocytes, or both mediate these actions of glucocorticoids is unknown. The goal of this study was to determine whether glucocorticoid action specifically on osteocytes is sufficient to mediate some of the negative impact of glucocorticoids on the skeleton. To do this we generated transgenic mice in which a hypersensitive mutant (M610L) of the glucocorticoid receptor (GR) is expressed specifically in osteocytes using the Dmp1 promoter. The GR_{M610L} mutant is activated in the presence of 5-10 fold lower glucocorticoid concentrations than the wild-type receptor. Therefore, osteocyte-specific expression of this mutant should increase the sensitivity of osteocytes, but not other cell types, to endogenous glucocorticoids. Quantitative RT-PCR analysis of mRNA isolated from transgenic mice confirmed bone specific expression of the DMPI-GR_{M610L} transgene. The dose-response curves of two known glucocorticoid target genes, GILZ and FKBP5, to dexamethasone were shifted to the left in osteocyte-enriched cortical bone cultures from transgenic mice compared to littermate controls confirming glucocorticoid hypersensitivity. MicroCT analysis revealed that cancellous bone in the femur and 4th lumbar vertebra was higher in transgenic mice compared to control littermates. These differences were observed in both sexes at 2 and 4 months of age. In contrast, cortical thickness measured at the midshaft of the femur was significantly lower in transgenic mice compared to wild-type mice at both ages and in both sexes. Consistent with reduced cortical bone thickness, transgenic mice displayed reduced bone strength, as measured by 3 point bending in the femur of 2 month old mice. These results demonstrate that activation of the glucocorticoid receptor specifically in osteocytes has positive effects on cancellous bone but negative effects on cortical bone and overall bone strength. Thus the negative impact of exogenous glucocorticoids on cortical bone may be mediated in part by actions on osteocytes where as their effects on cancellous bone may be independent of such actions.

Disclosures: Marilina Piemontese, None.

LB-MO0030

Romozumab (Sclerostin Antibody) Increases Wall Thickness in Remodeling Units in Cynomolgus Monkeys After 28 Weeks. Qing-Tian Niu, Rogely Boyce, Michael Ominsky*, Amgen Inc., USA

Romozumab (Romo), a sclerostin antibody, is a bone-forming agent under clinical investigation for the treatment of osteoporosis. Previous animal studies established Romo's ability to activate modeling-based formation, while its effects on remodeling-based bone formation were less clear. We examined the effects of Romo on bone remodeling using a kinetic reconstruction analysis of the formative site in lumbar vertebra from cynomolgus monkeys (cynos).

Male cynos (10-12 yr) were treated with either vehicle (Veh, n=8) or 30 mg/kg Romo (n=9) SC every 2 weeks for 28 weeks. Sequential fluorochrome labeling was performed from week 1 to 28, including tetracycline (Tet; weeks 4 and 10) and calcein (weeks 26 and 27.5). Kinetic reconstruction was performed (Steiniche et al., Bone 1992) on Villanueva-stained undecalcified sections of L3 vertebral bodies. Remodeling formative sites defined by an underlying scalloped cement line were sampled with a line grid and paired measurements of wall thickness (W.Th) and osteoid thickness (O.Th) were made. Final W.Th was measured in completed packets that contained

any label to provide an average effect across the treatment duration; those that contained Tet labels were separately evaluated to capture the early treatment effect. Final W.Th was also projected for packets near completion to reflect the treatment effect after 28 weeks.

After 28 weeks of Romo, BV/TV was increased from 28% in Vehicle to 46%, and active bone modeling sites were infrequently observed. Projected final W.Th for completing remodeling packets was significantly increased with Romo by 52% (57 vs 37µm in Veh). Similar W.Th values were found for completed packets reflecting the average treatment effect over 28 weeks (60 vs 33µm). In the Romo group, final W.Th in packets active from week 4-10 (containing both Tet labels) was 44% larger than projected final W.Th (82 vs 57µm), suggesting that the effects of treatment on W.Th were greatest early in the treatment period. Romo reduced eroded surfaces (ES/BS) by 64% (5.0 vs 1.8% in Vehicle), consistent with a reduction in remodeling space.

Together these results provide evidence of a positive effect of Romo on remodeling formative site in cyno vertebra. Greater W.Th and reduced remodeling space would contribute to the increases in bone mass during the period of active modeling-based formation as well as following self-regulation of bone formation with continued Romo administration.

*Disclosures: Michael Ominsky, Amgen; Amgen
This study received funding from: Amgen*

LB-MO0031

Effects of Ibuprofen Supplementation and Resistance Training on Bone and Marrow Properties in Postmenopausal Women. Whitney Duff*¹, Philip D. Chilibeck², Darren G. Candow³, Julianne J. Rooke², Riley S. Mason², Regina Taylor-Gjevre², Bindu Nair², Michael Szafron², Adam D.G. Baxter-Jones², Gordon A. Zello², Anthony M. Kehrig², Saija A. Kontalainen². ¹University of Saskatchewan, Canada, ²University of Saskatchewan, Canada, ³University of Regina, Canada

Fractures of the wrist in postmenopausal women are associated with low bone strength and bone adaptation has been linked to changes in marrow composition. Ibuprofen supplementation (400 mg) after resistance training sessions (3d/week, 9 months) has been shown to enhance hip areal bone mineral density in young women. The purpose of this study was to examine the effects of ibuprofen supplementation (400 mg) after resistance training sessions (3d/week, 9 months) on bone and marrow properties in postmenopausal women. Participants (n = 60, 64.8 ± 4.4y) were randomly assigned (double blind) to supervised resistance training or stretching (placebo-exercise), and ibuprofen or placebo (i.e. 4 groups) for 9 months. Baseline and post-intervention measurements included distal and shaft scans of the forearm and lower leg using pQCT (Stratec XCT2000). Outcomes for the radius and tibia at distal sites included: cross-sectional area, content, and density for total and trabecular bone as well as estimated strength in compression. Outcomes for shaft sites included: total area, and area, content, and density for cortical bone and marrow; estimated bone strength in torsion; and muscle area. Data was analyzed with SPSS using 3-factor ANOVA controlling for multiple comparisons (Bonferroni). Alpha level was 5% with custom hypothesis test for post-hoc analyses. There was an omnibus group effect. Resistance training combined with ibuprofen decreased distal radius total content (-1.6%) versus an increase for resistance training with placebo (0.6%) (p = 0.03). Stretching with ibuprofen increased distal radius total content (0.5%) (p = 0.05) versus a decrease for stretching with placebo (-1.35%). Resistance training with ibuprofen decreased radial shaft marrow content (-20.5%) versus an increase for resistance training with placebo (48.3%) (p = 0.01), with a trend for a decrease versus an increase in marrow density (-15.6%; 50.7%) (p = 0.06). Stretching with ibuprofen increased radial shaft marrow content (21.5%) and density (25.0%) versus a decrease for stretching with placebo (-42.9%; -36.4%) (p < 0.05). There were no interventional effects on remaining pQCT outcomes. Resistance training (without ibuprofen) or ibuprofen (without resistance training) increased bone content at the distal radius and marrow content at the radius shaft while combined interventions appeared to interfere with each other.

Supported by the Canadian Institutes of Health Research.

Disclosures: Whitney Duff, None.

LB-MO0032

Bisphosphonates and "Zebra lines": Relation to Fracture Risk and the Duration of Treatment in Osteogenesis Imperfecta. Jay Shapiro*, Evelise Brizola. Kennedy Krieger Institute, Johns Hopkins, USA

After 20 years of experience with pamidronate treatment in Osteogenesis Imperfecta (OI), uncertainty exists with regarding both the efficacy of extended treatment in fracture prevention and the recommended duration of treatment. Pamidronate treatment will initially decrease fracture rate but studies indicate that after 2-3 years the incidence of fractures tends to plateau. Bachrach and Ward (2009) suggested that in younger patients with OI, perhaps in a lower dose, bisphosphonate (BP) therapy should be continued until growth is fully or nearly complete. This recommendation is related to persistent risk factors and specifically to the risk of fracture at "BP-free zone" in the distal femur occurring with growth. BP induces "zebra lines" in the distal femur metaphysis. Harcke et al. (2012) proposed that zebra lines in patients with cerebral palsy, calcified zones of alternating high and low bone density, create a stress riser effect which could increase the risk of distal femur

fractures. We present a case illustrating the putative relation of zebra lines to femur fracture in OI. Case report: This 11 year old girl has type I OI, blue sclerae and multiple fractures. She completed 11 cycles of pamidronate treatment. Radiography of the right knee at age 8 year showed 5 residual zebra lines with a distal femur fracture just above the zone of zebra lines (Figure 1). Discussion: The risk of distal femur fracture in a “BP-free zone” is one leading argument for continuing BP treatment to the cessation of growth in children and adolescents with OI. This case illustrates the stress riser concept as contrasted with the “BP-free zone” postulate as a mechanism for distal femur fractures in BP- treated OI patients. Studies with *oimloim* model of OI indicate a delay of chondrocyte maturation to chondro-osseous lamellae following BP therapy. Antiresorptive BPs alter osteoclast activity at the growth plate leading to depressed bone remodeling and the formation of zebra lines with the stress riser risk for fracture. Conclusion: The case presented demonstrates a zone of increased fracture risk as previous reported in cerebral palsy cases. We propose this effect as more critical to injury than is the concept of a BP-free zone occurring with growth following cessation of initial treatment. Critical assessment of the relationship of zebra lines to the duration of BP treatment and the occurrence of distal femur fracture in OI is required.



Figure 1: Zebra lines and fracture

Disclosures: Jay Shapiro, None.

LB-MO0033

Melorheostosis: Whole Exome Sequencing Of An Associated Dermatoses Implicates Post-Zygotic Mosaicism Involving The KRAS Oncogene.

Michael P. Whyte^{*1}, Malachi Griffith², Lee Trani², Gary S. Gottesman¹, Susan Bayliss³, Kilannin Krysiak², William H. McAlister⁴, Brian A. Van Tine⁵, Katherine L. Madson¹, Vinieth N. Bijanki¹, Carol Brinson¹, Angie Nenninger¹, Steven Mumm⁶, Obi Griffith⁷, Elaine R. Mardis². ¹Center for Metabolic Bone Disease & Molecular Research, Shriners Hospital for Children, ²The Genome Institute, Washington University School of Medicine, ³Division of Dermatology, Washington University School of Medicine at Barnes-Jewish Hospital, ⁴Department of Pediatric Radiology, Mallinckrodt Institute of Radiology at St. Louis Children's Hospital, Washington University School of Medicine, ⁵Division of Medical Oncology, Washington University School of Medicine at Barnes-Jewish Hospital, ⁶Division of Bone & Mineral Diseases, Washington University School of Medicine at Barnes-Jewish Hospital, ⁷Division of Bone Marrow Transplant, Washington University School of Medicine at Barnes-Jewish Hospital

Melorheostosis (MEL) is the rare sporadic dysostosis featuring acquired areas of hyperostosis and osteosclerosis, often following a sclerotome, in one or more bones. Rarely, MEL becomes malignant. The etiology is unknown, but post-zygotic mosaicism is a favored hypothesis.

We studied a boy with MEL in his right ileum and femur (Figure A) with overlying scleroderma-like skin changes (Figure B) – an association some believe reflects a more widely distributed melorheostotic process. Additionally, he had a large epidermal nevus on his back (Figure C) - a dermatosis not associated with MEL but recently reported to harbor mosaic HRAS, NRAS, or KRAS mutations.

To explore for mosaicism underlying MEL in our patient, we performed whole exome sequencing (WES) of DNA from biopsies of both dermatoses, two areas of normal skin, and peripheral leukocytes. WES was conducted to ~100x average read depth (coverage) at every exon base position. Somatic variant calling, with four variant callers using all 20 possible pairwise combinations of the five separate DNA samples, was applied to identify any mutation(s) present in some but not all specimens. MEL bone was not investigated.

As expected for non-cancerous tissues, his overall mutation burden was exceptionally low. Only one high-confidence somatic variant emerged from the analyses – a heterozygous *KRAS* Q61H mutation (a well-established activating mutation) present in both skin lesions, but absent in his normal skin and blood. Interestingly, he and several other family members carried a heterozygous, in-frame, 24-base-pair deletion in the *LEMD3* gene. *LEMD3* mutation causes autosomal dominant Buschke-Ollendorff syndrome (BOS) and osteopoikilosis (OPK) featuring symmetrically distributed punctate osteosclerotic lesions where MEL is sometimes also present in an affected individual. This *LEMD3* deletion was detected in all four skin samples and blood at variant allele frequencies consistent with germline heterozygosity. However, he and other family members with the *LEMD3* mutation did not have the typical clinical or radiographic features of BOS or OPK, and *LEMD3* mutation does not underlie sporadic MEL. We also found in all five DNA samples two potentially interesting heterozygous germline mutations: a stop gain in *AMPD1*, and a frameshift in *MS4A12*.

In conclusion, the *KRAS* mutation in the scleroderma-like tissue overlying MEL of our patient implicates somatic mosaicism involving this oncogene in the etiology of MEL.



Figure

Disclosures: Michael P. Whyte, None.

LB-MO0034

Sclerostin Antibody Treatment Stimulates Bone Formation Without Increasing Bone Resorption to Normalize Bone Mass in Down Syndrome. Diarra Williams*¹, Sean Parham¹, Eric Schryver¹, Nisreen Akel¹, Jami Schmidt¹, Jessica Webber¹, Frances Swain¹, Dana Gaddy¹, Larry Suva². ¹Dept Orthopaedic Surgery UAMS, ²University of Arkansas for Medical Sciences, USA

A significant increase in the life expectancy of individuals with Down syndrome (DS) has been observed in recent decades. As such, skeletal complications such as osteopenia and bone fragility, previously not recognized in this population, have begun to appear. We have shown that this bone phenotype is associated with low bone turnover and decreased osteoblast activity, and not to the development of osteoporosis *per se*. Anti-resorptive agents, such as bisphosphonates, are frequently used to treat the low bone mass in people with DS, but the therapy is not directly treating the cause of the low bone mass and may in fact be contraindicated. New treatments which increase bone mass throughout the DS skeleton would therefore be highly beneficial. Sclerostin antibody (Scl-Ab) is a potential candidate anabolic therapy that functions by stimulating osteoblastic bone formation via the canonical Wnt signaling pathway, although the role of this pathway in the setting of low bone turnover is less clear. To determine the effect of Scl-Ab on the DS skeleton, 8 week old male Ts65Dn DS mice, trisomic for a portion of Mmu16 (analogous to Hsa21) that we have previously shown to also have low bone turnover, were treated with 3 weekly I.V. injections of 100 mg/kg Scl-Ab. Scl-Ab had significant anabolic effects by DXA and microCT in both age-matched controls (WT) as well as Ts65Dn mice, and led to increased trabecular and cortical bone formation at multiple skeletal sites. Importantly, Scl-Ab treatment led to the normalization of Ts65Dn BMD to WT levels in the whole body, distal femur and proximal tibia. Histologically, the striking anabolic activity was explained by significantly increased bone formation in Scl-Ab-treated mice, with no measurable differences in any measured *in vivo* osteoclast parameters. In *ex vivo* bone marrow cultures, Scl-Ab was able to significantly increase the recruitment of AP+ progenitors into the osteoblast lineage, resulting in increased AP+ colonies and osteoblastogenesis. In whole marrow or bone marrow macrophage (BMM) osteoclastogenic cultures, Scl-Ab did not change the differentiation of progenitors into osteoclasts. In conclusion, Scl-Ab was able to stimulate bone formation in a murine model of DS in the absence of increased osteoclastogenesis and bone resorption, and represents a potential new therapy to improve bone mass and reduce the fracture risk inherent in people with DS.

Disclosures: Diarra Williams, None.

LB-MO0035

Calcified Cartilage Islands in Mouse Bones. Victoria Ip¹, Zach Toth², Sarah McBride³. ¹Cornell University, ²Saint Louis University, ³Saint Louis University, USA

Bone's micro-scale structure differs greatly between humans and rodents, which can significantly affect strengthening mechanisms and limit findings' applicability to humans. Murine bones' lack of osteonal structure is a well-known example. Less obvious is an intracortical band of woven bone. The band's size and structure, which is indistinct using brightfield imaging, has prompted assumptions that it is unremodeled endochondral bone from early postnatal growth. Indeed, recent rat studies confirmed calcified cartilage islands within the band. To our knowledge, the same has not been shown in mice nor have the disorganized bone's origins been definitively proven. We hypothesize that, similar to rats, mouse long bones have cartilage islands within disorganized woven bone that is not evident on standard microCT (uCT), and this tissue is formed early in growth.

Twelve to 14 wk old male (n=4) and female (n=1) control mice generated for a previous study were used. Doxycycline (DOX) was administered via drinking water *in utero* to 3 weeks old. DOX, a fluorescent tetracycline, is typically used to repress Cre expression but also incorporates into actively mineralizing tissues. After euthanasia, both femora were harvested, fixed overnight, and scanned with uCT (cone beam, 12um resolution). Right femora midpoint paraffin sections were stained with alcian blue and picrosirius red to highlight cartilage and bone, respectively. Then polarized and brightfield imaging were used to quantify woven bone and cartilage islands. Left femora midpoint plastic sections were fluorescently imaged to quantify DOX labeled bone. To verify DOX labeling positive (DOX until 8 wks old, n=4) and negative (no DOX, n=4) controls were processed similarly (Fig 1). Paired t-tests compared the cartilage island locations (woven vs lamellar) and DOX labeled bone to woven bone area.

All samples had cartilage islands, although the number and percent area varied greatly (16 ± 8 islands, $0.1 \pm 0.3\%$). Remarkably, cartilage islands resided exclusively in the woven bone band (Fig 2). DOX labeling and woven bone patterns matched well and encompassed an almost identical cross sectional area. However, neither feature could be identified on uCT scans examined visually or by thresholding methods (Fig 3). In conclusion, young adult mice, like rats, have intracortical woven bone unremodeled from early growth. This tissue contains calcified cartilage islands which are indistinguishable from bone using typical uCT.

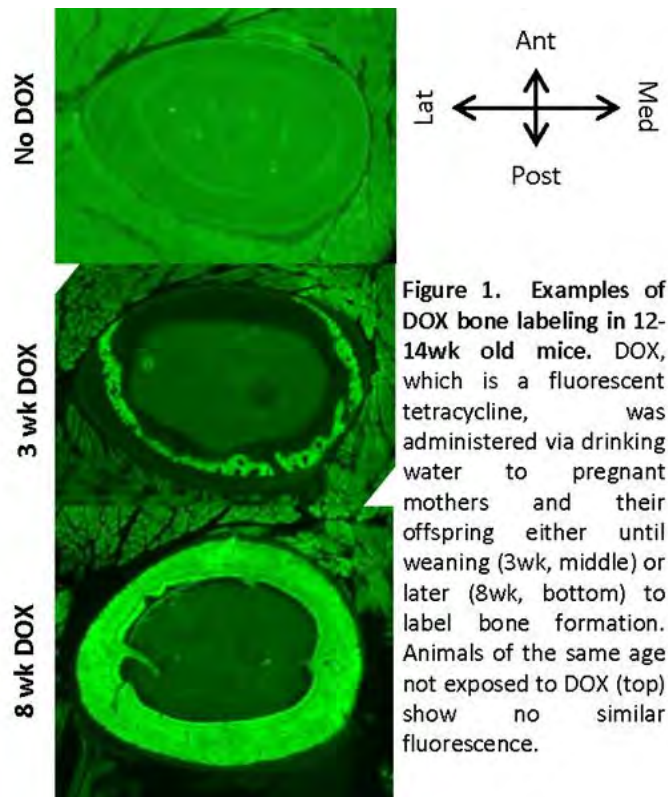


Figure 1. Examples of DOX bone labeling in 12-14wk old mice. DOX, which is a fluorescent tetracycline, was administered via drinking water to pregnant mothers and their offspring either until weaning (3wk, middle) or later (8wk, bottom) to label bone formation. Animals of the same age not exposed to DOX (top) show no similar fluorescence.

Figure 1

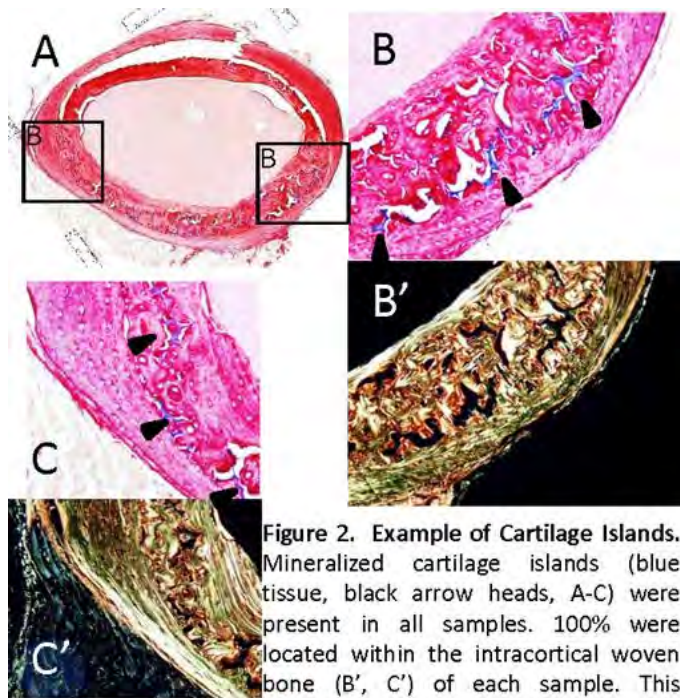


Figure 2. Example of Cartilage Islands. Mineralized cartilage islands (blue tissue, black arrow heads, A-C) were present in all samples. 100% were located within the intracortical woven bone (B', C') of each sample. This remained true even for animals as old as 30wks (data not shown).

Figure 2

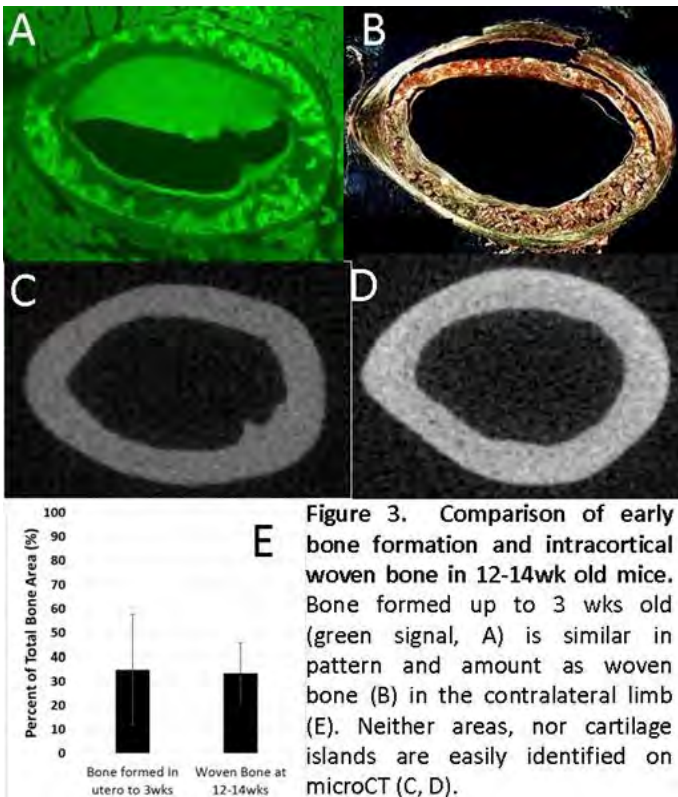


Figure 3

Disclosures: Sarah McBride, None.

This study received funding from: Saint Louis University

LB-MO0036

Kindlin-2 Controls TGF- β signaling and Sox9 Expression to Regulate Chondrogenesis. Guozhi Xiao^{*1}, Chuanyue Wu², Yumei Lai³, Ke Zhu³, Huiling Cao², Di Chen³. ¹Rush University Medical Center, USA, ²South University of Science & Technology of China, ³Rush University

The signals that control skeletogenesis are incompletely understood. Here we show that deleting Kindlin-2 in Prx1-expressing mesenchymal progenitors in mice causes neonatal lethality, chondrodysplasia, and loss of the skull vault. Kindlin-2 ablation reduces chondrocyte density by decreasing cell proliferation and increasing apoptosis, and disrupts column formation, thus impairing the formation of the primary ossification center and causing severe limb shortening. Remarkably, Kindlin-2 localizes to not only focal adhesions, but also to the nuclei of chondrocytes. Loss of Kindlin-2 reduces, while overexpression of Kindlin-2 increases, Sox9 expression. Furthermore, overexpression of Sox9 restores the defects in chondrogenic differentiation induced by Kindlin-2 deletion in vitro. Additionally, Kindlin-2 ablation inhibits TGF- β 1-induced Smad2 phosphorylation and chondrocyte differentiation. Finally, deleting Kindlin-2 in chondrocytes directly impairs chondrocyte functions, resulting in progressive dwarfism and kyphosis in mice. These studies uncover a previously unrecognized function for Kindlin-2 and a mechanism for regulation of the chondrocyte differentiation program and chondrogenesis.

Disclosures: Guozhi Xiao, None.